ZOOLOGICAL SCIENCE

An International Journal

VOLUME 4

1987

published by

The Zoological Society of Japan

CONTENTS
VOLUME 4

REVIEWS

ORIGINAL PAPERS

Physiology

Cell Biology

Genetics

Immunology

Biochemistry

Developmental Biology

Endocrinology

Morphology

Behavior Biology

Environmental Biology

Ecology

Taxonomy

Others

ISSN 0289-0003

Vol. 4 No. 1
February 1987

ZOOLOGICAL SCIENCE

PHYSIOLOGY
CELL and MOLECULAR BIOLOGY
GENETICS
IMMUNOLOGY
BIOCHEMISTRY
DEVELOPMENTAL BIOLOGY
REPRODUCTIVE BIOLOGY
ENDOCRINOLOGY
BEHAVIOR BIOLOGY
ENVIRONMENTAL BIOLOGY
ECOLOGY and TAXONOMY

published by **Zoological Society of Japan**

distributed by Business Center for Academic Societies Japan
VNU Science Press BV, Utrecht, The Netherlands

ZOOLOGICAL SCIENCE

The official Journal of the Zoological Society of Japan

ZOOLOGICAL SCIENCE is devoted to publication of original articles, reviews and communications in the broad field of Zoology. The journal was founded in 1984 as a result of unification of Zoological Magazine (1888–1983) and Annotationes Zoologicae Japonenses (1897–1983), the former official journals of the Zoological Society of Japan. ZOOLOGICAL SCIENCE appears bimonthly. An annual volume consists of six numbers more than 1000 pages including an issue containing abstracts of papers presented at the annual meeting of the Zoological Society of Japan.

MANUSCRIPTS OFFERED FOR CONSIDERATION AND CORRESPONDENCE CONCERNING EDITORIAL MATTERS should be sent to:

Dr. Seiichiro KAWASHIMA, Managing Editor, Zoological Science, Zoological Institute, Faculty of Science, Hiroshima University, 1–1–89 Higashisenda-machi, Naka-ku, Hiroshima 730, Japan, in accordance with the instructions to authors which appear in the first issue of each volume. Copies of instructions to authors will be sent upon request.

SUBSCRIPTIONS. ZOOLOGICAL SCIENCE is distributed free of charge to the members, both domestic and foreign, of the Zoological Society of Japan. To non-member subscribers within Japan, it is distributed by Business Center for Academic Societies Japan, 6–16–3 Hongo, Bunkyo-ku, Tokyo 113. Subscriptions outside Japan should be ordered from the sole agent, VNU Science Press BV, Europalaan 93, 3526 KP Utrecht, (postal address; P. O. Box 2093, 3500 GB Utrecht), The Netherlands. Subscription rates will be provided on request to these agents. New subscriptions and renewals begin with the first issue of the current volume.

[Publication of Zoological Science has been supported in part by a Grant-in-Aid for Scientific Publication from the Ministry of Education, Science and Culture, Japan.]

ZOOLOGICAL SCIENCE 4: 1–14 (1987)

REVIEW

Role of Oviducal Secretions in Mediating Gamete Fusion in Anuran Amphibians

CHIAKI KATAGIRI

Zoological Institute, Faculty of Science, Hokkaido University, Sapporo 060, Japan

INTRODUCTION

Mature unfertilized eggs of most animals are surrounded by extracellular coats or investments through which fertilizing sperm have to penetrate before fusing with the egg plasma membrane. These coats, composed mostly of glycoproteins with variable ultrastructures and molecular compositions, notably include the vitelline envelope or vitelline coat and the jelly coat in many invertebrates, and the zona pellucida in mammals. Studies on gamete fusion, particularly in echinoderms and mammals, have documented that these egg-investments are not a simple barrier for a fertilizing sperm but are obligatory participants in the process of sperm-egg fusion, playing such roles as specific binding sites for sperm or for inducing the acrosome reaction, etc. [1, 2]. In this context amphibians also provide a potentially good system, since a number of classical and recent studies have repeatedly shown that the jelly envelopes secreted by the oviduct are indispensable for sperm penetration into eggs [3, for earlier references]. However, the molecular bases for this jelly requirement in amphibian fertilization have been puzzling. In this paper, I will review first how this question has been challenged, and then I will summarize recent experiments, primarily from our laboratory, that have given a plausible explanation for a role of egg-jelly in anuran fertilization. Second, current studies implicating the functional significance of the non-jelly secreting portion of the oviduct will be discussed, to show how the oviduct of amphibians possesses an intriguing role in permitting sperm access to the egg. This discussion will be focussed mostly on anurans that have been studied more intensively than urodeles. References for studies on pertinent problems in urodeles can be found in other sources [4].

Received October 3, 1986

PRELIMINARIES TO FERTILIZATION

The ovulated eggs of anuran amphibians, surrounded by the vitelline coat or vitelline envelope[1] of several micrometers in thickness, are propelled towards the ostial openings of the oviduct by ciliary action and transported down the long reproductive tract to acquire several layers of jelly (Fig. 1). The eggs located in the expanded lowest portion of oviduct, i.e., ovisac or uterus, are regarded as mature, since eggs taken from coelom are not fertilizable, but fully jellied uterine eggs are fertilizable in high frequencies and undergo normal development. It may be assumed, therefore, that eggs acquire maturity during their passage down the oviduct. In fact, during transportation from ovary through coelom, oviduct to uterus, eggs undergo nuclear and cytoplasmic maturation. It has been shown, however, that the nuclear changes from germinal vesicle to second meiotic metaphase proceed quite independently from the location of eggs in the female reproductive tract. Thus, after initiating the germinal vesicle breakdown (GVBD), eggs may attain

[1] Designates the investment that is deposited around the oocytes during oogenesis, referred to as the vitelline membrane in the earlier literatures.

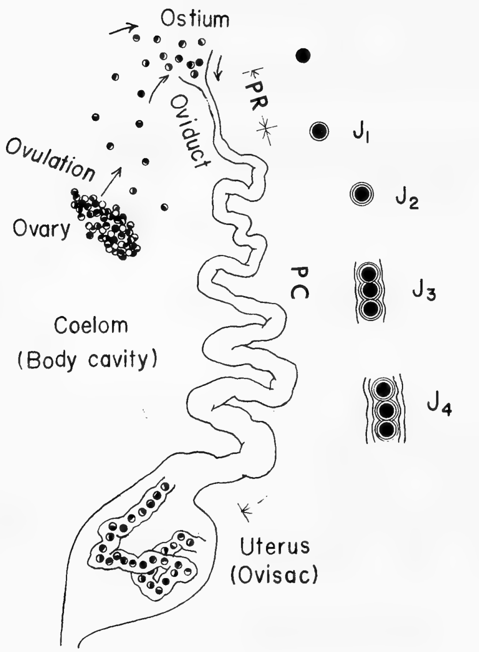

Fig. 1. The reproductive system of anuran female. The eggs released from the ovary to the coelom are moved by ciliary action towards the ostial opening of the oviduct, and pass through the non-jelly secreting pars recta (PR) and the jelly-secreting pars convoluta (PC) where they acquire several layers of jelly. The eggs located in the uterus are readily fertilizable upon insemination. J_1–J_4 denote jelly layers in the case of *Bufo japonicus*. The vitelline coat surrounding each egg is omitted.

metaphase of the second meiotic division even if they are forced to remain in the coelom by ligating the oviduct [5]. These eggs also attain cytoplasmic maturity as evidenced by their ability to undergo cortical granule exocytosis as well as to elicit an activation potential [6,7] in response to artificial stimuli. Extensive studies on the mechanism of oocyte maturation during the past two decades have established that the entire maturational events from the initiation of GVBD to completion of meiosis can be effected *in vitro* [8]. It seems clear that the major role of the oviduct in anurans is to mediate or support the sperm-egg interaction during the fertilization process.

EVENTS ASSOCIATED WITH SPERM ENTRY

Under natural conditions, anuran eggs are fertilized as soon as they are spawned in fresh water. Thus, unlike most urodeles [9], fertilization in anurans is external. Perhaps as an adaptation to this natural mating habit, spermatozoa of anuran amphibians are not motile in high ionic strength solution but become motile when the ionic strength is lowered. They are not only motile but are kept viable for several hours in hypotonic solutions osmotically equivalent to fresh water (e.g., 0.1–0.05 De Boer's or Ringer's solution ; for composition of De Boer's solution (DB), see legend for Fig.2). Hence, the usual method of

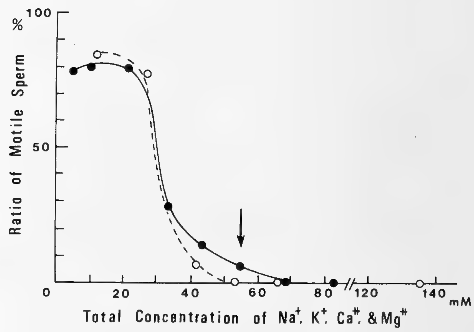

Fig. 2. Motility of *Bufo japonicus* sperm as a function of various cation concentrations in the surrounding media. Open circles, dilution of De Boer's solution (DB) consisting of 110 mM NaCl, 1.3 mM KCl and 1.3 mM $CaCl_2$; closed circles, dilutions of egg-jelly solubilized by UV-irradiation. Arrow indicates the total concentration in 0.5 DB. Data by Hosono and Ishihara (unpublished).

artificial fertilization in anurans consists of inseminating fully-jellied eggs freshly recovered from uterus with sperm suspended in 0.1–0.05 DB or Ringer. For the South African clawed frog *Xenopus laevis*, however, a slightly different method of artificial fertilization is adopted, because of a unique salt requirement by spermatozoa. The *X. laevis* sperm lose motility and fertilizing capacity rapidly in 0.05 DB, but are motile and remain viable in solutions with intermediate ionic strengths (e.g., 0.5 DB). Although fertilization is possible by inseminating

with sperm suspended in 0.05 DB as originally developed by Wolf and Hedrick [10], insemination with sperm suspended in 0.5 DB is more effective in successfully fertilizing *Xenopus* eggs [11, 12].

Fertilizing spermatozoa pass through several layers of jelly envelopes and the vitelline coat (VC) before fusing with the egg plasma membrane. Usually, it is 3–8 min after addition of sperm suspension that a fertilizing sperm is actually incorporated in the egg. During this short period, the jelly envelopes hydrate and swell rapidly. Observations on fresh material gametes (unpublished) reveal that a sperm arriving at the surface of the VC stands still for a while showing a boring movements and is incorporated in almost perpendicular to the surface of egg, leaving a swollen VC and a local accumulation of cortical cytoplasm [13, 14] (Fig. 3) at the site of sperm entry. Within seconds after the entry of sperm, the egg elicits a fertilization potential (or activation potential) including a rapid depolarization of the membrane potential, which is primarily due to the

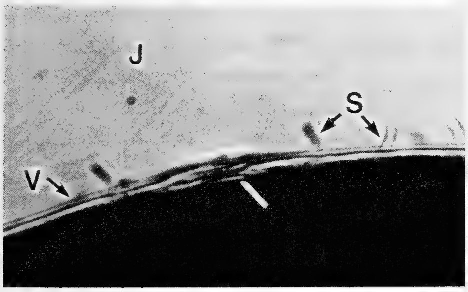

Fig. 3. Surface of the *Hyla arborea* egg 5 min after insemination, showing an accumulation of the cortical cytoplasm (arrow) at the site of sperm entry and a local swelling of vitelline coat (V) above it. S, sperm heads (out of focus); J, jelly coat.

opening of chloride channels [cf., 4]. There subsequently ensues a wave of cortical granule exocytosis that spreads from the site of sperm entry over the entire surface of the egg [14]. The cortical granule exudate alters the VC to become impenetrable by sperm, as most extensively studied in *X. laevis* [15]. Evidently these two events, the fertilization potential and the cortical granule exocytosis, constitute the fast and slow blocks to polyspermy in anurans. The problems related to the block to polyspermy in amphibians were recently reviewed by Elinson [4].

Regarding the reaction of sperm during the early phases of fertilization, two aspects are relevant to their passage through the egg envelopes. These include an acrosome reaction and a release of vitelline coat lysin. The acrosome reaction has so far been described only in two anurans, *Leptodactylus chaquensis* [16] and *Bufo japonicus*[2] [17]. For *L. chaquensis* the exact pattern of "acrosome breakdown", shown to be induced in a hypotonic medium, is not known. In *B. japonicus* the reaction involves the breakdown of the membrane-bounded acrosomal cap, thus exposing the inner membrane of the acrosomal cap which participates in the actual fusion with the egg plasma membrane (Fig. 4). It should be emphasized that sperm do *not* undergo this reaction at any point during the

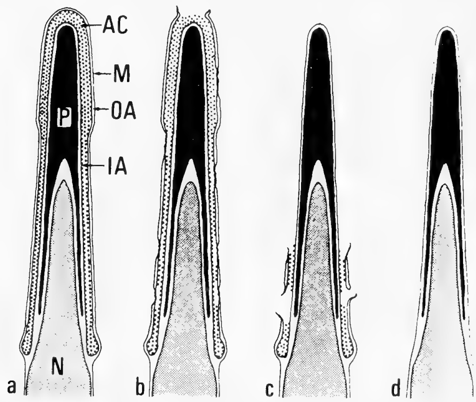

Fig. 4. A schematic illustration of the intact acrosome (a) and the acrosome reaction (b–d) in *Bufo japonicus*, showing the fusion of outer acrosomal membrane (OA) with the overlying plasma membrane (M), resulting in a release of the contents of acrosomal cap (AC) and exposure of the inner acrosomal membrane (IA). (Yoshizaki and Katagiri [17]. Reproduced by permission from Alan R. Liss Inc.)

passage through jelly, but those at the surface of or passing through the VC are definitely acrosome-reacted [16, 17]. The source of materials inducing the acrosome reaction will be discussed later.

[2] Previously referred to as *Bufo bufo japonicus* or *Bufo vulgaris formosus*. See Matsui [18] for the new nomenclature of this species.

There is evidence for the acrosomal localization of protease(s) in a number of anuran species, as defined by the formation of a "halo" on an artificial substrate (gelatin film). Although direct evidence is lacking for their involvement in the VC lysis, specific inhibitor studies employing this assay system revealed either a tryptic (*Rana pipiens,* [19–21]) or chymotryptic (*B. japonicus,* [22]) type of acrosomal proteases. The proteolytic activity that digests the VC of unfertilized eggs, but not of fertilized eggs, has been obtained by extraction of sperm with hypotonic medium (*B. arenarum,*[23]) or Triton X–100 (*B.japonicus,* [22]). The VC lysin isolated from the latter has a MW of 54,000 with occasional larger, polymeric forms observed. Its enzymatic properties are like the serine-protease chymotrypsin. It is able to lyse the VCs of some heterologous anuran species: such lytic activity correlates well with the cross-fertilizability by*Bufo* sperm. The relatively low specificity of sperm VC lysin in terms of heterologous VC hydrolysis is in contrast with the high species-specificity of hatching enzyme that is secreted by developing embryos to digest their own envelopes [24]. Most important in relation to the role of VC lysin in fertilization is that its release from individual sperm is highly correlated with the incidence of acrosome reaction, as discussed later. Besides the lysis of the VC, sperm may possibly possess other lytic activities in order to accomplish fertilization. Among these lytic activities is the dissolution of a special jelly component ("bouchon" or animal plug) by *Discoglossus pictus* sperm, which was one of the first demonstrations of acrosome-associated lytic activity in any species of sperm [25]. At present, it has not been unequivocally shown if fertilizing sperm use jelly-digesting enzyme(s) during their passage through the jelly envelopes.

ROLE OF EGG-JELLY

Fertilizing sperm first have to pass through the jelly-envelopes before making a fusion with the egg. The necessity for a fertilizing sperm to pass through jelly envelopes was indicated as early as in 1919 when Bataillon [26] showed that coelomic eggs exposed to sperm suspension were not fertilized despite their full ability to respond to parthenogenetic stimuli. Since then studies on a variety of species including both urodele and anuran amphibians confirmed that jelly-less eggs, either taken from the coelom or mechanically or chemically dejellied, cannot be fertilized when inseminated in water. Thus, just what role the egg-jelly plays has long been one of the major questions for understanding the mechanism of gamete-interactions in amphibians.

Properties of Egg-jelly

The jelly envelopes are made up of several layers of distinct composition and morphology which are highly variable according to the species or group of amphibians [27]. Chemical analyses have indicated their glycoprotein nature, with 60–70% carbohydrates and 30–40% proteins whose relative amount is variable according to species [28–30]. Their carbohydrate moiety is comprised of fucose, hexoses, a relatively large amount of hexosamines, and a small amount of sialic acid. Comprehensive analyses in *Xenopus laevis* revealed a total of 9 macromolecular components that are distributed differentially in 3 jelly layers [31]. Histochemical and analytical studies are available that implicate the difference in the glycoprotein composition of jelly layers [31–33], together with the specific localization of sulfated molecules in the innermost jelly layer [34].

Immunological analyses have demonstrated that jelly molecules include both species-specific configurations and components shared with other species or genera [35, 36]. Besides these, there are some antigenic components which are unique to particular layers of jelly [31, 35]. No studies, however, have elucidated the molecular nature of the antigenic determinants detected by conventional immunological techniques.

In evaluating the chemical analyses described above, it should be noted that the egg-jelly contains both the mechanically stable structural materials and soluble molecules which can easily diffuse away into surrounding medium. The relative amount of insoluble and soluble jelly materials may be variable according to the species of anurans. It seems that relatively larger amounts in jelly are soluble in toads (e.g., *Bufo arenarum,*[37]; *Bufo japonicus,* [30]) than in frogs

(*Ranas*, [3, 30]). In an extreme case as found in *B. arenarum*, repeated washings of eggs with water render them unfertilizable apparently due to the loss of soluble materials ("diffusible factor"), suggesting their importance for fertilization [38]. Chemical analyses in *B. japonicus* [30] revealed that carbohydrate and protein composition of water-soluble jelly materials is essentially the same as insoluble materials.

Egg-jelly as a Barrier for Sperm Penetration

Upon immersion of uterine eggs in salt solutions, hydration of jelly promptly begins. The adhesiveness and the degree of swelling in individual layers of jelly vary depending on the tonicity and the kinds of ions in the surrounding media. Generally, the jelly is more swollen and more adherent in lower salt solutions than in isotonic solutions, e.g., De Boer's or Ringer's solution. In parallel with the demonstration of the necessity of jelly in the fertilization process, it has repeatedly been shown that upon hydration in lower salt solutions, the eggs become refractory to fertilization, although they retain responsiveness to activation stimuli. The time required for the loss of egg-fertilizability after immersion in lower salt solutions is variable according to species of eggs, from 15—30 min (*R. chensinensis*, [39]; *X. laevis*, [10]) to 1 hr or more (*R. pipiens*, [3]; *B. bufo asiaticus*, [40]). There is ample evidence that this loss of fertilizability is accompanied by physicochemical changes in the particular layer of jelly envelopes that inhibit the migration of sperm through jelly. In *R. chensinensis* the blockade of sperm migration occurs both on the outermost and innermost layers, and these are ameliorated by treatment of jelly with trypsin [41]. A similar block in jelly of *X. laevis* [42] and *Hyla arborea* [43] is associated with an increased birefringence in a distinct middle layer of jelly, and this blockade in *X. laevis* is regained upon brief exposure to isotonic salt solution. It is emphasized that these changes of jelly accompanying the hydration in environmental conditions for normal fertilization decrease the actual number of sperm getting to the surface of VC, so that they function at least partly as a block to polyspermy.

Other lines of evidence point to the possible involvement of egg-jelly in preventing cross-fertilization. Although a large number of interspecific or intergeneric fertilizations are possible among amphibians [44], there are certain combinations where cross-fertilization does not occur. The block to heterologous sperm may occur at various steps preceding the actual gamete fusion, including the jelly layers, the VC, or the plasma membrane, depending on each combination. Of these the combinations between eggs of *Bufo japonicus* and sperm of *Rana* (*R. chensinensis, R. japonica,* and *R. nigromaculata*) are taken as examples where the jelly coat functions as a principal barrier for cross-fertilizability [36, 50]. The eggs of *Hyla arborea* are not fertilized by *R. chensinensis* sperm for the same reason [45]. Likewise, the eggs of *Xenopus borealis* are not fertilized by sperm of *X. laevis* because *laevis* sperm cannot penetrate the innermost jelly layer of *borealis* eggs. However, fertilization of *borealis* eggs with *laevis* sperm occurs if *borealis* eggs are enrobed with *laevis* jelly by transferring them to the oviduct of *laevis*. Alternatively, *laevis* eggs enrobed with *borealis* jelly cannot be fertilized with sperm of its own species but are still fertilized by *borealis* sperm [46].

Although the involvement of egg-jelly in preventing cross-fertilization is thus evident in certain crosses, the observed blockade of sperm migration in heterologous jelly cannot simply be ascribable to the lack of species-specific molecular interactions between sperm and the egg-jelly. Rather, in many cases the failure of sperm migration is more likely to be due to the incompatibility of the physical architecture of the egg-jelly. The *R. pipiens* eggs enrobed by *R. clamitans* jelly envelopes are not fertilized by *pipiens* sperm, but are fertilized when dejellied eggs are inseminated in the presence of soluble components ("egg-water") of *clamitans* egg-jelly [47].

Fertilizability of Oviducal Eggs

A number of experiments have been conducted to determine the fertilizability of the eggs taken from different levels of the oviduct, in an attempt to define what layers of jelly envelopes are indispensable for fertilization. Although the results in several species of amphibians favor the

general account that the fertilizability of eggs increases as they descend down the oviduct, it has not been easy to define an exactly specific jelly layer that is a prerequisite for fertilization. Experiments in *Xenopus laevis* indicated that the increase of fertilizability is gradual as the eggs travel down the oviduct, and there is no marked local rise correlated with a special jelly layer [48]. Other studies employing *Bufo japonicus* [49, 50], *B. arenarum* [51], and *Rana pipiens* [52] indicated that the rate of fertilization in eggs taken even from similar levels of the oviduct varied greatly according to the females used, the time after induction of ovulation, as well as the sperm concentration employed. Thus, in *B. japonicus* and *B. arenarum,* some batches of eggs taken from an upper portion of the oviduct may be fertilizable provided they are enrobed with a small amount of the inner second layer in addition to the innermost one. In other batches, however, eggs are not fertilizable until they are supplied with additional outer layers in the lower part of oviduct.

Apparently one of possible reasons for these variances is the maturity of eggs, as exemplified by the fact that the nuclear maturity of eggs bears no direct relation to the location of oocytes in the female reproductive tract. Under the conditions where eggs are mature enough to be responsive to artificial stimuli, results obtained in *Bufo* [50, 51] and *R. pipens* [3] seem to agree in showing that the innermost gelatinous jelly layer is not sufficient to support fertilization. On the other hand, the eggs were fertilized well even when they were enrobed only with the outer layer of jelly by bypassing the upper levels of the oviduct [3, 50]. The importance of outer jelly layers (J_3 or J_4 in *Bufo*; V3 in *R. pipiens*) deserves attention because of their possible relevance to retaining a diffusible factor that plays some essential role in supporting sperm entrance in eggs. The correlation of the loss of egg fertilizability with that of diffusible molecules has been particularly emphasized in studies with *B. arenarum* [53] and *R. pipiens* [3]. To summarize, studies on the fertilizability of eggs from various levels of oviduct have not given rise to conclusive results in understanding the role of jelly in fertilization. Re-evaluation of these studies should now be made in view of a more recent finding that the oviduct has roles other than the secretion of jelly materials, as discussed later.

Egg-jelly Factors Essential for Fertilization

A more potent approach to the question of how the egg-jelly functions in fertilization consists of inseminating dejellied uterine eggs in the presence of various jelly preparations. This assay system has the advantage of using eggs with homogeneous maturity, as well as the ease of applying jelly preparations after diverse chemical or physical modifications.

Eggs of *Bufo japonicus, B. arenarum, B. americanus, Hyla arborea*, and *Rana pipiens* obtained from the uterus and dejellied completely by KCN or NaCN are not fertilized when inseminated in 0.1 Ringer or 0.05 DB, but have proved to be fertilizable when inseminated in the presence of appropriate jelly preparations. The jelly materials that had been dissolved by cyanide and dialyzed to remove the cyanide ("dialyzed jelly") were highly effective in supporting fertilization of *B. japonicus* [54], *B. arenarum* [55], and *Hyla arborea* [45]. The nondialyzable fraction of jelly in *Xenopus laevis* which was solubilized by mercaptoethanol or UV-irradiation also supported fertilization of the eggs whose jelly was removed by sodium-sulfite to the extent that no fertilization occurred in 0.05 DB [56]. The other jelly material that supports fertilization of dejellied eggs of *B. japonicus* [30], *B. arenarum* [53], *B. americanus* [3], and *R. pipiens* [3] was obtained by shaking fully jellied uterine eggs in distilled water for 15–30 min ("diffusible factor": DF). The dialyzate but not the retentate after dialysis of DF retained a strong fertilization supporting activity in *B. arenarum* [53] and *B. japonicus* [30]. In *R. pipiens,* however, both dialyzate and retentate were required for insuring a high frequency of fertilization [3]. There is a possibility that a low activity of dialyzate in the *R. pipiens* DF was due to a relatively low concentration of the pertinent molecules. It was found additionally that in *B. japonicus* [30, 54, 57] synthetic polymers such as polyvinylpyrrolidone (PVP), dextran or Ficoll were effective in supporting fertilization of cyanide-dejellied eggs. The possibility that the observed results were ascribable to a small amount of jelly materials remaining

undissolved may be eliminated by the fact that the *Hyla arborea* eggs from which the vitelline coat in addition to jelly had been removed regained fertilizability only when inseminated in dialyzed jelly or PVP [45].

Assays on the fertilization-supporting activity of jelly preparations with dejellied eggs made it possible to inquire into the nature of factor(s) involved in the jelly. First, the egg-jelly played its biological role less species-specifically. The dialyzed jelly of *B. japonicus* and homogenized jelly of *R. chensinensis* were as effective as dialyzed jelly of the homologous species in supporting fertilization of dejellied *Hyla* eggs [45]. Dejellied eggs of *B. japonicus* were fertilized well in the presence of homogenized or trypsinized jellies from *R. chensinensis* or *R. japonica* [58], as well as of DF from *R. japonica* [30]. Likewise, DF from *R. pipiens* and *R. clamitans* were active in supporting fertilization of dejellied eggs from *B. americanus* and *R. pipiens,* respectively [3, 47]. Second, at least in *Bufo,* the active substances in jelly were regarded to be of small molecular weight since they were dialyzable, stable after boiling for 15 min [30], and remained active after extensive hydrolysis by pronase [54]. Gel-filtration on Sephadex G–25 gave a molecular weight of less than 500 for active molecules [30]. These observations, together with the observed lack of correlation of immunological cross-reactivity in jellies with cross-fertilizability between pertinent species [36], argued against the proposal that specific molecular interactions operating between jelly and sperm surface underlie the essential role of egg-jelly in fertilization process [35]. Third, experiments in *R. pipiens* [3] and *B. arenarum* [53] indicated that preincubation with jelly materials did not promote the fertilizing capacity of sperm, but rather the jelly or jelly factors must be present at the moment of sperm entrance in eggs. In this respect the state of sperm affected by jelly cannot be paralleled with capacitation in mammalian sperm [59].

The exact molecular entity in egg-jelly essential for its biological activity was further studied with *B. japonicus*, because of the ease with which large amounts of diffusible jelly materials can be collected [60]. The dialyzate from UV-irradiated jelly (UVJD) supported fertilization of dejellied eggs in a dose-dependent manner in a certain range of concentrations, but decreased its activity as its concentrations became higher. Surprisingly the fertilization-supporting activity of UVJD was retained even after ashing at 600°C for 16 hr, so that the involvement of organic substances was excluded from the biological activity concerned. To inquire as to the role of inorganic salts contained in biologically active preparations, concentrations of inorganic salts in UVJD were determined and a reconstituted salt solution (RSS) was prepared according to the composition of UVJD. RSS comprising 3.4 mM NaCl, 1.6 mM KCl, 0.33 mM $CaCl_2$, and 0.48 mM $MgCl_2$ proved to be equivalent to UVJD in insuring fertilization of dejellied eggs. Analyses of the relative role of individual salts in RSS revealed that what is important for its biological activity is to contain at least 1 mM Ca^{2+} and/or Mg^{2+}. Thus dejellied eggs are now fertilized in 0.05 DB supplemented with 1–5 mM $CaCl_2$ or $MgCl_2$ (0.05 DB contains $CaCl_2$ at 0.065 mM).

The finding of Ca^{2+} and/or Mg^{2+} as essential factor(s) for supporting fertilization of dejellied eggs is compatible with all the properties of active jelly preparations that have so far been described. A question then arises as to how the relatively high concentration of divalent cations in RSS is related to the heretofore mentioned biological function of jelly envelopes in fertilization. The answer to this question came when the ionic conditions in egg-jelly at the time of fertilization were evaluated in conjunction with the motility of sperm, as follows [60]. First, both dialysis and gel-filtration studies indicated that jelly has a unique property of retaining divalent cations preferentially to monovalent cations. Second, anuran sperm are not motile unless total cation concentration is less than 20–25 mM. Thus, the total cationic concentration in jelly envelopes of freshly laid eggs, measuring about 130 mM, is too high for adequate sperm motility. In fact, it was found that uterine eggs become fertilizable after contact with water and hydration for 2–3 min, when the salinity within the jelly is low enough to assure the motility of sperm. However, a simple dilution of physiological saline apparently results in divalent cation concentration (0.065 mM $CaCl_2$ in 0.05 DB) far below the level necessary for sperm-egg interac-

tions including the membrane fusion and acrosome reaction. An intriguing situation in jelly envelopes is that during the initial hydration process, both the dilution of total salinity and the maintenance of minimal essential divalent cations are effected, so that the environmental conditions necessary for successful sperm entrance into eggs are established.

ROLE OF THE OVIDUCAL PARS RECTA (PR)

Participation in Structural Alteration of VC

A puzzling result emerging from the experiments with the dejellied uterine egg bioassay was that jelly-less coelomic eggs, even though physiologically mature, are not or hardly fertilized under the conditions which support fertilization of dejellied uterine eggs. It was provisionally reasoned that the oviduct serves some additional roles to make eggs accessible to fertilizing sperm. Two series of experiments in early 70s revealed that a major barrier to fertilization of coelomic eggs resides in the VC. Coelomic eggs from *Rana pipiens* were successfully fertilized under the same conditions as for dejellied uterine eggs provided the VC had been either altered by treatment with trypsin or cyanide, or mechanically torn with forceps [61]. Likewise, coelomic eggs from *Bufo japonicus* were fertilized when the VC had been removed by pronase or hatching enzyme [57]. Similar experiments were extended also to *Xenopus laevis* [62]. Thus, these studies strongly suggested a new role of oviduct as altering the VC so as to be penetrable by sperm, rather than inducing the receptivity of the egg itself to sperm.

The evidence for the oviduct-induced alteration of the VC was first presented in *X. laevis* [63]. It was shown that the electron microscopically distinct bundles or filaments seen in the VC of coelomic eggs become evenly dispersed in oviducal or uterine eggs, in parallel with the acquisition of penetrability of isolated VC by sperm. This alteration was ascribed to the first 1 cm segment (1/20 of total length) of oviduct, since it occurred prior to addition of any jelly to the egg. Similar observations have been extended to the VC of other anurans, *R. japonica* [64], *B. japonicus* [65], and *B. arenarum* [66]. In *R. japonica* this fine structural alteration was accompanied by deposition of oviduct-derived carbohydrate materials as detected by PA-CrA-methenamine method. All these effects on the VC were observed either in the eggs that had passed through the first 1/20th portion of oviduct (pars recta, PR) or those incubated in the extracts from this tissue.

Electron microscopic observations of the PR cells in *B. japonicus* [65], *R. japonica* [64] and *X. laevis* [67] elucidated the unique epithelial cells that had been overlooked in a number of older observations on the amphibian oviduct [68, 69]. The non-ciliated epithelial cells in the PR possess electron-dense granules which are distinct from those in the jelly-secreting cells in more caudal levels of the oviduct, the pars convoluta (PC) (Fig. 5). The granules in PR cells are small in number during the hibernation period, increase in number significantly upon hormonal stimulation for ovulation, and almost disappear after oviposition. The acquisition in the VC of carbohydrate materials during passage of *R. japonica* [64] eggs through the PR is most probably ascribable to the secretion of PR granules. In *B. japonicus* [65] immunohistochemical studies showed a deposition of PR cell-specific antigen in the VC during passage of eggs through the PR. Thus, based on morphological criteria the effect of oviducal PR on the VC is two fold, *viz.*, a partial degradation and/or disorganization of filament bundles and a deposition of PR-derived substances within the filament bundles.

It should be added that in *Xenopus laevis,* the histologically defined PR comprises two distinct subportions, of which a more cephalic portion (PR1) is concerned with the structural alteration of the VC [67]. The caudal 1/5 portion (PR2) is involved in the formation of a fertilization layer (F-layer), as discussed later.

Molecular Basis for PR Function

Analyses of how the PR functions in the fertilization process have been undertaken using crude extracts of PR homogenates (PRE) from ovulating females (*Bufo*s, [65, 70]; *R. japonica,* [64]) or secretion fluids collected from ligated PR (*B. arenarum,* [70, 71]; *X. laevis,* [72]). In more

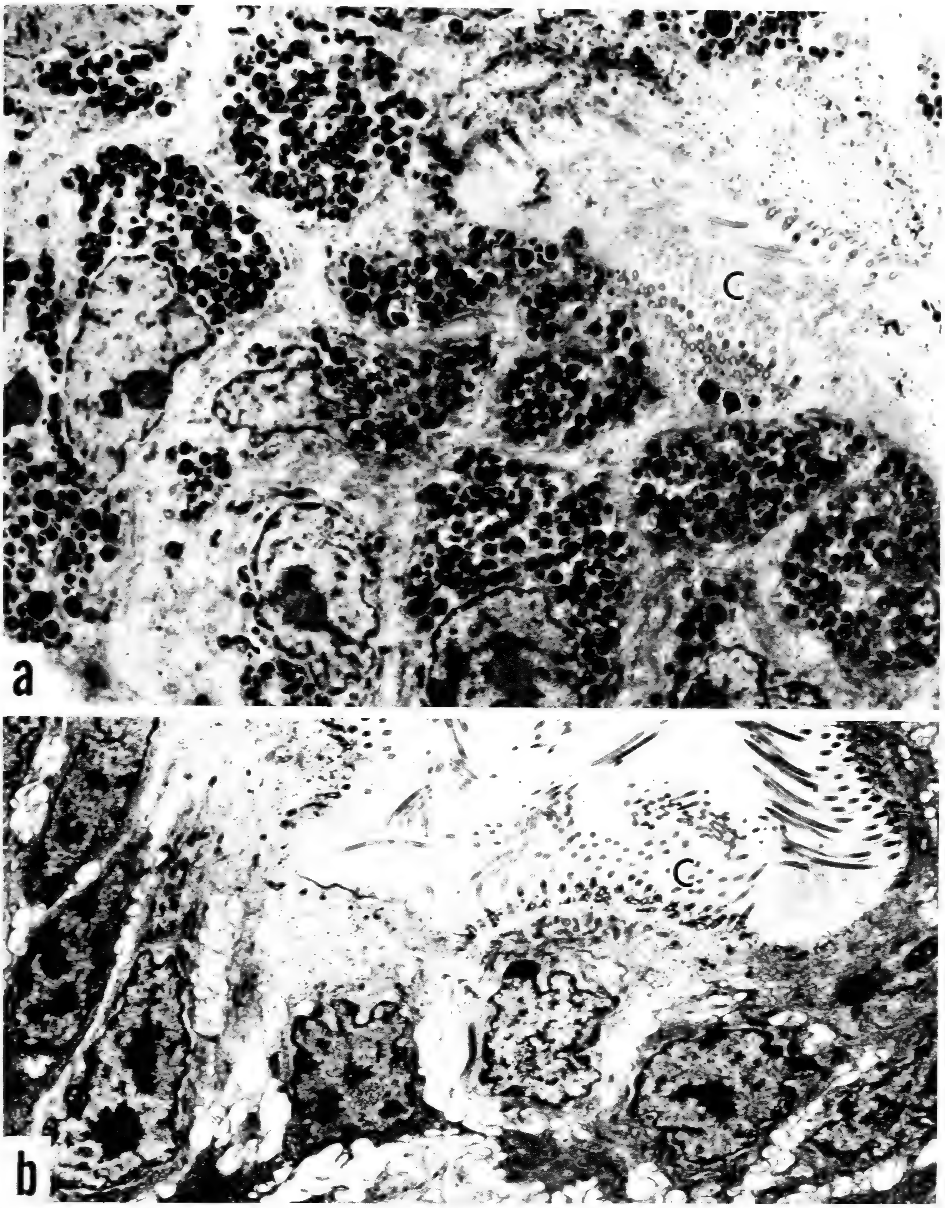

FIG. 5. TEM of non-ciliated epithelial cells in the pars recta of *Rana japonica*, before (a) and after (b) passage of several hundred eggs through this oviducal portion, showing the disappearance of electron-dense granules in (b). C, cilia.

recent studies with *B. japonicus* [73, 74], fairly pure PR granules (PRG) isolated by Percoll density gradient centrifugation proved to possess all the functions of the PR.

Most direct evidence for the involvement of PR in the fertilization process came from experiments in which coelomic eggs of *B. arenarum* [70, 71] and *B. japonicus* [65, 74] pretreated with PRE or PRG were shown to be fertilized well in the presence of diffusible jelly materials or RSS. Although a

preincubation time of 4 hr with PRE or PRG in contrast to a presumed 10–15 min residence in PR *in vivo* was necessary to obtain a high fertilizability in *B. japonicus,* this success of fertilization of coelomic eggs provided strong support for the notion that PR secretions render the VC penetrable by sperm.

Besides affecting the VC, the PR substances possess a striking activity for inducing an acrosome reaction in sperm. Treatment of coelomic eggs with PRE followed by addition of sperm in physiological saline resulted in the lysis of the VC (*B. japonicus,* [65]; *R. japonica,* [64]), despite a failure of fertilization due to the lack of jelly or RSS. Likewise, the supernatant solution of the PRE or PRG preincubated with sperm for 30 min has a strong VC lytic activity, accompanied by the induction of the acrosome reaction and a loss of VC lysin activity extractable from sperm [65]. Most probably the contents of PRG deposited in the VC function to induce an acrosome reaction and a release of VC lysin from individual sperm. This scheme is compatible with the TEM observation [17] that sperm passing through the jelly layers possess intact acrosomes, but those attaching to and passing through the VC are acrosome-reacted.

The molecular basis for the PR-induced structural transformation of VC has recently been the subject of intensive studies with *Bufo*s and *Xenopus*. It was shown in *B. arenarum* [71, 75] and *B. japonicus* [74] that the pretreatment of coelomic eggs with PRE or PRG renders the VC susceptible to the sperm lysin to the same degree as the VC of dejellied uterine eggs, as evidenced by a rapid dissolution of VC surrounding the eggs. Determinations of VC lysis *in vitro* indicated that the coelomic egg VC (CEVC) is not completely refractory to the sperm lysin as had been shown previously, but increases in susceptibility after treatment with PRE approximately 10 times [74]. A Ca^{2+}-dependent activity enhancing the CEVC susceptibility to sperm lysin has been partially purified from the PR of *B. arenarum* [75, 76]. The activity is of trypsin-like serine protease, as defined by its strong inhibition by SBTI and TLCK. These studies, combined with the observed increase in VC of both intrinsic fluorescence and the total number of 8 anilino-naphthalene binding sites, led Miceli *et al.* [77] to propose that the PR-induced transformation of VC includes a dissociation of some superficial peptides so that the site for sperm lysin attack is increased.

More recent studies with *B. japonicus* and *X. laevis* have provided new information as to how the PR affects the VC. SDS-PAGE analyses of *Bufo* VC protein revealed that in comparison with CEVC, uterine egg VC(UEVC) lacks 40–52 K glycoproteins concomitant with an increased

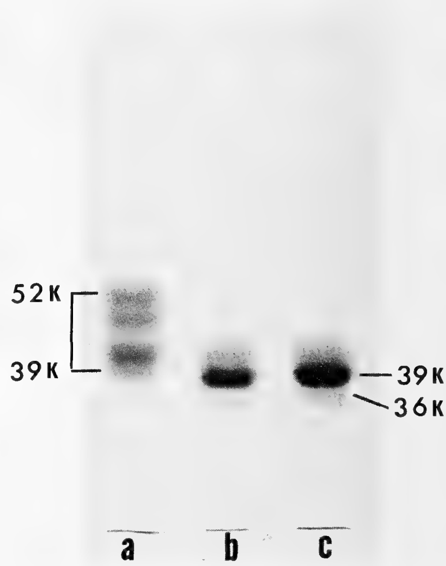

FIG. 6. SDS-PAGE analyses of vitelline coat proteins in *Bufo japonicus*, from coelomic egg (a), uterine egg (b), and coelomic egg treated with pars recta granule fraction (c). Numbers indicate molecular weights.

stainability of a 39 K glycoprotein and the appearance of a 36 K glycoprotein [74] (Fig. 6). Similar changes of VC proteins occur in *Xenopus,* where a 43 K glycoprotein in CEVC is converted to a 41 K in UEVC [78]. In both cases, the conversions can be induced upon incubation of coelomic eggs with PRG. Interestingly PRGs from *Bufo* and *Xenopus* share strong hydrolytic activities against synthetic substrates such as X-Arg-MCA and Val-Leu-Lys-MCA, and the incubation of coelomic eggs with heterologous PRGs between these two species results in specific glycoprotein changes in SDS-PAGE profiles of VC proteins in both reciprocal

combinations (unpublished observations). A proteolytic activity that induces a CEVC to UEVC type protein conversion has recently been partially purified from PRG of *B. japonicus* [91]. This activity, hydrolyzing preferentially Arg-MCA terminals in a highly Ca^{2+}-dependent manner, is inhibited by SBTI, leupeptin, PMSF and DFP, and thus shares properties in several respects with the trypsin-like enzyme obtained from *B. arenarum* [76]. It seems plausible that in the three species of anurans just discussed, the PR trypsin-like enzyme(s) is functioning to induce a partial degradation of VC proteins, so that the VC is accessible to sperm lysin.

It is clear that the PR serves two distinct roles, i.e., the induction of acrosome reaction and the partial hydrolytic degradation of VC proteins. Of these, the proteolytic degradation of CEVC proteins is evidently prerequisite for establishment of egg fertilizability, since the inhibition of the PRE-induced CEVC to UEVC changes by incubation of coelomic eggs with SBTI or leupeptin prevents the acquisition of egg fertilizability [74]. Once the VC glycoprotein changes have occurred, as in uterine eggs, treatment with trypsin inhibitors before insemination does not inhibit fertilization. It should be mentiond that the enzymatic partial hydrolysis of VC is not sufficient to ensure egg fertilizability, since no or only a low frequency of fertilization has been observed in the coelomic *Bufo* eggs whose VC had been altered by a partially purified PRG protease or the *Xenopus* PRG ([91]; unpublished observation). These last experiments are intriguing in that they suggest that the VC degrading and acrosome reaction inducing activities, both derived from PRG, can be studied as separate molecular entities.

Finally, mention should be made of an another intriguing example of oviducal contribution to fertilization process which has been uniquely developed in *Xenopus laevis*. Upon fertilization or artificial activation, the vitelline envelope (VE) of unfertilized *Xenopus* eggs is transformed into the fertilization envelope (FE) by acquiring an electron-dense layer (fertilization layer: F-layer) on the outer surface of the VE [79]. The F-layer is a protease- and mercaptoethanol-resistant precipitate that is formed as a Ca^{2+}-dependent agglutination involving both the cortical granule (CG)-derived lectin and its ligand of oviducal origin [15, 80]. Functionally, the F-layer provides a block to fertilizing sperm either mechanically or by masking sperm reactive sites on VE (a slow polyspermy block mechanism) [81, 82], as well as a molecular barrier to macromolecules released into perivitelline space from cortical granules [83, 84]. A CG lectin participating in the F-layer formation has been purified from CG exudates as a metalloglycoprotein of more than 500 K dalton that has a galactosyl sugar specificity for ligand binding [15, 84]. With regard to the ligand for CG lectin, the innermost jelly layer (J_1) has been implicated primarily based on its ability to undergo a precipitation reaction with the CG lectin both *in vivo* and *in vitro* [15, 31]. Recent studies, however, raise the possibility that the CG ligand is present as a prefertilization layer (PF-layer) localized on the outer surface of VE, as a secretion product from the lower 1/5 portion of PR [85, 86]. This proposal is based on the electronmicroscopic and immunohistochemical observations which indicate that molecules specific to the granules in PR2 epithelial cells are released and deposited on the VE. The exact origin of CG ligand, however, can be dual in view of the occurrence in an agarose plate of precipitation line between CG lectin and both PF-layer and J_1 materials, although in normal egg activation process the PF-layer occupies a potentially privileged position than the J_1 in reacting with the released CG lectin [84]. Whatever the exact source of CG ligand may be, PF-layer (PR2) or J_1(p. convoluta), the F-layer formation in *Xenopus* provides a unique model in which the oviducal secretions evidently participate in the slow but efficient polyspermy block mechanism. In other anurans, the oviduct does not seem to be involved in the formation of FE or fertilization coat, since the VC of activated coelomic eggs becomes refractory to the sperm lysin [22, 87].

CONCLUDING REMARKS

One of the basic concepts derived from studies on gamete interaction in amphibians is that the vitelline coat (VC) surrounding ovulated physiologically mature eggs acts as a barrier for sperm.

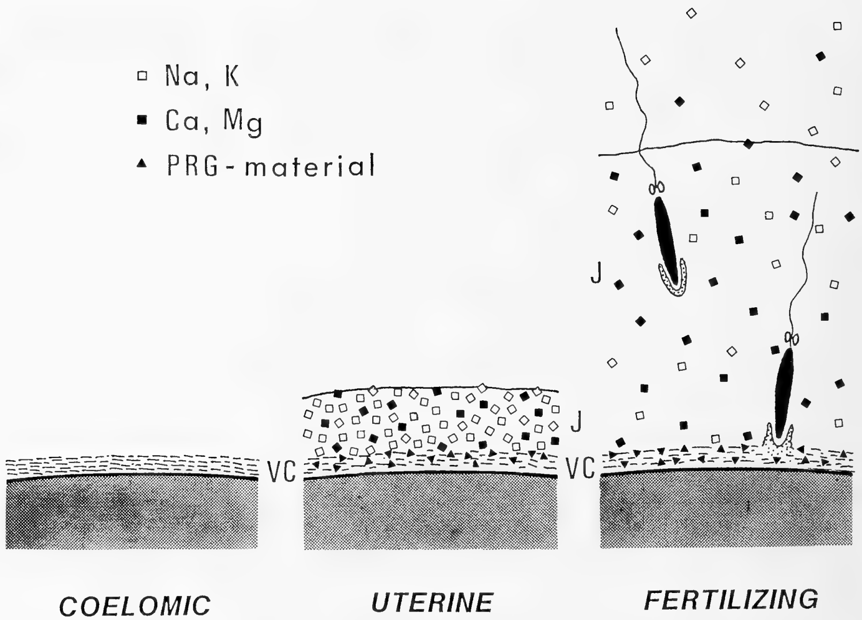

FIG. 7. Schematic illustration of alterations of the vitelline coat (VC) during passage of eggs through oviduct and the role of egg-jelly (J) in mediating sperm entry through the vitelline coat, based on studies in *Bufo japonicus*.

Figure 7 schematically illustrates how the secretions from the oviducal PR and PC in *Bufo japonicus* function to overcome this barrier. During the initial phase of fertilization, the unique nature of the jelly to hydrate and retain divalent cation assures both the motility and the minimal divalent cation requirement for gamete fusion. Sperm are acrosome-intact during passage through jelly, but undergo the acrosome reaction and release of VC lysin at the surface of the VC in response to the acrosome reaction-inducing substance of PR origin. By this time, the VC has become highly susceptible to sperm lysin due to a partial hydrolytic degradation by the PR protease, so that sperm may find a path through the VC.

According to this scheme, the role of jelly envelopes is simple enough to exclude the direct contribution of any macromolecules or organic substances and their localization in specific jelly layers. The scheme, however, does not rule out the possible involvement of the non-diffusible structural integrity of jelly, as emphasized in *B. arenarum* where the addition of non-diffusible jelly molecules to a diffusible jelly fraction enhances the rate of fertilization [38]. Studies are needed to determine whether or not the function of jelly as proposed here can be extended to other anurans and urodeles, In this connection, it will be of interest to learn as to how a specially differentiated component of jelly ("animal plug") in *Discoglossus pictus* eggs can restrict the site of sperm penetration [88].

In contrast with jelly, possible function of PR secretions are multiple, including the induction of a conformational change of VC and the acrosome reaction, as well as the enhancement of VC lytic activity. Of these, a hydrolytic degradation of VC by a trypsin-like enzyme is evidently associated with the increased susceptibility of the VC to the sperm lysin. In this respect, the VC exhibits three different states with respect to susceptibility to sperm lysin: less susceptible in coelomic eggs, highly susceptible in uterine eggs, and completely refractory in fertilized eggs. Studies on the molecular basis of the differential suceptibilities of the VC towards sperm lysin should aid in under-

standing the mechanism of action of pertinent enzymes including the hatching enzyme [24, 89, 90]. Compared with the trypsin-like enzyme, little is known about the molecular nature of acrosome reaction-inducing activity from PRG. There is evidence suggesting the involvement of carbohydrate moieties in fertilization process, as exemplified by concanavalin A(Con A) inhibition of fertilization in *Bufo*s [70, 74]. This observation is likely to be relevant to the inhibition by Con-A of the PRG-induced acrosome reaction (unpublished observation). Characterization studies of the PR-derived, acrosome reaction-inducing substance should be most promising.

From a comparative view, the vitelline coat of amphibians is homologous to the zona pellucida of mammals and the vitelline envelope of echinoderms, in the sense that it is deposited around the growing oocytes during oogenesis. However, in order to acquire the functional equivalence to mammalian or echinoderm counterparts, the amphibian vitelline coat has to be acted upon by secretory products of oviduct. Thus, the amphibian system provides a unique model to study the exact cellular source of molecules functioning in mediating gamete interactions, possibly together with their hormonal control.

ACKNOWLEDGMENT

I express my appreciation to Drs. J. Hosono, K. Ishihara, Y. Iwao, K. Takamune, and N. Yoshizaki, for their ingenious collaboration in pursuing studies with *Bufo japonicus*. My thanks are also due to Dr. J. L. Hedrick for his stimulating discussion and helpful comments to this article.

REFERENCES

1 Glabe, C. and Vacquier, V. D. (1978) Proc. Natl. Acad. Sci. U.S.A., **75**: 881–885.
2 Wasserman, P. M.,Florman, H. M. and Gerve, J. M. (1985) In "Biology of Fertilization". Ed. by C. B. Metz and A. Monroy, Vol. 2, Academic Press, New York, pp. 341–360.
3 Elinson, R. P. (1971) J. Exp. Zool., **176**: 415–428.
4 Elinson, R. P. (1986) Int. Rev. Cytol., **101**: 59–100.
5 Aplington, H. W., Jr. (1957) Ohio J. Sci., **57**: 91–99.
6 Iwao, Y., Ito, S. and Katagiri, Ch. (1981) Dev. Growth Differ., **23**: 89–100.
7 Iwao, Y. (1982) Dev. Growth Differ., **24**: 467–477.
8 Masui, Y. and Clarke, H. J. (1979) Int. Rev. Cytol., **57**: 185–282.
9 McLaughlin, E. W. and Humphries, A. A., Jr. (1978) J. Morphol ., **158**: 73–90.
10 Wolf, D. P. and Hedrick, J. L. (1971) Dev. Biol., **25**: 348–359.
11 Moriya, M. (1976) J. Fac. Sci. Hokkaido Univ. Ser. VI, **20**: 272–276.
12 Hollinger, T. G. and Corton, G. L. (1981) Gamete Res., **3**: 45–57.
13 Elinson, R. P. and Manes, M. E. (1978) Dev. Biol., **63**: 67–75.
14 Picheral, B. and Charbonneau, M. (1982) J. Ultrastruct. Res., **81**: 306–321.
15 Wyrick, R. E., Nishihara, T. and Hedrick, J. L. (1974) Proc. Natl. Acad. Sci. U.S.A., **71**: 2067–2071.
16 Raisman, J. S. and Cabada, M. O. (1977) Dev. Growth Differ., **19**: 227–232.
17 Yoshizaki, N. and Katagiri, Ch. (1982) Gamete Res., **6**: 343—352.
18 Matsui, M. (1984) Contriv. Biol. Lab. Kyoto Univ., **26**: 209–428.
19 Penn, A. and Gredhill, B. L. (1972) Exp. Cell Res., **74**: 285:288.
20 Elinson, R. P. (1974) Biol. Reprod., **11**: 406–412.
21 Elinson, R. P. (1971) J. Exp. Zool., **177**: 207–218.
22 Iwao, Y. and Katagiri, Ch. (1982) J. Exp. Zool., **219**: 87—95.
23 Raisman, J. S. and Barbieri, F. D. (1969) Acta Embryol. Exp., **1**: 17–26.
24 Katagiri, Ch. (1975) J. Exp. Zool., **1933**: 109–118.
25 Hibbard, H. (1928) Arch. Biol., **38**: 251–326.
26 Bataillon, E. (1919) Ann. Sci. Nat. Zool. Ser. 10, **3**: 1–38.
27 Salthe, S. N. (1963) J. Morphol., **113**: 161–171.
28 Folkes, B. F., Grant, R. A. and Jones, J. K. N. (1950) J. Chem. Soc.(440) part 3, 2136–2140.
29 Bolognani, L., Bolognani, A. M., Lusignani, F. R. and Zonta, L. (1966) Experientia, **22**: 601–603.
30 Katagiri, Ch. (1973) Dev. Growth Differ., **15**: 81–92.
31 Yurewicz, E. C., Oliphant, G. and Hedrick, J. L. (1975) Biochemistry, **14**: 3101–3107.
32 Freeman, S. B. (1968) Biol. Bull., **135**: 501–513.
33 Steinke, J. H. and Benson, D. G., Jr. (1970) J. Morphol., **130**: 57–66.
34 Hedrick, J. L., Smith, A. J., Yurewicz, E. C., Oliphant, G. and Wolf, D. P. (1974) Biol. Reprod., **11**: 534–542.
35 Shaver, J. R. (1966) Am. Zool., **6**: 75–87.
36 Katagiri, Ch. (1968) SABCO J., **4**: 33–43.
37 Barbieri, F. D. and Raisman, J. S. (1969)

Embryologia, **10**: 363–372.
38 Barbieri, F. D. and del Pino, E. G. (1975) Arch. Biol. (Bruxelles), **86**: 311–321.
39 Katagiri, Ch. (1961) J. Fac. Sci. Hokkaido Univ. Ser. VI, **14**: 606–613.
40 Tchou-Su and Wang, Y. L. (1956) Acta Exp. Biol. Sinica, **5**: 75–122.
41 Katagiri, Ch. (1962) Jpn. J. Zool., **8**: 365–375.
42 del Pino, E. G. (1963) J. Exp. Zool., **185**: 121–132.
43 Katagiri, Ch (1963) Zool. Mag., **72**: 23–28.
44 Moore, J. A. (1955) Adv. Genetics, **7**: 139–182.
45 Katagiri, Ch. (1966) J. Fac. Sci. Hokkaido Univ. Ser. VI, **16**: 77–84.
46 Brun, R. B. and Kobel, H. R. (1977) J. Exp. Zool., **201**: 135–138.
47 Elinson, R. P. (1974) J. Embryol. Exp. Morphol., **32**: 325–335.
48 Brun, R. P. (1974) Biol. Reprod., **11**: 513–518.
49 Kambara, S. (1953) Annot. Zool. Japon., **36**: 78–84.
50 Katagiri, Ch. (1965) J. Fac. Sci. Hokkaido Univ. Ser. VI, **15**: 633–643.
51 Barbieri, F. D. and Budeguer de Atenor, M. S. (1973) Arch. Biol. (Bruxelles), **84**: 501–511.
52 Glick, R. N. and Shaver, J. R. (1963) Exp. Cell Res., **32**: 615–618.
53 Barbieri, F. D. and Oterino, J. M. (1972) Dev. Growth Differ., **14**: 107–117.
54 Katagiri, Ch. (1966) Embryologia, **9**: 159–169.
55 Barbieri, F. D. and Raisman, J. S. (1969) Embryologia, **10**: 363–372.
56 Wolf, D. F. and Hedrick, J. L. (1971) Dev. Biol., **25**: 360–376.
57 Katagiri, Ch. (1974) J. Embryol. Exp. Morphol., **31**; 573–587.
58 Katagiri, Ch. (1967) Annot. Zool. Japon., **40**: 67–73.
59 Yanagimachi, R. (1978) Curr. Top. Dev. Biol., **12**: 83–105.
60 Ishihara, K., Hosono, J., Kanatani, H. and Katagiri, Ch. (1984) Dev. Biol., **105**: 435–442.
61 Elinson, R. P. (1973) J. Exp. Zool., **183**: 291–302.
62 Stewart-Savage, J. and Grey, R. D. (1984) Exp. Cell Res., **154**: 639–642.
63 Grey, R. D., Working, P. K. and Hedrick, J. L. (1977) J. Exp. Zool., **201**: 73–84.
64 Yoshizaki, N. and Katagiri, Ch. (1981) Dev. Growth Differ., **23**: 495–506.
65 Katagiri, Ch., Iwao, Y. and Yoshizaki, N. (1982) Dev. Biol., **94**:1–10.
66 Mariano, M. I., de Martin, M. G. and Pisano, A. (1984) Dev. Growth Differ., **26**: 33–42.
67 Yoshizaki, N. (1985) J. Morphol., **184**: 155–169.
68 Lee, P. A. (1967) J. Exp. Zool., **166**: 107–120.
69 Boisseau, C. (1973) J. Microsc., **18**: 341–358.
70 Cabada, M. D., Mariano, M. I. and Raisman, J. S. (1978) J. Exp. Zool., **204**: 409–416.
71 Miceli, D. C., Fernández, S. N., Raisman, J. S. and Barbieri, F. D. (1978) J. Embryol. Exp. Morphol., **48**: 79–91.
72 Bakos, M. and Hedrick, J. L. (1986) Zool. Sci., **2**: 934.
73 Katagiri, Ch. (1986) In " The Molecular and Cellular Biology of Fertilization : Gamete Interaction". Ed. by J. L. Hedrick, Plenum Press, New York, in press.
74 Takamune, K., Yoshizaki, N. and Katagiri, Ch. (1986) Gamete Res., **14**: 215–224.
75 Miceli, D. C., Fernández, S. N. and del Pino, E. J. (1982) Biochem. Biophys. Acta, **526**: 289–292.
76 Miceli, D. C. and Fernández, S. N. (1982) J. Exp. Zool., **221**: 357–364.
77 Miceli, D. C., Fernández, S. N. and Moreno, R. D. (1980) Dev. Growth Differ., **22**: 639–643.
78 Gerton, G. L. and Hedrick, J. L. (1986) J. Cell. Biochem. **30**: 341–350.
79 Grey, R. D., Wolf, D. P. and Hedrick, J. L. (1974) Dev. Biol., **36**: 44–61.
80 Wolf, D. P., Nishihara, T., Wert, D. M., Wyrick, R. E. and Hedrick, J. L. (1976) Biochemistry, **15**: 3671–3678.
81 Schmell, E. D., Gulyas, B. J. and Hedrick, J. L. (1983) In "Mechanism and Control of Animal Fertilization". Ed. by. J. F. Hartman, Academic Press, New York, pp. 365–413.
82 Grey, R. D., Working, P. K. and Hedrick, J. L. (1976) Dev. Biol., **54**: 52–60.
83 Nishihara, T. and Hedrick, J. L. (1977) Proc. Fed. Am. Soc. Exp. Biol., **36**: 811.
84 Yoshizaki, N. (1986) Dev. Growth Differ., **28**: 275–283.
85 Yoshizaki, N. and Katagiri, Ch. (1984) Zool. Sci., **1**: 255–264.
86 Yoshizaki, N. (1984) Dev. Growth Differ., **26**: 191–195.
87 Miceli, D. C., del Pino, E. J., Barbieri, F.D., Mariano, M. .I. and Raisman, J. S. (1977) Dev. Biol., **59**:101–110.
88 Campanella, C. (1975) Biol. Reprod., **12**: 439–447.
89 Urch, U. A. and Hedrick, J. L. (1981) J. Supramol. Struct. Cell. Biochem., **15**: 111–117.
90 Urch, U. A. and Hedrick, J. L. (1981) Arch. Biochem. Biophys., **206**: 424–431.
91 Takamune, K. and Katagiri, Ch. (1987) Dev. Growth Differ., **29**: in press.

ZOOLOGICAL SCIENCE 4: 15–22 (1987)

REVIEW

Ultrastructural Classification of Smooth Muscle Cells in Invertebrates and Vertebrates

AKIRA MATSUNO

Department of Biology, Faculty of Science, Shimane University, Matsue 690, Japan

INTRODUCTION

Ultrastructural studies on smooth muscle cells were begun in the 1960s, and have revealed characteristic structures in various organs and tissues of vertebrates as well as of invertebrates. These morphological studies have shown that there are several types of smooth muscle cells in each organ and tissue of the same animal [1–6], and that similar organs and tissues in different species of animals have different types of cells [7–10]. In this paper, I have attempted to classify the various smooth muscle cells by their ultrastructural characteristics. The relationship between the ultrastructure and function in various organs or tissues is also discussed.

CLASSIFICATION OF SMOOTH MUSCLE CELLS

It is possible to classify smooth muscle cells by size and the arrangement of myofilaments which are scattered in the main part of the cells. Smooth muscle cells were grouped into four types by the following markers: i) the diameter of the thick myofilament, ii) density of an arrangement of dense bodies, iii) the size of the cell, iv) other characteristics (structure of sacrcoplasmic reticulum (S. R.) systems, mitochondria, etc.). These markers made it possible to distinguish ultrastructural differences in the four types of smooth muscle cells. Ultrastructural characteristics of the four types of cells and their distributions in organs or tissues of several species of animals are listed in Table 1. The characteristics are also presented schematically in Figure 1.

Received September 22, 1986

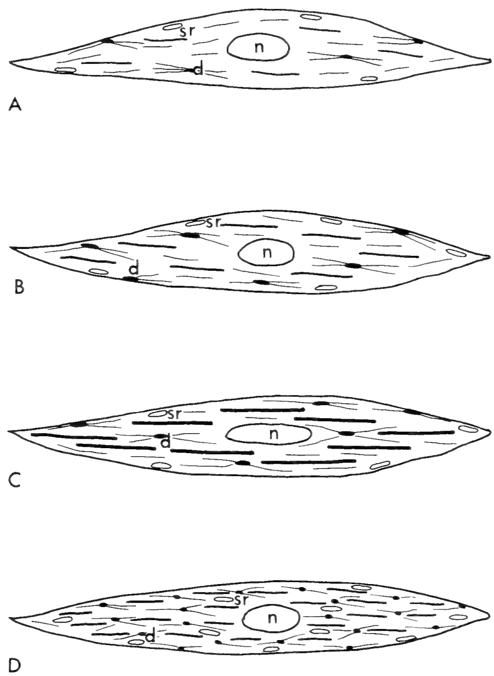

FIG. 1. Schematic representation of four types of smooth muscle cells. Note differences in diameter of thick myofilaments, number of dense bodies and their arrangements in the cell.

1) *A-type smooth muscle cell*

The A-type cells have thick myofilaments about 14 nm in diameter and thin myofilaments about 7

Table 1. Four types of cells with distribution in tissue or organ

Cell type	Diameter of thick myo-filament	Dense body and its arrangement	Sarcoplasmic reticulum	Animal	Tissue or organ	
A-type	–14 nm	small size; few in number; disordered	small size; distributed at periphery	*Stephanoscyphus*	tentacle	[18]
				Atorella	tentacle	[19]
				Tamanovalva	adductor	[17]
				Spondylus	adductor	[7]
				sea cucumber	body wall	[4]
				echinoid	spine	[1]
				echinoid	ovarian wall	[2]
				frog	intestine	[13]
				chicken	gizzard	[12]
				mouse	tunica	[16]
				guinea pig	taenia coli	[14]
				cat	urinary bladder	[15]
B-type	about 40 nm	large size; disordered	small size; distributed at periphery	*Atorella*	oral disc	[19]
				snail	body wall	[6]
				opisthobranchiate	sheathed muscle	[23]
				Dolabella	body wall	[26]
				Mytilus	byssus retractor	[24, 25]
C-type	60–120 nm	large size; few in number	small size; distributed at periphery	*Stephanoscyphus*	taeniol	[18]
				Atorella	taeniol	[19]
				Atrina	adductor	[10]
				Astarte	adductor	[27]
				Meretrix	adductor	[9]
				tellin	adductor	[8]
				Fragum	adductor	
D-type	14–40 nm	small size; sometimes regular arrangement	slightly developed	cuttlefish	intestine	[30]
				oligochaeta	intestine	[32]
				Phoronis	large vessel	[31]
				sea cucumber	intestine	[5]
				echinoid	ampulla	[3]

nm in diameter. The cells are generally small in size, and show an elongated spindle-shape. A nucleus is positioned in the central region and cell organelles in the periphery are not well developed.

Thick myofilaments sometimes disappear when the conditions of fixation are not suitable. Thus, they were not recognized in early investigations [11]. In chicken gizzard muscle cells, the thick myofilaments were observed only under conditions of low pH (6.6) during fixation [12, 13]. However, they were recognized in smooth muscle cells of guinea pig taenia coli even under usual conditions of fixation [14]. Now, thick myofilaments in this type of cell are universally observed under an electron microscope (Fig. 2). Thin myofilaments consist of actin and tropomyosin. Dense bodies are sometimes found connecting thin myofilaments. They appear in an elongated oval shape, and are small in size and number. The A-type cell is also found in the urinary bladder muscle of the cat [15], and tunica muscle of the mouse [16]. In invertebrates, the A-type cell was reported in many papers concerning the adductor muscle of *Spondylus cruentus* [7] and *Tamanovalva limax*

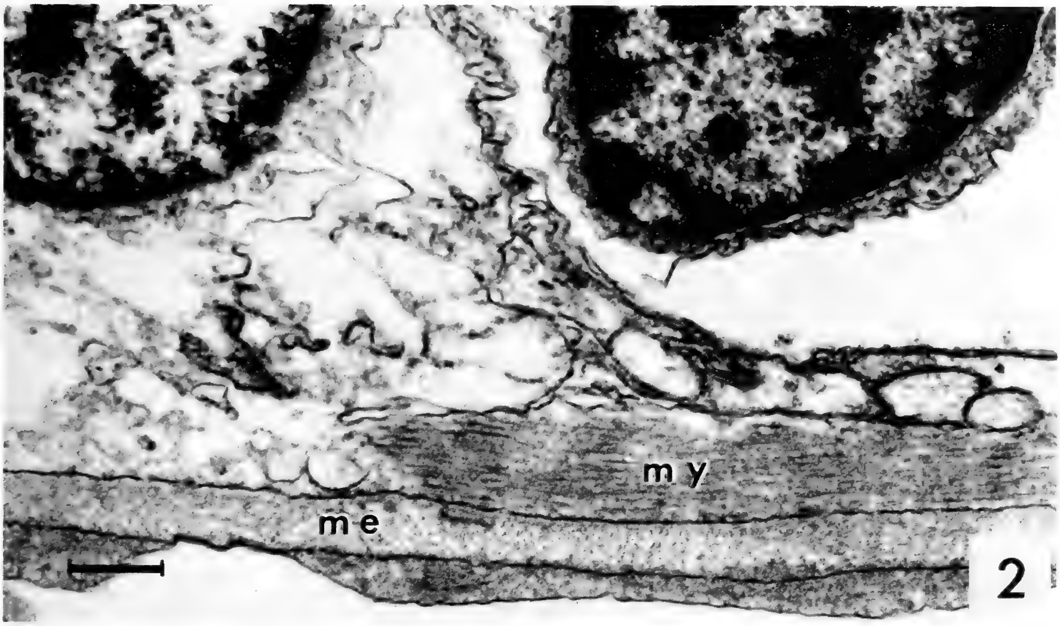

FIG. 2. A longitudinal-section of an A-type cell in the tentacle of *Atorella* polyp [19]. The epithelio-muscular cell (left) has a myofibril (my) near the mesoglea (me). The myofibril bears thick myofilaments small in size and thin ones running in parallel. Dense bodies are not shown in this figure. ×27,000, scale bar in the figure represents 0.5 μm.

[17]. The cells are also present in the spines and ovarian walls of an echinoid [1, 2], longitudinal muscles of the sea cucumber [4] and tentacle muscle of coelenterates, *Stephanoscyphus* [18] and *Atorella* [19].

Organs or tissues having the A-type cell are usually wall muscles of ducts in vertebrates which show repeated contraction-relaxations in a slow but long-lasting manner. On the other hand, in invertebrates, this type of cell is present in motive organs, exerting flexible and long-distanced contraction-relaxations.

The A-type cell is a rather primitive and inefficient type of smooth muscle cell for the following reasons : i) the arrangement of thick and thin myofilaments is not ordered, ii) dense bodies are small in number and their arrangement is not regular, and iii) the S. R. system in the cell is not well-developed.

2) *B-type smooth muscle cell*

The B-type cells have medium size (about 40 nm in diameter) thick myofilaments and thin myofilaments of 7 nm in diameter (Figs. 3 and 4). This type of cell is elongated in shape and tapers at both ends. It bears a nucleus in the center, and has cell organelles in the peripheral region showing a similar grade of development to the A-type cell. Dense bodies are large in size, but small in number. A thick myofilament similar in diameter in the oyster is shown to consist of a core of paramyosin with myosin at the surface [20], and it bears a regular periodicity of 13–17 nm intervals at its surface [21, 22].

Reports on this type of cell are mainly concerned with invertebrates and rarely with vertebrates. The B-type cell is frequently observed in invertebrate organs or tissues such as sheathed muscles of an opisthobranchiate mollusc [23], body wall muscles in the pond snail [6], anterior byssus retractor muscles of *Mytilus* [24, 25], longitudinal body wall muscles of *Dolabella* [26], and circular muscle in the oral disc of a coelenterate [19].

The B-type cell is the most popular type in motive organs of molluscs and echinoderms and is used to move or support their bodies. Upon

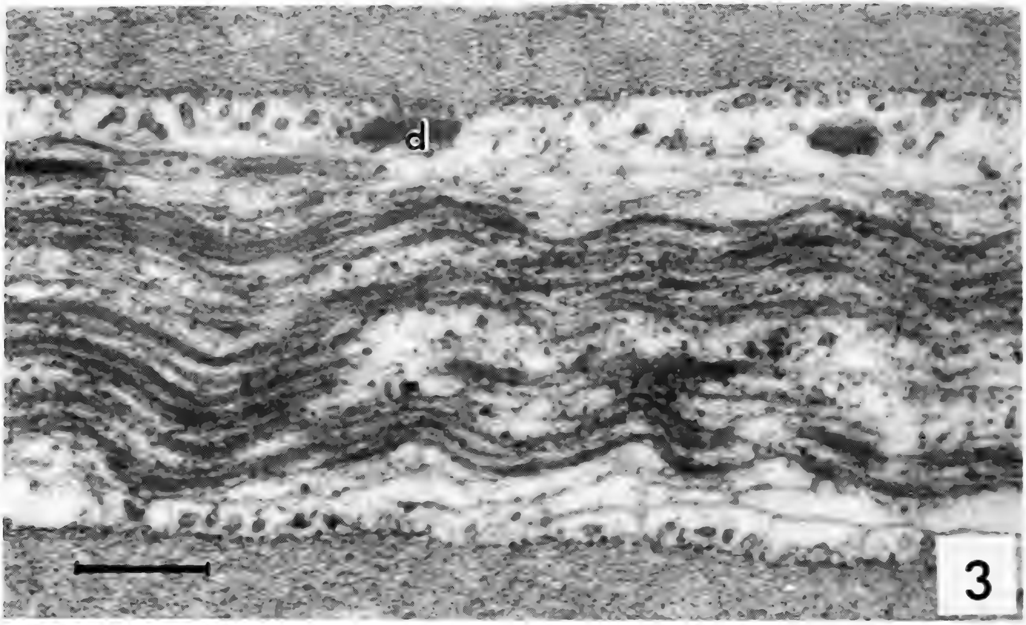

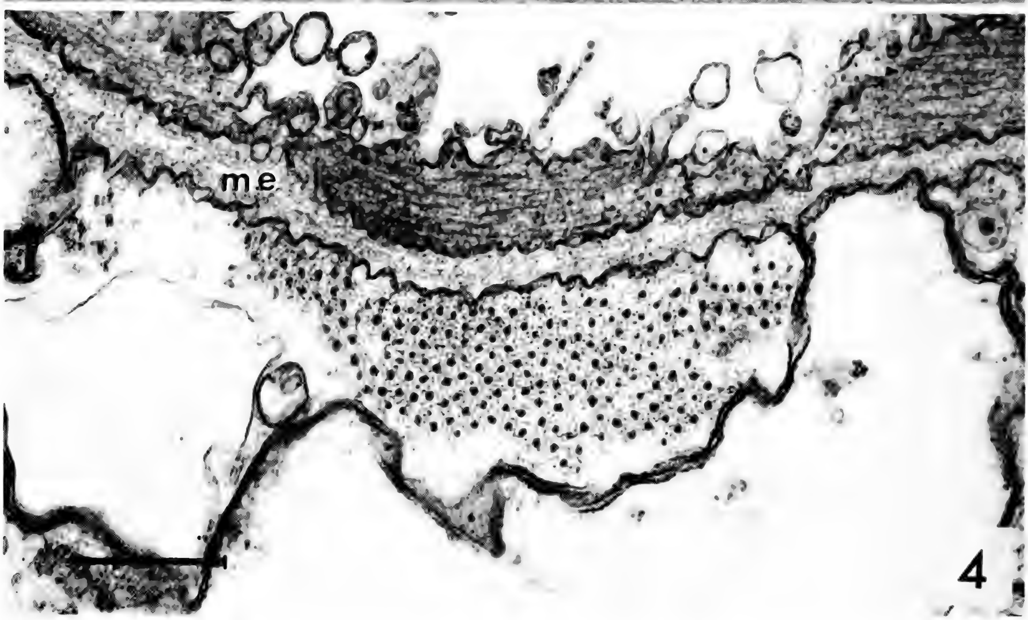

FIG. 3. A longitudinal-section of a B-type cell in the sheathed muscle of *Placobranchiate* [23]. Thick myofilaments (about 40 nm in diameter) run in parallel. d: dense body. ×39,200, scale bar represents 0.5 μm.

FIG. 4. A cross-section of a B-type cell in the oral disc of *Atorella* [19]. Thick myofilaments do not show a regular arrangement. me: mesoglea. ×46,300, scale bar represents 0.5 μm.

investigation of these motive tissues or organs, some of them showed "catch" contractions. The cell, therefore, seems to have two functions though they appear to be structurally similar. One of the functions is the "catch" contraction that is present in motive organs of gastropods or retractor muscles of bivalves. "Catch" contraction, however, is not so remarkble. The muscles are not very large in size and do not show specialized structures. The other function is the slow but mighty contraction that is observed in the most popular motive organs or tissues in molluscs and echinoderms.

3) *C-type smooth muscle cell*

The C-type cells have very thick (60–120 nm in diameter) myofilaments and thin myofilaments of 7 nm in diameter. The cell is large in diameter and long in length, and has a nucleus in its central region. Dense bodies are large in size, but small in number and are arranged in a disordered way. Tubules and S. R. systems are not fully developed. The very thick myofilaments bear a regular periodicity of paramyosin. Their length must be a few micra although they can not be traced from end to end. They taper at both ends. An array of thick myofilaments is not regular in cross-section, but run parallel to each other. Thick myofilaments sometimes appear in various sizes in a cross-section [27]. Their appearance may be a result of the disordered arrangement of thick myofilaments, that is, the thick ones may be cross-sections of the central portion of a thick myofilament and thin ones may be cross-sections of the terminal portion of the same thick myofilament. The thick myofilament shows a cored feature but does not show a tubular one (Figs. 5 and 6).

The C-type cells mainly investigated in adductors of bivalves, and are not reported in vertebrates. The exceptions are taeniols of coelenterate polyps of *Stephanoscyphus* [18] and *Atorella* [19]. A number of investigations were carried out in adductor muscles of a telline [8], *Meretrix* [9], *Atrina* [10] and *Fragum*.

The very thick myofilaments may be associated with "catch" contractions, as they are usually present in "catch" muscles [26, 27]. It has been discussed that the "catch" contraction might have some relation to paramyosin in the very thick myofilaments [28, 29]. The cell is a rather primitive type, as in the A- and B-type cells, since it has similar characteristics in its profile and intracellular structures except for its very thick myofilaments. The C-type cell must have developed a specialized course resulting in its mighty contraction and "catch"-mechanism for the following reasons: i) similar cells that show large profiles and have very thick myofilaments, are gathered in parallel in an adductor muscle, ii) the direction of cell contraction is limited by its very thick myofilaments, and iii) their very thick myofilaments are very long.

4) *D-type smooth muscle cell*

The D-type cells have thick myofilaments of various size (14–40 nm in diameter), thin myofilaments of 7 nm in diameter and many dense bodies. The cell generally appears small in cross-section. The cell is characterized by its dense distributions of dense bodies. Dense bodies connecting each thin myofilament measure to be about 0.2 μm in length [5]. They are generally arranged in an ordered way. Intervals between dense bodies are short. Cell organelles such as mitochondria or S. R. systems are more developed than those in A-, B- and C-types of cells (Figs. 7 and 8).

The D-type cell is reported only in muscles in invertebrates. The representative D-type cells are present in the intestinal walls of the sea cucumber [5] and cuttlefish [30], in an echinoid ampulla [3], in the large vessel of *Phoronis* [31], and in the longitudinal muscle of the intestine in *Branchiura* [32]. The D-type cell is the most developed and differentiated of the smooth muscle cells, and resembles the oblique-striated muscle cells. However, it is distinguishable by the following features: i) the arrangement of the dense bodies in the D-type cell is not as ordered as in oblique-striated muscle cells, ii) cell organelles, especially its S. R. systems, are not so well-developed. This type of a cell, however, facilitates speedy and repeated movements of organs and tissues of invertebrates. The pattern of movement may be related to the short intervals between dense bodies. The D-type cells must be employed in invertebrates instead of cross- or oblique-striated muscle cells to move quickly.

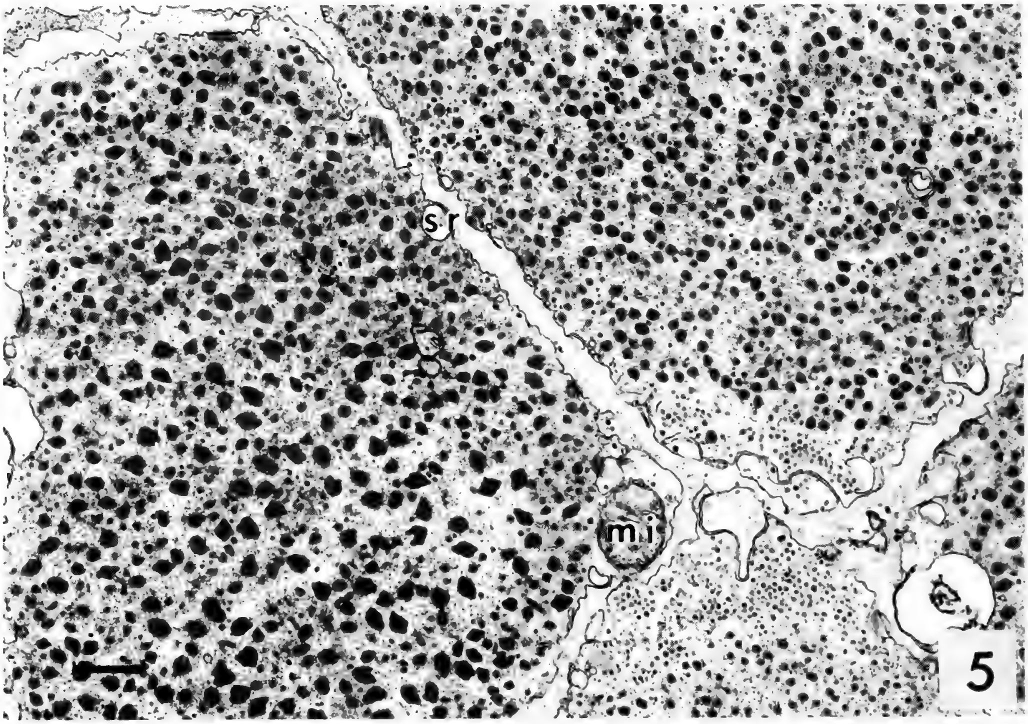

FIG. 5. A cross-section of a C-type cell in the adductor of *Meretrix*. Very thick myofilaments are shown. They appear as somewhat irregular circles in cross-section. mi: mitochondrion, sr: sarcoplasmic reticulum. $\times 15{,}800$, scale bar represents 0.5 μm.

FIG. 6. A longitudinal-section of thick myofilaments of a C-type cell in the adductor of *Fragum*. Very thick myofilaments bear regular periodicities, about 14.5 nm in interval. $\times 50{,}600$, scale bar represents 0.5 μm.

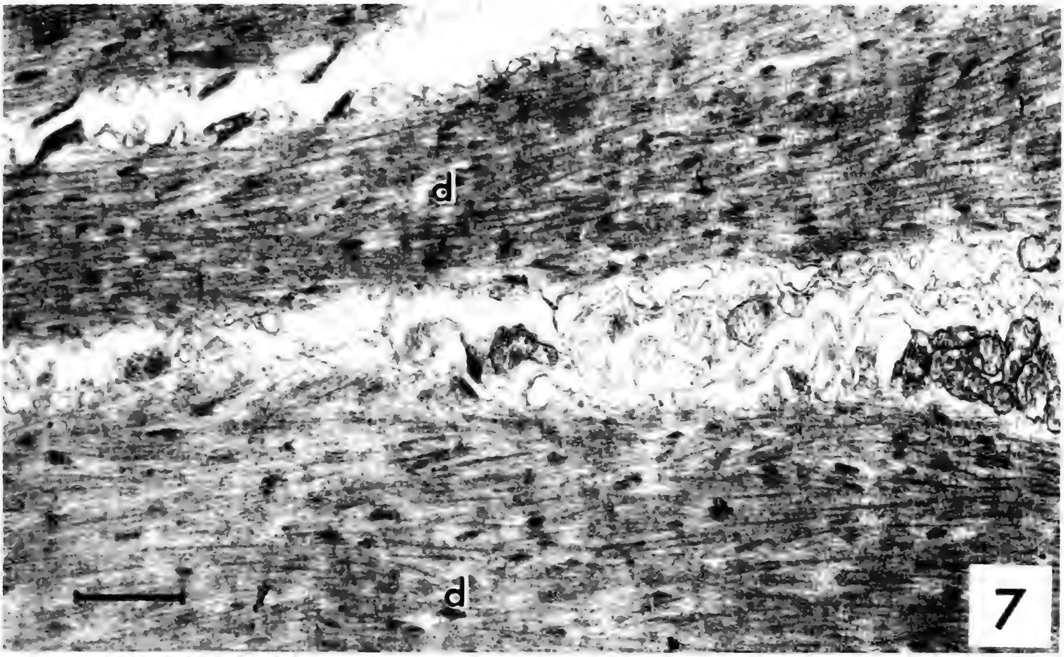

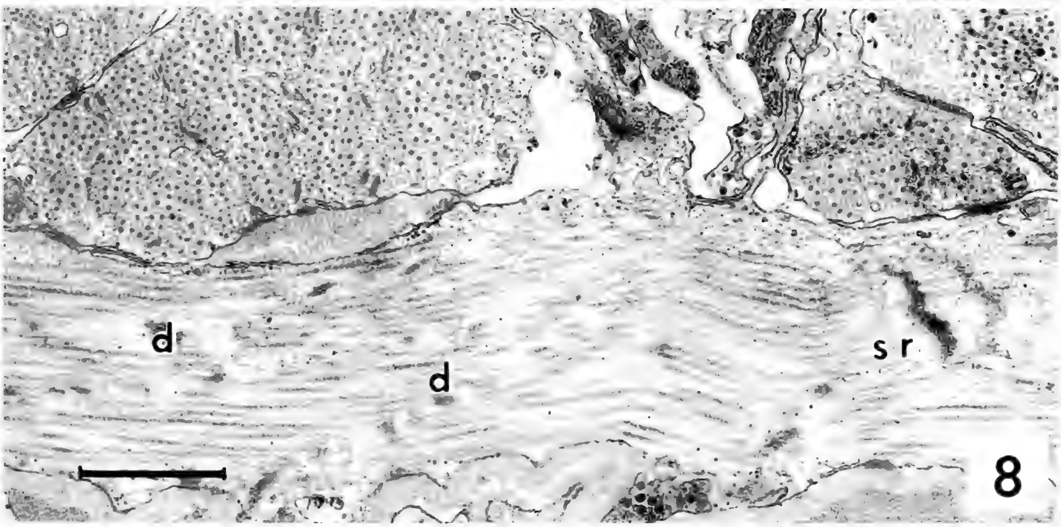

FIG. 7. A longitudinal-section of a D-type cell in the intestine of sea cucumber [5]. Many dense bodies (d) are scattered among myofilaments. Thick myofilaments are not large in size. ×15,800, scale bar represents 1 μm.

FIG. 8. A longitudinal-section of a D-type cell in the intestine of *Brachiura* [32]. Dense bodies (d) are shown in somewhat regular array. Sarcoplasmic reticular systems (sr) appear to be slightly developed. ×20,900, scale bar represents 1 μm.

COMMENTS

I should mention a special type of smooth muscle cell not listed in Table 1 . Smooth muscle cells in ascidians have ultrastructures similar to the A-type cell [33–35], but the cells show thoroughly different characteristics. They contain thin myofilament-linked regulatory systems of contraction in the same way as cross-striated muscle cells [33].

I have tried to classify smooth muscle cells from an ultrastuctural standpoint, and it is not clear whether the classification coincides with the one from the physiological and biochemical standpoints. I expect another classifications from other views. Very probably, they are not so different from the present classification.

ACKNOWLEDGMENTS

The author expresses his sincere thanks to Prof. K. Maruyama of Chiba University for his warm encouragement and critical advice on this manuscript. I am also indebted to Dr. S. Kawaguti, Prof. Emeritus of Okayama University for his critical advice during this work.

REFERENCES

1 Kawaguti, S. and Kamishima, Y. (1965) Biol. J. Okayama Univ.,**11**(1–2): 31–40
2 Kawaguti, S. (1965) Biol. J. Okayama Univ., **11** (3–4): 66–74.
3 Kawaguti, S. (1965) Biol. J. Okayama Univ., **11**(3–4): 75–86.
4 Kawaguti, S. and Ikemoto, N. (1965) Molecular Biology of Muscular Contraction, Igaku Shoin Ltd., pp. 610–613.
5 Kawaguti, S. (1964) Biol. J. Okayama Univ., **10** (1–2): 39–50.
6 Plesch, B. (1977) Cell Tissue. Res., **180**: 317–340.
7 Kawaguti, S. and Ikemoto, N. (1959) Biol. J. Okayama Univ., **5** (1–2): 73–87.
8 Kawaguti, S. and Ikemoto, N. (1961) Biol. J. Okayama Univ., **7** (1–2): 17–29.
9 Kawaguti, S. and Ikemoto, N. (1960) Biol. J. Okayama Univ.,**6** (1–2): 1–18.
10 Kawaguti, S. and Ikemoto, N. (1957) Biol. J. Okayama Univ., **3** (4): 248–268.
11 Panner, B. J. and Honig, C. R. (1967) J. Cell Biol., **35**: 303–321.
12 Kelly, R. E. and Rice, R. V. (1968) J. Cell Biol., **37**: 105–116.
13 Rosenbluth, J. (1971) J. Cell Biol., **48**: 174–188.
14 Nonomura, Y. (1968) J. Cell Biol., **39**: 741–745.
15 Kawaguti, S. and Ikemoto, N. (1957) Biol. J. Okayama Univ., **3** (3): 159–168.
16 Lane, B. P. (1965) J. Cell Biol., **27**: 199–213.
17 Kawaguti, S. and Yamasu, T. (1960) Biol. J. Okayama Univ., **6**(1–2): 61–70.
18 Kawaguti, S. and Yoshimoto, F. (1973) Biol. J. Okayama Univ., **16**(3–4): 47–66.
19 Matsuno, A. (1981) Annot. Zool. Japon., **54**: 171–181.
20 Elliott, A. (1974) Proc. R. Soc. Lond., B, **186**: 53–66.
21 Nonomura, Y. (1974) J. Mol. Biol., **88**: 445–455.
22 Elliott, A. (1979) J. Mol. Biol.,**132**: 323–341.
23 Kawaguti, S. (1968) Biol. J. Okayama Univ., **14**(1–2): 13–20.
24 Kawaguti, S. and Ikemoto, N. (1957) Biol. J. Okayama Univ., **3** (3): 107–122.
25 Sobieszek, A. (1973) J. Ultrastruct. Res., **43**: 313–343.
26 Sugi, H. and Suzuki, S. (1978) J. Cell Biol., **79**: 454–466.
27 Morrison, C. M. and Odense, P. H. (1974) J. Ultrastruct. Res., **49**: 228–251.
28 Ruegg, J. C. (1971) Rhysiol. Rev., **51**, Suppl. **1**: 201–248.
29 Johnson, W. H., Kahn, J. S. and Szent-Gyorgyi, A, G. (1959) Science, **130**: 160–161.
30 Kawaguti, S. (1964) Biol. J. Okayama Univ., **10** (3–4): 93–103.
31 Kawaguti, S. and Nakamichi, A. (1973) Biol. J. Okayama Univ., **16** (3–4): 73–82.
32 Naitoh, T. and Matsuno, A. (1985) Experientia, **41**: 370–372.
33 Toyota, N., Obinata, T. and Terakado. K. (1979) Comp. Biochem. Physiol., **62B**: 433–441.
34 Shinohara, Y. and Konishi, K. (1982) J. Exp. Zool., **221**: 137–142.
35 Terakado, K. and Obinata, T. (1986) Cell Tissue Res., in press.

ZOOLOGICAL SCIENCE 4: 23–30 (1987)

Phototactic Behavior of the Orb Weaving Spiders, *Argiope amoena* and *Nephila clavata*

Shigeki Yamashita[1] and Rieko Tuji

Department of Biology, Faculty of Science, Kyushu University, Fukuoka 812, Japan

ABSTRACT—Phototactic behavior of tethered orb weaving spiders which walked on a y-maze globe was investigated under open-loop conditions. On a dark background, the spiders tended to turn away from a test light given to the eyes (negative phototaxis). On a light background, however, the spiders tended to turn towards the test light (positive phototaxis). When a small light spot for background illumination was presented to only a portion of the eyes, the spiders showed a negative phototaxis to the test light. On the other hand, when the brain was illuminated through the cuticle covering it, the spiders showed a positive phototaxis to a test light given to the eyes. It is concluded that extraocular photoreceptors which should be present in the brain control the phototactic behavior of these spiders.

INTRODUCTION

Orb weaving spiders have four pairs of simple eyes arranged in two rows on the frontal part of the prosoma. The eyes of the orb weaving spiders, *Argiope,* have been studied morphologically [1, 2] and physiologically [3–6].

The present study was undertaken to examine the phototactic behavior of the orb weaving spiders and also to examine that phototactic behavior may be significantly affected by a kind of extraocular photoreceptor.

MATERIALS AND METHODS

Animals used in this study were female orb weaving spiders, *Argiope amoena* and *Nephila clavata*, which were collected in open fields. Individuals of both species ranged from 20–25 mm in body length, and from 1.2–1.7 g in weight.

The spider was held rigidly in space by a glass tube of about 1.5 mm diameter, waxed to the posterior part of the prosoma (Fig. 1A), or by a light guide of about 2 mm diameter waxed to the central part of the prosoma which was just above the brain (Fig. 1B). Then, the spider was given a y-maze globe with slightly lighter weight than that of the spider itself (about 0.8–1.2 g) to hold. Usually, 7–10 spiders were prepared at the same time, and only those spiders which showed spontaneous walking activity in a dim room were used for the experiments. From a total of about 250 spiders prepared, about 40 showed sufficient walking activity to enable them to be used in the experiments. These spiders made turns at y-arms one per every 2–10 seconds. However, most of them continued to show walking activity for less than two hours. We continued to make experiments as long as the spiders showed walking activity.

For test stimuli, two lights emitted from two 6–8 V tungsten filament lamps were passed through heat-absorbing filters and calibrated neutral density filters, and focused onto the tips of two light guides, respectively. One light guide was aimed horizontally at the frontal part of the prosoma from an angle of 45° clockwise to the body axis, and the other anticlockwise to the body axis. Thus, each test light illuminated the right or left eyes preferentially. The test light subtended a visual angle of about 2° at the spider eyes. The intensity of the test light without neutral density filters was referred to as unit intensity, and had a value of about 30 lux at the preparation.

Accepted June 26, 1986
Received May 23, 1986

[1] Present address: Biological Laboratory, Kyushu Institute of Design, Shiobaru, Fukuoka 815, Japan.

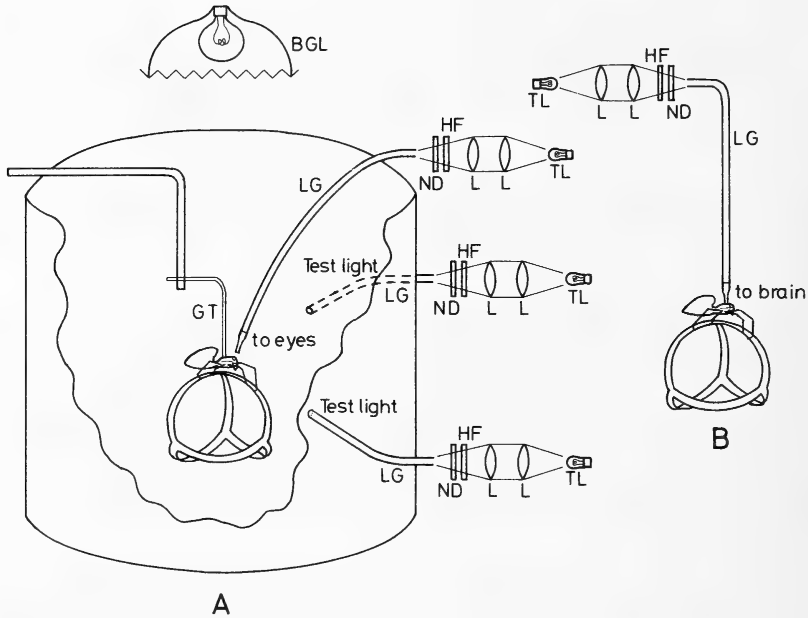

FIG. 1. Diagram of the experimental apparatus. The spider is fixed in the center of a 28 cm drum by a glass tube (A), or by a light guide (B). See text. TL, tungsten lamp; BGL, tungsten lamp for background light; LG, light guide; GT, glass tube; L, lens; ND, neutral density filter; HF, heat absorbing filter.

In most cases, spiders made 100–120 turns at y-arms for each test (each point on figures), half of them during illumination of the right eyes, plus a half during illumination of the left eyes. Successive illumination of the right and left eyes were performed in order to compensate for side preferences independent of visual stimulation. Prior to the start of each test run, spiders were adapted to each test light or background light for 5–10 min.

The turning reaction was defined as $P-N/P+N$, where P is the number of turns at y-arms directed towards the test light, and N is the number of turns directed away from the test light.

For background illumination, scattered light of a tungsten lamp placed over the spider was used (Fig. 1A). The intensity was controlled by changing the voltage of an electrical power source. For illumination of only a portion of the eyes or the brain, the light emitted from a tungsten lamp was passed through a heat-absorbing filter, calibrated neutral density filters and wedges, and then focused onto the tip of a light guide. The other tip of the light guide (about 2 mm in tip diameter) was positioned almost in contact with the eyes (Fig. 1A), or was touched onto the central part of the prosoma just above the brain (Fig. 1B). The light could illuminate the eyes or the brain, although it also illuminated the vicinity of the eyes or the brain. Blue light (440 nm peak wavelength) and green light (536 nm) were produced with interference filters. The half bandwidths of the blue filter was 38 nm, and that of the green was 14 nm.

To observe the movements of the y-maze globe in the dark, dim red light (edge filter, 50% value at 650 nm) was focused onto the globe. The red light was illuminated throughout the experiments.

RESULTS

Turning tendency in the absence of the test light

When the illumination intensity of background light was below 600 lux, spiders which walked on a y-maze globe made choices of y-arms at the rate of one time per every about 2–10 sec. The

relationship between choice frequency and background illumination could not be determined. However, when the background light intensity was over 600–1,000 lux, the choice frequency became very low, i.e. most spiders showed little walking activity.

Turning tendencies of spiders, to which no test light was presented, were observed under various background light intensities (Fig. 2). In this experiment, turning reaction was defined, for convenience, as R−L/R+L, where R is the number of turns towards right direction and L is that of left direction. As can be seen in Figure 2, both on the dark- and light-backgrounds, the value of the turning reaction for each spider was almost constant, although it varied from spider to spider. This observation shows that background light intensity has little effect on the spontaneous turning tendencies of spiders.

Changes in the phototactic behavior by background lightness

In Figure 3, the turning reactions of five spiders on the dark-background are plotted against the relative intensity of the test light. The spiders tend to turn away from the test light and this tendency becomes stronger as the stimulus intensity increases. It is obvious that the spiders show negative phototaxis on a dark-backgroud.

The negative phototaxis on a dark-background changed into positive phototaxis on a light-background. Figure 4 shows the responses of eleven spiders under various background light intensities. In this and following experiments, the intensity of the test light was restricted to −0.3 log units. On the dark-background, all spiders showed negative phototaxis. The tendency for a negative phototactic response decreased as the background became lighter, and at about 100–300 lux background, spiders did not show any phototaxis. When the background became still lighter than 100–300 lux, the spiders showed a positive phototaxis and this tendency was augmented as the background lightened.

To examine the role of each pair of eyes on the phototaxis, only one or two pairs of the eyes were left intact; all the other pairs were destroyed surgically and then covered with black paint. The

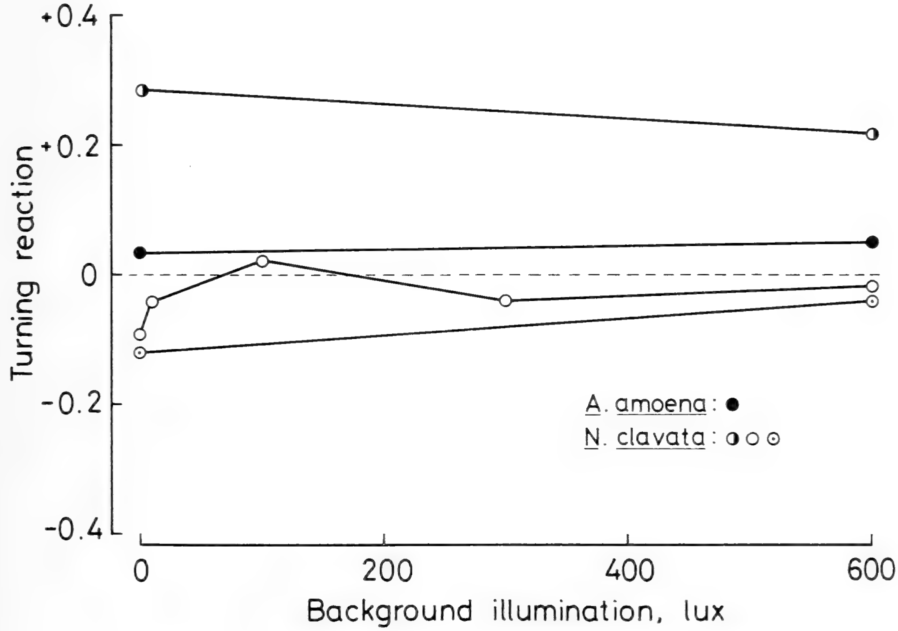

Fig. 2. Turning tendencies of one *Argiope* and three *Nephila* under various background light intensities. Each symbol represents a single spider.

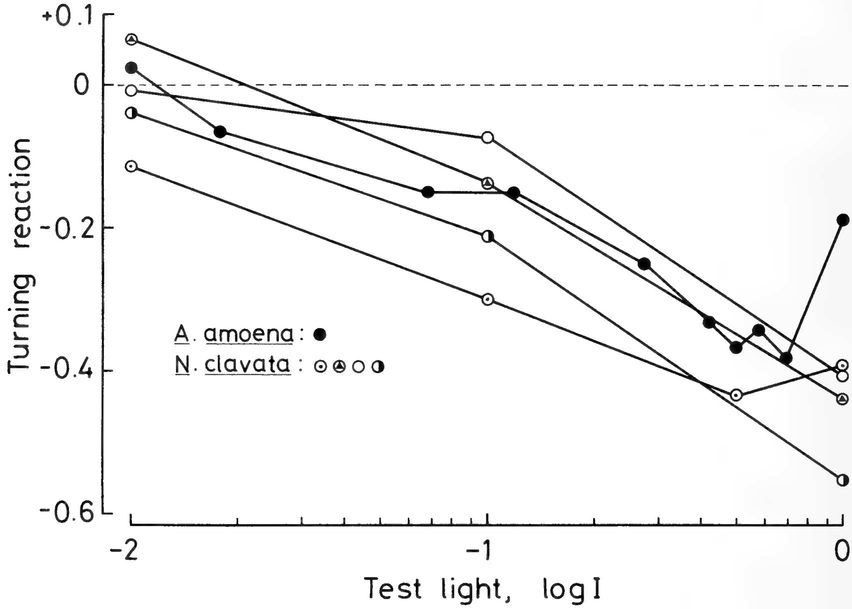

FIG. 3. Intensity-turning reaction curves for individual spiders on a dark-background.

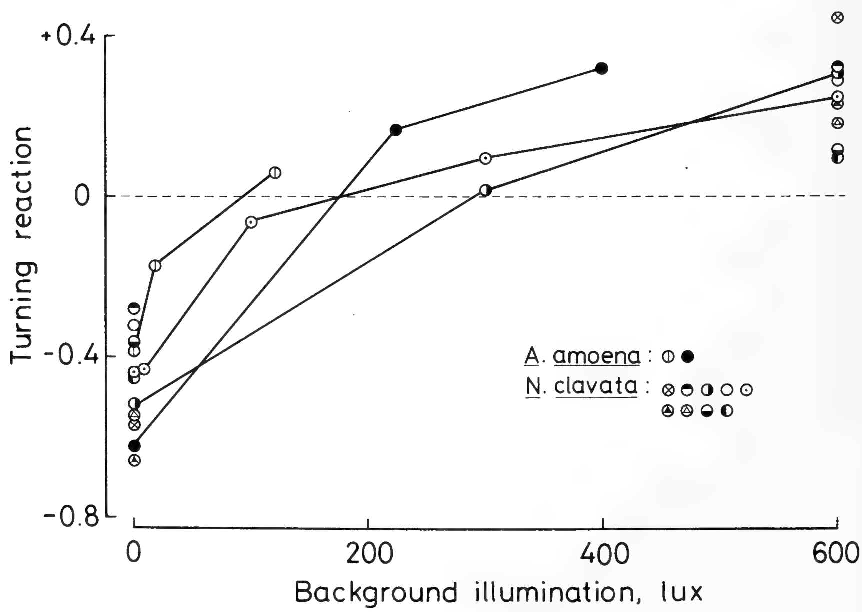

FIG. 4. Effects of background illumination on the phototactic response.

TABLE 1. Role of each pair of eyes on the phototactic responses on a dark-background and in light (600 lux)

Eyes	n	Turning reaction Dark-background	Turning reaction Light-background
All eyes	9	− 0.47 ± 0.12	+ 0.24 ± 0.11
AM eyes	2	− 0.36	+ 0.29
PM eyes	2	− 0.32	+ 0.20
AL and PL eyes	3	− 0.48	+ 0.22
No eyes	1	− 0.03	− 0.01

AM, anterior median; PM, posterior median; AL, anterior lateral; PL, posterior lateral. n= number of spiders tested. Mean (± S.D.) of turning reactions obtained from 1–9 spiders. In the experiments for the AM, PM, and AL and PL eyes, light guides which provided test stimuli were aimed at the AM, PM, and AL and PL eyes, respectively.

results are summarized in Table 1, where turning reactions obtained on the dark-background and on the light-background of 600 lux are shown. With one or two pairs of eyes, the spiders showed similar phototactic behavior to that of normal spiders, i.e. negative phototaxis on a dark-background and positive phototaxis on a light-background. However, when all of the eyes were blinded, no phototactic behavior was observed.

These observations show that the phototactic behavior of the spiders is induced by signals from the eyes, and that there are no significant differences in function among the four pairs of eyes with respect to phototactic behavior.

If the changes in phototaxis from negative to positive which are dependent on the background lightness is mediated by visual signals, then background illumination presented to only the eyes

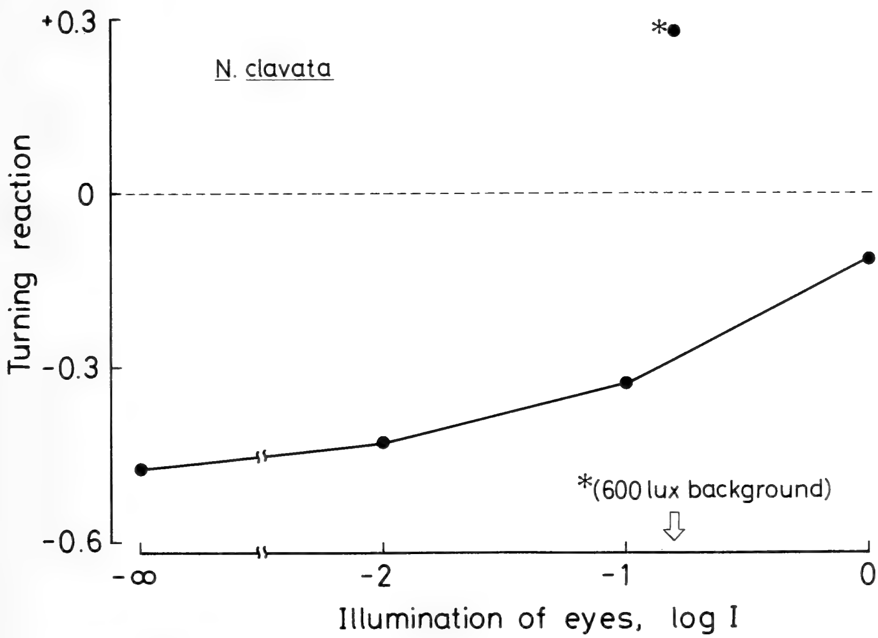

FIG. 5. Effects of illumination of the eyes on the phototactic response. The spider showed a positive phototaxis during illumination of the whole spider at 600 lux background (∗●), but a negative phototaxis during illumination of the eyes. Both ocular illumination of −0.8 log units (arrow) and whole illumination of 600 lux elicited similar ERGs in an AM eye.

should also change the phototaxis. To test this, a small light spot for background illumination was presented to a portion of the eyes. The light intensity of background illumination presented only to the eyes, and that presented to the whole spider were compared by recording ERGs from the AM eye under conditions similar to those used for the behavioral experiments. Both ocular illumination of -0.8 log units and whole illumination of 600 lux elicited similar ERGs in the AM eye. However, the effects of these two kinds of illumination on phototaxis were quite different. An example is shown in Figure 5. The spider showed positive phototaxis during illumination of the whole spider. However, it shows negative phototaxis during illumination of the eyes. These observations suggest that extraocular photoreceptors control the phototactic behavior of spiders.

Extraocular photoreceptors and phototaxis

Extraocular photoreceptors which take part in the phototaxis may be present in the brain. If this is true, spiders should show positive phototaxis during lighter illumination of the brain. The effects of illumination of the brain on the phototactic response are shown in Figure 6. On a dark-background, all spiders showed a negative phototaxis. As the intensity of cerebral illumination was increased, these spiders became positively phototactic. The light given to the brain diffused within the prosoma and part of the light reached the eyes, but it was small; ERGs elicited by cerebral illumination of intensity of 1.0 (Fig. 6) were smaller than those elicited by ocular illumination of about -1.6 log units (Fig. 5). It is, therefore, difficult to consider that the diffused light which reaches the eyes has direct effects on the changes in phototaxis from negative to positive.

These observations show that extraocular photoreceptors, presumably located in the brain, control the phototactic behavior of spiders.

The effects of blue, green and white light of equal energy on the brain are compared in Table 2. The intensities of light were corresponded to about one-tenth of the white light used in Figure 6. It was clear that blue light had a marked effect on the phototactic response. In contrast, green light had little effect. White light had an intermediate effect between that of blue and breen. These observa-

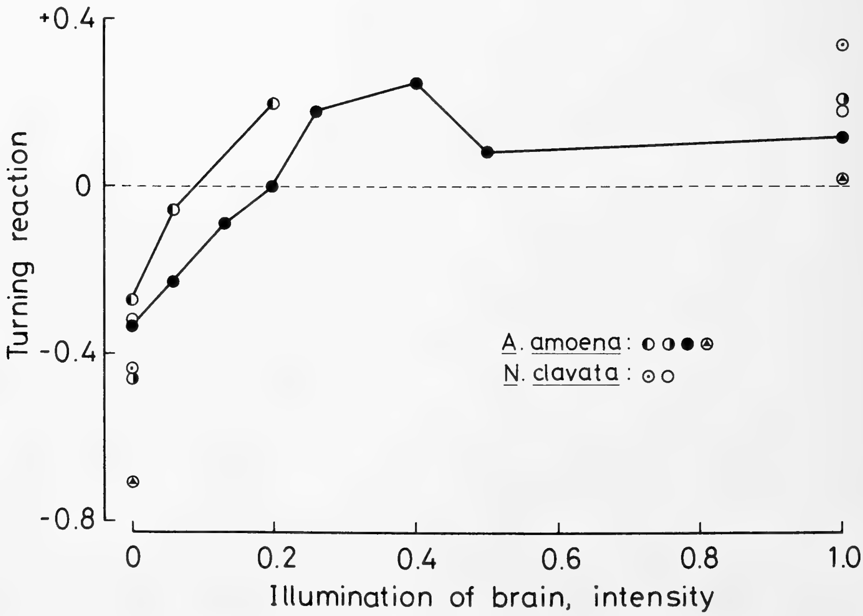

FIG. 6. Effects of illumination of the brain on the phototactic response.

TABLE 2. Effects of blue (440 nm), green (536 nm) and white light on the brain

Light to brain	None	Blue	Green	White
Turning reaction	−0.39	+0.18	−0.31	+0.04

Mean of turning reactions was obtained from two spiders.

tions suggest that the extraocular photoreceptors have a maximum sensitivity in the blue region.

DISCUSSION

In the present study, the brain was illuminated through the dorsal cuticle via a light guide. A dorsal view of the prosoma of *Argiope* and *Nephila* is shown in Figure 7. In both species, the central

FIG. 7. Drawings of the prosoma of *A. amoena* and *N.clavata*. All hairs covering the prosoma are removed.

part of the dorsal cuticle contains little pigments, although the area of the non-pigmented cuticle varied from spider to spider. The brain of the spider is located beneath the non-pigmented cuticle which transmits light. Yamashita and Tateda [5] reported that efferent neurons in the brain of *Argiope* are directly excitable by light. They have observed that illumination of the brain through the central part of the dorsal cuticle via a light guide increases the discharge rate of the cerebral photosensitive neurons which are recorded from the eye in the intact animal. It is, therefore, apparent that the light delivered by the light guide reaches the brain without significant diminution in intensity, although the light also illuminates other regions of the brain at the same time. We assume that extraocular photoreceptors are activated by light passing through the transparent area of dorsal cuticle.

The cerebral photosensitive neurons reported by Yamashita and Tateda [5] have a maximum sensitivity at about 420–440 nm. On the other hand, the eyes have maximum sensitivities at about 480–540 nm in the visible and at about 360 nm in the ultraviolet [3, 6]. As shown in the present study, blue light (440 nm peak-wavelength) had a marked effect on the phototactic response, but green light (536 nm) had little effect. These observations support the idea that extraocular photoreceptors control the phototactic behavior of the spiders, and suggest that the extraocular photoreceptors in the present study may be the cerebral photosensitive neurons reported by Yamashita and Tateda [5]. If this is true, the cerebral photosensitive neurons may be more directly involved in the dimming reaction than in phototaxis, since they respond markdly to a diminution in light intensity [5]. We have in fact observed that when the background light is turned off, the spiders tend to turn transiently towards the test light.

ACKNOWLEDGMENTS

This research was supported in part by grants from the Ministry of Education of Japan. The authors are deeply indebted to Dr. D. R. Stokes (Emory University, Atlanta, Georgia, U. S. A.) for his helpful discussion and comments on this manuscript, and also to Prof. H. Tateda (Kyushu University) for his helpful discussion throughout this work.

REFERENCES

1 Uehara, A., Toh, Y. and Tateda, H. (1977) Fine structure of the eyes of orb-weavers, *Argiope amoena* L. Koch (Aranea: Argiopidae). 1. The anteromedial eyes. Cell Tissue Res., **182**: 81:91.

2 Uehara, A., Toh, Y. and Tateda, H. (1978) Fine structure of the eyes of orb weavers, *Argiope amoena*

L. Koch (Aranea: Argiopidae). 2. The anterolateral, posterolateral and posteromedial eyes. Cell Tissue Res., **186**: 435–452.

3 Yamashita, S. and Tateda, H. (1978) Spectral sensitivities of the anterior median eyes of the orb web spiders, *Argiope bruennichii* and *A. amoena.* J. Exp. Biol., **74**: 47–57.

4 Yamashita, S. and Tateda, H. (1981) Efferent neural control in the eyes of orb weaving spiders. J. Comp. Physiol., **143**: 477–483.

5 Yamashita, S. and Tateda, H. (1983) Cerebral photosensitive neurons in the orb weaving spiders, *Argiope bruennichii* and *A. amoena.* J. Comp. Physiol., **150**: 467–472.

6 Yamashita, S. (1985) Photoreceptor cells in the spider eye: spectral sensitivity and efferent control. In "Neurobiology of Arachnids". Ed. by F. G. Barth, Springer-Verlag, Berlin-Heidelberg-New York-Tokyo, pp. 103–117.

ZOOLOGICAL SCIENCE 4: 31–35 (1987)

Dimming Reaction of the Orb Weaving Spider, *Argiope amoena*

Shigeki Yamashita[1]

Department of Biology, Faculty of Science, Kyushu University, Fukuoka 812, Japan

ABSTRACT—The reaction to the dimming of light in the tethered orb weaving spider which walked on a y-maze globe was investigated under open-loop conditions. The spiders tended to turn transiently towards the lighter direction after the dimming of light. It is suggested that cerebral photosensitive neurons play a role in the dimming reaction.

INTRODUCTION

Extraocular neural photoreceptors have been reported for many animals representing various invertebrate phyla and are reviewed by Yoshida [1]. Yamashita and Tateda [2] showed that the efferent neurons in the brain of orb weaving spiders, *Argiope amoena* and *A. bruennichii,* whose signals control the responses of the eyes, are directly sensitive to light. The discharge rate of the cerebral photosensitive neurons (the efferent neurons) increases transiently following the dimming of illumination of the eyes (the dimming reaction). Interaction of the cerebral photosensitive neurons and the eyes plays a role in increasing the dimming reaction [2, 3].

Prominent responses to the turning off and the dimming of light have been shown for the second order cells (I-cells) and the third order cells (A-cells) in the barnacle visual pathways [4, 5] and for the pallial nerve of *Spisula solidissima* [6]. The impulses generated in the A-cells of barnacles in response to dimming cause a withdrawal of the cirri and closure of the opercular plates [7–9]; impulses in the afferent axon of the pallial nerve of *Spisula* cause withdrawal of the siphon [6].

In orb-weaving spiders, impulses in the cerebral photosensitive neurons produced as a result of the interaction of the cerebral photosensitive neurons and the eyes may play a role in dimming reaction behavior. In the present study, reactions to the dimming of light in orb weaving spiders have been examined behaviorally.

MATERIALS AND METHODS

Female orb weaving spiders, *Argiope amoena,* collected in open fields were used throughout this study. Methods were similar to those described previously [10]. The spider was held rigidly in space and was given a ring or a y-maze globe to hold. For test stimuli, a couple of light emitted from two 6–8 V tungsten filament lamps was passed through heat-absorbing filters and focused onto the tips of two light guides, respectively. Initially, test light of similar intensity was simultaneously presented to the right and left eyes from two light sources of 45° clockwise and 45° anticlockwise to the body axis. The intensity of each test light was about 35 lux at the preparation. Reductions in light intensity were achieved by simultaneous introduction of neutral density filters into the two test light paths or were achieved by turning off one of the two test light; the other light was continued to illuminate the right or left eyes. In the latter case, the right test light and the left test light were turned off alternately in order to compensate for side preferences independent of visual stimulation. The duration of illumination was controlled by a mechanical shutter. Duration of the lighter period (illumination by two test light) was 2–5 min; the darker period (illumination by one test light), 2–4 min. The illumination cycle was repeated as long as each spider showed

Accepted July 8, 1986
Received May 23, 1986

[1] Present address: Biological Laboratory, Kyushu Institute of Design, Shiobaru, Fukuoka 815, Japan.

walking activity. However, most spiders showed walking activity only for less than 3–4 hr in a day. Each spider was tested for two or three days.

The turning reaction was defined as P−N/P+N, where P is the number of turns at y-arms directed towards a test light which was continued to illuminate the eyes after dimming, and N is the number of turns away from the test light. The turning reaction was averaged every 10 or 20 seconds. In most cases, spiders made, at least, 40 turns for each 10 or 20 seconds.

RESULTS

Walking activity following dimming

The changes in walking activity following diminution of the light intensity were examined for five spontaneous walking spiders. A typical example is shown in Figure 1. The spider walked on a ring at a speed of about 2.5 cm/sec before the dimming. Due to diminution of the light intensity, the spider stopped for a brief period, especially when the diminution was great. But then walking speed of the spider increased beyond the predimming level for less than 2–4 min. The increase was augmented as the diminution increased. In this spider, the maximum walking speed was about 6 cm/sec and occurred for 10–20 sec after a decrement of 1.0 log unit in intensity. The average value of the maximum walking speed for five spiders was 5.7 cm/sec, or 1.9 times faster than that before the dimming.

The increase in walking activity was also observed when only a portion of the eyes was exposed to a dimming light. However, illumination of the brain through the dorsal cuticle had little effect on walking activity [cf. 10]. It is unlikely, therefore, that cerebral photosensitive neurons play a direct role in controlling walking activity.

Turning reaction to dimming

The turning reaction following a diminution of light intensity was examined for eight spontaneous walking spiders. All of them tended to turn transiently towards the light (positive reaction) follwing a diminution of light intensity. Three examples are shown in figrure 2. The reaction was the most positive just after dimming and then it became weaker with time. Finally, all spiders

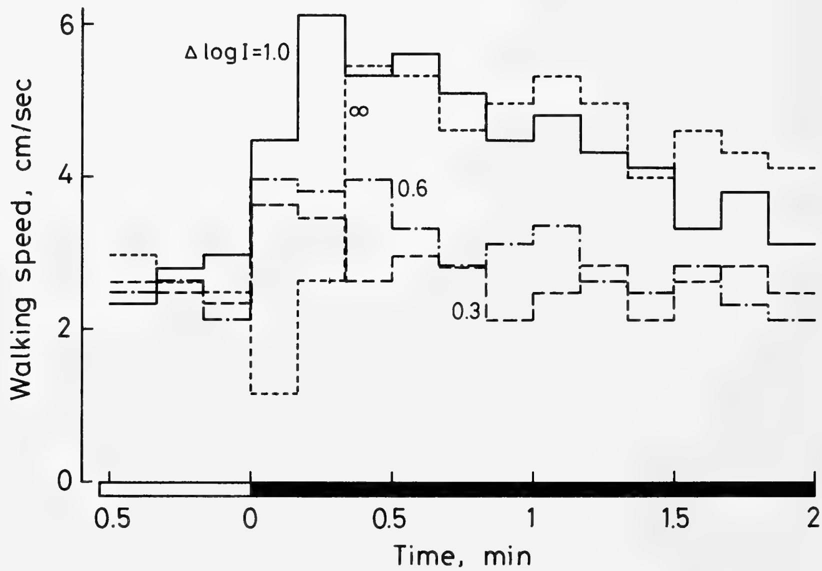

FIG. 1. Walking activity following dimming. Walking speed of one spider is plotted against the time after the beginning of 4 different decrements of light intensity. Decrement of lihgt intensity (△log I) is indicated for each curve in log units.

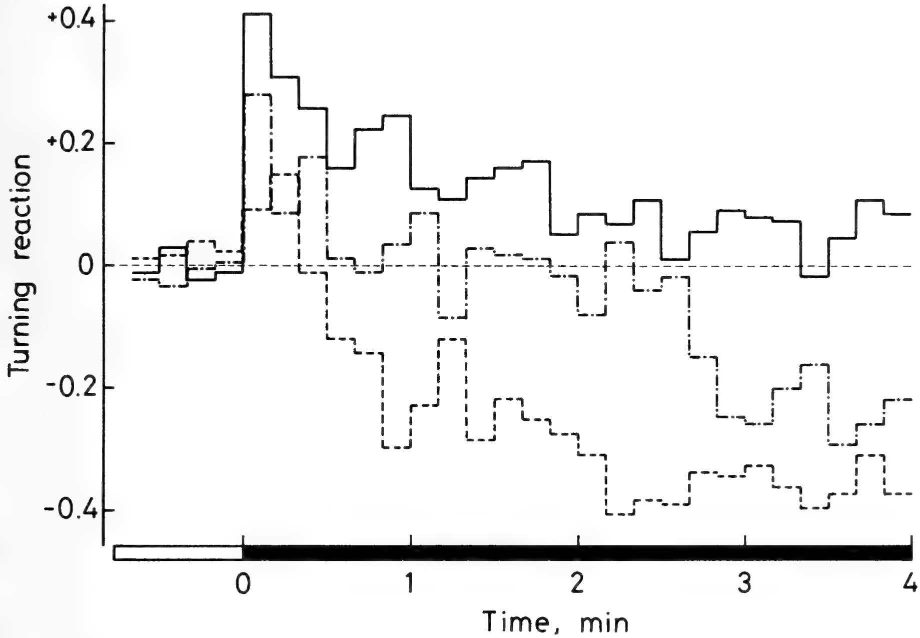

FIG. 2. Turning reactions to the dimming of light for three spiders. The reaction of each spider was tested for three days independently of time of day, when the spider showed spontaneous walking activity. Each curve represents one spider. Turning reaction is plotted against the time after the beginning of a decrement of light intensity.

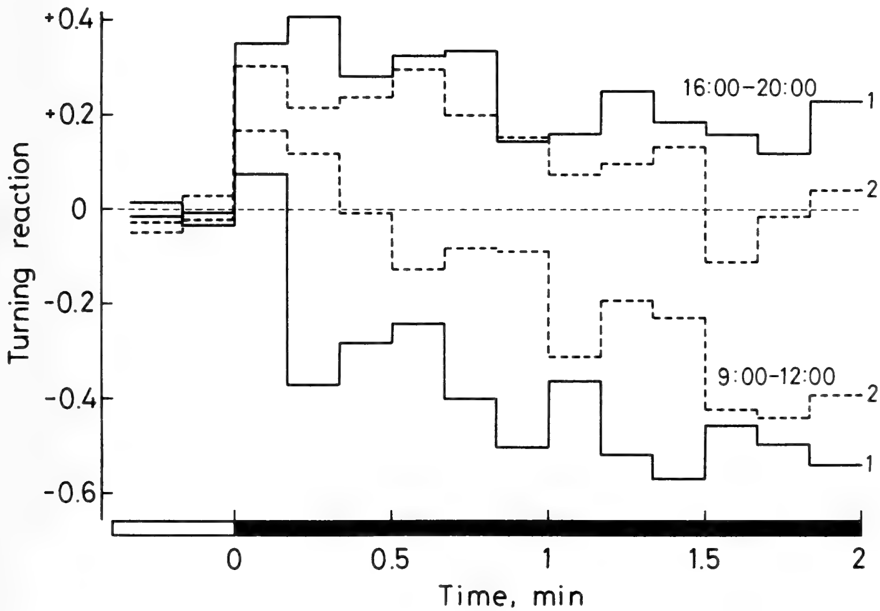

FIG. 3. Turning reaction of one spider to a dimming of light in the morning (9:00–12:00) and in the evening (16:00–20:00) for two days of the experiment. 1, first day; 2, second day.

tended to turn away from the light (negative reaction) [cf. 10]. As can be seen in Figure 2 , however, the maximum value of the positive reaction varied from spider to spider. For example, the spider which showed the largest positive reaction among the eight spiders examined (solid line in Fig. 2), achieved the maximum value of about 0.4 and the period of the positive reaction lasted at least two minutes. The spider did not show a clear negative reaction even within four minutes after dimming. However, when the turning reaction was examined five or more minutes after the dimming, this spider showed a negative reaction. On the other hand, one spider showed a smaller positive reaction (broken line in Fig. 2), with the maximum value of about 0.09 and a period of less than twenty seconds.

In one of eight spiders, it was observed that the dimming reaction varied with time of day (Fig. 3). The reaction of this spider was tested in the morning from 9:00 to 12:00 and in the evening from 16:00 to 22:00. For initial two days of the experiment, the spider showed a strong, positive reaction in the evening, but a weaker reaction in the morning. Unfortunately, this spider greatly reduced its walking activity on the third day. None of the other spiders showed sufficient walking activity both in the morning and in the evening. In the morning, an average value of the turning reaction for these seven spiders (P_t-N_t/P_t+N_t), obtained in the first twenty seconds after dimming was 0.19, and in the evening it was 0.28; where P_t and N_t are the total numbers of P and N made by the seven spiders. However, whether the orb weaving spiders show a diurnal periodicity of the dimming reaction could not be demonstrated.

DISCUSSION

Yamashita and Tuji [10] reported that the orb weaving spiders, *Argiope amoena* and *Nephila clavata,* which walked on a y-maze globe on a dark-background, tend to turn away from a light shown to the eyes (negative phototaxis), whereas they tend to turn towards the light during illumination of the brain (positive phototaxis). They concluded that extraocular photoreceptors which are likely to be present in the brain control the phototactic behavior, and suggested that the extraocular photoreceptors are the cerebral photosensitive neurons (the efferent neurons) reported by Yamashita and Tateda [2]. The cerebral photosensitive neurons responded markedly to a diminution in light intensity [2]. As shown in the present study, the spiders showed a prominent reaction to the dimming. The observation supports the idea that the extraocular photoreceptors reported by Yamashita and Tuji [10] are the cerebral photosensitive neurons reported by Yamashita and Tateda [2]. The cerebral photosensitive neurons showed a circadian oscillation in spike frequency with a period of approximately 22 hr under constant darkness [11]. As a result, the anterior median eye also showed a circadian oscillation of sensitivity with a period of approximately 22 hr [11, 12]. The maximun frequency of the efferent spikes in the optic nerve is seen in early period of the circadian " night" state. Later in the "night", efferent spike frequency becomes very low. Little or no efferent activity is present during the whole "day". If the cerebral photosensitive neurons take part in the dimming reaction, one would expect that spiders show a circadian oscillation of the dimming reaction as shown in Figure 3.

ACKNOWLEDGMENTS

This research was supported in part by grants from the Ministry of Education of Japan. The author wish to express his gratitude to Dr. D. R. Stokes (Emory Univ. USA) for his helpful discussion and comments on this manuscript. Gratitude is also extended to Prof. H. Tateda (Kyushu Univ.) for his helpful discussion.

REFERENCES

1 Yoshida, M. (1979) Extraocular photoreception. In"Handbook of Sensory Physiology, Vol. VII/6A: Comparative Physiology and Evolution of Vision in Invertebrates". Ed. by H. Autrum, Springer-Verlag, Berlin-Heidelberg-New York, pp. 581–640.

2 Yamashita, S. and Tateda, H. (1983) Cerebral photosensitive neurons in the orb weaving spiders, *Argiope bruennichii* and *A. amoena.* J. Comp. physiol., **150**: 467–472.

3 Yamashita, S. (1985) Photoreceptor cells in the spider eye: spectral sensitivity and efferent control. In "Neurobiology of Arachnids". Ed. by F. G.

Barth, Springer-Verlag, Berlin-Heidelberg-New York-Tokyo, pp. 103–117.

4 Stuart, A. E. and Oertel, D. (1978) Neuronal properties underlying processing of visual information in the barnacle. Nature, **275:** 287–290.

5 Oertel, D. and Stuart, A. E. (1981) Transformation of signals by interneurons in the barnacle's visual pathway. J. Physiol., **311:** 127–146.

6 Kennedy, D. (1960) Neural photoreception in a lamellibranch mollusc. J. Gen. Physiol., **44:** 277–299.

7 Gwilliam, G. F. (1963) The mechanism of the shadow reflex in Cirripedia. I. Electrical activity in the supraesophageal ganglion and ocellar nerve. Biol. Bull., **125**: 470–485.

8 Gwilliam, G. F. (1965) The mechanism of the shadow reflex in Cirripedia. II. Photoreceptor cell response, second-order responses, and motor cell output. Biol Bull., **129**: 244–456.

9 Gwilliam, G. F. (1976) The mechanism of the shadow reflex in Cirripedia. III. Rhythmical patterned activity in central neurons and its modulation by shadows. Biol. Bull., **151**: 141–160.

10 Yamashita, S. and Tuji, R. (1987) Phototactic behavior of the orb weaving spiders, *Argiope amoena* and *Nephila clavata*. Zool. Sci., **4**: 23–30.

11 Yamashita, S. and Tateda, H. (1981) Efferent neural control in the eyes of orb weaving spiders. J. Comp. Physiol. **143**: 477–483.

12 Yamashita, S. and Tateda, H. (1978) Spectral sensitivities of the anterior median eyes of the orb web spider, *Argiope bruennichii* and *A. amoena*. J. Exp. Biol., **74**: 47–57.

ZOOLOGICAL SCIENCE 4: 37–44 (1987)

Regulation by Intracellular Alanine of Water Transport across the Seawater Eel Intestine

MASAAKI ANDO

Laboratory of Physiology, Faculty of Integrated Arts and Sciences, Hiroshima University, Hiroshima 730, Japan

ABSTRACT—Using a new perfusion system, effects of L-alanine on the water transport across the seawater eel intestine were examined. Mucosal L-alanine (5 mM) stimulated the net Na^+, Cl^- and water fluxes under standard condition, accompanied by an increase in serosa-negativity of the transepithelial potential difference (PD). These enhancements were abolished in the presence of 0.01 mM furosemide, suggesting that L-alanine stimulates the Na^+–K^+–Cl^- transport and thus the water transport. After removing furosemide and L-alanine, however, the effects of L-alanine were evoked (after-effect), in spite of the absence of alanine on the bathing media, suggesting that L-alanine or its metabolite(s) act(s) from inside of the cells. This suggestion was supported by such findings as serosal L-alanine also enhanced the serosa-negative PD and the net water flux, and as a long latent period (20–30 min) was required before the effects of alanine appeared. Similar effects were observed after treatment with D-alanine, L-glutamine and L-glutamic acid, but not with other amino acids.

INTRODUCTION

It has been demonstrated recently that water absorption across the seawater eel intestine is mostly coupled to a Na^+–K^+–Cl^- transport system [1–3]. However, it is not clear yet how these transport systems are regulated. Recently we chanced to discover that the net water flux and the transepithelial potential difference (PD) across the seawater eel intestine decreased gradually with time when the serosal fluid was perfused, and that L-alanine stimulated these two parameters [4].

To determine how L-alanine acts on the seawater eel intestine, in the present study, effects of L-alanine on the net water and ion fluxes were examined in detail. The results indicate that L-alanine or its metabolite(s) stimulate(s) the Na^+–K^+–Cl^- transport, thus water transport, *via* acting from inside of the cells.

MATERIALS AND METHODS

Japanese cultured eels, *Anguilla japonica,* weighing about 200 g, were obtained from a commercial supplier and kept in seawater aquaria at 20°C for more than 1 week before use. They were decapitated and the intestine was excised. The outer muscle layers of the intestine were stripped off following our previous method [5]. After everting the intestine, a cylindrical polyester mesh was inserted into the middle part of the intestinal tube and the serosal side was perfused with the standard Ringer solution at a constant rate (around 173 μl/min). The effluent was collected every 10 min. Details of the apparatus for simultaneous measurement of net water flux and transepithal potential differnce (PD) are described previously [4].

The net water flux was calculated by subtracting the perfusion rate from the rate of effluent flow. Net ion fluxes were calculated from the difference between the products of ionic concentration and volume in each of the perfusate and the effluent as previously described [1]. Sodium and K^+ concentrations were measured with flame photometry (Hiranuma, FPF–2A) and Cl^- concentration was determined with a chloride counter (Hiranuma, CL–5M).

The standard Ringer solution contained (mM): 118.5 NaCl: 4.7 KCl; 3.0 $CaCl_2$: 1.2 $MgSO_4$; 1.2 KH_2PO_4; 24.9 $NaHCO_3$ (pH 7.3 on bubbled with

Accepted September 4, 1986
Received August 16, 1986

95% O_2–5% CO_2 gas mixture). Furosemide (Tokyokasei Co., Tokyo, Japan) or various amino acids (Katayama chemical Co., Osaka, Japan) was added to the mucosal side usually. At the end of the experiments, the intestine was cut longitudinally and spread on a graph paper; the surface area of the intestine was measured using a planimeter (Ushikata, 220L).

RESULTS

Effects of L-alanine in standard Ringer solution

Figure 1 illustrates typical effect of L-alanine on the PD and the net water flux. When 5 mM L-alanine was added into the serosal perfusate solution, the serosa-negative PD was enhanced gradually, after latent period of 20 min, and attained to a steady level after 50 min. The net water flux from mucosa to serosa was also accelerated in parallel with the enhancement of the serosa-negativity in the PD. After washing out the serosal alanine, the PD and the net water flux decreased gradually. When L-alanine (5 mM) was added into the mucosal fluid, the PD was initially depolarized only slightly (by 0.3±0.0 mV, N=8), and then began to increase in serosa-negativity gradually. The net water flux started to increase after the initiation of the increment in the serosa-negative PD; the latent period being 20–30 min. Both the PD and the net water flux continued to increase over 100 min. Further addition of L-alanine (5 mM) into the serosal fluid did not add to these increases. Therefore, it can be concluded that alanine is more effective from the mucosal side than from the serosal side.

Relationship between the mucosal L-alanine concentration and the PD or the net water flux is shown in Figure 2. After the PD reached a steady level in standard Ringer solutions, 0.1, 1.0, 5.0 and 10.0 mM alanine was added stepwise into the mucosal fluid. Until the concentration was raised to 5.0 mM, no enhancements of the PD and the net water flux were observed. When 5 mM L-alanine was added into the mucosal fluid, these two parameters increased gradually as cited above. Further addition of L-alanine (10 mM) into the mucosal or serosal fluid did not add to these

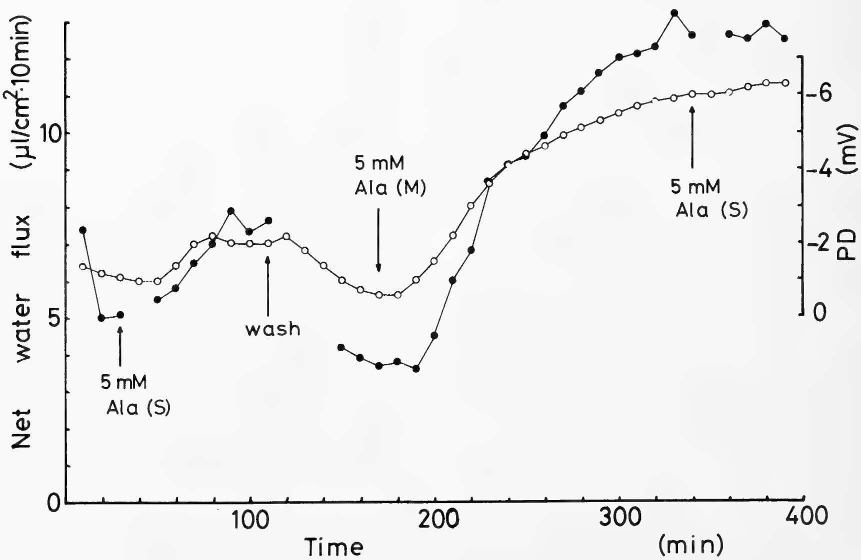

FIG. 1. Sidedness of the effects of L-alanine on the PD (○) and the net water flux (●). After bathing the intestine with standard Ringer solutions, 5 mM L-alanine was added into the serosal fluid (S); first arrow. At the second arrow, the serosal alanine was removed, and 5 mM L-alanine was added into the mucosal fluid (M) at the third arrow. Finally, both sides were applied with 5 mM L-alanine (fourth arrow).

increases. Therefore, following experiments were all made by 5 mM L-alanine.

To determine which ion flux contributes to the enhanced water flux, effects of 5 mM L-alanine on the net Na^+, K^+ and Cl^- fluxes were examined. As shown in Table 1, mucosal addition of L-alanine enhanced the net Na^+ and Cl^- fluxes by the same amount, and tended to increase the net K^+ flux only slightly. Since NaCl absorption across the seawater eel intestine is due to a coupled Na^+–K^+–Cl^- transport [1–3], it is likely that L-alanine enhances the Na^+–K^+–Cl^- transport and secondarily the water transport. Following results also support such an idea.

Effects of L-alanine in the presence of furosemide

Since the Na^+–K^+–Cl^- transport in the seawater eel intestine is known to be inhibited by mucosal application of furosemide [3], in the next experiments, effects of alanine were examined after abolishing the Na^+–K^+–Cl^- transport by furosemide (Fig. 3). When 0.01 mM furosemide was added into the mucosal fluid, the serosa-negative PD and the net water flux were dimin-

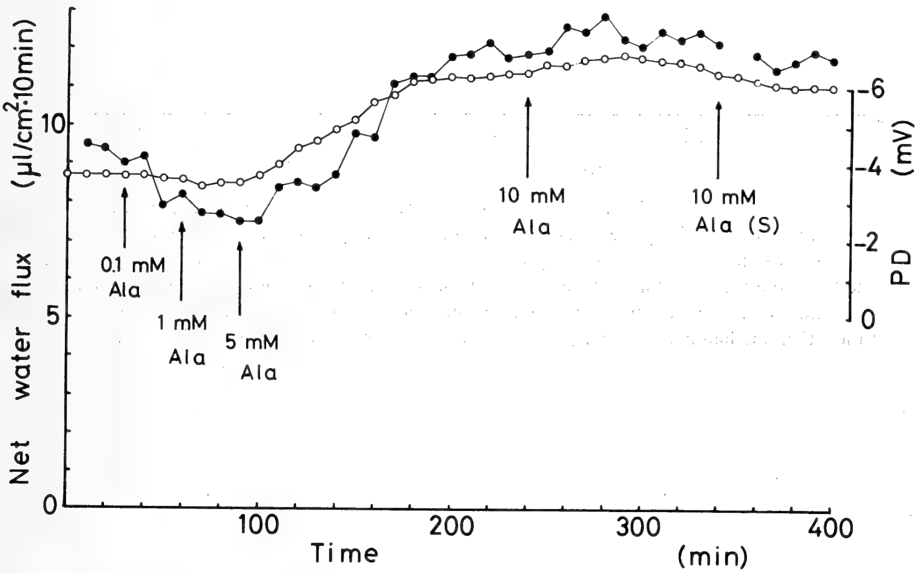

FIG. 2. Concentration-dependence of the effect of L-alanine on the PD (○) and the net water flux (●). Concentration of the mucosal L-alanine was increased stepwise from 0.1 to 10.0 mM, and the stimulatory effects were observed above 5 mM. (S) denotes that 10 mM L-alanine is added into the serosal fluid.

TABLE 1. Effects of L-alanine on the transepithelial potential difference (PD), net ion fluxes (J^{Na}_{net}, J^{K}_{net}, J^{Cl}_{net}) and net water flux ($J^{H_2O}_{net}$) across the seawater eel intestine

	PD (mV)	J^{Na}_{net}	J^{K}_{net} (μeq/cm^2·hr)	J^{Cl}_{net}	$J^{H_2O}_{net}$ (μl/cm^2·hr)
Control	-3.9 ± 0.3	10.0 ± 1.3	0.0 ± 0.1	8.4 ± 0.8	55.4 ± 5.2
L-alanine	-5.9 ± 0.6*	14.6 ± 1.1*	0.2 ± 0.2	12.9 ± 1.0**	80.3 ± 8.9*
Difference[a]	-2.0 ± 0.5	4.6 ± 1.4	0.3 ± 0.1	4.6 ± 1.0	24.8 ± 8.6

After bathing the intestine with the standard Ringer solution (control), 5 mM L-alanine was added into the mucosal fluid (L-alanine). Each value was obtained after the PD and net water flux reached a steady level. Values are means±S.E. for 5 fishes.
Difference from control values, * $P<0.05$, ** $P<0.01$ (paired *t*-test).
[a] Difference = L-alanine − control.

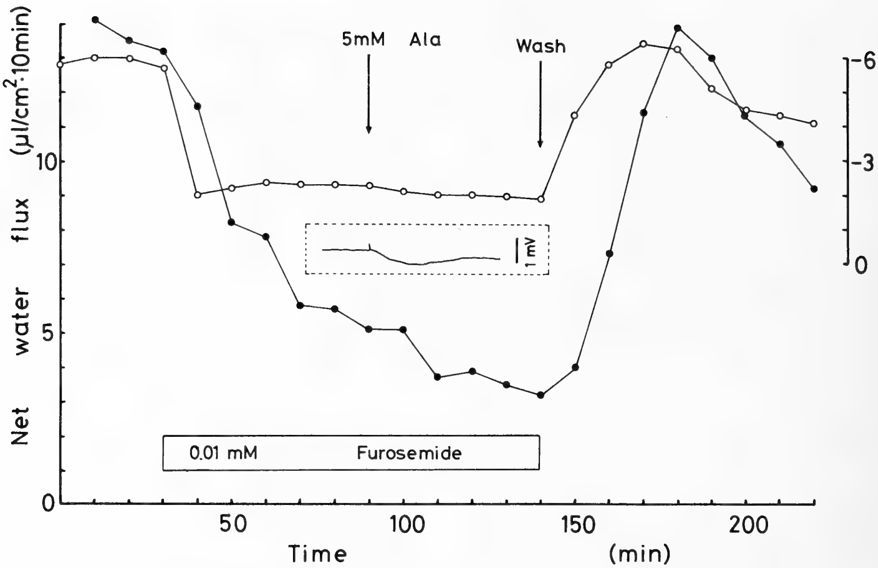

Fig. 3. A typical effect of L-alanine on the PD (○) and the net water flux (●) in the presence of furosemide. After bathing the intestine with standard Ringer solution, 0.01 mM furosemide was added into the mucosal fluid. In the presence of furosemide (open column), 5 mM L-alanine was added into the mucosal fluid (first arrow). At the second arrow, both of the mucosal alanine and furosemide were removed by rinsing the intestine twice with the standard Ringer solution. A trace of the PD immediately after addition of alanine is also shown in the inserted dotted column.

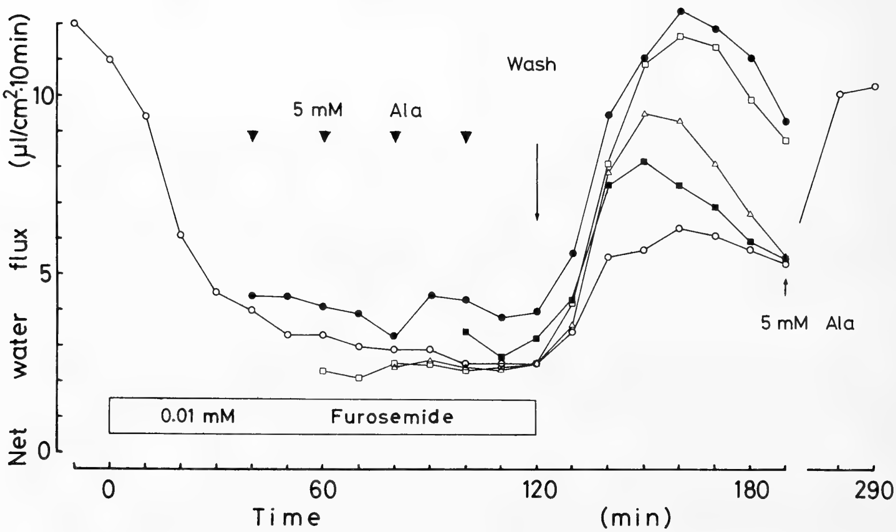

Fig. 4. After-effect of L-alanine on net water flux. After treatment with 0.01 mM furosemide, 5 mM L-alanine was added into the mucosal medium at 40 (●), 60 (□), 80 (△) or 100 min (■); arrow heads. At 120 min, both of the mucosal alanine and furosemide were removed by rinsing the intestine with the standard Rinder solution. As a control (○), furosemide was removed after treatment for 120 min without addition of alanine, and 5 mM L-alanine was applied into the mucosal fluid at 190 min. Each point represents the mean value. The number of preparations is indicated in the parentheses.

ished immediately to lower steady levels (around -2 mV and 4.0 $\mu l/cm^2 \cdot 10$ min respectively). In the presence of furosemide, no enhancement in the net water flux were induced by the addition of 5 mM L-alanine, whereas only the initial depolarization in the PD (0.3 ± 0.1 mV, N=6) was observed as in the absence of furosemide. When furosemide and alanine were removed by rinsing the intestine twice with the standard Ringer solution (alanine-free), both the PD and the net water flux were enhanced transiently. Since these two parameteres, especially in case of the net water flux, continue to decrease with time even in the initial control periods, these enhancements appear significant.

Figure 4 shows effects of pretreatment with L-alanine on the net water flux. With prolongation of the treatment time, higher net water flux was observed in spite of the absence of alanine in the bathing media. The maximal after-effect was obtained after the pretreatment with L-alanine for 60–80 min.

The serosa-negative PD was also enhanced with prolongation of the pretreatment with L-alanine (Fig. 5), and the maximal after-effect was obtained when the loading time with alanine was 60–80 min, similarly as in case of the net water flux.

Relationship between the loading time and the peak responses of the after-effect in the net water flux or the PD is shown in Figure 6. With prolongation of the loading time, the net water flux increased almost linearly. On the other hand, when 5 mM L-alanine was added into the mucosal fluid under the standard condition, thereafter the mucosal fluid containing L-alanine, the net water flux increased also linearly with time after latent period of 20 min (Fig. 6A, dotted line). Since these relations between the loading time and the net water flux were closely similar, irresperctive of the presence or absence of alanine in the medium, it is unlikely that L-alanine stimulates water transport *via* acting from outside of the cells. The peak after-effect of the serosa-negative PD also increased with prolongation of the loading time, and the relation was almost parallel to that obtained after addition of L-alanine to the mucosal side

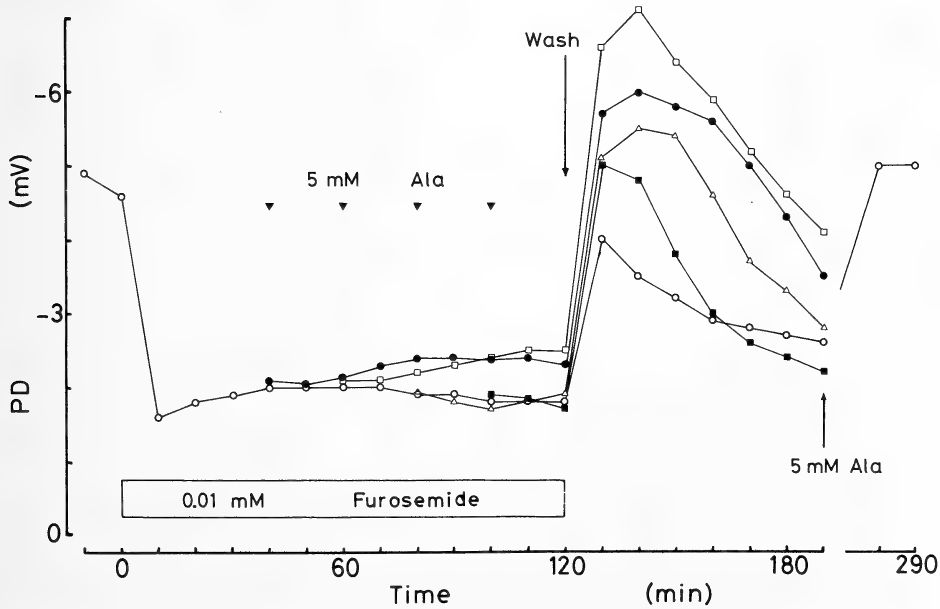

FIG. 5. After-effect of L-alanine on the PD. In the presence of 0.01 mM furosemide (open column), 5 mM L-alanine was added into the mucosal medium at 40 (●), 60 (□), 80 (△) or 100 min (■); arrow heads. At 120 min, both of the mucosal alanine and furosemide were removed. In control (○), 5 mM L-alanine was added into the mucosal fluid at 190 min. Each point represents mean value. The number of preparations is indicated in the parentheses.

(Fig. 6B, dotted line), whereas the serosa-negativity was lower in the presence of alanine.

Effects of other amino acids

Table 2 shows effects of various amino acids on the PD and the water flux. Among various amino acids examined, only L- and D-alanine, L-glutamine and L-glutamic acid enhanced the net water flux. In case of other amino acids, the net water flux continued to decrease as in the initial control period without such amino acids, thus they are represented by negative signs in Table 2. Even after treatment with these non-effective amino acids, a significant enhancement of the net water flux was induced by 5 mM L-alanine.

The effects on the PD seem to be composed of two phases, initial and final. An initial slight depolarization of the serosa-negative PD was observed immediately after addition of L-alanine (ΔPD$=0.3\pm0.0$ mV, N=8), D-alanine (0.1 ± 0.0 mV, N=4), L-serine (0.2 mV), or L-glutamine (0.1 ± 0.0 mV, N=3). Relatively large depolarization was observed after L-cysteine (1.8 mV), L-glutamic acid (1.0 ± 0.5 mV, N=4) or D-glutamic acid (2.6 ± 0.1 mV, N=3). On the other hand, an initial slight hyperpolarization was observed in case of L-leucine (ΔPD$=-0.5\pm0.2$ mV, N=3), D-glutamine (-0.9 ± 0.2 mV, N=3) or L-histidine (-0.6 ± 0.2 mV, N=3). Mucosal addition of mannitol (10 mM), as a control, showed neither initial depolarization nor hyperpolarization. After 100 min, however, only L- and D-alanine, L-glutamine

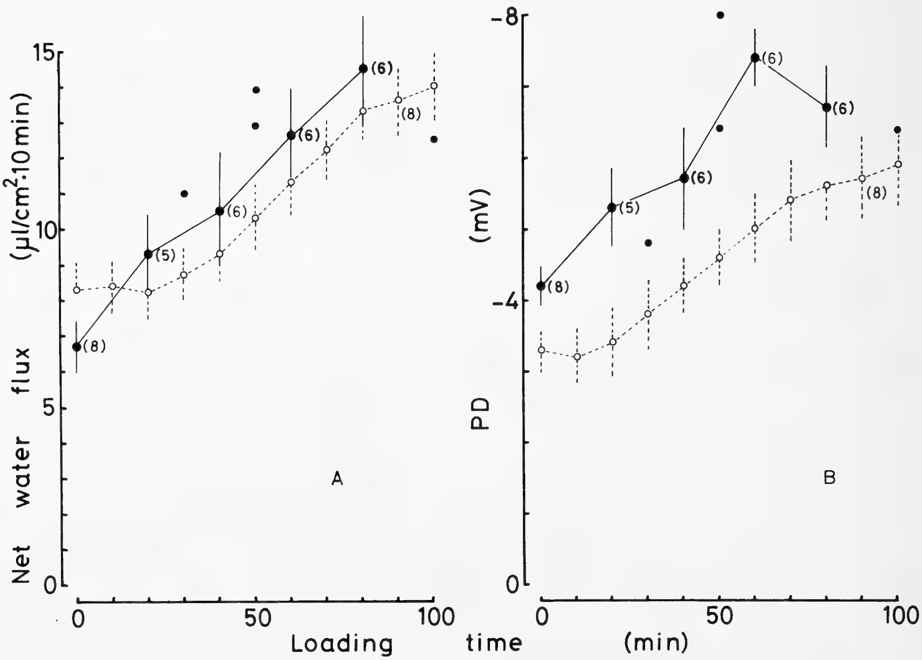

Fig. 6. Relations between the peak after-effects and the loading time. A. Peak after-effect of the net water flux as functions of the loading time. The peak after-effect (●) was obtained after removing both furosemide and alanine by rinsing with alanine-free Ringer solution in Fig. 4. For comparison, the time course of the net water flux after addition of alanine was shown as open circles, where 5 mM L-alanine was applied into the mucosal fluid at time zero, thereafter the mucosal medium containing L-alanine. B. Peak after-effect of the PD as functions of the loading time. The peak after-effect (●) was obtained after removing both furosemide and alanine in Fig. 5. Dotted line shows the time course of the PD after addition of 5 mM L-alanine into the mucosal fluid at time zero(○), thereafter the mucosal medium containing alanine. Each point and vertical bar indicate the mean and S.E., respectively. The number of preparations is indicated in the parentheses.

TABLE 2. Effects of various amino acids on the transepithelial potential difference (PD) and the net water flux ($J_{net}^{H_2O}$)

Amino acids	Concentration (mM)	N	ΔPD (mV)	$\Delta J_{net}^{H_2O}$ ($\mu l/cm^2 \cdot 10\,min$)
Glycine	10	3	0.1 ± 0.2	−4.3 ± 0.3
L-alanine	5	8	−2.8 ± 0.4	5.8 ± 0.9
D-alanine	10	4	−3.1 ± 0.3	4.2 ± 0.6
L-valine	10	5	0.5 ± 0.3	−2.4 ± 0.4
L-leucine	10	3	0.9 ± 0.7	−2.2 ± 0.4
L-norvaline	10	1	−0.4	−2.8
L-serine	10	1	−0.5	−3.0
L-cysteine	10	1	1.5	−4.6
L-methionine	10	1	0.8	−3.7
L-tryptophan	10	1	0.8	−1.1
L-proline	10	1	0.5	−3.1
L-asparagine	10	3	0.0 ± 0.4	−0.9 ± 1.2
L-glutamine	10	3	−4.2 ± 0.3	9.6 ± 1.2
D-glutamine	10	3	0.7 ± 0.4	−4.3 ± 1.2
L-glutamic acid	10	4	−3.0 ± 0.9	3.3 ± 1.6
D-glutamic acid	10	3	2.2 ± 0.4	−4.0 ± 1.7
L-aspartic acid	10	4	0.3 ± 0.2	−1.0 ± 0.4
L-lysine	10	3	0.1 ± 0.8	−3.4 ± 1.4
L-ornithine	10	3	0.9 ± 0.2	−2.4 ± 0.4
L-histidine	10	3	0.5 ± 0.1	−4.2 ± 0.2
β-alanine	10	1	−0.3	−2.1
γ-aminobutyric acid	10	1	0.0	−2.9

After bathing the intestine with standard Ringer solution, various amino acids was added into the mucosal fluid and the PD and the net water flux were measured every 10 min for 100 min. Results are given as mean ± S.E. Each value is presented as a difference (Δ) between the values before and 100 min after the addition of amino acid. Positive values represent depolarization in the PD and increase in the net water flux. Negative values represent hyperpolarization and decrease, respectively.

and L-glutamic acid enhanced the serosa-negativity (final phase), accompanied by the enhancement in the water flux.

DISCUSSION

The present study demonstrates that L-alanine stimulates the net Na^+, Cl^- and water fluxes under the standard condition (Table 1). Since the NaCl transport in the sea-water eel intestine is due to a coupled Na^+–K^+–Cl^- transport which contributes to the water absorption [1–3] these results suggest that L-alanine stimulates the Na^+–K^+–Cl^- transport, and secondarily water transport. This suggestion is supported by a finding that the enhancement of the net water flux induced by L-alanine is completely blocked by treatment with furosemide (Fig. 3), an inhibitor of the Na^+–K^+–Cl^- transport in the eel [3] or flounder [6] intestine. The enhancement of the serosa-negative PD can also be explained by the stimulated Na^+–K^+–Cl^- transport, because this cotransport system enhances intracellular accumulation of K^+ and Cl^- thus enhances K^+ efflux across the brushborder membrane and Cl^- efflux across the basolateral membrane, as explained in the flounder intestine [7].

After removing both furosemide and alanine, however, the effect of alanine (after-effect) were evoked (Figs. 4–6), suggesting that L-alanine or its metabolite(s) act(s) within the cells. This suggestion is further supported by such findings as serosal alanine also enhances the serosa-negative PD and the net water flux, whereas the enhancements are much smaller than those by mucosal alanine, and as a long latent period is required before the effects of mucosal alanine appear.

An initial depolarization of the PD was always observed immediately after addition of L-alanine into mucosal fluid, but its magnitude was too small (ca. 0.3 mV) to be analysed. Although a large depolarization has been demonstrated by L-leucine in the flounder intestine bathed with Cl^--free (replaced with gluconate) Ringer solution [8], such a large depolarization by L-leucine or L-alanine was not observed in the seawater eel intestine bathed with gluconate-Ringer solutions (unpublished observation). If the small depolarization in this study reflects the Na^+-alanine cotransport, the cotransport system seems to be refractory to furosemide, because a similar small depolarization is observed in the presence of furosemide and the after-effects of L-alanine are induced rapidly after removing furosemide (Figs. 3, 4 and 5B). The latter phenomenon indicates that L-alanine is already taken up into the cells. A parallel shift of the PD by the presence of alanine (Fig. 6B) may also be explained by the alanine-evoked potential.

ACKNOWLEDGMENT

This research was supported in part by Grant-in-Aid No. 58370047 from the Ministry of Education, Sciences and Culture, Japan.

REFERENCES

1 Ando, M. (1983) Potassium-dependent chloride and water transport across the seawater eel intestine. J. Membrane Biol., **73**: 125–130.

2 Ando, M. (1985) Relationship between coupled Na^+–K^+–Cl^- transport and water absorption across the seawater eel intestine. J. Comp. Physiol., **155**: 311–317.

3 Ando., M. and Utida, S. (1986) Effects of diuretics on sodium, potassium, chloride and water transport across the seawater eel intestine. Zool. Sci., **3**: 605–612.

4 Ando, M., Sasaki, H. and Huang, K. C. (1986) A new technique for measuring water transport across the seawater eel intestine. J. Exp. Biol., **122**: 257–268.

5 Ando, M. and Kobayashi, M. (1978) Effects of stripping off the outer layers of the eel intestine on salt and water transport. Comp. Biochem. Physiol., **61A**: 497–501.

6 Frizzell, R. A., Smith, P. L., Vosburgh, E. and Field, M. (1979) Coupled sodium-chloride influx across brush border of flounder intestine. J. Membrane Biol., **46**: 27–39.

7 Halm, D. R., Krasny, E. J. Jr. and Frizzell, R. A. (1985) Electrophysiology of flounder intestinal mucosa. *I. Conductance properties of the cellular and paracellular pathways.* J. Gen. Physiol., **85**: 843–864.

8 Thompson, K. A. and Kleinzeller, A. (1985) Glucose transport in intestinal epithelia of winter flounder. Am. J. Physiol., **248**: R573–R577.

ZOOLOGICAL SCIENCE 4: 45–52 (1987)

Comparison of Seawater and Fresh-water Eels for the Effects of L-alanine on Water Transport across the Intestine

Masaaki Ando, Yasuo Furukawa and Makoto Kobayashi

Laboratory of Physiology, Faculty of Integrated Arts and Sciences, Hiroshima University, Hiroshima 730, Japan

ABSTRACT—Using a new perfusion system, effects of L-alanine on the net water and ion fluxes across the intestine were examined *in vitro* in the seawater and fresh-water eels. In the seawater eel intestine, mucosal addition of 5 mM L-alanine stimulated the net water flux and the serosa-negative potential difference (PD), accompanied by an enhancement in the net Na^+ and Cl^- fluxes under the standard condition. On the other hand, in the fresh-water eel intestine the net water and ion fluxes were not affected significantly by the addition of alanine, indicating that alanine-sensitivity is enhanced by seawater adaptation of the eels. After injecting cortisol into the fresh-water eels, the alanine-sensitivity was enhanced to near the seawater levels, indicating that the alanine-sensitivity is regulated by cortisol. Furthermore, from the difference in the time course of the PD after setting each intestine isolated from seawater or fresh-water eels to the system, roles of alanine and cortisol in seawater adaptation of the eels are discussed.

INTRODUCTION

In the previous study, we developed a new system for measuring water transport across the intestine and found that L-alanine enhanced water absorption across the seawater eel intestine [1]. Furthermore, it has recently been demonstrated that the effect of L-alanine results from acting within the cells [2]: intracellular alanine stimulates water absorption in the seawater eel intestine.

Although it is well established in invertebrates that intracellular amino acids increase when they adapt to a hypertonic saline [3–5], in euryhaline teleosts it is still controversial whether intracellular amino acids increase [6, 7] or not [8] during seawater adaptation. Therefore, in the present study, the effects of L-alanine on the net water and ion fluxes across the intestine were compared between the seawater and fresh-water eels. The results obtained demonstrate that the seawater eel intestine is more sensitive to alanine than the fresh-water eel intestine, and that such an increment in the alanine-sensitivity is induced by cortisol.

Accepted September 4, 1986
Received August 19, 1986

MATERIALS AND METHODS

Japanese cultured eels, *Anguilla japonica* weighing about 200 g were obtained from a commercial supplier and kept in a fresh-water tank at 20°C for more than a week before use. Half of them were adapted to seawater (20°C) for more than a week. For assaying the effect of cortisol, cortisol (Schering) was injected intraperitoneally into the fresh-water eels at a dose of 0.5 mg/100 g body weight and the fish were sacrificed 24 hr after the injection. These eels were decapitated and the intestine was excised. The outer muscle layers of the intestine were stripped off following our previous method [9]. After everting the intestine, a cylindrical polyester mesh was inserted into the middle part of the intestinal tube. These operations were done on a cooled plate placed on ice: it took about 40 min. The serosal side of the intestine was perfused with the standard Ringer solution at a constant rate (ca. 173 μl/min), and the effluent was collected every 10 min. Details of the apparatus for simultaneous measurement of net water flux and transepithelial potential difference (PD) are described previously [1].

The net water flux was calculated by subtracting the perfusion rate from the rate of effluent flow.

Net ion fluxes were calculated from the difference between the products of ionic concentration and collected volume in each of the perfusate and the effluent as described previously [2, 10]. Sodium and K^+ concentration was measured with flame photometry (Hiranuma, FPF–2A) and Cl^- concentration was determined with a chloride counter (Hiranuma, CL–5M).

The standard Ringer solution contained (mM/l): 118.5 NaCl; 4.7 KCl; 3.0 $CaCl_2$; 1.2 $MgSO_4$; 1.2 KH_2PO_4; 24.9 $NaHCO_3$ (pH 7.3 on bubbled with 95% O_2–5% CO_2 gas mixture). For nutrient Ringer solution, 5 mM L-alanine or D-glucose (Katayama Chemical Co., Japan) was added to the standard Ringer solution. At the end of the experiments, the intestine was cut longitudinally and spread on a graph paper: surface area of the intestine was measured using a planimeter (Ushikata, 220L). All data are expressed as mean ± S.E.

RESULTS

Effects of nutrients

Figure 1 shows time course of the PD across the seawater and fresh-water eel intestine. In the seawater eels, higher serosa-negative PD (ca. −7 mV) was observed immediately after bathing the intestine with the standard Ringer solutions, but thereafter the serosa-negativity decreased gradually during perfusing the serosal side, suggesting that some essential substance(s) for maintaining the high level is/are lost from the seawater intestine during the perfusion. Glucose (5 mM) had no effect on the decline of the PD. When 5 mM L-alanine was added to the glucose Ringer solutions, however, the PD returned to the high level and remained at that high level. On the other hand, in the fresh-water eels the PD was less than −1 mV initially and then increased its negativity during the perfusion. The presence of glucose did

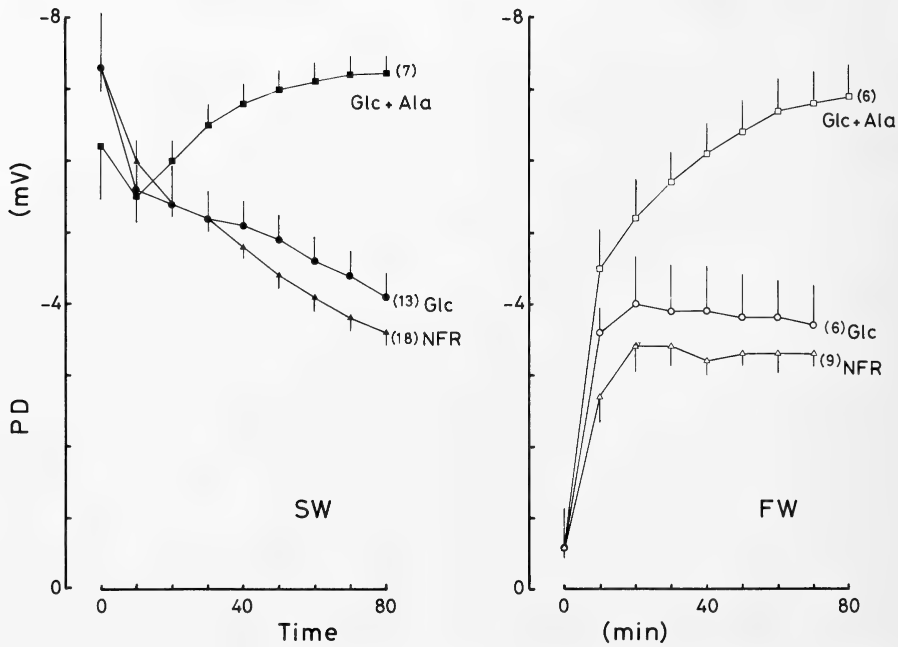

Fig. 1. Time course of the transepithelial potential difference (PD) across the seawater (SW) and fresh-water (FW) eel intestine. At time zero, the intestine was set to the apparatus and bathed with various Ringer solutions, such as nutrient-free (NFR), 5 mM D-glucose containing (Glc) or 5 mM D-glucose + 5 mM L-alanine containing (Glc + Ala) Ringer solutions, and then the serosal fluid started to be perfused. The number of preparations is indicated in the parentheses.

TABLE 1. Effects of D-glucose and L-alanine on the transepithelial potential difference (PD) and the net water flux ($J_{net}^{H_2O}$) across the intestine isolated from seawater (SW) or fresh-water (FW) eels

Adaptation	Nutrient (mM) Glucose	Alanine	PD (mV)	$J_{net}^{H_2O}$ (μl/cm^2·hr)
SW	0	0	-3.7 ± 0.3[a]	55.5 ± 4.0
	5	0	-4.1 ± 0.5	69.5 ± 9.0
	5	5	-7.4 ± 0.4*	87.3 ± 2.6*
FW	0	0	-3.3 ± 0.2	26.1 ± 1.3
	5	0	-3.6 ± 0.6	36.4 ± 5.8
	5	5	-7.0 ± 0.5*	39.0 ± 6.1

Each value was obtained under a nearly-steady state, more than 1 hr after bathing the preparation with each experimental solution.
Difference from control values under nutrient-free condition, * $P<0.001$ (Student *t*-test).
[a] Mean±S.E. (N=6).

TABLE 2. The effects L-alanine on the transepithelial potential difference (PD), net ion fluxes (J_{net}^{Na}, J_{net}^{K}, J_{net}^{Cl}) and net water flux ($J_{net}^{H_2O}$) across the seawater (SW), fresh-water (FW) or cortisol-injected fresh-water (FW+Cortisol) eel intestine

Adaptation	Condition	N	PD (mV)	J_{net}^{Na}	J_{net}^{K} (μeq/cm^2·hr)	J_{net}^{Cl}	$J_{net}^{H_2O}$ (μl/cm^2·hr)
SW	Control	9	-4.0 ± 0.3	9.5 ± 0.9	0.0 ± 0.1	8.0 ± 0.5	56.1 ± 4.1
	L-alanine		-6.1 ± 0.5**	13.8 ± 1.1**	0.1 ± 0.1	12.7 ± 0.6***	84.5 ± 5.2***
FW	Control	10	-3.6 ± 0.3	3.4 ± 0.3	0.0 ± 0.1	4.1 ± 0.7	20.9 ± 3.3
	L-alanine		-6.3 ± 0.5***	5.0 ± 0.7	0.1 ± 0.2	5.6 ± 0.9	33.7 ± 6.6
FW +Cortisol	Control	9	-5.1 ± 0.6	8.5 ± 1.1	-0.4 ± 0.1	7.6 ± 0.8	45.9 ± 4.8
	L-alanine		-7.9 ± 0.4**	11.3 ± 1.1*	-0.5 ± 0.2	11.1 ± 1.0*	65.5 ± 5.6*

After bathing the intestine with standard Ringer solutions (control), 5 mM L-alanine was added to the mucosal fluid (L-alanine). Each value (Mean±S.E.) was obtained after the PD and the net water flux reached a nearly-steady level.
Difference from control values, * $P<0.05$, ** $P<0.01$, *** $P<0.001$ (paired *t*-test).

not enhance the increment of the PD significantly, but alanine enhanced it gradually to near −7 mV. Under these three experimental conditions, the steady state values of the PD were closely similar to those in the seawater eels, respectively.

Table 1 summarizes the steady state values of the PD and the net water flux under various experimental conditions. In nutrient-free Ringer (NFR) solutions, the net water flux across the seawater eel intestine was almost twice as high as that in the fresh-water eels. The presence of alanine enhanced the net water flux in the seawater eels, but not in the fresh-water eels, whereas it enhanced the PD by the same amount in both the seawater and fresh-water eels. Glucose had no significant effects on these two parameters in both eels.

Effects of alanine

Since even 10 mM glucose has no effect on the PD and the net water flux [1], following experiments were restricted to clarify the effects of L-alanine. Figure 2 demonstrates that mucosal alanine plays a major role in the increment of the PD on both seawater and fresh-water eels. When alanine was added to the mucosal fluid after bathing the intestine with standard Ringer solutions, the PD depolarized initially by 0.2 ± 0.0 and 0.4 ± 0.1 mV (N=8) in the seawater and fresh-water eels respectively, thereafter the serosa-

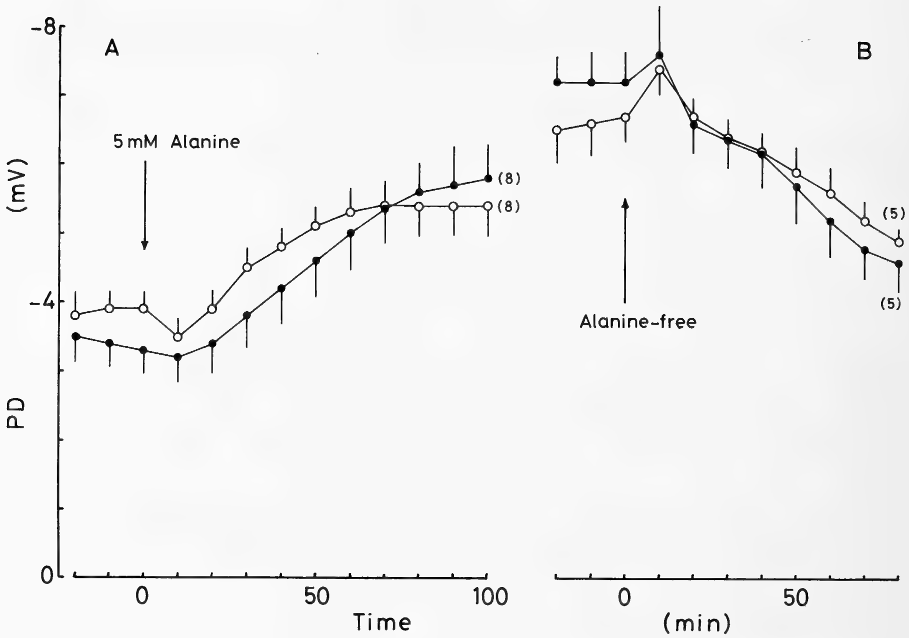

Fig. 2. The effects of L-alanine on the transepithelial potential difference (PD) across the seawater (●) or fresh-water (○) eel intestine. A. After bathing the intestine with standard Ringer solutions (nutrient-free), 5 mM L-alanine was added to the mucosal fluid at time zero. B. After bathing the intestine with glucose-alanine Ringer solutions which contain 5 mM D-glucose and 5 mM L-alanine, mucosal L-alanine alone was removed at time zero, while the serosal fluid still contained L-alanine and both fluids contained D-glucose. The number of preparations is shown in the parentheses.

negativity increased gradually. On the other hand, when mucosal alanine was omitted after bathing the intestine with glucose-alanine Ringer solutions, the PD hyperpolarized initially by 0.8 ± 0.3 and 0.8 ± 0.2 mV (N=5) in the seawater and fresh-water eels respectively, thereafter the serosa-negativity decreased gradually (Fig. 2B). After all, the time courses of the PD were almost identical in both the seawater and fresh-water eels.

The effects of mucosal alanine on the net water flux are shown in Figure 3. When 5 mM L-alanine was added to the mucosal fluid of the seawater eel intestine, the net water flux started to increase gradually after latent period of 20 min. When mucosal alanine was removed after bathing the intestine with glucose-alanine Ringer solutions, the net water flux increased initially but thereafter declined gradually (Fig. 3B). These time courses of the net water flux across the seawater eel intestine were in parallel to those in the PD. In the fresh-water eel intestine, in contrast, neither addition nor omission of alanine had no significant effect on the net water flux.

Effects of cortisol

Since it is well known that cortisol alters the fresh-water eel intestine to a seawater type [11, 12], in the next experiment, effects of alanine were examined in the cortisol injected fresh-water eels. Figure 4 shows the time course of the PD across the cortisol-treated fresh-water eel intestine. Immediately after bathing the intestine with Ringer solutions, about -3 mV was observed; an intermediate PD between fresh-water and seawater eels (cf. Fig. 1). Then the PD increased rapidly within 10 min. These initial increments in the serosa-negative PD were closely similar to those in the intact fresh-water eels, but the later phases were similar to those in the seawater eels.

Although alanine had no effects on the water

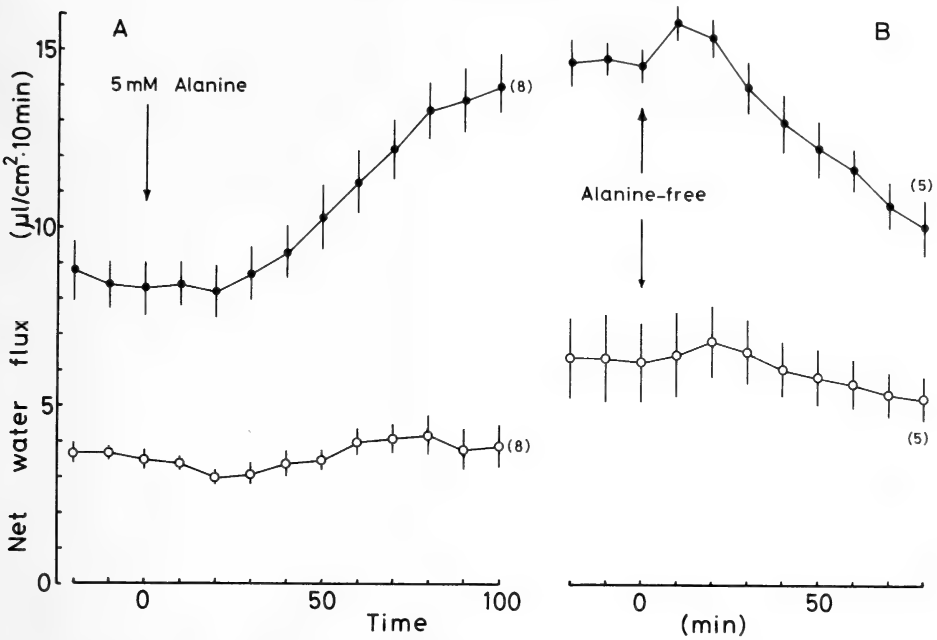

FIG. 3. The effects of L-alanine on the net water flux across the seawater (●) or fresh-water (○) eel intestine. A. After bathing the intestine with standard Ringer solutions, 5 mM L-alanine was added to the mucosal fluid (at time=0). B. After bathing the intestine with glucose-alanine Ringer solutions, mucosal alanine alone was omitted (at time=0). The number of preparations is indicated in the parentheses.

transport across the intact fresh-water eel intestine, it enhanced the net water flux after treatment with cortisol (Fig. 5). When 5 mM L-alanine was added to the mucosal standard Ringer solution, the net water flux increased gradually after latent period of 20 min and remained at the high level thereafter. On the other hand, omission of the mucosal L-alanine after bathing the intestine with glucose-alanine Ringer solutions, resulted in a decrease of the net water flux (Fig. 5B). These effects of alanine were essentially similar to those in the seawater eels, whereas the magnitude was slightly smaller.

Table 2 shows ion fluxes across the intestine isolated from seawater, fresh-water or cortisol-injected fresh-water eels, and also demonstrates the effects of alanine on their ion fluxes. In these three kinds of intestine, Na^+ and Cl^- were absorbed mainly from mucosa to serosa under the standard condition (control). Although a significant K^+ secretion from serosa to mucosa ($P<0.05$) was observed in the cortisol-injected fresh-water eels, it was negligibly small compared to the Na^+ and Cl^- fluxes. The NaCl absorption was two-fold higher in the seawater eels than that in the fresh-water eels, and cortisol-treatment mimicked the seawater adaptaion. Although the ion and water absorption across the cortisol-treated fresh-water eel intestine were slightly lower than those in the seawater eels, these differences were not statistically significant. When 5 mM L-alanine was applied, the NaCl absorption was enhanced significantly in the seawater and cortisol-injected fresh-water eels, but not significantly enhanced in the intact fresh-water eels, whereas it tended to increase.

DISCUSSION

The present study demonstrates that alanine-sensitivity in the water absoption across the intestine is enhanced by seawater adaptation of the eels. In the seawater eels, the net water flux was accelerated by mucosal L-alanine (Fig. 3), accom-

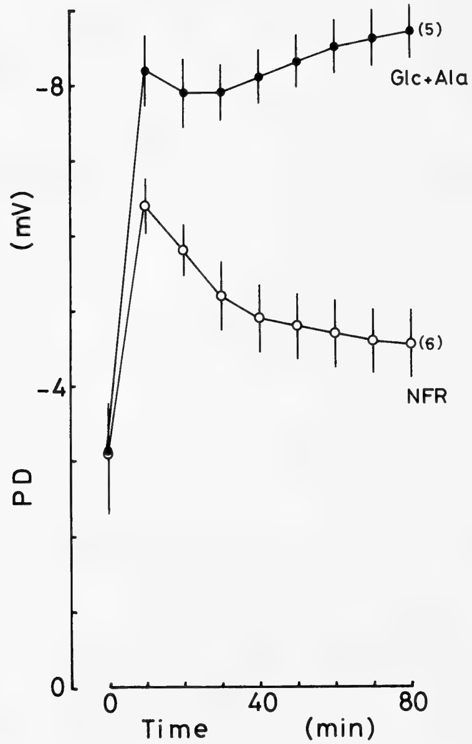

FIG. 4. Time course of the PD across the intestine isolated from cortisol-injected fresh-water eels. At time zero, the intestine was set to the apparatus and bathed with standard (NFR) or glucose-alanine (Glc +Ala) Ringer solutions, and then the serosal fluid started to be perfused. The number of preparations is indicated in the parentheses.

panied by an enhancement of net Na^+ and Cl^- fluxes (Table 2). On the other hand, in the fresh-water eel intestine alanine did not significantly enhance the net Na^+, Cl^- and water fluxes. Since the net Na^+, Cl^- and water fluxes in the seawater eel intestine are regulated by an intracellular alanine [2], the lack of alanine-effect in the fresh-water eels may indicate that in the fresh-water eels alanine content within the enterocyte can not reach to a seawater level. However, it is also possible that the ion transport systems are not developed enough to respond to an increment in the intracellular alanine in the fresh-water eels, even if the alanine content is identical to that in the seawater eels. Which possibility is plausible can not be determined from the present study; direct measurements of the amino acid content within the tissue are necessary.

Although the reasons why the effects of alanine are different between the seawater and fresh-water eels are not clear yet as cited above, the present results clearly indicate that the alanine-sensitivity of the eel intestine is regulated by cortisol: the alanine-effects in the fresh-water eels were enhanced to near the seawater level after treatment with cortisol (Fig. 5 and Table 2).

Although the serosa-negative PD in the fresh-water eels was also influenced by alanine similarly as in the seawater eels (Fig. 2 and Table 2), this potential change may be due to their high tissue resistance, because the tissue resistance in the fresh-water eel intestine is higher than that in the seawater eels [13], thus even a small current (= total net ion fluxes) can make a large PD across the fresh-water eel intestine. In fact, a slight increment of the net Na^+ and Cl^- fluxes was obtained after application of alanine to the fresh-water eel intestine, though not statistically significant (Table 2).

Perfusing the seawater eel intestine with standard Ringer solutions (NFR), the net water flux decreased gradually with time accompanied by a diminution of the PD (Fig. 1). This phenomenon can be explained by a loss of alanine or its metabolite(s) from the enterocytes, since addition of alanine restored these two parameters to their initial levels and omission of alanine diminished them (Figs. 2 and 3). On the analogy of the seawater eels, some essential substance(s) might be lost from the fresh-water eel intestine during perfusion, since the PD increased after the perfusion (Fig. 1) and the steady state value of the net water flux was six-fold higher (Table 1) than that in the sac preparation [9]. In addition, the net Na^+ and Cl^- fluxes in the fresh-water eels were also much higher (Table 2) than those described previously in the sac preparation [14, 15], whereas these previous measurements were performed in the intact intestine with muscle layers (not stripped). Although prolactin is well known to be an essential hormone for fresh-water adaptation of the teleost fish [16, 17], mammalian prolactin (0.5–1.0 U/ml) did not inhibit the PD and the net water flux in the fresh-water eel intestine *in vitro*

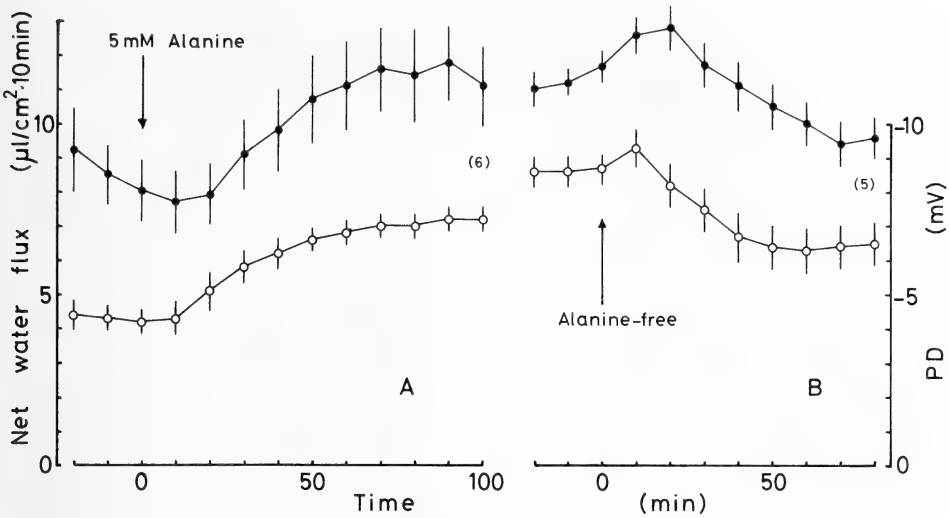

FIG. 5. The effects of L-alanine on the net water flux (●) and the PD (○) across the intestine isolated from the cortisol-injected fresh-water eels. After bathing the intestine with standard Ringer solution (NFR), 5 mM L-alanine was added to the mucosal fluid at time zero. B. After bathing the intestine with glucose-alanine Ringer solutions, mucosal alanine alone was omitted at time zero. The number of preparations is indicated in the parentheses.

(unpulished observation).

The initial rapid increase in the PD was also observed in the cortisol-treated fresh-water eels (Fig. 4). Although cortisol is well known to enhance the active Cl^- tranport [18], which contributes to the serosa-negative PD across the eel intestine, and to enhance the water absorption to the seawater levels [11, 12, 15], it must be noticed that these measurements are performed under a steady state condition, after enough equilibration period. The present result demonstrates that the effect of cortisol is not fully developed, at least immediately after isolating the intestine from the fresh-water living eels, but is induced in 10 min after bathing the intestine with salt solutions. To determine whether this induction is caused from a loss of an essential substance in the fresh-water eels or from a direct action of salt(s) to the luminal membrane of the enterocyte, further experiments are necessary.

ACKNOWLEDGMENT

We are grateful to Professor Tetsuya Hirano, Ocean Research Institite, University of Tokyo, for stimulating discussions. This research was supported in part by Gant-in-Aid No. 5870047 from the Ministry of Education, Sciences and Culture, Japan.

REFERENCES

1 Ando, M., Sasaki, H. and Huang, K. C. (1986) A new technique for measuring water transport across the seawater eel intestine. J. Exp. Biol., **122**: 257–268.

2 Ando., M. (1986) Regulation by intracellular alanine of water transport across the seawater eel intestine . Zool. Sci., **4**: 37–44.

3 Florkin, M. and Schoffeniels, E. (1969) Molecular Approaches to Ecology, Academic Press, New York.

4 Schoffeniels, E. and Gilles, R. (1970) Osmoregulation in aquatic arthropods. In "Chemical Zoology, Vol. 5". Ed. by M. Florkin and B. T. Scheer, Academic Press, New York, pp. 255–286.

5 Gilles, R. (1975) Mechanisms of iono and osmoregulation. In "Marine Ecology, Vol. 2". Ed. by Kinne, Wiley Interscience, New York, pp. 259–347.

6 Huggins, A. K. and Colley, L. (1971) The changes in the non-protein nitrogenous constituent of muscle during the adaptation of the eel *Anguilla anguilla* L. from fresh water to seawater. Comp. Biochem. Physiol., **38B**: 537–541.

7 Venkatachari, S. A. T. (1974) Effect of salinity

adaptation on nitrogen metabolism in the fresh water fish *Tilapia mossambica.* I. Tissue protein and amino acid levels. Marine Biol.,**24**: 57–63.

8 Goldstein, L. and Forster, R. P. (1970) Nitrogen metabolism in fishes. In "Comparative Biochemistry of Nitrogen Metabolism, Vol. 2 ". Ed. by J.W. Campbell, Academic Press, New York, pp. 495–518.

9 Ando, M. and Kobayashi, M. (1978) Effects of stripping off the outer layers of the eel intestine on salt and water transport. Comp. Biochem. Physiol., **61**A: 497–501.

10 Ando, M. (1983) Potassium-dependent chloride and water transport across the seawater eel intestine. J. Membrane Biol., **73**: 125–130.

11 Hirano, T. and Utida, S. (1968) Effects of ACTH and cortisol on water movement in isolated intestine of the eel, *Anguilla japonica.* Gen. Comp. Endocrinol., **11**: 373–380.

12 Ando, M. (1974) Effects of cortisol on water transport across the eel intestine. Endocrinol. Jpn., **21**: 539–546.

13 Ando, M., Utida, S. and Nagahama, H. (1975) Active transport of chloride in eel intestine with special reference to sea water adaptation. Comp. Biochem. Physiol., **51**A: 27–32.

14 Utida, S., Hirano, T., Oide, H., Ando, M., Johnson, D. W. and Bern, H. A. (1972) Hormonal control of the intestine and urinary bladder in teleost osmoregulation. Gen. Comp. Endocrinol., Suppl. **3**: 317–327.

15 Hirano, T., Morisawa, M., Ando, M. and Utida, S. (1976) Adaptive changes in ion and water transport mechanism in the eel intestine. In "Intestinal Ion Transport". Ed. by J.W.L. Robinson, MTP Press, Lancaster, pp. 301–317.

16 Bern, H. A. (1975) Prolactin and osmoregulation. Am. Zool., **15**: 937–948.

17 Bern, H. A. (1977) Some possible contributions of comparative endocrinology to mammalian and human endocrinology. Zool. Mag., **86**: 1–9.

18 Chen, T. S. T., Ando, M., Utida, S. and Huang, K. C. (1975) Ion fluxes and permeability studies of Japanese cultured eel inteatine. Fed. Proc., **34**: 470.

ZOOLOGICAL SCIENCE 4: 53–59 (1987)

Ultrastructural Studies on Developing Oblique-Striated Muscle Cells in the Cuttlefish, *Sepiella japonica* Sasaki

Akira Matsuno

Department of Biology, Faculty of Science, Shimane University, Matsue 690, Japan

ABSTRACT—Developmental changes in muscle cells located in the mantle of cuttlefish (*Sepiella japonica*) were investigated by electron microscopy. The circular muscle cells in the mantle, designated oblique-striated muscle cells, have peculiar myofilamental arrangements. Muscle cells observed in this work were taken from six stages (between stage 31 and 40) and larvae 48 hr after hatch. The differentiation of muscle cells can be divided into three phases: stages 31–36 (1st phase), stage 38 (2nd phase) and 24–48 hr after hatching (3rd phase). The ultrastructural characteristics in each phase are as follows. In the first phase, myofilaments are organized in the cytoplasm surrounded by endoplasmic reticular (E.R.) systems, and bundles constituted of thick and thin myofilaments appear. In the second phase, myofilamental bundles gradually become striated. Formation of the Z-body seems to be lead by tubular E.R. from E.R. systems under the cell membranes. In the last phase, bundles having A- and I-bands fuse into one thick bundle. The fusion was accompanied by the process which forms the Z-bodies into a line, and muscle cells are completed in this phase.

INTRODUCTION

The cuttlefish shows rather quick movements and they have well-developed muscles in the body wall or mantles. The well-developed muscles are classified as the oblique-striated muscle. They have regular myofilamental arrangements, alternating A- and I-bands in a direction towards the longitudinal axis of the cell, as seen in myofibrils of cross-striated muscle cells. In a rectangle section taken in that direction of the cell, sets of thick and thin myofilaments are arranged in an oblique pattern shifting their array among each other at a definite distance apart, thus the designation, oblique-striated muscle. In a cross-section, sets of myofilaments appear in a regular pattern as the myofibrils of cross-striated muscles [1].

Differentiations of cross-striated muscle cells have been already investigated by Obinata *et al.* [2] in chick embryos from the ultrastructural and biochemical standpoints. Fischman [3] and Shimada *et al.* [4] had investigated closely by electron microscope the processes of the formation of A- and I-bands in embryonic or cultured chick muscle cells. Another cross-striated type of epitherio-muscular cells in *Aurelia* showed somewhat peculiar processes as compared to the chick cross-striated muscle cells [5]. These reports have suggested that thin bundles of myofilaments having the A-band are formed first, then I-bands and Z-lines gradually appear.

I have attempted to reveal those processes in an oblique-striated muscle cell under the electron microscope as well as how and when the characteristic arrays of myofilaments appear. As a result, some differences in the developmental process between oblique-striated and cross-striated muscle cells have been observed.

Accepted August 18, 1986
Received June 23, 1986

MATERIALS AND METHODS

Embryos and larvae of the cuttlefish (*Sepiella japonica*) were used in this study. Embryos at stages 31, 33, 36, 38 and larvae 24 and 48 hr after hatching were successively fixed for electron microscopy. The stage of each embryo was estimated according to the "Table of Normal Embryonic Stage" [6] and in some cases upon advice from Dr. M. Yamamoto of the Marine Biological Labora-

tory of Okayama University.

Six stages of embryos and larvae were prefixed in a solution of 1.5% glutaraldehyde and 1.5% paraformaldehyde in 0.1 M cacodylate buffer (pH 7.3) at room temperature. After prefixation, they were rinsed with the buffer solution and arms and shells in the mantles were removed if necessary. They were then postfixed in a solution of 1% osmium tetroxide in 0.1 M phosphate buffer (pH 7.3) at 4°C. Fixed specimes were dehydrated in a series of ethanol and embedded in epoxy resin through n-butyl-glycidyl-ether.

Embedded specimens were cut into thin sections with glass or diamond knives. Sections were stained with saturated aqueous uranyl acetate and lead citrate. They were observed under a JEM 100 C-type electron microscope at magnifications ranging from 2,000–20,000.

RESULTS

Specimens in each stage were observed at the left side and middle portion of the mantle, where the muscle layer was thickest. The mantle of the cuttlefish consists of three muscular systems, the longitudinal muscle which runs longitudinally along the long axis of the mantle, the circular muscle, and the radial muscle, which runs transversely from the outer surface to the inner surface, crossing the circular one. Ultrastructural observations were carried out on the circular muscle cells in the mantle, and their ultrastructural characteristics are described separately at each stage. Observed muscle cells were the most well-developed ones in each stage, as cells did not develop simultaneously.

Stage 31: Muscle cells showed cell differentiation, and possessed a nucleus, scanty cytoplasm and undeveloped, scattered cell-organelles (Fig. 1). In this stage, a nascent myofilamental bundle was already observed. It was short in length and thin in diameter. The myofilamental bundle contained 3–7 thick myofilaments and showed no cross-striations, but thick and thin myofilaments were arranged roughly parallel in the bundle. The bundle was always surrounded by endoplasmic reticular (E. R.) systems (Fig. 1), suggesting that the myofilamental bundle might be organized in the cytoplasm surrounded by E. R. In this stage, one bundle was observed in a cell, but many were recognized in the advanced stages.

Stage 33: The general appearance of a cell in this stage was not so well-developed, but cell-organelles seemed somewhat advanced compared with those of the previous stage. The myofilamental bundle increased in diameter by 2–3 times compared with that of the previous stage (Fig.2). Myofilaments in the bundle were also increased in number, and their directions were not so regular but roughly parallel (Fig. 2) . The bundle was also surrounded by E. R. systems.

Stage 36: A muscle cell of this stage gradually was developing its cell-organelles. The myofilamental bundle was thicker than the one at the previous stage. The arrangement of myofilaments in the bundle was not so regular, that is, there were no A- or I-bands. Myofilaments ran parallel in the bundle (Fig. 3). The bundle showing an oval section of about 0.8 μm in major axis, were situated at a peripheral portion and ran along the long axis of the cell (Fig. 4).

Stage 38: A cell in this stage showed the most dynamic structural changes of all the stages examined. A longitudinal section of the mantle showed cross-sections of circular muscle cells and longitudinal sections of thin longitudinal and radial cells (Fig. 5). Longitudinal muscle cells ran below the inner and outer surfaces of the mantle in a longitudinal direction at definite intervals. Radial ones penetrated circular muscular layers from inside and outside of the mantle, and connected outer longitudinal muscles to inner longitudinal ones (Fig. 5). Almost all the cells in the circular muscle had myofilamental bundles in the peripheral regions. A nucleus in the central region, about 9 μm in diameter, was tapered toward the both ends. Myofilamental bundles were arranged in a disorderly way (Fig. 5). At this stage, a cross-striation-like structure was first clearly observed in a myofilamental bundle in longitudinal section (Fig. 6). As shown in Figure 6, tubular E. R. attached to both ends of the A-bands. They extended to the interspaces of the A-band and the neighboring one. The tubules ran in a zigzag line and contained electron dense materials in them. They originated from E. R. systems situated just

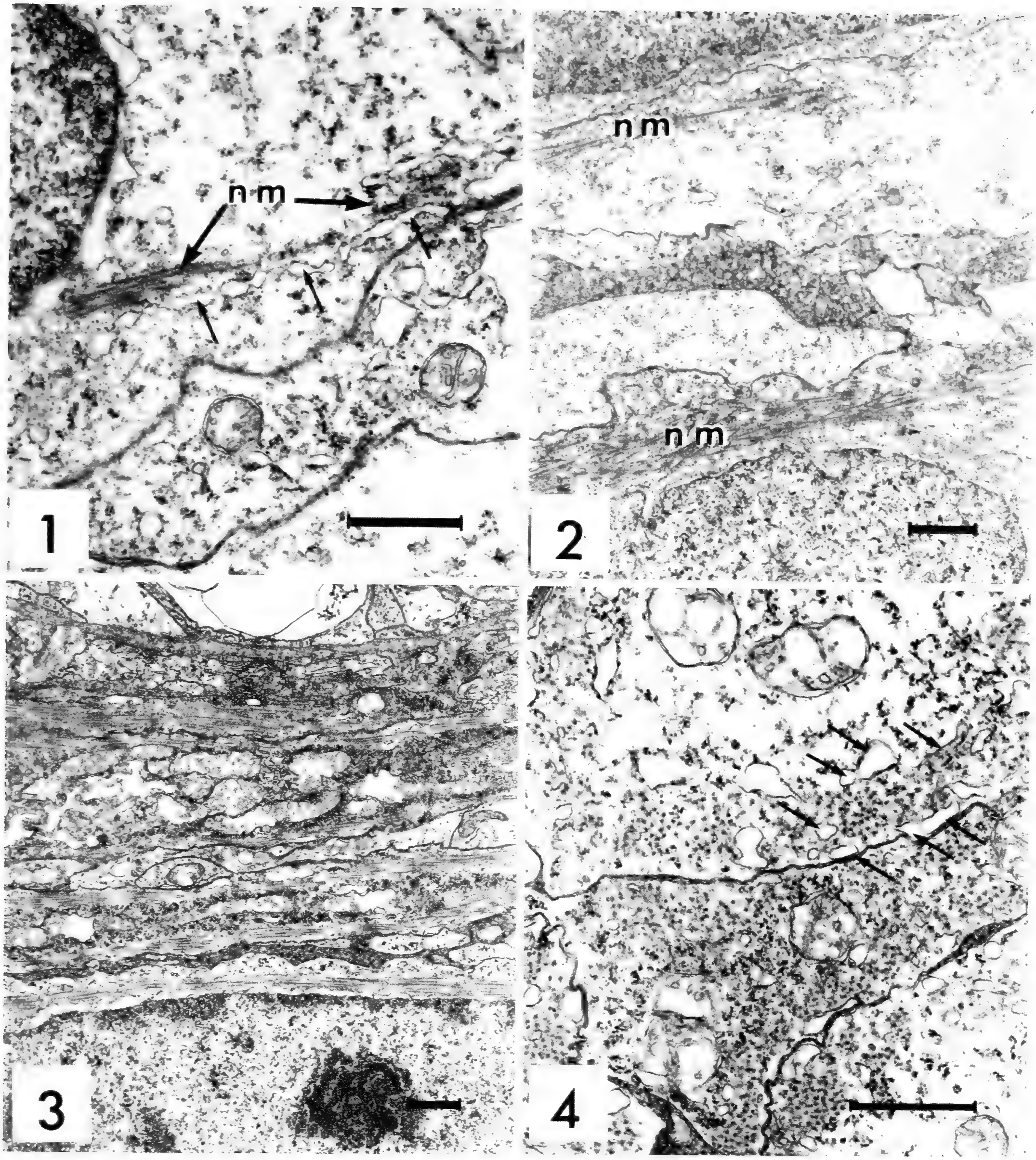

FIG. 1. A longitudinal section of muscle cells at stage 31. A nascent myofilamental bundle (nm) is shown near a nucleus. It is surrounded by E.R. systems (small arrows). ×16,700; scale bar, 1 μm.

FIG. 2. A longitudinal section of muscle cells at stage 33. Two nascent myofilamental bundles (nm) are shown. Bundles grow in size as compared to the one at the prvious stage. Myofilaments are arrayed in a disorderly way. They are surrounded by E.R. systems as at stage 31. ×10,200; scale bar, 1 μm.

FIG. 3. A longitudinal section of muscle cells at stage 36. Myofilamental bundles increase in length, but do not grow much in thickness. ×7,700; scale bar, 1 μm.

FIG. 4. A cross-section of muscle cells at stage 36. Myofilamental bundles surrounded by E.R. systems (arrows) are situated at the periphery of a cell. Thick myofilaments show a disordered arrangement. ×18,600; scale bar, 1 μm.

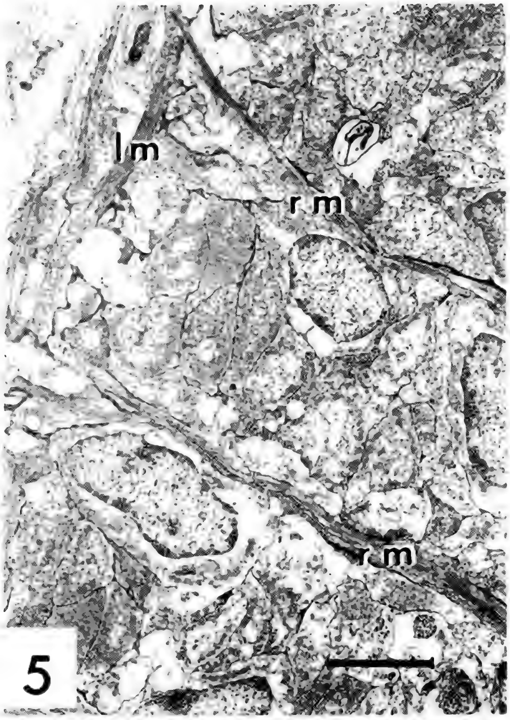

5

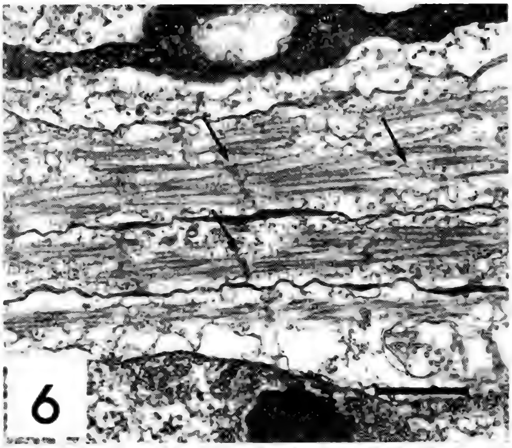

6

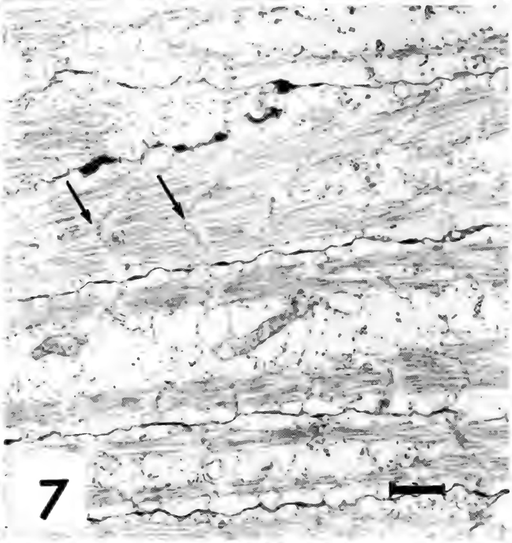

7

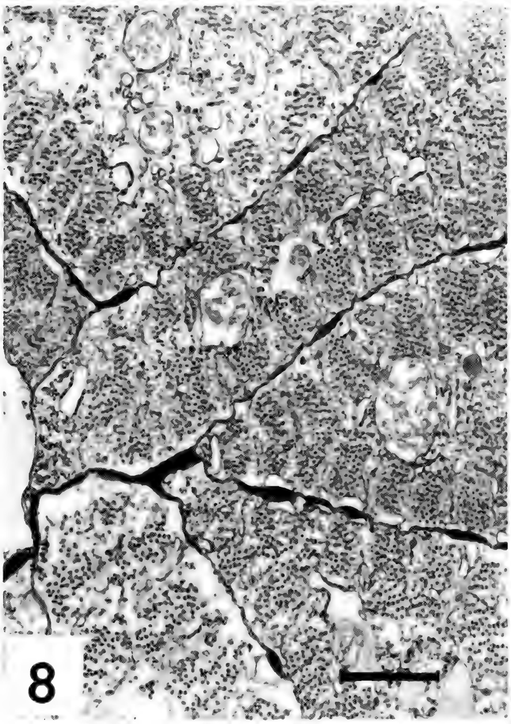

8

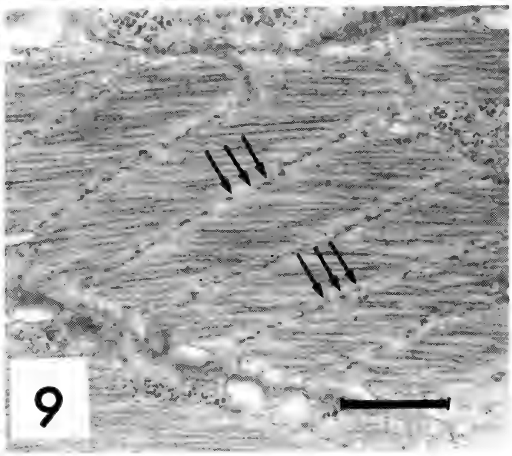

9

under the cell membranes, and the tubular portions extended to the myofilamental bundles. The tubules usually penetrated into the bundles, but in some cases, they reached other E. R. systems situated on the opposite side (Fig. 6). Thick myofilaments in the bundle measured about 24-35 nm in diameter, while thin ones measured about 7 nm. Thick and thin myofilaments in the bundle ran parallel to each other. Larvae began hatching at this stage and the next stage.

Larva 24 hr after hatching: Some myofilamental bundles having cross-striations gathered into one thick bundle at this stage. As shown in Figure 7, two thin bundles with A- and I-bands were present together at the one end of the cell. Because the two bundles were not simply united with each other and the connecting Z-bodies were fused into one line, the line of Z-bodies first appeared in a zigzag pattern (Fig. 7). Before the gathering began, E.R. systems surrounding the thin bundles had disappeared, and the newly reconstructed bundles became thick and ordered.

Larva 48 hr after hatching: Muscle cells were developed completely at this stage. In cross-section, cells appeared to be filled with myofilaments, and the cytoplasm disappeared except for the central region where there were a few mitochondria and other cell-organelles. Myofilaments rearranged to form regular units that stood one behind another along the long axis of the cell (Fig. 8). The regular units were surrounded by tubules and composed of 60–70 thick myofilaments (Fig. 8). In a longitudinal section, cells usually showed a regular oblique-striated pattern of myofilaments (Fig. 9). A-bands in the contracted state measured about 1.4 μm, and Z-bodies appeared alternately at a Z-line with a cross-section of tubules. These characteristic features were the same as the ones of an adult sepia (Fig. 9).

DISCUSSION

In the present study, the developmental course of the oblique-striated muscle cell has been traced succesively to determine how and when the charateristic array of myofilaments is started and formed. From observation, the process may be divided into three phases. The first phase is stages 31–36, the second 38 and the third 24–48 hr after hatching.

In the first phase, a thin and short myofilamental bundle is constructed at a peripheral region of the cell. The bundle includes two kinds of myofilaments that run roughly parallel to each other. The two kinds of myofilaments may be constructed by actin and myosin, respectively, judging from their diameters. Profiles of the bundle resemble previously reported nascent myofibrils of developing cross-striated muscle cells [2–4, 7, 9–12], and those of the lymph-heart [13]. However, the bundle seems rather thin in size as compared to the nascent myofibrils. It is inappropriate to regard the myofilamental bundle in oblique-striated muscle cells as a nascent "myofibril", because the bundle never grows into a myofibril as shown in cross-striated muscle cells. Myofilamental units in an oblique-striated muscle cell resemble a myofibril in cross-section, but they are not exactly true myofibrils.

FIG. 5. A cross-section of muscle cells at stage 38. Circular muscle cells show cross-sections, and longitudinal (lm) and radial muscle cells (rm) appear in longitudinal sections. Muscle cells (circular ones) are generally filled with myofilaments. ×3,000; scale bar, 5 μm.

FIG. 6. A longitudinal section of muscle cells at stage 38. Three myofilamental bundles are shown. They show striations divided by tubular E.R. (arrows). These striations become a line of sarcomeres. ×12,800; scale bar, 1 μm.

FIG. 7. A longitudinal section of muscle cells in a larva 24 hr after hatching. Two myofilamental bundles in a central cell are gathered into one thick bundle. Z-lines of the two bundles are arranged in a zigzag line in the thick bundle (arrows). ×7,700; scale bar, 1 μm.

FIG. 8. A cross-section of muscle cells in a larva 48 hr after hatching. Many myofilamental units appear in cells enclosed by E.R. systems. They appear regularly crossing cells at the short axis. ×13,800; scale bar, 1 μm.

FIG. 9. A longitudinal section of muscle cells in a larva 48 hr after hatching. Cells become fully developed and show structures completely similar to adults. Clear oblique-striated lines appear. Z-bodies and tubular E.R. appear alternately in the line (arrows). ×15,400; scale bar, 1 μm.

It is not clear which myofilaments, thick or thin, are formed first. However, it is believed that filament formation occurs in a limited area surrounded by E. R. systems as shown in Figure 1. This ia a very characteristic feature in the process of developing nascent myofilamental bundles of oblique-striated muscle cells. The bundle gets thicker and the number of myofilaments increases to about 60–70 thick myofilaments. These features resemble those of a nascent myofibril in myofilamental arrangements, that is, two kinds of myofilaments run parallel to each other but show no striated pattern, as reported previously [5].

In the second phase, a myofilamental bundle become cross-striated after the bundle increases in size. The procedure of cross-striation resembles that of cross-striated muscle cells; tubules from E. R. systems attach to the sites of myofibrils at lengths that correspond to an A-band. Allen and Pepe [7] suggested in regard to formation of the cross-striated pattern of developing chick embryos, that the transverse tubule was the first indication of a banding pattern. Similar investigations were reported on chick skeletal muscle *in vitro* [8]. On the contrary, Z-disk formations in stress-fiber were triggered by tubules during its formation [14]. Tubules originated from E. R. systems just under the cell membrane, and contained electron dense materials. They ran in zigzag lines to transverse the bundle. It is not clear whether or not the electron dense materials were secreted from the tubules. It appears that the materials may have some relation to the organization of Z-bodies.

The Z-band (Z-disk) of cross-striated muscle cells originated from dense-body-like structures which connect several thin myofilaments and resemble that of smooth muscle cells. The dense-bodies appeared side by side, in order to complete a Z-band [2–4]. In another case, Z-bands of a nascent myofibril of cross-striated muscle cells appeared in a complete structure at an early stage [3]. Epitherio-muscular cells in coelenterates have cross-striated myofibrils which possess Z-bands that remain at lines of dense bodies, but are not complete Z-disks as shown in cross-striated muscle cells [5]. The Z-bodies in cuttlefish muscle cells in the present study are arranged similar to the epitherio-muscular cell type, that is, the Z-band is constructed by a line of dense-bodies. Thus, the process where by the formation of Z-bodies is lead by tubular E.R. is remarkable in a nascent myofilamental bundle in oblique-striated muscle cells. A- and I - bands are organized completely in this phase.

In the last phase, muscle cells become complete, and the mantle constituted from these complete muscle cells show rhythmical pulsating contractions. Myofilamental bundles with A- and I-bands fuse into a thick bundle in the cell. Fusion progresses first from coupling the two bundles and then putting Z-bodies into a line with each other. E. R. systems of the two bundles disappear at this stage, and only tubular systems remain in the fused bundle. Bundles having different sizes of sarcomeres are also fused. The newly constructed thick myofilamental bundle shows a zigzag line of Z-bodies in longitudinal section. The zigzag lines are gradually rearranged into an oblique line, and the muscle cells are completed. These processes have not been previously reported in either oblique or cross-striated muscle cells.

ACKNOWLEDGMENTS

My sincere thanks to Prof. K. Maruyama of Chiba University for his helpful advice and critical reading of this manuscript. I am also indebted to Prof. M. Yoshida of the Marine Biological Labortatory of Okayama University for his encouragement and kindness in supplying the cuttlefish embryos and larvae.

REFERENCES

1 Kawaguti, S. (1963) Electron microscopy on the heart muscle of the cuttlefish. Biol. J. Okayama Univ., **9**: 27–40.
2 Obinata, T., Yamamoto, M. and Maruyama, K. (1966) The identification of randomly formed thin filaments in differentiating muscle cells of the chick embryo. Dev. Biol., **14**: 192–213.
3 Fischman, D. A. (1967) An electron microscope study of myofibril formation in embryonic skeletal muscle. J. Cell Biol., **32**: 557–575.
4 Shimada, Y., Fischman, D. A. and Moscona, A. A. (1967) The fine structure of embryonic chick skeletal muscle cells differentiated in vitro. J. Cell Biol., **35**: 445–453.
5 Matsuno, A. (1983) An electron microscopic study

on the development of cross-striated muscles in ephyrae of *Aurelia aurita*. Zool. Mag. Tokyo, **92**: 416–422.

6 Yamamoto, M. (1982) Normal stages in the development of the cuttlefish, *Sepiella Japonica* SASAKI. Zool. Mag. Tokyo, **91**: 146–157. (In Japanese)

7 Allen, E. R. and Pepe, F. A. (1965) Ultrastructure of developing muscle cells in the chick embryo. Am. J. Anat., **116**: 115–148.

8 Ezerman, E. B. and Ishikawa, H. (1967) Differentiation of the sarcoplasmic reticulum and T system in developing chick skeletal muscle in vitro. J. Cell Biol., **35**: 405–420.

9 Obinata, T., Yamamoto, M. and Maruyama, K. (1967) Morphological and biochemical studies on myofibrillar formation in developing chick embryo. Sci. Papers College General Educ. Univ. Tokyo, **17**: 95–120.

10 Shimada, Y. (1971) Electron microscope observations on the fusion of chick myoblasts in vitro. J. Cell Biol., **48**: 128–142.

11 Mair, W. G. P. (1981) Ultrastructure of developing human muscle. Biol. Neonate., **40**: 276–294.

12 Peng, H. B., Wolsosewick, J. J. and Cheng, P. C. (1981) The development of myofibrils in cultured muscle cells: A whole-mount and thin-section electron microscopic study. Dev. Biol., **88**: 121–136.

13 Markozashvili, M. I. and Rumyantsev, P. P. (1984) Ultrastructure of muscle fibers and cells synthesizing DNA in lymph heart of developing frogs and chick embryos. Cell Tissue Res., **238**: 369–379.

14 Dlugosz, A. A., Antin. P. B., Nachmias, V. T. and Holtzer, H. (1984) The relationship between stress fiber-like structures and nascent myofibrils in cultured cardiac myocytes. J. Cell Biol., **99**: 2268–2278.

ZOOLOGICAL SCIENCE 4: 61–72 (1987)

Effects of Calmodulin Antagonists on Motility and Acrosome Reaction of Sea Urchin Sperm

Fuyuki Iwasa[1], Yuko Hasegawa[1], Sumio Ishijima[1], Makoto Okuno, Toshiko Mohri and Hideo Mohri[2]

Department of Biology, University of Tokyo, Komaba, Meguro-ku, Tokyo 153, Japan

ABSTRACT—Effects of calmodulin antagonists on intact and demembranated sea urchin sperm were examined to elucidate possible functions of calmodulin in sperm motility and the acrosome reaction. Calmodulin antagonist W-7 immobilized intact sperm in artificial sea water (ASW), but did not affect motility of Nonidet-demembranated sperm. When sperm was exposed to W-7, oxygen consumption rate was reduced to 3.3% of control level and flagellar bending became non-propagating to the apical end. The acrosome reaction induced by egg jelly was inhibited concomitant with the loss of motility. W-7 also caused depolarization of sperm membrane. Such phenomena were dependent on amounts of the drug and occurred rather slowly. These effects of W-7 were reversible and canceled by exogenously added calmodulin. Theophilline partially canceled the immobilizing effect of W-7. In Na^{+}-free ASW, W-7 showed different effects, i.e. it reinitiated motility of immobilized sperm. Target(s) of W-7 and functions of calmodulin were considered based on the above results. If W-7 antagonized calmodulin, it seems that calmodulin has multiple functions in motility and the acrosome reaction of sea urchin sperm.

INTRODUCTION

Calcium ions (Ca^{2+}) function as an intracellular mediator of acrosome reaction and motility in sea urchin sperm [1]. The acrosome reaction, i.e. exocytosis of acrosomal vesicle and elongation of actin filaments (acrosomal process) is a prerequisite for fertilization in sea urchins. Egg jelly, the natural inducer of the acrosome reaction, is replaceable by Ca^{2+} ionophore A23187 [2], indicating that the reaction is triggered by an increase in intracellular Ca^{2+} concentration. Another important function of sperm is flagellar movement. In sea urchin sperm, patterns of flagellar bending of reactivated Triton-demembranated models change depending on Ca^{2+} concentration at demembranation and reactivation [3].

On the other hand, initiation or maintenance of motility requires cAMP-dependent phosphorylation of certain protein(s) in sperm of rainbow trout [4], sea urchin [5], dog [6], etc. There seems to be close relationship among regulations by cAMP and Ca^{2+} [7]. Presence of calmodulin in sea urchin sperm has been demonstrated [8]. A calmodulin antagonist, W-7 (N-(6-aminohexyl)-5-chloronaphthalenesulfonamide), inhibits the acrosome reaction of sea urchin sperm induced by egg jelly [9] and also immobilizes sea urchin sperm [10]. Another calmodulin antagonist, trifluoperazine (TFP), changes swimming pattern of dog sperm from straightforward to circular [6].

According to studies on effects of [^{3}H]-W-7 on CHO–K_1 cells, W-7 passes through the plasma membrane and distributes into the entire cytoplasm [11]. Although W-7 remains at low concentrations in the plasma membrane, it does not accumulate in the membrane or in the nucleus. When cells are replaced into media without W-7, the incorporated W-7 is released from the cells with time. One mole of calmodulin binds 3 moles of W-7 and its Kd is 11 μM, whereas affinity of W-5 (N-(6-aminohexyl)-naphthalenesulfonamide) for

Accepted August 18, 1986
Received June 26, 1986

[1] Present address: Suntory Institute for Biomedical Research for F. Iwasa, Life Science Laboratory, Showa Denko K. K. for Y. Hasegawa and National Institute for Basic Biology for S. Ishijima.

[2] To whom reprint requests should be addressed.

calmodulin is one eighth of that of W-7 [12].

In this study, we tried to elucidate possible functions of calmodulin in motility and the acrosome reaction of sea urchin sperm examining effects of calmodulin antagonists on live and Nonidet-treated sperm. We mainly used W-7 as a calmodulin antagonist and W-5 as its control.

MATERIALS AND METHODS

Materials

Sea urchin sperm was collected by injecting 0.5 M KCl into the coelomic cavity. *Hemicentrotus pulcherrimus* sperm were used for observation of the acrosome reaction, measurement of oxygen consumption, membrane potential and intracellular concentration of Ca^{2+}. Sperm of *H. pulcherrimus, Anthocidaris crassispina* and *Strongylocentrotus nudus* were used for observation of motility.

Artificial sea water

Compositions of artificial sea waters, ASW, Ca^{2+}-free ASW (CFASW), Ca^{2+}-free ASW containing EGTA (CF(G)ASW), Na^+-free ASW (NaFASW), Na^+, Ca^{2+}-free ASW (NaCFASW), Na^+, Ca^{2+}-free ASW containing EGTA (NaCF(G)ASW) are listed in Table 1.

Reagents

Calmodulin antagonists, W-7 and W-5 purchased from Rikaken Ltd., were dissolved in distilled deionized water (DDW) at 5 mM and aliquots were stored at −20°C until use. TFP was a gift from Yoshitomi Pharmaceutical Industries Ltd. TI233 (N^2-dancyl-L-arginine-4-t-piperazine amide) was a gift from Dr. M. Maruyama of Mitsubishi-Kasei Institute of Life Sciences. Theophilline was dissolved in DDW at 1 M. Calmodulin was purified from porcine brain by the method of Teo *et al.* [13]. BSA (bovine serum albumin) was a commercial Fraction V (Reheis Chemical Co., Phenix, USA). DiO-C_2-(5) (3,3′-diethyloxadicarbocyanine iodide) was dissolved in DDW and filtered through 0.45 μm nitrocellulose membrane before use. The concentration of the dye was determined by the absorption at 575 nm.

Quin-2 tetramethyl ester was purchased from Amersham, dissolved in dimethylsulfoxide at 3 mM and stored at −20°C. CCCP (carbonyl cyanide m-chlorophenylhydrazone) was dissolved in ethanol and stored at −20°C.

Observation of flagellar movement

One μl of semen was suspended in 200 μl of ASW, and after 30 sec 10 μl of the suspension was diluted into 500 μl of ASW containing various reagents. Observations were made using a phase contrast microscope (×200) without coverslip. In some cases, motility was recorded on video tapes. Sperm most actively swimming just beneath the open space were observed. Sperm motility was scored at 4 grades, i.e. swimming fast (++), swimming slowly (+), motile but not swimming (±) and immotile (−).

Observation of acrosome reaction

Semen was diluted 500 times with ASW, and W-7, W-5 or other reagent was added 30 sec after dilution. The acrosome reaction of sea urchin

Table 1. Compositions (mM) of artificial sea waters

	ASW	CFASW	CF(G)ASW	NaFASW	NaCFASW	NaCF(G)ASW
NaCl	458	474	458	—	—	—
Choline Cl	—	—	—	458	458	418
KCl	9.6	9.6	9.6	9.6	9.6	9.6
$MgCl_2$	48.5	48.5	48.5	48.5	48.5	48.5
$CaCl_2$	10.4	—	—	10.4	—	—
EGTA	—	—	10.0	—	—	10.0
EPPS[a]	10.0	10.0	10.0	10.0	10.0	10.0
pH	8.2	8.2	8.2	8.2	8.2	8.2

[a] N-(2-hydroxyethyl)-piperazine-N′-3-propanesulfonic acid.

sperm was induced by adding equal volume of "egg sea water" [9] to sperm suspension. One minute after the addition of "egg sea water", sperm were fixed with 3% glutaraldehyde in ASW. Fixed sperm were mounted on grids for electron microscopy, negatively stained with 1% uranyl acetate and observed under the Hitachi HS-9 electron microscope. Sperm were classified into 3 groups, that is, acrosome-reacted, not reacted and not distinct because of destruction or aggregation.

Demembranated sperm models

Nonidet models of sea urchin sperm were prepared by the method of Okuno and Brokaw [3]. Demembranation solution and reactivation solution were modified as follows. Nonidet demembranation solution: 0.15 M KCl, 20 mM Tris (Tris(hydroxymethyl)aminomethane)-HCl, 1 mM DTT (dithiothreitol), 0.04% (w/v) Nonidet P-40, 2 mM $MgCl_2$, 0 mM (for potentially asymmetrical model) or 5 mM (for potentially symmetrical model) $CaCl_2$, pH 8.2. Reactivation solution: 0.2 M KCl, 20 mM Tris-HCl, 2 mM $MgCl_2$, 1.8 mM EGTA (ethyleneglycol bis(2-aminoethyl ether)tetraacetic acid), 0–1.9 mM $CaCl_2$, 0.22 mM ATP, 1 mM DTT, 2% (w/v) polyethyleneglycol 6,000, pH 8.2.

Measurement of oxygen consumption

Oxygen consumption of sea urchin sperm was measured using a Clark type oxygen electrodes. Sperm concentration was approximately 1×10^8/ml and 50 μM W-7 or 10 μM KCN was added 2 min after the onset of measurement. At various intervals, small portions were withdrawn to examine sperm motility under the microscope.

Measurement of membrane potential

Relative values of membrane potential of sea urchin sperm were estimated using a fluorescent probe, 3,3′diethyloxadicarbocyanine iodide (diO-C_2-(5)). DiO-C_2-(5) is one of cyanine dyes, which are used for measurement of membrane potentials [14]. Cyanine dyes bind to biomembrane depending on its potential, and reduce their fluorescence intensity [15]. Five μl of semen was diluted in 1 ml of ASW and mixed with 1 ml of diO-C_2-(5) in ASW at certain intervals after semen dilution. Fluorescence intensity was measured using a Shimadzu fluorescence spectrophotometer RF-540 at excitation wavelength of 574 nm and emission wavelength of 595 nm.

Measurement of intracellular concentration of Ca^{2+}

Relative values of intracellular concentration of Ca^{2+}in sea urchin sperm were measured using Quin-2 by the method developed by Tsien [16]. Semen (0.2 ml) was mixed with 0.8 ml of ASW containing 0.1 mM $CaCl_2$ and 10 μl of 3 mM Quin-2 tetramethyl ester, and incubated for 30 min at room temperature. After the addition of 9 ml of ASW containing 0.1 mM $CaCl_2$, the mixture was further incubated for 30 min at 0°C. Sperm was then pelleted by centrifugation at 4,000 rpm with Tomy No.3 angle rotor for 5 min and again incubated for 30 min in 10 ml of ASW containing 0.1 mM $CaCl_2$ at 0°C. The last step was repeated once more. Measurement of fluorescence intensity was carried out by diluting pelleted sperm 200 times and at excitation wavelength of 339 nm and emission wavelength of 492 nm. Measurement of intracellular concentration of Ca^{2+} in Na^+-free ASW was done with the same procedure in NaFASW or NaCFASW instead of ASW containing 0.1 mM $CaCl_2$ or CFASW.

RESULTS

Effects of calmodulin antagonists on sperm motility and acrosome reaction

Calmodulin antagonists, W-7, TI233 and TFP at the concentrations of $1–5\times10^{-5}$ M, arrested flagellar beating of sea urchin sperm, whereas W-5 had no effect at the same concentration. Figure 1 shows changes in flagellar movement of *A. crassispina* sperm diluted 2×10^4 times in ASW and exposed to 25 μM W-7. Flagellar bending was gradually becoming non-propagating and observable only at proximal region of flagellum. Beat frequency dropped at that time, whereas amplitude did not change for longer period. Finally sperm became immotile with straightened flagellum.

W-7 also inhibited the acrosome reaction induced by egg jelly as previously reported [9]. In

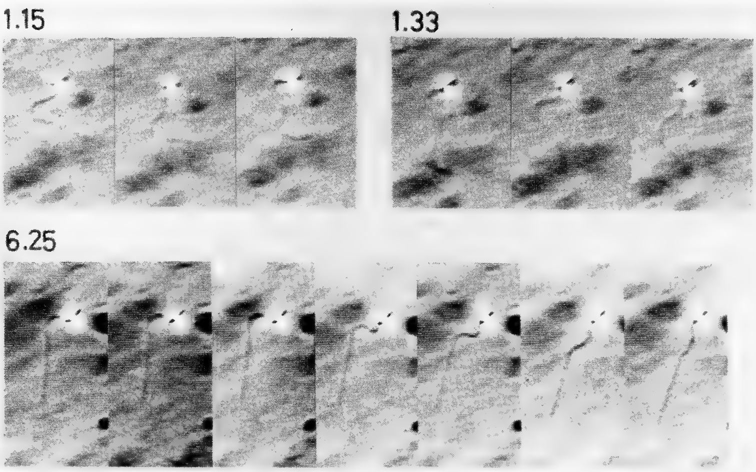

Fig. 1. Changes of flagellar movement of *A. crassispina* sperm exposed to W-7. Semen was diluted 2×10^4 times in ASW containing 25 μM W-7. Flagellar movement was recorded on a video tape. Numerals indicate min and sec after dilution.

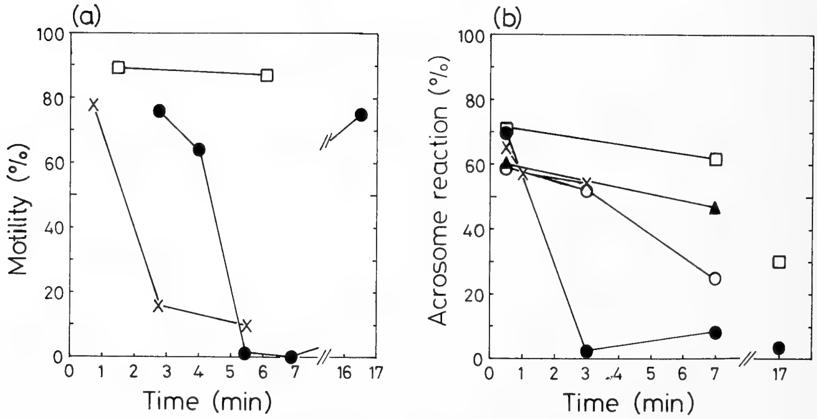

Fig. 2. Effects of W-7, W-5 and KCN on motility (a) and acrosome reaction (b) of *H. pulcherrimus* sperm. Semen was diluted 500 times in ASW containing various reagents. ●, 20 μM W-7; ▲, 20 μM W-7+20 μM calmodulin; ○, 20 μM W-5; ×, 50 μM KCN; □, none.

the present experiment, the time dependency of the inhibition and its relationship to inhibition of motility were examined. Figure 2 shows results of a typical experiment. *H. pulcherrimus* sperm were diluted 500 times in ASW containing 20 μM W-7, 20 μM W-5 or 50 μM KCN, and percentage of motile sperm (Fig. 2a) and percentage of acrosome-reacted sperm (Fig. 2b) were determined.

Concentration of sperm was 7×10^7/ml before the addition of "egg sea water". The effect of W-7 on the acrosome reaction was canceled by the addition of 20 μM calmodulin. W-5 was much less effective than W-7 in inhibiting the acrosome reaction. KCN inhibited motility, but not the acrosome reaction. The results indicate that targets of W-7 and KCN are different and that there is no direct relationship between motility and the acrosome reaction.

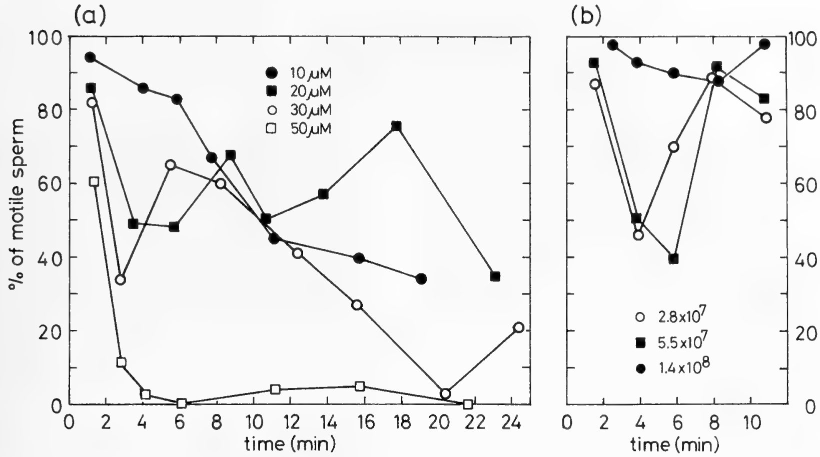

FIG. 3. Effect of W-7 on motility of *H. pulcherrimus* sperm. Percent motile sperm was counted (a) when semen was diluted to 4.7×10^7/ml at various concentrations of W-7 in ASW and (b) when *H. pulcherrimus* semen was diluted to various concentrations in ASW containing 20 μM W-7.

Calmodulin antagonists, W-7 and TFP at 50 μM, neither stopped flagellar movement nor changed the bending pattern of Nonidet-demembranated models of sea urchin sperm. It was the case for both potentially symmetrical and potentially asymmetrical models. The results show that W-7 does not affect motile systems in the axoneme.

Inhibition of the motility of *H. pulcherrimus* sperm in ASW by W-7 was dependent on concentration of W-7 and of sperm as shown as typical results in Figure 3. As will be described in the following section, an autonomous recovery of motility was observed at low concentrations of W-7. When the drug concentration was kept constant, the motility-inhibiting effect of W-7 became less prominent with increasing concentration of sperm. This was also true for KCN.

Recovery from the effects of calmodulin antagonists

Inhibition of flagellar bending by W-7 occurred independently of exogenous Ca^{2+}. *H. pulcherrimus* semen was diluted 2,000 times in ASW or CFASW containing 10 mM EGTA (CF(G)ASW). Sperm showed symmetrical bending in both media. When each suspension was diluted 10 times in corresponding ASW containing 50 μM W-7, sperm stopped motility in either case. Ten minutes after, 50 μM calmodulin was added to each suspension. Then sperm in ASW reinitiated motility, but sperm in CF(G)ASW did not. This result suggests that W-7 bound to intracellular calmodulin after the drug passed through the plasma membrane. The recovery by calmodulin from the effect of W-7 required exogenous Ca^{2+}. This indicates that intracellular concentration of W-7 decreased as calmodulin bound to W-7 extracellularly.

Figure 4a is a record on video tape of the recovery process of flagellar bending from inhibitory effect of W-7 by calmodulin. As calmodulin diffused, bending reinitiated at the proximal end of flagellum and propagated to the apical end. At that time, flagellar bending was symmetrical but beat frequency was too low to cause forward swimming. As time went on, so-called Ca^{2+} quiescent sperm [17] were frequently observed. Then beat frequency increased with asymmetrical bending. Some sperm became to show symmetrical bending with time, but others remained still asymmetrical. Thus the inhibition of motility by W-7 was reversible.

Theophilline is known to be an inhibitor of cyclic nucleotide phosphodiesterase and is effective on phosphodiesterase in sea urchin sperm (Dr. K. Ishida, personal communication). The exposure of *A. crassispina* sperm, immobilized by W-7, to 2 mM theophilline caused reinitiation of flagellar bending and in some sperm the bending prop-

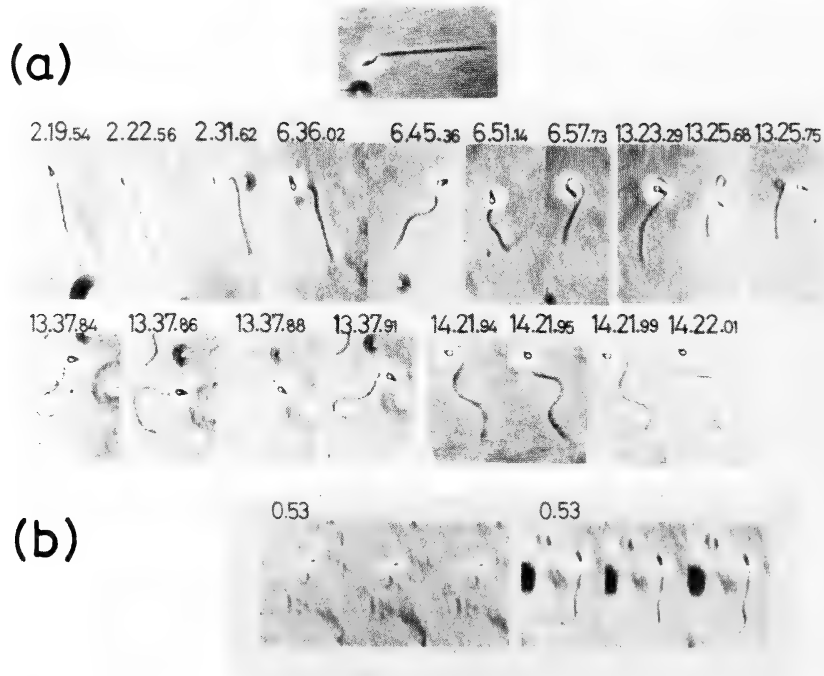

Fig. 4. (a) Recovery of flagellar beating of *A. crassispina* sperm from inhibitory effect of W-7 by calmodulin. *A. crassispina* semen was diluted 2×10^4 times in ASW containing 50 μM W-7. After the sperm ceased movement, calmodulin was added to the sperm suspension. Top figure represents a sperm immobilized by 50 μM W-7. Time (min, sec, 10^{-2} sec) after the addition of calmodulin is indicated. (b) Incomplete recovery of flagellar beating of *A. crassispina* sperm from inhibitory effect of W-7 by theophilline. Numerals are min and sec after the addition of theophilline.

agated. Loci of the reinitiation of bending were not always at the proximal end (Fig. 4b). The recovery by theophilline was incomplete because sperm did not show forward swimming and only continued slow bending for at least 20 min. The effect of theophilline was independent of exogenous Ca^{2+}. The recovery of motility by theophilline was not seen in *S. nudus* sperm. Recovery or canceling of the effect of W-7 on the acrosome reaction by theophilline was not observed.

Sperm immobilized by W-7 recovered their motility by merely diluting the sperm suspension with ASW. Figures 2a and 3 show that when the drug concentration was low, sperm reinitiated motility as time elapsed without any further treatments. It may be because the cells expel W-7 [11]. Nonidet-demembranated models prepared from the sperm immobilized by W-7 showed normal swimming after reactivation by ATP.

Effects of W-7 on sperm in Na^+-free ASW

Sea urchin sperm requires exogenous Na^+ for maintaining motility to eliminate H^+ produced by respiration in mitochondrion. NH_4Cl or NH_3 temporally elevates intracellular pH (pH_i) of immotile sperm and recovers motility in NaFASW [18].

When *A. crassispina* semen was diluted 1×10^4 times in NaFASW with or without 50 μM W-7, sperm were immotile in both cases. Ten mM NH_4Cl reinitiated motility of both sperm. Duration of motility was about 3 min in the absence of W-7 and about 30 sec in the presence of W-7. After the temporary movement ceased, 10 mM NH_4Cl was further added. Sperm in ASW without W-7 started to swim as before and third addition of

NH_4Cl was also effective, whereas sperm in ASW with W-7 did not move this time. On the other hand, NH_4Cl did not reinitiate motility of sperm immobilized by W-7 in ASW. Therefore, W-7 does not seem to stop flagellar movement by preventing elevation or lowering of pH_i.

Effects of W-7 on sperm in NaFASW were studied in more detail using *S. nudus* sperm. Sperm diluted 1×10^4 times were immotile with straightened flagella. When W-7 or W-5 was added 1 min after dilution, they had no effect. However, W-7 added 4 min after dilution reinitiated motility which lasted for 3–5 min. The pattern of immobilization in NaFASW with W-7 was different from that in ASW with W-7. Bending continued to propagate along the whole flagellum until it stopped. The pattern was similar in the case of NH_4Cl, although the patterns of initiation by W-7 and by NH_4Cl differed from each other in the following three points. 1) Recovery by W-7 occurred after some time had elapsed since sperm stopped motility in NaFASW, whereas this was not the case with NH_4Cl. 2) NH_4Cl reinitiated motility immediately, but W-7 had about 1 min lag time until reinitiation. 3) Although recovery by NH_4Cl was repeatable, recovery by W-7 occurred only once.

In NaFASW, duration of motility was 3–5 min with W-7, 10 min with NH_4Cl, but only about 2 min with both W-7 and NH_4Cl. When NH_4Cl was added to sperm immobilized in W-7, a small portion of sperm reinitiated motility which continued for about 1 min. Further addition of NH_4Cl had no effect.

W-5 had no reinitiation effect in contrast to W-7. However, about equimolar concentration of calmodulin did not cancel the effect of W-7. Contrary, calmodulin even prolonged the duration of motility. BSA in place of calmodulin in NaFASW containing W-7 also prolonged the swimming time. Immobilized sperm in Na^+, Ca^{2+}-free ASW containing 10 mM EGTA (NaCF(G)ASW) also reinitiated motility when W-7 was added. The effect was more remarkable than in NaFASW. Calmodulin prolonged the duration of swimming, although calmodulin does not seem to bind to W-7 extracellularly in this case.

Next we examined what happened after swimming in ASW. Semen was diluted 200 times in ASW and pelleted by centrifugation. When the pelleted sperm was diluted 1×10^4 times in NaFASW, sperm were immotile. NH_4Cl reinitiated motility reversibly, but W-7 scarcely recovered motility.

In summary, W-7 has two effects on sperm motility in NaFASW. Namely, W-7 stopped NH_4Cl-induced motility of sperm, and reinitiated motility of immotile sperm.

Oxygen consumption of sperm exposed to W-7

Oxygen consumption rates of sperm exposed to 50 μM W-7 or 10 μM KCN were measured using

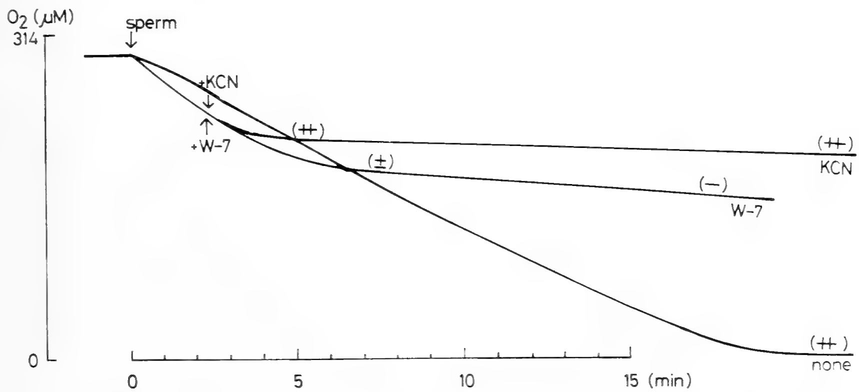

Fig. 5. Effects of W-7 and KCN on oxygen consumption rate of *H. pulcherrimus* sperm. Oxygen consumption was measured using suspensions of approximately 1×10^8 sperm/ml. Two min after the addition of sperm, 50 μM W-7 or 10 μM KCN was added. Motility is indicated as (−), (±) or (++).

oxygen electrodes. As shown in Figure 5, only 3.3% in the presence of W-7 and 1.8% in the presence of KCN of oxygen consumption as compared with control value were detected. Sperm exposed to W-7 became immotile about 5 min after the addition of W-7, whereas sperm in the presence of KCN swam actively in spite of the reduction in oxygen consumption (cf.[19]), although higher concentration of KCN such as 50 μM inhibited motility as described above. This means that the inhibition of respiration of sea urchin sperm does not necessarily lead to an inhibition of motility. The reduction of oxygen consumption by W-7 seems to be caused by the inhibition of motility.

Changes in membrane potential (Vm)

Relative values of membrane potential of sperm were estimated using a fluorescent probe, diO-C_2-(5). Our previous work [20] which measured membrane potential of sea urchin sperm using the dye gave the following conclusions. 1) Membrane potential of sea urchin sperm largely depends on concentration of Cl^-. 2) Depolarization is detected by adding "egg sea water" or A23187, which is observed as an increase in fluorescence intensity.

H.pulcherrimus sperm diluted 1×10^4 times in ASW became immotile 2–3 min after exposure to diO-C_2-(5). Duration of swimming was shorter as the dye concentration was higher. The measurement was completed within 30 sec after adding diO-C_2-(5) unless otherwise stated. Fluorescence intensity was settled as the dye was transferred from the solution to the sperm membrane.

Membrane potential of *H. pulcherrimus* sperm was measured in ASW, CF(G)ASW and NaFASW (Table 2). In these ASWs, increase of fluorescence intensity was detected when W-7 was added, indicating the depolarization of sperm membrane. Na^+, which also reinitiates sperm motility in NaFASW as NH_4Cl does, increased the fluorescence intensity to the level of that in ASW.

Depolarization of sea urchin sperm membrane in ASW caused by W-7 was further studied for

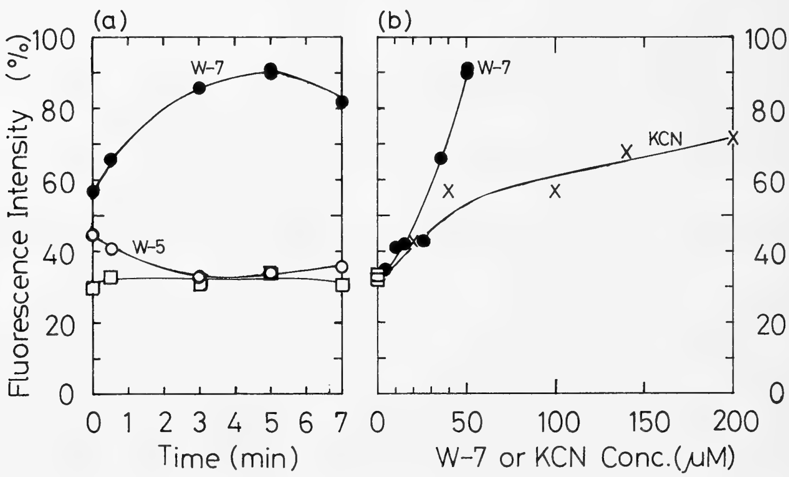

Fig. 6. Effects of calmodulin antagonists and KCN on fluorescence intensities of diO-C_2-(5) in sperm suspension. (a) Changes of fluorescence intensities after diluting *H. pulcherrimus* semen in ASW. Twenty μl of *H. pulcherrimus* semen was diluted in 4 ml of ASW with or without W-7. Fluorescence was measured 30 sec, 2 min, 5 min and 7 min after dilution by mixing 1 ml of each sperm suspension and equal volume of 0.1 μM diO-C_2-(5) in ASW. Fluorescence intensity at zero time was measured by diluting semen 400 times in 2 ml of 0.05 μM diO-C_2-(5) in ASW with or without W-7. ●, 50 μM W-7; ○, 50 μM W-5; □, none. (b) Fluorescence intensities after 5-min incubation of *H. pulcherrimus* sperm suspension. Semen of *H. pulcherrimus* was diluted 200 times in ASW containing 0, 5, 10, 15, 25, 35 or 50 μM W-7, and after 5 min incubation fluorescence intensities were measured by mixing equal volume of W-7 and 0.1 μM diO-C_2-(5) in ASW.

TABLE 2. Relative fluorescence intensities (%) of diO-C_2-(5) in sea urchin sperm suspensions

Reagent	ASW	CF(G)ASW	NaFASW
None	52[a]	<30	<30
50 μM W-7	95	97	76
50 μM W-5	61	59	40
50 μM KCN	60	55	n.d.[b]
10 mM NaCl	—	—	55

H. pulcherrimus semen was diluted 200 times in each ASW containing various reagents and mixed with equal volume of 0.2 μM diO-C_2-(5) in each ASW 4 min after dilution. Sperm suspensions diluted 200 times in NaFASW became immotile within 2 min.

[a] Fluorescence intensity in each ASW without sperm was taken as 100%.

[b] Not determined.

time dependency and dose dependency. Compared with control experiment, of which fluorescence intensity was nearly constant after dilution, W-7 gradually increased the fluorescene intensity. With W-5, on the other hand, values at zero time and 30 sec were somewhat higher than control, but almost the same as control thereafter (Fig. 6a).

Figure 6b shows that the fluorescence changed a little up to 25 μM of W-7 and remarkably increased above 25 μM. KCN did not increase the fluorescence at 25 μM and brought about 2-fold increase at 200 μM. Thus depolarization effect was greater with W-7 as compared with the effect of KCN. Similar depolarization to that caused by W-7 was observed when sperm suspension was exposed to CCCP, an effective uncoupler of oxidative phosphorylation, in ASW.

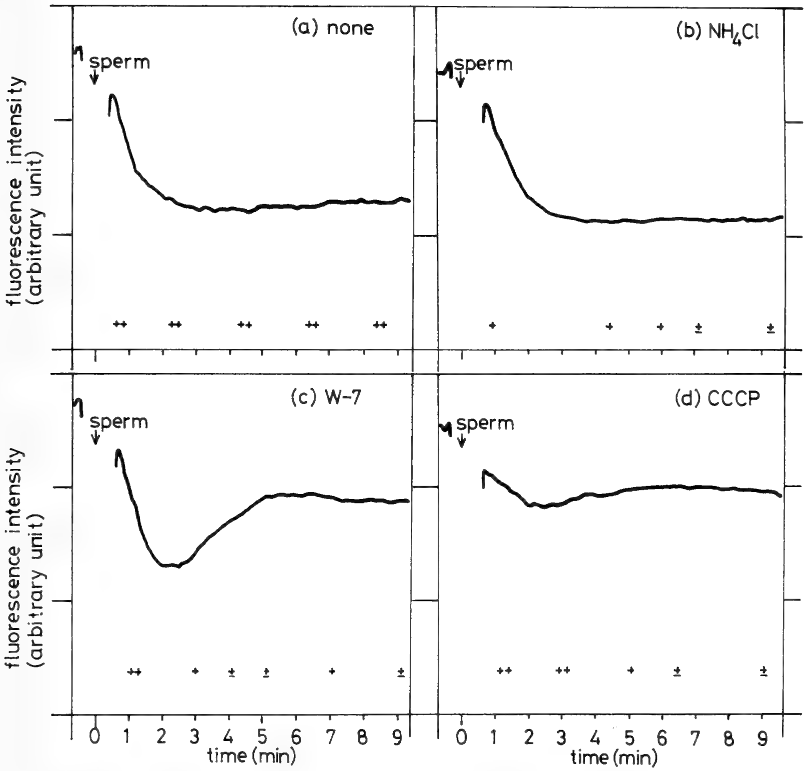

FIG. 7. Effects of NH_4Cl, W-7 and CCCP on membrane potential and motility of *H. pulcherrimus* sperm in ASW. At first, fluorescence of 0.05 μM diO-C_2-(5) in ASW was measured. Following reagents were contained in the above solution. (a) none, (b) 10 mM NH_4Cl, (c) 50 μM W-7, (d) 1×10^{-7} M CCCP. Next, changes in fluorescence intensities were recorded continuously after 400 times dilution of semen into each ASW. Motility of the same sperm suspension was evaluated as −, ±, + and ++.

After measuring the fluorescence intensities of 0.1 μM diO-C_2-(5) in ASW or NaFASW containing 10 mM NH_4Cl, 50 μM W-7 or $1-2\times10^{-7}$M CCCP, *H. pulcherrimus* sperm were diluted in each solution by 400 times (ASW) or 2,000 times (NaFASW) to record changes of fluorescence continuously (Figs. 7 and 8). Sperm motility was also observed. In ASW, NH_4Cl did not change membrane potential (Vm) and motility so much (Fig. 7b), but in NaFASW it raised Vm to the level of that in ASW concomitant with activation of motility (Fig. 8b). W-7 raised Vm and reduced motility in ASW (Fig. 7c). As mentioned previously, W-7 caused temporary movement in NaFASW. A rise in Vm was observed after such a movement (Fig. 8c). CCCP increased Vm as W-7 did in ASW, but the inhibition of motility by CCCP occurred more slowly than that by W-7 (Fig. 7d). On the other hand, a rise in Vm by CCCP in NaFASW was less than that by W-7, and reinitiation of motility was not observed (Fig. 8d).

Intracellular concentration of calcium ($Ca^{2+}{}_i$)

Finally the question as to whether W-7 changes $Ca^{2+}{}_i$ of sperm was examined. *H. pulcherrimus* sperm treated with Quin-2 were diluted 200 times in CFASW and fluorescence intensity was measured. Emission peak was shifted from 435 nm to 470 nm by hydrolysis of Quin-2 tetramethyl ester. Sperm were motile during the measurement. Fluorescence intensity of sperm suspension in CFASW (200 times diluted) changed little by the addition of calmodulin antagonists (data not shown).

We also measured $Ca^{2+}{}_i$ of sperm in NaFASW. *H. pulcherrimus* sperm treated with Quin-2 in NaFASW and diluted 200 times in this ASW were immotile, but reinitiated motility by 20 mM NH_4Cl. Emission peaks were found at 470 nm and 435 nm. The sperm was diluted in NaCFASW and the fluorescence intensity was measured. NH_4Cl reinitiated motility temporally, but did not change $Ca^{2+}{}_i$. Although W-7 also reinitiated motility in NaFASW, no change was found in $Ca^{2+}{}_i$ (data not shown).

In conclusion, W-7 does not seem to change $Ca^{2+}{}_i$. We could not find any parallel change of $Ca^{2+}{}_i$ to those of motility, the acrosome reaction or membrane potential.

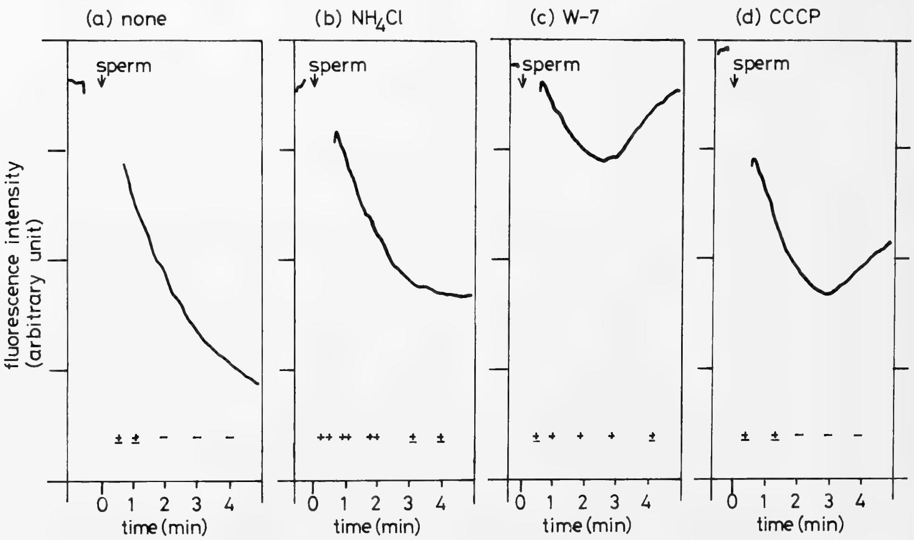

Fig. 8. Effects of NH_4Cl, W-7 and CCCP on membrane potential and motility of *H. pulcherrimus* sperm in NaFASW. Measurements were made as in Figure 7, except that dilution of semen was 2,000 times and that concentrations of diO-C_2-(5) and of CCCP were 0.1 μM and 2×10^{-7}M, respectively.

DISCUSSION

When sea urchin sperm were exposed to a calmodulin antagonist, W-7, in ASW, flagellar movement was arrested, the acrosome reaction failed to occur and sperm membrane was depolarized, although we could not really know which memberane was depolarized to what extent (see below). Inhibition of flagellar movement was also observed with other calmodulin antagonists, TI233 and TFP. These three phenomena were dependent on the amount of W-7, and occurred relatively slowly, that is, not instantaneously. It appears to take some time before W-7 reaches its targets. In contrast, no remarkable change was detected in $Ca^{2+}{}_i$. Therefore, W-7 does not seem to inhibit flagellar movement by raising Ca^{2+} concentration in the flagellum. Nor W-7 inhibits the acrosome reaction by preventing the increase of Ca^{2+} concentration in the sperm head. It should be noted, however, that only the average level of Ca^{2+} in sperm was estimated by using Quin-2. The obtained results do not exclude the possibility of local fluctuation of Ca^{2+} concentration within the cells.

Membrane potential measured may reflect mainly that of the inner mitochondrial membrane, because CCCP raised Vm in ASW. However, effects of NH_4Cl, W-7 and CCCP on Vm and sperm motility in ASW and NaFASW were different from each other. Therefore, it is not possible that W-7 functions only as an uncoupler of oxidative phoshorylation in mitochondria. Unlike W-7, CCCP had no inhibitory effect on repeated reinitiation of motility by NH_4Cl in NaFASW.

Concerning the effects of W-7 in ASW and NaFASW, the following two observations were made: W-7 stopped motility of sperm which had optimal pH_i and were motile; W-7 gave a temporary motility to sperm which had low pH_i and were immotile. Targets of W-7 in these two effects seem to be different. The effect of W-7 in NaFASW was not canceled by equimolar concentration of calmodulin, raising a question as to whether the effect came from the inhibition of sperm calmodulin by W-7. Such an effect was also observed in NaCF-(G)ASW.

In our preliminary experiments, changes in flagellar and ciliary movement caused by W-7 were also observed in golden hamster sperm and cilia of sea urchin embryos. W-7 affected only the principal bend of golden hamster sperm from the cauda epididymis leaving the reverse bend unaffected (cf. [21]), whereas W-5 had no such an effect. *H. pulcherrimus* embryos at mid-gastrula stage which show straightforward swimming with rotation were exposed to W-7, W-7 plus calmodulin or W-5. Among them, only W-7 changed motility pattern to either rotation or straight swimming only.

The results so far obtained suggest that W-7 has some targets in sperm concerning their flagellar movement. No direct evidence, however, has been obtained to indicate that they are calmodulin. Theophilline, a phosphodiesterase inhibitor, partially released sea urchin sperm from the inhibitory effect of W-7. If calmodulin is main target, the observation indicates involvement of calmodulin in regulation of cAMP content, because continuation of sea urchin sperm motility requires cAMP-mediated phosphorylation [5].

In sea urchin sperm, creatine phosphokinase seems to have a role to shuttle to mediate high energy phosphate between mitochondrion and tail [22]. If the enzyme is inhibited by dinitrofluorobenzene, flagellar bending is restricted to the proximal end near the mitochondrion and respiration rate is reduced to one third [22]. In the presence of W-7 in ASW, sea urchin sperm exhibited a similar restricted bending at the proximal region of the flagellum before the final arrest, although oxygen consumption was much reduced to 3.3% of the control. The result suggests the possibility that calmodulin participates in energy supply throughout the flagellum. Measurement of ATP and creatine phosphate content in sperm exposed and not exposed to W-7 revealed no significant differences between these two groups [23]. Furthermore, estimation of stiffness of the flagellum immobilized by W-7 according to the method of Okuno and Hiramoto [24] indicated that they are in a relaxed state [23]. Since lack of ATP results in a rigor state of the flagellum [25], the above result would mean that there remained the sufficient amount of ATP in the immotile flagellum.

ACKNOWLEDGMENTS

The authors wish to thank Dr. T. Kobayashi for teaching us measurements of membrane potential using fluorescent probe and for supplying the reagent and Ms. N. Niitsu-Hosoya for her help in measuring oxygen consumption. We also thank Drs. I. Nishida and M. Miyao for their helpful discussion.

This work was supported in part by Grants-in-Aid from the Ministry of Education, Science and Culture, Japan (Nos. 58340041 and 59480020) to H. M.

REFERENCES

1 Epel, D. (1978) Mechanism of activation of sperm and egg during fertilization of sea urchin gametes. In "Current Topics in Developmental Biology". Vol. 12. Ed. by A. A. Moscona and A. Monroy, Academic Press, Inc., New York, pp. 185–246.
2 Summers, R. G., Talbot, P., Keough, E. M., Hylander, B. L. and Franklin, L. E.(1976) Ionophore A23187 induces acrosome reactions in sea urchin and guinea pig spermatozoa (1). J. Exp. Zool., **196**: 381–385.
3 Okuno, M. and Brokaw, C. J. (1981) Effects of Triton-extraction conditions on beat symmetry of sea urchin sperm flagella. Cell Motility, **1**: 363–370.
4 Morisawa, M. and Okuno, M. (1982) Cyclic AMP induces maturation of trout sperm axoneme to initiate motility. Nature (London), **295**: 703–704.
5 Ishiguro, K., Murofushi, H. and Sakai, H. (1982) Evidence that cAMP-dependent protein kinase and a protein factor are involved in reactivation of Triton X-100 models of sea urchin and starfish spermatozoa. J. Cell Biol., **92**: 777–782.
6 Tash, J. S. and Means, A. .R. (1982) Regulation of protein phosphorylation and motility of sperm by cyclic adenosine monophosphate and calcium. Biol. Reprod., **26**: 745–763.
7 Tash, J. S. and Means, A. R. (1983) Cyclic adenosine 3′,5′ monophosphate, calcium and protein phosphorylation in flagellar motility. Biol. Reprod., **28**: 75–104.
8 Jones, H. P., Bradford, M. M., McRorie, R. A. and Cormier, M. J. (1978) High levels of a calcium-dependent modulator protein in spermatozoa and its similarity to brain modulator protein. Biochem. Biophys. Res. Commun., **82**: 1264–1272.
9 Sano, K. (1983) Inhibition of the acrosome reaction of sea urchin spermatozoa by a calmodulin antagonist, N-(6-aminohexyl)-5-chloro-1-naphthalene-sulfonamide (W-7). J. Exp. Zool., **226**: 471–473.
10 Sano, K. (1982) Ca requirement and effect of calmodulin inhibitor W-7 on sea urchin fertilization. Dev. Growth Differ., **24**: 406 (Abstract).
11 Oono, S. and Hidaka, H. (1981) Calmodulin sogaizai—Saibounai bunpu. In "Calmodulin". Ed. by H. Hidaka and S. Kakiuchi, Kodansha, Tokyo, pp. 137–139 (in Japanese).
12 Hidaka, H., Yamaki, T., Naka, M., Tanaka, T., Hayashi, H. and Kobayashi, R. (1980) Calcium-regulated modulator protein interacting agents inhibit smooth muscle calcium-stimulated protein kinase and ATPase. Mol. Pharmacol., **17**: 66–72.
13 Teo, T., Wang, T. H. and Wang, J. H. (1973) Purification and properties of the protein activator of bovine heart adenosine 3′, 5′-monophosphate phosphodiesterase. J. Biol. Chem., **248**: 588–595.
14 Hoffman, J. F.and Laris, P. C. (1974) Determination of membrane potentials in human and *Amphiuma* red blood cells by means of fluorescent probe. J. Physiol., **239**: 519–552.
15 Sims, P. J., Waggoner, A. S., Wang, C.-H. and Hoffman, J. F. (1974) Studies on the mechanism by which cyanine dyes measure membrane potential in red blood cells and phosphatidylcholine vesicles. Biochem., **13**: 3315–3330.
16 Tsien, R. Y. (1981) A non-disruptive technique for loading calcium buffers and indicators into cells. Nature (London), **290**: 527–528.
17 Gibbons, B. H. and Gibbons, I. R. (1980) Calcium-induced quiescence in reactivated sea urchin sperm. J. Cell Biol., **84**: 13–27.
18 Bibring, T., Baxandall, J. and Harter, C. C. (1984) Sodium-dependent pH regulation in active sea urchin sperm. Dev. Biol., **101**: 425–435.
19 Mohri, H. (1956) Studies on the respiration of sea-urchin spermatozoa I. The effect of 2,4-dinitrophenol and sodium azide. J. Exp. Biol., **33**: 73–81.
20 Kobayashi, T., Iwasa, F. and Mohri, H. (1981) Membrane potential change during acrosome reaction of sea urchin sperm. Zool. Mag., **90**: 416 (Abstract).
21 Ishijima, S. and Mohri, H. (1985) A quantitative description of flagellar movement in golden hamster spermatozoa. J. Exp. Biol., **114**: 463–475.
22 Thmbes, R. M. and Shapiro, B. M. (1985) Metabolite channeling: A phoshorylcreatine shuttle to mediate high energy phosphate transport between sperm mitochondrion and tail. Cell., **41**: 325–334.
23 Iwasa, F. (1985) Studies on functions of calmodulin in echinoderm eggs and sperm. D. Sc. Thesis, The University of Tokyo.
24 Okuno, M. and Hiramoto, Y. (1979) Direct measurements of the stiffness of echinoderm sperm flagella. J. Exp. Biol., **79**: 235–243.
25 Gibbons, B. H. and Gibbons, I. R. (1974) Properties of flagellar "rigor waves" formed by abrupt removal of adenosine triphosphate from actively swimming sea urchin sperm. J. Cell Biol., **63**: 970–985.

ZOOLOGICAL SCIENCE 4: 73–80 (1987)

Isolation of a *Paramecium tetraurelia* Mutant with Short Clonal Life-span and with Novel Life-cycle Features

Yoshiomi Takagi, Takako Suzuki and Chiaki Shimada

Department of Biology, Nara Women's University, Nara 630, Japan

ABSTRACT—We have isolated a mutant of *Paramecium tetraurelia* with a short clonal life-span, about one tenth that of the wild type stock. The short clonal life-span was coupled with senescent characteristics such as a low fission rate, a tendency to undergo autogamy even with excess food, and an intraclonal heterogeneity of division potential. However, the short clonal life-span of the mutant was coupled also with presenescent characteristics such as a high rate of food vacuole formation and excretion, high viability after autogamy, and the presence of autogamy-immaturity stage. It was normal also in its abilities to swim backward, to discharge trichocysts, and to divide the macronucleus properly. This mutant is, therefore, not a consistent senescence mutant but a mutant with conflicting life-cycle features in which presenescent and senescent characteristics are mingled. We can now expect to isolate additional mutants with altered life-cycle features, which will make it possible to use this protozoan species to study the genetic control of aging and life-span.

INTRODUCTION

Paramecium cells age and die as normal diploid cells from multicellular organisms such as humans, chickens and hamsters cultured *in vitro* age and die [1–5]. The maximum limit of the division potential is, in either case, species-specific and predictable; for example, it is about 250 fissions for *P. tetraurelia* [6] and about 600–700 fissions for *P. caudatum* [7–9] when conjugation or autogamy marks time zero. It is very likely, therefore, that the process of limiting the cellular or clonal life-span is somehow programmed, not being completely subject to stochastic events. One of the most useful ways to understand the programmed events of the complicated process may be the isolation of mutants involved in the events and the dissection of the process by breeding analysis. Although mutants with altered life-spans have been reported in several organisms [10–15], the advantage of the genetic analysis has not been fully exploited. In fruit flies or nematodes, which are suitable for genetic crosses, the organismic life-span, not the cellular life-span, can be the target of the analysis because of the postmitotic nature of their aging cells. In humans or chickens where cellular aging is evident, genetic crosses are impossible or difficult. In mice or rats where genetic crosses are easier, cells readily transform to immortal cell lines when transferred to *in vitro* culture so that cellular aging becomes elusive [16, 17]. In some fungi, which include mutants that have various division potentials or those that "senesce" [18], the life is basically immortal and thus appears to be irrelevant to cellular aging.

Paramecium has been a candidate for genetic analysis of aging and life-span [19], as *Paramecium* and related ciliates have been used for genetic analysis of clonal development [20–25]. But no mutants with short life-spans had been known, until some previously established mutants were found recently to be associated with short life-spans [26]. We wish to report here a newly isolated mutant that was screened for short life-span after chemical mutagenesis. The association revealed by Aufderheide and Schneller [26] was not seen in this mutant. This mutant expressed young and old characteristics simultaneously. In *P. tetraurelia,* the nuclear and cytoplasmic genetic background can be kept invariable through autogamies and the cells showing short life-span can be used for

Accepted August 9, 1986
Received July 7, 1986

genetic crosses. Thus, finding a short life-span mutant may open the way for genetic studies of aging and life-span.

MATERIALS AND METHODS

Cells

Wild-type stock 51 of *Paramecium tetraurelia* was used for mutagenesis and as a control culture. KL–DD6, a trichocyst non-discharging mutant carrying *nd242* gene [27], was provided by Dr. D. Nyberg of University of Illinois and used as another control culture.

Culture conditions

Culture medium was prepared after Sonneborn [28] with a modification of Cerophyl concentration; 10 g/l instead of 2.5 g/l was used. *Klebsiella pneumoniae* was inoculated 1–2 days before use.

Cultures were maintained in serial isolation lines with a single cell transfer daily or on alternate days. Ages of lines were given in $\log_2 n$ where n is the number of fission products. Plastic hemagglutination plates with 80 holes (Tomy Seiko, T–2) were used as culture vessels. The plates were sterilized before use by exposure to UV-light and covered with Saran wrap [29].

Cultures were kept at about 25°C unless otherwise specified.

Mutagenesis and screening

Cells in a logarithmic growth-phase were treated with 80 μg/ml N-methyl-N′-nitro-N-nitrosoguanidine for 1 hr. Then they were washed three times with fresh culture medium and suspended in small drops each including about 50 cells. The size of the culture drops was controlled to allow the cells to undergo one cell division. The additional cell division would be necessary to induce autogamy [30] but further divisions were avoided to minimize producing cells with the same genotype. After ascertaining autogamy in more than 95% of the sampled cells from each drop, the remaining cells were isolated into the holes of culture plates containing 0.5 ml culture medium. They were cultivated in isolation lines (primary lines) at 27–30°C, while the plate with the surplus cultures remaining after the first isolation was stored at 10–20°C. When some primary lines died before 50 fissions, secondary lines were reinitiated from the corresponding surplus cultures. Since the clonal life-span is coupled with the number of fissions rather than days [31], they should have remained younger. Therefore, we screened the secondary lines to determine if they might die again before 50 fissions.

RESULTS

Isolation of a mutant with short clonal life-span

Among 80 mutagenized lines, 69 died before the age of 50 fissions. Among the 69 early death lines, 23 remained alive in the corresponding surplus cultures in the stored plate. Among 23 secondary lines reinitiated, four lines died again before the age of 50 fissions. One of the four lines, however, named d4–SL4, escaped clonal extinction by means of autogamy. Figure 1 shows the survival curve of a d4–SL4 clone in contrast with that of a wild type stock 51 clone. For each clone, 20 lines were initiated from 20 cells of 100% autogamy cultures and cultivated in serial isolations without replacements. The average clonal life-span of the 20 d4–SL4 lines was 4 fissions and the maximum was 12 fissions; the stock 51 average was 150 fissions and the maximum 210 fissions. The extremely short clonal life-span of d4–SL4 was inherited through four succeeding autogamies (Fig. 2). Profiles of the survival curve were similar for the autogamous progeny of four generations, with life-spans of the fourth autogamous progeny being most variable ranging from 0 to 19. Besides these data, we have repeatedly ascertained the short clonal life-span of d4–SL4. Occasionally, however, some lines managed to live more than 50 fissions. From such lines, we initiated new isolation lines from a 100%-autogamy culture and maintained them with a complete check of autogamy: all but one of the daily fission products were sacrificed to examine if they had fragmented macronuclei. The maximal life-span of d4–SL4 so far examined in isolation cultures was 22 fissions, if the lines showing evidence of autogamy were excluded. Thus, d4–SL4 terminates its clonal

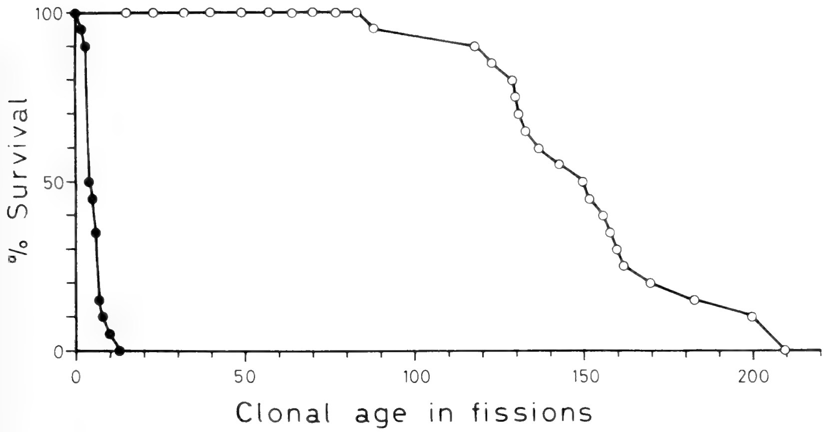

FIG. 1. Survival curves of mutantstock d4–SL4 (closed circles) and wild-type stock 51 (open circles). Clones were cultivated at 25±2°C in 20 isolation lines without replacements.

life-span either in early death or in autogamy.

In spite of the short life, the progeny viability of d4–SL4 was very high as shown in Figure 2, where most of the progeny showed an initial survival of 100%.

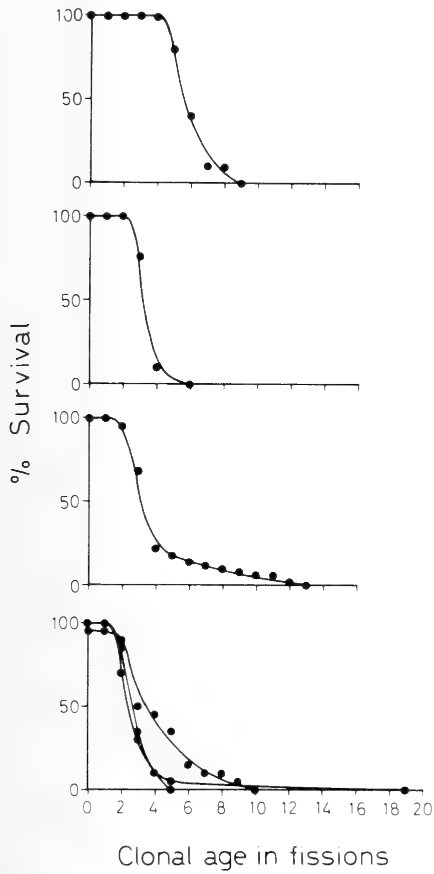

FIG. 2. Survival curves of four succeeding autogamous progeny of d4–SL4 from top to bottom. The number of isolation lines was 10, 30, 50, and 20 for each of four autogamous progenies, respectively. The fourth progeny were studied in 3 different exautogamous cultures with 20 isolation lines each.

Accompanying characteristics of d4–SL4

d4–SL4 is a slow divider. This is obvious in isolation cultures where fission rates were scored daily or on alternate days. In case of two clones in Figure 1, for example, the mean daily fission rate of stock 51 and d4–SL4 was 3.7 and 0.7, respectively during the first three days after autogamy, and 3.9 and 0.4, respectively during the next three day-interval.

d4–SL4 is prone to undergo autogamy. In isolation lines of wild-type stocks, autogamy is seldom seen in logarithmically growing surplus cultures, until they reach their final life-spans [32, Takagi and Nobuoka, unpublished]. In isolation lines of d4–SL4, however, cells with fragmented macronuclei indicative of autogamy were often detected in well-fed surplus cultures.

d4–SL4 is heterogeneous in division potential. All of the cells from a young wild-type culture are able to divide (homogeneous division potential) to produce the same number of cells not deviating

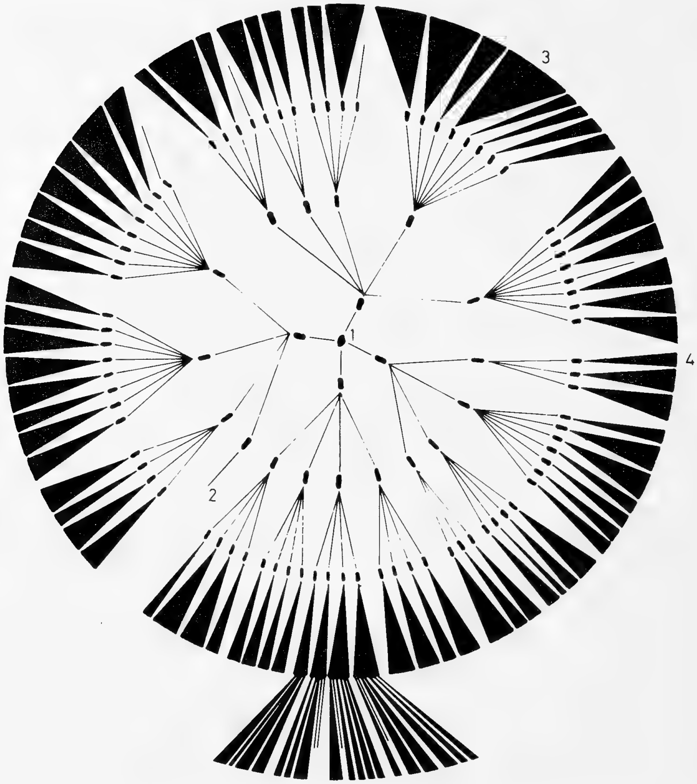

FIG. 3. Intraclonal heterogeneity of division potential in d4–SL4. A single cell of 3 fissions old (1) was allowed to divide for 12 days, during which all of the fission products were isolated every 3 days to follow the cell fate. Part of the 12th day-products were further isolated and allowed to divide for 3 more days. The number of cells produced on the 12th and 15th day was indicated in the relative length of the arch. For 12 days or during 4 isolations, there occurred heterogenous cell lineages; died (2), grew fastest (3), grew slowest (4), for example.

from 2^n where n is the number of cell divisions less than 4 (synchronous division) [7]. d4–SL4 cells often produced division products deviating from 2^n, including $n=0$ as exemplified in Figure 3. Starting with a single cell of three fissions old (1 in Fig. 3), we isolated all of the division products produced for three days; we repeated this procedure three times or, as for some products, four times. During four isolations or 12 days, the fastest- (3 in Fig. 3) and slowest-grown line (4 in Fig. 3) underwent 11.7 and 7.6 fissions, respectively. Some lines died during this interval (2 in Fig. 3, for example). Even in some 12th day products that had experienced relatively uniform divisions, intraclonal heterogeneity of division potential became evident on the 5th isolation or on the 15th day.

Characteristics sharing with wild-type stock

d4–SL4 is morphologically normal at a dissecting microscopic level.

d4–SL4 is normal in its capacity to discharge trichocysts. This was ascertained by dropping a saturated solution of picric acid on mutant cells. They discharged trichocysts regardless of the cell-cycle and life-cycle stages.

d4–SL4 is normal in its capacity to swim backward. This was ascertained by introducing mutant

cells into Ba^{2+} test-solution [33].

d4–SL4 can distribute the macronucleus properly to the daughter cells. Dividers were taken from log-phase cultures, stained with Dippell's solution [34], and examined under a compound microscope. The number of cells with improperly dividing macronuclei were two among 53 dividers in d4–SL4, and one among 55 dividers in stock 51. This difference can be regarded negligible from the standard of macronuclear misdividers [26].

d4–SL4 has a normal rate of food-vacuole formation. This was ascertained by counting black food vacuoles after 0.06% (final concentration) Rotring ink was introduced to log-phase cultures. The average rate of food-vacuole formation in six experiments was compared among three stocks, i.e., d4–SL4 of unidentified clonal ages, stock 51 of the clonal ages younger than 50 fissions, and KL–DD6 younger than 15 fissions (Fig. 4). There were no statistical differences among three stocks at any time (t-test, $p<0.01$).

d4–SL4 has a normal rate of food-vacuole excretion. This was ascertained by counting black food-vacuoles after the log-phase culture was first colored and then washed three hours later. Figure 5 shows the results of six experiments. The difference among three stocks at any time was insignificant (t-test, $p<0.05$).

d4–SL4 has an autogamy immaturity period. The autogamy immaturity period during which autogamy cannot be induced is the first stage of the clonal life-cycle following autogamy [1, 35]. In order to test a hypothesis that d4–SL4 may be a permanent senescence mutant truncating the early part of the life-cycle stages, cells of known ages were induced to undergo autogamy. In wild-type stock 51, no autogamy could be induced before 14 fissions, and 100% autogamy was possible after 21 fissions. In d4–SL4, we were able to induce autogamy in cells at the age of 7 fissions or more but failed in cells at the ages of 5 and 6 fissions.

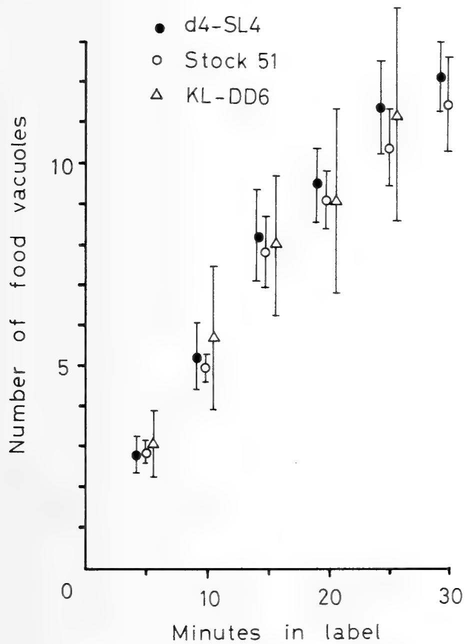

FIG. 4. Rate of the food-vacuole formation into 3 stocks. Cells were introduced in 0.06% Rotring ink and the number of black food vacuoles were scored every 5 min. Mean±SD of 6 experiments are shown.

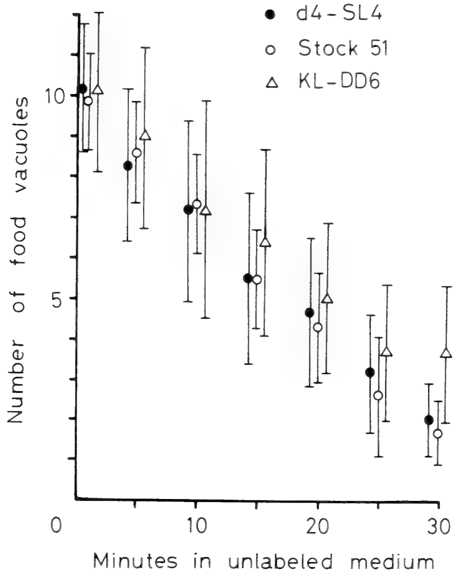

FIG. 5. Rate of the food-vacuole excretion in 3 stocks. Cells were preincubated in culture medium containing 0.06% Rotring ink for 3 hr to stain the food vacuoles black. After cells were washed three times by mild centrifugation, the number of food vacuoles was scored every 5 min. Mean±SD of 6 experiments are shown.

DISCUSSION

This is the first report on a mutant with a short clonal life-span that was isolated following mutagenesis. Clones with extremely short life-spans are known to occur commonly after conjugation or autogamy especially of aged cells; but they are all lethal and never established as a short life-span stock [35]. Short life-spans could result from any defective mutations in macronuclear genes which are essential to the clonal life of *Paramecium*. Since the macronucleus develops from mitotic products of the fertilization nucleus during autogamy and since all of the genetic loci become homozygous after autogamy [35], any defective changes even of the recessive type in the micronucleus would be expressed in the macronucleus after autogamy. The consequence should be a production of lethal clones with extremely short clonal life-spans. The present stock d4–SL4 was able to repeat the short clonal life-cycles starting with the autogamy-immaturity stage and with somewhat restored fission rates. Therefore, we can exclude the possibility that mutations in d4–SL4 are in the loci controlling key metabolic processes. This study shows that the clonal life-span can be extremely shortened keeping normal the micronuclear function to produce fertile progeny and also keeping normal the macronuclear functions to take food, excrete, swim, and respond to stimuli.

Many parameters characterize the senescent stage of the clonal life-cycle of *Paramecium* [4]. Although they do not necessarily come to an expression at the same time in all of the members of the clone, their expressions are more or less coordinated [36]. Low fission rate [1], low progeny viability after autogamy [29], intraclonal heterogeneity of division potential [7], a proneness to undergo autogamy in excess food [32], and the reduced rates of the food vacuole formation and excretion [32] are all characteristics of the senescent stage. Truly senescent cells expressing some of these characteristics would be expected to express also the others. But this was not true of d4–SL4. d4–SL4 might be considered young in the high progeny viability after autogamy and in the high rate of the food vacuole formation and excretion, while it might be considered old in its low fission rate, in its intraclonal heterogeneity of division potential, and in its autogamy-prone nature in excess food. d4–SL4 might be considered senescing early in that it has a short interval of autogamy immaturity and in that its low fission rate declines further in six days after autogamy. d4–SL4 is, therefore, not a uniformly senescent mutant but a mutant with conflicting life-cycle features in which presenescent and senescent characteristics are mingled.

Recently, Aufderheide and Schneller [26] found several stocks with short clonal life-spans among previously isolated *nd* (trichocysts non-discharging) mutants of *P. tetraurelia*. They further demonstrated that the short clonal life-spans were not associated with the inability to discharge trichocysts but rather were associated with the inability to divide the macronucleus properly. Unequal distribution of the macronucleus to the daughter cells is a senescent characteristic [36]. Perpetual unequal distribution could be a sufficient condition for the short clonal life-span, as discussed by Aufderheide and Schneller [26]; but it cannot be a necessary condition because no association between them was found in d4–SL4. Similarly, the factor that is responsible for the low fission rate could be responsible for the short clonal life-span in d4–SL4, although their association might not be found in other mutants. By isolating various life-cycle mutants, we may understand if two factors are dissectible and what is a necessary and sufficient condition for the short life-span. If we could find a short life-span mutant without any accompanying senescent characteristics, we might identify the genetic locus that controls the clonal life-span directly.

Breeding analysis on d4–SL4 is under investigation. The low fission rate is used as a tentative marker of the short life-span, because the determination of the life-span difference is a laborious work and because the short life-span of d4–SL4 is often perturbed by autogamy. Preliminary results suggest that the short life-span of d4–SL4 is inherited through the nucleus, not the cytoplasm: No segregation of the marker phenotype was found in F_1 progeny after conjugation between d4–SL4 and a wild-type stock, and segregation was

found in F_2 progeny after autogamy, with a marker gene indicating normal conjugation and autogamy. Although it is still a long way off to determine if the short life-span is dissectible from the low fission rate and how many genes are involved, we can now expect to isolate other mutants with altered life-cycle features and to perform the breeding analysis with a hope that we will have significant insights on how life-span is limited.

ACKNOWLEDGMENTS

This work was supported in part by a grant from the Itoh Science Foundation. We are grateful to Dr. P. Abhayavardhani for improving the manuscript.

REFERENCES

1 Sonneborn, T. M. (1954) The relation of autogamy to senescence and rejuvenescence in *Paramecium aurelia*. J. Protozool., **1**: 38–53.

2 Hayflick, L. and Moorhead, P. S. (1961) The serial cultivation of human diploid cell strains. Exp. Cell Res., **25**: 585–621.

3 Hayflick, L. (1977) The cellular basis for biological aging. In "Handbook of the Biology of Aging". Ed. by C. E. Finch and L. Hayflick, Van Nostrand Reinhold, New York, pp. 159–186.

4 Smith-Sonneborn, J. (1981) Genetics and aging in Protozoa. Int. Rev. Cytol., **73**: 319–354.

5 Raes, M. and Remacle, J. (1983) Ageing of hamster embryo fibroblasts as the result of both differentiation and stochastic mechanisms. Exp. Gerontol., **18**: 223–240.

6 Smith-Sonneborn, J. (1985) Aging in unicellular organisms. In "Handbook of the Biology of Aging", 2nd ed. Ed. by C.E.Finch and E.L.Schneider, Van Nostrand Reinhold, New York, pp.79–104.

7 Takagi, Y. and Yoshida, M. (1980) Clonal death associated with the number of fissions in *Paramecium caudatum*. J. Cell Sci., **41**: 177–191.

8 Karino, S. and Hiwatashi, K. (1981) Analysis of germinal aging in *Paramecium caudatum* by micronuclear transplantation. Exp. Cell Res., **136**: 407–415.

9 Karino, S. and Hiwatashi, K. (1984) Resistance of germinal nucleus to aging in *Paramecium*: Evidence obtained by micronuclear transplantation. Mech. Ageing Dev., **26**: 51–66.

10 Smith, J. R. (1978) Genetics of aging in lower organisms. In "The Genetics of Aging". Ed. by E. L. Schneider, Plenum, New York, pp.137–149.

11 Takeda, T., Hosokawa, M., Takeshita, S., Irino, M., Higuchi, K., Matsushita, T., Tomita, Y., Yasuhira, K., Hamamoto, H., Shimizu, K., Ishii, M. and Yamamuro, T. (1981) A new murine model of accelerated senescence. Mech. Ageing Dev., **17**: 183–194.

12 Dick, J. E. and Wright, J. A. (1984) Human diploid fibroblasts with alteration in ribonucleotide reductase activity, deoxyribonucleotide pools and in vitro lifespan. Mech. Ageing Dev., **26**: 37–49.

13 Brown, W. T. (1985) Genetics of human aging. Rev. Biol. Res. Aging, **2**: 105–114.

14 Johnson, T. E. (1985) Aging in *Caenorhabditis elegans*: Update 1984. Rev. Biol. Res. Aging, **2**: 45–60.

15 Lints, F. A. and Bourgois, M. (1985) Aging and lifespan in insects with special regard to *Drosophila*: Review 1982–1984. Rev. Biol. Res. Aging, **2**: 61–84.

16 Todaro, G. J. and Green, H. (1963) Quantitative studies of the growth of mouse embryo cells in culture and their development into established lines. J. Cell Biol., **17**: 299–313.

17 Meek, R. L., Bowman, P. D. and Daniel, C. W. (1980) Establishment of rat embryonic cells in vitro. Relationship of DNA synthesis, senescence, and acquisition of unlimited growth potential. Exp. Cell Res., **127**: 127–132.

18 Bertrand, H., Chan, B. S- S. and Griffiths, A. J. F. (1985) Insertion of a foreign nucleotide sequence into mitochondrial DNA causes senescence in *Neurospora intermedia*. Cell, **41**: 877–884.

19 Aufderheide, K. J. (1984) Cellular aging: An overview. In "Cellular Ageing". Ed. by H. W. Sauer, Karger, Basel, pp. 2–8.

20 Siegel, R.W. (1961) Nuclear differentiation and transitional cellular phenotypes in the life cycle of *Paramecium*. Exp. Cell Res., **24**: 6–20.

21 Siegel, R. W. (1967) Genetics of ageing and the life cycle in ciliates. Symp. Soc. Exp. Biol., **21**: 127–148.

22 Bleyman, L. K. and Simon, E. M. (1967) Genetic control of maturity in *Tetrahymena pyriformis*. Genet. Res. Camb., **10**: 319–321.

23 Bleyman, L. K. (1971) Temporal patterns in the ciliated protozoa. In "Developmental Aspects of the Cell Cycle". Ed. by I.L.Cameron, G.M.Padilla and A. M. Zimmer, Academic Press, New York, pp. 67–91.

24 Nanney, D. L. and Meyer, E. B. (1977) Traumatic induction of early maturity in *Tetrahymena*. Genetics, **86**: 103–112.

25 Myohara, K. and Hiwatashi, K. (1978) Mutants of sexual maturity in *Paramecium caudatum* selected by erythromycin resistance. Genetics, **90**: 227–241.

26 Aufderheide, K. J. and Schneller, M. (1985) Phenotypes associated with early clonal death in *Paramecium tetraurelia*. Mech. Ageing Dev., **32**: 299–309.

27 Nyberg, D. (1978) Genetic analysis of trichocyst discharge of the wild stocks of *Paramecium tetraure-*

lia. J. Protozool., **25**: 107–112.

28 Sonneborn, T. M. (1970) Methods in *Paramecium* research. In "Methods of Cell Physiology, Vol.4". Ed. by D. M. Prescott, Academic Press, New York, pp. 241–339.

29 Rodermel, S. R. and Smith-Sonneborn, J. (1977) Age-correlated changes in expression of micronuclear damage and repair in *Paramecium tetraurelia*. Genetics, **87**: 259–274.

30 Mikami, K. and Koizumi, S. (1983) Microsurgical analysis of the clonal age and the cell-cycle stage required for the onset of autogamy in *Paramecium tetraurelia*. Dev. Biol., **100**: 127–132.

31 Smith-Sonneborn, J. and Reed, J. C. (1976) Calendar life-span versus fission life-span of *Paramecium aurelia*. J. Gerontol., **31**: 2–7.

32 Smith-Sonneborn, J. and Rodermel, S. R. (1976) Loss of endocytic capacity in aging *Paramecium*. J. Cell Biol., **71**: 575–588.

33 Chang, S-Y. and Kung, C. (1973) Temperature-sensitive pawns: Conditional behavioral mutants of *Paramecium aurelia*. Science, **180**: 1197–1199.

34 Dippell, R. V. (1955) A temporary stain for *Paramecium* and other ciliate protozoa. Stain Technol., **30**: 69–71.

35 Sonneborn, T. M. (1974) *Paramecium aurelia*. In "Handbook of Genetics, Vol. 2". Ed. by R. C. King, Plenum, New York, pp. 469–594.

36 Takagi, Y. and Kanazawa, N. (1982) Age-associated change in macronuclear DNA content in *Paramecium caudatum*. J. Cell Sci., **54**: 137–147.

ZOOLOGICAL SCIENCE 4: 81–86 (1987)

Banding Karyotype of Korean Salamander: *Hynobius leechii* Boulenger[1]

SEI-ICHI KOHNO[2,6], MASAKI KURO-O[2], CHIKAKO IKEBE[3], REIKO KATAKURA[2], YASUHIRO IZUMISAWA[2], TADAO YAMAMOTO[4,7], HEI YUNG LEE[5] and SUH YUNG YANG[5]

[2]*Department of Biology, Faculty of Science, Toho University, Funabashi, Chiba 274, Japan,* [3]*Department of Biology, Faculty of General Education, Toho University, Funabashi, Chiba 274, Japan,* [4]*Buso High School, Yokohama, Kanagawa 222, Japan and* [5]*Department of Biology, Inha University, Inchon, Korea*

ABSTRACT—The chromosome constitutions of 56 embryos of *Hynobius leechii* from eight localities of Korea were analyzed by Giemsa staining, C-banding and R-banding. Banding patterns of 18 out of 28 chromosome pairs were identified by the analyses. The short arms of No. 10 chromosomes, each forming one negative R-band, showed intra-specific variations in size; The short arms of No. 10 chromosomes of the specimens from three northern localities (Sogumgang, Kangnung and Yangju) were larger than those from four southern localities (Kyeryongsan, Chupungryong, Kyonju and Chindo). The specimens from one locality (Chongson) between the northern and southern localities showed No. 10 chromosomes with large short arms and also those with small ones. The difference in the arm ratio of No. 10 chromosome between the specimens from three northern (large short arm) and four southern localities (small short arm) was statistically significant at <0.01 level. The size of the terminal band of the long arm of No. 2 chromosome in *H. leechii* (positive in C-banding and negative in R-banding) was larger than that in *H. nigrescens*. Except for these 2 bands and other minor intra-specific chromosome aberrations, no difference could be detected between *H. leechii* and *H. nigrescens* in the banding patterns of their 18 chromosome pairs identified.

INTRODUCTION

The genus *Hynobius* which is distributed in several countries of east Asia differentiates into many species, especially in Japan [1] and there are several studies available on karyotaxonomy of Japanese *Hynobius* [2–12]. These studies have reported that the diploid chromosome numbers of this genus are 40 (*H. retardatus*), 56 (*H. nebulosus* and other eight species) and 58 (*H. naevius* and other three). The karyotypes of the latter two (those with 56 and 58 chromosomes) are shown to be almost the same except for one additional small chromosome pairs in the species with 58 chromosomes. The chromosome number of most of the pond type species is 2n=56 [3–7, 9, 10, 14] whereas that of the mountain-brook type is 2n=58 [12].

In order to consider the process of differentiation of the genus *Hynobius*, the karyotype analysis of the Korean pond type salamander, *Hynobius leechii*, seemed to be indispensable to the search for the original karyotype of Japanese *Hynobius*. The chromosomes of *H. leechii* was studied by sectioning and Hematoxylin staining procedure by Makino in 1934, and the chromosome number of this species was reported to be 56 [13]. The Giemsa stained karyotype of this species was given by Chon [14]. However, there has been no report on the banding karyotype of this species.

In this paper, we would like to present the results of the karyotype analyses of this Korean *Hynobius*, *H. leechii*, by the newly improved chromosome banding methods for Urodela (C-

Accepted July 15, 1986
Received May 7, 1986

[1] This paper corresponds to "Cytogenetic studies of Hynobiidae (Urodela).V".
[6] To whom reprints should be requested.
[7] Deceased on November 2, 1985.

banding and R-banding) [8, 11].

MATERIALS AND METHODS

The embryos in egg-capsules of *Hynobius leechii* were collected from eight localities in Korea: Sogumgang, Kangnung, Yangju, Chongson, Kyeryongsan, Chupungryong, Kyongju and Chindo as shown in Figure 1. The detailed information on the number of the specimens collected from the eight localities and of the metaphases analyzed is summarized in Table 1.

The chromosome preparations were made according to the improved method of Ikebe and Kohno [4]; using whole embryos, 24 hr of 0.5% colchicine pretreatment, 30–40 min of hypotonic treatment in 15 times diluted Amphibian Ringer's after breaking embryos to pieces with a Pasteur pipette, fixation by fixative consisting of three parts of methanol and one part of acetic acid and air drying.

The C-banding slides were made according to the method by Sumner [15] with slight modifications.

The R-banding patterns were obtained by the method described by Kuro-o *et al.* [11]. The embryonal cells were cultured with BrdU (400 μg/ml) for 33 hr and the chromosome preparations were made by ordinary air drying method after the colchicine treatment. The slides were stained by FPG (Fluorescent plus Giemsa) staining procedure.

Fig. 1. Eight localities where the *Hynobius leechii* embryos were collected. 1. Sogumgamg, 2. Kangnung, 3. Yangju, 4. Chongson 5. Kyeryongsan, 6. Chupungryong, 7. Kyongju 8. Chindo.

RESULTS

Karyotype analyses were made in a total of 201 metaphases from 56 specimens in 20 egg capsules

Table 1. Numbers of the metaphases analyzed and of the specimens collected from eight localities in Korea

	Collection sites	Date of collection	No. of egg capsules	No. of metaphases / No. of embryos			
				Giemsa	C-banding	R-banding	Total
1	Sogumgang	Apr. '84	2	6/2	—	7/2	13/4
2	Kangnung	Apr. '85	1	5/2	3/2	4/2	12/4
3	Yangju	Mar. '84	3	10/4	15/6	22/9	47/19
4	Chongson	Apr. '85	3	11/3	8/2	6/4	25/7
5	Kyeryongsan	Apr. '85	2	10/3	5/1	7/3	22/6
6	Chupungryong	Mar. '85	3	10/3	5/2	7/4	22/7
7	Kyongju	Mar. '85	3	11/3	18/2	2/1	31/4
8	Chindo	Apr. '85	3	13/3	13/1	3/2	29/5
	Total		20	76/23	67/16	58/27	201/56

collected from eight localities as shown in Table 1: 76 metaphases from eight localities by the conventional Giemsa staining, 67 metaphases from seven localities by C-banding and 58 metaphases from eight localities by R-banding. The analyses of the conventional Giemsa stained karyotypes revealed the polymorphism of No. 10 chromosome (Fig. 2). The karyotypes which showed No. 10 chromosome pair with large short arms were found in the specimens from three out of eight localities, Sogumgang, Kangnung and Yangju. Those having No. 10 chromosome pair with small short arms were found in four localities; Kyeryongsan, Chupungryong, Kyongju and Chindo. The former specimens having No. 10 chromosome pair with large short arms were distributed in the northern part of Korea and the latter were found in the southern part of Korea. In the remaining one locality, Chongson, which was located between the northern and the southern parts, No. 10 chromosomes of both types were observed in the specimens collected. Three pairs of No. 10 chromosomes of the specimens from Yangju (large short arm) and another three pairs from Kyeryongsan

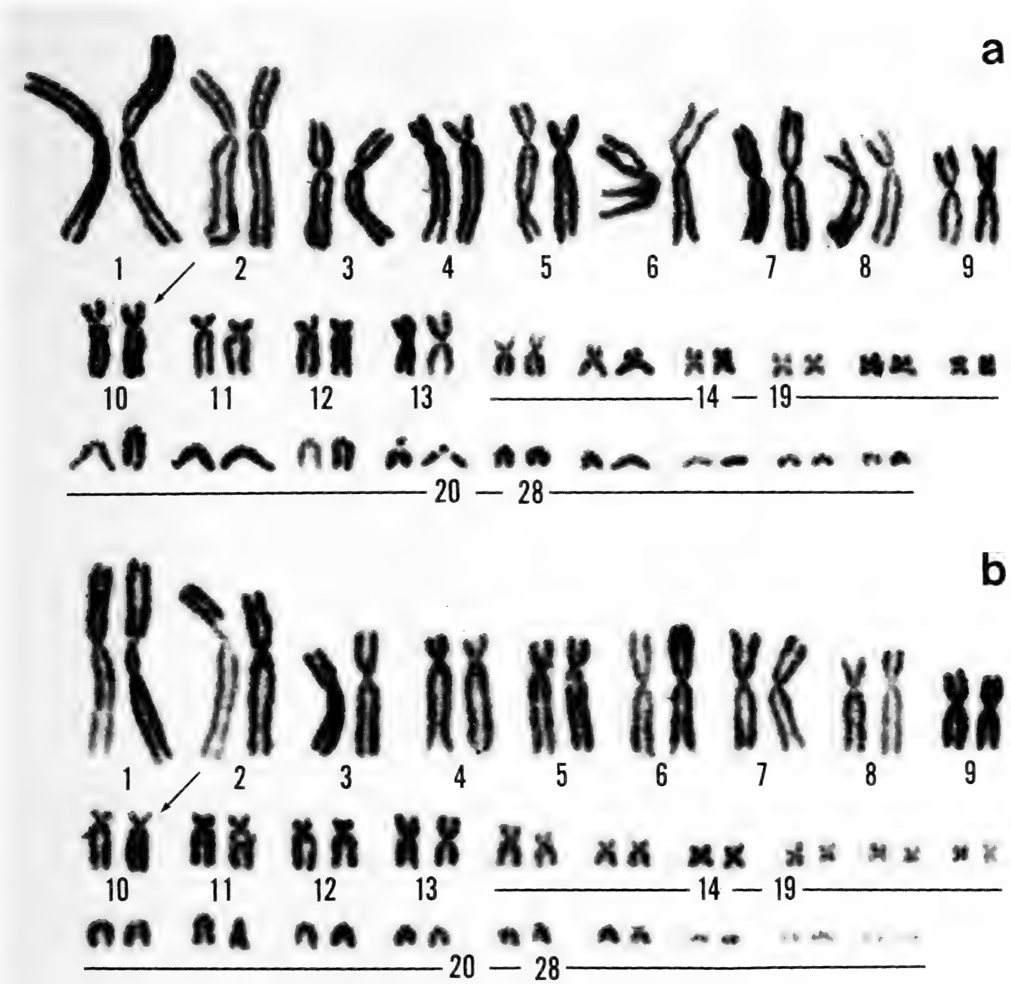

FIG. 2. Two conventional Giemsa staining karyotypes of *Hynobius leechii* collected from two localities (Yangju: a, Chindo: b). The arrows point out No. 10 chromosome pairs which show polymorphism in their short arms.

(small short arm), each pair being stained by the conventional Giemsa, C-banding and R-banding, respectively, were shown in Figure 3. The mean arm ratios of No. 10 chromosomes in the specimens from the eight localities are summarized in Table 2. The measurement of the arm ratios of No. 10 chromosomes, which have morphological similarities to Nos. 11 and 12, was made using R-banded chromosomes chosen at random. It may be necessary to note that the arm ratios of R-banded No. 10 chromosomes are somewhat smaller than those of Giemsa-stained ones because of the enlargement of their short arms due to the extreme uptake of BrdU.

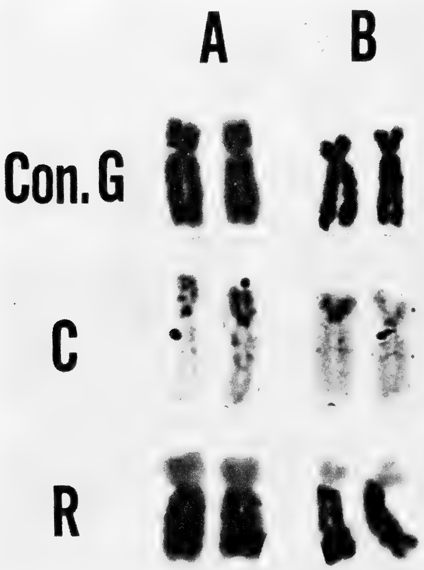

Fig. 3. No. 10 chromosome pairs of *Hynobius leechii* collected from 2 localities (Yangju: A, Kyeryongsan: B). The three pairs each stained by conventional Giemsa, C-banding and R-banding, respectively, are shown.

As shown in Table 2, the difference in the mean arm ratio of No. 10 chromosomes between the specimens from the three northern localities (Sogumgang, Kangnung and Yangju) and those from the four southern localities (Kyeryongsan, Chupungryong, Kyongju and Chindo) was statistically significant according to "t" test ($p<0.01$). The data from Chongson which located between the two groups mentioned above showed the medium value between those from the two areas.

Based on the R-banding and C-banding patterns, 18 out of 28 pairs of the chromosomes of this species could be identified. They were all of the large sized (Nos. 1–9) and medium-sized (Nos. 10–13) and 5 out of 15 small-sized (Nos. 14, 15, 20, 21 and 22) chromosome pairs (Fig. 4). Their banding patterns were identical to those reported on *Hynobius nigrescens* by Kuro-o *et al.* [11] except for the terminal band on the long arm of No. 2 chromosome; the band of *H. leechii* being larger than that of *H. nigrescens.*

In two out of 56 specimens from the eight localities, one numerical and two structural chromosome aberrations were observed: One specimen from Kangnung had 57 chromosomes due to trisomy of No. 13 chromosome. The other from Chindo had two chromosome aberrations,

Table 2. Mean arm ratios (long arm/short arm) of No. 10 chromosomes in *Hynobius leechii* collected from eight localities in Korea

	Collection sites	No. of measured chromosomes	Mean arm ratios ± S.D.	
1	Sogumgang	7	2.00 ± 0.27	
2	Kangnung	6	1.85 ± 0.17	1.95 ± 0.21
3	Yangju	20	1.99 ± 0.22	
4	Chongson	21	2.21 ± 0.28	
5	Kyeryongsan	21	2.44 ± 0.26	
6	Chupungryong	19	2.52 ± 0.20	
7	Kyongju	8	2.46 ± 0.21	2.48 ± 0.22
8	Chindo	25	2.49 ± 0.21	

FIG. 4. R-banding karyotype of *Hynobius leechii* from Yangju, with a C-banded chromosome being placed on the right side of each pair.

namely, a No. 21 chromosome with a large short arm, and a No. 1 chromosome with an atypical C-banding positive band on the long arm close to the centromere. The position of this band corresponded to that of a secondary constriction on the chromosome which was detected by the conventional Giemsa staining (Fig. 2).

DISUSSION

In the Korean Peninsula (the area being about 2/3 of Japan), only one species of the genus *Hynobius, H. leechii,* is found [1], whereas in Japan 14 species of the genus *Hynobius,* differentiated into pond type and mountain-brook type, are found [1, 10, 12]. In our chromosome observation of the specimens in the southern half area of the Korean Peninsula, the banding patterns of *H. leechii* were the same except for one band on the short arm of No. 10 chromosome. This band was positive in C-banding and negative in R-banding (Fig. 3), suggesting that this region (band) contains constitutive heterochromatin and scarcely includes structural genes. The terminal band on the long arm of No. 2 in *H. leechii* was also constitutive heterochromatin (Fig. 4) and was larger than those in *H. nigrescens* and *H. tokyoensis* reported by Kuro-o *et al.* [11] and Kohno *et al.* [8]. The intra- and inter-specific karyotypic variations in *H. leechii* we observed were only in heterochromatic ones, except for three chromosomal aberrations shown in the specimens from two localities.

The sizes of the short arms of the No. 10 chromosomes in the specimens from the southern part of this peninsula are supposed to have been reduced. In Japanese *Hynobius,* the sizes of the short arms of No. 10 chromosomes vary from none (*H. nebulosus*) [4, 7] to the size as large as the smaller ones in *H. leechii* (*H. tokyoensis* and others) [3–5, 7, 8, 10–12, 16]. The problem of

differentiation and karyotype evolution of this genus is going to be discussed elsewhere in connection with the morphological variations of the short arms of No. 10 chromosomes (Ikebe *et al.*, unpublished data).

As to the embryo from Kangnung, showing aneuploid karyotype (2n=57), it is not possible to state whether the embryo would have grown to be a normal adult or not, even though it did not show external morphological anomalies at the time of the observation. In our experience in karyotype analyses of *Hynobius* embryos, some hyperdiploid and hypodiploid embryos could be observed in other species, for example, in *H. tsuensis* (Ikebe *et al.*, unpublished data).

In order to study the presence of the aneuploidy in *H. leechii,* the screening of the karyotypes of adult populations should be carried out.

ACKNOWLEDGMENTS

The authors are grateful to Dr. T. Ishihara, National Institute of Radiological Sciences, Chiba, for his correcting and improving the manuscript. The authors are also grateful to Mr. Park, C. S. and Miss Lee, H. S. in Inha University for their assistance in collecting our materials.

This study was supported by a Grant-in-Aid for Scientific Research from the Ministry of Education, Science and Culture of Japan (No. 58540484).

REFERENCES

1 Sato, I. (1943) A Monograph on the Japanese Urodeles. Nippon Shuppan-sha Osaka, pp. 21–24, 27–40, 438–440. (In Japanese)

2 Makino, S. (1956) A review of the chromosome numbers in animals, Hokuryukan, Tokyo, pp. 143–144. (In Japanese)

3 Azumi, J. and Sasaki, M. (1971) Karyotypes of *Hynobius retardatus* Dunn and *Hynobius nigrescens* Stejneger. Chromosome Information Service, **12**: 31–32.

4 Ikebe, C. and Kohno, S. (1979) Cytogenetic studies of Hynobiidae (Urodela). I. Karyotypes of *Hynobius nebulosus nebulosus* (Schlegel) and *Hynobius nebulosus tokyoensis* Tago. Proc. Jpn. Acad., **55** B(9): 436–440.

5 Ikebe, C. and Kohno, S. (1979) Karyotypes of *Hynobius nigrescens* Stejneger and *Hynobius lichenatus* Boulenger. Chromosome Information Service, **27**: 13–15.

6 Morescalchi, A., Odierna, G. and Olmo, E. (1979) Karyology of the primitive salamanders, family Hynobiidae. Experientia, **35**:1434–1435.

7 Seto, T., Utsunomiya, Y. and Utsunomiya, T. (1983) Karyotypes of two representative species of Hynobiid salamanders, *Hynobius nebulosus* (Schlegel) and *Hynobius naevius* (Schlegel). Proc. Jpn. Acad., **59** B(7): 231–235.

8 Kohno, S., Ohhashi, T. and Ikebe, C. (1983) Cytogenetic studies of Hynobiidae (Urodela). II. Banding karyotype of *Hynobius tokyoensis* Tago. Proc. Jpn. Acad., **59** B(8): 271–275.

9 Seto, T. and Matsui, M. (1984) Karyotype of the Japanese salamander, *Hynobius abei.* Experientia, **40**:874.

10 Matsui, M., Seto, T. and Miyazaki, K. (1985) The karyotype of *Hynobius takedai* M. Matsui et Miyazaki, 1984, with comments on the karyotypic relationships among Japanese salamanders of the genus *Hynobius*. Jpn. J. Genet., **60**: 119–123.

11 Kuro-o, M., Ikebe, C. and Kohno, S. (1986) Cytogenetic studies of Hynobiidae (Urodela). IV. DNA replication bands (R-banding) for the genus *Hynobius* and the banding karyotype of *Hynobius nigrescens* Stejneger. Cytogenet. Cell Genet., (In press)

12 Ikebe, C., Yamamoto, T. and Kohno, S. (1986) Karyotypes of Japanese Hynobiid salamanders, *Hynobius kimurae* Dunn and *Hynobius boulengeri* (Thompson). Zool. Sci., **3**: 109–113.

13 Makino, S. (1934) The chromosomes of *Hynobius leechii* and *H. nebulosus*. Trans. Sapporo Nat. Hist. Soc., **13**: 351–354.

14 Chon, S. K. (1982) Studies on the karyotypes of the Korean Amphibians. Thesis of Master of Science, Inha University, Korea (In Korean with English Abstract). pp. 1–27.

15 Sumner, A. T. (1972) A simple technique for demonstrating centromeric heterochromatin. Exp. Cell Res., **75**: 304–306.

16 Ikebe, C., Kuro-o, M., Katakura, R., Kusada, S. and Kohno, S. (1984) Morphological variation of No. 10 chromosome in 9 pond type *Hynobius* from Korea and Japan. Zool. Sci., **1**: 899.

ZOOLOGICAL SCIENCE 4: 87–92 (1987)

Karyological Differentiation between Two Species of Mustelids, *Mustela erminea nippon* and *Meles meles anakuma*

Yoshitaka Obara

Department of Biology, Faculty of Science, Hirosaki University, Hirosaki 036, Japan

ABSTRACT—The karyotypes of the Japanese badger, *Meles meles anakuma,* were presented using conventional and differential staining. Its diploid number was 44, in accordance with Tsuchiya's observation. The sex determining system was XX for the female and XY for the male. Two of the five specimens studied herein carried a heteromorphic autosomal pair (B6) which was considered to have been produced by a deletion of a G-positive block.

The banded chromosomes of the badger were compared with those of the Japanese ermine, *Mustela erminea nippon,* with the aim of defining karyological differentiation between these two remotely related mustelids which belong to different subfamilies, Melinae or Mustelinae, respectively. A low grade of G-band homology was found between them, in agreement with a marked dissimilarity in their chromosome constitution. Over one-third of the total chromosome length hardly showed any G-band homology between the species.

The phylogenetic relationships of the Japanese mustelids were briefly discussed, introducing karyosystematic evaluation into the former taxonomic system.

INTRODUCTION

The karyotypes of the ermine, *Mustela erminea,* have been studied by several workers with the use of both conventional [1–3] and differential [4–6] staining. The Japanese ermine, *M. erminea nippon,* is almost identical with the continental taxa in the G- and C-banding patterns as well as in the diploid number and chromosome constitution [7–9].

On the other hand, the chromosomes of the Eurasian badger, *Meles meles,* have been studied only by conventional staining [1, 10–13]. Up to the present, no attempt has been made to compare the badger karyotypes with those of other mustelid species, even in conventionally stained materials. As to the Japanese taxon, *M. meles anakuma,* neither conventional nor banded karyotypes have been presented as yet, though its diploid number has been determined to be 44 by Tsuchiya [14].

In this paper the chromosomes of the Japanese mustelids, *Mustela erminea nippon* and *Meles meles anakuma,* were compared, making use of G- and C-banding methods, to estimate the intergeneric conservatism and/or variation of G- and C-banding patterns.

MATERIALS AND METHODS

Four adult specimens (one female and three males) of the Japanese badger, *Meles meles anakuma,* were captured alive near Mt. Nishimata, south of Hirosaki, Aomori Prefecture. The female specimen was pregnant when caught, and one male was retained from the pregnant specimen as chromosome material. Chromosome preparations were obtained from either bone marrow cells of the adult specimens or liver cells of the fetus. The two adult specimens of the Japanese ermine, *Mustela erminea nippon,* studied here are the same as those used in previous works [8–9]. The sampling procedure is almost the same as those previously reported [7, 15]. For G- and C-banding the ASG [16] and BSG [17] methods were adopted.

Two hundred and fifty two badger metaphases and 337 ermine ones were examined under the

Accepted August 26, 1986
Received July 4, 1986

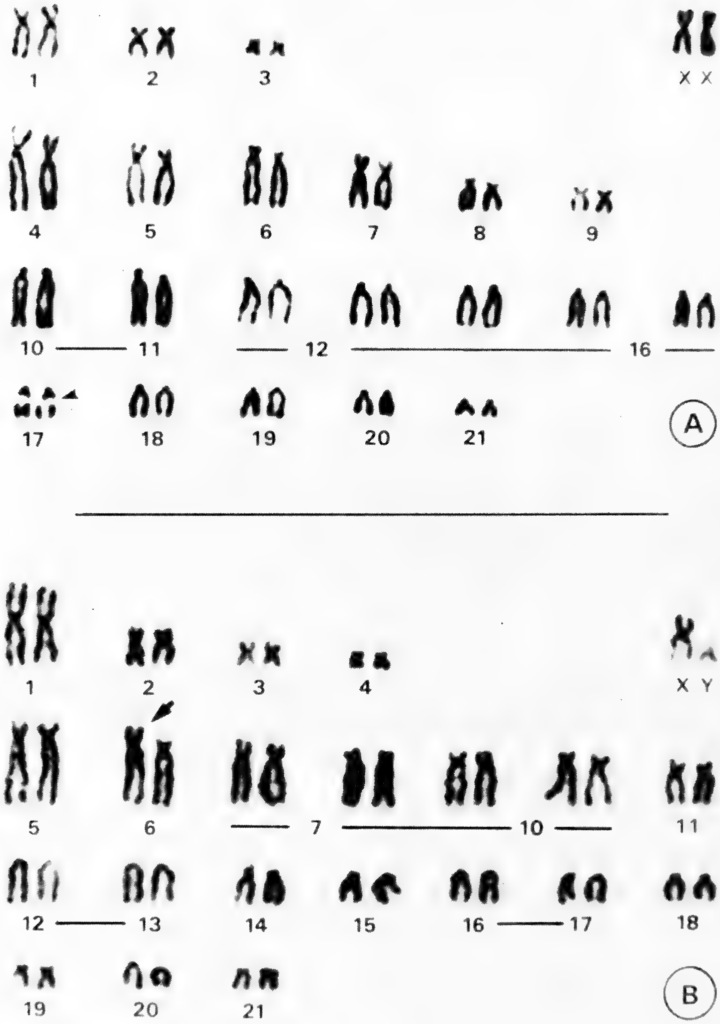

Fig. 1. Conventional karyotypes of a female Japanese ermine (A) and a male Japanese badger (B).

microscope to ascertain their diploid number of chromosomes. Twenty six conventionally stained, 16 G-banded and 17 C-banded metaphases were karyotyped in the former species and 30, 41 and 24 ones in the latter species.

RESULTS

The chromosome number was found to be 2n=44 in both species, but their chromosome constitutions differed greatly (Fig. 1). No. 17 of the ermine chromosomes (E17) carried a typical secondary constriction in the proximal region of its long arm (arrow head). Nos. 14 and 18 of the badger chromosomes (B14 and B18) carried very small satellites terminally in the short arm. The sex chromosomes, X and Y, were medium-sized metacentric and the smallest acrocentric in both

FIG. 2. G-banded (A) and C-banded (B) karyotypes of a male Japanese badger.

species. The short arms of the B6 homologue were apparently heteromorphic (arrow); the large one is submetacentric (SM) and the small one subtelocentric (ST). This heteromorphism was considered to be substantial in two (an adult female and its male fetus) of the five specimens, since it was detected in all the metaphases analysed, so far as these two specimens were concerned. The B6 homologue of the remaining three specimens was homologous for the SM element.

G- and C-banded karyotypes of the badger are shown in Figure 2. All the chromosomes, including morphologically similar ones, could be precisely identified by their G-banding patterns. The satellites were G- and C-negative. While the B6–SM element carried a large amount of C-heterochromatin (C-positive block) on the proximal half of its short arm, the B6–ST element carried no such large C-positive block on its short arm, just containing a small amount of centromeric C-heterochromatin. The C-positive block region was faintly stained as a G-negative segment when G-banded (arrows). The badger Y chromosome, forming more than one-third of its X chromosome ($38.63 \pm 0.68\%$) in length, seemed to be totally heterochromatic, thus being stained darkly by C-

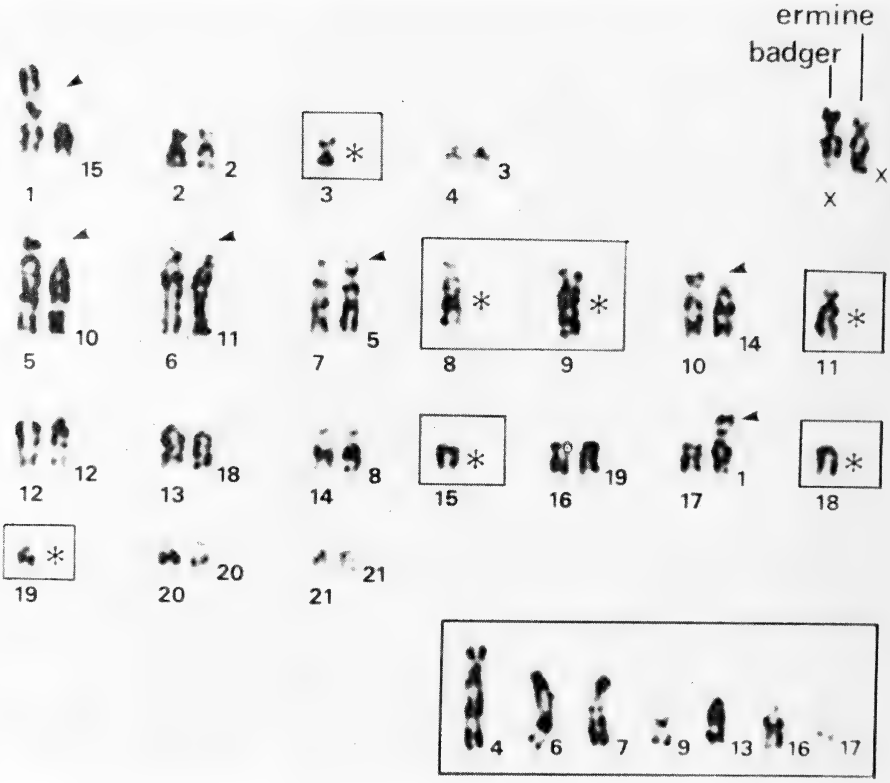

Fig. 3. Pair-matching of G-banded chromosomes between the Japanese ermine (right element of each pair) and the Japanese badger (left element of each pair). Unpaired ermine chromosomes were put together in the largest rectangle of the lowest right and seven badger chromosomes enclosed in the remaining small rectangles were left alone unpaired.

banding and faintly by G-banding. The ermine Y was also C-positive along its entire arm, but in size it was almost one-fifth of its X chromosome (20.46 ±0.91%) in length. A small interstitial C-band could always be detected on the short arm of B1, though it was liable to go unnoticed due to its small size. In addition to these non-centromeric C-bands, varying sizes of centromeric C-bands were observed in all of the chromosomes from deeply-stained large ones to faint small ones.

Figure 3 summarizes the pair-matching analysis, by side-by-side arrangement of the ermine and badger chromosomes which was made according to G-band homology. Nine pairs, including the X chromosome, showed one-to-one correspondence between species, and six badger chromosomes could only be paired partially with six ermine chromosomes mainly in the long arms. Arrow heads indicate unpaired segments. The remaining seven chromosomes hardly showed any G-band homology between species. These unpaired *non-homologous* chromosomes and chromosome segments amounted to about 36% of the haploid length of the ermine chromosomes. No information was available with respect to the interrelation of these unpaired parts.

The subtelocentric pair No. 11 of the ermine (E11) is known to have a large portion of C-heterochromatin on its short arm which is quite similar in its appearance to the C-positive block of B6 [8–9]. In view of this fact, the conventionally stained, and C-banded chromosome of E11 and B6 were compared in detail (Fig. 4). Their long arms share a common origin, as evident from their

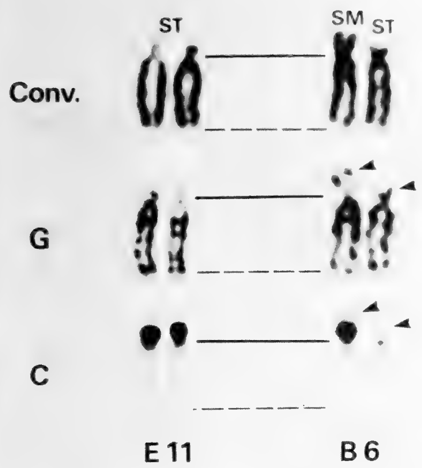

FIG. 4. Comparison of E11 and B6 chromosomes. Top: Conventinonally stained, Middle: G-banded, Bottom: C-banded. Arrow heads: Euchromatic segments on the short arms.

G-band homology. On the other hand, the short arms of E11 and B6–ST may be different in their origin in spite of their morphological similarity; the entire short arm of E11 consisted of C-heterochromatin, and in reverse the short arm of B6–ST was totally euchromatic. Based on the similarity in the size and location of their C-positive blocks, the short arm of E11 itself may correspond to the proximal half of the short arm of B6–SM.

DISCUSSION

In general, the mustelines show extensive interspecific variations of karyotypes [5, 18]. The Japanese mustelines, the Japanese ermine, the least weasel (LW) and the Japanese weasel (W), also show marked interspecific variation in number and structure of chromosomes [7–9]. Their karyological relationships could be explained by Robertsonian fusion and quantitative alteration of C-heterochromatin. These findings strongly suggest that G-banding patterns of these musteline species have been conserved within the genus in spite of their marked differentiation of karyotypes. The highly conservative nature of G-banding pattern was also detected between the ermine and the marten (M) which belong to different genera, *Mustela* and *Martes,* respectively (unpublished data). Their karyological relationship could be explained by three Robertsonian rearrangements, where the combination patterns of the chromosomes involved apparently differed from those found in the ermine and the least weasel, or the ermine and the Japanese weasel [8–9]. Such a high degree of G-band homology between *Mustela* and *Martes* may in itself imply a closeness of their phylogenetic relationship, though they can be regarded as remote relatives from their conventional karyotypes as well as from usual taxonomic criteria.

The badger chromosomes differed greatly from the ermine ones in both the chromosome constitution and the G-banding pattern. No G-band homology was found between these species in over a third of the haploid length of chromosomes. Such reduced G-band homology may directly reflect the remoteness of their phylogenetic relationship. According to the usual taxonomic criteria, the ermine is considered to be one of the more primitive froms and the badger is one of the more advanced ones among the mustelids. Based on this point of view, E15, E10 and E14 might have been involved, most probably through the Robertsonian fusion system, in the production of B1, B5 and B10, respectively, and by contraries the interrelation of B17 and E1 could be ascribed to the presence or absence of the short arm of E1, most probably being explicable by the Robertsonian fission system. It is also reasonable to consider that the B6–SM might have been formed by translocation of a euchromatic segment of unknown origin into the C-positive block, and the B6–ST by deletion of the C-positive block from the B6–SM. The heteromorphic pair B7 and E5 could be explained by a paracentric inversion in the short arm of E5.

The three Robertsonian fusions detected in the badger did not correspond in the combination of chromosomes involved to any of 7 Robertsonian fusions of three other mustelid species so far examined. Taking notice of E10 involved in the Robertsonian rearrangements, E10 and E16 corresponded to the long arm and short arm of LW1 in their G-banding pattern [9], E10 and E13 to

those of W1 [8], E10 and E21 to those of M9 (unpublished data) and E10 and an unknown element to those of B5. In the light of these findings, it is likely that these mustelid species have differentiated independently with one another from the ancestral ermine-like stock through different chromosome rearrangements. Among them, the badger has undergone the most intensive alteration of chromosomes, so that more than one-third of its genome length lacked G-band homology to any of the ermine chromosomes. These findings strongly suggest involvement of intricate and complicated rearrangements such as repeated inversions, compound translocations and their combinations during the course of their karyological differentiation. A high degree of karyological differentiation between the badger and the ermine is now well established based not only on the conventional staining but also on differential staining. Thus, the findings obtained here may support the appropriateness of the former taxonomic system in which the badger belongs to the subfamily Melinae and the other four species mentioned above to the subfamily Mustelinae. To understand the exact interrelation between these unpaired parts of chromosomes, closely related species such as hog-badger, stink badger, ferret badger, American badger and honey badger, all of which belong to the Melinae or Mellivorinae that is close to the Melinae, should be examined in detail, paying special attention to their G-band homology.

ACKNOWLEDGMENTS

The author wishes to express his gratitude to Professor Kazuo Saitoh, Faculty of Science, Hirosaki University, for his helpful advice and suggestions. Sincere thanks are also due to Professor Karl Fredga, Department of Genetics, University of Uppsala, for reading and revising the manuscript with expert criticism. This work was supported in part by a Grant-in-Aid for Scientific Research from the Ministry of Education, Science and Culture of Japan (No. 58540479).

REFERENCES

1 Fredga, K. (1967) Comparative chromosome studies of the family Mustelidae (Carnivora—Mammalia). Hereditas (Lund), **57**: 295.

2 Meylan, A. (1967) Les chromosomes de *Mustela erminea cicognanii* BONAPARTE (Mamm.—Carnivora). Can. J. Genet. Cytol., **9**: 569–574.

3 Hsu, T. C. and Benirschke, K. (1968) An atlas of mammalian chromosomes. Vol 2. Folio 80, Springer-Verlag New York Inc.

4 Grafodatsky, A. S., Volovuev, V. T., Ternovsky, D. V. and Radjabli, S. I. (1976) G-banding of the chromosomes in seven species of Mustelidae (Carnivora). Zool. J., **55**: 1704–1709 (in Russian with English summary).

5 Grafodatsky, A. S., Ternovsky, D. V., Isaenko, A. A. and Radjabli, S. I. (1977) Constitutive heterochromatin and DNA content in some mustelids (Mustelidae, Carnivora). Geneticka, **13**: 2123–2128 (In Russian with English summary).

6 Mandahl, N. and Fredga, K. (1980) A comparative chromosome study by means of G-, C- and NOR-bandings of the weasel, the pygmy weasel and the stoat (*Mustela,* Carnivora, Mammalia). Hereditas, **93**: 75–83.

7 Obara, Y. (1982) Comparative analysis of karyotypes in the Japanese mustelids, *Mustela nivalis namiyei* and *M. erminea nippon.* J. Mammal. Soc. Jpn., **9**: 59–69.

8 Obara, Y. (1985) G-band homology and C-band variation in the Japanese mustelids, *Mustela erminea nippon* and *M. sibirica itatsi.* Genetica, **68**: 59–64.

9 Obara, Y. (1985) Karyological relationship between two species of mustelids, the Japanese ermine and the least weasel. Jpn. J. Genet., **60**: 157–160.

10 Muldal, S. (1950) A list of vertebrates observed at Bayfordbury, 1949–1950. John Innes Hort. Inst., **41** (Ann. Rep.): 39–41.

11 Fredga, K. (1966) Chromosome studies in six species of Mustelidae and one of Procyonidae. Mammal. Chrom. Newsl., **21**: 145.

12 Omodeo, P. and Renzoni, A. (1966) The karyotype of some Mustelidae. Caryologia, **19**: 219–226.

13 Wurster, D. H. and Benirschke, K. (1968) Comparative cytogenetic studies in the order Carnivora. Chromosoma (Berl.), **24**: 336–382.

14 Tsuchiya, K. (1979) A contribution to the chromosome study in Japanese mammals. Proc. Jpn. Acad., **55** B (4): 191–195.

15 Obara, Y. and Miyai, T. (1981) A preliminary study on the sex chromosome variation in the Ryukyu house shrew, *Suncus murinus riukiuanus.* Jpn. J. Genet., **56**: 365–371.

16 Sumner, A. T., Evans, H. J. and Buckland, R. A. (1971) New technique for distinguishing between human chromosomes. Nature (Lond.) New Biol., **232**: 31–32.

17 Sumner, A. T. (1972) A simple technique for demonstrating centromeric heterochromatin. Exp. Cell Res., **75**: 304–306.

18 Bengtsson, B. O. (1980) Rates of karyotype evolution in placental mammals. Hereditas. **92**: 34–47.

ZOOLOGICAL SCIENCE 4: 93–97 (1987)

Acquired Resistance against *Microphallus pygmaeus* in the Laboratory Mouse

Rohani A. Ahmad, Brian L. James[1] and Alias B. Kamis[2]

Jabatan Zoologi, Universiti Kebangsaan Malaysia, 43600 Bangi, Malaysia, and [1]Department of Zoology, University College of Swansea, SA2 8PP, United Kingdom

ABSTRACT—Variations in worm burden indicate that Swiss albino and DBA/2 mice are more susceptible to infection by *Microphallus pygmaeus* than TO or C57BL/10 mice. The worm burden in outbred Swiss albino mice, however, has a much lower coefficient of variability than in the inbred DBA/2 strain. Susceptibility to infection decreases with age in all strains of mice. The worm burden is significantly lower in Swiss albino and C57BL/10 mice immunized by an oral primary infection, and in Swiss albino mice immunized by an intraperitoneal primary infection. Protection by oral immunization and by intraperitoneal injection persist for at least 12 days.

INTRODUCTION

Most literature covering study of acquired immunity in Digenea is concerned with parasites of human importance, namely *Schistosoma* spp. [1, 2] and of agricultural importance, namely *Fasiola hepatica* [3–6]. It is to be expected that these long-lived parasites which undergo migration through tissues of the mammalian hosts stimulate responses which induce a measure of protection against subsequent infection. The relative inefficiency of these responses in inducing protection may be attributed to the ability of the parasite to combat host defenses. In particular, all flukes are protected by the glycocalyx secreted by the syncytial tegument [7–9].

In contrast, it seemed unlikely that a short-lived gut parasite without a tissue stage in development, such as *Microphallus pygmaeus* would stimulate sufficient responses to induce protection against subsequent infection. Nevertheless, earlier work [11, 12] suggests that suppression of the host immune responses increases the worm burden of *M. pygmaeus* in mice.

It seemed appropriate therefore to examine if acquired immunity to *M. pygmaeus* as measured by a reduction in worm burden in the intestine could be induced in the laboratory mouse. Two methods of primary infection were employed, namely (a) a single oral infection of 2,000 metacercariae and (b) intraperitoneal injection of 2,000 metacercariae.

Accepted September 24, 1986
Received July 24, 1986
[2] To whom reprints should be requested.

METERIALS AND METHODS

Experimental host Mice used in the present investigations were maintained under conventional condition in the animal facility. The mice were housed in plastic cages (6 per cage), measuring 31 ×12×11 cm in a room at 18–22°C with 12 hr of flourescent lighting (between 22:30 and 10:30 hr). Food and water were available *ad libitum*.

Parasite The metacercariae of *M. pygmaeus* were obtained from daughter sporocysts in the haemocoel of the digestive gland of the primary molluscan host, *Littorina saxatilis tenebrosa* and kept for a short period in artificial sea water before being orally inoculated into mice.

Recovery of adult worm from mice After the required period postinoculation, the mice were killed, the whole of the small intestine quickly removed and placed in vial containing mammalian saline. The intestine was split opened lengthwise under saline and then incubated at 37°C for

25–30 min. The parasite migrated from the intestine into vial. Adult worms were counted with the aid of a microscope.

Statistics A student's *t* test or one way analysis of variance was done as appropriate on each set of data.

RESULTS

The susceptibility of four strains of mice to M. pygmaeus

A total of 72 male mice aged between 5 and 18 weeks were used, with 6 animals in each category. The four strains include 2 outbred strains, Swiss albino and TO and 2 inbred strains, DBA/2 and C57BL/10. The mice were infected with 1,000 metacercariae in 0.2 ml artificial sea water and the adult worms recovered 2 days post-inoculation and counted.

Swiss albino and DBA/2 mice are clearly more susceptible (Table 1) to infection by *Microphallus pygmaeus* than TO or C57BL/10 mice but the differences are significant ($P<0.05$) only with the former. The worm burden in outbred Swiss albino mice has a much lower coefficient of variability (Table 1) than in inbred DBA/2 mice and are thus more suitable for experimental purposes. The susceptibility to infection decreases with age in all strain of mice.

Acquired resistance against M. pygmaeus in 5 and 10 week old male Swiss albino and C57BL/10 mice induced by a primary oral infection of metacercariae

Twenty 5 week old and twenty 10 week old mice from each strain were given an oral primary infection of 2,000 metacercariae in 0.2 ml artificial sea water but 10 of each with 0.2 ml artificial sea water only. At 2 days post-primary infection (PPI), ten infected mice from each strain and age group were killed and the worm burden counted to confirm the existence of a viable primary infection. On the 12th day PPI when the primary infection was presumed to have terminated, 20 mice from each strain and age category, 10 preinfected with metacercariae and 10 only with sea water, were challenged with 1,000 metacercariae, the mice

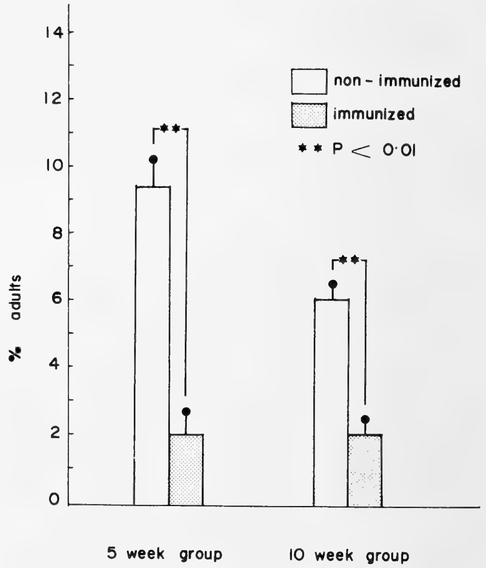

Fig. 1. Percentage (+SE) of adult *Microphallus pygmaeus* recovered 2 days post-challenged infection (PCI) from non-immunized and immunized 5 and 10 week old Swiss albino mice (n=10) given an oral primary infection of 2,000 metacercariae and challenged orally with 1,000 metacercaiae 12 days post-primary infection (PPI).

Table 1. Mean number (±SD) and coefficient of variability (C.V.) of adult *Microphallus pygmaeus* recovered two days post-inoculation from four strains of five to eighteen week old male mice (n=6) infected orally with 1,000 metacercariae

Strains	5 weeks old Mean±S.D.	5 weeks old C.V.(%)	10 weeks old Mean±S.D.	10 weeks old C.V.(%)	18 weeks old Mean±S.D.	18 weeks old C.V.(%)
Swiss	76.8 ± 16.6	21.6	68.5 ± 18.3	26.8	22.8 ± 8.0	34.9
TO	38.2 ± 30.8	80.6	37.8 ± 33.6	88.8	22.7 ± 19.7	87.1
DBA/2	84.2 ± 36.2	43.0	67.6 ± 21.0	31.0	64.0 ± 40.3	63.0
C57BL/10	54.8 ± 30.7	55.9	46.3 ± 23.1	49.9	38.8 ± 17.2	44.4

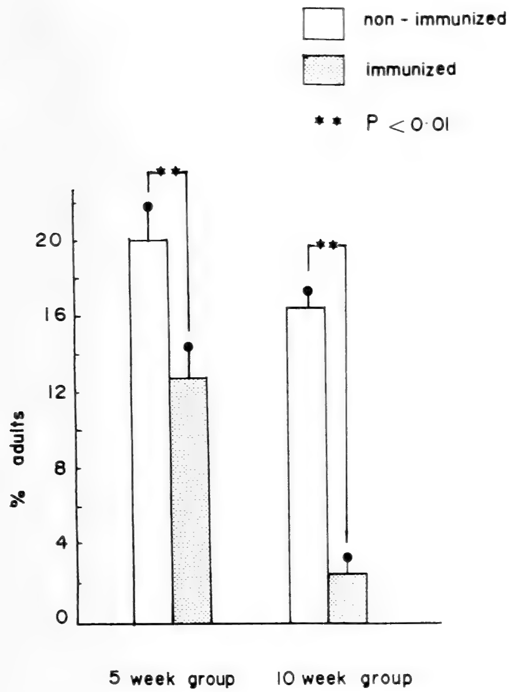

FIG. 2. Percentage (+SE) of adult *Microphallus pygmaeus* recovered 2 days post-challenged infection non-immunized and immunized 5 and 10 week old C57BL/10 mice (n=10) given a primary oral infection of 2,000 metacercariae and challenged orally with 1,000 metacercariae, 12 days post-primary infection (PPI).

were killed 2 days post-challenged infection and the worms counted in the usual manner.

The worm burden is significantly lower (P< 0.01) in 5 and 10 week old outbred male Swiss albino mice immunized by an oral primary infection of metacercariae than in unimmunized mice (Fig. 1). Similarly, the worm burden is lower (P< 0.01) in orally immunized than in unimmunized 5–10 week old male inbred C57BL/10 mice (Fig. 2).

Acquired resistance against M. pygmaeus in 5–6 week old male Swiss albino mice induced by intraperitoneal inoculation of metacercariae

Of the 40 mice used, 20 controls were injected intraperitoneally (IP) with 0.2 ml artificial sea water and 20 test animals with 2,000 living metacercariae in 0.2 ml artificial sea water using a 23 gauge needle.

On the 6th day post intraperitoneal injection, ten of the control groups and 10 of the rest animals were challenged orally with 1,000 metacercariae in 0.2 ml sea water. The mice were killed 2 days post challenge infection (PCI) and the adult Digenea counted. On the 12th day the remaining mice were challenged with 1,000 metacercariae and examined for parasites as above.

The worm burden is lower (P<0.01) in intraperitoneally immunized than in unimmunized 5 week old male Swiss albino mice. The extent of protection is not significantly altered from 6 days to 12 days (Fig. 3) after intraperitoneal injection.

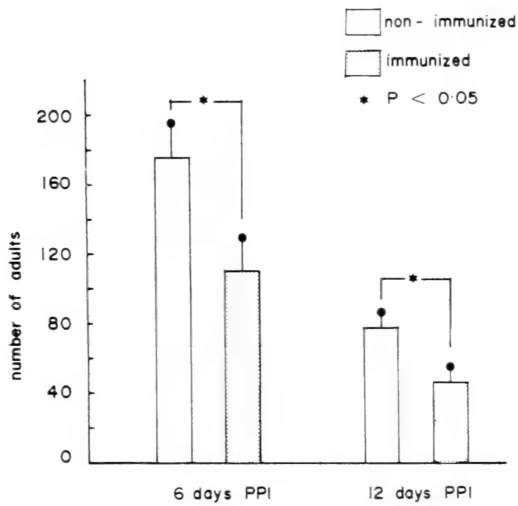

FIG. 3. Mean number (+SE) of adult *Microphallus pygmaeus* recovered 2 days PCI from non-immunized and immunized 5 week old Swiss albino mice (n=10) given an intraperitoneal primary infection with 2,000 metacercariae and challenged orally with 1,000 metacercariae 6 or 12 days post-primary infection (PPI).

DISUSSION

Variations in susceptibility to infection amongst various strains of mice may be attributed to genetic differences [13]. The relatively high mean recovery and coefficient of variability indicates that the outbred Swiss albino mouse is a suitable ex-

perimental host for *M. pygmaeus*.

The induction of a degree of persistent protection to a challenge infection by a relatively low single primary infection of healthy metacercariae is perhaps surprising for such a short-lived gut parasite which does no damage to the host. This result is, however, consistent with the earlier work [11, 14] which suggests that this parasite is responsive to the host immune system.

The protection afforded by the intraperitoneal injection of metacercariae is particularly relevant in this respect. The metacercariae degenerate and die within 24 hr, being surrounded by adhering macrophages [15]. It is significant that initially most macrophages adhere to the parasite in the neighbourhood of the oral and excretory orifices where most antigens are present. Similarly, Werheim and Hamada [16] observed that the infected larvae of *Nippostrongylus brasiliensis,* injected intraperitoneally into naive rats, were coated with adhering macrophages. Perez and Smithers [17] also found macrophages adhering to the surface membrane of *Schistosoma mansoni* and correlated this with protective immunity in the rat. In contrast, Engelkirt *et al.* [18] showed that mostly mast cells and eosinophils adhere to *Taenia taeniaeformis* in the peritoneal cavity of rats.

Previous workers have tried to induce immunity by injecting parasites, with a tissue phase in development, intraperitoneally, for example *Mesocestoides corti* [19] and *Fasciola hepatica* [20, 21]. According to White *et al* [19], the degree of resistance induced in C57BL/6 mice is independent of the route of inoculation. Doy and Hughes [20] reported a high degree of resistance in rats previously infected and challenged intraperitoneally. However, Rajasekariah and Howell [21] failed to find any significant difference in worm recovery between intraperitoneally challenged rats and their respective control. Further work is required before it is possible to deduce the mechanism of resistance to, or to identify the specific antibodies involved, in intestinal *M. pygmaeus* infection.

REFERENCES

1 Maddison, S. E., Slemenda, S. B., Chandler, F. M. and Kagan, I. G. (1981) Acquired immunity in B cell-deficient mice to challenge exposure following primary infection with *Schistosoma mansoni.* Am. J. Trop. Med. Hyg., **30**: 609–615.

2 Mahmoud, A. A. F., Warren, K. S. and Peters, P. A. (1975) A role for the eosinophil in acquired resistance to *Schistosoma mansoni* infection as determined by anti-eosinophil serum. J. Exp. Med., **142**: 805–813.

3 Doy, T. G., Hughes, D. L. and Harness, E. (1981) Hypersensitivity in rats infected with *Fasciola hepatica*: possible role in protection against a challenge infection. Res. Vet. Sci., **30**: 360–363.

4 Lang, B. Z. (1974) Host-parasite relationships of *Fasciola hepatica* in the white mouse. V. Age of fluke responsible for the induction of acquired immunity. J. Parasitol., **60**: 90–92.

5 Rajasekariah, G. R. and Howell, M. J. (1978) Acquired immunity to the trematode *Fasciola hepatica* in rats. Aust. J. Exp. Biol. Med. Sci., **56**: 747–756.

6 Smithers, S. R. (1976) Immunity to Trematoda infections with special reference to schistosomiasis and fascioliasis. In "Immunology of Parasitic Infections". Ed. by S. Cohen and E. H. Sadun, Blackwell Scientific Publications, Oxford, pp. 296–332.

7 Erasmus, D. A. (1972) The Biology of Trematodes, Edward Arnold, London.

8 Eramus, D. A. (1977) The host-parasite interface of trematodes. Adv. Parasitol., **15**: 201–242.

9 Lumsden, R. D. (1975) Surface ultrastructure and cytochemistry of parasitic helminths. Exp. Parasitol., **37**: 267–339.

10 Robinson, R.D. and Halton, D. W. (1983) Functional morphology of the tegument of *Corrigia vitta* (Trematoda: Dicrocoeliidae). Z. Parasitenkd., **69**: 319–333.

11 Ahmad, R. A., James, B. L. and Kamis, A. B. (1986) Retention and egg production of *Microphallus pygmaeus* in mice: the influence of the adrenal cortex. Z. Parasitenkd., **72**: 479–485.

12 Mills, A. R., Brain, P. E. and James, B. L. (1973) *Microphallus pygmaeus*: Effect of long-acting ACTH preparation on establishment and retention in alimentary canal of the mose. Exp. Parasitol., **34**: 251–256.

13 Wakelin, D. (1978) Genetic control of susceptibility and resistance to parasitic infection. Adv. Parasitol., **16**: 219–308.

14 Hameed, M. Z. (1971) Studies on larval Digenea from marine molluscs. Ph. D. thesis, University of Wales.

15 Ahmad, R. A. (1984) Studies on Marine Digenea in Experimental Hosts: *Microphallus pygmaeus* (Levinsen 1881) in the laboratory mouse. Ph. D. thesis, University of Wales.

16 Wertheim, G. and Hamada, G. (1980) *Nippostron-*

gylus brasiliensis: quantitative and qualitative aspects of larval destruction in the peritioneum of the rat. Isr. J. Med. Sci., **16**: 560–561.

17 Perez, H. A. and Smithers, S. R. (1977) *Schistosoma mansoni* in the rat: The adherence of macrophages to schistosomula *in vitro* after sensitization with immune serum. Int. J. Parasitol., **7**:315–320.

18 Engelkirk, P. G., Williams, J. F. and Signs, M. M. (1981) Interactions between *Taenia Taeniaeformis* and host cells *in vitro*: Rapid adherence of peritoneal cells to strobilocerci. Int. J. Parasitol., **11**: 463–474.

19 White, T. R., Thompson, R. C. A. and Penhale, W. J. (1982) A comparative study of the susceptibility of inbred strains of mice to infection with *Mesocestoides corti*. Int. J. Parasitol.,**12**: 29–33.

20 Doy, T. G. and Hughes, D. L. (1982) Evidence for two distinct mechanisms of resistance in the rat to reinfection with *Fasciola hepatica*. Int. J. Parasitol., **12**: 357–361.

21 Rajasekariah, G. R. and Howell, M. J. (1977) The fate of *Fasciola hepatica* metacercariae following challenge infection of immune rats. J. Helminthol., **51**: 289–294.

ZOOLOGICAL SCIENCE 4: 99–105 (1987)

A DNA Synthesis Inhibitory Peptide from Human Embryo Fibroblasts–Characterization of Biological Properties

Yasuji Okai[1,4], Shigeaki Ishizaka[2] and Uki Yamashita[3]

[1]*Tokyo Research Laboratories, Kyowa Hakko Kogyo Co., Machida, Tokyo 194,* [2]*Third Department of Internal Medicine, Nara Medical University, Kashiwara, Nara 634, and* [3]*Department of Immunology, University of Occupational and Environmental Health, Medical School, Fukuoka 807, Japan*

ABSTRACT—Low-molecular-weight inhibitory factors for lymphocyte DNA synthesis are known to be released from fibroblasts or fibroblast-like cells. Amongst these factors, 5 kDa peptide from human embyo fibroblasts strongly suppressed lymphocyte DNA synthesis when added at early periods after the lectin stimulation without causing a significat change in the lymphocyte viability. This peptide inhibited the lymphocyte DNA synthesis induced by interleukin 1, 2 or some mitogens. It also suppressed both the LPS-dependent polyclonal antibody (Ig M) production by B cells and the induction of hapten-reactive cytotoxic T cells. These results indicate that the 5 kDa peptide from human embryo fibrobalasts has a potential ability for the regulation of lymphocyte proliferation and functions.

INTRODUCTION

Lymphocyte reaction in immune responses are regulated by some soluble factors, which exhibit positive and negative effects on lymphocyte growth and functions. Previously, one of the authors (Y. O.) reported that some mammalian and insect cultured cells released low-molecular-weight peptides inhibitory to lymphocyte DNA synthesis [1–4]. However, the biological properties of these factors have not yet been elucidated extensively. Amongst these factors, the authors analyzed here the biological properties of the 5 kDa peptide derived from human embryo fibroblasts. This peptide inhibited the lymphocyte proliferative responses induced by interleukin 1, 2 or other mitogens, and suppressed both the cytotoxic T cell function and the antibody production by B cells.

Accepted July 22, 1986
Received May 8, 1986

[4] Present address and reprint requests: Laboratory of Molecular Oncology, Tsukuba Life Science Center, Yatabe, Tsukuba, Ibaragi 305, Japan.

MATERIALS AND METHODS

Cell culture

Human embryo fibroblast cell line was kindly donated from Dr. S. Gotoh (Department of Biochemistry, University of Occupational and Environmental Health, School of Medicine, Kitakyushu). The description of this cell line was found elsewhere [5]. The cells were grown in Eagle's minimum essential medium (MEM, Nissui Seiyaku Co., Tokyo) supplemented with 10% fetal calf serum (FCS, Gibco, Grand Island Biological Lab., New York) in 5% CO_2 95% air at 37°C. The cells became confluent in 4 days after a 1:4 splitting. The confluent cells were further cultured in a serum-free medium for 2 days to remove serum-derived materials. The serum-free medium was changed in every other day for two weeks and the pooled culture supernatant was served as a starting material to be examined. During this culture, the cell viability was not changed significantly.

Preparation of DNA synthesis inhibitory peptide

Two volumes of saturated ammonium sulphate solution were added to the culture medium (250 ml) and centrifuged at 12,000 $\times g$ at 15 min. The

precipitate was dissolved into 5 ml of 10 mM phosphate-buffered saline (PBS, pH 7.2), applied on a Sephadex G–100 column (Pharmacia, 1.8× 48 cm) and eluted with 10 mM phosphate buffer (pH 7.2) containing 50 mM NaCl at 5 ml per fraction. Some portion of the active fraction at less than 10 kDa of Sephadex G–100 chromatography was applied on CM Sephadex column (Pharmacia, 1×5 cm) and eluted with 10 mM phosphate buffer (pH 7.2) containing various NaCl concentrations. The active fraction of CM Sephadex chromatography was applied on a Sephadex G–25 column (Pharmacia, 1.4×90 cm) and eluted with PBS at 2.5 ml per fraction. The 5 kDa peptide was clearly separated at this purification step.

Assay for lymphocyte DNA synthesis

Thymocytes and splenocytes DNA syntheses were assayed according to the previous method [1, 2]. Thymocytes or splenocytes (5×10^5) from C3H/He mice (Shizuoka Experimental Animal Lab., Shizuoka) were cultured in 0.1 ml of RPMI 1640 medium (Nissui Seiyaku Co.) supplemented with 10% FCS in the presence of Concanavalin A (Con A, Sigma, 5 μg/ml) for 2 days. The cells were then labeled with 0.5 μCi of [^{3}H]TdR (5 Ci/mmol, Amersham, England) during the last one day. At the end of culture, trichloroacetic acid (TCA) was added at 10% in final concentration. The TCA-insoluble fraction was harvested on GF/C membrane filter (Whatman) and the radioactivity of the membrane was counted. Interleukin 1 (IL 1) was obtained from the culture medium conditioned by C3H/He mouse macrophages and partially purified by Sephadex G–100 and DEAE Sephadex A–25 columns (Pharmacia). Interleukin 2 (IL 2) was obtained from the culture medium conditioned by Con A-stimulated C3H/He mouse splenocytes and partially purified by Sephadex G–100 and DEAE Cellulose column chromatographies.

Induction and assay system of hapten-reactive cytotoxic T cells

Induction and assay were performed by the previous method [6]. Stimulator T cells were prepared by passaging C3H/He mouse spleen cells through a Nylon column. They were treated with mitomycin C (50 μg/ml, Kyowa Hakko Kogyo Co., Tokyo) at 37°C for 1 hr and then treated with 10 mM trinitrobenzen sulfonate for trinitrophenol (TNP)-coupling at 37°C for 10 min. Responder T cells were cultured with TNP-modified or unmodified stimulator T cells (2×10^6) in the presence or absence of spleen macrophages (2×10^6) in 2 ml of Peck-Click culture medium containing 10% FCS at 37°C for 5% CO_2 and 95% air for 5 days. In the ^{51}Cr release assay by cytotoxic T cells, X5563 plasmacytoma cells from C3H/He mice were used as target cells. *In vitro* sensitized T cells (5×10^5) were mixed with ^{51}Cr-labeled X5563 cells (1×10^4), which were modified with TNP at effector cell to target cell ratio of 50 : 1 in 0.2 ml of RPMI 1640 medium containing 10% FCS. After the mixed cell culture at 37°C for 5 hr in 5% CO_2 and 95% air, the culture supernatant was harvested with the aid of a Titertek collection system (Flow Labs, England) and the radioactivity on the filter was counted in a γ-counter. The percentage of specific lysis of target cells was calculated as: % specific lysis $=100 \times \dfrac{\text{experimental release} - \text{control release}}{\text{maximal release} - \text{control release}}$, where the maximal release was obtained by incubating ^{51}Cr-labeled target cells in 1% Nonidet P40 (Sigma Chemical Co.) and the control release was obtained by incubating target cells with unsensitized T cells.

Assay for antibody production by mouse lymphocytes

Assay for antibody production by mouse lymphocytes was performed according to the previous method [7]. Splenocytes (1×10^6) from DBA /2CrSlc mice (Shizuoka Experimental animal Lab.) were cultured for 4 days in 0.2 ml of RPMI 1640 medium supplemented with 10% FCS in the absence or presence of lipopolysaccharide (Sigma, 100 μg/ml) at different concentrations of 5 kDa inhibitory peptide. The number of IgM antibody-forming cells was determined by the plaque assay with protein A (Sigma). In brief, 25 μl of lymphocyte suspension mentioned above, 25 μl of a 1 : 8 suspension of protein A-coupled sheep red blood cells (SRBC), 25 μl of guinea pig complement (Boelinger) diluted at 1 : 6 were added to 0.5% agar (Difco)(0.2 ml) containing 0.05% DEAE dextran (Pharmacia). The cell mixture was plated

on a Petri dish, covered with a coverglass, incubated at 37°C for 4 hr and plaque forming cells (PFC) were counted.

RESULTS

The authors prepared 5 kDa peptide inhibitory to lymphocyte DNA synthesis from the serum-free culture medium conditioned by human embryo fibroblasts. The low-molecular-weight fraction at less than 10 kDa was separated from the conditioned medium by Sephadex G–100 column chromatography and this fraction was applied on a CM sephadex column. As shown in Figure 1, the major inhibitory activity was eluted at 500 mM NaCl. When the active fraction from CM Sephadex chromatography was further applied on a Sephadex G–25 column, the several inhibitory activities were observed (Fig. 2). Amongst these activities, the present study was focused on the major activity at 5 kDa. This fraction was characterized to be a heat-stable peptide as described in the previous report [3]. Although this peptide exhibited a strong inhibition on lymphocyte DNA synthesis, it did not change the viability of lymphocytes significantly (Table 1) suggesting that the 5 kDa peptide was not toxic for lymphocytes.

When the 5 kDa peptide was added to the lymphocyte culture at 0–5 hr after the lectin

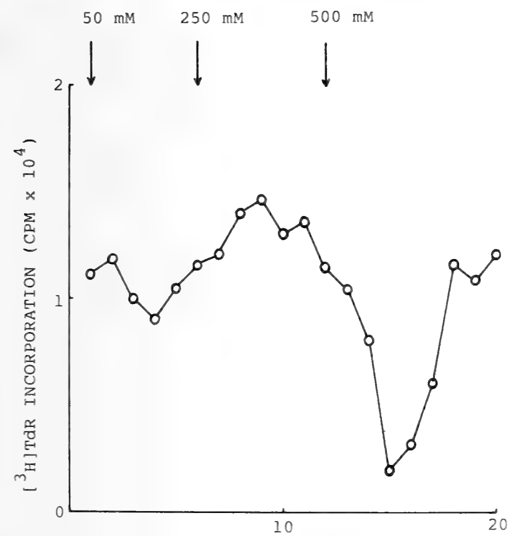

FIG. 1. Elution profile of the inhibitory activities for lymphocyte DNA synthesis of the culture medium in CM Sephadex column chromatography. The inhibitory activities at less than 10 kDa from Sephadex G–100 column chromatography were applied on a CM Sephadex column and eluted with 10 mM phosphate buffer containing various NaCl concentrations as shown in the figure. To remove the effect of the salts in the fractions on the assay for DNA synthesis, each fraction was diluted with 10 mM phosphate buffer to 5-fold and its activity was assayed,

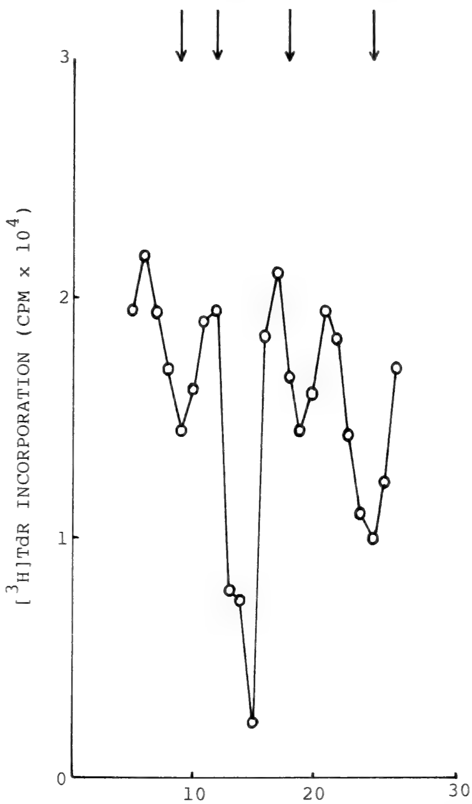

FIG. 2. Separation of 5 kDa peptide from other inhibitory activities by CM Sephadex G–25 column chromatography. The inhibitory activities of fraction 14–17 in Fig. 1 were concentated and applied on a Sephadex G–25 column and eluted with PBS as described in materials and methods. Arrows in the figure show the elution positions of molecular weight markers; cytochrome C (13 kDa), insulin (5.7 kDa), Bacitracin (1.5 kDa) and NaCl from the left to the right. The smallest activities at fraction 23–26 are derived from the contaminant salts.

stimulation, a remarkable inhibition of DNA synthesis was observed (Table 2). When the interval between the lectin-stimulation and peptide addition was prolonged to 10 hr, the inhibitory effect was slightly decreased and no significant suppression was detected any more when added at 30 hr after lectin-stimulation (Table 2). To analyze the action of this peptide on the cell membrane function, the authors examined the effect of this peptide on uridine and UTP incorporation in the activated lymphocytes. The incorporation during early periods after the addition of the peptide was decreased as compared with the activated lymphocytes without the peptide (data not shown). These findings are the same as those in 1 kDa inhibitory peptide reported previously [1].

Immune responses are regulated by some soluble factors. Amongst those, IL 1 and IL 2 have been known as typical stimulatory factors for lymphocyte proliferation and functions [8, 9]. The authors studied the effect of 5 kDa peptide on the lymphocyte DNA synthesis induced by IL 1, 2 or other mitogens. As can be seen in Figure 3, IL 1- or 2-induced thymocyte DNA synthesis in the presence of Con A was considerably suppressed by the addition of 5 kDa peptide. This peptide also suppressed the thymocyte DNA synthesis induced by Con A alone. In another experiment (data not shown), it could also suppress the LPS-induced DNA synthesis by B lymphocytes of a nude mouse. These results indicate that the 5 kDa peptide from human embryo fibroblasts exhibit the nonspecific suppressive effects on T and B lymphocyte DNA syntheses induced by IL 1, 2 and other mitogens.

Next, the authors studied the effect of this peptide on the biological functions of lymphocytes. The result on the antibody production by murine B lymphocytes was shown in Figure 4. A remarkable IgM production was induced by a polyclonal activator, LPS (100 μg/ml) and this IgM production was inhibited by the addition of the peptide in a dose-dependent manner (Fig. 4).

At last, the effect of the peptide on the hapten-reactive cytotoxic T cell function was analyzed. As indicated in Table 3, Nylon column-purified T cells alone did not show the cytotoxic T cell activity to TNP-coupled stimulator cells (1.2%). When the macrophages as accessory cells were added to the culture, a remarkable cytotoxic T cell activity was evidenced as the lysis of TNP-coupled tumor cells (X5563). The addition of the peptide to the culture considerably reduced this cytotoxic T cell activity induced by the macrophages. These findings indicate that the 5 kDa peptide from human embryo fibroblasts can repress both the activation of polyclonal antibody production by B cells and the induction of hapten-

TABLE 1. Effect of 5 kDa peptide on lymphocyte viability

	Viable cell numbers ($\times 10^5$) Control	+Peptide
Experiment 1	2.13	2.16
Experiment 2	2.26	2.18

Splenocytes (5×10^5) from C3H/He mice were cultured for 2 days in the absence or presence of the peptide (25 μl of fraction 13–15 in Fig. 2). The value in the table is an average of duplicate dye exclusion tests.

TABLE 2. Effect of 5 kDa peptide on lymphocyte DNA synthesis when added at different times after the lectin-stimulation

Added at (hr)	[^{3}H]TdR incorporation (CPM)	Relative activity (%)
untreated	13,260 ± 1,035	100.0
0	598 ± 16	4.5
5	799 ± 25	6.0
10	2,634 ± 581	19.8
30	10,892 ± 873	82.1

Splenocytes (5×10^5) from C3H/He mice were cultured in RPMI 1640 medium–10% FCS with Con A. The 5 kDa peptide (50 μl of fraction 13–15 in Fig. 2) was added at different times as indicated in table. The activity is expressed as the mean and standard error of triplicate assays.

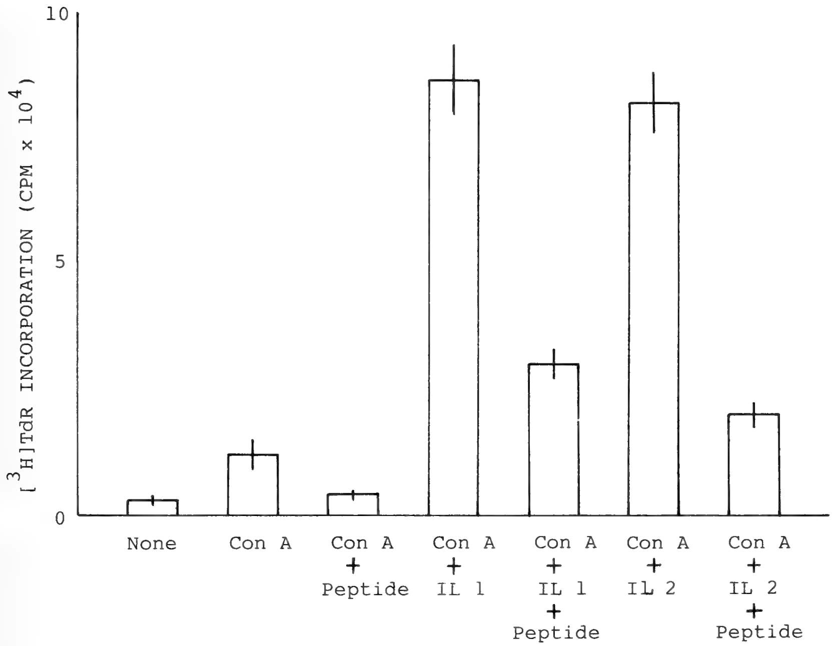

FIG. 3. Effects of 5 kDa peptide on the lymphocyte activation by IL 1, 2 and mitogen. C3H/He mouse thymocytes (5×10^5) were cultured in RPMI 1640–10% FCS in the absence or presence of 5 kDa peptide (25 μl of fraction 13–15 in Fig. 2) under the different experimental conditions as shown in the figure. The column and bar represent the mean and standard error of triplicate assays.

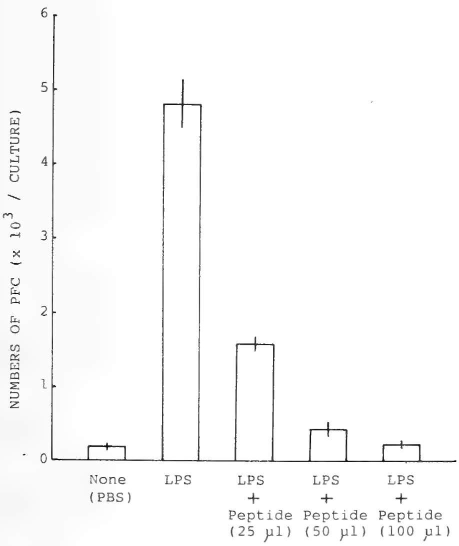

FIG. 4. Effect of 5 kDa peptide on IgM production by murine B lymphocytes. Splenocytes (1×10^6) from DBA mice were cultured for 4 days in agar culture system with various amounts of 5 kDa peptide (fraction 13–15 in Fig. 1) and IgM positive cells were counted by a protein A-PFC assay. The column and bar represent the activity of the mean and standard error of triplicate assays.

TABLE 3. Effect of 5 kDa peptide on the induction of hapten-reactive cytotoxic T cells

Added with	^{51}Cr Release (% Specific release)
none	1.2 ± 0.1
peptide	-1.4 ± 0.9
macrophages	80.0 ± 0.9
macrophages+peptide	43.4 ± 1.2

Nylon column-purified T cells (5×10^6) were cultured with TNP-modified T cells (2×10^6) in the absence or presence of 5 kDa peptide (25% in the culture mixture) and macrophages (2×10^6) at 37°C for 5 days. The induced cytotoxic T cell activity was detected by culturing with ^{51}Cr-labeled TNP-coupled X5563 cells as target. The value is expressed as the mean and standard error of triplicate assays.

reactive cytotoxic T cell function.

Judging from the results mentioned above, 5 kDa peptide from human embryo fibroblasts seems to suppress the overactivation of lymphocyte proliferation and functions and may be associated with the lymphocyte regulation in immune responses *in vivo*.

DISCUSSION

In this section, the authors discuss the biological significance of the peptide reported in this paper. First of all, fibroblast infiltrate into the inflammatory regions induced by the injury or infection together with neutrophils, macrophages and lymphocytes. The activated macrophages and lymphocytes release the soluble factors which stimulate fibroblast chemotaxis and proliferation [10–12]. In contrast, the authors previously elucidated that fibroblasts produce thymocyte-activating factors stimulating lymphocyte proliferation and functions [13–16]. In the present paper, the authors describes that fibroblasts release a low-molecular-weight peptide inhibitory to lymphocyte proliferation and function. These findings altogether suggest that fibroblasts have a potential ability for the regulation of lymphocyte proliferation and functions in the inflammatory reactions *in vivo*.

The similar peptides are also found in the culture medium of human and murine fibroblasts, insect fibroblastic cells and murine splenocytes: They have been evidenced to posess the similar biological and biochemical properties to those of the peptide in this paper [1–4]. These peptides can inhibit DNA synthesis of the producing cells themselves without affecting their viability, and the largest amount of the peptide is released into the culture medium at the confluent cell stage (data not shown). Thus it seems reasonable to infer that these peptides may play an important role in the growth regulation of fibroblasts or lymphocytes in an autocrine manner.

Another function of these peptides is a bactericidal activity: They have been known to cause lysis in some Gram-negative bacteria such as *E. coli* or *P. maltophilia* [1, 2]. Since the similar peptides are also found in mammalian serum and insect hemolymph [17–19], they seem to play a defense role against invading bacteria in the circulating system of the animal body.

In conclusion, the release of these peptides from fibroblasts seems to raise an interesting problem in the field of immunological regulation in vertebrates and invertebrates.

REFERENCES

1 Okai, Y. (1984) 3T3 fibroblasts release a low-molecular-weight inhibitory peptide of lymphocyte DNA synthesis into serum-free culture medium. Biochim. Biophys. Acta, **802**: 287–291.

2 Okai, Y. (1985) Insect fibroblast-like cells release inhibitory peptides of lymphocyte DNA synthesis into serum-free culture medium. Insect Biochem., **15**: 483–487.

3 Okai, Y. (1986) Heterogeneous molecular weight inhibitory factors for lymphocyte DNA synthesis from human embryo fibroblasts—two conversion pathways by trypsin-like protease(s). Zool. Sci., **3**: 271–276.

4 Okai, Y. (1984) Murine splenocytes release an inhibitory peptide of lymphocyte DNA synthesis into serum-free culture medium. Mol. Biol. Rep., **10**: 57–62.

5 Yanagisawa, K., Suenaga, Y., Nishio, K. and Gotoh, S. (1983) Establishment of a human diploid cell strain. J. Univ. Occup. Environ. Health (Kitakyushu), **5**: 49–54.

6 Yamashita, U. and Hamaoka, T. (1979) The requirement of Ia-positive accessory cells for the induction of hapten-reactive cytotoxic T lymphocytes *in vitro*. J. Immunol., **123**: 2637–2643.

7 Ishizaka, S. and Möller, G. (1982) Litium chloride induces partial responsiveness to LPS in nonresponder B cells. Nature, **299**: 365–366.

8 Mizel, S. B., Oppenheim, J. J. and Rosenstreich, D. L. (1978) Characterization of lymphocyte-activating factor (LAF) produced by a macrophage cell line, P388D$_1$ II. Biochemical characterization of LAF induced by activated T cells and LPS. J. Immunol., **120**: 1504–1508.

9 Mier, J. W. and Gallo, R. C. (1982) T cell growth factor. Limphokines, **6**: 137–163.

10 Leibovich, S. J. and Ross, R. (1975) The role of the macrophage in wound repair—a study with hydrocortisone and antimacrophage serum. Am. J. Pathol., **78**: 71–100.

11 Leibovich, S. J. and Ross, R. (1976) A macrophage-dependent factor that stimulates the proliferation of fibroblasts *in vitro*. Am. J. Pathol., **84**: 501–514.

12 Wahl, S. M. and Wahl, L. M. (1980) Modulation of fibroblast growth and functions by monokines and lymphokines. Lymphokines, **2**: 179–201.

13 Okai, Y., Tashiro, H. and Yamashita, U. (1982) 3T3 fibroblasts are stimulated by 12–O-tetradecanoyl-phorbol-13-acetate to produce thymocyte-activating factors. FEBS Lett., **142**: 93–95.

14 Okai, Y., Gotoh, S. and Yamashita, U. (1985) Thymocyte-activating factors from SV40-transformed human embryo fibroblasts. Immunol. Lett., 9: 153–159.

15 Okai, Y. (1985) A large-molecular-weight thymocyte-activation factors in extracellular matrix from SV40-transformed human embryo fibroblasts. Immunol. Lett., **11**: 63–68.

16 Okai, Y. and Yamashita, U. (1986) Human embryo fibroblast cell line produces factors to induce cytotoxic T lymphocytes. Zool. Sci., **3**: 765–771.

17 Okai, Y. (1985) DNA synthesis inhibitory peptides in mammalian serum and insect hemolymph. Mol. Biol. Rep., **10**: 123–128.

18 Okai, Y. (1985) Dual functions of DNA synthesis inhibitory peptide in fetal calf serum. Immunol. Lett., **9**: 229–223.

19 Okai, Y. (1985) A bactericidal substance in insect hemolymph strongly suppresses lectin-induced mammalian lymphocyte DNA synthesis. Zool. Sci., **2**: 663–669

ZOOLOGICAL SCIENCE 4: 107–114 (1987)

Myofibril Degradation by Tail Lysosomes from Metamorphosing Bullfrog Tadpoles

Ken-ichiro Kobayashi and Shiro Horiuchi

Life Science Institute, Sophia University, Chiyoda-ku, Tokyo 102, Japan

ABSTRACT—Myofibrils were degraded by a lysosomal fraction prepared from the tadpole tail of metamorphosing bullfrog, *Rana catesbeiana*. Myosin heavy chains and most of other myofibrillar proteins were hydrolyzed under both acidic pH and neutral pH, but actin was hydrolyzed only at acidic pH. The optimum pH of myofibril degrading activity was 3.4, and the second peak of the activity was observed at pH 5.4. The hydrolysis of myofibrillar proteins was inhibited by leupeptin, antipain and chymostatin at any pH examined, but at acidic pH the inhibition was not complete. Remaining activity was suppressed by pepstatin. Diisopropyl fluorophosphate and bestatin had no effect on the hydrolysis of myofibrillar proteins. Cysteine stimulated the hydrolysis of myofibrillar proteins. These results indicate that myofibril degradation by the lysosomal fraction must be due to the activity of a thiol proteinase(s), but cathepsin D may play a minor role in myofibril degradation. A thiol proteinase(s) possibly plays an essential role in the degeneration of tail muscle at metamorphosis.

INTRODUCTION

The tails of anuran tadpoles regress during metamorphosis by the action of thyroid hormone. In this process the tail muscle degrades and finally disappears. To elucidate the mechanism of muscle breakdown, ultrastructural changes in the regressing muscle had been thoroughly investigated [1–5]. These studies showed the formation of membrane bounded bodies called "sarcolytes" at the degeneration of muscle cells. During the formation of sarcolytes myofibrils are often cut into fragments and their striated structure is lost some degree. Then, sarcolytes are phagocytosed and degraded by mesenchymal macrophages which invade into muscle tissues.

These observations suggest the involvement of lysosomes in myofibril degradation by macrophages. However, it has been little known about what kind of lysosomal proteinases are responsible for the hydrolysis of myofibrillar proteins. Recently it was found that leupeptin, an inhibitor of thiol proteinases, suppressed the autolysis of tail muscle homogenates from metamorphosing tadpoles under acidic conditions [6]. This result suggests an important role of a lysosomal thiol proteinase(s) in myofibril degradation.

Accepted July 23, 1986
Received March 20, 1986

A lysosomal fraction isolated from the regressing tails of bullfrog tadpoles was shown to contain two acid proteinases, cathepsin D and a thiol proteinase [7]. This study attempted to identify a myofibril degrading enzyme(s) in the lysosomal fraction. A lysosomal preparation was incubated with myofibrils, and the hydrolysis of myofibrillar proteins was estimated by detecting peptide fragments on SDS-polyacrylamide gels and by measuring trichloroacetic acid (TCA)-soluble products fluorometrically. A myofibril degrading enzyme(s) was supposed to be a thiol proteinase from the inhibitory effect of proteinase inhibitors on myofibril degradation.

MATERIALS AND METHODS

Animals Tadpoles of bullfrog, *Rana catesbeiana,* were purchased from an animal supplier. They were maintained in an aquarium at 23°C and fed on boiled spinach. After the onset of metamorphosis they were transferred to the shallow water. Stages of development were defined according to the criteria described by Taylor and

Kollros [8].

Preparation of myofibrils Myofibrils were prepared from the tails of prometamorphic tadpoles (stages XVI–XVIII) in accordance with the method of isolating rabbit myofibrils [9]. This preparation was suspended in 0.039 M H_3BO_3–NaOH buffer (pH 7.1) containing 0.1 M KCl and 5 mM EDTA at a concentration of 2 mg protein/ml and stored at 4°C. Protein concentrations were measured by a dye-binding assay described by Read and Northcote [10] using bovine serum albumin as a standard.

Preparation of lysosomes Lysosomes were isolated from the whole tails of metamorphosing tadpoles (stages XXI and XXII) by gradient centrifugation using Percoll (Pharmacia Fine Chemicals AB) as reported previously [7]. In the present study Percoll was removed from a lysosomal fraction by centrifugation at 100,000 *g* for 90 min. A yellowish precipitate was collected, suspended in 10 mM MOPS–NaOH buffer (pH 6.8) and stored at −70°C until use. The activities of two acid proteinases, cathepsin D and a thiol proteinase, in this lysosomal fraction were measured using bovine hemoglobin (type IV, Sigma Chemicals Co.) as a substrate at pH 3.2 [11]. Specific activities of cathepsin D and a thiol proteinase were 10.4 units/mg protein and 7.4 units/mg protein respectively on the average of 10 preparations.

Myofibril degradation by lysosomes A myofibrillar preparation (0.3 mg protein) was incubated with 25 μmol of citric acid-sodium citrate buffer or Na_2HPO_4–NaH_2PO_4 buffer, 2.5 μmol of L-cysteine and a lysosomal fraction in the total volume of 0.5 ml at 25°C. A lysosomal fraction (about 10 μg protein) containing 0.2 unit of activity as the sum of cathepsin D and a thiol proteinase was used for each incubation mixture. Inhibitors tested were as follows: leupeptin, antipain, chymostatin, pepstatin and bestatin [12] (Peptide Institute, Inc.), and diisopropyl fluorophosphate (DIFP) (Sigma Chemicals Co.). The concentration of inhibitors in an incubation mixture was 25 μg/ml for leupeptin, antipain, chymostatin and bestatin, 0.25 μg/ml for pepstatin and 0.1 mM for DIFP.

Hydrolysis products of myofibrillar proteins were detected on SDS-polyacrylamide gels. SDS-polyacrylamide gel electrophoresis was performed according to the method of Laemmli and Favre [13]. To the incubation mixture 0.5 ml of solubilizing buffer (0.25 M Tris-HCl buffer, pH 6.8, containing 4% (w/v) SDS, 10% (v/v) β-mercaptoethanol and 20% (v/v) glycerol) was added at the end of incubation. The mixture was heated in a boiling water bath for 2 min, cooled by tap water and centrifuged at 1,500 *g* for 10 min. A supernatant was collected and one-tenth volume of bromphenol blue solution was added. Controls were prepared by adding a lysosomal fraction to the mixture just before heating. Samples (30 μl each) were applied on a 10% (w/v) polyacrylamide slab gel (10×14×0.1 cm), and electrophoresis was performed at 60 V until samples entered a separation gel and then at 120 V until the tracking dye migrated to the bottom of the gel. The gel was stained with 0.25% (w/v) Coomassie Brilliant Blue R–250 (Nakarai Chemicals, Ltd.) in methanol /acetic acid/water (5/1/5) and destained with the same solution but without the dye reagent. The gel was stored in 10% (v/v) acetic acid solution. Molecular weights of polypetide bands were estimated by use of a calibration protiein kit (Combithek, Boehringer Mannheim GmbH) consisting of α_2-macroglobulin (170 kDa), phosphorylase b (97.4 kDa), glutamate dehydrogenase (55.4 kDa), lactate dehydrogenase (36.5 kDa) and trypsin inhibitor (20.1 kDa).

Hydrolysis products of myofibrillar proteins were quantified fluorometrically. At the end of incubation period, 0.5 ml of 5% (w/v) TCA was added to the incubation mixture. The mixture was incubated for 20 min at 25°C and then centrifuged for 10 min at 10,000 *g*. The supernatant was collected and hydrolysis products in 0.2 ml of the supernatant were measured by the method of Böhlen *et al.* [14] using fluorescamine (Sigma Chemicals Co.). Controls were prepared by adding the lysosomal fraction immediately after the addition of TCA. The amount of TCA-soluble products was expressed as tyrosine equivalent using tyrosine as a standard.

RESULTS

Effect of pH A myofibrillar preparation was incubated with a lysosomal fraction in the range of pH 2.9 to 7.4 for 3 hr. After incubation hydrolysis products were detected by SDS-polyacrylamide gel electrophoresis (Fig. 1). Myofibrillar proteins were hydrolyzed most strongly at pH 3.4. Myosin heavy chains and actin, which have molecular weights of 180,000 and 45,000 respectively, and other myofibrillar components having lower molecular weights were hydrolyzed almost com-

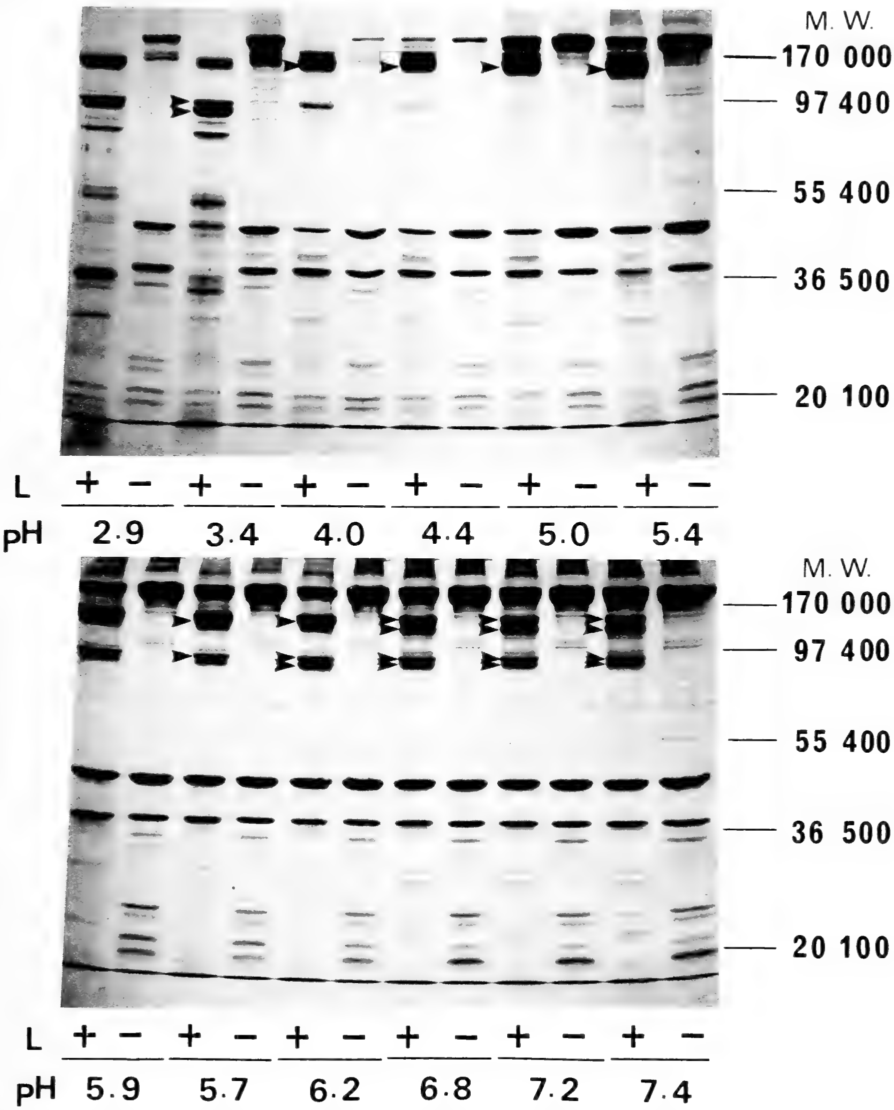

FIG. 1. Hydrolysis of myofibrillar proteins. Myofibrils were incubated in the presence (+) and absence (−) of a lysosomal fraction for 3 hr and then subjected to SDS-polyacrylamide gel electrophoresis as described in Materials and Methods. Incubation buffers used were 50 mM sodium citrate-citric acid buffer (pH 2.9–5.9) and 50 mM Na_2HPO_4–NaH_2PO_4 buffer (pH 5.7–7.4). The values of right margin indicate molecular weights of five marker proteins, which migrate to indicated positions. Arrowheads indicate the degrading products of myosin heavy chains.

pletely at this pH. The hydrolysis products of myosin heavy chains having molecular weights of 150,000, 97,000 and 90,000 were observed. At pH 2.9 and pH 3.4, a small amount of the hydrolysis products of myosin heavy chains was detected even in the absence of a lysosomal fraction. This hydrolysis was partly suppressed by leupeptin (data not shown), suggesting contamination of myofibrillar preparations by a thiol proteinase(s). In the range of pH 4.0 to 5.4, myofibrils were less degraded than at more acidic pH: myosin heavy chains and actin were hydrolyzed in part and the number of hydrolysis products on SDS-polyacrylamide gels decreased. In the range of pH 5.9 to 7.4, myosin heavy chains degraded into fragments with molecular weights of 135,000, 125,000, 93,000 and 89,000. On the other hand, actin did not show any sign of degradation. Most of other myofibrillar components disappeared even at neutral pH during incubation.

Figure 1 also shows that the amounts of proteins in control samples decreased remarkably between pH 2.9 and 4.4. This was because myofibrils tended to form insoluble aggregates under these conditions. After incubation without a lysosomal fraction 31% of myofibrillar proteins was recovered in solubilizing buffer at pH 2.9, 43% at pH 3.4, 28% at pH 4.0 and 32% at pH 4.4 (the mean of two experiments). In the range of pH 5.0 and 7.4, the values increased and reached into almost 100% above pH 6.4.

Myofibril degrading activity in a lysosomal fraction was quantified by measuring the amount of TCA-soluble products. As shown in Figure 2, the highest activity was observed at pH 3.4. This result agreed with that from SDS-polyacrylamide gel electrophoresis. The second peak of the activity was observed at pH 5.4, and the activity decreased gradually as pH increased.

Morphological observation Myofibrils disappeared immediately after mixing with acidic buffers (pH 2.9 and pH 3.4), suggesting dissocia-

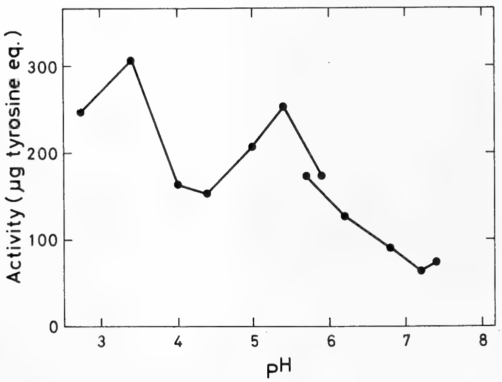

Fig. 2. Effect of pH on myofibril degrading activity. Myofibrils were incubated with a lysososmal fraction for 3 hr, and then TCA-soluble products were measured fluorometrically as described in Materials and Methods. Incubation buffers used were the same as those in Fig. 1.

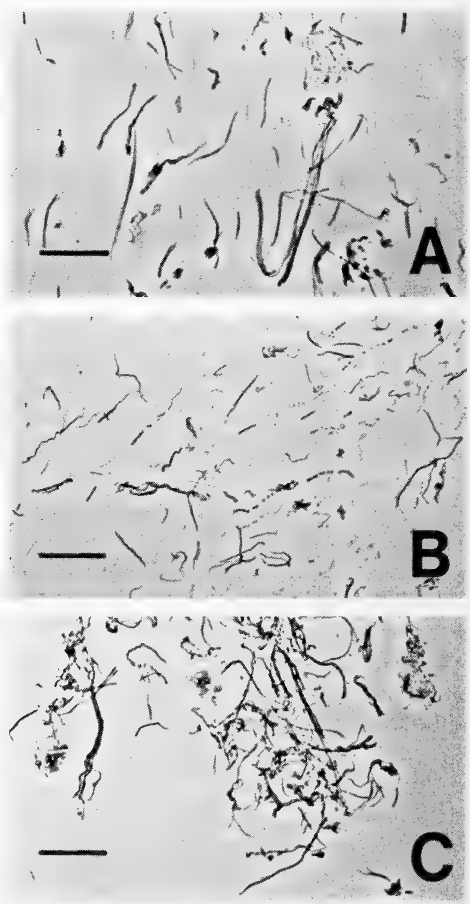

Fig. 3. Phase contrast micrograph of myofibrils. Myofibrils were incubated for 3 hr at pH 5.4 in the presence (B) and absence (C) of a lysosomal fraction. Zero time control (A) is also shown. Scale: 20 μm.

tion of myofibrillar components. Therefore morphological changes of myofibrils by a lysosomal fraction were observed at pH 5.4. As shown in Figure 3, myofibrils were cut into fragments after 3 hr incubation with a lysosomal fraction (Fig. 3B). On the contrary, myofibrils without a lysosomal fraction were not degraded but aggregated during incubation (Fig. 3C). Fragmentation of myofibrils was also observed at pH 6.8, but more slowly.

Effect of inhibitors A myofibrillar preparation was incubated with a lysosomal fraction in the presence of inhibitors and the effect of inhibitors on myofibril degradation was estimated by SDS-polyacrylamide gel electrophoresis (Fig. 4).

At pH 3.4, leupeptin, antipain and chymostatin, inhibitors of thiol proteinases, suppressed markedly the hydrolysis of myofibrillar proteins including myosin heavy chain and actin (Fig. 4A). And unusual products such as a peptide fragment below the band of actin appeared. On the other hand, pepstatin, an inhibitor of carboxyl proteinases, exhibited no inhibitory effect. Neither DIFP, an inhibitor of serine proteinases, nor bestatin, an inhibitor of aminopeptidases, were effective for the inhibition of myofibril degradation. These results showed that only thiol proteinase inhibitors could inhibit myofibril degrading activity when each inhibitor was used alone. However, pepstatin was shown to inhibit the activity which remained in the presence of leupeptin, because in the presence of both leupeptin and pepstatin myofibrillar proteins were hardly hydrolyzed.

At pH 5.4, the hydrolysis of myofibrillar proteins was inhibited by leupeptin, antipain and chymostatin, but not by pepstatin, DIFP and bestatin as well as at pH 3.4 (Fig. 4B). However, myofibril degradation which occurred in the presence of leupeptin at this pH was little suppressed by pepstatin and different from leupeptin-insensitive degradation at pH 3.4. Further inhibition of leupeptin-insensitive degradation was not achieved by either an increased amount of pepstatin (up to 12.5 μg/ml) or 0.1 mM DIFP (data not shown).

At pH 6.8, leupeptin, antipain and chymostatin

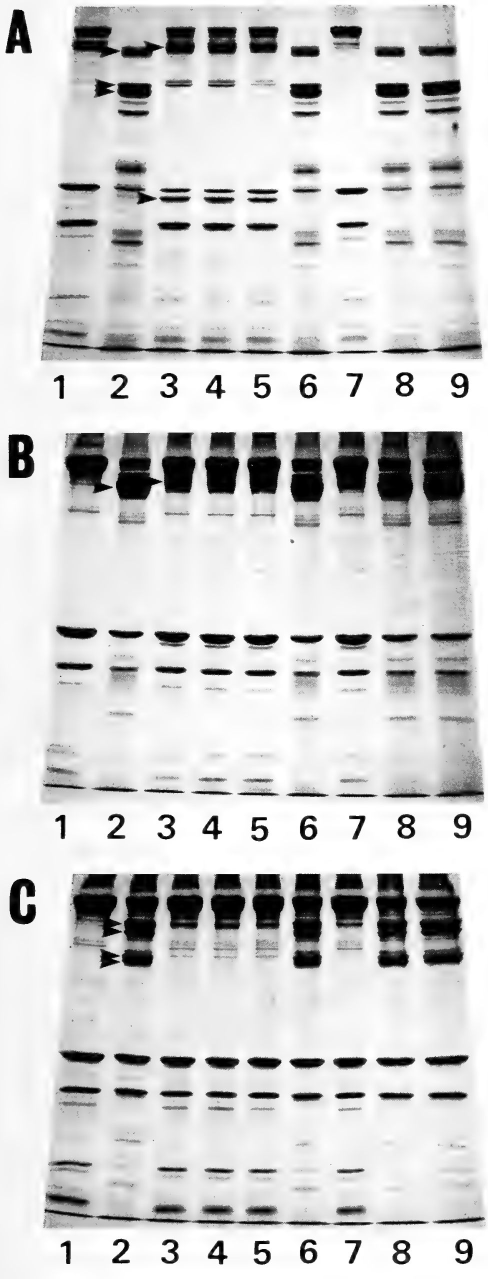

FIG. 4. Effect of inhibitors on hydrolysis of myofibrillar proteins at pH 3.4 (A), pH 5.4 (B) and pH 6.8 (C). Myofibrils were incubated for 3 hr with (lanes 2–9) or without (lane 1) a lysosomal fraction. Inhibitors added to incubation mixtures were as follows: no inhibitor (lane 2), leupeptin (lane 3), antipain (lane 4), chymostatin (lane 5), pepstatin (lane 6), leupeptin and pepstatin (lane 7), bestatin (lane 8) and DIFP (lane 9). Arrowheads indicate the degrading products of myofibrillar proteins.

inhibited myofibril degradation almost completely (Fig. 4C). Pepstatin did not show any effect in the presence and absence of leupeptin. DIFP and bestatin were not effective as well as at pH 3.4 and pH 5.4.

The effects of inhibitors on myofibril degradation was examined by measuring TCA-soluble products. Leupeptin suppressed 87% of myofibril degradation at both pH 3.4 and pH 5.4 (the mean of two experiments). Suppression by pepstatin was 8% at pH 3.4 and 3% at pH 5.4. In the presence of the two inhibitors 96% of myofibril degradation was suppressed at pH 3.4 and 92% at pH 5.4. These results confirmed that thiol proteinase inhibitors are potent inhibitors of myofibril degradation by lysosomes.

Effect of cysteine The above results suggested that a thiol proteinase(s) plays an important role in the degradation of myofibrils by a lysosomal fraction. Therefore, cysteine which had been known as an activator of a thiol proteinase in tadpole tails [11] was removed from incubation mixtures and the extent of myofibril degradation was compared to that in the presence of cysteine (Fig. 5). Stimulating effect of cysteine on the hydrolysis of myofibrillar proteins was remarkable at pH 6.8, moderate at pH 5.4 and slight at pH 3.4.

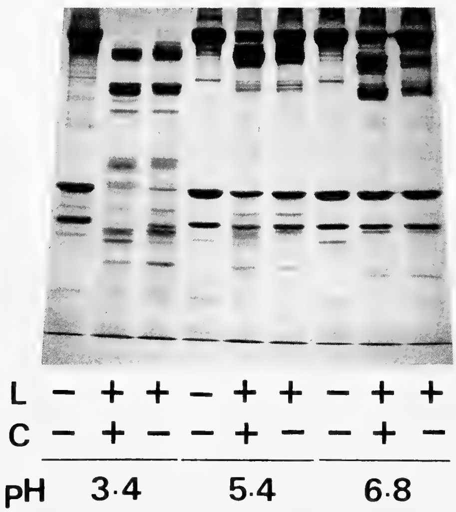

FIG. 5. Effect of cysteine on hydrolysis of myofibrillar proteins. Myofibrils were incubated for 3 hr in the presence (+) and absence (−) of 5 mM cysteine and a lysosomal fraction at pH 3.4, pH 5.4 and pH 6.8. C, cysteine; L, a lysosomal fraction.

DISCUSSION

Myofibrils were degraded by a lysosomal fraction from regressing tadpole tails especially at acidic pH (Fig. 1). Measurement of TCA-soluble products showed that myofibril degrading activity had two optimum pHs: the highest one was observed at pH 3.4 and the second highest was observed at pH 5.4 (Fig. 2). Myofibrils formed insoluble aggregates during incubation under acidic conditions, especially below pH 4.4. The decreased amount of myofibrils available as substrate may affect the activity of a lysosomal proteinase(s). Therefore it is not clear whether or not two acid proteinases with different pH optimum exist in a lysosomal fraction.

Localization of myofibril degrading activity in lysosomes was confirmed by the fact that a lysosomal fraction showed the highest specific activity among subcellular fractions (data not shown). A preliminary experiment showed that a lysosomal fraction isolated from the tails of prometamophic tadpoles degraded myofibrils as well as tail lysosomes from metamorphosing tadpoles, suggesting the presence of a similar proteinase in both growing and regressing tails.

Almost all of the myofibrillar proteins including myosin heavy chains and actin could be hydrolyzed by a myofibril degrading enzyme in a lysosomal fraction (Fig. 1). However, sensitivity to the attack of the proteinase was not identical among myofibrillar proteins. Myosin heavy chains seem to be more susceptible to the proteinase than actin, because myosin heavy chains were hydrolyzed at any pH examined but actin was hydrolyzed only at acidic pH.

Yoshizato and Nakajima [15] reported that the tail extract of metamorphosing bullfrog tadpoles contains a thiol proteinase, an actin-degrading enzyme. Recently the actin-degrading enzyme was purified and characterized [16, 17]. This enzyme hydrolyzed actin at pH 6.0 and formed a degrading product with molecular weight of 28,000. When the enzyme was incubated with myofibrils, myosin heavy chains were hydrolyzed in addition to actin. It is not clear now whether a thiol proteinase in

lysosomes is identical to the actin-degrading enzyme or not. However, actin was not hydrolyzed at around pH 6.0 in our present study. These two proteinases seem to be different from each other, but purification and characterization of the lysosomal enzyme is needed to clarify it.

A series of inhibitor experiments indicated that a thiol proteinase must be a major myofibril degrading enzyme in lysosomes. The stimulating effect of cysteine on myofibril degrading activity further supports that the activity is related to a thiol proteinase.

Unusual peptide fragments appeared in the presence of thiol proteinase inhibitors at pH 3.4 (Fig. 4A). And pepstatin inhibited the appearance of these products. Therefore this leupeptin-insensitive activity could be attributed to a carboxyl proteinase which has different substrate specificity from that of a thiol proteinase. When pepstatin was used alone, the result obtained from SDS-polyacrylamide gel electrophoresis was inconsistent with that from the measurement of TCA-soluble products: pepstatin did not affect the profile of peptide fragments on SDS-polyacrylamide gels but inhibited partly the formation of TCA-soluble products. The reasons why different results were obtained are not clear. In any case, a carboxyl proteinase is possibly a minor myofibril degrading enzyme in lysosomes.

Komukai *et al.* [6] recently observed that autolysis of tail muscle homogenates under acidic conditions was inhibited by leupeptin in metamorphosing bullfrog tadpoles. Pepstatin inhibited the autolysis only when both pepstatin and leupeptin were used together. These results correspond to the present results.

A lysosomal fraction contains two acid proteinases, a thiol proteinase and cathepsin D. A thiol proteinase which hydrolyzes myofibrillar proteins is probably identical to the thiol proteinase described by Kobayashi and Horiuchi [11] with respect to the optimum pHs of their activities and the effects of inhibitors and of cysteine. A carboxyl proteinase which hydrolyzed myofibrillar proteins is possibly cathepsin D [18]. Both activities of a thiol proteinase and cathepsin D increase in tails during metamorphosis [11, 19]. But physiological function of the two proteinases may be different from each other. Seshimo *et al.* [20] showed that triiodothyronine-induced tail fin regression *in vitro* was inhibited by pepstatin but not by leupeptin, antipain and chymostatin. This indicates an important role of cathepsin D in tail fin regression. On tail muscle degeneration, however, a thiol proteinase probably plays more important role than cathepsin D as discussed above.

Physiological function of lysosomal thiol proteinases on muscle degradation was suggested by Ishiura *et al.* [21], who proposed two-step mechanism of plasmocid-induced muscle degradation in rats. Plasmocid, a myotoxic agent, rapidly causes selective loss of α-actinin in muscle cells: this may be a non-lysosomal process. Subsequently macrophages invade into muscle tissues and phagocytose degraded muscle cells. Degradation of myofibrils in macrophages may be performed by cathepsins B and L, because macrophages were shown to contain a large amount of these thiol proteinases. These processes seem to resemble those of muscle degeneration in tadpole tails. Ultrastructural observations showed that muscle cells, in contrast to macrophages, contained only a little number of lysosomes even at metamorphic climax [2, 3, 5]. It is likely that a thiol proteinase in macrophages, which were shown to invade into muscle tissues and phagocytose sarcolytes in regressing tails [1–5], participates in the myofibril degradation.

ACKNOWLEDGMENT

This work was supported by Grant-in-Aid 58740359 from the Ministry of Education, Science and Culture, Japan and by The Science Research Promotion Fund from Japan Private School Promotion Foundation.

REFERENCES

1 Weber, R. (1964) Ultrastructural changes in regressing tail muscles of Xenopus larvae at metamorphosis. J. Cell Biol., **22**: 481–487.

2 Fox, H. (1972) Muscle degeneration in the tail of *Rana temporaria* larvae at metamorphic climax: an electron microscopic study. Arch. Biol. (Liège), **83**: 407–417.

3 Fox, H. (1975) Aspects of tail muscle ultrastructure and its degeneration in *Rana temporaria*. J.

Embryol. Exp. Morphol., **34**: 191–207.

4 Kerr, J. F. R., Harmon, B. and Searle, J. (1974) An electron-microscope study of cell deletion in the anuran tadpole tail during spontaneous metamorphosis with special reference to apoptosis of striated muscle fibres. J. Cell Sci. ,**14**: 571–585.

5 Watanabe, K. and Sasaki, F. (1974) Ultrastructural changes in the tail muscles of anuran tadpoles during metamorphosis. Cell Tissue Res., **155**: 321–336.

6 Komukai, M., Kobayashi, K. and Horiuchi, S. (1986) Autolysis in the tail muscles of metamorphosing tadpoles. Comp. Biochem. Physiol., **85B**: 55–59.

7 Kobayashi, K., Hara, M. and Horiuchi, S. (1985) Isolation of lysosomes from the tail of metamorphosing bullfrog tadpole. Comp. Biochem. Physiol., **81**B: 603–607.

8 Taylor, A. C. and Kollros, J. J. (1946) Stages in the normal development of *Rana pipiens* larvae. Anat. Rec., **94**: 7–23.

9 Perry, S. V. and Grey, T. C. (1956) A study of the effects of substrate concentration and certain relaxing factors on the magnesium-activated myofibrillar adenosine triphosphatase. Biochem. J., **64**: 184–192.

10 Read, S. M. and Northcote, D. H. (1981) Minimization of variation in the response to different proteins of the coomassie blue G dye-binding assay for protein. Anal. Biochem., **116**: 53–64.

11 Kobayashi, K. and Horiuchi, S. (1983) Lysosomal thiol proteinase in the tadpole tail of *Rana catesbeiana*: some properties and changes in the activity during metamorphosis. Zool. Mag., **92**: 130–137.

12 Umezawa, H. and Aoyagi, T. (1977) Activities of proteinase inhibitors of microbial origin. In “Proteinases in Mammalian Cells and Tissues”. Ed. by A. J. Barrett, Elsevier/ North-Holland Publishing Co., Amsterdam, pp. 637–662.

13 Laemmli, U. K. and Favre, M. (1973) Maturation of the head of bacteriophage T4. I. DNA packaging events. J. Mol. Biol., **80**: 575–599.

14 Böhlen, P., Stein, S., Dairman, W. and Udenfriend, S. (1973) Fluorometric assay of proteins in the nanogram range. Arch. Biochem. Biophys., **155**: 213–220.

15 Yoshizato, K. and Nakajima, Y. (1982) Actin degradation in the metamorphosing bullfrog tadpole tail. Dev. Growth Differ., **24**: 553–562.

16 Motobayashi, N. Y. and Yoshizato, K. (1986) Partial purification and characterization of an actin-degrading proteinase from the tail of metamorphosing tadpoles. Zool. Sci., **3**: 83–89.

17 Motobayashi, N. Y., Horiguchi, T. and Yoshizato, K. (1986) Mode of degradation of myofibrils and muscle tissues by the actin-degrading enzyme. Zool. Sci., **3**: 91–96.

18 Sakai, J. and Horiuchi, S. (1979) Characterization of cathepsin D in the regressing tadpole tail of bullfrog, *Rana catesbeiana*. Comp. Biochem. Physiol., **62**B: 269–273.

19 Sakai, J. and Horiuchi, S. (1979) Changes in cathepsin D activity in the tail of *Rana catesbeiana* larvae during spontaneous metamorphosis. Zool. Mag., **88**: 116–121.

20 Seshimo, H., Ryuzaki, M. and Yoshizato, K. (1977) Specific inhibition of triiodothyronine-induced tadpole tail-fin regression by cathepsin D-inhibitor pepstatin. Dev. Biol., **59**: 96–100.

21 Ishiura, S., Nonaka, I., Nakase, H., Tada, A. and Sugita, H (1984) Two-step mechanism of myofibrillar protein degradation in acute plasmocid-induced muscle necrosis. Biochim. Biophys. Acta, **798**: 333–342.

ZOOLOGICAL SCIENCE 4: 115–122 (1987)

Steroidogenic Activity of Isoelectric Gonadotropin Components in the Pituitary of Adult Male Newt, *Cynops pyrrhogaster pyrrhogaster*

SHIGEYASU TANAKA, MASA-AKI HATTORI[1] and KATSUMI WAKABAYASHI[1]

Department of Morphology and [1]Hormone Assay Center, Institute of Endocrinology, Gunma University, Maebashi 371, Japan

ABSTRACT—Biological activities of isoelectric GTH components in newt pituitary were studied using *in vitro* testosterone or cyclic AMP production by minced mature zone of newt testes. Seven isoelectric GTH components were prepared from adult male newt pituitaries by isoelectric focusing using pH 3.5–10 ampholites. These components showed receptor-binding activity to the *Anolis* testis. Among them, pIs of component F and G seemed to agree with those of *Ambystoma* FSH when estimated by its chromatographic behavior. These isoelectric GTH components were incubated with the minced testicular tissue at different tempeature (8, 20 or 35°C) for 3 hr in order to see their biological activity. The component F/G with pI 5.24 and 4.98 was effective in stimulating testosterone production similarly to the other five components which have alkaline to neutral pIs. When testes were incubated at 20°C, maximal steroidogenic activity was 7–17 times greater than basal activity without GTH, and a dose-response relationship was observed with GTH components. Furthermore, testosterone production increased as temperature increased. In contrast, regrardless of temperature, almost all the components stimulated cyclic AMP production at the highest doses tested (2–5 times over control). The relationship between steroidogenic activity and temperature was discussed.

INTRODUCTION

Bullfrog *Rana catesbeiana* pituitary has two chemically distinct gonadotropins (GTH) which show similar behavior to mammalian LH and FSH in ion-exchange chromatography, respectively [1–7]. Recently, available information on biological activities of these two GTHs has been accumulated [6–12]. However, with respect to other amphibians, especially in urodele species, many problems related to their biochemical and biological properties remain unsolved. We have previously examined isoelectric focusing (IEF) profiles of newt pituitary GTH activity in different reproductive states, employing *Xenopus* and *Anolis* radioreceptor assay (RRA), and found seasonal difference in the IEF profiles [13]. Furthermore, the IEF profiles of newt GTH were markedly different from those of bullfrog, suggesting a possible difference in biological properties between these species [13–15]. However, receptor-binding activity does not always reflect the biological activity [16–18]. Therefore, it was necessary to elucidate what kinds of biological properties each IEF component of newt pituitary GTH possesses. In the present study, testosterone and cyclic AMP production by minced newt testes were used to examine the biological activity. We also studied the influence of temperature on testosterone production, because temperature plays an important role in the steroidogenic effect of GTH on amphibian testes [for review, 19, 20].

Accepted July 22, 1986
Received June 18, 1986

MATERIALS AND METHODS

Isoelectric focusing (IEF) and separation of isoelectric components

Adult male newts *Cynops pyrrhogaster pyrrhogaster* were collected at an appointed station in Hayakawa, Niigata Prefecture in the middle of

July, 1983 (Experiment I) and again in July, 1984 (Experiment II). The pituitaries were removed immediately after collection, and then pituitary extracts were prepared by homogenizing approximately 175 glands (Experiment I) and 200 glands (Experiment II) with distilled water (DW), followed by freezing-thawing, and by centrifugation at 15,000 rpm for 20 min. The IEF fractionation was carried out on a 25 ml-column with Ampholine pH 3.5–10 (LKB Produkter) at 1% concentration in a sorbitol density gradient from 5 to 50%, according to the method described in the previous reports [13, 15]. IEF with the anode at the top of the column was run at 2–4°C for 4 days, the voltage applied being increased stepwise from 300 to 900 V. After focusing, 0.45-ml fractions were collected at a flow rate of 0.1 ml/min under simultaneous measurement of pH with a flow-through type of glass electrode (Fuji Kagaku Keisoku, SE 1600GC). The fractions containing GTH activity were detected by *Anolis* RRA (see below). Then, each fraction was dialysed against cold DW for 2 days after adding 1.5 ml of PBS containing 1% bovine serum albumin (PBS-BSA), and lyophilized. The materials were stored at −20°C until bioassay.

In vitro estimation of biological activity

The biological activity of isoelectric GTH components in the newt pituitary was measured by *in vitro* testosterone and cyclic AMP production in minced mature zone of newt testes containing androgen-secreting tissue [21, 22]. Testicular tissues were obtained from adult male newts collected in early November, 1983 (Experiment I) and late November, 1984 (Experiment II) at the same station as mentioned above. Newts were decapitated and only the mature zones of their testes were quickly excised. The testicular tissues were minced with scissors as small as possible in ice-cold Medium 199 (GIBCO Laboratories, Grand Island Biochemistry Company, Grand Island, NY) modified for amphibians containing 0.1% BSA (incubation medium). After centrifugation at 1,000 rpm for 15 min, the supernatant, containing spermatozoa, was removed by suction. This procedure was repeated three times to remove spermatozoa completely. The testicular tissue pellet was resuspended in the incubation medium. Incubations were performed at 8, 20 or 35°C in a 24-well tissue cluture cluster (Costar, Cambridge, MA) under an atmosphere of 95% O_2–5% CO_2 for 3 hr. The minced testicular tissue equivalent to approximately one-third of testis was incubated in triplicate in 0.5 ml of the incubation medium containing 0.5 mM 3-isobutyl-1-methylxanthine (Sigma) with or without varying doses of the GTH preparation. After incubation, 50 μl of 10% NaN_3 was added to each well to stop steroidogenesis. Each incubation medium was transferred to a glass culture tube and heated at 90°C for 10 min in the presence of 1 mM theophiline, then centrifuged at 3,000 rpm for 20 min. Testosterone and cyclic AMP in the supernatants were measured by radioimmunoassay using iodinated tracer, as previously described [23, 24].

Anolis radioreceptor assay (RRA)

Anolis RRA was performed with *Anolis* testicular homogenates as receptor fractions and ^{125}I-rat FSH as radioligand according to the described in the previous reports [13, 15]. ^{125}I-labeled rat FSH was prepared by radioiodination of NIADDK rat I–3 (supplied by the National Pituitary Agency and the Pituitary Hormones and Antisera Center, NIADDK, NIH) with lactoperoxidase according to the method of Miyachi *et al.* [25] with minor modification. Nonspecific binding was determined by incubation of the receptor fraction with iodinated tracer in the presence of 100 I.U. of pregnant mare serum gonadotropin (Sankyo Manufacturing Co.). Results were expressed as micrograms of NIADDK rat FSH I–3.

Statistical analysis

In *Anolis* RRA system, the inhibition curves obtained with isoelectric GTH components and standard preparation were linearized by the method of least squares on logarithmic amount of hormone preparations versus logit B/B_0, and their slopes were compared by Student's t-test or Cochran-Cox test.

RESULTS

Experiment I

Isoelectric GTH components

To obtain isoelectric GTH component preparations, pituitary extract from adult male newts collected in mid-July, 1983 was fractionated by IEF using pH 3.5–10 ampholites. When GTH activity was measured by *Anolis* RRA, seven peaks (three major peaks, two mediun peaks and two minor peaks) appeared in the alkaline to acidic pH region (Fig. 1). These components were designated for convenience as components A (pI 9.24), B (pI 8.75), C (pI 8.31), D (pI 7.53), E (pI 6.75), F (pI 5.24) and G (pI 4.98), respectively. This IEF profile was almost similar to that of the mid-July in the previous report [13]. Since the components F and G in the acidic pH region were also a very small amount, they were collected under one fraction as component F/G in the following experiment.

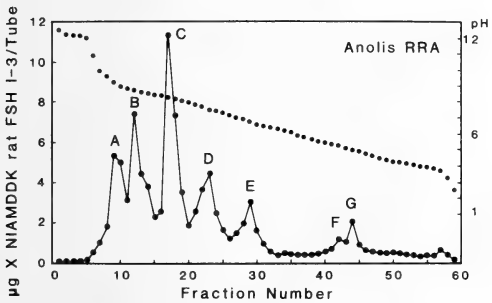

Fig. 1. Isoelectric focusing profile of gonadotropin in the pituitary extract of adult male newt captured in the mid-July, 1983. The fractions were assayed for GTH with *Anolis* RRA. Dots in the figure represent the pH of the fractions.

When the six isoelectric GTH components were assayed by *Anolis* RRA system in triplicates in several different dilutions, their inhibition curves were statistically parallel to the standard curve obtained with rat FSH, indicating that it is possible to express the relative amount of each component as *Anolis* testicular receptor-binding activity of NIADDK rat FSH I–3 (Table 1). In the following results, therefore, the relative potency represented the ratio of biological activity to receptor-binding activity (B: R).

Biological activity

In the present experiment using doses of the hormone ranging from 0.1 to 6.4 ng/well, all the components were effective in stimulating testosterone production (Fig. 2). Testosterone production was dose-dependently increased by each component. At the maximal dose (6.4 ng/well) of each component, testosterone produced by the minced testicular tissues was 5.19 ng/well (component A), 1.63 ng/well (B), 1.96 ng/well (C), 2.66 ng/well (D), 3.53 ng/well (E) and 3.14 ng/well (F/G). These values were 4–13 times greater than that without stimulation (0.40 ng/well). In addition, the component A with the highest pI showed the highest B: R ratio.

Experiment II

To elucidate the maximal response of testosterone production, higher doses of GTH preparation were used in the present experiment. Further-

Table 1. Inhibition curves of isoelectric GTH components

Species		R	Slope	S. E.	No. of Points
rat FSH		−0.986	−1.211	0.089	7
Component	A	−0.997	−1.185	0.061	4
	B	−0.976	−1.233	0.156	5
	C	−0.999	−1.306	0.024	4
	D	−0.953	−1.107	0.246	4
	E	−0.987	−1.243	0.099	6
	F/G	−0.980	−1.200	0.169	4

Slopes are from plots of logit % bound vs log of dilution factors or hormone concentration. All the slopes are not significantly different from the slope of rat FSH.

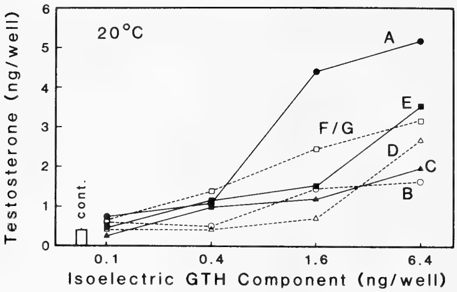

FIG. 2. Stimulation of *in vitro* testosterone production by the isoelectric GTH components obtained from newt pituitary extract in mid-July, 1983. Testes were from adult newts captured in early November. The minced testicular tissue equivalent to approximately one-third of a testis were incubated at 20°C for 3 hr in 0.5 ml of modified Medium 199 for amphibians with or without the GTH component. The hormonal dose of each component was expressed as the *Anolis* testicular receptor-binding activity of NIADDK rat FSH I–3. The points are means of triplicate incubations. The bar and vertical line represent the mean and SE of three controls.

more, incubation was carried out at different temperatures to examine the effects of temperature on steroidogenic activity. At the same time, cyclic AMP production was assayed.

Isoelectric GTH preparations were obtained by the same method as described in Experiment I. The IEF profile of newt pituitary GTH collected in mid-July, 1984 is shown in Figure 3. The pIs of the isoelectric GTH components were quite similar to those of Experiment I, although the relative amount of each component was somewhat different.

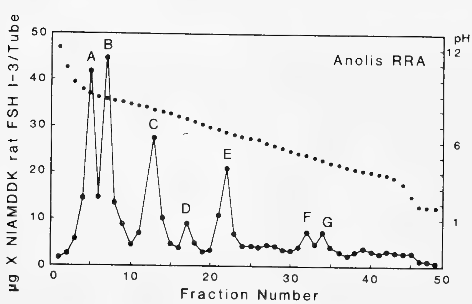

FIG. 3. Isoelectric focusing profile of gonadotropin in the pituitary extract of adult male captured in mid-July, 1984.

Effect of temperature on biological activity

a) Testosterone production

Since the available amount of each component was limited, the range of doses used in this experiment differed according to the component. When incubated at 35°C, the basal control level was 2.18±0.15 ng/well, and component F/G was the most potent of all the components tested

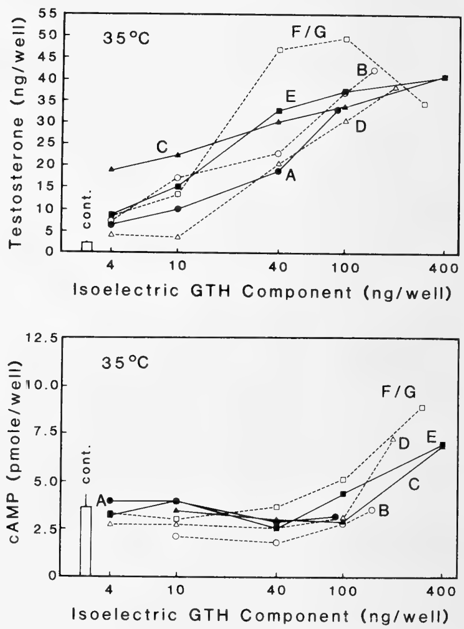

FIG. 4. Stimulation of *in vitro* testosterone and cyclic AMP production by minced testes in late November, 1984 with the isoelectric GTH components at 35°C. Incubation conditions and symbols are the same as those in Fig. 2.

(Fig. 4). The maximal steroidogenic activity of component F/G occurred at 100 ng/well (ca. 23 times over control), but at the highest dose (300 ng/well) testosterone production showed a slight decrease. The other five components showed maximal steroidogenic activity at the highest dose tested (ca. 15 to 20 times over control). Thus, there was no difference in potency among each isoelectric GTH component. In an incubation at 20°C, at the lower doses (4 to 10 ng/well) which are similar to those used in Experiment I, the component A with the greater

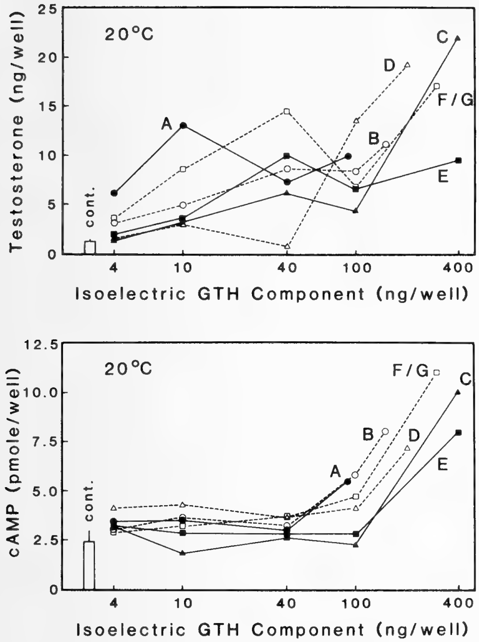

FIG. 5. Stimulation of *in vitro* testosterone and cyclic AMP production by minced testes in late November, 1984 with the isoelectric GTH components at 20°C. Incubation conditions and symbols are the same as those in Fig. 2.

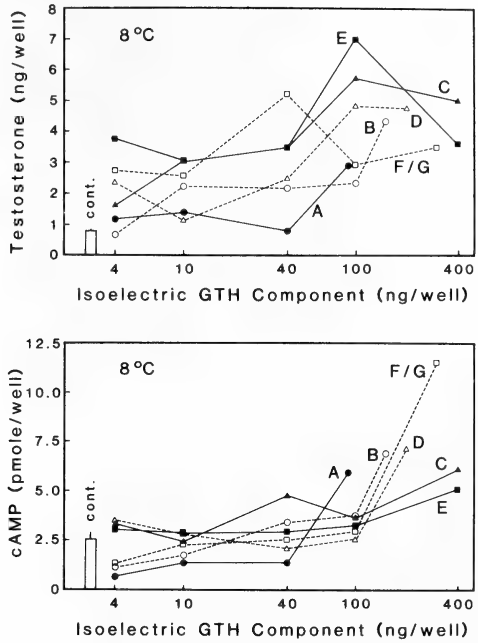

FIG. 6. Stimulation of *in vitro* testosterone and cyclic AMP production by minced testes in late November, 1984 with the isoelectric GTH components at 8°C. Incubation conditions and symbols are the same as those in Fig. 2.

alkaline pI value showed the highest stimulation in testosterone production (Fig. 5). In each of the isoelectric components maximal steroidogenic activity was 7–17 times as great as that without stimulation (1.29 ± 0.20 ng/well). When incubated at 8°C, the response was lower than at 20 and 35°C. Maximal steroidogenesis caused by the isoelectric GTH components was 3–9 times as much as that of control stimulation (0.79 ± 0.02 ng/well) (Fig. 6).

b) Cyclic AMP production

The effect of all the isoelectric GTH components on cyclic AMP production in the minced testicular tissue was measured (Figs. 4, 5 and 6). At 8 and 20°C, all the components stimulated cyclic AMP production only at the highest doses tested. The maximal response was only 2–5 times as great as that of the control (2.58 ± 0.31 pmol/well at 8°C and 2.45 ± 0.69 pmol/well at 20°C). At 35°C, a similar increase in cyclic AMP was noted in the four components except components A and B.

DISCUSSION

With respect to amphibian GTH, Licht and his co-workers have reported that pituitaries of both anuran and urodele species have two kinds of GTH which correspond to mammalian and avian LH and FSH, respectively (for review, [3, 26]). In the study on urodele *Ambystoma* LH and FSH, however, their biochemical and biological properties are not fully confirmed, because of difficulty of collecting their pituitaries in large quantities [27]. On the other hand, to observe all the components of GTH in as natural as possible and small amount of materials, we developed the IEF technique, coupled with RIA or RRA, and elucidated the IEF profiles of several amphibian GTH activity [13–15]. When newt pituitary extracts were fractionated by IEF, and GTH activity was measured by two RRA systems; one is *Xenopus* RRA, which is thought to be LH-specific, and the other is *Anolis* RRA, five GTH components appeared in the alkaline to neutral pH regoin, and

Xenopus RRA-positive components closely corresponded to *Anolis* RRA-positive ones [13]. On the other hand, in the IEF profiles of bullfrog GTH, *Xenopus* RRA-positive components were found in the alkaline pH region, whereas *Anolis* RRA-positive components were found in the neutral to acidic pH region [14, 15]. Thus both RRA-positive components were quite independent, indicating distinct separation of LH and FSH similar to that of mammalian and avian species. Therefore, it was estimated that the biological properties of newt GTH may be somewhat different from those of bullfrog LH and FSH. Furthermore, IEF profile of newt GTH varied depending on seasonal reproductive state; only in July when spermatogenesis was active, *Anolis* RRA gave one or two exceptional components in the neutral to acidic pH region [13]. Since the pIs of these additional components seemed to agree with those of *Ambystoma* FSH prepared by Licht *et al.* [27] when estimated by its chromatographic behavior, it was very interesting to elucidate whether or not all the components might possess steroidogenic activity.

First, in the present study, it was confirmed that IEF profiles of newt pituitary GTH in mid-July have two additional components F and G in the neutral to acidic pH region, which were obtained by *Anolis* RRA [13]. Secondly, it was clearly demonstrated that component F/G in the neutral to acidic pH region stimulated testosterone production similar to the other five components with alkaline to neutral pIs, when the biological activity of each component was examined on the basis of *in vitro* testosterone production in minced mature zone of newt testes captured in November. Thus, with respect to steroidogenic activity in the homologous testes, the specificity of each of the isoelectric components in newt pituitary GTH was not clearly distinct. However, this was in contrast to an earlier report that in secretion of *Ambystoma* testicular testosterone *Ambystoma* LH is about 50 times more potent than *Ambystoma* FSH, although *Ambystoma* FSH is not highly purified compared with LH [11].

In the range from 0.1 to 6.4 ng/well used in Experiment I, the components with the greatest alkaline pI value showed the highest B: R ratio, indicating that the hormonal actions of this component are efficiently amplified in the biological response to the final step. When incubated at 20°C in Experiment II, similar results were obtained in the lower dose range, but not at higher doses tested.

Since the testis of amphibians living temperate zone shows a discrepancy between spermatogenesis and steroidogenesis, depending on temperature, the importance of temperature to testicular function has been pointed out for a long time, and many studies have already been performed *in vivo* on the effect of temperature and gonadotropin upon testicular function (for review, [19]). Our previous study [20] on newt testes with mammalian LH and FSH has shown that FSH is more potent in stimulating spermatogenesis at the higher temperature (18°C), whereas LH is potent in testosterone production at the lower temperature (8°C), as well as the results in *Rana esculenta* [28] and *Triturus cristatus carnifex* [29]. In the present study, the incubation at 8 and 35°C in addition to 20°C was performed because our previous studies in respect to newt testicular function and environmental temperatures suggested that approximately 8°C is optimal for steroidogenesis, and 20°C for spermatogenesis [22, 30] and the temperature of 35°C seemed to be lethal for newt. We had expected that incubation at 8°C would result in the highest increase in testosterone production, but the present results indicated that testosterone production increases with increasing temperatures. Similar results were obtained in bullfrog although a significant decrease in androgen secretion was observed at 36°C [10]. On the other hand, Kubokawa and Ishii [31, 32] reported that gonadotropin receptor of newt testes has an optimal temperature of affinity for rat FSH between 15 and 20°C, but not around 37°C. These discrepancies might be due to differences in incubation time or seasonal fluctuations in the testicular sensitivity to GTHs.

It is well established that in mammals the action of GTHs in their target organ is mediated by cyclic AMP. In the present study, almost all the isoelectric GTH components at the highest dose significantly stimulated cyclic AMP production. Similar stimulation was found at three different

temperatures, suggesting that an increase in cyclic AMP production is not dependent on temperature. In the range of doses with no clear stimulation of cyclic AMP production, almost all the isoelectric GTH components stimulated testosterone production. This result may be consistent with the fact that in mammals receptor-occupation of less than 1% of the whole LH receptor is sufficient to elicit a maximal steroidogenic response in Leydig cells [33].

Recently, Abe [34] reproduced the differentiation of newt primary spermatocytes into spermatids *in vitro*, and moreover Nishikawa and Abe [35] demonstrated that the percentage of cell that progressed to an advanced stage is not increased by the addition of fetal bovine serum, ovine FSH, 5α-DHT and testosterone propionate at 22°C. On the other hand, secondary spermatogonia undergo some mitotic divisions *in vitro* but soon degenerate, which can be stimulated by neither mammalian FSH or LH [36]. Furthermore, Muller and Licht [37] reported that bullfrog LH as well as FSH stimulates the proliferation of spermatogonia in the frog testes. Hanaoka *et al.* [6] found that bullfrog FSH (acidic GTH–III, pI 6.2) stimulates only about 3 times as potently as bullfrog LH (basic GTH–IV, pI 9.3) the increase in testicular weight in hypophysectomized young *Xenopus*. Thus, there was no evidence indicating apparent FSH specificity for spermatogenesis. Therefore, it is possible that all the isoelectric components of newt pituitary GTH may stimulate some stages of the spermatogenic process. To clarify whether or not each isoelectric GTH component of newt pituitary with potency in testosterone production also stimulates spermatogenesis, further studies will be necessary.

ACKNOWLEDGMENTS

We are grateful to Professor K. Kurosumi of this Institute for his encouragement during this work. We are also grateful to Dr. Y. Hanaoka of the Institute for discussing this paper and Dr. A. F. Parlow of the Pituitary Hormones and Antirera Center and National Pituitary Agency, NIADDK for supplying rat FSH.

REFERENCES

1 Licht, P. and Papkoff, H. (1974) Separation of two distinct gonadotropins from the pituitary gland of the bullfrog *Rana catesbeiana*. Endocrinology, **94**: 1587–1594.

2 Papkoff, H., Farmer, S. W. and Licht, P. (1976) Isolation and characterization of luteinizing hormone from amphibian (*Rana catesbeiana*) pituitaries. Life Sci., **18**: 245–250.

3 Licht, P., Papkoff, H., Farmer, S. W., Muller, C. H., Tsui, H. W. and Crews, D. (1977) Evolution of gonadotropin structure and function. Recent Prog. Horm. Res., **33**: 169–248.

4 Takahashi, H. and Hanaoka, Y. (1981) Isolation and characterization of multiple components of basic gonadotropin from bullfrog (*Rana catesbeiana*) pituitary gland. J.Biochem., **90**: 1333–1340.

5 Takahashi, H. and Hanaoka, Y. (1985) Characterization of bullfrog gonadotropin molecules in comparison with mammalian hormones. In "Current Trends in Comparative Endocrinology". Ed. by B. Lofts and W. N. Holmes, Hong Kong Univ. Press., Hong Kong, pp. 187–188.

6 Hanaoka, Y., Hayashi, H. and Takahashi, H. (1984) Isolation and characterization of bullfrog gonadotropins. Gunma Symposia on Endocrinology, **21**: 63–77.

7 Takada, K. and Ishii, S. (1984) Purification of bullfrog gonadotropins: Presence of new subspecies of luteinizing hormone with high isoelectric points. Zool. Sci., **1**: 617–629.

8 Licht, P. and Crews, D. (1976) Gonadotropin stimulation of *in vitro* progesterone production in reptilian and amphibian ovaries. Gen. Comp. Endocrinol., **29**: 141–151.

9 Muller, C. H. (1977) *In vitro* stimulation of 5α-dihydrotestosterone and testosterone secretion from bullfrog testis by nonmammalian and mammalian gonadotropins. Gen. Comp. Endocrinol., **33**: 109–121.

10 Muller, C. H. (1977) Plasma 5α-dihydrotestosterone and testosterone in the bullfrog, *Rana catesbeiana*: Stimulation by bullfrog LH. Gen. Comp. Endocrinol., **33**: 122–132.

11 Muller, C. H and Licht, P. (1980) Gonadotropin specificity of androgen secretion by amphibian testes. Gen. Comp. Endocrinol., **42**: 365–377.

12 Gavaud, J., Licht, P. and Papkoff, H. (1979) *In vitro* stimulation of cyclic-AMP production in *Rana catesbeiana* ovaries by homologous gonadotropins. Gen. Comp. Endocrinol., **38**: 83–92.

13 Tanaka, S., Takikawa, H., and Wakabayashi, K. (1981) Seasonal variation in pituitary gonadotropin in the adult male newt, *Cynops pyrrhogaster pyrrhogaster,* revealed by isoelectric focusing technique

and radioreceptor assay. Endocrinol. Japon., **28**: 335–345.

14 Tanaka, S., Hanaoka, Y. and Wakabayashi, K. (1983) A homologous radioimmunoassay for bullfrog basic gonadotropin. Endocrinol. Japon., **30**: 71–78.

15 Tanaka, S., Park, M. K., Takikawa, H. and Wakabayashi, K. (1985) Comparative studies on the electric nature of amphibian gonadotropin. Gen. Comp. Endocrinol., **59**: 110–119.

16 Licht, P. and Midgley, A. R., Jr. (1976) *In vitro* binding of radioiodinated human follicle-stimulating hormone to reptilian and avian gonads: Radioligand studies with mammalian hormones. Biol. Reprod., **15**: 195–205.

17 Licht, P. and Midgley, A. R., Jr. (1976) Competition for the *in vitro* binding of radioiodinated human follicle-stimulating hormone in reptilian, avian and mammalian gonads by nonmammalian gonadotropins. Gen. Comp. Endocrinol., **30**: 364–371.

18 Licht, P. (1980) Relationship between receptor binding and biological activities of gonadotropins. In "Hormones, Adaptation and Evolution". Ed. by S. Ishii, T. Hirano and M. Wada. Japan Sci. Soc. Press, Tokyo/Springer-Verlag, Berlin, pp. 167–174.

19 Lofts, B. (1974) Reproduction. In "Physiology of the Amphibia II". Ed. by. B. Lofts, Academic Press, New York and London, pp. 107–218.

20 Tanaka, S. and Takikawa, H. (1984) Amphibian and reptilian gonadotropin: Biological activity. Gunma Symposia on Endocrinology, **21**: 37–61.

21 Imai, K. and Tanaka, S. (1978) Histochemical and electron microscopic observation on the steroid hormone-secreting cells in the testis of the Japanese red-bellied newt, *Cynops pyrrhogaster pyrrhogaster*. Dev. Growth Differ., **20**: 151–167.

22 Tanaka, S. and Iwasawa, H. (1979) Annual change in the testicular structure and sexual character of the Japanese red-bellied newt, *Cynops pyrrhogaster pyrrhogaster*. Zool. Mag., **88**: 295–305.

23 Hattori, M., Sakamoto, K. and Wakabayashi, K. (1983) The presence of LH components having different ratios of bioactivity to immunoreactivity in the rat pituitary glands. Endocrinol. Japon., **30**: 289–296.

24 Hattori, M. and Wakabayashi, K. (1983) Different profiles of isoelectric avian luteinizing hormone components in biological activity and immunoreactivity. Endocrinol. Japon., **30**: 551–560.

25 Miyachi, Y., Vaitukaitis, J. L., Nieschlag, E. and Lipsett, B. (1972) Enzymatic radioiodination of gonadotropins. J. Clin. Endocrinol., **34**: 23–28.

26 Licht, P. (1979) Reproductive endocrinology of reptiles and amphibians: Gonadotropins. Ann. Rev. Physiol., **41**: 337–351.

27 Licht, P., Farmer, S. W. and Papkoff, H. (1975) The nature of the pituitary gonadotropins and their role in ovulation in a urodele amphibian (*Ambystoma tigrinum*). Life Sci., **17**: 1049–1054.

28 Kort, E. J. M. de (1971) "Het interstitium testis bij de groene kikker, *Rana esculenta*: Een histometrisch en histochemisch onderzoek." Grafisch Bedrijf Fa. Lammers en Zn., Terborg.

29 Vellano. C., Sacerdote, M. and Mazzi, V. (1974) Effects of mammalian gonadotropins (FSH and LH) on spermatogenesis in the crested newt under different temperature conditions. Monitore Zool. Ital., **8**: 177–188.

30 Tanaka, S., and Takikawa, H. (1983) Seasonal changes in plasma testosterone and 5α-dihydroteststerone levels in the adult male newt, *Cynops pyrrhogaster pyrrhogaster*. Endocrinol. Japon., **30**: 1–6.

31 Kubokawa, K. and Ishii, S. (1980) Follicle-stimulating hormone (FSH) receptors in the testis of the newt, *Cynops pyrrhogaster*, and comparison of temperature dependency of the receptors with those of the vertebrates. Gen. Comp. Endocrinol., **40**: 425–433.

32 Kubokawa, K. and Ishii, S. (1984) Adaptation of testicular follicle-stimulating hormone receptors to ambient temperatures in vertebrates: Equilibrium analysis. Gen. Comp. Endocrinol., **54**: 277–282.

33 Dufau, M. L., Tsuruhara, T., Horner, K. A., Podesta, K. A. and Catt, K. J. (1977) Intermediate role of adenosine 3′: 5′-cyclic monophosphate and protein kinase during gonadotropin-induced steroidogenesis in testicular interstitial cells. Proc. Natl. Acad. Sci. USA, **74**: 3419–3423.

34 Abe, S. (1981) Meiosis of primary spermatocytes and early spermiogenesis in the resultant spermatids in newt, *Cynops pyrrhogaster in vitro*. Differentiation, **20**: 65–70.

35 Nishikawa, A. and Abe, S. (1983) Progression thoughout all stages of meiosis from the early prophase of newt primary spermatocytes *in vitro*. Dev. Growth Differ., **25**: 323–331.

36 Abe, S. and Tanaka, S. (1980) Behavior of the secondary spermatogonia of the newt, *Cynops pyrrhogaster* in *in vitro* culture. Dev. Growth Differ., **22**: 851–857.

37 Muller, C. H. and Licht, P. (1978) Gonadotropin control of testicular function in the anuran amphibian, *Rana pipiens*. In "Comparative Endocrinology". Ed by P.J.Gaillard and H.H.Boer, Elsevier/North-Holland, New York, pp. 85.

ZOOLOGICAL SCIENCE 4: 123–134 (1987)

Neuropeptide Y (NPY)-like Immunoreactive Neurons in the Brain and Pituitary of the Amphibian *Rana catesbeiana*

Daniel Cailliez[1], Jean-Michel Danger[1], Ann C. Andersen[1]
Julia M. Polak[2], Georges Pelletier[3], Kôsuké Kawamura[4],
Sakaé Kikuyama[4] and Hubert Vaudry[1,5]

[1]*Groupe de Recherche en Endocrinologie Moléculaire, UA CNRS 650, Unité Alliée à l'INSERM, Faculté des Sciences, Université de Rouen, 76130 Mont-Saint-Aignan, France,* [2]*Department of Histochemistry and Medicine, Royal Postgraduate Medical School, Hammersmith Hospital, London WI20HS, United Kingdom,* [3]*MRC Group in Molecular Endocrinology, Le Centre Hospitalier de l'Université Laval, Québec GIVG42, Canada, and* [4]*Department of Biology, School of Education, Waseda University, Tokyo 160, Japan*

ABSTRACT—The distribution of neuropeptide tyrosine (NPY) and the C-terminal peptide of the pro-NPY molecule (C-PON) was examined in the brain of the frog using the indirect immunofluorescence and the peroxidase-immunoperoxidase techniques. Very dense populations of perikarya containing simultaneously NPY- and C-PON-like immunoreactivity were localized in various regions of the brain, in particular in the pallium, the posterocentral nucleus of the thalamus, the mesencephalic tegmentum, the mesencephalic cerebellar nucleus, the dorsal and ventral infundibular nuclei and the preoptic nucleus. The co-existence of NPY- and C-PON-like material within the cell bodies indicates that frog NPY derives from a pro-hormone which exhibits a high degree of sequence homologies with mammalian pro-NPY. A dense network of nerve fibers containing NPY and C-PON immunoreactive material was found in the infundibular nuclei, coursing towards the internal zone of the median eminence and the pituitary stalk and terminating in the pars intermedia of the pituitary. The presence of a neuronal system containing simultaneously NPY and C-PON in the infundibulo-hypophyseal complex supports the view that these peptides may participate in the neuroendocrine regulation of the frog pituitary.

INTRODUCTION

Neuropeptide tyrosine (NPY) was isolated originally from porcine brain and sequenced by Tatemoto [1, 2]. This 36-amino acid peptide exhibits considerable sequence homologies with various peptides of the pancreatic polypeptide family mainly with peptide tyrosine-tyrosine (PYY) and avian pancreatic polypeptide (APP) [2]. Although the presence of these latter peptides has been initially reported in the central nervous system, there is now clear evidence that APP- and PYY-like immunoreactivities in the brain are actually due to authentic NPY [3]. Using immunohistochemical methods, NPY containing neurons have been localized in the brain of various mammalian species including rat [4–6], monkey [7, 8], and man [9–11]. Combination of radioimmunoassay with high performance liquid chromatography has established the identity of NPY in the brain [3, 12]. All these studies have shown that NPY has a widespread distribution and is present in extremely high concentrations, especially in the cerebral cortex and the hypothalamic area. Thus, it was postulated that NPY may act as both a neuromediator and a neurohormone [5, 13]. In sub-mammalian vertebrates, very few studies concerning the distribution of NPY have been reported. NPY has been localized and identified in the retina of the fish *Carassius auratus* [14] and in

Accepted September 30, 1986
Received July 31, 1986
[5] To whom reprints should be requested.

the central nervous system of the amphibian *Rana ridibunda* [15]. Recently the nucleotide sequence of the neuronal-specific gene encoding the NPY precursor molecule has been determined from human pheochromocytoma [16]. The deduced pre-pro-NPY amino acid sequence exhibits two potential sites for proteolytic cleavage which would generate three peptides: a 28 residue signal peptide, NPY and a C-terminal 30 amino acid peptide called C–PON [16]. Antisera have been raised against this cryptic peptide and co-localization of C–PON and NPY in the same neurons has been reported [17].

In the present study, we examined the distribution of NPY and C–PON immunoreactive neurons in the brain and pituitary of the amphibian *Rana catesbeiana* using both the indirect immunofluorescence and the peroxidase-antiperoxidase techniques.

MATERIALS AND METHODS

Tissue preparation

Adult bullfrogs (*Rana catesbeiana*) 300 g body weight were caught in April in their natural environment and maintained at constant temperature for one week. The fixation was performed by transcardial perfusion of a 4% paraformaldehyde solution in 0.1 M pH 7.3 sodium cacodylate buffer. The brains were carefully dissected and post-fixed in the same fixative for 4 hr. Then the tissues were washed overnight in a 5% sucrose solution and transferred to cacodylate buffer containing 10% sucrose. The brains were embedded and sectioned in a cryostat (Frigocut 2700, Reichert Jung). Consecutive sections (8 μm thick) were processed for the indirect immunofluorescence or the peroxidase-antiperoxidase immunohistochemical procedure. The slices were incubated overnight at 4°C in a humid atmosphere with antiserum to NPY or to C–PON at the respective working dilutions 1:600 and 1:200.

Antisera

Antibodies to NPY (n°4603) [9] were raised in rabbits by injection of a mixture of synthetic porcine NPY, methylated bovine serum albumine (BSA) and complete Freund's adjuvant. Antibodies to C–PON (n°JN8) [17] were raised in rabbits by injection of synthetic human C–PON coupled to BSA with glutaraldehyde.

Indirect immunofluorescence

The tissues were rinsed and incubated 1 hr with fluorescein-isothiocyanate-conjugated anti-rabbit γ-globulins (GAR/FITC; Nordic Labs) at the working dilution 1:60. The sections were rinsed, mounted in glycerol and examined under a Leitz Orthoplan microscope.

Peroxidase-Antiperoxidase (PAP)

The sections were rinsed and incubated for 1 hr with goat-anti-rabbit γ-globulins diluted 1:30 in Tris-HCl pH 7.6 buffer. The sections were rinsed and incubated for an additional hour with rabbit peroxidase-antiperoxidase solution (diluted 1:250) (Nordic Labs). The enzymatic activity was revealed using a diaminobenzidine (0.03%)-hydrogen peroxide (0.01%) mixture in Tris-HCl buffer. Finally the sections were rinsed, dehydrated, mounted and examined under a Leitz Orthoplan microscope.

Controls

No reaction product could be observed on control sections using normal rabbit serum as the primary antibody. Pre-incubation of the diluted NPY-antiserum with 10^{-6}M NPY resulted in the complete loss of staining. As synthetic C–PON was not available, it was impossible to perform additional control using pre-absorbed C–PON antibodies.

RESULTS

NPY and C–PON-immunoreactivities are widely distributed throughout the brain of the frog with remarkable co-distribution. The specificity of the immunoreaction was shown by a complete loss of staining after pre-absorbtion of the NPY antiserum with the homologous synthetic antigen 10^{-6}M and after substitution of the first antiserum for normal rabbit serum. The indirect immunofluorescence and the PAP procedures revealed C–PON and NPY immunoreactive perikarya and nerve fibers in

various brain regions (Fig. 1).

Stereotaxic mapping of the NPY and C–PON immunoreactivities is shown in Figure 2. Cell bodies are indicated as large filled circles and terminals are shown with small dots. The number of circles approximates the number of cells in a given section. Abbreviations according to Wada *et al.* [18] have been listed in legend to Figure 2.

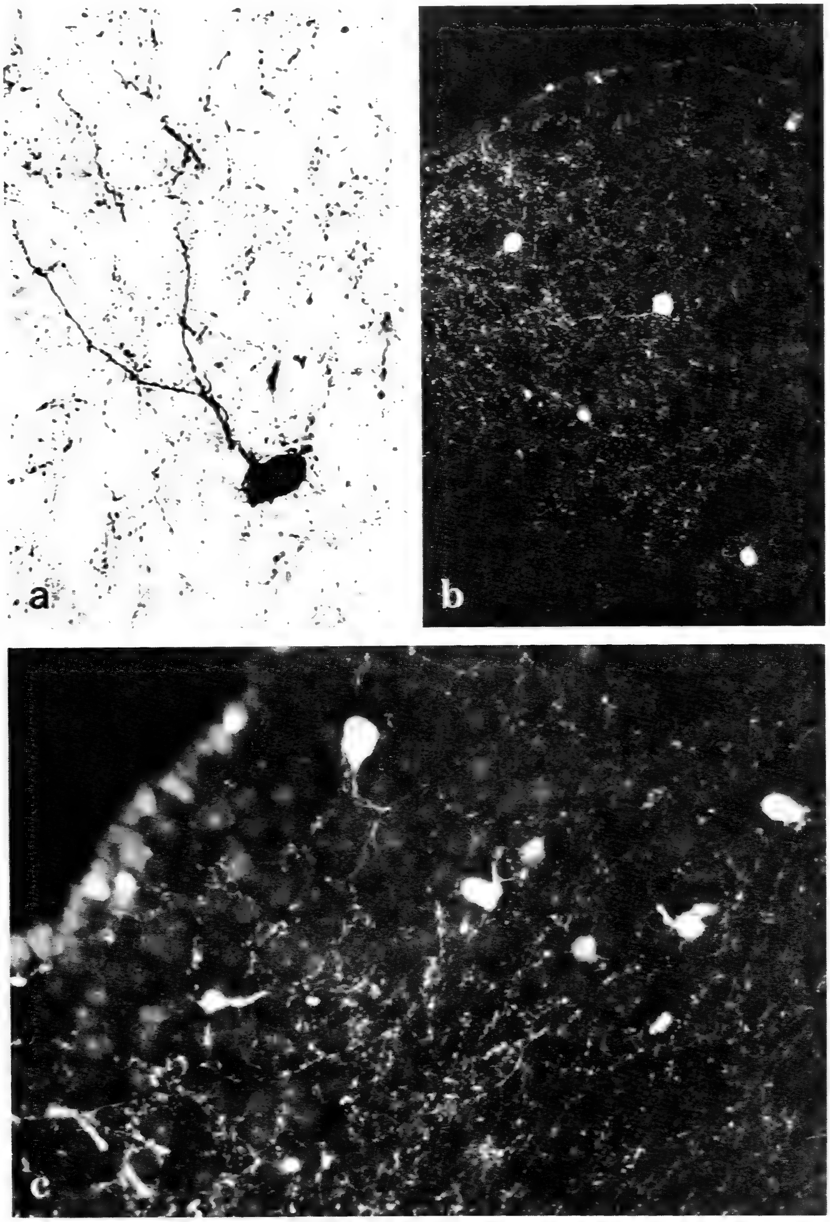

FIG. 1. (a) PAP technique reveals the dark-stained processes emanating from a C–PON immunoreactive cell body located in the infundibular nucleus (×500). (b, c) Immunofluorescence labelling of NPY containing perikarya and plexus of fibers in the medial (×525) and in the ventral pallium close to the lateral ventricle (×525).

Owing to the identical distribution of C–PON and NPY-containing fibers, only one schema depicting these fibers is shown on Figure 2.

Telencephalon

The dorsal (PD) and medial (PM) portion of the pallium showed numerous perikarya and varicose fibers containing NPY and C–PON. Both antisera showed a moderate number of cells in the pars medialis of the amygdala (Am) (Fig. 3) and in the posterior entopeduncular nucleus (NEP). Scarce cells were seen with NPY and C–PON antisera in the nucleus of the diagonal band of Broca (NDB). Axon processes emanating from cell bodies were visible (Fig. 1b, c).

Diencephalon

Both antisera revealed immunoreactive cells in the posterocentral nucleus of the thalamus (NPC) and in the ventromedial area of the thalamus (AVM). The dorsal (NID) (Fig. 4) and ventral (NIV) infundibular nuclei showed the greatest accumulation of cell bodies immunoreactive for NPY and C–PON. There were also cell bodies in the diencephalic extension of the interpeduncular nucleus (NIP) and in the preoptic nucleus (NPO) along the third ventricle. A dense accumulation of fibers was seen at the periphery of the dorsal habenular nucleus (NHD) and in the ventral infundibular nucleus (NIV). The most prominent NPY and C–PON bundle was found coursing from the infundibulum through the median eminence (ME) towards the pars intermedia (PI) of the pituitary.

Mesencephalon

The C–PON and the NPY antisera showed immunoreactive cell bodies and nerve fibers in the optic tectum. The highest density of immunoreactive perikarya was observed in the superficial grey layer (SGS). Positive perikarya could also be seen in the central (SGC) and periventricular grey (SGP) subdivisions. Immunoreactive fibers were seen in all the tectum subdivisions especially in the inner superficial white layer. Cells and fibers were also observed in other regions of the mesencephalon i.e. the dorsal (NAD) and ventral (NAV) parts of the anterior tegmentum and the part just posterior to the torus semicircularis (TS). Scarce nerve fibers were found in the reticular isthmic nucleus (NRIS). Conversely, no positive elements could be stained in the nucleus profundus

FIG. 2. Schematic drawing of frontal sections of the frog brain. Coordinates are taken from the topographic atlas of Wada *et al.* [18] and given in mm from the reference zero point defined as the anterior margin of the pars impar tecti mesencephali which is the apex of the angle formed by the junction of the dorsal midline of the two optic lobes. For convenience the drawings portray the left part of the brain. First half sections indicate the anatomical regions; the second ones describe the density and distribution of NPY and C–PON fibers; the third and the fourth ones show the location of NPY and C–PON perikarya respectively.
Abbreviations—AL: amygdala, pars lateralis, Am: amygdala, pars medialis, AC: anterior commissure, AVA: area ventralis anterior thalami, AVL: area ventrolateralis thalami, AVM: area ventromedialis thalami, CGL: corpus geniculatus laterale, E: epiphysis, GC: griseum centrale rhombencephali, LFB: lateral forebrain bundle, ME: median eminence, MFB: medial forebrain bundle, NAD: nucleus anterodorsalis tegmenti mesencephali, NAS: nucleus accumbens septi, NAV: nucleus anteroventralis tegmenti mesencephali, NBPC: bed nucleus of the pallial commissure, NCER: nucleus cerebelli, NDB: nucleus diagonal band of broca, NDLA: nucleus dorsolateralis anterior thalami, NDMA: nucleus dorsomedialis anterior thalami, NEP: nucleus entopeduncularis, NHD: nucleus habenularis dorsalis, NHV: nucleus habenularis ventralis, NID: nucleus infundibularis dorsalis, NIV: nucleus infundibularis ventralis, NIP: nucleus interpeduncularis, NLS: nucleus lateralis septi, NMNT: nucleus mesencephalicus nervi trigemini, NMS: nucleus medialis septi, NPC: nucleus posterocentralis thalami, NPL: nucleus posterolateralis thalami, NPO: nucleus preopticus, NR: nucleus rotundus, NRIS: nucleus reticularis isthmi, NRS: nucleus reticularis superior, NT: motor nucleus of the trigeminal nerve, OC: optic chiasma, ON: optic nerve, OT: optic tract, PaC: pallial commissure, PC: posterior commissure, PD: pallium dorsale, Pdis: pars distalis hypophysis, PI: pars intermedia hypophysis, PLd: pallium laterale, pars dorsalis, Plv: pallium laterale, pars ventralis, PM: pallium mediale, PN: pars nervosa hypophysis, SGC: stratum griseum centrale tecti, SGP: stratum griseum periventricularis tecti, SGS: stratum griseum supeficiale tecti, ST: striatum, STd: striatum, pars dorsalis, STv: striatum, pars ventralis, TS: torus semicircularis.

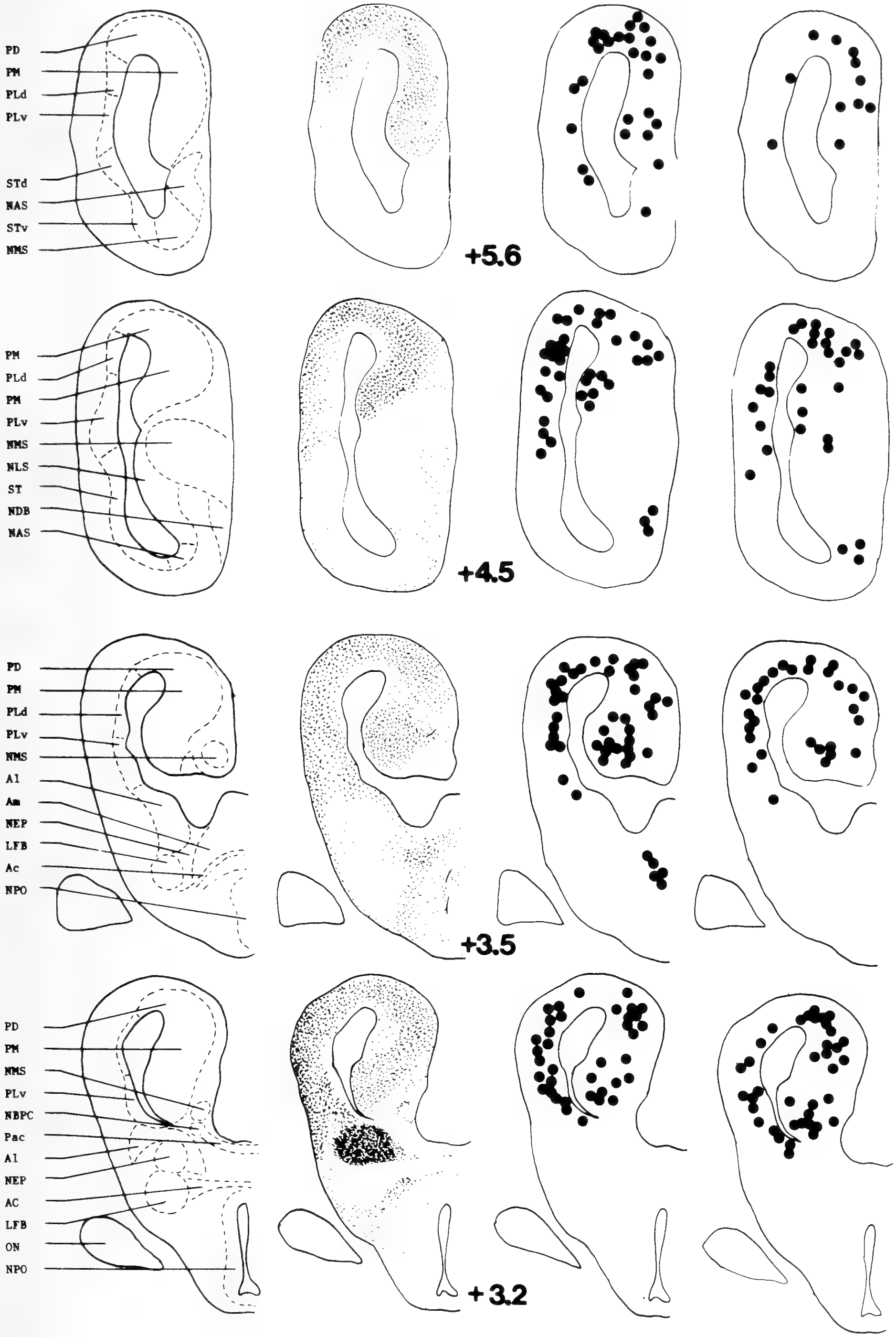
PD
PM
PLd
PLv
STd
NAS
STv
NMS
+5.6
PM
PLd
PM
PLv
NMS
NLS
ST
NDB
NAS
+4.5
PD
PM
PLd
PLv
NMS
Al
Am
NEP
LFB
Ac
NPO
+3.5
PD
PM
NMS
PLv
NBPC
Pac
Al
NEP
AC
LFB
ON
NPO
+3.2

Fig. 2–1

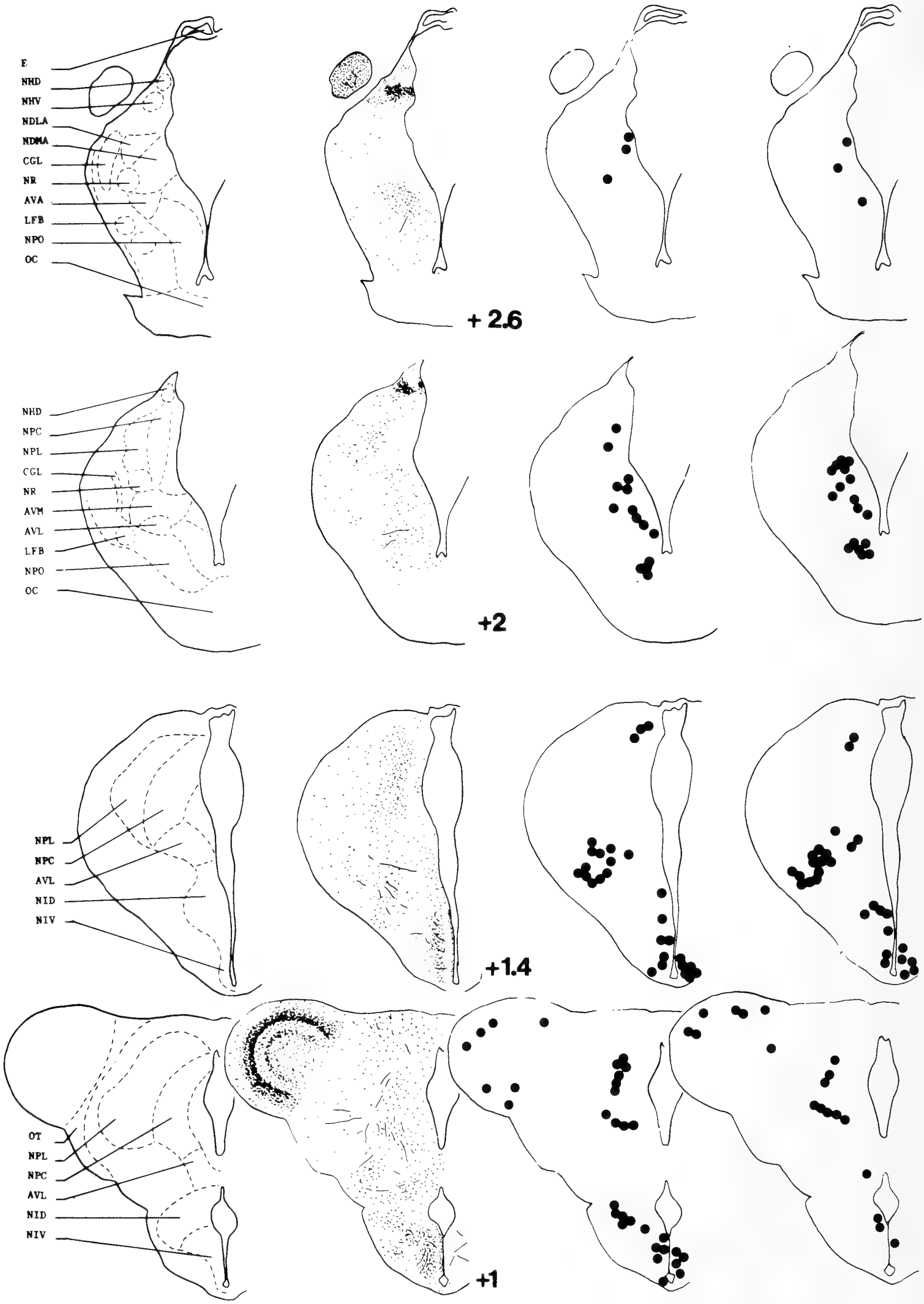
E
NHD
NHV
NDLA
NDMA
CGL
NR
AVA
LFB
NPO
OC
+ 2.6
NHD
NPC
NPL
CGL
NR
AVM
AVL
LFB
NPO
OC
+2
NPL
NPC
AVL
NID
NIV
+1.4
OT
NPL
NPC
AVL
NID
NIV
+1

Fig. 2–2

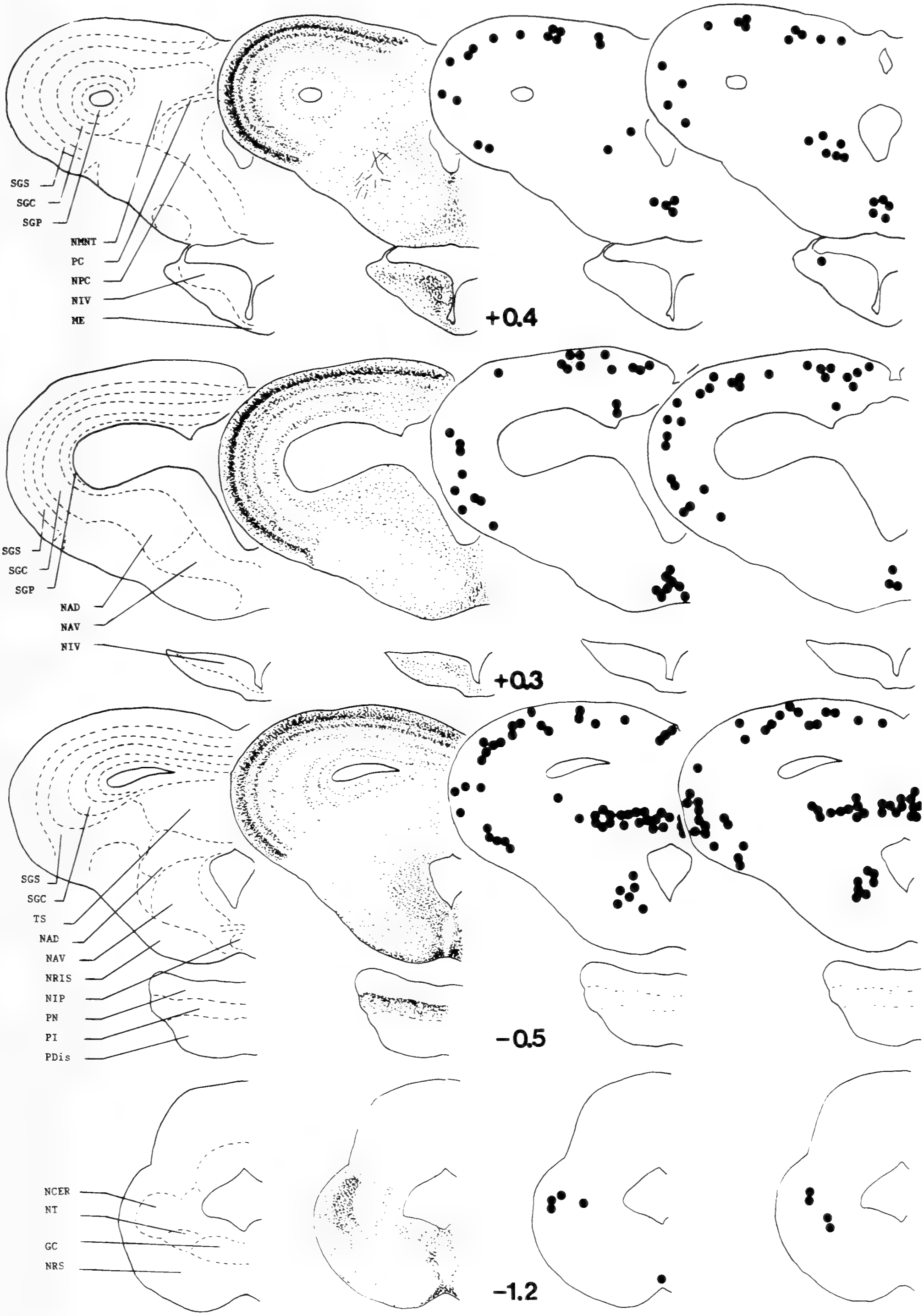
SGS
SGC
SGP
NMNT
PC
NPC
NIV
ME
+0.4
SGS
SGC
SGP
NAD
NAV
NIV
+0.3
SGS
SGC
TS
NAD
NAV
NRIS
NIP
PN
PI
PDis
−0.5
NCER
NT
GC
NRS
−1.2

FIG. 2–3

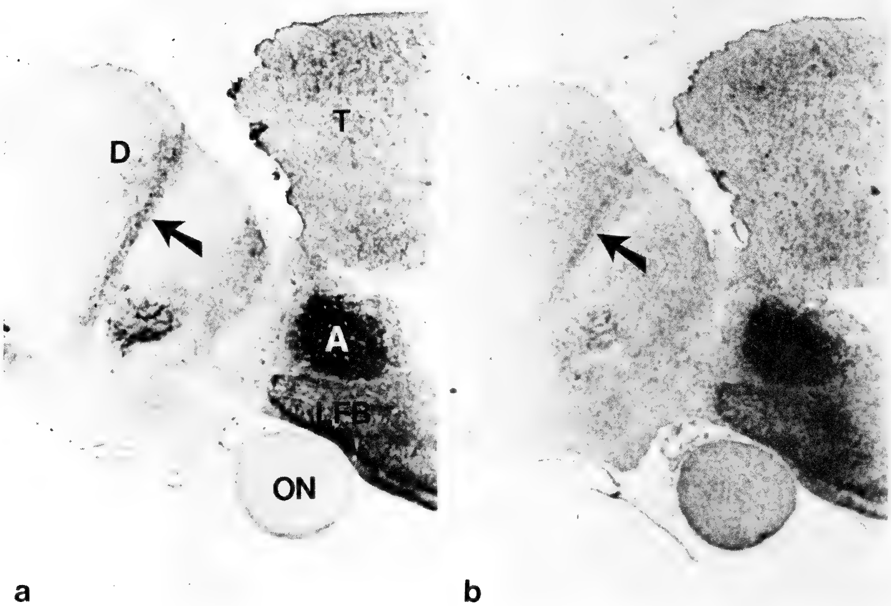

FIG. 3. Serial parasagittal sections of the posterior telencephalon (T) and the anterior diencephalon (D). Using the PAP technique, NPY (a) and C–PON (b) antisera show intense staining of fiber networks in the amygdala (A), the lateral forebrain bundle (LFB) and the anterior thalamus. This latter tract of fibers (arrow head) surrounds the habenular nuclei and courses downwards to the rostro-lateral infundibulum. (×20). ON: optic nerve.

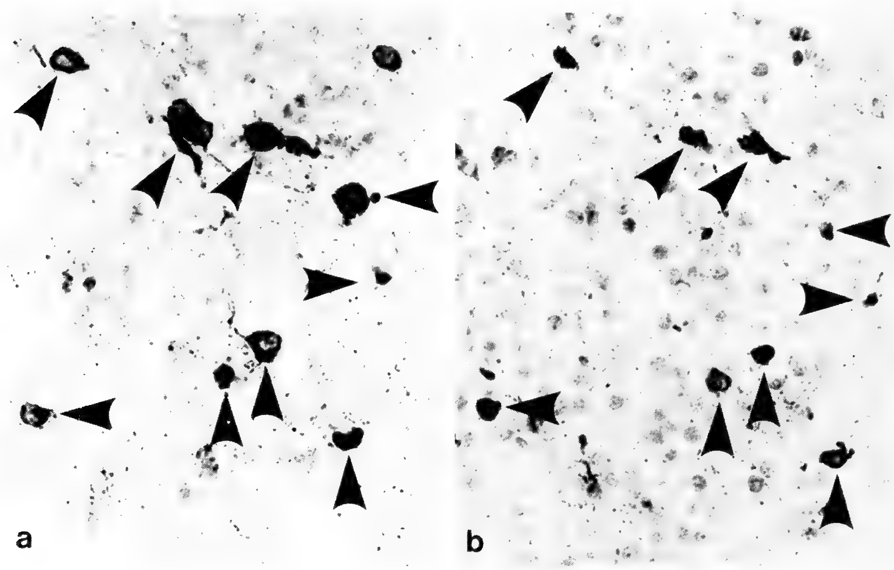

FIG. 4. Serial adjacent sections through the dorsal infundibular nucleus. The same cell bodies (arrow heads) are stained by NPY (a) and C–PON (b) antisera (×200).

mesencephali. In the posterior mesencephalon a moderate number of perikarya and fibers was observed in the interpeduncular nucleus (NIP). A dense accumulation of cells and fibers was seen in the cerebellar nucleus of the mesencephalon (NCER).

Metencephalon

The cerebellum was totally devoid of immunoreactivity to both antisera.

Rhombencephalon

Two dense tracts of C–PON and NPY-immunoreactive fibers were seen to run ventrally and dorsally in the medulla oblongata. However, no cell bodies were revealed in this brain region.

Pituitary

A dense plexus of C–PON and NPY immunoreactive fibers was seen in the pars intermedia (PI) close to the pars nervosa (PN) (Fig. 5). Immunoreactive terminals appeared to innervate most parenchymal cells of the pars intermedia. No immunoreactivities were seen in the pars distalis (Pdis) and only scarce nerve terminals were stained with C–PON and NPY antisera in the pars nervosa.

DISCUSSION

Specificity of the NPY-immunoreactive neurons, as is the case for all regulatory peptides, is not absolute. It cannot be ruled out that the NPY antiserum cross-reacts with structurally related peptides. By means of radioimmunoassays, we have shown that the cross-reactivities of our NPY antiserum with PYY and APP, two peptides which exhibit a high degree of sequence homologies with NPY, were 0.4% and 0.1% respectively [10]. However, it is important to stress that determination of the specificity of antisera by radioimmunoassay techniques does not necessarily agree with immunocytochemical results: immunocytochemistry represents a non competitive immunological system to detect covalently-linked antigens whereas radioimmunoassays measure the competition of soluble antigens with a radiolabelled tracer. Thus, although our radioimmunoassay results indicated that the antigenic determinant recognized by the NPY antiserum was the N-terminal region of the molecule (unpublished data), we cannot exclude that the antiserum contains an additional C-terminal-directed subpopulation of antibodies which would be detected only under the conditions of immunocytochemistry. Thus, it is not possible

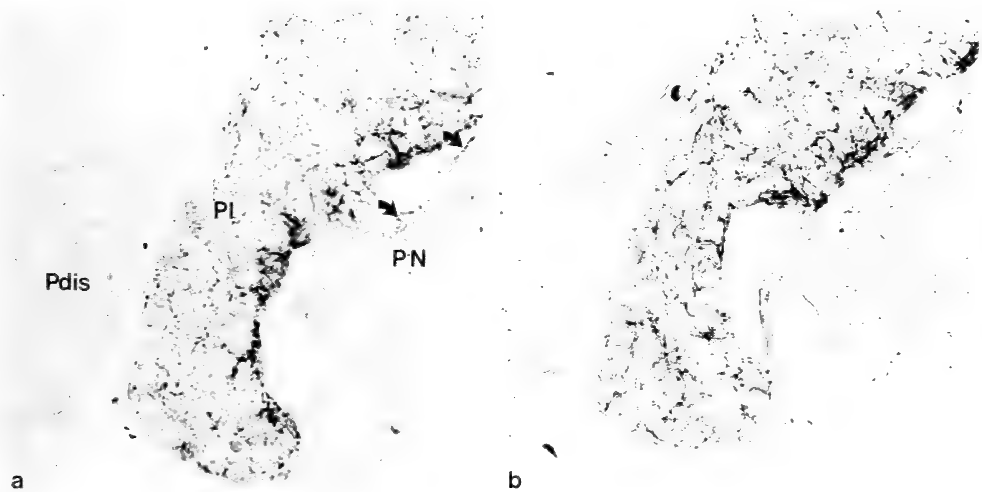

FIG. 5. Serial sections through the pituitary. NPY (a) and C–PON (b) nerve terminals are located in the pars intermedia (PI) being most abundant in the vicinity of the pars nervosa (PN). A few fibers are also present in the neural lobe, close to the intermediate lobe (arrows). The pars distalis (Pdis) is devoid of NPY or C–PON innervation (×240).

to exclude that NPY-related molecules exhibit higher cross-reactivity in the conditions of immunohistochemistry than in those of radioimmunoassays. In addition, other molecules structurally related to NPY may also account for the NPY-like immunoreactivity detected in the frog brain. In this respect, it is interesting to mention that APY, a regulatory peptide recently characterized in anglerfish pancreatic extracts exhibits 64% sequence homologies with porcine PYY [19]. The existence of such a molecule, as yet unknown, in the frog brain cannot be ruled out. Therefore a degree of caution is always warranted in interpreting immunohistochemical results and despite the fact that preabsorption of NPY antiserum with NPY completely abolished the immunohistochemical reaction, we refer to NPY immunoreactive neurons as "NPY-like" or "NPY-containing" cells.

This study demonstrates the widespread distribution of NPY-like neurons throughout the brain of the frog *Rana catesbeiana* with the greatest innervation in the pallium (considered comparable to the hippocampal area in mammals), the lateral amygdala, the entopeduncular nucleus and the diencephalon. These distributions are similar to those reported in another anuran species, *Rana ridibunda* [15]. In mammals several authors, found comparable distribution of NPY, in particular in the amygdaloid complex, the hippocampus and the medial basal hypothalamus. Taken together, the results of these studies, including the present one, suggest that in general NPY-containing neurons are distributed similarly in the brain of many vertebrate species.

No significant differences were found in the present study between the distributions of NPY immunoreactivity and C-PON immunoreactivity. In addition we often observed co-existence of NPY and C-PON in the same cell bodies. The fact that C–PON immunoreactivity occurs within NPY-positive neurons yields two important conclusions. i) NPY-like immunoreactivity detected in the frog brain most probably corresponds to authentic NPY, since structural differences are to be expected in the cryptic region of structurally related peptides which originate from distinct precursor molecules. To illustrate this assertion one may consider the three opioid precursors pro-opiomelanocortin, pro-enkephalin A and pro-dynorphin which generate the chemically related opioid peptides endorphins, enkephalins, dynorphin and α-neoendorphin, but exhibit no sequence homologies within the non-opioid regions of their molecule. ii) Both the NPY and C–PON domains of the pro-NPY molecule have been sufficiently preserved during evolution to make immunohistochemical detection of these neuropeptides possible.

The visualization of a dense plexus of NPY-containing fibers coursing from the infundibular region towards the internal zone of the median eminence, the pituitary stalk and the intermediate lobe of the pituitary suggests that NPY (and/or C–PON) might exert a hypophysiotropic function. This hypothesis has received strong support in that synthetic NPY was found capable of inhibiting alpha-melanotropin (α-MSH) release *in vitro* by neurointermediate lobe of *Rana ridibunda* [20]. More recently, NPY has been shown to inhibit α-MSH and β-endorphin secretion in another anuran species, *Xenopus laevis* [21]. Thus, it appears that in amphibians, NPY could play a physiological role in the inhibitory control exerted by the hypothalamus upon the intermediate lobe secretion. Whether C-PON is only a by-product generated during pro-NPY processing or whether it has a specific role of its own (e.g. modulation of the hypophysiotropic effect of NPY) remains to be determined.

It is interesting to note that noradrenergic fibers have been shown to innervate the intermediate lobe of the amphibian pituitary [22, 23] and that β-adrenergic agonists stimulate α-MSH release by isolated neurointermediate lobes [24]. In the brain of mammals, co-occurence of NPY and norepinephrine has been documented [25, 26]. Thus, possible co-existence of NPY (and C–PON) with noradrenaline in nerve terminals of the frog pars intermedia and possible modulation of β-adrenergic-induced α-MSH secretion deserve further investigation.

Quantification of NPY by radioimmunoassay in the brain of *Rana ridibunda* [15] has shown that, in addition to the diencephalon, the telencephalon and the mesencephalon contain high concentra-

tions of the peptide. Sephadex G–50 gel chromatography indicated that the immunoreactive component had a molecular weight similar to synthetic porcine NPY [15]. The abundance of NPY and C–PON containing neurons in the telencephalon and mesencephalon of *Rana catesbeiana* shown in the present study suggests that one of these peptides or both may have neurotransmitter or neuromodulator functions in the frog brain. This hypothesis is given strong support by the recent observation that perfusion of the brain of *Rana catesbeiana* with a solution containing NPY induced a dose-related reduction of cytochromes [27]. In addition, intracerebroventricular administration of NPY was found to elicit marked modification of the sexual [28] and feeding behavior [29–31] in mammals. Therefore, further studies are required to investigate the potential actions of NPY- and C–PON-like peptides in the brain of amphibians.

ACKNOWLEDGMENTS

This research was supported in part by research grants from INSERM (84–6020 and 86–4340), CNRS and France-Québec exchange program.

REFERENCES

1 Tatemoto, K., Carlquist, M. and Mutt, V. (1982) Neuropeptide Y a novel brain peptide with structural similarities to peptide YY and pancreatic polypeptide. Nature, **296**: 659–660.

2 Tatemoto, K. (1982) Neuropeptide Y: complete amino acid sequence of the brain peptide. Proc. Natl. Acad. Sci. USA, **79**: 5485–5489.

3 Di Maggio, D. A., Chronwall, B. M., Buchanan, K. and O'Donohue, T. L. (1985) Pancreatic polypeptide in rat brain is actually neuropeptide Y. Neuroscience, **15**: 1149–1157.

4 Allen, Y. S. and Adrian, T. E. (1983) Neuropeptide Y distribution in the rat brain. Science, **221**: 877–879.

5 Pelletier, G., Guy, J., Allen, Y. S. and Polak, J. M. (1984) Electron microscope immunocytochemical localization of neuropeptide Y (NPY) in the rat brain. Neuropeptides, **4**: 319–324.

6 Chronwall, B. M., Di Maggio, D. A., Massari, V. J., Pikel, V. M., Ruggiero, D. A. and O'Donohue, T. L. (1985) The anatomy of neuropeptide-Y-contaning neurons in the rat brain. Neuroscience, **15**: 1159–1181.

7 Hendry, S. H.C., Jones, E. G. and Emson, P. C. (1984) Morphology, distribution and synaptic relations of somatostatine and neuropeptide Y-immunoreactive neurons in rat and monkey neocortex. J. Neurosci., **4**: 2497–2517.

8 Smith, Y., Parent, A., Kerkérian, L. and Pelletier, G. (1985) Distribution of neuropeptide Y immunoreactivity in the basal forebrain and upper brainstem of the squirrel monkey (*Saimiri sciureus*). J. Comp. Neurol. **236**: 71–89.

9 Pelletier, G., Désy, L., Kerkérian, L. and Côté, J. (1984) Immunocytochemical localization of neuropeptide Y (NPY) in the human hypothalamus. Cell Tissue Res., **238**: 203–205.

10 Adrian, T. E., Allen, J. M., Bloom, S. R., Ghatei, M. A., Rossor, M. N., Roberts, G. W., Crow, T. J., Tatemoto, K. and Polak, J. M. (1983) Neuropeptide Y distribution in human brain. Nature, **306**: 584–596.

11 Dawbarn, D., Hunt, S. P. and Emson, P. C. (1984) Neuropeptide Y : regional distribution, chromatographic characterization and immunohistochemical demonstration in post-mortem human brain. Brain Res., **296**: 168 –173.

12 Lundberg, J. M., Terenius, L,. Hökfelt, T. and Tatemoto, K. (1984) Comparative immunohistochemical and biochemical analysis of pancreatic polypeptide-like peptides with special reference to presence of neuropeptide Y in central and peripheral neurons, J. Neurosci., **4**: 2376–2386.

13 O'Donohue, T. L., Chronwall, B. M., Pruss, R. M., Mezey, E., Kiss, J. Z., Eiden, L. E., Massari, V. J., Tessel, R. E., Pickel, V. M., Di Maggio, D. A., Hotchkiss, A. J. and Zukowska-Grogec, Z. (1985) Neuropeptide Y and peptide YY neuronal and endocrine systems. Peptides, **6**: 755–768.

14 Osborne, N. N., Patel, S., Terenghi, G., Allen, J.M., Polak, J. M. and Bloom, S. R. (1985) Neuropeptide Y (NPY)-like immunoreactive amacrine cells in retinas of frog and goldfish. Cell Tissue Res., **241**: 651–656.

15 Danger, J. M., Guy, J., Benyamina, M., Jégou, S., Leboulenger, F., Côté, J., Tonon, M. C., Pelletier, G. and Vaudry, H. (1985) Localization and identification of neuropeptide Y (NPY)-like immunoreactivity in the frog brain. Peptides, **6**: 1225–1236.

16 Minth, C. D., Bloom, S. R., Polak, J. M. and Dixon, J. E. (1984) Cloning, characterization and DNA sequence of human cDNA encoding neuropeptide tyrosine. Proc. Natl. Acad. Sci. USA, **81**: 4577–4582.

17 Gulbekian, S., Wharton, J., Hacker, G. W., Varndell, I. M., Bloom, S. R. and Polak, J. M. (1985) Co-localization of neuropeptide tyrosine (NPY) and its C-terminal flanking peptide (C–PON). Peptides, **6**: 1237–1243.

18 Wada, M., Urano, A. and Gorbman, A. (1980) A stereotaxic atlas for diencephalic nuclei of the frog *Rana pipiens*. Arch. Histol. Jpn. **43**: 157–173.

19 Andrew, P. C., Hawke, D., Shively, D. E. and Dixon, J. E. (1985) A nominated peptide homologous to porcine peptide YY and neuropeptide Y. Endocrinology, **116**: 2677–2681.

20 Danger, J. M., Leboulenger, F., Guy, J., Tonon, M. C., Benyamina, M., Martel, J. C., Saint-Pierre, S., Pelletier, G. and Vaudry, H. (1986) Neuropeptide Y in the intermediate lobe of the frog pituitary acts as an α-MSH-release inhibiting factor. Life Sci., **39**: 1183–1192.

21 Verburg-van Kemenade, L., Jenks, B., Danger, J. M., Saint-Pierre, S., Pelletier, G. and Vaudry, H. (1987) Evidence that an NPY-like peptide is a melanotropin-inhibiting factor in the pars intermedia of the amphibian *Xenopus laevis*. Peptides, in press.

22 Enemar, A. and Falck, B. (1965) On the presence of adrenergic nerves in the pars intermedia of the frog *Rana temporaria*. Gen. Comp. Endocrinol., **5**: 577–583.

23 Nakai, Y. and Gorbman, A. (1969) Evidence for doubly innervated secretory unit in the anuran pars intermedia. II. Electron microscopic studies. Gen. Comp. Endocrinol., **13**: 108–116.

24 Tonon, M. C., Leroux, P., Stoeckel, M. E., Jégou, S., Pelletier, G. and Vaudry, H. (1983) Catecholaminergic control of α-melanocyte-stimulating hormone (MSH) release by frog neurointermediate lobe in vitro: evidence for direct stimulation of α-MSH release by thyrotropin-releasing hormone. Endocrinology, **112**: 133–141.

25 Everitt, B. J., Hökfelt, , T., Terenius, L., Tatemoto, K., Mutt, V. and Goldstein, M. (1984) Differential co-existence of neuropeptide Y with catecholamines in the central nervous system of the rat. Neuroscience, **11**: 443–462.

26 Hökfelt, T., Lundberg, J. M., Lagercrantz, H., Tatemoto, K., Mutt, V., Lindberg, J., Terenius, L., Everitt, B. J., Fuxe, K., Agnati, L. and Goldstein, M. (1983) Occurence of neuropeptide Y (NPY)-like immunoreactivity in catecholamine neurons in the human medulla oblongata. Neurosci. Lett., **36**: 217–222.

27 Saito, T., Kanno, T., Tatemoto, K. and Mutt, V. (1983) Dose-related effect of neuropeptide Y stimulating respiratory chain in the bullfrog brain. Biomed. Res., **4**: 173–178.

28 Clark, J. T., Kalra, P. S. and Kalra, S. P. (1985) Neuropeptide Y stimulates feeding but inhibits sexual behavior in rats. Endocrinology, **117**: 2435–2442.

29 Stanley, B. G., Chin, A. S. and Leibowitz, S. F. (1985) Feeding and drinking elicited by central injection of neuropeptide Y: evidence for hypothalamic site(s) of action. Brain. Res. Bull., **14**: 521–524.

30 Stanley, B. G., Daniel, D. R., Chin, A. S. and Leibowitz, S. F. (1985) Paraventricular nucleus injections of peptide YY and neuropeptide Y preferentially enhance carbohydrate ingestion. Peptides, **6**: 1205–1211.

31 Levine, A. S. and Morley, J. E. (1984) Neuropeptide Y: a potent inducer of consummatory behavior in rats. Peptides, **5**: 1025–1029.

ZOOLOGICAL SCIENCE 4: 135–144 (1987)

Comparison of Reproductive Activities between Two Japanese Quail Lines Selected with Regard to Photoperiodic Gonadal Response

Hisao Honda, Tadashi Oishi[1] and Takao Konishi[2]

Kanebo Institute for Cancer Research, Tomobuchicho 1–5–90, Osaka 534, Japan

ABSTRACT—KR and KN lines of Japanese quail selected for photoperiodic gonadal response through five generations were maintained ten more generations with relaxed selection. Males of KR line have maintained their responsiveness of cloacal glands to "continuous light treatment (CLT)" by increasing the size of cloacal glands, while those of KN line have maintained irresponsiveness. Females of KR line maintained the trait to lay the first egg earlier in age than those of KN. Other characteristics noted are as follows: 1. Responses of cloacal glands in males (decrease in the size of cloacal glands) and oviposition in females (stop of the oviposition) to the light condition of short days were more distinct in KN than in KR line. 2. Females of KR line tend to lay foggy eggs (translucent milk-white material veils egg surface pattern of dark spots and patches). 3. Females of KR line have breast feathers with black dots all over, while black dots were restricted around the throat in females of KN. 4. The incubated eggs of KR line hatched earlier than those of KN. 5. Serum thyroxine (T_4) level was higher in KR than in KN under long photoperiod (LD 16:8) and normal temperature (23°C), but there was no difference in the serum triiodothyronine (T_3) level between two lines. 6. The birds of KR line grew faster, and their body weights were larger than those of KN line in generations with selection. The difference of body weight, however, disappeared after selection was relaxed.

INTRODUCTION

Two lines of Japanese quail (KR and KN lines) were established concerning the potency of reproduction under photoperiodic conditions [1]. In KR line, males responded to "continuous light treatment (CLT)" by increasing their cloacal gland size, and females laid eggs at earlier ages and between 08:00 and 14:00 under LD 16:8 (light on 01:00–17:00). In KN line, males were irresponsive to CLT, and females laid eggs at later ages and between 16:30 and 08:00. That is, the birds of KR line were more sensitive to photoperiodic manipulations in regard to their reproductive activities than those of KN line. These two lines were maintained for ten more generations with relaxed selection. In this report, we examined 1) whether genetical traits previously reported have been retained or not, 2) whether there is any difference in the short day photorefractoriness [2–4], a characteristic response of this species to short days, between these two lines, and 3) several other characteristics specific to each line.

Accepted September 18, 1986
Received July 7, 1986
Present address: [1]Department of Biology, Nara Women's University, Kitauoyanishi-machi, Nara 630, and [2]Aburabi Laboratories, Shionogi-Seiyaku Co., Ltd., Koka-cho, Koka-gun, Shiga 520–34, Japan.
[1] To whom reprints should be requested.

MATERIALS AND METHODS

Maintenance of lines

Breeding colonies (25 females and 12 males) of KR and KN lines of Japanese quail (*Coturnix coturnix japonica*) have been raised in large cages ($178^W \times 91^D \times 96^H$ cm). Eggs were collected and stored within limits of two weeks in a chamber where temperature was kept at 14°C and relative humidity at 80%. Eggs were then transferred to an incubator in which temperature and relative humidity were kept at 37°C and 60%, respectively. Eggs were turned every three hours. Rearing conditions of the birds after hatching were the

same as described previously [1].

Measurement

Incubation period until hatch was recorded. During incubation, eggs were placed separately in cotton wool on a plate to inhibit egg-to-egg contact, because the time of hatching synchronizes within an hour or two when the eggs are incubated in contact [5].

In females, the age at first egg was recorded individually. The number of eggs laid and the percentage of foggy eggs (translucent milk-white material veils egg surface pattern of dark spots and patches) were recorded. Breast feather pattern of black stipples was checked when the birds matured (The stippled feather pattern does not appear in males).

In males, the size of cloacal glands (width or volume) was measured before and after CLT (continuous light treatment of 32 hr on 42 days after hatching) with a caliper to check the responsiveness to CLT [1]. Volume of a cloacal gland was calculated by using a formula, volume=WLH/6, where W, L and H are width, length and height of a cloacal gland protrusion in cm, respectively.

In both males and females, responsiveness to short day treatments was examined by transferring them to an LD 8:16 photoperiod (light on from 10:00 to 18:00) from an LD 16:8 photoperiod (light on from 06:00 to 22:00) or by placing them under an LD 8:16 throughout the experimental periods.

Serum levels of triiodothyronine (T_3) and thyroxine (T_4) were measured by radioimmunoassay in both males and females. Radioimmunoassay kits (Eiken, Tokyo) for T_3 (I–LK12, cross reactivity with T_4 is less than 0.1%) and for T_4 (I–LK22, cross reactivity with T_3 is less than 0.1%) were used. Birds were reared for three weeks under respective condition (LD 16:8 and 23°C, LD 16:8 and 10°C or LD 8:16 and 23°C), and starved for about four hours before sacrificed. Blood was taken from 13:00 to 15:00 to avoid fluctuation of the data due to diurnal changes of the hormones. Average values were presented with standard errors (SE). For statistical analysis, we used the N88-basic programs [6]. Student's t-test, χ^2-test, two-way analysis of variance (ANOVA) and Duncan's multiple range test were employed.

Logistic analysis of body weight

Body weight was measured once every week and the difference in body growth between KR and KN lines was examined by logistic analysis as described elsewhere [7]. The increase of body weight was approximated by a logistic curve which was expressed by the analytical function, $w(t)=W_f/(1+\exp(-k(t-a)))$, where $w(t)$ is body weight at t days after hatching, W_f is the final body weight of a full grown body, and a is an inflection point of a logistic curve. The least square method by a personal computer was used to fit a logistic curve to average values of body weight at every measured ages (e.g., solid circles in Fig. 1). Then, we can obtain probable values of W_f, a and k. We note W_f for a parameter to indicate the final body weight.

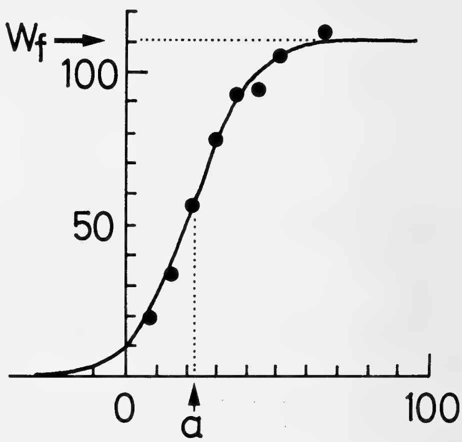

Fig. 1. An example of fitting of a logistic curve to the increase of body weight. Ordinate: body weight (g). Abscissa: age (days after hatching). A series of average values (population size, N=6–20) of body weight is plotted by solid circles. The logistic curve fitted to the data is characterized by W_f (final body weight), a (inflection point) and k. A gradient of the tangent of a curve at the inflection point is $k\ W_f/4$.

RESULTS

Characteristics noted in females

1. Age at first egg Age at first egg has been

TABLE 1. Average age[a] at first egg of each generation during maintenance of lines with relaxed selection[b]

Generation	No. of birds	KR line	No. of birds	KN line
F_5	38	42.2 ± 0.46	47	45.5 ± 0.51**
F_8	31	42.6 ± 0.52	24	47.7 ± 0.36***
F_9	54	42.0 ± 0.34	28	45.0 ± 0.86*
F_{10}	16	42.6 ± 0.74	25	47.2 ± 0.76**
F_{10}	31	44.2 ± 0.49	32	48.4 ± 0.51***
F_{11}	30	42.2 ± 0.61	31	49.3 ± 0.78***
F_{12}	29	43.3 ± 0.74	32	49.6 ± 0.62***
F_{13}	25	41.8 ± 0.59	25	43.0 ± 0.54
F_{14}	32	42.3 ± 0.65	31	47.5 ± 0.62***
Average	287	42.7 ± 0.23	275	47.0 ± 0.72***

a: Values are mean ± SE (days after hatching). b: Data of generations with selection (F_1–F_4) are presented in Table 3 in the previous paper [1]. Significant difference between KR and KN lines: * $P<0.05$, ** $P<0.01$, *** $P<0.001$.

recorded in every generation with relaxed selection and results are shown in Table 1. Two-way ANOVA showed that the difference in age at first egg among generations is not significant, but the difference between lines is highly significant ($P<0.002$). The average age at first egg of KR line is 4.3 days earlier than that of KN. Distribution of ages at first egg in F_{14} generation is shown in Figure 2 as an example.

2. Effect of short days Figure 3 shows the effect of alternation of long and short days on egg production. When the birds were transferred from

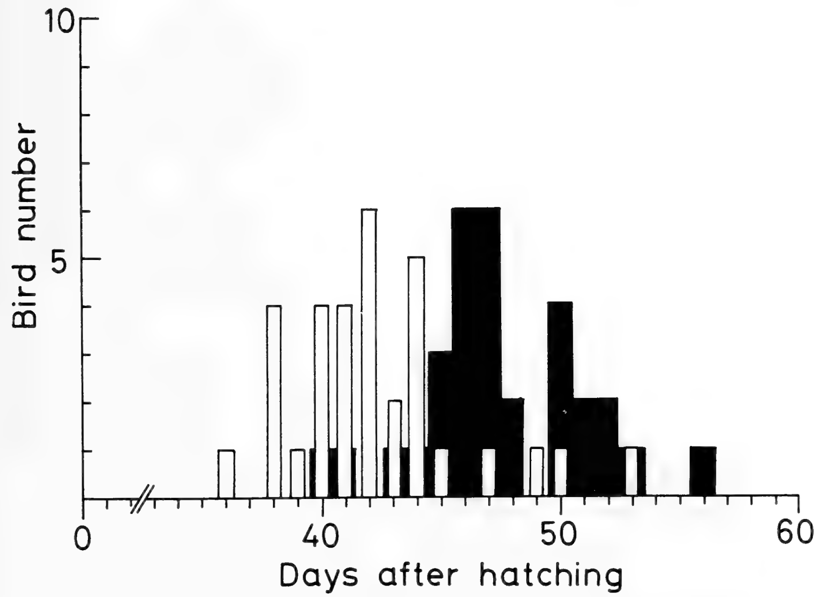

FIG. 2. Distributions of ages at first egg. Average ages with SE are 42.3±0.65 (N=32) days after hatching for KR line, and 47.5±0.62 (N=31) days for KN line. Data from birds of F_{14} generation. Open and solid bars indicate KR and KN lines, respectively.

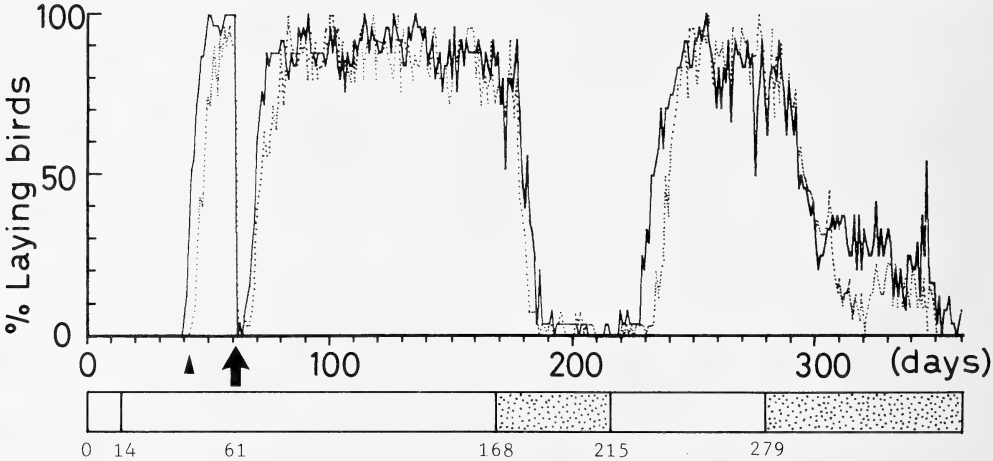

Fig. 3. Variation of the number of laying birds under alternate photoperiodic conditions. Ordinate: ratio (percentage) of laying birds to the total number of females in a day. Abscissa: age (days after hatching). Population sizes of females of KR and KN lines are from 24 to 32 and from 22 to 33, respectively. Solid and broken lines: birds of KR and KN lines, respectively. Photoperiodic conditions are shown at the bottom of the figure. Open areas: long days (LD 16:8) except for 0–14 days under continuous light. Stippled area: short days (LD 8:16). Solid arrow: date of inbreeding (61 days). Arrow head: days of first eggs. Data from F_{10} generation.

individual cages to large cages for inbreeding, they suddenly stop laying for about two weeks (arrow). When the birds were transferred from long days to short days at 168 days, they stopped laying soon. KR line stopped to lay eggs 1–2 days later than KN. When the birds were transferred from short to long days at 215 days, KR started to lay eggs about 6 days earlier than KN. This corresponds to the difference in the age at first egg (Fig. 2, arrow head in Fig. 3).

3. Ratio of the number of foggy eggs to that of normal ones There are two types of eggs, i.e., foggy eggs (upper three eggs in Fig. 4) and normal ones (lower three). The ratio of foggy eggs is 82.3% (the number of eggs examined, N=232) and 14.5% (N=249) for KR and KN, respectively. Chi-square test showed that the difference is highly significant ($P<0.01$).

4. Incubation periods until hatch Figure 5 shows frequency of hatching in every four hours during incubation. Incubation period for KR line was 5.7 hr shorter than that for KN (403.3 ± 1.0 hr for KR vs. 409.0 ± 1.1 hr for KN, $P<0.001$).

5. Breast feather pattern Females of KR line (left in Fig. 6) show distinct black stipples all over the breast. On the other hand, females of KN line (right) show stipples only around the throat. Quantitative data are shown in Table 2. The difference in breast feather pattern between KR and KN lines is highly significant ($P<0.01$, χ^2-test).

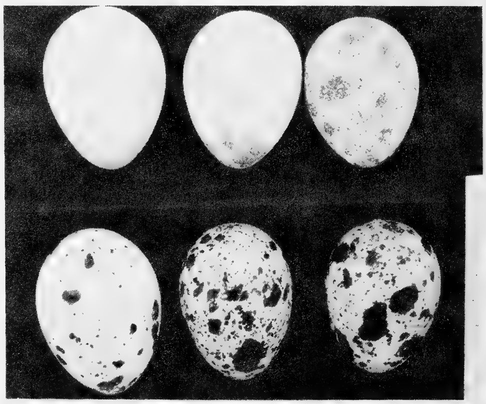

Fig. 4. Comparison between foggy and normal eggs. There are many dark spots and patches on the surface of normal eggs (lower three of the figure), and in foggy ones translucent milk-white material veils egg surface (upper three). The minimum scale of the measure on the right is in mm.

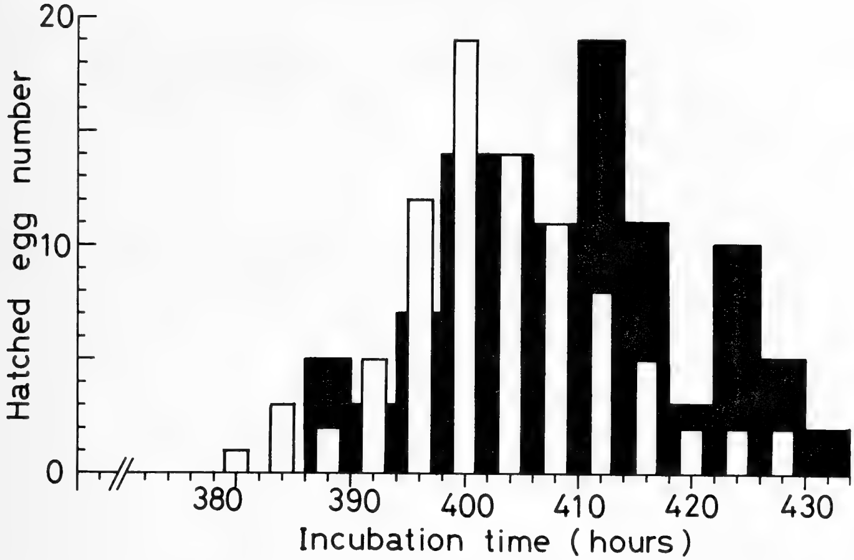

FIG. 5. Distribution of incubation periods until hatch. Ordinate: the number of hatched eggs in every four hours. Abscissa: incubation time (hours). Data from KR line (open bars) and KN line (solid bars) are shown. Average incubation periods with SE are 403.3±1.0 hr for KR line (N=86) and 409.0±1.1 hr for KN line (N=104, P<0.001). Data from F_9 generation.

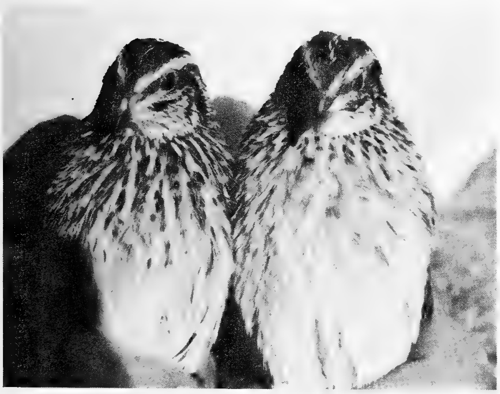

FIG. 6. Comparison of breast feather patterns between KR and KN lines. Distinct black stipples are all over the breast in females of KR line (left), forming a contrast to females of KN line (right) which show stipples only around the throat.

TABLE 2. The number[a] of females having each breast feather pattern

Pattern	KR line	KN line
Stipples all over	43	9
Intermediate	3	18
Stipples only around the throat	0	24
Total	46	51

a: Data from females of F_{14} and F_{15} generations.

Characteristics noted in males

1. Response of cloacal gland size to CLT

Growth rate of the cloacal gland in F_{12} generation was measured. Ratios of the cloacal gland size (width) after CLT to that before CLT were 1.46± 0.045 (N=20) for KR line, and 1.06±0.012 (N=18) for KN line (P<0.001). Thus, the genetical trait with selection, which was reported previously [1], has been retained after selection was relaxed.

2. Response of cloacal gland size to short days

Cloacal gland size was measured every week under alternate photoperiodic conditions. Individual records for KR and KN lines are shown in the upper part of Figure 7. Response patterns to short days are classified into three types (*a*, *b* and *c* at the lower part of Fig. 7). Type *a* does not respond to short days at all. Type *c* birds are

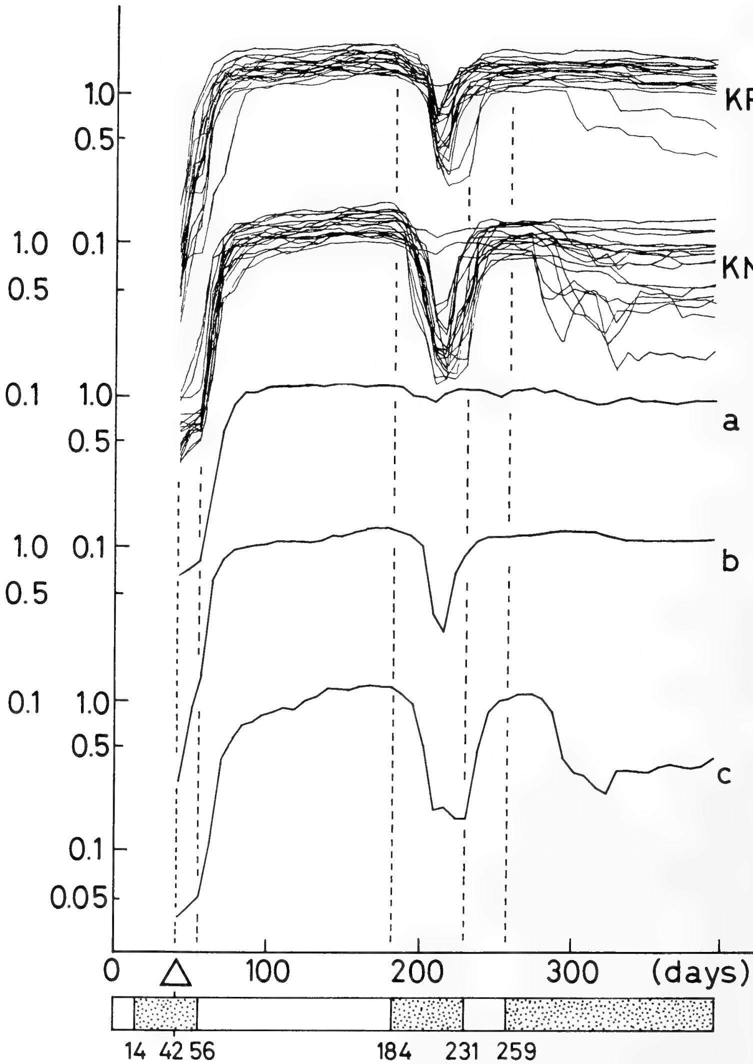

FIG. 7. Change of cloacal gland size under alternate photoperiodic conditions. Ordinate: cloacal gland volume in logarithm (cm^3). Abscissa: age (days after hatching). The size was measured every week. KR, KN: representation of volume change of individuals in superposition which belong to KR line (N=19) and KN line (N=18), respectively. a, b, c: volume change patterns of types a, b and c, respectively. Data from males of F_{12} generation. The bottom of the figure shows photoperiodic conditions as described in the legend of Fig. 3. The open arrow head indicates the date on which CLT was performed.

defined as those which respond to short days and reduce the cloacal gland volume to less than $0.5\,cm^3$. Type *b* responds to the second short day treatment but not to the third short day treatment. Table 3 indicates the number of birds of each type in KR and KN lines. There are more birds of type *b* in KR line than in KN line. In contrast, there are less birds of type *c* in KR than in KN line ($P<0.05$, χ^2-test).

3. Maturation under short days When

TABLE 3. The number[a] of males showing each type of response to alternate photoperiodic condition

Type[b]	KR line	KN line
Type a	1	2
Type b	16	9
Type c	2	7
Total	19	18

a: Data from males of F_{12} generation.
b: See Fig. 7.

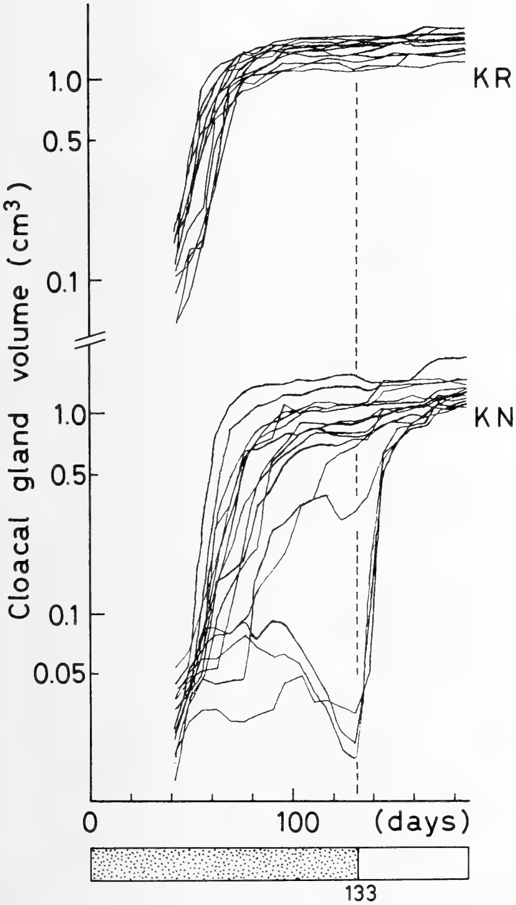

FIG. 8. Growth of cloacal glands under short days. The short day condition continues from the day of hatching until 133 days. KR, KN: representation of cloacal gland growth in superposition (13 and 16 individuals, respectively). See the legend of Fig. 7 for further explanation. Data from males of F_{13} generation.

quail were raised under short days, all the birds of KR line matured but 19% KN line did not mature (Fig. 8). Days required to attain half size of the maximum cloacal gland are 64.1 ± 1.33 days and 89.5 ± 6.08 days ($P<0.01$) for KR and KN, respectively.

4. Comparison of body growth between the two lines The body weight was recorded to be significantly larger in KR than in KN after selection (F_4 generaton) [1]. The body weight after relaxed selection (F_{12} and F_{13} generations) were measured under two rearing conditions as shown in Table 4. In either condition, differences of the body weight between KR and KN lines of F_{12} and F_{13} generations (25 and 32 days old) are small in comparison with differences between those of F_5 generation (28 days old). When the birds of 50 days old, at which the birds had fully grown, were compared, the difference of the body weight in F_{12} generation is also small. When the logistic analysis is applied to data of generations with selection (F_4 and F_5) and those after selection was relaxed (F_{12} and F_{13}), the final body weight of F_{12} and F_{13} generations did not show much differences (1–2 g) between KR and KN lines, while those of F_4 and F_5 generations showed greater differences (10–14 g) (Table 5). Although the logistic analysis has been done only on mean body weights, the results well coincide with those in Table 4. Thus, the trait of superiority in body weight in KR over KN has not been retained after selection was relaxed.

Serum levels of T_3 and T_4

The results are shown in Figure 9. Two-way ANOVA showed significant differences in T_3 levels between rearing conditions ($P<0.01$) and between lines ($P<0.05$) in males and between rearing conditions ($P<0.05$) in females. As shown in Figure 9a and b, serum level of T_3 does not differ between KR and KN lines under long days and 23°C. Under short days (23°C), the level of T_3 was higher than under long days (23°C) except for females of KR line. In the case of low temperature (10°C), the result was not definite.

The level of T_4 was low and close to the limit of detection by radioimmunoassay, and the level varied in each experiment. However, there was a definite tendency that the T_4 levels of males and

Table 4. Comparison of body weight between KR and KN lines

Rearing condition	Generation[a]	Age[b]	KR line[c]	KN line[c]
24L–8L[d]	5	28	76.3 ± 1.00 (33)	65.5 ± 0.86 (30)***
	12	25	66.9 ± 1.91 (20)	62.6 ± 1.11 (18)
	12	32	85.1 ± 1.60 (20)	82.0 ± 1.16 (18)
8L[e]	5	28	77.6 ± 1.01 (30)	66.9 ± 1.12 (32)***
	13	25	58.1 ± 1.77 (15)	58.2 ± 1.45 (17)
	13	32	77.8 ± 1.52 (15)	75.8 ± 1.76 (17)
24L–8L[d]	4	50	100.7 ± 1.53 (17)	88.1 ± 1.07 (25)***
	12	50	97.8 ± 1.38 (20)	96.9 ± 1.16 (18)

a: All data are from male birds. b: Days after hatching. c: Body weight in grams (mean ± SE). The number of birds is shown in parentheses. d: Birds were reared under LD 24 : 0 for the first 2 weeks and the photoperiod was changed to LD 8 : 16. e: Birds were reared under LD 8 : 16 throughout the experimental periods. Statistical difference between KR and KN lines: *** $P<0.001$.

Table 5. Final body weights in grams (W_f) obtained by logistic analysis[a]

Generation	KR line	KN line	Difference
F_4^b	110.4	96.5	13.9
F_5^c	95.5	84.0	11.5
F_{12}	106.8	104.7	2.1
F_{13}	101.8	100.9	0.9

a: Data from male birds. See "Materials and Methods" and Fig. 1 for the details of the analysis. b: Analyzed from the observed data by Konishi and Oishi [1]. c: Analyzed from the observed data by Konishi and Oishi (unpublished).

females in long days under 23°C were higher in KR than in KN line. Figure 9c and d shows the examples of the data obtained. Two-way ANOVA showed significant differences in T_4 levels between rearing conditions ($P<0.01$) and between lines ($P<0.05$) in males and between lines ($P<0.05$) in females. The value of males in long days under 23°C is significantly higher than those in short days under 23°C ($P<0.001$) and long days under 10°C ($P<0.01$). No remarkable difference was observed between conditions of short days (23°C) and long days (10°C).

DISCUSSION

KR and KN lines, which were selected for five generations and maintained for ten generations thereafter with relaxed selection, have retained the characteristics for photoperiodic gonadal response noted in our previous paper [1]. The birds of KR line have a high potency of reproduction, that is, males of KR line are easily stimulated to increase the size of cloacal glands by CLT, and females lay the first eggs earlier. In contrast, the cloacal gland size of KN males hardly increases after CLT, and females tend to stop laying eggs sooner when they are transferred from long to short days.

Superiority in body weight and growth rate in KR line over KN line [1] has not been maintained after selection was relaxed, i.e., we were unable to find any difference in body weight between KR and KN lines at F_{12} and F_{13} generations, because the body weight of KN line increased and reached the similar value as that of KR line after selection was relaxed. This is interesting in connection with the finding by Kawahara [8, 9] that unconscious selection of wild quail enhanced body growth and sexual maturation.

According to the response of cloacal glands to short photoperiods, three types were classified, i,e., type a: does not respond to short photoperiods, type b: responds to the second short photoperiod but not to the third short photoperiod, and type c: responds to the second and the third short photoperiods by showing a decrease of the cloacal gland volume to less than $0.5\,cm^3$. These types are comparable to types I, II and III in

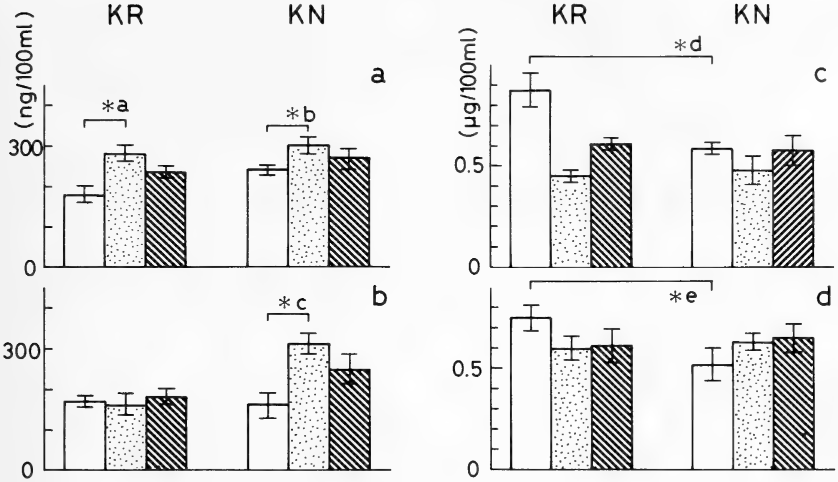

FIG. 9. Serum T_3 (a, b) and T_4 (c, d) concentrations. Open columns: long days (LD 16:8) and 23°C. Stippled columns: short days (LD 8:16) and 23°C. Striped columns: long days and 10°C. Vertical lines of each column represent SE. **a**: T_3 concentration (ng/100 ml) in males of KR and KN lines. **b**: T_3 concentration in females of KR and KN lines. **c**: T_4 concentration (μg/100 ml) in males of KR and KN lines. **d**: T_4 concentration in females of KR and KN lines. Population size: 6–15 for T_3, and 4–10 for T_4. *a: $P<0.005$, *b: $P<0.025$, *c: $P<0.005$, *d: $P<0.01$, *e: $P<0.05$.

our previous report [4]. That is, KR line includes more type I birds and KN line includes more type III birds, but one to one correspondence could not be established.

We found several other characteristics specific to each line, which had not been described in the previous paper [1], i, e., 1) females of KR line lay more foggy eggs, 2) females of KR line show more distinct dotted breast feathers than those of KN, and 3) incubation period required for hatching is several hours shorter in KR than KN line. It remains unsolved whether these characteristics correlate each other, whether these reflect the characteristics of wild and domesticated quails as suggested in our previous paper (1), or whether these reflect the habitats of different populations which were the ancestors of each line.

The results of serum T_3 concentration confirmed the previous paper [1], showing no statistical difference between KR and KN lines. Higher T_3 level in males under short than long photoperiods also confirmed the previous results [3]. Although serum T_4 concentration was low and varied among each experiment (some variations in the plasma T_4 level have been reported in birds [10, 11]), the level was always higher in KR than KN line under long days and 23°C. This is interesting in connection with the recent report by Follett and Nicholls [12]. They showed that the thyroid plays an important role in the gonadal response of Japanese quail to short days when the birds are transferred from long to short days, i.e., thyroidectomized males do not show the rapid testicular regression and moult which occur in controls and if T_4 is administered at certain period of the photoperiodic treatments normal regression does occur under short days. Therefore, the difference in the photoperiodic gonadal response between KR and KN lines might be attributable to the difference in the thyroid activity. In addition, as reviewed by Sharp and Klandorf [13], intimate interactions between day lengths, gonadal steroids and thyroid gland function in Galliform birds lead us to study the relation between thyroid and gonadal activity of KR and KN lines in future experiments.

ACKNOWLEDGMENTS

We are grateful to Professor Emeritus Masaru Kato of Kyoto University for his encouragement throughout this inverstigation. Thanks are also due to Messrs. Yoshio

Asai, Keiji Hara and Takaaki Himoto for their assistance in animal care and Ms. Kumiko Tanaka for her technical assistance on radioimmunoassay.

REFERENCES

1 Konishi, T. and Oishi, T. (1985) Characteristics of two lines of Japanese quail selected for response to "Continuous light treatment". Zool. Sci., **2**: 549–557.

2 Oishi, T. (1978) Effect of short days in the photoperiodic testicular response of Japanese quail. Environ. Cont. Biol., **16**: 35–40.

3 Oishi, T. and Konishi, T. (1978) Effects of photoperiod and temperature on testicular and thyroid activity of the Japanese quail. Gen. Comp. Endocrinol., **36**: 250–254.

4 Oishi, T. and Konishi, T. (1983) Variation in the photoperiodic cloacal response of Japanese quail: Association with testes weight and feather color. Gen. Comp. Endocrinol., **50**: 1–10.

5 Freeman, B. N. and Vince, M. A. (1974) Development of the Avian Embryo, Chapman and Hall, London.

6 Ishii, S. (1983) Programs of Statistical Methods for Biologists by N88-Basic, Baifukan, Tokyo. (in Japanese)

7 Honda, H., Tanaka, K., Minamino, T. and Konishi, T. (1982) Control of contour feather growth of Japanese quail. J.Exp. Zool., **220**: 311–319.

8 Kawahara, T. (1973) Comparative study of quantitative traits between wild and domestic Japanese quail (*Coturnix coturnix japonica*). Exp. Animals, **22** (Suppl.): 139–150.

9 Kawahara, T. (1976) History and useful characters of experimental strains of Japanese quail (*Coturnix coturnix japonica*). Exp. Animals, **25**: 351–354. (*in Japanese*)

10 Astier, H. (1980) Thyroid gland in birds: Structure and function. In "Avian Endocrinology". Ed. by A. Epple and M. H. Stetson, Acad. Press, New York, pp. 167–189.

11 Herbuté, S., Pintat, R., Parês, N., Astier, H. and Baylé, J. D. (1983) Comparison of plasma thyroxine levels following short exposure to cold and TRH administration in intact and pituitary autografted quail (*Coturnix coturnix japonica*). Gen. Comp. Endocrinol., **49**: 154–161.

12 Follett, B. K. and Nicholls, T. J. (1985) Influences of thyroidectomy and thyroxine replacement on photoperiodically controlled reproduction in quail. J. Endocrinol., **107**: 211–221.

13 Sharp, P. J. and Klandolf, H. (1985) Environmental and physiological factors controlling thyroid function in Galliforms. In "The Endocrine System and the Environment." Ed. by B. K. Follett, S. Ishii and A. Chandola, Japan Sci. Soc. Press, Tokyo/Spring-Verlag, Berlin, pp. 175–188.

ZOOLOGICAL SCIENCE 3: 145–150 (1986)

Structure, Innervation, Persistence, and Effects of Juvenile Hormone on the Prothoracic Glands in Adult *Blattella germanica* (L.) (Dictyoptera, Blattellidae)

LAKSHMI K. HAZARIKA and AYODHYA P. GUPTA[1]

Department of Entomology and Economic Zoology, Agricultural Experiment Station, Cook College, Rutgers University, New Brunswick, NJ 08903, USA

ABSTRACT—During a study of the structure, degeneration pattern, and effects of juvenile hormone on the integrity of adult prothoracic glands (PTGs) in *Blattella germanica* (Dictyoptera, Blattellidae), we found that the nymphal PTGs were characterized by the presence of interglandular bridges in addition to crossovers. The glands are innervated posteriorly by the prothoracic gland nerve, originating from the prothoracic ganglion. In adults, the PTGs, although degenerate, persist throughout the adult life, maintaining themselves as two nonglandular strands, composed of two muscle bands, and thick connective tissue sheath. The breakdown of the PTGs can be partially prevented by applying juvenile hormone (JH), suggesting that JH is necessary for maintaining the structural integrity of the PTGs.

INTRODUCTION

The prothoracic glands (PTGs) are nymphal structures, but in some dictyopterans they are present in the adults as well. After adult emergence, they gradually degenerate and break down, as reported in *Leucophaea maderae* [1, 2], *Periplaneta americana* [3], and *Nauphoeta cinerea* [4, 5]. It is believed that degeneration commences soon after adult emergence [2], owing to absence of JH [6], and is visible in the external appearance of the gland. It is also believed that the PTGs in the adults are endocrinologically non-functional [1]. The persistence of these so-called non-functional PTGs in adult cockroaches is an interesting phenomenon, since they disappear completely in adults of other insects. Therefore, the objectives of this study are to describe the gross anatomy and nervous innervation of the PTGs in the last (6th) instar nymphs, and their progressive degeneration and residual persistence in the adults, and the effects of JH on PTGs of adultoids of *Blattella germanica* L.

Accepted September 18, 1986
Received May 23, 1986
[1] To whom reprints should be requested.

MATERIALS AND METHODS

Insects

B. germanica colony was maintained at 28 ± 2°C on Purina lab chow and water. Sixth instar nymphs and adults of various ages were used in this study. Newly emerged male and female adults were separated each day from rearing jars and placed in groups of 15–20 individuals in Dixie cups with food and water. In this study, we used the PTGs of 5 adults for each of day 1 (which represented an adult immediately after emergence), day 7 (end of the first reproductive cycle), day 50 (about middle age), and day 120/150 (old age for male and female, respectively) to prove that the PTGs persisted throughout the adult life span. For scanning electron microscopic (SEM) observations, these PTGs were fixed *in toto* according to the method described below for histology. The fixed PTGs were air-dried, mounted on aluminium stubs, and coated with gold paladium for 2–4 min in a Technic sputterer. They were examined in a Hitachi S–510 SEM at

5 kV at different magnifications.

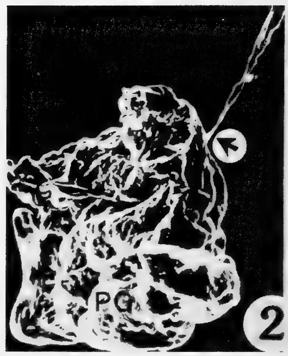

Fig. 1. Light micrograph of the prothoracic glands (PTG) of a 6th-instar female nymph showing the crossing over (X) and the interglandular bridge (arrow). ×400.

Fig. 2. Scanning electron micrograph showing the prothoracic gland nerve (PGN) (arrow) connected to the prothoracic ganglion (PG). The remaining nerves were cut during preparation. ×100.

Wholemount for gross anatomical study

Two-to-four hours prior to dissection, 6th-instar nymphs and adults were injected with 20 to 30 μl of 0.25% methylene blue in double-distilled water with the help of a 100 μl Hamilton syringe fitted with a 30-gauge needle. After cutting open the prothorax and neck ventrally in ice-cold physiological saline, 5 prothoracic ganglia (PG) attached with the blue-stained PTGs were also prepared after fixing *in toto* (as described in the following section) and whole-mounted in Permount or emersion oil for light microscopic observations. PTG-attached ganglia were also examined under the SEM.

Histology

PTGs from ten 6th instar nymphs and ten one-day-old adults were fixed *in toto* with 2.5% glutaraldehyde in sodium cacodylate buffer (pH 7.2) and postfixed in 1% osmium tetroxide in the same buffer (pH 7.2). They were then dehydrated in ethanol series and dealcoholized with propylene oxide. These tissues were used for preparing resin blocks with epon-araldite mixtures. One-to-two μm-thick sections were cut with Sorvall MT2–B Ultramicrotome. Sections were stained with basic fuchsin and couterstained with methylene blue. Composite diagrams were made through light microscopic observations.

Application of juvenile hormone analogue (JHA) and measurement of PTG widths

Two four-day-old 6th-instar nymphs were treated with two μl of 100 ppm R–20458 (6, 7-epoxy-1-(p-ethylphenoxy)-3, 7-dimethyl-trans-2-octene) in acetone on the dorsal side of the abdomen with an ISCO microapplicator fitted with a precalibrated 100 μl Hamilton syringe. The average widths of the two glands at their widest points were measured in normal adults (day-1, -7, -50, -120, and -150) and JHA-treated adultoids (day 1–3) according to [7].

RESULTS

The PTGs of *B. germanica* (L.) are a pair of irregularly shaped tissue bands (Fig. 1). They cross over each other anterior to the PG. Unlike the PTGs of other cockroach species so far studied, the PTGs of the 6th-instar nymph of *B. germanica* have an interglandular bridge (Fig. 1) below the crossing over. The histology of the bridge is similar to that of the gland.

Innervation of PTGs

At the base of the 4th peripheral nerve [8] of each side of the PG, a single nerve, the prothoracic gland nerve (PGN), arises and innervates the PTG of the respective side (Fig. 2). In examinations of

the methylene blue-stained PGN, we traced the nerve throughout the entire length of the PTG. The PGN appears to receive axons from the PG.

Histology of a nymphal PTG and interglandular bridge

The longitudinal section of gland (Fig. 3) and the bridge revealed the centrally located striated muscle, a nerve, fine branches of connective tissue, and cells with large nuclei. The boundaries of these cells are not well defined and the nuclei are of variable sizes and shapes, such as, long, elliptical, round and irregular. We did not observe any granules in the cytoplasm. As in *L. maderae* [1], we also observed in *B. germanica* that cells containing elliptical nuclei usually occupy the central part of the gland. Generally, at the broadest area of the gland, there are about 6 to 8 cells. Cytoplasm in the peripheral cells is abundant in comparison with that of the centrally located ones. The cup-shaped cavity with round extracellular basic fuchsin-stainable material can be seen in the cross section of the 6th-instar nymphal PTGs (Fig. 4). Trachea can be seen both externally and internally. A branch of the cephalic ventral longitudinal trachea (VLT) (ventral branch of the head [9]) tracheates the PTGs on both sides, appearing externally along the anterior 2/3 of their lengths. It enters and traverses internally in the remainder of the PTGs.

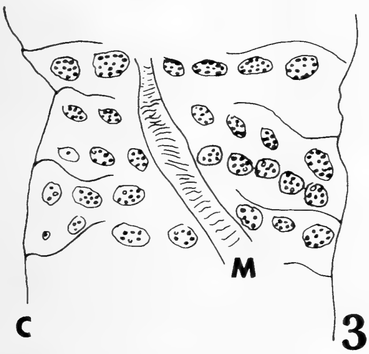

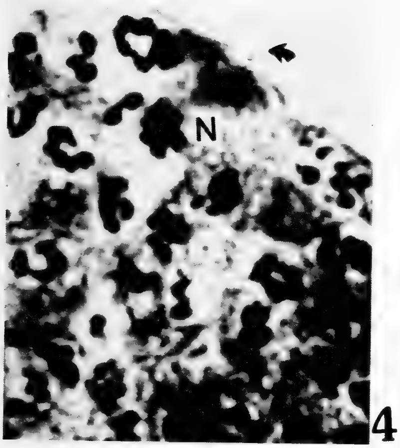

FIG. 3. Diagram of a longitudinal section through the center of a nymphal prothoracic gland. C: connective tissue sheath, M: muscle.

FIG. 4. Part of a cross section of a nymphal prothoracic gland showing the nuclei (N) and cup-shaped infolding (arrow). ×1,200.

Degeneration and persistence of PTGs in adults

The PTGs persist throughout the lifespan of male and female *B. germanica* adults (Fig. 5 and Table 1). However, they undergo degeneration,

TABLE 1. Comparision of PTG widths in nymphs and adults of *Blattella germanica* (L.)

Stages	N	Mean PTG widths* (in μm)	SD
6th Nym	5	138.60[a]	2.40
Adult			
1 day	5	79.20[b]	5.26
7 day	5	32.80[c]	2.16
50 day	5	15.40[d]	4.72
120 day	5	7.80[e]	2.58

* Means with the same letter are not significantly different at 0.05 level (Student-Newman-Keuls Test).

losing their glandular tissues within a few hours of adult emergence (<1-day old), which can be visualized from the cross section of a day-1-adult PTG (Fig. 6). During this process, the PTGs form lacunae or intercellular spaces and thickening and protrusion of the connestive tissue sheath. Subsequently, the lacunae disappear from the gland cavity and are replaced by thick connective tissue sheath. Consequently, the PTGs maintain their physical identity in the form of two nonglandular tissue strands, consisting of the muscle, trachea, and connective tissue.

When we compared the widths of the PTGs in

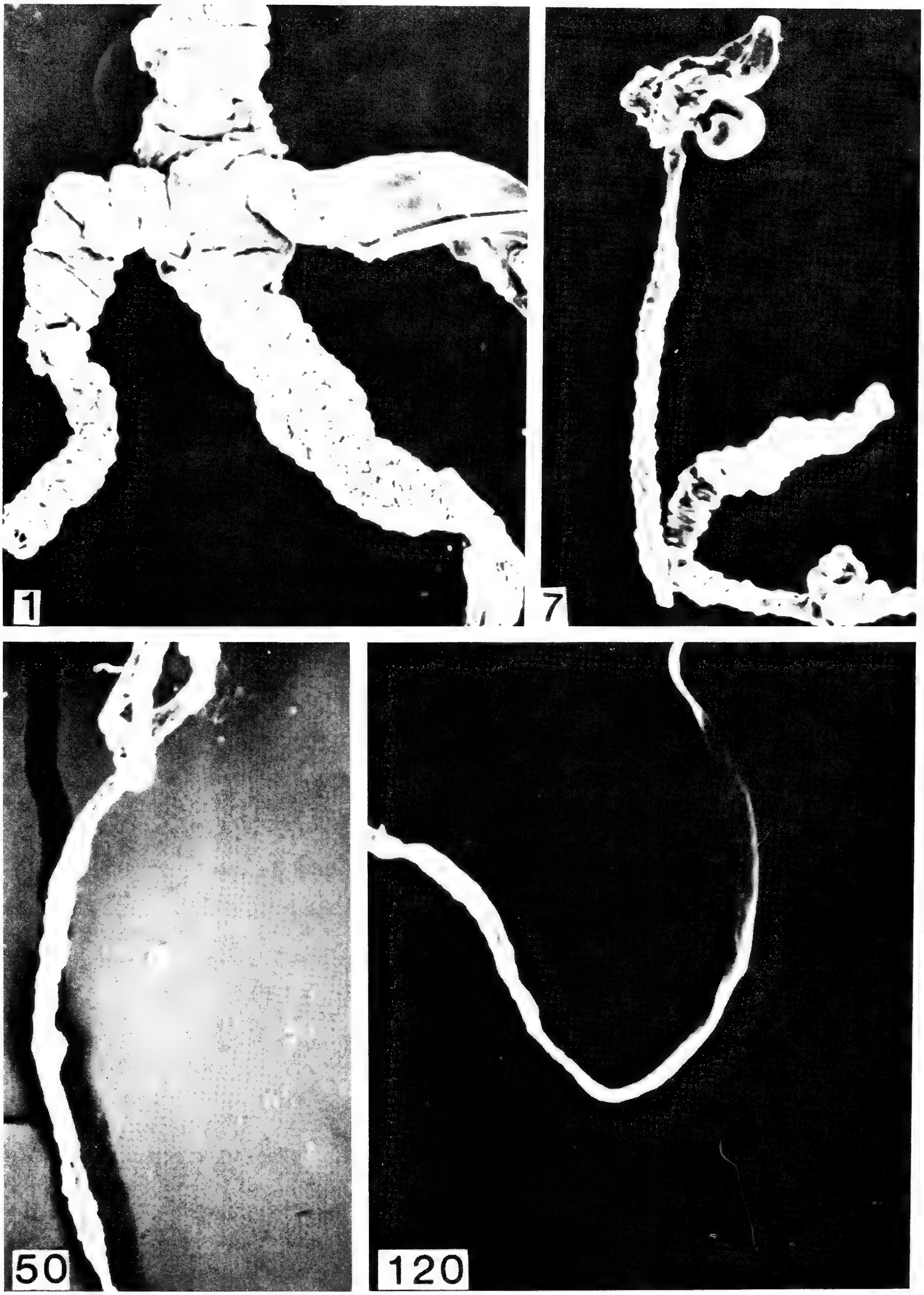

FIG. 5. Scanning electron micrographs of prothoracic glands of adults of various ages to show the reduction in size concommitant with advancement of ages. 1: 1-day-old adult, ×135. 7: 7-day-old adult, ×270. 50: 50-day-old adult, ×450. 120: 120-day-old adult, ×4,500. Though PTGs in micrographs 7 and 50 appear to be of same size, their magnifications are different.

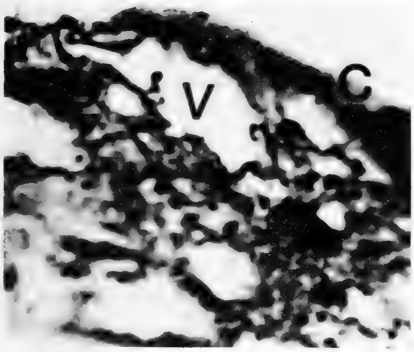

FIG. 6. Part of a cross section of a 1-day-old female adult PTG showing the lacunae (V), thick connective tissue sheath (C) and its branching (B) into the gland cavity. ×1,200.

6th-instar (day 6–7) nymphs and adults of various ages (Table 1), we found that they are significantly different from one another (P=0.05). The mean width of the PTG (8.2 μm) of the day-150-adult female (which is not shown in Table 1) was almost identical with that of the day-120-adult male. The widths of PTGs in the remaining adult females of ages, day-1, -7, and -50, were exactly identical with those of the male. Therefore, we did not consider them separately. Table 1 represents the mean PTG widths for both male and female adults.

Effect of JHA on adultoid PTGs

We found that JHA-treated adultoids of *B. germanica* contained almost nymphal-sized PTGs (in terms of widths) for 3 days after emergence (Table 2), which may be true for the remaining period of their short lifespan.

TABLE 2. PTG widths in JHA-treated adults of *Blattella germanica*

Age (Days)	N	Mean widths (in μm)	SD
1	11	118.74	27.1
2	9	102.04	47.86
3	7	123.91	60.2

DISCUSSION

As decribed previously, the PTG cross over anterior to the PG in *B. germanica*. The significance of the crossing over is, we believe, to provide mechanical support to the PTGs, since they are floating in the hemocoel between the gut dorsally and the ventral nerve cord ventrally. This is common in all dictyopterans so far studied. The presence of an interglandular bridge only in *B. germanica* is difficult to interpret; it might provide additional mechanical support. This kind of bridge has not been described in any other species. Considering the similarity in histology of the bridge with those of glands, we believe that the bridge may also be responsible for ecdysone synthesis.

The origin of the PGN in *B. germanica* in the PG has been observed also by scanning electron microscope (Fig. 2), in addition to the methylene blue-tracing technique. That the PG innervates the PTG via the PGN in *P. americana* [10] has been electrophysiologically documented [11] (for review see [12]).

In addition to the large nucleated cells in the gland periphery, the thickness of the connective tissues is indicative of the active nymphal state of the PTGs [1, 2]. A thin connective tissue sheath and its fine branches protruding into the gland cavity are characteristic features of nymphal PTGs, whereas, the thick connective tissue sheath and its branchings (Fig. 6) indicate the degenerating adult PTGs [1, 13].

Pronounced cup-shaped infoldings on the surface of the gland (Fig. 4) are essential for increasing surface area for exchange of materials [12, 14].

The significant differences in the widths of PTGs of the 6th-instar nymphs and adults of various ages (Table 2) has clearly demonstrated the difference in PTG sizes among those insects, presumably indicating the absence of growth of the PTG in adults. Persistence of such so-called endocrinologically nonfunctional glands in adult dictyopterans and *Aeshna* (Odonata) [15] may suggest a relationship between the two groups [1].

By applying JH exogenously at the critical stage of the last-instar nymph, one can prevent the degeneration of the PTGs in *B. germanica* adultoids and allow them to persists as nymphal-sized PTGs. From this finding, we can designate the day 2–4 of 6th instar nymphs as the critical stage, because those adults, which emerged as a result of

JH application on 6th-instar nymphs before or after this age (day 2–4), showed normal degenaration pattern of PTGs (personal observations). The differences in PTG widths between day-1-adults and -adultoids, and no difference in PTG widths between the 6th- instar nymphs and day-1 adultoids, strongly indicate that JH is essential in preserving the integrity of the PTGs.

ACKNOWLEDGMENTS

This paper is the New Jersey Agricultural Experiment Station Publication No. D–08112–14–86 supported by state funds, U.S. Hatch funds, and Rutgers Research Council. LKH was on sabbatical from Assam Agricultural University, Jorhat, India during this study on India Government Scholarship.

REFERENCES

1 Scharrer, B. (1948) The prothoracic glands of *Leucophaea maderae* (Orthoptera). Biol. Bull., **38**: 35–45.

2 Scharrer, B. (1966) Ultrastructural study of the regressing prothoracic glands of Blatterian insects. Z.Zellforsch., **69**: 1–21.

3 Bodenstein, D. (1953) Studies on the humoral mechanisms in growth and metamorphosis of the cockroach, *Periplaneta americana*. II. The function of the prothoracic glands and the corpus cardiacum. J. Exp. Zool., **123**: 413–433.

4 Radwan, W. A. (1977) The prothoracic glands in the cockroach, *Nouphoeta cinerea* (Olivier). II. Effect of JHA on histological structures of the gland. Bull. Soc. Entomol. Egypte, **61**: 91–98.

5 Radwan, W. A. and Novak, V. J. A. (1977) The prothoracic glands in the cockroach, *Nauphoeta cinerea* (Olivier). I. Histological studies of the glands in the last instar nymph and their degeneration in the adult insect. Bull. Soc. Entomol. Egypte, **61**: 79–89.

6 Lanzerin, B. (1975) Programming, induction, or prevention of the breakdown of the prothoracic gland in the cockroach, *Nauphoeta cinerea*. J. Insect Physiol., **21**: 367–389.

7 Hazarika, L. K. (1986) Hemocyte population changes and neuroendocrine complex in *Blattella germanica* (L.) (Dictyoptera: Blattellidae). Ph.D. Thesis, Rutgers University, New Brunswick, NJ.

8 Pipa, R. L. amd Cook, E. F. (1959) Studies on the hexapod nervous system. I. The peripheral distribution of the thoracic nerves of the adult cockroach, *Periplaneta americana*. Ann. Entomol. Soc. Am., **52**: 695–710.

9 Haber, V. R. (1926) The tracheal system to the German cockroach, *Blattella germanica* Linn. Bull. Brooklyn Entomol.Soc., 21: 61–92.

10 Chadwick, L. E. (1956) Removal of prothoracic glands from the nymphal cockroach. J. Exp. Zool., **131**: 291–306.

11 Richter, K. and Gersch, M. (1983) Electrophysiological evidence of nervous involvement of the prothoracic gland in the *Periplaneta americana*. Experientia, **39**: 917–918.

12 Pipa, R.L. (1983) Morphological considerations in the integration of nervous and endocrine systems. In "Endocrinology of Insects". Ed. by G. H. Downer and H. Laufer, Alan R. Liss, Inc., New York, pp. 39—53.

13 Scharrer, B. (1964) The fine structure of the Blatterian prothoracic glands. Z. Zellforsch., **64**: 301–326.

14 Dorn, A. and Romer, F. (1976) Structure and function of prothoracic glands and oenocytes in embryos and last larval instar of *Oncopeltus fasciatus* Dallas (Insecta, Hemiptera). Cell Tissue Res., **171**: 331–350.

15 Cazal, P. (1947) Recherches sur les glandes endocrines rétrocèrèbrales des Insects II. Odonates. Arch. Zool. Exp. Gén., **85**: 55–82.

ZOOLOGICAL SCIENCE 4: 151–158 (1987)

Long-lasting Effects of Orchiectomy and Its Preceding Procedures on Open Field Behavior in Male Mice

TAKEO MACHIDA, SHIHO ISO[1] and TETSUO NOUMURA[2]

Zoological Institute, Faculty of Science, Hiroshima University, Naka-ku, Hiroshima 730, [1]Biology Division, Tokyo Metropolitan Institute of Gerontology, Itabashi, Tokyo 173, and [2]Department of Regulation Biology, Faculty of Science, Saitama University, Urawa, Saitama 338, Japan

ABSTRACT—During the course of investigations aiming to clarify the role of androgen in the ontogeny of open field behavior in male mice, it was found that several manipulation stresses from transport to surgical castration exert long-lasting effects on measures of the behavior. Male mice of the ICR/SLC strain were divided into five groups, in stepwise addition of the following four treatments to the untreated controls: transport from animal room to laboratory, anesthetization with ether, operation of abdominal opening (sham-orchiectomy), and orchiectomy at 43 days of age. All animals were subjected to the open field test at 70–74 days of age. Scores of ambulation and rearing were the greatest in untreated controls and the smallest in orchiectomized mice, while those of grooming and defecation were the greatest in orchiectomized animals and the smallest in untreated controls. Scores of ambulation and rearing showed a tendency to decrease with addition of treatments. In contrast scores of grooming increased with addition of treatments. However, there were no significant differences in ambulation, rearing and grooming between orchiectomized and sham-orchiectomized animals. On the other hand, weight of adrenals increased with addition of treatments. Through 67 animals examined, adrenal weight negatively correlated with ambulation and positively interacted with grooming. These results indicate that orchiectomy and its preceding procedures at young adults exert long-term effects on later open field behavior in male mice and that orchiectomy itself exerts no significant influences on the open field behavior.

INTRODUCTION

Several aspects of sociosexual behavior of male rodents are markedly influenced by gonadal androgens (for review, see [1, 2]). In our preliminary experiments, we found that scores of ambulation and rearing in the open field were significantly smaller in orchiectomized mice than in intact animals but not significantly different from scores of sham-orchiectomized mice [3]. Similarly, significant difference was obtained in scores of defecation between intact male mice and sham-orchiectomized animals, although there were no differences between orchiectomized mice and sham-orchiectomized animals. It seems highly probable, therefore, that not only orchiectomy but also surgical operation itself and/or manipulation of animals preceding operation might act as stressors and cause some behavioral changes in male mice. Procedures of manipulating animals preceding operation of orchiectomy are divided into three steps: (1) transport of mice in the cage from animal room to laboratory, (2) anesthetization of animals with ether, and (3) operation of abdominal opening. In the present experiments, effects of these procedural steps on several measures of open field behavior were examined in male mice.

Accepted September 25, 1986
Received July 31, 1986

MATERIALS AND METHODS

Animals Sixty seven male mice of the ICR/SLC strain were used. All animals were obtained at 21 days of age from the Shizuoka Animal Breeding Laboratory, Hamamatsu, Japan. They

were housed in groups of four mice per cage and maintained on pelleted diet and water *ad libitum* in a temperature- ($22\pm2^\circ$C) and humidity- (50% R. H.) controlled animal room on a 14 hr/10 hr light-dark cycle (lights on at 0700).

Treatments At 43 days of age, all animals were randomly assigned to one of the following five groups: (1) untreated controls. Animals were left undisturbed in the animal room until the day of behavioral test. (2) transport. Animals were carried out of the animal room to laboratory. (3) anesthesia. Animals transported to laboratory were anesthetized with ether. (4) sham-orchiectomy. Animals transported to laboratory and anesthetized with ether were given an operation of sham-orchiectomy. (5) orchiectomy. Animals transported to laboratory and anesthetized with ether were orchiectomized. Animals that had been transported to laboratory were then carried back to animal room immediately after receiving above treatments.

Open filed test When animals reached 70 days of age, they were given open field test daily for five consecutive days. A detailed description of apparatus and procedures of the test has been reported elsewhere [4]. Briefly, a 45 cm square open field surrounded by walls of 20 cm high was constructed of acrylic plates, mat black in color. In each test, a sheet of black velvet paper, 45×45 cm in size, was placed on the floor of the open field. The floor of the field was divided into nine 15 cm square units by 1 mm white lines ruled on the velvet paper. The open field was lighted by a fluorescent light source ($20\,W\times2$) mounted 150 cm above the field.

In the daily test administered between 1030 and 1300 hours, each animal was gently removed from its home cage and placed in the center of the field and the following elements of behavior were measured for five minutes: (1) ambulation; number of squares entered by the animal, (2) rearing; number of standing upright on hind legs, (3) grooming; number of bouts of grooming and time in seconds spent grooming, and (4) defecation; number of fecal boli deposited.

After each test, animals were placed in a holding cage until all the occupants of the home cage had been tested.

Measurement of organ weight Two days after the end of open field test, animals were killed by overdose of ether and the adrenals and the preputial glands were dissected out and weighed.

Statistics Statistical analyses were performed by Mann-Whitney's U-test and Kruskal-Wallis test for multiple groups or using correlation coefflcient (r).

RESULTS

Cumulated scores for each measure of the open field behavior obtained over five days of testing are shown in Figures 1–3.

Scores of ambulation were significantly interacted with treatments (H cor (4)$=9.56$, $P<0.05$ by Kruskal-Wallis test, Fig. 1a). Mice of the untreated group exhibited significantly more active ambulation than those of the orchiectomized or the sham-orchiectomized group (U(14, 13)$=50$, $P<0.05$ between untreated and orchiectomized mice, and U (14, 17)$=67$, $P<0.05$ between untreated and sham-orchiectomized animals by Mann-Whitney's U-test), although there were no significant differences in ambulation between untreated and transported animals (U (14, 10)$=36$, $P>0.05$) or among transported, anesthetized, sham-orchiectomized and orchiectomized groups (H cor (3)$=3.25$, $P>0.3$). Through five groups, however, scores of ambulation showed somewhat decrease with addition of treatments.

On the other hand, scores of rearing failed to show any significant interaction with treatments (H cor (4)$=8.50$, $P>0.05$, Fig. 1b), although animals of the orchiectomized group exhibited significantly lower scores of rearing than the untreated controls (U (13, 14)$=39$, $P<0.05$). Nevertheless, scores of rearing decreased with addition of treatments, except for anesthetized animals.

Significant interaction with treatments was evident in number of bouts of grooming (H cor (4)$=$ 20.90, $P<0.001$, Fig. 2a). Orchiectomized animals exhibited significantly greater number of bouts of grooming than either anesthetized (U (13, 13)$=$ 33.5, $P<0.05$), transported (U (13, 10)$=10$, $P<$ 0.05), or untreated mice(U (13, 14)$=14.5$, $P<$ 0.05), although they failed to show significantly different numbers of bouts of grooming from

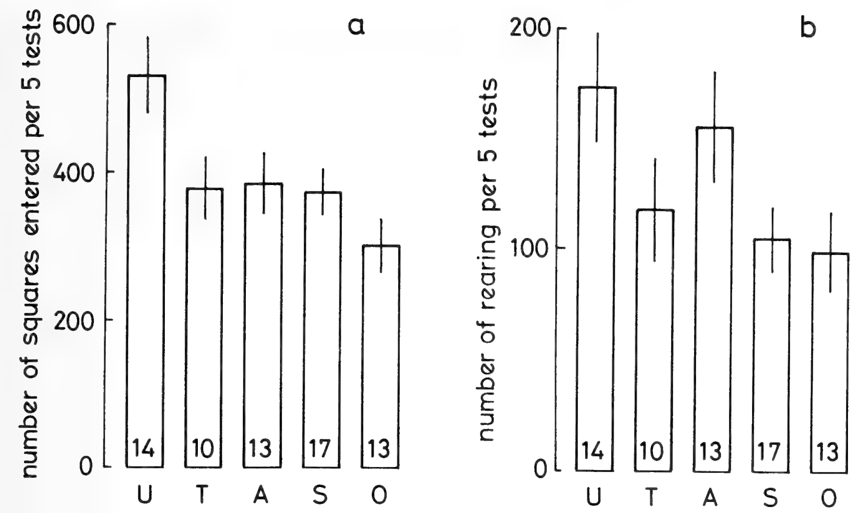

FIG. 1. Cumulated scores of ambulation (a) and rearing (b) obtained in the open field during 5 daily tests in male mice of different groups. U: ntreated, T:transported, A: nesthetized, S: sham-orchiectomized, O:orchiectomized. Each bar represents the mean ± standard error. Number of animals used is shown in each column. See text for statistical evaluation.

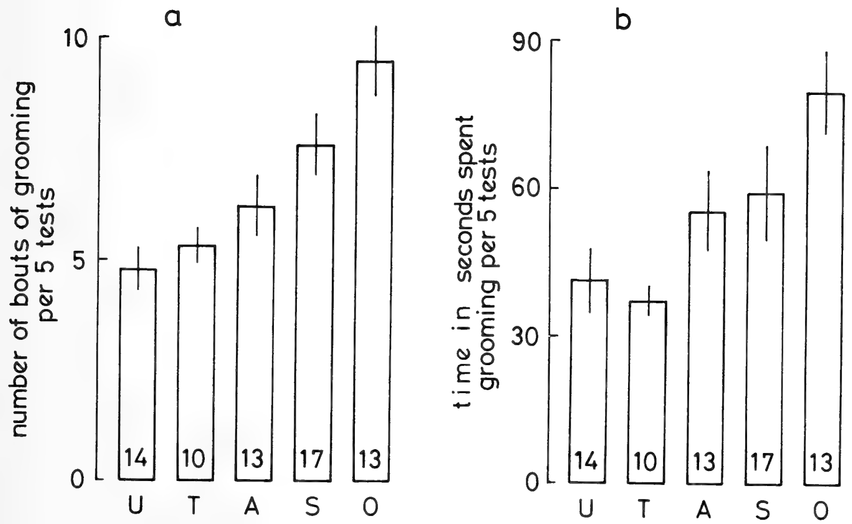

FIG. 2. Cumulated scores of number of bouts of grooming (a) and time in seconds spent grooming (b) obtained in the open field during 5 daily tests in male mice of different groups. See legend of Fig. 1 for details.

sham-orchiectomized animals (U (13, 17)=73, P> 0.1). Significant difference was similarly found in number of bouts of grooming between sham-orchiectomized and transported (U (17, 10)=40.5, P<0.05) or untreated animals (U (17, 14)=55, P<0.05). The number of bouts of grooming increased step by step with addition of treatments.

Duration of grooming likewise exhibited a significant interaction with treatments (H cor (4)= 15.28, P<0.01, Fig. 2b). Animals of the orchiecto-

mized group spent significantly longer time for grooming than those of either anesthetized (U (13, 13)=45, P=0.05), transported (U (13, 10)=8, P <0.05) or untreated group (U (13, 14)=32, P< 0.05), but failed to exhibit a significant difference in duration of grooming from sham-orchiectomized mice (U (13, 17)=82, P>0.1). Significant difference was achieved in scores of duration of grooming between sham-orchiectomized and transported animals (U (17, 10)=41.5, P<0.05). There were no significant differences, however, in duration of grooming among sham-orchiectomized, anesthetized and untreated animals (H cor (2)=3.86, P>0.1), and between transported and anesthetized (U (10, 13)=42, P>0.05) or untreated mice (U (10, 14)=64, P>0.1). Duration of grooming increased with addition of treatments, but not for transported. Scores of grooming were negatively interacted with ambulatory activity: correlation was significant between the number of bouts of grooming and the number of squares entered (r (67)=−0.39, P<0.005).

Statistically significant differences were obtained in scores of defecation among groups of different treatments (H cor (4)=13.34, P<0.01, Fig. 3). Animals of orchiectomized group eliminated significantly greater number of fecal boli than sham-orchiectomized, anesthetized or untreated animals (U (13, 17)=35, U (13, 13)=37.5, or U (13, 14)= 29, respectively, P<0.05). There were no significant differences in scores of defecation, however, between orchiectomized and transported groups (U(13, 10)=44, P>0.1) and among mice of untreated, transported anesthetized and sham-orchiectomized groups (H cor (3)=2.85, P>0.3).

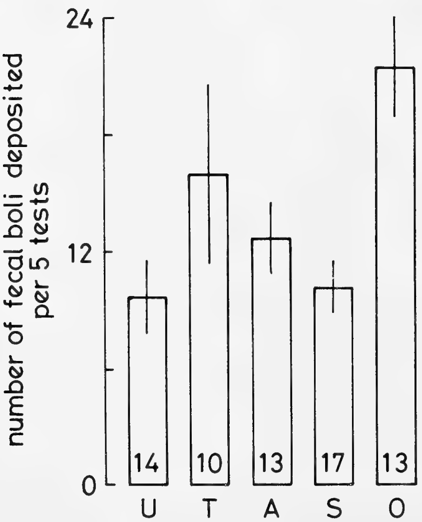

Fig. 3. Cumulated scores of defecation obtained in the open field during 5 daily tests in male mice of different groups. See legend of Fig. 1 for details.

Daily changes in several measures of the open field behavior during five days of testing were shown in Figure 4. In the five groups of different treatments, daily scores of ambulation invariably exhibited a significant decrease with repeated testings (r (70)=−0.37, r (50) =−0.47, r (65) = −0.44, r (85) =−0.39 and r (65)=−0.46 for untreated, transported, anesthetized, sham-orchiectomized and orchiectomized groups, respectively, P<0.005).

On the other hand, in scores of rearing, significantly negative correlation with days of testing was only found in the transported group (r (50)= −0.31, P<0.05), while no consistent correlation was obtained between scores of rearing and days of testing in the other four groups (r (70)=−0.13, r (65) =−0.17, r (85) =−0.16, and r (65) =−0.23 for untreated, anesthetized, sham-orchiectomized and orchiectomized groups, respectively, P> 0.05).

By contrast, daily scores of grooming tended to increase with repeated testing. Positive correlation was significant between duration of grooming and days of testing in the orchiectomized (r (65) = 0.42, P<0.001) and the anesthetized groups (r (65) =0.28, P<0.05). In the other groups, however, positive correlation between scores of grooming and the repeated testing failed to reach statistical significance (r (70)=0.12, P>0.1, r (50) =0.26, P >0.05, and r (85)=0.20, P>0.05 for untreated, transported and anesthetized groups, respectively.

Table 1 shows the body weight and the weights of adrenals and preputial glands in animals of different experimental groups. Significant interaction was obtained between the body weight and the different treatment two days after exposing five daily tests of behavior (H cor (4) =12.8, P<0.02). Orchiectomezed animals had significantly smaller body weight than mice of the untreated and the anesthetized groups (U (13, 14)=32, and (U (13,

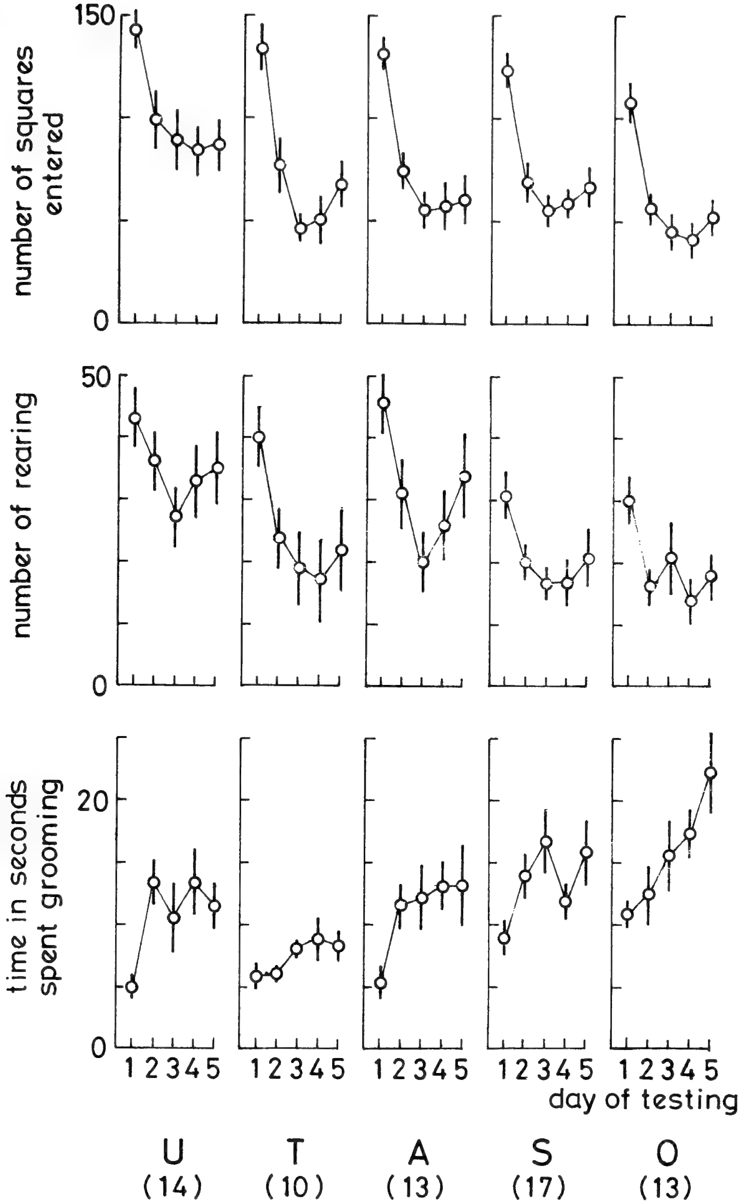

FIG. 4. Changes in scores of ambulation, rearing and grooming following daily testing in the open field. See legend of Fig. 1 for details.

13) =40, respectively, P<0.05). Sham-orchiectomized animals were likewise smaller than untreated controls (U (17, 14)=58, P<0.05). Through the five groups, the body weight decreased with the addition of treatments.

Weight of the adrenals was significantly interacted with treatments (H cor (4)=33.6, P<0.001). Adrenals of the orchiectomized animals were significantly heavier than those of anesthetized, transported and untreated mice (U (13, 13)=31.5, (U (13, 10)=1, and U (13, 14)=13, respectively, P <0.05), although there were no significant differ-

Table 1. Body weight and weights of adrenals and preputial glands in male mice of different experimental groups

Group (no. of mice)	Body weight (g)	Adrenals (mg/10 g B.W.)	Preputial gland (mg/10 g B.W.)
Untreated (14)	39.7±0.6	1.8±0.1	20.2±1.4
Transported (10)	38.4±0.6	1.8±0.1	20.8±0.9
Anesthetized (13)	38.8±0.7	2.2±0.1	20.9±2.3
Sham-orchiectomized (17)	37.4±0.6	2.4±0.1	19.4±1.3
Orchiectomized (13)	36.6±0.8	2.5±0.2	9.1±0.7

See text for statistical evaluation.

ences in the weight of adrenals between orchiectomized and sham-orchiectomized groups (U (13, 17)=63, P>0.05). Animals of the sham-orchiectomized group possessed significantly heavier adrenals than mice of the transported and the untreated groups (U (17, 10)=5.5, and U (17, 14)=32.5, P<0.05). Adrenals of the anesthetized animals were significantly heavier than those of the transported and the untreated mice (U (13, 10) = 22.5, and U(13, 14)=46, P<0.05). Adrenal weights increased with the addition of treatments.

On the other hand, weight of the preputial glands was significantly reduced by orchiectomy (orchiectomized vs. sham-orchiectomized mice, U (13, 17)=1, P<0.05). Among the other four groups with intact testes, however, no significant difference was found in the weight of preputial glands (H cor (3) =4.63, P>0.2).

Through 67 animals examined, significant correlations were obtained between measures of the open field behavior and the body weight or the weight of adrenals. Scores of ambulation exhibited a positive correlation with body weight and a negative correlation with adrenal weight (r (67)= 0.39, P<0.005, and r (67)=0.27, P<0.05, respectively). Significantly positive correlation was evident between the number of bouts of grooming and the weight of adrenals (r (67)=0.54, P< 0.001).

DISCUSSION

The present experiments clearly demonstrated that castration caused significant changes in measures of the open field behavior in male mice of the ICR/SLC strain. This is in good agreement with the reports of Broida amd Svare [5, 6] showing that locomotion in the home cage is significantly reduced by castration in males of the C57BL/6J, DBA/2J and Rockland-Swiss strains. However, in the present experiments, orchiectomized animals exhibited slightly smaller scores of ambulation than sham-orchiectomized mice. It seems therefore likely that removal of testes could exert only very small but no significant effect on male mice in lowering ambulatory activity in the open field. Similarly, the finding that orchiectomized animals exhibited slightly larger scores of grooming and defecation than sham-orchiectomized mice likewise indicates a minor involvement of testis in these measures of the open field behavior in male mice. Further experiments are required to clarify these differences.

It is well known that stimulation of animals in infancy results in significant modifications of behavioral responses in adulthood (for review, see [7, 8]). Although the literature unequivocally indicates that stimulation by handling for the first 20 days of life is most effective in inducing permanent changes in later behavior in rats and mice, Machida *et al.* [9] successfully restricted the effective period of infantile handling to the second 10 days after birth in mice: handling from 11 to 20 days of age, but not from 1 to 10 days, significantly elevated later activities of ambulation and rearing in male amd female mice. In the present experiments, a single exposure of male mice to orchiectomy and its preceding procedures at 43 days of age exerted significant influences on behavioral reactivities at 70 days of age. In this connection, Goodrcik [10] previously reported that gentling for

42-51 days of age significantly affected scores of grooming at 73 days of age in male rats. It is interesting that not only stimulation in infancy but also exposure to certain stimuli in later life produce long-term behavioral changes in animals.

In the present experiments, significant correlations were evident between measures of the open field behavior and the addition of treatments: scores of ambulation and rearing were significantly decreased with addition of treatments, while those of grooming and defecation were increased. On the other hand, it was found that addition of treatments at 43 days of age significantly decreased the body weight and increased the weight of adrenals at 76 days of age. It has been well known that exposure of immature rodents to stressful stimule, i.e., handling or electric shock, affects the later behaviors and the function of the hypothalamo-hypophyseal-adrenocortical (HHA) system [11, 12]. This manipulation also alters plasma levels of corticosterone in rats [11, 13]. Therefore, in the present experiments, there is every probability that four kinds of treatments acted as stressors, incited the function of HHA system and caused elevated secretions of adrenocorticotropic hormone (ACTH) and adrenocortical hormones which provoked long-term alterations of behavioral responses in later life. Determination of plasma titers of these hormones are required to confirm the probability.

It has been known that repeated exposure to the open field causes a decrease in ambulation and an increase in defecation and grooming in rats and mice (for review, see [14]). We have also reported a similar decrease in scores of ambulation and rearing and an increase in grooming following successive tesing in mice [4, 9, 15]. In the present experiments, five daily exposures to the open field caused a decrease in ambulation and rearing and an increase in grooming. The results are in good agreement with our and others' previous findings. In this connection, Nagy and Holm [16] found a significant increase in defecation following repeated testing in mice of the C3H strain. In our experiments, however, mice of the ICR/SLC strain eliminated a very small number of fecal boli in the open field and therefore we were unable to detect daily changes in defecation. It is apparent that defecation is not a valid measure for the ICR/SLC strain.

A significant negative correlation has well documented between defecation and ambulation in various strains of mice (for review, see [14]). Throughout 67 mice examined in this experiment, however, inverse correlation was evident between scores of grooming and ambulation. Correlation of ambulation with variables other than defecation has seldom been reported (for review, see [17]). This is the first to demonstrate significant inverse correlation of ambulation with grooming scores.

ACKNOWLEDGMENTS

This work was supported in part by a Grant for Life Science Research Project "Discovery of Factors Regulating Aging" from the Institute of Physical and Chemical Research to T. N.

REFERENCES

1 Hart, B. L. (1974) Gonadal androgen and sociosexual behavior of male mammals: A comparative analysis. Psychol. Bull., **81**: 383–400.

2 Lloyd, J. A. (1975) Social behavior and hormones. In "Hormonal Correlates of Behavior. Vol. 1. A Lifespan View". Ed. by B. E. Eleftheriou and R. L. Sprott, Plenum Press, New York, pp. 185–204.

3 Machida, T. (1985) Effects of androgen on spontaenous activities of male mice. Proc. Chugoku-Shikoku Branch, Zool. Soc. Japan, **37**: 24 (Abstract).

4 Machida, T., Matsumoto, K., Kobayashi, S. and Noumura, T. (1982) Age-associated changes in the open field behavior of male mice of the ICR/SLC strain. Zool. Mag., **91**: 263–271.

5 Broida, J. and Svare, B. (1983) Genotype modulates tetosterone-dependent activity and reactivity in male mice. Horm. Behav., **17**: 76–83.

6 Brioda, J. and Svare, B. (1984) Sex differences in the activity of mice: Modulation by postnatal gonadal hormones. Horm. Behav., **18**: 65–78.

7 Denenberg, V. H. (1964) Critical periods, stimulus input, and emotional reactivity: A theory of infantile stimulation. Psychol. Rev., **71**: 335–351.

8 Ader, R. (1975) Early experience: Emotinal behavior and adrenocortical function. In "Hormonal Correlates of Behavior. Vol. 1. A Lifespan View". Ed. by B. E. Eleftheriou and R. L. Sprott, Pleum Press, New York, pp. 7–33.

9 Machida, T., Kurando, T. and Tosaki, M. (1982) Effects of different periods of handling during

infancy on later open field behavior in mice. J. Sci. Hiroshima Univ., Ser. B, Div. 1, **30**: 259–270.

10 Goodrick, C. L. (1971) Variables affecting free exploration responses of male and female Wistar rats as a function of age. Dev. Psychol., **4**: 440–446.

11 Levine, S. (1962) Plasma free corticosteroid response to electric shock in rats stimulated in infancy. Science, **135**: 795–796.

12 Haltmeyer, G. C., Denenberg, V. H. and Zarrow, M. X. (1967) Modification of the plasma corticosterone response as a function of infantile stimulation and electric shock parameters. Physiol. Behav., **2**: 61–63.

13 Denenberg, V. H., Brumaghim, J. T., Haltmeyer, G. C. and Zarrow, M. X. (1967) Increased adrenocortical activity in the neonatal rat following handling. Endocrinology, **81**: 1047–1052.

14 Archer, J. (1973) Tests for emotionality in rats and mice: A review. Anim. Behav., **21**: 205–235.

15 Machida, T., Kobayashi, S. and Noumura, T. (1983) Effects of different sizes of postweaning grouping on open field behavior in male mice. J.Sci. Hiroshima Univ., Ser. B, Div. 1, **31**: 155–162.

16 Nagy, Z. M. and Holm, M. (1970) Open field behavior of C3H mice: Effect of early handling, field illumination and age at testing. Psychon. Sci., **19**: 273–274.

17 Walsh, R. N. and Cummins, R. A. (1976) The open-field test: A critical review. Psychol. Bull., **83**: 482–504.

ZOOLOGICAL SCIENCE 4: 159–166 (1987)

Geographic Variation in the Tail of the Japanese Salamander, *Hynobius lichenatus*, with Special Reference to Taxonomic Bearing

Masato Hasumi and Hisaaki Iwasawa

Biological Institute, Faculty of Science, Niigata University, Niigata 950–21, Japan

ABSTRACT—Tail vertebrae were observed radiographically in 283 males and 49 females of adult *Hynobius lichenatus* collected during the breeding season from 19 localities in northeastern Japan. The frequency of specimens with broken and regenerated tails was much higher when the sites of oviposition were in swifter flowing streams. The relative tail length of specimens with normal tails tended to be greater at higher latitude. It is difficult to distinguish externally most regenerated tails from normal tails. The dispersions of relative tail length, however, were remarkably greater in most localities when data from specimens with normal, questionable, and regenerated tails were used. It is, therefore, necessary to take notice of tail regeneration in the measurement of tail length for taxonomic purposes.

INTRODUCTION

Relative tail length, that is tail length/snout-vent length, is one of the diagnostic characters for study of intra- and interspecific variation in urodeles. Since tail-autotomization among salamanders is restricted to most plethodontids and some salamandrids [1], tail length of specimens with complete and unautotomized tails is used taxonomically in these urodelen species [2, 3]. As far as we know, however, there are no taxonomic papers that take into consideration regeneration following tail breakage in other urodeles.

Hynobius is a genus of the family Hynobiidae that contains the most primitive living salamanders [4]. *Hynobius lichenatus* is widely distributed in northeastern Honshu, the mainland of Japan. Sato [5] reported that this species had considerable geographic variation in morphology, but he did not provide enough data. We reinvestigated the taxonomic characters of this species in the minutest detail, taking into account the various localities, and drew some new conclusions. Variation in the length of the tail is dealt with in this paper.

Accepted August 1, 1986
Received March 11, 1986

MATERIALS AND METHODS

During the breeding seasons of 1983–1985, 283 adult males and 49 adult females of *Hynobius lichenatus* Boulenger were collected from sites of oviposition in nineteen localities in northeastern Honshu. Sample sites are shown in Table 1. Sample sites 16–19 nearly correspond to the southern limit of distribution for this species. The stream index for sites of oviposition, divided into five types, shows that the stream flows more rapidly at higher type numbers. Additionally, in sample site 8, salamanders were trapped in roadside ditches on their way to the natural site of oviposition.

As soon as possible after collection, animals were anesthetized with 0.01% *p*-aminobenzoic acid ethyl ester aq. and measured. All measurements were made to the nearest 0.1 mm with slide calipers. The specimens were then fixed in 10% formalin. The following morphological data were recorded: snout-vent length, measured from the tip of the snout to the posterior angle of the vent; tail length, from the posterior angle of the vent to the tip of the tail; and axilla-groin length, from the posterior angle of the forelimb to the anterior angle of the hindlimb. Proportions were represented as relative to snout-vent length.

Radiographs of all specimens were taken using

TABLE 1. Sample site, site of oviposition, stream index, and number of specimens used in this study

	Sample site (Altitude)	Oviposition site and stream index	No. of specimens	
			Male	Female
1)	Maedanome, Goshogawara-shi Aomori Pref. (320 m)	fountain, 2	2	0
2)	Kudoji, Hirosaki-shi Aomori Pref. (240 m)	fountain, 2	11	0
3)	Mt. Ajara-yama, Ohwani-machi Aomori Pref. (340 m)	fountain, 2	3	0
4)	Mase-keikoku, Hachimori-machi Akita Pref. (50 m)	roadside pool, 1	12	0
5)	Natsuzaka, Takko-machi Aomori Pref. (300 m)	roadside fountain, 2	15	0
6)	Kawamata, Tamayama-mura Iwate Pref. (180 m)	roadside stream, 3	18	0
7)	Hirukawa, Ohmagari-shi Akita Pref. (180 m)	fountain-flowing pond, 2	34	4
8)	Idosawa, Ichinoseki-shi Iwate Pref. (570 m)	*	13	12
9)	Yamanome, Ichinoseki-shi Iwate Pref. (120 m)	pool, 1	5	0
10)	Iragawa, Atsumi-machi Yamagata Pref. (100 m)	torrent, 5	7	0
11)	Hataya, Yamanobe-machi Yamagata Pref. (610 m)	fountain, 2	5	0
12)	Mt. Ninohji-dake, Shibata-shi Niigata Pref. (720 m)	swamp stream, 4	12	3
13)	Hibara, Kitashiobara-mura Fukushima Pref. (820 m)	fountain-flowing ditch, 3	9	4
14)	Yutagami, Tagami-machi Niigata Pref. (80 m)	torrent, 5	44	10
15)	Kamijoh, Kamo-shi Niigata Pref. (40 m)	fountain-flowing pool, 2	17	1
16)	Tanne, Kashiwazaki-shi Niigata Pref. (160 m)	torrent, 5	10	0
17)	Mt. Atema-yama, Tohkamachi-shi Niigata Pref. (800 m)	brook, 4	9	0
18)	Okushiobara, Shiobara-machi Tochigi Pref. (930 m)	brook, 4	9	3
19)	Fujiwara, Minakami-machi Gunma Pref. (740 m)	fountain-flowing ditch, 2	48	12

* See text.

SOFRON equipment (TYPE SRO–M50, SOKEN CO., LTD., Tokyo). The tail vertebrae observed were divided into four types as follows: a. externally broken tails, including obviously regenerated tails, with tail vertebrae half-cut the same as the broken parts; b. regenerated tails not distinguishable from normal tails externally but with partial or incomplete tail vertebrae (Fig. 1B, C); c. questionable tails with tail vertebrae somewhat abnormal but not partial; and d. normal tails with tail vertebrae normal and complete (Fig. 1A).

The presence of correlation between two variables was tested with Spearman's rank correlation coefficient. For statistical analysis of relative tail length, data from the specimens having normal tails (type d) were used. The significance between

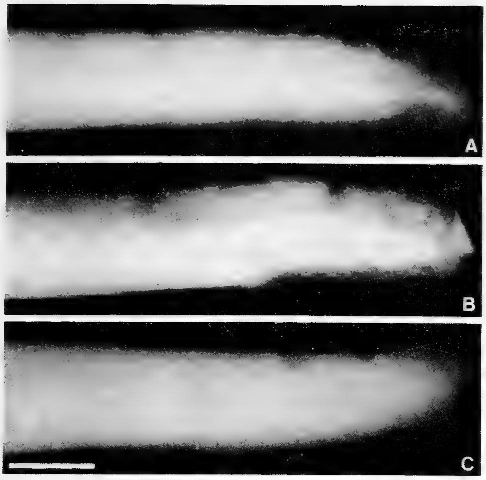

FIG. 1. Radiographs of tails: A. normal vertebrae; B. fragmentary vertebvrae; C. no vertebrae. Scale: 5 mm.

two sample means was tested with the median test.

For histological observations, regenerated tails were embedded in paraplast, sectioned serially at 8 μm, and stained with Delafield's hematoxylin and eosin.

RESULTS

Interpopulation variation was found in the ratios of the four types of tail vertebrae, and sexual difference in the ratios was also recognized in the specimens collected at sample sites 7, 12, and 14 (Fig. 2). The frequency of specimens with externally broken and regenerated tails was much higher where the sites of oviposition were the swifter flowing streams (Table 1 and Fig. 2). Animals with newly cut tails were not found among specimens having broken tails. No significant inverse correlation was found between the frequency of male specimens with broken and regenerated tails and the altitude ($r_s = -0.0725$, $\alpha = 0.05$; Table 1 and Fig. 2).

The mean relative tail length did not differ significantly ($\alpha = 0.05$) between males and females in sample site 7, but was significantly greater in males than in females in sample sites 8 ($P < 0.05$), 12 ($P < 0.05$), 13 ($P < 0.05$), 14 ($P < 0.02$), and 19 ($P < 0.005$) (Table 2). The relative tail length of this species tended to be greater at higher latitude (Tables 2 and 3). The mean relative tail length of the males in sample site 15 was significantly less than the means in other sites, except for sample sites 9 and 10 (Table 3). The absolute value of the relative tail length of the specimens collected in sample site 5 was the greatest of all (Tables 2 and 3). When data from specimens with normal, questionable, and regenerated tails were combined, the maximum and minimum relative tail lengths were 0.911 and 0.463, respectively, and these values were both found in males with regenerated tails (compare with the values shown in Table 2). The relative axilla-groin length was significantly ($P < 0.001$) greater in females (0.495 ± 0.014, mean $\pm$ SD) than in males (0.466 ± 0.014).

In the cross sections of the regenerated tails having no vertebrae, cartilage was observed to surround the spinal cord (Fig. 3A), while in the cross sections of the regenerated tails with fragmentary vertebrae, chondral cartilage or fragmentary bone tissue was seen (Fig. 3B).

DISCUSSION

1. The tail as a taxonomic character

Most salamanders seem to regenerate complete tails after suffering tail breakage, so it may be difficult to distinguish externally regenerated tails from normal tails. However, only herpetologists studying tail-autotomizable salamanders have pointed out the above-mentioned phenomenon [1, 6, 7]. In amputation-regeneration experiments on the tails of *Ambystoma* larvae, Holtzer *et al.* [8] showed that larvae regenerated all parts of the tail, but the lengths of the regenerated tails ranged from 20% to 35% below those of the controls.

It seems, however, that tail regeneration has not been taken into consideration in tail-unautotomizable salamanders, so that the lengths of tails including regenerated ones have been used for taxonomic comparison. Therefore, in most papers [9–14] in this field the relative tail length in each urodelen species shows a remarkable variation in comparison with other taxonomic characters, such as relative head length, trunk length, and axilla-groin length. In fact, when data from specimens

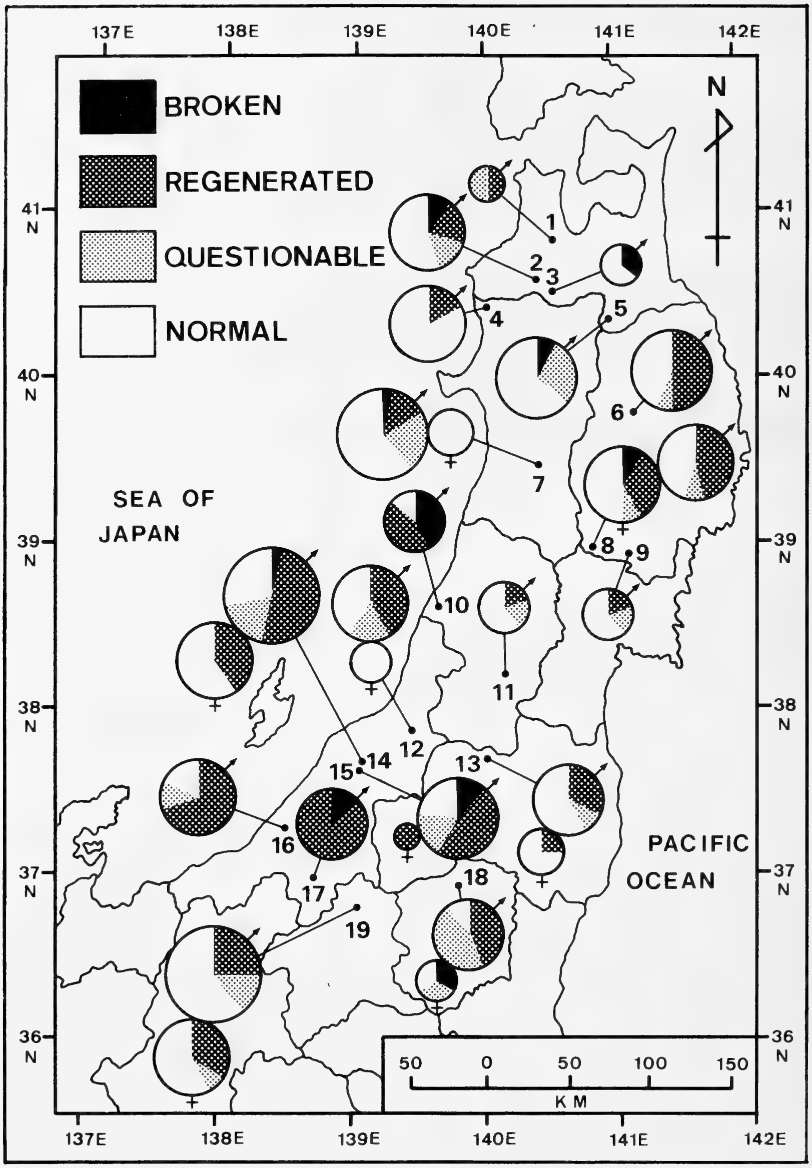

FIG. 2. The ratios of the four types of tail vertebrae in each sample site. The size of circles reflects sample size (See Table 1).

with normal, questionable, and regenerated tails are combined, the dispersions of relative tail length are greater and the means of relative tail length are less in most localities (Fig. 4).

The main reasons why relative tail length is significantly greater in males than in females may be that relative axilla-groin length is significantly greater in females than in males, and that breeding males have knife-edged tails so that the tails are longer. The relative lengths of many regenerated tails were less than those of normal tails, but the relative lengths of a few were greater. In addition,

TABLE 2. Geographic variation of relative tail length of specimens with normal tails

Sex	Sample site	No.	Mean snout-vent length ±2SE (range) (mm)	Mean relative tail length ±2SE (range)
	1	0		
	2	6	67.4±2.4 (63.9–71.6)	.804±.020 (.770–.844)
	3	2	59.6 (58.2–61.0)	.781 (.780–.782)
	4	10	61.9±0.7 (60.0–63.6)	.782±.018 (.742–.827)
	5	9	60.6±1.8 (56.7–66.1)	.827±.029 (.765–.890)
	6	8	67.9±2.7 (63.7–74.8)	.786±.037 (.700–.844)
	7	21	68.7±1.6 (63.0–76.1)	.795±.021 (.715–.877)
	8	6	58.8±2.4 (54.5–63.6)	.763±.014 (.750–.785)
	9	3	59.4±2.9 (56.8–61.7)	.724±.107 (.618–.793)
Male	10	1	67.8	.701
	11	3	63.5±5.5 (60.0–69.0)	.764±.032 (.732–.781)
	12	5	68.1±4.3 (63.0–73.8)	.802±.013 (.790–.828)
	13	5	57.4±1.9 (54.4–60.2)	.751±.017 (.728–.771)
	14	13	68.0±2.3 (61.8–75.2)	.766±.028 (.680–.846)
	15	4	67.6±2.2 (64.3–69.1)	.633±.034 (.607–.682)
	16	2	73.8 (73.0–74.6)	.786 (.764–.808)
	17	0		
	18	1	59.4	.795
	19	29	66.0±1.3 (58.1–74.1)	.760±.012 (.678–.820)
	7	4	67.0±3.2 (65.2–71.7)	.747±.050 (.715–.822)
	8	6	60.1±1.8 (57.6–62.8)	.724±.019 (.688–.759)
	12	3	68.9±5.4 (64.1–73.5)	.663±.032 (.637–.693)
Female	13	3	60.4±3.3 (58.7–63.7)	.672±.060 (.612–.705)
	14	6	69.6±3.7 (65.0–77.0)	.717±.022 (.678–.748)
	15	0		
	18	1	63.1	.658
	19	7	69.4±2.2 (65.9–73.9)	.695±.024 (.655–.738)

TABLE 3. Median test for the mean relative tail length ($\bar{x}$) of specimens with normal tails

	$\bar{x}$ min.																$\bar{x}$ max.
Sample site of males	15	(10)	9	13	19	8	11	14	(3)	4	(16)	6	(18)	7	12	2	5
Sample site of females	(18)	12	13	19	14	8	7										

Each category is arranged in linear as less value comes left. Each bar indicates the groups that the difference is not statistically significant ($\alpha=0.05$). However, the mean values of males in sample sites 19 and 4 are significantly less than the means in sample sites 4 and 2, respectively. Sample sites with no adequate number of specimens having normal tails are shown in parentheses.

the relative tail length showed a definite latitudinal variation, so it cannot always be determined from external observations that shorter tails must be regenerated ones.

In conclusion, it is necessary to take notice of tail regeneration, sexual difference, and latitudinal variation when cosidering tail length for taxonomic purposes.

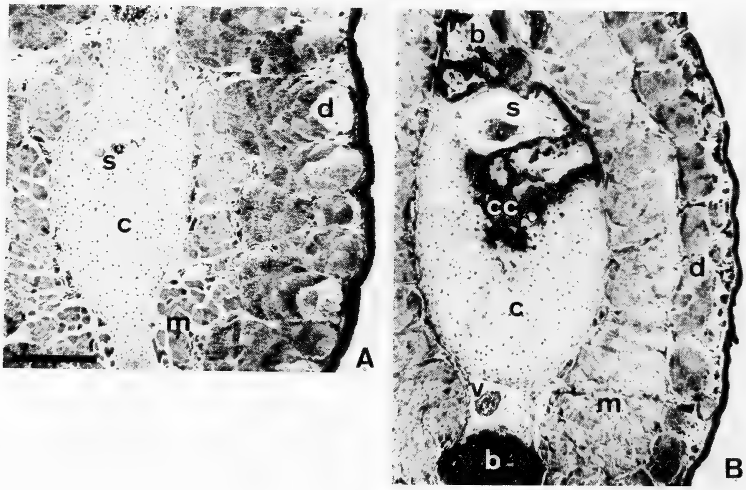

Fig. 3. Cross sections of regenerated tails: A. no vertebrae; B. fragmentary vertebrae. s: spinal cord, c: cartilage, cc: chondral cartilage, b: bone tissue, m: muscle, d: dermal gland, v: blood vessel. Scale: 0.5 mm.

2. Causes of tail breakage

The breakage of tails in tail-autotomizable salamanders was the result of traumatic events, such as attacks by predators, rock falls, entrapment, and so on [1].

Predators Previous investigators thought that tail autotomy in tail-autotomizable salamanders reflects predation pressure from any predator so long as the tail is attacked at least at some time [7, 15, 16]. The tails of tail-unautotomizable salamanders, too, may be injured by potential predators. So differential predation pressure ought to contribute to the differences in the ratios of the four types of tail vertebrae in *Hynobius lichenatus*. Shaffer [7] reported that snake densities (potential predators) were found to decrease with elevation, and a significant inverse correlation was found betweem tail loss and elevation; that is, tail loss and the regenerated tails were equivalent expressions. However, this correlation was not found in the present study.

Biting Kusano [17] suggested based on his observations on *Hynobius nebulosus tokyoensis* during the breeding season that tail breakage was

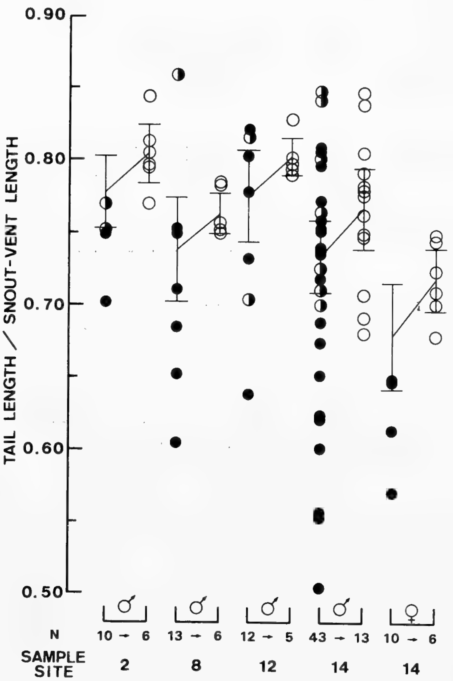

Fig. 4. Comparison of relative tail length. Left vertical lines indicate mean ± 2SE when data from specimens with normal, questionable, and regenerated tails are combined. Whereas right vertical lines indicate mean ± 2SE when only data from specimens having normal tails are used. Open circle: normal tail, semisolid circle: questionable tail, solid circle: regenerated tail.

the result of biting between breeding males, because the percentage of animals with cuts in the tail was higher in males than in females, and some breeding males which appeared in the pond were seen to lose their tail tips during their stay in the pond. It seems, however, that only tail tips or small parts of caudal fins would be lost in such cases.

Larval cannibalism Cannibalism during the larval period easily happens when larval density is high. It seems unlikely, however, that differential tail breakage resulted from cannibalism in the sites of oviposition, because the ratios of the four types of tail vertebrae differed according to sex.

Rapid stream The present results suggest that tail breakage in *Hynobius lichenatus* is due to rapid stream flow in most cases. During early spring thaw streams often overflow so rapidly that breeding adults may be carried away and injured because they are unable to resist the current. Moreover, the salamanders with just broken tails are even less able to resist and are carried away anew. Breeding males have knife-edged thin tails and stay longer in the stream, so they may be injured more frequently than females. It seems, however, that larvae are not so strongly influenced by the streams even in these sites, because the streams flow more slowly after the breeding season, except when there is occasional heavy rain. If tail breakage happens in the larval period, no difference according to sex would be found in the ratios of the four types of tail vertebrae. It is conceivable, therefore, that the breakage of tails usually happens to adults rather than to larvae.

At any rate, the causes of tail breakage in this species seem to be very complex.

3. Supplementary comments on the causes of tail breakage in three sample sites

Sample site 8 Roadside ditches in a forest were dug a year before the present collection, so tail breakage is not due falling into these ditches. A torrent was found near this site. Since the incidence of regenerated tails in the specimens collected at this site was quite high, the torrent may be the natural site of oviposition. However, because little difference according to sex was found in the ratios of the four types of tail vertebrae, it is also possible that the tails were injured during the construction of the road.

Sample site 15 This site is on either side of a railroad line and is almost a static body of water into which water from fountains flows. On both sides of the railroad line are vertical precipices 5 m high faced with blocks of stone. Thawing water cascades down from parts of the precipices during the breeding season, so it is conceivable that some salamaders fall down the precipices when they come to the site of oviposition, and some may fall down with the cascading water. These may be the causes of a higher frequency of specimens with regenerated tails in this site.

Sample site 19 This site is a roadside ditch 20 cm wide, and a body of water about 30 m long remains throughout the year because fountains flow into the ditch. More than 100 pairs of egg sacs were found in this ditch, and larval density was remarkably high. There was little difference according to sex in the ratios of the four types of tail vertebrae, and few specimens had severely broken tail vertebrae. It seems, therefore, that most tail breakage at this site is due to cannibalism of the tail in the larval period.

ACKNOWLEDGMENTS

We are grateful to Professor N. Nara of Hirosaki University for giving us information on the sites of oviposition. We are also grateful to Professor K. Kobayashi and Dr. I. Sasagawa of Nippon Dental University for the use of SOFRON equipment. We wish to express our gratitude to Professor K. Takata of Niigata University for his advice on statistical analysis.

REFERENCES

1 Wake, D. B. and Dresner, I. G. (1967) Functional morphology and evolution of tail autotomy in salamanders. J. Morphol., **122**: 265–306.

2 Brodie, E. D., Jr. (1970) Western salamanders of the genus *Plethodon*: systematics and geographic variation. Herpetologica, **26**: 468–516.

3 Crump, M. L. (1977) Intrapopulation and interspecific variation of "standard" morphological characters of four closely related South American salamanders (*Bolitoglossa*), with description of habitat preferences. Herpetologica, **33**: 415–426.

4 Dowling, H. G. and Duellman, W. E. (1973) Systematic herpetology: a synopsis of families and

higher categories. Hiss Publications, New York, p. 6.

5 Sato, I. (1943) Monogragh of Japanese tailed batrachians. Nippon Shuppan-sha, Osaka, pp. 106–119. (In Japanese)

6 Muchmore, W. B. (1955)Brassy flecking in the salamander *Plethodon c. cinereus,* and the validity of *Plethodon huldae.* Copeia, **1955**: 170–172.

7 Shaffer, H. B. (1978) Relative predation pressure on salamanders (Caudata: Plethodontidae) along an altitudinal transect in Guatemala. Copeia, **1978**: 268–272.

8 Holtzer, H., Holtzer, S. and Avery, G. (1955) An experimental analysis of the development of the spinal column. IV. Morphogenesis of tail vertebrae during regeneration. J. Morphol., **96**: 145–171.

9 Nambu, H. (1983) A preliminary note on the salamander (*Hynobius* sp.) found in Ooyama-machi, Toyama Pref., and Oumi-machi, Niigata Pref., Central Japan. Bull. Toyama Sci. Mus., **5**: 75–83. (In Japanese with English abstract)

10 Krebs, S. L. and Brandon, B. A. (1984) A new species of salamander (family Ambystomatidae) from Michoacan, Mexico. Herpetologica, **40**: 238–245.

11 Matsui, M. and Miyazaki, K. (1984) *Hynobius takedai* (Amphibia, Urodela), a new species of salamander from Japan. Zool. Sci., **1**: 665–671.

12 Morris, M. A. and Brandon, R. A. (1984) Gynogenesis and hybridization between *Ambystoma platineum* and *Ambystoma texanum* in Illinois. Copeia, **1984**: 324–337.

13 Nambu, H. (1984) Notes on Japanese salamander *Hynobius lichenatus* collected from a mixed egg-deposited pool in Minakami, Gunma Pref., Japan. Bull. Toyama Sci. Mus., **6**: 73–78. (In Japanese with English abstract)

14 Kraus, F. (1985) Unisexual salamander lineages in northwestern Ohio and southeastern Michigan: a study of the consequences of hybridization. Copeia, **1985**: 309–324.

15 Brodie, E. D., Jr., Johnson, J. A. and Dodd, C. K., Jr. (1974) Immobility as a defensive behavior in salamanders. Herpetologica, **30**: 79–85.

16 Dodd, C. K., Jr. and Brodie, E. D., Jr. (1976) Defensive mechanisms of neotropical salamanders with an experimental analysis of immobility and the effect of temperature on immobility. Herpetologica, **32**: 269–290.

17 Kusano, T. (1980) Breeding and egg survival of a population of a salamander, *Hynobius nebulosus tokyoensis* Tago. Res. Popul. Ecol., **21**: 181–196.

ZOOLOGICAL SCIENCE 4: 167–174 (1987)

The Sperm Length and the Internal Reproductive Organs of *Drosophila* with Special References to Phylogenetic Relationships

Fuyuo Hihara and Haruo Kurokawa[1]

Biological Institute, Ehime University, Matsuyama, Ehime 790, and
[1]Institute of Biological Sciences, The University of Tsukuba,
Ibaraki 305, Japan

ABSTRACT—Forty species of *Drosophila,* including 2 subfamilies, 7 genera, 10 subgenera, were examined for the sperm length in relation to the evolutionary trend. The sperm length varied broadly from 0.2 mm to about 10 mm among species of the family Drosophilidae. In the subfamily Drosophilinae to which many species belong, the more advanced genera and subgenera were clearly characterized by having longer sperm than the primitive ones. The lengths of the testis and the ventral receptacle (the sperm storage organ of the female) were highly correlated with the sperm length. This suggests that the non-homologous reproductive organs between sexes became to have a structural correlation along with the evolutionary processes due to a selection for the size of the sperm. All species examined were sorted into six classes to see whether or not the sperm length correlates with the number of spermatogonial divisions. Results showed that the species with smaller number of the spermatocytes per cyst generally produce the longer sperm. The sperm length, however, was very variable among species within the same class, showing that the number of spermatogonial divisions is not a definitive prerequisite to decide the sperm length. In contrast with this, the volume of the cytoplasm of the first spermatocytes just prior to the meiosis showed a high correlation with the sperm length in nine species, each belonging to either of the four different classes. The relation between the dose of the Y chromosome and the sperm length was discussed based on our results obtained here.

INTRODUCTION

The insects have sperm storage organs in the female to make her possible to fertilize numerous eggs without further copulations for a certain period of time. This type of the internal fertilization can avoid waste of the sperm. This may serve the purposes of the most insect species employing the strategy that the continuity of the species is chiefly dependent on high fecundity. The sperm storage organs of female, thus, are required to possess the structure and function favorable for the survival of the sperm without losing the ability of fertilization.

There have been several studies concerning the sperm length in *Drosophila* [1–3]. Hess and Meyer [4] showed the species difference of the sperm length among the five species of the *hydei* subgroup and *D. repleta* of the *repleta* subgroup. Members of the *obscura* species group have been known to produce the sperm with two or three different sizes in each individual [5–8]. Beatty and Sidhu [6] suggested that the variation in the sperm length among *Drosophila* might be related to their taxonomic positions. Thus, we can regard the sperm length as species-specific and considerably different among species.

In the present article, we report the lengths of the sperm, the testis and the ventral receptacle of 40 species of the family Drosophilidae with special references to the phylogenetic relationships. We also examined the relation between the sperm length and the number of spermatogonial divisions. The latter has a clear evolutionary trend that the more advanced species of *Drosophila* tend to show a smaller number of divisions [9].

MATERIALS AND METHODS

Two subfamilies, 7 genera, 10 subgenera including 40 species in total were examined for the

Accepted September 9, 1986
Received July 24, 1986

lengths of the sperm, the testis and the ventral receptacle (Table 1). Flies of the laboratory stocks were imaged on the usual food adding sufficient dry yeast, although the sperm length was proved not to be affected by the nutritional conditions [8]. Wild-caught flies were also used when the species were difficult to culture in the laboratory. Flies were dissected in Ephurussi-Beadle's Ringer solution. After removing the wall of the seminal vesicle, cover slip was put on the sperm which were free from the organ. A phase contrast microscope was used for the observation of the unstained sperm. Individual sperm was drawn by using camera lucida apparatus and measured by tracing with curvimeter on the whole length of the drawing. The lengths of the testis and the ventral receptacle were measured by the same methods.

The volume of the cytoplasm of the spermatocytes was calculated from the diameters of the cells and the nuclei. The mature spermatocytes which were clearly distinguished by the network structure of mitochondria surrounding the nucleus were chosen for the measure. The both spermatocytes of species to be measured and *D. melanogaster* were put together in a field under the microscope because the diameter changed gradually by the increasing pressure of the cover slip with the evaporation of the medium. The data from 20 spermatocytes in each species were used to obtain the means of the cell volume.

RESULTS

The sperm length

The means and the ranges of the sperm lengths of 40 species examined are listed in Table 1. The sperm length was highly variable among species of the family; two species of the subgenus *Scaptodrosophila* produce the shortest sperm, 0.21 and 0.32 mm, respectively, and *D. hydei* of the subgenus *Drosophila* produces the longest one reaching over 10 mm, being the other species range between these values. Because the sperm of *D. hydei* has a long end piece in its tail which is consisted only of the axial filaments and is frequently apt to be cut off under manipulations, the entire sperm length could hardly be measured.

In the subfamily Steganinae, number of species examined was so little that we could not speculate the phylogenetic relationships among them. Generally, species of this subfamily tend to produce the shorter sperm than the subfamily Drosophilinae; the sperm lengths of two species of the genus *Amiota* were both about 0.6 mm and those of three species of the genus *Leucophenga* were from 1.1 to 1.4 mm. The body sizes of the adults of five species in this subfamily were larger or nearly equal as compared with species of the subfamily Drosophilinae. Thus, the body size does not have a correlation with the sperm length. This fact is also applicable to species of the subfamily Drosophilinae; *D. immigrans*, for example, has nearly the same body size as *D. hydei* but its sperm length is much shorter than the latter (Table 1).

Among the subfamily Drosophilinae except for the genus *Drosophila*, two species of the genus *Scaptomyza* produce shorter sperm, a species of the genus *Mycodrosophila*, on the contrary, produces much longer one, although only one species, *M. shikokuana*, was concerned here. In the genus *Drosophila*, three species of the subgenus *Hirtodrosophila* were different in the sperm length; 0.36 mm in *D. qguadrivittata*, 2.78 mm in *D. alboralis* and 3.04 mm in *D. nokogiri*. The most members of this subgenus were not compiled in Table 1 because the data have not sufficiently been provided. However, it can be conjectured from our unpublished data that there is wide interspecific variation concerning the sperm length, reflecting that the *Hirtodrosophila* is composed of several species groups and subgroups which are widely diverged morphologically [10].

Eight species of the subgenus *Sophophora* being composed of five different species subgroups [11] show rather small difference among the species. Among these, three species, *D. ananassae* of the *ananassae* subgroup and *D. auraria* and *D. rufa* of the *montium* subgroup produce longer sperm than the others. In the subgenus *Drosophila*, the sperm length widely varies from 1.3 mm of *D. sternopleuralis* to about 10 mm of *D. hydei*.

Most species of the *immigrans* species group consistently produce the shorter sperm. In contrast with this, members of *robusta* (*D. sordidula, D. lacertosa*), *funebris* (*D. funebris*), *repleta* (*D.

Table 1. Summary information for the length (mm) of the sperm, the testis and the ventral receptacle in species of the family Drosophilidae

Species	Sperm Mean	Sperm Range	Testis	Ventral receptacle
Genus *Amiota*				
Subgenus *Amiota*				
dispina	0.64	0.58–0.76	—	—
Subgenus *Phortica*				
variegata	0.63	0.52–0.71	—	0.92
Genus *Leucophenga*				
Subgenus *Trichiaspiphenga*				
argentosa	1.38	1.15–1.50	3.60	—
Subgenus *Leucophenga*				
maculata	1.08	1.01–1.17	—	1.22
magnipalpis	1.16	0.97–1.33	3.85	1.55
Genus *Microdrosophila*				
Subgenus *Microdrosophila*				
purpulata	1.06	0.86–1.17	—	2.29
Genus *Mycodrosophila*				
shikokuana	5.32	5.08–5.46	—	9.41
Genus *Liodrosophila*				
aerea	2.47	2.17–2.84	—	6.78
Genus *Scaptomyza*				
pallida	0.31	0.28–0.33	2.42	1.50
graminum	0.58	0.52–0.65	—	1.68
Genus *Drosophila*				
Subgenus *Scaptodrosophila*				
coracina	0.21	0.20–0.23	0.76	—
throckmortoni	0.32	0.29–0.34	0.77	0.70
bryani	0.90	0.84–0.95	—	—
Subgenus *Hirtodrosophila*				
quadrivittata	0.36	0.35–0.37	—	0.53
alboralis	2.78	2.62–2.89	4.24	6.30
nokogiri	3.04	2.97–3.25	—	—
Subgenus *Dorsilopha*				
busckii	1.10	1.07–1.14	1.80	1.88
Subgenus *Sophophora*				
simulans	1.15	1.09–1.25	1.62	1.74
lutescens	1.52	1.19–1.66	2.42	4.43
melanogaster	1.81	1.63–1.97	2.41	3.76
ficusphila	1.84	1.64–1.92	—	3.11
suzukii	2.22	1.96–2.48	3.82	4.27
auraria	2.22	2.10–2.39	3.05	3.47
ananassae	2.30	2.25–2.38	3.96	6.26
rufa	5.37	5.35–5.39	6.24	7.22
Subgenus *Drosophila*				
sternopleuralis	1.29	1.23–1.39	2.65	2.65
immigrans	1.76	1.73–1.81	2.87	3.98
sulfrigaster	1.98	1.75–2.23	—	6.01
subtilis	2.02	1.96–2.06	2.97	—
curviceps	2.60	2.51–3.10	6.25	6.31
bizonata	2.77	2.52–3.11	3.55	4.14
brachynephros	2.87	2.71–3.09	3.86	5.50
histrio	3.23	3.16–3.28	5.14	7.21
pengi	3.71	3.59–3.86	6.23	6.64
nigromaculata	3.85	3.74–4.03	5.40	7.29
sordidula	5.24	5.09–5.37	7.62	6.67
lacertosa	5.44	5.26–5.66	8.44	8.93
virilis	6.47	6.18–7.51	8.39	8.18
funebris	8.29	7.06–9.92	10.50	12.97
hydei	≈10.0	—	28.77	47.20

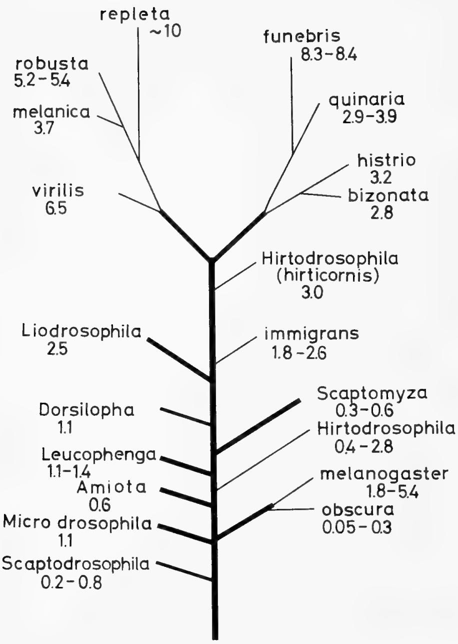

Fig. 1. Phylogenetic representation concerning the sperm length among the genera or the subgnera within the family Drosophilidae (the first letter capitalized) and the species groups of the genus *Drosophila*. For detailed explanations on phylogenetic treatments of the taxa, see Throckmorton [12].

hydei) and *virilis* (*D. virilis*) species groups produce the longer ones. The subgenus *Drosophila*, thus, consists of more various members concerning the sperm length than the subgenus *Sophophora*.

Figure 1 shows phylogenetic relationships relevant to the sperm length of the major taxa and groups within the family Drosophilidae. The phylogenetic tree adopted is mostly based on that presented by Throckmorton [12]. Evidently, the sperm length tends to become longer in advanced genera, subgenera or species groups as compared to primitive ones. It remained unknown, however, whether or not the sperm length can reflect a closer relationships among relatives within a certain species subgroup.

The lengths of the testis and the ventral receptacle

In the fourth column of Table 1, the testis lengths of 28 species are presented. There was an obvious correlation between the sperm and the testis length among 27 species examined ($r=0.948$, D.F.$=25$, $t=14.818$, $P<0.001$). As shown in Figure 2, the relative length of testis to the sperm length is about 1.5 when the sperm length exceeds 3 mm. However, it becomes larger when the sperm length is less than 3 mm. This implies that the spacial proportion of the elongating spermatid bundles to the whole length of the testis decreases as species have the shorter testis and *vice versa*.

The lengths of the ventral receptacle of female are shown in the last column of Table 1. The ventral receptacle consists of structurally two different parts, the basal and the folded or coiled ones. Most of the sperm stored is found in the latter part and, accordingly, the basal part is regarded to have a role of a passage of the sperm. Thus, the length of the folded or coiled part is indicative of structural correlation between the sperm and the ventral receptacle. But, the figures in this column were obtained by measuring the whole length of both parts, because the boarder was not exactly distinct.

In the most species, the length of the ventral receptacle was 1.5–3.0 times as much as that of the sperm. A high correlation was found between the sperm length and the total length of the ventral receptacle ($r=0.932$, D.F.$=31$, $t=13.366$, $P<0.001$). The length of the ventral receptacle is also highly correlated with that of the testis ($r=0.978$, D.F.$=23$, $t=22.607$, $P<0.001$). These high correlations well suggest that the sperm which accomplish their mission from male to female might be a predominant factor of the selection to determine the structure of the non-homologous organs between sexes.

Correlation between the sperm length and number of spermatocytes per cyst

Kurokawa and Hihara [9] reported that the more advanced forms of *Drosophila* tend to show a smaller number of spermatogonial divisions and, consequently, a smaller number of spermatocytes per cyst. Species listed in Table 1 were sorted into 6 classes by number of spermatocytes per cyst regardless of their taxonomic positions (Table 2). The 64 cell class comprises two species of the

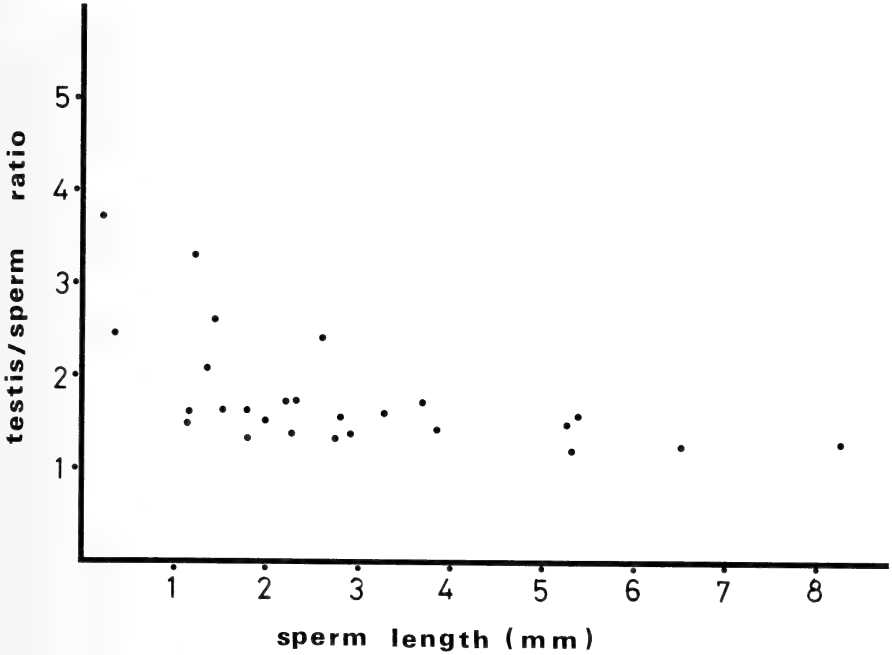

FIG. 2. Correlation between the sperm length (mm) and the ratio of the testis length to the sperm length. Each point corresponds to the species listed in Table 1.

TABLE 2. The mean sperm length among the classes sorted by the number of spermatocytes per cyst

Number of spermatocytes per cyst*	Number of species observed	Sperm length (mm)	
		Mean	Range
64	2	0.26	0.21–0.32
32	6	0.51	0.20–0.89
24	2	2.69	2.60–2.78
16	22	1.75	0.31–5.37
(16)**	(13)	(2.25)	(1.29–5.37)
12–14	2	4.48	3.71–5.24
7–8***	9	5.47	2.87–8.37

* Data from Kurokawa and Hihara [9].
** Figures in parentheses of the 16 cell class are obtained from 13 species limited to Genus *Drosophila*.
*** *D. hydei* was excluded from this class because precise sperm length could not be measured.

subgenus *Scaptodrosophila* and the 32 cell class includes *Microdrosophila purpurata, D(H). quadrivittata*, and four species of the *obscura* group, *D. obscura, D. bifasciata, D. imaii* and *D. pseudoobscura* all of which are not listed in Table 1 because they were reported before [8]. The 24 cell class comprises *D(H). alboralis* and D. *curviceps*.

The 16 cell class contains 22 species of many genera. Thirteen species of the genus *Drosophila* are also shown for comparison because the most species of the other classes are members of the genus *Drosophila*. The 12–14 cell class comprises *D. pengi* and *D. sordidula* and the 7–8 cell class contains eight species of the genus *Drosophila*.

Results presented in Table 2 clearly show a tendency that the mean sperm lengths of these classes increase as numbers of spermatocytes per cyst decrease. However, the length of the longest sperm of a given class frequently exceeds that of the shortest sperm of the next class as shown in the ranges. The sperm of *D. rufa* of the 16 cell class, for example, is much longer than that of *D. pengi* or *D. brachynephros* which belongs to the 12–14 and 7–8 cell class, respectively. Further, as shown in parenthesis in Table 2, the mean sperm length within the 16 cell class shifted remarkably when species of the genus *Drosophila* were chosen. Accordingly, number of spermatocytes per cyst might not be a definite prerequisite for decision of the sperm length, admitting that an indication that the sperm length increases in species with a smaller number of spermatocytes per cyst is in evidence.

Correlation between the sperm length and the cell volume of the mature spermatocyte

It is proved by more detailed observations that the volume of the mature spermatocytes is considerably different among species even if they have the same number of spermatocytes per cyst. A correlation between the sperm length and the cell volume of the mature spermatocytes just prior to the meiosis of nine species is shown in Figure 3. Both the values of the sperm length and the cell volume are relatively expressed on the basis of assigning a 1.0 to those of *D. melanogaster*. More strictly, the cell volume means the volume of the cytoplasm; the nuclear volume was deduced from the whole cell volume. When the whole cell volume was adopted, the correlation became somewhat indistinct.

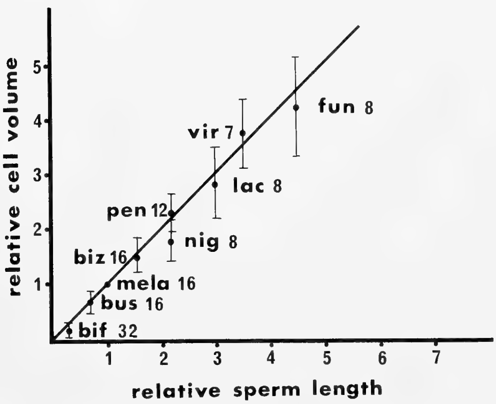

Fig. 3. Correlation between the relative sperm length and the relative cell volume with range in nine species of the genus *Drosophila*. bif; *D. bifasciata*, bus; *D. busckii*, mela; *D. melanogaster*, biz; *D. bizonata*, pen; *D. pengi*, nig; *D. nigromaculata*, vir; *D. virilis*, lac; *D. lacertosa*, fun; *D. funebris*. Figures after the species marks are the number of the first spermatocytes per cyst.

The relative cell volume of *D. busckii, D. melanogaster* and *D. bizonata* all belonging to the 16 cell class is 0.75, 1.00 and 1.30, respectively and obviously correlated with the relative sperm length of each species, 0.6, 1.0 and 1.6. In four species, *D. nigromaculata, D. lacertosa, D. virilis* and *D. funebris*, all belonging to the 7–8 cell class, a positive correlation between the relative sperm length and the relative cell volume is demonstrated as well. Although *D. pengi* is one of the species of the 12–14 cell class, both the sperm length and the cell volume are nearly equivalent to *D. nigromaculata* of the 7–8 cell class. These facts indicate that the sperm length would correlate more intimately to the cell volume than to the number of spermatocytes per cyst.

DISCUSSION

We examined for the sperm length of 40 species of *Drosophila* with special references to their phylogenetic relationships. Results obtained clearly indicate that the more advanced species tend to produce the longer sperm. This is in accordance with the study where four species of *Drosophila* were compared as concerned with the sperm length [3]. Our results also indicate that the cytoplasmic volume of the mature spermatocyte would have a primary cause in determination of the sperm length. This can be conjectured that large spermatocyte makes possible to increase the doses both of the ribosomes relating translation of sperm proteins and of the mitochondria forming mitochondrial derivatives of the sperm tail. Since elongating spermatids do not concern *de novo* synthesis of proteins [13], gene expression necessary for spermiogenesis might be accomplished in stages of spermatocyte. Although the sperm head becomes longer as the whole length of the sperm

increases [7, 14], the major part of the mature sperm is occupied by the tail which is consisted of the axoneme and the mitochondrial derivatives both being furnished by the materials from the cytoplasm of spermatocyte.

Our results obtained here well agreed with evidences presented by Virkki [15] for the beetle, the family Alticidae, where the number of spermatozoa had been stepwise reduced from the primitive to the modern forms, sometimes accompanied by an extra large size of spermatocytes.

In species of the *hydei* subgroup, sperm length have thought to be dependent on the Y chromosome dose; the sperm length varies from 1.2 mm for *D. nigrohydei* which has the smallest Y chromosome in this group, up to 6.6 mm for *D. hydei* which possesses the largest Y chromosome [4]. In *D. melanogaster* as well, males with a complete or a partial deficient Y chromosome, namely, XO, XY^S, XY^L, and with duplications of the Y chromosome, XYY, produce the sperm on the average 1.2, 1.3, 1.5 and 3.5 mm long, respectively [16]. These facts have led to regard the Y chromosome as one of the causative factors of the sperm elongation.

However, Gould-Somero *et al.* [17] reexamined the sperm length by means of duplicated Y chromosomes but were unable to repeat the observations by Hess and Meyer; clearly the presence of the extra Y chromosome *per se* was insufficient to elongate the length of the normal sperm of *D. melanogaster*.

On the bases of the facts mentioned above, we must regard that the role of the Y chromosome on the sperm elongation is remained obscure as yet. In the present study, we postulate a determinant role of the cytoplasmic volume of spermatocyte than the Y chromosome dose for the sperm elongation in *Drosophila*. The volume of mature spermatocyte might be partially dependent to the number of multiplication divisions of spermatogonia which is thought to be strictly regulated by a certain gene(s) in each species [9]. The final determinant of the volume of spermatocyte, however, remains uncertain.

In the present study, it can be affirmed that the length of the sperm is highly correlated with those of the internal reproductive organs of both sexes. Yanders and Perras [3] and Beatty and Sidhu [6] have already pointed out a close relation of the length between the testis and the ventral receptacle and they have a positive association with the sperm length in a limited species of *Drosophila*. Okada [10] gave a phylogenetic considerations on the subgenus *Hirtodrosophila* in which he assumed each set of character states to have been differentiated from a primitive to an advanced one. Steps of character differentiations of the testis and the ventral receptacle are: (1) banana-shaped, (2) with coils and with only a few small tite folds, (3) loosely and irregularly folded, (4) with proximal coils and distal folds, and finally, (5) with coil alone, respectively. We confirmed evolutionary changes in structures of these organs as proposed by him.

Physiological and behavioral changes of the inseminated female are affected by several factors transmitted from the male accessory gland but not by the sperm themselves [18]. This fact shows that the female reproductive tracts have two distinct functions; the storage role of the sperm accepted and the receptor role of the informative molecules related to the physiological changes of the reproductive system. Structural association of the inner reproductive organs between sexes might be a result of natural selection for the former function.

REFERENCES

1 Dobzhansky, Th. (1934) Studies of hybrid sterility. I. Spermatogenesis in pure and hybrid *Drosophila pseudoobscura*. Z. Zellforsch. Mikrosk. Anat., **21**: 169–223.

2 Cooper, K. W. (1950) Normal spermatogenesis in *Drosophila*. In "Biology of Drosophila". Ed. by M. Demerec, Wiley, New York, pp. 1–16.

3 Yanders, A. E. and Perras, J. P. (1960) Sperm length in four *Drosophila* species. Dros. Inf. Serv., **34**: 112.

4 Hess, O. and Meyer, G. F. (1963) Chromosome differentiations of the lampbrush type formed by the Y chromosome in *Drosophila hydei* and *Drosophila neohydei*. J. Cell Biol., **16**: 527–539.

5 Polikansky, D. (1970) Three sperm sizes in *D. pseudoobscura* and *D. persimilis*. Dros. Inf. Serv., **45**: 119–120.

6 Beatty, R. A. and Sidhu, N. S. (1970) Polymegaly of spermatozoan length and its genetic control. Proc. Roy. Soc. Edin., **B71**: 14–28.

7 Beatty, R. A. and Burgoyne, P. S. (1971) Size classes of the head and flagellum, of *Drosophila* spermatozoa. Cytogenetics, **10**: 177–189.

8 Kurokawa, H., Matsuo, Y. and Hihara, F. (1974) A study on sperm length and body size of *Drosophila bifasciata*. Annot. Zool. Japon., **47**: 140–146.

9 Kurokawa, H. and Hihara, F. (1976) Number of first spermatocytes in relation to phylogeny of *Drosophila* (Diptera: Drosophilidae). Int. J. Insect Morphol. Embryol., **5**: 51–63.

10 Okada, T. (1967) A revision of the subgenus *Hirtodrosophila* of the old world, with descriptions of some new species and subspecies (Diptera, Drosophilidae, *Drosophila*). Mushi., **41**: 1–36.

11 Bock, I. R. and Wheeler, M. R. (1972) The *Drosophila melanogaster* species group. Studies in Genetics VII. Univ. Texas. Publ., **7213**: 1–102.

12 Throckmorton, L. H. (1975) The phylogeny, ecology, and geography of *Drosophila*. In "Handbook of Genetics". Ed. by R. C. King, Plenum Press, New York and London, pp. 421–469.

13 Lindsley, D. L. and Grell, E. H. (1969) Spermiogenesis without chromosomes in *Drosophila melanogaster*. Genetics, **61**: Suppl. 1, 69–78.

14 Hauschteck-Jungen, E. and Mauer, B. (1976) Sperm dysfunction in sex ratio males of *Drosophila subobscura*. Genetica, **46**: 459–477.

15 Virkki, N. (1969) Sperm bundles and phylogenesis. Z. Zellforsch. Mikrosk. Anat., **101**: 13–27.

16 Hess, O. and Meyer, G. F. (1968) Genetic activities of the Y chromosome in *Drosophila* during spermatogenesis. Adv. Genet., **14**: 171–189.

17 Gould-Somero, M., Hardy, R. and Holland, L. (1974) The Y chromosome and sperm length in *D. melanogaster*. Exp. Cell Res., **87**: 397–398.

18 Hihara, F. (1981) Effects of the male accessory gland secretion on oviposition and remating in females of *Drosophila melanogaster*. Zool. Mag., **90**: 307–316.

ZOOLOGICAL SCIENCE 4: 175–181 (1987)

Two Peculiar Species of Corophiid Amphipods (Crustacea) from the Seto Inland Sea, Japan

AKIRA HIRAYAMA

Laboratory of Biology, Department of the Liberal Arts, Asia University, 5–24–10 Sakai, Musashino-shi, Tokyo 180, Japan

ABSTRACT—Two species of the genus *Corophium* (*Corophium lobatum* n. sp. and *C. sinense* Zhang, 1974) taken from the shallow water of the Seto Inland Sea are described and figured. *C. lobatum* n. sp. has the peculiar, fused urosome, and its uropod 2 arise from the base of the urosome instead of the distal part. This new species is clearly distinguished from the known corophiid amphipods by these characteristics. *C. sinense* Zhang, 1974, originally described from the Shangtung Peninsula, North China, is new to Japan. The specific characteristics of this species are observed in the mandibular palp that the terminal segment is reduced and directly attaches to the apex of the proximal one.

INTRODUCTION

During an assessement survey of the marine environment in the Seto Inland Sea, Japan, Mr. N. Sawada collected some specimens of peculiar amphipods from a sandy-mud bed of In-no-shima Island, Hiroshima Prefecture, and sent me for identification. Through a close exmination it became apparent that they were composed of two species of the genus *Corophium*. One species possesses a fused, laterally rounded urosome. This characteristic suggests that the species belongs to Section C of Crawford's system [2, 5, 6], but the uropod 2 of this species attaches to the laterobasal part of its urosome and is well developed. Such an uropod is not found among the corophiid amphipods previously known. On the basis of these characteristics, I will describe it in this paper as a new species of *Corophium*. The other species collected in the present survey is *Corophium sinense* Zhang, 1974 [8], originally described from the Shantung Peninsula, North China. This species, that is new to Japan, is redescribed also in this paper.

All the specimens here described are deposited in the collection of the Biological Laboratory, Department of the Liberal Arts, Asia University, Tokyo.

Corophium lobatum n. sp.
(Figs. 1–2)

Description of the holotype (*female*)

Body: Semicylindrical. Rostrum and eyes small. Pereonites subequal in size; coxae discontinuous in series. Pleonal epimeron 1 rounded, ventrally armed with 3 plumose long and short setae; pleonal epimeron 2 similar to epimeron 1 in form, twice in largeness, ventrally with 3 plumose setae; pleonal epimeron 3 1.5 times as broad as

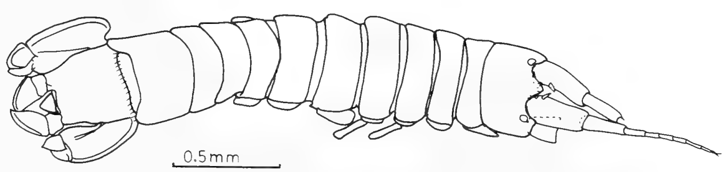

FIG. 1. *Corophium lobatum* n. sp. Holotype: female, 2.16 mm.

Accepted July 3, 1986
Received May 12, 1986

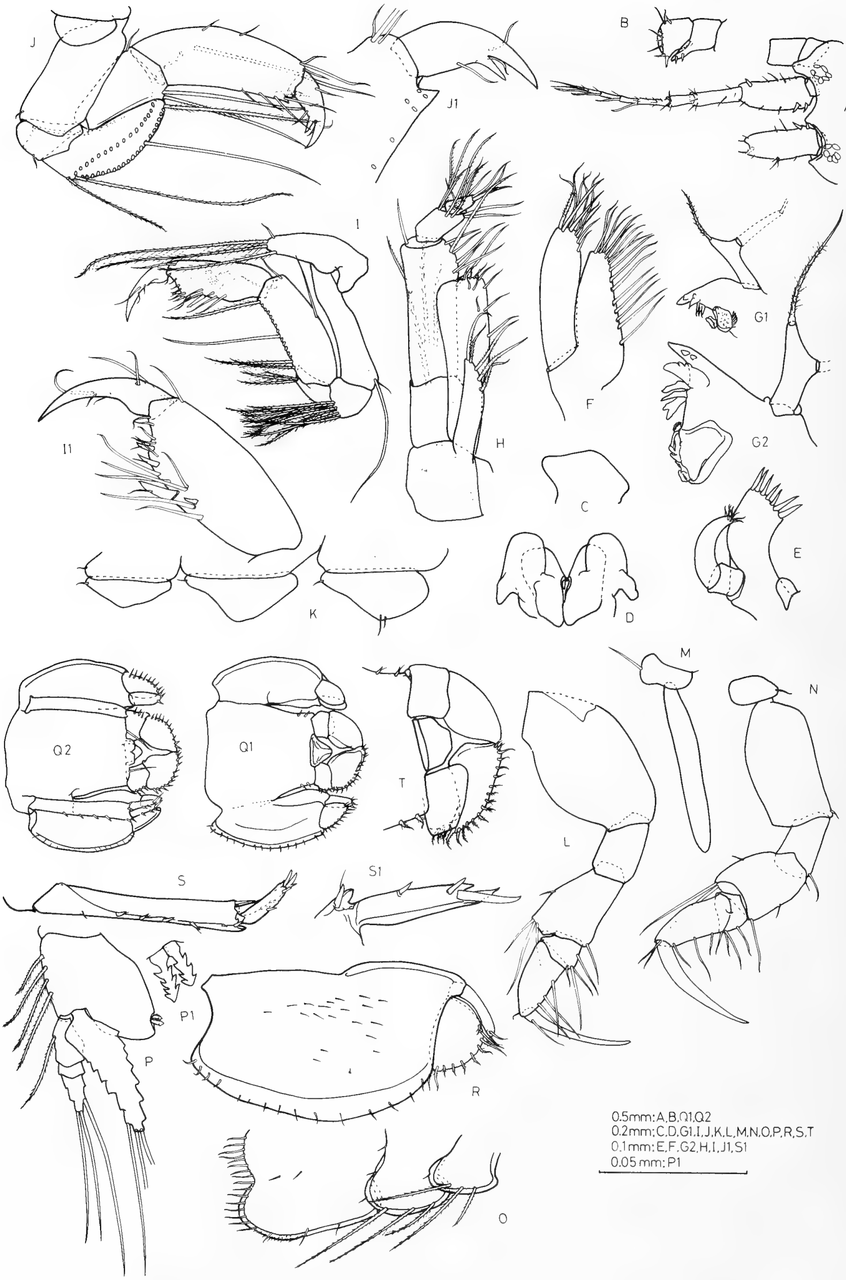

FIG. 2. *Corophium lobatum* n. sp. Holotype: female, 2.16 mm. A: Head and antenna 1. B: Antenna 2. C: Upper lip. D: Lower lip. E: Maxilla 1. F: Maxilla 2. G1: Right mandible. G2: Left mandible. H: Maxilliped. I and I1: Gnathopod 1. J and J1: Gnathopod 2. K: Coxae 5–7. L: Pereopod 1. M: Coxa 3 and gill. N: Pereoped 2. O: Pleonal epimera 1–3. P and P1: Pleopod 1. Q: Urosome in dorsal view. Q2: Urosome in ventral view. R: Uropod 1. S and S1: Uropod 2 and outer ramus (S1). T: Uropod 3 and telson.

epimeron 2, rounded and setaceous posteriorly, without plumose setae. Fused urosome even or slightly concave dorsally, provided with 2 spines on both laterodistal ends, anteroventrally with uropod 1 and anterolaterally with uropod 2.

Antennae: Antenna 1 about 1/3 as long as body length; segment 1 of peduncle armed with 2 inner-proximal and 1 outer-distal spines; flagellum 6-articulate, each segment excluding proximal and terminal ones provided with 1 aesthetasc. Both antennae 2 broken and only first two segments remained for each; segments 1–2 of penduncle equal in size, inner-distal process of segment 1 almost reaching apex of segment 2, armed with 2 spines, segment 2 inner-distally armed with 2 opposite spines.

Mouthparts: Mandibular process of lower lip medium. Inner plate of maxilla 1 rudimentary, lacking setae; outer plate provided with 7 tooth-like, simple spines; proximal segment of palp developed as corophiids, terminal segment provided with 8 apical small setae. Both plates of maxilla 2 equal in size, outer plate provided with 1 plumose seta on outer side of apex. Both mandibles similar to each other, provided with 3 accessory blades of which the proximal one is bifid; palp biarticulate, terminal segment attached to a slightly upper level against middle of the proximal one. Inner plate of maxilliped slender, provided with 4 pinnate setae on inner 1/3 part from apex; outer plate rectangular, reaching 1/3 point from palpal article 2, dispersively setaceous; palp 4-articulate, terminal segment half the length of segment 3, provided with 1 apical slender spine.

Gnathopod 1: Coxa 1 extending forward, slender, ventrally armed with 1 long pinnate seta. Propod shorter than carpus, palm oblique, armed with 2 spines, posterior margin medially armed with 1 pronounced and 1 smaller spines. Dactyl falcate, extending far beyond palm when closed; grasping margin smooth. *Gnathopod 2*: Corophiid-fashion. Carpus about 2/3 as long as merus. Propod almost as long as merus and carpus combined, produced posterodistally. Dactyl half the length of propod, grasping margin armed with 1 pronounced tooth.

Pereopods 1–2: Similar to each other. Merus prominently expanded and a little produced anterodistally. Carpus shorter than half the posterior length of merus. Dactyl falcate, slender, longer than merus and carpus combined. *Pereopods 3–5*: Coxae 5–7 similar to each other, subequal in size, armed with 1 posterodistal small seta. Other parts broken.

Pleopod 1: Peduncle subsquare, prominetly expanded backward, armed with 1 anterior plumose seta; rami unclearly segmented, inner ramus shorter than outer ramus; terminal swimming setae longer than rami.

Uropods: Uropod 1 slender, not extending beyond uropod 2; peduncle a little produced outer-distally, provided with 6 outer and 1 inner-distal spines; rami similar to each other, equal in size, 1/3 as long as peduncle, on outer margin armed with 2 spines, bifid apically, inner tooth more produced than the outer one, apical concavities armed with 1 pronounced spine. Uropod 2 lobate, broad, extending beyond peduncle of uropod 3, biramous; peduncle armed with marginal fringe; rami short, subequal in length, inner ramus slender, provided with 2 apical small setae, outer ramus semi-oval, broad, provided with 10 small, dispersively pinnate setae on outer and apical margins. Uropod 3 uniramous, lobate, shorter than half the length of uropod 2; peduncle broader than long, provided with 3 small pinnate setae on outer margin; rami leaf-like, provided with 14 small setae of which the greater part are pinnate, armed with 2 apical spines.

Telson: Very small, semi-oval, without setae.

Remarks

In the known corophiid amphipods, those species (Sections B and C [2, 5, 6] with fused urosome as that of the present new species) have longest and best developed uropod 1, and their uropod 2 is rather reduced and attaches to the upper part of the urosome. In contrast to them, the uropod 1 of the present new species is slender and not so developed, and its uropod 2 is well developed and attaches to the base of the urosome. Hence, the new species is clearly distinguishable from the other corophiids with fused urosome by these differences. On the other hand, the present new species has peculiar mandibular palp in which the terminal segment attaches to the middle of its

proximal one; this type has been known in only one species, *Corophium crassicorne* Bruzelius [1, 3, 5], that belongs to Section C of Crawford's system. The present new species would be closest to *C. crassicorne*.

Material examined

Holotype: Female, 2.16 mm. Type locality: Sandy bed in the shallow water of In-no-shima Island, Hiroshima Prefecture, Japan. Date: Aug. 1, 1984. Collector: Nobuo Sawada. Collection No.: Asia Univ. 3.

Corophium sinense Zhang, 1974
(Figs. 3–5)

Corophium sinense Zhang, 1974 [8], pp. 139–146.

Description of Female

Body: Depressed. Rostrum small, eyes invisible. Coxae discontinuous in series; pleonal epimera 1–3 gradually broadened at twice in turn, epimeron 3 provided with 1 posteroventral tooth; urosome segmented.

Antennae: In antenna 1, segment 1 of peduncle armed with 1 outer-distal spine, subequal to segment 2 in length; each segment of flagellum except for the terminal one provided with 1 aesthetasc. In antenna 2, segment 1 of peduncle provided with 1 bifid process, segments 2–3 lacking spines, segment 5 half the length of segment 4; flagellum biarticulate, terminal segment rudimentary.

Mouthparts: Mandibular process of lower lip rudimentary, inner lobe broad. Molar process rugose, provided with 1 short plumose seta; palp biarticulate, terminal segment reduced, directly jointed to the proximal one. Inner plate of maxilla 1 rudimentary, unarmed; outer plate with 6 bifid spines; palp biarticulate, proximal segment very small, apex of terminal segment with 2 opposite rows of 8 spines and 7 stiff setae. Plap of maxilliped 4-articulate, terminal segment much reduced, apically provided with 1 stout, long spine.

Gnathopod 1: Coxa 1 prominently produced forward, not attenuate, ventrally provided with 3 long plumose setae. Propod subequal to carpus in length; transverse palm a little produced forward, armed with many bifid spines. Dactyl extending beyond palm when closed, grasping margin finely pectinate on middle part. *Gnathopod 2*: Corophi-id-fashion. Dactyl falcate, nearly reaching the base of propod when closed, grasping margin unarmed with spines and teeth.

Pereopods 1–2: Similar to each other. Merus, propod and dactyl subequal in length. *Pereopods 3–4*: Similar to each other in form, pereopod 4 prominently longer than pereopod 3. Carpus about half the length of merus, extending postero-distally, armed with 1 pair of spines on outer side, 7 or 8 spines on outer-distal end gradually growing in length. Propod of peropod 3 provided with 1 locking spine. *Pereopod 5*: Broken.

Pleopod 1: Peduncle square, setaceous on outer margin; both rami equal in length, proximal segment of inner ramus dilated medially; terminal swimming setae 2/3 as long as rami.

Uropods: Uropod 1 extending beyond uropods 2–3; peduncle twice as long as inner ramus, 3 stout spines on inner margin gradually making larger, outer margin spinose; both rami spinose, especially inner ramus provided with 3 apical pronounced spines, outer ramus a little longer than inner ramus. Peduncle of uropod 2 a little longer than rami, provided with 1 inner-distal enormous spine; rami equal in length, marginally with many spines (6 or 7). Uropod 3 uniramous, half as long as uropod 2, peduncle as long as wide, dilated distally, both lateral margins armed with 5 spines respectively, outer spines stouter than inner ones;

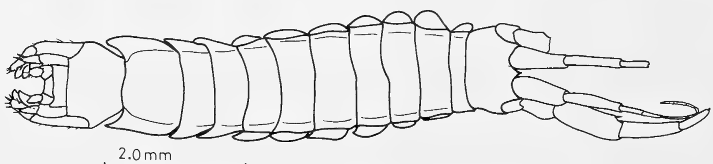

FIG. 3. *Corophium sinense* Zhang, 1974. Female, 6.83 mm.

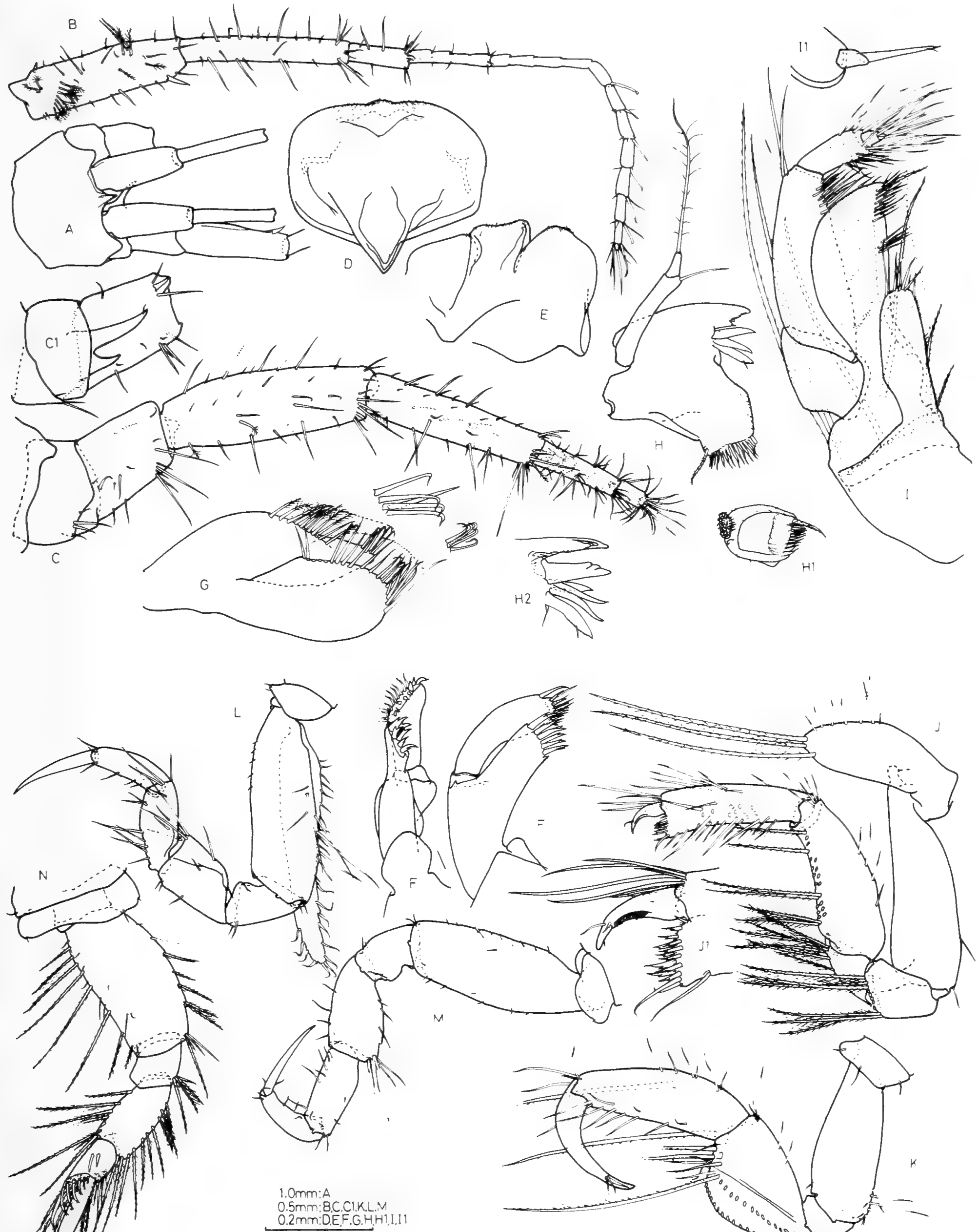

FIG. 4. *Corophium sinense* Zhang, 1974. Female, 6.83 mm. A: Head. B: Antenna 1. C and C1: Antenna 2. D: Upper lip. E: Lower lip. F: Maxilla 1. G: Maxilla 2. H and H1: Right mandible. H2: Left mandible. I and I1: Maxilliped. J and J1: Gnathopod 1. K: Gnathopod 2. L: Pereoped 1. M: Pereopod 2. N: Pereopod 3.

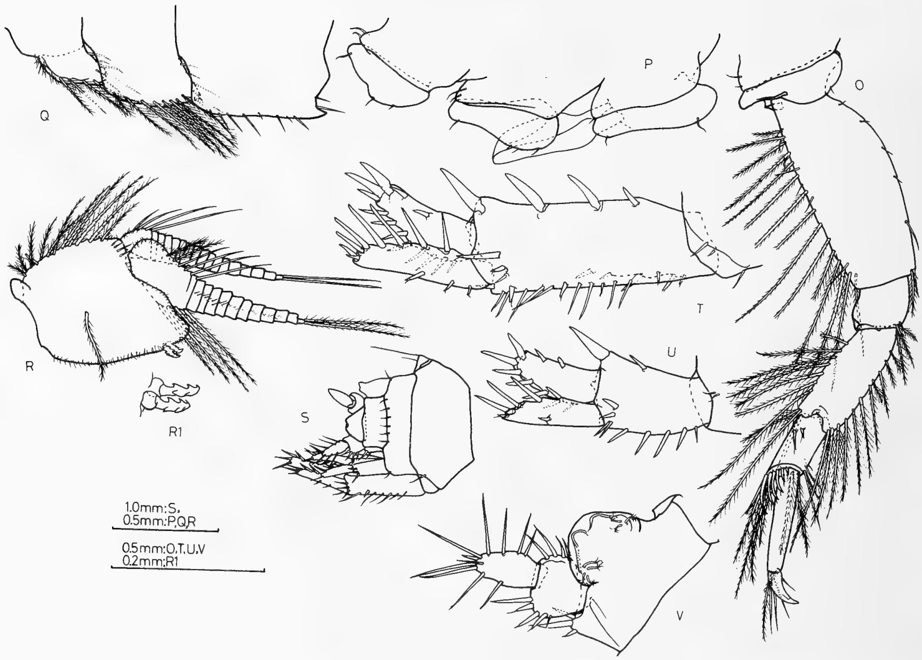

FIG. 5. *Corophium sinense* Zhang, 1974. Female, 6.83 mm. O: Pereopod 4. P: Coxae 5–7. Q: Pleonal epimera 1–3. R and R1: Pleopod 1. S: Urosome. T: Uropod 1. U: Uropod 2. V: Uropod 3 and telson.

ramus long elliptical, marginally armed with 10 stiff setae and 1 apical spine.

Remarks

The present specimens well agree with the female of *C. sinense* described by Zhang [8] from the Shantung Peninsula, North China, though several differences are observed. The Japanese specimens lack the prominent process that was found on the mid-medial face of the peduncular segment 1 of antenna 1 in Zhang's material, and the basal spine of the peduncular segment 1 on the antenna 1 found in the present specimens is not found in Zhang's; moreover, the peduncular segment 4 of antenna 2 is armed with one middle and one inner-distal spines in his specimens, but the present specimens lack them. It seems to me that these differences in the antennae 1–2 are mere local variation. As far as Zhang's figure and description are seen, the maxilliped palp of his material lacks one apical stout spine. He may have failed in observing the spine because it is masked by many setae. One more difference, though minor, is found in the pereopods: The carpus of peropods 1–2 of his material is longer than the propod, but the two segments are subequal in length in the present specimens.

Although I have not yet examined any specimen of the male of this species, Zhang [8] clearly demonstrated the presence of sexual dimorphism in the antenna 2 for his material from China. The combination of this sexual dimorphism and the segmented urosome is a characteristic of the member of Section A–1 of Crawford's system [2, 5, 6]. In addition to this character combination, this species has noticeable characteristics that the terminal segment of its mandibular palp is reduced instead of equal or subequal to the proximal one in length and attaches to the apex of the proximal one. The former character is known only in this species up to date, but the latter is known in *C. arenarium* Crawford, 1937 [2] and *C. orientale* Schellenberg, 1928 [4, 7], both of which belong to the same Section A–1 of Crawford's. *C. sinense* would be related to *C. arenarium* and *C. orientale*.

Material examined

Two females: One described and figured, 6.83 mm. Locality: Sandy-mud bed in the shallow water of In-no-shima Island, Hiroshima Prefecture, Japan. Date: Aug. 1 to 2, 1984. Collector: Nobuo Sawada. Collection No.: Asia Univ. 2.

ACKNOWLEDGMENTS

I wish to thank Mr. Nobuo Sawada of the Marine Ecological Research Co., Ltd., Ôsaka, for giving me the opportunity to examine the present materials and his personal communication with the figures. Thanks are also due to Dr. E. L. Bousfield of the National Museum of Canada for his critical reading of the manuscript and his comments. Further, I sincerely thank Dr. Yoshihide Suzuki of the Biological Laboratory, Asia University, for providing me with working facilities and for his critical comments on the manuscript.

REFERENCES

1 Bousfield, E. L. (1973) Shallow-water gammaridean Amphipoda of New England, Cornel Univ. Press, Ithaca, New. York. p. 312.

2 Crawford, G. I. (1937) A review of the amphipod genus *Corophium*, with notes on the British species. J. Mar. Biol. Assoc. U. K., **21**: 589–630.

3 Hirayama, A. (1984) Taxonomic studies on the shallow water gammaridean Amphipoda of West Kyushu, Japan. II. Corophiidae. Publ. Seto Mar. Biol. Lab., **29**: 1–29.

4 Schellenberg, A. (1928) Amphipoda in Cambridge Expedition to Suez Canal. Trans. Zool. Soc. London, **22**: 638–692.

5 Shoemaker, C. R. (1947) Further notes on the amphipod genus *Corophium* from the east coast of America. J. Wash. Acad. Sci., **37**: 47–63.

6 Shoemaker, C. R. (1949) The amphipod genus *Corophium* on the west coast of America. J. Wash. Acad. Sci., **39**: 66–82.

7 Stock, J. H. (1960) *Corophium volutator* forma *orientalis* Schellenberg, raised to specific rank. Crustaceana, **3**: 188–192.

8 Zhang, W. (1974) A new species of the genus *Corophium* (Crustacea, Amphipoda, Gammaridea) from the southern coast of Shantung Peninsula, North China. Stud. Mar. Scinica, **9**: 139–146.

ZOOLOGICAL SCIENCE 4: 183–186 (1987)

Three New Species of Avian Dilepidid Cestodes from Oita Prefecture, Japan[1]

Isamu Sawada and Giiti Kugi[2]

Biological Laboratory, Nara Sangyo University, Sango, Nara 636, and [2]Beppu City, Oita 874, Japan

ABSTRACT—Three new dilepidid cestodes were recorded from wild birds collected at Oita Prefecture, from December 1985 to March 1986. *Choanotaenia* (*Cholodkovskya*) *cylindrocephala* sp. n. from *Microscelis amaurotis amaurotis* is related to *C.* (*Cholodkovskya*) *unicoronata* (Fuhrmann, 1908) Matevosian, 1953 and *C.* (*Cholodkovskya*) *serivastavai* Mukherjee, 1965; but it differs from the former in the size of strobila, the shape of rostellar hooks and the form of cirrus, and from the latter in the size of rostellum, the length of rostellar hooks and the size of ovary. *Kowalewskiella grandihamata* sp. n. from *Turdus aureus aureus* differs from any of the five known species of the genus in the form, the length and the row of rostellar hooks, and the number of testes. *Paruterina oitana* sp. n. from *Otus scops japonicus* is related to but differs from *P. rauschi* Freeman, 1957, in the size of scolex and sucker, the length of rostellar hooks and the number of testes.

Since 1974, the authors have been examining cestodes parasitic on various wild animals collected in the Kyushu Districts, Japan. The present paper deals with cestodes obtained from wild birds at Oita Prefecture during the period from December 1985 to March 1986.

MATERIALS AND METHODS

All cestode specimens were obtained from the guts of the hosts and fixed in Carnoy's fluid for a few days. After being soaked in 45% acetic acid for about 1 hr for expanding, they were stored in 70% alcohol, and then stained with Delafield's hematoxylin, cleared in xylene and mounted in Canada balsam. Measurements are given in millimeters.

RESULTS

Choanotaenia (Cholodkovskya) cylindrocephala sp. n.

(Figs. 1–4)

A single specimen of this cestode was obtained from one brown-eared bulbul, *Microscelis amaurotis amaurotis,* collected at Yokoe-chô, Oita City, Oita Prefecture, on December 29, 1985.

Description: Small-sized dilepidid, worm length 38; maximum width 0.83, consisting of about 48 proglottids. Anterior proglottids much broader than long, but gradually proportion reversed, posterior ones being much longer than broad. Scolex nearly spherical, 0.42 long and 0.56 wide at level of suckers, distincly set off from neck. Suckers round, 0.245 in diameter. Rostellum pyriform, 0.301 by 0.140, armed with two alternate rows of 20 hooks. Hooks of two rows similar in shape, but attached at different levels. Hooks of anterior row larger, measuring 0.042 long; those of posterior row 0.039 long. Handle of hooks strong; guard small, bluntly round at its end, shorter than blade; blade sharpe at its end. Rostellar sac well-developed, extending almost to posterior margins of suckers, measuring 0.371 long and 0.182 wide.

Genital pore irregularly alternate, located a little anterior to middle of proglottid margins. Testes oval or spherical, numbering about 22–29, postovarian, lying in posterior half of proglottid. Cirrus sac thin-walled, measuring 0.084–0.091

Accepted July 9, 1986
Received June 12, 1986

[1] This paper corresponds to "Studies on the Helminth Fauna of Kyushu, Part 9"

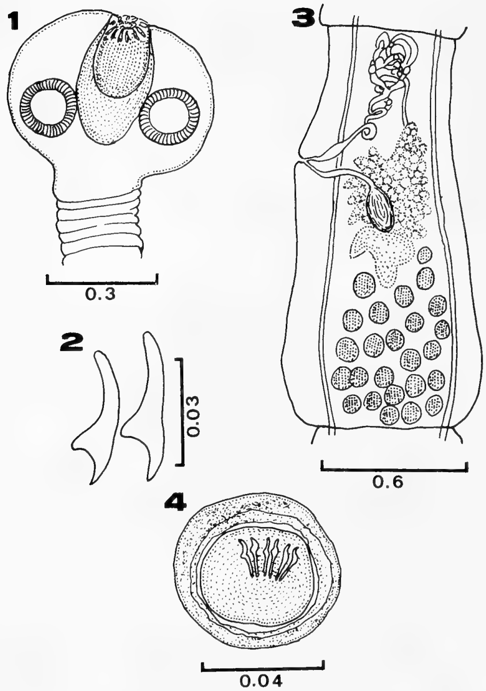

FIGS. 1–4. *Choanotaenia* (*Cholodkovskya*) *cylindrocephala* sp. n. 1: Scolex. 2: Rostellar hooks. 3: Mature proglottid. 4: Egg. Scale in mm.

long and 0.014 wide. Cirrus armed with minute spines. Ovary well-developed, bilobed, pretesticular, lying in middle of anterior half of proglottid. Poral lobe considerably smaller than aporal. Ovary bounded by longitudinal excretory canals, measuring 0.203–0.210 across. Vagina opening just posterior to getinal atrium and gradually expanding into a seminal receptacle measuring 0.070–0.091 by 0.043–0.056. Vitelline gland trilobate, measuring 0.084–0.070., just posterior to ovary.

Eggs spherical, 0.046–0.049 by 0.039–0.042, surrounded by four envelopes; outermost chorion thin, with smooth surface. Onchospheres spherical, 0.032–0.035 in diameter; embryonic hooks 0.014 long.

Host: Microscelis amaurotis amaurotis.

Site of infection: Small intestine.

Locality and date: Yokoe-chô, Oita City, Oita Prefecture; December 29, 1985.

Type specimen: Holotype: NSU Lab. Coll. No. 8601.

Remarks: Species of the genus *Choanotaenia* were divided into two groups by Wardle and McLeods (1952) [1]: one in which the rostellum has a single crown of rostllar hooks and the other in which the rostellum has a double crown of rostellar hooks. Matevosian (1954) [2] have divided the genus *Choanotaenia* Railliet, 1896, into two subgenera: *Choanotaenia, Choanotaenia* with one row of hooks on the scolex; *Cholodkovskya, Choanotaenia* with two rows of hooks. The present authors hold Matevosian's opinion. Each group comprises a large number of known species. So far as known to the authors, about 33 species of *C.* (*Cholodkovskya*) have been recorded from birds. Of these, the present new species most closely resembles *C.* (*Cholodkovskya*) *unicoronata* (Fuhrmann, 1908) Matevosian, 1954, from *Turdus merules* [3] in the number and length of rostellar hooks, and the number of testes; and *C.*(*Cholodkovskya) srivastavai* Mukherjee, 1965 from *Turdoides somervillei* [4] in the number of rostellar hooks and testes. However, the present new species differs from the former in the smaller size of the worm (37.1 vs. 220), the shape of rostellar hooks (handle bluntly round at its end vs. pointed) and the form of cirrus (armed vs. unarmed); and form the latter in the larger size of rostellum (0.301 by 0.140 vs. 0.13 by 0.10), the longer rostellar hooks (0.039–0.042 vs. 0.01–0.02) and the larger size of ovary (0.203–0.210 by 0.154–0.161 vs. 0.05–0.06 by 0.03–0.04).

Kowalewskiella grandihamata sp. n.
(Figs. 4–8)

Five specimens of the present form were obtained from one White's ground-thrush, *Turdus aureus aureus,* collected at Yokoe-chô, Oita City, Oita Prefecture, on January 23, 1986.

Description: Medium-sized dilepidid; strobila length 80–110; maximum width 2–2.5. Metamerism distinct, craspedote; margins serrate. Proglottid wider than long. Scolex 0.45–0.64 long and 0.63–0.73 wide, set off from neck. Suckers round, unarmed, 0.21–0.23 in diameter. Rostellum 0.28–0.38 long and 0.17–0.24 wide, armed with a double row of 28 hooks. Hooks of two rows

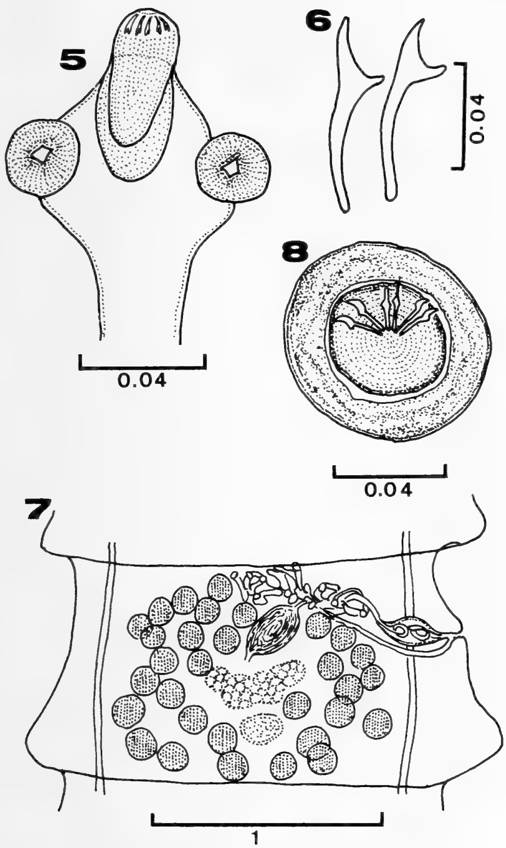

FIGS. 2–8 *Kowalewskiella grandihamata* sp. n. 5: Scolex. 6: Rostellar hooks. 7: Maure proglottid. 8: Egg. Scale in mm.

similar in shape, but attached at different levels. Hooks of anterior row larger, measuring 0.073; those of posterior row 0.068 long. Handle of hooks long, guard small, bluntly round at its end, shorter than blade; blade sharp at its end. Rostellar sac well-developed, 0.27–0.47 long and 0.17–0.27 wide. Neck 0.5 long and 0.2 wide.

Genital pore unilateral, located a little anterior to middle of proglottid margins. Testes 27–30 in number, encircling female organs, measuring 0.042–0.056 in diameter. Vas deferens much coiled, located in anterior poral third of proglottid, and joining to posterior edge of cirrus sac. Cirrus sac 0.070–0.091 long and 0.042 wide, extending behind lateral excretory canal. Vagina opening into genital atrium, extending to median field, parallel to cirrus sac, then enlarging, forming a seminal receptacle measuring 0.035–0.042 by 0.084. Ovary transversely elongated, measuring 0.105 across. Vitelline gland lobed structure, 0.021–0.035 by 0.014–0.021, situated just posterior to ovary. Eggs spherical 0.060–0.063 by 0.067–0.074, surrounded by four envelopes; outermost chorion thin, with smooth surface. Onchospheres spherical, 0.093 by 0.042; embryonic hooks 0.018 long.

Host: *Trudus aureus aureus.*

Site of infection. Small intestine.

Locality and date: Yokoe-chô, Oita City, Oita Prefecture; January 23, 1986.

Type specimen: Holotype: NSU Lab. Coll. No. 8902; Paratypes: No. 8603.

Remarks: The number of the species belonging to the genus *Kowalewskiella* Baczynska, 1914, amounts to five: *K. longiannulata* Baczynska, 1914 [5], *K. cingulifera* (Krabbe, 1869) Spassky, 1957 [6], *K. glareolae* (Burt, 1940) Lopez-Neyra, 1952 [7] and *K. stagnatilidis* (Burt, 1940) Lopez-Neyra, 1952 [7] and *K. hypoleucia* (Singh, 1952) Saxena, 1971 [8]. The present new species is distinct from any of the above-mentioned species in the form, length and row of rostellar hooks, and number of testes.

Paruterina oitana sp. n.
(Figs. 9–11)

One Japanese scop owl, *Otus scops japonicus,* collected at Asahi-chô, Beppu City, Oita Prefecture, on March 10, 1986, was found infected with six specimens of the present form. They were fully mature, but not gravid.

Description: Small-sized dilepidid; worm length 6–8; maximum width 0.5–0.7. Metamerism distinct, margins serrate. Mature proglottids wider than long. Scolex well-developed, 0.526 long and 0.650 wide, distinctly set off from neck. Rostellum 0.166 long and 0.221 wide when extended, armed with a double row of 44–45 hooks. Hooks of two rows similar in shape, but attached at different levels. Hooks of anterior row larger, measuring 0.070; those of posterior row 0.049 long. Handle of hooks long; guard small, round at its end, remarkably shorter than blade; blade sharp at its end. Suckers unarmed, 0.180–0.193 in diameter. Neck slender, 2.8 long and 0.3 wide.

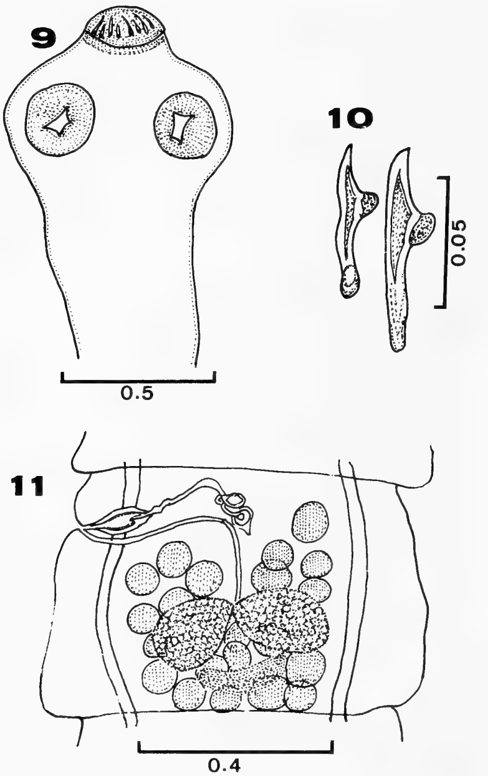

Figs. 9–11 *Paruterina oitana* sp. n. 9: Scolex. 10: Rostellar hooks. 11: Mature proglottid. Scale in mm.

Genital pore irrugularly alternating, located anterior to middle of proglottid margins. Cirrus sac pyriform, 0.091–0.112 long and 0.049 wide, extending beyond longitudinal excretory canals towards anterior border of proglottid. Vas deferens coiled, narrow, in anterior field of progloptid. Testes mostly ovoid, 22–23 per proglottid, arranged behind and in both anterolateral sides of female genitalia. Vagina posterior to cirrus sac, terminating in elongated seminal receptacle near ovarian isthmus. Ovary bilobed with each lobe measuring 0.063–0.091 long and 0.035 wide, located posterior half of proglottid. Vitellin gland 0.063–0.011 by 0.035, immediately post-ovarian.

Host: Otus scops japonicus.

Site of infection: Small intestine.

Locality and date: Asahi-chô, Beppu City, Oita Prefecture; March 10, 1986.

Type specimen: Holotype: NSU Lab. Coll. No. 8604; Paratypes : No. 8605.

Remarks: About 16 species of the genus *Paruterina* Fuhrmann, 1906 have been recorded from wild birds. Of these, two species; *P. otidis* Baczynska, 1914 [5] and *P. rauschi* Freeman, 1957 [9], were described from the Strigiformes. The present new species most closely resembles *P. rauschi* in the number of rostellar hooks and the position of genital pores. However, it differs from that species in the following characters: (1) larger scolex (0.526 by 0.650 vs. 0.150 by 0.225); (2) larger suckers (0.193 by 0.180 vs. 0.081–0.094 by 0.076–0.089); (3) longer rostellar hooks (0.049–0.070 vs. 0.030–0.042); and fewer number of testes (22–23 vs. 27–32).

REFERENCES

1 Wardle, R. A. and McLeod, J. A. (1952) The Zoology of Tapeworms, Univ. Minn. Press., New York. 780 pp.

2 Matevosian, E. M. (1954) Revision of cestode dilepidid system. Rabot. Gel'mintol., 75-Let. Skrjabin, 392–397. (Russian text)

3 Fuhrmann, O. (1908) Nouveaux Ténias d'oiseaux. Rev. Suisse Zool., **16**:27–73.

4 Mukherjee, R. P. (1965) On two new species of cestodes from babbler. J. Zool. Soc. India, **17**: 32–36.

5 Baczynska, H. (1914) Etudes anatomiques et histologiques sur quelques nouvelles espèces de cestodes d'oiseaux. Bull. Soc. Sci. Nat. Neuchâtel, **40**: 187–239.

6 Krabbe, H. (1869) Sidrag til Kundskab om Fuglenes Baendelorme. Kgl. Danske Videnska. Selskab, Skrifter, Naturvidenskab. Math. Afdel., **8**: 249–363.

7 Burt, D. R. R. (1940) Some new species of cestodes from Charadriiformes, Ardeiformes and Pelecaniformes in Ceylon. Ceylon J. Sci., **22**: 1–63.

8 Singh, K. S. (1952) Cestode parasites of birds. Ind. J. Helm., **4**:1–72.

9 Freeman, R. S. (1957) Life cycle and morphology of *Paruterina rauschi* n. sp. and *P. candelabraris* (Goeze, 1782) (Cestoda) from owls, and significance of plerocercoids in the oeder Cyclophyllidae. Can. J. Zool., **35**: 349–370.

ZOOLOGICAL SCIENCE 4: 187–191 (1987)

[COMMUNICATION]

The Intracellular Supporting Network in the Leydig Cells of Larval Salamander Skin

Seiji Kato and Kazushige Kurihara

Department of Anatomy, Medical College of Oita, Oita 879–56, Japan

ABSTRACT—The three-dimensional structure of the intracellular basket-like network, so-called Langerhans' net in the Leydig cells was studied in the epidermis of larval salamander, *Hynobius dunni* Tago by light and electron microscopy. The Langerhans' net consisted of irregularly arranged hexagonal mesh enclosing the entire cell. There were many mucous granules in the Leydig cell cytoplasm. These granules often attached to net with delicate spinous membranous processes. Our scanning electron micrographs seem to delineate the semischematic drawing of Hay. The fibers of the net were composed of filaments which might contain keratin-like substance. Leydig cells were attached to neighbouring epidermal cells at numerous points of the net fibers by desmosome. The Leydig cells increased in number and size during the course of larval life and then disappeared in the juvenile according to epidermal cornification after metamorphosis. Langerhans' net may function as a supporting cytoplasmic framework of the Leydig cell throughout the larval life.

INTRODUCTION

The Leydig cells first described as the "Schleimzellen" or mucous cells by Leydig [1] are detected between surface epidermal cells and basal cells in the larval salamander. These cells are characterized by large diameter, the presence of cytoplasmic mucous granules and unique peripheral supportive network (see review of Dawson [2]). Langerhans [3] observed a basket-like network at the peripheral cytoplasm of Leydig cell in the larval salamander. According to his findings, it was called Langerhans' net. The fine structures of the Langerhans' net as intracellular network have been studied in the larval salamanders, *Amblystoma punctatum* and *A. opacum* [4], *Salamandra salamandra* (L.) [5, 6], axolotls [7–9] and newt, *Taricha torosa* [10]. These studies provide information on fine structure of the nets in the Leydig cells and their development in the larval stage. Hay [4] further described semischematic drawing of a Leydig cell showing Langerhans' net in the whole mount of the skin with light microscope. To our knowledge, however, three-dimensional photographs of the Langerhans' net have not been directly shown. It is, therefore, of interest to delineate the spatial structure of the Langerhans' net in the salamander as a supporting cytoplasmic framework of the Leydig cell. We examined the spatial structure of the Langerhans' net by scanning electron microscopy with particular reference to the drawing of Hay [4]. The light and transmission electron microscopic observations of the net were also performed and the functions of the Langerhans' net and the Leydig cell were briefly discussed.

MATERIALS AND METHODS

Total thirty of larvae and juveniles of the salamander, *Hynobius dunni* Tago, were used in this experiment. Twenty larvae were fully grown ones of 45–50 mm in length. To investigate further growing fluctuation of Leydig cells before or after metamorphosis, the other ten, that is newly hatched larvae (10 mm), young larvae (25 mm) and juveniles three weeks after metamorphosis, were also examined. All specimens were raised from eggs at room temperature. For scanning electron microscopy, the dorsolateral skins from the middle

Accepted August 1, 1986
Received June 12, 1986

part of each specimen anesthetized with MS222 were fixed in 2.5% glutaraldehyde in 0.05 M sodium cacodylate buffer (pH 7.4) at 4°C for 2 hr. Internal surfaces of epidermal cells were exposed either by cutting with a razor blade or by cracking the tissue under liquid nitrogen. The fixed tissues were post-fixed and impregnated with osmium according to Murakami's tannic acid-osmium method [11]. All tissues were critical point dried. The specimens with or without further coating with gold (20 nm thick) were examined in a JSM–25S (JEOL) electron microscope. For transmission electron microscopy, aldehyde-fixed tissues were post-fixed in 1% osmium tetroxide at 4°C for 2 hr, dehydrated with a series of alcohol and embedded in epoxy resin (Taab Epon 812). Sections were cut with glass knives on a Reichert OmU 4. Ultrathin sections were stained with 6% uranyl acetate and lead citrate and examined in a JEM 300C electron microscope (JEOL). For light microscopy the tissues were fixed in neutral formalin and embedded in paraffin (melting point=42–44°C). Sections were subjected to alcian blue-PAS staining for mucopolysaccharide and keratin staining with orange G-methyleosin-anilin blue mixture according to Martinotti's method [12].

RESULTS AND DISCUSSION

Leydig cells in the epidermis of larval salamander, *Hynobius dunni* Tago, were also found between surface epidermal cells and basal cells in most body region as nearly continuous layers (Figs. 1 and 2) similar to those previously reported in other salamanders [7–9, 13] and newt [10]. The Leydig cells are characterized by a unique basket-like net, so-called Langerhans' net and the large granule. The net can be demonstrated only in the peripheral cytoplasm. Figures 3 and 4 show each one-half of the net in the view of inside and outside of Leydig cells respectively. The networks consist of branching fibers to form hexagonal meshes and enclose the entire cell. These micrographs indicate three-dimensional structure of the net and appear to correspond to the semischematic drawing of Langerhans' net described by Hay [4]. The hexagonal meshes of the net were 1.5–2.0 μm in diameter and irregularly arranged. Fibers of the net were 1.0 μm or less in diameter and were composed of filaments resemble to the tonofilaments of ordinary epidermal cells (Figs. 6,7 and 9). These fibers were stainable with anilin blue in orange G-methyleosin-anilin blue mixture for identification of keratin (Fig. 10). Hence, the fibers of the net seem to contain fibrous protein as a form of keratin. The filaments of the net were inserted into the desmosomal zones between Leydig cell and adjacent epidermal cell. Leydig cells were attached to neighbouring epidermal cells at numerous points by the narrow bridge of the fibers (Figs. 6 and 8). The sites of the attachment could be recognized as a desmosome similar to that between ordinary epidermal cells (Fig. 9). These fine structures of the net observed in our materials by transmission electron microscopy are essentially the same as previously reported in the other salamanders [4, 6] and newt [10]. Thus, the Langerhans' net may play a role in the function of the stability of Leydig cell shape and its connection to the adjacent epidermal cells as a cytoplasmic supporting framework during larval life. The Leydig cells were not found in the skin of newly hatched larvae but existed in the form of middle layer in the epidermis of young larvae. These cells increased in number during the course of larval life and formed two or three continuous layers in the epiderms of fully grown larvae. Then, the number of these cells diminished according to the cornification of outer epidermal layer during metamorphosis. In the juveniles three weeks after metamorphosis Leydig cells no longer existed as epidermal component (Fig. 5) and furthermore, large mucous gland with alcian blue-positive granules appeared under an epidermal cell layer. Similar changes in the distribution of Leydig cells were also found in other salamanders, *Hynobius nebulosus* and *Hynobius nigrescens* (unpublished data, Kato). Such growing fluctuations of Leydig cell number before and after metamorphosis have been said to be present in axolotl [7–9] and newt [10]. But, in the salamander, Rosenberg *et al.* [6] have reported that the number of Leydig cells in a unit area of epidermis declines from birth until after metamorphosis but cell hypertrophy reaches its peak near metamorphosis. There are differences in the growing fluctuations of Leydig cells

among urodeles.

The bulk of Leydig cells was occupied by a large number of granules varying in size, shape and electron density (Figs. 6 and 8). Most granules had an irregular limiting membrane. These granules of about 1.5 μm in diameter were PAS-positive, diastase resistant but alcian blue-negative. The granules were inside of the net (Figs. 3 and 4) and often attached to the net fibers with delicate spinous membranous processes. As for the function of Leydig cell, the early study [14] suggested that these cells secrete a fluid into the intercellular

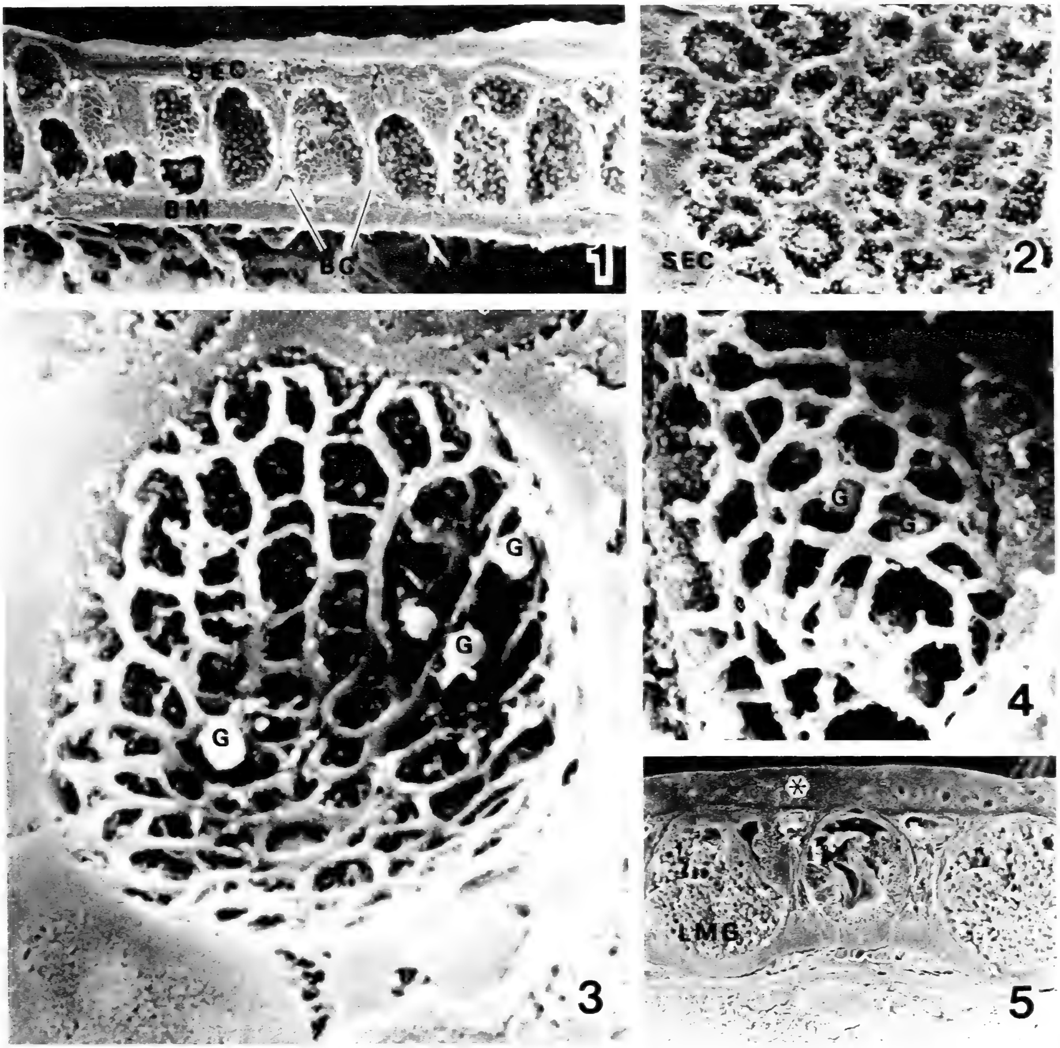

FIG. 1. Surface of dorsolateral epidermis of a fully grown larva cut vertically. The Leydig cells exist between surface epidermal cells (SEC) and basal cells (BC) near basement membrane (BM). ×310.

FIG. 2. Surface of the specimen cut horizontally. Leydig cells form nearly continuous layer under surface epidermal cells (SEC). ×510.

FIGS. 3 and 4. Freeze-cracked epidermal cells of the skin. Note Langerhans' nets and large granules (G) in the Leydig cell. Fig. 3 Inside view. ×5470. Fig. 4 Outside view. ×5660.

FIG. 5. Surface of juvenile skin cut vertically. Note large mucous glands (LMG) and no Leydig cells in the epidermis (asterisk). ×200.

spaces. On the other hand, Paulicki [15] reported that they secrete mucin in intercellular space and later Dawson [2] observed mucous secretion by Leydig cells. On the mucous secretion, Hay [4], Fährmann [7] and we also have detected evidences for mucosubstances in contrast to the reports of Warburg and Lewinson [13] and Rosenberg *et al.* [6]. Previously, Kelly [9] described cellular changes of the Leydig cells in the newt after various degree of desiccation. According to him, the physiological significance of Leydig cells seems not to involve mucous release onto outer surface of the skin but function as a water retaining cell for the substance in the intercellular space. As large mucous gland with alcian blue-positive granules already appear in the subepidermal layer of our material in the late larval stage, the granule in the Leydig cell may not be extruded in the outer surface of the epidermis but in the intercellular space to provide internal fluid preserve.

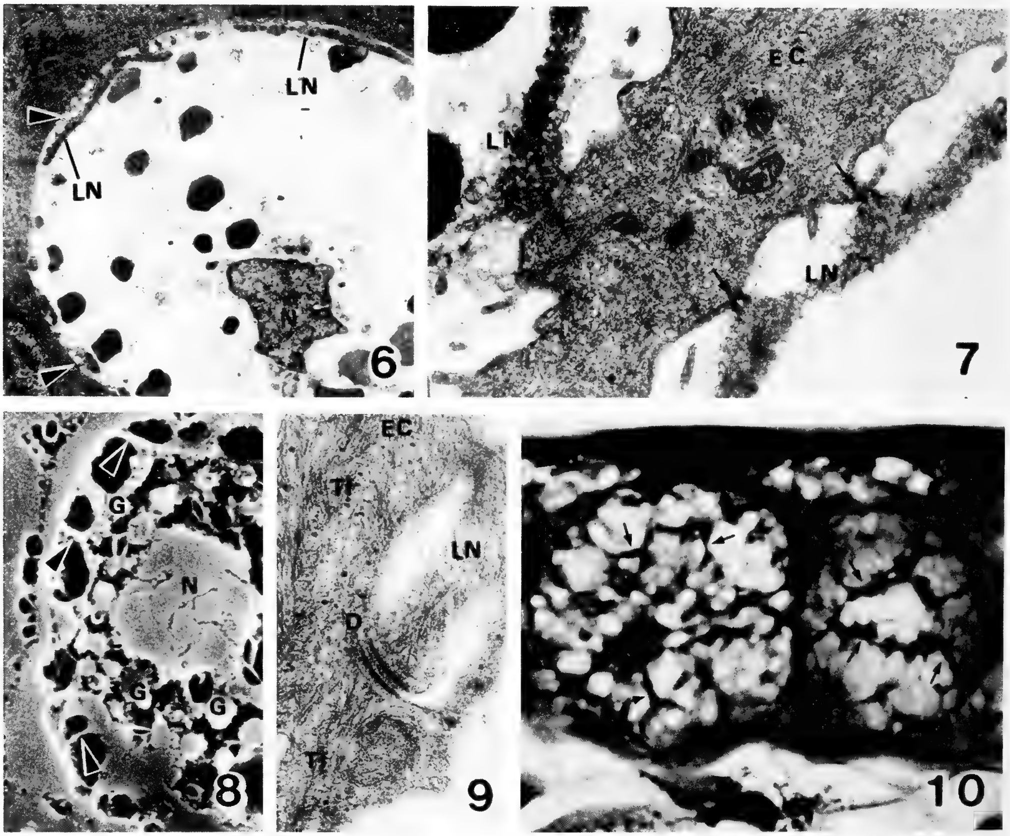

FIGS. 6 and 8. Section (Fig. 6) and freeze-cracked surface (Fig. 8) of the larval epidermis. A Leydig cell contains large granules (G) and Langerhans' net (LN) attached to neighbouring epidermal cells (EC) by narrow bridges (arrowheads). N: nucleus. ×1625, ×2200.

FIG. 7. Section of a Leydig cell. Filaments of Langerhans' net (LN) attach to neighbouring epidermal cells (EC) by desmosome-like structures (arrows). ×13,480.

FIG. 9. Higher magnification of desmosome (D) between Langerhans' net (LN) and adjacent epidermal cell (EC). Tonofilaments of the epidermal cell appear Tf. ×38,000.

FIG. 10. Paraffin section of the skin in the fully grown larva. The section is stained with orange G-methyleosin-anilin blue mixture for keratin. Note anilin blue-stainable net fibers (arrows) in the Leydig cells. ×670.

REFERENCES

1 Leydig, F. (1857) Lehrbuch der Histologie des Menschen und der Thiere, Hamm, G. Grotesche Buchhandlung (C. Müller)

2 Dawson, A. B. (1920) J. Morphol., **34**: 487–590.

3 Langerhans, P. (1873) Arch. Mikrosk. Anat., **9**: 745–752

4 Hay, E.D. (1961) J. Biophys. Biochem. Cytol., **10**: 457–463.

5 Greven, H. (1980) Z. Mikrosk. Anat. Forsch., **94**: 196–208.

6 Rosenberg, M., Lewinson, D. and Warburg, M. R. (1982) J. Morphol., **174**: 275–281.

7 Fährmann, W. (1971a) Z. Mikrosk. Anat. Forsch., **83**: 472–506.

8 Fährmann, W. (1971b) Z. Mikrosk. Anat. Forsch., **83**: 535–568.

9 Fährmann, W. (1971c) Z. Mikrosk. Anat. Forsch., **84**: 1–25.

10 Kelly, D. E. (1966) Anat. Rec., **154**: 685–700.

11 Murakami, T. (1974) Arch. Histol. Jpn., **36**: 189–193.

12 Martinotti, L. (1924) Z. Wiss. Mikrosk., **41**: 202–237.

13 Warburg, M. R. and Lewinson, D. (1977) Cell Tissue. Res., **181**: 369–393.

14 Pfitzner, W. (1880) Morphol. Jahrb., **6**: 469–526.

15 Paulicki, W. (1884) Arch. Mikrosk. Anat., **24**: 120–173.

ZOOLOGICAL SCIENCE 4: 193–196 (1987)

[COMMUNICATION]

Isolation of Spermatozoa, Their Ultrastructure, and Their Fertilizing Capacity in Two Frogs, *Rana japonica* and *Xenopus laevis*

NORIO YOSHIZAKI

Department of Biology, Faculty of General Education, Gifu University, Gifu 501–11, Japan

ABSTRACT—Spermatozoa were isolated by ultracentrifugation of a mixture of 70% Percoll solution and a sperm suspension prepared by macerating the testes of *Rana japonica* and *Xenopus laevis* frogs. After centrifugation, mature spermatozoa were layered at a density of 1.143 g/ml and mostly free from other types of cells, immature spermatozoa and subcellular organelles. Insemination by the isolated spermatozoa resulted in a rate of fertilization comparable to that by a crude sperm suspension. The isolated spermatozoa had the same morphological characteristics as those of mature spermatozoa in the testes. These results indicate that spermatozoa suffer no severe damage from the isolating procedure used.

INTRODUCTION

Having recently found secretory cells in a specific portion of the amphibian oviduct, I have postulated that the products of these cells induce the acrosome reaction of spermatozoa [1, 2]. Although the induction of the acrosome reaction by this substance(s) was confirmed in *Bufo* [2], ambiguity still remains whether the reaction is induced by this substance directly or mediated by other substances. This is because only crude sperm suspensions prepared by macerating the testes have so far been used in amphibian research. Absence of a paper relating with the metabolism and the motility of amphibian spermatozoa might also be due to the lack of a method to obtain a pure sperm preparation. So the purpose of the present study was to develop a method of isolating fertilizable spermatozoa from crude sperm suspensions. The effect of fractionation on the spermatozoa was checked by comparing the ultrastructures of fractionated spermatozoa with those of mature spermatozoa in the testes [3, 4].

Accepted September 19, 1986
Received July 23, 1986

MATERIALS AND METHODS

Sexually mature *Rana japonica* and *Xenopus laevis* frogs were purchased from dealers in Tokyo and Hamamatsu, respectively. Sperm suspensions were prepared by macerating excised testes in De Boer (DB) solution composing of 110 mM NaCl, 1.3 mM KCl and 1.3 mM $CaCl_2$ with pH adjusted to 7.3 by addition of $NaHCO_3$ [5]. After removing the coarse debris by brief centrifugation ($50 \times g$, 5 min), the suspension was divided into two portions, one-third to be used for the control experiment and two-thirds for the isolation experiment. The latter portion was centrifuged at $800 \times g$ for 5 min (4°C) and the precipitate was suspended in a 70% Percoll (Pharmacia Fine Chemicals) solution containing DB. After centrifugation of the mixture at $36{,}000 \times g$ for 60 min (4°C), the spermatozoa were layered at a density of 1.143 g/ml. Undissociated cell masses and blood cells were independently layered at a density lower than that and clearly separated from the spermatozoa. The spermatozoa were resuspended in DB and pelleted by ultracentrifugation at $100{,}000 \times g$ for 90 min (4°C).

Ovulation was induced by injecting frog pituitaries into the females of *Rana* [6] and human gonadotropic hormone into those of *Xenopus* [7].

FIGS. 1 and 2. Light micrographs of mature spermatozoa of *R. japonica* (Fig. 1) and *X. laevis* (Fig. 2), isolated by centrifugation through Percoll. Arrow indicates occasional contamination by abortive spermatozoa. Phase contrast.

TABLE 1. Fertilizing capacity of isolated spermatozoa of *R. japonica* and *X. laevis*

Species	% (mean±SD, n=5)[a] of eggs fertilized by	
	crude sperm	isolated sperm
R. japonica	97.6 ± 2.0	90.9 ± 1.3
X. laevis	93.2 ± 1.9	91.5 ± 2.4

a: At least 100 eggs were counted in each dish.

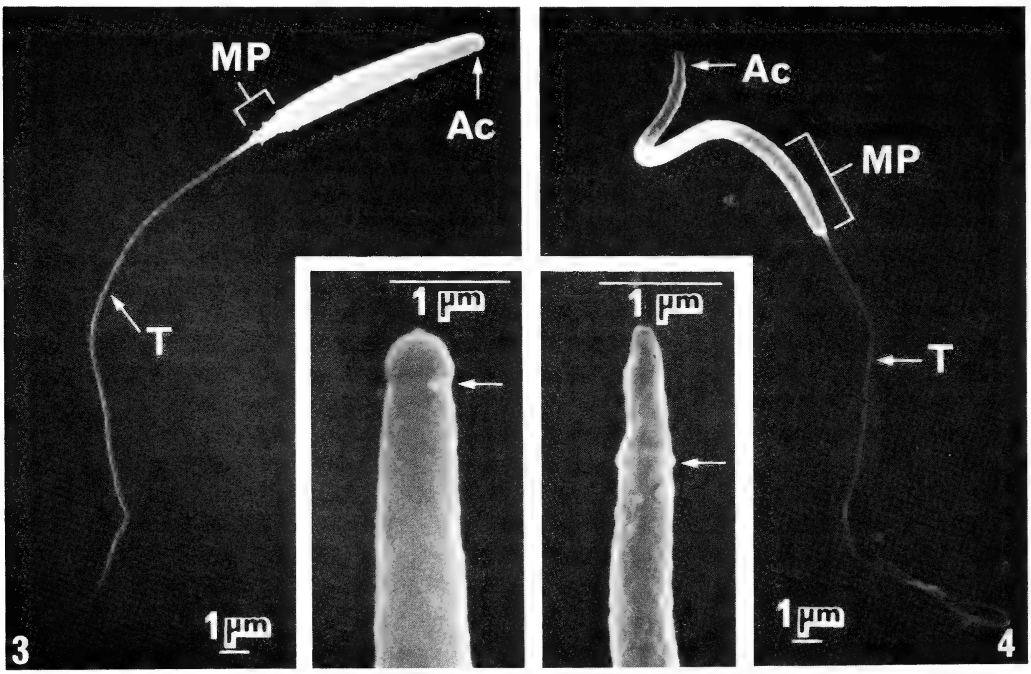

FIGS. 3 and 4. Scanning electron micrographs of isolated spermatozoa of *R. japonica* (Fig. 3) and *X. laevis* (Fig. 4). Insets show the posterior margin of the acrosome (arrows). Ac, acrosome; MP, middle piece; T, tail.

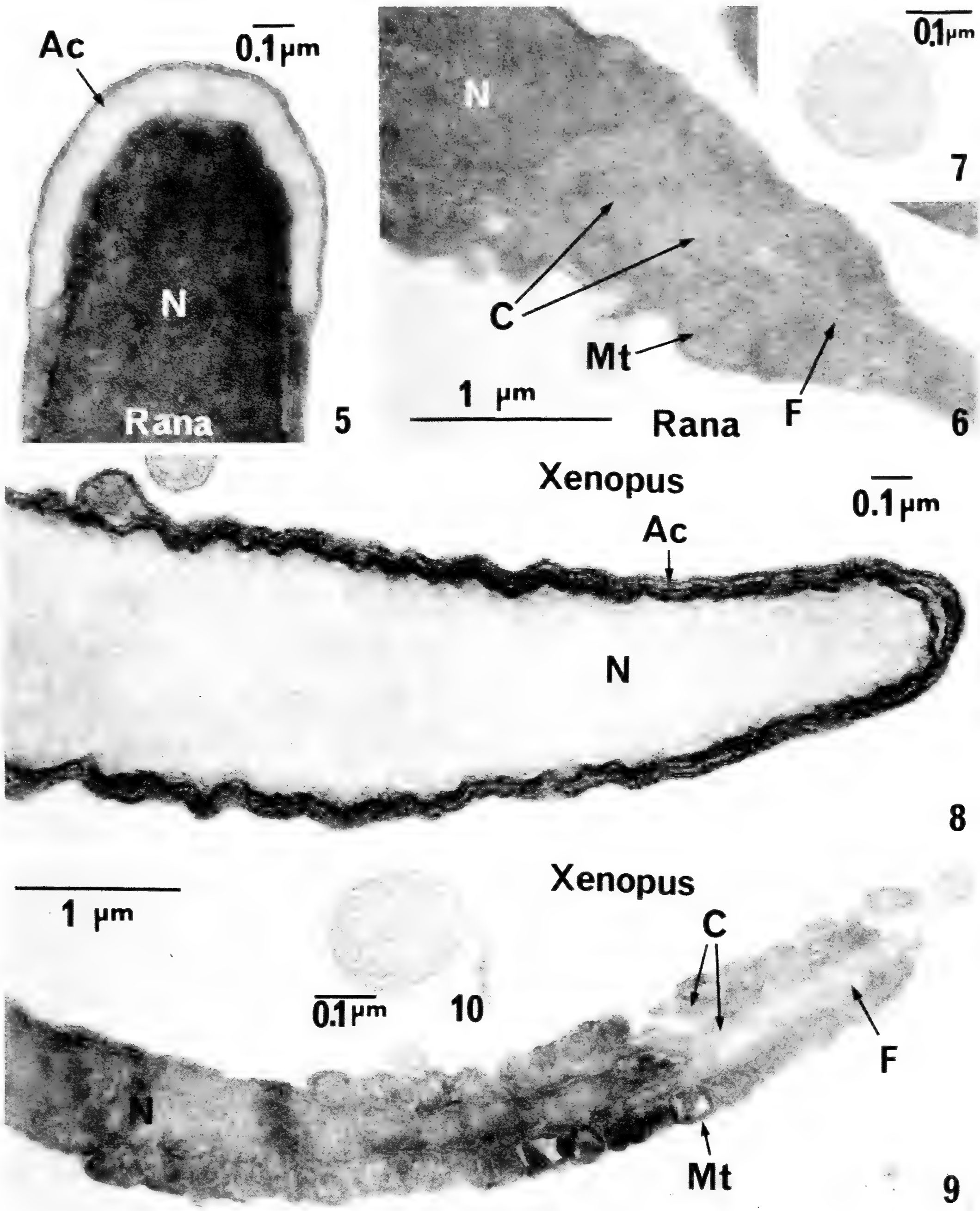

FIGS. 5–10. Transmission electron micrographs of isolated spermatozoa of *R. japonica* (Figs. 5–7) and *X. laevis* (Figs. 8–10). Acrosomes (Ac) are flattened and overlaid on the nuclei (N) (Figs. 5 and 8). The middle piece consists of posteriorly tapered nuclei, a pair of centrioles (C), axial filaments (F) extending from a centriole, and the mitochondria (Mt) surrounding them (Figs. 6 and 9). Cross sections of the flagella show a 9+2 axial filament complex (Figs. 7 and 10).

Artificial insemination was done according to the methods of Katagiri [5] and Moriya [8]. Sperm concentrations were adjusted to 10^7 cells/ml in 0.05 DB for *Rana* and 0.5 DB for *Xenopus*. This is a submaximal concentration of spermatozoa for successful fertilization in *Xenopus* [9]. Fertilization was measured by scoring the eggs in the morula stage.

For transmission and scanning electron microscopy, the spermatozoa were treated as mentioned previously [10].

RESULTS AND DISCUSSION

Figures 1 and 2 show the preparations of spermatozoa isolated from the testes of *Rana* (Fig. 1) and *Xenopus* (Fig. 2). The spermatozoa were mostly free from testicular tissues, immature spermatozoa and subcellular organelles of broken cells. Mature spermatozoa taken from the ureter of a hormonally stimulated male seem to have the same appearance. When the uterine eggs of *Rana* and *Xenopus* were inseminated by isolated spermatozoa of each species, the fertilization rate was comparable to that obtained by a crude sperm suspension (Table 1), suggesting that the procedure of isolating spermatozoa by the centrifugation through Percoll has no effect on sperm viability.

The isolated spermatozoa of *R. japonica* and *X. laevis* shared ultrastructural characteristics with the mature spermatozoa in the testes of *R. clamitans* [3] and *X. laevis* [4], respectively. The nuclei of the spermatozoa appear as elongated cylinders (Figs. 3 and 4). In *Xenopus,* they further take a helical form of about 1.5 revolutions. At the most anterior portion of the nuclei is an overlapping, flattened acrosome which extends approximately 0.4 μm in *Rana* and 1 μm in *Xenopus* (Figs. 5 and 8). The posterior margin of the acrosome is distinct in the scanning electron micrographs (Figs. 3 and 4). The middle piece of the spermatozoa is also externally distinguishable by uneven surface of the cell. The organelles contained in the middle piece are the posterior portion of the nucleus, which gradually tapers, a pair of centrioles, the axial filaments, which extend from a distal centriole, and the mitochondrial layer surrounding all of them (Figs. 6 and 9). The tails of both species consist of a 9+2 axial filament complex (Figs. 7 and 10). The cytoplasmic matrix in *Rana* has such high electron density that the boundary of each organelle seems indistinct.

It can be seen from these results that, according to the criteria of fertilizing capacity and morphology, spermatozoa isolated according to the method presented in this paper suffer no severe damage. Hence this method will enable us to investigate the physiological nature of spermatozoa, the knowledge of which is poor in amphibians.

REFERENCES

1 Katagiri, Ch., Iwao, Y. and Yoshizaki, N. (1982) Dev. Biol., **94**: 1–10.

2 Yoshizaki, N. and Katagiri, Ch. (1982) Gamete Res., **6**: 343–352.

3 Poirier, G. R. and Spink, G. C. (1971) J. Ultrastruct. Res., **36**: 455–465.

4 Reed, S. C. and Stanley, H. P. (1972) J.Ultrastruct. Res., **41**: 277–295.

5 Katagiri, Ch. (1961) J. Fac. Sci. Hokkaido Univ. Ser. VI. Zool., **14**: 607–613.

6 Yoshizaki, N. and Katagiri, Ch. (1981) Dev. Growth Differ., **23**: 495–506.

7 Yoshizaki, N. and Katagiri, Ch. (1984) Zool. Sci., **1**: 255–264.

8 Moriya, M. (1976) J. Fac. Sci. Hokkaido Univ. Ser. VI, Zool., **20**: 272–276.

9 Wolf, D. P. and Hedrick, J. L. (1971) Dev. Biol., **25**: 348–359.

10 Yoshizaki, N. (1985) J. Morphol., **184**: 155–169.

ZOOLOGICAL SCIENCE 4: 197–199 (1987)

[COMMUNICATION]

Suppressive Effect of Right-side Anterior Hypothalamic Lesion on Ovarian Compensatory Hypertrophy in Rats

Masaru Fukuda, Yumiko Nakano, Korehito Yamanouchi[1], Yasumasa Arai[1,2] and Hiroshi Furuya

Departments of Obstetrics and Gynecology, and [1]Anatomy, Juntendo University School of Medicine, Hongo, Bunkyo-ku, Tokyo 113, Japan

ABSTRACT—The development of ovarian compensatory hypertrophy (OCH) in the female rats with or without a unilateral anterior hypothalamic lesion was examined 2, 3 or 6 weeks after hemiovariectomy. OCH was effectively suppressed when the lesion was placed in the right anterior hypothalamus. However, the left-side anterior hypothalamic lesion failed to suppress the development of OCH, the rate being comparable to that in hemiovariectomized controls. This result indicates that right anterior hypothalamus seems to be responsible for the development of OCH and the function of the right anterior hypothalamus is hard to be replaced by the left side during 6-week postoperative period.

INTRODUCTION

The hypothalamus is thought to be responsible for the development of ovarian compensatory hypertrophy (OCH), because destruction of the region effectively suppresses OCH in rats [1]. Recently, we have reported that regardless of the side of hemiovariectomy, the lesion in the right anterior hypothalamus suppresses the development of OCH during 2-week postoperative period in rats, but the left side lesion has no effect [2]. According to Gerendai *et al.* [3], LH–RH (luteinizing hormone releasing hormone) content in the right side of the medial basal hypothalamus is higher than in the left side in female rats. Furthermore, the amount of LH–RH in the right medial basal hypothalamus is decreased significantly by the removal of both ovaries, when compared to that in the left side [4]. Cold stress increases LH–RH content only in the right hypothalamus in male rats [5]. These results suggest the possible right hypothalamic dominance in regulation of gonadotropin secretion. In the present study, in order to clarify whether the right side hypothalamic function in regulating OCH can be substituted by the left side during a longer post-hemiovariectomy period, the rate of OCH was examined at different periods (3 and 6 weeks) after the unilateral destruction of the anterior hypothalamus in female rats.

MATERIALS AND METHODS

Eighty-four female Wistar rats (210–300 g) housed under a controlled photoperiod (14:10 hr, L:D) and temperature (24–25°C) were used in the experiments. By means of a radiofrequency lesion generator (Radionics, Burlington, MA, USA), a unilateral lesion was made stereotaxically on either the right or left side of the anterior hypothalamus under ether anesthesia. At the same time, left ovary was removed and weighed. In addition, the animals without brain surgery were hemiovariectomized in the left side, as controls. Two, 3 or 6 weeks after surgery, fresh weight of the remaining (right) ovary was recorded for each rats. All ovarian weights were expressed as mg/100 g body wt. and the percentage relative hypertrophy of the remaining ovary constituted the response (OCH% =(remaining ovary−removed ovary)/removed

Accepted August 1, 1986
Received June 11, 1986

[2] To whom reprints should be requested.

TABLE 1. Effect of right- or left-side anterior hypothalamic lesion (RAHL or LAHL) on weight of the right-side ovary following left side hemiovariectomy

Term (wks)	Group	No. of rats	Body weight (g)	Ovarian weight (mg/ 100 g bw)	
				left	right
2	Control	9	259±7	16.7±1.2	23.8±1.3
	RAHL	8	248±12	16.5±1.0	18.1±1.3*
	LAHL	6	251±10	16.2±0.6	24.4±1.2
3	Control	9	278±10	16.0±0.8	22.4±1.2
	RAHL	13	257±5	16.9±0.6	19.5±1.1*
	LAHL	12	275±7	13.7±0.6	23.0±1.7
6	Control	5	321±8	12.5±0.7	22.5±1.2
	RAHL	10	307±9	13.4±0.9	15.5±1.7*
	LAHL	12	318±6	13.2±1.0	20.5±1.5

* P<0.05, vs. control and LAHL (*t*-test).

ovary×100). The precise localization of the hypothalamic lesions was verified after routine histological preparation.

RESULTS AND DISCUSSION

The results are summarized in Table 1 and Figure. 1. The mean weight of the remaining (right) ovary was significantly larger than that of the removed (left) ovary in control females at different intervals after the surgery (P<0.05, see Table 1). The mean OCH% was 45.0±8.2, 42.0±9.5 and 80.1±4.8 at 2, 3 and 6 weeks after surgery, respectively (Fig. 1). In the females with a lesion in the left anterior hypothalamus (LAHL), a significant increase in weight of the remaining ovary was also recognized, compared to that of the removed ovary (P<0.05). The mean OCH% in LAHL group in each post-hemiovariectomy period was comparable to that of control, being 50.8±5.1, 67.6±9.6 and 60.7±12.7 at 2, 3 and 6 weeks, respectively. In contrast to control and LAHL groups, the development of OCH in animals receiving the right side anterior hypothalamic lesion (RAHL) was markedly suppressed. The mean weight of the remaining ovary was not significantly different from that of the removed ovary (see Table 1). The mean OCH% of RAHL group (12.5±10.7) at 2 weeks was low when compared to that of control and LAHL groups. This inhibitory effect of RAHL on the development of OCH was still observed 3 and 6 weeks after surgery, the mean OCH% being 17.1±7.8 and 16.5±10.8, respectively. Histological examinations showed that RAHL and LAHL were centered in the medial anterior hypothalamus including the anterior hypothalamic nucleus. The lesions invaded the posterior part of the medial preoptic area in a number of animals. No damage was seen in the ventromedial-arcuate region in all operated females. In most cases, the periventricular gray of the anterior hypothalamus was left intact, but a partial damage was often found in the suprachiasmatic and/or paraventricular nucleus.

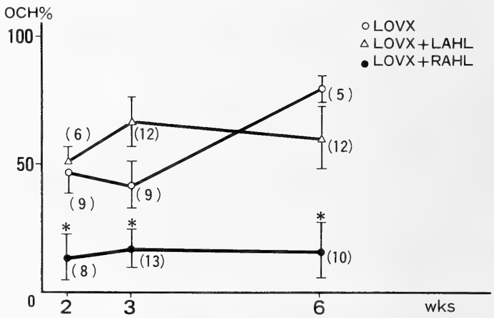

FIG. 1. Effect of the right- or left-side anterior hypothalamic lesion (RAHL or LAHL) on ovarian compensatory hypertrophy (OCH) following left-side hemiovariectomy (LOVX). The number in parentheses is the number of rats examined. The bar represents S.E. *P<0.05 vs. control and LAHL (*t*-test).

Present results confirmed our previous report that a lesion in the right anterior hypothalamus effectively suppressed the development of OCH 2 weeks after the surgery [2]. Furthermore, the impairment of OCH in the animals with a right anterior hypothalamic lesion could not recover 6 weeks after operation, even if their left anterior hypothalamus was left intact. Therefore, it is assumed that the function of the right anterior hypothalamus is hard to be replaced by the left side during 6-week-postoperative period. However, it is not known whether this is due to the left-right defference in LH-RH content in the medial basal hypothalamus in female rats [3]. If that is the case, the next problem is why available LH–RH in the left side hypothalamus cannot contribute to the development of OCH in the animals with RAHL. Further study is required to elucidate the precise role of the right anterior hypothalamus in regulating gonadotropin secretion during the development of OCH.

ACKNOWLEDGMENT

This study was supported by Grants-in-Aid to Y. A. from the Ministry of Education, Science and Culture of Japan.

REFERENCES

1 Flerko, B. and Bardos, V. (1961) Acta Endocrinol., **36**: 180–184.
2 Fukuda, M., Yamanouchi, K., Nakano, Y., Furuya, H. and Arai, Y. (1984) Neurosci. Lett., **51**: 365–370.
3 Gerendai, I., Rotsytein, W., Marchetti, B. and Scapagnini, U. (1979) In "Neuroendocrinology: Biological and Clinical Aspest. Proceedings of Sereno Symposia, vol. 19". Ed. by A. Polleri and R. Macleod, Academic Press, New York, pp. 97–102.
4 Gerendai, I. (1984) In "Cerebral Dominance—The Biological Foundations". Ed. by N. Geschwind and A. M. Galaburda, Harvard Univ. Press, Cambridge, pp. 167–178.
5 Bakalkin, G. Y., Tsibezov, V. V., Sjutkin, E. A., Veselova, S. P., Novilov, I. D. and Krivosheev, O. G. (1984) Brain Res., **296**: 361–364.

ZOOLOGICAL SCIENCE 4: 201–204 (1987)

[COMMUNICATION]

Prolactin Cells of *Clarias batrachus* in Response to Corpuscles of Stannius Extract Administration

SHYAM P. SRIVASTAV, KRISHNA SWARUP[1] and AJAI K. SRIVASTAV

Department of Zoology, University of Gorakhpur, Gorakhpur 273 009, India

ABSTRACT—Corpuscles of Stannius extract administration increased the activity of prolactin cells.

INTRODUCTION

Removal of corpuscles of Stannius (CS) causes a rise in serum calcium level [1–4] which is corrected by administration of CS extract [5–8]. This suggests that CS secrete hypocalcemic principle (s). So far, two hypocalcemic principles–'hypocalcin' [9] and 'teleocalcin' [10] have been reported from the CS. Recently, a PTH-like substance (parathyrin) has been localized immunocytochemically in the eel CS [11]. Extracts of CS have been found to be effective in inducing hypocalcemia in mammal [12], bird [13], amphibians [14] and intact fishes [2, 6, 9, 15, 16].

Induced hypocalcemia is met with an increased activity of parathyroid gland in tetrapods [17–19]. But in fishes, parathyroid gland is absent and in this group prolactin has specific hypercalcemic capacities [20–23]. There exists no earlier report regarding the response of administration of CS extract on prolactin cells in fish. In the present study, therefore, we have attempted to study such a response in a freshwater catfish, *Clarias batrachus*.

MATERIALS AND METHODS

Sixty adult male specimens of *Clarias batrachus* (23–27 cm/80–120 g) were collected locally during the first week of September and acclimatized to the laboratory conditions (temp. 23–25°C) for two weeks prior to use. They were then divided into two numerically equal groups–A and B.

Group A: Control fish received intraperitoneally 1 ml/100 g body weight of saline (0.6% NaCl solution; physiological saline) and were kept in tap water.

Group B: Experimental fish received intraperitoneally CS extract in a dosage of 5 mg/ml/100 g body weight and were maintained in tap water.

The CS used in this study were surgically removed from both sexes of adult *Clarias batrachus* (September–October is post-spawning period; in females during September the ovary displays large number of immature oocytes and unovulated mature oocytes in the process of resorption whereas in males the lobules show compactness, the interlobular septa become thick with numerous blood cells and the germ cells which are inactive during the period of functional maturity begin to divide). The glands were stored in ice and used almost immediately. Prior to use, the glands were weighed (weight of CS of average fish, 0.6 mg) and homogenized in ice-cold saline (0.6% NaCl solution). The homogenate was centrifuged for 10 min at 5,000 rpm and the supernatant was collected. Final volume of the supernatant was made up so that every 1 ml solution contained extract from 5 mg of CS.

Six specimens from each group were anaesthetized with MS 222 at 1/2, 1, 2, 4 and 6 hr following the injection and the blood samples were collected

Accepted September 22, 1986
Received May 19, 1986

[1] To whom correspondence should be sent.

by the sectioning of caudal peduncle. An initial sampling of blood (from 6 fish kept separately under similar conditions) was also taken before the start of the experiment (Zero hour). After clotting of the blood the sera were separated by centrifugation at 3,500 rpm and analysed for serum calcium level according to Trinder's [24] method. Pituitaries were fixed in aqueous Bouin's fluid and Bouin-Hollande fixative. After routine processing in graded series of alcohol and clearing in xylene, tissues were embedded in paraffin wax. Serial sections were cut at 4–6 μm and stained according to Herlant tetrachrome and Heidenhain's azan techniques.

The nuclear diameter was measured with the aid of ocular micrometer. Each nucleus was measured along its long and short axes and mean value was calculated. From each group 300 nuclei were measured at every interval (Fifty nuclei were measured from each fish). The data are presented as mean ± standard deviation of the mean. Differences in the serum calcium level and nuclear diameter among different groups were analysed by Student's t-test.

RESULTS

The serum calcium level, before the start of the experiment (Zero hour), was recorded as 9.77 ± 0.42 mg/100 ml.

In *C. batrachus,* CS extract administration evoked hypocalcemia after 1/2 hr which continued up to 1 hr. Thereafter, the serum calcium level increased progressively reaching the normal value after 4 and 6 hr of the initiation of the experiment (Fig. 1).

The prolactin cells of fish from group A (saline injected) showed no change in response to the treatment. The prolactin cells possessed indistinct boundaries, the nuclei, however, were distinct. The cytoplasm was noticed granular and azocarminophilic and erythrosinophilic in nature (Fig. 2).

The first perceivable change in the prolactin cells of specimens of group B (CS extract-treated) was observed at 2 hr as the gland exhibited degranulation and increase in nuclear size (Fig. 1). These changes were pronounced and the nuclei became hyperchromatic after 4 hr of the treatment (Fig. 3).

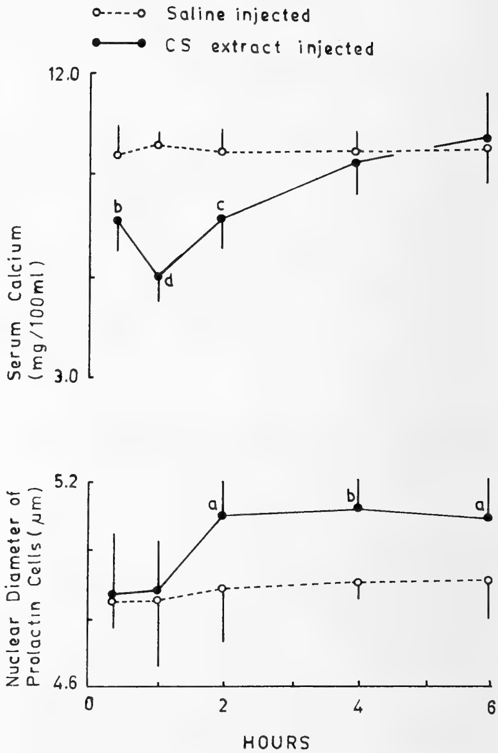

Fig. 1. Serum calcium level and nuclear diameter of prolactin cells after CS extract administration. a, b, c and d indicate significant differences compared with matching controls, $P<0.05$, $P<0.02$, $P<0.01$ and $P<0.001$, respectively.

Six hours after the initiation of the experiment, the prolactin cells showed recuperation and the nuclei had a tendency towards reduction in their size (Figs. 1 and 4).

DISCUSSION

In tetrapods, where parathyroids are the hypercalcemic glands, there is an increase in nuclear size to meet the induced hypocalcemia [17–19]. In *C. batrachus,* CS extract induced hypocalcemia renders prolactin cells to undergo similar changes (degranulation, increase in nuclear size and chromaticity i. e. increased synthesis and release of the hypercalcemic factor) at hour 2 which is maximum at hour 4. This is evidently to meet the hypocalcemic challenge and to restore the serum calcium

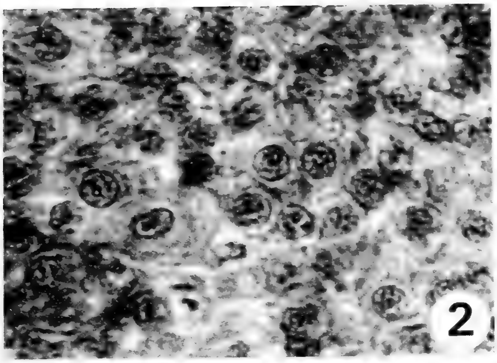

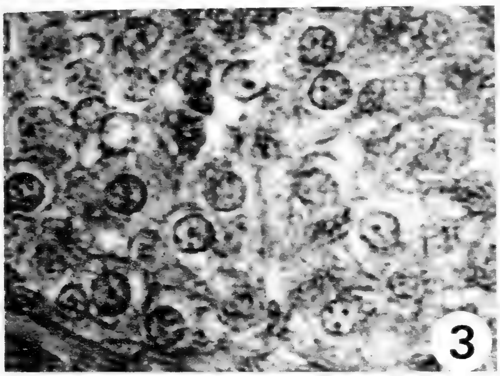

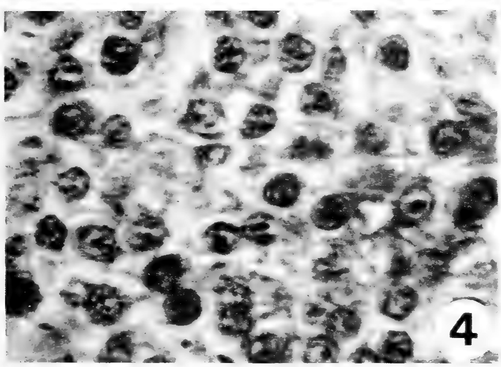

FIG. 2. Prolactin cells of saline-injected *C. batrachus* showing granular cytoplasm and well marked nuclei. Herlant tetrachrome. ×900.

FIG. 3. Prolactin cells of *C. batrachus* showing hyperchromatic nuclei and degranulation after 4 hr of CS extract administration. Herlant tetrachrome. × 900.

FIG. 4. Prolactin cells of *C. batrachus* showing recuperation of secretory granules after 6 hr of CS extract administration. Herlant tetrachrome. ×900.

level. Obviously, when the serum calcium level reaches normocalcemia at hour 6, the activity of these cells retards. These observations lend support to the suggestion of Pang *et al.* [7]"···the hypocalcemia caused by treatment with Stannius corpuscle homogenate might elicit the release of prolactin".

The present data suggest that calcium has a role in the regulation of prolactin secretion. Several reports agree with the present results showing that calcium levels in the blood and/or the environment are the main factors regulating the activity of prolactin cells [25–27]. Contrary to it, Olivereau and Olivereau [28] have suggested that sodium, and not calcium, plays a major role in the regulation of prolactin secretion. The reduced role of calcium in the regulation of prolactin cells has also been advocated by Ball *et al.* [29] and Olivereau *et al.* [30]. It has also been shown that the amount of prolactin released *in vitro,* by the*Tilapia* pituitary is not affected by the calcium concentration [31] but it is controlled by the osmotic pressure of the incubation medium [32].

ACKNOWLEDGMENT

The authors are thankful to M/S Sandoz Ltd., Basel for generous gift of MS 222 and UGC, New Delhi for financial assistance.

REFERENCES

1 Fontaine, M. (1964) C. R.Acad. Sci., **259**: 875–878.
2 Pang, P. K. T. (1971) J. Exp. Zool., **178**: 1–8.
3 Pang, P. K. T., Pang, R. K. and Sawyer, W. H. (1973) Endocrinology, **93**: 705–710.
4 Fenwick, J. C. (1976) Gen. Comp. Endocrinol., **29**: 383–387.
5 Chan, D. K. O., Rankin, J. C. and Chester Jones, I. (1969) Gen. Comp. Endocrinol., Suppl., **2**: 342–353.
6 Lopez, E. (1970). Z. Zellforsch. Mikrosk. Anat., **109**: 566–672.
7 Pang, P. K. T., Pang, R. K. and Griffith, R. W. (1975) Gen. Comp. Endocrinol., **26**: 179–185.
8 Kenyon, C. J., Chester Jones, I. and Dixon, R. N. B. (1980) Gen. Comp. Endocrinol., **41**: 531–538.
9 Pang, P. K. T., Pang, R. K. and Sawyer, W. H. (1974) Endocrinology, **94**: 548–555.
10 Ma, S. W. Y. and Copp, D. H. (1978) In "Comparative Endocrinology". Ed. by P. J. . Gaillard and H. H. Boer, Elsevier/North Holland Biomedical Press, Amsterdam, pp. 283–286.
11 Lopez, E., Tisserand-Jochem, E. M., Eyquem, A., Milet, C., Hillyard, C., Lallier, F., Vidal, B. and

MacLntyre, I. (1984) Gen. Comp. Endocrinol., **53**: 28–36.

12 Leung, E. and Fenwick, J. C. (1978) Can. J. Zool., **56**: 2333–2335.

13 Srivastav, A. K. and Swarup, K. (1982) Experientia, **38**: 869–870.

14 Pandey, A. K., Krishna, L., Srivastav, A. K. and Swarup, K. (1982)Experientia, **38**: 1314–1315.

15 Swarup, K. and Srivastav, S. P. (1982) J. Adv. Zool., **3**: 62–66.

16 Ogawa, H. and Sokabe, H. (1982) Gen. Comp. Endocrinol., **47**: 36–41.

17 Swarup, K. and Srivastav, A. K. (1981) Cell. Molec. Biol., **27**: 287–290.

18 Swarup, K. and Srivastav, A. K. and Tewari, N. P. (1979) Gen. Comp. Endocrinol., **37**: 541–545.

19 Krishna, L. and Swarup, K. (1985) Herpetologica, **41**: 65–70.

20 Pang, P. K. T., Schreibman, M. P., Balbontin, F. and Pang, R. K. (1978) Gen. Comp. Endocrinol., **36**: 306–316.

21 Olivereau, M. and Olivereau, J. (1978) Cell Tissue Res., **186**: 81–96.

22 Wendelaar Bonga, S. E., Grevan, J. A. A. and Mein, C. (1978) Gen. .Comp. Endocrinol., **34**: 91.

23 Wendelaar Bonga, S. E. and Van der Meij, J. G. A. (1980) Gen. Comp. Endocrinol., **40**: 342.

24 Trinder, P. (1960) Analyst, **85**: 889–894.

25 Wendelaar Bonga, S. E. (1978) Gen. Comp. Endocrinol., **34**: 265–275.

26 Wendelaar Bonga, S. E. (1978) In “Comparative Endocrinology”. Ed. by P. J. Gaillard and H. H. Boer, Elsevier/North Holland, Amsterdam, pp. 259–262.

27 Wendelaar Bonga, S. E. and Van der Meij, J. C. A. (1980) Gen. Comp. Endocrinol., **40**: 391–401.

28 Olivereau, M. and Olivereau, J. (1983) Cell Tissue Res., **229**: 243–252.

29 Ball, J. N., Uchiyama, M. and Pang, P. K. T. (1982) Gen. Comp. Endocrinol., **46**: 480–485.

30 Olivereau, M., Olivereau, J. M., Aimar, C., Chambolle, P. and Dubourg, P. (1983) Gen. Comp. Endocrinol., **52**: 51–55.

31 Grau, E. G., Nishioka, R. S. and Bern, H. A. (1979) Am. Zool., **19**: 875.

32 Grau, E. G., Nishioka, R. S. and Bern, H. A. (1981) Gen. Comp. Endocrinol., **45**: 406–408.

INSTRUCTIONS TO AUTHORS

ZOOLOCIGAL SCIENCE publishes contributions, written in English, in the form of (1) Reviews, (2) Articles, and (3) Communications of material requiring prompt publication. A *Review* is usually invited by the Editors. Those who submit reviews should consult with the Editor-in-Chief or the Managing Editor in advance. *Articles* of less than 6 printed pages and *communications* less than 3 printed pages will be published free of charge. Charges will be made for extra pages (7,000 yen/page). A *Communication* cannot exceed 4 printed pages. No charge will be imposed for invited reviews upto 15 printed pages. No free reprints of Articles and Communications are available. To the author of an invited review 50 reprints are provided gratis. Submission of papers from nonmembers of the Society is welcome. However, page charges (7,000 yen/pate) will be made to nonmembers.

A. SUBMISSION OF MANUSCRIPT

The manuscript should be submitted in triplicate, one original and two copies, each including all illustrations. Rough copies of line drawings and graphs may accompany the manuscript copies, but the two copies of continuous-tone prints (photomicrographs, etc.) should be as informative as the original. The manuscript should be sent to:

Dr. Seiichiro Kawashima, Managing Editor, Zoological Science, Zoological Institute, Faculty of Science, Hiroshima University, 1–1–89 Higashisenda-machi, Naka-ku, Hiroshima 730, Japan.

B. CONDITIONS

All manuscripts are subjected to editorial review. A manuscript which has been published or of which a substantial portion has been published elsewhere will not be accepted. It is the author's responsibility to obtain permission to reproduce illustrations, tables, etc. from other publications. Accepted papers become the permanent property of ZOOLOGICAL SCIENCE and may not be reproduced by any means, in whole or in part, without the written consent of both the Zoological Society of Japan and the authors(s) of the article in question.

C. ORGANIZATION OF MANUSCRIPT

The desirable style of the organization of an original paper is as follows: (1) Title, Authors(s) and Affiliation (2) Abstract (3) Introduction (4) Materials and Methods (5) Results (6) Discussion (7) Acknowledgments (8) References (9) Tables (10) Illustrations and Legends (11) Footnotes. The author is not obliged to adhere rigidly to this organization. He or she may modify the style when such modification makes the presentation clearer and more effective. In a Communication, combination of some of these sections is recommended. There is no restriction on the style of review articles.

D. FORM OF MANUSCRIPT

Manuscripts should be typewritten and double spaced throughout on one side of white typewriting paper with 2.5 cm margins on all sides. Abstract not exceeding 250 words, tables, figure legends and footnotes should be typed on separate sheets. All manuscript sheets must be numbered successively. The use of footnotes to the text is not recommended.

1. Title page

The first page of manuscript should contain title, authors' names and addresses of university or institution, abbreviated form of title (40 characters or less, including spaces), and name and address for correspondence. Authors with different affiliations should be identified by the use of the same superscript on name and affiliation. If one or more of the authors has changed his or her address since the work was carried out, the present address(es) to be published should be indicated in a footnote. In addition, a sub-field of submitted papers to be used as heading of an issue may be indicated in the first page. Authors are encouraged to choose one of the following: physiology, cell biology, molecular biology, genetics, immunology, biochemistry,

developmental biology, reproductive biology, endocrinology, behavior biology, ecology, phylogeny, taxonomy, or others (specify). However, the Editors are responsible for the choice and arrangement of headings.

2. Introduction

This section should clearly describe the objectives of the study, and provide enough background information to make it clear why the study was undertaken. Lenghty reviews of past literature are discouraged.

3. Materials and Methods

This section should provide the reader with all the information that will make it possible to repeat the work. For modification of published methodology, only the modification needs to be described with reference to the source of the method.

4. Results

Results should be presented referring to tables and figures, without discussion.

5. Discussion

The Discussion should include a concise statement of the principal findings, a discussion of the validity of the observations, a discussion of the findings in the light of other published work dealing with the same subject, and a discussion of the significance of the work. Redundant repetition of material in Introduction and Results, and extensive discussion of the literature are discouraged.

6. Statistical analysis

Statistical analysis of the data using appropriate methods is mandatory and the method(s) used must be cited.

7. References

References should be cited in the text by an Arabic numeral in square parentheses and listed at the end of the paper in numerical order. For example:

1 Takewaki, K. (1931) Oestrus cycle of female rat in prabiotic union with male. J. Fac. Sci. Imp. Univ. Tokyo, Sec. IV, **2**: 353–356.

2 Shima, A., Ikenaga, M., Nikaido, O., Takabe, H. and Egami, N. (1981) Photoreactivation of ultraviolet light-induced damage in cultured fish cells as revealed by increased colony forming ability and decreased content of pyrimidine dimers. Photochem. Photobiol., **33**: 313–316.

3 Hubel, O. and Wiesel, T. N. (1968) The functional architecture of the striated cortex. In “Physiological and Biochemical Aspects of Nervous Integration”. Ed. by F. D. Carlson, Prentice-Hall, New Jersey, pp. 153–161.

4 Campbell, R. C. (1974) Statistics for Biologists, Cambridge University Press, London, 2nd ed., pp. 59–61.

Titles of cited papers may be omitted in Reviews and Communications. The source of reference should be given following the commonly accepted abbreviations for journal titles (e.g., refer to ‘International List of Periodical Title Abbreviations’). The use of “in preparation”, “submitted for publication” or “personal communication” is not allowed in the reference list. “Unpublished data” and “Personal communication” should appear parenthetically following the name(s) in the text. Text citations to references with three or more authors should be styled as, e.g, Everett *et al.* [7].

E. ABBREVIATIONS

Abbreviations of measurement units, quantity units, chemical names and other technical terms in the body of the paper should be used after they are defined clearly in the place they first appear in the text. However, abbreviations that would be recognized by scientists outside the author’s field may be used without definition, such as SD, SE, DNA, RNA, ATP, ADP, AMP, EDTA, UV, and CoA. The metric system should be used for all measurements, and metric abbreviations (Table)

Table. Abbreviations for units of measure which may be used without definition

Length:	km, m, cm, mm, μm, nm, pm, etc.
Area:	km^2, m^2, cm^2, mm^2, μm^2, nm^2, pm^2, etc.
Volume:	km^3, m^3, cm^3, mm^3, μm^3, nm^3, pm^3, kl, liter (always spellout), ml, μl, nl, etc.
Weight:	kg, g, mg, μg, ng, pg, etc.
Concentration:	M, mM, μM, nM, %, g/l, mg/l, μg/l, etc.
Time:	hr, min, sec, msec, μsec, etc.
Other units:	A, W, C, atm, cal, kcal, R, Ci, cpm, dB, v, Hz, lx, $\times g$, rpm, S, J, IU, etc.

should, in general, be expressed in lower case without periods.

F. PREPARATIONS OF TABLES

Tables should only include essential data needed to show important points in the text. Each table should be typed on a separate sheet of paper and must have an explanatory title and sufficient explanatory material. All tables should be referred to in the text, and their approximate position indicated in the margin of manuscript.

G. PREPARATION OF ILLUSTRATIONS

All figures should be appropriately lettered and labelled with letters and numbers that will be at least 1.5 mm high in the final reproduction. Note the conventions for abbreviations used in the journal so that usage in illustrations and text is consistent. All figures should be referred to in the text and numbered consecutively (Fig. 1, Fig. 2, etc.). The figures must be identified on the reverse side with the author's name, the figure number and the orientation of the figure (top and bottom). The preferred location of the figures shold be indicated in the margin of the manuscipt. Illustrations that are substandard will be returned, delaying publication. Illustrations in color may be published at the author's expense.

1. Line drawings and graphs

Original artwork of high quality, glossy prints mounted on appropriate mounting card (less than 25×38 cm) should be submitted for reproduction. Author(s) may indicate size preference by making on the back of figures, such as "Do not reduce", "Two-column width" (no wider than 14.5 cm), or "One-column width" (no wider than 7 cm). Lines must be dark and sharply drawn. Solid black, white, or bold designs should be used for histograms. Xerox or any other copying mean may be used for the two review copies.

2. Continuous-tone prints

Three sets of continuous-tone prints (photomicrographs, etc.) must be submitted. One set for reproduction should be mounted on appropriate mounting card, and the other two for reviewers may be unmounted prints. Xerox or similar copies of photomicrogaphs are not acceptable for review purposes. The continuous-tone prints should be submitted preferably at the exact magnification which is to be used in the published papers and trimmed to conform to the page size (in no case should it exceed 14.5×20 cm). Press-on numbers should be applied to the lower right corner of individual prints. Letters (a, b, c, etc.) should be used for multiple parts of a single figure. If important structures will be covered by use of the lower right corner, identification may be applied in the lower left corner.

Reproduction of color photographs will have to be approved by the Editors. The extra costs of color reproduction will be charged to the authors.

3. Figure legends

Each figure should be accompanied by a title and an explanatory legend. The legends for several figures may be typed on the same sheet of paper. Sufficient detail should be given in the legend to make it intelligible without reference to the text.

H. PROOF AND REPRINTS

A galley proof and reprint order will be sent to the submitting author. The first proofreading is the author's responsibility, and the proof should be returned within 72 hours from the date of receipt (by air mail from outside Japan). The minimum quantity for a reprint order is fifty. Manuscript, tables and illustrations will be discarded after the editorial use unless their return is requested when the manuscript is accepted for publication.

Development Growth & Differentiation

Published by the Japanese Society of Developmental Biologists

The journal is devoted to the publication of original papers dealing with any aspects of developmental phenomena in all kinds of organisms, including plants and micro-organisms. Papers in any of the following fields will be considered: developmental genetics, growth, morphogenesis, cellular kinetics, fertilization, cell division, dormancy, germination, metamorphosis, regeneration and pathogenesis, at the biochemical, biophysical and analytically morphological levels; reports on techniques applicable to the above fields. At times reviews on subjects selected by the editors will be published. Brief complete papers will be accepted, but not preliminary reports.

Members of the Society receive the Journal free of charge. Subscription by institutions is also welcome.

Forthcoming Papers in DGD, Vol. 29, No. 1.

1. **REVIEW:** Y. Nagahama: 17α, 20β-dihydroxy-4-pregnen-3-one: A teleost maturation-inducing hormone
2. A. Fujiwara, K. Asami and I. Yasumasu: Induction of fertilization membrane formation and cyanide-insensitive respiration in sea urchin eggs by the treatment with dimethylsulfoxide followed by an incubation in an ice bath
3. J. H. Quertier, E. Baltus and J. Brachet: Cytological effects of heat-shocks on *Xenopus* oocytes and eggs
4. D. I. de Pomerai and A. Carr: Heat shock may relieve a post-transcriptional block on δ crystallin synthesis in cultures of chick embryo neuroretinal cells
5. K. Ishida, M. Okuno, S. Morisawa, T. Mohri, H. Mohri, M. Waku and M. Morisawa: Initiation of sperm motility induced by cyclic AMP in hamster and boar
6. K. Mitsunaga, Y. Fujino and I. Yasumasu: Probable role of allylisothiocyanate-sensitive H^+, K^+-ATPase in spicule calcification in embryos of the sea urchin, *Hemicentrotus pulcherrimus*
7. H. Kamai and T. Ohtaki: Pattern regulation of the leg disc of the fleshfly, *Sarcophaga peregrina*
8. S. Yasugi, K. Hayashi, K. Takiguchi, T. Mizuno, M. Mochii, R. Kodama, K. Agata and G. Eguchi: Immunological relationships among embryonic and adult chicken pepsinogens: A study with monoclonal and polyclonal antibodies
9. A. Picard, J.-C. Labbe, G. Peaucellier, F. le Bouffant, C. le Peuch and M. Doree: Changes in the activity of the maturation-promoting factor are correlated with those of a major cyclic AMP and calcium-independent protein kinase during the first mitotic cell cycles in the early starfish embryo

Development, Growth and Differentiation (ISSN 0012–1592) is published bimonthly by The Japanese Society of Developmental Biologists, Department of Biology, School of Education, Waseda University, Tokyo 160, Japan. 1987: Volume 29. Annual subscription U. S. $ 110.00 including air speed delivery except Japan. Application to mail at second class postage rate is pending at Jamaica, NY 11431, U. S. A.

Outside Japan: Send subscription orders and notices of change of address to Academic Press, Inc., Journal Subscription Fulfillment Department, 6277 Sea Harbor Drive, Orlando, FL 32887, U. S. A. Send notices of change of address at least 6–8 weeks in advance. Please include both old and new addresses. U. S. A. POSTMASTER: Send changes of address to *Development, Growth and Differentiation,* Academic Press. Inc., Journal Subscription Fulfillment Department, 6277 Sea Harbor Drive, Orlando, FL 32887, U. S. A.

In Japan: Send nonmember subscription orders and notices of change of address to Business Center for Academic Societies Japan, 16–3, Hongo 6-chome, Bunkyo-ku, Tokyo 113, Japan. Send inquiries about membership to Business Center for Academic Societies Japan,4–16, Yayoi 2-chome, Bunkyo-ku, Tokyo 113, Japan.

Air freight and mailing in the U. S. A. by Publications Expediting, Inc., 200 Meacham Avenue, Elmont, NY 11003, U. S. A.

(*Contents continued from back cover*)

Behavior Biology

Taxonomy

ZOOLOGICAL SCIENCE

VOLUME 4 NUMBER 1 **FEBRUARY 1987**

CONTENTS

(*Contents continued on inside back cover*)

Issued on February 15 *Printed by Daigaku Printing Co., Ltd., Hiroshima, Japan*

ISSN 0289-0003

Vol. 4 No. 2
April 1987

ZOOLOGICAL SCIENCE

PHYSIOLOGY
CELL and MOLECULAR BIOLOGY
GENETICS
IMMUNOLOGY
BIOCHEMISTRY
DEVELOPMENTAL BIOLOGY
REPRODUCTIVE BIOLOGY
ENDOCRINOLOGY
BEHAVIOR BIOLOGY
ENVIRONMENTAL BIOLOGY
ECOLOGY and TAXONOMY

published by Zoological Society of Japan

distributed by Business Center for Academic Societies Japan
VNU Science Press BV, Utrecht, The Netherlands

ZOOLOGICAL SCIENCE

The official Journal of the Zoological Society of Japan

ZOOLOGICAL SCIENCE is devoted to publication of original articles, reviews and communications in the broad field of Zoology. The journal was founded in 1984 as a result of unification of Zoological Magazine (1888–1983) and Annotationes Zoologicae Japonenses (1897–1983), the former official journals of the Zoological Society of Japan. ZOOLOGICAL SCIENCE appears bimonthly. An annual volume consists of six numbers of more than 1000 pages including an issue containing abstracts of papers presented at the annual meeting of the Zoological Society of Japan.

MANUSCRIPTS OFFERED FOR CONSIDERATION AND CORRESPONDENCE CONCERNING EDITORIAL MATTERS should be sent to:

Dr. Seiichiro KAWASHIMA, Managing Editor, Zoological Science, Zoological Institute, Faculty of Science, Hiroshima University, 1–1–89 Higashisenda-machi, Naka-ku, Hiroshima 730, Japan, in accordance with the instructions to authors which appear in the first issue of each volume. Copies of INSTRUCTIONS TO AUTHORS will be sent upon request.

SUBSCRIPTIONS. ZOOLOGICAL SCIENCE is distributed free of charge to the members, both domestic and foreign, of the Zoological Society of Japan. To non-member subscribers within Japan, it is distributed by Business Center for Academic Societies Japan, 6–16–3 Hongo, Bunkyo-ku, Tokyo 113. Subscriptions outside Japan should be ordered from the sole agent, VNU Science Press BV, Europalaan 93, 3526 KP Utrecht, (postal address; P. O. Box 2093, 3500 GB Utrecht), The Netherlands. Subscription rates will be provided on request to these agents. New subscriptions and renewals begin with the first issue of the current volume.

[Publication of Zoological Science has been supported in part by a Grant-in-Aid for Scientific Publication from the Ministry of Education, Science and Culture, Japan.]

ZOOLOGICAL SCIENCE 4: 209–222 (1987)

REVIEW

Gonadotropin Action on Gametogenesis and Steroidogenesis in Teleost Gonads

YOSHITAKA NAGAHAMA

Laboratory of Reproductive Biology, National Institute for Basic Biology, Okazaki 444, Japan

INTRODUCTION

The primary role of pituitary gonadotropin in the physiological regulation of gonadal function is well established. In most cases, however, gonadotropin action on gonadal development is not direct, but through the biosynthesis of gonadal steroid hormones which in turn mediate various stages of gametogenesis including oocyte growth (vitellogenesis), oocyte maturation, spermatogenesis and spermiation. Surprisingly little is known about the endocrine details of gonadal steroidogenesis in lower vertebrates. Over the past several years, a series of studies in our laboratory using several species of teleosts as experimental animals has provided important new information about the endocrine control of oocyte maturation in females and spermiation in males, and the interactions of gonadotropin with ovarian and testicular cell types and the mechanisms of its action. This article briefly reviews the endocrine control of vitellogenesis, oocyte maturation and spermiation in teleosts, and describes our recent data, mainly based on the amago salmon, *Oncorhynchus rhodurus,* on the mechanism by which gonadotropin exerts its action on the production of two major naturally occurring steroid hormones in salmonid reproduction, estradiol-17β and 17α, 20β-dihydroxy-4-pregnen-3-one (17α, 20β-diOHprog) (Fig. 1).

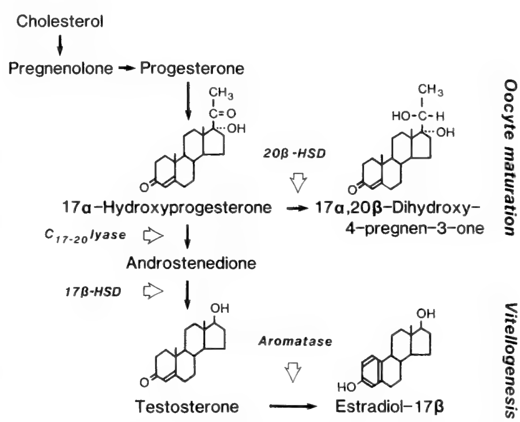

FIG. 1. Pathway of steroid biosynthesis in the ovary of salmonids. 17β-HSD, 17β-hydroxysteroid dehydrogenase; 20β-HSD, 20β-hydroxysteroid dehydrogenase.

GONADOTROPIN

It is well established that in teleosts, as in other vertebrates, pituitary gonadotropins are the major hormones which stimulate various ovarian activities. Although a number of biochemical studies have been conducted to purify piscine gonadotropins, the question of whether teleosts possess one or two types of gonadotropins in the pituitary gland is controversial at present. A glycoprotein-rich gonadotropin with a molecular weight of 25,000–40,000 (glycoprotein-rich "maturational" gonadotropin) has been purified in several teleosts [1, 2]. This type of gonadotropin has been reported to stimulate almost all gonadal activities including gametogenesis and steroidogenesis. We

Received December 23, 1986

purified a similar gonadotropin from the chum salmon, *Oncorhynchus keta*, pituitaries [3]. The molecular weight of this gonadotropin was estimated to be 38,000–40,000 by gel filtration, and that of the two distinct subunits, designated α and β, to be about 15,000 and 20,000 by SDS-polyacrylamide disc gel electrophoresis. The biological nature and peptide structure of this gonadotropin are very similar to those of other piscine glycoprotein gonadotropins.

There is now biochemical evidence that teleosts, similar to other higher vertebrates, probably possess two gonadotropins. Idler and his colleagues [2], who used affinity chromatography on Con A-Sepharose as one of the purification procedures, have isolated two gonadotropins, carbohydrate-rich "maturational" gonadotropin and carbohydrate-poor "vitellogenic" gonadotropin in several teleosts including chum salmon. This second gonadotropin has been reported to be responsible for the uptake of vitellogenin into the oocyte, although glycoprotein-rich gonadotropin itself has also been shown to mediate the uptake of the vitellogenin. More recently, two distinct carbohydrate gonadotropins have been identified, for the first time in any teleost, in chum salmon [4]. Physicochemical characterization of these two gonadotropins revealed that each consisted of two subunits. It is unknown, however, whether these two carbohydrate gonadotropins have different roles in the regulation of gonadal function in this species. Further data on the possibility of more than one gonadotropins in teleosts come from a number of morphological and histochemical studies which have shown that in some species at least, there are two distinct gonadotropin-secreting cells in the pituitary gland [5]. In this paper, the term gonadotropin is taken to refer to the glycoprotein-rich "maturational" gonadotropin.

HORMONAL REGULATION OF GAMETOGENESIS

A. Oocyte growth

After oogonia undergo proliferation by mitotic divisions, they become oocytes and enter a period of growth. During growth, the increase in oocyte size is very considerable. For example, in salmonids a young oocyte may be about 50 μm in diameter, and the fully developed egg is between 3.0 mm and 5.0 mm in diameter. Simultaneously with the growth the oocyte nucleus goes through the early stages of prophase but is arrested in diplotene stage of the first meiotic division.

The increase in oocyte size is due mainly to the accumulation of yolk proteins [6]. In teleosts, as in most other vertebrates, the site of synthesis of the precursor protein of yolk, vitellogenin, is the liver. A model of hormonal regulation of vitellogenesis in teleosts is provided in Figure 2. Estrogen, estradiol-17β in most cases, produced by the ovary under the influence of gonadotropin, is introduced

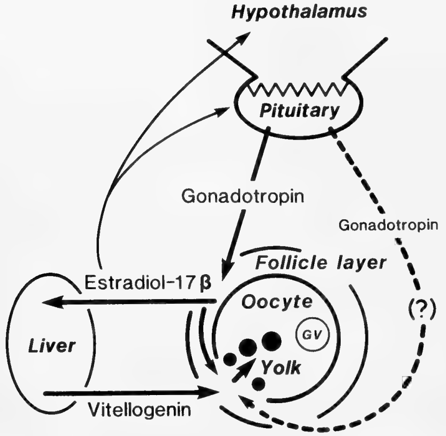

FIG. 2. Hormonal regulation of vitellogenesis in teleosts. (See the text for details).

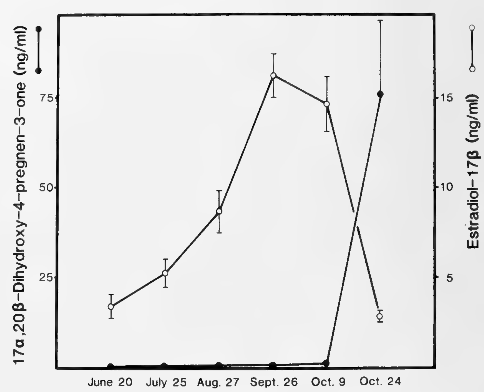

FIG. 3. Changes in plasma estradiol-17β and 17α, 20β-dihydroxy-4-pregnen-3-one levels during sexual maturation of amago salmon.

into the vascular system and stimulates the hepatic synthesis and secretion of vitellogenin. Vitellogenin is then selectively taken up from the bloodstream by developing oocytes. In all of the species studied so far, plasma concentrations of estradiol-17β have been reported to be high during the main vitellogenic growth period of the ovarian cycle [7, 8] (Fig. 3). It has been suggested that gonadotropin is involved in the process of incorporation of vitellogenin into the oocyte [9–11]. However, the endocrine details of this process are unknown and need to be investigated at the molecular level.

B. Oocyte maturation

Postvitellogenic oocytes are still physiologically immature in that they cannot be fertilized. For the oocytes to be fertilized they must undergo final oocyte maturation. This process is a prerequisite for successful fertilization and consists of the breakdown of the germinal vesicle (GVBD), chromosome condensation and extrusion of the first polar body (Fig. 4A, B, C). It is generally accepted that in lower vertebrates three major

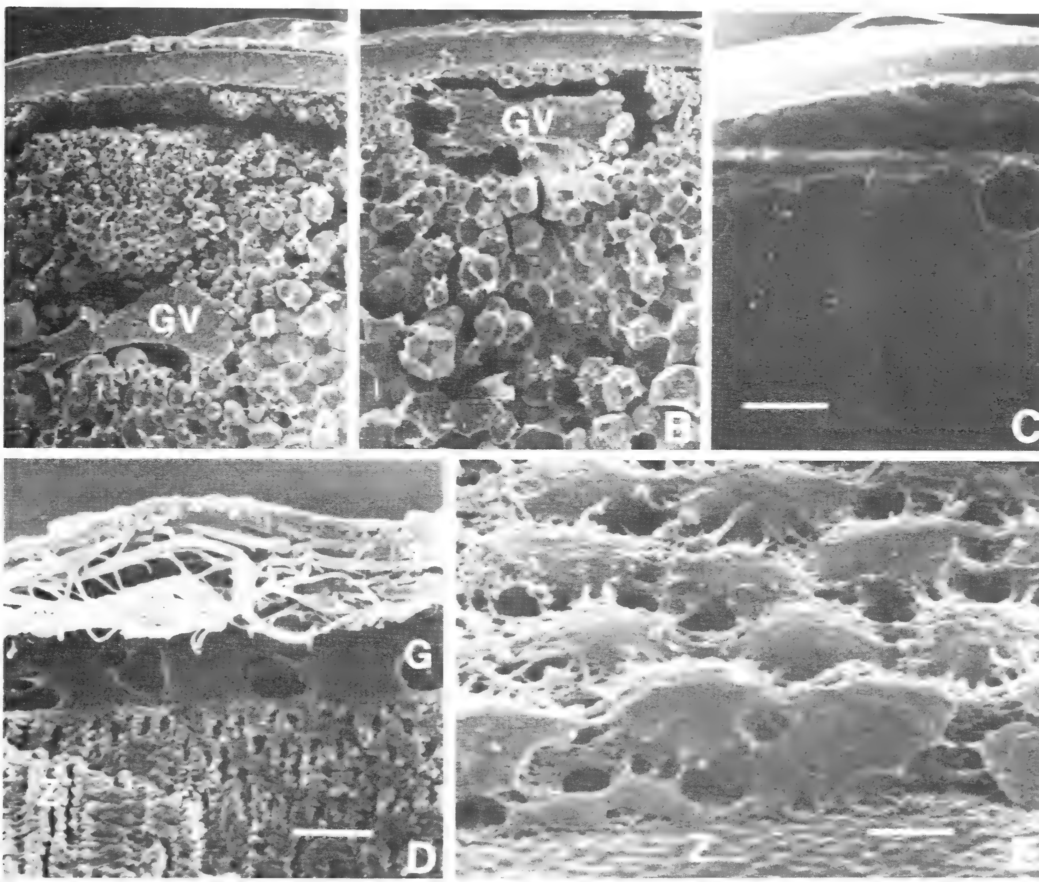

FIG. 4. Scanning electron micrographs of the fractured surface of rainbow trout oocytes during salmon gonadotropin-induced germinal vesicle breakdown *in vitro*. A, A fully grown immature oocyte with the germinal vesicle (GV) located halfway between the center and the oocyte periphery. F, ovarian follicle. B, An oocyte 24 hr after the onset of incubation with salmon gonadotropin. The germinal vesicle (GV) is located at the oocyte periphery. C, An oocyte 72 hr after the onset of incubation with salmon gonadotropin. Bar represents 100 μm. D, Scanning electron micrograph of the fractured surface of a rainbow trout ovarian follicle consisting of thecal layers (T), granulosa layers (G) and the zona radiata (Z). Bar represents 5 μm. E, Scanning electron micrograph of a granulosa layer preparation, consisting purely of granulosa cells. Z, zona radiata.

mediators, gonadotropin, maturation-inducing hormone and maturation-promoting factor, are involved in the induction of oocyte maturation [12–16]. These mediators function sequentially at the levels of the follicle layer, the oocyte surface and the oocyte cytoplasm (Fig. 5). The one exception to the intraovarian control of oocyte maturation in lower vertebrates appears to occur in the catfish, *Heteropneustes fossilis*. In this case, gonadotropin seems to stimulate the interrenal tissue to produce corticosteroids which in turn act on the oocytes to induce maturation [17].

It is now well established that in teleosts, the preovulatory surge of gonadotropin triggers a cascading series of biochemical events which lead to final oocyte maturation. An increase in gonadotropin levels during oocyte maturation and ovulation has been reported in several teleosts [2]. Follicle-enclosed full-grown postvitellogenic oocytes of some teleosts undergo GVBD *in vitro* when they are incubated with gonadotropin. However, denuded oocytes are incapable of responding to gonadotropin [16]. Cyanoketone, a specific inhibitor of 3β-hydroxy-Δ^5-steroid dehydrogenase, completely abolishes the maturational effects of gonadotropin and pregnenolone, but not of steroids such as progesterone or $17\alpha, 20\beta$-diOHprog [18]. Thus, the action of gonadotropin in inducing oocyte maturation appears to be

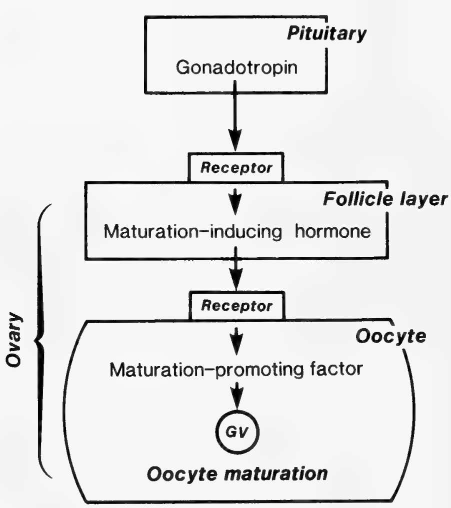

FIG. 5. Hormonal regulation of oocyte maturation in lower vertebrates. (See the text for details).

dependent on the synthesis of a secondary steroidal effector, maturation-inducing hormone.

In several teleosts, a variety of C21 steroids such as progesterone, 17α-hydroxyprogesterone, $17\alpha, 20\beta$-diOHprog, cortisol and deoxycorticosterone have been demonstrated to be effective in inducing meiotic maturation *in vitro* [16, 19–21]; among them, $17\alpha, 20\beta$-diOHprog has been reported to be the most effective steroid. C19 steroids, especially testosterone, have been shown to induce GVBD only at high concentrations. C18 steroids including estradiol-17β, are generally not effective in inducing oocyte maturation in teleost oocytes.

There have been no studies on the purification and characterization of the naturally occurring maturation-inducing hormone in any vertebrate. *In vitro* data described above strongly suggest that C21 steroids are responsible for the induction of oocyte maturation in teleosts. Recently, we purified and characterized the maturation-inducing hormone of amago salmon from media in which immature but fully grown folliculated oocytes of amago salmon had been incubated for 18–24 hr with partially purified chum salmon gonadotropin (SGA, Syndel Lab., Canada) [22].

Twenty separate fractions were obtained by the use of reversed-phase high performance liquid chromatography and their maturation-inducing activity was assessed by a homologous *in vitro* GVBD assay (Fig. 6A). Maturation-inducing activity was found only in one fraction which had a retention time coinciding exactly with $17\alpha, 20\beta$-diOHprog. The purity and final characterization of this active fraction were further confirmed by thin layer chromatography (Fig. 6B) and mass spectrometry with authentic $17\alpha, 20\beta$-diOHprog. Thus, the maturation-inducing hormone of amago salmon was identified as $17\alpha, 20\beta$-diOHprog (Fig. 1).

In collaboration with Dr. A. Kambegawa (Teikyo University), a specific radioimmunoassay for $17\alpha, 20\beta$-diOHprog was developed in our laboratory and has been applied to measure blood concentrations of this steroid during the sexual maturation of several species of salmonids [23–25]. In all of the species studied so far, $17\alpha, 20\beta$-diOHprog levels were low in vitellogenic females but were strikingly elevated in mature and

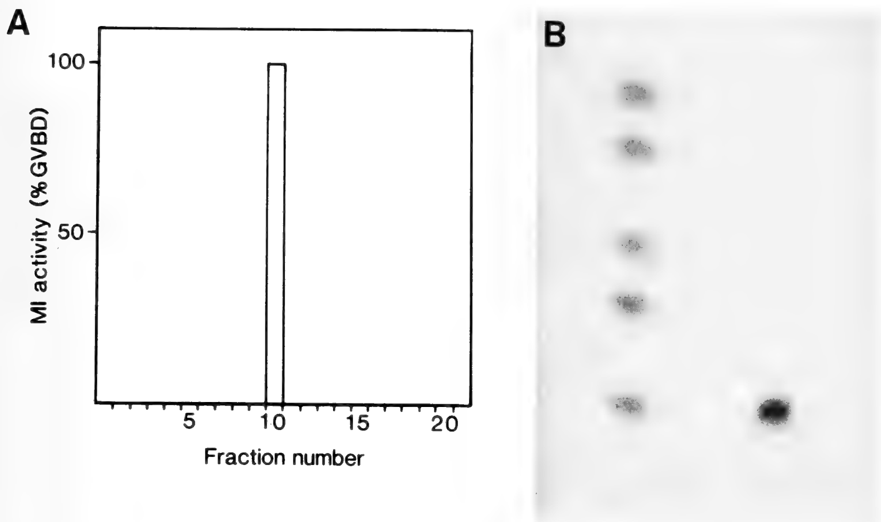

FIG. 6. Identification of maturation-inducing hormone of amago salmon. A, Maturation-inducing activity (MI) of various fractions of the 50% methanol phase of incubation media separated by high performance liquid chromatography. B, Thin layer chromatography of fraction 10 of the 50% methanol phase (right lane) and various steroid standards (left lane; from top to bottom, progesterone, androstenedione, 17α-hydroxyprogesterone, testosterone, 17α, 20β-dihydroxy-4-pregnen-3-one. The solvent system of benzene: acetone (4:1) was used). See [22] for details.

ovulated females (Fig. 3). The increase in plasma $17\alpha, 20\beta$-diOHprog levels correlated well with a dramatic rise in plasma gonadotropin levels [25]. In the masu salmon, *Oncorhynchus masou*, the peak of plasma $17\alpha, 20\beta$-diOHprog levels was observed 2–4 days prior to ovulation, coincident with the occurrence of GVBD in oocytes [24]. These data, together with those from other laboratories, indicate that $17\alpha, 20\beta$-diOHprog is the major naturally occurring maturation-inducing hormone common to several species of salmonids [26–32]. It is also possible that $17\alpha, 20\beta$-diOH-prog acts as an important steroidal mediator of oocyte maturation in several nonsalmonid teleosts [19, 20, 33–38].

C. Spermiation

In male salmonids, a marked increase in the relative amount of mature spermatozoa to total germ cells occurs during the later stages of spermatogenesis. Nonetheless, milt can not normally be collected from these fish. In addition, these spermatozoa do not seem to have the capacity to initiate motility. Spermiation generally occurs immediately before or during the spawning period when the majority of germ cells have completed spermatogenesis. Although the term spermiation is widely used by investigators in fish reproduction, the detailed morphological and physiological bases of this process are not known. In this review, spermiation is defined as the release of motile sperm from the genital pore by gentle pressure on the abdomen.

Spermiation has been considered to be under hormonal control. Injection of pituitary extracts or gonadotropins stimulates spermiation in several teleosts [39, 40]. It is generally assumed, however, that in teleosts exogenous gonadotropin does not act directly to induce spermiation but works in concert with testicular somatic elements to stimulate the production of steroidal mediator(s). In this connection, it was of great interest for us to measure plasma levels of maturation-inducing hormone, $17\alpha, 20\beta$-diOHprog. $17\alpha, 20\beta$-DiOH-prog levels were found to be low during the period of spermatogenesis and dramatically elevated at the time of spermiation in amago salmon [41]. The close association between high blood levels of 17α, 20β-diOHprog and spermiation has also been found in other salmonids [23, 28, 32, 42]. These

results suggest that $17\alpha, 20\beta$-diOHprog is involved in the process of spermiation in salmonids. This suggestion was strongly supported by our studies demonstrating that injections of $17\alpha, 20\beta$-diOHprog were effective in inducing *in vivo* spermiation in amago salmon about one month prior to the normal spawning period [43]. It was of further interest that gonadotropin action on spermiation was accompanied by a dramatic increase in blood levels of $17\alpha, 20\beta$-diOHprog [43]. Considered together, these results provide evidence to suggest that $17\alpha, 20\beta$-diOHprog is a testicular steroidal mediator of gonadotropin-induced spermiation in salmonids. Recently a similar suggestion has been made for goldfish [44].

MECHANISMS OF GONADAL STEROIDOGENESIS

The preceding findings led to the conclusion that in salmonids at least, two biologically important ovarian steroid hormones are estradiol-17β and $17\alpha, 20\beta$-diOHprog (Fig. 1). These findings permitted a study of the role of the follicle layer in the production of these two steroids. The ovarian follicle layer of teleosts, as in that of other vertebrates, consists of two major layers: the thecal layer, containing fibroblasts, capillaries, collagen fibers and large cells designated as special thecal cells, and the granulosa layer, composed of a single population of granulosa cells [45] (Fig. 4D). One of the major features of salmonid ovaries is that the follicles they contain are large, about 3–5 mm in diameter, and develop synchronously, an enormous advantage for biochemical studies, since a large number of follicles at the same stage of development can be obtained easily. The large size of the follicles has also facilitated the development of a simple dissection technique to separate the ovarian follicle of salmonids into two layers (thecal cell layer and granulosa cell layer) [46] (Fig. 4A), making it possible to elucidate the relative contributions of these layers and gonadotropin in the production of estradiol-17β and 17α, 20β-diOHprog in amago salmon and rainbow trout.

A. Ovarian estradiol-17β biosynthesis

1. *Two-cell type model*

In amago salmon, estradiol-17β levels in the plasma increase during vitellogenesis and rapidly decline prior to oocyte maturation. This seasonal pattern is reflected in the ability of the ovarian follicle to produce estradiol-17β in response to gonadotropin [8]. Using various follicular preparations obtained from vitellogenic amago salmon, we examined the effects of partially purified chinook salmon gonadotropin (SG–G100) or chum salmon gonadotropin (SGA) on estradiol-17β production. Both gonadotropins stimulated estradiol-17β production by intact follicles and thecal and granulosa layer co-culture preparations, but not by the isolated thecal or granulosa layers. These results indicated that both layers are necessary for gonadotropin-stimulated estradiol-17β production. In contrast, gonadotropins greatly stimulated testosterone production by thecal layers but only slightly stimulated testosterone production by the other follicular preparations. Incubation of granulosa layers with exogenous testosterone resulted in elevated estradiol levels, whereas isolated thecal layers incubated with testosterone produced relatively small amounts of estradiol-17β which should be attributed to contamination of thecal layer preparations with granulosa cells [8].

We further investigated the role of the thecal layer and the granulosa layer in estradiol-17β production using cyanoketone [47]. Thecal layers incubated with SG–G100 secreted large amounts of testosterone but not estradiol-17β into incubation medium. After incubation of granulosa layers in this medium estradiol-17β levels increased. Cyanoketone inhibited SG–G100-induced testosterone production of thecal layers and also inhibited estradiol-17β production by granulosa layers when they are incubated in this medium. However, addition of cyanoketone only to the granulosa layer incubations did not inhibit estradiol-17β production. Furthermore, *in vitro* incubation experiments with various steroids showed that granulosa layers have a limited capacity to metabolize exogenous pregnenolone, progesterone and 17α-hydroxyprogesterone.

Considering all of these data, a two-cell type

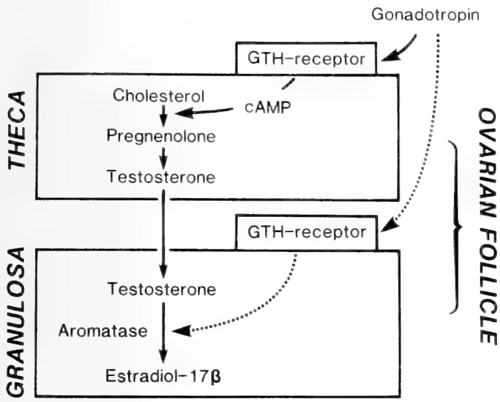

FIG. 7. Two-cell type model for the production of estradiol-17β in the ovarian follicle of salmonids. (See the text for details).

model in the production of follicular estradiol-17β has been proposed in amago salmon [8, 45, 48] (Fig. 7). In this model, the thecal layer, under the influence of gonadotropin, secretes aromatizable androgen, mainly testosterone, which is converted to estradiol-17β by granulosa layers. In a recent study we have found that the thecal layer from amago salmon and the granulosa layer from the rainbow trout, *Salmo gairdneri,* could produce the same effect as has been reported using combinations of thecal and granulosa layers from the same species. The reciprocal use of amago salmon granulosa and rainbow trout thecal layers is also effective (Nagahama, unpublished) (Fig. 8). This finding implies that there may be little species specificity of each of these cell layers among salmonids. This two-cell type model is the first report in lower vertebrates and of evolutionary interest considering the situation in mammals and birds. Since first proposed by Falck [49], numerous studies of isolated ovarian cell types from several mammalian species have attempted to elucidate the relative contributions of the various cells and gonadotropins in the overall process of estrogen biosynthesis. A two-cell type model similar to that in teleosts has been demonstrated in mammals [50], but in this case two kinds of gonadotropins, follicle-stimulating hormone (FSH) and luteinizing hormone (LH), are required, each of which acts upon separate follicular cell types. The theca interna cells, under the influence of LH, produce androgens that are transfered to granulosa cells, where, in the presence of FSH, they are converted to estrogens. In some larger mammals such as monkeys, the thecal

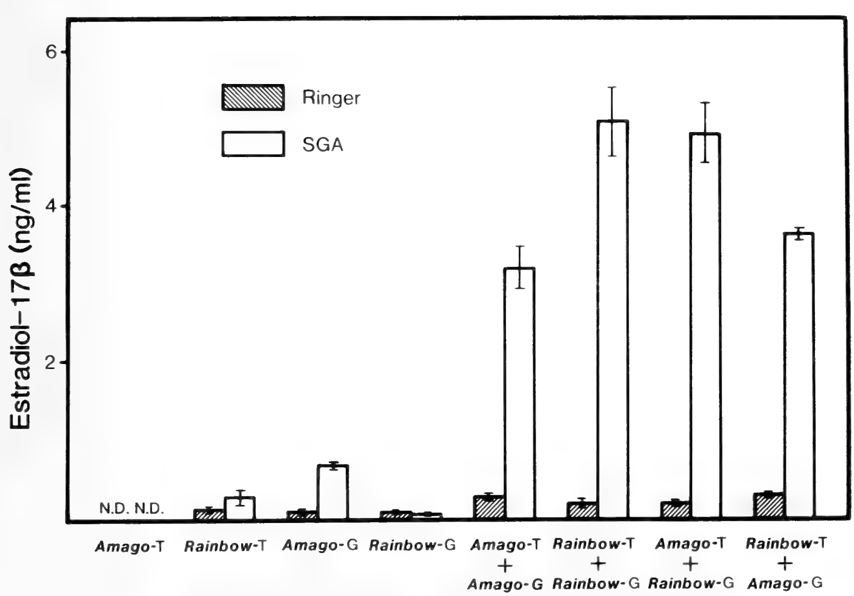

FIG. 8. The effect of various combinations of the thecal (T) and granulosa (G) layers from vitellogenic amago salmon and rainbow trout in response to 1 μg/ml chum salmon gonadotropin (SGA).

interna tissue is considered to be an additional source of estrogens. In the domestic hen, under gonadotropin stimulation progesterone is produced by the granulosa cells, most of this diffusing to the thecal cells where it is converted to estradiol-17β [51]. This is in sharp contrast to salmonids and mammals and thus be of evolutionary interest.

2. *Thecal layers*

Using biochemical methods, we have identified the aromatizable androgens produced by thecal layers in response to SG–G100. Thecal layers were incubated with SG–G100 and ether extracts of media from these incubates were fractionized (4.5 ml/fraction) by reversed-phase high performance liquid chromatography. Aromatase activity of each fraction was assessed by the capacity of isolated granulosa layers to produce estradiol-17β from exogenous testosterone. Among 27 fractions separated, one fraction produced large amounts of estradiol-17β when added to the granulosa layer incubation (Fig. 9A). This fraction had a retention time that coincided with authentic testosterone. Another fraction with a retention time coinciding with authentic androstenedione also produced estradiol-17β, but its production was much lower compared with the other fraction. The purity and final characterization of these fractions were confirmed by thin layer chromatography (Fig. 9B) and mass spectroscopy. Thus, we conclude that the major aromatizable androgen to be produced in the amago salmon thecal layer in response to gonadotropin is testosterone (Adachi and Nagahama, unpublished).

In vitro production of testosterone by the isolated thecal layer preparations obtained each month during vitellogenesis and oocyte maturation has revealed that the capacity of the thecal layer to produce testosterone in response to salmon gonadotropin gradually increased during the course of vitellogenic growth and peaked during the post-vitellogenic period; this capacity of thecal layers was maintained by the period of oocyte maturation

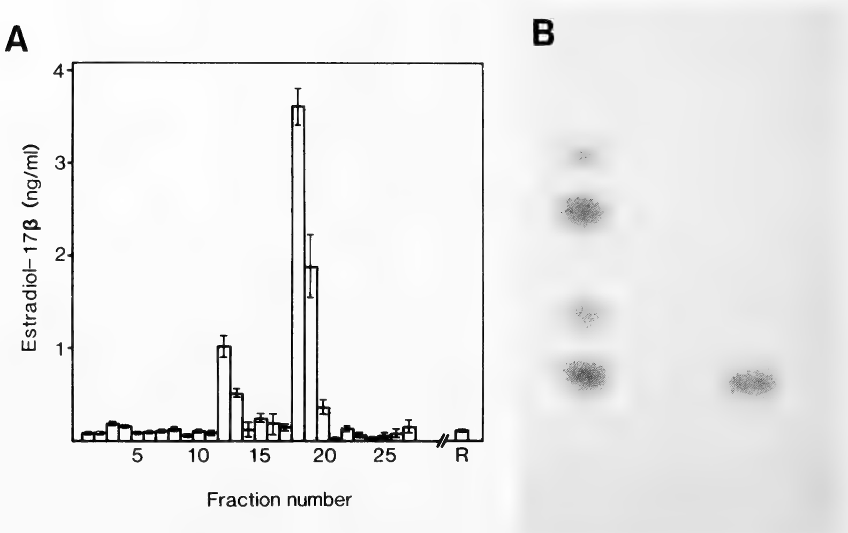

Fig. 9. Identification of aromatizable androgen produced by thecal layers of vitellogenic amago salmon. A, Aromatase activity of various fractions of the 50% methanol phase of incubation media separated by high performance liquid chromatography. Aromatase activity was assessed by the capacity of 10 isolated granulosa layers to produce estradiol-17β from 100 ng/ml exogenous testosterone. B, Thin layer chromatography of fractions 18 and 19 of the 50% methanol phase (right lane) and various steroid standards (left lane, from top to bottom, progesterone, androstenedione, 17α-hydroxyprogesterone and testosterone). The solvent system of benzene: acetone (4:1) was used. (See the text for details).

and ovulation. An identical seasonal pattern of stimulation of testosterone production was observed when thecal layers were incubated with forskolin and agents known to raise intracellular cyclic AMP (cAMP). These results are consistent with the general hypothesis that gonadotropin-induced testosterone production is mediated by the adenylate cyclase-cAMP effector system (Kanamori, unpublished). The site of gonadotropin action on the thecal layer remains unclear, but our recent *in vitro* data using steroid synthesis inhibitors suggest that its major site is on the pathway from cholesterol to pregnenolone.

3. Granulosa layers

The foregoing findings indicate the presence of aromatase enzymes in granulosa cells of amago salmon vitellogenic follicles. Aromatase activity increased during the period of vitellogenesis to reach a peak in late vitellogenesis, and then declined rapidly in association with the ability of the oocyte to mature in response to gonadotropin [52]. These findings, combined with our observations on the enhanced capacity of the thecal layer to produce testosterone in the postvitellogenic period, provide strong evidence that the decrease in the capacity of postvitellogenic follicles to produce estradiol-17β is due, in part, to the decrease in aromatase activity during the course of oocyte development. This is in contrast to the situation reported in the rat where the decreased secretion of estradiol-17β immediately after ovulation has been explained by a diminished supply of aromatizable androgens [53].

The mechanism of the induction or activation of the amago salmon granulosa cell aromatase system is unknown at this point. It is known that in certain mammals, one of the major roles of gonadotropin action on follicular estradiol-17β secretion is to stimulate aromatase activity; the most fundamental regulator is FSH [50]. However, very few studies have been conducted in non-mammalian species. As discussed above, isolated amago salmon granulosa cells have no capacity to produce testosterone and estradiol-17β from endogenous substrates in response to gonadotropin. Furthermore, there was no significant difference in estradiol-17β production by granulosa layers incubated with testosterone in the presence or absence of SG–G100 at any stage of follicle development [52]. In addition, pituitary homogenates from vitellogenic amago salmon were unable to induce aromatase activity (Kagawa, unpublished). Nevertheless, aromatase activity in granulosa cells increases during vitellogenesis to reach a peak in late vitellogenesis and thereafter rapidly declines in the postvitellogenic period.

In goldfish, human chorionic gonadotropin (HCG) slightly but significantly enhanced the conversion of exogenous testosterone to estradiol-17β by ovarian follicles at the primary yolk stage. Furthermore, forskolin, an adenylate cyclase activator, stimulated conversion of exogenous testosterone to estradiol-17β by vitellogenic follicles of goldfish even when cyanoketone was present in the medium [54]. Since cyanoketone completely blocked forskolin-induced endogenous production of estradiol-17β, the observed stimulated effects of forskolin can apparently be accounted for by an enhancement of endogenous aromatase activity in response to forskolin. Taken together, these results suggest that gonadotropin stimulates the induction of aromatase activation in goldfish vitellogenic follicles via an adenylate-cyclase-cAMP-dependent step. A similar situation seems to occur in the medaka, *Oryzias latipes* (Sakai and Nagahama, unpublished). In contrast, Sire and Depeche [55] reported that highly purified salmon glycoprotein maturational gonadotropin inhibited aromatase activity in pre- and early vitellogenic follicles of rainbow trout. Thus, the mechanisms by which aromatase activity in teleost ovarian follicles is regulated merit further investigation and are of evolutionary interest.

B. Ovarian $17\alpha, 20\beta$-diOHprog biosynthesis

1. Two-cell type model

The identification of the maturation-inducing hormone in salmonids as $17\alpha, 20\beta$-diOHprog permitted a study of the role of the follicle layer in the production of this hormone. $17\alpha, 20\beta$-DiOHprog production by intact follicles at different stages of development clearly showed that the capacity of the follicles to respond to gonadotropin by synthesizing and secreting this steroid is acquired immediately prior to the natural maturation period

[25]. Using isolation techniques similar to those used for the studies on follicular estradiol-17β production, three follicular preparations from postvitellogenic amago salmon and rainbow trout were incubated with or without chum salmon gonadotropin (SGA). 17α-Hydroxyprogesterone and 17α, 20β-diOHprog were measured by specific radioimmunoassay [48, 56].

In vitro production of 17α, 20β-diOHprog by co-culture preparations was remarkably enhanced by gonadotropin, but neither isolated thecal layers nor isolated granulosa layers were capable of producing substantial amounts of 17α, 20β-diOH-prog in response to gonadotropin. These *in vitro* data clearly indicate that the interaction of both thecal and granulosa layers is necessary for the production of 17α, 20β-diOHprog in response to gonadotropin. Measurement of 17α-hydroxyprogesterone concentrations of media from the same experiment revealed that isolated thecal layers produced large quantities of 17α-hydroxyprogesterone, but granulosa layers did not respond to gonadotropin. In contrast, levels of 17α-hydroxyprogesterone in media from co-culture incubations peaked at 12 hr and rapidly decreased concomitantly with a rapid rise in 17α, 20β-diOHprog levels. The presence of 20β-hydroxysteroid dehydrogenase (20β-HSD), the key enzyme involved in the conversion of 17α-hydroxyprogesterone to 17α, 20β-diOHprog (Fig. 1), has been demonstrated in the granulosa layers, since this layer produced 17α, 20β-diOHprog when incubated with exogenous 17α-hydroxyprogesterone. When all of these *in vitro* data are combined, a two-cell type model has been proposed for the first time in any vertebrate for the follicular production of maturation-inducing hormone, which is summarized in Figure 10. [48, 56]. In this model, the thecal layer produces 17α-hydroxyprogesterone that traverses the basal lamina and is converted to 17α, 20β-diOHprog by the granulosa layer where gonadotropin acts to enhance the activity of 20β-HSD. However, the extent to which thecal layers contribute to the production of 17α, 20β-diOHprog is still not clear, since in some cases thecal layer preparations produced this steroid in response to gonadotropin. Although our granulosa layer preparations are completely free of

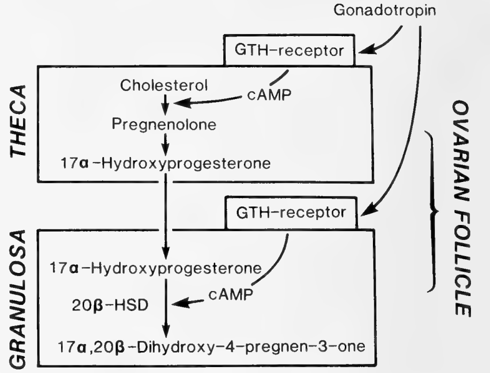

FIG. 10. Two-cell type model for the production of 17α, 20β-dihydroxy-4-pregnen-3-one in the ovarian follicle of salmonids. (See the text for details).

attached thecal layers, it is extremely difficult to obtain pure thecal layer preparations from postvitellogenic follicles.

2. *Thecal layers*

Studies of *in vitro* 17α-hydroxyprogesterone producton by thecal layers at different stages of development showed that the thecal layer only begins secreting 17α-hydroxyprogesterone immediately prior to the maturation of oocytes *in vitro*. Thus, in addition to 20β-HSD activation in the granulosa cells, the availability of 17α-hydroxyprogesterone may also play a major role in the enhancing action of gonadotropin on follicular biosynthesis of 17α, 20β-diOHprog (Kanamori, unpublished).

The first step of the stimulating effect of gonadotropin in the thecal layer appears to be receptor-mediated activation of adenylate cyclase and formation of cAMP, the major site of action probably occurring at the steroidogenic step between cholesterol and pregnenolone. Furthermore, gonadotropin-induced 17α-hydroxyprogesterone production by the thecal layer is abolished by cyclohexamide and puromycin, but not by actinomycin D and cordycepin, suggesting that stimulating effects of gonadotropin in the thecal layer require the synthesis of a new protein (Nagahama and Adachi, unpublished).

3. *Granulosa layers*

The granulosa cells of salmonids provide a

unique system in which to study gonadotropin regulation of a steroidogenic enzyme, in this case 20β-HSD, since precursor steroids cannot be produced by these cells; granulosa cells of amago salmon have little cholesterol side-chain cleavage activity. This allows the indirect quantification of 20β-HSD activity by the measurement of 17α, 20β-diOHprog production when these cells are incubated with exogenous 17α-hydroxyprogesterone [57, 58]. Granulosa cells obtained from full-grown follicles responded to gonadotropin by enhancing 20β-HSD activity when exogenous 17α-hydroxyprogesterone was added to the incubation medium. The action of gonadotropin on 20β-HSD enhancement was mimicked by forskolin, by dibutyryl cAMP (dbcAMP), but not dbcGMP, and by two phosphodiesterase inhibitors, theophylline and 3-isobutyl-1-methylxanthine [57]. Furthermore, gonadotropin and forskolin caused a rapid accumulation of cAMP with maximal levels at 30–60 min (Kanamori, unpublished). These findings are consistent with the view that cAMP is the second messenger of gonadotropin action.

In addition to cAMP, calcium appears to play an important role in the gonadotropin regulation of ovarian steroidogenesis in mammals. Recent evidence for the widespread role of calmodulin in the regulation of intracellular calcium led us to determine whether calmodulin was involved in the responses to gonadotropin and cAMP. For this purpose, three calmodulin inhibitors (trifluoroperazine, TFP, N-(6-aminohexyl)-1-naphthalenesulfonamide hydrochloride, W5 and N-(6-aminohexyl)-5-chloro-1-naphthalenesulfonamide, W7) were used, and the effects of these inhibitors on the gonadotropin-, cAMP- and forskolin-induced enhancement of 20β-HSD in the amago salmon granulosa cells have been investigated (Nagahama, unpublished). Both TFP and W7 strongly prevented SGA-, dbcAMP-, and forskolin-stimulated conversion of exogenous 17α-hydroxyprogesterone to 17α, 20β-diOHprog in a dose-dependent manner. W5 also inhibited 17α, 20β-diOHprog production, but was less effective than the other two inhibitors. These results suggest that calmodulin plays some role in the gonadotropin regulation of 20β-HSD activation in the amago salmon granulosa cell. The precise role and pathways through which calmodulin affects gonadotropin-induced 20β-HSD activation remain to be determined.

A very important question concerns the molecular mechanisms of granulosa cell 20β-HSD activation. We have examined the effects of cycloheximide, puromycin, actinomycin D and cordycepin on the production of 17α, 20β-diOHprog by chum salmon gonadotropin and dbcAMP in the amago salmon granulosa layer. When varying concentrations of one of the inhibitors were added to the incubation medium containing 17α-hydroxyprogesterone, stimulatory effects of SGA and dbcAMP on the production of 17α, 20β-diOHprog were significantly inhibited. Thus, effects of gonadotropin and dbcAMP upon both transcriptional and translational processes appear to be essential intermediate steps in the activation of 20β-HSD. Our time course studies further suggest that *de novo* synthesis of 20β-HSD *in vitro* in response to gonadotropin and dbcAMP occurs, and consists of gene transcriptional events within the first 6 hr of exposure to gonadotropin and dbcAMP and translational events 6–9 hr after exposure to gonadotropin and cAMP [58].

C. Testicular 17α, 20β-diOHprog biosynthesis

Incubation of testicular fragments from spermiating rainbow trout and amago salmon with gonadotropin (SGA) or 17α-hydroxyprogesterone resulted in a highly significant increase in 17α, 20β-diOHprog levels in the incubation medium [41]. These results indicate that the testis is the principal source of 17α, 20β-diOHprog biosynthesis. However, the testicular cell types responsible, as well as the intratesticular mechanisms involved in controlling testicular steroidogenesis in teleosts, remain unresolved. Therefore we investigated whether various testicular preparations of spermiating salmonids could produce two major testicular steroids, 11-ketotestosterone and 17α, 20β-diOHprog, in response to gonadotropin and 17α-hydroxyprogesterone [59]. Three different testicular preparations, intact testicular fragments, sperm-free testicular fragments, and isolated sperm from spermiating rainbow trout, were incubated in Ringer for 18 hr in the continuous presence or absence of SGA and 17α-hydroxypro-

gesterone. Both SGA and 17α-hydroxyprogesterone significantly stimulated 11-ketotestosterone by intact and sperm-free testicular fragments. Sperm preparations did not produce 11-ketotestosterone in any incubation condition. These results indicate that the site of 11-ketotestosterone production in the testis is its somatic cell elements. Whether 11-ketotestosterone production is limited only to Leydig cells or whether it also occurs in Sertoli cells is open to question, since our sperm-free testicular fragments included both Leydig cells and Sertoli cells.

Chum salmon gonadotropin also stimulated 17α, 20β-diOHprog production by intact testicular fragments, but not by sperm-free testicular fragments and sperm preparations (Fig. 11). 17α-Hydroxyprogesterone markedly stimulated 17α, 20β-diOHprog production by intact testicular fragments and sperm preparations, but not by sperm-free testicular preparations. A preliminary study with thin-layer chromatography has also shown that after incubation of sperm preparations with 17α-hydroxyprogesterone, 17α, 20β-diOHprog was identified as one of the major metabolites (Ueda and Nagahama, unpublished). Taken together, these results seem to indicate that the

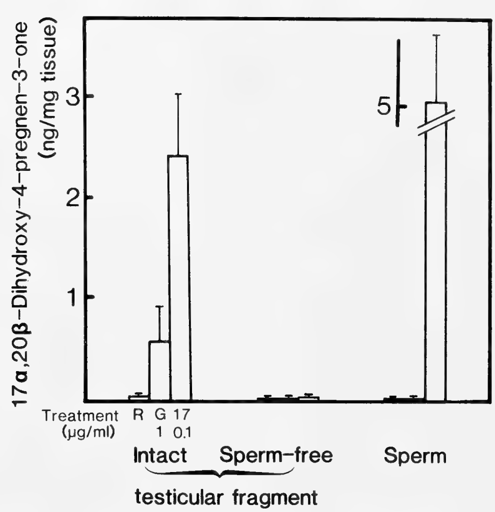

FIG. 11. *In vitro* production of 17α, 20β-dihydroxy-4-pregnen-3-one in response to chum salmon gonadotropin (SGA, G) and 17α-hydroxyprogesterone (17) by testicular fragments and isolated sperm. R, Ringer solution.

distribution of 20β-HSD in the amago salmon testis is limited only to sperm. It is a subject for further studies to define the cellular source of precursor steroids such as 17α-hydroxyprogesterone.

CONCLUSION

Inasmuch as 17α, 20β-diOHprog was identified as the major mediator of oocyte maturation, we now have two known biologically important mediators of oocyte growth and maturation in salmonids, estradiol-17β and 17α, 20β-diOHprog. It is now established a clear-cut synergism of ovarian thecal and granulosa layers for the production of these two steroid hormones. In both cases, the thecal layer is the site of precursor synthesis and the granulosa layer is the site of conversion of the precursors to the final products. Thus, normal growth and maturation of the oocyte depend upon a high degree of coordination of these layers. More complete understanding of the interactions of gonadotropin with ovarian somatic cells will provide new and important information about the endocrine activities of ovarian follicle cells in relation to oocyte growth and maturation. Our recent binding studies with [^{125}I]-chum salmon gonadotropin demonstrated specific binding to both thecal and granulosa layers from vitellogenic and postvitellogenic amago salmon follicles (Kanamori, unpublished). Certainly, studies on the temporal and functional nature of these bindings provide further insight into the mechanisms of interactions of gonadotropin with thecal and granulosa layers.

Endocrine details of vitellogenin uptake into the oocyte from the vascular system are not known. It is necessary to endeavor to investigate whether gonadotropin or other pituitary hormones have a mediator effect of this vitellogenin uptake by oocytes. As yet, we know very little about the mode of action of 17α, 20β-diOHprog to induce oocyte maturation. Since the site of 17α, 20β-diOHprog action is considered to be at or near the oocyte surface, further work must be performed to determine the identity and functional significance of the surface receptor of 17α, 20β-diOHprog.

17α, 20β-DiOHprog has also been shown to be

a major mediator of gonadotropin-induced spermiation in amago salmon and goldfish. A shift in the steroidogenic pattern from androgens to 17α, 20β-diOHprog seems to occur in the testis immediately prior to or during the spermiation period. Although the question of which cell type is the principal source of testicular production of $17\alpha, 20\beta$-diOHprog still remains unresolved, it is likely that the interaction of somatic cells and sperm is necessary. It is noteworthy that sperm contain 20β-HSD. These findings may be one of the best documented examples of the relationship between testicular steroidogenesis and male germ cell maturation in nonmammalian vertebrates, and will certainly provide the basis for a study at the molecular levels of hormonal regulation of male germ cell development.

ACKNOWLEDGMENTS

The studies from our laboratory described in this article have been aided in part by Grant-in-Aid for Special Project Research (Project Nos. 58119008 and 61134041) and scientific research from the Ministry of Education, Science and Culture, Japan.

REFERENCES

1 Burzawa-Gérard, E. (1982) Can. J. Fish. Aquat. Sci., **39**: 80–91.
2 Idler, D. R. and Ng, T. B. (1983) In "Fish Physiology". Ed. by W. S. Hoar, D. J. Randall and E. M. Donaldson, Academic Press, New York, Vol. IXA, pp. 187–221.
3 Ueda, H., Nagahama, Y. and Takahashi, H. (1984) Gunma Symp. Endocrinol., **21**: 21–35.
4 Kawauchi, H., Suzuki, K., Nagahama, Y., Adachi, S., Naito, N. and Nakai, Y. (1986) In "Pars Distalis of the Pituitary Gland—Structure, Function and Regulation". Ed. by F. Yoshimura and A. Gorbman, Elsevier Sci. Publ. B. V., pp. 383–390.
5 van Oordt, P. G. W. J. and Peute, J. (1983) In "Fish Physiology". Ed. by W. S. Hoar, D. J. Randall and E. M. Donaldson, Academic Press, New York, Vol. IXA, pp. 137–186.
6 Wallace, R. A. (1985) In "Developmental Biology". Ed. by L. W. Browder, Plenum Press, New York, Vol. 1, pp. 127–177.
7 Fostier, A., Jalabert, B., Billard, R., Breton, B. and Zohar, Y. (1983) In "Fish Physiology". Ed. by W. S. Hoar, D. J. Randall and E. M. Donaldson, Academic Press, New York, Vol. IXA, pp. 277–372.
8 Kagawa, H., Young, G. and Nagahama, Y. (1985) In "Salmonid Reproduction". Ed. by R. N. Iwamoto and S. Sower, Washington Sea Grant Program, University of Washington, Seattle, pp. 20–25.
9 Sundararaj, B. I., Nath, P. and Burzawa-Gérard, E. (1982) Gen. Comp. Endocrinol., **46**: 93–98.
10 Le Menn, F. and Burzawa-Gérard, E. (1985) Gen. Comp. Endocrinol., **57**: 23–36.
11 Ng, T. B. and Idler, D. R. (1983) In "Fish Physiology". Ed. by W. S. Hoar, D. J. Randall and E. M. Donaldson, Academic Press, New York, Vol. IXA, pp. 373–404.
12 Wasserman, M. J. and Smith, L. D. (1978) In "The Vertebrate Ovary". Ed. by R. E. Jones, Plenum Press, New York, pp. 443–468.
13 Masui, Y. and Clarke, H. J. (1979) Int. Rev. Cytol., **57**: 185–282.
14 Schuetz, A. W. (1979) J. Steroid Biochem., **11**: 695–699.
15 Kanatani, H. and Nagahama, Y. (1980) Biomed. Res., **1**: 273–291.
16 Goetz, F. W. (1983) In "Fish Physiology". Ed. by W. S. Hoar, D. J. Randall and E. M. Donaldson, Academic Press, New York, Vol. IXB, pp. 117–170.
17 Sundararaj, B. I., Goswami, S. V. and Lamba, V. (1979) J. Steroid Biochem., **11**: 701–707.
18 Young, G., Kagawa, H. and Nagahama, Y. (1982) J. Exp. Zool., **224**: 265–275.
19 Jalabert, B. (1976) J. Fish. Res. Board Can., **33**: 974–988.
20 Iwamatsu, T. (1980) J. Exp. Zool., **211**: 231–239.
21 Nagahama, Y., Hirose, K., Young, G., Adachi, S., Suzuki, K. and Tamaoki, B. (1983) Gen. Comp. Endocrinol., **51**: 96–105.
22 Nagahama, Y. and Adachi, S. (1985) Dev. Biol., **109**: 428–435.
23 Ueda, H., Hiroi, O., Hara, A., Yamauchi, K. and Nagahama, Y. (1984) Gen. Comp. Endocrinol., **53**: 203–211.
24 Yamauchi, K., Kagawa, H., Ban, M., Kasahara, N. and Nagahama, Y. (1984) Bull. Jpn. Soc. Sci. Fish., **50**: 2137.
25 Young, G., Crim, L. W., Kagawa, H., Kambegawa, A. and Nagahama, Y. (1983) Gen. Comp. Endocrinol., **51**: 96–105.
26 Idler, D. R., Fagerland, U. H. M. and Ronald, A. P. (1960) Biochem. Biophys. Res. Commun., **2**: 133–137.
27 Campbell, C. M., Fostier, A., Jalabert, B. and Truscott, B. (1980) J. Endocrinol., **85**: 371–378.
28 Fitzpatrick, M. S., Van Der Kraak, G. and Schreck, C. B. (1986) Gen. Comp. Endocrinol., **62**: 437–451.
29 Fostier, A., Breton, B., Jalabert, B. and Marcussi,

O. (1981) C. R. Acad. Paris, Ser. III, **293**: 817–820.
30 Hirose, K., Adachi, S. and Nagahama, Y. (1985) Bull. Jpn. Soc. Sci. Fish., **51**: 399–403.
31 Scott, A. P., Sheldrick, E. L. and Flint, A. P. E. (1982) Gen. Comp. Endocrinol., **46**: 444–451.
32 Truscott, B., Idler, D. R., So, Y. P. and Walsh, J. M. (1986) Gen. Comp. Endocrinol., **62**: 99–110.
33 Scott, A. P., MacKenzie, D. S. and Stacey, N. E. (1984) Gen. Comp. Endocrinol., **56**: 349–359.
34 Kagawa, H., Young, G. and Nagahama, Y. (1983) Bull. Jpn. Soc. Sci. Fish., **49**: 1783–1787.
35 Stacey, N. E., Peter, R. E., Cook, A. F., Truscott, B., Walsh, J. M. and Idler, D. R. (1983) Can. J. Zool., **61**: 2646–2652.
36 Kobayashi, M., Aida, K. and Hanyu, I. (1985) Bull. Jpn. Soc. Sci. Fish., **51**: 1085–1091.
37 Levavi-Zermonsky, B. and Yaron, Z. (1986) Gen. Comp. Endocrinol., **62**: 89–98.
38 Greeley, M. S., Jr., Calder, D. R., Taylor, M. H., Hols, H. and Wallace, R. A. (1986) Gen. Comp. Endocrinol., **62**: 281–289.
39 Clemens, H. P. and Grant, F. B. (1965) Copeia, **2**: 174–177.
40 Billard, R., Fostier, A., Weil, C. and Breton, B. (1982) Can. J. Fish. Aquat. Sci., **39**: 65–79.
41 Ueda, H., Young, G., Crim, L. W., Kambegawa, A. and Nagahama, Y. (1983) Gen. Comp. Endocrinol., **51**: 106–112.
42 Scott, A. P. and Baynes, S. M. (1982) In "Proceedings of the International Symposium on Reproductive Physiology of Fish". Ed. by C. T. T. Richter and H. J. Th. Goos, Pudoc. Wageningen, The Netherlands, pp. 103–106.
43 Ueda, H., Kambegawa, A. and Nagahama, Y. (1985) Gen. Comp. Endocrinol., **59**: 24–30.
44 Kobayashi, M., Aida, K. and Hanyu, I. (1986) Bull. Jpn. Soc. Sci. Fish., **52**: 755.
45 Nagahama, Y. (1983) In "Fish Physiology". Ed. by W. S. Hoar, D. J. Randall and E. M. Donaldson, Academic Press, New York, Vol. IXA, pp. 223–275.
46 Kagawa, H., Young, G., Adachi, S. and Nagahama, Y. (1982) Gen. Comp. Endocrinol., **47**: 440–448.
47 Young, G., Kagawa, H. and Nagahama, Y. (1982) Biomed. Res., **3**: 659–667.
48 Nagahama, Y. (1984) Gunma Symp. Endocrinol., **21**: 167–182.
49 Falck, B. (1959) Acta Physiol. Scand., **47**, Suppl. 163: 1–101.
50 Dorrington, J. H. and Armstrong, D. T. (1979) Recent Prog. Horm. Res., **35**: 301–342.
51 Huang, E. S., Rao, K. J. and Nalbandov, A. V. (1979) Biol. Reprod., **29**: 310–315.
52 Young, G., Kagawa, H. and Nagahama, Y. (1983) Biol. Reprod., **29**: 310–315.
53 Suzuki, K. and Tamaoki, B. (1980) Endocrinology, **107**: 2115–2116.
54 Tan, J. D., Adachi, S. and Nagahama, Y. (1986) Gen. Comp. Endocrinol., **63**: 110–116.
55 Sire, O. and Depeche, J. (1981) Reprod. Nutr. Dev., **21**: 715–726.
56 Young, G., Adachi, S. and Nagahama, Y. (1986) Dev. Biol., **118**: 1–8.
57 Nagahama, Y., Kagawa, H., Adachi, S. and Young, G. (1985) J. Exp. Zool., **236**: 371–375.
58 Nagahama, Y., Young, G. and Adachi, S. (1985) Dev. Growth Differ., **27**: 1213–1221.
59 Ueda, H., Kambegawa, A. and Nagahama, Y. (1984) J. Exp. Zool., **231**: 435–439.

ZOOLOGICAL SCIENCE 4: 223–232 (1987)

Effect of Host myo-Inositol Deficiency on *Hymenolepis diminuta* (Cestoda)

Muhammad M. Khan and Yuen K. Ip

Parasitology Laboratory, Department of Zoology, National University of Singapore, Kent Ridge, Singapore, 0511, Republic of Singapore

ABSTRACT—The absorption of myo-inositol and its incorporation into phosphatidylinositol by *Hymenolepis diminuta* in rats fed with normal pellets (Purina Laboratory Chow), were concentration and time dependent. Glucose uptake was similar in both groups of worms recovered from control and myo-inositol deficient rats. Deletion of myo-inositol from host diet caused no effect on the establishment of *H. diminuta* in its host. The worms obtained from rats fed with myo-inositol deficient diet were heavier in terms of wet weight than those from rats fed with control diet. No apparent difference in the length of the worms was noted. Compared to worms from rats fed with control diet, egg production was significantly higher ($P<0.01$) in those recovered from the rats fed with myo-inositol deficient diet. The patent period was reduced by one day in the worms parasitized in myo-inositol deficient rats. The infectivity of *H. diminuta* eggs was similar in both groups of worms.

INTRODUCTION

myo-Inositol appears to be an important carbohydrate for *Hymenolepis diminuta,* as the organism is synthesizing [1] and actively absorbing it [2]. It has been identified and shown to be unevenly distributed along the length of the worm [3]. Phosphatidylinositol is an essential constituent of biomembranes which is involved in transport phenomena. The cell membrane does not function satisfactorily if inositol lipids are not present in adequate concentration [4]. Formation of phosphatidylinositol from labelled ^{14}C-glucose, ^{14}C-palmitate and ^{32}P-orthophosphate has been established [1, 5]. However no published information is available for the formation of phosphatidylinositol from labelled ^{3}H-myo-inositol in *H. diminuta.* Thus one of the aims for the present investigation was to elucidate the pattern of absorption of myo-inositol and its incorporation into phosphatidylinositol in *H. diminuta.*

myo-Inositol is essential for the survival and growth of a number of microorganisms and mammalian cells in culture [6–9]. It has been reported that growth, development and reproduction of parasite may be markedly sensitive to the feeding activity, nutrient intake and digestive physiology of its host [10]. Several studies have been carried out to investigate the influence of host dietary carbohydrates, proteins and vitamins on the different aspects of growth and fecundity of *H. diminuta* [11–19]. However, no such information is available for myo-inositol. The present investigation was therefore undertaken to elucidate the effect of host diet, with or without myo-inositol, on the establishment, growth and reproduction of the parasite. In order to compare the physiological activities of the worms from control and myo-inositol deficient rats, glucose uptake studies were also performed.

Accepted October 3, 1986
Received August 16, 1986

MATERIALS AND METHODS

Male rats of the Sprague-Dawley strain weighing 100 to 130 g at the time of infection were used as definitive hosts in all experiments. Adult *Tenebrio* sp. served as intermediate host.

myo-Inositol uptake and its incorporation into phospholipids

Six rats were infected with 10 cysticercoids each.

Before and after infection, the rats were fed with water and food (Purina Laboratory Chow) *ad libitum*. Ten-day old worms were flushed from the excised gut with saline solution [20]. myo-Inositol uptake studies, with 10 worms in each incubation medium, were undertaken as described by Ip and Fisher [2]. Tritiated myo-inositol was used with specific activity adjusted to 2.5 μCi/μmol. Wet weight of the worms was recorded before the experimental incubation. Samples of parasites were homogenized and extracted according to Folch *et al.* [21]. The water washes from the Folch procedure as well as the water extract of the residue were combined. This fraction (water soluble fraction) contained free carbohydrates which were separated by paper chromatography. In order to study the incorporation of absorbed ^{3}H-myo-inositol into phospholipids, the washed total lipid fraction, obtained from the organic phase, was evaporated to dryness under nitrogen. Phospholipids were separated by thin layer chromatography.

Glucose uptake

Six rats were divided into two groups of three. Twenty cysticercoids were force-fed to each rat. Ten-day old worms for glucose uptake studies were prepared as described for the growth experiment. They were randomized, incubated and extracted according to Ip and Fisher [2]. Standard incubation conditions were two minutes. ^{14}C-Glucose (1 mM, 3 mM, 5 mM) was used with specific activity adjusted to 0.07 μCi/μmol. Uptake velocities were expressed in terms of μmol glucose absorbed/g ethanol extracted dry weight per 2 min.

Establishment, growth and reproduction of H. diminuta

Twenty or thirty cysticercoids, depending on the nature of the experiment, were force-fed to each rat host. The experimental rats were caged individually. Before and after infection, the rats were provided with water and food (Purina Laboratory Chow or Synthetic diets) *ad libitum*. Parasites were flushed from the excised guts with saline solution [20] at the end of the experimental period. Flushed parasites were washed in several changes of the same medium before any weight and length measurements were taken. All weighings were done to the nearest 0.1 mg. Worm lengths were determined after relaxing them in cold tap water for 45 min.

The synthetic diet was prepared according to Read *et al.* [22]. However, myo-inositol was deleted from it to prepare myo-inositol deficient diet. Water was added to the requisite amount of the dry material to make a thick paste. Freshly prepared diet was fed to the rats daily in clean and dry bowls *ad libitum*.

In order to study the effect on establishment of the parasite in the host, each of the two groups of three rats was fed with either the control or myo-inositol deficient diet. After two days, 30 cysticercoids were fed to each rat of both groups. The synthetic diets were continued for another five days followed by five days of normal pellets (Purina Laboratory Chow) to eliminate any possible effect of the diets on the growth of the parasite. The rats of both groups were then sacrificed. The worms, flushed from the excised gut with saline solution, were counted to determine the degree of infection.

To examine the effect of deleting myo-inositol from the diet on the growth of *H. diminuta* rats infected with 30 cysticercoids were fed with Purina Laboratory Chow during the first five days of infection to eliminate any possible diet effect on the establishment of the worms. After five days one group was fed myo-inositol deficient diet, whereas the other group received the control diet for another five days. Wet weight and length of these ten-day old worms were then determined.

To examine the effect of deleting myo-inositol from the host diet on reproduction of *H. diminuta*, six rats were infected with 20 cysticercoids each. These rats were maintained on their respective diets as for the growth experiment. To investigate the patent period, three faecal samples from each host of both groups were regularly examined every day beginning 13 days post infection. Egg counts were made for every 24 hr as described by Holmes [23]. At the end of the experiment (25 days postinfection) the worms were flushed from the excised gut with saline solution. Worms collected from each host were counted to establish rela-

tionship with egg production.

Infectivity of H. diminuta eggs

In order to determine the infectivity of the eggs obtained from the worms recovered from the control and myo-inositol deficient rats, beetles were starved for 24 hr at room temperature. Infection experiments were carried out in six small containers measuring 9 cm in diameter and 6 cm in height. Ten beetles were introduced into each container. To three containers, eggs from the worms recovered from control rats were administered, whereas the other three received eggs from the worms recovered from myo-inositol deficient rats. The eggs were offered according to the method of Voge [24]. The infectivity of *H. diminuta* eggs in the host was examined by beetle dissection after a period of two weeks as described by Voge [24].

Chromatographic Analyses

Water soluble fraction was reduced to dryness on a rotary evaporator *in vacuo* and the residue dissolved in a small volume of deionized water before passing through tandem columns of Dowex 50(H^+) and Dowex 2(OH^-). The resultant sample was dried and redissolved in small volume of deionized water. This sample was examined by paper chromatography on Whatman 3 MM paper as described by Gray and Frankel [25]. Carbohydrates were visualized with silver nitrate method of Trevelyan *et al.* [26].

Neutral lipids were separated from phospholipids by ice cold acetone. Phospholipids were separated into classes on Silica Gel G plates using two dimensional system of Rouser *et al.* [27]: chloroform/methanol/25% ammonia (65:35:5 v/v) followed by chloroform/acetone/methanol/acetic acid/water (10:4:2:2:1 v/v) in the second dimension. In the present work Silica Gel slurry was prepared by mixing 50 g of Silica Gel G (Merck) in 100 ml of deionized water. This slurry was applied to the glass plates (20×20 cm) at a thickness of 0.25 mm. Lipid spots were detected by exposing the developed plates to iodine vapours. The spots were identified by comparing with phospholipid standards obtained from Sigma Chemical Co.

Determination of radioactivity

All samples were counted for 10 min in an BETAmatic BASIC Liquid Scintillation Counter (KONTRON Analytical). Aliquots of water soluble fraction, containing ^{3}H-myo-inositol, were dried and mixed with Biofluor (NEN) for counting. Radioactive paper chromatograms were cut into 1 cm strips parallel to the origin. Each strip was then counted in a scintillation vial containing 10 ml of Liquifluor (NEN). Identified phospholipids were scraped from the plates into scintillation vials containing 1 ml of water and 10 ml of Biofluor. Radioactivity was determined as stated above.

Statistical analysis

Data presented graphically were plotted as least square regression lines wherever applicable. The data were analyzed statistically by Student's t-test for significant differences.

RESULTS

myo-Inositol uptake and its incorporation into phospholipids

These studies were carried out by incubating 10-day old worms with ^{3}H-myo-inositol at different concentrations and over different incubation periods to investigate the absorption and incorporation of myo-inositol into water soluble and lipid fractions. The observations were the result of single set of experiment. It is apparent from Figure 1 that the absorption of myo-inositol in water soluble fraction and the free myo-inositol, isolated from water soluble fraction by paper chromatography, was linear and constant with respect to time up to 4 hr of incubation. Its uptake also occurred in a concentration dependent manner (Table 1).

The incorporation of absorbed ^{3}H-myo-inositol into total phospholipid and phosphatidylinositol fractions was linear and constant as a function of time (Fig. 2). An early labelling of phosphatidylinositol was also observed. The incorporation of absorbed myo-inositol into total phospholipid and phosphatidylinositol fractions was non-linear with

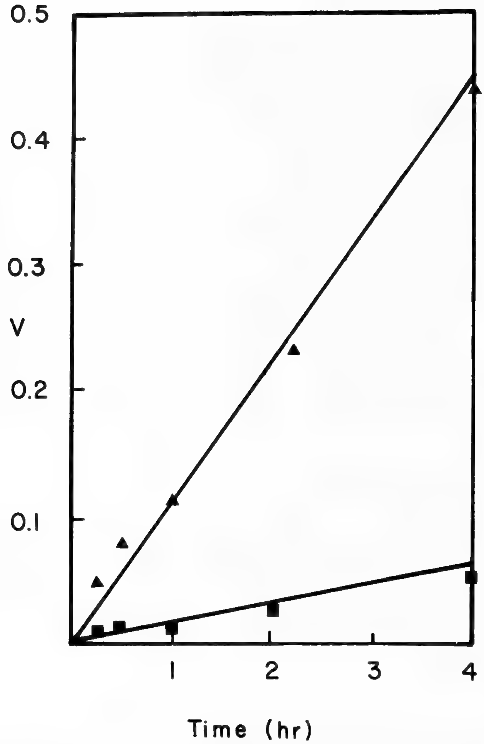

FIG. 1. Absorption of 0.1 mM ^{3}H-myo-inositol by *H. diminuta* as a function of time (hr). V= μmol/g wet weight. ▲=radioactivity in water soluble fractions; ■=radioactive myo-inositol isolated by paper chromatography from water soluble fractions.

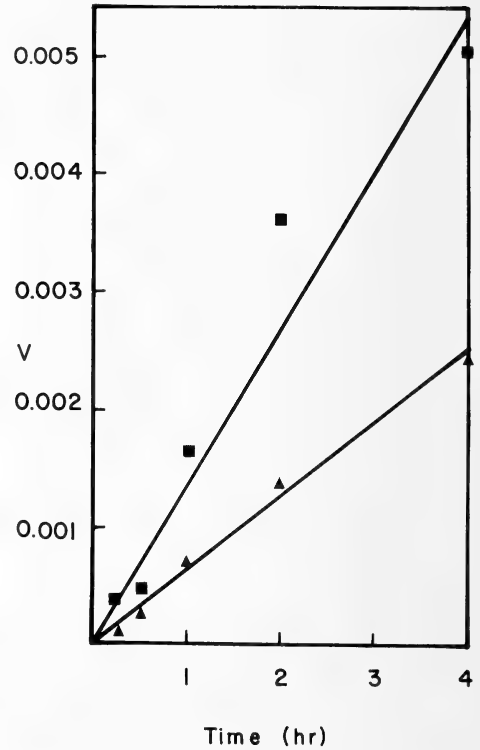

FIG. 2. Incorporation of 0.1 mM ^{3}H-myo-inositol into the total phospholipid and phosphatidylinositol fractions by *H. diminuta* as a function of time (hr). V= μmol/g wet weight. ■=total phospholipid; ▲=phosphatidylinositol.

TABLE 1. Rates of myo-inositol uptake; total phospholipid and phosphatidylinositol syntheses as a function of myo-inositol concentrations

Myo-inositol concentration (mM)	Total myo-inositol uptake μmol/g wet wt per 4 hr	Phosphatidylinositol synthesis % total myo-inositol uptake	Phosphatidylinositol synthesis % myo-inositol incorporated into the phospholipid fraction	Total phospholipid % total myo-inositol uptake
0.05	0.081	2.130	97.45	2.187
0.10	0.257	1.210	91.60	1.323
0.50	0.806	0.570	66.20	0.868
1.00	0.996	0.328	55.10	0.596
2.00	1.474	0.372	71.80	0.517

respect to myo-inositol concentration (Fig. 3). Lineweaver Burk transformation of the data (Fig. 4) revealed V_{max} values for total phospholipid and phosphatidylinositol fractions as 0.0086 and 0.005 μmol/g wet weight per 4 hr respectively. The respective K_m values were 0.186 and 0.086 mM.

It was expected that all radioactivity would be recovered in the phosphatidylinositol fraction.

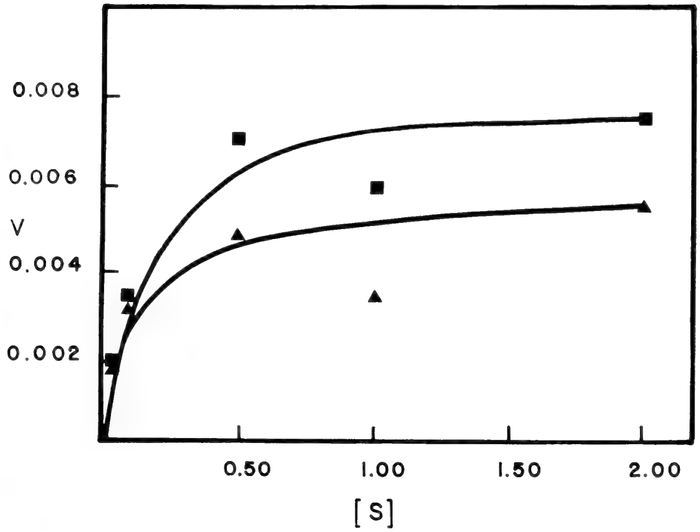

FIG. 3. Incorporation of ^{3}H-myo-inositol into the total phospholipid and phosphatidylinositol fractions by *H. diminuta* as a function of myo-inositol concentrations. V = μmol/g wet weight per 4 hr; S = myo-inositol concentration in mM; ■ = total phospholipid; ▲ = phosphatidylinositol.

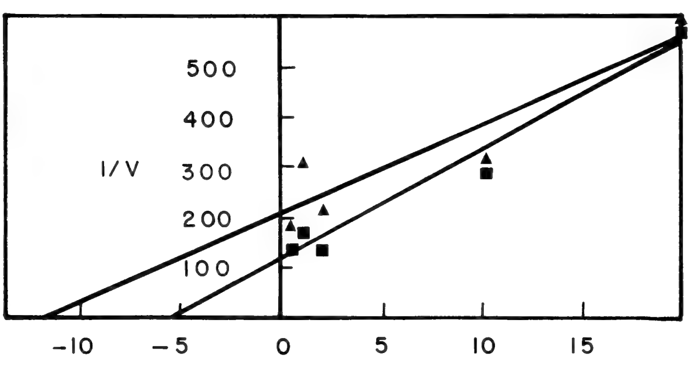

FIG. 4. Lineweaver-Burk plot of ^{3}H-myo-inositol incorporation into the total phospholipid and phosphatidylinositol by *H. diminuta* as a function of myo-inositol concentrations. V = μmol/g wet weight per 4 hr; S = myo-inositol concentration in mM; ■ = total phospholipid; ▲ = phosphatidylinositol.

However, when lipid fractions were subjected to two-dimensional thin layer chromatography, 97.45% and 91.6% of the total phospholipid radioactivities were attributed to phosphatidylinositol at 0.05 mM and 0.1 mM of substrate concentrations respectively. Whereas only 66.2%, 55.1% and 71.8% of the total phospholipid radioactivities were attributed to phosphatidylinositol at respective 0.5 mM, 1.0 mM and 2.0 mM of external myo-inositol concentrations (Table 1).

It is evident from Table 2 that increasing incubation time also increased total phospholipid and phosphatidylinositol syntheses from absorbed radioactive myo-inositol. However no change in phosphatidylinositol synthesis, expressed as percent myo-inositol incorporated into the phospholipid fraction, was noted. It was further observed that with increasing external myo-inositol concen-

TABLE 2. Rates of myo-inositol uptake; total phospholipid and phosphatidylinositol syntheses as a function of time at 0.1 mM ^{3}H-myo-inositol

Incubation time (hr)	Total myo-inositol uptake μmol/g wet wt	Phosphatidylinositol synthesis % total myo-inositol uptake	Phosphatidylinositol synthesis % myo-inositol incorporated into the phospholipid fraction	Total phospholipid % total myo-inositol uptake
1/4	0.049	0.279	37.60	0.742
1/2	0.073	0.366	61.70	0.592
1	0.112	0.615	39.10	1.592
2	0.221	0.616	37.50	1.640
4	0.447	0.551	48.10	1.144

trations the amount of radioactivity incorporated into the total phospholipid and phosphatidylinositol fractions relative to the quantity of absorbed radio-myo-inositol decreased (Table 1). The total myo-inositol absorbed by the worm was measured as the sum of water-soluble and total phospholipid radioactivities. The total myo-inositol uptake appeared to increase with respect to concentration and incubation time (Tables 1 and 2). The recovery of radioactivities in free myo-inositol, during 1/4, 1/2, 1.0, 2.0 and 4.0 hr of incubation, were 12.3%, 15.59%, 14.3%, 14.4% and 10.96% of the absorbed myo-inositol in the water soluble fraction respectively at 0.1 mM concentration. No attempt was made to identify the other radioactive metabolites.

Glucose uptake

In order to study biomembrane absorption activity in both groups of worms, glucose uptake studies were undertaken. It is evident from Table 3 that there was no apparent difference ($P>0.05$) in the absorption of ^{14}C-glucose at 1 mM, 2 mM and 3 mM of external glucose concentrations.

Establishment, growth and reproduction of H. diminuta

Deletion of myo-inositol from the diet appeared to have no effect on the establishment of the parasite in its host (Table 4).

The results of the experiment on growth (Table 5) demonstrated that the worms from the hosts fed with myo-inositol deficient diet were comparative-

TABLE 3. Absorption of ^{14}C-glucose by *Hymenolepis diminuta*

Glucose concentration (mM)	Uptake velocity [μmol/g ethanol extracted dry wt/2 min $\pm$ S.E. (n)]	
	Control group	myo-Inositol deficient group
1	14.12 ± 1.23 (3)	17.00 ± 1.27 (3)
3	15.40 ± 2.13 (3)	17.05 ± 0.76 (3)
5	15.28 ± 0.97 (3)	15.93 ± 2.32 (3)

TABLE 4. Effect of myo-inositol on the establishment of *Hymenolepis diminuta*

Diet group	Cysticercoids/rat	Average number of worms/rat ±S.E. (n)	Recovery % ±S.E.
Control	30	26.00±1.00 (3)	86.66± 3.33
myo-Inositol deficient	30	24.67±3.05 (3)	82.23±10.16

TABLE 5. Effect of myo-inositol on the growth of *Hymenolepis diminuta*

Diet group	Number of worms per host	Total wet weight (g)	Average wet weight (mg)	Average length per worm (cm) ± S.E.
Control	34	0.996	29.29	18.56 ± 3.38
Control	29	0.638	22.00	15.41 ± 1.92
Control	30	0.872	29.06	17.11 ± 2.35
myo-Inositol deficient	34	1.325	38.97	19.32 ± 1.86
myo-Inositol deficient	27	1.298	48.07	16.41 ± 4.15
myo-Inositol deficient	30	1.775	59.16	29.38 ± 2.77

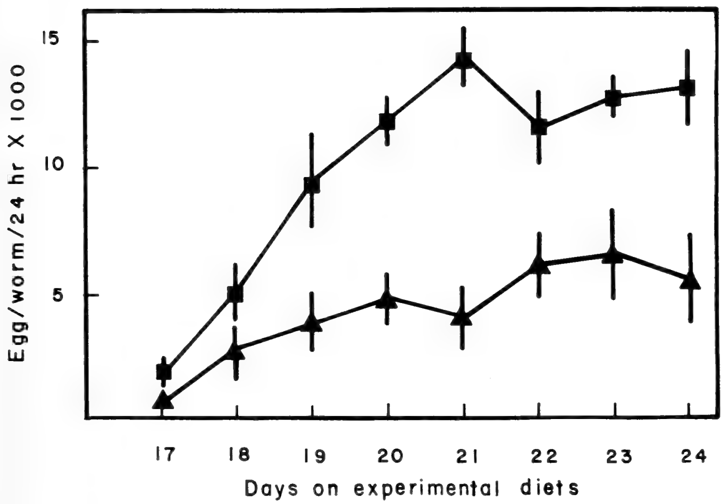

FIG. 5. Egg production of *H. diminuta* in control and myo-inositol deficient rats. ▲=control rats; ■=myo-inositol deficient rats. Vertical bars around the points show standard errors. Each point represents mean of three determinations.

ly heavier than those recovered from the hosts fed with control diet. This indicates that the growth of the worms was enhanced when myo-inositol was deleted from the host diet. No significant difference ($P>0.05$) in the length of worms was found when the hosts were presented diets with or without myo-inositol.

A comparison of rates of egg production from *H. diminuta* in rats fed with control or myo-inositol deficient diet is shown in Figure 5. Egg production in *H. diminuta* was remarkably higher when the rats were fed myo-inositol deficient diet. A considerable variation in daily egg output was observed. In the early period, a low level of egg output was noted in both groups of rats. A rapid rise in egg output was observed in both groups from the 18–21 day postinfection and stabilized with minor fluctuations thereafter. In the myo-inositol deficient rats, the *H. diminuta* egg output raised more rapidly than in the rats fed with control diet. The worms from the myo-inositol deficient rats gained patency 15 days postinfection. However, the patency was delayed by one day for worms parasitizing rats fed with control diet.

Infectivity of H. diminuta eggs

Beetles examination after a period of two weeks revealed no significant difference in the infectivity of *H. diminuta* eggs, obtained from both groups of rats.

DISCUSSION

The function of myo-inositol in higher vertebrates has been suggested as a vitamin, a phos-

phate storage agent, a phosphagen and the most important of all, as a component of phospholipids. Best *et al.* [28] reported the lipotropic function of myo-inositol in rats regardless of the type of fats used. It is therefore possible for myo-inositol to affect the physiology of *H. diminuta* through its functions discussed above.

The present study confirms the observations of Ip and Fisher [2] that myo-inositol uptake in *H. diminuta* involves, at least in part, a mediated process (Table 1). The absorption of myo-inositol was observed to be time (Fig. 1) and concentration dependent (Table 1). In order to study the fate of absorbed myo-inositol, water soluble fractions obtained as a function of time were subjected to paper chromatography. Only 10.96% to 15.59% myo-inositol was recovered from these fractions indicating that it was being rapidly metabolised. Other radioactive metabolites were not identified.

The incorporation of absorbed myo-inositol into the total phospholipid and phosphatidylinositol fractions were also linear with respect to time (Fig. 2). Total phospholipid and phosphatidylinositol syntheses, when expressed as percent synthesis of total myo-inositol uptake, revealed similar phenomenon (Table 2). However, there was no change in the amount of radioactivity of phosphatidylinositol relative to the quantity of myo-inositol incorporated into the phospholipid fraction (Table 2). The incorporation of absorbed myo-inositol into the lipid fractions was also found to be concentration dependent (Fig. 3). In order to study the incorporation of ^{3}H-myo-inositol into different classes of phospholipids, the lipid fractions were analyzed by thin layer chromatography. The recovery of phosphatidylinositol, when expressed as percent synthesis of total myo-inositol uptake or of myo-inositol incorporated into phospholipid fraction, was highest at lowest myo-inositol concentration. It, however, decreased with the increase in external myo-inositol concentration (Table 1). At higher concentrations the lower recovery of phosphatidylinositol could be due to the metabolism of myo-inositol to some other compounds.

H. diminuta can absorb and metabolize glucose [29–33]. Since myo-inositol is an important component of biomembrane, glucose uptake studies were therefore undertaken to examine the biomembrane activity in the worms. The results indicated that there was no difference in glucose uptake in worms under both conditions. Hence there may not be significant changes in the lipid components of the membrane that would affect the membrane transport processes. Ginger and Fairbairn [1] reported synthesis of myo-inositol and its incorporation into phospholipids from glucose in *H. diminuta*. It is possible that the worm can maintain its membrane syntheses for growth and reproduction with its limited capability of forming inositol from glucose. Similarly, deletion of myo-inositol from the host diet appeared to have no effect on the establishment of the worms in its host.

It is evident from Table 5 and Figure 5 that the growth and egg production of *H. diminuta* were enhanced with myo-inositol deficient diet. Such condition also resulted in the reduced time to their patency. Esotcott [6], Beadle [7] and Eagle *et al.* [9] indicated that myo-inositol was essential for the survival and growth of microorganisms. Stimulation of growth by myo-inositol has been observed in higher animals [8]. Hayashi *et al.* [34] reported that the growth rate of the rats maintained on the myo-inositol deficient diet did not differ from that of the control rats. Addis and Chandler [13] observed that the addition of myo-inositol in the basic diet, deficient in B_1 and B_2 complex, did not significantly alleviate the stunting effect caused by such vitamin deficiency. However, such conclusions were drawn basing only on the length of the worms. The present study indicated that the growth and egg production were, in fact, markedly increased when myo-inositol was omitted from the host diet. This was in contrast to the results of earlier workers [6–9] who considered myo-inositol as a growth factor in microorganisms and higher animals.

The stimulating effect of male dog bile on the egg output of *H. diminuta* in both male and female rats had been reported by Beck [15]. Goodchild [35] observed that bile was necessary for normal growth and development of adult *H. diminuta* in the rat host. Robert [36] reported that *H. diminuta* required bile salts for its normal development. It is now well established that triacylglycerol and

cholesterol levels in liver were markedly raised in the rats maintained on the basal diet without myo-inositol [34]. It is therefore possible that during the syntheses of bile acids and salts from the elevated cholesterol level in the liver, an alteration in the intestinal physiology favourable to *H. diminuta* might have occurred, which increased the growth and egg production of the worms.

In the present study we found that both growth and egg production in *H. diminuta* were retarded in the presence of myo-inositol. However, it does not imply that *H. diminuta* has no requirement for myo-inositol. It is definitely an important component of biomembrane. Bly [37] reported increase of peristaltic activity in the stomach and small intestine of dogs in the presence of myo-inositol which may produce a transitry cathartic effect. Such effect may interfere with the growth and development of *H. diminuta* as a gut parasite. There are other vitamins which either have no effect on the establishment and growth of *H. diminuta* or retard its growth. Choline or pantothenate deficient diets have no effect on the establishment or growth of this worm [19]. Addition of riboflavin in the host diet, however, causes retardation in its growth [19]. Although these vitamins do not favour the growth of this parasite, it still needs them as nutritional requirement [19].

Figure 5 displayed the pattern of egg production of *H. diminuta* in the presence or absence of myo-inositol from the host diet. The retardation of growth and in egg production in worms from rats fed with control diet as compared to those from myo-inositol deficient rats indicates the existence of a less favourable environment in the former hosts. The day to day variations in egg counts in both groups of rats were due to the shedding of gravid proglottids at irregular intervals. In the early period, 17 and 18 days postinfection, a low level of egg output occurred. It happened only when the worms were just beginning to shed gravid proglottids. The higher rate of egg production by worms from myo-inositol deficient rats was very obvious from the 18 days postinfection. However, the infectivities of *H. diminuta* eggs from both groups of rats were similar, indicating that myo-inositol deficiency in the diet neither affects its hatchability nor normal development.

ACKNOWLEDGMENTS

This project is supported by a grant RP 145/82 from the National University of Singapore.

REFERENCES

1 Ginger, C. D. and Fairbairn, D. (1966) Lipid metabolism in the helminth parasites. II. The major origins of the lipids of *Hymenolepis diminuta* (Cestoda). J. Parasitol., **52**: 1097–1107.

2 Ip, Y. K. and Fisher, F. M., Jr. (1982) Membrane transport of inositol by *Hymenolepis diminuta* (Cestoda). J. Parasitol., **68**: 53–60.

3 Ip, Y. K. and Fisher, F. M., Jr. (1982) Quantitative determination of inositol by *Hymenolepis diminuta* (Cestoda). J. Parasitol., **68**: 593–598.

4 Michell, R. H. (1979) Inositol phospholipids in membrane function. Trans. Biochem. Sci., **4**: 128–131.

5 Webb, R. A. and Mettrick, D. F. (1971) Pattern of incorporation of ^{32}P into the phospholipids of the rat tapeworm *Hymenolepis diminuta.* Can. J. Biochem., **49**: 1209–1212.

6 Esotcott, E. V. (1928) Wilder's Bios, the isolation and identification of "Bios I". J. Phys. Chem., **32**: 1094–1111.

7 Beadle, G. W. (1944) An inositolless mutant strain of *Neurospora* and its use in bioassays. J. Biol. Chem., **156**: 683–689.

8 McIntire, J. M., Schevergerl, B. S. and Eluejhem, C. A. (1944) The nutrition of the cotton rat (*Sigmodon hispidus hispidus*). J. Nutr., **27**: 1–9.

9 Eagle, H., Oyama, V. I., Levy, M. and Freeman, A. E. (1956) myo-Inositol as an essential growth factor for normal and malignant human cells in tissue culture. Nature, **128**: 845–847.

10 Mettrick, D. F. and Podesta, R. B. (1974) Ecological and physiological aspects of helminth-host interactions in the mammalian gastrointestinal canal. In "Advances in Parasitology". Ed. by B. Dawes, Academic Press, London, **12**: 183–278.

11 Hager, A. (1941) Effects of dietary modifications of host rats on the tapeworm *Hymenolepis diminuta.* Iowa State Coll. J. Sci., **15**: 127–153.

12 Chandler, A. C. (1943) Studies on the nutrition of tapeworms. Am. J. Hyg., **37**: 121–130.

13 Addis, C. J., Jr. and Chandler, A. C. (1944) Studies on the vitamin requirements of tapeworms. J. Parasitol., **30**: 229–236.

14 Addis, C. J., Jr. and Chandler, A. C. (1946) Further studies on the vitamin requirements of tapeworms. J. Parasitol., **32**: 581–584.

15 Beck, J. W. (1952) Effect of diet upon singly established *Hymenolepis diminuta* in rats. Exp.

Parasitol., **1**: 46–59.

16 Roberts, L. S. and Mong, F, N. (1973) Developmental physiology of cestodes. XIII. Vitamin B_6 requirement of *Hymenolepis diminuta* during *in vitro* cultivation. J. Parasitol., **59**: 101–104.

17 Hall, A. (1983) Dietary protein and the growth of rats infected with the tapeworm *Hymenolepis diminuta*. Br. J. Nutr., **49**: 59–65.

18 Keymer, A., Crompton, D. W. T. and Singhvi, A. (1983) Mannose and the "crowding effect" of *Hymenolepis* in rats. Int. J. Parasitol., **13**: 561–570.

19 Platzer, E. G. and Robert, L. S. (1970) Developmental physiology of cestodes. VI. Effect of host riboflavin deficiency on *Hymenolepis diminuta*. Exp. Parasitol., **28**: 393–398.

20 Read, C. P., Rothman, A. H. and Simmons, J. E., Jr. (1963) Studies on the membrane transport, with special reference to parasite-host integration. Ann. N. Y. Acad. Sci., **113**: 154–205.

21 Folch, J., Lees, M. and Sloane-Stanley, G. H. (1957) A simple method for the isolation and purification of total lipids from animal tissues. J. Biol. Chem., **226**: 497–509.

22 Read, C. P., Schiller, E. L. and Phifer, K. (1958) The role of carbohydrates in the biology of cestodes. V. Comparative studies on the effects of host dietary carbohydrates on *Hymenolepis* spp. Exp. Parasitol., **7**: 198–216.

23 Holmes, J. C. (1970) The effect of crowding on fecundity of *Hymenolepis diminuta* . In "Experiments and Techniques in Parasitology". Ed. by A. J. Macinnis and M. Voge, D. H. Freeman and Co., San Francisco, pp. 49–50.

24 Voge, M. (1970) Laboratory maintenance of parasites. In "Experiments and Techniques in Parasitology". Ed. by A. J. Macinnis and M. Voge, D. H. Freeman and Co., San Francisco, pp. 130–131.

25 Gray, H. E. and Fraenkel, G. (1953) Fructomaltose, a recently discovered trisaccharide isolated from honeydew. Science, **118**: 304–305.

26 Trevelyan, W. E., Procter, D. P. and Harrison, J. S. (1950) Determination of sugars on paper chromatograms. Nature, **166**: 444–445.

27 Rouser, G., Kritchevsky, G. and Yamamoto, A. (1967) Column chromatographic and associated procedures for separation and determination of phosphatides and glycolipids. In "Lipid Chromatographic Analysis". Vol. I. Ed. by G. Y. Marinetti, Marcel Dekker Inc., New York, pp. 99–162.

28 Best, C. H., Ridout, J. H., Patterson, J. M. and Lucas, C. C. (1951) A statistical evaluation of the lipotropic action of inositol. Biochem. J., **48**: 448–452.

29 Laurie, J. S. (1957) The *in vitro* fermentation of carbohydrates by two species of cestodes and one acanthocephala. Exp. Parasitol., **6**: 245–260.

30 Read, C. P. and Rothman, A. H. (1958) The role of carbohydrates in the biology of cestodes. VI. The carbohydrates metabolized *in vitro* by some cyclophyllidean species. Exp. Parasitol., **7**: 217–223.

31 Phifer, K. (1960) Permeation and membrane transport in animal parasites : The absorption of glucose by *Hymenolepis diminuta*. J. Parasitol., **46**: 51–62.

32 Phifer, K. (1960) Permeation and membrane transport in animal parasites : Further observations on the uptake of glucose by *Hymenolepis diminuta*. J. Parasitol., **46**: 137–144.

33 Overturf, M. (1966) *In vivo* and *in vitro* uptake and distribution of C^{14}-glucose by *Hymenolepis diminuta*. Comp. Biochem. Physiol., **17**: 705–713.

34 Hayashi, E., Maeda, T. and Tomita, T. (1974) The effect of myo-inositol deficiency on the lipid metabolism in rats. I. The alteration of lipid metabolism in myo-inositol deficient rats. Biochim. Biophys. Acta, **360**: 134–145.

35 Goodchild, C. G. (1958) Growth and maturation of the cestode *Hymenolepis diminuta* in bileless hosts. J. Parasitol., **44**: 352–362.

36 Roberts, L. S. (1980) Development of *Hymenolepis diminuta* in its definitive host. In "Biology of the Tapeworm *Hymenolepis diminuta*". Ed. by H. P. Arai, Academic Press, New York, pp. 357–423.

37 Bly, C. H., Heggeness, E. W. and Naset, E. S. (1943) The effect of pantothenic acid and inositol added to whole wheat bread on evaculation time, digestion and absorption in the upper gastrointestinal tract of dogs. J. Nutr., **26**: 161.

ZOOLOGICAL SCIENCE 4: 233–242 (1987)

Morphometrical Features of Rod Outer Segments in Relation to Visual Acuity and Sensitivity in the Retina of *Rana catesbeiana*

YOSHIHIKO TSUKAMOTO

Department of Anatomy, Hyogo College of Medicine, Mukogawa, Nishinomiya, Hyogo 663, Japan

ABSTRACT—Morphometry of the rod outer segment in the bullfrog retina was performed to clarify the structural bases of functional local specialization along the vertical meridian. The length, cross-sectional area, and density of the outer segments showed distinct differences between the red and green rods, between the central and peripheral parts, and between the dorso-central and ventro-central portions. The outer segments of red rods are always longer than those of neighboring green rods in all locations, while the cross-sectional areas are nearly equal. The red and green rod outer segments are smaller in length and in cross-sectional area, and higher in density at the periphery than at the center, in both the dorsal and ventral retinas. On the other hand, when measured at about 2 mm from the optic disc, they are larger in length, smaller in cross-sectional area, and higher in density at the dorso-central retina than at the ventro-central retina. At the dorso-central "area centralis", although the diameter of the rod outer segment decreases (being accompanied with the increase in density), the increase in length complements the decrease in diameter. Since the volume of the outer segment decreases little, visual acuity is thought to increase with almost no decrease in sensitivity. The above findings are substantiated by observations of the thickness and angular spread of the retina using whole eyes embedded in celloidin.

INTRODUCTION

The bullfrog retina has been noted to have local specialization. The content of visual pigments is two the three times greater in the dorsal than in the ventral retina [1, 3]. Vitamin A_2-based pigments are much denser in the dorsal retina (porphyropsin zone) [1–4]. The consequent changes in the spectral sensitivity are considered to adapt to the environmental light [1]. In addition, the environmental influences on the bullfrog retina are thought to differ in light intensity between the dorsal and ventral halves. This is suggested by the fact that macrophages in the subretinal space are more abundant in the ventral than in the dorsal retina [5].

The area centralis is shaped like a crescent and lies above the optic disc in *Rana* [6, 7]. The topographic map of ganglion cells indicates that the area centralis extends horizontally like a streak in the dorso-central part of the bullfrog retina. The peak densities of photoreceptors and ganglion cells are located about 2 mm dorsal to the horizontal meridian [8]. This may largely contribute to the functional differences between the dorsal and ventral retina of the bullfrog.

Although the density of photoreceptors is related to visual acuity, it does not offer any information about sensitivity. The morphological parameter related to sensitivity is the volume of the photoreceptor outer segment which contains the visual pigments. It has been recently shown that the area with the highest concentration of visual pigments is located 3–4 mm just dorsal to the optic disc and is shaped like a semicircular band [3]. Since visual acuity and sensitivity are both important functions but generally contradic-

Accepted October 29, 1986
Received September 19, 1986

tory, the relationship of them in the bullfrog area centralis is interesting.

In this report, first, the retinal thickness and angular spread are surveyed using bullfrogs with different sizes. Second, the length, cross-sectional area, cell density and other parameters of the red and green rod outer segments (ROS) are examined along the vertical meridian of the retina. It will be shown that in the area centralis the larger length of the outer segment compensates its smaller cross-sectional area, thus keeping its volume constant.

MATERIALS AND METHODS

Preparations and preliminary fixation

Adult bullfrogs (*Rana catesbeiana*), 12–14 cm in length, were used under room light after more than 5 hr of illumination. Two syringe needles, passing through the anterior and posterior poles of the cornea, were inserted as far as the vitreous body, while the eyeball was held by the upper jaw, which had been removed by decapitation. The intraocular perfusion of the fixative was carried out with a syringe, using one of the two holes as an inlet, the other as an outlet. After 10 min of this preliminary fixation, the eye was gently enucleated. One of two different fixative solutions was used from this step, as described below.

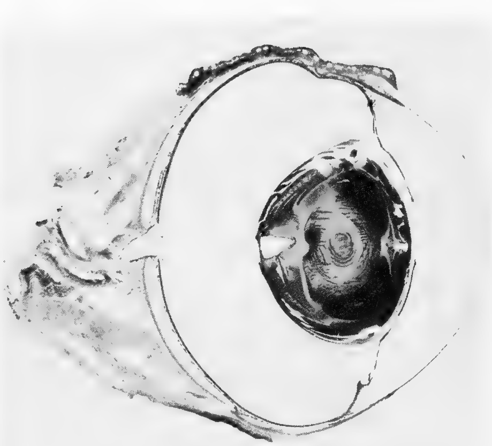

FIG. 1a. Photomicrograph of vertical section of a bullfrog left eye, embedded in celloidin, cut into a 20 μm thick section, and stained with Cason's Mallory Heidenhain. Upper side is dorsal.

Whole eyes embedded in celloidin

For embedding the whole eye in celloidin resin, a solution of 3% glutaraldehyde, 1% paraformaldehyde, 2% $CaCl_2$, and 2% $MgCl_2$ in 0.1 M cacodylate (pH 7.4) was used as the fixative. The eye was immersed in the fixative overnight following the above-mentioned preparation. It was dehydrated in ethanol with graded percentages, for one day at each concentration, and substituted by a dehydrated ethyl ether and ethanol mixture. After immersion in 2%, 4%, 8% celloidin for 3–4 weeks each, the sample was transferred to 10% celloidin which was gradually hardened for 3 months. The eye was vertically sectioned with a steel knife, and 20–30 μm thick sections passing through the optic disc along the meridional line were obtained. The sections were stained according to Cason, a modification of Azan staining (Mallory-Heidenhain).

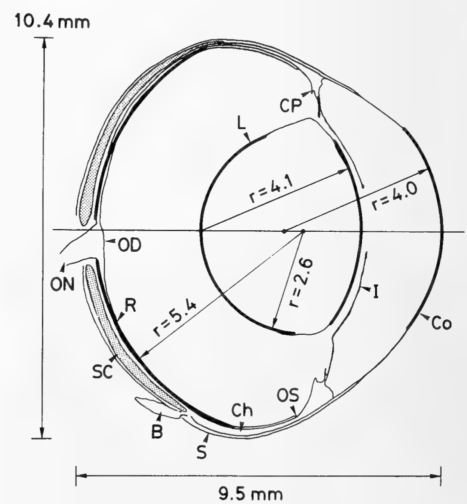

FIG. 1b. Diagram of vertical section of the bullfrog eye shown in Fig. 1a. R, retina; Ch, choroid; S, Sclera; SC, scleral cartilage; B, blood vessel; OD, optic disc; ON, optic nerve; Co, cornea; I, iris; CP, ciliary pappilla; OS, ora serrata. Most part of the cornea, the anterior and posterior lens surfaces, and the retina are regarded as arcs of the circles having their centers on the optic axis (horizontal line). Their radii (r) are shown in units of *mm*. The intersection of the retina and the optic axis is regarded as the retinal center. Optic disc is located 0.3 mm ventrally.

After the eyeballs were embedded in celloidin, the horizontal and vertical diameters of the sclera showed only 1–3% of shrinkage. The retina, which is stiffly attached to the choroid and sclera complex, is thought to hardly change in length in the tangential direction. However, it was possible that a considerable shrinkage might occur in a radial direction.

Pieces of retina embedded in Araldite

For embedding pieces of retina in epoxy-resin, 2% OsO_4 in 0.1 M phosphate buffer (pH 7.4) was used as the fixative. After the above-mentioned preparation, the anterior parts of the eye were removed. The posterior hemisphere was divided into quadrants by horizontal and then vertical sectionings. Tissues were furthermore immersed in the fixative for 1.5 hr. Strips of retina (1.5–2 mm in width) along the meridional line were cut out from the dorsal and ventral halves. Each strip was cut into 5–7 rectangular pieces. One angle of each piece was cut off for reference of direction. These pieces were numbered, separately dehydrated and embedded in Araldite. Three retinas from different frogs, denoted as retina 1 (right eye), 2 (right eye), and 3 (left eye) in the following, were used for morphometry of the ROS along the vertical meridian. The sections of 0.5 μm in thickness were cut in radial (retina 1 and 2) and tangential (retina 1 and 3) directions, and stained

TABLE 1. Comparison in parameters of occular apparatus between two bullfrogs A and B at different growth stages

	Frog A	Frog B
body length and weight	12 cm and 200 g	14 cm and 300 g
meridional length of the retina	16.7 mm	19.2 mm
angle encompassing the retina	173°	188°
radius of curvature of the retina	5.4 mm	5.7 mm
eye ball:		
$\frac{\text{equatorial dia.}}{\text{axial dia.}}=\text{ratio}$	$\frac{10.4\text{ mm}}{9.5\text{ mm}}=1.09$	$\frac{11.5\text{ mm}}{10.5\text{ mm}}=1.10$
lens:		
$\frac{\text{equatorial dia.}}{\text{axial dia.}}=\text{ratio}$	$\frac{6.3\text{ mm}}{4.1\text{ mm}}=1.5$	$\frac{5.6\text{ mm}}{3.7\text{ mm}}=1.5$

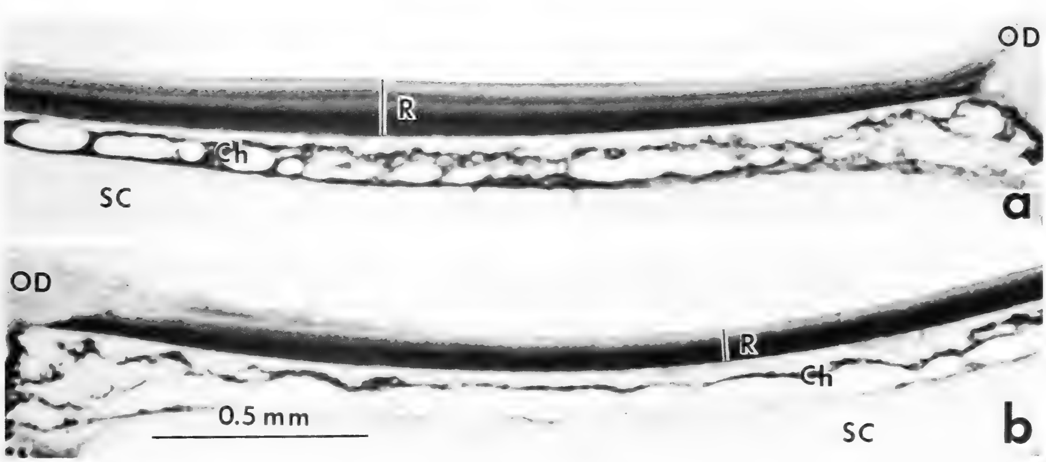

FIG. 2. Parts of the retina shown in Fig. 1a, dorsal (a) and ventral (b) to the optic disc. Abbreviations are the same as in Fig. 1b. The thickness of the retina, indicated by bars, is about 2 times greater in the dorsal than in the ventral.

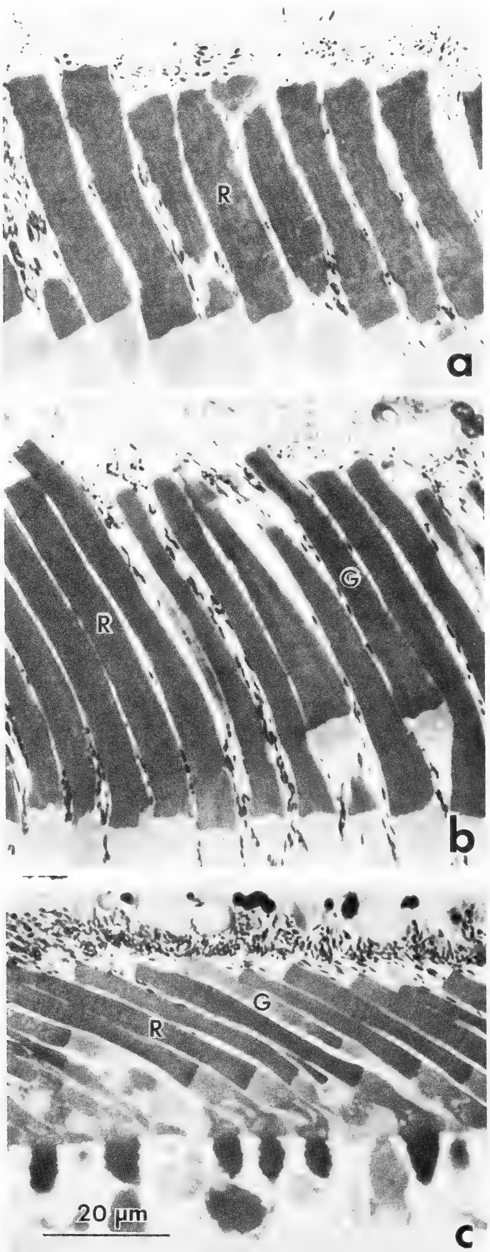

FIG. 3. Light micrographs of ROS in longitudinal section taken from three different areas in a retina; (a) about 2.5 mm ventral to the center, (b) about 2 mm dorsal to the center, and (c) close to the dorsal *ora serrata*, at the same magnification. R, red rod; G, green rod.

with toluidine-blue for light microscopy. In particular, for the retina 1, radial sectioning was followed by reembedding and tangential sectioning. Ultrathin sections were also obtained for electron microscopy with the cutting plane transverse to the ROS. These sections were stained with uranyl acetate and lead citrate.

During processing of Araldite embedding, the retina was estimated to shrink 7–12% in a tangential direction.

Microscopy and measurements

Zeiss Ultraphot and Olympus Vanox light microscopes were used with plan-apochromat objective lenses of 20 ×, 40 ×, 100 × (oil). Sections of the whole eye were photographed with a Nikon Multiphoto camera. An electron microscope (JEM-100CX) was used at 80 kV.

Morphological measurements were carried out on enlarged photographs. The length of tortuous lines, and the sectional area of cells, were calculated with a microcomputer (Sord M243) linked to a digitizer (Summagraphics, Bit Pad One). All the data are presented in this paper with no correction for shrinkage.

RESULTS

Morphology of the whole eye

The vertical section of a whole eye gives general morphology of the ocular apparatus of the bullfrog eyeball (Fig. 1). Morphometric parameters of the left eyes of two male bullfrogs with body lengths of 12 and 14 cm are compared (Table 1). The inner aspect of the sclera is made of hyaline cartilage. This cartilage is thickest at the posterior pole and extends anteriorly close to the equatorial plane. The eye and its lens are greater in the frog with the greater body weight [9]. The meridional length of the retina is also greater in the larger eye. This is based on two factors. The radius of curvature of the retina and the angle encompassing the retina are both greater in the larger eye. On the other hand, the ratios of the equatorial versus the axial diameter in the eyeball and in the lens are almost constant. Their shapes are regarded to be homologous.

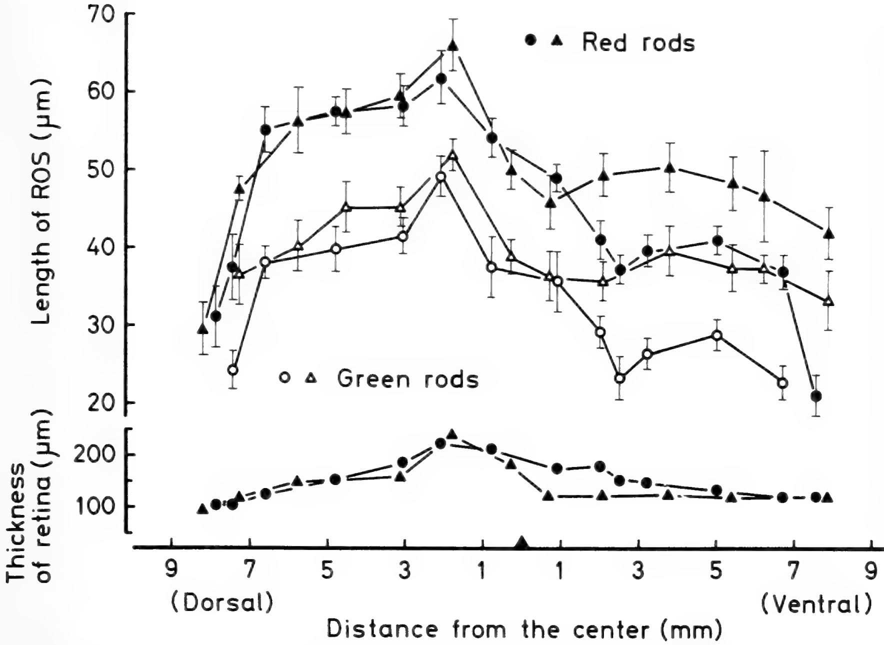

FIG. 4. *Upper*) Vertical variations in the length of red (closed) and green (open) ROS in retinas 1 (circle) and 2 (triangle) from two bullfrogs. The maximal length is given at about 2 mm dorsal to the center, such as retina 1: red=62 ± 4, green=49 ± 3, and retina 2: red=66 ± 3, green=52 ± 2. The length is prominently short at 1–3 mm ventral to the center, such as retina 1: red=37 ± 2, green=23 ± 3, and retina 2: red=46 ± 4, green =36 ± 3. It becomes shorter toward the periphery, e.g. reaching 21 ± 3 (retina 1, red) at 7.4 mm ventral to the center, and 24 ± 3 (retina 1, green) at 7.7 mm dorsal to the center. (Mean ± standard deviation in units of μm. The number of counts is 20 for red rods and 10 for green rods at each position). The margins are located 8.4 mm dorsal and ventral to the center in both retinas 1 and 2. *Lower*) The thickness of the retina is greatest at about 2 mm dorsal to the center, such as retina 1: 220 μm, retina 2: 240 μm. It has the smallest value of about 100 μm at the margin. The data are obtained from the retinas embedded in Araldite.

Retinal thickness and the length of ROS

The thickness of the retina is given by the distance from the inner limiting membrane to the basement of the pigment epithelium. The retina has the greatest thickness at about 2 mm dorsal to the center, which is one and a half to two times larger than that at about 2 mm ventral to the center (Figs. 2 and 4, below; the retinal center is defined as the intersection of the retina and the optic axis as shown in Fig. 1b). The retina becomes thinner toward the periphery.

The discrimination of the red and green ROS in radial section is based on the differences in their lengths and the position of their basal ends; the green ROS is shorter and located to the scleral side as compared with the red ROS (Fig. 3). Since it is often difficult to find the green ROS near the *ora serrata*, no data are displayed for them in this location. The lengths of the red and green ROS are also greatest at about 2 mm dorsal to the center, and prominently short at 1–3 mm ventral to the center. Their lengths become shorter toward the periphery, reaching the minimal values at the margin (Fig. 4, upper).

The cross-sectional area and the density of ROS

Cross sections of the red and green ROS are observed by electron microscopy at the height where they both appear. The sectional planes have been adjusted so as to be perpendicular to the long axis of the ROS. The red and green ROS in cross section can be discriminated on electron micrographs by cues of the number and depth of disc

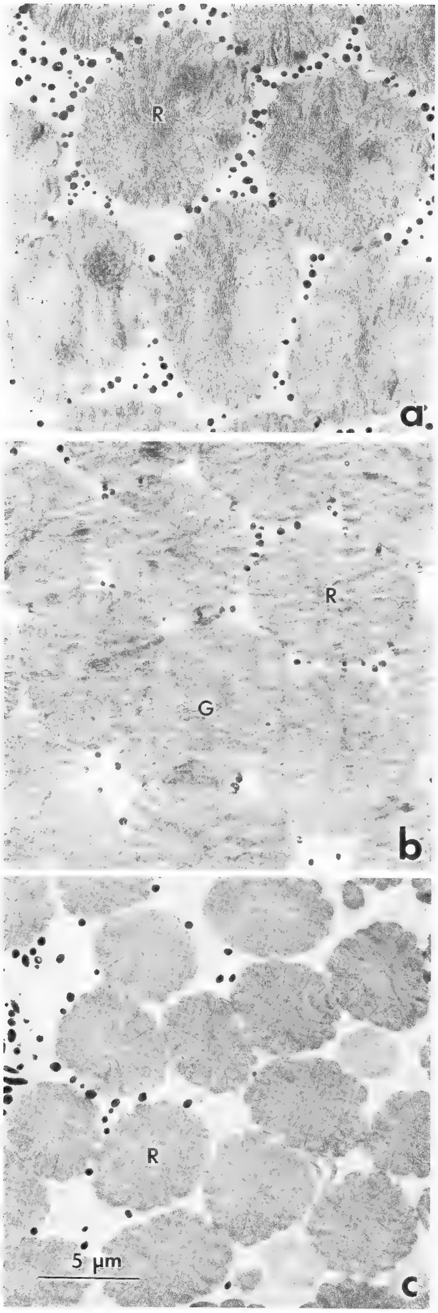

Fig. 5. Electron micrographs of ROS in cross section taken from three different areas in a retina; (a) about 3 mm ventral to the center, (b) about 2 mm dorsal to the center, and (c) near the dorsal *ora serrata*, at the same magnification. R, red rod; G, green rod.

incisures [10]; the disc incisures of the red rod are greater in number and longer in depth than those of the green rod (Fig. 5). The sectional areas of the red and green ROS are prominently small at 2–3 mm dorsal to the center, showing valley-like curves in the vertical variation. In contrast, these values are greatest at 2–4 mm ventral to the center. Their sectional areas tend to become smaller in more peripheral portions, reaching the minimal values at the margin (Fig. 6).

The densities of the red and green ROS have peaks at 2–3 mm dorsal to the center. On the other hand, their densities are almost constant in the ventral retina. Extremely close to the margin, it is often difficult to discriminate the green rods from the red ones. The density totaling both types of rods tends to increase sharply near the *ora serrata* in both the dorsal and ventral retinas (Fig. 7, upper). No prominent differences are found in the density ratio of red rods to green rods (R/G ratio) between the dorsal and ventral retinas. While the R/G ratio varies moderately from 5.4 to 7.3 in the central retina, it has a tendency to increase to some extent close to the margin (Fig. 7, below).

DISCUSSION

Features in relation to the bullfrog growth

The body length and the eye-lens weight of bullfrogs are parameters showing the degree of their growth [9, 12]. Clear correlations are observed by Makino-Tasaka *et al.* [3] between the body length and the contents of protein, visual pigment, and dopamine in the bullfrog retina. In the present study, also, both the eyeball and the retina are greater in size in the larger bullfrog. The growth of the retina seems to be related to the increases in both the radius of curvature and the angle encompassing the retina. An increase in the angle encompassing the retina means that the *ora serrata* moves anteriorly. This suggests that the retinal field in the vicinity of the *ora serrata* is capable of growing [9]. The ROS small in both length and cross-sectional area are present in the extreme peripheral retina. These ROS are thought to be in the process of growing. Adult bullfrogs

range from 12 to 18 cm in body length [12]. Since relatively juvenile adult bullfrogs (12 and 14 cm) are used for the present study, it is reasonable that their organs have some growing activities.

According to Duke-Elder [6], the lens in the tadpole, like that of fish, is spherical and close to the cornea; in the adult frog it moves posteriorly and becomes somewhat flattened in an antero-posterior direction. The value of 1.3 has been quoted as the ratio of the equatorial versus the axial diameter of the lens in a certain kind of frog (Rabl, 1898 in [6]). The value of 1.5 is obtained as this ratio for the bullfrog lens in the present study. The bullfrog lens is distinctly far from a sphere; its anterior surface is prominently flat.

The volume of ROS and the content of visual pigment

The data represented by filled circles in Figures 4 and 6 of both the length and cross-sectional area of the ROS were derived from the same retina (retina 1). The product of the mean length and the mean cross-sectional area of the red ROS at each position on the meridional line of the retina gives the mean volume. In the central half of the retina, the mean volumes of the red ROS approximately

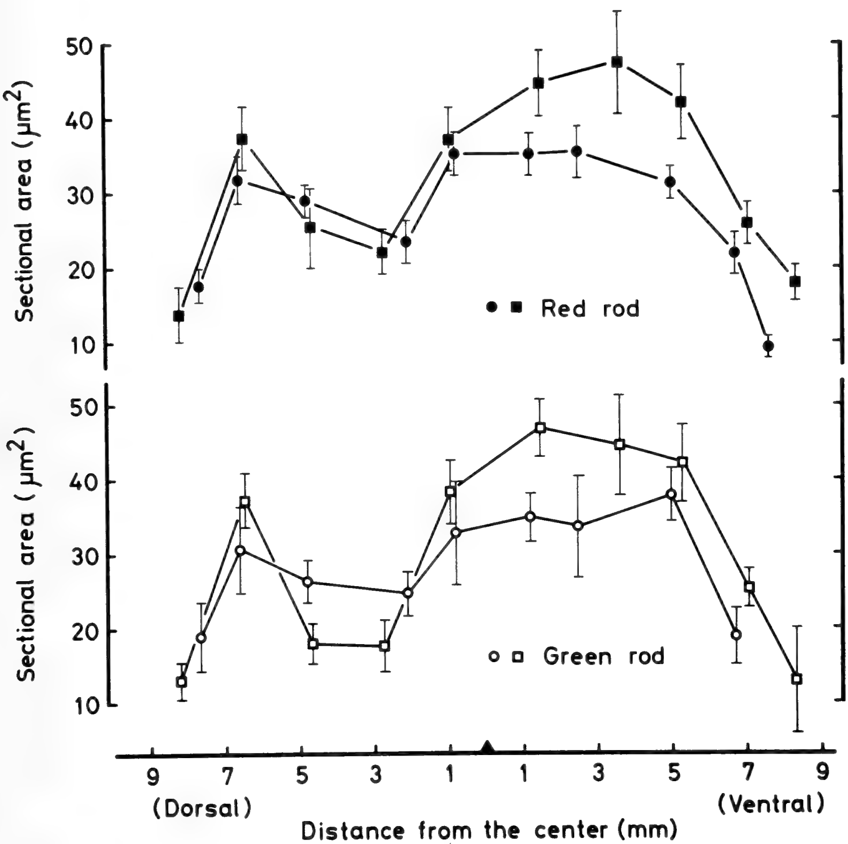

FIG. 6. Vertical variation in the sectional area of red (closed, upper) and green (open, lower) ROS in retinas 1 (circle) and 3 (rectangular) from different bullfrogs. The maximal area is given at 2–5 mm ventral to the center, such as retina 1: red$=36\pm4$, green$=38\pm4$, and retina 3: red$=47\pm7$, green$=47\pm4$. The area is prominently small at 2–3 mm dorsal to the center, such as retina 1: red$=24\pm3$, green$=25\pm3$, and retina 3: red$=22\pm3$, green$=18\pm4$. It becomes smaller toward the periphery, e.g. reaching 9 ± 2 (retina 1, red) at 7.4 mm ventral to the center, and 13 ± 3 (retina 3, green) at 8.4 mm dorsal to the center. The margins are located 8.9 mm dorsal and ventral to the center in the case of retina 3. (Mean$\pm$standard deviation in units of μm^2. The number of counts is 20 for red rods and 10 for green rods at each position).

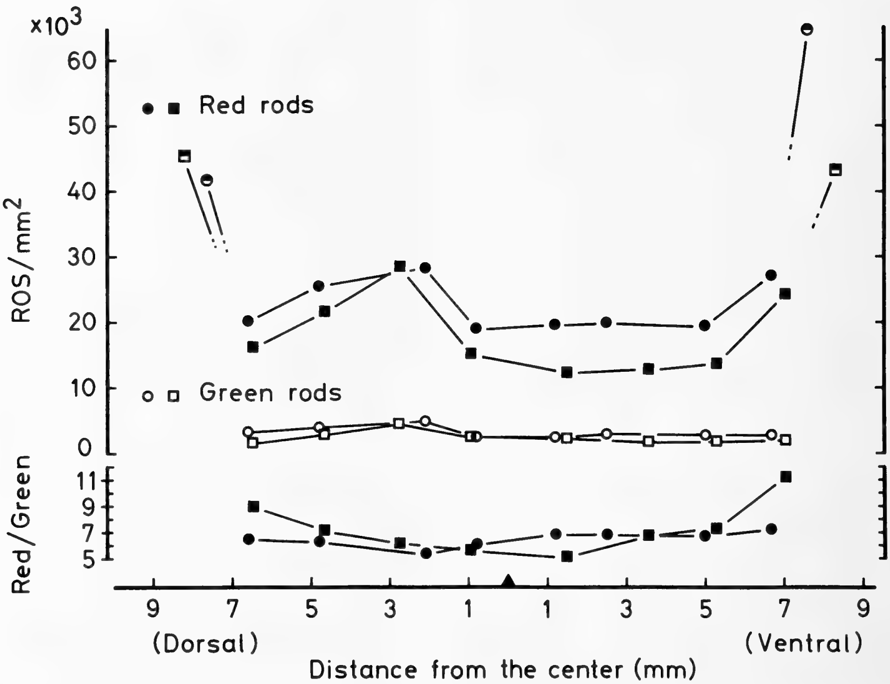

FIG. 7. *Upper*) Vertical variation in the density of red (closed, upper) and green (open, lower) ROS in retinas 1 (circle) and 3 (rectangular). The maximal density is given at 2–3 mm dorsal to the center, such as retina 1: red=28, green=5, and retina 3: red=29, green=4.5. The density is rather small at 2–5 mm ventral to the center, such as retina 1: red=17, green=2.5, and retina 3: red=13, green=2. It sharply increases at the extreme margin, where discrimination of the green rod from the red rod is difficult. Therefore the values totaling both types of rods are displayed with half-closed symbols, e.g. reaching 45 (retina 3) at 8.4 mm dorsal to the center, and 65 (retina 1) at 7.4 mm ventral to the center. (units: $10^3/\mathrm{mm}^2$). *Lower*) The ratio of red to green rods ranges from 5.4 to 7.3 between the dorsal and ventral locations about 5 mm distant from the center. It increases near the margin, e.g. reaching 12 (retina 3) at 6.9 mm ventral to the center.

range from 1,500 to 1,800 μm^3 (Fig. 8, upper). Their differences, less than 20%, are rather small compared with those of the mean lengths and sectional areas.

When the mean volume of the red ROS is multiplied by the mean density at each position given in Figure 7, the product indicates the red ROS volume per unit area (mm^2) (Fig. 8, lower). The pattern illustrated by these values is quite similar to the meridional profile in the topographic map of visual pigment in the bullfrog retina [3]. The red ROS volume per unit area is about two times as great in the dorsal as in the ventral areas. This coincides with the observation of Reuter *et al.* [1] that the number of visual pigment molecules per unit area is two to three times as great in the dorsal as in the ventral areas, assuming the relation that the content of visual pigment is proportional to the ROS volume.

The area centralis

The ROS volume can be considered to have a close relationship to visual sensitivity. On the other hand, the density of the ROS is one of the determining factors of visual acuity. The ROS are "slender" and high in density in the dorsal areas but are "stocky" and low in density in the ventral areas of the bullfrog retina. In the area centralis a few millimeters dorsal to the optic disc, the ROS show a peak in density and are reciprocally small in sectional area. Since the increase in length complements the decrease in cross-sectional area, the volume of the ROS decreases little. It is suggested that visual acuity increases with almost no decrease

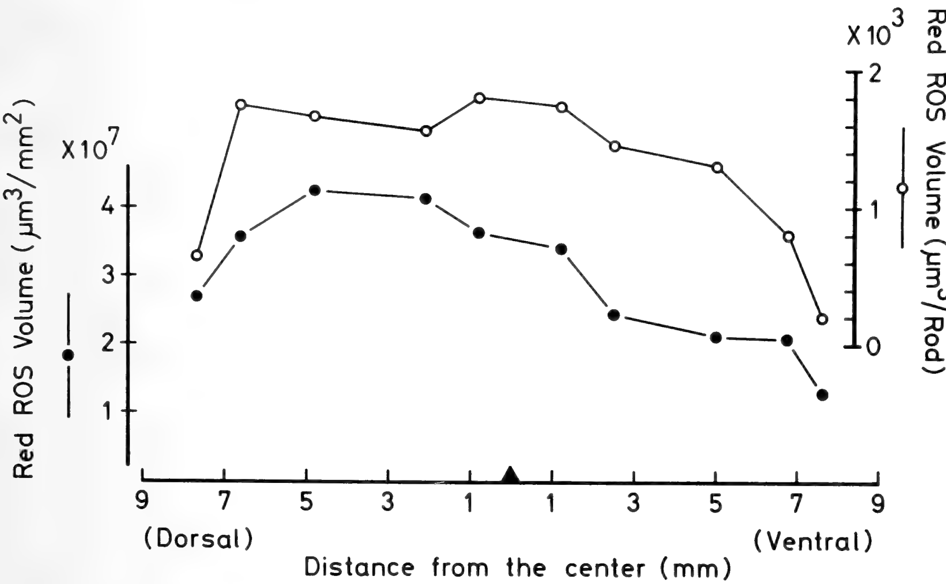

FIG. 8. *Upper*) Estimated volume of a red ROS along the vertical meridian of a retina. Each value is obtained by multiplying the mean length (μm) and the mean sectional area (μm^2) of the red ROS at each position. *Lower*) Estimated total volume of red ROS in a unit area of mm^2. Each value is obtained by multiplying the mean volume of the red ROS (μm^3) and the mean density (1/mm^2) at each position.

in sensitivity in the area centralis.

Cone outer segments are well known to be thinner and longer in the fovea centralis than in the other regions of avian, reptile, and primate retinas [13, 14]. The volume of the outer segment seems to be equalized by the inverse relationship between its length and thickness in the same manner as described above. A layer of photoreceptors is thought to make the "primal sketch" [15] of an outer object in the planar pattern of their responses. Both form and color recognitions ultimately depend on the "primal sketch". Equal sensitivity is probably essential for the comparison among neighboring photoreceptor units. If the sensitivity of the same type of photoreceptor differs from unit to unit even in the neighborhood, the intensity pattern of the outer object would be misdescribed or a special mechanism for correction would be needed. The equalization of the outer segment volume is considered to be one factor for designing an efficient and reliable array of light intensity-coding units in living retinas.

ACKNOWLEDGMENTS

The author thanks Dr. C. J. Karwoski, University of Georgia, and Dr. T. Suzuki, Department of Pharmacology, for their helpful comments on the manuscript, Prof. S. Kanda and Dr. Y. Yamada for their continual encouragement, and Ms. M. Wada for her excellent technical assistance.

REFERENCES

1 Reuter, T. E., White, R. H. and Wald, G. (1971) Rhodopsin and porphyropsin fields in the adult bullfrog retina. J. Gen. Physiol., **58**: 351–371.

2 Tsin, A. T. C. and Beatty, D. D. (1980) Visual pigments and vitamins A in the adult bullfrog. Exp. Eye Res., **30**: 143–153.

3 Makino-Tasaka, M., Suzuki, T., Nagai, K. and Miyata, S. (1985) Spatial distribution of visual pigment and dopamine in the bullfrog retina. Exp. Eye Res., **40**: 767–778.

4 Makino-Tasaka, M., Nagai, K. and Suzuki, T. (1983) Seasonal variation of the vitamin A_2-based visual pigment in the retina of adult bullfrog, *Rana catesbeiana*. Vision Res., **2**: 199–204.

5 Eckmiller, M. S. and Steinberg, R. H. (1981) Localized depigmentation of the retinal pigment epithe-

lium and macrophage invasion of the retina in the bullfrog. Invest. Ophthalmol. Vis. Sci., **21**: 369–393.

6 Duke-Elder, S. (1958) The eye in evolution. In "System of Ophthalmology". Vol. 1, Ed. by S. Duke-Elder, Henry Kimpton, London, pp. 333–351.

7 Gordon, J. and Hood, D. C. (1976) Anatomy and physiology of the frog retina. In "The Amphibian Visual System". Ed. by K. V. Fite, Academic Press, New York, pp. 29–86.

8 Fite, K. V. and Scala, F. (1976) Central visual pathways in the frog. In "The Amphibian Visual System". Ed. by K. V. Fite, Academic Press, New York, pp. 87–118.

9 Bruggers, R. L. and Jackson, W. B. (1974) Eye-lens weight of the bullfrog (*Rana catesbeiana*) related to larval development, transformation, and age of adults. Ohio J. Sci., **74**: 282–286.

10 Tsukamoto, T. and Yamada, Y. (1982) Light-related morphological changes of outer segment membranes from lamellae to tubules and two kinds of wavy configurations in the frog visual cells. Exp. Eye Res., **34**: 675–694.

11 Negishi, K., Drujan, B. D. and Laufer, M. (1980) Spatial distribution of catecholaminergic cells in the fish retina. J. Neurosci. Res., **5**: 621–635.

12 Iwasawa, H. (1979) The Care and Regulation of Laboratory Animals and their Practice. Ed. by T. Imamichi, K. Takahashi and T. Nobunaga, Soft Science Co., Tokyo, pp. 554–556. (in Japanese)

13 Cajal, S. L. (1893) La Retine des Vertebres. La Cellule. **9**: 125–255. In "R. W. Rodieck: The Vertebrate Retina." D. Maguire and R. W. Rodieck, transl. Freeman, San Francisco, pp 775–904.

14 Polyak, S. L. (1957) The Retina. Univ. Chicago Press, Chicago.

15 Marr, D. (1976) Early processing of visual information. Philos. Trans. R. Soc. Lond. **B275**, 483–524.

ZOOLOGICAL SCIENCE 4: 243–257 (1987)

Mechanism of Light Reflection in Blue Damselfish Motile Iridophore[1]

HIROAKI KASUKAWA, NORIKO OSHIMA and RYOZO FUJII[2]

Department of Biology, Faculty of Science, Toho University, Miyama, Funabashi, Chiba 274, Japan

ABSTRACT—Using split-fin preparations of the blue damselfish, *Chrysiptera cyanea,* analyses were made on the mechanism of light reflectivity in the iridophores, which have recently been disclosed to be motile, being regulated by the sympathetic nervous system. A rather steep spectral peak of the reflected light is apparently due to the multilayered thin-film interference phenomenon of the "non-ideal" type. If a skin specimen was equilibrated in the physiological saline, the spectral peak of light reflected from the iridophores stood around 380 nm (near-ultraviolet region), but could be shifted towards longer wavelength up to 530 nm by adrenergic stimuli. Reverse changes were aroused by the effect of adenosine, which has lately been shown to be the co-transmitter of chromatic fibers to antagonize the action of the true transmitter, norepinephrine. A hypotonicity of the bathing media also gave rise to a shift of the wave-band up to about 600 nm. These observations indicate that the shift of the peak towards longer or shorter wavelengths may be due to the simultaneous increase or decrease in the distance between adjoining reflecting platelets within a stack of them. Functional significance of the iridophores in skin coloration characteristic to this species of fish was discussed in conjunction with the unique architecture of the cells and with the supplemental role of underlying melanophores.

INTRODUCTION

Iridophores are light-reflecting chromatophores, rather commonly found in the dermis of many poikilothermal vertebrates, and are known to take predominant role in producing the metallic luster or whitish tone of the integument. Recent fine structural observations have revealed that, in these cells, large platelets ran parallel to each other, forming stacks of them [1–3].

Being crystalline structures mainly composed of guanine, the vertebrate iridophore platelets have very high refractive index of about 1.93 [4], and are consequently very highly reflective in the watery vehicle, the cytoplasm. The refractive index of the latter should be somewhat above that of the water, being about 1.37, as recently estimated, for example, on sea-urchin eggs by Hiramoto *et al.* [5].

The reflectivity for a single interface can be given by the Fresnel's equation:

$$r^2=(n_b-n_a)^2/(n_b+n_a)^2,$$

where r^2 is the reflectivity, i.e. the proportion of incident energy reflected (r: the amplitude reflection coefficient), while n_a and n_b are defined as the refractive indices of materials consisting two phases. Usually, n_b is used for representing the higher one for convenience. At the guanine-cytoplasm interface, the reflectivity is calculated in such a way to be about 0.029, when we adopt 1.37 and 1.93 for n_a and n_b, respectively. r can thus be calculated to be a strikingly high value of about 0.17. These circumstances can effectuate a very high reflectance of the structure containing a number of parallel interfaces.

Actually, the light reflection in the iridophores which contain a number of platelets has also been considered by a few workers. Using the sprat (*Clupea sprattus*) scales, for instance, Denton and Land [6] have shown that the cellular reflectivity is due to the multiple thin-film interference phe-

Accepted December 6, 1986
Received November 4, 1986

[1] This paper is dedicated to Professor H. Kobayashi on the occasion of his retirement from the Faculty of Science, Toho University.

[2] To whom requests for reprints should be addressed.

nomenon. Furthermore, they explained the silvery layers in the scale of the sprat and the herring, *C. harengus*, as the structures to display the so-called "ideal" multilayer thin-film interference phenomenon for an effective reflector of light [7]. There, the optical thickness (i.e., the refractive index multiplied by the actual thickness) of the reflecting platelets and that of the cytoplasmic sheet intervening the adjacent platelets are almost the same, being about one-quarter of a wave length of a spectral peak of light reflected from the iridophores.

In this system, the spectral peak becomes very wide, and the reflectivity so high, resulting in the silvery glitter of the body surface, quite often like a mirror. It has further been pointed out that such architectures displaying the ideal interference phenomenon are rather abundantly found in the surface structures of animals [6, 7].

In case that the above-mentioned conditions can not be applied, the reflection should be "non-ideal". Examining electron-micrographs taken by former researchers, in fact, we could frequently find the presence of too thin reflecting platelets as to form the ideal layers. There, the interference should be of a non-ideal type.

Quite recently, on the other hand, we have found peculiar iridophores in the skin of the blue damselfish, reflective colors of which varied upon neural stimulation [8, 9]. As the common name signifies, these fish species normally display characteristic cobalt-blue coloration, which we have presumed to be due mainly to the reflective properties of the iridophores. Under certain ethological or stressful conditions, the fish change their hue rapidly to dark with some shade of violet, or sometimes to greenish tone. Some structural changes have naturally been assumed in the iridophores. Our electron-microscopic observations indicated that, in these iridophores, there are a number of stacks of reflecting platelets, although the spatial arrangement is quite different from that in any other light reflecting cells reported to date [8]. We came to a conclusion that the color change is due to a simultaneous change in the distance between adjoining reflecting platelets constituting a stack of them. Thus, the cellular motility of the damselfish iridophores is of an entirely new type known hitherto throughout living organisms.

To understand subcellular optical events and the significance of colorations characteristic to this fish, we tried to analyse quantitatively the light reflection of the iridophores under variously stimulated conditions. Part of the results of the present work has been reported briefly [10].

MATERIALS AND METHODS

The blue damselfish, *Chrysiptera cyanea* (Quoy et Gaimard), was used as the experimental material. Being very popular coral-reef fish for home aquariums, they could easily be obtained from local commercial sources. Adult forms having body lengths between 45 and 60 mm were selected

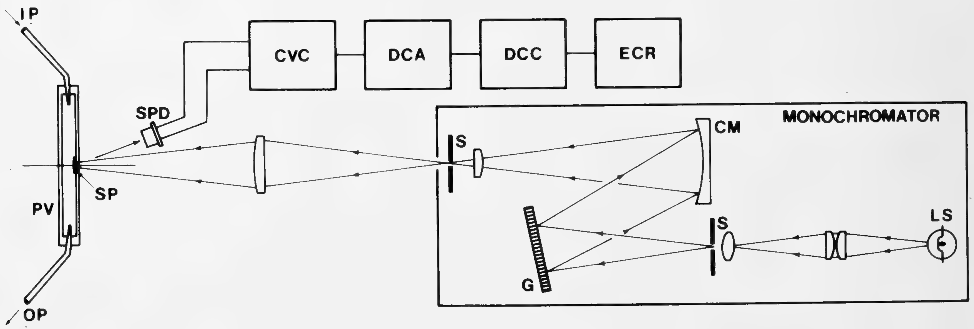

Fig. 1. Diagram of the setup for measuring spectral reflectance of ultraviolet-to-visual light region of the surface of a skin piece, employing a monochromator as the light source. CM: concave surface mirror, CVC: current-to-voltage converter, DCA: direct-current amplifier, DCC: DC-component compensator, ECR: electronic chart recorder, G: grating, IP: inlet pipette for perfusing solution, LS: light source, OP: outlet pipette for perfusing solution, PV: perfusion vessel, S: slit, SP: skin preparation, SPD: silicon photodiode.

for the present purpose.

In this study, split dorsal-fin pieces were exclusively used, which were prepared according to the method described in a previous paper [11]. These pieces were prepared in a physiological solution of the following composition (mM): NaCl 125.3, KCl 2.7, $CaCl_2$ 1.8, $MgCl_2$ 1.8, D-glucose 5.6, Tris-HCl buffer 5.0 (pH 7.2). Iridophores and/or melanophores on their web skin were observed, photographed, and sometimes recorded with their motile responses on a microscope equipped both with epi-illumination and usual transmission optical systems (Optiphot, XT–BD, with CF–BD plan objective lenses; Nikon, Tokyo) [12].

For measuring the spectrum of light reflected from the iridophores, two different assemblies of instruments were put to use. In the first system, a monochromator (High-Intensity Grating Monochromator, Shimadzu-Bausch & Lomb, Kyoto) was employed as an incident light source (Fig. 1). The beam condensed through a long focal length (100 mm) quartz lens was projected on a piece of split fin preparation and the light reflected from it was caught with a silicon photodiode (S1226–5 BQ, Hamamatsu Photonics, Hamamatsu), which was sensitive enough to light-rays of ultraviolet (UV) through visual light region. The wavelength of light emitted from the monochromator was changed from 200 to 700 nm. In the UV range from 200 to 350 nm, a deuterium lamp was used as a light source, whereas a tungsten lamp was employed for generating longer wavelength rays. The wavelength was manually changed at intervals of 5 nm, and the reflectance was recorded on a paper chart recorder (SP–G3C, Riken Denshi, Tokyo) by a photoelectrical method as partly modified from the original one by Oshima and Fujii [12]. By using a rectangular field stop, the area to be irradiated was restricted to about 7.6 mm^2 (2.0×3.8 mm) which fit with the dimension of a split dorsal-fin preparation.

Another measuring system was a commercial item called the Spectro-Multichannel Photo-Detector (MCPD–100, Otsuka Electronics, Osaka) which enabled us to measure the spectral characteristics very rapidly (Fig. 2). Being operated by an equipped personal computer system (PC–9801VM2, Nippon Electric, Tokyo), this apparatus, using a photodiode array (1024 channels), could measure the light spectrum ranging from 220 to 800 nm within a short period of 25 msec through 20 sec. In the present measurements, a 500-msec range was exclusively employed for sampling. In this system, a quartz fiber-optics was adopted for light irradiation and measurement. Of the two optical fiber assemblies, each of which being consisted of a number of fine glass fibers, one was led to the light source (deuterium lamp for 220–350 nm; halogen lamp for 350–800 nm) and the other to a photoelectric transducer. At the other ends of the two sets, fibers were appropriately mingled to form the bottom half of the letter, Y. From the cut and ground end there, the source light was emitted, and the rays reflected

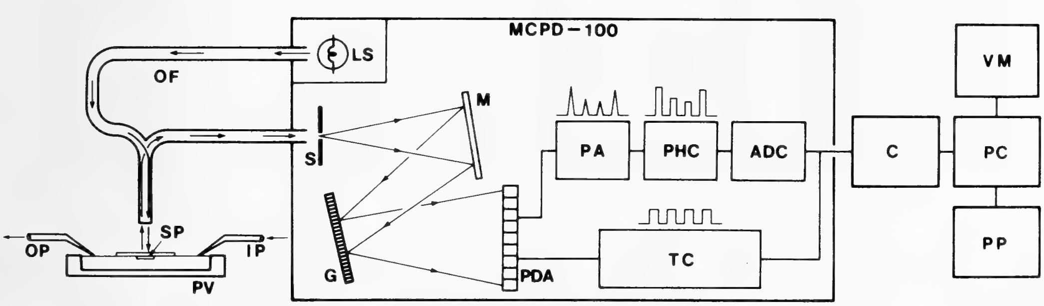

FIG. 2. Diagram of the setup for measuring rapidly the spectral reflectance of near ultraviolet-to-visual light region, using a photodiode-array detection system, MCPD-100 (Otsuka Electronics, Osaka). ADC: analog-to-digital converter, C: controller, G: grating, IP: inlet pipette for perfusing solution, LS: light source, M: mirror, OF: optical fiber assembly, OP: outlet pipette for perfusing solution, PA: pre-amplifier, PC: personal computer, PDA: 1024-channel photodiode aray, PHC: peak hold circuit, PP: X–Y plotter printer, PV: perfusion vessel, S: slit, SP: skin preparation, TC: triggering circuit, VM: video monitor.

from the specimen were introduced into the fiber-assembly again. That is, the angle between the incident and the reflected rays could practically be regarded to be 0°. The total area of the cross section of the fiber assembly was about 20 mm^2. In order to minimize the angle of incidence, however, the area from which light-rays emitted was restricted to ca. 0.9 mm^2 (0.55×0.65 mm). In each measurement, data concerned were processed by the attached computer and immediately registered on an X-Y plotting recorder (MC–920, Otsuka Electronics).

A standard reflecting white paper (reflectance, ca. 90%; Japan Color Research Institute, Tokyo) or a compressed sheet of fine crystals of $MgCO_3$ (Nakarai Chemicals, Kyoto) was adopted as a full reflector control in using the monochromator or the MCPD system, respectively. When measuring optical properties within the UV region, quartz products were rightly chosen for lenses, cover slips and slide glasses.

In an attempt to see the light-reflecting characteristics of swollen iridophores, hypotonic media were used to bathe a skin preparation. For this purpose, a saline solution whose osmotic pressure was lowered by decreasing the NaCl concentration to 100, 80, 60, 40 or to 20 mM was employed. In preparing such a medium, all other components than NaCl were left unchanged from the recipe of the primary physiological saline. The tonicity of the solution was calculated on the rightful assumption that all the salts were totally dissolved. The hypotonic solutions having following osmolarities were used (mOsm): 231.8, 191.8, 151.8, 111.8 and 71.8. Incidentally, the tonicity of the primary saline was calculated to be 282.4 mOsm. Using the dark-field epi-illumination microscope mentioned above, the states taken by iridophores in these solutions were observed and/or monitored photoelectrically on a paper chart recorder (EPR–10B; slightly remodelled to meet our request to have chart-driving speeds of 10 and 20 mm/min by the manufacturer, Toa Electronics, Tokyo) [12]. In this series of tonicity experiments either the above-mentioned monochromator or the MCPD system was put to use for determining the spectrum of light reflected from the iridophores.

In some experiments, an electric stimulator (SEN–3201; Nihon Kohden, Tokyo) was used to excite the sympathetic fibers controlling chromatophore motility. The method was essentially the same as that described in a previous paper [13]. When a chemical stimulation was adopted to induce the coloring response of varying grades delicately, a K^+-rich saline containing either 10, 20, 25, 30, or 50 mM K^+ was used to irrigate the skin piece. In those solutions, the Na^+ concentration was compensatorily lowered to keep the tonicity unchanged.

The drugs used were norepinephrine hydrochloride (Sankyo, Tokyo), tolazoline hydrochloride (Yamanouchi Pharmaceutical, Tokyo), adenosine (Kohjin, Tokyo), phenoxybenzamine hydrochloride (Nakarai Chemicals, Kyoto). The stock solutions of these drugs were diluted with the physiological saline or one of the experimental solutions immediately before use.

All the experiments were carried out at a room temperature between 19 and 24°C.

RESULTS

Preliminary observations

As shown in Figure 3A, the normal coloration of the blue damselfish is cobalt-blue, but not so shiny. The spectral peak reflected from the integument of such a fish takes its position around 465 nm. Under certain ethological conditions, e.g. in fear, they loose their remarkable hue, becoming dark violet (Fig. 3B). Then, the peak of the wave-band is located on about 380 nm, and the skin hardly reflects visible rays. Sometimes, such as when they are feeding, the fish show a different reaction, i.e. their body surface displays greenish tone (Fig. 3C). The spectral peak at that time stands at around 500–530 nm. These distinguishing colorations are manifested by the overspread presence in the integument of simple dermal chromatophore units, each of which consists of a melanophore and numbers (10–20) of small overlying iridophores in a monolayer [8, 11].

We recognized in the present study that some parts of the body surface of the material lacked the iridophores. In the distal part of the caudal half of the dorsal fin, for instance, only melanophores

FIG. 3. Typical body colorations displayed by the blue damselfish, *Chrysiptera cyanea*. A: normal, characteristic cobalt-blue coloration commonly observable among most fish in a school. B: dark violet phase observable during excitement darkening or in one or a few fish (probably social outcasts) in a group. C: greenish phase observable in some ethological encounters, such as those in fear, or during handling (excitement blanching). Photographs were taken immediately after taking a fish out of the water. Body length: 48 mm.

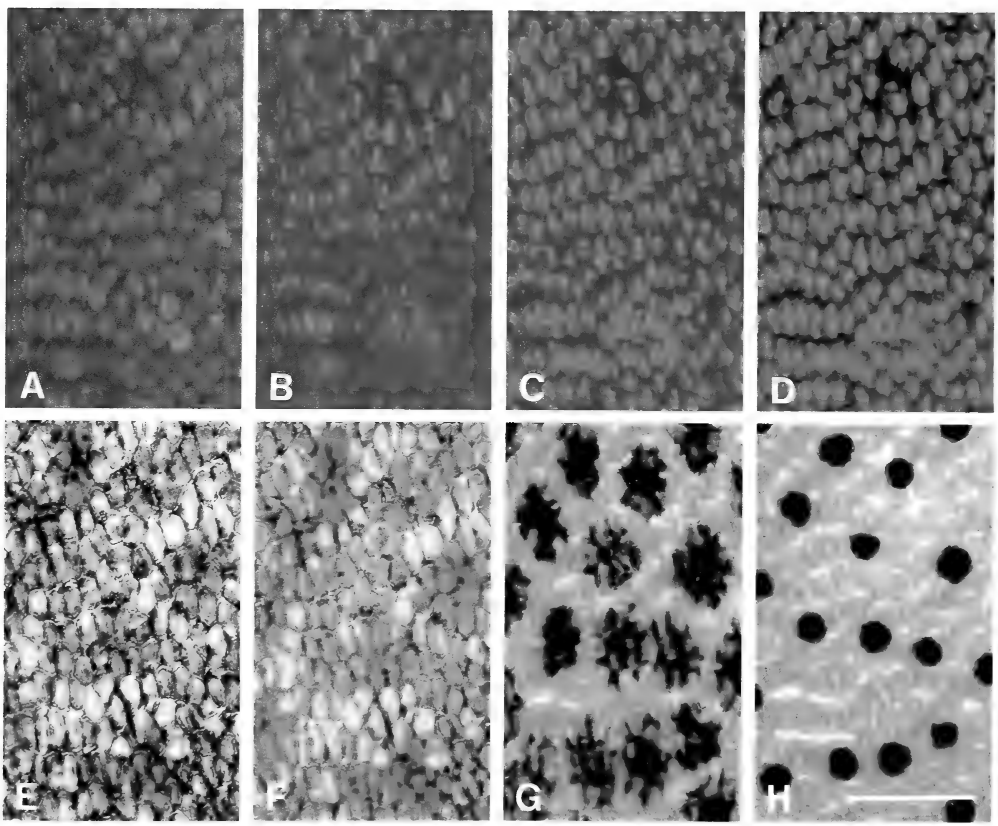

FIG. 4. Photomicrographs showing four stages of iridophores (upper row; taken with a dark-field epi-illumination optics) and melanophores (lower row; with a transmission optics) of the blue damselfish as induced by electrical nervous stimulation or by norepinephrine solution. All photographs were taken on the same field on an isolated split dorsal-fin piece. For details of the methods, see text. A and E: Equilibrated in physiological saline. B and F: After 3-min volley of biphasic square pulses (10 V in strength, 1.0 msec in duration) at 0.2 Hz. C and G: after stimulation with pulses of the same parameters, but at 0.5 Hz. D and H: 3 min after the application of 5×10^{-6} M norepinephrine. Scale bar: 50 μm.

exist. Such parts reflected practically no light. These observations provide a further support for the view that the iridophores are predominantly responsible for the light reflectivity of the integumental tissue.

Based primarily on pharmacological analyses on split dorsal-fin preparations, we have lately shown that the motile responses of the iridophores are solely under the control of sympathetic nervous system being unaffected by any endocrine principles known hitherto to control the motility of chromatophores [9]: The iridophores which had previously been brought to a transparent or "cleared" state by equilibrating the carrier skin piece in the physiological saline became "colored" upon stimulation of chromatic nerves or by applying sympathomimetic substances. More precisely speaking, the shift of the spectral peak of the reflecting light up to green via violet and blue is essentially due to the neurally evoked response of the iridophores. Such a change in the state of iridophores has lately been defined as the "coloring" response, while the reverse process taking place in the simple saline or induced actively by adenosine, the co-transmitter substance of the sympathetic pigment-motor fiber, was designated as the "clearing" response [9, 10]. The transparent, the maximally colored and two intermediate stages of iridophores photographed under incident light illumination are exhibited in color in Figure 4, which also includes four transmission photomicrographs in the lower row showing states assumed by melanophores.

We have already shown that norepinephrine gives rise to the coloring response of the iridophores dose-dependently, and that the maximal degree of the response could be reached by the amine at above 5×10^{-6}M [9]. An elevated K^+ concentration in the bathing medium also caused the same response but through the liberation of catecholamine neurotransmitter from neural elements around the iridophores [14]. The ion also acted dose-dependently. We found, in addition, that tolazoline, a known alpha-adrenergic blocker, could bring about a moderate coloring response of the iridophores. In consideration of the intrinsic alpha-blocking action of the drug, the observed reaction seemed to be rather strange. However, the observed action may be considered as a side-effect, i.e. an adverse, agonistic action possessed by the antagonist itself, because the moderate melanosome-aggregating effect of the same drug on guppy melanophores has been explained by the same mode of action [15]. By making good use of these agents, we have been able to investigate optical characteristics of motile iridophores in the following sections.

Reflection in motile iridophores

Using the MCPD system, the spectral characteristics of light reflected from the iridophores were studied, and the results of a typical series of measurements are shown in Figure 5.

As mentioned earlier, the iridophores assume a transparent state, when the excised skin preparation was equilibrated in the physiological saline. The peak of the wave-band was about 380 nm, as shown in the curve A in the figure. We recognized that the peak was rather low within the region of near-UV, and further that the reflection within the visible-ray domain, i.e. above 400 nm, was very low and practically flat.

When chromatic nerves were stimulated electrically, the spectral peak reflected from the iridophores moved towards longer wavelengths, and the results of a series of measurments are typically exhibited in Figure 5. As seen in curves A through H of the figure, the wave peak progressively moved towards longer wavelengths up to 513 nm upon stimulation. It was also recognizable here that the reflectance became higher with the progress of the response.

Within two minutes after the application of 5×10^{-6}M norepinephrine, on the other hand, the iridophores became almost maximally colored. At that time, the spectral peak was found shifted to about 530 nm, i.e. green. The reflection in the near-UV region was no longer detectable. Even when the duration and/or the strength of norepinephrine stimulation were increased, the spectral parameters remained essentially unchanged. That is, the maximal response attainable under usual conditions is green.

Examining spectral curves on variously treated *in vitro* preparations, we then tried to quantify the relation of the magnitude of the coloring responses

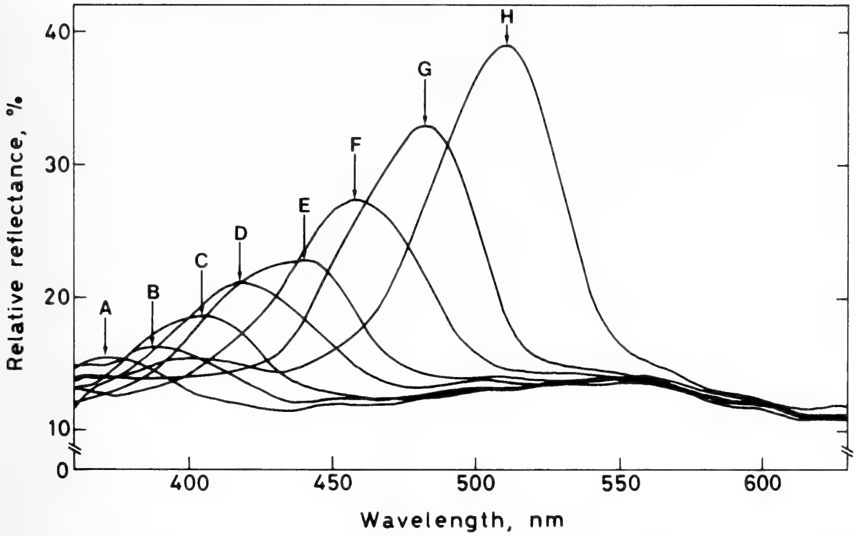

FIG. 5. Typical recordings showing spectral reflectance changes with the progress of coloring response of iridophores elicited by electrical nervous stimulation (biphasic square pulses, 10 V in strength, 1.0 msec in duration, 1 Hz). Spectral curve A was recorded in physiological saline, while those from B to H were obtained at 12, 29, 35, 41, 46, 50 and 60 sec after the initiation of stimuli, respectively. The wave peak moved from 372 to 388, 404, 420, 440, 458, 482 and finally to 510 nm, progressively. Arrows indicate positions of the peaks of those spectral reflectance curves.

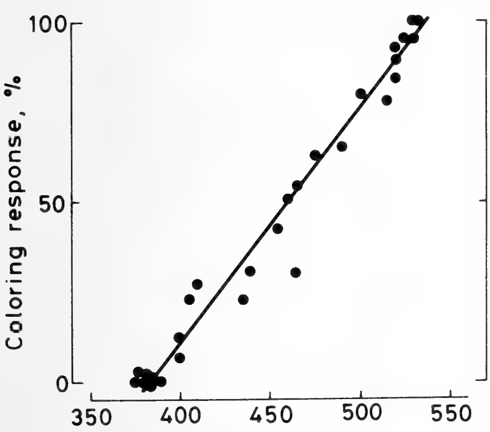

FIG. 6. Relationship between the spectral peak wavelength and the magnitude of coloring response of damselfish iridophores. Each plot was obtained on different split-fin preparation. The coloring responses at varying levels were induced by norepinephrine, tolazoline or increased K^+ at various strengths. Abscissa, wavelength of the spectral peak in nm. Ordinate, magnitude of response as a percentage of the level of full coloring response attained during a 5-min application of 5×10^{-6} M norepinephrine at the end of each series of measurement.

to the position of the spectral peak. The measurements were made by the monochromator system, and the results were shown in Figure 6, where the magnitude of the coloring response was plotted against the wavelength of the peak. The linear regression was calculated as follows:

$$y=0.655x-251$$

where y is the grade of the coloring response in percentage, and x is the wavelength of the peak in nm. It was found that, while y proceeds from 0 to 100, x changes from 383 to 536.

Then, we studied the effect of changing the angle of incidence of light hitting the plane of the body surface on the spectrum of the reflected light. The skin preparations in which iridophores assumed the maximally and sustained colored state by treating with 5×10^{-6} M norepinephrine were exclusively employed, since the strongest and stable reflectivity could be obtained. In the actual measurements using the MCPD–100 system, the inclination of the skin piece was appropriately varied in reference to the direction of light-rays emitted from the rigidly fixed light-guide setup. When the incident rays were perpendicular to the

plane of the skin preparation, the angle of incidence was justly defined as 0°. In this particular series of measurements, the spectral peak wavelength in this geometrical condition was found to be 530 nm, as exhibited in Figure 7. The incident angle was then increased up to 40°. Between each group, one way analysis of variance showed no significant difference. That is, the spectral peak of the reflected light was found to stand practically unmoved disregarding the angle of incidence.

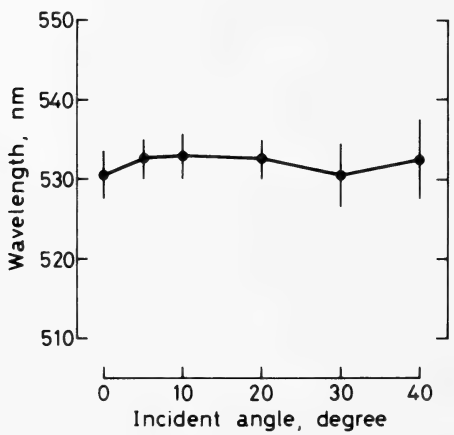

FIG. 7. Relationship of the angle of incident light-beam to the spectral peak wavelength of the light reflected from iridophores in a damselfish skin piece. A full coloring response of the cells had previously been induced by 5×10^{-6} M norepinephrine. Angle of incidence varied from 0 to 40°. Each point is the mean of 5 measurements on different animals. Vertical lines indicate SE.

Hyposmotic effect on iridophore reflectivity

As expected, a decrease in the osmolarity of the solution bathing a skin preparation induced coloring of the iridophores. For example, the iridophores exhibited a moderate coloring response, when the normal saline (282.4 mOsm) was replaced with a little hyposmotic solution of 191.8 mOsm, as displayed in Figure 8. The rate of the response to the hypotonicity, however, was significantly lower than that elicited by sympathomimetic substances of supramaximal strengths in the normal saline. In the left part of this particular recording, the rapid and pronounced response to norepinephrine at 5×10^{-6} M is exhibited as a control. The hypotonicity (191.8 mOsm)-induced response shown around the middle was about half as large as the maximal level caused by the amine of the mentioned strength. With a further lowering of the tonicity of the media, the magnitude of the response progressively increased, and the response became even larger than that attainable by the amine alone (control response), when the tonicity was lowered to 151.8 mOsm (cf. Table 1).

Using the MCPD–100 system, then, the effects of the hyposmolarity on the spectrum of light reflected from the iridophores were investigated more quantitatively. The data obtained were summarized in Table 1. Evidently, the spectral peak shifted towards the longer wavelengths as the tonicity was decreased. Within the region of the tonicity decrease exhibited in Table 1, the phenomenon was quite reversible and reproducible, although a further decrease in it infallibly caused the rupture of the cells, resulting in the irreversibility of the phenomenon. The lowest tonicity within the limit of reversibility was as low as 71.8 mOsm. At that time, the peak was rising at about 600 nm, and the skin piece assumed yellow with a dash of orange color. As referred to in Table 1, the spectral peak in the maximally colored state induced by norepinephrine was about 530 nm (green). By lowering the tonicity of the bathing fluid, therefore, the spectral peak could be brought into the region much longer in wavelength than when norepinephrine alone was added to the normal saline.

So far, alpha adrenoceptors have been known to be solely responsible for mediating physiologically the coloring response of the cells [9]. In the next trial, therefore, influences of adrenergic blocking agents of alpha type, i.e. phentolamine and phenoxybenzamine, on the coloring response-inducing effect of hypotonicity were examined. The results were that neither of them had any influence. These observations apparently exclude the possibility that the hypotonic effect is mediated by adrenoceptors or by the liberation of adrenergic neurotransmitter from the neural elements around the effector cells.

TABLE 1. Effects on the wavelength of the spectral peak reflected from motile iridophores of the blue damselfish, *Chrysiptera cyanea*, of the hypotonicity of the medium, and the influence of norepinephrine (NE) and adenosine (AS) on the former's action

$[Na^+]$ in test solution* (mM)	Tonicity (mOsm)	Wavelength of spectral peak** (nm)		
		In simple saline	$+10^{-4}$ M AS	$+5\times10^{-6}$ M NE
125.3 (Control)	282.4	376.0±5.48	372.0± 4.47	534.4± 4.39
100.0	231.8	434.8±10.38	422.4±11.35	546.8± 2.77
80.0	191.8	492.2±16.77	463.8±13.65	558.2± 3.03
60.0	151.8	562.4± 6.35	542.0±13.65	574.4± 3.91
40.0	111.8	581.8± 5.40	588.0± 3.39	592.8± 2.28
20.0	71.8	596.4± 7.92	586.8± 8.79	595.2±10.85

* Other components (mM): KCl 2.7, $CaCl_2$ 1.8, $MgCl_2$ 1.8, D-glucose 5.6, Tris-HCl buffer 5.0 (pH 7.2).

** Each value is the mean of 5 measurements followed by SE.

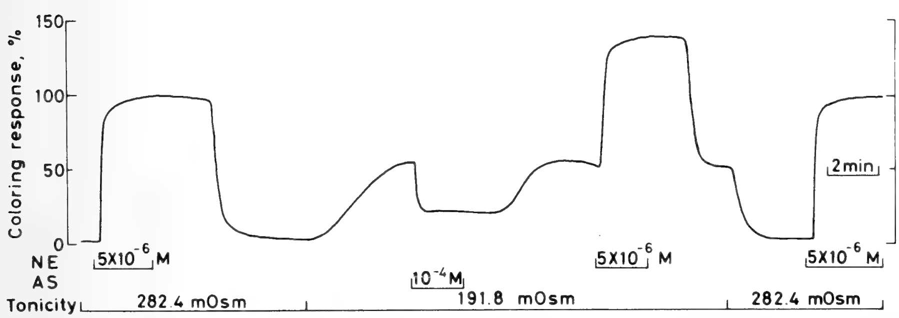

FIG. 8. Typical recording showing the coloring response-inducing action of the hypotonicity (191.8 mOsm) on damelfish motile iridophores, and the influences of 10^{-4} M adenosine (AS) and 5×10^{-6} M norepinepherine (NE) added to the same medium. Abscissa: time. Ordinate: magnitude of coloring response in percentage, taking maximal coloring response to 5×10^{-6} M NE in the normal saline (282.4 mOsm) as 100%.

Norepinephrine and adenosine effects in hypotonicity

We have already shown that either the coloring response or the reverse process, i.e. the clearing response, of the motile iridophores was induced by the true neurotransmitter, norepinephrine, or the co-transmitter, adenosine, from the same fibers, respectively [9]. In solutions, whose osmolarity was lowered variously, therefore, the effects of those neural substances were examined. The photoelectric recording displayed in Figure 8 includes parts showing their effects under a hypotonic condition. Again, the maximal coloring response to 5×10^{-6} M norepinephrine seen in the left part could be employed as the control, which was followed by a moderate coloring response induced by changing the medium to a hyposmotic saline (191.8 mOsm). Then, 10^{-4} M adenosine was added to the same medium. A large clearing response developed quickly. The nucleoside's effect was quite reversible. Then, 5×10^{-6} M norepinephrine was added to the hypotonic saline. The moderately colored state was soon augmented to the level apparently beyond that attained by the amine of the same strength in the isotonic saline.

The results of a number of such measurements were statistically treated and summarized in Table 1. Evidently, the spectral curves shifted towards longer wavelengths as the tonicity of the medium was lowered. It is also clear that both adenosine and norepinephrine retained their actions even in the hypotonic media. The effects of adenosine was the most remarkable in 191.8-mOsm saline, and

fell to some degree upon further decrease in the tonicity. On the other hand, the shift of the spectral peak by norepinephrine decreased in proportion to the decrease of the tonicity. At osmolarities below 111.8 mOsm, neither adenosine nor norepinephrine showed influences.

DISCUSSION

Reviewing past morphological and functional observations as well as theoretical treatments of the relevant optics, Huxley [16] and then Land [7] elaborately discussed the light reflection from multilayered structures often found in the surface specializations of many animal species. The reader may refer to these articles especially when a certain phenomenon in which he or she is interested must be dealt with theoretically.

In the case of the multilayered thin-film system, the highest reflectivity at a given wavelength (λ) is known to be actualized when the alternately arranged, optically "less dense" (with suffix "*a*") and "denser" ("*b*") layers have the same and definite optical thickness (i.e. the refractive index (n) multiplied by the actual thickness (d)), which equals a quarter of wavelength of the reflective ray. That is, the so-called "ideal" multilayer interference occurs when both $n_a d_a$ and $n_b d_b$ are equal to $\lambda/4$. The interference under such conditions should truly be constructive, yielding an extremely effective reflective surfaces. For instance, the architecture of the reflecting stack in the iridophores of a clupeid fish has been shown to fit this "ideal" system [17]. Applying the interference microscopy to the iridophore inclusions from a sprat scale, Denton [18] actually showed that the platelets had an exceedingly uniform thickness of ca. 100 nm, and that the cytoplasmic sheets between the crystals were about 135 nm thick. The optical thickness of either layer was shown to be practically identical, being about 180 nm.

The above authors have also treated of the "non-ideal" system, where $n_a d_a$ is not identical with $n_b d_b$ [7, 16]. In addition, Bone and Denton [19] and Denton and Land [20] have presented observations on teleostean iridophores which may be explainable in terms of the "non-ideal" interference phenomenon. For example, the latter investigators reported that the spectral peak of light reflected from the iridophores shifted from ca. 650 nm to ca. 515 nm, when the bathing normal saline for marine teleosteans was replaced with the solution in which the salt concentrations were doubled. The tonicity change should not have influenced the thickness of the crystalline platelets. Thus, the optical change may safely be ascribable to the dehydration-induced thinning of the cytoplasmic layer sandwitched between the platelets. They further claimed that, when the cells were equilibrated in the isotonic saline, the situation was actually "ideal". Upon exposure to hypertonicity, the system proceeded to a non-ideal state, where the decreased $n_a d_a$ naturally became unequal to $n_b d_b$. These changes, however, are by no means physiological, but are experimentally induced processes.

Based mainly on the fine structural observations on the iridophores of the present material, the blue damselfish, *Chrysiptera cyanea,* we have reported lately that the reflecting platelets were too thin as to produce the ideal-type interference, and further suggested that the characteristic hue displayed by the fish should be due to the interference of the non-ideal nature, being far from the "constructive" interference [8]. In the present study, we could further corroborate our former assumption: By making use of modern optical means, it was definitely proven that the iridophores are motile, and that the essence of motility is the simultanenous change in the distance of platelets contiguous with each other in all the piles of them within the cells. All our observations to date on the present material indicate evidently that the reflection in the iridophores is explainable in terms of the multilayer interference of the "non-ideal" type.

Quite recently, Iga and Matsuno [21], while working on the freshwater goby, *Odontobutis obscura,* reported that iridophores on their scales are motile. Like many other chromatophore types dealt with by many researchers, these cells are dendritic, and a number of minute reflecting platelets in the cytoplasm disperse from or aggregate into the perikarya in response to neural or hormonal principle. There, the multilayer interference can not be applicable to the mass of

randomly oriented platelets. The incident rays are reflected by the simple scattering like in a leucophore. According to the current terminology of the chromatophores [22], the cells studied by those workers may more properly be classified into the leucophores.

Lythgoe and Shand [23] also reported that iridophores which were responsible for the beautiful blue-green tint of their characteristic longitudinal stripe in the neon tetra, *Paracheirodon innesi,* might be motile. The stripe shows circadian color changes, varying to deep violet at night. According to them, the cells change their configuration at the transition of color. A rather narrow peak of the spectrum from these iridophores may be due to the interference of the "non-ideal" type. However, the structural organization of the cell as well as the regulatory mechanisms for the cellular motility are quite different from those reported by us on the blue damselfish [8, 9]. Later, the workers on the neon tetra have come to the conclusion that the spacing of the platelets may change daily, being triggered by the action of light on the rhodopsin-like molecules contained in the light-reflecting cells themselves [24].

Huxley [16] and Land [7] soundly described that, in the non-ideal interference, the mean wavelength of the reflectance is given as follows:

$$\lambda = 2\,(n_a d_a + n_b d_b)$$

As mentioned earlier in the Introduction, 1.37 and 1.93 may be adopted for n_a and n_b, respectively. Reflecting platelets of this material have been estimated on transmission electron micrographs to be not more than 5 nm thick [8]. Substituting these values into the above equation, the following equation may be offered for estimating the cytoplasmic spacing in nm:

$$d_a = \lambda / 2.74 - 7.04$$

When the body surface assumes the cobalt-blue color (the spectral peak: ca. 465 nm), the cytoplasmic layer between platelets is calculated to be 163 nm thick. We have learned in the study that the spectral peak of light reflected from the iridophores could be moved experimentally between 380 and 530 nm. For producing those changes, the thickness of the cytoplasmic sheet should vary within the region between 132 and 186 nm, theoretically (Table 2). That is, when the coloring response in the iridophores proceeds from 0 to 100%, the net increase in the spacing should be about 54 nm, while the rate of increase is 42%. When the skin coloration changes from the characteristic cobalt-blue to dark violet hue, and to green, the estimated rates of decrease and increase in the spacing thickness may be approximately 19 and 14%, respectively.

It has also been shown that when the optical thicknesses of two alternate layers are different, both the maximal reflectance and the bandwidth of the principal spectral peak decrease depending upon the grade of the difference [7, 16]. Actually, the reflectance of the blue damselfish skin is much lower than that of the silvery trunk or belly skins of

TABLE 2. Summary of the relation of skin colors to motile activities of the iridophores and melanophores in the dermis of the blue damselfish, *Chrysiptera cyanea*

Chromatic state of animal	Normal	Excitement darkening	Excitement pallor
Skin hue	Cobalt-blue	Dark violet	Light green
Peak wavelength (nm)	465	380	530
Calculated distance between guanine platelets (nm)	163	132	186
Increase in distance from normal (%)	—	−19	+14
Coloring response of iridophore (%)	52	0	100
Aggregation response of melanophore (%)	24	0	100

a number of teleosteans, including, for instance, the sprats, sardines, cutlasses, silvery smolts of salmonids, where the "ideal" interference by large paralleled platelets has been confirmed to occur for the high reflectivity.

One may call to mind that the colorations assumed by the blue damselfish are "fluorescence-like". This is especially specious when the fish are characteristic cobalt-blue. Of course, any colors of the tegument do not belong to the fluorescence. In the latter, the radiating rays are commonly restricted within a narrow range of spectrum. The present measurements disclosed clearly that, alike the fluorescence, the spectral peaks of the reflected light were always sharp, if compared with those from the colored surfaces of many other organisms from which the light-rays are absorbed and scattered. In other words, the chroma (saturation) of the blue damselfish coloration is very high, according to the terminology of the Munsell color system, which is being widely used to describe characteristics of colors. That is, the hues assumed by this species of fish are much "purer" than those displayed by many other common fishes. Those optical characteristics may afford additional strong supports for the conclusion that the coloration of the iridophores is based on the "non-ideal" multilayer thin-film interference phenomenon, and that the motility of the cell is due to the alteration of the spacing between the thin platelets.

In the present study, it was clearly shown that the hyposmolarity of the bathing medium shifted the spectral peak of the reflection from the iridophores towards longer wavelengths. It was further shown that norepinephrine or adenosine could bring about additive chromatic effects on the cells which had previously been under the influence of the hypotonicity. That is, the spectral shifts induced by the hypotonicity may be a passive and simply osmotic process, being entirely different from the sequences initiated by the interaction between pigment-motor ligands and membrane-bound receptors. The latter events are of course physiological ones, normally operating in the control of the chromatophore motility *in vivo*. Preliminary studies have led us to conclude that the tubulin-dynein system is involved in this process (Oshima and Fujii, to be published), although the detailed explanations for the cellular motility still remain to be the subject of future research.

Another point worthy to be noted here is that, at a certain degree of the response, the spectral peak did not shift, even when the angle of incidence was varied (cf. Fig. 7). We conclude that this is certainly due to the characteristic arrangement of the piles of reflecting platelets in the motile iridophores; the axes of many piles dispose radially from the nucleus which locates around the apical part of the non-dendritic cell [8]. If the parallel light-rays project on the surface of the skin from a certain incident angle, the piles whose axes are almost parallel with the rays are dominantly responsible for the reflective interference. We have already known through morphological studies that such piles are always present in every iridophore in the skin [8, 9]. The piles with the axes forming a sufficiently small angles with the incident rays may be concerned with the reflection to a lesser degree by a small number of platelets within each stack. Those having axes crossing with a larger angle with the direction of the rays are practically irrelevant to the reflection, since the number of platelets becomes too small for producing an effective interference. Even under such an artificial condition of being irradiated by parallel rays unidirectionally any part of skin can reflect light macroscopically, since, as mentioned above, every iridophore contains at least one or few piles among many of them ready for reflecting incident rays, i.e. only a small part within the area occupied by an iridophore is reflective [8]. Consequently, the fractional area of light reflection becomes small, resulting in the weak net reflectance of the skin. In their habitat, i.e. under the coral sea water, on the other hand, the fish receive scattered blue light-rays from every quarter. Thus, the incident rays from near the observer are reflected rather effectively and definitely towards the latter by the mechanism we are now concerned. Against the blue background deep in the sea water, therefore, the fish are rather faintly visible with the characteristic bluish hues with the higher chroma.

An important problem to be discussed next is that the black-pigment containing melanophores underlying the iridophores must have a sup-

plemental but very important role in producing the characteristic hues, especially in increasing chroma value of the coloration. The dark sheet of light-absorbing melanin may certainly be serviceable in decreasing the intensity of stray light coming from inside the body of the small fish. If there were no dark layers, the light coming out through the skin is inevitably filtered by the iridophore layer, tending to assume a hue complementary to the intrinsic reflective one, i.e. reddish, yellowish or greenish tone, when the iridophores reflect blue green, cobalt-blue or violet rays, respectively. The same dark sheet should also be useful in preventing rays to invade the body, thus leading to a reduction of stray light-rays under the tegument.

When melanosomes are so well dispersed as to fill dendritic processes of the melanophore, furthermore, each iridophore becomes light-insulated from the adjacent ones, because, as already described by us elsewhere [8, 9], peripheral halves of the processes are bent and inserted into the space among the iridophores to form screens partitioning each of them off. Stray light from the adjacent cells may thus be shut off by the dark wall. Such architectural features may certainly enhance the chroma or the purity of the colorations displayed by the integument.

When the melanosomes aggregate into the melanophoral perikarya, such as when the fish is in the excitement pallor or when the *in vitro* skin piece is adrenergically stimulated, the iridophores become rather easily accessible by the stray light-rays both from their bottom and sides. Under such a condition, a considerable amount of diffused and scattered rays from both the dermal side and the surrounding iridophores may actually penetrate the iridophore, resulting in the lightening of the skin. Furthermore, the hues complementary to the reflective peaks of the iridophores are added as the stray light-rays pass through the iridophore layer. Consequently, the broadening of the spectral peak of the reflectance occurs, and the skin assumes greenish white hue. Above explanations on the reflective characteristics of the blue damselfish skin are comprehensively summarized in Table 2.

We have just shown that the characteristic colorations and their changes of a blue damselfish species, *Chrysiptera cyanea*, are predominantly due to the motile activities of the iridophores present in the uppermost part of the dermis in a single layer. It should also be stressed here that the changes are entirely graded or continuous in term of the wavelength within the region between the near UV and the green. Rather incredibly, those are resulted entirely from a physical phenomenon, i.e. the thin-film interference, being totally independent of the changes in the spectral absorption characteristics of certain pigmentary substances. In such a way, the blue damselfish iridophores possess an extremely elaborate machinery within them to realize the remarkable but subtle changes of skin coloration. As one of almost terminally evolved motile cell types, we may be able to compare this optical effector cell even to the striated muscle cell, which has universally been believed to be the most sophisticated mechanism for fulfilling its part, i.e. very fast and effective production of tension. Such an exquisite optical mechanism has never been reported before in any sort of biological structures. Thus, we dare to categorize the motility of the iridophores of the material to be of an entirely new type.

The presence of such motile iridophores as described here is not restricted to this particular species of fish. Up to the present time, for instance, we have actually found very similar ones in a closely related species belonging to the same genus, the yellowtail blue damselfish, *C. hemicyanea* (Weber), and in the heavenly damselfish, *Pomacentrus coelestis* Jordan et Starks (Kasukawa *et al.*, unpublished observations). At least within the genera *Chrysiptera* and *Pomacentrus*, both belonging to the family Pomacentridae (damselfishes), therefore, one may safely suppose that some other unexamined species possess the iridophores of the same category.

On the other hand, our preliminary survey also indicates that such unique iridophores are not existing in many fishes even if they were taxonomically included into the so-called damselfish group (the family Pomacentridae). Instead, those fishes possess immotile iridophores which are quite identical with those found and described almost ubiquitously among many teleostean families [7, 18, 22]. The role of such iridophores among the

assemblage of chromatophores in the color manifestations of some damselfish species will be given in a separate article (Kasukawa and Oshima, to be published).

What a signification or an advantage do the characteristic hues and their changes have in the life of the blue damselfish? We like lastly to consider this interesting ethological problem, which should at the same time be an extremely important one for the fish themselves in fulfilling their strategy for survival.

Using the herring, *Clupea harengus*, for instance, Denton and Nicol [17] have shown that iridophores existing in the skin must take a decisive role in camouflaging the fish against the marine blue background. Their morphological studies indicated that iridophores were present widely over the trunk, and that all the reflecting platelets within them were arranged very parallel with the median plane of the body, i.e. in the sagittal planes. When the fish is swimming normally, therefore, the platelets were very perpendicular to the plane of the sea surface. Thus, the body surface can be likened to a vertically held mirror.

In the sea, the light intensity is of course higher from above and lower from below, although not so much like in the air. On the other hand, the horizontal components of the intensity are much more even in the water, since light-rays are scattered at the rough surface and inside the sea water. That is, the fish receives rays from both sides nearly equally. It is easily understandable, therefore, that, when an observer sees the fish swimming on the same level, the mirror equivalent reflects the light of the same intensity and color, resulting in the invisibleness of the organism.

If the observer looks at the fish at a certain angle, either of depression or of elevation, both the rays reflected at the body surface and those directly reaching the eyes by passing close to the fish have practically the same intensity and the spectrum, since both groups of rays have practically the same absolute value of the angle in reference to the vertical reflective plane. Thus, the image of the fish becomes obscure against the oceanic blue, as if it were not there. This type of optics explaining the cryptic coloration may be applicable to oceanic migratory fishes very commonly [7, 18].

According to the results of our morphological as well as optical investigations, the participation taken by the blue damselfish iridophores must be quite different from the above explanation. Everywhere on the skin, the iridophores reflect light-rays but only those incident from the directions close to the position of the observer, as we have just discussed here. The reflectivity is low and much restricted to a narrow range within the spectrum depending upon the periodicity of the iridophore platelets assumed at that time. Thus, the mirror effect as explained above in the migratory fishes can not be applied.

So far as we are aware, no observations have been recorded up to the present time on the ethological significance of characteristic colorations of the species or of those closely related. We have made only few preliminary investigations into these subjects, too. Therefore, it may be too early to speculate the problem. But, we dare to presume that the rather faint but highly saturated coloration assumed by them must be a signal coloration or more properly the recognition one for other individuals of the same species. Among the corals, the cobalt-blue color should be very conspicuous. Conversely, the same color might be useful as the crytic means when they are apart from the coral reef to escape from their predators. There, the blue tint may be useful in concealing themselves into the marine blue water. Further works are justly needed to establish the roles of their characteristic colorations as well as of their extraordinary rapid changes amid their beautiful habitat.

ACKNOWLEDGMENTS

We thank Professor T. Kajiwara, Department of Chemistry, Professor M. Shimazu and some other members of the Department of Physics, for their helpful discussion on the optical problems. This work was supported by Grants-in-Aid for Scientific Research from the Ministry of Education, Science and Culture of Japan. The monochromator employed was procured by the amount supplementary to the Makoto Seiji Memorial Prize to R. F., 1983.

REFERENCES

1 Kawaguti, S. (1965) Electron microscopy on iridophores in the scale of the blue wrasse. Proc. Japan Acad., **41**: 610–613.

2 Kawaguti, S. and Kamishima, Y. (1966) Electron microscopy on the blue back of a clupeid fish, *Harengula zunasi*. Proc. Japan Acad., **42**: 389–393.

3 Kawaguti, S. and Kamishima, Y. (1966) A supplementary note on the iridophore of the Japanese porgy. Biol. J. Okayama Univ., **12**: 57–60.

4 Hachisu, S. (1975) Nacreous pigments. Prog. Organic Coatings, **3**: 191–220.

5 Hiramoto, Y., Shimoda, S. and Shoji, Y. (1979) Refractive index of the protoplasm in sea urchin eggs. Dev. Growth Differ., **21**: 141–153.

6 Denton, E. J. and Land, M. F. (1967) Optical properties of the lamellae causing interference colours in animal reflectors. J. Physiol. (London), **191**: 23–24P.

7 Land, M. F. (1972) The physics and biology of animal reflectors. Prog. Biophys. Mol. Biol., **24**: 75–106.

8 Oshima, N., Sato, M., Kumazawa, T., Okeda, N., Kasukawa, H. and Fujii, R. (1985) Motile iridophores play the leading role in damselfish coloration. In "Pigment Cell 1985: Biological, Molecular and Clinical Aspects of Pigmentation". Ed. by J. Bagnara, S. N. Klaus, E. Paul, and M. Schartl, Univ. Tokyo Press, Tokyo, pp. 241–246.

9 Kasukawa, H., Oshima, N. and Fujii, R. (1986) Control of chromatophore movements in dermal chromatic units of blue damselfish—II. The motile iridophore. Comp. Biochem. Physiol., **83C**: 1–7.

10 Kasukawa, H., Oshima, N. and Fujii, R. (1985) Optical analyses of reflection in the motile iridophores of blue damselfish. Zool. Sci., **2**: 885.

11 Kasukawa, H., Sugimoto, M., Oshima, N. and Fujii, R. (1985) Control of chromatophore movements in dermal chromatic units of blue damselfish—I. The melanophore. Comp. Biochem. Physiol., **81C**: 253–257.

12 Oshima, N. and Fujii, R. (1984) A precision photoelectric method for recording chromatophore responses *in vitro*. Zool. Sci., **1**: 545–552.

13 Fujii, R. and Novales, R. R. (1969) The nervous mechanism controlling pigment aggregation in *Fundulus* melanophores. Comp. Biochem. Physiol., **29**: 109–124.

14 Oshima, N., Kasukawa, H. and Fujii, R. (1985) Effects of potassium ions on motile iridophores of blue damselfish. Zool. Sci., **2**: 463–467.

15 Fujii, R. and Miyashita, Y. (1975) Receptor mechanisms in fish chromatophores—I. Alpha nature of adrenoceptors mediating melanosome aggregation in guppy melanophores. Comp. Biochem. Physiol., **51C**: 171–178.

16 Huxley, A. F. (1968) A theoretical treatment of the reflexion of light by multi-layer structures. J. Exp. Biol., **48**: 227–245.

17 Denton, E. J. and Nicol, J. A. C. (1965) Reflexion of light by external surfaces of the herring, *Clupea harengus* . J. Mar. Biol. Assoc. U. K., **45**: 711–738.

18 Denton, E. J. (1970) On the organization of reflecting surfaces in some marine animals. Philos. Trans. R. Soc. London, Ser. B, **258**: 285–313.

19 Bone, Q. and Denton, E. J. (1971) The osmotic effects of electron microscope fixative. J. Cell Biol., **49**: 571–581.

20 Denton, E. J. and Land, M. F. (1971) Mechanism of reflexion in silvery layers of fish and cephalopods. Proc. R. Soc. London, Ser. B, **178**: 43–61.

21 Iga, T. and Matsuno, A. (1986) Motile iridophores of a freshwater goby, *Odontobutis obscura*. Cell Tissue Res., **244**: 165–171.

22 Fujii, R. (1969) Chromatophores and pigments. In "Fish Physiology". Ed. by W. S. Hoar and D. J. Randall, Vol. 3, Academic Press, New York, pp. 307–353.

23 Lythgoe, J. N. and Shand, J. (1982) Changes in spectral reflexions from the iridophores of the neon tetra. J. Physiol. (London), **325**: 23–34.

24 Lythgoe, J. N. and Shand, J. (1984) Action spectra for the iridophore light response in the neon tetra. Photochem. Photobiol., **40**: 551–553.

ZOOLOGICAL SCIENCE 4: 259–264 (1987)

Meiosis in the Japanese Gryllacridid *Anoplophilus acuticercus* Karny 1931 (Orthoptera Saltatoria, Rhaphidophoridae): Amphitelic Orientation of the X and Supernumerary Chromosome(s)

Alejo Mesa and Beatriz Goñi[1]

[1]*Departamento de Biologia, Instituto de Biociências, Universidade Estadual Paulista "Julio de Mesquita Filho" UNESP, 13500 Rio Claro, Sao Paulo, Brasil, and* [2]*Department of Biology, Tokyo Metropolitan University, Setagaya-ku, Tokyo 158, Japan*

ABSTRACT—The karyotype of the Japanese rhaphidophorid *Anoplophilus acuticercus* exhibits a male chromosome number of 33, comprising six pairs of metacentric or submetacentric autosomes, ten pairs of acrocentric autosomes and a submetacentric X chromosome. The sex determining mechanism is of the XO(male)-type. One of the two individuals studied had one, the other two supernumerary chromosomes. Both the X and the S's orientate amphitelically in metaphase I and anaphase I, and are reintegrated into one of the daughter nuclei as a single undivided mass of chromatin at telophase I. This meiotic behavior was observed in all the nuclei of both the studied specimens. A tentative reconstruction of the history of Rhaphidophoridae taking into account the karyological data compatible with a recent systematic classification is proposed. The chromosome number of *A. acuticercus* suggests no clear relationship with Rhaphidophorini, where it has been assigned. As an alternative, the morphology and arboreal habits of *A. acuticercus* suggest a close relationship to *Gammarotettix* in the Gammarotettigini.

INTRODUCTION

The Rhaphidophoridae is a worldwide family of wingless gryllacridoid saltatorial Orthoptera. In recent classifications it is divided into five subfamilies: Macropathinae, Ceuthophilinae, Dolichopodinae, Tropidschiinae and Rhaphidophorinae [1]. All Japanese rhaphidophorids belong to the last-named subfamily, which includes three tribes: Gammarotettigini, with one genus in western North America; Rhaphidophorini, with a number of Asiatic genera including *Diestrammena* and *Tachycines,* each having species in Japan; and Troglophilini, comprising the circum-Mediterranean *Troglophilus* with seven described species and the Japanese *Anoplophilus* with three.

Doubts have been expressed by Hubbell (personal communication) as to whether *Anoplophilus* belongs in the Troglophilini; in his opinion it is probably a member of the Gammarotettigini. With the intent of investigating this problem using a karyological approach, the senior author visited Japan in the summer of 1985 in a successful attempt to obtain living specimens of *Anoplophilus*. In this paper the karyotype of *A. acuticercus* is analyzed and its significance in relation to the other known rhaphidophorid karyotypes is considered. Certain unusual features in it relating to the amphitelic orientation of the X and supernumerary chromosome(s) in the first meiotic division are described and discussed.

MATERIALS AND METHODS

Five females and two males of *Anoplophilus acuticercus* Karny 1931 (determined by T. H. Hubbell) were collected in Honshu, Saitama Prefecture, Chichibu District, in the vicinity of the Mitsuminejinja Shrine near Ropeway Station at an elevation of 1100 m, on 9 August, 1985. They were all taken at night along trails in the forest, resting

Accepted October 6, 1986
Received May 23, 1986

on tree trunks.

Two male specimens (J2 and J3) were dissected in the field and the testes were fixed in a mixture of pure ethanol and glacial acetic acid (3:1 in volume ratio). Semipermanent slides were prepared by squashing follicular testes in a drop of lactoacetic orcein 0.5% after approximately one minute of softening in acetic acid 45%.

RESULTS

Both the studied individuals of *A. acuticercus* exhibit a basic karyotype of 2n=33, comprising 16 pairs of autosomes and an X chromosome. The sex-determining mechanism is of the XO(male)-type. Specimen J2 has two relatively large but sligthly unequal supernumerary (S) chromosomes (Fig. 1a), while J3 has only one (Fig. 1c). The autosomes comprise six pairs of metacentric or submetacentric chromosomes and ten pairs of acrocentrics (Fig. 1a). The X and the S's seem to be submetacentric, although the morphology of each chromosome could not be ascertained with certainty. The S chromosomes are univalent, and their arrangement at metaphase I (MI) is amphitelic (Fig. 2a). The same arrangement is shown by the X chromosomes. As anaphase I (AI) proceeds the S's and the X remain in the equatorial plate until the beginning of telophase (Fig. 2b). At last moment, S and X join together into a single

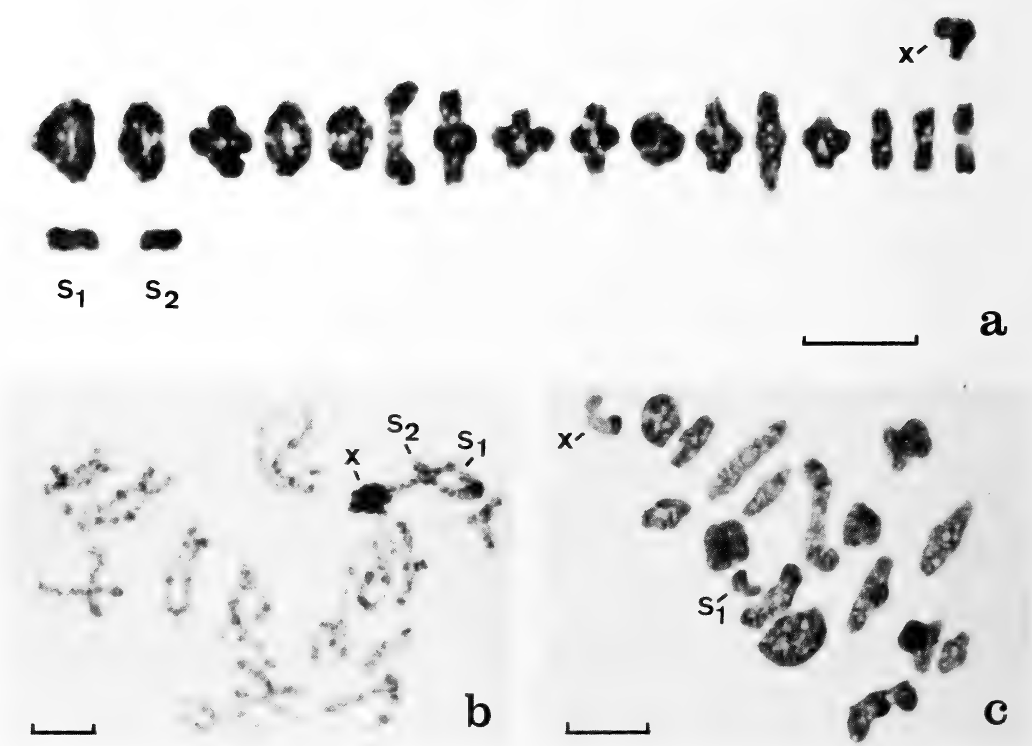

FIG. 1. Metaphase and diplotene chromosomes of *A. acuticercus*. a) First metaphase of specimen J2 with bivalents (six of them formed by metacentric or submetacentric autosomes plus 10 acrocentric pairs) arranged in decreasing order of size. b) Diplotene of specimen J2 with two S chromosomes; note the nonhomologous association involving the X and S's chromosomes. c) Metaphase I of specimen J3 with a single S chromosome. Bar=10μm.

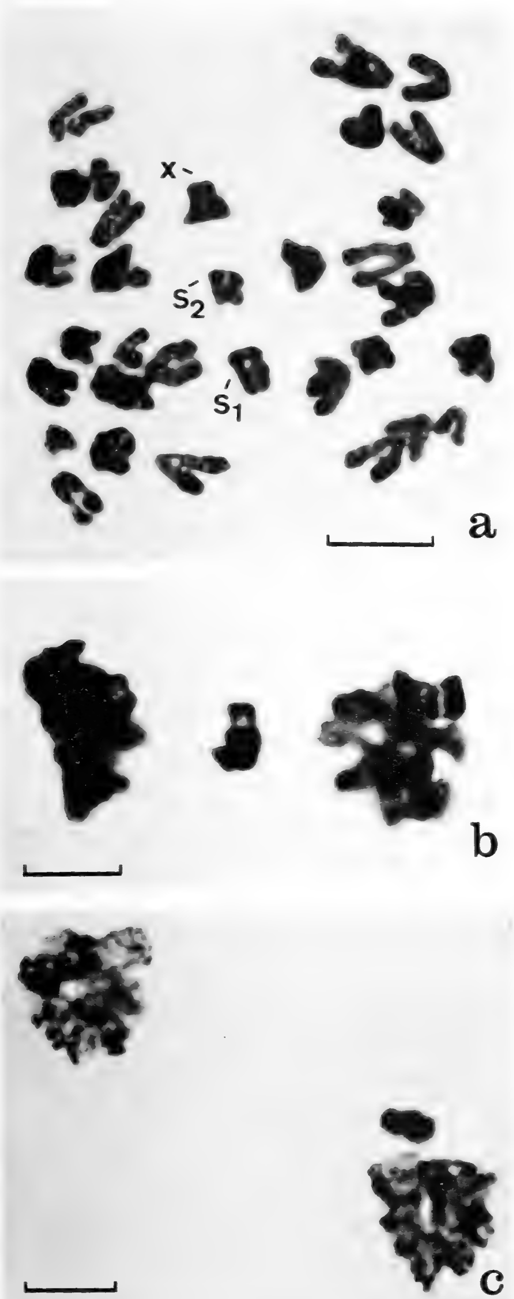

FIG. 2. Anaphase and telophase chromosomes of *A. acuticercus*. a) First anaphase of specimen J2 with amphitelic orientation of both X and S's. b) The X and S's chromosomes clustered in a single mass of chromatin during early telophase I. c) Late telophase I showing X+S's mass of chromatin approaching one of the daughter cell nuclei. Bar=10μm.

mass of chromatin and start a fast movement toward one of the daughter cells (Fig. 2c), being apparently incorporated normally into the nucleus instead of being eliminated in the cytoplasm. At pachytene and diplotene (Fig. 1b) the X remains strongly heteropycnotic, while S_1 and S_2 are also heterochromatic but stain less deeply. X, S_1 and S_2 remain connected throughout the prophase stage in the majority of nuclei (Fig. 1b).

DISCUSSION

First anaphase division is subject to several variables. It depends to some extent on the previous coorientation of the unsplit centromeres of the associated chromosomes in the metaphase configurations. The simultaneous orientation of two centromere halves of a chromosomes to the same pole is called syntelic while the orientation to different poles is called amphitelic. The first event is normally restricted to AI while the second occurs at AII [2]. When amphitelic orientation of univalents (including the X) occurs in MI and AI, either of the two kinds of events may follow. In the first case the two centromeres start to move toward opposite poles, pulling the respective chromatids which remain connected by a bridge of chromatin [3, 4]. In the alternative event the univalents lag behind in the equational plate without any poleward movement of their centromeres during anaphase stage. When the nuclei enter telophase the lagging chromosomes may finally move rapidly toward one of the poles to be integrated into one of the nuclei, or else may be eliminated into the cytoplasm in the form of micronuclei [5].

In species with localized centromeres, normal reductional division of the chromosomes takes place in AI. An exception to this rule occurs in species of the coleopterous family Lampyridae, where the X always divides equationally in AI and reductionally in all AII [6, 7]. Amphitelic orientation of univalents at MI and even equational division at AI, however rare, have been occasionally reported in some species [8–11]. Univalent autosomes, originated in accidental asynapsis or in meiosis of hybrids or polysomic cells, as well as the X chromosome in XO males, are obvious

candidates for misdivision. In some cases the delay of amphitellically oriented univalents to divide equationally may lead to a failure of the cell to divide, and as a result to the production of unreduced second division products [8, 9]. This is not what happens in *A. acuticercus*, however, where the first meiotic division proceeds normally.

In three instances of misdivision of the X chromosome observed in our laboratories the individuals also carried S chromosomes. This coincidence opens into a question whether the presence of supernumerary chromosome may cause irregularities in the orientation of univalent chromosomes at meiosis. In *Passalus perplexus*, a passalid beetle, Martins [3] observed that S and X oriented amphitelically in some AI, and that after a period of lagging in the equatorial plate the sister chromatids went to opposite poles though remained connected by a thin thread of chromatin. Mesa [4] observed a similar behavior of the X and S chromosomes in some AI nuclei of two specimens of the grasshopper *Daguerreacris tandiliae*. In *A. acuticercus* the situation is different. The X and S's remain amphitelically oriented in the equatorial plate, forming at the end of MI a single mass of chromatin which at the last moment moves rapidly to be integrated into one of the daughter nuclei. This belated incorporation prevents the formation of gametes that all lack an X, which would result in an all-male progeny.

Karyological information about species of Rhaphidophoridae is not extensive except for the circum-Antarctic Macropathinae, in which group the majority of the species have been studied and the ancestral chromosome number determined to be $2n♂=45$ [12–16]. Among the Dolichopodinae (comprising the genera *Dolichopoda, Hadenoecus* and *Euhadenoecus*), some species of the first-named genus possess chromosome numbers ranging from $2n♂=28$ to 35 [17–20]. In *Hadenoecus cumberlandicus* and *Euhadenoecus insolitus*, Lamb [21] found the number in bisexual populations to be $2n♂=34+XY$ and $2n♀=34+XX$; in parthenogenetic populations of both these species the females have the same chromosome number as those of the bisexual ones. Chromosome data have been published on only two Ceuthophilinae: *Ceutophilus* sp. with $2n♂=37$ [22] and *C. maculatus* (as *latebricola*) with $2n♂=37-39$ [23]. Chromosome data on Rhaphidophorinae are also few. Only two members of the tribe Rhaphidophorini have been examined: *Diestrammena japanica* and *Tachycines asynamorus*, both with $2n♂=57$, the X metacentric, and the autosomes "rod-shaped". The first was studied by Makino [24] from specimens collected near Lake Shikotsu in Hokkaido, Japan, and the latter by Mohr and Ecker [25] from specimens taken in a greenhouse in Oslo, Norway, where it has recently become established. In the Troglophilini only two species have been reported upon: *Troglophilus cavicola* with $2n♂=21$ [26] and *T. neglectus* with $2n♂=17$ [19]. Nothing is known of the chromosomes of half dozen species of the western North American genus *Gammarotettix*, at present the only member of the tribe Gammarotettigini, or of *Tropidischia xanthostoma*, restricted to the western edge of North America and the only species of the only genus of the subfamily Tropidischiinae.

If high chromosome number is indicative of primitiveness in the Orthoptera, then the Rhaphidophorini have the most primitive ancestral karyotype not only among the gryllacridoid Orthoptera but indeed among all sexually reproducing Saltatoria for which data are available. However, Hubbell and Norton [1] concluded that the Macropathinae are in most respects the most primitive living rhaphidophorids. They pointed out that in addition to shared apomorphic characters and sole occupancy of the Gondwanaland fragments that attest to the monophyletic origin of the subfamily, its taxa exhibit the largest assemblage of primitive (pleisomorphic) features to be seen in any of the subfamilies.

A tentative reconstruction of the history of the Rhaphidophoridae, compatible with that proposed by Hubbell and Norton [1] but taking into account the karyological evidence, is as follows: An ancestral pre-rhaphidophorid stock already existed in the Triassic (approximately 200 million years ago), prior to the division of Pangaea. In that stock the chromosome number 57–58 was probably common. When Pangaea split up, a species or a group of closely related species with $2n♂=45$ remained in Gondwanaland, most of the descendants of which have preserved that basic karyotype down to

the present. The same conservatism is manifest in their morphology. In Laurasia most of the lineages evolved toward a reduction in the chromosome number, but a few of them may have maintained the old 57–58 karyotype and given rise to the modern Rhaphidophorini. It is, however, also possible that the chromosome number 57 observed in Rhaphidophorini has been derived from lower numbers by pericentric inversion and centric fission cycles. A search among the more than one hundred unstudied species of this tribe could help to settle this question.

The chromosome number of *Anoplophilus acuticercus* is too low to suggest direct relationship with the Rhaphidophorini and too high to make probable any close relationship to *Troglophilus*. Whether or not *Anoplophilus* belongs with *Gammarotettix* in the Gammarotettigini, as suggested by its morphology and arboreal habits, cannot now be determined. The validity of such an assignment must await the cytological analysis of the latter genus (*Gammarotettix*).

ACKNOWLEDGMENTS

The authors are indebted to Dr. T. H. Hubbell of the University of Michigan for identifying the species studied, reviewing published information on the genus for us and critical reading on the manuscript, and Drs. T. Yamasaki and Y. N. Tobari of the Tokyo Metropolitan University for constructive comments on the manuscript (T. Y.) and for providing us with field collecting materials. This work was sponsored by the CNP_q PIG (Conselho Nacional de Pesquisa, Programa Integrado de Genetica) and the CNP_q Research Fellowship (Processo 30 1315/80) grants to the senior author and by a grant from the Ministry of Education, Science and Culture, Japan to B. Goñi.

REFERENCES

1 Hubbell, T. H. and Norton, R. M. (1978) The systematics and biology of the cave-crickets of the North American tribe Hadenoecini (Orthoptera Saltatoria, Ensifera, Rhaphidophoridae, Dolichopodinae). Misc. Publ. Mus. Zool. Michigan Univ., **156**: 1–156.

2 Sybenga, J. (1975) Meiotic Configurations. Springer-Verlag, Berlin, Heidelberg & New York.

3 Martins, V. G. (1982) Citogenética de dezenove especies de Scarabaeoidea (Treze Passalidae e seis Scarabaeidae) (Coleoptera). M. Sc. Thesis, Universidade Estadual Paulista "Julio de Mesquita Filho" UNESP, Rio Claro, São Paulo, Brasil, 62 pp.

4 Mesa, A. (1984) The chromosomes of a relict species of eumastacid: *Daguerreacris tandiliae* Decamp and Lieberman 1970 (Orthoptera, Eumastacoidea, Morseinae). Rev. Brasil. Genet., **7**: 219–229.

5 Morrison, J. W. (1953) Chromosome behavior in wheat monosomes. Heredity, **7**: 203–217.

6 Stevens, N. M. (1909) Further studies on the chromosomes of the Coleoptera. J. Exp. Zool., **6**: 101–113.

7 Smith, S. G. and Maxwell, D. E. (1953) Post-reduction of the X-chromosome and complete chiasma interference in the Lampyridae (Coleoptera). Can. J. Zool., **31**: 179–192.

8 John, B. and Henderson, S. A. (1962) Asynapsis and polyploid in *Schistocerca paranensis* . Chromosoma, **13**: 111–147.

9 John, B. and Lewis, R. (1965) Genetic speciation in the grasshopper *Eyprepocnemis plorans* . Chromosoma, **16**: 308–344.

10 John, B. and Lewis, R. (1965) The meiotic system. Protoplasmatologia, **16**: 1–335.

11 Lewis, R. and John, B (1959) Breakdown and restoration of chromosome stability following inbreeding in a locust. Chromosoma, **10**: 589–618.

12 Mesa, A. (1965) Karyology of four Chilean species of gryllacridids of the genus *Heteromallus* (Orthoptera, Gryllacridoidea, Rhaphidophoridae). Occas. Papers Mus. Zool., Michigan Univ., **640**: 1–13.

13 Mesa, A. (1970) The chromosomes of two species of the genus *Australotettix* Richards (Gryllacridoidea, Macropathinae). J. Aust. Entomol. Soc., **9**: 7–10.

14 Mesa, A. and Mesa, R. S. de (1971) Citología y evolución en Macropathinae (Orthoptera, Gryllacridoidea, Rhaphidophoridae). Rev. Peru. Entomol., **14**: 220–224.

15 Mesa, A., Ferreira, A. and Mesa, R. S. de (1968) The karyotype of some Australian species of Macropathinae (Gryllacridoidea, Rhaphidophoridae). Chromosoma, **24**: 456–466.

16 Mesa, A., Ferreira, A. and Mesa, R. S. de (1969) The chromosomes of three Australian species of gryllacridids (Gryllacridoidea, Rhaphidophoridae). Rev. Peru. Entomol., **14**: 220–224.

17 Saltet, P. (1959) La formule chromosomique de *Dolichopoda linderi* Duf. (Orthoptera, Rhaphidophoridae). C. R. Acad. Sci. Paris, **248**: 851–853.

18 Saltet, P. (1960) La formule chromosomique de *Dolichopoda palpata* e *D. bolivari* (Orthoptera, Rhaphidophoridae). C. R. Acad. Sci. Paris, **250**: 2612–2614.

19 Saltet, P. (1967) La formule chromosomique de l'Orthoptere *Troglophilus neglectus* (Rhaphidophoridae). C. R. Acad. Sci. Paris, **265**: 1313–1316.

20 Baccetti, B. (1958) Osservazioni caryologiche sulle *Dolichopa italiane*. Redia, **43**: 315–327.

21 Lamb, Y. R. (1975) Cytogenetic studies of parthenogenetic and bisexual populations in two species of cave cricket. Proc. North. Cent. Branch Entomol. Soc. Am., **30**: 103.

22 Stevens, N. M. (1912) Supernumerary chromosomes and synapsis in *Ceutophilus* (sp.?). Biol. Bull., **22**: 4–6.

23 Thompson, C. (1911) The spermatogenesis of an orthopteran *Ceutophilus latebricola* Scudder with special reference to the accessory chromosome. 30th Rep. Michigan Acad. Sci., 97–104.

24 Makino, S. (1931) The chromosomes of *Diestrammena japonica* Karny, an orthopteran. Zool. Mag., **43**: 635–645.

25 Mohr, O. L. and Ecker, R. (1934) The grasshopper *Tachycines asynamorus,* a new animal for cytological purposes. Cytologia, **5**: 384–390.

26 Baccetti, B. (1961) Cariologia di populazioni partenogenetiche e bisesuate de *Troglophilus cavicola* Koll. IX Int. Kongr. Entomol. Wein.

ZOOLOGICAL SCIENCE **4**: 265–276 (1987)

Examinations of Spindle Structures Modified by T-1, the Mitotic Arrester

Tomohiko J. Itoh, Hidemi Sato and Akio Kobayashi[1]

Sugashima Marine Biological Laboratory, School of Science, Nagoya University, Sugashima-cho, Toba-shi, Mie 517, and
[1]Department of Agricultural Chemistry, Faculty of Agriculture, Okayama University, Tsushima naka 1–1–1, Okayama 700, Japan

ABSTRACT—The process of inducing barrel-shaped spindle (B-spindle) in fertilized eggs of sea urchins, *Hemicentrotus pulcherrimus* and *Pseudocentrotus depressus*, was examined. By elecron microscopy, the microtubule organizing centers (MTOCs) of the spindle poles were seen to be dispersed into many MTOCs and appeared spread out both in sections of whole dividing eggs or isolated mitotic apparatus(MA), supporting our previous conclusion that T-1 alters the distribution pattern of MTOCs. Spindle assembly in eggs, which were first pulse-treated with T-1 and then inseminated after various time intervals, was examined with the polarizing microscope. We confirmed that a 5 min exposure to T-1 was sufficient to produce typical B-spindles when the drug concentration was above 4.2×10^{-7} M in *H. pulcherrimus* and 1.3×10^{-6} M in *P. depressus*. Although the birefringence(BR) of spindle decreased with higher concentrations of T-1, the decrease was inversely proportional to the length of the interval between brief T-1 application and fertilization. However, the spindle never reverted to the normal spindle form. Suppression of pronuclear migration, which was also induced by T-1 treatment, could be reduced by increasing the time interval. Application of 30% D_2O to B-spindle rapidly induced an increase in spindle BR and in spindle dimensions but did not restore the spindle to the original shape of untreated spindles. These results indicate that the T-1 dependent alteration of spindle morphology is very difficult to reverse and this effect is independent of the inhibitory effect of the drug on microtubule assembly. We believe that T-1 is a novel molecule which alters the spindle configuration by affecting the centrosome.

INTRODUCTION

Mitotic poisons have played an important role in the analyses of the functional and structural basis of spindle assembly [1]. For instance, colchicine and its derivatives, *Vinca* alkaloids, griseofulvin and nocodazole have been applied as inhibitors of tubulin polymerization, whereas taxol has been used to prevent microtubule disassembly. Information accumulated by using such mitotic poisons has mainly related to the behavior of microtubule assembly because the major effect of these poisons is to disturb the *in vivo* tubulin polymerization/depolymerization equilibrium.

Additional information has been obtained by shifting various physical parameters such as temperature and hydrostatic pressure [2–4], or by the partial substitution of D_2O for enviornmental H_2O [5–7]. In previous works [8–10], Takahashi and Sato showed that D_2O converts unpolymerizable tubulin molecules to a polymerizable state in dividing cells. Although the use of D_2O is a powerful tool in the examination of spindle assembly in living cells, the results of *in vitro* tubulin polymerization experiments with D_2O [11] did not coincide with those from the *in vivo* experiments. This discrepancy may be due to the presence *in*

Accepted October 8, 1986
Received September 4, 1986

Abbreviations Used
EGTA, ethyleneglycol-bis-(2-aminoethyl ether)-*N, N, N′, N′*-tetraacetic acid; PIPES, piperazine-*N, N′*-bis(2-ethanesulfonic acid; TAME, p-tosyl-L-arginine methylester HCl; B-spindle, barrel-shaped spindle; BR, birefringence; ASW, artificial sea water; FSW, filtered sea water; MA, mitotic apparatus; MTOCs, microtubule organizing centers.

vivo of unidentified molecule(s) not found *in vivo*. One may be able to identify and characterize these molecules by using certain molecular probes.

T-1 (2-hexyl-5-propyl-1-3-benzene diol), which can be isolated from the culture medium of *Pseudomonas* sp., is known to alter the spindle morphology of sea urchin eggs causing, (i) a shortening of pole to pole distance, (ii) a straightening of the spindle microtubules, (iii) a spreading of the polar regions and (iv) a shrinking of the aster size. This modified spindle has been previously termed a "barrel-shaped spindle (B-spindle)" [12,13]. T-1 has also been reported to suppress microtubule assembly both *in vivo* and *in vitro*, although spindle morphology is altered without a concurrent decrease in spindle birefringence [14]. Thus, we thought that T-1 affected, in particular, the spatial arrangement of MTOCs in the spindle poles and the centrosome, independent of its inhibitory effect on microtubule assembly. The centrosome is considered to be a kinetic organelle which governs the shape of the mitotic apparatus during cell division [15]. The drug T-1 may play a key role in uncovering additional clues useful in determining the molecular basis of the system regulating spindle morphology.

In this paper, we follow the induction of B-spindle by T-1 in sea urchin egg. We describe our electron microscopic observations of the polar region of B-spindle which verify our idea that the centrosome is modified by T-1. We also follow the formation of B-spindle in eggs which were pulse-treated by T-1 before and after fertilization and observe the effects of D_2O on the B-spindle. The latter experiments were done in order to determine whether B-spindle induction is independent of the modulation of microtubule assembly.

MATERIALS AND METHODS

Materials and chemicals

All chemicals were purchased from commercial sources and were of certified reagent grade. Mature gametes of Japanese autumn sea urchin, *Pseudocentrotus depressus* and winter sea urchin, *Hemicentrotus pulcherrimus*, were used and handled as described before [14].

Electron Microscopy

Dividing sea urchin eggs were fixed according to the method of Hirano *et al.* [16]. This fixation medium consisted of 0.1 M phosphate buffer (pH 6.9), 0.1 M sucrose, 10 mM EGTA, 5 mM $MgSO_4$, 2.5% glutaraldehyde, 1% paraformaldehyde and 300 μg/ml saponin.

Mitotic apparatus (MA) was isolated as described before [14] and fixed as follows. The isolation medium for MA consisted of 10 mM PIPES (pH 6.9), 5 mM EGTA, 1 mM $MgSO_4$, 1 mM TAME, 20% glycerol and 1% Nonidet P-40. Immediately after isolation, MA was fixed with 2.5% glutaraldehyde in glycerol free MA isolation medium for 60 min. The fixed MA was washed with glycerol free MA isolation medium three times then treated with 0.2% tannic acid in 0.1 M phosphate buffer (pH 6.9) containing 0.5 mM $MgSO_4$ for 120 min. They were washed three more times with this mixture and postfixed with OsO_4 on ice for 60 min.

Both eggs and MA were dehydrated through a graded series of ethanol, *en bloc* stained with lead acetate [17] and embedded in Quetol 651 resin [18]. *En bloc* staining was used as a routine procedure to increase contrast.

Thin sections 80–100 nm in thickness were cut with a diamond knife on Porter-Blum MT2B ultramicrotome. After being placing on a collodion coated 200 mesh grid, the sections were stained with uranyl acetate and lead citrate. In some cases, serial sections were made and mounted on collodion- and carbon-coated single slot grids. HITACHI H-300 electron microscope operated at 60 kV was routinely used. The mitotic stages were identified from the distribution pattern of the chromsomes.

T-1 Pulse treatment

Eggs were treated with T-1 before or after fertilization. In the former case, unfertilized eggs were collected in conical tubes by hand centrifugation and gently suspended for 5 min in artificial sea water (ASW) containing various concentrations of T-1. After washing with filtered sea water (FSW) three times, the pulse-treated eggs were transferred to a watch glass and allowed to settle until

fertilization. Eggs were fertilized by adding a drop of diluted sperm.

When eggs were treated with T-1 after fertilization, they were first fertilized in a watch glass and allowed to develop for 30 to 40 min. After the pronuclei fused, eggs were collected and treated with T-1 in ASW in the way as the T-1 pretreated eggs. In both cases, spindles were stabilized at the metaphase stage as described before [14], and examined under polarizing microscope.

In some cases, stabilized eggs were treated with 10 μg/ml of ethidium bromide for 10 min in order to observe the chromosomes. After washing the eggs with stabilizing medium, eggs were examined under an Olympus BH-RFL epifluorescence microscope (Olympus Optical Co., Tokyo) equipped with a dichroic mirror (BH-DMV) and a 570 nm cut-off barrier filter. A high pressure mercury arc lamp (Osrum HBO 100 W, Berlin-München, West Germany) was used as the illuminating source. Fluorescence was induced by exciting ethidium bromide with 300–350 nm light.

Application of D_2O to T-1 treated eggs

Because D_2O is known to increase the assembly of spindle microtubule [6, 7], we examined the effect of D_2O on microtubule assembly in the B-spindles of T-1 treated eggs using the following procedure. T-1 was applied to fertilized eggs between the pronuclear fusion stage and the break down of the nuclear envelop, and the eggs were allowed to develop until metaphase. In metaphase, eggs were transferred to 30%(v/v) D_2O ASW and suspended for 2 min. Then, the spindles were stabilized. In some cases, fertilized eggs at prometaphase were treated with T-1 containing 30% D_2O ASW for 5–8 min and then the spindles were stabilized.

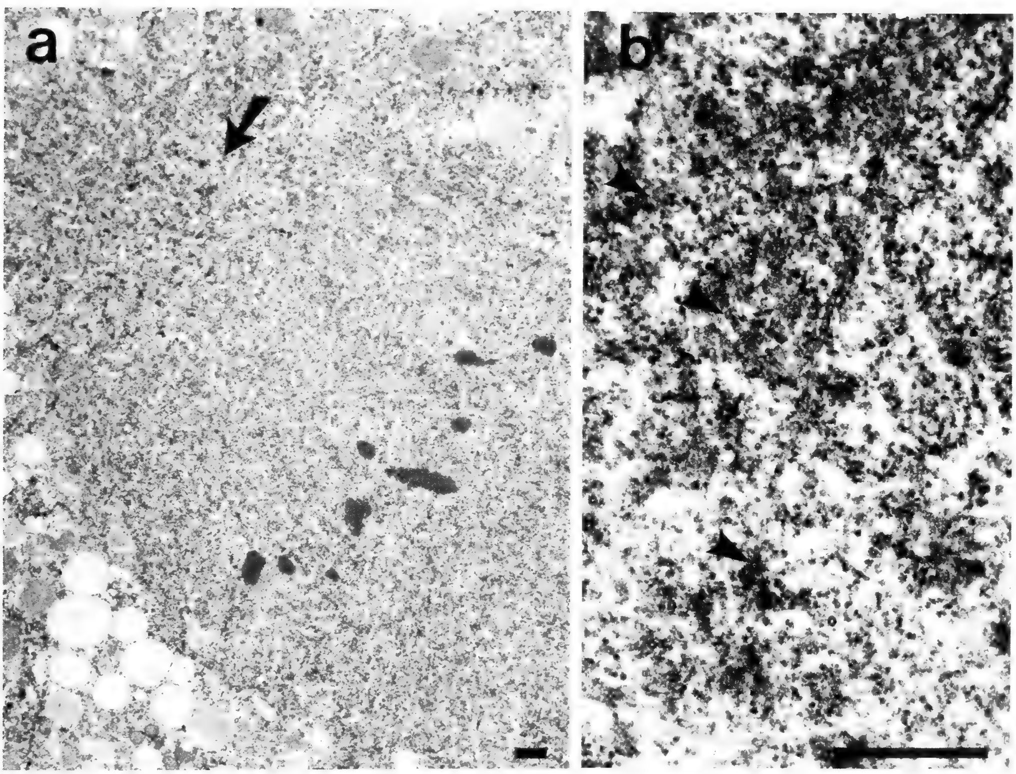

FIG. 1. Electron micrographs of a B-spindle induced by 8×10^{-7} M T-1 in an egg of *H. pulcherrimus*. (a) A half spindle in early anaphase at low magnification. Note the slightly electron dense materials dispersed at the polar region perpendicular to the axis of the B-spindle (indicated by an arrow). Bar = 1 μm. (b) High magnification of the polar region in Fig. 1a. Arrowheads indicate MTOCs. bar = 0.5 μm.

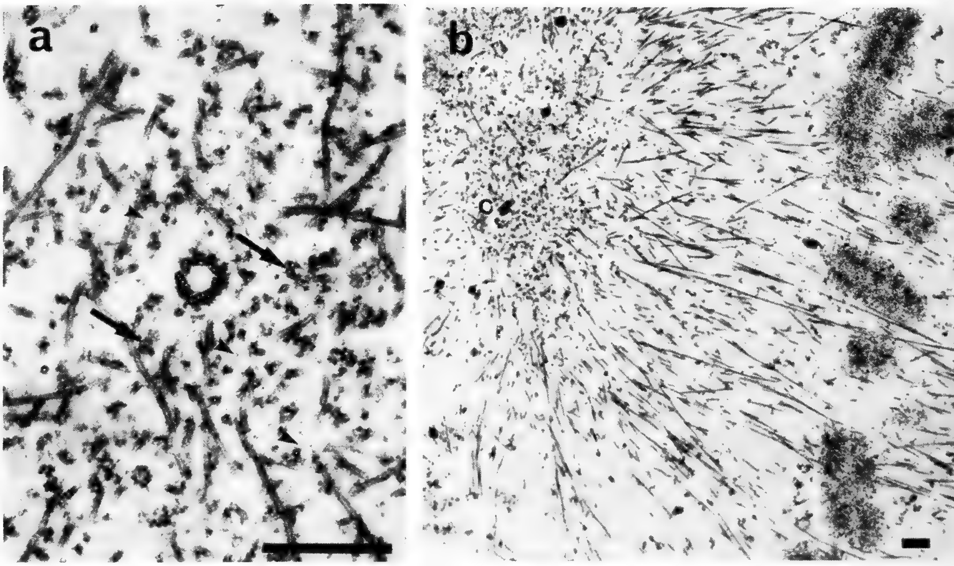

Fig. 2. Electron micrographs of isolated MA from *H. pulcherrimus* eggs. (a) The center of the polar region of a normal spindle. Arrows indicate short microtubules which do not extend into adjacent sections and were commonly seen in the polar region. Arrowheads indicate minute filamentous bridge structures. bar=0.5 μm. (b) A half B-spindle in metaphase. The "bridge-rich region" in the spindle pole is observed as a slightly darker area at low magnification. A centriole (c) exists at the center of this region. bar=0.5 μm.

RESULTS

Ultrastructure of the polar region of the B-spindle

The improved fixation method developed in this laboratory [16] allowed us to obtain the excellent preservation of spindle structures as well as associated membranous components in dividing eggs of the sea urchin, *H. pulcherrimus*. Electron dense amorphous material was always seen in the polar regions of the spindle as reported previously [16]. This amorphous material was composed of aggregated clusters of tiny granules. Many microtubules terminated in it and appeared to radiate out from it to various directions. As shown in Figure 1a, B-spindle excluded yolk granules and mitochondria just as normal spindles do. Though the distribution pattern of the microtubules was rather difficult to detect at low magnifications, we could identify the spindle axis from the position of the chromosomes. The amorphous material turned out to be distributed in a cloud perpendicular to the axis of the B-spindle. This material did not form a compact aggregate as it does in normal spindles, but rather was in a dispersed state. As shown in Figure 1b, however, these dispersed granules could also act as MTOCs. In a series of cross sections of B-spindle, we confirmed that the MTOCs in the polar region were dispersed and formed a disk.

To analyze the distribution pattern of microtubules within a B-spindle, isolated MA from dividing eggs of sea urchin, *H. pulcherrimus,* were examined. In the polar region of isolated MA, the majority of spindle microtubules were radially oriented. As shown in Figure 2a, many short and fragmented microtubules were seen in this region (indicated by arrows). Instead of granules, many filamentous bridges were commonly seen in the polar region which appeared to connect neighbouring microtubules each other. At low magnification (Fig. 2b), this "bridge-rich region" could be easily distinguished from other areas because of its slightly darker contrast. We considered the possibility that this region could contain an altered centrosome from the isolated MA. The centrosome of the B-spindle in metaphase appeared to be in a spread or flattened form and perpendicularly

oriented to the spindle axis. The centriolar pair was always located at the middle of the centrosomal area. The components of centrosome from isolated MA such as the filamentous bridges did not have the same appearance as in the sections of preserved eggs. However, the dispersed state of the MTOCs observed in both specimens is consistent with the results obtained from light microscopy as reported before [14]. The electron dense spots whose diameter are around 0.1 to 0.2 μm are artifacts induced during the *en bloc* staining and probably correspond to secondary deposits of lead carbonate.

A three dimensional reconstruction made from serial sections of an isolated B-spindle clearly showed that the centrosome of this B-spindle has a flat or spread appearance (Fig. 3). We also found that the microtubules radiating out from this region were gathered together as loose bundles containing both kinetochore and non-kinetochore microtubules.

FIG. 3. Three-dimensional reconstruction of a half B-spindle at the onset of anaphase. Microtubules, chromosomes and bridge-rich regions were traced through four adjacent sections, bar=1 μm.

T-1 pulse treatment on fertilized eggs

The minimum dose of T-1 inducing B-spindle formation was slightly different for the two species of sea urchins. Eggs of *P. depressus* were less sensitive to T-1 than those of *H. pulcherrimus*; the minumum dose required to induce B-spindle formation in *P. depressus* eggs was 1.3×10^{-6}M and 4.2×10^{-7}M for *H. pulcherrimus*. B-spindle could be induced by pulsing eggs of both species with T-1 if the fertilized eggs were treated with T-1 ASW for 5 min after the stage of syngamy formation. The BR of the spindle decreased as the T-1 concentration increased in the same manner as in the immersion experiments described before [14].

When T-1 pulsed eggs were allowed to develop, mitotic spindles formed sequentially in the first, second, third and fourth division with a slight delay as compared to control eggs. The spindles were still barrel-shaped during these cell cycles. These observations indicated that T-1 did not inhibit the replication cycle of centrosomal components during the cell cycles despite the morphological modification of the centrosome. However, cytokinesis was frequently inhibited and cleavage did not occur until the fourth division. It has been suggested that the position of the cleavage furrow is controlled by the cortical ends of the astral microtubules [19]. The asters of B-spindle are tiny, containing short microtubules which do not extend into the cortex. Therefore, the suppression of cleavage by T-1 might be attributed to the lack of microtubules ending in the cortex. In the fourth division, cleavage furrows formed all at once but were randomly oriented, yielding irregular blastomeres.

T-1 pulse treatment on unfertilized eggs

To examine the reversibility of T-1 effect, we followed the assembly of spindles in eggs which were treated with T-1 for 5 min before fertilization and then, after standing for 5 to 240 min, were inseminated. B-spindles could be induced using a concentration of T-1 above 4.2×10^{-7}M for *H. pulcherrimus* (Fig. 4). The BR of the B-spindle in eggs fertilized following a pulse of T-1 decreased in

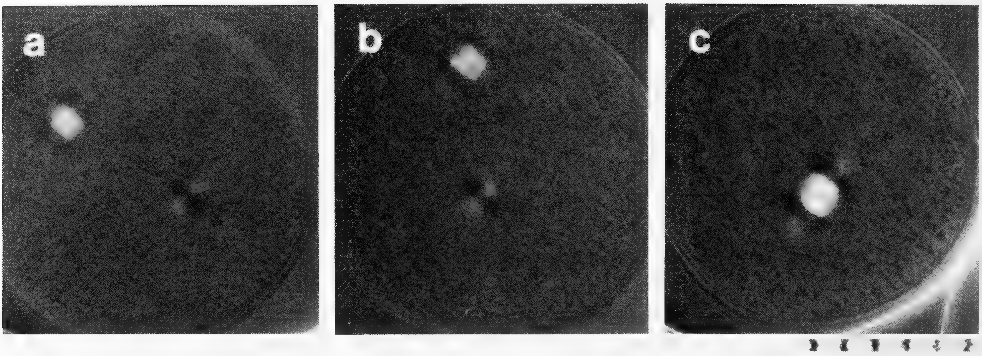

Fig. 4. B-spindle induced in eggs of *H. pulcherrimus* pulsed with T-1 (2.1×10^{-6} M) before fertilization. Eggs are fertilized (a) 5 min, (b) 60 min and (c) 240 min after application of T-1. When the interval between pretreatment and fertilization is short (5 to 60 min), the B-spindle is situated in the periphery of the egg and a cytoaster frequently existed beside the B-spindle. 1 div. = 10 μm.

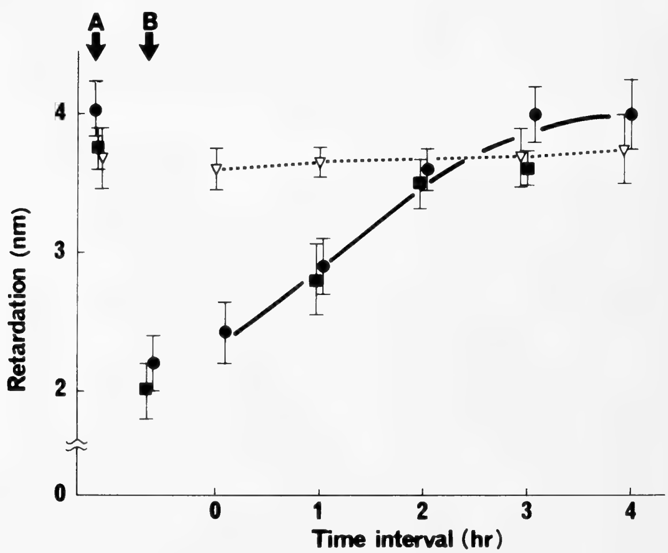

Fig. 5. BR recovery in B-spindles induced by pulse-treating eggs of *H. pulcherrimus* with T-1. The point below arrow A represents the BR of control spindle and those below arrow B, the BR of B-spindle induced by T-1 applied after the syngamy formation. Different symbol shapes correspond to the diferent batches of eggs. The x-axis indicates the length of the interval between T-1 treatment and fertilization. The y-axis indicates the amount of BR in the center of the half spindle. The T-1 concentration used was 4.2×10^{-7} M (open symbols) or 2.1×10^{-6} M (closed symbols). The sample number for each point ranges from 18 to 20 eggs.

inverse proportion to the increase of T-1 concentrations (Fig. 6). When pretreated eggs were fertilized 60 to 240 min after a highly concentrated T-1 pulse, the T-1 induced decrease in BR was less and less apparent as the time of the chase increased. With the 240 min chase, the BR attained normal levels. However, the modified B-spindle morphology persisted and did not revert to the normal spindle shape. With lower concentrations of T-1, the BR was not altered while the change in spindle shape continued to occur. These results showed that T-1 is more effective in

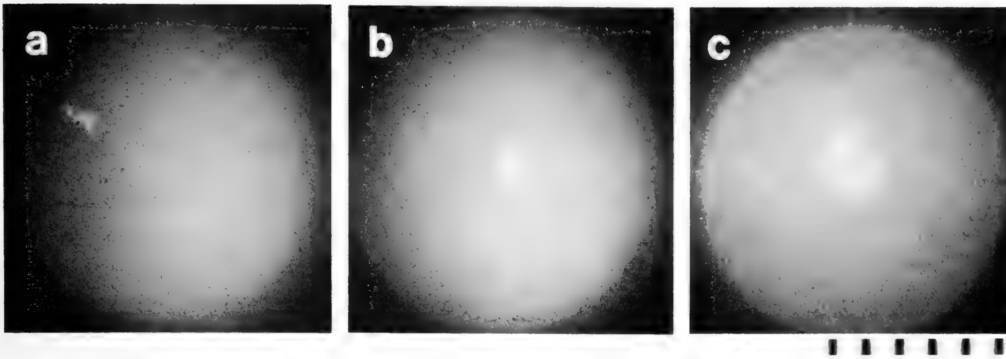

FIG. 6. Observation of chromosomes in T-1 pulse treated eggs of *H. pulcherrimus* by fluorescent microscopy. Photographs of (a) and (b) were taken from the same egg at different depth of focus. This egg was fertilized 5 min after the pulse treatment. The chromosomes in photograph (a) are located on a metaphase plate and those in (b) are dispersed, suggesting that the clusters in (a) come from the male pronuclei and the cluster in (b) come from the female pronuclei. In almost all the eggs observed, the two clusters of chromosomes were not in the same focal plane. Egg (c) was fertilized 180 min after pulse treatment. Under these conditions, one still sees two separate chromosomal clusters but the distance between them is less and the clusters are usually observed in the same focal plane. One is in the metaphase state and the other in the dispersed state. The T-1 concentration during the pulse treatment for this egg was 2.1×10^{-6} M. 1 div. = 10 μm.

modifying the morphology of the centrosome and inducing B-spindle formation than in reducing spindle BR.

Suppression of syngamy formation by T-1 pulse treatment

When eggs were treated with T-1 before fertilization, B-spindles were not formed in the center of eggs but in the peripheral region. A cytoaster was frequently seen beside the B-spindle (Fig. 4). This raises a question. Is pronuclear migration also disturbed by T-1 pulse treatment and is this effect, again, independent of B-spindle assembly? To answer this question, the location of chromosomes in prometaphase or metaphase was followed by staining the DNA with ethidium bromide. When eggs were washed briefly from 5 to 60 min before fertilization, two chromosomal clusters were seen in each egg in the majority of cases as shown in Figure 6a, b. In many cases, one cluster appeared to be located on a metaphase plate whereas the other one consisted of randomly situated chromosomes. The presence of two chromosomal clusters suggests that T-1 pulse treatment disturbs pronuclear migration. According to Sluder and Rieder [20], when the migration and fusion of pronuclei are inhibited in sea urchin eggs, only centrosomes associated with the male pronucleus organize a bipolar spindle. Thus, it is probable that spindles assembled in eggs treated by T-1 before fertilization were organized by centrosomes derived from the male pronucleus.

The percentage of eggs forming two chromosomal clusters decreased with an increase in the

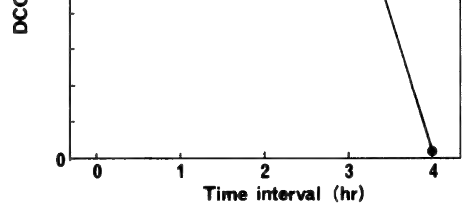

FIG. 7. The proportion of eggs which contain double chromosomal clusters (DCC) vs. the length of time interval between T-1 pulse and fertilization. X-axis indicates time interval length and y-axis indicates the proportion of eggs which contain DCC. Eggs were observed under the fluorescent microscope after staining chromosomes with ethidium bromide. The sample number at each point ranges from 160 to 200 eggs.

time between the T-1 pulse treatment and fertilization (Fig. 7). As shown in Figure 6c, the cluster to cluster distance also appears to decrease with increasing time between the T-1 pulse and fertilization. When eggs were fertilized 240 min after T-1 pulse-treatment, the separation of the two chromosomal clusters was hardly detectable, if it occurred at all during first spindle assembly. Instead, the usual metaphase chromosome plate as seen in untreated cells formed in the center of the egg. These results suggest that T-1 pulse treatment suppresses pronuclear migration. Because this T-1 inhibitory effect was reversible as is the reduction of spindle BR in T-1 treated cells, we presume that the suppression of normal pronuclear migration may be related to the disturbance of microtubule assembly in the sperm aster.

Effects of D_2O on B-spindle

Because D_2O is an agent which directly promotes microtubule polymerization both *in vivo* and *in vitro* [6, 7, 11], we can rapidly increase microtubule assembly with the proper concentrations of D_2O. Therefore, eggs pretreated with T-1 were immersed in 30% D_2O to determine if there is any relationship between the extent of microtubule assembly and B-spindle induction. Because spindle shape often becomes abnormal at higher concentrations of D_2O, we chose a rather intermediate concentration. According to Takahashi and Sato [8], 33% D_2O was enough to show the reversibility of the isotope effects in *H. pulcherrimus* eggs. At this concentration, the effects of the D_2O was reversible and could be repeated. This concentration was high enough to increase the extent of microtubule assembly both in normal spindle and in B-spindle. When eggs were kept in D_2O, further development was retarded compared to the control. As shown in Table 1, when eggs were treated with 30% D_2O, the B-spindle responded with an increase in BR. The whole shape of the B-spindle became more spherical. Both the length and the width of spindle increased but the length to width ratio hardly changed and its value stayed around 1.0. Astral rays also grew but the dispersed aster did not change (Fig. 8). The increase in the BR and in the dimensions of the B-spindle and the astral rays is clearly due to the isotope effects of D_2O on spindle microtubule assembly. The rounding of spindle shape could be due to the increased number of microtubules within the restricted regions of the B-spindle. These results indicate that D_2O can affect microtubule assembly in T-1 treated spindles. However, the normal shape of the spindle could not be restored merely by increasing microtubule polymerization.

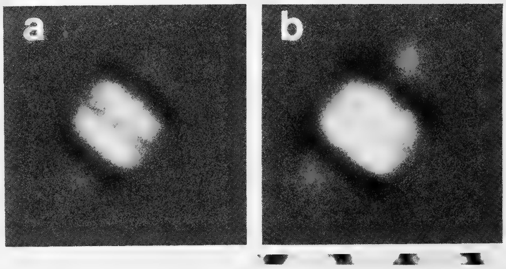

FIG. 8. Effect of D_2O on B-spindle in eggs of *H. pulcherrimus*. (a) A B-spindle induced with 2.1×10^{-6} M T-1 applied after pronuclear fusion. (b) A B-spindle treated with 30% D_2O for 2 min in metaphase. Note that the length and width of the B-spindle are increased but that the structure of spindle is not at all restored to the original form of untreated spindle. 1 div. = 10 μm.

DISCUSSION

In an earlier paper, we considered the possibility

TABLE 1. Change in BR of B-spindle with D_2O

No.	Control	T-1	T-1+D_2O*	Species
1	3.66 ± 0.14 (16)	2.42 ± 0.29 (20)**	4.18 ± 0.49 (20)**	*H. pulcherrimus*
2	3.72 ± 0.27 (20)	2.33 ± 0.26 (20)**	3.54 ± 0.23 (20)**	*H. pulcherrimus*
3	3.71 ± 0.16 (14)	3.73 ± 0.13 (12)***	4.21 ± 0.27 (12)***	*P. depressus*

* D_2O concentration is 30%. **T-1 concentration is 2.1×10^{-6} M. *** T-1 concentration is 1.3×10^{-6} M. Numbers in parentheses show the number of examined spindles.

that the induction of B-spindle formation in sea urchin eggs by T-1 is not due to the inhibitory effect of T-1 on microtubule assembly [14]. The morphological modification of the spindle may be dependent on the redistribution of the MTOCs which normally form the spindle poles. In this article, we intend to determine the cause of the induction of B-spindles.

We employed an electron microscopic technique which gave improved ultrastructural preservation to observe the MTOCs of the B-spindle. We saw that the centrosomes in the B-spindle were spread out and a granular material was dispersed perpendicular to the spindle axis in sections of preserved eggs. In sections of isolated MA, a number of minute filamentous bridges which appeared to connect neighbouring microtubules were commonly observed in the polar regions in place of granules. These might be a residual skeletal components of the centrosome which remained throughout the MA isolation procedure. The granules commonly observed in sections of whole eggs were probably lost during the process of spindle isolation.

Endo *et al.* [21] saw clusters of granular material in the polar regions of MA of *H. pulcherrimus* eggs and called them microtubule organizing granules (MTOGs). The cluster of granules seen in this article did not appear similar to the MTOGs observed by Endo *et al.* because the MTOGs are denser than and their size is three to four times larger than the clusters in the polar region of the B-spindle. However, the conditions under which the eggs were fixed and sectioned were different in the two cases. Furthermore, T-1 might induce the clusters of granules to disperse and change in shape and size, and therefore, the altered appearance of the granules might be ascribed to the effect of T-1 on the centrosome.

The results of the electron microscopic examination of B-spindles were in good agreement with those from light microscopy [14]. However, it should be noted that distinctly different spindle pole morphologies were seen in these two different microscopic techniques. The dispersed polar centrosome of the B-spindle appeared as a strand of beads in light microcopy [14], but these aggregates were not the same size when seen with electron microscopy. This discrepancy may be due to an artifact caused by specimen modifications which occur during its preparation for light or electron microscopy. The distribution of microtubules appeared to be unaltered by fixation and dehydration since the microtubules were observed to be gathered in loose bundles similar to that seen by light microscopy (compare Figure 5 in ref. [14] to Figure 3 in present article).

Recently, Schatten *et al.* [22] found that the poles of acentriolar spindles in mouse oocytes and eggs were spread out and that the spindle were typically barrel-shaped. In contrast, the centrosomes of normal metaphase spindles in sea urchin eggs are more compact. We believe that one purpose of centrioles may be to gather pericentriolar materials into one location, thus producing a centrosomes with a compact shape during metaphase. Although the centrioles are always located in the center of centrosomes in B-spindle as they are in normal spindle, the morphology of the B-spindles and its dispersed, flattened ellipsoid centrosomes resembles to that of mouse oocytes or mouse eggs. We suggest that the centrioles in B-spindle cannot behave as proper kinetic centers for spindle assembly and cannot properly gather the MTOCs together during metaphase due to the influence of T-1.

Next, we attempted to separate the T-1 dependent modification of spindle shape from its inhibitory effect on microtubule assembly. Because spindle BR directly reflects the number of oriented microtubules within the spindle [23], the results obtained from the T-1 pulse experiments are interpreted as following. The reduction in the population density of microtubules following a highly concentrated pulse of T-1 was accompanied by an alteration of the centrosomal configuration. However, the reduction in the number of microtubules induced by the T-1 pulse was abolished when the interval between the pulse and fertilization was increased, whereas there was no change in microtubular length or in the dispersal of the kinetic centers from which microtubules were assembled. Because the microtubule population density could be restored by increasing the length of time between the T-1 pulse and fertilization, we consider the T-1 dependent disturbance of microtubule

assembly to be reversible.

The migration of male and female pronuclei and the formation of pronuclei were also suppressed when eggs were treated with high concentrations of T-1. Again, this suppression was abolished by leaving the eggs unfertilized for more than 180 min after the T-1 pulse. Because the migration of pronuclei is considered to be tightly coupled to sperm aster formation and microtubule assembly [24, 25], these results are a further indication that the inhibition of microtubule assembly within the sperm aster by T-1 can be readily reversed.

The results of our work is comparable with that obtained by Sluder and Rieder [20]. They have shown that pulsing sea urchin eggs with Colcemid before fertilization is enough to suppress microtubule assembly, while the UV irradiation reverses the effects of the Colcemid. They believe that the long term suppression of microtubule assembly by the pulse of Colcemid was due to the high affinity between tubulin molecules and Colcemid. We suggest that the T-1 dependent suppression of microtubule assembly may also be the result of a similarly tight T-1-tubulin interaction. Despite the similarity between the effect of T-1 and Colcemid, the mechanism of T-1 dependent suppression of pronuclear migration may not be identical to that of Colcemid, especially when considering the different way the eggs recover from the effects of each drug.

The T-1 dependent induction of B-spindle is not reversible. This suggests that the morphological modification of spindle by T-1 could be mediated by a different mechanism than that which produces the inhibitory effect on microtubule assembly. The effects of D_2O on B-spindle clearly indicate that the inhibition of microtubule assembly does not cause modification of the spindle structure by T-1. D_2O is a useful reagent for producing an increase in the amount of polymerized tubulin [6, 7, 11], and the effect of D_2O on tubulin polymerization is considered to be due to an increase in proportion of polymerizable tubulin subunits in the living cells [8–10]. In this case, the employment of D_2O enhances microtubule assembly. If we use other chemical reagents such as taxol, which bind to tubulin and thereby increase microtubule assembly, the binding of that reagent may competitively interfere with the binding of T-1. This competition may produce side effects which make the results difficult to understand.

If the reduction in microtubule assembly caused by T-1 is necessary for the formation of B-spindle, then these modified B-spindle configuration should be restored by adding D_2O. If the spreading of the centrosome was a result of the partial inhibition of microtubule assembly, then D_2O might induce the MTOCs in the centrosomal regions to retract into the compact morphology of the control centrosome. However, the addition of D_2O to the B-spindle did not alter the dispersed state of its polar centrosomes or its reduced length to width ratio. The BR and dimensions of the B-spindle were increased without a reversion to the normal structure of the spindle, instead changing to an enlarged barrel-shape. Astral fiber length also increased by the application of D_2O. These results indicated that the isotope effects of D_2O on B-spindle microtubules were similar to those on normal spindles. The modified spindle configuration was never converted to the normal shape although D_2O promoted the assembly of microtubules. We believe, therefore, that the T-1 dependent alteration of spindle structure is not due to its effect on microtubule assembly.

Sato and Sato [26] have reported the effect of T-1 on dividing endosperm cells of *Haemanthus katharinae*. In this case, high concentrations of the drug mainly affected the spindle BR, but no alteration of the poles occurred, even when using higher concentrations of T-1. These effects can be explained as due to the absence of a centrosome in the endosperm of *H. katharinae*. T-1 could not modify the spindle configuration by affecting the centrosome because of the absence of centrosome. Only the secondary effect of the drug, that of modulating microtubule assembly, could be detected. Indeed, the T-1 induced change in the plant spindle can be reversed by washing, suggesting that T-1 affects only microtubule assembly. Based on these data, we suggest that T-1 affects in particular the MTOCs of the centrosome.

In conclusion, we believe that the main effect of T-1 on the induction of B-spindle is to directly cause the dispersion of the MTOCs within the centrosome. Although the inhibitory effect of T-1

on microtubule assembly was reversible, the modified spindle could not be converted to a normal morphology, suggesting that T-1 may irreversibly modulate the distribution pattern of the kinetic centers on which microtubules assemble. For this reason, we believe that T-1 will be uniquely useful in the examination of the molecular basis of the physiology of the centrosome and of what determines spindle morphology. We suggest that T-1 binds to some cellular component(s) which participates in the control of the structure of the centrosome, and thereby alters the overall morphology of the spindle. Our next goal is to identify and characterize these regulatory molecules using both biochemical and physiological procedures.

ACKNOWLEDGMENTS

The authors are most grateful to Drs. Makoto Fukumoto and Koichi H. Kato of the College of General Education, Nagoya City University for the use of their electron microscope and for their various helpful suggestions on electron microscopy technique. We also thank Dr. Hiroshi Hayashi of the Institute of Molecular Biology, Nagoya University for critically reading this manuscipt, Dr. Elena McBeath for her help for editing of this manuscript, and Mr. Yoshiharu Murata and Kuzaki Fishermen's Cooperative Association for supplying us with sea urchins.

TJI appreciates the general support from fellowships of the Japan Society for the Promotion of Science for Japanese Junior Scientists.

This work was supported by several Grant- in- Aids for Scientific Research provided from the Ministry of Education, Science and Culture, Japan, whose numbers are 57380016, 58340042, 58380026, 59390006 and 61790232.

REFERENCES

1 Dustin, P. (1984) Microtubules, Springer-Verlag, Berlin, Heidelberg, New York, Tokyo, 2nd ed., pp. 482.

2 Inoué, S. (1959) Motility of cilia and the mechanism of mitosis. Rev. Mod. Phys., **31**: 402–408.

3 Stephens, R. E. (1973) A thermodynamic analysis of mitotic spindle equilibrium at active metaphase. J. Cell Biol., **57**: 133–147.

4 Salmon, E. D. (1975) Pressure-induced depolymerization of spindle microtubules. II. Thermodynamics of in vivo spindle assembly. J. Cell Biol., **66**: 114–127.

5 Inoué, S. and Sato, H. (1967) Cell motility by labile association of molecules. The nature of mitotic spindle fibers and their role in chromosome movement. J. Gen. Physiol., **50**: 259–292.

6 Sato, H. (1975) The mitotic spindle. In "Aging Gamates". Ed. by J. Blandau, S. Karger AG, Basel, pp. 19–49.

7 Sato, H., Kato, T., Takahashi, T. C. and Ito, T. (1982) Analysis of D_2O effect on in vivo and in vitro tubulin polymerization and depolymerization. In "Biological Functions of Microtubules and Related Structures". Ed. by H. Sakai, H. Mohri and G. G. Borisy, Academic Press, New York, pp. 211–226.

8 Takahashi, T. C. and Sato, H. (1982) Thermodynamic analysis of the effect of D_2O on mitotic spindles in developing sea urchin eggs. Cell Struct. Funct., **7**: 349–357.

9 Takahashi, T. C. and Sato, H. (1984) Effects of heavy water (D_2O) on the length of the mitotic period in developing sea urchin eggs. Cell Struct. Funct., **8**: 357–365.

10 Takahashi, T. C. and Sato, H. (1984) Yields of tubulin paracrystals, vinblastine-crystals, induced in unfertilized and fertilized sea urchin eggs in the presence of D_2O. Cell Struct. Funct., **9**: 45–52.

11 Itoh, T. J. and Sato, H. (1984) The effect of deuterium oxide (^2H_2O)) on the polymerization of tubulin in vitro. Biochim. Biophys. Acta, **800**: 21–27.

12 Kobayashi, A., Hino, T., Umeyama, K. and Kawazu, K. (1985) Chemical studies on microtubule assembly regulators of microbial origin. 27th Symposium on the Chemistry of Natural Products, Hiroshima. Symposium Papers, pp. 343–350.

13 Sato, H., Kobayashi, A. and Itoh, T. J. (1985) The mitotic arresters; Molecular probes to examine the spindle assembly. In "Cell Motility. II. Mechanism and Regulation". Ed. by H. Ishikawa, S. Hatano and H. Sato, Univ. Tokyo Press, Tokyo, pp. 357–370.

14 Itoh, T. J., Sato, H. and Kobayashi, A. (1986) T-1 dependent barrel-shaped spindle induction in the sea urchin eggs and the role of T-1 in microtubule assembly. Zool. Sci., **3**: 255–264.

15 Mazia, D. (1984) Centrosomes and mitotic poles. Exp. Cell Res., **153**: 1–15.

16 Hirano, K-I., Masuda, M. and Sato, H. (1984) Ultrastructural study of asters induced by microinjection with sperm centriolar fraction in sea urchin eggs. Dev. Growth Differ., **26**: 435–444.

17 Kushida, H. (1966) Block staining with lead acetate. J. Electorn Microscopy, **15**: 90–92.

18 Kushida, H. (1975) Hardness control of the Quetol 651 cured block. J. Electron Microscopy, **24**: 299.

19 Conrad, G. W. and Rappaport, R. (1981) Mechanism of cytokinesis in animal cells. In "Mitosis/ Cytokinesis". Ed. by A. M. Zimmerman and A. Forer, Academic Press, New York, pp. 365–396.

20 Sluder, G. and Reider, C. L. (1985) Experimental separation of pronuclei in fertilized sea urchin eggs: Chromosomes do not organize a spindle in the absence of centrosomes. J. Cell Biol., **100**: 897–903.

21 Endo, S., Toriyama, M. and Sakai, H. (1985) Microtubule organizing granules (MTOGs) in mitotic sea urchin egg. In "Cell Motility. II. Mechanism and Regulation". Ed. by H. Ishikawa, S. Hatano and H. Sato, Univ. Tokyo Press, Tokyo, pp. 403–414.

22 Schatten, H., Schatten, G., Mazia, D., Balczon, R. and Simerly, C. (1986) Behavior of centrosomes during fertilization and cell division in mouse oocytes and in sea urchin eggs. Proc. Natl. Acad. Sci. USA, **83**: 105–109.

23 Sato, H., Ellis, G. W. and Inoué, S. (1975) Microtubular origin of mitotic spindle form birefringence. Demonstration of the applicability of Wiener's equation. J. Cell Biol., **67**: 501–517.

24 Schatten, G. and Schatten, H. (1981) Effects of motility inhibitors during sea urchin fertilization. Exp. Cell Res., **135**: 311–330.

25 Hiramoto, Y., Hamaguchi, M. S., Nakano, Y. and Shoji, Y. (1984) Colcemid UV-microirradiation method for analyzing the role of microtubules in pronuclear migration and chromosome movement in sand-dollar eggs. Zool. Sci., **1**: 29–34.

26 Sato, Y. and Sato, H. (1985) Effect of the mitotic arrester on the spindle assembly in dividing endosperm cells of *Haemanthus katharinae*. Cell Struct. Funct., **10**: 540.

ZOOLOGICAL SCIENCE 4: 277–283 (1987)

Novel Cytotoxic Factors from Tumor Virus-transformed Human Embryo Fibroblasts

YASUJI OKAI[1]

Tokyo Research Laboratories, Kyowa Hakko Kogyo Co., Ltd., Machida, Tokyo 194, Japan

ABSTRACT—The author found novel growth-inhibiting factors in the culture medium conditioned by SV40-transformed human embryo fibroblasts. They were separated by gel filtration, ion exchange and lectin-affinity column chromatographies from the culture medium and characterized to be a protein or glycoprotein which exhibiting the drastic cytotoxic effect on certain untransformed and transformed cell lines. They were inactivated by the addition of endogenous growth-promoting factors from the same transformed cells. The properties of the factors are compared with those of the other factors reported previously and the biological significance of the factors is discussed from the aspect of the cell growth regulation.

INTRODUCTION

The cell proliferation is regulated by various growth factors [1]. Amongst these factors, transforming growth factor α (TGFα) is produced from various tumor virus-transformed cells which confers the transformed phenotype on normal cells [2] and TGFβ is produced from normal or transformed cells which synergistically potentiates the effect of TGFα and epidermis growth factor (EGF).

In this paper, the author will describe the partial purification and characterization of novel growth regulating factors from tumor virus-transformed human cell line. They exhibited a remarkable inhibition of DNA synthesis and a drastic cytotoxic activity in various cultured cell lines. They are compared with the other factors reported previously and the biological significance of the factors is discussed.

MATERIALS AND METHODS

Cell culture

Normal human embryo fibroblast cell line (YH-1) was obtained from a 2-month-old embryo and they are transformed by SV40 at generation 19 as described previously [4]. The cells were grown in Eagle's minimum essential medium (MEM) supplemented with 10% fetal calf serum (FCS, GIBCO, Grand Island Biological Lab., New York) in 5% CO_2 and 95% air at 37°C. The medium was changed every other day and the culture was split by a 1:4 ratio every fourth day.

Partial purification of the cytotoxic factor from the conditioned medium

The recovered medium conditioned by SV40-transformed cells was concentrated with 60% saturation with ammonium sulphate and the precipitate was spun down by a Hitachi RP–20 rotor at 16,000 rpm for 15 min. The sample was applied on a Sephadex G–100 column (Pharmacia, 1.8×48 cm) and eluted with 10 mM phosphate-buffered saline (PBS, pH 7.2) at 5 ml per fraction. Then, the active fractions of Sephadex G–100 chromatography were dialyzed against 10 mM Tris-HCl buffer (pH 7.5) and applied on a DEAE Sephadex A–25 column (Pharmacia, 0.8×5 cm). After washing the column with 10 mM Tris-HCl buffer, it was eluted with a Tris-HCl buffer-containing different NaCl concentrations (0–500 mM). The active fraction of DEAE Sephadex A–25 chromatography was applied on a Concanavalin A (Con A) -Sepharose column (Pharmacia, 0.8×3 cm) and

Accepted October 3, 1986
Received May 8, 1986

[1] Present Address: Lab. of Molecular Oncology, Tsukuba Life Science Center, Yatabe-Machi, Tsukuba-Gun, Ibaragi 305, Japan.

eluted with PBS and PBS supplemented with 0.3 M α-methyl-D-mannoside (α-mM, Sigma).

Assay for DNA synthesis and proliferation

Mammalian cultured cells (1×10^4) (Balb/c 3T3, YH–1, SV40-transformed YH–1, PC 10, SK 28, KB, Flow 7,000, GM 258, K 562, IMR 90, L 132, L 929, T3M–1, Namarva and Wish) were suspended in 0.1 ml of RPMI 1640 medium supplemented with 10% FCS and 0.1 ml of test solution was added. After the cells were cultured for 15 hr at 37°C in 5% CO_2 and 95% air, they were incubated for further 5 hr in the presence of 1 μCi of [^{3}H] TdR (5 Ci/mmol, Amersham, England). The culturing was stopped by the addition of trichloroacetic acid (TCA) in 10% and TCA-insoluble fraction was collected on a GF/C membrane filter (Whatman Co.) by an aid of a cell harvester. The membrane was washed with 5% TCA and ethanol, dried and its radioactivity was counted in a Beckman scintillation counter. For the assay of cell proliferation activity, the number of viable cells in 10 randomly selected microscopic fields was counted by a dye exclusion test with 0.1% trypan blue. The average cell number per microscopic field was expressed as the cell proliferation activity.

Analysis of physicochemical and biochemical properties of the cytotoxic factor

Heat treatment was carried out at 56°C for 30 min and pH stability was analyzed in 50 mM acetate buffer (pH 4.0) and 50 mM Tris-HCl buffer (pH 10.0) for 5 hr at 4°C. After the treatment, the sample was dialyzed against PBS and its activity was assayed. Freezing at −70°C and thawing were repeated twice. Enzyme digestion was performed by bovine pancreas trypsin (Sigma) or proteinase K (Merck) at 50 μg/ml for 30 min. To remove the effects of the exogenously added enzymes on the assay system, soy bean trypsin inhibitor (Sigma) was added to the digest at a final concentration of 50 μg/ml after the trypsin treatment. Proteinase K was separated from the factor's fractions by a Sephadex G–100 column chromatography, because the proteinase K was positioned at more than 20–30 KDa.

RESULTS

As a preliminary experiment, the medium conditioned by SV40-transformed human embryo fibroblasts was added to the culture of Balb/c 3T3 fibroblasts, the cell growth was considerably enhanced as compared with that in the fresh medium supplemented with 10% FCS (data not shown). When the medium was concentrated and applied on a Sephadex G–100 column, the several stimulating activities for DNA synthesis of Balb/c 3T3

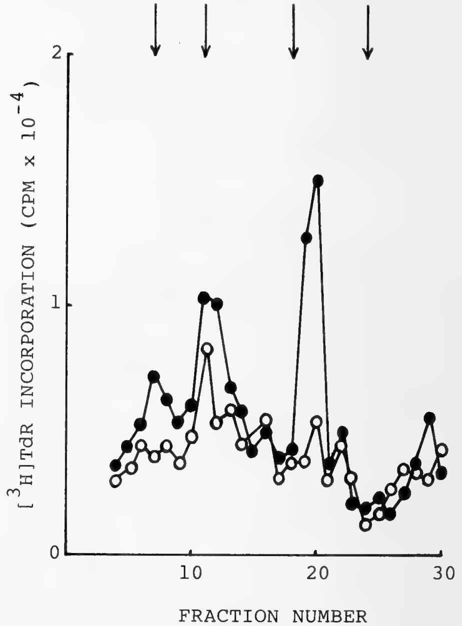

FIG. 1. DNA synthetic activities of Balb/c 3T3 fibroblasts in the culture medium conditioned by SV40-transformed human embryo fibroblasts in Sephadex G–100 column chromatography.
The fresh medium supplemented with 10% FCS or the conditioned medium from SV40-transformed cells was recovered, concentrated, applied on a Sephadex G–100 column and eluted with PBS at 2.5 ml per each fraction. Open and closed circles show the DNA synthetic activities of Balb/c 3T3 fibroblasts in the fractions from the fresh medium supplemented with 10% FCS and the conditioned medium from SV40-transformed cells. Upper arrows in the figure represent the elution positions of molecular weight markers: blue dextran 2,000 (void volume), bovine serum albumin (67 KDa), cytochrome C (13 KDa) and bacitracin (1.5 KDa) from the left to the right.

fibroblasts were observed at void volume, 30–70 KDa and about 10 KDa (closed circles in Fig. 1). Amongst these activities, the major 30–70 KDa activities were also observed in the fresh medium supplemented with 10% FCS (open circles in Fig. 1) and the activity at void volume was considerably shifted to the position at about 10 KDa by a high salt treatment (1 M NaCl) (data not shown). Thus, the author focused here the attention to the dominant activity at about 10 KDa in Figure 1. The 10 KDa stimulating activity from the Sephadex G–100 chromatography was dialyzed, applied on a DEAE Sephadex A–25 column, eluted with the buffer containing NaCl at various concentrations and the stimulating activity in the fractions was examined. As shown in Figure 2, three major stimulating activities for DNA synthesis were found in the fractions at 0–50, 50–150 and 300–500 mM NaCl. Unexpectedly, a strong inhibitory activity for DNA synthesis was separated in

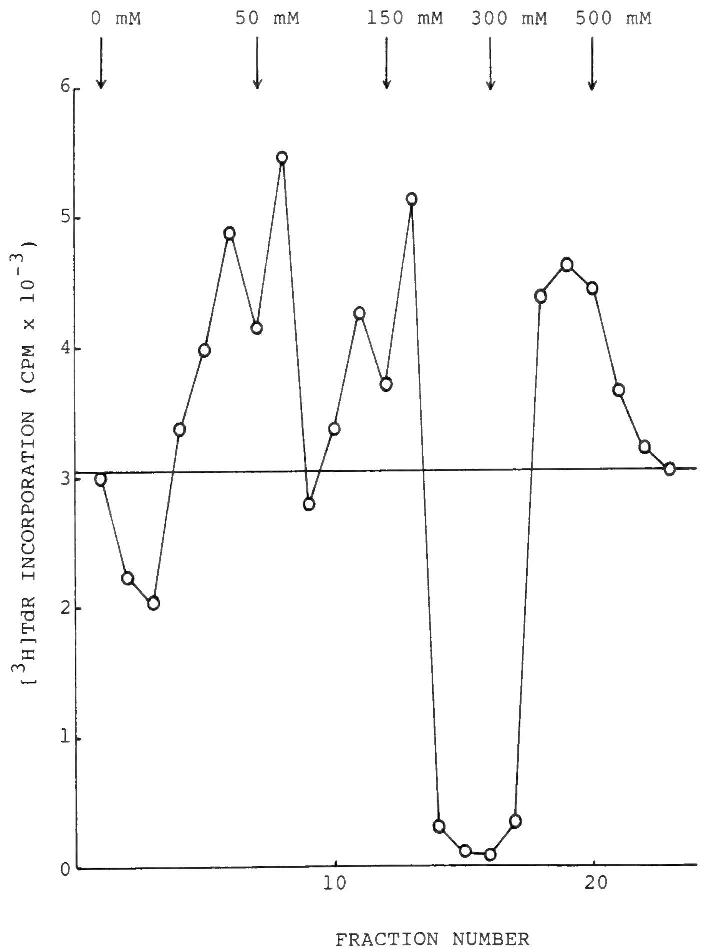

FIG. 2. DNA synthetic activities of Balb/c 3T3 fibroblasts in 10 KDa fraction of the culture medium analyzed by DEAE Sephadex A–25 column chromatography.
The fractions at 19–20 in Fig. 1 were dialyzed against 10 mM phosphate buffer, applied on a DEAE Sephadex A–25 column and eluted with 10 mM phosphate buffer containing various NaCl concentrations as shown in the figure. Open circles show the DNA synthetic activities of Balb/c 3T3 fibroblasts. Each fraction was previously dialyzed against PBS to remove the salts in the fraction and its activity was assayed. The horizontal bar shows the control activity by PBS.

the fractions at 150–300 mM NaCl from the other stimulating factors (Fig. 2). When the cell growth activities in the same fractions of DEAE Sephadex A–25 column chromatography were assayed, a similar elution profile was obtained: Three growth-promoting activities were eluted at the positions similar to those found in DNA synthesis assay and one strong inhibitory activity was eluted at 150–300 mM NaCl (Fig. 3). This inhibitory activity was due to a cytotoxic effect: When examined microscopically, number of the adherent viable cells remarkably decreased and the most cells were lysed. This cytotoxic activity could not be detected in the fresh medium supplemented with FCS. A relatively weak activity was observed in the culture medium conditioned by normal human embryo fibroblasts (YH–1) (data not shown). Then it can be concluded that the cytotoxic activity is specific to the medium conditioned by the SV40-transformed cells.

Next, the author analyzed the biochemical and physicochemical properties of the cytotoxic activity. The activity was resistant to heat treatment (56°C for 30 min) and to freezing and thawing. It was also stable in an acidic (pH 4.0) or basic (pH 10.0) environment (Table 1). The activity was considerably inactivated by proteinase K, but slightly by trypsin (Table 1). In addition, the cytotoxic activity was separated into two fractions, pass-through and bound fractions by a Con A affinity column chromatography (Fig. 4). These results suggest that the cytotoxic activity is associated with a heat stable protein or glycoprotein.

At last, the author studied the effect of the factor on various mammalian cultured cells (Table 2). The SV40-transformed human embryo fibroblasts which produce the factors were very sensitive to the factors and more than 90% of DNA synthesis was inhibited. A similar high sensitivity was found in YH-1 (untransformed human embryo

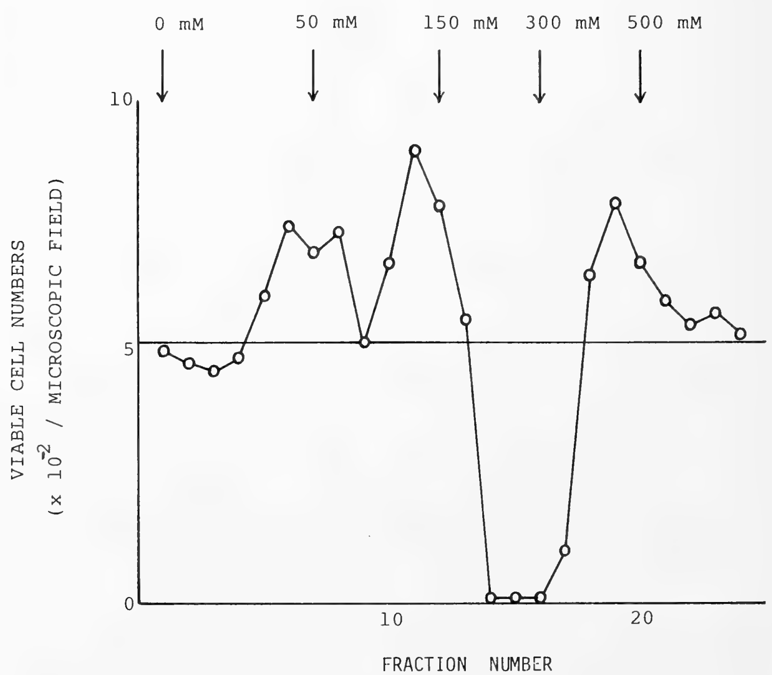

FIG. 3. Cell growth activities of Balb/c 3T3 fibroblasts in 10 KDa fraction of the culture medium analyzed by DEAE Sephadex A–25 column chromatography.
The effect by the same fractions in Fig. 2 on the number of viable cells in Balb/c 3T3 fibroblasts was assayed by a dye exclusion test with trypan blue. Open circles show the average number of viable cells per microscopic field and the horizontal bar is the value in the PBS control.

TABLE 1. Biochemical and physicochemical properties of the cytotoxic factor

	[^{3}H]TdR Incorporation (CPM)
Control	2839 ± 210
+Factor treated with	
None	56 ± 5
Heat (56°C, 30 min)	69 ± 10
pH 4.0	75 ± 13
pH 10.0	48 ± 4
Freezing and thawing	81 ± 12
Trypsin	237 ± 29
Proteinase K	2080 ± 268

The radioactivity is shown as the mean and standard error of triplicate assays.

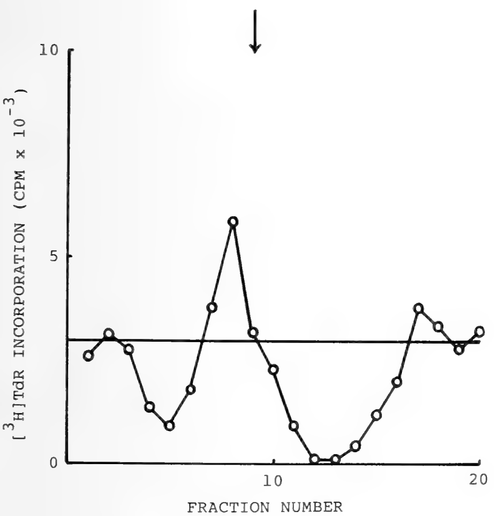

FIG. 4. The cytotoxic factors are eluted in the unbound and bound fractions of a Con A-Sepharose column chromatography.
The active fractions at 14–17 in Fig. 2 were dialyzed against PBS, applied on a Con A-Sepharose column and eluted with PBS, and PBS with 0.3 M α-methyl-D-mannoside (α-mM), successively. The arrow indicates the addition of α-mM. The fraction with PBS containing α-mM was dialyzed against PBS and its activity was assayed. The horizontal bar is the activity of the PBS control.

TABLE 2. Effects of cytolytic factor on various cultured cells

Cell strain	Origin	Sensitivity
YH-1	human embryo fibroblast	+++
SV40-transformed YH-1		+++
3T3	murine fibroblast	+++
PC 10	human epidemoid carcinoma	+++
SK 28	human melanoma	+++
KB	human epimoid carcinoma	++
Flow 7000	human foreskin fibroblast	++
GM 258	human embryo fibroblast	++
K 562	human erythroleukemia cell	+
IMR 90	human embryo fibroblast	+
L 132	human embryo lung cell	+
L 929	murine fibrosarcoma	−
T3M-1	human carcinoma	−
Namarwa	human lymphoblastoid cell	−
Wish	human amniotic cell	−

DNA synthesis inhibition, +++: more than 90%, ++: 50–90%, +: less than 50%, −: no change

fibroblast), PC 10 (epimoid carcinoma) and SK 28 (melanoma). The next high sensitivity (50–90% inhibition) was found in KB (epimoid carcinoma), Flow 7,000 (foreskin fibroblast) and GM 258 (embryo fibroblast) cells. K 562 (erythroleukemia cell), IMR 90 (lung fibroblast) and L 132 (embryo lung cell) cells were relatively resistant (less than 50% inhibition). No significant inhibitory effect was observed in T3M-1 (carcinoma), Namarva (lymphoblast) and Wish (amniotic cell) cells.

The cytotoxic activity derived from the culture medium of SV40-transformed human embryo fibroblasts was cytotoxic to the same cells (Table 2). The reason why the cells can grow and become confluent in the conventional culture was found in the fact that this cytotoxic activity was inactivated by the growth-promoting factors derived from the same transformed cells: As shown in Figure 5, the isolated cytotoxic factor was represented as a single inhibitory activity at about 10 KDa in Sephadex G-100 column chromatography (open circles). When the growth-promoting factors in Figure 2 were combined, mixed with the cytotoxic factor and applied on a Sephadex G-100 column, the cytotoxic factor was inactivated, and even reversely, some stimulating activities were observed at void volume, 30–70 KDa and about 10 KDa (closed circles in Fig. 5). The larger stimulating activities were derived from the aggregates of 10 KDa activities.

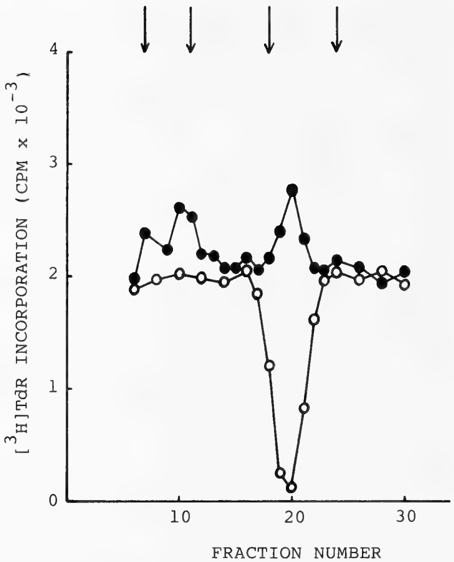

Fig. 5. The effect by the cytotoxic factor was inactivated by the growth-promoting factors.
The active fraction of the cytotoxic factor in Fig. 2 was incubated with (closed circles) and without (open circles) the growth-promoting factors at 4°C for 30 min and applied on a Sephadex G–100 column as performed in Fig. 1. The growth-promoting activities in Fig. 2 (Fractions at 6, 8, 11, 13, and 19) were combined, concentrated with 60% saturated ammonium sulphate and added to the cytotoxic factor. Upper arrows in the figure are the same as in Fig. 1.

DISCUSSION

The results mentioned above suggest that a novel regulating factor for cell growth is released from SV40-transformed human embryo fibroblasts. This factor showed the cytotoxic effects on certain transformed and untransformed cell lines, but its activity was inactivated by the growth-promoting factors from the same transformed cells.

Some cytotoxic or growth-inhibiting factors from mammalian cells have been reported. First of all, lymphotoxic (LT) and tumor necrosis factor (TNF) are released from the lymphocytes or monocytes and they exhibit the cytotoxic or cytostatic effects on certain transformed cell lines [5–8]. A considerable homology exists in their amino acids and DNA sequences [9, 10]. Their molecular weights are estimated to be 25 KDa and 17 KDa by means of their DNA clonings [9, 10] and aggregate as the forms larger than 40–50 KDa [5–8]. They show little or no anticellular activities on primary cell culture or normal cell strains such as primary human embryo fibroblasts or mouse 3T3 fibroblasts [5–8]. On the other hand, the factor obtained in this study was estimated to be about 10 KDa by a gel filtration chromatography under the conventional buffer condition and show the cytotoxic effect on some transformed and untransformed cell lines including normal human embryo fibroblasts and 3T3 fibroblasts. Therefore, the further analysis is required, the present factor is considered to be different from LT or TNF.

Tumor cell growth-inhibiting factors (TIFs) were reported and they inhibit the growth of various tumor cell lines, but stimulate normal human foreskin fibroblasts and epithelial cells in monolayer cultures [11, 12]. The effects by the factors are not cytotoxic, but reversible when the affected cells are no longer exposed to the factors. On the contrary, the factor in the present paper showed the irreversible cytotoxic effect on untransformed and transformed cell lines and did not exhibit the stimulating activity for the proliferative response of human embryo fibroblasts.

TGFβ is a potent stimulator of growth in soft agar of ancholage-dependent cells including human fibroblasts and also a potent growth inhibitor for human foreskin keratinocytes and certain human cancer cell lines [13]. This inhibition is not cytotoxic in nature, but reversible which is different from the inhibition by the factor in this paper.

Tumor degenerating factor (TDF) was found in the culture medium of normal human embryo fibroblasts [14]. It has a basic charge property and does not bind to DEAE Sephadex column. It causes a morphological change on KB, HeLa and other cell lines [14]. It can cause neither significant inhibition to DNA synthesis nor cytotoxic effect (personal communication by Dr. A. Tanaka, Kyoto Prefecture University of Medicine).

The author reported the heterogeneous molecular weight inhibitory factors for DNA synthesis from the serum-free culture medium conditioned by normal human embryo fibroblasts (YH-1 cells) [15]. Although they show a strong inhibition to

DNA synthesis in normal fibroblasts or lymphocytes, the cell viability is not changed. In addition, the production of the cytotoxic factor in this paper was very weak in the culture medium of normal human embryo fibroblasts.

Thus it may be concluded that a novel cytotoxic factor is released from the SV40-transformed human embryo fibroblasts which exhibits the cytotoxic effect on certain untransformed and transformed cell lines and that the action of this factor is counteracted by the growth-promoting factors from the some transformed cells.

Although the more detailed study is required, the existence of this cytotoxic factor in tumor virus-transformed human embryo fibroblasts seems to serve an interesting problem concerning the cell survival, growth and death in untransformed and transformed cells.

ACKNOWLEDGMENTS

The author would like to thank Miss S. Kurata for her technical assistance and Dr. N. Fujiyoshi for his encouragement in Tokyo Research Laboratories of Kyowa Hakko Kogyo Co.

REFERENCES

1 Holley, R. W. (1980) Control of animal cell proliferation. J. Supramol. Struct., **13**: 191–197.

2 Delarco, J. E. and Todaro, G. J. (1978) Growth factors from a murine sarcoma virus-transformed cells. Proc. Natl. Acad. Sci. USA, **75**: 4001–4005.

3 Roberts, A. B., Frolik, C. A., Anzano, M. A. and Sporn, M. B. (1983) Transforming growth factors from neoplastic and nonneoplastic tissues. Fed. Proc., **42**: 2621–2626.

4 Yanagisawa, K., Suenaga, Y., Nishio, K. and Gotoh, S.(1983) Establishment of human diploid cell strain. J. Univ. Occup. Eniron. Health (Kitakyushu), **5**: 49–54.

5 Aggarwal, B. B., Moffat, B. and Harkins, R. N. (1984) Human lymphotoxin – Production by a lymphoblastoid cell line, purification, and initial characterization. J. Biol. Chem., **259**: 686–691.

6 Ruddle, N. H., Powell, M. B. and Conta, B. S. (1983) Lymphotoxin, a biologically relevant model lymphokine. Lymphokine Res., **2**: 23–31.

7 Williamson, B. D., Carswell, E. A., Rubin, B. Y., Prendergast, J. S. and Old, L. J. (1983) Human tumor necrosis factor produced by human B cell lines : Synergistic cytotoxic interaction with human interferon. Proc. Natl. Acad. Sci. USA, **80**: 5397–5401.

8 Ruff, M. R. and Gifford, G. E. (1981) Tumor necrosis factor. Lymphokines, **2**: 235–272.

9 Gray, P. W., Aggarwal, B. B., Benton, C. V., Bringman, T. S., Henzel, W. J., Jarrett, J. A., Leung, D. W., Moffat, B., Ng, P., Svedersky, L. P., Palladino, M. A. and Nedwin, G. E. (1984) Cloning and expression of cDNA for human lymphotoxin, a lyohokine with tumor necrosis activity. Nature, **312**: 721–724.

10 Pennica, D., Nedwin, G. E., Hayflick, J. S., Seeburg, P. H., Derynck, R., Palladino, M. A., Kohr, W. J., Aggarwal, B. B. and Goeddel, D. V.(1984) Human tumor necrosis factor : precursor structure, expression and homology to lymphotoxin. Nature, **312**: 724–729.

11 Iwata, K. K., Fryling, C. M., Knett, W. B. and Todaro, G. J.(1985) Isolation of tumor cell growth-inhibiting factors from a human rhabdomyosarcoma cell line. Cancer Res., **45**: 2689–2694.

12 Fryling, C. M., Iwata, K. K., Johnson, P. A., Knott, W. B. and Todaro, G. J.(1985) Two distinct tumor cell growth-inhibiting factors from a human rhabdomyosarcoma cell line. Cancer Res., **45**: 2695–2699.

13 Moses, H. L., Tucker, R. F., Loef, E. B., Coffey, R. J., Halper, J. J. and Shipley, G. D.(1985) Type-β transforming growth factor is a growth stimulator and a growth inhibitor. In "Cancer Cells, Vol. 3". Ed. by J. Feramisco, B. Ozanne and C. Stiles, Cold Spring Harbor Lab., New York, pp. 65–71.

14 Tanaka, A., Matsuoka, H., Uemura, H., Kakui, Y., Imanishi, T., Nishino, H. and Imanishi, J.(1985) Production and characterization of tumor-degenerating factor. J. Natl. Cancer Inst., **74**: 575–581.

15 Okai, Y.(1986) Heterogeneous molecular inhibitory factors for lymphocyte DNA synthesis from human embryo fibroblasts – two conversion pathways by a trypsin-like protease(s). Zool. Sci., **3**: 271–276.

ZOOLOGICAL SCIENCE 4: 285–292 (1987)

Two-dimensional Polyacrylamide Gel Analysis of Papilloma and Normal Skin Proteins in Newt

KAZUNORI SHIMADA, HIROMICHI KOYAMA[1] and MAKOTO ASASHIMA[2]

Department of Biology, Yokohama City University, 22–2 Seto, Kanazawa-ku, Yokohama 236, and [1]Department of Anatomy, School of Medicine, Yokohama City University, Urafune-cho, Minami-ku, Yokohama 232, Japan

ABSTRACT—The protein patterns of papilloma found in Japanese newt *Cynops pyrrhogaster* were compared with those of the nontumourous skin of the same animal by two-dimensional (2-D) gel electrophoresis method. There were 11 protein spots specific to the skin. Almost all of them were detected also in skin derived from different regions of normal adult male and female. On the other hand, 7 protein spots specific to papilloma were detected. The papilloma-specific spots were detected neither in the skin, lung and liver of normal adult newt, the skin of normal larvae, nor the presumptive ectodermal region of embryo. One of the 11 spots specific to adult skin coincided with one of the spots of normal larval skin. Two unique spots were identified in the larval skin. Such appearance of these tissue specific proteins suggests that the cell transformation involves a disdifferentiative but not dedifferentiative process.

INTRODUCTION

Little attention has been paid to the tumors of amphibians, as compared to those of the higher vertebrates. This is due to the fact that not much is known about the variety of tumors among this group, and also because amphibians are possessed of such unique characteristics as a strong regenerating ability, hibernation and metamorphosis which are not shared by other vertebrates [1, 2].

We have been conducting a clinical laboratory study of papilloma-bearing Japanese newts, *Cynops pyrrhogaster*, collected in Niigata and Iwate prefectures. Differences in the geographical and seasonal abundance of the papilloma, and the effects of temperature on the growth of the papilloma have been reported [3, 4]. However, no comparison or analysis has been made as to the biochemical natures of papilloma and normal skin. Biochemical studies of Lucké renal carcinoma in the *Rana pipiens* frog revealed the appearance of tumor specific proteins after the transformation of normal renal tissues [5, 6]. As papilloma are thought to consist of transformed epidermal cells [7], it is possible that such tumor specific proteins are present also in the papilloma of newts. We, therefore, conducted the study on the protein pattern of Japanese newt papilloma by means of 2-D polyacrylamide gel electrophoresis. The protein pattern of newt papilloma was determined and then compared with those of normal adult and larval skin, and those of embryonic presumptive ectoderm, in order to examine whether or not tumor specific protein exists in the papilloma of the newt.

MATERIALS AND METHODS

Sample preparation

The material used was Japanese newt *Cynops pyrrhogaster* collected in Iwate prefecture in the autumn of 1984. Female newts, approx. 110 mm in body length, with papilloma (ca. 2 mm in diameter) on their dorsal surface were selected. Each newt was anesthetized with 0.02% MS–222 in water, and its papilloma was removed with a fine scalpel (Fig. 1). The dissected segment of papillo-

Accepted November 7, 1986
Received August 19, 1986
[2] To whom reprints should be requested.

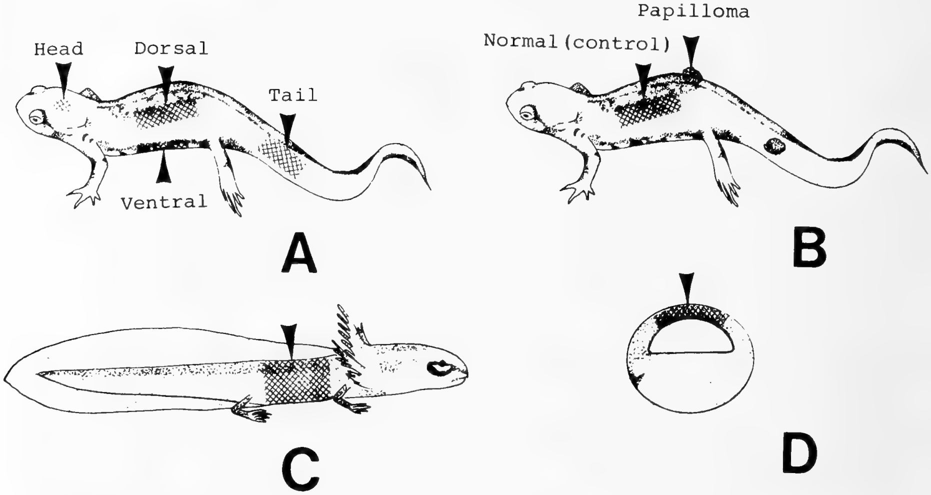

FIG. 1. Schematic diagram of source materials. Skins (or presumptive ectoderm) were taken as controls from shaded areas. A; normal adult (male and female). B; adult female newt bearing papilloma. C; larval newt (stage 55). D; early gastrula (stage 10).

ma was cleaned at room temperature in Holtfreter's solution (HS) [8]. Blood cells and muscle tissue were removed. They were twice washed with HS. Cleaned papilloma tissues were homogenized at 0°C in a lysis buffer containing 8 M urea, 5% Ampholine pH 3–10 (LKB, Sweden), 5% β-mercaptoethanol and 2% NP–40 (Sigma, USA) [9]. The homogenate was left standing at room temperature for 5 hr, and then centrifuged at $3{,}000 \times g$ for 30 min, and the supernatant was obtained as papilloma sample.

For a control, papilloma-free skin with dermis was taken from the dorsal surface of the same newt from which papilloma had been removed (Fig. 1). At the same time, skin samples were obtained from the dorsal region of normal male newts, body length ca. 100 mm, and from 4 different regions (head, dorsal, ventral and tail; Fig. 1) of normal female newts, body length ca. 110 mm. Lung and liver tissue of normal female newts also were used. These samples were processed as described for the papilloma sample.

Larvae at stage 55 [10] before metamorphosis were also anesthetized with MS–222. Larval skin samples were prepared after removal of fins. A part of the body (Fig. 1) between the anterior and posterior limbs was removed with a fine scalpel and the skin was removed from it in HS, with forceps. Presumptive ectoderm was prepared from early gastrula after the jelly envelope and vitelline membrane were removed (Fig. 1).

All the samples were stored at −15°C until use. The samples were thawed at room temperature, precipitated with trichloracetic acid (TCA), and then the concentration of protein was determined by the method of Lowry *et al.* [11].

2-D Polyacrylamide gel electrophoresis

The basic process followed the method described by O'Farrell [12, 13]. The first-dimension (1-D) featured polyacrylamide gel and isoelectric focusing, and SDS polyacrylamide gel was used in the second-dimension (2-D). The acrylamide stock solution contained 30% acrylamide in total concentration, i.e., 29.2% acrylamide (BIORAD, USA) and 0.8% bis-acrylamide (BIORAD, USA).

1-D Isoelectric focusing gels (8 M urea, 3.5% acrylamide, 2% NP–40, 5% Ampholine pH 3–10, 0.015% ammonium persulfate, 0.1% TEMED: N, N, N′, N′-tetramethylethylenediamine) were cast to a length of 12 cm in 2.5 mm i.d. ×13 cm long glass tubes, overlayed with distilled water to form the uniformly flat surface, and allowed to polymerize at room temperature for 5 hr. After prerunning at 200 V for 15 min, at 300 V for 30 min and at

400 V for 30 min, in this sequence, each gel was loaded with a sample, usually containing 0.02 mg of proteins. Electric focusing was carried out at 400 V for 14 hr, followed by at 800 V for 30 min. Gels were removed from the glass tubes and shaken in an SDS sample buffer (10% glycerol, 5% β-mercaptoethanol, 0.0625 M Tris-HCl pH 6.8, 2.3% SDS) for 60 min.

The 2-D separation gel used was 12 cm-wide, 11 cm-high and 1 mm-thick 7.5% acrylamide gel with 0.375 M Tris-HCl, pH 8.8, 1% SDS, 0.078% ammonium persulfate and 0.075% TEMED. After polymerization of the separation gel, a 1 cm-high stacking gel (3% acrylamide, 0.125 M Tris-HCl pH 6.8, 1% SDS, 0.1% ammonium persulfate and 0.1% TEMED) was added onto it. The SDS sample buffer was wiped off from each equalized 1-D gel and this was fixed onto polymerized 2-D gel with a hot agar mixture (1% Agarose in SDS sample buffer) containing a slight amount of bromophenolblue. The gels were set in an electrophoresis apparatus (Atto Co., Ltd., Tokyo) with a buffer (0.025 M Tris, 0.1% SDS and 0.192 M glycine) and was run for 270–300 min at 20 mA/gel until the dye front reached 10 mm from the bottom of the gel. As a standard protein, actin (Sigma, USA) was run in the 2-D gel.

Silver staining

The 2-D separation gel was fixed in a mixture of 50% methanol and 10% acetic acid, shaken for 1 hr, washed three times in distilled water for a total of 45 min, and then immersed into a silver stainer (0.776% $AgNO_3$, 0.0756% NaOH and 0.392% NH_4OH) [14] and shaken for 15 min. The gel was then rinsed twice for 3 min each in distilled water and transferred to a developer (0.005% citrate and 0.019% formaldehyde). When spots became sufficiently visible, the developer was replaced with a double volume of a fixer to terminate staining.

Photography and drying

Stained gels were photographed with Neopan F ASA 32 (Fuji) using transmission light, and then dried for one day between sheets of cellophane. Both the photographs and the dried gels were used to analyze the protein spots.

RESULTS

In our modification of the method of O'Farrell, the pH 4–9 range of the first dimension was broader than that in the original method [12, 13].

When actin monomer was subjected to electrophoresis, the isoelectric point was pH 4.8 and Rf value 0.64. As the constantly detectable spot of probable actin in our experiments showed similar values (isoelectric point pH 4.8; Rf value 0.65), it was reasonable to use this spot as an actin marker spot.

Comparison between normal skin and papilloma

As shown in Figure 2, the proteins of normal skin and papilloma were separated by the 1-D gel in the range of pH 4 to 9. The arrow followed by "A" indicates a probable actin spot, and this spot was used as a marker in the present analysis. There was an average of 300 spots detected in both normal skin and papilloma. At least 11 and 7 spots were detected only in normal skin and papilloma, respectively. The former will be referred to as skin specific spots (SSSs) and the latter as papilloma specific spots (PSSs). The staining intensity of each spot was diverse.

Regional difference of protein patterns of skin

Of the 11 SSSs, spot numbers 1, 2, 3, 4, 7, 8, 9 and 10 were detected in the dorsal, ventral, head and tail skin in normal adult female (Table 1), although some region specific spots were detected (spot patterns not shown in figures). No spot from these materials corresponded to any of the PSSs (Table 2).

Difference by sex

The 11 SSSs were also found in the dorsal skin of normal adult male, but no PSSs were detected (Tables 1 and 2). There were no significant differences between spot patterns of males and females (data not shown).

Comparison with larval skin

There were fewer spots in larval skin than in adult skin, or an average of about 200 (Fig. 3A). One spot corresponding to SSSs was observed (Fig. 3A, 9). Two spots not detected in any other

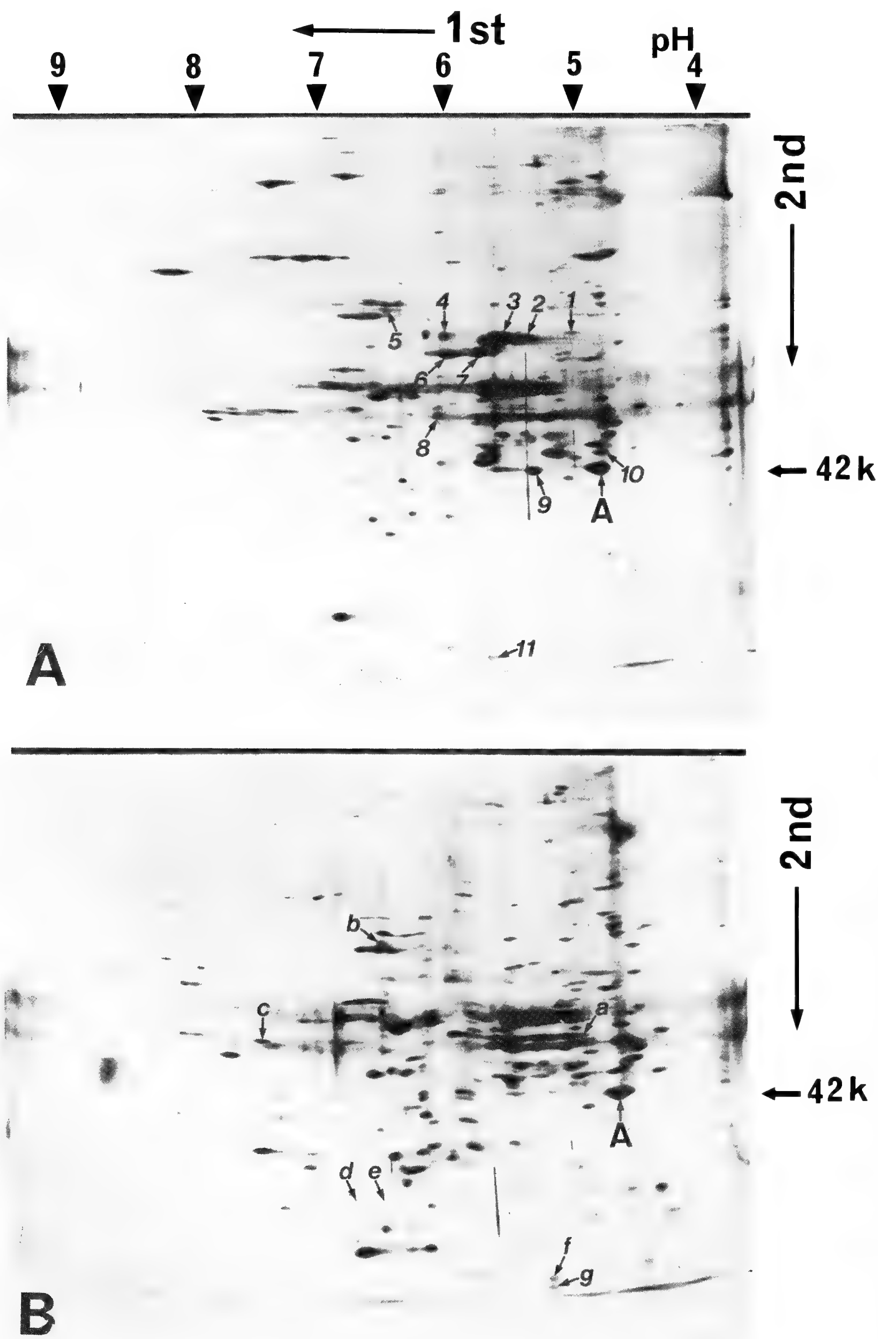

FIG. 2. 2-D Gel protein pattern of skin (A) and papilloma (B) of adult female. "A" indicates the spot of actin. Numbers 1 to 11 in (A) indicate skin specific protein spots (SSSs). Letters a to g in (B) indicate papilloma specific protein spots (PSSs).

TABLE 1. Comparison of skin specific spots among various materials

Materials \ Spot number	1	2	3	4	5	6	7	8	9	10	11
Papilloma-bearing adult (f)											
papilloma	−	−	−	−	−	−	−	−	−	−	−
skin dorsal	+	+	+	+	+	+	+	+	+	+	+
Normal adult											
skin dorsal (f)	+	+	+	+	±	+	+	+	+	+	+
ventral (f)	+	+	+	+	±	+	+	+	+	+	+
head (f)	+	+	+	+	+	−	+	+	+	+	−
tail (f)	+	+	+	+	+	+	+	+	+	+	+
dorsal (m)	+	+	+	+	+	+	+	+	+	+	+
lung (f)	−	−	−	−	−	−	−	−	−	−	−
liver (f)	−	−	−	−	−	−	−	−	−	−	−
Larval skin (st. 55)	−	−	−	−	−	−	−	−	+	−	−
Ectoderm (st. 10)	−	−	−	−	−	−	−	−	−	−	−

1–11; skin specific spots, f; female, m; male.

TABLE 2. Comparison of papilloma specific spots among various materials

Materials \ Spot number	a	b	c	d	e	f	g	LSS	actin
Papilloma-bearing adult (f)									
papilloma	+	+	+	+	+	+	+	−	+
skin dorsal	−	−	−	−	−	−	−	−	+
Normal adult									
skin dorsal (f)	−	−	−	−	−	−	−	−	+
ventral (f)	−	−	−	−	−	−	−	−	+
head (f)	−	−	−	−	−	−	−	−	+
tail (f)	−	−	−	−	−	−	−	−	+
dorsal (m)	−	−	−	−	−	−	−	−	+
lung (f)	−	−	−	−	−	−	−	−	+
liver (f)	−	−	−	−	−	−	−	−	+
Larval skin (st. 55)	−	−	−	−	−	−	−	+	+
Ectoderm (st. 10)	−	−	−	−	−	−	−	−	+

a–g; papilloma specific protein spots, f; female, m; male, LSS; larva specific protein spots.

samples were larva specific spots (Fig. 3A, L). Except for these larva specific spots, the spot pattern of larval skin corresponded to that of adult skin.

Comparison with presumptive ectoderm

This tissue demonstrated even fewer spots than larval skin, the average being 100 (Fig. 3B). The total protein content of this sample used was as 5 times (0.1 mg) as in Figures 2 and 3A. Except for the appearance of two large spots at pH 7–8 and extending from high MW to low MW, which is probably indicating yolk protein, all spots detected in presumptive ectoderm corresponded to those found in adult skin and no PSSs were found. Tables 1 and 2 summarize the occurrence of SSSs and PSSs in the subject materials.

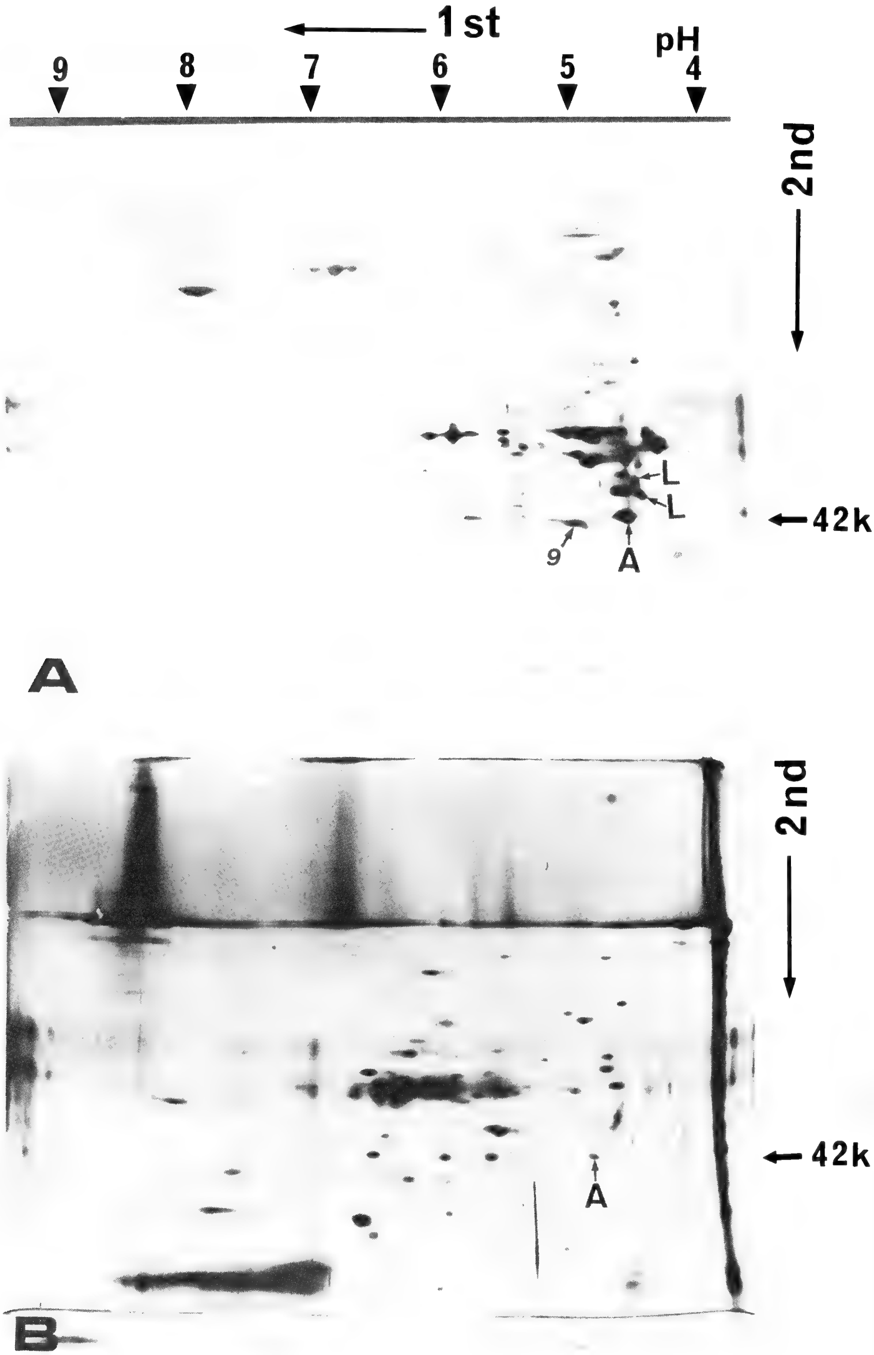

FIG. 3. 2–D Gel protein patterns of larval skin (A) and presumptive ectoderm (B). "A" indicates the spot of actin. "9" in (A) is similar to spot found in adult skin. "L" marks in (A) indicate larva specific protein spots.

DISCUSSION

There were averages of 300 of protein spots detected in adult dorsal skin, 200 in larval skin (stage 55), and 100 in presumptive ectoderm of embryo (stage 10). The 11 spots specific to adult skin (SSSs) were found. We believe that regional differences in spot patterns are of minor significance. There was negligible difference by sex, and the SSSs were common to both gender.

A comparison of the spot patterns in skin and in papilloma resulted in the identification of 7 papilloma specific spots (PSSs). These were not detected in normal adult skin, larval skin or presumptive ectoderm. It would, therefore, concern that the appearance of PSSs indicates the presence of virus-associated proteins [3], changes in the basement membrane [15], or increase of lysosomes [15] and so on. There is a necessity for further study of the functional role of these PSSs in papilloma cells.

In some kinds of tumor, cellular transformation is regarded as a consequence of cell dedifferentiation [16, 17]. Another view of transformation is that it is a disdifferentiative process [18, 19]. Fetalization is one example of the former. The fetalized state of tumor cells involves the production of carcinoembryonic proteins (CEP) such as α-fetoprotein. In mammals the CEP can be usually detected in the embryonic tissues and not in the normal adult tissues. However, the CEP reappear in the transformed adult tissues [20, 21]. We carried out this study to examine whether proteins of larval or embryonic skin reappear in the transformed skin of adult newts. The results did not prove the appearance of CEP type proteins in papilloma. Instead, some papilloma specific proteins (PSSs), not shared by the skins of normal adult and of juvenile, were detected. Considering both the disappearance of SSSs and the occurrence of PSSs in papilloma, the transformation of normal epidermal cells into papilloma cells seems to be a disdifferentiative process, but not included into fetalization. In some hepatomas, occurrence of disdifferentiative transformation is characterized by, for instance, the presence of isoenzymes of other tissue type [22].

A comparison of the spots found in adult newt, larva and embryo in our study suggested that the number of spots increases along with the development from embryo to adult. Except for the two unique spots found in larval skin, the spot pattern included that of the embryo, and the spot pattern of the larva was included in that of the adult newt. As the process of development advances, the structure and functions of the newt become more complex.

ACKNOWLEDGMENTS

We are thankful to Dr. S. Togashi for his technical advice on 2-D gel electrophoresis. This work was supported in part by a Grant-in-Aid for Cancer Research from the Ministry of Education, Science and Culture of Japan (#60010019).

REFERENCES

1 Waddington, C. H. (1935) Cancer and the theory of organizers. Nature, **135**: 606–608.

2 Asashima, M. and Oinuma, T. (1985) Amphibian tumors. Oncologia, **13**: 99–114.

3 Asashima, M., Komazaki, T., Satou, C. and Oinuma, T. (1982) Seasonal and geographical changes of spontaneous skin papillomas in the Japanese newt *Cynops pyrrhogaster*. Cancer Res., **42**: 3741–3746.

4 Asashima, M., Oinuma, T., Matsuyama, H. and Nagano, M. (1985) Effects of temperature on papilloma growth in the newt, *Cynops pyrrhogaster*. Cancer Res., **45**: 1198–1205.

5 Nace, G. W. and Ostrovsky, D. S. (1977) Frog lysozyme. IV. Isozymes of lysozyme and the Lucké renal adenocarcinoma. J. Natl. Cancer Inst., **58**: 453–454.

6 Rubin, M. L. and Nace, G. W. (1966) The virus inhibiting action of a lysozyme present in normal frogs but lacking in tumor frogs and eggs. Am. Zool., **6**: 510.

7 Asashima, M. and Oinuma, T. (1982) Transplantation and injection of skin papilloma fragments in newts (*Cynops pyrrhogaster*). J. Fac. Sci., Univ. Tokyo, Sec IV., **15**: 151–158.

8 Holtfreter, J. (1934) Über die Verbreitung induzierender Substanzen und ihre Leistungen im *Triton*-Keim. Roux's Arch. Entwicklungsmech. Org., **132**: 307–383.

9 Meuler, D. C., and Malacinski, G. M. (1984) Protein synthesis patterns during amphibian embryogenesis. In "Molecular Aspects of Early Development". Ed. by G. M. Malacinski and W. H. Klein, Plenum Press, New York and London, pp. 267–288.

10 Okada, Y. K. and Ichikawa, M. (1974) Normal table of *Triturus pyrrhogaster* (revised). Jpn. J. Exp. Morphol., **3**: 1–6.

11 Lowry, O. H., Rosebrough, N. J., Farr, A. L. and Randall, R. J. (1951) Protein measurement with the Folin phenol reagent. J.Biol. Chem., **193**: 265–275.

12 O'Farrell, P. H. (1975) High resolution two-dimensional electrophoresis of proteins. J. Biol. Chem., **250**: 4007–4021.

13 O'Farrell, P. Z., Goodman, H. H. and O'Farrell, P. H. (1977) High resolution two-dimensional electrophoresis of basic as well as acidic proteins. Cell, **12**: 1133–1142.

14 Oakley, B. R. Kirsh, D. R., and Morris, N. R. (1980) A simplified ultra-sensitive silver stain for detecting proteins in polyacrylamide gels. Anal. Biochem., **105**: 361–363.

15 Asashima, M. and Komazaki, S. (1980) Spontaneous progressive skin papilloma in newts (*Cynops pyrrhogaster*). Proc. Japan Acad., **56** (10): 638–642.

16 Greenstain, T. P. (1954) Biochemistry of Cancer, Academic Press, New York, pp. 1–653.

17 Suda, M., Tanaka, T., Yanagi, S., Hayashi, S., Imamura, K. and Taniuchi, K. (1972) Dedifferentiation of enzymes in the liver of tumor-bearing animals. In "Gann Monograph on Cancer Research, Vol. 13". Ed. by S. Weinhouse and T. Ono, Univ. Tokyo Press, pp. 79–93.

18 Meezan, E., Wu, H. C., Black, P. H. and Robbins, P. W. (1969) Comparative studies on the carbohydrate-containing membrane components of normal and virus-transformed mouse fibroblasts. II. Separation of glycoproteins and glycopeptides by Sephadex chromatography. Biochemistry, **8**: 2518–2524.

19 Sugimura, T., Matsushima, T., Kawachi, T., Togure, K., Tanaka, N., Miyake, S., Hozumi, M., Sato, S. and Sato, H. (1972) Disdifferentiation and decarcinogenesis—the isozyme patterns in malignant tumors and membrane changes of cultured tumor cells. In "Gann Monograph on Cancer Research, Vol. 13". Ed. by S. Weinhouse and T. Ono, Univ. Tokyo Press, pp. 31–45.

20 Hirai, H., Nishi, S. and Watanabe, H. (1973) Chemical studies of AFP's of human and several other animals. Tumor Res., **8**: 11–16.

21 Nishi, S. and Hirai, H. (1976) Radio-immuno assay of carcinoembryonic antigen and its related antigens by the sandwich methods. In "Oncodevelopmental Gene Expression". Ed. by W. H. Fishman and S. Sell, Academic Press, London, pp. 567–572.

22 Weinhouse, S. and Ono, T. (1974) Isonezymes and Enzyme Regulation in Cancer (Gann Monograph on Cancer Research, Vol.13), Univ. Tokyo Press, pp. 1–322.

ZOOLOGICAL SCIENCE 4: 293–299 (1987)

Localization of Catecholaminergic Nerves in Larval Echinoderms

Yoko Nakajima

Department of Biology, Keio University, Hiyoshi, Yokohama 223, Japan

ABSTRACT—Localization of catecholaminergic nerves in three classes of echinoderms, the echinopluteus of *Hemicentrotus pulcherrimus,* the bipinnaria of *Asterias amurensis* and the auricularia of *Stichopus japonicus,* was studied by means of a glyoxylic acid fluorescence histochemistry and electron microscopy. A continuous fibrous structure, which emitted strong blue-green fluorescence characteristic of catecholamines, was clearly observed along the ciliary bands in the specimens treated with glyoxylic acid. A few cells in the lower lip of the mouth also exhibited prominent fluorescence. In addition, intensely fluorescing cell bodies were found along the ciliary bands of upper and anal lobes of bipinnaria and auricularia.

These regions with strong fluorescence correspond to the sites where nerve bundles and ectoneural cells were identified by electron microscopy. Since these nerves are found in close association with ciliary bands, it is suggested that the nervous system controlling ciliary movements is catecholaminergic.

In contrast, glyoxylic acid treatment evoked weak yellow or very faint fluorescence in the preoral area of the echinopluteus and in the upper lip of the auricularia, respectively, in spite of the presence of a large number of nerve cells and a bundle of axons. This appears to be an indication that some ectoneural cells contain neurotransmitters other than catecholamines.

INTRODUCTION

Locomotion and feeding of larval echinoderms rely on water current produced by ciliary movements. Earlier physiological studies suggest that the ciliary movements in some echinoplutei (*Strongylocentrotus droebachiensis* and *Psammechinus miliaris*) are under the control of nervous system [1, 2]. Histochemical localization of cholinesterases and biogenic amines was studied by Ryberg [3, 4] using enzymatic and formaldehyde-induced fluorescence methods in echinopluteus, but the insufficiency of the resolution made it difficult to identify the neuronic elements at cellular level. Burke described the development and ultrastructure of nerve cells in the larvae of two species of sea urchin *Strongylocentrotus purpuratus* and *Dendraster excentricus,* and the starfish *Pisaster ochraceus* [5–8], and more recently, ultrastructure of several types of ectoneural cells, which probably have sensory function, was studied by the present author in the plutei of *Hemicentrotus pulcherrimus, Mespilia grobulus,* and *Temnopleurus toreumaticus* [9, 10]. However, the development and the anatomy of entire network of nervous system in larval echinoderms still remain to be elucidated.

The present investigation was undertaken to demonstrate the occurrence of catecholaminergic nerves in the larvae of three species of echinoderms that belong to three representative classes of the phylum. The glyoxylic acid fluorescence method for the specific visualization of catecholamines [11] was employed for the histochemical localization, and nerve cells and axons were identified by elecron microscopy.

MATERIALS AND METHODS

Larval echinoderms

The pluteus of the sea urchin, *Hemicentrotus pulcherrimus,* the bipinnaria of the starfish, *Asterias amurensis,* and the auricularia of the sea cucumber, *Stichopus japonicus,* were used.

Accepted October 7, 1986
Received July 31, 1986

The adults of *Hemicentrotus pulcherrimus* were supplied from the Misaki Marine Biological Station (Kanagawa Pref.) and the Tateyama Marine Laboratory (Chiba Pref.). Unfertilized eggs were obtained by an injection of 0.5 M KCl into the adult body cavity and inseminated artificially. The larvae were raised in filtered sea water or in artificial sea water (Jamarin U, Osaka) at 13–17°C with gentle agitation.

Adult starfish *Asterias amurensis* were supplied from the Tateyama Marine Laboratory. Ovaries were excised and treated with 10^{-6} M 1-methyladenine [12]. Obtained mature eggs were artificially inseminated. The planktonic larvae of the starfish were kept in Petri dishes at 17–20°C without agitation.

The adults of *Stichopus japonicus* were collected at the Mikawa Bay (Aichi Pref.) and around the Miura Peninsula (Kanagawa Pref.). Among three color variants (red, blue and black colored integument), red and blue varieties were used in this study. Naturally spawned or artificially inseminated gametes were employed. The auricularia were kept in Petri dishes at 20–23°C.

Larvae of all three species were fed with *Cheatoceros gracillis*.

Histochemical localization of catecholamines

The glyoxylic acid fluorescence technique [11] improved by Sharpe and Atkinson [13] was employed with a slight modification. Larvae were immersed in 2% glyoxylic acid (Merck) in 0.2 M phosphate buffer, pH 7.0, for 30 sec to 2 min. After a brief rinse in the same buffer, samples were mounted on slides and dried with a hair drier, and then heated for 2 min on a hot plate at 100°C. The specimens were sealed in liquid paraffin and observed with epi-fluorescence microscope (Nikon Fluophot). A filter with the maximum emission at 410–440 nm was employed.

Electron microscopy

Larvae were fixed in a mixture of 2% glutaraldehyde and 1% osmium tetroxide in 0.45 M sodium acetate buffer, pH 6.4, for 30 to 60 min at room temperature. After dehydration through a graded series of alcohol, samples were embedded in epoxy resin. Ultrathin sections were stained with uranyl acetate and lead citrate and observed in a JEOL 100S electron microscpe with an accelerating voltage at 80 kV.

RESULTS

Hemicentrotus pulcherrimus

The fluorescence micrographs of echinopluteus treated with glyoxylic acid are shown in Figure 1. Fluorescence was most prominent in a continuous fibrous structure along the ciliary bands of arms and perioral area (Fig. 1a). The fluorescing, continuous fiber became visible at first at early

FIG. 1. Glyoxylic acid-treated *Hemicentrotus pulcherrimus* plutei.
(a) An 18 day-old pulteus, ventral view. Note fluorescence along the ciliary bands of arms and perioral area. ala: anterolateral arm, m: mouth, poa: postoral arm. ×220.
(b) A 2 day-old early pluteus. A fluorescent fiber (arrow) appears along the ciliary band. ×240.
(c) Fluorescing cell bodies align along the lower lip (*), between postoral and anterolateral arms (arrowhead), in the peripheral region of the pylorus (doulde arrow), and the anus (arrow). Dark spots are pigment cells. A 30 day-old pluteus. A: anus, E: esophagus, P: proctodium, S: stomach. ×360.

FIG. 2. Glyoxylic acid-treated *Asterias amurensis* bipinnarias.
(a) A 16 day-old bipinnaria, ventral view. A continuous fibrous structure along the ciliary bands shows strong fluorescence. Fluorescent cell bodies are prominent along the preoral and anal loops. ×160.
(b) A 35 hr-gastrula shows a fluorescent cell with dendritic processes (arrow) in the anterior part of the embryo. ×160.
(c) Anterior part of a 20 day-old bipinnaria shows a fibrous network of glyoxylic acid-induced fluorescence. ×220.

FIG. 3. Glyoxylic acid-treated *Stichopus japonicus* auricularias.
(a) A 4 day-old auricularia. Note fluorescence along ciliary bands. arrow: fluorescence cells in lower lip. × 130.
(b) A 2 day-old auricularia shows fibrous fluorescence along the ciliary bands. ×110.
(c) Higher magnification of ciliary band. ×610.

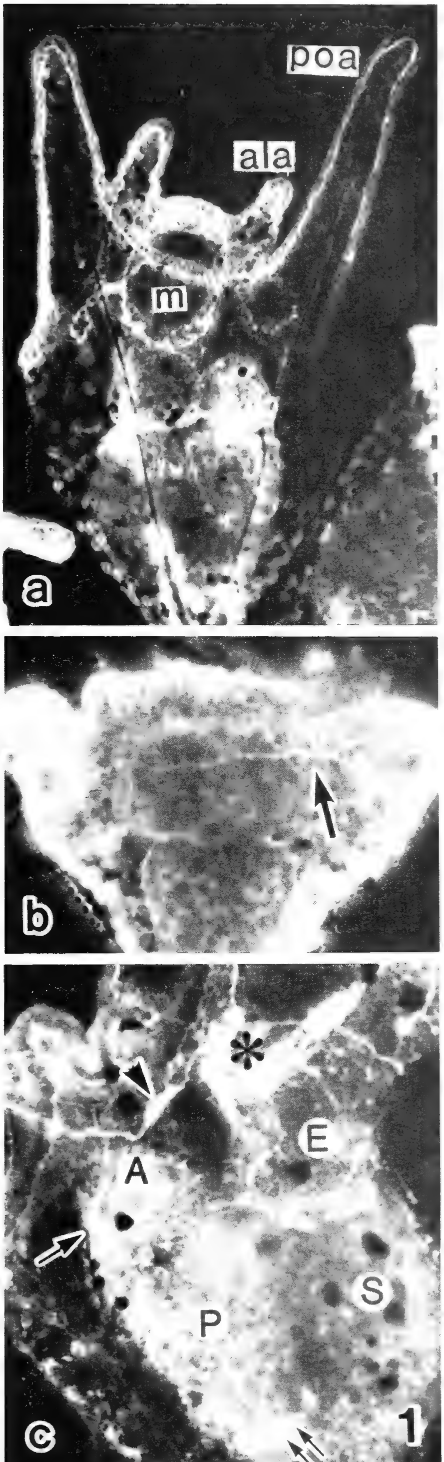
poa
ala
m
a
b
*
E
A
P
S
c
1

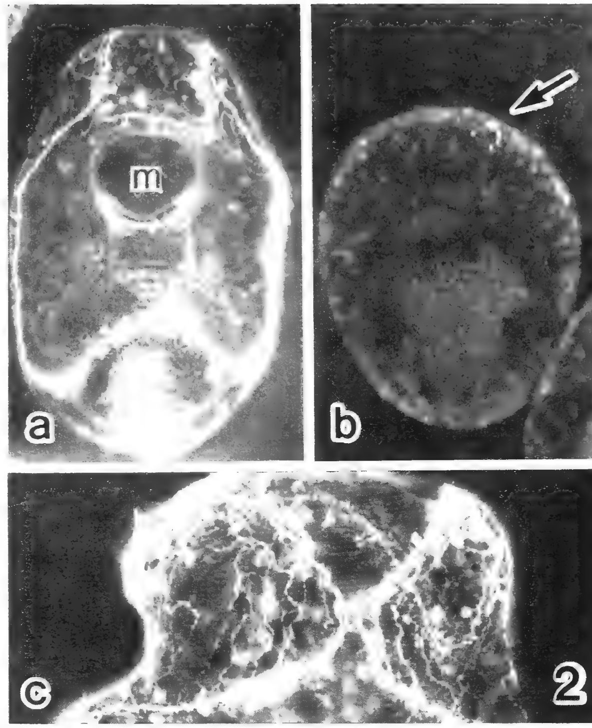
m
a
b
c
2

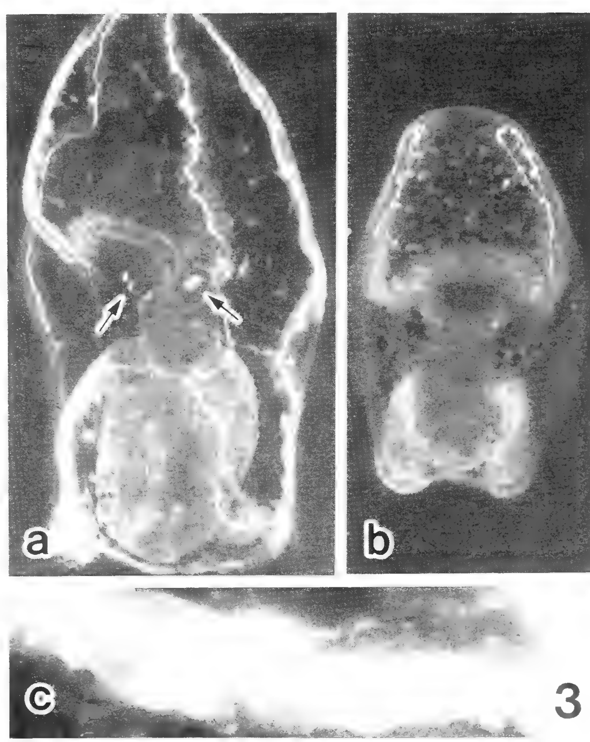
a
b
c
3

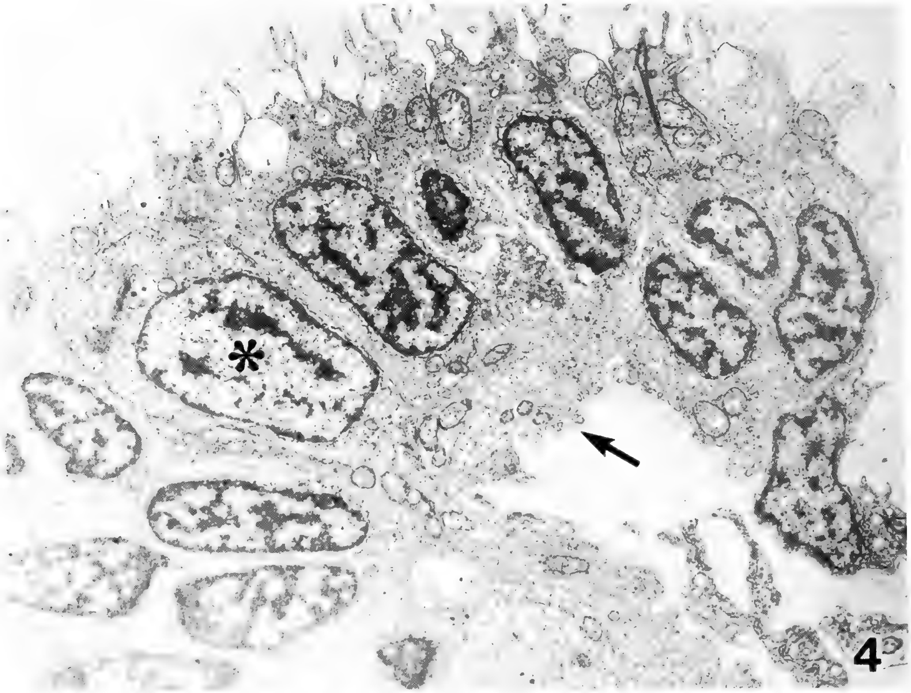
4

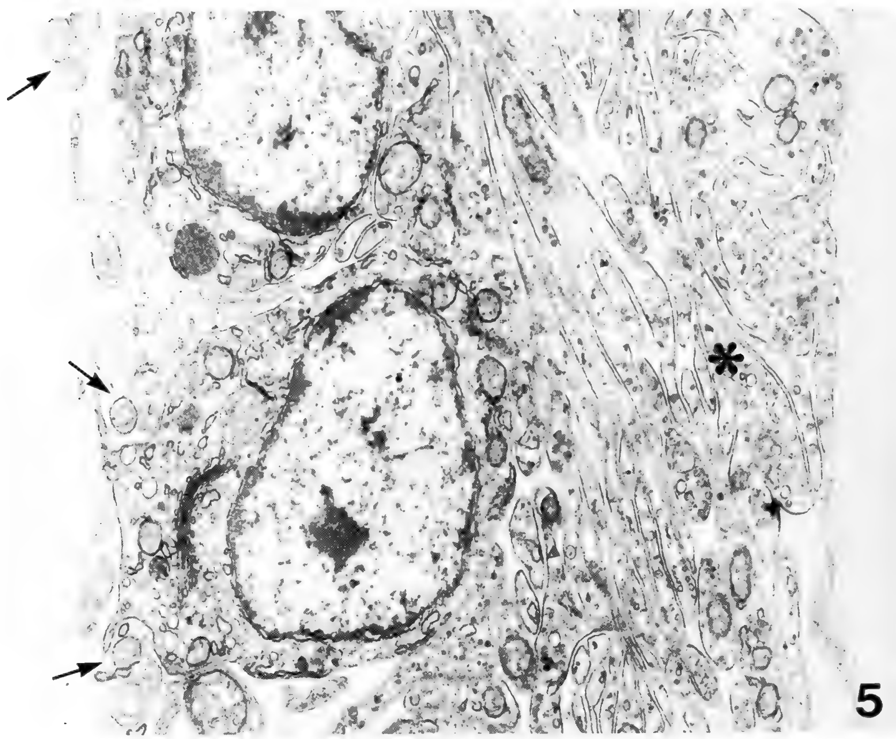
5

pluteus stage (Fig. 1b). This main fluorescing 'tract' branched out thin filaments toward the squamous epithelium of the arms, body wall, and circumoesophageal regions. Moreover, intensely fluorescing cell bodies were seen aligning along the lower lip. Fluorescent cell bodies were also located between the postoral and anterolateral arms, and in the peripheral regions of the pylorus and the anus (Fig. 1c). A small number of fluorescent cell bodies were also observed in the ciliary bands of the arms. Electron microscopically, a large bundle of axons was observed along the proximal end of the ciliary band where the main fluorescent tract was demonstrated by the glyoxylic acid method. The other places in which glyoxylic acid induced blue-green fluorescence also corresponded to the loci where ectoneural cells and nerve bundles were identified by electron microscopy (Fig. 4).

In the preoral area, a filamentous network with weak yellow fluorescence, different from blue-green fluorescence of catecholamines, was induced by the glyoxylic acid treatment. A large number of nerve cells and bundle of axons were present in this region (Fig. 5).

Asterias amurensis

As in the echinopluteus, a continuous fibrous structure with strong blue-green catecholamine fluorescence was distinct in the glyoxylic acid-treated bipinnaria (Fig. 2). This fluorescing fiber which was consisted of bundle of fine filaments was apparently in association with the ciliary band. Several cell bodies in ciliary bands of the preoral and anal loops emitted intense fluorescence, and joined to the main fluorescent tract with a fine filaments (Fig. 2a). A few cell bodies and bundle of filaments with fluorescence were also observed in the upper and lower lips. The fibrous network showing strong blue-green fluorescence in the squamous epithelium of anterior part of the larva was characteristic of this species. This network appeared to originate from a fluorescent cell with dendritic processes developed in the anterior part of the squamous epithelium of 35 hr-old gastrula (Fig. 2b). The fibers in the network had varicosities and merged into main fluorescent tract (Fig. 2c). These fluorescing structures corresponded to the nervous elements observed in electron microscopy. Figure 6 shows the ultrastructure of axonal bundles frequently encountered in the upper part of the squamous epithelium.

Stichopus japonicus

A ruffled bundle of filaments with blue-green fluorescence appeared in a direct association with the ciliary bands, and a few strongly fluorescing cell bodies were observed in the ciliary bands of the upper lobe and the lower lip of auricularia (Fig. 3a, c). The network of catecholaminergic nerves was almost completed in 2 day-old auricularia (Fig. 3b), while in 24 hr-old gastrulae, nervous system was not demonstrated by the glyoxylic acid treatment (micrograph not shown). Ultrastructurally, neuronal cells with axonal projections were observed in the ciliary bands. Figure 7 depicts one of these catecholaminergic cells appeared in the ciliary band of the upper lobe. Although a large bundle of axons was observed along the ciliary band of the upper lip (Fig. 8), only faint fluorescence was induced in this region by the glyoxylic acid treatment.

DISCUSSION

For the histochemical localization of catecholamines, the glyoxylic acid method employed in this investigation has been reported to give a higher resolution than the formaldehyde technique both in tissue and whole mount preparations [13]. Furthermore, blue-green fluorescence induced by glyoxylic acid is found to be specific to catecholamines [11].

In all specimens examined in the present study, glyoxylic acid produced distinct blue-green fluorescence in nerve bundles located in the ciliary bands. During development, the appearance of the fluorescing fibers and the formation of ciliary

FIG. 4. Ultrastructure of ciliary band of upper lip of a 33 day-old pluteus. A nerve cell (*) extends an axonal process. The nerve tract (arrow) consists of a large number of axons. ×6,000.

FIG. 5. Two ectoneural cells with coiled cilia (arrow) and axons (*) in preoral ciliary patch. 33 day-old, early 8 armed pluteus. ×14,400.

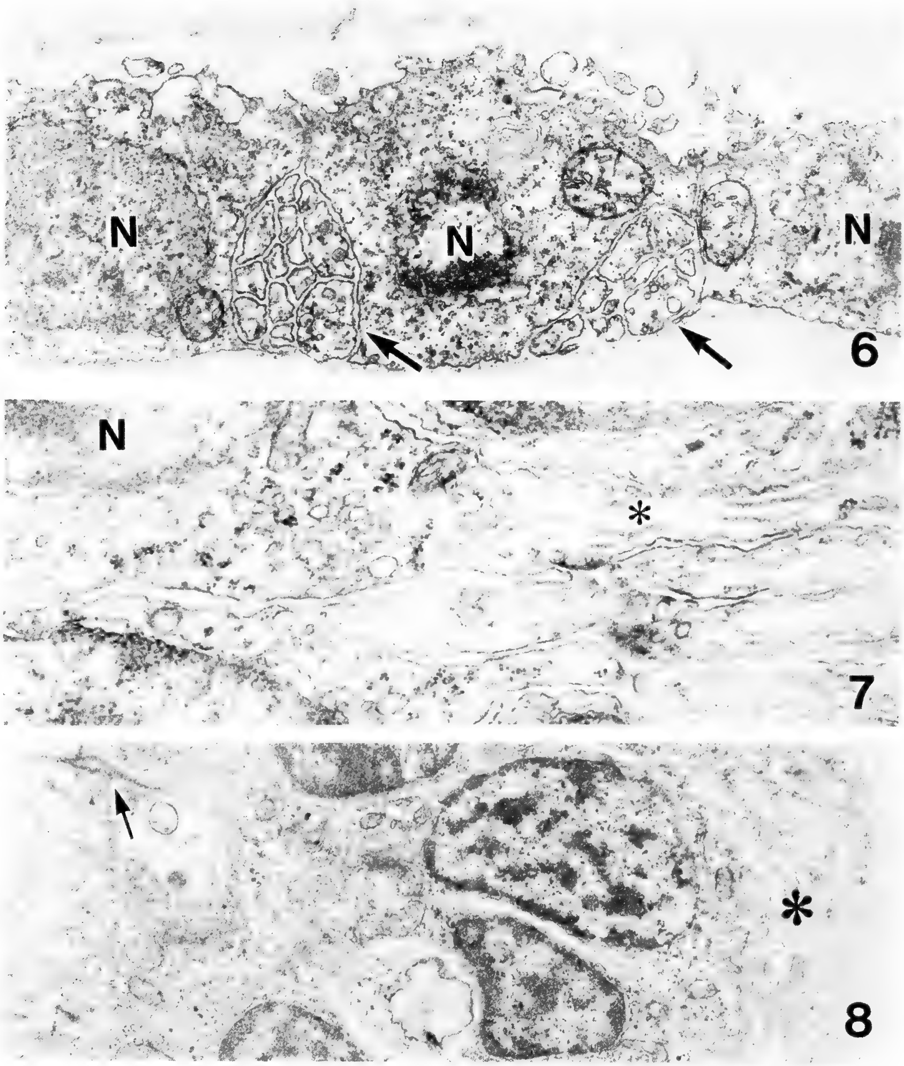

FIG. 6. Ultrastructure of squamous epithelium of a 20 day-old bipinnaria. N: nucelus, arrow: bundle of axons. ×15,500.

FIG. 7. Basal part of upper lobe ciliary band of a 6 day-old auricularia. A nerve cell extends an axon (*) toward a nerve bundle. ×22,200.

FIG. 8. Nerve cell in the ciliary band of upper lip (oral hood) of a 10 day-old auricularia. arrow: ciliary rootlet, (*): nerve bundle. ×7,700.

bands took place almost simultaneously in sea urchin and sea cucumber, while in the starfish, a single precusor cell appeared early in late gastrula in the anterior part of squamous epithelium. The localization and the development of nervous elements, ascertained by fluorescence and electron microscopy, indicate that the ciliary bands are innervated by catecholaminergic nerves.

In preoral area of echinopluteus, a ciliary patch that composed of a large number of ectoneural cells with coiled cilia and a large bundle of axons are observed [9]. Glyoxylic acid induced a filamen-

tous network of weak yellow fluorescence indicating that the nerve cells in this region contain neurotransmitter(s) other than catecholamines. This yellow fluorescing region appears to correspond to the apical part of larval *Strongylocentrotus purpuratus* where the presence of serotonin was recently demonstrated by Bisgrove and Burke using an indirect immunofluorescence microscopy (personal communication). During development, these serotonergic neuroblasts are first detected in animal plate of the late gastrula. Moreover, in the larval form of the sea cucumber, *Parastichopus californicus,* Burke and his collaborators [14] have reported the occurrence of serotonergic nerve cells at their apical tip.

In the auricularia of *Stichopus japonicus* observed in this study, a few weakly fluorescing cells scattered sparingly in the apical portion. Fluorescence was not distinct compared to that found in the preoral area of the echinopluteus. Another example in which nervous structure with faint glyoxylic acid induced fluorescence was observed was the upper lip (oral hood) of auricularia. These are probably the examples of the nerves in which neurotransmitter(s) other than catecholamines or serotonin is involved, although the nature of the neurotransmitter is totally unknown at this moment. Further studies to identify the neurotransmitters in larval echinoderms, and detailed analyses on the possible anatomical divergence of the nervous system in different classes remain to be carried out.

ACKNOWLEDGMENTS

The author thanks the directors and the members of the Misaki Marine Biolological Station and the Tateyama Marine Laboratory for supplies of *Hemicentrotus pulcherrimus* and *Stichopus japonicus,* and *H. pulcherrimus* and *Asterias amurensis* respectively. The author thanks the staff of Aichi Prefectural Fisheries Experimental Station, Owari Branch and Aichi Prefectural Farming Fisheries Center for generous supplies of *S. japonicus* and advice on handling of the animals.

She is grateful to Drs. K. Dan, T. Yanagisawa, M. Obika, and M. Ikeda for valuable suggestions during the course of this study and critical reading of the manuscript.

REFERENCES

1 Mackie, G. O., Spencer, A. N. and Strathmann, R. (1969) Electrical activity associated with ciliary reversal in an echinoderm larva. Nature, **223**: 1384–1385.

2 Gustafson, T., Lundgren, B. and Treufeldt, R. (1972) Serotonin and contractile activity in the echinopluteus. Exp. Cell Res., **72**: 115–139.

3 Ryberg, E. (1973) The localization of cholinesterases and nonspecific esterases in the echinopluteus. Zool. Scripta, **2**: 163–170.

4 Ryberg, E. (1974) The localization of biogenic amines in the echinopluteus. Acta Zoologica, **55**: 179–189.

5 Burke, R. D. (1978) The structure of the nervous system of the pluteus larva of *Strongylocentrotus purpuratus.* Cell Tissue Res., **191**: 233–247.

6 Burke, R. D. (1983) Development of the larval nervous system of the sand dollar, *Dendraster excentricus.* Cell Tissue Res., **229**: 145–154.

7 Burke, R. D. (1983) Neural control of metamorphosis in *Dendraster excentricus.* Biol. Bull., **164**: 176–188.

8 Burke, R. D. (1983) The structure of the larval nervous system of *Pisaster ochraceus* (Echinodermata: Asteroidea). J. Morphol., **178**: 23–35.

9 Nakajima, Y. (1986) Presence of a ciliary patch in preoral epithelium of sea urchin plutei. Dev. Growth Differ., **28**: 243–249.

10 Nakajima, Y. (1986) Development of the nervous system of sea urchin embryos: Formation of ciliary bands and the appearance of two types of ectoneural cells in the pluteus. Dev. Growth Differ., **28**: 531–542.

11 Lindvall, O. and Bjorklund, A. (1974) The glyoxylic acid fluorescence histochemical method: a detailed account of the methodology for the visualization of central catecholamine neurons. Histochemistry, **39**: 97–127.

12 Kanatani, H. (1969) Induction of spawning and oocyte maturation of 1-metyladenine in starfishes. Exp. Cell Res., **57**: 333–337.

13 Sharpe, M. J. and Atkinson, A. D. (1980) Improved visualization of dopaminergic neurons in nematodes using the glyoxylic acid fluoresence method. J. Zool., Lond., **190**: 273–284.

14 Burke, R. D., Brand, D. G. and Bisgrove, B. W. (1986) Structure of the nervous system of the auricularia larva of *Parastichopus californicus.* Biol. Bull., **170**: 450–460.

ZOOLOGICAL SCIENCE 4: 301–306 (1987)

In vitro Spermatids Formation from Diapausing Pupal Spermatogonia of the Cabbage Armyworm, *Mamestra brassicae* L. (Lepidoptera; Noctuidae)

TOSHIAKI SHIMIZU

Laboratory of Insect Physiology and Toxicology, The Institute of Physical and Chemical Research, Wako, Saitama 351–01, Japan

ABSTRACT—A cell monolayer originating from diapausing *Mamestra brassicae* pupal testicular peritoneal sheath was cultured in modified Grace's medium containing 20-hydroxyecdysone. To investigate whether the cell sheet and its conditioned medium can support spermatogonial development, spermatogonial cysts were cultured on the cell sheet in the conditioned medium, in which the newly formed cell sheet from the testicular peritoneal sheath had been cultured for 3 days. It was found the apparently morphogenically early spermatids are induced without passing over spermatocysts stages.

INTRODUCTION

Spermiogenesis has been induced when spermatocysts were co-cultured with testis in Grace's medium alone [1]. This medium conditioned by testes seems to contain unknown factors from the testes. Recently, it was suggested that unknown testicular factors which promote spermiogenesis are released from pre-cultivated testes of *Mamestra brassicae* [2]. In addition, the author was able to induce spermiogenesis in medium in which degenerating testes with a newly formed cell sheet had been pre-cultivated for 5 days [3].

Spermatogenesis is induced *in vitro* only when the medium contains macromolecular factors (MFs) as demonstrated by Kambysellis and Williams [4, 5]. However, development from spermatogonial cysts to spermatocysts (~256 spermatocytes) is difficult to obtain in our experimental medium.

In this report, spermatid formation from spermatogonia of diapausing pupae of the cabbage armyworm, *Mamestra brassicae* is investigated.

Accepted October 23, 1986
Received September 10, 1986

MATERIALS AND METHODS

Insect

Testes used for cultivation were dissected from diapausing pupae (just pupated) of *Mamestra brassicae* which were reared on an artificial diet under a 12:12 photoperiod at 20°C.

Culture of the peritoneal sheaths

The culture methods used in the experiments were the same as those described previously [5, 6]. Testicular epithelium (wall) cosists of the peritoneal sheath and follicle epithelium. Testicular peritoneal sheath extending from the testis was cultivated in Grace's medium or modified Grace's medium. Modified Grace's medium by Yunker *et al.* [7] contains 1% bovine serum albumin fraction V, 7% fetal bovine serum and 10% whole egg ultrafiltrate. Ten μg/ml of 20-hydroxyecdysone was added to aliquots of both media. In each culture vessel containing 20 μl of medium, one testis was cultured for 7 days in an incubator maintained at 22°C.

Replacement of medium

Seven days after culture of the intact testis, a cell sheet originating from the peritoneal sheath developed on the glass surface and this "cell sheet"

was then studied. The cell sheets which remained after the testis degenerated have been cultivated for one month by replacing old medium with fresh medium every three days.

Culture of spermatogonia on the newly formed cell sheet

To investigate whether the cell sheet and its medium have an ability to induce spermatogonial development, "naked" spermatocysts and spermatogonial cysts were added to the medium. These "naked" spermatocysts and spermatogonial cysts were obtaind from testes from diapausing pupae (just pupated) by dissecting the testis with a pair of fine needles. Then, development of "naked" spermatocysts and spermatogonial cysts was observed for 14 days.

RESULTS

Culture of peritoneal cell sheet

Testes from diapausing pupae were cultured in Grace's medium containing 20-hydroxyecdysone for 7 days, forming a cell sheet on the glass surface from the testicular peritoneal sheath. This contiguous cell sheet (monolayer) from the degenerating testis was cultivated for over one month with changing old medium with fresh medium (Fig. 1). The cells in this cell sheet contained many granules which surrounded the nucleus-like structure (vesicle). Cell membrane of each cell was barely visible under the microscope, but the intercellular space between cells was more clear. There are no nuclei in this newly formed cell sheet, but only spherical vesicles of 7.0–17.5 μm were observed. Similar results were obtained in modified Grace's medium containing 20-hydroxyecdysone. However, testes cultuerd in Grace's medium or modified Grace's

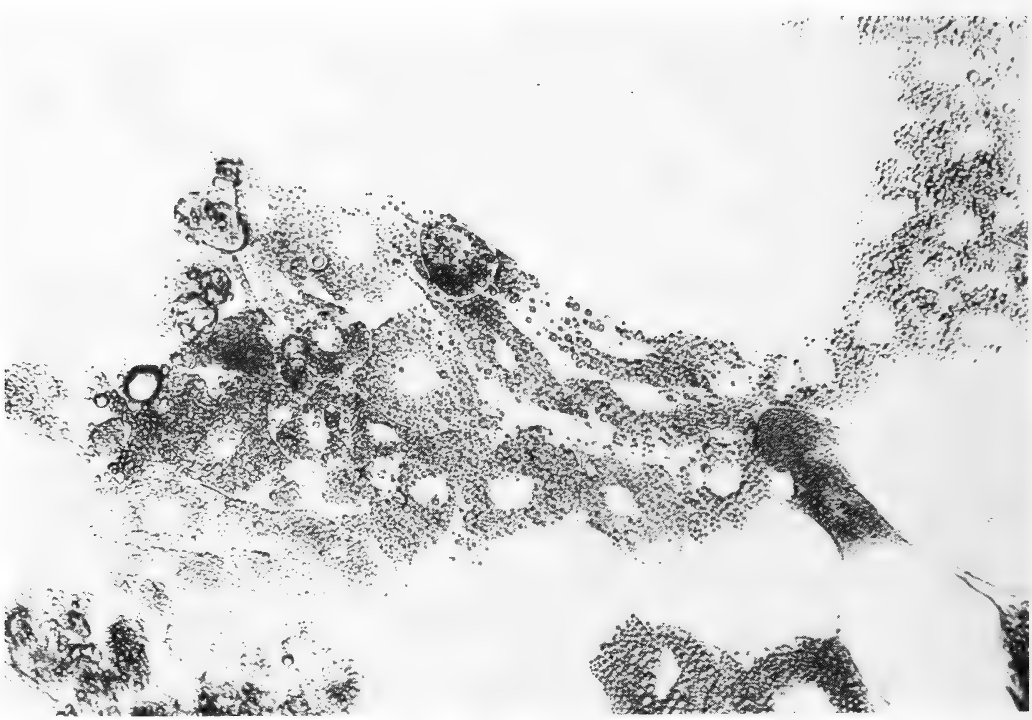

FIG. 1. Newly formed cell sheets from the testes incubated in modified Grace's medium containing 20-hydroxyecdysone. (×273).

medium in the absence of hormone did not form this cell sheet. The newly formed cell sheet in the Grace's medium containing hormone degenerated when the medium was changed into hormone-free Grace's medium or modified Grace's medium. The cell sheet degenerated within 3 days after removal of hormone in Grace's medium, and the cell sheet detached from the glass surface. In other words, Grace's medium containing 20-hydroxyecdysone supports cell migrations from the peritoneal sheath and the formation of the cell sheet in monolayer. This cell sheet and the conditioned medium were used for cultivation of spermatocysts and spermatogonial cysts.

Spermatocysts and spermatogonial cysts from diapausing pupae were cultured on the cell sheet in conditioned medium to assess the ability of the cell sheet and the conditioned medium to induce spermatogonial development, since no spermatid formation can be induced in the germinal cysts of the diapausing pupae in hormone-free medium.

Spermatid formation

When "naked" spermatocysts and spermatogonial cysts were cultivated for 14 days on the cell sheet in the conditioned medium, the spermatocysts developed into spermatids and consequently became elongated spermatocysts [3], while the spermatogonial cysts developed into early spermatids in the present experiment. In comparison with the size of normal spermatogonial cysts (32 cells) (Fig. 2), the spermatocysts developed in culture were one-half in the size (16 cells) (Fig. 3). The

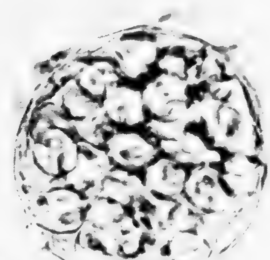

FIG. 2. A normal spermatogonial cyst consisting of about 32 cells. (×328). This spermatogonium was cultivated for 2 days in modified Grace's medium containing 20-hydroxyecdysone.

FIG. 3. Morphogenically early spermatids developed from spermatogonia (16 cells) in culture. (×328). The spermatogonial cysts (SGC) were cultivated on the testicular peritoneal cell sheet in the conditioned medium in which degenerated testes with the remaining cell sheet were cultured for 3 days. These 16 cells were estimated from the size of spermatogonial cyst (32 cells) in Fig. 2. Three spermatogonial cysts (A, B, C) were obtained from three different cultures.

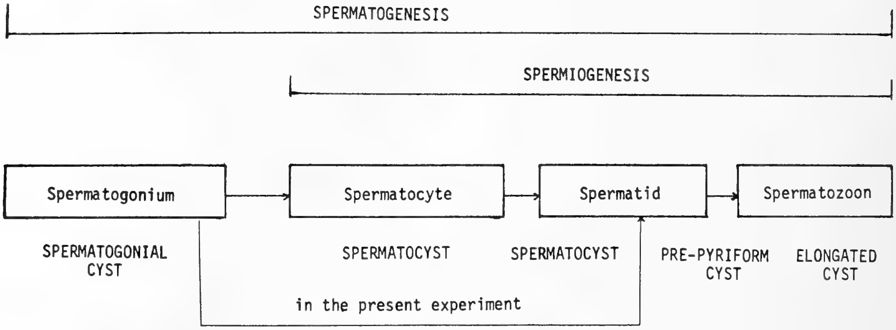

FIG. 4. A figure representing precocious spermatid formation, spermiogenesis and spermatogenesis.

axial filaments were oriented to the center of the lumen. Cells which differentiated into morphogenically early spermatid were present in the central part of the spermatogonial cysts than in peripheral part (Fig. 3). Generally, spermatogonia develop into early spermatids via spermatocytes (Fig. 4). However, in the present experiment, the spermatogonia developed into early spermatids, but no further trace of development was observed. The newly formed spermatids survived for 14 days.

On the other hand, the spermatogonial cysts degenerated within 3 days from the onset of culture in Grace's medium or modified Grace's medium even in the presence of 20-hydroxyecdysone.

In other observations, spermatogonial cyst envelopes (wall) enlarged (as shown in Fig. 5) when cultured for 7 days on the cell sheet in modified Grace's medium containing 20-hydroxyecdysone, but showed no further development in longer cultivation. It was observed that two spermatogonia developed and other spermatogonia degenerated and/or escaped into surrounding medium through the cyst membrane (Fig. 5).

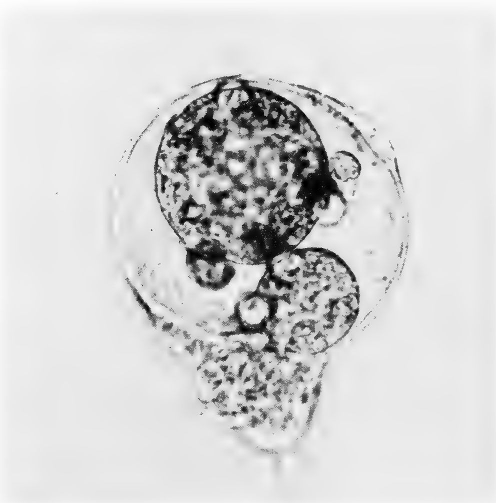

FIG. 5. Enlarged spermatogonial wall (envelope) and two grown spermatogonia. Other spermatogonia were degenerated and/or had passed through the cyst membrane into the surrounding medium. (×328).

DISCUSSION

Spermatid formation

Differentiation from spermatogonia to early spermatids could be induced after 5 days by culturing spermatogonial cysts on newly formed cell sheets, but the spermatogonia did not reach the spermatid elongation stage. Spermatogonial cysts (~64 cells) failed to develop into elongated cysts having elongated cyst envelopes, while spermatocysts (256 spermatocytes) developed into elongated spermatozoa in the same medium [3]. The spermatogonial wall (envelope) was activated when co-cultivated with this cell sheet. That is to say, the wall was modified by receiving slight changes in the physiological properties of the cyst membrane (Fig. 5). From the morphogenic appearance of early spermatids in the present experiment, the developmental process from spermatogonia to spermatid may be not homologous to some of the normal cyto-differentiation processes in the testes. Generally, spermatogonia (~64

cells) form spermatids via spermatocysts (256 spermatocytes). It is difficult to transform spermatocytes into spermatids *in vitro* during spermatogenesis. Whether spermatid elongation can be induced from the stage of 128 spermatocytes in the testis *in vitro* is an unresolved question.

Even in modified Grace's medium containing bovine serum albumin fraction V, fetal bovine serum and 20-hydroxyecdysone, spermiogenesis and spermatogenesis were not observed. In *Drosophila* spermatogonial cells, no changes or slight changes were found in the K-medium [8]. There is a possibility that a cell sheet factor may be present which can induce a testicular factor released from the testicular sheath for development of spermatogonia. In addition, a maintenance factor of the spermatogonial cysts in the conditioned medium seems to be important for differentiation. Although cyclic AMP level in the non-diapausing pupal testis was high, c-AMP content in the conditioned medium with a cell sheet was low ($<$ 0.62 pMol/ml) (unpublished data).

Role of peritoneal cell sheet

Loeb *et al.* [9] and Loeb [10] demonstrated that the testis sheath *in vitro* is the site of ecdysteroid synthesis in larvae of the tobacco budworm, *Heliothis virescens*. Therefore, it was of interest to determine whether this cell sheet synthesizes ecdysone or not (cf. Shimizu *et al.* [11]). It is obvious from the present experiment that maintenance of the cell sheet requires ecdysteroid. Although it was suggested that cell sheet has the ability to cause differentiation or maintenance of spermatogonia, the actual biological function of this cell sheet is not clear.

The phenomena observed in these experiments suggest that the testicular sheath (peritoneal cell sheet) plays an important role in the development of spermatocysts [3] and spermatogonial cysts. It is well known that mammalian Sertoli cells play an important role in development of the spermatocysts. The migration patterns of Sertoli cells (epithelial-type cells) have been closely investigated *in vitro* [12]. In insects, the role of Sertoli-like cells in the testis is not clear. However, macromolecular factors possibly of hemocyte origin are necessary to induce differentiation [4, 5]. We suggest that a testicular factor which promotes spermiogenesis may be released from the precultivated testes of *Mamestra brassicae* [1, 2]. Furthermore, spermiogenesis is induced by a newly formed cell sheet [3]. Further, the author speculated that the cell sheet functions in a manner similar to that of mammalian Sertoli cells.

ACKNOWLEDGMENTS

The author is indebted to Dr. N. Agui, The National Institute of Health, and Dr. L. R. Whisenton, The University of North Carolina, for their critical reading of the manuscript.

REFERENCES

1 Shimizu, T. and Yagi, S. (1978) Hormonal effect on cultivated insect tissues. IV. The role of testis in spermiogenesis of the cabbage armyworm, *Mamestra brassicae, in vitro*. Appl. Entomol. Zool., **13**: 278–282.

2 Shimizu, T. (1986) Medium for *in vitro* spermiogenes of diapausing pupal spermatocytes of *Mamestra brassicae* (Insecta, Lepidoptera, Noctuidae). Zool. Sci., **3**: 203–206.

3 Shimizu, T. (1986) Culture of the peritoneal sheath from the diapausing cabbage armyworm (*Mamestra brassicae*) pupal testis. Zool. Sci., **3**: 309–313.

4 Kambysellis, M. and Williams, C. M. (1971) *In vitro* development of insect tissues. I. A macromolecular factor prerequisite for silkworm spermatogenesis. Biol. Bull., **141**: 527–540.

5 Kambysellis, M. and Williams, C. M. (1971) *In vitro* development of insect tissues. II. The role of ecdysone in the spermatogenesis of silkworms. Biol.Bull., **141**: 541-552.

6 Yagi, S., Kondo, E. and Fukaya, M. (1969) Hormonal effect on cultivated insect tissues. I. Effect of ecdysterone on cultivated testes of diapausing rice stem borer larvae (Lepidoptera; Pyralidae). Appl. Entomol. Zool., **4**: 70–78.

7 Yunker, C. E., Vaughn, J. L. and Cory, J. (1967) Adaptation of an insect cell line (Grace's Antheraea cells) to medium of insect hemolymph. Science, **155**: 1565–1566.

8 Kuroda, Y. (1974) Spermatogenesis in pharate adult testes of *Drosophila* in tissue cultures without ecdysones. J. Insect Physiol., **20**: 637–640.

9 Loeb, M. J., Woods, C. W., Brandt, E. P. and Bořkovec, A. B. (1982) Larval testes of the tobacco budworm: A new source of insect ecdysteroids. Science, **218**: 896–898.

10 Loeb, M. J. (1986) Ecdysteroids in testis sheath of

Heliothis virescens larvae: An immunocytological study. Arch. Insect Biochem. Physiol., **3**: 173–178.

11 Shimizu, T., Moribayashi, A. and Agui, N. (1985) *In vitro* analyses of spermiogenesis and testicular ecdysteroids in the cabbage armyworm, *Mamestra brassicae* L. (Lepidoptera: Noctuidae). Appl. Entomol. Zool., **20**: 56–61.

12 Tung, P. S. and Fritz, I. B. (1986) Extracellular matrix components and testicular peritubular cells influence the rate and pattern of Sertoli cell migration *in vitro*. Dev. Biol., **113**: 119–134.

ZOOLOGICAL SCIENCE 4: 307–313 (1987)

Variations in Hemocyte Populations during Various Developmental Stages of *Blattella germanica* (L.) (Dictyoptera, Blattellidae)

LAKSHMI K. HAZARIKA and AYODHYA P. GUPTA

Department of Entomology and Economic Zoology, Agricultural Experiment Station, Cook College, Rutgers University, New Brunswick, NJ 08903, USA

ABSTRACT—During various developmental stages of *Blattella germanica* (Dictyoptera: Blattellidae), total- and differential-hemocyte counts (THCs and DHCs, respectively) were determined in order to correlate qualitative and quantitative changes in hemocyte populations with ontogenic development. We found that THCs increased linearly as *B. germanica* developed from one instar to the next, until it became an adult. A similar pattern of qualitative change (DHC) of hemocyte population occurred for plasmatocytes (PLs), granulocytes (GRs), and oenocytoids (OEs). By contrast, the prohemocytes (PRs) and coagulocytes (COs) did not increase linearly during development.

INTRODUCTION

Ecdysis, circadian rhythm, nutrition, diapause, starvation, and wounds are all known to alter hemocyte populations in insects (see reviews in Gupta [1, 2]). Several authors have reported both qualitative (differential hemocyte counts, DHCs) and quantitative (total hemocyte counts, THCs) changes in various insects [1]. During our studies of the effects of insect growth regulators on hemocyte populations in various developmental stages of the German roach, *Blattella germanica* (L.) and the possible role of hemocytes as carriers of growth hormones [2], we found not only a progressively linear increase in the THCs, as we expected, but also in the DHCs, especially of the plasmatocytes (PLs) and the granulocytes (GRs). Gupta [2,3] designated the PLs and GRs as *immunocytes,* because of their ability to distinguish between "self" and "nonself" tissues. Although trimodal [4] and bimodal [5] frequencies in hemocyte populations have been reported in *Gryllus assimilis pennsylvanicus* and *Periplaneta americana,* respectively, as far as we know, a continuously linear increase throughout the developmental period of any insect has not been reported. In this study, we report such an increase in *B. germanica.*

Accepted October 29, 1986
Received September 12, 1986

MATERIALS AND METHODS

Cockroaches were maintained at $28\pm2^\circ$C on Purina Laboratory chow and water in 12L:12D cycle, except when handled; they have been in culture at Rutgers University for over 35 years. Nymphs were sexed according to Ross and Cochran [6]. We determined the THCs and DHCs at the "mid stage" of each instar, except the 1st and the adult, in a known hemolymph volume. With the exception of the 1st instar nymphs, which molt to the next instar within a few hours, all instars and the adults that were used, were 48-hour old, a stage that we designate as the "mid stage" for convenience. Because the 1st-, 2nd-, and 3rd-instar nymphs were too small to be bled individually for adequate hemolymph samples, hemolymph from 10 nymphs from each of the 1st, 2nd, and 3rd instars was pooled separately into known volumes (1 μl) of phosphate-buffered saline (PBS of GIBCO, Grand Island, New York) with 0.1% citric acid and 0.5% EDTA, by puncturing their abdomens. We determined the THCs and DHCs for each of the three instars from these hemolymph pools [7, 8]. For the remaining 4th, 5th, and 6th instars and the adults, the THCs and DHCs were determined per mm^3 by bleeding the

roaches through the antennae and legs.

Since the THCs, and DHCs of different stages were not normally distributed, we transformed them into log 10 values for performing ANOVA, Linear Regression Analysis, and Duncan's Multiple Range Test (alpha=0.05).

RESULTS AND DISCUSSION

The total hemocyte counts (THCs)

The mean THCs±SE are shown in Table 1. It is obvious that they continuously increase throughout the developmental period and reach their peak in the adult. The mean THCs that we observed in *B. germanica* adults (Table 1) are almost comparable to those observed by Tauber and Yeager [9]. The continuous increase in THC during each developmental stage in *B. germanica* (Table 1) is similar to the findings of Wheeler [10] in *P. americana,* and Bahadur and Pathak [16] in *Halys dentata.*

Although the THCs were lower in the female 1st-, 2nd-, 4th-, and 5th-instar nymphs, those in the 3rd- (P=0.0005) and 6th- (P=0.0028) instars and adults (P=0.0001) were significantly higher, compared with those in the male. There is a significant difference in the THCs between the two sexes in the adults, as previously reported for *Mantis* and *Ameles* (Mantidae) [11] and for *Schistocerca* [12]. During development of an insect, a series of allometric changes occurs at both biochemical and morphological levels [13]. Tanaka [14] has reported that in *B. germanica,* the 3rd instar is the critical instar, after which the nymph regulates the adult body size. The higher THC counts in the female 3rd instar in our study seems to suggest that the "midstage" 3rd-instar nymphs perhaps regulate their hemocyte production and circulating hemocyte population differentially between male and female. Ross [15], Ross and Cochran [6], Tanaka [14] as well as our own observations have shown that the female 6th-instar nymphs and adults are larger in body size than their male counterparts. The adult male *B. germanica* is slender and lighter in color than the female [15]. It is likely that the 6th-instar female nymphs possess certain regulatory mechanisms that control the larger body size and enhanced hemopoiesis and hemocyte differentiation and probably other physiological processes, including the differential gonadal development (unpublished observation). The latter would demand greater nutrient, and hormonal transport from the hemolymph to the ovaries, and hemocytes may be the likely carriers.

The logs of THCs of various developmental stages, which were significantly different from one

TABLE 1. Comparisons of THCs in the developmental stages of *Blattella germanica* (L.)

Stage	Sex	Sample size	Mean log (THC)	Mean (SE)
1	M	10	2.813	651^{g} (7)
	F	14	2.798	629^{g} (13)
2	M	10	2.94	874^{f} (30)
	F	14	2.894	792^{f} (32)
3	M	10	3.124	1334^{e} (24)
	F	14	3.246	1799^{j} (111)
4	M	10	3.362	2303^{d} (35)
	F	14	3.323	2142^{d} (111)
5	M	10	3.937	8649^{c} (133)
	F	14	3.908	8139^{c} (263)
6	M	10	3.986	9695^{b} (165)
	F	14	4.111	13346^{i} (983)
adult	M	15	4.231	17248^{a} (754)
	F	14	4.392	25154^{h} (1418)

Duncan's Multiple Range Test for log (THC) at alpha=0.05. For each sex, means with the same letter are not significantly different. M=males, F=females, THC=total hemocyte count, SE=standard error.

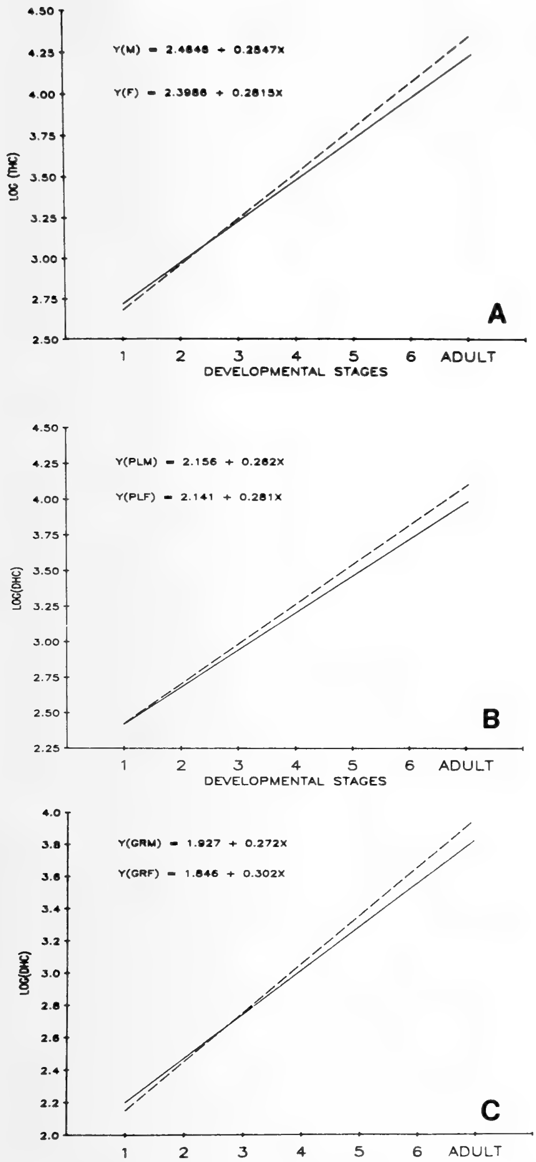

FIG. 1 A. Total hemocyte counts of male (Y(M)=— with r^2=0.96, P = 0.0001) and female (Y(F)= --- with r^2=0.95, P=0.001) *Blattella germanica* as a function of developmental stage.

FIG. 1 B. Differential plasmatocyte counts of male (Y(PLM)=—with r^2=0.95, P=0.001) and female (Y(OLF)= --- with r^2=0.96, P = 0.001) *Blattella germanica* as a function of developmental stage.

FIG. 1 C. Differential granulocyte counts of male (Y(GRM)=—with r^2=0.95, P=0.001) and female (Y(GRF)=—with r^2=0.96, P = 0.001) *Blattella germanica* as a function of developmental stage.

another (P=0.05) (Table 1), were analyzed by the Linear Regression Analysis, and when plotted against stages, resulted into two straight lines for both male and female *B. germanica* (P=0.001) (Fig. 1A). This showed not only a gradual, but a linear increase of THCs (log THCs) during development. We beleive that a linear increase in hemocyte populations occurs probably concomitantly with an increasing demand for nutrient supply during development, cellular defense, production of immunologic factors (such as hemagglutinins, antimicrobial, antiviral factors), and supply of tyrosine and phenoloxidase for sclerotization and recognition of nonself tissue [3]. The linear increase of hemocytes at a given time of each stage (e.g., "mid stage", Fig. 1A), in addition to trimodal in *Gryllus* [4] and bimodal in *Periplaneta* [5] or cyclic in *Halys* ([16] and for review see Shapiro [17]) is probably a widespread phenomenon in insects, yet to be explored.

Differential hemocyte counts (DHCs)

The mean DHCs and their log 10 values for PLs, GRs, prohemocytes (PRs), coagulocytes (COs), and oenocytoids (OEs) are shown in Tables 2 and 3. The log 10 (DHCs) values for all the above hemocyte types were analyzed by Linear Regression Analysis; each mean log value, when plotted against the developmental stages, resulted into two straight lines, male and female, for each of the PLs (Fig. 1B), the GRs (Fig. 1C) and the OEs (Fig. 2). PRs and COs were not recognized to have any linearity because they had $r^2 \leq 0.75$.

The differential counts of PLs also were significantly different among developmental stages in both sexes, with the exception of the female 3rd- and 4th- and the male 5th- and 6th-instar nymphs (Tables 2 and 3).

Like those of the THCs, the GR counts of each developmental stage not only increase linearly, but differ significantly from one another (Tabled 2 and 3). The mean differential counts of the PLs and GRs are slightly higher in the male 1st-, 2nd-, 4th-, and 5th-nymphal instars, but those of the female 3rd-, and 6th-nymphal instars and adults are significantly higher ($P \leq 0.05$), compared with those in the male. The continuous and linear increases of PLs and GRs probably correspond to

Table 2. Comparisons of DHCs in the developmental stages of female *Blattella germanica*

Stage	Hemocyte types CO	GR	OE	PL	PR
1	14.32* ±2.3 1.1^{d}	179.94 ±6.7 2.25^{k}	9.77 ±1.1 0.96^{o}	258.74 ±7.3 2.41^{u}	189.08 ±4.5 2.28^{z}
2	21.29 ±1.3 1.28^{d}	262.71 ±3.4 2.42^{j}	11.12 ±1.4 1.02^{o}	519.62 ±22.9 2.71^{t}	34.78 ±2.6 1.53^{y}
3	38.42 ±7.2 1.52^{c}	538.9 ±50.0 2.71^{i}	31.5 ±5.1 1.45^{n}	1230.57 ±85.3 3.07^{s}	92.86 ±7.2 1.96^{y}
4	37.06 ±5.0 1.53^{c}	753.21 ±25.1 2.87^{h}	25.13 ±3.0 1.38^{n}	1197.99 ±57.9 3.07^{s}	75.6 ±13.1 1.81^{y}
5	428.62 ±35.7 2.62^{b}	3095.6 ±199.4 3.48^{g}	167.55 ±28.4 2.17^{m}	4374.61 ±235.6 3.64^{r}	380.62 ±60.5 2.54^{x}
6	718.71 ±74.5 2.84^{a}	5027.99 ±74.5 3.68^{f}	245.31 ±38.3 2.34^{m}	7774.18 ±660.9 3.87^{g}	618.81 ±63.1 2.77^{w}
adult	482.46 ±110.2 2.60^{b}	9746.53 ±787.2 3.98^{e}	399.86 ±57.1 2.56^{l}	12347.98 ±1210.8 4.08^{p}	1139.57 ±187.1 2.99^{v}

* First row of each stage represents the mean, the second row standard error, and the the third row the log transformed mean. Sample size = 10. Log (mean DHCs) with the same letters are not significantly different from each other (Duncan's Test, alpha = 0.05). DHC = differential hemocyte count, CO = coagulocyte, GR = granulocyte, OE = oenocytoid, PL = plasmatocyte, PR = prohemocyte.

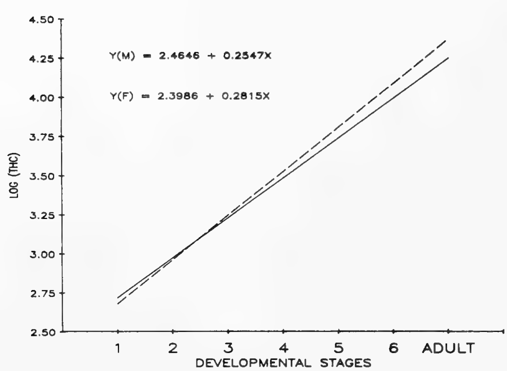

Fig. 2. Differential oenocytoid counts of male (Y(OEM) = — with $r^2 = 0.80$, $P = 0.01$) and female (Y(OEF) = --- with $r^2 = 0.85$, $P = 0.01$) *Blattella germanica* developmental stage.

growing demand for cellular immunity as *B. germanica* progresses its development through various instars. In fact, Ragyalis [18] suggested that each ontogenic stage in *Acantholyda posticalis* has specific hemocyte composition to meet its developmental needs. Because the effectiveness of phagocytosis, encapsulation, and other related defense mechanisms, is primarily a result of the available circulating immunocyte population (PLs and GRs, [2, 3]), it is reasonable to suggest that larger the PL and the GR populations, the stronger the cellular defense. Apparently, the effectiveness of phagocytosis and encapsulation differs from one developmental stage to another (for review see Gupta [2]). We believe that this differential defense capability of an insect during development is largely due to the differential population of the circulating PLs and GRs, and possibly of the OEs.

It is reasonable to assume that the early immature instars (for example, 1st-instar nymphs of *B. germanica*) are immunologically less competent, because they have comparatively fewer PLs and GRs. They are likely to succumb more readily to pathogen attack as well as susceptible to biologi-

TABLE 3. Comparisons of DHCs in the developmental stages of male *Blattella germanica*

Stage	Hemocyte type CO	 GR	 OE	 PL	 PR
1	15.58* ±1.2 1.15^{c}	207.04 ±12.7 2.31^{j}	16.74 ±2.9 1.15^{n}	264.04 ±8.2 2.42^{s}	147.8 ±12.1 2.16^{y}
2	58.45 ±8.0 1.72^{b}	281.82 ±10.9 2.45^{i}	24.99 ±2.2 1.38^{m}	473.9 ±27.5 2.67^{r}	34.71 ±2.8 1.53^{x}
3	63.65 ±6.7 1.72^{b}	398.92 ±10.9 2.6^{h}	23.98 ±3.3 1.34^{m}	801.67 ±37.1 2.9^{g}	67.37 ±9.1 1.77^{w}
4	63.65 ±13.4 1.72^{b}	765.47 ±37.1 2.88^{g}	27.4 ±2.8 1.42^{m}	1391.05 ±61.5 3.14^{p}	55.73 ±10.7 1.67^{w}
5	272.28 ±58.0 2.35^{a}	3129.59 ±73.1 3.49^{f}	94.69 ±7.8 1.97^{l}	4812.84 ±149.3 3.68^{o}	340.51 ±44.4 2.49^{v}
6	389.52 ±40.3 2.56^{a}	3852.14 ±217.7 3.58^{e}	185.13 ±24.1 2.23^{k}	4783.68 ±183.0 3.68^{o}	484.59 ±70.1 2.65^{tu}
adult	341.68 ±51.6 2.48^{a}	6414.77 ±436.7 3.8^{d}	209.48 ±25.9 2.3^{k}	8608.1 ±453.9 3.93^{n}	617.3 ±130.1 2.71^{t}

* First row of each stage represents the mean, the second row standard error, and the third row the log transformed mean. Sample size=10. Log (mean DHCs) with the same letters are not significantly different from each other (Duncan's Test, alpha=0.05). DHC=differential hemocyte count, CO=coagulocyte, GR=granulocyte, OE=oenocytoid, PL=plasmatocyte, PR=prohemocyte.

cally active substances, including insecticides and insect growth regulators (IGRs). For example, when the 1st- and 2nd-instar nymphs were allowed to feed on IGRs-treated food pellets, they died within a few days without molting ([19, 20] and unpublished observation), in comparison with controls (acetone-treated food pellets). Lower PL- and GR counts as well as THC in these instars may partly contribute to their mortality directly or indirectly by reducing their immunity or by failing to undergo ecdysis [19, 20].

As shown earlier, the linear OE counts seem to correlate with the higher demand for nutrient supply as *B. germanica* advances in its development; OEs supposedly carry proteins in the cockroach, *Gromphadorhina portentosa* [21].

Compared with the male 5th and 6th instars, the corresponding female instars had significantly higher CO counts (Tables 2 and 3). The penultimate and ultimate female nymphal instars probably require higher COs in comparison with those of males. Considering the presence of significant differences in CO counts among various developmental stages, it is possible that there is a differential coagulative capability and prophenoloxidase-carrying capacity among them (Tables 2 and 3). This, however, needs confirmation. Although the differential counts of COs were lower in the female 1st-, 3rd-, and 4th-instar nymphs, those of the 2nd-instar male (P=0.0004) were significantly higher, compared with those in the female (Tables 2 and 3). This sexual dimorph-

ism in CO counts in an early instar is hard to explain. However, we believe that maximum differentiation of hemocytes is presumably very pronounced in the 2nd-instar nymphs, including a dimorphic differentiation in this developmental stage. As shown in the subsequent discussion of the PR counts, a similar differentiation pattern of PRs was also observed. The circulating population of COs during development does not seem to be progressively linear during development; however, in the event of injury their numbers may increase to stop bleeding as a result of coagulation.

In addition to increasing continuously only in the 5th- and 6th-instar nymphs and adults of both sexes (Tables 2 and 3), the PR counts were also significantly different from one another (among 5th-, 6th-instar nymphs and adults) and also among other developmental stages (P=0.0001). However, the 1st-instar nymphs had significantly higher PR counts (Tables 2 and 3) than the 2nd-, 3rd- and 4th-instar nymphs. The latter two had insignificantly different PR counts between them. The non-linear distribution of the PR counts suggests that perhaps there are three phases of PR differentiation during the development of *B. germanica*: 1) The relatively higher counts in the 1st instar indicate that PRs are still being produced. 2) The significantly lowest counts in the 2nd instar suggest that the PRs are undergoing transformation into PLs and other types. 3) The transformation process is completed in the 3rd- and 4th-instar nymphs, as suggested by the insignificant differences in the PR counts between these instars. These suggestions are also supported by the mean percent data. A steady increase in THC during the 5th- and 6th-instar nymphs, and adults (Fig. 1A and Tables 1, 2 and 3) contributes probably to a similar steady increase in PR counts during those developmental stages.

Correlation between THC and DHC

The rates of increase of PLs and GRs are almost identical to those of THCs, suggesting strong correlation between THCs and DHCs of PLs and GRs. With the exception of PRs and COs, there is a linear increase for PLs, GRs and OEs. The significant differences between the stages of *B. germanica* for GRs and PLs (with a slight variation in case of PLs) and also an exactly similar sexual dimorphism in THCs and DHCs of PLs and GRs, strongly suggest a positive correlation between the THCs and DHCs of the major hemocyte types. The PLs and GRs represent almost more than 70–80% of THCs in all the developmental stages; thus, they determine the total quantitative picture of the hemocyte populations in any of the seven developmental stages.

ACKNOWLEDGMENTS

This paper is the New Jersey Agricultural Experiment Station Publication No. D–08112–12–86, supported by state funds, U. S. Hatch funds, and Rutgers Research Council. LKH was on sabbatical leave from Assam Agricultural University, Jorhat, India, during this study on a Government of India fellowship.

REFERENCES

1 Gupta, A. P. (1979) Insect Hemocytes, Cambridge Univ. Press, Cambridge.

2 Gupta, A. P. (1985) Cellular elements in the hemolymph. In “Comprehensive Insect Physiology, Biochemistry and Pharmacology”. Ed. by G.A. Kerkut and L. I. Gilbert, Pergamon Press, Oxford, Vol. 3, pp. 402–451.

3 Gupta, A. P. (1986) Arthopod Immunocytes: identification, structure, functions, and analogies to the functions of vertebrate B- and T-lymphocytes. In “Hemocytic and Humoral Immunity in Arthropods”. Ed. by A. P. Gupta, Wiley & Sons, New York, pp. 3–59.

4 Tauber, O. E. and Yeager, J. F. (1934) On the total blood (hemolymph) cell count of the field cricket, *Gryllus assimilis pennsylvanicus* Burm. Iowa State Coll. J. Sci., **9**: 13–24.

5 Smith, H. W. (1938) The blood of the cockroach, *Periplaneta americana* L. Cell structure and degeneration, and cell counts. Studies on contact insecticides. Tech. Bull. New Hampshire. Agric. Exp. Stn., **71**: 1–23.

6 Ross, M. H. and Cochran, D. G. (1960) A simple method for sexing nymphal German cockroaches. Ann. Entomol. Soc. Am., **53**: 550–551.

7 Gupta, A. P. and Sutherland, D. J. (1968) Effect of sublethal doses of chlordane on the hemocytes and midgut epithelium of *Periplaneta americana*. Ann. Entomol. Soc. Am., **61**: 910–918.

8 Gupta, A. P. (1979) Identification key for hemocyte types in hanging drop preparation. In “Insect Hemocytes.” Ed. by A. P. Gupta, Cambridge Univ. Press, Cambridge, pp. 527–529.

9 Tauber, O. E. and Yeager, J. F. (1935) On the total hemolymph (blood) cell counts of insects. I. Orthoptera, Odonata, Hemiptera, and Homoptera. Ann. Entomol. Soc. Am., **28**: 229–240.

10 Wheeler, R. E. (1963) Studies on the total hemocyte count and hemolymph volume in *Periplaneta americana* (L.) with special reference to the last molting cycle. J. Insect Physiol., **9**: 223–235.

11 Arvy, L., Gabe, M. and Lhoste, J. (1949) Contribution a l'étude morphologique du sang de Mantidea. Rev. Can. Biol., **8**: 184–200. (original not seen)

12 Webley, D. P. (1951) Blood cell counts in the African migratory locust (*Locusta migratoria migratorioides*). Proc. R. Entomol. Soc. Lond., **A26**: 25–37.

13 Kunkel, J. G. (1981) A minimal model of metamorphosis: fat body competence to respond to juvenile hormone. In "Current Topics in Insect Endocrinology and Nutrition". Ed. by G. Bhaskaran, S. Friedman and J. Rodrigues, Plenum, New York, pp. 102–129.

14 Tanaka, A. (1981) Regulation of body size during larval development in the German cockroach, *Blattella germanica*. J. Insect Physiol., **27**: 587–592.

15 Ross, M. H. (1929) The life history of the German cockroach. Trans. Illinois., St. Acad. Sci, **21**: 84–93.

16 Bahadur, J. and Pathak, J. P. N. (1971) Changes in the total hemocyte counts of the bug, *Halys dentata* under certain conditions. J. Insect Physiol., **17**: 329–334.

17 Shapiro, M. (1979) Changes in hemocyte populations. In "Insect Hemocytes." Ed. by A. P. Gupta, Cambridge Univ. Press, Cambridge, pp. 475–523.

18 Ragyalis, A. K. (1982) Physiological and biochemical changes in *Acantholyda posticalis* hemolymph during ontogeny: 1. Cell morphology. Liet. Tsr. Mokslu Akad. Darb. Ser. C Biol. Mokslai., **0** (4): 69–78. (Abstract; original not seen)

19 Das, Y. T. (1975) Effects of juvenile hormone analog on the German cockroach, *Blattella germanica* (L.) (Dictyoptera: Blattellidae). Ph. D. dissertaion in Entomology, Rutgers University, New Brunswick, NJ.

20 Masner, P., Hangartner, W. and Suchy, M. (1975) Reduced titres of ecdysone following juvenile hormone treatment in the cockroach, *Blattella germanica*. J. Insect Physiol., **21**: 1755–1765.

21 Gupta, A. P. (1985) The identity of the so-called crescent cell in the hemolymph of the cockroach, *Gromphadorhina portentosa* (Schaum) (Dictyoptera: Blaberidae). Cytologia, **50**: 739–746.

ZOOLOGICAL SCIENCE 4: 315–321 (1987)

Growth and Maturation of Ovaries in Isolated Abdomens of *Bombyx mori*: Response to Ecdysteroids and Other Steroids

Eiji Ohnishi

Department of Biology, Faculty of Science, Nagoya University, Chikusa-ku, Nagoya 464, Japan

ABSTRACT—Studies on ovaries in isolated pupal abdomens of *Bombyx mori* revealed that they remained in an immature state, but could be stimulated to develop by injection of ecdysteroids. The stimulatory activity of ecdysone was dose-dependent and the process of vitellogenesis of ecdysone-stimulated isolated abdomens, as judged from electrophoretograms of major egg proteins, was comparable with that in normal pupae. Various ecdysteroids differing in the numbers and positions of their hydroxyl groups were examined for their stimulatory activities in comparison with that of ecdysone or 20-hydroxyecdysone. From the results it was concluded that the hydroxyl group at C–2, C–20, and C–22 has an enhancing effect, whereas that at C–24, C–25 and C–26 has an inhibitory effect. Several C_{18}, C_{19} and C_{21} steroids of vertebrate hormone type and their related compounds were also examined for possible ovary stimulatory activity. However, no activity was shown following the injection of these compounds.

INTRODUCTION

The growth and maturation of insect ovaries are under hormonal control. In the majority of species, ovaries are immature in adults at emergence and become functional after a period ranging from several days to several months. In insects of this type, juvenile hormone seems to play a central role in the maturation of the ovaries [1]. In species belonging to the Saturniidae and Bombycidae, ovaries maturate during the pupal period and adults are able to copulate and lay eggs immediately after emergence. In insects of these families, ecdysteroids seem to replace the function of juvenile hormone, which in itself plays no role [2].

In the commercial silkworm, *Bombyx mori,* it has been shown that ovaries in the isolated abdomens remain in an immature state, but can be stimulated to develop upon injection of ecdysteroids [3, 4]. Such isolated abdomens seem to be a versatile model system for the study of ecdysteroid action on ovarian maturation.

In the present study, the stimulatory effect of ecdysone was re-examined in more detail and the effect of various ecdysteroids and steroids of vertebrate hormone type were compared for their activity.

Accepted December 22, 1986
Received December 9, 1986

MATERIALS AND METHODS

Isolation of pupal abdomens, injection of steroids and dissection of ovaries

The method of preparing isolated pupal abdomens was the same as that reported previously [4]. Steroids or steroid derivatives were dissolved in warmed isopropanol and the solution was diluted 5 to 10 times with deionized water just before injection. In cases of strictly water-insoluble materials, a 1/10 volume of olive oil was included in the the isopropanol solution and the emulsion resulting upon dilution with water was injected immediately after vigorous agitation. Seven days after injection, ovaries were dissected out into 1% NaCl solution containing 10^{-3} M sodium diethyldithiocarbamate. The latter compound was included in order to suppress melanization of isolated ovaries. The isolated ovaries were placed on wetted tissue paper in a plastic container and kept

in cold until weighed.

SDS-polyacrylamide gel electrophoresis

Polyacrylamide gel electrophoresis in the presence of sodium dodecyl sulfate was performed according to the method of Laemmli [5]. Several oocytes were removed from mature ovaries and homogenized with 10 parts of Tris-buffered saline (20 mM Tris-HCl, pH 7.4, containing 150 mM NaCl). The homogenate was centrifuged at 10,000 $\times g$ for 10 min and an aliquot of the supernatant was placed on the top of the gel. The electrophoresis was done at a current of 25 mA per slab for 2 hr. The proteins in the gel were stained with Coomassie brilliant blue [6].

Chemicals

Ecdysone was obtained from Simes s.p.a and 20-hydroxy-ecdysone was a gift from Dr. T. Takemoto, Tokushima Bunri University. Ponasterone A was from Takeda Pharmaceutical Co. and inokosterone from Rhoto Pharmaceutical Co. Abutasterone was sent by Dr. A. I. Da Rocha, University of California at San Diego. 2-Deoxyecdysone, 2-deoxy-20-hydroxyecdysone and 2, 22-dideoxy-20-hydroxyecdysone were extracted and purified from the ovaries of *Bombyx mori* [7]. 22(R)-Hydroxycholesterol, 5-pregnen-3β, 20β-diol, 17β-estradiol-3-(β-D-glucoside), and 17β-estradiol-17-(α-D-glucoside) were provided by Drs. N. Ikekawa and Y. Fujimoto. 5-Pregnen-3β, 20β-diol was also given by Dr. K. Suzuki of the National Institute of Radiological Sciences. Pregnenolone, progesterone, estradiol-17α, estradiol-17β, 17β-estradiol benzoate, estrone, and testosterone were the products of Sigma Chemical Co.

RESULTS

Dose-dependency of ovarian development on the injected ecdysone and the maturity of the ecdysone-stimulated ovaries

The increase in the fresh weight of a pair of ovaries, removed from each injected abdomen after 7 days' incubation, was taken as a measure of the development of stimulated ovaries. As shown in Figure 1, ecdysone was effective at a dose of 0.5 μg and the effect was dose-dependent up to a level of 5 μg per abdomen. When ecdysone was injected in amounts exceeding 10 μg per abdomen, the injected abdomens were filled with mature ovaries after 7 days and scanty fat body remained.

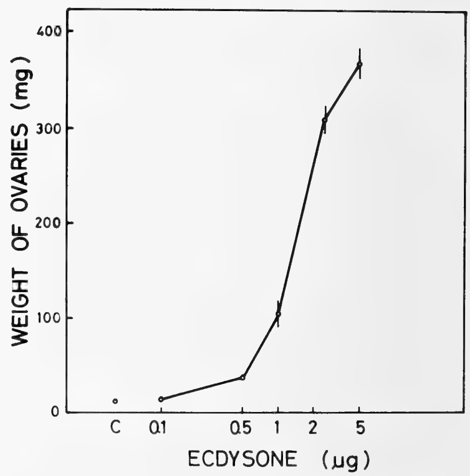

Fig. 1. Dose-response curve of ecdysone. Ecdysone was injected into isolated pupal abdomens and the fresh weight of a pair of ovaries in each abdomen was weighed after 7 days' incubation. Each point represents an average value of 7 to 10 samples, with standard deviation. Ordinate: weight of a pair of ovaries in milligrams. Abscissa: dose of injected ecdysone in micrograms. C: control.

In order to clarify the process of vitellogenesis in the ecdysone-stimulated ovaries, the compositions of the major egg proteins were analyzed by SDS-gel electrophoresis. The electrophoretograms (not shown) of the ecdysone-injected ovaries showed major bands of heavy and light chains of vitellogenin, 30 K-proteins and egg-specific protein [8]. This pattern was essentially the same as that found in normal ovaries. Thus, vitellogenesis in the ecdysone-stimulated isolated pupal abdomens seemed to be comparable to that in normal mature pupae.

In further attempt to gain an insight into the degree of maturity of the stimulated ovaries, the ecdysone-stimulated ovaries were heat-treated (46 $\pm$0.5°C, 18 min) to induce artificial parthenogenesis [9]. After the heat-treatment, eggs were maintained at 20$\pm$0.5°C to allow embryonic de-

velopment to occur. About half of the treated eggs exhibited red to purple coloration about 3 days after the treatment, indicating the initiation of embryonic development. Most of them became first instar larvae with fully pigmented setae. However, none of them hatched out from their chorions, indicating that their embryonic development had been impaired.

Stimulatory activity of Bombyx ooecdysteroids

The ovaries of *Bombyx mori* accumulate several ecdysteroids (ooecdysteroids) characteristic to the ovaries and eggs [7]. These ecdysteroids were isolated from the ovaries and purified to a chromatographically pure state. Concentrations of the ecdysteroids were estimated on the basis of their optical densities at 243 nm in ethanol. In each experiment, ecdysone or 20-hydroxyecdysone was injected at several doses into the isolated abdomens of the same batch and the dose-response curves were compared in order to estimate the stimulatory activities of the test samples relative to that of ecdysone or 20-hydroxyecdysone.

2-Deoxyecdysone, one of the major ooecdysteroids in *Bombyx,* had about 1/5 the activity of that of ecdysone (Fig. 2A). 2, 22-Dideoxy-20-hydroxyecdysone, which has been identified only in *Bombyx* ovaries [10], has negligible activity up to the dose of 36 μg per abdomen (Fig. 2B). 2-Deoxy-20-hydroxy-ecdysone, most abundantly found in *Bombyx* ovaries, had about 1/3 of the activity of ecdysone, or 1/5 of the activity of 20-hydroxyecdysone (Fig. 2C).

Stimulatory activity of phytoecdysteroids

Ponasterone A (20-hydroxy-25-deoxyecdysone) exhibited quite high activity, being about twice as active as ecdysone (Fig. 3A). Inokosterone (20, 26-dihydroxy-25-deoxyecdysone) showed an activity comparable with that of 20-hydroxy-ecdysone (Fig. 3A), indicating that the hydroxyl group at C-26 has a similar effect to that at C-25. Abutasterone (20, 24-dihydroxyecdysone) [11] had a slightly lower activity than 20-hydroxyecdysone (Fig. 3B).

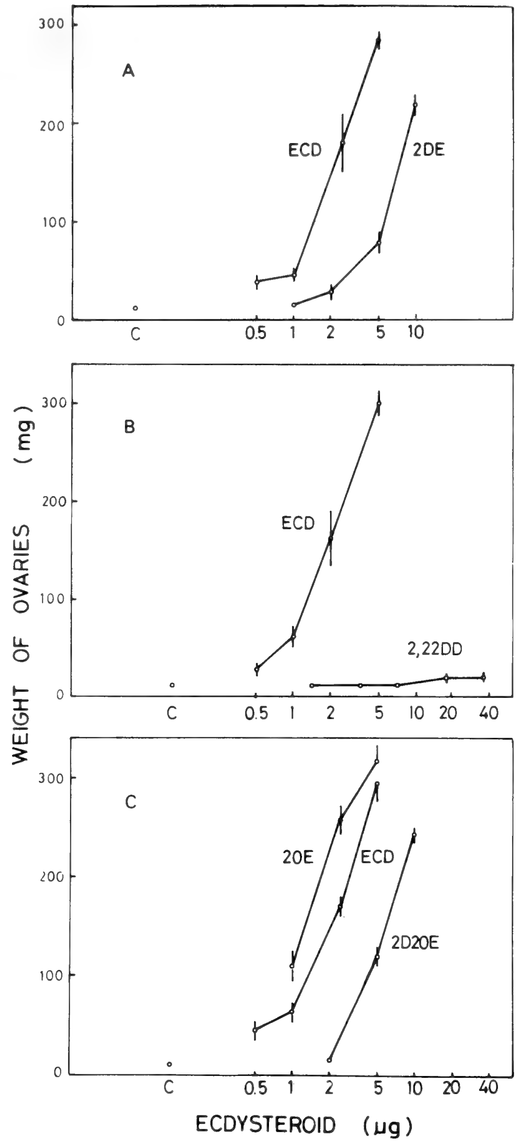

FIG. 2. Dose-response curves of *Bombyx* ooecdysteroids. A: 2-deoxyecdysone (2DE) and ecdysone (ECD). B: 2, 22-dideoxy-20-hydroxyecdysone (2, 22DD) and ecdysone (ECD). C: 2-deoxy-20-hydroxyecdysone (2D20E), ecdysone (ECD) and 20-hydroxyecdysone (20E). For other explanations, see legend for Fig. 1.

Effect of vertebrate steroid hormones and related compounds

The following steroids and steroid conjugates were examined for their possible stimulatory activ-

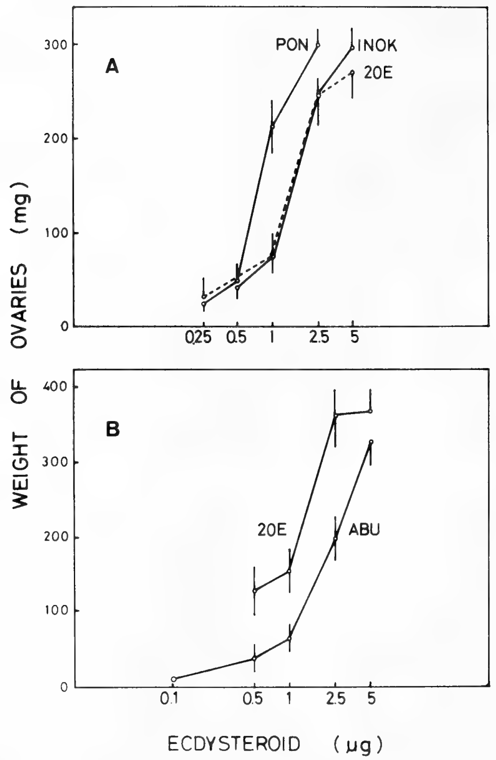

FIG. 3. Dose-response curves of phytoecdysteroids. A: ponasterone A (PON), inokosterone (INOK) and 20-hydroxyecdysone (20E). B: abutasterone (ABU) and 20-hydroxyecdysone (20E). For other explanations, see legend for Fig. 1.

ity at doses up to 40 μg per abdomen: 22(R)-hydroxycholesterol, progesterone, pregnenolone, 5-pregnen-3β, 20β-diol (2 samples), estradiol-17α, estradiol-17β, estrone, testosterone, 17β-estradiol benzoate, 17β-estradiol-3-(β-D-glucoside) and 17β-estradiol-17-(α-D-glucoside). As summarized in Table 1, all of these compounds gave negative results.

DISCUSSION

The gonadotropic activity of prothoracic gland hormone was first demonstrated in the classic experiment performed by Williams using isolated abdomens of the saturniid *Hyalophora cecropia* [12]. By transplantation of the activated prothoracic glands into the isolated abdomens, he was able to show that the recipients not only expressed imaginal characteristics but also laid several eggs. This clearly indicated that the ovaries in the abdomens had become fully mature.

In *Bombyx mori,* Sakurai and Hasegawa [3] showed that ovaries in isolated pupal abdomens could be stimulated by injection of ponasterone A and that the fresh weights of the stimulated ovaries roughly parallelled the doses of the injected ecdysteroid. We also observed, using isolated pupal abdomens, that the injection of 20-hydroxyecdysone not only stimulated ovarian development, but also induced the accumulation of

TABLE 1. Effect of injection of steroids of vertebrate hormone type and their related compounds on ovary development

Injected compounds and doses of injection (μg)	Weight of ovaries (mg) mean ± S. D.
Expt. 7Au6	
estradiol-17β	
40	11.9 ± 0.9
20	11.9 ± 1.3
10	9.3 ± 1.1
testosterone	
40	13.6 ± 1.7
20	11.5 ± 1.0
10	10.3 ± 1.2
estrone	
40	10.5 ± 0.7
20	11.4 ± 0.9
10	10.4 ± 1.3

TABLE 1. (Continued)

Injected compounds and doses of injection (μg)	Weight of ovaries (mg) mean $\pm$ S. D.
estradiol-17α	
40	11.8 ± 1.0
20	11.4 ± 1.0
10	10.5 ± 1.0
17β-estradiol benzoate	
40	12.0 ± 1.8
20	11.9 ± 2.2
10	10.2 ± 1.0
control	11.1 ± 0.7
Expt. 2Jn6	
estradiol-17α-glucoside	
40	9.0 ± 1.5
20	7.8 ± 1.1
10	9.0 ± 1.8
4	8.2 ± 1.3
5-pregnen-3β, 20β-diol*	
40	9.1 ± 1.3
20	8.9 ± 0.6
10	10.4 ± 1.6
control	8.6 ± 1.3
Expt. 12Jn6	
estradiol-3β-glucoside	
40	10.6 ± 0.9
20	10.6 ± 0.7
10	9.8 ± 1.0
5-pregnen-3β, 20β-diol**	
40	9.4 ± 1.4
20	8.1 ± 1.1
10	10.2 ± 2.4
22(R)-hydroxycholesterol	
40	9.4 ± 0.9
20	9.5 ± 0.7
10	9.7 ± 1.1
control	9.3 ± 0.7
Expt. 26Jn6	
pregnenolone	
40	10.5 ± 2.9
20	8.0 ± 0.6
10	9.4 ± 1.1
progesterone	
40	10.0 ± 0.8
20	8.5 ± 0.6
control	8.4 ± 1.1

The effect was determined by examining the fresh weight of a pair of ovaries isolated 7 days after injection.

* sample from Dr. K. Suzuki. ** sample from Dr. Y. Fujimoto.

ecdysteroids in the ovaries [4, 13]. Upon re-examination of the dose-effect of ecdysteroids, we found a quite typical dose-response relationship. Thus, comparison of stimulatory activities among various ecdysteroids differing in the number and position of their hydroxyl groups was shown to be possible.

2-Deoxyecdysone exhibited about 1/5 of the activity of ecdysone, indicating that the hydroxyl group at C-2 has a significant effect. Also, 2, 22-dideoxy-20-hydroxyecdysone, which is also one of major ooecdysteroids in *Bombyx,* exhibited quite low activity, showing that the hydroxyl group at C-22 is requisite for the activity. These results seem to suggest that these major ecdysteroids lacking hydroxyl group at C-2 are not the active forms, but rather the precursors of active compounds. 20-Hydroxyecdysone, which is a rather minor component in *Bombyx* ovaries, was twice as active as ecdysone, indicating that the hydroxyl group at C-20 has an enhancing effect. Consistent with the report of Sakurai and Hasegawa [3], and with the results of other studies employing cultured cells [14] or imaginal disks of *Drosophila* [15], ponasterone A was more active than ecdysone and 20-hydroxyecdysone. Together with the results of the experiments using inokosterone and abutasterone, it can be concluded that the hydroxyl group at the termini of the side chain of ecdysteroids has some inhibitory effect. These differences in activity among the ecdysteroids should be expected to be a reflection of the structure of the binding site(s) of the target cells in the isolated abdomens.

Steroids of vertebrate hormone type, and their related compounds, were tried for possible ovarian stimulatory activity. Estradiol-17β, a vertebrate female sex hormone, has been identified in the ovaries of *Bombyx mori* [16]. In an *in vitro* system of isolated *Bombyx* ovaries, estradiol has been shown to be converted into several metabolites including its two glucosides, 17β-estradiol-3-(β-D-glucoside) and 17β-estradiol-17-(α-D-glucoside) [17]. However, estradiol and its derivatives including these two glucosides exhibited no ovary-stimulatory activity in the present study. In the tobacco hornworm, *Manduca sexta,* Thompson and his colleagues [18] demonstrated the efficient conversion of [^{14}C] cholesterol into the glucoside of 5-pregnen-3β, 20β-diol and further showed the presence of this glucoside in intact pupae. These facts seemed to suggest the presence in insects of metabolic activities yielding C_{21} steroids from cholesterol. However, in the present study, examination of the ovary-stimulatory activity of several C_{21} steroids including 5-pregnen-3β, 20β-diol, produced negative results. Thus the significance of the presence of C_{18} and C_{21} steroids in insect ovaries remains for future study.

The hormonal regulatory mechanism of insect ovarian maturation seemed to be variable among species. In most species, maturation is stimulated by juvenile hormone with or without concomitant action of neurohormones. In *Bombyx mori,* the scheme seems to be rather simple. Mizuno [19] has shown through his experiments using debrained pupae and isolated pupal abdomens, that prothoracic gland hormone secreted in the early pupal period stimulates ovarian maturation and that neurohormone seems to play no role. The present experiments have thus confirmed the above scheme and extended the previous findings.

ACKNOWLEDGMENTS

The author wishes to thank Dr. S. Y. Takahashi and Mr. K. Soma for their skilful technical assistance and to Dr. O. Yamashita for his valuable advice. He is also indebted to Dr. T. Takemoto, Tokushima Bunri University, to Drs. N. Ikekawa and Y. Fujimoto, Tokyo Institute of Technology, Dr. A. I. Da Rocha of University of California at San Diego, and to Dr. K. Suzuki, National Institute of Radiological Sciences, for their gift of steroids. The present study was supported by grants Nos. 60304009 and 61540517 from the Ministry of Education, Science and Culture.

REFERENCES

1 Koeppe, J. K., Fuchs, M., Chen, T. T., Hunt, L. H., Kovalick, G. E. and Briers, T. (1985) The roles of juvenile hormone in reproduction. In "Comprehensive Insect Physiology, Biochemistry and Pharmacology". Ed. by G. A. Kerkut and L. I. Gilbert, Pergamon Press, Oxford, New York & Toronto, Vol. 8, pp. 165–204.

2 Hagedorn, H. H. (1985) In "Comprehensive Insect Physiology, Biochemistry and Pharmacology". Ed. by G. A. Kerkut and L. I. Gilbert, Pergamon Press,

Oxford, New York & Toronto, Vol. 8, pp. 205–262.

3 Sakurai, H. and Hasegawa, K. (1969) Response of isolated pupal abdomens of silkworm, *Bombyx mori* L., to injected ponasterone A (Lepidoptera: Bombycidae). Appl. Entomol. Zool., **4**: 59–65.

4 Chatani, F. and Ohnishi, E. (1976) Effect of ecdysone on the ovarian development of *Bombyx* silkworm. Dev. Growth Differ., **18**: 481–484.

5 Laemmli, U. K. (1970) Cleavage of structural proteins during the assembly of the head of bacteriophage T_4. Nature, **227**: 680–685,

6 Weber, K., Pringle, J. and Osborn, M. (1972) Measurement of molecular weight by electrophoresis on SDS acrylamide gel. In "Methods in Enzymology". Ed. by C. H. W. Hirs and N. Timasheff, Academic Press, New York & London, Vol. 26, pp. 3–27.

7 Ohnishi, E., Mizuno, T., Ikekawa, N. and Ikeda, T. (1981) Accumulation of 2-deoxyecdysteroids in ovaries of silkworm, *Bombyx mori.* Insect Biochem., **11**: 155–159.

8 Takahashi, S. Y. (1986) Studies on the phosphorylation of ovarian proteins from the silkworm, *Bombyx mori*: Identification of band 2 protein as egg-specific protein. Insect Biochem., **17**: 141–152.

9 Sakaguchi, B. (1978) Method for artificial parthenogenesis. In "The Silkworm: An Important Laboratory Tool". Ed. by Y. Tazima, Kodansha, Tokyo, p. 21.

10 Ikekawa, N., Ikeda, T., Mizuno, T., Ohnishi, E. and Sakurai, S. (1980) Isolation of a new ecdysteroid, 2, 22-dideoxy-20-hydroxyecdysone from the ovaries of the silkworm, *Bombyx mori.* Chem. Commun., **1980**: 448–449.

11 Pinheiro, M. L. B., Filho, W. W., Da Rocha, A. I., Porter, B. and Wenkert, E. (1983) Abutasterone, an ecdysone from *Abuta velutina.* Phytochem., **22**: 2320–2321.

12 Williams, C. M. (1952) Physiology of insect diapause. IV. The brain and prothoracic glands as an endocrine system in the cecropia silkworm. Biol. Bull., **103**: 120–138.

13 Ohnishi, E. and Chatani, F. (1977) Biosynthesis of ecdysone in the isolated abdomen of the silkworm, *Bombyx mori.* Dev. Growth Differ., **19**: 67–70.

14 Maroy, P., Dennis, R., Beckers, C., Sage, B. A. and O'Connor, J. D. (1978) Demonstration of an ecdysteroid receptor in a cultured cell line of *Drosophila melanogaster.* Proc. Natl. Acad. Sci. USA, **75**: 6035–6038.

15 Yund, M. A., King, D. S. and Fristrom, J. W. (1978) Ecdysteroid receptors in imaginal disks of *Drosophila melanogaster.* Proc. Natl. Acad. USA, **75**: 6039–6043.

16 Ohnishi, E., Ogiso, M., Wakabayashi, K., Fujimoto, Y. and Ikekawa, N. (1985) Idetification of estradiol in the ovaries of the silkworm, *Bombyx mori.* Gen. Comp. Endocrinol., **60**: 35–38.

17 Ogiso, M., Fujimoto, Y., Ikekawa, N. and Ohnishi, E. (1986) Glucosidation of estradiol-17β in the cultured ovaries of the silkworm, *Bombyx mori.* Gen. Comp. Endocrinol., **61**: 394–401.

18 Thompson, M. J., Svoboda, J. A., Lusby, W. R., Rees, H. H., Oliver, J. E., Weirich, G. F. and Wilzer, K. R. (1985) Biosynthesis of a C_{21} steroid conjugate in an insect. The conversion of [^{14}C] cholesterol to 5-[^{14}C] pregnen-3β, 20β-diol glucoside in the tobacco hornworm, *Manduca sexta.* J. Biol. Chem., **260**: 15410–15412.

19 Mizuno, T. (1982) Control of accumulation of ecdysteroids in ovaries of the silkworm, *Bombyx mori.* Zool. Mag., **91**: 12–17.

ZOOLOGICAL SCIENCE 4: 323–329 (1987)

Annual Changes in Plasma and Testicular Androgen in Relation to Reproductive Cycle in a *Japalura* Lizard in Taiwan

Ruai-Huei Chen, Jun-Yi Lin, Yuh-Lin Yu[1],
and Hsien Yu Cheng[2]

Department of Biology, Tunghai University, Taichung, [1]Institute of Zoology, Academia Sinica, Taipei, and [2]Department of Zoology, National Taiwan University, Taipei, Taiwan, R.O.C.

ABSTRACT—Male *Japalura mitsukurii formosensis* are reproductively active from emergence in March through July. Plasma and testicular androgen levels in association with all other reproductive activities decline dramatically in July–August to a minimum in August–September. A sudden surge of testicular androgen level dissociated from plasma androgen level observed near the end of spermatogenic cycle appears to be involved in the control of decline of the spermatogenesis. After the regression, spermatogenesis, interstitial cells and Sertoli cells began to recrudesce and peak prior to hibernation. However, accessory sex organs weights, testicular androgen level and plasma androgen level still remained low after the regression until the emergence in March. The plasma androgen level was more positively correlated with recrudescence of spermatogenic activity. The increased testicular androgen level appeared more coincided with high spermiogenesis and also with high mating activity.

INTRODUCTION

Numerous studies of the male reproductive cycle in lizards demonstrate changes in size and histology of the testes and accessory sexual organs, and androgen production [1–4]. However, the correlation between androgen production and the testicular cycle is less well documented [5–8], and such fundamental research is necessary to answer questions on the nature of endocrine physiology in nonmammals and the evolution of vertebrate hormone structure [9, 10]. The objectives of the present study on *Japalura mitsukurii formosensis* are to provide information on seasonal changes of androgen levels in plasma and testis and to correlate annual androgen levels in plasma and testis with the phases of the spermatogenic cycle.

MATERIALS AND METHODS

Lizards were collected monthly from the woods of mainly *Acacia confusa,* on the campus of Tunghai University, Taichung, Taiwan (24°10′N, 120°35′E; elevation 180 m), from March 1982 to March 1983. Only adult males with snout-vent length (SVL) greater than 65 mm were used for the analysis [11, 12].

All individuals were anesthetized with ether within three hours of capture. Their weight and SVL were measured to the nearest 0.1 g and 0.1 mm, respectively. Blood samples (0.4–0.7 ml) were drown from the inferior vene cava near its entry in the heart, then placed into heparinized tubes. The blood was immediately centrifuged and plasma (0.2–0.45 ml) was frozen and stored at −20°C for androgen analysis. The testes and the accessory sexual organs including epididymis, vas deferens and kidney were removed and weighed to the nearest 0.1 mg. The right testis was fixed in Bouin's solution for histological examination, and the left testis was frozen and stored for the androgen analysis in the tissues.

Androgen concentrations in plasma and testis were measured by radioimmunoassay methods modified from Wingfield and Farner [13] and Anderson *et al.* [14], as described previously by Yu *et al.* [15]. The modified procedure quantitated

Accepted November 11, 1986
Received September 22, 1986

total androgen, since a chromatographic separation of androgens was omitted. The assay was sensitive to 10 pg of testosterone per assay tube. Standard and samples produced parallel displacement of tritiated testosterone. The between-assay coefficient of variation was 13.4% and the within-assay coefficient of variation was 3.8%. Recovery of tritiated testosterone and unlabelled testosterone standards added to plasma or testis homogenates was about 94%.

The specificity of testosterone antiserum used for this assay was described previously [14]; it cross-reacted with dihydrotestosterone, androstenedione, and androstenediol at 90%, 12%, and 11%, respectively, relative to testosterone (100%), and had negligible cross-reactivities with other test steroids. The concentration of androgen in the sample was expressed as testosterone equivalent extrapolated from the standard curve.

Paraffin-embedded testes were sectioned at 6 μm and stained with Harris's hematoxylin and eosin. The diameters of seminiferous tubules, the thickness of germinal epithelium, Sertoli cell nuclear diameter and interstitial cell nuclear diameter were measured with ocular micrometer to the nearest 0.1 μm. The number of cellular layers of germinal epithelium, Sertoli cells around the peripheral regions of the seminiferous tubules and maximal amount of interstitial cells in the intertubular area were estimated from counts directly under the microscope. Values presented for each variable are the averages of the 10 measurements for each testis. Reproductive stages were judged from the spermatogenetic process outlined in Table 1.

RESULTS

A total of 146 adult males were used in this study. The monthly mean SVL of the samples was similar in all months (ANOVA, p=0.87) and ranged from 75.0 mm to 79.1 mm (Table 2).

In 1982, first emergence was observed on March 12 and was March 19 in 1983. Individuals entered hibernation in late November or early December in 1982. Males emerge from hibernation about 2 weeks before females [11, 16]. In 1982, during the 12 days following the first emergence, 124 males and 21 females were observed (5.9:1). In 1983, during the same period, 62 males and 24 females were observed (2.5:1). After March in both year, sex ratio appeared to be 1:1.

The monthly data on the testis weights, accessory sex organ weights and histological observations of the testes including the diameters of seminiferous tubules, the thickness of germinal epithelium, Sertoli cell nuclear diameter and interstitial cell nuclear diameter, the number of

Table 2. Monthly means (±SEM) of the weights in testis and accessory sex organs, androgen epithelium, germinal layer number, and nuclear diameters and numbers in interstitial cells and

Month	N	Snout-vent length (mm)	Testis weight (mg/pair)	Accessory sex organs weight (mg)	Androgen concentration: Testis (ng/testis)	Androgen concentration: Blood plasma (ng/ml)	Seminiferous tubules diameter (μm)
1982							
Mar	14	79.1±0.9	125.0± 7.8	119.5±4.7	3.50±0.70	2.41±0.43	301.8± 7.8
Apr	16	77.8±0.6	135.8± 3.5	114.8±3.6	6.55±1.35	2.27±0.79	279.2± 8.1
May	17	77.6±0.5	122.2± 4.7	115.6±3.1	7.00±0.91	1.18±0.26	292.0± 7.1
Jun	15	75.5±1.2	91.7± 6.9	112.9±5.9	19.42±4.80	1.58±0.44	273.8± 8.4
Jul	15	75.5±1.2	91.3± 7.9	106.5±6.2	29.27±5.47	0.35±0.09	292.8± 7.6
Aug	18	75.3±0.8	17.1± 2.7	91.5±4.6	2.45±0.45	0.16±0.03	99.7± 5.9
Sep	14	76.5±0.9	19.3± 2.7	73.0±4.2	1.33±0.25	0.17±0.02	134.7±11.5
Oct	14	75.5±0.8	74.8± 5.6	76.1±3.0	2.38±0.29	0.40±0.09	247.0± 5.8
Nov	12	78.3±0.8	156.4±10.4	90.2±4.4	0.62±0.16	0.63±0.42	317.8± 8.1
1983							
Mar	10	76.9±1.0	143.3± 6.6	119.9±6.1	5.74±1.58	7.10±2.35	298.8± 7.6

TABLE 1. Spermatogenic stages during reproductive cycles in *Japalura mitsukurii formosensis*

Stage	Testicular spermatogenic condition
1	only spermatogonia, few or no spermatocytes, no lumen.
2	primary spermatocytes present, few or no secondary spermatocytes, few or no lumen.
3	secondary spermatocytes abundant, few or no spermatids.
4	all stages of spermatogenesis present, spermatids abundant, few or no spermatozoa.
5	all stages of spermatogenesis present and abundant. No or few spermiogenesis.
6	all stages of spermatogenesis present and abundant. Spermiogenesis occurs.
7	spermatozoa abundant but spermatids and spermatocytes greatly reduced.

cellular layers of germinal epithelium, the number of Sertoli cells and of interstitial cells are summarized in Table 2, and they all showed a similar corresponding pattern of reproductive cycle. Adult males of this species showed a distinct spermatogenic cycle (Table 3), and were reproductively active from March (right after emergence) to July. The testis weight decreased in August and September, then recrudesced in October and reached the maximum size in November. The diameters of seminiferous tubules, the thickness of germinal epithelium, Sertoli cell nuclear diameter and interstitial cell nuclear diameter also dropped in August but their recrudescence occurred in September, one month ahead of the recrudescence of testis weights. The accessory sex organ weights declined in September, one month later than the regressoin of testis weight and remained low or increased slightly in the pre-hibernation period (October to November). The male reproductive pattern of *J. m. formosensis* in this study was in close agreement with the previous finding by Cheng and Lin [11].

Monthly changes of plasma androgen concentration showed a distinct cycle with the highest concentration in late March, immediately after emergence (Table 2). Thereafter, the plasma androgen level declined, although remaining relatively high (greater than 1.1 ng/ml) until June, then dropped sharply to below 0.5 ng/ml in July, and reached the minimum level (0.16 ng/ml) in August. Plasma androgen level remained low during the pre-hibernation period. Testicular androgen level, measured per testis, was moderate at emergence and increased to the maximum level in July (Table 2). The July peak of testicular

concentrations in testis and plasma, diameters of seminiferous tubules, thickness of germinal
Sertoli cells in *Japalura mitsukurii formosensis*

Germinal layer thickness (μm)	Germinal layer number (N)	Sertoli cell No./tubule (N)	Sertoli cell Nuclear diameter (μm)	Interstitial cell No./intertubular area (N)	Interstitial cell Nuclear diameter (μm)
61.7±3.1	11.6±0.5	18.9±0.7	5.06±0.13	4.8±0.2	4.95±0.10
55.2±1.6	11.6±0.5	19.2±0.7	4.90±0.12	5.0±0.3	4.74±0.11
59.5±2.2	11.8±0.4	20.4±0.5	4.88±0.08	5.1±0.1	4.88±0.15
58.5±4.9	11.7±0.9	16.6±0.7	5.07±0.23	4.9±0.4	4.71±0.29
52.6±1.2	9.5±0.4	17.1±0.6	5.23±0.15	5.0±0.2	4.87±0.17
15.3±1.6	2.4±0.2	7.4±0.8	4.31±0.18	3.1±0.2	3.99±0.05
40.7±3.6	6.3±0.5	12.9±1.2	4.49±0.11	3.2±0.2	4.02±0.17
74.1±2.4	13.0±0.5	16.4±0.6	5.02±0.10	3.9±0.2	4.18±0.10
83.1±3.0	16.5±0.5	22.8±0.7	5.28±0.12	5.0±0.2	4.43±0.13
63.8±1.8	12.2±0.7	17.3±0.6	5.12±0.17	4.6±0.2	5.12±0.16

TABLE 3. Percent distribution of spermatogenic stages in *Japalura mitsukurii formosensis*

Month	N	Stages 1	2	3	4	5	6	7
Mar	14	—	—	—	—	—	100	—
Apr	16	—	—	—	—	—	100	—
Mar	17	—	—	—	—	—	100	—
Jun	16	—	—	—	—	—	68.8	31.2
Jul	15	—	—	—	—	—	40.0	60.0
Aug	18	100	—	—	—	—	—	—
Sep	14	28.6	71.4	—	—	—	—	—
Oct	14	—	7.1	85.8	7.1	—	—	—
Nov	12	—	—	—	58.3	41.7	—	—

TABLE 4. The means (±SEM) of testis weight, accessory sex organs weight and androgen concentrations in testis and plasma at different spermatogenic stages in *Japalura mitskurii formosensis*

Stage	N	Testis weight (mg/pair)	Accessory sex organs weight (mg)	Androgen concentration Testis (ng/testis)	Androgen concentration Plasma (ng/ml)
1	22	16.2± 2.2	87.8±4.4	2.10±0.40	0.15±0.02
2	11	25.3± 4.4	74.2±4.3	1.70±0.26	0.23±0.04
3	12	74.8± 6.3	77.2±3.1	2.37±0.34	0.38±0.10
4	8	144.1±16.6	87.2±7.0	0.94±0.34	0.82±0.63
5	5	159.7± 3.5	92.4±2.4	0.57±0.65	0.43±0.12
6	64	124.2± 4.7	116.8±4.4	11.34±4.95	1.92±0.34
7	14	87.3± 8.5	102.8±6.8	21.90±4.48	0.83±0.31

androgen concentration dropped sharply to the minimum in August, and remained low during the pre-hibernation period (Table 2). Both plasma and testicular androgen level were higher at the time of emergence than prior to hibernation period (Table 2).

Changes in testicular weight, accessory sex organ weights, testicular and plasma androgen concentrations were correlated with spermatogenic stages (Table 4). Plasma and testicular androgen levels were relatively high during the peak of spermatogenesis and spermiation (stage 6) in the breeding season. Testicular androgen level reached the highest level when the germinal epithelium started to regress (stage 7) in June and July. However, plasma androgen concentration regressed to a relatively low level (Tables 1, 3, and 4).

DISCUSSION

The concordance of the present data with the previous finding [11] indicates a consistent timing of the reproductive cycle in male *J. m. formosensis*. Males emerge from hibernation in March with the testis and accessory sex organs ready for further spermiogenesis. In March plasma androgen concentration is at the highest level but testicular androgen concentration level is still relatively low (Table 2). Matings occur mainly from April through June [16] as the testicular androgen concentration is at increasing phase (Table 2). The plasma androgen declined steadily, coincided with the regression of testicular weights during mating period (March through June, Table 2, Fig. 1). In contrast, testicular androgen rised markedly with an increase in spermiogenesis

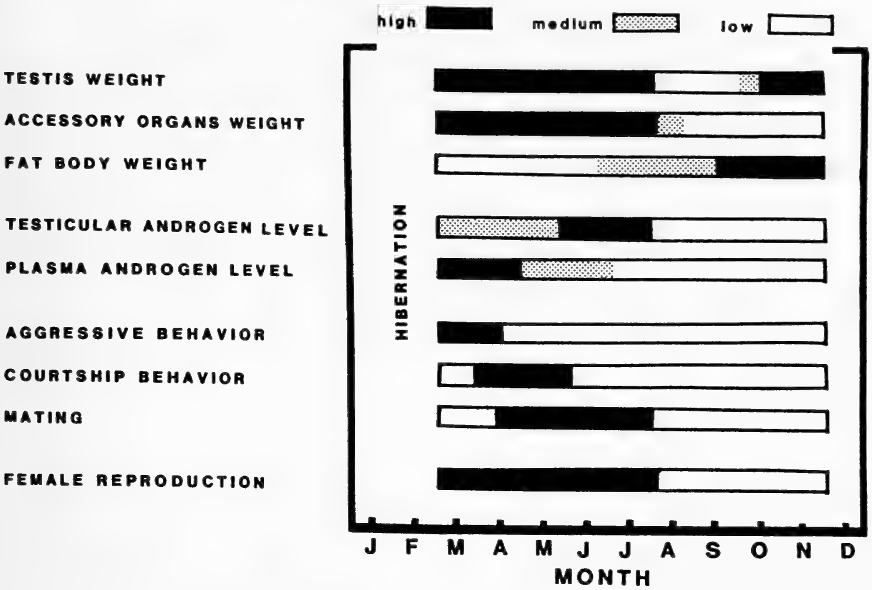

FIG. 1. A summary of annual reproductive pattern of *Japalura mitsukurii formosensis*. The variables are: testis weight, high>90 mg, medium≤90 mg and>30 mg, low≤30 mg; accessory sex organs weights, high>100 mg, medium≤100 mg and >80 mg, low≤80 mg; fat body weight (male), high>200 mg, medium≤200 mg and>100 mg, low≤100 mg; testicular androgen level, high>10 ng/testis, medium≤10 ng/testis and>3 ng/testis, low≤3 ng/testis; blood plasma androgen level, high>2 ng/ml, medium≤2 ng/ml and>1 ng/ml, low≤1 ng/ml; aggressive behavior, courtship behavior, and mating, high=active months, low=non-active months; female reproduction, high=occurrence of enlarged follicles or oviducal eggs, low=absence.

(Tables 2 and 4). During June–July, some individuals possessed regressing testes (spermatogenetic stage 7, Tables 1 and 3). Thereafter, all the reproductive activities drop dramatically in July–August, and reached the minimum in August–September (Table 2). All individuals collected in August were spermatogenetically inactive (stage 1, Tables 1 and 3). During pre-hibernation, the activities of testicular tissues including interstitial cells and Sertoli cells start to accelerate (Tables 2, 3, and 4). Accessory sex organs weights, testicular androgen and plasma androgen remain low after the regression (Table 2, Fig. 1).

Interstitial cells and Sertoli cells have been proposed as the major sites of steroid biosynthesis in the reptilian testis [17, 18]. In general, during the breeding season, high plasma and testicular androgen levels were accompanied with a numerical increase and large nuclear diameter of interstitial cells and Sertoli cells (Table 2). However, plasma androgen and testicular androgen were at the lowest level during the whole pre-hibernation period as testicular activities began to increase in September–October and reached the highest level before entering hibernation in November (Table 2). The evidence shows that both testicular and plasma androgen level are not associated with the recrudescence phase of the testicular activities. This disassociation pattern is not concordant with the findings of the previous studies on other lizards [5, 6]. The functional meaning of the hypertrophication of interstitial cells and Sertoli cells during this pre-hibernation period is obscure. The main cause responsible for the resumption of the spermatogenesis is still an open question. The level of androgen needed in the initiation of spermatogenic recrudescence may be quite low (about 10% of the maximum) in this lizard [18, 19]; or like epitestosterone, other than androgen, may involve in this testicular recrudescence [10].

In reptiles, unlike endotherms, the ambient temperature may play a key role in modulating the pattern of the annual reproductive rhythm [5, 20–22]. A marked drop in testicular androgen level

(in November) prior to hibernation may be due to a progressive inactivity of the steroidogenic tissue in response to decreasing temperature and, perhaps, also to shortening photoperiods [5]. The unexpected drop of androgen concentration in testicular and plasma tissues as the spermatogenesis reached relatively high level (stage 5; Tables 1 and 4), may be explained owing to their occurrence in November prior hibernation (Table 3).

Discrepancies between testicular and plasma androgen levels have been observed and discussed in other lizards [5–7]. A similar finding with a sudden surge of testicular androgen level dissociated with plasma androgen level in this lizard during the termination of spermatogenesis (Table 2, Fig. 1) indicates further that steroid hormones might play an important part in the control of decline of spermatogenesis [7, 23].

Increase in plasma androgen was observed to be related to mating season [5, 24]. Increase in testicular androgen was observed to be associated with recrudescent spermatogenesis [5, 6]. However, our data indicated that it was the plasma androgen level which was more positively associated with recrudescence of spermatogenic activity (Table 4). The testicular androgen level showed depressed as the spermatogenic activity recrudescent, although the testicular androgen concentration dramatically increased as the spermatogenic activity reached the peak (stage 6). Furthermore, the androgen level continually surged even as the spermatogenic activity had started to regress (Table 4). In this lizard, the increase of testicular androgen level appeared more coincided with high spermiogenesis activity and also with high mating activity (Table 4, Fig. 1).

ACKNOWLEDGMENTS

Thanks are to the Department of Laboratory Medicine, University of Washington, Seattle, USA, for the supply of testosterone antiserum, and to the Institute of Botany, Academia Sinica, for the use of the liquid scintillation spectrometer. The manuscript was completed while HYC held a Smithsonian postdoctoral fellowships. For critical comments on the manuscript, we are greateful to George Zug.

REFERENCES

1 Fox, H. (1977) The urinogenital system of reptiles. In "Biology of the Reptilia". Ed. by C. Gans, Academic Press, New York, pp. 1–157.

2 Callard, I. P., Callard, G. V., Lance, V., Bolaffi, J. L. and Rosset, J. S. (1978) Testicular regulation in nonmammlian vertebrates. Biol. Reprod., **18**: 16–43.

3 Crews, D. (1979) Endocrine control of reptilian reproductive behavior. In "Endocrine Control of Sexual Behavior". Ed. by C. Beyer, Raven Press, New York, pp. 167–222.

4 Crews, D. (1979) Neuroendocrinology of lizard reproduction. Biol. Reprod., **20**: 51–73.

5 Arslan, M., Libo, J., Zaidi, A. A., Jalali, S. and Quzi, M. H. (1978) Annual androgen rhythm in the spiny-tailed lizard, *Uromastix hardwicki*. Gen. Comp. Endocrinol., **36**: 16–22.

6 Coutry, Y. and Dufaure, J. P. (1979) Levels of testosterone in the viviparous lizard (*Lacerta vivipara jacquin*). Gen Comp. Endocrinol., **39**: 336–342.

7 Courty, Y. and Dufaure, J. P. (1980) Levels of testosterone, dihydrotestosterone, and androstenedione in the plasma and testis of lizard (*Lacerta vivipara jacquin*) during the annual cycle. Gen. Comp. Endocrinol., **42**: 325–333.

8 McPherson, R. J., Roots, L. R., McGrege, R. III, and Marion, K. R. (1982) Plasma steroids associated with seasonal reproductive changes in a multiclutched freshwater turtle, *Sternotherus odoratus*. Gen. Comp. Endocrin., **48**: 440–451.

9 Licht, P., Papkoff, H., Farmer, S. W., Muller, C. H., Tsui, H. W. and Crews, D. (1977) Evolution in gonadotropin structure and function. Rec. Prog. Horm. Res., **33**: 169–248.

10 Bourne, A. R., Taylor, J. L. and Watson, T. G. (1985) Identification of epitestosterone in the plasma and testis of the lizard *Tiliqua* (*Trachydrosaurus*) *rugosa*. Gen. Comp. Endocrinol., **58**: 394–401.

11 Cheng, H. Y. and Lin, J. Y. (1977) Comparative reproductive biology of the lizards, *Japalura swinhonis formosensis, Takydromus septentrionalis* and *Hemidactylus frenatus* in Taiwan. I. Male reproductive cycle. Bull. Inst. Zool., Academia Sinica (R.O.C.), **16**: 107–120.

12 Cheng, H. Y. and Lin, J. Y. (1978) Comparative reproductive biology of the lizards, *Japalura swinhonis formosensis, Takydromus septentrionalis* and *Hemidactylus frenatus* in Taiwan. II. Fat body and liver cycles of the males. Bull. Inst. Zool., Academia Sinica (R.O.C.), **17**: 67–74.

13 Wingfield, J. C. and Farner, D. S. (1975) The determination of five steroids in avian plasma by radioimmunoassy and competitive protein-binding. Ster-

oids, **26**: 311–327.

14 Anderson, P. H., Fukushima, K. and Schiller, H. S. (1975) Radioimmunoassay of plasma testosterone, with use of polyethylene glycol to separate antibody-bound and free hormone. Clin. Chem., **21**: 708–714.

15 Yu, J. Y. L., Chang, T. Y., Hsu, H. K., Liao, C. F. and Wan, W. C. M. (1981) Androgen/testosterone synthesis by the dissociated testicular cells from mice of different ages in response to rat LH stimulation *in vitro*. Bull. Inst. Zool., Academia Sinica (R.O.C.), **20**: 57–65.

16 Lin, J. Y. (1979) Ovarian, fat body and liver cycles in the lizard *Japalura swinhonis formosensis* in Taiwan (Lacertillia:Agamidae). J. Asian Ecol., **1**: 29–38.

17 Lofts, B. (1972) The Sertoli cell. Gen. Comp. Endocrinol., Suppl., **3**: 636–648.

18 Lofts, B. and Bern, H. A. (1972) The functional morphology of steroidogenic tissues. In "Steroids in Nonmammalian Vertebrates". Ed. by D. R. Idler, Academic Press, New York, pp.6–36.

19 Lofts, B. (1968) Patterns of testicular activity. In "Perspectives in Endocrinology". Ed. by E. J. W. Barrington, and C. Barker-Jorgensen, Academic Press, New York.

20 Licht, P. (1972) Envrionmental physiology of reptilian breeding cycles: Role of temperature. Gen. Comp. Endocrinol., Suppl., **3**: 477–488.

21 Pearson, A. K., Tsui, H. W. and Licht, P. (1976) Effect of temperature on spermatogenesis, on the production and action of androgens and on the ultrastructure of gonadotropic cells in the lizard *Anolis carolinensis*. J. Exp. Zool., **195**: 291–304.

22 Cheng, H. Y. (1986) Internal rhythms and the mechanisms in the regulation of annual reproductive and energetic patterns in lizards. Tunghai Journal, **27**: 565–590.

23 Johnson, L. and Jacob, J. S. (1984) Pituitary activity and reproductive cycle of male *Cnemidophorus sexlineatus* in West Tennessee. J. Herpetol., **18**: 396–405.

24 Bourne, A. R. and Seamark, R. F. (1975) Seasonal changes in 17-hydroxysteroids in the plasma of a male lizard (*Tiliqua rugosa*). Comp. Biochem. Physiol., **50B**: 535–536.

ZOOLOGICAL SCIENCE 4: 331–337 (1987)

Effects of Intracranially Implanted Cholecystokinin and Substance P on Serum Concentrations of Gonadotropins, Prolactin and Thyroid Stimulating Hormone in the Rat

HARUKO UEMURA, ATSUHIKO HATTORI[1], MASARU WADA[1] and HIDESHI KOBAYASHI[2]

Biological Laboratory, Kanagawa Dental College, Yokosuka, Kanagawa 238, [1]Department of General Education, Tokyo Medical and Dental University, Ichikawa, Chiba 272, and [2]Department of Biology, Faculty of Science, Toho University, Funabashi, Chiba 274, Japan

ABSTRACT—A cannula containing a mixture of cholecystokinin-4 (CCK-4) and cholesterol (1:1 or 5:3 by weight) and one containing a mixture of substance P (SP) and cholesterol (1:1) were implanted into the median eminence of male rats. CCK-4 reduced serum LH but not FSH, PRL and TSH concentrations; SP reduced serum TSH but not LH, FSH and PRL concentrations, according to measurements made 4–5 days following the implantations. CCK-4 implanted into the ventromedial or arcuate nucleus failed to have any effect on serum LH concentration. It is thus concluded that CCK-4 inhibits the release of LH, and SP inhibits the release of TSH, probably by inhibiting LHRH and TRH secretion from their respective axon terminals in the median eminence.

INTRODUCTION

The presence of the gastrin-cholecystokinin family of peptides (G-CCK) and substance P (SP) has been demonstrated by radioimmunoassay (RIA) in the hypothalamus of mammals (G-CCK: [1, 2]; SP: [3]) and pigeons (SP: [4]). Furthermore, the axon terminals of these substances have been shown immunohistochemically in the median eminence (ME) of mammals (G-CCK: [5]; SP: [6, 7, 10]) and lower vertebrates (G-CCK: [8]; SP: [9–11]). Thus, G-CCK and SP may possibly be essential to the regulation of the secretion of hypothalamic releasing or release-inhibiting hormones from the ME. To gain confirmation of this, various studies have been conducted on the effects of G-CCK and SP on the release of adenohypophysial hormones. Intraventricular injections of COOH-terminal octapeptide of CCK (CCK-8) [12] and gastrin [13] inhibited release of luteinizing hormone (LH), but CCK-8 stimulated it when implanted in the medial preoptic area in rats [14]. Further, intraventricularly injected SP stimulated LH and prolactin (PRL) secretion in rats [15] but had no influence on the release of LH or follicle-stimulating hormone (FSH) in the rhesus monkey [16]. It is thus apparent that these findings are at variance with each other.

Intraventricularly administered substances diffuse into nervous tissue and affect neurons near the ventricle, thus making it difficult to identify the site of action of the substances. In the present study, in order to find a particular site that is affected, a cannula containing the COOH-terminal tetrapeptide of CCK (CCK-4) or SP was chronically implanted into the ME. In addition, a cannula containing CCK-4 was implanted into the arcuate (AR) or hypothalamic ventromedial (HVM) nucleus, since G-CCK is found in these nuclei [2, 5, 21]. Then the serum concentrations of LH, FSH, PRL and thyroid-stimulating hormone (TSH) were estimated by RIA.

MATERIALS AND METHODS

Male rats of the Wistar-Imamichi strain, 8 to 10 weeks of age (220–290 g), were used. The animals

Accepted December 15, 1986
Received November 20, 1986

were housed in an air-conditioned room at about 24°C under a 12 hr photoperiod (07:00–19:00) and had free access to water and food obtained from a commercial source. CCK-4 and SP (both from Peptide Institute, Inc.) were used for the implantation. CCK-4 was chosen among G-CCK for implantation, since it is known that CCK-4 interacts with CCK receptors in the rat brain [17]. For their implantation into the brain, CCK-4 and cholesterol were mixed well in a small glass-mortar with a pestle at a ratio of 1:1 or 5:3 by weight. SP and cholesterol were mixed in the same way at a ratio of 1:1. About 7–10 mg of each mixture or cholesterol alone was packed into a steel cannula of 0.35 mm in inner diameter. Each rat was anesthetized with Nembutal and fixed to a stereotaxic instrument. A cannula was then implanted stereotaxically into the brain, guiding its tip so that it would contact the desired hypothalamic sites, with the aid of X-rays. In the ME, the tip of a cannula containing CCK-4, SP or cholesterol was placed to contact with or just beneath the ependymal layer (Fig. 1). Furthermore, a cannula containing CCK-4 was implanted so that its tip would be in the center of the right AR or HVM (Fig. 1). It has already been demonstrated that substances mixed with cholesterol packed into a cannula, which is then implanted into the brain, diffuse out from the tip of the cannula for a certain period of time [18–20]. Rats implanted with a cannula containing either cholesterol or a piece of nylon thread of 0.3 mm in diameter served as cholesterol or blank controls. They were implanted into the same sites as those of the experimental rats. Animals without any implantation were also killed to serve as intact controls. The details of the implantation technique have been described in an earlier paper [19]. Four or 5 days after the operation, the rats were decapitated and blood samples were collected from the trunk between 10:00 and 11:00. Serum was separated by centrifugation at 2,000 rpm for 20 min and stored at −80°C until hormone assay. At the time of decapitation, a piece of hypothalamic tissue hit by the tip of the cannula was dissected out and fixed in Bouin's fluid. Paraffin sections were cut at 14 μm in thickness and stained with hematoxylin and eosin. The loci of the cannula tips in the hypothalamus were examined microscopically. Data were collected only from rats in which the cannula tip was situated at the desired position. Serum concentrations of LH, FSH, PRL and TSH were determined in triplicate with RIA kits supplied by the National Hormone and Pituitary Program. Reference standards for the assays were NIADDK rat LH-RP-1, rat FSH-RP-2, rat PRL-RP-1 and rat TSH-RP-1. Concentrations of these hormones were expressed in terms of LH-NIH-S1, FSH-RP-2, PRL-RP-1 and TSH-RP-1, respectively. The data were statistically analyzed by the Student's t-test and Cockran-Cox method.

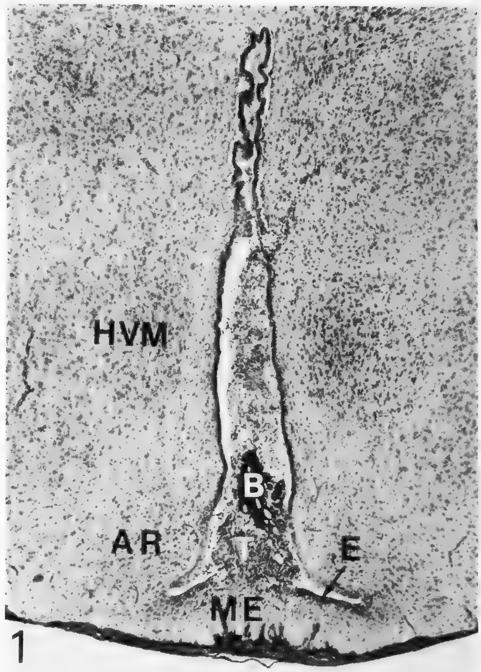

Fig. 1. Frontal section of basal hypothalamic region of a rat implanted with a cannula containing cholesterol into the median eminence (ME). The tissue was fixed in Bouin's fluid after the cannula was removed. The tip of the cannula was placed just beneath the ependymal layer. AR: arcuate nucleus, B: blood, E: ependymal layer, HVM: hypothalamic ventromedial nucleus, T: a tissue mass consisted mostly of ependymal, glial and some phagocytic cells. ×45.

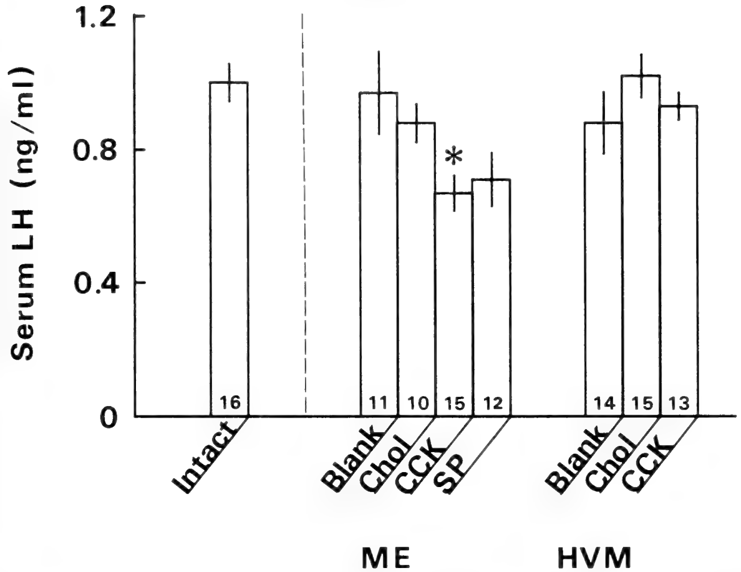

FIG. 2. Serum LH concentrations 4 or 5 days following the implantation of a cannula containing a piece of nylon thread (Blank), cholesterol (Chol), a mixture of CCK-4 and cholesterol at 5:3 by weight (CCK) or a mixture of SP and cholesterol at 1:1 (SP). Each column with vertical line shows mean and SE. Number of rats of each group is shown at the bottom of the column. ME: median eminence, HVM: hypothalamic ventromedial nucleus. * Significant ($p<0.05$) compared with the cholesterol control rats (Student's *t*-test).

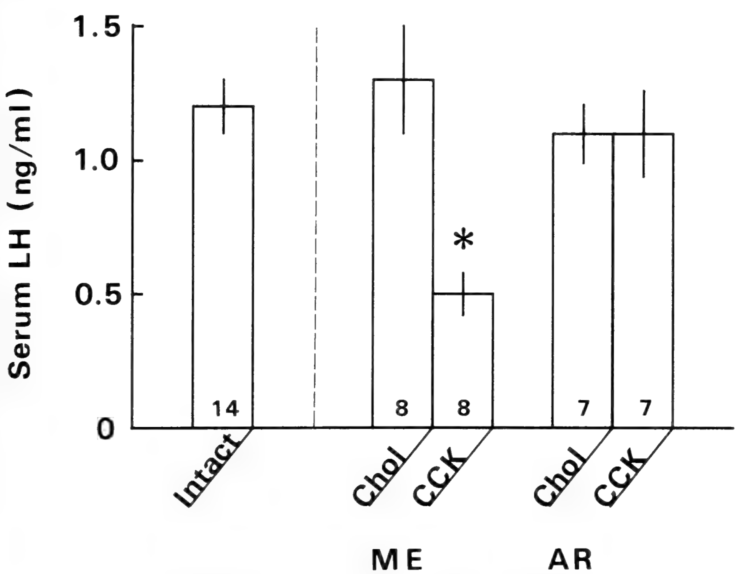

FIG. 3. Serum LH concentrations 4 or 5 days following the implantation. AR: arcuate nucleus. In this experiment, a mixture of CCK-4 and cholesterol at 1:1 (CCK) was used. Other abbreviations are the same as those in Fig. 2. * Significant ($P<0.05$) compared with the cholesterol control rats (Cockran-Cox method).

RESULTS

Effects of operation: Concentrations of serum LH, FSH, PRL and TSH in rats of cholesterol and blank controls were not significantly different from intact controls, irrespective of implantation sites (Figs. 2 to 6). These findings indicate that implantation of a cannula or cholesterol into the

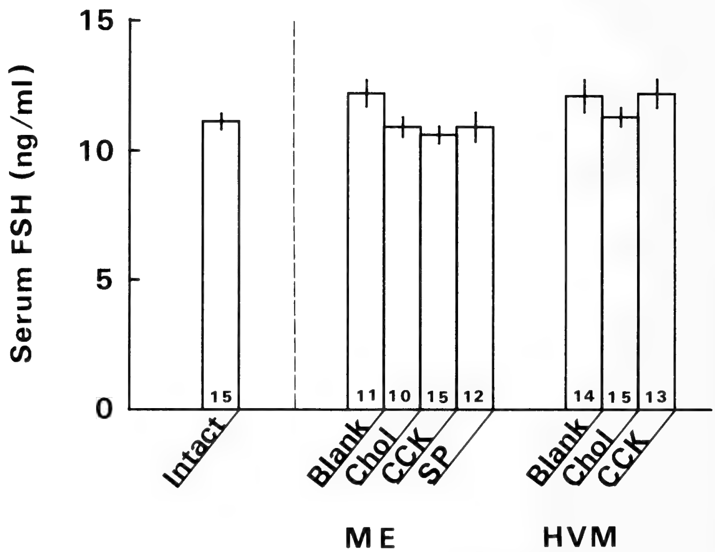

Fig. 4. Serum FSH concentrations 4 or 5 days following the implantation. Abbreviations are listed in Fig. 2. No effects were observed on FSH levels by any implantation.

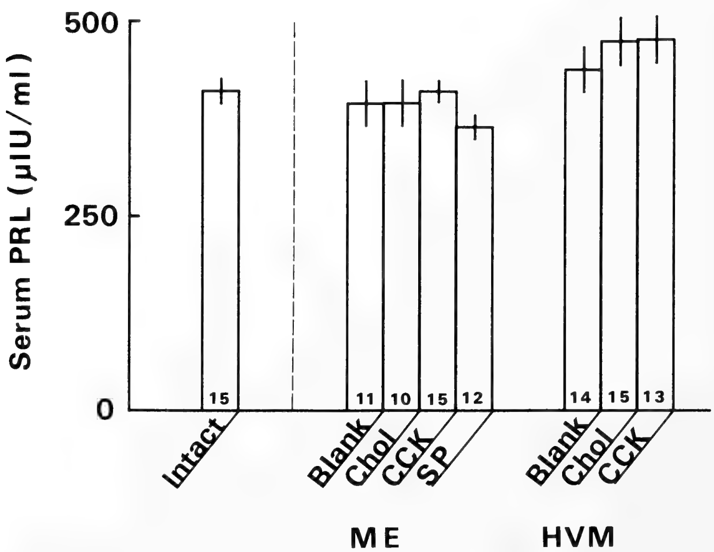

Fig. 5. Serum PRL concentrations 4 or 5 days following the implantation. Abbreviations are the same as those in Fig. 2. No effects were observed on PRL levels by any implantation.

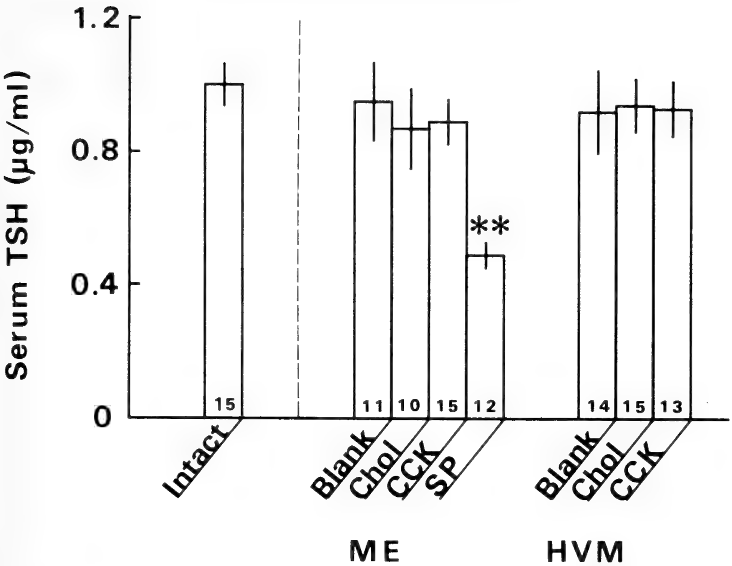

FIG. 6. Serum TSH concentrations 4 or 5 days following the implantation. Abbreviations are the same as those in Fig. 2. ** Significant ($P<0.01$) compared with the cholesterol control rats (Student's *t*-test).

brain has no effect on the release of LH, FSH, PRL and TSH. Therefore, data obtained from experimental rats were compared only with cholesterol controls.

Serum LH concentration: Two series of experiments were carried out: (1) implantation of CCK-4 plus cholesterol (5:3) in the ME and HVM (Fig. 2) and (2) implantation of CCK-4 plus cholesterol (1:1) in the ME and AR (Fig. 1). The serum LH concentration of rats implanted with CCK-4 into the ME was lower than that of cholesterol controls ($P<0.05$) (Figs. 2 and 3). Implantation of CCK-4 into the HVM (Fig. 2) or AR (Fig. 3) has no effect on serum LH concentration. In rats implanted with SP in the ME, the serum LH concentration was not significantly different from that of cholesterol controls (Fig. 2).

Serum FSH and PRL concentrations: Implantations of CCK-4 plus cholesterol (5:3) in both the ME and HVM and SP in the ME caused no change in the serum concentrations of FSH and PRL, compared with cholesterol controls (Figs. 4 and 5).

Serum TSH concentration: The implantation of a cannula containing CCK-4 plus cholesterol (5:3) had no effect on the concentration of serum TSH, whereas SP implantation into the ME reduced remarkably the serum TSH level ($P<0.01$), compared with cholesterol controls (Fig. 6).

DISCUSSION

In the present study, serum LH concentration decreased when CCK-4 was implanted into the ME. Vijayan *et al.* [12] reported that LH secretion was inhibited by CCK-8 injected intraventricularly in ovariectomized rats. This reduction of LH secretion may possibly be explained by the assumption that CCK-8 acted on the ME. This explanation is also supported by the observation that CCK-immunoreactive fibers are present in the ME [5].

Two possible mechanisms may be considered for the inhibitory effects of CCK-4 implanted in the ME on serum LH. (1) CCK-4 affects nerve terminals containing LH-releasing hormone (LHRH) in the ME causing reduced LHRH secretion, and (2) CCK-4 drains into the capillaries of the primary plexus, reaching the adenohypophysis to inhibit LH release. However, the second possibility seems unlikely, since CCK-8 had no effect on the release of LH from the hemipituita-

ries of rats *in vitro* [12]. Rather, it is probable that CCK acted on LHRH axons at least in the ME in such a way as to inhibit the release of LHRH, resulting in reduced LH concentration in the serum.

Since gastrin and CCK-8 share biologically active COOH-terminal tetrapeptide (CCK-4), they may have similar actions to that of CCK-4 within the ME. CCK-8, CCK-4 and gastrin have been demonstrated by RIA to be present in the porcine hypothalamus [1]. Further, intraventricularly administered CCK-8 and gastrin were actually found to reduce LH secretion [12, 13]. It thus remains to be determined which peptides physiologically functions to reduce LHRH release, CCK-8, CCK-4 or gastrin.

In our experiments, CCK-4 implanted in the HVM and AR at the right side of the hypothalamus had no effect on serum LH concentration, although the presence of many G-CCK immunoreactive fibers in the HVM [5] and relatively high concentration of G-CCK in the AR [2] have been reported. It is probable that the HVM and AR at the left side may have compensated for possible inhibition of LHRH release by CCK-4 or G-CCK in these regions may not be involved in the release of LHRH.

Serum concentrations of FSH, PRL and TSH were not affected by CCK-4 implantation in the HVM or ME of male rats. However, according to Vijayan *et al.* the intraventricular injection of gastrin reduced serum concentrations of PRL and TSH [13] and the intraventricular injection of CCK-8 reduced TSH secretion, but not FSH and PRL secretion [12] in ovariectomized rats. The differences between their results and ours may possibly be ascribed to differences in sites of action, duration of action, concentrations of substances administered and animal sex.

Implantation of SP into the ME caused a remarkable decrease in serum TSH in the present study. Vijayan and McCann [22], however, failed to observe such an inhibitory effect of intraventricular SP on TSH release in rats. This discrepancy may be explained by differences in experimental design, especially the mode of SP administration. The present data indicate SP implanted into the ME may possibly interfere with release of TSH-releasing hormone (TRH) through interactions that may occur between SP and TRH axons within the ME. SP immunoreactive fibers have been shown to be present in the internal and external layers of the rat ME [23, 24].

Electron microscopic examination has demonstrated SP terminals projecting into the perivascular space of the capillaries of the primary plexus of the rat ME [24]. Thus, SP may be released into the portal vessels and reach the adenohypophysis to bring about a reduction in TSH release, as suggested by Tsuruo *et al.* [24]. In the *in vitro* experiments, however, SP did not alter the release of TSH from the hemipituitaries of ovariectomized rats *in vitro* [22]. On the basis of the present data, it appears most likely that SP acts on TRH fibers in the ME to reduce TRH release.

SP implanted into the ME had no effect on the serum concentrations of LH, FSH and PRL in the present study. The absence of any effect of intraventricularly injected SP (100 μg) on the release of LH and FSH has been observed in normal female rhesus monkeys [16]. However, SP (2 μg) injected into the third ventricle stimulated LH and PRL secretion in ovariectomized rats [15]. Differences in reported data may be due to particular sites of action, dose amounts of SP and animal hormonal status. To achieve greater consistency in the results obtained, further experimentation on such aspects as implantations of mixtures of SP and cholesterol at different ratios should be carried out.

ACKNOWLEDGMENTS

Prof. K. Wakabayashi (Institute of Endocrinology, Gunma University) is gratefully acknowledged for his valuable advice in conducting the hormone measurements and permitting use of his laboratory facilities. We thank Dr. Y. Okawara for help in the preparation of the manuscript. The present research was supported by a Grant-in-Aid for Scientific Research from the Japan Ministry of Education, Science and Culture.

REFERENCES

1 Rehfeld, J. F (1978) Localization of gastrins to neuro- and adenohypophysis. Nature, **271**: 771–773.

2 Beinfeld, M. C., Meyer, D. K., Eskay, R. L, Jensen, R. T. and Brownstein, M. J. (1981) The dis-

tribution of cholecystokinin immunoreactivity in the central nervous system of the rat as determined by radioimmunoassay. Brain Res., **212**: 51–57.

3 Brownstein, M. J., Mroz, E. A., Kizer, J. S., Palkovits, M. and Leeman, S. E. (1976) Regional distribution of substance P in the brain of the rat. Brain Res., **116**: 299–305.

4 Reubi, J. C. and Jessell, T. M. (1978) Distribution of substance P in the pigeon brain. J. Neurochem., **31**: 359–362.

5 Lorén, I., Alumets, J., Håkanson, R. and Sundler, F. (1979) Distribution of gastrin and CCK-like peptides in rat brain. An immunocytochemical study. Histochemistry, **59**: 249–257.

6 Hökfelt, T., Pernow, B., Nilsson, G., Wetterberg, L., Goldstein, M. and Jeffcoate, S. L. (1978) Dense plexus of substance P immunoreactive nerve terminals in eminentia medialis of the primate hypothalamus. Proc. Natl. Acad. Sci. USA, **75**: 1013–1015.

7 Stoeckel, M. E., Porte, A., Klein, M. J. and Cuello, A. C. (1982) Immunocytochemical localization of substance P in the neurohypophysis and hypothalamus of the mouse compared with the distribution of other neuropeptides. Cell Tissue Res., **223**: 533–544.

8 Rehfeld, J. F., Goltermann, N., Larsson, L.-I., Emson, P. M. and Lee, C. M. (1979) Gastrin and cholecystokinin in central and peripheral neurons. Fed. Proc., **38**: 2325–2329.

9 Gaudino, G. and Fasolo, A. (1980) Substance P-related peptides in the hypothalamus of Amphibia. Cell Tissue Res., **211**: 241–250.

10 Ho, R. H. and DePalatis, L. R. (1980) Substance P immunoreactivity in the median eminence of the North American opossum and domestic fowl. Brain Res., **189**: 565–569.

11 Mikami, S. and Yamada, S. (1984) Immunohistochemistry of the hypothalamic neuropeptides and anterior pituitary cells in the Japanese quail. J. Exp. Zool., **232**: 405–417.

12 Vijayan, E., Samson, W. K. and McCann, S. M. (1979) *In vivo* and *in vitro* effects of cholecystokinin on gonadotropin, prolactin, growth hormone and thyrotropin release in the rat. Brain Res., **172**: 295–302.

13 Vijayan, E., Samson, W. K. and McCann, S. M. (1978) Effects of intraventricular injection of gastrin on release of LH, prolactin, TSH and GH in conscious ovariectomized rats. Life Sci., **23**: 2225–2232.

14 Kimura, F., Hashimoto, R., Kawakami, M. (1983) The stimulatory effect of cholecystokinin implanted in the medial preoptic area on luteinizing hormone secretion in the ovariectomized estrogen-primed rat. Endocrinol. Jpn., **30**: 305–309.

15 Vijayan, E. and McCann, S. M. (1979) *In vivo* and *in vitro* effects of substance P and neurotensin on gonadotropin and prolactin release. Endocrinology, **105**: 64–68.

16 Eckstein, N., Wehrenberg, W. B., Louis, K., Carmel, P. W., Zimmermann, E. A., Frantz, A. G. and Ferin, M. (1980) Effects of substance P on anterior pituitary secretion in the female rhesus monkey. Neuroendocrinology, **31**: 338–342.

17 Saito, A., Sankaran, H., Goldfine, I. D. and Williams, J. A. (1980) Cholecystokinin receptors in the brain: characterization and distribution. Science, **208**: 1155–1156.

18 Matsui, T. (1967) Effects on the rat estrous cycle of implants of norepinephrine placed in the median eminence. Annot. Zool. Japon., **40**: 74–81.

19 Uemura, H. and Kobayashi, H. (1971) Effects of dopamine implanted in the median eminence on the estrous cycle of the rat. Endocrinol. Jpn., **18**: 91–100.

20 Uemura, H. and Kobayashi, H. (1974) Effects of norepinephrine and dibenamine implanted in the median eminence on the estrous cycle of the rat. Horm. Res., **5**: 89–111.

21 Larsson, L.-I. and Rehfeld, J. F. (1979) Localization and molecular heterogeneity of cholecystokinin in the central and peripheral nervous system. Brain Res., **165**: 201–218.

22 Vijayan, E. and McCann, S. M. (1980) Effects of substance P and neurotensin on growth hormone and thyrotropin release *in vivo* and *in vitro*. Life Sci., **26**: 321–327.

23 Ljungdahl, Å., Hökfelt, T. and Nilsson, G. (1978) Distribution of substance P-like immunoreactivity in the central nervous system of the rat—I. Cell bodies and nerve terminals. Neuroscience, **3**: 861–943.

24 Tsuruo, Y., Kawano, H., Nishiyama, T., Hisano, S. and Daikoku, S. (1983) Substance P-like immunoreactive neurons in the tuberoinfundibular area of rat hypothalamus. Light and electron microscopy. Brain Res., **289**: 1–9.

ZOOLOGICAL SCIENCE 4: 339–347 (1987)

Biochemical Study on the Taxonomic Situation of the Sea-urchin, *Pseudocentrotus depressus*

NORIMASA MATSUOKA

Department of Biology, Faculty of Science, Hirosaki University, Hirosaki 036, Japan

ABSTRACT—There are two conflicting views on the taxonomic situation of an endemic Japanese species of sea-urchin, *Pseudocentrotus depressus,* from the morphological standpoint. One is the generally accepted view that the species is a member of the family Toxopneustidae, and another that it is included in the family Strongylocentrotidae. My previous immunological study by enzyme inhibition test strongly suggested the close affinity between *P. depressus* and the Strongylocentrotidae. For further clarifying quantitatively the phylogenetic position of *P. depressus,* I examined the phylogenetic relationships among seven species of the two families, Toxopneustidae and Strongylocentrotidae, of the order Echinoida by electrophoretic analyses of 15 different enzymes. The biochemical dendrogram for the seven species constructed from the Nei's genetic distances between species showed the following: (1) *P. depressus* is more closely related to the family Strongylocentrotidae than to the family Toxopneustidae. (2) Among the three species of the Toxopneustidae, *Toxopneustes pileolus* is more closely related to *Pseudoboletia maculata* than to *Tripneustes gratilla.* (3) The three species of the Strongylocentrotidae (*Strongylocentrotus intermedius, Strongylocentrotus nudus* and *Hemicentrotus pulcherrimus)* endemic to Japan are very closely related to one another, and the two species of the genus *Strongylocentrotus* showed the highest affinity among the seven species examined here. These results are strongly supported by several molecular and non-molecular evidences. It is concluded from the present electrophoretic study that *P. depressus* is a member of the family Strongylocentrotidae. This study also suggested that the three Strongylocentrotids may have been descended from the common ancestor with *P. depressus* in the Pliocene.

INTRODUCTION

The echinoid taxonomy has been extensively studied by many workers mainly from the morphological and/or paleontological standpoint [1–8]. However, various taxonomic systems have been proposed and there is much disagreement as to the echinoid phylogeny, owing to the different interpretations about the morphological characters used when speculating the phylogenetic relationships among echinoids.

On the other hand, during the last 10 to 15 years, studies in phylogenetics and evolutionary biology have been revitalized by the application of techniques from molecular biology. Protein sequencing, immunology, electrophoresis, DNA hybridization and sequence analysis of mitochondrial DNA are among the molecular techniques used in phylogenetic studies. Such biochemical approaches make possible for us to estimate the phylogenetic relationships among taxa quantitatively with the common parameters such as enzymes and DNA. It is important to introduce such biochemical approaches into the field of echinoid taxonomy with much controversy, and to compare the results with the proposals from the morphological considerations.

The sea-urchin, *Pseudocentrotus depressus,* is one of the endemic Japanese species and forms a single genus of its own. The species characterized by the reddish and flat body is commonly found in shallow water other than Hokkaido and the Pacific coasts of Tohoku, and it has often been used in developmental and cellular biology. Although the genus *Pseudocentrotus* was established by Mortensen [9] on a single Japanese species, *Toxocidaris depressus* A. Agassiz, 1863, its taxonomic situation

Accepted October 13, 1986
Received September 6, 1986

has been much disputed. Mortensen [10] included *P. depressus* in the family Toxopneustidae based on the morphological similarities of the globiferous pedicellaria and the body skeleton of the larva. His taxonomic system has been widely accepted by many workers [e.g., 5–7]. However, they recognize that the species is the most specialized of all the members in the Toxopneustidae, because it is considerably different from the other Toxopneustids in many morphological characters as described previously [11].

On the other hand, Clark [1, 12] did not accept this genus, and referred the species to the genus *Strongylocentrotus* of the family Strongylocentrotidae because of its polyporous ambulacra. Thus, the taxonomic situation proposed by Mortensen and by Clark to *Pseudocentrotus depressus* are quite different: the Toxopneustidae and the Strongylocentrotidae, respectively.

In the previous study, I examined immunologically the phylogenetic relationships among 19 species of sea-urchins belonging to the four families of the order Echinoida by using the enzyme inhibition method with anti-*Strongylocentrotus intermedius* G6PD (glucose-6-phosphate dehydrogenase) antibody [13, 14]. The immunological results strongly suggested the close affinity between *Pseudocentrotus depressus,* which is generally included in the family Toxopneustidae, and the members of the family Strongylocentrotidae. Recently, in parallel with the immunological study, I have also examined the phylogenetic relationships among the four members of the family Toxopneustidae by the electrophoretic analyses of various enzymes [11]. The biochemical dendrogram within the Toxopneustidae constructed from the allozyme data showed that *P. depressus* is strongly differentiated from the other Toxopneustids.

In the present study, with the background noted above, I have attempted to establish the biochemical dendrogram for the seven members of the two families, Toxopneustidae and Strongylocentrotidae, of the order Echinoida by the electrophoretic analyses of various enzymes in order to more clarify its taxonomic situation which *P. depressus* is more closely related to the members of the Toxopneustidae or those of the Strongylocentrotidae.

MATERIALS AND METHODS

The sea-urchins examined in this study were the four species of the family Toxopneustidae: *Toxopneustes pileolus, Tripneustes gratilla, Pseudoboletia maculata* and *Pseudocentrotus depressus,* and the three species of the family Strongylocentrotidae: *Strongylocentrotus intermedius, Strongylocentrotus nudus* and *Hemicentrotus pulcherrimus.* The specimens of Toxopneustidae were the same as those used in my previous electrophoretic study [11]: *T. pileolus, T. gratilla* and *P. maculata* collected from the coast near the Sesoko Marine Science Center of Ryukyu University, Okinawa Prefecture, and *P. depressus* from the coast near the Fukaura Marine Biological Laboratory of Hirosaki University, Aomori Prefecture, in July 1983. *S. nudus* and *S. intermedius* were provided through the courtesy of the Asamushi Marine Biological Station of Tohoku University, Aomori Prefecture, in September 1983 and in December 1983, respectively. *S. intermedius* collected from the coast near the Oshoro Marine Biological Station of Hokkaido University in September 1982 were also used in this study. *H. pulcherrimus* were collected from the same locality as *P. depressus* in July 1983. Immediately after collection, the guts and gonads were extracted from these specimens and exhaustively washed in filtered sea water. They were then frozen on dry ice and transported to the laboratory at Hirosaki University, where they were stored at -80°C until used.

Polyacrylamide gel electrophoresis was carried out by the same method as described previously [11]. The following 15 different enzymes were assayed, using supernatants of tissue homogenates: alcohol dehydrogenase (ADH), glucose-6-phosphate dehydrogenase (G6PD), hydroxybutyrate dehydrogenase (HBDH), malate dehydrogenase (MDH), malic enzyme (ME), octanol dehydrogenase (ODH), sorbitol dehydrogenase (SDH), xanthine dehydrogenase (XDH), hexokinase (HK), tetrazolium oxidase (TO), glutamate oxaloacetate transaminase (GOT), acid phosphatase (ACPH), alkaline phosphatase (ALK), esterase (EST) and amylase (AMY). The enzymes

other than HK and GOT are the same as those assayed in the previous electrophoretic study on the Toxopneustidae [11]. G6PD, HK and GOT were assayed with the extract of the gonad, and for the remaining enzymes the extract of the gut was used. The stain mixtures for HK and GOT were prepared according to Shaw and Prasad [15] and Marcus [16], respectively. Stain recipes for other enzymes were those described previously [11]. Data from 12 individuals per species were used to characterize the band pattern of each enzyme.

RESULTS

The electrophoretic patterns of the 15 different enzymes observed in and among the seven species of two families are shown in Figure 1. Those other than HK and GOT in the four species of Toxopneustidae are the same as reported previously [11]. From these band patterns, 20–21 loci were obtained in each species. In the course of this study, HBDH could not be scored in *S. nudus,* although the cause of this enzymatic inactivity was not known. The major features of variation in the 15 enzymes are summarized as follows.

Six enzymes: G6PD, HBDH, SDH, HK, GOT and ACPH exhibited a single band of activity and were monomorphic, all but SDH varying interspecifically.

ADH in *S. nudus* and ODH in *S. intermedius* showed single- and triple-banded phenotypes. This variation was interpreted as a diallelic system at a single locus coding for a dimeric protein, with single-banded patterns corresponding to the homozygous state, and triple-banded patterns to the heterozygous state. The two enzymes in other species were monomorphic.

In ALK, single- and double-banded phenotypes were observed in the three Toxopneustids with the exception of *P. depressus.* This variation was interpreted as a diallelic system at a single locus coding for a monomeric protein.

ME in the three species of Toxopneustidae with the exception of *P. depressus* consistently appeared as two active bands, the faster band of these showing strong activity. *P. depressus* and the three species of Strongylocentrotidae exhibited only a single ME active band. The two and one band pattern were interpreted as the products of different alleles at a single locus. In contrast with ME, XDH in the three species of Toxopneustidae except *P. depressus* consistently appeared as a single active band and in the remaining four species two active bands exhibited. No intraspecific variation of these enzymes was detected in any of the seven species.

MDH in *S. intermedius* and *H. pulcherrimus* showed two active bands, the slower band of these showing strong activity. Other five species exhibited only a single MDH active band. This enzyme requiring NAD as co-enzyme showed higher activity that ME which is NADP-specific MDH. It was also monomorphic in each species.

TO was presented as several bands and grouped into three zones. Within the middle zone there was strong TO activity (TO-2), single- and double-banded phenotypes were obseved in *T. gratilla* and the Oshoro population of *S. intermedius,* which was interpreted as representing homozygosity and heterozygosity at a single locus coding for a monomeric protein. As the enzyme in the Asamushi population of *S. intermedius* gave diffuse gel patterns, the electrophoretic data of TO in the species was obtained from the Oshoro population. The all other enzymes of the species were analysed in the Asamushi population. TO-1 and TO-3 were monomorphic in each species.

EST activity was detected as several bands which were grouped into three zones. The middle zone (EST-2) consisted of a single heavily stained band in *P. depressus, S. nudus* and *H. pulcherrimus,* and two heavily staining bands in the remaining four species. These two distinct band patterns were interpreted as the products of different alleles at a single locus, as well as in ME, MDH and XDH. *H. pulcherrimus* did not exhibit the band of EST-1. The band of EST-3 in *S. nudus* showed slower mobility than those in other species. Although a few faint bands appeared in some species, these bands did not show reproducibility and could not be defined genetically.

AMY activity was also detected as several bands. These were assumed to be the products of three different genetic loci (AMY-1, AMY-2 and AMY-3). Among these, a single band in the middle zone (AMY-2) showed the strong enzyma-

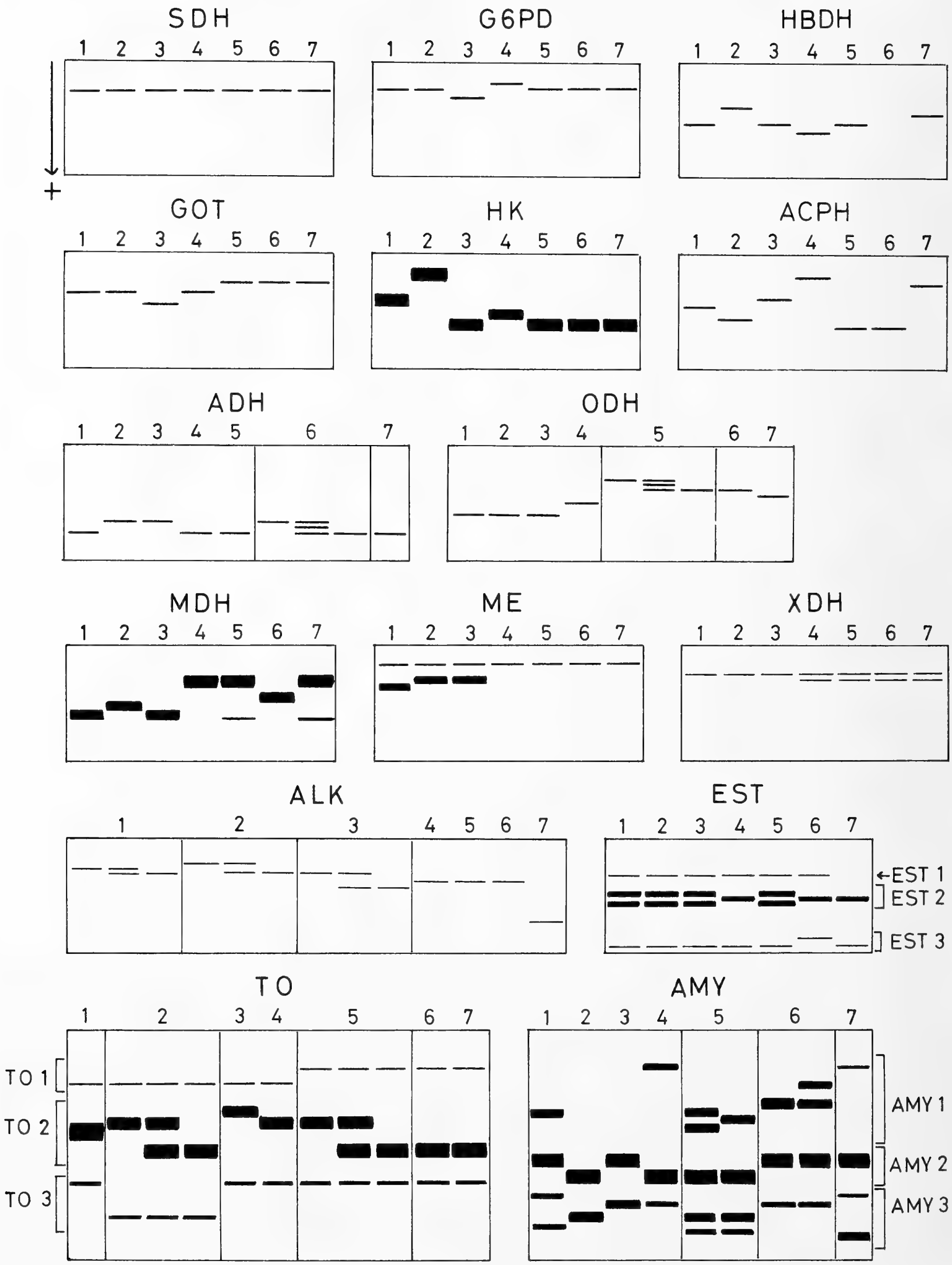

Fig. 1. Electrophoretic patterns of 15 different enzymes in seven species of two families, Toxopneustidae and Strongylocentrotidae. For each enzyme the origin is at the top and the direction of mobility toward the bottom. Presumptive loci are numbered downwards from 1, starting with that nearest the origin (i.e., of lowest electrophoretic mobility). 1=*Toxopneustes pileolus*, 2=*Tripneustes gratilla*, 3=*Pseudoboletia maculata*, 4=*Pseudocentrotus depressus*, 5=*Strongylocentrotus intermedius*, 6=*Strongylocentrotus nudus*, 7=*Hemicentrotus pulcherrimus*. HBDH in *S. nudus* could not be detected.

tic activity. Polymorphism was observed in AMY-1 of *S. intermedius* and *S. nudus*.

The allele frequencies for all loci in these seven species are given in Table 1. Based on these data, the genetic identity (I) and genetic distance (D) between each species were calculated by the method of Nei [17]. Table 2 presents the matrices of I and D values between all pairs of species examined. From this table, it can be seen that the D values among the three Strongylocentrotids are as small as that between *T. pileolus* and *P. maculata* and fall within the range of about 0.4–0.6. On the other hand, the D values between the three Strongylocentrotids and the three Toxopneustids other than *P. depressus* are considerably large (above 1.0). Figure 2 shows the biochemical phylogenetic tree for these seven sea-urchin species constructed from the genetic distance matrix of Table 2 using the unweighted pair-group arithmetic average (UPGMA) clustering method of Sneath and Sokal [18]. The biochemical dendrogram indicates the following: (1) The seven species examined are divided into the two large clusters. One is consisted of the three species of the Toxopneustidae (*T. pileolus, P. maculata* and *T. gratilla*) and another consisted of *P. depressus* of the Toxopneustidae and the three species of the Strongylocentrotidae (*S. intermedius, S. nudus*

TABLE 1. Allele frequencies at various enzyme loci in the four species of Toxopneustidae and the three species of the Strongylocentrotidae

Locus	*Tp*	*Tg*	*Pm*	*Pd*	*Si*	*Sn*	*Hp*
ADH	b	a	a	b	b	a (0.75) b (0.25)	b
G6PD	b	b	c	a	b	b	b
HBDH	c	a	c	d	c	—	b
MDH	d	c	d	a	e	b	e
ME	c	b	b	a	a	a	a
ODH	e	e	e	d	a (0.67) b (0.33)	b	c
SDH	a	a	a	a	a	a	a
XDH	a	a	a	b	b	b	b
HK	b	a	d	c	d	d	d
TO-1	b	b	b	b	a	a	a
TO-2	c	b (0.46) d (0.54)	a	b	b (0.58) d (0.42)	d	d
TO-3	a	b	a	a	a	a	a
GOT	b	b	c	b	a	a	a
ACPH	d	e	c	a	f	f	b
ALK	b (0.10) c (0.90)	a (0.29) c (0.71)	c (0.25) e (0.75)	d	d	d	f
EST-1	a	a	a	a	a	a	—
EST-2	b	b	b	a	b	a	a
EST-3	b	b	b	b	b	a	b
AMY-1	c	—	—	a	d (0.29) e (0.71)	b (0.08) c (0.92)	a
AMY-2	a	b	a	b	b	a	a
AMY-3	a	d	c	c	e	c	b

Alleles are correspondingly lettered from "a". The value in parenthesis represents the frequency of each allele in population. *Tp*=*Toxopneustes pileolus*, *Tg*=*Tripneustes gratilla*, *Pm*=*Pseudoboletia maculata*, *Pd*=*Pseudocentrotus depressus*, *Si*=*Strongylocentrotus intermedius*, *Sn*=*Strongylocentrotus nudus*, *Hp*=*Hemicentrotus pulcherrimus*.

TABLE 2. Genetic identities (above diagonal) and genetic distances (below diagonal) among seven sea-urchin species

Species	1	2	3	4	5	6	7
1. *Toxopneustes pileolus*	—	0.471	0.542	0.335	0.395	0.314	0.287
2. *Tripneustes gratilla*	0.753	—	0.474	0.314	0.327	0.222	0.172
3. *Pseudoboletia maculata*	0.612	0.747	—	0.288	0.348	0.345	0.240
4. *Pseudocentrotus depressus*	1.094	1.158	1.245	—	0.472	0.418	0.381
5. *Strongylocentrotus intermedius*	0.929	1.118	1.056	0.751	—	0.629	0.562
6. *Strongylocentrotus nudus*	1.158	1.505	1.064	0.872	0.464	—	0.570
7. *Hemicentrotus pulcherrimus*	1.248	1.760	1.427	0.965	0.576	0.562	—

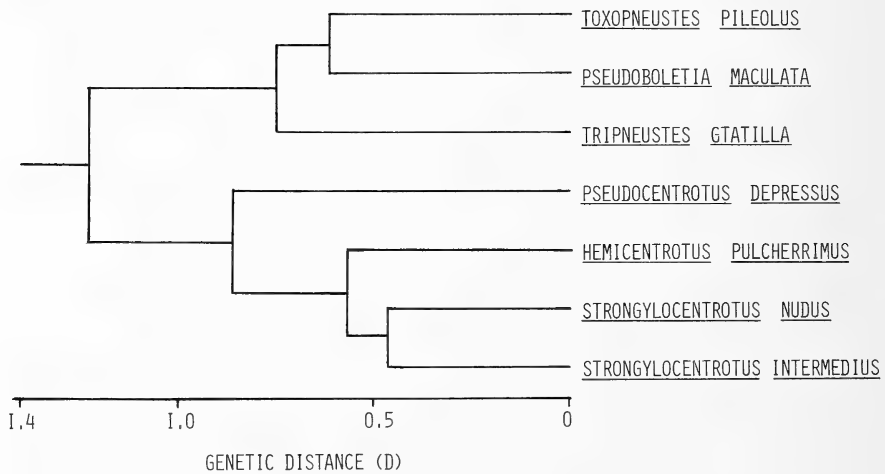

FIG. 2. A biochemical dendrogram showing the phylogenetic relationships among seven sea-urchin species, based on Nei's (1972) genetic distances.

and *H. pulcherrimus*). The mean genetic distance between these two clusters is considerably large (D =1.230) (2) Among the three Toxopneustids, *T. pileolus* is more closely related to *P. maculata* (D =0.612) than to *T. gratilla* (D=0.753). (3) The three Strongylocentrotids are closely related to one another and the mean genetic distance is D= 0.534. Among these, the two members of the genus *Strongylocentrotus* (*S. intermedius* and *S. nudus*) are the most closely related (D=0.464). (4) *P. depressus,* which is included in the family Toxopneustidae, is more closely related to the members of the family Strongylocentrotidae than to those of the family Toxopneustidae.

The proportion of polymorphic loci (P) was in the range of 0–14.3%, with a mean of 6.3%, and the mean heterozygosity per locus (H), in the range of 0–6.4%, with a mean of 2.3%.

DISCUSSION

With the exception of the phylogenetic position of *P. depressus* the biochemical dendrogram shown in Figure 2 is largely compatible with the generally accepted taxonomic system established by morphological studies. The three Toxopneustids other than *P. depressus* and the three Strongylocentrotids are clearly divided into two large clusters, and it shows the phylogenetic value of electrophoretic data at the family level. With respect to the phylogenetic relationships among the three species of Toxopneustidae (*T. pileolus, T. gratilla* and *P. maculata*) which are widely distributed in the Indo-West Pacific region, the

electrophoretic data show that *P. maculata* is more closely related to *T. pileolus* than to *T. gratilla*. The result is strongly supported by morphological and chromosomal studies. Mortensen [10] pointed out the close affinity between the two genera, *Pseudoboletia* and *Toxopneustes*, in the Toxopneustidae from morphological considerations. Further, Shingaki and Uehara [19] reported that *P. maculata* is more similar to *T. pileolus* than to *T. gratilla* in their karyotypes: the diploid chromosome number is 42 in *P. maculata* and *T. pileolus*, but 36 in *T. gratilla*. On the other hand, Clark [1, 12] referred *P. maculata* to the family Strongylocentrotidae because of its polyporous ambulacra. The phylogenetic position of *P. maculata* shown in the biochemical dendrogram is apparently inconsistent with the view of Clark.

With respect to the phylogenetic relationships among the three species of Strongylocentrotidae, the electrophoretic data show that the two species of the genus *Strongylocentrotus* (*S. intermedius* and *S. nudus*) are more closely related to each other ($D=0.464$) than they are to *H. pulcherrimus* ($D=0.576$, 0.562). The relationship is well consistent with that inferred from morphological studies. *H. pulcherrimus* had long been included in the genus *Strongylocentrotus*, but Mortensen [20] established a single new genus, *Hemicentrotus*, on the endemic Japanese species by considering the morphological differences between the species and the other Strongylocentrotids in ambulacral plate and spicule. The geographical distributions of these three species may also reflect their relationships. *S. intermedius* and *S. nudus*, which are endemic Japanese species, are commonly found in the northern sea of Japan. On the other hand, *H. pulcherrimus* is not commonly found in Hokkaido where is the most northern district of Japan, although it is widely distributed in Japanese seas from northern Honshu to southern Kyushu. The electrophoretic data also show that the I values obtained among the three Strongylocentrotids are relatively large (about 0.6) and *H. pulcherrimus* is very closely related to the genus *Strongylocentrotus* (Table 2). The similar result is also obtained by the other comparative biochemical studies. Suzuki *et al.* [21] reported that the amino acid composition of respiratory stimulating egg jelly peptides obtained from *S. intermedius* was quite similar to that of *H. pulcherrimus*. Further, Poltaraus and Antonov [22] showed by the DNA hybridization test that the degree of divergence of the unique DNA sequences of *S. intermedius* against the DNAs from *S. nudus* and *H. pulcherrimus* are approximately equal. These biochemical results do not appear to be conflict with the view of the earlier echinoid taxonomists [e.g., 1, 12] that *H. pulcherrimus* is a member of the genus *Strongylocentrotus*.

The present electrophoretic result on the phylogenetic position of *P. depressus* is not consistent with the generally accepted taxonomic system proposed by Mortensen [10] from morphological studies. The biochemical dendrogram shown in Figure 2 clearly shows that *P. depressus* is more closely related to the membres of the family Strongylocentrotidae than to those of the family Toxopneustidae. There are several molecular and non-molecular evidences that strongly support the electrophoretic result: My previous immunological study strongly suggested the close phylogenetic relationship between *P. depressus* and the Strongylocentrotidae [13, 14]. In addition, Poltaraus and Antonov [22] suggested their close relationships by comparing the unique DNA sequences of *S. intermedius* separated from repetitive sequence with the DNAs from other sea-urchin species with the DNA hybridization technique. As non-molecular evidence, Noguchi [23] reported that *P. depressus* and *S. intermedius* can successfully hybridize in the cross fertilization test. The close affinity between *P. depressus* and the Strongylocentrotidae was also proposed by the earlier echinoid taxonomist, Clark [1, 12], from morphological considerations. From the zoogeographical standpoint, the distributional range of *P. depressus* overlaps much more widely with those of the three Strongylocentrotids than with those of the other three Toxopneustids. Namely, the three Toxopneustids (*T. pileolus*, *T. gratilla* and *P. maculata*) are widely distributed in the Indo-West Pacific region, while *P. depressus* and the three Strongylocentrotids are endemic Japanese species: their distributional ranges are confined to the seas around Japan [7].

Putting these various evidences together, it is

concluded that *Pseudocentrotus depressus* is a member of the family Strongylocentrotidae. In a previous paper [13], I described that *P. depressus* might be a member of the genus *Strongylocentrotus*. However, the present electrophoretic study showed that the mean genetic distance (D=0.812) between *P. depressus* and the genus *Strongylocentrotus* was larger than those (D=0.612, 0.747, 0.753) observed among the three different genera of Toxopneustidae. The value is also comparable to those observed between different genera of many other animals [24]. Considering the present electrophoretic data and the morphological differences between *P. depressus* and the genus *Strongylocentrotus* in larva and globiferous pedicellaria, it seems reasonable to conclude that *P. depressus* should be included in the family Strongylocentrotidae as a distinct genus from the genus *Strongylocentrotus*. During the preparation of this paper, I have known that Shigei [25] has modified his previous taxonomic system [7] and transferred *P. depressus* from the family Toxopneustidae to the family Strongylocentrotidae, although the reason for it is not described in detail. I agree to his modification on the taxonomic situation of the species. However, I do not agree to his view that the Toxopneustidae and the Strongylocentrotidae belong to the different suborders (Temnopleurina and Echinina, respectively), because my previous immunological study [13, 14] strongly suggested the close affinity between these two families.

The biochemical dendrogram (Figure 2) shows not only their phylogenetic relationships, but also the sequence of their evolutionary divergences. According to Nei [26], genetic distance (D) corresponds well with the divergence time (T) from the common ancestor, and T of two taxa can be estimated by $T=5\times10^6D$ (year). Applying this equation to the biochemical dendrogram constructed from the D values, each divergence time may be calculated as follows: Toxopneustidae and Strongylocentrotidae, 6.2 million years ago (MY); *P. depressus* and the three Strongylocentrotids, 4.3 MY; the three Toxopneustids, 3–4 MY and the three Strongylocentrotids, 2–3 MY. Nisiyama [5] estimated from the fossil evidence that the origins of the genus *Pseudocentrotus* and *Strongylocentrotus* might date back to the Miocene and to the Pliocene, respectively. The molecular estimation of divergence time is roughly consistent with the palaeontological data. As already mentioned, *P. depressus* has both morphological characters of the Toxopneustidae and of the Strongylocentrotidae. Namely, the globiferous pedicellaria and the body skeleton of larva are characteristic in Toxopneustidae, and the polyporous ambulacral plate and the shallow gill-slit are characteristic in Strongylocentrotidae. Considering these biochemical, morphological, palaeontological and zoogeographical evidences, the following evolutionary process might be inferred: The ancestral form of *P. depressus* diverged from the primitive Toxopneustids in the Miocene. Thereafter, during the Pliocene, the three Strongylocentrotids have been descended from the ancestral form of *P. depressus* which developed independently some morphological characters of the Strongylocentrotidae with those of the Toxopneustidae conserved, and have diversified in the seas around Japan.

ACKNOWLEDGMENTS

I am grateful to the Asamushi Marine Biological Station, Tohoku University, the Sesoko Marine Science Center, Ryukyu University, the Oshoro Marine Biological Station, Hokkaido University, Dr. S. Kubota, Department of Zoology, Hokkaido University, and Mr. M. Matsuoka, Department of Sociology, Nihon University, for their kind help in collecting the sea-urchin specimens. This study was supported in part by a Grant-in-Aid (Grant No. 60740424) from the Ministry of Education, Science and Culture of Japan.

REFERENCES

1 Clark, H. L. (1925) A Catalogue of the Recent Sea-Urchins (Echinoidea) in the Collection of the British Museum (Natural History). London.

2 Mortensen, T. (1928–1951) A Monograph of the Echinoidea, C. A. Reitzel, Copenhagen, Vol. 1–15.

3 Durham, J. W. and Melville, R. V. (1957) A classification of echinoids. J. Paleontol., **31**: 242–272.

4 Philip, G. M. (1965) Classification of echinoids. J. Paleontol., **39**: 45–62.

5 Nisiyama, S. (1966) The echinoid fauna from Japan and adjacent regions, Part I. Palaeontol. Soc. Japan Spec. Pap., No. 11.

6 Nisiyama, S. (1968) The echinoid fauna from Japan

and adjacent regions, Part II. Palaeontol. Soc. Japan Spec. Pap., No. 13.

7 Shigei, M. (1974) Echinoids. In "Systematic Zoology". Ed. by T. Uchida, Nakayama Book Company, Tokyo, Vol. 8b, pp. 208–332. (In Japanese).

8 Smith, A. (1984) Echinoid Palaeobiology. George Allen & Unwin, London.

9 Mortensen, T. (1903) The Danish Ingolf-expedition, Echinoidea (Part I), **4**: 1–198.

10 Mortensen, T. (1943) A Monograph of the Echinoidea, C. A. Reitzel, Copenhagen, Vol. 3, Part 2, pp. 382–545.

11 Matsuoka, N. (1985) Biochemical phylogeny of the sea-urchins of the family Toxopneustidae. Comp. Biochem. Physiol., **80B**: 767–771.

12 Clark, H. L. (1912) Hawaiian and other Pacific Echini. Mem. Mus. Comp. Zool. Harv., **34**: 205–383.

13 Matsuoka, N. (1980) Immunological relatedness of sea-urchin glucose 6-phosphate dehydrogenases: Phylogenetic implication. Comp. Biochem. Physiol., **66B**: 605–607.

14 Matsuoka, N. (1986) Further immunological study on the phylogenetic relationships among sea-urchins of the order Echinoida. Comp. Biochem. Physiol., **84B**: 465–468.

15 Shaw, C. R. and Prasad, R. (1970) Starch gel electrophoresis of enzymes: A compilation of recipes. Biochem. Genet., **4**: 297–320.

16 Marcus, N. H. (1977) Genetic variation within and between geographically separated populations of the sea urchin, *Arbacia punctulata*. Biol. Bull., **153**: 560–576.

17 Nei, M. (1972) Genetic distance between populations. Am. Nat., **106**: 283–292.

18 Sneath, P. H. A. and Sokal, P. R. (1973) Numerical Taxonomy. Freeman, San Francisco.

19 Shingaki, M. and Uehara, T. (1984) Chromosome studies in the several species of sea urchin from Okinawa. Zool. Sci., **1**: 1008. (In Japanese).

20 Mortensen, T. (1942) New Echinoidea (Camarodonta): Preliminary notice. Vidensk. Meddel. fraden Nathist. Foren., Köbenhavn, **106**: 225–232.

21 Suzuki, N., Hoshi, M., Nomura, K. and Isaka, S. (1982) Respiratory stimulation of sea urchin spermatozoa by egg extracts, egg jelly extracts and egg jelly peptides from various species of sea urchins: Taxonomical significance. Comp. Biochem. Physiol., **72A**: 489–495.

22 Poltaraus, A. B. and Antonov, A. S. (1984) Interspecies divergence of unique DNA sequences of the sea urchin *Strongylocentrotus intermedius* (AGASS.) and their homologues in the genomes of some echinoderms and ascidia. Biochemistry (USSR), **49**: 1529–1537. (In Russian with English summary).

23 Noguchi, M. (1982) The phenotype of hybrids of *Pseudocentrotus depressus* and *Strongylocentrotus intremedius*. Zool. Mag., **91**: 409. (In Japanese).

24 Ayala, F. J. (1975) Genetic differentiation during speciation. In "Evolutionary Biology". Ed. by T. Dobzhansky, M. K. Hecht and W. C. Steere, Plenum Press, New York, pp. 1–78.

25 Shigei, M. (1986) The Sea Urchins of Sagami Bay. Maruzen, Tokyo. (In Japanese and English).

26 Nei, M. (1975) Molecular Population Genetics and Evolution. North-Holland, Amsterdam.

ZOOLOGICAL SCIENCE 4: 349–365 (1987)

The Larval Stages of *Pagurus brachiomastus* (Thallwitz, 1892) (Crustacea: Anomura) Reared in the Laboratory

Kooichi Konishi and Rodolfo Quintana

Zoological Institute, Faculty of Science, Hokkaido University, Sapporo 060, Japan

ABSTRACT—The larval stages of the hermit crab *Pagurus brachiomastus* (Thallwitz) are described and illustrated. Under the laboratory conditions of 15°C temperature and 35 ppt salinity, the present species passes through one prezoeal, four zoeal and one megalopal stages. The first megalopa was obtained 23 days after the hatching; a late megalopa was observed in the cultures after 35 days. Morphological characterisics of larvae of the present species are compared with those of pagurid crabs hitherto known from Hokkaido, especially with previous Kurata's descriptions of planktonic larvae.

INTRODUCTION

The anomuran fauna of Hokkaido is different from that of other areas of Japan in having a relatively small number of species, and a relatively high percentage (ca. 66%) of paguroids (=Paguridae+Lithodidae) species [1]. Kurata [2] reported some larval stages of the family Paguridae, based mainly on planktonic material, but specific identification of these larvae remains unknown. Planktonic paguroid larvae have also been reported by Makarov [3] from western Kamchatkan shelf. The first complete larval description from laboratory-reared material was given by Kurata [4] for *Pagurus geminus* McLaughlin (as *P. samuelis* (Stimpson). Recently larval studies on pagurid species have been made by Hong [5–7] based on larval material from Korean waters, and by Ivanov [8] on those from northern Pacific; some of these species are common to the Japanese fauna.

However the larval information on pagurid crabs of Japan is not yet satisfactory for identification of planktonic amomuran larvae; e.g. of the 51 described species of the family Paguridae, published description of all larval stages have been given for only 12% of this family.

The complete larval development of *Pagurus brachiomastus* (Thallwitz), one of the most common hermit crabs from northern Japan is reported in the present study; a discussion on the morphological characteristics of the zoeas of the family Paguridae of Japan, especially on Kurata's [2] larval description, is also given.

MATERIALS AND METHODS

One ovigerous female of *P. brachiomastus,* inhabiting in a shell of *Buccinum* sp., was collected from Akkeshi, eastern Hokkaido, on 31 May 1984, and maintained in aerated sea water until hatching occurred on 19 June 1984. Larvae were reared in 200 ml glass beakers, 20 zoeas per beaker at 15°C temperature and 35 ppt salinity. Newly-hatched *Artemia* nauplii were given as food, and cultures were checked daily.

Larvae and exuviae of each stage were fixed with 5% formalin, rinsed briefly in distilled water, and then preserved in 70% ethanol; these specimens were transferred to 50% glycerin solution before dissection; in some cases, specimens were treated with 2% KOH in order to make them translucent; exuviae were stained with methylene blue.

Drawings and measurements were made with the aid of a camera lucida and ocular micrometer. The carapace length (=CL) was measured from the tip of rostrum to the mid-posterior margin of carapace. The numbering of the telsonal posterior processes follows to Pike and Williamson [9], and

Accepted October 24, 1986
Received September 30, 1986

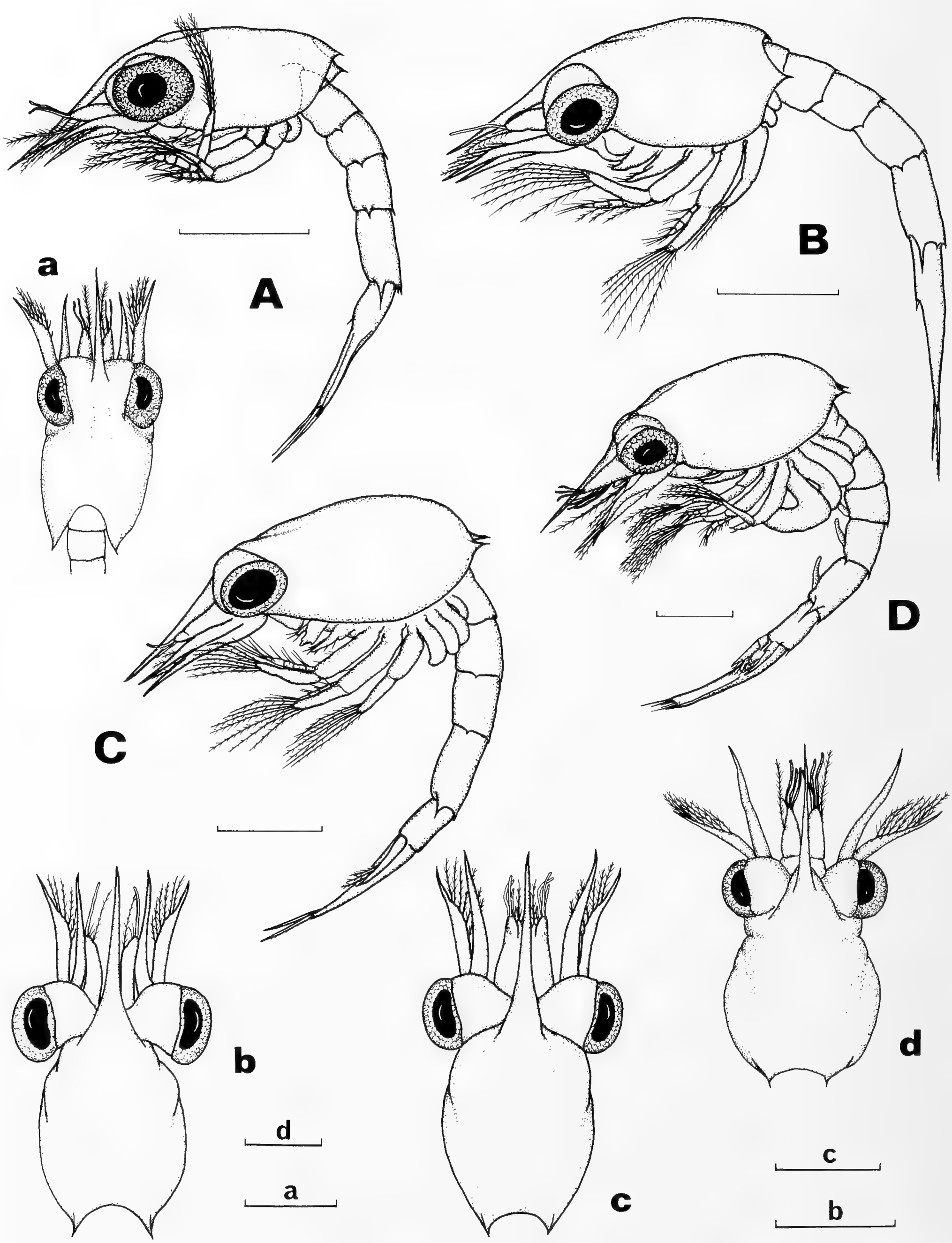

FIG. 1. *Pagurus brachiomastus* (Thallwitz). Complete specimens of zoeal stages I–IV (A–D), lateral view; a–d, carapace, dorsal view. Scale bars=0.5 mm.

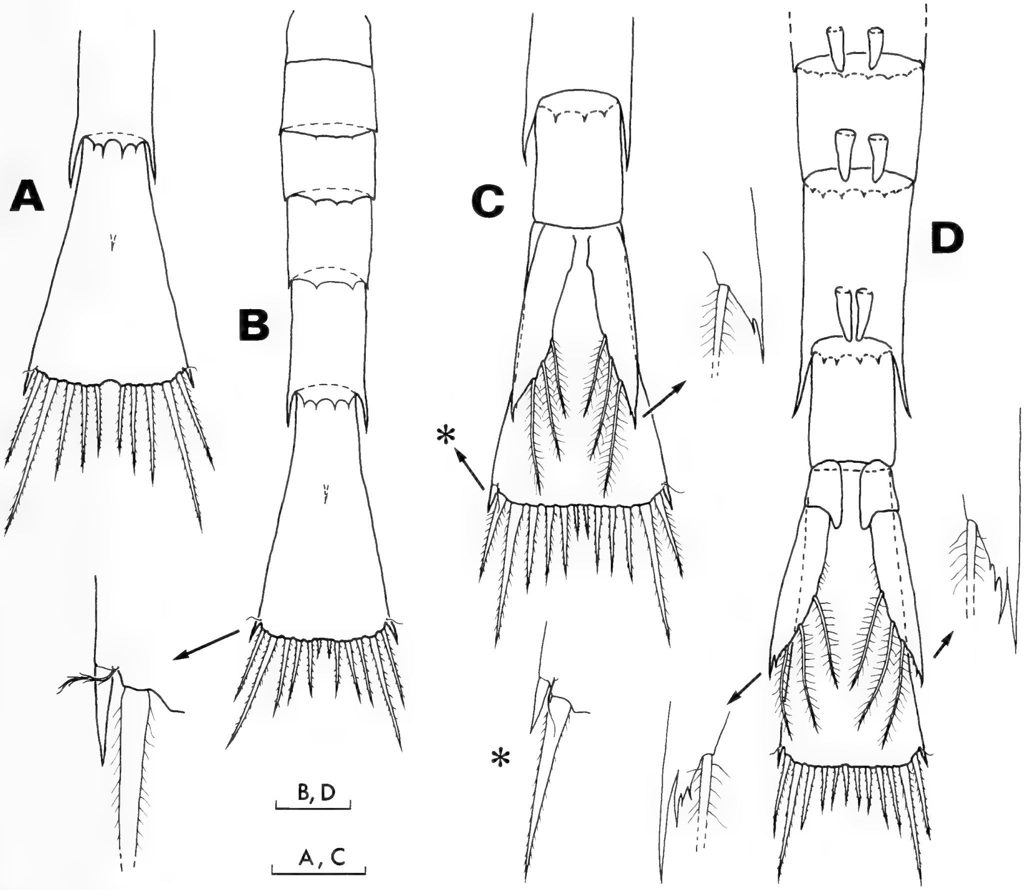

FIG. 2. *Pagurus brachiomastus* (Thallwitz). Abdomens and telsons of zoeal stages I–IV (A–D). Scale bars=0.2 mm.

the setation of each appendage is presented from proximal to distal.

RESULTS

P. brachiomastus hatches as a prezoeal stage, few minutes before moulting to the first zoeal stage. A recent paper on this short-duration stage of this and allied species was given by Quintana and Konishi [10].

Only 4 megalopas were obtained in the present study; these were used for further dissections and observations, therefore no crab stages are included in the following descriptions.

Descriptions of the Larvae

First zoea

Duration: 7–9 days.

Dimension: CL=0.74–0.80 mm (mean 0.77 mm; 10 specimens).

Carapace (Fig. 1A and a): With a well developed rostrum and short spines on posterolateral margins; pointed rostrum, slightly longer than antennae. Eyes sessile.

Abdomen (Fig. 2A): Consists of 5 somites and a telson; second through fifth somite with dorsal and lateral spines, and pleopod buds absent. Telson elongate, with 7 posterior processes on each furca; outermost a stout and smooth process; second

process very fine; third through seventh elongate, serrated; fourth process longest; an anal spine present.

Antennule (Fig. 3A): Uniramous, unsegmented process; 2 long aesthetascs and 2 simple setae; a long subterminal plumose seta also present.

Antenna (Fig. 4A): Biramous; exopod (=scale) with one short and 5 long plumose setae; endopod unarmed, fused with protopod; protopod with a stout, serrated spine on distal end.

Mandible (Fig. 5A): Asymmetrical with irregular teeth ; no palp.

Maxillule (Fig. 6A): Coxal endite with 5 plumose and 2 setae; basal endite with 2 stout spines and 2 setae, each of the stout spines bearing cuneate spinules. The three-segmented endopod with one short simple seta proximally (rarely 2), one long simple seta on the second, and 3 terminal setae on the distal segment.

Maxilla (Fig. 7A): Coxal endite bilobed, proximal lobe with 5 and distal lobe with 4 plumose setae; basal endite also bilobed, proximal lobe with 5 and distal lobe with 4–5 setae; endopod bears 7 setae arranged in two groups as 3+4; scaphognathite with 5 soft plumose setae along anterior margin.

Maxilliped 1 (Fig. 8A): Coxa unarmed. Basis setae arranged laterally as 1+2+3+3; endopod 5-segmented with a setation of 2–3, 2, 1, 2, 4+I (I =dorsal plumose seta); first through third segment has 5–7 fine setules on outer side ; exopod with 4 long natatory setae distally.

Maxilliped 2 (Fig. 9A): Coxa without setae. Basis with 1+2 setae laterally; endopod 4-segmented, setal arrangement of 2, 2, 2, 4+I; second and third segment with numerous fine setules; exopod as in the maxilliped 1.

Maxilliped 3 (Fig. 10): Uniramous, unarmed bud.

Second zoea

Duration: 4–7 days.

Dimension: CL=0.85–0.90 mm (mean 0.88 mm; 9 specimens).

Carapace (Fig. 1B and b): Eyes stalked.

Abdomen (Fig. 2B): Telson with an additional, short posterior process medially. The fine second process with setules, as observed under high magnification (as shown in figure).

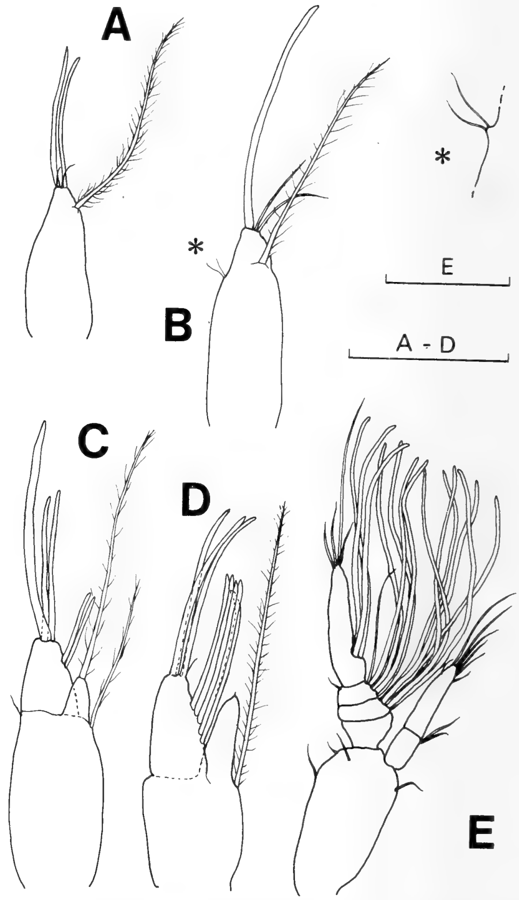

Fig. 3. *Pagurus brachiomastus* (Thallwitz). Antennules of zoeal stages I–IV (A–D) and of megalopa (E). Scale bars=0.2 mm.

Antennule (Fig. 3B): One aesthetasc, 2 simple and one large plumose setae, and 2 minute setules subterminally.

Antenna (Fig. 4B): Exopod with 6 marginal setae; abnormal form, as that shown in Figure 4B′, was rarely observed.

Mandible (Fig. 5B): Increased in number of teeth.

Maxillule (Fig. 6B): Four spinulose stout spines and 2 setae on basal endite; endopod without minute setules on the proximal segment. Otherwise unchanged.

Maxilla (Fig. 7B): Endopod with 2+4 setae; scaphognathite fringed with 7 soft plumose setae.

Maxilliped 1 (Fig. 8B): Basis with 7 (occasional-

ly 8) setae; setal arrangement of endopod: 2+I (occasionally 3+I), 2+I, 1+I, 2, 4+I; exopod with 7 terminal natatory setae.

Maxilliped 2 (Fig. 9B): Basis unchanged; endopod with setation of 2, 2+I, 2+I, 4+I; exopod as in the maxilliped 1.

Maxilliped 3 (Fig. 10B): Exopod 2-segmented, with 6 terminal natatory setae; no endopod.

Pereiopods: Visible as buds beneath the carapace, as shown in Figure 1B.

Third zoea

Duration: 5–8 days.

Dimension: CL=0.95–1.10 mm (mean 1.05 mm; 6 specimens).

Carapace (Fig. 1C and c): No remarkable changes.

Abdomen (Fig. 2C): Sixth abdominal somite and uniramous uropods present ; exopod of uropod with 3 plumose setae along inner margin and a bifid spine distally, as shown in figure. Fourth telsonal process still articulated and longest; the second process is a simple setule.

Antennule (Fig. 3C): Two tiers of aesthetascs: the subterminal with 2 and distal with 3 longer aesthetascs, unequal in length. Endopod as a bud, carrying one long, plumose seta apically; protopod with a seta and a setule on its distal portion.

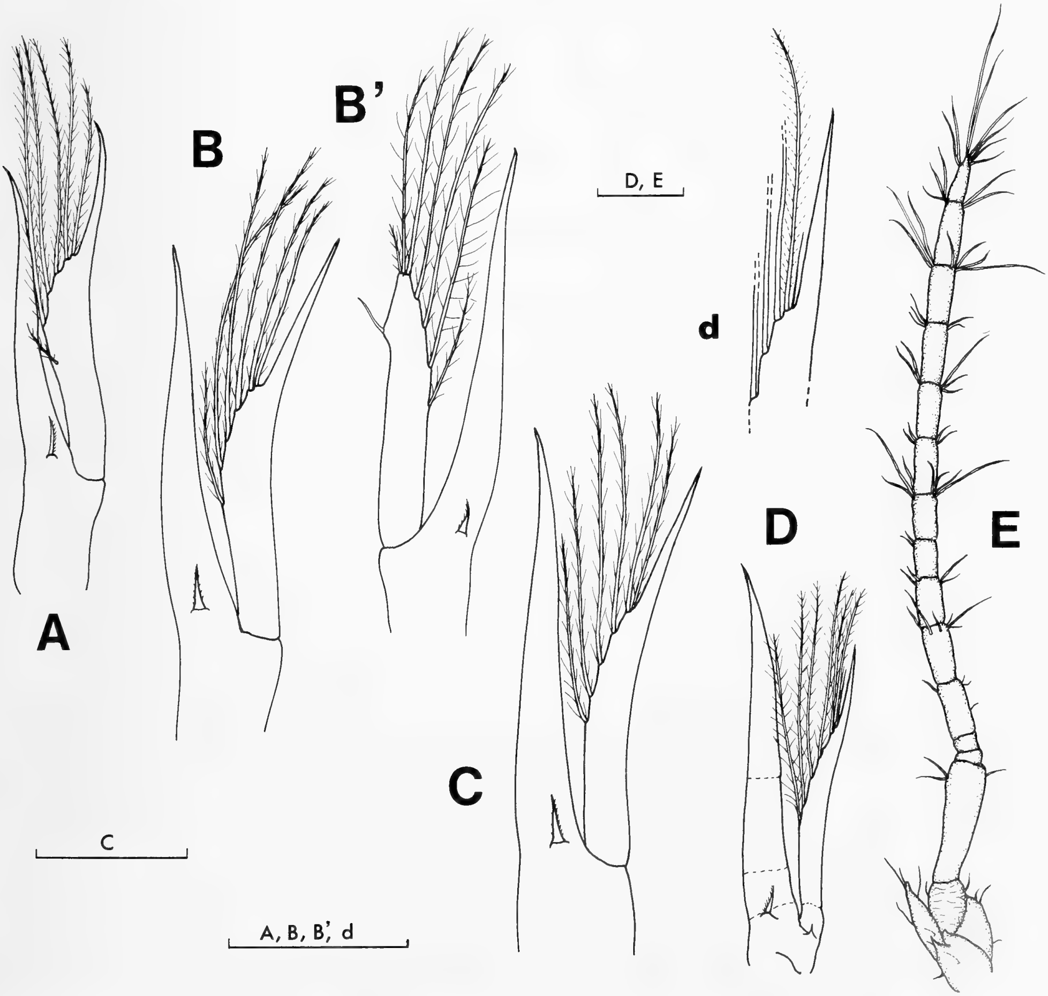

FIG. 4. *Pagurus brachiomastus* (Thallwitz). Antennae of zoeal stages I–IV (A–D) and of megalopa (E). B′, abnormal antenna of a second zoea; d, detail of apical portion of exopod, fourth zoea. Scale bars=0.2 mm.

Antenna (Fig. 4C): Tip of endopod exceeds that of expopod.

Mandible (Fig. 5C): No remarkable changes.

Maxillule (Fig. 6C): Setation of coxal and basal endites as in the previous stages; endopod with 1, 1, 3 setae.

Maxilla (Fig. 7C): Setation of coxal, basal endites, and endopod as in the second zoea; scaphognathite with 10 soft plumose setae.

Maxilliped 1 (Fig. 8C and c): Basis setation 1+1+3+3; endopod 3+I, 2+I, 1+I, 2, 4+I; exopod with 7 natatory setae as in the second zoea.

Maxilliped 2 (Fig. 9C and c): Setation unchanged.

Maxilliped 3 (Fig. 10C): Now biramous; endopod short, with a terminal plumose setae; exopod with 7 natatory setae.

Pereiopods (Fig. 10F): Present as buds, and visible beneath the carapace (Fig. 1C).

Fourth zoea

Duration: 7–11 days.

Dimension: CL=1.23–1.45 mm (mean 1.34 mm; 6 specimens).

Carapace (Fig. 1D and d): Lateral regions somewhat swollen.

Abdomen (Fig. 2D): Uropods with rudimentary endopod; exopod terminating in a quadrifid spine. Pleopod buds elongate.

Antennule (Fig. 3D): Exopod with 3 terminal and 5 subterminal aesthetascs, and a setule distally; endopod without seta; protopod with a long distal seta.

Antenna (Fig. 4D): Endopod indistinctly 3-segmented; exopod with 6 long setae and a shorter distal setule (Fig. 4d).

Mandible (Fig. 5D): Palp present as a bud.

Maxillule (Fig. 6D): Coxal endite with 8 setae; basal endite with 6 cuneated spines; endopod with 2 setules on the proximal segment, as shown in figure.

Maxilla (Fig. 7D): Endopod carries 3+5 setae; scaphognathite with 12–14 soft plumose setae. Otherwise unchanged.

Maxilliped 1 (Fig. 8D and d): Basis with 2+5+3 setae; exopod with 8 natatory setae.

Maxilliped 2 (Fig. 9D and d): Basis unchanged; endopod with 2, 2+I, 1+I, 4+I setae; exopod as in the maxilliped 1.

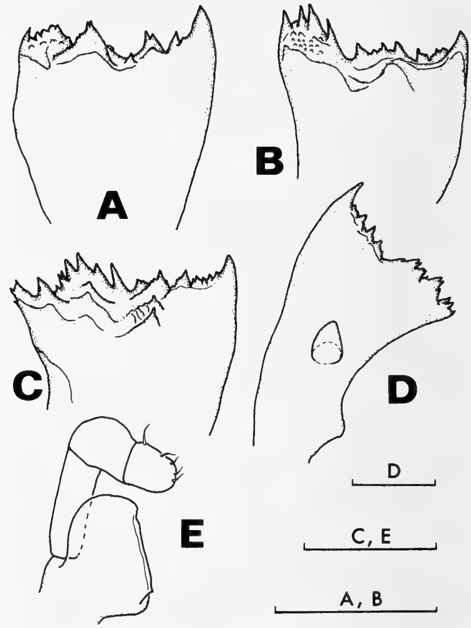

FIG. 5. *Pagurus brachiomastus* (Thallwitz). Mandibles of zoeal stages I–IV (A–D) and of megalopa (E). Scale bars=0.1 mm.

Maxilliped 3 (Fig. 10D): Endopod with 2 setae.

Pereiopods (Fig. 10G): More developed than in the previous stage, but indistinctly segmented; pereiopod 1 apparently chelate. Rudiments of branchiae basally, as shown in figure.

Megalopa

Duration: Undetermined.

Dimension: CL=1.01–1.19 mm (mean 1.11 mm; 4 specimens).

Carapace (Fig. 11A and B): Rostrum reduced to a blunt end; posterolateral carapace spines absent. Ocular peduncles with small acicles basally.

Abdomen (Fig. 11A): Second through fifth somite with biramous pleopods; each endopod with 2 terminal hooks (Fig. 12b); 8–9, 8–9, 9, 7 natatory plumose setae on exopods of pleopods 2–5 (Fig. 12B–D). Telson oval, with 8 posterior long setae, and short setae on surface. Uropods subequal; basis with a distal outer seta; endopod with 4 corneous granules and 2 subterminal setae; exopod armed with 10–11 long, plumose setae, 3–4 fine,

simple setae and 8–9 marginal corneous granules (Fig. 2A).

Antennule (Fig. 3E): Peduncle 3-segmented (the two proximal segments not drawn). Inner flagellum 2-segmented; 2 setae on proximal and 7 setae on distal segment. Outer flagellum 4-segmented with 6, 4, 3 aesthetascs on second through fourth segment; penultimate and distal segments with 1 and 4 setae respectively.

Antenna (Fig. 4E): Peduncle with 5 segments and a flagellum (=endopod) 13-segmented, each segment with 2–7 distal setae except for the proximal (=0), second (=0), and distal (=8) segments. Acicle (=exopod) well-developed, with 5 short setules.

Mandible (Fig. 5E): Palp 3-segmented, 4–5 spinules on the distal segment.

Maxillule (Fig. 6E): Coxal endite with 7 setae; basal endite with 13–15 short spines, 4 setae and a setule; endopod as an unarticulated, unarmed lobe.

Maxilla (Fig. 7E and e): Coxal endite with 5 setae on each lobe; basal endite with setae 8 on the proximal and 9 on the distal lobe; endopod unsegmented, with a subterminal setule. Scaphognathite with 32 soft plumose setae.

Maxilliped 1 (Fig. 8E): Basis 2-lobed; 3–4 plumose setae and a spinule on the proximal, 13–14 setae on the distal lobe. Endopod and exopod reduced, without setae.

Maxilliped 2 (Fig. 9E): Endopod 4-segmented, with 3–4 terminal setae on the distal segment; occasionally 2 setae on the penultimate. Exopod with 4–5 long plumose setae distally.

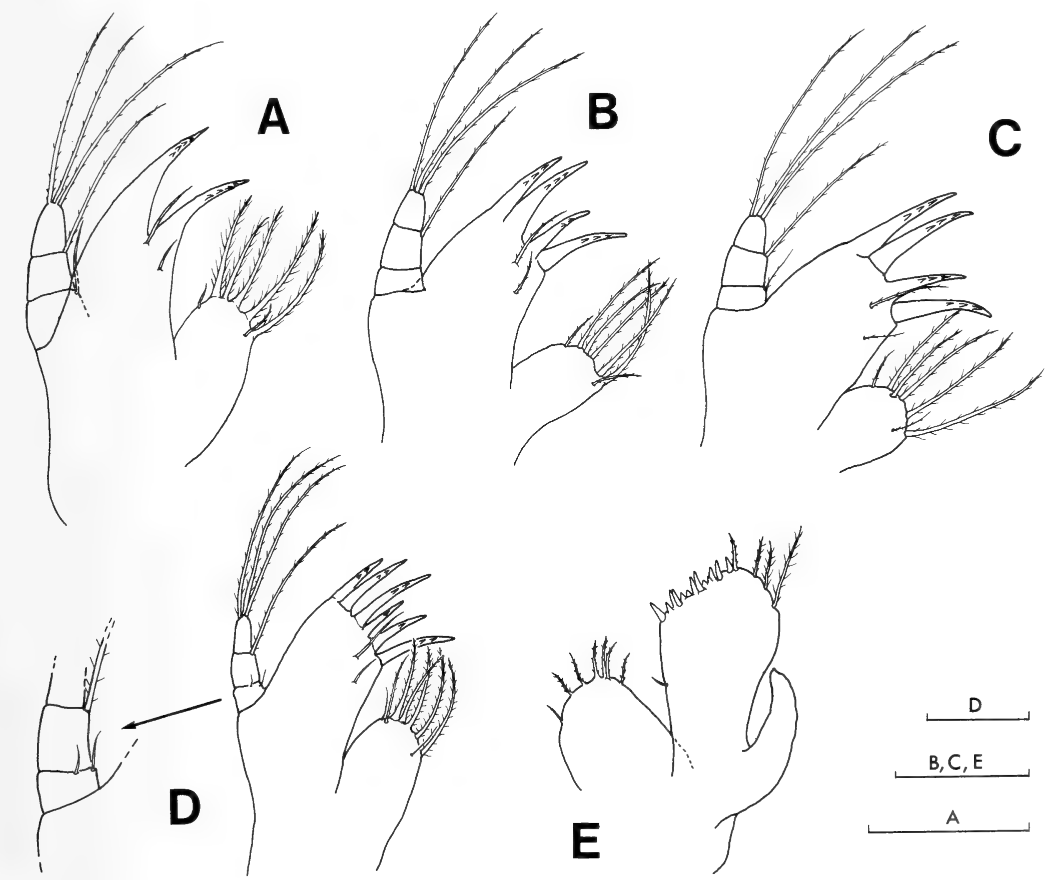

FIG. 6. *Pagurus brachiomastus* (Thallwitz). Maxillules of zoeal stages I–IV (A–D) and of megalopa (E). Scale bars=0.1 mm.

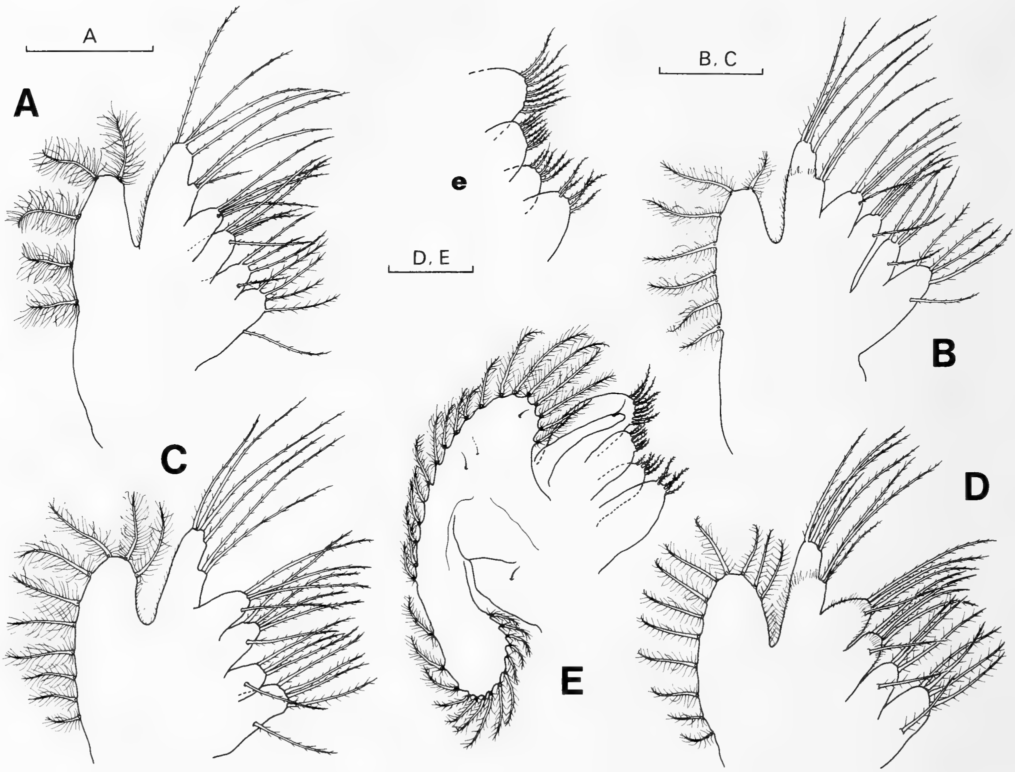

Fig. 7. *Pagurus brachiomastus* (Thallwitz). Maxillae of zoeal stages I–IV (A–D) and of megalopa (E). Scale bars =0.1 mm.

Maxilliped 3 (Fig. 10E): Endopod 5-segmented, providing with stout serrated spines and numerous setae on penultimate and distal segment; exopod 2-segmented with 4–6 terminal long plumose setae on the distal, and a seta on the proximal segment.

Pereiopod 1 (Fig. 11C): Right cheliped slightly larger than left; a pair of conspicuous ventral tubercules of merus of adult crabs absent at this stage.

Pereiopods 2 and 3 (Fig. 11D and E): Adult-like walking legs.

Pereiopod 4 (Fig. 11F and f): Subchelate, flattened distally; propodus broad, armed with 5 corneous tubercules and setae, and dactylus with 3 stout spines and setae.

Pereiopod 5 (Fig. 11G and g): Propodus and dactylus with 17 and 3 distal tubercules, respctively. Four long, and several short setae emerge from propodus; the longest is approximately two times the length of carpus-dactylus.

DISCUSSION

Fourteen species of the family Paguridae have been recorded from Hokkaido coastal waters [1]; larvae of this family are abundant in the meroplankton of the area. From a practical point of view, it is interesting to compare the larvae of the present species with those of other species of the coasts of Hokkaido. Although the zoeas of the paguroid family Lithodidae closely resemble those of the genus *Pagurus,* and are also found in this area, lithodid zoeas are distinguished by several diagnostic features [13–15]. Previous larval works have revealed first or complete larval stages in 7 species among the Paguridae [2, 4–6, 8, 11, 12] (see also Table 1).

From the plankton of Hokkaido, Kurata [2]

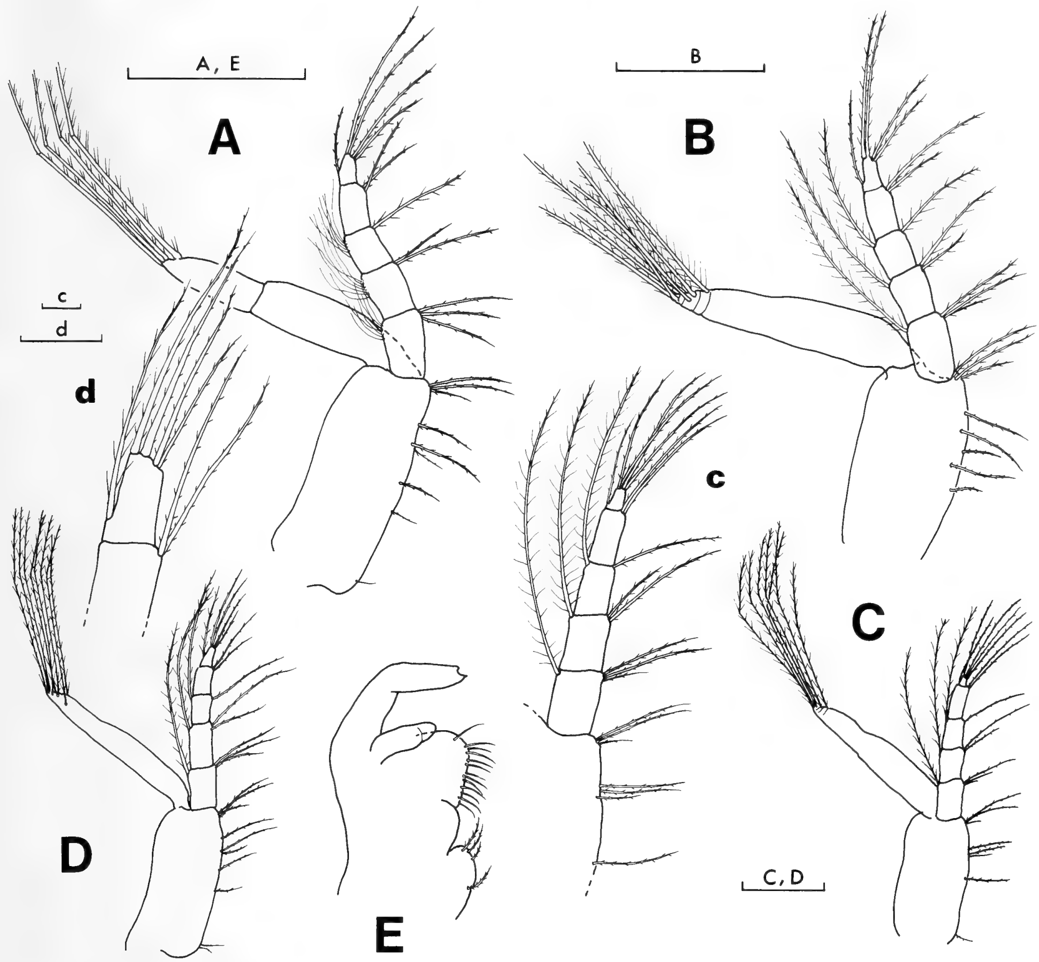

FIG. 8. *Pagurus brachiomastus* (Thallwitz). Maxillipeds 1 of zoeal stages I–IV (A–D) and of megalopa (E); c, d, details of endopods of third and fourth zoea, respectively. Scale bars indicate 0.2 mm for A–E, and 50 μm for c and d.

recognized 17 and 6 kinds of pagurid zoeas and megalopas, respectively. Using main zoeal characteristics, i.e. carapace, antenna and abdomen, some of Kurata's undetermined zoeas are compared with those of laboratory-reared materials as summarized in Table 1. His zoeal species "N. 1" and "N. 10" (or "N. 11") seem to belong to *Pagurus hirsutiusculus* (Dana) and *Labidochirus splendescens* (Owen), respectively, except for the carapace lengths. However, no other Kurata's zoeal species correspond to previously described pagurid zoeas both in their dimensions and setations of antennal exopods. The zoeas of *P. brachiomastus* are similar to those of species "N. 3" and "N. 9" in having 6 setae on antennal exopod, but these zoeas are different from the present species as follows: the carapace lengths are larger than *P. brachiomastus,* and the inner lateral lobe of antennal exopod is not well-developed. It has been known that cultured larval specimens tend to be smaller than planktonic specimens [15, 16], but discrepancies such as found in antennal exopod, one of stable characteristics, make it difficult to identify the zoeas. It is probable that

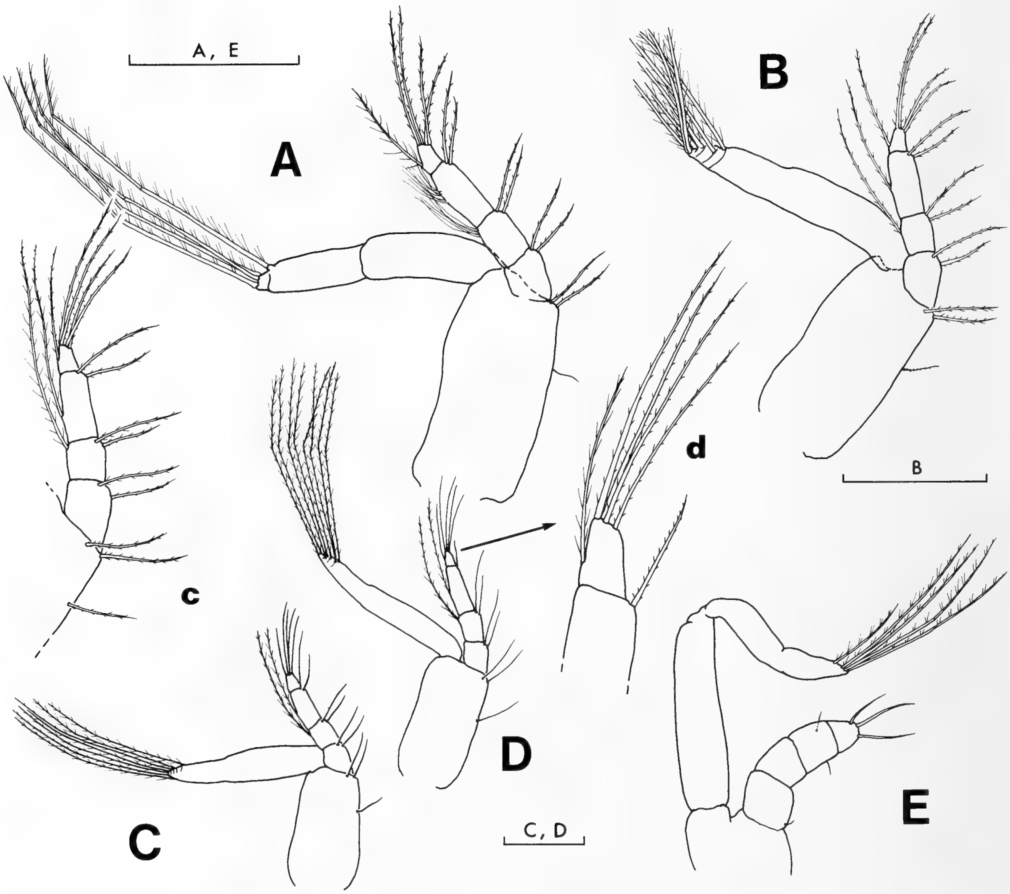

Fig. 9. *Pagurus brachiomastus* (Thallwitz). Maxillipeds 2 of zoeal stages I–IV (A–D) and of megalopa (E); c, d, details of endopods of third and fourth zoea, respectively. Scale bars = 0.2 mm.

both such undertermined zoeas and those constructed from plankton overlap each other, in having been described a same larval stage as different species, or in having been attributed to another allied family, since the total number of them exceeds that of pagurid crabs which are usually distributed in the region of Hokkaido so far as known. On the other hand, ecological study has been poorly carried out on larval distributional pattern on the coast of Japan in the Paguridae; therefore, we cannot reject the possibility that larvae of some pagurid species from southern areas can be transported to Hokkaido by the warm current of Tsushima.

Table 2 shows comparison of morphological characteristics of megalopas between Kurata's species and those of known pagurid species. Among them, species "G–1" is quite different from the remainders; indeed, later Kurata [18] assigned this megalopa to one species of *Paguristes* (family Diogenidae). Otherwise, none of the megalopas from laboratory cultures corresponds to the 5 remaining Kurata's undetermined megalopas in morphological features. For example, such large megalopal specimens as found in species "G–3" and "G–4" have been unknown from cultured *Pagurus* larvae. Since no detailed description of each appendage was given for these planktonic megalopas, and variation between planktonic and cultured specimens has been poorly

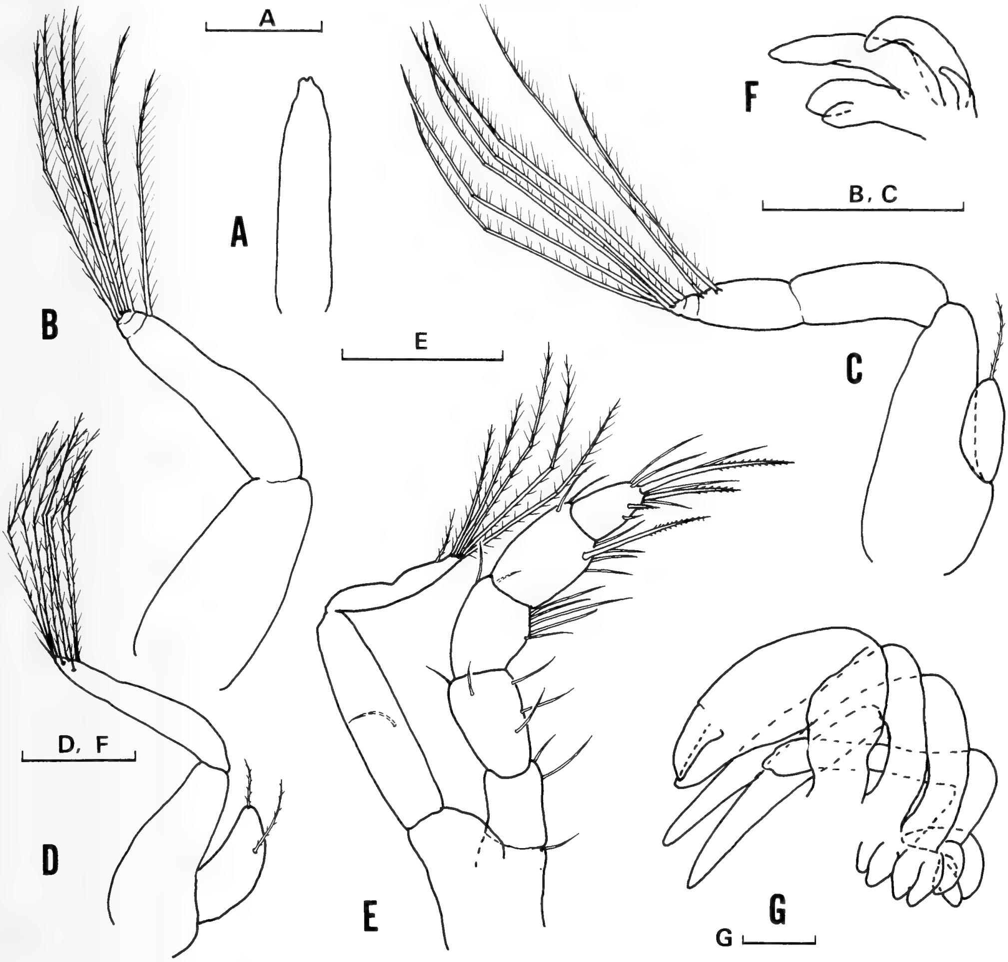

FIG. 10. *Pagurus brachiomastus* (Thallwitz). Maxillipeds 3 of zoeal stages I–IV (A–D) and megalopa (E); F, G, rudiments of pereiopods of third and fourth zoeal stage, respectively. Scale bars=0.2 mm, except 0.1 mm for A.

studied in megalopal stage, complete identification of species is uncertain at present.

Future laboratory-rearing larval studies will promote information on their true larval-adut relationships.

MacDonald *et al.* [19] divided larvae of *Pagurus* into two groups in 12 larval features. Pike and Williamson [9] added a third group, with the inclusion of *P. anachoretus* Risso and *P. kulkarnii* Sankolli, and recently Roberts [20] gave evidences for a fourth group, to accommodate *P. longicarpus* Say. Consequently the *Pagurus* larvae consist of 4 groups, A–D arranged by 9 zoeal and 2 megalopal characteristics. Based on Roberts' grouping, most of pagurid larvae of Japan, i.e. *P. middendorffii* Brandt, *P. dubius* (Ortmann), *P. geminus, Labidochirus splendescens,* and including our *P. brachiomastus* are members of Group A according to the following larval features: 1) the antennal and uropodal endopod lacking seta, 2) the sixth abdominal somite without median dorsal spine, 3) the mandibular palp present in last zoeal stage, and 4) the antenna of megalopa longer than pereiopod 1. However, the 4th telsonal process of those species is articulated throughout zoeal stages, and is the largest among the telsonal

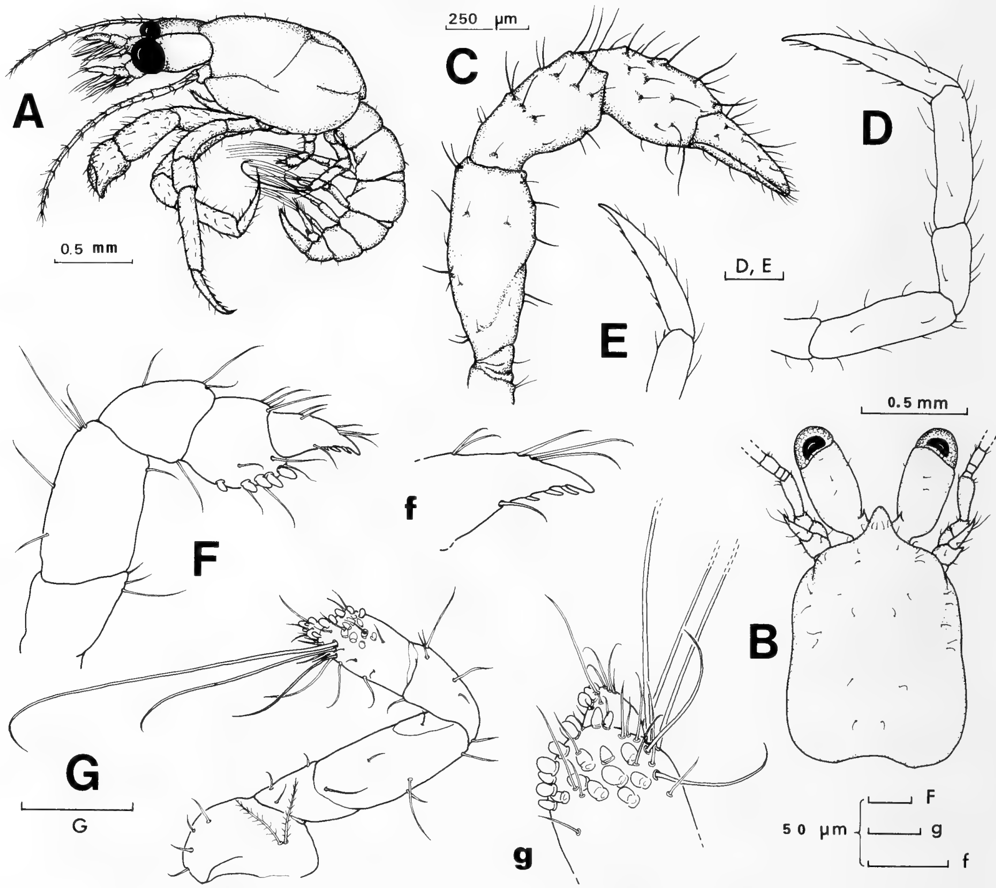

FIG. 11. *Pagurus brachiomastus* (Thallwitz), megalopa. A, complete specimen, lateral view; B, carapace, dorsal view; C–G, pereiopods 1–5; f, g, distal portion of pereiopods 4 and 5, respectively. Scale bars=0.2 mm for D,E,G; others, as indicated.

processes. Furthermore, *P. lanuginosus* and *P. hirsutiusculus* are similar to Group C, but the antennal exopod of the former two species is unarmed. At present, among Japanese *Pagurus* species, only *P. similis* shares all larval characteristics mentioned for Group B. Thus, this grouping of *Pagurus* larvae should be re-examined to avoid exceptions as those indicated.

ACKNOWLEDGMENTS

The authors are grateful to Prof. F. Iwata of Hokkaido University for his encouragement and critical reading of the manuscript. We thank to the staff of the Akkeshi Marine Biological Station for providing facilities for collection of ovigerous females. Thanks are also due to Prof. S. Miyake of Kyushu Sangyo University for identification of adult hermit crabs.

REFERENCES

1 Miyake, S. (1982) Japanese crustacean decapods and stomatopods in color. Vol. I. Macrura, Anomura, and Stomatopoda. Hoikusha, Osaka. 261 pp. 56 pls. (In Japanese).

2 Kurata, H. (1964) Larvae of decapod Crustacea of Hokkaido. 5. Paguridae (Anomura). Bull. Hokkaido Reg. Fish. Res. Lab., **29**: 24–48. (In Japanese, with English abstract).

3 Makarov, R. R. (1967) Larvae of shrimps, hermit-crabs and crabs of West Kamchatkan shelf and their distribution. Natl. Lending Libr. Sci. Technol., Boston Spa, Yorkshire, England, 199 pp.

4 Kurata, H. (1968) Larvae of Decapoda Anomura of

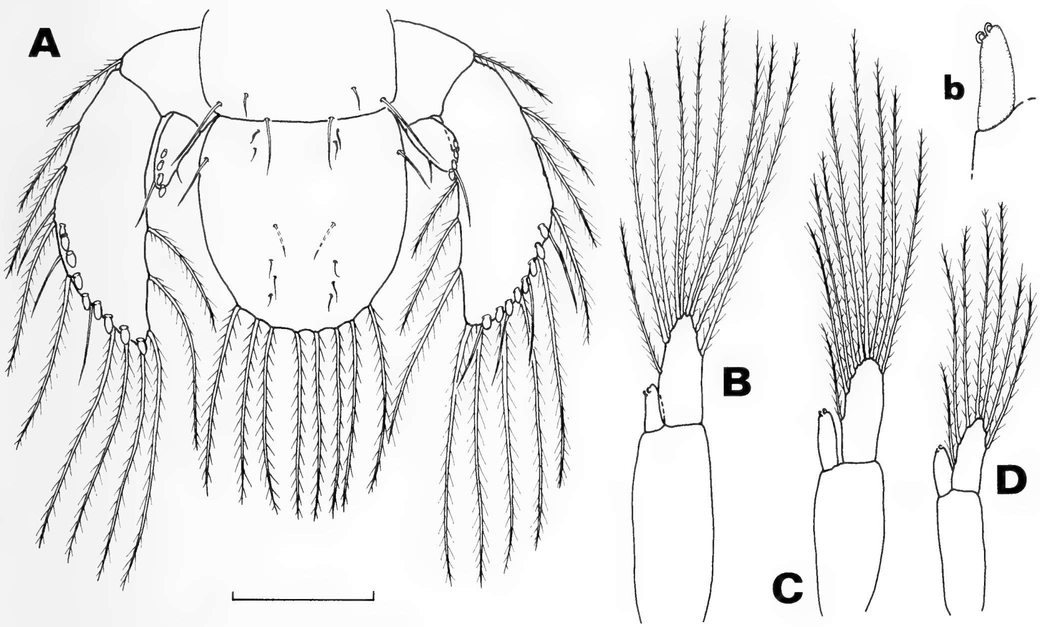

FIG. 12. *Pagurus brachiomastus* (Thallwitz), megalopa. A, telson and uropods; B–D, 1st, 3rd and 4th pair of pleopods (=pleopod 2, 4, and 5); b, endopod of pleopod 2. Scale bars=0.2 mm.

Arasaki, Sagami Bay—I. *Pagurus samuelis* (Stimpson) (Paguridae). Bull. Tokai Reg. Fish. Res. Lab., **55**: 265–269. (In Japanese, with English abstract).

5 Hong, S. Y. (1969) The larval development of *Pagurus lanuginosus* de Haan (Crustacea, Anomura) reared in the Laboratory. Bull. Kor. Fish. Soc., **2**: 1–15.

6 Lee, B. D., and Hong, S. Y. (1970) The larval development and growth of decapod crustaceans of Korean waters. I. *Pagurus similis* Ortmann (paguridae, Anomura). Publ. Mar. Lab. Pusan Fish. Coll., **3**: 13–26.

7 Hong, S. Y. (1981) The larvae of *Pagurus dubius* (Ortmann) (Decapoda, Paguridae) reared in the laboratory. Bull Natl. Fish. Univ. Busan, **21**: 1–11.

8 Ivanov, B. G. (1979) A contribution to the biology of hermit crabs of the North Pacific. 2. The first larval stages of some species reared in the laboratory (Crustacea, Decapoda, Paguridae). Zool. Zhur., **58**: 977–985. (In Russian, with English abstract).

9 Pike, R. B., and Williamson, D. I. (1960) Larvae of decapod Crustacea of the families Diogenidae and Paguridae from the Bay of Naples. Pubbl. Staz. Zool. Napoli, **31**: 493–552.

10 Quintana, R. and Konishi, K. (1986) On the prezoeal stages: observations on three *Pagurus* species (Decapoda, Anomura). J. Nat. Hist., **20**: 837–844.

11 Fitch, B. M. and Lindgren, E. W. (1979) Larval development of *Pagurus hirsutiusculus* (Dana) reared in the laboratory. Biol. Bull., **156**: 76–92.

12 Nyblade, C. F. and McLaughlin, P. A. (1975) The larval development of *Labidochirus splendescens* (Owen, 1839) (Decapoda, Paguridae). Crustaceana, **29**: 271–289.

13 Kurata, H. (1964) Larvae of decapod Crustacea of Hokkaido. 6. Lithodidae (Anomura). Bull. Hokkaido Reg. Fish. Res. Lab., **29**: 49–65. (In Japanese, with English abstract).

14 Haynes, E. B. (1984) Early zoeal stages of *Placetron wosnessenskii* and *Rhinolithodes wosnessenskii* (Decapoda, Anomura, Lithodidae) and review of lithodid larvae of the northern North Pacific Ocean. Fish. Bull., **82**: 315–324.

15 Konishi, K. (1986) Larval development of the stone crab, *Hapalogaster dentata* (De Haan, 1844) (Crustacea: Anomura: Lithodidae) reared in the laboratory. J. Fac. Sci. Hokkaido Univ. Ser. VI, Zool., **24**: 155–172.

16 Le Roux, A. (1966) Le développement larvaire de *Porcellana longicornis* Pennant(Crustacé Décapode Anomoure, Galatheide). Cah. Biol. Mar., **7**: 69–78.

17 Roberts, M. H. (1968) Larval development of the decapod *Euceramus praelongus* in laboratory culture. Chesapeake Sci., **9**: 121–130.

18 Kurata, H.(1968) Larvae of Decapoda Anomura of Arasaki, Sagami Bay—III. *Paguristes digitalis* (Stimpson) (Diogenidae). Bull. Tokai Reg. Fish. Res. Lab., **56**: 181–186. (In Japanese, with English

TABLE 1. Comparison of main morphological characteristics between Kurata's zoeal species

Species	Carapace (Z1–4) Lengths (mm) Z1	Z2	Z3	Z4	PLS
Species N. 1	1.56–1.76	2.18–2.27	2.7–3.0	3.2–3.4	short
Species N. 2	—	1.98	2.76	3.1	short
Species N. 3	—	—	2.5	—	short
Species N. 4	—	2.40	2.40–2.60	3.2	short
Species N. 5	—	—	—	4.2–4.6	short
Species N. 6	1.76	2.40–2.52	3.1	3.8	short
Species N. 7	—	2.52	3.5	5.0	short
Species N. 8	2.1–2.2	2.7	3.3	—	short
Species N. 9	1.7	1.9	2.6	3.7	short
Species N. 10	2.94	3.4–4.1	5.6–5.8	6.9	long
Species N. 11	2.8	3.9	4.5	5.5	long
Species N. 12	—	1.9	—	—	short
Species N. 13	1.8	—	—	—	short
Species N. 14	—	2.22	2.88	—	short
Species N. 15	1.22	1.65	1.95	2.46	short
Species N. 16	—	3.4	—	—	short
Species N. 17	—	3.05	—	3.35	short
Pagurus					
brachiomastus	0.74–0.80	0.85–0.90	0.95–1.10	1.23–1.45	short
dubius	0.47–0.52	0.57–0.65	0.78–0.83	0.80–0.89	short
geminus	1.2	1.5	1.8	2.2	short
hirsutiusculus	1.4	1.4	1.7	2.3	short
lanuginosus	1.34–1.47	1.60–1.72	1.95–2.09	2.15–2.20	short
middendorffi	1.24	1.75	2.16	2.5	short
similis	1.94	2.12	2.33	2.69	—
trigonocheirus	2.7–2.9	—	—	—	short
Labidochirus					
splendescens	2.5–2.7	3.5–3.9	4.9–5.5	5.8–6.9	long
splendescens	2.8	—	—	—	long

a, articulated; d, developed; ex, expanded type; f, fused with telson; s, subterminal spine; sl, spines; –, unarmed; —, no data; *, this study.

and hitherto known zoeas of the family Paguridae of Japan

Antenna (Z1)			Abdomen (Z1)	Telson (Z3–4)	Source of material	Reference
Exopod		Endopod	5th somite PLS	4th process		
Seta	Shape	Tip				
4(5)	sl	–	short	a	P	[2]
7	sl	–	long	a	P	[2]
6	sl	–	long	a	P	[2]
7	sl	–	long	a	P	[2]
8	sl	–	long	a	P	[2]
7	sl	–	long	a	P	[2]
8	sl	–	long	a	P	[2]
8	sl	1s	long	a	P	[2]
6	sl	–	long	a	P	[2]
9–10	sl	1s	long	a	P	[2]
10–12	sl	–	long	a	P	[2]
7	ex	–	long	–	P	[2]
8	ex	–	long	–	P	[2]
10	ex	–	long	a	P	[2]
7	ex	–	long	a	P	[2]
10	ex	–	long	–	P	[2]
10	ex	–	long	a	P	[2]
6	ex	–	long	a	L	*
5	ex	1s	long	a	L	[7]
6	ex	1s	long	a	L	[4]
5	sl	–	short	a	L	[11]
5	ex	–	long	a	L	[5]
6	sl	–	long	a	P+L	[2]
10	ex	2t	short	f	L	[6]
8	sl	1s	long	a	L	[8]
8	sl	–	long	a	L	[12]
8	sl	–	long	–	P	[8]

slender type; t, terminal setae; L, laboratory-reared; P, plankton; PLS, postero-lateral

Table 2. Comparison of main morphological characteristics between Kurata's megalopal species and hitherto known megalopas of the family Paguridae of Japan

Species	Carapace		Antenna			Length of A2, P1	Telson	Pereiopod (cheliped)	Source of material	Reference
	Length (mm)	Ocular acicle	Flagelum	Exopod			Posterior process			
			Segment	Tip	Length					
Species G-1	0.82	–	4	p	long	A2=P1	16	left=right	P	[2]
Species G-2	1.9	+	20	p	long	A2>P1	8	left<right	P	[2]
Species G-3	3.8	+	16	p	long	A2>P1	8	left<right	P	[2]
Species G-4	4.3	+	23	p	long	A2>P1	8	left<right	P	[2]
Species G-5	1.74	+	20	r	short	A2>P1	8	left<right	P	[2]
Species G-6	1.4	+	10–11	r	short	A2>P1	8	left<right	P	[2]
Pagurus										
brachiomastus	1.01–1.09	+	13	p	medium	A2>P1	8	left<right	L	*
dubius	0.52–0.58	?	11	r	?	A2>P1	8	left<right	L	[7]
geminus	1.2	–	10	r	short	A2>P1	8	left<right	L	[4]
hirsutiusculus	1.3	?	12–14	r	short	A2>P1	6	left<right	L	[11]
lanuginosus	2.01–2.05	?	11	r	long	A2>P1	6	left<right	L	[5]
similis	1.54	+	11	p	long	A2<P1	8	left<right	L	[6]
Labidochirus										
splendescens	2.3–2.4	+	47–49	r	medium	?	8	left<right	L	[12]

A2, antenna; P1, pereiopod 1 (=cheliped); p, pointed; r, rounded; L, laboratory-reared; P, plankton; ?, no data; long=exceeding the 4th peduncular segment, medium=just reaching the tip of 4th peduncular segment, and short=not exceeding the 4th peduncular segment. *, this study.

abstract).

19 MacDonald, J. D., Pike, R. B. and Williamson, D. I. (1957) Larvae of British species of *Diogenes, Pagurus, Anapagurus* and *Lithodes* (Crustacea, Decapoda). Proc. Zool. Soc. London, **128**: 209–257.

20 Roberts, M. H. (1970) Larval development of *Pagurus longicarpus* Say reared in the laboratory, I. Description of larval instars. Biol. Bull., **139**: 188–202.

ZOOLOGICAL SCIENCE 4: 367–373 (1987)

Spongicola levigata sp. nov., a New Shrimp Associated with a Hexactinellid Sponge from the East China Sea (Decapoda, Stenopodidae)

KEN-ICHI HAYASHI and YASUKI OGAWA[1]

Department of Aquaculture and Biology, Shimonoseki University of Fisheries, Shimonoseki, Yamaguchi 759–65, and [1]Faculty of Applied Biological Science, Hiroshima University, Fukuyama, Hiroshima 720, Japan

ABSTRACT—A new stenopodid shrimp, *Spongicola levigata* sp. nov., is described and illustrated from specimens associated with hexactinellid sponges in the East China Sea.–It is a small species, measuring only 8.3–11.8 mm in body length of the mature female.–This species is unique in the entirely smooth carapace and abdomen, and the lack of telsonal dorsal spines near the articulation with the sixth abdominal somite.–Its affinities with related species and sexual distinctions are discussed.

INTRODUCTION

Six unusual specimens of the stenopodidean shrimp were recently examined. They were found in spongocoels of a certain species of the hexactinellid sponge collected from the East China Sea in about 200 m. This type of sponge is usually known to house a commensal shrimp, *Spongicola venusta* De Haan; in fact, that commensal was collected together during the cruise. The present unusual shrimps are referred to a species of the genus *Spongicola* but their size is much smaller, only 1/3 or 1/4 the length of *S. venusta,* and it apparently represents an undescribed species. The type-series has been deposited in the collection of the Shimonoseki University of Fisheries, Shimonoseki.

MATERIALS

TYPE: Holotype, male, East China Sea, 30°44.7′N, 127°48.3′E, about 200 m deep, 14 June 1978, 13:44–16:30, otter trawl, Koyo Maru, O. Tabeta and K. Hayashi leg. Paratypes, 1 male, 3 ovigerous females and 1 female, collected with holotype.

Accepted October 21, 1986
Received September 9, 1986

DESCRIPTION

Spongicola levigata sp. nov.
(Figs. 1–4)

Diagnosis: Rostrum completely smooth on dorsal and ventral margins, or provided with 1–4 dorsal and 1 ventral processes, all step-like. Carapace glabrous and smooth, lacking grooves and spines. Abdominal terga entirely smooth. Pleura of first to fifth somites broadly rounded without marginal spines. Telson lacking dorsal spines near base, but 3 pairs present on dorsal longitudinal ridges. Chela of third pereopod broad with serration or irregularity on upper and lower margins. Dactyli of fourth and fifth pereopods biunguiculate.

Description: Shell of soft, somewhat membraneous texture. Body slender and glabrous, abdomen rather depressed (Fig. 1).

Rostrum short, falling short of end of first antennular segment (Fig. 2*a*); directed downward or slightly curved downward; triangular in dorsal view, its base considerably wide; distally pointed obtusely; dorsal margin bearing few step-like processes, and ventral margin with one similar process or occasionally entirely smooth. Carapace 4 times as long as rostrum; glabrous and smooth, without any grooves and spines on surface, ante-

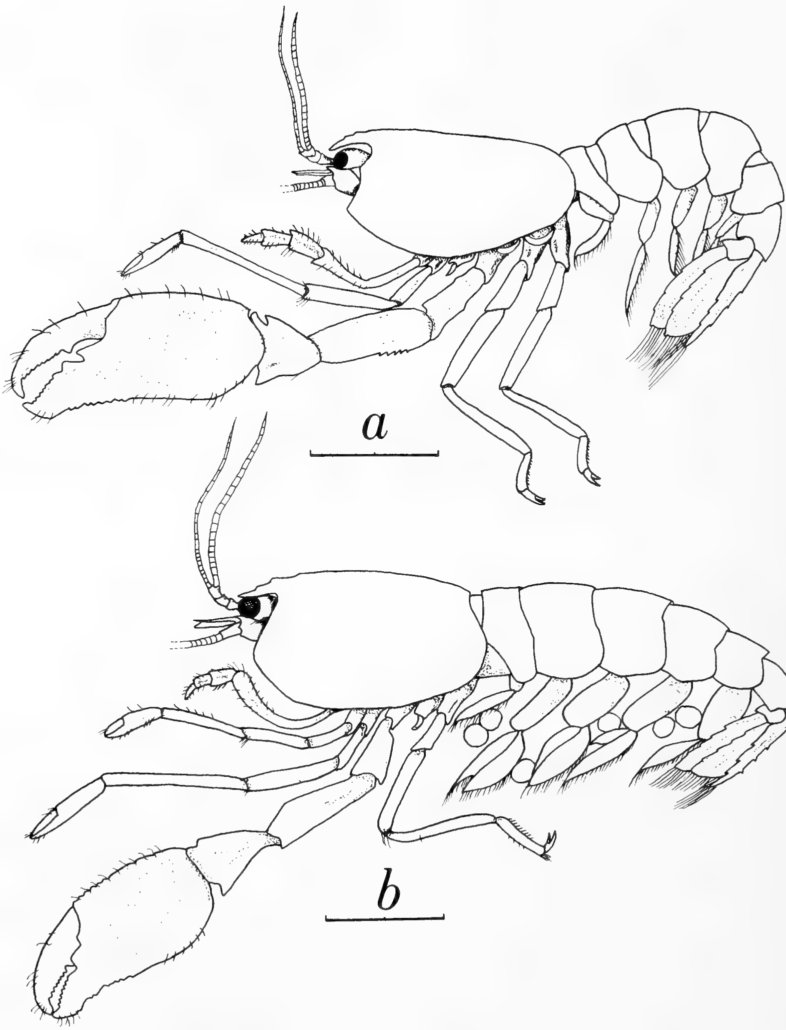

FIG. 1. *Spongicola levigata* sp. nov. from the East China Sea. *a*, Holotype, male, 2.8 mm in cl; *b*, paratype, ovigerous female, 3.2 mm in cl. Scales 2.0 mm.

rior margin also smooth; suborbital or antennal angle obtusely pointed; pterygostomial angle rounded or rectangular, not spiniform (Fig. 2*b*).

Abdomen smooth; first to fifth terga glabrous, sixth tergum with few setae; pleura of first to fifth somites broadly rounded without marginal spines; no spiniform process on sixth somite. Telson broadly lance-shaped, 1.5 times as long as broad, slightly narrowed at base; dorsal surface with pair of longitudinal ridges, each bearing 3 large, posteriorly directed spines; lateral margin with 2–4 pairs of distinct spines; posterior margin fringed with long setae and provided with 3 tiny spines, 2 subterminal flanking median terminal (Fig. 2*c*).

Eyes comparatively large, eyestalk mesially with few spinules near cornea (Fig. 2*a*). Antennular peduncles simply elongate; basal segment more than twice as long as second segment; stylocerite small, ending in sharp point. Antennal scale broad and semi-circular, about twice as long as broad; outer margin almost straight, with 4 or 5 spinules on anterior half, terminal one largest; inner margin

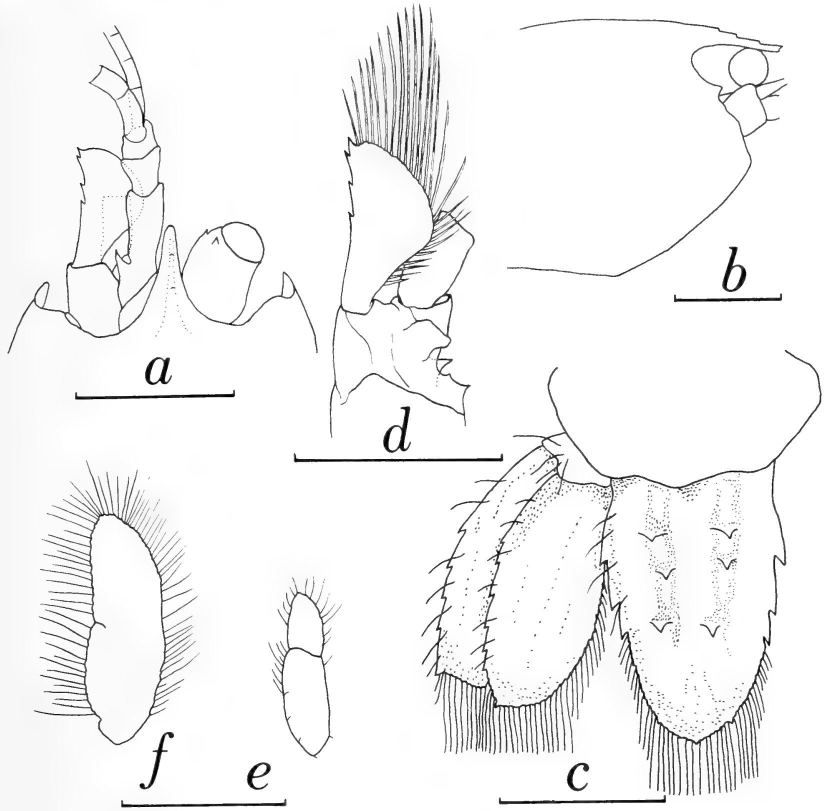

FIG. 2. *Spongicola levigata* sp. nov. *a, c, e,* male holotype, 2.8 mm in cl; *b, d, f,* paratype, ovigerous female, 3.2 mm in cl. *a,* Anterior part of body, dorsal view; *b,* anterior part of body in lateral view; *c,* tail fan, right uropod removed; *d,* left antenna; *e,* right first pleopod; *f,* right second pleopod. Scales 1.0 mm.

strongly convex; long setae on inner and distal margins; basicerite dorsomesially with quadrate flap, ventromesially with conspicuous spine near base of carpocerite (Fig. 2*d*).

Mandible with 3-segmented palp; incisor and molar processes fused with each other (Fig. 3*a, b*). Palp of first maxilla slender and simple with 2 apical and few subapical setae (Fig. 3*c*). Palp of second maxilla long and slender; 2 endites each bilobed (Fig. 3*d*). Palp of first maxilliped unilobed with feeble median notch; epipod large and bilobed; distal endite large and unequally bilobed; proximal endite small and unilobed (Fig. 3*e*). Second maxilliped with 5-segmented endopod; epipod bilobed, small globular podobranch present (Fig. 3*f*). Third maxilliped rather stout, especially merus and ischium, setae on distal three segments rigid; epipod slender and partly twisted, exopod extremely short, only bud-like (Fig. 3*g*).

First pereopod slender and chelate; fingers finely pectinate on distal 1/4 of cutting edge; palm about 1.5 times as long as fingers; carpus slightly longer than merus, bearing small subterminal spine on inner side (Fig. 4*a, b*). Second pereopod similar in shape to first pereopod but larger and longer; palm twice as long as fingers; carpus 1.5 times as long as merus (Fig. 4*c*). Third pereopod strongest, sparsely provided with short setae on chela, slightly shorter than body length; lower margin of chela serrate on distal 2/3 of length; upper margin smooth or faintly serrate; fingers distally curving inward, crossing, each ending in sharp point; opposable margin of movable finger with prominent median tooth fitting to large opposing con-

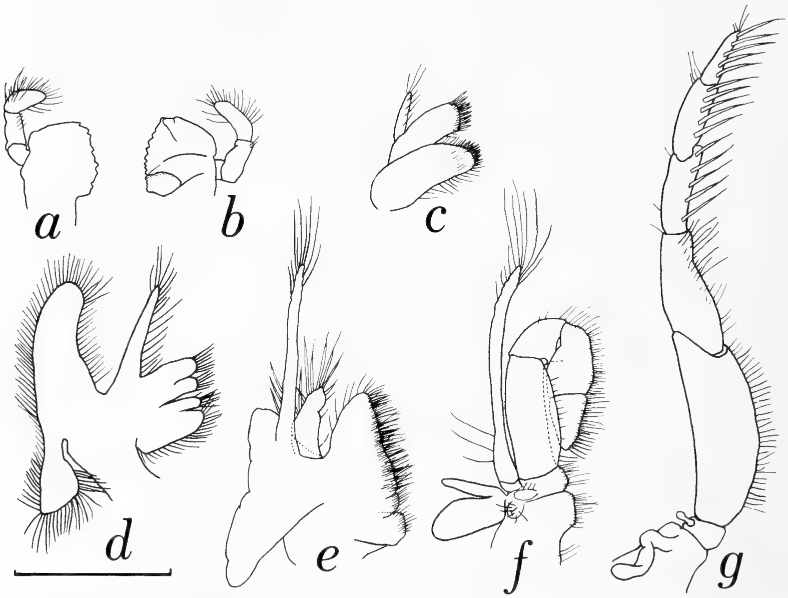

FIG. 3. Mouthparts of *Spongicola levigata* sp. nov. (right side), paratype, ovigerous female, 3.2 mm in cl. *a*, mandible, ventral view; *b*, same, dorsal view; *c*, first maxilla, ventral view; *d*, second maxilla, ventral view; *e*, first maxilliped, ventral view; *f*, second maxilliped, ventral view; *g*, third maxilliped, outer view. Scale 1.0 mm.

cavity; cutting edges distal to snapping part armed with several quadrangular teeth; palm rather massive, roughly quadrate or slightly longer than broad, width as long as dactylus; carpus triangular in lateral view, anterior margin pointed at upper and lower ends; merus armed with 5 spines on posteromedian margin in male, spineless in female; ischium with small spine at anterodistal end (Fig. 4*d, e*). Fourth and fifth pereopods similar, long and slender, sparsely setose; dactylus short, simply biunguiculate, penultimate tooth articulated; propodus 2.5 times as long as dactylus and half as long as carpus, bearing 8–12 spines on posterior margin; carpus slightly longer than merus, armed with 2 small but sharp spines on posterodistal end (Fig. 4*f, g*).

Branchial formula as shown below. Epipods absent from fifth pereopods; exopods well developed on first and second maxillipeds, rudimental on third maxillipeds, absent from pereopods.

	Maxillipeds			Pereopods				
	1	2	3	1	2	3	4	5
Pleurobranchs	—	1	1	1	1	1	1	1
Arthrobranchs	—	1	2	2	2	2	2	—
Podobranchs	—	1	—	—	—	—	—	—
Epipods	1	1	1	1	1	1	1	—
Exopods	1	1	r	—	—	—	—	—

First pleopods in male small, composed of 2 segments and feebly setose (Fig. 2*e*), those in female largely unilobed, and fully setose (Fig. 2*f*). Second to fifth pleopods bilobed, each fringed with long setae. Endopod and exopod of uropod each with weak longitudinal dorsal ridge, bearing long setae on inner and distal margins; endopod armed with 4–7 spines on distal 2/3 of outer margin, terminal spine larger; exopod with 6–10 spines on distal half of outer margin, terminal spine relatively large (Fig. 2*c*).

Color: Body almost transparent; cornea light brown.

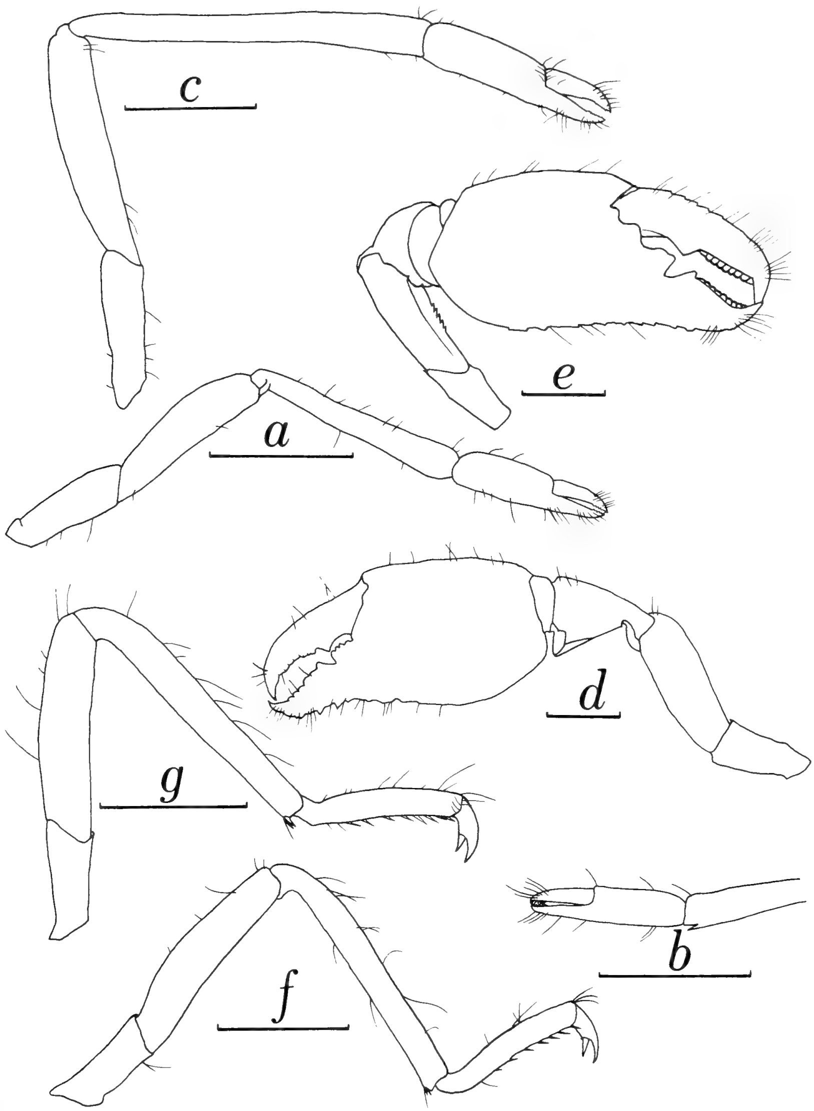

FIG. 4. Pereopods of *Spongicola levigata* sp. nov. *a–d, g,* paratype, ovigerous female, 3.2 mm in cl; *e, f,* male holotype, 2.8 mm in cl. *a,* right first pereopod, outer view; *b,* chela and anterior part of carpus of same, inner view; *c,* right second pereopod, outer view; *d,* left third pereopod, outer view; *e,* right third pereopod, outer view; *f,* right fourth pereopod, outer view; *g,* right fifth pereopod, outer view. Scales 1.0 mm.

Measurements: Holotype, male, 10.0 mm in body length excluding rostrum (BL), 2.8 mm in carapace length excluding rostrum (CL), 9.8 mm in length of right third pereopod. Paratypes, 1 male, 8.8 mm in BL, 2.9 mm in CL; 4 females, 8.3–11.8 mm in BL, 2.7–3.4 mm in CL; smallest ovigerous female, 8.3 mm in BL. Subglobular eggs, 0.4–0.6 mm in diameter.

DISCUSSION

In spite of having the glabrous smooth integu-

ment, the present species may be referred to a species of the genus *Spongicola*. As mentioned by Holthuis [7] and Bruce and Baba [4], *Spongicola* bears well-developed exopods in the first two maxillipeds but rudimental one in the third maxillipeds. Recently Saint Laurent and Cleva [15] slightly modified this definition to include *S. inflata,* which has a normal, well-developed exopod on the third maxillipeds. The gill formula of the present species is exactly the same as shown by Holthuis [7] for *Spongicola* and differs from those of the related genera, *Spongicoloides* [11], *Spongiocaris* [4] and the recently erected *Paraspongicola* [15]. The glabrous, smooth integument unique to the present species is, however, shared with some species of *Spongicoloides* [7, 11]. The chela of the third pereopod in this species also represents the feature of *Spongicola.*

The known species and subspecies of the genus *Spongicola* retain several teeth or spines on the rostrum and carapace, with rather fair regularity. In most of the species, the rostrum bears a few to several dorsal and a single ventral spines; the carapace is also provided on each side with 1 postrostral, 1 hepatic, 1 antennal, and some small spines on both the anterior margin and the pterygostomial region directly inside of it. The present new species, however, is entirely devoid of the carapacial spines and grooves. Even the antennal or suborbital angle is reduced to an obtuse process. The dorsal margin of the rostrum bears a few step-like processes, none of which ends in a sharp point; occasionally they are absent, even the ventral marginal one.

In almost all species of *Spongicola,* the abdominal pleura are more or less serrated marginally, and telson bears 2 pairs of spines near the articulation with the sixth abdominal somite, in addition to the dorsal pairs on the longitudinal carinae [1, 7, 14, 15]. In the present new species such spines or processes are barely recognizable, only excepting the last mentioned ones.

The sexual distinctions in this species are apparent in the third pereopods and the first pleopods. In the male about 5 spines are distinct on the posteromedian margin of the third pereopods, while they are absent in the female. The first pleopod is a single lobe without articulation in the female, instead of being composed of 2 segments in the male; the marginal setae in the female are longer and more numerous in the female.

Like the other members of this genus as well as the related genera [2, 4, 7, 9, 15], the present new species is a symbiont of the deep-sea glass sponge. All of the present type series were obtained from the spongocoels of a hexactinellid sponge, probably *Euplectella oweni* Herklots and Marshall. Four of them were found in a pair in 2 different host sponges. The female is larger than the paired male; in one pair the female is 11.8 mm in body length and the male is 10.0 mm and in the other pair the female is 10.8 mm and the partner is 8.8 mm.

Other examples of this sponge found in the same trawl haul accommodated the other common stenopodid, *S. venusta* De Haan; a total of 18 (6 pairs and 6 singles) specimens were collected. *S. venusta* was recorded from Japan, Korea, the East China Sea and the Philippines at the depths of 174–315 m [3, 5–8, 10, 12, 13, 15, 16]. *S. levigata* and *S. venusta* may be readily distinguished from each other at the field by the size difference. The former is only 1/3 or 1/4 of the latter and is probably the smallest among the species of this genus, being only 8.3 mm in body length of the smallest ovigerous female.

ACKNOWLEDGMENTS

We thank Dr. K. Baba of the Kumamoto University, Kumamoto, Japan, for his critical review of the manuscript.

REFERENCES

1 Alcock, A. (1901) A descriptive catalogue of the Indian deep-sea Crustacea Decapoda Macrura and Anomala, in the Indian Museum. Being a revised account of the deep-sea species collected by the Royal Indian Marine Survey Ship Investigator. pp. 1–286, i–iv, pls. 1–3.

2 Baba, K. (1983) *Spongicoloides hawaiiensis,* a new species of shrimp (Decapoda: Stenopodidea) from the Hawaiian Islands. J. Crust. Biol., **3**: 477–481.

3 Bate, C. S. (1888) Report on the Crustacea Macrura collected by H.M.S., Challenger during the years 1873–76. Rep. Voy. Challenger, Zool., **24**: i–xc, 1–

942, pls. 1–150.

4 Bruce, A. J. and Baba, K. (1973) *Spongiocaris*, a new genus of stenopodidean shrimp from New Zealand and South African waters, with a description of two new species (Decapoda, Natantia, Stenopodidea). Crustaceana, **25**: 153–170.

5 Fujino, T. and Miyake, S. (1970) Caridean and stenopodidean shrimps from the East China and the Yellow Seas (Crustacea, Decapoda, Natantia). J. Fac. Agr., Kyushu Univ., **16**: 237–312.

6 De Haan, W. (1833–1850). Crustacea. In "P. F. von Siebold: Fauna Japonica sive descriptio animalium, quae in itinere per Japoniam, jussu et auspiciis superiorum, qui summum in India Batava Imperium tenent, suscepto, annis 1823–1830 collegit, notis, observationibus et adumbrationibus illustravit". i–xvii, i–xxxi, 1–244, pls. 1–55, A–Q, 1, 2.

7 Holthuis, L. B. (1946) The Decapoda Macrura of the Snellius Expedition. 1. The Stenopodidae, Nephropsidae, Scyllaridae and Palinuridae. Biological results of the Snellius Expedition XIV. Temminckia, **7**: 1–178.

8 Kim, H. S. (1977) Macrura. Illustrated Flora and Fauna of Korea, **19**: 1–414, pls. 1–56.

9 Kubo, I. (1943) A new commensal shrimp, *Spongicola japonica* n. sp. Annot. Zool. Japon., **21**: 90–94.

10 Miers, E. J. (1878) On species of Crustacea living within the Venus's flower-basket (*Euplectella*) and in *Meyerina claviformis*. J. Linn. Soc. Lond., Zool., **13**: 506–512, pl. 24.

11 Milne Edwards, A. and Bouvier, E. L. (1909) Les peneides et Stenopodides. Reports on the results of dredging, under the supervision of Alexander Agassiz, in the Gulf of Mexico (1877–78), in the Caribbean Sea(1878–79) and along the Atlantic coast of the United States (1880), by the U. S. Coast Survey Streamer "Blake". XLIV. Mem. Mus. Comp. Zool., Harvard, **27**: 177–274, pls. 1–9.

12 Ortmann, A. (1890) Die Decapoden-Krebse des Strassburger Museums, mit besonderer Berucksichtigung der von Herrn Dr. Doderlein bei Japan und bei den Liu-Kiu-Inseln gesammelten und z. Z. im Strassburger Museum aufbewahrten Formen. I. Theil. Die Unterordnung Natantia Boas. Zool. Jahrb., Syst., **5**: 437–542, pls. 36, 37.

13 Parisi, B. (1919) I Decapodi Giapponesi del Museo di Milano. VII. Natantia. Atti Soc. Ital. Sci. Nat., **58**: 59–99, pls. 3–6.

14 Rathbun, M. J. (1906) The Brachyura and Macrura of the Hawaiian Islands. Bull. U. S. Fish. Comm., **23**: 827–930, pls. 3–24.

15 Saint Laurent, M. de and Cleva, R. (1981) Crustaces decapodes: Stenopodidae. In Resultats de la Campagne Musorstom. 1. Philippines (18–28 Mars 1976), 1 (7). Mem. ORSTOM, **91**: 151–188.

16 Yokoya, Y. (1933) On the distribution of decapod crustaceans inhabiting the continental shelf around Japan, chiefly based upon the materials collected by S.S. Soyo-Maru, during the years 1923–1930. J. Coll. Agr., Tokyo Imp. Univ., **12**: 1–126.

ZOOLOGICAL SCIENCE 4: 375–378 (1987)

Notes on the Genus *Sasanychus* Ehara, New Status, with Description of A New Species from Hokkaido (Acarina, Tetranychidae)

SHÔZÔ EHARA and TETSUO GOTOH[1]

Biological Institute, Faculty of Education, Tottori University, Tottori 680, and
[1]Laboratory of Applied Entomology, Faculty of Agriculture, Ibaraki University, Ami, Ibaraki 300–03, Japan

ABSTRACT—The subgenus *Sasanychus* Ehara in the genus *Panonychus* Yokoyama was elevated to a full genus. A mite, so far referred to "stipeless-egg form" of *P.* (*S.*) *akitanus* Ehara, was described under the name *S. pusillus* n. sp. from *Sasa apoiensis* Nakai in Tomakomai, Hokkaido.

INTRODUCTION

The subgenus *Sasanychus* was created by Ehara [1] in the genus *Panonychus* Yokoyama to accomodate a new species *akitanus* taken from *Sasa* sp. in Akita Prefecture. Recently, it was reported by Gotoh [2, 3] that in *P.* (*S.*) *akitanus* there were two forms differing in egg shape, micro-habitat preference, overwintering stage, diapause characteristics and voltinism. Moreover, the two forms were experimentally confirmed to be reproductively isolated [4].

On close examination we have come to the conclusion that one of the two forms, "stipeless-egg form", is not assigned to *akitanus* but to a new species. In this paper the new species is described and illustrated from *Sasa apoiensis* Nakai in Tomakomai, Hokkaido. Further, the subgenus *Sasanychus* is raised here to genus.

Genus *Sasanychus* Ehara, new status

Panonychus (*Sasanychus*) Ehara, 1978 [1], p. 88.

Type-species: *Panonychus* (*Sasanychus*) *akitanus* Ehara.

Two pairs of para-anal setae present. Dorsal idiosomal setae not set on tubercles. Hysterosoma with transverse striae on the dorsocentral area. Empodium claw-like, with 3 pairs of proximoventral hairs that are similar in length and set at a nearly right angle with claw. Two sets of duplex setae on tarsus I adjacent to each other. Tibia I with 9 tactile setae; tibia II with 8 tactile setae.

Sasanychus akitanus Ehara

Panonychus (*Sasanychus*) *akitanus* Ehara, 1978 [1], p. 88, Figs. 1–11.

Sapporo population of *Panonychus akitanus*: Gotoh, 1986 [2], p. 125; 1986 [3], p. 137.

Stiped-egg form of *Panonychus akitanus*: Gotoh, 1986 [3], p. 149; 1986 [4], p. 153.

Female Dark green. Measurements in μm: body length (including rostrum) 463, body width 273; lengths of setae: P_1 80.7±0.5*, P_2 130.5±1.8, P_3 92.0±1.2, H 106.0±1.3, C_1 114.5±1.1, C_2 113.1±0.9, C_3 108.1±1.6, L_1 112.3±1.2, L_2 118.3 ±1.3, L_3 113.6±1.3, I 94.7±0.6, O 86.8±0.8, CL 64.5±0.7, PA 50.4±1.1; distances: P_1–P_1 81.4±0.6, P_2–P_2 91.6±0.7, C_1–C_1 78.7±1.9, C_2–C_2 81.5 ±1.1, C_3–C_3 58.4±1.3. Length ratio P_3/body=0.197±0.005, H/body=0.229±0.005, L_2/body=0.256±0.005, L_3/body=0.245±0.004. The number of setae and solenidia (in parentheses) on leg podomeres: femora 10–7–4–3, genua 5–5–4–4, tibiae 9(1)–8–6–7, tarsi 14(1)+2 dupl. −13(1)+1 dupl. −10(1)−10(1).

Accepted December 6, 1986
Received November 8, 1986

* Mean±S. E., n=10.

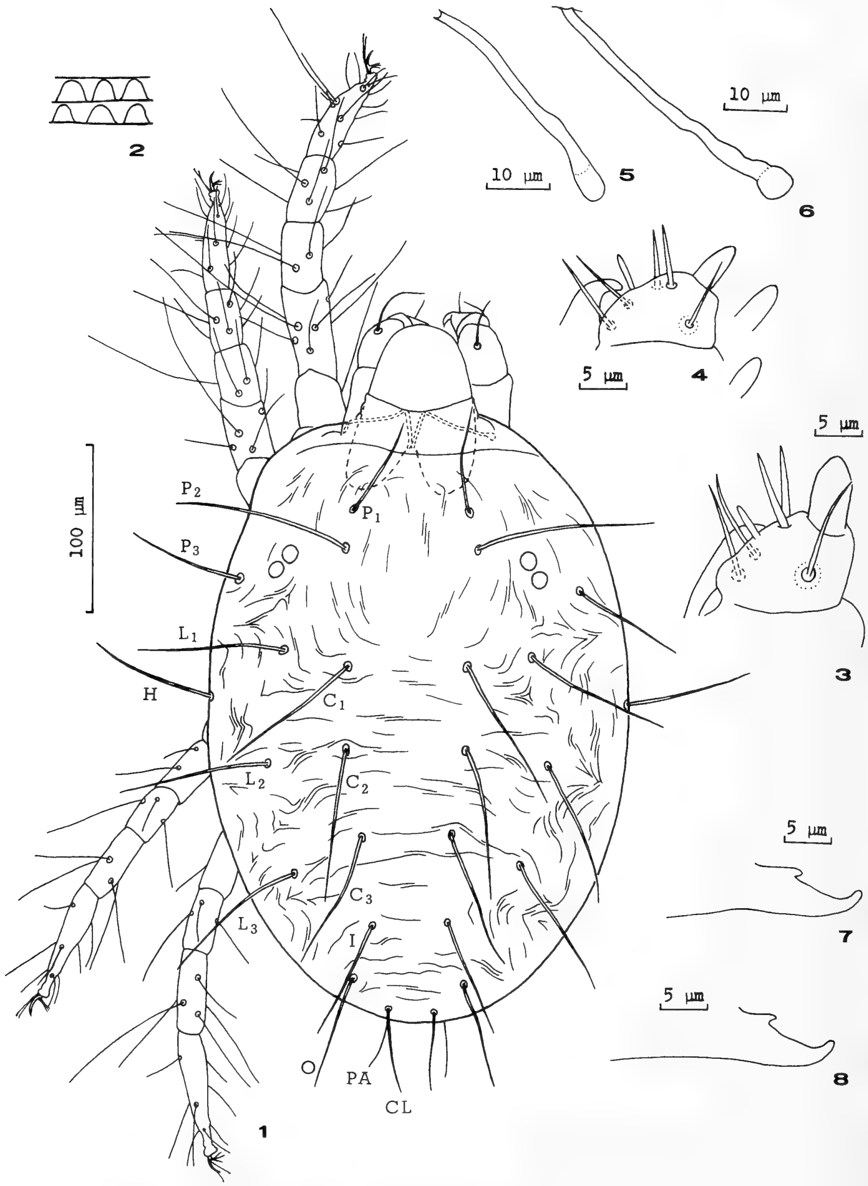

FIGS. 1–8. *Sasanychus pusillus* n. sp. 1: Dorsum of female. 2: Lobes on dorsal hysterosomal striae (schematic). 3: Distal segment of palpus of female. 4: Distal segment of palpus of male, showing variation of terminal sensillum. 5–6: Peritremes of female. 7–8: Aedeagi.

Male Measurements in μm: body length (including rostrum) 344, body width 160; lengths of setae: P_1 67.1±0.7, P_2 92.6±1.0, P_3 75.3±1.3, H 82.7±1.0, C_1 86.3±1.2, C_2 83.1±0.9, C_3 75.3±0.5, L_1 81.5±0.9, L_2 88.5±1.0, L_3 84.0±0.8, I 66.0±1.1, O 56.6±1.0, CL 35.3±1.0, PA 31.7±1.6. The number of setae and solenidia (in parentheses) on leg segments: femora 10–7–4–3, genua 5–5–4–4, tibiae 9(3)–8–6–7, tarsi 13(3)+2 dupl. −13(1)+1 dupl. −10(1)−10(1).

Specimens examined In addition to the type-series (type locality: Nishi-senboku, Akita Pref., Honshu), the following specimens from Hokkaido have been examined: Four ♂♂ and 5 ♀♀, Hokkaido Univ. campus, Sapporo, 9–IX–1983 (S. Ehara and T. Gotoh), on *Sasa senanensis* (Franchet et Savatier) Rehder; 4 ♂♂ and 4 ♀♀, 9–IX–1983 (S. Ehara and T. Gotoh), bred in Inst. of Appl. Zool., Hokkaido Univ., originally collected on Hokkaido Univ. campus, V–1983 (T. Gotoh), on *Sasa senanensis*; 5 ♂♂ and 13 ♀♀, Hokkaido Univ. campus, VII~VIII–1985 (Y. Saitô), on *Sasa senanensis*.

Distribution Hokkaido, Honshu.

Remarks The redescription is based on the type-series, but the measurements nearly accord with those for the specimens from the Hokkaido University campus, Sapporo.

Sasanychus pusillus Ehara et Gotoh, n. sp.
(Japanese name: Hime-midori-hadani)
(Figs. 1–12)

Tomakomai population of *Panonychus akitanus*: Gotoh, 1986 [2], p. 125; 1986 [3], p. 137.

Stipeless-egg form of *Panonychus akitanus*: Gotoh, 1986 [3], p. 149; 1986 [4], p. 153.

Female Body blackish green. Idiosoma with dorsal setae slender, pubescent, longer than distances between consecutive setae. Dorsal hysterosomal striae with lobes rounded apically. Peritremes dilated distally. Genital flap with mostly transverse striae; area immediately anterior to flap with longitudinal striae. Palpus with terminal sensillum approximately twice as long as wide; dorsal sensillum much smaller, slender. Measurements in μm: body length (including rostrum) 416, body width 250; lengths of setae: P_1 64.7±0.7, P_2 103.7±1.0, P_3 67.0±0.5, H 70.6±1.0, C_1 90.8±0.6, C_2 88.2±0.7, C_3 82.7±1.0, L_1 86.0±0.8, L_2 88.8±1.2, L_3 87.0±0.9, I 73.2±0.9, O 64.5±0.8, CL 45.6±0.6, PA 38.9±0.8; distances: P_1–P_1 70.2 ±0.8, P_2–P_2 77.2±0.6, C_1–C_1 71.3±1.2, C_2–C_2 71.8±0.8, C_3–C_3 53.5±0.9. Length ratio P_3/body =0.161±0.004, H/body=0.170±0.005, L_2/:body =0.214±0.005, L_3/body=0.210±0.004. The number of setae and solenidia (in parentheses) on

FIGS. 9–12. *Sasanychus pusillus* n. sp. 9: Tarsus and tibia I of female. 10: Tarsus and tibia II of female. 11: Tarsus and tibia I of male. 12: Tarsus and tibia II of male.

leg segments: femora 10–7–4–3, genua 5–5–4–4, tibiae 9(1)–8–6–7, tarsi 14(1)+2 dupl. –13(1)+1 dupl. –10(1)–10(1). Tarsus I with 5 tactile setae and 1 solenidion proximal to duplex setae; tarsus II with 3 tactiles and 1 solenidion proximad of duplex setae.

Male Aedeagus bent dorsad; the shaft with a prominent process near basilar lobe, the distal upward part nearly straight, terminating in a round tip. Palpus with terminal sensillum slender; dorsal sensillum shorter, very slender. Empodium I with the middle pair of hairs strong, the ventral pair weak, and the dorsal pair similar to the middle or ventral one. Measurements in μm: body length (including rostrum) 318, body width 158; lengths of setae: P_1 53.2±1.2, P_2 83.3±1.4, P_3 58.0±1.1, H 57.7±1.2, C_1 68.3±1.1, C_2 66.7±0.5, C_3 62.6±1.0, L_1 69.0±0.9, L_2 68.4±1.0, L_3 69.0±1.3, I 50.3±1.0, O 41.2±0.6, CL 24.0±0.7, PA 22.1±0.9. The number of setae and solenidia (in parentheses) on legs: femora 10–7–4–3, genua 5–5–4–4, tibiae 9(3)–8–6–7, tarsi 12(3)+ 2 dupl. –11(1)+ 1 dupl. –10(1)–10(1). Tarsus I with 3 tactile setae and 3 solenidia proximal to duplex setae; tarsus II with 1 tactile seta and 1 solenidion well proximal to duplex setae.

Type-series Holotype: ♂, Takaoka, Tomakomai, Hokkaido, 7–VIII–1982 (T. Gotoh), on *Sasa apoiensis* Nakai. Paratypes: 6 ♂♂ and 19 ♀♀, with the above data; 6 ♂♂ and 30 ♀♀, 9–IX–1983 (S. Ehara and T. Gotoh), bred in Inst. of Appl. Zool., Hokkaido Univ. [host in laboratory, *S. apoiensis* and occasionally *S. senanensis* (Franchet et Savatier) Rehder], originally collected at Takaoka, Tomakomai, 13–VII–1983 (T. Gotoh), on *S. apoiensis*.

The type-series is deposited in the Biological Institute, Faculty of Education, Tottori University.

Distribution Hokkaido.

Remarks The female of *Sasanychus pusillus* closely resembles that of *S. akitanus* but differs from the latter in having the dorsal idiosomal setae noticeably shorter (*t*-test, $P<0.001$ for each seta). The former is smaller in body size than the latter, but the length ratios of setae P_3, H, L_2 and L_3 to body are distinctly smaller in *pusillus* (*t*-test, $P<0.001$).

Further, the male of *pusillus* is characterized by having tarsus II with one tactile seta and one solenidion proximal to duplex setae; in the male of *akitanus* tarsus II has three tactiles and one solenidion on the area. In addition, the male tarsus I of *pusillus* has three tactiles and three solenidia proximal to the duplex setae, instead of four tactiles and three solenidia. The aedeagus of *pusillus* is distinctive in that the distal upward part is not undulate and ends in a round tip, and the dorsal margin of the shaft bears a prominent process, whereas in *akitanus* the distal part is slightly sigmoid and has a truncate tip, and the shaft is smooth dorsally.

S. pusillus overwinters as eggs on *Sasa apoiensis* Nakai in Tomakomai, while *akitanus* overwinters both as eggs and female adults on *Sasa senanensis* (Franchet et Savatier) Rehder in Sapporo [2, 3]. The eggs of *pusillus* are deficient in a dorsal stipe, but those of *akitanus* have a distinct dorsal stipe [3]. Moreover, there is the obvious post-mating reproductive isolation between the two species [4].

ACKNOWLEDGMENTS

We wish to express our gratitude to the following gentlemen for their kind and much help: Dr. H. Mori and Dr. Y. Saitô (Institute of Applied Zoology, Hokkaido University), Dr. K. Ishigaki (Tomakomai Experimental Forest of Hokkaido Univ.), Dr. K. Takahashi (Hokkaido Institute of Public Health), Dr. Y. Ohta (School of General Education, Tottori Univ.), and Dr. S. Okuyama (Laboratory of Plant Pathology, Ibaraki Univ.). This study was supported by a Grant-in-Aid for Scientific Research from the Ministry of Education, Science and Culture, Japan (No. 61560054).

REFERENCES

1 Ehara, S. (1978) A new genus and a new subgenus of spider mites from northern Japan (Acarina: Tetranychidae). J. Fac. Educ. Tottori Univ., Nat. Sci., **28**: 87–93.

2 Gotoh, T. (1986) Life-cycle variation in *Panonychus akitanus* Ehara (Acarina: Tetranychidae). Exp. Appl. Acarol., **2**: 125–136.

3 Gotoh, T. (1986) Local variation in overwintering stages of *Panonychus akitanus* Ehara (Acarina: Tetranychidae). Exp. Appl. Acarol., **2**: 137–151.

4 Gotoh, T. (1986) Reproductive isolation between the two forms of *Panonychus akitanus* Ehara (Acarina: Tetranychidae). Exp. Appl. Acarol., **2**:153–160.

ZOOLOGICAL SCIENCE 4: 379–380 (1987)

[COMMUNICATION]

Lamprey Connectin

Yoshiharu Itoh, Di Hua Hu, Kazuyo Ohashi, Sumiko Kimura and Koscak Maruyama

Department of Biology, Faculty of Science, Chiba University, Chiba 260, Japan

ABSTRACT—In lamprey skeletal muscle, only α-connectin, mother molecule of connectin, but not β-connectin was detected in an SDS gel electrophoresis. Lamprey connectin was identified by an immunoblot technique using antisera against chicken breast muscle connectin. Immunofluorescent observations showed that connectin is located at A–I junction regions of a sarcomere as in chicken or rabbit skeletal muscle.

Connectin is an elastic filamentous protein of a huge molecular weight (3000 kDa) in striated muscle, linking myosin filaments to Z discs in a sarcomere (for a review, see [1]). In a comparative survey, it has been shown that connectin is widely distributed among vertebrate striated muscles from fishes to mammals [2, 3]. However, cyclostomes were not investigated.

In the present study, connectin was also detected in lamprey skeletal muscle by SDS gel electrophoresis and by immunoblot and immunofluorescence techniques using anti-chicken connectin. Interestingly, only α-connectin, mother molecule of connectin, was present in freshly sacrified lamprey muscles. In all the muscles of other vertebrates so far examined, β-connectin coexisted together with α-connectin [2].

MATERIALS AND METHODS

Live lamprey was obtained in a local market. Skeletal muscles were cut out, immediately ground in an SDS solution and electrophoresed using 1.8% polyacrylamide as described before [2]. Immunoblot and immunofluorescence procedures were carried out as reported previously, using antisera against chicken breast muscle connectin [4].

Accepted November 26, 1986
Received November 13, 1986

RESULTS AND DISCUSSION

An SDS gel electrophoresis pattern clearly showed that there is only one main band corresponding to connectin in lamprey breast muscle

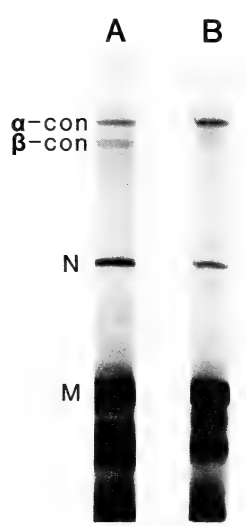

Fig. 1. SDS gel electrophoresis pattern of lamprey skeletal muscle proteins. A total SDS extract was elctrophoresed as described by Hu *et al.* [2], using 1.8% polyacrylamide gels. A, chicken breast muscle; B, lamprey skeletal muscle. α-, β-con, connectin; N, nebulin; M, myosin heavy chain.

(Fig. 1B). Note that there are distinct doublet bands (β-, and β'-connectins) in chicken breast muscle in addition to α-connectin (Fig. 1A). The electrophoretic mobility of lamprey connectin was almost the same as that of chicken breast muscle α-connectin, suggesting the molecular weight of approximately 3 million [5]. It is to be added that nebulin was recognized in lamprey skeletal muscle as well as in chicken (Fig. 1).

To identify the lamprey connectin, an immunoblot technique was adopted. The electrophoresed bands were transferred onto a nitrocellulose sheet followed by the treatment with antisera against chicken breast muscle connectin. The connectin band was detected by the binding of fluorescent antisera against chicken immunoglobulin. As shown in Figure 2, only the slowest band corresponding to α-connectin reacted with anti-connectin. It should be emphasized that anti-chicken connectin crossreacts with lamprey connectin. Therefore, there is not any specificity in anti-connectin so far as vertebrate muscles are concerned. Previously, it was reported that anti-chicken connectin reacts with frog connectin [6].

It has been repeatedly described that polyclonal antibodies against connectin strongly bind the A–I junction region of a sarcomere [1, 4]. An indirect immunofluorescence microscopy confirmed this localization of connectin in cyclostomes striated muscle (Fig. 3). As seen in Figure 3, both edges of an A band were fluorescent. Central region, 1 μm long, of an A band (1.5 μm), and also Z disc area were not stained with anti-connectin. These staining patterns were due to specific locations of antigenic sites on connectin filaments in register in a relaxed sarcomere (cf. [1]).

The present work demonstrated that there is α-connectin alone in lamprey (cyclostomes) skeletal muscle. This is very unique, because β-connectin, proteolytic product of α-connectin, is always present togther with α-connectin in other vertebrate striated muscles including a variety of fishes [7].

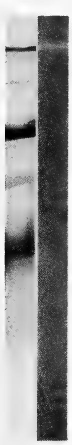

FIG. 2. Immunoblot pattern of lamprey skeletal muscle connectin. A total SDS extract was used. Left, Coomasee brilliant blue stained pattern; Right, stained with an antiserum against chicken breast muscle connectin [6].

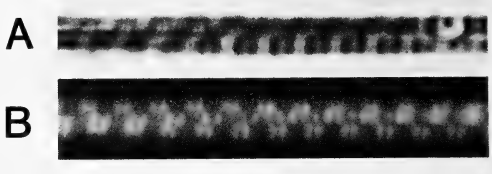

FIG. 3. Immunofluorescent pattern of lamprey skeletal myofibrils treated with antisera against chicken breast muscle connectin. A, phase contrast microscopic image; B, fluorescent microscopic image. Bar, 10 μm.

ACKNOWLEDGMENT

This work was supported by a grant from the Ministry of Education, Science and Culture to "Molecular Biological Studies on Marine Animal Muscles" at Chiba University.

REFERENCES

1 Maruyama, K. (1986) Int. Rev. Cytol., **104**: 81–114.
2 Hu, D. H., Kimura, S. and Maruyama, K. (1986) J. Biochem., **99**: 1485–1492.
3 Locker, R. H. and Wild, D. J. C. (1986) J. Biochem., **99**: 1473–1484.
4 Maruyama, K., Sawada, H., Kimura, S., Ohashi, K., Higuchi, H. and Umazume, Y. (1984) J. Cell Biol., **99**: 1391–1397.
5 Maruyama, K., Kimura, S., Yoshidomi, H., Sawada, H. and Kikuchi, M. (1984) J. Biochem., **95**: 1423–1433.
6 Maruyama, K., Yoshioka, T., Higuchi, H., Ohashi, K., Kimura, S. and Natori, R. (1985) J. Cell Biol., **101**: 2167–2172.
7 Seki, N. and Watanabe, T. (1984) J. Biochem., **95**: 1161–1167.

ZOOLOGICAL SCIENCE 4: 381–383 (1987)

[COMMUNICATION]

Disappearance of Immunoglobulin G in Endodermal Cells in Non-Immunized Murine Yolk Sac Placenta towards Parturition

KIYOSHI SHIMIZU and MASAMI HOKANO

Department of Anatomy, Tokyo Medical College, Shinjuku-ku, Tokyo 160, Japan

ABSTRACT—Immunoglobulin G in the endodermal cell of yolk sac placenta of non-immunized mouse exisited on day 16 of pregnancy but most of it disappeared on day 18 of pregnancy. Disappearance of immunoglobulin G in mouse was similar to that in rat.

INTRODUCTION

Immunoglobulin G (IgG) is the only immunoglobulin that is incorporated into the circulating system of fetus. The yolk sac placenta is the transporting site of passive immunity from mother to fetus in mouse and rat [1]. In mouse, IgG production is stimulated by substance or factor from fetus [2] and increases towards parturition [3]. A transmission of IgG from mother to fetus increases towards parturition [4].

Antibodies produced after immunization with horseradish peroxidase in female rat before mating are uptaken by visceral endodermal cells of yolk sac placenta and stored in it's apical vacuoles during mid pregnant period [5–7]. Most of these antibodies in the vacuoles, however, is degraded by lysosomal enzymes towards parturition and thus disappears [7]. Since similar disappearance of IgG in the murine endodermal cells towards parturition has been unknown, we observed IgG in the endodermal cells of non-immunized mouse with immunohistochemical method.

Accepted December 2, 1986
Received October 23, 1986

MATERIALS AND METHODS

Animals used were female mice of the IVCS strain. They were reared under 12L: 12D and given food and water *ad libitum*. At 8 weeks of age they were mated. They were examined every morning for the presence of a copulatory plug and day when the pulg was found was desingned as day 0 of pregnancy. In this strain the pregnant period was 19 days. The uterine horn was removed, fixed in 10% buffered formalin, embedded in paraffin and cut in sections 3 μm thick.

The anti-mouse IgG (heavy and light chains), anti-sheep γ-globulin, sheep-peroxidase anti-peroxidase (PAP) and sheep whole serum was obtained from Cappel laboratory. Abbreviations of the antibodies are as follows; anti-mouse IgG, sheep antiserum to mouse IgG; anti-sheep γ-globulin, rabbit antiserum to sheep γ-globulin; PAP, sheep anti-peroxidase IgG conbined with horseradish peroxidase.

Endogenous peroxidase in the sections was destroyed by exposure to absolute alcohol with contained H_2O_2 (10%, V/V). The sections were exposed to sheep whole serum (1:200) or anti-mouse IgG (1:200) for 30 min at room temperature. Then they were washed three times in phosphate-buffered saline (PBS, pH 7.2), incubated in anti-sheep γ-globulin (1:10) for 30 min at room temperature. After three-fold washing in PBS, the sections were reincubated in PAP (1:50) for 30 min at room temperature.

The sites of antibody were determined histochemically, using 3, 3′-diaminobentizine solution

[8] for 5 min and counterstained with hematoxylin. When exposed to sheep whole serum (control staining), the specific stain was not found in the sections.

RESULTS AND DISCUSSION

On day 16 of pregnancy, IgG was found in the endodermal cells, being heaviest in the apical vacuole (Fig. 1a). IgG positive cells were located

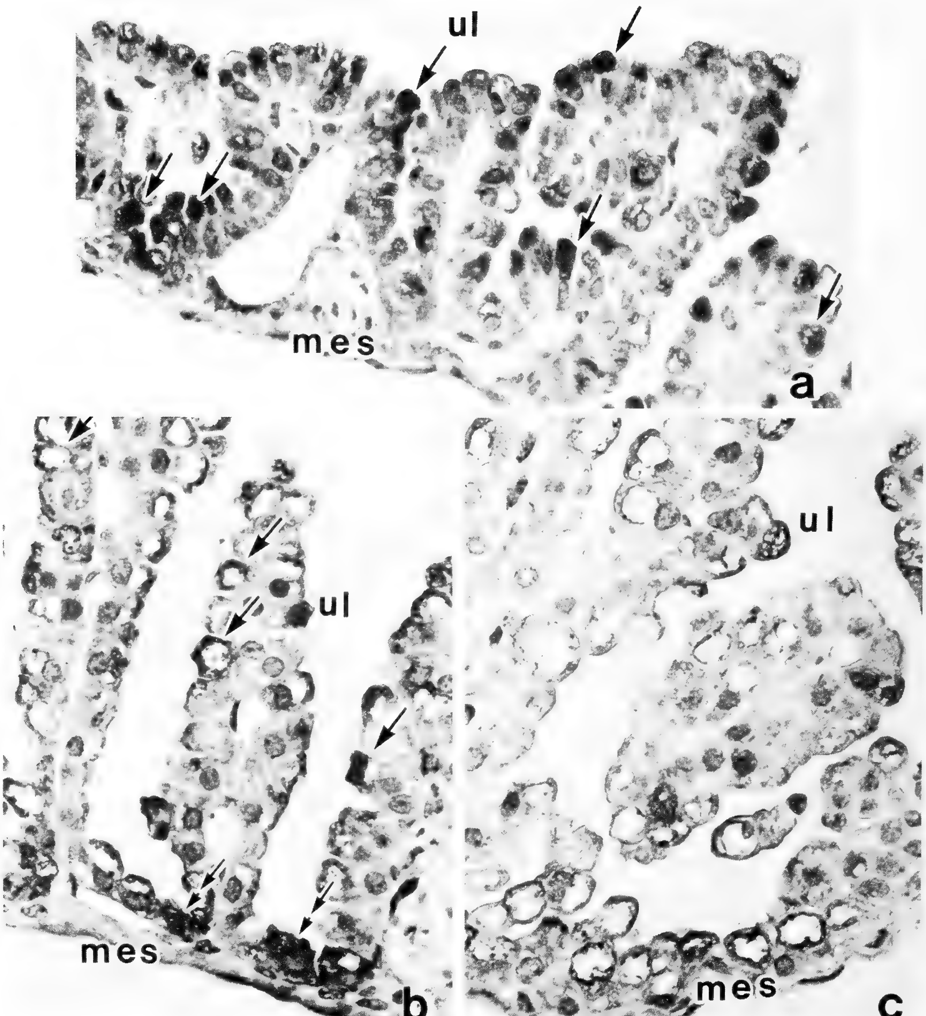

FIG. 1. IgG in the endodermal cells on day 16 (a), 17 (b), or 18 (c) of pregnancy (PAP method).

(a) IgG positive endodermal cells (arrows) scattered in the visceral endoderm. IgG exsisted in apical large vacuoles (×530).

(b) Most of IgG in apical vacuoles of the endodermal cells disappeared. A little IgG remained in a rim of apical vacuoles (arrows). There were some IgG positive cells (double arrows) in the bottom of villi. (× 530).

(c) There were no IgG positive cells in the bottom of villi. Disappearance of IgG in apical vacuoles of the endodermal cells became clearer from that on day 17 of pregnancy. (×530).

mes; mesothelium. ul; uterine lumen.

in scattered groups of the visceral endoderm. On day 17 of pregnancy, villi became tall and the endodermal cell hypertrophied. Most of IgG in the apical vacuoles disappeared and a little IgG remained in a rim of vacuoles (Fig. 1b). In bottom of villi, there were some IgG positive cells. The endodermal cells hypertrophied more on day 18 than on day 17 of pregnancy. IgG in the apical vacuoles disappeared more on day 18 than day 17 of pregnancy (Fig. 1c). There was no IgG positive cell on day 18 of pregnancy. These observations indicated that IgG in the endodermal cells of murine yolk sac placenta disappeared towards parturition and that this disappearance of IgG was similar to that in rat [7].

Both biochemical [9] and histochemical [10] methods show that activity of lysosomal enzymes in the endodermal cells becomes high towards parturition. Since large quantities of materials uptaken by the endodermal cells are degraded by lysosomal enzymes for a source of amino acid for protein synthesis by fetus [11, 12], IgG in the endodermal cells may be degraded as materials for protein synthesis by fetus. The transporting route that conveys endocytosed materials from apical to deep portion within the endodermal cells establishes towards parturition [13, 14], suggesting that IgG is transported by this route and thus IgG is not degraded by lysosomal enzymes towards parturition when a transmission of IgG becomes high [4].

REFERENCES

1 Brambell, F. W. R. (1970) Front. Biol., **18**: 80–101.

2 Carter, J. and Dresser, D. W. (1985) J. Reprod. Fertil., **74**: 535–542.

3 Carter. J. and Dresser, D. W. (1983) Immunology, **49**: 481–490.

4 Appleby, P. and Catty, D. (1983) J. Reprod. Immunol., **5**: 203–213.

5 LaLiberté, F., Mucchielli, A., Ayraud, W. and Masseyeff, R. (1981) Am. J. Reprod. Immunol., **1**: 345–351.

6 Mucchielli, A., LaLiberté, F. and LaLiberté, M.-F. (1983) Placenta, **4**: 175–184.

7 Jollie, W. P. (1985) J. Reprod. Immunol., **7**: 261–274.

8 Graham, R. C. and Karnovsky, M. J. (1966) J. Histochem. Cytochem., **14**: 291–302.

9 Beck, F. F., Lloyd, J. B. and Griffiths, A. (1967) J. Anat., **101**: 461–478.

10 Padykula, H. A. (1958) J. Anat., **92**: 118–129.

11 Freeman, S. J., Beck, F. and Lloyd, J. B. (1983) J. Embryol. Exp. Morphol., **73**: 307–315.

12 Freeman, S. J. and Lloyd, J. B. (1983) J. Embryol. Exp. Morphol., **73**: 307–315.

13 Lambson, R. O (1966) Am. J. Anat., **118**: 21–52.

14 Seibel, W. (1974) Am. J. Anat., **140**: 213–236.

ZOOLOGICAL SCIENCE 4: 385–386 (1987)

[COMMUNICATION]

Karyotype of a Gekkonid Lizard, *Cosymbotus platyurus*, from Sabah, Borneo, Malaysia

Hidetoshi Ota, Masafumi Matsui[1], Tsutomu Hikida, and Toshitaka Hidaka

Department of Zoology, Faculty of Science, and [1]Biological Laboratory of Yoshida College, Kyoto University, Sakyo, Kyoto 606, Japan

ABSTRACT—Both sexes of the gekkonid lizard *Cosymbotus platyurus* from Sabah, Borneo, have 46 diploid chromosomes. All chromosomes are telocentric and their sizes vary gradually. There are neither sexually dimorphic nor heteromorphic pairs. Possible karyological differentiation in the species is discussed.

INTRODUCTION

The family Gekkonidae consists of approximately 85 genera, of which only about one-fourth has been karyologically investigated [1, 2]. The genus *Cosymbotus* comprises two species from the Asian tropics, *C. platyurus* and *C. craspedotus* [3]. The fromer species is a common house dweller, widely ranging throughout South Asia and Indo-Australian Archipelago, and its karyotype has been reported by De Smet [2]. A single karyological information available is, however, inadequate, only being based on a single male from an unknown locality [2].

We have examined the karyotypes for both sexes of *Cosymbotus platyurus* from North Borneo and obtained a result slightly different from the previous report.

MATERIALS AND METHODS

Two adult males and one adult female were collected from Kota Kinabalu, Sabah, Malaysia, and were brought to the laboratory where they were intraperitoneally injected with 0.1 ml of colchicine solution (2 mg/ml) per gram of body weight. Thirty hours after the injection, the femur bone marrows were taken out, treated with hypotonic solution and fixed in Carnoy's solution. Metaphase chromosome spreads were obtained by an air-dry method and stained with Giemsa.

Accepted October 20, 1986
Received September 30, 1986
[1] To whom requests of reprints should be addressed.

RESULTS AND DISCUSSION

Sixteen cells from two males and eight from one female possessed 46 diploid chromosomes, all of which were telocentric. The chromosomes showed a continuous size variation and did not form distinct size groups (Fig. 1). No heteromorphic pair was observed in either sex, and no sexually dimorphic pair was found, either. De Smet [2] also counted 46 chromosomes in a male *Cosymbotus platyurus* from an unknown locality, but he found three large pairs being subtelocentric. The reason for the discordant results is unknown, but it is possible that the male examined by De Smet [2] had been obtained from a locality other than Borneo, and that the karyotypes may differ geographically.

The diploid number of chromosomes in the gekkonids hitherto examined ranges from 32 to 46, and *Cosymbotus platyurus* has the largest number as with several species of *Hemidactylus* [4, 5]. Gorman [1] noted that the typical gekkonid karyotype primarily consists of a graded series of telocentric chromosomes without discrete macro- and microchromosomes. These typical features

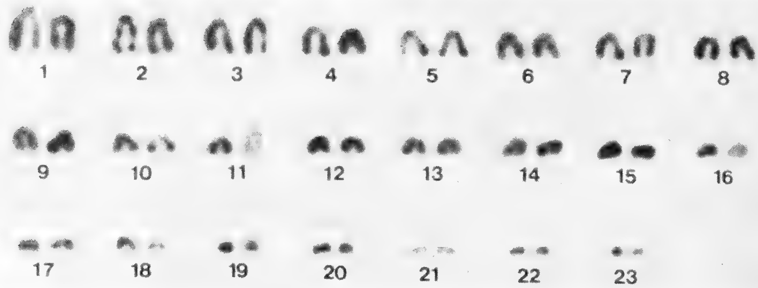

FIG. 1. Karyotype of male *Cosymbotus platyurus* from Kota Kinabalu, Sabah, Borneo. ×1700.

well apply to the karyotype of *Cosymbotus platyurus* examined here.

Considerable karyological differentiation among widely ranging geckos has been reported for several genera [e.g., 6–11]. In some cases, morphologically identical forms have differential karyotypes and have been tentatively treated as "chromosomal races" [8]. In other cases, however, detailed morphological analyses revealed the presence of several cryptic species [12]. As noted above, *Cosymbotus platyurus* is widespread throughout a large part of Tropical Asia, and the presence of karyotypic differentiation in this species was suggested. It is, therefore, necessary to karyologically investigate further specimens from various localities of its range.

ACKNOWLEDGMENTS

We thank S. Ishihara for literature. Field trips to Borneo were financed by a Grant-in-Aid for Scientific Research (Overseas Scientific Survey) from the Japan Ministry of Education, Science and Culture (60041037).

REFERENCES

1 Gorman, G. C. (1973) In "Cytotaxonomy and Vertebrate Evolution". Ed. by A. B. Chiarelli and E. Capanna, Academic Press, New York, pp. 349–424.

2 De Smet, W. H. O. (1981) Acta Zool. Pathol. Antverp., **76**: 35–72.

3 Wermuth, H. (1965) In "Das Tierreich". Ed. by R. Mertens, W. Henning and H. Wermuth, Walter de Gruyter & Co., Berlin, pp. 21–22.

4 Nakamura, K. (1932) Cytologia, **3**: 156–168.

5 Makino, S. and Momma, E. (1949) Cytologia, **15**: 96–108.

6 King, M. and Rofe, M. R. (1976) Chromosoma, **54**: 75–87.

7 King, M. (1977) Aust. J. Zool., **25**: 43–57.

8 King, M. (1978) Herpetologica, **34**: 216–218.

9 King, M. (1983) Aust. J. Zool., **30**: 723–741.

10 Darevsky, I. S., Kupriyanova, L. A. and Roshchin, V. V. (1984) J. Herpetol., **18**: 277–284.

11 Moritz, C. (1986) Syst. Zool., **35**: 46–67.

12 King, M. (1983) Amphibia-Reptilia, **4**: 147–169.

ZOOLOGICAL SCIENCE 4: 387–390 (1987)

[COMMUNICATION]

Immunoreactive Angiotensin II in the Corpuscles of Stannius of the Rainbow Trout, *Salmo gairdneri*

CHIFUMI YAMADA and HIDESHI KOBAYASHI[1]

Department of Biology, Faculty of Science, Toho University, Funabashi, Chiba 274, Japan

ABSTRACT—The localization of immunoreactive angiotensin II (AII) in the corpuscles of Stannius (CS) was examined in five species of freshwater teleosts, the rainbow trout, *Salmo gairdneri,* the biwa trout, *Oncorhynchus masou,* the Japanese char, *Salvelinus leucomaenis,* the carp, *Cryprinus carpio* and the goldfish, *Carassius auratus.* An AII-like substance was found in the cells of CS of the rainbow trout. In four other species, AII-immunoreactivity could not be detected.

INTRODUCTION

The corpuscles of Stannius (CS) situated near or in the kidney of ganoids and teleosts are considered to constitute an endocrine gland on the basis of various observations. Histologically, granules in the cells of CS are stained with Bowie's staining, which also stains granules containing renin in the juxtaglomerular cells of the teleostean kidney [see 1]. Electron microscopically, CS cells contain many proteinous granules [2–5]. Pharmacologically, Chester Jones *et al.* [6] reported extracts of CS of the European eel, *Anguilla anguilla,* to possess pressor activity such as that of renin. Sokabe *et al.* [7] and Ogawa and Sokabe [8] have also described that homogenate of CS contains a substance showing renin-like activity in several species of teleosts. Further, chemically, [Asp^1, Val^5, Asn^9] angiotensin I (AI) and [Asn^1, Val^5, Asn^9] AI were found to be produced by incubating tissue extracts of CS and kidney with homologous plasma in the chum salmon, *Oncorhynchus keta* [9] and [Asn^1, Val^5, His^9] AI in the Japanese goosefish, *Lophius litulon* [10]. Thus, it is clear that CS contain a renin-like enzyme. This raises a question as to whether this enzyme produces angiotensin II (AII) in the same cells of CS, since it has been demonstrated that renin and AII coexist in gonadotrophs in the rat [11]. In the present study, the presence of AII, a member of the renin-angiotensin system, was examined immunohistochemically in the CS of five species of fresh water teleosts.

MATERIALS AND METHODS

Tissue preparations

The rainbow trout, *Salmo gairdneri* (about 20 cm in total length), the biwa trout, *Oncorhynchus masou* (about 20 cm), the Japanese char, *Salvelinus leucomaenis* (about 20 cm), the carp, *Cyprinus carpio* (about 40 cm) and the goldfish, *Carassius auratus* (about 10 cm) were obtained commercially in the spring and summer. Following decapitation, CS were quickly removed from the kidney and fixed in Bouin's solution overnight. Tissue preparations were dehydrated through a series of ethanols, cleared in xylol and embedded in paraffin. Six or eight μm thick sections were made.

Immunohistochemistry

An antiserum to AII raised by Yamaguchi [12] against synthetic Asp^1-$Ileu^5$-AII in rabbits was

Accepted December 12, 1986
Received November 20, 1986

[1] To whom request of reprints should be addressed.

used for the immunohistochemistry. This antiserum was fully cross-reactive with Asp^1-Val^5-AII [12] and Asn^1-Val^5-AII (Okawara, unpublished data), both of which are teleostean type AII [9, 13, 14].

Deparaffinized tissue preparations were immunostained according to the peroxidase-anti-peroxidase method of Sternberger *et al.* [15]. After incubation in 0.3% H_2O_2 for 30 min, the tissue preparations were rinsed in 0.1 M phosphate-buffered saline (PBS; pH 7.2) containing 0.3% Triton X–100 for 15 min and incubated in AII antiserum diluted at 1:1000 overnight at 4°C. They were then washed in 0.1 M PBS containing 0.3% Triton X–100 and incubated for 90 min at room temperature in goat anti-rabbit IgG (Polysciences Inc.) diluted at 1:200. After being washed in 0.1 M PBS containing 0.3% Triton X–100, they were incubated in peroxidase-anti-peroxidase complex (Dako Corp. or Cappel Laboratories) diluted at 1:200 for 90 min at room temperature. Staining was carried out by incubating the sections in a solution of 0.02% 3, 3′-diaminobenzidine (DAB) in 0.05 M Tris buffer (pH 7.6) containing 0.006% H_2O_2 for 10–15 min at room temperature. To examine the specificity of the immunoreaction by AII antiserum, immunostaining with AII antiserum preabsorbed by Asn^1-Val^5-AII (20 μg/ml antiserum; Hypertensin Ciba) was performed.

RESULTS

There are 4 to 6 CS in the rainbow trout. CS belong to Type IV as defined by Krishnamurthy and Bern [16] and are comprised of many small lobes. Each lobe consists of a number of incomplete lobules (Fig. 1). Cells showing AII-immunoreactivity were observed singly (Fig. 1) or in clusters (Fig. 2) among the cells of the lobules (Fig. 2) . Some AII-immunoreactive cells were observed to have cytoplasmic projections (Fig. 3). The intensity of AII-immunoreactivity and number of AII-immunoreactive cells varied with the individual. The AII-immunoreactivity observed in the rainbow trout was abolished when AII antiserum was preincubated with AII. Thus, the immunoreaction is thought to be specific to AII. In some trout specimens, no AII-immunoreactive cells were detected in CS. No AII-immunoreactivity was detected in the CS of the

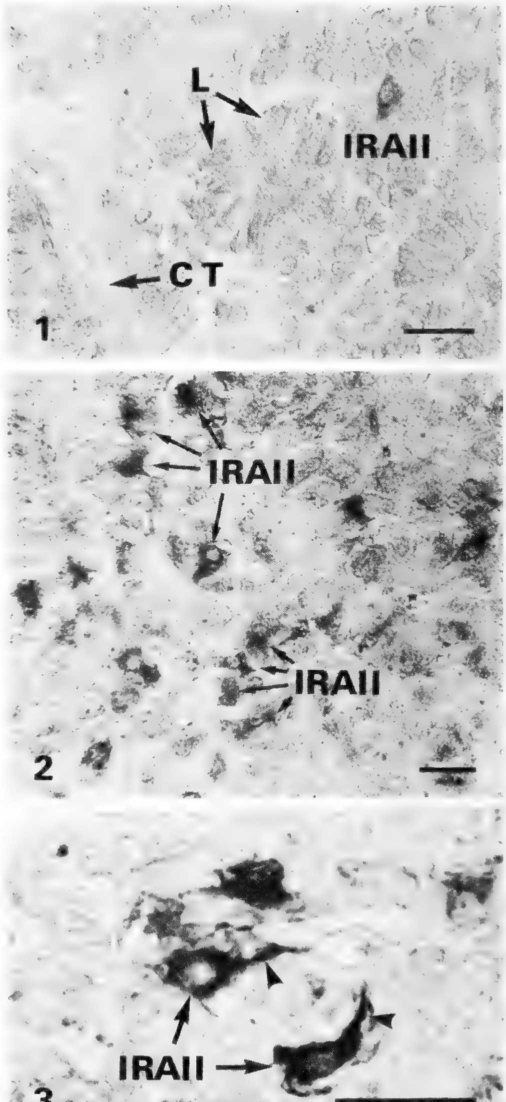

Fig. 1. Corpuscles of Stannius of the rainbow trout, *Salmo gairdneri,* containing an AII-immunoreactive cell (IRAII). L, lobule. CT, connective tissue between lobes. Scale, 20 μm.

Fig. 2. AII-immunoreactive cells (IRAII) in loose clusters in the CS of the rainbow trout. Scale, 20 μm.

Fig. 3. Some AII-immunoreactive cells (IRAII) with cytoplasmic projections (arrow heads). Scale, 20 μm.

four other species.

DISCUSSION

In the present study, immunoreactive AII was first demonstrated in the CS of the rainbow trout, *Salmo gairdneri*. However, in the biwa trout, the Japanese char, the carp and the goldfish, no AII was detected immunohistochemically. It is not clearly understood why the CS of these fishes fail to show AII-immunoreactivity, but there is the possibility that the amount of AII-like substance in CS cells is too small to be detected by the present immunohistochemical techniques in these four species. Also, the antiserum used in the present study may possibly have been unable to cross-react with AII in the CS of the four species of fish. By using different fixatives, sectioning techniques and antisera or radioimmunoassay, AII-like substance may be detected. It is important to clarify whether AII is present in the cells of CS in fish in general.

Since AII-immunoreactive cells in CS of the rainbow trout have cytoplasmic projections, they apparently belong to the type 2 cells with projections described by Wendelaar Bonga *et al.* [17] in the threespined stickleback, *Gasterosteus aculeatus* and also correspond to AF-negative cells in the rainbow trout [16]. However, Aida *et al.* [18, 19] consider type 2 cells likely to be different physiological stages of type 1 cells in the Coho salmon, *Oncorhynchus kisutch*. It is thus difficult to confirm whether AII-immunoreactive cells belong to type 1 or type 2 at the present time. Cells containing AII-like substance observed in the rainbow trout were not many in number and most of the cells in CS were not immunoreactive to the AII antiserum used. Thus, these immunoreactive cells with AII antiserum may possibly be a cell type distinct from type 1 or 2.

A renin-like enzyme in CS has been suggested on the basis of histological [see 1] and pharmacological findings [6–8]. Recently, angiotensins were chemically found to be produced by incubating extracts of CS with plasma in the chum salmon [9] and the Japanese goosefish [10]. In the present study, AII itself was immunohistochemically found in the cells of CS in the rainbow trout. The presence of AII-like substance in the CS of species other than the rainbow trout is now being examined using the same and different techniques. The physiological significance of immunoreactive AII in CS is not clear at the present time. However, the AII-like substance produced in CS likely functions locally in CS rather than systemically, since its amount in CS may be very small, based on a report that in the carp, the crucian carp and the Japanese goosefish, amount of renin in CS is far less than that in the kidney [7]. AII in CS cells may regulate intracellularly the secretion of CS hormones.

The CS of the eel were recently found to synthesize and secrete a mammalian parathyroid-like hormone called parathyrin of CS (PCS), by immunofluorescence techniques, to be located in the cytoplasm of all cells in CS [20]. Whether the CS of the rainbow trout contain PCS or not is not known at the present. If they do, it would be of interest to examine the distribution of AII-like substance and PCS in CS.

ACKNOWLEDGMENTS

The authors are grateful to Dr. Ken-ichi Yamaguchi, Department of Physiology, Niigata University School of Medicine, for a supply of AII antiserum. This study was supported by Grant-in-Aid for Scientific Research from the Ministry of Education, Science and Culture of Japan.

REFERENCES

1 Oguri, M. and Sokabe, H. (1974) Bull. Jpn. Soc. Sci. Fish., **40**: 545–549.
2 Oguri, M. (1966) Bull. Jpn. Soc. Sci. Fish., **32**: 903–908.
3 Fujita, H. and Honma, Y. (1967) Z. Zellforsch., **77**: 175–187.
4 Ogawa, M. (1967) Z. Zellforsch., **81**: 174–189.
5 Cohen, R. S., Pang, P. K. T. and Clark, N. B. (1975) Gen. Comp. Endocrinol., **27**: 413–423.
6 Chester Jones, I., Henderson, I. W., Chan, D. K. O., Rankin, J. C. and Mosley, W. (1966) J. Endocrinol., **34**: 393–408.
7 Sokabe, H., Nishimura, H., Ogawa, M. and Oguri, M. (1970) Gen. Comp. Endocrinol., **14**: 510–516.
8 Ogawa, M. and Sokabe, H. (1982) Gen. Comp. Endocrinol., **47**: 36–41.
9 Takemoto, Y., Nakajima, T., Hasegawa, Y., Watanabe, T. X., Sokabe, H., Kumagae, S. and Sakakibara, S. (1983) Gen. Comp. Endocrinol., **51**: 219–227.

10 Hasegawa, Y., Watanabe, T. X., Nakajima, T. and Sokabe, H. (1984) Gen. Comp. Endocrinol., **54**: 264–269.

11 McKenzie, J. C., Naruse, K. and Inagami, T. (1985) Anat. Rec., **212**: 161–166.

12 Yamaguchi, K. (1981) Acta Endocrinol., **97**: 137–144.

13 Hayashi, T., Nakayama, T., Nakajima, T. and Sokabe, H. (1978) Chem. Pharm. Bull., **26**: 215–219.

14 Hasegawa, Y., Nakajima, T. and Sokabe, H. (1983) Biomed. Res., **4**: 417–420.

15 Sternberger, L. A., Hardy, P. H., Cuculis, J. J., Jr. and Meyer, H. G. (1970) J. Histochem. Cytochem., **18**: 315–333.

16 Krishnamurthy, V. G. and Bern, H. A. (1969) Gen. Comp. Endocrinol., **13**: 313–335.

17 Wendelaar Bonga, S. E., Greven, J. A. A. and Veenhuis, M. (1976) Cell Tissue. Res., **175**: 297–312.

18 Aida, K., Nishioka, R. S. and Bern, H. A. (1980) Gen. Comp. Endocrinol., **41**: 296–304.

19 Aida, K., Nishioka, R. S. and Bern, H. A. (1980) Gen. Comp. Endocrinol., **41**: 305–313.

20 Lopez, E., Tisserand-Jochem, E-M., Eyquem, A., Milet, C., Hillyard, C., Lallier, F., Vidal, B. and MacIntyre, I. (1984) Gen. Comp. Endocrinol., **53**: 28–36.

ZOOLOGICAL SCIENCE 4: 391–394 (1987)

[COMMUNICATION]

Phosphocalcic Response of Stannius Corpuscles Extract in the Freshwater Snake, *Natrix piscator*

N. Hasan, S. Das, Ajai K. Srivastav and Krishna Swarup[1]

Department of Zoology, University of Gorakhpur, Gorakhpur-273009, India

ABSTRACT—The effect of i.p. injection of aqueous extract of Stannius corpuscles (2.5, 5 and 10 mg/100 g b. wt.) on serum calcium and inorganic phosphorus levels was investigated in the freshwater snake, *Natrix piscator* over a period of 8 hr. This treatment evokes hypocalcemia and hypophosphatemia with a return to control.

INTRODUCTION

The corpuscles of Stannius(CS) are putative endocrine glands located on the kidneys of holostean and teleostean fishes. Recently, they have aroused considerable interest for their role in calcium homeostasis. Stanniectomy in teleosts brings forth hypercalcemia [1–3]. The hypocalcemoc factor (s) released from CS are hypocalcin [4] and teleocalcin [5]. A PTH-like substance (parathyrin) has also been localized immunocytochemically in the eel CS [6].

Recently, it has been reported that CS extract induces hypocalcemia in non-piscine vertebrates i.e. mammal [7], bird [8] and amphibia [9, 10]. So far, there exists no information regarding the effect of CS extract on the serum calcium and inorganic phosphorus levels of reptiles. This tempted us to undertake such a study in the freshwater snake, *Natrix piscator*.

MATERIALS AND METHODS

The CS used in this study were surgically removed from both sexes of the adult freshwater catfish, *Heteropneustes fossilis*. These glands were stored in ice and used almost immediately. The glands were weighed wet and homogenized in ice-cold saline (0.9% sodium chloride solution). The homogenate was centrifuged (5000 rpm for 10 min) and the supernatant was collected.

Forty eight individuals of the freshwater snake (*Natrix piscator*, b. wt. 150–200 g) were maintained under laboratory conditions for 1 week prior to use. They were then divided into 4 numerically equal groups – Group A, injected with saline only (0.2 ml/100 g b. wt.); Group B, injected with extract of 2.5 mg CS/100 g b. wt.; Group C, injected with extract of 5 mg CS/100 g b. wt.; Group D, injected with extract of 10 mg CS/100 g b. wt. All injections were given i.p. In all the groups the volume of the injection was the same (0.2 ml/100 g b. wt.). The blood samples were always collected after slight ether anesthesia. An initial sample of blood (zero hour) was taken from group A. Multiple sampling of blood from groups A–D were taken serially after 0.5, 1, 2, 4, 6 and 8 hr following the injection. There are 12 individuals in each group. From 6 individuals (at each interval 6 determinations from separate individual) blood for the analysis of serum calcium level was taken, similarly from the other 6 individuals (at each interval 6 determinations from separate individual) blood for the analysis of serum inorganic phosphorus level was taken. The serum calcium and inorganic phosphorus levels were measured according to Trinder's [11] and Fiske and Subbarow's [12] methods, respectively.

Accepted October 6, 1986
Received June 30, 1986

[1] To whom reprints should be requested.

Differences between the values of serum calcium and inorganic phosphorus levels among the snakes injected either with saline (group A) or CS extract (groups B, C and D) were evaluated using Student's t-test.

RESULTS

The initial values (zero hour) of serum calcium and inorganic phosphorus are 11.7±0.10 and 6.9 ±0.40 mg/100 ml, respectively.

The serum calcium levels of saline injected specimens (group A) at different time intervals have been shown in Figure 1.

The serum calcium level of the specimens of group B (extract of 2.5 mg CS/100 g b. wt.) exhibits no change at 0.5 hr. At 1 hr a perceivable hypocalcemic effect is noticed which continues up

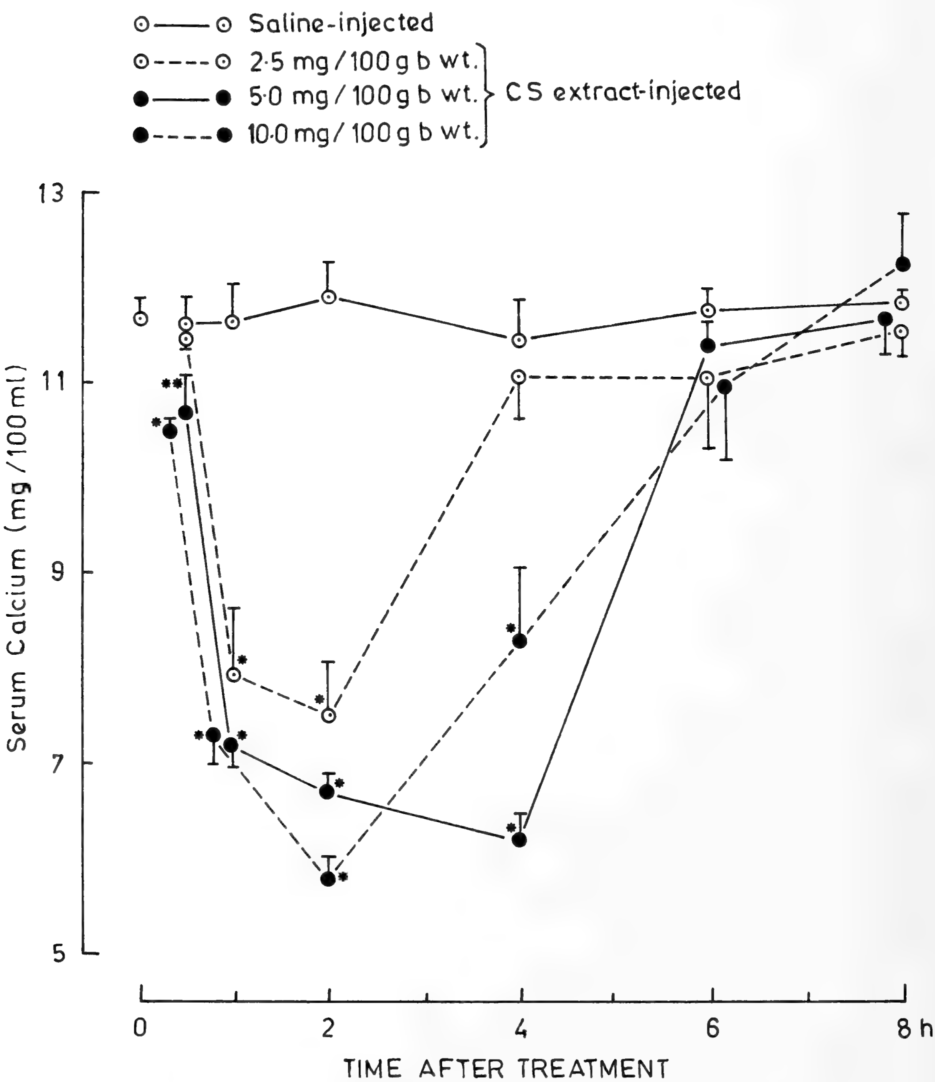

FIG. 1. Changes in the serum calcium level after administration of saline and CS extract. Each point indicates mean±SD of 6 determinations. * and ** represent significant responses, $p<0.001$ and $p<0.01$, respectively.

to 2 hr. There after, the values show a tendency towards normocalcemia (Fig. 1).

In group C (extract of 5 mg CS/100 g b. wt.) hypocalcemia is perceived ealier i.e. at 0.5 hr which progressively increases till 4 hr following the treatment (Fig. 1). Thereafter, the serum calcium level becomes normal at 6 and 8 hr.

In group D (extract of 10 mg CS/100 g b. wt.), the hypocalcemia is perceived after 0.5 hr. This response gets exaggerated up to 2 hr. This is followed by a rise in the serum calcium level ultimately approaching normocalcemia between 6 and 8 hr (Fig. 1).

The serum inorganic phpsphorus levels of the specimens of group A (saline injected) at different time intervals have been shown in Figure 2.

In group B hypophosphatemic effect of CS extract has been noticed at 0.5 hr which gradually increases till 1 hr following the administration. From 2 hr onwards the hypophosphatemic effect decreases till the close of the experiment (Fig. 2).

In group C the hypophosphatemic effect increases progressively from 0.5 hr up to 4 hr following the treatment (Fig. 2). Thereafter, the values tend to become normal. However, the hypophosphatemic effect of CS extract is significant till the close of the experiment.

In group D, the hypophosphatemic effect has been noticed at 0.5 hr. This response persists throughout the experiment (Fig. 2).

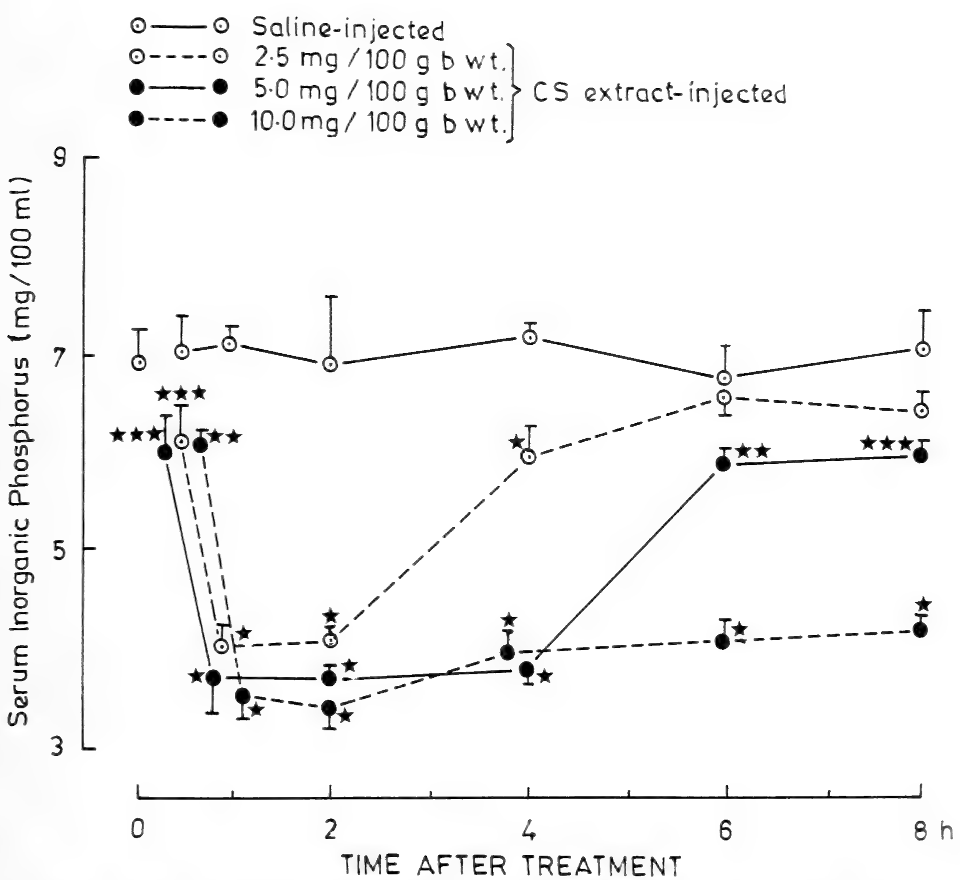

FIG. 2. Changes in the serum inorganic phosphorus level after administration of saline and CS extract. Each point indicates mean ± SD of 6 determinations. *, ** and *** represent significant responses $p<0.001$, $p<0.01$ and $p<0.02$, respectively.

DISCUSSION

The present study shows that CS extract induces hypocalcemia in freshwater snake, *Natrix piscator*. The hypocalcemic effect in *N. piscator* derives support from the observations on non-piscine vertebrates – mammal [7], bird [8] and amphibia [9, 10]. However, reports of the effect of CS extract administration on serum calcium of mammals are contradictory. Pang (cited by Leung and Fenwick[7]) did not find any hypocalcemic action in rats in the CS from cod or killifish and Copp (cited by Leung and Fenwick[7]) obtained similar results when he tested salmon CS in rats. Moreover, CS extract of bullhead failed to induce hypocalcemia in rats although eel CS extract is effective on rats [7]. Ma and Copp [13] have reported the ineffectiveness of teleocalcin on rats. On the contrary, Milet *et al.* [14] have reported hypercalcemia after CS extract administration.

There seems to be no report regarding the effect of CS extract administration on the serum inorganic phosphorus from non-piscine vertebrates except that of Milet *et al.* [10] which reports hypophosphatemia in *Xenopus laevis*.

The present study describes hypocalcemic and hypophosphatemic effects of CS extract in *N. piscator* which is the first report from reptiles.

ACKNOWLEDGMENTS

One of us (KS) is thankful to UGC, New Delhi for providing financial assistance for this study.

REFERENCES

1 Fontaine, M. (1964) C.R. Acad. Sci., **259**: 875–878.

2 Chan, D. K. O. (1972) Gen. Comp. Endocrinol., Suppl., **3**: 411–420.

3 Kenyon, C. J., Chester Jones, I. and Dixon, R. N. B. (1980) Gen. Comp. Endocrinol., **41**: 531–538.

4 Pang, P. K. T, Pang, R. K. and Sawyer, W. H. (1974) Endocrinology, **94**: 548–555.

5 Ma, S. W. Y. and Copp, D. H. (1978) In"Comparative Endocrinology". Ed. by P. J. Gaillard and H. H. Boer, Elsevier/ North-Holand Biomedical Press, Amsterdam, pp. 283–286.

6 Lopez, E., Tisserand-Jochem, E. M., Eyquem, A., Milet, C., Hillyard, C., Lallier, F., Vidal, B. and MacIntyer, I. (1984) Gen. Comp. Endocrinol., **53**: 28–36.

7 Leung, E. and Fenwick, J.C. (1978) Can. J. Zool., **56**: 2333–2335.

8 Srivastav, Ajai K. and Swarup, K. (1982) Experientia, **38**: 869–870.

9 Pandey, A. K., Krishna, L., Srivastav, Ajai K. and Swarup, K. (1982) Experientia, **38**: 1314–1315.

10 Milet, C., Buscaglia, M., Chartier, M. M., Martelly, E. and Lopez, E. (1984) Gen. Comp. Endocrinol., **53**: 497.

11 Trinder, P. (1960) Analyst, **85**: 889–894.

12 Fiske, C. H. and Subbarow, Y. (1925) J. Biol. Chem., **66**: 375–400.

13 Ma, S. W. Y. and Copp, D. H. (1982) In "Comparative Endocrinology of Calcium Regulation". Ed. by C. Oguro and P. K. T. Pang, Japan Scientific Societies Press, Tokyo, pp. 173–179.

14 Milet, C., Lopez, E., Chartier, M. M., Martelly, E., Lallier, F. and Vidal, B. (1979) In "Molecular Endocrinology". Ed. by I. MacIntyre and M. Szelke, Elsevier/North Holland Biomedical Press, Amsterdam, pp. 341–348.

ANNOUNCEMENT

Optical Approaches to the Dynamics of Cellular Motility

Marine Biological Laboratory Centenary Symposium

A Symposium in Honor of Robert D. Allen

October 5–8, 1987 at Marine Biological Laboratory, Woods Hole, MA

Monday, October 5: (8:00 P.M.–) Wine and cheese party and demonstrations of optical equipment by manufacturers.

Tuesday, October 6: *Morning*: Introductory remarks: N. Kamiya (Okazaki).

Optical Techniques in Cell Biology: Chairmen: D. L. Taylor and S. Inoué

G. Nomarsky (Antony, France): Contrast Enhancement and Imaging in Light Microscopy; *S. Inoué (MBL, Woods Hole)*: Video Microscopy; *D. L. Taylor (Carnegie-Mellon, Pittsburgh)*: Optical Studies of the Chemistry of Living Cells; *D. A. Agard (UC Med, San Francisco)*: Optical Sectioning Microscopy; *T. Yanagida (University of Osaka)*: Direct Observation of Molecular Motility by Light Microscopy.

Afternoon: *Amoeboid Movement and Cytoplasmic Streaming*: Chairman: J. Condeelis

N. Kamiya (Okazaki): Cytoplasmic Streaming; *J. Condeelis (Einstein, NYC)*: Amoeboid Chemotaxis; *M. Schliwa (UC, Berkeley)*: Regulation of Directionality of Cell Locomotion; *J. Hartwig (Mass. General, Harvard)*: Pseudopod Extension in Macrophages; *G. Oster (UC, Berkeley)*: Biophysics of the Leading Lamella.

Evening: Talks and demonstrations by equipment manufacturers (Swope Center). *R. Wicks (PMI Corp.)* Ultralow Light Imaging Optical Microscopy; *Zeiss Representative*: Conformal Laser Scanning Microscopy (remainder of program to be arranged).

Wednesday, October 7: *Morning*: *Mitosis*: Chairman: L. I. Rebhun

Y. Hiramoto (Tokyo): Micromanipulation Studies of Dividing Cells; *E. W. Salmon (UNC, Chapel Hill)*: Microtubule Dynamics and Chromosome Movement; *A. Bajer (UO, Eugene)*: Comparison of Turnover of Plant and Animal Tubulin in Higher Plant Cells; *L. I. Rebhun and R. Palazzo (U. Va., Charlottesville)*: *In Vitro* Approaches to Spindle Function; *W. C. Cande UC, Berkeley)*: *In Vitro* Studies of The Mechanism of Anaphase Spindle Elongation.

Afternoon: *Poster Session.*

Evening: *Motility in Other Systems*; Chairman: K. Edds

N. S. Allen (Wake Forest, NC): Intracellular Particle Motions in Plant Cells; *R. Hard (SUNY-Buffalo)*: Control of Ciliary Metachrony in Newt Lungs; *J. Hayden (Sienna College, NY)*: Regulation of Organelle Translocation in Fibroblasts; *J. Lafountain (SUNY, Buffalo)*: Chromosome Movements During Meiotic Prophase; *C. Izzard (SUNY, Albany)*: Cell-Substrate Interactions and Cellular Movement in Fibroblasts.

Thursday, October 8: *Morning*: *Microtubule Dynamics*: Chairman: R. Sloboda

R. Sloboda and S. Gilbert (Dartmouth, Hanover): Vesicle-Microtubule Interactions During Axoplasmic Transport; *J. Travis (Vassar, Poughkeepsie) and S. Bowser (N.Y. State Dept. Health, Albany)*: Microtubule-Associated Motility in Allogromia (Foraminifera); *T. T. Chen (Wayne State, Detroit)*: Analysis of Particle Translocation in Goldfish Xanthophores; *P. Satir (Enstein, NYC)*: Dynein As a Microtubule Translocator; *H. Hotani (Kyoto University)*: Darkfield Studies of Microtubule Assembly and Disassembly.

Afternoon: *Axoplasmic Transport*: Chairman: D. Weiss

D. Weiss (Munich) and G. Langford (UNC, Chapel Hill): Microtubule-Based Particle Transport in Squid Axoplasm; *Richard Smith (Edmonton, Canada)*: Motion Analysis of Bidirectional Organelle Movement; *Anthony Breuer (Cleveland Clinic, Cleveland)*: Intraaxonal Organelle Traffic Analysis in Human Nerve; *Bruce Schnapp (MBL, Woods Hole)*: Mechanochemistry of Microtubule Translocators; *Richard Weisenberg (Temple, Philadelphia)*: Microtubule Gelation-Contraction *In vitro*: A Model for Slow Axoplasmic Transport.

Evening: Dinner and Concert.

Registration and Housing: The registration fee is $75. Housing is limited and will be assigned in order of receipt of application. Deadline for housing and meal plan is July 1, 1987. Forms and information may be obtained by writing:

Robert Day Allen Symposium
P. O. Box 477
Woods Hole, MA 02543 USA

Abstracts may be submitted for inclusion in the poster session and will be published in Cell Motility and Cytoskeleton. Information on preparation of abstracts will be sent with application forms for registration. Final date for abstract submission will be June 15, 1987.

Development Growth & Differentiation

Published by

the Japanese Society of Developmental Biologists

The journal is devoted to the publication of original papers dealing with any aspects of developmental phenomena in all kinds of organisms, including plants and micro-organisms. Papers in any of the following fields will be considered: developmental genetics, growth, morphogenesis, cellular kinetics, fertilization, cell division, dormancy, germination, metamorphosis, regeneration and pathogenesis, at the biochemical, biophysical and analytically morphological levels; reports on techniques applicable to the above fields. At times reviews on subjects selected by the editors will be published. Brief complete papers will be accepted, but not preliminary reports.

Members of the Society receive the Journal free of charge. Subscription by institutions is also welcome.

Papers in DGD, Vol. 29, No. 2. (Apr. 1987)

Development, Growth and Differentiation (ISSN 0012-1592) is published bimonthly by The Japanese Society of Developmental Biologists, Department of Biology, School of Education, Waseda University, Tokyo 160, Japan. 1987: Volume 29. Annual subscription U. S. $ 110.00 including air speed delivery except Japan. Application to mail at second class postage rate is pending at Jamaica, NY 11431, U. S. A.

Outside Japan: Send subscription orders and notices of change of address to Academic Press, Inc., Journal Subscription Fulfillment Department, 6277 Sea Harbor Drive, Orlando, FL 32887, U. S. A. Send notices of change of address at least 6–8 weeks in advance. Please include both old and new addresses. U. S. A. POSTMASTER: Send changes of address to *Development, Growth and Differentiation,* Academic Press. Inc., Journal Subscription Fulfillment Department, 6277 Sea Harbor Drive, Orlando, FL 32887, U. S. A.

In Japan: Send nonmember subscription orders and notices of change of address to Business Center for Academic Societies Japan, 16–3, Hongo 6-chome, Bunkyo-ku, Tokyo 113, Japan. Send inquiries about membership to Business Center for Academic Societies Japan,4–16, Yayoi 2-chome, Bunkyo-ku, Tokyo 113, Japan.

Air freight and mailing in the U. S. A. by Publications Expediting, Inc., 200 Meacham Avenue, Elmont, NY 11003, U. S. A.

(*Contents continued from back cover*)

ZOOLOGICAL SCIENCE

VOLUME 4 NUMBER 2 **APRIL 1987**

CONTENTS

(*Contents continued on inside back cover*)

INDEXED IN:
Current Contents/LS and AB & ES,
Science Citation Index,
ISI Online Database,
CABS Database

Issued on April 15
Printed by Daigaku Printing Co., Ltd.,
Hiroshima, Japan

ISSN 0289-0003

Vol. 4 No. 3

June 1987

ZOOLOGICAL SCIENCE

An International Journal

PHYSIOLOGY
CELL and MOLECULAR BIOLOGY
GENETICS
IMMUNOLOGY
BIOCHEMISTRY
DEVELOPMENTAL BIOLOGY
REPRODUCTIVE BIOLOGY
ENDOCRINOLOGY
BEHAVIOR BIOLOGY
ENVIRONMENTAL BIOLOGY
ECOLOGY and TAXONOMY

published by **Zoological Society of Japan**

distributed by Business Center for Academic Societies Japan
VNU Science Press BV, Utrecht, The Netherlands

ZOOLOGICAL SCIENCE

The official Journal of the Zoological Society of Japan

The Zoological Society of Japan:
Toshin-building, Hongo 2–27–2, Bunkyo-ku, Tokyo 113, Japan. Tel. (03) 814–5675

ZOOLOGICAL SCIENCE is devoted to publication of original articles, reviews and communications in the broad field of Zoology. The journal was founded in 1984 as a result of unification of Zoological Magazine (1888–1983) and Annotationes Zoologicae Japonenses (1897–1983), the former official journals of the Zoological Society of Japan. ZOOLOGICAL SCIENCE appears bimonthly. An annual volume consists of six numbers of more than 1000 pages including an issue containing abstracts of papers presented at the annual meeting of the Zoological Society of Japan.

MANUSCRIPTS OFFERED FOR CONSIDERATION AND CORRESPONDENCE CONCERNING EDITORIAL MATTERS should be sent to:

Dr. Seiichiro KAWASHIMA, Managing Editor, Zoological Science, Zoological Institute, Faculty of Science, Hiroshima University, 1–1–89 Higashisenda-machi, Naka-ku, Hiroshima 730, Japan, in accordance with the instructions to authors which appear in the first issue of each volume. Copies of INSTRUCTIONS TO AUTHORS will be sent upon request.

SUBSCRIPTIONS. ZOOLOGICAL SCIENCE is distributed free of charge to the members, both domestic and foreign, of the Zoological Society of Japan. To non-member subscribers within Japan, it is distributed by Business Center for Academic Societies Japan, 6–16–3 Hongo, Bunkyo-ku, Tokyo 113. Subscriptions outside Japan should be ordered from the sole agent, VNU Science Press BV, Europalaan 93, 3526 KP Utrecht, (postal address; P. O. Box 2093, 3500 GB Utrecht), The Netherlands. Subscription rates will be provided on request to these agents. New subscriptions and renewals begin with the first issue of the current volume.

[Publication of Zoological Science has been supported in part by a Grant-in-Aid for Scientific Publication from the Ministry of Education, Science and Culture, Japan.]

ZOOLOGICAL SCIENCE 4: 395–410 (1987)

REVIEW

The Variety and Distribution of the FMRFamide-Related Peptides in Molluscs

David A. Price, Noel W. Davies, Karen E. Doble
and Michael J. Greenberg[1]

C. V. Whitney Laboratory, University of Florida, Rt. 1, Box 121, St. Augustine, FL 32086, U.S.A.

INTRODUCTION

Peptide families, like societal kinships, are perceived in terms of morphological, functional, and geneological similarities. Moreover, both sorts of families are poorly delimited, since they comprise a network of relationships extending, from an elementary unit, outward to other existing individuals (or peptides), and backward in time through ancestral lineages. Therefore, although peptide families are often discussed, the underlying concepts remain variable and vague. Since this review is a description of a peptide family, we thought to introduce it with a clarification of our hierarchical terminology.

First, the fundamental unit in peptide associations is the *intragene family,* a set of peptides with similar sequences, all processed from one precursor encoded by a single gene. The sets of enkephalin-containing (EC-) peptides processed from pre-pro-enkephalins A and B are each examples of such fundamental families [1].

Second, within any species, a number of peptides may be clearly related structurally, but be derived from two or more precursors. Such groups are *intraspecific families,* and examples include: the set of EC-peptides generated from 3 precursors in any mammal [1]; the pancreatic polypeptide-related peptides (PP-RPs; including PP, NPY and PYY) in pig [2]; and the ELH-like peptides from two precursors in *Aplysia californica* [3].

Third, homologous peptides from closely related species usually have very similar sequences, but as species and their ancestries become dissimilar, so often do their peptides. Thus, bovine and porcine PP differ by only one residue out of 36, whereas bovine and anglerfish PP have only 16 residues in common [4]. Still, *intraphyletic peptide families* are readily recognized, even when the number of residues common to all members is relatively small. A case in point is the family of 8 peptides related to pigment concentrating hormone of prawns and adipokinetic homone of insects which has only three invariant common residues (pGlu^1, Phe^4, and Trp^8) [5]. *Interphyletic,* or even *universal families* have been proposed [6], but are very difficult to define.

Finally, the functions of peptides are not a consideration in these definitions for, although members of intragene families may have a common function, the functions attributed to related peptides become increasingly heterogeneous at higher hierarchical levels.

In this review, we consider an emerging intraphyletic family of molluscan peptides related to FMRFamide (Phe-Met-Arg-Phe-NH_2). We summarize the major and minor components of this family and their phylogenetic distribution; we describe a methodological key to the characterization of the member peptides, and present some new, exemplary, data about the family in the snail *Helix aspersa*. In the end, we speculate about the ancestry of this peptide family and about its extension to other phyla.

Received February 14, 1987

[1] To whom reprints should be requested.

MAJOR FMRFamide-RELATED PEPTIDES (FaRPs)

FMRFamide

FMRFamide had its origin in several observations that ganglion extracts from various molluscs would increase the force of contraction of isolated hearts of venerid clams, and that this excitation was not inhibited by the serotonin antagonists methysergide and 2-bromo-d-lysergic acid diethylamide [7–9]. Frontali *et al.* [10] began to purify this cardioactivity by gel chromatography with Sephadex G–15. Four cardioexcitatory peaks were separated from the well-studied molluscan neurotransmitters, and one of them — peak C, which was retained on the column and eluted just after the salt volume — occurred in every species tested in all of the major groups of molluscs; and it was a potent cardioexcitor and antiarrhythmic agent [8, 9]. The source of this activity was sought, with persistance and vigor, in the ganglia of *Macrocallista nimbosa,* the sunray venus clam, and was finally identified as the tetrapeptide, FMRFamide [11]. FMRFamide has since proven to be ubiquitous in Mollusca and an invariably major component of FMRFamide-like immunoreactivity in that phylum (Table 1).

The pulmonate heptapeptides

Studies on the FMRFamide-like activity in the ganglia of *Helix aspersa* started soon after the isolation of FMRFamide, and the first was an attempt to localize FMRFamide to identifiable neurones using bioassay [12]. This investigation led to the preliminary conclusion that FMRFamide itself is not present in *Helix,* but is replaced by a novel FMRFamide analog with a modified N-terminal and considerably more potency on the *Helix* heart than the parent peptide [13]. Using HPLC for fractionation and radioimmunoassay for detection, three major peaks of FMRFamide immunoreactivity were detected in *Helix* ganglia [14]. Attention was focused on the most retained (i.e., non-polar) one, which was identified, finally, as a heptapeptide with an N-terminal pyroglutamyl residue [14]. The amino acid sequence of this peptide is: pGlu-Asp-Pro-Phe-Leu-Arg-Phe-NH_2 (pQDPFLRFamide), the methionyl residue of FMRFamide being replaced by leucine, and it is, indeed, much more potent than FMRFamide on the *Helix* heart [15]. The remaining two major peaks in *Helix* are FMRFamide and a partially characterized analog of pQDPFLRFamide, observations that will be discussed below in some detail.

Several additional species of pulmonate snails and slugs have since been examined. In each case, the extracts contain three major FaRPs in roughly equal quantities. One of these is always FMRFamide, as mentioned above; the others are all heptapeptides analogous to pQDPFLRFamide (Table 1). The common heptapeptide sequence is X-DPFLRF-NH_2, and peptides with pGlu, Gly, Ser and, probably, Asn as the N-terminal residue have been idetified thus far (Table 1).

Although only a small number of species has been sampled, a clear difference has emerged between the heptapeptides of the two major orders of Pulmonata — the Basommatophora (mostly limnic snails) and the Stylommatophora (mostly terrestrial snails and slugs). First, in the stylommatophoran pulmonates—represented in Table 1 by *Helix,* three other snails from disparate families, and the slug *Limax maximus* — one of the pair of heptapeptides is always pQDPFLRFamide; the other is indeterminate (Table 1). Moreover, the chromatographic peaks of stylommatophoran heptapeptides are easily distinguished (see section on Methodology, below).

Among the basommatophorans, two species have been studied in some detail: the false limpet *Siphonaria pectinata,* a primitive member of the order [16], and the more advanced snail *Lymnaea stagnalis* [17]. These two species representing the upper and lower ends of the phylogenetic range, as well as other lymnaecean snails that have been tested, all contain the Gly^1 analog GDPFLRFamide as one of their two heptapeptides (Table 1). Thus, GDPFLRFamide appears to be characteristic of the Basommatophora. As to the second heptapeptide in this pulmonate order, the Ser^1 and the Asn^1, have been identified; but pQDPFLRFamide has never been detected in a limnic snail (Table 1). The basommatophoran heptapeptides are also characteristically difficult to resolve, and thus to characterize (see section on Methodology,

TABLE 1. Major and minor FMRFamide-related peptides (FaRPs) in molluscs

CLASS SUBCLASS Order *Species*	Major FaRPs			Minor FaRPs		
	FMRFamide	Heptapeptides[a] (X-DPFLRFamide)				
		1°	2°	FLRFamide	Others	Refs.
POLYPLACOPHORA						
Acanthopleura granulata	+	—ni—		ni		d
BIVALVIA						
PTERIOMORPHIA						
Geukensia demissa	+	—ni—		+		[19]
HETERODONTA						
Macrocallista nimbosa	+			ni		[11]
GASTROPODA						
PROSOBRANCHIA						
Mesogastropoda						
Pomacea paludosa	+	—ni—		+	SGFLRF	[19]
Neogastropoda						
Busycon contrarium	+	—ni—		+		[19]
OPISTHOBRANCHIA						
Aplysia brasiliana	+	—ni—		ni		[20]
Aplysia californica	+	—ni—		+*	nt-GYLRFa*	[21]
PULMONATA						
Basommatophora						
Siphonaria pectinata	+	Gly	Asn	ni		[16]
Lymnaea stagnalis	+	Gly	Ser	ni		[17]
Stagnicola palustris	+	—c—		ni		[19]
Helisoma sp.	+	Gly	ni	ni		d
Stylommatophora						
Strophocheilus oblongus	+	pGlu	c	ni		d
Succinea campestris	+	pGlu	c	ni		[19]
Limax maximus	+	pGlu	c	ni		[18]
Helix aspersa	+	pGlu	Asn[b]	ni		[15], d
Cepaea nemoralis	+	pGlu	c	ni		[19]
CEPHALOPODA						
Octopus vulgaris	+	—ni—		+	YGGFMRFamide	[26, 43]
Octopus bimaculoides	+	—ni—		+	ni	[46]

+ Unambiguous identification.
ni Sought but not identified.
* Predicted from gene sequence.
[a] Where heptapeptides were identified, the N-terminal residue (X-) is listed. The primary heptapeptide (1°) is characteristic of the order; the 2° heptapeptide is not.
b Prediction based on amino acid composition and homology.
c Unresolved peak eluting on HPLC (ACN/TFA system) with Ser-, Asn, and Gly-DPFLRFamide.
d Previously unreported.

below).

MINOR FaRPs

A number of minor immunoreactive peaks always occur in chromatograms of ganglion extracts. Some appear to be FMRFamide analogs secreted in small amounts, some may arise as artifacts of purification, and some may be processing intermediates.

FLRFamide

This peptide was discovered in the mesogastropod, *Pomacea paludosa,* the apple snail. *Pomacea* contains very large quantities of FMRFamide-like immunoreactivity in its ganglia: several hundred picomoles per snail. Most of this immunoreactivity is due to FMRFamide, but the Leu^2 analog FLRFamide is also present at 10–20% the level of the parent peptide [19]. FLRFamide has since been identified in several other molluscs, including bivalves, cephalopods, and always at the same low levels (Table 1). This tetrapeptide is difficult to identify in most animals, not only because it is present in small amounts, but also because it is less reactive in the radioimmunoassay (see Methodology section below).

Although FMRFamide was easily characterized in the opisthobranch *Aplysia braziliana,* FLRFamide was not detected [20]. Yet the FMRFamide precursor in *Aplysia californica* does appear to generate one copy of FLRFamide [21]. FLRFamide has also never been detected in a pulmonate, but nothing is yet known about the gene or precursor in these organisms. These gaps in our information will be discussed toward the end of this review.

SGFLRF

This is the tentative sequence for another, very small peak of immunoreactivity from *Pomacea.* Notwithstanding the low immunoreactivity, the amino acid levels were high enough to determine a composition —Ser, Pro, Phe_2, Leu, Arg— so this peak is probably not amidated [19].

YGGFMRFamide

Met-enkephalin-Arg^6-Phe^7 (YGGFMRF) was first discovered in the adrenal chromaffin granules and in the striatum of the ox [22], and has been reported to occur in molluscs [23]. Although YGGFMRF has no effect as an agonist on the standard bioassay for FMRFamide, its C-terminally amidated analog is approximately equipotent with FMRFamide [24, 25].

A peak of FMRFamide-like immunoreactivity eluting with YGGFMRFamide was detected in ganglion extracts from *Octopus vulgaris* [26]. Its identification as YGGFMRFamide was based on its immunoreactivity with various antisera, its HPLC retention times in various solvents, and its activity in an opiate binding assay (Table 1).

Artifacts of purification

FMRFamide is susceptible to oxidation, but the oxidized peptide has only slight biological activity and may not be detected by bioassay. However, oxidized FMRFamide is still immunoreactive, and can be separated from the unoxidized peptide on HPLC, if gradient elution is used. Deliberate oxidation of *Helix* ganglion extracts with hydrogen peroxide showed that the FMRFamide peak behaved as expected for authentic FMRFamide; i.e., the peak at the normal elution time for FMRFamide disappeared, and the peak at the position of oxidized FMRFamide increased [15]. This shift of the peak with oxidation, or the appearance of both peaks as a doublet, are good, practical indicators of the occurrence of FMRFamide.

In an analysis of ganglion extracts from the pulmonate *Lymnaea stagnalis,* Ebberink *et al.* [17] detected the unamidated forms of the two major heptapeptides in a single batch of material. A conservative interpretation of this observation is that the heptapeptides were enzymatically deamidated during the purification. This notion is supported by the diminished height of the immunoreactive heptapeptide peak in the same preparation.

Another peak that might be expected to arise during the purification of pulmonate extracts is one containing Pro-Phe-Leu-Arg-Phe-NH_2. This peptide could arise from the cleavage of the extremely acid-labile Asp-Pro bond of the heptapeptides.

THE INTRAPHYLETIC FAMILY

The phylogenetic distribution of major and minor FaRPs within the Phylum Mollusca is summarized diagrammatically in Figure 1. The heterogeneity of the intraphyletic family, due primarily to the taxonomic restriction of the pulmonate heptapeptides, is evident. Also clear, however, is that the picture in Figure 1 is incomplete in two ways.

First, some minor classes —Aplacophora, Polyplacophora, and Scaphopoda— have been ignored or inadequately studied, primarily because of practical considerations such as supply or size. More critical is the absence of information about peptides in taxa closer to the divergence of the three gastropod subclasses. For example, a study of the families Onchidiidae and Veronicellidae, which are considered systellommatophoran pulmonates by some authors [28] and gymnophilan opisthobranchs by others [29] should be particularly rewarding.

Second, although the characterizations of SGFLRF in Mesogastropoda, and of YGGFMRFamide in Cephalopoda, are not complete, their occurrence does suggest that a variety of minor FaRPs are widely distributed in molluscs and await discovery. Some new information about minor FaRPs in *Helix* is set out below (and Table 1).

METHODOLOGY

The identification of a particular peptide depends, not only upon the species and tissue examined, but also upon the methods of extraction and purification followed and the bioassay used to monitor these procedures. Therefore, we review

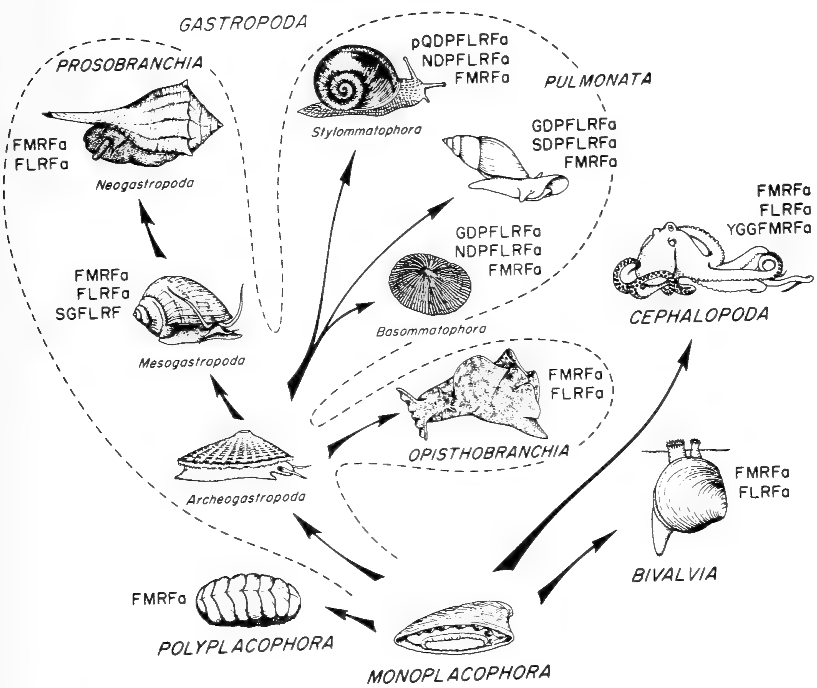

FIG. 1. The distribution of FMRFamide-related peptides in the Mollusca, showing, especially, the ubiquity of FMRFamide and the delimited occurrence of the pulmonate heptapeptides (general sequence, X-DPFLRFamide). The phylum is assumed to radiate from primitive molluscs similar to tryblidian monoplacophorans. An archeogastropod is pictured to provide continuity, but no member of this subclass has been examined for its peptides. a, amide.

in brief the specific steps involved in characterizing the FMRFamide-related peptides of molluscs.

Assay systems: bioassay

The classical clam heart assay [30] was used throughout the identification of FMRFamide, but the isolated radula protractor of *Busycon contrarium,* prepared as first described by Hill [31], was also introduced and increasingly relied upon. The radula protractor muscle is not only very sensitive to FMRFamide, but is also much more selective than the clam heart [32]; e.g., this muscle is contracted by FMRFamide and its analogs, but by few other substances, and especially not by 5-hydroxytryptamine (5-HT), a ubiquitous major component of molluscan ganglion extracts. Moreover, the radula protractor muscles from small *Busycon* can be isolated in a microbath and used to assay very small volumes of material [33].

Other molluscan hearts, muscles, muscular organs, and nerve cells respond to FMRFamide, and the structure-activity relations (SAR) of the peptide have been studied on some of them [34–36]. But most of these preparations are neither sufficiently sensitive nor convenient to serve as bioassays. In any event, radioimmunoassay (RIA) has become the system of choice for monitoring the purification of FMRFamide-like peptides.

Assay systems: radioimmunoassay

Several RIAs for FMRFamide, using different antisera, were developed soon after the tetrapeptide was sequenced [e.g., 37–41], but only one of them has been used to identify all of the new molluscan FMRFamide-like peptides [41]. This antiserum was raised to a conjugate of thyroglobulin with YGGFMRFamide. The rationale for doing this was that, since the peptide could only be conjugated through its N-terminal, the glycyl residues would serve as a spacer, extending the C-terminal FMRFamide sequence away from the protein carrier and allowing more specificity for the peptide hapten. The expected result was realized: the antiserum, in contrast to ones made to conjugates of FMRFamide itself, recognizes (though not equally) all of the residues in the FMRFamide sequence.

The cross-reactivity of the antiserum has been studied in detail and compared with those of other antisera [41, 42]. Three of its features have especially contributed to the analysis of chromatographic data (illustrations in Table 2): 1) The antiserum is unusually specific for the N-terminal phenylalanyl residue; even the substitution of a tyrosine in this position drastically lowers the cross-reactivity. 2) Analogs extended at the N-terminal are more reactive in the RIA than is FMRFamide itself, especially if the extension has a glycyl residue analog. Other antisera, and most bioassays, react with extended peptides about as strongly as with FMRFamide, or slightly worse [41]. 3) Substitutions for the methionyl residue tend to be relatively benign; in particular, oxidation of the methionine or its replacement with a leucyl residue has relatively little effect on immunoreactivity.

TABLE 2. Immunoreactivity of selected synthetic peptides in an RIA for FMRFamide

Peptide sequence	Cross-reactivity*
FMRFamide	1.00
FLRFamide	.25
YMRFamide	.007
FMRYamide	.002
YGGFMRFamide	50.0
YGGFLRFamide	10.0
pQDPFLRFamide	2.0
SDPFLRFamide	.6
GDPFLRFamide	.6

* Relative to FMRFamide taken as 1.00.

Extraction

In most peptide investigations, an early purification step can be achieved through the judicious choice of a species from which very large ganglia (or other tissues) can be dissected cleanly and conveniently. In contrast, phylogenetic studies (e.g., on the evolution of a peptide family) place special demands on extraction methods; the procedures must apply to any relevant species, no matter how small, heavily shelled, or otherwise inconveniently constructed.

Acetone has proven to be a very salutory extraction medium. If the ganglia can be dissected out, the FaRPs will be extracted with a sufficient

degree of purity that gel filtration can be eschewed, and high perfomance liquid chromatography (HPLC) performed directly (details below). More important, significant quantities of immunoreactive FMRFamide can be recovered simply by steeping whole animals, with their shells, in acetone at $-4^{\circ}C$. Recently, we were able to characterize the three major FaRPs in the primitive pulmonate snail *Siphonaria pectinata* by extracting thousands of these abundant, but very small organisms [16].

Notwithstanding the success of acetone marination, other methods such as acid extraction have also been used to isolate FMRFamide-like peptides with good results [43].

Gel chromatography

Although this methodology would seem to have been rendered obsolete by HPLC, fractionation on Sephadex G–15 remains a useful component in the purification of FaRPs (Fig. 2A). The major advantage is that all of the known peptides in this family elute together, with good recovery, in the classic peak C of Frontali *et al.* [10], thereby effecting an early and impressive purification. Still, in instances when a very clean dissection has been possible, gel filtration is omitted. In such cases, the extracts are injected directly onto an HPLC column (e.g., Waters C18 Radial Pak) and eluted with an ammonium acetate/n-butanol buffer system. If the extract is clean enough, this chromatographic step can separate out several major and minor peaks (method and example in Fig. 3A).

HPLC: a chromatographic key

The identification of the components of peak C by HPLC may require two steps, with the procedure and results dependent on the taxon of the sample species. The possibilities and their outcomes are summarized in Figure 2, a kind of methodological key.

The first step is reverse-phase HPLC with elution in a gradient system (ACN/TFA) comprising 0.072% trifluoroacetic acid (TFA, the aqueous solvent) and 80% acetonitrile with the same concentration of TFA (ACN, the organic solvent; details of the ACN/TFA system in Fig. 2 and [16]). When extracts of non-pulmonate molluscs are chromatographed in this system, FMRFamide and oxidized FMRFamide appear as a pair of immunoreactive peaks, and FLRFamide occurs in a very small peak (Fig. 2Bi), sometimes only a shoulder. A similarly unambiguous result obtains when a stylommatophoran extract is chromatographed in the ACN/TFA system: the immunoreactive peaks of pQDPFLRFamide and the second heptapeptide are well separated and both are equal in height to the FMRFamide peak (Fig. 2Biii).

Basommatophoran extracts in the ACN/TFA system, however, yield a single immunoreactive peak in addition to, and about twice as large as, that of FMRFamide plus oxidized FMRFamide (Fig. 2Bii). This result is caused by the virtual coelution of GDPFLRFamide (i.e., the basommatophoran characteristic) and all other heptapeptides except pQDPFLRFamide which is never found in basommatophorans. The two heptapeptides can be resolved by HPLC with elution in another gradient system (ACN/PO_4) comprising 5 mM sodium phosphate, pH 7.0, and acetonitrile (details in Fig. 2 and [16]). The ACN/PO_4 system clearly separates GDPFLRFamide from its Asn^1 analog in *Siphonaria* (Fig. 2Ci), or from its Ser^1 analog in *Lymnaea* (Fig. 2Cii).

THE FMRFamide-RELATED PEPTIDES OF *HELIX*

The ganglion extracts of *Helix aspersa* were the first to be examined after FMRFamide was discovered, and it was in this snail that the first pulmonate heptapeptide to be sequenced—pQDPFLRFamide— was identified. Nevertheless, the second heptapeptide in *Helix* has not yet been characterized, and most of the minor immunoreactive peaks have never been analyzed. Recently, however, we purified 400 circumoesophageal ganglionic rings, dissected out of snails in St. Andrews, Scotland. The results of this study, reported here, have given us further insight into the FMRFamide-like peptides of *Helix* and the evolution of the peptide family.

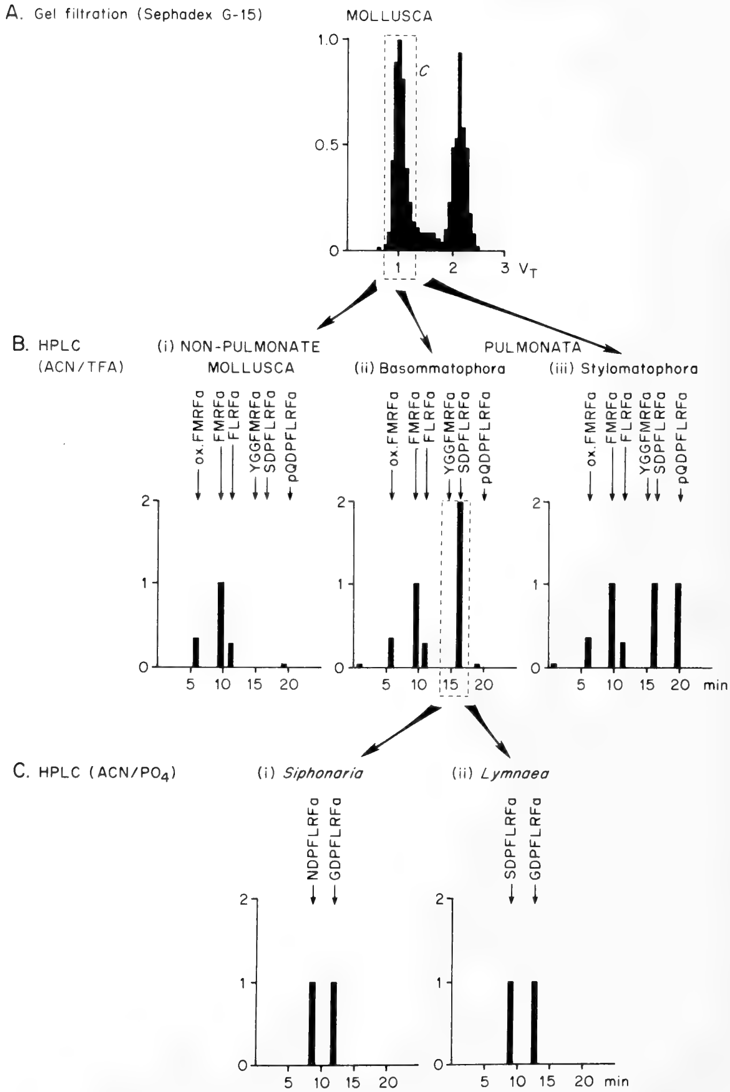

Fig. 2. A diagrammatic scheme for purifying and characterizing FMRFamide-related peptides (FaRPs) from molluscan ganglion extracts, including a set of idealized chromatographic profiles characteristic of particular taxa. The profiles are plots of FMRFamide-like immunoreactivity with time. A: The extract is applied to G–15 and eluted with 0.1 M acetic acid. B: Immunoreactive peak C, comprising fractions that elute at one column volume (V_T), is applied to reverse-phase HPLC, and eluted with a solvent system including acetonitrile (ACN) and trifluoroacetic acid (TFA). The nonpulmonate FaRPs (Bi), and those of stylommatophoran pulmonates (Biii), are resolved in the ACN/TFA system; basommatophoran heptapeptides are not (Bii). C: The complex immunoreactive peak of basommatophoran heptapeptides can be resolved by HPLC in a solvent system containing acetonitrile and phosphate buffer (Ci and Cii). The buffer systems are described in the text and the legend for Fig. 3, as well as [16].

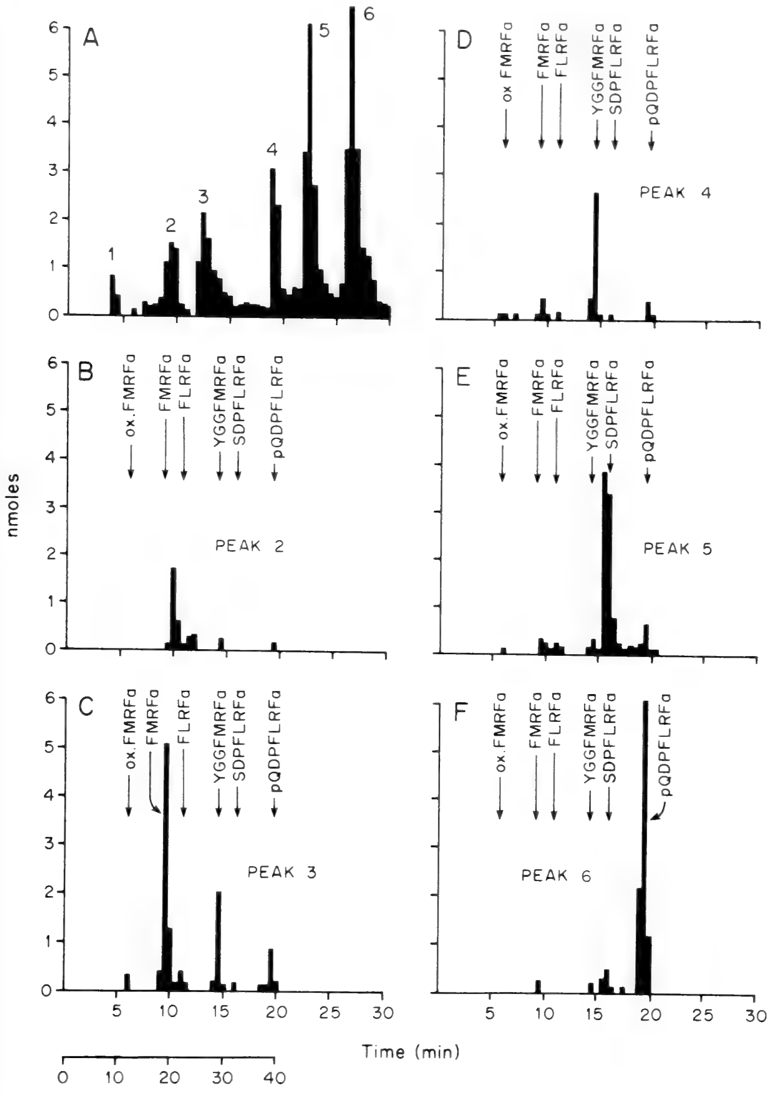

FIG. 3. Purification and chromatographic identification of an acetone extract of snail (*Helix aspersa*) ganglia. A: HPLC fractionation on a Waters C18 Radial-Pak column; elution with a solvent system consisting of 0.5 M ammonium acetate, in 0.1 M acetic acid (pH 5.5), and n-butanol. The butanol was first held constant at 4% (10 min), and was then increased to 8% over 20 min. The solvent was pumped at 4 ml/min; 0.5 min fractions were collected. The FMRFamide-like immunoreactivity in each fraction (plotted on the ordinate) was determined from radioimmunoassay (RIA) of an aliquot. The six major peaks of immunoreactivity are labeled (1–6), and these designations are used in B–D: The six peaks were separately pooled and lyophilized and re-chromatographed. HPLC was on a Waters C18 Microbondapak column; elution with a gradient (12–40% over 30 min) of acetonitrile in 6 mM trifluoroacetic acid. Solvent flow, 2 ml/min; fractions, 0.5 min. Immunoreactivity was measured by RIA, and UV absorbance was monitored at 210 nm. The positions of several standards, determined in separate but similar runs, are indicated.

Extraction

Each ganglionic ring was dropped into acetone as soon as it was removed from the animal in Scotland, and the mixture was kept frozen until it was brought to St. Augustine, Florida, for further processing. The well-travelled acetone was decanted, centrifuged, and the supernatants saved. The ganglia were then homogenized (Polytron) in aqueous acetone (80%), the mixture centrifuged, and the acetone removed from the combined supernatants on a rotary evaporator. The small volume of aqueous solution left in the flask was forced through a C18 cartridge (Waters Sep-Pak) which was washed with water and the active material then eluted with methanol. The methanol was also removed by rotary evaporation, and the residue was taken up in water for injection directly onto the HPLC column (ammonium acetate/butanol system). This, then, is an instance of a clean dissection obviating a preliminary fractionation on Sephadex G–15.

Purification

Six, clear, immunoreactive peaks (labeled 1–6 in Fig. 3A) were the major features in the elution pattern of this first HPLC step. *Peak 1* eluted at the expected position of oxidized FMRFamide and was not further characterized.

Peaks 2 and 3 both eluted near the position of FMRFamide itself. Either peak could have contained FMRFamide, but they were well-resolved, so we kept them separate and re-chromatographed each with the ACN/TFA buffer system (Fig. 3A, B). This new separation showed that the bulk of the material eluting with FMRFamide is in Peak 3 (Fig. 3C), but there also appears to be some in Peak 2 (Fig. 3B).

The fractions constituting the two peaks were hydrolyzed and the amino acid composition of each fraction analyzed. The fractions that appeared to contain FMRFamide in peak 3 had, in fact, the composition expected of the tetrapeptide (e.g., 3–19 in Table 2). In fact, this composition completes the identification of FMRFamide in *Helix aspersa*; previous characterizations had been based only on the elution times of the oxidized and unoxidized peptides [15, 44].

The results of re-chromatographing peak 2 were not so clear (Fig. 3B). The largest peak, at about 10 min, included the small amount of FMRFamide occurring in peak 2, but contained very low levels of amino acids. In contrast, the minor peak of immunoreactivity, comprising fractions 23 and 24, which eluted near the position of FLRFamide, contained high levels of a small number of amino acids. The composition, Asx_2, Pro_1, Tyr_1, Leu_1, Arg_1, Phe_1 (Table 2; 2–24), however, is not consistent with the minor peak being FLRFamide. Moreover, the immunoreactivity observed was low: only 2% of that to have been expected were FLRFamide present at the level suggested by the amino acid analysis. Finally, since FLRFamide elutes after FMRFamide in the ammonium acetate/butanol system, it should have appeared (had it been present) in peak 3, rather than in peak 2.

When peak 4 from the butanol system was re-chromatographed with the ACN/TFA buffer system, a large peak of immunoreactivity resulted (Fig. 3D), but its component fractions contained no corresponding peak of amino acids. Thus, this peak could be an RIA artifact [44], but it might also represent a substance with considerably more immunoreactivity than FMRFamide.

Peak 5, upon re-fractionation, yielded a clear peak of immunoreactivity (Fig. 3E) with a coincident peak of UV absorbance (not shown) and high amino acid levels (Table 3, 5–32). The analysis is not unambiguous, but the most reasonable composition —Asx_2, Pro_1, Phe_2, Leu_1, Arg_1— is identical to that determined for an analogous heptapeptide peak in *Siphonaria pectinata* [16]. Moreover, it is also similar to the composition of the minor peak in peak 2, except that, in the latter, a tyrosinyl residue replaces one of the phenylalanines (compare 5–32 with 2–24 in Table 3).

Finally, when the most retained peak in the ammonium acetate/butanol system —peak 6— was re-chromatographed in the ACN/TFA system, the elution time corresponded well to the previously characterized heptapeptide, pQDPFLRFamide (Fig. 3F).

Summary of Helix FaRPs

Price [14] had previously shown that *Helix* ganglia contain three major peaks of FMRFamide-

TABLE 3. Amino acid analysis of peak immunoreactive fractions from *Helix aspersa*

Amino acid	Fraction 3–19[a]		Fraction 2–24[a]		Fraction 5–32[a]	
	nmol	ratio	nmol	ratio	nmol	ratio
Phenylalanine	1.543	1.83(2)	3.132	1.18(1)	3.505	1.70(2)
Arginine	.873	1.03(1)	2.654	1.00(1)	2.082	1.01(1)
Aspartic Acid	.141	.17(0)	5.124	1.93(2)	2.910	1.41(1–2)
Proline	.117	.14(0)	2.622	.99(1)	2.057	1.00(1)
Leucine	.205	.24(0)	2.832	1.07(1)	2.450	1.19(1)
Methionine	.845	1.00(1)	.192	.07(0)	.435	.21(0)
Tyrosine	.072	.09(0)	1.940	.73(1)	.192	.09(0)
Glycine	.129	.15(0)	.977	.39(0)	.567	.28(0)
Serine	.150	.18(0)	.757	.29(0)	1.144	.56(0)

[a] An extract of ganglia was fractionated on HPLC (ammonium acetate/butanol system). The 6 peaks were then rechromatographed (TFA/ACN system) (see Fig. 3). Fractions 19, 24 and 32, from rechromatographed peaks 3, 2 and 5, respectively, were hydrolyzed, and the amino acids analyzed.

like immunoreactivity. One of them is FMRFamide and another is the classic heptapeptide pQDPFLRFamide [15]. The remaining major peak (peak 5, Fig. 3E) still eludes full characterization. But we hypothesize that it is the heptapeptide Asx-DPFLRFamide, a sequence also proposed for its analog in *Siphonaria pectinata* which was discussed earlier in this review.

The two minor peaks in *Helix* ganglia differ from the major peaks in that their levels of immunoreactivity are not equivalent to the levels of peptide determined by amino acid analysis. One of these minor peaks (fractions 23 and 24 in re-chromatographed peak 2; Fig. 3) is much less immunoreactive than FMRFamide although the peptide levels are similar. In contrast, peak 4 contains little peptide, and thus seems to be more immunoreactive than FMRFamide. The characteristics of the antiserum used in the RIA (Table 2) suggest that a *decrease* in immunoreactivity would reflect some change in the tetrapeptide core of FMRFamide. An *increase* in immunoreactivity would be brought about by changes in the molecule (e.g., N-terminal extension) that would make it more like YGGFMRFamide, the antigen to which the antiserum was raised. If the minor peak of peak 2 had the sequence: Asx-DPYLRF-NH_2, suggested by its composition (Table 3; 2–24), it would (in spite of the N-terminal elongation) surely be less immunoreactive due to the substitutions of the leucyl and, especially, the tyrosinyl residues (see Table 2). Peak 4 is considered further, below.

FMRFamide GENES AND PRECURSORS

The Aplysia precursor

The inhomogeneity evident in the intraphyletic family of FMRFamide-related peptides should be explicable in terms of the precursors of the constituent intragene families. To date, however, only one FMRFamide precursor, that from *Aplysia californica,* has been studied. The gene encoding this precursor has been cloned and its sequence determined [21]. The precursor (Fig. 4A) is about 600 amino acids long and contains: 28 putative copies of the FMRFamide sequence, one copy of FLRFamide, and one copy of another peptide ending in -Gly-Tyr-Leu-Arg-Phe-NH_2 (designated nt-GYLRFa to indicate that it is at the n-terminal of the precursor and is amidated).

The number of functional copies of FMRFamide arising from this precursor is still in question because many of the sequences would have to be processed out by cleavage at a single lysine residue, a mechanism unknown for other peptide precursors [45]. However, the report of Lehman *et al.* [20], that FMRFamide was the only identifiable FaRP in *Aplysia* ganglion extracts, is consistent

with FLRFamide and nt-GYLRFa being very minor components of the intraspecific family.

The basic molluscan precursor

One striking feature of the *Aplysia* gene (and the precursor it encodes) is its high content of

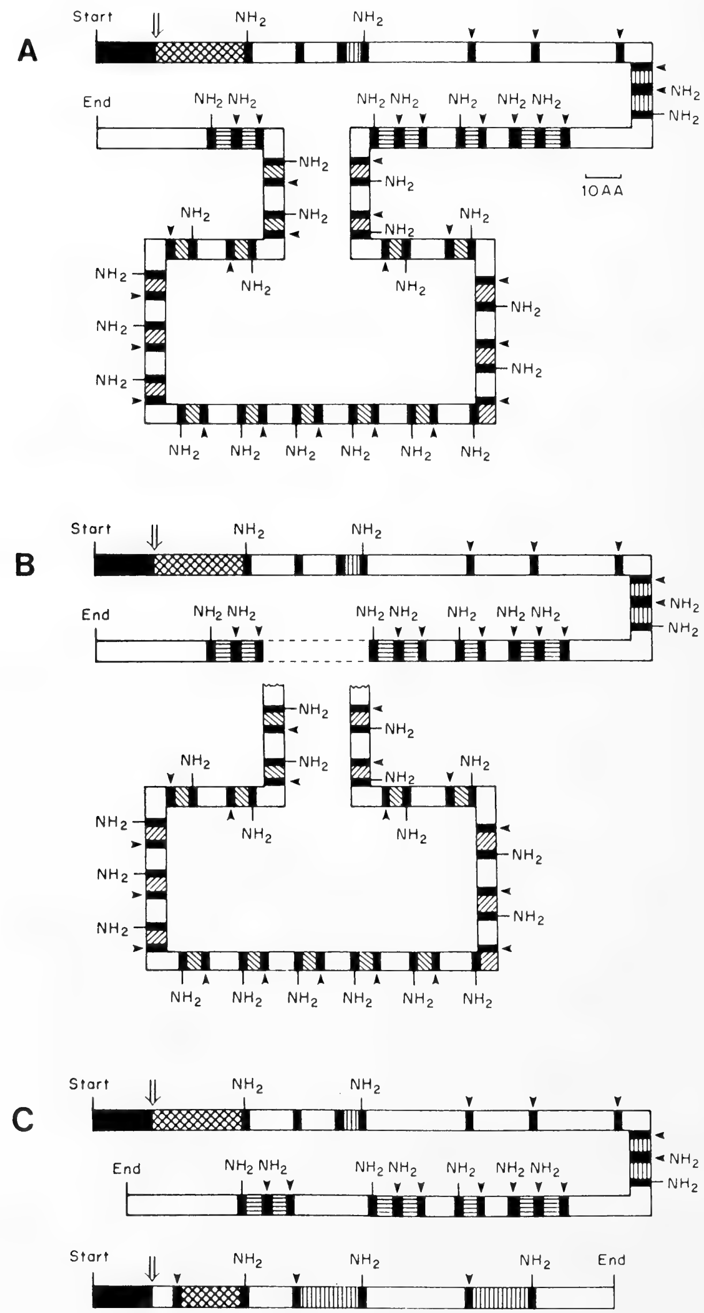

repetitive sequences (Fig. 4a; [21]). Long stretches of the precursor are composed of repeated 15 or 16 amino acid segments, each containing one FMRFamide sequence. Many of the repeats are identical at the amino acid level, and several are even completely identical at the nucleotide level. These repeats must represent relatively recent iterative events, and we can therefore approximate the ancestral gene by simply deleting the segments containing most of the similar repeats (Fig. 4B). This gene encodes a truncated precursor containing FLRFamide and nt-GYLRFa, but fewer than ten copies of FMRFamide.

Such a precursor would account reasonably well for the ratio of FMRFamide to FLRFamide seen in both a prosobranch, *Pomacea paludosa* [19], and in two species of octopods, *Octopus bimaculoides* [46] and *Octopus vulgaris* [43]. This correlation therefore supports our proposition that the back-extrapolation in Figure 4B resembles the basic molluscan precursor, which is conserved in modern bivalves, cephalopods and most gastropods, and is ancestral to the opisthobranch and pulmonate precursors.

The number of FMRFamide-related peptides actually processed from the putative basic molluscan precursor—e.g., three distinct peptides as in *Aplysia,* or only the two (FMRFamide and FLRFamide) detected to date—remains unknown. However, Price [19] reported the occurrence, in *Pomacea,* of a minor peptide which appeared to be SGFLRF (Table 1); and K. H. Voigt has found other FLRFamide-related peptides in *Octopus* (personal communication). We conclude, therefore, that the proposed basic precursor probably contains at least as many distinct peptides as that of *Aplysia*.

The pulmonate precursor

If we assume that our analysis of the minor peaks of *Helix* is both correct and applicable to all pulmonate species, and if we add those data to our information about the major immunoreactive peaks of pulmonates (Table 3), we find that the family of FMRFamide-related peptides in the Subclass Pulmonata falls into two branches, as follows. The *heptapeptide branch* contains three FLRFamide analogs, all present at about equal levels: XDPFLRFamide, X※DPFLRFamide, and X※DPYLRFamide (e.g., in *Helix,* X is pGlu, and X※ is Asn). As described above, the first two are much more immunoreactive than the third which is the minor peak of fraction 2 of *Helix* (Fig. 3B). What we will call the *basic branch* of the family contains FMRFamide and a highly immunoreactive peptide present at very low levels (*Helix* peak 4, Fig. 3D). Of these two branches, it is the heptapeptide one that is novel and that distinguishes the pulmonate FaRP family from those of the other molluscs.

The precursor proteins in the pulmonates, and the genes that encode them, are completely unknown at present. Nevertheless, a reasonable conjecture about the molecular basis for the pulmonate family is possible. We propose that the pulmonates contain two distinct genes and precur-

FIG. 4. Hypothetical representation of the FMRFamide precursors in molluscs and their derivation by back-extrapolation from the known *Aplysia* precursor. A: The FMRFamide precursor of *Aplysia* redrawn from [21]. The initiation methionine at the N-terminal is labeled "Start," and the following hydrophobic signal sequence is solid black. The large arrow shows where the signal sequence is cleaved from the precursor, and the nt-GYLRFa peptide follows immediately (cross-hatched). The bold black bars are basic amino acid residues, potential processing points. Simple cleavage points are at the small arrows; cleavage sites with amidation signals (glycyl residue) are indicated by NH_2. The single copy of FLRFamide is vertically hatched. Copies of FMRFamide in the unique (basic) region of the precursor are horizontally hatched; those in the iterative regions are diagonally hatched. The bends in the diagram have no physical meaning. B: Hypothetical basic molluscan FMRFamide precursor. The most iterative region of the *Aplysia* precursor has been deleted, leaving FLRFamide, and about 10 copies of FMRFamide. (All symbols are as in A.) C: Two hypothetical precursors accounting for the FMRFamide-related peptides of *Helix* and other pulmonates. One precursor is presumed to be similar to the basic molluscan precursor (upper diagram). It yields FMRFamide, FLRFamide and an analog of nt-GYLRFa (possibly peak 4 of *Helix*). The second precursor, unique to the pulmonates, produces three heptapeptides, two immunoreactive (in *Helix,* pQDPFLRFamide and putative NDPFLRFamide) and one poorly immunoreactive (putative NDPYLRFamide from *Helix* peak 2). (All symbols as in A.)

sors giving rise to the two branches of the peptide family (Fig. 4C). (The alternative notion, that a single precursor gives rise to all of the pulmonate peptides, ignores both the minor peaks of immunoreactivity and observations that the relative sizes of the various peaks vary markedly from tissue to tissue [44]).

First, a precursor resembling the conserved basic molluscan precursor will produce multiple copies, about ten, of FMRFamide. We suggest that it also produces a peptide with the partial sequence -GFLRFamide. This peptide —a close analog of nt-GYLRFa in the *Aplysia* precursor— would have a greatly enhanced immunoreactivity and, therefore, though its concentration would be about one tenth that of FMRFamide, it would appear to be more abudant. This peptide would account for fraction 4 of *Helix* (see Fig. 3A, D). Finally, the basic precursor should also give rise to a single copy of FLRFamide, a peptide not yet detected due to its scarcity and low immunoreactivity. Clear demonstrations of FLRFamide at a level one tenth that of FMRFamide, and of the proposed -GFLRFamide, would go far toward confirming this portion of the hypothesis.

The origin of a distinct heptapeptide gene is not at all clear. Two bits of evidence—that the heptapeptides are all FLRFamide analogs, and that the phenylalanyl residue is replaced with a tyrosine in both the pulmonate heptapeptide of low immunoreactivity (X※DPYLRFamide) and the nt-GYLRFa peptide of *Aplysia*—suggest that the heptapeptide gene could have arisen by duplication from the N-terminal portion of the basic molluscan gene. Alternatively, the heptapeptide gene, rather than being unique to the pulmonates, may occur in all molluscs. Its products might not have been detected for two reasons: they might be expressed at low levels, or they might be processed in a non-immunoreactive form (i.e., unamidated). An example of the latter possibility might be the putative peptide SGFLRF in *Pomacea* [19].

THE INTERPHYLETIC FAMILY

FMRFamide, *sensu stricto,* has been unambiguously identified in a variety of molluscan species (Table 1), but never convincingly in any non-mollusc. Indeed, until very recently, the few non-molluscan FMRFamide-like peptides sequenced have only had the final two residues of the C-terminal [47, 48] —or at most the final three [49, 50]— in common with either FMRFamide or FLRFamide.

Within the last several months, however, three very FMRFamide-like peptides have been sequenced in non-molluscs, and they are all N-terminally extended analogs of FLRFamide. One of these peptides is pGlu-Asp-Val-Asp-His-Val-FLRF-NH_2 (leucomyosuppressin), isolated from extracts of cockroach heads [51]. Two other peptides, characterized from the pericardial glands of the American lobster, are: Ser-Asp-Arg-Asn-FLRF-NH_2 and Thr-Asn-Arg-Asn-FLRF-NH_2 [52]. That these closest non-molluscan analogs of FLRFamide occur in the Arthropoda, a protostomous phylum with close affinities to the molluscs, is strongly suggestive of an interphylum peptide family.

The novel arthropodan peptides most resemble the two molluscan peptides that are processed out of the N-terminus of the *Aplysia* precursor; i.e., nt-GYLRFa and FLRFamide. Moreover, the N-terminus is especially lacking in obvious redundancies and would thus appear to be the oldest part of the precursor. We therefore speculate that the primeval "FMRFamide" precursor present in the common ancestor of the molluscs and arthropods had only FLRFamide-related sequences.

ACKNOWLEDGMENTS

This work was supported by NIH grant HL28440 to M. J. G. The assistance of Louise MacDonald, Lynn Milstead and Jim Netherton in preparing the manuscript is gratefully acknowledged. We would like to thank all the kind people who supplied us with animals: Y. Grimm-Jørgensen, T. Audesirk, Harvey Blankespoor, and especially R. A. Koch. We are even more in debt to collaborators who supplied us with dissected tissue, including: A. G. M. Bulloch, C. P. Jaeger and G. A. Cottrell. We thank E. A. Kravitz for sending us prepublication copies of manuscripts from his laboratory, and K. H. Voigt for keeping us informed of progress in his laboratory on the peptides of *Octopus*. This is contribution 258 from the Tallahassee, Sopchoppy and Gulf Coast Marine Biological Association.

REFERENCES

1 Douglass, J., Civelli, O. and Herbert, E. (1984) Ann. Rev. Biochem., **53**: 665–715.

2 Emson, P. C. and De Quidt, M. E. (1984) Trends in Neurosci., **7**: 31–35.

3 Scheller, R. H., Jackson, J. F., McAllister, L. B., Rothman, B. S., Mayeri, E. and Axel, R. (1983) Cell, **32**: 7–22.

4 Andrews, P. C., Hawke, D., Shively, J. E. and Dixon, J. E. (1985) Endocrinol., **116**: 2677–2681.

5 Gade, G. and Rinehart, K. L., Jr. (1986) Biochem. Biophys. Res. Comm., **141**: 774–781.

6 LeRoith, D., Shiloach, J., Heffron, R., Rubinovitz, C., Tanenbaum, R. and Roth, J. (1985) Can. J. Biochem. Cell Biol., **63**: 839–849.

7 Hill, R. B. and Welsh, J. H. (1966) In "Physiology of Mollusca", Vol. 2. Ed. by K. M. Wilbur and C. Y. Yonge. Academic Press, New York, pp. 125–174.

8 Agarwal, R. A., Ligon, P. J. B. and Greenberg, M. J. (1972) Comp. Gen. Pharmacol., **3**: 249–260.

9 Greenberg, M. J., Agarwal, R. A., Wilkens, L. A., and Ligon, P. J. B. (1973) In "Neurobiology of Invertebrates, Tihany 1971". Ed. by J. Salanki, Akademiai Kiado, Budapest, pp. 123–142.

10 Frontali, N., Williams, L. and Welsh, J. H. (1967) Comp. Biochem. Physiol., **22**: 833–841.

11 Price, D. A. and Greenberg, M. J. (1977) Science, **197**: 670–671.

12 Cottrell, G. A., Price, D. A. and Greenberg, M. J. (1981) Comp. Biochem. Physiol., **70C**: 103–107.

13 Greenberg, M. J. and Price, D. A. (1980) In "Peptides: Integrators of Cell and Tissue Function". Ed. by F. E. Bloom, Raven Press, New York, pp. 106–127.

14 Price, D. A. (1982) Comp. Biochem. Physiol., **72C** 325–328.

15 Price, D. A., Cottrell, G. A., Doble, K. E., Greenberg, M. J., Jorenby, W., Lehman, H. K. and Riehm, J. P. (1985) Biol. Bull., **169**: 256–266.

16 Price, D. A., Cobb, C. G., Doble, K. E., Kline, J. K. and Greenberg, M. J. (1987) Peptides, **8**: (in press).

17 Ebberink, R. H. M., Price, D. A., van Loenhout, H., Doble, K. E., Riehm, J. P., Geraerts, W. P. M. and Greenberg, M. J. (1987) Peptides, **8**: (in press).

18 Krajniak, K. G., Greenberg, M. J., Doble, K. E. and Price, D. A. (1985) Amer. Zool., **25**: 15A.

19 Price, D. A. (1986) Amer. Zool., **26**: 1007–1015.

20 Lehman, H. K., Price, D. A. and Greenberg, M. J. (1984) Biol. Bull., **167**: 460–466.

21 Taussig, R. and Scheller, R. H. (1986) DNA, **5**: 453–462.

22 Stern, A. S., Lewis, R. V., Kimura, S., Rossier, J., Gerber, L. D., Brink, L., Stein, S. and Udenfriend, S. (1979) Proc. Natl. Acad. Sci. USA, **76**: 6680–6683.

23 Leung, M. K. and Stefano, G. B. (1984) Proc. Natl. Acad. Sci. USA, **81**: 955–958.

24 Greenberg, M. J., Painter, S. D. and Price, D. A. (1981) Nuropeptides, **1**: 309–317.

25 Greenberg, M. J., Lambert, S. M., Lehman, H. K. and Price, D. A. (1986) In "Handbook of Comparative Opioid and Related Neuropeptide Mechanisms", Vol. 1. Ed. by G. B. Stefano, CRC Press, Boca Raton, pp. 93–101.

26 Voigt, K.-H. and Martin, R. (1986) In "Handbook of Comparative Opioid and Related Neuropeptide Mechanisms", Vol. 1. Ed. by G. B. Stefano, CRC Press, Boca Raton, pp. 127–138.

27 Walsh, K. A., Ericsson, L. H., Parmelee, D. C. and Titani, K. (1981) Ann. Rev. Biochem., **50**: 261–284.

28 Solem, A. (1978) In "Pulmonates, Vol. 2A, Systematics, Evolution and Ecology". Ed. by V. Fretter and J. Peake, Academic Press, New York, pp. 49–97.

29 Keen, A. M. (1971) Sea Shells of Tropical West America, 2nd ed., Stanford Univ. Press.

30 Welsh, J. H. and Taub, R. (1948) Biol. Bull., **95**: 346–353.

31 Hill, R. B. (1958) Biol. Bull., **115**: 471–482.

32 Greenberg, M. J. (1983) In "Molluscan Neuroendocrinology". Ed. by J. Lever and H. H. Boer, North Holland Publ. Co., New York, pp. 190–196.

33 Nagle, G. T. and Greenberg, M. J. (1982) Comp. Biochem. Physiol., **71C**: 101–105.

34 Painter, S. D., Morley, J. S. and Price, D. A. (1982) Life Sci., **31**: 2471–2478.

35 Kobayashi, M. and Muneoka, Y. (1986) Comp. Biochem. Physiol., **84C**: 349–352.

36 Muneoka, Y. and Saitoh, H. (1986) Comp. Biochem. Physiol., **85C**: 207–214.

37 Dockray, G. J., Vaillant, C. and Williams, R. G. (1981) Nature, **293**: 656–657.

38 Weber, E., Evans, C. J., Samuelsson, S. J. and Barchas, J. D. (1981) Science, **214**: 1248–1251.

39 O'Donahue, T. L., Bishop, J. F., Chronwall, B. M., Groome, J. and Watson, W. H. (1984) Peptides, **5**: 563–568.

40 Boer, H. H., Schot, L. P. C., Veenstra, J. A., and Reichelt, D. (1980) Cell Tissue Res., **213**: 21–27.

41 Price, D. A. (1983) In "Molluscan Neuroendocrinology". Ed. by J. Lever and H. H. Boer, North Holland Publ. Co., New York, pp. 184–190.

42 Dockray, G. J. (1985) J. Neurochemistry, **45**: 152–158.

43 Voigt, K.-H., Hirt, R., Kiehling, C. and Martin, R. (1987) In "Neurobiology, Molluscan Models". Ed. by H. H. Boer, W. P. M. Geraerts and J. Joose,

Mon. Kon. Ned. Akad. Wetensch., North Holland Publ. Co., Amsterdam, (in press).

44 Lehman, H. K. and Price, D. A. (1987) J. Exp. Biol., (in press).

45 Schaefer, M., Picciotto, M. R., Kreiner, T., Kaldany, R.-R., Taussig, R. and Scheller, R. H. (1985) Cell, **41**: 457–467.

46 Price, D. A. (1987) In "Neurobiology, Molluscan Models". Ed. by H. H. Boer, W. P. M. Geraerts and J. Joose, Mon. Kon. Ned. Akad. Wetensch., North Holland Publ. Co., Amsterdam, (in press).

47 Yang, H.-Y.T., Fratta, W., Majane, E. A. and Costa, E. (1985) Proc. Natl. Acad. Sci. USA, **82**: 7757–7761.

48 Grimmelikhuijzen, C. J. P. and Graff, D. (1986) Proc. Natl. Acad. Sci. USA, **83**: 9817–9821.

49 Dockray, G. J., Reeve, J. R. Jr., Shively, J., Gayton, R. J. and Barnard, C. S. (1983) Nature, **305**: 328–330.

50 Nachman, R. J., Holman, G. M., Haddon, W. F. and Ling, N. (1986) Science, **234**: 71–73.

51 Holman, G. M., Cook, B. J. and Nachman, R. J. (1986) Comp. Biochem. Physiol., **85C**: 329–333.

52 Trimmer, B. A., Kobierski, L. A. and Kravitz, E. A. (1987) J. Comp. Neurol., (submitted).

ZOOLOGICAL SCIENCE 4: 411–425 (1987)

REVIEW

Tumors in Amphibia

MAKOTO ASASHIMA, TSUTOMU OINUMA[1] and V. BENNO MEYER-ROCHOW[2]

Department of Biology, Yokohama City University, Seto 22–2, Kanazawa-ku, Yokohama 236, [1]Department of Anatomy, Miyazaki Medical College, Kiyotake, Miyazaki 889–16, Japan, and [2]Department of Biological Sciences, University of Waikato, Hamilton, New Zealand

INTRODUCTION

Amphibians, together with reptiles and fishes, are poikilothermic (or ectothermic) animals and are often referred to as lower vertebrates. The principal body structures and organs of lower vertebrates, however, are the same as those of the higher vertebrates such as birds and mammals. It is not surprising, therefore, that tumors of amphibians with regard to the organs affected by the tumor, the morphology of the tumors and the relationships between factors of tumorigenesis and tumor formation, are basically the same as those of other vertebrates, including the human being. Many investigators have been studying tumors mainly in mammals and this, no doubt, has increased our knowledge concerning tumors; but at the same time aspects of comparative oncology within different vertebrate classes have been somewhat neglected despite a certain amount of solid fundamental works [1–4].

Recognising the unique position of amphibians as animals of both aquatic and terrestrial habitats we and others before us [5–16] have been looking for tumors, their causes, their growth patterns, etc. in these animals for quite some time now. Although amphibians have long been used as suitable material for various lines of research within the subject of biology, e.g. experimental embryology, biochemistry, genetics and cell biology, the number of reports on tumors in amphibia is relatively small. In mammals, birds and fishes, on the other hand, many different kinds of tumors have been studied and the number of reports is larger.

There are two major explanations for the small number of reports on amphibian tumor. One is that investigators, who have used amphibians as experimental material for all kinds of research, may not specifically have looked for tumors and, thus, may not have reported them [17]. Tumors could have been overlooked and if investigators, dealing with amphibians, had carefully examined the internal organs of amphibia, various types of tumors could possibly have been found. The other explanation is that amphibians do suffer less from tumor, because they may have some specific tumor-repelling system which makes it especially hard for a tumor to form in their bodies. In short, they may be different from all other vertebrates with regard to tumors [18, 19]. If such a characteristic or something in the nature of amphibians is present that prevents tumors from forming or proliferating we have to identify these forces and relate them to the characteristic way of life of amphibians. For example, amphibians can live both in water and on land; they highly depend on the changes of the environment; as adults they are entirely carnivorous, etc. In addition to the ability to adapt to the environment, they have other characteristics such as metamorphosis during development and, especially in urodela, a remarkably strong ability to regenerate lost or damaged parts of the body. When we consider

Received February 9, 1987

tumors of amphibians in relation to their unique biological characteristics, on the one hand, and their similarity to human neoplasms on the other [5]. Amphibians may perhaps turn out to be particularly suitable material for tumor investigation. Already Khudoley has been calling *Rana temporaria* "a new experimental animal in cancer research" [20]. The one amphibian tumor that has been well investigated and has been known for decades is renal adenocarcinoma in *Rana pipiens* first reported by Lucké in 1934 [21]. In addition to furthering our knowledge of tumor generally, the purpose of our study on tumor of amphibians is to recognise common problems in cancer research and to study the biological nature of tumor by making use of the unique biology of one group of vertebrates: amphibians.

Recently, papillomata in the newt *Cynops pyrrhogaster* and tumors in *Xenopus laevis* have been found and investigated. In this review we intend to summarize what is known about tumors in amphibia, concentrating on studies of renal adenocarcinoma in *Rana,* papilloma in *Cynops* and tumors in *Xenopus.*

REPORTS ON SPONTANEOUS TUMORS

The number of reports on spontaneous tumors in amphibians is smaller than that dealing with tumors in mammals, birds and fishes. For exam-

TABLE 1. List of spontaneous tumors in anurans (—1986)

Species	Tumors (number of animals)	Sites
Rana pipiens	osteogenic sarcoma (1), adenocarcinoma (many) carcinoma (6), teratoma (1), lymphosarcoma (3), liposarcoma (2), epithelioma (1), hepatoma (2), mesothelioma (2), carcinosarcoma (1), rhabdomyosarcoma (1), plasmacytoma (1), cystoadenocarcinoma (1), squamous cell carcinoma (7), papilloma (1)	thigh, kidney, lung, fat body, muscle, ovary, spleen, bladder, viscera, skin, liver, dermal glands,
Rana esculenta	carcinoma (1), fibroma (1), adenoma (1), hepatoma (1), adenocarcinoma (1), hypernephroma (1), sarcoma (1)	buccal cavity, kidney, ovary, leg, liver
Rana catesbeiana	adenocarcinoma (2), neurosarcoma (1) adenoepithelioma (2)	skin, sacral plexus, kidney
Rana clamitance	myxosarcoma (1)	tail
Rana temporaria	melanoma (1), epithelioma (1) cystadenocarcinoma and cystadenopapilloma (7)	skin
Rana arvalis	adenoma (1)	skin
Rana ridibunda	cystadenocarcinoma and cystadenopapilloma (16)	skin
Rana chensinensis	tumor-like displasias (many)	limb
Bufo bufo	capsulated tumor (1), fibroma (8), lipoma (1)	kidney, skin, bladder
Bufo calamita	adenocarcinoma (1)	lung
Bufo marinus	adenoma (1)	parotid gland
Bufo boreas	fibroma (1)	muscle
Ceratophrys ornata	fibrosarcoma (1)	leg, kidney
Dendrobates pumilio	erythrophoroma (1)	viscera, skin
Hyla meridionalis	guanophoroma (1)	skin
Hyla arborea	xanthophoroma (1)	skin
Xenopus laevis	lymphosarcoma (3), carcinoma (1), fibroma (1), adenocarcinoma (3), fibromata (1), nephroblastoma (1), lipoma (1), papilloma (1), adenoma (1), melanoma (8), neuroma (3)	kidney, pelvis, face, under skin, viscera, head, skin, liver, orbit
Xenopus fraseri	lymphosarcoma (2)	viscera

TABLE 2. List of spontaneous tumors in urodeles (—1986)

Species	Tumors (number of animals)	Sites
Andrias japonica	fibroma (2), carcinoma (1), fibroma (1)	limb, testis, under skin
Ambystoma opacum	mixed tumor (1)	skin
Ambystoma tigrinum	papilloma (1), fibroma (2), melanoma (1), melanocytoma (1), myxofibroma (1)	skin
Ambystoma mexicanum	melanoma (4), lymphosarcoma (3), melanosarcoma (1), epithelioma (1), adenocarcinoma (1), neuroepithelioma (2) teratoma (1), testicular tumor (16)	skin, mouth, tail, testis
Amphiuma tridactylum	leiomyoma (1)	lung
Necturus maculosus	adenocarcinoma (1)	kidney
Triturus cristatus	adenocarcinoma (1), melanoma (1)	skin gland, skin
Triturus alpestris	carcinoma (4), epithelioma (1)	skin
Triturus vulgaris	chondroma (1), fibroma (25)	skin
Cynops (=*Triturus*) *pyrrhogaster*	lymphosarcoma (1), sarcoma (5), papilloma (many), nephroblastoma (1)	viscera, liver, skin, kidney
Notophthalmus viridescens	mesenchymal tumor (1), neuroblastoma (1)	skin, under skin, neck
Cryptobranchus alleganiensis	adenoma (1)	testis

ple, Effron *et al.* examined tumors by necropsy and by histology in various species of wild animals which had died in the San Diego Zoological Garden and in the Wild Animal Park region from 1964 to 1976 [22]. They found tumors in 2.75% of 3,127 mammals, 1.89% of 5,957 birds and 1.90% of 1,233 reptiles, but they did not detect any tumors in amphibia (0% of 198).

The number of reports on spontaneous tumors in amphibians known to us up until 1986 is about 491 cases involving 18 species of anurans and about 253 cases involving 12 species of urodeles. Relevant data are listed in Tables 1 and 2. The known amphibian tumors are dealt with in some excellent reviews [8, 11, 17, 22–28]. The number of reports in anurans is greater than that in urodeles which according to Brunst [29] is merely a reflection of the greater extent to which anurans are used in research. In some anuran species like *Rana pipiens, Rana esculenta* and *Xenopus laevis* several kinds of tumor were reported; the same holds true for the urodele species *Ambystoma tigrinum, Ambystoma mexicanum* and *Cynops pyrrhogaster*. These species are frequently used as experimental material in biology. Amongst the tumors listed in Tables 1 and 2, there are some reports dealing with precancerous changes and tumors in *Rana*. Tumors in intersubspecific and interspecific hybrids have also been reported, e.g. in *Xenopus laevis laevis* × *Xenopus laevis victorianus* and *Rana pipiens* × *Rana palustris*. Lymphosarcoma has been found in the viscera of the former frog, which was produced by nuclear transplantation. The tumor in the latter was teratocarcinoma in the testes. The reported tumors were classified into six types; epithelioma, mesenchymal tumor, pigment tumor, blood cell tumor, central nervous system tumor and reproductive organ tumor. Epithelial tumors such as adenocarcinoma, adenoma, and papilloma accounted for nearly half of all reports. Epithelial tumors are thought to be related to the fact that amphibians have many glands in the skin and that the skin is covered by a thin *stratum corneum*. Mesenchymal tumors, such as fibroma, lipoma and smooth muscle tumor, made up about a quarter of the total. Tumors of pigment cells, hematopoietic cells, and gonads could also be encountered. Tumors of the central nervous system were reported once each in anurans and urodeles. It is very rare that the same type of tumor has been found in many animals of the

same species, but renal adenocarcinoma in the leopard frog *Rana pipiens* (Lucké renal tumor) and papilloma in the Japanese newt *Cynops pyrrhogaster* (newt papilloma) are exceptions and have been found in very large numbers. These tumors will be discussed later.

Recently, a few reports on the incidence of spontaneous tumors in amphibians have been published. Khudoley and Mizgireuv collected 320 specimens of *Rana temporaria* and 978 *Rana ridibunda* in the Leningrad region and found tumors in 7 and 16 frogs, respectively [30]. There were one to seven tumors in each frog and the tumors were all cystadenopapillomata or cyst-adenocarcinomas originating from mucous glands. Infiltrations were not found in most animals, but a metastasis was found in one frog. Mizgireuv *et al.* collected many frogs and toads in three regions of Southern Sakhalin [31]. They found tumor-like dysplasiae of osteochondrous tissue of hind limbs in *Rana chensinensis*. With 11.5% out of 1,095 frogs the highest incidences of the dysplasiae were observed in point A, a place polluted with the sewage effluent of a paper factory; in points B and C the figures were 5.5% of 3,651 and 0% of 1,614, respectively. Oinuma *et al.* observed large tumors in the dorsal region of four adult females of the African clawed frog (*Xenopus laevis*) [32]. The tumor-bearing frogs were found in amongst about 20,000 adults which were bred in artificial ponds. Surprisingly, no tumors were seen in about 10,000 larvae and 5,000 juvenile frogs. The tumors of the four frogs were similar to each other and were thought to be melanomas and neuromas. In urodeles, Counts *et al.* reported a mixed tumor in a male *Ambystoma opacum* [33]. The number of collected animals was not clear. The tumor was composed of epithelial cells and mesenchymal cells and it appeared rather benign. Khudoley and Eliseiv found a melanoma in the skin of one out of 272 axolotls (*Ambystoma mexicanum*) of 5 months old [34]. This tumor proliferated and metastasized during breeding. Counts *et al.* captured about 300 newts (*Notophthalmus viridescens*) and found a neuroblastoma in one newt [35]. A cyst of connective tissue was observed and the tumor occurred under the skin.

Deformations and abnormal growth in amphibians have repeatedly been reported [36, 37]. In 1969 Rostand and Darré suggested that deformations such as brachymelia, polymelia, and polydactylism in *Rana esculenta* could have been caused by a teratogenic virus, which was carried by certain species of fish like tench and eel [38]. These two authors, thus, appear to have been one of the first to recognise the connection between virus and abnormal regeneration. Other possible causes of abnormal growth must, of course, not be completely discounted [37].

FREQUENCY OF TUMOR OCCURRENCE

We have seen in the preceding section that some kinds of tumor in anurans and urodeles are nothing new and have been known for quite a while. However, the types of tumor which could be used or have been used as detailed experimental material for detailed investigations are very few in number. The three kinds among them which we shall discuss one by one are Lucké renal adenocarcinoma in anurans, melanoma and neuroma in the African clawed frog *Xenopus,* and newt papilloma in urodeles. An important point to consider is also the artificial tumorigenesis in amphibians using carcinogenic materials.

1. Lucké renal tumor

Lucké renal tumor is an adenocarcinoma in the kidney of the leopard frog (*Rana pipiens*) and was first reported by Lucké in 1934 [21]. Since then, this tumor has been investigated as a model of tumors in lower vertebrates. Lucké renal tumor appears spontaneously at a relatively low frequency (less than 13%) in one kidney alone or on both sides. Almost no metastases to other organs were observed. However, when the frogs were kept in a laboratory (at about 22°C) for a long period the incidence of spontaneously appearing tumors increased by about 50%, and metastases to lung or liver became recognisable. The origin of the tumor cells is considered to be the epithelium of the urinary tubule, since microvilli were often observed in the tumor cells. The transplantation to healthy frogs is possible. When the tumor fragment was implanted into the anterior chamber of the eye, the transplants proliferated very rapid-

ly [39, 40] and might induce formation of a tumor in the kidney of the host.

McKinnell *et al.* examined seasonal fluctuations of the Lucké renal tumor from 1965 to 1968 [41, 42]. They collected a total of 3,367 frogs from the wild in spring, summer and autumn, and found that the tumor-bearing frogs were most numerous in spring and autumn (average 5.0% and 4.4%, respectively), but considerably less so in summer (0.14%). As for the reason of the rare appearance of tumorous frogs in summer, McKinnell *et al.* considered that the tumor-bearing frogs were easily captured by their predators and, thus, showed a lower survival rate, but they could not exclude the possibility that death of sick animals or spontaneous regression of the tumor were additional, important factors involved. McKinnell *et al.* [42] collected a total of 1,363 frogs at 15 localities in Minnesota and it became obvious that the frequency of the tumorous frogs depended not only on seasons as described above, but also on the specific region in Minnesota from which the frogs came. In spring or autumn collections, tumor-bearing frogs made up 0.9–14.0% in 9 out of 15 regions, but no tumor-bearing frog was found in any of the other 6 regions.

Thereafter, McKinnell *et al.* turned towards the phenomenon of decreasing numbers of tumor-bearing frogs in Minnesota [43, 44]. In the regions where many tumor-bearing frogs had appeared in the springs and autumns of the years 1966–1975, they captured 685 frogs in 1977 and 1,216 in 1978 and 1979, but not one tumor-bearing frog was found. Nowadays it appears to be difficult to find renal adenocarcinoma in *R. pipiens* from the wild, but a full explanation why this should be so remains to be put forward.

2. *Tumor in Xenopus laevis*

Throughout the world the African clawed frog (*Xenopus laevis*) has been used as an experimental animal for a wide range of biological investigations. However, as stated in Table 1, reports on tumors number only 24 cases. This figure seems to indicate a very low incidence. Oinuma *et al.* examined the frequency of tumor in *Xenopus* bred in an artificial pond in 1983 and 1984 [32]. In the first examination, they found four tumor-bearing frogs in a population of about 20,000 frogs (0.02%). But following re-examination 7 months later, no tumor-bearing frog could be found at all. Compared with the cases of Lucké renal tumor or newt papilloma the frequency of tumor in *Xenopus* is really considerably depressed. Considering Lucké renal tumor and newt papilloma, normal frogs or newts kept with tumor-bearing animals of the same species in the same water tank for a long period (about a year) developed the tumor with high regularity (more than 50%). However, as for the tumor of the African clawed frog, it did not occur in normal animals for at least a year. It seems that the infection is related to a virus and that the path of the infection takes in *Xenopus* is different from that of Lucké tumor or newt papilloma. In tissue sections of the tumor in *Xenopus,* many mature pigment cells were observed among the tumor cells. The DOPA test was carried out on the tumorous tissue, and positive results were obtained [28]. Based on these results and the long term-cultivation of these cells [45], the tumors in *Xenopus* were thought to be melanomas and neuromas.

3. *Newt papilloma*

Papillomata are occasionally found in the skin of the Japanese newt, *Cynops pyrrhogaster.* The tumors may be found anywhere on the body surface but preferably occur on the tail, back, and limbs. This tumor, which is also called epithelioma, was first reported from one case each by Honma and Murakawa [46] and Bryant [47]. Since then newt papilloma has been found in large numbers in a variety of species (e.g. *Diemictylus viridescens*: [48]; *Triturus alpestris*: [49]; *T. cristatus*: [10, 50]) and presently newt papilloma as well as Lucké renal tumor is considered to represent important material for the investigation of amphibian tumor [51–56]. As newt papilloma often regresses and disappears during breeding, it may turn out to be very suitable material to analyse the mechanisms involved in the spontaneous regression of the tumor. Newt papilloma grows by proliferation of epithelial cells of the tumor region, but metastases have not been observed in any organs other than the skin.

Asashima *et al.* collected newts at specific localities in Niigata prefecture from autumn of 1979 to autumn of 1983 and have examined the seasonal changes of the papilloma [53, 54].

The total number of newts collected was 28,630 and the frequency of papilloma-bearing newts among the collected newts was monitored for every season. Papilloma-bearing newts were numerous only in autumn (1.9–7.9%) whereas in spring, summer and winter (0.16–0.32%, 0.47–0.50% and 0.48–0.50%, respectively) they were far less frequent. Though males tended to be affected more commonly than females, it is not clear if there really is a sex-related difference in the abundance of papilloma. Seasonal peaks in papilloma-bearing newts not only occurred in Niigata but in definite regions of other prefectures (Yamagata and Iwate), too.

The incidence of Lucké renal tumor was high in two seasons per annum, namely, spring and autumn, but that of newt papilloma was high only in autumn. The reason for this difference is not easy to understand.

Besides seasonal changes in the abundance of papilloma-bearing newts, geographical variations of the tumor frequency in autumn from 1980 to 1985 have also been examined [53, 54]. Newts from 16 prefectures in Japan were collected and examined whether they had papillomata or not. Papilloma-bearing newts were numerous in Aomori, Iwate, Yamagata and Niigata prefectures (1.3–7.9%), less numerous in Yamanashi, Gifu, and Shimane (0.7–2.6%), and least numerous in Chiba, Shizuoka, Aichi, Kochi, Okayama, Nagasaki, Saga, Kumamoto and Miyazaki (0–0.6%). More newts from the North and West side of Japan than from Southern and Eastern parts suffered from papillomas. To complicate the picture, there are prefectures like Kochi and Shizuoka in which papilloma-bearing newts were found in some years but apparently seemed absent in others.

THE RELATION BETWEEN TUMOR AND ONCOGENETIC FACTOR

1. *Oncogenic virus*

The existence of viruses in amphibian tumors has been proved in some cases. It became evident, for example, that Lucké renal tumor was caused by a virus [3, 8]. In newt papilloma, too, virus particles were detected [51, 53] and spontaneous tumors have successfully been transmitted by experiment (e.g. in *Pleurodeles waltii*: [57]). In *Xenopus* lymphosarcoma virus particles were detected and infection experiments gave equally positive results. Particles resembling viruses were also present in *Xenopus* melanoma. Fish-born viruses were thought to be involved in abnormal growth of appendages in *Rana esculenta* [38].

For Lucké renal tumor there no longer exists any doubt that it is caused by a virus [35, 58, 59]. Lucké on the basis of the following observations had already suggested that the tumor was caused by a virus; the acidophilic inclusion bodies existed in the nucleus of the tumor cells and resembled those agents responsible for *herpes* infection [21]. When glycerinated or dried tumor was inoculated to another, healthy leopard frog, the tumor appeared regularly soon after [58]. At present, this virus is known as Lucké herpes virus. Though the virus was present in most instances, there were cases in which it was not found. Rafferty noticed that the virus was found in tumors of frogs captured in winter, but not in summer material [40]. Subsequently the virus was observed by electron microscopy in the renal tumor of a frog captured in winter, and in the tumor of a frog kept at low temperature in the laboratory.

Actually, when seven tumor-bearing frogs in hibernation were exposed to a higher temperature (20–22°C), many inclusion-body containing cells were observed at first but later they were broken and the residues of cells and virus particles were flushed out into the urinary tubules. Seven days later, cells that did not contain any inclusion-bodies were to be observed in the tumor [60]. On the other hand, when frogs were captured before they entered a lake for hibernation and they were put in a cage and experimentally immersed in the

lake [61], the virus was not found in the tumor before the frogs entered the lake, but began to appear seven days later so that more than a month later all the tumors contained viruses. The water temperature in the lake was 5–9°C. Even though tumor-bearing frogs were kept at low temperature in the laboratory, a similar result could not be obtained. Thus, the maturation of the virus appears to occur at low temperature while the proliferation of the tumor cells requires higher temperature. The encapsulation of Lucké herpes virus is a hibernation-related phenomenon in nature. Though the virus is not found in tumors of the summer-type, it is believed that the virus genome is contained in the tumor cells in a masked or latent state [40].

When frog larvae were reared segregated from early stages of development, the frequency of tumor formation was almost the same as that found in the field. The infection by virus from a tumor-bearing frog to another healthy animal may occur at an early period of development [40]. Furthermore, such an infection seems to occur perhaps in spring, the season of spawning and embryonic development. Horizontal infections might well represent one pathway for the spread of the disease, because experiments with transmitting infections have been successful.

Generally, to know whether a virus is a tumor agent, transplantation experiments have to be carried out successfully. Cultured cells will have to be infected with the virus and their transplantability has to be affirmed. In Lucké tumor, it has been proved that the virus was the etiological agent on the basis of virus isolation, transplantation and cell culture studies [96].

Tweedell separated the tissue of frog renal tumor into cell organelle fractions which were kept under low temperature [62]. Each fraction was injected to sterilized early embryos or hatching larvae. In embryos injected with the mitochondrial fraction, tumors were formed in the pronephros or mesonephros in large numbers (13–92%) during or after metamorphosis. In the embryos injected with the microsomal fraction, tumors were also induced in the metamorphosing larvae or in juvenile frogs (0–50%). These newly created tumors were proliferating renal adenocarcinomas. Furthermore, Mizell separated the mitochondrial fraction of the tumor into several fractions by the zonal centrifugation method and obtained a fraction which readily induced the growth of tumors when it was injected into early embryos [63]. The establishment of cell lines originating from the virus-induced pronephric tumor was performed by Tweedell and Williams [64]. Primary explants obtained from normal pronephri of larvae were cultured *in vitro* and the cells were infected with herpes virus obtained from adult tumors. These cells were cultured for three passages and the mitochondria-herpes virus fraction was obtained from these cells. Then frog embryos were inoculated with the fraction. When the embryos developed and became tadpoles, the tumor was formed in pronephros or mesonephros. Dissociated cells were obtained from this tumor, cultured, and two cell lines PNRT 4 and PNRT were established. More than 85% of these cells were epitheloid and the rest was fibroblastic.

Naegele *et al.* examined whether Lucké herpes virus fulfilled Koch-Henle postulates [65]. According to Koch-Henle postulates, the experiment was separated into 4 steps. (1) Herpes virus was associated with kidney tumor of frog adult. (2) A cell fraction, containing virus, was obtained from the tumor. Tail-bud embryos were infected with this fraction and allowed to develop until tadpoles. Tumors were induced in pronephros or mesonephros of these tadpoles at a high frequency (about 62%). (3) Then the tissue fragments of the induced tumor were cultured. If the tissue was kept at 7.5°C, herpes virus was detected in the nucleus, but if kept at 22°C, the virus was not found. (4) Cultured tissue fragments were homogenised and centrifuged. Early embryos were inoculated with the supernatant and were allowed to develop. Tumors were not induced in animals inoculated with the cell extract kept at 22°C, but readily so (64.7%) when they received the cell extract kept at 7.5°C. Herpes virus was detected in the newly formed tumor. It had oncogenic activity and it was the same virus isolated from the tumor of wild adult frogs.

Nace *et al.* found an antigen "X" by immunoelectrophoresis and fluorescent antibody techniques, which was contained in normal cells

but was absent from tumor cells. The antigen X was identified as a lysozyme [66]. There were at least eight isozymes in the normal kidney of adult frogs. One of them always existed, three were absent from the tumor and others were variably distributed. Since frog lysozyme was thought to possess activity against frog herpes virus [67], the hypothesis was advanced that the absence of an isozyme of lysozyme was linked to the virus infection and the subsequent initiation of the growth of the tumor.

Next, as for the newt papilloma, the existence of virus particles was confirmed in the tumor by Pfeiffer *et al.* [51] and Asashima *et al.* [53]. Which type of virus group this virus belonged to has not been clearly established yet. This virus resembles the herpes virus and Lucké herpes virus in regard to size and morphology but it is entirely possible that newt papilloma virus belongs to the group of iridoviridae [68]. Because the virus is often observed to proliferate in the cytoplasm of papilloma cells, the core of the virus particle must be large and the form of the virus a 6-edged body. This has to suffice to determine the nature of this virus and the nature and size of nucleic acid of this virus. Isolation of it will be required.

In newts papilloma transplantation experiments were successfully carried out [69]. When tumor fragments were implanted under the skin of healthy newts, tumors were formed in the skin of 17% of the hosts within a year. The tumorous tissue was then homogenized. When this homogenate was used for inoculation in newts collected at Kumamoto prefecture, a region where tumor-bearing newts had not been found previously, tumors did occur in 10.0–15.8% of these newts. In these transplantation studies, the frequency of tumor formation was higher than that of the control experiments and that of newts captured from nature. During the study of tumor homogenate injection, it became obvious that we did not know whether all the cells of the tumor were destroyed completely, but at least it appears to be the generally accepted view now that some factor(s) contained in the tumor cells induce the tumor.

Differences in the protein patterns of papilloma and normal skin tissues of the Japanese newt *Cynops pyrrhogaster* were studied by the two-dimensional (2–D) gel electrophoresis method. Also compared were protein patterns of skin derived from different regions of the same body and that from male and females. Groupings of 11 protein spots specific to normal skin and 7 protein spots specific to papilloma were detected [70]. The papilloma specific protein spots were not detected in the normal skin of adult newts, the skin of larvae, the presumptive ectodermal region of embryos, or such organs as the lung and liver. There were some differences regionally, but none by sex. One of the 11 spots specific to normal skin of adult newts was found to coincide with one in the spot grouping of larval skin. Two unique spots were identified in normal larval skin. The possibility exists that the appearance of papilloma specific proteins indicates the presence of virus associated proteins.

Virus particles were also seen in at least two cases of tumors of *Xenopus laevis*. In the first case, virus particles were detected in lymphosarcoma by electron microscopy [71]. A cell free extract containing the virus of this tumor could induce tumor formation. This infectious virus was about 0.05 μm in size. In the second case, a virus was found in a melanoma of *Xenopus laevis* [32]. The virus particles were often found in large number in the nucleus of a tumor cell, and in some cells, it was observed, that the inside of the nucleus was filled with virus, which would actually spill over into the cytoplasm. The virus found in the melanoma of *Xenopus* was considered to be herpes virus judging by its morphology, size and situation of the core.

The existence of virus associated with tumor in amphibians must, therefore, be regarded as factual. From now on amphibian virus-associated tumors could provide material for the analysis of tumorigenesis, cell transformation and cell differentiation and for the comparative study of the virology of tumor.

2. *The effects of carcinogens*

A large number of abiotic causes for tumorous growths have become recognised, notably ionising radiation and chemicals. The latter may exert their effectiveness directly or indirectly through food

uptake and the production of carcinogenic breakdown-products.

When a carcinogenic chemical, known to induce tumor in mammals and fish following exposure to a small quantity or dose of it, is given to amphibians, the probability of inducing tumor is generally low [27, 28, 72].

Methylcholanthrene (MC), which is known to induce skin tumor when applied to the skin of mice and which induces sarcoma when injected subcutaneously, exerts an effect that is broadly the same in both anurans and urodeles. 3, 4-Benzopyrene (BP) showed similar results. BP induces only skin tumors in urodeles but tumors of internal organs in anurans. Though hepatoma was induced with dimethylnitrosoamine (DMNA), diethylnitrosoamine (DENA), benzidine and aflatoxin in anurans, no hepatoma was formed with these carcinogens in urodeles.

It is thought that urodeles have strong internal resistance to the hepatoma-causing carcinogens. The authors examined newts (*Cynops pyrrhogaster*) which were bred in water containing a carcinogen such as 4-nitroquinoline-1-oxide (4-NQO), N-methyl-N′-nitro-N-nitrosoguanidine (MNNG) or DMNA for a long period (a year), but no tumor formation was found in any organ of these newts (data not shown). It is suggested that urodeles possess some kind of system which minimises the effect of the carcinogens.

Regeneration phenomena are known to occur in urodeles following amputation of a limb or the tail. Though a carcinogen such as MNNG or 4-NQO was administered into the regeneration blastema, no tumor formation was observed and the differentiation itself proceeded normally, though various abnormalities (=morphological malformations) occurred. This problem will be discussed later.

It seems certain that amphibians, and in particular urodeles, are less sensitive towards carcinogens than other vertebrates. Since urodeles are the least sensitive, they could possibly serve in conjunction with their strong regeneration capacity as a convenient experimental animal in the study of the mechanisms of cellular resistance against carcinogens.

BIOLOGY OF TUMOR CELLS

The last published work of the Nobel laureate Hans Spemann, the discoverer of the organiser in the amphibian embryo, dealt with the tumor problem [73]. He transplanted the organiser region of gastrula stage embryos onto the liver of the adult newt *Triton taeniatus* and finally found the tumor cells resembling those of teratocarcinoma near the transplanted area of the newt. Following this experiment, many other investigators have used the amphibian tumor cells to study aspects of cell differentiation.

1. The relation between regeneration and tumor cells

In amphibians, the number of reports on spontaneous tumors is less than that for other vertebrates, and the resistance of amphibians towards chemicals, which in other animals are known to possess strong carcinogenic activity, seems to be very high. If it is true that in amphibians tumors have greater difficulty to form, then this may well be related to the strong regeneration potential of amphibians. Urodeles, in particular, have an enormous capacity for regeneration. When limbs, tail, or lens are amputated or removed, the powers of regeneration in each amputated area begin to work to reconstruct the original morphology. Dedifferentiation, proliferation, redifferentiation and morphogenesis occur in the amputated region, which eventually is restored to the former state. Tumor cells, however, escape from the contact of normal cells and from the control in normal tissues, and they proliferate independently and abnormally ignoring the order of the surrounding tissue. Though the cells in the "regeneration field" proliferate abnormally, their degree of freedom is minimised by the effect of the "regeneration field" in the rest of the amputated region, which is also involved in the process of normal cell differentiation.

It is known that in urodeles, such as newts, normal tissue dedifferentiates first before the new specific structure is reconstructed in the regeneration process [74]. Perhaps this was one of the reasons why Jonas [75] argued, though not totally unopposed [76], that the process of regeneration

could be seen as a kind of cancerous growth. Whether true tumor cells can be converted to normal cells if placed in the "regenerating field" is, of course, an interesting and important problem.

Rose and Wallingfold transplanted the tissue fragment of frog renal tumor into the limb of the newt *Triturus viridescens* [77]. After the transplant took hold and infiltrated the newt limb, the limb of the host was amputated leaving the tumor. In subsequent histological observations, frog cells were distinguished from newt cells by the size of the nucleus and the difference in stainability with haematoxylin. The results showed that regeneration occurred in the normal way in all cases, and that transplanted cells originating from frog tumor differentiated into muscle, cartilage and fibrous connective tissue and freely mingled with and spread in the host tissues. The cells of the renal tumor were epithelial in origin, but they apparently differentiated into many other directions. The results, however, remain controversial, since a reinvestigation, carried out by Ruben [78] gave negative results, i.e., the transplants kept their own characteristic tubuli *renalis* (=or uriniferous tubule) structures during regeneration and had not mixed with other tissues.

There was an interesting report that urodele epithelial tumor induced by treatment with MC differentiated into normal tissue spontaneously [79] but it is not clear to what extent the tumor disappeared or became differentiated. Recently, Tsonis [80] using newt papilloma, examined the effects of the presence of a tumor on the process of limb regeneration and the behaviour of the tumor cells in the regenerated tail. He observed that although the differentiation proceeded normally, the formation of the regenerative cone became retarded in tumor-bearing newts. When the tail with a tumor was amputated through the tumor, the tumor cells covered the surface of the wound but did not mix with normal epithelium and did not invade the blastema.

The problem of redifferentiation of tumor cells into normal tissue in the regenerating field needs to be reinvestigated. A clear distinction of transplanted tumor cells from host cells in transplantation studies is paramount for the correct interpretation of the results. Furthermore we need to give attention to the question whether tumor cells can be incorporated at all in the regeneration process.

The effects of chemical carcinogens on regeneration have been examined. Urodela obviously have a high resistance against carcinogens, and malformations rather than tumors occurred as a response. Tsonis and Eguchi treated forelimb blastema with a crystal of various carcinogens (about 5 μg), e.g. MNNG, 4-NQO, MC or BP for 7 days after amputation [81–83]. These carcinogens were not able to arrest the regeneration completely, but abnormal bones were formed or the regeneration was delayed. Abnormal limb regeneration can be classified into several types. For example, complete deficiency of both ulna and radius; abnormal regeneration and polymorphism of carpal bones, metacarpal bones and phalanges of fingers; hypertypic limb regeneration, and incomplete limb regeneration. Normally newts have four fingers in the forelimb and five in the hindlimb. When the left hindlimb was amputated and a small crystal of 4-NQO was put into 7-day blastema, the regenerated limb, developed an abnormal 6-fingered polymorphism, but a tumor was not formed.

The effects of carcinogens such as 4-NQO or MNNG on the cells of newt blastema are different from those on normal cells of other vertebrates. In newts the carcinogens show no carcinogenic activity, but only cause changes in cell movement or cell behaviour in the blastema. The blastema cells of newt are very resistant and stable against carcinogens. The relationship between the action mechanism of carcinogens in the regeneration process of urodeles and the reaction of blastema cells in the regeneration field provides the tumor scientist with a unique experimental system.

It is known that the iris in an eye also has strong regeneration power. When the lens is removed from an eye of a newt, cells of the upper part of the iris dedifferentiate, proliferate, form a lens vesicle, and bring about the regeneration of the lens. At this time, a strong carcinogen was administered into an eye ball after the removal of the lens. But, once again, no tumor was formed

as in the case of limb regeneration. Though only one lens is regenerated in normal regeneration, several lenses were regenerated following the administration of a carcinogen. The lens, regenerated while being treated with a carcinogen, is normal with regard to lens differentiation and transparency, but it seems almost impossible for the eye to function properly, considering there are several lenses in an eye [84]. This experimental system is very interesting if one desires to study the mechanisms of cell differentiation and cell reaction affected by carcinogens in lens regeneration.

2. *Nuclear transplantation and potency of cell differentiation*

Studies have been performed by means of the nuclear transplantation technique to determine whether the nucleus of a tumor cell possessed latent pluripotency and whether it had genes which enabled it to differentiate into various types of normal cells, tissues and organs. King and DiBerardino transplanted a nucleus from a Lucké renal tumor cell into an anucleated egg [85]. The nucleus was obtained from either proliferated tumor cells of primary tumorous tissue which were implanted into the anterior chamber, or from cells which were cultured *in vitro* for a short period. Out of the eggs with nuclear transplants, 1–5% reached the normal blastula state. In some of them development proceeded to late neurula and even larval state.

On the other hand, when the donor nuclei originated from normal kidney cells 3% of the eggs reached the blastula. The capacity to continue the process of cleavage was similarly developed in the nuclei from the tumor. However, when nuclei from blastula or gastrula were used as donors, 37% of all embryos reached the state of blastula and 40% of them developed into normal larvae. As for the arrest of the development, at some stage, of the embryos with nuclear transplants, it was shown that the chromosomes divided abnormally during the early stages of development and that the embryos, thereafter, failed to develop normally [86]. Although abnormal chromosomes occur frequently in embryos which developed from nuclei that originated from a differentiated cell, abnormal chromosomes were relatively rare in embryos which originated from nuclear transplants of undifferentiated cells. From these observations it was concluded that abnormal chromosomes in embryos coming from nuclear transplants reflected the degree of differentiation of donor nuclei prior to transplantation.

Then, to unambiguously show pluripotency of renal tumor nuclei, the nuclei were marked and made identifiable by being triploid [87, 88]. Since the nuclei of the host cells were diploid, the distinction between host nuclei and transplanted tumor nuclei was possible. First, triploid early embryos were obtained by the technique of low temperature treatment. These triploid embryos were infected with Lucké herpes virus. Embryos which proceeded development and yielded tumor cells in the pronephros were obtained. Next, the triploid tumor cell nuclei were injected into anucleated eggs. Then the eggs that had received triploid tumor nuclei proceeded development, but no tumor at all was formed. Moreover, to clarify these results, the nuclei from cultured triploid renal carcinoma cells were also transplanted [88].

Eggs with transplanted nuclei developed in such a way that 47% of them became blastulae, 17% and 20% became gastrulae and neurulae, respectively, and 3% developed into swimming larvae. The nuclei of these embryos were all triploid, and histologically, the cells differentiated into all organs of the body such as brain, spinal cord, optic cup and lens, somites, pronephros, midgut and so on. These results suggest that the nucleus of a tumor cell is genetically multipotent and can differentiate reversibly. Thus, using the nucleus of Lucké renal tumor cell, normal cloned larvae could be obtained. This is not only an important result, which agrees with observations on plant tumors [89] but also demonstrates a convenient experimental approach to study the expression of pluripotency of tumor cells and their ability to redifferentiate.

3. *Effects of temperature*

It has already been described that both in Lucké renal tumor and in newt papilloma, the abundance of the tumor depended notably on the

season [41–44, 52–56]. One of the causes of the seasonal change in tumor appearance is thought to be temperature. Especially, since amphibians are poikilothermic animals, they represent a convenient material to study the changes of tumor cells by means of alteration of temperature. In homoiothermic animals such as mammals, although it is possible to change the temperature regionally or even that of the whole body for a short period, it is difficult to change the body temperature from higher temperature to lower for any length of time. Amphibians allow such experiments to be performed and it is then possible to investigate the effects of temperature on the tumor, the regulatory mechanisms of the body and the properties of the virus.

Newts with papillomata of moderate size (2.5–3.5 mm in diameter) were chosen. They were divided into five experimental groups of different temperature conditions (4, 10, 13, 25 and 30°C) and bred under these controlled temperatures, while the diameters of the tumors were measured weekly [55, 56, 90]. As a control, papilloma-bearing newts were bred outdoors in the shade. The size of the tumor tended to increase gradually at 10°C and 13°C which are temperatures similar to those present in autumn, but it decreased notably both at 4°C (lower temperature) and at 25 and 30°C (higher). Newts have the ability to attenuate the tumor in their bodies; depending on changes in environmental temperature, they may even possess the ability to cure themselves and have the tumor regress.

Interestingly, the tumor regression occurred at both lower and higher temperatures, but it was found by histological examination that the way the regression occurred was different at both temperatures. At the higher temperature end the regression occurred more vigorously at 30°C than at 25°C. The size of the papilloma began to decrease soon after the animal was placed in the higher temperature. Cells of the upper layer of the tumor keratinized more actively than that of normal epidermis, i.e., shedding off tumor cells and size-reduction of tumor mass took place simultaneously. On the other hand, under conditions of the lower temperature movement of cells into the dermal layer was observed though tumor cells necrosed in part. The movement of cells was found at the earlier period soon after the change in temperature (within 4 weeks). However, the apparent size of the tumor did not become reduced in this early period. The reduction in size began after two months, and the tendency of the tumor to regress became more intense than at the higher temperature condition.

Generally, epithelial cells proliferate in the papilloma, but important changes in the dermal and pigment layers are lacking. However, at lower temperature, the number of cells in the epithelium decreased and simultaneously, that of the pigment layer increased. A down-growth of the epithelioma cells was observed at 4°C (low temperature treatment) [91]. The effects of temperature became evident much earlier. The mitotic index was strongly affected within as early as one week after the onset of temperature treatment. In the newts kept at 4°C or 30°C, the mitotic indices remained low (0.03–0.27) throughout the experimental periods, whereas under mild temperature conditions (10°C), the mitotic index of papilloma cells became significantly higher than at other temperatures. It is evident that the mitotic indices are closely related to the size of the newt papilloma [91].

When newts with regressing papillomata, caused by exposing them to lower or higher temperatures, were once again maintained at middle temperatures (10°C or 13°C), the tumor cells began to proliferate and increase the size of the tumor again. The growth of this tumor can be controlled or regressed reversibly by the effects of temperature. In addition to this effect, it has occasionally been observed that newts are likely to possess another method for curing a tumorous growth.

Generally, the tumor regresses gradually by depending on the change of temperature, but in some newts the mass of tumor disappeared almost abruptly from their bodies. This phenomenon may represent a form of "spontaneous therapy of tumor" in newts. It may be called "tumor cut-off" and could be comparable to the casting off of the tail in a lizard [74], and may be the most efficient method, and certainly fastest, to deal with a tumor. Practically, the process is achieved by

blood vessels being clogged up by blood cells and the subsequent prevention of the blood flow through the tumorous tissue. As a result, tumor cells necrose entirely and the mass of the tumor is removed from the root.

When it became obvious that newt papilloma is influenced by changes in temperature, it was thought that amphibians could serve as experimental material to study tumor regression, especially aspects of change and movement in tumor cells, and the contribution of virus in tumorous growth. However, to date almost no study has been performed with such objectives. For biochemical analysis, diamine and polyamine levels in spontaneous skin papilloma of newt were determined. In the papilloma putrescine was most abundant among the polyamines being nearly 5 times higher than that in the control skin [92].

Tumor bearing leopard frogs and the virus are not found in nature during summer. However, the latent existence of a virus can be confirmed by cold temperature treatment. Lucké renal tumor is, therefore, also thought to be a convenient system to analyse the effects of temperature on tumor cells and the role that the virus plays. Back to newts, it was pointed out earlier that they had papillomata predominantly in autumn, whereas Lucké renal tumor was present in large numbers twice a year, namely in spring and in autumn. If papillomas in newts would be controlled by means of temperature as the only causation factor, newt tumor ought to appear both in spring and in autumn. However, as the frequency of the tumor is actually low in spring, it suggests that factors promoting the tumor are not only temperature alone but others like, for example, hormones, growth factors or properties of the virus, too. As yet the different roles of these factors are not fully understood.

There is proof of the close relationship between temperature and cell motility and the cell movement of tumor cells. McKinnell *et al.* observed the distribution of microtubules in the cytoplasm of Lucké renal tumor cells, the established cell line PNKT–4B, the primary culture of renal tumor and, as a control, normal kidney cells of tadpole [93]. The cultures were kept at 20°C or 28°C and the microtubules were observed by the immunofluorescence method. In all of the three cultures, the microtubules were distributed regularly from the centre of the cell to the periphery, but when the cultures were kept at 7°C the distribution of microtubules in the tumor cells became irregular while normal cells remained unaffected. The microtubules of tumor cells quite unlike those of certain dermal cells in fish [94] become disordered by low temperature treatment similar to the disorder of microtubules seen in normal cells after application of a microtubule inhibitor. In Lucké renal tumor, metastasis formation occurs commonly at 28°C (77%), but much more rarely at low temperature (6%). It has also been suggested that the collagenase secreted by Lucké tumor *in vitro* explants degradated type 1 collagen at 30°C and was having an effect similar to that of temperature during metastasis formation [95]. However low levels of collagenase were also released at room temperature.

In those studies meant to illuminate the effects of temperature in newt papilloma the observed cell movements did not always agree with the results obtained on Lucké renal tumor. Nonetheless, amphibian tumor cells are excellent material to study the mechanisms of tumor formation, the complicated movement of cells at tumor growth and the phenomenon of regression. We are, therefore, convinced that human cancer research can only gain from the work, presently undertaken in various labs around the world, on amphibian tumor and regeneration.

ACKNOWLEDGMENTS

We are grateful to Professor Emeritus G. Nace of Michigan University for his suggestions.

REFERENCES

1 Krontovsky, A. (1916) Comparative and Experimental Pathology of Tumors, Kiev, Bacteriol. Inst., (In Russian).

2 Sheremetieva, E. A. (1938) Rep. Inst. Zool., Acad. Sci. Ukr. S. S. R., **12**: 37–61 (In Russian).

3 Lucké, B. and Schlumbarger, H. G. (1949) Physiol. Rev., **29**: 91–126.

4 Duryee, W. R., Long, M. E., Taylor, H. C., McKel-

way, W. P. and Ehrmann, R. L. (1960) Science, **131**: 276–280.
5 Brunst, V. V. and Roque, A. L. (1967) J. Natl. Cancer Inst., **38**: 193–204.
6 Hadji-Azimi, I. and Fischberg, M. (1967) Rev. Suisse Zool., **74**: 641–645.
7 Hadji-Azimi, I. and Fischberg, M. (1971) Cancer Res., **31**: 1594–1599.
8 Mizell, M. (1969) Biology of Amphibian Tumor, Springer, Berlin, Heidelberg & New York, pp. 1–484.
9 McKinnell, R. G. and Ellis, V. L. (1972) Cancer Res., **32**: 1154–1159.
10 Wirl, G. (1972) Arch. Geschwulstforsch., **40**: 111–115.
11 Balls, M. and Clothier, R. H. (1974) Oncology, **29**: 501–519.
12 Khudoley, V. V. and Eliseiv, V. V. (1979) J. Natl. Cancer Inst., **63**: 101–104.
13 Khudoley, V. V., Anikin, I. V., Sirenko, O. A. and Pliss, G. B. (1979) Vopr. Onkol. (Leningrad), **25**: 70–75 (In Russian).
14 Eliseiv, V. V. and Khudoley, V. V. (1980) Vopr. Onkol. (Leningrad) **26**: 70–71 (In Russian).
15 Jaenisch, W. and Schmidt, T. (1980) Arch. Geschwulstforsch., **50**: 253–265.
16 McKinnell, R. G., DiBerardino, M. A., Blumenfeld, M. and Bergad, R. D. (1980) Results and Problems in Cell Differentiation, **11**: Differentiation and Neoplasia, Springer-Verlag, Berlin, Heidelberg & New York, 310 pp.
17 Schlumberger, H. G. and Lucké, B. (1948) Cancer Res., **8**: 657–753.
18 Waddington, C. H. (1935) Nature, **135**: 606–608.
19 Needham, J. (1936) Proc. R. Soc. B, **29**: 1577–1626.
20 Khudoley, V. V. (1982) Bull. Exp. Biol. Med., **92**: 1084–1085.
21 Lucké, B. (1934) Am. J. Cancer, **20**: 352–379.
22 Effron, M., Griner, L. and Benirschke, K. (1977) J. Natl. Cancer Inst., **59**: 185–198.
23 Balls, M. (1962) Cancer Res., **22**: 1142–1154.
24 Reichenbach-Klinke, H. and Elkan, E. (1965) II. Diseases of Amphibian, Acad. Press, New York.
25 Dawe, C. J., Harshbarger, J. C., Kondo, S., Sugimura, T. and Takayama, S. (1981) Phyletic Approaches to Cancer. Proc. 11th Int. Symp. Princess Takamatsu Cancer Res. Fund., Japan Sci. Soc. Press, Tokyo.
26 Okada, T. S. (1979) Cancer Cells, UP Biology Ser. 36, Tokyo Univ. Press, Tokyo, pp. 1–128 (In Japanese).
27 Kimura, I. (1984) Current Encyclopedia of Pathology, **9c**: 304–318, Nakayama-shoten, Tokyo (In Japanese).
28 Asashima, M. and Oinuma, T. (1985) Oncologia, **13**: 99–114 (In Japanese).
29 Brunst, V. V. (1968) Exp. Cell Res., **53**: 401–409.
30 Khudoley, V. V. and Mizgireuv, I. V. (1980) Neoplasma, **27**: 289–293.
31 Mizgireuv, I. V., Flax, N. L., Borkin, L. J. and Khudoley, V. V. (1984) Neoplasma, **31**: 175–181.
32 Oinuma, T., Seki, M. and Asashima, M. (1984) Proc. Jpn Acad., **60B**: 265–268.
33 Counts, C. L. III., Wilson, C. T. and Taylor, R. W. (1975) Herpetologica, **31**: 422–424.
34 Khudoley, V. V. and Eliseiv, V. V. (1979) J. Natl. Cancer Inst., **63**: 101–103.
35 Counts, C. L. III. (1980) Herpetologica, **36**: 46–50.
36 Woitkewitsch, A. A. (1959) Natürliche Mehrfachbildungen an Froschextremitäten. VEB Gustav Fischer Verlag.
37 Meyer-Rochow, V. B. and Koebke, J. (1986) Zool. Anzeiger, **217**: 1–13.
38 Rostand, J. and Darré, P. (1969) C. R. Soc. Biol., **163**: 2033–2034.
39 Lucké, B. and Schlumbarger, H. (1936) J. Exp. Med., **70**: 257–268.
40 Rafferty, K. A. Jr (1964) Cancer Res., **24**: 169–185.
41 McKinnell, R. G. and McKinnell, B. K. (1968) Cancer Res., **28**: 440–444.
42 McKinnell, R. G. (1969) In "Biology of Amphibian Tumors". Ed. by M. Mizell, Springer-Verlag, Berlin, pp. 254–260.
43 McKinnell, R. G., Gorham, E., Martin, F. B. and Schaad, J. W. IV. (1979) J. Natl. Cancer Inst., **63**: 821–824.
44 McKinnell, R. G., Gorham, E. and Martin, F. B. (1980) Am. Midl. Nat., **104**: 402–404.
45 Asashima, M., Sasaki, T. and Takuma, T. (1986) Proc. Jpn. Acad., Ser. B, **62**: 307–310.
46 Honma, Y. and Murakawa, S. (1967) Annot. Zool. Japon., **40**: 211–214.
47 Bryant, S. V. (1973) Cancer Res., **33**: 623–625.
48 Burns, R. E. and White, H. J. (1971) Cancer Res., **31**: 826–829.
49 Darquenne, J. and Matz, G. (1971) Bull. Soc. Zool. Fr., **96**: 352–353.
50 Rose, F. L. and Harschbarger, J. C. (1977) Science, **196**: 315–317.
51 Pfeiffer, C. J., Nagai, T., Fujimura, M. and Tobe, T. (1979) Cancer Res., **39**: 1904–1910.
52 Asashima, M, and Komazaki, S. (1980) Proc. Jpn. Acad., Ser. B., **56**: 638–642.
53 Asashima, M., Komazaki, S., Satou, C. and Oinuma, T. (1982) Cancer Res., **42**: 3741–3746.
54 Asashima, M. (1983) Animal and Nature, **13**: 15–19.
55 Asashima, M., Oinuma, T., Matsuyama, H. and Nagano, M. (1985) Cancer Res., **45**: 1198–1205.

56 Asashima, M. and Koyama, H. (1986) Jpn. J. Hyperthermic. Oncol., **2**: 359–370.

57 Placais, D. (1974) Bull. Soc. Zool. Fr., **99**: 283–295.

58 Lucké, B. (1938) J. Exp. Med., **68**: 457–468.

59 Mizell, M., Stackpole, C. W. and Halpern, S. (1968) Proc. Soc. Exp. Biol. Med., **127**: 808–814.

60 Zambernard, J. and Vatter, A. E. (1966) Cancer Res., **26**: 2148–2153.

61 McKinnell, R. G., Ellis, V. L., Dapkins, D. C. and Steven, L. N. Jr (1972) Cancer Res., **32**: 1729–1733.

62 Tweedell, K. S. (1967) Cancer Res., **27**: 2042–2052.

63 Mizell, M. (1969) In "Biology of Amphibian Tumors". Ed. by M. Mizell, Springer-Verlag, Berlin, pp. 1–25.

64 Tweedell, K. S. and Williams, D. C. (1976) J. Cell Sci., **22**: 385–395.

65 Naegele, R. F., Granoff, A. and Darlington, R. W. (1974) Proc. Natl. Acad. Sci., **71**: 830–834.

66 Nace, G. W. and Ostrovsky, D. S. (1977) J. Natl. Cancer Inst., **58**: 453–454.

67 Rubin, M. L. and Nace, G. W. (1966) Am. Zool., **6**: 510.

68 Hirayasu, T., Iwamura, Y. and Asashima, M. (1987) (to be submitted).

69 Asashima, M. and Oinuma, T. (1982) J. Fac. Sci. Univ. Tokyo, Sec IV., **15**: 151–158.

70 Shimada, K., Koyama, H. and Asashima, M. (1987) Zool. Sci., **4**: 287–294.

71 Balls, M. and Ruben, L. N. (1968) Prog. Exp. Tumors Res., **10**: 238–260.

72 Balls, M. and Ruben, L. N. (1964) Experientia, **21**: 241–296.

73 Spemann, H. (1942) Wilhelm Roux' Arch. Entwicklungsmech. Org., **141**(4): 693–769.

74 Alibardi, L. and Sala, M. (1983) Atti Mem. Acad. Patavita Sci. Lett. ed Atti, **95** (Pt II: Scienze Matematiche e Naturali): 101–151.

75 Jonas, A. D. (1985) Orientierungshilfen zur Psychotherapie in der Allgemeinpraxis-archaische Relikte in Psychosomatischen Symptomen (pp. 92–97). Edition Materia, Medica, Verlag Socio-medico, Grafelfing.

76 Meyer-Rochow, V. B. (1985) Selecta, **27**, 2309.

77 Rose, S. M. and Wallingford, H. M. (1948) Science, **107**: 457.

78 Ruben, L. N. (1956) J. Morphol., **98**: 389–404.

79 Seilern-Aspang, F. and Kratochwil, K. (1962) J. Embryol. Exp. Morphol., **10**: 337–353.

80 Tsonis, P. A. (1984) Can. J. Zool., **62**: 2681–2685.

81 Tsonis, P. A. and Eguchi, G. (1981) Differentiation, **20**: 52–60.

82 Tsonis, P. A. and Eguchi, G. (1982) Dev. Growth Differ., **24**: 183–190.

83 Tsonis, P. A. and Eguchi, G. (1983) Dev. Growth Differ., **25**: 201–210.

84 Eguchi, G. and Watanabe, K. (1973) J. Embryol. Exp. Morphol., **30**: 63–71.

85 King, T. J. and DiBerardino, M. A. (1965) Ann. N. Y. Acad. Sci., **126**: 115–126.

86 DiBerardino, M. A. and King, T. J. (1965) Dev. Biol., **11**: 217–242.

87 McKinnell, R. G., Deggins, B. A. and Labat, D. D. (1969) Science, **165**: 394–396.

88 DiBerardino, M. A., Mizell, M., Hoffner, N. J. and Friesendorf, D. G. (1983) Differentiation, **23**: 213–217.

89 Braun, A. C. (1965) Sci. Am., **213**: 75–83.

90 Asashima, M. (1984) Oncologia, **11**: 147–150.

91 Asashima, M., Seki, M., Kanno, H. and Koyama, H. (1986) Proc. Jpn. Acad., Ser. B., **62**: 83–86.

92 Matsuzaki, S., Kurabuchi, S. and Inoue, S. (1985) Zool. Sci., **2**: 131–134.

93 McKinnell, R. G., DeBruyne, G. K., Mareel, M., Tarin, D. and Tweedell, K. S. (1984) Differentiation, **26**: 231–234.

94 Obika, M. and Meyer-Rochow, V. B. (1986) Cell Tissue Res., **244**: 339–343.

95 Ogilvie, D. J., McKinnell, R. G. and Tarin, D. (1984) Cancer Res., **44**: 3438–3441.

96 Lunger, P. D., Darlington, R. W. and Granoff, A. (1965) N. Y. Acad. Sci., **126**: 289–314.

ZOOLOGICAL SCIENCE 4: 427–431 (1987)

Proposed Tertiary Olfactory Pathways in a Teleost, *Carassius auratus*

Ken Ohnishi

Department of Physiology, Nara Medical University, Kashihara, Nara 634, Japan

ABSTRACT—Projection fields of the secondary olfactory terminal fields in the goldfish (*Carassius auratus*) were studied using retrograde axonal transport of horseradish peroxidase (HRP). The cell bodies within the ipsilateral lateral and posterior secondary olfactory terminal fields were labeled retrogradely after the injection of HRP into the medioposterior region of area dorsalis telencephali pars dorsalis (mpDd). The cell bodies within the hypothalamic secondary olfactory terminal field were labeled retrogradely after the injection of HRP into the posterior region of area dorsalis telencephali pars medialis (pDm). These anatomical results suggest that the mpDd and pDm in the goldfish probably form part of the tertiary olfactory projection fields.

INTRODUCTION

In the teleostean olfactory systems, the neural pathways of the secondary olfactory fibers have been studied by many investigators not only anatomically [1–10] but also electrophysiologically [11] for understanding of the evolution of the vertebrate central nervous systems. The projection fields of the fibers revealed in these studies are essentially very similar among different species. In the goldfish, *Carassius auratus,* Ichikawa [5], Bartheld *et al.* [1] and Levine and Dethier [7] have pointed out that the secondary olfactory fibers project bilaterally to three main telencephalic regions: (1) ventral area surrounding the dorsal aspects of the medial olfactory tract (medial terminal field of Ichikawa [5]); (2) medioventral region of area dorsalis telencephali pars lateralis (lateral terminal field of Ichikawa [5]); (3) posteroventral region of area dorsalis telencephali pars lateralis (posterior terminal field of Ichikawa [5]) and one diencephalic region: nucleus posterior tuberis, NPT, (hypothalamic terminal field of Bartheld *et al.* [1]). However, projections of the secondary olfactory terminal fields in the telencephalic hemispheres of teleosts have not been investigated as yet except for Murakami *et al.* [8]. To examine whether the higher olfactory terminal fields exist or not in teleosts, axon terminal fields of the neurons within lateral, posterior and hypothalamic terminal field were examined using retrograde labeling with horseradish peroxidase (HRP).

MATERIALS AND METHODS

Sixty goldfish (*Carassius auratus*), 10 to 13 cm in length, obtained from a commercial dealer were used. The animals were anesthetized by putting them in a small tank containing 0.1% tricaine methanesulfonate (MS 222) and then positioned in the stereotaxic apparatus slightly modified from that of Peter and Gill [12]. During surgery, the animals were respired by circulating aerated tap water containing 0.05% MS 222 through the gill. The dorsal part of the skull was removed with a dental drill and the brain was exposed under a dissecting microscope. HRP injection into the surface layer of the telencephalon was performed by the insect pin method. An insect pin (No. 000) coated with a small amount of HRP paste was manually inserted into the desired site at the surface layer of the telencephalon [13]. After survival times of 3 days in a water tank at 20–25°C, the animals were anesthetized with MS 222 and

Accepted January 21, 1987
Received December 25, 1986

then perfused through the conus anteriosus with 0.6% saline followed by a solution of 4% glutaraldehyde in 0.1 M phosphate buffer (pH 7.4). The brain was removed from the skull and postfixed in the same buffer solution containing 10% sucrose for 24 hr. Frontal 50 μm thick sections were cut on a cryostat while referring to the atlas of Peter and Gill [12]. The present terminology was after this reference [12]. The HRP reaction with tetramethylbenzidine was processed according to the procedure of Mesulam [14]. The sections mounted on the gelatin-coated slide were counterstained with 1% neutral red.

RESULTS AND DISCUSSION

HRP injections were performed in twelve regions of the telencephalic surface layer divided into the anterior, anteromedial, medioposterior and posterior region of area dorsalis telencephali pars lateralis (Dl), dorsalis (Dd) and medialis (Dm), respectively. At the injection site, the diffusion of HRP was confined to a region of about 300 μm in diameter. After the injection into the mpDd, a large number of labeled cells were observed densely in the ipsilateral medioventral (Fig. 1 C and D) and posteroventral region of Dl (Fig. 1 E and F) and precommissural medioposterior region of area dorsalis telencephali pars centralis (Dc), (Fig. 1 B and C). The labeled cells in the posteroventral region of Dl were 5 to 7 μm in diameter (Fig. 3 a and b). A few labeled cells were also observed sparsely in the ipsilateral medioposterior region of Dl (Fig. 1 B), Dd (Fig. 1 C) and Dm (Fig. 1 B–D) and posterior region of Dm (Fig. 1 E and F). No labeled cells were observed in the

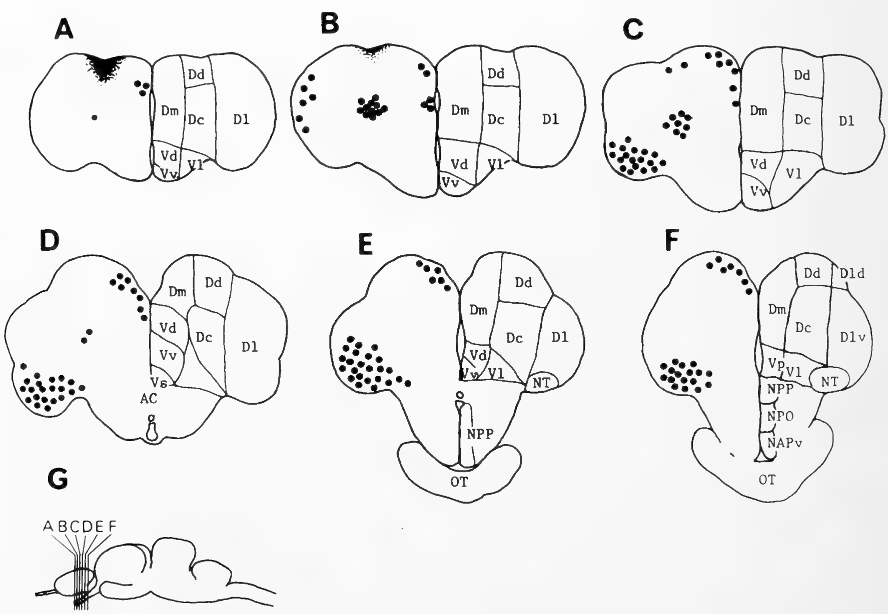

Fig. 1. A–F. The distribution of labeled cells in the telencephalon after injection of HRP into the mpDd. Blackened area and surrounding stippled area indicate the injection site and diffusion area of HRP, respectively. Each solid circle marks the location of several labeled cells. AC, anterior commissure; Dc, area dorsalis telencephali pars centralis; Dd, area dorsalis telencephali pars dorsalis; Dl, area dorsalis telencephali pars lateralis; Dld, area dorsalis telencephali pars lateralis dorsalis; Dlv, area dorsalis telencephali pars lateralis ventralis; Dm, area dorsalis telencephali pars medialis; NAPv, nucleus anterioris periventricularis; NPO, nucleus preopticus; NPP, nucleus preopticus periventricularis; NT, nucleus tenia; OT, optic tract; Vd, area ventralis telencephali pars dorsalis; Vl, area ventralis telencephali pars lateralis; Vp, area ventralis telencephali pars postcommissuralis; Vs, area ventralis telencephali pars supracommissuralis; Vv, area ventralis telencephali pars ventralis. G. Levels of A–F.

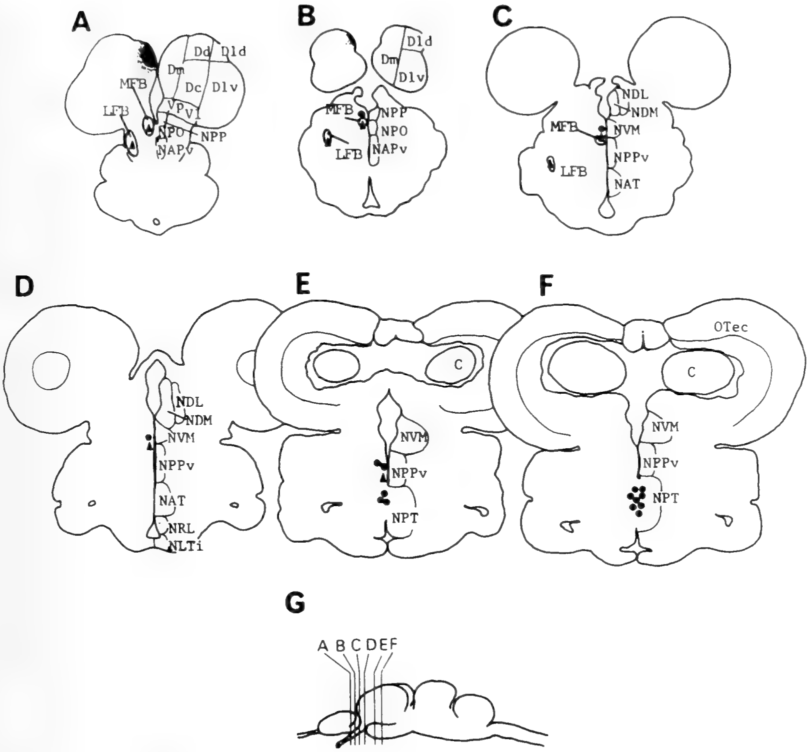

FIG. 2 A–F. The distribution of labeled cells in the telencephalon and diencephalon after injection of HRP into the pDm. Filled triangles indicate labeled axons. C, cerebellum; LFB, lateral forebrain bundle; MFB, medial forebrain bundle; NAT, nucleus anterior tuberis; NDL, nucleus dorsolateralis thalami; NDM, nucleus dorsomedialis thalami; NLTi, nucleus lateralis tuberis pars inferioris; NPPv, nucleus poterioris periventricularis ventralis; NRL, nucleus recessus lateralis; NVM, nucleus ventromedialis thalami; OTec, optic tectum. G. Levels of A–F. See Fig. 1 for further explanations.

medial terminal field. The medioventral and the posteroventral region of Dl in the goldfish has been reported to receive the secondary olfactory fibers from the olfactory bulb [1, 5, 7]. Consequently, the labeled cells in the medioventral and posteroventral region of Dl probably make a connection with the secondary olfactory fibers. After the injection into pDm, retrogradely labeled cells were mostly observed in the NPT (Fig. 2 E and F) and few labeled cells in the nucleus preopticus periventricularis (Fig. 2 B and E) and nucleus ventromedialis thalami (NVM, Fig. 2 C and D). The labeled cells in the NPT were very small and they were less than 3 μm in diameter (Fig. 3 c and d). Labeled axons were also observed in the medial forebrain bundle running ventral area of nucleus preopticus periventricularis and NVM (Fig. 2 A–E) and some in the lateral forebrain bundle (Fig. 2 A and B). No labeled cells were observed in the medial, lateral or posterior terminal field. The NPT receives secondary olfactory fibers from the olfactory bulb in the goldfish [1, 7]. Thus, the labeled cells in the NPT probably connect with the secondary olfactory fibers. HRP injections into other regions scarcely led to retrograde labeling of cells in the medial, lateral, posterior or hypothalamic terminal field.

Mammalian central olfactory neural pathways can be divided into two main routes, direct projection from the secondary olfactory terminal field to the tertiary olfactory terminal field in the telencephalon [15–19] and another nondirect projection via diencephalon to the telencephalon [19–23]. However, in teleosts only direct projection is

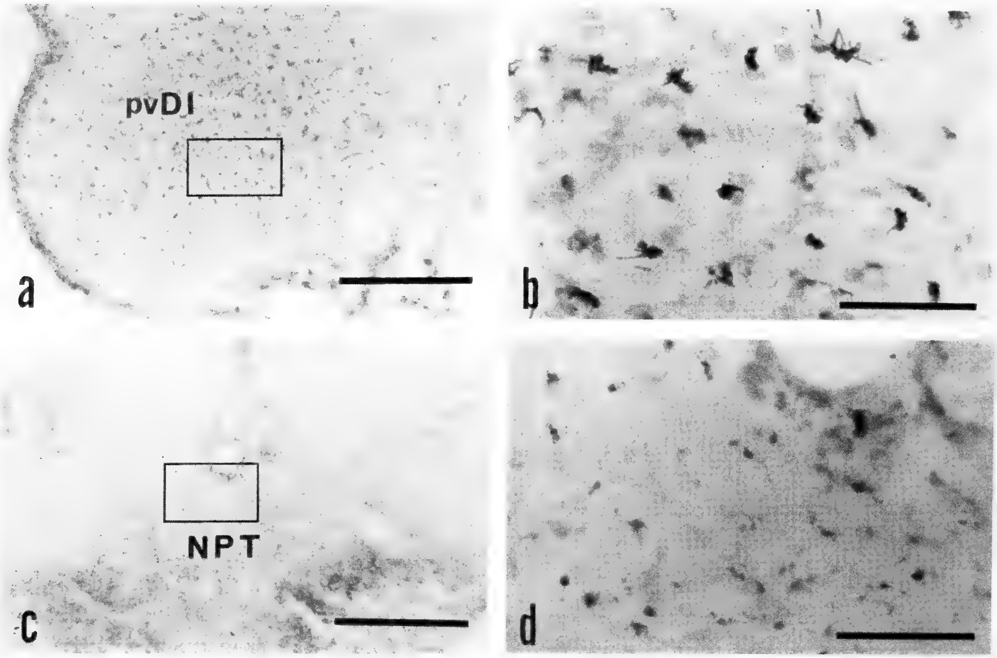

FIG. 3. a and b. Labeled cells in posteroventral region of area dorsalis telencephali pars lateralis (pvDl) after HRP injection into medioposterior region of area dorsalis telencephali pars dorsalis (mpDd). c and d. Labeled cells in nucleus posterior tuberis (NPT) after HRP injection into posterior region of area dorsalis telencephali pars medialis (pDm). The outlined area of a and c is shown at a higher magnification in b and d, respectively. Scale bar=300 μm (a and c), 75 μm (b and d).

known [8]. In the present study, nondirect projection via diencephalon was revealed for the first time in the teleostean olfactory system. This suggests that not only in mammals but also in teleosts two main olfactory routes exist. In the nondirect projection in the monkey, the hypothalamus receives the tertiary olfactory fibers from the secondary olfactory terminal field (piriform cortex) and projects to the telencephalic area (lateroposterior orbitofrontal cortex) [22]. Compared with this pathway, the route via the hypothalamus in the goldfish is more simple. The hypothalamus receives directly fibers from the olfactory bulb not via the secondary olfactory terminal field and projects to the telencephalic area. These results lead to the proposition that the central olfactory nervous systems become more complex with evolution. This view will be confirmed when olfactory projections of olfactory bulb-hypothalamus-telencephalon are detected in lower vertebrates such as amphibians and reptiles.

Murakami *et al.* [8] have detected in the rockfish, *Sebastiscus marmoratus,* retrogradely labeled cells in the ipsilateral posterior terminal field after HRP injection into ventral region of the Dm and concluded the region as the tertiary olfactory terminal field. The projection field of the posterior terminal field in the goldfish was the ipsilateral mpDd. This discrepancy may result from method differences. In present study, since HRP injections were strictly limited to the surface layer of the telencephalon, the projections to the inner parts of the telencephalon, i.e. ventral region of Dm, Dc, medial region of Dl and area ventralis telencephali, were not examined. Thus, the possibility of the projections to the inner parts from the secondary olfactory terminal fields, especially the medial terminal field whose projection area are not detected, remain unclear. Furthermore, compared with projections of the secondary olfactory fibers, those of the tertiary olfactory fibers may differ greatly with the species. To prove

this hypothesis, investigations on the higher olfactory projections, i.e. projections of the secondary olfactory terminal fields in other teleostean species, are required.

REFERENCES

1 Barthɇld, C.S., Meyer, D.L., Fiebig, E. and Ebbesson, S.O.E. (1984) Central connections of the olfactory bulb in the goldfish, *Carassius auratus.* Cell Tissue Res., **238**: 475–487.

2 Bass, A.H. (1981) Olfactory bulb efferents in the channel catfish, *Ictalurus punctatus.* J. Morphol., **169**: 91–111.

3 Ebbesson, S.O.E., Meyer, D.L. and Scheich, H. (1981) Connections of the olfactory bulb in the piranha (*Serrasalmus nattereri*). Cell Tissue Res., **216**: 167–180.

4 Finger, T.E. (1975) The distribution of the olfactory tracts in the bullhead catfish, *Ictalurus nebulosus.* J. Comp. Neurol., **161**: 125–142.

5 Ichikawa, M. (1975) The central projections of the olfactory tract in the goldfish, *Carassius auratus.* J. Fac. Sci. Univ. Tokyo, **13**: 257–263.

6 Ito, H. (1973) Normal and experimental studies on synaptic patterns in the carp telencephalon, with special reference to the secondary olfactory termination. J. Hirnforsch., **14**: 237–253.

7 Levine, R.L. and Dethier, S. (1985) The connections between the olfactory bulb and the brain in the goldfish. J. Comp. Neurol., **237**: 427–444.

8 Murakami, T., Morita, Y. and Ito, H. (1983) Extrinsic and intrinsic fiber connections of the telencephalon in a teleost, *Sebastiscus marmoratus.* J. Comp. Neurol., **216**: 115–131.

9 Oka, Y. (1980) The origin of the centrifugal fibers to the olfactory bulb in the goldfish, *Carassius auratus*: An experimental study using the fluorescent dye primuline as a retrograde tracer. Brain Res., **185**: 215–225.

10 Scalia, F. and Ebbesson, S.O.E. (1971) The central projections of the olfactory bulb in a teleost (*Gymnothorax funebris*). Brain Behav. Evol., **4**: 376–399.

11 Fujita, I., Satou, M. and Ueda, K. (1984) A field-potential study of centripetal and centrifugal connections of the olfactory bulb in the carp, *Cyprinus carpio* (L.). Brain Res., **321**: 33–44.

12 Peter, R.E. and Gill, V.E. (1975) A stereotaxic atlas and technique for forebrain nuclei of the goldfish, *Carassius auratus.* J. Comp. Neurol., **159**: 69–102.

13 Finger, T.E. (1978) Cerebellar afferents in teleost catfish (Ictaluridae). J. Comp. Neurol., **181**: 173–182.

14 Mesulam, M.-M. (1978) Tetramethylbenzidine for horseradish peroxidase neurohistochemistry: A non-carcinogenic blue reaction-product with superior sensitivity for visualizing neural afferents and efferents. J. Histochem. Cytochem., **26**: 106–177.

15 Allison, A.C. (1953) The morphology of the olfactory system in the vertebrates. Biol. Rev., **8**: 195–244.

16 Gerfen, C.R. and Clavier, R.M. (1979) Neural inputs to the prefrontal agranular insular cortex in the rat: Horseradish peroxidase study. Brain Res. Bull., **4**: 347–353.

17 Harberly, L.B. and Price, J.L. (1978) Association and commissural fiber systems of the olfactory cortex of the rat. I. Systems originating in the piriform cortex and adjacent areas. J. Comp. Neurol., **178**: 711–740.

18 Krettek, J.E. and Price, J.L. (1977) Projections from the amygdaloid complex to the cerebral cortex and thalamus in the rat and cat. J. Comp. Neurol., **172**: 687–722.

19 Potter, H. and Nauta, W.J.H. (1979) A note on the problem of olfactory associations of the orbitofrontal cortex in the monkey. Neuroscience, **4**: 361–367.

20 Giachetti, I. and MacLeod, P. (1977) Olfactory input to the thalamus: Evidence for a ventroposteromedial projection. Brain Res., **125**: 166–169.

21 Powell, T.P.S., Cowan, W.M. and Raisman, G. (1965) The central olfactory connexions. J. Anat., **99**: 791–813.

22 Tanabe, T., Yarita, H., Iino, M., Ooshima, Y. and Takagi, S.F. (1975) An olfactory projection area in orbitofrontal cortex of the monkey. J. Neurophysiol., **38**: 1269–1283.

23 Yarita, H., Iino, M., Tanabe, T., Kogure, S. and Takagi, S.F. (1980) A transthalamic olfactory pathway to orbitofrontal cortex in the monkey. J. Neurophysiol., **43**: 69–85.

ZOOLOGICAL SCIENCE 4: 433–439 (1987)

Gonad Response to γ-Aminobutyric Acid in the Sea Urchin

NOBUAKI TAKAHASHI

Marine Biomedical Institute, Sapporo Medical College, Higashirishiri, Hokkaido 097–01, Japan

ABSTRACT—In the sea urchin, *Strongylocentrotus intermedius,* gonad response to γ-aminobutyric acid (GABA) was examined by indirect measurements of gonad contraction. (1) Mechanical response was noted to increase with gonad growth. Young growing gonads showed small response but for maturing, ripe and post-spawning specimens, the response was large. (2) Two different GABA responses on the part of maturing, ripe and post-spawning gonads, and young and growing gonads were thus in evidence. In the former, there were both phasic and rhythmical contractions but in the latter, only phasic contraction. (3) GABA response was also noted to vary according to sex. In the female, the appearance of rhythm was high, but low in the male. (4) The duration of GABA response was about 20 min in maturing and ripe gonads. (5) The threshold concentration of GABA response was 0.01 mM. The 50% effective and maximal doses were 0.1 mM and 10 mM, respectively. (6) The sites of action of GABA injected at a concentration of 10 mM were examined. GABA acted directly on the gonads. The generator inducing phasic and rhythmical contraction is discussed.

INTRODUCTION

Several studies for obtaining gametes from sea urchins have already been performed, such as those involving the use of mechanical damage [1], potassium [1–3] and calcium [1] ions, electrical shock [4–7], acetylcholine [8], and the radial nerve factor [9, 10]. However, no report has so far appeared on a physiological triggering mechanism for gamete shedding in sea urchins.

The injection of γ-aminobutyric acid (GABA) into sea urchins was recently found to induce gamete release [11]. The threshold concentration of GABA for spawning was noted to be about 0.01 mM and the optimal for 100% spawning, to exceed 0.1 mM. The initiation time of release following the injection was about 12 sec. Thus GABA spawning is a rapid phenomenon. In the present research, this matter was examined in greater detail by measuring the mechanical response of gonads toward GABA. Portions of this work recently appeared in abstract form [12].

Accepted January 8, 1987
Received November 15, 1986

MATERIALS AND METHODS

Animals

Sea urchins (*Strongylocentrotus intermedius*) were collected from the coast of Rishiri Island off northern Hokkaido throughout the year. The animals were kept at our laboratory in an aquarium provided with running seawater until use.

Seawater

Modified van't Hoff seawater (ASW) (462 mM NaCl; 9 mM KCl; 9 mM $CaCl_2$; 36 mM $MgCl_2$; 17 mM $MgSO_4$; 20 mM Tris-HCl, pH 8.2) was used as the basal incubation medium. K^+-rich ASW contained KCl at the concentration of 500 mM. NaCl was removed. The composition of other ions was the same as ASW. GABA ASW was made by adding γ-aminobutytic acid (Nakarai Chemicals Ltd.) at various concentrations to ASW.

Apparatus

Okada *et al.* [13] reported the central part of gonads at the time of spawning to increase in height and termed this height change as potential

difference (PD). The present study also uses this term as well as some of their procedures.

The sea urchins were first fixed with large forceps. On the oral side of each specimen, a hole 3 cm in diameter was opened by cutting the shell test with solid scissors. A small hole 5 mm in diameter on a portion of the remaining test was made by a dental drill. The animal was fixed by placing one foot of the forceps into a small hole and pinching the test (Fig. 1i).

The PD of the gonads was measured by a strain guage (Fig. 1c; SB–1TH, Nihon Koden). The strain guage was horizontally set and connected to a straw. At a certain point on the horizontally set straw, it was then placed perpendicularly and cut vertically in half with its top made rectangular. It was placed perpendicularly on the central part of the gonad (Fig. 1j). The PD measurement was amplified (Fig. 1b; RP–3, Nihon Koden) and recorded on an ink-writing oscillograph (Fig. 1d; Nihon Koden).

Solution exchange was carried out by withdrawing the old solution through the straw inserted in the body cavity (Fig. 1h) and then introducing the new solution through a 10 ml pipette (Fig. 1g).

Recording

The recording was performed at room temperature which varied from 18 to 25°C. The Aristotle's lantern and oesophagus were removed from the sea urchin. In experiments on the action site of GABA, the oral and aboral intestines were also removed by forceps. The animal was fixed and immersed up to the equator into filtered natural sea water in a large beaker (Fig. 1i and e). Soon after the animal had been fixed, its body cavity was filled with coelomic fluid or ASW by pipette. The straw was placed on the gonad and the siphon in the central portion of the body cavity. In that state, the sea urchin was left for 30 min. When the gonad was immersed in ASW, exchange of ASW was carried out two or three times during this period. After the 30 min, the gonads were treated with GABA for 10 min (Fig. 2). The PD induced by GABA was designated as PD_G and the GABA was removed. The gonad

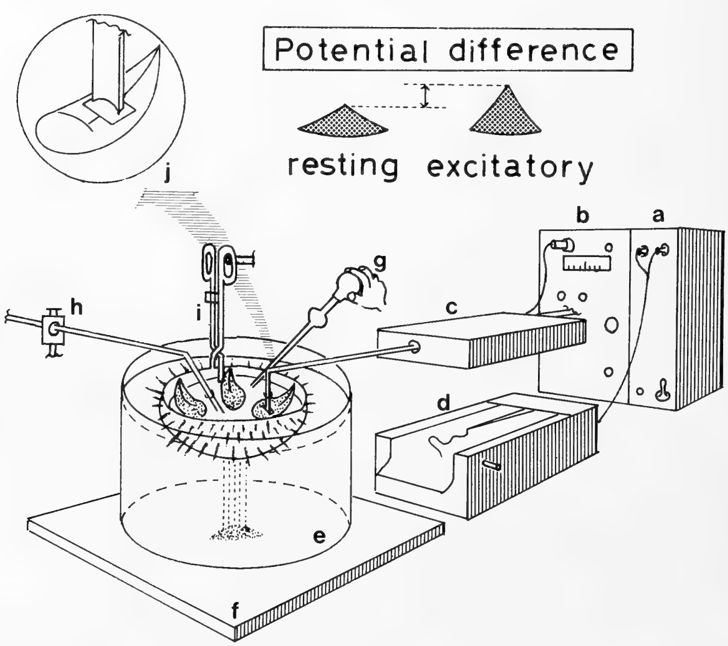

FIG. 1. Apparatus for measuring potential differences in sea urchin gonads. a, main amplifier; b, carrier amplifier; c, strain guage; d, ink-writing oscillograph; e, beaker; f, lab jacks; g, pipette; h, siphon; i, forceps; j, magnification of straw cut vertically in half, with the top made rectangular.

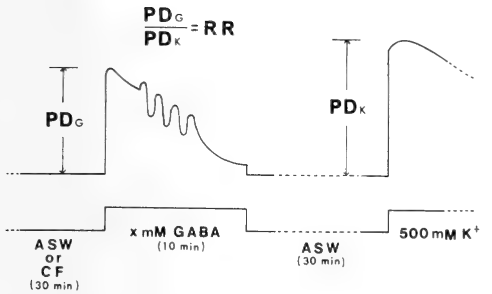

FIG. 2. Method for recording. ASW, artificial sea water; CF, coelomic fluid; PD_G, potential difference induced by GABA; PD_K, potential difference by 500 mMK^+; RR, relative response.

was washed two or three times in ASW and then left for 30 min. This was followed by treatment with K^+-rich ASW. The resulting PD was designated as PD_K. The relative value of PD_G against PD_K was designated as the relative response, RR.

Histology

To observe gonoduct and gonopore structures, the sea urchin was first placed in decalcified solution for about one week to adequately soften the test. The solution contained 5 ml nitric acid, 10 ml formalin and 85 ml distilled water. The decalcified sea urchin was cut into small pieces, which were then washed in running water. The gonaoduct and gonopore segments were embedded in paraffin according to the usual method and sectioned and stained with hematoxylin-eosin.

The silver-staining method for nerve cells was carried out as follows: small pieces of gonad were fixed with 10% formalin for 6 hr followed by washing in running water for 4 hr. Five drops of ammonia water were added to the solution containing the pieces. Twenty-four hours later, they were transferred to a 1.5% silver nitrate solution at 38°C and left for 5 days. The pieces were then placed in a reducing solution consisting of 100 ml distilled water, 15 ml formalin and 1 g hydroquinone. This was followed by embedding in paraffin by the usual method. After sectioning and removal of the paraffin, they were dehydrated and observed without stain.

RESULTS

Mechanical response

Contraction mode and sex differences Mechanical response to GABA was generally of two types. The response in young and growing gonads showed smooth phasic contraction (Fig. 3a). That in maturing, ripe and post-spawning gonads indicated oscillating rhythmical contraction superimposed on phasic contraction (Fig. 3b). Response to GABA ceased at about 20 min (Fig. 4). The time from the start of contraction to its peak was approximately 40 sec. Both small and large oscillations in rhythmical contraction were noted. On some occasions, rhythm could be observed to a small degree near the peak of the phasic contraction (Fig. 3a). Usually, large

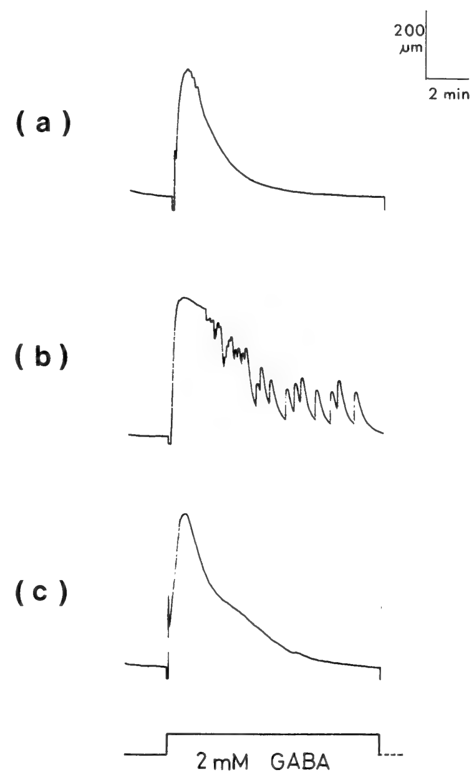

FIG. 3. Response to 2 mM GABA. a, a phasic contraction in growing ovary; b, a rhythmical contraction in addition to phasic contraction in the descending phase of a mature ovary; c, a phasic contraction in a testis.

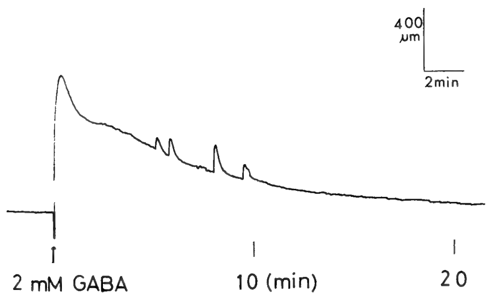

FIG. 4. Mechanical response induced by 2 mM GABA, in a mature ovary. Gonad response ceased at 20 min.

rhythm could be easily detected in females with mature ripe gonads. Males displayed only phasic contraction in response to GABA (Fig. 3c). Thus, response to GABA varies according to sex.

Seasonal variation Seasonal variation of GABA response was observed. RRs in January (1 mM GABA), May (2 mM) and July (2 mM) were 0.89 ± 0.08 (mean $\pm$ SEM), 0.60 ± 0.11 and 1.03 ± 0.08, respectively. RR in April through June was usually low. In Rishiri Island, the average weight of one lobule from a gonad was 0.86 g in May and 1.39 in July in sea urchins 4–5 cm in diameter. Since one lobule in post-spawning and young gonads is usually 0.32 g, the gonads in May were apparently in the growing stage, thus accounting for the response in gametogenic gonads. RR in July was significantly higher than in May ($P<0.01$). This high RR exceeding 1.0 may possibly have been due in part to the abundant release of gametes during the time when the gonads were treated with GABA.

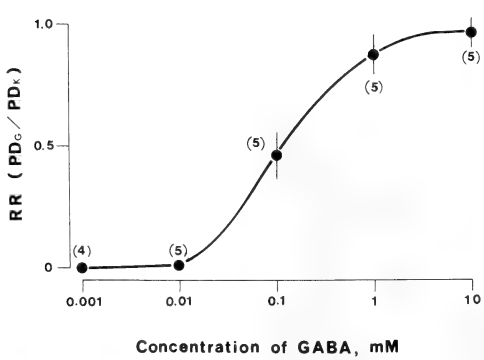

FIG. 5. Dose-response curve of gonad contraction by GABA. Abscissa, concentration of GABA (mM); ordinate, relative response (RR). Points and vertical bars are means $\pm$ SEM. The number of preparations examined is shown in parentheses. 10 mM GABA corresponds to 0.96 RR.

Dose-response

Dose-response in the present study is represented as the response of PD toward GABA relative to that toward 500 mM K^+. The experiment was performed in February, when the gonads appeared to be in the post-spawning stage and the average weight of one lobule was 0.32 g for sea urchins 4–5 cm in diameter. PD peaks were measured as RR. In Figure 5, the threshold concentration is 0.01 mM. The 50% effective dose appeared near 0.1 mM and maximal one, 10 mM. The RR in 10 mM GABA was 0.96.

Site(s) of action

Aboral nerve system The aboral nerve sys-

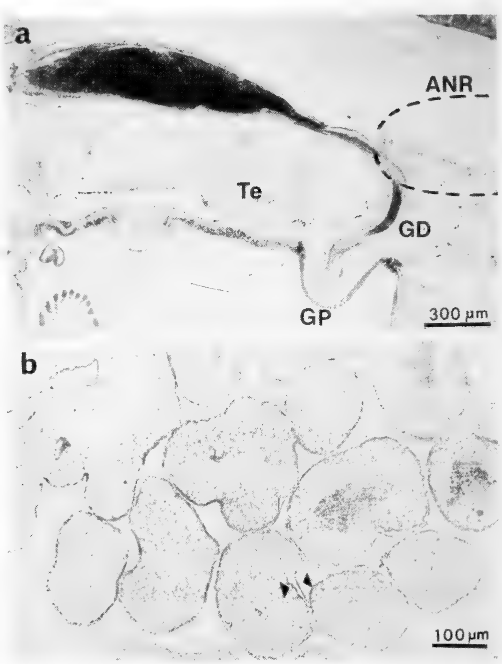

FIG. 6. (a) Histology of male sea urchin reproductive system. The test is decalcificated. ANR, aboral nerve ring; GD, gonoduct; GP, gonopore; Te, test. Dotted line indicates a supposed place of aboral nerve ring. (b) Testis stained with silver. Both layers in the gonad wall are stained (two arrow heads).

tem appears to be composed of nerve cells and fibers in the nerve ring surrounding the anus, those in the gonoduct and those in the gonad wall. The gonad wall in this animal is composed of three layers, outer coelomic epithelium (visceral peritoneum), middle connective tissue with muscle cells and nerve cells, and an inner germinal layer [14]. Silver-staining indicated two layers of nerve cells, one just beneath the outer coelomic epithelium and the other in the middle connective tissue (Fig. 6b). Some of the nerve cells in the gonad are also possibly associated with those in the gonoduct. As can be seen from Figure 6a, the gonoduct passes through the test and opens to the outside of the gonopore. At the point where the gonoduct enters the test, the nerve process in the gonoduct divides into two branches. By conjugating circularly with branches originating from each of the five lobules in the gonad, the aboral nerve ring is formed and surrounds the anus.

Site(s) of action The experiment was performed in March, at the time gonads were in the resting stage. The RR for 10 mM GABA was 0.8 (Fig. 7, control in b). To study the site(s) of action of injected GABA, three different experiments were carried out. The first experiment was conducted to determine if a supposed action site was the aboral nerve ring. One lobule was separated from the other four in a gonad by cutting nervous branches at both sides of the gonoduct with a surgical knife (Fig. 7, I in a). If the site is actually the aboral nerve ring, no GABA response should occur. In the second experiment, since the gonoduct consisted of several kinds of cell, one lobule was removed from the gonoduct with surgical knife (Fig. 7, II in a). In this experiment, the supposed site was found to be the gonoduct. In the third experiment, since the gonad was in contact with the peritoneum, one gonad was separated from the surroundings by cutting the peritoneum and border of the gonoduct (Fig. 7, III in a). The supposed site was the gonad. The RR of three different experiments exhibited no significant difference with that of the control (Fig. 7b), indicat-

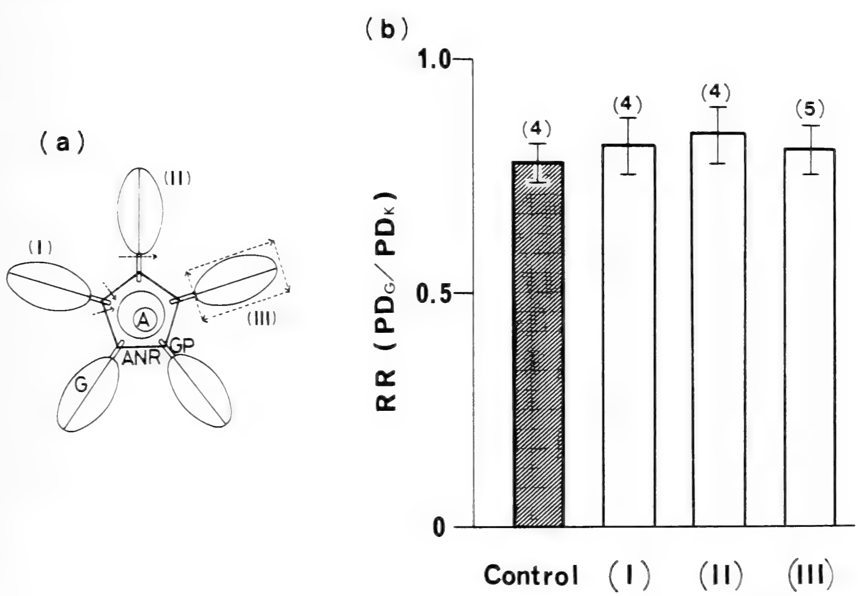

FIG. 7. Site(s) of action of injected GABA. (a) Three different experiments (I, II and III) were carried out. Arrows indicate surgical knife cut. A, anus; ANR, aboral nerve ring; G, gonad; GP, gonopore. (b) The results obtained by (a) are shown in the columns. The number of preparations examined appears in parentheses. Abscissa, results for control and each experiment (I, II and III); ordinate, relative response (RR).

ing GABA to likely act directly on the gonad. When separating the gonad from the peritoneum and gonoduct (Fig. 7, III in a), small rhythmical contractions but no large ones were noted by gonad.

DISCUSSION

It is well established that starfish spawning is triggered by the release of gonad-stimulating substances (GSS) from supporting cells in nervous tissue containing radial nerves [15]. Recently, Shirai and co-workers [16] found two kinds of peptides with GSS action in *Asterias amurensis.* A water extract of radial nerves in the sea cucumber is capable of inducing the spawning of the same species and is possibly a peptide [17]. In the sea urchin, radial nerve water extract has also been reported to bring about gamete shedding [9, 10]. Iwata and Fukase [8] found that acetylcholine, as a neuro-transmitter, induces sea urchin spawning. Recently, gamete shedding in the sea urchin has been observed to occur by injecting GABA [11]. The inhibitory substances depressing spawning activity are known to be present in coelomic fluid [18]. The sea urchin thus begins releasing gametes by washing ceolomic fluid with natural seawater. These substances have been identified as L-glutamic acid and aspartic acid [19], possible neuro-transmitters. Thus, sea urchin spawning appears to be associated particularly with a certain substance(s) from nervous tissue.

The final step in gamete shedding is a contraction of smooth muscle in the gonad wall. Since a ripe gonad in the sea urchin is easily injured in the course of an operation, the extent of gonadal contraction can be determined indirectly by measuring PD. Along with its development and maturation, the mechanical response of a gonad to GABA increases. Moreover, maturing and ripe ovaries display both phasic and rhythmical contraction while young and growing ovaries, only phasic contraction. GABA response is likely to vary according to sex differences. The time required for mechanical response due to GABA in maturing sea urchins is about 20 min. On the dose-response curve, the threshold, 50% effective, and maximal concentrations are 0.01 mM, 0.1 mM and 10 mM, respectively. Our surgical experimental data indicated that GABA acted directly on the gonad and induced contraction and spawning. Thus, the presence of GABA-responding nerve cells in the gonad appears to induce sea urchin spawning.

Recently, it has been reported that the five lobules of sea urchin gonads contract synchronously and rhythmically through the aboral nerve system [13]. Okada *et al.* [13] suggested that the gonoduct generated this rhythm. From the data of the present study, it is evident that a lobule separated from the surroundings is also capable of inducing small but not large rhythm. This in turn appears to result in contraction of the gonad itself and vibration of the rhythmical contraction of the other four lobules. The generator of this rhythm should be studied cytologically.

In conclusion, gonad response to GABA appears to be both phasic and rhythmical contractions, each possibly originating from a different generator. That is, phasic contraction was noted to occur throughout the year, and rhythmical contraction, at the time of gonad maturation. Gonad contraction and spawning appear to be explained quite well if at least two different generators are assumed to be operative. At any rate, GABA appears to act on both these different generators.

ACKNOWLEDGMENTS

The author is grateful to Dr. M. Takahashi, Sapporo Medical College, and Professor M. Yoshida, Okayama University, for their valuable comments. He also thanks Professor K. Kikuchi, President of Sapporo Medical College, and Professor K. Takahashi, Sapporo Medical College, for their encouragement throughout the course of this work. This work was supported by a grant from the Hokkaido Newspaper Office for Social and Natural Scientific Research.

REFERENCES

1 Palmer, L. (1937) The shedding reaction in *Arbacia punctulata.* Physiol. Zoöl., **10**: 352–367.

2 Harvey, E. B. (1939) A method of determining the sex of *Arbacia*, and a new method of producing twins, triplets and quadruplets. Biol. Bull., **77**: 312.

3 Harvey, E. B. (1940) A note on determining the sex of *Arbacia punctulata*. Biol. Bull., **79**: 363.

4 Iwata, K. S. (1950) A method of determining the sex of sea urchins and of obtaining eggs by electric stimulation. Annot. Zool. Japon., **23**: 39–42.

5 Harvey, E. B. (1952) Electrical method of "sexing" *Arbacia* and obtaining small quantities of eggs. Biol. Bull., **102**: 284.

6 Harvey, E. B. (1953) A simplified electrical method of determining the sex of sea urchins and other marine animals. Biol. Bull., **105**: 365.

7 Iwata, K. S. (1962) A simplified electrical method of determining the sex of sea urchins. Zool. Mag., **71**: 301–302.

8 Iwata, K. S. and Fukase, H. (1964) Artificial spawning in sea urchins by acetylcholine. Biol. J. Okayama Univ., **10**: 51–56.

9 Cochran, R. C. and Engelmann, F. (1972) Echinoid spawning induced by a radial nerve factor. Science, **178**: 423–424.

10 Cochran, R. C. and Engelmann, F. (1976) Characterization of spawning-inducing factors in the sea-urchin, *Strongylocentrotus purpuratus*. Gen. Comp. Endocrinol., **30**: 189–197.

11 Takahashi, N. (1986) The spawing of the sea-urchin, *Strongylocentrotus intermedius,* by γ-aminobutyric acid. Bull. Japan. Soc. Sci. Fish., **52**: 2041.

12 Takahashi, N. (1986) Gamete shedding by sea urchins in response to γ-aminobutyric acid. Dev. Growth Differ., **28**: 384.

13 Okada, Y., Iwata, K. S. and Yanagihara, M. (1984) Synchronized rhythmic contractions among five gonadal lobes in the shedding sea urchins: coordinative function of the aboral nerve ring. Biol. Bull., **166**: 228–236.

14 Kawaguchi, S. (1965) Electron microscopy on the ovarian wall of the echinoid with special references to its muscles and nerve plexus. Biol. J. Okayama Univ., **11**: 66–74.

15 de Angelis, E., Viglia, A. Watanabe, T., Shirai, H., Kubota, J. and Kanatani, H. (1972) Presence of granules containing gonad-stimulating substance in starfish radial nerve. Annot. Zool. Japon., **45**: 16–21.

16 Shirai, H., Bulet, P., Kanatani, H., Kondo, N., Imai, K., Isobe, M., Goto, T.and Kubota, I. (1985) Purification of gonad-stimulating substance in starfish. Zool. Sci., **2**: 912.

17 Maruyama, Y. K. (1985) Holothurian oocyte maturation induced by radial nerve. Biol. Bull., **168**: 249–262.

18 Okada, Y. and Iwata, K. S. (1985) A substance inhibiting rhythmic contraction of the gonad in the shedding sea urchin. Zool. Sci., **2**: 805–808.

19 Nogi, H. and Yoshida, M. (1984) Inhibitory substance of rhythmic contraction in sea urchin gonad. Zool. Sci., **1**: 873.

ZOOLOGICAL SCIENCE **4**: 441–446 (1987)

Gonad Response to Calcium and a Comparison of the Effects of Calcium, Potassium, Acetylcholine and γ-Aminobutyric Acid on the Sea Urchin Gonad

NOBUAKI TAKAHASHI AND MASAKI TAKAHASHI

Marine Biomedical Institute, Sapporo Medical College, Higashirishiri, Hokkaido 097–01, Japan

ABSTRACT—Gonad response to calcium and the effects of calcium, potassium, acetylcholine (ACh) and γ-aminobutyric acid (GABA) on the gonads of the sea urchin, *Strongylocentrotus intermedius* were studied on the basis of measurements of the potential difference (PD). Rhythmical contraction due to Ca^{2+} occurred at a concentration exceeding 50 mM and its frequency increased as the concentration rose above this. In mature gonads, rhythmical contraction lasted for over an hour. Among four stimuli, ACh initiated threshold-contraction at the lowest concentration, 10^{-8} or 10^{-7} M. In relative response (RR) indicating the PD of a certain stimulation against that of 500 mM K^+, the RR of GABA and K^+ reached 1.0 but Ca^{2+} and ACh saturated near 0.8. Ca^{2+} and GABA induced both rhythmical and smooth phasic contraction while K^+ and ACh, only smooth long lasting contraction. The response to 50 mM K^+ and 50 mM Ca^{2+} persisted for more than an hour but that toward 2 mM GABA and 2 mM ACh, only about 20 min.

INTRODUCTION

Palmer [1] indicated that, on dropping potassium chloride directly onto a gonad surface, visible steady contraction of the gonad wall resulted and following the injection of this salt, a genital substance was released with force from all five pores. At the time of this observation, he devised a procedure for obtaining sea urchin gametes. He also found that a drop of isotonic calcium chloride on a gonad surface appeared to cause the wall to contract and relax in a rhythmical manner and the injection of this salt to cause characteristic rhythmical shedding followed by the complete release of genital substance from the gonads. In the preceding papers, γ-aminobutyric acid (GABA) was found to induce rhythmical as well as phasic contraction of the sea urchin gonad and gamete shedding [2, 3]. This prompted the authors to examine again gonad rhythmical contraction using calcium. In the present study, measurements were made of rhythmical contraction induced by calcium. Calcium, potassium, acetylcholine (ACh) and GABA were compared for their ability to bring about gonad response.

Accepted January 8, 1987
Received November 15, 1986

MATERIALS AND METHODS

Animals

Sea urchins (*Strongylocentroturs intermedius*) were collected from the coast of Rishiri Island off northern Hokkaido during all seasons of the year. The animals were kept at our laboratory in an aquarium provided with running seawater until use.

Seawater

Modified van't Hoff seawater (ASW) (462 mM NaCl; 9 mM KCl; 9 mM $CaCl_2$; 36 mM $MgCl_2$; 17 mM $MgSO_4$; 20 mM Tris-HCl, pH 8.2) was used as the basal incubation medium. Ca^{2+}-rich ASW was prepared at various concentration of Ca^{2+}, using $CaCl_2$ in place of NaCl to maintain isotonicity. K^+-rich ASW was prepared in a similar manner. ACh (Sigma Chemical Co.) and GABA (Nakarai Chemicals Ltd.) seawater solutions were made by the addition of various concentrations of each chemicals to ASW.

Apparatus

The apparatus used in the present study is described in the preceding paper [2].

Recording

The recording was carried out at room temperature which varied from 18 to 25°C.

To measure gonad contraction, namely potential difference (PD) devised by Okada *et al.* [4], a hole 3 cm in diameter was made on the oral side of each sea urchin with solid scissors followed by the removal of Aristotle's lantern and the oesophagus by forceps. The animal was subsequently fixed by pinching the test with large forceps and immersed up to its equator in filtered natural seawater in a beaker and soon after, the body cavity was filled with ASW. The straw previously cut vertically in half and connected to a strain guage (SB–1TH, Nihon Koden) was placed on a gonad and the siphon in the central portion of body cavity. The gonad was allowed to remain in this state for 30 min; during which time the ASW was changed two or three times. The gonad was first treated with a stimulant at a concentration of x mM until immediately following a peak of induced contraction (Fig. 1). The gonad was washed, placed in ASW solution and 30 min later, the same treatment was repeated but at a stimulant concentration of y mM (Fig. 1). This was followed by washing the gonad and placing it in ASW for 30 min. It was finally treated with 500 mM K^+ ASW. Mechanical response by 500 mM K^+ was designated as $PD_{500K \text{ or } K}$ The relative value of PD_{St} (stimulant) against PD_K was represented by relative response (RR). In this way, the two RRs of one preparation were measured.

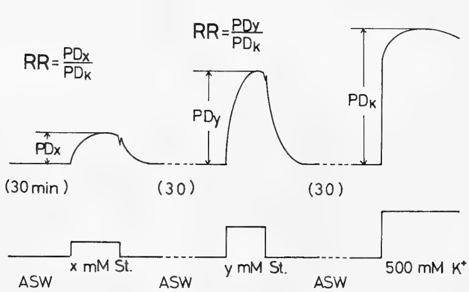

FIG. 1. Method for measuring relative response (RR). In a gonad, two RRs were measured at different concentrations of a stimulant. Immediately after PD peak was reached, the gonad was washed and immersed in ASW for 30 min. ASW, artificial sea water; PD, potential difference; St., stimulant.

RESULTS

Ca^{2+} effects

Dose-response experiment This experiment was conducted in March. The average weight of one lobule in a gonad was 0.28 g and from external observation, it appeared to be in the resting state. The first recording was generally performed at a low Ca^{2+} concentration and the second, at a high concentration. The filled circles in Figure 2 indicate the occurrence of rhythmical contraction superimposed on phasic one. The highest peak of rhythmical contraction was measured. The Ca^{2+} concentration inducing a threshold-contraction was about 20 mM. At about 100 mM, the dose-response curve indicated saturation of gonad response to Ca^{2+} with an RR of 0.74. The 50% effective dose ranged from 30 mM to 40 mM Ca^{2+}. For generation of rhythm, the threshold-contraction was induced at a concentration of 40 mM Ca^{2+}.

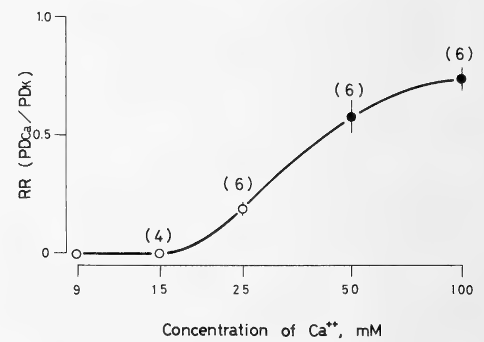

FIG. 2. Dose-response curve of potential difference (PD) by Ca^{2+}. Filled circles indicate rhythmical contraction. Points and vertical bars are means ± SEM. The number of preparations assayed appears in the parentheses. Abscissa, concentration of Ca^{2+} (mM); ordinate, relative response (RR).

Contraction mode Figure 3 a and b were recorded using the same ovary. The sea urchin

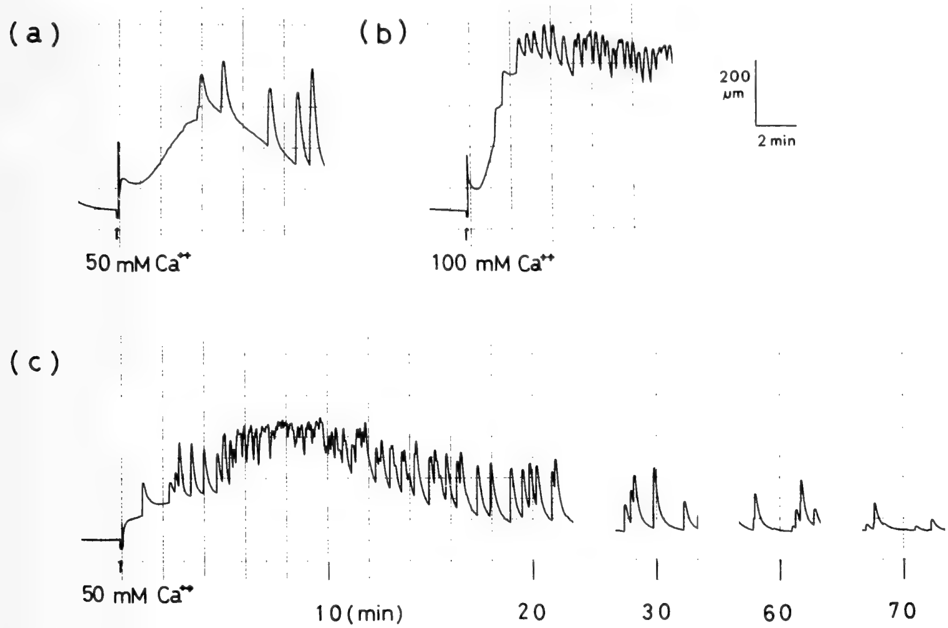

FIG. 3. Several features of PD by Ca^{2+}. Frequency of rhythm was noted to rise with increase in Ca^{2+} concentration. (a) 50 mM Ca^{2+}; (b) 100 mM Ca^{2+}. All time course of rhythmical contraction by 50 mM Ca^{2+} is shown in (c). The rhythm continued for 70 min.

from which it came spawned in response to over 50 mM Ca^{2+}. The frequency of the rhythm increased with Ca^{2+} concentration. The initiation of rhythm occurred more quickly at 100 mM than at 50 mM. Rhythm was greater at 50 mM than at 100 mM, since, owing to its high frequency at 100 mM Ca^{2+}, it became superimposed on itself. All the time courses of rhythmical contraction induced by 50 mM Ca^{2+} are shown in Figure 3c. The highest frequency was noted within 6–8 min. The contraction continued for 70 min following immersion of the gonad in the Ca^{2+}-rich ASW and then ceased. Generally, the rhythm in young gonad did not occur easily.

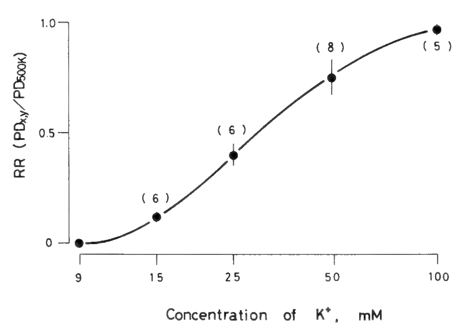

FIG. 4. Dose-response curve of potential difference (PD) by K^{+}. Points and vertical bars are means ± SEM. The number of preparations assayed appears in parentheses. Abscissa, concentration of K^{+} (mM); ordinate, relative response (RR).

K^{+} effects

Dose-response experiment The experiment was carried out in March. The average weight of one lobule was 0.34 g and the gonads appeared to be either in the resting or young stage. At 100 mM, gonad RR was maximium (Fig. 4). The threshold concentration ranged from 9 mM to 15 mM, with the 50% effective dose being 30 mM. Response difference according to sex could not be detected.

Contraction mode Although, when a few drops of 0.5 KCl were added to coelomic fluid, the sea urchin gonad induced rhythmical contraction [4], K^{+}-rich ASW prepared at various concentrations of K^{+} generally failed to produce any rhythm. Contraction due to K^{+} at concentration exceeding 100 mM was noted to be quite active but

to be followed by a state of rigor. That is, gonad relaxation was rendered impossible by K^+ treatment. The contraction produced by K^+ at 50 mM is shown in Figure 6a. To bring about the relaxation of the gonad, one hour was required. No rhythm could be observed.

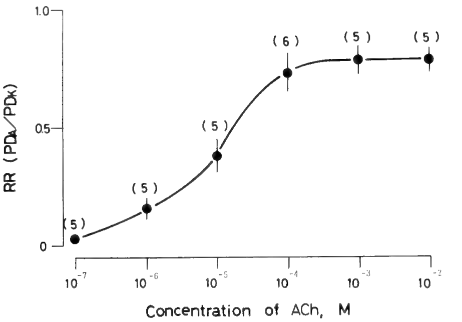

FIG. 5. Dose-response curve of potential difference (PD) by ACh. Points and vertical bars are means ±SEM. The number in parentheses is number of preparations assayed. Abscissa, concentration of ACh (M); ordinate, relative response (RR).

ACh effects

Dose-response experiment This experiment was performed in March. The average weight of one lobule was 0.27 g. The gonads appeared to be in the resting stage. The threshold contraction-concentration was 10^{-8} to 10^{-7} M (Fig. 5). RR at concentrations exceeding 10^{-4} M ACh was saturated at a value of 0.8. The 50% effective dose was about 10^{-5} M. Sex difference could not be detected.

Contraction mode No rhythmical contraction occurred at any ACh concentrations used. Relaxation of contraction by high ACh concentra-

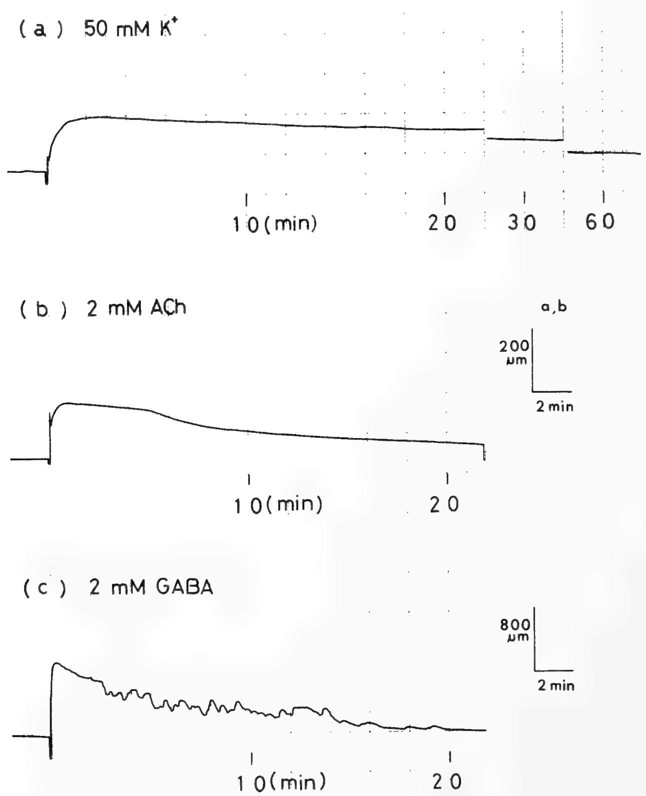

FIG. 6. Potential difference (PD) for each of three stimuli. (a) 50 mM K^+; (b) 2 mM ACh; (c) 2 mM GABA. Time course of PD in 50 mM K^+ was about one hour and that of ACh and GABA (2 mM) was about 20 min.

tion (2 mM) was possible, as evident from Figure 6b. The gonad was a testis and sperm continued to be released for 15 min. ACh contractions generally terminated within 20 min.

GABA effects

Dose-response experiment The data presented here have already been presented in the preceding paper [2]. Dose-response is shown in Figure 7. The threshold, 50% effective, and maximal doses were 0.01 mM, 0.1 mM and 10 mM GABA, respectively.

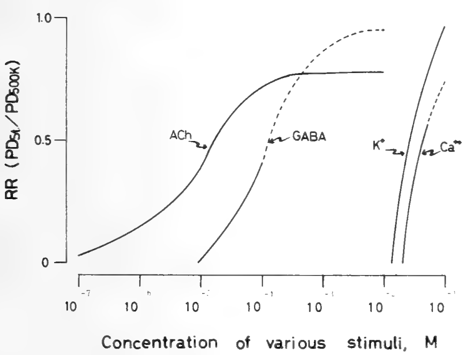

FIG. 7. Dose-response curves of potential difference (PD) by Ca^{2+}, K^+, ACh and GABA, on the same co-ordinate. Dotted lines indicated rhythmical contraction. Abscissa, concentration of stimuli; ordinate, relative response (RR).

Contraction mode The type of GABA contraction has already been presented in Figure 4 of the preceding paper, but in the present research as well, the contraction was found to be rhythmical (Fig. 6c). This was noted in July. Response to GABA ceased in 20 min.

DISCUSSION

Ca^{2+} response

Palmer [1] found that, on placing a drop of isotonic calcium chloride on the surface of a gonad of *Arbacia punctulata*, its wall appeared to contract and relax rhythmically. The data of the present research confirm this observation. The rhythmical contraction of a gonad of *Strongylocentrotus intermedius* was recorded with an oscillograph. Also, in his investigation, following an injection of $CaCl_2$, a definite relation between Ca^{2+} concentration and both the time prior to visible shedding and duration of the shedding reaction could be clearly discerned. In the present study, rhythm frequency was observed to increase with Ca^{2+} concentration. The rate of increase in PD was also found to do the same. In regard to gamete shedding in response to Ca^{2+}, Palmer found the average time interval between an injection of $CaCl_2$ and gamete shedding to depend on sex type. The time of sperm shedding for a 1 ml injection of 0.3 M $CaCl_2$ was 18 sec and that of egg shedding, 95 sec. In the present *in vitro* experiments, such variation according to sex could not be detected. Threshold concentration and rate of increase in calcium contraction were the same for both male and female. Rhythmical contraction also occurred at the same concentration (50 mM) in both sexes. The absence of any variation according to sex may possibly have been due to the conditions of the *in vitro* experiment and/or individual species differences.

Comparison of response to Ca^{2+}, K^+, ACh and GABA

Dose-response curves for Ca^{2+}, K^+, ACh and GABA appear on the same co-ordinate in Figure 7. The dotted line indicates rhythmical contraction. The threshold concentration of ACh is lower than that of the others. RR in the case of GABA and K^+ was as much as 1.0 but that in Ca^{2+} and ACh, 0.8. The duration of response to K^+ and Ca^{2+} was in proportion to their concentration and more than an hour. But for GABA and ACh, the duration was about 20 min. GABA and Ca^{2+} induced both rhythmical and phasic contraction but K^+ and ACh, only slow phasic or long lasting contraction.

The gonad displayed at least two kinds of contraction with or without rhythm. Consequently, it may be considered that contractions are produced by at least two different types of generators, one inducing smooth phasic and the other, rhythmical contraction. The present data show the first type of generator to be influenced by K^+, ACh and GABA and the second, by Ca^{2+} and GABA. Generation in one case appears to involve stable reactions with various stimuli regardless of

the season but the latter is apparently influenced by season since the number of such reactions was noted to increase with gonad maturation. This confirms the possibility of at least different types of generators.

Certain muscles of echinoderm are known to be responsive to ACh. In the lantern retractor muscle of the sea urchin, ACh at a concentration of 10^{-5}M has been found almost invariably to produce powerful contraction which persists with hardly any change for at least 80 min [5]. Moreover, the sea urchin oesophagus has been shown to contract through the action of ACh. Thus, although neuro-muscular transmission in the sea urchin is generally considered cholinergic, the gonad wall responds to GABA as well as ACh [2, 7]. The wall is composed of three layers, outer coelomic epithelium (visceral peritoneum), middle connective tissue with muscle and nerve cells, and an inner germinal layer [8]. The middle layer is further divided into five sub-layers, outer connective tissue, a muscle layer, central connective tissue, a nerve plexus, and inner connective tissue. Davis [9] showed nerve cell processes are present between the visceral peritoneum and the outer connective tissue. Thus, the muscles constitute one layer but the nerves, two layers in the gonad wall of the sea urchin [2]. The one muscle layer may possibly be controlled by various types of nerves whose determination should be made so as to gain an understanding of the spawning mechanism in the sea urchin.

ACKNOWLEDGMENTS

The authors are grateful to Professor K. Kikuchi, President of Sapporo Medical College, and Professor K. Takahashi, Sapporo Medical College, for their encouragement throughout this work. This work was supported by a grant from the Hokkaido Newspaper Office for Social and Natural Scientific Research (N. T).

REFERENCES

1 Palmer, L. (1937) The shedding reaction in *Arbacia punctulata*. Physiol. Zoöl., **10**: 352–367.

2 Takahashi, N. (1987) Gonad response to γ-aminobutyric acid in the sea urchin. Zool. Sci., **4**: 433–439.

3 Takahashi, N. (1986) The spawning of the sea-urchin, *Strongylocentrotus intermedius*, by γ-aminobutyric acid. Bull. Japan. Soc. Sci. Fish., **52**: 2041.

4 Okada, Y., Iwata, K. S. and Yanagihara, M. (1984) Synchronized rhythmic contractions among five gonadal lobes in the shedding sea urchins: coordinative function of the aboral nerve ring. Biol. Bull., **166**: 228–236.

5 Boltt, R. E. and Ewer, D. W. (1963) Studies on the myoneural physiology of Echinodermata. V. The lantern retractor muscle of *Parechinus*: responses to drugs. J. Exp. Biol., **40**: 727–733.

6 Florey, E. and McLennan, H. (1959) The effects of factor I and of gamma-aminobutyric acid on smooth muscle preparations. J. Physiol., **145**: 66–76.

7 Nogi, H. and Yoshida, M. (1984) Inhibitory substance of rhythmic contraction in sea urchin gonad. Zool. Sci., **1**: 873.

8 Kawaguchi, S. (1965) Electron microscopy on the ovarian wall of the echinoid with special references to its muscles and nerve plexus. Biol. J. Okayama Univ., **11**: 66–74.

9 Davis, H. (1971) The gonad wall of Echinodermata: a comparative study based on electron microscopy. MSc Thesis, Univ. of California, San Diego, 90 pp.

ZOOLOGICAL SCIENCE 4: 447–450 (1987)

The Mediation of Cyclic AMP in Octopaminergic Modulation at Neuromuscular Junctions of the Mealworm, *Tenebrio molitor*

OSAMU HIDOH[1] and JUN-ICHI FUKAMI[1, 2]

Institute of Agriculture and Forestry, University of Tsukuba, Sakura-mura, Ibaraki 305, and [2]Laboratory of Insect Toxicology, Institute of Physical and Chemical Research, Wako, Saitama 351, Japan

ABSTRACT—The possibility that there is mediation of cyclic AMP in the octopaminergic modulation of neuromuscular transmission was examined. Octopamine (1 μM) potentiated the amplitude of neurally-evoked excitatory junctional potentials (EJPs) at the neuromuscular junctions on the ventral longitudinal muscle of the mealworm, *Tenebrio molitor*. Although lower doses of octopamine (0.01 μM) or cyclic AMP (100 μM) had no effects on EJPs, the amplitude of EJPs was potentiated by these compounds when the phosphodiesterase activity was inhibited with simultaneous application of phosphodiesterase inhibitor, isobutyl-1-methylxanthine (IBMX, 10 μM). No effects of octopamine, cyclic AMP or IBMX on the time constant of the decay phase of the EJPs and the resting membrane potentials were observed. The results support the presynaptic mediation of cyclic AMP in octopaminergic modulation at neuromuscular junctions.

INTRODUCTION

Octopamine is a multifunctional biogenic amine, believed to be a neurotransmitter, a neurohormone and a neuromodulator in the insect nervous system [1, 2]. Glutaminergic neuromuscular transmission is well modulated by this amine. Presynaptic action of octopamine enhances the neuromuscular transmission in the locust [3], in *Manduca* [4], resulting in the potentiation of the amplitude of excitatory junctional potentials (EJPs) and contributing to the potentiation of twitch tension [3, 5].

There is growing evidence that adenosine 3′, 5′-cyclic monophosphate (cyclic AMP) plays a role as cellular mediator in the nervous system. Octopamine is widely distributed in insect nervous system [1, 6] and specific increase in cyclic AMP induced by octopamine has been reported in various neural tissues [7–13]. These observations suggest that a broad variety of octopaminergic actions is mediated via a second messenger system [14, 15].

It seems, therefore, that there is mediation of cyclic AMP in the modulatory action of octopamine at neuromuscular junctions in insects. The present work was undertaken to examine the mediation of cyclic AMP by using phosphodiesterase inhibitor, isobutyl-1-methylxanthine (IBMX) [16].

MATERIALS AND METHODS

Larvae of the mealworm (*Tenebrio molitor*) were used. The neuromuscular preparation employed was similar to that described by Yamamoto and Washio [17]. The ventral longitudinal muscle fibers of an abdominal segment were exposed by slitting open the larvae along the dorsal midline and removing the alimentary canal and fat bodies. The dissected animal was mounted on a perfusion chamber made of Sylgard Resin (Dow-Corning Co.) and was continuously perfused with *Tenebrio* saline containing 70 mM NaCl, 30 mM KCl, 14.4 mM $MgCl_2$, 0.6 mM $CaCl_2$, 445 mM glucose and 5 mM HEPES. The pH of this saline was adjusted to 7.2 with NaOH. Octopamine HCl and adenosine 3′, 5′-cyclic monophosphate (cyclic AMP)

Accepted December 25, 1986
Received November 18, 1986
[1] Present address: Laboratory of Biology, Meiji College of Pharmacy, Setagaya, Tokyo 154, Japan.

were obtained from Sigma Chemical Co. Isobutyl-1-methylxanthine (IBMX) was obtained from Aldrich Chemical Co. These chemicals were dissolved in the saline.

Intracellular recordings from a ventral muscle fiber were made with a glass microelectrode filled with 3 M KCl (5–10 MΩ). To elicit EJPs, the motor nerve innervating the ventral muscle was stimulated at a point close to the segmental ganglion with square pulses of 0.1 msec duration using a pair of fine Ag-hook electrodes. Sixteen EJPs evoked at 2 Hz were averaged to estimate their amplitude, the time constant of single exponential decay phases and resting membrane potentials. These averaging treatments were performed every one minute.

All experiments were carried out at room temperature (24–26°C).

RESULTS

The effects of treatments were examined by three parameters: the amplitude of EJPs, the time constant of their single exponential decay phase and resting membrane potentials. Neurally-evoked EJPs showed no facilitation properties when they were evoked at 2 Hz. Results obtained are summarized in Table 1. Time constant of single exponential decay phase and resting membrane potentials were unchanged with all treatments.

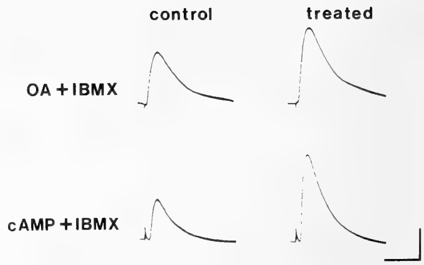

FIG. 1. Action of octopamine, cyclic AMP and IBMX on neurally-evoked EJPs. Sixteen EJPs evoked at 2 Hz were averaged before (control) and 5 min after (treated) the onset of the treatments. Upper two traces were treated with 0.01 μM octopamine and 10 μM IBMX. Lower two traces were treated with 100 μM cyclic AMP and 10 μM IBMX. Calibration: 5 mV, 20 msec.

Phosphodiesterase inhibitor, IBMX, added to perfusate at a concentration of 10 μM (designated as 10 μM IBMX treatment) had no effect on EJP amplitude. Lower doses of octopamine (0.01 μM octopamine treatment) also had no effect. In contrast, these two compounds applied at the same time (0.01 μM octopamine plus 10 μM IBMX treatment) modulated neuromuscular transmission. The amplitude of EJPs was significantly potentiated; the upper two traces in Figure 1 represent this action. The time course comparing 0.01 μM octopamine treatment with 0.01 μM octopamine plus 10 μM IBMX treatment is drawn in Figure 2 A. Treatment by octopamine alone did

TABLE 1. The effects of octopamine, cyclic AMP and IBMX on the neurally-evoked EJPs

Treatment	EJP amplitude (mV) control/treated	Time constant (ms) control/treated	Resting potential (mV) control/treated	N
OA (1 μM)	8.2±1.7/14.9±2.3*	17.8±4.0/17.5±3.8	−48.6±2.3/−48.1±2.6	5
OA (1 μM) +IBMX (10 μM)	8.2±1.6/13.8±2.3*	16.2±2.4/17.1±2.8	−50.0±1.9/−49.1±2.3	6
OA (0.01 μM)	8.8±1.6/ 8.7±1.3	12.0±0.4/12.8±0.2	−49.2±2.0/−48.7±1.6	5
OA (0.01 μM) +IBMX (10 μM)	7.1±1.4/ 9.9±1.3*	12.0±0.7/13.0±0.6	−48.2±1.5/−48.5±1.9	5
cAMP (100 μM)	12.1±1.1/12.9±0.5	16.0±2.3/15.2±2.2	−49.2±2.0/−48.8±2.2	5
cAMP (100 μM) +IBMX (10 μM)	8.3±1.3/12.3±1.4*	15.5±2.1/14.5±2.3	−49.8±1.4/−48.5±1.3	6
IBMX (10 μM)	8.6±1.2/ 8.8±1.7	13.0±0.4/12.6±0.5	−51.2±2.5/−48.9±2.1	5

Each value is the mean and S.E. just before (control) and 5 min after (treated) the onset of the treatments. * indicates the mean is significantly increased at $P<0.01$ by a paired-sample *t*-test. OA: octopamine. cAMP: cyclic AMP. IBMX: isobutyl-1-methylxanthine.

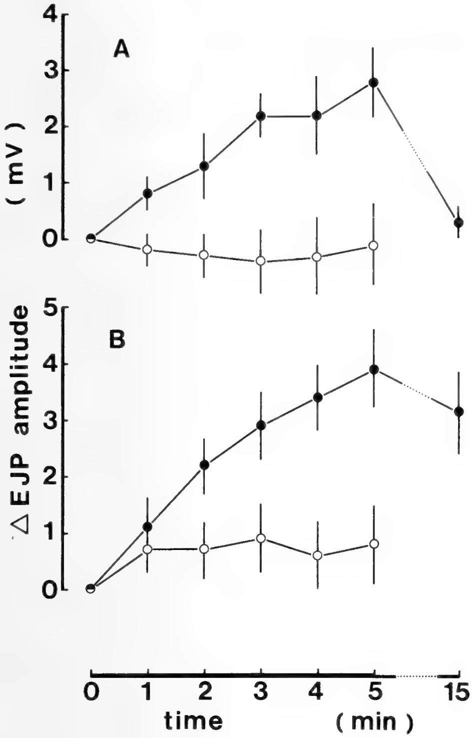

FIG. 2. Time courses of the effect on the EJP amplitude by octopamine, cyclic AMP and IBMX. A: 0.01 μM octopamine (○) and 0.01 μM octopamine plus 10 μM IBMX (●) were added to the perfusate for 5 min. B: 100 μM cyclic AMP (○) and 100 μM cyclic AMP plus 10 μM IBMX (●) were added to the perfusate for 5 min. Each point represents the mean of difference of the EJP amplitude obtained from 5 or 6 determinations; vertical bars represent S.E.

not potentiate EJP amplitude, whereas octopamine plus IBMX resulted in gradual potentiation.

The results were different in the case of octopamine (1 μM) and IBMX(10 μM). EJPs were potentiated both by 1 μM octopamine treatment and 1 μM octopamine plus 10 μM IBMX treatment. Potencies inducing potentiation between these two conditions exhibited the same strength. Amplitude of EJPs increased by 6.7 ± 1.6 mV (n=5) with treatment of 1 μM octopamine alone and by 5.6 ± 0.9 mV (n=6) with 1 μM octopamine plus 10 μM IBMX treatment (means and S. E.) (Table 1). These values were not different by two sample *t*-test.

The action of cyclic AMP had similarities with the potentiating action of octopamine (0.01 μM). One hundred μM cyclic AMP treatment was not effective, whereas 100 μM cyclic AMP plus 10 μM IBMX treatment potentiated the amplitude of EJPs; the lower two traces in Figure 1 represent potentiating action by this treatment. As in the case of 0.01 μM octopamine plus 10 μM IBMX treatment, the time course of potentiating action is drawn in Figure 2B, and also shows the gradual increase by 100 μM cyclic AMP plus 10 μM IBMX treatment.

DISCUSSION

Presynaptic action of octopamine has been revealed by an increase in the frequency of miniature EJPs (MEJPs) at neuromuscular junctions in locust extensor tibiae muscle [3]. Although major changes in cyclic AMP levels occur postsynaptically, octopamine increases cyclic AMP levels in this neuromuscular preparation [12]. Elevation of cyclic AMP levels by phosphodiesterase inhibitors [18, 19] and by a series of cyclic AMP analogues [19] causes an increase in the frequency of MEJPs, showing similarities of action and time course of octopamine on presynaptic terminals. The elevation of cyclic AMP levels by octopamine in the presynaptic terminals is likely to affect transmitter release by the cyclic AMP-dependent protein kinase, changing the calcium levels [20].

At *Tenebrio* neuromuscular junctions, octopamine-induced potentiation of EJP amplitude is contributed to the increase of quantal contents which are estimated by extracellularly-recorded EJP failures, whereas the frequency of MEJPs is not affected by octopamine [21]. These actions suggest the enhancement of calcium accumulation that is associated with the impulse invasion into the presynaptic terminals.

In the present study, the amplitude of EJPs was potentiated by 0.01 μM octopamine plus 10 μM IBMX treatment but not by treatment with 0.01 μM octopamine alone, suggesting that octopamine elevates cyclic AMP levels in the presynaptic terminals. Even 0.01 μM octopamine may elevate cyclic AMP levels; the elevation, however, is so slight that the natural phosphodiesterase inacti-

vates cyclic AMP. If this inactivation is inhibited by IBMX, the elevation is sufficient that cyclic AMP exerts potentiating action. In the case of cyclic AMP treatment, the same event related to phosphodiesterase may occur. The elevation of cyclic AMP by 1 μM octopamine treatment may exceed an optimum level, so that 1 μM octopamine plus 10 μM IBMX treatment potentiates the amplitude of EJPs in the same way as 1 μM octopamine alone.

The mediation of cyclic AMP is also suggested by the similar time courses of octopamine and of cyclic AMP treatments shown in Figure 2, and by similar effects on the amplitude of EJPs but not on the time constant of decay phase or the resting membrane potentials.

Our results support the presynaptic mediation of cyclic AMP in octopaminergic modulation at insect neuromuscular junctions. It is important to point out that neurally-evoked transmitter release is enhanced by the cyclic AMP-mediated octopaminergic action, because this release is closely concerned with muscle contraction.

REFERENCES

1 Evans, P. D. (1980) Biogenic amines in the insect nervous system. Adv. Insect Physiol., **15**: 317–473.

2 Orchard, I. (1982) Octopamine in insects: neurotransmitter, neurohormone, and neuromodulator. Can. J. Zool., **60**: 659–669.

3 O'Shea, M. and Evans, P. D. (1979) Potentiation of neuromuscular transmission by an octopaminergic neurone in the locust. J. Exp. Biol., **79**: 169–190.

4 Klaassen, L. W. and Kammer, A. E. (1985) Octopamine enhances neuromuscular transmission in developing and adult moths, *Manduca sexta*. J. Neurobiol., **16**: 227–243.

5 Evans, P. D. and O'Shea, M. (1978) The identification of an octopaminergic neurone and modulation of a myogenic rhythm in the locust. J. Exp. Biol., **73**: 235–260.

6 Evans, P. D. (1978) Octopamine distribution in the insect nervous system: distribution, synthesis and metabolism. J. Neurochem., **41**: 562–568.

7 Nathanson, J. A. and Greengard, P. (1973) Octopamine-sensitive adenylate cyclase: evidence for a biological role of octopamine in nervous tissue. Science, **180**: 308–310.

8 Harmer, A. J. and Horn, A. S. (1977) Octopamine sensitive adenylate cyclase in cockroach brain: effects of agonists, antagonists and guanylyl nucleotides. Mol. Pharmacol., **13**: 512–520.

9 Bodnaryk, R. P. (1979) Characterization of an octopamine-sensitive adenylate cyclase from insect brain (*Mamestra configurata* Wlk). Can. J. Biochem., **57**: 226–232.

10 Bodnaryk, R. P. (1979) Identification of specific dopamine- and octopamine-sensitive adenylate cyclases in the brain of *Mamestra configurata* Wlk. Insect Biochem., **9**: 155–162.

11 Bodnaryk, R. P. (1979) Basal, dopamine- and octopamine-stimulated adenylate cyclase activity in the brain of the moth, *Mamestra configurata*, during its metamorphosis. J. Neurochem., **33**: 275–282.

12 Evans, P. D. (1984) A modulatory octopaminergic neurone increases cyclic nucleotide levels in locust skeletal muscle. J. Physiol., **348**: 307–324.

13 Orchard, I. and Lange, A. B. (1986) Pharmacological profile of octopamine receptors on the lateral oviduct of the locust, *Locusta migratoria*. J. Insect Physiol., **32**: 741–745.

14 Bodnaryk, R. P. (1982) Biogenic amine-sensitive adenylate cyclases in insects. Insect Biochem., **12**: 1–6.

15 Evans, P. D. (1985) Biogenic amines and messenger systems in insects. In "Approaches to New Leads for Insecticides". Ed. by H. C. von Keyserlingk, A. Jager, and C. von Szczepanski, Springer-Verlag, Berlin & Heidelberg, pp. 117–131.

16 Beavo, J. A., Rogers, N. L., Crofford, O. B., Hardman, J. G., Sutherland, E. W. and Newman, E. V. (1970) Effects of xanthine derivative on lipolysis and on adenosine 3′, 5′-monophosphate phosphodiesterase activity. Mol. Pharmacol., **6**: 597–603.

17 Yamamoto, D. and Washio, H. (1979) The inhibitory action of L-glutamic acid esters on the insect neuromuscular junction. Comp. Biochem. Physiol., **63C**: 75–80.

18 Fahim, M. A. and Usherwood, P. N. R. (1983) Effects of c-AMP, caffeine, theophyline, and vinblastine on spontaneous transmittrer release at locust nerve-muscle junctions. J. Neurobiol., **14**: 391–397.

19 Evans, P. D. (1984) The role of cyclic nucleotides and calcium in the mediation of the modulatory effects of octopamine on locust skeletal muscle. J. Physiol., **348**: 325–340.

20 Greengard, P. (1976) Possible role for cyclic nucleotides and phosphorylated membrane proteins in post-synaptic actions of neurotransmitters. Nature, **260**: 101–108.

21 Hidoh, O. and Fukami, J. (1987) Presynaptic modulation by octopamine at a single neuromuscular junction in the mealworm (*Tenebrio molitor*) J. Neurobiol., (In press).

ZOOLOGICAL SCIENCE 4: 451–454 (1987)

Diamine Oxidase Activities in Catfish Tissues

TAKESHI KUMAZAWA and OSAMU SUZUKI

Department of Legal Medicine, Hamamatsu University School of Medicine, 3600 Handa-cho, Hamamatsu 431–31, Japan

ABSTRACT—Diamine oxidase (DAO) activity was measured in the brain, intestine, kidney, liver and skin of the siluroid catfish, *Parasilurus asotus,* with putrescine and cadaverine as substrates. The activity was found in the intestine and skin, but no detectable activities were found in other tissues. The apparent Km values for putrescine in the intestine and skin were 85.5 μM and 89.1 μM, respectively; those for cadaverine in the intestine and skin were 152.1 μM and 123.0 μM, respectively. Substrate specificity was tested for the intestinal enzyme, and the highest activity was found with putrescine, cadaverine and 1,3-propanediamine, followed by 1,7-heptanediamine and 1,6-hexanediamine.

INTRODUCTION

Diamine oxidase (DAO; EC 1.4.3.6.) catalyzes the oxidative deamination of both histamine and diamines, such as putrescine and cadaverine [1]. Its distribution is wide among plants, microorganisms and vertebrates [2]. In the present study, we report the distribution of DAO in various tissues of the catfish and its characterization. Although the characteristics of DAO have been reported for a few teleostean species [3, 4], no report on DAO appeared for the catfish, and this is also the first demonstration of DAO existence in animal skins.

MATERIALS AND METHODS

Chemicals

Acetylcadaverine-2HCl, acetylputrescine-HCl, agmatine-H_2SO_4, cadaverine-2HCl, 1,2-ethylenediamine-2HCl, 1,7-heptanediamine, 1,6-hexanediamine, histamine-2HCl, homovanillic acid, horseradish peroxidase (type 1), pargyline-HCl, 1,3-propanediamine-2HCl, putrescine-2HCl, spermidine-3HCl and spermine-4HCl were obtained from Sigma Chemical (St. Louis, MO); ornithine from Kanto Chemical (Tokyo); arginine-HCl and histidine-HCl from Nippon Rikagakuyakuhin (Tokyo); ethylamine from Tokyo Kasei Kogyo (Tokyo); lysine-HCl from Yoneyama Chemical (Osaka); hydrogen peroxide from Mitsubishi-Gasukagaku (Tokyo). Other common chemicals used were of the highest purity commercially available.

Animals

Both sexes of the siluroid catfish, *Parasilurus asotus*, were used as experimental materials. Fishes with body lengths of about 25 cm were selected for experiments. After decapitation, the brain, liver, kidney, intestine and skin were rapidly removed and frozen at −80°C until assayed.

Assays

The tissues were homogenized, and the crude homogenates were used as enzyme source. DAO activities were assayed fluorometrically by the method of Suzuki and Matsumoto [5]. The assay mixture (total 0.6 ml) contained 0.1 ml of potassium phosphate buffer solution (final concentration 0.08 M), 0.1 ml of horseradish peroxidase solution (0.5 mg/ml), 0.1 ml of homovanillic acid solution (1.0 mg/ml), 0.1 ml of the homogenate, 0.1 ml of substrate solution and 0.1 ml of distilled water. The pH of the buffer solution was adjusted to 7.4 in view of the physiological conditions. After incubation at 30°C for 30 min, the

Accepted February 10, 1987
Received January 14, 1987

enzyme activities were stopped by adding 2.0 ml of 0.1 N NaOH. The fluorescence intensity was measured with excitation at 323 nm and emission at 426 nm. As blank tests, assay mixtures without substrates are incubated; the substrates are mixed after adding the NaOH solution. Internal standards should be taken by adding appropriate amounts of hydrogen peroxide to the mixtures prior to incubation. The effect of temperature on DAO reaction was examined with the catfish intestinal enzyme with putrescine and cadaverine as substrates. Assay mixture with 0.08 M potassium phosphate buffer solutions (pH 7.4) covering 0–60°C were used. The highest activity was found at 30°C with both substrates. From this results, we carried out DAO assay at 30°C. When experiments for substrate specificity were made, the enzyme was incubated in the presence of 0.1 mM pargyline to suppress the contamination of mitochondrial monoamine oxidase.

TABLE 1. Diamine oxidase activities in catfish tissues

Tissue	DAO activity (n mole H_2O_2 formed/g wet tissue/30 min)	
	Putrescine	Cadaverine
Intestine	1138 ± 3	1185 ± 4
Skin	124.3 ± 18.4	84.2 ± 14.1
Liver	N. D.	N. D.
Kidney	N. D.	N. D.
Brain	N. D.	N. D.

DAO activities were measured with 0.5 mM putrescine and cadaverine as substrates. Values are expressed as means of 7 experiments ± S. E. N. D., Not detected.

RESULTS

The effect of pH was examined with the intestinal enzyme with putrescine and cadaverine as substrates. The optimal pH with putrescine was 6.8 and that with cadaverine was 6.5.

Table 1 shows DAO activities in the brain, liver, kidney, intestine and skin of the catfish with putrescine and cadaverine as substrates. DAO

TABLE 2. Apparent *K*m values of DAO in catfish intestine and skin

Substrate	*K*m (μM)	
	Intestine	Skin
Putrescine	85.5	89.1
Cadaverine	152.1	123.0

*K*m values were determined graphically from Lineweaver-Burk plots with 5–6 substrate concentrations assayed in duplicate upon a single enzyme source prepared from the pooled tissues of 7 catfishes.

TABLE 3. Substrate specificity of DAO in catfish intestine

Substrate (final 0.5 mM)	Relative activity (%)
Putrescine	100
Cadaverine	100
Spermidine	1.2
Spermine	0
1, 2-Ethylenediamine	2.1
1, 3-Propanediamine	99.0
1, 6-Hexanediamine	55.6
1, 7-Heptanediamine	97.9
Agmatine	9.7
Histamine	10.3
Acetylputrescine	15.1
Acetylcadaverine	31.4
Ethylamine	0
Ornithine	0
Lysine	0
Arginine	0
Histidine	0

The relative activities with each substrate represent the means obtained from duplicate determinations upon a single enzyme source prepared from the pooled tissues of 7 catfishes. The incubation mixtures contained 0.1 mM pargyline.

activities were found only in the intestine and skin. The activities in the intestine were about 9- and 13-fold higher than that in the skin when putrescine and cadaverine were used as substrates, respectively.

Apparent *K*m values for putrescine and cadaverine were measured in catfish intestine and skin (Table 2). The values for putrescine and cadaverine were similar between the intestine and skin.

Substrate specificity was tested for their oxidation by DAO in catfish intestine (Table 3). DAO showed the highest activity toward putrescine, cadaverine and 1, 3-propanediamine, followed by 1, 7-heptanediamine and 1, 6-hexanediamine.

DISCUSSION

In the present study, the highest DAO activity was found in the intestine of the catfish. The highest activity in the intestine is commonly observed for many vertebrates, such as man, rabbit, guinea-pig, rat, mouse and hen [6–10]. In other organs, however, there are obvious differences in its distribution among different species. The kidney contains a relatively high DAO activity in mammalian species, such as man, pig, dog and cat [7, 9]; while renal activities are low or not detectable in rodents and birds [7–10]. The DAO activity in the liver can be detected only in a few animal species, such as dog, guinea-pig and hen [7, 10]. In the present study, DAO activity of catfish brain could not be detected by the fluorometric method. By use of much more sensitive radioisotopic methods, however, the presence of DAO was demonstrated in the central nervous system of a few fish species [3].

Some acetylpolyamines have been reported to be present in human urine, blood and rat tissues [11–13], and not to be end products but intermediates for further reactions [14, 15]. In the present study, both acetylputrescine and acetylcadaverine could be oxidized with appreciable activities by catfish intestinal DAO. The acetylpolyamines probably present in fish tissues and their metabolic regulation by DAO are subjects to be explored in the future.

The most probable function of DAO in the intestine seems to be detoxification of toxic diamines present in the diet or produced by bacterial flora. The second function of the intestinal DAO was proposed by Luk *et al.* [16]; DAO is related to maturation and turnover of mucosal cells.

An appreciable DAO activity was also found in catfish skin (Table 1). This is the first demonstration of existence of DAO in animal skins. The nature of fish epidermis is different from those of other vertebrates; they are composed of mucinous tissues [17–19], and similar to intestinal epithelial tissues [19–21] in morphology and function, though they do not function as the site of active absorption. The catfish epidermal cells seem very active in renewal, differentiation and secretion of mucosubstances like intestinal mucosal cells. Thus the presence of an appreciable DAO activity in catfish skin seems to be very reasonable.

REFERENCES

1 Gorkin, V. Z. (1983) Substrate specificity of amine oxidases. In “Amine Oxidase in Clinical Research”. Pergamon Press, Oxford, pp. 95–107.

2 Zeller, E. A. (1963) Diamine oxidases. In “The Enzymes”. Ed. by P. D. Boyed, H. Lardy and K. Myrback, Vol. 8, Academic Press, New York, pp. 313–335.

3 Burkard, W. P., Gey, K. F. and Pletscher, A. (1963) Diamine oxidase in the brain of vertebrates. J. Neurochem., **10**: 183–186.

4 Matsumiya, M. and Otake, S. (1983) On the diamine oxidase in the pyloric caeca and the intestine of common mackerel *Scomber japonicus* . Bull. Jpn. Soc. Sci. Fish., **49**: 1695–1699.

5 Suzuki, O. and Matsumoto, T. (1986) Purification and properties of diamine oxidase from human kidney. Biogenic Amines, in press.

6 Bieganski, T., Kusche, J., Lorenz, W., Hesterberg, R., Stahlknecht, C-D. and Feussner, K-D. (1983) Distribution and properties of human intestinal diamine oxidase and its relevance for the histamine catabolism. Biochim. Biophys. Acta, **756**: 196–203.

7 Waton, N. G. (1956) Studies on mammalian histidine decarboxylase. Br. J. Pharmacol., **11**: 119–127.

8 Shaff, R. E. and Beaven, M. A. (1976) Turnover and synthesis of diamine oxidase (DAO) in rat tissues. Studies with heparin and cycloheximide. Biochim. Biophys. Acta, **25**: 1057–1062.

9 Cotzias, G. C. and Dole, V. P. (1952) The activity of histaminase in tissues. J. Biol. Chem., **196**: 235–242.

10 Bieganski, T. and Ulatowska, M. A. (1983) Diamine oxidase in the hen. Agents and Actions, **13**: 257–262.

11 Seiler, N. and Knödgen, B. (1979) Determination of the naturally occurring monoacetyl derivatives of di- and polyamines. J. Chromatogr., **164**: 155–168.

12 Dolezalova, H., Sepita-Klauco, M., Kucera, J., Uchimura, H. and Hirano, M. (1978) Monoacylcadaverines in the blood of schizophrenic patients. J. Chromatogr., **146**: 67–76.

13 Seiler, N., Al-Therib, M. J. and Knödgen, B. (1973) Occurrence of monoacetylputrescine in vertebrate tissue. Hoppe-Seyler's Z. Physiol. Chem., **354**: 589–590.

14 Bolkenius, F. N. and Seiler, N. (1981) Acetylderivatives as intermediates in polyamine catabolism. Int. J. Biochem., **13**: 287–292.

15 Seiler, N., Bolkenius, F. N., Knödgen, B. and Mamont, D. (1980) Polyamine oxidase in rat tissues. Biochim. Biophys. Acta, **615**: 480–488.

16 Luk, G. D., Bayless, T. M. and Baylin, S. B. (1980) Diamine oxidase (Histaminase). A circulating marker for rat intestinal mucosal maturation and integrity. J. Clin. Invest., **66**: 66–70.

17 Whitear, M. (1970) The skin surface of bony fishes. J. Zool., Lond., **160**: 437–454.

18 Harris, J. E., Watson, A. and Hunt, S. (1973) Histochemical analysis of mucous cells in the epidermis of brown trout *Salmo trutta* L. J. Fish Biol., **5**: 345–351.

19 Yamada, K. (1975) Morphochemical analysis of mucosubstances in some epithelial tissues of the eel (*Anguilla japonica*). Histochemistry, **43**: 161–172.

20 Curry, E. (1939) The histology of the digestive tube of the carp (*Cyprinus carpio communis*). J. Morphol., **65**: 53–78.

21 Weinreb, E. L. and Bilstad, N. M. (1955) Histology of the digestive tract and adjacent structures of the rainbow trout, *Salmo gairdneri irideus* . Copeia, **3**: 194–204.

ZOOLOGICAL SCIENCE 4: 455–464 (1987)

Experimental Myopia and Glaucoma in Chicks

Tadashi Oishi, Jean K. Lauber[1] and Jerry Vriend[2]

Department of Biology, Nara Women's University, Nara 630, Japan,
[1]Department of Zoology, University of Alberta, Edmonton, Canada,
and [2]Department of Anatomy, University of Manitoba, Winnipeg, Canada

ABSTRACT—The ocular response of the developing chick to several parameters of the light environment constitutes a useful model system for studies of experimental myopia and glaucoma. We explored the roles of long photoperiod and light intensity extremes in setting a pathological course for the developing eye.

Chicks reared under continuous light developed increased eye weight, globe enlargement, decreased corneal diameter, reduced anterior chamber depth, and flat cornea, all effects associated with light-induced avian glaucoma (LIAG). Exposure to very dim light also caused eye enlargement (dim light buphthalmos, DLB), but with less pronounced anterior segment lesions. Under very bright light, globe enlargement was less severe. The LIAG and DLB syndromes appear to be additive, and are probably distinct from one another.

INTRODUCTION

Domestic chicks reared under continuous light (24L/0D) develop eye enlargement, but with retarded anterior segment growth, and eventual blindness, a condition we have called light-induced avian glaucoma (LIAG) [1–3]. Several aspects of LIAG have been explored, and a number of lesions associated with the syndrome have been recorded [4], but the primary lesion remains obscure. Very long photoperiods, e.g., 22L/2D or 23L/1D, cause LIAG changes as severe, or almost as severe, as those occurring under 24L/0D [5, 6]. One of the aspects of LIAG is eventual elevation of intraocular pressure (IOP), the diagnostic finding which permits use of the designation "glaucoma". When refraction has been monitored during development of LIAG, these eyes show early hypermetropia (presumably due to reduced corneal curvature), then develop the myopia which would be expected with axial lengthening of the eyeball [2, 7].

Even when rearing has *not* been under continuous, or almost continuous light, myopia may ensue under several other environmental conditions. Thus, very dim light [8], or spectrally restricted light (also dim), even diurnal [9], also causes buphthalmos. The pattern of eye lesions differs somewhat from those of LIAG, and in particular, high IOP has not been recorded at any age so far tested. Thus, we have not used the term glaucoma for this condition, but instead refer to it as dim light buphthalmos (DLB). Corneal flattening is minimal or absent in DLB (when the lighting schedule has been diurnal) [10], and eye enlargement, including axial lengthening, may be even more extreme than in LIAG, Thus, there is every reason to expect myopia, and this has been confirmed in at least ond study [11]. Nevertheless, in both their etiology and in several physical and physiological findings, LIAG and DLB can be shown to be separate and distinct phenomena. When chicks are reared under continuous light which is also very dim, as in the present study, the LIAG and DLB effects are superimposed, and eye enlargement is extreme.

A third eye enlargement syndrome has been described when chicks are reared in complete darkness (0L/24D), or almost complete darkness (2L/22D or 1L/23D) [6, 10, 12]. Some caution is

Accepted February 9, 1987
Received December 25, 1986

necessary in interpreting the results of such experiments, because what may seem to a human observer to be a "total darkness" protocol may still involve sufficient light to precipitate DLB in chicks. Thus, a seemingly trivial light leak, a pilot light, a photographer's "safelight", or a glowing brooder element could flaw an intended 0L/24D protocol.

However, it does appear that there is a separate 0L/24D-induced eye enlargement phenomenon, although it has not been so well documented as DLB and LIAG, and we have, as yet, only the most subjective guess as to the threshold between "light" and "no light", in the chick's preception. Whether or not the 0L/24D chicks would be myopic is a moot point, since vision is probably severely impaired during a prolonged stay in complete darkness.

Yet another class of eye-affecting environmental factors is exemplified by "lid closure myopia" and related phenomena. We found, in early experiments, that covering one eye, with or without suturing the lids, caused specific responses, including eye enlargement, in that eye only [13]. Meanwhile the environmental lighting condition (e.g., 24L/0D, or dim) had its systemic effect on both eyes, the lid closure effect being additive to the photoenvironment effect [10]. There have recently been a number of studies on the lid suture myopia model, both in chicks and on several mammals in which a similar syndrome has been described [14, and references therein]. In addition, some variations on the theme have been employed, involving, for instance, "altered visual experience", or the use of vision-restricting goggles or lenses [15–17].

Our exploration of the lid suture myopia phenomenon in chicks, against the background of other myopia-inducing, glaucoma-inducing and/or buphthalmos-inducing factors, will be the subject of a subsequent paper. Here we attempt to distinguish between light intensity effects and photoperiod effects on the size and dimensional parameters of the chick eye. Elsewhere we have dealt with the possible involvement of melatonin in the same system(s) [18], and with the roles of adrenocortical and/or gonadal hormones in relation to LIAG and DLB syndrome [19, 20].

METERIALS AND METHODS

Domestic chicks of the Hubbard strain (fast growing, broiler type) were obtained on day of hatch from a commercial hatchery, and reared in floor pens at the University of Alberta Biosciences Animal Services Farm. During the early weeks, temperature was kept at recommended levels for young chicks by electric brooder heaters which emitted no visible light. Other environmental conditions, especially with respect to light intensity and photoperiod, were strictly controlled. Before the experiments began, chicks were kept under control lighting conditions for the first four days after hatching, so that they could learn the position of the food and water supply, which were thereafter always put in the same locations. This is a necessary precaution if chicks are to be reared later in complete darkness or very dim light. Food (chick starter crumbles) and water were available *ad libitum*.

Five experimental treatments (P, Q, R, S, T) were used in the first experiment, as outlined in Table 1. In the second experiment, four of these treatments (PP–SS) were retained unchanged (except for numbers of chicks), but room T was replaced by treatment UU. In all lighted rooms, light was supplied by incandescent bulbs in overhead fixtures, so placed in the four quadrants of the room that the entire 3.7 m$\times$3.7 m floor space was more or less evenly illuminated at bird height. Light intensity was measured before the beginning of Expt. I with an ISCO spectroradiometer (Instrumentation Specialties Co., Lincoln, Nebr.), wavelength being set sequentially at 50 nm intervals, from 400 to 650 nm. The area under the light intensity curve so generated was determined for 50 nm bandwidths, and multiplied by the luminosity weighting factor at mid-bandwidth, to arrive at an approximate value for the total light (in lux) to which the chicks were exposed.

Of the photoperiods chosen, 12L/12D (lights on 0800–2000), as used in Expts. I/P and II/PP, was considered to be the control treatment, while 23L/1D (dark 0700–0800), as used in rooms Q, QQ, R, RR, S and SS, was considered to be "almost-continuous light", an environmental rearing condition expected to produce LIAG [6]. The

TABLE 1. Summary of Experimental Treatments

Expt/Group	Photoperiod	Lights on (MST)	Light intensity	$\mu W/cm^{2*}$	n(N)†
I/P (control)	12L/12D	0800–2000	10 lux	0.025	10 (50)
I/Q	23L/ 1D	0800–0700	10 lux	0.025	10 (50)
I/R (dim)	23L/ 1D	0800–0700	1.0 lux	0.003	10 (50)
I/S (bright)	23L/ 1D	0800–0700	5000 lux	0.86	10 (50)
I/T	1L/23D	0800–0900	0.25 lux	0.001	10 (50)
II/PP (cont.)	12L/12D	0800–2000	10 lux	(as above)	12 (38)
II/QQ	23L/ 1D	0800–0700	10 lux	" "	14
II/RR (dim)	23L/ 1D	0800–0700	1.0 lux	" "	11 (31)
II/SS (bright)	23L/ 1D	0800–0700	5000 lux	" "	14 (14)
II/UU	0L/24D	(not at all)	—	—	10

† (N)=additional chicks used in a larger experiment.
*=peak at 550 nm.

one hour of darkness was introduced in these experiments to provide a daily time signal, in case any cyclic phenomena should otherwise "free run" under constant conditions.

Of the light intensities chosen for the present experiments, 10 lux at bird height was designated the control value; this amount of light, comparable to what we have used in previous LIAG experiments [3], was provided by four 60 W frosted bulbs hung at approximately 2 m, in the four quadrants of a 3.7m×3.7m room. Treatment R and RR, at 1.0 lux, are here described as dim light [8], provided by four 7.5 W bulbs, lightly coated with black spray paint, and hung 2 m from the floor in a similar 3.7 m×3.7 m room. The bright light treatments S and SS, at over 5000 lux [6], were achieved with 16 reflector floodlamps, 150 W each, hung at approximately 1.2 m from the floor, and evenly spaced throughout a 3.7 m× 3.7 m room. All light bulbs were replaced with new ones once a month, to forestall burnouts which might affect the results.

In treatment UU of Expt. II, we aimed to achieve total darkness, a condition not quite accomplished in our treatment T of Expt. I. Whereas in room T, one hour of very dim light (<0.25 lux) was scheduled each morning (0800–0900) to provide an opportunity for personnel to replenish food and water, in treatment UU we eliminated even this amount of light, by use of several light-tight environment chambers, placed in turn in a light-controlled room. Each chamber measured 61 cm×61 cm×41 cm high, and was made of sheet aluminum, with light-baffled ventilation ports. Four to five chicks were started in each chamber, but these numbers were reduced (to forestall overcrowding) to two per chamber by four weeks of age. After an initial four-day "learning period", these chicks were serviced in complete darkness. Brooder heat was supplied by passing the positive pressure airflow to the chambers first through a coil of copper tubing, which was in turn wrapped with electric heating tape and an insulating layer of asbestos.

During the seventh week after hatching, chicks of Expt. I were bled (5–6 ml, by cardiac puncture), then sacrificed by sudden decapitation. All of the Expt. I chicks on which we report here were sacrificed at midday, from approximately 1200–1400 hrs. These Expt. I chicks were part of a much larger series (60 birds per room) from which we obtained blood samples on a "round-the-clock" schedule: the corticosterone and melatonin radioimmunoassay for which this plasma was saved have been reported separately [18, 19]. Both eyes were enucleated immediately postmortem, trimmed of fat and extraorbital muscles, weighed, and photographed in front and side view (Fig. 1), for later measurement of dimensional parameters. Figure 2 shows the parameters measured on these photographs of freshly enucleated eyes. Each eye was then bisected equatorially

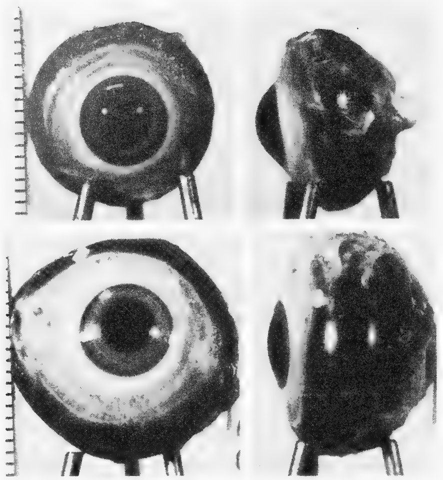

FIG. 1. Front and side views of enucleated right eyes. Above, diurnal control chick (Group PP); below, chick reared under continuous light (Group QQ). Light intensity was 10 lux for both. Note greatly enlarged globe and flat cornea in the LIAG eye.

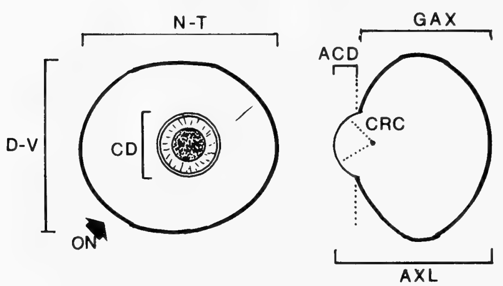

FIG. 2. Diagrammatic representation of front and side view of right eye photographs, showing the parameters measured. To maintain orientation, the optic nerve (ON) stump was positioned at 8 o'clock. D–V=dorsoventral equatorial diameter, N–T=nasotemporal equatorial diameter, AxL=axial length (meridional diameter), GAX=globe axis, AcD=anterior chamber depth, CD=corneal diameter, CRC=corneal radius of curvature.

with a sharp razor blade, the retinal half frozen over dry ice for later biochemical studies, and the anterior segment fixed in Bouin's fluid for later histology. Adrenals and testes were also weighed and saved to Bouin's.

Expt. II chicks were bled then sacrificed, this time by overdose of Nembutal, during their sixth weeks of age, half at 1000–1200 hrs, and half at 2200–2400 hrs (lights on 0800–2000 hrs for diurnal birds). Thereafter, the same tissues were taken, and the same procedures followed, as for Expt. I.

For statistical analysis, we used the MINITAB software program [21], via a terminal interacting with the University of Alberta Amdahl 5860 mainframe computer. Analysis of variance, Student's t-test (independent samples), paired t-test and product-moment correlation analysis were employed.

RESULTS

Eye enlargement, measured as increased eye weight (above and beyond that which could be ascribed to normal growth), occurred under each of the several experimental lighting regimes employed (Figs. 1 and 3, Table 2). Overall, there was an 18.5% increase (Expt. II) in eye weight which could be attributed to continuous light (the LIAG effect). When the continuous light was also of low intensity, the increase in eye size was 30.4% over controls (Expt. I). The dim light effect was significantly greater than the LIAG effect alone (e.g., $p<0.001$ for R vs. Q). Eye enlargement also occurred under continuous bright light, although it was less dramatic: 16.0%

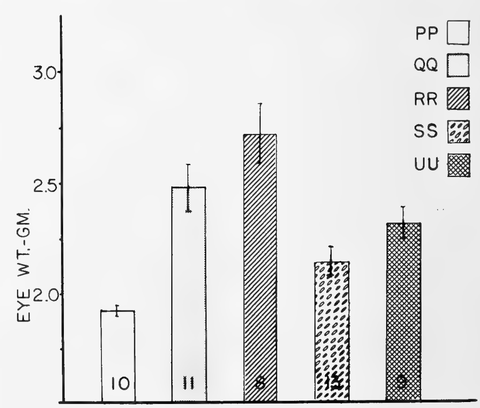

FIG. 3. Bar graph showing eye weight at 6 weeks of age, in chicks reared under control conditions (PP), or one of four different environmental lighting treatments in Expt. II. For further explanation of the environmental conditions set for this experiment, see text and Table 1. *Relative* eye weight (g/kg B.W.) for the same birds is shown in Table 2. Error bars indicate ±SEM.

TABLE 2. Eye parameters in chicks reared under several light regimes

Group(n)	Rel. EWt[†]	D–V[††]	N–T	AxL	AcD	CD	CRC
			Experiment I—7 weeks old				
P (9)	1.12 ±0.035	16.48 ± 0.24	16.59 ± 0.27	12.64 ± 0.23	2.02 ±0.08	7.42 ±0.29	4.35 ±0.07
Q (10)	1.07 ±0.025	17.21* ± 0.19	17.48* ± 0.17	13.06 ± 0.11	1.15*** ±0.11	6.45* ±0.20	5.14** ±0.17
R (8)	1.46*** ±0.053	19.24*** ± 0.37	18.69*** ± 0.13	14.63*** ± 0.29	1.25*** ±0.13	6.91 ±0.34	5.87*** ±0.20
S (7)	1.30** ±0.036	17.41** ± 0.15	17.68* ± 0.25	12.66 ± 0.22	0.89*** ±0.05	6.33* ±0.25	5.989*** ±0.24
T (10)	1.36*** ±0.052	18.90*** ± 0.22	18.51*** ± 0.16	13.69** ± 0.18	1.04*** ±0.11	6.59 ±0.30	5.40*** ±0.14
			Experiment II—6 weeks old				
PP (10)	1.35 ±0.042	16.41 ± 0.06	16.71 ± 0.09	13.03 ± 0.12	2.17 ±0.06	7.67 ±0.09	5.23 ±0.09
QQ(11)	1.60* ±0.076	17.61*** ± 0.26	18.10*** ± 0.28	13.22 ± 0.26	1.25*** ±0.07	7.20** ±0.12	6.44*** ±0.11
RR(8)	1.61** ±0.064	18.30*** ± 0.29	18.34*** ± 0.35	13.94*** ± 0.17	1.38*** ±0.05	7.53 ±0.11	6.64*** ±0.13
SS (13)	1.45 ±0.052	16.62 ± 0.16	17.28** ± 0.17	12.60 ± 0.19	1.25*** ±0.04	6.96*** ±0.05	6.16*** ±0.12
UU(9)	1.67** ±0.068	17.21** ± 0.18	17.50** ± 0.17	12.68 ± 0.17	1.23*** ±0.08	7.11*** ±0.09	5.97*** ±0.12

† g/Kg body wt±SEM.
†† all D–Vs, N–Ts etc. in mm±SEM. Dorsoventral (D–V) diameter, nasotemporal (N–T) diameter, axial length (AxL), anterior chamber depth (AcD), corneal diameter (CD) and corneal radius of curvature (CRC), all in mm±SEM.
* significantly different from control, $p<0.05$.
** $p<0.01$
*** $p<0.001$.

over controls in Expt. I and 7.4% in Expt. II (Table 2). In both experiment there was a significant positive correlation ($p<0.05$) between body weight and eye weight, but eye weight differences could not be explained by body growth alone: relative eye weight showed a similar pattern of response under the several lighting regimes (Table 2).

The size of the globe increased with eye weight, as shown by both dorsoventral (D-V) and nasotemporal (N-T) equatorial diameters (Table 2). The third eye diameter, axial length (AxL), showed a less pronounced increase, but when AxL minus anterior chamber depth was calculated, (here called GAX, the globe axis), a highly significant degree of correlation ($p<0.01$) with eye weight was seen (Fig. 4). In comparisons of GAX across groups (Fig. 5) the greatest increase was in 23L/1D dim light ($p<0.001$ for R vs. P,

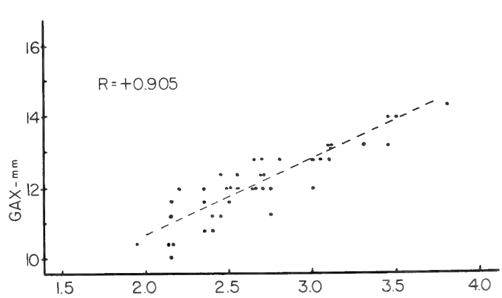

FIG. 4. Correlation of globe axis (see Fig. 2) with eye weight in 7 week-old chicks of Expt. I. All photoperiod and light intensity groups are included.

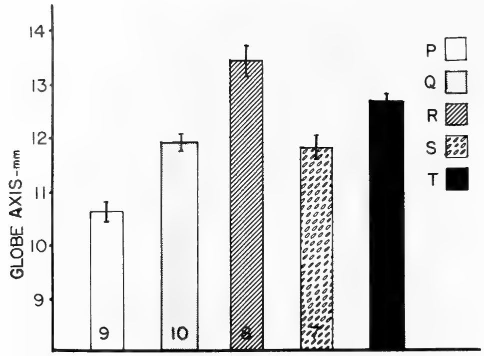

FIG. 5. Globe axis diameter (GAX, see Fig. 2) in 7 week-old chicks of Expt. I, reared under several different lighting regimes. For explanation of P, Q, R, S, T, see text and Table 1.

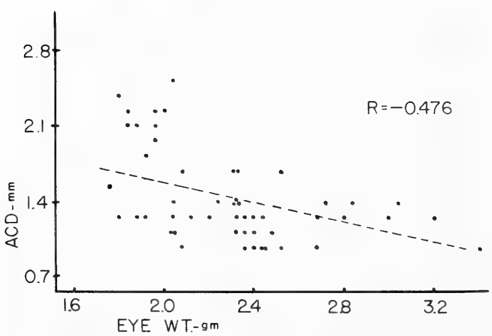

FIG. 6. Correlation of anterior chamber depth with eye weight in 6 week-old chicks of Expt. II. Shallow anterior chamber is characteristic of light-induced avian glaucoma (LIAG).

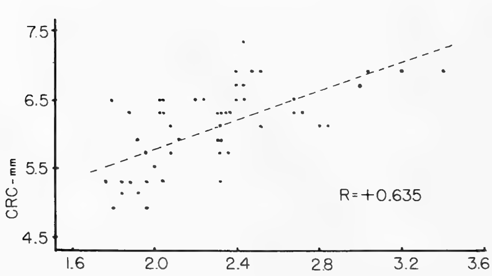

FIG. 7. Correlation of corneal radius of curvature with eye weight in 6 week-old chicks of Expt. II. The cornea is flattened in the enlarged eyes of chicks with LIAG.

and also for RR vs. PP). For the other groups as well, GAX was significantly above control values,

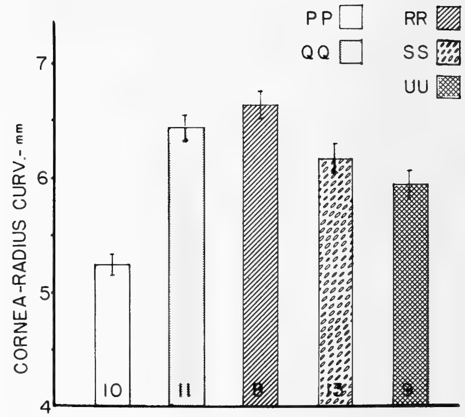

FIG. 8. Bar group showing the degree of corneal flattening in Exp. II chicks reared to 6 weeks under several different lighting schedules, as outlined in the text and Table 1.

but at the same time, significantly less than under dim light (e.g., $p<0.05$ for S vs. R; $p<0.001$ for SS vs. RR) (see also Table 2).

With respect to the corneal parameters anterior chamber depth (AcD), corneal diameter (CD), and corneal radius of curvature (CRC) (ref. Fig. 2), the differential responses to continuous light, and to light intensity extremes, further distinguished chicks in the several lighting regimes from one another, as well as from diurnal controls (Table 2). Overall, there was a modest, but significant ($p<0.01$), negative correlation between AcD and eye weight (Fig. 6), and a strong positive correlation of CRC with eye weight ($p<0.001$) (Fig. 7). Comparison of the CRC responses across the several groups (Fig. 8) reveals that all showed some degree of corneal flattening, but this was most pronounced in LIAG+DLB subjects (groups R and RR); ($p<0.001$ for each experimental group vs. controls, but not significant for comparisons of experimental groups with one another).

DISCUSSION

While the correlations between globe dimensions and eye weight were all positive, as might be predicted in a growing system, the relationship between eye weight and the several corneal para-

meters was more complex. Because the front and the back of the eye responded differently, and possibly independently, to several permutations of the light environment employed here, the responses of the anterior and posterior segments of the eye are discussed separately below.

The posterior segment

Influence of photoperiod: The pronounced eye enlargement which occurred here in chicks reared under continuous light is to be expected in LIAG, and confirms several previous studies [1, 3]. Also as expected, body weight was increased in 23L/1D vs. 12L/12D chicks. The eye enlargement was, however, not simply a reflection of this accelerated growth rate: comparison of eye weight relative to body weight showed the same trends as for absolute eye weights.

The enlarged eyes of 23L/1D chicks displayed highly significant differences from controls in both D-V and N-T equatorial diameters; at this age, the N-T value was usually the larger of the two. The third diameter we measured, on side view photos of enucleated eyes, was AxL: this dimension was slightly, though not dramatically, increased in LIAG vs. control eyes (both 10 lux). However, the cornea was also changing shape in 23L/1D eyes (see below), and this tended to negate the overall axial increase. When globe axis (ref. Fig. 2) was plotted, the difference between LIAG and control eyes was highly significant. Nevertheless, in both LIAG and control eyes, this dimension remains the smallest of the three diameters; i.e., the chick's eye is not so nearly spherical as is the human eye, the globe being considerably flattened meridionally.

Influence of light intensity: Treatments R and S were designed to test the effects of several extremes of light intensity on the photosensitivity of the developing eye. In comparing our groups R and S with treatment Q, and all with the diurnal control P, it is important to remember that chicks in all three of these experimental groups (Q, R, S) were reared under 23L/1D, or almost-continuous light: the LIAG symptoms would thus be expected, and did indeed develop (Q and QQ). In dim light of such long photoperiod (R and RR), as compared to Q or QQ, body weight was almost the same (although much greater than in P or PP controls), while eye weight of dim-lighted subjects was even greater than in "normal" intensity (10 lux) light of the same photoperiod. The low level of light intensity set for room R (1.0 lux) was not unlike that we have employed previously in "dim light" experiments [8, 10], which led us to first use the designation "dim light buphthalmos" (DLB). It is also similar to "dim light" intensity levels used by Harrison *et el.* [9, 11], who also reported eye enlargement even in diurnal chicks. The R vs. Q comparison, of eye weight and/or dimensional parameters, suggests an additive response, the DLB eye enlargement superimposed on the LIAG effects. This supports a suggested explanation we proffered based on several previous smaller experiments, although in the earlier cases we had included also a diurnal dim light treatment, to better separate the two effects [8, 10]. In every instance, the resulting eye enlargement pattern was consistent with the view that continuous light, leading to LIAG, and dim light, producing DLB, call forth separate and distinct responses in the eye, differing not only in their etiology, but also thier pathological course.

The response of chicks to the bright light treatment S or SS was somewhat enigmatic. In body weight and in eye weight, S chicks seemed to be intermediate between diurnal controls and LIAG birds. Thus under 5000 lux, eye weight was significantly *greater* than for control ($p<0.001$ for SS vs. PP), but significantly *less* than at 10 lux ($p<0.05$ for SS vs. QQ), and also significantly *less* than at 1.0 lux ($p<0.01$ for SS vs. RR), even though all three experimental groups were reared under continuous light. Likewise, in the dimensional parameters D-V, N-T and GAX, values recorded for S chicks were somewhat *higher* than for controls ($p<0.01$ for most parameters). At the same time, these globe dimensions were significantly *less* than those recorded for chicks in dim light. In a previous experiment which closely resembled the present one, one of us also found that under 24L/0D at 5000 lux, the expected LIAG eye enlargement was suppressed [6].

The anterior segment

Influence of photoperiod: Corneal diameter (CD) was significantly smaller in LIAG eye, as compared with diurnal controls. This was also as expected, and confirms previous findings in LIAG. In this connection, we have also previously shown that the cornea in LIAG is damaged, leaking lactic dehydrogenase into the aqueous [4], and that growth of the cornea (as evidenced by mitotic counts in the corneal epithelium) is impaired in LIAG [22]. In the present Expt. I, mean number of dividing cells per standard field was reduced by almost half in Q compared with P; whereas there was a photoperiod-driven rhythm in normal eyes, with a scotophase peak, this rhythm was damped in all 23L/1D birds (Q, R, S). Our report on corneal mitotic rates has been published separately [18], but the above preliminary finding is included here as well, because it confirms that growth of the cornea is suppressed in the LIAG syndrome.

Decreased corneal curvature (i.e., high CRC) is an early finding in LIAG, as evidenced either by measured radius of curvature of the corneal surface, or by +D refractive error [2]. In the present series, we confirmed a reduction in AcD and a dramatic increase of CRC, in LIAG chicks at 6–7 weeks of age. Comparison of AxL and GAX measurements confirms that, while the cornea is becoming flatter, the globe is, in fact, enlarging axially [1, 8].

Reduced corneal curvature would tend toward hyperopia (which was indeed found at 3–4 weeks of age in several earlier studies where refractions were done) [2, 7]. However, the overall eye enlargement of LIAG, and especially the increase in GAX, finally overrides the effect on refraction expected from the early anterior segment changes, and this soon results in a net myopia, of increasing severity with age (up to −9D at 6 weeks in one of our previous series) [2].

Influence of light intensity: Whereas light intensity differences appeared to have a less dramatic effect than photoperiod on the globe of the eye, consideration of the corneal parameters reveals a different picture of the effects of light intensity extremes. The corneal flattening as characteristic of LIAG also occurred in both bright and dim light of 23L/1D. However, the CD and AcD effects, as compared with controls, were most pronounced (i.e., the values were smallest) in bright light, and least pronounced (though still most significant) in dim light. The CD reduction, in fact, fell just short of significance in groups R and RR (DLB) chicks. CRC was also significantly different in bright light as compared to dim light, in both experiments ($p<0.05$ for R vs. Q, and also for S vs. Q). Likewise, in an earlier study, CD and AcD were even more reduced under 5000 lux than in 150 lux (both continuous light) [6].

Because we did not have a diurnal dim light treatment in the present Expt. I or II, we must look elsewhere to see what might have been expected: earlier experiments showed that dim light of a diurnal photoperiod induces globe enlargement but not corneal flattening [10]. This suggests that whatever increase in CRC occurred here can be attributed to LIAG, not DLB.

Rearing in constant darkness: As noted earlier, Treatment T was intended as a "complete darkness" protocol, although we felt obliged to allow 1 hr/day of very dim light, to facilitate servicing. There was no question but that these birds found access to food and water: their mean body weight was above average at the time of sacrifice. Eye weight was 28.8% greater in these chicks ($p<0.001$ for T vs. P), a similar and only slightly less pronounced response than that seen in 23L/1D dim light. In the dimensional parameters as well, the responses of group T and group R birds were quite similar, and of approximately the same magnitude, when both were compared to controls. The CRC constitutes a possible exception: corneal flattening was less pronounced in T vs. P than in R vs. P. These results of dark-rearing echo the findings in several other studies involving a complete darkness protocol [6, 12]. Nevertheless it is tempting to view our T treatment as a kind of "super dim light" treatment but different in one key respect from Treatment R, in that the photoperiod was not long, but in fact, very short (and possibly perceived by the Group T chicks as diurnal?).

Comparison of the T chick response in Expt. I

will the UU response under 0L/24D in Expt. II suggests, however, that these two treatments cannot be equated. Let it be assumed for the moment that in the UU environment chambers we did indeed achieve total darkness, in the chick's perception. The UU vs. control comparison reveals that the eyes were significantly enlarged in total darkness ($p<0.001$ for UU vs. PP), and the dimensional parameters correspondingly increased; however, none of these globe dimensions were as great as in QQ or RR. The reductions in AcD and in CD were not remarkable in treatment UU, either. From the CRC, however, one sees that the flattening of the cornea was less pronounced in UU than in T, each compared to its own control (P or PP), as well as to Q, R and S responses.

Because of the persistent question as to whether either of the "total darkness" environments we provided was indeed so perceived by the subjects, we do not yet feel able to draw conclusions about the effects of constant darkness on chick eye parameters.

In summary, in this study we document, and distinguish between, several effects of light on the developing avian eye. Eye enlargement, and increases in the several globe diameters, are characteristic of both light-induced avian glaucoma (LIAG), brought on by rearing in continuous light, and dim light buphthalmos (DLB). When the environmental light is both continuous and dim, the effects on the posterior segment of the eye are additive. When the continuous light is instead very bright (5000 lux), globe enlargement is less extreme than under light of "normal" intensity (10 lux). Of the three globe diameters measured, globe axis (GAX) shows the closest correlation with eye weight, and would be the best predictor of eye enlargement.

In the front of the eye, the small flat cornea and shallow anterior chamber of LIAG are less pronounced in DLB, even when the dim light is continuous. Some differences, especially of the anterior segment parameters, in responsiveness to light intensity extremes support the conclusion that light intensity effects and photoperiod effects constitute separate and distinct influences on the growing eye. We also investigated eye development under conditions of complete darkness, but interpretation of these results is uncertain because, we believe, of the difficulty in achieving absolute darkness, which will be so perceived by the avian subjects.

The domestic chick used in these studies constitutes a particularly useful research subject, for several reasons. Relative to body size, the eyes of birds tend to be large, and are of considerable importance to their owners (i.e., the chick is highly vision-dependent). The LIAG system, especially, provides the investigator with a valuable model system for glaucoma and myopia research: this condition can be easily brought on at the will of the investigator, it follows a predictable course, it permits manipulations which would be impossible or unacceptable with human subjects, and it presents eyes available for detailed study during a long preglaucoma period. All of these are luxuries not afforded the clinical researcher working with human subjects.

Since both glaucoma and myopia are clinical entities of some importance for human sufferers, the availability to the investigator of animal models for these vision-threatening conditions presents unique opportunities for both basic and pragmatic research.

ACKNOWLEDGMENTS

This research was supported by a grant (to JKL) from the Natural Sciences and Engineering Research Council of Canada, and by a Visiting Scientist grant (to TO) from the Alberta Heritage Foundation for Medical Research.

REFERENCES

1 Lauber, J. K. and McGinnis, J. (1965) Eye lesions in domestic fowl reared under continuous light. Vision Res., **6**: 619–626.

2 Lauber, J. K., Boyd, J. E. and Boyd, T. A. S. (1970) Intraocular pressure and aqueous outflow facility in light-induced avian buphthalmos. Exp. Eye Res., **9**: 181–187.

3 Lauber, J. K. and Kivett, V. K.(1981) Environmental control of the rearing conditions and early preglaucomatous lesions in chicks. Exp. Eye Res., **32**: 501–509.

4 Kinnear, A., Lauber, J. K. and Boyd, T. A. S. (1974) Genesis of light-induced avian glaucoma.

Invest. Ophthalmol., **13**: 872–875.

5 Lauber, J. K., McLaughlin, M. A. and Chiou, G. C. Y. (1985) Timolol and pilocarpine are hypotensive in light-induced avian glaucoma. Can. J. Ophthalmol., **20**: 147–152.

6 Oishi, T. and Murakami, N. (1985) Effects of duration and intensity of illumination on several parameters of the chick eye. Comp. Biochem. Physiol., **81A**: 319–323.

7 Shiraki, K., Sotani, T., Oishi, T. and Okuzawa, I. (1981) Effects of continuous light and continuous darkness on the eyes of chicks (in Japanese). Fol. Ophthalmol. Japonica, **32**: 1157–1163.

8 Lauber, J. K. and Kinnear, A. (1979) Eye enlargement in birds induced by dim light. Can. J. Ophthalmol., **14**: 265–269.

9 Harrison, P. C., Bercovitz, A. B. and Leary, G. A. (1968) Development of eye enlargement of domestic fowl subjected to low intensity light. J. Biometeorol., **12**: 351–358.

10 Chiu, P. S. L., Lauber, J. K. and Kinnear, A. (1975) Dimensional and physiological lesions in the chick eye as influenced by the light environment. Proc. Soc. Exp. Biol. Med., **148**: 1223–1228.

11 Bercovitz, A. B., Harrison, P. C. and Leary, G. A. (1972) Light-induced alterations in growth pattern of the avian eye. Vision. Res., **12**: 1253–1259.

12 Osol, G., Schwartz, B. and Foss, D. C. (1986) The effects of photoperiod and lid suture on eye growth in chickens. Invest. Ophthalmol. Vis. Sci., **27**: 255–260.

13 Lauber, J. K., McGinnis, J. and Boyd, J. (1965) Influence of miotics, Diamox and vision occluders on light-induced buphthalmos in domestic fowl. Proc. Soc. Exp. Biol. Med., **120**: 572–575.

14 Yinon, U. (1984) Myopia induction in animals following alteration of the visual input during development: a review. Curr. Eye Res., **3**: 677–690.

15 Wallman. J., Turkel, J., and Trachtman, J. (1978) Extreme myopia produced by modest change in early visual experience. Science, **201**: 1249–1251.

16 Hodos, W. and Kuenzel, W. J. (1984) Retinal image degradation produces ocular enlargement in chicks. Invest. Ophthalmol. Vis. Sci., **25**: 652–659.

17 Hayes, B. P., Fitzke, F. W., Hodos, W. and Holden, A. L. (1986) A morphological analysis of experimental myopia in young chickens. Invest. Ophthalmol. Vis. Sci., **27**: 981–991.

18 Lauber, J. K., Oishi, T. and Vriend, J. (1986) Plasma melatonin rhythm lost in preglaucomatous chicks. J. Ocular Pharmacol., **2**: 205–213.

19 Lauber, J. K., Vriend, J. and Oishi, T. (1986) Plasma corticosterone in chicks reared under several lighting schedules. Comp. Biochem. Physiol., **86A**: 73–78.

20 Oishi, T. and Lauber, J. K. (1986) Light, experimental avian myopia and the role of the suprarenals. J. Ocular Pharmacol., **2**: 139–146.

21 Ryan, T. A., Joiner, B. L. and Ryan, B. F. (1976) MINITAB Student Handbook, Duxbury Press, Boston, Mass.

22 Oishi, T. (1984) Circadian mitotic rhythm in chick corneal epithelium. J. Interdisc. Cycle Res., **15**: 281–288.

ZOOLOGICAL SCIENCE 4: 465–474 (1987)

Cytochalasin B Affects Selectively the Marginal Cells of the Epithelial Sheet in Culture

SHIGEO TAKEUCHI

Zoological Institute, Faculty of Science, University of Tokyo, 7–3–1, Hongo, Bunkyo-ku, Tokyo 113, Japan

ABSTRACT—The epithelial spreading is a fundamental one among morphogenetic movements. To know the mechanism generating force for spreading, the effect of cytochalasin B (cytB) on the corneal epithelium in culture was investigated. Four μg/ml of cytB inhibited completely the epithelial spreading and, at the same time, altered selectively the shapes of marginal cells: they shrinked at leading lamella and retracted quickly leaving fine tails behind, in which the bundles of F-actin were disintegrated to be numbers of fragments, while most of the other cells kept their shapes unchanged, along the cell borders of which F-actin distributed as before the treatment of cytB. The high sensitivity of the marginal cells to cytB led us to consider that F-actin was incessantly polymerized and taken into the intracellular organs generating force which enabled the marginal cells to locomote outwards, and that the outward locomotion, as a main force, spread entire epithelium.

INTRODUCTION

When the body surface of higher animals was injured, the epithelial cells started to migrate and spread quickly over the denuded area as a coherent cell sheet, and ceased the movement after the closure of wound. The locomotion of epithelial cells, as one of fundamental cellular movements in morphogenesis, has attracted the interest of many authors [see 1, 2].

The marginal cells of epithelial sheets in culture were flattened and formed leading lamella at the free end, where they attached to the substratum with both focal and close contacts [1, 3–5]. Lamellipodia, filopodia or microspikes were protruded from the leading edges, accompanying ruffling or blebbing [6], as like as in the fibroblastic cells [7–9]. In the leading lamella of epithelial cells, bundles of microfilaments or of actomyosin were reported to be aligned in a way quite similar with those in fibroblasts [1, 10]. We could therefore assume that the contraction of actomyosin systems in the marginal cells was a main force for the epithelial spreading as in the locomotion of fibroblasts [11]. In order to know more precisely the mechanism of epithelial spreading, cytochalasin B (cytB), the drug known as an inhibitor of actin filament formation since Schroeder [12], was applied to the cultured epithelia. Both shapes of cells and alignment of bundels of F-actin, as well as an inhibition of spreading of epithelial sheets, were altered remarkably. Above all, the marginal cells were affected most conspicuously. The results lead us to accept the hypothesis that the marginal cells are mainly responsible for epithelial spreading. The entire epithelium was pulled outwards with the marginal cells in which the bundles of F-actin were structuralized incessantly for generating force for the outward locomotion. The details of the observation and the discussion on the subject will be presented in this communication.

MATERIALS AND METHODS

The eggs of white leghorn obtained commercially were incubated for 8 days at 38°C.

Millipore filters (MF), PH or RA (Millipore Co.), pore sizes of which are 0.3 μm and 1.2 μm respectively, were used for substrata. They will be referred as 0.3 MF and 1.2 MF, characterized by numerals expressing pore size.

The cover slip (24×24 mm) cleaned for culture

Accepted February 10, 1987
Received December 10, 1986

use (Matunami Glass Inc.) was used as a substratum for an epithelium.

1) *Isolation of the epithelium* More than 200 sheets of corneal epithelium were isolated in the ordinary procedures using 1 mM ethylenediaminetetraacetic acid (EDTA) in calcium and magnesium free Tyrode solution. The details were presented in a previous paper [13].

2) *Culture methods* Each isolated epithelium was combined with a piece of 0.3 MF or 1.2 MF, explanted onto the surface of normal Wolff-Haffen's medium [14] or that containing cytochalasin B (Sigma Co., 4, 0.4, or 0.04 μg/ml in a final concentration, cytB–W–H), gelled in a hollow in a glass block. After covered with glass slide and sealed with melted paraffin, the explant was incubated for 24, 48, or 96 hr at 38°C. CytB–W–H was prepared as follows: 1% agar in Gey's solution, donor horse serum (Flow Lab.), 50% embryonic extract of 9-day chick embryos, which contained cytB in a concentration of 19, 1.9, or 0.19 mg/ml, and Penicillin G–K (Meiji Pharm. Co., 20,000 units/ml) were mixed in a ratio, 7:3:3:1 in volume. CytB was primarily dissolved in dimethylsulfoxide (DMSO) and diluted in embryonic extract. As a result, cytB–W–H contained inevitably 2%, at most, of DMSO in a final concentration. The effect of DMSO was checked in the epithelia cultured on W–H containing 2% DMSO alone.

Fifty or more sheets of corneal epithelia were explanted onto the surface of cover glass with a small drop of L-15 medium (Leibowitz, L15, Gibco Co.) supplemented with 20% of donor horse serum (Flow Lab.), covered with hollow slide, sealed with melted paraffin and incubated at 38°C. After 24 hr of primary culture, only the epithelium started to spread along the glass surface was transferred into filming slide with a L-15 medium contained 4 μg/ml of cytB and 20% of horse serum (cytB–L-15) and observed under a phase-contrast microscope, the stage of which was kept at 38°C. The rest of epithelium attached not firmly enough to the glass surface was cultured for another 24 hr at 38°C in Petri dish with a large amount of L-15 medium. The epithelium which began to spread was served for cytB treatment as described above.

3) *Quantitative assessment* The epithelia cultured on MF for 48 or 96 hr with cytB–W–H were fixed with Bouin's fluid for 2 hr. After a thorough elimination of picric acid with 70% ethanol, they were stained *in toto* with Meyer's hematoxylin and eosin, dehydrated through a series of graded alcohol, cleared with xylene and mounted on slide glass with balsam and cover glass.

A ratio between the area of epithelium before and after the culture was used as the index of migratory activity. The details were presented in the previous report [13].

4) *Scanning electron microscopy* (*SEM*) More or less than 10 samples were selected at random from each of 8 groups of culture (two types of MF, and four kinds of cytB–W–H in concentration of cytB) at 24, 48, or 96 hr of culture and fixed with 2.5% glutaraldehyde (Taab. Co.) in 0.1 M cacodylate buffer (pH=7.2, c-buffer) for 2 hr at 0°C. Rinsed three times and overnighted in 0.1 M c-buffer at 4°C, they were postfixed with 1% OsO_4 in 0.1 M c-buffer for 2 hr at 0°C, dehydrated through a series of graded ethanol at 0°C and, immediately or after stocked for several days in the refrigerator, dried in a critical point dryer (Hitachi HII) using liquid CO_2 as a medium. After coated with gold in an ion coater (Eiko Co.), the epithelium was observed with Hitachi S430 scanning electron microscope.

5) *NBD-Phallacidin staining* The epithelia cultured on MF for 24, 48, or 96 hr and those on the glass surface, treated or not treated with cytB, were fixed with 3.5% of neutral formalin in phosphate buffered saline (pH=7.2, PBS) for 30 min at 20°C, rinsed several times in PBS, placed on the bottom of Petri dish, and immersed in a drop of NBD-Phallacidin (NBD-Ph, Wako Pure Chem. Indust.) solution, in which 2 units of NBD-Ph were solved in PBS, for 2 hr at 20°C in the moist and dark chamber. After the treatment, they were rinsed several times in PBS to eliminate free NBD-Ph, mounted on slide glass with PBS-glycerine (1:1 in volume) and covered with cover slip.

6) *Optics* A phase-contrast microscope and a microscope equipped with epifluorescent apparatus and with objective lenses free from autofluorescence (UHF ×20, UHF ×40, and UHF

×100, the last two, for oil immersion, Olympus Co.) were used. For microphotography with the fluorescent microscope, Tri-X films (ISO=400, Kodak) were adopted, which were developed with Super prodol (Fuji Co.) for 7 min at 20°C to enhance the sensitivity from ISO 400 to 800. With the phase-contrast microscope, Neopan F (ISO=32, Fuji Co.) was used without a special treatment.

RESULTS

1. Quantitative assessment of the effect of cytB on epithelial spreading

CytB suppressed completely epithelial spreading. In a concentration more than 10 μg/ml, the epithelial cells hardly survived (data not shown). In 4 μg/ml of cytB, in spite of healthy appearance of cells in histological survey, the migratory index (MI) was 1.2±0.2 (an average of 15 cases ± a standard deviation) in the epithelia cultured for 96 hr in combination with 0.3 MF, which was one-sixth of that in the epithelia cultured on normal W–H (7.9±2.3, 10 samples). The value did not differ significantly from that in the epithelia cultured on normal W–H in combination with 1.2 MF (1.1±0.2, 15), showing complete stop of spreading. Even in a low concectration (0.04 μg/ml), cytB still worked inhibitory: the MI was 3.3 ±1.4 [14], approximately as half as that in those cultured on normal W–H. On W–H containing 2% DMSO alone, the MI (6.0±1.2, 10) differed not significantly from that in those on normal W–H in combination with 0.3 MF at 96 hr of culture. These results were summarized in Table 1. As the cytB in the concentration of 4 μg/ml suppressed the epithelial spreading most effectively, and without giving severe damage to cells, the concentration was used in this series of experiments.

2. The early changes of the marginal cells when transferred into the medium containing cytB

CytB was observed to affect at first in the marginal cells within 5 min after the epithelium was transferred into cytB–L-15. They swelled up slightly and their leading lamella were narrowed at their width. Then the cells began to retract but some parts of the distal end still attached firmly to the glass surface. As the result, fine thread-like cytoplasmic bridges were left behind, and the more the cell body retracted, the longer the bridges became (Figs. 1 and 3a). It was noteworthy that the leading lamella never took "arborized" forms as in the fibroblastic cells treated with cytB [15–18]. The retraction of the margin attained to a maximum about 40 min after the application of cytB, and kept the state for several hours (Fig. 1). The retracted marginal cells in cytB–L-15 for 2 hr could restart to develop the leading lamella and to migrate within 30 min after brought back to a normal L-15 medium.

3. SEM observation on the epithelia cultured for more than 24 hr on cytB–W–H

Almost all of the epithelial marginal cells cultured on cytB–W–H in combination with 0.3 MF lost the leading lamella to be a hemisphere in shapes (Fig. 2d). Some had poor leading lamella

TABLE 1. The effect of cytochalasin B on the epithelial spreading

Culture medium	Substratum	No. of samples	Migratory index (Av. ±s.d.)
W–H	0.3 MF	10	7.9±2.3
W–H+DMSO	0.3 MF	10	6.0±1.2
W–H+2% DMSO+0.04 μg/ml cytB	0.3 MF	14	3.3±1.4
W–H+2% DMSO+0.4 μg/ml cytB	0.3 MF	12	1.9±0.6
W–H+2% DMSO+4 μg/ml cytB	0.3 MF	15	1.2±0.2
W–H	1.2 MF	15	1.1±0.1

W–H: Wolff-Haffen's medium. DMSO: dimethylsulfoxide. Av. ±s.d.: Average±standard deviation.

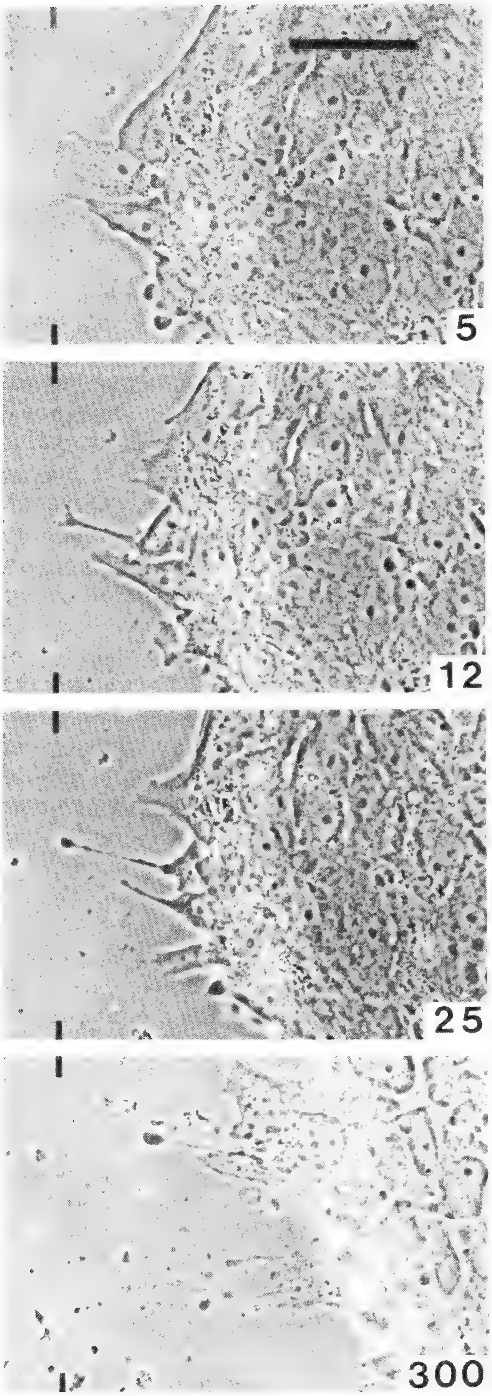

with many blebs at the edges (Fig. 2a) as in the aggregated fibroblasts in a medium containing cytB [19], suggesting no sufficient expansion occurred in the cells [20]. Those on W–H without cytB, in contrast, were flat and had well developed leading lamella, from which filopodia, lamellipodia, micro-filopodial processes, blebs or ruffles were protruded as reported before [21] (Fig. 2c).

The submarginal cells elongated along the direction in parallel with the marginal line and had microvilli on top as in those cultured on normal W–H, suggesting weak or no effect of cytB on them (Fig. 2a).

The inner area differed from place to place in the effect of cytB: Most of places were kept intact. Some still kept regular polygonal shapes, but swelled up slightly, or tended to break contacts with the neighbours to be a fibroblast-like cell on the surface of epithelium (Fig. 2b).

In the epithelium combined with 1.2 MF, the effect of cytB was not clear. Neither the marginal, submarginal nor the inner cells changed conspicuously in their figures on cytB–W–H: The marginal cells scarcely attached to MF and not spread at all, quite similar with those cultured in combination with 1.2 MF on normal W–H (Fig. 2d).

4. *The distribution pattern of F-actin in the epithelial cells in the presence of cytB*

In the cytoplasmic bridges left behind the retracted marginal cells (Figs. 1 and 3a), there were numbers of small fragments bound with NBD-Ph scattered (Fig. 3b). Similar fragments of fluorescence were recognized also at perinuclear region in the inner cells (Fig. 3d). Most of marginal cells cultured for more than 24 hr on cytB–W–H in combination with 0.3 MF had hemispherical edges, in which the fluorescence of NBD-Ph was recognized faintly only along cell membrane. By contrast, on normal W–H, the

Fig. 1. The process of marginal retraction in the epithelium in cytB–L-15. The numerals at right end in each figure indicate the time after the epithelium was transferred into cytB–L-15. The thick black bar on the top figure, 50 μm. The thin bars in each mark the fixed points on the glass surface.

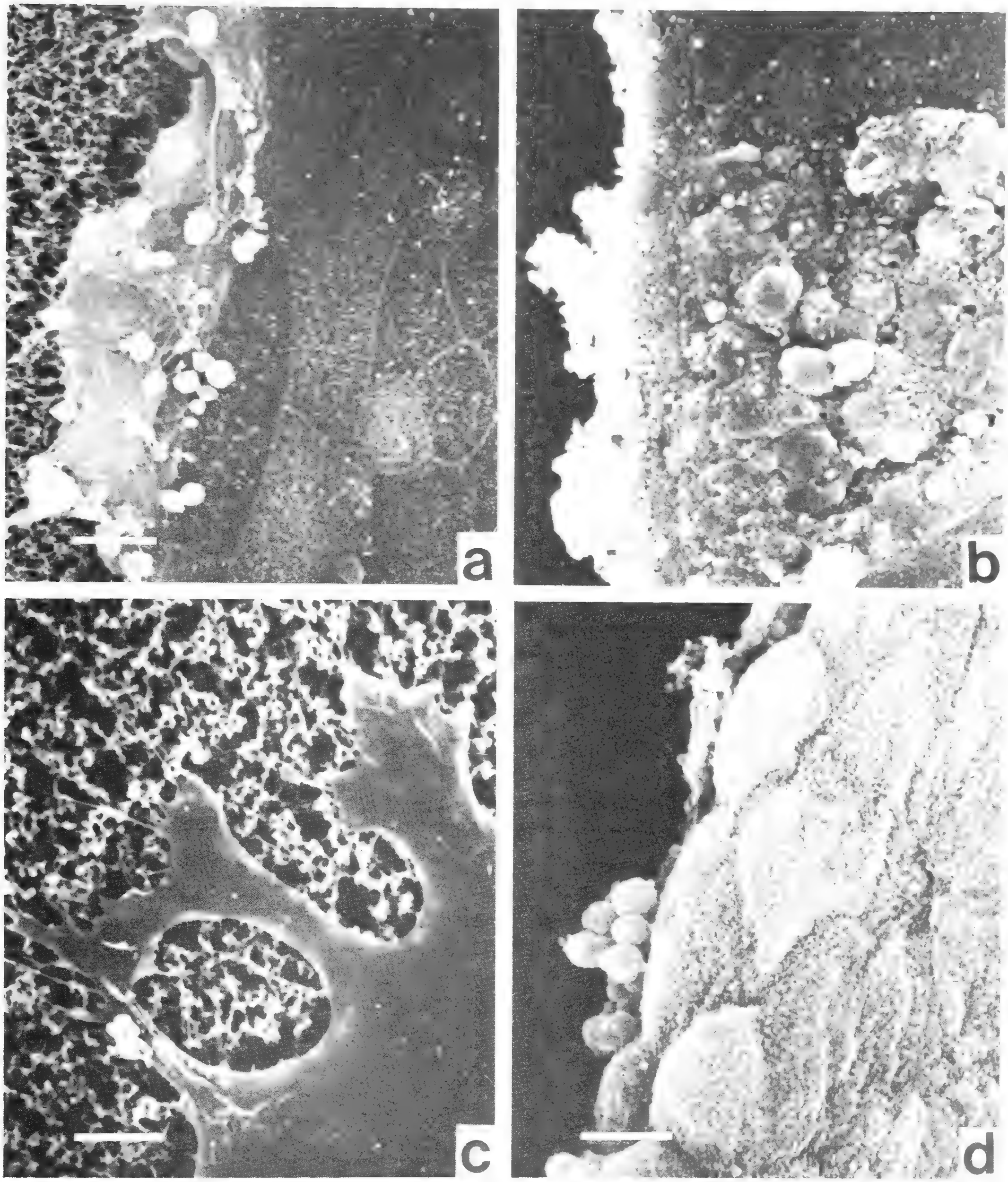

FIG. 2. The epithelial cells observed with an SEM.

a. The marginal cells in the epithelium combined with 0.3MF and cultured for 12 hr on cytB–W–H. In comparison with Fig. 2c below, the retraction of margin and bleds are marked. The white bar, 10 μm.

b. The submarginal cells and the inner of the epithelium combined with 0.3MF and cultured for 48 hr on cytB–W–H. The marginal cells retracted completely. Some of inner cells were swelled and loosened connection among them. The white bar, 10 μm.

c. The marginal cells combined with 0.3MF and cultured for 24 hr on normal W–H. Note the leading lamella spread in flat. The white bar, 5 μm.

d. The marginal cells in the epithelium cultured for 24 hr, in association with 1.2MF, on cytB–W–H. The white bar, 5 μm.

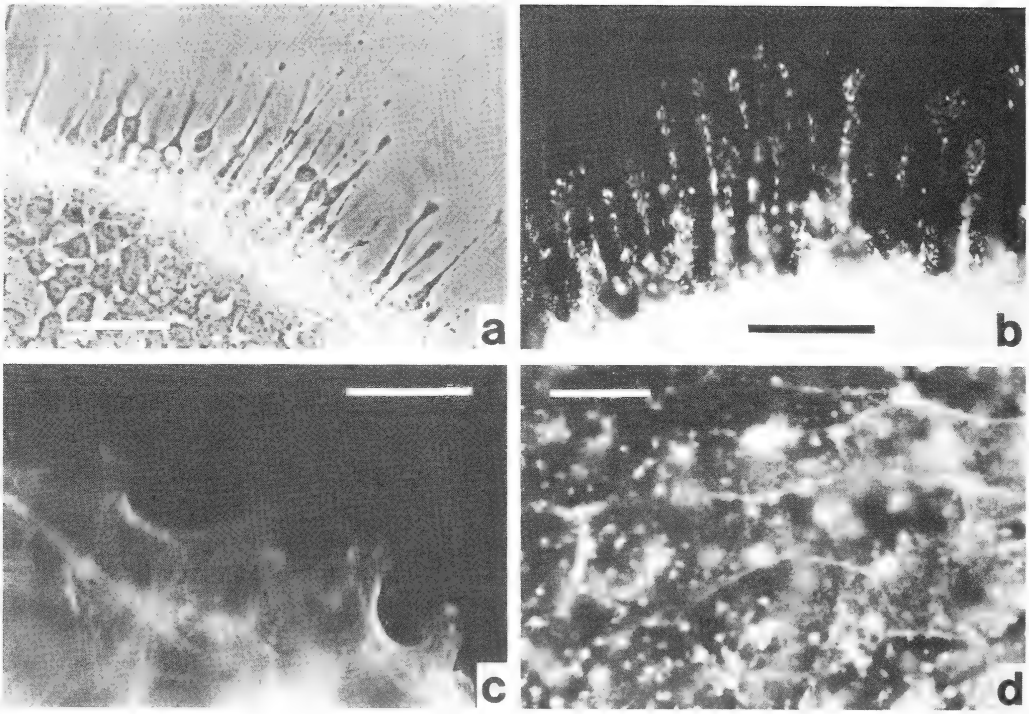

FIG. 3. The epithelial cells cultured on the glass surface.

a. The fine thread-like leading lamella in the epithelial marginal cells after 4 hr of culture in cytB–L-15. The white bar, 50 μm.

b. The small aggregates of F-actin in the thread-like leading lamella in the epithelial cells cultured for 4 hr in cytB–L-15. Compare with the alignment of F-actin bundles in the well developed leading lamella in Fig. 3c below. The black bar, 50 μm.

c. The alignment of bundles of F-actin fibers in the marginal cells cultured for 24 hr in association with 0.3 MF on normal W–H. The white bar, 50 μm.

d. F-actin fibers in the inner cells of the epithelium cultured for 4 hr in cytB–L-15. Note F-actin fibers are aligned along cell borders. The white bar, 20 μm.

bundles of NBD-Ph were observed to run through cell body from a cytocenter to the leading edges. The distribution pattern was similar with that of microfilaments observed with the aid of a transmission electron microscope [1] and also with that of actin filaments observed with the indirect immunofluorescence method using anti-actin antibody ([10] and Takeuchi, unpublished).

In the leading lamella once lost from the marginal cell in the presence of cytB and recovered in a normal medium, the NBD-Ph positive filaments were radially aligned, running through the leading lamella as in the cells not treated with cytB (Fig. 3c). The recovery of NBD-Ph positive filaments was confirmed in both the epithelia cultured on MF on cytB–W–H for 72 hr and those on the glass surface in cytB–L-15 for 2 hr.

In the inner cells, the bundles of NBD-Ph positive filaments were aligned along the polygonal borders as in the intact epithelium [22] without noticeable changes after the application of cytB, suggesting no effect of cytB on them (Fig. 3d). Apart from the border, however, many flakes of NBD-Ph were recognized to be scattered at perinuclear region (Fig. 3d).

DISCUSSION

The effect of cytB on the epithelial spreading

was evident (Table 1). This agreed with the results that the movement of corneal epithelium of newt was arrested with ctyB or cytD [23].

In the epithelia, spreading of which was inhibited, the marginal cells were most severely deformed with cytB, even cultured on a substratum smooth enough to permit spreading: they lost the leading lamella to be hemisphere in shapes as those cultured on the rough surface without cytB [16]. The deformation began soon after the epithelium was transferred into cytB–L-15 (Figs. 2 and 3a). It could, therefore, be said that the inhibition of epithelial spreading was mainly due to the loss of locomotory activity in the marginal cells accomapnied with the deformation. How did cytB act on the cells to bring about deformation or to disrupt the locomotory activity?

The action of cytB on actin filaments

There is a variety of elucidation reporting about the mode of action of cytB: CytB bound to one end of an actin filament to block further association of actin monomers [24–29]. CytB inhibited nucleation of F-actin, so that the formation of actin filaments was delayed [30]. CytB inhibited annealing of F-actin to suppress further elongation [31]. Besides, ctyB was reported to inhibit gelation of actin [26, 30, 32–34]. MacLean-Fletcher and Pollard [30] insisted the inhibition of actin-network formation might be more important in living cells than that of actin elongation. Schliwa [35] pursued the changes in the cytoskeletal system under the presence of cytB. Within minutes, cytB disrupted the cytoskeletal networks by severing the filaments into small fragments. At the next, cytoplasmic contraction, though disorganized and uncontrolled, occurred to form dense foci (aggregates of filamentous materials). A series of changes ended at a state, where the cytoskeletal system was disintegrated completely.

NBD-Ph was reported to associate specifically with F-actin [36]. According to this, the flakes observed in the marginal cells in cytB–L-15, were considered as aggregates of disintegrated F-actin derived from the bundles in the leading lamella as reported by Schliwa [35] (Fig. 3c), or considered as myoid bundles which were assumed to be contracted microfilamentous apparatus at the cell cortex reported by Miranda *et al.* [37]. Whichever the nature of the flakes might be, it was sure that the bundles of F-actin in the cells were disintegrated completely. The problems are how, specifically in the marginal cells, the F-actin bundles were disorganized, especially at early phase, and how the F-actin bundles were reformed and aligned in accopany with restoration of the leading lamella.

The early changes in the marginal cells, when the epithelial sheet was immersed in cytB–L-15

The marginal cells were narrowed very quickly at the leading lamella, when cytB was applied (Fig. 2). This suggested the structure or the machanism keeping the leading lamella flat was most sensitive to cytB.

Heath [38] reported that there were networks called as dorsal cortical microfilament sheath (DCMS) in the leading lamella of fibroblastic cells under locomotion. The DCMS consisting of actin and other contractile proteins were recycled from disintegration to reassociation to spread the leading lamella. The DCMS was moved backwards along dorsal surface of the leading lamella and decomposed to be cytoplasmic sol, which were pushed forwards to the leading edges to be reformed as DCMS. Considering similarity of the epithelial cells in locomotory activities to the fibroblastic cells [1, 6], the DCMS was assumed to work also on the leading lamella of epithelial cells. In the presence of cytB, the DCMS could not be structuralized because F-actin polymerization was inhibited. This might be a reason why the leading lamella was sensitive to cytB and narrowed themselves at first.

There might be another explanation for the mode of action of cytB to the leading lamella. According to Godman *et al.* [39, 40], F-actin was dissociated with actin-binding proteins with cytB and aggregated with myosin as in superprecipitation. This might bring about a general contraction of the leading lamella.

The mode of action of cytB in living cells will be elucidated more comprehensively when the behavior of actin *in situ* is fully understood.

The late changes in the marginal cells, the elongation of cytoplasmic bridges

The initial shrinkage of width in the leading lamella was followed by elongation of it. It was observed to be elongated straight, not so "arborized" as in the fibroblastic cells treated with cytB [15–18]. This might be explained as follows: after the bundles of F-actin were disintegrated with cytB, the marginal cells could not pull any more the rest of epithelial cells outwards but were, in reverse, pulled inwards, too strongly to permit the slack in the cytoplasmic bridge, by elastic force of themselves and/or of neighbouring cells which had counterbalanced tension arisen inevitably in them. Some parts in the leading edge stuck firmly to the substratum worked as supporting points against the recoiling force. Thus, the more the cells retracted, the longer the cytoplasmic bridges became. This hypothesis was agreed with the reports presented previously: there was strong tension at the marginal area of epithelial sheet in culture. The margin retracted to a considerable extent, when the contacts of marginal cells with the glass surface were disrupted mechanically [41]. Furthermore, the tension accelerated the epithelial spreading seemingly by enhancing the transition of the epithelial cells from a stationary state to a motile [42]. The focal contacts [3] were candidates for the supporting points which stuck firmly to the substratum. Indeed, the focal contacts were recognized in the epithelial marginal cells [1, 10]. Some of these contacts remained even in the presence of cytB to work as supporting points against the recoiling force.

Stability of F-actin filaments

It was quite queer that the bundles of F-actin along borders of the inner cells could not be disintegrated with cytB, while those at perinuclear region were broken down to be small flakes (Fig. 3d). Based on the action of cytB discussed above, the intact bundles were considered to be in a stationary state in which neither polymerization nor disintegration occurred. At the perinuclear region of the inner cells or at the leading lamella of marginal cells, in contrast, F-actin filaments were maintained in an equilibrium between incessant association of actin monomers with one end and decomposition at another end as discussed by Brenner and Korn [25]. Füchtbauer *et al.* [43] confirmed this in both the fibroblastic cells and the epithelial cells. Capping proteins for F-actin, when injected into the cells in culture, disintegrated the microfilaments at the site where the focal contacts were formed, causing shrinkage of the cells. According to them, actin monomers were always taken into filaments at the focal contacts.

Summerizing the points, the bundles of F-actin were newly aligned only at such active parts in cells as the leading lamella which generated force for works. In the marginal cells which were responsible for generating force for epithelial spreading, F-actin might be always polymerized and the bundles of them might be aligned along tension in order to work most effectively in accordance with formation of firm contacts between cell and substratum.

These results supported our "two step hypothesis" that tried to elucidate how the stationary epithelial cells acquired motility (Takeuchi, unpublished): the stationary cells were pulled outwards and under tension, at the first step, the bundles of microfilaments along cell border were discomposed completely and, at the second step, the components were reconstructed to be aligned along the direction of tension through cell body to the leading edge which generated force for locomotion. Only cytB-sensitive microfilaments were, therefore, observed in the marginal cells that made the transition from a stationary state to motile.

REFERENCES

1 Heath, J. P. (1982) Adhesions to substratum and locomotory behaviour of fibroblastic and epithelial cells in culture. In "Cell Behaviour", Ed. by R. Bellair, A. Curtis and G. Dunn, Cambridge Univ. Press, Cambrige, pp. 77–108.

2 Trinkaus, J. P. (1984) Cells into Organs. The Forces That Shape the Embryo, Prentice-Hall, Englewood Cliffs, New Jersey, 543 pp.

3 Izzard, C. S. and Lochner, L. R. (1976) Cell-to-substrata contacts in living fibroblasts: An interference reflexion study with and evaluation of the technique. J. Cell Sci., **21**: 129–160.

4 Radice, G. P. (1980) The spreading of epithelial cells during wound closure in *Xenopus* larvae. Dev. Biol., **76**: 26–46.

5 Radice, G. P. (1980) Locomotion and cell-substratum contacts of *Xenopus* epidermal cells *in vitro* and *in situ*. J. Cell Sci., **44**: 201–223.

6 DiPasquale, A. (1975) Locomotory activity of epithelial cells in culture. Exp. Cell Res., **94**: 191–215.

7 Abercrombie, M., Heaysman, J. M. and Pegrum, S. M. (1970) The locomotion of fibroblasts in culture. I. Movements of leading edge. Exp. Cell Res., **59**: 393–398.

8 Abercrombie, M., Heaysman, J. M. and Pegrum, S. M. (1970) The locomotion of fibroblasts in culture. II. Ruffling. Exp. Cell Res., **60**: 437–444.

9 Abercrombie, M., Heaysman, J. E. and Pegrum, S. M. (1970) The locomotion of fibroblasts in culture. III. Movements of particles on the dorsal surface of the leading lamella. Exp. Cell Res., **62**: 389–398.

10 Billig, D., Nicol, A., McGinty, R., Cowin, P., Morgan, J. and Garrod, D. (1982) The cytoskeleton and substratum adhesion in chick embryonic corneal epithelial cells. J. Cell Sci., **57**: 51–71.

11 Isenberg, G., Rathke, P. C., Hulsmann, N., Franke, W. W. and Wohlfarth-Bottermann, K. E. (1976) Cytoplasmic actomyosin fibrils in tissue culture cells. Direct proof of contractility by visualization of ATP-induced contraction in fibrils isolated by laser microbeam dissection. Cell Tissue Res., **166**: 427–443.

12 Schroeder, T. E. (1970) The contractile ring. Fine structure of dividing mammalian (HeLa) cells and the effects of cytochalasin B. Z. Zellforsch. Mikrosk. Anat., **109**: 431–449.

13 Takeuchi, S. (1976) Wound healing in the cornea of the chick embryo. III. The influence of pore size of Millipore filters on the migration of isolated epithelial sheets in culture. Dev. Biol., **51**: 49–62.

14 Wolff, Et. and Haffen, K. (1952) Sur une méthode de culture d'organes embyronnaires *in vitro*. Texas Rep. Biol. Med., **10**: 463–472.

15 Sanger, J. W. (1974) The use of cytochalasin B to distinguish myoblasts from fibroblasts in cultures of developing chick striated muscle. Proc. Natl. Acad. Sci. USA., **71**: 3621–3625.

16 Miranda, A. F., Godman, G. C., Deitch, A. D. and Tanenbaum, S. W. (1974) Action of cytochalasin D on cells of established lines. J. Cell Biol., **61**: 481–500.

17 Atlas, S. J. and Lin, S. (1978) Dihydrocytochalasin B. Biological effects and binding to 3T3 cells. J. Cell Biol., **76**: 360–370.

18 Bliokh, Z. L., Domnina, L. V., Smolyaninov, V. A., Vasiliev, J. M. and Gelfand, I. M. (1980) Spreading of fibroblasts in medium containing cytochalasin B: Formation of lamellar cytoplasm as a combination of several functionally different processes. Proc. Natl. Acad. Sci. USA., **77**: 5919–5922.

19 Van der Schueren, B., Cassiman, J. J. and van der Berghe, H. (1978) Modulation of the effect of colchicine and cytochalasin B on fibroblast aggregates by the substratum. J. Cell Sci., **31**: 353–367.

20 Erickson, C. A. and Trinkaus, J. P. (1976) Microvilli and blebs as sources of reserve surface membrane during cell spreading. Exp. Cell Res., **99**: 375–384.

21 Takeuchi, S. (1983) Would healing in the cornea of the chick embryo. V. An observation and quantitative assessment of the cell shapes in the isolated corneal epithelium during spreading *in vitro*. Cell Tissue Res., **229**: 109–127.

22 Owaribe, K., Araki, M., Hatano, S. and Eguchi, G. (1979) Cell shape and actin filaments. In "Cell Motility: Molecules and Organization". Ed. by S. Hatano, H. Ishikawa and H. Sato, Univ. Tokyo Press, Tokyo, pp. 491–500.

23 Yamanaka, H and Eguchi, G. (1981) Regeneration of the cornea in adult newt: Overall process and behavior of epithelial cells. Differ., **19**: 84–92.

24 Brown, S. S. and Spudich, J. A. (1979) Cytochalasin inhibits the rate of elongation of actin filament reagents. J. Cell Biol., **83**: 657–662.

25 Brenner, S. L. and Korn, E. D. (1979) Substichiometric concentrations of cytochalasin D inhibit actin polymerization. Additional evidence for an F-actin treadmill. J. Biol. Chem., **254**: 9982–9985.

26 Lin. D. C. and Lin, S. (1980) Cytochalasins inhibit actin gelation by binding to filament ends. J. Cell Biol., **87**(2–2): 213a.

27 Flanagan, M. D. and Lin, S. (1980) Cytochalasins block actin filament elongation by binding to high affinity sites associated with F-actin. J. Biol. Chem., **255**: 835–838.

28 Lin, D. C. Tobin, K. D., Grumet, M. and Lin, S. (1980) Cytochalasins inhibit nuclei-induced actin polymerization by blocking filament elongation. J. Cell Biol., **84**: 455–460.

29 Brown, S. S. and Spudich, J. A. (1981) Mechanism of action of cytochalasin: Evidence that it binds to actin filament ends. J. Cell Biol., **88**: 487–491.

30 MacLean-Fletcher, S. and Pollard, T. D. (1980) Mechanism of action of cytochalasin B on actin. Cell, **20**: 329–341.

31 Maruyama, K., Hartwig, J. H. and Stossel, T. P. (1986) Cytochalasin B and the structure of actin gels. II. Further evidence for the splitting of F-actin by cytochalasin B. Biochim. Biophys. Acta, **626**: 449–450.

32 Weihing, R. R. (1976) Cytochalasin B inhibits actin-

related gelation of HeLa cell extract. J. Cell Biol., **71**: 303–307.

33 Pollard, T. D. (1976) The role of actin in the temperature-dependent gelation and contraction of extracts of *Acanthamoeba*. J. Cell Biol., **68**: 579–601.

34 Hartwig, J. H. and Stossel, T. P. (1979) Cytochalasin B and structure of actin gels. J. Mol. Biol., **134**: 539–553.

35 Schliwa, M. (1982) Action of cytochalasin D on cytoskeletal networks. J. Cell Biol., **92**: 79–91.

36 Barak, L. S., Yocum, R. R., Nothnagel, E. A. and Webb, W. W. (1980) Fluorescence staining of the actin cytoskeleton in living cells with 7-nitrobenz-2-oxa-1, 3-diazole-phallacidin. Proc. Natl. Acad. Sci. USA., **77**: 980–984.

37 Miranda, A. F., Godman, G. C. and Tanenbaum, S. (1974) Action of cytochalasin D on cells of established lines. II. Cortex and microfilaments. J. Cell Biol., **62**: 406–423.

38 Heath, J. P. (1983) Direct evidence for microfilament-mediated capping of surface receptors on crawling fibroblasts. Nature, **302**: 532–534.

39 Godman, G., Woda, B. and Kolberg, R. (1980) Redistribution of contractile and cytoskeletal components induced by cytochalasin. I. In Hmf cells, a nontransformed fibroblastoid line. Eur, J. Cell Biol., **22**: 733–744.

40 Godman, G. Woda, B. and Kolberg, R. (1980) Redistribution of contractile and cytoskeletal components induced by cytochalasin. II. In HeLa and HEp2 cells. Eur. J. Cell Biol., **22**: 745–754.

41 DiPasquale, A. (1975) Locomotion of epithelial cells. Factors involved in extension of the leading edge. Exp. Cell Res., **95**: 425–439.

42 Takeuchi, S. (1979) Wound healing in the cornea of chick embryo. IV. Promotion of the migratory activity of isolated corneal epithelium in culture by the application of tension. Dev. Biol., **70**: 232–240.

43 Füchtbauer, A., Jockusch, B. M., Maruta, H., Kilimann, M. W. and Isenberg, G. (1983) Disruption of microfilament organization after injection of F-actin capping proteins into living tissue culture cells. Nature, **304**: 361–364.

ZOOLOGICAL SCIENCE 4: 475–481 (1987)

Retinal and 3-Dehydroretinal in the Egg of the Clawed Toad, *Xenopus laevis*

Takaharu Seki, Shigechika Fujishita, Masami Azuma[1] and Tatsuo Suzuki[2]

Department of Health Science, Osaka Kyoiku University, Hirano Campus, 1–6–7 Nagaremachi, Hiranoku, Osaka 547, [1]Department of Health Science, Osaka Kyoiku University, 4–88 Minamikawahoricho, Tennojiku, Osaka 543, and [2]Department of Pharmacology, Hyogo College of Medicine, 1–1 Mukogawacho, Nishinomiya, Hyogo 663, Japan

ABSTRACT—Retinals in the egg of the clawed toad, *Xenopus laevis,* were extracted and the composition of the geometric isomers was analysed by using high-performance liquid chromatography. Nearly equal amounts of retinal (all-*trans* and 13-*cis*) and 3-dehydroretinal (all-*trans* and 13-*cis*) were present at the total quantity about 50 pmol/egg. In the eggs of other frogs, *Rhacophorus schlegelii* and *Rhacophorus arboreus,* only retinal was contained at the quantity about 50 pmol/egg. Retinyl ester and carotenoids in the *Xenopus* eggs were scarce, and retinols, 3-hydroxyretinals or 11-*cis* isomers of retinals were undetectable in them.

Retinals in the *Xenopus* eggs were suggested to be present in a protein-bound form through the Schiff base linkage, for after reduction by $NaBH_4$ neither retinol nor retinyl-product could be found in the organic solvent layer.

The metabolic pathways forming the egg retinals are discussed on the basis of retinyl ester and carotenoids found in the *Xenopus* ovary.

INTRODUCTION

In animal kingdom, diversity of visual pigments has been ensured by both the variety of the protein and the prosthetic moieties. On the basis of the prosthetic moiety, three kinds of visual pigments can be classified: rhodopsin (and iodopsin), porphyropsin (and cyanopsin) and xanthopsin [1], containing 11-*cis* retinal, 11-*cis* 3-dehydroretinal and 11-*cis* 3-hydroxyretinal [2–4], respectively. How an animal obtained the capacity to use one or a few of the multiformular visual pigments is an interesting problem to be clarified in relation to an adaptation of the animal to the environmental conditions. For this purpose, a clawed toad, *Xenopus laevis*, is one of the excellent materials because this toad contains porphyropsin as a principal visual pigment [5] and can be reared easily in a laboratory under controlled conditions, e.g. on food of the known retinoid composition. Furthermore, it can be induced to lay fertile eggs by administration of gonadotrophic hormone at any time of year [6], and the change of retinoid composition during the development of eggs into tadpoles can be examined precisely by using high-performance liquid chromatography (HPLC). At the beginning of the study, we analysed retinoids and carotenoids in the frog eggs and ovary. Retinoids in the egg of frogs in another suborder (*Rhacophorus arboreus* and *R. schlegelii*) were also analysed.

MATERIALS AND METHODS

Pairs of *X. laevis* were kindly supplied by Dr. Takasaki (Osaka Kyoiku Univ.) or purchased from Hamamatsu Seibutsu Kyozai Co., Ltd. (Shizuoka, Japan). They were reared at 25°C and fed with porcine liver twice a week. The eggs of

Accepted December 26, 1986
Received October 20, 1986

X. laevis were induced to breed by injection of chorionic gonadotrophic hormone (Gonatropin; Teikoku Zoki Ltd., Tokyo) to a pair [6], 300 IU to female and 150 IU to male. In some cases, unfertilized eggs were bred, but no difference was found between fertilized and unfertilized eggs in the results reported here. In order to facilitate handling, the jelly layer was removed by immersing the eggs in 1% sodium thioglycolate, pH 9–10 [7]; the presence of the jelly layer did not affect the results. A lump of eggs of *R. schlegelii* was collected at a rice field and that of *R. arboreus* at a local pond both in Fukui Prefecture on 22 June, 1986. Eggs of *R. arboreus* hatched on the next day, and so the abdominal parts, where the yolk was retained, of the tadpoles were collected and analysed.

Two methods were applied to extract retinoids from eggs. For the extraction of retinal as oxime [8, 9], the procedure described previously [4] was used. For the extraction of nonderivertized retinal, the formaldehyde method [10] was used with minor modification. Two hundreds of eggs were homogenized, in a Potter-Elvehjem homogenizer with a motor-driven teflon pestle, in 5 ml of 90% aqueous methanol containing 1.2 M formaldehyde. After standing at room temperature for 5 min, 10 ml of 6 M formaldehyde was added and the retinoids were extracted with 10 ml of dichloromethane and 20 ml of *n*-hexane by centrifugation at 3500 rpm for 5 min. The extraction with dichloromethane/*n*-hexane was repeated three times.

Reduction of retinal into retinol by sodium borohydride($NaBH_4$), formation of retinaloximes with hydroxylamine (NH_2OH) and saponification of retinyl ester were performed by the described methods [11].

Retinoids and carotenoids were analysed on a Hitachi 655 HPLC system equipped with a 6×150 mm column of YMC–PACK A–012–3 S–3 SIL (particle size 3 μm; Yamamura Chemical Laboratories Co., Ltd., Kyoto) with an eluent, 8% diethylether-0.08% ethanol in *n*-hexane, or with a 4×250 mm column of LiChrosorb SI–60 (5 μm; Merck, Darmstadt, FRG) with the eluents, 15% diethylether-0.15% ethanol in *n*-hexane followed by 50% diethylether-0.5% ethanol in *n*-hexane. The flow rate was at 2 ml/min. Absorbance at 350 nm was monitored with a Hitachi 638–41 UV-detector and at 450 nm with a 875–UV detector (Japan Spectroscopic Co., Ltd., Tokyo). Quantities of retinaloxime and 3-dehydroretinaloxime were estimated from the peak height of the *syn* isomers of the equimolar mixture of standard oximes [12]. Absorption spectra were measured with a Hitachi 200–20 spectrophotometer equipped with a X–Y recorder (RY–101; Rikadenkikogyo Co., Ltd., Tokyo).

All operations were carried out under red light exceeding 610 nm.

RESULTS AND DISCUSSION

The elution profile of the standard oximes (Fig. 1A) shows the peaks of *syn* and *anti* 11-*cis* retinaloximes (1, 1′), 11-*cis* 3-dehydroretinaloximes (2, 2′) all-*trans* retinaloximes (3, 3′) and all-*trans* 3-dehydroretinaloximes (4, 4′). Figure 1B shows the elution profile of retinoids extracted from eggs of *R. schlegelii*, indicating the peaks corresponding to all-*trans* retinaloximes (3, 3′) and 13-*cis* retinaloximes (5, 5′). In Figure 1C, a typical chromatogram of retinoids extracted from the eggs of *X. laevis* is shown. The several peaks in Figure 1C were assigned to all-*trans* retinaloximes (3, 3′), all-*trans* 3-dehydroretinaloximes (4, 4′), 13-*cis* retinaloximes (5, 5′) and 13-*cis* 3-dehydroretinaloximes (6, 6′). Peaks corresponding to 11-*cis* isomers of retinaloximes and 3-dehydroretinaloximes, or retinol and 3-dehydroretinol were not detected in the egg extracts. The existence of 3-hydroxyretinaloximes was examined by changing the eluent from 8% ethylether-0.08% ethanol in *n*-hexane to 50% ethylether-0.5% ethanol in *n*-hexane [4], but any peaks due to 3-hydroxyretinaloximes were undetectable.

For further analysis of retinals in the *Xenopus* eggs, the formaldehyde method was applied to the extraction of retinals. Figure 2 shows an elution profile of retinal isomers on HPLC; the peaks attributable to 13-*cis* and all-*trans* isomers of retinal (1, 5), and those of 3-dehydroretinal (2, 6) are observed, accompanied with small peaks (3, 4) probably due to 9-*cis* isomers of retinal and

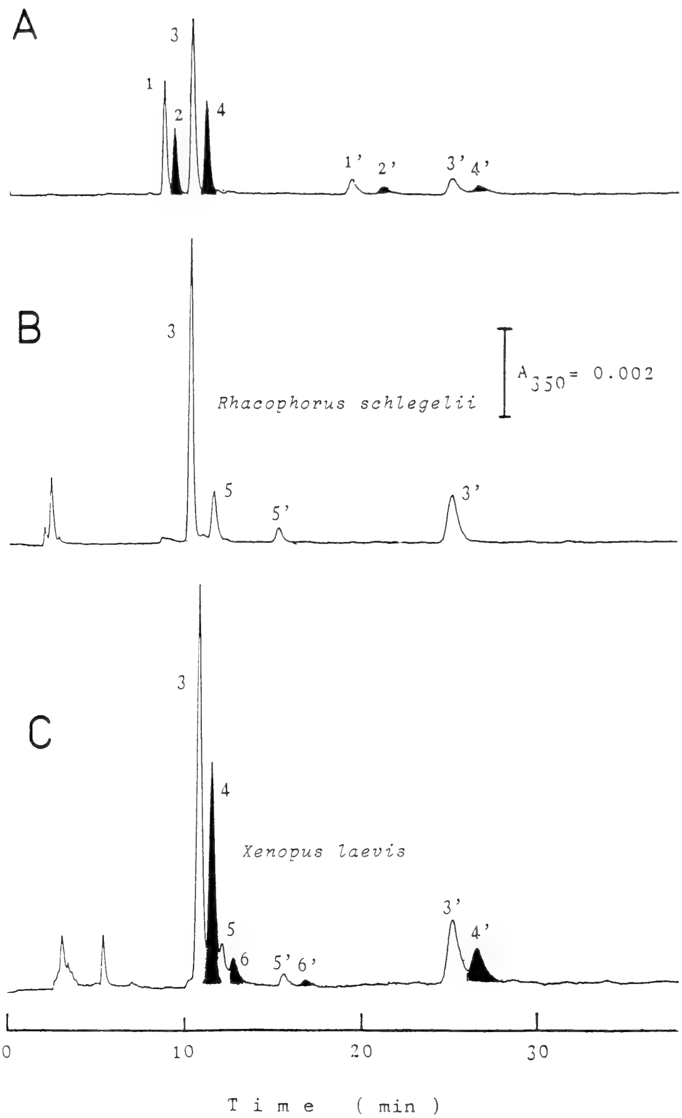

FIG. 1. High-performance liquid chromatograms of (A) standard oximes of retinal and 3-dehydroretinal, (B) retionids extracted from eggs of *R. schlegelii* and (C) those of *X. laevis* by the oxime method. Standard oximes contain *syn* and *anti* 11-*cis* retinaloximes (1, 1′), 11-*cis* 3-dehydroretinaloximes (2, 2′), all-*trans* retinaloximes (3, 3′) and all-*trans* 3-dehydroretinaloximes (4, 4′) at 50 pmol each. (B) shows the peaks with the retention times similar to those of all-*trans* retinaloximes (3, 3′) and 13-*cis* retinaloximes (5, 5′), and (C) exhibits the peaks corresponding to all-*trans* retinaloximes (3, 3′), all-*trans* 3-dehydroretinaloximes (4, 4′), 13-*cis* retinaloximes (5, 5′)and 13-*cis* 3-dehydroretinaloximes (6, 6′). HPLC conditions; column: YMC–PAC A–012–3 S–3 SIL, 4×150 min, mobile phase: 8% diethylether-0.08% ethanol in *n*-hexane, flow rate: 2 ml/min, and detection: absorbance at 350 nm.

3-dehydroretinal. Identification of the peak substances was further carried out with the measurements of absorption spectra and the chemical reactivities. Three fractions corresponding to peaks 1 and 2 (fraction 1), peak 5 (fraction 2) and peak 6 (fraction 3) in Figure 2 were collected.

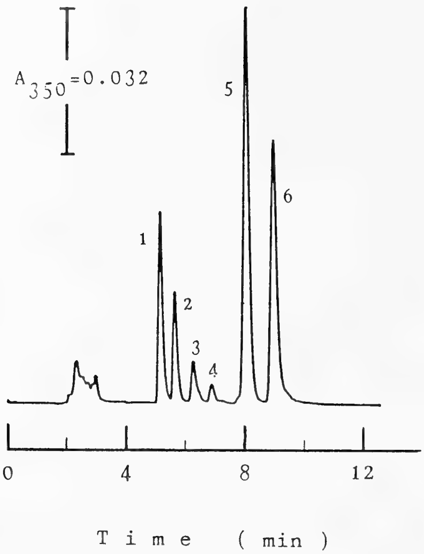

FIG. 2. The elution profile of retinoids extracted from 200 eggs of *X. laevis* by the formaldehyde method and chromatographed on HPLC. The peaks with the retention times similar to those of 13-*cis* retinal and 13-*cis* 3-dehydroretinal (1, 2), 9-*cis* retinal and 9-*cis* 3-dehydroretinal (3, 4) and all-*trans* retinal and all-*trans* 3-dehydroretinal (5, 6) are obvious. HPLC conditions are same as those of Fig. 1.

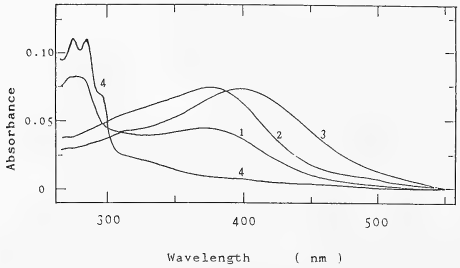

FIG. 3. Absorption spectra of the peak substances shown in Fig. 2. The fractions corresponding to peaks 1 and 2 (curve 1), peak 5 (curve 2), peak 6 (curve 3) and the substances eluting out around solvent front (curve 4) in Fig. 2 were collected, redissolved in 1 ml of ethanol and the absorption spectra of the fractions were measured. Curve 4 was diluted 5 times before spectrophotometry.

Figure 3 shows the absorption spectra of these fractions in ethanol. Fraction 2 shows the absorption maximum at 380 nm (curve 2) and fraction 3 at 400 nm (curve 3), indicating that the former is all-*trans* retinal and the latter all-*trans* 3-dehydroretinal. Fraction 1 shows the absorption spectrum (curve 1) due to the mixture of 13-*cis* retinal, 13-*cis* 3-dehydroretinal and some contaminating material with the absorption maximum around 280 nm. The fractions used for spectral analysis were assayed by HPLC after treatment with NH_2OH or $NaBH_4$. By reaction with NH_2OH, the fraction 1 was converted to a mixture of 13-*cis* isomers of retinaloxime and 3-dehydroretinaloxime, the fraction 2 to all-*trans* retinaloxime and the fraction 3 to all-*trans* 3-dehydroretinaloxime. The treatment with $NaBH_4$ converted the retinal isomers to corresponding retinol isomers. From these results it is concluded that all-*trans* and 13-*cis* isomers of retinal and 3-dehydroretinal are included in the egg of *X. laevis*.

An existing state of the retinals in the *Xenopus* egg was examined by using $NaBH_4$ [cf. 13]. To a homogenate of eggs in 67 mM phosphate buffer, pH 6.7, were added $NaBH_4$ grains and then the retinoids in the homogenate were extracted by the oxime method or formaldehyde method. The organic solvent layer (dichloromethane/*n*-hexane) was collected and analysed by HPLC, spectrophotometry and fluorometry. On HPLC analysis, no peaks corresponding to retinol or 3-dehydroretinol were detected, suggesting that the retinals are not present in free forms that could be reduced to retinols by $NaBH_4$ [13]. The measurement of absorption and fluorescence spectra did not show any retinol or *N*-retinyl-product in the organic solvent layer. These results suggest strongly that the retinal and 3-dehydroretinal in eggs exist as a complex with some protein by forming the Schiff base. The Schiff base compound of retinal and protein is converted to *N*-retinyl-protein by $NaBH_4$, which can not be extracted into the organic solvent layer. Plack and Kon [14] have reported that the retinals in fish eggs [14] and in hen's eggs [15] are present in such a way that the characteristic properties are masked, probably because they are bound to a lipid and protein.

In order to examine the presence of retinyl ester, the materials eluting at the solvent front on HPLC (Fig. 2) were collected and analysed by measurement of absorption spectrum (curve 4 in

TABLE 1. Amounts and composition of geometrical isomers of retinals in frog eggs

Frogs	Retinal (pmol/egg) all-*trans*	Retinal (pmol/egg) 13-*cis*	3-Dehydroretinal (pmol/egg) all-*trans*	3-Dehydroretinal (pmol/egg) 13-*cis*	Sum (pmol/egg)
Xenopus laevis	23.6	2.6	25.0	3.1	54.3
Rhacophorus schlegelii	44.2	6.3	n.d.	n.d.	50.5
Rhacophorus arboreus	53.4	n.d.	n.d.	n.d.	53.4

n.d.: not detectable.

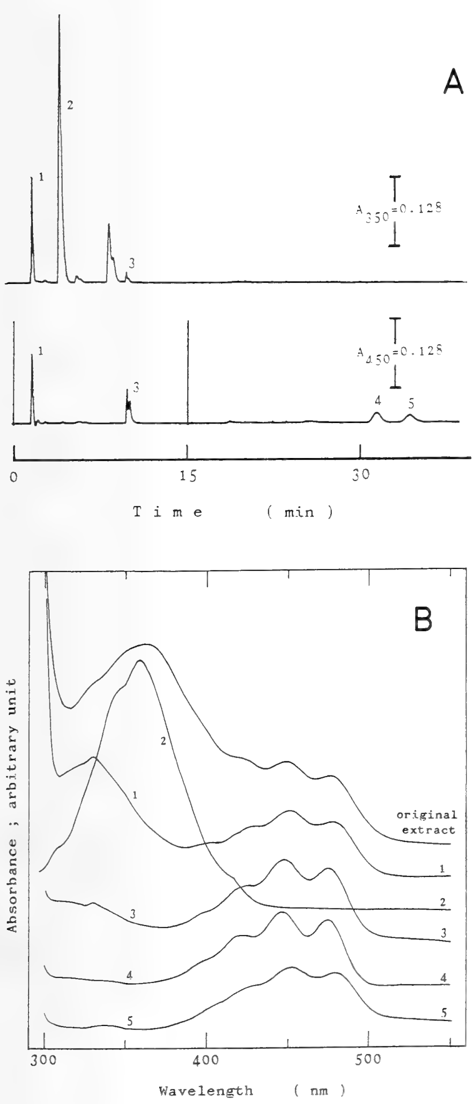

Fig. 3). The main absorption maxima were present at 275 and 285 nm, and the absorbance around 330 nm was about 20% that at 285 nm. Saponification of the substance caused only small decrease in HPLC peaks at the solvent front and induced very small peaks due to retinol isomers. The amount of retinyl esters, if any, must be scarce in the egg of *X. laevis*. Curve 4 in Figure 3 also shows that little carotene is present in the egg.

As was shown in Figure 1B, the egg of *R. schlegelii* contains all-*trans* and 13-*cis* isomers of retinal as the main stock of retinoids; retinyl ester (at the solvent front) seems to be present but the amount might be far less than that of retinal. The yolk of *R. arboreus* also contains all-*trans* retinal as the main stock of retinoids. In any case, *Rhacophorus* eggs contain no 3-dehydroretinal. Table 1 shows the composition and amount of retinal isomers contained in an egg of the three species of frogs. All the frogs contain about 50 pmol retinal(s) per egg, and in the case of *X. laevis* neary equal amounts of retinal and 3-

FIG. 4. Retinoids and carotenoids in a ovary of *X. laevis*. A, elution profiles of an extract obtained from the ovary by the oxime method and analysed on HPLC equipped with two detectors monitoring absorbances at 350 nm (upper) and at 450 nm (lower). Under this HPLC conditions (column: LiChrosorb SI-60, 4×250 mm, eluent: 15% diethylether-0.15% ethanol in *n*-hexane for 15 min followed by 50% diethylether-0.5% ethanol in *n*-hexane, and flow rate: 2 ml/min), the peaks of *syn* all-*trans* retinaloxime and 3-dehydroretinaloxime are cochromatographed (peak 2). B, absorption spectra of the original extract from the ovary and the peak substances separated by HPLC (peaks 1, 2, 3, 4 and 5 in A).

dehydroretinal are present. Plack and Kon [16] have reported that the egg of *Rana temporalia* contains retinal (1.72 mg/g dry matter) and that the proportion of 3-dehydroretinal is 11%, using the Carr-Price method improved by Plack [17].

An interesting problem of the egg retinals is their metabolic origin. To investigate the precursor of the egg retinals, retinoids and carotenoids in the ovary of *X. laevis* were extracted by the oxime method and analysed on HPLC with two detectors monitoring absorbances at 350 and 450 nm (Fig. 4A). The elution profile detected at 350 nm (upper in Fig. 4A) shows a peak at the solvent front (peak 1) besides the peaks of retinaloximes (peak 2); under the eluent conditions, *syn* all-*trans* retinaloxime and *syn* all-*trans* 3-dehydroretinaloxime are not separated. Figure 4A also shows the absence of 3-hydroxyretinal in the ovary [cf. 4]. The elution profile detected at 450 nm (lower in Fig. 4A) shows some peaks suggesting the presence of carotenoids including xanthophyll (peaks 4 and 5) which have higher polarity than carotene. Figure 4B shows the absorption spectra of the peak substances shown in Figure 4A (peaks 1, 2, 3, 4 and 5). Curve 1 shows the absorption bands around 330 nm and in the visible region suggesting the presence of retinyl ester and carotene, respectively. Curve 2 shows the absorption spectrum of retinaloximes, and curves 3, 4 and 5 show the characteristic spectra of carotenoids [cf. 18]. Now, two possible metabolic pathways forming egg retinals can be considered. One is the oxidation of retinol and 3-dehydroretinol, which should have been transported from the liver to the ovary, producing retinal and 3-dehydroretinal, respectively. Another is the formation of retinals from carotenoids. Gawienowski *et al.* [19] have reported that β-carotene is converted to retinal by slices of bovine corpus luteum. In the frog ovary, where both retinals and carotenoids are found, such an enzyme as carotene cleavage enzyme [20, 21] may function to produce retinals from carotenoids.

The change of the retinoid composition in the *Xenopus* egg during developement is now under investigation; the amount and the composition of retinals in the abdomen of the tadpoles remain almost constant till about stage 38. Bridges *et al.* [5] have shown that the visual pigment of *Xenopus* tadpole becomes detectable from stage 39. The retinals in the egg must be a reservoir for the precursor of visual pigment chromophores. The transport and the metabolic change of egg retinals into visual pigment chromophores in the eye is a subject of further investigation.

ACKNOWLEDGMENTS

The authors thank Dr. H. Takasaki (Osaka Kyoiku Univ.) for her kind supply of pairs of *Xenopus laevis* and for advices on rearing them. We thank also Drs. M. Ito, K. Tsukida (Kobe Women's College of Pharmacy) and Y. Kito (Osaka Univ.) for their discussions. This study was supported, in part, by a Grant-in-Aid for Scientific Research from the Ministry of Education, Science and Culture of Japan (No. 61740420 to T. Seki).

REFERENCES

1 Vogt, K. (1983) Is the fly visual pigment a rhodopsin? Z. Naturforsch., **38c**: 329–333.

2 Vogt, K. and Kirschfeld, K. (1984) Chemical identity of the chromophore of fly visual pigment. Naturwissenschaften, **71**: 211–213.

3 Tanimura, T., Isono, K. and Tsukahara, Y. (1986) 3-Hydroxyretinal as a chromophore of *Drosophila melanogaster* visual pigment analyzed by high-pressure liquid chromatography. Photochem. Photobiol., **43**: 225–228.

4 Seki, T., Fujishita, S., Ito, M., Matsuoka, N., Kobayashi, C. and Tsukida, K. (1986) A fly, *Drosophila melanogaster*, forms 11-*cis* 3-hydroxyretinal in the dark. Vision Res., **26**: 255–258.

5 Bridges, C. D. B., Hollyfield, J. G., Witkovsky, P. and Gallin, E. (1977) The visual pigment and vitamin A of *Xenopus laevis* embryos, larvae and adults. Exp. Eye Res., **24**: 7–13.

6 Nieukoop, P. D. and Faber, J. (1956) Normal Table of *Xenopus laevis* (Daudin). North-Holland, Amsterdam.

7 Sakai, M. and Kubota, H. Y. (1981) Cyclic surface changes in the non-nucleate egg fragment of *Xenopus laevis*. Dev. Growth Differ., **23**: 41–49.

8 Groenendijk, G. W. T., De Grip, W. J. and Daemen, F. J. M. (1980) Quantitative determination of retinals with complete retention of their geometric configuration. Biochim. Biophys. Acta, **617**: 430–438.

9 Suzuki, T. and Makino-Tasaka, M. (1983) Analysis of retinal and 3-dehydroretinal in the retina by high-pressure liquid chromatography. Anal.

Biochem., **129**: 111–119.

10 Suzuki, T., Fujita, Y., Noda, Y. and Miyata, S. (1986) A simple procedure for the extraction of the native chromophore of visual pigments: the formaldehyde method. Vision Res., **26**: 425–429.

11 Bridges, C. D. B. and Alvarez, R. A. (1982) Measurement of the vitamin A cycle. In "Methods in Enzymology", Vol. 81, Biomembranes. Ed. by L. Packer, Academic Press, New York, pp. 463–485.

12 Makino-Tasaka, M. and Suzuki, T. (1986) Quantitative analysis of retinal and 3-dehydroretinal by high-pressure liquid chromatography. In "Methods in Enzymology", Vol. 123, Vitamins and coenzymes. Ed. by F. Chytil and D. B. McCormick, Academic Press, New York, pp. 53–61.

13 Seki, T. (1984) Metaretinochrome in membranes as an effective donor of 11-*cis* retinal for the synthesis of squid rhodopsin. J. Gen. Physiol., **84**: 49–62.

14 Plack, P. A., Kon, S. K. and Thompson, S. Y. (1959) Vitamin A_1 aldehyde in the eggs of the herring (*Clupea harengus* L.) and other marine teleosts. Biochem. J., **71**: 467–476.

15 Plack, P. A. (1960) Vitamin A_1 aldehyde in hen's eggs. Nature, **186**: 234–235.

16 Plack, P. A. and Kon, S. K. (1961) A comparative survey of the distribution of vitamin A aldehyde in eggs. Biochem. J., **81**: 561–570.

17 Plack, P. A. (1961) The colorimetric reaction between vitamin A_2 aldehyde and antimony trichloride. Biochem. J., **81**: 556–561.

18 Zechmeister, L. (1962) *Cis-trans* Isomeric Carotenoids, Vitamins A and Arylpolyenes, Springer, Wien.

19 Gawienowski, A. M., Stacewicz-Sapuncakis, M. and Longley, R. (1974) Biosynthesis of retinal in bovine corpus luteum. J. Lipid Res., **15**: 375–379.

20 Goodman, D. S. and Huang, H. S. (1965) Biosynthesis of vitamin A with rat intestinal enzymes. Science, **149**: 879–880.

21 Olson, J. A. and Hayaishi, O. (1965) The enzymatic cleavage of β-carotene into vitamin A by soluble enzymes of rat liver and intestine. Proc. Natl. Acad. Sci., USA., **54**: 1364–1370.

ZOOLOGICAL SCIENCE 4: 483–487 (1987)

Chromosome Numbers in 8 Japanese Species of Sea Urchins

KYOKO SAOTOME

Yokohama City Institute of Health, Takigashira, 1–2–17, Isogo, Yokohama 235, Japan

ABSTRACT—Chromosome numbers were examined in 8 Japanese species of sea urchins. In Regularia, *Glyptocidaris crenularis* belonging to the order Arbacioida had chromosome number of 2n =44 and *Temnopleurus hardwickii, Pseudocentrotus depressus, Strongylocentrotus nudus, Hemicentrotus pulcherrimus* and *Anthocidaris crassispina* belonging to the order Echinoida all showed chromosome numbers of 2n=42. On the other hand, in Irregularia, both *Scaphechinus mirabilis* and *Astriclypeus manni* belonging to the order Clypeasteroida had chromosome number of 2n=46. The chromosome numbers were found to be the same in the species belonging to the same order but differ among three different orders. Arbacioida, Echinoida and Clypeasteroida had chromosome numbers of 2n=44, 2n=42 and 2n=46, respectively.

INTRODUCTION

The echinoid fauna is especially abundant in Japan [1–4] and about 160 species have been ascertained by Shigei [4]. Systematic study on the echinoids has been carried out from the morphological viewpoint, whereas unsolved systematic problems still remain [3]. In the last ten years, biochemical approach has been tried in echinoid phylogeny [5–8] and the biochemical data have been compared with the phylogenetic relationship based on morphological criteria. On the other hand, cytogenetical technique is also considered to provide valuable information for echinoid taxonomy [9]. However, chromosomal reports about Japanese echinoids are too few to discuss systematic problems [10–12]. The reason for inactivity in chromosome study may be that sea urchins have many chromosomes of small size and that clear metaphase plates are not constantly obtained by sectioning method [10] or squash method [11, 12] used so far. Therefore, an air-drying method has been developed to obtain well-spread chromosome preparation from the morula or the early blastula [13].

In this paper, chromosome numbers in 8 species determined by the air-drying method [13] will be discussed concerning echinoid taxonomy.

Accepted January 29, 1987
Received December 16, 1986

MATERIALS AND METHODS

Materials *Glyptocidaris crenularis, Temnopleurus hardwickii*, and *Strongylocentrotus nudus* were provided by the Asamushi Marine Biological Station, Tohoku University. *Pseudocentrotus depressus* was obtained from Tsushima, Nagasaki Prefecture and *Scaphechinus mirabilis* from the Ushimado Marine Laboratory, Okayama University. *Hemicentrotus pulcherrimus, Anthocidaris crassispina* and *Astriclypeus manni* were supplied by the Misaki Marine Biological Station, University of Tokyo.

Eggs and sperm were obtained by injecting 0.3 ml of 0.01 M acetylcholine chloride into body cavity of adult sea urchins. More than five pairs of males and females were used for preparation.

Methods Chromosome preparations were made using the embryos at the morula or the early blastula stage according to the air-drying method previously described [13] with the following modification: 1) Ca-Mg-free sea water [13] or 1 mM 3-amino-1, 2, 4-triazole [14] was used to remove fertilization membrane, 2) division was inhibited by colcemid [13] or colchicine, and 3) concentration of colchicine (0.1–1.0 mg/ml) and hypotonic KCl solution (0–0.075 M) was changed according to species.

RESULTS

Figure 1 shows metaphase plates of 8 species of sea urchins and distribution of the diploid chromosome numbers is summarized in Table 1.

Glyptocidaris crenularis (Fig. 1A) showed chromosome number of 2n=44 in 76.7% of the 73 cells examined (Table 1). Chromosome numbers of *Temnopleurus hardwickii* (Fig. 1B), *Pseudocentrotus depressus* (Fig. 1C), *Strongylocentrotus nudus* (Fig. 1D), *Hemicentrotus pulcherrimus* (Fig. 1E) and *Anthocidaris crassispina* (Fig. 1F) were found to be all 2n=42, and the percentage of cells with 2n=42 was 74.0% in 100 cells, 87.1% in 70 cells, 81.2% in 101 cells, 91.7% in 192 cells and 77.2% in 92 cells examined, respectively (Table 1). Both *Scaphechinus mirabilis* (Fig. 1H) and *Astriclypeus manni* (Fig. 1G) showed the chromosome number of 2n=46 and percentage of cells with 2n =46 was 94.0% in 100 cells and 81.1% in 90 cells examined, respectively (Table 1).

DISCUSSION

In this paper, the clear metaphase plates which are beyond comparison with the metaphase plates already reported about Japanese echinoids [10, 12] have been obtained in many species and chromosome numbers have been exactly counted (Fig. 1).

The chromosome size of sea urchins ranged from about 0.7 μm of the smallest size in *Temnopleurus hardwickii* (Fig. 1B) to about 5 μm of the largest one in *Glyptocidaris crenularis* (Fig. 1A) of the present paper, with a reservation that the chromosomes tend to contract in colchicine or colcemid.

In the distribution of the diploid chromosome numbers (Table 1), the percentage of cells showing the mode was more than 80% in *Pseudocentrotus depressus, Strongylocentrotus nudus, Hemicentro-*

TABLE 1. Distribution of the diploid chromosome numbers in 8 species of sea urchins

Species	Total No. of cells (%)	Chromosome numbers <40	40	41	42	43	44	45	46	47	47<	[2n]
Glyptocidaris	73	1	1	0	3	7	56	2	1	0	2	44
crenularis	100%	1.4	1.4	0	4.1	9.6	76.7	2.7	1.4	0	2.7	
Temnopleurus	100	3	1	12	74	5	3	0	0	0	2	42
hardwickii	100%	3.0	1.0	12.0	74.0	5.0	3.0	0	0	0	2.0	
Pseudocentrotus	70	2	2	4	61	1	0	0	0	0	0	42
depressus	100%	2.9	2.9	5.7	87.1	1.4	0	0	0	0	0	
Strongylocentrotus	101	2	4	10	82	0	0	0	1	1	1	42
nudus	100%	2.0	4.0	9.9	81.2	0	0	0	1.0	1.0	1.0	
Hemicentrotus	192	3	2	7	176	2	2	0	0	0	0	42
pulcherrimus	100%	1.6	1.0	3.6	91.7	1.0	1.0	0	0	0	0	
Anthocidaris	92	3	4	12	71	2	0	0	0	0	0	42
crassispina	100%	3.3	4.3	13.0	77.2	2.2	0	0	0	0	0	
Scaphechinus	100	0	0	0	0	0	2	2	94	1	1	46
mirabilis	100%	0	0	0	0	0	2.0	2.0	94.0	1.0	1.0	
Astriclypeus	90	0	0	1	2	0	4	8	73	1	1	46
manni	100%	0	0	1.1	2.2	0	4.4	8.9	81.1	1.1	1.1	

FIG. 1. Metaphase plates of 8 species of sea urchins. A) *Glyptocidaris crenularis,* B) *Temnopleurus hardwickii,* C) *Pseudocentrotus depressus,* D) *Strongylocentrotus nudus,* E) *Hemicentrotus pulcherrimus,* F) *Anthocidaris crassispina,* G) *Astriclypeus manni,* and H) *Scaphechinus mirabilis.* Bar, 5 μm.

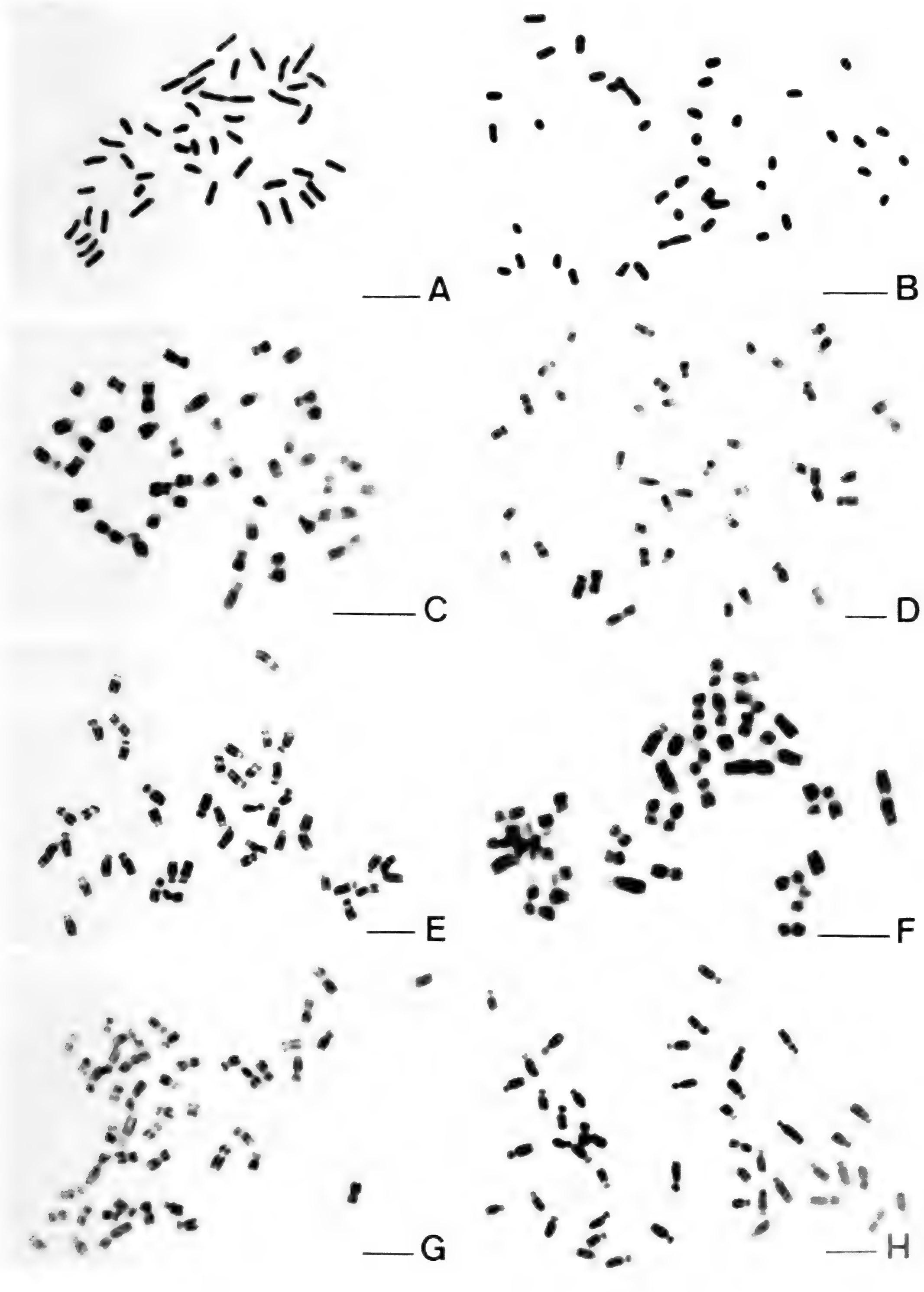
A
B
C
D
E
F
G
H

tus pulcherrimus, *Scaphechinus mirabilis* and *Astriclypeus manni* but was in the level of 70% in *G. crenularis*, *T. hardwickii* and *Anthocidaris crassispina*. The reason for a relatively low percentage in the latter species may be that chromosomes flow out on air-drying owing to weakness of cell membrane after hypotonic treatment.

Chromosome numbers (2n=42) of *H. pulcherrimus* and *A. crassispina* by the air-drying method of this paper were consistent with those reported by Nishikawa [12] using squash method in testis.

Nine species, including *Clypeaster japonicus* described previously [13] and 8 species in this paper (Table 1), can be divided into three groups on the basis of the chromosome numbers; the first group has 2n=44, consisting of *G. crenularis*, the second one has 2n=42, including *T. hardwickii, P. depressus, S. nudus, H. pulcherrimus* and *A. crassispina*, and the third one has 2n=46, containing *S. mirabilis, A. manni* and *C. japonicus*. When the relationship among the three groups in the light of classification from morphological standpoint was examined, the difference in chromosome number well corresponded to the difference in systematic order of Shigei [3]; the first, the second and the third groups corresponded to the order Arbacioida of Regularia, the order Echinoida of Regularia and the order Clypeasteroida of Irregularia, respectively. The chromosome numbers, therefore, were found to be the same in the species belonging to the same order but differ among three different orders; Arbacioida, Echinoida and Clypeasteroida. Concerning foreign echinoids, *Arbacia punctulata* [15, 16] and *Arbacia lixula* [9] belonging to the order Arbacioida have chromosome number of 2n=44, and *Sphaerechinus granularis* [9], *Psammechinus microtuberculatus* [9] and *Paracentrotus lividus* [17] belonging to the order Echinoida have 2n=42. These data coincided with the present results. In the comparison, the previous data obtained by sectioning method were excluded for low reliability [18].

Concerning chromosome numbers, Arbacioida, Echinoida and Clypeasteroida have respectively 2n=44, 2n=42 and 2n=46, as already noted. Colombera *et al.* [19] has reported chromosome number of *Cidaris cidaris* belonging to Cidaroida as 2n=44, with reserve, because of insufficient numbers examined (20 metaphase plates) and the chromosome number of *Diadema setosum* belonging to Diadematoida has been reported as 2n=44 by Shingaki and Uehara [20].

On the other hand, concerning echinoid phylogeny based on morphological viewpoint, although there are various disagreements in detail [3, 21–23], it is generally considered that Cidaroida is a primitive group, from which Diadematoida and Arbacioida have evolved and that Echinoida and Clypeasteroida are newer groups, the former being descended from Arbacioida [3]. Further, Shigei [3] has proposed from the morphological and paleontological standpoints that Irregularia separated from Regularia on the way of evolution from Cidaroida to Arbacioida after Diadematoida branched off (Fig. 2). If chromosome numbers of Cidaroida and Diadematoida are taken as 2n=44 in spite of knowledge of a single species, diagram of phylogeny based on chromosome numbers may be drawn like Figure 2. In the diagram, there may be at least three chromosome evolutions; 1) Diadematoida (2n=44) and Arbacioida (2n=44) have evolved from Cidaroida (2n

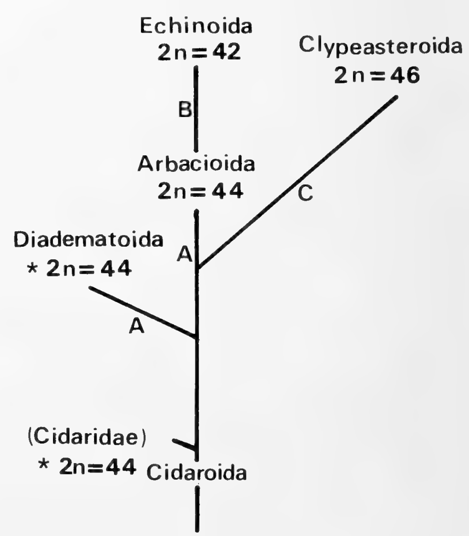

Fig. 2. Phylogeny of echinoids based on chromosome numbers. The scheme was drawn according to the phylogenetic diagram of Shigei [3] with simplification. *Diploid chromosome number from the knowledge of a single species.

=44) without change in chromosome number (A of Fig. 2), 2) chromosome number has decreased from 2n=44 to 2n=42 in the evolution from Arbacioida (2n=44) to Echinoida (2n=42) (B of Fig. 2) and 3) chromosome number has increased from 2n=44 to 2n=46 in the evolution from Regularia to Clypeasteroida (2n=46) of Irregularia (C of Fig. 2). The mechanism about decrease and increase in chromosome number is still unknown. Though Robertsonian rearrangement may be considered concerning the mechanism, comparison of arm number, banding pattern and karyotype will be necessary to solve it. Karyotype analysis is now in progress.

ACKNOWLEDGMENTS

The author expresses her gratitude to Prof. Emer. K. Dan of Tokyo Metropolitan University and to Dr. M. Shigei, University of Tokyo, for valuable discussion. Thanks are also due to the staff of the Marine Biological Stations of the University of Tokyo, Tohoku University and Okayama University and to Waseda University for their kind supply of materials.

REFERENCES

1 Nisiyama, S. (1966) The echinoid fauna from Japan and adjacent regions. Part I. Palaeontol. Soc. Japan, Spec. Pap., No. 11.
2 Nisiyama, S. (1968) The echinoid fauna from Japan and adjacent regions. Part II. Palaeontol. Soc. Japan, Spec. Pap., No. 13.
3 Shigei, M. (1974) Echinoids. In "The Systematic Zoology 8 (2)—Echinoderms". Nakayama Book Company, Tokyo, pp. 208–332. (In Japanese)
4 Shigei, M. (1986) The Sea Urchins of Sagami Bay. Maruzen Co., Ltd., Tokyo.
5 Nagaoki, S and Isono, N. (1981) Free amino acids in unfertilized sea urchin eggs. Hiyoshi Sci. Rev. (Keio Univ.), **16**: 93–110. (In Japanese)
6 Suzuki, N., Hoshi, M., Nomura, K. and Isaka, S. (1982) Respiratory stimulation of sea urchin spermatozoa by egg extracts, egg jelly extracts and egg jelly peptides from various species of sea urchins: Taxonomical significance. Comp. Biochem. Physiol., **72A**: 489–495.
7 Matsuoka, N. (1985) Biochemical phylogeny of the sea-urchins of the family Toxopneustidae. Comp. Biochem. Physiol., **80B**: 767–771.
8 Matsuoka, N. (1986) Further immunological study on the phylogenetic relationships among sea-urchins of the order Echinoida. Comp. Biochem. Physiol., **84B**: 465–468.
9 Colombera, D. (1974) Chromosome evolution in the phylum Echinodermata. Z. Zool. Syst. Evol.-forsch., **12**: 299–308.
10 Makino, S. and Niiyama, H. (1947) A study of chromosomes in echinoderms. J. Fac. Hokkaido Univ. Ser. VI, Zool., **9**: 225–232.
11 Makino, S. and Alfert, M. (1954) To the question of somatic reduction divisions in sea urchin micromeres. Experientia, X/**12**: 489–490.
12 Nishikawa, S. (1961) Notes on the chromosomes of two species of echinoderms, *Hemicentrotus pulcherrimus* and *Anthocidaris crassispina*. Zool. Mag., **70**: 425–428. (In Japanese)
13 Saotome, K. (1982) A method for chromosome preparation of sea urchin embryos. Stain Technol., **57**: 103–105.
14 Showman, R. M. and Foerder, C. A. (1979) Removal of the fertilization membrane of sea urchin embryos employing aminotriazole. Exp. Cell Res., **120**: 253–255.
15 Auclair, W. (1965) The chromosomes of sea urchins, especially *Arbacia punctulata*; A method for studying unsectioned eggs at first cleavage. Biol. Bull., **128**: 169–176.
16 German, J. (1966) The chromosomal complement of blastomeres in *Arbacia punctulata*. Chromosoma (Berl.), **20**: 195–201.
17 Colombera, D., Venier, G. and Vitturi, R. (1977) Chromosome and DNA in the evolution of echinoderms. Biol. Zbl., **96**: 43–49.
18 Makino, S. (1950) A Review of the Chromosome Numbers in Animals. Hokuryukan, Tokyo, pp. 31–33. (In Japanese)
19 Colombera, D., Vitturi, R. and Zanirato, L. (1977) Chromosome number of *Cidaris cidaris* . Acta Zool. (Stockh.), **58**: 185–186.
20 Shingaki, M. and Uehara, T. (1984) Chromosome studies in the several species of sea urchin from Okinawa. Zool. Sci., **1**: 1008. (Abstract, In Japanese)
21 Mortensen, T. (1928–1952) A Monograph of the Echinoidea. Vol. 1–15. C. A. Reitzel, Copenhagen.
22 Durham, J. W. and Melville, R. V. (1957) A classification of echinoids. J. Paleontol., **31**: 242–272.
23 Philip, G. M. (1965) Classification of echinoids. J. Paleontol., **39**: 45–62.

ZOOLOGICAL SCIENCE 4: 489–496 (1987)

Twin Formation in *Xenopus laevis* Eggs Centrifuged before First Cleavage

Mutsuki Kunieda and Masami Wakahara[1]

Zoological Institute, Faculty of Science, Hokkaido University, Sapporo 060, Japan

ABSTRACT—Twin formation was studied in the fertilized *Xenopus* eggs by means of low speed centrifugation ($15\text{–}30 \times g$) for a short period (20 sec to 5 min) before first cleavage. Dejellied eggs were embedded in gelatin with a vertical orientation (animal pole up), but randomly oriented with reference to the sperm entrance site. They were then spun with the centrifugal force vector at right angles to the animal-vegetal axis. When the eggs were centrifuged at T=0.3–0.6 (30–60% of the time interval to first cleavage), a large number of twin embryos developed, whereas when centrifuged after T=0.7 twin embryos were almost never obtained. Morphological features of the twin embryos were briefly described. They showed a rather continuous spectrum from almost normal to completely double-axes embryos. The twin embryos were tentatively grouped into 6 categories based on the degree of twinning. Twin embryos with clear double-axes were divided into 3 groups in regard to the spatial relationships between the two axes. All double-axes embryos developed from the gastrulae which had shown two blastoporal lips. Possible mechanisms of twinning are discussed in terms of a postcentrifugal modification of the localization of the "dorsal determinants" which specify the future dorsal side of the embryos.

INTRODUCTION

It is well known that an amphibian egg can produce two complete embryos after separation of the blastomeres at the 2-cell stage [1]. This leads us to conclude that an amphibian egg has an ability to produce two complete sets of axial structures, including such dorsal axial structures as notochord, neural tube and somites. In fact, several experimental treatments of amphibian eggs are known to cause twin formation: Delayed fertilization (overripeness of eggs) in *Rana pipiens* [2]; rotation of eggs in *R. nigromaculata* [3] and *Xenopus laevis* [4–6]; and centrifugation of eggs in *Bufo vulgaris* [7] and *X. laevis* [5, 8, 9]. If an amphibian egg has the ability to produce two complete sets of axial strucutres, a regulation must naturally occur to insure that a single axial structure rather than two axes normally develops. Thus, analysing the twin by means of centrifugation or egg rotation will aid in understanding the development of dorsal-ventral polarity and also will provide information concerning the regulation of pattern formation in normal development.

We have recently succeeded to demonstrate possible existence of the "dorsal determinants", which specify the future dorsal side of the embryos, in fertilized *Xenopus* eggs by means of cytoplasmic withdrawal experiments [10]. At present, it seems much important to know the behavior of the "determinants" during the first cell cycle to elucidate the mechanisms of the establishment of the dorsal-ventral polarity in amphibian eggs. Twin formation by centrifugation is expected to be a biological tool for analysing the localization of the "dorsal determinants".

In this paper, we first describe the morphological features of twin embryos developed from the centrifuged *Xenopus* eggs, and then describe the conditions of centrifugation for obtaining twin embryos. The results obtained support the view that the postcentrifugal modification of the localization of the "dorsal determinants" which specify the future dorsal side of the embryos [10] causes

Accepted January 21, 1987
Received November 8, 1986
[1] To whom reprints should be requested.

the twin formation.

MATERIALS AND METHODS

Source of embryos

The two colonies of *Xenopus laevis* which are maintained in our laboratory, J and HD groups [11] were used. Eggs from hormone-stimulated female were rinsed briefly with Steinberg's solution and then inseminated with a testis homogenate. Eggs and embryos were usually maintained at 15°C unless mentioned otherwise [12]. Eggs before first cleavage were staged according to the fraction of the interval between fertilization (T=0) and first cleavage (T=1.0) at the time of the relevant manipulation. Embryos were staged according to Nieuwkoop and Faber [13].

Embedment of eggs in gelatin

Twenty minutes after fertilization eggs were dejellied in 2.5% thioglycolic acid (pH 8.2) and washed four times in 10% Steinberg's solution. Nine percent gelatin was prepared according to Black and Gerhart [14], with some modifications: penicillin G potassium (100 IU/ml) and streptomycin sulfate (0.1 mg/ml) were added instead of gentamycin. Approximately 40 eggs were pipetted at once into molten 9% gelatin (25°C) and then tranferred to a plastic dish (Falcon 1008) containing 2.5 ml molten gelatin. Almost all eggs maintained their normal, vertical orientation (animal pole up) in the molten gelatin. The fewer eggs which had rotated or inverted when tranferred were quickly oriented with forceps to orient the animal pole up. Eggs were aligned approximately along the center line of the dish so that all the eggs could be exposed to the similar centrifugal forces. After the eggs were arranged the dish was placed on an ice-chilled copper plate for 2 min and then placed in a 15°C water bath for 10 min to complete the solidification of the gelatin.

Centrifugation of embedded eggs

Dishes with eggs were mounted on a holder made from a plastic centrifuge tube. The holders were placed on the swing rotor of a clinical centrifuge and spun at 15°C. The duration of centrifugation indicated below included only the time while the given centrifugal forces were operating (i.e. acceleration and deceleration periods of approximately 1 min were not included in the "duration"). The centrifugal force vector was at right angles to the animal-vegetal axis of the eggs. Since the eggs were not oriented to bring the sperm entrance site (SES) to the same direction when embedded in the gelatin, the centrifugal force vector varied from egg to egg with respect to the SES.

Observation of embryos

After centrifugation eggs were incubated at 15°C in the normal, vertical orientation (animal pole up) in gelatin. When the embryos developed to stage 4 (8-cell stage) they were freed from the gelatin by incubating the dish in 35°C water bath for a short period (1–2 min). Embryos freed from gelatin were washed twice with 10% Steinberg's solution. Developing embryos were periodically observed until they developed to stage 29. Dead and abnormal (except for twinning) embryos were discarded. Eggs and embryos were fixed with a modified Bouin-Holland or Smith's fixative. Serial sections of 8 μm thick were stained with Delafield's hematoxylin and eosin.

RESULTS

Brief description of morphological features of twin embryos which developed from centrifuged eggs

As a starting point for experimental analysis, a general description of the morphological features of twin embryos which developed from centrifuged *Xenopus* eggs was given. Although Black and Gerhart [9] described in detail the conditions of centrifugation for obtaining twin embryos, there has been no systematic description on twin embryos developed from the centrifuged eggs.

Approximately 400 "twin embryos" (which included complete and incomplete double-axes embryos and single-axis embryos with a "wide" sucker; cf. "imbalanced embryos" of Cooke [6]) were obtained. They showed a continuous spectrum in external and internal morphology from

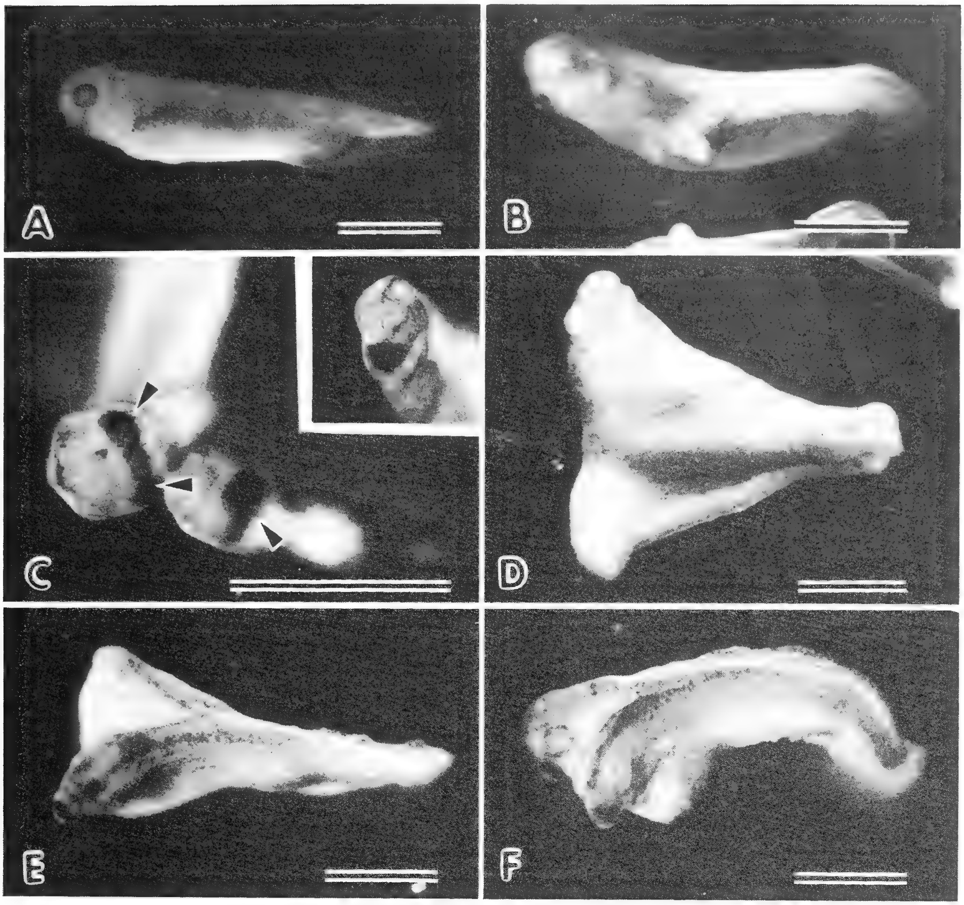

FIG. 1. Typical external views of the "twin embryos" developed from the eggs centrifuged before first cleavage, showing 6 types of twinning, which were divided tentatively based mainly upon the external morphological features. (A) Normal control embryo. Lateral view. (B), Type 1, almost normal but displaying a small protuberance. Lateral view. (C), Type 2, single-axis embryo but containing an apparent wide sucker (an arrowhead). Type 3, single-axis embryo but containing two distinct suckers (two arrowheads). Compare with normal control embryo (inset). Frontal view. (D) Type 4, double-axes embryo with no distinct sucker. Lateral view. (E), Type 5, double-axes embryo one of which contains a distinct sucker, but the other lacks a sucker. Dorsolateral view. (F), Type 6, double-axes embryo both of which show distinct suckers respectively. Lateral view. Bars: 1 mm.

almost normal to complete double-axes. We divided these embryos into the following 6 categories, based mainly upon the external morphological features (Fig. 1):

Type 1: almost normal (single-axis) embryos, but displaying a small protuberance similar to a secondary embryo (Fig. 1B).

Type 2: almost normal (single-axis) embryos, but containing a wide sucker (Fig. 1C).

Type 3: single-axis embryos with two distinct suckers (Fig. 1C).

Type 4: double-axes embryos with no distinct sucker (Fig. 1D).

Type 5: double-axes embryos, one of which contains a distinct sucker but the other lacks a sucker (Fig. 1E).

Type 6: double-axes embryos both of which show distinct suckers (Fig. 1F).

Of these 6 types, only Types 4, 5 and 6 showed complete duplication of external dorsal axial struc-

tures. Internal inspections revealed, however, similar indication of duplication of dorsal axial structures (such as somites) even in Types 1, 2 and 3 embryos. Thus, all embryos that showed the morphological features described above (Type 1–Type 6) were tentatively designated as "twin embryos".

Figure 2 shows typical internal structures of several twin embryos. In general, Type 6 twins (two axes–two suckers) contained two complete sets of dorsal axial structures in the half with the sucker and one incomplete set of the axial struc-

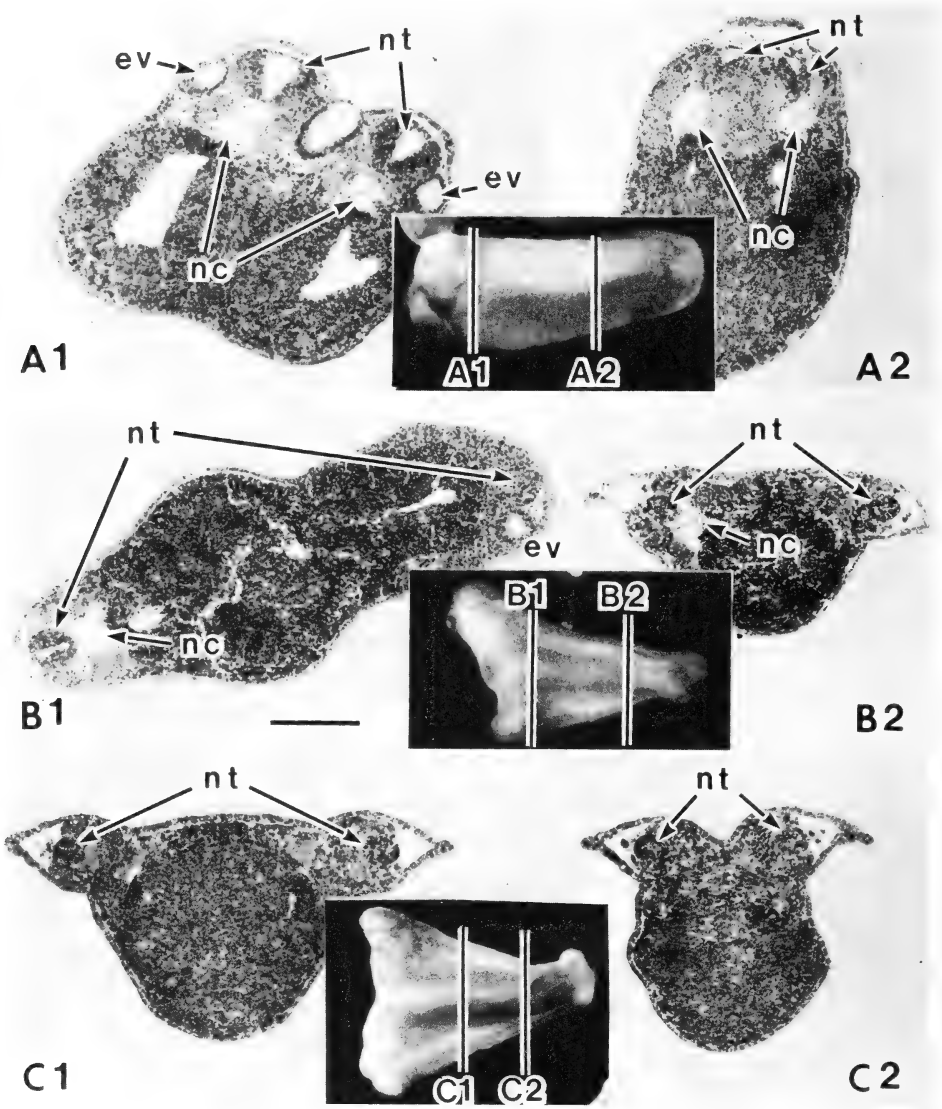

FIG. 2. Internal structures of twin embryos developed from the centrifuged eggs. The level of the sections was indicated in the inserted figures. (A), Type 6 twin (two axes—two suckers), showing two distinct neural tubes (nt) and notochords (nc). (B), Type 5 twin (two axes—one sucker), showing two neural tubes but one distinct notochord. (C), Type 4 twin (two axes—no sucker), showing two neural tubes but no distinct notochord. ev, ear vesicle. Bar: 100 μm.

tures in the other half. The notochord was underdeveloped in this half and so only one intact notochord was observed in the histological sections (Fig. 2B). Similarly, Type 4 twins (two axes-no sucker) showed two incomplete sets of dorsal axial structures: notochordal structures were underdeveloped, but neural tube-like structures were usually developed in both halves of the embryo (Fig. 2C).

Spatial relationships between the two axes were different among embryos regardless of the type of the twinning. Typically, twin embryos were divided into three groups; face-to-face (Fig. 2B), side-by-side (Fig. 2A) and in between (Fig. 2C). The spatial relationship depended upon the original location of the two dorsal lips of the blastopores, or the direction of the invaginations (Fig. 3). Face-to-face twins originated from the embryos which had shown the two dorsal lips just opposite to each other (Fig. 3C). Side-by-side twins were derived from the embryos which had had two distinct dorsal lips on one side of the embryo (Fig. 3B).

Relationship between centrifugation conditions and frequency of twin formation

Eggs were centrifuged at T=0.4–0.6 with two centrifugal forces (15 and 30×*g*) for different periods to establish optimal conditions of centrifugation for obtaining twin embryos (Table 1). The centrifugal force vector was at right angles to the animal-vegetal axis. The data in Table 1 represent 6 experiments using 3 different females. As controls, 384 eggs were embedded in gelatin but not centrifuged. They were freed from the gelatin after stage 4 and maintained in 10% Steinberg's solution thereafter in the same fashion as the centrifuged embryos. Approximately half of them were alive at stage 29. Only one embryo from 384 eggs (0.2% of eggs used or 0.5% of embryos alive at stage 29) twinned. In contrast, many twinned embryos developed from centrifuged eggs: 46 twins (13.6% of eggs centrifuged or 31.1% of the embryos alive at stage 29) developed from 339 eggs centrifuged at 30×*g* for 1 min. Although variations in survival and frequency of twin formation were considerably large from one experiment to another, it was clear that low speed centrifugation caused twin formation. When the eggs were spun at 15×*g* for 1 min or 5 min, a high frequency twinning occurred. At a higher centrifugal force (30×*g*) shorter periods of centrifugation (20 sec or 1 min) was sufficient for high frequency twinning.

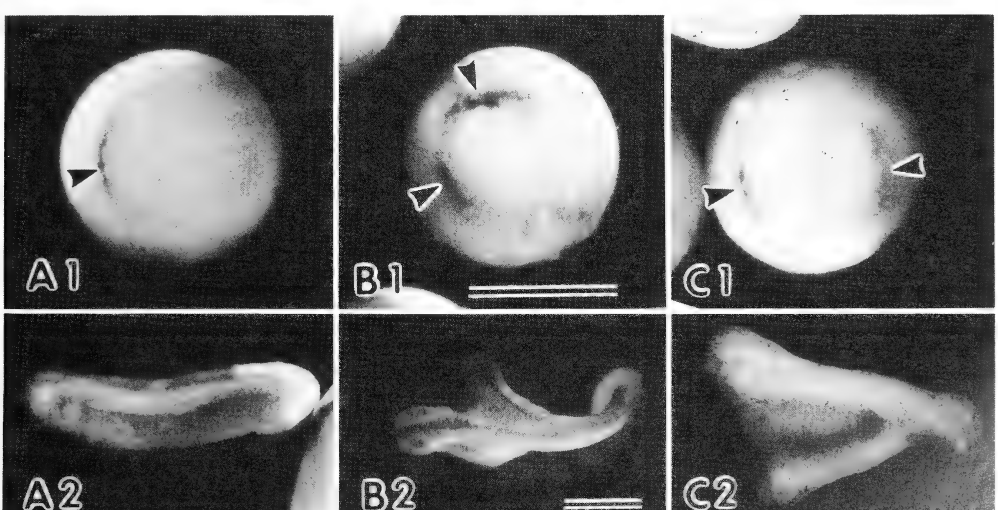

FIG. 3. Bottom views of the early gastrula embryos, showing the spatial relationship of two dorsal lips of the blastopore (upper, arrowheads) and the resulting tailbud embryos (bottom). (A), Normal control. (B), Typical "side-by-side" type twin. (C), Typical "face-to-face" type twin. Bars: 1 mm.

TABLE 1. Frequency of twin formation under various centrifugation conditions*

Conditions of centrifugation		No. of eggs centrifuged	No. of embryos at stage 29 alive	twinnned
$1\times g$	0 min	384	187 (48.7%)	1 (0.5%)**
	20 sec	331	64 (19.3%)	4 (6.3%)
$15\times g$	1 min	257	108 (42.0%)	25 (23.1%)
	5 min	153	34 (22.2%)	7 (19.3%)
	20 sec	335	88 (26.3%)	17 (19.3%)
$30\times g$	1 min	339	148 (43.7%)	46 (31.1%)
	5 min	161	9 (5.6%)	1 (11.1%)

* Fertilized *Xenopus* eggs from 6 different females were centrifuged at T=0.4–0.6, with a centrifugal force vector at right angles to the animal-vegetal axis.

** Percent live embryos at stage 29 which displayed twinning.

Stage sensitivity of the egg to centrifugation

In a previous study [14], the exact stage sensitivity of the egg to centrifugal effects on modification of the orientation of *Xenopus* embryonic axis was determined during first cell cycle, showing three different phases of the centrifugal effects; prior to T=0.4, during T=0.4–0.7 and after T=0.7. Thus, we attempted to determine the stage sensitivity of the egg to centrifugal effects on the twin formation. Eggs were centrifuged at $15\times g$ for 5 min at various periods in the first cell cycle. The centrifugal force vector was at right angles to the animal-vegetal axis of the eggs. Figure 4 shows data summarized from 6 experiments using 6 different females. Although there were wide variations in the rate of twin formation among the experiments, it was clear that twin embryos developed largely from eggs centrifuged in the period of T=0.3–0.6. No twin embryos were observed from eggs centrifuged after T=0.7.

DISCUSSION

It is clear that low speed centrifugation (15 or $30\times g$) at right angles to the egg's animal-vegetal axis causes twin formation in *Xenopus laevis* embryos. The results reported here are consistent with the recent studies by Black and Gerhart [9]. Thus, a fertilized *Xenopus* egg has an ability and probably materials to produce two complete sets of the body plan.

Since every twin embryo was always developed

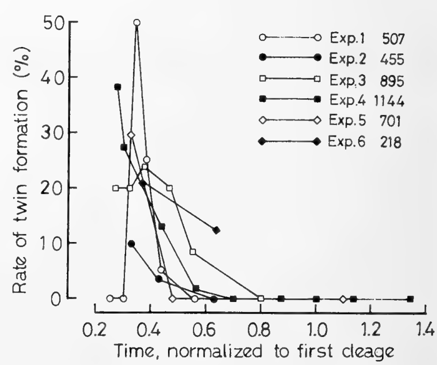

FIG. 4. Stage sensitivity of *Xenopus* eggs to centrifugation on the twin formation. Fertilized eggs from 6 different females were centrifuged ($15\times g$ for 5 min) at various periods in the first cleavage, with a centrifugal force vector at right angles to the animal-vegetal axis of the eggs. Number on right-top indicates the numbers of eggs centrifuged in each experiment. No twin embryos were observed from eggs centrifuged after T=0.7.

from the gastrula which showed two dorsal lips and furthermore the spatial relationship between the two axes of twin embryos depended upon the original location of the two blastoporal lips (Fig. 3), twin formation relates inevitably to the problems how and where the dorsal lip is specified, or more generally, of the establishment of the dorsal-ventral polarity during the early development of embryos. Because the place where cells of the blastopore start to invaginate is known to make the future dorsal side without exceptions [10], the location of the dorsal lip can serve as a manifestation of the ultimate dorsal-ventral polarity. In this respect, the dorsal-most vegetal cells of the 32- or 64-cell *Xenopus* embryo are reported to contain a set of determinants which enable them to induce neighboring cells to undertake dorsal axis formation [15, 16]. Furthermore, the dorsal-vegetal cells of the 8-cell embryo are known to receive already an ability to form dorsal axial structures [17, 18]. Provided that the set of "dorsal determinants", which are recently demonstrated to exist in fertilized *Xenopus* eggs by means of cytoplasmic withdrawal experiments [10], specifies the location of the dorsal lip, twin formation by centrifugation is considered to be involved in altered localization of the "dorsal determinants" after centrifugation of egg. That is, normal arrangements of the egg cytoplasm are modified by centrifugation or post-centrifugal rearrangements or the egg contents [14]. Presumably, a bifurcation of the "dorsal determinants" occurs. However, the mechanisms involved in the modification of the localization or partitioning of the "dorsal determinants" by centrifugation is complex and still remained to be clarified.

Recent studies have clearly demonstrated that centrifugations cause a stage-specific modification of the dorsal-ventral polarity: When centrifuged before T=0.4, the future dorsal side is specified in the centrifugal side of the eggs but in the centripetal side of the eggs after T=0.4 centrifugation, irrespectively of the sperm entry site [14]. Centrifugation between T=0.4–0.45 causes twin formation [9]. This stage-specific effect of centrifugation for obtaining twin embryos was confirmed in this work (Fig. 3). Presumably, the stage-specific effects of centrifugation on the modification of the future dorsal-ventral polarity are involved in the drastic changes in the cytoplasmic consistency during the first cell cycle of the fertilized eggs [19].

This is the first description of the morphological diversity of twin embryos developed from the centrifuged eggs. As illustrated in Figures 1 and 2 they showed a rather continuous spectrum in external and internal morphology from an almost normal to a complete double-axes embryos. This variability in twinning is probably due to the degree and localization to which bifurcation of the dorsal determinants after the centrifugation occurs: When the "dorsal determinants" are divided evenly into two groups of the vegetal blastomeres at 32- or 64-cell embryo [15, 16], complete double-axes embryos will result, whereas uneven partitioning of the "determinants" results in incomplete twin embryos. Spatial relationship between two axes was also shown to be continuous from face-to-face to side-by-side twin (Fig. 3). When the "determinants" are divided into just opposite to each other face-to-face twin will result, whereas partitioned into two distinct sites on one side of the egg results in side-by-side twin. Twin embryos developed from the centrifuged eggs were divided into 6 categories to allow further quantitative analyses of the centrifugal effects on twinning and the modification of the "dorsal determinants".

ACKNOWLEDGMENTS

We are grateful to Prof. G. M. Malacinski (Indiana University, Bloomington, Indiana) for his critical reading of the manuscript and valuable discussions. Supported, in part, by Grants-in-Aid for Scientific Research from the Ministry of Education, Science and Culture of Japan (60440100, 60540452).

REFERENCES

1 Kageura, H. and Yamana, K. (1983) Pattern regulation in isolated halves and blastomeres of early *Xenopus laevis*. J. Embryol. Exp. Morphol., **76**: 221–234.

2 Witschi, E. (1952) Overripeness of the egg as a cause of twinning and teratogenesis: A review. Cancer Res., **12**: 763–786.

3 Kubota, T. (1967) A regional change in the rigidity of the cortex of the egg of *Rana nigromaculata* following extrusion of the second polar body. J.

Embryol. Exp. Morphol., **17**: 331–340.

4 Kirschner, M., Gerhart, J. C., Hara, K. and Ubbels, G. A. (1980) Initiation of the cell cycle and establishment of bilateral symmetry in *Xenopus* eggs. Symp. Soc. Dev. Biol., **38**: 187–215.

5 Gerhart, J., Ubbels, G. A., Black, S., Hara, K. and Kirschner, M. (1981) A reinvestigation of the role of the grey crescent in axis formation in *Xenopus laevis*. Nature, **292**: 511–516.

6 Cooke, J. (1986) Permanent distortion of positional system of *Xenopus* embryo by brief perturbation in gravity. Nature, **319**: 60–63.

7 Motomura, I. (1935) Determination of the embryonic axis in eggs of amphibia and echinoderms. Sci. Rep. Tohoku Univ. (Ser. 4), **10**: 211–245.

8 Young, R. S., Deal, P. H., Souza, K. A. and Whitfield, O. (1970) Altered gravitational field effects on the fertilized frog egg. Exp. Cell Res., **59**:267 –271.

9 Black, S. D. and Gerhart, J. C. (1986) High-frequency twinning of *Xenopus laevis* embryos from eggs centrifuged before first cleavage. Dev. Biol., **116**: 228–240.

10 Wakahara, M. (1986) Modification of dorsal-ventral polarity in *Xenopus laevis* embryos following withdrawal of egg contents before first cleavage. Dev. Growth Differ., **28**: 543–554.

11 Katagiri, Ch. (1978) *Xenopus laevis* as a model for the study of immunology. Dev. Comp. Immunol., **2**: 5–14.

12 Neff, A. W., Wakahara, M., Jurand, A. and Malacinski, G. M. (1984) Experimental analyses of cytoplasmic rearrangements which follow fertilization and accompany symmetrization of inverted *Xenopus* eggs. J. Embryol. Exp. Morphol., **80**: 197–224.

13 Nieuwkoop, P. D. and Faber, J. (1956) Normal Table of *Xenopus laevis* (Daudin), North-Holland Publ., Amsterdam.

14 Black, S. D. and Gerhart, J. C. (1985) Experimental control of the site of embryonic axis formation in *Xenopus laevis* eggs centrifuged before first cleavage. Dev. Biol., **108**: 310–324.

15 Gimlich, R. L. and Gerhart, J. C. (1984) Early cellular interactions promote embryonic axis formation in *Xenopus laevis*. Dev. Biol., **104**: 117–130.

16 Gimlich, R. L. (1985) Cytoplasmic localization and chordamesoderm induction in the frog embryo. J. Embryol. Exp. Morphol., **89**: Suppl., 98–111.

17 Kageura, H. and Yamana, K. (1984) Pattern regulation in defect embryos of *Xenopus laevis*. Dev. Biol., **101**: 410–415.

18 Kageura, H. and Yamana, K. (1986) Pattern formation in 8-cell composite embryos of *Xenopus laevis*. J. Embryol. Exp. Morphol., **91**: 79–100.

19 Elinson, R. P. (1983) Cytoplasmic phases in the first cell cycle of the activated frog egg. Dev. Biol., **100**: 440–451.

ZOOLOGICAL SCIENCE 4: 497–521 (1987)

A Histological Survey on the Development of Circumventricular Organs in Various Vertebrates

KAZUHIKO TSUNEKI

Department of Biology, Shimane University, Matsue, Shimane 690, Japan

ABSTRACT—The development of various circumventricular organs was studied histologically in the lamprey, smelt, catfish, guppy, salamander, frog, lizard, chick, and mouse. The circumventricular organs that appear first in ontogeny are usually the pineal and subcommissural organ. The neurohypophysis (median eminence and neural lobe) also differentiates relatively early in ontogeny. These epithalamic and hypothalamic organs may be fundamental circumventricular organs of vertebrates. Roughly speaking, the choroid plexuses, paraphysis, and paraventricular organ differentiate at about the same time as the neurohypophysis does. The organum vasculosum laminae terminalis, subfornical organ, and area postrema differentiate much later in ontogeny. The developmental sequence of the circumventricular organs roughly corresponds to the phylogenetic development of these organs in a series of vertebrates.

INTRODUCTION

The ventricular surface of the vertebrate brain is specialized at several places as circumventricular organs (CVOs) [1]. In previous papers [2, 3], I surveyed the occurrence of various CVOs in a series of vertebrates, paying special attention to lower groups, and discussed the phylogeny of these organs. In these papers, however, I did not refer to the ontogeny of the CVOs. Nevertheless, the pertinent description and discussion on the development of these organs in various vertebrates are obviously indispensable for understanding the overall morphological and evolutionary characteristics of the CVO system in vertebrates. This study is an attempt to describe concisely the development of various CVOs in several representative vertebrates and to discuss the characteristics of the development of these organs.

In this paper, all CVOs in the brains of various vertebrates are together dealt with. This treatment is apparently necessary for relevant comparisons among organs and among animals. There are a large number of papers dealing with the development of the CVOs, especially in higher vertebrates. However, most papers deal with a single organ in a single species (e.g. the development of the hypophysis in the mouse, the development of the pineal in the chick, and so on). This kind of detailed work focusing on a particular aspect is of course important to characterize each organ in each animal, but does not necessarily allow adequate comparisons among organs and among animals. For appropriate comparisons, all organs should be examined in various vertebrate groups chronologically under the same viewpoint. This kind of comparison is aimed in this paper. The result may serve as a bird's-eye view on the developmental patterns of the vertebrate CVOs. The review of the literature is kept in minimum, because it is obviously not the purpose of this study and is not indispensable either for the present purpose. The numerous references on the topic may be found in extensive reviews such as Studnička [4], Bargmann [5], Wingstrand [6], Leonhardt [1], and Vollrath [7].

Accepted December 29, 1986
Received October 30, 1986

MATERIALS AND METHODS

The development of the following 10 species was examined: the brook lamprey, *Lampetra reissneri*; the smooth dogfish, *Mustelus manazo*; the Japanese smelt, *Hypomesus nipponensis*; the Far Eastern catfish, *Silurus asotus*; the guppy, *Poecilia reticulata*; the hynobiid salamander, *Hynobius*

nebulosus; the ranid frog, *Rana japonica*; the lacertid lizard, *Takydromus tachydromoides*; the domestic chick, *Gallus gallus*; and the albino mouse, *Mus musculus*.

In *Lampetra reissneri*, fertilized eggs were obtained through natural spawning of mature adults in a laboratory aquarium. Fractions of embryos and larvae were fixed at appropriate intervals (Table 1). Developmental stages were determined according to the criteria made for *Petromyzon marinus* [8]. In addition, larvae (ammocoetes) of about 10 cm in total length were collected from a river and their heads were fixed.

In *Mustelus manazo*, intra-uterine embryos were obtained from a pregnant female of 88 cm in total length. These embryos were about 7 cm in total length and possessed well developed external gills. These were only dogfish embryos that were available for this study (Table 2).

In *Hypomesus nipponensis*, fertilized eggs were obtained by artificial insemination (dry method). They were attached to the nylon mesh and kept in a laboratory tank. Eight developmental stages of embryos and larvae were studied (Table 3).

In *Silurus asotus*, fertilized eggs were obtained through natural spawning of mature adults in the laboratory aquarium. Ten developmental stages of embryos and larvae were examined (Table 4). In addition to these materials reared in the laboratory, juveniles of about 15 mm in total length were captured from a river and their heads were fixed.

In *Poecilia reticulata* (flamingo variety), pregnant females of varying degrees of bulging and darkening of the belly were sacrificed and the embryos were taken out and fixed. In addition to the embryos, swimming larvae of two different stages were examined (Table 5).

In *Hynobius nebulosus*, egg sacs were collected from a pool and were kept in a laboratory tank. Developmental stages were determined according to the illustrations of embryos and larvae of *Hynobius nigrescens* by Usui and Hamsaki (*sic*, probably Hamasaki) [9] (Table 6). However, accurate determination of stages was often difficult, because the illustrations made by Usui and Hamsaki are not accompanied by the literal description. The present determination is urged to be somewhat tentative.

In *Rana japonica*, egg masses were collected from the rice field and were kept in a laboratory tank. Developmental stages were determined according to Tahara [10, 11] (Table 7). In addition to these materials reared in a laboratory, small frogs shortly after metamorphosis (about 15 mm in head-trunk length) were collected from the field and their heads were fixed.

In *Takydromus tachydromoides*, naturally deposited eggs were obtained from a laboratory terrarium. These eggs were carefully transferred from the terrarium to the Petri dish of which floor was covered with moist cotton and left there for further development. Developmental stages were determined according to the criteria made for *Lacerta vivipara* [12] (Table 8).

In *Gallus gallus* (White Leghorn strain), fertilized eggs were incubated at about 38°C. Developmental stages were determined according to Hamburger and Hamilton [13] (Table 9). In addition, the brains of chicks of eight days after hatching and adult hens were fixed.

In *Mus musculus* (ICR strain), newly pregnant females were sacrificed at appropriate intervals and the intra-uterine embryos were taken out. Developmental stages were determined according to Theiler [14] (Table 10). In addition, the brains of postnatal mice of three and seven days old and adult mice were fixed.

All materials were fixed in Bouin's solution, embedded in paraffin, and serially sectioned at 6 or 7 μm. Both sagittal and transverse serial sections were prepared at all stages of all species except for *Takydromus tachydromoides* in which the number of materials was not sufficient. In this species, transverse sections were prepared at every stage, but sagittal sections were made only in a few stages. The sections were stained with paraldehyde fuchsin (AF) and Masson-Goldner's method.

RESULTS

The results are shown in Tables 1 to 10. In the following sections, the developmental characteristics of the CVOs are described briefly in each species. The detailed cytological description of the development of the CVOs is not attempted. The aspects which are obvious from the tables are not

repeated in the text. The CVOs of adult individuals of *Lampetra, Mustelus, Hypomesus, Silurus, Poecilia, Hynobius, Rana*, and *Takydromus* are described in a previous paper [2]. Abbreviations are given in the legend following Table 1. Busy readers may skip Results, but see Tables and go to Discussion and Summary.

The brook lamprey, Lampetra reissneri (Table 1)

Hypothalamic structures In early stages, the ventrocaudal floor of the III ventricle (infundibulum) consists of a single layer of ependymal cells. At stage 16^+, small nerve fiber bundles appear under the ependymal layer. The fiber layer becomes thicker and is stained with AF at stages 17 and 18, thus constituting the neural lobe (NL) (Fig. 1). At these stages, the ventral surface of the NL is supplied with sinusoid vessels, but is not underlain by the pars intermedia-component of adenohypophysial tissue. The median eminence

TABLE 1. Development of circumventricular organs in the brook lamprey, *Lampetra reissneri*

Stage[1)]	Days after fertilization (22–25°C)	Total length (mm)	(ME)	NL	(OVLT)	P	PP	SCO	SD	MeCP	MCP
12	6		−	−	−	−	−	−	−	−	−
13	7		−	−	−	−	−	−	−	−	−
14	8	2.0–2.8[2)]	−	−	−	±	−	−	−	−	−
15	10	3.5–5.0	−	−	−	+	±	−	−	−	−
16^-	11	5.0–6.0	−	−	−	+	+	±(*)	−	−	−
16^+	15	6.0–6.5	−	±	−	+	+	+*	−	−	−
17	21	7.5–8.2	±	+*	−	+	+	+*	−	−	±
18	31	7.8–8.2	±	+*	−	+	+	+*	−	±	±
Ammocoetes		ca. 100	+	+*	±	+	+	+*	±	+	+
Adult		ca. 170	+	+*	+	+	+	+*	+	+	+

1) Stages were determined according to Piavis [8]. Stage 12=head stage, stage 13=prehatching stage, stage 14=hatching stage, stage 15=pigmentation stage, stage 16=gill-cleft stage, stage 17=burrowing stage, stage 18=larva stage.

2) Crown-rump length (mm).

Notes to Tables 1 to 10.

A mark + means that the organ is differentiated. A mark − means that the organ is not differentiated. A mark ± means that the organ is differentiating. An asterisk means that the organ is distinctly stained with AF. An asterisk in parentheses means that the organ is faintly stained with AF. An abbreviation in parentheses such as (OVLT) means that the organ does not show a typical mammalian pattern of differentiation even in adults (see [2]). Brackets include organs that cannot be clearly separated from each other. Data for adults from Tables 1 to 8 were taken from Tsuneki [2]. A horizontal bar in Table 8 indicates the boundary between embryos and adults. Horizontal bars in the other tables indicate the boundary between embryos and larvae (juveniles) and the boundary between larvae and adults. As shown in each table, temperatures under which embryos and larvae were reared are within a certain range in poikilothermal animals. Since the development of *Lampetra, Hypomesus, Silurus, Hynobius, Rana,* and *Takydromus* was studied in the earlier half of the year (mainly in spring), lower temperatures in the range indicate the temperatures for the earlier development (in earlier weeks or months) and higher temperatures in the range indicate the temperatures for the later development (in later weeks or months) in each species.

Abbreviations are as follows: AP, area postrema; DCP, diencephalic choroid plexus; FO, frontal organ; MCP, myelencephalic choroid plexus; ME, median eminence; MeCP, mesencephalic choroid plexus; NL, neural lobe; OVLT, organum vasculosum laminae terminalis; PA, paraphysis; PE, parietal eye; P, pineal; PP, parapineal; PVO, paraventricular organ; SCO, subcommissural organ; SD, saccus dorsalis; SFO, subfornical organ; SV, saccus vasculosus; TCP, telencephalic choroid plexus; VT, velum transversum.

(ME) is not developed in the larvae even at stage 18. At stages 17 and 18, the hypothalamic floor above the adenohypophysial cell cord consists of a single layer of ependymal cells. The rostral part of this floor is also provided with small subependymal nerve fiber bundles and is slightly protruding into the III ventricle. The floor is separated from the underlying adenohypophysial cell cord only by an AF-positive connective tissue sheet.

Epithalamic structures The first anlage of the pineal appears at stage 14 as a shallow epithalamic evagination of ependymal cells. However, the ependymal cells of the evagination still contain yolk granules. At stage 15, the evagination takes a clear omega-shaped structure. The pineal lumen becomes smaller as the development proceeds. At stage 16^+, the pineal is located above the habenular and posterior commissures. The dorsal wall of the pineal is much thinner than the ventral wall. In later stages (stages 17 and 18), the pineal moves slightly rostrally, but it still does not differentiate a stalk (Fig. 2). At these stages, AF-positive intraluminal processes are distinct.

The parapineal appears at stage 16^- as a small aggregation of cells around the rostroventral corner of the pineal. At stages 16^+, 17, and 18, the parapineal is a flattened sac formed by a single layer of cells (Fig. 2). The lumen is indistinct. In

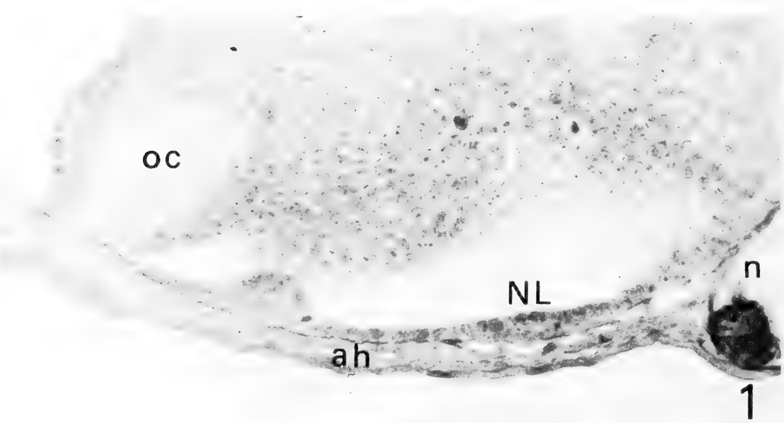

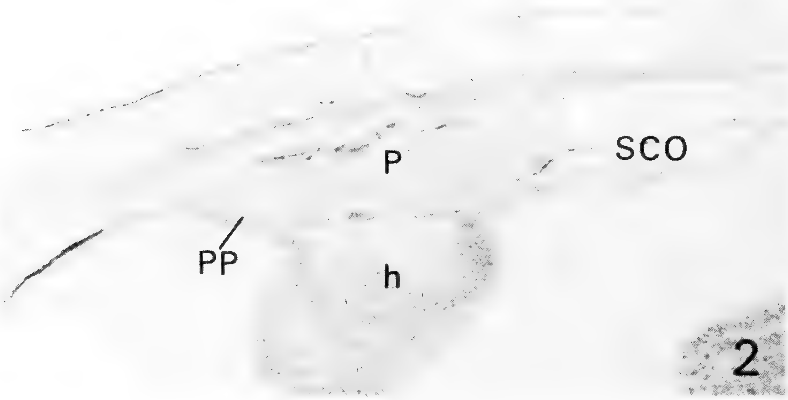

FIG. 1. Sagittal section of the hypothalamo-hypophysial region of a stage 17 larva of *Lampetra reissneri*. ah, adenohypophysis; n, notochord; oc, optic chiasma. ×500. The left is rostral in this and all following figures of sagittal sections.

FIG. 2. Sagittal section of the pineal complex of a stage 17 larva of *Lampetra reissneri*. Note AF-positive structures in the pineal (P). h, habenula; PP, parapineal. ×500.

young larvae, the parapineal is very small compared to its relative size in adults. The subcommissural organ (SCO) is stained with AF earlier than the NL. (The earlier differentiation of the SCO than the NL is corroborated by the pseudoisocyanin-fluorescence study in *Lampetra planeri* [15].)

The dorsal ependymal roof of the cerebral ventricle consists of cuboidal ependymal cells and does not show any histological specialization and thus the paraphysis and the saccus dorsalis (SD) are virtually absent in larvae even at stage 18.

Choroid plexuses The mesencephalic and myelencephalic ventricular roofs consist of a single layer of ependymal cells. At stage 15, they still contain yolk granules. In all stages up to 18, the roofs are not folded and thus they are not considered as the typical choroid plexus (CP). The ependymal cells are consistently cuboidal or flat. Blood vessels investing the roofs increase gradually. It is thus hard to say exactly when the cells differentiate into the CP cells. In ammocoetes larvae (ca. 10 cm), both the mesencephalic and

TABLE 2. The occurrence of circumventricular organs in 7 cm-embryos of the smooth dogfish, *Mustelus manazo*

ME	NL	SV	OVLT	PVO	P	SCO	PA	SD	[VT	DCP	TCP]	SFO	MCP	AP
+	+	−	−	+	+	+*	+	+	+	+	+	−	+	−

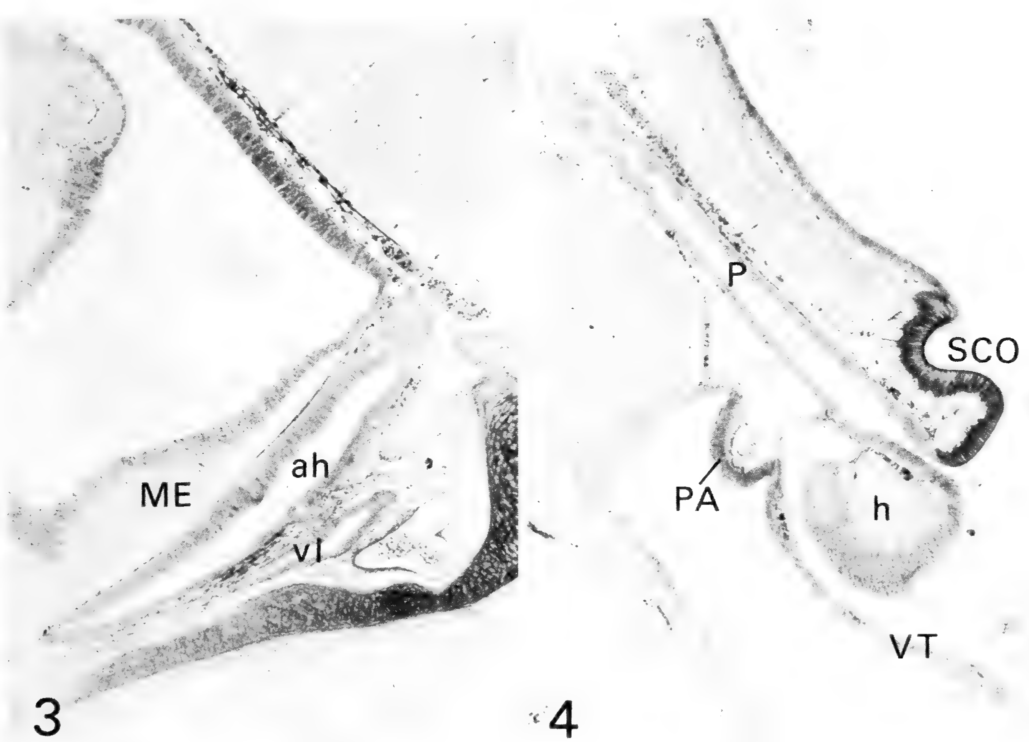

FIG. 3. Sagittal section of the hypothalamo-hypophysial region of a 7 cm-long embryo of *Mustelus manazo*. The dorsocaudal wall of the third ventricle represents the incipient SV. The ventral lobe (vl) is still clearly connected to the main part of adenohypophysis (ah). ×50.

FIG. 4. Sagittal section of the epithalamus of a 7 cm-long embryo of *Mustelus manazo*. The ependymal sheet of velum transversum (VT) form some folding in other sections of this series. h, habenula; PA, paraphysis; P, pineal. ×50.

myelencephalic ependymal roofs are folded and thus are considered as the CP.

The smooth dogfish, Mustelus manazo (Table 2)

Hypothalamic structures The ME is thick and possesses a well developed fiber layer (Fig. 3). The ventral surface of the ME is straight and is apposed to the sac-like adenohypophysis. The ME and adenohypophysis are separated from each other only by an AF-positive connective tissue sheet and sporadic capillaries. The NL is small and possesses a thin fiber layer. It is not stained with AF, but its ventral surface is well vascularized. The caudal and caudolateral walls of the infundibular recess consist of several layers of cells (Fig. 3). They are well covered with sinus-like capillaries and may represent the anlage of the saccus vasculosus (SV). However, typical coronet cells are not yet detected and the walls are too thick to be designated as the SV.

Both the lateral and posterior recesses of the III ventricle are partly contoured with columnar ependymal cells and thus the paraventricular organ (PVO) is already differentiated.

Epithalamic structures The pineal is a long straight tube directed dorsorostrally (Fig. 4). The end-vesicle is slightly dilated. The velum transversum (VT) is developed and projects several small ependymal processes into the ventricle. Therefore, it approaches the condition of the diencephalic choroid plexus (DCP). In front of the VT, there is a thick ependymal sheet. It consists of a few dense layers of cells and may represent the incipient paraphysis (Fig. 4).

Choroid plexuses In the lateral ventricle, the telencephalic choroid plexus (TCP) is well developed. The TCP caudally transforms into the DCP-like VT. These two structures are distin-

Table 3. Development of circumventricular organs in the smelt, *Hypomesus nipponensis*

Stage[1]	Days after fertilization (12–14°C)	Total length (mm)	[ME	NL]	SV	PVO	P	SCO	SD	VT	(TCP)	(MCP)
A	5		—	—	—	—	+	—	—	—	—	—
B	7		—	—	+	—	+	—	—	—	—	—
C	9		—	—	+	—	+	—	—	—	—	—
D	11		—	—	+	—	+	±	—	—	—	—
E	13	5.0	—	±	+	±	+	±	—	—	—	±
F	15	5.0–5.5	—	±	+	+	+	+	—	—	—	±
G	19	6.1–6.3	—	±	+	+	+	+	—	—	±	±
H	26	6.5–7.0	—	±	+	+	+	+	—	—	±	±
Adult		ca. 110	+	+*	+	+	+	+*	+	+	+	+

[1] Stage A=the eye not conspicuously pigmented, the body making a complete turn around the yolk mass, stage B=the eye distinctly pigmented, the body surrounding the yolk in less than one and half turn, stage C=the body surrounding the yolk in more than one and half turn, stage D=prehatching stage, stage E=shorty after hatching.

Fig. 5. Sagittal section of the pituitary region of a stage C embryo of *Hypomesus nipponensis*. Note the well developed SV. The adenohypophysis (ah) is partly embedded in the hypothalamus. ×500.

Fig. 6. Sagittal section of the pineal (P) region of a stage C embryo of *Hypomesus nipponensis*. pc, posterior commissure. ×500.

Fig. 7. Sagittal section of the pituitary region of a stage F larva of *Silurus asotus*. ah, adenohypophysis. ×380.

Fig. 8. Sagittal section of the pineal (P) region of a stage F larva of *Silurus asotus*. Note AF-positive structures in the pineal lumen. ×380.

Fig. 9. Transverse section of the OVLT of a stage E embryo of *Poecilia reticulata*. An arrow indicates a blood vessel. ×440.

Fig. 10. Sagittal section of the epithalamus of a stage G larva of *Poecilia reticulata*. The DCP is not fully differentiated even in adults. An asterisk indicates the habenular commissure. ×500.

guished topologically, but they actually represent a continuous ependymal structure.

The myelencephalic choroid plexus (MCP) is a large dorsal evagination of the ependymal wall of the IV ventricle. It is already well folded. The most caudal roof of the IV ventricle represents a small pouch-like posterior tela.

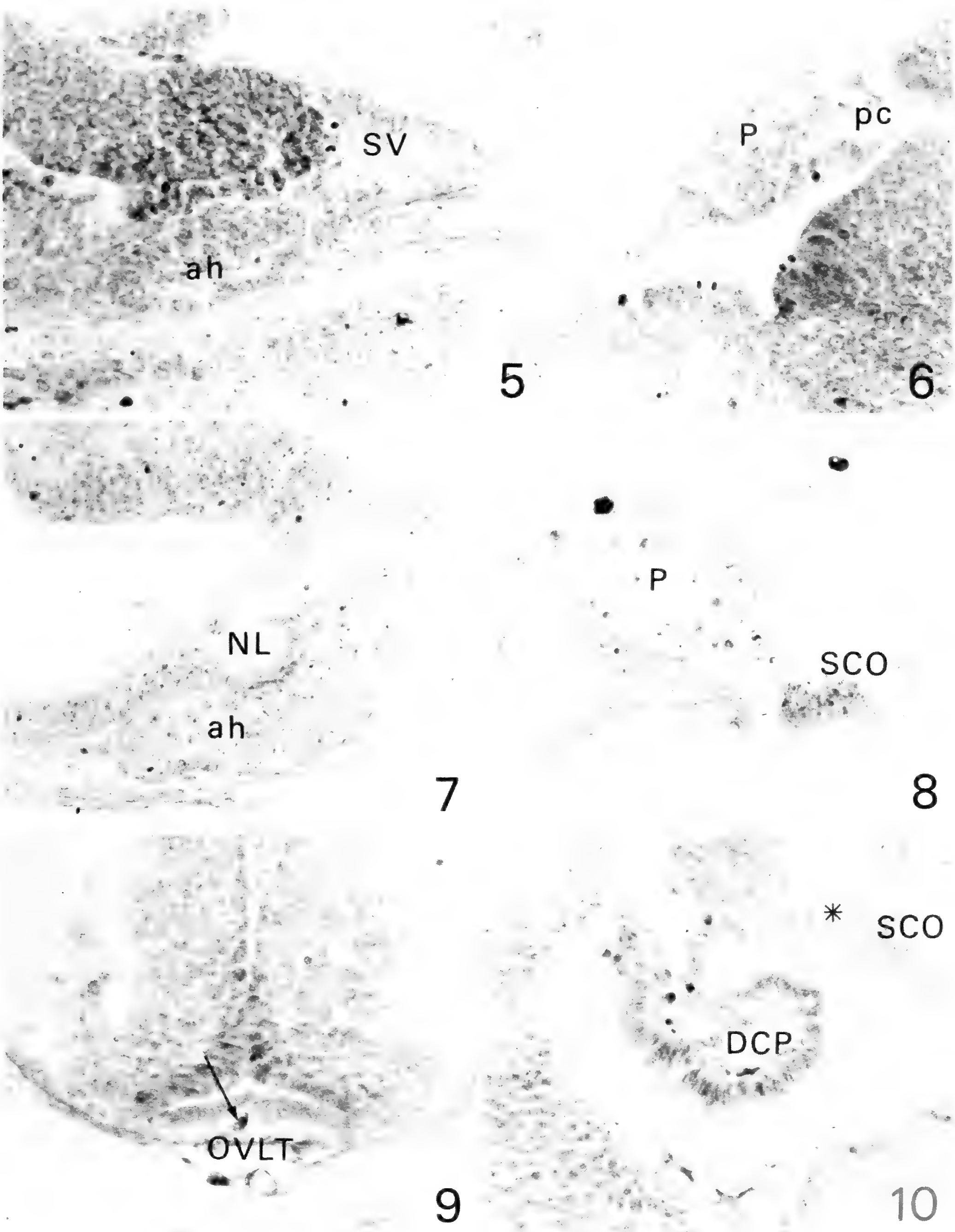

The smelt, Hypomesus nipponensis (Table 3)

Although eight stages from embryos to larvae were studied during 22 days, histological differentiation of the CVOs was slow, probably because of low water temperatures.

Hypothalamic structures In larvae, the adenohypophysis, except for the ventral surface, is embedded in the hypothalamus just as encountered in some adult gobiid teleosts. The neural tissue overlying the adenohypophysis may represent the neurohypophysis, but it does not differentiate as such in the larvae studied. However, a thin sheet of tissue above the caudal part of the adenohypophysis consists of nerve fibers and may represent an initial stage of differentiation of the NL. The adenohypophysis and the surrounding neural tissue (the future neurohypophysis) are consistently separated by a connective tissue sheet.

The caudal end of the infundibular recess is covered with columnar cells in stage A embryos. It appears like a cup which opens rostrally. In stage B and C embryos, the cells of the cup possess a light, abundant, apical cytoplasm and the cup itself differentiates as the SV (Fig. 5). In larvae, the SV takes the form of a flattened sac extending laterally. The lumen of the sac is occupied by flocculent material. The vascularization is not prominent. In larvae, the SV is even larger than the adenohypophysis in size, especially in its width. (In adult *Hypomesus*, the SV is also a large organ.)

Epithalamic structures The pineal is present as early as in stage A embryos. Throughout the embryonic and larval periods, the pineal lumen is not distinctly open, but is occluded by AF-positive droplet-like structures (incipient outer segment?). In embryos, the pineal is located above the intercommissural area (Fig. 6), but in larvae the pineal is located mainly above the SCO. (In adults, the pineal is extended far rostrally.) The differentiation of the SCO is so gradual that it is difficult to determine the exact time of definite appearance.

Choroid plexuses The roof of the ventriculus impar telencephali is formed by a simple ependymal sheet. In front of the habenular commissure, the ependymal cells are low columnar in later larvae and may represent the tela chorioidea telencephali or a combination of this structure either with the VT or the SD. The VT and SD themselves are not differentiated in the larvae studied.

The dorsal wall of the IV ventricle consists of flat ependymal cells in embryos, but consists of cuboidal or low columnar ependymal cells in larvae. In later larvae, it may represent a tela chorioidea myelencephali.

See Tsuneki [2] for terminology on the choroid plexus and its related structures. (An ependymal sheet consisting of flat cells is called a tela membranosa, a straight or slightly undulating ependymal sheet consisting of cuboidal or columnar cells is called a tela chorioidea, and a tufted or highly folded ependymal sheet consisting of cuboidal or columnar cells is called a choroid plexus.)

The catfish, Silurus asotus (Table 4)

Hypothalamic structures In embryos and early larvae, the ventral hypothalamus and adenohypophysis are apposed, but are clearly separated by an AF-positive connective tissue sheet. In stage E embryos, a small mass of cells appears at the ventrocaudal part of the infundibulum where the NL differentiates later. The NL is stained with AF already at its initial stage of differentiation (stage F) (Fig. 7). The ME appears to differentiate slightly later than the NL, although these two components of the neurohypophysis cannot be clearly separable even in adults.

At stage F, the SV differentiates as a round sac. During the larval period, the SV is almost as large as the adenohypophysis. (It stands in high contrast to adults where the SV is much smaller than the adenohypophysis.) The organum vasculosum laminae terminalis (OVLT) is not clearly differentiated in larvae, although the ventromedial wall of the preoptic recess is slightly bulging into the recess in later larvae.

Epithalamic structures At stage C, the distinct pineal appears as an evagination of the dorsal wall of the III ventricle. Although the pineal lumen is patent in some larvae (Fig. 8), it is not distinct in the other larvae and the center of the pineal is irregularly occupied by the AF-positive

TABLE 4. Development of circumventricular organs in the catfish, *Silurus asotus*

Stage[1]	Days after fertilization (17–24°C)	Total length (mm)	[ME	NL]	SV	OVLT	PVO	P	SCO	(DCP)	(TCP)	(MCP)
A	1		—	—	—	—	—	—	—	—	—	—
B	2		—	—	—	—	—	±	—	—	—	—
C	3		—	—	—	—	—	+	—	—	—	—
D	4	5.5–6.0	—	—	—	—	—	+	+	—	—	—
E	5	6.2	—	±	—	—	—	+	+*	—	±	—
F	7	6.5–7.0	±	+*	+	—	±	+	+*	—	+	—
G	9	8.0–8.5	±	+*	+	—	+	+	+*	—	+	+
H	11	8.5–8.8	±	+*	+	—	+	+	+*	—	+	+
I	15	8.0–8.5	±	+*	+	—	+	+	+*	—	+	+
J	20	8.5	±	+*	+	—	+	+	+*	—	+	+
Juvenile		15	+	+*	+	±	+	+	+*	—	+	+
Adult		ca. 520	+	+*	+	+	+	+	+*	+	+	+

[1] Stage A=the body not surrounding the yolk mass completely, stage B=the body completely surrounding the yolk, stage C=immediately after hatching, stage D=the eye barely visible, barbel rudiments, stage E=the eye distinct, many melanophores on the body, stage F=barbels elongated.

TABLE 5. Development of circumventricular organs in the guppy, *Poecilia reticulata*

Stage[1]	Days after fertilization (26–27°C)	Total length (mm)	[(ME)	NL]	OVLT	PVO	P	SCO	(DCP)	(MCP)
A			—	—	—	—	+	—	—	—
B			—	—	—	—	+	+	—	—
C			+	+(*)	±	+	+	+	—	—
D			+	+*	±	+	+	+(*)	±	±
E		7.1–8.2	+	+*	+	+	+	+*	±	±
F	1	7.5–7.7	+	+*	+	+	+	+*	±	±
G	5	8.1–8.7	+	+*	+	+	+	+*	+	±
Adult		ca. 45	+	+*	+	+	+	+*	+	+

[1] Stage A=the body surrounding the half of the yolk mass, the eye slightly pigmented, stage B=rudiments of pectoral and anal fins visible, stage C=a membrane completely covering the head, stage D=a small round window in the membrane at the top of the head, the body completely surrounding the yolk, fin rays in the pectoral, anal, and caudal distinct, stage E=a small yolk mass visible externally, fin rays appearing in the dorsal, stage F=immediately after hatching, the yolk mass not visible externally, fin rays developed in all fins including the pelvic.

droplet-like structures. In younger larvae, the pineal is located on the intercommissural area, without a distinct stalk. In later larvae, the pineal is gradually extended rostrally and it differentiates a short stalk.

Choroid plexuses The tela chorioidea telencephali which consists of cuboidal ependymal cells is distinguished as such in the larvae later than stage F. The tela chorioidea myelencephali is differentiated in the rostral part of the dorsal wall of the IV ventricle at stage G. In earlier stages, the roof of the IV ventricle entirely consists of flat ependymal cells.

The guppy, Poecilia reticulata (Table 5)

Hypothalamic structures The neurohypophysis differentiates in stage C embryos. In stage D embryos, the caudal part of the neurohypophysis, that may correspond to the NL, is already distinctly stained with AF. The entire neurohypophysis is well vascularized before birth. (Ichikawa *et al.* [16] also noted that the neurohypophysis of *Poecilia* (=*Lebistes*) *reticulata* is stained with AF before birth.) The SV is not discernible in embryos and larvae.

In stage B embryos, the ventral wall of the preoptic recess (future OVLT) consists of a single layer of ependymal cells, but is vascularized meningeally. In stage C embryos, thin bundles of nerve fibers appear under the ependymal layer. In stage E embryos, the nerve fiber layer is vascularized as well as the ventral surface (meninx) (Fig. 9).

Epithalamic structures The pineal develops as an evagination of the dorsal wall of the III ventricle in stage A embryos. It gradually increases in size. The lumen is indistinct throughout the stages studied, and it is partially occluded by AF-positive droplet-like structures. The pineal stalk is short even in stage G larvae. (See Omura and Oguri [17] for the ultrastructural development of the pineal photoreceptor cells in *Poecilia*.)

Choroid plexuses The ependymal cells in front of the habenular commissure is cuboidal in stage B embryos and are columnar in stage C embryos. The ependymal sheet invaginates as a sac into the ventricle in stage D embryos. As the development proceeds, the sac is dilated and may represent the incipient DCP (Fig. 10).

The rostrodorsal wall of the IV ventricle consists of columnar ependymal cells in stage C embryos, and it is slightly invaginates into the ventricle in stage D embryos. The invagination is incomplete and does not form an intraventricular sac even in stage G larvae.

The salamander, Hynobius nebulosus (Table 6)

Hypothalamic structures At stage 46, the infundibulum (future NL) is composed of a single layer of ependymal cells. At stage 49, small bundles of nerve fibers appear in the future NL. In the ME, small bundles of nerve fibers are recognizable at stages 56 and 62.

At stage 46, the ependymal cells located around the sulcus hypothalamicus possess a relatively ample cytoplasm and irregular ventricular protrusions. These cells may form the incipient PVO. The differentiation of this organ is slow and gradual.

Table 6. Development of circumventricular organs in the salamander, *Hynobius nebulosus*

Stage[1)]	Total length (mm)	ME	NL	PVO	P	SCO	PA	DCP	TCP	SFO	MCP
24	3.3	−	−	−	−	−	−	−	−	−	−
29	3.9	−	−	−	−	−	−	−	−	−	−
33	6.2	−	−	−	±	−	−	−	−	−	−
36	9.5	−	−	−	+	−	±	−	−	−	−
39	11	−	−	−	+	+(*)	+	−	−	−	−
43	12	−	−	±	+	+(*)	+	−	±	−	−
46	15	−	−	±	+	+(*)	+	+	+	−	−
49	17	−	±(*)	+	+	+(*)	+	+	+	−	±
56	19	±	+*	+	+	+*	+	+	+	−	+
62	25	±	+*	+	+	+*	+	+	+	−	+
Juvenile[2)]	27	±	+*	+	+	+*	+	+	+	−	+
Adult	89	+	+*	+	+	+*	+	+	+	+	+

1) Stages were determined according to Usui and Hamsaki [9]. Embryos were kept in water of about 9°C and larvae were kept in water of about 10 to 24°C.

2) Salamanders shortly after metamorphosis (4.5 months after hatching).

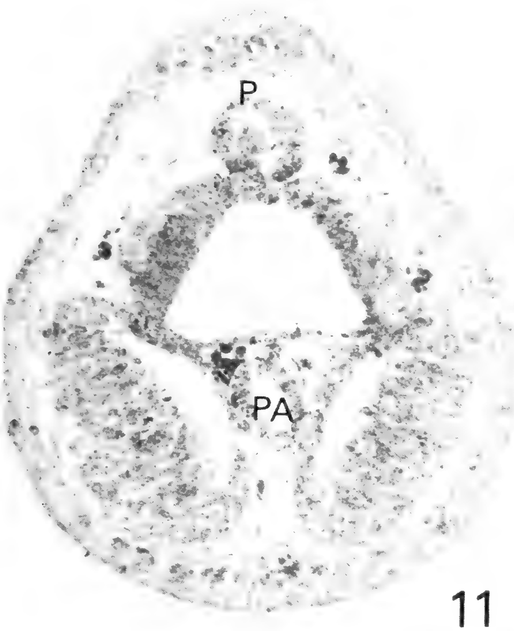

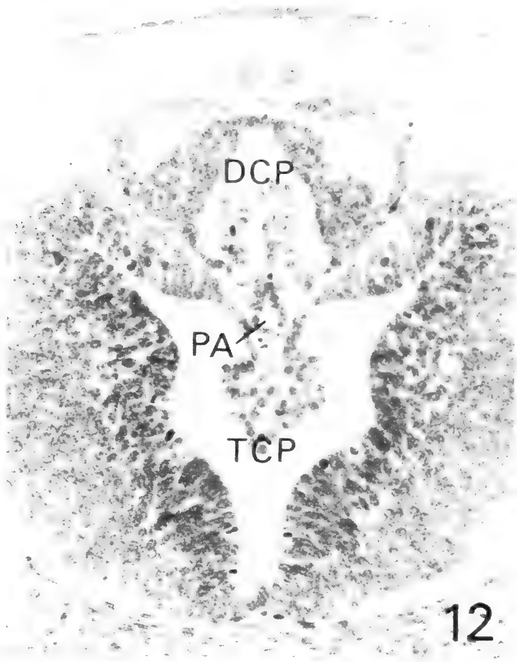

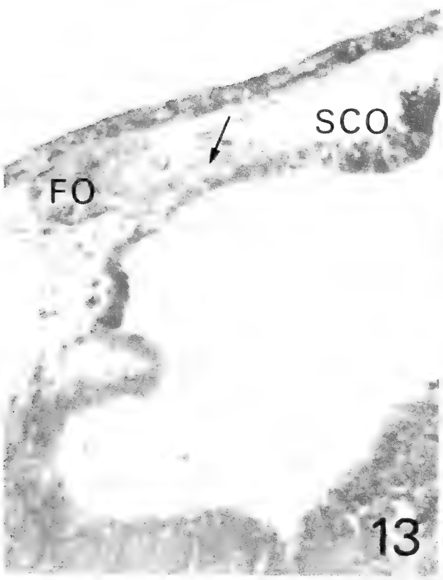

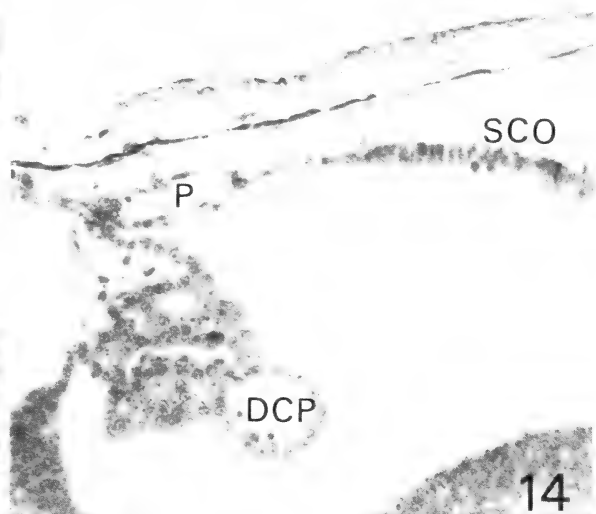

FIG. 11. Transverse section of the brain of a stage 39 embryo of *Hynobius nebulosus*. In this section, the lateral ventricles appear below the third ventricle because of the cranial flexure of the embryo. PA, paraphysis; P, pineal. ×120.

FIG. 12. Transverse section of the brain of a stage 46 larva of *Hynobius nebulosus*. PA, paraphysis. ×120.

FIG. 13. Sagittal section of the epithalamus of a stage 24 larva of *Rana japonica*. An arrow indicates the pineal anlage. The incipient DCP is seen as a ventricular protrusion below the frontal organ (FO). ×190.

FIG. 14. Sagittal section of the epithalamus of a stage 26 larva of *Rana japonica*. The frontal organ moves rostrally outside the scope of this figure. P, pineal. ×190.

Epithalamic structures At stage 33, a shallow omega-shaped evagination appears in the dorsal wall of the III ventricle. This structure represents the initial differentiation of the pineal. Although the pineal anlage appears in the intercommissural area, the pineal is slightly caudally dislocated during the development in high contrast to the rostrally extended pineal of piscine vertebrates. Thus, in the older larvae of *Hynobius* it is located mainly on the rostral part of the SCO.

At stage 36, the anlage of the paraphysis appears as a shallow evagination in front of a VT-like structure. At stage 39, the anlage becomes a rostrally directed, large, simple sac (Fig. 11). At stage 43, it is elongated and tube-like in appearance. At stage 56, the tip of the tube is divided into saccules and thus the structure indeed appears paraphysis-like. At stages 56 and 62, the ependymal cells of the paraphyseal stalk are more densely arranged than those of the paraphyseal saccules.

Choroid plexuses The DCP appears as paired ventricular protrusions at stage 46 (Fig. 12). The cuboidal ependymal cells cover the vascularized core of the protrusion. At stage 56, the DCP becomes a median structure which is probably due to a fusion of the pair. At this stage, the ependymal cells are rather flat. (Even in adults, the ependymal cells of the CP are flat. In most vertebrates, however, the ependymal cells of the CP are cuboidal. The flat ependymal cells in *Hynobius* may be related to the unusually large size of nuclei in this species as well as in other urodeles [18].) The anlage of the TCP appears at stage 43. It is a median ventricular protrusion. In the following stages, it becomes a glomerulus-like in appearance (Fig. 12). At stage 56, the TCP protrudes into the lateral ventricle and its ependymal cells become lower in height.

The ependymal sheet covering the IV ventricle becomes undulant at stage 49. At stage 56, the MCP differentiates at the rostrolateral region. At stage 62, the entire ependymal roof of the IV ventricle well differentiates as the MCP except for the most caudal part, which represents the simple posterior tela.

In *Hynobius nebulosus* as well as the other species, developmental stages were selected at some intervals. Therefore, even if a certain structure is described to appear at a certain stage, it is quite possible that such a structure actually appears between this stage and a preceding stage

TABLE 7. Development of circumventricular organs in the frog, *Rana japonica*

Stage[1)]	Total length (mm)	ME	NL	(OVLT)	PVO	P	FO	SCO	PA	DCP	SFO	MCP
17	4	−	−	−	−	−	−	−	−	−	−	−
19	5	−	−	−	−	+		−	−	−	−	−
20	6	−	−	−	−	+		−	−	−	−	−
21	7	−	−	−	−	+		−	−	−	−	−
22+	9	−	−	−	−	+	+	±	−	±	−	−
24	10	−	−	−	−	+	+	+(*)	−	±	−	−
25	12	−	±	−	±	+	+	+(*)	−	+	−	+
26	16	±	±(*)	−	±	+	+	+*	±	+	−	+
28	26	+	+*	−	±	+	+	+*	+	+	−	+
32	37	+	+*	−	+	+	+	+*	+	+	−	+
Juvenile frog	15	+	+*	−	+	+	+	+*	+	+	±	+
Adult frog	36	+	+*	+	+	+	+	+*	+	+	+	+

1) Stages were determined according to Tahara [10, 11]. Embryos and larvae were kept in water of temperatures of 13 to 17°C.

examined.

The frog, Rana japonica (Table 7)

Hypothalamic structures The ME starts to differentiate around stage 26. It consists of a single layer of cuboidal ependymal cells and a thin nerve fiber layer. The NL starts to differentiate at about stage 25 to 26. At these stages, the nerve fiber layer is very thin.

In the ventral wall of the preoptic recess, the subependymal fiber layer is scarcely found in tadpoles and thus the OVLT is not differentiated histologically in larvae. In frogs shortly after metamorphosis, a thin nerve fiber layer appears but the organ is still barely specialized.

Epithalamic structures The common anlage of the pineal and frontal organ appears as a shallow omega-shaped evagination at stage 19. At stages 20 and 21, it is a rather parenchymatous structure. The anlage is elongated rostrocaudally at stage 22^+. The rostral swelling differentiates into the frontal organ and the caudal stalk into the pineal (Fig. 13). The anlage is clearly separated into the frontal organ and the pineal at stage 26, although they are connected by a slender nerve. The pineal bears a distinct lumen after stage 26. At stage 28, the frontal organ is a balloon-like structure with a distinct lumen. In later tadpoles, the frontal organ becomes nearly parenchymatous and moves rostrally. In frogs shortly after metamorphosis, it is located in the dermis right above the olfactory bulb.

In stage 26 tadpoles, a small ependymal sac develops rostrodorsally to the DCP. It may be an anlage of the paraphysis. In stage 32 tadpoles, it is divided into saccules. In tadpoles, the paraphysis is a more or less evaginated structure. In frogs shortly after metamorphosis, the caudal part of the paraphysis is situated in the III ventricle (invaginated), being covered by the DCP.

Choroid plexuses The TCP is not found at any stages of development. In stage 22^+ and 24 tadpoles, the anlage of the DCP forms a plate-like ventricular invagination. The anlage becomes an irregularly shaped invagination at stage 25, but its ependymal cells are not yet differentiated as typical ependymal cells of the CP. The ependymal cells gradually increase in amount of the cytoplasm

TABLE 8. Development of circumventricular organs in the lacertid lizard, *Takydromus tachydromoides*

Stage[1)]	Days after oviposition[2)]	ME	NL	(OVLT)	PVO	P	PE	SCO	PA	DCP	TCP	(SFO)	MCP	(AP)
29^+	4	–	–	–	–	+		–	–	–	–	–	–	–
30^+	7	…[3)]	…	–	–	+		–	–	–	–	–	–	–
32^-	11	…	…	±	–	+	+	+*	+	SD	–	–	–	–
33^-	14	…	…	±	–	+	+	+*	+	SD	±	–	±	–
35^-	18	±	±	–	±	+	+	+*	+	SD	+	–	+	–
37^-	21	+	+	–	+	+	+	+*	+	SD	+	–	+	–
39	26	+	+(*)	–	+	+	+	+*	+	+	+	±	+	–
40	31	+	+*	–	+	+	+	+*	+	+	+	+	+	±
Adult	180	+	+*	+	+	+	+	+*	+	+	+	+	+	+

1) Stages were determined according to Dufaure and Hubert [12]. Stage 29^+=forelimb bud stub-like, the eye slightly pigmented, stage 30^+=the eye moderately pigmented, stage 32^-=the elbow distinct, stage 33^-=no scleral papillae yet, distal forelimb flanged, stage 35^-=scleral papillae 9, tympanic membrane differentiated, webbed palm, no scales, stage 37^-=distal fingers pigmented, body scales differentiating, dorsal rostrum slightly pigmented, stage 39=no scales on eye-lid, head scales differentiating, claw and body scales pigmented, lower eye-lid reaching the lens, stage 40=lower eye-lid scaled, head scales differentiated.

2) Eggs were left under room temperatures (25–30°C)

3) These blanks could not be filled, because sagittal sections were not available and transverse sections available, which were cut obliquely because of the cranial flexure, were not suitable to observe the infundibulum.

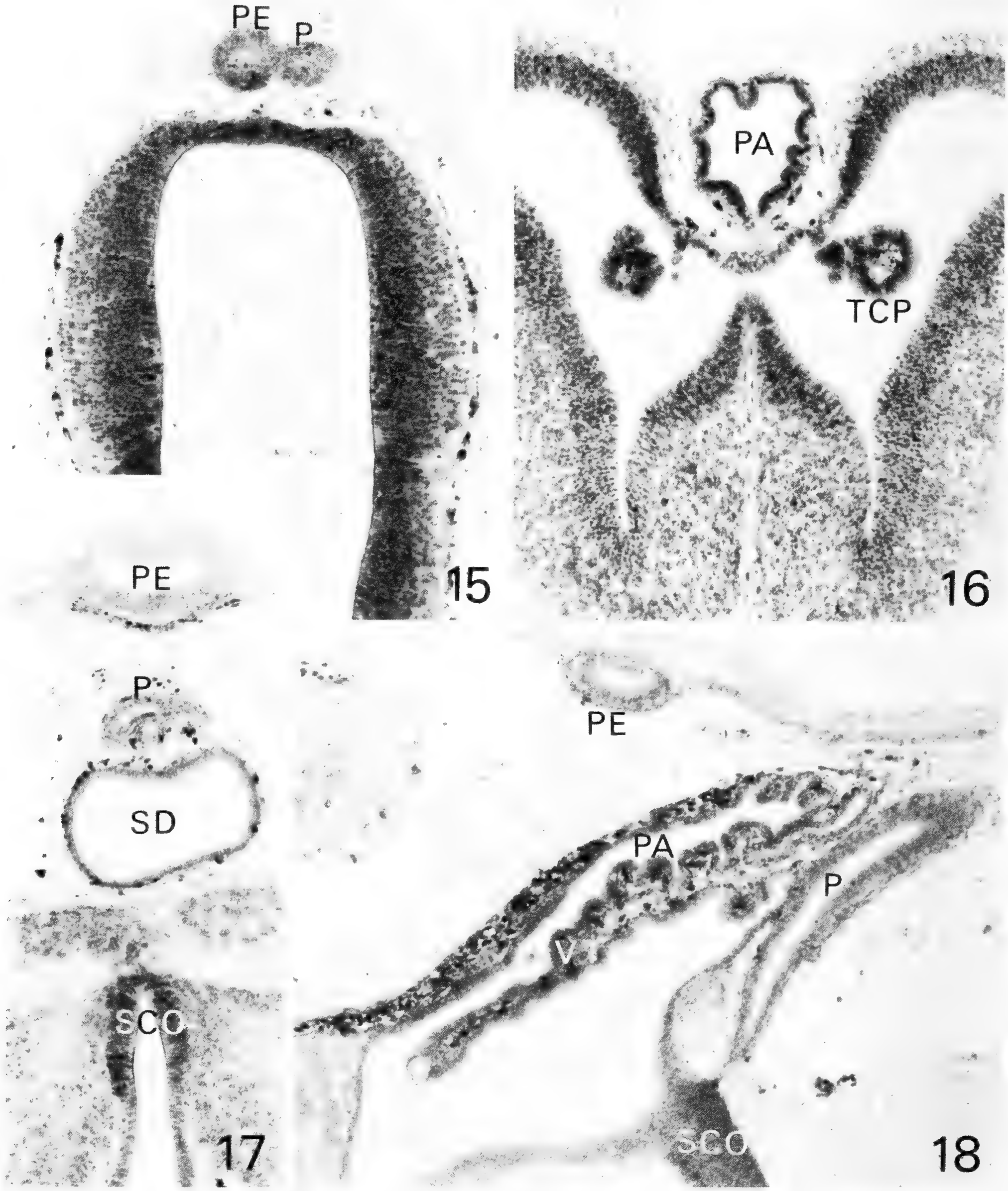

FIG. 15. Transverse section of the epithalamus of a stage 32⁻ embryo of *Takydromus tachydromoides*. At this level of section, the parietal eye (PE) parallels the pineal (P). ×120.

FIG. 16. Transverse section of the telencephalon of a stage 33⁻ embryo of *Takydromus tachydromoides*. PA, paraphysis. ×120.

FIG. 17. Transverse section of the pineal complex of a stage 37⁻ embryo of *Takydromus tachydromoides*. PE, parietal eye; P, pineal; SD, saccus dorsalis. ×120.

FIG. 18. Sagittal section of the epithalamus of a stage 39 embryo of *Takydromus tachydromoides*. The ventrocaudal wall of velum transversum (VT) differentiates as the DCP. PA, paraphysis; PE, parietal eye; P, pineal. ×120.

and they transform into histologically typical CP cells by stage 28 (Fig. 14).

In stage 24 tadpoles, the wall covering the IV ventricle partially consists of cuboidal ependymal cells. The sheet of these ependymal cells becomes undulant at stage 25. At stage 26, these ependymal undulation invaginates into the IV ventricle medially to form the MCP. It becomes gradually complex in the degree of ependymal folding.

The lacertid lizard, Takydromus tachydromoides (Table 8)

Hypothalamic structures At stage 35^-, the neurohypophysis is not well differentiated. In stage 37^- embryos, the ME is well differentiated with the nerve fiber layer of moderate thickness. In these embryos, the NL is also well formed, although the nerve fiber layer is not distinct. (Oota and Sakurai [19, 20] studied the development of the hypophysis of *Takydromus tachydromoides*. According to them, the ME differentiates by stage 38 both light and electron microscopically.)

The distinct OVLT is not recongnizable in embryos. In stage 32^- and 33^- embryos, however, a prominent reversed-omega-shaped structure is found in the region where the OVLT might appear. This structure is not particularly vascularized and becomes indistinct in later embryos.

Epithalamic structures Both the pineal and parietal eye appear to develop as a common evagination from the intercommissural area. It is found as early as in stage 29^+ embryos. In stage 32^- embryos, the proximal portion (future pineal) lies somewhat left to the distal portion (parietal eye) (Fig. 15). In stage 33^- embryos, both the parietal eye and the pineal are located in the median plane, the parietal eye being rostral and the pineal being caudal. They are gradually separated as the development proceeds.

The anlage of the paraphysis appears as a rostrodorsal evagination in stage 32^- embryos. The wall of the evagination is made up of stratified ependymal cells (Fig. 16). In stage 35^- embryos, the paraphyseal wall is composed of a single layer of ependymal cells and is dorsally covered by capillaries. In stage 39 embryos, the paraphysis is a rather small ependymal tube which is slightly wrinkled.

Choroid plexuses In stage 32^-, 33^-, and 37^- embryos, a large evaginated dome is found in front of the habenular commissure. The wall of the dome consists of a single layer of ependymal cells (Fig. 17). The ependymal cells are cuboidal to low columnar and possess a round nucleus and apical cilia. These cells are histologically similar to those of the CP, but the dome itself may be identified as the SD. The DCP appears first in stage 39 embryos (Fig. 18). Even in these embryos, however, the structure is rather reminiscent of the VT of piscine vertebrates. In stage 32^- embryos, a small swelling is detected in the region where the TCP develops later. The swelling becomes knob-like in stage 33^- embryos (Fig. 16). Although it is underlain by capillaries, the ependymal cells are columnar and contain an oblong nucleus; thus they cannot be considered as the typical CP cells. The ependymal nuclei of the TCP are still oblong in stage 35^- and 37^- embryos, but become roundish in stage 39 embryos.

The development of the MCP is gradual. At stage 35^-, the rostrolateral ependymal wall of the IV ventricle projects into the ventricle, thus differentiates into the MCP. In the embryos later than stage 37^-, the dorsal wall of the IV ventricle also contributes to the formation of the MCP.

The chick, Gallus gallus (Table 9)

Hypothalamic structures In earlier embryos (stages 25 to 30), the putative ME consists of a thick ependymal layer and a thin nerve fiber layer. As the development proceeds, the ependymal layer becomes thinner and the fiber layer becomes thicker. The outer layer of the anterior ME is stained with AF in the embryos later than stage 41. In the embryos before stage 38, the adenohypophysis is rather closely apposed to the ventral surface of the ME. In the embryos later than stage 39^+, however, the adenohypophysis is separated from the ME by a large amount of intervening loose connective tissue and blood vessels.

In stage 28^+ embryos, a small outgrowth of the infundibulum forms the future NL. The initiation of the outgrowth is noticed even in stage 25 embryos. The infundibulum becomes gradually deeper in stage 30 to 35^- embryos, but it consists of columnar ependymal cells almost exclusively.

TABLE 9. Development of circumventricular organs in the chick, *Gallus gallus*

Stages[1)]	Days[2)]	ME	NL	(OVLT)	PVO	P	SCO	PA	DCP	TCP	(SFO)	MCP	AP
18	3	–	–	–	–	+	–	–	–	–	–	–	–
21^+	4	–	–	–	–	+	–	–	–	–	–	–	–
25	5	–	–	–	–	+	+	±	–	–	–	–	–
28^+	6	±	±	–	–	+	+*	+	–	–	–	±	–
30	7	±	±	–	–	+	+*	+	–	±	–	±	–
32^+	8	+	+	–	–	+	+*	+	+	+	–	+	–
35^-	9	+	+	–	±	+	+*	+	+	+	–	+	–
36	10	+	+	–	±	+	+*	+	+	+	–	+	–
38	12	+	+	–	+	+	+*	+	+	+	–	+	–
39^+	14	+(*)	+*	–	+	+	+*	+	+	+	–	+	±
41	16	+*	+*	–	+	+	+*	+	+	+	–	+	±
42	18	+*	+*	±	+	+	+*	+	+	+	–	+	±
44	20	+*	+*	±	+	+	+*	+	+	+	–	+	+
8 days old chick		+*	+*	±	+	+	+*	+	+	+	±	+	+
Adult hen		+*	+*	+	+	+	+*	+	+	+	+	+	+

1) Stages were determined according to Hamburger and Hamilton [13].
2) Days after the onset of incubation.

The peripheral fiber layer becomes discernible by stage 38.

In the embryos examined, the OVLT is not well differentiated, although the lamina terminalis itself is distinct and consists of ependymal and nerve fiber layers.

Epithalamic structures The hollow outgrowth of the pineal is noticed as early as in stage 18 embryos. The first sign of follicle formation in the distal part of the pineal is discernible in stage 25 embryos. As the development proceeds, the pineal becomes larger and larger. The stalk becomes slender and slender.

In front of the future DCP, a thick ependymal sheet dorsally evaginates very early in ontogeny (stages 25 and 28^+). The ependymal cells of the sheet are columnar and stratified. In stage 30 embryos, the evagination is distinct (Fig. 19). It gradually becomes parenchymatous except for the tubular stalk. This structure may be identified as the paraphysis. It does not grow as the surrounding brain tissues. Therefore, it is relatively large in earlier embryos, but relatively small in later embryos (Fig. 20). The paraphysis is still found in the postembryonic chicks and adult hens, although the stalk becomes indistinct.

Choroid plexuses In stage 28^+ and 30 embryos, a large dome appears between the habenular region and the paraphysis. The dome consists of columnar ependymal cells and is vascularized dorsally. It may be considered as the SD. In stage 32^+ embryos, the rostral part of the dome extends short protrusions into the III ventricle, thus manifesting the first sign of the DCP formation. In stage 38 embryos, the caudal part of the dome also forms the DCP. The ependymal cells become typical CP cells by this stage. The first sign of the formation of the TCP is noticed in stage 30 embryos. In these embryos, however, the ependymal sheet is thick and ependymal cells are stratified. Therefore, it cannot be identified as the CP yet, although it projects into the lateral ventricle. The ependymal sheet is still thick in stage 32^+ embryos, although the protrusion is well folded. In stage 38 embryos, the ependymal cells are single-layered and are considered as typical CP cells.

The ependymal cells covering the IV ventricle are cuboidal and covered with capillaries as early as in stage 25 embryos. The ependymal cells are low columnar in stage 28^+ and 30 embryos. The ependymal sheet irregularly projects into the

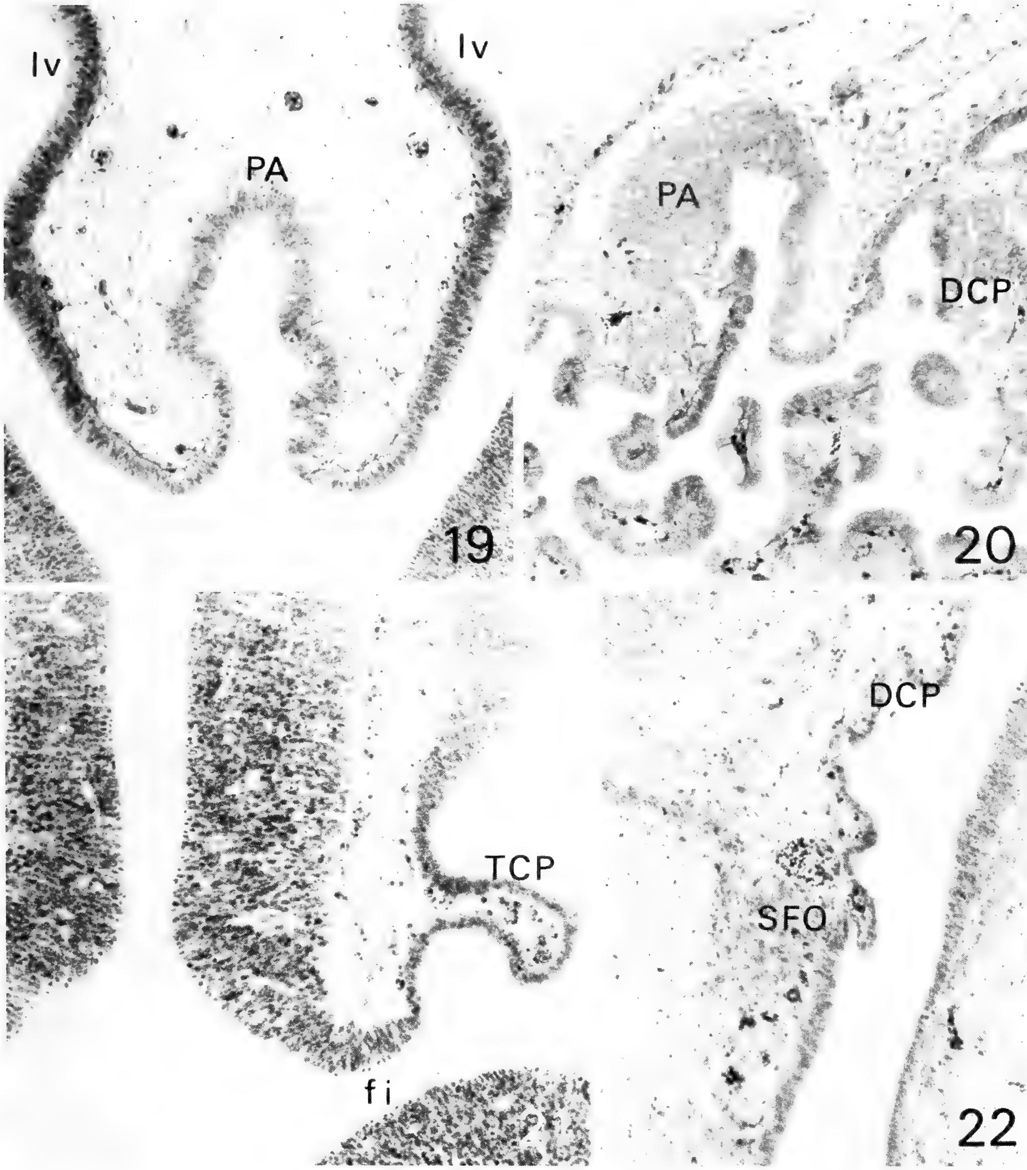

FIG. 19. Transverse section of the paraphysial evagination (PA) of a stage 30 embryo of *Gallus gallus*. lv, lateral ventricle. ×120.

FIG. 20. Sagittal section of the paraphysis (PA) and DCP of a stage 39^+ embryo of *Gallus gallus*. The paraphysis is parenchymatous except for the stalk. ×120.

FIG. 21. Transverse section of the anlage of TCP of a stage 21 embryo of *Mus musculus*. fi, foramen interventriculare. ×120.

FIG. 22. Sagittal section of the SFO of a stage 25 embryo of *Mus musculus*. ×120.

mouse are very popular laboratory animals and there are many references on the development of CVOs in these animals. In this section, some relevant references are cited. (The citation is far from comprehensive.)

In the chick, the development of the neurohypophysis was well described by Wingstrand [21]. Daikoku *et al.* [22] studied the differentiation of

ventricle in stage 32^+ embryos, thus forming the MCP.

References Except for *Poecilia*, the above poikilothermal vertebrates are either Asian or Japanese species and the development of their CVOs is scarcely studied. However, the chick and mouse are very popular laboratory animals and there are many references on the development of CVOs in these animals. In this section, some relevant references are cited. (The citation is far from comprehensive.)

In the chick, the development of the neurohypophysis was well described by Wingstrand [21]. Daikoku *et al.* [22] studied the differentiation of the hypothalamo-hypophysial system with an electron microscope. According to them, the development of portal vessels initiates on day 6.5 and nerve terminals in the ME contain cored vesicles on day 7.5 for the first time. Vigh *et al.* [23] noted that the PVO appears histologically at stage 34 and it shows monoamine fluorescence at stage 36.

Staging chick embryos, Hamburger and Hamilton [13] noted that the pineal becomes a distinct knob at stage 17. Calvo and Boya [24] reported that the pineal evaginates by stage 19. Ultrastructural differentiation of the pineal was described by Omura [25]. Ziegels [26] noted that the secretory activity of the SCO appears on the 7th day. According to Wingstrand [27], Gomori-positive material appears in the SCO on the 6th day and in the NL on the 13th or 14th day. Stockem and Weber [28] reported that the paraphysis appears 4 days after incubation. Malik and Singh [29] noted that the primordium of the TCP and DCP appears on day 6 and the MCP appears on day 7 of incubation. With an aid of a scanning electron microscope, El-Gammal [30, 31] described that the ependymal surface of the DCP distinctly differentiates at 11 days and that of the TCP at 9 days.

The mouse, Mus musculus (Table 10)

Hypothalamic structures In stage 21 embryos, the future ME is provided with a scant fiber layer. In stage 23 embryos, the ME is provided with an ample fiber layer. In stage 18 embryos, a shallow infundibular outgrowth forms the incipient NL. In stage 20 embryos, the outgrowth is deeply evaginated and may be termed as the NL although the nerve fiber layer is not well differentiated. In stage 25 embryos, the parenchyma of the NL is well developed and vascularized, although AF stainability is faint.

The differentiation of the OVLT is gradual. In stage 25 embryos, the thick ependymal layer is underlain by a thin nerve fiber layer. The ventral surface is moderately vascularized. The fiber layer becomes gradually thicker.

Epithalamic structures The pineal is a simple shallow outgrowth in stage 20 embryos. It becomes omega-shaped in stage 21 embryos. Its ependymal cells are columnar and histologically

TABLE 10. Development of circumventricular organs in the mouse, *Mus musculus*

Stage[1)]	Days of gestation	ME	NL	OVLT	P	SCO	DCP	TCP	SFO	MCP	AP
15^+	9	−	−	−	−	−	−	−	−	−	−
18	10	−	±	−	−	−	−	−	−	−	−
20	11	−	+	−	±	−	−	−	−	−	−
21	12	−	+	−	+	±	−	±	−	+	−
23	14	+	+	±	+	+	±	+	−	+	±
25	16	+	+(*)	±	+	+	+	+	+	+	±
26	18	+	+*	±	+	+	+	+	+	+	+
3 days old baby		+	+*	+	+	+	+	+	+	+	+
7 days old baby		+	+*	+	+	+(*)	+	+	+	+	+
Adult		+	+*	+	+	+(*)	+	+	+	+	+

1) Stages were determined according to Theiler [14].

similar to those of the SCO. In stage 23 embryos, the pineal becomes a caudodorsally elongated pocket. In stage 25 embryos, the pineal consists of the hollow stalk and the parenchymal end-portion, thus approaching the adult condition. The SCO differentiates at about stages 21 to 23. In mice, the SCO is poorly stained with AF even in adults.

Choroid plexuses The first sign of differentiation of the DCP is observed in stage 23 embryos. The low columnar ependymal cells form a rugged sheet. In stage 25 embryos, the ependymal cells are cuboidal and contain a stout nucleus. The ependymal sheet becomes folded. In the lateral ventricle, a small ependymal protrusion is found in stage 21 embryos, but the ependymal cells are densely aggregated and do not appear to be characteristic ependymal cells of the CP (Fig. 21). In stage 23 embryos, the protrusion becomes finger-like and thus differentiates as the TCP.

The ependymal sheet covering the IV ventricle scarcely undulates in stage 20 embryos. It protrudes into the ventricle in stage 21 embryos. The invaginated rostrolateral part is finger-like in appearance, but the caudomedial part is a simple sheet without a ventricular protrusion or folding. In stage 23 embryos, the medial part also is folded.

In stage 21 embryos, erythrocytes are nucleated. In stage 23 embryos, most erythrocytes are not nucleated, but there are still some nucleated erythrocytes. In stage 25 embryos, all erythrocytes are not nucleated. Thus, the enucleation from erythrocytes roughly corresponds to histological differentiation of the CPes.

Subfornical organ and area postrema The subfornical organ (SFO) is differentiated in stage 25 embryos (Fig. 22). The columnar ependymal cells are densely arranged and stratified. The parenchyma is crowded with cells and capillaries. As the development proceeds, the ependymal cells become lower in height and are lined up in a single layer. The development of the area postrema (AP) is gradual. In later embryos, the AP contains many parenchymal cells and capillaries.

References In describing the general developmental sequences of mouse embryos, Theiler [14] noted that the infundibular recess becomes distinct at stage 18. Beauvillain [32] reported that the ME differentiates ultrastructurally during 14 to 18 days. According to Gross and Baker [33], gonadotropin-releasing hormone is detectable immunohistochemically both in the ME and OVLT on the 17th day.

Theiler [14] noted that the pineal anlage evaginates at stage 20. With a Golgi method, Castañeyra-Perdomo *et al.* [34] reported that the SCO differentiates at embryonic day 14. Graumann [35] described the paraphysis in embryos of 15 to 16 mm length. Theiler [14] noted that the CP projects into the lateral and the IV ventricle at stage 21. According to Zaki [36], the TCP appears on the 13th postconception day.

DISCUSSION AND SUMMARY

There are apparent limitations in this study. First, the time when the organ has just appeared was judged not necessarily objectively. In this study, if the rudimentary organ appears histologically different from the surrounding regular brain tissue, it was judged to be differentiated as a CVO in most cases. However, the embryonic organs do not appear suddenly at a certain stage. It was not always easy to determine whether the organ is differentiating or not at the very beginning of its development. Second, all what I did in this study is only routine light microscopic histology. Detailed studies relying on electron microscopy, enzyme histochemistry, and immunohistochemistry of biologically active substances were not carried out. The development of blood-brain barrier was not examined either. It is apparent that some different results might be obtained if these detailed studies would be performed. As a matter of fact, however, the results of the present light microscopic study in *Gallus* and *Mus* are not very different from the results of detailed electron-microscopic or histochemical studies as noted in the section of *References*. The primary purpose of this study is to make an overall framework concerning the histological development of the vertebrate CVOs and is to compare the developmental sequences among organs and among animals under the same viewpoint. For these fundamental purposes, the present elementary study may not be inadequate. Although histological differentiation may not be necessarily parallel to

functional differentiation, here I am concerned with purely histological differentiation of CVOs both in terms of ontogeny and phylogeny of vertebrates.

Developmental stage at the time of hatching or birth

Hatching or birth is a critical event in the life history of animals, but the developmental stages when animals hatch out or are born are quite different among animals as the result of different life strategies employed by each species. *Lampetra* and *Silurus* hatch out at a very young stage. In these animals, virtually no CVOs appear in the embryonic period. *Hypomesus* also hatch out at a young stage, and only the SV and pineal are histologically discernible in embryos. On the contrary, *Poecilia* are born at a well developed stage and most CVOs are differentiated during the intra-ovarian period. *Hynobius* hatch out at a more developed stage than *Rana*: in the latter only the pineal complex is recognizable in embryos. Both *Takydromus* and *Gallus* hatch out at a well developed stage. Most of their CVOs are developed during the embryonic period. The same applies to *Mus*, although newborn mice externally appear much immature than newly hatched *Takydromus* and *Gallus*.

The neurohypophysis (median eminence=ME and neural lobe=NL)

These structures were identified mainly by the development of the subependymal nerve fiber layer. In most animals studied, the NL differentiates slightly earlier than the ME. In anamniotes studied, the appearance of the ME roughly corresponds to the appearance of AF stainability of the nerve fibers of the NL. In amniotes studied, the appearance of the ME precedes the appearance of AF stainability of the NL.

The NL is present in all vertebrates. The ME is also present in all vertebrates, although the ME of cyclostomes and advanced teleosts is not typical in terms of vascularization and anatomical relations to the NL [2, 3]. Possibly reflecting the phylogenetic antiquity and ubiquitousness of the NL and ME, these organs, especially the NL, differentiate relatively early in ontogeny in most animals. Their development is usually preceded only by the pineal, SCO, and paraphysis.

The saccus vasculosus (SV)

As adults, *Lampetra* and *Poecilia* do not possess the SV, whereas *Mustelus, Hypomesus*, and *Silurus* possess it [2]. The SV does not appear in embryos and larvae of *Lampetra* and *Poecilia* at any stage. Therefore, the absence of the SV in these animals is primary and is not due to the loss during ontogeny. Von Mecklenburg [37] also noted that the SV does not exist in embryos of *Esox* which had been known to lack the SV as adults. The adult *Hypomesus* possess a large and well developed SV. In this species, the SV appears very early in ontogeny. Its appearance is preceded only by the pineal. The adult *Silurus* possess a relatively small SV. In this species, the SV appears much later than the pineal. In *Hypomesus* and *Silurus*, the degree of final development of the SV appears to be correlated to the time of differentiation of the anlage during ontogeny. The adult *Mustelus* possess a moderately developed SV. In this dogfish, the development of the SV is preceded even by the neurohypophysis.

Considering the results in *Hypomesus* and *Silurus*, it may be said that the earlier differentiation of the SV results in the more developed SV in adults. However, the SV is well developed, atrophied, or even absent among a wide variety of teleosts and therefore the relation between phylogeny and ontogeny of the SV cannot be well documented in this study which dealt with only a few species. The literature on the histogenesis of the SV is reviewed by Dorn [38].

The organum vasculosum laminae terminalis (OVLT)

Among the species studied, only *Silurus, Poecilia*, and *Mus* possess a well differentiated OVLT as adults [2]. The OVLT of the other species is poorly developed histologically even in adults and, reasonably, it is hardly detectable in their embryos and larvae. In the mid-embryonic stages of *Takydromus*, the ventral wall of the preoptic recess is somewhat specialized, but such a specialized region disappears in later embryonic stages. This transient structure may not have a direct significance in the development of the OVLT.

In *Silurus*, the appearance of the OVLT is very late. This observation is in accord with the study in adults which showed that only large individuals possess a well differentiated OVLT [2]. On the contrary, the OVLT of *Poecilia* develops quite early in ontogeny. This may be related to the large size of this organ in adults. In *Mus*, the development of the OVLT is slow. It fully differentiates histologically only after birth.

The relation between phylogeny and ontogeny of the OVLT cannot be well documented, because this organ is well developed in phylogenetically remote groups but are histologically indistinct in many groups and ontogenetically differentiates quite differently even in the same group (*viz. Silurus* vs. *Poecilia*).

The paraventricular organ (PVO)

The adult *Lampetra* and *Mus* do not possess the PVO. No traces of the PVO is noticed in the embryos of these two animals. Therefore, the absence of the PVO in *Lampetra* and *Mus* may be primary and not be the secondary loss during the course of ontogeny.

In most animals studied, the appearance of the PVO roughly corresponds to that of the neurohypophysis. In *Hynobius*, however, the PVO differentiates earlier than the neurohypophysis and in *Gallus* the PVO differentiates later than the neurohypophysis. As adults, the PVO of amphibians and reptiles is better developed than that of birds [2]. The relatively late ontogenetic differentiation of the PVO in *Gallus* may be related to the relatively poor development of this organ in adults. Vigh-Teichmann *et al.* [39] also have shortly described the development of the PVO in several species of vertebrates.

Except for cyclostomes and mammals, the PVO ubiquitously occurs in vertebrates, although this organ is not well differentiated histologically in the lungfish and caecilian [2]. Possibly reflecting this phylogenetic antiquity, the PVO differentiates relatively early in ontogeny in most non-mammalian gnathostomes.

The pineal and parapineal

Ontogenetically, the pineal usually appears first among all CVOs. Only in *Mus*, the appearance of the pineal anlage is preceded by that of the NL. In this study, however, the appearance of the pineal was judged by the initiation of the omega-shaped epithalamic evagination rather than histological differentiation. Indeed, possibly photoreceptive outer segment-like intraluminal protrusions, which are usually stained weakly with AF, appear much later than the appearance of the omega-like evagination. However, even if we admit the tendency to have evaluated the pineal appearance slightly earlier than in the other CVOs, it still might be considered that the pineal is the CVO that differentiates first during ontogeny. The utmost importance of the pineal is also inferred from the phylogenetic survey which showed that the pineal is found in all vertebrate groups except for sporadic secondary degeneration or loss [3, 7].

In *Lampetra*, the parapineal is very small in early stages of development, but it still precedes the other CVOs (except for the pineal) in appearance. In *Rana*, the anlage of the possibly parapineal-equivalent frontal organ cannot be separable from the pineal anlage before stage 21. In *Takydromus*, the anlage of the parapineal-equivalent parietal eye cannot be separable from the pineal anlage before stage 30^{+}. In both species, however, the separation of the parapineal-equivalent structure occurs quite early in ontogeny. These observations suggest that the parapineal is an ancient CVO as the pineal although the parapineal has been lost in many extant vertebrates. It may be noteworthy that in parapineal-possessing animals such as *Lampetra, Rana*, and *Takydromus* initial differentiation of the SCO roughly coincides with the separation of the parapineal from the pineal.

The development of the pineal complex has been extensively studied in reptiles [40–42]. See also review articles cited in Introduction for numerous references on the pineal development in various vertebrates.

The subcommissural organ (SCO)

The appearance of the SCO was determined by the differentiation of the columnar ependymal cells under the posterior commissure. Although this differentiation is quite gradual and these ependymal cells are not distinctly stained with AF

at early stages of differentiation, the SCO should be considered as the very early differentiating CVO. In most animals studied, the appearance of the SCO is preceded only by the pineal complex (*Lampetra, Silurus, Poecilia, Rana*, and *Takydromus*) or roughly coincides with the appearance of the paraphysis (*Hynobius* and *Gallus*). In *Hypomesus*, the SCO develops later than the SV. In *Mus*, the SCO develops slightly later than the NL. Even in these two species, however, the development of the SCO is not retarded at all. AF stainability of the SCO also precedes that of the NL except for *Poecilia* and *Mus*.

There are some mammals (man, for example) that do not possess a distinct SCO as adults. Even in these mammals, the SCO is developed at least at some embryonic stages [43]. From an ontogenetic viewpoint, the SCO may be considered as the most fundamental CVO as well as the pineal. The essential importance of the SCO is conjectured also from the phylogenetic study which showed that the SCO is the most ancient CVO of chordates [2, 44].

The paraphysis

In three teleostean species studied, the paraphysis is absent even as adults [2]. In *Mustelus*, the paraphysis is small both in embryos and adults. (See Ariëns Kappers [45] for the problem on the paraphysis in the embryonic chondrichthyans.) In *Hynobius*, the paraphysis appears very early in ontogeny, being preceded only by the pineal. In *Rana*, the paraphysis appears rather late, being preceded by the DCP. The paraphysis is most well developed in amphibians among vertebrates [2] and therefore its late appearance in *Rana* is somewhat peculiar. In *Takydromus*, the paraphysis appears early in ontogeny. In *Gallus*, it also appears quite early in ontogeny. Both in *Takydromus* and *Gallus*, the appearance of the paraphysis precedes that of the CP. In *Gallus*, however, the paraphysis degenerates in posthatching chicks and therefore its embryonic development may be considered as a transitory manifestation of an old reptilian character. The embryonic *Mus* lacks the paraphysis as in the adult *Mus*. Some authors described the paraphysis in embryonic mice [35], but the structure is indistinct in any case. In the other mammalian embryos, the paraphysis is extremely atrophied or virtually absent [46, 47].

Although the paraphysis has been paid little attention from a functional viewpoint, its very early appearance at least in some tetrapods suggests that the paraphysis was a fundamental CVO in the early evolution of tetrapods.

The development of the paraphysis was concisely reviewed in various vertebrates by Ariëns Kappers [48].

The choroid plexus (CP)

As adults, both *Silurus* and *Poecilia* possess a weakly developed DCP. Adult *Hypomesus* do not possess the DCP, but possess a simple VT [2]. In larval *Hypomesus*, the VT is not developed but this may be attributable to the young stages of the larvae studied. In *Silurus*, the DCP is not formed even in 15 mm long larvae. In this catfish, the DCP must develop much later in ontogeny. Indeed, 33 mm long *Silurus* still does not differentiate an ependymal folding characteristic to the CP [2]. On the contrary, the DCP differentiates rather early in *Poecilia*, although it is merely a ball-like intraventricular protrusion throughout the life. In teleosts, the TCP is not a typical CP, but a simple ependymal sheet consisting of cuboidal or columnar ependymal cells (tela chorioidea telencephali). In *Silurus*, the transition from flat to cuboidal ependymal cells occurs quite early in ontogeny. In teleosts, the tela chorioidea myelencephali also differentiates from a flat ependymal sheet called the tela membranosa myelencephali. In *Hypomesus*, the tela chorioidea myelencephali differentiates slightly earlier than the tela chorioidea telencephali. In *Silurus*, the order of differentiation is reversed.

As adults, the TCP is found in *Hynobius, Takydromus, Gallus*, and *Mus*, but it is absent in *Rana* among tetrapod species studied in this paper [2]. Both the DCP and MCP are present in all adult tetrapod species studied. In three amniote species (*Takydromus, Gallus*, and *Mus*), the order of differentiation of three kinds of CP is roughly as follows; the MCP, TCP, and DCP. The DCP of *Takydromus* differentiates as the SD in the early embryonic stages. Since the SD is a piscine CVO, its occurrence in embryonic tetrapods may be

considered as the manifestation of the phylogenetic vestige inherited from their ancestors. In amphibians, the developmental order of CPes is different from that in amniotes. In *Hynobius*, the TCP differentiates first, then the DCP, and finally the MCP. In *Rana*, the DCP also differentiates slightly earlier than the MCP. In amphibians, the development of the CPes was described in *Rana temporaria* [49], *Xenopus laevis* [50], and in some other species.

In all vertebrates including the lamprey, the MCP or tela chorioidea myelencephali differentiates from a single layer of epithelium (tela membranosa myelencephali). In fishes and amphibians, the tela chorioidea telencephali and DCP appear to differentiate also from a single-layered ependymal sheet. In amniotes (*Takydromus, Gallus*, and *Mus*), however, the anlage of the DCP and TCP is a ventricular protrusion of which wall is rather thick and is usually composed of a few layers of cells (pseudostratified?). Histogenesis of the TCP and DCP is thus somewhat different between anamniotes and amniotes.

It might be assumed that the MCP is the most fundamental CP of vertebrates, because it is most widely distributed in a series of vertebrates [2] and ontogenetically appears earlier than the more rostral CP in amniotes. As far as the present tetrapod species are concerned, the TCP appears to predominate over the DCP, because the TCP differentiates earlier than the DCP except for *Rana* that does not differentiate the TCP at all. The relatively early appearance of the DCP in *Rana* may compensate the absence of the TCP in this species.

The subfornical organ (SFO)

The SFO is developed only in higher vertebrates. Even among them, only mammals possess a well differentiated organ with many parenchymal capillaries [2]. Indeed, even in advanced embryos and larvae of *Hynobius, Rana, Takydromus*, and *Gallus*, the SFO is not at all detectable or scarcely differentiated. On the contrary, the SFO is differentiated already in the embryonic period in *Mus*. In these respects, the SFO is similar to the OVLT. Both phylogenetically and ontogenetically, the SFO development appears to culminate in mammals.

The area postrema (AP)

The adult *Mustelus* possesses a moderately developed AP [2], but embryos studied do not show the differentiation as the AP. In these embryos, most CVOs are already differentiated. Therefore, the AP must be an organ that differentiates quite late in ontogeny.

Among the tetrapods examined, the AP of adult *Takydromus* is poorly developed, the AP of adult *Gallus* is moderately developed, and the AP of adult *Mus* is well developed. Possibly reflecting these developmental degrees in adults, the AP is not differentiated yet in *Takydromus* embryos, but it is differentiating in late embryos of *Gallus* and *Mus*. Among vertebrates, only mammals possess a well differentiated AP, SFO, and OVLT [2]. In *Mus*, the development of these three organs occurs almost simulateously only in the late period of the embryonic life. These organs are considered as relatively young organs, especially ontogenetically.

Conclusions

The CVO that first appears in the embryonic brain is the pineal complex (pineal and parapineal if present) and the SCO in most species studied. Since the pineal and SCO are very old organs also phylogenetically, these organs are considered as the most fundamental CVOs of vertebrates. In the vertebrate hypothalamus, three neurohemal organs are present; the ME, NL, and OVLT. The first two are phylogenetically very old organ and appear relatively early in ontogeny. Even in the ancient vertebrates, the pineal and the neurohypophysis might have been indispensable CVOs as an epithalamic sensory CVO and a hypothalamic secretory CVO, respectively.

In gnathostomes, both the PVO and paraphysis are old organs phylogenetically. They also appear rather early in ontogeny. The paraphysis is especially an early differentiating organ and might be an important CVO in lower tetrapods. In homoiotherms, however, these organs are fundamentally obsolete. In birds, the paraphysis appears to be distinct only in embryos and in mammals both the paraphysis and PVO appear to

be lost even in embryos.

In teleosts, the CP is not differentiated as a folded organ, but the CP must be a fundamental CVO of vertebrates. In tetrapods, three kinds of CP (TCP, DCP, and MCP) are consistently developed (except for the absence of the TCP in anurans) and they appear rather early in ontogeny. In very early embryos, however, the CP is not indispensable for the production of cerebrospinal fluid, because in these embryos the ventricles are large but the CP is not yet formed.

The SFO is a young organ both phylogenetically and ontogenetically at least in terms of histological differentiation. The OVLT and AP are also considered as young organs from an ontogenetical viewpoint, although they are not necessarily young organs in a phylogenetic sense. The primitive vertebrates and early embryos apparently manage to live without these three organs.

ACKNOWLEDGMENTS

I would like to express my sincere thanks to Professor Masami Ouji for his continuous advice and encouragement. This work was partly supported by Grant-in-Aid from the Ministry of Education, Science and Culture of Japan.

REFERENCES

1 Leonhardt, H. (1980) Ependym und circumventrikuläre Organe. In "Handbuch der Mikroskopischen Anatomie des Menschen, IV/10". Ed. by A. Oksche and L. Vollrath, Springer, Berlin, pp. 177–666.

2 Tsuneki, K. (1986) A survey of occurrence of about seventeen circumventricular organs in brains of various vertebrates with special reference to lower groups. J. Hirnforsch., **27**: 441–470.

3 Tsuneki, K. (1986) A histologic survey of diencephalic circumventricular organs in teleosts with special reference to osteoglossomorphs. Jpn. J. Ichthyol., **33**: 27–38.

4 Studnička, F. K. (1905) Die Parietalorgane. In "Lehrbuch der vergleichenden Mikroskopischen Anatomie der Wirbeltiere, V". Ed. by A. Oppel, Gustav Fischer, Jena.

5 Bargmann, W. (1943) Die Epiphysis cerebri. In "Handbuch der mikroskopischen Anatomie des Menschen, VI/4". Ed. by W. V. Möllendorff, Springer, Berlin, pp. 309–502.

6 Wingstrand, K. G. (1966) Comparative anatomy and evolution of the hypophysis. In "The Pituitary Gland, 1". Ed. by G. W. Harris and B. T. Donovan, Univ. Calif. Press, Berkeley, pp. 58–126.

7 Vollrath, L. (1981) The pineal organ. In "Handbuch der mikroskopischen Anatomie des Menschen, VI/7". Ed. by A. Oksche and L. Vollrath, Springer, Berlin.

8 Piavis, G. W. (1971) Embryology. In "The Biology of Lampreys, 1". Ed. by M. W. Hardisty and I. C. Potter, Academic Press, London, pp. 361–400.

9 Usui, M. and Hamsaki, M. (1939) Tafeln zur Entwicklungsgeschichte von *Hynobius nigrescens* Stejneger. Zool. Mag. (Tokyo), **51**: 195–206.

10 Tahara, Y. (1959) Table of the normal developmental stages of the frog, *Rana japonica*. I. Early development (stages 1–25). Jpn. J. Exp. Morphol., **13**: 49–60.

11 Tahara, Y. (1974) Table of the normal developmental stages of the frog, *Rana japonica*. II. Late development (stages 26–40). Mem. Osaka Kyoiku Univ., III, **23**: 33–53.

12 Dufaure, J. P. and Hubert, J. (1961) Table de développement du lézard vivipare: *Lacerta (Zootoca) vivipara* Jacquin. Arch. Anat. Microsc. Morphol. Exp., **50**: 309–327.

13 Hamburger, V. and Hamilton, H. L. (1951) A series of normal stages in the development of the chick embryo. J. Morphol., **88**: 49–92.

14 Theiler, K. (1972) The House Mouse. Development and Normal Stages from Fertilization to 4 Weeks of Age, Springer, Berlin.

15 Sterba, G., Pfister, Cl. and Naumann, W. (1965) Über den Beginn der Neurosekretion und der Sekretion des Subkommissuralorgans bei Neunaugenembryonen. Z. Mikrosk. -Anat. Forsch., **74**: 33–38.

16 Ichikawa, T., Kobayashi, H., Zimmermann, P. and Müller, U. (1973) Pituitary response to environmental osmotic changes in the larval guppy, *Lebistes reticulatus* (Peters). Z. Zellforsch., **141**: 161–179.

17 Omura, Y. and Oguri, M. (1971) The development and degeneration of the photoreceptor outer segment of the fish pineal organ. Bull. Jpn. Soc. Sci. Fish., **37**: 851–860.

18 Tsuneki, K. (1986) Evolution of the nuclear size of cerebellar granular cells in vertebrates with special references to fishes and amphibians. Zool. Sci., **3**: 885–892.

19 Oota, Y. and Sakurai, K. (1983) The embryonic development of the hypothalamo-hypophysial system in the lizard, *Takydromus tachydromoides*. Rep. Fac. Sci., Shizuoka Univ., **17**: 65–75.

20 Oota, Y. and Sakurai, K. (1984) Ultrastructural studies on the embryonic development of the hypothalamo-hypophysial system in the lizard, *Takydromus tachydromoides* . Rep. Fac. Sci.,

Shizuoka Univ., **18**: 45–59.

21 Wingstrand, K. G. (1951) The Structure and Development of the Avian Pituitary, Gleerup, Lund.

22 Daikoku, S., Ikeuchi, C. and Nakagawa, H. (1974) Development of the hypothalamo-hypophysial unit in the chick. Gen. Comp. Endocrinol., **23**: 256–275.

23 Vigh, B., Tar, E. and Teichmann, I. (1968) The development of the paraventricular organ in the White Leghorn chicken. Acta Biol. Acad. Sci. Hung., **19**: 215–225.

24 Calvo, J. and Boya, J. (1978) Embryonic development of the pineal gland of the chicken (*Gallus gallus*). Acta Anat., **101**: 289–303.

25 Omura, Y. (1977) Ultrastructural study of embryonic and post-hatching development of the pineal organ of the chicken (Brown Leghorn, *Gallus domesticus*). Cell Tissue Res., **183**: 255–271.

26 Ziegels, J. (1977) Etude histochimique de l'organe sous-commissural du Poulet au cours du développement. C. R. Soc. Biol., **171**: 1306–1308.

27 Wingstrand, K. G. (1953) Neurosecretion and antidiuretic activity in chick embryos with remarks on the subcommissural organ. Ark. Zool., **6**: 41–67.

28 Stockem, W. and Weber, W. (1966) Zur vergleichenden Entwicklungsgeschichte der Paraphyse bei Vögeln. Z. Anat. Entwickl. -Gesch., **125**: 101–118.

29 Malik, M. R. and Singh, S. (1980) Histogenesis and mode of growth of choroid plexus in chick embryos. J. Anat. Soc. India, **29**: 1–5.

30 El-Gammal, S. (1981) The development of the diencephalic choroid plexus in the chick: a scanning electron-microscopic study. Cell Tissue Res., **219**: 297–311.

31 El-Gammal, S. (1983) Regional surface changes during the development of the telencephalic choroid plexus in the chick. A scanning-electron microscopic study. Cell Tissue Res., **231**: 251–263.

32 Beauvillain, J.-C. (1973) Structure fine de l'eminence médiane de souris au cours de son ontogenese. Z. Zellforsch., **139**: 201–215.

33 Gross, D. S. and Baker, B. L. (1977) Immunohistochemical localization of gonadotropin-releasing hormone (GnRH) in the fetal and early postnatal mouse brain. Am. J. Anat., **148**: 195–216.

34 Castañeyra-Perdomo, A., Meyer, G. and Ferres-Torres, R. (1983) Development of the subcommissural organ in the albino mouse (a Golgi study). J. Hirnforsch., **24**: 363–370.

35 Graumann, W. (1950) Zelldegeneration im Telencephalon medium und Paraphysenentwicklung bei der weißen Maus. Z. Anat. Entwickl. -Gesch., **115**: 19–31.

36 Zaki, W. (1981) Ultrastructure of the choroid plexus and its development in the mouse. Z. Mikrosk. -Anat. Forsch., **95**: 919–935.

37 Von Mecklenburg, C. (1974) The development of saccus vasculosus in two teleosts. Acta Zool. (Stockh.), **55**: 137–148.

38 Dorn, E. (1955) Der Saccus vasculosus. In "Handbuch der mikroskopischen Anatomie des Menschen, IV/2". Ed. by W. V. Möllendorff and W. Bargmann, Springer, Berlin, pp. 140–185.

39 Vigh-Teichmann, I., Vigh, B. and Aros, B. (1969) Phylogeny and ontogeny of the paraventricular organ. In "Zirkumventrikuläre Organe und Liquor". Ed. by G. Sterba, Gustav Fischer, Jena, pp. 151–154.

40 Trost, E. (1953) Die Entwicklung, Histogenese und Histologie der Epiphyse, der Paraphyse, des Velum Transversum, des Dorsalsackes und des subcommissuralen Organs bei *Anguis fragilis, Chalcides ocellatus* und *Natrix natrix* . Acta Anat., **18**: 326–342.

41 Oksche, A. (1965) Survey of the development and comparative morphology of the pineal organ. Prog. Brain Res., **10**: 3–29.

42 Quay, W. B. (1979) The parietal eye–pineal complex. In "Biology of the Reptilia, 9. Neurobiology A". Ed. by C. Gans, R. G. Northcutt and P. Ulinski, Academic Press, London, pp. 245–406.

43 Olsson, R. (1961) Subcommissural ependyma and pineal organ development in human fetuses. Gen. Comp. Endocrinol., **1**: 117–123.

44 Sterba, G., Fredriksson, G. and Olsson, R. (1983) Immunocytochemical investigations of the infundibular organ in amphioxus (*Branchiostoma lanceolatum* ; Cephalochordata). Acta Zool. (Stockh.), **64**: 149–153.

45 Ariëns Kappers, J. (1957) On the problem of the presence of a paraphysis cerebri in selachians. Pubbl. Staz. Zool. Napoli, **29**: 41–70.

46 Warren, J. (1917) The development of the paraphysis and pineal region in Mammalia. J. Comp. Neurol., **28**: 75–135.

47 Krabbe, K. H. (1936) Studies on the existence of a paraphysis in mammalian embryos. Brain, **59**: 483–493.

48 Ariëns Kappers, J. (1982) The paraphysis cerebri. In "Comparative Correlative Neuroanatomy of the Vertebrate Telencephalon". Ed. by E. C. Crosby and H. N. Schnitzlein, Macmillan, New York, pp. 249–265.

49 Wolff, F. (1962) Funktionell-histologische Studien am Plexus chorioideus von *Rana temporaria* L. unter besonderer Berücksichtigung der Sekretionsfrage. Z. Zellforsch., **57**: 63–105.

50 Lametschwandtner, A., Laminger, A. and Adam, H. (1983) Development and differentiation of the brain ventricular system in tadpoles of *Xenopus laevis* (Daudin) (Amphibia, Anura). Z. Mikrosk. -Anat. Forsch., **97**: 265–278.

ZOOLOGICAL SCIENCE 4: 523–528 (1987)

Involvement of Angiotensin II in Water Intake in the Japanese Eel, *Anguilla japonica*

Yuji Okawara, Takeo Karakida, Masahiro Aihara, Ken'ichi Yamaguchi[1] and Hideshi Kobayashi[2]

Department of Biology, Faculty of Science, Toho University, Funabashi, Chiba 274, and [1]Department of Physiology, School of Medicine, Niigata University, Niigata, Niigata 951, Japan

ABSTRACT—When Japanese eels, *Anguilla japonica,* were transferred from fresh water to sea water (SW), they started drinking within 15 min, though not copiously, and no increase in plasma angiotensin II (AII) could be observed for at least 120 min following transfer. Significant increases in both drinking rate and plasma AII level were observed 10 hr after transfer to SW and further increases occurred 1 to 3 days after transfer. Water intake of eels maintained in SW for 10 days was inhibited by single intraperitoneal injections of SQ14225 (1 mg/fish), an inhibitor of the enzyme which converts angiotensin I into AII. These findings suggest that endogenous plasma AII is not related to water intake observed for at least 120 min after transfer, but is physiologically involved in the mechanism regulating the water intake observed after 10 hr of transfer to SW.

INTRODUCTION

The administration of angiotensin II (AII) has been found to induce drinking in most vertebrate species [1–4, 6, see 5 for a review], except amphibians [2, 6]. However, the involvement of endogenous plasma AII in the mechanism regulating physiological water intake is not yet fully understood. In the present study, the Japanese eel was used, since it has been demonstrated that they drink copiously immediately after transfer from fresh water (FW) to sea water (SW) [7, 8] and ingest SW constantly when adapted to SW [9]. First, the changes in circulating AII were compared to water intake at various time intervals after transfer of eels from FW to SW. Second, an attempt was made to reduce plasma AII in SW-adapted eels by treatment with SQ14225 (an inhibitor of the conversion of angiotensin I (AI) into AII) in order to examine whether water intake would be consequently affected.

Accepted December 18, 1986
Received December 11, 1986
[2] To whom requests of reprints should be addressed.

MATERIALS AND METHODS

Japanese eels, *Anguilla japonica* (160–240 g), cultured in Taiwan and imported to Japan, were purchased from a commercial source. Seven to ten eels were kept without food in an aquarium containing about 70 liters of well aerated FW or SW at about 25°C for several days before use. Five to six polyvinyl tubes (i.d. = 6 cm, length = 40 cm) were placed at the bottom of the aquarium as hiding place for the eels. All experiments were performed in either June or August.

Measurement of water intake

Water intake was measured by the phenol red (PR) method of Smith [11] and Oide and Utida [9] with some modifications, as detailed earlier [4]. Briefly, the eels were immersed in PR (0.004%)-containing FW (PR-FW) or SW (PR-SW) for certain periods. After sacrifice, the stomach and intestine were removed and the PR was rinsed out with 5 ml of 0.75% NaCl solution. Fat and protein were removed from the rinse by petroleum ether and trichloroacetic acid (TCA), respectively. The amount of PR in the rinse was determined by a

spectrophotometer (Hitachi model 101) at a wave length of 550 nm. The stomach and intestine of FW eels were treated in the same way and the values obtained served as blank values. The blank value was subtracted from experimental values obtained from PR-FW or PR-SW eels. The equivalent amount of water ingested was calculated from these values. Smith [11] and Oide and Utida [9] did not use petroleum ether and TCA, but the use of petroleum ether and TCA in this procedure is important. For example, water intake was $15.0 \pm 4.5\,\mu l/100\,g$ (n=5) for 60 min following transfer of FW eels to SW when measured following treatment with these chemicals, but $46.6 \pm 2.1\,\mu l/100\,g$ (n=4) without treatment. Thus, without TCA and petroleum ether, some unidentified substances in the gut other than PR interfered with the photometric values. It was also confirmed that these chemicals have no effect on the PR.

Determination of plasma AII and hematocrit

Trunk blood (approximately 2 ml) was collected individually after decapitation and placed in heparinized ice-chilled centrifuge tubes containing 0.1 ml of 0.125 M Na_2EDTA, 0.025 M o-phenanthroline and 0.2% neomycin sulphate [12]. Extraction and radioimmunoassay of AII were carried out according to the method of Yamaguchi [13]. The antiserum used was raised against Asp^1–$Ileu^5$–AII and crossreacted 100% with Asp^1–Val^5–AII [14] and Asn^1–Val^5–AII (Okawara, unpublished data), both native AIIs of the Japanese eel [15]. A small amount of blood was used for microhematocrit determinations. In some cases, the AII values were corrected for changes in the hematocrit as described previously [16].

Experiment I. Observation for a period of 1 to 2 hr following transfer of FW eels to SW

Thirty FW-adapted eels were transferred into PR-SW, while hiding in the polyvinyl tubes. Groups of seven or eight eels each were killed 15, 30, 60 and 120 min following the transfer. Another ten eels kept in FW were transferred to PR-FW and killed 60 min later. These eels served as controls. Water intake, hematocrit and plasma AII concentration were measured in all fish. The experiments were repeated twice using thirty-eight and eighteen eels.

In order to examine the possible effects of the handling stress, one more experiment was conducted using twelve eels. Six eels were kept in an aquarium [30(D)×45(W)×10(H) cm] constantly supplied with aerated FW. Three polyvinyl tubes were available for every two eels. The FW was drained gently from the aquarium through an opening at the bottom. Then the opening was closed and PR-SW was introduced into the vessel. This process required about 2 min. The aquarium was supplied constantly with aerated PR-SW. The six eels were killed 15 min after the introduction of PR-SW. The remaining six eels were treated in the same way and killed 60 min after the introduction of PR-SW. Water intake was measured in all fish.

Experiment II. Observation for a period of 3 days following transfer of FW eels to SW

Twenty-nine FW-adapted eels were transferred to SW and groups of six to eight eels were killed 10 hr and 1, 2, and 3 days following SW immersion. The eels were transferred while in the polyvinyl tubes, and exposed to the PR-SW only 1 hr before sacrifice. We did not immerse eels into PR-SW for more than 2 hr, because when freshwater eels were transferred to PR-SW, they started excreting PR from the gut beginning at 2 hr after the transfer.

To measure plasma AII and hematocrit, another thirty FW eels were transferred to SW without PR. Five to ten of these eels were killed 10 hr and 1, 2, and 3 days following SW immersion. The data of the control eels in Experiment I were used as control values.

Experiment III. Effects of SQ14225 on water ingestion of SW-adapted eels

After 10 days of adaptation to SW, each of seven eels was netted and placed in a plastic bag. SQ14225 (captopril, Sankyo Co. Tokyo, 1 mg/0.1 ml/fish) dissolved in 1.3% NaCl solution was singly injected ip through the bag. The eels were then immediately transferred to PR-SW. Water intake was measured after 30 min. The control eels (n=8) were injected with the same volume of the vehicle.

Statistical analysis

The data of hematocrit and plasma AII were first analyzed by the Kruskal-Wallis test. The groups showing a significant difference at the 95% confidence limit were further compared by the Mann-Whitney U-test (Experiment I and II). Water intake values were analyzed by the Mann-Whitney test (Experiment II and III).

RESULTS

Experiment I. Observation for a period of 1 to 2 hr following transfer of FW eels to SW

The control PR-FW eels ingested no water during a 60 min observation period (Table 1). However, eels ingested 2.9, 19.5, 17.0 and 37.5 μl/100 g, in 15, 30, 60 and 120 min, respectively, following the exposure to SW (Table 1).

Similar results were obtained in two repetitions of this experiment. In one, eels ingested 0.3 ± 0.2 (n=10), 0.9 ± 0.5 (n=10), 20.9 ± 8.2 (n=10) and 79.2 ± 21.2 μl/100 g (n=8), in 15, 30, 60 and 120 min, respectively, after the transfer. In the other experiment, the intake was 7.6 ± 1.4 (n=9) and 13.4 ± 3.9 μl/100 g (n=9), in 15 and 60 min, respectively, following the transfer.

In the experiment, where FW was replaced without removing the fish from the aquarium, the eels ingested 2.2 ± 0.9 (n=6) and 11.8 ± 5.2 μl/100 g (n=6), in 15 and 60 min, respectively. The two different transfer procedures used in Experiment I were found to yield similar results.

Plasma AII concentrations showed no significant change throughout the experiment. The hematocrit values at 15 and 120 min after transfer were significantly lower than the controls or at other time intervals (Table 1). Recalculation of the plasma AII levels at 15 and 120 min, taking hematocrit values into consideration, according to the method of Okawara *et al.* [16] yielded values of 61.9 ± 8.1 and 43.9 ± 10.0 pg/ml, respectively. These values were not significantly different from control values.

Experiment II. Observation for a period of 3 days following transfer of FW eels to SW

Water intake in the final 1 hr before sacrifice 10 hr after transfer to SW increased significantly (4.7 ± 2.2 μl/100 g, n=7). It increased remarkably to 56.1 ± 14.2 μl/100 g (n=8) one day after the transfer. A further increase in water intake was noted after 2 days, reaching a rate of 264.0 ± 49.9 μl/100 g (n=8). However, no further increase could be observed on the following day (Fig. 1).

The plasma AII concentration had already increased significantly at 10 hr following transfer (77.6 ± 11.2 pg/ml, n=8) and a further increase occurred at day 2 (96.9 ± 15.6 pg/ml, n=9). This high level was maintained up to the end of the

TABLE 1. Water intake, plasma AII and hematocrit values following transfer of FW eels, *Anguilla japonica* to SW

Time period in PR-SW (min)	Number of eels	Water intake[a] (μl/100 g)	Plasma AII[a] (pg/ml)	Hematocrit[a] (%)
control (60 min in PR–FW)	10	-2.4 ± 0.6[b]	52.5 ± 5.2	36.2 ± 1.4
15	7	2.9 ± 0.5	55.1 ± 6.6	28.9 ± 1.9*
30	8	19.5 ± 7.5	57.8 ± 7.4	34.1 ± 0.8
60	7	17.0 ± 7.3	42.1 ± 5.8	38.2 ± 1.7
120	8	37.5 ± 11.0	40.7 ± 9.4	29.7 ± 2.6*

[a] Water intake was measured for a specified time period and plasma AII and hematocrit were determined at given times of SW exposure.

[b] Mean ± standard error.

* $p < 0.05$, compared with control values.

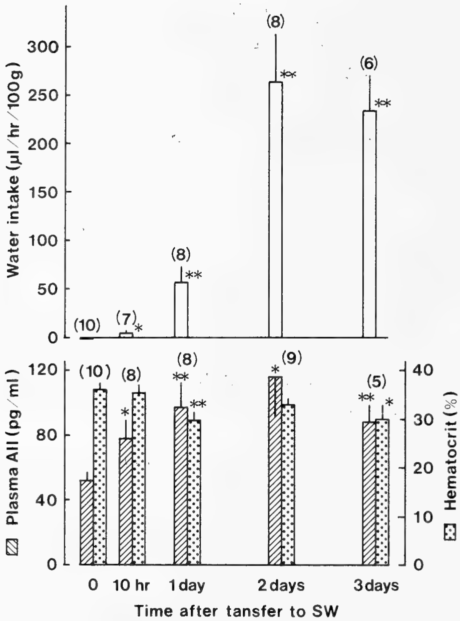

FIG. 1. Changes in drinking rate, plasma AII and hematocrit following transfer of FW eels to SW (Experiment II). Values at 0 time (control) are those obtained in Experiment I. Numbers of eels are indicated in parentheses. Each column represents the mean±SE. The amount of water ingested was measured for the last hour of 10 hr and 1, 2 and 3 days after immersion in SW. *, $p<0.05$ and **, $p<0.01$, as compared with the control.

third day (116.9±25.1 pg/ml, n=5) (Fig. 1). The hematocrit decreased significantly at day 1 (29.6±2.1%, n=8) and at day 3 (29.9±3.1%, n=5) after the transfer. Recalculation of the plasma AII levels at these time points, taking hematocrit values into consideration, according to the method of Okawara *et al.* [16] yielded values of 104.7±18.0 and 95.8±11.3 pg/ml, respectively. These values were also significantly different from control values.

Experiment III. Effects of SQ14225 on the water ingestion of SW-adapted eels

Water intake of the control eels adapted to SW for 10 days was 57.3±14.3 μl/100 g (n=7) within 30 min following the vehicle injections and that of eels injected with SQ14225 (1 mg/ fish) was 1.7±1.4 μl/100 g (n=8). The difference was significant ($p<0.01$).

DISCUSSION

In the present experiments, the Japanese eels did not ingest water while in FW. This is in agreement with the results of Oide and Utida [9] and Hirano [6]. We observed only marginal water ingestion (less than 20.7 μl/100 g), during the first one hour after transfer to SW. However, there are several reports indicating that eels ingest water copiously immediately after transfer from FW to SW [7, 8, 17]. Hirano [7] and Takei *et al.* [8] used oesophagus-cannulated eels and measured water intake with a drop counter. Kirsch and Mayer-Gostan [17] used intact eels and measured water intake using an isotope. The present experiments were conducted on intact eels, measuring water intake by the phenol red method. The difference between our data and those of other investigators may be due to difference in technique, species and source of eels. However, it may be interesting to measure plasma AII concentration at the time when copious drinking is observed, although it is said that the copious drinking is induced by Cl^- reflex [7].

In the present experiment, eels started drinking water soon after being transferred to SW, but the amounts of water intake were small in two of the experiments, even after 120 min. During this period, plasma AII concentrations did not change. Thus, plasma AII may not be involved in inducing water intake immediately after the transfer to SW. This hypothesis is consistent with the observation that renin activity in the eels transferred from FW to SW increased between 0.5 and 8 hr after the transfer [18].

Takei *et al.* [8] observed that a vigorous drinking immediately after the transfer was inhibited by preinjection of SQ14225. Their data suggest the involvement of plasma AII in the vigorous drinking induced by Cl^- reflex, but there is the possibility that SQ14225 inhibited such drinking through some unidentified mechanisms other than the inhibition of converting enzyme.

Water intake and plasma AII both significantly increased 10 hr after transfer. After this, water intake increased in parallel with that of plasma AII concentration. These findings suggest the possible involvement of plasma AII in water intake

observed 10 hr after transfer to SW.

Our results show that SQ14225 curtailed water intake of eels maintained in SW for 10 days. It may be hypothesized, therefore, that AII is involved in the physiological mechanism regulating natural water intake in SW adapted eels. This hypothesis is in agreement with the observations that infusion of SQ14225 inhibited water intake of SW-adapted euryhaline flounder [19] and that administration of SQ20881, another converting enzyme inhibitor, reduced water intake of the SW-adapted euryhaline killifish [20]. Furthermore, SQ14225 also reduced natural water intake in mammals [see 5 for a review] and in Japanese quail [1]. Nevertheless, Beasley *et al.* [21] reported that SQ14225 did not attenuate basal water intake in certain obligatory marine fish such as the winter flounder and the longhorn sculpin. It is possible that stenohaline SW fish such as the winter flounder and the longhorn sculpin may regulate basal drinking through mechanisms independent of the renin-angiotensin system. Further studies using freshwater, marine and euryhaline fishes are needed to clarify this point.

ACKNOWLEDGMENTS

We are grateful to Professor Tetsuya Hirano, Ocean Research Institute, University of Tokyo, Professor Zvi Yaron, Department of Zoology, Tel Aviv University and Dr. Yoshio Takei, Department of Physiology, Kitasato University for their valuable suggestion and discussion during the preparation of this manuscript. This investigation was supported by a Grant-in-Aid for Scientific Research from the Ministry of Education, Science and Culture of Japan.

REFERENCES

1 Kobayashi, H. and Takei, Y. (1982) Mechanisms for induction of drinking with special reference to angiotensin II. Comp. Biochem. Physiol., **71A**: 485–494.

2 Kobayashi, H., Uemura, H., Wada, M. and Takei, Y. (1979) Ecological adaptation of angiotensin-induced thirst mechanism in tetrapods. Gen. Comp. Endocrinol., **38**: 93–104.

3 Kobayashi, H., Okawara, Y., Maitra, S., Sinhahkim, A. and Ghosh A. (1982) Further studies on angiotensin II-induced drinking in birds. J. Yamashina Inst. Ornithol., **14**: 137–142.

4 Kobayashi, H., Uemura, H., Takei, Y., Itatsu, N., Ozawa, M. and Ichinohe, K. (1983) Drinking induced by angiotensin II in fishes. Gen. Comp. Endocrinol., **49**: 295–306.

5 Fitzsimons, J. T. (1979) The Physiology of Thirst and Sodium Appetite, Cambridge Univ. Press, Cambridge/London/New York/Melbourne, pp. 285–288.

6 Hirano, T., Takei, Y. and Kobayashi, H. (1978) Angiotensin and drinking in the eel and the frog. In "Osmotic and Volume Regulation". Ed. by C. B. Jorgensen and E. Skadhauge, Munksgaard, Copenhagen, pp. 123–128.

7 Hirano, T. (1974) Some factors regulating water intake by eel, *Anguilla japonica*. J. Exp. Biol., **61**: 737–747.

8 Takei, Y., Uemura, H. and Kobayashi, H. (1985) Angiotensin and hydromineral balance: with special reference to induction of drinking behavior. In "Current Trends in Comparative Endocrinology". Ed. by B. Loft and W. N. Holmes, Hong Kong Univ. Press, Hong Kong, pp. 933–936.

9 Oide, H. and Utida, S. (1968) Absorption and excretion in the Japanese eel. Marine Biol., **1**: 172–177.

10 Takei, Y., Hirano, T. and Kobayashi, H. (1979) Angiotensin and water intake in the Japanese eel, *Anguilla japonica*. Gen. Comp. Endocrinol., **38**: 466–475.

11 Smith, H. W. (1931) The absorption and excretion of water and salts by the elasmobranch fishes. II. Marine elasmobranchs. Am. J. Physiol., **98**: 296–310.

12 Düsterdieck, G. and McElwee, G. (1976) Estimation of angiotensin II concentration in human plasma by radioimmunoassay. Some applications to physiological and clinical states. Eur. J. Invest., **2**: 32–38.

13 Yamaguchi, K. (1981) Effect of water deprivation on immunoreactive angiotensin II levels in plasma, cerebroventricular perfusate and hypothalamus of the rat. Acta Endocrinol., **97**: 137–144.

14 Takei, Y., Okawara, Y. and Kobayashi, H. (1987) Mechanisms regulating drinking in the Japanese quail, *Coturnix coturnix japonica*. In "Progress in Avian Osmoregulation". Ed. by M. R. Hughes and A. C. Chadwick, Leeds Philosophical and Literary Society Ltd., Leeds. (in press)

15 Hasegawa, Y., Nakajima, T. and Sokabe, H. (1983) Chemical structure of angiotensin formed with kidney renin in the Japanese eel, *Anguilla japonica*. Biomed. Res., **4**: 417–420.

16 Okawara, Y., Karakida, T., Yamaguchi, K. and Kobayashi, H. (1985) Diurnal rhythm of water intake and plasma angiotensin II in the Japanese quail (*Coturnix coturnix japonica*). Gen. Comp.

Endocrinol., **58**: 89–92.

17 Kirsch, R. and Mayer-Gostan, N. (1973) Kinetics of water and chloride exchanges during adaptation of the European eel to sea water. J. Exp. Biol., **58**: 105–121.

18 Sokabe, H., Oide, H., Ogawa, M. and Utida, S. (1973) Plasma renin activity in Japanese eels (*Anguilla japonica*) adapted to SW or in dehydration. Gen. Comp. Endocrinol., **38**: 466–475.

19 Carrick, A. and Balment, R. J. (1983) The renin-angiotensin system and drinking in the euryhaline flounder, *Platichthys flesus*. Gen, Comp. Endocrinol., **51**: 423–433.

20 Malvin, R. L., Schiff, D. and Eiger, S. (1980) Angiotensin and drinking rates in the euryhaline killifish. Am. J. Physiol., **239**: R31–R34.

21 Beasley, D., Shier, D. N., Malvin, R. L. and Smith, G. (1986) Angiotensin-stimulated drinking in marine fish. Am. J. Physiol., **250**: R1034–R1038.

ZOOLOGICAL SCIENCE 4: 529–534 (1987)

Cyclic CMP Alters Squirrel Monkey (*Saimiri sciureus*) Luteal Cell Structure via Cyclic AMP-Dependent Mechanisms

PHILIP J. CHAN[1]

Department of Obstetrics and Gynecology, University of Medicine and Dentistry of New Jersey School of Osteopathic Medicine, 401 Haddon Ave., Camden, New Jersey 08103, U.S.A.

ABSTRACT—Cyclic cytidine monophosphate (cCMP) is a pyrimidine nucleotide that is not as well-known as the other intracellular messengers such as cyclic adenosine monophosphate (cAMP). The present study was undertaken to determine if cCMP functions to alter cultured luteal cell morphology and if the mechanism involves cAMP. Adult female squirrel monkeys of Guyanan origin were administered daily single i.m. injections of FSH (follicle-stimulating hormone) for 4 days followed by hCG (human chorionic gonadotropin) on the fourth day. Luteal cells were aspirated from ovarian corpora lutea 64 hr after hCG by laparoscopy. The cells were dispersed, washed and cultured in individual center-well petri dishes for 48 hr at 37°C in 5% CO_2 in air. The test compounds (10 μM each), dbcCMP, dbcAMP, dbcGMP, dbcCMP and 6 mM imidazole, or control media were added at the start of culture. At the end of the incubation period, the cells were fixed in methanol and stained with Giemsa stain. The data indicated that dbcCMP restructured the polygonal luteal cells into small narrow-shaped cells with minimal cytoplasm in a manner similar to dbcAMP. However, when imidazole, a phosphodiesterase stimulator, was also present, the cells retained the polygonal shape. Dibutyryl cGMP at the concentration tested did not affect luteal cell morphology. The results suggest that dbcCMP alters the squirrel monkey luteal cell morphology in a manner similar to dbcAMP and that the process requires intracellular cAMP.

INTRODUCTION

Cyclic nucleotides are a class of intracellular compounds [1–3] which are involved in mediating hormone action and regulating cellular events such as the assembly of microtubules [4, 5] and microfilament cell processes [6]. The role of cAMP and cGMP as intracellular second messengers is well-documented [2, 3, 7, 8].

At the present time, there have been no reports on the function of cCMP in the regulation of cell morphology and progesterone synthesis. Cyclic CMP is a pyrimidine compound, in contrast to cAMP and cGMP which are purine compounds. Studies in other cell types indicate that cCMP activates protein kinases [9], hemoglobin synthesis [10], modulates cell proliferation and increases phosphodiesterase activity in fast growing hepatoma cells [11]. The present study was carried out to define the action of cCMP, in relation to cAMP and cGMP, on squirrel monkey luteal cell morphology. The objective is to determine if cCMP alters cell morphology and to examine the mechanism involved in the transformation.

MATERIALS AND METHODS

Adult female squirrel monkeys (*Saimiri sciureus*) of Guyanan origin (Buckshire Corp., Perkasie, PA) weighing between 600 g and 750 g were housed individually in stainless steel flush-type cages. The animals were kept indoors on a 12L:12D cycle and fed a commercial monkey feed and water *ad libitum*. The hormonal-stimulating regimen [12] consisted of administering the female monkeys with 4 days of follicle-stimulating hormone (FSH-P, Burns-Biotec Laboratories Inc., Omaha, NE) at a daily dosage of 1 mg intramuscu-

Accepted January 19, 1987
Received November 19, 1986

[1] Present address: Department of Obstetrics and Gynecology, Oral Roberts University School of Medicine, City of Faith, 8181 S. Lewis, Tulsa, Oklahoma 74104, U.S.A.

larly followed by a single i.m. injection of 250 IU human chorionic gonadotropin (hCG, APL Ayerst Laboratories, New York, NY) on the final day of FSH treatment. It has been shown that there is no seasonal effect on squirrel monkey oocyte development and that follicle cells such as luteal cells may be harvested at any time of the year [13]. At 64 hr after hCG treatment, the squirrel monkeys were anesthetized (15 mg ketamine/animal i.m.) and laparoscoped. The luteal cells were aspirated from the corpora lutea in the ovaries using a 1 ml tuberculin syringe fitted with a 25 gauge needle. The cells were dispersed into the culture medium, gently minced, washed and pipetted into the center well of individual Falcon #3037 petri dishes and incubated as low-density cultures at 37°C in a moist atmosphere of 5% CO_2 in air. The test compounds, 10 μM each of dbcCMP, dbcAMP, dbcGMP, dbcCMP plus 6 mM imidazole or control media were added at the start of culture. After 48 hr of incubation, the cells were fixed in methanol and stained with Giemsa stain [14]. Photomicrographs of the stained cells in the different treatments were taken and analyzed using the Zeiss Videoplan computerized image analyzer as described below.

Culture medium

The culture medium consisted of Medium 199 with 25 mM HEPES buffer, Earle's salts and L-glutamine (GIBCO, Grand Island, New York) and 75 mg/l penicillin and 75 mg/l streptomycin. The medium was filtered through a 0.22 micron syringe filter (Nalgene Co., Rochester, NY) and supplemented with 20% filtered and heat-inactivated fetal bovine serum (HyClone, Logan, UT).

Videoplan computerized image analysis

Morphometric measurements of the photomicrographs of the cells were quantitated using the Zeiss Videoplan computerized image analyzer equipped with statistical software. The image analyzer operated by translating the movements of the tracing of the outline of selected two-dimensional objects using an electronic input pen placed on a magnetized tabloid. The area and perimeter of the nucleus and individual cell outline were measured. The data collected were expressed as mean ± S. E. For convenience, the units of measurement were in arbitrary units. The actual perimeter in microns may be calculated by multiplying each value by 0.2545. In the case of the area value, multiplying each area value by 0.0648 should provide the actual value in square microns.

Statistical analysis

Differences in the perimeter and area measurements were tested for significance using the Dunnett's t-test for comparisons with the control with heterogeneous variance and unequal treatment sample sizes. A $P<0.05$ value was considered significant.

RESULTS

The presence of 10 μM dbcCMP in the media resulted in a significant reduction ($P<0.01$) in the cross-sectional area of the squirrel monkey luteal cell (Table 1). The cross-sectional area of the nucleus of the dbcCMP-treated cell was also significantly smaller in comparison with the control cell nucleus. When the cAMP-specific phosphodiesterase stimulator, imidazole, was present along with dbcCMP, the cells did not show the characteristic reduction in cell shape. Light microscopic observations of the cells revealed differences in shape of dbcCMP-treated and control luteal cells (Fig. 1). The control cells were polygonal-shaped while the dbcCMP-treated cells were small and narrow-shaped with less cytoplasm. The dbcCMP cells also appeared to have less pseudopod formation and less granular cytoplasm compared with the control cells. Some of the dbcCMP-treated cells had a wide spindle-shaped appearance. We did not observe any other cell types along with the cultured luteal cells. When imidazole was present along with dbcCMP (Fig. 2), the luteal cell morphology was similar to the control cell morphology and did not have the small narrow-shaped appearance characteristic of dbcCMP-treated cells.

The luteal cells became smaller and narrow-shaped when 10 μM dbcAMP was added to the culture media (Fig. 3). The decrease in cell shape and structure was significant ($P<0.001$) in comparison with the control (Table 1). The cross-

TABLE 1. The effect of cyclic nucleotides on the morphology of squirrel monkey (*Saimiri sciureus*) luteal cells *in vitro*

Treatment	Mean area of cell nucleus (sq. units)	Mean area of entire cell (sq. units)
Control	73.7±4.6 (27)	628.5±36.2 (22)
10 μM dbcCMP	58.6±4.0 (28)[a]	451.0±34.6 (33)[b]
10 μM dbcCMP+ 6 mM imidazole	75.6±2.3 (32)	603.3±50.7 (22)
10 μM dbcAMP	52.0±4.0 (33)[b]	396.6±25.1 (26)[b]
10 μM dbcGMP	73.0±3.7 (26)	701.6±42.4 (23)

[a] Significant difference from respective control ($P<0.05$).
[b] Significant difference from respective control ($P<0.01$).
Values are expressed as mean±S.E. (sq. arbitrary units).
Values in parentheses indicate number of cells.

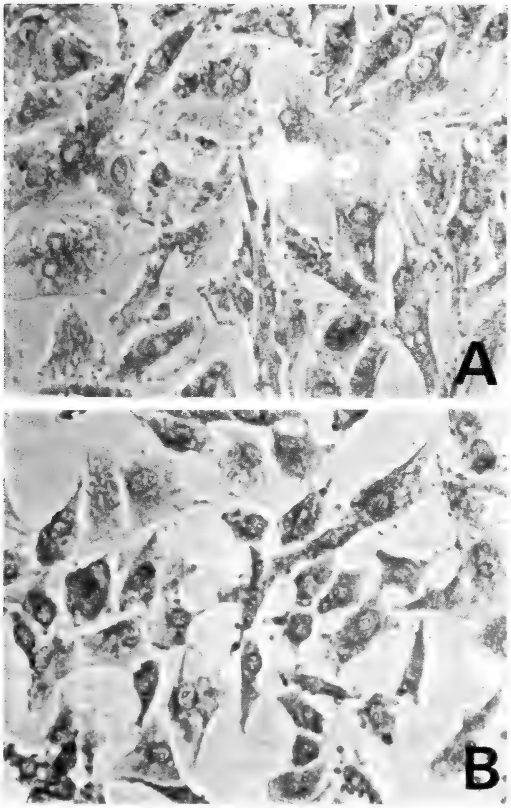

FIG. 1. The morphology of squirrel monkey luteal cells growing in low-density cultures after 48 hr of incubation in either control media (A) or in the presence of 10 μM dbcCMP (B). Note the decreased cell size and reduced cytoplasm in the dbcCMP-treated cells. Magnification ×400, phase contrast.

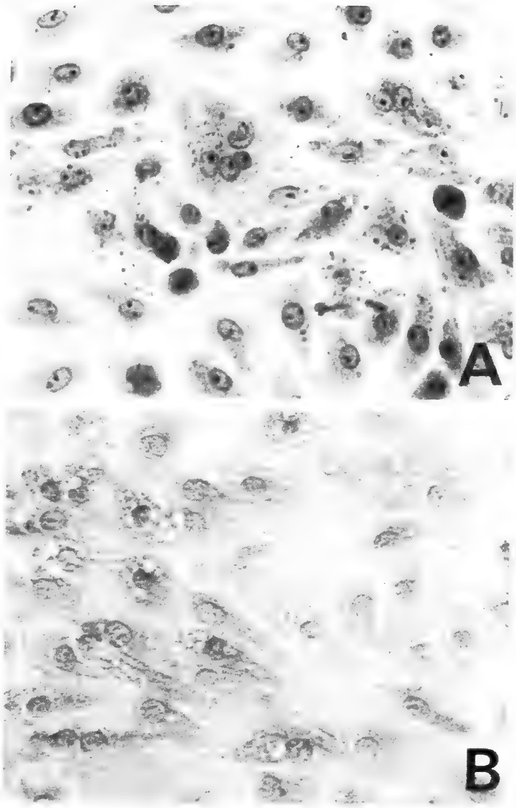

FIG. 2. Two views of squirrel monkey luteal cells in low-density cultures after 48 hr of incubation in the presence of 10 μM dbcCMP and 6 mM imidazole; light microscopy (A) and phase contrast (B). Magnification ×400.

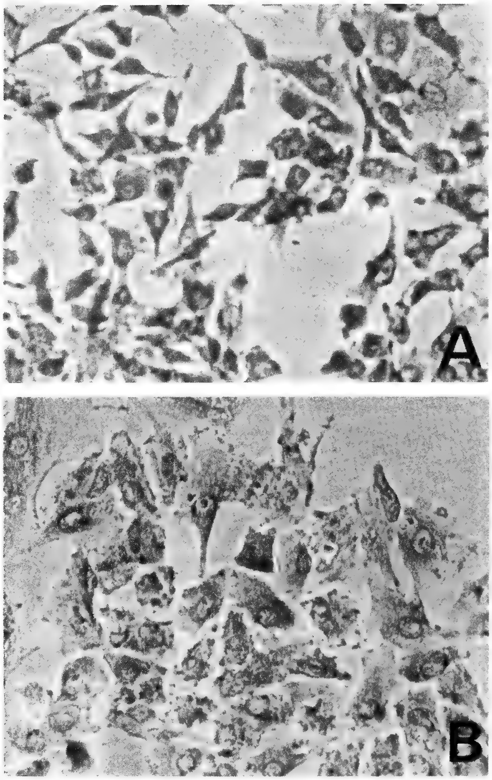

FIG. 3. The effect of 10 μM dbcAMP (A) or 10 μM dbcGMP (B) on the morphology of squirrel monkey luteal cells in low-density cultures after 48 hr of incubation. Magnification ×400, phase contrast.

sectional area of the cell nucleus was also decreased by the dbcAMP treatment. Some of the cells showed a pronounced spindling effect. In contrast, the addition of 10 μM dbcGMP to the cultures did not have an effect on cell morphology (Fig. 3). An analysis of the cross-sectional area of the dbcGMP-treated luteal cells also did not reveal any significant differences from control cells (Table 1).

DISCUSSION

This report is the first demonstration of *in vitro* cultured squirrel monkey (*Saimiri sciureus*) luteinized granulosa cells or luteal cells. In the present study, we have demonstrated that the action of dbcCMP on the alteration of the morphology of cultured squirrel monkey luteal cells is similar to the action of dbcAMP on these cells. This suggests that the function of cCMP may be similar to cAMP. The size of the luteal cell soma and nucleus are both decreased by dbcCMP and dbcAMP treatment. Our observation that dbcAMP alters the luteal cell morphology is supported by studies showing the same effect in other cell types such as fibroblasts [6, 15, 16] and granulosa cells [17, 18]. The alteration in cell size by cAMP and by other compounds that increase intracellular cAMP such as luteinizing hormone (LH) has been correlated to active steroidogenesis in the cell [17] and may involve reorganization of the tubulin and intermediate filaments [18, 19] through calmodulin-mediated mechanisms [20]. We surmise that cCMP may be involved in the control of steroidogenesis in luteal cells because of the similarity of dbcCMP-treated cells and dbcAMP-treated cells. The synthesis of progesterone by the squirrel monkey luteal cells will be examined in a future experiment.

There is very little information on the role of cCMP in the cell. Cyclic CMP is a pyrimidine compound, unlike cAMP and cGMP which are purine compounds. A related compund, cytidine-3′-monophosphate is a ribonuclease inhibitor and it is possible that cCMP may also function as such. The role of cCMP in other cell activities such as stimulating cancer cell proliferation has been reported [21, 22]. A study done on pigeon crop-sac mucosal epithelial cells suggests a role of cCMP as a mediator in the proliferation of cells [23]. The activity of cCMP-phosphodiesterase (PDE) has been shown to be high in slow growing hepatoma cells and low in rapidly-dividing cells [24] and the cCMP-PDE appears to be a separate and different PDE from the cAMP-specific PDE [25]. Another study suggested a role of cCMP in stimulating hemoglobin synthesis [10] probably via protein kinases [9]. In this study we postulate a role of cCMP in the control of steroidogenesis in luteal cells.

The action of dbcCMP on squirrel monkey luteal cells can be inhibited by imidazole, a cAMP-specific PDE stimulator implying that the mechanism of action of dbcCMP requires intracellular cAMP. We cannot exclude the possibil-

ity that the imidazole may be stimulating PDE to inactivate both intracellular cAMP and exogenous dbcCMP, although this argument is weak because it has been shown that dibutyryl cyclic nucleotide analogues are resistant to degradation by PDE [26]. It is possible that the role of cCMP is to be a mediator or co-factor for cAMP-induced cell shape changes, calcium-mediated events and steroidogenesis.

In this study, we also tested dbcGMP because certain concentrations of cGMP appear to affect intracellular cAMP production [27]. Our data indicated that dbcGMP was not involved in the alteration of luteal cell morphology. It appears that cGMP does not play a role in the physiological processes in the squirrel monkey luteal cell.

The results of the present study suggest that cCMP alters the squirrel monkey luteal cell morphology in a manner similar to cAMP and that the process requires intracellular cAMP.

ACKNOWLEDGMENTS

This research was supported in part by the Foundation of the University of Medicine and Dentistry of New Jersey.

REFERENCES

1 Michelson, A. M. (1983) The Chemistry of Nucleosides and Nucleotides, Academic Press, New York, NY, pp. 1–40.

2 Robison, G. A., Butcher, R. W. and Sutherland, E. W. (1971) Cyclic AMP, Academic Press, New York, NY, pp. 1–51.

3 Sutherland, E. W. (1972) Studies on the mechanism of hormone action. Science, **177**: 401–407.

4 Garland, D. L. (1979) CAMP inhibits the in vitro assembly of microtubules. Arch. Biochem. Biophys., **198**: 335–337.

5 Means, A. R., Tash, J. S., Chafouleas, J. G., Lagace, L. and Guerriero, V. (1981) Regulation of the cytoskeleton by Ca^{++}-calmodulin and cAMP. Ann. N. Y. Acad. Sci., **383**: 69–84.

6 Willingham, M. C. and Pastan, I. (1975) Cyclic AMP and cell morphology in cultured fibroblasts. J. Cell Biol., **67**: 146–159.

7 Goldberg, D. L., Haddox, M. K., Hartle, D. K. and Hadden, J. W. (1972) The biological role of cyclic 3′, 5′-guanosine monophosphate. Proc. 5th Int. Congr. Pharmacol, Krager, Basel, pp. 149–169.

8 Goldberg, D. L. and Haddox, M. K. (1977) Cyclic GMP metabolism and involvement in biological regulation. Ann. Rev. Biochem., **46**: 823–896.

9 Vardanis, A. (1980) A unique cyclic nucleotide-dependent protein kinase. J. Biol. Chem., **255**: 7238–7243.

10 Canas, P. E. and Congote, L. F. (1982) Effects of cyclic nucleotides on hemoglobin synthesis in fetal calf liver cells in culture. Can. J. Biochem., **60**: 1–7.

11 Wei, J. W. and Hickie, R. A. (1983) Decreased activities of cyclic CMP phosphodiesterase in Morris hepatomas having varying growth rates. Int. J. Biochem., **15**: 789–796.

12 Dukelow, W. R. (1970) Induction and timing of single and multiple ovulations in the squirrel monkey (*Saimiri sciureus*). J. Reprod. Fertil., **22**: 303–309.

13 Chan, P. J. and Dukelow, W. R. (1984) Variations in squirrel monkey responses with seasonal and environmental conditions. Zool. Sci., **1**: 471–476.

14 Freshney, R. I. (1983) Characterization. In "Culture of Animal Cells". Ed. by R. I. Freshney, Alan R. Liss, Inc., New York, pp. 159–161.

15 Hsie, A. W., Jones, C. and Puck, T. T. (1971) Further changes in differentiation state accompanying the conversion of CHO cells to fibroblastic form by dibutyryl adenosine 3′, 5′-monophosphate and hormones. Proc. Natl. Acad. Sci. USA, **68**: 1648–1652.

16 Johnson, G. S., Friedman, R. M. and Pastan, I. (1971) Restoration of several morphological characteristics of normal fibroblasts in sarcoma cells treated with adenosine-3′: 5′-cyclic monophosphate and its derivatives. Proc. Natl. Acad. Sci. USA, **68**: 425–429.

17 Lawrence, T. S., Ginzberz, R. D., Gilula, N. B. and Beers, W. H. (1979) Hormonally induced cell shape changes in cultured rat ovarian granulosa cells. J. Cell Biol., **80**: 21–36.

18 Soto, E. A., Kliman, H. J., Strauss, J. F. III, Paavola, L. G. (1986) Gonadotropins and cyclic adenosine 3′, 5′-monophosphate (cAMP) alter the morphology of cultured human granulosa cells. Biol. Reprod., **34**: 559–569.

19 Herman, B. and Albertini, D. F. (1984) A time-lapse videoimage intensification analysis of cytoplasmic organelle movement during endosome translocation. J. Cell Biol., **98**: 565–576.

20 Chan, P. J. and Dukelow, W. R. (1985) Calmodulin level changes associated with cyclic AMP treatment in cultured squirrel monkey oocytes and sperm. Zool. Sci., **2**: 219–223.

21 Bloch, A. (1975) Isolation of cytidine 3′, 5′-monophosphate from mammalian tissues and body fluids and its effects on leukemia L1210 cell growth in culture. Adv. Cyclic Nucleotide Res., **5**: 331–338.

22 Bloch, A., Dutschman, G. and Maue, R. (1974) Cytidine 3′, 5′-monophosphate. II. Initiation of leukemia L1210 cell growth in vitro. Biochem. Biophys. Res. Commun., **59**: 955–959.

23 Anderson, T. R., Mayer, G. L. and Nicoll, C. S. (1982) Cyclic nucleotides and the control of epithelial cell proliferation: Cyclic CMP may be a partial mediator of the response of the pigeon crop-sac to prolactin. J. Cyclic Nucleotide Res., **7**: 225–234.

24 Wei, J. W. and Hickie, R. A. (1983) Decreased activities of cyclic CMP phosphodiesterase in Morris hepatomas having varying growth rates. Int. J. Biochem., **15**: 789–796.

25 Cheng, Y. C. and Bloch, A. (1978) Demonstration in leukemia L-1210 cells of a phosphodiesterase acting on 3′: 5′ cyclic CMP but not on 3′: 5′-cyclic AMP or 3′: 5′-cyclic GMP. J. Biol. Chem., **253**: 2522–2524.

26 Kaukel, E., Mundhenk, K. and Hilz, H. (1972) N6-monobutyryl adenosine 3′: 5′ monophosphate as the biologically active derivative of dibutyryl adenosine 3′: 5′ monophosphate in Hela 53 cells. Eur. J. Biochem., **27**: 197–200.

27 Whitfield, J. F., Boynton, A. L., Macmanus, J. P., Sikorska, M. and Tsang, B. K. (1979) The regulaiton of cell proliferation by calcium and cyclic AMP. Mol. Cell. Biochem., **27**: 155–179.

ZOOLOGICAL SCIENCE 4: 535–542 (1987)

Entrainment of Cricket Circadian Activity Rhythm after 6-Hour Phase-Shifts of Light-Dark Cycle

Kenji Tomioka and Yoshihiko Chiba

Environmental Biology Laboratory, Biological Institute, Yamaguchi University, Yamaguchi 753, Japan

ABSTRACT—Adult crickets *Gryllus bimaculatus* show a circadian locomotor rhythm peaking early in the dark fraction of 12-h light to 12-h dark cycle (LD). Reentrainability of the locomotor rhythm to 6-h delayed or advanced LD was investigated in 68 crickets under a constant temperature of 26°C with three different illumination levels, i.e. 10, 100 and 400 lux. The LD was shifted by either lengthening or shortening of the light fraction. More cycles were needed for reentrainment in phase-advance than in phase-delay. Decrements of light intensity increased the cycles needed in both phase-delay and phase-advance. When the LD was shifted by 6-h in either direction, the LD masked the rhythm dependently on the phase of the rhythm, either inducing or inhibiting the activity; the strongest masking was observed in the subjective night. Interestingly, a second peak was developed to form a double peaked activity pattern after phase-shifting in 31 animals, more frequently when the illumination level was 10 lux. The results are discussed mainly in relation to effects of LD on the circadian rhythm.

INTRODUCTION

Circadian rhythms, freerunning with a period of about 24-h under constant conditions, synchronize to certain environmental 24-h cycles (zeitgeber). The most powerful zeitgeber is light-dark cycles; reentrainment of the rhythm by its phase shifts revealed its efficacy in entrainment [1]. In addition, photic informations related to the LD, bypassing the circadian pacemaker, modulate waveforms of the overt rhythms. The modulation, termed masking effect [2], has been profoundly studied in mammals such as rats [3] and squirrel monkeys [4]. Thus, behavioral rhythms under LD may reflect pacemaker-dependent effects of light as well as masking effects.

The cricket *G. bimaculatus* shows clear circadian activity rhythm peaking in the light fraction as nymph but in the dark fraction as adult [5]. A series of surgical and electrophysiological experiments [6–10] has revealed that the rhythm is controlled by a circadian system composed of bilateral optic lobe pacemakers, a secondary oscillatory system outside of the lobes, and the compound eye as the necessary source of photoreceptive information for entrainment. The activity rhythm of crickets with optic nerves severed, therefore, freeruns because of a lack of photic information. However, we found that the rhythm of the optic nerve severed animals eventually resynchronized to the LD without any sign of forced phase-shifting [7]. Our explanation for this was that the reentrainment was attributable to the nerve regeneration which was not so sufficiently completed that the zeitgeber information conveyed was too weak to force the rhythm to resynchronize by abrupt phase-shifting; in other words, light was felt subjectively too weak.

The present experiment was carried out to investigate the reentrainment of the cricket activity rhythm to 6-h phase-shifted LDs with three different illumination levels (10, 100, and 400 lux). The results revealed that the entraining ability of LD depends on light intensity, supporting our previous explanation. In addition, it was shown that the phase-shifting of LD often induced a double peaked activity pattern as well as circadian phase-dependent maskings.

Accepted December 22, 1986
Received August 4, 1986

MATERIALS AND METHODS

All experiments were carried out with male crickets, *Gryllus bimaculatus* which were taken from our laboratory colonization kept under 12-h light to 12-h dark cycle (LD 12:12, L: 06^{00}–18^{00}) and a constant temperature of 26 ± 0.5°C, hereafter called the standard conditions. Locomotor activities were recorded individually with an actograph with a rocking substratum whose movement caused by a moving animal was sensed by a microswitch connected to an event-recorder (Yokogawa, XP–490) and a digital printer (Chino, Procos–V).

Phase-shift experiments included studies with three illumination intensities, bright-LD (L: about 400 lux), medium-LD (L: about 100 lux) and dim-LD (L: about 10 lux), and with 22, 23 and 23 animals, respectively. Lighting was manipulated with the use of 20 W cool white fluorescent lamps which were programed to produce an LD of 12-h of light and 12-h of darkness per day. Light intensity was adjusted either by changing the number of lamps or by shading them. Temperature was 26 ± 0.5°C. Six-hour phase-shifts of LD were carried out by either lengthening or shortening the light fraction.

RESULTS

In the cricket *Gryllus bimaculatus*, diurnally peaked activity rhythm is reversed to peak nocturnally 3 to 5 days after the imaginal molt [5]. The endogenous rhythm reversal [5] could be

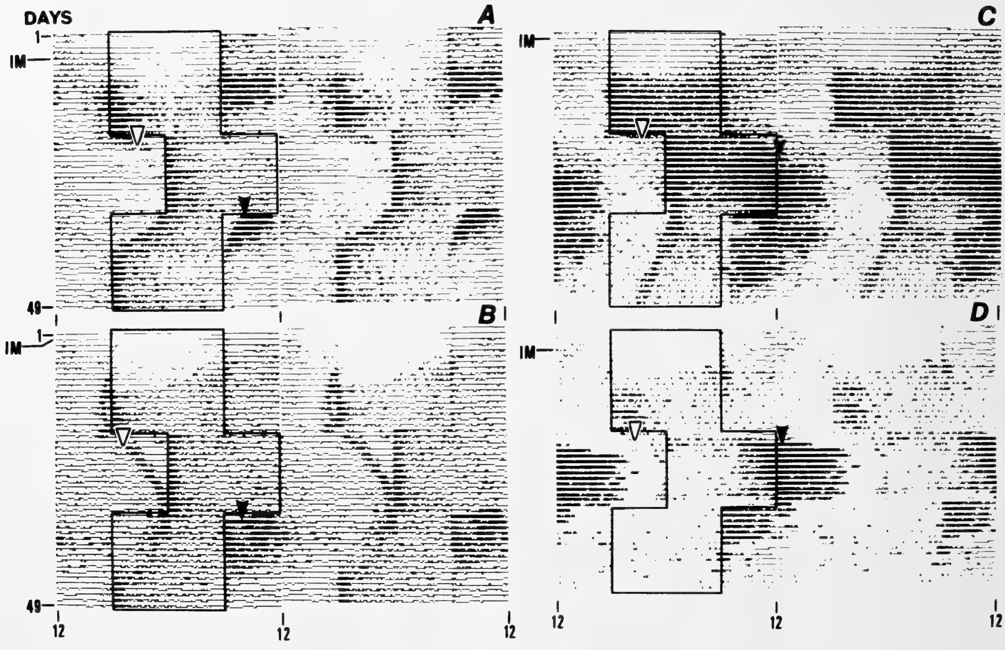

Fig. 1. Double plotted activity records of 4 crickets showing a reentrainment to the shifted LD 12:12 with 10 lux. Lighting conditions are indicated in the left half of the figure: brackets show a dark fraction. IM, imaginal molt. The animals were diurnal in nymphal stage, but became nocturnal a few days after the imaginal molt. At the early stage of the rhythm reversal, an intense activity occurred to form a double peaked activity in A. In response to a 6-h delayed LD, a slowly delaying (open arrow heads) and an immediately synchronized component occurred. The latter seems to be a positive masking effect of lights-off. After phase-shifts of LD, a second component either being restricted in the light fraction or spreading widely from late night to midday appeared (arrow heads). The second component either disappeared with the completion of reentrainment (A, B) or persisted for weeks (C, D).

observed under the three LDs of different illumination levels; daily locomotor activity was initiated at lights-on in nymphal stage and at lights-off in adults (Figs. 1–3). At the early stage of the reversal, an intense activity often occurred at lights-on to make a double peaked activity together with the newly developed nocturnal peak, but, in most cases, this lights-on activity became to terminate earlier day after day and

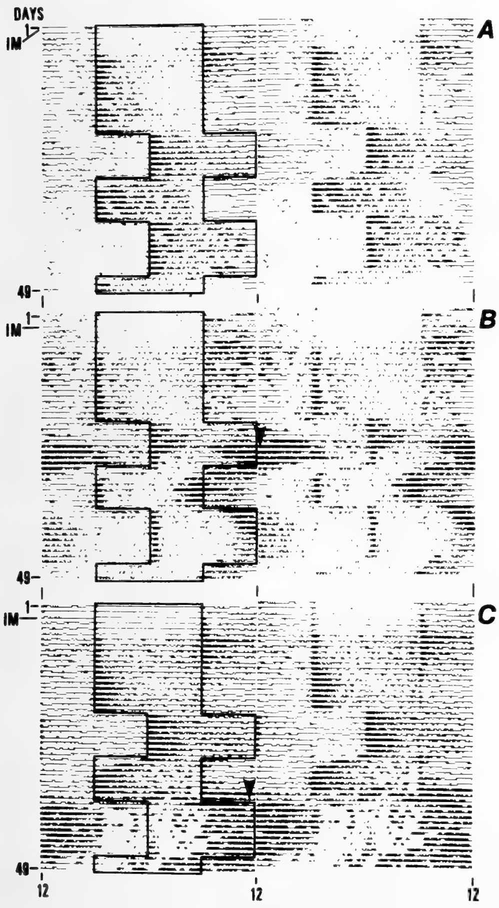

FIG. 2. Double plotted activity records of 3 crickets under phase-shifting of LD 12:12 of 100 lux. Brackets show a dark phase. IM, imaginal molt. The animals were reentrained by shifted LDs. An animal shown in A consistently exhibited a single peaked nocturnal activity, while other two animals shown in B and C exhibited a second activity component (arrow heads) which extended from late at night to about midday.

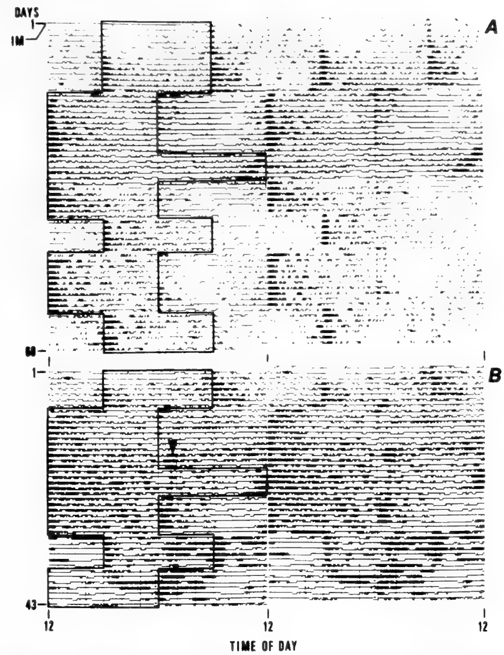

FIG. 3. Double plotted activity records of two crickets under various lighting conditions with illumination level of 400 lux. Brackets show a dark phase. IM, imaginal molt. A single nocturnal component consistently occurred in A, whereas a second component (arrow) was developed to produce a double peaked pattern in B.

eventually disappeared (example: Fig. 1A). The LD was first phase-shifted, at the earliest, 4 days after the establishment of the nocturnal rhythm and was done repeatedly. Figures 1–3 exemplify the activity recording of fully entrained animals.

In dim-LD, two kinds of activity peaks were clearly observed after a 6-h delay of the LD (Fig. 1); one occurred in synchrony with the new LD from the very beginning and the other (open arrow heads in Figure 1) moved backward slowly to attain resynchronization in several days. The latter was less prominent in most cases, and almost disappeared in higher illumination levels (Figs. 2 and 3). In view of the masking effect of LD, the slowly moving peak may be endogenous under circadian control and receives sometimes inhibitory effect (negative masking) of light, whereas the other peak may be regarded as exogenous, being induced by lights-off (positive masking). Thus, we adopted this slowly moving

Table 1. Transient cycles after 6-h delay- and advance-shift under different intensities of illumination

Illumination level (lux)	Transient cycles (days)	
	delay	advance
400	2.27±1.12 (15)	3.50±0.76 (18)
100	2.76±1.11 (21)	4.26±0.71 (19)
10	6.00±2.33 (17)	10.70±3.20 (10)

Numerals in brackets indicate the number of animals used for estimating the values.

Table 2. Activity patterns during phase shifting under different intensities of illumination

Illumination level (lux)	N	No. of animals with	
		single peaked nocturnal rhythm	double peaked rhythm
400	22	15	7 (7)
100	23	15	8 (6)
10	22	6	16 (14)
Totals	67	36	31 (27)

Numerals in brackets indicate the number of animals showing a second component broadened from late at night to midday.

activity onset for estimating the transient cycles (number of cycles required for reentrainment). Animals showing obscure onsets were excluded from data.

The number of transient cycles varied with the direction of shifts and with the light intensity: it was shorter in delay-shifts (ANOVA, $P<0.01$) and in higher light intensity (ANOVA, $P<0.01$) (Table 1). The asymmetry-effects of delay- and advance-shifts and the light intensity dependency of the transient cycles conform to results obtained from other nocturnal animals [cf. 1].

In addition to these activity peaks related with lights-off, a peak (second component) was sometimes developed at lights-on, as the LD was shifted, to make a double peaked activity in all illumination levels (arrow head in Figs. 1, 2B, C and 3B). This second component often broadened from late at night to midday and sometimes merged with the nocturnal peak (Figs. 1C, D, 2B, C and 3B). Table 2 summarizes the relationship between the occurrence of double peaked activity and the light intensity. The occurrence of the second component depended on the light intensity (chi-square test, $P<0.01$): the lower the light intensity was, the greater the number of animals with the second component was. In 4 out of 31 animals which developed the double peaked activity, the second component occurred only during the 6-h phase-advance and was restricted in the light fraction. It's offset advanced keeping pace with the nocturnal peak, but it's onset never entered the dark fraction. The component thus disappeared on the completion of reentrainment of the rhythm (Fig. 1A, B). The remaining 27 animals showed the broadened second component which persisted for weeks and resynchronized to the shifted-LD with several transient cycles (Figs. 1C, D, 2B, C and 3C). The component, however, sometimes later became to be restricted in the light fraction and was often observed to be synchronized with the lights-on (Fig. 1C, D). On the basis of these facts, the broadened second component seems to be regulated by a combination of an endogenous pacemaker causing an activity preceding lights-on and the LD as an exogenous zeitgeber inducing lights-on activity (i.e. positive masking effect of light). In some animals the nocturnal component became very faint or even disappeared to form an almost diurnal pattern by the second component (Figs. 1D and 2C).

Of the 68 animals examined, one animal from the dim-LD series failed to synchronize to the LD, showing a freerunning rhythm consistently (Fig. 4). The LD, however, modulated the rhythm in two ways: (1) the relative coordination, which is a phenomenon that the rhythm changes the freerunning period systematically dependently on the phase-angle relationship between the LD

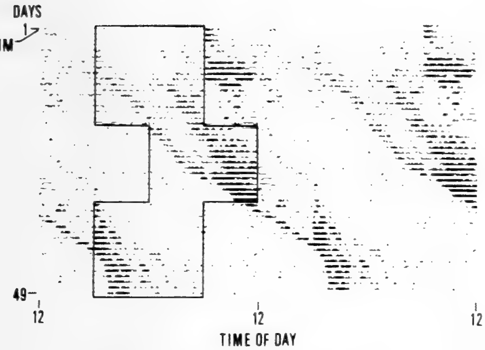

FIG. 4. Double plotted activity record of a cricket showing a freerunning rhythm under shifting LD 12:12 with 10 lux. A bracket indicates a dark phase. IM, imaginal molt. The freerunning activity started with two peaks in the dark phase, which later fused in a single component. The period of the rhythm was shortened when the onset of activity occurred early in the dark phase. The positive masking occurred at lights-on after 6-h advance of LD on day 33.

and it, being explained to occur when zeitgeber is below but near the threshold for entrainment and (2) the positive masking effect. The freerunning rhythm started with two activity components in the night (around day 10), and the components merged around day 28 as the second component reached the lights-on. The relative coordination was evident after first and second phase-shifting; the rhythm freeran with shorter period when the onset of the activity occurred early in the dark onset. The masking effect was seen after 6-h advance of LD on day 33. Thereafter, an activity component appeared at lights-off, being intensified with the passage of day while the freerunning component approached the lights-off. These results suggest that the LD of 10 lux might be below but near the threshold for entrainment in this particular animal.

DISCUSSION

1. *Entrainment*

We proposed previously a view that, in the crickets with regenerated-optic nerves, the LD being felt subjectively very weak could not force the rhythm to phase-shift abruptly, but entrain it [7]. One of the purposes of this study was to see whether the view was effective for intact crickets.

The number of transient cycles was shown to depend on both the light intensity and the direction of the shift: it was longer in low light intensity and in advance-shifts (Table 1). In dim-LD with a illumination level of 10 lux, the most animals showed the adult nocturnal peak gradually advancing or delaying to synchronize the newly phased LD without abrupt phase shifting (Fig. 1A, B). In addition, some of them needed extremely long transient cycles for resynchronization (Fig. 1C) and one failed to entrain (Fig. 4). The evidence implies the illumination level of 10 lux is near threshold level for entrainment of the rhythm. These results are consistent with our previous view [7], suggesting that the entraining ability of LD depends on the amount of information about it being conveyed to the circadian pacemaker.

The asymmetry-effect of delay and advance shifts observed in the cricket, where the delay-shifts completes faster than advance, is commonly seen in nocturnal animals, such as rats [11] and flour beetles [12]. The opposite occurs in diurnal animals: chaffinches [13] and lizards [14]. Wever [15] proposed a mathematical model simulating various properties of circadian rhythms to explain a relation between the freerunning period and the transient cycles. According to his model, there is a "natural period" of about 24.5-h at which advance- and delay-shifts last equally long. With longer period advances last longer than delays; with shorter period the opposite occurs. The model seems to be effective for *G. bimaculatus*, where the freerunning period in constant dim light (LL) of 10 lux as adult is 25.49 ± 0.49 (mean $\pm$S.D.)-h [5].

2. *Double peaked activity rhythm*

About 45% of the cricket developed the double peaked activity with the adult nocturnal and the second components after phase-shifting. The occurrence of the pattern was low in LD with higher light intensity (Table 2), suggesting that the LD with higher illumination level entrains the circadian system more stably. Involvement of endogenous control in the double peaked activity

is evident by the fact that both of the two activity components showed transients before completion of the reentrainment to the newly phased LD no matter whether either of the components disappeared (Figs. 1 and 2B).

A double peaked pattern was also observed at the early stage of the rhythm reversal. This pattern is similar to that after the 6-h phase-advance in a following respect: an intense lights-on activity, which was restricted in the light fraction, became to terminate earlier day after day and eventually disappeared (example: Fig. 1A). The similarity may suggest that these two double peaked activities share a common physiological mechanism.

That the activity peak occurs twice in one circadian cycle has been reported for some animals. Whether the peaks are underlain by separate oscillations has called much attention of researchers, because the kinetic analyses sometimes suggest that they are of physiologically different nature (the mosquitoes *Aedes aegypti* [16], *Culex pipiens molestus* [17], *Culiseta incidens* [18], the silkmoth *Hyalophora cecropia* [19], the New Zealand weta *Hemideina thoracica* [20], the cricket *Teleogryllus commodus* [21], the hamster *Mesocricetus auratus* [22]). Recently results of lesion experiments appeared in both vertebrates and invertebrates, strengthening the view of 'separate oscillations'; unilateral ablation of the candidate pacemaker tissue eliminates the double peaked activity to make a single peaked rhythm in the hamster [23] and in the cricket (*T. commodus*) [24]. The other view is that one circadian pacemaker controls the two peaks, being adopted where no physiological difference can be detected between the peaks (the cockroach *Periplaneta americana* [25]).

The circadian system of *G. bimaculatus* is suggested to be composed of three constituents, i.e. the circadian pacemakers in the bilateral optic lobes, a driven system outside the optic lobe regulating locomotor activity under control from the pacemaker, and the compound eye as a photoreceptor for entrainment [10]. The two peaks of the double peaked activity here seem to be driven by a common pacemaker. The facts arguing this statement are that the two peaks resynchronized to the newly phased-LD in similar time courses and that the double peaked activity survived unilateral removal of the lobe [26]. However, to clarify the entire physiological mechanism underlying the cricket's double peaked activity, further critical study is deserved.

3. *Masking effect of LD*

The activity pattern is controlled essentially by endogenous mechanism but receives exogenous modification from LD cycle. This effect of LD which operates independently of its effects on the endogenous circadian system was classically termed "masking effect" [2]. The present study revealed that the LD induced "positive" or "negative" masking dependently on the phase of the circadian rhythm. Negative masking occurred as more or less potent inhibition of the delaying nocturnal component when the first half of the subjective night phase (the night phase for the circadian pacemaker) was exposed to light after 6-h phase-delay of the LD (Figs. 1 and 2). Positive masking, as lights-on activity, however, was induced by exposure of the second half of the subjective night phase to the light by 6-h advance of the LD (Fig. 1A, B). The positive masking action of light decreased cycle by cycle, disappearing with completion of re-entrainment. Lights-off also induces a positive masking at the subjective night when the first half of the subjective night was exposed to light (cf. Figs. 1A–C and 4). In summary, the most effective phase for the masking of the LD is the subjective night phase of the circadian activity rhythm.

The circadian phase dependence of masking action of light has been investigated profoundly for some vertebrate species: such as the nocturnal prosimian *Galago crassicaudatus* [27], the rat [3], the diurnal squirrel monkey *Saimiri sciureus* [4] and the chicken [28]. The most effective circadian phase for masking action of light seems to be variable among species. In *Galago* and *Saimiri* light is most effective in the subjective day [4, 27], whereas the opposite is effective in nocturnal rats [3]. The masking of chicken brain temperature rhythm is maximal on both the ascending and descending slopes of the rhythm [28]. The characteristic circadian phase dependency of masking in

each species may have an adaptive value in that animals can respond properly to light given at unexpected time.

ACKNOWLEDGMENTS

This work was supported by grants from Ministry of Education, Science and Culture of Japan.

REFERENCES

1 Aschoff, J., Hoffmann, K., Pohl, H. and Wever, R. (1975) Reentrainment of circadian rhythms after phase shifts of the zeitgeber. Chronobiologia, **2**: 23–78.

2 Aschoff, J. (1960) Exogenous and endogenous components in circadian rhythms. Cold Spring Harbor Symp. Quant. Biol., **25**: 11–27.

3 Borbely, A. A. and Huston, J. P. (1974) Effects of two-hour light-dark cycles on feeding, drinking and motor activity of the rat. Physiol. Behav., **13**: 795–802.

4 Gander, P. H. and Moore-Ede, M. C. (1983) Light-dark masking of circadian temperature and activity rhythms in squirrel monkeys. Am. J. Physiol., **245**: R927–R934.

5 Tomioka, K. and Chiba, Y. (1982) Post-embryonic development of circadian rhythm in the cricket, *Gryllus bimaculatus*: a rhythm reversal. J. Comp. Physiol., **147**: 299–304.

6 Tomioka, K. and Chiba, Y. (1982) Persistence of circadian ERG rhythm in the cricket with optic tract severed. Naturwissenschaften, **69**: 395–396.

7 Tomioka, K. and Chiba, Y. (1984) Effects of nymphal stage optic nerve severance or optic lobe removal on the circadian locomotor rhythm of the cricket, *Gryllus bimaculatus*. Zool. Sci., **1**: 385–394.

8 Tomioka, K. and Chiba, Y. (1985) Optic lobe-compound eye system in cricket: a complete circadian system. J. Interdiscipl. Cycle Res., **16**: 73–76.

9 Tomioka, K. and Chiba, Y. (1986) Circadian rhythm in the neurally isolated lamina-medulla complex of the cricket, *Gryllus bimaculatus*. J. Insect Physiol., **32**: 745–755.

10 Tomioka, K. (1985) Residual circadian rhythmicity after bilateral lamina-medulla removal or optic stalk transection in the cricket, *Gryllus bimaculatus*. J. Insect Physiol., **31**: 653–657.

11 Halberg, F., Nelson, W., Runge, W. J., Schmitt, O. H., Pitts, G. and Reynolds, O. E. (1971) Plans for orbital study of rat biorhythms. Results of interest beyond the biosatellite program. Space Life Sci., **2**: 437–471.

12 Chiba, Y., Cutkomp, L. K. and Halberg, F. (1973) Circadian oxygen consumption rhythm of the flour beetle, *Tribolium confusum*. J. Insect Physiol., **19**: 2163–2172.

13 Aschoff, J. and Wever, R. (1963) Resynchronization der Tagesperiodik und Zeitgeberperiodik. Z. vergl. Physiol., **46**: 321–335.

14 Fischer, K. (1961) Untersuchungen zur Sonnenkompassorientierung und Laufaktivität von Saragdeidechsen, (*Lacerta viridis* Laur). Z. Tierpsychol., **18**: 450–470.

15 Wever, R. (1966) The duration of re-entrainment of circadian rhythms after phase-shifts of the Zeitgeber. J. Theor. Biol., **13**: 187–201.

16 Taylor, B. and Jones, M. D. R. (1969) The circadian rhythm of flight activity in the mosquito *Aedes aegypti* (L.): The phase-shifting effects of light-on and light-off. J. Exp. Biol., **51**: 59–70.

17 Chiba, Y., Kubota, M. and Nakamura, Y. (1982) Differential effects of temperature upon evening and morning peaks in the circadian activity of mosquitoes, *Culex pipiens pallens* and *C. pipiens molestus*. J. Interdiscipl. Cycle Res., **13**: 55–60.

18 Clopton, J. R. (1984) Mosquito circadian and circa-bi-dian flight rhythms: a two-oscillator model. J. Comp. Physiol., **155**: 1–12.

19 Truman, J. W. (1974) Physiology of insect rhythms. IV. Role of the brain in the regulation of the flight rhythm of the giant silkmoth. J. Comp. Physiol., **95**: 281–296.

20 Christensen, N. D. and Lewis, R. D. (1982) The circadian locomotor rhythm of *Hemideina thoracica* (Orthoptera; Stenopelmatidae): the circadian clock as a population of interacting oscillators. Physiol. Entomol., **7**: 1–13.

21 Wiedenmann, G. and Loher, W. (1984) Circadian control of singing in crickets: two different pacemakers for early-evening and before-dawn activity. J. Insect Physiol., **30**: 145–151.

22 Pittendrigh, C. S. and Daan, S. (1976) A functional analysis of circadian pacemaker in nocturnal rodents. V. Pacemaker structure: A clock for all seasons. J. Comp. Physiol., **106**: 333–353.

23 Pickard, G. E. and Turek, F. W. (1982) Splitting of the circadian rhythm of activity is abolished by unilateral lesions of the suprachiasmatic nuclei. Science, **215**: 1119–1121.

24 Wiedenmann, G. (1983) Splitting in a circadian activity rhythm: the expression of bilaterally paired oscillators. J. Comp. Physiol., **150**: 51–60.

25 Wiedenmann, G. (1980) Two peaks in the activity rhythm of cockroaches controlled by one circadian pacemaker. J. Comp. Physiol., **137**: 249–254.

26 Tomioka, K. and Chiba, Y. (1985) Modification of circadian waveform by 6-hr phase shifts of LD cycle in the cricket, *Gryllus bimaculatus*. Zool. Sci., **2**: 1000.

27 Randorph, M. (1971) Role of light and circadian rhythms in the nocturnal behavior of *Galago crassicaudatus*. J. Comp. Physiol. Psychol., **1**: 115–122.

28 Aschoff, J. and Paul, U. von S. (1976) Brain temperature in the unanesthetized chicken: its circadian rhythm of responsiveness to light. Brain Res., **101**: 1–9.

ZOOLOGICAL SCIENCE 4: 543–549 (1987)

Relationship Between Daily Variation of Locomotor Activity and That of Plasma Corticosterone Levels in the Newt, *Cynops pyrrhogaster pyrrhogaster*

Atsuhiko Chiba and Kiyoshi Aoki

Life Science Institute, Sophia University, 7-1 Kioi-cho, Chiyoda-ku, Tokyo 102, Japan

ABSTRACT—The daily variation of locomotor activity and that of plasma corticosterone levels were investigated in the newt, *Cynops pyrrhogaster pyrrhogaster*. Under LD 12:12 (Light on 07:00, off 19:00), the newts were active chiefly during the light period, and the daily variation of locomotor activity clearly showed a biphasic pattern. Plasma corticosterone levels increased during the dark period and reached a maximum value just prior to the light period just as is observed in diurnal mammals. The daily variation of plasma corticosterone levels also showed a biphasic pattern and virtually paralleled that of locomotor activity. If the light-dark cycle was reversed (Light on 19:00, off 07:00) by doubling the first light period, the daily patterns of both locomotor activity and of plasma corticosterone levels were also reversed within 7 days. These results suggest that, in the newt, the daily variation of plasma corticosterone levels is closely associated with that of locomotor activity at least under the light-dark cycles of LD 12:12.

INTRODUCTION

A number of studies have established that in mammals, the circadian rhythms of plasma glucocorticoid levels are closely linked to their rest-activity cycles including their sleep-wake and fasting-eating cycles [1–10]. In non-mammalian species, however, several studies have been carried out to investigate the daily variations of plasma glucocorticoid levels [11–14]. The relationship between the levels of these hormones and the rest-activity cycles, however, was not precisely examined in non-mammalian studies.

Corticosterone is the major glucocorticoid secreted by the adrenal gland of amphibians [15, 16]. The existence of a daily rhythm of plasma corticosterone has already been demonstrated in frogs living freely in their natural habitat [14]. Recently, the present authors have succeeded in a long-term recording of the locomotor activity in the newt, *Cynops pyrrhogaster pyrrhogaster*, under experimental conditions [17].

In the present study, the writers recorded the locomotor activity and measured the plasma corticosterone levels in *Cynops* to clarify the relationship between the daily variation of locomotor activity and that of plasma corticosterone levels under experimental conditions.

Accepted February 4, 1987
Received January 7, 1987

MATERIALS AND METHODS

Animals

Adult female newts, *Cynops pyrrhogaster pyrrhogaster*, over 50 mm in snout-vent length were purchased from commercial suppliers in Tokyo from March to October. Prior to the following investigations, all animals were maintained for at least a month in aquaria at 22°C under a controlled light-dark cycle of LD 12:12 (Light on 07:00, off 19:00). Food was scattered in the aquaria once a week.

Locomotor activity recordings

Four newts were housed per small plastic recording box (17 cm long, 8.5 cm wide) which was placed separately in a light-tight container. Water was maintained in the recording box at 1.5 cm depth and it was continuously circulated

through a gravel filter. The container had on its ceiling a 4 W fluorescent lamp, which was connected to an automatic timing device to control the photoperiod. The intensity of the light was adjusted to 50 lux at the surface of the water by inserting pieces of thin paper beneath the lamp. The temperature of both water and air in the container was kept at 22°C. No food was given throughout the experiment. The newts were initially kept under a normal light-dark cycle of LD 12:12 (Light on 07:00, off 19:00) and subsequently exposed to a reversed light-dark cycle (Light on 19:00, off 07:00) achieved by doubling the first light period.

Locomotor activity (counts/5 min) of the newts in each recording box was recorded by an infrared photoswitch (NT–10, Takenaka Electronic Industrial Co., Ltd.) connected to a micro-computer. The beam of the photoswitch was adjusted so that it would be located just below the surface of the water and also be directed along the longitudinal axis of the recording box. The signals were generated when the newts moved and intercepted the beam. The number of the signals was recorded as an index of locomotor activity.

For visual display, time series of locomotor data were computer-plotted to simulate Esterline Angus recorder actogram. The authors have already recorded previously the locomotor activity from the recording box containing a single newt each and have obtained the actogram in the same manner as the present investigation. These former actogram clearly showed locomotor rhythms entrained to LD 12:12 and free-running in constant darkness (Fig. 1).

In an experimental series to investigate the relation to plasma glucocorticoid level, the daily variation of locomotor activity was determined under the normal light-dark cycle two days before the light-dark reversal, and on the 1st, 3rd, 5th and 7th day under the reversed lighting regimen; the counts of locomotor activity were summed up every two hours over a 24 hr-period, beginning at 10:00 a.m., and expressed as a relative locomotor activity (percentage) to the mean 24 hr-activity of the last 7 days under LD 12:12 (Fig. 3).

Measurement of plasma corticosterone

For measurement of plasma corticosterone, the newts were divided into two groups. In order to keep approximately the same density as in locomotor activity recording, each group consisting of 20 to 25 newts was housed per plastic tank (37 cm long, 21 cm wide) which was placed separately in a light-tight container. Water for the tank and illumination in the container were also supplied in the same manner as in the locomotor activity recording. The temperature of both water and air in the container was maintained at 22°C. No food was given throughout the experiment. The first group was kept under the normal light-dark cycle

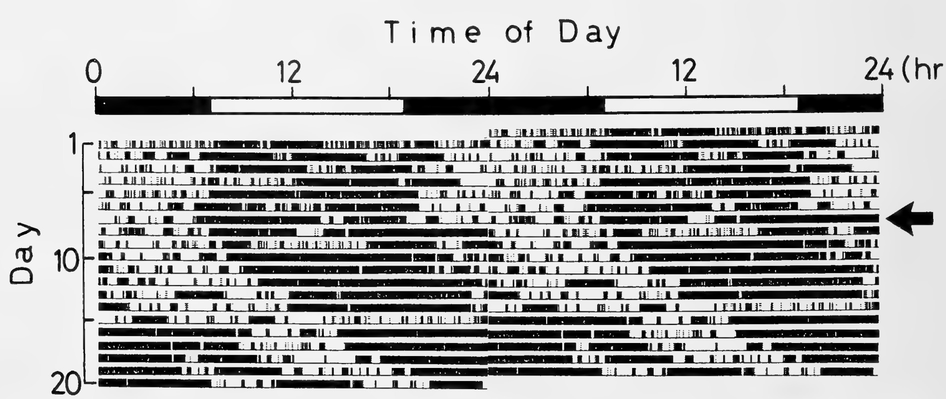

FIG. 1. A sample of the locomotor activity record of one recording box containing a single newt. To aid in visual inspection the record has been duplicated and arranged 48 hr-time base. The newt was initially entrained to a light-dark cycle of LD 12:12 (Light on 07:00, off 19:00) diagrammed at the top of the figure. On the indicated day, the newt was placed in constant darkness.

for at least two weeks and then sacrificed. The 2nd group was exposed to the reversed light-dark cycle after being kept under the normal light-dark cycle for at least two weeks, and then sacrificed on the 7th day of the reversed lighting regimen.

An average of 3 newts in each group were sacrificed every 4 hr over a 24 hr-period, beginning at 10:00 a.m., by decapitation within 30 sec after removal from the tank. The effluent blood from each newt was collected in heparinized tubes and was then immediately centrifuged to obtain the plasma sample.

The amount of corticosterone was determined by a radioimmunoassay employing an antibody for corticosterone (Miles Yada Ltd.) and [1, 2, 6, 7–^{3}H] corticosterone (91 Ci/mmol, The Radiochemical Centre Amersham). Methylene chloride was added to each plasma sample. The mixture was shaken on a Vortex mixer, then centrifuged, and the organic phase was evaporated by a stream of nitrogen gas. The dried material was reconstructed in benzene: methanol (85:15, vol: vol) and subjected to chromatography on Sephadex LH–20 column (0.9×25 cm) in a solvent system of benzene: methanol (85:15, vol: vol). The fraction containing corticosterone was collected and evaporated by a stream of nitrogen gas. The residue was dissolved in 0.05 M Tris HCl buffer (pH 8.0) containing 0.1 M NaCl, 0.1% NaN_3 and 0.1% bovine serum albumin and incubated with labelled corticosterone and the antibody. Dextran-coated charcoal was used to separate the bound from the free hormone. The least detectable amount of the assay was 0.08 ng/ml plasma. The inter-assay and intra-assay coefficient of variation was 13.6% and 4.0%, respectively. For statistical analysis, the Student's *t* test was employed.

The procedure described above was repeated until a sample size of 4 for locomotor recording, and a sample size of more than 9 per each point during the 24 hr-period for blood collection were obtained.

RESULTS

Under the normal light-dark cycle (LD 12:12), the newts were active chiefly during the light period (Fig. 2). The daily locomotor activity began before the onset of light and ended at the light to dark transition. After the light-dark reversal, the phase of the daily onset of locomotor activity gradually delayed and finally shifted approximately 12 hr from that seen under the normal light-dark cycle. On the other hand, the locomotor activity ended at the end of the light period from the initiation of the reversed lighting regimen. In all samples of the activity records, the rest-activity cycles were almost completely reversed within 7 days after the light-dark re-

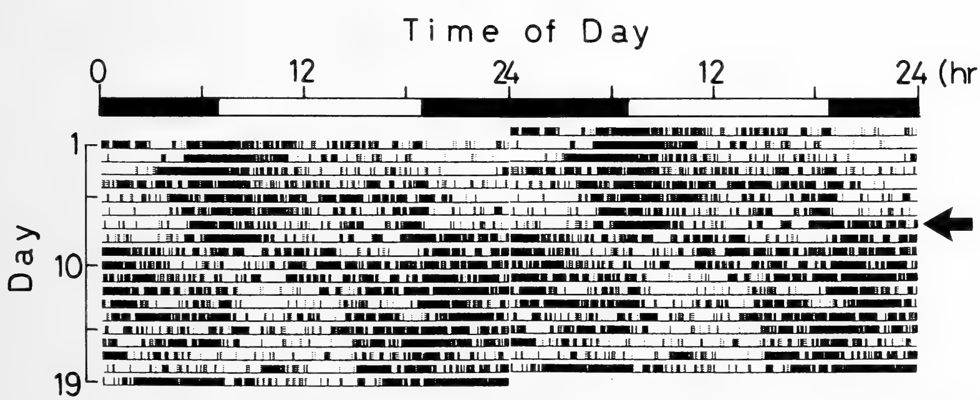

FIG. 2. A sample of the locomotor activity record of one recording box containing 4 newts. To aid in visual inspection the record has been duplicated and arranged on 48 hr-time base. The newts were initially entrained to a light-dark cycle of LD 12:12 (Light on 07:00, off 19:00) diagrammed at the top of the figure. On the indicated day, light period was continued for 24 hr from 07:00 till 07:00 and the reversed light-dark cycle was started.

versal.

The daily variation of locomotor activity under the normal light-dark cycle clearly showed a biphasic pattern (Fig. 3A). The amount of locomotor activity peaked sharply just before the onset of light and then decreased during the first half of the light period. The second peak appeared near the end of the light period. The lowest amount of activity was observed around the middle of the dark period.

On the 1st, 3rd and 5th day after the light-dark reversal, the locomotor activity rhythms were still in the transient period leading to the new phase, and the daily patterns of locomotor activity were atypical (Fig. 3B–D). On the 7th day, the same pattern as observed under the normal light-dark cycle was shown with the phase shifting approximately 12 hr (Fig. 3E).

Under the normal light-dark cycle, the daily variation of plasma corticosterone levels also showed a biphasic pattern (Fig. 3A). The plasma corticosterone increased during the dark period and reached a maximum value at 06:00 just prior to the light period. The value at 06:00 was significantly higher ($p<0.02$) than the value at 22:00. During the light period, the plasma corticosterone decreased one time but then increased again showing a smaller peak (not significant) at the end of the light period (at 18:00). The minimum value was observed in the early part of the dark period (at 22:00).

On the 7th day after the light-dark reversal, the daily pattern of plasma corticosterone levels was similar to that demonstrated under the normal light-dark cycle (Fig. 3E). The plasma corticosterone increased during the dark period of the reversed light-dark cycle and reached the maximum value at 18:00 just prior to the light period. The value at 18:00 was significantly higher ($p<0.05$) than the value at 10:00. During the light period, the plasma corticosterone had decreased once slightly and then showed a second peak (not significant) as shown under the normal light-dark cycle. This peak, however, appeared around the middle of the light period (at 02:00) instead of at the end. Then the level dropped to the minimum value in the early part of the dark period (at 10:00).

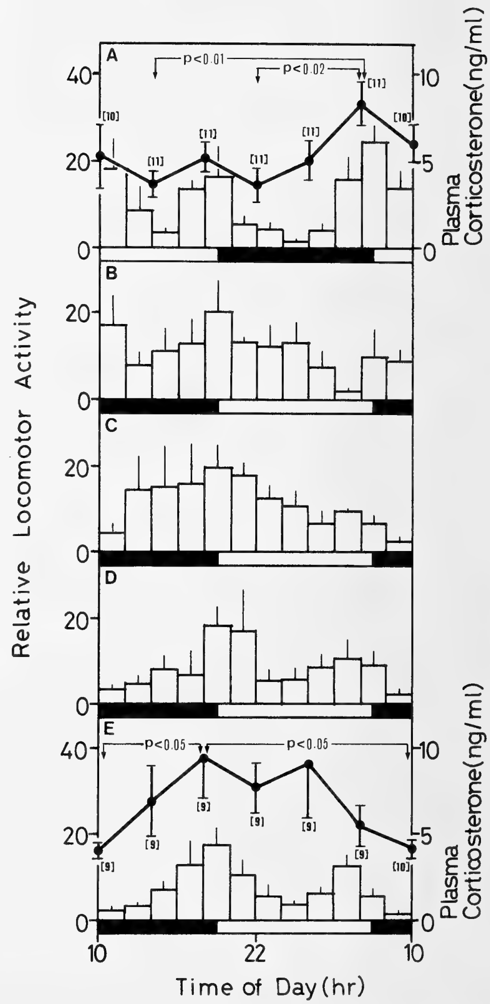

Fig. 3. (A) The daily variation of plasma corticosterone levels and that of locomotor activity in the newts adapted to a normal light-dark cycle of LD 12:12 (Light on 07:00, off 19:00), and (B) in the newts on the 1st, (C) the 3rd, (D) the 5th and (E) the 7th day under a reversed light-dark cycle (Light on 19:00, off 07:00). Each point (A, E) represents the mean ± SEM of plasma corticosterone levels, and number in brackets indicates the number of sampled animals. A significant difference is indicated in figures. Each column (A–E) represents the mean ± SEM of relative locomotor activity of 4 recording boxes. Each box contained 4 newts. The light-dark cycles are diagrammed at the bottom of each figure.

Under the reversed light-dark cycle, the phases of both the maximum and the minimum value of the plasma corticosterone levels on the 7th day had already shifted approximately 12 hr from those recorded under the normal light-dark cycle.

DISCUSSION

It has been established that in diurnal mammals the peak values of plasma glucocorticoid levels are observed early in the morning [18–24] and in nocturnal species late in the afternoon [1, 25]. In non-mammalian species, however, the relationship between the daily variation of plasma glucocorticoid levels and that of locomotor activity has not been precisely described [11–14].

It has been reported that in amphibians, circadian rhythms of locomotor activity are not clearly evident and that a large amount of "noise" is observed in their activity records [26, 27]. However, the authors have recently investigated the circadian rhythms of locomotor activity in the *Cynops*, and these rhythms were clearly day-active under light-dark cycles of LD 12:12 (Fig. 1). In the present study, the actogram from those recording boxes containing 4 female newts each has also demonstrated that these newts were clearly day-active (Fig. 2). The plasma corticosterone increased during the dark period and reached the maximum value just prior to the light period just as is observed in diurnal mammals (Fig. 3A, E). This similarity between mammals and the newt may suggest that a similar mechanism for glucocorticoids secretion exists in both classes of vertebrates. In the newts, the daily variation of locomotor activity clearly showed a biphasic pattern, while that of plasma corticosterone levels had only one significant peak (Fig. 3A, E). The daily variation of plasma corticosterone levels, however, virtually paralleled that of locomotor activity both under the normal light-dark cycle and after the adaptation to the reversed light-dark cycle (Fig. 3A, E). These data indicate that the daily variation of plasma corticosterone levels is closely associated with that of locomotor activity in the newts as well as in mammalian species.

It has been reported that in rats the circadian rhythms in both rest-activity and plasma corticosterone were altered concomitantly under various lighting conditions including constant darkness and constant light [8]. The plasma corticosterone levels tended to increase when they were asleep or during inactive periods, and the levels tended to decrease when they were during active periods regardless of lighting conditions [8]. Further, several authors have suggested that the alteration in the circadian rhythms of locomotor activity, such as that induced by the restriction of feeding, might act as a predominant zeitgeber of the circadian rhythms of the pituitary-adrenal system rather than the light-dark cycle [4–6, 8, 28]. In the newts, the results presented in Figure 3 demonstrated that a change in the phase of the locomotor activity rhythm was accompanied by a change in that of the plasma corticosterone rhythm. The present authors' results, however, do not answer the question as to whether the daily rhythm of plasma corticosterone levels is synchronized predominantly by that of locomotor activity rather than by the imposed light-dark cycle.

In amphibians, it has been reported that in a natural environment during midsummer spawning period, plasma corticosterone levels of European green frogs were higher during the night when the frogs developed an important activity associated with the various components of sexual behavior, yet they were usually active throughout the day in this season [14]. The spontaneous locomotor activity recorded in the present study might be composed of various facets of activity. The newts might be demonstrating sexual behavior under the given experimental conditions. Therefore, the authors did not exclude the possibility of the circadian rhythms in the pituitary-adrenal system in the newts being linked definitely to the rhythms of the activity associated with some components of sexual behavior. In addition, for non-domesticated animals such as newts, exposure to experimental conditions may have some effects on both behavior and plasma corticosterone levels. For instance, it was recently shown in male rough-skinned newts that the exposure to stressful stimuli elevated the levels of plasma corticosterone and inhibited sexual behavior [29]. From this

point of view, it would be of great interest to examine, in newts, the relationship between plasma corticosterone levels and specific types of locomotor activity.

ACKNOWLEDGMENTS

We thank Dr. W. Heiligenberg for helpful discussion and criticism of the manuscript and Dr. S. Kikuyama for reviewing it. We are also grateful to Dr. M. Kikuchi for extensive technical assistance with the experiments. This work was supported by 58540473 Grant-in-Aid for Scientific Research from the Ministry of Education, Science and Culture of Japan.

REFERENCES

1 Halberg, F., Peterson, R. E. and Silber, R. H. (1959) Phase relations of 24-hour periodicities in blood corticosterone, mitoses in cortical adrenal parenchyma, and total body activity. Endocrinology, **64**: 222–230.

2 Perkoff, G. T., Eik-Nes, K., Nugent, C. A., Fred, H. L., Nimer, R. A., Rush, L., Samuels, L. T. and Tyler, F. H. (1959) Studies of the diurnal variation of plasma 17-hydroxy-corticosteroids in man. J. Clin. Endocrinol. Metab., **19**: 432–443.

3 Orth, D. N., Island, D. P. and Liddle, G. W. (1967) Experimental alteration of the circadian rhythm in plasma cortisol (17-OHCS) concentration in man. J. Clin. Endocrinol. Metab., **27**: 549–555.

4 Krieger, D. T. (1974) Food and water restriction shifts corticosterone, temperature, activity and brain amine periodicity. Endocrinology, **95**: 1195–1201.

5 Holley, D. C., Beckman, D. A. and Evans, J. W. (1975) Effect of confinement on the circadian rhythm of ovine cortisol. J. Endocrinol., **65**: 147–148.

6 Moberg, G. P., Bellinger, L. L. and Mendel, V. E. (1975) Effect of meal feeding on daily rhythms of plasma corticosterone and growth hormone in the rat. Neuroendocrinology, **19**: 160–169

7 Gibbs, F. P. (1976) Correlation of plasma corticosterone levels with running activity in the blinded rat. Am. J. Physiol., **231**: 817–821.

8 Morimoto, Y., Arisue, K. and Yamamura, Y. (1977) Relationship between circadian rhythm of food intake and that of plasma corticosterone and effect of food restriction on circadian adrenocortical rhythm in the rat. Neuroendocrinology, **23**: 212–222.

9 Takahashi, K., Inoue, K. and Takahashi, Y. (1977) Parallel shift in circadian rhythms of adrenocortical activity and food intake in blinded and intact rats exposed to continuous illumination. Endocrinology, **100**: 1097–1107.

10 Honma, K. and Hiroshige, T. (1978) Internal synchronization among several circadian rhythms in rats under constant light. Am. J. Physiol., **235**: R 243–R 249.

11 Boehlke, K. W., Church, R. L., Tiemeier, O. W. and Eleftheriou, B. E. (1966) Diurnal rhythm in plasma glucocorticoid levels in channel catfish (*Ictalurus punctatus*). Gen. Comp. Endocrinol., **7**: 18–21.

12 Singley, J. A. and Chavin, W. (1971) Cortisol levels of normal goldfish, *Carassius auratus* L., and response to osmotic change. Am. Zool., **11**: 653.

13 Redgate, E. S. (1974) Neural control of pituitary-adrenal activity in *Cyprinus carpio*. Gen. Comp. Endocrinol., **22**: 35–41.

14 Leboulenger, F., Delarue, C., Belanger, A., Perroteau, I., Netchitailo, P., Leroux, P., Jegou, S., Tonon, M. C. and Vaudry, H. (1982) Direct radioimmunoassays for plasma corticosterone and aldosterone in frog. I. Validation of the methods and evidence for daily rhythms in a natural environment. Gen. Comp. Endocrinol., **46**: 521–532.

15 Carstensen. H., Burgers, A. C. J. and Li, C. H. (1961) Demonstration of aldosterone and corticosterone as the principal steroids formed in incubates of adrenals of the American bullfrog (*Rana catesbeiana*) and stimulation of their production by mammalian adrenocorticotropin. Gen. Comp. Endocrinol., **1**: 37–50.

16 Macchi, I. A. and Phillips, J. G. (1966) In vitro effect of adrenocorticotropin on corticoid secretion in the turtle, snake, and bullfrog. Gen. Comp. Endocrinol., **6**: 170–182.

17 Aoki, K., Kikuchi, M. and Chiba, A. (1984) The role of the pineal organ in circadian rhythm of the newt. In "Animal Behavior: Neurophysiological and Ethological Approaches". Ed. by K. Aoki, S. Ishii and H. Morita, Japan Scientific Societies Press, Tokyo, pp. 243–251.

18 Bliss, E. L., Sandberg, A. A., Nelson, D. H. and Eik-Nes, K. (1953) The normal levels of 17-hydroxycorticosteroids in the peripheral blood of man. J. Clin. Invest., **32**: 818–823.

19 Migeon, C. J. French, A. B., Samuels, L. T. and Bowers, J. Z. (1955) Plasma 17-hydroxy-corticosteroid levels and leucocyte values in the rhesus monkey, including normal variation and the effect of ACTH. Am. J. Physiol., **182**: 462–468.

20 Harwood, C. T. and Mason, J. W. (1956) Effects of intravenous infusion of autonomic agents on peripheral blood 17-hydroxycorticosteroid levels in the dog. Am. J. Physiol., **186**: 445–452.

21 Peterson, R. E. (1957) Plasma corticosterone and hydrocortisone levels in man. J. Clin. Endocrinol.

Metab., **17**: 1150–1157.

22 Zolovick, A., Upson, D. W. and Eleftheriou, B. E. (1966) Diurnal variation in plasma glucocorticosteroid levels in the horse (*Equus caballus*). J. Endocrinol., **35**: 249–253.

23 McNatty, K. P., Cashmore, M. and Young, A. (1972) Diurnal variation in plasma cortisol levels in sheep. J. Endocrinol., **54**: 361–362.

24 Leshner, A. I., Toivola, P. T. K. and Terasawa, E. (1978) Circadian variations in cortisol concentrations in the plasma of female rhesus monkeys. J. Endocrinol., **78**: 155–156.

25 Guillemin, R., Dear, W. E. and Liebelt, R. A. (1959) Nychthemeral variations in plasma free corticosteroid levels of the rat. Proc. Soc. Exp. Biol. Med., **101**: 394–395.

26 Binkley, S., Adler, K. and Taylor, D. H. (1973) Two methods for using period length to study rhythmic phenomena. J. Comp. Physiol., **83**: 63–71.

27 Demian, J. J. and Taylor, D. H. (1977) Photoreception and locomotor rhythm entrainment by the pineal body of the newt, *Notophthalmus viridescens* (amphibia, urodela, salamandridae). J. Herpetol., **11**(2): 131–139.

28 Krieger, D. T. and Hauser, H. (1978) Comparison of synchronization of circadian corticosteroid rhythms by photoperiod and food. Proc. Natl. Acad. Sci. USA, **75**: 1577–1581.

29 Moore, F. L. and Miller, L. J. (1984) Stress-induced inhibition of sexual behavior: Corticosterone inhibits courtship behaviors of a male amphibian (*Taricha granulosa*). Horm. Behav., **18**: 400–410.

ZOOLOGICAL SCIENCE 4: 551–555 (1987)

The Effects of Preputialectomy on Aggression in Male Mice

Susumu Hayashi

Department of Biology, Faculty of Education, Kagoshima University, Kagoshima 890, Japan

ABSTRACT—To investigate the relationship between preputial glands and aggression, male mice underwent one of the following three surgeries, bilateral (XX), unilateral (PX) or sham (PP) preputialectomy. The mice were paired off and placed for 14 days in cages which were divided by a wire net barrier. The pair was permitted to come into contact with each other periodically. Social behavior during removal of the barrier was observed. PP–PP, PP–PX and PP–XX pairs showed vigorous aggressive behavior than PX–PX, XX–XX and PX–XX pairs. PP males were more apt to become dominant than PX or XX males. It was concluded that the preputial gland affects the aggressive behavior of its owner.

INTRODUCTION

The preputial glands of male mice have been frequently implicated in olfactory communication. Male preputial odors attract females [1–4]. It has also been suggested that there is a relationship between preputial odors and aggressive behavior. Preputial sebum that has been applied to a castrated male promotes attacks by a conspecific male [5, 6]. These findings, however, are concerned with the pheromonal function of preputial odors which act on conspecific recipients other than donors. There are very few reports which deal with the reactions of animals to their own odors [7]. This may be partly because the pheromonal concept implies transmission of olfactory information from one animal to a second animal and partly because the effects of an animal's own odors are likely to be confused with motivational changes.

The present investigation intended to study the relationship between aggressive behavior and the preputial glands which may affect conspecifics including its owner. For this purposes the glands were bilaterally or unilaterally segregated in some male mice and sham operations were performed in others.

Accepted February 12, 1987
Received November 20, 1986

GENERAL MATERIALS AND METHODS

Mice (*Mus musculus*) of the ICR–JCL strain were used. They were housed in groups of 5 or 6 in plastic cages ($23\times16\times12$ cm), and received food and water *ad lib.* in a light and temperature controlled room. When the males were 110–140 days of age, they were isolated for 11 days. On the 10th day of isolation, they were anesthetized with sodium pentobarbital and underwent one of three surgeries, a bilateral preputialectomy (XX), a unilateral preputialectomy (PX) or a sham operation (PP). Each male was placed together with an assigned male for 14 days from the day after the surgery in a cage divided by a wire net barrier, inhibiting tactile responses between cohabitants. The barrier was removed for the first 24 hr and for 26 min daily from the 3rd to 14th day of cohabitation. Social behavior such as attacks, bites or mounts were recorded while the barrier was removed. These behaviors were counted as one bout when the animals parted from each other regardless of the duration time of the behavior. Attacks and bites were put together as aggressive behaviors.

In preliminary experiments, the activities of male mice were observed with ANIMEX before and after the surgery. Although the activities weakened slightly immediately after the surgery, they were restored after 24 hr. There were no

significant differences among the motor activities of PP and XX males after the surgery.

EXPERIMENT I

Methods

Males used in this experiment were paired with an animal which underwent the same kind of surgery. Males of about half the pairs (7 PP–PP pairs, 7 PX–PX pairs and 8 XX–XX pairs) were familiar with each other because they had been fed in the same cage from weaning (28 days old) up until isolation. The other pairs were comprised of males who were unfamiliar with each other (10 PP–PP pairs, 13 PX–PX pairs and 8 XX–XX pairs). In addition, preputial glands removed from the males of unfamiliar XX–XX and PX–PX pairs were freed from fatty and connective tissues, the fluid content gently sqeezed out, and the wet weight measured. The remaining preputial glands of PX–PX pairs and PP–PP pairs were removed immediately after cohabitation and weighed.

Results

Results are shown in Table 1. Dominant-subordinate relationships were established in almost every pair by the 3rd day of cohabitation, and there were no changes in social status throughout the remaining observation period. Dominant males of both familiar and unfamiliar

TABLE 1. Social behaviors exhibited by paired males in the same preputial state during cohabitation (26 min×12 day)

Pair		N	Dominance	Aggression	Mount
				Median (Range)	Median (Range)
familiar	PP–PP	7	Dominant	80 (18–123)	2 (0–12)
			Subordinate	0 (0– 6)	0 (0– 0)
	PX–PX	7	Dominant	21 (3– 26)	0 (0– 5)
			Subordinate	3 (0– 10)	0 (0– 1)
	XX–XX	8	Dominant	7 (2– 34)	1 (0– 6)
			Subordinate	1 (0– 11)	0 (0– 3)
unfamiliar	PP–PP	10	Dominant	45 (33–127)	8 (0–52)
			Subordinate	0 (0– 10)	0 (0–10)
	PX–PX	13	Dominant	19 (0– 48)	13 (2–46)
			Subordinate	0 (0– 6)	1 (0–25)
	XX–XX	8	Dominant	32 (3– 44)	48 (10–82)
			Subordinate	0 (0– 6)	2 (0–14)

TABLE 2. Comparison of preputial weight (Mean±SE)

Pair	Segregation	Dominance	Weight (mg)
PP–PP	after Cohabitation	Dominant	62.4±8.3[a]
		Subordinate	41.9±3.3
PX–PX	before Cohabitation	Dominant	21.5±1.6*
		Subordinate	15.9±1.3*
	after Cohabitation	Dominant	27.7±2.6*
		Subordinate	19.9±2.3*
XX–XX	before Cohabitation	Dominant	39.9±6.0
		Subordinate	31.6±2.5

* Weight of a unilateral gland.
[a] Mean±standard error.

PP–PP pairs were more aggressive than those of PX–PX or XX–XX pairs (Mann-Whitney U-test; $P<0.01$). Although the number of aggressive behaviors displayed by PX and XX males was less than that of PP males, there was no qualitative difference among them. Concerning aggression, unfamiliar pairs were more active than familiar pairs only when the preputial glands were removed bilaterally. The remarkable difference between familiar and unfamiliar groups was a mounting behavior. The behavior was mainly displayed by unfamiliar pairs ($P<0.01$), and with dominant XX males showing the highest frequency ($P<0.05$).

In regard to preputial weight, the glands removed from dominant males of PP–PP and PX–PX pairs after cohabitation were heavier than those of subordinate ones (t-test, PP–PP; $t=2.33$, $P<0.05$, PX–PX; $t=2.22$, $P<0.05$) as shown in Table 2. The glands increased in weight during cohabitation because the preputial weight of a dominant PI male after the cohabitation was heavier than that before cohabitation (Wilcoxon matched-pairs signed-ranks test, $T=4$, $N=13$, $P<0.01$). Although it was not as marked as in the dominant male, the weight of the preputial gland of a subordinate male increased, too ($T=11$, $N=11$, $P<0.05$).

EXPERIMENT II

In Exp. I, dominant males of PP–PP pairs were more aggressive than PX or XX males. The difference could be accounted for in two ways. PP males may provoke aggressive behavior in a cohabitant more than PX or XX males. Alternatively, PP males were motivationally more aggressive than PX or XX males. To clarify this point, Exp. II was performed.

Methods

Male mice which had undergone one of three surgeries as in Exp. I were placed with an unfamiliar male of a different preputial condition. Fourteen PP–XX pairs, 11 PP–PX pairs and 9 PX–XX pairs were used and the other procedures were the same as in Exp. I.

Results

As shown in Table 3, PP males showed more aggressive behaviors than cohabitants when they were paired with XX males ($P<0.01$) or PX males ($P<0.05$), although 3 XX males and 2 PX males dominated the PP cohabitants. In PX–XX pairs, 6 PX and 3 XX males became dominant.

DISCUSSION

It was reported that preputial odors provoke aggressive behaviors in recipients [5, 6]. In this experiment, however, neither XX males of PP–XX pairs nor PX males of PP–PX pairs showed aggressive behaviors toward a cohabitant although they were the recipients of preputial odors. They retained a lower status than a PP male. These results suggest that a preputialectomy decreases aggressivity in the excised mouse. In other words the preputial gland may maintain the aggressiveness of its owner. The reduction of aggressivity in PX–XX, PX–PX and XX–XX pairs seemed to be attributable to a decline in aggressive motivation rather than a decline of aggression inducing stimuli.

McKinney and Christian [8] found that PP–XX

TABLE 3. Social behaviors exhibited by paired males in different preputial states

Pair	N	Males	Aggression	Mount
			Median (Range)	Median (Range)
PP–PX	11	PP	54 (0–183)	7 (0–29)
		PX	0 (0–138)	0 (0–20)
PP–XX	14	PP	33 (0–179)	3 (0–41)
		XX	0 (0– 50)	0 (0– 3)
PX–XX	9	PX	14 (0– 85)	9 (0–27)
		XX	1 (0– 63)	1 (0–16)

pairs exhibited more fights than PP–PP or XX–XX pairs. Their findings were not consistent with those of the present experiment, due perhaps, to a methodological difference. They observed only 15 min of cohabitation and it was in the early stages of establishing dominance. In the present experiment, however, observation did not commence until 48 hr after the start of cohabitation and consequently most social orders were established by the beginning of observation.

Bronson and Marsden reported that preputial glands of dominant males are heavier than those of subordinate ones, and that preputial glands of subordinate males are lighter than isolated males [9]. These individual variations in preputial weight are partly induced by social environment; a mouse with heavier preputial glands does not necessarily dominate one with lighter glands. Cohabitation with a strange male increases the preputial weight. Although it occurs without physical contact (prevented by a wire net barrier), it is much more effective when the barrier is removed periodically [10]. Preputial glands of dominant males increased markedly in the present experiment. This is in accord with previous findings [9, 10]. However, preputial glands of subordinate males also increased in weight although the increase was not as marked as in dominant males. Bronson and Marsden housed 2 male mice in a cage for 2 weeks without a barrier, while the mice of the present experiment came into physical contact with each other for only 26 min a day. Preputial growth of subordinate males would probably not occur without a partition.

Aggressive behaviors were displayed only by dominant males. Considering that preputial glands seem to maintain aggressivity, the glands may play an important role in social order.

Mugford [11] observed that pairs of preputialectomized males spent less time on aggression with one another than did pairs composed of sham operated males. He attributed the reduction of aggressive behaviors to operation trauma and lack of pheromonal stimulus. In the present investigation, cohabitation began on the day following the operation. It cannot be denied that surgery may have imposed some pain or stress which could indirectly influenced aggression. However, it did not seem to disturb comparative studies because PP males were not intact but underwent sham operations and the frequency of social behaviors (aggression and mounts) exhibited by unfamiliar PP–PP pairs was comparable to that of XX–XX pairs. Any other social behaviors as grooming, chasing and so on were rarely observed in this experimental situation. In addition, activities observed with ANIMEX did not reveal any differences among PP, PX and XX males.

Recently, Wiesler *et al.* [12] and Novotny *et al.* [13] studied the function of substances in urine such as 2-(*sec*-butyl)-4, 5-dihydrothiazole and dehydro-*exo*-brevicomin, both of which are not contained in preputial secretions. They observed that the substances act as aggression-inducers, sex-attractants, and estrous-inducers. On the other hand, it is well known that preputial odors attract female mice, and there are some reports about preputial sebum which promotes the attack of opponents. Those substances contained in urine and preputial secretions may be effective as cues which indicate maleness without particular meaning.

Mounting behavior between males, which was very similar to the mounting behavior between a male and a female except intromission, was displayed mainly by dominant males regardless of their preputial state. Although the meaning of the mounting between males was not determined, the difference between familiar and unfamiliar pairs suggested that individual recognition prevented mounting behavior. XX–XX males showed the most frequent mounting behavior among unfamiliar pairs. This seems to be caused not only by a reduction in agonistic motivation but also by a decline in the maleness of a cohabitant.

Preputial materials stimulate the owner of the glands. It is probably olfactory stimuli that affect the owner, considering the other functions of the preputial glands, although this must be confirmed by impairing olfactory pathways.

REFERENCES

1 Bronson, F. H. and Caroom, D. (1971) Preputial

gland of the male mouse: Attractant function. J. Reprod. Fertil., **25**: 279–282.

2 Hayashi, S. and Kimura, T. (1973) Responses of normal and neonatally estrogenized female mice to the odor of males. Sci. Pap. Coll. Gen. Educ. Univ. Tokyo, **23**: 39–43.

3 Hayashi, S. (1979) A role of female preputial glands in social behavior of mice. Physiol. Behav., **23**: 967–969.

4 Hayashi, S. (1985) A preputial odor imprinted on female mice. J. Ethol., **3**: 89–91.

5 Jones, R. B. and Nowell, N. W. (1973) Effects of preputial and coagulating gland secretions upon aggressive behavior in male mice: a confirmation. J. Endocrinol., **59**: 203–204.

6 Homady, M. H. and Brain, P. F. (1982) Effects of marking with preputial gland material on the attack directed towards long-term castrates by isolated males. Aggress. Behav., **8**: 137–140.

7 Kimura, T and Hagiwara, Y. (1984) Responses of male and female laboratory mice to the odor of conspecifics of the same sex: Effects of previous isolation and gruping. J. Ethol., **2**: 121–126.

8 McKinney, E. D. and Christian, J. J. (1970) Effect of preputialectomy on fighting behavior in mice. Proc. Soc. Exp. Biol. Med., **134**: 291–293.

9 Bronson, F. H. and Marsden, H. M. (1973) The preputial gland as an indicator of social dominance in male mouse. Behav. Biol., **9**: 625–628.

10 Hayashi, S. (1986) Effects of a cohabitant on preputial gland weight of male mice. Physiol. Behav., **36**: 299–300.

11 Mugford, R. A. (1973) Intermale fighting affected by home cage odors of male and female mice. J. Comp. Physiol. Psychol., **84**: 289–295.

12 Wiesler, D. P., Schwende, F. J., Carmack, M. and Novotny, M. (1983) Structural determination and synthesis of a chemical signal of the male state and a potential multipurpose pheromone of the mouse *Mus musculus*. J. Org. Chem., **49**: 882–884.

13 Novotny, M., Harvey, S., Jemiolo, B. and Alberts, J. (1985) Synthetic pheromones that promote inter-male aggression in mice. Proc. Natl. Acad. Sci. USA, **82**: 2059–2061.

ZOOLOGICAL SCIENCE 4: 557–561 (1987)

Annual Ovarian, Fat Body and Liver Cycles of the Grass Lizard *Takydromus stejnegeri* in Taiwan

HSIEN YU CHENG and JUN YI LIN[1]

Department of Zoology, National Taiwan University, Taipei, Taiwan 107, and [1]Department of Biology, Tunghai University, Taichung, Taiwan 400, R. O. C.

ABSTRACT—The female *Takydromus stejnegeri* in Taiwan has a definite breeding season from March to August. Most females produced two clutches but a few females may produce one or three clutches a year. The number of eggs per clutch for most clutches was 2 (with range from 1 to 4). The clutch size increased significantly during the breeding season. The smallest and largest mature females were 41 mm and 57 mm in snout-vent length, respectively. Most newly hatched individuals (<25 mm in snout-vent length) occur from May to September.

Fat body size was inversely correlated with reproduction. The mean liver weights peak in June. Both annual mean liver and fat body weights of *T. stejnegeri* females were similar to those of males during this same period.

INTRODUCTION

During the past ten years, a wealth of data has accumulated on annual reproductive and lipid storage patterns in both temperate and tropical lizards [1–7]. However, the reproductive and energetic biology of most lizards remains poorly known, particularly for insular populations in the Pacific region [8]. The paucity of reproductive and energetic data on tropical and subtropical Asian lizards has been one of the obstacles to a fuller understanding of evolutionary strategies of saurian reproduction and energetics [9–11]. The present study reported here was made as part of our comparative study on reproductive and energetic biology of lizards in Taiwan, a subtropical Pacific island.

MATERIALS AND METHODS

Lizards were collected monthly from November 1975 to December 1976. An additional collection was made on April 27, 1977. Individuals for this study were collected from grassy field and cultivated area of sugarcane and sweet-potato around the Tunghai University campus, Taichung, Taiwan (24°10′N; elevation 180 meters) during midday (from 11:30 am to 2:00 pm) when their activities were at the peak.

Specimens were etherized within two hours after capture, weighed to the nearest 0.01 g and their snout-vent length (SV-length) measured to the nearest 0.1 mm. Each specimen was then made a small abdominal cut and preserved in 10% formalin for further examinations. Livers and fat bodies were, thereafter, removed and weighed to the nearest 1 mg. Yolked follicles, oviducal eggs, and corpora lutea were counted. Yolked follicles and oviducal eggs were then weighed to the nearest 0.1 mg and their greatest diameter was measured to the nearest 0.1 mm. Females were classified as reproductive when they contained either oviducal eggs or bright yellow ovarian follicles greater than 1.8 mm in diameter.

To minimize the influence of SV-length on the results [12], only a relatively narrow range of adult SV-lengths was included for analyses. The metereological data of Taichung City (9 km from Tunghai campus; 83.8 m above sea level) were obtained from the Central Weather Bureau, Taipei, and shown in a Cheng and Lin's article [13].

Accepted February 14, 1987
Received December 23, 1986

RESULTS

The smallest and largest mature females were 41.0 mm and 56.8 mm SV-length, respectively. However, samples (n=10) contained only one mature individual with the 41.0–43.5 mm SV-length class. This mature individual derived from the March sample. Thus, also to minimize the influence of the SV-length on the results, 43.6 mm SV-length was chosen as the smallest female adult size used in the analyses. From November 1975 to December 1976, a total of 105 females of *T. stejnegeri*, larger than 43.6 mm in SV-length, were collected. The overall yearly mean SV-length for adult females was 48.6 mm. The monthly SV-length means were similar among all months (ANOVA, p=0.90) and ranged from 44.4 mm to 51.6 mm.

Reproduction

In 1976, almost all (>90%) adult females captured from March through August were classified as reproductive (N=75, Fig. 1). The number of reproductively active females declined sharply in September, and reached the lowest level (0%) in late September (the samples of this month were collected on September 28). No yolked follicles or oviducal eggs were observed among the thirty adult females sampled during September to December 1976 and November 1965 to February 1976 (Fig. 1).

During 1976, most females produced two clutches. By May and June, the majority (68%) of the adult females contained both yolked follicles and oviducal eggs or both yolked follicles and corpora lutea. A few females may produce three clutches or merely one clutch. Because females containing oviducal eggs occurred in mid-March and would have oviposited in late March or early April, these females would have had nearly five months for reproduction, long enough to produce a second and perhaps a third clutch. The mean time necessary to produce a clutch was estimated to be two months. Females would reach maturity in every month during the breeding season but most females achieve their mature size from late breeding season (July-August) to the early period of the next breeding season (March or April). The younger adult (reaching maturity in late breeding season) unlikely could produce more

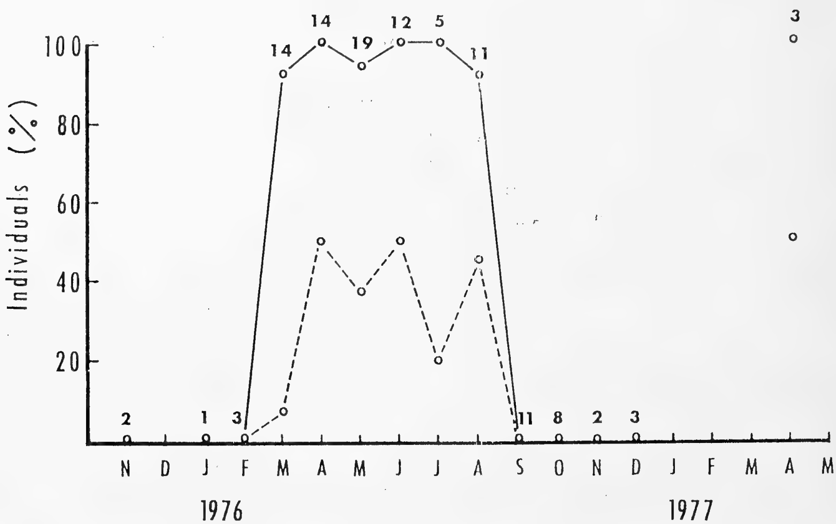

FIG. 1. Monthly changes in the reproductive state of adult females (SV-length>43 mm) from November 1975 to December 1976 (with additional data on April 1977). Solid line shows the percentage of each sample that contained yolked follicles, oviducal egg or both; dashed line shows the percentage of each sample that contained oviducal eggs. Sample size is shown above each month.

than one clutch during that year. To sum up, many females produced their first clutch in late April and May and a second clutch in July and August. A few females may produced a first clutch in late March-early April, a second clutch in June, and a third clutch in August. Younger females may produce only one clutch in August.

The mean number of eggs for all clutches was 2.2 as estimated by the mean number of ovarian yolked follicles (N=43; range: 1–4; mode=2) or by the mean number of oviducal eggs (N=27; range: 1–4; mode=2). Cluth size had no significant correlation with SV-length. However, only females larger than 53 mm in SV-length had clutch size of four eggs. The clutch size of three eggs occurred only in the females larger than 46 mm SV-length.

The number of eggs for the first clutch was 2.0 (N=15) as estimated by the mean number of oviducal eggs of females collected during March, April and May. This was lower than the mean number 2.33 (N=12) for the second or the last clutch of the adults collected during June, July and August.

Sizes of oviducal eggs, both weights and maximum diameters, were very similar in eggs of the same clutch; but between females there was considerable variation. Maximum oviducal egg diameters ranged from 5.8 to 11.9 mm. No females with oviducal eggs less than 10.1 mm in diameter had yolked follicles at the same time.

Inter-uterine migration of eggs was found to have occurred in 14% of gravid females with no apparent bias toward the right or left oviduct. there was a slight difference between the numbers of oviducal eggs in the right and the left oviducts (1.18 vs. 0.93, favoring the right).

The mean incubation time of oviducal eggs (n=3) was 32 days. All eggs were incubated at room temperature (25–28°C). The mean hatchling SV-length was 20.8 mm. Maturity was estimated to occur between 9 to 12 months of age.

Livers and fat bodies

Monthly mean liver weights were at higher level from March through September with a peak in June. During the late fall and winter, the monthly means of liver weights were low (Fig. 2).

No considerable fat bodies occurred in the spring and summer months. The marked increase in sizes of fat bodies occurred in September after the end of the breeding activities and reached the peak in October and November. The weight of fat bodies decreased markedly in winter to their lowest size in March (Fig. 2).

DISCUSSION

The female *T. stejnegeri* in Taiwan has a definite breeding season from March to August (Fig.

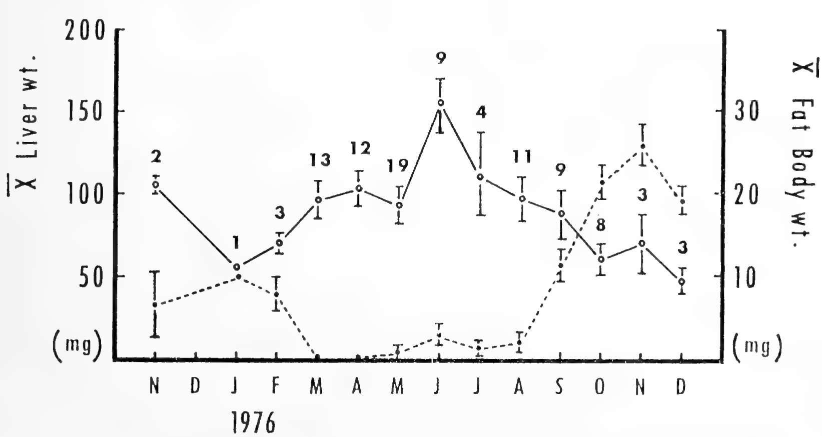

FIG. 2. Monthly changes of liver and fat body weights of adult females from November 1975 to December 1976. Solid line indicates mean liver weight changes; dashed line indicates mean fat body weight changes. Vertical lines show plus and minus one standard error about the means; numbers are sample sizes.

1). Most females produced two clutches but a few females may have produced three clutches or merely one clutch during the 1976 breeding season. The female *T. stejnegeri* in Taiwan, as *T. tachydromoides* in Japan [14], has a multiple-brooded cyclic reproductive pattern. The earliest clutches were laid in March or early April, and the last clutches were laid in early September. Since the incubation time is about one month, the hatchings are expected to occur from May to early October and this is concordant with observations of recently hatched young (<25 mm in SV-length) occurring from May to September.

The reproductive cycle of male *T. stejnegeri* during the same period was reported by Cheng and Lin [13]. The testicular changes in weight showed that *T. stejnegeri* had a distinct reproductive cycle: mainly reproductively active during the spring and summer, and quiescent in September and October. During the winter, male *T. stejnegeri* had a potential for breeding; i.e., accessory organs were hypertrophied and spermiation occurred [13]. However, no breeding activities of female *T. stejnegeri* occurred during the same period of the winter. In *T. stejnegeri*, females cease their reproductive activities while the males still show reproductive potential, as in some species of lizards such as *Leiolopisma rhomboidalis* (Scincidae) [15], *Agama agama* (Agamidae) [16, 17], and *Hemidactylus frenatus* (Gekkonidae) in Taiwan [4].

The number of eggs per clutch was found to increase slightly but significantly during the second half of the 1976 reproductive season. Since the second clutch began development during the middle of the rainy season, it appears likely that an increased food supply during that time would allow for greater investment in reproduction. Several studies have demonstrated a positive correlation between rainfall and food abundance or lizard growth [18, 19]. The possibility that this increase in egg number was due to a general increase in the size of individual lizards in the population or sampling bias, was eliminated by an examination of the mean SV-length of each month's samples. There was essentially no difference in the mean SV-length between combined spring (March, April and May) and combined summer (June, July and August) samples.

The cyclical lipid storage and utilization system is an important adaptation in lizards to seasonal fluctuation of the environment for reproduction or winter dormancy [9]. All lizards with a cyclical lipid storage and utilization system are expected to be cyclical breeders. Both liver and fat body weights have been used as indices of body lipid content and consequently stored energy [20].

Fat body size in both sexes of *T. stejnegeri* was essentially inversely correlated with reproduction, though some accumulation of fat occurred while reproductive activities were still taking place. The absence of fat bodies during spring and summer probably did not result from physiological inability to accumulate energy or from the shortage of food. It appears more likely that reduced size of fat bodies is due to the high expenditure of energy for breeding activities and to the reduction of foraging time during the breeding season.

Liver is probably an intermediary organ for both the storage and utilization of lipids, especially for the reproductive purpose [21, 22]. The peak of the mean liver weight occurred in June, suggesting that June was the end of intense reproductive effort allowing the energy accumulation for lipid storage to begin (Figs. 1 and 2). As to the precise role of the liver functions, further experiments are needed.

Although climate at study areas is subtropical, the annual reproductive and energetic patterns of *T. stejnegeri* and the other two species of lizards studied in Taiwan are more similar to the patterns found in temperate lizards. Even the house gecko, *Hemidactylus frenatus*, shows a definite breeding season in Taiwan, although it has a continuous reproductive pattern in Java [3, 13, 20, 23]. In the present species (*T. stejnegeri*) and the other species studied (*Japalura swinhonis*), vitellogenesis begins in spring and continues untill mid-summer, followed by a period of the reproductive quiescence and rapid build-up of fat reserves prior to winter [4, 20, 25]. In general, this pattern fits the reproductive strategy described by Tinkel *et al.* [25] of early maturing, relatively small clutch sized, mutiple-brooded lizards.

ACKNOWLEDGMENTS

This study was partially suported by a grant from the National Science Council (NSC75–0201–B002–29 to HYC) of the Republic of China and a grant from the Taipei Zoological Garden (to JYL). The facilities for the computer word processing and calculation were provided by the Department of Zoology of National Taiwan University. Figures were prepared by Tsai Tsan-Dung.

REFERENCES

1 Fitch, H. S. (1982) Reproductive cycles in tropical reptiles. Occas. Papers Mus. Nat. Hist. Univ. Kansas, **96**: 1–53.

2 Guillette, L. J. and Sullivan, W. P. (1985) The reproductive and fat body cycles of the lizard, *Sceloporus formosus*. J. Herpetol., **19**: 474–480.

3 Lin, J. Y. and Cheng, H. Y. (1984) Ovarian cycle in the house gecko, *Hemidactylus frenatus*, in Taiwan with reference to food stress in winter. Bull. Inst. Zool., Academia Sinica, **23**: 21–28.

4 Lin, J. Y. and Cheng, H. Y. (1986) Annual reproductive and lipid storage patterns of the agamid lizard, *Japalura swinhonis mitsukurii* in southern Taiwan. Bull. Inst. Zool., Academia Sinica, **25**: 13–23.

5 McKinney, R. B. and Marion, K. R. (1985) Reproductive and fat body cycles in the male lizard, *Sceloporus undulatus*, from Alabama, with comparisons of geographic variation. J. Herpertol., **19**: 208–217.

6 Vitt, L. J. (1983) Reproduction and sexual dimorphism in the tropical Teiid lizard *Cnemidophorus ocellifer*. Copeia, **1983**: 359–366.

7 Vitt, L. J. and Goldberg, S. R. (1983) Reproductive ecology of two tropical iguanid lizards: *Tropidurus torquatus* and *Platynotus semitaeniatus*. Copeia, **1983**: 131–141.

8 Schwaner, T. D. (1980) Reproductive biology of lizards on the American Samoan Islands. Occas. Papers Mus. Nat. Hist. Univ. Kansas, **86**: 1–53.

9 Derickson, W. K. (1976) Lipid storage and utilization in reptiles. Am. Zool., **16**: 711–723.

10 Pianka, E. R. (1976) Natural selection of optimal reproductive tactics. Am. Zool., **16**: 775–748.

11 Stearns, S. C. (1976) Life-history tactics: a review of ideas. Q. Rev. Biol., **51**: 3–47.

12 Atchley, W. R.,Gaskins, C. T., and Anderson, D. (1976) Statistical properties of ratios. I. Empirical results. Syst. Zool., **25**: 137–148.

13 Cheng, H. Y. and Lin, J. Y. (1977) Comparative reproductive biology of the lizards, *Japalura swinhonis formosensis, Takydromus septentrionalis*, and *Hemidactylus frenatus* in Taiwan. I. Male reproductive cycles. Bull. Inst. Zool., Academia Sinica, **16**: 107–120.

14 Telford, S. R. (1969) The ovarian cycle, reproductive potential, and structure in a population of Japanese lacertid, *Takydromus tachydromoides*. Copeia, **1969**: 548–567.

15 Wilhoft, D. C. (1963) Gonadal histology and seasonal changes in the tropical Australian lizard *Leiolopisma rhomboidalis*. J. Morphol., **113**: 185–204.

16 Chapman, B. M. and Chapman, R. F. (1964) Observations on the biology of the lizard *Agama agama* in Ghana. Proc. Zool. Soc. Lond., **143**: 121–132.

17 Marshall, A. L. and Hook, R. (1960) The breeding biology of equatorial verterbrates: reproduction of the lizard *Agama agama lionotus* Boulenger at Lat. 0°01′N. Proc. Zool. Soc. Lond., **134**: 197–205.

18 Ballinger, R. E. (1977) Reproductive strategies: food availability as a source of proximal variation in a lizard. Ecology, **56**: 628–635.

19 Stamps, J. A. (1977) Rainfall, moisture and dry season growth rates in *Anolis aeneus*. Copeia, **1977**: 415–419.

20 Cheng, H. Y. and Lin, J. Y. (1978) Comparative reproductive biology of the lizards, *Japalura swinhonis formosensis, Takydromus septentrionalis* and *Hemidactylus frenatus* in Taiwan. II. Fat body and liver cycles of the males. Bull. Inst. Zool., Academia Sinica, **16**: 107–120.

21 Hahn, W. E. (1967) Estradiol-induced vitellogenesis and concomitant fat mobilization in the lizard *Uta stansburiana*. Comp. Biochem. Physiol., **23**: 83–93.

22 Reddy, P. R. K. and Prasad, M. R. N. (1972) Seasonal variations in the pattern of lipids in the sexual segment of kidney and liver of the Indian house lizard, *Hemidactylus flaviviridis* Ruppell. Comp. Biochem. Physiol., **41A**: 63–76.

23 Church, G. (1962) The reproductive cycles of the Javanese house geckos, *Cosymbotus platyurus, Hemidactylus frenatus,* and *Peropus multilatus*. Copeia, **1962**: 262–269.

24 Lin, J. Y. (1979) Ovarian, fat body and liver cycles in the lizard *Japalura swinhonis formosensis* in Taiwan (Lacertilia: Agamidae). J. Asian Ecology, **1**: 29–38.

25 Tinkle, D., Wilber, H. M., and Tilley, S. G. (1970) Evolutionary strategies in lizard reproduction. Evolution, **24**: 55–74.

ZOOLOGICAL SCIENCE 4: 563–567 (1987)

Advertisement Calls of Two Taiwan Microhylid Frogs, *Microhyla heymonsi* and *M. ornata*

MITSURU KURAMOTO

Department of Biology, Fukuoka University of Education, Munakata, Fukuoka 811-41, Japan

ABSTRACT—The advertisement calls of two Taiwan microhylid frogs, *Microhyla heymonsi* and *M. ornata,* were analyzed with sound spectrograph to clarify acoustic characteristics and a possible cause of acoustic divergence. The calls of the two species were composed of a series of pulse groups (notes). Several notes constituted distinct note groups in *M. heymonsi,* while no such note groups were involved in *M. ornata*. In *M. heymonsi* the note lasted longer, pulses in a note were fewer, and pulses were repeated more slowly than in *M. ornata,* but the energy distribution and wave form were quite similar in both species. These indicate that the calls of the two sympatric species have diverged essentially in temporal features, not in frequency features. Between populations of *M. ornata* from Taiwan and those of the Ryukyu Islands, considerable differences were found in temperature relationships of temporal acoustic features.

INTRODUCTION

Acoustic features of anuran amphibians reflect the phylogenetic relationships, that is, closely related species should have similar acoustic features as a consequence of their common descent. From the function of anuran calls, however, it is expected that the acoustic features have diverged to maximize the efficiency in attracting conspecific females. Thus, sympatric species have distinct specific calls even if they are closely related to each other. Selection will favor for acoustic divergence where two species with similar calls are sympatric [1].

Four frog species of the family Microhylidae occur in Taiwan [2], but no acoustic works have been performed. In this study I analyzed advertisement calls of two species, *Microhyla heymonsi* and *M. ornata,* to clarify the species-specificity in their acoustic features. The two species occur widely in southeastern Asia and resemble each other in their size, shape, and habitat, but differ in larval morphology [3]. In Taiwan, *M. heymonsi* is confined to the southern half where it is sympatric with *M. ornata,* while the latter ranges to the northern half and to the Ryukyu Islands. By comparing the acoustic features of the two species with each other and with those of Thailand and the Ryukyu Islands reported previously [4, 5], a possible cause of acoustic divergence is suggested.

Accepted December 25, 1986
Received August 8, 1986

MATERIALS AND METHODS

Advertisement calls of *M. heymonsi* were recorded at Manchou (Pingtung Co.) and Chiahsien (Kaohsiung Co.) and those of *M. ornata* at Manchou, Chiahsien, Chi-an (Hualien Co.), Mucha and Nankang (Taipei City) from 1976 through 1984. All calls were recorded in the field with casette tape recorders (Sony TC–1015, TC–1051 and TCM–100) and the sounds were analyzed with sound spectrographs (Rion SG–09 and Kay Sona-Graph 7800). Air temperature records were taken near the calling males. Male specimens obtained from these localities were 20–23 mm in snout-vent length.

The calls of the two species were composed of a series of pulse groups. In the following, "note" means a pulse group, "note length" the time from the beginning of the first pulse to the beginning of the last pulse in a note, "note interval" the time from the beginning of a note to the beginning of

the next note, and "note gap" the time from the end of a note to the beginning of the next note. Significance tests used were *t*-test and *F*-test.

RESULTS

The mean length of advertisement calls of *M. heymonsi* from Manchou (25.5°C) was 15.5 sec and consisted of about 18 notes (N=42). The mean values for *M. heymonsi* from Chiahsien (24.5°C) were 22.1 sec and 17 notes (N=20). In some calls notes were repeated with a regular interval, but in others some of the notes formed distinct note groups consisting of two, three, four and more notes (Figs. 1A and 2A–2C). Accordingly, whole call structures can be described as 1-1-1-1-1-1-1-1, 1-1-1-2-2-4-3-4-2 and so on, where each figure indicates the number of notes constituting a note group. Every call began with a series of single notes which may or may not be followed by several multi-note groups. For the sake of convenience, a note which does not form a multi-note group is regarded as constituting a single-note group.

Generally the notes in a multi-note group were longer, contained more pulses and showed faster

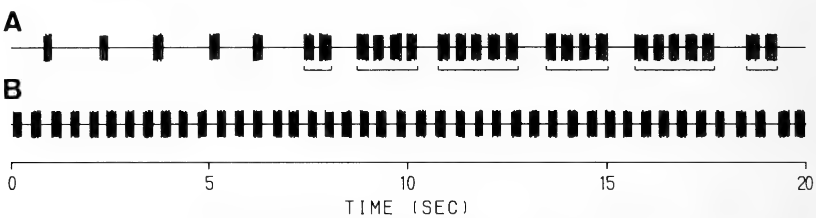

FIG. 1. Diagrammatic representation of pulse patterns of a whole call of *M. heymonsi* (A) and a part of a call of *M. ornata* (B). Vertical bars represent pulses. Multi-note groups in *M. heymonsi* are underlined.

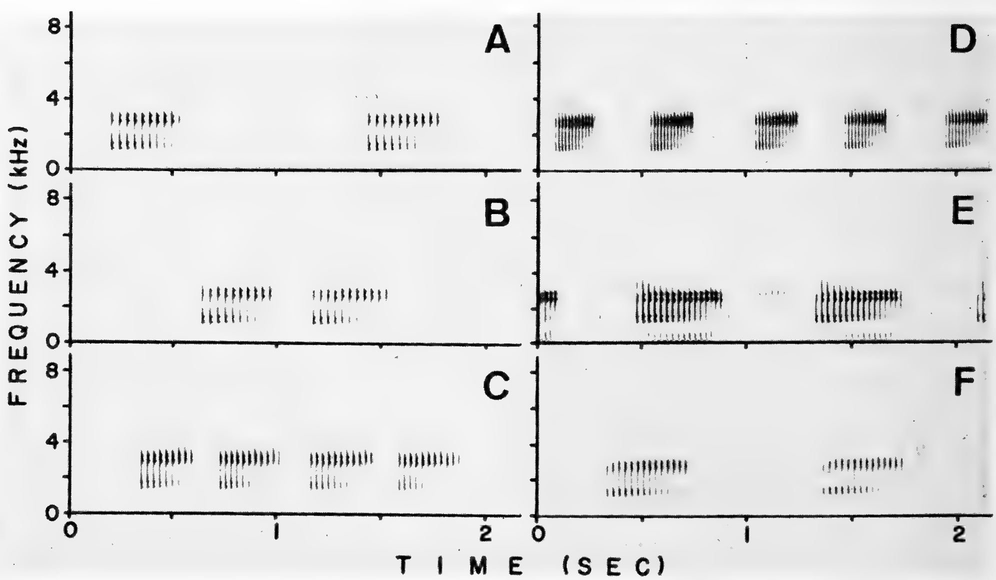

FIG. 2. Sound spectrograms of advertisement calls of *M. heymonsi* (A–C) and *M. ornata* (D–F) analyzed with 300 Hz filter. (A) Two successive single-note groups and (B) a 2-note group recorded at Chiahsien, 24.5°C. (C) A 4-note group recorded at Manchou, 25.5°C. *M. ornata* calls are from Manchou, 25.5°C (D), Mucha, 22°C (E), and Nankang, 18.5°C (F).

TABLE 1. Temporal characteristics of pulse groups (notes) in advertisement calls of *M. heymonsi* and *M. ornata* (m±SD)

Type of note group	Note	Manchou (25.5°C) N	Note length (sec)	No. pulse	Pulse rate (pulse/sec)	Chiahsien (24.5°C) N	Note length (sec)	No. pulse	Pulse rate (pulse/sec)
M. heymonsi									
1-note		21	0.17±0.05	6.1±1.4	30.8±1.9	19	0.32±0.04	9.8±1.0	27.3±0.4
2-note	1st	11	0.24±0.04	8.4±1.0	30.5±1.2	6	0.32±0.03	9.8±0.8	27.9±0.4
	2nd	11	0.27±0.02	9.5±0.7	31.7±1.5	6	0.37±0.02	11.5±0.6	28.8±0.4
3-note	1st	10	0.27±0.02	9.0±0.7	30.0±1.0	2	0.34±0.03	10.5±0.7	28.0±0.4
	2nd	10	0.29±0.03	10.0±0.9	31.4±1.5	2	0.38±0.01	12.0±0.0	28.7±0.6
	3rd	10	0.29±0.02	10.1±0.9	31.2±1.9	2	0.41±0.03	12.5±0.7	28.3±0.3
M. ornata		14	0.20±0.01	12.8±0.6	58.7±1.8	16	0.25±0.02	13.4±0.9	50.1±0.9

pulse repetition rate than the notes in a single-note group (Table 1). These tendencies were more evident in the latter notes within a note group. Note gaps (0.17–0.19 sec in Manchou and 0.21–0.22 sec in Chiahsien) did not differ significantly between various kinds of multi-note groups ($P<0.05$). In the calls from Manchou the gaps between multi-note groups (0.68–0.69 sec) were significantly shorter than those between single-note groups (1.09 sec, $P<0.01$).

The dominant frequencies were at about 3 kHz in Manchou and at about 2.8 kHz in Chiahsien calls. They were the second harmonic bands with fundamental frequencies of 1.5 and 1.4 kHz, respectively. Sound energy was concentrated between 1–4 kHz (Fig. 3A). The wave form of pulses (Fig. 3C) was regular and symmetric with a sharp rise time.

The advertisement calls of *M. ornata* were recorded in several localities at various air temperatures. The calls were much longer than those of *M. heymonsi*, and often lasted for a few minutes and involved more than a hundred notes. As in *M. heymonsi*, the calls of *M. ornata* were composed of notes, but the notes were repeated at a regular interval without forming note groups (Fig. 1B). More pulses were involved in a note and the pulse rate was much faster in *M. ornata* than in *M. heymonsi* when compared at the same temperature (Fig. 2D, Table 1). Note intervals and note gaps were short compared with those of *M. heymonsi*. Dominant frequencies, about 2.7 to 3 kHz, and energy distribution (Fig. 3B) and the wave form of pulses (Fig. 3D) were similar to those of *M. heymonsi*, although the rise time was longer than that of *M. heymonsi*.

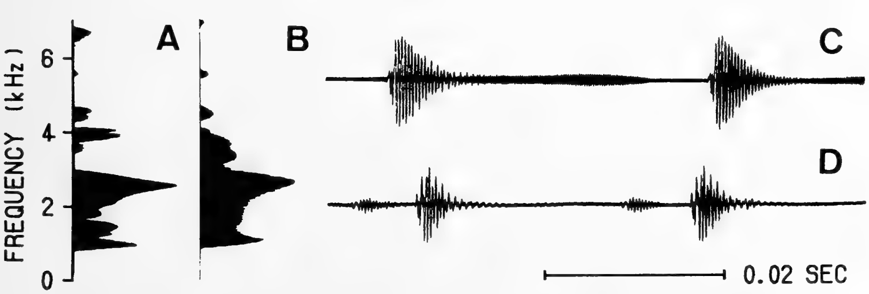

FIG. 3. Power spectrums (45 Hz filter) and wave forms of a pulse in advertisement calls of *M. heymonsi* recorded at Chiahsien, 24.5°C (A, C), and *M. ornata* recorded at Nankang, 18.5°C (B, D). Abscissa in A and B is relative intensity.

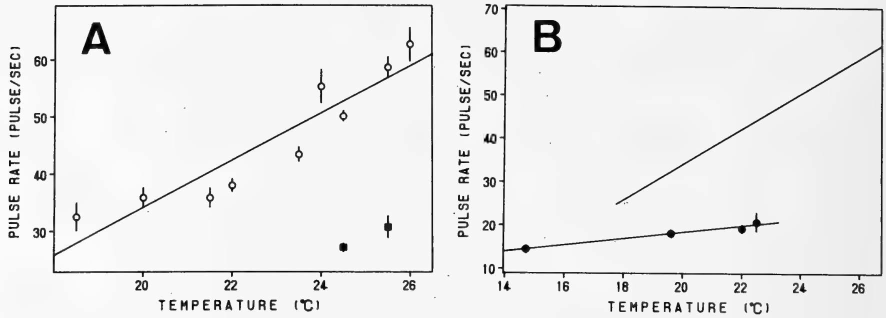

FIG. 4. Correlation between air temperature and pulse rate in advertisement calls of *M. ornata* from Taiwan (A), and from the Ryukyu Islands (B). Mean pulse rates are indicated by hollow circles in *M. ornata* of Taiwan and solid circles in *M. ornata* of the Ryukyus. Vertical bars represent one standard deviation on both sides of the mean. Solid squares in A are mean values for *M. heymonsi* and upper line in B is the regression for Taiwan *M. ornata* given in A.

When two males of *M. ornata* were calling in close proximity, the notes were given always alternately, never synchronously or overlapping. Note intervals were longer in alternately emitted calls than singly emitted ones. At 22°C the note interval was 0.84 ± 0.10 sec (m±SD, N=5) in the former, while 1.07 ± 0.03 sec (N=8) in the latter, the difference being highly significant ($P<0.01$). Note length and pulse rate did not differ in either situations.

Pulse rate was directly, and note interval and note length were inversely, correlated with air temperature (Fig. 2D–2F). Linear regression equations were $P=4.12T-48.32$ (Fig. 4A), $I=-0.07T+2.38$, and $L=-0.02T+0.74$ where P is pluse rate (pulse/sec), I is note interval (sec), L is note length (sec) and T is temperature (°C), differences of the regression coefficients from 0 being highly significant ($P<0.01$) in the former two and significant ($P<0.05$) in the last. The number of pulses and dominant frequency were temperature-independent.

DISCUSSION

Acoustic features as revealed by sound spectrograms seem very distinct between *M. heymonsi* and *M. ornata* at nearly the same temperature (cf. Fig. 2A and 2D). However, the calls of *M. heymonsi* at high temperatures are quite similar to those of *M. ornata* at low temperatures (cf. Fig. 2A and 2F). Pulses constitute distinct notes, and the frequency constitution and wave form are essentially identical in both species. These results indicate that *M. heymonsi* and *M. ornata* share many acoustic features, and suggest that they have derived from a common ancestral stock, probably rather recently. Obviously, acoustic divergence in the two species has occurred mainly in two temporal features, pulse rate and note group formation. Another microhylid *M. inornata* from south Taiwan (Yu, personal communication) and from Thailand [4] has quite different vocalization.

In Manchou and Chiahsien, *M. heymonsi* and *M. ornata* called simultaneously in the same place. It is obvious that the females discriminate the calls of conspecific males from those of the other species in these situations. Among the acoustic parameters examined, pulse rate should be the most important cue for species discrimination because the other parameters differ only slightly. Gerhardt [6], applying synthetic calls to the American treefrog *Hyla versicolor*, demonstrated that the pulse-repetition rate is critical for species discrimination. Since pulse rate is a function of temperature, the female's, as well as the male's auditory system should be adjusted in some way so as to offset the temperature effects. Note groups may be used as a cue for species discrimination, too. Multi-note groups seemed to become predominant over single-note groups as the breeding season of *M. heymonsi* proceeded, like multi-note calls of *Rhacophorus taipeianus*

and multi-pulse calls of *Polypedates leucomystax* [7].

Among the *M. ornata* populations here examined, only Manchou and Chiahsien populations are sympatric with *M. heymonsi*. Because no acoustic data were available for *M. ornata* of Manchou and Chiahsien at below 24.5°C, it could not be confirmed whether regressions of temperature and pulse rate or note interval differed between sympatric and allopatric populations of *M. ornata* with *M. heymonsi*.

Heyer [4] reported the *M. heymonsi* calls from Thailand recorded at 28°C. Note length (0.48 sec) and pulse rate (23 pulses/sec) are much longer and much slower, respectively, than those of the Manchou population at 25.5°C. The call of *M. ornata* from Thailand recorded at 25–28°C [4] has a note length of 0.23–0.31 sec, pulse number 10–18, and a pulse rate of 53–60 pulses/sec. Comparisons of these data with those of Taiwan populations indicate that the parameters of *M. ornata* are similar, while those of *M. heymonsi* differ considerably between the two areas. The acoustic divergence of the two species seem to be more pronounced in Thailand probably due to character displacement, the phenomenon exemplified in several other frogs [8, 9].

By contrast, the *M. ornata* populations of the Ryukyu Islands [5] have different acoustic characteristics from those of Taiwan. The mean note length is longer and the mean pulse number in a note is fewer in Ryukyu than in Taiwan populations. The relationship of temperature and pulse rate is on a distinct regression, $P=0.74T+3.55$ (Fig. 4B), the difference between the regression coefficients of Taiwan and the Ryukyus being highly significant ($P<0.01$). Apparently the Ryukyu populations of *M. ornata* have temporal acoustic features distinct from Taiwan and Thailand populations, although their body sizes are similar. Since *M. ornata* is the only microhylid in the Ryukyu Islands, there has been no selective pressure which may shift the temperature relationships of temporal acoustic features.

ACKNOWLEDGMENTS

A part of this study was financed from the National Science Council, Republic of China. Professors K.-H. Chang and F.-J. Lin, Zoological Institute, Academia Sinica, R. O. C., provided help when I was staying in the Institute in 1982 and 1984. Professor Y. Minamide, Department of Special Education, and Professor S. Ikeura, Department of Foreign Languages, Fukuoka University of Education, offered their facilities for sound analysis.

REFERENCES

1 Bogert, C. M. (1960) The influence of sound on the behavior of amphibians and reptiles. In "Animal Sounds and Communication". Ed. by W. E. Lanyon and W. N. Tavolga, AIBS Publ. No. 7, Washigton, D. C., pp. 137–320.

2 Lue, K.-Y. and Chen, S.-H. (1985) The Amphibians of Taiwan. C.-H. Chang, Publisher, Taiwan, 190 pp. (In Chinese)

3 Pope, C. H. (1931) Notes on amphibians from Fukien, Hainan, and other parts of China. Bull. Am. Mus. Nat. Hist., **61**: 397–611.

4 Heyer, W. R. (1971) Mating calls of some frogs from Thailand. Fieldiana: Zool., **58**: 61–82.

5 Kuramoto, M. (1977) Mating calls of the frog, *Microhyla ornata*, from the Ryukyu Islands. Bull. Fukuoka Univ. Educ., Pt. III, **26**: 91–93.

6 Gerhardt, H. C. (1978) Temperature coupling in the vocal communication system of the gray tree frog, *Hyla versicolor*. Science, **199**: 992–994.

7 Kuramoto, M. (1986) Call structures of the rhacophorid frogs from Taiwan. Sci. Rep. Lab. Amph. Biol., Hiroshima Univ., **8**: 45–68.

8 Fouquette, M. J., Jr. (1975) Speciation in chorus frogs. I. Reproductive character displacement in the *Pseudacris nigrita* complex. Syst. Zool., **24**: 16–23.

9 Littlejohn, M. J. and Loftus-Hills, J. J. (1968) An experimental evaluation of premating isolation in the *Hyla ewingi* complex (Anura: Hylidae). Evolution, **22**: 659–663.

ZOOLOGICAL SCIENCE 4: 569–574 (1987)

Notes on the Evolutionary Systematics of the Genus *Corophium*

Akira Hirayama

Laboratory of Biology, Department of the Liberal Arts, Asia University, 5–24–10 Sakai, Musashino-shi, Tokyo 180, Japan

ABSTRACT—Crawford's convenient division of the corophiid amphipods based on the urosome and antenna 2 has been basically accepted in spite of other important characteristics observed in the mandibular palp and the dactyl of gnathopod 2. A new evolutionary system is presented for the corophiid amphipods, which reflects variations of the mandibular palp and the presence of teeth on the dactyl of gnathopod 2.

INTRODUCTION

The genus *Corophium* is one of the most advanced groups of gammaridean Amphipoda [1, 2] and about 60 species are hitherto known in this genus. The first division in this genus was created by Crawford [3] in 1937 based on the urosome and antenna 2, and his basic proposal has subsequently been accepted by several workers [4–10]. Though convenient, evolutionary changes in both of these organs are not reflected in their systems. Moreover, variations of the mandibular palp (Fig. 1A) and the presence of teeth on the dactyl of gnathopod 2 have been ignored in their systems as potential taxonomic tools. Therefore, I present here a preliminary new system for the genus *Corophium* that reflects the evolutionary changes in the mandibular palp and the dactyl of gnathopod 2.

NOTES ON THE KEY CHARACTERISTICS IN THE GENUS *COROPHIUM*

Crawford's proposal [3] for systematic division of the genus *Corophium* was systematized by Shoemaker [8] for the corophiid species from America, as follows:

Section A: Segments of urosome separate.
1. Antenna 2, segment 4, different between male and female.
2. Antenna 2, segment 4, alike in male and female.

Section B: Segments of urosome fused; uropods 1 and 2 inserted in notches on the margins.
1. Antenna 2, segment 4, different between male and female.
2. Antenna 2, segment 4, alike in male and female.

Section C: Segments of urosome fused; uropods 1 and 2 attached ventrally; lateral margins of urosome without notches.
1. Antenna 2, segment 4, different between male and female.
2. Antenna 2, segment 4, alike in male and female.

These characteristics are very important when specific evolution within the genus *Corophium* is analysed. In this system, the changes observed in antenna 2 presumably occur in the corophiid amphipods subsequent to the formation of these three types of urosome (Sections A, B and C). However, as both types of antenna 2 are observed in each section based on the urosome, it is reasonable to consider that both morphological evolutions occurred in parallel or that at least one morphological changes did not occur subsequent to the other. Therefore, these morphological changes must be treated as an independent element in the evolutionary system of corophiid amphipods.

In antenna 2 of the corophiid amphipods, I recognize the sexually dimorphic and the sexually

Accepted January 19, 1987
Received May 19, 1986

similar types as Crawford [3] and Shoemaker [11] did, and, in this paper, the former is designated as the "D" type and the latter the "A" type. Antenna 2 in the males of both the types and in the female of type A has the robust peduncular segment 4 distally armed with tooth-like processes, and the female antenna 2 in type D is feebleer than in the male one and lacks the tooth-like processes.

The urosome in the corophiid amphipods can be divided into two types, one with a segmented urosome (Section A) and the other with a fused urosome (Section B and C), according to Crawford's proposal, and the latter can be further subdivided. However, as evolutionary changes in the urosome advanced in such a direction that the scar of fused segments faded away, its change became continuous and made it difficult to clearly classify all fused urosomes into the above Sections B and C. Therefore, I set up the intermediate type (F2 in Fig. 1B) between the F1 and F3 type, each of which corresponds to Sections B and C in Shoemaker's system, and the evolutionary change of the urosome is surmised as shown in Figure 1B. Moreover, the F3a type represents a urosome deviated from the F3 one in Figure 1B, as this deviative urosome is observed in *C. lobatum* [12].

The mandibular palp in corophiid amphipods is first divided into the triarticulate type (P1t in Fig. 1A) and the biarticulate type based on the number of segments (Fig. 1A). The latter is apomorphic and has probably been derived from the former with the consequence that the proximal segment lacking a terminal seta in the triarticulate mandibular palp was degenerated or fused with the penultimate one, because the terminal setae on two distal segments of triarticulate mandibular palpi were observed in the same position of the corresponding segments in the biarticulate one. This idea can be easily accepted because of the fact that the plesimorphic genus *Paracorophium*, which is closely related to the genus *Corophium*,

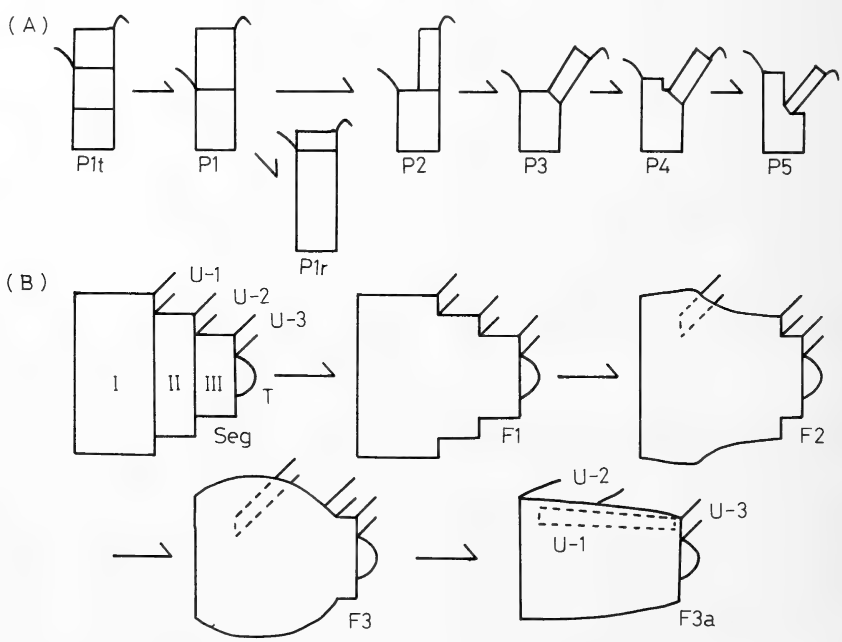

FIG. 1. Schemata of the evolutionary changes in the mandibular palp (A) and the urosome (B). P1: direct and ordinarily articulate type. P2: one side type. P3: angulate type. P4: angulate and produced type. P5: middle type. Seg: segmented urosome. F: fused type. F1: notched type. F2: intermediate type. F3: rounded type. F3a: aberrant type of rounded urosome. t: triarticulate. r: terminal segment reduced. I, II and III: urosomites 1–3. U–1, U–2 and U–3: uropods 1–3. T: telson.

has a triarticulate palp [4, 13]. The biarticulate type is further subdivided into two types; one with a reduced terminal segment (P1r in Fig. 1A) and the other with equal or subequal segment length. The former has been observed only in *C. sinense* [12, 14] to date and was probably derived from the usually biarticulate one (P1) because both the types, P1r and P1, are usually articulate and are comparatively equal to each other in the proportion of the proximal segment to the mandible in length [10, 12, 14]. In the latter type, with the equal or subequal segment length, we can observe various positions of the terminal segment attached to the proximal one in a series. Therefore, we can estimate the evolutionary change of these mandibular palpi as P1→P2→P3→P4→P5 in Figure 1A under the series of these various positions.

NOTES ON THE CLASSIFICATION SYSTEM IN GENUS *COROPHIUM*

The three organs, antenna 2 in both sexes, urosome and mandibular palp, were described and figured in only 24 of about 60 known corophiid species [3–19] except for the male antenna 2 of *C. volutator japonicum* [15] and *C. lobatum* [12], in which the sexual dimorphism of antenna 2 is inferred from the morphology of the female antenna 2. *C. volutator japonicum* is sexually similar in antenna 2 because its female has the antenna 2 of the male type [15]; *C. lobatum* is sexually dimorphic because the peduncular segment 4 of female antenna 2 is rather feeble and is not provided distally with tooth-like processes (Fig. 2). Therefore, I will attempt to create an evolutionary system for the genus *Corophium* based on these 24 species.

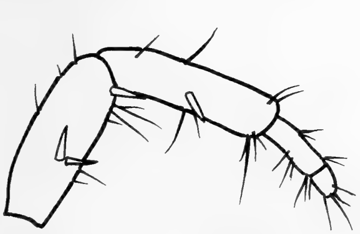

FIG. 2. Antenna 2 in a *Corophium lobatum* female. (Personal communication with N. Sawada.)

First, it is necessary to find the most plesimorphic species-group in the genus *Corophium*. These 24 species can be largely divided into two groups, one group with segmented urosomes and the other with fused urosomes (Fig. 3). It is most likely that the latter was derived from the former according to the evolutionary change of the urosome (Fig. 1B). This idea can be easily accepted due to the fact that the former possesses plesimorphic mandibular palpi (P1t, P1r, P1 and the intermediate type between P2 and P3 in Fig. 1A) and the latter possesses apomorphic mandibular palpi (P3, P4, and P5 in Fig. 1A) (Fig. 3). In the former group, the most plesimorphic known species is *C. aquafuscum* which has a triarticulate mandibular palp and a sexually similar antenna 2 [4, 13]. However, I think that this species derived from the main evolutionary flow of the corophiid amphipods, because it has teeth on the dactyl of gnathopod 2 and these teeth are absent in corophiid amphipods with plesimorphic mandibular palpi (Fig. 3). Therefore, I set up the present ancestral species (A–S–P1t) with the ordinarily triarticulate mandibular palp, the segmented urosome, the dactyl of gnathopod 2 without teeth and the sexually similar antenna 2. I further suppose that the most plesimorphic subgroup (A–S–P1, *C. volutator* [5, 10]) in the corophiid species with biarticulate mandibular palp arose from this ancestral subgroup according to the proximal segment of the triarticulated mandibular palp degenerated or fused with the penultimate one.

Next, I constructed evolutionary pathways in the corophiid species with a biarticulate mandibular palp. This evolutionary flow advanced in two groups: one group with sexually similar antenna 2 and the other with sexually dimorphic antenna 2. The former went to the A–S–P2 or P3 subgroup (*C. volutator japonicum* [15]) through the A–S–P2 one in the group with segmented urosome according to the evolutionary change of the mandibular palp from P1 type to the intermediate type between the P2 and P3 types. This flow further reached the A–T–P3–F1 subgroup (*C. ouklandense* [9]) (Fig. 3) according to morphological change from the segmented urosome to the most plesimorphic fused urosome, F1 (Fig. 1B).

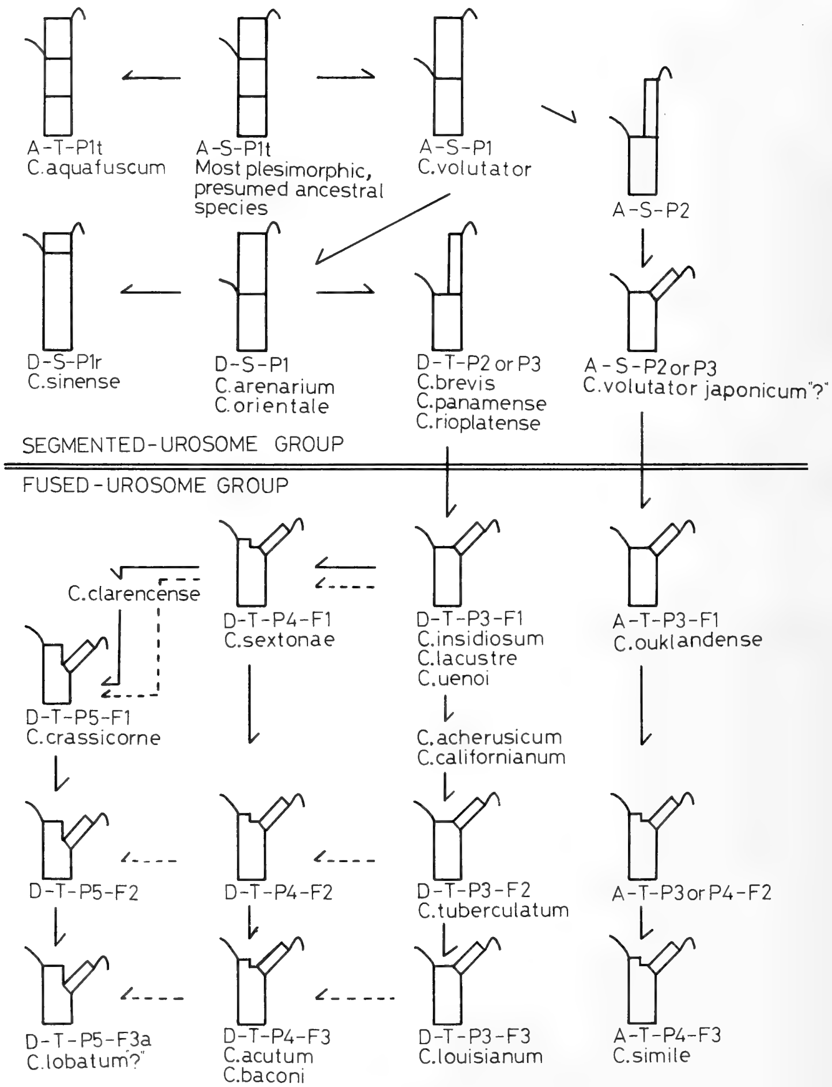

FIG. 3. Evolutionary schema of the genus *Corophium*. A: antenna 2, alike in the two sexes. D: antenna 2, different between the two sexes. S: smooth on the grasping margin of dactyl in gnathopod 2. T: grasping maring of gnathopod 2 with teeth or spines. P1, P1t, P1r, P2, P3, P4, P5, Seg, F1, F2, F3 and F3a: see Fig. 1. "?": supposed type of antenna 2. ⟶ and --→ : evolutionary pathways; refer to the text for explanation of these solid and broken lines.

In this evolutionary flow, the morphological change of the mandibular palp from the intermediate type between the P2 and P3 to the P3 type spontaneously occurred. This flow in the group with the fused urosome finally reached the most apomorphic A–T–P4–F3 subgroup (*C. simile* [5, 7, 8]) through the A–T–P3 or P4–F2 one. The latter is subdivided into two pathways at the D–S–P1 subgroup (*C. arenarium* [3, 7] and *C. orientale* [10, 19]); one pathway had the ordinarily segmented mandibular palp and the other had various positions of the terminal segment attached to the proximal segment. In the former pathway, we can permit the evolutionary flow

from the D–S–P1 subgroup to the D–S–P1r one (*C. sinense* [12, 14]) according to the side pathway of the mandibular palp from the P1 type to the P1r type (Fig. 1A), but we cannot hypothesize further pathways in this flow, as we have not found variations of the ordinarily segmented mandibular palp and this mandibular palp in the group with fused urosome. The latter pathway went to the D–T–P2 or P3 subgroup (*C. brevis* [9], *C. panamense* [9] and *C. rioplatense* [8]) in the group with segmented urosome during the evolutionary change of the mandibular palp from the P1 type to the intermediate one between the P2 and P3 types, and further reached the D–T–P3–F1 subgroup in the group with fused urosome according to evolutionary changes in the urosome and mandibular palp as well as those in the flow with the sexually similar antenna 2. This flow is supported by the fact that the teeth on the dactyl of gnathopod 2 are present in the D–T–P2 or P3 subgroup and all subgroups with fused urosome.

Lastly, we will consider the evolutionary pathways in the group with fused urosome and sexually dimorphic antenna 2. In this group, we can set up 9 subgroups by combining the three types of fused urosome (F1, F2 and F3) with the P3, P4 and P5 type in the mandibular palp. Seven of these 9 subgroups and 3 intermediate species have been found to date (Fig. 3). In the evolutionary pathways among these 9 subgroups, two schema can be shown for each of the following assumptions: 1) that the evolutionary change in the urosome occurred subsequent to the formation of three types in the mandibular palp; 2) that the change in both organs occurred in a reverse order. If we accept the former assumption, we will be able to show the pathways drawn with a solid line in Figure 3. That is, after the formation of three subgroups, D–T–P3–F1 (*C. insidiosum* [5, 8], *C. lacustre* [5, 7, 8] and *C. uenoi* [18]), D–T–P4–F1 (*C. sextonae* [3, 7]) and D–T–P5–F1 (*C. crassicorne* [5, 7, 8, 15]), and the intermediate species, *C. clarencense* [9], between the D–T–P4–F1 and the D–T–P5–F1 subgroups, the D–T–P3–F1 one evolved to the D–T–P3–F3 one (*C. louisianum* [8]) through two intermediate species, *C. acherusicum* [3, 5, 7, 8] and *C. californianum* [9], and the D–T–P3–F2 one (*C. tuberculatum* [5, 8]); the D–T–P4–F1 one to the D–T–P4–F3 one (*C. acutum* [5, 7, 8] and *C. baconi* [9]) through the D–T–P4–F2 one; the D–T–P5–F1 one to the D–T–P5–F3a one (*C. lobatum* [12]) through the D–T–P5–F2 one. Reversely, if the latter assumption is accepted, we will be able to show the pathways drawn with a broken line in Figure 3. That is, after the formation of three subgroups, D–T–P3–F1, D–T–P3–F2 and D–T–P3–F3, the D–T–P3–F1 one evolved to the D–T–P5–F1 one through the D–T–P4–F1 one and the intermediate species, *C. clarencense*; the D–T–P3–F2 one to the D–T–P5–F2 one through the D–T–P4–F2 one; the D–T–P3–F3 one to the D–T–P5–F3a one through the D–T–P4–F3 one.

As mentioned above, I intended to present a new evolutionary system for the corophiid amphipods in this paper based on four morphological features, antenna 2, urosome, mandibular palp and dactyl of gnathopod 2, but this system is incomplete. Difficulties are caused by the insufficient information provided in many poorly described species. In order to improve the present systematics of the genus *Corophium*, many known corophiid species must be redescribed, new species need to be described and figured and new key characteristics must be found to provide more insight into the classification of corophiid amphipods.

ACKNOWLEDGMENTS

I wish to thank Dr. E. L. Bousfield of the National Museum of Canada for his useful comments. Thanks are also due to Dr. Y. Suzuki of the Biological Laboratory, Asia University, for providing me with facilities to work and for his critical comments on the manuscript. I am grateful to Mr. N. Sawada of the Marine Ecological Research Co. Ltd., Osaka, for his personal communication concerning *Corophium lobatum* and for allowing me to use a drawing (Fig. 2) in this paper.

REFERENCES

1 Barnard, J. L. (1973) Revision of the Corophiidae and related families (Amphipoda). Smithson. Contr. Zool., **151**: 1–27.

2 Myers, A. A. (1981) Amphipoda Crustacea. I. Family Aoridae. Mem. Hourglass Cruises, **5**(5): 1–75.

3 Crawford, G. I. (1937) A review of the amphipod genus *Corophium* with notes on the British species. J. Mar. Biol. Assoc. U. K., **21**: 589–630.

4 Boesch, D. F. and Diaz, R. J. (1974) New records of peracarid crustaceans from oligohaline waters of the Chesapeake Bay. Chesapeake Sci., **15**: 56–59.

5 Bousfield, E. L. (1973) Shallow water gammaridean Amphipoda of New England, Cornell Univ. Press, Ithaca, N. Y., 312 pp.

6 Hurly, D. E. (1954) Studies on the New Zealand amphipodean fauna. No. 7. Family Corophiidae, including a new species of *Paracorophium*. Trans. R. Soc. New Zealand, **82**: 431–460.

7 Lincoln, R. J. (1979) British Marine Amphipoda: Gammaridea, Chaucer Press, 658 pp.

8 Shoemaker, C. R. (1947) Further notes on the amphipod genus *Corophium* from the east coast of America. J. Wash. Acad. Sci., **37**: 47–63.

9 Shoemaker, C. R. (1949) The amphipod genus *Corophium* on the west coast of America. J. Wash. Acad. Sci., **39**: 66–82.

10 Stock, J. H. (1952) Some notes on the taxonomy, the distribution and the ecology of four species of the amphipod genus *Corophium* (Crustacea, Malacostraca). Beafortia, **21**: 1–10.

11 Shoemaker, C. R. (1934) Two new species of *Corophium* from the west coast of America. J. Wash. Acad. Sci., **24**: 356–360.

12 Hirayama, A. (1987) Two peculiar species of corophiid amphipods (Crustacea) from the Seto Inland Sea, Japan. Zool. Sci., **4**: 175–181.

13 Heard, R. W. and Sikora, W. B. (1972) A new species of *Corophium* Latreille, 1806 (Crustacea: Amphipoda) from Georgia brackish waters with some ecological notes. Proc. Biol. Soc. Wash., **84**: 467–476.

14 Zhang, W. (1974) A new species of the genus *Corophium* (Crustacea, Amphipoda, Gammaridea) from the southern coast of Shangtung Peninsula, North China. Stud. Mar. Sinica, **9**: 139–146.

15 Hirayama, A. (1984) Taxonomic studies on the shallow water gammaridean Amphipoda of west Kyushu, Japan. II. Corophiidae. Publ. Seto Mar. Biol. Lab., **29**: 1–92.

16 Ledoyer, M. (1977) Contribution à l'etude de l'écologie de la faune vagile profonde de la Méditerranée Nord occidentale. 1. Les gammarides (Crustacea, Amphipoda). Bull. Mus. Civ. Stor. Nat. Verona, **4**: 321–421.

17 Stebbing, T. R. R. (1906) Amphipoda I: Gammaridea. Das Tierreich, **21**: 1–806.

18 Stephensen, K. (1932) Some new amphipods from Japan. Annot. Zool. Japon., **13**: 487–501.

19 Stock, J. H. (1960) *Corophium volutator* forma *orientalis* Schellenberg, raised to specific rank. Crustaceana, **3**: 188–192.

ZOOLOGICAL SCIENCE 4: 575–578 (1987)

[COMMUNICATION]

Number and Size of Eggs in the Three Emerald Damselflies, *Lestes sponsa, L. temporalis* and *L. japonicus* (Odonata: Lestidae)[1]

MAMORU WATANABE and YASUYO ADACHI

Department of Biology, Faculty of Education, Mie University, Tsu-shi, Mie 514, Japan

ABSTRACT—Females of the emerald damselflies, *Lestes sponsa, L. temporalis* and *L. japonicus*, were captured in the wild and their reproductive organs were observed. The number of mature eggs was rather constant during their reproductive ages at about 200, 100 and 100 in *L. sponsa, L. temporalis* and *L. japonicus*, respectively. The egg maturation seemed to occur continuously after a particular developmental stage of adult female. The mature egg size of *L. temporalis* was more than two times of that of other species and decreased with age. The realized fecundity seemed to be the largest in *L. sponsa*.

INTRODUCTION

The reproductive biology of the emerald damselflies, *Lestes* spp., has been focussed upon the mating behaviour in relation to sperm precedence [1], the life history [2–4], and the adult movements [5]. However, there have been no reports on the fecundity and oviposition pattern of these damselfly species. Since these species deposit eggs in tandem with male, it may be difficult to obtain eggs from females under laboratory condition. By dissection of feral females, Watanabe and Adachi [6] have already clarified the fecundity and estimated the number of eggs actually deposited by a damselfly, *Copera annulata*, which also shows oviposition behaviour in tandem. In this paper, we attempt to clarify the fecundity of the emerald damselflies, *L. sponsa, L. temporalis* and *L. japonicus*, by counting the number of eggs in ovaries of feral adults by dissection.

Accepted January 26, 1987
Received December 13, 1986

[1] Comparative Ecological Studies of Coenagrionoidea in Woodlands V.

MATERIALS AND METHODS

Three species of the emerald damselflies were collected in Mie and Shizuoka Prefectures both in the warm-temperate zone of Japan. Because of low density of *L. sponsa* in these prefectures, supplementary females were collected in Fukushima Prefecture. All females were captured during various behaviours, e.g. feeding, roosting, tandem flight and ovipositing, from June to October in 1985. Females were put into 50% ethyl alcohol, as soon as they were netted. The condition and the length of their hind wings and abdomen were recorded. They were classified into seven age classes (T, I, II, P, M, MM, and MMM) mainly by the colour of the abdomen [6]. The former four age classes are regarded as immature females. The latter three are at the reproductive stages, in which the females show mating and ovipositing behaviours.

All the dissected females were examined for the number of eggs remaining in the ovaries. The height, the width and the length of the bursa copulatrix were measured for calculation of its volume as a spheroid. Eggs in the ovaries were classified into three categories, i.e. mature, submature and immature eggs, as the case of *C. annulata* [6]. Volume of the mature egg was also calculated as an oval.

The number of mature and submature eggs was

counted directly. Since immature eggs were not divided individually under a microscope, we were not able to evaluate the number. Instead, we assessed the abundance of immature eggs in the ovaries by four degrees: r, +, ++ and +++, denoting rare, a few, common and abundant, respectively. All means are reported with standard errors.

RESULTS AND DISCUSSION

Thirty-six females of *L. sponsa*, 62 of *L. temporalis* and 73 of *L. japonicus* were collected in the field and dissected. Since there were no size variations with the ages collected (F-test, $P>0.1$), all of the data were pooled. The lengths of the abdomen and the hind wings were 31.9 ± 0.1 mm and 24.3 ± 0.3 mm in *L. sponsa*, 36.9 ± 0.1 mm and 26.9 ± 0.5 mm in *L. temporalis* and 31.6 ± 0.1 mm and 22.0 ± 0.1 mm in *L. japonicus*, respectively.

Newly emerged females (age T) had little fat body in the cavity of the abdomen. The fat body enlarged toward the age M and then decreased. Such a change in quantity of the fat body was also observed in *C. annulata* [6].

At age T, the bursa copulatrix was of a thin ellipsoidal shape. The volume was about 0.02, 0.05 and 0.02 mm^3, in *L. sponsa, L. temporalis* and *L. japonicus*, respectively (Fig. 1). The sizes were the same during ages I and II in all species. They became thicker in age P (about 0.1–0.2 mm^3), but no sperm was found in them. In mature females (M), the bursa copulatrix became oval shape with filled sperms (Fig. 2). The shape and the size of the bursa copulatrix were similar with each other among these three species. The volume was rather constant after the age M. This fact suggests that male emerald damselflies may remove the sperm of previous males and inseminate with a similar volume, because multiple matings are the rule in mature females as reported by Waage [1]. About 1 mm^3 was the maximum volume of the bursa copulatrix in all species. The volume was ten more times larger than that of *C. annulata* [6].

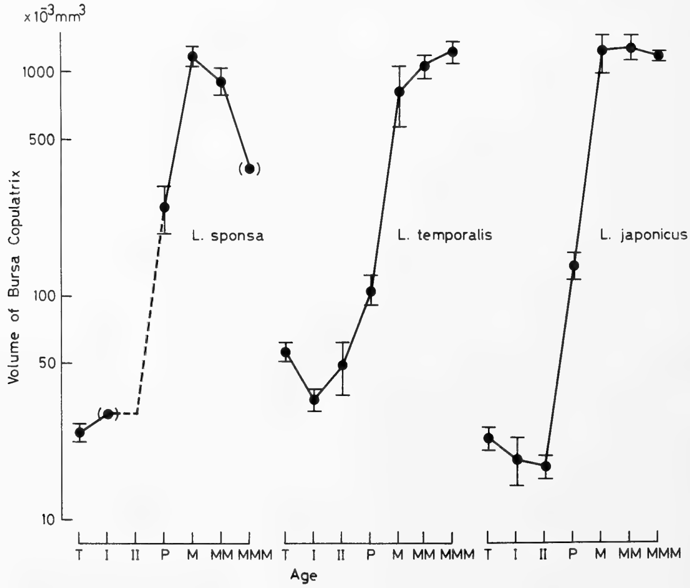

FIG. 1. Change in the volume of the bursa copulatrix in relation to female age. Sample size was 2, 1, 1, 10, 12, 9 and 1 in *L. sponsa* (left), 13, 14, 6, 11, 5, 6 and 7 in *L. temporalis* (middle) and 9, 10, 9, 19, 6, 10 and 10 in *L. japonicus* (right), in age classes of T, I, II, P, M, MM and MMM, respectively. Broken line shows the estimated volume in the age II of *L. sponsa,* because the bursa copulatrix was damaged during the dissection.

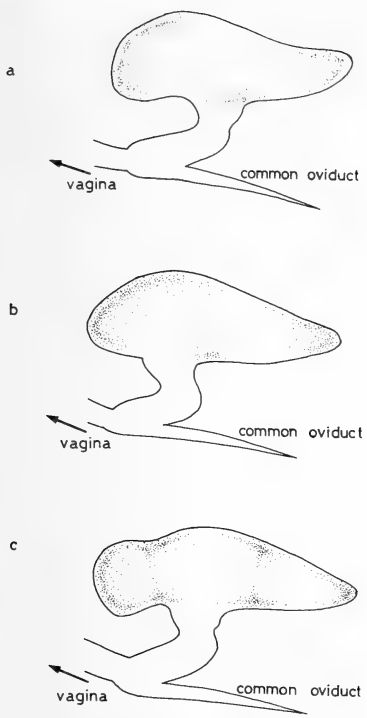

FIG. 2. Illustration of bursa copulatrix filled by sperm in a mature female of (a): *L. sponsa,* (b): *L. temporalis* and (c): *L. japonicus.*

The abundance of immature eggs increased with age significantly ($r^2=0.23$, $p<0.001$ in *L. temporalis*; $r^2=0.32$, $p<0.001$ in *L. japonicus*), but was not significant ($r^2=0.02$, $p>0.2$) in *L. sponsa* (Fig. 3). Submature eggs appeared at age P in *L. sponsa* and *L. temporalis*, while those were observed at age M in *L. japonicus*. Except the number of eggs in age MMM of *L. sponsa*, the submature eggs of all species increased according to the reproductive ages.

Mature eggs of *L. sponsa* and *L. temporalis* were found after age P, while those of *L. japonicus* appeared after age M. Little difference in the egg number between age M (or P) and MMM was observed in each species. The number was rather constant at about 200, 100 and 100 in *L. sponsa, L. temporalis* and *L. japonicus*, respectively. Thus, it is expected that the number of mature eggs is maintained throughout the reproductive period (M to MMM). This shows that egg maturation occurred continuously during their reproductive ages in the emerald damselfly. An increase in number of immature eggs with the age also supports that the number of mature eggs is generated after oviposition.

Volume of matured eggs in *L. temporalis* decreased significantly (t-test, $P<0.005$) with the age (Table 1). An egg at the age MMM had a volume of about 75% of that at the age P. The egg of *L. tempolaris* was the largest. The decrease in egg volume was also observed in *L. sponsa* (t-test, $P<0.005$), though the difference between maximum (age P) and minimum (age MM) volume was about 1.13 times. On the other hand, no egg size variation with age was found in *L. japonicus*, egg volume of which was the smallest among three species. Although we have already reported the smaller eggs deposited by older females of *C. annulata* [6], its adaptive significance still remained unknown.

In general, the decrease of egg size is assumed to be due to the decrease in yolk content [7]. In the butterfly such as *Pararge aegeria*, neither egg survival nor larval survival is correlated with the egg size [8]. However, there was no report on the possible difference in hatchability, length of larval period or survival rate of larvae between larger and smaller eggs in damselfly species. It is likely that females of *L. temporalis* increase their fecundity by depositing smaller eggs at an older age, at which they probably counteracted their shorter life-expectancy with deterioration of fat body. In *L. japonicus* smaller egg size may be due to less yolk content. Considering lowest mature egg number in ovaries of each female, the fecundity might be the smallest among these species. On the other hand, either egg size or the size variation of *L. sponsa* was intermediate. The realized fecundity seemed to be the largest, because the mature egg number in ovaries per female was double of that in other species. Further studies regarding the oviposition pattern of the emerald damselfly are needed to explain the relationship between egg size and female age.

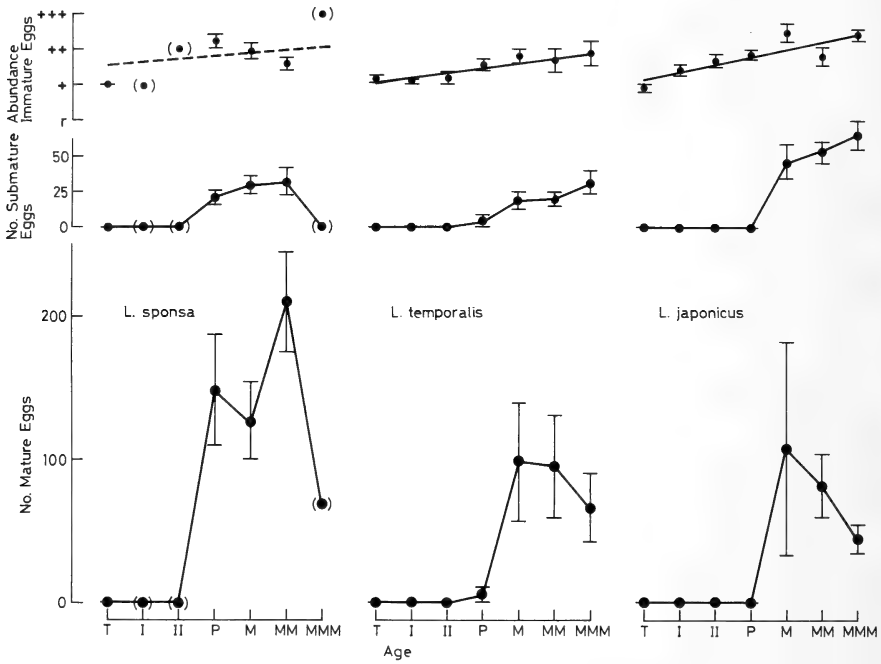

FIG. 3. Change in the quantity of immature eggs (upper) and the number of submature (middle) and mature (lower) eggs in relation to female age of *L. sponsa* (left), *L. temporalis* (middle) and *L. japonicus* (right). See Fig. 1 for sample size in each age class.

TABLE 1. Change in egg volume with age in three emerald damselfly species ($\times 10^{-2}$ mm^3, $\pm$SE)

	P	M	MM	MMM	
L. sponsa	3.45±0.04 (80)	3.24±0.03 (110)	3.06±0.04 (90)	3.34±0.09 (10)	P<0.005
L. temporalis	6.09±0.13 (10)	5.11±0.10 (10)	5.01±0.08 (56)	4.66±0.06 (70)	P<0.005
L. japonicus	—— —	2.40±0.05 (60)	2.61±0.03 (100)	2.66±0.05 (91)	n.s.

( ): number of mature eggs counted.

ACKNOWLEDGMENTS

We wish to express our sincere thanks to Dr. K. Ueda for critical reading, and to Mr. N. Ohsawa for a technical assistance. This study was partly supported by the Grant-in-Aid for Encouragement of Young Scientists, No. 60740356 from the Ministry of Education, Science and Culture of Japan.

REFERENCES

1 Waage, J. K. (1982) Odonatologica, **11**: 201–209.
2 Gower, J. L. and Kormondy, E. J. (1963) Ecology, **44**: 398–402.
3 Pickup, J., Thompson, D. J. and Lawton, J. H. (1984) Odonatologica, **13**: 451–459.
4 Lutz, P. E. (1968) Ecology, **49**: 576–579.
5 Utzeri, C., Carchimi, G., Falchetti, E. and Belfiore, C. (1984) Odonatologica, **13**: 573–584.
6 Watanabe, M. and Adachi, Y. (1987) Odonatologica, **16** (in press).
7 Kimura, K. and Tsubaki, Y. (1985) Appl. Entomol. Zool., **20**: 500–501.
8 Wiklund, C. and Persson, A. (1983) Oikos, **40**: 53–63.

ANNOUNCEMENT

CUPT P. RICHTER PRIZE IN PSYCHONEUROENDOCRINOLOGY

The International Society of Psychoneuroendocrinology (ISPNE) invites submission of manuscripts for the Curt P. Richter Prize 1988. The award includes an honorarium of US $ 1,000 (sponsored by Pergamon Press) and a travel grant of up to US $ 1,000 (offered by the Society) to the 19th International Congress of the ISPNE in Groningen, The Netherlands, August 22 to 26, 1988, where the prize will be awarded. The winning paper will automatically be considered for publication in the Journal "Psychoneuroendocrinology".

Manuscripts should be submitted in quadruplicate to:

Gerhard Langer, M.D.
Associate Professor of Psychiatry
Secretary of the ISPNE

The deadline for submission is January 31, 1988.

All submissions will be screened by a committee of established psychoneuroendocrinologists. Before submission of manuscript, for detailed information please contact the Secretary of the ISPNE, Gerhard Langer, M. D., Associate Professor of Psychiatry, Department of Psychiatry, University of Vienna, Waehringer Guertel 18–20, A–1090 Vienna, Austria.

Development Growth & Differentiation

Published by
the Japanese Society of Developmental Biologists

The journal is devoted to the publication of original papers dealing with any aspects of developmental phenomena in all kinds of organisms, including plants and micro-organisms. Papers in any of the following fields will be considered: developmental genetics, growth, morphogenesis, cellular kinetics, fertilization, cell division, dormancy, germination, metamorphosis, regeneration and pathogenesis, at the biochemical, biophysical and analytically morphological levels; reports on techniques applicable to the above fields. At times reviews on subjects selected by the editors will be published. Brief complete papers will be accepted, but not preliminary reports.

Members of the Society receive the Journal free of charge. Subscription by institutions is also welcome.

Papers in DGD, Vol. 29, No. 3. (June 1987)

Development, Growth and Differentiation (ISSN 0012–1592) is published bimonthly by The Japanese Society of Developmental Biologists, Department of Biology, School of Education, Waseda University, Tokyo 160, Japan. 1987: Volume 29. Annual subscription U. S. $ 110.00 including air speed delivery except Japan. Application to mail at second class postage rate is pending at Jamaica, NY 11431, U. S. A.

Outside Japan: Send subscription orders and notices of change of address to Academic Press, Inc., Journal Subscription Fulfillment Department, 6277 Sea Harbor Drive, Orlando, FL 32887, U. S. A. Send notices of change of address at least 6–8 weeks in advance. Please include both old and new addresses. U. S. A. POSTMASTER: Send changes of address to *Development, Growth and Differentiation,* Academic Press. Inc., Journal Subscription Fulfillment Department, 6277 Sea Harbor Drive, Orlando, FL 32887, U. S. A.

In Japan: Send nonmember subscription orders and notices of change of address to Business Center for Academic Societies Japan, 16–3, Hongo 6-chome, Bunkyo-ku, Tokyo 113, Japan. Send inquiries about membership to Business Center for Academic Societies Japan,4–16, Yayoi 2-chome, Bunkyo-ku, Tokyo 113, Japan.

Air freight and mailing in the U. S. A. by Publications Expediting, Inc., 200 Meacham Avenue, Elmont, NY 11003, U. S. A.

(*Contents continued from back cover*)

Taxonomy

ZOOLOGICAL SCIENCE

VOLUME 4 NUMBER 3 **JUNE 1987**

CONTENTS

(*Contents continued on inside back cover*)

INDEXED IN:
Current Contents/LS and AB & ES,
Science Citation Index,
ISI Online Database,
CABS Database

Issued on June 15
Printed by Daigaku Printing Co., Ltd.,
Hiroshima, Japan

ISSN 0289-0003

Vol. 4 No. 4

August 1987

ZOOLOGICAL SCIENCE

An International Journal

PHYSIOLOGY
CELL and MOLECULAR BIOLOGY
GENETICS
IMMUNOLOGY
BIOCHEMISTRY
DEVELOPMENTAL BIOLOGY
REPRODUCTIVE BIOLOGY
ENDOCRINOLOGY
BEHAVIOR BIOLOGY
ENVIRONMENTAL BIOLOGY
ECOLOGY and TAXONOMY

published by Zoological Society of Japan

distributed by Business Center for Academic Societies Japan
VNU Science Press BV, Utrecht, The Netherlands

ZOOLOGICAL SCIENCE

The official Journal of the Zoological Society of Japan

The Zoological Society of Japan:
Toshin-building, Hongo 2–27–2, Bunkyo-ku,
Tokyo 113, Japan. Tel. (03) 814–5675

ZOOLOGICAL SCIENCE is devoted to publication of original articles, reviews and communications in the broad field of Zoology. The journal was founded in 1984 as a result of unification of Zoological Magazine (1888–1983) and Annotationes Zoologicae Japonenses (1897–1983), the former official journals of the Zoological Society of Japan. ZOOLOGICAL SCIENCE appears bimonthly. An annual volume consists of six numbers of more than 1000 pages including an issue containing abstracts of papers presented at the annual meeting of the Zoological Society of Japan.

MANUSCRIPTS OFFERED FOR CONSIDERATION AND CORRESPONDENCE CONCERNING EDITORIAL MATTERS should be sent to:

Dr. Seiichiro KAWASHIMA, Managing Editor, Zoological Science, Zoological Institute, Faculty of Science, Hiroshima University, 1–1–89 Higashisenda-machi, Naka-ku, Hiroshima 730, Japan, in accordance with the instructions to authors which appear in the first issue of each volume. Copies of INSTRUCTIONS TO AUTHORS will be sent upon request.

SUBSCRIPTIONS. ZOOLOGICAL SCIENCE is distributed free of charge to the members, both domestic and foreign, of the Zoological Society of Japan. To non-member subscribers within Japan, it is distributed by Business Center for Academic Societies Japan, 6–16–3 Hongo, Bunkyo-ku, Tokyo 113. Subscriptions outside Japan should be ordered from the sole agent, VNU Science Press BV, Europalaan 93, 3526 KP Utrecht, (postal address; P. O. Box 2093, 3500 GB Utrecht), The Netherlands. Subscription rates will be provided on request to these agents. New subscriptions and renewals begin with the first issue of the current volume.

[Publication of Zoological Science has been supported in part by a Grant-in-Aid for Scientific Publication from the Ministry of Education, Science and Culture, Japan.]

ZOOLOGICAL SCIENCE 4: 579–591 (1987)

REVIEW

The Importance of Inducing Factors for Determination, Differentiation and Pattern Formation in Early Amphibian Development

Horst Grunz

Department of Zoophysiology, FB 9 (Biologie) University GHS Essen, Universitätsstr., 4300 Essen 1, FRG

INTRODUCTION

It is generally accepted that the amphibian embryo is one of the best studied eucaryotic systems in developmental biology. Since now absolutely new methods (fluorescent cell lineage markers, highly purified or homogeneous morphogenetic factors, monoclonal antibodies, electrofusion of amphibian cells, techniques of genetic engineering) are available, the molecular processes, including the expression of regional and tissue specific genes, of the fairly well described morphological and morphogenetic events during embryogenesis can be further studied in detail. A growing number of scientists focus their interest on molecular processes during amphibian oogenesis, cleavage, embryonic induction and pattern formation. An increasingly favoured species is the South African clawed frog, *Xenopus laevis,* since its eggs can be obtained under laboratory conditions throughout the whole year. Of special importance are the mechanisms of gene expression and gene regulation during early embryonic development. Powerful tools are now available to study such events also in the very complex amphibian embryo [1, 2]. This holds true also for the problem of early embryonic induction. Although an overwhelming amount of data from many laboratories is available, the exact molecular mechanisms of embryonic induction are still obscure. Therefore it is highly desirable to get a better understanding of processes responsible for mesoderm formation, midblastula transition [3] and induction of the central nervous system. It should be pointed out that most of those processes are basic topics in cell biology and molecular genetics. Therefore, those results in amphibians can be considered to be closely related to embryonic events in higher vertebrates, which are less suitable for many studies because of technical or ethic (human embryo) reasons.

Accepted March 10, 1987

PECULIARITIES IN THE *XENOPUS* EMBRYO

Since *Xenopus laevis* is now frequently used for embryological and biochemical studies, first I like to mention basic results, which were achieved in our laboratory. In contrast to *Triturus* species or *Ambystoma mexicanum* the jelly coat of *Xenopus laevis* or *X. borealis* is removed by culture medium containimg cysteine hydrochloride or other disulfide cleaving agents [4]. K. Buiting in our lab could show that a prolonged treatment of early gastrulae with cysteine hydrochloride results in malformations of the head area of the swimming larvae. If early gastrulae are treated with cysteine longer than 10 min, we got defects of the olfactory placodes, eyes or the whole brain area (synophthalmia, cyclopia, Figs. 1 and 2). Therefore the procedure should be performed under strictly controlled conditions. We recommend the following standard conditions: 3.5% cysteine hydrochloride in Holtfreter solution, pH 7.35 at 20°C for 10 min; Holtfreter solution: 0.059 M NaCl, 0.00067

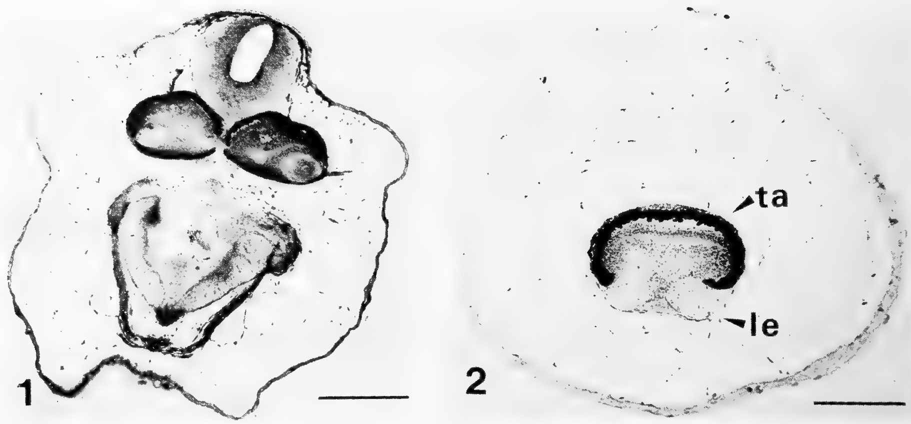

FIG. 1. Transversal section of the head area of an embryo, which was treated in the early gastrula stage with cysteine hydrochloride for 13 min. The larva has formed two fused eyes (synophthalmia). Bar: 0.1 mm.

FIG. 2. Transversal section of the head area of an embryo, which was treated in the early gastrula stage with cysteine hydrochloride for 16 min. The larva has formed a cyclopic eye with two lenses. ta: tapetuum, le: lens. Bar: 0.1 mm.

M KCl, 0.0009 M $CaCl_2 \cdot 2H_2O$). In addition we emphasize the macroscopical control, since variations in the thickness of the jelly coat of different spawns require a shorter or prolonged treatment. After artificial insemination, however, the jelly coat of 2–4-cell stages can be removed within 3–4 min under the same experimental conditions. Also in biochemical experiments, using cleavage stages up to the early tadpole stage, control embryos should be raised up to stage 46 [5] to find out negative effects of cysteine. Malformations (reduced size of the eyes) can easily be identified in the stereomicroscope. It must be pointed out that malformations of the head area can be caused by various substances [6–9]. Although it can be speculated that the defects are correlated with impaired morphogenetic movements and abnormal formation of the prechordal plate, responsible for the induction of the archencephalic brain area [10], the exact mechanism of action of cysteine at the molecular level is not known.

In contrast to *Triturus* species (urodela) the ectoderm of *Xenopus* similar to other anura consists of several distinct cell layers [11], which mechanically can be separated by fine very flexible glass needles with a possible tip diameter less than 2 μm. Also in the upper blastopore lip an outer and deep layer can be distinguished [12]. Nieuwkoop and Florschütz [13] have postulated that only the deep layers develop into mesodermal derivatives, while the superficial cell sheet is thought to have epidermal character. Preliminary results of U. Koch in our laboratory indicate that also the outer ectoderm possess a weak capacity to differentiate into mesoderm.

Another peculiarity in *Xenopus* should be shortly mentioned. If inducer substances in pellet form (inducers bound to biologically inactive γ-globulin) are implanted into the blastocoel of early gastrulae (implantation method after Spemann and Mangold [14]; Fig. 3a2), the pellet is later found in most larvae within the intestine. In contrast to the situation in *Triturus* species the pellet does not come into contact with the competent presumptive belly epidermis, which is a prerequisite for inductions. Another effect is the unspecific formation of additional tail structures, probably caused by the mechanical splitting of the inducing archenteron during invagination by the implanted material. This effect can even be observed with pellets of γ-globulin without any neuralizing or mesodermalizing activity. Therefore the implantation technique cannot be recommended for *Xenopus laevis*. In contrast the sandwich-technique [15] is an excellent test-method also for *Xenopus* (Fig. 3b).

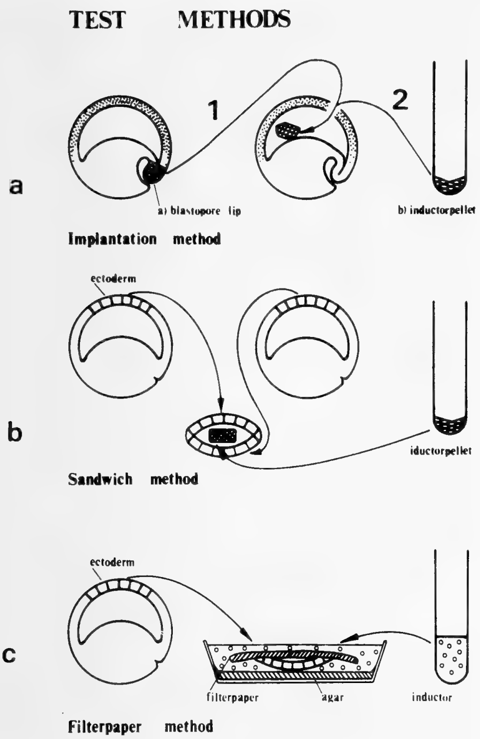

FIG. 3. Diagrammatic representation of 3 important test methods: a) implantation-technique after Mangold, a1) implantation of blastopore lip into the blastocoel of an early gastrula, a2) implantation of an inducer pellet, b) sandwich-technique after Holtfreter, c) test method for soluble agents. The filter-paper prevents the curling up of the ectoderm. The hanging drop culture technique is shown elsewhere (Tiedemann, [23]).

THE IMPORTANCE OF MORPHOGENETIC FACTORS FOR THE EARLY EMBRYONIC DEVELOPMENT

Spemann and Hilde Mangold could show in their famous implantation experiment in 1924 (Fig. 3a1) that a certain area of the embryo (the upper blastopore lip) is able to induce a secondary axis in a host embryo. Therefore Spemann called this part of the embryo "organizer". Its role in embryogenesis is described in detail elsewhere [16, 17]. The interest of embryologists focussed on the question, which factors located in the blastopore lip are responsible for the induction process of the central nervous system. Since morphogenetic factors are present in the embryo in very low concentrations, the isolation of those neuralizing factors was not successful for long time. The same holds true for endoderm or mesoderm inducing factors. They will induce in competent ectoderm notochord, somites, pronephros, intestine etc. Crude factors could be isolated from guinea pig bone marrow [18, 19]. However, a vegetalizing factor, protein in nature (molecular weight 13,000 Daltons), was isolated from chicken embryos and was purified to homogeneity [20]. Also from swimmbladder a factor with mesodermalizing activity was partially purified [21]. Also crude neuralizing factors could be obtained from amphibian embryos [22]. Recently a mesodermalizing factor was found in conditioned medium of a *Xenopus laevis* cell line (XTC-Cells) by Smith, London. All the just mentioned factors (in solution or bound to biologically inert protein) can be tested by the implantation method, sandwich-technique or hanging-drop-culture [23]. In all three test methods or slightly modified techniques competent ectoderm is the target for the inducing factors (Fig. 3). Depending on the different biological activity of the inducing factors, the ectoderm, which in normogenesis forms epidermis [24], differentiates into endodermal, mesodermal or neural differentiations [11, 25, 26]. Of interest was the observation that certain lectins (Concanavalin A (Con A) and *Ulex europeus* agglutinin) will evoke neural inductions in competent ectoderm [25–31]. It can be speculated that those lectins mimic the action of the "natural" neuralizing factors, which are thought to interact with specific receptors (glycoproteins) on the plasmamembrane of the reacting tissue (ectodermal target cells). There are strong indications that the internalization is not a prerequisite for the biological function of neuralizing factors [32]. It should be pointed out that the competent ectoderm must be triggered by certain threshold concentrations of the inducer (Con A) to form neural tissues [27]. Apparently not only the quality but also the quantity of receptors on the plasmamembrane of the target cells play a crucial role in the realisation of neural structures [28, 33]. We could show that the superficial layer of the competent ectoderm of *Xenopus laevis,* which binds much less Con A than the deep layer, is unable to form neural structures.

On the other hand, the deep layer of the ectoderm of the late gastrula, which has lost its competence to react to neuralizing stimuli, binds similar amounts of Con A as competent early gastrula ectoderm (deep layer) [33]. These data support the view that the loss of competence is not correlated with a change in the amount of receptors, but more likely with intracellular regulatory events at the genome level.

POSSIBLE ROLE OF IONS AND CYCLIC AMP IN EMBRYONIC INDUCTION AND THE PROBLEM OF AUTONEURALIZATION

By Holtfreter [34] it was shown that amphibian ectoderm can form neural structures under unphysiological conditions without any interaction with a specific inducer. Recently Hildegard Tiedemann found that HEPES-containing medium also induces neural structures [35]. Also phorbolester is a potent substance to evoke neural structures in competent ectoderm [36]. Normal culture conditions, which are without effect in other species (*Triturus alpestris* or *Xenopus laevis*), can cause autoneuralization in *Ambystoma mexicanum* (Axolotl). It is well known that neuralization in contrast to mesodermalization can be evoked by unspecific treatment of ectoderm with different substances except lithium chloride. One explanation for such effects was that a certain amount of cells of the ectoderm piece was fully or partially impaired by the treatment, which will liberate inducing substances and will induce the remaining unaffected cells [37]. It could be argued that after Con A treatment the tissue is also damaged. However, neither Takata's group nor ours did find necrotic cell material in the explants. Therefore the effect of Con A could be considered as an activation of processes, which are more closely related to the natural inducers. It could be assumed that the different neural inducing substances have the activity in common that they interact on the same or a succeeding link in the chain of molecular events, leading to neural induction and differentiation. This could hold true also for the neuralizing effect of phorbolester [36]. On the other hand we cannot support the view that ions or cyclic AMP are involved in the inducing processes as primary signals. We could show that cyclic AMP has no neuralizing effect in *Tritutus alpestris* or *Xenopus laevis* species, which in contrast to *Ambystoma* are very resistant against treatments, leading to autoneuralization in *Ambystoma*. Therefore, data describing neuralization in *Ambystoma* after the treatment with cAMP or other substances must be discussed with great caution. By experiments using vegetalizing factor and calciumionophore A 23187 the exclusive role of ions as primary signals for embryonic induction can be ruled out [29, 38]. On the other hand ions Ca^{++} are important cofactors in signal transduction, for example, the activation of proteinkinase C [39], which could play part in the process of neural induction and differentiation.

INFORMATION TRANSFER AND COMMUNICATION BETWEEN EMBRYONIC CELLS

The central nervous system is formed by the interaction between the invaginating chordamesoderm and the overlaying neuroectoderm, which forms the neural plate. It could be shown by transfilter experiments that free migrating factors are transmitted from the inducing chordamesoderm to the reacting ectoderm [40]. It is likely that those factors are released from the inducing chordamesoderm by exocytosis into the intercellular space between the chordamesoderm and the ectodermal target cells [41]. Those neuralizing factors then could interact with specific receptors on the plasmamembrane of the target cells. That the neuralizing factors in contrast to the vegetalizing factor apparently must not be internalized to become biologically active can be concluded from experiments with factors, which were prevented from internalization by the binding to sepharose beads [27, 32, 42]. The isolation and characterization of neural factors from *Xenopus laevis* is described in detail elsewhere [22]. On the basis of earlier and recent data obtained in our laboratory it can be postulated that the transmission between inducing and reacting tissue takes place by short distance transport [43]. Together with Dr. Tacke in my laboratory it could be shown that there must be established a close juxtaposition

between inducing upper blastopore lip (chordamesoderm) and reacting ectoderm for the realization of neural structures. At least 75% of the ectodermal cells must come into close contact with the chordamesodermal cells. This process is time dependent. If the chordamesoderm of *Xenopus laevis* is removed from the sandwich within 3 hr (cell contact area below 75%) no or only small amount of neural structures is formed. These data will be published in detail elsewhere. Furthermore we could document that a close association of combined inducing and reacting tissues is realized in various species (*Triturus vulgaris, Rana esculenta* and *Xenopus laevis*) after different periods of time. Earlier data (Grunz, unpublished results) could show that chordamesoderm of *Ambystoma* takes up close cell-to-cell contacts to reacting ectoderm much faster than recombinants of *Triturus alpestris*. These data may explain why chordamesoderm of *Ambystoma* induces neural structures after 5 min contact with ectoderm, while in *Triturus vulgaris* chordamesoderm needs 4 hr to trigger the reacting ectoderm [44, 45]. A long distance diffusion of inducing factors is unlikely because of the following reasons. During the gastrulation process an unlimited transport of neuralizing factors, released from the invaginating chordamesoderm, could induce not only the neuroectoderm but also the presumptive epidermis after migration of the inducers through the blastocoel. Furthermore already during cleavage mesoderm inducing factors released from the vegetal blastomeres could not only trigger the presumptive marginal zone to form the mesoderm, but also the animal pole material (presumptive ectoderm) after crossing the blastocoel. However, there exists also the possibility that secreted inducers are inactivated by inhibitors present in the blastocoel. The data so far available support the view that inducing factors exert their biological activity after short distance migration in areas of close juxtaposition of inducing and reacting tissue.

It is likely that a critical number of cells within a piece of ectoderm must be stimulated with a certain threshold concentration for the realization of neural structures. It is highly probable that the susceptibility for the neuralizing or other inducing factors also depends on critical phases of the cell cycle, which corresponds to the exposition of specific receptors for inducing signals and endocytotic processes, important for the recycling of receptors [33]. On the basis of our experiments with combined upper blastopore lip and ectoderm it seems unlikely that only one or few cells are triggered first, which in turn will stimulate their neighbours. Presumably in the first step a critical number of cells must be stimulated. However, we don't exclude the possibility of secondary cell interactions (cell communication within the same germ layer) including the still obscure molecular processes of homoiogenetic induction [46–51]. That every competent ectodermal cell within the same sandwich apparently cannot react on the same inducing signal in the same way, can be concluded from the fact that always different cell types are formed in the mesodermal or neural induced tissue.

IMPORTANCE OF THE EXTRACELLULAR MATRIX FOR EARLY EMBRYOGENESIS

Boucaut and coworkers and the group of Nakatsuji in Japan could show that extracellular matrix proteins (fibronectin and laminin), covering the blastocoelic side of the ectoderm, are important as contact guidance for the invaginating chordamesoderm [52, 53]. When specific antibodies directed against fibronectin are injected into the blastocoel of blastulae the gastrulation movements are inhibited [54]. In the early neurula stage also glucosaminoglycans are present in the intercellular gap between chordamesoderm and neural plate [41]. However, it can be excluded that those polysaccharides and the fibrillar high molecular weight proteins are themselves responsible for the neural induction. Together with Boucaut's group we could show that the binding of anti-fibronectin (anti-FN) to ectoderm does not prevent neural induction, when anti-FN-treated ectoderm was combined with upper blastopore lip in the sandwich-technique [55]. These data indicate that the extracellular matrix proteins in normogenesis are responsible for the close juxtaposition of inducing and reacting tissue only, a prerequisite for the short distance transport of neuralizing factors. Those factors, proteins in nature, have presumably

a much smaller molecular weight than the fibrillar extracellular matrix proteins.

THE ROLE OF VEGETALIZING AND MESODERMALIZING FACTORS IN EARLY EMBRYOGENESIS

A vegetalizing factor with endodermal and mesodermal inducing activity has been isolated from chicken embryos and was purified to homogeneity. Its chemical features and its biological activity are described in detail elsewhere [20, 56]. We could show that this factor is able to trigger competent ectoderm to form endodermal and mesodermal derivatives [25]. Also neural structures were formed under certain conditions by the ectoderm, treated with vegetalizing factor. However, those differentiations are thought to be formed by secondary cell interactions [47–49]. A similar factor could be present in the vegetal half of amphibian embryo. We know from our earlier experiments that in the 8-cell-stage-embryo the differentiation potentials of the 4 animal blastomeres differ significantly from the 4 vegetal blastomeres [57]. By more detailed studies [58–60] could be shown that all blastomeres of the 8-cell-stage-embryo possess distinct developmental capacities. The results show that very early in amphibian development there exist already specific animal/vegetal and dorsal/ventral and also lateral gradients [61]. Nieuwkoop demonstrated that the mesodermal marginal zone including the upper blastopore lip is formed by the interaction of the vegetal with the animal blastomeres of early cleavage and blastula stages [62]. Asashima [63] found that the vegetal material of the mid blastula stage possesses the highest mesodermal inducing capacity. Gurdon and colleagues demonstrated that within 3 hr after combination of material of the vegetal and the animal hemispheres of early blastulae the activation of actin genes takes place [64]. By transfilter experiments we could show that mesodermal inducing factors are passing through Nucleopore filter pores of 0.4 μm from isolated vegetal pole material to ectodermal target cells. By electron microscopy we could exclude that cell protrusions have penetrated into the Nucleopore filter pores. Therefore also cell contacts between the inducing and the reacting tissue could be ruled out [65]. Those experiments convincingly show that gap junctions are not relevant for the primary steps in mesodermal induction. Therefore the asymmetric malformations, observed especially in the head area of larvae after injection of antibodies directed against the 26 KDa gap junction protein in blastomeres of 8- to 32-cell stages of *Xenopus laevis,* must be considered as a result of inhibition of secondary steps (control of cell proliferation, cell cycle etc.) [29, 66, 67]. Since gap junctions are thought to permit the exchange of molecules up to 1 KDa only, it is unlikely that inducing factors (molecular weight over 10,000 Da) are transmitted from cell to cell via gap junctions. As a working hypothesis we suggest that a mesodermalizing factor is exported from the vegetal pole material and will interact with receptors of cells of the presumptive mesodermal zone of the embryo. Of interest was our observation that in the transfilter experiments single animal cap formed ventral mesodermal derivatives (heart structures, coelomic epithelium, and blood cells), while aggregates of 4 or 6 animal caps differentiated into dorsal mesodermal structures (notochord, somites and neural tube). Because of the increase of the initial cell mass of the reacting ectoderm the differentiation pattern is shifted from ventral to dorsal mesodermal structures [47, 65]. The experiments of Boterenbrood and Nieuwkoop [68] indicate that the ventral and lateral endoderm induces ventral mesodermal structures, while the dorsal endoderm evokes dorsal mesodermal derivatives. They concluded from their results that the difference in mesodermal inducing capacity of the dorsal mesoderm as against the lateral and ventral mesoderm is probably purely quantitative in character. From our data it could be concluded that in addition to the inducing capacity of the inducing tissue several other parameters are controlling the realization of a certain differentiation pattern, i.e. the initial cell mass, inducer concentration, incubation time, size of the contact zones of the recombinants, and phase of competence.

It should be mentioned that we tried to isolate the mesodermalizing factor from supernatant of vegetal pole material of early blastula by binding to Heparin-Sepharose. However, so far we were

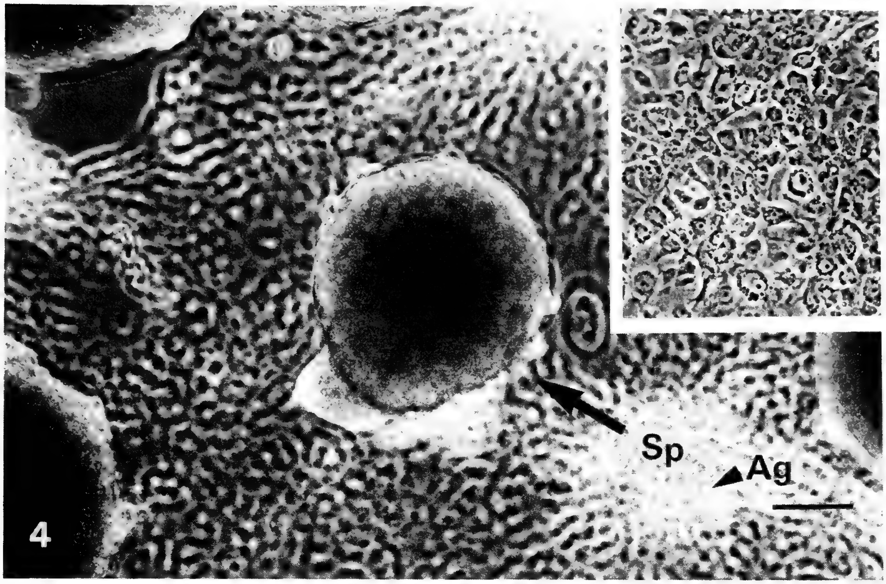

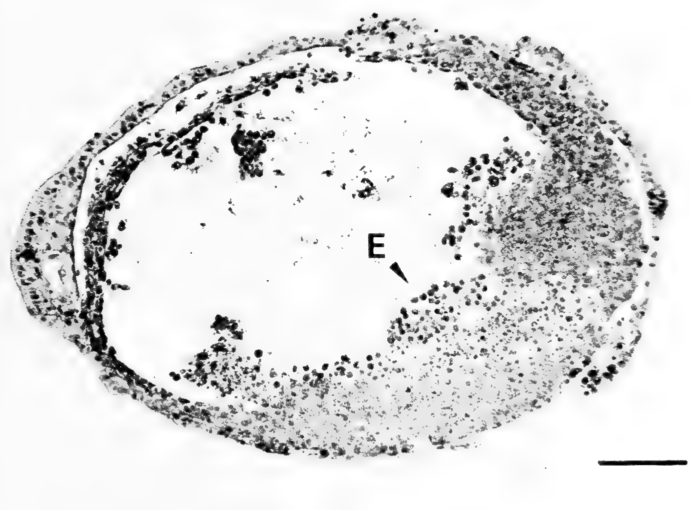

FIG. 4. Confluent layer of XTC-cells of *Xenopus laevis*. Several days after confluency also aggregates (Ag) and freely floating spheres (Sp) can be observed. The monolayer is out of focus. Inset: Focus on the monolayer of the XTC-cells. Bar: 0.1 mm.

FIG. 5. A small sphere of XTC-cells (compare with Fig. 4) was wrapped by late blastula ectoderm (sandwich-method) and cultured for 5 days at 17°C. The explant has formed blood cells (E) and coelomic epithelium. Similar differentiations were formed by gastrula ectoderm, treated for 1/2 hr with XTC-conditioned medium. Late blastula ectoderm after incubation with 50 μg/ml FGF for 10 min differentiates in similar way. Bar: 0.1 mm.

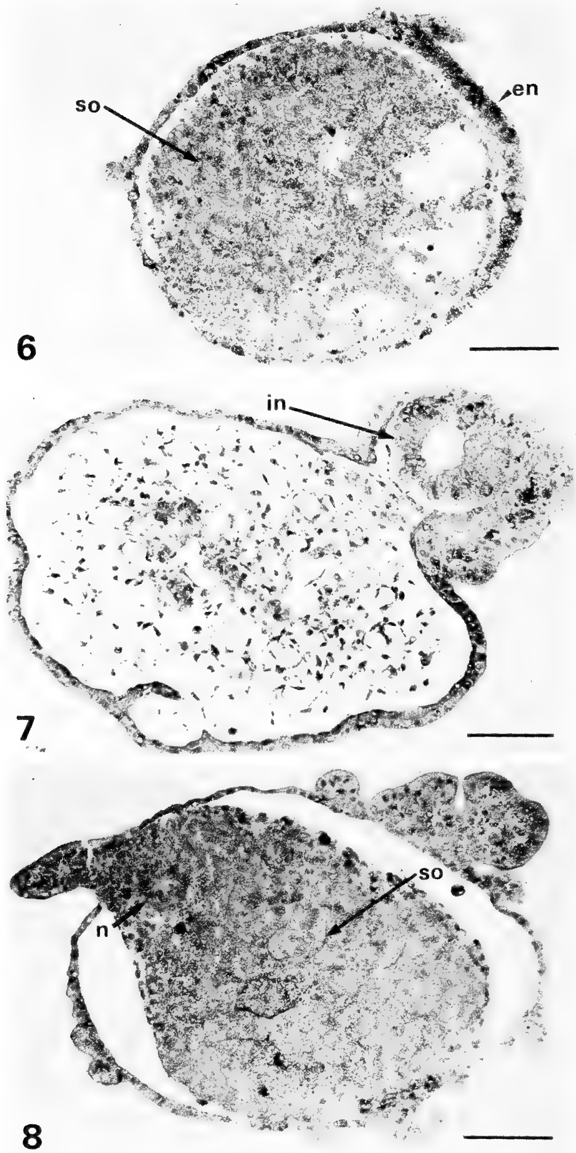

Fig. 6. Differentiations formed by late blastula ectoderm, treated for 20 min with 50 μg/ml FGF. Somites (so) and peripheral endoderm (en) can be seen. Bar: 0.1 mm.

Fig. 7. Differentiations formed by late blastula ectoderm, treated for 40 min with 50 μg/ml FGF. The explant has formed intestine (in), mesenchyme and blood cells (not present in this section). Bar: 0.1 mm.

Fig. 8. Differentiations formed by late blastula ectoderm, treated for 40 min with 50 μg/ml FGF. The explant has differentiated into somites (so) and neural tube (n). Similar differentiations have formed after the treatment of blastula ectoderm with XTC-conditioned medium (supernatant of XTC-cultures). Bar: 0.1 mm.

not successful. It can be suggested that the inducer is present in very low concentrations only or/and it is inactivated during the different steps of isolation.

Dr. Slack, London, has reported that fibroblast growth factor (FGF) induces ventral mesodermal structures in competent ectoderm [69]. However, we could show by the treatment of ectoderm of middle blastulae with very high concentrations of FGF (50 μg/ml) (Boehringer, Mannheim) for 10–60 min that this growth factor is also able to evoke dorsal mesodermal structures (Fig. 8). When the ectoderm of middle blastulae is incubated for relatively long period (2 hr), the explants develop in yolk-rich spheres. Similar results we obtained with high concentrations of vegetalizing factor [25]. The tissue could be identical with undifferentiated endoderm. The histotypic differentiation of endoderm depends on the presence of mesodermal derivatives [70]. This fact is corroborated by the observation that shorter incubation time of ectoderm with FGF (5–10 min) results not only in the differentiation of ventral mesodermal structures (Fig. 5), but in few cases also into endodermal derivatives, i.e. intestine and endodermal epithelium (Figs. 6 and 7).

Another mesodermalizing factor could be isolated by Smith, London, from the supernatant (conditioned medium) of a confluent layer of a *Xenopus*-cell line (XTC-cells) [71]. He could show that ectoderm, treated with the conditioned medium, differentiates into dorsal mesodermal structures (notochord, somites and neural tube) [72]. However, when we used early gastrula ectoderm instead of blastula ectoderm ventral mesodermal and endodermal structures are also formed after short incubation period (Fig. 5) (Tacke and Grunz, unpublished results). It should be mentioned that the XTC-cells after confluency form compact freely floating spheres (Fig. 4). These small aggregates can be wrapped by competent ectoderm (sandwich method). It is of interest that the ectoderm is stimulated by the XTC-aggregates to form ventral mesodermal (blood cells, coelomic epithelium and intestine) and muscle structures as well (Figs. 5 and 8). Therefore the factor from XTC-cells or FGF cannot be considered as specific ventral or dorsal mesodermalizing factor, respectively [73]. So far it is not clear whether two different (a dorsal and a ventral mesodermalizing factors) inducers are present in the dorsal and the ventral vegetative material of the intact embryo. We know that the basic FGF-factor, purchased from Boehringer, Mannheim, which we used for our experiments, still contains other components. So far we cannot exclude that these factors are also biologically active. The HPLC-purification and the test of the different fractions are in progress (joint experiments with Dr. Tiedemann, Berlin).

It could be speculated that homogeneous vegetalizing factor, XTC-factor and FGF contain similar domains, which are responsible for the biological activity. This could be concluded from the fact that all three factors are able to initiate the formation of endoderm or vegetal and dorsal mesoderm. Besides certain structural differences all three factors could contain specific amino acid sequences.

It could be argued that all three factors give a similar primary vegetalizing signal, followed by secondary cell interactions (activation of mesodermalizing factors), which will cause the formation of mesodermal derivatives, which in turn will induce neural structures under certain experimental conditions.

It is known that FGF can be bound to Heparin-Sepharose. In preliminary experiments we could show that after addition of Heparin-Sepharose CL-6B to conditioned medium (supernatant of confluent layers) of XTC-cells (1 ml gel to 4 ml supernatant) the inducing activity of the XTC-inducer(s) is not fully abolished. We obtained in 25% of the cases mesodermal inductions. This could mean that in contrast to FGF there is only a weak affinity of XTC-factor(s) to Heparin-Sepharose. However, we found no inductions at all, when we added Con A-Sepharose to the XTC-conditioned medium and treated competent ectoderm with the supernatant. This could mean that XTC-factor contains α-D-mannoside or/and α-D-glucoside residues. In contrast the fraction with the highest mesodermal inducing capacity isolated from carp swimmbladder does not bind to Con A-Sepharose [21].

CONCLUSIONS AND PERSPECTIVES

There are known several vegetalizing (mesodermalizing) factors, protein in nature, which can be obtained in highly purified form. This holds true for the FGF and the factor(s) from XTC-cells. The amino acid sequence has already been described for the pituitary basic FGF and the acidic bovine brain FGF [74]. Since large quantities of conditioned medium (supernatant of confluent cultures) of XTC-cells can be obtained, a further purification and characterization of XTC-mesodermalizing factor(s) can be expected. Next steps would include the cloning of vegetalizing (mesodermalizing) and neuralizing factors. Since the factors, just mentioned, mimic the biological effects of the genuine factors present in the embryo, it can be suggested that they contain similar domains, which are important for the biological activity. The exact mode of the induction process could also be studied with specific antibodies directed against the inducers. Furthermore other modern techniques (for example electro-cellfusion, adapted to amphibian cell material [75]) will be useful for studies on cytoplasmic/nuclear interrelationships including gene regulation.

These homogeneous proteineous inducing factors will be powerful tools for studies of the chain of molecular events, which take place during the determination of cells and pattern formation in early embryogenesis, closely related to differential gene expression.

ACKNOWLEDGMENT

Supported by the Deutsche Forschungsgemeinschaft (Schwerpunkt "Steuerung der Differenzierung von ein- und wenigzelligen eukaryontischen Systemen") and, in part, by the University GHS Essen.

We thank Sabine Effenberger for the preparation of the histological sections.

REFERENCES

1 Sargent, T. G. and Dawid, I. B. (1983) Differential gene expression in the gastrula of *Xenopus laevis*. Science, **222**: 135–139.

2 Miyatani, S., Winkles, J. A., Sargent, T. D. and Dawid, I. G. (1986) Stage-specific keratins in *Xenopus laevis* embryos and tadpoles: The XK81 gene family. J. Cell Biol., **103**: 1957–1965.

3 Newport, J. and Kirschner, M. (1982) A major developmental transition in early *Xenopus* embryos: I. Characterization and timing of cellular changes at the midblastula stage. Cell, **30**: 675–686.

4 Gusseck, D. J. and Hedrik, J. L. (1971) A molecular approach to fertilization. I. Disulfide bonds in *Xenopus laevis* jelly coat and a molecular hypothesis for fertilization. Dev. Biol., **25**: 337–347.

5 Nieuwkoop, P. D. and Faber, J. (1956) Normal Table of *Xenopus laevis* (Daudin). North Holland, Amsterdam.

6 Stockard, C. R. (1909) The artificial production of one-eyed monsters and other defects, which occur in nature, by the use of chemicals. Anat. Rec., **3**: 167–173.

7 Stockard, C. R. (1909) The development of artificially produced cyclopean fish. "The magnesium embryo". J. Exp. Zool., **6**: 285–337.

8 Adelmann, H. (1936) The problem of cyclopia. Part I. Quart. Rev. Biol., **11**: 161–183.

9 Adelmann, H. (1936) The problem of cyclopia. Part II. Quart. Rev. Biol., **11**: 284–305.

10 Mangold, O. (1931) Das Determinationsproblem. Dritter Teil. Das Wirbeltierauge in der Entwicklung und Regeneration. Ergeb. Biol., **7**: 193–403.

11 Asashima, M. and Grunz, H. (1983) Effects of inducers on inner and outer gastrula ectoderm layers of *Xenopus laevis*. Differentiation, **23**: 157–159.

12 Keller, R. E. (1981) An experimental analysis of the role of bottle cells and the deep marginal zone in gastrulation of *Xenopus laevis*. J. Exp. Zool, **216**: 81–101.

13 Nieuwkoop, P. and Florschütz, P. (1950) Quelques caracteres speciaux de la gastrulation et de la neurulation de l'oeuf de *Xenopus laevis*, Daud. et de quelques autres Anoures. Arch. Biol. (Liege), **61**: 113–150.

14 Spemann, H. and Mangold, H. (1924) Über Induktion von Embryonalanlagen durch Implantation artfremder Organisatoren. Wilhelm Roux' Arch. Entwicklungsmech. Org., **100**: 599–638.

15 Holtfreter, J. (1933) Nachweis der Induktionsfähigkeit abgetöteter Keimteile. Isolations- und Transplantationsversuche. Wilhelm Roux' Arch. Entwicklungsmech. Org., **128**: 584–633.

16 Nakamura, O. and Toivonen, S. (1978) Organizer–A Milestone of a Half-Century from Spemann. Biomedical Press, Elsevier/North-Holland.

17 Nieuwkoop, P. D., Johnen, A. G. and Albers, B. (1985) The epigenetic nature of early chordate development. Inductive interactions and competence. Cambridge University Press, Cambridge, London.

18 Yamada, T. (1958) Induction of specific differentiation by samples of proteins and nucleoproteins in the isolated ectoderm of *Triturus gastrulae*. Experientia, **14**: 81–87.

19 Yamada, T. (1961) A chemical approach to the problem of the organizer. In "Advances in Morphogenesis, Vol. 1". Ed. by M. Abercrombie and J. Brachet, Academic Press, New York, pp. 1–53.

20 Born, J., Hoppe, P., Schwarz, W., Tiedemann, H., Tiedemann, H. and Wittmann-Liebold, B. (1985) Embryonic inducing factor: Isolation by high performance liquid chromatography and chemical properties. Biol. Chem. Hoppe-Seyler's, **366**: 729–735.

21 Asashima, M., Nakano, H., Matsunaga, K., Hashimota, K. and Shimada, K. (1986) Purification of mesodermal inducing substance and protein synthesis using this material. In "Cellular Endocrinology: Hormonal Control of Embryonic and Cellular Differentiation". Ed. by. G. Serrero and J. Hayashi, Alan R. Liss, Inc., New York, pp. 55–66.

22 Janeczek, J., Born, J., Hoppe, P., Schwarz, W., Tiedemann, H. and Tiedemann, H. (1986) Informative molecules and induction in early embryogenesis. In "Cellular Endocrinology: Hormonal Control of Embryonic and Cellular Differentiation". Ed. by. G. Serrero and J. Hayashi, Alan R. Liss, Inc., New York, pp. 11–24.

23 Tiedemann, H. (1986) Test of embryonic factors: advantages and disadvantages of different procedures. In "Cellular Endocrinology. Hormonal Control of Embryonic and Cellular Differentiation". Ed. by G. Serrero and J. Hayashi, Alan R. Liss, Inc., New York, pp. 25–34.

24 Grunz, H. (1973) The ultrastructure of amphibian ectoderm treated with an inductor or actinomycin D. Wilhelm Roux' Arch., **173**: 283–293.

25 Grunz, H. (1983) Change in the differentiation pattern of *Xenopus laevis* ectoderm by variation of the incubation time and concentration of vegetalizing factor. Wilhelm Roux' Arch., **192**: 130–137.

26 Grunz, H. (1983) Early embryonic induction in amphibians, a model system of the information transfer between cells. In "Developmental Biology", An Afro-Asian Perspective. Ed. by. S. C. Goel and R. Bellairs, pp. 73–86.

27 Takata, K., Yamamoto, K. Y. and Ozawa, R. (1981) Use of lectins as probes for analyzing embryonic induction. Roux' Arch. Dev. Biol., **190**: 92–96.

28 Grunz, H. (1985) Effect of Concanavalin A and vegetalizing factor on the outer and inner ectoderm layers of early gastrulae of *Xenopus laevis* after treatment with Cytochalasin B. Cell Differ., **16**: 83–92.

29 Grunz, H. (1985) Information transfer during embryonic induction in amphibians. J. Embryol. Exp. Morphol., **89**: Suppl., 349–363.

30 Gualandris, L., Duprat, A. M. and Rouge, P. (1987) Cross-linking of membrane glycoconjugates is not a sufficient condition for neural induction by Con A. Cell Differ., (in press).

31 Takata, K. (1985) A molecular profile of the receptor responsive to the neural-inducing signals in the amphibian competent ectoderm. Zool. Sci., **2**: 443–453.

32 Born, J. Hoppe, P., Janeczek, J., Tiedemann, H. and Tiedemann, H. (1986) Covalent coupling of neuralizing factor from *Xenopus* to Sepharose beads: no decrease of inducing activity. Cell Differ., **19**: 97–101.

33 Tacke, L., and Grunz, H. (1986) Electron microscopy study of the binding of Con A-gold to superficial and inner ectoderm layers of *Xenopus laevis* in correlation to the neural inducing activity of this lectin. Roux' Arch. Dev. Biol., **195**: 158–167.

34 Holtfreter, J. (1944) Neural differentiation of ectoderm through exposure to saline solution. J. Exp. Zool., **95**: 307–340.

35 Tiedemann, H. (1986) The molecular mechanism of neural induction: neural differentiation of *Triturus* ectoderm exposed to hepes buffer. Roux' Arch. Dev. Biol., **195**: 399–402.

36 Davids, M., Loppnow, B., Tiedemann, H. and Tiedemann, H. (1987) Neural differentiation of amphibian gastrula ectoderm exposed to phorbolester. Roux' Arch. Dev. Biol., **196**: 137–140.

37 Chuang, H. H. (1955) Untersuchungen über die Reaktionsfähigkeit des Ektoderms mittels sublethaler Cytolyse. J. Acad. Sinica, **4**: 151–186.

38 Siegel, G., Grunz, H., Grundmann, U., Tiedemann, H. and Tiedemann, H. (1985) Embryonic induction and cation concentrations in amphibian enbryos. Cell Differ., **17**: 209–219.

39 Nishizuka, Y. (1984) The role of protein kinase C in cell surface signal transduction and tumor promotion. Nature, **308**: 693–698.

40 Saxen, L. (1961) Transfilter neural induction of amphibian ectoderm. Dev. Biol., **3**: 140–152.

41 John, M., Janeczek, J., Born, J., Hoppe, P., Tiedemann, H. and Tiedemann, H. (1983) Neural induction in amphibians. Transmission of a neuralizing factor. Roux's Arch. Dev. Biol., **192**: 45–47.

42 Born, J., Grunz, H., Tiedemann, H. and Tiedemann, H. (1980) Biological activity of the vegetalizing factor: decrease after coupling to polysaccharide matrix and enzymatic recovery of active factor. Roux's Arch., **189**: 47–56.

43 Grunz, H. and Staubach, J. (1979) Cell contacts between chorda-mesoderm and the overlaying neuroectoderm (presumptive central nervous system) during the period of primary embryonic induction in amphibians. Differentiation, **14**: 59–65.

44 Johnen, A. G. (1956) Experimental studies about the temporal relationships in the induction process. I. Experiments on *Amblystoma mexicanum*. Proc. Acad. Sci. Amst., ser. C, **59**: 554-561.

45 Johnen, A. G. (1956) Experimental studies about the temporal relationships in the induction process. II. Experiments on *Triturus vulgaris*. Proc. Acad. Sci. Amst., ser. C, **59**: 652–660.

46 Nishijima, K., Noda, S., Kurihara. K. and Sasaki, N. (1978) Differentiation of partially mesodemalized ectoderm; homoiogenetic and heterogenetic induction by primarily induced part of the ectoderm. Dev. Growth Differ., **20**: 275–281.

47 Grunz, H. (1979) Change of the differentiation pattern of amphibian ectoderm after the increase of the initial cell mass. Wilhelm Roux' Arch., **187**: 49–57.

48 Asahi, K., Born, J., Tiedemann, H. and Tiedemann, H. (1979) Formation of mesodermal pattern by secondary inducing interactions. Wilhelm Roux' Arch., **187**: 231–244.

49 Minuth, M. and Grunz, H. (1980) The fromation of mesodermal derivatives after induction with vegetalizing factor depends on secondary cell interactions. Cell Differ., **9**: 229–238.

50 Albers, B. (1985) Kompetenz als entscheidender Faktor bei der räumlichen Begrenzung der Neuralanlage (*Ambystoma mexicanum*). Ph. D. Thesis, Köln.

51 Grunz, H., Born, J., Tiedemann, H. and Tiedemann, H. (1986) The activation of a neuralizing factor in the neural plate is correlated to its homoiogenetic inducing activity. Roux' Arch. Dev. Biol., **195**: 464–466.

52 Boucaut, J. C. and Darribere, T. (1983) Fibronectin in early amphibian embryos. Cell Tissue Res., **234**: 135–145.

53 Nakatsuji, N., Hashimoto, K. and Hayashi, M. (1985) Laminin fibrils in newt gastrulae visualized by the immunofluorescent staining. Dev. Growth Differ., **27**: 639–643.

54 Boucaut, J. C, Darribere, T., Boulekbache, H. and Thiery, J. P. (1984) Prevention of gastrulation but not neurulation by antibodies to fibronectin in amphibian embryos. Nature, **307**: 364–367.

55 Grunz, H., Darribère, T. and Boucaut, J. C. (1987) Binding of anti-fibronectin to early amphibian ectoderm does not result in inhibition of neural induction under *in vitro* conditions. Roux' Arch. Dev. Biol., **196**: 203–209.

56 Geithe, H.-P., Asashima, M., Asahi, K., Born, J., Tiedemann, H. and Tiedemann, H. (1981) A vegetalizing inducing factor—Isolation and chemical properties. Biochim. Biophys. Acta, **676**: 350–356.

57 Grunz, H. (1977) The differentiation of the four animal and the four vegetal blastomeres of the eight-cell-stage of *Triturus alpestris*. Wilhelm Roux' Arch., **181**: 267–277.

58 Kageura, H. and Yamana, K. (1983) Pattern regulation in isolated halves and blastomeres of early *Xenopus laevis*. J. Embryol. Exp. Morphol., **74**: 221–234.

59 Kageura, H. and Yamana, K. (1986) Pattern farmation in 8-cell composite embryos of *Xenopus laevis*. J. Embryol. Exp. Morphol., **91**: 79–100.

60 Yamana, K. and Kageura, H. (1987) Reexamination of the "regulative development" of amphibian embryos. Cell Differ., **20**: 3–10.

61 Scharf, S. R. and Gerhart, J. C. (1980) Determination of the dorsal-ventral axis in eggs of *Xenopus laevis*: Complete rescue of UV-impaired eggs by oblique orientation before first cleavage. Dev. Biol., **79**: 181–198.

62 Nieuwkoop, P. D. (1969) The formation of the mesoderm in urodelean amphibians. I. Induction by the endoderm. Wilhelm Roux' Arch., **162**: 341-373.

63 Asashima, M. (1975) Inducing effects of the presumptive endoderm of successive stages in *Triturus alpestris*. Wilhelm Roux' Arch., **177**: 301–308.

64 Gurdon, J. B., Mohun, J., Brennan, S. and Cascio, S. (1985) Actin genes in *Xenopus* and their developmental control. J. Embryol. Exp. Morphol., **89**: (Suppl.), 125–136.

65 Grunz, H. and Tacke, L. (1986) The inducing capacity of the presumptive endoderm of *Xenopus laevis* studied by transfilter experiments. Roux's Arch. Dev. Biol., **195**: 467–473.

66 Warner, A. E., Guthrie, S. C. and Gilula, N. B. (1984) Antibodies to gap-junctional protein selectively disrupt junctional communication in the early amphibian embryo. Nature, **311**: 127–131.

67 Tseng, M.-P. Chuang (1986) On the cellular communication of amphibian embryogenesis. In "Cellular Endocrinology: Hormonal Control of Embryonic and Cellular Differentiation". Ed. by G. Serrero and J. Hayashi, Alan R. Liss, Inc., New York, pp. 35–44.

68 Boterenbrood, E. C. and Nieuwkoop, P. D. (1973) The formation of the mesoderm in urodelean amphibians. IV. Its regional induction by the endoderm. Wilhelm Roux' Arch. Dev. Biol., **173**: 319-332.

69 Slack, J. M. W., Darlington, B. G., Heath, J. K. and Godsave, S. F. (1987) Mesoderm induction in early *Xenopus* embryos by heparin-binding growth factors. Nature, **326**: 197–200.

70 Okada, T. S. (1960) Epithelio-mesenchymal relationships in the regional differentiation of the digestive tract in the amphibian embryo. Roux' Arch. Dev. Biol., **152**: 1–21.

71 Pudney, M., Varma, M. G. R. and Leake, C. J. (1973) Establishment of a cell line (XTC-2) from

South African clawed frog, *Xenopus laevis*. Experientia, **29**: 466–467.

72 Smith, J. C. (1987) A mesoderm-inducing factor is produced by a *Xenopus* cell line. Development, **99**: 3–14.

73 Dale, L., Smith, J. C. and Slack, J. M. W. (1985) Mesoderm induction in *Xenopus laevis*: a quantitative study using a cell lineage label and tissue-specific antibodies. J. Embryol. Exp. Morphol., **89**: 289–312.

74 Esch, F., Baird, A., Ling, N., Ueno, N., Hill, F., Denoroy, L., Klepper, R., Gospodarowicz, D., Böhlen, P. and Guillemin, R. (1985) Primary structure of bovine pituitary basic fibroblast growth factor (FGF) and comparison with the amino-terminal sequence of bovine brain acidic FGF. Proc. Natl. Acad. Sci. USA, **82**: 6507–6511.

75 Grunz, H. and Tacke, L. (1986) Embryonic induction in amphibians. In "New Discoveries and Technologies". Ed. by. H. C. Slavkin, Alan R. Liss Inc., New York, pp. 135–138.

ZOOLOGICAL SCIENCE 4: 593–606 (1987)

REVIEW

The Derivation of Terrestrial Cave Animals

SHUN-ICHI UÉNO

Department of Zoology, National Science Museum (Nat. Hist.), Shinjuku, Tokyo 160, Japan

INTRODUCTION

It was believed for more than a century that terrestrial cave animals were derived from ancestors which had entered into limestone caves, colonized there and adapted themselves to various environmental factors peculiar to the underground world. All the eminent biospeologists in former times, including Viré [1], Racovitza [2], Jeannel [3, 4] and Vandel [5], did not throw any doubt on this point. The situation did not change even after the Second World War and all the biospeological studies were confined in calcareous areas, although considerable development was achieved in this field of science, not only in taxonomic and zoogeographic studies but also in the ecology and physiology of cave animals.

On the other hand, aquatic cave animals were already known from outside calcareous areas near the end of the last century [6]. Various kinds of phreatic animals, mostly eyeless and colourless, were subsequently found, first from wells [7, 8] and then from interstitial waters along rivers and seashores [9]. In Japan, the first phreatic animal, a planarian, was found in November 1889 from a well at Ichigaya in Tokyo and was described in 1916 [10]. Following this lead, subterranean species of freshwater worms, water-mites and isopod and amphipod crustaceans were recorded in the next two decades, mostly from wells dug or driven into alluvial layers distant from karstic terrains [11]. Similar data were rapidly accumulated in the 1950's and 1960's, and it became a common knowledge that so-called aquatic cave animals, at least most of small-sized ones, originated in the interstitial zone irrespective of the geological nature of the areas concerned. It is, therefore, incredible that no biospeologists suspected the existence of terrestrial cavernicoles in non-calcareous areas.

In the past decade or so, however, our concept of terrestrial cave animals has made a drastic change, and now we are fully aware of the fact that they are not confined to limestone caves but widely occur wherever environmental condition is suitable for their existence. They have not been met so far in pure granitic terrains, alluvial plains and small oceanic islands, but these blanks seem to have been caused either from ecological reasons or from existence of extrinsic barriers to dispersal of their ancestors. The purpose of the present review is to delineate the process of recent development in the study of terrestrial cavernicoles, and to demonstrate what is the original habitat of most terrestrial troglobionts. Since the upper hypogean fauna of the Japanese Islands has not yet been thoroughly studied, the following account is mainly based on better known groups with relatively numerous species, especially on trechine beetles.

An abstract of the present paper was already published in a previous volume of this journal [12], and a concise outline of the recent development of Japanese biospeology was given in the Tenth Anniversary Special Volume of the Speleological Society of Japan [13].

Received February 18, 1987

BIOSPEOLOGICAL STUDY OF LAVA CAVES

In 1968, the National Parks Association of Japan and the Japanese National Subcommittee for the

Conservation of Terrestrial Animals in the International Biological Program organized a joint project for investigating the natural history of Mt. Fuji-san [14]. Since this volcano is famous not only for its beautiful shape but also for the abundance of lava tubes, study of the cave fauna was taken up in the project, and its execution was entrusted to me. I was, however, rather reluctant to accept the responsibility, because it was generally believed that lava caves were not sufficiently old to develop

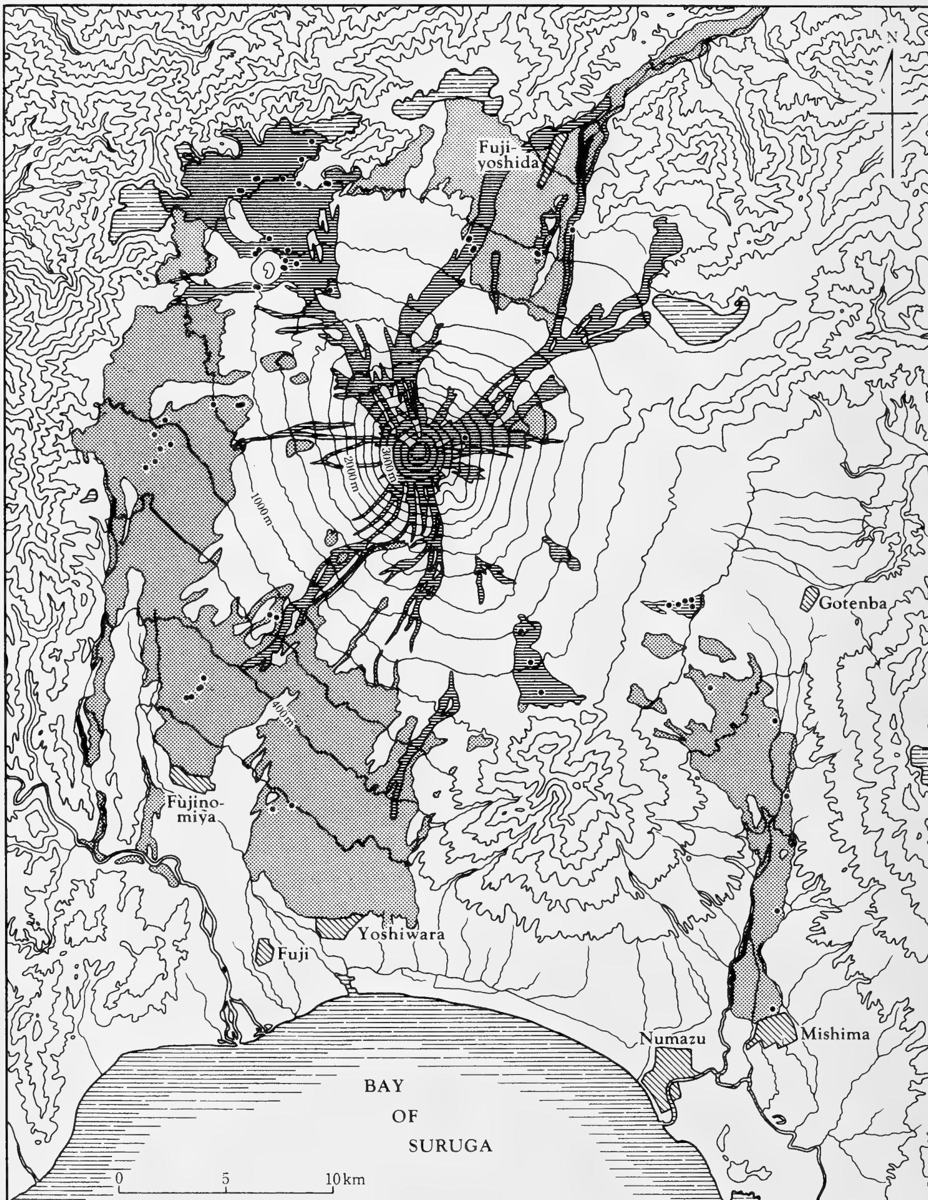

Fig. 1. Map showing the distribution of lava caves (including complex tree-molds) in the Fuji area; young lava flows are indicated by horizontal hatching; old ones are shown by fine dots; middle-aged lavas are omitted.

specialized cavernicoles. This belief was founded on the data that all but one of the lava caves theretofore examined were sterile and devoid of troglobionts. Nevertheless, I myself had to undertake the task, as I was unable to find anyone willing to study the supposedly meagre fauna of lava caves.

Before the new project was drawn up, there had been two biologists who had taken a particular interest in the lava cave fauna of Mt. Fuji-san. They were Hajime S. Torii [15, 16] and Masao Kumano [17], both of whom considered that some clue for clarifying the origin and adaptation of cave animals could be obtained by a comparative study between the fauna of old lava caves and that of young ones. Neither of them succeeded in accomplishing an expected result, but their working hypothesis seemed to make a good starting point. And thus, I commenced my own investigation along the same line as that of Kumano.

With the consistent support of expert cavers, my study progressed systematically and rapidly, and soon I became aware of the fundamental error of our former belief. Excepting frozen ones, most lava caves in the Fuji area were inhabited by certain terrestrial animals, especially by spiders and millipedes. Those found in young caves usually did not show appreciable morphological modification adaptive to subterranean life, whereas those occurring in old ones were often highly modified and similar to species previously known only from limestone caves. The faunal discrepancy was so decisive that the age difference between young and old caves appeared to bear on the differentiation of cave animals.

Many young caves in the Fuji area are developed in a lava flow spouted in 864 on the northwestern side of the volcano, that is, they are about 1,100 years old, while older caves lie in southeastern, southern and western lava flows 8,000–13,000 years old (Fig. 1). Therefore, there is a lapse of 7,000–12,000 years between the birth of old caves and that of young ones. However, 10,000 years or so did not seem sufficiently long for differentiation of troglobiontic animals, and besides, all the troglobionts found in Fuji lava caves belong to groups, whose members are widely distributed in the neighbouring areas. If we regard them as morphologically modified independent of their relatives, we cannot explain the close similarity between lava cave forms and limestone cave ones, unless very unusual parallel evolution could have taken place between them. Thus, I had to seek for other factors than mere age to account for the faunal difference between old and young caves.

Examining the ecological data amassed during the course of cave explorations, I realized that there was a definite difference in environmental conditions between old and young caves [18]. Young caves are mostly composed of bare lava and devoid of soil, and the climate is usually subject to

FIG. 2. A habitat of troglobionts in an old lava cave (Komakado-kaza-ana Cave) at the southeastern foot of Mt. Fuji-san. Photo by Takanori Ogawa.

diurnal and seasonal fluctuations because of the porous nature of the rock. On the contrary, old caves are more or less covered with layers of soil and frequently have muddy floors; the climate is usually stable throughout the year as in limestone caves (Fig. 2). It is therefore evident that the former is not suited for the habitats of highly specialized cavernicoles, especially of such soil-dependent animals as chthoniid pseudoscorpions and trechine beetles.

When it is created, a lava cave is completely bare. As time goes by, its roof becomes gradually eroded, forested and finally covered with thick layers of humus and soil. This coating keeps the underground climate stable and protects the environment from substantial changes. On the other hand, the soil gradually percolates into the cave with rain water, accumulates on the floor, and fills up small voids in the rock. For this reason, old caves are always wet and often have shallow pools of groundwater. The presence of soil is also indispensable for the existence of many specialized cavernicoles, since autotrophic microorganisms living in the clay or silt deposits synthesize certain vitamins in the absence of light and serve as the nutrition of young cavernicoles [5, 19]. After all, habitats suitable for specialized cavernicoles are yielded only in old caves.

It was necessary to see whether the existence of troglobionts in environmentally stabilized lava caves is peculiar to the Fuji area or universally observed. Accordingly, we extended our studies to all the areas in which lava caves were known, that is, the Island of Daikon-jima on Lake Nakaumi in western Honshu, Aso Volcano in central Kyushu, the Satsuma Peninsula in southwestern Kyushu, and the Island of Fukué-jima of the Gotôs off the western coast of Kyushu. The results of the explorations accorded well with that obtained in the Fuji area, almost all the old caves examined having been inhabited by highly specialized cavernicoles (Fig. 3) [20, 21]. It was confirmed beyond doubt that the controlling factor in the lava cave fauna was the environmental conditions, not simply the age of the caves concerned.

The biospeological importance of lava caves was subsequently recognized by Howarth, who discovered many extraordinary troglobionts on the Island of Hawaii [22]. All these troglobionts belong to groups autochthonous to the island group and have become differentiated under the tropical climate, so that they cannot be directly compared with temperate forms. Howarth's study is, however, important in clarifying that a specialized cave fauna can exist wherever there is a suitable environment for colonization and adaptation [23].

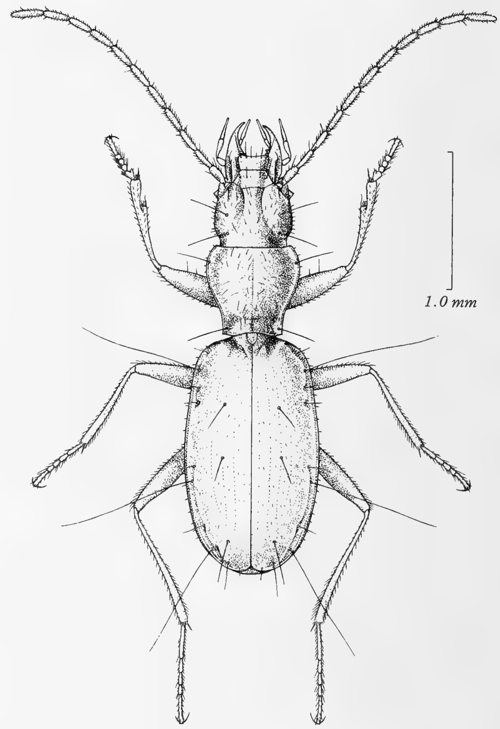

Fig. 3. *Gotoblemus ii* S. Uéno, a specialized anophthalmic trechine beetle endemic to old lava caves on the Island of Fukué-jima of the Gotôs off the western coast of Kyushu.

Next problem to be cleared up was to determine whether or not the troglobionts extant in lava caves had evolved after the eruption of lava flows bearing the caves concerned. It was difficult to approach the subject directly from the data obtained by the studies of lava cave inhabitants. Fortunately, however, a new light was shed from a different direction and led us to a new field of biospeology.

BIOSPEOLOGICAL STUDY OF ARTIFICIAL CAVES

In the autumn of 1970, when I was still in an inextricable maze of lava cave problems, an anophthalmic trechine beetle was discovered by Masahisa Ohrui in an abandoned adit of a gold mine on the Izu Peninsula [24]. After a careful examination, it became apparent that the beetle was a new species closely related to a lava cave inhabitant endemic to the southeastern foot of Mt. Fuji-san (Fig. 4). Subsequent investigations revealed that the adit had an interesting fauna very similar to that of old caves in the Fuji area. Most important was the discovery of an eyeless spider called *Falcileptoneta caeca*, which was common between the two areas [25].

The location of the gold mine was not very far from the nearest lava flow in the Fuji area, but was still more than 20 km distant in a bee-line. Besides, the geological feature of the intervening area was very intricate and not comparable to relatively simple calcareous terrains or lava fields. If the troglobiontic spiders extant in the two areas became independently differentiated from a common ancestor, they could not be perfectly identical with each other, even though a striking parallelism could have taken place. Therefore, certain underground routes passable for the spider must exist between Fuji and Izu however implausible it seemed to be. This inference was also supported by the fact that the mine adit was only 100–150 years old, or much younger than the youngest known lava cave in the Fuji area. No troglobiont could have undergone an appreciable morphological modification within such a short time.

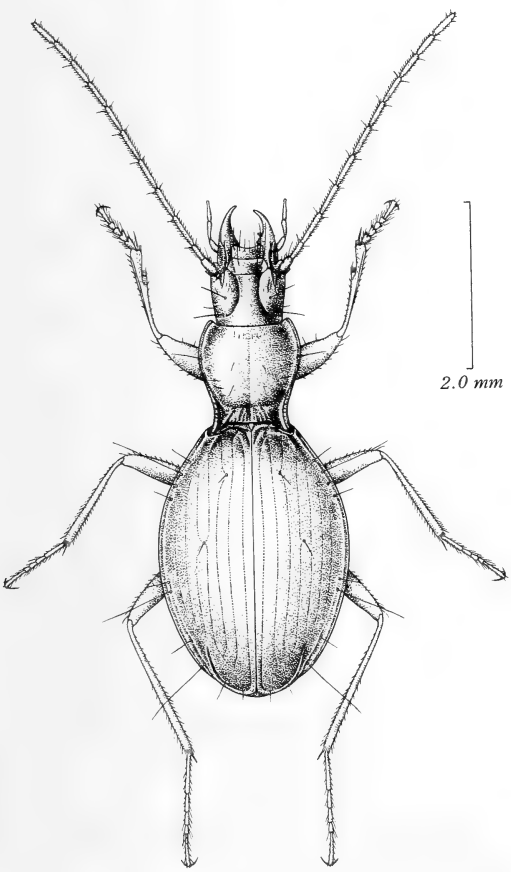

FIG. 4. *Trechiama ohruii* S. Uéno, an anophthalmic trechine beetle first found in an old gold mine on the Izu Peninsula.

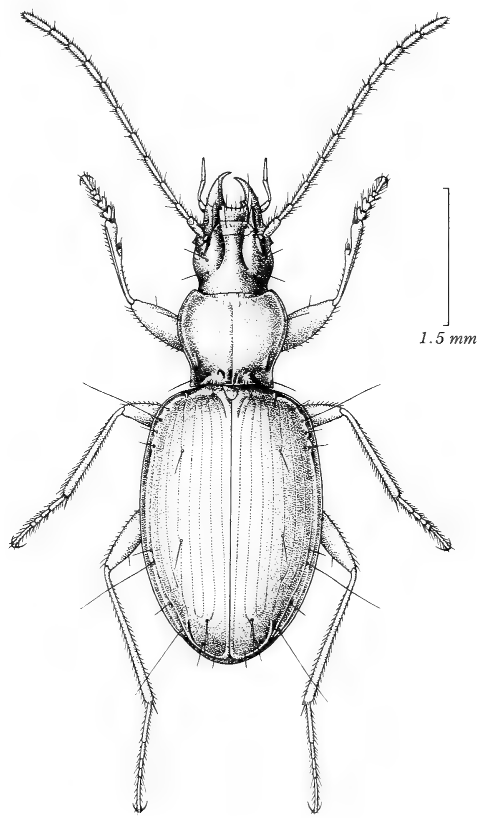

FIG. 5. *Trechiama echigonis* S. Uéno, an anophthalmic trechine beetle first discovered from the upper hypogean zone of Central Japan.

Five years prior to the discovery of the mine fauna on the Izu Peninsula, Kintaro Baba discovered an anophthalmic trechine beetle, which was in every respect troglobiontic, from the narrow fissures of shale about 2 m below the surface (Fig. 5) [26]. In our present concept, the habitat of this beetle is typically upper hypogean, but at that time I was unable to distinguish it from the endogean domain, although I was much surprised at its unusual depth. The realization that artificial cavities could harbour specialized fauna directed my eyes once again to the importance of Baba's discovery. Similar environment under the earth might well be the original habitat of terrestrial troglobionts found in the mine adit.

It was, however, not easy to dig deep holes into the ground for searching for minute animals of considerable rarity. An easier way to obtain the same result seemed to me to be the faunal investigation of artificial cavities already dug into the ground by someone else, and most abundant of them seemed to be mine adits of various kinds. Besides, there were several records suggestive of a promising future of this project. In 1954, Shigeru Nomura examined an abandoned mercury mine in eastern Kyushu and found that its fauna was very similar to those of nearby limestone caves [27]. Though lying in a calcareous area, the adit itself

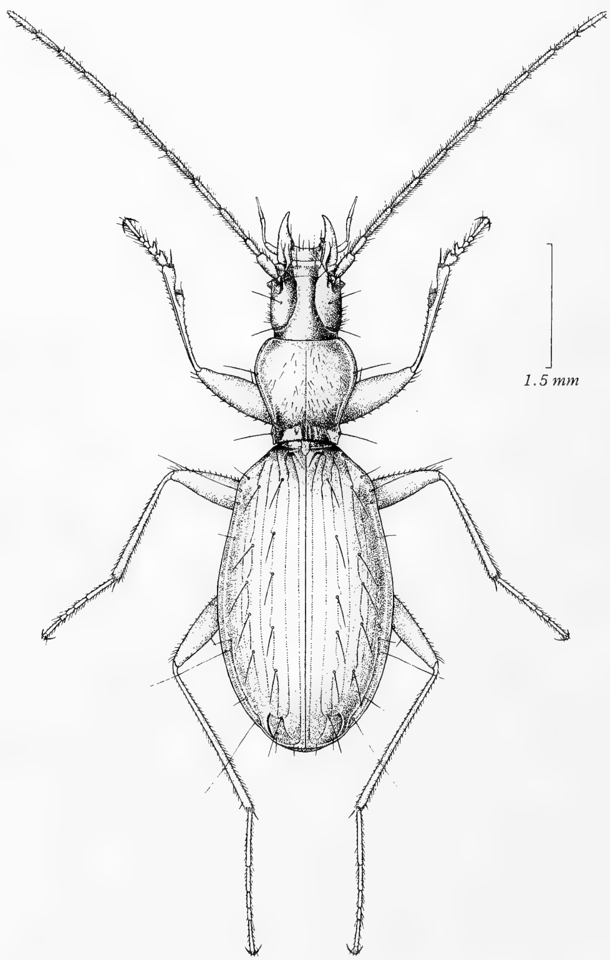

FIG. 6. *Chaetotrechiama procerus* S. Uéno, a very remarkable anophthalmic trechine beetle hitherto known only from an abandoned mine in southwestern Shikoku.

was dug into a small hill mainly composed of chert. In the following year, I myself paid a visit to that area and examined the adit in question and two other adits of another mine, all of which were found rich in specialized fauna [28, 29]. At about the same time, J. Balazuc and J. Demaux explored a hematite mine in southern France, reporting that it harboured various terrestrial troglobionts [30]. However, all these findings were made in either calcareous terrains or their vicinities, so that their importance in biospeology was overlooked, until a rich troglobiontic fauna was found in the gold mine on the Izu Peninsula widely distant from any calcareous areas. Standing on a new solid ground, we started in a renewed study of mine fauna with the hope of pursuing the origin of terrestrial cavernicoles.

As in the case of the faunal study of Fuji lava caves, our exploration of artificial cavities progressed systematically and rapidly, but at first the results were not so good as expected. We had to endure repeated disappointment and almost gave up the whole plan. After a few years of painstaking efforts, however, we finally located several mines rich in specialized cavernicoles, first in the vicinities of Kyoto and Osaka, and then in the Island of Shikoku (Fig. 6). Once fertile mines were found, subsequent researches became much easier, and a large quantity of new materials were rapidly accumulated.

We are now fully aware of the fact that specialized hypogean faunas are found in various kinds of artificial cavities including mines, underground shelters, conduits, prospecting adits at dam sites, and so on. The age of the cavities is not significant with the faunas, since highly specialized troglobionts are found in old adits 100 or more years old as well as in very young ones that were dug only 2 or 3 years before. Moreover, their existence are not directly dependent on the nature of rocks into which the cavities in question are dug; igneous and metamorphic rocks are equally suitable to sedimentary ones [31, 32]. However, most favourable are such clastic rocks as mudstones, shales, schists and breccias. Tuff mines are also frequently, but not always, good for habitats of specialized cavernicoles. On the other hand, pure granite is always devoid of specialized fauna; this was one of the main reasons why our investigation of mine fauna was not successful at the beginning.

It is apparent at present that the sterility of granitic cavities is mainly ascribed to ecological causes. When eroded, pure granite only produces pure sand, so that granitic cavities are usually devoid of clay or silt indispensable for the existence of many terrestrial cavernicoles. The situation is similar to that observed in young lava caves which are almost always bare and very clean. The sterility of granitic terrains was also confirmed later by the study of the upper hypogean fauna, as will be described in the following chapter.

RECOGNITION OF THE UPPER HYPOGEAN ZONE

Alongside of the faunal investigation of artificial cavities, we tried a more direct method of finding out terrestrial troglobionts from their supposed natural habitats, that is, excavation from the surface. This was a laborious and time-consuming work, so that its progress was slow and expected results were not gained for some time. After 1975, however, we were able to locate several places inhabited by anophthalmic trechine beetles, and realized that they were always met on or near the bedrock beneath thick layers of soil. Though scanty, these data seemed to indicate that terrestrial troglobionts could be regularly found in narrow spaces just above the bedrock, and if so, we could locate their habitats more easily by looking for such spots as the overlying soil mantle was relatively thin.

Keeping this in mind, we continued our searches for anophthalmic trechines mainly in the vicinities of Lake Biwa-ko, because that area was rather easily accessible and looked promising judged from the data obtained by cave explorations. Our expectation was soon realized, especially by the painstaking efforts of Yoshiaki Nishikawa, who alone discovered six new species of anophthalmic trechines from outside caves between the autumn of 1978 and the summer of 1980. They were described in 1980, together with other species, in a revision of the trechine beetles belonging to the group of *Trechiama ohshimai* [33]. Of the twenty-two species recognized in this paper, six were then

known only from caves of some kind (two of the six were later found in extra-cave habitats), thirteen were obtained from the underground habitats we specially looked for, and the remaining three were taken from both inside and outside caves. Thus, it was proved beyond all reasonable doubt that so-called troglobiontic trechines were not confined in caves but widely occurred in narrow spaces between the soil layer and the bedrock. At that time, I regarded this habitat as the lowest zone of the endogean domain, though it was unusually deep and looser than ordinary endogean environment.

In the same year, Juberthie and his colleagues published the result of their study on the fauna of a zone below the deepest layer of the soil, concluding that terrestrial cavernicoles were not confined in calcareous terrains but widely distributed in the shale and crystalline rock areas [34, 35]. They considered that the extra-cave environment suitable for the existence of terrestrial troglobionts was a zone extending just above the bedrock, which was characterized by its high porosity due to the presence of fissures and interconnecting spaces. Because of this feature and of the regular occurrence of troglobionts, they distinguished the zone from the endogean domain and named it "le milieu souterrain superficiel".

Their conclusion perfectly accorded with ours, though the methods of approach were different. While we dug out eyeless animals directly from their habitats, they dug holes into the ground, inserted baited traps and attracted troglobionts. The latter method was not very successful in Japan though we tried it later, probably because of the low population density of Japanese forms.

One of the most important achievements made by the French scholars was the discovery of undoubted connections between a limestone cave and the milieu souterrain superficiel. This was made at Moulis on the Pyrénées in southern France, where a subterranean laboratory had been established in a limestone cave. Placing baited traps in a scree on the hillside above the laboratory cave, they obtained four troglobiontic species of bathysciine beetles; two of them were native to the area, but the other two were imported species which had escaped from terraria and settled down in the cave [36, 37]. This was an irrefutable proof that the extent of their habitat was not restricted to the cave itself but spread out all over the milieu souterrain superficiel.

At present, it is indisputable that many terrestrial cave animals distributed in temperate regions originated in the milieu souterrain superficiel, or the upper hypogean zone. Specialized upper hypogean fauna exists from near the seashore to the height of at least 2,000 m (Figs. 7 and 8). It has been unknown in certain areas, for instance, pure granitic terrains and alluvial plains. The former is sterile because it is usually sandy and devoid of clay or silt. However, terrestrial troglobionts may survive even on granitic hills, if there are certain oases suitable for their existence. An example is Zôzu-san in northeastern Shikoku, which is a small granitic hill largely devoid of upper hypogean fauna. In spite of such an unfavourable condition, an anophthalmic trechine beetle endemic to the hill occurs in the upper hypogean zone in a small andesitic gully on its northeastern slope [38]. The sterility of alluvial plains can be ascribed to the

FIG. 7. A schistous gully on Okuminagawa-yama in central Shikoku, which harbours an anophthalmic trechine beetle of the genus *Ishikawatrechus*.

FIG. 8. Excavation of an upper hypogean habitat of an *Ishikawatrechus* on Okuminagawa-yama.

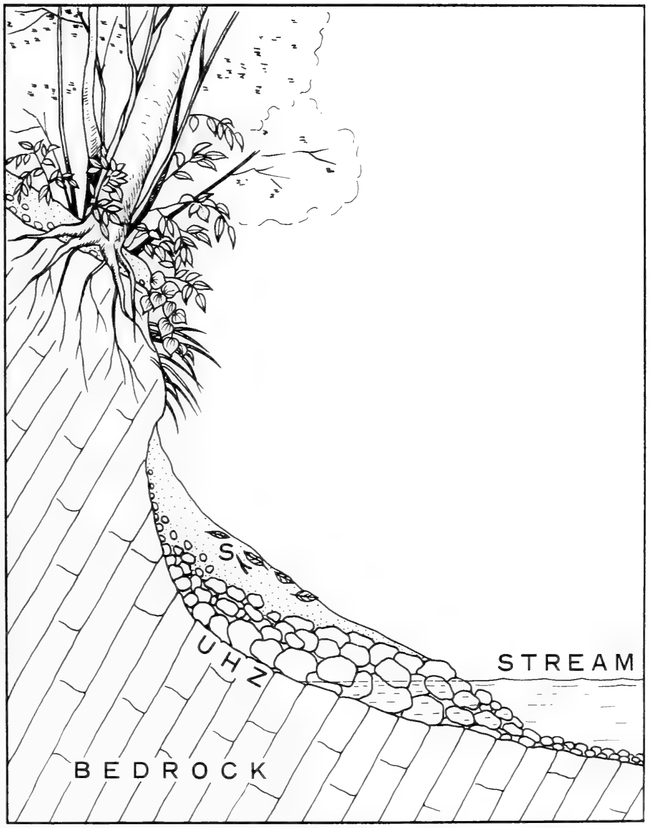

FIG. 9. Schematic cross section of a colluvium showing the habitat of troglobionts. UHZ–upper hypogean zone; S–soil layer.

absence of continuous spaces under the earth.

To our present knowledge, upper hypogean habitats of terrestrial troglobionts can be located without much difficulty in small gullies or at the sides of moderate-sized streams (Fig. 9). They are invariably found beneath colluvia emplaced under steep slopes and fed by seepages. The thickness of the soil mantle is usually 50 cm or more, but where the mantle is thinner, terrestrial troglobionts can be met at the depth of only 10–20 cm. Unfortunately, however, favourable colluvia are not very common, and once they are excavated, their recovery cannot be expected within a short time. Besides, population density of Japanese troglobionts is much lower than that of continental forms. This makes procuration of adequate materials very difficult. We know that specialized upper hypogean fauna exists over most of the Japanese Islands and that it consists of various groups of terrestrial troglobionts, but most of them have not yet been studied even taxonomically. For instance, white eyeless polydesmid millipedes have been known from many stations in West Japan, but always from a single female which is useless for taxonomic study. Only the exception is trechine beetles, which are, though also rare, fairly well known through my own efforts and unfailing collaborations of many friends of mine.

After the discoveries made in Japan and France, upper hypogean fauna was also found in Romania [39]. It has been unknown in the United States [40], but must exist there, especially on the Appalachian Mountains where a very rich cave fauna has been reported. Recent discovery of an anophthalmic trechine beetle in an abandoned coal mine in Kentucky is an infallible indication of its existence [41].

CONCLUDING REMARKS

Terrestrial cavernicoles comprise many groups of animals derived from various sources. Recent investigations of tropical and subtropical cave faunas have shown that there exist relatively few but very interesting terrestrial troglobionts in the tropics [42, 43]. Derivation of those tropical troglobionts may not be the same as that of temperate ones; for instance, herbivorous cixiid homopterans [44] and extremely long-legged reduviid heteropteran [45], both from Hawaiian lava caves, may have entered underground through the spaces around tree roots, and small eyeless cockroaches of the Ryukyu Islands [46] may have colonized limestone caves through porous coral reefs.

However, a great majority of terrestrial troglobionts occur in the temperate areas of both the Northern and Southern Hemispheres, and most of them seem to originate in the upper hypogean zone. Since they are invariably hygrophilous, they probably have their roots in ripicolous ancestors, which lived under stones on water edges of narrow streams. Their colonization in the upper hypogean zone may have been initiated by dispersal along seepages, debouchures of which usually attract various hygrophilous animals, especially in drier seasons. Continuous spaces in the upper hypogean zone, or intricate microcaverns, are equivalent to caves in an ordinary sense for such minute creatures as insects and other terrestrial arthropods. We have to realize clearly that "caves", which are defined as "underground cavities large enough to permit human entrance", are an artificial concept not applicable to small animals.

The above conclusion cannot be applied to all terrestrial troglobionts even in the temperate zone. Notable exceptions are those derived from endogean ancestors and from pholeophilous ones. Cavernicoles of endogean origin can be recognized by a thickset or parallel-sided body form and relatively short appendages (Fig. 10). Their close relatives are always found in the endogean domain, not in the upper hypogean zone. Probably descended from humicolous ancestors, these endogean animals may have found their way into depths of soil layer. Most of them remain there nowadays, but there are some that have penetrated deeper and settled down in caves. Contrary to the cave animals of endogean origin, descendants of pholeophiles, mostly represented by guanobionts, usually do not show high specialization adaptive to subterranean life. They have become cavernicolous only because deposits of bats' guano are found in caves. There are, however, exceptions like the springtails belonging to the *Aphoromma–Coecoloba* group, which are all troglobiontic and have

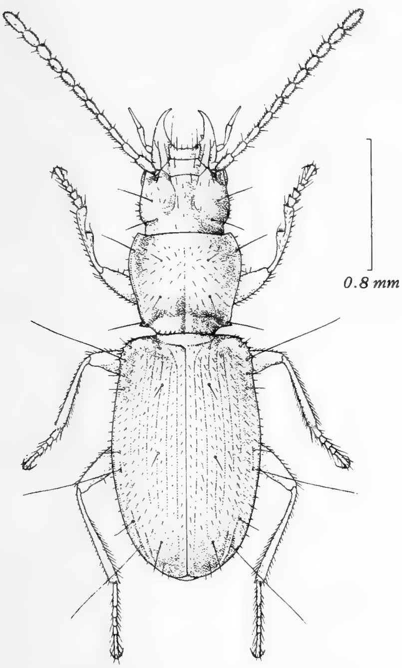

FIG. 10. *Stygiotrechus nishikawai* S. Uéno from Gonjiana Cave/Mine on the Kii Peninsula, an anophthalmic trechine beetle derived from an endogean ancestor.

undergone intensive allopatric speciation [47].

The realization that most terrestrial troglobionts occurring in temperate areas originated in the upper hypogean zone has broadened the scope of biospeology to a considerable extent. We can now fill in wide blanks in our knowledge about the distribution of terrestrial cave animals, which was formerly gained by the investigation of sporadically distributed limestone caves and lava tubes. In the Japanese Islands, about 130 species of anophthalmic trechine beetles have been known from natural caves and endogean habitats. Faunal investigation of artificial cavities and the upper hypogean zone has already doubled the number, and new findings are still being accumulated at a considerable speed. Many new species have been found in such areas wholly devoid of natural caves as the eastern part of the Chûgoku Hills in western Honshu [48] and coastal area on the Japan Sea side of central Honshu (unpublished data). Accordingly, we can analyse phylogeny and distribution of Japanese trechines on a much sounder basis than before (Fig. 11).

The discovery of the upper hypogean fauna has also revealed that terrestrial troglobionts occur in such areas as were immersed by Pleistocene transgressions. Endemic species are commonly found in such areas immersed in the early Pleistocene as the Hokuriku District, Niigata region and the Mogami-gawa drainage area in northeastern Honshu, which indicates that their speciation must have taken place after the subsequent regression. Even in certain areas immersed in the last Interglacial Age, there sometimes occur endemic trechine beetles and other arthropods. These evidences, together with the fact that many troglobionts are endemic to lava flows only 8,000–13,000 years old, suggest that the speciation of troglobionts must have progressed much more rapidly than it is generally supposed. Barr cited previous authors' calculations that 100,000–1,000,000 generations would be required for accomplishment of the loss of eyes, considering that troglobionts had colonized caves as late as the Last Interglacial, about 300,000 years ago [49]. Based upon the data on reproductive isolation and genetic distance, Sbordoni has surmised that the time required for speciation in caves is rather long, possibly not less than 5×10^5–10^6 years [50]. I am not in a position to argue if the calculations presented by these authors are correct or not, as I am not a geneticist, but I am fully satisfied that colonization of caves including microcaverns and subsequent speciation of troglobionts usually took place after the Last Interglacial Age. Preadaptation to subterranean existence may require a longer time, so that the calculations cited above may include it if they are really correct.

Recently, Juberthie proposed a new definition of the subterranean environment, describing that it consists of all the intercommunicating cavities of various sizes isolated from the surface and characterized by the total darkness and relatively stable climatic condition [51]. He then developed his idea and built up a hypothesis on the colonization of caves by terrestrial troglobionts and their subsequent isolation and speciation [52]. His discussion seems largely reasonable, although his explanation of the role of glacial–interglacial climatic changes seems to me better interpreted as

FIG. 11. Maps showing the distribution of anophthalmic trechine beetles in Japan. Map A is based solely on the species known from limestone caves. Map B is drawn from our present knowledge enlarged by the discoveries of mine and upper hypogean faunas; the blank at the southeastern part of the Island of Shikoku was to some extent filled after the manuscript of this paper had been sent to the press.

that of stadial–interstadial ones in the Last Glacial Age. Anyway, biospeology has made a considerable progress by the discovery of the upper hypogean fauna, but there still remain many other problems not yet cleared up. It is to be hoped that more intensive studies will be made from different

aspects of cave animals so as to develop the biospeology in a harmonious way.

REFERENCES

1 Viré, A. (1900) La Faune Souterrain de France. 159 pp. J.-B. Baillière et fils, Paris.

2 Racovitza, É. G. (1907) Essai sur les problèmes biospéologiques. Biospéologica, I; Arch. Zool. exptl. gén., (IV), **6**: 371–488.

3 Jeannel, R. (1926) Faune cavernicole de la France, avec une étude des conditions d'existence dans le domaine souterrain. Encycl. ent., **7**: 1–334, 15 pls. Paul Lechevalier, Paris.

4 Jeannel, R. (1943) Les fossiles vivants des cavernes. L'Avenir de la Science, (n. s.), (1): 1–321, 12 pls. Gallimard, Paris.

5 Vandel, A. (1964) Biospéologie—La Biologie des Animaux Cavernicoles. XVIII+619 pp. Gauthier-Villars, Paris.

6 Vejdovský, F. (1882) Thierische Organismen der Brunnenwässer von Prag. 70 pp., 8 pls. Selbstverlag, Prag.

7 Spandl, H. (1926) Die Tierwelt der unterirdischen Gewässer. Speläologische Monographien, **11**: I–XII+1–235. Speläologisches Institut, Wien.

8 Chappuis, P. A. (1927) Die Tierwelt der unterirdischen Gewässer. Die Binnengewässer, **3**: i–v+1–175, 4 pls. E. Schweizerbart, Stuttgart.

9 Delamare Deboutteville, C. (1960) Biologie des Eaux Souterraines Littorales et Continentales. 740 pp., 2 folders. Hermann, Paris.

10 Ijima, I. and Kaburaki, T. (1916) Preliminary descriptions of some Japanese triclads. Annot. zool. japon., **9**: 153–171.

11 Uéno, S.-I. (1957) Blind aquatic beetles of Japan, with some accounts of the fauna of Japanese subterranean waters. Arch. Hydrobiol., Stuttgart, **53**: 250–296, 3 pls.

12 Uéno, S.-I. (1985) The derivation of terrestrial cave animals. Zool. Sci., Tokyo, **2**: 852.

13 Uéno, S.-I. (1986) Recent development of biospeology in Japan. J. speleol. Soc. Japan, 10th Anniv. spec. Vol., 17–23. (In Japanese, with English summary.)

14 Uéno, S.-I. (1971) The fauna of the lava caves around Mt. Fuji-san. I. Introductory and historical notes. Bull. natn. Sci. Mus., Tokyo, **14**: 201–218, pls. 1–4.

15 Torii, H. S. (1962) A consideration of the distribution of some troglobionts of Japanese caves III. Jpn. J. Zool., **13**: 423–440.

16 Torii, H. S. (1965) Die Lavahöhlen am Fuße des Fudschijama (Japan) und deren Tierwelt. Die Höhle, Wien, **16**: 18–24.

17 Kumano, M. (1943) The animals of the lava caves around Mt. Fuji. Hakubutsugaku Zasshi, Tokyo, **39** (73): 51–56. (In Japanese.)

18 Uéno, S.-I. (1971) Notes on the lava cave fauna of Mt. Fuji. Fuji-san: Results co-op. sci. Surv. Fuji, 752–759. Fuji Kyuko, Tokyo. (In Japanese, with English summary.)

19 Caumartin, V. (1959) Quelques aspects nouveaux de la Microflore des cavernes. Annls. Spéléol., **14**: 147–157, pl. 5.

20 Uéno, S.-I. and Morimoto, Y. (1970) The fauna of the insular lava caves in West Japan. I. General account. Bull. natn. Sci. Mus., Tokyo, **13**: 443–454, 1 folder, 1 pl.

21 Uéno, S.-I. (1977) The fauna of the lava caves in the Far East. Proc. 6th int. Congr. Speleol., Olomouc 1973, **5**: 237–242.

22 Howarth, F. G. (1972) Cavernicoles in lava tubes on the Island of Hawaii. Science, Washington D.C., **175**: 325–326.

23 Howarth, F. G. (1980) The zoogeography of specialized cave animals: a bioclimatic model. Evolution, Lawrence, **34**: 394–406.

24 Uéno, S.-I. (1972) A new anophthalmic *Trechiama* (Coleoptera, Trechinae) found in an old mine of the Izu Peninsula, Central Japan. Annot. zool. japon., **45**: 111–117.

25 Yaginuma, T. (1972) The fauna of the lava caves around Mt. Fuji-san. IX. Araneae (Arachnida). Bull. natn. Sci. Mus., Tokyo, **15**: 267–334.

26 Uéno, S.-I. (1972) A new endogean *Trechiama* (Coleoptera, Trechinae) from the northern side of Central Japan. Annot. zool. japon., **45**: 42–48.

27 Nomura, S. (1959) On the fauna of lime-stone caves in Ôita Prefecture (9). Collect. & Breed., Tokyo, **21**: 174–175, 177. (In Japanese, with English title.)

28 Uéno, S.-I. (1959) A new troglobiontic trechid found in the mines of central Kyushu. Mem. Coll. Sci. Univ. Kyoto, (B), **26**: 285–290.

29 Uéno, S.-I. (1960) A new species-group of the genus *Rakantrechus* (Coleoptera, Harpalidae). Mem. Coll. Sci. Univ. Kyoto, (B), **27**: 37–44.

30 Balazuc, J. (1962) Troglobies des cavités artificielles. Spelunca (4° Sér.), Mém., (2): 104–107.

31 Uéno, S.-I. (1977) The biospeleological importance of non-calcareous caves. Proc. 7th int. speleol. Congr., Sheffield 1977, 407–408.

32 Uéno, S.-I. and Kashima, N. (1978) An Introduction to Speleology. Exploring the Underground World in Darkness. Blue Backs, B-361. 233 pp. Kodansha, Tokyo. (In Japanese.)

33 Uéno, S.-I. (1980) The anophthalmic trechine beetles of the group of *Trechiama ohshimai*. Bull. natn. Sci. Mus., Tokyo, (A), **6**: 195–274.

34 Juberthie, C., Delay, B. and Bouillon, M. (1980) Sur l'existence d'un milieu souterrain superficiel en

zone non calcaire. C. R. Acad. Sci. Paris, (D), **290**: 49–52.

35 Juberthie, C., Delay, B. and Bouillon, M. (1980) Extension du milieu souterrain en zone non-calcaire: Description d'un nouveau milieu et de son peuplement par les Coléoptères troglobies. Mém. Biospéol., **7**: 19–52.

36 Juberthie, C. and Delay, B. (1981) Ecological and biological implications of the existence of a "superficial underground compartment". Proc. 8th int. Congr. Speleol., Bowling Green 1981, **1**: 203–206.

37 Juberthie, C., Bouillon, M. and Delay, B. (1981) Sur l'existence du milieu souterrain superficiel en zone calcaire. Mém. Biospéol., **8**: 77–93.

38 Uéno, S.-I. (1981) New anophthalmic *Trechiama* (Coleoptera, Trechinae) from northern Shikoku, Japan. J. speleol. Soc. Japan, **6**: 11–18.

39 Juberthie, C., Delay, B., Decou, V. and Racoviţă, Gh. (1981) Premières données sur la faune des microespaces du milieu souterrain superficiel de Roumanie. Trav. Inst. Spéol. "Émile Racovitza", **20**: 103–111.

40 Barr, T. C., Jr. and Holsinger, J. R. (1985) Speciation in cave faunas. Ann. Rev. Ecol. Syst., **16**: 313–337.

41 Barr, T. C., Jr. (1986) An eyeless subterranean beetle (*Pseudanophthalmus*) from a Kentucky coal mine (Coleoptera: Carabidae: Trechinae). Psyche, Cambridge, **93**: 47–50.

42 Howarth, F. G. (1973) The cavernicolous fauna of Hawaiian lava tubes, 1. Introduction. Pacif. Ins., **15**: 139–151.

43 Peck, S. B. (1977) Recent studies on the invertebrate fauna and ecology of sub-tropical and tropical American caves. Proc. 6th int. Congr. Speleol., Olomouc 1973, **5**: 185–194.

44 Fennah, R. G. (1973) The cavernicolous fauna of Hawaiian lava tubes, 4. Two new blind *Oliarus* (Fulgoroidea: Cixiidae). Pacif. Ins., **15**: 181–184.

45 Gagné, W. C. and Howarth, F. G. (1975) The cavernicolous fauna of Hawaiian lava tubes, 7. Emesinae or thread-legged bugs (Heteroptera: Reduviidae). Pacif. Ins., **16**: 415–426.

46 Asahina, S. (1974) The cavernicolous cockroaches of the Ryukyu Islands. Mem. natn. Sci. Mus., Tokyo, (7): 145–156, pl. 18.

47 Yosii, R. (1956) Monographie zur Höhlencollembolen Japans. Contr. biol. Lab. Kyoto Univ., (3): i+1–109+*1–22,* 50 pls.

48 Uéno, S.-I. (1985) The group of *Trechiama oni* (Coleoptera, Trechinae) —its distribution and differentiation—. Mem. natn. Sci. Mus., Tokyo, (18): 163–198.

49 Barr, T. C., Jr. (1968) Cave ecology and the evolution of troglobites. Evol. Biol., New York, **2**: 35–102.

50 Sbordoni, V. (1982) Advances in speciation of cave animals. Mechanisms of Speciation, ed. by C. Barigozzi, 219–240. Alan R. Liss, New York.

51 Juberthie, C. (1983) Le milieu souterrain: étendue et composition. Mém. Biospéol., **10**: 17–65.

52 Juberthie, C. (1984) La colonisation du milieu souterrain; théories et modèles, relations avec la spéciation et l'évolution souterraine. Mém. Biospéol., **11**: 65–102.

ZOOLOGICAL SCIENCE 4: 607–611 (1987)

Frequency Block in the Giant Axons of a Sabellid Worm, *Pseudopotamilla occelata*

Takashiro Higuchi, Hiroyuki Nakamura[1], Katsuhiko Sawauchi[1] and Hiroshi Okumura[1,2]

Department of General Education, Higashi-Nippon-Gakuen University, Ishikari-Tobetsu, Hokkaido 061–02, and [1]Akkeshi Marine Biological Station, Hokkaido University, Akkeshi, Hokkaido 088–11, Japan

ABSTRACT—In the sabellid worm, *Pseudopotamilla occelata,* there is a graded decrease in the capacity for the conduction of action potentials along the giant axons. Failure of a faithful conduction of successive action potentials under a constant frequency stimulation, namely, the frequency block, occurs near the mid-body position. All action potentials are eventually blocked in an area posterior to this. These phenomena require neither a special geometry of the axon nor the effects of the accumulation of much preceding axon activity. It is likely that there are gradual changes in the properties of the membrane along the axon. Temporal changes in the properties of the membrane are also involved in the mechanism of the frequency block.

INTRODUCTION

Body contraction in the sabellid worm, *Pseudopotamilla occelata*, during the rapid withdrawal reflex occurs in the anterior half of the body. End-to-end shortening is never observed. This phenomenon is caused by the conduction block of single action potentials in the giant axons, whose activity induces the contractions of segmental longitudinal muscles, at the mid-body [1].

Conduction block of single action potentials in the giant axons of this worm does not require any special geometrical features of the axons. Although isthmus-like structures within the giant axon in the mid-body position (around the 40th body segment) are characteristic, the conduction block occurs in a region anterior to these structures, and does often in a region of uniform geometry [1]. Thus, in this worm, it appears that the low safety factor for conduction is not dependent upon geometrical factors such as a sudden increase in the membrane surface area [2–5] or axonal bifurcation [6–10].

Current injection experiments on the giant axons of this worm have revealed that an area of low safety factor for conduction was relatively large around the apparent site of the conduction block of single action potentials [1]. Following this result, we demonstrate in this papaer a frequency block which develops towards the site of the conduction block of single action potentials, and show that there is an inherent gradient in the ability to conduct action potentials along the giant axons of *Pseudopotamilla occelata*.

MATERIALS AND METHODS

Sabellid worms, *Pseudopotamilla occelata*, were obtained near the Marine Biological Station of Hokkaido University (Akkeshi, Hokkaido) and maintained in an aquarium in circulating sea water (at 10–15°C) before use. Experiments were carried out on semi-dissected worms pinned in a chamber filled with natural sea water. Worms having 100–140 body segments (each segment of ca. 1 mm in length) were selected for experiments. The first nine segments form the head and thorax,

Accepted March 26, 1987
Received February 17, 1987
[2] Present address: Department of Biology, Japan Women's University, Mejirodai, Bunkyo-ku, Tokyo 112, Japan.

and the remainder form the abdomen. The giant axons in the dorsomedial position within the ventral nerve cord were exposed, by removing the body wall on the dorsal surface and overlying digestive tract, from the posterior half of the thorax to the middle of the abdomen. The axons were stimulated extracellularly in the thorax by twin or bursts of rectangular current pulses (50–100 μsec in duration). Action potentials were recorded intracellularly, with KCl-filled glass microelectrodes (10–20 MΩ in resistance), and successively at several points along the giant axon. After the electrophysiological experiments, the specimens were fixed in Bouin's fluid. Serial transverse sections (10 μm in thickness) were cut and stained with hematoxylin-eosin solution and observed under the light microscope.

RESULTS

Previous experiments [1] have shown that the region of the conduction block of single action potentials was effectively restricted to an area between the 20th and the 40th body segments. This experimental result also indicated that the single action potentials could consistently be conducted within the anterior part of the abdomen.

A gradual developement of a frequency block along the giant axon was found to occur in the anterior part of the abdomen. In response to electrical stimulation of giant axons, a train of three action potentials with an interspike interval of 10 msec were elicited (Fig. 1A). Control responses were recorded in the 13th segment. In most cases the frequency block occurred more posterior to the 15th segment. Faithful conduction of all action potentials was observed in the 18th segment. The amplitude of the last (the third) action potential decreased posteriorly. In the 21st segment, a reduced potential, which was due to the electrotonic spread of the blocked action potential, was observed. The second potential was blocked in the 23rd segment, resulting in successful conduction of only the first action potential beyond this point. The remaining action potential (the first action potential) was then blocked in the 30th segment. The geometrical features of this axon, reconstructed from serial sections around the

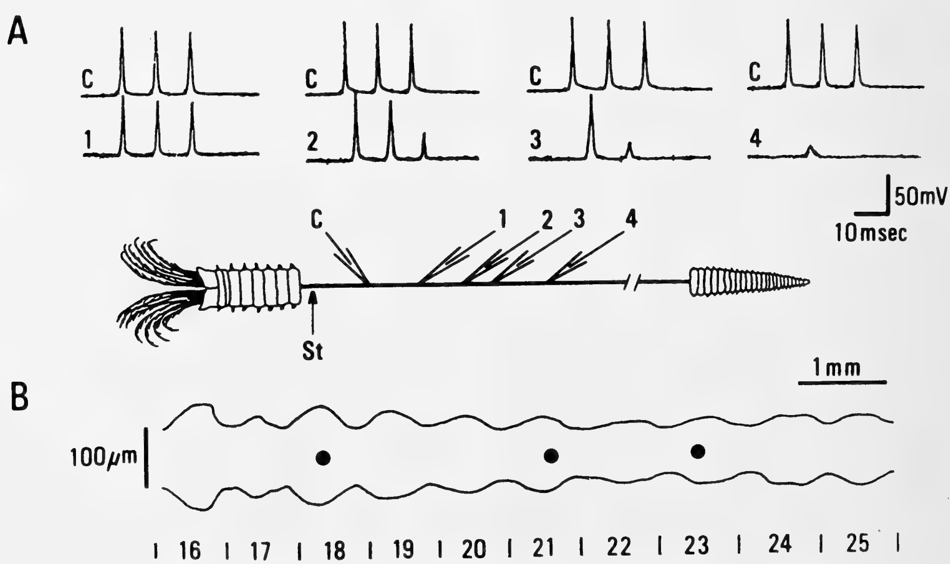

Fig. 1. (A) Frequency block of the giant axon, and schematic representation of the arrangement of external stimulation (St) and intracellular recordings. Control responses (C) were recorded in the 13th segment. Each pair of control response and the response in the 18th (1), 21st (2), 23rd (3) or 30th (4) segment were recorded simultaneously. (B) Giant axon geometry around the region of the frequency block. Recording sites of 1–3 are indicated by closed circles. Numbers below the axon indicate the body segment.

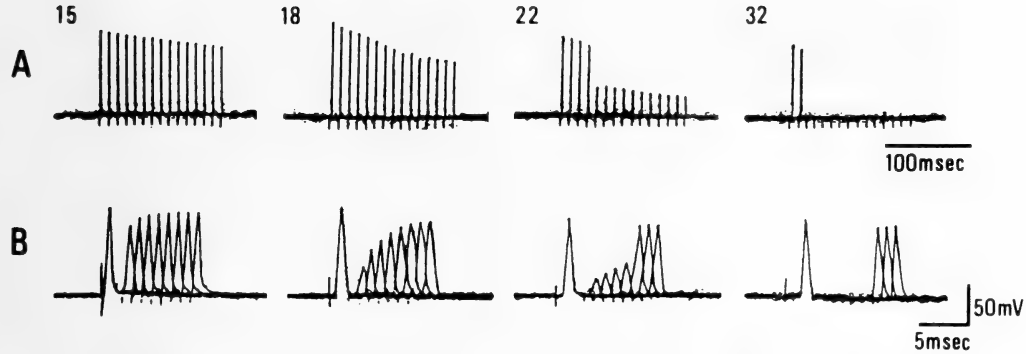

FIG. 2. Train and twin pulse experiments. (A) Responses to a train of pulses with a 10 msec interpulse interval. Numbers indicate the body segment where recordings were performed. (B) Responses to twin pulses with varying intervals in each segment corresponding to those in A.

recording region (Fig. 1B), show only regular repetition of segmental constrictions, which are natural features of the giant axons of sabellid worms [11]. No special geometrical features could be observed which may be responsible for the frequency block.

The responses at four different points along the giant axon to both trains of pulses (15 pulses with an interpulse interval of 10 msec) and twin pulses with varying intervals are shown in Figure. 2. In the 15th segment, the train of 15 action potentials could still be recorded, although a gradual decrease in the amplitude of the action potentials was observed. A refractory period of approximately 2 msec was measured in this segment. In the 18th segment, all of the action potentials in the train were still recorded, but the gradual decrease in the amplitude was enhanced. The twin pulse experiment in this segment showed the prolongation of the relative refractory period. The frequency block clearly occurred at some point between the 18th and the 22nd segment. Only the initial four action potentials were conducted to the 22nd segment. The remaining action potentials were blocked possibly near the 22nd segment since the electrotonically spreading potentials were relatively large. In this region, the refractory period was prolonged to 7 msec. Electrotonic potentials with a delay of 3–6 msec between the two pulses also indicated that the region of refractoriness was near the recording site. No more than the first two action potentials were conducted to the 32nd segment. In this segment there were no electrotonic potentials, indicating that the region of refractoriness was far from the recording microelectrode. Although development of the frequency block increased from the 22nd to the 32nd segment, there was no further prolongation of the refractory period in that region.

In all of the preparations used (20 animals), the frequency block was consistently observed in a region anterior to the apparent site of the conduction block of single action potentials. There was some variation in the development of the frequency block along the axon between animals. When the interpulse interval was 10 msec, the number of action potentials which could be conducted along the axon reduced linearly in some preparations and non-linearly in other ones.

DISCUSSION

On the basis of the results of the present and previous studies [1], the giant axon in the anterior half of *Pseudopotamilla* has been divided into three areas with reference to the capacity for the conduction of action potentials (Fig. 3B). They have been named (1) normal, (2) frequency blocking, and (3) blocking areas. In the normal area, which encompassed the head and thoracic segments to approximately the 15th segment, the giant axons show general characteristics commonly observed in many other axons. On the other hand, all action potentials were completely blocked in

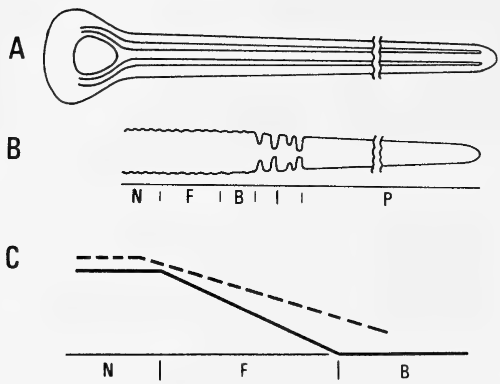

FIG. 3. Schematic representation of the giant axons of *Pseudopotamilla occelata*. (A) Diagram of a pair of giant axons. (B) Enlarged diagram of one of the giant axons in the abdomen. N: normal area. F: frequency blocking area. B: blocking area. I: region of isthmus-like structures. P: giant axon in the posterior half of the body. (C) Schematic representation of a decrease in the capacity for the conduction (solid line) and hypothetical reduction in the density of sodium channels (dotted line) along the giant axon. Note that a gradual decrease in the density of sodium channels occurs from the end of the normal area, and develops continuously over the frequency blocking and the blocking area.

the blocking area, around the 30th segment (20th–40th segment). In the frequency blocking area, namely, the area between the normal and the blocking areas, single action potentials could consistently propagate, but the frequency block of a train of action potentials developed gradually towards the blocking area. Although the boundaries of these areas were not distinct and varied from preparation to preparation, a gradual change in the capacity for conduction along the axon was commonly observed.

One common characteristic of both the conduction block of single action potentials and the frequency block, which has by now been demonstrated in several species, is that the axons have a zone with a special geometry [2, 5–7]. A second common feature is that the conduction block appears following stimulation at high frequency producing an accumulation of extracellular potassium ions [5, 9]. However, on the basis of the histological study, the first possibility must be excluded as a possible mechanism for the frequency block since the block occurs in an area of uniform geometry. The second feature must also be excluded since the occurrence of the frequency block was independent of the accumulation of extracellular potassium ions produced by preceding axon activity.

In the previous paper [1], it was hypothesized that the conduction block of single action potentials might be induced by changes in the properties of the membrane, such as a reduction in the density of sodium channels [12, 13], and that the isthmus-like structures were secondary features associated with a change of membrane structure which was in turn responsible for the change in membrane properties. A gradual development of the frequency block may also be explainable if the density of sodium channels gradually decreases along the axon towards the blocking area (Fig. 3C). This assumes that both the frequency block and the conduction block of single action potentials are induced by the same factors, and that the frequency blocking area and blocking area are continuous, although there is a gradient in the degree of the change in membrane excitability.

It is likely that the mechanism of the frequency block in this animal involves not only a local change in the membrane properties but also a temporal change in membrane excitability. The twin pulse experiment (Fig. 2) showed that the refractory period was 7 msec in both the 22nd and the 32nd segments. However, pulse trains in which the interpulse interval was 10 msec led to the block of action potentials after the first four and the first two action potentials in the 22nd and the 32nd segments respectively. This suggests that there is a cumulative effect of the preceding axon activity on the recovery of the membrane excitability. In a few preparations we observed a restoration of conduction during the spike train, i.e. intermittent conduction block (our unpublished data). Although the data are lacking, it is possible that the effects of the preceding action potentials, other than the accumulation of extracellular potassium ions, may be closely related to the local change of the membrane properties.

This worm has a great capacity for regeneration. When the worm is cut at the mid-body position, the head and thorax regenerate from the cut end of

the posterior half. Giant axons also regenerate to form the giant system in the head and thorax. The responses to current injection across the giant axon membrane during the course of this regeneration are similar to those around the blocking area in the intact animal, namely, rise of the threshold depolarization and fall of the amplitude of the action potential in both cases [1, 14]. It is therefore conceivable that the phenomena observed during this study may be the result of changes in the membrane properties of the giant axons.

ACKNOWLEDGMENT

The authors wish to thank Dr. P. L. Newland, Hokkaido University, for his reading and correcting of the manuscript.

REFERENCES

1 Higuchi, T., Nakamura, H., Sawauchi, K. and Okumura, H. (1986) Withdrawal reflex and conduction block in the giant axon of a sabellid worm (*Pseudopotamilla occelata*). J. Exp. Biol., **126**: 433–444.

2 Parnas, I., Spira, M. E., Werman, R. and Bergmann, F. (1969) Nonhomogeneous conduction in giant axons of the nerve cord of *Periplaneta americana*. J. Exp. Biol., **50**: 635–649.

3 Mellon, D. and Kaars, C. (1974) Role of regional cellular geometry in conduction of excitation along a sensory neuron. J. Neurophysiol., **37**: 1228–1238.

4 Castel, M., Spira, M. E., Parnas, I. and Yarom, Y. (1976) Ultrastructure of region of a low safety factor in inhomogeneous giant axon of the cockroach. J. Neurophysiol., **39**: 900–908.

5 Spira, M. E., Yarom, Y. and Parnas, I. (1976) Modulation of spike frequency by regions of special geometry and by synaptic inputs. J. Neurophysiol., **39**: 882–899.

6 Parnas, I. (1972) Differential block at high frequency of branches of a single axon innervating two muscles. J. Neurophysiol., **39**: 909–923.

7 Grossman, Y., Spira, M. E. and Parnas, I. (1973) Differential flow of information into branches of a single axon. Brain Res., **64**: 379–386.

8 Hatt, H. and Smith, D. O. (1976) Synaptic depression related to presynaptic conduction block. J. Physiol., **259**: 367–393.

9 Smith, D. O. (1980) Mechanisms of action potential propagation failure at site of axon branching. J. Physiol., **301**: 243–259.

10 Smith, D. O. (1980) Morphological aspects of the safety factor for action potential propagation at axon branch points in the crayfish. J. Physiol., **301**: 261–269.

11 Mellon, D., Treherne, J. E., Lane, N. J., Harrison, J. B. and Langley, C. K. (1980) Electrical interactions between the giant axons of a polychaete worm (*Sabella penicillus* L.). J. Exp. Biol., **84**: 119–136.

12 Smith, D. O. (1977) Ultrastructural basis of impulse propagation failure in a nonbranching axon. J. Comp. Neurol., **176**: 659–670.

13 Raymond, S. A. and Lettvin, J. Y. (1978) Aftereffects of activity in peripheral axons as a clue to nervous coding. In "Physiology and Pathology of Axons". Ed. by S. G. Waxman, Raven Press, New York, pp. 203–225.

14 Higuchi, T., Nakamura, H., Okumura, H. and Sawauchi, K. (1983) Propagation of action potentials in giant axons of sabellid worms, *Pseudopotamilla occelata*. Zool. Mag., **92**: 526. (In Japanese)

ZOOLOGICAL SCIENCE 4: 613–620 (1987)

Electron Microscopic Observations of the Alveolar Brush Cell of the Bullfrog

Toshiaki Gomi, Akihiko Kimura, Hiromasa Tsuchiya, Takeshi Hashimoto, Kazuyoshi Higashi[1] and Shozo Sasa[1]

Department of Anatomy, School of Medicine, Toho University, Tokyo 143, and [1]Department of Histology, Kanagawa Dental College, Yokosuka 238, Japan

ABSTRACT—The alveolar brush cells of bullfrogs were observed by scanning electron microscope (SEM) and transmission electron microscope (TEM). SEM showed brush cells with long, thick, unique microvilli of ca. 80–90 in number, existing in concave cavities in the capillary network. TEM showed slightly expanded cylindrical (columnar) brush cells. They were constricted in the area directly below the free cell surface of the lateral side of the cell, resulting in a flask or pear shape. Marked junctional complexes were found in the constricted part of the cells. The microvilli were about 0.8–1.0 μm in length and about 0.15–0.25 μm in diameter. A large number of fine filaments extended from the top of the microvilli to the supranuclear region. Vesicles, and granules which had moderate electron density and various shapes were found from near the free cell surface to the supranuclear region. The most characteristic feature of brush cells is the presence of companion cells, which have osmiophilic lamellated bodies and poorly developed cell organs. From these morphological characteristics, our study suggested the possibility that the alveolar brush cells might have sensory or chemoreceptive functions in spite of the fact that it includes no nerve ending in addition to their absorptive or secretory functions.

INTRODUCTION

Rhodin and Dalhamn [1] were the first to study the rat tracheal epithelium with an electron microscope. They were also the first to report the existence of non-ciliated cells with brush borders consisting of well-developed microvilli, and they named this cell the "brush cell". Thereafter, many researchers reported the existence of brush cells in the respiratory system; these cells have been found in the nasal cavity [2–5], larynx [6], trachea and bronchi [7–14]. However, since Low [15], a large number of authors have studied the ultrastructure of the alveoli [16–21], while there are only a few reports on alveolar brush cells, the third kind of alveolar epithelial cell, other than the epithelial cells of Type I and Type II. Meyrick and Reid [12], Luciano *et al.* [22], Hijiya *et al.* [23] and Scheuermann *et al.* [24] reported on those of rats, Scheuermann and Timmermans [25] on those of red eared turtles, and Gomi [26] on those of striped snakes. We previously reported briefly that alveolar brush cells exist in bullfrogs [27]. We then made a further study in which a scanning electron microscope (SEM) and a transmission electron microscope (TEM) were used to identify brush cells among the alveolar epithelial cells. We observed the ultrastructure of these cells very carefully, and obtained some interesting findings. Here we compare the ultrastructure of the brush cells we observed with that reported in earlier reports, and we include some discussion on their functions.

MATERIALS AND METHODS

Commercially available adult male bullfrogs (*Rana catesbeiana*) were used. Their body weights were about 200–250 g.

Accepted March 16, 1987
Received November 5, 1986

After being rendered unconscious by a blow to the head, they were thoractomized, and the lungs were quickly extracted. The extracted organs were sliced into sections of 1–2 mm square (for TEM) and 5–6 mm square (for SEM), and the specimens were fixed in 2% glutaraldehyde buffered with 0.1M sodium cacodylate (pH 7.4, at 4°C) for 2 hr. At the beginning of pre-fixation, deaeration of the specimens was carried out using an aspirator or an injection syringe. Thereafter, the specimens were rinsed with the same buffer, and post-fixation was achieved with a treatment of 1% osmium tetroxide (at 4°C) for 1.5 hr.

Specimens for SEM After fixation, dehydration with ethanol was done. Specimens were dried to the critical point with isoamyl acetate, and after they were dried thoroughly they were attached to a stub with silver conducting paint for double evaporation using carbon and platinum-paradium. They were examined and photographed at an acceleration voltage of 15 kV using a JXA–50A (JEOL).

Specimens for TEM After fixation, dehydration with ethanol was performed. The specimens were embedded in Epon by ordinary methods, after which they were thinly sectioned with a diamond knife, and this was followed by electron-staining with uranyl acetate and lead citrate. Observation was then carried out with a JEM–100B (JEOL) under an accelerating voltage of 80 kV and with an H–600 (HITACHI) under an accelerating voltage of 75 kV.

RESULTS

Observation by SEM With SEM we could see that brush cells had long and thick microvilli of a unique form (Figs. 1–3), which clearly distinguished them from other epithelial cells. Brush cells existed in the concave cavities of the capillary network. The form of their microvilli was clearly different from that of microvilli of other epithelial cells covering the capillary. Brush cells had about 80–90 microvilli of uneven heights. They were protuberant in the center.

Observation by TEM The alveolar brush cells were slightly expanded cylinders (columnar), and constricted in the area directly below the free cell surface of the lateral side of the cell resulting in a flask or pear shape (Figs. 4–6). The upper part of the cell cytoplasm slightly expanded to the alveolar lumen. As for the form of connection with the adjoining cells, marked junctional complexes existed in the area where cells were constricted directly below the free cell surface (Figs. 4a, 5a, 7 and 8), while lateral interdigitation was found in the lower area (Fig. 6). The microvilli were about 0.8–1.0 μm in length and about 0.15–0.25 μm in diameter. Inside these unique microvilli, numerous fine filaments extended from the top to the supranuclear region of the cytoplasm (Figs. 4a, 5a, 7 and 8). Most bundles of filaments ran, and were markedly developed, along the central long axis of the brush cells.

Vesicles existed in apical cytoplasm between filament bundles near the free cell surface, with their orifices found in the cellular surface between microvilli (Figs. 5a and 7). Vacuoles existed in lateral side of the apical cytoplasm (Fig. 4a). Granules, which had moderate electron density and different forms ranging from almost round to comma-shaped beads, were present in the region extending from the area near the free surface to the supranuclear region (Figs. 4a and 8). Oval to long rod-shaped mitochondria, endoplasmic reticula and free ribosomes and microtubules existed in the supranuclear region (Figs. 4a, 5a, 7 and 8). Immediately above the nucleus, oval lysosomes and Golgi apparatus existed (Figs. 5a and 7). Golgi apparatus was composed of several lamellae, and both edges of the lamellae expanded substantially in some Golgi apparatus (Fig. 7). Glycogen granules were scattered throughout the cytoplasm, except for the area where filaments developed in the top of the central long axis of the brush cells (Figs. 4–6). Microtubules were present at the supranuclear region where filament bundles became sparse (Fig. 4a).

The nucleus occupied about a third to a half of the cell, and was omnipresent in the base of the cytoplasm with a concave, irregular form. The chromatin of the nucleus aggregated in the periphery of the karyoplasm, and usually a nucleolus was observed (Figs. 4–6).

On one side of the adjacent cells, the very thin cytoplasmic processes of the alveolar epithelial

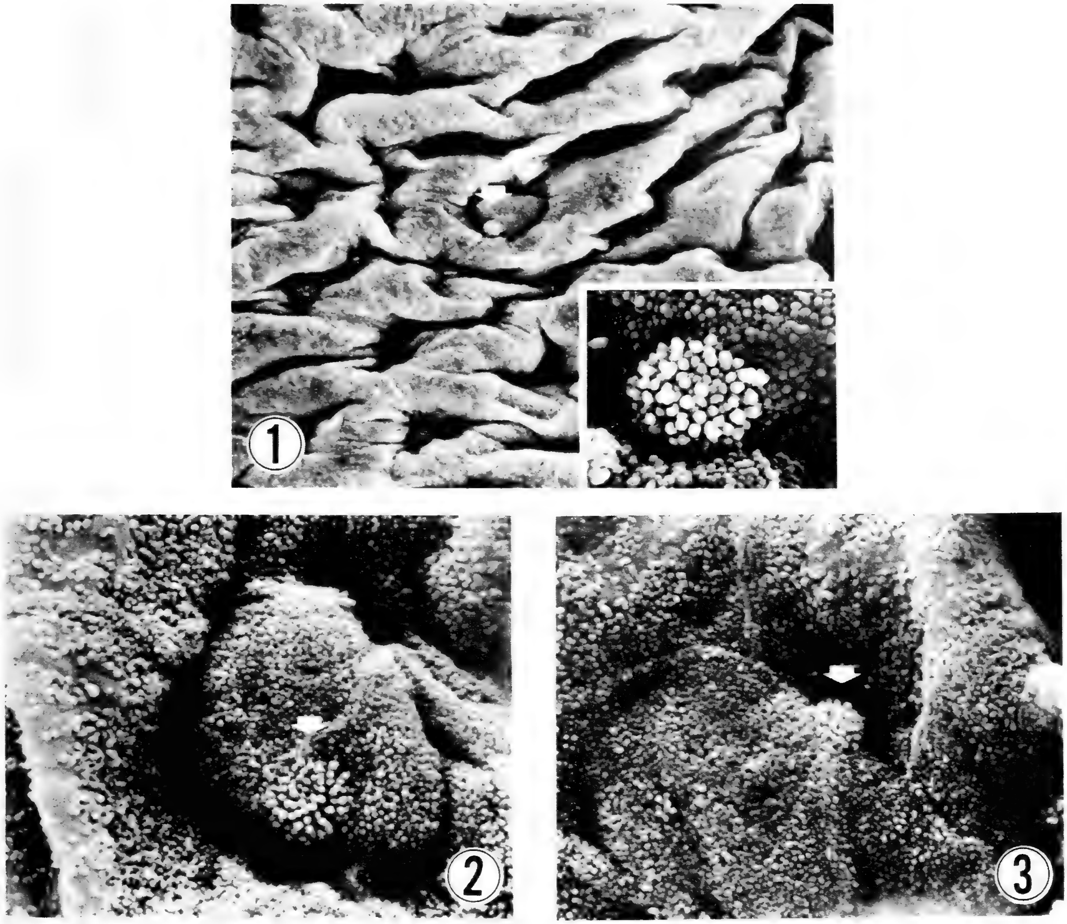

FIGS. 1–3. Alveolar brush cells (arrow) are seen here in concave cavities of the capillary network. Long, thick and unique microvilli, about 80–90 in number, can be seen protruding into the alveolar lumen.
(Inset: High magnification of the alveolar brush cell in Fig. 1).
(Fig. 1 ×1400, Inset ×12200, Fig. 2 ×7000, Fig. 3 ×6000)

cells, which continuously covered the capillary, extended further to cover the upper side of the brush cells. The other side neighbored with a cell that was a slightly expanded, cylinder-shaped cell (companion cell) in most cases (Figs. 4–6). Most of the cytoplasm of this companion cell was occupied by an irregularly-shaped nucleus, and contained only a few osmiophilic lamellated bodies (Figs. 5 and 6). Cell organs were poorly developed, and mitochondria, rough endoplasmic reticula and free ribosomes were scattered in the cytoplasm. Most of these cells extended very thin cytoplasmic processes onto the neighboring capillary (Figs. 4–6). Between companion cells and brush cells, a very small intercellular space existed in most cases (Figs. 4 and 6), but sometimes there was a slightly expanded intercellular space between the lower parts of their bodies (Fig. 5).

DISCUSSION

On the surface of the alveolar brush cell, there were long, thick and peculiar microvilli, and fine filaments characteristically extending from the top of the microvilli to the supranuclear region of the cytoplasm, which phenomenally differentiated it from other alveolar epithelial cells.

As we previously reported, brush cells are oval

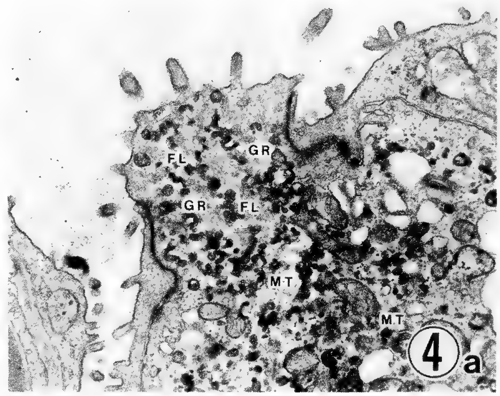

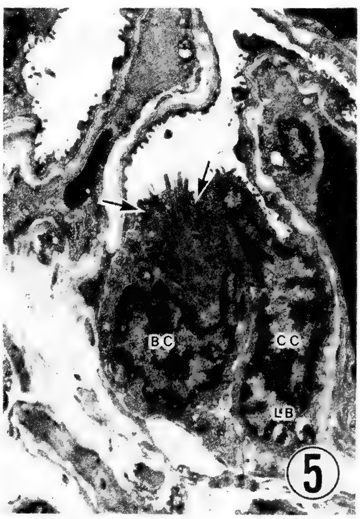

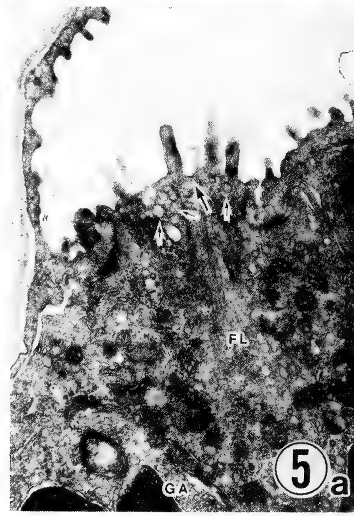

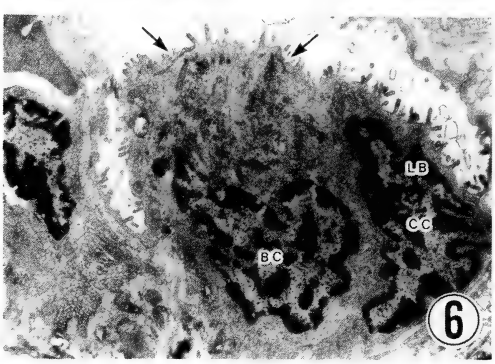

FIGS. 4–6. Flask-shaped (pear-shaped) alveolar brush cells (BC) showing marked junctional complexes (arrows) near the free cell surface. Each alveolar brush cell is accompanied by a companion cell (CC). Most of the companion cells contain only a few osmiophilic lamellated bodies (LB) (5, 6). Sometimes there is a slightly expanded intercellular space (*) between the lower parts of companion cell and brush cell (5).
(Fig. 4 ×3100, Fig. 5 ×3500, Fig. 6 ×5200)

(spherical), expanding toward the both sides of the cell [27]. Besides their oval shape, this study found some brush cells that were slightly expanded and cylinder-shaped. This suggests that the shape of brush cells is not fixed, but varies with function, which would account for the different forms of brush cells that have been found in other organs and tissues. Numerous fine filaments in the long

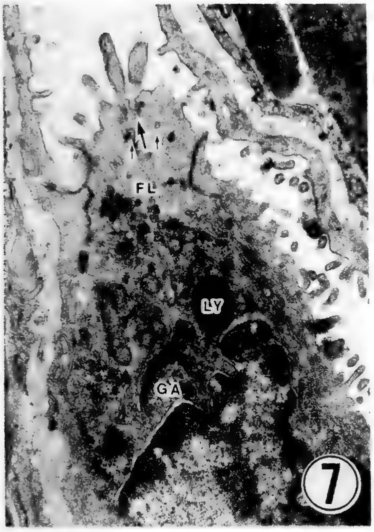

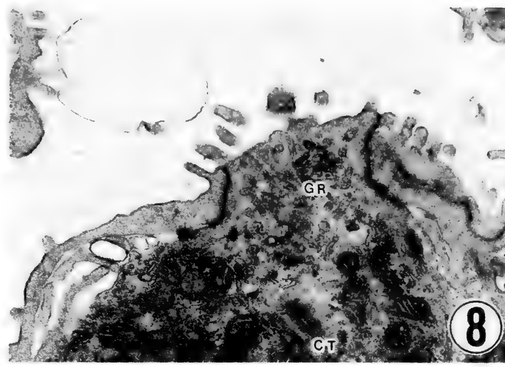

Figs. 4a, 5a, 7 and 8. High magnification of the supranuclear regions of the alveolar brush cells. Figs. 4a, 5a in the facing page are high magnification of Figs. 4 and 5.

Long, thick and unique microvilli can be seen protruding from the cell surface into the alveolar lumen. Inside these unique microvilli, there are numerous fine filaments (FL) extending from the top to the supranuclear region (4a, 5a, 7). In addition to filaments, there are vesicles (arrows) (5a, 7), vacuoles (4a), granules (GR) (4a, 8), mitochondria (5a, 7, 8), Golgi apparatus (GA) (5a, 7), endoplasmic reticula, free ribosomes, glycogen granules (7, 8), lysosomes (LY) (7), microtubules (MT) (4a) and a centriole (CT) (8) in the cytoplasm. The orifice of a vesicle can be seen at the cell surface (thick arrow) (5a, 7).
(Fig. 4a ×12200, Fig. 5a ×13600, Fig. 7 ×9800, Fig. 8 ×13600)

axis of the cell shrink depending on the function of the cell, which may change the shape of the entire cell.

On one side of the adjacent cells, the very thin cytoplasmic processes of the alveolar epithelial cells covered the upper side of the brush cells. The other side neighbored with a companion cell. Meyrick and Reid [12] and Hijiya *et al.* [23] reported that brush cells neighbor the very thin cytoplasmic processes of the Type I cell (squamous lining type) and the Type II cell including osmiophilic lamellated bodies (cuboidal secretion type). Most companion cells that were found in this study possessed the features of both Type I and Type II alveolar cells, which are usually found in the alveolar epithelial cells of the lungs of higher animals.

Luciano and Reale [28] reported that there is a very small intercellular space between brush cells and adjacent cells. A number of lateral interdigitations penetrate deep in the adjacent cells to form desmosomes with the adjacent cells, which differs from our result. This study showed that a very small intercellular space existed between most brush cells and companion cells, while there was a somewhat larger intercellular space between the lower parts of some brush cells and their companion cells. Differences in cellular activity may be responsible for the expansion or shrinkage of intercellular space.

Various theories have been proposed concerning the function of brush cells; including that they are undifferentiated cells [6–8, 29], that they have an absorptive function [1, 12, 30], and that they are receptors [11, 12, 23, 31]. Rhodin [7], Spoendlin [6], Leeson [8], and Johnson and Young [29] stated that brush cells are undifferentiated cells. However, we do not think this is true for the following reasons: 1) numerous filament bundles do not exist in undifferentiated cells [28], and 2) cell organs develop poorly in undifferentiated cells. Rhodin and Dalhamn [1] and Meyrick and Reid [12] suggested that brush cells are absorption cells, because they resemble absorption cells of the

intestinal epithelium in that they have a brush border. However, Luciano and Reale [28] negated this when they reported that they did not found any trace of horseradish peroxidase in the cytoplasm of brush cells in the gallbladder to which those substances were applied. On the other hand, Qwarnström and Hand [30] stated that horseradish peroxidase that was applied to the main excretory duct of the submandibular glands of rats was absorbed by brush cells. Our study showed vesicles existing from apical cytoplasm between filament bundles near the free cell surface to the supranuclear region, with their orifices existing on the cellular surface between microvilli. Almost round to comma-shaped bead granules that had moderate electron density existed with these vesicles and vacuoles in the supranuclear region. This study did not clearly show whether or not these granules were secretory granules, but the fact that these granules were located only in the supranuclear region, as well as their form, suggest a possibility that they may have an absorptive function, as mentioned above, or a secretory function. Concerning the function of the brush cell, Luciano *et al.* [11] reported that the tracheal brush cell in rats is a chemoreceptor, since it forms an afferent synapse with a dendrite, i.e., the epithelio-neural junctions; they also suggested that the alveolar brush cell might have a chemoreceptive function, since its shape, though the nerve ending had not found, was the same as that of the tracheal brush cell. Meyrick and Reid [12] also support the chemoreceptive function idea. According to Hijiya *et al.* [23], administration of Bleomycin increased the number of alveolar brush cells, and SEM pictures revealed that the microvilli were protruding toward the alveolar duct, not from the top of the cell, but from the side, and that a structure considered to be of unmyelinated nerve fibers was found near the basement membrane of this cell, thus possibly having the activities of a kind of chemoreceptor. According to the observation by Higashi *et al.* [31] of brush cells in the gallbladder, the microvilli and cell organs of the brush cells had a similar shape to the type I taste cell of the taste buds [32], in the base of which basal cells exist. From these results, they suggested that the brush cells act as receptors, and the basal cells have some functional relationship with the brush cells. In the alveolar brush cell of the bullfrog, the form of the microvilli and the presence of filaments, microtubules, granules and vesicles in cytoplasm resemble that of the type I taste cell of the taste buds [33]. Moreover, the alveolar brush cell resembles the fifth cell type of the olfactory epithelium in that the upper part of the cell cytoplasm slightly expanded to the alveolar lumen, unique microvilli protruded from the surface of the cell, a large number of fine filaments extended from the top of the microvilli to the supranuclear region, and it has marked junctional complexes near the free cell surface at the constricted part [34]. Andres [3] reported that sensory nerve fibers entered the olfactory epithelium and synapsed with this fifth cell type.

This study suggested that the alveolar brush cells in bullfrogs might have sensory or chemoreceptive functions besides their absorptive and secretory functions already described. Long, thick microvilli of a unique form protruded from the cell surface, and the upper part of the cytoplasm expanded to the alveolar lumen. These observations, combined with the report published by Hijiya *et al.* [23] in which SEM pictures revealed that the microvilli were protruding toward the alveolar duct, not from the top of the cell but rather from the side, suggest that the brush cells are shaped so as to be convenient to receive any information from a substance that may be present in the alveolar lumen, for example, a stream of air that reached the alveoli. Furthermore, the fact that the shape of the alveolar brush cell is quite similar to that of tracheal brush cell, which possesses epithelio-neural junctions, and that the shape of the alveolar brush cell is entirely similar to the type I cell of taste buds and to the fifth cell type of the olfactory epithelium suggest the possibility that the alveolar brush cells might have sensory or chemoreceptive functions in spite of the fact that it includes no nerve ending; it also suggested that there is a close relationship between the brush cells and their adjacent cells, which in turn suggests that the brush cells may receive information on the secretion of osmiophilic lamellated bodies that acts as a surfactant involved in the essence of gas exchange and the lamination of the blood-air barrier (expan-

sion of alveoli).

A summary of this paper was presented at the 11th International Congress on Electron Microscopy.

REFERENCES

1 Rhodin, J. and Dalhamn, T. (1956) Electron microscopy of the tracheal ciliated mucosa in rat. Z. Zellforsch., **44**: 345–412.

2 Brettschneider, H. (1958) Elektronenmikroskopische Untersuchungen an der Nasenschleimhaut. Anat. Anz., **105**: 194–204.

3 Andres, K. H. (1969) Der olfaktorische Saum der Katze. Z. Zellforsch., **96**: 250–274.

4 Adams, D. R. and Wiekamp, M. D. (1984) The canine vomeronasal organ. J. Anat., **138**: 771–787.

5 Adams, D. R. (1986) The bovine vomeronasal organ. Arch. Histol. Japon., **49**: 211–225.

6 Spoendlin, H. (1959) Elektronenmikroskopische Untersuchungen am respiratorischen Epithel der oberen Luftwege. Pract. Oto-rhino-laryngol., **21**: 484–498.

7 Rhodin, J. (1959) Ultrastructure of the tracheal ciliated mucosa in rat and man. Ann. Otol. Rhinol. Laryngol., **68**: 964–974.

8 Leeson, T. S. (1961) The development of the trachea in the rabbit, with particular reference to its fine structure. Anat. Anz., **110** (Suppl.): 214–223.

9 Watson, J. H. L. and Brinkman, G. L. (1964) Electron microscopy of the epithelial cells of normal and bronchitic human bronchus. Am. Rev. Resp. Dis., **90**: 851–866.

10 Konrádová, V. (1966) The ultrastructure of the tracheal epithelium in rabbit. Folia Morphol., **14**: 210–214.

11 Luciano, L., Reale, E. and Ruska, H. (1968) Über eine „chemorezeptive" Sinneszelle in der Trachea der Ratte. Z. Zellforsch., **85**: 350–375.

12 Meyrick, B. and Reid, L. (1968) The alveolar brush cell in rat lung – a third pneumonocyte. J. Ultrastruct. Res., **23**: 71–80.

13 Jeffery, P. K. and Reid, L. (1975) New observations of rat airway epithelium: a quantitative and electron microscopic study. J. Anat., **120**: 295–320.

14 Allan, E. M. (1978) The ultrastructure of the brush cell in bovine lung. Res. Vet. Sci., **25**: 314–317.

15 Low, F. N. (1952) Electron microscopy of the rat lung. Anat. Rec., **113**: 437–450.

16 Scheuermann, D. W. and De Groodt-Lasseel, M. H. A. (1981) Comparative ultrastructural exploration of the alveoli in the normal lung. Verh. Anat. Ges., **75**: 307–341.

17 Gomi, T. (1983) Electron microscopic studies on the alveolar epithelial cells of the striped snake (*Elaphe quadrivirgata*). J. Med. Soc. Toho, **29**: 577–593.

18 Hashimoto, T., Gomi, T., Kimura, A. and Tsuchiya, H. (1983) Light and electron microscopic study of the lung of the giant salamander, *Megalobateracus japonicus davidanus*. J. Med. Soc. Toho, **29**: 724–733.

19 Bartels, H. and Welsch, U. (1984) Freeze-fracture study of the turtle lung: 2. Rod-shaped particles in the plasma membrane of a mitochondria-rich pneumocyte in *Pseudemys (Chrysemys) scripta*. Cell Tissue Res., **236**: 453–457.

20 Kimura, A., Gomi, T., Tsuchiya, H., Fujita, H. and Hashimoto, T. (1984) Comparative anatomical observation on the lung blood-air barrier of vertebrates. Acta Anat. Nippon., **59**: 516.

21 Matsumura, H. and Setoguti, T. (1984) Electron microscopic studies of the lung of the salamander, *Hynobius nebulosus*: I. A scanning and transmission electron microscopic observation. Okajimas Folia Anat. Jpn., **61**: 15–31.

22 Luciano, L., Reale, E. and Ruska, H. (1969) Bürstenzellen im Alveolarepithel der Rattenlunge. Z. Zellforsch., **95**: 198–201.

23 Hijiya, K., Okada, Y. and Tankawa, H. (1977) Ultrastructural study of the alveolar brush cell. J. Electron Microsc., **26**: 321–329.

24 Scheuermann, D. W., Van Meir, F. and De Groodt-Lasseel, M. H. A. (1980) Ultrastructural study of alveolar brush cells in normal and terbutaline treated rats. Electron Microscopy (Proc.), **2**: 138–139.

25 Scheuermann, D. W. and Timmermans, J. P. (1982) Peculiar observations with the scanning electron microscope in the pulmonary epithelium of the fresh water turtle. Abst. 10th Int. Congr. Electron Microsc., Hamburg, No. 3, 597–598.

26 Gomi, T. (1982) Electron microscopic studies on the alveolar brush cell of the striped snake (*Elaphe quadrivirgata*). J. Med. Soc. Toho, **29**: 481–489.

27 Gomi, T., Murakami, K. and Kitazawa, Y. (1980) The lung epithelium of lower vertebrates. J. Med. Soc. Toho, **27**: 674–680.

28 Luciano, L. and Reale, E. (1979) A new morphological aspect of the brush cells of the mouse gallbladder epithelium. Cell Tissue Res., **201**: 37–44.

29 Johnson, F. R. and Young, B. A. (1968) Undifferentiated cells in gastric mucosa. J. Anat., **102**: 541–551.

30 Qwarnström, E. E. and Hand, A. R. (1982) A light and electron microscopic study of the distribution and effects of water-soluble radiographic contrast medium after retrograde infusion into the rat submandibular gland. Arch. Oral Biol., **27**: 117–127.

31 Higashi, K., Takano, K. and Sasa, S. (1982) Ultrastructural aspects of the brush cell of the mouse

gallbladder. Zool. Mag. (Tokyo), **91**: 158–164.

32 Takeda, M. and Hoshino, T. (1975) Fine structure of taste buds in the rat. Arch. Histol. Japon., **37**: 395–413.

33 Fujimoto, S. (1984) In "Human Histology, vol. 7. Sense Organs: Gustatory Organ". Ed. by E. Yamada and H. Hashimoto, Asakura Shoten, Tokyo, pp. 43–64.

34 Okano, M. (1984) In "Human Histology, vol. 7. Sense Organs: Olfactory Organ". Ed. by E. Yamada and H. Hashimoto, Asakura Shoten, Tokyo, pp. 1–31.

ZOOLOGICAL SCIENCE 4: 621–626 (1987)

Karyotype Analysis of Two Japanese Salamanders, *Hynobius nebulosus* (Schlegel) and *Hynobius dunni* Tago, by Means of C-banding[1]

Chikako Ikebe, Ken-ichi Aoki[2] and Sei-ichi Kohno[2]

Department of Biology, Faculty of General Education, and [2]Department of Biology, Faculty of Science, Toho University, Funabashi, Chiba 274, Japan

ABSTRACT—The karyotypes of *Hynobius nebulosus* from Nagasaki-shi (Nagasaki Prefecture) and Minabe-cho (Wakayama Pref.), and those of *H. dunni* from Takamori-cho (Kumamoto Pref.) and Oita-shi (Oita Pref.) were analyzed by the conventional Giemsa-staining and C-banding methods using their embryos. Intraspecific chromosome variations were detected in chromosomes 1, 5, 8, 10 and 13 of *H. nebulosus* and in chromosome 20 of *H. dunni*. C-banding patterns of 17 identified chromosome pairs (chromosomes 1–13 and 4 pairs of small-sized chromosomes) of *H. nebulosus* and *H. dunni* were similar, except for the variant bands.

INTRODUCTION

The two pond type hynobiid salamanders, *Hynobius nebulosus* and *Hynobius dunni*, are considered to be phylogenetically close because of similar morphological characters in egg-capsules, larvae and adults [1–3]. *H. nebulosus* is distributed widely in the western part of Japan including the Kinki, Chugoku, Shikoku and Kyushu districts, while *H. dunni* is distributed only in the Kyushu district [1–3].

Chromosome analyses of *H. nebulosus* and *H. dunni* have been performed by Makino [4, 5] and Sato [6] in the 1930s, using the testis-sectioning method, and the diploid chromosome numbers of both species were reported as 56. Recently, the conventional Giemsa-stained karyotypes of *H. nebulosus* and *H. dunni* were described by Morescalchi [7] and Morescalchi *et al.* [8], though the shape of small-sized chromosomes of their karyotypes was still not clear. The conventional Giemsa-stained karyotypes of *H. nebulosus* from the Chugoku and Kinki districts were also described by Ikebe and Kohno [9], and those from other sites in the Chugoku district by Seto *et al.* [10]. However, the banded karyotype has been reported only in *H. nebulosus* from Nagasaki-shi by Kuro-o *et al.* using R-banding method [11].

In the present paper, the karyotypes of *H. nebulosus* and *H. dunni* from two localities were analyzed by the conventional Giemsa-staining and C-banding methods using embryos. Intraspecific chromosome variations were detected in both species.

MATERIALS AND METHODS

Materials used in this study were late tail-bud stage embryos. The specimens of *H. nebulosus* were collected in Nagasaki-shi (Nagasaki Prefecture in the Kyushu district) and Minabe-cho (Wakayama Pref. in the Kinki). Those of *H. dunni* were collected in Takamori-cho (Kumamoto Pref. in the Kyushu) and Oita-shi (Oita Pref. in the Kyushu). Detailed data from these two species are summarized in Table 1.

The methods of chromosome preparation have been described previously [9, 12], and the C-banding was accomplished by the BSG method [13].

The chromosomes were designated following the nomenclature for centromeric position on

Accepted March 31, 1987
Received January 20, 1987

[1] This paper corresponds to "Cytogenetic Studies of Hynobiidae (Urodela). VII".

Table 1. Sites and years of collection of *Hynobius nebulosus* and *Hynobius dunni*, and numbers of egg-capsules, metaphases and embryos analyzed

Species	Collection site & year	No. of egg-capsules	No. of metaphases / No. of embryos		
			Giemsa	C-banding	Total
H. nebulosus	Nagasaki-shi '82, '83, '84	4	19 / 9	43 / 16	62 / 23
	Minabe-cho '85	2	24 / 7	37 / 7	61 / 10
H. dunni	Takamori-cho '80, '82	5	16 / 9	——	16 / 9
	Oita-shi '86	1	34 / 9	20 / 4	54 / 9

chromosomes by Levan *et al.* [14].

RESULTS

Two conventional Giemsa-stained karyotypes of *H. nebulosus* from Nagasaki-shi and Minabe-cho are shown in Figures 1 and 3, respectively. A C-banded karyotype of *H. nebulosus* from Nagasaki-shi is shown in Figure 2. All embryos analyzed from two localities had 56 chromosomes as a diploid set, in agreement with previous data [4, 6–10].

Some structural chromosome variations were detected in the karyotypes from the two localities. The morphology of chromosome 10 from Nagasaki-shi was subtelocentric, while that from Minabe-cho was acrocentric, in agreement with previous data of *H. nebulosus* [7, 9, 10]. Secondary constrictions were observed in the long arm of chromosome 1 and the short arm of chromosome 8 in specimens from Nagasaki-shi. In chromosome pairs 1 and 8, all three possible combinations, namely homomorphic pair with the secondary constriction, homomorphic pair without the secondary constriction and heteromorphic pair with and without the secondary constriction, were observed. The secondary constriction in the long arm of chromosome 5 was observed in specimens from Minabe-cho. We observed the chromosome pair 5 only in two combinations, namely heteromorphic pair with and without the secondary constriction and homomorphic pair without the secondary constriction.

Intraspecific variations in chromosomes 5, 8, 10 and 13 of *H. nebulosus* are shown in Figure 4. Chromosome 5 from Minabe-cho specimens and chromosome 8 from Nagasaki-shi specimens had a C-positive band corresponding to the region of the secondary constriction. In the two chromosomes without secondary constrictions, no C-positive band was observed in that region. We could not ascertain whether or not the secondary constriction in the long arm of chromosome 1 from Nagasaki-shi specimens corresponded to the C-positive band. As to chromosome 10, the specimen from Nagasaki-shi showed C-positive bands in the short arm and in the centromere region, and those from Minabe-cho showed C-positive bands in the centromere region and in the proximal region of the long arm. The lengths of the C-positive bands of the specimens from these two localities were almost the same. Chromosome 13 from Minabe-cho specimens had an especially dark C-positive band near the terminal end of the long arm. This band was not detected by the conventional Giemsa-staining method. We observed all three possible combinations in chromosome pair 13 by C-banding analysis, namely homomorphic pair with this band, homomorphic pair without the band and heteromorphic pair with and without the band.

A conventional Giemsa-stained karyotype and a C-banded karyotype of *H. dunni* from Oita-shi are shown in Figures 5 and 6. All embryos analyzed from the two localities had a diploid set of 56 chromosomes, which corresponded to previous data [5–8]. Six of 9 embryos from Takamori-cho and 4 of 9 embryos from Oita-shi had the same karyotype shown in Figure 5. The remaining 3 embryos from Takamori-cho

FIG. 1. A conventional Giemsa stained karyotype of *Hynobius nebulosus* from Nagasaki-shi.

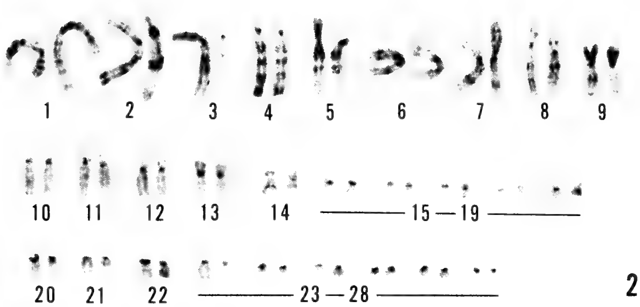

FIG. 2. A C-banded karyotype of *Hynobius nebulosus* from Nagasaki-shi.

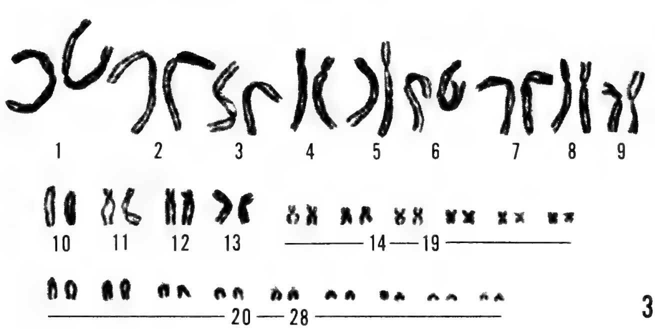

FIG. 3. A conventional Giemsa-stained karyotype of *Hynobius nebulosus* from Minabe-cho.

and 5 embryos from Oita-shi had a submetacentric marker chromosome which was slightly smaller than the midium-sized chromosomes (10–13), and one acrocentric small-sized chromosome was absent. We consider the karyotype which has no marker chromosome as

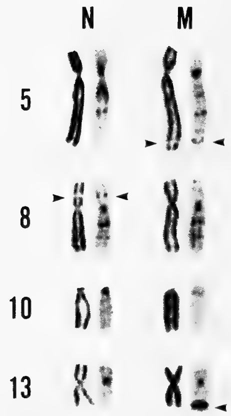

FIG. 4. Chromosomes 5, 8, 10 and 13 of *Hynobius nebulosus* from Nagasaki-shi (N) and Minabe-cho (M). The left hand chromosomes from specimens in each locality were stained by the conventional Giemsa-staining method and the right hand chromosomes by C-banding method. Arrowheads indicate the secondary constrictions and the variant bands.

typical of *H. dunni.* C-banding analyses of 4 embryos from Oita-shi revealed that this marker chromosome originated in chromosome 20. As shown in Figure 7, one of chromosomes 20 is absent and the long arm of the marker chromosome had the same C-banding pattern as chromosome 20. The centromere region of the marker chromosome stained darker than that of chromosome 20.

Comparing the karyotype of *H. dunni* with that of *H. nebulosus*, we detected some interspecific variations. The secondary constriction was not detected in *H. dunni.* The small-sized chromosomes (14–28) consisted of 5 meta- or submetacentric and 10 acrocentric pairs in *H. dunni*, while there were 6 meta- or submeta-centric and 9 acrocentric pairs in *H. nebulosus*. Chromosome 10 of *H. dunni* was subtelocentric as was that of *H. nebulosus* from Nagasaki-shi.

C-banding patterns of all the 17 identified chromosome pairs (chromosomes 1–13 and 4 pairs of small-sized chromosomes) of *H. dunni* were similar to those of *H. nebulosus*, except for the variant bands on chromosomes 5, 8 and 13 of *H. nebulosus*.

DISCUSSION

This study indicates that intraspecific chromosome variations exist in both *H. nebulosus* and *H. dunni.* These variations are related to the C-positive region. The difference in chromosome 10 of *H. nebulosus* between Nagasaki-shi specimen and Minabe-cho specimen revealed to be pericentric inversion of the C-positive segment. The variant bands on chromosomes 5, 8 and 13 of *H. nebulosus* were C-positive. The variant bands on chromosomes 5 and 8 corresponded to the secondary constrictions; however, that on chromosome 13 did not correspond to the secondary constitution and stained especially intensely by C-banding method. Thus, the variant band on chromosome 13 may be different from those on chromosomes 5 and 8 at the molecular level. The short arm of the marker chromosome of *H. dunni* stained as deeply as the C-positive region of the long arm of chromosome 20. The short arm of the marker chromosome might have arisen by tandem duplication of the C-positive region in chromosome 20.

It suggests that the C-positive region contains constitutive heterochromatin and scarcely includes structural genes. As all embryos used in this study developed normally to the late tail-bud stage as judged by their external morphology, C-positive variant bands of these two species apparently did not affect their development.

By comparing the karyotypes of *H. nebulosus* in the present study with those of *H. nebulosus* previously published [9, 10], a difference in the constitution of the small-sized chromosomes (14–28) was detected. We observed 6 meta- or submeta-centric and 9 acrocentric pairs in the present study, as opposed to 7 meta- or submeta-centric and 8 acrocentric pairs [9] and 5 meta- or submeta-centric and 10 acrocentric pairs [10] in previous studies. In *H. nebulosus* from Nara-shi (Nara Pref. in the Kinki), Izumo-shi (Shimane Pref. in the Chugoku) and Sakaide-shi (Kagawa Pref. in the Shikoku), we observed the same constitution of the small-sized chromosomes as that in *H. nebulosus* from Nagasaki-shi and Minabe-cho in the present study (Ikebe *et al.*, unpublished data). Therefore, the typical con-

FIG. 5. A conventional Giemsa-stained karyotype of *Hynobius dunni* from Oita-shi.

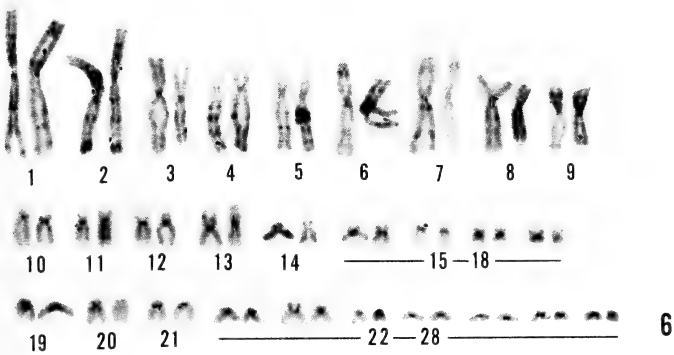

FIG. 6. A C-banded karyotype of *Hynobius dunni* from Oita-shi.

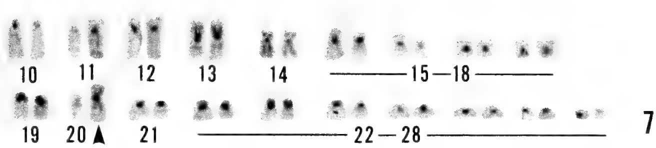

FIG. 7. A partial C-banded karyotype of *Hynobius dunni* from Oita-shi. An arrowhead indicates the marker chromosome.

stitution of the small-sized chromosomes in *H. nebulosus* may be 6 meta- or submeta-centric and 9 acrocentric pairs.

The C-banding patterns of chromosomes 1–13 (except for the variant bands) of *H. nebulosus* and *H. dunni* were compared with the previously published C-banding data of *H. tokyoensis* from Yokose (Saitama Pref.), Yokosuka (Kanagawa Pref.) and Chosei (Chiba Pref.) [15]. *H. tokyoensis* has sometimes been regarded as subspecies of *H. nebulosus* [2, 3]. While the C-banding patterns of *H. nebulosus* and *H. dunni* were similar, those of *H. tokyoensis* differed from the patterns in these two species in chromosomes 2 and 10. The differences in chromosomes 2 and 10 between *H. nebulosus* and *H. tokyoensis* were already detected by R-banding analysis [11]. On the basis of the karyological studies, the phylogenetic rela-

tionships between *H. nebulosus* and *H. dunni* appear to be closer than those between *H. nebulosus* and *H. tokyoensis*.

ACKNOWLEDGMENTS

We are grateful to the following people for their help in collecting specimens: Mr. M. Itoh, Mr. M. Miyamoto, Mr. K. Numata and Mr. S. Tamai. This study was supported by a Grant-in-Aid from the Ministry of Education, Science and Culture, Japan (No. 58540484).

REFERENCES

1 Sato, I. (1943) A Monograph on the Japanese Urodeles, Nippon Shuppan-sha, Osaka, pp. 41–84. (In Japanese)

2 Nakamura, K. and Ueno, S.-I. (1963) Japanese Reptiles and Amphibians in Colour, Hoikusha, Osaka, pp. 6–8. (In Japanese)

3 Thorn, R. (1968) Les Salamandres d'Europe, d 'Asie et d 'Afrique du Nord, Paul Lechevalier, Paris, pp. 43–49, 58–59. (In French)

4 Makino, S. (1934) The chromosomes of *Hynobius leechii* and *H. nebulosus*. Trans. Sapporo Nat. Hist. Soc., **13**: 351–354.

5 Makino, S. (1935) The chromosomes of *Hynobius dunni* and *H. kimurae*. Jpn. J. Genet., **10**: 243–244. (In Japanese, with English Résumé)

6 Sato, I. (1936) On the chromosomes in some hynobiid salamanders from southern Japan. J. Sci. Hiroshima Univ., Ser. B, Div. 1, **4**: 143–154.

7 Morescalchi, A. (1973) Cytotaxonomy of the Amphibia. In "Cytotaxonomy and Vertebrate Evolution". Ed. by A. B. Chiarelli and E. Capanna, Academic Press, London & New York, pp. 240–244.

8 Morescalchi, A., Odierna, G. and Olmo, E. (1979) Karyology of the primitive salamanders, family Hynobiidae. Experientia, **35**: 1434–1435.

9 Ikebe, C. and Kohno, S. (1979) Cytogenetic studies of Hynobiidae (Urodela). I. Karyotypes of *Hynobius nebulosus nebulosus* (Schlegel) and *Hynobius nebulosus tokyoensis* Tago. Proc. Japan Acad., **55B**: 436–440.

10 Seto, T., Utsunomiya, Y. and Utsunomiya, T. (1983) Karyotypes of two representative species of hynobiid salamanders, *Hynobius nebulosus* (Schlegel) and *Hynobius naevius* (Schlegel). Proc. Japan Acad., **59B**: 231–235.

11 Kuro-o, M., Ikebe, C. and Kohno, S. (1987) Cytogenetic studies of Hynobiidae (Urodela). VI. R-banding patterns in five pond-type *Hynobius* from Korea and Japan. Cytogenet. Cell Genet., **44**: 69–75.

12 Kohno, S., Kuro-o, M., Ikebe, C., Katakura, R., Izumisawa, Y., Yamamoto, T., Lee, H. Y. and Yang, S. Y. (1987) Banding karyotype of Korean salamander: *Hynobius leechii* Boulenger. Zool. Sci., **4**: 81–86.

13 Sumner, A. T. (1972) A simple technique for demonstrating centromeric heterochromatin. Exp. Cell Res., **75**: 304–306.

14 Levan, A., Fredga, K. and Sandberg, A. A. (1964) Nomenclature for centromeric position on chromosomes. Hereditas, **52**: 201–220.

15 Kohno, S., Ohhashi, T. and Ikebe, C. (1983) Cytogenetic studies of Hynobiidae (Urodela). II. Banding karyotype of *Hynobius tokyoensis* Tago. Proc. Japan Acad. **59B**: 271–275.

ZOOLOGICAL SCIENCE 4: 627–634 (1987)

The Distribution of A and B Blood Group Antigens in Tissues of the Frog, *Rana catesbeiana*

Masayoshi Kaiho and Ikuo Ishiyama

Department of Forensic Medicine, Faculty of Medicine, Tokyo University, Hongo, Tokyo 113, Japan

ABSTRACT—The distribution of blood group antigens A and B in tissues of the frog, *Rana catesbeiana,* was demonstrated by light and electron microscopic immunohistochemistry. Antigen B was localized on blood cells and vascular endothelium throughout the body. This distribution pattern is similar to that of human ABO blood group substances. This was not, however, the case for A antigen, which was specifically localized in the pancreas and adult epidermis. These facts clearly indicate that the expression of antigen A is not the allelomorph to that of antigen B in the bullfrog. In the pancreas, antigen A was confined to the excretory acinar cells. Their secretory granules and plasmalemma showed the reaction.

INTRODUCTION

Glycoproteins and glycolipids are generally present in animal cell membranes, and they extrude carbohydrate chains with a specific sequence on the cell surface [1]. They have been suggested to be closely related to differentiation phenomena because some differentiated cells or tissues can be distinguished based on differential lectin bindings [2]. In addition, marked changes in carbohydrates are known to occur in malignant cells [1]. It has also been reported that the alteration of the cell surface carbohydrates seems to be responsible for changes in cell adhesion properties and cellular interactions.

The antigen on the red cell surface is usually referred to as a blood group when it is possessed by only some individuals of a species. The most popular examples are antigens of the ABO system in man. The biological significance of the blood group antigens is not clearly understood, but it is well known that they are composed of glycoproteins or glycolipids [1]. Although the substances of the human ABO blood group system are found most commonly on erythrocytes, they are also distributed in some other kinds of cells and tissues including the endothelium, mucous epithelium and mucus secretions [3–10]. Furthermore, the antigens of the ABO system are not confined to human bodies, but are widely distributed in other animals [11, 12] and even in some kinds of bacteria [13, 14].

Yada and Yamazawa [15] and Yada *et al.* [16] reported the presence of the antigen B on blood cells and in many other tissues of the frog, *Rana catesbeiana*, by the absorption and mixed agglutination tests. Antigen A was also found to occur in trace amounts in the cloaca and epidermis of the adult bullfrog. These findings suggest the possibility that A and B antigens are simultaneously present in different cells or tissues in the same body.

This is not the case in human bodies because, phenotypes A and B are in the relation of allelomorphs in man and the A and/or B antigens are normally expressed in the same site in the body. Although the histological localization of the blood group antigens in human and rodent tissues has been described by light and electron microscopic immunohistochemistry [3, 5–10, 12, 17], no such study has been made with regard to frog tissue. In the present study, we examined the immunohistochemical demonstration of A and B antigens in bullfrog tissues to investigate the above-mentioned possibility.

Accepted February 27, 1987
Received October 31, 1986

MATERIALS AND METHODS

An anuran amphibian bullfrog, *Rana catesbeiana*, was used in this study. Adult male and female frogs and tadpoles (stages 15–23) of this species were obtained in fields near Tokyo. They were pithed and dissected to expose the heart. For conventional light microscopy and immunohistochemistry, the animals were perfused from the heart with a frog Ringer's solution and then with 10% neutralized formalin. The excised organs and tissues were further fixed by immersion in fresh fixative and embedded in paraffin. The A and B antigens were immunohistochemically detected in 4 μm sections according to the method of Nakane and Pierce [18] with some modificatins. Deparaffinized sections were immersed in 0.3% H_2O_2 in methanol and then treated with normal serum (goat or rabbit, diluted 1:10 with phosphate buffered saline (PBS; pH 7.4). Thereafter, they were incubated with anti-A antiserum (rabbit, Takeda) or anti-B antiserum (goat, Takeda), and further reacted with peroxidase-labeled antirabbit IgG (goat, Dako) or anti-goat IgG (rabbit, Dako). Primary antisera and peroxidase-labeled second antibody were diluted 1:5 and 1:25, respectively, with PBS. After the diaminobenzidine (DAB) reaction, some sections were counterstained with hematoxylin. For electron microscopic immunocytochemistry, tissues were fixed by perfusion with a fixative containing 2% paraformaldehyde and 1% glutaraldehyde in 0.1 M cacodylate buffer (pH 7.4) and further immersed in fresh fixative for an hour at 4°C. Subsequently, they were treated with 0.1 M NH_4Cl in PBS [19] for 30 min and then 15 μm thick sections were cut with a Microslicer DTK-1000 (Dosaka EM). The sliced sections of the pancreas were treated with bovine serum albumin (BSA; Sigma) solution (1% in PBS). Thereafter, they were incubated in anti-A antiserum (1:5) for an hour at 20°C and then in protein A-colloidal gold (15 nm) complex solution (1:20 with PBS containing 1% BSA; Janssen Pharmaceuticals) for 20 min. The section of the liver, on the other hand, were treated with normal rabbit serum (1:10) and then in peroxidase labeled antigoat IgG solution (1:20) for 20 min. After rinse, peroxidase was histochemically detected by the DAB reaction. Following thorough washing in PBS, both sections were postfixed in 1% OsO_4 and embedded in an Epon mixture. Thereafter, specimens were processed and observed according to the routine method [20].

In control experiments, anti-A or anti B antisera, which had been adsorbed with human erythrocytes of the respective blood groups, were used in the primary incubation in both light and electron microscopic immunohistochemistry.

RESULTS

Based on the previous data [15, 16] indicating that B antigen is distributed widely in the body of the bullfrog, we first surveyed the distribution of the antigen in the liver, pancreas, kidney, spleen, gallbladder, testis, stomach, heart and skin from adult frogs and tadpoles light microscopically. Consequently, we found that the B antigen is distributed on blood cells and vascular endothelial cells throughout the body (Fig. 1a). Not only the erythrocytes, but all free cells in the blood vessels were positive. In addition, macrophages in the spleen and in intestine of metamorphosing tadpoles (Stages 20–23) and the sperm in adult testes expressed the antigenicity. Light microscopically, only the outer surface of the blood cells appeared to be stained. But in the case of macrophages and endothelial cells, their cell bodies seemed to be stained (Fig. 1a). Kupffer's cells in the liver

Fig. 1. Light micrographs showing the distribution of antigen B in an adult frog liver. Sections were immunohistochemically treated with anti-B antiserum (1a) or with control antiserum (1b) and counterstained with hematoxylin. ×1,200. In Fig. 1a, the DAB reaction product is localized on the blood cell surface (arrowhead) and sinusoidal endothelium. Kupffer's cells are indicated by arrows.

Fig. 2. Electron microscopic demonstration of antigen B in an adult frog liver. The luminal surface (double arrows) of the endothelial cell (E) is more densely stained than the other side (arrow) facing Disse's space. The hepatocyte (H) is negative. Antibodies or reagents were thought to have surely reached the surface of the hepatocytes, because continuity between the external part and Disses's spaces is certain at the fractured site (arrowhead). ×14,000.

contained dense materials regarded as the secondary lysosomes in their cytoplasm (Fig. 1b), but the brown color of the peroxidase reaction could be distinguished from the material, and it was decided that these cells were positive for the B antigen. The liver parenchymal cells lie almost in contact with the positive sinusoidal endothelial cells. Therefore, it was difficult to decide at the

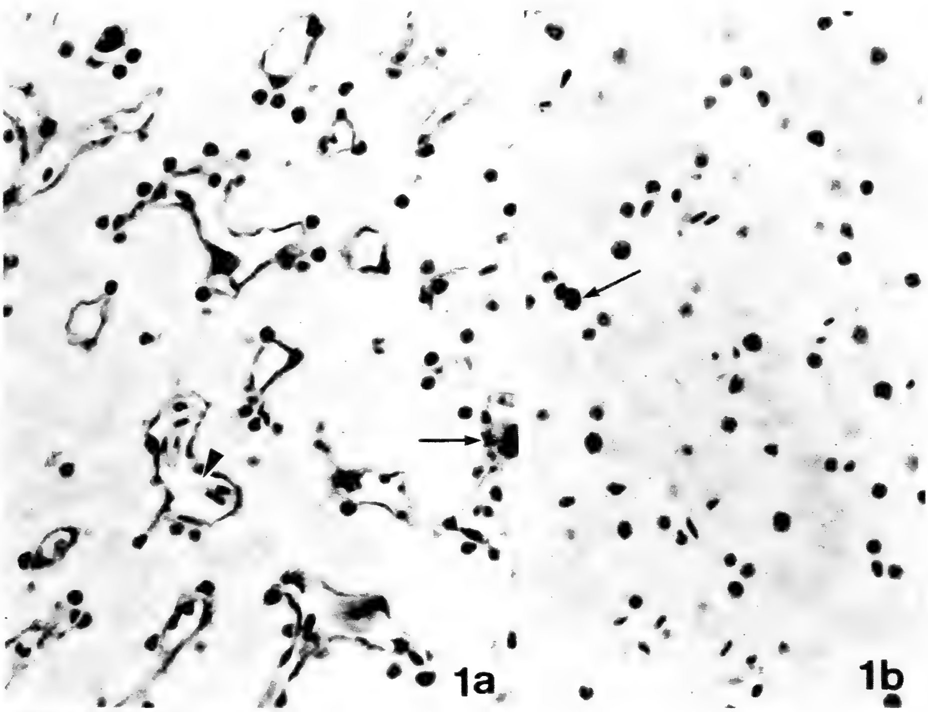

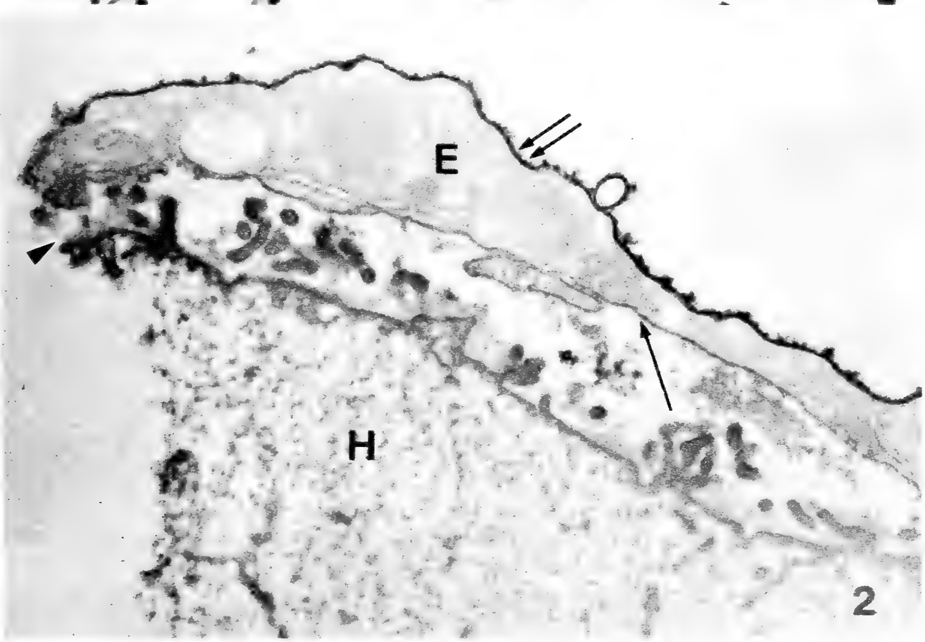

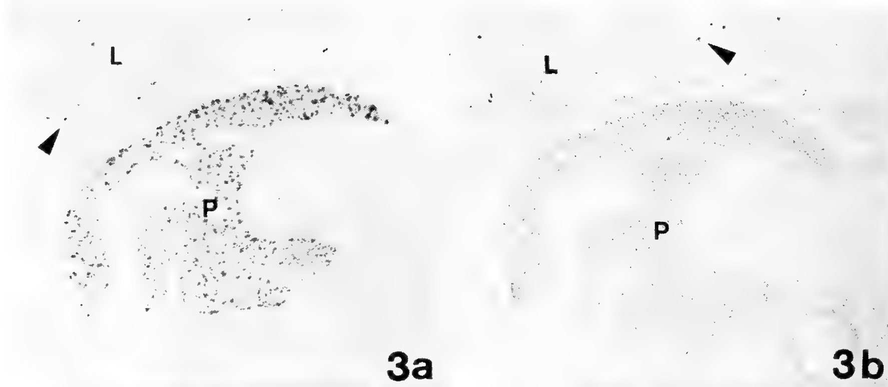

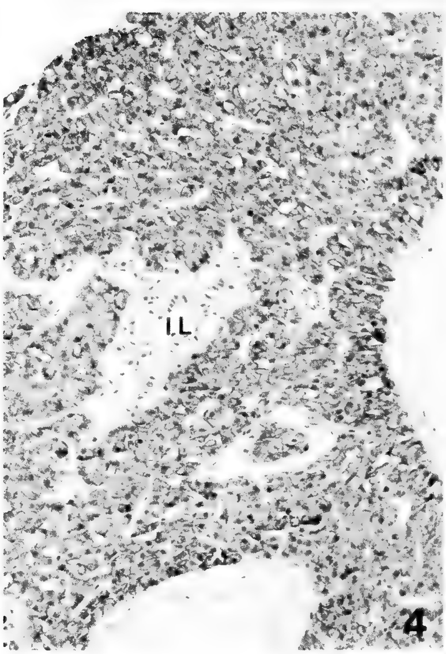

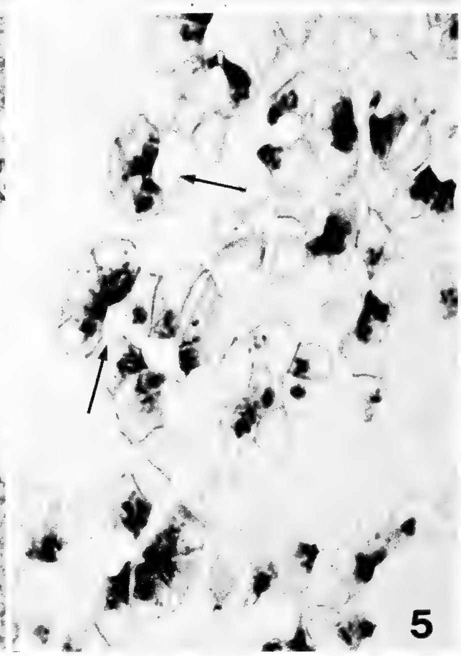

FIG. 3. Light micrographs of serial sections treated with anti-A antiserum (Fig. 3a) and control antiserum (Fig. 3b), respectively. The section in Fig. 3b was counterstained with hematoxylin. Tadpole liver (L) and pancreas (P) are contained in the section, but positive reaction is observed only on the pancreas (Fig. 3a). Dark dots as seen on the liver portion (arrowheads) are secondary lysozomes in Kupffer's cells. ×120.

FIG. 4. A part of a tadpole pancreas. The antigen A was immunohistochemically detected. The section was counterstained with hematoxylin. Most regions except for the islet of Langerhans (IL) and connective tissue area are positively stained. ×300.

FIG. 5. Distribution of antigen A in an adult frog pancreas in larger magnification (×1,200). The reaction is confined to exocrine acinar cells. The surface and secretory granules of the acinar cells are stained. The centroacinar cells (arrows) are not stained.

light microscopic level whether the parenchymal cell surface facing the Disse's space were positive or not. To clarify this problem, we attempted to demonstrate B antigen in the liver electron microscopically. As a result, we confirmed that the hepatocytes were negative (Fig. 2). In addition, the endothelial cell surface facing the Disse's space was more weakly stained than the luminal

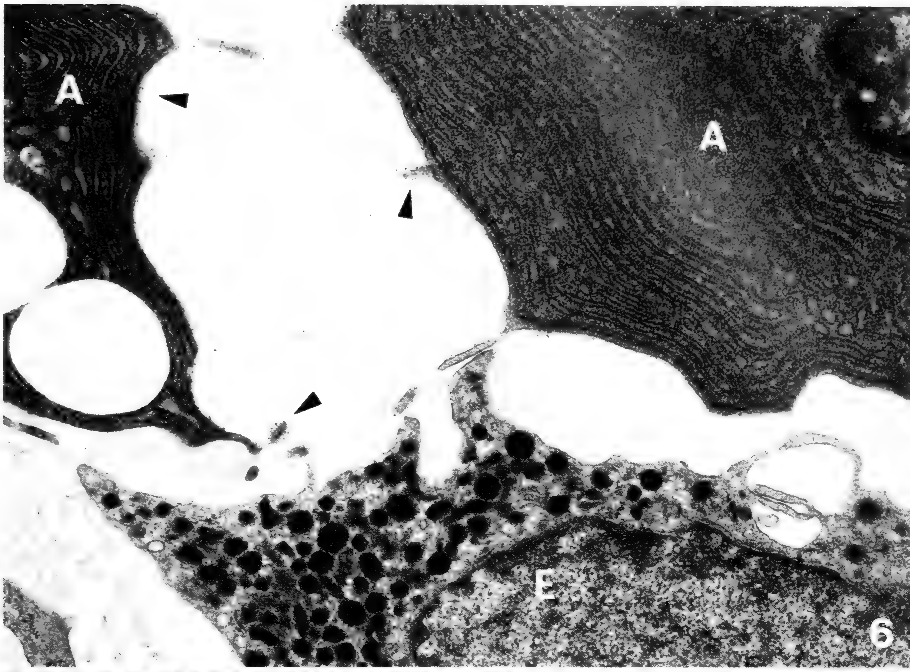

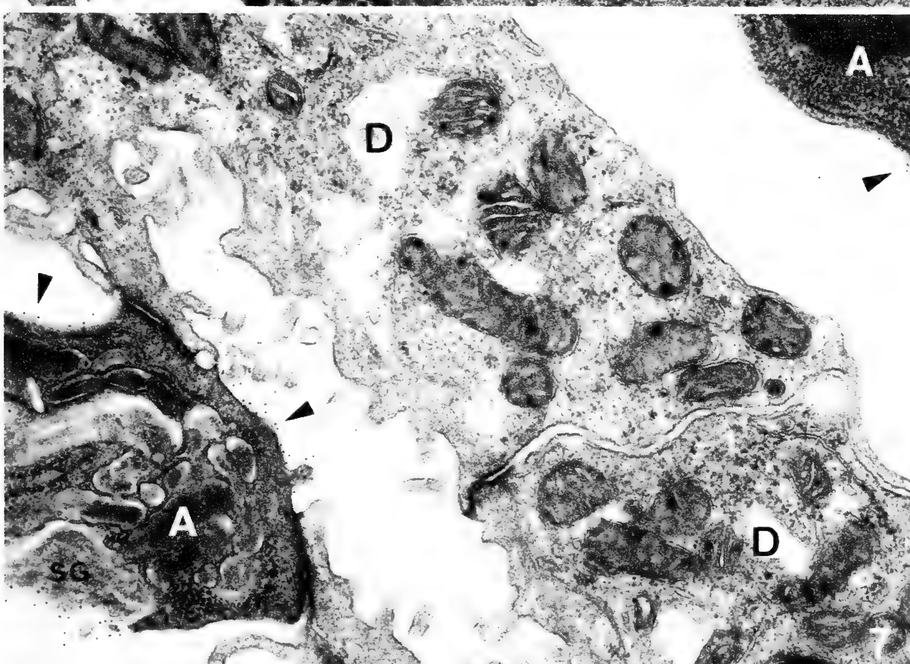

FIG. 6. Electron micrograph to show the localization of antigen A in the adult frog pancreas. Colloidal gold particles (arrowheads) are distributed on the surface of exocrine acinar cells (A), but not on the endocrine cell (E). ×17,000.

FIG. 7. The basal (upper right) and apical (lower left) parts of acinar cells and two duct cells (D) are observed. Colloidal gold particles (arrowheads) are localized on the apical and basolateral surface of acinar cells and on a secretory granule (SG), which are supposed to have been fractured during the slicing procedure of the material. Duct cells are not labeled. ×21,000.

surface. In our method, glutaraldehyde was employed in the fixation procedure, and it was impossible to demonstrate the intracellular location of antigens, possibly because reagents could not penetrate the well fixed plasmalemma.

The same organs or tissues as listed above were also examined for A antigen, and we recognized the positive reaction only in the pancreas (Fig. 3a) and epidermis in adult frogs. In tadpoles also, the pancreas expressed the antigenicity, but the epidermis was negative. (The detailed results concerning the epidermis will be presented in a separate paper.)

In the pancreatic tissues, many kind of cells, such as endocrine cells, exocrine acinar cells, centroacinar cells, duct cells, connective tissue cells etc., are present. Among them, only the exocrine acinar cells were stained, the other cells being negative (Figs. 3–5). The surface of the acinar cells and secretory granules contained in their cytoplasm were ascertained to be positive. We further investigated the localization of A antigen in pancreatic acinar cells electron microscopically. Interestingly, all surface areas involving both the apical and basolateral sides were positive (Figs. 6 and 7). The presence of the antigen in the secretory granules was confirmed by the labeling of fractured ones (Fig. 7). The limited distribution of the antigen in the excretory acinar cells was also confirmed. All the above-presented results concerning the localization of A and B antigens were proved specific by the control experiments, which were performed using antisera absorbed with A or B group blood cells.

DISCUSSION

In the present study, we demonstrated the distribution of blood group A and B antigens in frog tissues by the light and electron microscopic immunohistochemistry. An antigenicity is generally thought to be carried by the antigen determinant part of a molecule. Therefore, it should be emphasized that what we detected were the A and B antigens, and not the blood group substances themselves. According to our results, B antigen was localized on the blood cells and endothelium of blood vessels throughout the body. This pattern of distribution is similar to that of human blood group substances in the human body [4–7, 9, 10]. Based on this distribution similarity between the two species, antigen B in the bullfrog is thought to play still not fully clarified roles comparable to human blood group substances.

So far as we have observed (more than 10 animals were tested), all the tadpole and adult bullfrog individuals had only B antigen on their erythrocytes, in contrast to the fact that A and/or B, or no antigen(s) are expressed on human erythrocytes according to the corresponding blood groups of A, B, AB or O. We have no data at present as for the presence of their own blood group(s) in the frogs.

The results concerning the distribution of A antigen were of much interest. It was confined to the pancreas and adult epidermis. The existence of blood group antigens in the pancreas or epidermis has previously been described by some workers in man and rodents [3, 12, 21]. In the case of the bullfrog, only the exocrine acinar cells were stained with anti-A antiserum in the pancreas, and no other components were positive. Antigen B was also present in the pancreas, but it was localized on the endothelial cells as mentioned above and not on the acinar cells. From these observations, it is clear that A and B antigens are expressed in different sites in the bullfrog body. This fact indicates that A and B antigens in this animal cannot be regarded as allelomorphs to each other. This means that the expression of the A antigen in the frog is possibly a phenomenon with no phylogenetical relation to human blood group substance. In man, A and B substances are known to be synthesized from a common precursor (H substance). Therefore, it seems important to make clear whether the two antigens in the frog are synthesized in a similar way. We are now proceeding our investigation along this line.

The pancreas contains many kinds of cells. The excretory portion is composed of three different types of cells—acinar, centroacinar and duct cells. Among them, only the acinar cells expressed the A antigen, although the three cell types appear to arise from a morphologically

homogeneous cell population in the developing pancreatic rudiment [22]. We further examined the expression of A antigens in pancreatic organogenesis during the early (external gill stage) development of the bullfrog larva and confirmed its simultaneous appearance with the formation of the secretory granules in the acinar cells (unpublished observations). From these findings, the specific expression of the A antigen in the acinar cells appears to be closely related to their differentiation. Similar results indicating that specific saccharides are expressed in the exocrine acinar cells have been presented in the rodent pancreas with the use of lectins [23].

According to the present results, the antigen A-positive sites in acinar cells were the plasmalemma and secretory granules. The plasmalemma of epithelial cells is thought to be divided by tight junctions into two spatially and functionally separate regions comprised of the apical and basolateral zones. Exocytosis in acinar cells normally occurs solely in the former [24]. It was, therefore, surprising that the apical- and basolateral-plasmalemmal zones both reacted with the anti-A antibody.

Maylie-Pfenninger and Jamieson [25] reported similar findings in dispersed rodent pancreatic acinar cells. According to them, lectins labeled both the apical and basolateral zones uniformly. In their experiments, however, artifactitious effects of cell dissociation conditions in the plane of the membrane were considered [26]. In our study, we used intact tissue. Thus, our data indicate that some kind of cell surface saccharides (A antigen determinants) are uniformly distributed on the surface of acinar cells even in the intact pancreas. It is also suggested, at the same time, that the A antigen probably does not participate in the secretion phenomena (exocytosis) of these cells.

From the observation that the central region of the secretory granule was labeled, secretory materials are thought to have a moiety with the A antigenicity. However, we cannot decide whether the limiting membranes of the secretory granules are positive or not, but the possibility cannot be ruled out that the A antigen is synthesized on the cisternal surface of the intracellular membrane system and conveyed to the apical surface via the process of exocytosis of secretory granules [27, 28].

The antigens A are, therefore, considered to be carried by at least two different kinds of molecules, a membrane-bound type and a nonbound type, that are contained in the secretory granules. Why these different molecules with identical antigenicity are coexpressed in the acinar cells is not yet known. With regard to their chemical nature, both of them are thought to be glycoproteins, because glycolipids appear to be extracted by the dehydration process with ethanol [25], and excretory substances in the pancreas are glycoproteins in nature. However, additional studies using proteolytic enzymes such as papain are required to confirm this point conclusively.

Carbohydrate moieties of blood group substances are known to be composed of branched sequences of saccharides and are synthesized stepwise by several glycosyltransferases [29]. An antibody specific to a blood group substance appears to recognize such a sequence. Thus, antibodies are regarded to have higher specificities than lectins, which recognize only one or two terminal saccharides. In practice, we have experienced that a lectin of *Helix promatia* which recognizes the terminal saccharide (GalNAc) of A substance staines wider regions than the anti-A antiserum.

To our knowledge, not very many studies concerning the cell surface molecules using antibodies have been performed [3, 12]. We recommend their use, in addition to lectins, for the detection of cell surface saccharides in the field of cell and developmental biology.

REFERENCES

1 Hakomori, S. (1981) Glycosphingolipids in cellular interaction, differentiation and oncogenesis. Ann. Rev. Biochem., **50**: 733–764.

2 Watanabe, M., Muramatsu, T., Shirane, H. and Ugai, K. (1981) Discrete distribution of binding sites for *Dolichos biflorus* agglutinin (DBA) and for peanut agglutinin (PNA) in mouse organ tissues. J. Histochem. Cytochem., **29**: 779–790.

3 Dabelsteen, E., Vedtofte, P., Hakomori, S. and Young, W. W. (1982) Carbohydrate chains specific for blood group antigens in differentiation of human

oral epithelium. J. Invest. Dermatol., **79**: 3–7.

4 Davison, I. and Stejskal, R. (1972) Tissue antigens A, B and H in health and disease. Haematologia, **6**: 177–184.

5 Glynn, L. E. and Holborow, E. J. (1959) Distribution of blood group substances in human tissues. Br. Med. Bull., **15**: 150–153.

6 Holborow, E. J., Brown, P. C., Glynn. L. E., Hawes, M. D., Gresham, G. A., O'Breien, T. F. and Cooms, R. R. A. (1960) The distribution of the blood group A antigen in human tissues. Br. J. Exp. Pathol., **41**: 430–437.

7 Szulman, A. E. (1960) The histological distribution of blood group substances A and B in man. J. Exp. Med., **111**: 785–800.

8 Szulman, A. E. (1962) The histological distribution of the blood group substances in man as disclosed by immunofluorescence. II. The H antigen and its relation to A and B antigens. J. Exp. Med., **115**: 977–996.

9 Szulman, A. E. (1965) The ABH antigens in human tissues and secretions during embryonal development. J. Histochem. Cytochem., **13**: 752–754.

10 Szulman, A. E. (1971) The histological distribution of the blood group substances in man as disclosed by immunofluorescence. Human Pathol., **2**: 575–585.

11 Joysey, V. C. (1959) The relation between animal and human blood groups. Br. Med. Bull., **15**: 158–164.

12 Reibel, J., Dabelsteen, E., Hakomori, S., Young, W. W. and Mackenzie, I. C. (1984) The distribution of blood group antigens in rodent epithelia. Cell Tissue Res., **237**: 111–116.

13 Iseki, S. (1952) Blood group substances in bacteria. Gumma J. Med. Sci., **1**: 7.

14 Springer, G. F., Williamson, P. and Brandes, W. C. (1961) Blood group activity of gram-negative bacteria. J. Exp. Med., **113**: 1077–1093.

15 Yada, S. and Yamazawa, K. (1962) Distribution of the ABO blood group antigens in various tissues of *Rana catesbeiana*. Jpn. J. Legal Med., **16**: 62–64.

16 Yada, S., Yamazawa, K. and Mori, S. (1962) The ABO blood group antigens in various tissue cells of *Rana catesbeiana* shown by mixed agglutination. Jpn. J. Legal Med., **16**: 233–237.

17 Hinglais, N., Bretton, R., Rouchon, M., Oriol, R. and Bariety, J. (1981) Ultrastructural localization of blood group A antigen in normal human kidneys. J. Ultrastruct. Res., **74**: 34–45.

18 Nakane, P. K. and Pierce, B. (1967) Enzyme-labeled antibodies for the light and electron microscopic localization of tissue antigens. J. Cell. Biol., **33**: 307–318.

19 Roth, J. (1983) The colloidal gold marker system for light and electron microscopic cytochemistry. In "Techniques in Immunocytochemistry, Vol. 2". Ed. by G. R. Bullock and P. Petrusz, Academic Press, London, pp. 217–284.

20 Kaiho, M. Nakamura, T. and Kumegawa, M. (1975) Morphological studies on the synthesis of secretory granules in convoluted tubules of mouse submandibular gland. Anat. Rec., **183**: 405–420.

21 Ito. N., Nishi, K., Nakajima, M., Matsuda, Y., Ishitani, A., Mizumoto, J. and Hirota, T. (1986) Localization of blood group antigens in human pancreas with lectin-horseradish peroxidase conjugates. Acta Histochem. Cytochem., **19**: 205–218.

22 Pictet, R. and Rutter, W. (1972) Development of the embryonic endocrine pancreas. In "Handbook of Physiology, Sect. 7. The Endocrine Pancreas, Vol. 1". Ed. by D. F. Steiner and N. Freinkel, Am. Physiol. Soc., Washington, D. C., pp. 25–66.

23 Maylie-Pfenninger, M. F., Doyle, C. M. and Jamieson, J. D. (1977) Differential lectin receptor appearance during the development of the pancreas. J. Cell Biol., **75**: 67a.

24 Jamieson, J. D. and Palade, G. E. (1977) Production of secretory proteins in animal cells. In "International Cell Biology". Ed. by B. R. Brinkley and K. R. Porter, The Rockefeller University Press, New York, pp. 308–317.

25 Maylie-Pfenninger, M. F. and Jamieson, J. D. (1979) Distribution of cell surface saccharides of pancreatic cells. II Lectin-labeling patterns on mature guinea pig and rat pancreatic cells. J. Cell Biol., **80**: 77–95.

26 Pisam, M. and Ripoche, P. (1976) Redistribution of surface macromolecules in dissociated epithelial cells. J. Cell Biol., **71**: 907–920.

27 Leblond, C. P. and Bennett. G. (1977) Role of the Golgi apparatus in terminal glycosylation. In "International Cell Biology". Ed. by B. R. Brinkley and K. R. Porter, The Rockefeller University Press, New York, pp. 326–336.

28 Pestalozzi, D. M., Hess, M. and Berger, E. G. (1982) Immunohistochemical evidence for cell surface and Golgi localization of galactosyltransferase in human stomach, jejunum, liver and pancreas. J. Histochem. Cytochem., **30**: 1146–1152.

29 Watkins, W. M. (1977) The glycosyltransferase products of the A, B, H and Le genes and their relationship to the structure of the blood group antigens. 5th Int. Convoc. Immunol., Buffalo, N. Y., pp. 134–142.

ZOOLOGICAL SCIENCE 4: 635–639 (1987)

Further Observations on Division Pattern of Binucleate Fish Embryonic Cells

SETSURO MIZUKAMI

Depatment of Biological Science, Yamanashi Gakuin University, Sakaori 2-4-5, Kofu 400, Japan

ABSTRACT—In order to study changes in physiological and cytological properties of embryonic cells during embryogenesis of the killifish, *Oryzias latipes,* blastomeres were dissociated from morula and blastula stage embryos in Yamamoto's saline solution. During the following division of the isolated cells, about 30% of them failed in cytokinesis, resulted in formation of a cell with two individual nuclei or binucleate cell. When further divisions of the binucleate cells were observed, a binucleate cell divided into either four daughter cells with one nucleus each (Type A), three daughter cells, two of them with a nucleus each and a cell with two individual nuclei (Type B), two daughter cells with two individual nuclei each (Type C), or gave rise to a cell with four individual nuclei (Type D). Relationship of the frequency of occurrence of each of these four types with the developmental stages at which the cells were dissociated was examined. The frequency of Type-A division pattern decreased with the progress of developmental time. Instead, the frequency of Type D increased during the period from the late morula to the late blastula stage.

INTRODUCTION

In a series of experiments [1–8], I have been studying formation of binucleate cells in dissociated fish embryonic cells, nuclear fusion in the binucleate cells, and further divisions of the binucleate cells. Blastomeres are easily dissociated in Yamamoto's saline solution from morula and blastula stage embryos of the teleost, *Oryzias latipes* [4]. When isolated embryonic cells are brought into physical contact each other within about 30 sec after dissociation, cell fusion could be induced in more than half of the paired cells [4, 6], resulting in formation of a cell with two nuclei or binucleate cell. Binucleate cell formation is also induced by abortive mitosis, in which normal karyokinesis is followed by incomplete cytokinesis [1, 2, 8]. When I observed further behavior of two nuclei during interphase of the binucleate cells, I discovered a frequent fusion of the two individual nuclei in the cell [2, 3]. In addition, it was noticed that there are four types of division pattern in binulceate cells [5] (cf. Fig. 1).

In this study, I examined whether the frequency of occurrence of four types of division pattern is correlated with developmental stages at which the cells are dissociated. The result clearly showed an existence of a certain correlation between them.

MATERIALS AND METHODS

Developing eggs of the orange-red variety of the medaka, *Oryzias latipes*, were used in this study. Handling of eggs, dechorionation and dissociation of blastomeres were carried out as described previously [4]. After dechorionation, whole blastoderms of the morulae and blastulae were mechanically dissociated into their constituent cells with sharp watchmaker's forceps. The medium used was Yamamoto's saline solution [9]. (0.75% NaCl, 0.02% KCl, 0.02% $CaCl_2$, 0.002% $NaHCO_3$, pH 7.4). Fish blastoderm at these stages consists of cells of the enveloping layer, deep cells and cells of the periblast [10]. Only deep cells were used in this study. The whole procedure of cell dissociation, followed by

Accepted February 16, 1987
Received December 19, 1986

observation of the formation of binucleate cells and further divisions of the induced binucleate cells was performed in a deep depression glass slide with the aid of an inverted microscope, without exchanging the medium, at room temperature (23–28°C). Although in the saline solution dissociated cells showed surface adhesivity to the glass substrate or to each other, the adhesivity of cells was not so great that cells could not be dissociated or handled. Skillful handling allowed nearly complete cell dissociation without injuring cells.

If the isolated cells were brought into physical contact each other within 30 sec after dissociation, cell fusion could be easily induced [3, 4, 6], resulted in formation of binucleate cells. On the other hand, binucleate cells were also formed by abortive cytokinesis [1, 2, 8]. In this study, division pattern of binucleate cells formed by abortive mitosis was exclusively followed.

RESULTS

Blastomeres were dissociated from morulae and blastulae during interphase of divisions (Fig. 1a). Several minutes after dissociation, division of the isolated cells began. The nuclear membrane became invisible (Fig. 1b), followed by reappearance of two nuclei (Fig. 1c). Usually, the karyokinesis is followed by normal cytokinesis. However, in nearly 30% of the cells, the cleavage furrow progressed to some extent but did not completely divided the cell (Fig. 1c). Instead, the furrow was retracted, resulting in formation of a binucleate cell or a cell with two separate nuclei in the protoplasm (Fig. 1d). Sometimes, pseudopodia appeared on the surface of dividing cells and they played important roles in the process of binucleate cell formation [e.g., 2]. When the cleavage furrow advanced to about a half of the cell diameter, hyaline pseudopodia were produced on the surface. The pseudopodia tended to rotate around the cell circumference. During the "circus movement" of pseudopodia, the dividing cell, passing through various shapes, transformed into a binucleate cell. During the following interphase, two individual nuclei frequently closed each other (Fig. 1e), and sometimes they

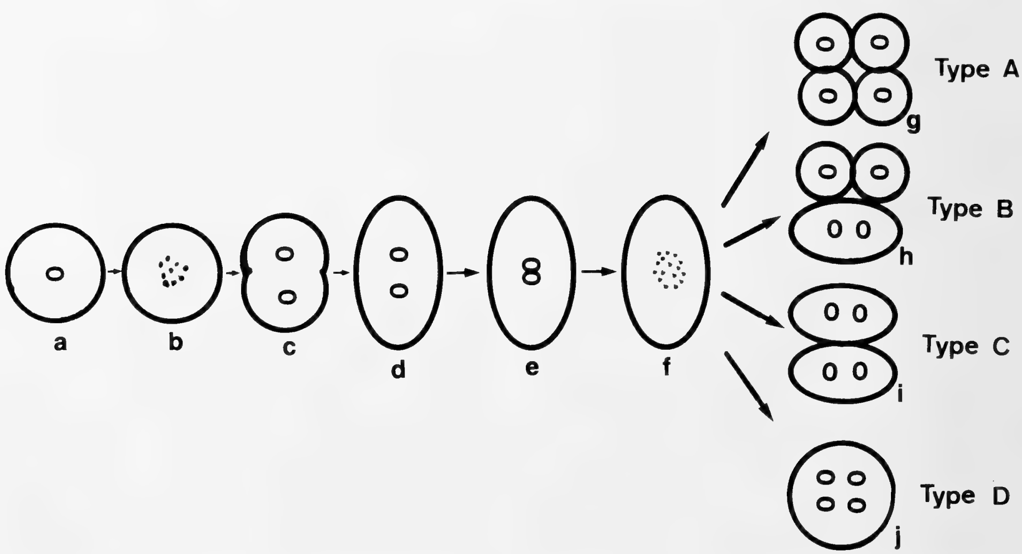

FIG. 1. Schematic representation of formation of a binucleate cell by abortive mitosis from a single dissociated fish-embryonic cell (a–d), and four types of division pattern of the binucleate cells (e–j). In Type A (g), a binucleate cell divides into four daughter cells with one nucleus each. In Type B (h), a binucleate cell divides into three daughter cells, two with one nucleus each and one with two nuclei because of an additional abortive mitosis. In Type C (i), a binucleate cell divides into two daughter cells, each with two nuclei. In Type D (j), a binucleate cell fails in cytokinesis again, but four nuclei appear in the same protoplasm.

coalesced together [3].

About 15 min after formation of binucleate cells, the nuclear membrane disappeared again, starting the next cycle of karyokinesis (Fig. 1f). About several minutes thereafter four individual nuclei became visible. However, the extent of cytokinesis varied, producing four types of daughter cells. As schematically shown in Figure 1, in the first case, a binucleate cell divided at a time into four daughter cells with one nucleus each (I designated this pattern of division as Type A; Fig. 1g, Fig. 2A). In the second case, a binucleate cell divided into three daughter cells, two of which had one nucleus each and the other had two individual nuclei (Type B; Fig. 1h, Fig. 2B). In the third case, a binucleate cell divided into two daughter cells with two individual nuclei each (Type C; Fig. 1i, Fig. 2C). In the fourth case, a binucleate cell failed in cytokinesis again, resulting in production of a cell with four separate nuclei in the protoplasm (Type D; Fig. 1j, Fig. 2D).

In order to examine whether the frequency of occurrence of each of the four division patterns mentioned above is correlated with the developmental stages at which the cells are originated, blastomeres were dissociated from late morulae, early blastulae and late blastulae. At each de-

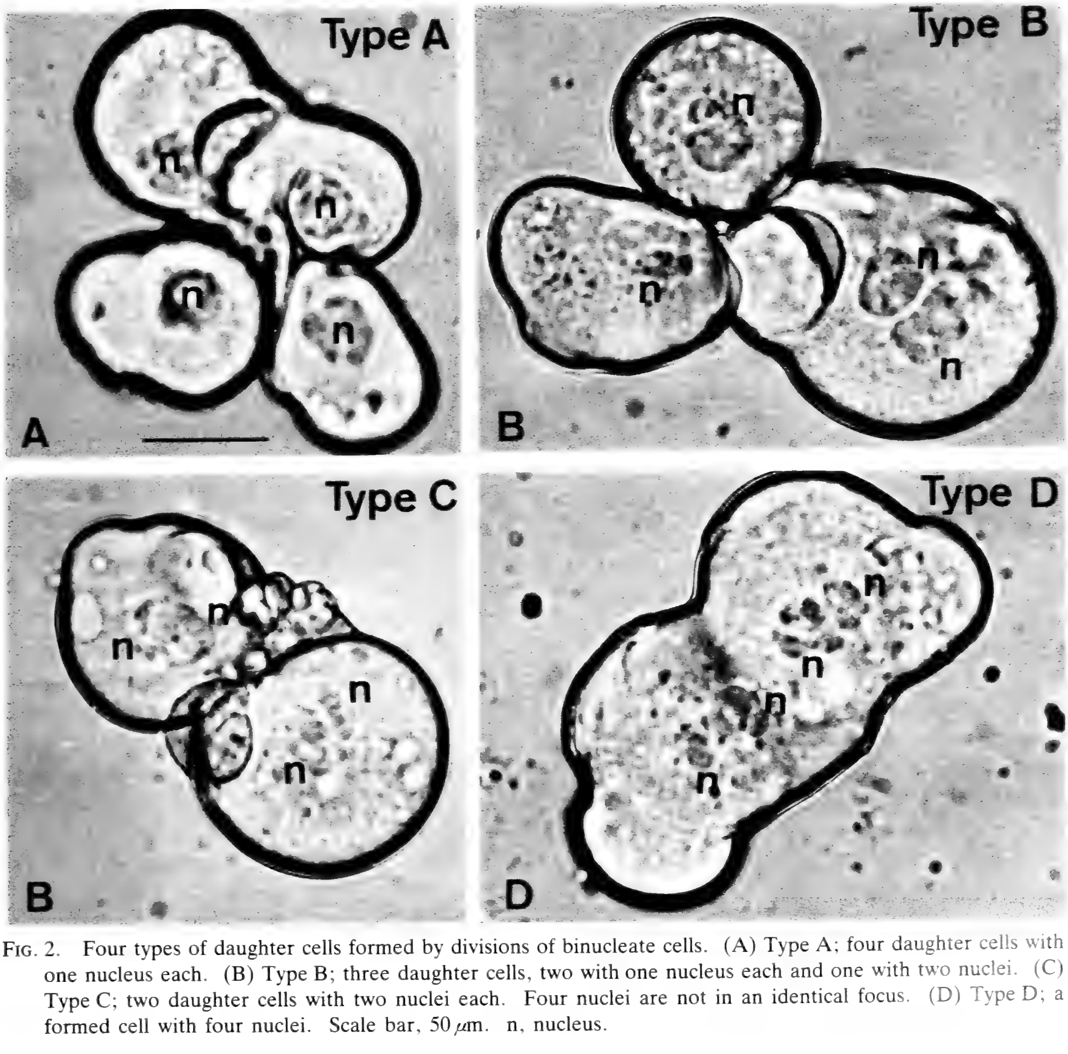

FIG. 2. Four types of daughter cells formed by divisions of binucleate cells. (A) Type A; four daughter cells with one nucleus each. (B) Type B; three daughter cells, two with one nucleus each and one with two nuclei. (C) Type C; two daughter cells with two nuclei each. Four nuclei are not in an identical focus. (D) Type D; a formed cell with four nuclei. Scale bar, 50 μm. n, nucleus.

TABLE 1. Frequency of occurrence of four types of division pattern in binucleate cells originated from three different stages of development

Stages	No. of cells examined	Types of division pattern			
		A	B	C	D
Late morula	221	89 (40.2%)	20 (9.0%)	67 (30.3%)	45 (20.3%)
Early blastula	233	39 (16.7%)	27 (11.6%)	92 (39.5%)	75 (32.1%)
Late blastula	236	25 (10.5%)	22 (9.3%)	71 (30.0%)	118 (50.0%)

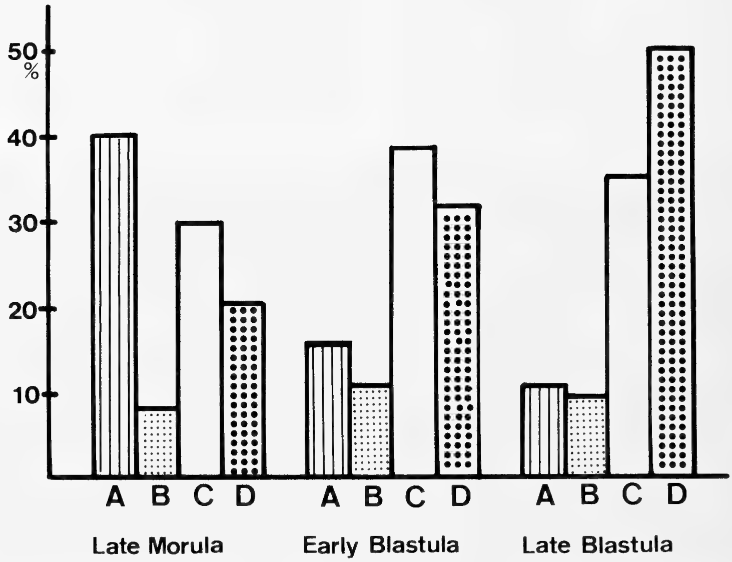

FIG. 3. Frequencies of occurrence of the four types of division pattern of binucleate cells originated from the late morulae, early blastulae and late blastulae, respectively. The ordinate indicates percentages of occurrence of four types of division pattern, while the abscissa shows the three developmental stages at which cells are dissociated. The frequency of Type-A division pattern decreases with the progress of developmental time. Instead, the frequency of Type-D division pattern increases from the late morula stage to the late blastula stage. Frequencies of Type-B and Type-C division patterns are rather constant during the period.

velopmental stage, more than 200 binucleate cells were examined. The results were summarized in Table 1 and Figure 3.

Nearly 40% of binucleate cells formed by abortive mitosis of dissociated cells which originated from the late morulae, showed Type-A division pattern. About 9% and 30% of them showed Type B and Type C pattern, respectively. Type-D division pattern was observed in about 20% of them.

In binucleate cells derived from the early blastulae, the frequency of occurrence of Type A decreased; only 16.7% of them showed this pattern. Instead, the number of Type D pattern increased; nearly 32% of them showed this pattern. This inclination continued as development proceeded. In binucleate cells originated from late blastulae, about half of them showed Type-D division pattern, whereas only 10% of them showed Type A pattern (Table 1, Fig. 3).

The frequencies of Type B and Type C were rather constant during the period examined. Type-B division pattern occurred in nearly 10% of the cells, irrespective of the developmental stages. Nearly 30% of them showed Type C pattern, although the frequency increased to a-

bout 39% at the early blastula stage (Table 1, Fig. 3).

DISCUSSION

As clearly shown in this study, the frequency of occurrence of Type A division pattern decreased with the developmental time. Instead, that of Type D increased as development proceeded. This may be related to development of motile activities of embryonic cells. Kageyama [11] reported that the surface of blastomeres of medaka embryos begins to undulate gently at the early morula stage and that blebs or pseudopodia appear at the early blastula stage. He also reported that at the mid-blastula stage blebs or pseudopodia are found in most of the blastomeres [11]. These surface activities of the cells are thought to be involved in morphogenetic movements of fish embryos [10, 11]. As described previously [2], pseudopodia are sometimes associated with abortive mitosis, resulting in formation of binucleate cells. That is, an increase of the cell-surface activities might bring about the increase of frequency of Type-D division pattern of the binucleate cells, where abortive mitosis took place again. In other words, the increase of Type D pattern may be reflected by changes during embryogenesis of physiological properties of blastomeres, although the detail mechanism is a subject of further investigation.

Polyploidy cells induced by artificial fusion with HVJ usually retained the polyploidy at least during the following several divisions [12]. As discussed in a previous paper [5], in the case of fused nuclei in binucleate fish embryonic cells, the cells recovered the diploidy from the polyploidy-like condition during the following division. This may be one of features of embryonic cells.

ACKNOWLEDGMENTS

I thank Dr. Noriyuki Satoh of Kyoto University for discussion and help in preparing the manuscript.

REFERENCES

1 Mizukami, S. (1971) On the formation of cells with double nucleus in isolated embryonic cells of *Oryzias latipes* (Japanese Medaka). Zool. Mag., **80**: 132–136.

2 Mizukami, S. (1976) Binucleate formation in isolated embryonic cells in the teleost, *Oryzias latipes*. Annot. Zool. Japon., **49**: 120–130.

3 Mizukami, S. (1978) Fusion of dissociated embryonic cells in the teleost, *Oryzias latipes*. III. Nuclear fusion during interphase in the fused cells. Cell Struct. Funct., **3**: 275–277.

4 Mizukami, S. (1979) Fusion of dissociated embryonic cells in the teleost, *Oryzias latipes*. II. On factors affecting the induction of spontaneuos fusion. Zool. Mag., **88**: 17–23.

5 Mizukami, S. (1981) Fusion of dissociated embryonic cells in the teleost, *Oryzias latipes*. V. Divisions of fused nuclei. Zool. Mag., **90**: 251–253.

6 Mizukami, S. and Satoh, N. (1977) Fusion of dissociated fish embryonic cells. J. Embryol. Exp. Morphol., **40**: 265–270.

7 Mizukami, S. and Satoh, N. (1979) Fusion of dissociated embryonic cells in the teleost, *Oryzias latipes*. IV. Changes in cell surface morphology related to this fusion: A scanning electron microscope study. Cell Struct. Funct., **4**: 45–49.

8 Shirakami, K. and Mizukami, S. (1965) Cytoembryological studies of amphibians. V. On the origin, fate, and biological significance of the "doublenucleus". Mem. Fac. Lib. Arts & Ed., Yamanashi Univ., **16**: 133–138.

9 Yamamoto, T. (1975) "Medaka (Killifish)", Biology and Strains. Keigaku Publ. Co., Tokyo.

10 Trinkaus, J. P. (1963) The cellular basis of *Fundulus* epiboly. Adhesivity of blastula and gastrula cells in culture. Dev. Biol., **7**: 513–532.

11 Kageyama, T. (1977) Motility and locomotion of embryonic cells of the medaka, *Oryzias latipes*, during early development. Dev. Growth Differ., **19**: 103–110.

12 Ringertz, N. R. and Savage, R. E. (1976) Cell Hybrids. Academic Press, New York.

ZOOLOGICAL SCIENCE 4: 641–648 (1987)

Speract Binds Exclusively to Sperm Tails and Causes an Electrophoretic Mobility Shift in a Major Sperm Tail Protein of Sea Urchins

Norio Suzuki, Masanori Kurita, Ken-ichi Yoshino and Masaaki Yamaguchi

Noto Marine Laboratory, Kanazawa University, Ogi, Uchiura, Ishikawa 927–05, Japan

ABSTRACT—Intact spermatozoa, sperm heads and sperm tails of the sea urchin *Hemicentrotus pulcherrimus* were incubated with various concentrations of synthetic speract. The results of bioassay of the residual respiration stimulation activity in the supernatant obtained from each incubation mixture showed that more than 99% of speract in the original solution bound to sperm tails as well as intact spermatozoa, but little to sperm heads. Speract caused a mobility change of a major high-molecular weight sperm tail protein in *H. pulcherrimus* or *Anthocidaris crassispina* on SDS-polyacrylamide gels.

INTRODUCTION

It is known that sea urchin egg jelly contains small peptides which affect sperm respiration and motility. These include speract and its derivatives and resact. Speract (Gly-Phe-Asp-Leu-Asn-Gly-Gly-Gly-Val-Gly) is a peptide isolated from the egg jelly of *Hemicentrotus pulcherrimus* and *Strongylocentrotus purpuratus* [1–4]. The egg jelly of the sea urchins, *H. pulcherrimus, Anthocidaris crassispina* and *Lytechinus pictus,* contains several speract derivatives ([Thr^5]-speract, [Ser^5]-speract, [Thr^5, Gln^{10}]-speract and Des-Gly^1-[Thr^5, Gln^{10}]-speract) [1, 5, 6]. Speract and its derivatives not only stimulate sperm respiration and motility but also cause a transient increase in sperm cGMP concentrations [2, 6]. A peptide named resact (Cys-Val-Thr-Gly-Ala-Pro-Gly-Cys-Val-Gly-Gly-Gly-Arg-Leu-NH_2) has been purified from the egg jelly of the sea urchin *Arbacia punctulata* [7, 8]. Resact has recently been shown to be a potent chemoattractant for *A. punctulata* spermatozoa [9]. Like speract, resact increases the cGMP levels, respiration, and motility of *A. punctulata* spermatozoa [7, 8]. Both resact and speract are species specific, although the physiological events measured appear to be the same.

We have shown that exposing *A. punctulata* spermatozoa to resact results in a change in the electrophoretic mobility (from 160,000 to 150,000) of a major sperm membrane protein [8]. This protein has been purified to homogeneity and identified as guanylate cyclase [9–14]. Sea urchin spermatozoa contain extremely high guanylate cyclase activity, and this enzyme is localized in the plasma membrane of the flagellum [15, 16]. Guanylate cyclase in the flagellum membrane has been reported to exist as a phosphorylated glycoprotein [12–14]. At fertilization, the enzyme looses 15 phosphate groups per molecule. The loss of phosphate groups is postulated to cause a shift in the mobility of guanylate cyclase on SDS-polyacrylamide gels from 160,000 daltons to 150,000 daltons [13]. In this paper we report that speract binds exclusively to sperm tails and it induces a mobility change of high molecular weight protein in sperm tails.

Accepted February 19, 1987
Received January 7, 1987

MATERIALS AND METHODS

Experimental animals and chemicals

Sea urchins, *H. pulcherrimus* and *A. crassispina,* were collected at Japan Sea Coast (Tsukumo Bay) near Noto Marine Laboratory. Artificial sea water (ASW) containing 454 mM NaCl, 9.7 mM KCl, 24.9 mM $MgCl_2$, 9.6 mM $CaCl_2$, 27.1 mM $MgSO_4$, 4.4 mM $NaHCO_3$ and 10 mM tris (hydroxymethyl) aminoethane (Tris) or N-(2-acetamido)-2-aminoethane sulfonic acid (ACES) was prepared in the laboratory. Sodium dodecyl sulfate (SDS) (95% pure material), Tris, ACES and, molecular weight standards for gel electrophoresis (MW–SDS–200 kit) were purchased from Sigma Chemical Co. Speract was custom synthesized for us by Peptide Institute, Inc., Osaka.

Gamete collection and determination of respiration rates

Spermatozoa obtaind by intracoelomic injection of 0.5 M KCl were collected "dry" at room temperature and stored on ice at approximately 630 mg (wet weight)/ml until use.

Respiration rates were determined at 20°C using a Yanagimoto PO–100A oxygen consumption recorder in 3.0 ml capacity chamber fitted with a Clark type electrode at 20°C. Dry sperm (18.9 mg wet weight/30 μl) was added to 2.96 ml of ASW (pH 6.8). After recording stable basal respiration rates for several minutes, samples (10 μl) were added. The new respiration rates were determined over the next 3 min. When respiratory stimulation activity of speract solution incubated with intact spermatozoa, sperm heads or sperm tails was determined, 2.97 ml of supernatant obtained by centrifugation of the incubation mixture was added to the chamber and then dry sperm (18.9 mg wet weight/30 μl) was added. The initial rate of sperm respiration was calculated from the tangent to the slope recorded after the onset of experiment. Respiration rates were determined by assuming the solubility of pure O_2 at 1 atm to be 234 nmoles/ml of ASW at 20°C.

Preparation of sperm tails and sperm heads

Spermatozoa (usually 10–15 ml of dry sperm) were diluted with 250 vol of ice cold ASW and centrifuged at 1,000×*g* for 5 min at 4°C. The supernatant was then centrifuged at 5,000×*g* for 30 min at 4°C. The sperm pellet was suspended in 20 vol of ice cold ASW and homogenized in ice bath with a 50 ml Dounce homogenizer fitted with a teflon pestle [17, 18]. About 15–20 strokes were enough to detach the tails from the heads as monitored by phase-contrast microscopy. The homogenate was centrifuged at 1,000×*g* for 30 min at 4°C to pellet the sperm heads. The sperm head fraction was suspended in 100–150 ml of ice cold ASW and centrifuged at 2,000×*g* for 30 min at 4°C. The resultant pellet (sperm heads) was used for experiments. The supernatant containing tails was centrifuged at 6,000×*g* for 30 min at 4°C, and the resultant pellet was suspended in 100–150 ml of ice cold ASW. The suspension was centrifuged at 2,000×*g* for 30 min at 4°C and the supernatant was centrifuged at 6,000×*g* for 30 min at 4°C. The resultant pellet (sperm tails) was used for experiments. Phase-contrast microscopy was used routinely to monitor the extent of contamination by sperm heads in the tail fraction. As shown in Figure 1, contamination by intact spermatozoa in the head and tail fractions and sperm heads in the tail fraction was little.

Other methods

To prepare samples for electrophoresis, spermatozoa (18.9 mg wet weight) were incubated with or without various concentrations of speract in normal ASW. At 1 min, the reaction was stopped by the addition of trichloroacetic acid (final concentration of 10%) and the samples were centrifuged at 10,000×*g* for 30 min at 4°C. The resultant pellet was resuspended in ice cold 90% (v/v) acetone and then centrifuged. The pellet was resuspended in ice cold acetone. After centrifugation, the acetone layer was removed and the pellet was lyophilized. Then, 10% SDS (200–300 μl) was added to the residue, and the mixture was placed in a boiling water bath for 5 min and vortexed vigorously. This procedure was repeated until the solution became clear. For

electrophoresis, 10 μg of sperm protein was added per lane. Electrophoresis on a 5.5% polyacrylamide slab gel was performed in the presence of SDS according to Laemmli [19]. The gel was subsequently stained by the method of Morrissey [20]. The molecular weight of proteins was calculated from the relative mobility of co-electrophoresised standards (myosin, rabbit muscle, Mw 205,000; β-galactosidase, *E. coli*, Mw 116,000; phosphorylase b, rabbit muscle, Mw 97,400; albumin, bovine plasma, Mw 66,000 and albumin, egg, Mw 45,000). Protein was determined by the method of Lowry *et al.* according to Schacterle and Pollack's modification [21, 22].

RESULTS

Respiratory stimulation activity of speract solution incubated with or without intact spermatozoa, sperm heads or sperm tails

As shown in Figure 2 (control), speract half-maximally stimulated *H. pulcherrimus* spermatozoan respiration at 0.2 nM. This is comparable to reported values [2, 4]. Spermatozoa (18.9 mg wet weight) were incubated with various concentrations of speract in 3 ml of ASW (pH 6.8) for 3 min at 20°C and then the mixtures were centrifuged at 10,000$\times g$ for 30 min at 0°C to remove spermatozoa. The resultant supernatant was assayed for the respiration stimulation activity. The supernatant obtained from incubation of spermatozoa with lower than 3.72×10^{-9} M of speract showed the decreased activity for respiration stimulation compared with the corresponding control speract solutions (Fig. 2, intact spermatozoa). Intact speract was recovered from the supernatant. When the resultant sperm pellet was extracted by 70% ethanol, no speract fragments were found in the extracts. Results obtained by the same experiments using sperm heads or sperm tails are shown in Figure 2 (sperm heads and sperm tails). In these experiments, the added amount of sperm heads or sperm tails was equivalent to that of intact spermatozoa based on the amount of protein. A sperm head contained 83% protein of intact spermatozoon. When sperm heads were used for incubation with various concentrations of speract, the resultant supernatant showed almost the same respiration stimulation activity as that of the corresponding control solution while the supernatant obtaind from the incubation mixtures of sperm tails exhibited similar stimulation activity to that with intact spermatozoa. These results

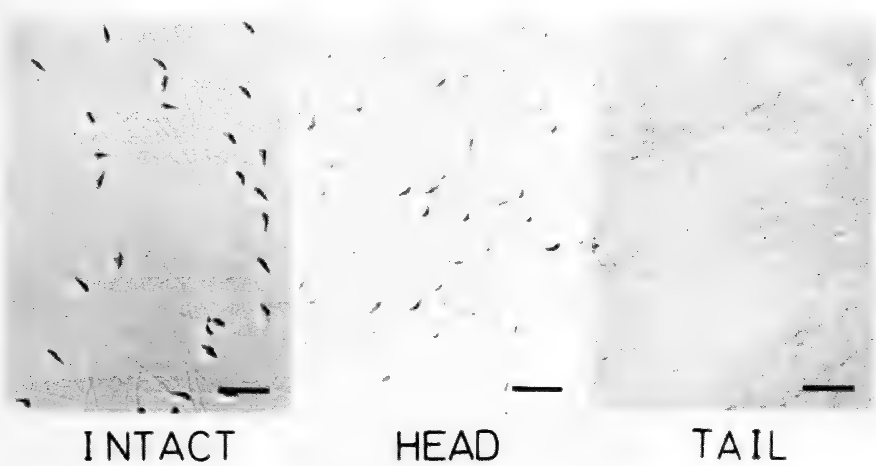

FIG. 1. Phase-contrast microscopic photographs of intact spermatozoa, isolated sperm heads and tails of *H. pulcherrimus*. Bars indicate 100 nm.

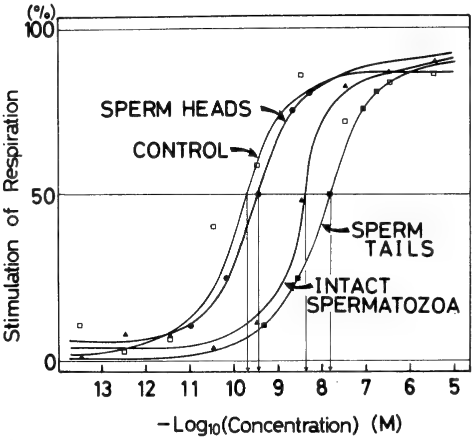

FIG. 2. Respiration stimulating activity of various concentrations of speract before or after incubation with *H. pulcherrimus* spermatozoa, sperm heads or sperm tails. ——□——, supernatant from incubation mixture without intact spermatozoa; ——■——, supernatant from incubation mixture with sperm tails; ——●——, supernatant from incubation mixture with sperm heads; ——▲——, supernatant from incubation mixture with intact spermatozoa.

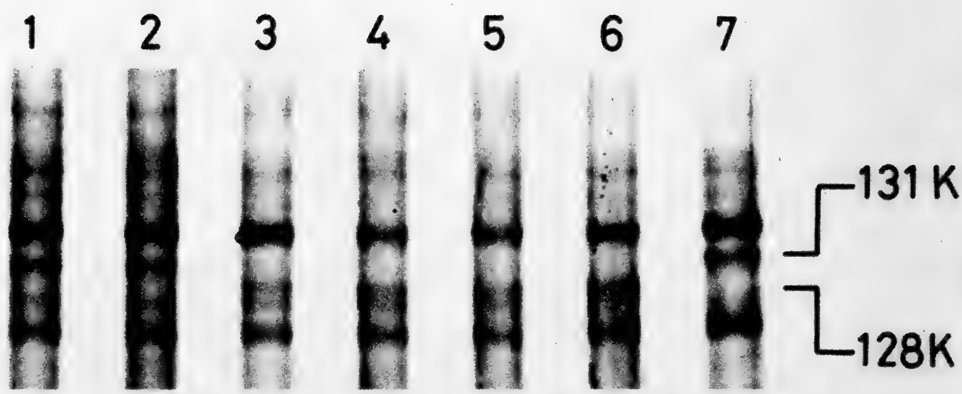

FIG. 3. The effect of various concentrations of speract on the mobility of a high-molecular weight protein of *H. pulcherrimus* spermatozoa. 1, 1.12×10^{-10} M; 2, 1.12×10^{-9} M; 3, 1.12×10^{-8} M; 4, 1.12×10^{-7} M; 5, 1.12×10^{-6} M; 6, 1.12×10^{-5} M; 7, none.

strongly suggest that speract binds exclusively to sperm tails but not or less to sperm heads.

SDS-polyacrylamide gel electrophoresis of sea urchin spermatozoa, sperm heads and sperm tails treated with or without speract

When *H. pulcherrimus* spermatozoa were treated with synthetic speract higher than 1.12×10^{-8} M in normal ASW, one new major protein

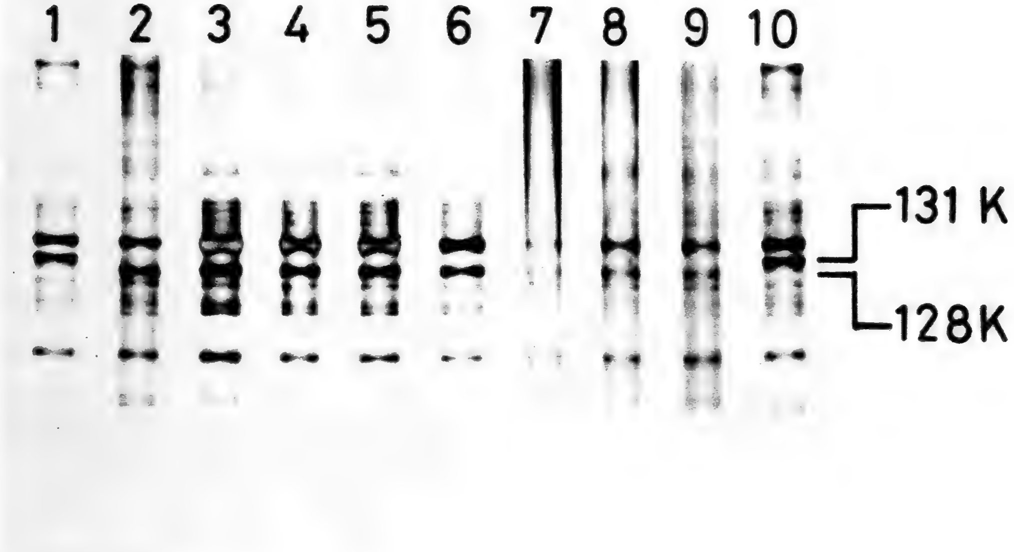

FIG. 4. The effect of speract on the mobility of a high-molecular weight protein of *H. pulcherrimus* spermatozoa, sperm heads or sperm tails. 1, intact spermatozoa without speract; 2, intact spermatozoa with speract (1.12×10^{-9}M); 3, sperm tails with speract (1.12×10^{-14}M); 4, sperm tails with speract (1.12×10^{-9}M); 5, sperm tails with speract (1.12×10^{-5}M); 6, sperm tails without speract; 7, sperm heads with speract (1.12×10^{-9}M); 8, sperm heads with speract (1.12×10^{-5}M); 9, sperm heads without speract; 10, intact spermatozoa without speract.

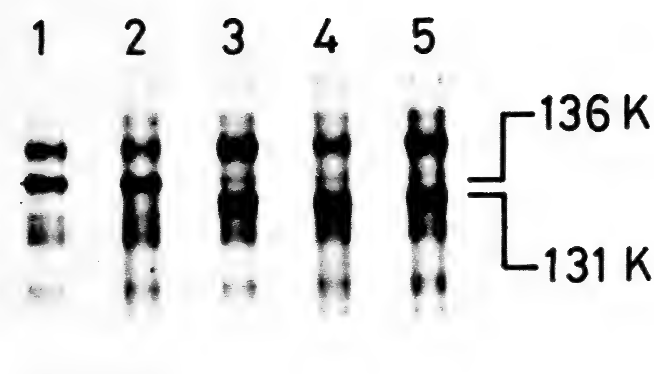

FIG. 5. The effect of various concentrations of speract on the mobility of a high-molecular weight protein of *A. crassispina* spermatozoa. The concentrations of speract used in each lane were as follows: 1, none; 2, 3.74×10^{-9}M; 3, 3.74×10^{-8}M; 4, 3.74×10^{-7}M; 5, 3.74×10^{-6}M.

appeared at an apparent molecular weight of 128,000 which was not found in spermatozoa treated without speract (Fig. 3). Intact spermatozoa without speract had a protein molecular weight of which was 131,000. Treatment of spermatozoa lower than 1.12×10^{-9} M of speract resulted in no change in the mobility of any sperm proteins on an SDS-polyacrylamide gel. The 128,000 dalton protein was found as a major protein in sperm tails isolated in normal ASW, while it was faintly detected in sperm heads (Fig. 4). The 131,000 dalton protein was not detected in sperm tails or sperm heads. However, when sperm tails were isolated in acidified ASW (pH 5.6), the 131,000 dalton protein was detected in sperm tails as a major protein and the 128,000 dalton form was not found (not shown).

As shown in Figure 5, in *A. crassispina* spermatozoa treated with speract, a new protein whose mass is 131,000 daltons was observed on an SDS-polyacrylamide gel. This protein was not found in spermatozoa without speract, which had a protein with the molecular weight of 136,000. The conversion of the 136,000-molecular weight form to 131,000 dalton form in *A. crassispina* spermatozoa occurred completely with 3.74×10^{-8} M of speract. The 131,000 dalton protein was exclusively found in isolated sperm tails (not shown).

DISCUSSION

It has been reported that radiolabeled speract binds specifically and in a saturable manner to *S. purpuratus* spermatozoa [23]. Although we did not use labeled peptide, our results presented here also showed that speract binds to *H. pulcherrimus* sperm cells (Fig. 2, intact spermatozoa). In the experiments, we biologically determined the amounts of unbound speract. When a fixed amount (18.9 mg wet weight) of spermatozoa was incubated with speract lower than 3.72×10^{-9} M, the residual respiration stimulation activity of speract in the supernatant of the incubation mixture was about one-hundredth of the corresponding control speract solution. This suggests that more than 99% speract in the original solution was bound to intact spermatozoa. The spermatozoa did not seem to digest speract since no speract fragments were found and intact speract was obtained from the supernatant by HPLC after 70% ethanol extraction of the samples. The same results were obtained from experiments with sperm tails (Fig. 2, sperm tails), while experiments with sperm heads showed that almost all speract molecules remained in the supernatant, suggesting that speract incubated with the sperm heads did not bind to the heads. These results indicate that speract binds exclusively to sperm tails but not or little to sperm heads. Although the procedure we used here is not accurate enough for determination of binding numbers of speract to sperm cells, it seems to have some advantages compared with the method using labeled speract. It is more simple and economical and it does not need to use tyrosine-substituted speract or Bolton-Hunter adduct of speract which might be troublesome for the bindings because of a large molecule at the N-terminal part of speract.

As shown in Figures 3, 4 and 5, speract induced an electrophoretic mobility change (from 131,000 to 128,000 in *H. pulcherrimus* and from 136,000 to 131,000 in *A. crassispina*) in a major sperm protein. This results is essentially the same as that obtained from *L. pictus* spermatozoa treated with speract derivatives [6]. When sperm tails were isolated from *H. pulcherrimus* spermatozoa in normal ASW (pH 8.0), there was no detectable protein band on a SDS-polyacrylamide gel at an apparent molecular weight of 131,000. The sperm tails possessed the 128,000 dalton protein, which was found in intact spermatozoa treated with speract. It is known that H^+ concentration in sperm cells is higher than that in normal ASW [24]. Speract has been shown to induce Na^+/H^+ exchange across the plasma membrane of sea urchin spermatozoa [25]. It is possible that H^+ concentrations in sperm tails would be changed by exposing the cut end of the tail to lower H^+ concentrations in ASW. In this connection, it should be stressed that when sperm tails were isolated in acidified ASW (pH 5.6), the 131,000 dalton protein was detected as a major protein in *H. pulcherrimus* sperm tails. These suggest that the mobility shift observed in a major sperm protein may be triggered by alkalinization in

sperm cells induced by speract.

Ward and Vaquier have reported that the shift in electrophoretic mobility and concomitant loss of phosphate can be induced *in vitro* by calf intestinal alkaline phosphatase [10]. The increased mobility is thought to result from increased binding of SDS. Our results show that speract induces the increased mobility of a high molecular weight protein and the protein localizes exclusively in sperm tails (Fig. 4). It is known that a specific protein phosphatase involves in dephosphorylation of many proteins [28]. Although it is not proved yet, we presume that the electrophoretic mobility shift of a sperm tail protein from 131,000 daltons to 128,000 daltons is a result of dephosphorylation of the protein and a specific protein phosphatase involves in the process.

It has been reported that resact, another sperm activating peptide purified from the egg jelly of the sea urchin, *A. punctulata*, causes a mobility shift in a major sperm membrane protein which was identified as guanylate cyclase [8, 11, 12]. The enzyme has been reported to be localized in sperm flagellar membrane [15, 16]. Guanylate cyclase in *A. punctulata* has been suggested to be a receptor for resact [26]. The protein observed here may represent guanylate cyclase, although this is not proven. From the experiments on *S. purpuratus* spermatozoa incubated with radiolabeled speract analogue and a chemical crosslinking reagent, Dangott and Garbers have suggested that a speract receptor is a glycoprotein whose molecular mass is 77,000 daltons as estimated by SDS-polyacrylamide gel electrophoresis [27]. This suggests that receptors for sperm activating peptides are different from one species to another or the molecular weight of guanylate cyclase is different in different species. To solve this we are now purifying several proteins from sperm flagellar membrane.

ACKNOWLEDGMENTS

We wish to thank Mr. T. Shinya and Mr. M. Matada for collecting the sea urchins. This work was supported by research grants to N. S. from the Ministry of Education, Science and Culture of Japan (No. 59540471 and No. 60480022).

REFERENCES

1 Suzuki, N., Nomura, K., Ohtake, H. and Isaka, S. (1981) Purification and the primary structure of sperm activating peptides from the jelly coat of the sea urchin eggs. Biochem. Biophys. Res. Commun., **99**: 1238–1244.

2 Garbers, D. L., Watkins, H. D., Hansbrough, J. R., Smith, A. and Misono, K. S. (1982) The amino acid sequence and chemical synthesis of speract and of speract analogues. J. Biol. Chem., **257**: 2734–2737.

3 Suzuki, N., Hoshi, M., Nomura, K. and Isaka, S. (1982) Respiratory stimulation of sea urchin spermatozoa by egg extracts, egg jelly extracts and egg jelly peptides from various species of sea urchins: taxonomical significance. Comp. Biochem. Physiol., **72A**: 489–495.

4 Suzuki, N., Ohizumi, Y., Yasumasu, I. and Isaka, S. (1984) Respiration of sea urchin spermatozoa in the presence of a synthetic jelly coat peptide and ionophores. Dev. Growth Differ., **26**: 17–24.

5 Nomura, K., Suzuki, N., Ohtake, H. and Isaka, S. (1983) Structure and action of sperm activating peptides from the egg jelly of a sea urchin, *Anthocidaris crassispina*. Biochem. Biophys. Res. Commun., **117**: 147–153.

6 Shimomura, H., Suzuki, N. and Garbers, D. L. (1986) Derivatives of speract are associated with the eggs of *Lytechinus pictus* sea urchins. Peptide, **7**: 491–495.

7 Suzuki, N. and Garbers, D. L. (1984) Stimulation of sperm respiration rates by speract and resact at alkaline pH. Biol. Reprod., **30**: 1167–1174.

8 Suzuki, N., Shimomura, H., Radany, E. W., Ramarao, C. S., Ward, G. E., Bentley, J. K. and Garbers, D. L. (1984) A peptide associated with eggs causes a mobility shift in a major plasma membrane protein of spermatozoa. J. Biol. Chem., **259**: 14874–14879.

9 Ward. G. E., Brokaw, C. J., Garbers, D. L. and Vaquier, V. D. (1985) Chemotaxis of *Arbacia punctulata* spermatozoa to resact, a peptide from the egg jelly layer. J. Cell Biol., **101**: 2324–2329.

10 Ward, G. E. and Vaquier, V. D. (1983) Dephosphorylation of a major sperm membrane protein is induced by egg jelly during sea urchin fertilization. Proc. Natl. Acad. Sci., USA, **80**: 5578–5582.

11 Ward, G. E. Garbers, D. L. and Vaquier, V. D. (1985) Effects of extracellular egg factors on sperm guanylate cyclase. Science, **227**: 768–770.

12 Ward, G. E., Moy, G. W. and Vaquier, V. D. (1986) Phosphorylation of membrane-bound guanylate cyclase of sea urchin spermatozoa. J. Cell Biol., **103**: 95–101.

13 Vaquier, V. D. and Moy, G. W. (1986) Stoichiometry of phosphate loss from sea urchin sperm guany-

late cyclase during fertilization. Biochem. Biophys. Res. Commun., **137**: 1148–1152.

14 Radany, E. W., Gerzer, R. and Garbers, D. L. (1983) Purification and characterization of particulate guanylate cyclase from sea urchin spermatozoa. J. Biol. Chem., **258**: 8346–8351.

15 Gray, J. P. and Drummond, G. I. (1976) Guanylate cyclase of sea urchin sperm: subcellular localization. Arch. Biochem. Biophys., **172**: 31–38.

16 Sano, M. (1976) Subcellular localizations of guanylate cyclase and 3:5-cyclic nucleotide phosphodiesterase in sea urchin sperm. Biochim. Biophys. Acta, **428**: 525–531.

17 Lee, H. C. (1985) The voltage-sensitive Na^+/H^+ exchange in sea urchin spermatozoa flagellar membrane vesicles studied with an entrapped pH probe. J. Biol. Chem., **260**: 10794–10799.

18 Tombes, R. M. and Shapiro, B. M. (1985) Metabolite channeling: A phosphocreatine shuttle to mediate high energy phosphate transport between sperm mitochondrion and tail. Cell, **41**: 325–334.

19 Laemmli, U. K. (1970) Cleavage of structural proteins during the assembly of the head of bacteriophage T4. Nature, **257**: 680–685.

20 Morrissey, J. H. (1981) Silver stain for proteins in polyacrylamide gels: A modified procedure with enhanced uniform sensitivity. Anal. Biochem., **117**: 307–310.

21 Lowry, O. H., Rosebrough, N. J., Farr, A. L. and Randall, R. J. (1951) Protein measurement with the Folin phenol reagent. J. Biol. Chem., **193**: 265–275.

22 Schacterle, G. R. and Pollack, R. L. (1973) A simplified method for the quantitative assay of small amounts of protein in biologic material. Anal. Biochem., **51**: 654–655.

23 Smith, A. and Garbers, D. L. (1983) The binding of an I^{125}-speract analogue to spermatozoa. In "Biochemistry of Metabolic Processes". Ed. by D. L. F. Lennon, F. W. Stratman and R. N. Zalten, Elsevier Biomedical, New York, pp. 15–18.

24 Christen, R., Schackmann, R. W. and Shapiro, B. M. (1982) Elevation of the intracellular pH activates respiration and motility of sperm of the sea urchin, *Strongylocentrotus purpuratus*. J. Biol. Chem., **257**: 14881–14890.

25 Hansbrough, J. R. and Garbers, D. L. (1981) Sodium-dependent activation of sea urchin spermatozoa by speract and monensin. J. Biol. Chem., **256**: 2235–2241.

26 Shimomura, H., Dangott, L. G. and Garbers, D. L. (1986) Covalent coupling of a resact analogue to guanylate cyclase. J. Biol. Chem., (in press).

27 Dangott, L. J. and Garbers, D. L. (1984) Identification and characterization of the receptor for speract. J. Biol. Chem., **259**: 13712–13716.

28 Ingebritsen, T. S. and Cohen, P. (1983) Protein phosphatases: Properties and role in cellular regulation. Science, **221**: 331–338.

ZOOLOGICAL SCIENCE 4: 649–656 (1987)

Purification and Structure of Mosact and Its Derivatives from the Egg Jelly of the Sea Urchin *Clypeaster japonicus*

Norio Suzuki, Masanori Kurita, Ken-ichi Yoshino, Hiroko Kajiura[1], Kohji Nomura[2] and Masaaki Yamaguchi

Noto Marine Laboratory, Kanazawa University, Ogi, Uchiura, Ishikawa 927–05, [1]National Institute for Basic Biology, Okazaki 444, and [2]Department of Biochemistry, Tokyo Metropolitan Institute of Gerontology, 35–2 Sakaecho, Itabashi-ku, Tokyo 173, Japan

ABSTRACT—Peptides (mosact and its derivatives) associated with the eggs of the sea urchin, *Clypeaster japonicus,* which stimulate *C. japonicus* sperm respiration rate but neither *Anthocidaris crassispina* nor *Glyptocidaris crenularis* sperm respiration rate, were purified and their amino acid sequences were determined. The sequences of mosact, Des-Gln^6, Asn^7-[His^6]-mosact and Des-Gln^6, Asn^7-[Phe^6]-mosact were found to be Asp-Ser-Asp-Ser-Ala-Gln-Asn-Leu-Ile-Gly, Asp-Ser-Asp-Ser-Ala-His-Leu-Ile-Gly and Asp-Ser-Asp-Ser-Ala-Phe-Leu-Ile-Gly, respectively. Mosact and its derivatives half-maximally stimulate *C. japonicus* sperm respiration rate at 0.5 nM at slightly acidic pH values (6.6–6.8) and cause a shift in the apparent molecular weight (126,000–123,000) of a sperm plasma membrane protein at extracellular pH value of 8.0. Sodium ions were essential for the formation of 123,000 dalton protein.

INTRODUCTION

The sea urchin egg jelly is composed mainly of polysaccharide-protein complex which is separated into a sialoglycoprotein and a fucose polysaccharide [1–3]. The latter is considered to induce the sperm acrosome reaction [3]. In addition to these major macromolecular components, the egg jelly contains several oligopeptides so-called sperm activating peptides [4–11]. These include speract (Gly-Phe-Asp-Leu-Asn-Gly-Gly-Gly-Val-Gly) and its derivatives ([Thr^5]-speract: Gly-Phe-Asp-Leu-Thr-Gly-Gly-Gly-Val-Gly; [Ser^5]-speract: Gly-Phe-Asp-Leu-Ser-Gly-Gly-Gly-Val-Gly; Des-Gly^1-[Thr^5, Gln^{10}]-speract: Phe-Asp-Leu-Thr-Gly-Gly-Gly-Val-Gln; [Thr^5, Gln^{10}]-speract: Gly-Phe-Asp-Leu-Thr-Gly-Gly-Gly-Val-Gln) and resact (Cys-Val-Thr-Gly-Ala-Pro-Gly-Cys-Val-Gly-Gly-Gly-Arg-Leu-NH_2). Speract stimulates sperm respiration with concomitant Na^+/H^+ exchange across the sperm plasma membrane and increases the concentrations of cAMP and cGMP in sperm cells [12, 13]. Resact which is specific for *Arbacia punctulata* spermatozoa has been reported to cause a shift in the apparent molecular weight of guanylate cyclase in the sperm membrane of *A. punctulata* with dephosphorylation of the enzyme [10, 13–17]. Recently resact was identified to act as a potent chemoattractant for *A. punctulata* spermatozoa [18].

We have reported previously that the egg jelly of the sea urchin *C. japonicus* contains a respiration stimulating peptide(s) specific for *C. japonicus* spermatozoa [19]. The peptide named mosact causes a mobility change (from 126,000 daltons to 123,000 daltons) of the sperm protein of *C. japonicus*. Here we purify and present the amino acid sequence of the peptide and its derivatives.

Accepted February 19, 1987
Received January 7, 1987

MATERIALS AND METHODS

Experimental animals and chemicals

Sea urchins, *Clypeaster japonicus, Hemicentrotus pulcherrimus* and *Anthocidaris crassispina,* were collected at Japan Sea Coast (Tsukumo Bay) near Noto Marine Laboratory. The sea urchin *G. crenularis* was collected at the Aomori Bay near the Asamushi Marine Biological Station. Artificial sea water (ASW) containing 454 mM NaCl, 9.7 mM KCl, 24.9 mM $MgCl_2$, 9.6 mM $CaCl_2$, 27.1 mM $MgSO_4$, 4.4 mM $NaHCO_3$ and 10 mM tris (hydroxymethyl) aminoethane (Tris) or 10 mM N-(2-acetamido)-2-aminoethane sulfonic acid (ACES) was prepared in the laboratory. Na^+-free ASW had the same composition except that choline chloride was substituted for NaCl and $NaHCO_3$ was for $KHCO_3$. Sodium dodecyl sulfate (SDS) (95% grade material), Tris, ACES and molecular weight standards for gel electrophoresis (MW–SDS–200 kit) were obtained from Sigma Chemical Co. Acetonitrile (ACN) of liquid chromatography grade and trifluoroacetic acid (TFA) were from Wako Pure Chemical Co. Speract was custom synthesized for us by Peptide Institute, Inc., Osaka. [Thr^5]-speract and [Ser^5]-speract were purified from the egg jelly of *H. pulcherrimus* and *A. crassispina,* respectively. Synthetic resact and synthetic Des-Gln^6, Asn^7-[Asn^1, His^6]-mosact (Asn-Ser-Asp-Ser-Ala-His-Leu-Ile-Gly) were generous gifts from Dr. H. Shimomura and Dr. D. L. Garbers, respectively. Other reagents were of analytical grade.

Gamete collection and determination of respiration rates

Spermatozoa or eggs were obtained by intracoelomic injection of 0.5 M KCl. Eggs were colleted in sea water and then treated with acidified sea water (pH 5.0) to remove the jelly coat rapidly. Spermatozoa were collected "dry" at room temperature and stored on ice at approximately 330 mg (wet weight)/ml until use.

Respiration rate of sea urchin spermatozoa was determined as described previously [19].

Isolation of sperm heads and tails

Spermatozoa (usually 10–15 ml of dry sperm) were diluted with 250 vol of ice cold ASW and centrifuged at $1,000\times g$ for 5 min at 4°C. The supernatant was then centrifuged at $5,000\times g$ for 30 min at 4°C. The sperm pellet was suspended in 20 vol of ice cold ASW and homogenized in an ice bath with a 50 ml-Dounce homogenizer fitted with a teflon pestle [20, 21]. About 15–20 strokes were enough to detach the tails from the heads as monitored by phase-contrast microscopy. The homogenate was centrifuged at $1,000\times g$ for 30 min at 4°C to pellet the sperm heads. The sperm head fraction was suspended in 100–150 ml of ice cold ASW and centrifuged at $2,000\times g$ for 30 min at 4°C. The resultant pellet (sperm heads) was used for experiments. The supernatant fraction containing tails was centrifuged at $6,000\times g$ for 30 min at 4°C, and the pellet was suspended in 100–150 ml of ice-cold ASW. The suspension was centrifuged at $2,000\times g$ for 30 min at 4°C and the supernatant was centrifuged at $6,000\times g$ for 30 min at 4°C. The resultant pellet (sperm tails) was used for experiments. Phase-contrast microscopy was used routinely to monitor the extent of contamination by sperm heads in the tail fraction. In some experiments, Na^+-free ASW was used for preparation of sperm heads and tails.

Preparation of sperm plasma membrane

Dry sperm were washed twice with millipore-filtered sea water (MFSW) by centrifugation at $2,000\times g$ for 15 min at 4°C. The sperm pellet was suspended in 20 vol of MFSW containing 20 mM Tris-HCl (pH 9.0), 2 mM benzamidine-HCl, 0.01% (w/v) streptomycin sulfate and 0.01% (w/v) penicillin G [22]. The suspension was incubated for 12 hr at 4°C and then centrifuged at $7,000\times g$ for 30 min at 4°C. The supernatant was collected and re-centrifuged under the same conditions. The second $7,000\times g$ supernatant was then centrifuged at $105,000\times g$ for 60 min at 4°C to pellet the sperm plasma membrane.

Purification of mosact and its derivatives from C. japonicus egg jelly

The egg jelly solution of *C. japonicus* was mixed

with a 2-fold volume of 95% ethanol and then centrifuged at 10,000×*g* for 30 min at 4°C. The supernatant fraction was concentrated under reduced pressure and delipidated by chloroform extration. The sample was then lyophilized. The residue was dissolved in distilled water. Mosact and its derivatives were purified by sequential high pressure liquid chromatographies.

High pressure liquid chromatography (HPLC)

HPLC was performed using a Shimadzu model 6A chromatography system with octyl columns (Shimpack C–8 Prep, 10 μm, 20×250 mm for step-wise elution; Unisil C–8, 5 μm, 4.6×250 mm for gradient elution). The column effluent was monitored for absorbance at 225 nm using a Shimadzu model SPD–6AV spectrophotometer equipped with a variable wavelength detector. In general, separations were carried out using a combination of the following programs:

Program I: flow rate was 9.9 ml/min, the column (Shimpack C–8 Prep) was equilibrated with 5% ACN in 0.1% TFA in water and eluted for 15 min, and then eluted for next 15 min with 60% ACN in 0.1% TFA.

Program II: flow rate was 1.0 ml/min, the column (Unisil C–8) was equilibrated with 10% ACN in 0.1% TFA and eluted for 10 min, followed by a linear gradient from 10% ACN to 50% ACN in 0.1% TFA over a 50-min time period.

Amino acid and sequence analysis

Amino acid analysis was carried out with an automatic amino acid analyzer Hitachi 835–50 after hydrolysis with constant-boiling HCl. Normally, 2–5 nmoles of peptide were hydrolyzed. Sequence analysis was performed by automated Edman degradation using a 470A Protein Sequencer (Applied Biosystems, Inc.) with 100 pmoles of peptide.

Other methods

Polyacrylamide gel electrophoresis was performed essentially as described by Laemmli [23]. A gel was run for 8 hr at 10 mA/slab gel at room temperature. The gel was subsequently stained by the method of Morrissey [24]. Protein was determind by the method of Lowry *et al.* according to Schacterle and Pollack's modification [25, 26].

RESULTS

Purification of mosact and its derivatives

The egg jelly solution was obtained by the treatment of *C. japonicus* eggs with acidified (pH 5.0) sea water for 15 min and by centrifugation to remove eggs. Five liters of the egg jelly solution were mixed with 10 liters of 95% ethanol and the suspension was then centrifuged at 10,000×*g* for 30 min at 4°C. The resultant supernatant fluid was concentrated with a rotary evaporator at 50°C. The concentrated sample after being centrifuged to remove salt was delipidated by chloroform extraction and then lyophilized. The residue was dissolved in a minimum volume of distilled water and filtered through a millipore-filter (0.45 μm). The filtrate was applied onto a Shimpack C–8 Prep column equilibrated with 5% ACN in 0.1% TFA. The column was eluted first with equilibrating solvent for 5 min and then eluted according to Program I. The fractions were assayed for their ability to stimulate sperm respiration rate. The fractions eluted with 60% ACN in 0.1% TFA were found to contain respiration stimulation activity (Fig. 1A). The fractions were pooled and lyophilized. The residue was dissolved in 10% ACN in 0.1% TFA and was further purified by repeated HPLC with a Unisil C–8 column using Program II (Fig. 1B–H). Three active materials were obtained.

Amino acid composition and sequence

The purified peptides were analyzed for amino acid composition. As shown in Table 1, peptide b was consisted of 10 amino acids while peptide a and c contained 9 amino acids, respectively. Peptide b had the same amino acid composition of the peptide named as mosact in our previous report [19]. The compositions of peptide a and c were similar to that of peptide b while peptide a had three residues of aspartic acid and one residue of glutamic acid and peptide c contained one residue of phenylalanine. These peptides were then subjected to sequence analysis. The sequences of peptide a and c were similar to that of

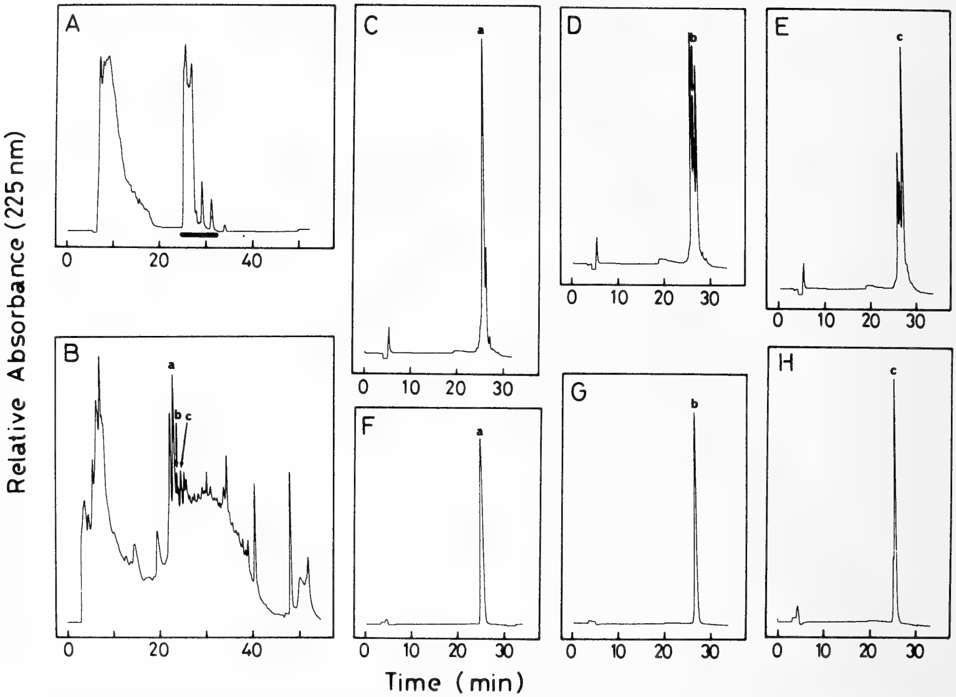

Fig. 1. High pressure liquid chromatographs of peptides. A: Elution profile of crude extracts. Crude extracts were injected onto a reverse-phase (Shimpack C–8 Prep, 20×250 mm) column. Program I was used for elution. Solid bar indicates active fractions; B: Further purification of the active fractions on a reverse-phase (Unisil C–8) column. Program II was used for elution. Fractions indicated by a, b and c were active and used for further purification; C–H: Re-HPLC of the active fractions (a, b and c). Elution conditions used were the same as Fig. 1B.

Table 1. Amino acid compositions and sequences of sperm activating peptides obtained from *Clypeaster japonicus* egg jelly

	Peptide a	Peptide b	Peptide c
Asp	2.080 (2)	2.604 (3)	2.054 (2)
Ser	1.914 (2)	1.778 (2)	1.880 (2)
Glu	—	0.718 (1)	—
Gly	1.215 (1)	1.148 (1)	1.239 (1)
Ala	1.063 (1)	0.987 (1)	1.020 (1)
Ile	1.000 (1)	1.000 (1)	1.000 (1)
Leu	1.115 (1)	1.040 (1)	1.092 (1)
Phe	—	—	1.128 (1)
His	0.935 (1)	—	—
Total residue	(9)	(10)	(9)

Peptide a (Des-Gln^6, Asn^7–[His^6]-mosact) Asp–Ser–Asp–Ser–Ala–His–Leu–Ile–Gly
Peptide b (mosact) Asp–Ser–Asp–Ser–Ala–Gln–Asn–Leu–Ile–Gly
Peptide c (Des-Gln^6, Asn^7–[Phe^6]-mosact) Asp–Ser–Asp–Ser–Ala–Phe–Leu–Ile–Gly

peptide b (mosact), thus being named as mosact derivatives to be Des-Gln[6], Asn[7]-[His[6]]-mosact and Des-Gln[6], Asn[7]-[Phe[6]]-mosact, respectively. However, when the sequence of peptide c was determined, cycle 6 resulted in no identifiable amino acid and phenylalanine was not detected at any cycle. Sixth residue of the peptide was assigned to phenylalanine since the amino acid analysis data clearly showed that the peptide contained one phenylalanine residue. To confirm the sequence, the peptide was synthesized by liquid phase methods with phenylalanine as the sixth residue. The synthesized peptide had the following amino acid composition: Asp (1.0), Ser (1.9), Gly (1.0), Ala (1.1), Ile (1.0), Leu (1.1) and Phe (0.9) and the following sequence: Asp-Ser-Asp-Ser-Ala-Phe-Leu-Ile-Gly. The synthesized peptide also stimulated *C. japonicus* sperm respiration rate at the same concentration as the native peptide (Fig. 2)

Respiration stimulation

Mosact and its derivatives stimulated sperm respiration rates at slightly acidic pH values. The effect was specific for *C. japonicus* spermatozoa.

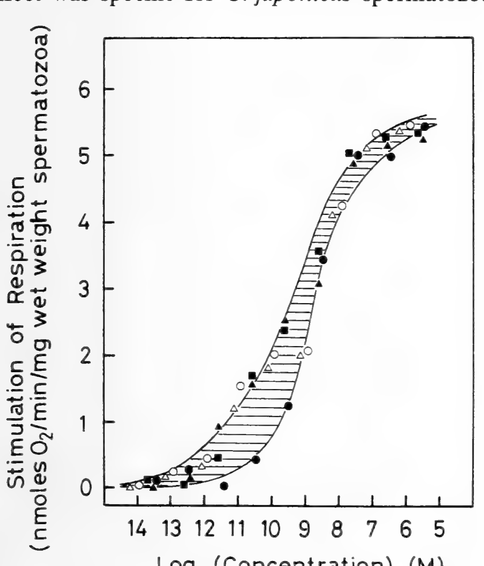

FIG. 2. The effect of mosact (▲), Des-Gln[6], Asn[7]-[Phe[6]]-mosact (○), Des-Gln[6], Asn[7]-[His[6]]-mosact (■), synthetic Des-Gln[6], Asn[7]-[Phe[6]]-mosact (●) and synthetic Des-Gln[6], Asn[7]-[Asn[1], His[6]] (△) on *C. japonicus* sperm respiration rates.

Mosact and its derivatives were half-maximally active at about 0.5 nM on the stimulation of *C. japonicus* sperm respiration rate (Fig. 2). These peptides did not show this effect on *A. crassispina*, *H. pulcherrimus* or *G. crenularis* spermatozoa. Speract and its derivatives such as [Ser[5]]-speract and [Thr[5]]-speract at concentrations as high as 10 μM failed to elevate respiration rate of *C. japonicus* spermatozoa.

SDS-polyacrylamide gel electrophoresis of proteins of intact spermatozoa, sperm heads, sperm tails and sperm plasma membrane

Crude mixtures of *C. japonicus* egg factors caused a mobility shift of a sperm protein on a SDS-polyacrylamide gel [19]. When *C. japonicus* spermatozoa were incubated in normal ASW (pH 8.0) with various concentrations of mosact for 1 min the high molecular weight of a protein of the spermatozoa shifted from about 126,000 daltons to 123,000 daltons (Fig. 3). Mosact failed to cause any detectable mobility change in the other proteins of *C. japonicus* spermatozoa. About 735 nM mosact were enough to cause the complete mobility change of the protein.

Sodium ions are essential for respiration stimulation by speract [8, 12] and for that by mosact (not shown). Spermatozoa were washed in Na^+-free ASW (pH 8.0) and then incubated in Na^+-free ASW (pH 8.0) with mosact for 1 min. Mosact failed to cause the mobility change of the 126,000 daltons protein (Fig. 4). The continued incubation of sperm cells for 1 hr showed no mobility change of the protein.

Sperm heads (nucleus and mitochondrial midpiece) were separated from sperm tails and sperm plasma membrane fraction was prepared by the procedure of Podell *et al.* [23]. These fractions (sperm heads, sperm tails and plasma membrane) were analyzed by SDS-polyacrylamide gel electrophoresis after incubation of spermatozoa in normal ASW (pH 8.0) with or without mosact (Fig. 5). On a per-mg-of-protein basis, the 123,000 dalton protein derived from the modification of 126,000 dalton protein was found exclusively in the sperm tails and sperm plasma membrane fractions.

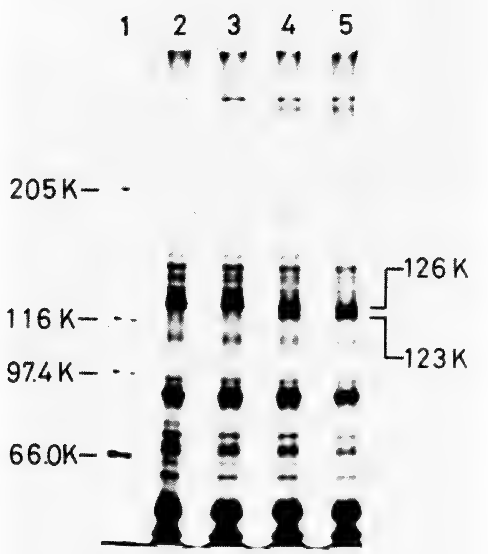

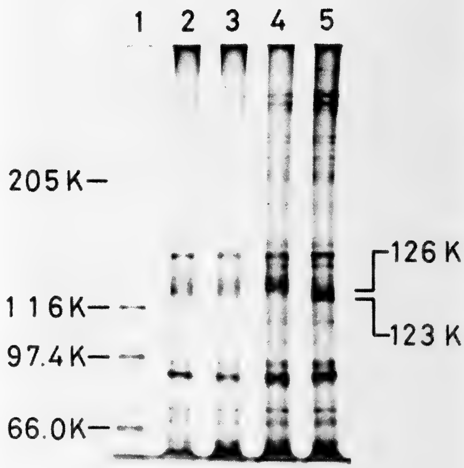

Fig. 3. The effect of various concentrations of mosact on the mobility of a high-molecular weight protein of spermatozoa. *C. japonicus* spermatozoa were incubated at 20°C with various concentrations of mosact in normal ASW (pH 8.0) (lane 2: none; lane 3: 7.35×10^{-9}M; lane 4: 7.35×10^{-8}M; lane 5: 7.35×10^{-6}M). At 1 min of incubation, the reaction was stopped by the addition of trichloroacetic acid (final concentration of 10%). Then the samples for SDS-polyacrylamide gel electrophoresis were prepared as described previously [19]. Approximately 10 μg of sperm proteins were added per lane. The lane 1 shows co-electrophoresis of molecular weight standards (myosin, rabbit muscle, MW 205,000; β-galactosidase, *E. coli,* MW 116,000; phosphorylase b, rabbit muscle, 97,400; albumin, bovine plasma, MW 66,000).

Fig. 4. The effect of mosact on the appearance of 123,000 dalton sperm protein in the presence or absence of Na^+. *C. japonicus* spermatozoa were incubated at 20°C with or without mosact (7.35×10^{-6}M) in the presence or absence of Na^+. At 1 min of incubation the reaction was stopped by the addition of trichloroacetic acid (final concentration of 10%). The sample preparation for SDS-polyacrylamide gel electrophoresis and the electrophoresis were the same as described in the legend of Fig. 3. Approximately 8 μg of sperm proteins were added to lane 2 (without mosact in Na^+-free ASW) and lane 3 (with mosact in Na^+-free ASW). Approximately 10 μg of sperm proteins were added to lane 4 (without mosact in normal ASW) and lane 5 (with mosact in normal ASW). The lane 1 shows co-electrophoresis of molecular weight standards.

DISCUSSION

The egg jelly of *C. japonicus* which belongs to the order Clypeasteroida contains three sperm activating peptides named as mosact and its derivatives (Des-Gln^6, Asn^7-[His^6]-mosact and Des-Gln^6, Asn^7-[Phe^6]-mosact). The primary structures of mosact and its derivatives are similar to each other, but completely different from speract, [Thr^5]-speract or [Ser^5]-speract which were previously characterized from the sea urchins, *H. pulcherrimus* [4], *Strongylocentrotus purpuratus* [5] and *A. crassispina* [7], respectively. They are also different from resact which was purified from *A. punctulata* egg jelly [10]. *H. pulcherrimus, S. purpuratus* and *A. crassispina* belong to the order Echinoida and spermatozoa from these species are activated by speract, [Thr^5]-

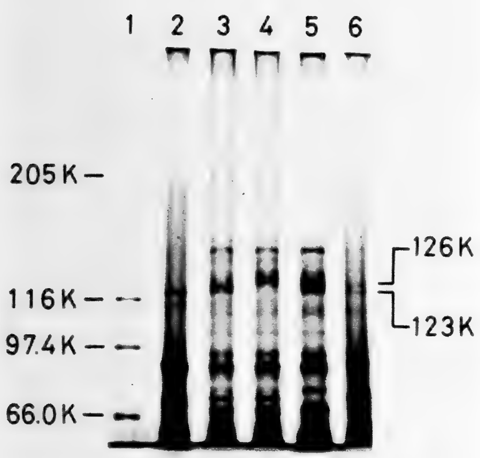

FIG. 5. SDS-polyacrylamide gel electrophoresis of sperm membrane, sperm tails, sperm heads and intact spermatozoa. Intact spermatozoa were incubated at 20°C with or without mosact (7.35×10^{-6} M) in normal ASW for 1 min. Samples for electrophoresis were prepared as described in the legend of Fig. 3. SDS-polyacrylamide gel electrophoresis was performed according to Laemmli's procedure [23]. Approximately 10 μg of proteins was added to each lane (lane 1: molecular weight standards; lane 2: sperm membrane without mosact; lane 3: intact spermatozoa with mosact; lane 4: intact spermatozoa without mosact; lane 5: sperm tails without mosact; lane 6: sperm heads without mosact).

speract and [Ser^5]-speract, respectively. *A. punctulata* belongs to another order Arbacioida which also includes *G. crenularis*. Speract and its derivatives activate neither *A. punctulata* spermatozoa nor *G. crenularis* spermatozoa. Mosact and its derivatives do not stimulate sperm respiration of *H. pulcherrimus*, *A. crassispina* and *G. crenularis*. These support a theory that peptides isolated from the eggs of one taxonomic order may interact with sperm cells of other species within the same order, but not within another order [6].

Mosact not only stimulates spermatozoan respiration rate but also causes the appearance of a newly-stained protein whose mass is 123,000 daltons as estimated by SDS-polyacrylamide gel electrophoresis. In previous studies, a membrane protein identified as guanylate cyclase was shown to change in apparent molecular weight from 160,000 to 150,000 in response to resact in *A. punctulata* spermatozoa [10, 14, 15]. The protein observed here located dominantly in sperm tails and is found in sperm membrane as a major protein. However, the protein remains to be identified.

The formation of the 123,000 dalton protein by mosact requires sodium ions. It may suggest that the protein involves in the stimulation of sperm respiration by mosact, since a sperm activating peptide, speract, requires sodium ions for the respiration stimulation action [8, 12]. But this may be controversial by the fact that the conversion of a 126,000 dalton protein to 123,000 dalton protein requires 50–100 fold concentrations of mosact as compared with the respiration stimulation.

Although resact, speract and mosact do not crossreact with receptors of spermatozoa of the opposite species, the physiological events measured appear to be the same [4, 6, 9–11, 19]. This extends a theory that the apparent coevolution of peptide and receptor is due to the necessity of the resultant physiological responses [11].

The egg jelly peptides show many physiological activities such as respiration stimulation, increasing cGMP and cAMP concentrations, the conversion of a high molecular weight sperm membrane protein to a lower molecular weight one and chemoattractant action. At present time, we do not know which is the key function of the peptides. This remains to be determined.

ACKNOWLEDGMENTS

The authors wish to thank Dr. D. L. Garbers at Vanderbilt University School of Medicine for preliminary sequence analysis of mosact and its derivatives. We also wish to thank Mr. T. Shinya and M. Matada for collecting and culturing sea urchins. We express our appreciation to the Asamushi Marine Biological Station for kindly supplying the sea urchin *Glyptocidaris crenularis*. This work was supported by research grants to N.S. from the Ministry of Education, Science and Culture of Japan (No. 59540471 and No. 60480022).

REFERENCES

1 Isaka, S., Hotta, K. and Kurokawa, M. (1970) Jelly coat substances of sea urchin eggs. I. Sperm isoagglutination and sialopolysaccharide in the jelly. Exp. Cell Res., **59**: 37–42.

2 Ishihara, K., Oguri, K. and Taniguchi, H. (1973) Isolation and characterization of fucose sulfate from jelly coat glycoproteins of sea urchin egg. Biochim. Biophys. Acta, **320**: 628–634.

3 SeGall, G. K. and Lennarz, W. J. (1979) Chemical characterization of the component of the jelly coat from sea urchin eggs responsible for induction of the acrosome reaction. Dev. Biol., **71**: 33–48.

4 Suzuki, N., Nomura, K., Ohtake, H. and Isaka, S. (1981) Purification and the primary structure of sperm activating peptides from the jelly coat of the sea urchin eggs. Biochem. Biophys. Res. Commun., **99**: 1238–1244.

5 Garbers, D. L., Watkins, H. D., Hansbrough, J. R., Smith, A. and Misono, K. S. (1982) The amino asid sequence and chemical synthesis of speract and of speract analogues. J. Biol. Chem., **257**: 2734–2737.

6 Suzuki, N., Hoshi, M., Nomura, K. and Isaka, S. (1982) Respiratory stimulation of sea urchin spermatozoa by egg extracts, egg jelly extracts and egg jelly peptides from various species of sea urchins: taxonomical significance. Comp. Biochem. Physiol., **72A**: 489–495.

7 Nomura, K., Suzuki, N., Ohtake, H. and Isaka, S. (1983) Structure and action of sperm activating peptides from the egg jelly of a sea urchin, *Anthocidaris crassispina*. Biochem. Biophys. Res. Commun., **117**: 147–153.

8 Suzuki, N., Ohizumi, Y., Yasumasu, I. and Isaka, S. (1984) Respiration of sea urchin spermatozoa in the presence of a synthetic jelly coat peptide and ionophores. Dev. Growth Differ., **26**: 17–24.

9 Suzuki, N. and Garbers, D. L. (1984) Stimulation of sperm respiration rates by speract and resact at alkaline extracellular pH. Biol. Reprod., **30**: 1167–1174.

10 Suzuki, N., Shimomura, H., Radany, E. W., Ramarao, C. S., Ward, G. E., Bentley, J. K. and Garbers, D. L. (1984) A peptide associated with eggs causes a mobility shift in a major plasma membrane protein of spermatozoa. J. Biol. Chem., **259**: 14874–14879.

11 Shimomura, H., Suzuki, N. and Garbers, D. L. (1986) Derivatives of speract are associated with the eggs of *Lytechinus pictus* sea urchins. Peptide, **7**: 491–495.

12 Hansbrough, J. R. and Garbers, D. L. (1981) Sodium-dependent activation of sea urchin spermatozoa by speract and monensin. J. Biol. Chem., **256**: 2235–2241.

13 Repaske, D. R. and Garbers, D. L. (1983) A hydrogen ion flux mediates stimulation of respiratory activity by speract in sea urchin spermatozoa. J. Biol. Chem., **258**: 6025–6029.

14 Ward, G. E. and Vacquier, V. D. (1983) Dephosphorylation of a major sperm membrane protein is induced by egg jelly during sea urchin fertilization. Proc. Natl. Acad. Sci., **80**: 5578–5582.

15 Ward, G. E., Garbers, D. L. and Vacquier, V. D. (1985) Effects of extracellular egg factors on sperm guanylate cyclase. Science, **227**: 768–770.

16 Ward, G. E., Moy, G. W. and Vacquier, V. D. (1986) Phosphorylation of membrane-bound guanylate cyclase of sea urchin spermatozoa. J. Cell Biol., **103**: 95–101.

17 Vacquier, V. D. and Moy, G. W. (1986) Stoichiometry of phosphate loss from sea urchin sperm guanylate cyclase during fertilization. Biochem. Biophys. Res. Commun, **137**: 1148–1152.

18 Ward, G. E., Brokaw, C. J., Garbers, D. L. and Vacquier, V. D. (1985) Chemotaxis of *Arbacia punctulata* spermatozoa to resact, a peptide from the egg jelly layer. J. Cell Biol., **101**: 2324–2329.

19 Suzuki, N. and Yamaguchi, M. (1986) Species specific respiratory stimulation of sea urchin (*Clypeaster japonicus*) spermatozoa by an egg associated factor. Zool. Sci., **3**: 801–806.

20 Lee, H. C. (1985) The voltage-sensitive Na^+/H^+ exchange in sea urchin spermatozoa flagellar membrane vesicles studied with an entrapped pH probe. J. Biol. Chem., **260**: 10794–10799.

21 Tombes, R. M. and Shapiro, B. M. (1985) Metabolite channeling: A phosphocreatine shuttle to mediate high energy phosphate transport between sperm mitochondrion and tail. Cell, **41**: 325–334.

22 Podell, S. B., Moy, G. W. and Vacquier, V. D. (1984) Isolation and characterization of a plasma membrane fraction from sea urchin sperm exhibiting species specific recognition of the egg surface. Biochim. Biophys. Acta, **778**: 25–37.

23 Laemmli, U. K. (1970) Cleavage of structural proteins durinig the assembly of the head of bacteriophage T4. Nature, **257**: 680–685.

24 Morrissey, J. H. (1981) Silver stain for proteins in polyacrylamide gels: A modified procedure with enhanced uniform sensitivity. Anal. Biochem., **117**: 307–310.

25 Lowry, O. H., Rosebrough, N. J., Farr, A. L. and Randall, R. J. (1951) Protein measurement with the Folin phenol reagent. J. Biol. Chem., **193**: 265–275.

26 Schacterle, G. R. and Pollack, R. L. (1973) A simplified method for the quantitative assay of small amounts of protein in biologic material. Anal. Biochem., **51**: 654–655.

ZOOLOGICAL SCIENCE 4: 657–664 (1987)

Germ Cell Kinetics in Gonadal Development in the Toad *Bufo japonicus formosus*

Akihiko Tanimura and Hisaaki Iwasawa

Biological Institute, Faculty of Science, Niigata University, Niigata 950–21, Japan

ABSTRACT—The sexual difference in the number of germ cells in primordial gonads of *Bufo japonicus* was investigated. The sexual difference in the number was not clear in larvae of stage 41 when sexual differentiation of the gonad itself was occurring. The difference was first recognized on the 6th day after metamorphosis in the gonads propers, and on the 18th day in Bidder's organs. The number was significantly larger in females. A rapid increase in the proliferation of secondary gonia was occurring in female gonads on the 6th day. It is conceivable that in toads the cause of the appearance of a sexual difference in the number is due to a remarkable proliferation of secondary gonia in female gonads.

INTRODUCTION

Hardisty [1] reviewed the sexual difference in the number of germ cells in larval and neonatal periods of vertebrates, and pointed out that the number is larger in males in mammals and birds, and in females in anamniotes. He also suggested that the cytodifferentiation and proliferation of germ cells depend on the cortico-medullary induction in gonadal primordia. However, the cause of the appearance of this sexual difference is not clear yet.

Toads, irrespective of sex, have rudimentary ovaries, Bidder's organs, between the fat body and gonad proper. Therefore, toads are an interesting material for the study of sexual differentiation. We suggested the sexual difference in oogenic activity in Bidder's organs of young toads [2]. In the present paper, the sexual difference in Bidder's organ and the difference between the ovary and Bidder's organ are shown quantitatively, and a dependence of sexual difference in the number of germ cells upon the oogenic activity is elucidated.

MATERIALS AND METHODS

Egg strings of *Bufo japonicus formosus* were collected in a suburb of Niigata City. Larvae and young toads derived from these eggs were reared at 18 ± 1°C. The animals were fed on commercial fish meal during the larval period, and on small insects thereafter. Gonadal regions of these larvae and young toads were fixed in Bouin's solution at various intervals after hatching (Tables 1 and 2). These were serially sectioned transversely in paraffin into 5 μm thicknesses, and stained with Masson trichrome. In order to determine the developmental stages of the larval specimens, Ichikawa and Tahara's normal table of development [3] was used.

Germ cells in gonads and Bidder's organs were classified into 5 stages, i.e., primary gonia, secondary gonia, oocytes in leptotene-pachytene, oocytes in diplotene and auxocyte-like cells. The number of germ cells in each stage was counted, and the obtained data were divided by the diameter of each stage of germ cells/thickness of sections + 1 for the revise of overlapping. The results obtained were tested statistically for significance by paired *t*-test, Duncan's new multiple range test or Mann-Whitney's *U*-test.

RESULTS

Number of germ cells in gonad proper

The sexual differentiation of gonads occurred at

Accepted April 8, 1987
Received March 9, 1987

TABLE 1. Number of germ cells

Developmental stages (Days after metamorphosis)	Days after hatching	Number of animals: male	Number of animals: female	Total: male	Total: female	Primary gonia: male	Primary gonia: female	Secondary gonia: male	Secondary gonia: female
		indifferent		indifferent		indifferent		indifferent	
34	6	6		75± 8		75± 8		0	
34	8	6		74± 3		74± 3		0	
38	12	6		188±29		188±29		0	
40	18	6		261±34		261±34		0	
41	22	6		540±56		540±56		0	
41	26	4	4	458± 48	713± 160	458± 48	713±160	0	0
42	30	5	4	714± 88	953± 152	714± 88	915±140	0	38± 23
43	34	3	4	958± 23	1121± 147	958± 23	984±100	0	129± 49
45 (0)	39	4	4	2576±215	2875± 857	2576±215	2102±459	0	762± 431
(6)	45	4	4	** 1872±520	5531± 352	1859±510	2153±356	10±10	3069± 155
(12)	51	4	4	* 3325±734	11385±2111	3325±734	2032±272	0	7716±1754
(18)	57	4	4	* 2043±188	12989±2996	* 2016±176	1506±205	26±26	3369± 695
(24)	63	4	4	* 3803±312	21209±2516	* 3794±316	1961±645	10±10	4973±1044
(30)	69	4	2	** 5017±897	16137±1439	5017±897	1751±835	0	3311± 678

Sexual difference: * $0.01<p<0.05$, ** $p<0.01$.

TABLE 2. Number of germ cells

Developmental stages (Days after metamorphosis)	Number of animals: male	Number of animals: female	Total: male	Total: female	Primary gonia: male	Primary gonia: female	Secondary gonia: male	Secondary gonia: female
	indifferent		indifferent		indifferent		indifferent	
34	6		41± 4		41± 4		0	
34	6		48± 6		48± 6		0	
38	6		107±12		107±12		0	
40	6		132±29		132±29		0	
41	6		298±32		255±21		43±13	
41	4	4	344± 61	422± 117	248± 37	321± 60	88± 28	97± 92
42	5	3	669± 105	528± 171	480± 76	377±132	145± 46	86± 36
43	3	4	* 1141± 108	700± 73	576±121	374± 24	354± 84	201± 53
45 (0)	4	5	2520± 889	2021± 671	1569±529	1080±352	535±360	497±219
(6)	4	4	2189± 77	3467± 487	1071±343	1001±163	415±189	714±414
(12)	4	4	3290±1123	5830±1508	1191±226	1088±205	1358±878	2830±777
(18)	4	4	* 3452± 493	5798± 817	986±134	822±139	1264±219	1613±347
(24)	4	4	* 4296± 566	7958±1382	** 1607±430	633± 92	1028±224	1690±158
(30)	4	2	5151± 429	8122±1810	1211±158	886± 61	1507±319	2713±625

Sexual difference: * $0.01<p<0.05$, ** $p<0.01$.

(mean ± SE) in gonads

Oocytes (leptotene-pachytene)		Oocytes (diplotene)		Mitotic index of primary gonia (%)	
male	female	male	female	male	female
indifferent		indifferent		indifferent	
0		0		0.0	
0		0		0.0	
0		0		1.6±0.6	
0		0		1.8±0.5	
0		0		2.2±0.4	
0	0	0	0	2.0±0.2	2.1±0.3
0	0	0	0	1.7±0.5	2.0±0.4
0	8± 7	0	0	3.5±0.8	3.4±0.3
0	11± 7	0	0	1.3±0.2	1.6±0.1
0	309± 149	0	0	1.7±0.3	2.6±0.4
0	1637± 510	0	0	** 0.8±0.1	1.5±0.1
0	8112±2716	0	1± 1	1.1±0.2	1.7±0.4
0	14048±1578	0	228±116	0.6±0.2	1.2±0.3
0	10279± 123	0	796±197	0.9±0.2	1.2±0.2

(mean ± SE) in Bidder's organs

Oocytes (leptotene-pachytene)		Oocytes (diplotene)		Auxocyte-like cells		Mitotic index of primary gonia (%)	
male	female	male	female	male	female	male	female
indifferent		indifferent		indifferent		indifferent	
0		0		0		0.0	
0		0		0		0.0	
0		0		0		1.0±0.4	
0		0		0		2.3±1.0	
0		0		0		2.3±0.4	
0	0	0	0	8± 3	5± 5	3.0±0.7	1.8±0.7
1± 1	2± 2	0	0	44± 13	64± 16	2.6±0.5	3.1±0.5
17± 4	39± 18	0	0	193± 60	87± 26	3.0±0.5	3.4±0.8
49± 20	73± 34	0	0	367± 31	371±102	1.1±0.5	1.3±0.1
222± 53	371± 93	0	0	482±214	383± 62	1.5±0.2	2.1±0.5
481±274	1556± 484	0	0	260± 97	357± 79	1.3±0.3	0.9±0.1
* 844±284	2932± 622	49±31	73± 28	309± 57	358±121	0.6±0.1	1.4±0.4
** 1283±304	5120± 964	65±18	239±101	263± 24	275± 59	0.9±0.1	1.4±0.5
2168±245	3721±1197	* 58±31	514±118	207± 49	288± 44	1.1±0.1	1.2±0.1

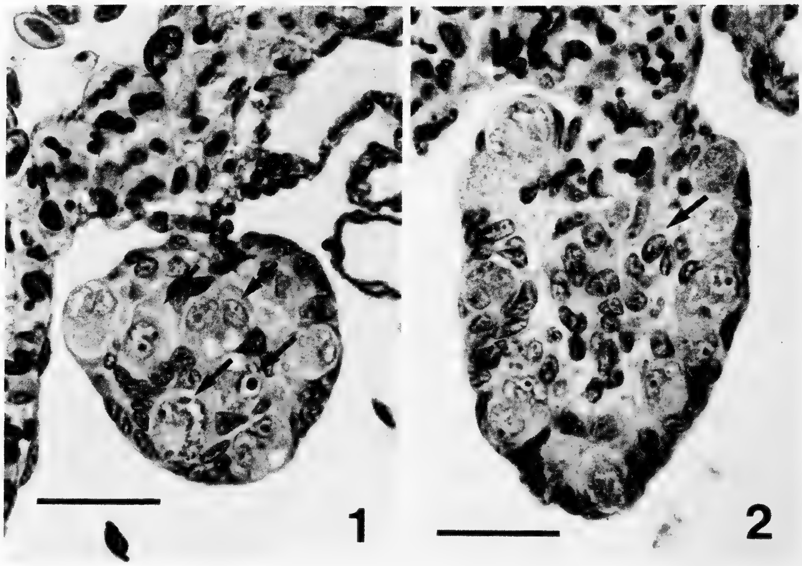

Figs. 1 and 2. Cross sections of gonads. 1. Male gonad at stage 41. Germ cells are seen in the medulla (arrow). 2. Female gonad at stage 43. Medulla shows a degenerative figure (arrow). Scales: 30 μm.

stage 41 (26 days after hatching) (Figs. 1 and 2), when the number of germ cells (primary gonia) in female gonads tended to be larger than in male ones, but it was not significant statistically. The remarkable sexual difference in the number of germ cells was seen from the 6th day after metamorphosis (Table 1), and the total number of germ cells in female gonads (ovaries) was significantly larger than that in male gonads (testes). The mitotic index of primary gonia tended to be higher in ovaries during this period. Furthermore, a large number of secondary gonia and oocytes were seen in the ovaries (Fig. 4). In the testes, on the other hand, a few secondary gonia were found, and no spermatocytes were seen (Fig. 3). In the ovaries, primary gonia remarkably gave rise to secondary gonia, so the number of primary gonia tended to be relatively larger in the testes.

Number of germ cells in Bidder's organ

Some germ cells in Bidder's organ grew into auxocyte-like cells without any meiotic nuclear change (Figs. 5 and 6). These auxocyte-like cells appeared in stage 41 (26 days after hatching), and the number of these cells increased until the 6th day after metamorphosis, though the number did not change thereafter (Table 2). No sexual difference in the number of auxocyte-like cells was found at all. Normal gonial cells were seen in the peripheral region of Bidder's organ, and these entered meiosis at stage 45 (the time of completion of metamorphosis). In females, secondary gonia and oocytes appeared earlier in Bidder's organ than in the gonad proper (ovary). The sexual difference in the number of germ cells in Bidder's organ was recognized at stage 43. The total number of germ cells in male Bidder's organ was significantly larger than the number in female one, and the difference was due to the number of gonial cells. From the 18th day after metamorphosis on, however, the total number of germ cells, the number of secondary gonia and the number of oocytes in Bidder's organ were significantly larger in females, and the mitotic index of primary gonia also tended to be higher in females. As a result of the more active formation of secondary gonia from primary gonia in females, the number of primary gonia tended to be larger in males. The difference in the mitotic index of primary gonia between the gonad proper and Bidder's organ was not recognized except in female toads on the 12th day after metamorphosis.

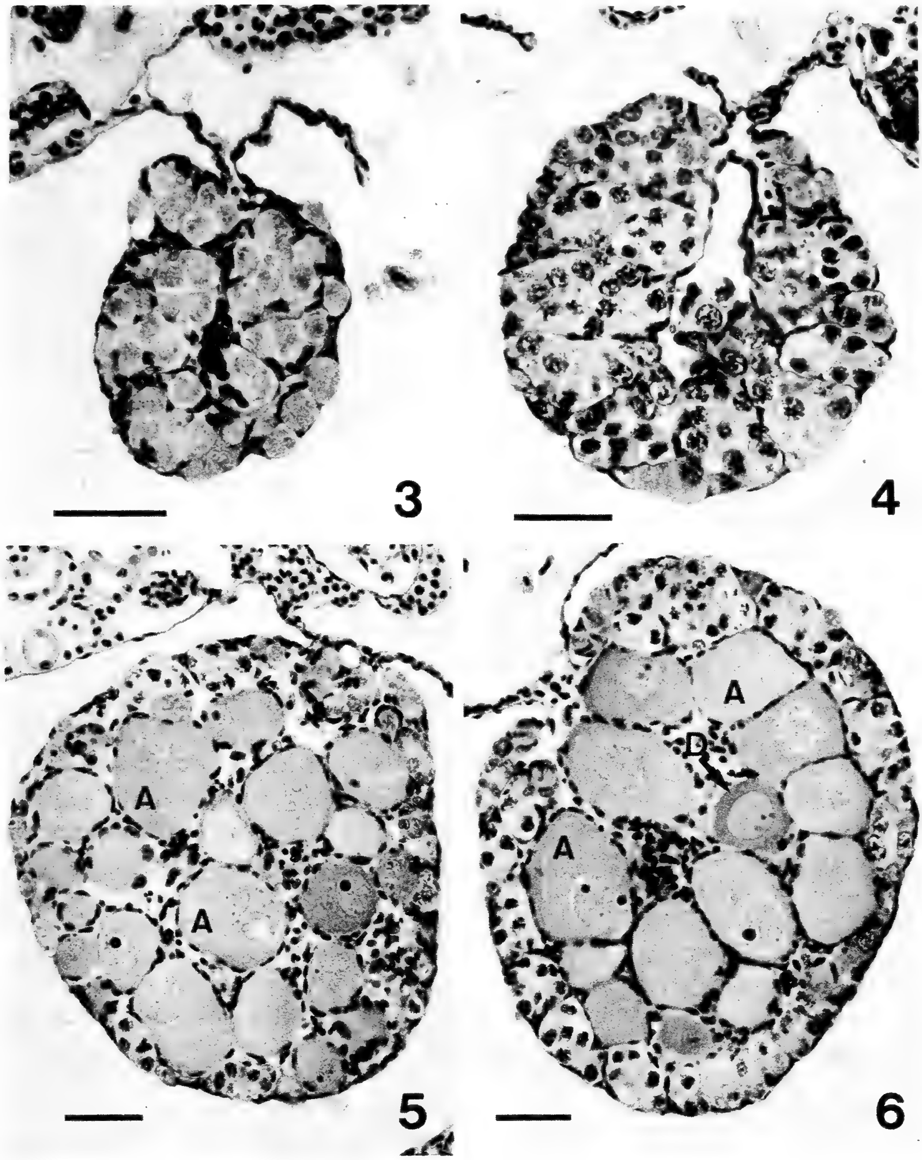

FIGS. 3–6. Cross sections of gonads and Bidder's organs on 24th day after metamorphosis. 3. Male gonad (testis). 4. Female gonad (ovary). 5. Male Bidder's organ. 6. Female Bidder's organ. A: auxocyte-like cell, D: degenerating auxocyte-like cell. Scales: 50 μm.

Oogenic activities in the ovary and Bidder's organ in females

The number of secondary gonia and oocytes (oogenic cells) accounted for the total number of germ cells (percentage of oogenic cells) was significantly lower in the gonad proper (ovary) than in Bidder's organ at stage 43 (Fig. 7). A rapid increase in the percentage of oogenic cells, which indicates that the active formation and proliferation of secondary gonia, was seen from just after metamorphosis to the 12th day. Furthermore, the number of oocytes accounted for the number of oogenic cells (percentage of oocytes) was signif-

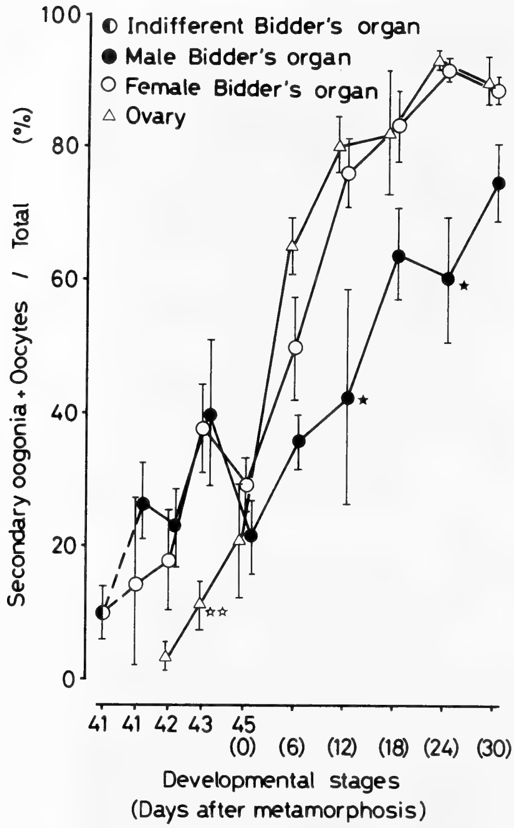

FIG. 7. Percentage of oogenic cells in the ovary and Bidder's organ. Mean±SE. Sexual difference: ★ $0.01<p<0.05$. Difference between ovary and Bidder's organ: ☆ $0.01<p<0.05$, ☆☆ $p<0.01$.

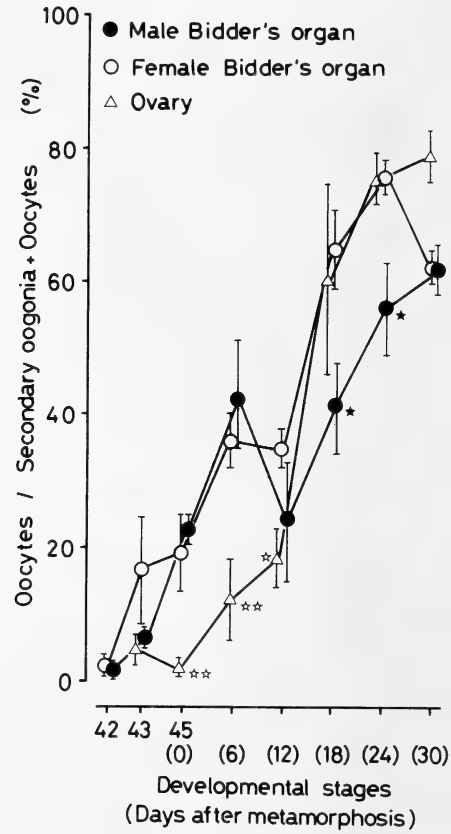

FIG. 8. Percentage of oocytes in the ovary and Bidder's organ. Mean±SE. Sexual difference: ★ $0.01<p<0.05$. Difference between ovary and Bidder's organ: ☆ $0.01<p<0.05$, ☆☆ $p<0.01$.

icantly lower in the ovary than in Bidder's organ until the 12th day (Fig. 8). The rapid increase in the percentage of oocytes, which indicates that the active formation of oocytes, was seen from 12th to the 24th day.

The rapid increase in the above-mentioned percentage was not seen in male Bidder's organ.

DISCUSSION

The sexual difference in the number of germ cells has been known in *Rana nigromaculata* [4] and *Xenopus laevis* [5, 6]. In these species, the sexual difference in the number of germ cells was recognized at the time of gonadal sex differentiation, and the number was significantly larger or tended to be larger in females. In *Bufo japonicus formosus,* on the other hand, the sexual difference in the number of germ cells was not yet clear at the time of sex differentiation of gonads, and was recognized on the 6th day after metamorphosis, and the number was larger in females. A slightly higher mitotic index of primary gonia was noticed in ovaries, and a large number of secondary gonia and oocytes were seen in the ovaries. A similar phenomenon was seen in Bidder's organs on the 18th day. Therefore, in toads the main cause of the appearance of a sexual difference in the number of germ cells is due to a remarkable proliferation of secondary gonia in female gonads.

Kobayashi [4] and Yamaguchi and Iwasawa [6] pointed out a positive relationship between the

occurrence of sexual difference in the number of germ cells and the initiation of oogenesis in some anuran species, and Satoh and Egami [7] reported the same phenomenon in the teleost *Oryzias latipes*. On the other hand, Beaumont and Mandl [8] suggested that in the rat a high rate of mitotic activity of primordial germ cells may set in earlier in male gonads. Furthermore, in birds, a rapid increase in the number of the gonial cells takes place in the gonadal medulla at the time of sex differentiation in males [9].

Wartenberg [10] reviewed that the dark cells which originate from the mesonephros exert an influence on the development of gonads and the initiation of meiosis in mammals. He also pointed out the existence of somatic cells which have a similar influence on developing gonads in birds, though the origin of these cells is not yet clear [11, 12]. In fish, on the other hand, Kanamori *et al.* [13] reported that interrenal or mesonephric cells did not influence gonadal development. It has been suggested that in anurans both the cortex and medulla in gonadal primordia originate from the coelomic epithelium [14–16]. From the above-mentioned facts, it can be said that some types of somatic cells which take part in the gonadal development may exert an influence on the proliferation of germ cells.

In the present study, a rapid increase in the formation and proliferation of secondary gonia and the initiation of meiosis were seen in the ovary and Bidder's organ in females. On the other hand, no similar increase was seen in Bidder's organ in males. It is likely, therefore, that such activities in females were influenced by some substances produced by the somatic cells which differentiated around the germ cells. The regulatory mechanism of these oogenic activities is not clear from the present study. The hormonal control of oogonial proliferation and meiosis has not been sufficiently elucidated in amphibians [17]. In mammals, the existence of meiosis-preventing and inducing substances has been pointed out [18]. Further studies in this field are needed in amphibians.

ACKNOWLEDGMENTS

This work was supported in part by a Grant-in-Aid for Scientific Research to H. I. (No. 59340049) from the Japanese Ministry of Education, Science and Culture.

REFERENCES

1 Hardisty, M. W. (1967) The number of vertebrate primordial germ cells. Biol. Rev., **42**: 265–287.

2 Tanimura, A. and Iwasawa, H. (1986) Development of gonad and Bidder's organ in *Bufo japonicus formosus*: Histological observation. Sci. Rep. Niigata Univ., Ser. D, **23**: 11–21.

3 Ichikawa, M. and Tahara, Y. (1966) Normal table of development of the toad, *Bufo bufo japonicus*. In "Vertebrate Embryology". Ed. by M. Kume, Baifukan, Tokyo, pp. 178–195. (In Japanese)

4 Kobayashi, M. (1975) Sexual and bilateral differences in germ-cell numbers in the course of the gonadal development of *Rana nigromaculata*. Zool. Mag., **84**: 109–114. (In Japanese with English abstract)

5 Ijiri, K. and Egami, N. (1975) Mitotic activity of germ cells during normal development of *Xenopus laevis* tadpoles. J. Embryol. Exp. Morphol., **34**: 687–694.

6 Yamaguchi, K. and Iwasawa, H. (1981) Histological studies on gonadal development and sexual difference in germ cell number in *Xenopus laevis*. Zool. Mag., **90**: 456 (Abstract in Japanese).

7 Satoh, N. and Egami, N. (1972) Sex differentiation of germ cells in the teleost, *Oryzias latipes*, during normal embryonic development. J. Embryol. Exp. Morphol., **28**: 385–395.

8 Beaumont, H. M. and Mandl, A. M. (1963) A quantitative study of primordial germ cells in the male rat. J. Embryol. Exp. Morphol., **11**: 715–740.

9 Witschi, E. (1956) Development of Vertebrates, W. B. Saunders Co., Philadelphia, pp. 298–313.

10 Wartenberg, H. (1983) Structural aspects of gonadal differentiation in mammals and birds. Differentiation, **23** (suppl.): 64–71.

11 Lepori, N. G. (1980) Sex Differentiation, Hermaphroditism and Intersexuality in Vertebrates including Man, Piccin Medical Books, Padua, pp. 149–165.

12 Merchant-Larios, H., Popova, L. and Reyss-Brion, M. (1984) Early morphogenesis of chick gonad in the absence of mesonephros. Dev. Growth Differ., **26**: 403–417.

13 Kanamori, A., Nagahama, Y. and Egami, N. (1985) Development of the tissue architecture in the gonads of the medaka *Oryzias latipes*. Zool. Sci., **2**: 695–706.

14 Merchant-Larios, H. and Villalpando, I. (1981) Ultrastructural events during early gonadal development in *Rana pipiens* and *Xenopus laevis*. Anat.

Rec., **199**: 349–360.

15 Iwasawa, H. and Yamaguchi, K. (1984) Ultrastructural study of gonadal development in *Xenopus laevis*. Zool. Sci., **1**: 591–600.

16 Tanimura, A. and Iwasawa, H. (1986) Formation and following morphogenic change of gonadal medulla in the toad *Bufo japonicus formosus*. Zool. Sci., **3**: 1067 (Abstract).

17 Tokarz, R. R. (1978) Oogonial proliferation, oogenesis, and folliculogenesis in nonmammalian vertebrates. In "The Vertebrate Ovary". Ed. by R. E. Jones. Plenum Press, New York, pp. 145–179.

18 Gondos, B. and Byskov, A. G. (1981) Germ cell kinetics in the neonatal rabbit testis. Cell Tissue Res., **215**: 143–151.

ZOOLOGICAL SCIENCE 4: 665–673 (1987)

Preliminary Study on the Pattern of Gonadal Development of the Sea Urchin, *Diadema setosum*, off the Coast of Singapore

REIJI HORI, VIOLET P. E. PHANG and TOONG JIN LAM

Department of Zoology, National University of Singapore, Singapore 0511, Singapore

ABSTRACT—Eighteen collections of the sea urchin, *Diadema setosum*, were made from coral reefs of islands off the coast of Singapore from July 1982 to July 1983. On each occasion 9–36 sea urchins were collected. A total of 459 sea urchins were collected and induced to spawn with isotonic KCl solution after which samples of the gonads were dissected from each individual for histological observations to study oogenesis and spermatogenesis. The number of males exceeded that of females in 14 of the 18 collections. Some animals of both sexes could be induced to spawn throughout the period. Thus, within the 12 month period studied, spawning was continuous but peak percentage of induced spawning was observed in October when all the individuals of both sexes were induced to spawn. The process of gonadal maturation was categorized histologically into four stages in the testis and five stages in the ovary. Gametogenesis was asynchronous. The optimal stage for induction of spawning appeared to be stage III for males and stage V for females. There was no obvious lunar reproductive rhythm nor was there clear correlation between frequency of induced spawning and total monthly rainfall.

INTRODUCTION

The sea urchin, *Diadema setosum,* is widely distributed in Indo-Pacific sea waters [1]. The reproductive pattern of the animal in the temperate zone is limited to a certain period of the year. According to Yoshida [2], animals from Japan spawn only once a year during summer; those from the Misaki bay in the south coast spawn during full moon but those from Seto, also in the south coast spawn during the hemi-lunar period [3].

At the edge of the tropics, the species spawns during the summer months when sea temperatures are above 25°C [1, 4–6]. There have been several discussions on the lunar periodicity of the animal in the edge of the tropics. Fox [7, 8] found there was a lunar periodicity of *D. setosum* in the Red Sea at Suez. During the breeding season, the animals spawned at full moon and became again full of ripe eggs or sperm at the next full moon. However, Mortensen [1] could not confirm Fox's observations, finding that near Suez ripe specimens could be obtained irrespective of the full moon. In a later investigation, Mortensen [9] reported that, in the case of other populations in this region, there was not much support for a lunar periodicity and considered that the periodicity in *D. setosum* near Suez is a rare exception. Later studies by Pearse [5, 6] showed that reproduction of *D. setosum* in the gulf of Suez and the northern Red Sea was not related to lunar periodicity thus giving support to Mortensen's conclusion [9]. On the other hand, Pearse [5] reported that gametogenesis was synchronous among individuals of *D. setosum* from 5 equatorial localities in central West-Pacific, and spawning occurred rhythmically, more or less monthly during the spawning period without any relation to lunar phases. Other investigations [10–12] showed that spawning occurred throughout the year in the tropics where sea temperatures were nearly always above 25°C. It would appear that reproduction of this species does not show a constant pattern but may vary according to geographical locality, sea temperature, lunar cycle and other environmental condi-

Accepted April 9, 1987
Received September 2, 1986

tions. The main purpose of the present study is to obtain preliminary information on spawning frequency and the synchrony of reproduction of *D. setosum* off the coasts of Singapore. The maturation process of the gonads was also studied histologically.

MATERIALS AND METHODS

From July 1982 to July 1983 samples of *D.setosum* were collected monthly or fortnightly from the area including three islands, Pulau Sakeng, Pulau Hantu and Pulau Sakra off the southern coast of Singapore (Fig. 1). These islands are located within 8 km from each other. The sea urchins could be found to a depth of 6 metres. The dates of the collections were made to coincide with the full moon, half moon or new moon. The sample size for each collection consisted of 9–36 animals. The surface water temperature was taken at each collection and variation between surface and bottom temperature was found to be less than 1°C. A total of 459 specimens was collected. The width of the test of each animal was measured with a ruler after the spines were trimmed. The width ranged from 4.0–8.0 cm. The sea urchins were dissected within a day after collection. The animals were opened around the peristome and the lantern of Aristotle and the body fluid were removed.

For each individual, a small middle portion of the gonad was collected, fixed in Bouin's solution for 24 hr, sectioned at 7 μm and stained with haematoxylin and eosin. After the gonadal biopsy, each sea urchin was placed upside down in a beaker filled with sea water at room temperature (23–25°C) and induced to spawn by pouring isotonic 5/9 M KCl solution into the coelomic cavity. As soon as the male started to release milky sperm into the sea water, the KCl solution in the coelomic cavity was removed and the animal was transferred to an empty beaker for sperm collection. The volume of the seminal fluid was measured 30 min after transferring to the empty beaker. The female induced to spawn was left to stand on the beaker filled with sea water for 30 min, for all the eggs to sink to the bottom of the

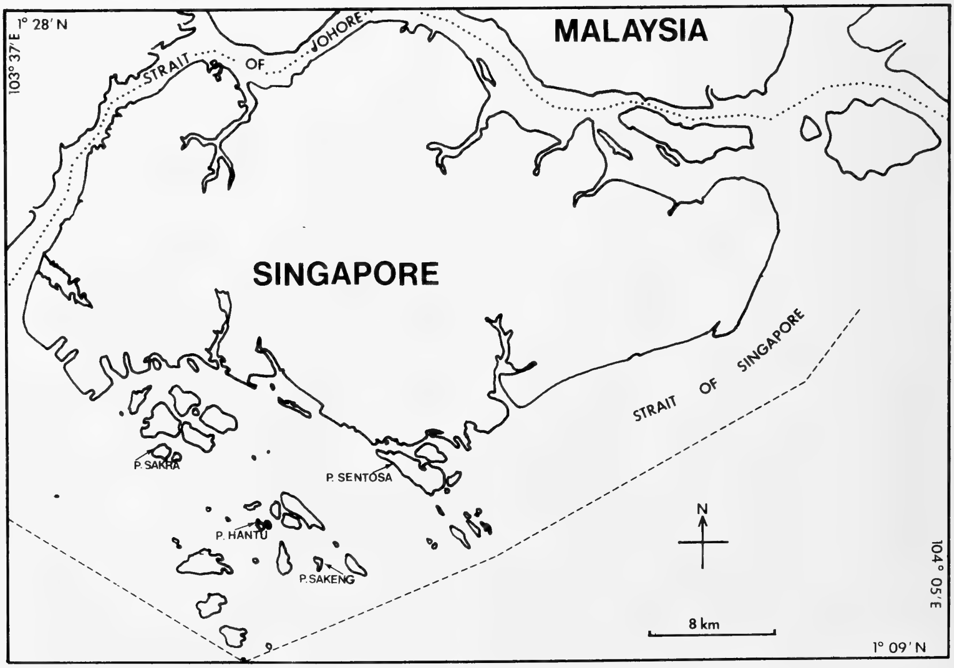

Fig. 1. The locations of collecting *Diadema setosum* and the station of the Meteorological Service of Singapore (Pulau Sentosa).

beaker. The supernatant sea water was carefully removed. The eggs were rinsed twice with sea water and transferred to a glass cylinder. The volume of the egg suspension was also measured 30 min after transferring to the cylinder. The critical volumes of seminal fluid and egg suspension to confirm the induction of spawning were 0.5 ml and 1 ml, respectively. Microscopic examinations of samples with volumes below the critical values showed that there were only fragments of gonadal epithelia, and small amount of spermatozoa or immature eggs. In samples with volumes exceeding the critical levels there were much more spermatozoa and mature eggs. The maximum volumes of the seminal fluid and egg suspension from fully mature gonads could amount to as much as 10 ml and 50 ml, respectively. If spawning was not induced, a small piece of the gonad was collected and a smear was made on a glass slide for microscopic examination to determine sex.

Data of total monthly rainfall[1] were obtained from the station of the Meteorological Service of Singapore at Pulau Sentosa which lies within the area where the sea urchins were collected.

RESULTS

1. Gonads

There appeared to be no difference in gross appearance between the testis and ovary. The general condition of the gonads varied greatly among individuals as was found by Pearse [5]. The color of gonads ranged from pale cream, beige, pale yellow, yellow brown to brown, with no relation to sex. Young immature gonads tended to be soft and smooth. Other gonads were large, firm and glandular but the size was not indicative of their maturity. However none of the gonads were found to be very hard as reported by Kobayashi and Nakamura [3] for *D. setosum* in Seto, Japan.

TABLE 1. Number of male and female of *Diadema setosum* from each collection

Date, time and place of collection	Surface sea water temperature (°C)	Male	Female	Total	Sex ratio No. of male / No. of female
15 July 1982 1,30 pm P. Hantu	31.0	15	9	24	1.67
31 Aug. 1982 10,00 am P. Sakra	30.5	12	9	21	1.33
8 Oct. 1982 9,30 am P. Sakeng	29.0	8	6	14	1.33
10 Oct. 1982 1,00 pm P. Hantu	29.5	12	6	18	2.00
9 Nov. 1982 10,00 am P. Sakeng	29.5	7	10	17	0.70
22 Dec. 1982 1,00 pm P. Sakra	28.5	15	8	23	1.88
30 Dec. 1982 11,00 am P. Sakeng	27.0	22	10	32	2.20
30 Jan. 1983 1,00 pm P. Sakeng	28.0	25	5	30	5.00
27 Feb. 1983 1,00 pm P. Sakra	30.0	18	12	30	1.50
16 Mar. 1983 10,00 am P. Sakeng	30.5	22	9	31	2.44
31 Mar. 1983 10,00 am P. Sakeng	30.0	13	17	30	0.76
28 Apr. 1983 11,00 am P. Sakeng	29.5	21	8	29	2.63
13 May 1983 1,00 pm P. Sakra	29.5	16	8	24	2.00
18 May 1983 10,00 am P. Sakeng	29.5	4	5	9	0.80
28 May 1983 0,30 pm P. Sakra	28.5	19	11	30	1.73
19 June 1983 10,00 am P. Sakeng	29.0	20	16	36	1.25
26 June 1983 10,30 am P. Sakeng	29.0	17	14	31	1.21
25 July 1983 10,00 am P. Sakeng	29.5	8	22	30	0.36
Total	(average) 29.3	274	185	459	(average) 1.71

[1] The Data were referred from Monthly Abstracts of Observations, the Meteorological Service of Singapore, 1982 and 1983.

2. Sex ratio

The sex of the animal could not be simply distinguished externally because there was variation in the pattern surrounding the genital pore. It could only be distinguished by spawning or by microscopic examination of gonadal smears. The sex of each animal in all collections was determined (Table 1). The sex ratio (number of males divided by number of females) was greater than 1 in 14 of the 18 samples. In the sample collected in January, the number of males was 5 times of that of females. Of the total of 459 animals, 60% were males and 40% females.

3. Spawning pattern

Induced spawning occurred in some males and females collected throughout the period of investigation. Thus spawning was continuous within the 12 month period studied (Tables 2 and 3). There did not appear to be a correlation between the proportion of animals spawning and the phase of the lunar cycle. The average percentage of males induced to spawn was greater than that of females. The number of males induced to spawn generally exceeded those which did not except for 5 collections on 16 March, 13, 18 and 28 May, and 19 June 1983. For the two samples collected in October 100% spawning of both sexes was observed. There was also 100% spawning of females in the sample collected on 30 January.

Figure 2 shows the percentage of monthly spawning of males and females, and total monthly rainfall at Pulau Sentosa from July 1982 to July 1983. In Singapore the rainy season occurs in the period between October and January and minor wet season occurs around April and May. There did not appear to be any clear relationship between percentage of induced spawning and total monthly rainfall for the period studied.

4. Histological Analysis

To study the process of spermatogenesis and oogenesis, histological sections of 459 animals were examined. Fox [7] divided the process of gonadal maturation of *D. setsum* into 5 stages

Table 2. The number of males of *Diadema setosum* induced to spawn and percentage of individuals in different stages of spermatogenesis

Lunar phase	Date of collection	Total	No. induced to spawn	% induced to spawn	Stages of spermatogenesis (%) I	II	III	IV
H	15 July 1982	15	12	80	7	13	67	13
F	31 Aug. 1982	12	10	83	0	25	67	8
H	8 Oct. 1982	8	8	100	0	12	76	12
N	18 Oct. 1982	12	12	100	0	17	75	8
H	9 Nov. 1982	7	4	57	14	29	57	0
H	22 Dec. 1982	15	14	93	0	20	67	13
F	30 Dec. 1982	22	15	68	14	18	59	9
F	30 Jan. 1983	25	16	64	4	40	52	4
F	27 Feb. 1983	18	16	88	6	16	67	11
N	16 Mar. 1983	22	10	45	5	50	40	5
F	31 Mar. 1983	13	10	76	0	31	69	0
F	28 Apr. 1983	21	13	62	0	38	57	5
N	13 May 1983	16	7	44	6	50	38	6
H	18 May 1983	4	1	25	0	50	50	0
F	28 May 1983	19	6	32	11	53	31	5
H	19 June 1983	20	8	40	35	30	35	0
F	26 June 1983	17	11	65	12	29	53	6
F	25 July 1983	8	7	88	12	25	50	12
Average		274 (total)	180 (total)	67.2	7.0	30.4	56.1	6.5

F: full moon, H: half moon, N: new moon.

TABLE 3. The number of females of *Diadema setosum* induced to spawn and percentage of individuals in different stages of oogenesis

Lunar phase	Date of collection	Total	No. induced to spawn	% induced to spawn	Stages of oogenesis (%) I	II	III	IV	V
H	15 July 1982	9	3	33	22	11	33	11	22
F	31 Aug. 1982	9	6	67	0	11	22	33	33
H	8 Oct. 1982	6	6	100	0	0	0	33	67
N	18 Oct. 1982	6	6	100	0	0	0	50	50
H	9 Nov. 1982	10	6	60	0	10	20	50	20
H	22 Dec. 1982	8	7	88	0	0	13	38	50
F	30 Dec. 1982	10	7	70	0	0	20	30	50
F	30 Jan. 1983	5	5	100	0	0	0	20	80
F	27 Feb. 1983	12	6	50	0	8	8	50	34
N	16 Mar. 1983	9	4	44	0	0	22	56	22
F	31 Mar. 1983	17	10	59	0	12	12	38	38
F	28 Apr. 1983	8	4	50	0	12	18	41	29
N	13 May 1983	8	3	38	0	13	13	38	38
H	18 May 1983	5	2	40	0	20	20	40	20
F	28 May 1983	11	4	36	9	18	18	36	18
H	19 June 1983	16	6	37	0	12	25	44	19
F	26 June 1983	14	7	50	14	7	21	36	21
F	25 July 1983	22	7	32	5	23	32	18	22
Average		185 (total)	99 (total)	58.6	2.8	8.7	16.5	36.8	35.2

F: full moon, H: half moon, N: new moon.

while Yoshida [2] into 9. Pearse [13] divided the maturation process of *Echinometra mathaei* into 6 stages. For this study we found it more convenient to categorize the process into 4 stages in the testis (Fig. 3) and 5 stages in the ovary (Fig. 4).

Testis

Stage I. (Fig. 3a) Cells which are well-stained with eosin occupy the majority of the testicular lobes. The testis looks solid. Among haematoxylin-stained spermatogonia, some are scattered in the centre of the testicular lobe and the rest are found in the periphery of the testis forming considerable number of masses.

Stage II. (Fig. 3b) The number of spermatogonia which are well-stained with haematoxylin increases and they gradually move to the central area of the testicular lobe. A narrow empty space (lumen) can be found in the centre of the testicular lobe. A few spermatozoa are observed in the lumen.

Stage III. (Fig. 3c) The space of the lumen is expanded. The wall of the lumen becomes thinner and consists of few layers of epithelium. The lumen is filled with large numbers of mature spermatozoa. This stage corresponds to the full mature stage of spermatogenesis. By isotonic KCl solution, artificial spawning of spermatozoa is easily induced at this stage.

Stage IV. (Fig. 3d) The lumen in the centre of the testicular lobes is almost empty. The wall of the testicular lobes becomes thicker and few haematoxylin-stained spermatozoa are observed in the lumen. Considerable numbers of spermatozoa are found surrounding the testicular lobes. Completely degenerated testis has not been observed from histological sections of all the specimen examined during this investigation.

Ovary

Stage I. (Fig. 4a) In the periphery of the ovarian lobe, a few young oogonia stained with haematoxylin are observed. The diameter of the oogonia is 10–15 μm. The rest of the ovarian lobe is occupied with eosin-stained cells and the ovary itself is compact.

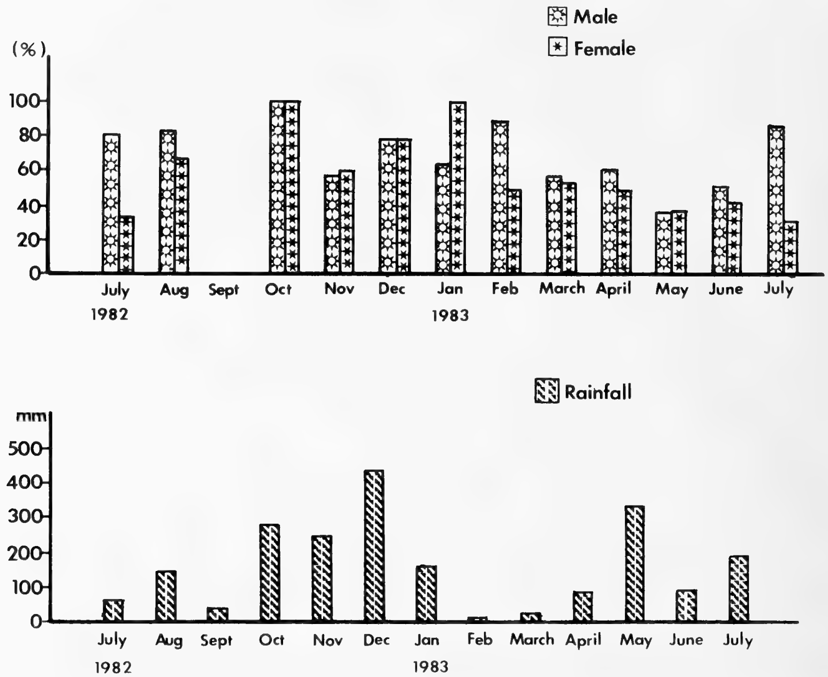

Fig. 2. Percentage of monthly spawning of male and female *Diadema setosum* and total monthly rainfall at Pulau Sentosa from July 1982 to July 1983.

Stage II. (Fig. 4b) Oogonia have a tendency to increase in size and to migrate from the periphery to the centre of the ovarian lobe where the ovarian cavity will be eventually formed and where the oogonia develop into young oocytes. The germinal vesicle cannot be recognized in the young oocytes.

Stage III. (Fig. 4c) Several large oocytes with a big germinal vesicle appear at this stage. The ovarian cavity is not yet clearly defined. Some of the oocytes are found near the undefined ovarian cavity while the rest was still in the periphery of the ovarian lobe. There may be a tendency for the oocytes to migrate to the ovarian cavity during the maturation period.

Stage IV. (Fig. 4d) The wall of the ovarian cavity is still thick. Small-sized oocytes with a germinal vesicle occupy the wall of the ovarian cavity. The ovarian cavity has not yet expanded widely but a considerable number of mature eggs are found in it.

Stage V. (Fig. 4e) The ovary is in a fully mature state. The epithelium becomes thinner and consists of single or double layers inside of which very few small oocytes are embedded. The wide ovarian cavity is filled with many mature ova. Ovaries with empty or degenerated ovarian cavity have not been found in this investigation.

There is little uniformity in stages of gametogenesis of both testes and ovaries among different individuals in each sample (Tables 2 and 3). The gonads of most of the animals were in stages II or III for the testis (except the sample collected on 19 June, where 35% of testes were in stage I) (Table 2) and stage IV or V for the ovary (except two samples on 15 July 1982 and 25 July 1983 where more than 30% of ovaries were in stage III) (Table 3). Thus gametogenesis was asynchronous throughout the year.

DISCUSSION

Orton [14] proposed that changing sea temperature was the major cause of seasonality of reproduction in marine animals. Yonge [10] from

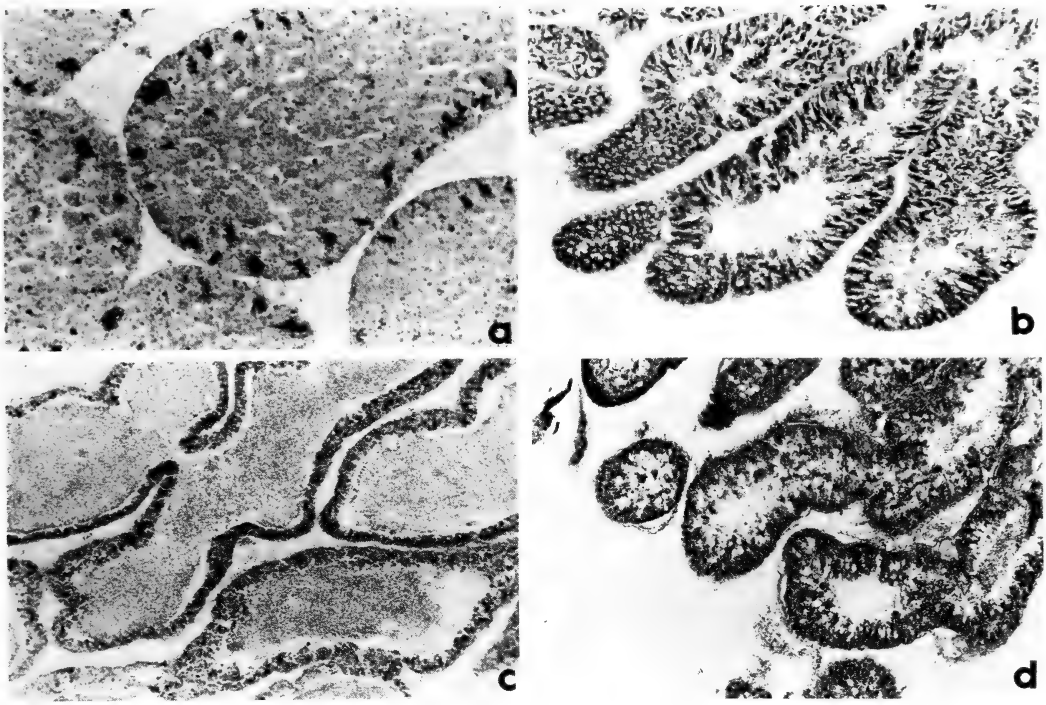

FIG. 3. Cross sections of the testis in *Diadema setosum*. a and b; immature testes, c; fully mature testis, d; testis after spawning. a; ×450, b, c and d; ×350.

studies of marine invertebrates along the Great Barrier Reef categorized invertebrates into two groups according to whether lower or higher temperatures limit their reproductive activities. He included *D. setosum* in the higher temperature group and assumed that the critical temperature was 25°C. Thus in the tropics where sea temprature are nearly always above 25°C, spawning is continuous, as found in *D. setosum* by Yonge [10], Pearse [11, 15] and Tuason and Gomez [12]. During the period under study, the surface sea water temperature ranged from 27°C to 31°C and variation between surface and bottom temperature was less than 1°C. Spawning in *D. setosum* from Singapore waters was also found to be continuous but there was maximum induced spawning in the month October for both sexes.

Yoshida [2] found that in *D. setosum* from Misaki, Japan gametogenesis was well synchronized. He described transitional changes of maturation and classified spermatogenesis and oogenesis into 9 stages. According to him, the transitional changes are continuous, that is, after spawning the gonads gradually degenerate until they arrive at a completely degenerated stage which he called the "post-spawning stage". The animals then resume the maturation process and arrive at the fully mature state the next summer. The post-spawning stage corresponds to "Class 5" of Fox's description [7]. Among 274 males and 185 females studied histologically no individual was found with completely degenerated gonads corresponding to Stage IX of Yoshida [2]. Considering the asynchronous gametogenesis of *D. setosum* in tropical waters, the authors are inclined to believe that the sea urchins in this region recover functions of the gonads before they become completely degenerated; this may be due to tropical conditions such as continuous high temperature of the sea water which is always greater than 25°C.

According to Yoshida [2], *D. setosum* spawns once a year during full moon in Misaki, Japan. Kobayashi and Nakamura [3] reported that this species in Seto, Japan had a hemi-lunar periodicity

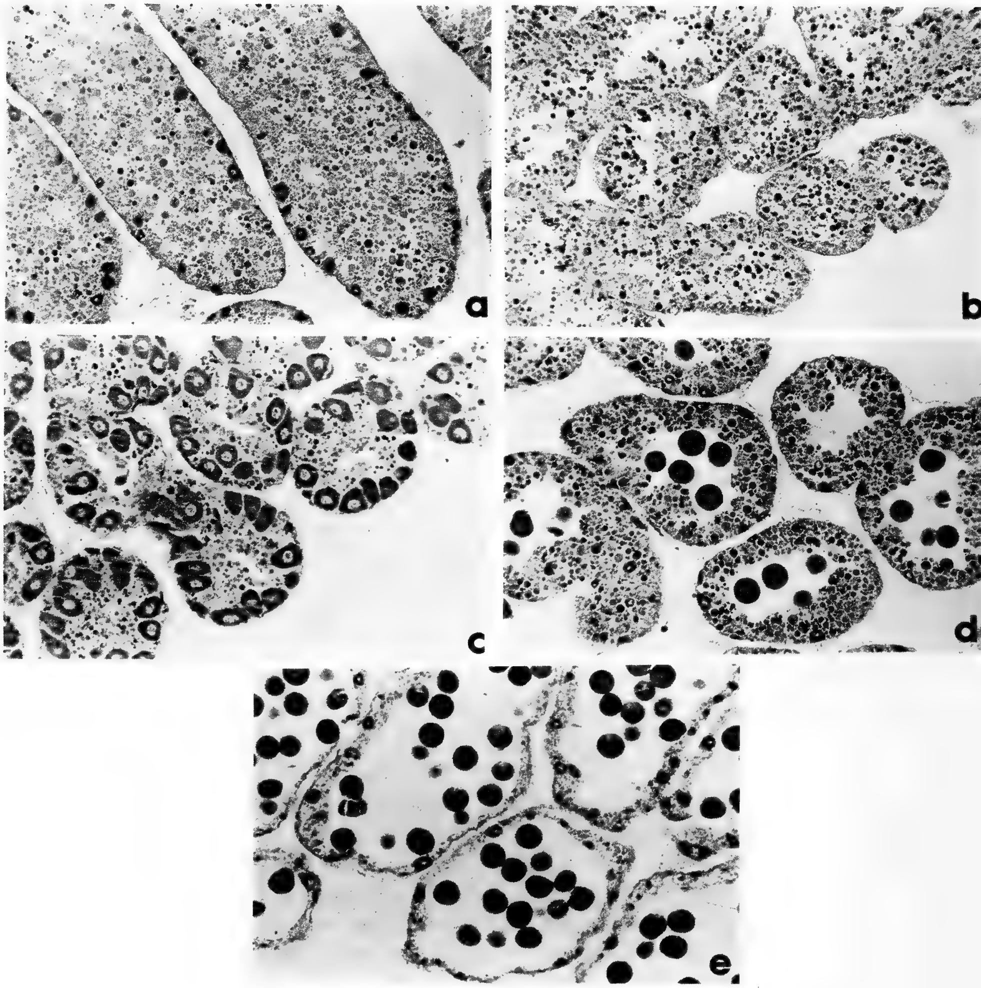

Fig. 4. Cross sections of the ovary in *Diadema setosum*. a, b and c; immature ovaries, d; almost mature ovary, e; fully mature ovary. a; ×450, b, c, d and e; ×350.

with spawning around the full moon and new moon. Thus in animals living in higher latitudes gametogenesis is synchronous and the reproductive activity is very much restricted [5]. The spawning period is not only limited to the summer month but is also related to the lunar phases.

Reproduction of *D. setosum* in tropical waters in the southern area of Singapore appeared to bear little relationship to the lunar cycle as found by Korringa [16] and Pearse [5, 6]. There was lack of gametic synchrony among individuals of each sample in the present study. Since the animals were collected near three islands offshore of Singapore located within 8 km from each other, the feature of spawning may represent that in this area. The cycle of maturation, therefore, may occur several times in a year and the gonads do not become completely degenerate after each spawning. This differs from the findings of Pearse [6] who reported close gametic synchrony among individuals within each population but a lack of synchrony between different populations in central West-Pacific. As the spawning pattern was affected by a critical sea temperature of around

25°C, lunar phases, accumulation of nutrients in the gonads and other environmental conditions [13, 17], the spawning rhythm in the central West-Pacific populations may be intermediate between temperate and tropical types.

Every year in Singapore, the rainy season due to the north-east monsoon occurs in the period between October and January. Another minor wet season due to the south-west monsoon occurs around April and May. Peak percentage of induced spawning was found in October, which is the beginning of the north-east monsoon period. Basing on the assumption that monsoon rains trigger off spawning, another peak of induced spawning would be expected during the south-west monsoon period but there was no corresponding peak during April and May. There was also 100% spawning of females in the sample collected on 30 January which was the end of the north-east monsoon period, although sample size was only five. Hence, there does not appear to be any clear relationship between percentage of induced spawning and the total monthly rainfall during the period studied (Fig. 2). Further and more detailed studies of animals in Singapore covering a longer period of time are needed to clarify the relationships between frequency of spawning and the amount of rainfall and also other environmental factors.

Artificial spawning with isotonic KCl in the present study is unnatural. KCl causes contraction of gonadal tissues of the animal which forces the release of the gametes into the sea water. However, such artificial procedure would be close to natural spawning when fully mature gametes are involved. Comparing the number of individuals induced to spawn with the results of histological examination of gametogenesis (Tables 2 and 3), the optimal stage for induction of spawning appeared to be stage III for males and stage V for females.

REFERENCES

1 Mortensen, Th. (1937) Contribution to study of the development and larval forms of the echinoderms. III. Kgl. Dansk. Vidensk. Selsk. Skr. Naturv. Math. Ser. 9, **7** (1): 1–65.

2 Yoshida, M. (1952) Some observations on the maturation of the sea urchin *Diadema setosum*. Annot. Zool. Japon., **25**: 265–271.

3 Kobayashi, N. and Nakamura, K. (1967) Spawning periodicity of sea urchins at Seto. II. *Diadema setosum*. Publ. Seto Mar. Biol. Lab., **15**: 173–184.

4 Stephenson, A. (1934) The breeding of reef animals. Part II. Invertebrates other than corals. Gt. Barrier Reef Exped. 1928–1929, Sci. Rep., **3**: 247–272.

5 Pearse, J. S. (1968) Patterns of reproduction in 4 species of Indo-Pacific echinoderms. Proc. Indian Acad. Sci. Sec. B, **67**: 247–279.

6 Pearse, J. S. (1970) Reproductive periodicities of Indo-Pacific invertebrates in the Gulf of Suez. III. The echinoid *Diadema setosum* (Leske). Bull. Mar. Sci., **20**: 697–720.

7 Fox, H. M. (1924) Lunar periodicity in reproduction. Proc. Roy. Soc. Lond. Ser. B, **95**: 523–550.

8 Fox, H. M. (1924) The spawning of echinoids. Proc. Camb. Phil. Soc. Biol. Sci., **1**: 71–74.

9 Mortensen, Th. (1938) Contribution to study of the development and larval forms of the echinoderms. IV. Kgl. Dansk. Vidensk. Selsk. Skr. Naturv.Math. Ser. 9, **7** (3): 1–59.

10 Yonge, C. M. (1924) The biology of reef-building corals. Gt. Barrier Reef Exped. 1928-1929, Sci. Rep., **1**: 353–389.

11 Pearse, J. S. (1974) Reproductive patterns of tropical reef animals: Three species of sea urchins. Proc. 2nd Int. Coral Reef Symp., **1**: 235–240.

12 Tuason, H. Y. and Gomez, E. D. (1979) The reproductive biology of *Tripneustes gratilla* Linnaeus (Echinoidea: Echinodermata) with some notes on *Diadema setosum* Leske. Proc. Int. Symp. Mar. Biogeogr. Evol. Southern Hemisphere, **2**: 707–716.

13 Pearse, J. S. (1969) Reproductive periodicities of Indo-Pacific invertebrates in the Gulf of Suez. II. The echinoid *Echinometra mathaei* (de Blainville). Bull. Mar. Sci., **19**: 580–613.

14 Orton, J. H. (1920) Sea temperature, breeding and distribution in marine animals. J. Mar. Biol. Ass. U. K., **12**: 339–366.

15 Pearse, J. S. (1975) Lunar reproductive rhythms in sea urchins. A review. J. Interdiscipl. Cycle Res., **6**: 47–52.

16 Korringa, P. (1947) Relations between the moon and periodicity in the breeding of marine animals. Ecol. Monogr., **17**: 347–381.

17 Iliffe, T. M. and Pearse, J. S. (1982) Annual and reproductive rhythms of the sea urchin *Diadema antillarum* (Philippi) in Bermuda. Int. J. Invert. Reprod., **5**: 139–148.

ZOOLOGICAL SCIENCE 4: 675–681 (1987)

Extrahypothalamic Projection of Immunoreactive Vasotocin Fibers in the Brain of the Toad, *Bufo japonicus*

YOJI JOKURA[1] and AKIHISA URANO[2]

Department of Regulation Biology, Faculty of Science, Saitama University, Urawa, Saitama 338, Japan

ABSTRACT—Extrahypothalamic projection of vasotocin (AVT) fibers in the brain of the toad (*Bufo japonicus*) was examined immunohistochemically by the avidin-biotin-peroxidase complex (ABC) method. Immunoreactive AVT perikarya are localized in the nucleus preopticus pars magnocellularis. The AVT neurons send their immunoreactive varicose fibers to many discrete brain regions, such as the limbic cortex, the thalamus, the optic tectum and the lower brain stem, in addition to the neurohypophysis. A dense network of AVT fibers was found in the septal nuclei and the anterior part of the preoptic nucleus. AVT fibers which run postero-dorsad project to the nucleus posterocentralis thalami, the nucleus posterodorsalis tegmenti mesencephali, and the nucleus isthmi. Meanwhile, AVT fibers which run through in the dorsal infundibular region and then the mesencephalic reticular formation are distributed in the medulla oblongata. These findings suggest that AVT acts as a neuromodulator or a local hormone in the toad brain.

INTRODUCTION

It is well established that, in anuran amphibians, vasotocin (AVT) has both antidiuretic and vasopressor effects. In addition, AVT shows pronounced effects on reproductive behavior in *Rana pipiens* [1] and *Taricha granulosa* [2]. In *T. granulosa,* AVT may be involved in control of sexual behavior by acting neurons in the central nervous system [3]. We have shown in the toad brain that vasotocin neurons project their varicose axons into the anterior part of the preoptic nucleus (APON) which is considered to be the triggering center for male mate calling behavior in anuran amphibians [4]. These results suggest that AVT neurons transmit APON neurons peptidergic information concerned with initiation of sexual behavior.

In mammalian brains, the distributions of various neurohormones including arginine-vasopressin (AVP) are not confined only in the hypothalamo-neurohypophyseal system. They are widely distributed throughout in discrete brain loci [5]. Ultrastructural studies showed that axon endings of immunoreactive (ir) luteinizing hormone-releasing hormone (LHRH) fibers [6] and ir-AVP ones [7] form synapses and synaptoid contacts with other neurons. Further, varicose LHRH fibers form en passant synapses in the preoptic area of the guinea pig [6]. Therefore, it is probable in amphibian brains that, in addition to the APON and the neurohypophysis, AVT neurons send their fibers to many extrahypothalamic regions.

In this study, we examined immunohistochemically the extrahypothalamic distribution of AVT fibers in the toad brain to learn whether AVT neurons project their axons to the loci which are related to control of mating behavior. Further, we have tried to elucidate phylogenetically fundamental distributional pattern of AVT in the vertebrate brain, since the amphibian brain is considered to show fundamental structural organization of the vertebrate brain [8].

Accepted March 28, 1987
Received February 25, 1987

[1] Present Address: Tochigi First Lab., Kaou Co., Akabane, Ichikai-machi, Haga-gun, Tochigi 321–34, Japan.

[2] To whom reprints should be requested.

MATERIALS AND METHODS

Adult toads (*Bufo japonicus*) of both sexes, body weight ranging from 117 to 303 g, and body

length (snout to vent) from 11.9 to 14.1 cm, were used. These animals were either obtained from an animal supplier in late September or were captured at the breeding season. Three animals, which were obtained from an animal supplier in late November, were used for immunohistochemical staining of thick frozen sections.

Immunohistochemical procedure

Distribution of AVT was immunohistochemically localized in paraffin sections and thick frozen sections that were cut either transversally, sagittally or horizontally to determine exact loci where ir-AVT fibers were found. As for immunohistochemical staining of vasotocin in the paraffin sections of the toad brain, details of fixation, tissue preparation and immunohistochemical procedure, in which the Vectastain ABC kit (Vector) was used, have been described previously [9, 10].

For the staining of thick frozen sections, the brains were fixed by transcardial perfusion with a fixative solution containing 1% glutaraldehyde, 2% paraformaldehyde and 4% sucrose in 0.1 M phosphate buffer (pH 7.4). The brains were removed, postfixed in the same fixative at 4°C overnight, and were washed in 0.1 M phosphate buffer. Frozen sections were cut at 50 μm, and were washed in 0.1 M phosphate buffered saline (pH 7.4) at room temperature for 30 min. Then, they were stained immunohistochemically by use of the Vectastain ABC kit. The sections were first incubated with the primary antiserum in a reaction medium at 4°C for 12–16 hr. The solution for incubation contained anti-arginine-vasopressin

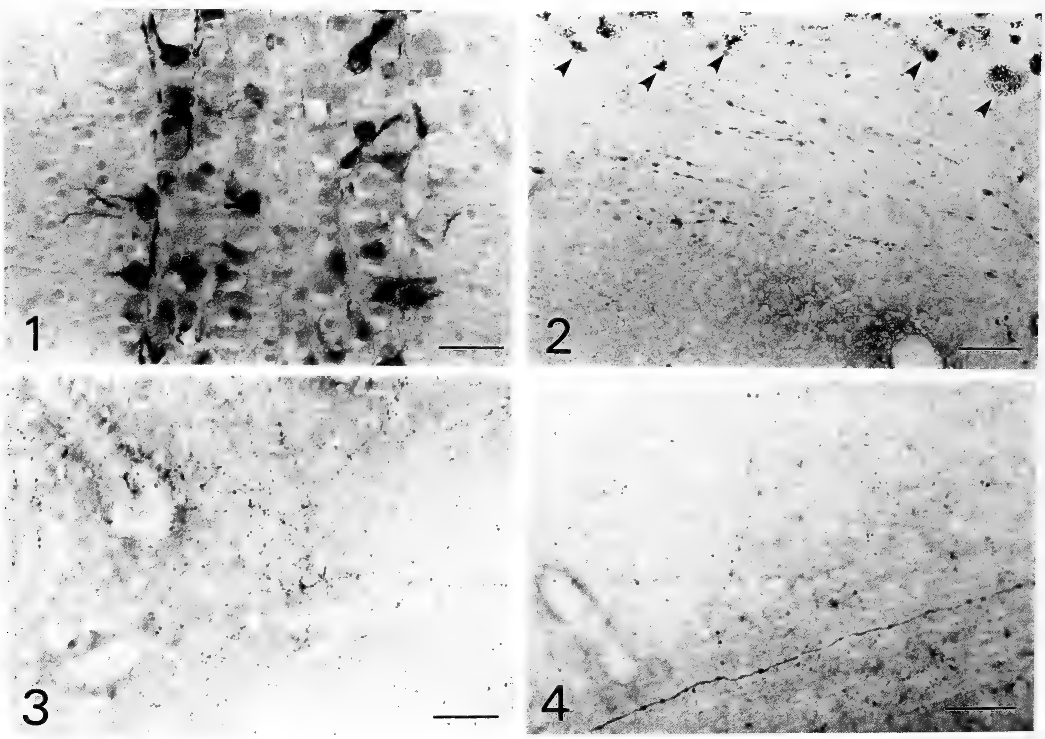

Fig. 1. Ir-vasotocin perikarya in the nucleus preopticus pars magnocellularis. Transversal paraffin section. Scale, 40 μm.

Fig. 2. Ir-vasotocin fibers travelling in the nucleus infundibularis dorsalis. Arrowheads indicate melanin granules. Sagittal frozen section. Scale, 40 μm.

Fig. 3. Plexus of ir-vasotocin fibers in the region anterior to the nucleus isthmi. Thick sagittal frozen section. Scale, 40 μm.

Fig. 4. Ir-vasotocin fibers in the floor of the medulla oblongata. Thick sagittal frozen section. Scale, 40 μm.

serum (1: 8000 dilution, Bioproducts), which cross-reacts completely with vasotocin but not with mesotocin (cross reactivity, 0.3%), in 0.1% Triton X–100 dissolved in 0.1 M phosphate buffered saline (PBS–T). After the incubation with the primary antiserum, the sections were washed in PBS–T at room temperature for 30 min, incubated with biotinylated anti-rabbit Ig-G for 1 hr, and were washed in PBS–T. Afterward, the tissue sections were incubated in the avidin-biotin-peroxidase complex in PBS–T for 30 min. After a few rinses, they were incubated in DAB solution including 0.05% 3, 3′-diaminobenzidine (Sigma) and 0.01% hydrogen peroxide for 10 min, washed briefly in phosphate buffer, and were mounted on slide glasses with 40% ethanol containing 0.75% gelatin. They were then dehydrated, and were cover-slipped with Permount (Fisher). The tests for specificity of immunohistochemical staining followed the previous study [4, 9].

Nissl stained tissue sections were refered to for describing precise localization of ir-AVT. Nomenclatorial usage in this paper is basically those in *Rana pipiens* [11] and *Bufo japonicus* [9].

RESULTS

Distribution of ir-AVT perikarya and fibers

As was described previously [4, 9], ir-AVT perikarya are localized in the ventral (VMC) and dorsal (DMC) magnocellular parts of the preoptic nucleus (Figs. 1 and 5). Beaded or varicose ir-AVT fibers were widely distributed among the discrete extrahypothalamic loci in the limbic system and the brain stem (Figs. 2–4). They were not found in the dorsal and anteroventral regions of the telencephalon. The extrahypothalamic ir-AVT projections can be classified roughly into three groups according to their destinations (see Fig. 5). Neither notable seasonal variation nor sexual difference was found in the distribution of ir-AVT fibers in this study.

Projection to the telencephalon (Figs. 5–8)

A part of ir-AVT fibers emanating from the VMC project to the posteromedial region of the telencephalon, principally to the nuclei medialis septi and lateralis septi. Ir-AVT fibers are sent out to these loci mainly through the white matter including the medial forebrain bundle which surrounds the neuronal cell mass of the APON. A

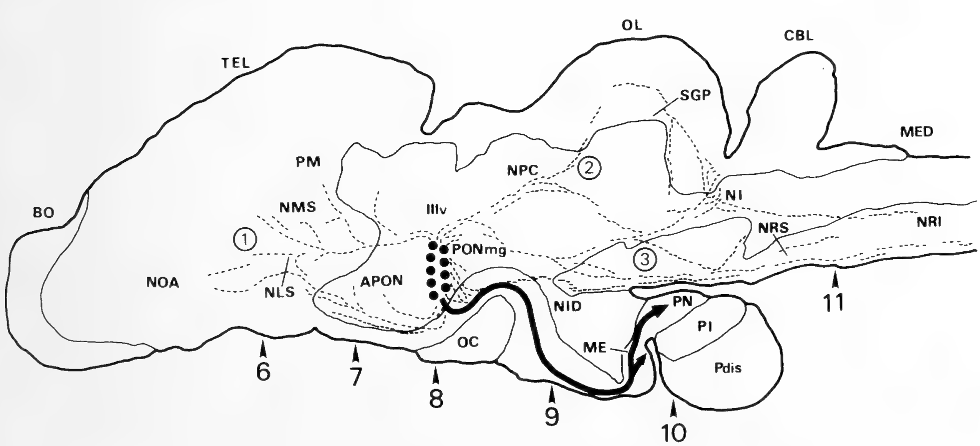

FIG. 5. Diagram of the mid-sagittal plane of the toad brain illustrating the distribution of ir-vasotocin fibers (broken lines) and ir-vasotocin perikarya (filled circles). The thick line shows the hypothalamo-neurohypophyseal vasotocinergic tract. Each numbered arrowhead shows the level of drawings (Figs. 6–11) illustrating the distribution of ir-vasotocin fibers and perikarya. Ir-vasotocin fibers are assembled into three projection groups: 1, projection to the telencephalon; 2, to the thalamus and the tectum; and 3, to the brain stem.

considerable number of varicose ir-AVT fibers that diverge from the projection to the telencephalon innervate into the APON and the amygdala medialis. Scattered ir-AVT fibers were often found in the pallium mediale and the nucleus of the diagonal band of Broca. The ir-AVT fibers found in the telencephalon have a varicose form, however, they rarely show Herring bodies which are frequently observed in the magnocellular preopticoneurohypophyseal neurosecretory system.

Projection to the thalamus and the tectum (Figs. 5, 8–9).

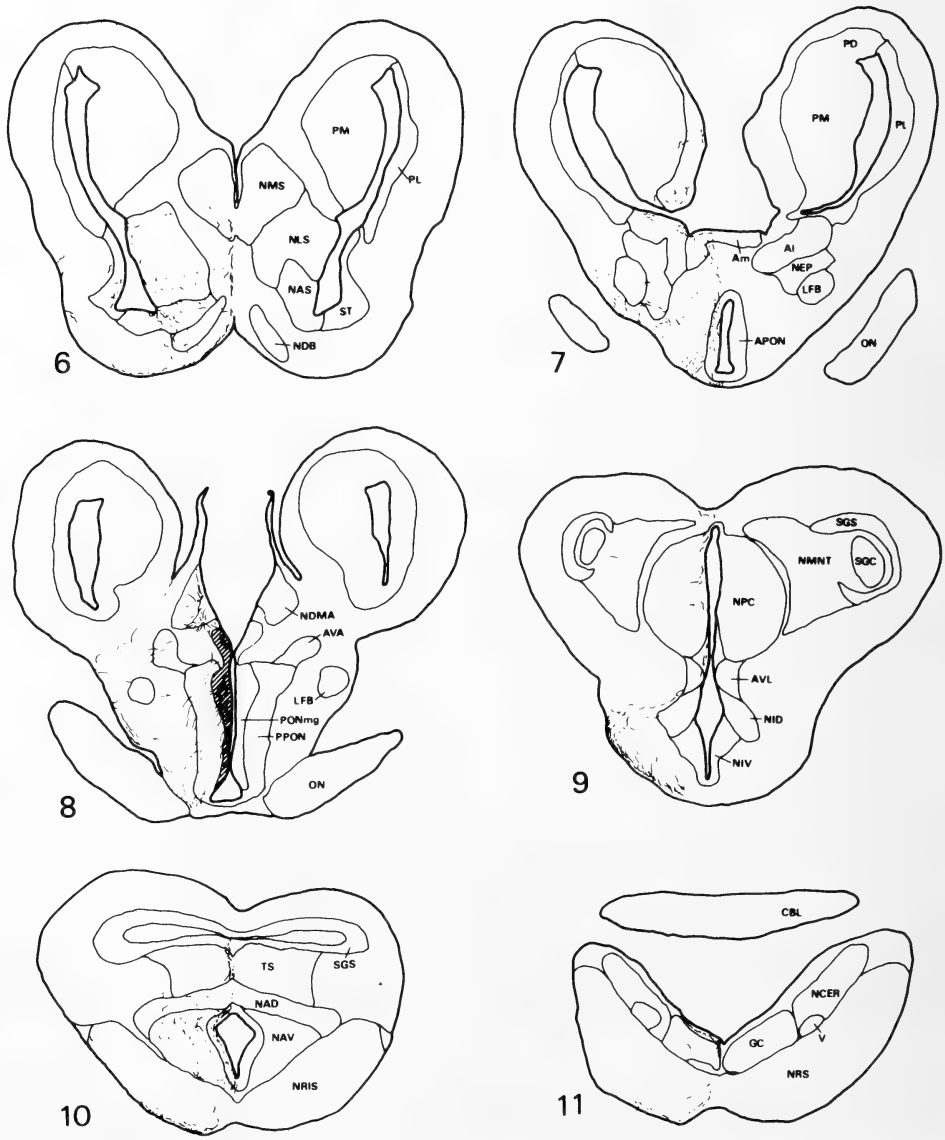

Figs. 6–11. Diagrammatic camera lucida drawings illustrating the distribution of ir-vasotocin fibers and perikarya (filled circles). The hatched area in Fig. 8 shows the region in which dense ir-vasotocin fibers were observed.

Many fibers arising from both the VMC and DMC run posterodorsad to the dorsomedial thalamic region, and are distributed mainly in the nuclei dorsomedialis anterior thalami and posterocentralis thalami. A few ir-AVT fibers further proceed posteriad to terminate in the optic tectum.

Projection to the brain stem (Fig. 5, 10–11).

Ir-AVT fibers which project to the brain stem arise from ir-AVT neurons in the VMC. They initially proceed laterad into the white matter in the preoptic region. Then, they turn their destination caudad to the direction of the lower brain stem with many ir-AVT fibers that project to the neurohypophysis. Thereafter, the fibers projecting to the brain stem diverge from the preoptico-neurohypophyseal tract around the dorsal infundibular region. A few beaded ir-AVT fibers are localized in the nucleus infundibularis dorsalis (Fig. 2). Many ir-AVT fibers run down to the mesencephalic tegmentum. They project to the nuclei posterodorsalis tegmenti mesencephali and isthmi, and further to the griseum centrale rhombencephali. A considerable number of fine beaded fibers gather together to form a plexus in the region anterior to the nucleus isthmi (Fig. 3). Some fibers which emanate from this plexus proceed dorsad to the stratum griseum tecti. Many ir-AVT fibers which run posteriad through the white matter in the floor of the mesencephalon were also found (Fig. 4). These fibers, which diverge from the fiber group destining to the isthmic region at the level caudal to the dorsal infundibular region, reach the rhombencephalic reticular formation, and proceed further toward the spinal cord.

DISCUSSION

The present study showed that ir-AVT fibers are distributed widely among many extrahypothalamic loci in the toad brain. Such regions are the limbic cortex, the thalamus, the optic tectum, the isthmic region and the lower brain stem.

The distributional pattern of extrahypothalamic ir-AVT fibers in the toad brain seems to be homologous to those described in the brains of other vertebrate classes. In the rat and the monkey, vasopressin neurons, the mammalian counterpart of AVT neurons, project their immunoreactive fibers to the hippocampus, the septum, the amygdala and the preoptic area. They

Abbreviations for Figs. 5–11.

Al	amygdala, pars lateralis
Am	amygdala, pars medialis
APON	anterior part of the preoptic nucleus
AVA	area ventralis anterior thalami
AVL	area ventrolateralis thalami
BO	bulbus olfactorius
CBL	cerebellum
GC	griseum centrale rhombencephali
LFB	lateral forebrain bundle
ME	median eminence
MED	medulla oblongata
NAD	nucleus anterodorsalis tegmenti mesencephali
NAS	nucleus accumbens septi
NAV	nucleus anteroventralis tegmenti mesencephali
NCER	nucleus cerebelli
NDB	nucleus of the diagonal band of Broca
NDMA	nucleus dorsomedialis anterior thalami
NEP	nucleus entopeduncularis
NI	nucleus isthmi
NID	nucleus infundibularis dorsalis
NIV	nucleus infundibularis ventralis
NLS	nucleus lateralis septi
NMNT	nucleus mesencephalicus nervi trigemini
NMS	nucleus medialis septi
NOA	nucleus olfactorius anterior
NPC	nucleus posterocentralis thalami
NRI	nucleus reticularis inferior
NRIS	nucleus reticularis isthmi
NRS	nucleus reticularis superior
OC	optic chiasma
OL	optic lobe
ON	optic nerve
PD	pallium dorsale
Pdis	pars distalis hypophysis
PI	pars intermedia hypophysis
PL	pallium laterale
PM	pallium mediale
PN	pars nervosa hypophysis
PONmg	preoptic nucleus, pars magnocellularis
PPON	posterior part of the preoptic nucleus
SGC	stratum griseum centrale tecti
SGP	stratum griseum periventricularis tecti
SGS	stratum griseum superficiale tecti
ST	striatum
TEL	telencephalon
TS	torus semicircularis
IIIv	third ventricle
V	motor nucleus of the trigeminal nerve

project further to the thalamus, the superior colliculus, and the several pontine and medullary nuclei [12]. A similar immunohistochemical distributional pattern of ir-AVT fibers was observed in the brain of the lizard *Gekko gecko* [13] and the eel *Anguilla japonica* (Fujiwara *et al.*, unpublished). A radioimmunoassay study of microdissected brain areas of rough-skinned newts also showed a similar distributional pattern of AVT [14]. These results indicate that the patterns of extrahypothalamic projections of AVT and vasopressin are fundamentally homologous in all vertebrate classes.

Immunoelectron microscopic studies demonstrated the presence of synapses containing neurophypophysial hormones in the rat brain [7, 15]. In the previous study, we showed that LHRH and AVT fibers may contact synaptically with APON neurons [4]. It is therefore highly probable that, in the toad brain, the extrahypothalamic AVT fibers form ordinary and/or en passant synapses with neurons in the loci where AVT fibers were localized. As was discussed in our previous paper [4], beaded or varicose ir-AVT fibers traveling through the white matter may form such synapses with dendrites of many central neurons, because in the amphibian brain many neurons located in the medial cell mass develop their dendritic fields in the adjacent white matter [8, 16]. Since neurohypophysial hormones could excite unit-spike activity of neurons in the rat supraoptic and paraventricular nuclei [17, 18], the eel preoptic nucleus [19] and the toad APON (Fujita and Urano, unpublished), vasotocin may facilitate activity of many central neurons as a neuromodulator or a local hormone. The latter possibility is supported by the fact that AVP of 10^{-9} M, comparable to effective doses of AVP for peripheral targets, could excite rat paraventricular neurons [18]. However, physiological roles of vasotocinergic transmission in the anuran brain are not clear at present, although an involution in reproductive behavior has been suggested as is described in the introduction.

The present study showed that vasotocin fibers are distributed in the loci concerned with reproductive behavior. Such regions are the limbic cortex, the preoptic area, the optic tectum and the central gray. In the limbic cortex, a considerable number of ir-AVT fibers were found in the septal nuclei, and also in the nucleus of the diagonal band of Broca. These regions contain the majority of ir-LHRH neurons in the toad brain [4, 10]. A similar projection of vasopressin fibers was found in the organum vasculosum lamina terminalis in the mammalian brain where many ir-LHRH perikarya are localized [12]. In the eel, vasotocin fibers were found in the preoptic region (Fujiwara *et al.*, unpublished). Meanwhile, ir-LHRH fibers project to the VMC in the toad brain [20]. These observations suggest that the LHRH-ergic and vasotocinergic neurosecretory systems are mutually connected, and that they interact on each other for controlling sexual behavior.

ACKNOWLEDGMENT

We thank Dr. T. Ichikawa, Tokyo Metropolitan Institute for Neurosciences, for his kind help and technical advice. A part of this study was supported by research grants from the Ministry of Education, Science and Culture, Japan.

REFERENCES

1 Diakow, C. (1978) Hormonal basis for breeding behavior in female frog: vasotocin inhibits the release call of *Rana pipiens*. Science, **199**: 1456–1457.

2 Moore, F. L. and Zoeller, R. T. (1979) Endocrine control of amphibian sexual behavior: Evidence for a neurohormone-androgen interaction. Horm. Behav., **13**: 207–213.

3 Moore, F. L. and Miller, L. J. (1983) Arginine vasotocin induces sexual behavior of newts by acting on cells in the brain. Peptides, **4**: 97–102.

4 Jokura, Y. and Urano, A. (1985) Projections of luteinizing hormone-releasing hormone and vasotocin fibers to the anterior part of the preoptic nucleus in the toad, *Bufo japonicus*. Gen. Comp. Endocrinol., **60**: 390–397.

5 Buijs, R. M. (1985) Extrahypothalamic pathways of a neurosecretory system: their role in neurotransmission. In "Neurosecretion and the Biology of Neuropeptides." Ed. by H. Kobayashi, H. A. Bern and A. Urano, Japan Sci. Soc. Press, Tokyo /Springer-Verlag, Berlin, pp. 279–286.

6 Silverman, A. J. (1983) Luteinizing hormone-releasing hormone (LHRH) synapses in the diagonal band (DBB) and preoptic area (POA) of the

guinea pig. Soc. Neurosci., **9**: 1182 (abstract).
7 Buijs, R. M. and Swaab, D. F. (1979) Immunoelectron microscopical demonstration of vasopressin and oxytocin synapses in the limbic system of the rat. Cell Tissue Res., **204**: 355–365.
8 Herrick, C. J. (1948) The Brain of the Tiger Salamander, *Ambystoma tigrinum*. The University of Chicago Press, Chicago.
9 Takami, S., Jokura, Y. and Urano, A. (1984) Subnuclear organization of the preoptic nucleus in the toad, *Bufo japonicus*. Zool. Sci., **1**: 759–770.
10 Jokura, Y. and Urano, A. (1985) An immunohistochemical study of seasonal changes in luteinizing hormone-releasing hormone and vasotocin in the forebrain and the neurohypophysis of the toad, *Bufo japonicus*. Gen. Comp. Endocrinol., **59**: 238–245.
11 Wada, M., Urano, A. and Gorbman, A. (1980) A stereotaxic atlas for diencephalic nuclei of the frog, *Rana pipiens*. Arch. Histol. Jpn., **43**: 157–173.
12 Zimmerman, E. A., Nilaver, G., Hou-yu, A. and Silverman, A. J. (1984) Vasopressinergic and oxytocinergic pathways in the central nervous system. Fed. Proc., **43**: 91–96.
13 Stoll, C. J. and Voorn, P. (1985) The distribution of hypothalamic and extrahypothalamic vasotocinergic cells and fibers in the brain of a lizard, *Gekko gecko*: presence of a sex difference. J. Comp. Neurol., **239**: 193–204.
14 Zoeller, R. T. and Moore, F. L. (1986) Arginine vasotocin immunoreactivity in hypothalamic and extrahypothalamic areas of an amphibian brain. Neuroendocrinology, **42**: 120–123.
15 Theodosis, D. T. (1985) Oxytocin-immunoreactive terminals synapse on oxytocin neurons in the supraoptic nucleus. Nature, **313**: 682–684.
16 Urano, A. (1984) A Golgi-electron microscopic study of anterior preoptic neurons in the bullfrog and the toad. Zool. Sci., **1**: 89–99.
17 Baker, J. L. (1977) Physiological roles of peptides in the nervous system. In "Peptides in Neurobiology". Ed. by H. Gainer, Plenum Press, New York, pp. 295–343.
18 Inenaga, K. and Yamashita, H. (1986) Excitation of neurones in the rat paraventricular nucleus in vitro by vasopressin and oxytocin. J. Physiol., **370**: 165–180.
19 Sugita, R. and Urano, A. (1986) Responses of magnocellular neurons in *in vitro* eel preoptic nucleus (PONmg) to acetylcholine, catecholamines, vasotocin, isotocin, angiotensin, and Na^+. Zool. Sci., **3**: 1081 (abstract).
20 Jokura, Y. and Urano, A. (1986) Extrahypothalamic projection of luteinizing hormone-releasing hormone fibers in the brain of the toad, *Bufo japonicus*. Gen. Comp. Endocrinol., **62**: 80–88.

ZOOLOGICAL SCIENCE 4: 683–692 (1987)

A Circadian Aspect of the Photoperiodic Time-measurement on the Basis of the Larval-ecdysis Rhythm in the Small Copper Butterfly, *Lycaena phlaeas daimio* Seitz

Katsuhiko Endo and Mariko Shibata

Environmental Biology Laboratory, Biological Institute, Faculty of Science, Yamaguchi University, Yamaguchi 753, Japan

ABSTRACT—The present study was aimed at showing how the circadian clock controlling the timing of larval ecdysis is entrained to light/dark (L/D) cycles in the small copper butterfly, *Lycaena phlaeas daimio* Seitz. In addition, experiments were made to investigate how the circadian clock is related to the time-measurement of photoperiods in this butterfly.

Larval ecdysis occurred in a specific zone of L/D cycles. The zone was determined by the secretion of prothoracicotropic hormone (PTTH) preceding the larval ecdysis by 32 hr at 25°C. The preparatory period was shortened to 29 hr at 30°C, but the secretion of PTTH occurred in almost the same zone of L/D cycles at these two different temperatures. Furthermore, when a group of larvae were held in 4L–20D and transferred to continuous darkness (DD), they showed a significant rhythm of larval ecdysis in DD following the transfer. The timing of larval ecdysis-zone was advanced (or delayed), when the night was interrupted by a supplementary light pulse of 0.5-hr (or 1-hr). In 4L–20D, a specific 6-hr zone may exist, in which spring morph development is prevented by a supplementary light pulse of 0.5-hr.

The results suggest that time-resetting of the circadian clock controlling the timing of PTTH-secretion may occur at light-on and light-off, respectively. The circadian clock itself or an oscillator entrained by the circadian clock is supposed to play a significant role in the time-measurement of photoperiod in *L. phlaeas daimio*.

INTRODUCTION

In many multivoltine insects, diapause and determination of seasonal morphs are governed by photoperiod and temperature existing during certain developmental stages [1, 2]. The physiological system underlying the photoperiodic control involves a functional component measuring day- or night-length. However, when each species of insects was subjected to either a skeleton photoperiod consisting of two light-pulses or light/dark (L/D) cycles of non-24-hour, they were found to show a wide diversity of the responses to the photoperiods [3, 4].

For explaining the diversities in the responses to the photoperiods, several models have been proposed by previous workers on the basis of circadian rhythm study [3–8]. The diversities could be mostly explained on the basis of these models, but there have remained many speculations yet to be studied.

Larval ecdysis occurs in a particular zone of L/D cycles in several lepidopteran insects. The timing of larval ecdysis has been shown to be determined by the secretion of the prothoracicotropic hormone (PTTH) [9, 10]. That is, a specific zone exists in L/D cycles in which the PTTH-secretion is allowed to occur. The timing of the allowed zone for PTTH-secretion has been speculated to be determined by a physiological (circadian) system involving circadian oscillator(s) or hourglass (es) [9, 10].

In the small copper butterfly, *Lycaena phlaeas daimio* Seitz, determination of seasonal morphs —spring, intermediate and summer morphs—has

Accepted February 20, 1987
Received October 9, 1986

been shown to be controlled by photoperiod and temperature during the larval and/or early pupal stages [11, 12]. The physiological system underlying the photoperiodic control involves a neuroendocrine system secreting the summer-morph-producing hormone [13].

The present study was aimed at assessing whether or not the PTTH-secretion preceding the larval ecdysis is gated by a circadian system in *L. phlaeas daimio*. Then, the investigation was extended to see how the circadian clock controlling the timing of larval ecdysis is entrained to L/D cycles and related to the photoperiodic time-measurement in this butterfly.

MATERIALS AND METHODS

Animals Eggs and larvae of *L. phlaeas daimio* were divided into groups (n=200–250 for each group) and were held in either a petridish ($\phi 9 \times 2$ cm^3) or a container of transparent plastic ($\phi 9 \times 5$ cm^3). They were placed in an L/D cycle of either a complete or an asymmetrical skeleton photoperiod at 20°C or 25°C. The larvae were fed on leaves of *Rumex acetosa* which were exchanged daily.

The petridishes and the rearing containers were placed in a photoperiod-controlled cabinet ($62 \times 39 \times 23$ cm^3 or $62 \times 39 \times 110$ cm^3) and were illuminated by a 10-W or 20-W white fluorescent tube which was controlled by a 24-hr time-switch. In the light period, light intensity was provided at about 400 lux to the petridishes or to the rearing containers.

Photoperiodic regimens In the complete photoperiods, the light period was changed depending on the groups at 2-hr increments from 2L–22D (alternating 2-hr light and 22-hr dark periods) to 18L–6D. In the asymmetrical skeleton photoperiods, the dark component of 4L–20D was interrupted by a light pulse of 0.5 hr. Then, the time of the light pulse was delayed from one group to the next at a 1-hr interval so that different groups received the light pulse at different times of night.

Besides, to know how much the timing of larval ecdysis is changed in response to a single light-pulse, larvae were reared under 4L–20D, exposed to a night-interruption of 1 hr on the first night of the 2nd larval ecdysis and transferred to DD.

Timing of larval ecdysis *L. phlaeas* larvae stopped feeding at about 20 hr before larval ecdysis and their head was bent downwards to form an oval posture (head capsule slippage stage). Larvae of the oval form were selected from a stock culture with a red-light illumination less than 5 lux twice a day and were put in a latticework-plate of wood and paper. They were held in continuous light and photographed at a 0.5-hr interval to see how many larvae underwent larval ecdysis in each 0.5-hr period of the day. In each group, larval ecdysis from the 3rd to the 4th instar occurred for a 3- to 4-day period. The rhythmicity of larval ecdysis was analyzed by the method of least-square cosin fitting (LSCF) [14]. When the larval ecdysis was judged to occur with a rhythm of 24 hr, the acrophase-time of the best fitting cosin was obtained and the time was regarded as the acrophase-time of larval ecdysis. Subsequently, the time at which the larval ecdysis occurred at minimum frequency within the day (the minimum frequency-time) was determined. Then, the numbers of ecdysed larvae were added from the minimum frequency-time to the next and the times at which the percentage of ecdysed larvae reached 20% and 80% were recorded. The times are described hereafter as T–20% and T–80%.

To assess whether the larval ecdysis occurs with a rhythm in continuous darkness (DD) following L/D cycles, various stages of larvae were transferred to DD from 4L–20D. The peaks of larval ecdysis were punctuated one after another at the minimum frequency-time, and the gravity-time of each peak of larval ecdysis was obtained together with T–20% and T–80%.

Neck-ligature of larvae Larvae were raised from the egg stage under 4L–20D at 25°C or at 30°C. Newly molted 3rd-instar larvae (day 0) were selected from the stock culture and were divided into groups (n=50–70). The neck was ligatured at a 2-hr interval. The surgery began 14 hr (or 6 hr) after dawn on day 0 at 25°C (or at 30°C) and continued for 2 days. Five (or four) days later at 25°C (or 30°C), the neck-ligatured (decapitated) larvae were observed for the production of 4th-instar cuticle.

Criteria for the classification of seasonal

morphs Classification of the seasonal morphs was based on the number of red scales in the 4th and 7th red spots distributed along the central line of the dorsal side of anterior wing. The classification was carried out in each butterfly by using a method of confident ellipse [8].

RESULTS

The timing of larval ecdysis in the complete photoperiods

Firstly, ecdysis from the 3rd to 4th instar was examined in groups of larvae (n=200–250) to see whether or not larval ecdysis occurs in a specific zone of L/D cycles in the complete photoperiods. The photoperiods examined varied from 2L–22D to 18L–6D with photophases differing by 2 hr (25°C).

Larval ecdysis was found to occur in a specific zone of the L/D cycles in most regimens (Fig. 1). The zone covered approximately an 8-hr period beginning at about 2 hr before dawn in 2L–22D. When the light period became longer, the acrophase-time of larval ecdysis came to on an almost parallel line (0.4-hr delay/2 hr against dawn in LSCF-analysis) with a line connecting the dawn. Furthermore, the other three indices characterizing the larval ecdysis-zone—T–20% (the beginning time), T–80% (the end time) and the minimum frequency-time—were delayed (or advanced) in a fashion almost parallel to the shift of the acrophase-time. When larvae were subjected to 18L–6D, the larval ecdysis occurred with no significant rhythm ($P>0.05$).

The results indicated that *L. phlaeas daimio* has a specific zone of 5–8 hr in which they undergo larval ecdysis in photoperiods with a photophase shorter than 16 hr. The timing of larval ecdysis may be determined so that the zone comes to on an almost parallel zone with the connecting line of dawn.

The timing of the larval ecdysis in the asymmetrical skeleton photoperiods of 4L–20D

To investigate how the larval ecdysis-zone changes in response to the night-interruption, groups of larvae were subjected to the asymmetrical skeleton photoperiods of 4L–20D at 25°C. The night-interruption (supplementary light pulse) of 0.5-hr was delayed depending on the groups at 1-hr intervals and the timing of larval ecdysis was

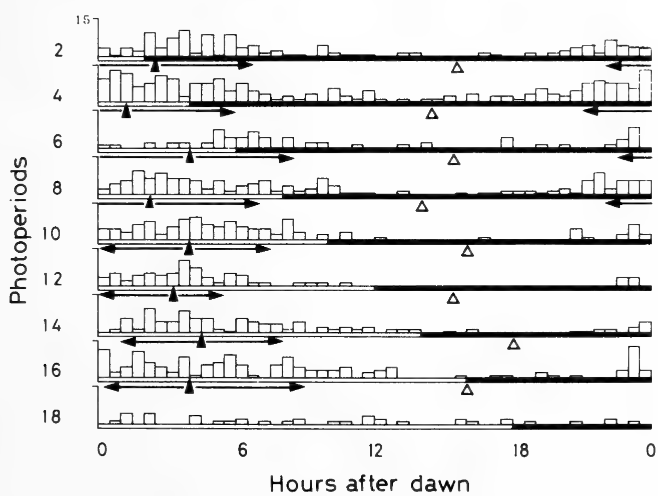

FIG. 1. Fluctuating pattern in the number of ecdysed larvae in the complete photoperiods. Each histogram shows the number of ecdysed larvae in each 0.5-hr period of the day. Solid and open bars show dark and light periods, respectively. Double sided arrows indicate the larval ecdysis-zone between T–20% and T–80%. Solid and open triangles show the acrophase-time and the minimum frequency-time of larval ecdysis, respectively.

examined in each group.

When the night-interruption fell in an 11-hr zone following dusk, the timing of larval ecdysis was delayed (Fig. 2). The delay occurred in the minimum frequency-time, but it was not clear in the acrophase-time, with 0.4-hr/1-hr light-pulse delay. The maximum delay of 4-hr was recorded in the minimum frequency-time when the night-interruption fell on at 11 hr after dusk (the end-point of the first 11-hr zone following dusk). The larval ecdysis-zone was advanced in response to the night-interruption falling on in an 8-hr zone preceding dawn. The maximum advance of 6-hr was recorded by the night-interruption coming to at 14 hr after dusk. Thereafter, the advance of the acrophase-time as well as that of the other indices became gradually smaller (0.7 hr/1 hr in LSCF-analysis).

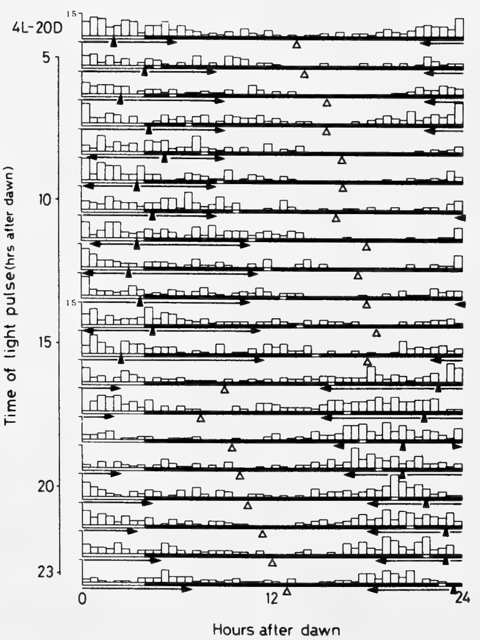

FIG. 2. Fluctuating pattern in number of the ecdysed larvae in the asymmetrical skeleton photoperiods of 4L–20D. Each histogram shows the number of ecdysed larvae in each 0.5-hr period of the asymmetrical skeleton photoperiods at 25°C. Double-sided arrows indicate the larval ecdysis-zone between T–20% and T–80%. Solid and open triangles show the acrophase-time and the minimum frequency-time, respectively.

The results indicate that the timing of larval ecdysis may be changed when the night is interrupted by a supplementary light pulse. However, the night of 4L–20D may be divided into two zones depending on the response of the larval ecdysis-zone. The first zone covers an 11-hr period following dusk, in which the larval ecdysis-zone was delayed by night-interruption. But, in the second zone covering an 8-hr period preceding dawn, the larval ecdysis-zone was advanced.

The timing of the prothoracicotropic hormone (PTTH)-secretion for larval ecdysis from the 3rd to the 4th instar

To know how much time the PTTH-secretion precedes the larval ecdysis in *L. phlaeas daimio,* the neck of the 3rd instar larvae was ligatured at 25°C and 30°C. The surgery was started on the first day of the 3rd instar (day 0) and made for 2 days at a 2-hr interval.

As is summarized in Figure 3, a small proportion (2%) of larvae producing the 4th-instar cuticle appeared when the neck was ligatured at mid-night on day 0 at 25°C. However, neck-ligatured larvae which produced the cuticle of the 4th instar increased when the surgery was made at and later than 18 hr after the dawn on day 0. The percentage of the cuticle-producing larvae rose continuously until the increment once stopped at 60% at the end of light period on day 1. The percentage began to rise again a few hours after the dusk to reach about 100% at mid-night on day 1 at 25°C.

At 30°C, a low percentage of larvae already produced the 4th-instar cuticle when the neck was ligatured 2 hr after dusk on day 0. The proportion of the cuticle-producing larvae began to rise earlier than in those held at 25°C and the percentage reached near 90% at dusk on day 1. However, increment in percentage of the cuticle-producing larvae became almost zero for a few hours following dusk on day 1 as in those held at 25°C.

In intact (control) insects, larval ecdysis began to occur on day 1 and ended on day 3 at 25°C (or on day 2 at 30°C). They formed two or three peaks in larval ecdysis. The peaks of the PTTH-secretion seemed to precede the corresponding peaks of larval ecdysis by about 32 hr at 25°C. The time period may be shortened to 29 hr when the rearing

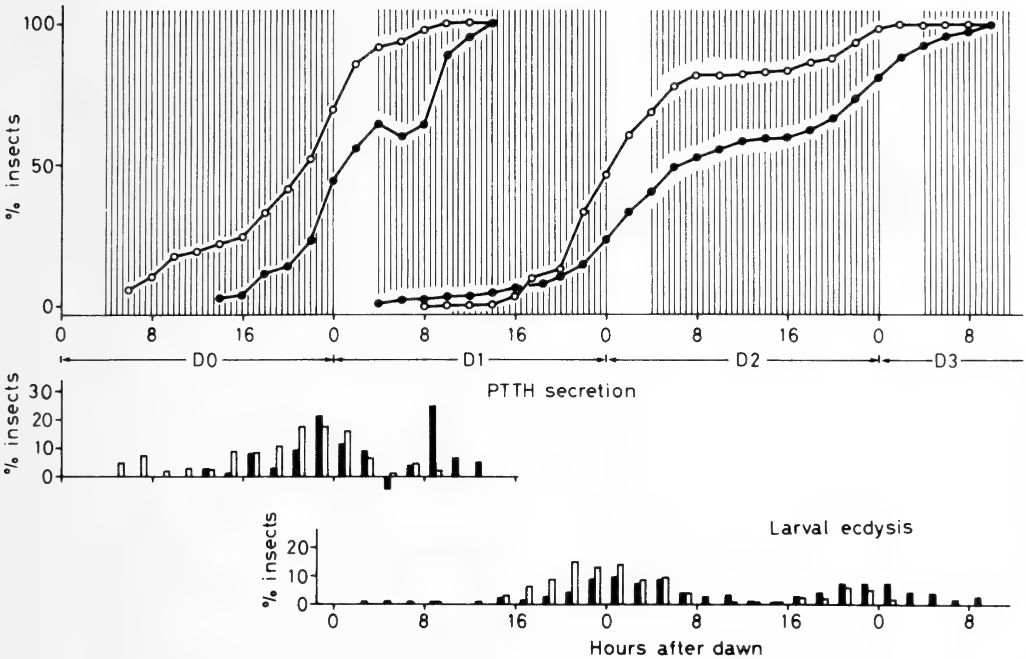

FIG. 3. The response of the 3rd instar larvae to neck-ligature as a function of the time of operation at 25°C and 30°C. Upper panel: Solid and open circles (left) show the cumulative percentage of neck-ligatured larvae producing the cuticle of the 5th instar at 25°C and 30°C, respectively. Solid and open circles drawn on right-side show the cumulative percentage of intact larvae undergoing larval ecdysis at 25°C and 30°C, respectively. Straight lines show dark periods. Lower panel: Open (or solid) histograms show the increments in percentage of neck-ligatured larvae producing the cuticle of 4th instar at 2-hr intervals and those in percentage of intact larvae undergoing larval ecdysis in each 0.5-hr period of the day at 30°C (or 25°C), respectively.

temperature rises to 30°C. However, the allowed zone for PTTH-secretion is judged to cover about the same zone of L/D cycles at these two different temperatures.

Rhythmicity of larval ecdysis in DD following L/D cycles

To clarify whether or not the larval ecdysis occurs with the rhythm in DD following L/D cycles, larvae were raised from the egg stage under 4L–20D and were transferred to DD by extending the scotophase from day 0 of the 2nd to day 3 of the 3rd instar. Larval ecdysis was examined and the time of PTTH-secretion was obtained by subtracting 32 hr from the observed time of ecdysis after DD-transfer. The histograms of Figure 3 represent the time of PTTH-secretion, the data of which were pooled according to the time elapsed after DD-transfer.

As is evident from Figure 4, larval ecdysis occurred with rhythms in DD following the transfer. Periodical cycles of a little shorter than 24 hr (23.6 hr?) was obtained when the analysis was made on larvae undergoing larval ecdysis on the days following the 2nd day of DD (Fig. 4).

The results indicate that a circadian (or hourglass) clock determining the timing of PTTH-secretion (or larval ecdysis) may exist in *L. phlaeas daimio*. As a result, larval ecdysis occurs with a rhythm of circadian cycles in DD following L/D cycles. However, the rhythm of larval-ecdysis may be damped in DD as it becomes long.

Phase response of the PTTH-secretion zone against one night-interruption

To clarify how the timing of the PTTH-secretion zone is changed by one night-interruption (a light pulse), larvae were raised from the egg stage under

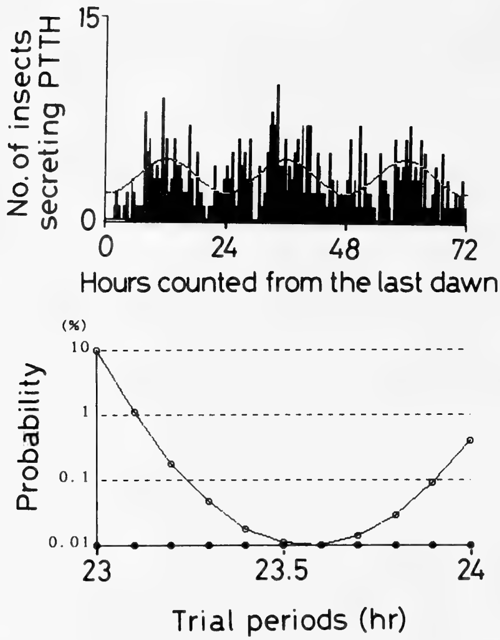

FIG. 4. Fluctuations in the number of larvae determined to undergo larval ecdysis (upper panel) and time period of its rhythm in DD (lower panel). Each histogram (upper panel) shows the approximate timing of PTTH-secretion (at which time larvae is determined to undergo larval ecdysis). A waved line represents the best fitting cosin of the cycles of 23.5-hr. Open and solid bars on the abscissa indicate light and dark periods, respectively. Solid and open circles (lower panel) show the fittness (P) and the relative error to the cosin tried to fit.

4L–20D at 25°C, divided into groups (n=250–300) on the first day of the 3rd instar, transferred to DD from the next scotophase, and exposed to a light pulse (night-interruption) of 1 hr at different times with a 2-hr interval. The time of larval ecdysis was observed and the minimum frequency-time of larval ecdysis was calculated. The timing and the minimum frequency-time for PTTH-secretion were obtained by subtracting 32 hr from these data and shown in Figure 5.

The minimum frequency-time of PTTH-secretion did not change by the night-interruption falling on in a 4-hr period following dusk. However, the minimum frequency-time was advanced when the night was interrupted at and later than 6 hr after dusk. The maximum advance in the minimum frequency-time of PTTH-secretion (12 hr) was recorded, when the night-interruption fell on at 8 hr after dusk. Thereafter, the advance of the minimum frequency-time became smaller almost steadily (0.7 hr/1 hr in LSCF-analysis) as the time of light pulse was delayed.

Based on the response of the minimum frequency-time of PTTH-secretion, the night of 4L–20D may be divided into two zones as proved by the experiments of the asymmetrical skeleton photoperiods. But, the first zone covers, at this time, about a 6-hr period, in which the minimum frequency-time was independent of the night-interruption. In the second zone covering the

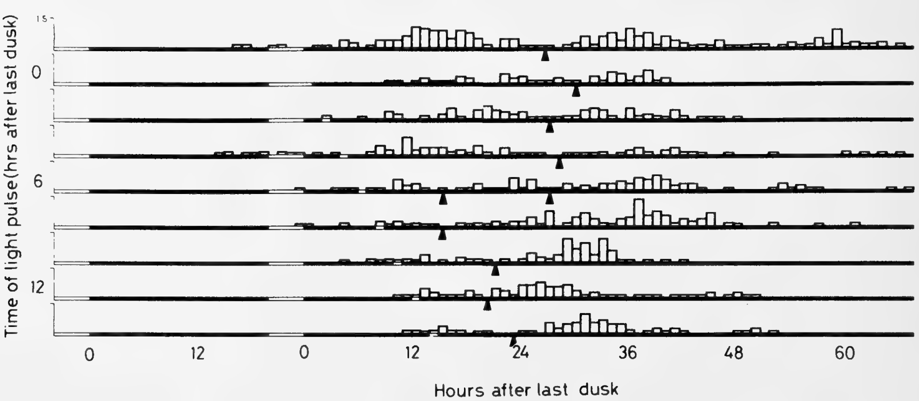

FIG. 5. The phase response of the minimum frequency-time of PTTH-secretion representing as a function of the time of night-interruption. Each histogram shows the number of larvae which are determined to undergo larval ecdysis in each 1-hr period of the day. Solid triangles show the minimum frequency-time of PTTH-secretion (?). Open and solid bars show the photoperiodic regimens.

following 13-hr period, the minimum frequency-time is advanced by the night-interruption in the same manner as the groups subjected to the asymmetrical skeleton photoperiods.

Photoperiodic response curves of seasonal-morph determination in the complete and the asymmetrical skeleton photoperiods

To investigate how the incidence of the spring morphs is changed by daylength or by a supplementary light pulse of 0.5 hr, groups of larvae (n=200–250) were raised from the egg stage under either a complete or an asymmetrical skeleton photoperiod of 4L–20D at 25°C. In the complete photoperiods, length of the light period was changed depending on the groups at 2-hr increments, whereas, in the asymmetrical skeleton photoperiods, the night-interruption of 0.5-hr was delayed at 1-hr intervals. Then, the incidence of spring-morph adults was examined in each group.

When larvae were subjected to photoperiods with a photophase shorter than 11 hr, the majority

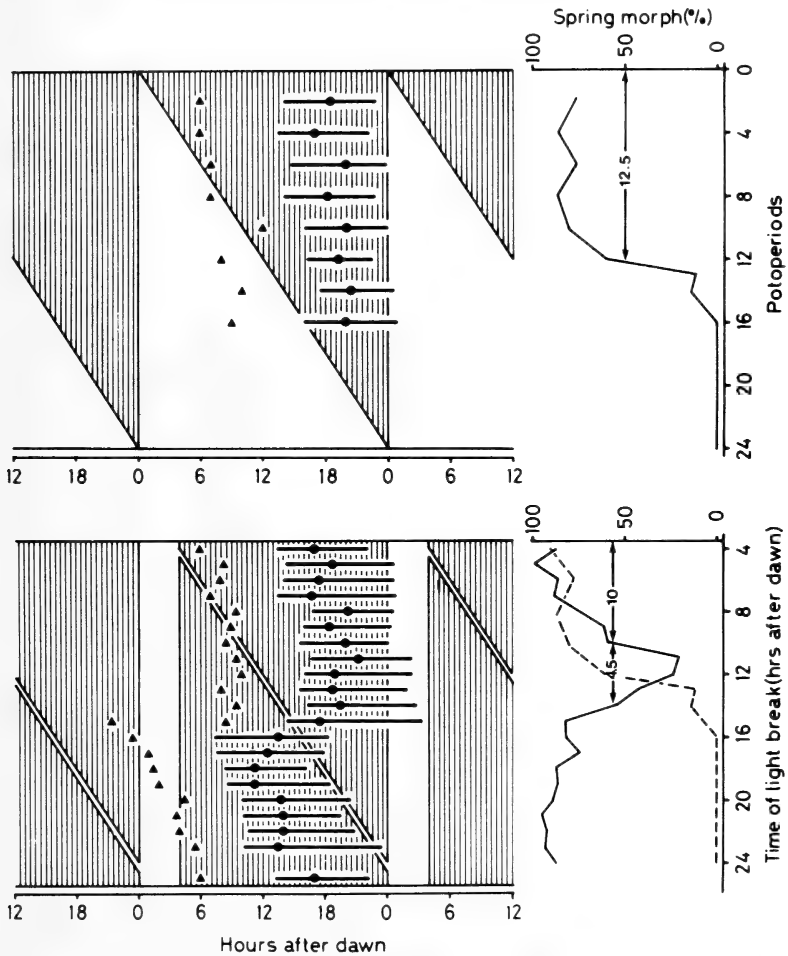

FIG. 6. The allowed zone for PTTH-secretion and photoperiodic response curves represented on the complete and the asymmetrical skeleton photoperiods. Left panels: Solid circles with bars show the acrophase-time and the allowed zone for PTTH-secretion preceding those of larval ecdysis by 32 hr at 25°C. Solid triangles show the minimum frequency-time of PTTH-secretion. Thin straight lines indicate the dark periods. Right panels: Solid lines (upper and lower panels) show the photoperiodic response curves of spring-morph determination, while a broken line (lower panel) shows the response curve obtained in the corresponding daylengths of the complete photoperiods.

(80–95%) of them developed into spring morphs and the rest (5–20%) developed into intermediate morphs. On the other hand, in regimens with a photophase longer than 14 hr, they developed into summer (75–80%) and intermediate (10–20%) morphs in addition to some spring morphs (2–3%). The critical daylength preventing spring-morph development in 50% insects (the short- to the long-day) was about 12 hr 30 min at 25°C (Fig. 6: upper panel).

In the asymmetrical skeleton photoperiods of 4L–20D, spring-morph development was prevented by a supplementary light pulse of 0.5-hr, when if fell on in about 6-hr zone beginning at about 9 hr after dawn (light-on of the main light period). The maximum prevention of 80% was recorded when the night-interruption fell on at 12 hr after dawn. Two critical daylength in induction of the spring morphs existed in the asymmetrical skeleton photoperiods of 4L–20D. They were 10 hr (the short- to the long-day) and 14 hr 30 min (vice versa) at 25°C. The critical daylength of 10 hr (the short- to the long-day) was shorter than that of the complete photoperiods (12 hr 30 min) by 2 hr 30 min (Fig. 6: lower panel).

The results indicated that *L. phlaeas* larvae may measure the length of light-(or dark-)period with an error of less than 1 hr. The critical daylength resulting in the 50%-prevention of spring-morph development is at about 12 hr 30 min in the Yamaguchi strain of *L. phlaeas daimio*. In the photoperiod of 4L–20D, a specific 6-hr zone beginning at around 9 hr after dawn may exist, in which the incidence of spring morphs is lowered by a supplementary light pulse of 0.5-hr. Furthermore, the critical daylength (the short- to the long-day) is shortened to 10 hr in the asymmetrical skeleton photoperiods of 4L–20D.

DISCUSSION

The timing mechanism of larval ecdysis

In *L. phlaeas daimio,* larval ecdysis occurs in a specific zone of L/D cycles. The timing of larval ecdysis-zone is found to be delayed at 0.4-hr intervals against dawn when photoperiod was changed at 2-hr increments (Fig. 1). The larval ecdysis occurs with rhythms in DD following L/D cycles (Fig. 3). However, the rhythm is dampted gradually in DD as day goes by as has been shown in several other insects [9, 10]. The periodical cycles of the larval ecdysis (or PTTH-secretion) rhythm in DD is judged to be about 24-hr (23.6-hr in LSCF-analysis) in this lycaenid butterfly.

This evidence suggests that the timing of larval ecdysis is controlled by a circadian oscillator(s) or hourglass(es). Therefore, larval ecdysis occurs with a rhythm of ca. 24-hr cycles in DD following L/D cycles, but the rhythm is damped in DD as day goes by.

The timing of larval ecdysis is supposed to be determined by the timing of the PTTH-secretion in *L. phlaeas daimio* in the same manner as has been demonstrated in several other lepidopteran insects [9, 10, 13].

The timing of PTTH-secretion for larval ecdysis

Based on the evidence of neck-ligature experiments, the peaks of PTTH-secretion are found to precede the corresponding peaks of larval ecdysis by 32 hr at 25°C (Fig. 3), where the allowed zone for PTTH-secretion may exist in *L. phlaeas daimio.* The timing of the allowed zone is supposed to be determined by a temperature-compensated circadian system since the PTTH-secretion occurred at 30°C in approximate by the same zone of L/D cycles as in those held at 25°C (Fig. 3).

Third instar larvae of *L. phlaeas daimio* are found to require about the same preparatory period (32 hr) as those of *Manduca sexta* for larval ecdysis [9]. The time period is shorter than the period demonstrated in *Papilio xuthus* (34 hr) by 2 hr [13]. The *L. phlaeas* preparatory period seemed to be shortened to 29 hr at 30°C.

How is the circadian clock entrained to L/D cycles in the complete and the asymmetrical skeleton photoperiods in L. phlaeas daimio?

An insect is supposed to have plural oscillators or plural hourglasses. They may be entrained by master oscillator and mostly synchronized to the environmental cycles in 24-hr L/D-cycles [9, 10]. The timing of the allowed zone for PTTH-secretion may be determined by a physiological

system involving the oscillator(s) [9, 10]. The same supposition may be applicable for *L. phlaeas* mechanism determining the timing of PTTH-secretion. According to this supposition, the allowed zone can be regarded as indicating where an approximate phase of the master oscillator comes to on the photoperiodic regimens as has been speculated in several other insects [9, 10].

In *L. phlaeas daimio,* each index of the allowed zone for PTTH-secretion (T–20%, T–80%, the acrophase-time and the minimum frequency-time) may be located on a different phase of the circadian oscillator as speculated in the case of *P. xuthus* [13]. Each index of larval ecdysis-zone comes to on parallel lines in the complete photoperiods when light period is changed at 2-hr increments (Fig. 6). However, the parallel lines connecting the same indices have a small angle with the line connecting dawn (delay of index /extension of light period=0.2) (Fig. 1). The angle of the lines is significantly smaller than those of *P. xuthus* (delay of index/extention of light period=0.5) ($P<0.01$) [13].

Furthermore, in the asymmetrical skeleton photoperiods, the *L. phlaeas* indices of larval ecdysis-zone were found to show different behaviors against night-interruption from those of *P. xuthus*: each index of *P. xuthus* shows a response in almost the same manner against either main light period or a supplementary light pulse [13]. In contrast, the indices of *L. phlaeas daimio* showed the response against the two light pulses (4-hr and 0.5-hr) in the same manner as those held in the complete photoperiods (Fig. 6: upper and lower panels). That is, the light period may be regarded as starting at light-on of the main light pulse of 4-hr (or a supplementary light pulse of 0.5-hr), whereas it may be regarded as ending at light-off of the supplementary light pulse of 0.5-hr (or the main light period of 4-hr) in *L. phlaeas daimio.*

Here, we could not provide enough evidence to solve the question why the two species of insects showed the different responses to the night-interruption in the asymmetrical skeleton photoperiods. The difference is supposed to be due to the differences of the nature of circadian clocks between these two different species.

Furthermore, in *L. phlaeas daimio,* synchronization of the circadian clock to the environment is supposed to be achieved in two steps; the first rough adjustment may be made at dawn by advancing it and the subsequent fine adjustment may be done at dusk by delaying it for several days.

The supposition is based on the evidence of phase response experiments. That is, the larval ecdysis-zone was advanced in the same manner as the groups held in the asymmetrical skeleton photoperiods by one night-interruption falling on in a 12-hr period preceding dawn. However, the larval ecdysis-zone did not show any response (phase advance or phase delay) against one night-interruption even when it fell on in a 7-hr period following dusk (Fig. 5), in which the ecdysis-zone was delayed by the night-interruption in the asymmetrical skeleton photoperiods (Fig. 2).

How is the circadian clock related to time-measurement of photoperiod in L. phlaeas daimio?

The time-measurement system underlying the photoperiodic control of seasonal-morph determination is thought to involve (or to work with the close assistance of) a circadian clock(s) and speculated to measure day- or night-length to see whether or not the light period exceeds a critical length [3–8].

The present evidence about the photoperiodic control of seasonal-morph determination—shortening of the critical daylength and existence of the specific 6-hr zone in which the short-day effect is eliminated by a supplemetary light pulse—may be mostly explained on the model of external coincidence [5, 7]. On this model, a photosensitive phase eliminating the short-day effects is speculated to exist at around the end time of the allowed zone for PTTH-secretion. When the light period is extended to the length longer than 12.5 hr, the circadian (photosensitive?) phase comes out into light period. In the asymmetrical skeleton photoperiods, the circadian phase (the end time of the allowed zone for PTTH-secretion) showed a larger delay against dawn (0.4 hr/1 hr) than in the complete photoperiods (0.2 hr/1 hr). As the results, the circadian phase is supposed to come out into main light period of 4 hr when night was interrupted in a 6-hr period beginning at 10 hr

after dawn.

A gradual shift of seasonal morphs occuring at around critical daylength of the complete photoperiods is supposed to be caused by the nature of circadian clock in *L. phlaeas daimio*. The supposition is based on an evidence that the same phase of circadian clock comes to on a line having a small angle (0.2 hr/1 hr) with the connecting line of dawn in the complete photoperiods. If the photosensitive phase in which the short-day effect is elliminated by an exposure to light is circadian, the phase is supposed to gradually come out from the group to the next into light period in the complete photoperiods (Fig. 6).

Here, we could not provide any direct evidence with respect to the photosensitive phase in which spring-morph development is prevented by a exposure to light in *L. phlaeas daimio*. The circadian phase on which the photosensitive phase is located in *L. phlaeas daimio* may be identified by further study.

ACKNOWLEDGMENT

The authors wish to express their sincere gratitude to Professor Y. Chiba and to Professor A. Okajima of Yamaguchi University for advice and valuable suggestions during the course of this work.

REFERENCES

1 Müller, H. J. (1955) Die Saisonformenentbildung von *Araschnia levana*, ein photoperiodish gesteuerter Diapause-effekt. Naturwissenschaften, **42**: 134–135.

2 Danilevskii, A. S. (1961) Fotoperiodism i sezonne razvitie nasekomykh. Lzd. Leningradskogo Universiteta, Leningrad.

3 Saunders, D. S. (1966) Insect Clock, Pergamon Press, Oxford, 297 pp.

4 Beck, S. D. (1980) Insect Photoperiodism, 2nd ed., Academic Press, New York.

5 Bünning, E. (1960) Circadian rhythms and time measurement in photoperiodism. Cold Spring Harbor Symp. Quant. Biol., **25**: 245–256.

6 Pittendrigh, C. S. (1960) Circadian rhythm and the circadian organization of living systems. Cold Spring Harbor Symp. Quant. Biol., **25**: 158–184.

7 Pittendrigh, C. S. and Minis, D. H. (1964) The entrainment of circadian oscillators by light and their roles as photoperiodic clock. Am. Nat., **98**: 261–294.

8 Tyschenko, V. B. (1966) Two-oscillator model of the physiological mechanism of insect photoperiodic reaction. Zhur. obshch. Biol., **27**: 209–222.

9 Truman, J. W. (1972) Physiology of insect rhythm. I. Circadian organization of the endocrine events underlying the moulting cycle of larval tobacco hornworms. J. Exp. Biol., **57**: 805–820.

10 Fujishita, M. and Ishizaki, H. (1981) Circadian clock and prothoracicotropic hormone secretion in relation to the larval-larval ecdysis rhythm of saturniid *Samia cynthia ricini*. J. Insect Physiol., **27**: 121–128.

11 Sakai, T. and Masaki, S. (1965) Photoperiod as a factor causing seasonal forms in *Lycaena phlaeas daimio* Seitz. Konchu, **33**: 275–283.

12 Endo, K., Maruyama, Y. and Sasaki, K. (1985) Environmental factors controlling seasonal morph determination in the small copper butterfly, *Lycaena phlaeas daimio* Seitz. J. Insect Physiol., **31**: 525–532.

13 Endo, K. and Kamata, Y. (1985) Hormonal control of seasonal-morph determination in small copper butterfly, *Lycaena phlaeas daimio* Seitz. J. Insect Physiol., **31**: 701–706.

14 Halberg, F., Johnson, E. A., Nelson, W., Runge, W. and Southern, R. (1972) Autorhythmometry: procedures for physiological self-measurements and their analysis. Physiol. Teach., **1**: 1–11.

15 Nakahama, K. and Endo, K. (1986) Time-measurement system underlying the photoperiodic control of pupal diapause in the swallowtail, *Papilio xuthus* L.: A trial for the application of the external coincidence model. Zool. Sci., **3**: 837–846.

ZOOLOGICAL SCIENCE 4: 693–697 (1987)

Mating Aggregation in the Japanese Treefrog, *Rhacophorus arboreus* (Anura: Rhacophoridae): a Test of Cooperation Hypothesis

Eiiti Kasuya, Hideko Shigehara and Mariko Hirota

Laboratory of Biology, Faculty of Education, Niigata University, 2–8050 Ikarasi, Niigata 950–21, Japan

ABSTRACT—The hypothesis that the relationship among males in one female–multiple male aggregations in mating and oviposition of the foam-making rhacophorid frogs is cooperative was tested in the Japanese treefrog *Rhacophorus arboreus*. Joining males were not observed beating the foam with their hind limbs. The size of foam nest tended to increase with the body size of female, but was not correlated with the number of joining males. The duration of oviposition was correlated with the number of joining males but not with the body size of the paired female and male. These results were inconsistent with the hypothesis that the relationship among males in the one female–multiple male aggregations is cooperative.

INTRODUCTION

Contrasting with conflicts among males at the scene of mating, cooperation among males during mating has been rarely reported, except cases where the high degree of relatedness among males is expected (e.g. [1]). However, in some foam-nesting rhacophorid treefrogs, the relationships among males in one female–multi male mating aggregations have been described as cooperative (e.g. [2] for *Chiromantis rufescens*; [3] for *Rhacophorus arboreus*). Following Coe [2], Wilson [4] considered a one female–three male aggregation of the African rhacophorid *Chiromantis rufescens* reported by Coe as a case of "cooperative breeding". In their review on the sperm competition in amphibians, however, Halliday and Verrell [5] pointed out that there is no evidence for Wilson's interpretation except the observation that all the males in the aggregation moved their hind limbs and contributed to the formation of the foam nest.

The behavioral sequences of mating of foam-nesting rhacophorid treefrogs in one female–multi male mating aggregations are: the pair in amplexus and some other males (hereafter referred to joining males) arrive at the oviposition site (joining males sometimes arrive after the female begins oviposition). Only one male is in the amplexus position. The female secretes a fluid from which the foam nest is constructed and oviposits eggs into it. The female (and males in a few reports) beats the secretion and constructs the foam nest. After oviposition, the female and males leave the constructed foam nest.

In the present paper, we test two sub-hypotheses ("a larger nest hypothesis" and "less susceptibility of predation hypothesis", [2]) derived from the assumption that the male–male relationship in one female–multiple male mating aggregations is cooperative in the Japanese treefrog *R. arboreus*.

MATERIALS AND METHODS

The observations were made from May to July, 1984, at the 'Hyoutan' pond (26 m×8 m) in Iwamuro, Niigata, Japan (altitude about 200 m). Frogs were captured by hand or with a handy net, and were individually marked with colored waist bands for later identification [6]. We measured the snout-vent length (body size, hereafter) and weight of each frog. Observations at night were made with a 6V battery head lamp which seemed not to disturb the behavior of frogs. We observed

Accepted March 3, 1987
Received December 9, 1986

the behavior of solitary females and pairs in amplexus and that of males approaching the observed females or pairs under observation. The length and width of newly deposited foam nest were measured (the method of [7]) with a ruler. The product of length and width was used for the size measurement of foam nest and called it 'size' of foam nest hereafter.

RESULTS

During foam nest construction, we observed no males of beating the foam with their hind limbs (swimming-like behavior) apart from passive movements when the hind limbs of females touched those of males. In all the instances (n=14), beating of the foam with hind limbs was done by females.

There is no significant correlation between the size of foam nest and the number of males in a mating aggregation ($r=-0.194$, $0.8>P>0.5$, $n=11$) (Fig. 1).

The size of foam nest is not significantly correlated with the body size of the female ($r=0.451$, $0.05<P<0.1$, $n=16$, Fig. 2), although there is a trend suggesting the female body size is one of factors governing the size of the foam nest. There is no significant correlation between the size of foam nest and the body size of the male in amplexus ($r=0.042$, $P>0.8$, $n=9$, Fig. 3).

There is no correlation between the number of males in a mating aggregation and the body size of the male in amplexus ($r=-0.039$, $P>0.8$, $n=10$) nor the size of the female ($r=0.263$, $0.5>P>0.4$,

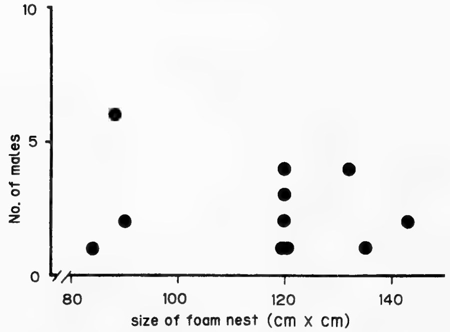

FIG. 1. The relationship between the size of foam nest and the number of males in mating aggregation.

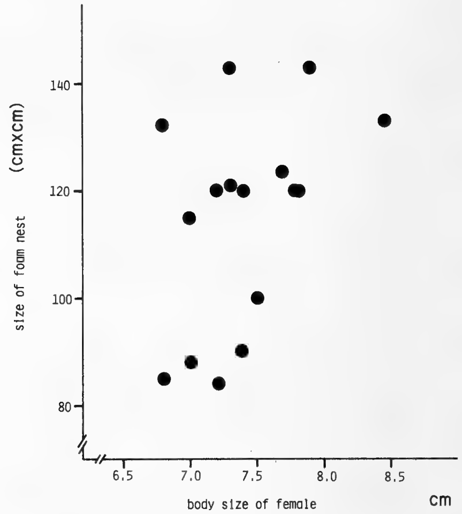

FIG. 2. The relationship between the size of foam nest and the body size (snout-vent length) of the female.

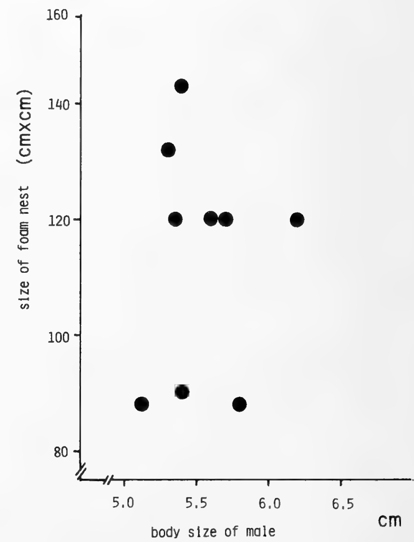

FIG. 3. The relationship between the size of foam nest and the body size (snout-vent length) of the male in amplexus.

$n=11$).

Figures 4 and 5 show the relationships between the duration of oviposition (from the beginning of construction of foam nest, i.e. the swimming movement of hind limbs of female, to the leaving of the female) and the number of males in mating

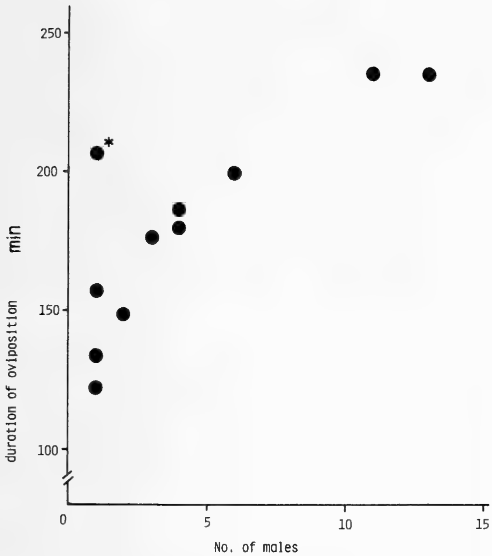

FIG. 4. The relationship between the duration of oviposition (from the beginning of foam nest construction to the departure of the female) and the number of males.
asterisk: the amplexus posture of male (grip of his fore limbs) was incomplete.

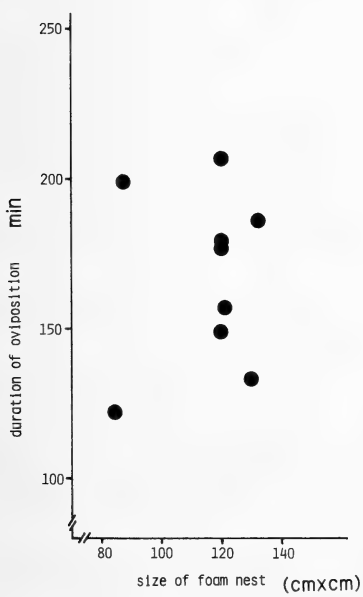

FIG. 5. The relationship between the duration of oviposition (from the beginning of foam nest construction to the leaving of the female) and the size of foam nest.

aggregation and the size of foam nest, respectively. There is a significantly positive correlation between the duration of oviposition and the number of males ($r=0.820$, $P<0.05$, $n=11$) (Fig. 4). However, the correlation between the duration of oviposition and the size of foam nest is not significant (Fig. 5, $r=0.077$, $P>0.8$, $n=9$). The correlation between the duration of oviposition and the body size of female is also not significant ($r=0.134$, $0.8>P>0.5$, $n=10$).

DISCUSSION

First, we test the following two sub-hypotheses derived from the main hypothesis that the male–male relationship in mating aggregations is cooperative. They are "a larger nest hypothesis" [2]: the advantage of using more than one male is that a larger nest can be constructed (and thus a larger number of offspring can be reared), and "less susceptibility of predation hypothesis" [2]: the advantage of using more than one male is that the assistance by a larger number of males render a female less susceptible to predation because the oviposition activity leaves the female exhausted.

The first sub-hypothesis predicts the positive correlation between the size of foam nest and the number of males. However, this is inconsistent with the result of Figures 1 which shows weakly negative (not significant) correlation between them. The results of Figures 1 and 2 suggest that the factor responsible for the size of foam nest is not the number of males but the body size of female.

The second sub-hypothesis is not directly tested because we did not measure the degree of exhaustion of females after oviposition. We use the duration of oviposition as a substitute. Furthermore, the duration of oviposition seems to be a reasonable index of susceptibility of predation during oviposition. *R. arboreus* was preyed by predators including snakes during oviposition (e.g. Kinefuchi, personal communication). The results of Figures 4 and 5 show that the duration of oviposition is strongly positively correlated with the number of males and is not correlated with the size of foam nest.

Therefore, both sub-hypotheses of the coopera-

tion hypothesis are not consistent with the results of the present study.

The cooperation hypothesis is not consistent with the observation by Saitou and Kumaki (unpublished) that the hatchability of eggs in cases of one female–multi male mating aggregations is similar to that in oviposition by a single pair in amplexus (96.4% and 98.6%, respectively). Furthermore, Kato [8] reported that all the males in mating aggregation secrete sperm with both direct and microscopic observations.

We propose alternative hypothesis, "sperm competition hypothesis", for explaining the significance of one female–multi male mating aggregation in foam-making rhacophorids based on the results of the present study. This suggests that one female–multi male mating aggregations are formed as a consequence of selfish activities of joining males, i.e. releasing sperm into the foam and fertilizing eggs by his own sperm. Because interruption of the oviposition is costly for both female and male of the pair, and because the male in the amplexus can not use his fore limbs [5], both female and male of the pair can not effectively counteract other males which approach the pair to release sperm into the foam. In this hypothesis, the joining of males is regarded as detrimental for both the male and female in amplexus. For the female, the joining males increase the duration of oviposition and hence increase the susceptibility of predation. For the male, they decrease the number of eggs fertilized by his sperm and increase his susceptibility of predation. The "sperm competition" hypothesis is consistent with the results of the present study.

Males joining the mating aggregation do not increase the size of the foam nest (Fig. 1). The size of foam nest is not correlated with the body size of male in amplexus nor the number of males (Fig. 3), but there is a trend between the foam nest and the body size of female (Fig. 2). The activities of males are not responsible for the size of foam nest. It suggests that the body size of female determines the size of the foam nest. The joining of males is costly in terms of the duration of oviposition (Figs. 4 and 5). The activities of joining males in mating aggregation are thus considered to be obstructing the constructing behavior of female rather than assisting it. In the present study, this is a natural conclusion because we did not observe the swimming-like behavior of hind limbs of males in mating aggregations. This does not mean, however, that the male–male relationship is cooperative in species in which the swimming-like behavior of males is observed (e.g. [2, 7]). In such species, the swimming-like behavior of males can be interpreted either as cooperative behavior or selfish one to increase the chance of fertilization of eggs by his sperm.

In conclusion, the selective significance of one female–multi female mating aggregation in foam-making rhacophorids is better explained by selfishness of males than by cooperation of males, as in the context of reproductive behavior of other anurans (e.g. [9]).

ACKNOWLEDGMENTS

We are indebted to A. Arak for his critical reading of the manuscript. Thanks are also due to K. Kinefuchi, Y. Kishi, K. Maekawa, S. Tsurumaki and M. J. West-Eberhard for useful comments. T. Saitou and T. Kumaki showed us their unpublished data. We are grateful to members of our laboratory for their assistance.

REFERENCES

1 Bertram, B. C. R. (1976) Kin selection in lions and in evolution. In "Growing Points in Ethology". Ed. by P. P. G. Bateson and R. A. Hinde, Cambridge Univ. Press, Cambridge, pp. 281–301.

2 Coe, M. J. (1967) Co-operation of three males in nest construction by *Chiromantis rufescens*. Nature, **214**: 112–113.

3 Matsui, M. (1980) Breeding behavior of some Japanese anurans. Collection and Breeding, **42**: 132–135.

4 Wilson, E. O. (1975) Sociobiology. Belknap Press of Harvard Univ. Press, Cambridge, Mass.

5 Halliday, T. R. and Verrell, P. A. (1984) Sperm competition in amphibians. In "Sperm Competition and the Evolution of Animal Mating Systems". Ed. by R. L. Smith, Academic Press, Orlando, Florida, pp. 487–508.

6 Emlen, S. T. (1968) A technique for marking anuran amphibians for behavioral studies. Herpetologica, **24**: 172–173.

7 Coe, M. J. (1974) Observations on the ecology and breeding biology of the genus Chiromantis. J. Zool., Lond., **172**: 13–34.

8 Kato, K. (1956) Ecological notes on the green frogs during the breeding season. 2. Breeding habit and others. Jpn. J. Ecol., **6**: 57–61.

9 Arak, A. (1983) Male-male competition and mate choice in anuran amphibians. In "Mate Choice". Ed. by P. Bateson, Cambridge Univ. Press, Cambridge, pp. 181–210.

ZOOLOGICAL SCIENCE 4: 699–709 (1987)

What is *Scopura longa* Uéno, 1929 (Insecta, Plecoptera)? A Revision of the Genus[1]

Shigekazu Uchida[2] and Hiroki Maruyama[3]

Department of Natural History, Faculty of Science, Tokyo Metropolitan University, Setagaya, Tokyo 158, and [3]Laboratory of Entomology, Tokyo University of Agriculture, Setagaya, Tokyo 156, Japan

ABSTRACT—*Scopura prolifera* Kawai is synonymized with *S. longa* Uéno. *S. longa* sensu Kawai, 1974 is redescribed as a new species, *S. montana* Maruyama. Two new species, *S. bihamulata* Uchida and *S. quattuorhamulata* Uchida, are described from Hokkaido. One more new species, *S. laminata* Uchida, is described from Korean nymphs. These species are distinguished from one another by one or more characters: male and female genitalia, lateral margin of adult nota and epiproct of male nymph.

Scopura Uéno, 1929 [1] is the only genus of the family Scopuridae Uéno, 1935 [2], which is endemic to Japan and Korea. It comprises peculiar wingless stoneflies with many primitive morphological features [3, 4]. The first species, *S. longa* Uéno, 1929, on which the present genus was established, was described from nymphs collected by the lake Towada-ko, northern Honshu [1]. Subsequently, the first adult of *Scopura* was collected in 1930 at Takeshi-tôge, Nagano-ken, central Honshu, and described as *longa* by Uéno in the next year [5]. Then, *longa* was considered to occur in Honshu, Hokkaido and Korea [6–8]. But *longa* in this broad sense was not based on the detailed comparative studies of adults from different localities, which were seldom collected except those from central Honshu. In 1974, Kawai divided *longa* into two species by describing the second species, *S. prolifera,* from Sado Is. on the Sea of Japan [9]. He found clear differences between *prolifera* and his "*longa*" in male genitalia which were figured with a key to the species. According to his distribution map, "*longa*" occurs in most parts of Honshu but *prolifera* is restricted to Sado Is. and Ibaraki-ken, Honshu.

However, he was unable to find a nymphal character which distinguishes these two species from each other, and therefore left the nymphs from Hokkaido and Korea unidentified, where no adult had been collected. Moreover, it is uncertain if he examined the adult male from the type locality of *longa* by the lake Towada-ko, because he did not show the locality of examined specimens of his "*longa*". Accordingly, it is problematic that he assigned the adults from most parts of Honshu to *longa*.

We found an important nymphal character of *Scopura* species in the epiproct of the male nymph, and succeeded to acquire many adults from the type locality of *longa* by rearing nymphs. They are clearly assigned to *longa* by a nymphal characteristic of their epiprocts which was described and figured in the original description. Comparison of the adults from the type locality with those from Sado Is. made it clear that *S. prolifera* Kawai is a junior synonym of *S. longa* Uéno, and that the "*longa*" of Kawai [9] is an unnamed species. The

---

Accepted March 31, 1987
Received December 6, 1986

[1] Parts of this paper were presented at the annual meetings of the Entomological Society of Japan, Kantô Branch, Tokyo, December 1982, December 1983 and the Entomological Society of Japan, Tsukuba, October 1984.

[2] Present address: Limnologische Flußstation des Max-Planck-Instituts für Limnologie, Postfach 260, D 6407 Schlitz, Germany.

[3] Present address: Nihon Tokushu Noyaku Seizo K. K., Osaka Branch Office, Furukawa-Osaka Bldg., 1-29, Dojimahama 2-Chome, Kita-ku, Osaka-shi, Osaka 530, Japan.

distribution of *longa* is confined to Sado Is. and northern Honshu, whereas the unnamed species occurs only in central Honshu. We also acquired the adults from Hokkaido by rearing. They belong to two new species which are clearly distinguished from each other and from the two species of Honshu by the genitalia and the epiproct of the male nymph. The adult of Korean *Scopura* has not been collected yet. However, the epiprocts of male nymphs from south Korea indicate that they also represent a new species which is the fifth one of the genus.

Specimens used in this study are deposited in the collection of the National Science Museum, Tokyo (NSMT), the Laboratory of Entomology, Tokyo University of Agriculture (TUA), the Limnologische Flußstation des Max-Planck-Instituts für Limnologie, Schlitz (LFS) and the senior author (SU).

Localities where only nymphs were collected are not stated in detail in this paper. They will be published elsewhere with the depository of specimens.

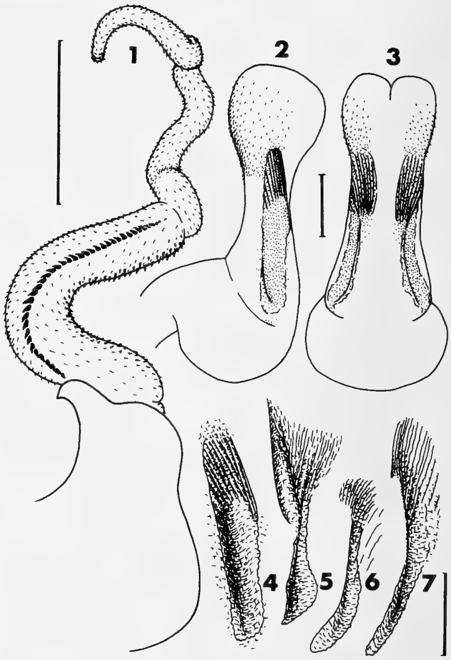

FIGS. 1–7. Internal sac of epiproct and penis — 1, *Scopura longa* from Wainai, internal sac of epiproct, everted, lateral view; 2–3, *S. montana* sp. nov. from Mitô-san, everted penis, lateral (2) and ventral (3) views; 4–7, lateral sclerites on penes of *S. montana* sp. nov. from Mitô-san (4), *S. longa* from Wainai (5), *S. bihamulata* sp. nov. (6) and *S. quattuorhamulata* sp. nov. (7). Scales, 0.5 mm.

Genus **Scopura** Uéno, 1929

Scopura Uéno, 1929 [1], 124. Type species: *Scopural longa* Uéno, original design. and monotypy.

Generic characters of *Scopura* were described by authors (see [10]) as the characters of *S. longa* in a broad sense. Kawai [9] distinguished the following characters (1–3) of species from the generic ones, to discriminate *prolifera* from his "*longa*":

1) projection at the base of male cercus,
2) male epiproct,
3) armature of penis.

We accept his distinction of characters and add the following (4–8) to the characters of species:

4) epiproct of male nymph,
5) lateral margins of adult thoracic nota,
6) male abdominal tergum 9,
7) vagina,
8) hairs and sclerites around the opening of vagina.

We present here some generic features which have never or insufficiently been described.

Male Paraproct weakly sclerotized, simple, covered with fine spinules and curved dorsally with rounded tip. "Internal sac of epiproct" (Fig. 1, ="Epiproctblase" of Zwick [4]) eversible, armed with teeth and spinules. Basal part of the sac thick, with a pair of dorso-lateral rows of strong teeth and with ventral scattered teeth; apical part slender, gradually tapered to tip. The whole sac densely covered with small spinules. The sac has no particulars that could serve species distinction, but exhibits minor geographical variation in the number of ventral teeth. The penis (Figs. 2 and 3) consists of basal everted and apical armed (not everted) parts; the apical part with a pair of lateral sclerites (Figs. 4–7) and with fine spinules on the apical expansion around the gonopore. Apical part of the lateral sclerite with many fine longitudinal folds; but basal part without fold, concave and forming a longitudinal trough.

Female General color paler than in male. Lateral margin of pronotum (Figs. 14–19) with a

hump. Vagina (Figs. 57–59, 61) with an irregularly branched accessory gland attached to the anterior part of its dorsal side. Distal end of oviduct irregularly folded, connected to apical end of vagina which bears a small sclerite ventrally; the folded part remains after KOH treatment.

Nymph The female nymph, from young (ca. 10 mm long) to mature ones, is distinguished from the male one by a central notch on abdominal sternum 8 [11]; the notch moves from the anterior margin of the sternum in young nymphs to its posterior part in mature ones. Epiproct and paraproct each with a thread of tapered gill, but the mature male nymph lacks that of the epiproct. The gills persist in adult females, but are reduced in the male.

Scopura montana Maruyama, sp. nov.

(Japanese name: Mine-towada-kawagera)
(Figs. 2, 4, 8, 9, 14, 15, 20, 24, 25, 30, 31, 36, 37, 42, 45, 54, 57, 62, 68 and 69)

Scopura longa: Uéno, 1931 [5]: 40, fig. 3. In part (adult).
Scopura longa: Kawai, 1967 [7]: 4, 178, figs. 105–108.
Scopura longa: Zwick, 1973 [4]: 167, fig. 57.
Scopura longa: Kawai, 1974 [9]: 275, fig. 2, D–F.
Additional references: *Scopura longa,* [2, 12, 13, 14, 15, 16].

Material Types: Holotype ♂ with exuvia (NSMT), Mitô-sawa at 1270 m, Mitô-san, Hinohara-mura, Tokyo, nymph collected 1.x emerged 11–12.x.1984, S. Uchida; Paratypes, 8♂7♀ (1♂1♀, TUA; 3♂2♀, LFS; 4♂4♀, SU), same locality, 1.x.1984, nymph collected 1.x emerged 6–9.x.1984, 1.xi.1984, S. Uchida. Additional specimens: Ishikawa, Yoshinodani-mura, Chûgû, nymph collected 6.x emerged 12.xi–11.xii.1982, T. Ito and S. Uchida, 1♂3♀ (SU); Shizuoka, Honkawane-chô, Tekari-dake at 2380 m, 14.x.1980, S. Uchida and N. Morihiro, 5♂1♀ (Specimens reported by [14]: 2♂, LFS; 3♂1♀, SU); Shizuoka-shi, Tekari-dake at ca. 2400 m, 13.x.1980, N. Morihiro, 1♂ (Specimen reported by [14]; LFS) Nagano, Tobira-tôge, 11.x.1982, M. Hasegawa, 1♀ (TUA); Iiyama, 23.x.1960, collector?, 2♂1♀ (LFS); Otari-mura, Tsugaike, 10.x.1982, M. Hasegawa, 1♂ (TUA); Ômachi-shi, Nakatsuna at 950 m, nymph collected 9.viii emerged 6–18.x.1982, S. Uchida, 12♂2♀ (6♂, LFS; 6♂2♀, SU); Niigata, Itoigawa-shi, Renge-onsen, nymph collected 12.viii emerged 6–16.x.1982, S. Uchida, 1♀ (SU); Kanagawa, Tsukui-machi, Kasagi-zawa at 1290 m, 4.xi.1980, S. Uchida, 17♂3♀ (Specimens reported by [15]: 6♂1♀, LFS; 11♂2♀, SU); Tokyo, Hinohara-mura, Mitô-san, nymph collected v, ix emerged 28.ix–8.x.1981, H. Maruyama and A. Mase, nymph collected 2.v emerged ix–x. 1982, H. Maruyama, A. Mase and T. Okayama, 2♂4♀ (TUA), 25.x.1985, H. Saito, 1♀ (SU); Okutama-machi, Kawanori-yama, 30.x.1983, K. Takahashi, 1♂ (TUA); Yamanashi, Enzan-shi, Ichinose, 1.x.1984, nymph collected 1.x emerged 1–5.x.1984, 8.x.1984, nymph collected 8.x emerged 8–15.x.1984, S. Uchida, 13♂8♀ (3♂3♀, LFS; 10♂5♀, SU); Tateno-sawa at 1700 m near Syôgen-tôge, 18.xi.1985, S. Uchida, 1♂2♀ (SU); Daibosatsu-tôge, nymph collected 23.v, 29.vi emerged ix.1983, A. Mase, H. Maruyama, R. Terakoshi, C Tobiyama and M. Furukawa, 12♂9♀ (TUA); Tabayama-mura, Hiryû-san, Waru-dani at 1750 m, 22.xi.1984, S. Uchida, 1♂ (SU); Gumma, Minakami-machi, Doai, 27.x.1982, T. Torii, 1♀ (SU); Katashina-mura, Tokura, nymph collected 10.ix emerged ix-x.1982, H. Maruyama, 1♂ (TUA); Tochigi, Nikkô-shi, Hantsuki-yama, nymph collected 12.vi emerged 14–20.ix.1982, A. Mase, H. Maruyama, M. Watanabe and R. Terakoshi, 3♂1♀ (TUA); 968 nymphs (138 nymphs, TUA; 97 nymphs, LFS; 733 nymphs, SU) from Ishikawa, Shizuoka, Nagano, Niigata, Tokyo, Yamanashi, Gumma, Tochigi and Fukushima.

The name *longa* is presumed to have been applied to this species by authors [3, 17, 28, etc.] who treated the *Scopura* from central Honshu (see *longa*). But their material was not accessible for re-examination and most of these authors did not describe the characteristics of this species.

The male *longa* of Uéno [5] is assigned to this species, because he described long posterior projections on the lateral margins of meso- and metanota. Kawai [7, 9] and Zwick [4] also show clearly the characteristics of this species in their descriptions and figures of male genitalia.

Male Body 13–25 mm long. Anterior projection on lateral margin of mesonotum (thick arrows in Figs. 8 and 9) slightly shorter than posterior one (fine arrows); anterior one of metanotum (thick

arrows) nearly as long as posterior one (fine arrows). Abdominal tergum 9 (Fig. 20) without spinule patch; postero-mesal part somewhat membranous. Epiproct (Figs. 42 and 45) with a pair of hooks, which project dorsally and curve anteriorly to terminate in pointed tips; the hooks are cylindrical and bear spinules on the dorsal side near the tips. Internal sac of epiproct opens dorsally between hooks; anterior side of its opening sclerotized, with spinules. Projection at the base of cercus (Figs. 24, 25, 30, 31, 36 and 37) directed

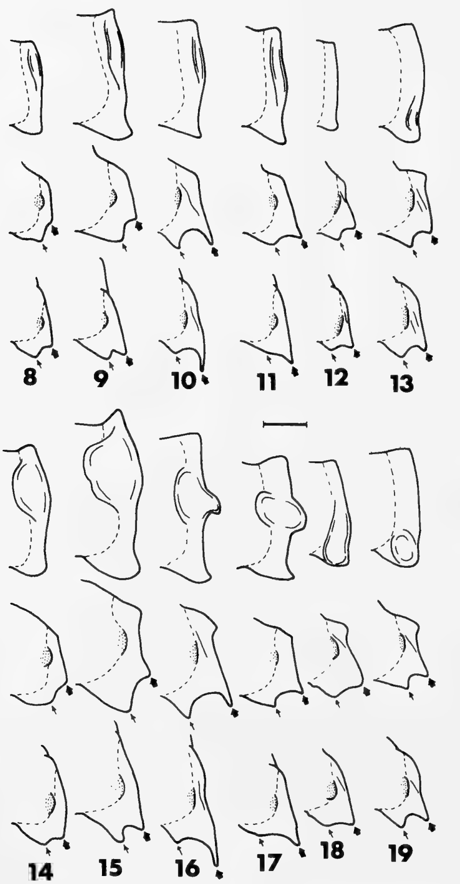

FIGS. 8–19. Lateral margins of thoracic nota: top, pronota; middle, mesonota; below, metanota: 8–13, male; 14–19, female — 8–9, 14–15, *Scopura montana* sp. nov. from Tekari-dake (8, 14) and Mitô-san (9, 15); 10–11, 16–17, *S. longa* from Yamizo-san (10, 16) and Wainai (11, 17); 12, 18, *S. bihamulata* sp. nov.; 13, 19, *S. quattuorhamulata* sp. nov. Scale, 1 mm.

dorso-mesally with a rounded tip which bears many spinules. Lateral sclerite on penis (Fig. 4) strongly sclerotized, somewhat broad and weakly folded; fine folds on its apical part directed basally to ventral side. Apical expansion of penis (Figs. 2 and 3) with spinules on dorsal and lateral side, but not on ventral side.

Female Body 25–35 mm long. Lateral margin of pronotum (Figs. 14 and 15) with a hump on anterior part; the hump is elongate and extends longitudinally. Projections on lateral margin of meso- and metanota (Figs. 14 and 15) similar to those in male in relative length of the anterior (thick arrows) and posterior (fine arrows) projections, but all of them are longer than those of male. Hind margin of abdominal sternum 8 (Fig. 54) shallowly concave. The membrane between vaginal opening and sternum 9 without or at most with a few hairs. Vagina (Fig. 57) large, 1.4–1.6 mm wide at its opening.

Male nymph Epiproct (Fig. 62) with a pair of sclerotized knobs dorsally; mesal part between the knobs flat and sclerotized.

Scopura longa Uéno, 1929
(Japanese name: Towada-kawagera)
(Figs. 1, 5, 10, 11, 16, 17, 21, 26, 27, 32, 33, 38, 39, 43, 44, 46–48, 51, 55, 58, 63 and 69)

Scopura longa Uéno, 1929 [1]: 125. Holotype: a nymph, Wainai by the lake Towada-ko, Akita-ken, northern Honshu, deposited in the collection of Dr. T. Kawai (Nara).

Scopura prolifera Kawai, 1974 [9]: 275. Holotype ♂, Myôken-zan, Sado Is. on the Sea of Japan, deposited at the National Science Museum, Tokyo. Syn. nov.

Additional references: *Scopura longa,* [5], details of type locality; *S. prolifera,* [16].

Material Niigata, Sado Is., Kanai-machi, Myôken-zan, nymph collected 10–11.ix emerged 24–30.ix.1983, H. Maruyama and A. Mase, 3♂6♀ (TUA); Ibaraki, Kita-ibaraki-shi, Hanazono-san, nymph collected 6.ix emerged 4–11.x. 1982, H. Maruyama and A. Mase, 1♂3♀ (TUA); Daigo-machi, Yamizo-san, nymph collected 7–8.vi emerged 1.x–5.xi.1981, N. Gokan, T. Nagashima and H. Maruyama, nymph collected 6.ix emerged 13–27.ix.1982, H. Maruyama and A. Mase, 3♂4♀ (TUA); Akita, Kosaka-machi, Wainai by

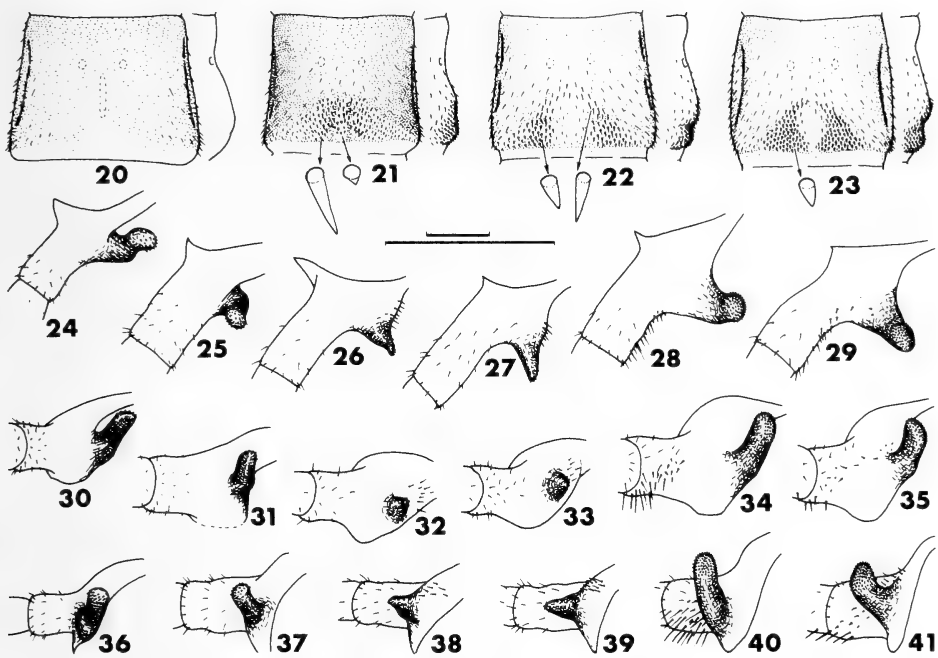

Figs. 20–41. Male abdominal tergum 9 (20–23), dorsal views with lateral views, and the bases of cerci (24–41), dorsal views (24–29), posterior views (30–35) and inside views (36–41) — 20, 24–25, 30–31, 36–37, *Scopura montana* sp. nov. from Nakatsuna (24, 30, 36) and Mitô-san (20, 25, 31, 37); 21, 26–27, 32–33, 38–39, *S. longa* from Sado Is. (26, 32, 38) and Wainai (21, 27, 33, 39); 22, 28, 34, 40, *S. bihamulata* sp. nov.; 23, 29, 35, 41, *S. quattuorhamulata* sp. nov. Scales, 1 mm.

the lake Towada-ko, nymph collected 11.ix emerged 14.x.1982, H. Maruyama, 1♂4♀ (TUA); 21.ix.1984, nymph collected 21.ix emerged 21.ix–2.x.1984, S. Uchida, 44♂33♀ (5♂7♀, LFS; 39♂26♀, SU); 166 nymphs (63 nymphs, TUA; 32 nymphs, LFS; 71 nymphs, SU) from Niigata, Ibaraki, Fukushima, Yamagata, Iwate, Akita and Aomori.

This name was previously used for all species of the genus from Honshu, Hokkaido and Korea [8, 10]. Kawai [9] erroneously used this name for the population of central Honshu. According to our study, *longa* occurs only in Sado Is. and northern Honshu (Fig. 69). Therefore, most workers of *Scopura* have presumably applied the name *longa* to other species, mostly to *montana* from central Honshu where the genus was intensively studied.

Uéno [1] described a mesal knob on the dorsal side of the epiproct of the male nymph in detail. It is clear enough to assign this species to *longa*. Kawai [9] also showed clearly some of the characteristics of this species in his description of *prolifera*.

Male Body 18–25 mm long. Anterior projection on lateral margin of mesonotum (thick arrows in Figs. 10 and 11) longer than posterior one (fine arrows); anterior one of metanotum (thick arrows) far longer than posterior one (fine arrows). Abdominal tergum 9 (Fig. 21) with a postero-mesal patch of long spinules, but those in the central light part are short. Epiproct (Figs. 43, 44, 46–48 and 51) with a mesal sclerotized hook at dorsal tip, which curves anteriorly and forms a blunt tip; spinules scattered on dorsal side before the hook. Internal sac of epiproct opens postero-dorsally behind the hook; lateral side of its opening with a pair of sclerotized lobes, which bear spinules postero-dorsally. The lobes of the material from the type locality (Figs. 48 and 51) are less produced than those from Sado Is. (Figs. 43 and 46) and Yamizo-san (Figs. 44 and 47). Projection at the base of cercus (Figs. 26, 27, 32, 33, 38 and 39)

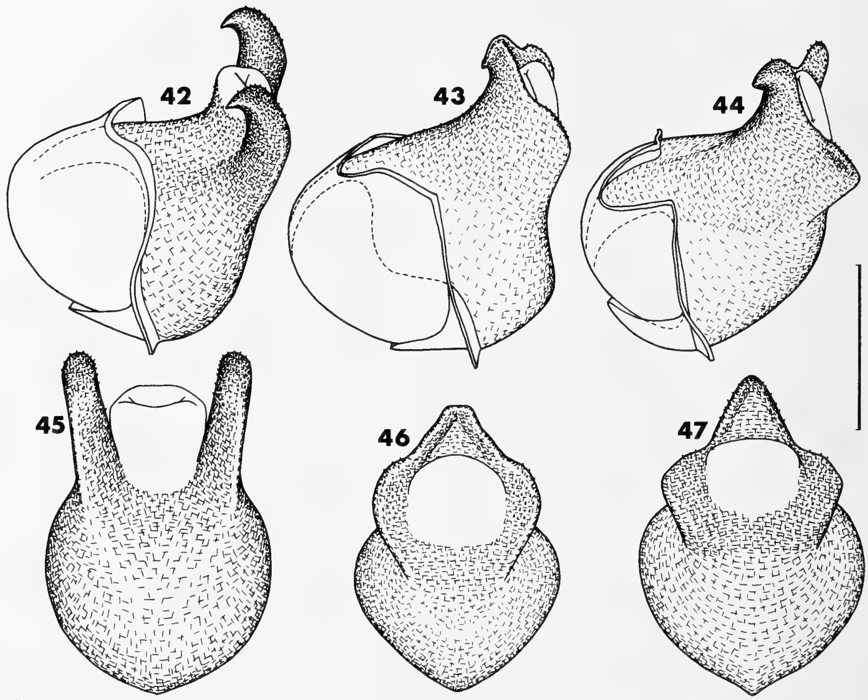

FIGS. 42–47. Male epiprocts, dorso-lateral (42–44) and posterior (45–47) views — 42, 45, *Scopura montana* sp. nov. from Mitô-san; 43–44, 46–47, *S. longa* from Sado Is. (43, 46) and Yamizo-san (44, 47). Scale, 0.5 mm.

directed posteriorly, with a pointed (specimens from Sado Is., Figs. 26, 32 and 38) or rounded (those from the type locality, Figs. 27, 33 and 39) tip which bears some spinules; dorso-mesal side of the base of the projection with hairs. Lateral sclerite on penis (Fig. 5) strongly sclerotized, constricted in median part and strongly folded; fine folds on its apical part directed basally to dorsal side. Apical expansion of penis with spinules on all sides around the gonopore.

Female Body 23–40 mm long. Lateral margin of pronotum (Figs. 16 and 17) with a hump on median part, which is positioned transversely and is produced laterally. Projections on lateral margins of meso- and metanota (Figs. 16 and 17) similar to male in relative length of anterior (thick arrows) and posterior (fine arrows) projections, but all of them longer than those of male. Hind margin of abdominal sternum 8 (Fig. 55) deeply concave. The membrane between vaginal opening and sternum 9 with many hairs, which point anteriorly. Vagina (Fig. 58) smaller than in *montana,* 1.2–1.3 mm wide at its opening.

Male nymph Epiproct (Fig. 63) with a mesal sclerotized knob dorsally; both sides of the knob also sclerotized, rounded, but never produced to knobs nor swellings as in *montana, bihamulata* and *laminata.*

Scopura bihamulata Uchida, sp. nov.
(Japanese name: Futakagi-towada-kawagera)
(Figs. 6, 12, 18, 22, 28, 34, 40, 49, 52, 56, 59, 64 and 69)

Material Types: Holotype ♂ with exuvia (NSMT), Asari-tôge, 600 m, Otaru-shi, Hokkaido, nymph collected 18.vii emerged 17–23.ix. 1984, S. Uchida; Paratype, ♀, same locality, nymph collected 18.vii.1984 emerged 2–8.x.1985, S. Uchida (SU). Additional specimens: 45 nymphs (32 nymphs, LFS; 13 nymphs, SU) from Sapporo-shi and Otaru-shi, Hokkaido.

Male Body 22 mm long. Lateral projections

on thoracic nota (Fig. 12) poorly developed; anterior ones of meso- and metanota (thick arrows) longer than those of *montana* and *quattuorhamulata* but shorter than those of *longa,* in relation to the posterior ones (fine arrows). Abdominal tergum 9 (Fig. 22) with a pair of spinule patches posteriorly; the posterior spinules shorter than the anterior ones. Epiproct (Figs. 49 and 52) with a pair of strong hooks, which are spread like fans. Dorsal margin of the hook forming an elongate disk with spinules; the disk extends anteriorly to a pointed tip. Internal sac of epiproct opens dorsally between the hooks; anterior side of its opening sclerotized without spinules. Projection at the base of cercus (Figs. 28, 34 and 40) directed dorso-mesally, with a rounded tip which bears dense spinules. Lateral sclerite on penis (Fig. 6) weakly sclerotized, slender and weakly folded; fine folds on its apical part directed basally to dorsal side. Apical expansion of penis with spinules on all sides around the gonopore.

Female Body 22 mm long. Lateral margin of pronotum (Fig. 18) with a hump on posterior part, which is longitudinally elongate. Projections on lateral margins of meso- and metanota (Fig. 18) similar to those of *longa,* but less pointed. Hind margin of abdominal sternum 8 (Fig. 56) not concave, with a pair of sclerotized humps. The membrane between vaginal opening and sternum 9 with two lip-like folds; the anterior one without hairs, but the posterior one with many hairs; the mesal hairs shorter than the lateral ones. Vagina (Fig. 59) short but as wide as in *longa,* 1.2 mm wide at its opening, with a dorsal sclerite which tapers anteriorly.

Male nymph Epiproct (Fig. 64) with a pair of dorso-lateral sclerotized swellings which are produced dorsally; the swellings far larger than the knobs of *montana.*

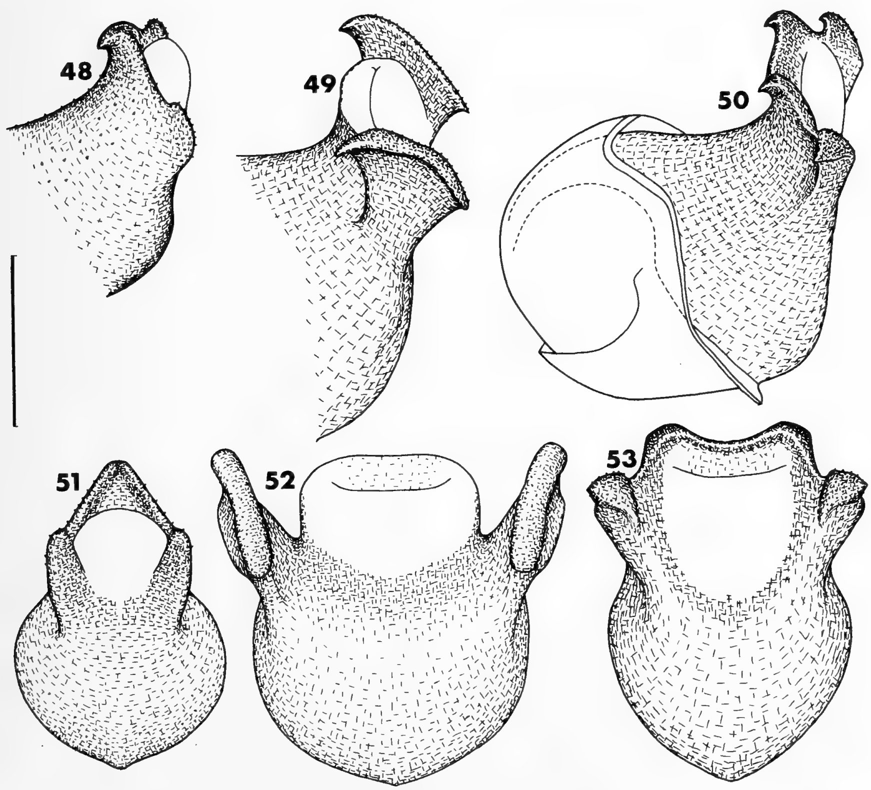

FIGS. 48–53. Male epiprocts, dorso-lateral (48–50) and posterior (51–53) views — 48, 51, *Scopura longa* from Wainai; 49, 52, *S. bihamulata* sp. nov.; 50, 53, *S. quattuorhamulata* sp. nov. Scale, 0.5 mm.

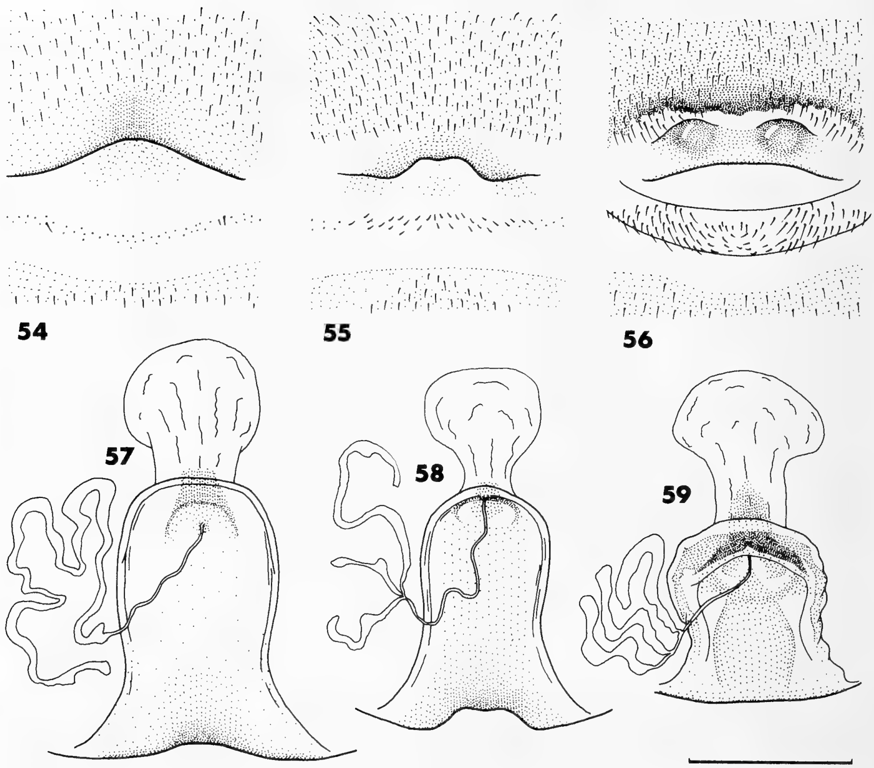

Figs. 54–59. Female abdominal sterna 8 and 9 (54–56) and vagina (57–59) — 54, 57, *Scopura montana* sp. nov. from Mitô-san; 55, 58, *S. longa* from Wainai; 56, 59, *Scopura bihamulata* sp. nov. Scale, 1 mm.

Scopura quattuorhamulata Uchida, sp. nov.
(Japanese name: Yotsukagi-towada-kawagera)
(Figs. 7, 13, 19, 23, 29, 35, 41, 50, 53, 60, 61, 65 and 69)

Material Types: Holotype ♂ with exuvia (NSMT), small stream into Niikappu-ko, 450 m, 1.5 km WNW of Niikappu-dam, Niikappu-chô, Hokkaido, nymph collected 19.ix emerged 19–20. ix.1984, S. Uchida and R. Kuranishi; Paratypes, 6♂10♀ (1♂1♀, TUA; 2♂4♀, LFS; 3♂5♀, SU), same data. Additional specimens: 48 nymphs (21 nymphs, LFS; 27 nymphs, SU) from Otoineppu-mura and Niikappu-chô, Hokkaido.

Male Body 18–25 mm long. Anterior projections on lateral margins of meso- and metanota (thick arrows in Fig. 13) longer than those of *montana* but shorter than those of *longa* and *bihamulata,* in relation to the posterior ones (fine arrows). Abdominal tergum 9 (Fig. 23) with a pair of spinule patches posteriorly; the spinules uniformly short excepting some long ones at the anterior end of the patch. Epiproct (Figs. 50 and 53) with four small hooks; a mesal pair before the opening of the internal sac, another lateral pair on its lateral sides. The mesal hooks curve anteriorly whereas the lateral ones curve antero-laterally; all tips of the hooks pointed. Projection at the base of cercus (Figs. 29, 35 and 41) directed dorsally, mesally and posteriorly, with a rounded tip which bears dense spinules. Lateral sclerite on penis (Fig. 7) strongly sclerotized, slender but broad in apical part, moderately folded; fine folds on its apical part directed basally to dorsal side. Apical expansion of penis with spinules on all sides around the gonopore.

Female Body 22–30 mm long. Lateral margin of pronotum (Fig. 19) with a hump on posterior

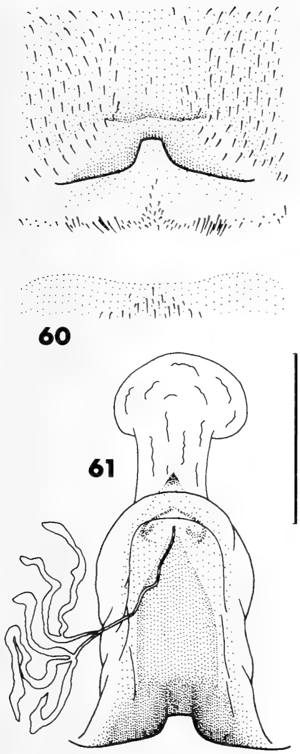

Figs. 60–61. Female abdominal sterna 8 and 9 (60) and vagina (61) of *S. quattuorhamulata* sp. nov. Scale, 1 mm.

end, which is oval with the longitudinal axis. Projections on lateral margins of meso- and metanota (Fig. 19) similar to those of *montana,* but anterior projections (thick arrows) slightly longer in relation to posterior ones (fine arrows). Hind margin of abdominal sternum 8 (Fig. 60) more deeply concave than in *longa.* The membrane between vaginal opening and sternum 9 with many hairs; the mesal hairs shorter than the lateral ones. Vagina (Fing. 61) nearly as large as in *longa,* 1.2 mm wide at its opening, with a dorsal sclerite which tapers anteriorly.

Male nymph Epiproct (Fig. 65) without knob nor swelling, smoothly rounded and sclerotized dorso-laterally.

Scopura laminata Uchida, sp. nov.
(Figs. 66, 67 and 69)

Material Types: Holotype, a male nymph (NSMT), small stream beside the temple Pukdae-sa, ca. 1200 m, Odae-san, Kangwon-do, Korea, 10.vi.1983, S. Uchida; Paratypes, 9 male nymphs (1 nymph, TUA; 4 nymphs, LFS; 4 nymphs, SU), same data. Additional specimens: 74 nymphs (14 nymphs, LFS; 60 nymphs, SU) from Chiri-san, Kyŏngsangnam-do and the type locality, Korea.

Adult Unknown.

Male nymph Epiproct (Figs. 66 and 67) with a pair of lateral membranous swellings which are produced posteriorly and with a dorso-mesal sclerite which is produced dorsally with a transversely elongated small concavity at its center. The swellings of the specimens from Chiri-san (Fig. 66) are smaller than those from the type locality (Fig. 67)

KEYS TO THE SPECIES OF *SCOPURA*

The adult of *laminata* is not known.

Male

1. Epiproct with a mesal hook (Figs. 43, 44 and 48) .... *longa*
– Epiproct with one or two pairs of hooks (Figs. 42, 49 and 50) 2
2. Epiproct with two pairs of hooks (Fig. 50) .... *quattuorhamulata*
– Epiproct with one pair of hooks (Figs. 42 and 49) 3
3. Hooks of epiproct cylindrical (Fig. 42) .... *montana*
– Hooks of epiproct fan-shaped (Fig. 49) .... *bihamulata*

Female

1. Lateral margin of pronotum with a hump

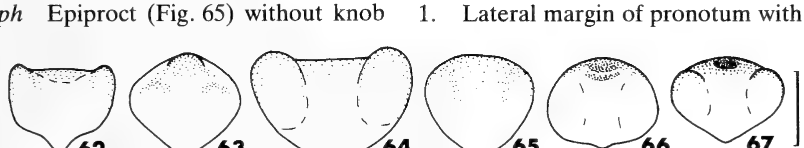

Figs. 62–67. Epiprocts of male nymphs, posterior views — 62, *Scopura montana* sp. nov.; 63, *S. longa*; 64, *S. bihamulata* sp. nov.; 65, *S. quattuorhamulata* sp. nov.; 66–67, *S. laminata* sp. nov. from Chiri-san (66) and Odae-san (67). Scale, 0.5 mm.

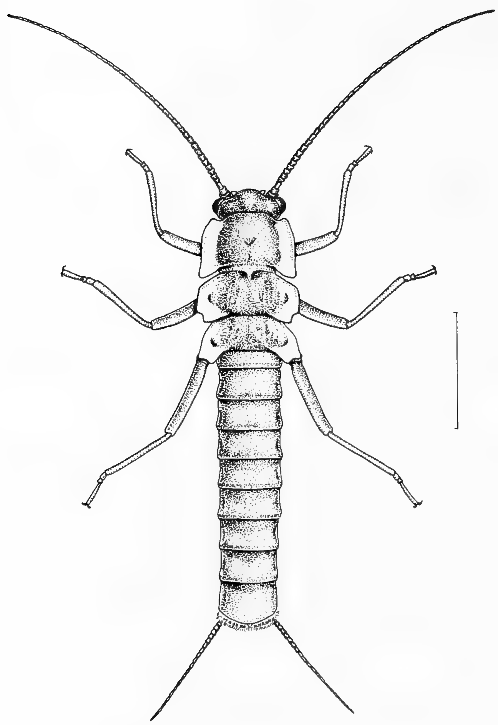

FIG. 68. *Scopura montana* Maruyama, sp. nov., female, habitus. Scale, 5 mm.

on anterior or median part (Figs. 14–17) 2
- Lateral margin of pronotum with a hump on posterior part (Figs. 18 and 19) 3

2. Lateral margin of pronotum with a longitudinally elongate hump on anterior part (Figs. 14 and 15)........................... *montana*
- Lateral margin of pronotum with a transversely elongate hump on median part (Figs. 16 and 17).............................. *longa*

3. Lateral margin of pronotum with a longitudinally elongate hump on posterior part (Fig. 18)................................. *bihamulata*
- Lateral margin of pronotum with an oval hump on posterior end (Fig. 19) .... *quattuorhamulata*

Male nymph

1. Epiproct without knob nor swelling (Fig. 65)................................ *quattuorhamulata*
- Epiproct with knob(s) or swellings (Figs. 62–64, 66 and 67) 2

2. Epiproct with a mesal knob (Fig. 63)... *longa*
- Epiproct with a pair of knobs or swellings (Figs. 62, 64, 66 and 67).......................... 3

3. Epiproct with a pair of small knobs dorsally (Fig. 62) .... *montana*
- Epiproct with a pair of large swellings dorso-laterally or laterally (Figs. 64, 66 and 67) 4

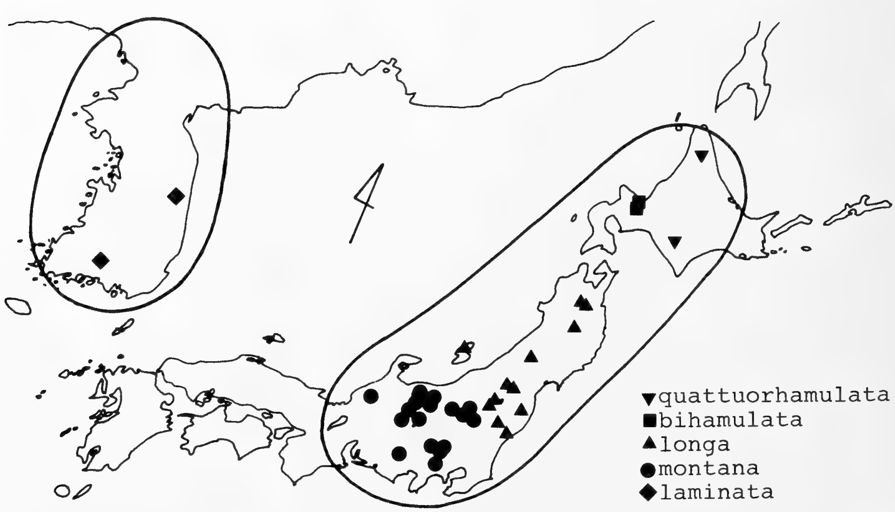

FIG. 69. Distribution of *Scopura* species. Solid lines represent the approximate distribution of the genus (from [8] and our material).

4. Swellings of epiproct sclerotized, produced dorsally, without produced sclerite between the swellings (Fig. 64).... *bihamulata*
– Swellings of epiproct membranous, produced posteriorly, with a mesal sclerite which is produced dorsally between the swellings (Figs. 66 and 67)............. *laminata*

ACKNOWLEDGMENT

We are very grateful to Professors R. Ishikawa, T. Yamasaki (Tokyo Metropolitan University), H. Sawada and Y. Watanabe (Tokyo University of Agriculture) and Dr. S. Asahina (Tokyo) who gave us helpful advice and encouragement throughout this study. Professor T. Kawai (Nara Women's University) kindly provided valuable literature and helpful information on this study. We are also grateful to Priv.-Doz. Dr. P. Zwick (Limnologische Flußstation des Max-Planck-Instituts für Limnologie) for his critical reading of the manuscript and to many people given in the text for their gift of specimens used in this study.

REFERENCES

1 Uéno, M. (1929) Studies on the stoneflies of Japan. Mem. Coll. Sci. Kyoto Imp. Univ., Ser. B, **4**: 97–155, pl. 24.
2 Uéno, M. (1935) Plecoptera. In, "Aquatic Animals of the Azusa-gawa River System and Kamikôchi". Iwanami, Tokyo, pp. 30–51. (In Japanese.)
3 Illies, J. (1962) Das abdominale Zentralnervensystem der Insekten und seine Bedeutung für Phylogenie und Systematik der Plecopteren. Ber. 9. Wandervers. Dtsch. Entomol., Berlin, **45**: 139–152.
4 Zwick, P. (1973) Plecoptera, phylogenetisches System und Katalog. Das Tierreich, **94**: xxxii+465 pp.
5 Uéno, M. (1931) Two apteral stoneflies, *Capnia nivalis* and *Scopura longa*. Kontyû, Tokyo, **5**: 38–46, pl. 2. (In Japanese.)
6 Uéno, M. (1938) Recorded localities of *Scopura longa* Uéno (Plecoptera, Scopuridae). Mushi, Fukuoka, **11**: 201–203. (In Japanese.)
7 Kawai, T. (1967) Plecoptera. Fauna Japonica. Biogeographical Society of Japan, Tokyo, 211 pp.
8 Komatsu, T. (1970) Localities of *Scopura longa* Uéno (Plecoptera) in Japan and Korea. New Insect, **14**: 14–28. (In Japanese.)
9 Kawai, T. (1974) The second species of the genus *Scopura* (Plecoptera, Scopuridae). Bull. Natl. Sci. Mus., Tokyo, **17**: 275–281.
10 Komatsu, T. (1970) Bibliography of *Scopura longa* Uéno (Plecoptera). New Insect, **14**: 29–36. (In Japanese.)
11 Kohno, M. (1951) Notes on *Scopura longa* Uéno of Aizu, Fukushima-pref. (1), (2). Collect. & Breed., Tokyo, **13**: 49–54, 128–130. (In Japanese.)
12 Uéno, M. (1938) Scopuridae, and aberrant family of the order Plecoptera. Ins. Matsum., Sapporo, **12**: 154–159.
13 Kobayashi, M. (1981) New locality of *Scopura longa* Uéno. Nat. Hist. Rept. Kanagawa, Yokohama, **2**: 45–46. (In Japanese.)
14 Uchida, S. (1981) Benthic animals of mountain streams in the Oi-gawa Genryubu wilderness area. In "Conservation Reports of the Oi-gawa Genryubu Wilderness Area in the Southern Japanese Alps, Central Japan". Nature Conservation Society of Japan, Tokyo, pp. 295–319. (In Japanese.)
15 Uchida, S. (1984) Distribution of the large stoneflies in Tanzawa mountains. Nat. Hist. Rept. Kanagawa, Yokohama, **5**: 17–25. (In Japanese.)
16 Zwick, P. (1980) Plecoptera (Steinfliegen). Handbuch der Zoologie, Berlin, **4** (2) 2/7: 115 pp.
17 Kohno, M. (1937) Notes on *Perlodes yarizawana* Uéno and *Scopura longa* Uéno. Mushi, Fukuoka, **9**: 116–119.
18 Komatsu, T. (1956) On the imago, egg and first instar of *Scopura longa* Uéno. New Entomol., Ueda, **5**: 13–21, 1 pl. (In Japanese.)

ZOOLOGICAL SCIENCE 4: 711–720 (1987)

Taxonomic Notes on Coenomyiidae (Insecta: Diptera)[1]

AKIRA NAGATOMI

Entomological Laboratory, Faculty of Agriculture, Kagoshima University, Kagoshima 890, Japan

ABSTRACT—A list of Coenomyiidae of the world is prepared and some notes are given to certain species. A brief review is presented to the recent literature on taxonomy, mouthparts, genitalia, biology, immature stages, and distribution in N. America.

RECENT LITERATURE ON TAXONOMY

Nagatomi and Saigusa [1] revised the Coenomyiidae of Japan. Later, Nagatomi [2–4] defined the extent and limit of Coenomyiidae and in these papers, the genera *Glutops* and *Pseudoerinna* (=*Bequaertomyia*) are excluded and the genus *Dialysis* is newly combined with the Coenomyiidae. James (in McAlpine *et al.* [5]) put the genera *Arthropeas, Coenomyia,* and *Dialysis* in the Coenomyiinae of the Xylophagidae.

Webb [6–8] revised the Nearctic *Dialysis, Coenomyia,* and *Arthropeas,* respectively. Webb and Lisowski [9] found the larva and pupa of *Dialysis fasciventris* from N. America, and reinforced the assignment of *Dialysis* into the Coenomyiidae.

Webb [10] erected a new genus *Napemyia* from N. America, a close relative of *Dialysis.* Nagatomi [11] revised the genus *Odontosabula,* adding two new species from Japan, and Nagatomi and Nagatomi [12] revised the genus *Arthropeas.*

Oldroyd [13] revised the genus *Coenomyia* and recognized three component species, that is, *basalis* (=*comans*) (Japan), *bituberculata* (Himalayas), and *ferruginea* (Europe and N. America). Weinberg and Bächli [14] doubted the specific validity of *Coenomyia basalis* and *C. bituberculata* and considered that "this genus includes a single species". However, *basalis* and *bituberculata* seem to be valid species as shown in this paper.

Accepted March 25, 1987
Received January 21, 1987

[1] Fifth supplement to Nagatomi [17] on Male Genitalia of the Lower Brachycera (Diptera).

RELATED FAMILIES AND THEIR AGES

The Coenomyiidae belong to the Xylophagidae s. lat. which include the Rachiceridae, Xylophagidae, Exeretoneuridae, Heterostomidae, and possibly Pantophthalmidae. The Xylophagidae s. lat. are comprised in the Stratiomyioidea, together with the Stratiomyidae and Xylomyidae (=Solvidae). The sister group of the Stratiomyioidea is the Tabanoidea consisting of the Pelecorhynchidae, Rhagionidae, Athericidae, and Tabanidae. The scheme above is chiefly derived from Hennig [15], Nagatomi [16], and McAlpine *et al.* [5].

Within the Xylophagidae s. lat., the Coenomyiidae are most closely related to the Heterostomidae and Exeretoneuridae, each of which include only one genus. *Heterostomus* was removed from the Rhagionidae (Nagatomi [16–18]), and *Exeretoneura* from the Nemestrinidae (Nagatomi [16, 17]).

Mackerras [19] wrote, "the distribution of the genus (=*Exeretoneura*) in Tasmania and on the mountains of Eastern Australia suggests that its nearest relatives will probably be found in South America". The nearest relative in question will be *Heterostomus* known from Chile. For geographical distribution of the Xylophagidae s. lat., see Nagatomi [20].

Mackerras [21] discussed the composition and distribution of the fauna of Australia and put *Exeretoneura* into the archaic element, which is "a small element, consisting of primitive animals that have evidently survived with little change since Palaeozoic or early Mesozoic times".

If Mackerras' assumption is correct as to the age of *Exeretoneura,* almost the same will apply to *Heterostomus.*

The genera of Coenomyiidae are obviously more advanced than *Exeretoneura* and *Heterostomus,* but their origins seem to be old too, judging from morphological evidence, although *Dialysis* is apparently younger than other genera of Coenomyiidae.

FAMILY CHARACTERISTICS

The family characteristics of Coenomyiidae were given by Nagatomi [2], to which some notes are added.

Palpus is 1 or 2 segmented in *Arthropeas* species according to individual. It is always 1-segmented in other genera.

Midventral part of fused basistyles (=area corresponding to sternum 9 or hypandrium) has a large desclerotized or membranous area in *Dialysis iwatai* (after Nagatomi [17]) and 8 Nearctic species of *Dialysis* (after Webb [6]), as in other genera of Coenomyiidae. However, the midventral membranous area (="ventral opening") is absent in *Dialysis kesseli* and *Napemyia illinoensis* (after Webb [6, 10]).

MOUTHPARTS AND GENITALIA

Nagatomi and Soroida [22] discussed the structure of the mouthparts of the orthorrhaphous Brachycera and described and illustrated those of five genera (and 5 species) of Coenomyiidae. They [22] wrote, "the mouthparts of Therevidae (based on 4 genera and 4 species) are similar to those of Coenomyiidae and may be difficult to distinguish from the latter, although the systematic positions of these two families are evidently very distant".

After the Therevidae, the mouthparts of Coenomyiidae may be similar to those of Rhagionidae (some genera), Vermileonidae (*Vermileo*), Nemestrinidae (*Hirmoneura*), and Hilarimorphidae (*Hilarimorpha*), of which the last two (or three) families belong to the Asilomorpha.

It may be said that the structure of the mouthparts in the families or genera above are generalized or primitive among the orthorrhaphous Brachycera, apart from the absence of mandibles.

The described and illustrated genitalia of the genera of Coenomyiidae are seen in the literature given below.

Male genitalia: *Anacanthaspis,* Nagatomi and Saigusa [1]; *Arthropeas,* Webb [8], and Nagatomi and Nagatomi [12]; *Coenomyia,* Nagatomi and Saigusa [1], Webb [7], Weinberg and Bächli [14], and Nagatomi [17]; *Dialysis,* Hardy [23], Webb [6], and Nagatomi [17]; *Napemyia,* Webb [10]; *Odontosabula,* Nagatomi and Saigusa [1], and Nagatomi [17].

Some errors must be pointed out to Nagatomi [17] as follows.

P. 114, line 9 under Genus *Dialysis,* read "mid-anterior", for "mid-posterior."

P. 115, line 10 (in *Odontosabula gloriosa),* read "dorso-posterior" for "dorso-anterior."

In Figure 26 by Nagatomi [17] as to *Coenomyia basalis,* there is "a large mid-anterior membranous or desclerotized part which is not shorter than posterior sclerotized part." This part was interpreted as dorsal plate (=dp), but seems to be aedeagal dorso-anterior plate (=adp).

The male genitalia of *Anacanthaspis bifasciata japonica* are described and illustrated in the forthcoming chapter.

Female genitalia: *Arthropeas,* Webb [8]; *Coenomyia,* Nagatomi and Iwata [24], and Webb [7]; *Dialysis,* Nagatomi and Iwata [24], and Webb [6]; *Odontosabula,* Nagatomi and Iwata [24].

In the genitalia of Coenomyiidae, no definite distinguishing characters are found among genera in both sexes.

The male genitalia in each family of the Xylophagidae s. lat. are very distinctive, but are similar between Coenomyiidae and Rhagionidae (which does not belong to the Xylophagidae s. lat.). However, Nagatomi [17] wrote, "the genera of Coenomyiidae, which are almost identical with one another in male genitalia, may easily be separated from each genus of Rhagionidae, which may be characteristic in the details of male genitalia."

On the other hand, the female genitalia are similar among the Xylophagidae s. lat. (except the Pantophthalmidae), although those of each family may be separated (see the keys in Nagatomi and

Iwata [24, 25]).

Webb [6] shows in *Dialysis* that the endophallus (=anterior bar of aedeagus) and "endophallic hilt" (=correctly endophallic supporting sclerite) (=aedeagal dorso-anterior sclerite) vary in shape with species.

BIOLOGY AND IMMATURE STAGES

Very little is known of the biology of Coenomyiidae. It is introduced below. *Arthropeas sibiricum*: "The larvae develop in the soil of spruce-fir forests." (after Krivosheina [26]); *Coenomyia ferruginea*: "Adults feed on fluid matter or the nectar of flowers (Malloch, 1917). ... Larvae have been collected in a field some distance from timber or in decaying wood (Malloch, 1917) and from silty clay loam (pH 4.6) in Connecticut in a red oak and sugar maple forest (C. T. Maier, personal communication). The larvae are predaceous and feed upon white grubs and other insect larvae (Malloch, 1917)." (after Webb [7]); *Dialysis fasciventris*: "The larvae were collected from the top 5 cm of soft organic soil in a beech and sugar maple forest in Vermilion County in eastern Illinois. Six larvae were collected from 42 soil samples (each sample 890 sq. cm), giving an average abundance of 1.57 larvae per square meter." (after Webb and Lisowski [9]).

I observed a swarm of *Dialysis iwatai,* flying low in the air, of which some male individuals were captured by net. It was early in the morning (something past seven), on July 29, 1977 at Ichinose, Mt. Haku, Ishikawa Prefecture, Honshu.

The literature on the larval and pupal stages of Coenomyiidae is as follows: *Arthropeas sibiricum* (larva): Krivosheina [26, 27]; *Coenomyia ferruginea*: Beling (1880) (larva and pupa), Brauer (1883) (larva), Hart (1898) (pupa), Malloch (1917) (larva and pupa), Greene (1926) (pupa), Peterson (1951) (larva), James (in McAlpine *et al.,* 1981) (larva), and Webb (1983a) (larva and pupa) (after Hennig [28], and Webb [7]); *Dialysis fasciventris* (larva and pupa): Webb and Lisowski [9].

A comparison of the morphological characters of the pupal stages of *Coenomyia* and *Dialysis* and that of the larval stages of the three genera above are summarized in Tables 1–2 by Webb and Lisowski [9], who thus reinforced the grouping of these three genera into the family Coenomyiidae. Judging from Table 2 by Webb and Lisowski, it is almost certain that *Arthropeas* occupies an intermediate position between *Coenomyia* and *Dialysis* and it is not deniable that *Arthropeas* is more similar phylogenetically to *Coenomyia* than to *Dialysis*.

The biology and immature stages of *Heterostomus* and *Exeretoneura,* close relatives of Coenomyiidae, are not known.

DISTRIBUTION IN NORTH AMERICA

The North American Coenomyiidae may be broadly divided in geographical distribution into eastern and western species, which are shown below, according to Webb [6–8, 10] who prepared a very useful distributional map in each species.

Eastern species: *Arthropeas americanum; Coenomyia ferrugines; Dialysis* species such as *elongata, fasciventris* and *rufithorax; Napemyia illinoensis*.

Western species: *Arthropeas magnum; Dialysis* species such as *aldrichi, dispar, kesseli, lauta, mentata* and *reparta*.

Coenomyia ferruginea, an eastern species, is also distributed in Europe. *Arthropeas americanum,* an eastern species, is closely related to *sibiricum* (which is distributed in Siberia, N. China, N. Korea, and Tibet) and *sachalinense* (Sakhalin). These three species are common in several structural characters and different from *magnum,* a western species.

PHYLOGENETIC RELATIONSHIPS AMONG GENERA

The matter titled above must be analized, but there are few definite plesiomorphic or apomorphic characters which are determined as such in the genera of Coenomyiidae. A number of combinations of the relationships are able to imagine, but only one thing is right and it is difficult to determine. However, one possibility is presented in Figure 1 and the key to genera by Nagatomi [2] is here modified according to more

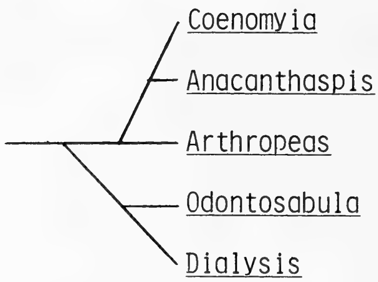

FIG. 1. Possible phylogenetic relationships among the genera of Coenomyiidae.

possible synapomorphic characters.

KEY TO GENERA OF COENOMYIIDAE
(modified from Nagatomi [2])

1. Hind femur not longer than mesonotum and scutellum combined (plesiomorphic); body somewhat slender (in *Arthropeas americanum)* to robust 2
– Hind femur distinctly longer than mesonotum and scutellum combined (apomorphic); body slender........................ 4

2(1). Antennal segment 1 distinctly longer than wide and segments 1+2 over 1/2 as long as flagellum (apomorphic); head distinctly narrower than thorax (apomorphic).................................... 3
– Antennal segment 1 about as long as wide and segment 1+2 less than 1/2 as long as flagellum (as in *Dialysis* and *Odontosabula*) (plesiomorphic); head nearly as wide as thorax (as in *Dialysis* and *Odontosabula*) (plesiomorphic) .... *Arthropeas*

3(2). Scutellum unarmed, much wider than long, and its hind margin distinctly concave at middle and consisting of two, more or less rounded portions (apomorphic); vein M_4 arising from discal cell at or near m-cu crossvein (as in *Arthropeas, Dialysis,* and *Odontosabula*) or sometimes arising from m-cu crossvein (plesiomorphic); eye bare or practically so (as in *Arthropeas, Dialysis,* and *Odontosabula*) (plesiomorphic); abdomen widest at segment 3 or 4 (apomorphic) ....*Anacanthaspis*
– Scutellum trapezoidal or semicircular and with a pair of spine-like processes (which become small and inconspicuous in *C. bituberculata* Enderlein) (plesiomorphic); vein M_4 arising from discal cell much beyond m-cu crossvein and distance between bases of M_2 and M_3 roughly as long as that between bases of M_3 and M_4 (apomorphic); eye distinctly pilose (apomorphic); abdomen widest at segment 2 or 3 (plesiomorphic)......................... *Coenomyia*

4(1). Antennal segment 3 annulated, porrect, and subulate (as in *Anacanthaspis, Arthropeas,* and *Coenomyia)* (plesiomorphic); 4th posterior cell widely open and anal cell narrowly open or closed at wing margin (as in *Anacanthaspis, Arthropeas,* and *Coenomyia*) (plesiomorphic); scutellum with a pair of spine-like processes (which are longer than in *Coenomyia*); female front broader toward antenna (as in *Anacanthaspis, Arthropeas,* and *Coenomyia*) (plesiomorphic) .... *Odontosabula*
– Antennal segment 3 conical and with a long arista (apomorphic); 4th posterior cell (when M_3 is present) and anal cell closed before wing margin (sometimes the latter closed at wing margin) (apomorphic); scutellum unarmed (as in *Arthropeas)*; female front nearly parallel-sided (apomorphic) .... *Dialysis*

LIST OF COENOMYIIDAE

A list of Coenomyiidae is presented below and some notes are given to certain species. The synonyms given by Kertész [29] are omitted.

Genus ***Anacanthaspis*** Röder

Anacanthaspis Röder, 1889, Wien Ent. Ztg., **8**: 8. Type species: *Anacanthaspis bifasciata* Röder, 1889 from Siberia (Amur).

For diagnosis of *Anacanthaspis,* see Nagatomi and Saigusa [1] and Nagatomi [3].

Anacanthaspis contains only one species, consisting of *A. bifasciata bifasciata* Röder, 1889 from E. Siberia and Manchuria and *A. bifasciata japonica* Shiraki, 1932 from Japan (Honshu).

Shiraki [30] distinguished *bifasciata japonica* from *bifasciata bifasciata* "by the wing-patterns and by the proportionally long second joint of the antennae."

Anacanthaspis bifasciata Röder

Anacanthaspis bifasciata Röder, 1889, Wien Ent. Ztg., **8**: 8. Type locality: Siberia (Amur).

There are 1♂, 1♀ from Manchuria (=NE. China) (=*bifasciata bifasciata*) which differ from the description of *bifasciata japonica* (based on 7♂♂, 1♀ from Honshu (Yamanashi and Nagano Pref.)) by Nagatomi and Saigusa [1].

Between the continental and the Japanese forms, the difference in wing pattern may be of subspecific importance. It remains undetermined whether or not the differences in head structure and the relative lengths of leg segments are significant, simply because the material examined is small.

Description of *bifasciata bifasciata,* based on 1♂, 1♀ from Manchuria is given below.

Male. Head: pile on cheek partly black; relative lengths of antennal segments 1, 2, and segment 3+flagellum 100: 86: 329 (measured along midinner surface) and segment 1, 1.1 times as long as wide (in *bifasciata japonica* 1.3–1.5 times).

Thorax: pile on mesonotum and scutellum partly black.

Legs: hairs on coxa and femur chiefly black; relative lengths of segments (excluding coxa and trochanter) of fore leg 223:261:100:39:29:23:48, of mid leg 229:245:81:32:26:23:48, of hind leg 335:332:103:39:29:23:45 and in hind leg, relative thickness of femur, tibia, and tarsal segments 1–3, 52:35:23:19:16.

Wing: 1st and 2nd basal cells without any darkened basal spot, and anal cell and axillary not darkened.

Abdomen: pile in middle of terga 2–3 may be black.

Genitalia: not examined.

Length: body 12.3 mm; wing 10.7 mm; fore basitarsus 1.2 mm.

Female. Head: hairs on head wholly black; in 1 specimen measured, width of one eye on a mid line from a direct frontal view equals distance from antenna to median ocellus (in *bifasciata japonica* 1.2 times), and 0.8 times width of face at lowest portion from a direct frontal view (in *bifasciata japonica* 1.1 times); width of front just above antenna 1.6 times that at median ocellus (in *bifasciata japonica* 1.8 times); space between antennae 0.7 times width of ocellar triangle (in *bifasciata japonica* 0.5 times); antenna 1.4 times distance from antenna to median ocellus (in *bifasciata japonica* 1.7 times); relative lengths of antennal segments 1, 2, and segment 3+flagellum (measured along midinner surface) 100:100:325 (in *bifasciata japonica* 100:71:247); antennal segment 1, 1.1 times as long as wide (in *bifasciata japonica* 1.4 times).

Thorax: hairs on mesonotum and scutellum chiefly black; pile on lower parts of metapleura black (as well as that on propleura).

Legs: relative lengths of segments of fore leg 247:274:100:32:29:24:47, of mid leg 262:265:82:29:29:21:44, of hind leg 371:362:115:38:32:?:? and in hind leg, relative thickness of femur, tibia, and tarsal segments 1–3, 56:35:26:21:21.

Wing: 1st and 2nd basal cells without any darkened basal part, and anal cell and axillary not darkened.

Length: body (with ovipositor) 15.2 mm; wing 12.2 mm; fore basitarsus 1.3 mm.

Distribution. E. Siberia and Manchuria.

Specimens examined: 1♂, 1♀, Ersentientze, Manchuria, 15. vi. 1941, V. N. Alin.

Anacanthaspis bifasciata japonica Shiraki (Fig. 2)

Anacanthaspis bifasciata var. *japonica* Shiraki, 1932, Trans. Nat. Hist. Soc. Formosa, **22**: 489. Type locality: Honshu (Kamikochi or Ibuki).

This subspecies was redescribed and illustrated by Nagatomi and Saigusa [1].

Some notes are given to the male genitalia, of which dorsal aspect is here illustrated (Fig. 2). Their ventral aspect, and the dorsal aspect of tergum 9, cerci, and sternum 10 were figured by Nagatomi and Saigusa [1]. Basistyle bluntly attenuate distally; dististyle (from dorsal or ventral

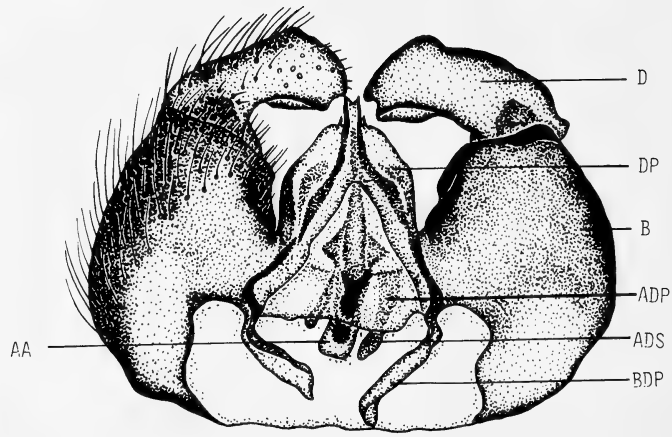

FIG. 2. *Anacanthaspis bifasciata japonica,* ♂. Genitalia (excluding tergum 9, cerci, and sternum 10), dorsal view. AA, anterior bar of aedeagus; ADP, aedeagal dorsoanterior plate; ADS, aedeagal dorsoanterior sclerite; B, basistyle; BDP, basistylar dorsoinner anterior process; D, dististyle; DP, dorsal plate.

view) widest before apex; anterior bar of aedeagus almost parallel-sided; anterior margin of dorsal plate deeply concave horizontally and its midanterior part transparent; dististyle with dorsal haris which are absent on inner apical part and outer basal part, and with ventral hairs which are absent on midinner part except inner margin; basistyle haired, except dorsoinner basal part and area corresponding to sternum 9; tergum 9 at posterior part, cerci, and sternum 10 at ventrtal surface with hairs.

Distribution. Japan (Honshu).

Genus ***Arthropeas*** Loew

Arthropeas Loew, 1850, Stettin. Entomol. Zeitg., **9**: 304. Type species: *Arthropeas sibirica* Loew. By monotypy.

For diagnosis of *Arthropeas,* see Nagatomi [3] and Webb [8]. Leonard [31] and Webb [8] revised the North American species and Nagatomi and Nagatomi [12] reviewed the species from Far East and N. America.

americanum Loew, 1861, Berl. Entomol. Zeits., 5, p. 316 — Northern Wisconsin; "Virginia to Maine and west to Minnesota" (after Webb [8]).

magnum Johnson, 1913, Can. Ent., **15**: 11 — Manitoba; Manitoba to Oregon (after Webb [8]).

sachalinense Matsumura, 1916, Thous. Ins. Jpn., Addit., **2**: 361 — Sakhalin.

sibiricum Loew, 1850, Stettin. Entomol. Zeitg., **9**: 305 — Siberia; Siberia, China, and Korea.

var. *fenestrale* Malloch, 1932, Stylops, **1**: 119 — Tibet (Tatsienlu, 8,900 feet).

var. *semifuscum* Malloch, 1932, Stylops, **1**: 119 — Tibet (Ja-Ze Pass, 16,000–17,150 feet).

Genus ***Coenomyia*** Latreille

Coenomyia Latreille, 1796, Precis d. caract. génér. d. Ins. p. 159. Type species: *Musea ferruginea* Scopoli (subsequent monotypy by Latreille, 1802).

For diagnosis of *Coenomyia,* see Oldroyd [13] and Nagatomi and Saigusa [1].

Coenomyia basalis Matsumura

Coenomyia basalis Matsumura, 1915, Kontyu-bunruigaku, Part 2, p. 47. Type locality: Japan.

Coenomyia apicalis Matsumura, 1915, Kontyu-bunruigaku, Part 2, p. 47. Type locality: Japan.

Coenomyia comans Enderlein, 1927, SitzBer. Ges. naturf. Fr. 1927, p. 47. Type locality: Japan.

Coenomyia japonica Séguy, 1955, Boll. Lab. Ent. agr. Portici, **14**: 290. Type locality: Japan.

Matsumura [32, 33] described this species twice as "*Coenomyia basalis* sp. n". In 1915 he [32] gave the name *basalis* for ♀ and *apicalis* for ♂ and in 1916 he [33] used the name *basalis* in the text and *grandis* by mistake in the explanations of appended figures.

This species was redescribed by Nagatomi and Saigusa [1].

Shiraki [30] synonymized *basalis* with *ferruginea*. Weinberg and Bächli [14] noticed considerable colour variations of legs and abdomen within *ferruginea* and found no difference in the male genitalia between *ferruginea* and *basalis*. However, it seems that *basalis* differs specifically from *ferruginea* in the following respects: antenna and palpus in both sexes distinctly longer than in *ferruginea*; hairs on eye and occiput near cerebrale in both sexes and those on male mesonotum much longer than in *ferruginea*; eyes of male not contiguous but separated; pair of knobs at midposterior margin of mesonotum in both sexes somewhat larger than in *ferruginea*. In *basalis* antenna (1) 1.2–1.4 times in ♂ and (2) 1.8–1.9 times in ♀, and palpus (3) 0.9–1.2 times in ♂ and (4) 1.4–1.7 times in ♀ distance from antenna to median ocellus respectively; width of ♀ front just above antenna (5) 0.6–0.7 times and that at median ocellus (6) 0.3–0.4 times half width of head from a direct frontal view respectively. Whereas in *ferruginea,* (1) 0.9 times, (2) 0.9 times, (3) 0.6 times, (4) 0.8 times, (5) 0.7 times, and (6) 0.4 times respectively.

The width of ♀ front is not different significantly between *basalis* and *ferruginea*. We have seen 9♂♂, 6♀♀ of *basalis* from Japan and 1♂, 1♀ of *ferruginea* from N. America.

Distribution. Japan (Hokkaido, Honshu, Shikoku, and Kyushu).

Coenomyia bituberculata Enderlein

Coenomyia bituberculata Enderlein, 1921, Mitt. Zool. Mus. Berlin, **10**: 213. Type locality: Sikkim.

This species was redescribed in detail by Oldroyd [13]. Pair of spine-like processes on scutellum become small, inconspicuous tubercles in *bituberculata*. "Wings (fig. 5) show a distinct difference in shape from other two species" (after Oldroyd [13])".

Distribution. Sikkim, Tibet, and Nepal.

Coenomyia ferruginea Scopoli

Musca ferruginea Scopoli, 1763, Entomol. Carniol., p. 340. Type locality: Europe.

For synonyms, see Leonard [31] and Oldroyd [13]. This species was redescribed in detail by Leonard [31], Oldroyd [13], and Webb [7].

Distribution. Europe and North America.

Genus ***Dialysis*** Walker

Dialysis Walker, 1850, Ins. Saund., Dipt. 1, p. 4. Type species: *Dialysis dissimilis* Walker, 1850 (from N. America). By monotypy.

Triptotricha Loew, 1872, Berl. Ent. Zeits., **14**: 59. Type species: *Triptotricha lauta* Loew, 1872 (from California). By designation of James, 1965.

For diagnosis of *Dialysis,* see Leonard [31], Nagatomi [3], and Webb [6]. The North American species were revised by Leonard [31] and Webb [6]. A revision of the Formosan and Japanese species is necessary. The list of the Nearctic species given below is quoted from James [34] and Webb [6]. A total of 12 known species are distributed as follows: N. America (9 species), Japan (2), and Formosa and S. China (1).

aldrichi Williston, 1895, Kans. Univ. Quart., **3**: 265 — Idaho; California to British Columbia east to Idaho.

arakawae Matsumura, 1916, Thous. Ins. Jpn. Addit., **2**: 351 — Japan (Honshu); Japan (Honshu and Shikoku).

cispacifica Bezzi, 1912, Ann. Mus. Nat. Hung., **10**: 444 — Formosa; Formosa and S. China.

dispar Bigot, 1879, Ann. Soc. Ent. France, ser. 5, **9**: 197 — California; California to British Columbia.
  disparilis Bergroth, 1879, Wien. Ent. Zeitg., **8**: 296 — British Columbia.

elongata (Say), 1823, J. Acad. Nat. Sci. Phila., **3**: 41 (*Stygia*) — Pennsylvania; Georgia to Quebec.
  dissimilis Walker, 1850, Insecta Saundersiana Dipt. 1, p. 4 — North America.

fasciventris (Loew), 1874, Berl. Ent. Zeits., **18**: 380 (*Triptotricha*) — Pennsylvania; "North Carolina and Tennessee to New York west to eastern Kansas."

iwatai Nagatomi, 1953, Mushi, **25**: 13 — Japan (Honshu).

kesseli Hardy, 1948, Wasmann Coll., **7**: 129 — California.

lauta (Loew), 1872, Berl. Ent. Zeits., **16**: 59 (*Triptotricha*) — California.
  discolor (Loew), 1874, Berl. Ent. Zeits., **18**: 379 (*Triptotricha*) — San Francisco.

mentata Webb, 1978, J. Kansas Ent. Soc., **51**: 424 — California; California to Washington.

reparta Webb, 1978, J. Kansas Ent. Soc., **51**: 428 — California.

rufithorax (Say), 1823, J. Acad. Nat. Sci. Phila., **3**: 36 (*Leptis*) — Pennsylvania; "northern Florida to

Pennsylvania and New Jersey, west to southern Illinois."

Genus *Napemyia* Webb

Napemyia Webb, 1983, Proc. Entomol. Soc. Wash., **85**: 822. Type species: *Napemyia illinoensis* Webb, 1983 (from Illinois), by original designation.

This genus contains only one species. Judging from the original description and illustrations, *Napemyia* is very similar to *Dialysis* but differs from the latter by having the side of face haired, posterior margin of sternum 10 (="ventral plate of proctiger") narrowly concave at middle, area corresponding to sternum 9 (=hypandrium) without a desclerotized area (="ventral opening"), and wing without thyridium. Webb [6] wrote as to *Dialysis kesseli,* "basistyle (Fig. 4) without ventral opening", which is present in other 8 Nearctic species of *Dialysis*. It is suspected whether or not the distinguishing characters above are of generic value. However, *Napemyia* is retained as a distinct genus at present.

Napemyia illinoensis Webb

Napemyia illinoensis Webb, 1983, Proc. Entomol. Soc. Wash., **85**: 823. Type locality: Illinois (Vermilion County).

The original description of this species was based on a single male specimen. The female is unknown. Webb [10] wrote, "I have made several trips each year for the last six years and have not collected additional specimens, nor have I found additional specimens in 67 museum, university, and private collections that I have examined".

Distribution. N. America (Illinois).

Genus *Odontosabula* Matsumura

Odontosabula Matsumura, 1905, Thous. Ins. Jpn., **2**: 78. Type species: *Odontosabula gloriosa* Matsumura, 1905 from Japan (Kyushu). By monotypy.

Stratioleptis Pleske, 1925, Encyc. ent. B. II. Dipt., **2**: 182. Type species: *Stratioleptis czerskii* Pleske, 1925 from East Siberia. By monotypy.

For diagnosis of *Odontosabula,* see Nagatomi and Saigusa [1] and Nagatomi [3].

Nagatomi [11] revised this genus and wrote, "this genus is distributed in East Siberia, Manchuria, Korea, and Japan (Honshu and Kyushu) and contains 5 species, that is, *czerskii, decora* sp. n., *gloriosa* (=*pleskei*), *fulvipilosa* sp. n. and *licenti.* But *licenti* is possibly a synonym of *czerskii.* It is not necessarily certain whether the distinction is specific or subspecific among them".

Odontosabula czerskii (Pleske)

Stratioleptis czerskii Pleske, 1925, Bull. Soc. ent. France, 1925: 166 or Encyc. ent B. II. Dipt., **2**: 182. Type locality: East Siberia ("Province Littorale").

It is necessary to examine the type specimen or the specimens from the type locality for exact identification of *czerskii.* Nagatomi [11] described and illustrated 1♂, 4♀♀ from Korea (Quelpart I.) as *czerskii.* Some additional notes are given below, based on 4 female specimens whose collecting data were given in Nagatomi [11].

Width of ocellar triangle 0.7–1.0 times as wide as long and that of front almost fits the description of *decora* mentioned in this paper.

Distribution. East Siberia, NE. China (=Manchuria), and Korea.

Odontosabula decora Nagatomi

Odontosabula decora Nagatomi, 1985, Kontyu, **53**: 220. Type locality: Japan (Fukui Pref., Honshu).

Some additional notes are given below, based on 8 female specimens whose collecting data were given in Nagatomi [11].

Width of one eye on a mid line from a direct frontal view 0.9–1.1 times width of front just abvove antenna; width of ocellar triangle 1.0–1.2 times its length; width of front at median ocellus 1.8–2.0 times width of ocellar triangle, 0.6–0.7 times width of front just above antenna, and 0.6–0.8 times distance from antenna to median ocellus.

There is additional 1♂, Norikura Kôgen (1,800 m), Nagano Pref., 25. vii. 1979, K. Ôhara.

Distribution. Japan: Honshu (Fukui, Ishikawa, and Nagano Prefectures).

Odontosabula fulvipilosa Nagatomi

Odontosabula fulvipilosa Nagatomi, 1985, Kontyu, **53**: 223. Type locality: Japan (Yamagata Pref., Honshu).

The female structural characters of *decora* given in this paper almost apply to *fulvipilosa.* In 4♀♀ measured, width of one eye on a mid line from a

direct frontal view 1.1–1.3 times width of front just above antenna; width of ocellar triangle 0.9–1.1 times its length; width of front at median ocellus 1.8–2.1 times width of ocellar triangle.

There is additional 1♀ (Yumoto, Nikko, 27. vii. 1984, T. Kumazawa) which is newly recorded from Tochigi Prefecture. In this specimen, anterior black border of tergum 2 is wider than its posterior yellowish brown border (as in *decora*) and sternum 3, except posterior narrow border, dark brown to black (as in *decora*).

Distribution. Japan: Honshu (Yamagata, Tochigi, Nagano, and Gifu Prefectures).

Odontosabula gloriosa Matsumura

Odontosabula gloriosa Matsumura, 1905, Thous. Ins. Jpn., **2**: 78. Type locality: Japan(Kyushu).
Stratioleptis pleskei Séguy, 1926, Encyc. ent. B. II. Dipt., **3**: 11. Type locality: Japan (Kyushu).

The female structural characters of *decora* given in this paper almost apply to *gloriosa* (N=10).

There is 1♀ (6. v. 1966, K. Kusigemati) which is newly recorded from Amami Ôshima.

Distribution. Japan: Kyushu (Fukuoka, Ôita, Kumamoto, Miyazaki, and Kagoshima Prefectures) and Amami Ôshima.

Odontosabula licenti (Séguy)

Stratioleptis licenti Séguy, 1952, Rev. fr. Ent., **19**: 243. Type locality: Manchuria ("Kirin").

It is possible that *licenti* is a synonym of *czerskii*.

Distribution. NE. China (=Manchuria).

CONCLUDING REMARKS

1. A brief review is given to the recent literature on taxonomy, mouthparts, genitalia, biology, immature stages, and distribution in N. America.

2. Phylogenetic relationships among the genera are discussed, and one possibility is shown in Figure 1.

3. *Anacanthaspis bifasciata* is redescribed. *Anacanthaspis bifasciata japonica* is perhaps valid as subspecies on the basis of the wing marking.

4. The validity of the 2 *Coenomyia* species, i.e. *basalis* and *bituberculata* is not deniable at present.

5. The genus *Napemyia* may be a synonym of *Dialysis*, because the distinguishing characters are slight. However, it is hasty to treat so now.

6. It was observed that a swarm of *Dialysis iwatai* (♂♂) flew low in the air early in the morning.

7. A list of Coenomyiidae is prepared.

ACKNOWLEDGMENTS

I express my deepest respect for the late Dr. Mortimer D. Leonard and Dr. D. Elmo Hardy, whose works have influenced me very much. My sincere thanks are offered to Dr. Paul H. Arnaud, Jr. (California Academy of Sciences, San Francisco), Dr. D. W. Webb (Illinois Natural History Survery, Champaign), Mr. T. Kumazawa, and Mr. K. Ôhara (Tokushima Prefectural Office) for their generous gift or loan of material. Professor T. Saigusa (College of General Education, Kyushu University, Fukuoka) has helped me in many ways. His help is greatly appreciated.

REFERENCES

1 Nagatomi, A. and Saigusa, T. (1970) The Coenomyiidae of Japan (Diptera). Mem. Fac. Agric. Kagoshima Univ., **7**: 257–292.
2 Nagatomi, A. (1975) Definition of Coenomyiidae (Diptera). I. Diagnoses of the family. Proc. Japan Academy, **51**: 452–456.
3 Nagatomi, A. (1975) Definition of Coenomyiidae (Diptera). II. Genera of the family. Proc. Japan Academy, **51**: 457–461.
4 Nagatomi, A. (1975) Definition of Coenomyiidae (Diptera). III. Genera excluded from the family. Proc. Japan Academy, **51**: 462–466.
5 McAlpine, J. F., Peterson, B. V., Shewell, G. E., Teskey, H. J., Vockeroth, J. R. and Wood, D. M. (1981) Manual of Nearctic Diptera. Res. Br., Agric. Can. Monogr., 27(1), 674 pp.
6 Webb, D. W. (1978) A revision of the Nearctic genus *Dialysis* (Diptera: Rhagionidae). J. Kans. Entomol. Soc., **51**: 405–431.
7 Webb, D. W. (1983) The genus *Coenomyia* (Diptera: Coenomyiidae) in the Nearctic region and notes on generic placement. Proc. Entomol. Soc. Wash., **85**: 653–664.
8 Webb, D. W. (1983) A revision of the Nearctic species of *Arthropeas* (Diptera: Coenomyiidae). Proc. Entomol. Soc. Wash., **85**: 737–747.
9 Webb, D. W. and Lisowski, E. A. (1983) The immature stages of *Dialysis fasciventris* (Loew) (Diptera: Coenomyiidae). Proc. Entomol. Soc. Wash., **85**: 691–697.
10 Webb, D. W. (1983) A new genus and species of

Nearctic Coenomyiid (Diptera: Coenomyiidae). Proc. Entomol. Soc. Wash., **85**: 822–825.

11 Nagatomi, A. (1985) The genus *Odontosabula* (Diptera, Coenomyiidae). Kontyû, Tokyo, **53**: 216–228.

12 Nagatomi, A. and Nagatomi, H. (1987) A revision of *Arthropeas* (Diptera, Coenomyiidae). Kontyû, Tokyo. (in press)

13 Oldroyd, H. (1966) Notes on *Coenomyia* Latreille (Diptera: Coenomyiidae). Beitr. Ent., **16**: 953–963.

14 Weinberg, M. and Bächli, G. (1984) The review of some families of the infraorder Asilimorpha (Diptera) from the collections of the museum of Zürich University. Travaux du Muséum d'Histoire naturelle Grigore Antipa, **25**: 191–201.

15 Hennig, W. (1973) Ordung Diptera (Zweiflügler). Handb. Zool., 4(2), 2/31 (Lfg. 20), pp. 1–337. Berlin.

16 Nagatomi, A. (1977) Classification of lower Brachycera (Diptera). J. nat. Hist., **11**: 321–335.

17 Nagatomi, A. (1984) Male genitalia of the lower Brachycera (Diptera). Beitr. Ent., **34**: 99–157.

18 Nagatomi, A. (1985) Redescription of *Heterostomus curvipalpis* (Diptera, Heterostomidae) and some notes on my paper of the male genitalia of the lower Brachycera (Diptera). Kontyû, Tokyo, **53**: 699–710.

19 Mackerras, I. M. (1925) The Nemestrinidae (Diptera) of the Australasian region. Proc. Linn. Soc. N. S. W., **50**: 489–561.

20 Nagatomi, A. (1982) Geographical distribution of the lower Brachycera (Diptera). Pac. Insects, **24**: 139–150.

21 Mackerras, I. M. (1970) Composition and distribution of the fauna. In "The Insects of Australia". Ed. by Division of Entomology, CSIRO, Melbourne Univ. Press, pp. 187–203.

22 Nagatomi, A. and Soroida, K. (1985) The structure of the mouthparts of the orthorrhaphous Brachycera (Diptera) with special reference to blood sucking. Beitr. Ent., **35**: 263–368.

23 Hardy, D. E. (1948) New and little known Diptera from the California Academy of Sciences Collection (Rhagionidae and Dorilaidae). Wasmann Coll., **7**: 129–137.

24 Nagatomi, A. and Iwata, K. (1976) Female terminalia of lower Brachycera (Diptera). I. Beitr. Ent., **26**: 5–47.

25 Nagatomi, A. and Iwata, K. (1978) Female terminalia of lower Brachycera (Diptera). II. Beitr. Ent., **28**: 263–293.

26 Krivosheina, N. P. (1967) Comparative characteristics of the larva of *Arthropeas sibilica* Loew (Diptera, Xylophagidae). Zool. Zhurnal, **46**: 954–956. (in Russian)

27 Krivosheina, N. P. (1971) The family Glutopidae, Fam. n. and its position in the system of Diptera Brachycera Orthorrhapha. Ent. Obozr., **50**: 681–694. (in Russian)

28 Hennig, W. (1952) Die Larvenformen der Dipteren, Vol. 3. 628 pp. Akademie-Verlag, Berlin.

29 Kertész, K. (1908) Catalogus dipterorum hucusque descriptorum. Vol. 3, 367 pp. Hungarian National Museum, Leipzig, Budapest.

30 Shiraki, T. (1932) Some Diptera in the Japanese Empire, with descriptions of new species (3). Coenomyiidae. Trans. Nat. Hist. Soc. Formosa, **22**: 487–492.

31 Leonard, M. D. (1930) A revision of the Dipterous family Rhagionidae (Leptidae) in the United States and Canada. Mem. Am. Ent. Soc., **7**: 1–181.

32 Matsumura, S. (1915) Kontyu-bunruigaku (=Taxonomic Entomology). Part 2. Keiseisha, Tokyo.

33 Matsumura, S. (1916) Thousand Insects of Japan, Additamenta 2. Keiseisha, Tokyo.

34 James, M. T. (1965) Family Rhagionidae. In "A Catalog of the Diptera of America North of Mexico". Ed. by A. Stone, C. W. Sabrosky, W. W. Wirth, R. H. Foote, and J. R. Coulson, U. S. Dept. of Agriculture, Washington, D. C. pp. 342–348.

ZOOLOGICAL SCIENCE 4: 721–729 (1987)

Further Studies on Cestodes of Japanese Bats, with Descriptions of Three New Species of the Genus *Vampirolepis* (Cestoda: Hymenolepididae)[1]

Isamu Sawada

Biological Laboratory, Nara Sangyo University, Sango, Nara 636, Japan

ABSTRACT—Three new and three known species of hymenolepidid cestodes are recorded from bats collected at various places in Japan in 1986. *Vampirolepis rikuchuensis* sp. n. from *Myotis hosonoi* from Ichinohe-chô, Iwate Prefecture, closely resembles *V. ogaensis* Sawada, 1974, but differs from it in smaller rostellar hooks (0.018 vs. 0.021 mm), thicker outermost chorion (tough vs. thin), surface structures of eggs (smooth vs. rough) and position of genital pores (located a little anterior to middle vs. middle). *V. kaguyae* sp. n. from *M. frater kaguyae* from the same locality, closely resembles *V. yoshiyukiae* Sawada, 1980, but differs from it in larger suckers, larger rostellum, larger rostellar sac, and longer rostellar hooks (0.032 vs. 0.0245 mm). *V. yakushimaensis* sp. n. from *Murina aurata ussuriensis* from Yakushima, Kagoshima Prefecture closely resembles *V. iriomotensis* Sawada, 1983, but differs from it in shape of ovary (pentalobate or hexalobate vs. trilobate), morphological feature of egg inner membrane (provided with polar filaments vs. no polar filaments) and longer embryonic hooks (0.018 vs. 0.014 mm).

INTRODUCTION

As a continuation of my serial studies on the cestode parasites of the Japanese bats, the present paper reports three new and three known hymenolepidid cestodes from bats collected at various localities, except Hokkaido and Shikoku, in Japan in 1986.

MATERIALS AND METHODS

The bats were captured alive and autopsied immediately at the collecting sites (Fig. 1). Their alimentary canals were cut open to extract endoparasites as soon as possible and fixed in Carnoy's fluid and bought back to my laboratory. After being soaked in 45% acetic acid for about 1 hr for expanding, they were stored in 70% alcohol. Cestodes obtained from these alcohol-preserved guts were stained with alcohol-hydrochloride-carmine, dehydrated in alcohol, cleared in xylene, and mounted in Canada balsam. Measurements are given in millimeters.

Accepted March 26, 1987
Received February 23, 1987

[1] This paper corresponds to "Helminth Fauna of Bats in Japan XXXVII".

RESULTS

The localities and dates of bats examined and cestodes obtained are shown in Table 1.

Vampirolepis Spassky, 1954
Vampirolepis rikuchuensis sp. n.
(Figs. 2–5)

From June 17 to July 7, 1986, five specimens of Hosono's whistered bat, *Myotis hosonoi,* were captured by Mukooyama around street lamps at Ichinohe-chô, Iwate Prefecture. On dissection, one of them was found infected with two mature and one juvenile specimens of this cestode.

Description: Medium-sized hymenolepidid; mature worms 24–43 in length and 0.8–1.1 maximum width. Metamerism distinct, margins serrate. Proglottids wider than long. Scolex 0.245–0.280 long and 0.273–0.287 wide, not sharply demarcated from strobila. Rostellum pyriform, 0.126 long by 0.070–0.091 wide, armed with a crown of 29–30 spanner-shaped hooks measuring 0.018 long. Hook handle long and attenuate; guard

TABLE 1. Localities and dates of bats examined and their cestode parasites in 1986

Host species / Cave and locality[1]	Date	Number of bats: examined	infected	%	Cestode species
Rhinolophidae					
(1) *Rhinolophus cornutus cornutus*					
8) Mizunashi-dô, Maebaru-chô, Fukuoka Pref.	Oct. 19	10	0	0	
10) Gongenyama-dô, Himeto-machi, Kumamoto Pref.	Dec. 7	16	9	56	*Vampirolepis isensis*
11) Disused air-raid shelter, Nishinoomote-shi, Tanegashima, Kagoshima Pref.	Dec. 11	11	2	18	*V. isensis*
12) Sea-eroded cave, Minamitane-chô, Tanegashima, Kagoshima Pref.	Dec. 25	2	1	50	*V. isensis*
(2) *Rhinolophus cornutus orii*					
14) Abandoned mine, Ryugô-son, Amamiôshima, Kagoshima, Pref.	July 28	13	3	23	*V. isensis*
15) Raceway, Yamato-son, Amamiôshima, Kagoshima, Pref.	July 29	10	0	0	
16) Disused air-raid shelter, Kakeroma, Amamiôshima, Kagoshima, Pref.	July 30	1	0	0	
(3) *Rhinolophus pumilus*					
18) Abandoned mine, Nago-shi, Okinawa Pref.	July 25	25	0	0	
20) Onaga-dô, Gushichan-son, Okinawa Pref.	July 24	20	0	0	
(4) *Rhinolophus ferrumequinum nippon*					
2) Snow tunnel, Ooyama-chô, Toyama Pref.	July 25	1	1	100	*Hymenolepis rashomonensis*
4) Deserted house, Jôhana-chô, Toyama Pref.	Aug. 2	7	5	75	*H. rashomonensis*
6) Abandoned mine, Ikeda-shi, Ôsaka Pref.	Nov. 9	1	1	100	*H. rashomonensis*
8) Mizunashi-dô	May 24	10	7	70	*H. rashomonensis*
10) Gongenyama-dô	Dec. 7	1	1	100	*H. rashomonensis*
Vespertilionidae					
(5) *Miniopterus schreibersii fuliginosus*					
5) Abandoned mine, Shiga-chô, Ishikawa Pref.	Aug. 15	5	0	0	
	Oct. 28	5	2	40	*V. hidaensis*
9) Disused air-raid shelter, Misumi-chô, Kumamoto Pref.	Dec. 7	5	3	60	*V. hidaensis*
10) Gongenyama-dô	Dec. 7	5	2	40	*V. hidaensis*
(6) *Miniopterus schreibersii blepotis*					

17) Erabu-dô Chinan-chô, Okinoerabu, Kagoshima Pref.	July 28	10	0	0	
19) Itokazu-dô Tamagusuku-son, Okinawa Pref.	July 31	10	1	10	*V. hidaensis*
(7) *Myotis hosonoi*					
1) Street lamps Ichinohe-chô, Iwate Pref.	June 17–July 1	5	2	40	*V. rikutsuensis* sp. n.
3) Forest Ooyama-chô, Toyama Pref.	July 30	1	0	0	
(8) *Myotis frater kaguyae*					
1) Street lamps	June 17–20	5	1	20	*V. kaguyae* sp. n.
3) Forest	July 30	1	1	100	*V.* sp. (juvenile, unidentified)
(9) *Murina aurata ussuriensis*					
13) Abandoned gold mine Kamiyaku-chô, Yakushima, Kagoshima Pref.	Dec. 26	1	1	100	*V. yakushimaensis* sp. n.
(10) *Murina leucogaster hilgendorfi*					
7) Abandoned mine Nose-chô, Ôsaka Pref.	Nov. 9	1	0	0	

[1] Locality numbers correspond to those in Fig. 1.

prominent, round at its end, slightly shorter than blade; blade sharp at its end. Rostellar sac slightly elongate, 0.189 long by 0.133–0.161 wide, extending posterior to suckers. Suckers discoid, 0.091–0.105 in diameter.

Genital pores unilateral, located a little anterior to the middle of proglottid margin. Testes three in number, ovoid, 0.098–0.112 long by 0.056–0.070 wide, arranged in a transverse row, one poral and two aporal. Cirrus sac club-shaped, attaining a size of 0.154 long by 0.042 wide, filled with internal seminal vesicle measuring 0.070–0.077 long by 0.035 wide. External seminal vesicle 0.112 long by 0.065 wide. Ovary transversely elongate, 0.308–0.315 wide, located anterior half of proglottid. Vagina opening in genital atrium, extending medially, then enlarging and forming seminal receptacle. Seminal receptacle 0.070–0.077 long by 0.049–0.056 wide. Vitelline gland compactly lobate, 0.140 by 0.056, located posterior to ovary. Uterus arising directly from ovarian lobe as a lobed sac, gradually enlarging, filling all available space in senile proglottids. Eggs spherical or ellipsoidal, 0.049–0.053 by 0.042–0.046, surrounded by four envelopes; outermost chorion thick and with smooth surface. Onchospheres spherical 0.032–0.035 in diameter; embryonic hooks 0.014 long.

Type host: *Myotis hosonoi* Imaizumi, 1954.

Site of infection: Small intestine.

Type locality and date: Ichinohe-chô, Iwate Prefecture; June 17, 1986.

Type specimen: Holotype: NSU Lab. Coll. No. 8701. Paratypes: 8702.

Remarks: The present new species, *V. rikuchuensis* closely resembles *V. ogaensis* Sawada, 1974 [1] from *Rhinolophus ferrumequinum nippon* in the shapes of scolex, rostellum, rostellar sac and rostellar hooks. However, it differs from *V. ogaensis* in smaller rostellar hooks (0.018 vs. 0.021), thicker outermost chorion of eggs (tough vs. thin), the surface structure of eggs (smooth vs. rough) and the position of genital pores (located a little anterior to the middle vs. the middle).

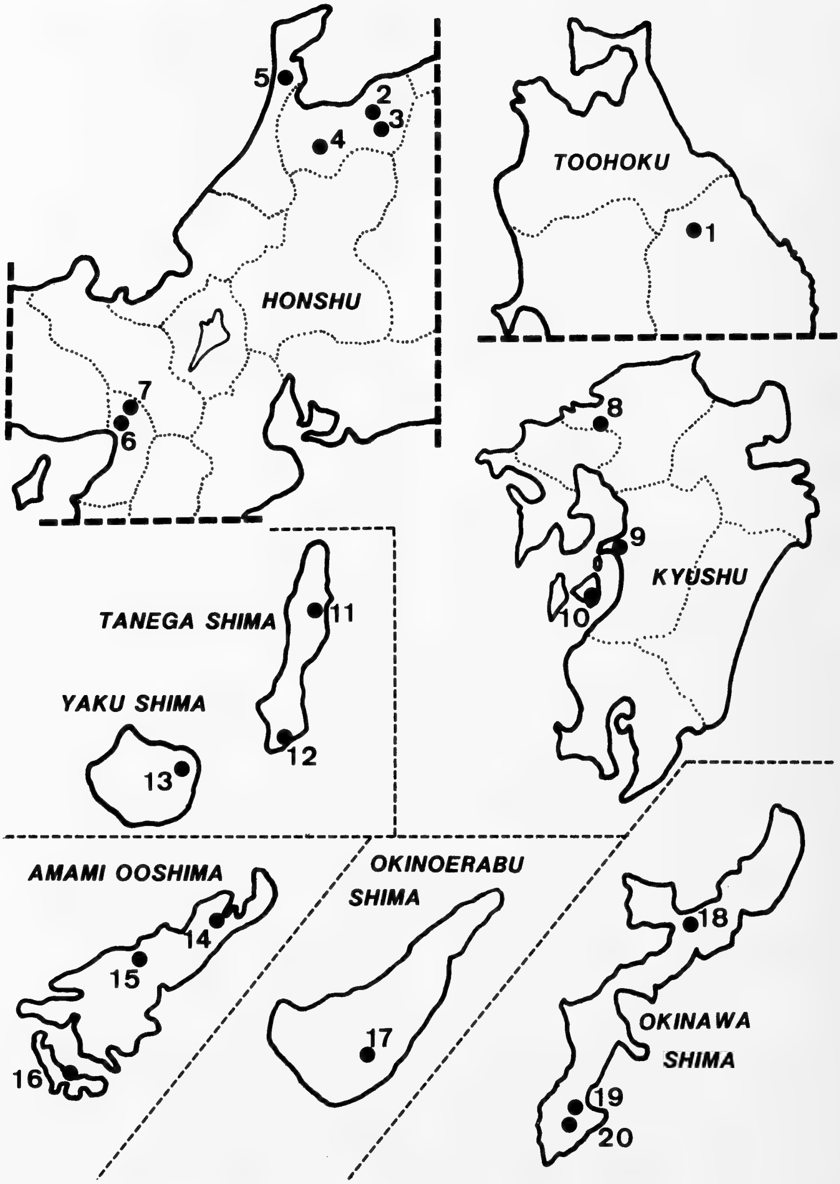

FIG. 1. Map showing the collection sites of bats. For the locality number, see Table 1.

Vampirolepis kaguyae sp. n.

(Figs. 6–9)

Of five long-leged whistered bat, *Myotis frater kaguyae,* captured by Mukooyama around street lamps at Ichinohe-chô, Iwate Prefecture, June 17 to 20, 1986, one was found infected with one mature specimen of this cestode.

Description: Medium-sized hymenolepidid; strobila length 45; maximum width 1.6. Metamerism distinct, craspedote, margins serrate. Proglottids wider than long. Scolex 0.280 long by 0.135

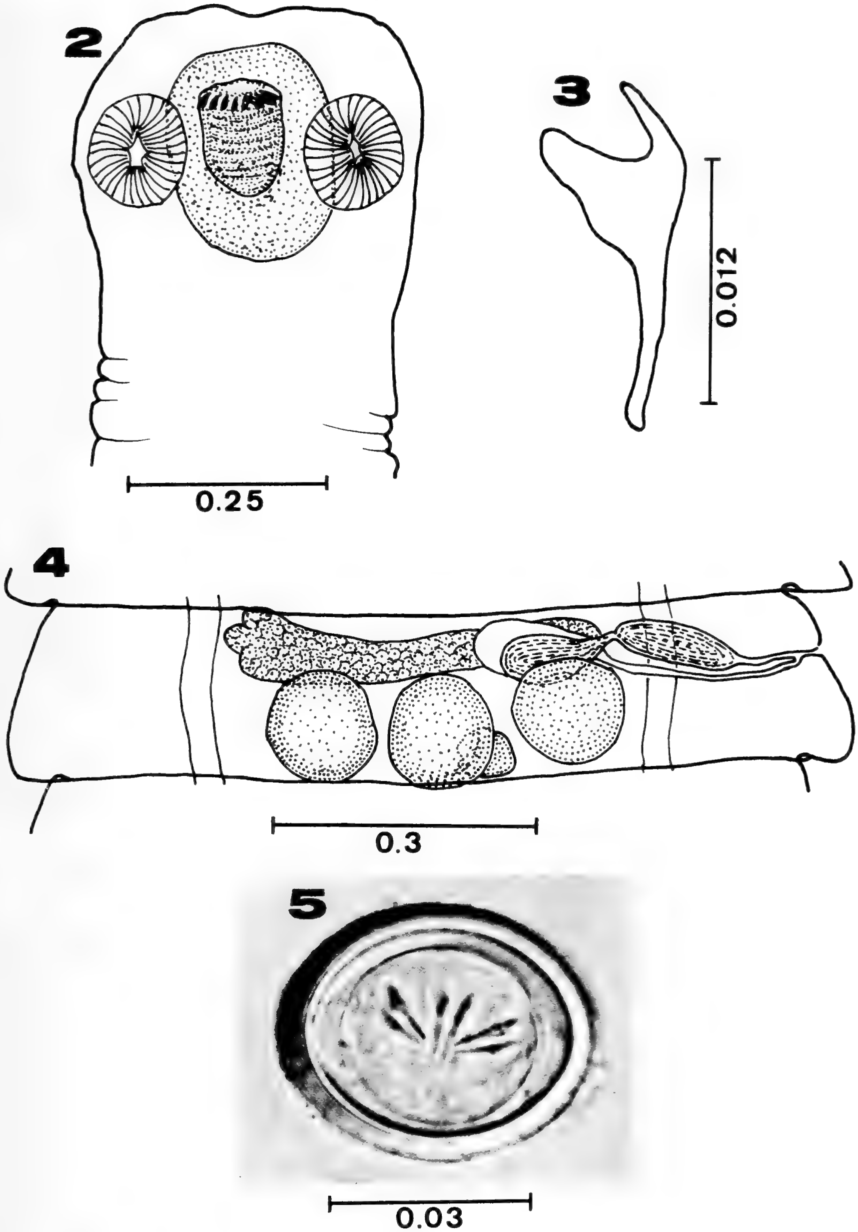

FIGS. 2–5. *Vampirolepis rikuchuensis* sp. n.
2: Scolex. 3: Rostellar hooks. 4: Mature proglottid, dorsal view. 5: Ripe egg. Scales in mm.

wide, slightly set off from neck. Rostellum pyriform, 0.140 long and 0.112 wide, armed with a single row of 35 spanner-shaped hooks measuring 0.032 long. Hook handle long, attenuate; guard prominent, round at its end, slightly shorter than blade; blade sharp at its end. Rostellar sac 0.217 long by 0.182 wide, when the rostellum is invaginated. Suckers round, 0.105 in diameter.

Genital pores unilateral, located a little posterior to the middle of proglottid margins. Testes

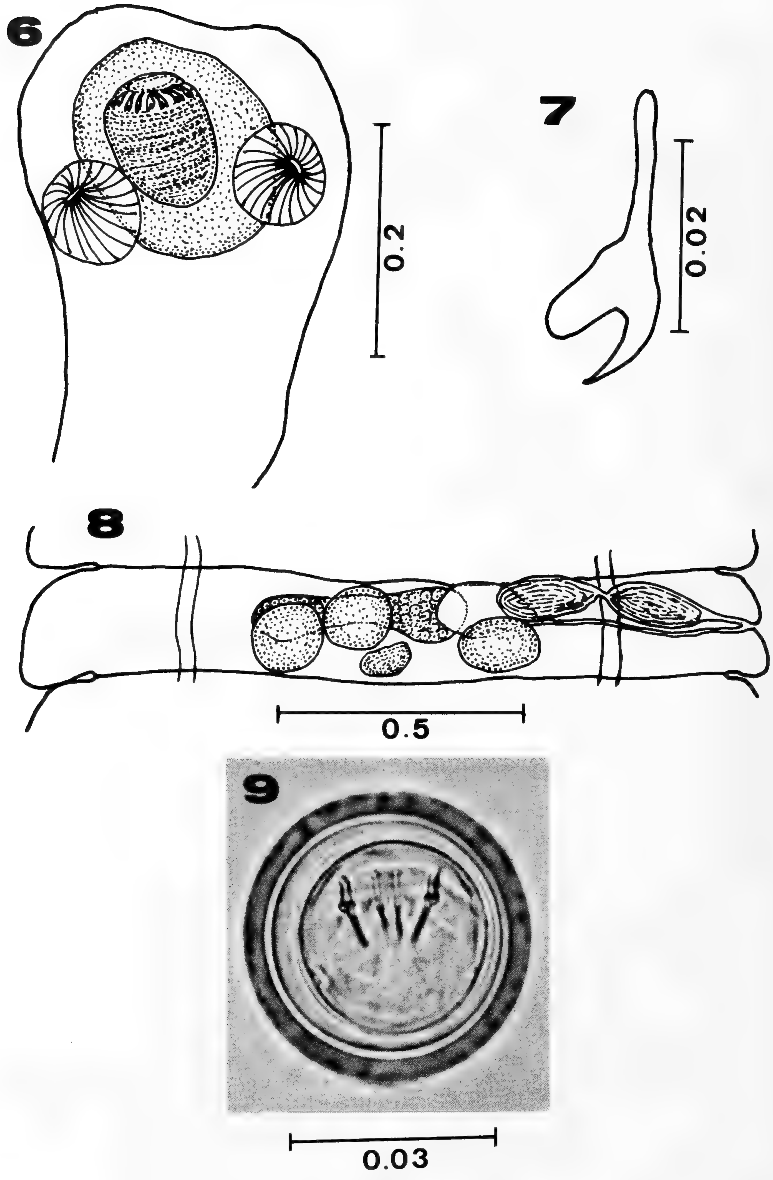

FIGS. 6–9. *Vampirolepis kaguyae* sp. n.
6: Scolex. 7: Rostellar hook. 8: Mature proglottid, dorsal view. 9: Ripe egg. Scale in mm.

three in number, spherical, 0.077–0.091 long by 0.063–0.077 wide, arranged in a transverse row, one poral and two aporal. Cirrus sac slightly elongate, 0.154–0.175 long and 0.049–0.056 wide, extending to longitudinal excretory canals. Internal seminal vesicle 0.112–0.119 long by 0.049–0.056 wide, enlarging to fill proximal portion of cirrus sac. External seminal vesicle slightly elongate, 0.104–0.175 long by 0.070–0.77 wide, extending to poral testis and dorsal to seminal receptacle. Vagina opening in genital atrium, extending to median field, then enlarging to

forming voluminous seminal receptacle measuring 0.112–0.133 long by 0.070–0.084 wide. Ovary transversely elongate, 0.280–0.287 wide. Vitelline gland compact, directly posterior to ovary, 0.077–0.091 long by 0.035–0.049 wide. Eggs spherical, 0.042 in diameter, surrounded by four envelopes; outermost chorion thick and with smooth surface. Onchospheres spherical, 0.028 in diameter; embryonic hooks 0.011 long.

Type host: *Myotis frater kaguyae* Imaizumi, 1956.

Site of infection: Small intestine.

Type locality and date: Ichinohe-chô, Iwate Prefecture: June 17, 1986.

Type specimen: Holotype NSU Lab. Coll. No. 8703.

Remarks: The present new form, *V. kaguyae,* closely resembles *V. yoshiyukiae* Sawada, 1980 [2] from the same species bat collected at Oze, Gunma Prefecture, in the shape and number of rostellar hooks. However, it differs from *V. yoshiyukiae* in larger suckers (0.105 in diameter vs. 0.056–0.070), larger rostellum (0.140 by 0.112 vs. 0.070 by 0.056), larger rostellar sac (0.217 by 0.180 vs. 0.046 by 0.054), and longer rostellar hooks (0.032 vs. 0.0245).

Vampirolepis yakushimaensis sp. n.
(Figs. 10–14)

On December 26, 1986, one lesser tube-nosed bat, *Murina aurata ussuriensis,* was collected in an abandoned gold mine at Kamiyaku-chô, Yakushima, Kagoshima Prefecture. The bat was found infected with 13 mature specimens of this cestode. The cestode is the first to be reported from this species bat from Japan.

Description: Small-sized hymenolepidid; mature worms 25–30 long and 1.0–1.2 maximum wide. Metamerism distinct, craspedote, margins serrate. Scolex clavate, 0.105–0.154 long and 0.259–0.315 wide, not sharply demarcated from strobila. Rostellum 0.049–0.077 long and 0.063–0.084 wide, armed with a single circle of 28–35 spanner-shaped hooks measuring 0.021 long. Hook handle slender; guard prominent, round at its end, slightly shorter than blade; blade remarkably sharp at its end. Rostellum retractable into rostellar sac measuring 0.119–0.140 long and 0.119–0.126 wide. Unarmed suckers round, 0.070–0.084 in diameter. Neck region behind scolex 0.22–0.28 long and 0.28 wide. Mature and gravid proglottids much broader than long.

Genital pores unilateral and located a little anterior to middle. Testes three in number, subspherical, 0.070–0.084 long by 0.084–0.105 wide, arranged in a form of triangle, one poral and two aporal, not in contact with longitudinal osmoregulatory canals laterally. Cirrus sac cylindrical, 0.154–0.270 long and 0.032–0.056 wide, positioned anteromedial from genital atrium, extending beyond osmoregulatory canals. Internal seminal vesicle 0.124–0.138 long by 0.056 wide, occupying almost whole of cirrus sac. External seminal vesicle 0.111–0.126 long by 0.042–0.055 wide. Ovary pentalobate or hexalobate, 0.182–0.189 wide. Vitelline gland lying posterior to ovary, irregularly lobate, 0.028–0.035 long by 0.070–0.077 wide. Seminal receptacle saccate, 0.126–0.140 long by 0.070–0.084 wide, overlapping poral testis. Uterus arising directly from ovarian lobes as a lobe sac, gradually enlarging, filling whole gravid proglottid. Ripe eggs elliptical; outermost chorion thin, 0.056–0.060 in major axis and 0.042–0.046 in minor axis; inner membrane 0.032–0.035 by 0.028–0.032, with at each pole a round projection provided with polar filaments. Onchospheres subspherical, 0.025–0.028 by 0.028–0.032; embryonic hooks 0.018 long.

Type host: *Murina aurata ussuriensis* Ognev, 1913.

Site of infection: Small intestine.

Type locality and date: Kamiyaku-chô, Yakushima, Kagoshima Prefecture; December 26, 1986.

Type specimen: Holotype: NSU Lab. Coll. No. 8704. Paratypes: No. 8705.

Remarks: The present new species, *V. yakushimaensis* closely resembles *V. iriomotensis* Sawada, 1983 [3] from *Rhinolophus imaizumii* in the number and length of rostellar hooks. However, it differs from *V. iriomotensis* in the shape of ovary (pentalobate or hexalobate vs. transversely elongated and trilobate), the morphological feature of egg inner membrane (provided with polar filaments vs. no polar filaments) and in longer embryonic hooks (0.018 vs. 0.014).

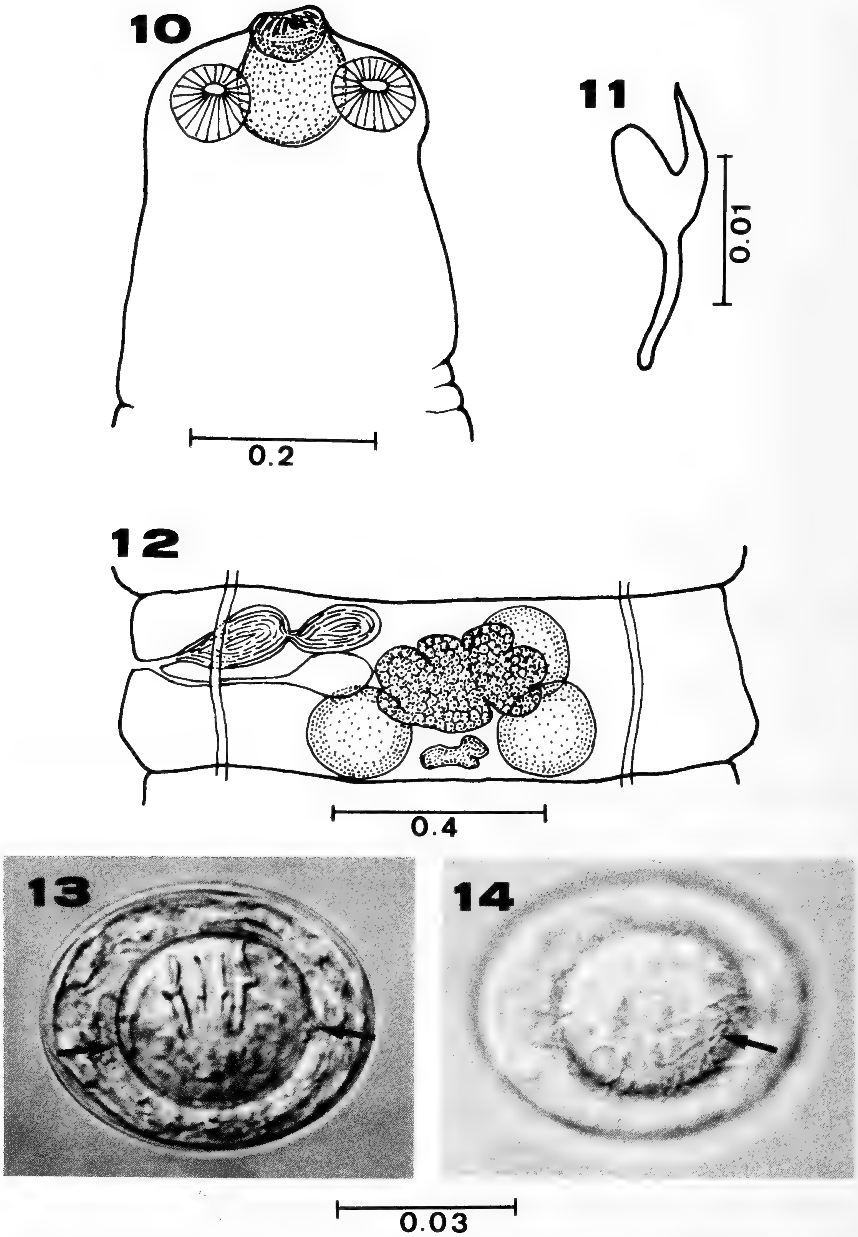

FIGS. 10–14. *Vampirolepis yakusimaensis* sp. n.

10: Scolex. 11: Rostellar hook. 12: Mature proglottid, ventral view. 13: Ripe egg, showing a projection (arrow) of the inner membrane provided with polar filaments. 14: Ripe egg, showing polar filaments (arrow). Scale in mm.

Vampirolepis isensis Sawada, 1966 [4]

Host: *Rhinolophus cornutus cornutus* and *R. c. orii*. For localities, see Table 1 and Figure 1.

Vampirolepis hidaensis Sawada, 1976 [5]

Host: *Miniopterus schreibersii fliginosus* and *M. s. blepotis*. For localities, see Table 1 and Figure 1.

Hymenolepis Weinland, 1858
Hymenolepis rashomonensis Sawada, 1972 [6]

Host: *R. ferrumequinum nippon*. For localities, see Table 1 and Figure 1.

ACKNOWLEDGMENTS

This study was supported by a Grant-in-Aid for Scientific Research from the Ministry of Education, Science and Culture, Japan, and a grant from the Nissan Science foundation. I am indebted to Mr. Mitsuru Mukooyama (Sannohe High School) for supplying the alimentary canals of bats; and to Mr. Masashi Harada (Laboratory of Experimental Animals, Osaka City University Medical School), Dr. Kimitaka Funakoshi (Department of Anatomy, Faculty of Medicine, Kyushu University), Mr. Teruo Irie (Kumamoto Education Center) and Mr. Masahide Nakaji (Gyokusen-dô, Okinawa) for their generous cooperation.

REFERENCES

1 Sawada, I. (1974) Helminth fauna of bats in Japan XV. Annot. Zool. Japon., **47**: 103–106.

2 Sawada, I. (1980) Helminth fauna of bats in Japan XXII. Annot. Zool. Japon., **53**: 194–201.

3 Sawada, I. (1983) Helminth fauna of bats in Japan XXIX. Annot. Zool. Japon., **56**: 209–220.

4 Sawada, I. (1966) On a new tapeworm, *Vampirolepis isensis* found in bats with the table of the morphological features of tapeworms in *Vampirolepis*. Jpn. J. Med. Sci. Biol., **19**: 51–57.

5 Sawada, I. (1976) Helminth fauna of bats in Japan II. Jpn. J. Parasitol., **16**: 103–106.

6 Sawada, I. (1976) Helminth fauna of bats in Japan XI. Bull. Nara Univ. Educ., **21**: 27–30.

ZOOLOGICAL SCIENCE 4: 731–734 (1987)

[COMMUNICATION]

Origin of Binucleate Cells in the Neural Gland of the Ascidian *Halocynthia roretzi* (Drasche)

Mizuho Ogawa, Kiyoshi Terakado[1] and Jin Okada

Department of Biology, Faculty of Liberal Arts and Science, and [1]Department of Regulation Biology, Faculty of Science, Saitama University, Urawa, Saitama 338, Japan

ABSTRACT—The origin of binucleate cells in the neural gland of the simple Ascidian, *Halocynthia roretzi* (Drasche) was examined by light- and electron-microscopy. The central area of dorsal wall of the gland is a simple columnar epithelium composed of rather compact mono-nucleate cells. Peripheral to the center of the dorsal wall, however, the epithelium expands and becomes stratified containing binucleate cells. The binucleate cells seem to proliferate in this limited area of the dorsal epithelium and slough off into the lumen of the gland to form a loose parenchymatous tissue.

INTRODUCTION

Many investigators have examined possible endocrine functions of the neural complex, reasoning that there is a definite structural similarity between the vertebrate hypothalamus-pituitary-Rathke's pouch pattern and the tunicate cerebral ganglion-neural gland-neural gland duct pattern [1]. Recently, cells containing immunoreactive substances have been demonstrated after incubation with antisera raised against some mammalian pituitary and gastrointestinal hormones [2–5]. However, the true function or functions of the neural gland remain uncertain.

In an earlier paper we reported that most of the cells of the neural gland in *Halocynthia* are binucleate [6]. However, the origin of these binucleate cells remained uncertain as does their significance in the neural gland and indeed the function of the neural gland itself.

Accepted April 22, 1987
Received March 26, 1987

The aim of the present work is to describe the origin of binucleate cells in the neural gland of the ascidian *Halocynthia roretzi.*

MATERIALS AND METHODS

Specimens of the ascidian *Halocynthia roretzi* were purchased from the market in February and every other month for a year. They were kept in aquaria for at least 2 days before use. After dissection, the neural glands were fixed in Bouin's or Zenker's solution, then dehydrated, embedded in paraffin and sectioned at 6 μm using routine procedures.

For electron microscopy, small pieces of the neural gland were excised and immediately fixed with 2% OsO_4 in 0.15 M collidine buffer (pH 7.3) at 4°C for 1 hr. They were dehydrated in graded concentrations of ethanol and embedded in epoxy resin. Thin sections were cut with glass knives, doubly stained with aqueous uranyl acetate and lead citrate, and examined with a Hitachi H 700H electron microscope operated at 100 KV.

RESULT

The neural gland of *Halocynthia roretzi* appears to be composed of acinous lobules. The dorsal wall of the neural gland is composed of a simple columnar epithelium. The same epithelium not only extends dorso-posteriorly as a dorsal cord, but also connects anteriorly with a neural gland duct opening into the pharyngeal cavity via a

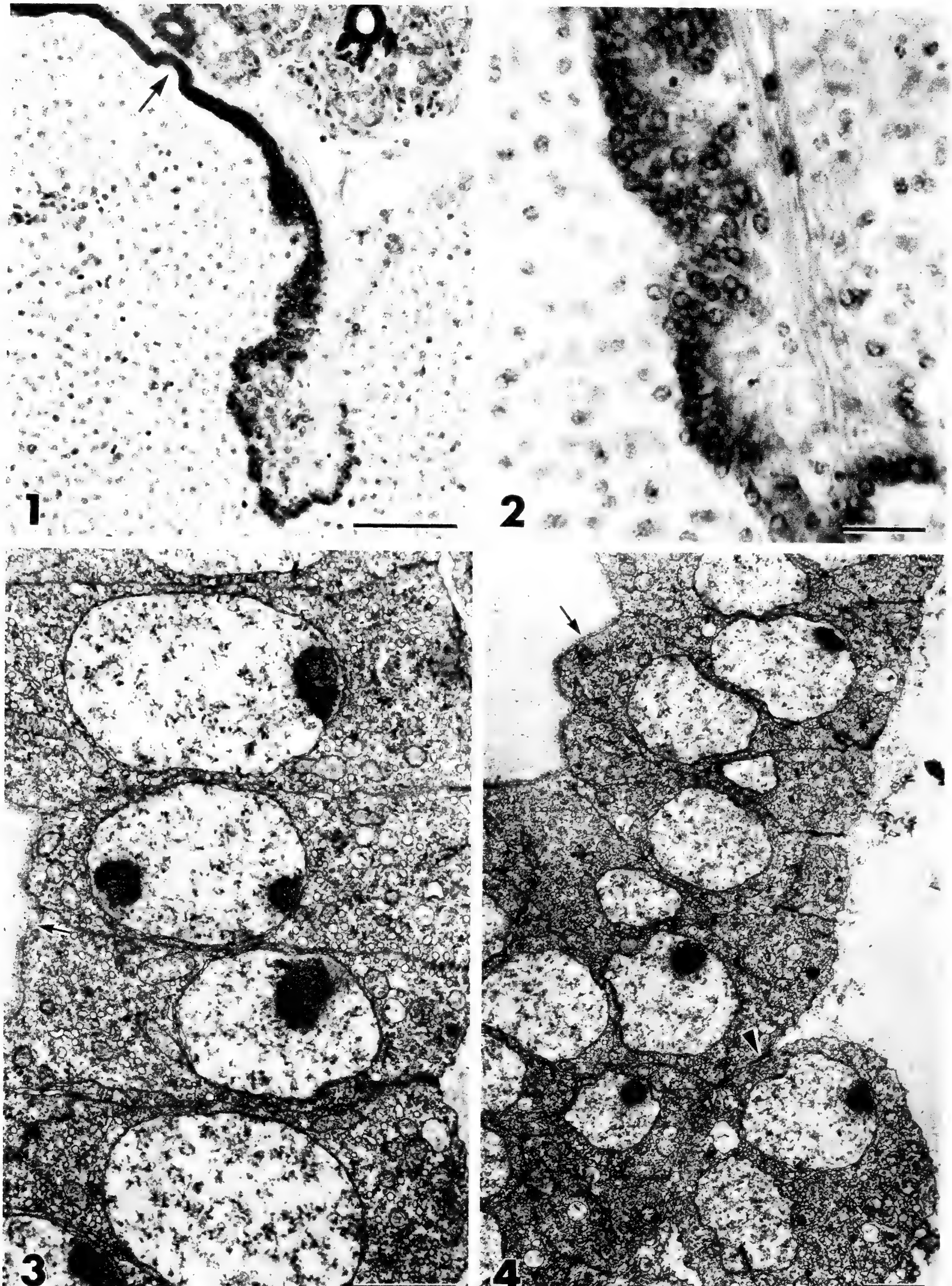
1
2
3
4

ciliated funnel. The opposite, ventral wall of the gland, is surrounded by a thin cell layer and a connective tissue.

The central area of the dorsal epithelium is composed of simple columnar, rather compact and mono-nucleate cells (Fig. 1). These mono-nucleate epithelial cells are relatively high columnar (about 10 μm high) with an oval nucleus; they are held together laterally. No mitotic figures were observed in this area. By electron-microscopy, these cells show a relatively small Golgi body, some small mitochondria and vesicles, and a poorly developed terminal bar; they lack microvilli (Fig. 3). Some cells contained two nucleoli located on the opposite sides of the nucleus. In contrast to the free surface, the surface of basal membrane was covered with a diffuse coating.

Peripheral to the center of dorsal wall, the epithelium expands and becomes irregularly stratified. In this region binucleate cells are observed (Fig. 2). By electron-microscopy, the simple columnar epithelium is seen to be gradually transformed into a pseudostratified form in the areas around the center of the dorsal wall; the transformed cells lack uniformity and binucleate cells are encountered (Fig. 4). Some of the cells lose their connection with the free surface and become round in shape. These rounded cells are also binucleated with some mitochondria and vesicles.

No seasonal change occurs in these epithelial features so far examined.

DISCUSSION

It has been reported that the epithelium of the neural gland undergoes cyclical changes of activity. In the neural gland of *Ciona intestinalis,* according to Georges [7–9], there are two different morphological phases, showing 24 hours rhythmical secretory cycle: a loose reticulated form (epithelial structure) and an expanded compact form (mesenchymal structure).

Whether or not the neural gland of *Halocynthia* shows such a circadian rhythm is not known at present. However, in the adults examined in this study, the neural gland was filled with binucleate cells appearing like parenchymatous tissue with a compact form at every season so far examined.

The central region of the dorsal epithelium is composed of simple columnar, mono-nucleate cells. However, peripheral to the center of the dorsal epithelium, binucleate cells are observed. How the binucleate cells arise in the limited area of the dorsal epithelium remains uncertain. No mitotic figures were observed in the present study. Although the lumen of the gland was filled with binucleate cells, no cell division was observed. At present it is believed that the binucleate cells originate in a limited, peripheral area of the dorsal epithelium and slough off into the lumen of the gland to form loose parenchymatous tissue. In some sense, the neural gland seems to be classified into a holocrine gland.

The available data still do not show whether the neural gland is homologous with the pituitary of vertebrate. The possible role of the neural gland, therefore, requires further study.

ACNOWLEDGMENTS

We wish to express our gratitude to Prof. W. S. Hoar, University of British Columbia, for his encouragement and critical reading of the manuscript.

FIG. 1. Cross section of the neural gland. Arrow shows the center of dorsal epithelium from which the dorsal cord branches. Dense, tubular structures seen on the upper side of the figure are cut-planes of the dorsal cord. Scale, 50 μm.

FIG. 2. High magnification of the area surrounding the central region of dorsal epithelium. Binucleate cells occur here. Scale, 20 μm.

FIG. 3. Electron-micrograph of the central region of dorsal epithelium, being a typical simple columnar epithelium. Arrow shows the basement membrane. Scale, 2 μm.

FIG. 4. Electron-micrograph of the area peripheral to the central region of dorsal epithelium, expanding and turning into a stratified epithelium. There is a binucleate cell (under right hand corner) just sloughing from the epithelium, but a poor terminal bar is still existent (arrowhead). Arrow shows the basement membrane. Scale, 2 μm.

REFERENCES

1 Goodbody, I. (1974) Adv. Mar. Biol., **12**: 1–149.

2 Pestarino, M. (1984) Gen. Comp. Endocrinol., **54**: 444–449.

3 Pestarino, M. (1984) Acta Zool. (Stockh.), **65**: 113–118.

4 Pestarino, M. (1985) Gen. Comp. Endocrinol., **60**: 293–297.

5 Pestarino, M. (1985) Cell Tissue Res., **24**: 497–500.

6 Ogawa, M., Orikasa, C. and Terakado, K. (1985) Zool. Sci., **2**: 213–217.

7 Georges, D. (1970) C. R. Acad. Sci. Paris, **270**: 3137–3140.

8 Georges, D. (1971) Acta Zool. (Stockh.), **52**: 257–273.

9 Georges, D. (1978) In "Comparative Endocrinolgy". Ed. by P. J. Gaillard and H. H. Boer, Elsevier/North Holland Biomedical Press, Amsterdam, pp. 161–164.

ZOOLOGICAL SCIENCE 4: 735–737 (1987)

[COMMUNICATION]

Asynchronous Expression of Alleles at the Alcohol Dehydrogenase Locus during *Oryzias* Hybrid Development

Jack S. Frankel

Department of Zoology, Howard University, Washington, D.C. 20059, U.S.A.

ABSTRACT—The expression of alleles encoding the enzyme alcohol dehydrogenase (ADH; EC 1.1.1.1) was investigated in *Oryzias melastigma, O. javanicus* and in *O. melastigma* ♀ × *O. javanicus* ♂ hybrids by acrylamide gel electrophoresis. It was not possible to investigate the expression of ADH in reciprocal hybrids as these fry failed to develop past the stage of embryonic body formation. The delay in appearance of isozymes of paternal ADH subunit composition is suggestive of an incompatibility between maternal cytoplasmic regulatory factors and the paternal regulative element.

INTRODUCTION

The expression of gene loci during development is both the result of, and impetus for, cellular differentiation and specialization. The appearance of specific enzymes during embryogenesis reflects metabolic and, thus, biochemical changes associated with increasing developmental complexity. Furthermore, since different enzymes have distinct physiological roles, their expression during development may indicate times of unique metabolic requirements in certain cells, tissues or organs. While many enzymes have general "housekeeping" functions, serving basic metabolic needs in most cells and, therefore, usually found throughout embryogenesis, others are restricted spatially and/or temporally; appearing in specifiic tissues at specific times during development. Enzymes exhibiting such tissue and/or temporal specific patterns have been the focal point of numerous ontogenetic studies [1–19].

Isozymes have proven to be ideally suited to studies designed to analyze patterns of allelic expression during interspecific hybrid development [6–8, 12–14, 20–22]. Genetic variation in parental alleles, reflected in isozymes with different electrophoretic mobilities, permits the determination of the temporal expression of maternal and paternal contributions toward development. In instances where a delay or total repression of paternal isozyme expression occurs, the asynchronous activation of alleles is attributed to incompatibilities of the maternal species effector molecules with the paternal gene; thereby reducing the efficiency of allelic recognition and delaying activation [16]. The present communication reports on the activation and expression of the gene locus encoding alcohol dehydrogenase (ADH; EC 1.1.1.1) in *Oryzias javanicus, O. melastigma* and their hybrid.

Accepted April 10, 1987
Received March 6, 1987

MATERIALS AND METHODS

Healthy adults of *O. javanicus* and *O. melastigma* were obtained from Mid-Atlantic Distributors, Inc., Springfield, VA, USA. Intra- and interspecific embryos were obtained by artificial fertilizations under conditions and procedures described by Iwamatsu *et al.* [23], except that fishes were incubated in fingerbowls measuring 105 mm in diameter and 45 mm in depth.

At selected stages/times during development, pre- and posthatching, intra- and interspecific fishes were collected and screened electrophoretically for the presence of ADH activity. The ADH patterns of the hybrids were compared with those of intraspecific fry at corresponding times during

development (posthatching). In determining the temporal spacing of ADH gene expression, fry were sampled at 2-hr intervals. The time indicated for the appearance of a given ADH isozyme is an average of four separate observations. Individual observations varied no more than + or − 2 hr from their mean. For each assay, individual fry were randomly chosen from a time-monitored fingerbowl and homogenized at 4°C in a 0.01 M K_2PO_4/0.3 mM EDTA solution adjusted to pH 7.0 with 0.01 M KH_2PO_4. Fifty percent homogenates, by volume, were prepared for all samples. Homogenates were centrifuged for 10 min at 4°C in a Beckman 152 Microfuge. Twenty-μl aliquots of the clear supernatant were electrophoresed. Liver tissue was excised from adult fishes decapitated after immobilization in ice water. Tissue samples were prepared for electrophoresis as described for fry samples.

Electrophoresis was conducted employing an acrylamide gel vertical slab system (E. C. Apparatus Co.), maintained at 4°C by a recirculating water bath (Lauda K-2/R, Brinkman Instruments). Six percent acrylamide gels were run at 300 volts for 5 hr using the 0.155 M tris-citrate (pH 7.0) buffer system of Shaw and Prasad [24]. Gels were stained with an incubation medium from Shaw and Koen [25], and fixed in 7% acetic acid.

RESULTS AND DISCUSSION

The ADH phenotypes of liver tissue for *O. melastigma, O. javanicus* and the *O. melastigma* ♀ × *O. javanicus* ♂ hybrid are shown (Fig. 1). As has been observed in a previous investigation on the interspecific hybridization of *O. javanicus* and *O. melastigma* [23], *O. javanicus* eggs inseminated with *O. melastigma* sperm failed to develop past embryonic body formation and, as a result, it was not possible to determine the timing of ADH expression in these hybrids. ADH is dimeric in nature, being encoded in the majority of vertebrates at a single gene locus [3, 8–11, 26, 27]. The enzyme occurs at its highest concentrations in liver, but has also been reported to be present to a lesser extent in stomach and kidney [3, 26].

Zymograms of ADH of *O. javanicus* and *O. melastigma* exhibit single, cathodal zones of en-

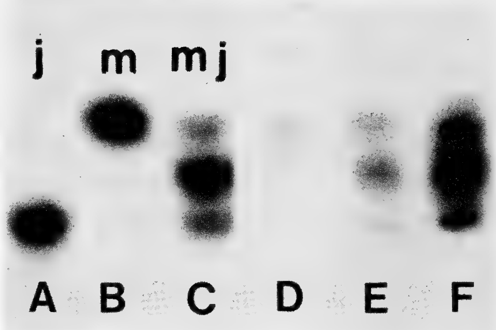

FIG. 1. Zymogram of *Oryzias* ADH isozymes of liver tissue and fry samples. Channel A—*O. javanicus* liver. Channel B—*O. melastigma* liver. Channel C—*O. melastigma* ♀ × *O. javanicus* ♂ hybrid liver. Channel D—hybrid fry at 104 hr posthatching (p. h.). Channel E—hybrid fry at 122 hr p.h. Channel F—hybrid fry at 134 hr p.h.

zymatic activity, restricted in expression to liver (Fig. 1, channels A and B, respectively). The zymogram of the hybrid displays both *O. melastigma* and *O. javanicus* homodimers, along with a heterodimer of intermediate electrophoretic mobility (Fig. 1, channel C). Evidence of *Adh* locus expression in intraspecific *O. javanicus* and *O. melastigma* fry was observed at 100 and 104 hr posthatching (p.h.), respectively, by the initial appearance of ADH activity on the gel. By 128 hr p.h., ADH activity of intraspecific fry appeared to reach a maximum level. However, zymograms of hybrid fry at 104 hr p.h. exhibited a zone of maternally derived ADH along with an extremely faint zone of activity corresponding to the hybrid allodimer (Fig. 1, channel D). The paternal homodimer was not detected at this time. Hybrid zymograms at 122 hr p.h. showed two distinct zones of ADH activity corresponding to the maternally derived homodimer and the hybrid allodimer, along with a faint zone of activity corresponding to the paternal homodimer (Fig. 1, channel E). Zymograms of hybrid fry at 134 hr p.h. (Fig. 1, channel F) revealed an ADH pattern indicative of a 1 : 2 : 1 ratio in the concentrations of the three isozymes; suggestive of full expression of *Adh* alleles of maternal and paternal origin. It would seem that at the time when the *Adh* locus is expressed in intraspecific *Oryzias* fry (104 hr p.h.), preferential expression of the *melastigma* allele

occurs in the *O. melastigma* ♀ × *O. javanicus* ♂ hybrid.

The marked temporal shift in the expression of the paternal *Adh* allele in the *Oryzias* hybrid is consistent with the observed effects of gene regulatory divergence among species [17]. As has been noted in other studies [21, 22], both developmental abnormalities at the morphological level and aberrant expression of allelic isozymes in differentiated tissues increase concomitantly with the greater evolutionary distance of the parental species used in forming a given hybrid. Indeed, the asymmetrical developmental response of reciprocal *Oryzias* hybrids is suggestive of a "significant" degree of gene divergence between *O. melastigma* and *O. javanicus*.

In conclusion, the observations from the present study are in keeping with reports on ADH expression in other hybrids [8, 11, 26, 27] and support postulated mechanisms of allelic expression [16, 18] where alleles of maternal origin effectively interact with maternally derived effector molecules, whereas alleles of paternal origin may interact less effectively, if at all. Indeed, allelic asynchrony during *Oryzias* hybrid development may be a consequence of varying degrees of affinity between maternal regulatory molecules and maternal and paternal regulative elements controlling the expression of structural gene loci.

ACKNOWLEDGMENT

The author thanks Joan Ann Frankel for her help with the photography.

REFERENCES

1 Holmes, R. S. and Whitt, G. S. (1972) Biochem. Genet., **4**: 471–480.
2 Lindahl, R. and Mayeda, K. (1973) Comp. Biochem. Physiol., **45B**: 265–273.
3 Shaklee, J. B., Champion, M. and Whitt, G. S. (1974) Dev. Biol., **38**: 356–382.
4 Champion, M. J. and Whitt, G. S. (1976) J. Exp. Zool., **196**: 263–282.
5 Champion, M. J. and Whitt, G. S. (1976) Biochem. Genet., **14**: 723–737.
6 Hart, N. H. and Cook, M. (1976) Comp. Biochem. Physiol., **54B**: 357–364.
7 Frankel, J. S. and Hart, N. H. (1977) J. Hered., **68**: 81–86.
8 Frankel, J. S. (1978) J. Hered., **69**: 57–58.
9 Frankel, J. S. (1980) J. Hered., **71**: 430–431.
10 Frankel, J. S. (1981) Comp. Biochem. Physiol., **70B**: 643–644.
11 Frankel, J. S. (1983) J. Hered., **74**: 311–312.
12 Frankel, J. S. and Wilson, R. V. (1985) Comp. Biochem. Physiol., **80B**: 463–466.
13 Frankel, J. S. (1985) Comp. Biochem. Physiol., **81B**: 635–639.
14 Frankel, J. S. (1985) Comp. Biochem. Physiol., **82B**: 413–417.
15 Philipp, D. P., Childers, W. F. and Whitt, G. S. (1979) J. Exp. Zool., **210**: 473–488.
16 Philipp, D. P., Parker, H. R. and Whitt, G. S. (1983) In "Isozymes: Current Topics in Biological and Medical Research". Ed. by M. C. Rattazzi, J. C. Scandalios and G. S. Whitt, Alan R. Liss, New York, Vol. X, pp. 193–237.
17 Whitt, G. S. (1981) Am. Zool., **21**: 549–572.
18 Whitt, G. S. (1983) In "Isozymes: Current Topics in Biological and Medical Research". Ed. by M. C. Rattazzi, J. C. Scandalios and G. S. Whitt, Alan R. Liss, New York, Vol. X, pp. 1–40.
19 Frankel, J. S. and Wilson, R. V. (1984) Comp. Biochem. Physiol., **78B**: 179–182.
20 Whitt, G. S., Cho, P. and Childers, W. F. (1972) J. Exp. Zool., **179**: 271–282.
21 Whitt, G. S., Childers, W. F. and Cho, P. (1973) J. Hered., **64**: 55–61.
22 Whitt, G. S., Philipp, D. P. and Childers, W. F. (1977) Differentiation, **9**: 97–109.
23 Iwamatsu, T., Watanabe, T., Hori, R., Lam, T. J. and Saxena, O. P. (1986) Zool. Sci., **3**: 287–293.
24 Shaw, C. R. and Prasad, R. (1970) Biochem. Genet., **4**:297–320.
25 Shaw, C. R. and Koen, A. L. (1968) In "Chromatographic and Electrophoretic Techniques". Ed. by I. Smith, John Wiley, New York, Vol II, p. 347.
26 Hitzeroth, H., Klose, J., Ohno, S. and Wolf, U. (1968) Biochem. Genet., **1**: 287–300.
27 LeVine, J. P. and Haley, L. E. (1975) Biochem. Genet., **13**: 435–446.

ZOOLOGICAL SCIENCE 4: 739–742 (1987)

[COMMUNICATION]

Cloning of Stage Specific Gene Sequences from a cDNA Library Representing Poly(A)$^+$RNA of Sea Urchin Prism-Embryos

Koji Akasaka, Masanori Taira[1], Tsugio Shiroya and Hiraku Shimada

Zoological Institute, Faculty of Science, University of Tokyo, Hongo, Tokyo 113, and [1]Department of Biochemistry, Chiba University School of Medicine, Inohana, Chiba 280, Japan

ABSTRACT—A cDNA library was constructed using poly(A)$^+$RNA from sea urchin embryos (*H. pulcherrimus*) at the prism stage. Four cDNA clones corresponding to the RNA population abundant at the prism stage but rare at the morula stage were selected by differential hybridization technique. The relative abundance of individual RNAs were measured by Northern hybridization analysis. The size of the RNA population represented by these cloned cDNAs was small in the unfertilized eggs, decreased further until blastula stage, and thereafter, increased sharply. However, the different RNA species started to increase in their amount at different developmental stages. Moreover, the amount of each of these RNA species fluctuated in a different manner.

INTRODUCTION

It has been reported that the RNA synthesis is not necessarily needed for the development of sea urchin embryos up to the blastula stage [1], and that most of the genes become active at the gastrula stage [2]. The mechanisms of the onset of gene activation during early development have not been clarified as yet. To study the molecular mechanism of the regulation of gene expression during blastula-gastrula transition of the sea urchin development, we constructed a cDNA library and selected the genes which mRNAs begin to accumulate at the stage of blastula-gastrula transition.

Accepted April 18, 1987
Received January 26, 1987

MATERIALS AND METHODS

Embryo culture

Eggs and sperm of *Hemicentrotus pulcherrimus* were collected by artificial spawning induced with a 0.5 M KCl solution. Eggs were fertilized and developed in filtered sea water at 15°C.

Preparation of RNA

Total cellular RNA was isolated from embryos by the guanidinium/hot phenol method [3]. Polyadenylated RNAs were isolated by oligo(dT)-cellulose chromatography [4].

Preparation of a library of cloned cDNAs from H. pulcherrimus prism embryos (λHpPR library)

DNA complementary to the polyadenylated RNA of the prism embryo was prepared by the use of reverse transcriptase [5]. Double-stranded cDNA was formed in a DNA synthesizing system containing *E. coli* ribonuclease H and DNA polymerase I [6]. Construction of a cDNA library in λgt10 was carried out according to the methods developed by Huynh *et al.* (7). *E. coli* C600hfl$^+$ was used as a host.

Preparation of cDNA probe

Polyadenylated RNA from morula-stage or prism-stage embryos was used for the synthesis of cDNA probes. The primary single stranded cDNA copies were synthesized using reverse transcriptase

in the presence of a random primer [8] and [α–^{32}P] dCTP. cDNA probes were obtained after the hydrolytic removal of RNA from the RNA–DNA hybrids by incubating with 0.6 N NaOH at 37°C for 1 hr.

Isolation of phage recombinants containing stage-specific gene and preparation of the cDNA from the clones

The library was screened by the method of plaque hybridization using morula-cDNA probes and prism-cDNA probes. Each of the stage-specific clones was amplified and isolated from the culture medium [9]. The cloned DNAs were extracted with phenol/chloroform, digested with EcoRI and then electrophoresed on a low melting-point-temperature agarose. The cDNAs were extracted from the gel slices with hot phenol and precipitated with ethanol.

RNA determination

To eliminate the color development by uronic acid and sialic acid, polysaccharides were removed from the samples by ethanol precipitation after hydrolysis with 0.3 N KOH. A 10% trichloroacetic acid-insoluble fraction of 5×10^4 eggs or embryos was defatted with ethanol and ether, and then hydrolized with 0.3 N KOH at 37°C for 12 hr to liberate ribonucleotides. After neutralizing the pH of the hydrolysate with 0.3 N $HClO_4$, polysaccharides were precipitated with two volumes of ethanol. The amount of RNA in the supernatant was determined by the orcinol-$FeCl_3$ method [10].

Northern blot hybridizations

Ten microgram each of total cellular RNA prepared from the embryos at various stages using the guanidinium/hot phenol method [3] was electrophoresed on formaldehyde-agarose gels and transferred to nitrocellulose filters [11]. Then RNA was immobilized on nitrocellulose filters and hybridized with nick-translated cDNA clones.

RESULT AND DISCUSSION

Preparation of a cDNA library from prism embryos

To construct a library of cDNA clones which were expected to contain the RNA species that accumulated during development, the total cellular RNA was prepared from prism embryos. About 1.5 mg of RNA was obtained from 1 ml of prism embryos. The amount of poly(A)$^+$RNA obtained after oligo(dT)cellulose column (1 ml) chromatography was 30 μg, which corresponds to 2% of the total cellular RNA. The cDNA library was constructed from 40 ng of the double-stranded cDNA as described in Materials and Methods, yielding 6×10^6 plaques.

Screening of stage specific genes

About 2×10^3 clones were plated out on *E. coli* C600hfl$^+$. The screening was carried out by differential plaque hybridization using the morula-cDNA and the prism-cDNA as probes. Among the prism-stage specific clones, four clones (λP1, λP2, λP3 and λP16) were selected and purified for further analysis.

λP16 contained only one EcoRI fragment of cDNA (0.6 kb), while two size classes of the EcoRI fragment were found in the cDNA inserts of λP1, λP2 and λP3. The predicted sizes of the fragment by gel mobilities were 1.1 kb and 0.53 kb in λP1, 1.3 kb and 0.48 kb in λP2, and 0.80 kb and 0.36 kb in λP3. It is not clear at present whether the presence of two fragments in one cDNA clone reflects the multiple EcoRI sequences in a stretch of mRNA or different fragments recombined incidentally during the ligation process. The EcoRI fragments were tentatively designated here as λP1–1.1, λP1–0.53, λP2–1.3, λP2–0.48, λP3–0.80, λP3–0.36 and λP16–0.60.

Northern analysis

Prior Northern analyisis, the RNA content of sea urchin embryos during development was determined. The amount of RNA was about 0.1 ng per embryo at all the stages examined in this experiment. It seems that the fraction of newly synthesized RNA was negligibly small in comparison with that of stored RNAs. As any significant changes in the RNA content of the embryos were not observed during development, a definite amount of RNA (10 μg) was loaded on each slots.

Total RNA was extracted from the embryos at nine different developmental stages, and subjected

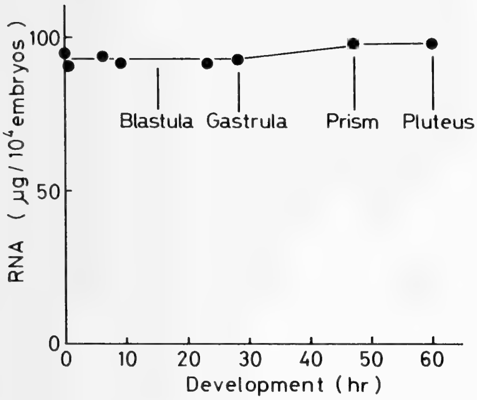

FIG. 1. Ontogenic change in RNA content of embryos during early development of *H. pulcherrimus*. The amount of RNA was assayed as described in the Materials and Methods.

to Northern analysis as described in Materials and Methods. Since the λP3–0.36 probe scarcely hybridized with RNA from the embryos at any stages examined, it was difficult to determine the relative content of this RNA species, and the further experiments were carried out using the other clones.

There was a single size class of mRNA corresponding to each clone with molecular lengths predicted by gel mobilities of 1.7 kb (λP1–1.1), 1.7 kb (λP1–0.53), 2.0 kb (λP2–1.3), 2.0 kb (λP2–0.48), 1.8 kb (λP3–0.80) and 0.9 kb (λP16–0.60). The relative intensity of the bands in Northern blots was quantified by microdensitometric scanning of the autoradiograms (Table 1). Unfertilized eggs contained the RNA which hybridized with all of the clones used as probes, though the content of these mRNA species per egg was small. The intensity of hybridization decreased until the embryos reached the 32-cell or unhatched-blastula stage. RNAs corresponding to λP1–0.53, λP2–1.3, λP2–0.48 and λP16–0.60 began to increase at the unhatched-blastula stage while RNAs corresponding to λP1–1.1 and λP3–0.38 started to increase later at the hatched-blastula stage. The concentration of RNAs corresponding to λP1–0.53, λP2–1.3 and λP2–0.48 RNA decreased once at the mesenchyme-blastula stage and then increased again. It seems that the RNAs detected in the early stages of development may be derived from the maternal stored mRNAs and those found in the later stages correspond to newly synthesized RNAs. Generally, the level of RNAs represented by the present clones decreased by the blastula stage and thereafter increased sharply. However, the onset of the increase in the individual RNA species occurred at differnt developmental stages, and the amount of each RNA species fluctuated in a different manner. The reproducibility of the data shown in Table 1 was confirmed by two to three separate experiments. It seems that the accumulation of the different RNA species is under a different pattern of control.

TABLE 1. Abundance of individual mRNA species during development

Clone	λP1–1.1	λP1–0.53	λP2–1.3	λP2–0.48	λP3–0.80	λP16–0.60
Stage	Percentage of specific RNA content in prism stage					
Oocyte	1.3	0.60	1.0	1.8	15	13
2-cell	0.57	0.28	0.72	0.73	12	2.2
32-cell	0.56	0.15	0.56	0.61	6.0	1.3
Unhatched blastula	0.51	1.2	4.0	3.0	0.47	2.1
Hatched blastula	9.8	23	27	27	10	12
Mesenchyme blastula	17	15	17	18	27	43
Gastrula	45	32	45	56	57	96
Prism	100	100	100	100	100	100
Pluteus	95	69	86	75	80	94

The intensities of the bands in Northern blots were quantified by densitometry of the autoradiograms.

The stage-specific difference in the complexity of the mRNA population during sea urchin development has been clearly shown by Galau *et al.* [12], suggesting that the expression of many kinds of genes is switched on-and-off during embryogenesis. Though the sea urchin genes for histone [13], actin [14] and collagen [15] have been cloned, the mechanism underlying the stage specific expression of these genes during development has not been elucidated. In the present study, we have constructed a cDNA library from the sea urchin embryos at prism stage, and cloned some of the genes which mRNAs show a stage-specific mode of accumulation. Shepherd *et al.* have previously selected the stage-specifically expressed genes from a cDNA library of sea urchin embryos by colony differential hybridization using *in vivo* [^{32}P]labeled RNA [16]. This method, however, seems inefficient for the screening of these genes. Here we have employed the plaque differential hybridization technique using *in vitro* [^{32}P]labeled cDNAs for screening of the genes more effectively. The cDNA clones obtained in the present experiment would be helpful for the molecular study of the regulation of gene expression during blastula-gastrula transition.

ACKNOWLEDGMENTS

We would like to thank Professor Masamiti Tatibana of the Chiba University for his encouragement. The present study was supported by Grant-in-Aid 61304009 for Scientific Research from the Japan Ministry of Education, Science and Culturte.

REFERENCES

1 Giudice, G., Mutolo, V. and Donatuti, G. (1968) Wilhelm Roux' Arch. Entwicklungsmech. Org., **161**: 118–128.

2 Giudice, G. (1986) The Sea Urchin Embryo. Springer-Verlag, Berlin, Heidelberg, New York, Tokyo.

3 Feramisco, J. R., Helfman, D. M., Smart, J. E., Burridge, K. and Thomas, G. P. (1982) J. Biol. Chem., **257**: 11024–11031.

4 Aviv, H. and Leder, P. (1972) Proc. Natl. Acad. Sci. USA, **69**: 1408–1412.

5 Verma, I. M., Temple, G. F., Fan, H. and Baltimore, D. (1972) Nature (New Biol.), **235**: 163–167.

6 Gubler, U. and Hoffman, B. J. (1983) Gene, **25**: 263–269.

7 Huynh, T. V., Young, R. A. and Davis, R. W. (1984) In "DNA Cloning". Ed. by D. M. Glover, IRL Press, Oxford, Washington DC, Vol. 1, pp. 49–78.

8 Taylor, J. M., Illmensee, R. and Summers, J. (1976) Biochim. Biophys. Acta, **442**: 324–330.

9 Yamamoto, K. R., Alberts, B. M., Benzinger, R., Lawhorne, L. and Treiber, G. (1970) Virology, **40**: 734–744.

10 Mejbaum, W. (1936) Z. Physiol. Chem., **258**: 117–120.

11 Lehrach, H., Diamond, D. Wozney, J. M. and Boedtker, H. (1977) Biochemistry, **16**: 4743–4751.

12 Galau, G. A., Klein, W. H., Davis, M. M., Wold, B. J., Britten, R. J. and Davidson, E. H., (1976) Cell, **7**: 487–505.

13 Mauron, A., Kedes, L., Hough-Evans, B., R. and Davidson, E. H. (1982) Dev. Biol., **94**: 425–434.

14 Merlino, G. T., Water, R. D., Moore, G. P. and Kleinsmith, L. J. (1981) Dev. Biol., **85**: 505–508.

15 Venkatesan, M., Pablo, F., Vogeli, G. and Simpson, R. T. (1986) Proc. Natl. Acad. Sci. USA, **83**: 3351–3355.

16 Shepherd, G. W., Rondinelli, E. and Nemer, M. (1983) Dev. Biol., **96**: 520–528.

ZOOLOGICAL SCIENCE 4: 743–746 (1987)

[COMMUNICATION]

Met-Enkephalin-like Immunoreactivity in the Nervous System of *Helix aspersa*

Trinidad Ortiz, Joaquín Piñero and Rafael Coveñas

Departamento de Biología Celular de la Facultad de Biología, Universidad de Sevilla, Avd. Reina Mercedes s/n, 41012-Sevilla, Spain

ABSTRACT—By means of indirect immunocytochemical method, met-enkephalin-like immunoreactivity was demonstrated in the cerebral and visceral ganglia of the snail, *Helix aspersa*. Immunoreactive neurons and nerve fibers of the neuropile were located in the ganglia.

INTRODUCTION

Enkephalin and β-endorphin were demonstrated in the neurons of the earthworm by Alumet *et al.* [1]. Rémy and Dubois [2] also reported that β-endorphin immunoreactive cell bodies exist in the subpharyngeal ganglion of the earthworm and since then there have been investigations that have established the existence of immunocytological detection of methionine-enkephalin-like neuropeptides in invertebrates [1].

In molluscs, by immunocytochemistry, met-enkephalin has been localized in the cerebral and pedal ganglia of *Lymnea stagnalis,* in the pedal ganglia of *Mytilus edulis* and *Octopus vulgaris* nerves [3, 4]. On the other hand, enkephalin-like immunoreactivity in a pulmonate gastropod, *Achatina fulica,* has been demonstrated [5].

In *Helix aspersa,* Williamson and Emson [6], in extracts of the nervous tissue, have detected met-enkephalin by radioimmunoassay. In the present study, we have localized met-enkephalin-like material by indirect immunocytochemical method in the perikarya and fibers of the snail *Helix aspersa*.

Accepted March 16, 1987
Received December 27, 1986

MATERIALS AND METHODS

The snails, *Helix aspersa,* were collected from Aljarafe, south Spain region, in October. Cerebral and visceral ganglia were removed and fixed for 2–4 hr in paraformaldehyde in 0.15M phosphate buffer at pH 7.4 containing 0.342% L-lysine and 0.055% sodium periodate, embebbed in paraffin and cut serially at 7 μm. All the sections were treated for 10 min with 10% H_2O_2 in methanol, to inactivate endogenous peroxidase activity before incubation with immunohistochemical reagents. Several sections were pretreated for 20 min at 37°C in a solution of pepsin (4mg/ml), in 0.01N HCl, to eliminate background reaction.

The sections were stained according to the immunoperoxidase indirect method. Met-enkephalin antibodies were prepared as previously described by Arluison *et al.* [7]. Briefly, the peptide was coupled to haemocyanin with glutaraldehyde and injected repeatedly every month into rabbits. Antibodies were purified from collected sera by affinity chromatography onto a met-enkephalin–CH–sepharose 4B column. With the radioimmunoassay conditions of Cesselin *et al.* [8], we found that the met-enkephalin antibodies presently used exhibited only very limited cross-reactivity with other peptides: 0.4% with leu-enkephalin, 1.7% with β-endorphin, less than 0.01% with substance P, cholecystokinin-octapeptide, vasoactive intestinal peptide, dynorphin and FMRF-amide.

The sections were incubated for 20 hr in a solution containing met-enkephalin-antiserum ($1:10^3$), Triton X–100 (0.3%) and normal goat

serum (1%) in 0.15M phosphate buffer at pH 7.4.

The site of antigen-antibody reaction was revealed by goat anti-rabbit IgG, labelled with peroxidase, at a concentration of 1:250. The specificity of the reactions was verified by a) omitting the first antiserum in the incubation medium and b) by using a previously absorbed antiserum with excess of antigen (250μg of met-enkephalin in 1 ml of antiserum diluted to 1:10^3) for 24 hr at 4°C.

RESULTS

Met-enkephalin-like immunoreactivity (ELI) was found in the nervous system of the adult *Helix aspersa.* Many neuronal cell bodies of different sizes were seen in the cerebral ganglia. Here, the perikarya showed intense enkephalin immunoreactivity and several axonic eminences were also immunostained (Figs. 1 and 2).

In the visceral ganglion several cell bodies showed enkephalin-like immunoreactivity as well as the fibers in the neuropile (Figs. 3 and 4).

The majority of ELI cell bodies presented a narrow peripheral band of immunoreactivity (Fig. 5), but also, some neurons showed immunoreactivity in whole cytoplasm (Fig. 4). The enkephalin immunoreactive material appears in granular form.

Both nuclei and fibers did not show significant immunoreactivity in control sections (Figs. 6 and 7).

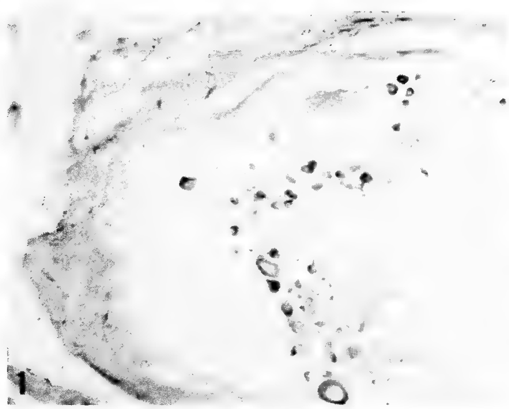

FIG. 1. Cerebral ganglion. Met-enkephalin-like immunoreactive cell bodies. ×200.

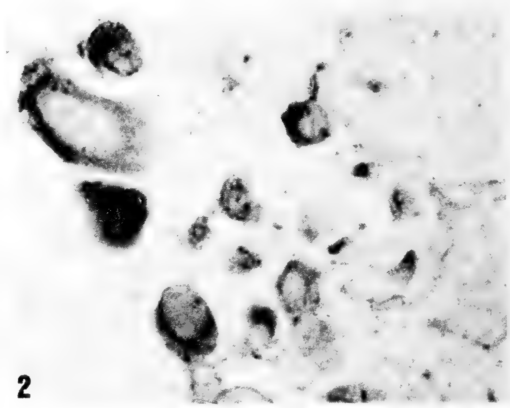

FIG. 2. Cerebral ganglion. Higher magnification reveals darkly immunoreactive perikarya. ×500.

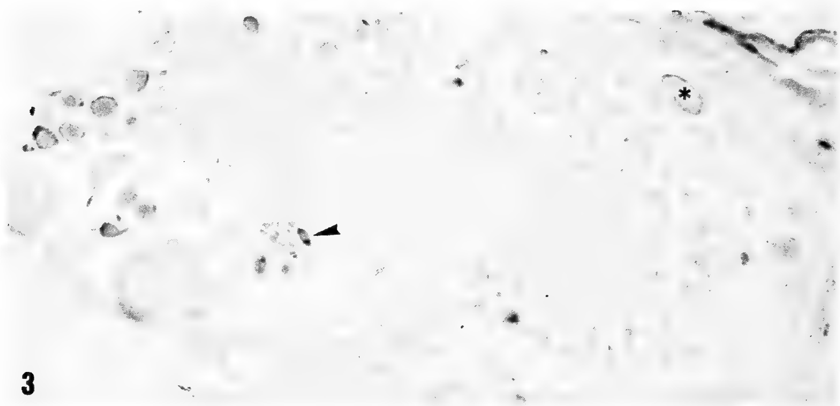

FIG. 3. Visceral ganglion. Small (◄) and medium (*) size cell bodies showing immunoreactivity. ×100.

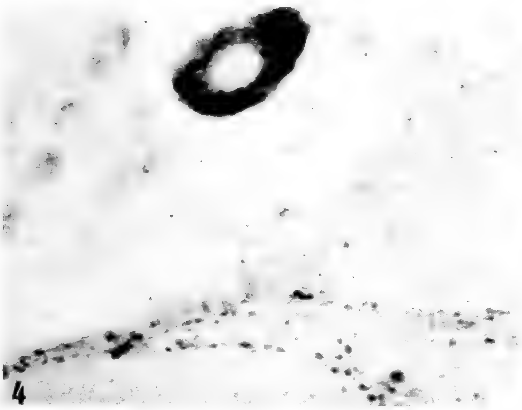

FIG. 4. Visceral ganglion. Enkephalin-like immunoreactivity in whole cytoplasm and fibers in the neuropile. ×500.

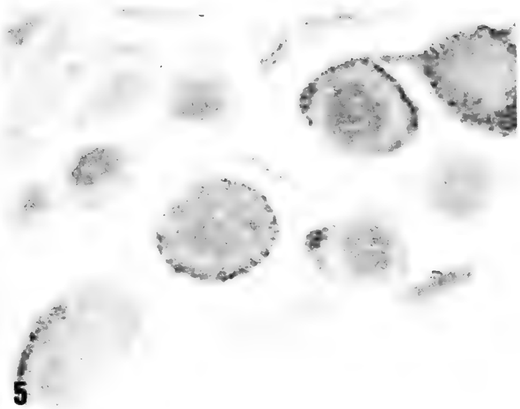

FIG. 5. Visceral ganglion. Higher magnification of narrow peripheral band of immunoreactivity. ×500.

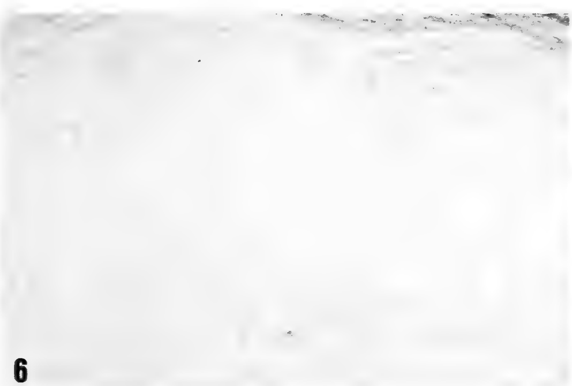

FIG. 6. Visceral ganglion. Section treated with preabsorbed antiserum showing no immunoreactivity. ×100.

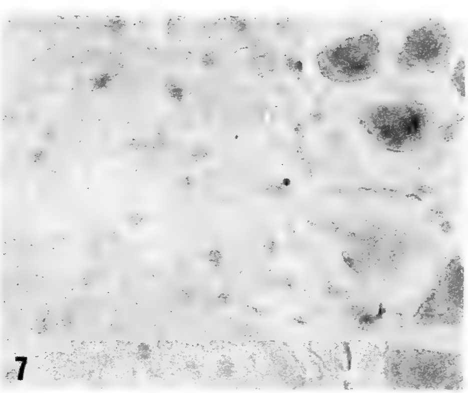

FIG. 7. Visceral ganglion. Magnification from the neuropile demonstrating no ELI fibers. ×500.

DISCUSSION

In the last few years, at various times, the presence of neuronal peptides in molluscs has been demonstrated [3, 4, 9]. However, by immunocytochemical methods, the enkephalin was only found in the pedal ganglia of *Mytilus edulis* [4] and in the nerves of *Octopus vulgaris* [10]. In this paper, we describe the population of peptidergic neurons containing met-enkephalin-like substance in the cerebral and visceral ganglia of *Helix aspersa*.

Many recent studies have demonstrated the functional role that the met-enkephalin plays in vertebrates, indicating that it can be related to stress-analgesia, inhibiting nociceptive neurons located in the dorsal horn of the spinal cord [7, 11]; however, up to now, the function of this in molluscs has been a subject of controversy. In *Helix pomatia* it has been demonstrated that an increase of met-enkephalin increases the level of dopamine and so also increases the dopaminergic nervous transmission [12]. Gromov *et al.* [13] have demonstrated that enkephalin altered the effect of acetylcholine on postsynaptic acetylcholine receptors in the neurons of *Helix pomatia*. This suggests that opioid peptides take part in the regulation of synaptic transmission of some biogenic amines.

Also, a naloxone-reversible action of met-enkephalin on the activity of single identified

neurons in *Helix pomatia* has been reported [14]. The study of Salanki *et al.* [9] strongly suggests that substance P has its own receptors in *Helix pomatia,* and also suggests that substance P and met-enkephalin antagonizes each other activity by separate mechanisms. This suggests that some of the activities of both peptides, substance P and met-enkephalin, occur in invertebrates in the same way as in mammals. However, the analysis of nervous systems like that of the snail, to gain more precise understanding of concepts such as neurotransmission and neuromodulation, may prove to be a good means for providing the answer to many questions, such as how different neuropeptides act.

REFERENCES

1 Alumets, J., Hakanson, R., Sundler, F. and Thorell, J. (1979) Nature, **279**: 805–806.

2 Rémy, Ch. and Dubois, M. P. (1981) Cell Tissue Res., **218**: 271–278.

3 Schot, L. P. G., Boer, H. H., Swaab, D. F. and Van Noorden, S. (1981) Cell Tissue Res., **216**: 373–378.

4 Stefano, G. B. and Martin, R. (1983) Cell Tissue Res., **230**: 147–153.

5 Van Noorden, S. (1980) Gen. Comp. Endocrinol., **40**: 375–379.

6 Williamson, M. E. and Emson, P. C. (1982) Biochem. Soc. Trans., **10**: 384–385.

7 Arluison, M., Conrath-Verrier, M., Tauc, M., Mailly, P., De la Manche, I. S., Cesselin, S., Bourgoin, S. and Hamon, H. (1983) Brain Res. Bull., **11**: 555–571.

8 Cesselin, F., Hamon, M., Bourgoin, S., Buisson, N. and Devitry, F. (1982) Neuropeptides, **2**: 351–369.

9 Salanky, J., Vehouszky, A. and Stefano, G. B. (1983) Comp. Biochem. Physiol., **75C**: 387–390.

10 Martin, R., Frösch, D., Kiehling, C. and Voigt, K. H. (1981) Neuropeptides, **2**: 141–150.

11 Basbaum, A. I. and Fields, H. L. (1984) Ann. Rev. Neurosci., **7**: 309–380.

12 Juel, C. (1982) Neuropharmacology, **21**: 1301–1303.

13 Gromov, L. A., Krivorotov, S. V. and Skryma, R. N. (1983) Neuroscience, **8**(4): 855–860.

14 Stefano, G. B., Vadasz, I. and Hiripi, L. (1980) Experientia, **36**: 666–667.

ZOOLOGICAL SCIENCE 4: 747–749 (1987)

[COMMUNICATION]

A Method of Measuring the Volume of Soft Tissue

Eiji Yoshioka

Seto Marine Biological Laboratory, Kyoto University,
Shirahama, Wakayama 649–22, Japan

ABSTRACT—A convenient method for measuring the volume of soft tissue is reported. The volume can be calculated from the area × the thickness if it is flattened evenly. This was tried successfully for the gonad of chiton *Acanthopleura japonica* using a metal frame of 1 mm thickness. On the example of the chiton's gonads, the calculated volume as well as the wet weight was shown to be correlated to the dry weight and the volume can be taken as a quantity of the tissue.

When dealing with the majority of small invertebrates, it is not an easy task to measure the weight of the organ, and a most precise balance and a laboratory free of vibrations are often necessary. Nevertheless, the wet weight is not so reliable because the extra water on the organ cannot be removed uniformly and with certainty. Desiccation of the material for taking the dry weight naturally makes it unsuited as an histological sample. In these respects, the volume is thought to be a good indicator of the size of the tissue. The rough volume can be grasped visually, but to measure it quantitatively some device must be introduced. In this paper, a method for measuring the volume of tissue, for example, as the numerator quantity of the gonad index is reported. The gonad of the chiton, *Acanthopleura japonica* was used for the experiment, which was easily separated from other tissues and so was appropriate for this method.

A gonad placed on a glass slide was soaked in sea water, the isotonic medium to the body fluid of the marine invertebrate, to avoid problems which may result from osmotic pressure and drying. A metal frame of 1 mm thickness was secured encircling it and a cross-ruled glass slide for plankton counting was pressed over it so as to make the gonad evenly 1 mm thick (Fig. 1). The area the gonad covered was measured against the 1 mm lattice. When the gonad is large enough, the number of the lattice points it covers may be counted, which mathematically appropriates the number of squares divided into the area of the gonad (for example, 22 points in the case shown in Fig. 1). The volume of the gonad was calculated simply by multiplying the area (in mm^2) by the thickness (1 mm). The wet weight of the gonad was measured after excess water was removed with filter paper, and its dry weight was measured after desiccation (90°C, 6 hr) to 10 mg.

Figure 2 showed the relationships of the dry weight of the gonad to its volume and wet weight. The dry weight is generally admitted to be the most meaningful value among the three as an expression of the substantial size of the gonad. According to the values of correlation coefficient (r), the volume was shown to be correlated to the dry weight as well as the wet weight was shown.

The balance used in this study (Parkin Elmer; Autobalance AD-2) is very expensive and requires careful handling. However, the apparatus here described is proof against rough handling in the field, and the cross-ruled glass slide is easily obtained from oceanographic warehouses or planktological laboratories. Moreover, the procedure of measuring the volume does not damage the organ for histological preparation. The thickness of the inserted frame and the square size of cross-rule can be modified to measure various organs of different sizes.

Accepted March 16, 1987
Received February 17, 1987

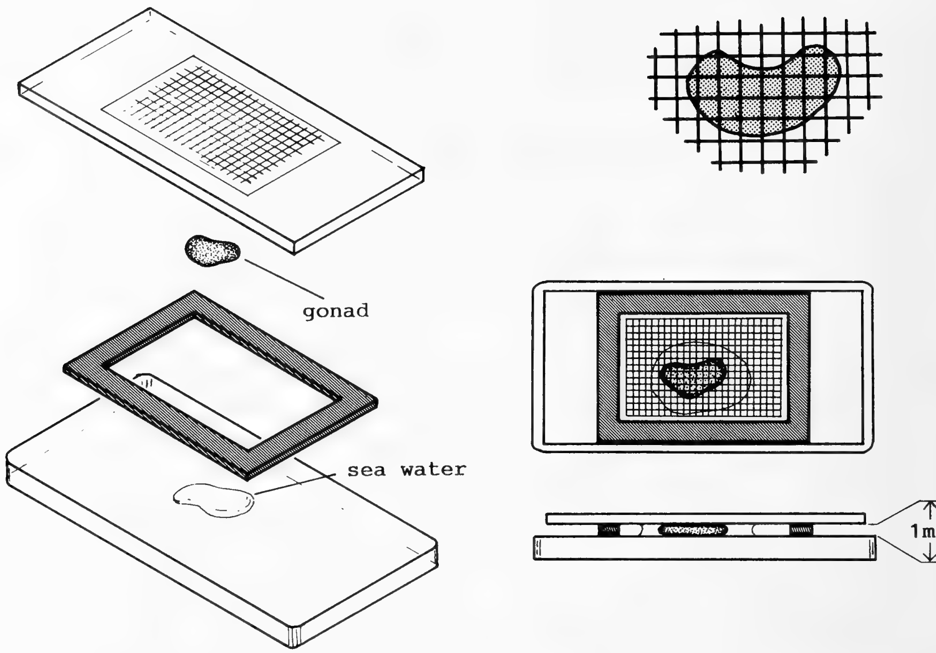

FIG. 1. The apparatus and procedure for measuring the volume of the gonad.

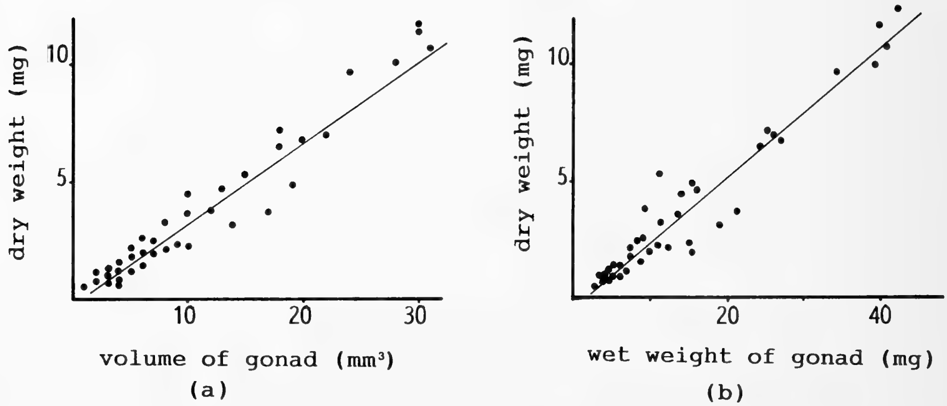

FIG. 2. The relationships of the dry weight to the volume (a), and to the wet weight (b) of the gonad of the chiton *Acanthopleura japonica*. (a) r=0.970; (b) r=0.963.

As Grant and Tyler [1] pointed out, studies of invertebrate reproduction are expensive in both time and money. Many researchers of invertebrate reproduction use the gonad index, or the ratio of wet or dry weight of gonad to the total animal weight, as the indicator of reproductive activity [2]. The method in this study, as expected, allows studies in reproductive biology to be effectively and economically carried out.

REFERENCES

1 Grant, A. and Tyler, P. A. (1983) Int. J. Invertebr. Reprod., **6**: 259–269.

2 Giese, A. C. and Pearse, J. S. (1979) In "Reproduction of Marine Invertebrates, Vol. 1". Ed. by A. C. Giese and J. S. Pearse, Academic Press, New York, pp. 1–49.

An Invitation to Join the Zoological Society of Japan

The Zoological Society of Japan was founded in 1878 for the purpose of discussing and exchanging information pertaining to the biology of animals. The society holds annual meetings, regional meetings and publishes the journal *Zoological Science* and a newsletter.

Membership is open to any individual who has sent the application form to the society. The annual dues are ¥ (Yen) 9,500 for full members and ¥ (Yen) 7,500 for student members. The *Zoological Science* and the newsletter are sent to all members as a part of their dues.

Details of the society and its activities can be obtained from its business office (Zoological Society of Japan, Toshin Building, Hongo 2–27–2, Bunkyo-ku, Tokyo 113, Japan).

Telephone: Tokyo (03) 814–5675

Secretary of the Society

MEMBERSHIP APPLICATION FORM
ZOOLOGICAL SOCIETY OF JAPAN

(Telephone: Tokyo (03) 814–5675)

APPLICATION FOR: ☐ STUDENT MEMBERSHIP
☐ FULL MEMBERSHIP
☐ CHANGE FROM STUDENT TO FULL MEMBERSHIP

NAME ☐ DR. ☐ MR. ☐ MISS ☐ MRS. ☐ MS. ______________________

POSITION ______________________ INSTITUTION ______________________

MAILING ADDRESS ______________________

____

TELEPHONE (AREA CODE ____) ______________________

SPECIALIZED AREA 1. ________ 2. ________ 3. ________

______________________ ______________________
(Date) (Signature)

Please forward completed application form to:

Secretary of the Zoological Society of Japan, Toshin Building, Hongo 2–27–2, Bunkyo-ku, Tokyo 113, Japan.

Development Growth & Differentiation

Published by

the Japanese Society of Developmental Biologists

The journal is devoted to the publication of original papers dealing with any aspects of developmental phenomena in all kinds of organisms, including plants and micro-organisms. Papers in any of the following fields will be considered: developmental genetics, growth, morphogenesis, cellular kinetics, fertilization, cell division, dormancy, germination, metamorphosis, regeneration and pathogenesis, at the biochemical, biophysical and analytically morphological levels; reports on techniques applicable to the above fields. At times reviews on subjects selected by the editors will be published. Brief complete papers will be accepted, but not preliminary reports.

Members of the Society receive the Journal free of charge. Subscription by institutions is also welcome.

Papers in Vol. 29, No. 4. (August 1987)

Development, Growth and Differentiation (ISSN 0012–1592) is published bimonthly by The Japanese Society of Developmental Biologists, Department of Biology, School of Education, Waseda University, Tokyo 160, Japan. 1987: Volume 29. Annual subscription U. S. $ 110.00 including air speed delivery except Japan. Application to mail at second class postage rate is pending at Jamaica, NY 11431, U. S. A.

Outside Japan: Send subscription orders and notices of change of address to Academic Press, Inc., Journal Subscription Fulfillment Department, 6277 Sea Harbor Drive, Orlando, FL 32887, U. S. A. Send notices of change of address at least 6–8 weeks in advance. Please include both old and new addresses. U. S. A. POSTMASTER: Send changes of address to *Development, Growth and Differentiation,* Academic Press. Inc., Journal Subscription Fulfillment Department, 6277 Sea Harbor Drive, Orlando, FL 32887, U. S. A.

In Japan: Send nonmember subscription orders and notices of change of address to Business Center for Academic Societies Japan, 16–3, Hongo 6-chome, Bunkyo-ku, Tokyo 113, Japan. Send inquiries about membership to Business Center for Academic Societies Japan,4–16, Yayoi 2-chome, Bunkyo-ku, Tokyo 113, Japan.

Air freight and mailing in the U. S. A. by Publications Expediting, Inc., 200 Meacham Avenue, Elmont, NY 11003, U. S. A.

(*Contents continued from back cover*)

ZOOLOGICAL SCIENCE

VOLUME 4 NUMBER 4 **AUGUST 1987**

CONTENTS

(*Contents continue on inside back cover*)

INDEXED IN:
Current Contents/LS and AB & ES,
Science Citation Index,
ISI Online Database,
CABS Database

Issued on August 15
Printed by Daigaku Printing Co., Ltd.,
Hiroshima, Japan

ISSN 0289-0003

Vol. 4 No. 5

October 1987

ZOOLOGICAL SCIENCE

An International Journal

PHYSIOLOGY
CELL and MOLECULAR BIOLOGY
GENETICS
IMMUNOLOGY
BIOCHEMISTRY
DEVELOPMENTAL BIOLOGY
REPRODUCTIVE BIOLOGY
ENDOCRINOLOGY
BEHAVIOR BIOLOGY
ENVIRONMENTAL BIOLOGY
ECOLOGY and TAXONOMY

published by Zoological Society of Japan

distributed by Business Center for Academic Societies Japan
VNU Science Press BV, Utrecht, The Netherlands

ZOOLOGICAL SCIENCE

The official Journal of the Zoological Society of Japan

The Zoological Society of Japan:
Toshin-building, Hongo 2–27–2, Bunkyo-ku,
Tokyo 113, Japan. Tel. (03) 814–5675

ZOOLOGICAL SCIENCE is devoted to publication of original articles, reviews and communications in the broad field of Zoology. The journal was founded in 1984 as a result of unification of Zoological Magazine (1888–1983) and Annotationes Zoologicae Japonenses (1897–1983), the former official journals of the Zoological Society of Japan. ZOOLOGICAL SCIENCE appears bimonthly. An annual volume consists of six numbers of more than 1000 pages including an issue containing abstracts of papers presented at the annual meeting of the Zoological Society of Japan.

MANUSCRIPTS OFFERED FOR CONSIDERATION AND CORRESPONDENCE CONCERNING EDITORIAL MATTERS should be sent to:

Dr. Seiichiro KAWASHIMA, Managing Editor, Zoological Science, Zoological Institute, Faculty of Science, Hiroshima University, 1–1–89 Higashisenda-machi, Naka-ku, Hiroshima 730, Japan, in accordance with the instructions to authors which appear in the first issue of each volume. Copies of INSTRUCTIONS TO AUTHORS will be sent upon request.

SUBSCRIPTIONS. ZOOLOGICAL SCIENCE is distributed free of charge to the members, both domestic and foreign, of the Zoological Society of Japan. To non-member subscribers within Japan, it is distributed by Business Center for Academic Societies Japan, 6–16–3 Hongo, Bunkyo-ku, Tokyo 113. Subscriptions outside Japan should be ordered from the sole agent, VNU Science Press BV, Europalaan 93, 3526 KP Utrecht, (postal address; P. O. Box 2093, 3500 GB Utrecht), The Netherlands. Subscription rates will be provided on request to these agents. New subscriptions and renewals begin with the first issue of the current volume.

[Publication of Zoological Science has been supported in part by a Grant-in-Aid for Scientific Publication from the Ministry of Education, Science and Culture, Japan.]

ZOOLOGICAL SCIENCE 4: 751–761 (1987)

REVIEW

Fine Structure of Ascidian Smooth Muscle

KIYOSHI TERAKADO

Department of Regulation Biology, Faculty of Science, Saitama University, Urawa 338, Japan

I. INTRODUCTION

The body-wall muscle of the ascidian *Halocynthia roretzi* is a vertebrate-type (paramyosin-free type) smooth muscle [1], possessing an actin-linked regulatory system of contraction, which is the case with that of vertebrate striated muscle. In this review, observations on the structural organization of the ascidian smooth muscle, with special reference to contractile structures, will be discussed, and comparisons are made between the organization of vertebrate smooth and striated muscles (for vertebrate smooth muscle, see ref. [2–5]).

II. GENERAL ARCHITECTURE

The body-wall muscle consists of two layers, an inner longitudinal layer and an outer circular one [1]. Both layers of muscle consist of numerous bands of muscle separated from each other by a thick layer of connective tissue filaments. Each band is about 50–150 μm in width and contains about 10–100 bundles of muscle fibers. Each bundle is further composed of several muscle cells arranged longitudinally and is completely covered by a thin layer of connective tissue filaments and a basement membrane (Fig. 1) [6]. The cells within each bundle are arranged side by side in very close proximity, in a type of simple apposition and behave like a single cell at contraction. This grouping of cells into bundles in the ascidian smooth muscle contrasts with the situation in most vertebrate smooth muscles which consist of individual cells separated by collagen fibrils and the basal lamina. These recent findings indicate that the bundles of cells, rather than the individual cells, are the structural and functional units in the muscle tissues.

Received May 25, 1987

III. CELLULAR FEATURES

1. Multiple Nuclei

The cells in the body-wall muscle are very long, cylindrical structures, tapering at each end. Most individual, isolated cells are about 1.5–2 mm in length and fixed cells are about 1.3–1.7 mm in length. Each cell contains about 20–40 nuclei, the number being proportional to the length of the cell [6]. Multinucleate smooth muscle cells, which are very rare in vertebrates and invertebrates, were found first in the ascidian smooth muscle [7], and their presence was confirmed in the same material by Shinohara and Konishi [8] by a three-dimensional reconstruction method. Aside from the ascidian body-wall muscle, the giant smooth muscle cells of ctenophores are the only known examples of such multinucleate smooth muscle cells [9, 10]. The presence of multiple nuclei is apparently related to elongation of the cells, as in the case of vertebrate skeletal muscles, but the mechanism for the generation of multiple nuclei remains to be clarified.

2. Myofilaments

Recent ultrastructural studies of smooth muscle revealed that both actin and myosin are persistently present in filamentous form. Thick (myosin) and thin (actin) filaments are about 14–16 nm and

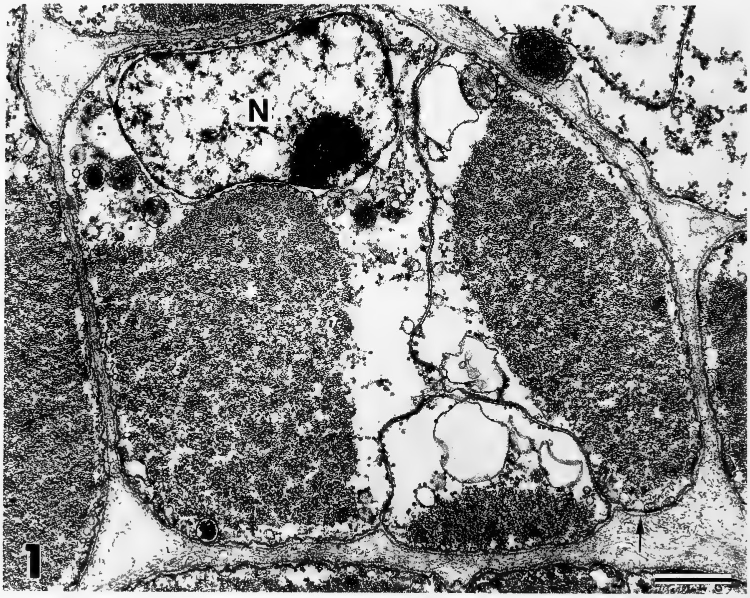

FIG. 1. Cross-section of a small bundle of muscle fibers from the outer layer of the ascidian body-wall muscle (double fixation). Glycogen particles have been lost from the cytoplasmic matrix. Basement membrane (arrow) and connective tissue filaments fully cover the bundles of fibers, but not individual cells. Contractile elements tend to lie toward the outer surface of the bundle. Bar, 1 μm. (From Terakado and Obinata [6]).

6–7 nm in diameter, respectively, which are dimensions very similar to those of vertebrate smooth and striated muscles. In transverse sections of relaxed muscle cells, the population densities of thick and thin filaments are about 220–330 and 1300–2300 filaments per μm^2, respectively (Fig. 2) [6]. The former value is much higher than in vertebrate smooth muscles, but is lower than in striated muscles (Table 1). The latter value is nearly identical to that in vertebrate smooth muscles. The ratio of thick to thin filaments is about 1:6, which is intermediate between the ratios of those filaments in vertebrate smooth and striated muscles. The thick filaments are often arranged in a quasi-rectangular or quasi-hexagonal lattice; each thick filament is always surrounded by a single row of 5–9 thin filaments, to produce a rosette in transverse section (Fig. 2, inset) [6]. The distances between the thick filaments arranged in the lattice are about 30–50 nm, distances more similar to those in striated muscles than those in vertebrate smooth muscles.

Cross-bridges, with a repeat period of 14.5 nm or 29 nm, between thick and thin filaments, can also be identified. In smooth muscles, it was noted sometime ago that the identification of cross-bridges in sections is generally difficult, presumably because of the less regular alignment and greater spacing between adjacent thick filaments, in addition to other reasons [11]. The ease with which cross-bridges can be observed in the present material probably reflects the population density of thick filaments which is much higher than in vertebrate smooth muscles. The periodicity of about 14.5 nm is identical with the results from X-ray diffraction [12, 13], optical diffraction [14], and electron-microscopic observations of isolated native and synthetic myosin filaments [13].

The exact length of the thick filaments has not been determined in smooth muscles. In the ascidian smooth muscle, the length appears to be about 2–2.4 μm, based on the length of A-zone (see below) and on measurements of some long filaments in longitudinal sections (Fig. 3) [6].

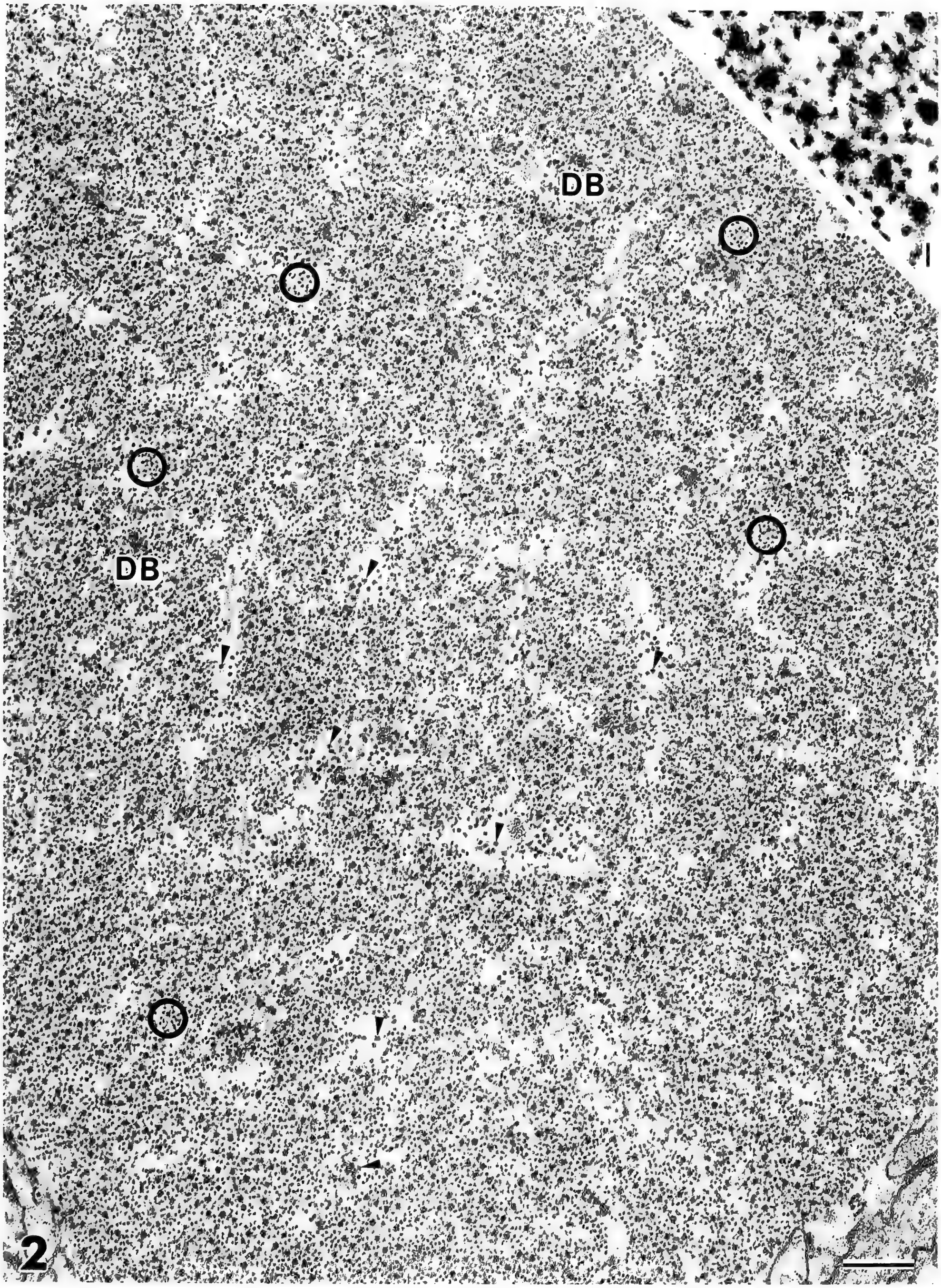

FIG. 2. Cross-section of a cell from the outer layer of the ascidian body-wall muscle in a relaxed state. Dense bodies (DB) are oval structures in which numerous thin filaments are evident. Groups of thin filaments (circled), having diameters similar to those of the dense bodies, are also found. Intermediate filaments (arrowheads) either lie between the groups of thick and thin filaments or are associated with the dense bodies. Note the abundance of thick filaments. Bar, 0.2 μm. Inset: Each thick filament is surrounded by a single row of several thin filaments. Cross-bridges are seen between them. Bar, 20 nm. (From Terakado and Obinata [6]).

This value is similar to that estimated from intermediate high voltage electron microscopy [15]. However, isolated thick filaments from guinea pig taenia coli are of variable length, but most are less than 3 μm in length [14]. However, thick filaments of smooth muscles are evidently longer than those of striated muscles. The exact length of thin filaments has also been unsettled. The isolated, native, thin filaments of the ascidian smooth muscle are about 1–2 μm long as measured by electron microscopy, and 1.4–2.2 μm in solution, as estimated by a flow birefringence method [1]. In some vertebrate smooth muscles, isolated thin filaments have been found to be at least 1.2 μm [16] and as much as 4 μm [17] long. It has not been ascertained whether the variability in length of isolated filaments is a result of fragmentation during isolation procedures, or whether it reflects true variability among filaments. Other possible reasons for the variability in length may be related to differences in tissues and/or species, and cannot yet be eliminated.

3. Contractile Apparatus

Presence of myofibrils in smooth muscle cells was suggested by earlier observations under the light microscope (see [4]). However, such fibrillar structures have not commonly been noted by electron microscopy, in spite of the great number of investigations; these structures are only found in trypsinized cells or in trypsinized and detergent-treated cells (see [4]). It is probable that the proteolytic and/or detergent treatments enhance the fibrillar structures by extraction of some filaments. In the ascidian smooth muscle, distinct fibrillar structures (myofibrils) with a diameter of

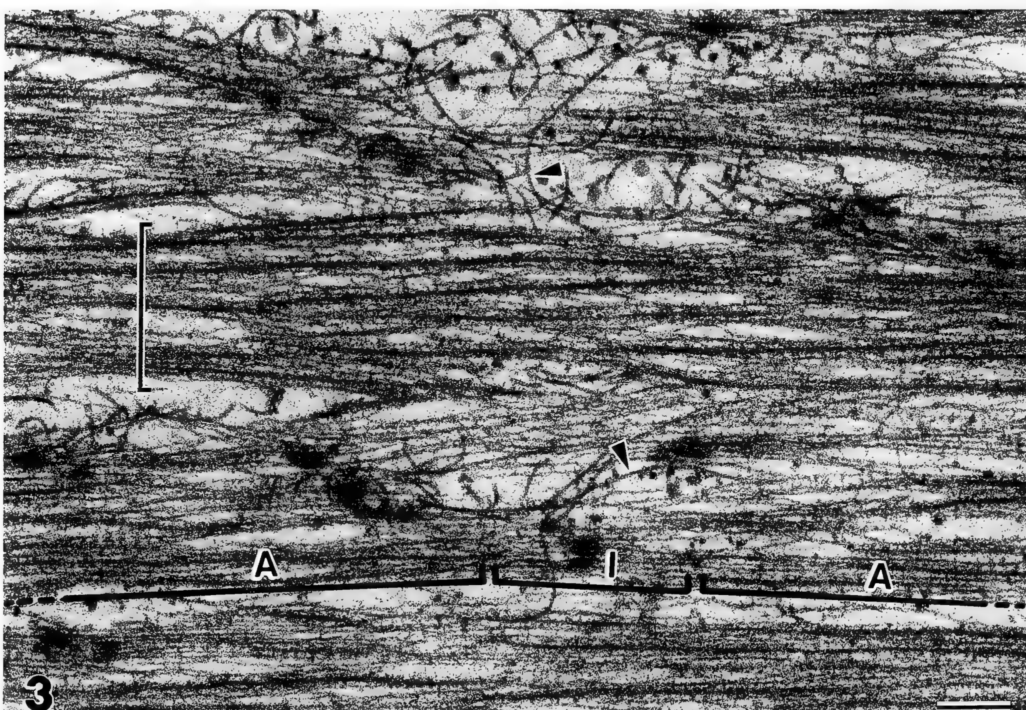

Fig. 3. Longitudinal-section of part of a group of myofibrils from a cell of the outer layer, showing formation of an A–I zone. Thin filaments which emerge from dense bodies are inserted into small groups of thick filaments (A) on both sides of an I-zone (I). Intermediate filaments run through spaces in the continuous network of myofibrils and run across myofibrils along I-zones exclusively (arrowheads). Bracket indicates width of a single myofibril. Bar, 0.2 μm.

about 0.2–0.6 μm are observed without such treatments, and are seen more easily in contracted cells. The myofibrils are repeatedly branched and fused, and run along almost the total length of the cell. They are separated from each other by interfibrillar spaces and a network of intermediate filaments which run through the spaces (Fig. 3) [6]. Dense bodies, with a diameter of about 0.06–0.1 μm, are evenly scattered throughout the myofibrils, but very often the dense bodies are located near the lateral surface of the myofibrils. From these structural features, it is apparent that the myofibrils exist as distinct structural units of the contractile elements in the ascidian smooth muscle cells, and presumably such is also the case in vertebrate smooth muscles.

Within the myofibrils, sub-groups of more regularly aligned, parallel, thick and thin filaments can be identified (Fig. 3) [6]. In longitudinal sections, it can be seen that the thin filaments are inserted into both sides of the dense bodies, and that the thin filaments which emerge from the dense bodies enter into adjacent groups of thick filaments on both sides, to form a sarcomere-like structure (Fig. 3) [6]. In a given sarcomere-like structure, the group of thick filaments (with the inserted thin filaments) is termed the A-zone, and the group which contains only thin filaments is termed the I-zone, by analogy with the A- and I-bands of myofibrils of striated muscle, even though they are not arranged exactly in parallel. A dense body lies in the center of each I-zone. However, areas containing thick filaments exclusively (H-zone) are not found. The A-zone is about 2.2–2.5 μm in length and 0.1–0.2 μm in width in the relaxed state. The length of the I-zone is about 1–2 μm. In transverse sections, many groups of about 25–50 thin filaments, which are apparently cut-planes of the I-zones, can be identified (Fig. 2) [6].

In vertebrate smooth muscles, the association between dense bodies and thin filaments, which suggests that the cytoplasmic dense bodies are functionally equivalent to the Z-bands of striated muscle, was proposed sometime ago but has only recently been unequivocally demonstrated [18, 19].

The finding of an A–I band pattern [6, 18], together with the association of thin filaments with dense bodies, indicates that the minimum functional units of the contractile apparatus in smooth muscle are the sarcomere-like structures, which consist of interdigitating thick and thin filaments with attached dense bodies.

Dense patches (surface dense bodies) on the cell surface, where the thin and intermediate filaments are attached, vary greatly in shape and in the extent of differentiation, from area to area and from cell to cell. In general, in cells of the outer circular muscle, the dense patches are only thin, narrow layer of cell surface with indistinct borders, and, therefore, it seems that the thin filaments are attached to a lesser extent to the lateral surface of the middle part of these cells. However, in cells of the inner longitudinal muscle, the inner surface of the cell membrane is richly covered with dense fibrous material, which increases in abundance toward the tapering ends of the cells, and to which numerous thin filaments are attached.

With respect to establishment of the association of thin filaments with dense bodies, an important question arises concerning the presence or absence of "free" thin filaments which do not associate with cytoplasmic dense bodies or surface dense patches. From the ratio of the cut-plane area of a sarcomere-like structure to that of a myofibril, calculated from the widths of myofibrils (about 0.2–0.6 μm) and sarcomere-like structures (about 0.1–0.2 μm), it seems that there may be about 2–16 sarcomere-like structures in the cut-plane of a single myofibril. This value is very similar to the number of groups of 25–50 thin filaments (about 3–13) in a cut-plane of a single myofibril, calculated from the ratio of number of thin filaments in a group of thin filaments (25–50) to the number of thin filaments in a myofibril (72–650, estimated from population density, $2300/\mu m^2$, in areas excluding interfibrillar spaces). This agreement means that the number of thin filaments in a single I-zone corresponds to that in a single sarcomere-like structure, and that practically all the thin filaments are attached to dense bodies. From this, it is further suggested that the thin filaments emerged from opposing dense bodies are not much overlapped (or separated) in the central region of the sarcomere-like structure in relaxed state, if

they have a definite length. This is compatible, in a large measure, with the lengths of isolated, native, thin filaments [1].

In spite of the fact that practically all thin filaments are presumed to be attached to the dense bodies, many "excess" thin filaments, which do not participate in the formation of rosettes, occur between the rosettes and around the lattices of thick filaments in transverse sections (Fig. 2). This result may be explained as follows. Since most thick filaments do not lie in isolation, but are predominantly arranged in quasi-rectangular [11] or quasi-hexagonal lattices, in which each thick filament is surrounded by a single row of about 7 (mean value) thin filaments which form a rosette in transverse section (Fig. 2, inset) [6], some "excess" thin filaments, of which the number would depend on the size of the thick filament lattice, should be present. However, such a clear separation of thin filaments into rosette-forming and "excess" filaments is unlikely in such a system. The observed "excess" of thin filaments may actually be due, in a large measure, to the partial association of each thin filaments with a thick filament(s), which may occur to a variable extent (Fig. 4) [6].

From these data, a tentative model of the sarcomere-like structure in the smooth muscle cell has been proposed [20]. In this model, each thin filament is partially associated with two or more thick filaments, via cross-bridges. At contraction, the sarcomere-like structure shortens from about 3.5–4.5 μm to about 2.5 μm, as a result of the shortening of the I-zone. This reduction in length indicates the presence of a sliding filament mechanism as a fundamental aspect of smooth muscle contraction.

4. Intermediate Filaments

It is well known that intermediate filaments in smooth muscles occur in significant quantity and associate with dense bodies [6, 14, 15, 18, 19, 21–26]. Recent investigations [6, 15, 18, 19] have provided further evidence that the dense bodies

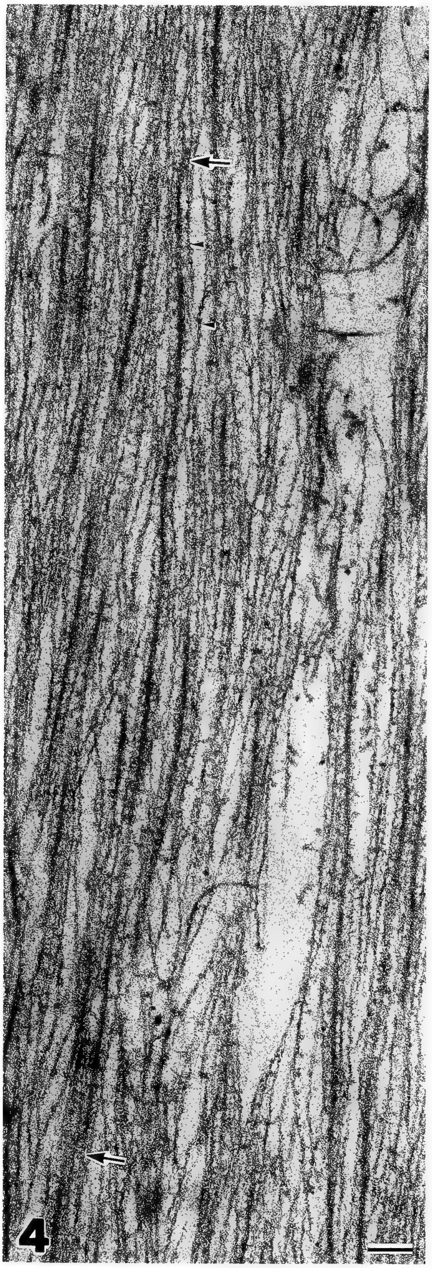

Fig. 4. Longitudinal-section of part of myofibrils from a cell of the outer layer, showing the presence of a long thick filament (arrows indicate both ends). Cross-bridges occur along the entire length of the thick filament. By contrast, each thin filament associates only partially with a thick filament(s). Arrowheads indicate thin filaments partially associated with two thick filaments in different regions. Bar, 0.1 μm. (From Terakado and Obinata [6]).

are not only the sites of lateral attachment for intermediate filaments, but are also the sites of attachment of thin actin filaments, through which the contractile apparatus is mechanically integrated within the smooth muscle cells. Nevertheless, the relationship between the localization or passage of intermediate filaments and the actual organization of the contractile apparatus was not well understood, mainly because of the paucity of information about the structure of the contractile apparatus of smooth muscle cells. In the ascidian smooth muscle, an extensive network of intermediate filaments, which interconnect the cytoplasmic dense bodies and connect the dense bodies to the cell surface, is easily visualized in double-fixed, tannic acid-stained preparations.

The intermediate filaments are approximately 9–10 nm in diameter and usually occur in groups in interfibrillar spaces (Fig. 2) [6]. A small number of intermediate filaments is also present in the intrafibrillar spaces. In transverse sections, there are about 35–65 (mean value 50) intermediate filaments per μm^2 of the area occupied by filaments (about 2.5% of all filamentous components). The number of intermediate filaments attached to the dense bodies varies greatly from 3 to 20 (mean value 9). In general, large numbers of intermediate filaments are attached to the dense bodies which are located on the surface of myofibrils, but fewer filaments are attached to the dense bodies in the interior of the myofibrils. The patterns of interconnection between the dense bodies also vary, apparently because of the irregular arrangement of dense bodies in the myofibrils. The network of filaments runs through spaces in the network of myofibrils, connecting them longitudinally, obliquely and transversely in the vicinity of the dense bodies, to form an intimately associated, dual network. In their transverse passage, the intermediate filaments run across myofibrils, along the I-zones exclusively, interconnecting successive dense bodies (Fig. 3).

The attachment of intermediate filaments to dense bodies does not neccessarily occur along the long axis from one end to the opposite end, but is frequently partial and oblique, and occasionally transverse. Furthermore, in most cases, the filaments associate with only one side of the lateral surface of dense bodies. The predominantly one-sided association of intermediate filaments with cytoplasmic dense bodies is different from that in vertebrate smooth muscles, where intermediate filaments often form a circle around the dense body in transverse sections [15, 18, 25]. The one-sided association seen in the ascidian smooth muscle seems to be primarily related to the organization of distinct myofibrillar structures and the predominant interfibrillar passage of intermediate filaments, which makes possible the lateral, one-sided association of the filaments with dense bodies. Such a mode of association may be effective for the establishment of an efficient contractile apparatus, since the non-contractile, intermediate filaments are clearly separated from the contractile apparatus, although the filaments are associated laterally in the regions of the dense bodies. Thus, the intermediate filaments should disturb only minimally the cycles of contraction and relaxation and remain folded and unfolded in interfibrillar spaces [6].

The transverse and oblique interconnection of neighboring myofibrils or sarcomere-like structures in the regions of the dense bodies, and the longitudinal interconnection of adjacent dense bodies by the network of intermediate filaments, reveal close similarities in structure and possibly in function to striated muscles (see [27]). The most probable explanation for such a continuous network of intermediate filaments in the ascidian smooth muscle cells may be that it is involved in the mechanical maintenance of the ordered arrangement of the contractile apparatus, and that it acts to facilitate the restoration of the original arrangement after contraction, via the intimate association of the network with the organized contractile apparatus and the cell surface.

5. Sarcoplasmic Reticulum

Sarcoplasmic reticulum is poorly differentiated in the cells of ascidian smooth muscle and is almost absent in the filamentous area. However, many small tubules and oval vesicles are characteristically found just beneath the cell membrane. The tubular elements of the sarcoplasmic reticulum are agranular, with filamentous material in the lumen, and are always coupled to the cell membrane.

TABLE 1. A comparison of some structural characteristics of the ascidian smooth muscle with those of vertebrate smooth and striated muscles

	Ascidian smooth muscle	Vertebrate smooth muscle	Vertebrate striated muscle (Skeletal m., Cardiac m.)
Tissue architecture	consists of bundles of cells	mostly consists of individual cells*	consists of individual cells
Cell length	1–2 mm, 0.2 mm [8]	0.1–0.5 mm	1–50 mm, 0.05–0.1 mm
Cell width	5–20 μm, 10–30 μm [8]	2–20 μm	10–100 μm, 5–20 μm
Number of nuclei per cell	20–40	1	hundreds to thousands, 1
Population density of nuclei	2/100 μm	(0.2–1/100 μm)	3–10/100 μm, (0.5–1/100 μm)
Localization of nuclei	Cell periphery	Center of a cell	Cell periphery, Center of a cell
Contractile apparatus	Myofibril (0.2–0.6 μm wide)	Myofibril (0.3–0.5 μm) [14, 29] (generally not identified)	Myofibril (0.5–2 μm)
Minimum unit of contractile apparatus	Sarcomere-like structure (3.5–4.5 μm in length, and 0.1–0.2 μm in width)	Sarcomere-like structure [18] (2.5–3.8 μm in length) [15]	Sarcomere (2–3 μm in length)
Thick (myosin) filaments			
Diameter	14–16 nm, 18–20 nm [8]	12–18 nm	12–16 nm
Length	2–2.4 μm	mostly less than 3 μm [14] 2.2 μm [15], 2 μm [30]	1.6 μm
Population density	220–330 (mean 270)/μm²	160/μm² [11], 80–150/μm² [31]	350–450/μm²
Periodicity of lateral projection	14.5 nm	14–14.4 nm	14.3 nm
Stability	labile	labile	stable
Thin (actin) filaments			
Diameter	6–7 nm, 8 nm [8]	6–7 nm	6–7 nm
Length	1–2 μm or 1.4–2.2 μm [1]	at least 1.2 μm [16], up to 4 μm [17]	1.0 μm
Population density	1300–2300/μm²	1000–2400/μm²	900–1100/μm²
Ratio of thick to thin filaments	1:6	1:10–15 [11, 14, 15, 32–35] 1:25–30 [30]	1:2.5
Interval of localization of troponin	38 nm [36]	——	38 nm
Attachment sites	Dense bodies, cell surface and vesicles	Dense bodies and cell surface (dense plaques) [18], [19]	Z-bands and cell surface
Stability	relatively stable	relatively stable	stable

TABLE 1. (Continued)

	Ascidian smooth muscle	Vertebrate smooth muscle	Vertebrate striated muscle Skeletal m. Cardiac m.
Distance between thick filaments	30–50 nm	60×80 nm [37]	45 nm [38]
Distance between thick and thin filaments	18–26 nm	25.7±5.9 nm [11]	10–20 nm [38]
Dense bodies	oval, 0.06–0.1 μm wide	0.1 μm wide and 0.3–1.5 μm long [18]	——
Mitochondria	few in number located in cell periphery	many, located in perinuclear region and cell periphery	abundant between myofibrils and beneath the sarcolemma
Sarcoplasmic reticulum	poor, mostly coupled to the cell membrane	generally poor	highly differentiated, attached closely to myofibrils
Intermediate filaments	abundant interconnect dense bodies	abundant interconnect dense bodies	limited in quantity interconnect adjacent Z-bands
Mode of association with dense bodies	predominantly one-sided	surrounded [15, 18, 25]	(surrounded)
Content of glycogen particles	enormous	varied	high
(Regulatory system)	actin-linked (troponin-tropomyosin system) [1]	actin-linked (leiotonin- or caldesmon-tropomyosin system) or myosin-linked (phosphorylation-dephosphorylation system of a myosin light chain)	actin-linked (troponin-tropomyosin system)

Data about the ascidian smooth muscle, unless indicated, are taken from Terakado and Obinata [6]. All data for vertebrate smooth and striated muscles, unless indicated, are taken from textbooks and review articles.

* Avian feather muscles are an exception and consist of bundles of cells [28].

The coupled elements of the sarcoplasmic reticulum are sometimes continuous with uncoupled elements which are often granular. Vesicles that open to the cell surface, which are common in cells of vertebrate smooth muscle, are rarely found. Oval vesicles are also found in groups in the perinuclear region.

Information on the structure of ascidian smooth, vertebrate smooth and vertebrate striated muscles is summarized in Table 1.

IV. SUMMARY

1) The cells of the ascidian smooth muscle are multinuclear. Each cell contains 20–40 nuclei, the number of nuclei being proportional to the length of the cell.
2) The population density of thick filaments and the ratio of thick to thin filaments in the ascidian smooth muscle are intermediate between those in vertebrate smooth and striated muscles.
3) The contractile apparatus consists of numerous myofibrils which are separated from each other by a network of intermediate filaments.
4) The myofibrils further consist of many irregularly arranged, sarcomere-like structures.
5) Almost all the thin filaments are attached to the dense bodies, and the thin filaments which emerge from dense bodies associate partially with thick filaments via cross-bridges.
6) Most or all of the dense bodies are interconnected by intermediate filaments in networks, through which the myofibrils are folded in each cell, in a manner that permits the cycles of contractions and relaxations to be minimally disturbed.
7) The agranular, tubular elements of sarcoplasmic reticulum are situated just beneath the cell surface coupled to the cell membrane.

REFERENCES

1 Toyota, N., Obinata, T. and Terakado, K. (1979) Comp. Biochem. Physiol., **62B**: 433–441.
2 Shoenberg, C. F. and Needham, D. M. (1976) Biol. Rev., **51**: 53–104.
3 Somlyo, A. P. and Somlyo, A. V. (1977) In "Excitation-Contraction Coupling in Smooth Muscle". Ed. by R. Casteels, T. Godfraind and J. C. Reugg, Elsevier/North Holland, New York, pp. 317–322.
4 Small, J. V. and Sobieszek, A. (1980) Int. Rev. Cytol., **64**: 241–306.
5 Fay, F. S., Rees, D. D and Warshaw, D. M. (1981) In "Molecular Structure and Function", Vol. 4. Ed. by E. E. Bitter, John Wiley and Sons, New York, pp. 79–130.
6 Terakado, K. and Obinata, T. (1987) Cell Tissue Res., **247**: 85–94.
7 Terakado, K. and Obinata, T. (1977) Zool. Mag., **86**: 491. (Abstract, In Japanese)
8 Shinohara, Y. and Konishi, K. (1982) J. Exp. Zool., **221**: 137–142.
9 Hernandez-Nicaise, M.-L., Mackie, G. O. and Meech, R. W. (1980) J. Gen. Physiol., **75**: 79–105.
10 Hernandez-Nicaise, M.-L., Nicaise, G. and Malaval, L. (1984) Biol. Bull., **167**: 210–228.
11 Somlyo, A. P., Devine, C. E., Somlyo, A. V. and Rice, R. V. (1973) Phil. Trans. R. Soc. Lond., **B265**: 223–229.
12 Lowy, J., Vibert, P. J., Haselgrove, J. C. and Poulsen, F. R. (1973) Proc. R. Soc. Lond., **B265**: 191–196.
13 Shoenberg, C. F. and Haselgrove, J. C. (1974) Nature, **249**:152–154.
14 Small, J. V. (1977) J. Cell Sci., **24**: 327–349.
15 Ashton, F. T., Somlyo, A. V. and Somlyo, A. P. (1975) J. Mol. Biol., **98**: 17–29.
16 Panner, B. J. and Honig, C. R. (1967) J. Cell Biol., **35**: 303–321.
17 Marston, S. B. and Smith, C. W. J. (1984) J. Musc. Res. Cell Motility, **5**: 559–575.
18 Bond, M. and Somlyo, A. V. (1982) J. Cell Biol., **95**: 403–413.
19 Tsukita, S., Tsukita, S. and Ishikawa, H. (1983) Cell Tissue Res., **229**: 233–242.
20 Terakado, K. (1986) J. Electron Microsc., **35**, Suppl. 4: 3117–3118.
21 Campbell, G. R., Uehara, Y., Mark, G. and Burnstock, G. (1971) J. Cell Biol., **49**: 21–34.
22 Cooke, P. H. and Chase, R. H. (1971) Exp. Cell Res., **66**: 417–425.
23 Uehara, Y., Campbell, G. R. and Burnstock, G. (1971) J. Cell Biol., **50**: 484–497.
24 Cooke, P. H. and Fay, F. S. (1972) J. Cell Biol., **52**: 105–116.
25 Cooke, P. (1976) J. Cell Biol., **68**: 539–556.
26 Small, J. V. and Sobieszek, A. (1977) J. Cell Sci., **23**: 243–268.
27 Price, M. G. and Sanger, J. W. (1983) In "Cell and Muscle Motility", Vol. 3. Ed. by R. M. Dowben and J. M. Shay, Plenum Press, New York, pp. 1–40.
28 Drenckhahn, D. and Jeikowski, H. (1978) Cell Tissue Res., **194**: 151–162.
29 Small, J. V. (1974) Nature, **249**: 324–327.

30 Tsukita, S., Tsukita, S., Usukura, J. and Ishikawa, H. (1982) Eur. J. Cell Biol., **28**: 195–201.

31 Heumann, H.-G. (1973) Phil. Trans. R. Soc. Lond., **B265**: 213–217.

32 Devine, C. E. and Somlyo, A. P. (1971) J. Cell Biol., **49**: 636–649.

33 Heumann, H.-G. (1971) Cytobiologie, **3**: 259–281.

34 Bois, R. M. (1973) Anat. Rec., **177**: 61–78.

35 Somlyo, A. V., Butler, T. M., Bond, M. and Somlyo, A. P. (1981) Nature, **294**: 567–569.

36 Endo, T. and Obinata, T. (1981) J. Biochem., **89**: 1599–1608.

37 Rice, R. V., McManus, G. M., Devine, C. E. and Somlyo, A. P. (1971) Nature, **231**: 242–243.

38 Huxley, H. E. (1957) J. Biophys. Biochem. Cytol., **3**: 631–647.

ZOOLOGICAL SCIENCE 4: 763–779 (1987)

REVIEW

Cell Rearrangement in Morphogenesis

RAY KELLER

Department of Zoology, University of California at Berkeley, Berkeley, CA 94720, U.S.A.

INTRODUCTION

There is strong evidence that tissue cell rearrangement, the local repositioning of cells with respect to one another, plays a major role in metazoan morphogenesis. Cell rearrangement is defined here, after Fristrom's definition [1], as the local repositioning of cells with respect to one another, such that the overall shape of the tissue array is changed (Fig. 1). This rearrangement may be passive, accomodating the changes in embryonic shape generated by other mechanisms, or active, resulting in new arrays and driving the overall change in shape of the cell population. Rearrangement is likely to be a major morphogenetic process in those situations where cell populations undergo dramatic changes in shape which are not reflected in the shapes of individual cells, and cannot be attributed to oriented cell divisions or cell death (see p. 109 of [2]; [3]).

Cell rearrangement is a common phenomenon. It has been shown by indirect morphometric data to occur during *Drosophila* imaginal disc evagination [1], during neurulation in amphibians [4], during epiboly in amphibians [5, 6], and during segment shortening in insect metamorphosis [7, 8]. It also occurs during pronephric duct elongation [9], during teleost epiboly [10], during *Hydra* regeneration [11, 12], during secondary elongation of the sea urchin archenteron [13, 14], and during scale primordia alignment in the moth wing [15]. It has been analyzed directly with time-lapse micrography of cell behavior during amphibian gastrulation and neurulation [16–18], during notochord formation in ascidians [19] and amphibians [17, 18], and during teleost epiboly [20]. In some of these systems, cell rearrangement appears to be a passive accomodation to external forces, wheras in others it appears to be an active, force-generating morphogenetic process.

Cell rearrangement is a powerful and efficient mechanism of generating changes in tissue form. A short movement on the part of individual cells, between adjacent cells, exercised over the whole population, can produce dramatic effects. For example, if the cells in a 2×5 array actively intercalate themselves between their neighbors to form a 1×10 array, no cell actively moves more than a cell diameter but some in the population

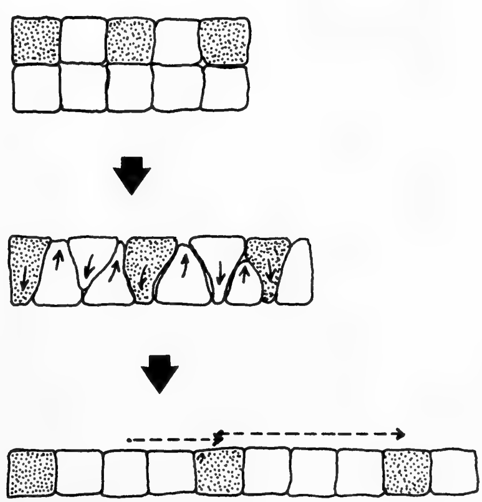

FIG. 1. A schematic diagram shows how local cell rearrangement can produce large changes in shape of the cell population. From Keller [21] with permission.

Received June 20, 1987

may be displaced great distances with respect to one another by virtue of their membership in the tissue array (Fig. 1). Although these endogenously driven transformations in tissue shape have prominent roles in embryogenesis and have fascinated generations of embryologists, their mechanism has remained obscure [21].

In this paper, I will review the major features of what is known about the occurrence, the function, and the mechanism of cell rearrangement in several systems.

REARRANGEMENT WITHIN THE PLANE OF AN EPITHELIAL SHEET

In this type of rearrangement, epithelial cells connected to one another by a circumapical junctional complex, exchange neighbors within the plane of the epithelium during a tissue deformation in which the epithelial sheet takes part. These situations appear to be of two types: those in which the epithelial cells generate the force for tissue deformation and those in which the epithelial sheet passively deforms.

Enveloping Layer Cells Rearrange to Accomodate Changes in Shape of the Embryo during Teleost Fish Epiboly

The following is based on the work of Kageyama [10] on *Oryzias latipes* and Keller and Trinkaus [20, 22] on *Fundulus heteroclitus.* In the development of these teleost fish, cleavage is incomplete, resulting in a cap of cells at one end and uncleaved yolk at the other. The cap is composed of a surface layer of epithelial cells, called the enveloping layer, and a deep mass of non-epithelial cells. At its margin, the enveloping layer is connected to the unsegmented portion of the egg, the yolk syncytial

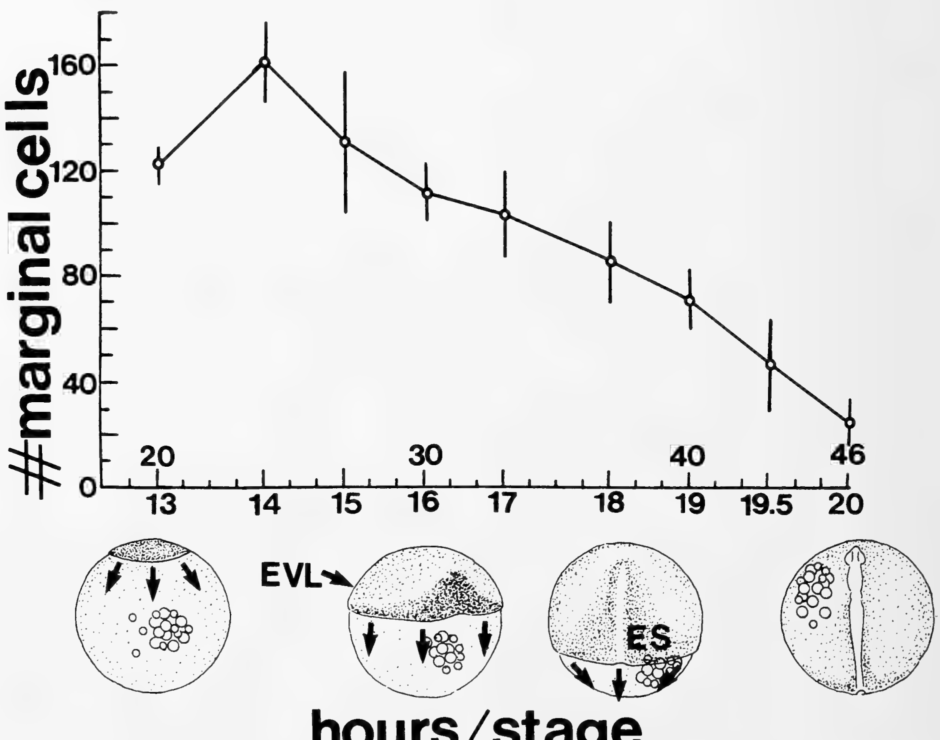

FIG. 2. The number of marginal cells of the enveloping layer (EVL) of *Fundulus* is plotted against hours and developmental stage. The arrows show movement of the margin of the EVL. The embryonic shield (ES) is darkly shaded. Modified from Keller and Trinkaus [20] with permission.

layer. As gastrulation occurs, the enveloping layer undergoes epiboly and spreads vegetally over the yolk while the deep cells collect on the dorsal side and make an embryonic shield from which the embryo will be derived (Fig. 2). This epiboly occurs by spreading and thinning of the original population of cells since few, if any, cells are added by cell division [23]. The marginal and submarginal regions of the enveloping layer must increase their circumference as they pass from near the animal pole toward the equator and decrease their circumference as they pass beyond the equator and approach the vegetal pole.

Cell counts in silver-stained blastoderms [10, 22] show decreased numbers of marginal cells during epiboly (Fig. 2), and direct time-lapse cinemicrography shows that marginal cells decrease their boundary with the yolk syncytial layer, lose contact with it, and then recede from the margin [20] (Fig. 3). The adjacent cells on either side to come into contact immediately, and thus the continuity of the epithelial sheet is never broken. Submarginal cells likewise rearrange by separating from one another along the animal-vegetal axis and allowing cells on either side come into contact simultaneously [20] (Fig. 3). As the connection between two submarginal cells or a marginal cell and the yolk syncytial layer narrows, the apices of the cells become rounded, phase-dense, and convex in profile. When separation occurs, no apical protrusive activity is seen in the case of marginal separations, but "flowers" of apical microvilli appear, immediately adjacent to the sites of submarginal separation.

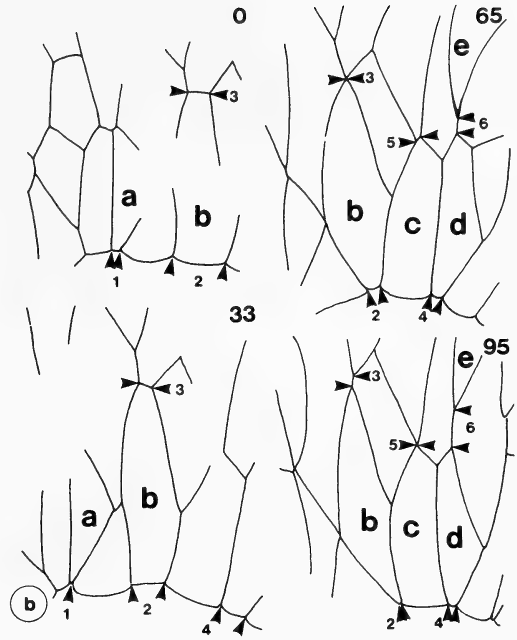

FIG. 3. Progress of the rearrangement of marginal and submarginal cells is shown in line tracings of time-lapse recordings of the EVL at 0, 33, 65, and 95 minutes. The margin of the EVL is below in all figures. Note the narrowing of the boundary of cells a, b and d with the yolk syncytial layer (pointers #1, #2, and #4). Note also that cell b narrows its common boundary with the cell above it and eventually separates from it (pointer #3). From Keller and Trinkaus [20] with permission.

The cells of the enveloping layer are attached to one another and to the yolk syncytial layer by a circumapical junctional complex consisting of continuous tight junctions, desmosomes, and gap junctions [23, 24]. Thus this epithelial sheet forms a high resistance physiological barrier [25], one that is even nearly impermeable to water [26]. Nevertheless, these epithelial cells can and do exchange neighbors in the course of epiboly. Thus the junctional complex has the seemingly imcompatible properties of allowing relative movement of cells and maintaining a physiological barrier. But such incongrous properties might be expected of embryonic epithelial sheets, which at once must protect the *milieu interieur* and at least permit, if not actually generate the dramatic changes in shape of morphogenesis. This is particularly true of *Fundulus,* an esturine fish, which must develop in a variety of salinities.

The enveloping layer is under meridional and circumferential tension, and thus its component cells might respond to these tensions by moving past one another. Alternatively, the cells may actively participate in bringing about their own rearrangement with appropriate motile activity at their basal surfaces. They do bear underlapping protrusions at their basal ends [23, 24]; whether or not these protrusions function in rearrangement is not known.

Passive Epithelial Cell Rearrangement Accomodates Convergence and Extension of the Dorsal Marginal Zone during Xenopus Gastrulation

The dorsal marginal zone of the amphibian embryo undergoes extreme narrowing (convergence) and elongation (extension) in the course of gastrulation and neurulation. Time-lapse cinemicrography of this region of the gastrula and neurula shows that the superficial epithelial cells rearrange to form a longer, narrower array [16] (Fig. 4). As the marginal zone elongates, the apices of the individual cells also elongate and then return to their original isodiametric shape as they rearrange. Such behavior suggests a passive rearrangement in response to stretching by external forces. In fact, the underlying deep cell population produces the force for convergence and extension [27, 28]. However, the junctions in the marginal zone epithelium may be specialized to allow cell rearrangement. Epithelial cells from the animal cap, a region which normally does not undergo convergence and extension, will show convergence and extension when grafted to the dorsal marginal zone, but in contrast to the native epithelium of this region, the grafted cells elongate greatly and tear apart from one another in an apparent reluctance to rearrange [27]. Research should be done to determine if the junctional complex is uniform throughout the gastrula or whether it is specialized in some fashion in those regions destined to undergo rearrangement.

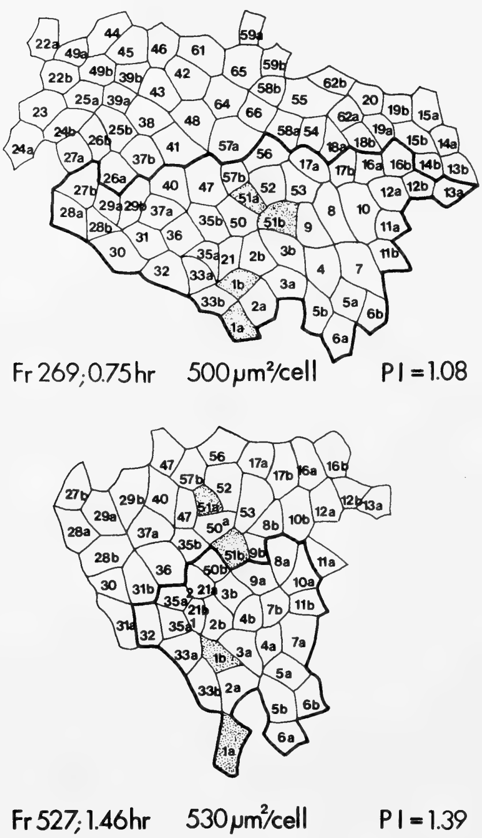

FIG. 4. Tracings of cell apices in the dorsal marginal zone of a *Xenopus* gastrula, as they appear in time-lapse cinemicrography at 0.75 hours and 1.46 hours, shows the rearrangement of these epithelial cells (shaded cells) as the region undergoes convergence (narrowing) and extension (lengthening). The axis of convergence is horizontal; the axis of extension is vertical. From Keller [16] with permission.

Active Epithelial Cell Rearrangement May Function in Tissue Elongation during Newt Neurulation

During neurulation in the urodele amphibian, the neural anlage undergoes an elongation that is important in transforming its originally circular outline into a keyhole shape [4] and may contribute to neural tube closure as well [29]. The neural anlage consists of two regions, the notoplate, which lies immediately superficial to the notochord, and the neural plate, which lies lateral to the notoplate and superficial to the somitic mesoderm. The boundary of the notoplate and neural plate seems to play a special organizing role in producing the elongation of the neural anlage. This boundary elongates during neurulation, probably by a mechanism in which cells in the interior of the notoplate move outward to the notoplate-neural plate boundary and thus elongate the boundary [30]. Jacobson [29, 30] favors the notion that this movement is driven by adhesive relationships along the boundary; his idea is that the notoplate-neural plate interface is a region of maximum adhesion and the notoplate cells move to attach themselves to this favorable adhesive boundary. Jacobson *et al.* [31] proposed that this movement is driven by a "cortical tractor" mechanism in which a fountainoid flow of cell

cortex and adhesions to other cells would function to move cells between one another. In the case of the notoplate cells, their lateral surfaces would be the only ones free to engage in cortical tractoring, because of motility-inhibiting contacts at their other surfaces, and thus they would tend to intercalate in the plane of the epithelium. Lamellipodia, sometimes spanning 3 or 4 cell diameters, have been seen among these cells [31]. It is worth noting that isolated amphibian cells are notorious for showing amoeboid locomotion of one type or another, during which they may exert traction on the substratum by movement of the cortex [32, 33]. The cortical tractor is in many ways an elaboration of this well-travelled observation.

Active Cell Rearrangement Brings about Evagination of the Drosophila Imaginal Disc

Although cell rearrangement was suggested on indirect evidence in early work (see p. 109 of [2]) and implied in the results of others [34, 35], its modern definition and the revival of serious interest in it as a morphogenetic mechanism is largely due to the pioneering work of Fristrom and her colleagues [1, 3, 36, 37] on the role of cell rearrangement in evagination of the *Drosophila* imaginal disc. The leg imaginal discs of *Drosophila* consist of a monolayered epithelium forming a circular "disc" of concentric folds. After exposure to B-ecdysone *in vitro,* the discs evaginate to form a leg structure resembling, in general form, a cylindrical tube. The geometry of such a transformation involves decreasing the circumference and increasing the length of the disc such that it forms a cylinder, with more peripheral parts of the disc (prospective proximal parts of the leg) showing greater change in shape. The cells maintain specialized junctional contacts throughout the process [3]. Cell division is not necessary for the process of evagination since it occurs in the absence of DNA synthesis [38] and in the presence of colchicine [3]. Likewise cell death does not account for the change in shape [3]. Theoretically, a fixed number of cells could either change their shape or their arrangement to produce such a shape change of the cell population. Fristrom [1] found that the latter was the case. In the basitarsal region, which is the easiest to analyze, the number of cells comprising the circumference decreases and the number of cells comprising the length increases, with little or no change in cell shape. In the tarsus the number of circumferential cells is reduced to three fifths the original (Fig. 5) and in the tibia to less than half the original number. Moreover, the number of cells does not change significantly. Analysis of cell contacts shows that unlike adult epidermal cells, the cells of the disc show departures from strict hexagonal packing during rearrangement, with more cells having 5 and 7 neighbors instead of 6.

Little is known of the actual cell motility involved in rearrangement of these epithelial cells other than the fact that in time-lapse videomicrography they show more pulsatile activity throughout the period of rearrangement than earlier (Dr. D. Fristrom, personal communication). It seems likely that this activity may have some function in rearrangement but there is no direct evidence that this is the case or how it works. Trypsin (0.1%) will accelerate the rate of evagination *in vitro* but the mechanism of action is not known [39]; the chracteristic septate junctions are found in trypsin-accelerated discs, so it does not appear to be a simple loosening of junctions.

Ultrastructural work by Fristrom [37] has shown how the individual cells maintain a junctional seal at their apical ends while exchanging neighbors. Each cell is viewed as having a lateral surface, or contact domain, with each adjacent cell (Fig. 6).

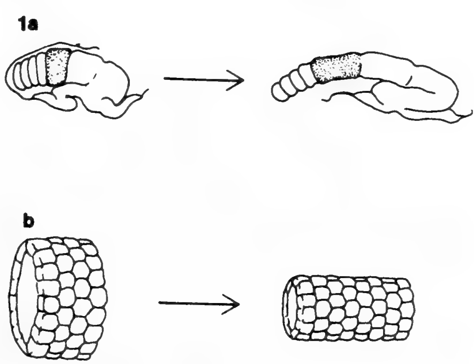

FIG. 5. Schematic diagrams show the transition from partly evaginated to fully evaginated leg imaginal disc (1a) and the corresponding change in the arrangement of the cells in the first tarsal segment (b). From Fristrom [37] with permission.

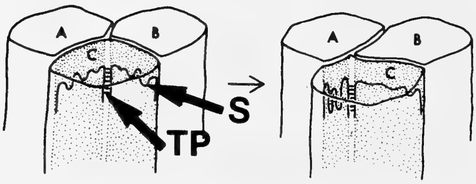

FIG. 6. Fristrom's scheme for redistribution of septa during cell rearrangement is shown diagramatically. Cell B is intercalating between cells A and C. The contact domains are shaded and the septate junctions (s) and tricellular plug (tp) are indicated. Note that the septa adjust to the decreasing width of the contact domain between cells A and C by folding and to the increasing width of the contact domain between cells B and C by unfolding. The tricellular plug forms a seal between the extensions of the septate down the margins of the contact domains where three cells meet. From Fristrom [37] with permission.

As expected, each contact domain has a septate junction forming a band immediately beneath the apex of the cell, but contrary to expectation, these junctions turn basally and run along the lateral edge of the contact domain (Fig. 6). The space where three cells join is occupied by a tricellular plug, a structure consisting of electron-dense ladder-like arrays of lenticular bars (Fig. 6). According to Fristrom's model, neighbor exchange occurs by adjacent cells decreasing their common contact domain; as they do so, the septate junctions fold. As the contact domain nears zero, and exchange of vertices involving the tricellular plugs would have to occur, and it is not yet clear how this might occur.

Active Cell Rearrangement Functions in Secondary Invagination of the Sea Urchin Archenteron

Sea urchin embryos show two phases of archenteron formation. Primary invagination involves the bending the vegetal plate to form a short stubby archenteron, spanning one third to one half the diameter of the blastocoel. During secondary invagination, the archenteron narrows and extends across the blastocoel to the animal region, where it attaches to the ectoderm on the ventral side of the embryo and later forms the mouth. In this second phase of invagination, secondary mesenchyme cells send out long filipodia, which contact the underside of the ectoderm. These were thought to develop tension and stretch the archenteron into its elongate shape (see [40] for a review).

The evidence that archenteron elongation involves active cell rearrangement is based on several facts. Ettensohn [13] showed that archenteron elongation is accompanied by a decreased number of cells in any transverse cross-section, a fact that must be attributed to a cell rearrangement. Moreover, the junctional complex linking these cells at their apices remained intact during the cell rearrangement. Mechanical simulations of pulling by filopodia on the roof of the blastocoel showed that if this were the sole mechanism of archenteron elongation, the blastocoel roof should deform and the archenteron should acquire a shape not seen in embryos [14]. Moreover, the archenteron shows elongation to nearly normal lengths in lithium chloride-induced exogastrulae, in which the archenteron is directed outward into the medium where secondary mesenchyme cells are not in position to exert traction on the archenteron [14]. Recently, Hardin has killed the secondary mesenchyme cells with a laser microbeam at the end of primary invagination and found that the archenteron nevertheless elongates (Jeff Hardin, personal communication). Thus it seems that a major part of the force producing elongation is generated within the archenteron, and that the process underlying elongation may involve active cell rearrangement. Archenteron elongation does not require DNA synthesis or cell division [41].

Given that cell rearrangement functions in archenteron elongation, how do the cells rearrange themselves? Gustafson and Kinnander [42] and Kinnander and Gustafson [43] recorded pulsatile activity at the basal ends of the archenteron cells, but this protrusive activity could not be resolved. There are stage-specific changes in the type of protrusions and cell shapes in the archenteron (Hardin and Benson, personal communication). Early in secondary elongation, the basal ends of the cells bear large lamellipodia oriented toward the archenteron tip and overlapped shingle-fashion (Fig. 7; Hardin and Benson, personal communication; [44, 45]). As elongation procedes, the lamellipodia disappear and the cells become more rounded and are connected by short, basal protru-

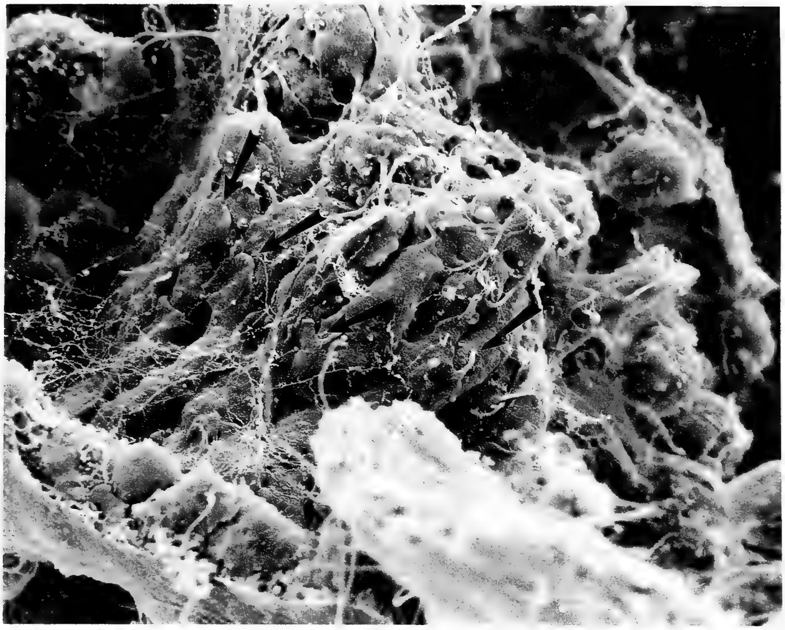

FIG. 7. Early in secondary invagination of the sea urchin gastrula, archenteron cells show elongation parallel to the long axis of the archenteron and have large basal lamellipodia (pointers) overlapping the basal ends of cells nearer the closed end of the archenteron (upper right of photograph). The micrograph was provided by Jeff Hardin. Magnification is ×200.

sions. Then, toward the end of secondary invagination, the cells again elongate slightly. How these changes in protrusive activity and cell shape function in rearrangement, if at all, is not known. Undoubtedly changes in the cytoskeleton or in the adhesions of these cells to one another underlies the observed changes in protrusive activity. Whatever these might be, intact microtubules do not appear to be necessary for archenteron elongation or cell rearrangement [46].

Epithelial Feet May Function in Cell Rearrangement during Formation of Scale Spacing Patterns in the Manduca Wing

Epithelial cell rearrangement may be mediated by filopodia during the formation of rows of scale primordial cells in the development of the wing of the moth *Manduca sexta* [15]. The pupal wing of this organism consists of two epithelial monolayers closely applied to one another and initially composed of morphologically homogeneous cells. By two and half days after pupation, when the epithelium retracts from the overlying cuticle, two cell types are seen–smaller general epithelial cells of the wing and larger scale primordial cells fated to form scale and socket cells by subsequent divisions. After the primordial scale cells are freed from the cuticle, they begin shifting their positions within the epithelial sheet and transform their initially random distribution into rows parallel to the anterior-posterior axis of the wing (Fig. 8). As they rearrange, the scale primordial cells become polarized, with their anterior and posterior edges being longer than their proximal and distal edges. Moreover, during this period from day 2.5 to 4, these cells, and the general epithelial cells as well, form basal filopodia in all directions and contact cells as far as several cell diameters away (Fig. 8). In the fifth day, the basal filopodia become aligned along the anterior-posterior axis of the wing, and by the end of day 5, the rearrangment is complete and all basal filopodia are retracted.

In this case of cell rearrangement, modulation of junctions appears to occur. The epithelial cells lose most of their hemidesmosomal connections with the underlying basal lamina, and the basal

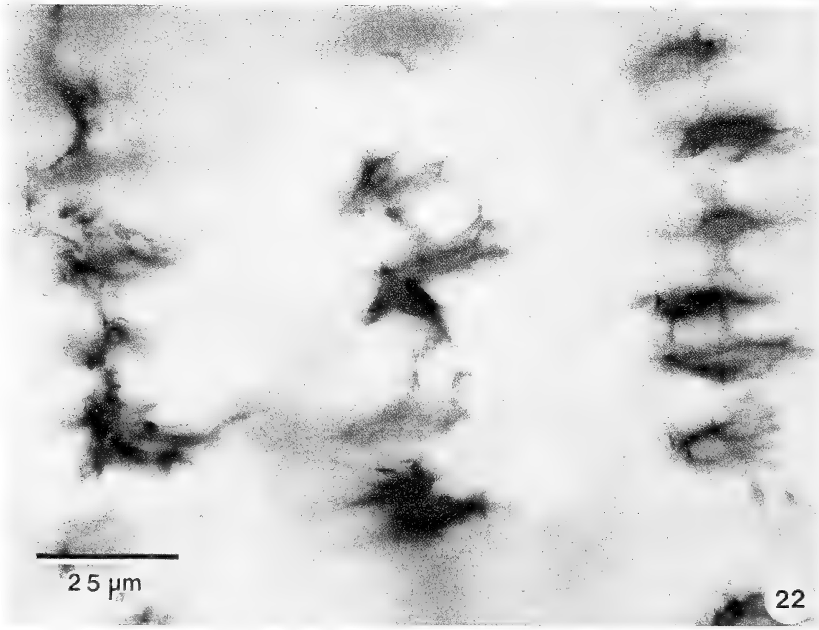

FIG. 8. A whole mount of the upper epithelial monolayer of a *Manduca* wing, stained by the procedure of Locke and Huie [7, 8] shows the primordial scale cells that have begun to align in regularly spaced rows oriented perpendicular to the proximal distal axis of the wing. Anterior is at the top, proximal is to the right. At this stage (day 4) the protrusions of the cell margins extend both between rows and along transverse rows. From Nardi and Magee-Adams [15] with permission.

lamina becomes highly convoluted perhaps as a result of pulling filopodia during rearrangement. Later in development the epithelial cells reestablish contact with the cuticle and a smooth basal lamina. Interestingly, the generalized epithelial cells also show numerous short filopodia on their apical surfaces during the period of cell rearrangement, whereas the scale primordial cells do not.

Nardi and Magee-Adams [15] suggest that these basal filopodia function to generate the physical forces that bring about rearrangement and perhaps impose the control necessary to bring cells into such precise alignment. Since the filopodia span from one to several cell diameters, both short and long range interactions are possible by direct contact [15]. These workers favor the notion that cells rearrange within the epithelium until cells of similar or identical adhesive values are maximized to form the most stable arrangement, which in the case of the moth wing is a series of anterior-posterior bands. They point out that this notion is consistent with the evidence that there is a proximal-distal adhesive gradient in the wing [47, 48], with the fact that alignment and homotypic contacts of protrusions occur at the end of rearrangement, and that the density of primordial scale cells is maximized, relative to earlier states, within a transverse row in the final state.

Epidermal Feet in Pupal Segment Morphogenesis

Research by Locke and Huie [7, 8] and Locke [49] suggests that specialized protrusions or "epidermal feet" at the basal ends of insect epidermal cells play a role in driving the cell rearrangement that occurs during abdominal segment shortening in *Calpodes ethlius* (Lepidoptera). During the last larval (5th) stage in this insect, the body of the animal shortens to 60 percent of its previous length as a result of the shortening of individual segments. This shortening can not be explained as the elastic recoil of the inflated larval segments as hemolymph pressure is

reduced and thus appears to require generation of new axial forces. It is accompanied by epidermal cell rearrangement [49]. The epidermal cells show protrusions of their basal margins which undergo a sequence of stage-specific changes in morphology. Initially, the epidermal cells have a typical polygonal morphology and bear a few short basal protrusions. Then numerous protrusions form at their basal ends, which extend across adjacent cells to form an interlaced fringe around each cell. Thus several layers of feet form between the basal ends of the cells and the basal lamina beneath the epidermis. However, all the protrusions are connected by hemidesmosomes to the basal lamina and are mechanically united by desmosomes connecting them to one another and to adjacent cells. These protrusions contain axially oriented microtubules and microfilaments. Initially, the epidermal feet are distributed uniformly in all directions but later they become progressively longer and oriented axially. Some cells show polarity as well, with the anteriorly directed feet being more finely divided. As the segment begins to shorten, the feet straighten and appear to lose some of their branching, and the epidermal cells become columnar. Finally, the feet shrink back to the basal perimeter of the cell and form a slightly stellate basal apron. The relative shortening of the segment occurs by cell rearrangement, since all the component cells are isodiametric at the start and at the end of the process.

As the cells begin to rearrange, the original junctions seems to be maintained, and the margins of the cells are pulled into extensions to accomodate the shift in relative positions of the cells. Later, the junctions are broken down and new stable connections made between cells. As the feet shorten the basal lamina forms folds, presumably due to compression. A new basal lamina then appears to form below the stabilized pupal cell arrangement. Locke [49] has some evidence that the initiation, extension, and retraction of the epidermal feet may be controlled by ecdysteroid levels. The epidermal feet are not found in larval moults but only in the moult generating the pupa, during which segment shortening occurs. Thus there appears to be strong circumstantial evidence that segment shortening involves an active rearrangement of component epidermal cells, probably driven by the protrusion, attachment and retraction of epidermal feet.

Changes in Proportions of the Body Column of Hydra Involve Cell Rearrangement

The *Hydra* body column consists of two epithelial cell layers, the ectoderm and the endoderm, separated by a non-cellular mesogleal layer. The epithelia are attached to the mesogleal layer by basal muscle processes aligned parallel to the body axis in the ectoderm and perpendicular to it in the endoderm [51]. In regeneration of *Hydra* from isolated fragments of the body column, or in normal asexual reproduction by budding, changes in body form occur which cannot be attributed to cell division (see [51]), nor to permanent change in cell shape [11, 52].

Bode and Bode [12] have made a detailed study of the reshaping of the body column during regeneration. Pieces of body tissue of various sizes and numbers of cells parallel and perpendicular to the long axis of the body column were excised, allowed to heal into a sphere, and monitored in subsequent stages for changes in axial and circumferential cell number, shape of individual cells, and shape of the regenerating body column. Pieces of approximately the same cell number but differing in initial dimensions were compared. These classes of explants were studied: circumferential rectangles (long dimension along the body circumference), squares, and axial rectangles (long dimension along the length of the body column) (Fig. 9). Instead of forming short fat cylinders, intermediate cylinders, and tall narrow cylinders as might be expected from their original shapes, after 6 days these pieces formed cylinders of the same proportions with the same cell arrangements (Fig. 9). This was undoubtedly accomplished by cell rearrangement. Remimiscent of what was seen in *Drosophila* imaginal disk evagination, the rearrangement of cells in *Hydra* regenerates was accompanied by increased numbers of cells having 4, 5 and 7 neighbors rather than the usual 6. The explant affected the proportions of the regenerated body column, with small pieces being shorter and wider than large pieces. This difference is related to the presence of a head. Those without

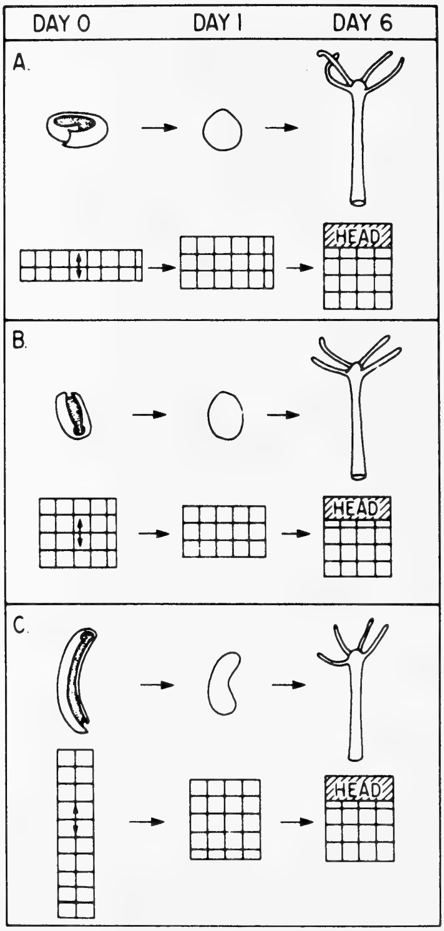

Fig. 9. These diagrams show cell rearrangements in the ectoderm during regeneration of pieces of *Hydra* of nearly the same size but different shapes. The shapes are: (A) circumferential rectangle, (B) square, and (C) axial rectangle. The cell rearrangement is shown schematically with each block representing a 5 by 5 array of cells. From Bode and Bode [12] with permission.

heads remain spherical whereas those with heads form cylinders with a constant ratio of head diameter to body diameter for all regenerate sizes. The head consists of a larger part of the total tissue mass in small regenerates.

Thus the reproportioning of the regenerating body column of *Hydra* during regeneration occurs by cell rearrangement, although it is not known how the cells move between one another. A likely possibility is that these cells use their basal muscle processes to bring about these movements [50, 53], perhaps in a manner similar to the proposed function of the epidermal feet in insects. The fact that the head appears to control the diameter of the body cylinder, a parameter determined by cell arrangement, suggests that the head controls cell rearrangement. Bode and Bode [12] favor the notion that a gradient of adhesive differences can drive conversion of an epithelial sheet into a cylinder [54]. There is, in fact, evidence consistent with the notion of an adhesive gradient in *Hydra:* cells in the upper part of the body column are small in area and columnar, suggesting strong lateral adhesions, whereas those in the lower part of the body have large areas and are squamous in shape, suggesting weaker lateral adhesions [12].

INTERCALATION OF NONEPITHELIAL CELLS INTO AN EPITHELIAL SHEET

Intercalation of Deep Cells into the Superfical Epithelial Layer during Epiboly

Hatta [34] noted in histological sections of the lamprey embryo that the animal cap was transformed from a double-layered structure to a single-layered one in the course of epiboly. Moreover, this appeared to occur by gradual interdigitation of the tapered, adjacent ends of the two tiers of cells until the deep cells had intercalated themselves into the outer layer. Such behavior implies the entry or ingression of nonepithelial cells into an epithelial sheet.

Holtfreter [32] contended that a similar phenomenon occurs during epiboly in the urodele amphibian, based on his observation that the animal cap region is initially dark and later becomes lighter in color, in consequence of the intercalation of deep, non-pigmented cells between the darker epithelial cells to form a single layer. This is in fact the case. Surface cells marked with Bolton-Hunter reagent in the blastula stage are later joined in this layer by unlabelled cells that must have been deep when the surface cells were marked [6]. It is not known how nonepithelial cells manage to insinuate themselves between epithelial cells, despite the fact that the latter are presumably

connected to one another by circumapical junctional complexes. The nonepithelial cells are presumably able to invade an epithelial layer and, after doing so, become true epithelial cells themselves. These events deserve further study.

Intercalation of Inner Cell Mass Cells into the Trophectoderm of Mouse Blastocyst

Work by Cruz and Pedersen [55] and Winkel and Pedersen (personal communication) shows that the same phenomenon occurs in the mouse blastocyst. The mouse blastocyst consists of an outer, epithelial monolayer, the trophectoderm, and a nonepithelial region, the inner cell mass. The inner cell mass is located eccentrically, immediately beneath the trophectoderm, and consists of several layers of cells. Cells of the polar trophectoderm (trophectoderm immediately above the inner cell mass), marked with a cell lineage tracer, were found to be displaced peripherally, at later stages, away from the polar trophectoderm into the mural trophectoderm [55]. These workers proposed that inner cell mass cells were moving outward into the polar trophectoderm and displacing those cells already there. Winkel and Pedersen (personal communication) produced proof of this; they labelled inner cell mass cells and found that these nonepithelial cells, or their progeny, move outward and intercalate themselves into the epithelial polar trophectoderm.

BOUNDARY SHORTENING METHOD OF ANALYZING BEHAVIOR OF CELLS IN A MONOLAYER

Honda and his associates [56–61] have developed the boundary shortening (BS) method to analyze the behavior of cells in monolayers. This method may be useful in analyzing cell rearrangement. The BS procedure predicts how much shortening of the boundaries of cells in a monolayer is possible, and it involves using a computer to perform iterations of a boundary shortening procedure beginning with outline tracings of cell perimeters. In each iteration, the total length of five boundaries, the common boundary between two cells and the two sides adjacent to this boundary on both of its ends, are shortened without changing the areas of the polygons involved (see [60]). The procedure is repeated, selecting cell boundaries at random, until no further significant shortening occurs. The amount of shortening, *s*, is expressed as a fraction of the original boundary length. In analysis of cultured epithelial and nonepithelial cells, the former were found to have small *s* values and the latter large ones [60]. These workers developed two other useful parameters, a *motility area* and a *motility center*. The former is the area swept out by marginal fluctuations of the cell over a period of time as a fraction of total area, and the latter is displacement of the apparent center of gravity of the cell outline over that period of time; the two show high correlation. On the basis of these parameters, these investigators classified the cells into several categories: stable tensile monolayers (small motility and *s* values); stable non-tensile monolayers (small motility and large *s* values); and fluctuating monolayers (large motility and *s* values).

These parameters have been used to monitor developmental changes in epithelia. The starfish embryo changes from a non-tensile to a tensile state in the course of formation of the blastula [58], and during wound healing in the corneal endothelium the endothelium shows a transient change from tensile to non-tensile state [57]. Honda and his coworkers propose that cell rearrangement occurs by boundary shortening. As healing occurs the cells are deformed; the circumapical microfilament system actively contracts, shortening the boundaries and resulting in neighbor changes. Computer simulations, using the boundary shortening procedure and allowing vertex changes, mimic the cell rearrangement seen in the cornea.

In an analysis of cell patterns in the bird oviduct, Honda and others [61] were able to conclude that boundary shortening and adhesive differentials between two types of cells are sufficient to produce a stereotyped repacking of cells. The immature oviduct epithelium of the Japanese quail consists of two cell types, large ciliated cells (C cells) and smaller gland cells (G cells) arrayed in a kagome (star) pattern in which the former are surrounded by the latter (Fig. 10). This pattern matures to

form a rectangular block pattern resembling a checkerboard but deformed towards a honeycomb pattern (Fig. 10). On theoretical grounds, the authors argue that the modified checkerboard pattern is a result of strong adhesion between unlike cells and boundary contraction. Using computational analysis they were able to estimate the value of the difference of adhesion between like and unlike cells. Using this parameter and the BS procedure, they successfully simulated the generation of the rectangular pattern from the kagome pattern. This work makes specific predictions about how relatively simple modulations of adhesion and contraction can maintain or generate complex patterns of cell arrangement in a monolayer. Such an approach should be equally productive when applied to other systems.

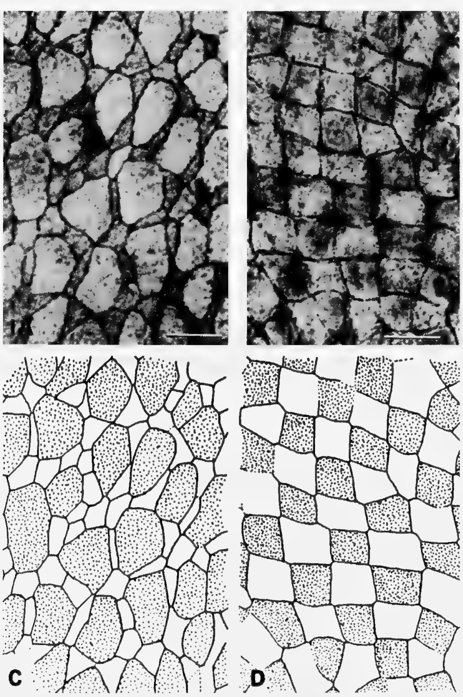

FIG. 10. Light micrographs show the luminal surface of an immature oviduct epithelium (1A) and a mature oviduct epithelium (B) after staining with silver-nitrate to reveal the boundaries of the cells. Corresponding line drawings show the large C cells (stippled) surrounded by G cells (unstippled) in the kagome pattern of the immature oviduct (C) and in the rectangular pattern of the mature oviduct (D). The bar is 10 μm. From Honda *et al.* [61] with permission.

REARRANGEMENT OF NONEPITHELIAL CELLS DURING MORPHOGENESIS

Deep Cells Actively Intercalate To Form a Longer, Narrower Array during Gastrulation and Neurulation of the Xenopus Embryo

As mentioned above, the deep, nonepithelial cells of the dorsal marginal zone of anuran amphibian *Xenopus laevis* appear to be the active cell population in producing narrowing (convergence) and elongation (extension) of this region of the embryo during gastrulation and neurulation [17, 18, 27, 28]. Both the involuting and noninvoluting parts of the dorsal marginal zone show convergence and extension. The deep cells of the involuting marginal zone are prospective mesodermal cells [62]. Tracing cells with a cell lineage tracer showed that the deep cells rearrange to form a narrower, longer array during convergence and extension, and direct time-lapse cinemicrography of explants of the dorsal marginal zone showed that the deep cells actively move between one another to form a longer, narrower array [17, 18]. Such intercalation occurs from the midgastrula stage and continues through neurulation. Intercalation involves pulsatile advance and retraction of the deep cell margins, which results in gradual movement of cells between their neighbors. During notochord formation in the early neurula stage, the notochord cells extend protrusions transverse to the long axis of the notochord and gradually intercalate (Fig. 11); ultimately each cell spans nearly the entire diameter of the notochord. Deep cells are connected to one another by numerous filiform and lamelliform protrusions which are undoubtedly involved in the intercalation process. Individudal cells may move rapidly between others by using large lobopodia formed and advanced by the amoeboid-type cytoplasmic flow described by Holtfreter [33] and others, but this is a rare event [45]. It is not known what agents direct the intercalation to be mediolateral and thus result in a longer, narrower array.

The dorsal noninvoluting marginal zone also

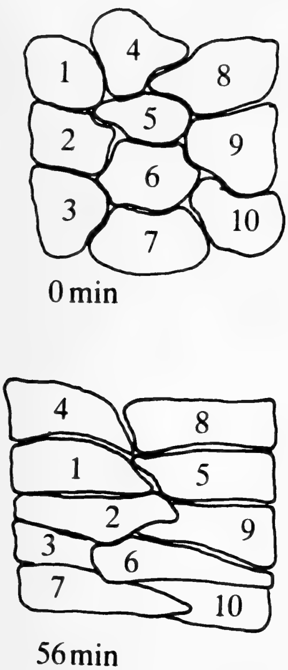

FIG. 11. Tracings of cells from time-lapse films of the dorsal mesoderm in explants of *Xenopus* gastrulae, show three rows of notochord cells rearranging to form two rows of cells during the development of the notochord. The long axis of the notochord is vertical. From Keller *et al.* [17] with permission.

shows convergence and extension, but the underlying cellular activities may be different from those occurring in the involuting marginal zone. Convergence and extension in the noninvoluting and involuting dorsal marginal zones involve different cell morphologies; the rate of extension is greater in the former; the convergence and extension of the former is dependent on basal contact with itself or with dorsal mesoderm (Keller and Danilchik, unpublished results). This latter property makes it impossible to observe cellular behavior directly in the noninvoluting marginal zone, since in order to do so the basal surface must be exposed. Thus we know little about the motility of the cells in this region. It does appear, however, that there are two different mechanisms of convergence and extension in the *Xenopus* gastrula and neurula.

Intercalation of deep cells also occurs during epiboly of the *Xenopus* gastrula. Several layers of deep cells of the animal cap and noninvoluting marginal zone intercalate between one another to form fewer layers of greater area [5]. Although it is important in generating the increased area during epiboly, nothing is known about the mechanism of this intercalation.

Notochord Cells Rearrange during Morphogenesis of the Ascidian

The ascidian embryo offers good material for the study of cell rearrangement because the clarity of the embryo allows direct observation of morphogenesis. After blastopore closure the notochord rudiment in the ascidian lies above the dorsal lip of the closed blastopore. The notochord narrows and elongates by a process similar to that seen in the amphibian. The component cells elongate transverse to the long axis of the notochord, become wedge-or spindle-shaped and intercalate to form a single row of rectangular cells [19, 63]. The rearrangement of the notochord cells occurs with a pulsatile advance and retraction of the tapered protrusions at the medial borders of these intercalating cells [19]. Here, as in the amphibian, nothing is known about how this protrusive activity is organized, but this organism warrants further study, given the simplicity of its notochord and its favorable optical properties.

Pronephric Duct Cells Rearrange during Elongation of the Rudiment

The development of the pronephric duct in urodele amphibians has been described in detail by Poole and Steinberg [9]. The pronephric duct rudiment consists of an oblong tissue mass which segregates from the adjacent mesoderm near the ventral boundary of somites 2 through 7 in the early tailbud stage. Thereafter it narrows and elongates posteriorly to reach nearly twice its original length. Vital dye marking experiments show that its elongation is due to reshaping of the component tissue rather than recruitment of additional tissue along its route. Morphometric analysis shows that the duct narrows from about 6 to 8 cells in diameter to 2 or 3 cells in diameter in the course of its elongation, without significant change in size or shape of the component cells. The posterior tip of the duct, which leads its migration, has lamellipodia, lobopodia, and filopodia in

intimate contact with the mesoderm at the ventral edges of the somites, and results of experiments in which the duct rudiment was grafted to abnormal positions are consistent with the notion that its tip migrates in response to a gradient of adhesion in the lateral mesoderm [64, 65]. Although the migration of the tip makes a major contribution to the guidance of the duct, it is not clear to what extent the component cells in the body of the duct are passively rearranged as a result of tension generated by the duct tip, or whether these cells actively rearrange and contribute to the forces bringing about elongation of the duct. It would seem that the minimum contribution of cell rearrangement to duct elongation would be to allow elongation in response to the tension generated by the cells at the tip.

Interestingly, cell rearrangement may play another role in duct elongation. Gillespie and Armstrong [65] found that the lateral mesoderm is temporarily transformed from two layers of cuboidal cells to one layer of columnar cells as the duct migrates across it. These changes in height and number of cell layers occur as a wavefront over the entire lateral mesoderm. These authors suggest that such changes may be related to the apparent adhesive gradient controlling the direction of migration of the duct tip.

MECHANISMS OF CELL REARRANGEMENT

There are Probably Several Mechanisms of Cell Rearrangement

Although cell rearrangement is not understood in any system, there is enough evidence to suggest that several mechanisms exist. Cell rearrangement in the moth wing and insect segment epidermis differs in detail from that seen in the sea urchin archenteron and the insect imaginal disc, even though the rearrangement occurs in epithelial sheets in all cases. In the first two cases, the long filiform protrusions apparently involved in displacing the cells undergo one or at most a few cycles of extension and retraction, whereas in the last two cases there is rapid, pulsatile activity. In the gastrulation of *Xenopus* there are at least two mechanisms of convergence and extension, which appear to generate active, force-producing cell rearrangement by different rules of cell motility. The intercalation of nonepithelial cells into an epithelial sheet during amphibian and lamprey epiboly and during blastocyst development in mice undoubtedly differs from intercalations involving only epithelial cells or nonepithelial cells. Undoubtly there are similarities of underlying cellular behavior in these various types of cell rearrangement, but at present there is not enough evidence to know what these are, beyond the obvious and trivial ones, or to evaluate their significance.

Motile Activity, Orientation, Directionality, and Adhesion

These properties of cells are undoubtedly involved directly or indirectly in cell rearrangement. Cells undergoing rearrangement are connected by filiform or lamelliform protrusions. In the case of the insect epidermal cells, cell rearrangement seems to involve one cycle of extension, perhaps across many cell diameters, attachment, and retraction of protrusions. The same may be true in the case of the primordial scale cells. In *Xenopus,* pulsatile protrusive activity repeated on the order of minutes appears to be involved in cell rearrangement, and the same is true of notochord cells in the ascidian. It is worth considering the possibility that mechanisms of rearrangement fall into two categories: those which involve one or a few cycles of extension, attachment, and retraction of protrusions over great distances; and those which involve rapidly repeated cycles of short-range protrusive activity.

In some cases, such as the insect epidermis, the displacement of cells during rearrangement undoubtedly involves contraction of protrusions which have become attached to surfaces of other cells some distance away. In other cases, such as the deep cells of *Xenopus,* advance of the cell by cytoplasmic flow may be involved. On the other hand, Honda and his associates have argued cogently that a general, circumferential contraction of the cell margin can function in cell rearrangement by the boundary shortening mechanism. On the limited evidence available, it seems likely that several kinds of motile activity are likely to be involved in the various types of cell

rearrangement, or in various aspects of a single type of rearrangement, and that the mechanical context in which these activities are exercised may be as important as the character of the activity itself. More data on the motile activity involved in cell rearrangement is badly needed; we have time-lapse records of actual cell rearrangement at reasonably high resolution only in the ascidian notochord, the cornea during wound healing, the fish enveloping layer, and the deep and superficial cells of *Xenopus* gastrulae. None of these systems have been analyzed in sufficient detail.

Cell rearrangement appears to be an oriented process (cell rearrangement along an axis, in either direction) and may be directional (cell rearrangement in one direction along an axis) as well. In the imaginal disc and in the sea urchin archenteron the orientation of rearrangement is circumferential. In the *Xenopus* gastrula rearrangement appears to be directional and generally towards the dorsal side. In the moth wing it is exercised in the proximal-distal axis and thus produces aligned cell in anterior-posterior rows. In the notochord, intercalation of the central cells is oriented at right angles to the long axis with activity at either end; those notochord cells at the notochord-somitic mesoderm boundary show directed intercalation, with all activity confined to their inner ends. In this case, the notochord boundary may exert a polarizing influence. In most cases, however, it is not known whether oriented intercalation results from a bias in the direction of protrusive activity, or from a bias in the motile effectiveness of certain protrusions over others. If protrusive activity is biased, is this bias an intrinsic property of the cell, perhaps based on its cytoskeletal organization, or is it a bias imposed on the cell by its extracellular environment, such as the extracellular matrix or a diffusible chemotactic molecule? Another possibility is differential adhesion within a heterogeneous population of cells. Mittenthal and Mazo [54] have proposed a model for the conversion of a disc into a cylinder, based on blocks of cells which have differential adhesion for one another and within which cells are free to rearrange, but between which they cannot. Related ideas involve collection of cells at boundaries of greater adhesiveness and thus enlarging the boundary [12, 15, 30]. The timing of disassembly of old adhesions and the formation of new ones during neighbor exchange is also an important unresolved issue in most systems. It is clear that rearrangement can occur even among epithelial cells joined with sealing tight or septate junctions.

In general, there are many ideas about how cell rearrangement works. Some of these ideas, if not correct themselves, may lead to others that are useful. But there is too little direct information about the intercellular adhesions, and the nature, organization, and timing of motile activity during cell rearrangement. Thus there is little evidence on which to decide among current ideas or to suggest new ones. Given the prevalence and importance of cell rearrangement in development, these basic questions of mechanism should be pursued with vigor.

ACKNOWLEDGMENTS

Many thanks to Paul Wilson and Jeff Hardin for their insightful comments, and to Paul Tibbetts for help in preparing the manuscript. This was prepared under the support of NIH Grant HD18979 to the author.

REFERENCES

1 Fristrom, D. (1976) The mechanism of evagination of imaginal discs of *Drosophila melanogaster*. III. Evidence for cell rearrangement. Dev. Biol., **54**: 163–171.

2 Waddington, C. H. (1940) Organizers and Genes. Cambridge University Press, Cambridge.

3 Fristrom, D. and Fristrom, J. (1975) The mechanism of evagination of imaginal discs of *Drosophila melanogaster*. I. General considerations. Dev. Biol., **43**: 1–23.

4 Jacobson, A. and Gordon, R. (1976) Changes in the shape of the developing nervous system analyzed experimentally, mathematically and by computer simulation. J. Exp. Zool., **197**: 191–246.

5 Keller, R. E. (1980) The cellular basis of epiboly: A SEM study of deep cell rearrangement during gastrulation in *Xenopus laevis*. J. Embryol. Exp. Morphol., **60**: 201–234.

6 Smith, J. and Malacinski, G. M. (1983) The origin of the mesoderm in an anuran, *Xenopus laevis*, and a urodele, *Ambystoma mexicanum*. Dev. Biol., **98**: 250–254.

7 Locke, M. and Huie, P. (1981) Epidermal feet in insect morphogenesis. Nature, **293**: 733–735.

8 Locke, M. and Huie, P. (1981) Epidermal feet in pupal segment morphogenesis. Tissue Cell, **13**: 787–803.

9 Poole, T. and Steinberg, M. (1981) Amphibian pronephric duct morphogenesis: segregation, cell rearrangement and directed migration of the *Ambystoma* duct rudiment. J. Embryol. Exp. Morphol., **63**: 1–16.

10 Kageyama, T. (1982) Cellular basis of epiboly of the enveloping layer in the embryo of the Medaka, *Oryzias latipes*. II. Evidence for cell rearrangement. J. Exp. Zool., **219**: 241–256.

11 Graf, L. and Gierer, A. (1980) Size, shape and orientation of cells in budding hydra and regulation of regeneration in cell aggregates. Wilhelm Roux's Arch., **188**: 141–151.

12 Bode, P. M. and Bode, H. R. (1984) Formation of pattern in regenerating tissue pieces of *Hydra attenuata*. III. The shaping of the body column. Dev. Biol., **106**: 315–325.

13 Ettensohn, C. A. (1985) Gastrulation in the sea urchin embryo is accompanied by the rearrangement of invaginating epithelial cells. Dev. Biol., **112**: 383–390.

14 Hardin, J. D. and Cheng, L. Y. (1986) The mechanisms and mechanics of archenteron elongation during sea urchin gastrulation. Dev. Biol., **115**: 490–501.

15 Nardi, J. and Magee-Adams, S. M. (1986) Formation of scale spacing patterns in a moth wing. I. Epithelial feet may mediate cell rearrangement. Dev. Biol., **116**: 278–290.

16 Keller, R. E. (1978) Time-lapse cinemicrographic analysis of superficial cell behavior during and prior to gastrulation in *Xenopus laevis*. J. Morphol., **157**: 223–248.

17 Keller, R. E., Danilchik, M., Gimlich, R. and Shih, J. (1985) Convergent extension by cell intercalation during gastrulation of *Xenopus laevis*. In "Molecular Determinants of Animal Form. UCLA Symposium on Molecular and Cellular Biology, New Series", Vol. 31. Ed. by G. M. Edelman, Alan R. Liss, New York, pp. 111–142.

18 Keller, R. E., Danilchik, M., Gimlich, R. and Shih, J. (1985) The function of convergent extension during gastrulation of *Xenopus laevis*. J. Embryol. Exp. Morphol., **89**: Suppl., **89**: 185–209.

19 Miyamoto, D. M. and Crowther, R. (1985) Formation of the notochord in living ascidian embryos. J. Embryol. Exp. Morphol., **86**: 1–17.

20 Keller, R. E. and Trinkaus, J. P. (1987) Rearrangement of enveloping layer cells without disruption of the epithelial permeability barrier as a factor in *Fundulus* epiboly. Dev. Biol., **120**: 12–24.

21 Keller, R. E. (1986) The cellular basis of amphibian gastrulation. In "Developmental Biology: A Comprehensive Synthesis, Vol. 2, The Cellular Basis of Morphogenesis". Ed. by L. Browder, Plenum Press, New York, pp. 241–327.

22 Keller, R. E. and Trinkaus, J. P. (1982) Cell rearrangement in a tightly joined epithelial layer during *Fundulus* epiboly. J. Cell Biol., **95**: 325a.

23 Betchaku, T. and Trinkaus, J. P. (1978) Contact relations, surface activity, and cortical microfilaments of marginal cells of the enveloping layer and of the yolk syncytial and yolk cytoplasmic layers of *Fundulus* before and during epiboly. J. Exp. Zool., **206**: 381–426.

24 Trinkaus, J. P. and Lentz, T. (1967) A fine structural study of cytodifferentiation during cleavage, blastula and gastrula stages of *Fundulus heteroclitus*. J. Cell Biol., **32**: 121–138.

25 Bennett, M. V. L. and Trinkaus, J. P. (1970) Electrical coupling of embryonic cells by way of extracellular space and specialized junctions. J. Cell Biol., **44**: 592–610.

26 Dunham,P. B., Cass, A., Bennett , M. V. L. and Trinkaus, J. P. (1970) Water permeability of *Fundulus* eggs. Biol. Bull., **139**: 420–421.

27 Keller, R. E. (1981) An experimental analysis of the role of the bottle cells and the deep marginal zone in gastrulation of *Xenopus laevis*. J. Exp. Zool., **216**: 81–101.

28 Keller, R. E. (1984) The cellular basis of gastrulation in *Xenopus laevis*: Active, postinvolution convergence and extension by mediolateral interdigitation. Am. Zool., **24**: 589–603.

29 Jacobson, A. G. (1981) Morphogenesis of the neural plate and tube. In "Morphogenesis and Pattern Formation". Ed. by T. G. Connelly, L. L. Brinkley and R. M. Carlson, Raven Press, New York, pp. 233–263.

30 Jacobson, A. G. (1985) Adhesion and movement of cells may be coupled to produce neurulation. In "The Cell in Contact: Adhesions and Junctions as Morphogenetic Determinants". Ed. by G. M. Edelman and J.-P. Thiery, John Wiley and Sons, New York, pp. 49–65.

31 Jacobson, A., Oster, G., Odell, G. and Cheng. L. (1986) Neurulation and the cortical tractor model for epithelial folding. J. Embryol. Exp. Morphol., **96**: 19–49.

32 Holtfreter, J. (1943) A study of the mechanics of gastrulation. Part I. J. Exp. Zool., **94**: 261–318.

33 Holtfreter, J. (1947) Structure, motility, and locomotion in isolated embryonic amphibian cells. J. Morphol., **79**: 27–62.

34 Hatta, S. (1907) Gastrulation in *Petromyzon*. J. Coll. Sci. Imp. Univ. Tokyo, **21**: 3–44.

35 Holtfreter, J. (1944) A study of the mechanics of gastrulation. Part II. J. Exp. Zool., **95**: 171–212.

36 Fristrom, D. and Chihara, C. (1978) The mecha-

nism of evagination of imaginal discs of *Drosophila melanogaster*. V. Evagination of disc fragments. Dev. Biol., **66**: 564–570.

37 Fristrom, D. (1982) Septate junctions in imaginal discs of *Drosophila melanogaster*: A model for the redistribution of septa during cell rearrangement. J. Cell Biol., **94**: 77–87.

38 Fristrom, J. W., Logan, W. R. and Murphy, C. (1973) The synthetic and minimal culture requirements for evagination of imaginal discs of *Drosophila melanogaster in vitro*. Dev. Biol., **33**: 441–456.

39 Fekete, E., Fristom, D., Kiss, I. and Fristrom, J. W. (1975) The mechanism of evagination of imaginal discs of *Drosophila melanogaster*. II. Studies on trypsin-accelerated evagination. Wilhelm Roux' Archiv. Entwicklungsmech. Org., **178**: 123–138.

40 Gustafson, T. and Wolpert, L. (1967) Cellular movement and contact in sea urchin morphogenesis. Biol. Rev., **42**: 442–489.

41 Stephens, L., Hardin, J., Keller, R. and Wilt, F. (1986) The effects of aphidicolin on morphogenesis and differentiation in the sea urchin embryo. Dev. Biol., **118**: 64–69.

42 Gustafson, T. and Kinnander, H. (1956) Microaquaria for time-lapse cinematographic studies of morphogenesis in swimming larvae and observations on gastrulation. Exp. Cell Res., **11**: 36–57.

43 Kinnander, H. and Gustafson, T. (1960) Further studies on the cellular basis of gastrulation in the sea urchin larva. Exp. Cell Res., **19**: 276–290.

44 Ettensohn, C. A. (1985) Mechanisms of epithelial invagination. Q. Rev. Biol., **60**: 289–307.

45 Keller, R. E. and Hardin, J. D. (1987) Cell behavior during active cell rearrangement: Evidence and speculations. J. Cell Sci., (in press).

46 Hardin, J. D. (1987) Archenteron elongation in the sea urchin is a microtubule-independent process. Dev. Biol., **121**: 253–262.

47 Nardi, J. and Kafatos, F. C. (1976) Polarity and gradients in lepidopteran wing epidermis. I. Changes in graft polarity, form, and cell density accompanying transposition and reorientation. J. Embryol. Exp. Morphol., **36**: 469–487.

48 Nardi, J. and Kafatos, F. C. (1976) Polarity and gradients in lepidopteran wing epidermis. II. The differential adhesiveness model: Gradient of a non-diffusible cell surface parameter. J. Embryol. Exp. Morphol., **36**: 489–512.

49 Locke, M., (1985) The structure of epidermal feet during their development. Tissue Cell, **17**: 901–921.

50 Otto, J. (1977) Orientation and behaivor of epithelial cell muscle processes during *Hydra* budding. J. Exp. Zool., **202**: 307–322.

51 Campbell, R. D. (1967) Tissue dynamics of steady-state growth in *Hydra littoralis*. I. Patterns of cell division. Dev. Biol., **15**: 487–502.

52 Campbell, R. D. (1968) Cell behavior and morphogenesis in hydroids. In Vitro, **3**: 22–32.

53 Campbell, R. D. (1980) Role of muscle processes in hydra morphogenesis. In "Developmental and Cellular Biology of Coelenterates". Ed. by P. Tardent and R. Tardent, Elsevier/North Holland, New York, pp. 421–428.

54 Mittenthal, J. and Mazo, R. (1983) A model for shape generation by strain and cell-cell adhesion in the epithelium of an arthropod leg segment. J. Theor. Biol., **100**: 443–483.

55 Cruz, Y. P. and Pedersen, R. A. (1985) Cell fate in the polar trophectoderm of mouse blastocysts as studied by microinjection of cell lineage tracers. Dev. Biol., **11**: 73–83.

56 Honda, H. and Eguchi, G. (1980) How much does the cell boundary contract in a monolayered cell sheet? J. Theor. Biol., **84**: 575–588.

57 Honda, H., Ogita, Y., Higuchi, S. and Kani, K. (1982) Cell movements in a living mammalian tissue: long-term observation of individual cells in wounded corneal endothelia of cats. J. Morphol., **174**: 23–39.

58 Honda, H., Dan-Sohkawa, M. and Watanabe, K. (1983) Geometrical analysis of cells becoming organized into a tensile sheet, the blastular wall, in the starfish. Differentiation, **25**: 16–22.

59 Honda, H. (1983) Geometrical models for cells in tissues. Int. Rev. Cytol., **81**: 191–248.

60 Honda, H., Kodama, R., Takeuchi, T., Yamanaka, H., Watanabe, K. and Eguchi, G. (1984) Cell behavior in a polygonal cell sheet. J. Embryol. Exp. Morphol., **83**: Suppl., 313–327.

61 Honda, H., Yamanaka, H. and Eguchi, G. (1986) Transformation of a polygonal cellular pattern during sexual maturation of the avian oviduct epithelium: computer simulation. J. Embryol. Exp. Morphol., **98**: 1–19.

62 Keller, R. E. (1976) Vital dye mapping of the gastrula and neurula of *Xenopus laevis*. II. Prospective areas and morphogenetic movements in the deep region. Dev. Biol., **51**: 118–137.

63 Cloney, R. A. (1964) The development of the ascidian notochord. Acta Embryol. Morphol. Exp., **7**: 111–130.

64 Poole, T. and Steinberg, M. (1982) Evidence for the guidance of pronephric duct migration by a craniocaudally traveling adhesion gradient. Dev. Biol., **92**: 144–158.

65 Gillespie, L. L. and Armstrong, J. B. (1986) Morphogenetic waves in the development of the lateral mesoderm in the Mexican axolotl (*Ambystoma mexicanum*) and their relationship to pronephric duct migration. J. Exp. Zool., **237**: 327–338.

ZOOLOGICAL SCIENCE 4: 781–788 (1987)

Geotactic Behavior in *Paramecium caudatum* I. Geotaxis Assay of Individual Specimen

Koji Taneda

Department of Biology, Faculty of Science, Kochi University, Akebonocho 2–5–1, Kochi 780, Japan

ABSTRACT—Geotactic behavior of an individual specimen of *Paramecium caudatum* was examined by analyzing its swimming path in a vertical glass tube. The path was recorded by means of a specially designed apparatus. The specimen swam upward to the top of the tube and stayed there (negative geotaxis), when the glass tube was thicker than 1.8 mm in its inner diameter. In thinner tube the specimen did not show the negative geotaxis, because upward orientation of the specimen was somehow inhibited in the tube. Inhibition of ciliary activity caused a decrease in the upward swimming velocity. This seems to indicate that the upward orientation of the specimen is independent of the ciliary activity. Change in hydrostatic pressure on the specimen did not affect the geotactic behavior. Thus a hydrostatic pressure difference between upper and lower portion of the specimen can not be a cause for the upward orientation of the specimen. Change in the hydrostatic pressure with time was also eliminated from possible causes for the negative geotaxis. The specimen showed negative geotaxis in a heavy water-containing solution, whose specific gravity was larger than that of the specimen. In highly viscous solution, frequent occurrence of ciliary reversal in a downward orienting specimen caused its negative geotaxis.

INTRODUCTION

Many ciliated and flagellated protozoans exhibited negative geotaxis. Since specific gravity of the cells is usually higher than their surrounding medium, they exhibit negative geotaxis with expenditure of energy. Several hypotheses for the mechanism of the negative geotaxis have been proposed [1–4]. All the hypotheses were based on the analysis of distribution of the cells in gravity field. For better understanding of the mechanism it is important to know locomotor behavior of an individual organism in gravity field.

Present paper will deal with precise description of swimming behavior of a single specimen of *Paramecium caudatum* in a vertical glass tube. The effects of some environmental factors on the behavior will also be presented. Some hypotheses proposed by previous workers will be confuted on the basis of present findings.

Accepted June 6, 1987
Received October 18, 1985

MATERIALS AND METHODS

Specimens of *Paramecium caudatum* (wild type) were cultured in bacterized (*Klebsiella aerogenes*) dried lettuce infusion at 22–24°C. The specimens were washed with a diluted Herbst's modified artificial sea water (ASW), which was osmotically equivalent to 2 mM NaCl and buffered to pH 7.2–7.4 with $NaHCO_3$. All the chemicals examined were dissolved in the diluted ASW. In some experiments heavy water (D_2O; C. E. N. Sacley, France, 99.8%) was substituted for natural water. Specimens obtained from various cultures with different culture age were rinsed with the diluted ASW at least three times. As shown in Figure 1, a single specimen was pipetted into the bottom of a vertical glass tube (T1; 15 cm in length) filled with a test solution through a thin glass tube (O; 3 mm in inner diameter, 5 mm in length) branched at the bottom of T1. The specimen (C) in the tube was observed through a magnifying glass with a horizontal mark line (L). The swimming specimen in the tube was tracked by moving the line along the tube. The movement

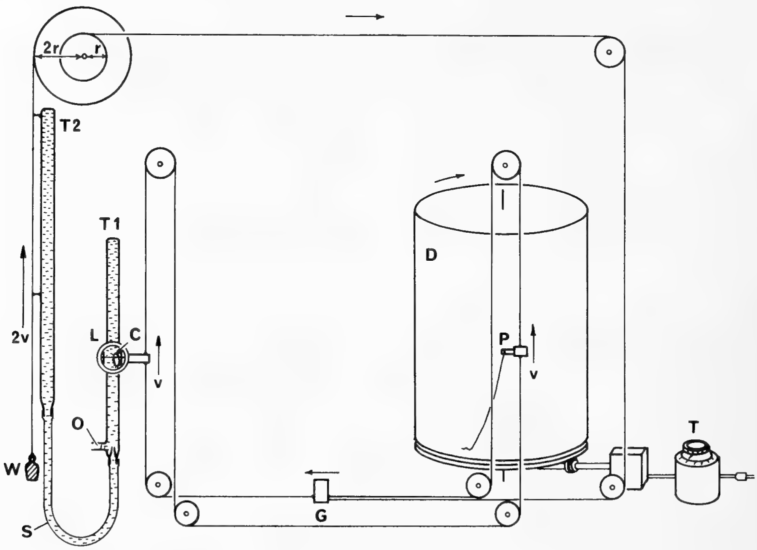

FIG. 1. Schematic representation of the experimental set-up for recording the swimming behavior of an individual specimen of *Paramecium caudatum*. T1; a vertical glass tube where a single specimen of *Paramecium* (C) is introduced through an opening (O). Position of *Paramecium* in the tube is followed by moving a small magnifying glass with a horizontal mark line (L) through which the specimen is observed. G; a finger-grip for moving the magnifying glass. The movement of the glass is recorded on a paper on a kymograph drum (D) by means of a pen (P). T; a transformer for adjusting rotation rate of the drum (1.5 cm/min). T2; a vertical glass tube connected to T1 with silicone rubber tube (S) for applying extra hydrostatic pressure to the specimen. The tube is kept lay down when the extra hydrostatic pressure is not needed. See the text for details. W; a weight for smooth movement of pulley-systems.

of the line was transferred into vertical movement of a recording pen (P) by a pulley-system to record the movement of the specimen on a sheet of section paper lapped around a kymograph drum (D). Running speed of the drum was adjusted to be 1.5 cm/min by a voltage controller (T). Other details of the experimental methods will be described in Results section. All the experiments were performed at room temperature ranging from 18°C to 25°C.

RESULTS

Effect of thickness of the glass tube on the swimming behavior

A series of experiments was carried out to examine influence of bore size of the glass tube on swimming behavior of a specimen in the tube. Some typical results on the specimens obtained from 6-day culture are shown in Figure 2. When

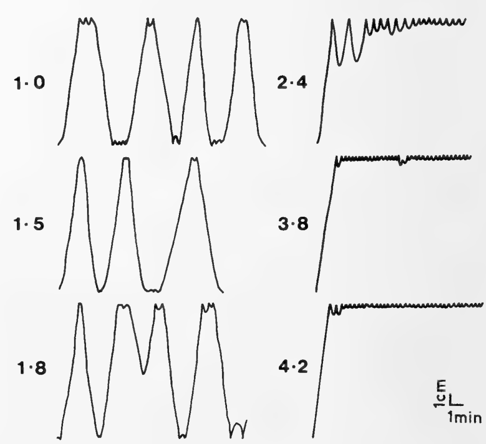

FIG. 2. Influence of bore size of the glass tube on the swimming behavior of *P. caudatum* in the tube. Each record represents time-change in the position of a single specimen in the tube. The specimens were obtained from 6-day culture. Each number indicates inner diameter of the glass tube in mm.

inner diameter of the tube was thinner than 1.8 mm, the specimen swam upward and downward alternatively over the full length of the tube. In a glass tube thicker than 2.4 mm the specimen swam upward to the top of the tube then turned downward, but soon began to swim upward again. Thus they tended to stay near the upper portion of the tube (negative geotaxis). In the following experiments the geotactic behavior was examined in a glass tube of 4.2 mm in inner diameter.

Effect of culture age on the swimming behavior

Swimming behavior in the vertical tube was examined in several specimens with different culture age. Typical results are shown in Figure 3. The specimens in the logarithmic growth phase (1–3-day culture) exhibited weak negative geotaxis, while those in the early stationary phase (6–7-day culture) showed strong negative geotaxis. In order to show degree of the negative geotaxis quantitatively, period of time when the specimen was present in upper 1/5 portion of the tube during 30-min observation was determined and expressed in percentage (Gs). Moreover, the period of time from the moment when a specimen at the top of the tube began to swim downward to the moment when it reoriented upward (Td) was measured. Td corresponds to the tendency of the specimen to swim downward. In Figure 4 mean values of Gs and Td obtained from 5 measurements with 5 different specimens were plotted against culture age together with the growth curve of the specimens in the culture. Gs was minimum in 1–2-day culture, increasing gradually and reached its maximum in 6–7-day culture. Td was inversely related with Gs, e.g., it was maximum in 1–2-day culture, while minimum in 6–7-day culture.

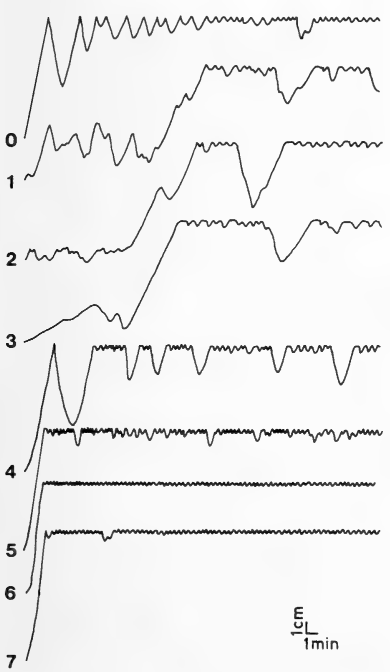

FIG. 3. Effect of the culture age on the swimming behavior of *P. caudatum* in a vertical tube with inner diameter of 4.2 mm. Each record represents time-change in the position of a single specimen in the tube. Each number indicates the culture age in day.

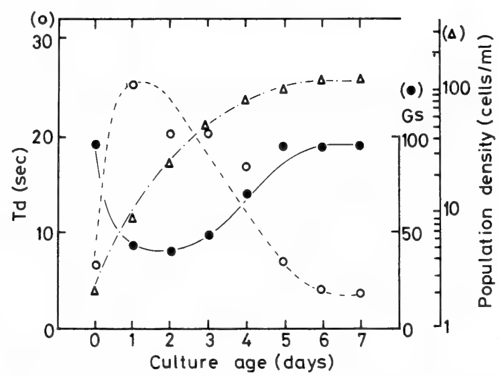

FIG. 4. Relation of the culture age with degree of the negative geotaxis (Gs; solid circles) and with tendency of the specimen of *P. caudatum* to downward swimming (Td; open circles) in the vertical tube. For the definitions of Gs and Td see the text. Cell density in the culture (open triangles) is also presented as a function of the culture age.

Effect of starvation on the swimming behavior

When the specimens had been kept unfed, the negative geotaxis became unconspicuous. As shown in Figure 5, tendency of the specimen to stay in the upper portion of the tube decreased with starvation period. Changes in both Gs and Td with starvation period are shown in Figure 6. Td increased slightly by 4-day starvation and greatly after then. Gs decreased to zero in 4-day starvation.

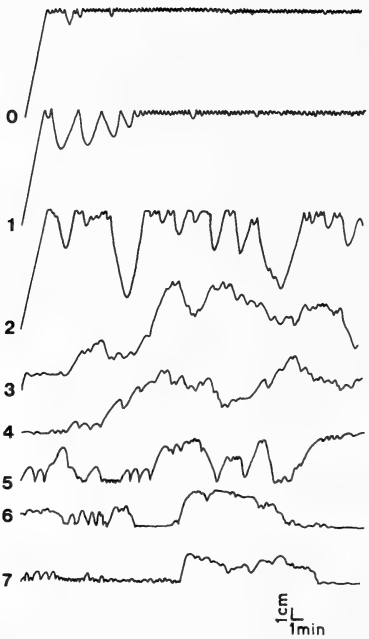

FIG. 5. Effect of starvation on the swimming behavior in the specimen of *P. caudatum* obtained from 6-day culture. Each record represents the position of a single specimen in the vertical tube. Each number indicates period of starvation in day.

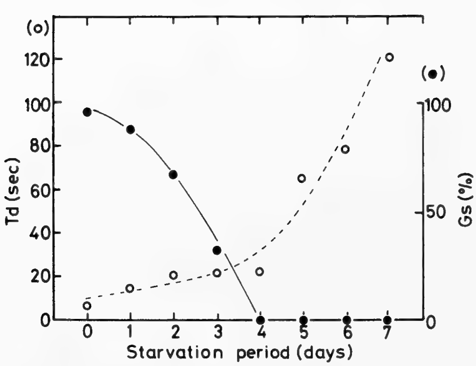

FIG. 6. Relation of the period of starvation (days) with Gs (solid circles) and Td (open circles) of *P. caudatum* in the vertical glass tube. See the legend of Fig. 4.

Effects of hydrostatic pressure and of density of the external solution on the swimming behavior

Hydrostatic pressure on the specimen in the tube decreases as the specimen swim upward. In order to examine a possible dependency of the negative geotaxis on the decrease in the hydrostatic pressure with time, the experimental apparatus was arranged so that the pressure increased as the specimen swam upward. As shown in Figure 1, the glass tube, T1, was connected to another glass tube, T2. T2 moved upward twice as fast as the swimming speed of the specimen in T1 by means of a pulley-system, so that the hydrostatic pressure on the specimen increased with the specimen swam upward. The increased hydrostatic pressure can be removed suddenly by laying T2 down. Three typical examples of geotactic behavior of the specimens under the influence of increasing the hydrostatic pressure are shown in Figure 7. The behavior was essentially similar to that in normal case, where the pressure decreased as the specimen swam upward (Figs. 3–6). The specimens stayed at the top of the tube even after removing the increased hydrostatic pressure.

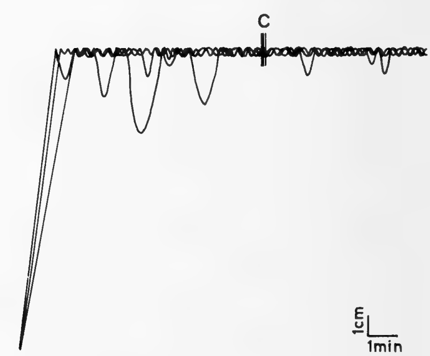

FIG. 7. Time-change in the position of a single specimen of *P. caudatum* in the vertical tube under the influence of increasing the hydrostatic pressure. C indicates the time when the extra hydrostatic pressure was removed.

In order to examine the resistance hypothesis for the negative geotaxis proposed by Davenport [3], behavior of the specimens in a solution with a density higher than that of *Paramecium* (d=1.04) was examined. Heavy water (d=1.10) was employed to make the density of the solution higher. Viscosity of the solution was almost the same with that of normal solution. When the specimens were transferred into the solution, their swimming speed decreased gradually with time and finally

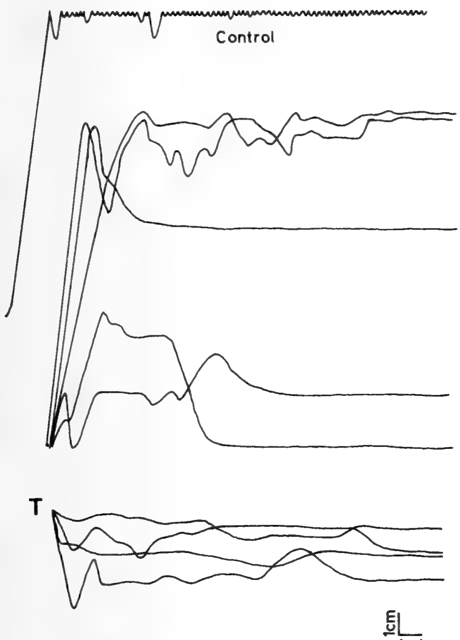

FIG. 8. Time-change in the position of a single specimen of *P. caudatum* in the vertical tube filled with a heavy water-containing solution. Upper record (control); the time-change in the normal water test solution. Middle records; the specimens were introduced into the bottom of the tube. Lower records (T); the specimens were introduced into the top of the tube.

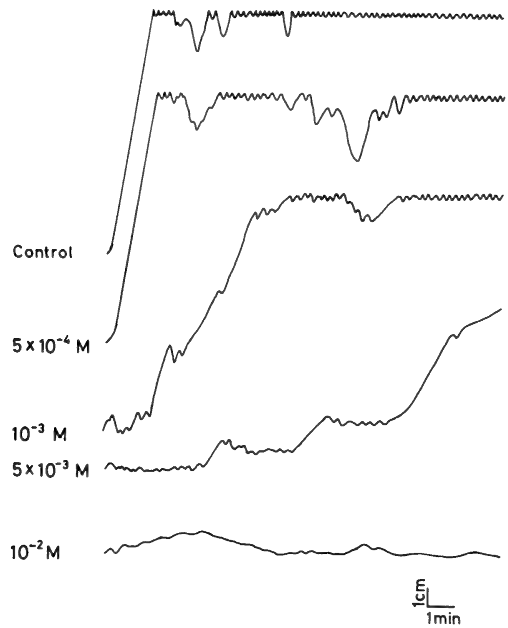

FIG. 9. Concentration effect of NaN_3 on the time-change in the position of a single specimen of *P. caudatum* in the vertical tube.

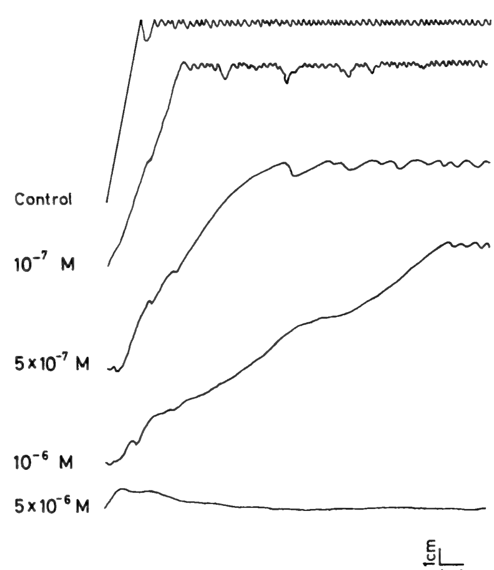

FIG. 10. Concentration effect of $NiSO_4$ on the time-change in the position of a single specimen of *P. caudatum* in the vertical tube.

they stopped the swimming. As shown in Figure 8, some specimens showed clear negative geotaxis. When the specimens were introduced into top of the tube instead of into bottom[1], they did not show clear tendency to swim downward (lower records labelled as T in Fig. 8).

Effects of NaN_3 and other inhibitors of motility

The effect of NaN_3, a metabolic inhibitor, on the geotaxis of *Paramecium* was examined. As shown in Figure 9, NaN_3 produced little effect on the geotaxis when its concentration was below 5×10^{-3} M. With increasing NaN_3 concentration upward swimming velocity of the specimen decreased gradually. However, tendency of the

[1] Introduction of the specimen into the top of the tube was performed by turning the glass tube; T1 (see Fig. 1) upside down, so that the opening (O) for introducing the specimen was located at the top of the tube.

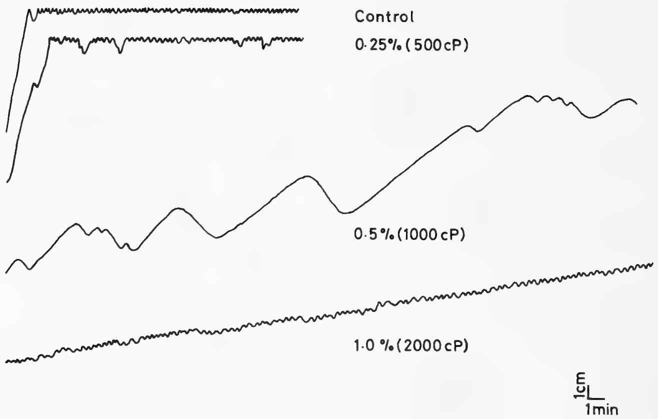

FIG. 11. Concentration (%) effect of methylcellulose on the time-change in the position of a single specimen of *P. caudatum* in the vertical tube. An approximate value of the viscosity of each solution is presented in parenthesis.

specimen to go upward remained even in a solution with 5×10^{-4} M NaN_3. The specimen stopped its swimming in a solution with NaN_3 higher than 10^{-3} M. It consequently did not show the upward swimming.

Effect of an addition of $NiSO_4$ or methylcellulose into the external solution on the geotaxis was examined and compared with that of NaN_3. Ni^{2+} ions are well known to inhibit ciliary beating and thereby decrease swimming velocity [5]. Methylcellulose decreases swimming velocity of the specimen due to increased viscosity. Some typical results are shown in Figures 10 (Ni^{2+}) and 11 (methylcellulose). The specimen showed negative geotaxis in the presence of Ni^{2+} or methylcellulose. The upward swimming velocity of the specimen decreased with increasing the concentration of Ni^{2+} or methylcellulose. The negative geotaxis in a solution with high concentration of Ni^{2+} or methylcellulose became unconspicuous due to decreased swimming velocity.

The specimens in a highly viscous methylcellulose-containing solution (2000 cP) migrated upward slowly, while they showed frequent alternation of upward and downward swimming (Fig. 11, the lowest trace). In order to understand the mechanism for the negative geotaxis in the highly viscous medium, frequency of ciliary reversal was determined in a specimen oriented either upward or downward in a methylcellulose solution. A

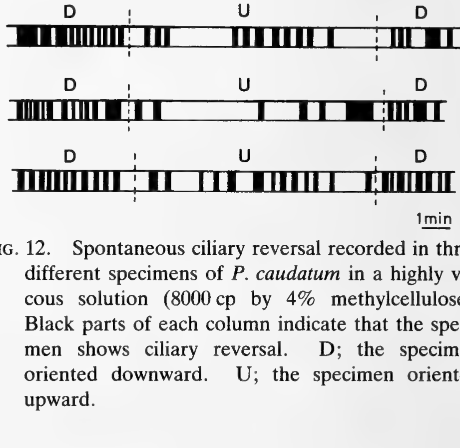

FIG. 12. Spontaneous ciliary reversal recorded in three different specimens of *P. caudatum* in a highly viscous solution (8000 cp by 4% methylcellulose). Black parts of each column indicate that the specimen shows ciliary reversal. D; the specimen oriented downward. U; the specimen oriented upward.

specimen was introduced into a small hanging drop of 4% methylcellulose solution (8000 cP) and placed on a stage of a horizontal microscope. The specimen was oriented upward or downward by rotating the stage. Three typical results are shown in Figure 12. The downward-oriented specimens showed ciliary reversal more frequently than the upward-oriented specimens.

DISCUSSION

Bean [6] found that *Chlamydomonas* did not show negative geotaxis in a thin glass tube, because of restriction of turning of the cell in the tube. Inhibition of the negative geotaxis of

Paramecium in a thin glass tube seems to be also due to restriction of its turning in the tube (Fig. 2). An increase in degree of the negative geotaxis, Gs, with culture age was correlated with a decrease in Td (Fig. 4). A decrease in Gs by starvation was correlated with an increase in Td (Fig. 6). A decrease (increase) in Td corresponds to an increase (decrease) in the probability that the specimen swimming downward turns upward. The present findings, therefore, confirmed the previous idea that the upward orientation of the specimen is an important factor for its negative geotaxis [6].

Four hypotheses have been proposed for the mechanism of the negative geotaxis in protozoans as reviewed by Kuznicki [7]. According to the pressure hypothesis by Jensen [2], a small difference in hydrostatic pressure between the upper and lower portions of the organism causes the negative geotaxis, because ciliary activity is assumed to be higher when the pressure is higher. However, Lyon [8] demonstrated that a change in the hydrostatic pressure as small as the hydrostatic pressure difference between upper and lower portions of *Paramecium* did not produce change in the ciliary activity. Present finding that the negative geotaxis is not affected by subjection of the specimen to an increasing hydrostatic pressure as it moved upward (Fig. 6) denies a possibility that decrease in the hydrostatic pressure with time causes the negative geotaxis. An abrupt decrease in the hydrostatic pressure did not affect the negative geotaxis. This finding is also unfavorable to the pressure hypothesis.

In order to understand the mechanisms by which the negative geotaxis, positive centrotaxis and negative rheotaxis are governed, Davenport [3] proposed the resistance hypothesis. According to his hypothesis, *Paramecium* orients and moves in a direction so as its energy consumption to be the highest. Since *Paramecium* is heavier than its surrounding water, upward swimming requires more energy than downward swimming. It was found that the specimens of *Paramecium* showed clear negative geotaxis in the heavy water solution with a density higher than that of *Paramecium* (Fig. 8). This finding is unfavorable to the resistance hypothesis. Platt [9] and Lyon [5] reported that ciliates such as *Paramecium* and *Spirostomum* exhibited negative geotaxis in a gum-arabic containing high density medium. This is also unfavorable to the resistance hypothesis.

Kanda [4] and Lyon [5] proposed the statocyst hypothesis for the negative geotaxis of *Paramecium*. They assumed that inclusions (granules, crystals or food vacuoles) and nuclei of the cell of *Paramecium* play a role essentially similar to the statolith in metazoan statocyst. Mechanical stimulation of inner surface of the cell membrane by the cell inclusions or nuclei might produce upward orientation of the specimen. In a methylcellulose-containing viscous solution the specimens migrated upward, while they showed frequent alternation of upward and downward swimming (Fig. 11). The specimens oriented downward in the viscous solution showed change in the swimming direction more frequently than those oriented upward (Fig. 12). This apparently causes denser distribution of the specimens in the upper portion of the tube. As shown in Figure 11, swimming velocity was higher in the specimens oriented downward than upward. The viscous resistance experienced by the specimen with its anterior end is presumably larger when it swims downward, and thereby produces more frequent ciliary reversal due to activation of mechanosensitive Ca channels in the anterior membrane [10]. This mechanism for the negative geotaxis is, however, applicable only to the case in highly viscous solution. Ciliary reversal was not necessary for establishing the negative geotaxis. Specimens of the CNR mutant [11], which is incapable of showing ciliary reversal, also exhibited the negative geotaxis as normal specimens did.

All the three hypotheses mentioned above involve some stimulus-transduction mechanisms in the cell. They therefore can be classified as physiological hypotheses.

According to Bean [6] negative geotaxis in *Chlamydomonas* was inhibited by NaN_3. The inhibition, however, was found to occur before motility of the cell was inhibited. Thus he assumed a gravity-force-sensory mechanism for the upward orientation of the cell which is more sensitive to NaN_3 than the motile mechanism. However, in *Paramecium* the negative geotaxis was inhibited in parallel with inhibition of ciliary motile activity by NaN_3 or by Ni^{2+} ions (Figs. 9 and 10).

Present results are not favorable to all the three hypotheses except for the case in a highly viscous medium. Verworn [1], Dembowsky [12, 13] and recently, Fukui and Asai [14] proposed the mechanical hypothesis. According to them, the posterior end of *Paramecium* is heavier than the anterior end. Thus a force which orients the specimen upward is produced in a gravity field. Applicability of this hypothesis will be discussed in the succeeding paper.

ACKNOWLEDGMENT

The author wishes to express his thanks to Professor Y. Naitoh of Tsukuba University for critical reading of the manuscript.

REFERENCES

1 Verworn, M. (1889) Psychophysiologische Protistenstudien, G. Fischer Verlag, Jena.

2 Jensen, P. (1893) Über den Geotropismus niederer Organismen. Pflüger's Arch. Gesamte Physiol., **53**: 428–480.

3 Davenport, Ch. B. (1897) Experimental Morphology, Macmillan Co., New York.

4 Kanda, S. (1914) On the geotropism of *Paramecium* and *Spirostomum*. Biol. Bull., **26**: 1–24.

5 Kuznicki, L. (1963) Reversible immobilization of *Paramecium caudatum* evoked by nickel ions. Acta Protozool., **6**: 301–312.

6 Bean, B. (1977) Geotactic behavior of *Chlamydomonas*. J. Protozool., **24**: 394–401.

7 Kuznicki, L. (1968) Behavior of *Paramecium* in gravity fields. I. Sinking of immobilized specimens. Acta Protozool., **6**: 109–117.

8 Lyon, E. P. (1904) On Jensen's theory of geotropism in *Paramecium*. Am. J. Physiol., **13**: 15–16.

9 Platt, J. B. (1899) On the specific gravity of *Spirostomum, Paramecium* and the tadpole in relation to the problem of geotaxis. Am. Nat., **33**: 31–38.

10 Naitoh, Y. and Eckert, R. (1969) Ionic mechanism controlling behavioral response of *Paramecium* to mechanical stimulation. Science, **164**: 963–965.

11 Takahashi, M. and Naitoh, Y. (1978) Behavioural mutants of *Paramecium caudatum* with defective membrane electrogenesis. Nature, **271**: 656–659.

12 Dembowski, J. (1929) Die Vertikalbewegungen von *Paramecium caudatum*. I. Die Lage des Gleichgewichtscentrumus in Körper des Infusors. Arch. Protistenkd., **66**: 104–132.

13 Dembowski, J. (1929) Die Vertikalbewegungen von *Paramecium caudatum*. II. Einfluss einiger Aussenfaktoren. Arch. Protistenkd., **68**: 215–260.

14 Fukui, K. and Asai, H. (1980) The most probable mechanism of the negative geotaxis of *Paramecium caudatum*. Proc. Japan Acad., Ser. B., **56**: 172–177.

ZOOLOGICAL SCIENCE 4: 789–795 (1987)

Geotactic Behavior in *Paramecium caudatum* II. Geotaxis Assay in a Population of the Specimens

Koji Taneda, Seiji Miyata[1] and Akiko Shiota

Department of Biology, Faculty of Science, Kochi University, Akebonocho 2-5-1, Kochi 780, Japan

ABSTRACT—The negative geotaxis exhibited by the specimens of *Paramecium caudatum* in an assay tube was examined. The negative geotaxis was conspicuous in the specimens from 1–2-day culture. Number of the Ni^{2+}-immobilized specimens which oriented upward in a solution with the specific density identical with that of the specimen during centrifugation was the highest in the specimens showing the highest negative geotaxis. However, no difference in the number of the upward-oriented specimens was found between two groups of the specimens, one from upper half and the other from lower half of the assay tube. This suggests less important role of the gravity-buoyancy torque in the negative geotaxis. Anterior half of the specimens showing negative geotaxis was thinner than posterior half. However, no difference in the cell shape was found between two groups of the specimens, one from upper half and the other from lower half of the assay tube. This indicates that a torque produced by difference in the drag force between the anterior and posterior halves of the specimen is not an essential factor for the negative geotaxis. The propulsion-gravity model is a remaining probable candidate for the mechanism of the negative geotaxis.

INTRODUCTION

In the preceding paper, we examined swimming path of an individual specimen of *Paramecium caudatum* in a vertical glass tube to analyze its geotactic behavior. Our results could not be satisfactorily explained on any physiological hypotheses, such as the pressure hypothesis [1], the resistance hypothesis [2] and the statocyst hypothesis [3]. We, therefore, examined applicability of physiological hypotheses to the geotactic distribution of the specimens of *Paramecium* in a vertical tube. To examine if the specific density is different between the anterior and the posterior halves of the specimen, orientation of Ni^{2+}-immobilized specimens [4] subjected to a centrifugal force was determined. The difference, if it presents, causes upward orientation of the specimen in the gravity field. We also determined the cell shape to examine the difference in the drag force between the anterior and the posterior halves of the specimen as a possible cause for the upward orientation of the specimen. We found that neither the gravity-buoyancy model of Verworn [5], which was recently supported by Fukui and Asai [6], nor the drag-gravity model of Roberts [7] was explainable for our results.

Accepted Jnue 6, 1987
Received October 18, 1985

[1] Present Address: Toyama Chemical Industry, Toyama 930, Japan.

MATERIALS AND METHODS

Specimens of *Paramecium caudatum* (strain G-3) were cultured in a test tube filled with bacterized (*Klebsiella aerogenes)* lettuce infusion at 22–24°C. Specimens obtained from culture were washed three times with a standard saline solution [8] containing 1 mM KCl, 1 mM $CaCl_2$ and 1 mM Tris-HCl (pH 7.2), and kept equilibrated in the solution for more than 10 min prior to experimentation.

Geotactic behavior of an individual specimen was examined by the method similar to that described in the previous paper [9]. Geotactic distribution of a population of the specimens was quantitatively determined by the following methods. Suspension of the specimens (10 cells /ml) was introduced into a vertical glass tube (3 cm

in inner diameter, 30 cm in length), and kept for a given period of time. The suspension in the tube was divided into two fractions, e.g. upper and lower halves, and the number of the specimens in each fraction was counted. Then the geotaxis index (Gt) was calculated according to Bean [10]. Gt is defined as:

$$Gt=\frac{Nb-(Nb+Nt)/2}{(Nb+Nt)/2},$$

where Nt is number of the specimens in the upper fraction, and Nb is that in the lower fraction.

All the experiments were done at a constant temperature of $24\pm1°C$. Some details of the experimental procedures will appear in Results section.

RESULTS

Geotactic responses in an individual specimen

Swimming path of the specimens obtained from different cultures with different culture age (1–5 days) in the vertical tube was recorded. As shown in Figure 1, the specimens from 1- or 2-day culture introduced into the bottom of the vertical tube swam upward to the top of the tube and stayed there (negative geotaxis). Most of the specimens from 3-day culture showed upward and downward swimming alternately over the full length of the glass tube. Some specimens from 4-day culture first showed negative geotaxis then showed downward swimming to the bottom of the tube and

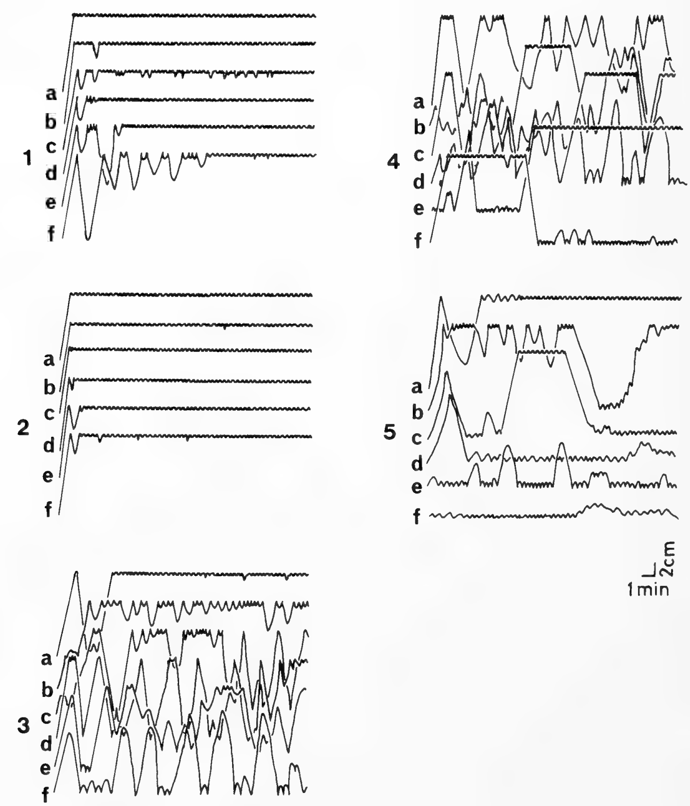

Fig. 1. Swimming path of an individual specimen of *Paramecium caudatum* in a vertical tube. Five groups of the specimens from 5 different cultures with different culture age (1–5-day; indicated by corresponding numbers at the left of each group of the records) were examined. Each group consists of 6 different specimens (labeled a–f).

stayed there (positive geotaxis), as shown in Figure 1, 4–f. Some of them showed first positive and then negative geotaxis (Fig. 1, 4–e). Number of specimens to show the positive geotaxis increased in 5-day culture (Fig. 1, 5–d, e, f).

Geotactic responses in a population of the specimens

Time-change in distribution of the specimens in the geotaxis-assay tube was examined. Homogeneous suspension of the specimens was introduced into the tube and kept undisturbed for various period of time (1–20 min). Then, the negative geotaxis index (−Gt) was determined. Time-change in −Gt is shown in Figure 2. −Gt increased quickly and reached a definite saturated level (0.84) in 5 min. Therefore, determination of −Gt was carried out after 10-min assay. Thigmotaxis of the specimen was not observable in the present assay condition.

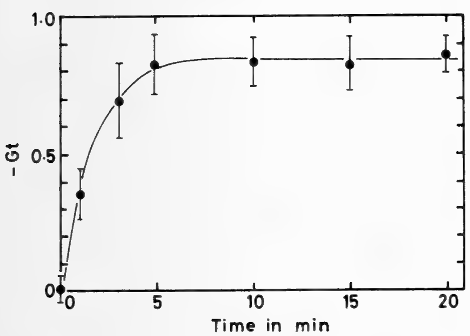

FIG. 2. Time-change in the negative geotaxis index (−Gt) of a populaiton of the specimens of *P. caudatum*. Each point is the mean obtained from 5 measurements with the specimens from 2-day culture. Vertical bars; standard deviations of the mean.

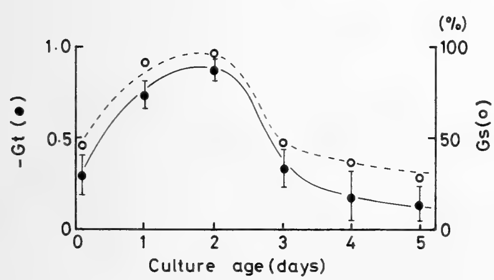

FIG. 3. Change in the negative geotaxis index (−Gt) of a population of *P. caudatum* as a function of culture age (day).

Change in −Gt as a function of culture age is shown in Figure 3. −Gt reached its maximum value (0.87) by the 2nd day of culture, then decreased to zero on the 5th day. The change in −Gt with culture age appears to correspond to the geotactic activity in each individual specimen of the population (see Fig. 1). To find correlation between the individual behavior and populational behavior, geotactic activity of individual specimen (Gs) was calculated from the data presented in Figure 1 according to Taneda [9], and the value was compared with Gt. Gs corresponds to the probability that the specimen stay in upper half of the assay tube. As shown in Figure 3, Gs changed with culture age in parallel with −Gt.

Orientation of Ni-immobilized specimens under influence of a centrifugal force

In order to examine localized difference in the specific density of the protoplasm in the cell as a possible cause for the upward orientation in the negative geotactic specimens, they were first immobilized by Ni^{2+} (0.0075% $NiSO_4$, w/v), then introduced into a vessel ($40\times20\times1$ mm^3) with a solution whose specific density was adjusted to be the same with that of the specific density was adjusted to be the same with that of the specimen (d=1.042) by adding gum arabic. They were subjected to a centrifugal force of 110 G for 30 sec. Then, the direction in which the anterior end of the specimen pointed was determined by the aid of a horizontal microscope. As shown in the upper left inset of Figure 4, a circle around each specimen was divided into 9 directional divisions (A to I) with reference to direction of the centrifugal force (an arrow labelled with g). Percent number of the specimens which pointed in each directional division was counted, and shown in Figure 4. As shown in the figures, most of the specimens from 1- or 2-day culture pointed their anterior end upward. Number of the upward-oriented specimens decreased with culture age, and the specimens from 4- or 5-day culture oriented more or less at random.

If the upward-oriented specimens swim upward

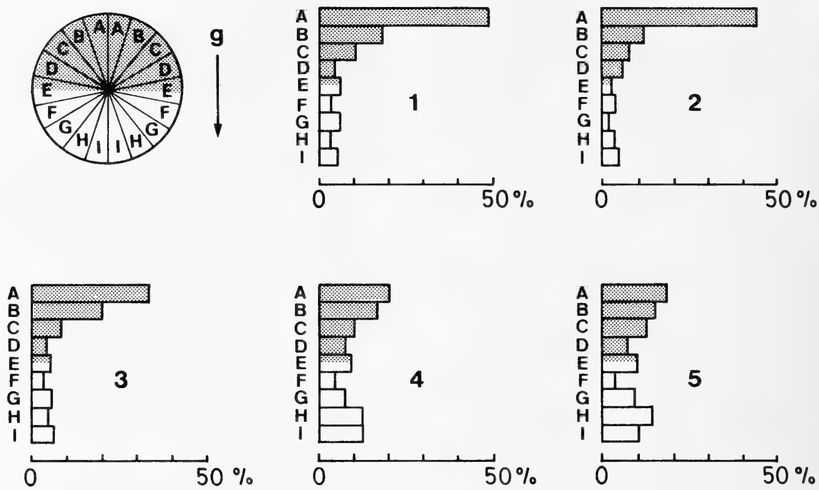

FIG. 4. Frequency distributions of the orientation of the Ni^{2+}-immobilized specimens of *P. caudatum* under the influence of a centrifugal force (110 G). Shaded columns show the specimens oriented upward. The number in each histogram shows the culture age in day. See the text for the details.

and stay in upper half of the tube, and the downward-oriented specimens swim dowanward and stay in lower half of the tube when their cilia beat, the geotaxis index of the non-motile population of the specimens, Gp, which corresponds to Gt in motile population, can be formulated as:

$$Gp = \frac{Nd-(Nu+Nd)/2}{(Nu+Nd)/2},$$

where Nd is number of the specimens oriented downward and Nu that oriented upward. $-$Gp was calculated from the data shown in Figure 4 and plotted against the culture age as shown in Figure 5. Change in $-$Gt with culture age was also

FIG. 5. Change in the geotaxis index in a population of the specimens of *P. caudatum* as a function of culture age (day). Open circle; the negative geotaxis index calculated from the data in Fig. 6 ($-$Gp). Solid circle; negative geotaxis index calculated from actual distribution of the specimens in the assay tube ($-$Gt).

presented in Figure 5 (open circles). Gt in this figure was determined with the specimens from the culture, with which determination of Gp was made. Both $-$Gp and $-$Gt were highest in the specimens from 1- or 2-day culture. However, each value of $-$Gt did not coincide with each corresponding value of $-$Gp.

In the next series of experiments, the specimens in the assay tube was divided into two groups, one presents in upper half and the other in lower half of the tube, after they were kept in the tube for more than 10 min. The specimens in each group was immobilized by Ni^{2+}, immersed into the gum arabic-containing solution and subjected to a centrifugal force (110 G) for 30 sec. Then their spacial orientation was determined. As shown in Figure 6, the distribution pattern of the orientation was identical between the two groups.

Change in the cell shape with culture age

In order to examine relationship between cell shape and geotactic activity, change in cell shape with culture age was determined. Specimen of *Paramecium* is cylinder-shaped. Thickness of the cylinder is different between anterior and posterior half of the specimen. We, therefore, measured radius of a cross section of the cell cylinder at the levels of both anterior and posterior contractile

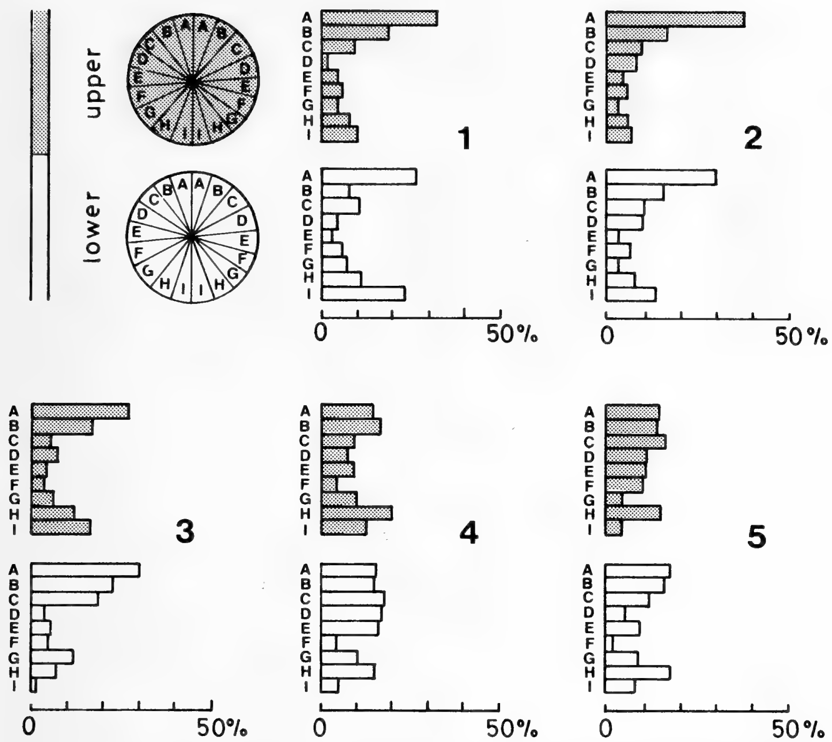

Fig. 6. Frequency distribution of the orientation of Ni^{2+}-immobilized specimens of *P. caudatum* under the influence of a centrifugal force (110 G). Open column; obtained with the specimens collected from the lower half of the assay tube. Shaded columns; obtained with the specimens collected from the upper half of the assay tube. Each number in each histogram shows the culture age. For further explanation, see the text.

vacuoles (r_a; at the anterior, r_p; at the posterior vacuole). The difference between the squares of the radii ($r_a^2-r_p^2=\Delta r^2$) was used to characterize the cell shape. When the value is negative (positive), the anterior half of the specimen is thinner (thicker) than its posterior half. Δr^2 was determined in 200 specimens from a single culture. The frequency distribution of Δr^2 for different cultures with different culture age is shown in Figure 7. Δr^2 was negative for most of the specimens from 1–2-day culture. Number of the specimens whose Δr^2 was positive tended to increase with culture age. More than half of the specimen from 5-day culture showed positive Δr^2. This indicates that the cell shape changes from its original thinner anterior-shape to thinner posterior-shape with culture age.

The specimens from 4-day culture in the assay tube were separated into two groups, one present in the upper half and the other in the lower half of the tube after they were kept in the tube for more than 10 min. Δr^2 value was determined with 200 specimens from each group and presented as a histogram (lower parts of Fig. 7). Distribution patterns of the cell shape were almost identical between these two groups.

DISCUSSION

Three physical models for the mechanism of negative geotaxis in free swimming microorganisms have been proposed: 1) the gravity-buoyancy model of Verworn [5], 2) the drag-gravity model of Roberts [7] and 3) the propulsion-gravity model of Winet and Jahn [11].

We determined the orientation of Ni^{2+}-immobilized specimens in a solution with a specific density identical with that of the specimen, under

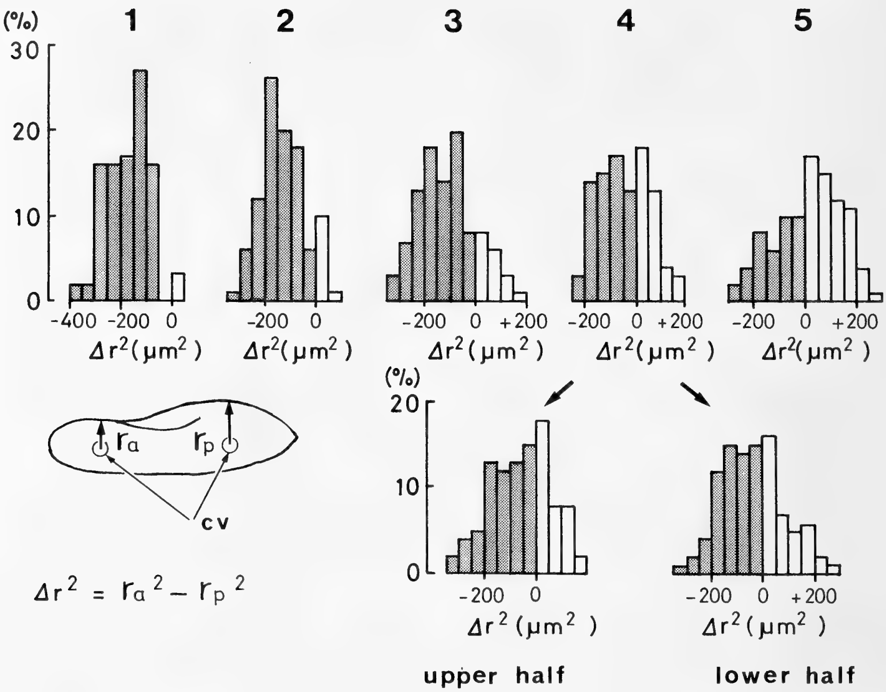

FIG. 7. Change in the shape of the specimens of *P. caudatum*. The change is presented as a change in the frequency distribution pattern of the Δr^2 value. See the lower left inset for the definition of Δr^2. Negative value of Δr^2 (shaded columns) shows that the anterior half of the specimens is thinner than the posterior half. For further explanation, see the text.

the influence of centrifugal force (110 G). As shown in Figure 4, number of the upward-oriented specimens, which are heavier in their posterior region, was larger in a population of the specimens showing stronger negative geotaxis. The geotaxis index (Gp) calculated on the assumption that the upward-oriented specimens stay in the upper half of the assay tube, while the downward-oriented specimens in the lower half of the tube, was almost identical with the geotaxis index (Gt) calculated from actual distribution of the specimens in the tube (Fig. 5). These findings are favorable to the gravity-buoyancy model for the negative geotaxis. However, our findings that histogram for the orientation of the immobilized specimens was almost identical between the two groups of the specimens, one obtained from the upper half and the other from the lower half of the assay tube (Fig. 6) indicates that the upward orientation of the specimens due to the gravity-buoyancy torque is not essential factor for the negative geotaxis.

We also determined Δr^2 which characterizes the cell shape. Δr^2 is proportional to the anterior and the posterior halves of the specimen due to difference in their sizes. As shown in Figure 7, Δr^2 changed in close association with change in the geotactic activity of the specimens. This is favorable to the drag-gravity model for the negative geotaxis. However, the histogram for Δr^2 was almost identical between two groups of the specimens, one from the upper half and the other lower half of the assay tube (see lower portion of Fig. 7). This finding strongly suggests that the cell shape is not essential factor for the negative geotaxis.

It is interesting to note that some specimens from 4-day culture showed sudden change from negative to positive geotaxis or *vice versa* (Fig. 1). According to the gravity-buoyancy model, such change should be accompanied by a sudden reversal of the portions for the center of gravity

and for the center of buoyancy in the cell. The most probable cause for such reversal is redistribution of food vacuoles in the cell. However, our observation (unpublished) proved that the food vacuoles were hardly seen in the specimens from 4-day culture. Sudden change in the cell shape is a possible cause for the change in the polarity of the geotaxis. This, however, is not examined yet.

The remaining propulsion-gravity model seems to be more reasonable for explanation of the geotactic behavior in the specimens of *Paramecium*. Examination of the model will appear in the succeeding paper.

ACKNOWLEDGMENT

We thanks Professor Y. Naitoh, University of Tsukuba, for valuable comments on the manuscript.

REFERENCES

1 Jensen, P. (1893) Über den Geotropismus niederer Organismen. Pflüger's Arch. Gesamte Physiol., **53**: 428–480.

2 Davenport, Ch. B. (1897) Experimental Morphology, Macmillan Co., New York.

3 Kanda, S. (1914) On the geotropism of *Paramecium* and *Spirostomum*. Biol. Bull., **26**: 1–24.

4 Kuznicki, L. (1963) Reversible immobilization of *Paramecium caudatum* evoked by nickel ions. Acta Protozool., **6**: 301–312.

5 Verworn, M. (1889) Psychophysiologische Protistenstudien, G. Gischer Verlag, Jena.

6 Fukui, K. and Asai, H. (1980) The most probable mechanism of the negative geotaxis of *Paramecium caudatum*. Proc. Japan Acad., Ser. B., **56**: 172–177.

7 Roberts, M. (1970) Geotaxis in motile microorganisms. J. Exp. Biol., **53**: 687–699.

8 Naitoh, Y. and Eckert, R. (1972) Electrophysiology of the ciliate Protozoa. In "Experiments in Physiology and Biochemistry", Vol. V. Ed. by G. A. Kerkut, Academic Press, London, pp. 17–38.

9 Taneda, K. (1987) Geotactic behavior in *Paramecium caudatum*. I. Geotaxis assay in individual specimen. Zool. Sci., **4**: 781–788.

10 Bean, B. (1977) Geotactic behavior of *Chlamydomonas*. J. Protozool., **24**: 394–401.

11 Winet, H. and Jahn, T. L. (1974) Geotaxis in protozoa. I. A propulsion-gravity model for *Tetrahymena* (Ciliata). J. Theor. Biol., **46**: 449–465.

ZOOLOGICAL SCIENCE 4: 797–801 (1987)

The Structure and Innervation of a New Muscle in the Tailfan of the Crayfish, *Procambarus clarkii*

Philip L. Newland

Zoological Institute, Faculty of Science, Hokkaido University, Sapporo 060, Japan

ABSTRACT—The structure and innervation of a newly discovered muscle in the exopodite of the crayfish, *Procambarus clarkii,* were examined using histochemical and electrophysiological techniques. Based on the histochemical detection of the specific activity of ATPase, the muscle was found to contain only lightly stained fibres typical of the crustacean slow type. Muscle fibres were often divided into separate subunits and had sarcomere lengths of 6–10 μm. The muscle was innervated by one excitatory axon from the second root of the sixth ganglion, and one inhibitory axon from the third root. Both the excitatory and inhibitory axons produced small junction potentials which exhibited facilitation and summation characteristic of crustacean slow muscles.

INTRODUCTION

The uropods, the paired terminal appendages of decapod crustaceans, are involved in a great variety of behavioural acts. In recent years considerable attention has focused on the uropods in terms of the muscles and the organization of their innervation [1, 2], their patterns of activation during postural movements [3] and their role in different behaviour patterns [4]. Unlike many crustacean joints that move in a single plane, such as the joints between the basal segments of the antennae [5, 6], the joints between the telson and the protopodite, and the protopodite and exopodite are mobile in a number of planes, resulting in complex movements. These movements range from a phasic streamlining of the tailfan during the extension phase of the swimming cycle [7], to slow postural movements made during steering [8].

The work of both Larimer and Kennedy [1, 2] and Takahata *et al.* [3] on crayfish, provide the most recent descriptions of the underlying musculature producing movements of the uropods. However, this work was restricted in the number of muscles examined in the protopodite and exopodite. Previous experiments (Newland, unpublished data) have shown that a new, previously undescribed muscle was located in the exopodite of the crayfish. This paper describes the structure and physiology of this new muscle.

Accepted May 6, 1987
Received February 10, 1987

MATERIALS AND METHODS

Freshwater crayfish, *Procambarus clarkii* (Girard), of both sexes (10 to 12 cm in length) were used for experiments. These animals were maintained in large aquaria and were fed regularly.

Crayfish abdomen were pinned ventral side up in a small bath containing cooled physiological saline [9]. To expose the muscle, the cuticle around the insertion was cut on three sides and a small patch of cuticle was removed. The adductor muscle was displaced laterally to allow access to the new muscle for recording. The sixth abdominal ganglion was also exposed, and the sensory bundles of the second and third roots, and the entire fourth root were cut. A small oil-hook electrode was placed on the motor nerve innervating the new muscle for extracellular recording of motor activity or stimulation. The second and third roots were stimulated using oil-hook electrodes with square wave pulses of 0.01–0.1 ms duration at various frequencies. For intracellular recordings of muscle potentials, glass microelectrodes filled with 3 M KCl and of 10–15 mΩ resistance were used. All signals were amplified and plotted using a signal

processor (Nihon-Kohden Addscope) and X–Y plotter (Rikadenki).

The procedure used for the characterization of the uropod muscles for the specific activity of ATPase was based on that of Ogonowski and Lang [10]. In brief, the uropods, telson and sixth abdominal segment were removed and quickly frozen in isopentane with liquid nitrogen. The tissues were then blocked in O. C. T. compound (Miles Scientific Co.) and mounted on the chuck of a cryostat. Serial sections of 25 μm were cut and picked up on slides coated with chrome alum-gelatine, and air-dried for 30–60 min before staining. The staining procedure used was as described by Ogonowski *et al.* [11]. Measurements of the sarcomere lengths were made directly on freshly dissected preparations which were teased apart on a microscope slide. Fibres were viewed under Nomarski optics on an Olympus Vanox microscope which was calibrated with an ocular micrometer.

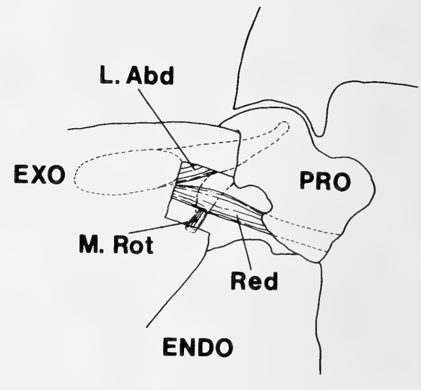

Fig. 1. Diagram showing the position of the medial rotator (M. Rot) in the exopodite (EXO) relative to the lateral abductor (L. Abd) and reductor (Red) muscles. The adductor has been omitted for clarity. The new muscle originates on a small sclerite between the exopodite and protopodite (PRO) and inserts on the ventral surface of the exopodite. The endopodite (ENDO) is also shown. Ventral view. Scale bar, 2 mm.

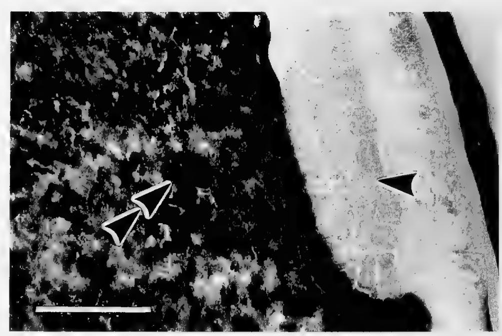

Fig. 2. Histochemical identification of 2 uropod muscles stained for the activity of myofibrillar ATPase. The new muscle (single arrowhead) stains lightly indicating the presence of slow fibres. The adductor (double arrowheads) is more intensely stained, typical of fast muscle fibres. Horizontal section through the tailfan. Some of the muscle fibres can be seen to be divided into subunits. Scale bar, 0.25 mm.

RESULTS

General morphology

Each of the previous studies on the uropod musculature has adopted a different nomenclature for the uropod muscles. In this study the nomenclature of Larimer and Kennedy [1] is used.

The location of the newly discovered muscle is shown in Figure 1. The muscle, which is relatively small in size (named here the Medial Rotator), originates on a large sclerite between the exopodite and the protopodite on the dorsal surface at its posterior margin, and inserts on the ventral surface of the exopodite. In animals of the size range used in these experiments this muscle was about 1.5 mm long and 0.5 mm in diameter. It was composed of about 15 separate fibres (Fig. 2), which were often subdivided into closely connected subunits, typical of crustacean slow muscles [12, 13]. Sarcomere lengths were determined for different regions of the muscle, and were found to be similar in all regions examined. The sarcomere lengths had a mean of 7.26 ± 0.21 μm.

When stained for myofibrillar ATPase activity, the new muscle showed a uniform light staining compared to that of the fast fibres of the adductor muscle which showed an intense dark staining (Fig. 2). The activity of myofibrillar ATPase is 2–3 times greater in crustacean fast muscles than in slow muscles [11, 14]. Consequently the fast fibres stain much more intensely.

Innervation

Stimulation of the second motor root of the sixth ganglion close to the muscle, with an increasing intensity, excited firstly an inhibitory axon followed at a higher intensity by an excitatory axon (Fig. 3). A further increase in the stimulus intensity, above that necessary to stimulate the excitatory axon, failed to recruit additional axons. Recording from different fibres of the muscle showed that all had a similar pattern of innervation. Separate stimulation of root 2 and root 3 showed that the excitor was recruited by stimulation of root 2, whereas the inhibitor was recruited by stimulation of root 3 (Fig. 4). Simultaneous stimulation of both roots often resulted in an inhibition of the excitatory junction potentials (Fig. 4). The inhibitory axon crossed from the motor branch of root 3 to that of root 2 in an area where both motor branches were in close proximity within the protopodite.

Resting potentials of the muscle fibres ranged

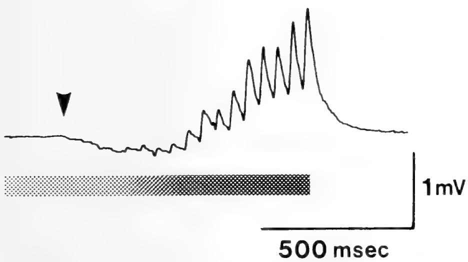

FIG. 3. Intracellularly recorded responses of the new muscle to electrical stimulation of its motor nerve with an increasing stimulus intensity. An inhibitory response is followed at a higher stimulus intensity by an excitatory response. Stimulus intensity increases linearly from left to right during the period indicated by the shaded bar (1–8 V). The beginning of the response is marked with an arrowhead. Stimulus frequency, 20 Hz.

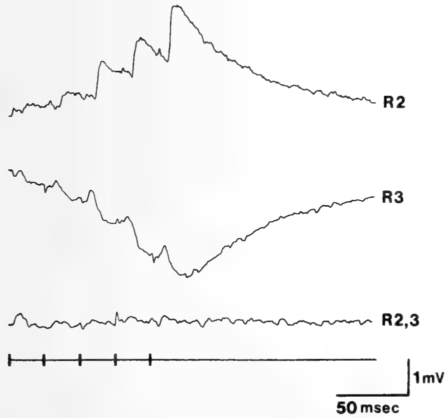

FIG. 4. Excitatory and inhibitory responses of the new muscle to electrical stimulation of different motor roots of the sixth ganglion. Upper trace, root 2 stimulation at 9.5 V (R2); second trace, root 3 stimulation at 7.5 V (R3); third trace, simultaneous stimulation of both root 2 and root 3 at 9.5 V (R2, 3). Lower trace, stimulus monitor. Stimulation of both roots results in an inhibition of ejps. Marked facilitation and summation are evident for both ejps and ijps. Stimulus frequency, 40 Hz.

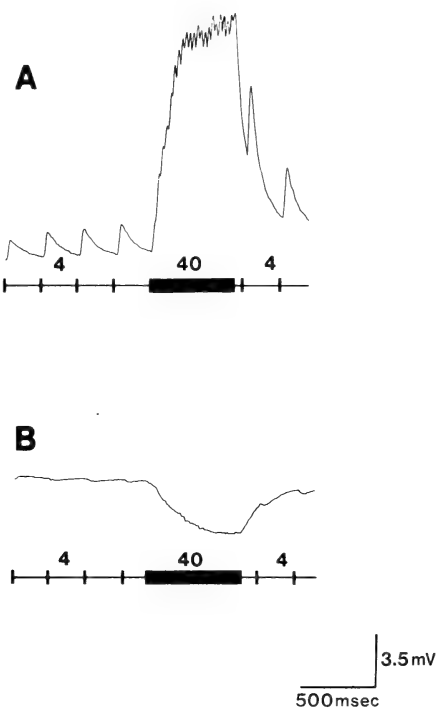

FIG. 5. Intracellularly recorded responses of the new muscle to continuous stimulation. A. Response to root 2 stimulation (7 V). B. Response to root 3 stimulation (7 V). Stimulus frequency was changed from 4 Hz to 40 Hz, and back to 4 Hz at the times indicated by the stimulus markers (lower trace of A and B). On returning to 4 Hz, post-tetanic potentiation of ejps and ijps was clearly evident. Summation and facilitation can be observed by comparing responses at 4 Hz and 40 Hz.

from −56 to −68 mV and had a mean of −64 mV. Single stimuli to root 2 resulted in small excitatory junction potentials of about 1 mV in amplitude. At stimulus frequencies greater than 4 Hz marked facilitation and summation occurred. Maximum facilitation was reached at 40 Hz where individual ejps were about 2 mV in amplitude (Fig. 5A). Summation of these ejps produced membrane depolarizations ranging from about 3 mV at 10 Hz, to 14 mV at 40 Hz.

Inhibitory junction potentials were, in general, much smaller than ejps (Fig. 5B). The largest ijps recorded at a stimulus frequency of 4 Hz were −0.35 mV in amplitude. In most cases little facilitation of these potentials occurred even at frequencies up to 40 Hz. Summation of ijps was observed at stimulus frequencies above 10 Hz, producing membrane hyperpolarizations of about −4 mV at 40 Hz.

When the stimulus frequency was reduced from a high to a low frequency, marked post-tetanic potentiation of both the ejps and ijps was observed (Fig. 5). This effect was most evident when the frequency during tetanic stimulation was between 20 Hz and 40 Hz.

DISCUSSION

In terms of structure and physiology, this new muscle exhibits characteristics that are typical of slow or tonic crustacean muscle fibres. It has muscle fibres which are divided into closely connected subunits in cross section [12], and long sarcomere lengths which are comparable to those of other tonic muscles [1, 13, 15]. Staining for ATPase activity supports this data showing all fibres to be of the slow type [10, 11]. Typical of uropod slow muscles, the junction potentials recorded never gave rise to spikes [1].

The uropods move about three axes of rotation: promotion/remotion, flexion/extension and rotation. The muscles bringing about these movements have therefore been categorised into three groups acting in these three planes [1, 3]. Based on the line of action of this new muscle, it is likely that contraction of the muscle would raise the posterior edge of the exopodite closing it on the endopodite, while the leading edge of the exopodite blade would be brought downward, tending to "cup" or rotate the exopodite blade. Therefore, the muscle has been named the medial rotator.

In view of the discovery of this new muscle, it seems possible that the interpretation of the electrical records in previous work may have led to inaccuracies in the identification of the origins of motor axons. For example, stimulation of root 2 near the muscle (Fig. 3) suggests that the inhibitory and excitatory axons both exit the sixth ganglion through root 2. However, separate stimulation of root 2 and 3 near the sixth ganglion shows that this is misleading, and that the excitatory axon actually exits through root 2, while the inhibitory axon exits through root 3 (Fig. 4). The work of Larimer and Kennedy [1] describes a clear separation of the axons in the second and third roots of the sixth abdominal ganglion. The root 2 motor neurones only innervate the closer muscles (the remotors), while the root 3 motor neurones only innervate the opener muscles (the promotors). It is not clear from the previous study exactly where the electrical activity was monitored in order to determine the origin of the motor neurones. Without monitoring this activity close to the ganglion and near the target muscle it is not possible to describe with absolute certainty, the origin of the motor neurones of these two roots. It remains to be determined how many axons actually cross; however, from the data presented here, we now know that at least one axon does cross from one root to the other. Therefore, it may be necessary to re-examine the innervation of the uropod muscles which are innervated by the second and third roots in order to clarify their origins.

ACKNOWLEDGMENTS

I am grateful to Professor M. Hisada for critically reading an early draft of this manuscript and to M. Takahashi for his help with the muscle histochemistry. This work was supported by a fellowship from the Japan Society for the Promotion of Science.

REFERENCES

1 Larimer, J. L. and Kennedy, D. (1969) Innervation patterns of fast and slow muscle in the uropods of

crayfish. J. Exp. Biol., **51**: 119–133.

2 Larimer, J. L. and Kennedy, D. (1969) The central nervous control of complex movements in the uropods of crayfish. J. Exp. Biol., **51**: 135–150.

3 Takahata, M., Yoshino, M. and Hisada, M. (1985) Neuronal mechanisms underlying crayfish steering behaviour as an equilibrium response. J. Exp. Biol., **114**: 599–617.

4 Newland, P. L. (1985) The control of escape behaviour in the Norway lobster, *Nephrops norvegicus*. Ph. D. Thesis, University of Glasgow, Scotland.

5 Vedel, J.-P. (1980) The antennal motor system of the rock lobster: competitive occurrence of resistance and assistance reflex patterns originating from the same proprioceptor. J. Exp. Biol., **87**: 1–22.

6 Vedel, J.-P. and Monnier, S. (1983) Reflex reversal resulting from active movements in the antenna of the rock lobster. J. Exp. Biol., **101**: 121–133.

7 Webb, P. W. (1979) Mechanics of escape responses in crayfish (*Orconectes virilis*). J. Exp. Biol., **79**: 245–263.

8 Yoshino, M., Takahata, M. and Hisada, M. (1980) Statocyst control of the uropod movements in response to body rolling in crayfish. J. Comp. Physiol., **139**: 243–250.

9 Van Harreveld, A. (1936) A physiological solution for freshwater crustaceans. Proc. Soc. Exp. Biol. Med., **34**: 428–432.

10 Ogonowski, M. M. and Lang, F. (1979) Histochemical evidence for enzyme differences in crustacean fast and slow muscle. J. Exp. Zool., **207**: 143–151.

11 Ogonowski, M. M., Lang, F. and Govind, C. K. (1980) Histochemistry of lobster claw-closer muscles during development. J. Exp. Zool., **213**: 359–367.

12 Parnas, I. and Atwood, H. L. (1966) Phasic and tonic neuromuscular systems in the abdominal extensor muscles of the crayfish and rock lobster. Comp. Biochem. Physiol., **18**: 701–723.

13 Sherman, R. G. and Atwood, H. L. (1971) Structure and neuromuscular physiology of a newly discovered muscle in the legs of the lobster, *Homarus americanus*. J. Exp. Biol., **176**: 461–474.

14 Lehman, W. and Szent-Györgyi, A. G. (1975) Regulation of muscular contraction: Distribution of actin and myosin control in the animal kingdom. J. Gen. Physiol., **66**: 1–30.

15 Lang, F., Govind, C. K. and Costello, W. J. (1978) Experimental transformation of muscle fiber properties in lobster. Science, **201**: 1037–1039.

ZOOLOGICAL SCIENCE 4: 803–811 (1987)

Changes in Blood Volume after Hemorrhage and Injection of Hypertonic Saline in the Conscious Quail, *Coturnix coturnix japonica*

YOSHIO TAKEI and IPPEI HATAKEYAMA

Department of Physiology, Kitasato University School of Medicine, 1–15–1 Kitasato, Sagamihara, Kanagawa 228, Japan

ABSTRACT—Continuous changes in blood volume after hemorrhage or injection of hypertonic NaCl solution were measured in the conscious quail, *Coturnix coturnix japonica.* Initially, an intravenous injection of 0.1 ml of 2.5% Evans blue was made into birds, and the rate of disappearance of the dye from the circulation more than 10 hr after injection was estimated by fitting the concentrations in plasma measured prior to the 10 hr point to a dual exponential function. The estimated dye concentrations fell within 95% confidence intervals of 3.7–6.9% from the measured values for 4 hr. Then, the change in blood volume was calculated in different birds from changes in the dye concentration in plasma and in the hematocrit, after hemorrhage or injection of hypertonic saline was applied 10 hr after injection of dye. It was found that the response of blood volume to 1 ml of hemorrhage, which amounted to 12.5% of total blood, was quick; blood volume overshot the level prior to hemorrhage within 15 min. Blood volume also responded quickly to an intravenous injection of 0.1 ml of 7% NaCl, which theoretically increases Na concentration of extracellular fluids by 3.6%; blood volume increased immediately after injection, and the maximal increase was attained after 45 min. These changes in blood volume were compatible with the changes in the hematocrit, blood pressure and plasma Na concentration after hemorrhage or injection of hypertonic saline.

INTRODUCTION

It is generally accepted that volemic regulation of body fluid in terrestrial animals is achieved primarily by drinking (input) and urinary excretion (output). Thus, it is a common practice in the study of volemic regulation to measure continuously those parameters that influence drinking and production of urine after manipulation of hydromineral balance [1]. These parameters are blood volume, plasma osmolality, plasma electrolyte concentrations, blood pressure, and plasma levels of hormones which are involved in hydromineral metabolism. We reported recently that the quail drank in response to hemorrhage or an intravenous injection of hypertonic NaCl solution [2, 3]. Since drinking is regulated primarily by blood volume, plasma osmolality and plasma angiotensin II concentration [4], we attempted to measure these parameters continuously after hemorrhage and injection of hypertonic saline. We could measure plasma osmolality and plasma angiotensin II concentration continuously, but we could not find a technique suitable for continuous measurement of blood volume in such small animals as quail whose blood volume is less than 10 ml.

The present study was undertaken, first, to establish a reliable technique for continuous measurement of blood volume. The technique should be sensitive enough to be applicable to small animals such as the quail. Evans blue was used as a tracer to determine plasma volume, since this dye binds strongly to plasma proteins and, thus, leaves the circulation slowly [5]. Then the technique was applied to measurements of changes in blood volume that follow hemorrhage or injection of hypertonic saline in the conscious quail. The changes in blood pressure and plasma Na concentration were also measured after these procedures to evaluate the reliability of the

Accepted May 15, 1987
Received April 18, 1987

measurements.

MATERIALS AND METHODS

Animals

Male Japanese quail, *Coturnix coturnix japonica,* aged 3 weeks, were purchased from a quail farm (Suzukei, Toyohashi) and kept, 5 to a cage ($45 \times 45 \times 90$ cm), under a natural photocycle in August, September and October, in Japan, at 22 ± 1°C. Commercial quail diet containing 150 mEq/kg of Na (Nippon Haigo Shiryo, Yokohama), and tap water were given *ad libitum,* unless otherwise specified. The birds were acclimated to these conditions for longer than 2 weeks before use, and weighed 108 ± 8 g (mean $\pm$ SD, $n=34$) at the time of experiment.

Surgery

For measurements of blood volume and plasma Na concentration, the quail were anesthetized by an intraperitoneal (ip) injection of Nembutal (40 mg/kg), and a U-shaped polyethylene catheter (o. d.: 0.8 mm) was inserted cephalad into the right external jugular vein by 4 cm. The tip of the catheter was located at the neck region where blood was constantly circulating. For measurements of blood pressure, quail were lightly anesthetized by an ip injection of urethane (0.3 g/kg), and a polyethylene catheter (o. d.: 0.61 mm) was inserted caudad through the right external jugular vein into the atrium, and another polyethylene catheter (o. d.: ca. 1 mm) made from a thicker catheter by heating and pulling, was inserted caudad into the right common carotid artery. Less than 0.05 ml of blood was lost during each surgery. The jugular catheter was filled with saline containing calcium heparin (10 U/ml) when not in use.

Experimental protocol

Pilot experiment After more than 18 hr of postoperative recovery, 0.1 ml of 2.5% Evans blue (Wako Pure Chemical., Tokyo) in 0.9% NaCl was injected in 10 sec through the jugular catheter, and followed by a flush with 0.1 ml of 0.9% NaCl. Dead space in the catheter was approximately 0.03 ml. Blood samples (50 μl) were taken just before injection of dye and at 0.25, 0.5, 0.75, 1, 3, 6, 9, 10, 11, 12, 13, 14 and 24 hr after the injection. Blood was collected directly into heparinized hematocrit tubes, and the blood that remained in the catheter was reintroduced into the circulation with 0.03 ml of heparinized saline. After measurement of the hematocrit, 10 μl of plasma was diluted into 0.5 ml of distilled water in duplicate. Absorbances at 624 nm were determined in a spectrophotometer (Hitachi 124) with a microcuvette. The linearity of the dilution curve had been confirmed. Plasma collected before injection of dye was used as a plasma blank for spectrophotometry. Nielsen and Nielsen [6] pointed out considerable variations of the absorbance at 620 nm in the human plasma collected consecutively from the same subject. Thus, they recommended to correct each dyed plasma sample measured at 620 nm with the blank absorbance of the same sample which was calculated from the absorbance at 740 nm. However, we did not make the correction in this experiment, because we measured absorbances of diluted plasma samples at 620 nm which were collected from 3 birds on the time schedule mentioned above without injection of the dye, and found that the absorbance was small and consistent (0.0017 ± 0.0004, mean $\pm$ SD, $n=42$).

The rate of disappearance of dye from the circulation more than 10 hr after injection was then estimated by fitting the absorbances measured before the 10 hr time point to a dual exponential function ($A_t = ae^{-\alpha t} + be^{-\beta t} + c$), where A_t is the absorbance at time t, and a, b, c, α and β are constants. A constant (c) was added to the function because the dye remaining in the circulating blood as long as 5 days after injection, as observed in the present study, appeared to be assumable as a constant during the experimental period of 24 hr. The fitting was done with a 3-step *regula falsi* method which was principally based on the "peeling" method [7]. The outline of the 3-step *regula falsi* method was:

(1) The constant, c, of the dual exponential function was determined by fitting the later set of data before the 10 hr point to a single exponential function with a constant ($A_t = de^{-\gamma t} + c$), where d and γ are dummy parameters. The later sets of

data were those measured 1–10 hr, 3–10 hr, and 6–10 hr after injection of dye.
(2) The constants, a and α, were determined by fitting the earlier set of data to a single exponential function ($A_t - c = ae^{-\alpha t}$), where c is now constant. The earlier sets of data were those measured 0.25–0.5 hr, 0.25–0.75 hr, 0.25–1 hr, and 0.25–3 hr after injection of dye.
(3) The constants, b and β, were determined by fitting all data before the 10 hr point (0.25–10 hr) to a single exponential function ($A_t - c - ae^{-\alpha t} = be^{-\beta t}$), where a, α and c are now constant.
The fitting to a single exponential function at each step was done by the *regula falsi* method. The computer program was written in APL and run on an IBM 4341 computer. The program will be supplied on request. Among all combinations of earlier and later sets of data, the best combination was selected with a criterion that the data more than 10 hr after injection of dye could be estimated best, that is, squares sum of relative residuals (estimated value/measured value−1) on 11–24 hr data was minimal. An example that shows a fitness of the estimated absorbances to the measured values is illustrated in Figure 1a.

Change in blood volume after hemorrhage or injection of 7% NaCl Blood samples (50 μl) were collected up to 10 hr after injection of dye, according to the time schedule described for the pilot experiment. Immediately after the sampling at 10 hr, hemorrhage (0.5 or 1 ml) was induced (n=4 each) or 0.1 ml of 7% NaCl was injected intravenously (n=4), both of which procedures were followed by injection of 0.03 ml of heparinized saline. Samples of blood were taken 0.25, 0.5, 0.75, 1, 2, 3, 4 and 14 hr after each procedure. An example that shows a deviation of the absorbances from the estimated values after injection of 7% NaCl is illustrated in Figure 1b. Time controls (n=4) were prepared for the birds that were induced to hemorrhage in which no procedure was applied at 10 hr and blood samples were collected on the same time schedule as described above. As controls for the birds that were injected with 7% NaCl, 4 birds were injected with 0.1 ml of 0.9% NaCl at 10 hr. Water was withheld for 4 hr after each procedure to eliminate the influence by induced water intake on blood volume. Plasma

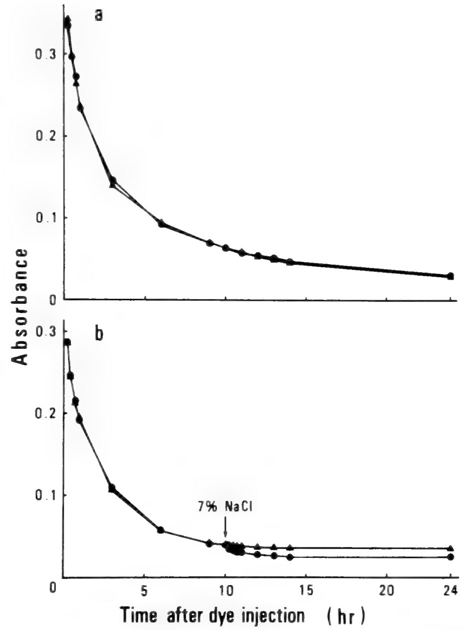

FIG. 1. a. An example of the fitness of estimated absorbances of Evans blue (▲) to the measured values (●) in a quail, after intravenous injection of the dye. The estimation was made with the best combination data measured prior to the 10 hr point as described in the text. The multiple correlation coefficient was 0.999.
b. An example that exhibited a deviation of absorbances, measured after intravenous injection of 0.1 ml of 7% NaCl (●), from the estimated values (▲) in a quail. The multiple correlation coefficient was 0.962.

volume after the treatment (PV′) was calculated by the equation: $PV' = PV \times A_e / A'$, where PV is plasma volume before treatment, A_e and A' are absorbances estimated and measured after the treatment, respectively. PV was determined by the equation: $PV = 5(A_r - A_r')/(A_0 - A_b)$, where A_r, A_r', and A_b are absorbances of a reference standard, a blank for the reference, and the plasma blank, respectively. A_0 was determined by extrapolating the data measured between 0.25 and 1 hr to time 0 with a single exponential function ($A_t = ae^{-\alpha t} + b$) with a *regula falsi* method. The reference standard was prepared by additions of 0.1 ml of the 2.5% dye solution and 0.1 ml of 0.9% NaCl to 5 ml of 1% bovine serum albumin (BSA, Wako Pure Chemical., Tokyo) in 0.9% NaCl.

One percent BSA in 0.9% NaCl was used as the blank for the reference. Blood volume was calculated by correction of the plasma volume with hematocrit. The hematocrit was not corrected for trapped plasma. The change in blood volume was also calculated from changes in hematocrit alone (hematocrit method) to allow comparison with the present method employing Evans blue.

Measurements of blood pressure and Na concentration in plasma Changes in blood pressure was monitored following 1 ml of hemorrhage, and intravenous injection of 0.1 ml of 0.9 or 7% NaCl in the lightly anesthetized quail. The hemorrhage (n=4) and the injection of NaCl solutions (n=5) were made in different birds. The signal from the transducer was amplified by a carrier amplifier (Type 3126, Yokogawa Electric Works Ltd.) and recorded by a pen recorder (Rectigraph 85, San-ei Instrument Co. Ltd.), while the signal after amplification was also stored in a data recorder (R–260, TEAC) for further analyses.

Concentrations of Na ions in plasma were measured 0, 0.25, 0.5, 0.75, 1, 2, 3, 4 and 14 hr after 0.5 ml of hemorrhage, 1 ml of hemorrhage, or intravenous injection of 0.1 ml of 7% NaCl. Controls were prepared for each procedure as described for the measurement of blood volume. According to the above time schedule, 30 μl of blood was collected into heparinized hematocrit tubes (Terumo), centrifuged, and 2 μl of plasma was diluted in 4 ml of double distilled water in duplicate. The concentration of Na ions was determined with an atomic absorption spectrophotometer (Hitachi 180–80). Double distilled water collected in the hematocrit tube was diluted as above, and used as a blank for plasma samples. The absorbance of the blank was always less than 0.1% of that of diluted plasma samples.

Statistical analyses

All results are expressed as means$\pm$SD or $\pm$95% confidence interval. In order to make clearer the change in blood volume after hemorrhage or injection of hypertonic saline, the change in each bird was expressed in terms of a ratio to the initial blood volume, and mean of the initial blood volume was given in the text. Since blood volume and concentration of Na ions in plasma at each time point after hemorrhage or injection of hypertonic saline are not independent on each other, the data concerning changes with time in blood volume and plasma Na concentration were treated as time-series data and analyzed *en bloc* by the sign test or Hotelling T-test [8]. Statistical significance and rejection of null hypothesis were achieved when $P<0.05$. All computations were carried out with an IBM 4341 computer using an APL interpreter.

RESULTS

Plasma volume in water-replete quail was 4.75 ± 1.03 ml/bird (n=34). Blood volume, corrected by the hematocrit ($40.7\pm5.9\%$, n=34), was 8.04 ± 1.56 ml/bird or 7.47 ± 1.47 ml/100 g body weight (n=34).

Pilot experiment

The concentrations of dye more than 10 hr after injection were estimated best when the 0.25–0.5 hr and 3–10 hr data were applied to the dual exponential function as earlier and later sets of data, respectively, as described in Materials and Methods. The mean deviations of the estimated concentrations of dye from the measured values were −0.5, 4.9, 2.9, 10.5 and 34.7% after 1, 2, 3, 4, and 14 hr of estimation, respectively. The time-series analysis by the Hotelling test showed that the values thus estimated were biased significantly towards values greater than the measured values. Therefore, the estimated values were corrected by the deviation at each time point for calculations of the changes in blood volume, in the following experiments. The estimated values thus corrected fell within 95% confidence intervals of ±3.7, ±5.6, ±6.9, ±6.6 and $\pm16.0\%$ from the measured values after 1, 2, 3, 4 and 14 hr of estimation, respectively.

Changes in blood volume

Blood volume returned to the level prior to hemorrhage between 1 and 2 hr after withdrawal of 0.5 ml of blood (6.2% of total blood volume), while recovery from hemorrhage was quicker (within 15 min) after larger volume (1 ml) of hemorrhage (Fig. 2a, b). The time-series analysis

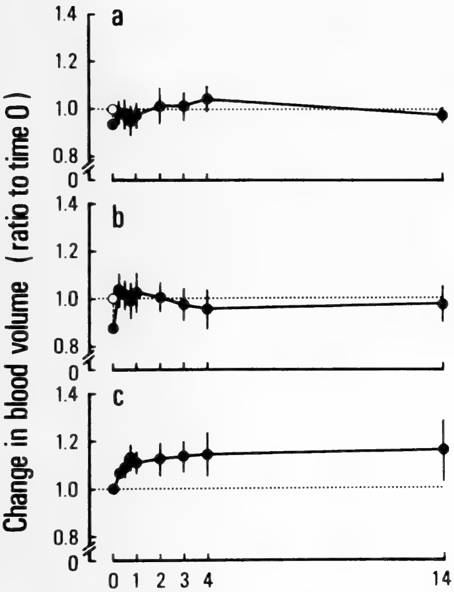

FIG. 2. Time course of change in blood volume after (a) 0.5 ml of hemorrhage, (b) 1 ml of hemorrhage, and (c) intravenous injection of 0.1 ml of 7% NaCl, calculated from changes in the concentration of Evans blue in plasma and in the hematocrit in the quail (n=4 each). Changes in blood volume were expressed in terms of ratios to the values before treatments. Average blood volumes before treatment were (a) 7.24±1.08 ml, (b) 8.26±0.51 ml, and (c) 7.77±0.32 ml. The changes after hemorrhages and injection of 7% NaCl were corrected by mean changes in time controls and 0.9% NaCl-injected controls, respectively. Values are means± SD.

showed that the level of blood volume for 14 hr after hemorrhage was greater than the level just after hemorrhage, but was not different from the level prior to hemorrhage in both groups subjected to 0.5 and 1 ml of hemorrhage. There was no significant change in blood volume in time controls.

Blood volume increased immediately after intravenous injection of 0.1 ml of 7% NaCl, and the maximal increase of 12.5% was achieved after 45 min (Fig. 2c). The increase became smaller thereafter but the level was still greater than the level prior to injection after 14 hr. The increase for 14 hr after injection was statistically significant. In controls injected with 0.1 ml of 0.9% NaCl, there was a transitory increase in blood volume due to the volume of saline injected, but the blood volume returned to the level prior to injection within 1 hr.

Hematocrit method for determination of changes in blood volume

The pattern of changes in blood volume after hemorrhage determined by the hematocrit alone was similar to that determined by the present method that employs Evans blue (Fig. 3a, b). However, the initial increase appears to be greater by the hematocrit method, and blood volume overshot the previous level within 15 min after both 0.5 and 1 ml of hemorrhage (Fig. 3a). Blood volume appeared scarcely to increase during the 1 hr period after intravenous injection of 0.1 ml of

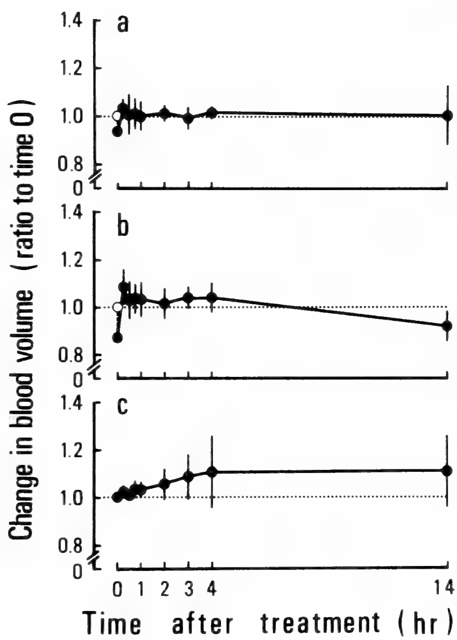

FIG. 3. Time course of change in blood volume after (a) 0.5 ml of hemorrhage, (b) 1 ml of hemorrhage, and (c) intravenous injection of 7% NaCl, calculated from the change in hematocrit alone, in the quail (n=4 each). The data were obtained from the same birds as in Fig. 2. Changes in blood volume after hemorrhages and injection of 7% NaCl were expressed in terms of ratios to the values before treatments, and corrected by the changes in corresponding controls as detailed in Fig. 2. Values are means±SD.

7% NaCl, when the change was determined by the hematocrit method (Fig. 3c). Blood volume increased thereafter and the maximal increase was 10% 14 hr after injection.

Change in blood pressure

The mean blood pressure of the quail lightly anesthetized with urethane was 117.8±13.8 mm Hg (n=14). Blood pressure decreased by 40.0±9.9% (n=4) after 1 ml of hemorrhage, but the level was restored in 11.6±4.0 min. Blood pressure increased by 35.3±3.0% (n=5) after intravenous injection of 0.1 ml of 7% NaCl and returned to the level prior to injection in 6.8±2.3 min. In 4 of 5 cases, blood pressure decreased further below the pre-injection level thereafter. In controls injected with 0.9% NaCl, the increase in blood pressure was 13.0±2.8% (n=5), which disappeared in 1.5±0.5 min.

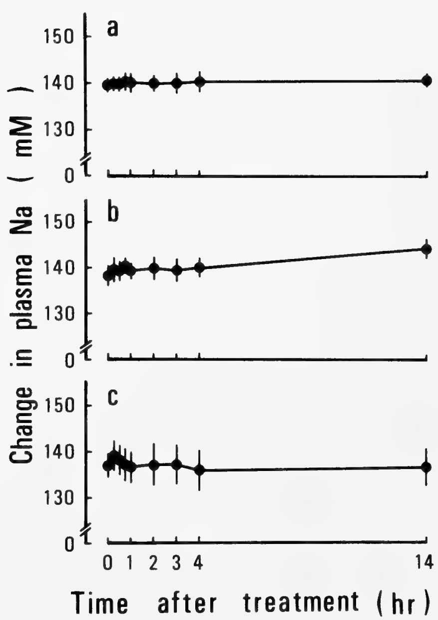

FIG. 4. Time course of change in plasma Na concentration after (a) 0.5 ml of hemorrhage (n=5), (b) 1 ml of hemorrhage (n=5), and (c) intravenous injection of 0.1 ml of 7% NaCl (n=6) in the quail. Changes in Na concentration after hemorrhage and injection of 7% NaCl was corrected by the mean changes in time controls and 0.9% NaCl-injected controls, respectively. Values are means±SD.

Change in concentration of Na ions in plasma

The concentration of Na ions in plasma in intact birds was 139.4±4.7 mM (n=17). Plasma Na concentrations tended to increase after both 0.5 and 1 ml of hemorrhage (Fig. 4a, b). The time-series analysis showed that the increase for 14 hr was statistically significant in both groups. The levels of Na ions returned to normal 45 min after intravenous injection of 0.1 ml of 7% NaCl, which theoretically increases Na concentration in extracellular fluids by 3.6%. The level decreased further below the pre-injection level thereafter (Fig. 4c). Thus, the time course of change in plasma Na concentration for 14 hr was not significantly different from the normal level after injection of 7% NaCl. The levels of Na ions in plasma did not change in time controls for hemorrhage, and in controls injected with 0.9% NaCl.

DISCUSSION

Two techniques have, thus far, been established for continuous measurement of blood volume. The first method consists of the injection of a known amount of ^{51}Cr-tagged red blood cells into the circulation, with a continuous monitoring of radioactivity in an extracorporeal arterio-venous shunt loop, and has been tested in anesthetized dogs [9, 10] and conscious rats [11]. This technique enables continuous monitoring of blood volume in its true sense, but, due to a considerable volume of blood required for external circulation, it cannot be applied to the quail which has only 8 ml of blood. The other technique follows the change in blood volume by means of the changes in hematocrit and concentration of hemoglobin [12]. This technique scarcely disturbs homeostasis of the animal and, thus, is suitable for use in the human in whom experimental manipulations should be avoided [13]. However, accurate measurement is impossible if red blood cells are released from the storage sites during the experiment. This technique has been applied to the sheep fetus, in which release of red blood cells is not significant [14]. In adult mammals, however, the spleen is known to act as a blood reservoir and, even in splenectomized dogs, red blood cells are released into the

circulation after injection of vasoactive drugs [15].

In the present study, we attempted to monitor the change in blood volume by measuring both plasma volume and hematocrit at the same time. Evans blue was used as a tracer for measurement of plasma volume, because it has been shown to bind strongly to plasma proteins and scarcely to escape from the vascular space [5]. In the present study, however, Evans blue seems to disappear rather quickly from the circulation as illustrated in Figure 1. This is partly because we injected a considerable amount of dye (2.5 mg/bird) to ensure high absorbance 10 hr after injection of dye (0.060 ± 0.002 after 1/51 dilution, $n=20$), and thus dyes unbound to plasma proteins might escape from the circulation during the initial phase after injection. Our preliminary experiment using polyacrylamide gel electrophoresis showed, however, that all the dyes bound to plasma proteins within 15 min after injection of this amount of dye into the quail (Takei and Ihara, unpublished observation). Thus, the quick disappearance of dye appears to be due to a high metabolic rate in birds. We adopted a dual exponential function to simulate the disappearance of dye from circulation, because semi-log plot of the disappearance curve resulted in a diagonal line which signifies an involvement of two exponential terms, and because two major routes of excretion of the dye have been reported in mammals, the reticulo-endothelial system and the liver [5]. In fact, fitting all the data measured during the 24 hr period to the dual exponential function invariably produced multiple correlation coefficients of more than 0.998 in the pilot experiment of this study. Furthermore, spleens and livers of the quail were found to be stained deep blue at post-experimental autopsy.

It seems that ^{51}Cr-tagged red blood cells might be a better tracer for monitoring the change in blood volume, because the decay of the tracer should be slower and, thus, the estimation of future decay could be made with a greater accuracy than in the case of Evans blue. However, in many institutions like ours, the use of radioactive materials in *in vivo* studies are strictly limited because of the lack of facilities to dispose of experimental animals contaminated with radioactive materials. On the other hand, the present technique could be utilized in the laboratories equipped only with a spectrophotometer and a microcomputer. Thus, the present technique has an advantage to be utilized in almost any laboratories.

It has been shown that the estimation of the dye concentration could be made within the range of 6.9% from the measured values for 4 hr with more than 95% confidence, while hemorrhage and injection of 7% NaCl caused much greater changes in the dye concentration. In view of this fact, this technique seems to be reliable. For the accurate measurement, however, the rate of disappearance of dye from the circulation should not be modified by hemorrhage or injection of hypertonic saline. Thus, we will discuss below the reliability of the present measurement in relation to this problem by comparing the change in blood volume with changes in hematocrit, blood pressure and plasma Na concentration after hemorrhage and injection of hypertonic saline.

It is rather surprising that blood volume overshot the previous level within 15 min after 1 ml of hemorrhage. This overshot was also observed when the change in blood volume was assessed by changes in hematocrit alone. Stallone and Braun [16] examined the validity of hematocrit as an indicator for the change in blood volume in the domestic fowl, and found that the change in blood volume measured by hematocrit alone after isosmotic volume expansion or hemorrhage was similar to the change measured by ^{51}Cr-labeled red blood cells. Furthermore, the present study showed that blood pressure returned to the normal level within 15 min after 1 ml of hemorrhage. We also observed that, 15 min after hemorrhage, blood flooded from the jugular catheter more vigorously than before hemorrhage, indicating that venous pressure was elevated due to an increased expansion of volume in this low pressure side of the circulation. These observations support the quick restoration of blood volume after hemorrhage. In other avian species, it is shown that blood volume restored quickly after 10 and 20% of hemorrhage in the domestic fowl [16], because the maximal decrease in hematocrit was completed 5 min after each hemorrhage. In the pigeon,

Kaufman and Peters [17] showed that plasma volume was restored within 4 hr after hemorrhage when the change was measured by the change in hematocrit.

Blood volume increased immediately after injection of 7% NaCl, and the maximal increase was 12.5% after 45 min. Ruch and Hughes [18] also reported that in a few species of birds, the volume of extracellular fluid increased immediately after an intravenous injection of hypertonic NaCl solution. The increase in Na concentration in extracellular fluid should be 3.56% after injection of 0.1 ml of 7% NaCl; extracellular Na concentration is 139.4 mM (present study) and extracellular space is approximately 23% of body weight in birds [19]. If injected excess Na ions were diluted only by practically Na-free cellular fluid and all the cellular water entered the vascular space, and if no Na ions were excreted during that time, the increase in blood volume should be 10.2%. Thus, the maximal increase in blood volume in the present study is more than the maximal increase expected theoretically. One interpretation of this result is that the excretion of the dye was stimulated after injection of hypertonic saline due to increases in volume and pressure of blood, which results in a false increase in blood volume. However, blood pressure rather decreased more than 7 min after injection of 7% NaCl as shown in the present study. Thus, another interpretation is that decreased blood pressure stimulated an influx of interstitial fluid into the vascular space. This interpretation also explains the sustained increase in blood volume for 14 hr after injection of the hypertonic saline, although the data at 14 hr are not so reliable as those by 4 hr after injection. On the other hand, the maximal increase in blood volume was attained 45 min after injection of 7% NaCl, which coincides well with the restoration of plasma Na concentration to normal that occurs 45 min after injection. The blood volume scarcely increased for 1 hr after injection of 7% NaCl when the change was measured by hematocrit alone. This result may be due to a release of red blood cells after the hyperosmotic volume expansion.

The present study showed that, when an acute reduction of blood volume was induced in the quail, the compensation of blood volume exceeded the previous reduction. The degree and rate of the compensation were greater as the reduction was greater. It is also shown that, when an acute increase in plasma Na ions was induced in the quail, the increase in blood volume was more than that required to dilute the increased Na ions to the previous level. These excess responses to exogenous acute alterations seem to occur often in many biological systems, when the system possesses a mechanism to respond quickly to the alterations. For instance, Drischel [20] reported that, when glucose was injected into the circulation, blood glucose level rather decreased after a brief increase for a few minutes in the rat. These phenomena are generally termed ‘rebound phenomenon’ [21], or ‘overcompensation’ in the cybernetic terms. It is likely that the responses of blood volume to hemorrhage and injection of hypertonic saline in the quail of the present study may exemplify these phenomena.

ACKNOWLEDGMENTS

The authors express their appreciation to Dr. Toshiro Sato, Department of Internal Medicine, Kitasato University School of Medicine, and to Dr. Tetsuya Hirano, Ocean Research Institute, University of Tokyo, for their critical reading of the manuscript. We also thank Ms. Junko Okubo and Sanae Nishida for technical assistance. This investigation was supported in part by a Grant-in-Aid from the Ministry of Education, Science and Culture, Japan (574307).

REFERENCES

1 Guyton, A. C., Hall, J. E., Manning, R. D., Jr., Norman, R. A., Jr., and DeClue, J. W. (1978) A systems analysis of volume regulation. In “Osmotic and Volume Regulation”. Ed. by C. B. Jørgensen and E. Skadhauge, Munksgaard, Copenhagen, pp. 283–294.

2 Kobayashi, H. and Takei, Y. (1982) Mechanisms for induction of drinking with special reference to angiotensin II. Comp. Biochem. Physiol., **71A**: 485–494.

3 Takei, Y., Uemura, H. and Kobayashi, H. (1985) Angiotensin and hydromineral balance: With special reference to induction of drinking behavior. In “Current Trends in Comparative Endocrinology”. Ed. by B. Lofts and W. N. Holmes, Hong Kong Univ. Press, Hong Kong, pp. 933–936.

4 Fitzsimons, J. T. (1972) Thirst. Physiol. Rev., **52**: 468–561.

5 Gregersen, M. I. and Rawson, R. A. (1959) Blood volume. Physiol. Rev., **39**: 307–342.

6 Nielsen, M. H. and Nielsen, N. C. (1962) Spectrophotometric determination of Evans blue dye in plasma with individual correction for blank density by a modified Gaeblers method. Scan. J. Clin. Lab. Invest., **14**: 605–617.

7 Mancini, P. and Pilo, A. (1970) A computer program for multiexponential fitting by the peeling method. Comput. Biomed. Res., **3**: 1–14.

8 Hotelling, H. (1936) Relations between two sets of variables. Biometrika, **28**: 321–377.

9 Leonard, J. I. and Abbrecht, P. H. (1974) A method for continuously monitoring blood volume. J. Appl. Physiol., **36**: 506–508.

10 Tanaka, Y., Morimoto, T., Miki, K., Nose, H. and Miyazaki, M. (1981) On-line control of circulating blood volume. Jpn. J. Physiol., **31**: 427–431.

11 Nose, H., Morita, M., Yawata, T. and Morimoto, T. (1986) Continuous determinantion of blood volume on conscious rats during water and food intake. Jpn. J. Physiol., **36**: 215–218.

12 Dill, D. B. and Costill, D. L. (1974) Calculation of percentage changes in volumes of blood, plasma, and red cells in dehydration. J. Appl. Physiol., **37**: 247–248.

13 Hubbard, R. W., Matthew, W. T., Horstein, D., Francesconi, R., Mager, M. and Sawka, M. N. (1984) Albumin-induced plasma volume expansion: Diurnal and temperature effects. J. Appl. Physiol., **56**: 1361–1368.

14 Brace, R. A. (1983) Blood volume and its measurement in the chronically catheterized sheep fetus. Am. J. Physiol., **244**: H487–H494.

15 Baker, C. H. (1965) Blood reservoirs in the splenectomized dog. Am. J. Physiol., **208**: 485–491.

16 Stallone, J. N. and Braun, E. J. (1986) Osmotic and volemic regulation of plasma arginine vasotocin in conscious domestic fowl. Am. J. Physiol., **250**: R644–R657.

17 Kaufman, S. and Peters, G. (1980) Regulatory drinking in the pigeon, *Columba livia*. Am. J. Physiol., **239**: R219–R225.

18 Ruch, F. E., Jr. and Hughes, M. R. (1975) The effect of hypertonic sodium chloride injection on body water distribution in ducks (*Anas platyrhynchos*), gulls (*Larus glauchscens*) and roosters (*Gulls domesticus*). Comp. Biochem. Physiol., **52A**: 21–28.

19 Skadhauge, E. (1981) Osmoregulation in Birds, Springer Verlag, Berlin, Heidelberg and New York, p. 5.

20 Drischel, H. (1956) Blutzukerregelung. In "Regelungsvorgänge in der Biologie". Ed. by H. Mittelstaedt, Verlag R. Oldenborg, München, pp. 60–75.

21 Sherrington, C. S. (1939) Selected Writings of Sir Charles S. Sherrington. Ed. by D. Denny-Brown, Hamish Hamilton, London.

ZOOLOGICAL SCIENCE 4: 813–818 (1987)

Cryoprotection of Medaka Embryos During Development

Nozomi Arii, Kaori Namai, Fujiya Gomi
and Tohru Nakazawa[1]

Department of Biology, Faculty of Science, Toho University, Funabashi, 274, Japan

ABSTRACT—In order to establish a method for the cryopreservation of experimental animals, a determination of optimal conditions for the freezing was performed by using medaka (*Oryzias latipes*) embryos. Since dimethyl sulfoxide (DMSO) had no influence on embryonic development even following its treatment at low temperature, it thus qualifies as a cryoprotectant. Treatment of embryos with Ringer containing DMSO caused a transient decrease in the volume of embryos but the DMSO appeared to permeate gradually into the embryos as shown from the recovery of its volume. Survival rates after freezing were greatly affected by the concentration of DMSO, duration of DMSO-treatment, rate and final temperature of freezing and developmental stages of the embryos. The highest survival, 57.1% after freezing at a temperature as low as −40°C, was obtained by pretreatment with 2 M DMSO/Ringer for 5 hr. When frozen slowly below −20°C, survival rates declined. A rapid freezing rate blow −20°C, however, resulted in high survival rates. Embryos at the gastrula stage showed the highest tolerance toward freezing among the embryonic stages examined from 8 cell stage to 23 somite stage.

INTRODUCTION

The cryopreservation of living organisms has recently been developed from a single cell to multicellular system, particularly at the early stages of development. In the cryopreservation, however, cells are damaged severely during freezing and thawing. Particularly rapid freezing causes destruction of cell organelles due to the formation of ice inside the cells owing to insufficient dehydration of intracellular free water. Slow freezing induces denaturation of protein by high salinity due to gradual dehydration of the protoplasm. Freezing may also result in inactivation of structural proteins by osmotic stress or dissociation of S–S bonds. To avoid such intracellular freezing, an appropriate cooling rate is necessary.

Cryopreservation of mouse embryos was first carried out by Whittingham *et al.* [1] in 1972. Subsequently that cryopreservation of other mammalian embryos such as those of rat [2] and rabbit [3] have also been reported. However, only a few reports are available on the cryopreservation of nonmammalian embryos. Only the embryos of rainbow trout [4] and medaka [5, 6] have been subjected to low temperature.

In this study, medaka (*Oryzias latipes*) embryos were used to develop a reproducible method for the cryopreservation of nonmammalian embryos. A general method of cryopreservation should facilitate an understanding of the mechanism of embryonic development and the preservation of strains for long periods of time. In the present paper, a freezing procedure involving less damage to medaka embryos was investigated with special attention to the treatment of cryoprotectant and freezing rates.

MATERIALS AND METHODS

1. *Medaka embryos*

Medaka (*Oryzias latipes*) were kept in an aquarium under controlled conditions of light (14 hr light and 10 hr darkness) and temperature (about 26°C). Fertilized eggs were collected from female abdomens 1 hr following the beginning of the light period and incubated in modified Yama-

Accepted May 28, 1987
Received April 25, 1987

[1] To whom reprints should be requested.

moto's Ringer solution (127.3 mM NaCl, 2.56 mM KCl, 1.83 mM $CaCl_2$ and 1 mM 3-(N-morpholino)propanesulfonic acid; pH 7.3) [7]. Embryonic stages were determined according to the table of developmental stage of medaka [8].

Freezing of embryos

The embryos were treated with Ringer solution containing DMSO and then 10 embryos each together with the DMSO-Ringer solution were transferred into a 0.5 ml plastic straw tube (Fuji Kogyo KK). Numbers of embryos used for each value in experiments were 30 to 200. Straws were inserted in a plastic test tube filled with ethanol followed by cooling with a program freezer (MINI-COOL, CFPO, France). The freezing rate was monitored by a recorder connected to a thermocouple situated in a plastic straw. The embryos were cooled at a rate of −1°C/min from room temperature to 10°C and then at a rate of −2°C/min to −6°C (Fig. 1). Seeding was introduced by touching the straws with forceps previously cooled in liquid nitrogen. Following the seeding, the embryos were kept at −7°C for a period of 30 min. Freezing rates of −0.3°C/min and −10°C/min were used to proceed from −7°C to −20°C and from −20°C to −50°C, respectively. Below −50°C, the embryos were again cooled at a rate of −0.3°C/min.

Thawing of embryos

The frozen embryos were thawed in tap water at 19°C. DMSO was removed from the embryos following thawing by adding successively 2 ml, 2 ml and 4 ml of Ringer solution to 2 ml of thawed DMSO/Ringer solution every 20 min. Eventually, all the solutions were replaced completely by fresh Ringer. The thawed embryos were then incubated at 26°C for about 7 days until hatching. Survival rates were estimated in a comparison between normal embryos which developed to the hatching and the total number of used embryos.

RESULTS

Effects of DMSO on the normal development of medaka embryos

An examination was first performed to determine if DMSO had any effect on the development of medaka embryos. Embryos at gastrula stage (stage 15) were immersed in Ringer containing 2 M DMSO (DMSO/Ringer) for 1 to 40 hr and survival rates were estimated at the time of hatching against control embryos (Fig. 2). Over 90% of the embryos were always found to survive regardless of the length of time of DMSO treatment. It is thus evident that 2 M DMSO/Ringer had no effect on the normal development of embryos.

Permeability of DMSO into embryos

DMSO is known to be a highly permeable

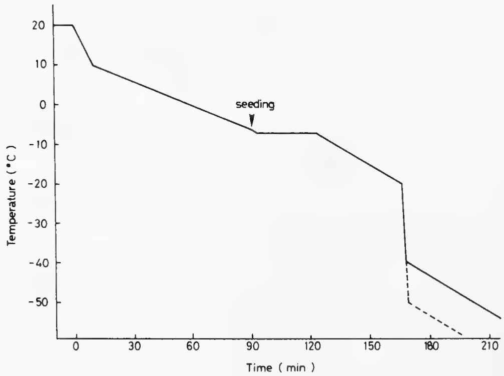

Fig. 1. Diagram of the freezing process of medaka embryos using a program freezer.

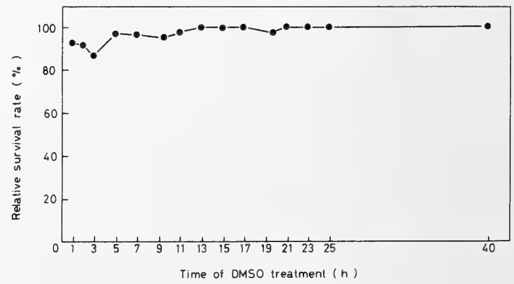

Fig. 2. Effects of DMSO treatment on the normal development of medaka embryos. Embryos at gastrula stage were immersed in Ringer containing 2 M DMSO. The percentage of embryos which normally developed up to time of hatching in the presence of DMSO against that without DMSO is shown on the ordinate.

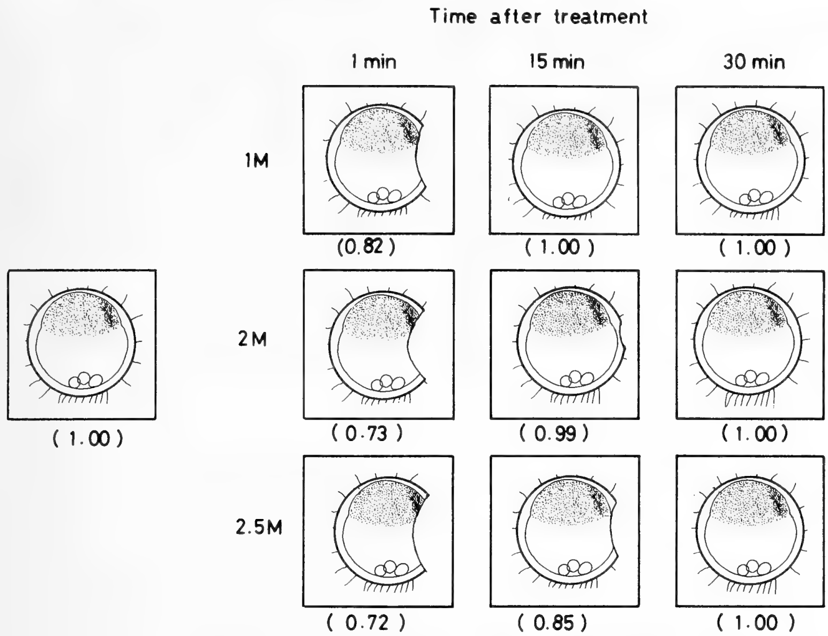

FIG. 3. Changes in the morphology of embryos during treatment with DMSO. Embryos treated with 1 M, 2 M and 2.5 M DMSO/Ringer are shown at 1, 15 and 30 min, respectively, following treatment. The relative diameter of egg (diameter without DMSO is 1.00) is represented in parentheses.

substance. Its permeability into medaka embryos was investigated by observing morphological changes in embryos following their immersion in 1 M, 2 M and 2.5 M of DMSO/Ringer. Figure 3 shows sketches of embryos after this treatment. Since the volume of embryos decreased just after being transferred into DMSO/Ringer, embryos were considered to be dehydrated as a result of the high concentration of surrounding DMSO solution. Thereafter shrunk embryos recovered gradually to their original volume. The embryos might be equilibrated with DMSO by its influx into them. The periods required for recovery to original volume were 7.5 min, 13.2 min and 20.3 min in the presence of 1 M, 2 M and 2.5 M DMSO/Ringer, respectively. The higher the DMSO concentration, the longer should be used the period required to reach equilibrium. Higher concentrations of DMSO caused greater shrinkage of embryos. According to these results, DMSO may reversibly penetrate into the embryos. DMSO could be used as a cryoprotective agent toward medaka embryos.

Effects of DMSO concentration on freezing

The effects of DMSO concentration on embryo survival during the freezing process were studied. Embryos at the gastrula stage were treated with 1 M, 2 M and 2.5 M DMSO/Ringer for 5 hr. The embryos thus treated were frozen at −20°C, −30°C and −40°C. After reaching these temperatures, the embryos were thawed and incubated until hatching following removal of DMSO. The survival rates are shown in Figure 4. At every temperature, the highest survival was noted in the presence of 2 M DMSO. At −40°C, living embryos could be found only in 2 M DMSO /Ringer. Without DMSO treatment, however, all the embryos died when frozen at −20°C. This indicates positively that DMSO is an effective cryoprotectant.

Effects of the freezing rate on survival

Effect of DMSO treatment on the freezing rate of embryos was examined. Embryos at the gastrula stage pretreated with 2 M DMSO for 5 hr

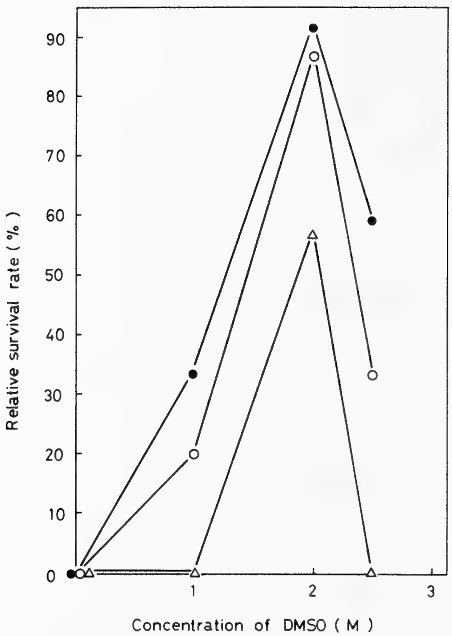

Fig. 4. Effects of DMSO concentration on survival of embryos. Embryos at gastrula stage were treated with 2 M DMSO/Ringer for 5 hr and then cooled. Embryos were thawed after reaching −20°C (closed circles), −30°C (open circles) and −40°C (open triangles). A rapid freezing rate (−10°C/min) was used to attain temperatures lower than −20°C. Relative survival is expressed as the proportion of normally developed embryos up to the time of hatching following freezing against normally developed embryos without freezing.

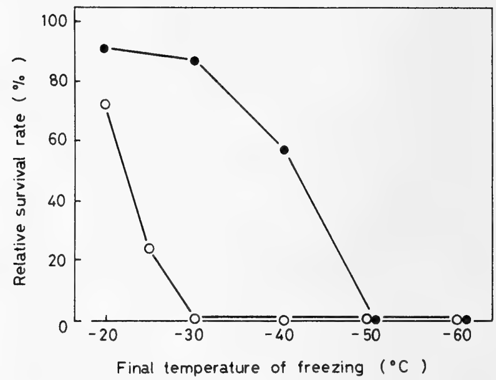

Fig. 5. Effect of final temperature on survival of embryos. Embryos at the gastrula stage were treated with 2 M DMSO/Ringer for 5 hr. Embryos were cooled at a rate of −1°C/min from room temperature to 10°C and −0.2°C/min from 10°C and −0.2°C/min from 10°C to −6°C. Seeding was introduced at −6°C followed by freezing again at a rate of −0.3°C/min from −7°C to −20°C. From −20°C, the embryos were frozen at two different rates, ○—○, −0.3°C/min and ●—●, −10°C/min to −50°C and −0.3°/min below −50°C.

were frozen at −20°C to −60°C. After every drop of 10°C, the embryos were thawed and their survival rate was determined. As shown in Figure 5, the survival rate of embryos declined abruptly below −20°C by a slow freezing rate of −0.3°C/min (the survival rate was 72.4% at −10°C and 22.2% at −25°C). However, survival was greater by a rapid freezing rate of −10°C/min (the survival rate was 86.7% at −30°C and 57.1% at −40°C).

Stage sensitivity to freezing during development

Changes in survival rate following freezing at various stages of development were investigated (Fig. 6). Examinations were stages 5 to 6 (8- to 16-cell), stages 10 to 13 (blastula), stages 14 to 16

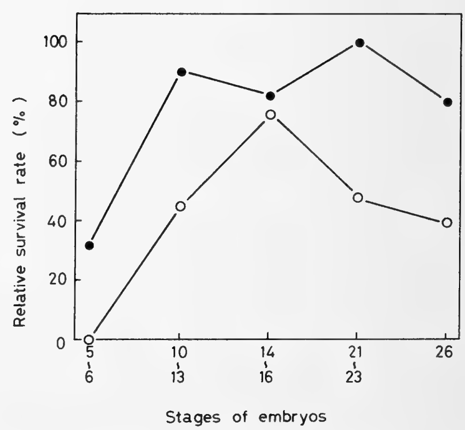

Fig. 6. Survival of embryos after freezing at different stages of development. Embryos at stages 5 to 6 (8- to 16-cell), stages 10 to 13 (blastula), stages 14 to 16 (gastrula), stages 21 to 23 (6- to 12-somite) and stage 26 (23-somite) were treated with 2 M DMSO for 5 hr and then frozen. After being frozen at −20°C (closed circles) and at −30°C (open circles), the embryos were thawed and incubated up to the time of hatching.

(gastrula), stages 21 to 23 (6- to 12-somite) and stage 26 (23-somite). Maximal survival was noted at stages 14 to 16 at a freezing temperature of −30°C. Survival rates were higher at both blastula and 6- to 12-somite stages than at gastrula stage at −20°C. Embryos at 8- to 16-cell stages showed considerably lower survival rates. Embryos at this early stage may be quite sensitive to DMSO, because considerable number of DMSO-treated embryos died. Without freezing, only 15.1% of the embryos treated with DMSO at 8- to 16-cell stages were able to hatch in contrast of 96.7% of the embryos treated at gastrula stage.

DISCUSSION

In the present study, maximal survival of medaka embryos after being frozen was obtained following pretreatment with Ringer solution containing 2 M DMSO for 5 hr and freezing stepwise at two different rates; slowly proceeding to −20°C and rapidly going below −20°C. The embryos thawed after such freezing developed normally through hatching.

Embryos treated in DMSO/Ringer shrank soon after the start of treatment but recovered their original volume within a few minutes. They developed normally in the same manner as non-treated embryos. It thus appears that DMSO effectively dehydrates embryos. Embryos without treatment of DMSO before freezing died possibly as a result of physical destruction of cells due to the formation of ice within the cells, if dehydration was insufficient during rapid cooling to −10°C. The concentration of cryoprotectant, mode of the addition, and duration and temperature of the treatment are known to be factors affecting on the survival of embryos to a considerable degree. The suitability of a cryoprotectant varies among species of animals. In this study, treatment with 2 M DMSO/Ringer was found most suitable for cryoprotection.

According to Whittingham *et al.* [1], seeding at −3.5°C to −4.5°C is one of the reasons accounting for successful cryopreservation in mouse embryos. In the present study, a seeding temperature of −6°C was used. Seeding caused to form ice in the content of straw tube, as making reduce physical stress by its formation following supercooling and avoid intracellular freezing. A temperature jump due to latent heat was observed in the case of no seeding, but it was not recognized by seeding, thus confirming indirectly that seeding prevents supercooling.

In the case of mouse embryos, cryopreservation was possible by freezing at a rate as slow as −0.33°C/min to −196°C [1, 9]. Survival rates of medaka embryos decreased considerably from −20°C, becoming 0% at −30°C freezing at a rate of −0.3°C/min (Fig. 4). By freezing more rapidly from −20°C, however, surviving embryos were obtained. After being dehydrated during slow freezing, the embryos showed lesser extent of damage since the crystals of intracellular ice formed by rapid freezing may not provide osmotic stress. During rapid freezing, DMSO may protect proteins from high salinity and cellular structures from osmotic stress.

Medaka embryos underwent a change in tolerance toward low temperatures during development (Fig. 5). They apparently have lesser tolerance at early stages when blastomeres are large but greater tolerance at later stages when blastomeres are smaller in sizes. The latter situation may be due to the greater ease of dehydration in smaller blastomeres or changes in the permeability of blastomeres during development.

Living organisms can be preserved for long periods of time only in liquid nitrogen (−196°C) [10, 11]. Since medaka embryos are large in diameter and contain considerable amounts of lipid, they may thus have low tolerance toward freezing due to the difficulty for sufficient dehydration to take place. In order to determine optimal freezing conditions permitting embryos to survive after being frozen at −196°C, biochemical nature of embryos should be examined.

ACKNOWLEDGMENT

The authors are grateful to Dr. Takeshi Yamada, Division of Biology, National Institute of Radiological Sciences, for allowing use of the program freezer.

REFERENCES

1 Whittingham, D. G., Leibo, S. P. and Mazur, P. (1972) Survival of mouse embryos frozen to -196°C and -269°C. Science, **178**: 411–414.

2 Utsumi, K. and Yuhara, M. (1974) Survival of frozen rat embryos, freezing and storage of rat blastocyst by dry ice alcohol. Sci. Rep. Fac. Agric., Okayama Univ., **44**: 24–27.

3 Bank, H. and Mauzer, R. R. (1974) Survival of frozen rabbit embryos. Exp. Cell Res., **89**: 188–196.

4 Haga, Y. (1982) On the subzero temperature preservation of fertilized eggs of rainbow trout. Bull. Japan. Soc. Sci. Fish., **48**: 1569–1572.

5 Onizuka, N., Kato, K. and Egami, N. (1983) Freezing of whole-body of medaka (*Oryzias latipes*). Biomed. Gerontol., **7**: 111–112. (In Japanese)

6 Onizuka, N. and Egami, N. (1985) Effects of γ-irradiation of fish embryos under frozen conditions on survival and hatching. Zool. Sci., **2**: 411–413.

7 Gilkey, J. C. (1983) Roles of calcium and pH in activation of eggs of the medaka fish, *Oryzias latipes*. J. Cell Biol., **97**: 669–678.

8 Matsui, K. (1949) Illustration of the normal course of development in the fish, *Oryzias latipes*. Japan. J. Exp. Morphol., **5**: 33–42. (In Japanese)

9 Leibo, S. P., Mazur, P. and Jacknowisky, S. (1973) Factors affecting the survival of frozen-thawed mouse embryos. Cryobiol., **10**: 509.

10 Utsumi, K., Yuhara, M. and Yamada, M. (1978) Viability of frozen two-cell eggs and blastocysts in rat. Cryobiol., **15**: 689.

11 Willadsen, S. M., Polge, C., Rowson, L. E. A. and Moor, R. M. (1976) Deep freezing of sheep embryos. J. Reprod. Fertil., **46**: 151–154.

ZOOLOGICAL SCIENCE 4: 819–823 (1987)

Excitatory and Inhibitory Neuromuscular Transmission in Fish Red Muscle

Tohoru Hidaka and Tokuji Miyahara[1]

Department of Biology, Faculty of General Education, and [1]Faculty of Science, Kumamoto University, Kumamoto 860, Japan

ABSTRACT—Three types of the electrical responses, the excitatory junction potential (ejp), the inhibitory junction potential (ijp) and the diphasic junction potential which was composed of ejp followed by ijp, were recorded to a single nerve stimulation in the red muscle of a pectoral fin of a silver carp, *Carassius auratus*. Some physiological and pharmacological properties of these junction potentials, especially of ijp, were examined. During the time course of the hyperpolarization brought about by ijp the membrane conductance increased to about 1.5 times of control. By passing the conditioning hyperpolarization, the equilibrium potential of ijp was measured to be approximately −107 mV at the resting potential of −74 mV. In the resting muscle, the spontaneously arising miniature excitatory junction potential (mejp) and miniature inhibitory junction potential (mijp) could be recorded from the same muscle fiber. Nicotinic antagonist of acetylcholine (ACh) receptor, *d*-tubocurarine (*d*-TC), suppressed ijp and anticholinesterase, neostigmine, augmented and prolonged it. Muscarinic antagonist, atropine, had no effects on ijp. From the results, it was suggested that this muscle was innervated by two separate, excitatory and inhibitory, nerves and the transmission would be mediated by the nicotinic action of ACh.

INTRODUCTION

Two types of muscle fiber, namely white (fast) and red (slow) muscle fibers, are known in vertebrate skeletal muscles. Differences in structure and electrical properties between both muscle types have been investigated in many vertebrate species (see Morgan and Proske [1] for a review), since the slow muscle system was described in the frog [2, 3]. In the fish, two muscle systems were reported in hagfish [4–7], elasmobranch [8–10] and teleost [11–14]. It was observed that the red muscle of the freshwater teleost did not generate a propagating spike and generated only the depolarizing junction potential by the nerve stimulation [11]. Similar observation was obtained in the red muscle of the pectoral fin of a silver carp [13]. In this muscle, the excitatory junction potential (ejp) was recorded in response to the nerve stimulation and the spike initiation was very rare. Also, the miniature excitatory junction potential (mejp) could be recorded in the resting muscle. Although the spike was not generated, this muscle could develop tension by ejp. That is, the critical membrane potential level required to produce tension was exceeded by the depolarization attained by ejp [13].

In the present experiment, we report that, in addition to ejp and mejp, the hyperpolarizing, inhibitory junction potential (ijp) could be recorded by the nerve stimulation and the miniature inhibitory junction potential (mijp) was observed in the resting muscle of the red muscle of a silver carp. Furthermore, it was intended to investigate some physiological and pharmacological properties of the neuromuscular transmission, especially of ijp.

MATERIALS AND METHODS

Preparations of the red muscle, *M. levator pinnae pectoralis,* together with its nerve (Th. 1 and Th. 2) were made from a silver carp, *Carassius auratus*. The methods for dissecting the muscle and the nerve were the same as those described

Accepted May 27, 1987
Received May 1, 1987

previously [12]. The preparation fixed on a Silgard plate was placed in a chamber of about 5 ml in volume and was perfused constantly with physiological saline at a rate of about 5 ml/min. The saline consisted of (mM): NaCl, 129.6; KCl, 2.7; $CaCl_2$, 1.8, and was adjusted to pH 7.3 with 2.5 mM $NaHCO_3$. The methods for recording the membrane potential and for stimulating the nerve were also described [12]. Glass microelectrodes were filled with 1 M K-citrate, instead of KCl used in the previous study, their resistance varying from 10 to 30 MΩ. The nerve was stimulated by a suction electrode of about 0.1 mm in orifice, made from glass pipette. The response to the nerve stimulation was elicited by supramaximal stimulus, except for the record illustrated in Figure 2. To change the membrane potential level and to measure the membrane conductance, the bridge methods were used. The following drugs were used; *d*-tubocurarine (*d*-TC, Sigma), neostigmine methylsulfate (Sigma) and atropine (Nakarai Chemicals). All experiments were performed at room temperature (18–25°C).

RESULTS

Figure 1 shows the different types of the responses recorded from the red muscle of pectoral fin of a silver carp. In response to single nerve stimulation, ejp (a), ijp (b) and diphasic junction potential (c) which was composed of ejp followed by ijp were elicited from the different muscle fibers. In this Figure, ejp (a1, 2) and ijp (b1, 2) of the different duration were shown. As shown in Figure 1c, while the amplitude and the duration of ejp were almost the same, the duration of ijp was different (c1, 2). In the most muscle fibers

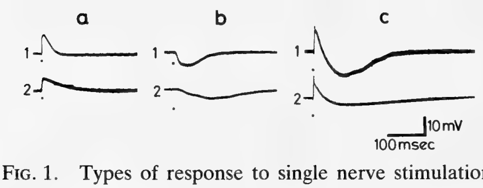

FIG. 1. Types of response to single nerve stimulation. a; ejp, b; ijp, c; diphasic junction potential. Note longer duration of 2 than of 1 in each record. Records taken from different muscle fibers. Dots in this, Figs. 2, 5 and 7 indicate nerve stimulation.

examined, ijp lasted longer than ejp. The amplitude and the duration of three types of the junction potentials were not the same from fiber to fiber. One of reasons why such difference arose might result from the different distance between the neuromuscular junction and the recording electrode inserted.

The junction potentials elicited at different stimulus intensities were illustrated in Figure 2. Records shown in a and b were taken from different muscle fibers. Only ejp (a1) and ijp (b1) were elicited at lower stimulus intensity and the diphasic junction potentials (a 2 and b 2) were elicited at higher intensity.

The reversal potential of ijp was determined by

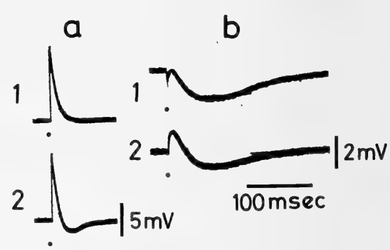

FIG. 2. Effects of increasing stimulus intensity on junction potentials. Low stimulus intensity elicited only ejp (a1) and ijp (b1). As intensity increased, diphasic junction potentials were elicited (a 2 and b 2).

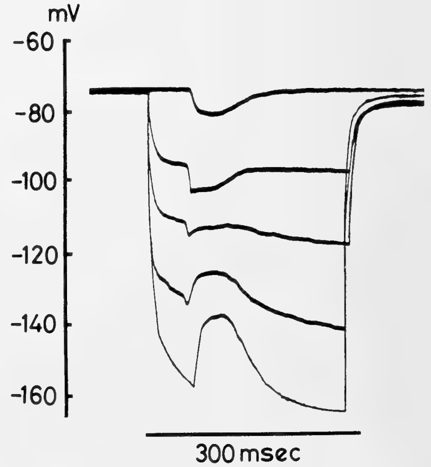

FIG. 3. Effects of hyperpolarizing the membrane on ijp. Traces of photographs were superimposed.

passing conditioning hyperpolarizing current pulses using a bridge circuit method. As shown in Figure 3, the amplitude of ijp was decreased by hyperpolarizing the membrane and reversed its polarity at a critical membrane potential level. This membrane potential level might be the equilibrium potential of ijp. The amplitude of the reversed ijp was increased by further hyperpolarization. The relation between the amplitude of ijp and the membrane potential was approximately linear (Fig. 4). From this relation, the equilibrium potential of ijp was determined to be approximately −107 mV, when the resting potential was −74 mV in this particular fiber.

The change in the effective resistance of the membrane during the generation of ijp was measured by passing constant inward current of 4 nA (Fig. 5). The input resistance decreased by 26.5% at the maximal hyperpolarization attained during the generation of ijp. From results shown in Figures 4 and 5, it was suggested that the generation of ijp was due to the increase in the membrane permeability to ion(s), although it was not attempted to analyze the ionic mechanism involved in the generation of ijp in the present study.

It was reported in the previous experiment that only mejp was recorded in the resting muscle fiber [13]. In the present study, the spontaneously occurring mijp, in addition to mejp, could be recorded, although the generation of mijp was

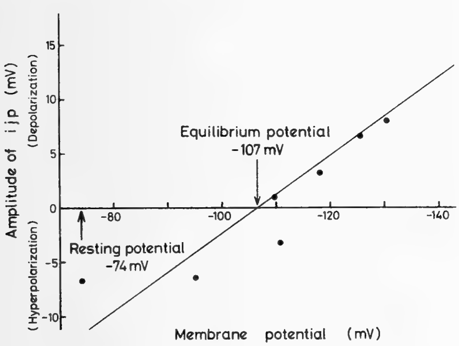

FIG. 4. Relation between the amplitude of ijp and the membrane potential. Abscissa; displacement of the membrane potential from its resting level (mV), ordinate; amplitude of ijp (mV).

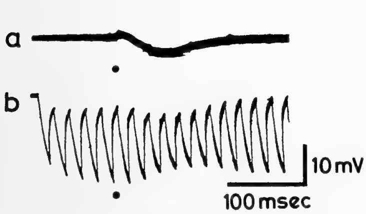

FIG. 5. Change in the membrane conductance during the generation of ijp. a, ijp without the application of current pulses. b, changes in electrotonic potentials during the generation of ijp were measured by the application of inward current pulses (4 nA, 10 msec, 100 Hz).

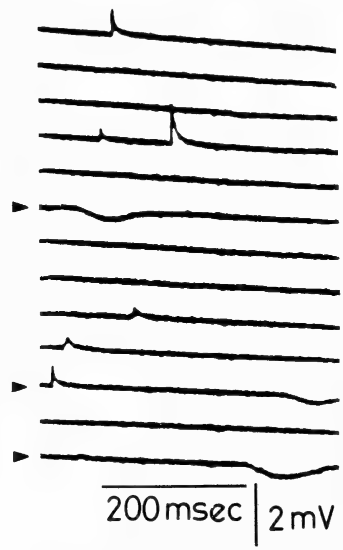

FIG. 6. An example of mejp and mijp (seen on sweeps marked with the arrowhead). The continuous record taken from the same muscle fiber.

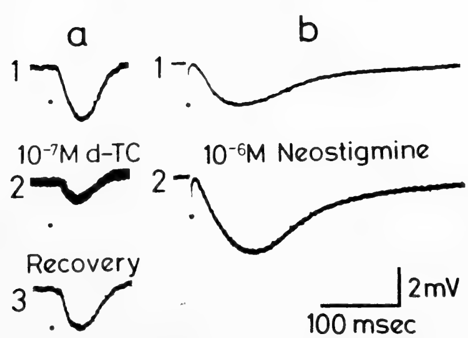

FIG. 7. Effects of *d*-TC and neostigmine on ijp. a1 and b1; control. a2; 17 min after 10^{-7} M *d*-TC, a3; recovery 42 min after washing. b2; 16 min after 10^{-6} M neostigmine. No recovery 120 min after washing (not shown).

very rare in comparison with that of mejp (Fig. 6). Figure 6 shows a particular example in which both mejp and mijp were observed in the same muscle fiber. It is noted that the time course of mijp is much slower than that of mejp.

To reveal the nature of the chemical transmitter mediating ijp, the effects of some chemical agents on ijp were investigated. Figure 7 shows that after the application of 10^{-7} M *d*-TC, ijp decreased to about 30% (a 2) of control (a1), while 10^{-6} M neostigmine, anticholinesterase, augmented and prolonged ijp (b 2). Atropine at a concentration of 10^{-5} M did not exhibit any noticeable effects on ijp.

DISCUSSION

It has been generally accepted that at least two kinds of fiber types are present in vertebrate skeletal muscle. These are termed fast and slow, phasic and tonic or white and red muscles, respectively. There are many morphological and physiological differences between two muscle types. Morgan and Proske [3] reviewed the difference between the fast and slow muscle fibers in vertebrates. In fish, it was described that the white muscle produced the propagating action potential, whereas the red muscle did not produce it and generated the non-propagating ejp in response to the nerve stimulation [11]. Similar findings were also reported in the red muscle of a silver carp [13].

In the present experiment, it was demonstrated in the red muscle of a silver carp that the hyperpolarizing ijp as well as ejp was elicited by the nerve stimulation and that mejp and mijp were recorded in the resting muscle fibers. Also, the nerve stimulation initiated the diphasic junction potential composed of ejp followed by ijp (Figs. 1 and 2). However, the occurrence of ijp, diphasic junction potential and mijp were very rare in comparison with that of ejp and mejp. These results might indicate that this muscle receives double innervations from the excitatory and inhibitory nerves and that the inhibitory innervation is much fewer than the excitatory one. This seems to be one of reasons why ijp and mijp were overlooked in the previous study [13]. The present results would be the first demonstration that ijp and mijp were recorded in vertebrate skeletal muscle.

From the results that ijp was suppressed by *d*-TC, the nicotinic antagonist of ACh receptor, and was augmented by neostigmine, the anticholinesterase (Fig. 7), the neuromuscular transmission of this muscle would be cholinergic. The nature of the receptor would be nicotinic, because atropine, the muscarinic cholinergic antagonist, did not affect ijp. Equilibrium potential of ijp was determined to be approximately -107 mV at the resting potential of -74 mV (Fig. 4) and the increase in the membrane conductance was observed during the generation of ijp (Fig. 5). This might indicate that the increase in the permeability of the membrane to ion(s) is involved in the generation of ijp. In this study, however, the ionic mechanism to produce ijp has not been investigated. This is now in progress.

The term ijp has been proposed for the hyperpolarizing potential of the red muscle fiber recorded in the present experiment. The inhibitory innervation has been revealed in the mammalian smooth muscle [15] and the skeletal muscle of crustacea [16] and insect [17]. In these nerve-muscle preparations, it was demonstrated that the stimulation of the inhibitory nerve and the resulting ijp caused the inhibition of the mechanical response of the muscle. However, ijp recorded in the present experiment has not yet been shown to inhibit the initiation of ejp and consequently to suppress the mechanical response of the red muscle of a silver carp. The peripheral neuromuscular mechanism by which ejp, ijp and perhaps their combination might control the mechanical activity of this muscle must be elucidated further.

REFERENCES

1 Kuffler, S. W. and Vaughan Williams, E. M. (1953) Small-nerve junction potentials. The distribution of small motor nerves to frog skeletal muscle, and the membrane characteristics of the fibres they innervate. J. Physiol., **121**: 298–317.

2 Kuffler, S. W. and Vaughan Williams, E. M. (1953) Properties of the "slow" skeletal muscle fibres of the frog. J. Physiol., **121**: 318–340.

3 Morgan, D. L. and Proske, U. (1984) Vertebrate

slow muscle: Its structure, pattern of innervation, and mechanical properties. Physiol. Rev., **64**: 103–169.

4 Anderson, P., Jansen, J. K. S. and Løyning, Y. (1963) Slow and fast muscle fibres in the Atlantic hagfish (*Myxine glutinosa*). Acta Physiol. Scand., **57**: 167–179.

5 Teräväinen, H. (1971) Anatomical and physiological studies on muscles of lamprey. J. Neurophysiol., **34**: 954–973.

6 Korneliussen, H. (1973) Dense-core vesicles in motor nerve terminals. Monoaminergic innervation of slow non-twitch muscle fibers in the Atlantic hagfish (*Myxine glutinosa,* L.)? Z. Zellforsch., **140**: 425–432.

7 Nicolaysen, K. (1976) Spread of the junction potential in the T-system in hagfish slow muscle fibres. Acta Physiol. Scand., **96**: 50–57.

8 Bone, Q. (1972) The dogfish neuromuscular junction: Dual innervation of vertebrate striated muscle fibres? J. Cell Sci., **10**: 657–665.

9 Kryvi, H. (1977) Ultrastructure of the different fibre types in axial muscles of the sharks *Etmopterus spinax* and *Galeus melastomus*. Cell Tissue Res., **184**: 287–300.

10 Stanfield, P. R. (1972) Electrical properties of white and red muscle fibres of the elasmobranch fish *Scyliorhinus canicula*. J. Physiol., **222**: 161–186.

11 Takeuchi, A. (1959) Neuromuscular transmission of fish skeletal muscles investigated with intracellular microelectrode. J. Cell. Comp. Physiol., **54**: 211–220.

12 Hidaka, T. and Toida, N. (1969) Biophysical and mechanical properties of red and white muscle fibres in fish. J. Physiol., **201**: 49–59.

13 Hidaka, T. and Toida, N. (1969) Neuromuscular transmission and excitation-contraction coupling in fish red muscle. Japan. J. Physiol., **19**: 130–142.

14 Davey, D. F., Mark, R. F., Marotte, L. R. and Proske, U. (1975) Structure and innervation of extraocular muscles of *Carassius*. J. Anat., **120**: 131–147.

15 Burnstock, G., Campbell, G. and Rand, M. J. (1966) The inhibitory innervation of the taenia of the guinea-pig caecum. J. Physiol., **182**: 504–526.

16 Grundfest, H., Reuben, J. P. and Rickles, W. H., Jr. (1959) The electrophysiology and pharmacology of lobster neuromuscular synapse. J. Gen. Physiol., **42**: 1301–1323.

17 Usherwood, P. N. R. and Grundfest, H. (1965) Peripheral inhibition in skeletal muscle of insects. J. Neurophysiol., **28**: 497–518.

ZOOLOGICAL SCIENCE 4: 825–832 (1987)

Surface Movement in the Region of the Cleavage Furrow of Amphibian Eggs

TSUYOSHI SAWAI

Department of Biology, Faculty of General Education, Yamagata University, Yamagata 990, Japan

ABSTRACT—During cleavage of amphibian eggs, a pale surface without pigment granules appears on both sides of the deepening furrow in the middle stage of furrow formation and extends during the late stage of furrowing. The process of appearance and extension of the pale surface was examined by observing the behavior of carbon particles attached to the surface of the furrow region of eggs of the newt, *Cynops pyrrhogaster*. The pale surface was formed relatively rapidly in the middle stage of furrowing by extensive stretching of the surface of the small, narrow initial furrow. Subsequently, the area of the pale surface gradually increased mainly from the bottom of the deepening furrow. As the surface increased, the pale surface gradually shifted toward boundary of the pigmented and the unpigmented surface. The contractility of the cortex along the cleavage plane was also examined. The cortex of the furrow plane is known to be greatly constricted in the early phase of furrow formation. Observations showed that the contraction was temporarily arrested in the late phase of furrowing, but was taken up again about 15 min later, eventually dividing eggs into two blastomeres.

INTRODUCTION

In the amphibian egg, the mechanism of cleavage furrow formation has been studied mainly by microsurgical methods with optical microscopy or electron microscopy. Studies at the optical level have revealed details of surface movements in eggs during cleavage, by techniques such as cortical transplantation [1–3], use of surface markers [4–7] or time-lapsed cinematography [6, 8]. These investigations have shown directly that the cleavage furrow is formed by contraction of the cortex in the cleavage plane. On the other hand, studies at the electron microscopic level have shown that a bundle of microfilaments is localized beneath the surface along the furrow [9–13], and that this bundle is mainly composed of actin filaments [14].

These studies have mainly been directed to analysis of events during early stage of furrow formation, and have resulted in understanding of systematic and dynamic aspects of morphological events. In addition, very recently biochemical aspects of amphibian cleavage have been studied (Mabuchi *et al.*, unpublished). These studies have established that cytokinesis of amphibian eggs is brought about by cortical contraction caused by actin-myosin interaction, at least in the early phase, as in smaller eggs or tissue cells (cf. reviews, [15–18]).

Unlike the early phase of furrowing, the late phase is poorly understood, although it has been studied extensively both morphologically [7, 8, 19, 20] and ultrastructurally [12, 21–25]. Therefore, further studies are required at various levels and by various methods on the late stage of furrow formation.

In the present work, we investigated furrow formation in the late phase of the first cleavage of living newt eggs with special reference to the source of membrane for increasing the furrow surface, the site of surface growth and contractility of the bottom of the furrow.

MATERIALS AND METHODS

Spawning of fertilized eggs of the newt, *Cynops pyrrhogaster,* was stimulated by injecting about 80 i.u. of chorionic gonadotropin (Gonatropin, Teikoku Zoki, Tokyo) every other day into the

Accepted June 5, 1987
Received May 7, 1987

abdomen of females which had taken up spermatophores. The jelly coat of eggs was removed by treatment with about 1.5% sodium thyoglycollate (pH 10) [cf. 26], and the vitelline membrane was stripped off with two pairs of watchmaker's forceps. The naked eggs were put into a shallow depression in agar gel coated dishes containing modified Holtfreter's saline (NaCl 3.5 g, KCl 0.05 g, $CaCl_2$ 0.1 g, HEPES 1.1 g, Kanamycin sulfate 0.1 g, H_2O 1000 ml, pH 7.3) [27]. Their surface was marked by small carbon particles as described previously [4] by placing a glass tube containing a suspension of carbon particles in saline on the agar bed over the egg. Unattached particles were washed off, and the eggs were finally put in an agar bed and photographed every 5 min under a dissection microscope, at room temperature (18–25°C). The behavior of the carbon particles on the egg surface was analyzed from enlarged prints.

RESULTS

During cytokinesis in amphibians, a pale surface appears at both sides of the cleavage furrow, and this area gradually increases during division. This process cannot be observed in eggs enveloped in a jelly coat and a vitelline membrane, but is easily visible on freeing the eggs from these membranes. In the present experiments on eggs without the egg membranes, the first cleavage stage was arbitrarily divided into four phases on the basis of the appearance of the furrow region: early, middle, late and final stages. The early stage was the period from the appearance of the initial furrow with double stripes (Fig. 1A) through wrinkle formation on both sides of the furrow and their disappearance (Fig. 1B, C), to depigmentation on the sides of the furrow. The middle stage was the period from the formation of a pale surface to its full extension, during which the furrow extended to surround about two-thirds of the egg circumference and its bottom deepened (Fig. 1D–F). The late stage was the period from the time when the opened white area reached a maximum until the furrow bottom became invisible by deep invagination, while the furrow came to surround the whole egg and the ring-shaped furrow somewhat deepened (Fig. 1F). The final stage was the period when the exposed white region became slightly closed and division was completed (Fig. 1G). The last stage was characterized by accumulation of pigments along the boundary of the pigmented and unpigmented surfaces. The present study was mainly performed in the first three stages.

Surface movement in the early to the middle stage

The movement of carbon particles attached to the initial furrow and its vicinity was traced by examination of pale-surface formation (Fig. 2). First the distance between particles located inside the double stripes (Fig. 2A, particles no. 3, 4) was seen to shorten (Fig. 2A–C). Subsequently, the particles moved away from the bottom of the furrow, and became situated on the pale surface when the furrow region changed from a pigmented to an unpigmented surface (Fig. 2D–F). Particles

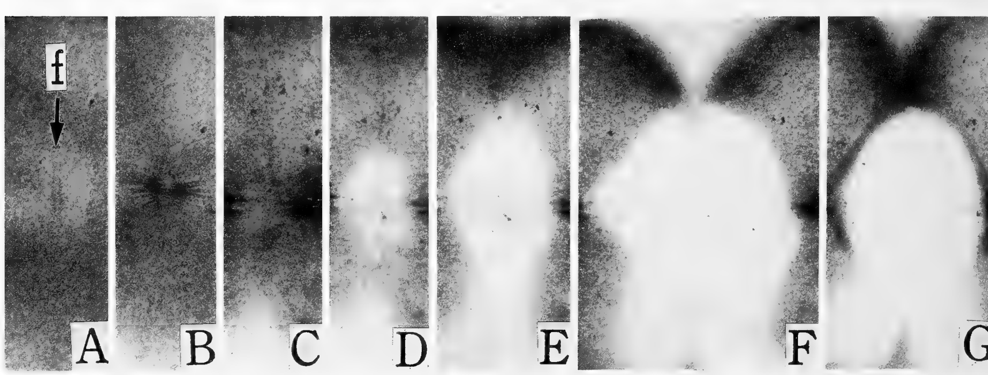

FIG. 1. Four stages in furrow formation in the animal hemisphere: early (A–C), middle (D–F), late (F) and final stages (G). f in A: double striped initial furrow. Time (min): A–B, 10; B–F, 20 in each; F–G, 40. ×27.

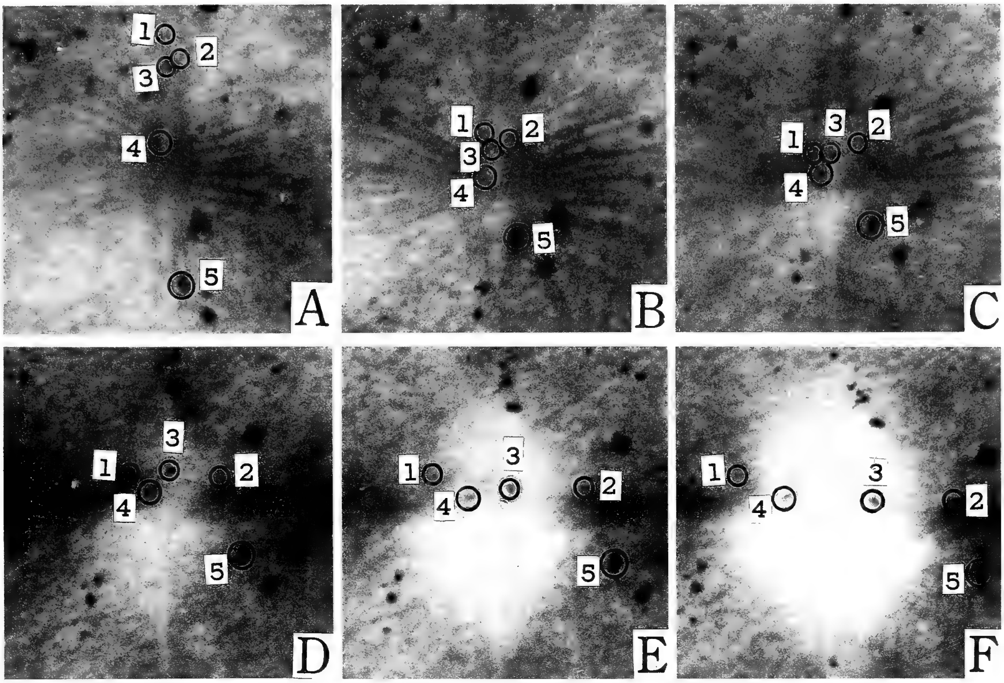

FIG. 2. Surface movement in the furrow region during the early and middle stages. Five particles are circled to show their movement: nos. 1, 3 and 4, inside the two stripes; no. 2, on the stripe, and no. 5, outside the stripe. Time: 5 min in each. ×70.

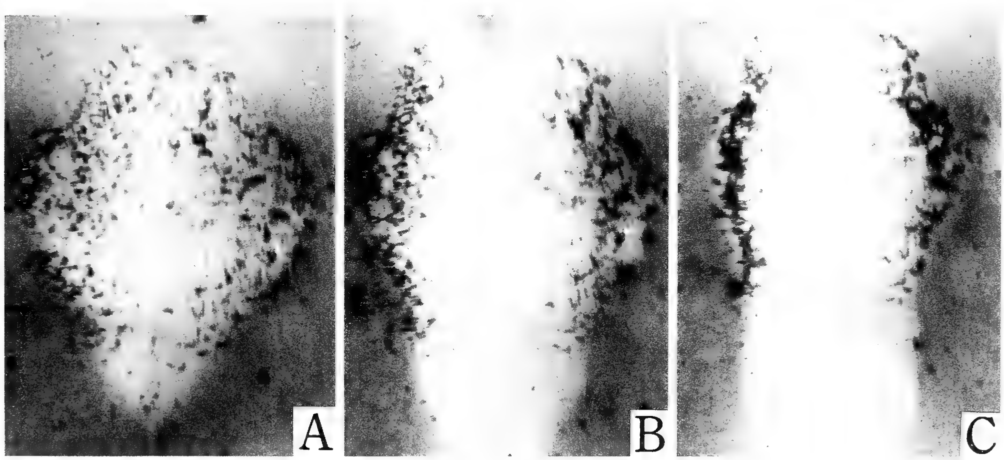

FIG. 3. Particle movement on the pale surface. The sequential movements of numerous particles attached to the pale surface are shown in A, B and C, respectively. Time: 10 min in each. ×40.

on the initial furrow usually showed this movement, but a few remained on the base of the furrow without shifting.

The particles attached to the stripe or outside it (Fig. 2, no. 2, 5) remained located on the pigmented surface during and after formation of the pale surface, and never moved to the new surface. This feature has recently been reported by Ohshima and Kubota [25].

These results confirmed that the early furrow

was formed by marked contraction of the cortex in the cleavage plane, and indicated newly that the pale surface was formed by remarkable extension of the pigmented surface of the narrow initial furrow of about 50 μm width. The distance between particles no. 1 and 2 is about 40 times more in Figure 2F than in Figure 2B.

Surface movement during the middle to late stages

The surface movement in the furrow region after the appearance of the pale surface was examined by tracing the behavior of particles attached to it. Figure 3 shows an outline of particle movement on the pale surface during the middle and late stages of furrowing. Almost all particles gradually shifted toward a boundary of the pigmented and the unpigmented surfaces, and they ultimately accumulated in the vicinity of the border (Fig. 3C). The particles did not move out beyond the borderline. The detailed movement of particles on the pale surface are shown schematically in Figures 4–6. Figure 4 shows typical findings on the movement of particles perpendicular to the furrow in the middle stage. Almost all particles gradually moved toward the boundary of the pigmented and unpigmented surfaces away from the furrow base (Fig. 4, particles no. 1–3, 5–9). But a few particles on the furrow bottom remained there (Fig. 4, no. 4). Similar movement of particles was seen in the late stage (Fig. 5).

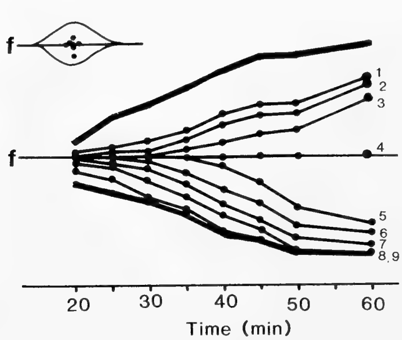

Fig. 4. Graphic representation of particle movement on the pale surface in the middle stage, in the direction perpendicular to the cleavage plane. The top figure shows the rough positions of a cluster of particles on the pale surface at the time when the study was started. The movements of nine particles (1–9) are traced. All the particles except no. 4 shifted away from the furrow bottom (line f). Particle no. 4 remained at the bottom. The two thick outer curves show the border between the pigmented and unpigmented surface. Time: min after the appearance of the furrow.

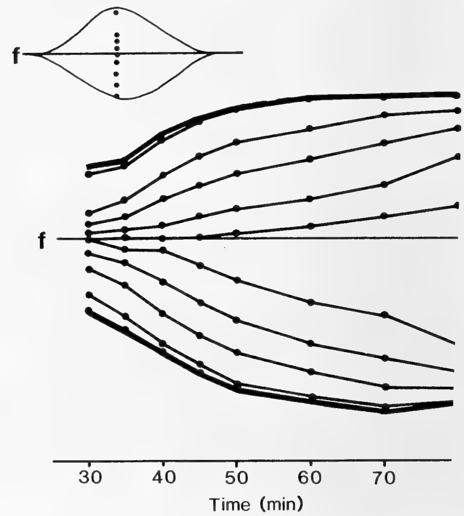

Fig. 5. Graphic tracing of movements of particles on the pale surface during the middle and late stages in the direction perpendicular to the cleavage plane. The explanation is as for Fig. 4.

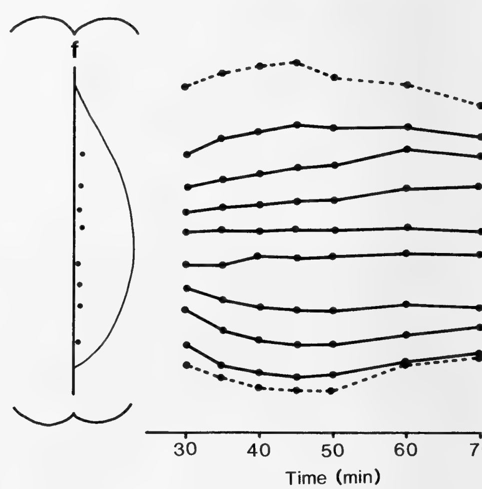

Fig. 6. Graphic representation of particle movement on the pale surface in the direction parallel to the cleavage plane in the late stage. Particles moved slightly in parallel. The dotted lines indicate the position of the edge of the pale area at the furrow bottom. Other explanations are as for Fig. 4.

These movements of particles indicated that the cell membrane was added at the bottom of the furrow and the surface moved toward the border region of the two kinds of surfaces and accumulated there.

Figure 6 shows traces of movement of eight particles along the furrow bottom in the direction parallel to the furrow in the late stage. The particles showed little movement in this direction. Similar slight movement was observed in the region distant from the furrow bottom.

Surface movement at the bottom of the furrow from the early to late stages

As described above, in almost all embryos the carbon particles attached to the initial furrow or the bottom of the deepening furrow gradually shifted from it with progress of cleavage. Therefore, continuous tracings of movement of particles in the furrow base were possible in only a few cases.

Figure 7 shows an example of the movement of

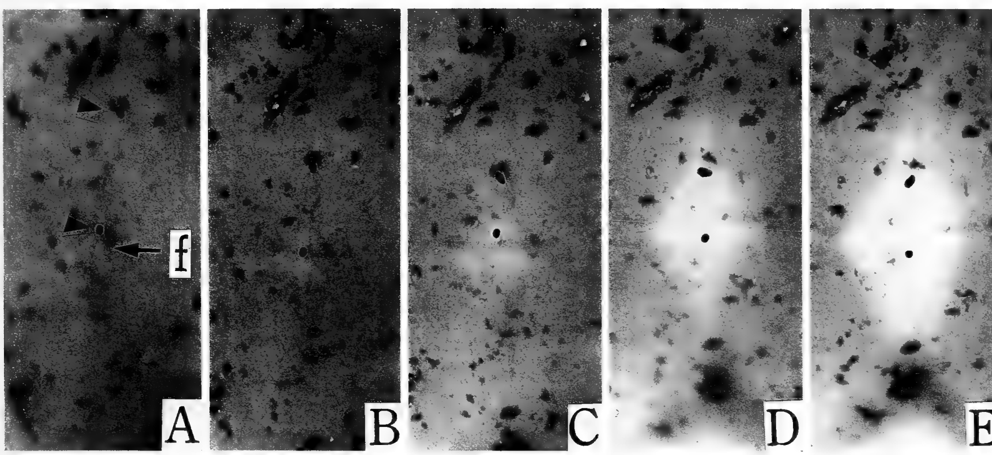

FIG. 7. Change of the distance between two particles attached to the furrow bottom. The two particles are marked (arrow-head). The distance between them decreased in the early stage of furrowing (A–C), but later increased (C–E). f: furrow. Time (min): A–C, 5 and C–E, 10 in each. ×31.

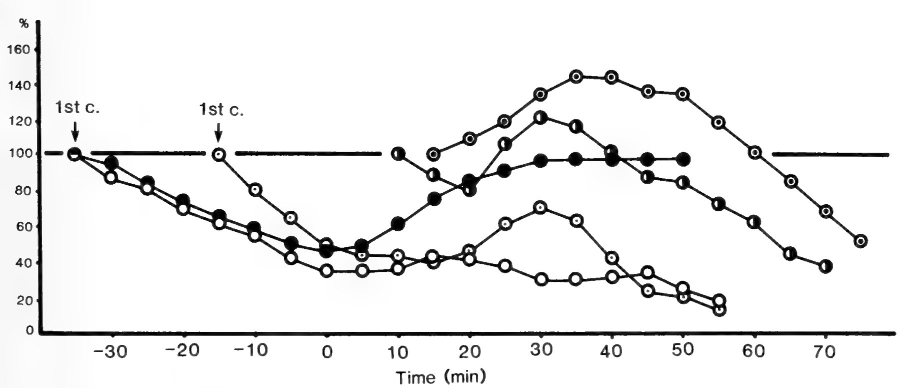

FIG. 8. Graphic representation of the change in distance between two particles attached to the furrow bottom. Ordinate: change in distance as a percentage for the initial value. Abscissa: times in min before (−) and after (+) the appearance of the pale surface. Measurements were started at the time of initiation of the first cleavage, in three cases (1st c), and after pale surface formation in two cases.

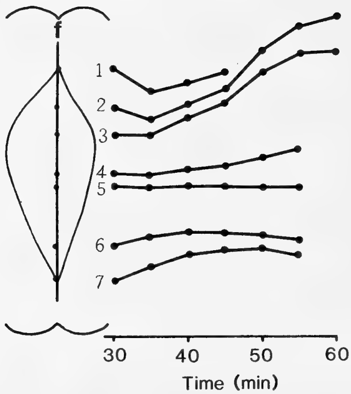

Fig. 9. Graphic tracing of movements of seven particles in the furrow bottom (f) in the late stage. Time: min after the onset of the first cleavage.

two particles on the furrow bottom from the early to middle stage. In such cases, change in the distance between two particles was measured (Fig. 8). This distance steadily shortened until the appearance of the pale surface (Figs. 7A–C and 8). In the subsequent phase of expansion of the pale surface, this shortening was temporarily arrested and in fact the distance slightly increased (Figs. 7C–E and 8). Then, contraction occurred again at about the time when the advancing tips of the furrow reached the vegetal pole. Figure 9 shows the movements of seven particles in the furrow bottom. In this case, many particles were attached to the furrow bottom of one egg, and the seven remained there for some time, although almost all eventually shifted away. The distance between two adjacent particles shortened on the two sides near the advancing tips of furrow (particles no. 1–2, 6–7), but lengthened in the centre of the furrow (particles no. 3–4, 4–5).

DISCUSSION

The process of pale-surface formation and its enlargement during cleavage of newt eggs were examined. The pale surface was formed by extreme expansion of the narrow region of pigmented surface between two stripes of the initial furrow, and successive growth of the pale surface occurred mainly in the region along the bottom of the deepening furrow. Simultaneously with increase in the surface area in the bottom of the furrow, the pale surface gradually shifted toward the boundary of the pigmented and the unpigmented surfaces, and accumulated near their border.

Schechtman [19] concluded from studies of vital staining that the pale surface was formed by expansion of the pigmented surface. In the present study, this expansion was found to be restricted to a small area of about 50 μm width which was demarkated by the two stripes of the initial furrow. Electron microscopy has shown that the egg surface of the initial furrow has more protrusions than the region outside the furrow [1, 22], and that when the furrow surface becomes unpigmented, its surface becomes relatively smooth [11, 22, 23]. These findings support the idea that increase in the membrane in the furrow region depends at least in part on the pre-existing zygote surface through a process such as flattening of surface projections. On the other hand, Selman and Waddington [8] and Zotin [20] postulated from cytological observations that the pale furrow surface was formed by addition to the pigmented surface of cell membrane that was newly constructed within the egg along the cell plate. Their postulation was supported by electron microscopic studies showing the presence of abundant membrane-bound vesicles under the furrow surface and their fusion to the furrow wall [1, 12, 21, 23]. Recently this idea has also been supported by results on radioiodination of surface proteins of *Xenopus* eggs [7].

These results on the source of membrane for pale surface formation probably imply that the change from the pigmented surface to the pale one is brought about by both expansion of the zygote surface and addition of cytoplasmic precursors.

Singal and Sanders [23] reported from ultrastructural observations on *Xenopus* eggs that growth of the pale surface in the late phase of furrowing was due to addition of membrane vesicles at two sites, the leading edge and lateral walls of the deepening furrow. Moreover, Byers and Armstrong [7] recently reported from optical studies on *Xenopus* eggs that the furrow surface grew in the region along the boundary of the pigmented and unpigmented surfaces. The present experiment showed directly that membrane

growth occurred mainly at the bottom of the deepening furrow, and that the plae surface gradually shifted toward the boundary of the two kinds of surfaces, accumulating at the boundary. The accumulated excess membrane protruded from the egg surface, forming eaves-structures. These structures seemed to be the same as the ridges [11] or lamellipodia [25] observed by electron microscopy. In the egg enveloped in egg membranes, these structures must function in connecting tightly adjacent blastomeres and conceal the furrow, but in the egg freed from the egg membrane, this connection would be inhibited by flattening of the eggs by gravity.

The base of the furrow of cleaving amphibian eggs always contains pigment granules and looks like a thin pigmented thread even after the appearance of the pale surface. Schechtman [19] and Byers and Armstrong [7] reported that the dark thread was derived from the pigmented surface of the zygote, i.e., a part of the initial furrow surface. Their reports are consistent with the present observation that some carbon particles remained on the furrow bottom. Ultrastructural studies have shown that the microfilamentous bundle is a contractile system in cytokinesis of large cells such as the amphibian egg as well as in small eggs and tissue cells. The present study confirmed the contraction of the cortex in the furrow region in the early furrowing stage. But, results showed that in the late stage, the contraction at the furrow base was temporarily arrested and instead slight stretching occurred. This result may be interpreted as follows. During unilateral division of the large amphibian egg, the initial furrow is formed by contraction of an arc of the filament bundle in the cortical layer of the animal pole. Probably, the contractile arc is extended by the bundle arrangement at the advancing tips of the furrow. When the arc becomes long in the middle to late stage, active contraction occurs mainly in the region of the two tips of the furrow. This contractile force pulls the surface of the central region of the furrow bottom toward the tips, temporarily arresting shrinking and instead causing stretching. When the furrow reaches the vegetal pole and a contractile ring is established round the whole egg, the ring contracts evenly, dividing the zygote into two blastomeres. Of these events, it is doubtful, however, whether stretching of the furrow surface in the late stage actually occurs during natural cleavage of the egg with the egg coats, in which the furrow region is closed by the tight contact of blastomeres.

ACKNOWLEDGMENT

This work was supported by a Grant-in-Aid for Project Research from the Ministry of Education, Science and Culture of Japan (58340042) to Y. Hiramoto.

REFERENCES

1 Sawai, T. (1974) Furrow formation on a piece of cortex transplanted to the cleavage plane of the newt egg. J. Cell Sci., **15**: 259–267.

2 Sawai, T. (1976) Movement of the cell surface and change in surface area during cleavage in the newt's egg. J. Cell Sci., **21**: 537–551.

3 Sawai, T. (1980) On propagation of cortical factor and cytoplasmic factor participating in cleavage furrow formation of the newt's egg. Dev. Growth Differ., **22**: 437–444.

4 Sawai, T. (1982) Wavelike propagation of stretching and shrinkage in the surface of the newt's egg before the first cleavage. J. Exp. Zool., **222**: 59–68.

5 Sawai, T. (1984) Surface movement in the first cleavage stage of newt egg. Zool. Sci., **1**: 427–432.

6 Sawai, T. and Oda, T. (1983) Movement of the cell surface in the first cleavage stage in the newt egg. Bull. Yamagata Univ., Nat. Sci., **10**: 385–392.

7 Byers, T. J. and Armstrong, P. B. (1986) Membrane protein redistribution during *Xenopus* first cleavage. J. Cell Biol., **102**: 2176–2184.

8 Selman, G. G. and Waddington, C. H. (1955) The mechanism of cell division in the cleavage of the newt's egg. J. Exp. Biol., **32**:700–733.

9 Bluemink, J. G. (1970) The first cleavage of the amphibian egg. An electron microscope study of the onset of cytokinesis in the egg of *Ambystoma mexicanum*. J. Ultrastruct. Res., **32**: 142–166.

10 Bluemink, J. G. (1971) Cytokinesis and cytochalasin-induced furrow regression in the first cleavage zygote of *Xenopus laevis*. Z. Zellforsch. Mikrosk. Anat., **121**: 102–126.

11 Selman, G. G. and Perry, M. M. (1970) Ultrastructural changes in the surface layers of the newt's egg in relation to the mechanism of its cleavage. J. Cell Sci., **6**: 207–227.

12 Kalt, M. R. (1971) The relationship between cleavage and blastocoel formation in *Xenopus laevis*. II.

Electron microscopic observation. J. Embryol. Exp. Morphol., **26**: 51–61.

13 Kubota, T. (1979) Mechanism of cleavage of newt eggs. J. Cell Sci., **37**: 39–45.

14 Perry, M. M., John, H. A. and Thomas, N. S. T. (1971) Actin-like filaments in the cleavage furrow of newt egg. Exp. Cell Res., **65**: 249–253.

15 Schroeder, T. E. (1981) Interrelations between the cell surface and the cytoskeleton in cleaving sea urchin eggs. In "Cytoskeletal Elements and Plasma Membrane Organization". Ed. by G. Poste and G. L. Nicolson, Elsevier/North Holland, Amsterdam, pp. 169–216.

16 Conrad, G. W. and Rappaport, R. (1981) Mechanisms of Cytokinesis. In "Mitosis/Cytokinesis". Ed. by A. M. Zimmerman and A. Forer, Academic Press, New York, pp. 365–396.

17 Karasiewicz, J. (1981) Electron microscope studies of cytokinesis in metazoan cells. In "Mitosis/Cytokinesis". Ed. by A. M. Zimmerman and A. Forer, Academic Press, New York, pp. 419–436.

18 Mabuchi, I. (1986) Biochemical aspects of cytokinesis. Int. Rev. Cytol., **101**: 175–213.

19 Schechtman, A. M. (1937) Localized cortical growth as the immediate cause of cell division. Science, **85**: 222–223.

20 Zotin, A. I. (1964) The mechanism of cleavage in amphibian and sturgeon eggs. J. Embryol. Exp. Morphol., **12**: 247–262.

21 Bluemink, J. G. and De Laat, S. W. (1973) New membrane formation during cytokinesis in normal and cytochalasin B-treated eggs of *Xenopus laevis*. I. Electron microscope observations. J. Cell Biol., **59**: 89–108.

22 De Laat, S. W. and Bluemink, J. G. (1974) New membrane formation during cytokinesis in normal and cytochalasin B-treated eggs of *Xenopus laevis*. II. Electrophysiological observations. J. Cell Biol., **60**: 529–540.

23 Singal, P. K. and Sanders, E. J. (1974) An ultrastructural study of the first cleavage of *Xenopus* embryos. J. Ultrastruct. Res., **47**: 433–451.

24 Sanders, E. J. and Singal, P. K. (1975) Furrow formation in *Xenopus* embryos. Involvement of the Golgi body as revealed by ultrastructural localization of thiamine pyrophosphatase activity. Exp. Cell Res., **93**: 219–224.

25 Ohshima, H. and Kubota, T. (1985) Cell Surface changes during cleavage of newt eggs: scanning electron microscopic studies. J. Embryol. Exp. Morphol., **85**: 21–31.

26 Shinagawa, A. (1986) Close correlation of the periodicities of the cleavage cycle and cytoplasmic cycle in early newt embryos. Dev. Growth Differ., **28**: 251–257.

27 Okamoto, M. (1972) A method for the removal of the jelly and vitelline membrane from the embryos of *Xenopus laevis*. Dev. Growth Differ., **14**: 37–41.

ZOOLOGICAL SCIENCE 4: 833–838 (1987)

Activity Changes in Myosin ATPase during Metamorphosis of Fruitfly

SUMIKO TAKAHASHI and KOSCAK MARUYAMA

Department of Biology, Faculty of Science, Chiba University, Chiba 260, Japan

ABSTRACT—The K^+-ATPase activity of a crude myosin preparation of *Drosophila* was low in larval stage, decreased at pupation, gradually increased during pupal stage, and abruptly increased within 5 hr after the emergence of adult fly. Purity examinations, however, revealed that larva and pupa myosins were heavily contaminated with other proteins. Highly purified preparations showed that both the K^+- and Ca^{2+}-ATPase activities of larva myosin were appreciably higher than those of actively flying adult fly, and pupa myosin had the enzyme activities of half a level as compared with those of larva or adult myosins. Two dimensional gel electrophoresis revealed that myosin light chains undergo changes during metamorphosis of the fruitfly.

INTRODUCTION

Many insects undergo metamorphosis where remarkable changes in muscular function occur. In 1954, one of the present authors reported that myosin ATPase activities of housefly larva and pupa were low, and increased suddenly at the emergence of adult fly [1]. At that time, a suitable method for purity test was not available. In 1962, Levenbook and his associates [2] described that myosin ATPase activity of blowfly larva was only slightly lower than that of adult fly. Schlieren patterns showed that larva myosin was contaminated with tropomyosin, but not adult one, suggesting that ATPase activity of larva myosin was rather comparable with that of adult myosin. Recently, characterization of *Drosophila* adult and larva myosin light chains has been performed by Takano-Ohmuro and her collaborators ([3]; for a review, see [4]).

The present work has been attempted aiming at elucidation of changes in myosin ATPase activities during metamorphosis of *Drosophila* fruitfly.

MATERIALS AND METHODS

Materials

Drosophila melanogaster was reared in our laboratory. The wild strain was kindly supplied by Prof. Y. Hotta of the University of Tokyo.

Accepted June 2, 1987
Received April 16, 1987

Methods

Preparation of myosin Crude myosin was prepared from 200 insects. Whole larva, pupa, and fly were homogenized in a solution (0.1 M KCl, 1 mM EDTA, 0.1 mM phenylmethylsulfonyl fluoride (PMSF), leupeptin, 10 μg/ml, and 10 mM Tris-HCl, pH 7.0) and centrifuged at $8000 \times g$ for 5 min. The sediment was washed once more. The precipitate was extracted with 2 ml of a salt solution (0.6 M KCl, 1 mM $NaHCO_3$, 0.1 mM PMSF, leupeptin, 10 μg/ml, and 10 mM EDTA) for 1 hr at 0°C. The supernatant after centrifugation at $10{,}000 \times g$ for 10 min was used. For purification of myosin, washed sediments of 10–20 g of larvae, 30–50 g of pupae or 3–5 g of flies were extracted with a salt solution (0.6 M KCl, 10 mM $NaHCO_3$, 3 mM ATP, 10 mM pyrophosphate, and 2 mM $MgCl_2$) for 30 min at 0°C. The supernatant was diluted with 20 vol. of cold water and myosin was precipitated by centrifugation for 10 min at $8{,}000 \times g$. The precipitate was dissolved in 0.6 M KCl containing 1 mM $NaHCO_3$. These dissolution and dilution-precipitation procedures were repeated twice. The final myosin solutions were clarified by a centrifugation for 20 min at $10{,}000 \times g$.

ATPase measurements Myosin ATPase activities were assayed by measuring Pi liberated from ATP according to Martin and Doty [5], and expressed as

μmoles Pi/mg/min. Myosin was incubated for 2–5 min at 25°C in the presence of 1 mM ATP, 3 mM $CaCl_2$, 0.1 M KCl and 10 mM imidazole buffer, pH 6.0 (Ca^{2+}-ATPase) or of 1 mM ATP, 1 M KCl, 10 mM EDTA, and 10 mM imidazole buffer, pH 8.0 (K^+-ATPase).

SDS gel electrophoresis SDS gel electrophoresis was carried out according to Weber and Osborn [6], using 7.5% polyacrylamide gels.

Two dimensional gel electrophoresis Two dimensional gel electrophoresis (first, isoelectric focusing and second, SDS gel electrophoresis) was performed as reported by Takano-Ohmuro *et al.* [3].

RESULTS

Activity changes of crude myosin ATPase during life span of fruitfly

Figure 1 summarizes the changes in myosin K^+-ATPase activity during life span of the fruitfly. K^+-ATPase action of myosin was measured to avoid Mg^{2+}- or Ca^{2+}- enhanced activities of any contaminated ATPases in crude preparations. Larva myosin ATPase activity was moderate, decreased on pupation, and remarkably increased at the emergence of adult fly. The ATPase activity elevated twice within 5 hr after the emergence of fly. This sudden increase during early stages of adult life in ATPase activity was repeatedly confirmed. The high level of ATPase activity remained constant during adult life until the end, where a notable decline occurred just before death.

The above mentioned changes were in agreement with the data with housefly reported 30 years ago [1]. However, on examination of purities of the myosins used, it turned out that both larva and pupa myosin preparations were heavily contaminated with proteins other than myosin (Fig. 2). Even adult myosin preparation contained actin and other proteins. Note that the Ca^{2+}-ATPase activity of larva myosin preparation was almost the same as that of pupa one, although the K^+-ATPase activity of the former was higher than the latter. Mg^{2+}-ATPase activities were to a small extent in all the cases.

Comparison of ATPase activities of larva, pupa, and adult myosin

Myosin was purified from full grown larva, pupae (approximately 6 days and 8 days after hatch) and adult fly of *Drosophila* by the procedure rountinely carried out in this laboratory [7].

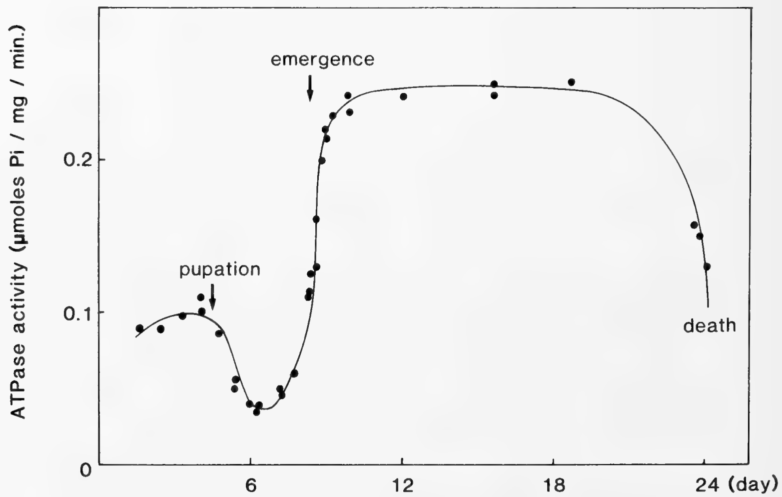

FIG. 1. Changes in K^+-ATPase activities of crude myosin preparations during life span of the fruitfly. Assay conditions: 1 M KCl, 10 mM EDTA, 1 mM ATP and 10 mM imidazole buffer, pH 8.0, 25°C.

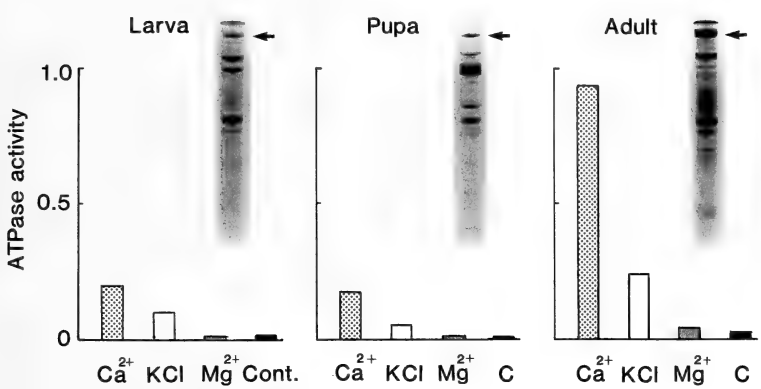

FIG. 2. Comparison of ATPase activities of crude myosin preparations from fruitfly larva, pupa, and adult fly. Assay conditions: 0.1 M KCl, 3 mM $CaCl_2$ or 1 mM $MgCl_2$ (none for control), 1 mM ATP and 10 mM imidazole buffer, pH 6.0, 25°C. For KCl-ATPase, see conditions in Fig. 1. Arrows in SDS gel electrophoresis patterns (7.5% polyacrylamide gels) indicate myosin heavy chains.

As seen in Figure 3, myosin heavy chain and two species of light chains were main bands in all the preparations, although slight contaminations were detected in SDS gel electrophoresis. Surprisingly, the larva myosin ATPase activities were even higher than that of adult myosin in both Ca^{2+}- and K^+- activated enzyme actions (Fig. 4). The pupa myosin ATPase activities at an early stage were significantly lower than those of larva or adult myosin. However, at a late stage, pupa myosin ATPase activities became closer to those of adult one. It is to be noted that even pupa Ca^{2+}-ATPase activity (0.8 μmoles/mg/min) was higher than that of rabbit skeletal myosin (0.5 μmoles/mg/min) under similar conditions (cf. [7]).

Effects of pH on the myosin ATPase activities were compared between larva and adult preparations. As seen in Figure 5, the K^+-ATPases were not much influenced by pH, the maximal being around pH 8.0 for both myosins. On the other hand, the Ca^{2+}-ATPase activities showed a biphasic pH dependence (Fig. 6). The optimal pH of adult myosin (pH 6.0) was slightly different from that of larval myosin (pH 5.8). In both cases, the ATPase levels were higher for larval myosin than for adult one (Figs. 5 and 6).

Light chains of larva, pupa, and adult myosins

In Figure 3, the presence of light chains of approximately 30 kDa and 20 kDa was recognized in all the *Drosophila* myosins. Takano-Ohmuro *et al.* classified *Drosophila* myosin light chains into fibrillar (adult thorax) type (Lf1, Lf2 and Lf3) and tubular (larva muscle and adult leg muscle) type (Lt1, Lt2 and Lt3) [3]. Chain weights are as follows: Lf1, 34 kDa; Lf2, 30 kDa and Lf3, 20 kDa; Lt1, 31 kDa; Lt2, 30 kDa and Lt3, 20 kDa, respectively.

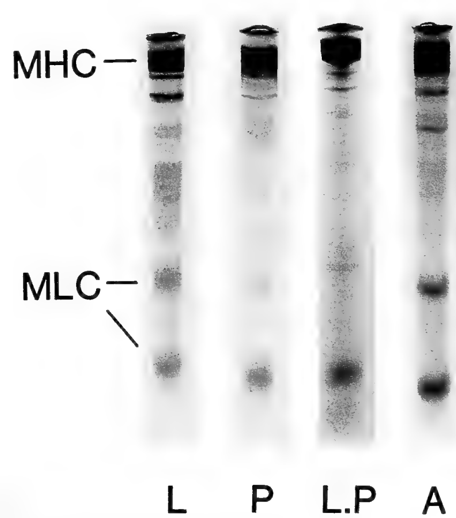

FIG. 3. SDS gel electrophoresis patterns of purified myosin preparations from fruitfly larva, pupae and adult fly. L, larva; P, early pupa; L. P, late pupa; A, adult. MHC, myosin heavy chains; MLC, myosin light chains.

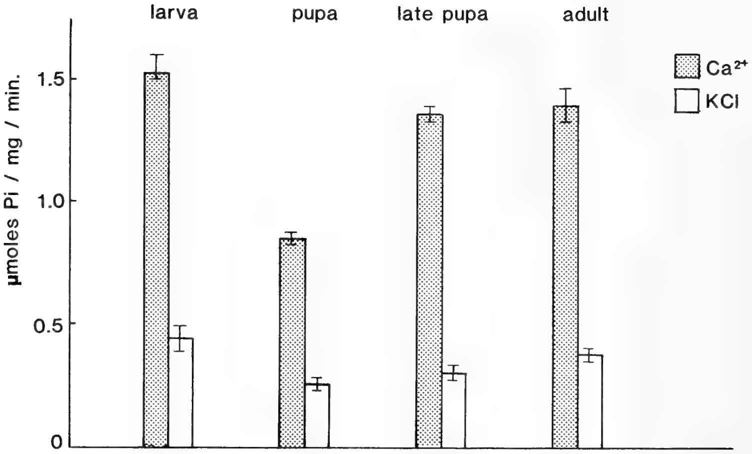

FIG. 4. Comparison of ATPase activities of purified myosin preparations from fruitfly larva, pupae and adult fly. Assay conditions, as in Fig. 2.

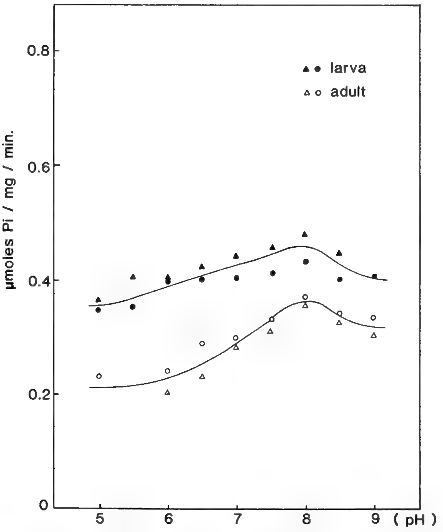

FIG. 5. pH-activity curves of myosin K^+-ATPases from fruitfly larva and adult. Assay conditions, as in Fig. 2.

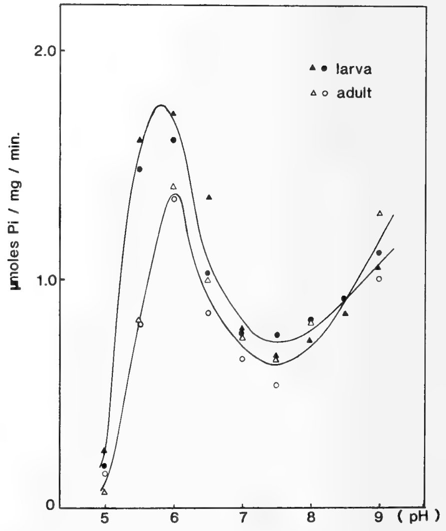

FIG. 6. pH-activity curves of myosin Ca^{2+}-ATPases from fruitfly larva and adult. Assay conditions, as in Fig. 2.

Therefore, the present myosin preparations were subjected to 2 dimensional electrophoresis to distinguish each light chain. As shown in Figure 7, Lt1, Lt2 and Lt3 were identified in larva and pupa myosins. In adult myosin, Lf2 (=Lt2) and Lf3 (=Lt3) were detected. However, Lf1 was not detected in purified adult myosin preparations (Fig. 7) for unknown reasons, although it was present in crude preparations (Fig. 8). It is suggested that larva and pupa myosins were mainly tubular type and adult myosin was largely fibrillar type although the latter contained tubular type, too. This was the same as late pupa myosin.

During the analyses with adult myosin light chains, it was observed that there existed an additional spot at the acidic side of Lf2 in crude

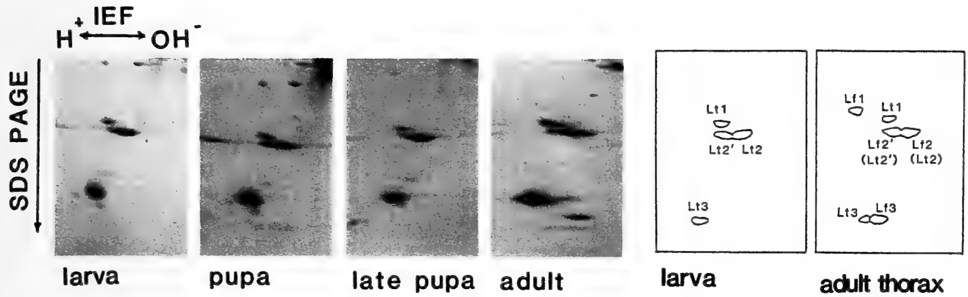

FIG. 7. Two dimensional gel electrophoresis patterns of myosin light chains of fruitfly larva, pupa and adult fly. IEF, isoelectric focusing; SDS PAGE, SDS gel electrophoresis patterns. For terminology, see ref. [3]. Schematic patterns are reproduced from Takano-Ohmuro *et al.* [3].

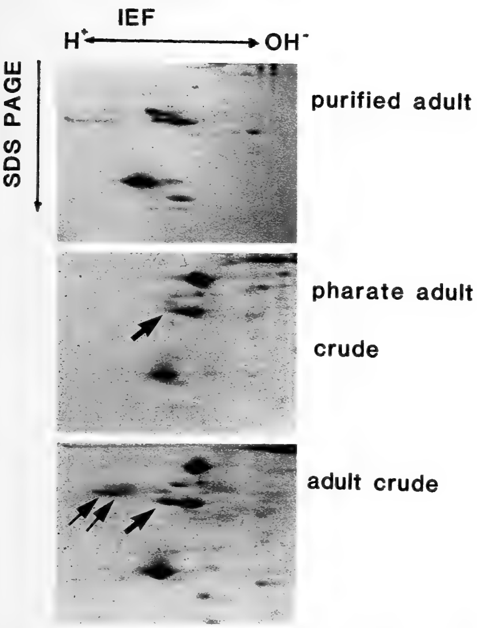

FIG. 8. Two dimensional gel electrophoresis patterns of myosin light chains of fruitfly adult myosin preparations. Double arrow indicates Lf1 in adult crude preparation (not detected in purified preparation).

prepartions, it decreased purified preparations (Fig. 8). This spot may correspond to Lf2′ called by Takano-Ohmuro *et al.* [3]. Furthermore, this spot was not present even in a crude myosin preparation of pharate adults (just before emergence of fly), as seen in Figure 8. This spot may be phosphorylated light chain, as observed in cricket thoracic myosin (27′ kDa LC) [8].

DISCUSSION

The present work completely denies the previous view that myosin ATPase activity of slowly moving larva of Diptera was low and that of actively flying adult was high, first reported by Maruyama [1]. That false observation was entirely due to heavier impurity of larva myosin preparations, as evident in the present study (cf. Figs. 2, 3, and 4). Purified myosin from larva showed even higher Ca^{2+}- or K^{+}-ATPase activities than those of adult fly. This was already suggested by Kominz *et al.* [2] using less purified blowfly myosin. It is more difficult to purify larva myosin than adult one, probably because the myosin content is much smaller in the former: approximately 3–5 mg of myosin was obtained from 10–20 g of larva in comparison with the similar yield from 3–5 g of adult fly. According to morphological investigations ([9]; for a review, see [10]), there are visceral and intersegmental striated muscles in larva. We have observed striation of larval muscles under microscope. Takano-Ohmuro *et al.* [3] adopted Snodgrass' classical terminology: tubular (larval muscles, adult leg muscles) and fibrillar (indirect flight muscle), and showed that there are distinct differences in light chains between tubular and fibrillar types of myosin. The present work has confirmed the results of Takano-Ohmuro *et al.* and extended that the ATPase activity of tubular myosin is slightly higher than that of fibrillar myosin. Maruyama *et al.* [11] described that Ca^{2+}-dependent Mg^{2+}-ATPase activity of water-bug tubular (leg) actomyosin was markedly higher

than that of fibrillar (indirect flight) actomyosin. However, judging from pH dependence of both K^+- and Ca^{2+}-ATPase activities, the properties of larva and adult myosins appeared to be similar to each other (Figs. 5 and 6).

The decrease in myosin ATPase activity during pupation requires a careful investigation, because larval muscles largely undergo "histolysis" and then differentiation of fibrillar muscle starts ([12]; cf. [10]). The sudden increase in the myosin ATPase activity within a few hours after emergence of adult fly is noteworthy. The newly emerged adult cannot fly, and gets flight ability within a few hours in good parallel with the increase in ATPase activity. Similar increase in myofibrillar Ca^{2+}-ATPase activity was observed with honeybee thoracic muscle, a few days after emergence accompanied with gain of flight ability [13]. It is of special interest to test whether the post-hatch increase in myosin ATPase activity is due to phosphorylation of myosin light chains (Lf2) or not (cf. [8]). In fact, in crude myosin preparation from actively flying adult, there was an additional spot, possibly phosphorylated Lf2, which was not present in crude myosin from pharate adult before emergence (Fig. 8). There is a possibility that phosphorylated light chain was dephosphorylated during purification procedures. It is highly desirable to get myosin with phosphorylated light chain and to compare its ATPase activities with those of myosin with dephosphorylated light chain.

Finally, it should be mentioned that there was a significant decrease in myosin ATPase occurred in aged adults, as shown in Figure 1. This was not due to any increased amount of contaminants. The decrease in myosin ATPase activity of aged muscle may be of some importance from gerontological point of view (cf. [4]).

REFERENCES

1 Maruyama, K. (1954) The activity change of actomyosin ATPase during insect metamorphosis. Biochim. Biophys. Acta, **14**: 264–285.

2 Kominz, D. R., Maruyama, K., Levenbook, L. and Lewis, M. S. (1962) Tropomyosin, myosin and actin from the blowfly, *Phormia regina*. Biochim. Biophys. Acta, **63**: 106–116.

3 Takano-Ohmuro, H., Hirose, G. and Mikawa, T. (1983) Separation and identification of *Drosophila* myosin light chains. J. Biochem., **94**: 967–974.

4 Maruyama, K. (1985) Biochemistry of muscle contraction. In "Comprehensive Insect Physiology, Biochemistry and Pharmacology", Vol. 10. Ed. by G. A. Kerkut and L. I. Gilbert, Pergamon Press, Oxford, pp. 487–498.

5 Martin, J. B. and Doty, D. M. (1949) Determination of inorganic phosphate. Anal. Chem., **21**: 965–967.

6 Weber, K. and Osborn, M. (1969) The reliability of molecular weight determinations by dodecyl sulfate-polyacrylamide gel electrophoresis. J. Biol. Chem., **244**: 4406–4412.

7 Tanikawa, M., Ueyama, A. and Maruyama, K. (1986) Instability of insect myosin ATPase activity and its protection. Comp. Biochem. Physiol., **86B**: 63–65.

8 Takano-Ohmuro, H., Tanikawa, M. and Maruyama, K. (1986) Phosphorylation of cricket myosin light chain and Mg^{2+}-activated actomyosin ATPase activity. Zool. Sci., **3**: 715–717.

9 Goldstein, M. A. and Burdette, W. J. (1971) Striated visceral muscle of *Drosophila melanogaster*. J. Morphol., **34**: 315–334.

10 Crossley, A. C. (1978) The morphology and development of the *Drosophila* muscular system. In "The Genetics and Biology of *Drosophila*", Vol. 26. Ed. by M. Ashburner and T. R. F. Wright, Academic Press, New York, pp. 499–560.

11 Maruyama, K., Tregear, R. T. and Pringle, J. W. S. (1968) The calcium sensitivity of ATPase activity of myofibrils and actomyosins from insect flight and leg muscles. Proc. Roy. Soc. (London), **169B**: 229–240.

12 Shafiq, S. A. (1963) Electron microscopic studies of the indirect flight muscles of *Drosophila melanogaster* II. Differentiation of myofibrils. J. Cell Biol., **17**: 363–374.

13 Sakagami, S. F. und Maruyama, K. (1956) Aktivitätsänderung der Adenosintriphosphatase im Flugmuskel der Bienenarbeiterinnen während ihres ersten Imaginallebens. Z. vergl. Physiol., **39**: 21–24.

14 Takahashi, A., Philpott, D. E. and Miquel, J. (1970) Electron microscopic studies on aging *Drosophila melanogaster*. III. Flight muscle. J. Gerontol., **25**: 222–228.

ZOOLOGICAL SCIENCE 4: 839–847 (1987)

Meiotic Divisions and Early-Mid-Spermiogenesis from Cultured Primary Spermatocytes of *Xenopus laevis*

Shin-Ichi Abé and Shoji Asakura

Department of Biology, Faculty of Science, Kumamoto University, Kurokami 2-chome, Kumamoto 860, Japan

ABSTRACT—Dissociated primary spermatocytes from *Xenopus laevis* were cultured in dishes coated with poly-L-lysine. Single primary spermatocytes in metaphase which attached to the dish were marked and their extent of differentiation was observed with phase contrast microscopy. The primary spermatocytes completed first and second meiotic divisions and produced quadruplets of round spermatids within a day. The spermatids formed flagella and acrosomes; later the acrosomes condensed. Finally, the spermatids elongated and the round nuclei were situated on one side of the cells. However, nuclear elongation did not occur. Electron microscopic observation revealed that round mitochondria assembled around the nuclei of spermatids when the acrosomes were formed. Sometimes cell fusion occurred in pairs of secondary spermatocytes and among quadruplets of spermatids. The efficiency of differentiation to the stage of the formation of flagella and acrosomes in spermatids was greater than 90%. About 60% of the spermatocytes advanced to the stage of elongated spermatids. The possible contribution of Sertoli cells to the promotion of differentiation was examined by reducing the number of Sertoli cells to less than 10 per culture. Under these conditions differentiation proceeded at a very high efficiency. The time schedule of differentiation *in vitro* was obtained at 22°C: from telophase I to telophase II, about a day; interphase II, about 18 hr; from telophase II to acrosome formation in spermatids, about 1.3 days; from telophase II to acrosome condensation, about 5.6 days; from telophase II to elongated spermatids, about 7.7 days.

INTRODUCTION

An *in vitro* culture of spermatogenic cells that supports spermatogenesis would provide an excellent means to analyze the mechanisms of spermatogenesis. Recently, the culture of amphibian spermatogenic cells has been refined. In the newt [1–3], single primary spermatocytes cultured within collagen matrix completed two meiotic divisions resulting in four round spermatids which formed flagella, acrosomes, rings and neckpieces [1, 3]. Also single spermatids cultured within collagen matrix elongated their nuclei [2, 3]. However, cytoplasmic shedding and the final stages of chromatin condensation did not occur. In *Xenopus laevis,* Risley and Eckhardt [4] and Risley [5] demonstrated that leptotene-zygotene spermatocytes advanced to pachytene spermatocytes, and some zygotene and most pachytene-diplotene spermatocytes progressed through meiotic divisions. The resultant round spermatids formed flagella and acrosomes and displayed cytoplasmic shedding and partial chromatin condensation. However, spermatid nuclear elongation and the final stages of chromatin condensation did not occur.

Risley [5] observed spermatogenic cells cultured in cell suspension and counted the numbers of each cell type as differentiation proceeded. The disadvantage of cell suspension is that it is almost impossible to follow the fate of individual single primary spermatocytes. Hence, it is difficult to observe cytological changes which occur consecutively in individual cells during spermatogenesis. It is also difficult to determine the efficiency of differentiation and the exact time that is required for cells to progress from one stage to another. To circumvent these difficulties, we cultured *Xenopus* primary spermatocytes on poly-L-lysine-coated

Accepted April 23, 1987
Received March 16, 1987

culture dishes to which the cells adhered firmly. We followed single primary spermatocytes in metaphase that were marked and determined the stage and efficiency of differentiation that they attained, as well as the length of time required to reach a respective stage.

MATERIALS AND METHODS

Cell culture of spermatogenic cells on poly-L-lysine(pLL)-coated dishes

Testes from one or two adult *Xenopus laevis* were minced with scissors and dissociated into single cells by incubation for 3 hr at 22°C in 5 ml of 0.2% collagenase (type I, Sigma) prepared in 70% Leibovitz-15 (L–15) medium, pH 7.4 (1.043 g L–15 medium powder (GIBCO) was dissolved in 100 ml deionized, triple-distilled water containing 10 mM HEPES, 10,000 IU of penicillin and 10 mg of streptomycin). Then, 0.1 ml of 0.1% DNase I (Sigma) was added and the cells were incubated for an additional 15 min. After gentle pipetting, the resultant cell suspension was filtered through Nitex filters (100 μm and then 50 μm pore size) and the cells were collected by centrifugation. The sedimented cells were washed in OR2 (a balanced salt solution) [6], suspended in 8% Metrizamide (Analytical grade, Nyegaard & Co., Norway) in OR2 solution and centrifuged at $10,000 \times g$ for 20 min. The supernatant contained spermatocytes, early-mid stage spermatids and a small number of Sertoli cells [5]. The cells were washed twice in OR2 and then once in 70% L–15 medium. In a plastic culture dish (3.5 cm in diameter) $2\text{–}10 \times 10^4$ cells were plated. For observation through an oil immersion lens, 6.0 cm plastic dishes whose central areas (about 10 cm^2) had been replaced with coverslips were used. The culture dishes were previously coated with 0.1% pLL (Sigma, M. W. 14,000–27,000) and incubated overnight. Before inoculation of cells, the dishes were washed three times with OR2. After the cells settled (1–2 hr after inoculation), the medium was replaced with 60% L–15 medium supplemented with 10% fetal bovine serum. This medium was prepared by dissolving 0.894 g of L–15 powder in 90 ml of deionized, triple-distilled water to which antibiotics and 10 ml of fetal bovine serum were added. The HEPES was dissolved to be 10 mM and pH of the medium was adjusted to be 7.4. Fetal bovine serum (Lot. No. KC300135), obtained from KC Biological Inc., U. S. A., was previously heat-inactivated (55°C, 30 min) and dialyzed against OR2 overnight.

In order to separate spermatogenic cells from Sertoli cells, the cell suspension was plated in plastic culture dishes lacking the coating of pLL. On the next day, Sertoli cells adhered firmly to the bottom of the dish, whereas spermatocytes and round spermatids did not. The supernatant was collected, centrifuged and the cells were plated in culture dishes coated with pLL. After the cells settled, the medium was replaced with 60% L–15 medium supplemented with fetal bovine serum.

Cultures were maintained in a dark incubator at 22°C. On the next day following the inoculation, single primary spermatocytes in metaphase were marked on the undersurface of the dish with a pen and observed. Medium was changed every 3 or 4 days.

Electron microscopy

Cultured cells were fixed in 2.0% glutaraldehyde (Nakarai) in OR2, pH 7.4 for 1 hr at room temperature, postfixed in 1.0% OsO_4 (Nakarai) in M/15 phosphate buffer, pH 7.4 for 30 min at 4°C, and dehydrated by passage through a graded series of ethanols. The cells were embedded in Epok 812 (Oken Shoji, Japan) and the resin was polymer-

Fig. 1. Phase contrast photomicrographs showing two meiotic divisions and spermiogenesis in *Xenopus laevis in vitro*. Oil immersion lens was used. Bar indicates 10 μm.
a. A primary spermatocyte in metaphase. b. Telophase I of a primary spermatocyte. c. Interphase of a pair of secondary spermatocytes derived from a primary spermatocyte. d. Metaphase II. e. Telophase II. f. A quadruplet of round spermatids. g. Round spermatids in which large acrosomes were formed. Ac, acrosome; Nu, nucleus. h. Spermatid with a condensed acrosome. Fl, flagellum. i. Elongated spermatid with a round nucleus. j. The same cell as (i) but focus is slightly different from (i). Arrows indicate a dark line along the posterior part of the nuclear envelope which should be a cluster of round mitochondria.

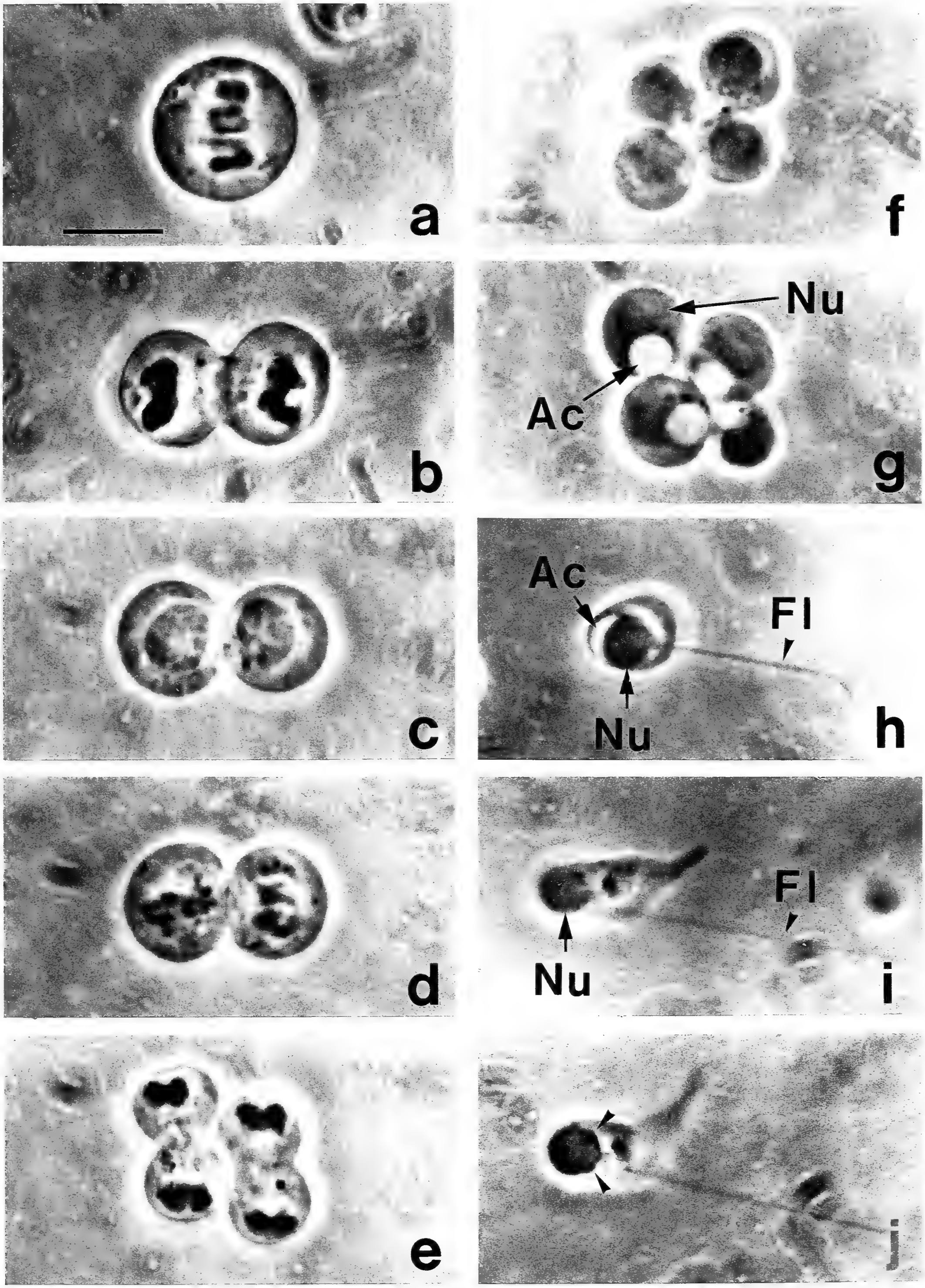
a
b
c
d
e
f
Nu
Ac
g
Ac
Fl
Nu
h
Fl
Nu
i
j

ized. A small area containing the marked cells was cut out, stripped off the plastic dishes, and mounted on supporting blocks. Ultra-thin sections were made with a Porter-Blum microtome MT–1, stained with aqueous uranyl acetate followed by lead citrate, and examined under a JEM 100C electron microscope.

RESULTS

Differentiation of primary spermatocytes

Primary spermatocytes in metaphase (Fig. 1a) completed the first division within a couple of hours (Fig. 1b) and formed pairs of secondary spermatocytes. During interphase II, the nuclei appeared homogeneous (Fig. 1c). The secondary spermatocytes proceeded through metaphase II (Fig. 1d) and telophase II (Fig. 1e) and formed quadruplets of round spermatids (Figs. 1f and 2). Soon, a flagellum developed in each round spermatid (Fig. 3). Small vacuoles appeared in the cytoplasm (Fig. 3) and became larger and fewer. Finally, after a couple of days, a round transparent acrosome, attached over a considerable area of the nuclear envelope, formed in each spermatid (Figs. 1g and 4). The diameter of the acrosome was almost the same as that of the nucleus. Some spermatids disappeared in a few days but most survived. After about a week, the acrosome began to condense (Figs. 1h and 5) and the cells assumed an elongated shape. Then the acrosome completely condensed (Fig. 1i, j). Flagella attained the length of 20–40 μm after one week's culture and did not increase after an additional week. A round nucleus was located in one side of the cell.

Electron microscopic observations revealed an interesting behavior of the mitochondria in spermatids. Just after the second division, small round mitochondria were scattered throughout the cytoplasm (Fig. 2). Within a day after the second division, some mitochondria assembled around the nucleus (Fig. 3). When the large acrosome was formed, most of the round mitochondria attached to the nuclear envelope (Fig. 4). During acrosome condensation (Fig. 5) and spermatid elongation, the mitochondria remained attached to the nuclear envelope. Phase contrast microscopic observation revealed a dark line along the posterior half contour of the nuclear envelope (Fig. 1j). The dark line should represent the cluster of round mitochondria attached to the posterior part of the nuclear envelope. In the cytoplasm of the elongating spermatid, membraneous structures and some microtubules were observed.

After first meiotic division, cell fusion between paired secondary spermatocytes frequently occurred. An average of 16% of primary spermatocytes (149 cells) in three experiments fused after first meiotic division. Likewise, fusion among spermatids frequently occurred following the second meiotic division. Thirty percent of secondary spermatocytes (189 cells) which had not fused after the first division fused after the second division. The fused spermatids differentiated normally except that a single large acrosome formed in a fused cell.

Efficiency of differentiation

The fate of 138 primary spermatocytes in metaphase from three experiments is summarized in Figure 6. More than 90% of the primary spermatocytes completed the first and second divisions and differentiated into round spermatids which formed flagella and acrosomes. About 70% of the initial primary spermatocytes formed spermatids with condensing acrosomes and about 60% advanced to elongated spermatids. Thus, differentiation progressed at a very high efficiency.

Differentiation at a very high efficiency could be due to some factor(s) which might be secreted from Sertoli cells in culture. In order to exclude the possible effect of Sertoli cells on the differentiation of spermatocytes or spermatids, Sertoli cells were removed from cultures as described in Materials and Methods. Before removal, the percentage of the Sertoli cells per inoculum was about 2% (1×10^3 Sertoli cells per inoculum of

Fig. 2. Electron microscopic photograph of a round spermatid a couple of hours after the second meiotic division. Bar indicates 1 μm. Arrows indicate round mitochondria through Fig. 2–Fig. 5.

Fig. 3. Fused spermatids. About 20 hr after the second meiotic division. Some small vacuoles appeared. Fl, flagellum.

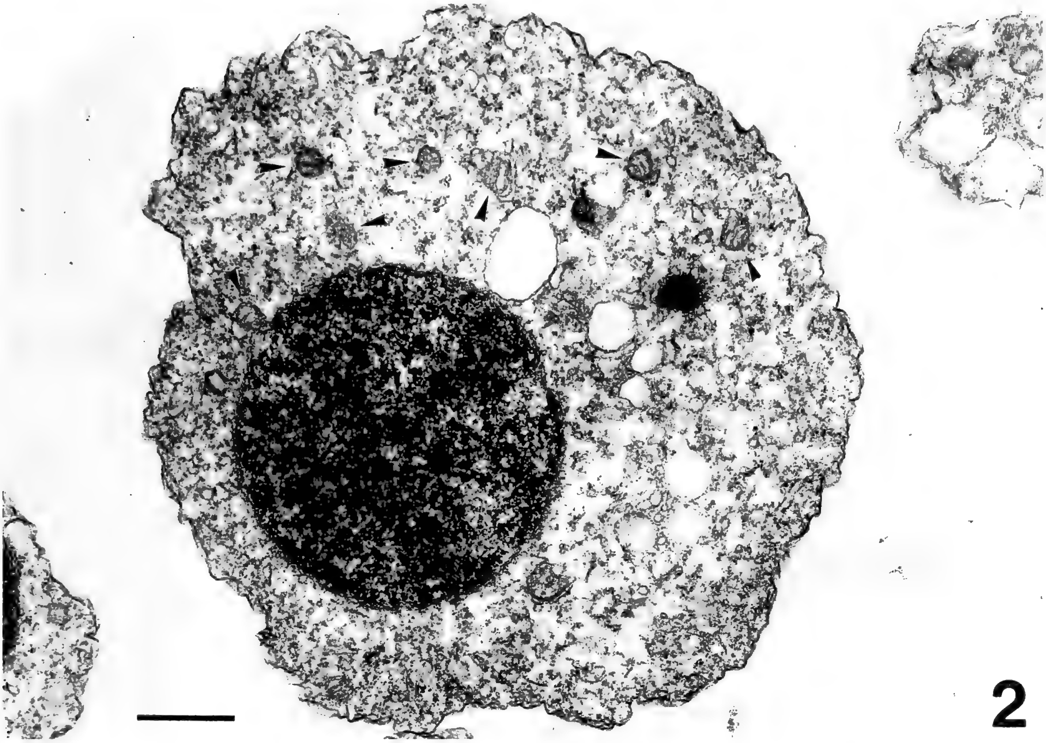
2

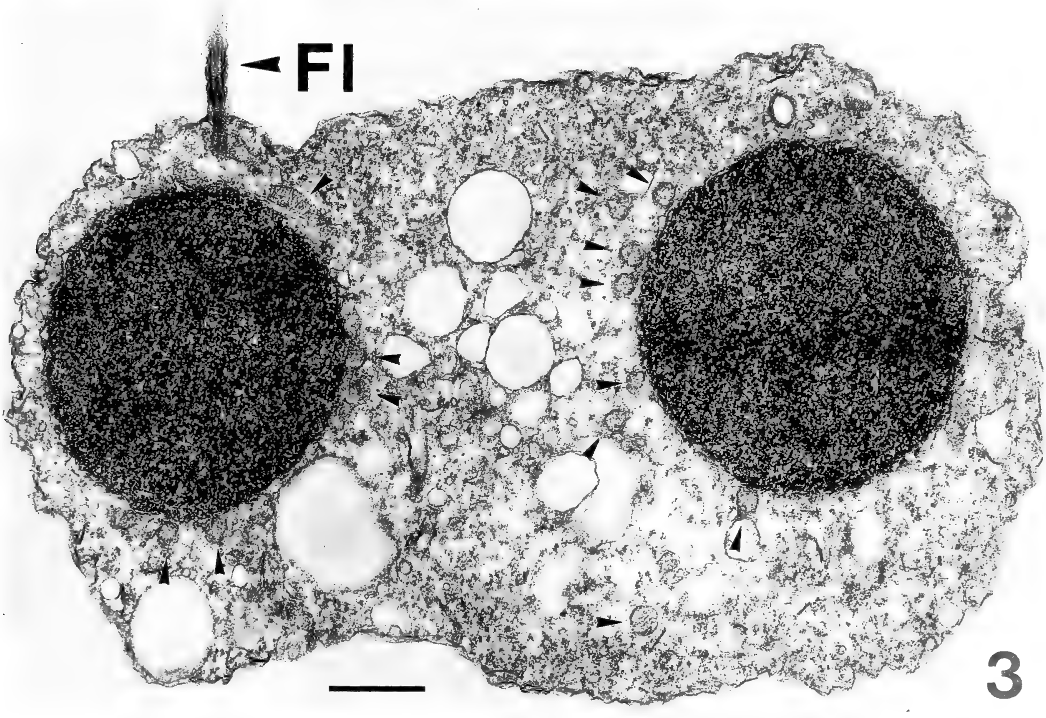

3

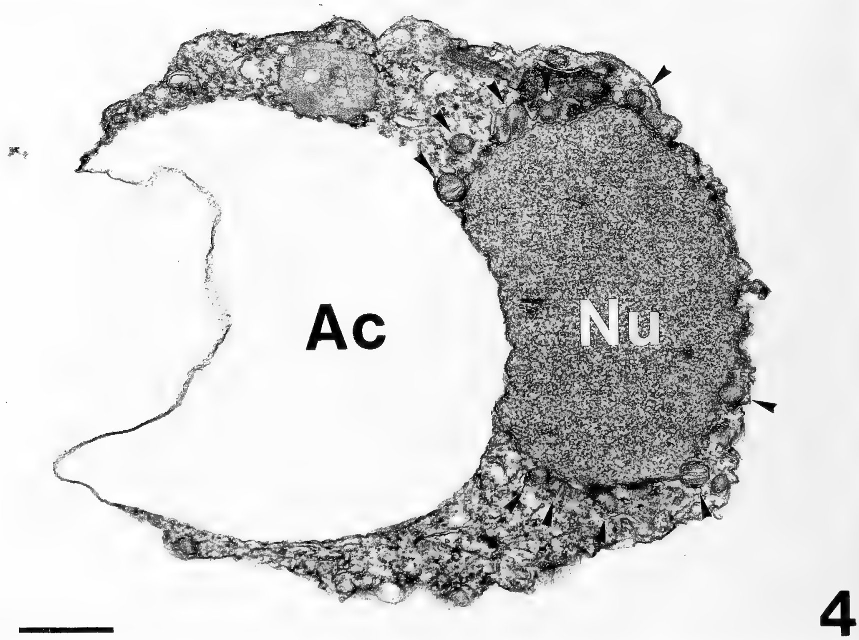

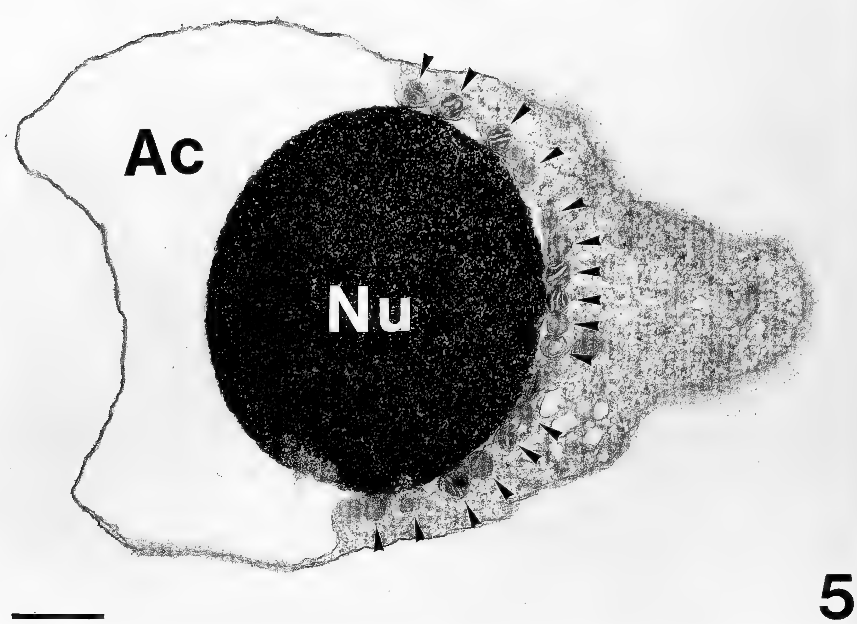

Fig. 4. A round spermatid with a large acrosome. Ac, acrosome; Nu, nucleus. Bar indicates 1 μm.
Fig. 5. A round spermatid with a condensed acrosome.

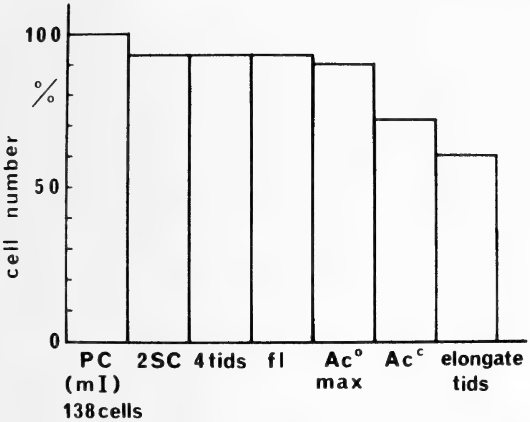

FIG. 6. The percentage of differentiated cells resulting from primary spermatocytes in metaphase. PC, primary spermatocytes in metaphase; 2SC, pairs of secondary spermatocytes; 4 tids, quadruplets of round spermatids; fl, spermatids with flagella; Ac° max, spermatids each with a large acrosome; Ac^c, spermatids with condensed acrosomes; elongate tids, elongated spermatids. In this graph, a pair of secondary spermatocytes and a quadruplet of spermatids derived from a primary spermatocyte were counted as one cell.

5×10^4 cells). After removal, the number of Sertoli cells was lower than 10 per dish. Even when very few Sertoli cells were present, differentiation proceeded at almost the same efficiency compared to those cultures that contained large numbers of Sertoli cells. Thus, the differentiation of spermatids *in vitro* does not require substantial numbers of Sertoli cells.

Time schedule of differentiation

The initially marked primary spermatocytes were observed at constant intervals and the time required for the progression of cells from one stage to another was obtained. From the primary spermatocyte to the formation of the acrosome in spermatids the changes were rapid and observations were made every 1–3 hr. Following the formation of the acrosome, the changes were very slow and the cells were observed every 10 hr. The period between telophase I and telophase II extended about a day (Table 1). Interphase II lasted about 18 hr. Within 3 hr following telophase II, a short motile flagellum (about 1 μm) developed in each round spermatid. Within about 1.3 days after telophase II the complete formation of the acrosome occurred. About 7–8 days were required for the completion of the acrosome condensation and the elongation of the spermatids.

DISCUSSION

The fate of individual primary spermatocytes of *Xenopus laevis* that attached to pLL-coated culture dishes was observed with phase contrast microscopy. We obtained direct evidence that each spermatocyte completed two meiotic divisions and the resultant quadruple round spermatids formed flagella and acrosomes. The acrosomes condensed, the cells elongated and the nuclei were situated on one side. Nuclear elongation, however, did not occur even after a prolonged culture period. Our results are similar to those of Risley who used different medium and cultured the cells in suspension [5].

We also observed by electron microscopy that

TABLE 1. Time schedule of spermatogenesis in *Xenopus laevis* at 22°C *in vitro*

Period	Average time ±S.D.	No. of cells examined
telophase I ~ telophase II	22.2 ± 3.6 hr	42 cells
interphase II	17.8 ± 3.8	39
telophase II ~ acrosome formation	31.3 ± 9.5 (1.3 ± 0.4 days)	36
telophase II ~ acrosome condensation	135.1 ± 18.3 (5.6 ± 0.8)	48
telophase II ~ elongate spermatids	185.2 ± 22.4 (7.7 ± 0.9)	23

round mitochondria in acrosomal spermatids attached to the posterior part of the nuclear envelope. Clearly, this phenomenon is the primary step toward mitochondrial assembly in the middle piece of mature sperm. What is the mechanism to assemble the mitochondria in the region close to the nuclear envelope?: Do microtubules transport them to the nuclear envelope? Or does the nuclear envelope attract the mitochondria by exposing some substances on the nuclear envelope? It needs a further study to answer these questions.

The possibility that Sertoli cells promote the differentiation of spermatocytes by secreting some factors into culture media was examined by reducing the presence of Sertoli cells to less than 10 per culture. Nevertheless, differentiation proceeded at an efficiency similar to that in cultures containing high numbers of Sertoli cells. This result suggests that Sertoli cells are not required *in vitro* for spermatogenesis from the stage of primary spermatocytes in metaphase to elongated spermatids. The function of Sertoli cells in spermatogenesis of *Xenopus laevis* remains to be elucidated.

The efficiency of differentiation was very high. More than 90% of the primary spermatocytes developed into spermatids with flagella and acrosomes. This efficiency of differentiation in *Xenopus* is comparable to that obtained in primary spermatocytes of the newt [7].

The time schedule of *Xenopus* spermatogenesis *in vitro* was obtained at 22°C. According to Kalt [8] who studied *Xenopus* spermatogenesis *in vivo,* the most rapidly maturing cells in the testis spend one day in meiotic division and 12 days in spermiogenesis at 18°C. The time schedule of our cells *in vitro* is comparable to that *in vivo*.

In our current studies with *Xenopus,* we used pLL to attach cells to the culture dishes. Various molecular weights of pLL were tested for their effect on viability and differentiation of cells; pLL with molecular weight lower than 27,000 had no inhibitory effect on meiotic divisions and differentiation of spermatids. But, pLL with high molecular weights (47,000, 90,000 and 120,000) was toxic to the cells.

It should be noted that cell fusion frequently occurred between secondary spermatocytes and between spermatids when cells were cultured in pLL-coated dishes. However, cell fusion rarely occurred when the cells were cultured in suspension in the dishes uncoated with pLL. Thus, cell fusion appears to be aided by pLL. Polycation polyarginine also induces fusion between sea urchin eggs [9]. In a fused spermatid differentiation proceeded normally except for the acrosome formation; even when a cell contained 2 or 4 nuclei, a single acrosome larger than normal was formed. How such a single acrosome is formed in a fused cell is now under investigation.

Previously, we showed in the newt that single primary spermatocytes completed two meiotic divisions and differentiated into round spermatids that formed flagella, acrosomes, rings and neckpieces [1]. Thus, we have shown that L–15 medium supports meiotic divisions and early-mid-spermiogenesis *in vitro* in both the newt and *Xenopus laevis* of which mature sperms are entirely different in size and shape from each other.

One of the differences observed in spermatogenesis *in vitro* between *Xenopus* and the newt is that the flagellar length in *Xenopus* is shorter (20–40 μm) than that in the newt (100–400 μm) [1]. Another difference is that the acrosome in the *Xenopus* spermatid is as large as the nucleus and easily observed by phase contrast microscopy, whereas the acrosome in the newt is small and not easily observed. Also, in the *Xenopus* spermatid mitochondria attached to the posterior part of the nuclear envelope when the acrosome was formed. However, in the newt acrosomal spermatids, mitochondria were scattered throughout the cytoplasm. These results correctly reproduce the difference in *in vivo* spermatogenesis between both species [10–16].

Since the culture of dissociated spermatogenic cells in *Xenopus* and the newt has been refined, future studies on the differences between newt and *Xenopus* spermatogenesis *in vitro* at the cellular and molecular levels should provide insight into the regulatory mechanisms governing the flagellar formation, acrosome formation, and the assemblage of mitochondria in the middle piece of the mature sperm.

ACKNOWLEDGMENTS

We thank Professor Marie A. DiBerardino (The Medical College of Pennsylvania) for editing this manuscript. This work was supported by a Research Grant from the Ministry of Education, Science and Culture of Japan (no. 60540467) and grants from the Ito Science Foundation and Naito Science Foundation to S. A.

REFERENCES

1 Abé, S.-I. (1981) Meiosis of primary spermatocytes and early spermiogenesis in the resultant spermatids in newt, *Cynops pyrrhogaster, in vitro.* Differentiation, **20**: 65–70.

2 Abé, S.-I. and Uno, S. (1984) Nuclear elongation of dissociated newt spermatids in vitro and their shortening by antimicrotubule agents. Exp. Cell Res., **154**: 243–255.

3 Abé, S.-I. (1987) Differentiation of spermatogenic cells from vertebrates *in vitro.* Int. Rev. Cytol., **109**: 159–209.

4 Risley, M. S. and Eckhardt, R. A. (1979) Evidence for the continuation of meiosis and spermiogenesis in in vitro cultures of spermatogenic cells from *Xenopus laevis* (1). J. Exp. Zool., **207**: 513–520.

5 Risley, M. S. (1983) Spermatogenic cell differentiation *in vitro.* Gamete Res., **4**: 331–346.

6 Wallace, R. A., Jared, D. W., Dumont, J. N. and Sega, M. W. (1973) Protein incorporation by isolated amphibian oocytes. III. Optimum incubation conditions. J. Exp. Zool., **184**: 321–334.

7 Nishikawa, A. and Abé, S.-I. (1983) Progression throughout all stages of meiosis from the early prophase of newt primary spermatocytes *in vitro.* Dev. Growth Differ., **25**: 323–331.

8 Kalt, M. R. (1976) Morphology and kinetics of spermatogenesis in *Xenopus laevis.* J. Exp. Zool., **195**: 393–408.

9 Bennett, J. and Mazia, D. (1981) Interspecific fusion of sea urchin eggs. Surface events and cytoplasmic mixing. Exp. Cell Res., **131**: 197–207.

10 Kalt, M. R. (1973) Ultrastructural observations on the germ line of *Xenopus laevis.* Z. Zellforsch., **138**: 41–62.

11 Reed, S. C. and Stanley, H. P. (1972) Fine structure of spermatogenesis in the South African clawed toad *Xenopus laevis* Daudin. J. Ultrastruct. Res., **41**: 277–295.

12 Meves, F. (1897) Ueber Structur und Histogenese der Samenfaden von *Salamandra maculosa.* Arch. Mikrosk. Anat. Entwickl., **50**: 110–141.

13 Barker, K. R. and Biesele, J. J. (1967) Spermateleosis of a salamander *Amphiuma tridactylum* Cuvier. A correlated light and electron microscope study. Cellule, **57**: 91–118.

14 Picheral, B. (1972) Les elements cytoplasmiques au cours de la spermiogenese du Triton *Pleurodeles waltlii* Michah. I. La genese de l'acrosome. Z. Zellforsch., **131**: 347–370.

15 Picheral, B. (1972) Les elements cytoplasmiques au cours de la spermiogenese du Triton *Pleurodeles waltlii* Michah. II. La formation du cou et l'evolution des organites cytoplasmiques non integres dans le spermatozoide. Z. Zellforsch., **131**: 371–398.

16 Picheral, B. (1972) Les elements cytoplasmiques au cours de la spermiogenese du Triton *Pleurodeles waltlii* Michah. III. L'evolution des formations caudales. Z. Zellforsch., **131**: 399–416.

ZOOLOGICAL SCIENCE 4: 849–854 (1987)

Plasma Thyroid Hormone Levels in Metamorphosing Larvae and Adults of a Salamander, *Hynobius nigrescens*

Shintaro Suzuki

Department of Comparative Endocrinology, Institute of Endocrinology, Gunma University, Maebashi 371, Japan

ABSTRACT—Plasma thyroxine (T_4) and 3, 5, 3′-triiodothyronine (T_3) were measured by radioimmunoassay (RIA) in metamorphosing larvae, metamorphosed animals, and adults of a salamander, *Hynobius nigrescens*. At the onset of metamorphosis the plasma T_4 was at an undetectable level. As metamorphosis proceeded, the plasma T_4 gradually increased and reached its highest level (1.96 ng/ml) at the metamorphic climax, accompanied with striking regression of a dorsal fin and sudden reduction in the size of gills. Thereafter, the plasma T_4 decreased towards the end of metamorphosis. The plasma T_3 of these metamorphosing larvae was detected only at the metamorphic climax. In the animals tested two weeks after metamorphosis, the plasma T_4 level increased again. In the adults which were collected before spawning, the plasma T_4 level was 0.34–5.77 ng/ml, although the plasma T_4 was undetectable after spawning. Plasma T_3 was undetectable in any of the adults collected. These results from metamorphosing larvae resemble those reported in anuran tadpoles. However, the data from metamorphosed animals and adults suggest that there is a positive correlation between thyroid activity and molting and the spawning behavior in the aquatic habitat.

INTRODUCTION

Thyroid hormones are indispensable for amphibian metamorphosis and it has been suggested that a gradual rise in the circulating thyroid hormone level is necessary for anuran metamorphosis [1–4]. Recently, it has been reported that the plasma thyroid hormone level rose sharply at the onset of metamorphic climax and fell towards the end of metamorphosis [5–10]. In urodeles, in which the metamorphic events seem to be much less striking than in anurans, the data available thus far are fragmentary [11, 12] and the plasma thyroid hormone levels have not been elucidated in relation to distinct metamorphic stages.

In the present communication, we report plasma thyroid hormone levels in the metamorphosing larvae of the Japanese salamander, and also refer to the plasma thyroid hormone levels both in the metamorphosed animals and in the adults before and after spawning to define the role of thyroid hormones.

Accepted June 2, 1987
Received March 9, 1987

MATERIALS AND METHODS

Animals The eggs of the Japanese salamander, *Hynobius nigrescens* Stejneger, were collected from a pond in a mountain region in Gunma Prefecture. After hatching, the larvae were kept at 20 ± 2°C in well water and were fed with a living *Tubifix* twice a week. The developmental stages were determined from the normal table (sketches) reported by Usui and Hamasaki [13] (UH stages 62 to 66), and two stages (stages 67 to 68) by the time of completion of metamorphosis were added to the UH stages. Larvae were anesthetized with MS222 (tricaine methanesulfonate, Sankyo Co., Tokyo), and blood samples were pooled into heparinized capillaries after cutting the ventral aorta. After centrifugation the plasma was stored at -60°C for RIA. The animals kept for two weeks after metamorphosis were also used for measurement of thyroid hormones. The body length and weight of these animals were 4.6–5.0 cm and 0.7–1.0 g, respectively. Adult salamanders with a body weight ranging 7.4–14.1 g were collected from the same pond during the breeding season in March. These adults collected before

spawning were kept in the laboratory for two days and blood samples were taken for the measurement of thyroid hormones. Some of the blood samples from the remainder were also obtained at one day after spontaneous spawning in the laboratory. Some adults were collected from the same pond after spawning. Blood samples were collected from these larvae and adults between 11:00 a.m. and 2:00 p.m.

Radioimmunoassay Plasma T_4 and T_3 were measured by appropriate RIA methods [14, 15], as described previously [9]. [^{125}I] T_4 (1250 μCi/μg) and [^{125}I] T_3 (1200 μCi/μg) were purchased from New England Nuclear, U.S.A. Antisera for T_4 and T_3 were prepared by immunizing rabbits with their conjugates with bovine serum albumin, and used at a final dilution of 1:3000 and 1:2500, respectively. The cross reactivities of these antisera were 0.1% (T_4 antiserum to T_3) and 0.14% (T_3 antiserum to T_4). For duplicate RIA determination, T_4 and T_3 in 100 μl plasma were extracted with 1 ml of ethanol [6]. The minimum detectable level was estimated to be 0.2 ng/ml for T_4 and 0.15 ng/ml for T_3.

RESULTS

Identification of developmental stages in metamorphosing larvae

The developmental stages of metamorphosing larvae and some characteristics are shown in Table 1, with corresponding stages of *Ambystoma maculatum* [16]. At UH stage 62, slight shrinkage of the dorsal fin and gill platelets was observed. However, the body length and body weight of the larvae continued to increase with the growth of the forelimbs (UH stages 63 to 64). At UH stage 65, the regression of the dorsal fin reached to halfway between the forelimbs and hindlimbs, and conspicuous shrinkages of gill platelets were observed. After this stage, the operculum began to fuse to head, with rapid regression of dorsal fin and gills. At UH stage 66, a striking puffing of eyelids and the formation of square-jaws were observed in these larvae. Their gills changed into nubbins, and the regression of the dorsal fin reached the joints of the hindlimbs. At stage 67, the head shape changed into that of the adult due to rapid regression of the hyobranchial skeleton. Complete fusion of the operculum and the first molting were observed in the larvae. Thereafter, small pieces of tail fin disappeared and many white spots emerged on the dark brown skin of the larvae (stage 68). Within a few days or a week, metamorphosed animals began to feed again. After the first molting at stage 67, regular molting with a cycle of 2.4 days was observed for at least two months. The body length and weight of these metamorphosing larvae increased to the UH stage 65. However, a rapid decrease in body weight was observed at the end of metamorphosis (Fig. 1(B)).

Table 1. Developmental stages and some external characteristics of metamorphosing larvae of *Hynobius nigrescens*, and corresponding stages of *Ambystoma maculatum*

Hynobius Developmental stage	Some external characteristics	*Ambystoma* Developmental stage
62	Onset of shrinkages of dorsal fin and gill platelets; puffing of eyelids	56
64	Shrinkages continuing; striking wrinkles and undulating tail fin	
65	Regression of dorsal fin reaching to halfway between forelimbs and hindlimbs	
66	Regression of dorsal fin as far back as hindlimbs; small gill pieces existing	57
67	Disappearance of gill pieces; complete fusion of opercular fold; change in head shape due to rapid regression of hyobranchial skeleton; small pieces of tail fin existing; 1st molting of entire skin	58
68	Gular fold almost smoothing out; disappearance of tail fin; sudden increase in number of white spots on the dark skin	59

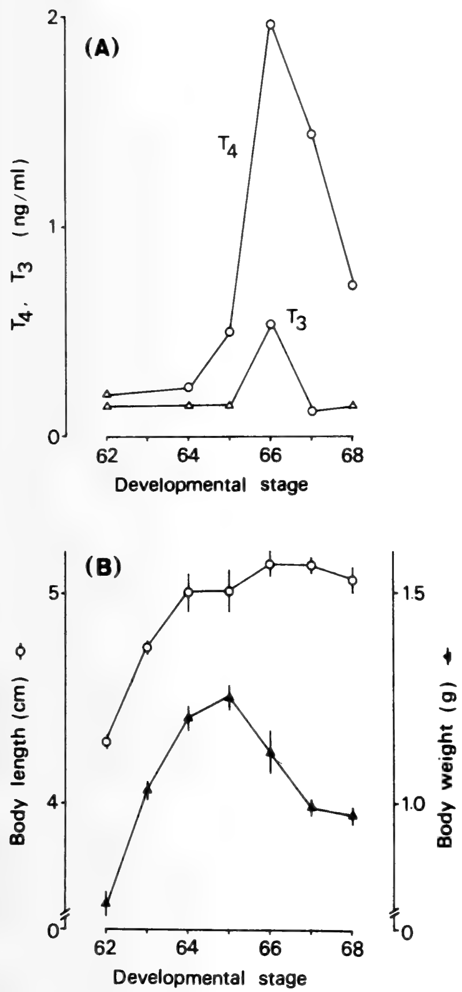

Fig. 1. Plasma T_4 and T_3 levels (A), and changes in body length and weight (B) during metamorphosis of *Hynobius nigrescens*. Symbols (△) in Fig. 1 (A) show undetectable levels of T_4 and T_3. Each point in Fig. 1 (B) shows the mean value ± standard error (n=10).

Plasma T_4 and T_3 levels in metamorphosing larvae and metamorphosed animals

Plasma T_4 and T_3 levels in both metamorphosing larvae and animals kept two weeks after metamorphosis are shown in Table 2. The plasma T_4 was undetectable at the onset of metamorphosis (UH stage 62). As metamorphosis proceeds, its plasma T_4 gradually increased (UH stage 64, 0.23 ng/ml) and reached its highest level (UH stage 66, 1.96 ng/ml) at the metamorphic climax when remarkable regression of gills and dorsal fin is observed. Thereafter, the T_4 values decreased towards the end of metamorphosis. In the animals which were kept for two weeks after metamorphosis, the plasma T_4 value was 1.32 ng/ml.

On the other hand, the plasma T_3 level was undetectable at the early stages of metamorphosis (UH stages 62, 64 and 65). At the metamorphic climax (UH stage 66) the plasma T_3 value was 0.54 ng/ml. Thereafter, the plasma T_3 decreased and reached an undetectable level at stage 68 (Fig. 1(A)). In the animals two weeks after metamorphosis, the plasma T_3 was at an undetectable level.

Table 2. Plasma T_4 and T_3 levels in *Hynobius nigrescens* at various developmental stages

Developmental stage	Number of animals	T_4 (ng/ml)	T_3 (ng/ml)
62	23	—*	—**
64	50	0.23	—**
65	27	0.50	—**
66	39	1.96	0.54
67	21	1.44	0.11
68	15	0.71	—**
Metamorphosed animals***	29	1.32	—**

* Not detectable, $T_4 < 0.2$ ng/ml
** Not detectable, $T_3 < 0.15$ ng/ml
*** Animals kept for two weeks after metamorphosis

TABLE 3. Plasma T_4 and T_3 levels in the adult salamanders, *Hynobius nigrescens* before and after spawning

	Animal number	Sex	Body length (cm)	Body weight (g)	T_4 (ng/ml)	T_3 (ng/ml)
Animals before spawning	1	F	16.2	10.0	0.34	—**
	2	F	13.5	9.6	5.77	
	3	M	14.3	9.6	1.24	—**
	4	M	15.2	11.6	1.87	—**
	5	M	14.0	10.3	2.51	
	6	M	14.0	13.0	2.14	—**
Animals after spawning	7	F	16.0	7.6	—*	—**
	8	F	12.7	7.9	—*	—**
	9	F	14.2	10.9	—*	
	10	M	15.2	11.2	—*	—**
	11	M	16.0	14.1	—*	
	12	M	12.3	7.4	—*	—**

* Not detectable, $T_4<0.2$ ng/ml
** Not detectable, $T_3<0.15$ ng/ml

Plasma T_4 and T_3 levels in the adult salamanders

Plasma T_4 and T_3 in the adults were measured before and after spawning. As shown in Table 3, in all adults collected before spawning, the plasma T_4 values changed greatly from 0.34 to 5.77 ng/ml. However, after spawning the plasma T_4 was at an undetectable level. T_4 value was also undetectable in adults collected from the same pond after spawning. In all adults tested at the same time, the plasma T_3 was undetectable both before and after spawning. No significant sex differences in the plasma levels of T_4 and T_3 were found.

DISCUSSION

Until now, plasma thyroid hormones in metamorphosing larvae of several urodeles have been measured by RIA [11, 12]. Plasma T_4 values in metamorphosing larvae of *Ambystoma gracile* (30 ng/ml) were much higher than those in both non-metamorphosing larvae and metamorphosed animals (below 10 ng/ml) [11]. Larras-Regard *et al.* [12] classified the metamorphosing larvae of *Ambystoma tigrinum* into three groups (beginning, middle, and end of metamorphosis) according to the metamorphic stage. They found a significant elevation of plasma T_4 levels only during metamorphosis, although T_4 values fluctuated considerably in different animals. Plasma T_4 values reached the highest level at the end of metamorphosis (1–15 ng/ml). However, T_3 levels were much higher at the middle than at the end of metamorphosis (0.98–1.95 ng/ml). In particular, they observed high plasma T_3, although plasma T_4 was undetectable in several metamorphosing animals. The present results obtained in the metamorphosing larvae of *Hynobius* clearly showed that a slight increase in plasma T_4 is found at the early stages of metamorphosis and plasma T_4 reached its highest level at the metamorphic climax, accompanied with striking regression of the dorsal fin and gills. Thereafter, the plasma T_4 level fell towards the end of metamorphosis. The circulating T_3 level in metamorphosing animals was very low and detected only at climactic stages. These changes in the plasma T_4 and T_3 during metamorphosis of the salamander *Hynobius* resemble those found in anuran tadpoles [5–10]. It seems that a gradual rise in plasma thyroid hormone levels is required for early metamorphosis, and a decrease is observed at the end of metamorphosis even in urodeles.

It was reported that molting in urodeles is

influenced by thyroid function and the frequency of molting is determined by the level of thyroid activity [17–19]. In the present study it was shown that the level of plasma T_4 in metamorphosed animals which were continuing a cyclic molting was much higher than that in larvae which had just completed metamorphosis (stage 68). This result suggests that the higher plasma T_4 level is a prerequisite to frequent molting in metamorphosed animals.

Larras-Regard *et al.* [12] reported the plasma T_4 and T_3 levels in adult *Ambystoma tigrinum*. In seven of these animals, plasma T_4 and T_3 levels were below the limits of detection (T_4, below 0.5 ng/ml; T_3, below 0.05 ng/ml). In one animal the plasma T_4 level was quite elevated (5.2 ng/ml), but plasma T_3 was not detected. In neotens of the same species, Norris *et al.* [20] found circannual changes in plasma T_4 levels. The plasma T_4 was at a much higher level (5.4–5.5 ng/ml) from November to March (prespawning) and decreased to its minimum level (2.2 ± 0.31 ng/ml) from June to September (postspawning). They emphasized antagonistic roles in thyroid function and reproductive events such as gonadal development in these animals. In the present study it was shown that plasma T_4 values for adult *Hynobius* in prespawning were much higher than those in postspawning. There was no significant change in the amounts of total serum proteins among these adults (unpublished data, mean$\pm$standard error: prespawning, 19.3 ± 0.4 mg/ml; postspawning, 18.9 ± 2.6). From the results of Norris *et al.* [20] and our results, it appears likely that the thyroid function of the adult salamanders is more active in prespawning.

In newly metamorphosed *Ambystoma tigrinum*, Duvall and Norris [21] found that plasma T_4 levels are significantly higher in animals displaying spontaneous land preference than in those displaying water preference. It is assumed therefore that the higher thyroid activity found in *Hynobius* kept in the laboratory for two weeks after metamorphosis may also reflect their land preference. On the other hand, the adult *Hynobius* migrates to water only during the breeding season and returns to the terrestrial life after laying its eggs. Therefore, in these animals it seems that the role of thyroid hormone should be considered in controlling changes in habitat. Recently, Moriya [22] found that prolactin-treated salamanders, *Hynobius retardatus,* sink to the bottom of the water, although the control salamanders that do not receive prolactin float near the surface. Moreover, Moriya and Dent [23] reported the effect of prolactin and T_4 on habitat choice, the specific gravity of the whole body and osmotic pressure of serum in the newt, *Notophthalmus viridescens*. They showed that the animals move from water to land, and both specific gravity and serum osmolality are decreased when they are immersed in a solution containing T_4. As already mentioned above, we found a conspicuous difference in plasma T_4 between the prespawning and the postspawning *Hynobius,* both of which are staying in the water. It seems likely that thyroid activity is in some fashion correlated with spawning behavior in the aquatic habitat.

ACKNOWLEDGMENTS

I express my gratitude to Professor M. Suzuki of our Institute, for his valuable suggestions during this work. Thanks are also due to Mr. T. Kakegawa and Mr. T. Narita, for their technical assistance.

REFERENCES

1 Etkin, W. (1935) The mechanisms of anuran metamorphosis. I. Thyroxine concentration and the metamorphic pattern. J. Exp. Zool., **71**: 317–340.
2 Etkin, W. (1968) Hormonal control of amphibian metamorphosis. In "Metamorphosis". Ed. by W. Etkin and L. I. Gilbert, North-Holland Publ. Co., Amsterdam, pp. 313–348.
3 Just, J. J. (1972) Protein-bound iodine and protein concentration in plasma and pericardial fluid of metamorphosing anuran tadpoles. Physiol. Zool., **45**: 143–152.
4 Dodd, M. H. I. and Dodd, J. M. (1976) The biology of metamorphosis. In "Physiology of the Amphibia", Vol. 3. Ed by B. Lofts, Academic Press, New York and London, pp. 467–599.
5 Leloup, J. and Buscaglia, M. (1977) La triiodothyronine, hormone de la metamorphose des amphibiens. C. R. Acad. Sci., Ser. D, **284**: 2261–2263.
6 Miyauchi, H., LaRochelle, F. T., Jr., Suzuki, M., Freeman, M. and Frieden, E. (1977) Studies on thyroid hormones and their binding in bullfrog tadpole plasma during metamorphosis. Gen. Comp. Endocrinol., **33**: 254–266.

7 Regard, E., Taurog, A. and Nakashima, T. (1978) Plasma thyroxine and triiodothyronine levels in spontaneously metamorphosing *Rana catesbeiana* tadpoles and in adult anuran amphibia. Endocrinology, **102**: 674–684.

8 Mondou, P. M. and Kaltenbach, J. C. (1979) Thyroxine concentrations in blood serum and pericardial fluid of metamorphosing tapoles and of adult frogs. Gen. Comp. Endocrinol., **39**: 343–349.

9 Suzuki, S. and Suzuki, M. (1981) Changes in thyroidal and plasma iodine compounds during and after metamorphosis of the bullfrog, *Rana catesbeiana.* Gen. Comp. Endocrinol., **45**: 74–81.

10 Weil, M. R. (1986) Changes in plasma thyroxine levels during and after spontaneous metamorphosis in a natural population of the green frog, *Rana clamitans.* Gen. Comp. Endocrinol., **62**: 8–12.

11 Eagleson, G. W. and McKeown, B. A. (1978) Changes in thyroid activity of *Ambystoma gracile* (Baird) during different larval, transforming, and postmetamorphic phases. Can. J. Zool., **56**: 1377–1381.

12 Larras-Regard, E., Taurog, A. and Dorris, M. (1981) Plasma T_4 and T_3 levels in *Ambystoma tigrinum* at various stages of metamorphosis. Gen. Comp. Endocrinol., **43**: 443–450.

13 Usui, M. and Hamasaki, M. (1939) Tafeln zur Entwicklungsgeschichte von *Hynobius nigrescens* Stejneger. Zool. Mag., **51**: 192–206 (In Japanese).

14 Larsen, P. R. (1972) Direct immunoassay of triiodothyronine in human serum. J. Clin. Invest., **51**: 1939–1949.

15 Larsen, P. R., Dockalova, J., Sipula, D. and Wu, F. M. (1973) Immunoassay of thyroxine in unextracted human serum. J. Clin. Endocrinol. Metab., **37**: 177–182.

16 Ballard, W. W. (1972) Characterization of developmental stages. Part VI. Salamander. In "Biological Data Book", Vol. 1. Ed. by P. L. Altman and D. S. Dittmer, Fed. Am. Soc. Exp. Biol., U. S. A., pp. 185–189.

17 Jørgensen, C. B. and Larsen, L. O. (1960) Hormonal control of moulting in amphibians. Nature, **185**: 244–245.

18 Clark, N. B. and Kaltenbach, J. C. (1961) Direct action of thyroxine on skin of the adult newt. Gen. Comp. Endocrinol., **1**: 513–518.

19 Larsen, L. O. (1976) Physiology of molting. In "Physiology of the Amphibia", Vol. 3. Ed. by B. Lofts, Academic Press, New York and London, pp. 53–100.

20 Norris, D. O., Duvall, D., Greendale, K. and Gern, W. A. (1977) Thyroid function in pre- and post-spawning neotenic tiger salamanders (*Ambystoma tigrinum*). Gen. Comp. Endocrinol., **33**: 512–517.

21 Duvall, D. and Norris, D. O. (1980) Stimulation of terrestrial substrate preferences and locomotor activity in newly transformed tiger salamanders (*Ambystoma tigrinum*) by exogenous or endogenous thyroxine. Anim. Behav., **28**: 116–123.

22 Moriya, T. (1982) Prolactin induces increase in the specific gravity of salamander, *Hynobius retardatus,* that raises adaptability to water. J. Exp. Zool., **223**: 83–88.

23 Moriya, T. and Dent, J. N. (1986) Hormonal interaction in the mechanism of migratory movement in the newt, *Notophthalmus viridescens.* Zool. Sci., **3**: 669–676.

ZOOLOGICAL SCIENCE 4: 855–860 (1987)

Proliferation of Prolactin Cells in the Rat: Effects of Estrogen and Bromocryptine

SUMIO TAKAHASHI and SEIICHIRO KAWASHIMA

Zoological Institute, Faculty of Science, Hiroshima University, Naka-ku, Hiroshima 730, Japan

ABSTRACT—The mitosis of prolactin (PRL) cells was immunohistochemically identified in colchicine-treated rats. The administration of estrogen increased the mitotic activity of PRL cells and serum PRL levels in male rats, while bromocryptine, a dopamine agonist, blocked the estrogen-mediated increase in mitotic activity and PRL levels. In female rats, bromocryptine treatment in the early afternoon of 2nd day of diestrus and proestrous day, which should block the increase in serum PRL level in the evening of proestrous day, decreased the mitotic activity of PRL cells at estrus, which was very high in non-treated females. These results suggest that the proliferation of PRL cells was closely associated with PRL release from the pituitary gland.

INTRODUCTION

Mitotic prolactin (PRL) cells were immunohistochemically and electron microscopically identified in intact rats [1, 2]. The mitotic activity of PRL cells varied with the estrous cycle, and the mitotic index at estrus was higher than those at other stages of the cycle [3]. Estrogen treatment stimulated and ovariectomy decreased the mitotic activity of PRL cells [3, 4].

Estrogen is a stimulatory agent on PRL release. In the course of estrogenic stimulation, the synthesis of PRL-messenger RNA (mRNA) began to increase 12 hr after estrogen treatment and further increased over the next 48 hr [5]. Pituitary PRL concentration and DNA synthesis also rose at 30 hr after estrogen treatment [6]. Earlier study found that the number of mitotic cells was increased during the second day after estrogen treatment, although the cell types undergoing mitosis were not identified in this study [7]. Chronic estrogen treatment induced an increase in the number of immunohistochemically identified PRL cells [8–10]. Yamamoto *et al.* [9] recently found the increase in PRL mRNA content per PRL cell as assessed by the *in situ* hybridization in chronic estrogen-treated rats. However, little has been known about the time-related changes of the mitosis of PRL cells and serum PRL levels after estrogen treatment, and the first aim of the present study was to solve this problem.

Dopamine agonists, such as ergocryptine and bromocryptine, inhibited the syntheses of PRL mRNA and PRL, and the release of PRL [11, 12]. Bromocryptine also inhibited DNA synthesis and mitosis in the pituitary cells in estrogen-treated rats [13, 14]. In this conjunction, the second aim of the present study was to examine the effects of dopamine agonist, bromocryptine (CB–154), on the mitosis of PRL cells in estrogen-treated male rats and intact female rats exhibiting normal estrous cycles to clarify the relationship between PRL secretion and mitosis. The mitotic PRL cells were observed immunohistochemically in colchicine-treated rats throughout the present study.

Accepted May 9, 1987
Received April 14, 1987

MATERIALS AND METHODS

Animals

Adult male and female rats (about 60 days of age) of the Wistar/Tw strain were used. They were housed in a temperature-controlled room with a 12-hr light (06:00–18:00) and 12-hr dark cycle, and given rat chow (Clea Japan Inc., Tokyo)

and water *ad libitum*. In female rats vaginal smears were recorded daily for at least two weeks before the experiments.

Estrogen treatment

Intact male rats were given a single subcutaneous injection of 50 μg estradiol-17β (E_2, Sigma, St. Louis) dissolved in 0.1 ml sesame oil. This dose was chosen from the data of our previous experiments [4]. These rats were killed at 0, 3, 6, 24, 36, 48, 72 or 96 hr after the treatment for the observations of the mitotic PRL cells. Rats given sesame oil only served as controls (0, 48 and 96 hr). For serial blood samplings, other rats were similarly given E_2 or oil, and blood samples were collected from the jugular vein under light ether anesthesia on the same schedule as for mitosis observations.

Bromocryptine treatment

Intact male rats were given a single subcutaneous injection of E_2, and 24 or 42 hr later they were subcutaneously given bromocryptine (CB–154, Sandoz, Ltd., Basel) at a dose of 4 mg/kg. Bromocryptine was dissolved in a minimal amount of 100% ethanol and diluted with 0.9% saline to the final concentration of 2 mg/ml. Final ethanol concentration did not exceed 1%. Vehicle-treated rats served as controls. All rats were killed 48 hr after E_2 treatment. About half of them were used for the observation of the mitosis, and the remaining animals were used for the measurement of serum PRL levels.

Intact female rats were given bromocryptine at a dose of 4 mg/kg on 2nd day of diestrus (15: 00 hr), proestrous day (15: 00 hr) or estrous day (10: 00 hr). Vehicle-treated rats served as controls. All rats were killed in the afternoon of estrous day (16: 00 hr).

Immunohistochemistry and counting of mitotic PRL cells

Colchicine (Wako Pure Chemical Industries, Ltd., Osaka) was injected intraperitoneally at a dose of 1 mg/kg. Three hours later, between 16: 00 and 18: 00, the rats were killed by decapitation. The pituitary glands were quickly removed and fixed in Bouin's fluid. Horizontal paraffin sections 6 μm thick were cut. Immunohistochemical staining was performed according to PAP method of Sternberger *et al.* [15], using rabbit antiserum to rat prolactin (NIADDK-anti-rat prolactin S–7). Immunospecificity of the antiserum to rat PRL was checked in a previous report [3]. Peroxidase activity was demonstrated by the reaction with 3, 3′-diaminobenzidine tetrahydrochloride. After the immunohistochemical staining, sections were counterstained with hematoxylin. Sections near the horizontal medial plane were selected for histometry, because in a preliminary study the value from the horizontal medial plane represents the mean value of PRL cell population of three different levels of horizontal planes. The total number of anterior pituitary cells in colchicine-arrested metaphase and the number of immunoreactive mitotic cells (mitotic PRL cells) were counted. In the sections used for the differential mitotic cell counting, the area of anterior pituitary glands was measured using a tablet digitizer MG 200–1 (Mutoh Kogyo, Tokyo). The mitotic index is expressed as the number of mitoses per mm^2 of section. The sectional area of 1 mm^2 contained about 10,000 cells in 60-day-old rats.

Radioimmunoassay of PRL

Blood samples were collected under light ether anesthesia from the jugular vein or the decapitated trunks. PRL levels were measured using the NIADDK RIA kit. The data were expressed as ng/ml of NIADDK-rat-prolactin RP–2.

Statistics

Statistical analyses of differences were performed with Student's t test.

RESULTS

Mitotic index of PRL cells and serum PRL levels in estrogen-treated male rats

E_2 significantly increased the mitotic indices of PRL cells and the total anterior pituitary cells 36 hr after the injection, and the significantly high mitotic activity lasted until 96 hr (Fig. 1). At 6, 36, 48, 72 and 96 hr after the E_2 injection the mitotic

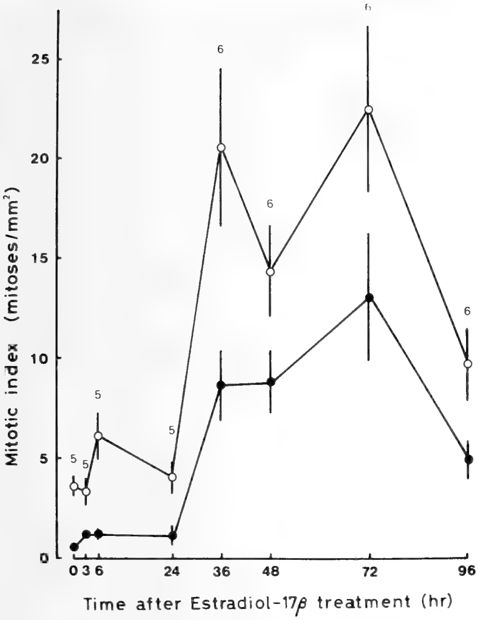

FIG. 1. Mitotic index of prolactin cells (●) and total pituitary cells (○) after estradiol-17β (50 μg) injection. The mitotic index in vehicle-treated controls was described in the text. The numbers on each point depict the numbers of rats, and the bars indicate the standard errors of means.

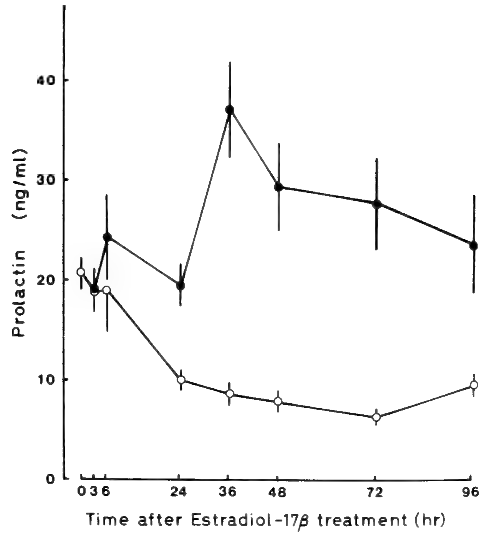

FIG. 2. Serum prolactin concentration in male rats given estradiol-17β (50 μg, 7 rats, ●) or sesame oil (6 rats, ○). The value at 0 hr is the composite data of estradiol-17β-treated rats and vehicle-treated rats (n=13). The bars depict the standard errors of means.

index of total cells including PRL cells was significantly greater than that at the time of injection ($P<0.05$, at 6 hr; $P<0.01$ at 36, 48, 72 and 96 hr), and that of PRL cells was higher at 36, 48, 72 and 96 hr than that at the time of injection ($P<0.01$, in all comparisons). In vehicle-treated controls the mitotic indices of PRL cells and total cells (n=the number of rats) were 1.4 ± 0.3 (PRL cells) and 4.0 ± 0.8 (total cells) (n=5) at 0 hr, 0.6 ± 0.1 and 2.6 ± 0.5 (n=5) at 48 hr, and 1.5 ± 0.3 and 4.0 ± 0.3 (n=6) at 96 hr, respectively. E_2 significantly increased serum PRL levels 36 hr after the injection and maintained the elevated PRL levels until 96 hr (Fig. 2). In vehicle-treated controls, on the other hand, PRL levels tended to decrease during the successive blood samplings, and the significant differences in serum PRL levels between estrogen-treated rats and vehicle-treated rats were observed at 36, 48, 72 and 96 hr ($P<0.001$, at 36, 48 and 72 hr; $P<0.05$, at 96 hr).

Effect of bromocryptine on the mitotic index of PRL cells and serum PRL levels in estrogen-treated rats

Bromocryptine injection at 24 hr after E_2 treatment blocked the E_2-induced increase in the mitotic index of PRL cells, while bromocryptine injection at 42 hr after E_2 was not effective on this parameter (Table 1). Mitotic indices of cells other than PRL cells were not influenced by bromocryptine injection. Serum PRL levels significantly decreased when bromocryptine was injected either 24 or 42 hr after E_2 treatment.

Effect of bromocryptine on the mitosis of PRL cells in intact female rats

Mitotic index of PRL cells was observed at 16:00 hr of estrous day, which has proved to be maximal during the estrous cycle [3]. Bromocryptine treatment on 2nd day of diestrus (15:00 hr) or proestrous day (15:00 hr) significantly decreased

TABLE 1. Effect of bromocryptine (CB–154) on the mitosis of PRL cells and serum PRL level in estrogen-treated male rats

Treatment	Time at CB–154 treatment (hr)	Mitotic index (mitoses/mm^2) PRL cell	Mitotic index (mitoses/mm^2) Other cells	Serum PRL level (ng/ml)
Control	24[1)]	12.1±2.9[a]	13.9±2.3 (7)[b]	80.3±16.4 (8)
CB–154	24	3.9±0.6*	11.7±2.7 (5)	11.1± 1.5** (8)
Control	42[1)]	10.9±1.7	13.1±2.2 (5)	78.6±11.4 (7)
CB–154	42	12.9±4.4	8.4±1.9 (5)	12.1± 2.5** (7)

a: Mean±S.E.M., b: The number in parentheses indicates the number of rats.
1): CB–154 or vehicle was injected 24 or 42 hr after E_2 injection. All animals were killed 48 hr after E_2 treatment.
Difference from matched controls: *P<0.05, **P<0.001.

TABLE 2. Effect of bromocryptine (CB–154) on the mitosis of PRL cells in intact female rats at estrus

Treatment	Day of treatment	No. of rats	Mitotic index (mitoses/mm^2) PRL cell	Mitotic index (mitoses/mm^2) Other cells
Control	2nd day of diestrus	5	58.2±9.5[a]	13.4±3.5
CB–154		5	1.4±0.7**	3.6±1.0*
Control	Proestrous day	5	29.7±4.0	16.7±2.9
CB–154		5	1.9±0.2**	3.5±0.4*
Control	Estrous day	6	31.0±2.2	19.3±3.2
CB–154		6	32.5±5.0	18.7±3.5

a: Mean±S.E.M.
Difference from matched controls: *P<0.05, **P<0.001.

the mitotic indices of PRL cells and other pituitary cells (Table 2). On the other hand, bromocryptine treatment at estrus 6 hr before autopsy failed to affect the mitotic indices of PRL cells and other cells.

DISCUSSION

Mitotic PRL cells were immunohistochemically shown in the present study. The result in the present study indicates that the proliferation of PRL cells is closely associated with PRL release from the pituitary gland. Davies *et al.* [13], Lloyd *et al.* [14] and Jahn *et al.* [16] previously presented the evidence that PRL release was accompanied by the increases in DNA synthesis and the number of mitotic cells in the pituitary glands. However, the cell types of the mitotic cells were not verified in their reports. Immunohistochemical observations after colchicine treatment in the present study showed that the increase in the mitotic activity of total pituitary cells in estrogen-treated rats could be explained partly by the increase in the mitotic activity of PRL cells.

The sharp increase in the mitotic activity of PRL cells at estrus in female rats [3] was associated with the elevation in serum PRL levels in the afternoon of proestrous day (proestrous PRL "surge") as shown in Neill *et al.* [17]. In the present study, bromocryptine treatment in intact female rats in the early afternoon of 2nd day of diestrus and the morning of proestrous day inhibited the increase in the mitotic activity of PRL cells along with that of other cell types at estrus. The same dose of

bromocryptine as used in female rats effectively blocked the estrogen-induced PRL release 24 hr later in male rats (the present study) and also in estrogen-treated female rats [11]. Therefore, the present bromocryptine treatment in female rats at 15:00 hr of 2nd day of diestrus could be effective in blocking the proestrous PRL surge in the following day. In estrogen-treated male rats, bromocryptine decreased the mitotic activity of PRL cells as shown in female rats, but did not affect the proliferation of other cell types in male rats. The difference between sexes may be explained if some of the immunonegative cells in intact female rats are PRL cells. However, the verification of this view should await future study.

The proestrous PRL "surge" is ovarian estrogen and hypothalamic dopamine dependent [17, 18]. Plasma estrogen began to rise from the afternoon of 2nd day of diestrus and reached a peak in the afternoon of proestrous day, and plasma PRL level started to rise 3 hr after the estrogen peak [19]. Similarly, the increase in the mitotic activity of PRL cells at estrus was ovary dependent, because ovariectomy on 2nd day of diestrus or proestrous day blocked this increase [3]. It is well known that dopamine is the physiological PRL-inhibitory hormone [18]. The dopamine concentration in the portal blood is lower at proestrus compared with that at other states of the estrous cycle [20]. This low dopamine level on proestrous day is another factor of the proestrous PRL "surge" and the elevation of the mitotic activity of PRL cells. Thus, the PRL secretion and proliferation of PRL cells are regulated by the two factors, estrogenic stimulation and dopaminergic inhibition.

The changes in the mitotic activity of total pituitary cells after estrogen treatment were in good agreement with the earlier report by Hunt [7]. The significant increase in the mitotic activity of total pituitary cells and PRL cells at 36 hr after estrogen treatment in male rats may be regarded as a mimic of the increase in the mitotic activity of PRL cells in intact female rats at estrus. However, the effect of estrogen treatment on serum PRL levels and the mitotic activity of PRL cells continued until 96 hr later. The decrease in serum PRL levels in vehicle-treated controls may be due to the procedure of sequential blood sampling, although the significant difference in serum PRL levels between estrogen-treated rats and vehicle-treated rats was apparent during the course of samplings after 36 hr. In female rats, the mitotic activity of PRL cells, and estrogen levels rapidly decreases after estrus [3, 19], and these changes were associated with the fluctuation in serum PRL levels. Based on the fact that the decrease in the mitotic activity of PRL cells and the decrease in estrogen and PRL levels are all well correlated, the long-lasting effects of E_2 on male rats in the present study might indicate that the injected dose was large enough to maintain the high mitotic activity and PRL level for longer period.

Bromocryptine failed to affect the mitotic activity of PRL cells if given 6 hr before autopsy in estrogen-treated male or intact female rats. Similarly, ovariectomy on the morning of estrous day was without effect on the mitotic activity of PRL cells 6 hr later [3]. Such ineffectiveness suggests that the mitotic process had already been in progress at the time of these treatments.

Estrogen may stimulate the proliferation of pituitary cells other than PRL cells, because estrogen increased the mitotic activities of pituitary cells which were immunohistochemically negative to anti-rat PRL serum. The possibility is not ruled out that the mechanism of cell proliferation, which is dependent on serum estrogen levels but independent of serum levels of PRL, may exist in the pituitary cell population.

ACKNOWLEDGMENTS

We wish to thank Drs. W. Weidmann and H. Friedli, Sandoz Ltd., Basel for providing bromocryptine. We also wish to thank Dr. S. Raiti, and National Hormone and Pituitary Program, NIADDK for the supply of PRL RIA kit. This study was supported in part by a Grant-in-Aid for Scientific Research from the Ministry of Education, Science and Culture, Japan.

REFERENCES

1 Sato, S. (1980) Postnatal development, sexual difference and sexual cyclic variation of prolactin cells in rats: special reference to the topographic affinity to a gonadotroph. Endocrinol. Jpn., **27**: 573–583.

2 Shirasawa, N. and Yoshimura, F. (1982) Immunohistochemical and electron microscopical studies of

mitotic adenohypophysial cells in different ages of rats. Anat. Embryol., **165**: 51–61.

3 Takahashi, S., Okazaki, K. and Kawashima, S. (1984) Mitotic activity of prolactin cells in the pituitary glands of male and female rats of different ages. Cell Tissue Res., **235**: 497–502.

4 Takahashi, S. and Kawashima, S. (1986) Mitotic potency of prolactin cells in the pituitary gland in rats. In "Pars Distalis of the Pituitary Gland—Structure, Function and Regulation". Ed. by F. Yoshimura and A. Gorbman, Elsevier Science Publishers B. V., Amsterdam, pp. 497–501.

5 Seo, H., Refetoff, S., Vassart, G. and Brocas, H. (1979) Comparison of primary and secondary stimulation of male rats by estradiol in terms of prolactin synthesis and mRNA accumulation in the pituitary. Proc. Natl. Acad. Sci. USA, **76**: 824–828.

6 Jacobi, J., Lloyd, H. M. and Meares, J. D. (1977) Onset of oestrogen-induced prolactin secretion and DNA synthesis by the rat pituitary gland. J. Endocrinol., **72**: 35–39.

7 Hunt, T. E. (1947) Mitotic activity in the anterior hypophysis of ovariectomized rats after injection of estrogen. Anat. Rec., **97**: 127–137.

8 Takahashi, S. and Kawashima, S. (1981) Responsiveness to estrogen of pituitary glands and prolactin cells in gonadectomized male and female rats. Annot. Zool. Japon., **54**: 73–84.

9 Yamamoto, N., Seo, H., Suganuma, N., Matsui, N., Nakane, T., Kuwayama, A. and Kageyama, N. (1986) Effects of estrogen on prolactin mRNA in the rat pituitary. Analysis by in situ hybridization and immunohistochemistry. Neuoendocrinology, **42**: 494–497.

10 Perez, R. L., Machiavelli, G. A., Romano, M. I. and Burdman, J. A. (1986) Prolactin release, oestrogens and proliferation of prolactin-secreting cells in the anterior pituitary gland of adult male rats. J. Endocrinol., **108**: 399–403.

11 Brooks, C. L. and Welsch, C. W. (1974) Reduction of serum prolactin in rats by 2 ergot alkaloids and 2 ergoline derivatives: a comparison. Proc. Soc. Exp. Biol. Med., **146**: 863–867.

12 Maurer, R. A. (1980) Dopaminergic inhibition of prolactin synthesis and prolactin messenger RNA accumulation in cultured pituitary cells. J. Biol. Chem., **255**: 8092–8097.

13 Davies, C., Jacobi, J., Lloyd, H. M. and Meares, J. D. (1974) DNA synthesis and the secretion of prolactin and growth hormone by the pituitary gland of the male rat: effects of diethylstilboestrol and 2-bromo-ergocryptine methanesulphonate. J. Endocrinol., **61**: 411–417.

14 Lloyd, H. M., Meares, J. D. and Jacobi, J. (1975) Effects of oestrogen and bromocryptine on in vivo secretion and mitosis in prolactin cells. Nature, **255**: 497–498.

15 Sternberger, L. A., Hardy, P. H., Jr., Cuculis, J. J. and Meyer, H. G. (1970) The unlabeled antibody enzyme method of immunohistochemistry. Preparation and properties of soluble antigen-antibody complex (Horseradish peroxidase-antihorseradish peroxidase) and its use in identification of spirochetes. J. Histochem. Cytochem., **18**: 315–333.

16 Jahn, G. A., Machiavelli, G.A., Kalbermann, L. E., Szijan, I., Alonso, G. E. and Burdman, J. A. (1982) Relationships among release of prolactin, synthesis of DNA and growth of the anterior pituitary gland of the rat: effects of oestrogen and sulpiride. J. Endocrinol., **94**: 1–10.

17 Neill, J. D., Freeman, M. E. and Tillson, S. A. (1971) Control of the proestrous surge of prolactin and luteinizing hormone secretion by estrogens in the rat. Endocrinology, **89**: 1448–1453.

18 MacLeod, R. M. (1976) Regulation of prolactin secretion. In "Frontiers in Neuroendocrinology, Vol. 4". Ed. by L. Martini and W. F. Ganong, Raven Press, New York, pp. 169–194.

19 Smith, M. S., Freeman, M. E. and Neill, J. D. (1975) The control of progesterone secretion during the estrous cycle and early pseudopregnancy in the rat: prolactin, gonadotropin and steroid levels associated with rescue of the corpus luteum of pseudopregnancy. Endocrinology, **96**: 219–226.

20 Ben-Jonathan, N., Oliver, C., Weiner, H. J., Mical, R. S. and Porter, J. C. (1977) Dopamine in hypophysial portal plasma of the rat during the estrous cycle and throughout pregnancy. Endocrinology, **100**: 452–458.

ZOOLOGICAL SCIENCE 4: 861–865 (1987)

Effects of Two Juvenile Hormone Analogs (R–20458, RO203600) and Three Juvenile Hormones (JH 1, JH 2, JH 3) on the External Morphology and Length of the Spiculum Copulatus (SC) in the Male German Cockroach, *Blattella germanica* (L.) (Dictyoptera: Blattellidae)

Christine M. Wheeler and Ayodhya P. Gupta

Department of Entomology and Economic Zoology, Cook College, New Jersey Agricultural Experiment Station, Rutgers University, New Brunswick, N. J. 08903, U.S.A.

ABSTRACT—The spiculum copulatus (SC) of adult male *Blattella germanica* (Dictyoptera: Blattellidae) is a robust, pollex-shaped cuticular process characterized by an irregularly sculptured exterior, no membranous articulation and numerous sensilla trichoidea. It is crucial for copulation to occur. The insect growth regulator (R–20458, RO203600, and Juvenile Hormones 1, 2 and 3)-treated SCs showed various degrees of distortion to the exterior surface and a significant reduction in length for all treatments.

INTRODUCTION

Various sensory structures, important in receiving tactile and/or chemical information during the mating behavior of cockroaches, have been investigated in one or both sexes of *Periplaneta americana* [1–3], *Blattella germanica* [4], *Leucophaea maderae* [5], and *Diploptera punctata* [6]. Another unusual sensory structure, first discovered by Sreng [7] and later independently reported and designated as the spiculum copulatus (SC) by Ramaswamy *et al.* [8], plays a major role in the mating behavior of male *B. germanica*. During the stereotyped mating sequence of males, the tergal glands, located beneath the modified 7th and 8th abdominal terga, release an attractant concurrently with male wing-raising; the female mounts the male and ingests these attractants [4, 8, 9]. While feeding, the female stimulates this sensory structure (140–200 μm long) which is located between the anterior and posterior pairs of tergal gland orifices on the 7th abdominal tergum, and is invested with numerous bifurcate and trifurcate sensilla. Prodding of the SC with an insect pin caused arching and extension of the abdomen in 87% of all males tested [8], whereas heat cauterization of this structure resulted in failure of 68.3% of the males to elicit this behavior after female feeding; it was concluded from this that the SC is crucial for copulation to occur.

Reductions in the number of sensilla on the antennae and/or maxillary and labial palps of juvenile hormone-treated male *L. maderae* [10], *P. americana* [11] or female *B. germanica* [12] have been reported; in these cases, mating was prevented. No one has reported the juvenile hormone effects on the SC in male *B. germanica*; a structure critical for copulation. We describe the normal morphology of the SC and report the effects of two juvenile hormone analogs (JHAs) (R–20458, RO203600) and three juvenile hormones (JH 1, JH 2, JH 3) on the external morphology and length of the SC.

MATERIALS AND METHODS

German cockroaches were selected from a laboratory colony maintained at 25°C under a photoperiod of 12 hr per day and reared on Purina laboratory chow and water. Thirty (1 to 3-day-old) 6th (last) instar males were treated topically with

Accepted May 27, 1987
Received March 30, 1987

0.2 μg/insect of R–20458 (6, 7-epoxy-1-(p-ethylphenoxy)-3, 7-dimethyl-trans-2-octene) (2 μl), 2.5 μg/insect RO203600 (6, 7-epoxy-3-methyl-7-ethyl-1-(3, 4-methylenedioxyphenoxy)-2-octene) (5 μl), 2 μg/insect Juvenile Hormone 1 (JH 1) (methyl-10, 11-epoxy-7-ethyl-3, 11-diemthyl-2, 6-tridecadienoate, cis/trans mixture) (2 μl), 2 μg /insect Juvenile Hormone 2 (JH 2) (2 μl), 7.5 μg/insect Juvenile Hormone 3 (JH 3) (6 μl) or 2, 5 or 6 μl of acetone, respectively (controls). After adult emergence, 7th abdominal terga from both treated and control groups were excised and processed for light and scanning electron microscopy [12]. Changes in spur morphology were noted and the lengths of 30 individual SCs for each treatment were determined using an ocular micrometer calibrated by means of a 2 mm reference stage micrometer. Comparisons were made between the treated and control groups with respect to SC length (Analysis of Variance (ANOVA); Duncan).

RESULTS

Based on our present SEM studies and earlier work [8], the SC is a robust, pollex-shaped cuticular process, which is rigidly connected to the integument that separates the left and right anterior and posterior pairs of tergal gland orifices on the 7th abdominal tergum. The SC is characterized by an irregularly sculptured exterior (Fig. 1A–C); it lacks a membranous articulation and its width varies throughout its length (approximately 60 μm at the base and 4 μm at the apex). With the help of SEM studies, and the morphological [12] and nomenclatural [2] descriptions, we have characterized the sensilla on the SC as sensilla trichoidea. To simplify the morphological descriptions, we have divided the SC into three regions: the apical (Fig. 1A), central (Fig. 1B), and basal (Fig. 1C) regions. The narrow distal area of the apical region (approximately 20 μm long) tapers to a blunt rotundate apex (Fig. 1A) and lacks sensilla; a wider proximal area (approximately 33 μm long) contains a few sensilla (Fig. 1A). The central region, narrower than the proximal area of the apical region and 33 μm long, has several nodules and numerous sensilla trichoidea (Fig. 1B) on its

Fig. 1. Montage showing full length of SC. ×1,500. A. Apical area showing blunt, rotundate apex (upper white arrow) and wide proximal area (lower white arrow). B. Central region with nodules (white arrow). C. Basal region.

surface. The broad basal region (55 μm long) is continuous with the cuticle (Fig. 1C).

All five treatments resulted in various degrees of distortion in SCs, rendering the three SC regions indistinguishable from one another (Fig. 2A–F); JHA-treated SCs showed the greatest distortion (Fig. 2B–C). Since the analogs are not the natural compound in the insect and they are not easily metabolized, their effects may be more potent. The irregularly sculptured surface of normal SCs was replaced by a relatively smooth exterior in the stump-like, R–20458-treated (Fig. 2B) and pyriform, RO203600-treated SCs (Fig. 2C). One hundred percent of all males with JH-induced abnormalities had distorted, pyramiform SCs with compressed, blunt apices bent to one side, giving a slightly geniculate appearance to the distal end of the SC (Fig. 2D–F). Unlike normal SCs, the JHA- and JH-treated SCs were broad at the base and progressively narrowed toward the apices, with JHA-treated SCs having obtuse, severed apices.

TABLE 1. Effect of JHAs and JHs on spiculum copulatus length of male *B. germanica*

Treatment	Spiculum length (μm) (Mean ± S.D.)
Acetone Control	144.7 ± 19.4 a
R–20458	37.7 ± 5.5 b
RO203600	53.6 ± 5.9 c
JH 1	56.1 ± 7.6 c
JH 2	87.7 ± 32.2 d
JH 3	94.2 ± 8.0 d

Numbers followed by the same letter are not significantly different at the p=0.05 level (ANOVA; Duncan).

From the measurements reported in Table 1 and the scanning electron micrographs (Fig. 2A–F), there is a significant reduction in SC length for all treatments (R–20458, RO203600 and JH 1, 2 and 3), compared with the control. JH 1-treated SCs were significantly shorter than JH 2-treated SCs (ANOVA; Duncan). The JH 1 titer in the nymph is higher than JH 2, which may explain the significant difference in the lengths of the JH 1- and 2-treated SCs.

DISCUSSION

Application of two juvenile hormone analogs (R–20458, RO203600) and three juvenile hormones (JH 1, 2 and 3) to 6th (last) instar male *B. germanica* results in a 35 to 65% reduction in the length of the SC (Table 1). R–20458 was the most potent with the SC reduced by 65%. Apparently, JH-induced changes in the length or morphology of the SC does not interrupt the mating sequence of *B. germanica* males, as long as the neural mechanism to the structure remains intact. In another study, we found also that JH-treated males showed a reduction in sensilla number on the 7th terga, the tergum involved in mating, without interruption in the mating sequence. The male may not require a certain quantity of specific sensilla types for mating; their mating sequence requires contact between the sexes and pheromone perception is short range so that successful stimuli reception may occur with only a few sensory receptors.

Previous reports [8] have shown that *B. germanica* males, whose SCs were heat cauterized, reinitiated precopulatory behaviors, but were unreceptive to copulation and thus not able to arch and extend the abdomen. Although no electrophysiological recordings were done, they suggest that once the female tergal feeding begins, the subsequent mating behaviors are released by mechanoreceptive or tactile stimuli; the SC and its sensilla may be an innervated mechanoreceptor.

That the SC may function as an innervated mechanoreceptor is further substantiated by a report on the behavioral responses of abdominal vibration receptors (AVRs) in *P. americana* males, which are involved in detecting cuticular vibrations [13]. It was found that the *P. americana* AVRs respond to mouthpart movements on the cuticle and suggested that in those cockroaches, which require female tergal feeding in the courtship sequence, AVRs may be present and could function as female position detectors. It is possible that the SC, a cuticular extension containing a concentrated group of mechanoreceptive sensilla, is functioning like an AVR, capable of detecting the correct position of the female during courtship.

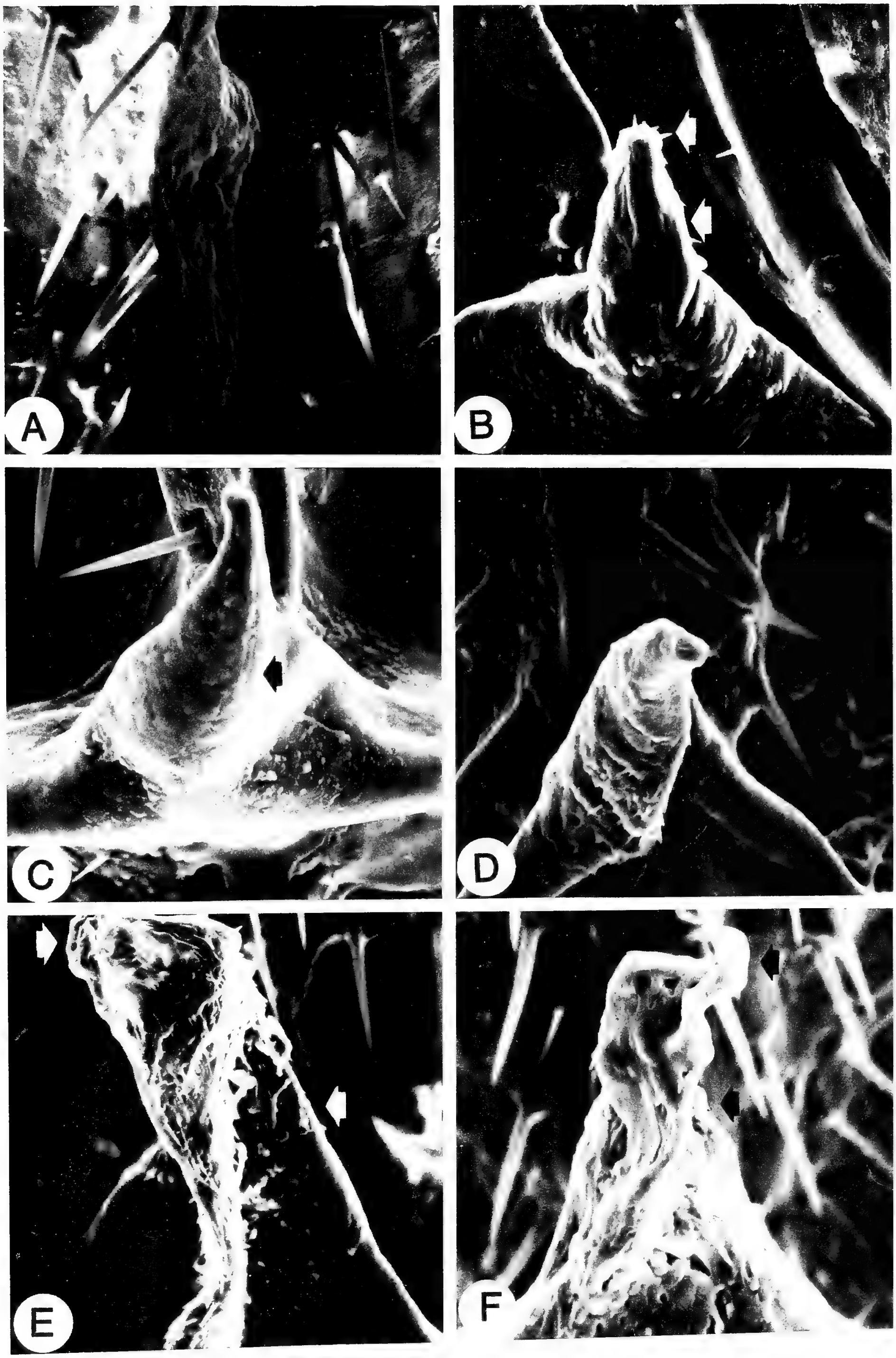
A
B
C
D
E
F

ACKNOWLEDGMENT

This report is the New Jersey Agricultural Experiment Station Publication No. 08125-21-86 supported by state and U.S. Hatch funds and Rutgers Research Council.

REFERENCES

1 Schafer, R. J. (1973) Postembryonic development in the antenna of the cockroach, *Leucophaea maderae*: Growth, regeneration and development of the adult pattern of sense organs. J. Exp. Zool., **183**: 353–364.

2 Schafer, R. and Sanchez, T. V. (1973) Antennal sensory system of the cockroach, *Periplaneta americana*: Postembryonic development and morphology of the sense organs. J. Comp. Neurol., **149**: 335–354.

3 Schaller, D. (1978) Antennal sensory system of *Periplaneta americana*: Distribution and frequency of morphologic types of sensilla and their sex-specific changes during postembryonic development. Cell Tissue Res., **191**: 121–139.

4 Roth, L. M. and Willis, E. R. (1952) A study of cockroach behavior. Am. Middl. Nat., **47**: 66–129.

5 Engelmann, F. (1960) Hormonal control of mating behavior in an insect. Experientia, **16**: 69–70.

6 Stay, B.and Roth, L. M. (1956) The reproductive behavior of *Diploptera punctata* (Blattaria: Diplopteridae). Proc. 10th Int. Congr. Entomol., **2**: 547–552.

7 Sreng, L. (1976) Les glandes tergales du male de *Blattella germanica* L. (Insecte Dictyoptere). Ultrastructure, development, chimie de la secretion. These de troisieme Cycle, Univ. Dijon, France.

8 Ramaswamy, S. B., Gupta, A. P. and Fowler, H. G. (1980) External ultrastructure and function of the "spiculum copulatus" (SC) of the German cockroach, *Blattella germanica* (L.) (Dictyoptera: Blattellidae). J. Exp. Zool., **214**: 287–292.

9 Roth, L. M. (1969) The evolution of the male tergal glands in the Blattaria. Ann. Entomol. Soc. Am., **62**: 176–208.

10 Schafter, R. J. (1977) The nature and development of sex attractant specificity in cockroaches of the genus *Periplaneta*. III. Normal intra- and inter-specific behavioral responses and responses of insects treated with juvenile hormone. J. Exp. Zool., **199**: 73–84.

11 Schafter, R. and Sanchez, T. V., (1974) Juvenile hormone inhibits differentiation of olfactory sense organs during postembryonic development of cockroaches. J. Insect Physiol., **20**: 965–974.

12 Ramaswamy, S. B. and Gupta, A. P. (1981) Sensilla of the antennae and the labial and maxillary palps of *Blattella germanica* (L.) (Dictyoptera: Blattellidae): Their classification and distribution. J. Morphol., **168**: 269–279.

13 Florentine, G. J. (1968) Response characteristics and probable behavioral roles for abdominal vibration receptors of some cockroaches. J. Insect Physiol., **14**: 1577–1588.

FIG. 2. SEM micrographs of normal and treated SCs. ×600. A. Normal SC. B and C. R-20458-treated and RO203600-treated SCs showing smooth exteriors (lower white and black arrows) and obtuse apices (upper white and black arrows). D and E. JH 1- and JH 2-treated SCs showing the distorted surfaces (lower black and white arrows) and geniculate distal ends with compressed apices (upper black and white arrows). F. JH 3-treated SC with distorted surface (lower black arrow) and geniculate distal end with compressed, hook-shaped apex (upper black arrow).

ZOOLOGICAL SCIENCE 4: 867–873 (1987)

Sex Difference in the Early Histopathological Changes of the Kidney in Wistar/Tw Rats

Win Win Yee and Seiichiro Kawashima

Zoological Institute, Faculty of Science, Hiroshima University, Hiroshima 730, Japan

ABSTRACT—Early signs of histopathological changes of the kidney were detected at 3 months of age in male rats and at 9 months of age in female rats of the Wistar/Tw strain. Criteria for early lesions include the enlargement of Bowman's capsule space and glomerular capillary walls, slight mesangial thickening and the formation of few casts in the renal tubules. Enlargement of Bowman's capsule space in male rats was 1.6 times of that in female rats at 3, 6 and 9 months of age. Moreover, in male rats 50% of glomeruli were affected at 3 months of age and about 90% at 13 months. In contrast, in female rats the percentage of affected glomeruli was only about 40% at 9 months of age. The enlargement of Bowman's capsule space and the incidence of affected glomeruli were closely related with age and sex of rats. However, there were no significant changes in water metabolism up to 13 months of age. Degenerated glomeruli counted about 20% of the total glomeruli in male rats at 13 months of age, but those were very few in female rats. Thus, the marked changes of renal function in male rats at more advanced ages may be related to the high percentage of glomerular degeneration.

INTRODUCTION

Kobayashi and Kawashima [1, 2] and Kawashima and Kobayashi [3] reported that polydipsia and polyuria, with the decrease in urinary electrolyte concentration, occurred in male rats of the inbred Wistar/Tw strain at the age of about 17 months. However, polydipsia and polyuria occurred significantly later in female rats than in males [4]. These senile changes in water and electrolyte metabolism are the consequences of retardation in renal function, because spontaneous kidney disease is common in rats of this substrain as well as in old rats maintained in other laboratories [5–11]. In male Wistar/Tw rats frequent occurrence of degenerated glomeruli, enlargement of Bowman's capsule space and marked increase in hyaline cast in the renal tubules were the features at the age of 17–18 months, while the histopathological changes were less pronounced in female rats of the same age ([12] and their unpublished observations). Furthermore, Kawashima *et al.* [13] suggested that definite sex difference in water metabolism may be due to the difference in the onset of degenerative changes of the kidney.

The aim of the present study is to know the early signs of histopathological changes of the kidney and whether there are sex differences at younger ages.

MATERIALS AND METHODS

Male and female rats of the Wistar/Tw strain raised in this laboratory were used in the present study. They were housed in a temperature-controlled room at a 12-hr light (6:00–18:00) and 12-hr dark cycle, with free access to laboratory chow (CA-1, Clea Japan Inc.) and tap water. At 1, 3, 6, 9 and 13 months of age, five male and five female rats each were used for the measurements of water intake and urinary volume. For the measurement, rats were kept individual for 3 days in aluminum metabolic cages in which the urine could be collected without contamination with feces.

After the measurement the animals were killed by decapitation. The kidneys, after weighing, were cut into several frontal pieces. Superior, medial and inferior parts of the kidney were fixed

Accepted May 23, 1987
Received March 26, 1987

in Bouin's fluid and embedded in paraplast. Frontal sections were cut at 8 μm thickness and divided into two series. A series of sections were stained with hematoxylin and eosin, and the other series, with periodic acid Schiff (PAS). Histoquantitative studies were carried out only on the medial parts of the kidney. The space of Bowman's capsules in sections cut at the plane of renal corpuscle including the vascular and urinary poles was measured with the aid of an image analyzer connected with a computer (Mutoh Industry Ltd., Tokyo). In each kidney the total number of glomeruli and the number of affected glomeruli were counted in a total of 18 sections at different levels (each section shows more than 150 glomeruli). The affected glomeruli were expressed as percentage as applied by Elema and Arends [14]. The affected glomeruli showed various degrees of lesions from sclerosis to complete degeneration. The severity of lesions was increased as a function of age.

Progressive glomerulonephrosis (PGN) was used as the general term for the age-related kidney lesions in the present study. Initial signs of PGN

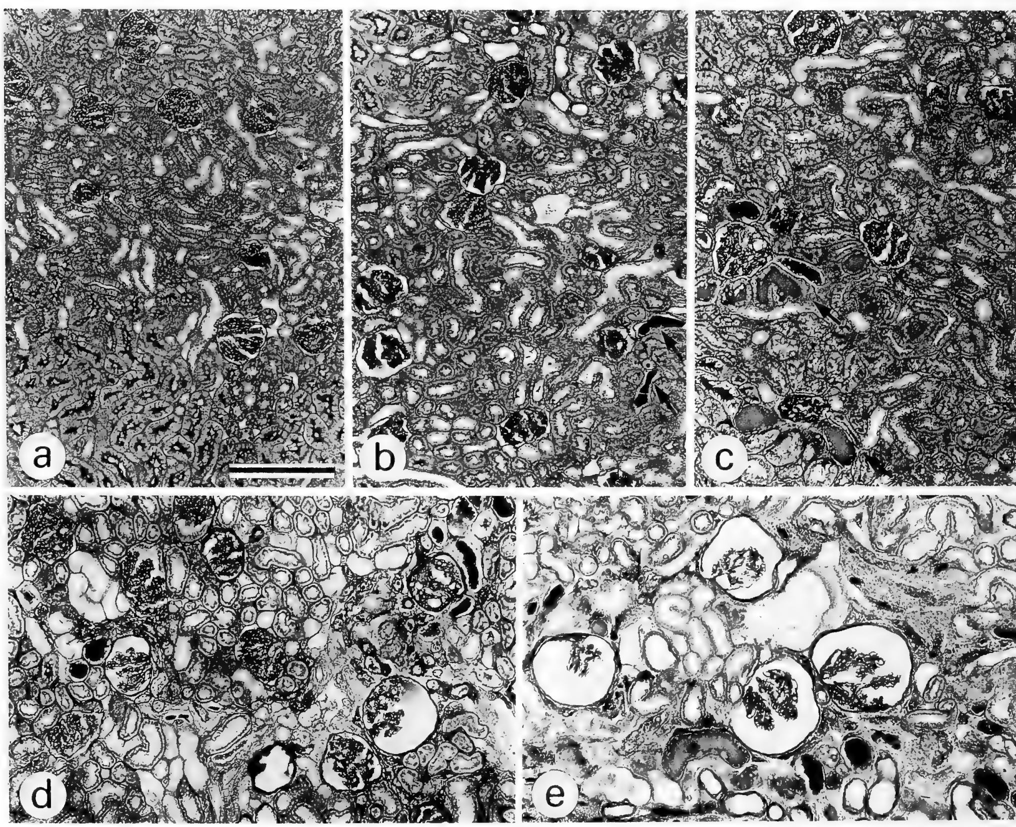

FIG. 1. Grades for histopathological changes of the kidney of Wistar/Tw rats. PAS preparations. Scale: 0.5 mm.

a. Normal. Glomeruli are compact and tubules are devoid of PAS-positive casts.
b. Grade 1. Irregularly thickened Bowman's capsule space with thickened glomerular capillary wall and tubules with some casts (arrows).
c. Grade 2. Dilated tubules with casts (arrows).
d. Grade 3. Degenerated glomeruli associated with enlargement of Bowman's capsule space. Most of the tubules are filled with casts.
e. Grade 4. Adhesion of glomerular tufts to Bowman's capsule, dilated tubules and tubules filled with large amount of casts.

were based on criteria described in several papers [6, 15–17] and PGN was arbitrarily graded from 1 to 4. The grading system was generally based on Coleman *et al.* [16]. However, as their criteria for early pathological changes did not fit well to our materials, we have rated the changes with some modifications as follows.

Grade 1: The earliest lesion. Presence of irregularly thickened Bowman's capsule space with thickened glomerular capillary wall and slight mesangial thickening in some glomeruli. A few casts were present in Henle's loop preferentially in the region at the cortico-medullary junction (Fig. 1a). The casts were strongly PAS-positive, and the kidneys without any PAS-positive cast were classified as normal.

Grade 2: Presence of scattered dilated tubules lined by flattened epithelium with hyaline casts particularly at the cortico-medullary junction (Fig.1b).

Grade 3: Presence of large casts throughout the renal tubular system, the atrophy of capillary tufts and the degeneration of some glomeruli. Enlargement of most of the Bowman's capsule space (Fig. 1c).

Grade 4: In addition to exaggerated Grade 3 lesions, the adhesion of glomerular tufts to Bowman's capsules with wide-spread glomerulosclerosis (Fig. 1d).

Bowman's capsule space and the number of affected glomeruli were measured in all kidneys.

The statistical analyses between two groups of rats were performed by Kruskal-Wallis and Mann-Whitney U tests. The relationship between the weight of the kidney and the Bowman's capsule space was analyzed by coefficients of rank correlation.

RESULTS

Daily water intake and urinary volume

Water intake was the greatest at 3 months of age in both sexes than at other ages (Fig. 2). After 3 months water intake decreased in female rats, while in male rats water intake was almost constant until 9 months of age and it slightly decreased at 13 months. The urinary volume decreasd steadily as a function of age in females after 3 months of age. However, in male rats daily urinary volume was almost constant between 3 and 9 months of age but decreased at 13 months (Fig. 2) (3 vs. 13 months, $P<0.005$).

Incidence of progressive glomerulonephrosis (PGN)

In male rats the initial lesions (Grade 1) were first detected at 3 months of age (Table 1) and

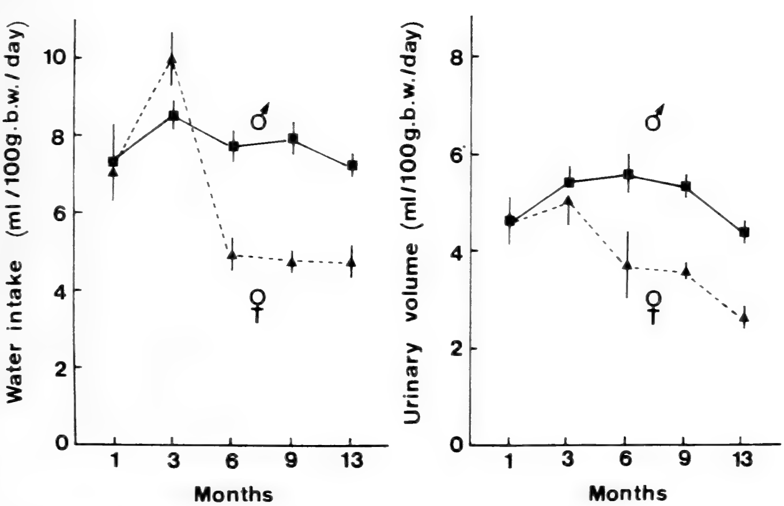

FIG. 2. Age-related changes in daily water intake and urinary volume of Wistar/Tw rats of both sexes. Vertical bars indicate standard errors of means. Each point depicts the mean of 5 rats.

TABLE 1. Incidence of progressive glomerulonephrosis (PNG) in male and female Wistar/Tw rats at various ages

Sex	Age (months)	No. of rats	Incidence				
			Normal	Grade 1	Grade 2	Grade 3	Grade 4
Male	1	5	5	—	—	—	—
	3	5	1	4	—	—	—
	6	5	—	—	5	—	—
	9	5	—	—	—	3	2
	13	5	—	—	—	—	5
Female	1	5	5	—	—	—	—
	3	5	5	—	—	—	—
	6	5	4	1	—	—	—
	9	5	—	5	—	—	—
	13	5	—	—	5	—	—

definite lesions of Grade 2 developed at 6 months of age. Grade 4 lesions were observed in two out of five male rats at 9 months and all rats at 13 months of age (Table 1). In contrast, in female rats the kidney was affected only slightly until 6 months of age. Initial lesions were observed at 9 months. The definite lesions of Grade 2 were encountered at 13 months of age (Table 1). Thus, male rats showed earlier the development of PGN after 3 months than female rats.

Figure 3 illustrates the incidences of affected glomeruli and degenerated glomeruli in the kidney of rats at various ages. In male rats about 50% of glomeruli were affected at 3 months of age and about 90% at 13 months. The incidence of affected glomeruli significantly increased only at 9 months in female rats to about 40%. The increase in percentage of degenerated glomeruli occurred at 9 months in male rats (about 20%). However, in female rats degenerated glomeruli were very few even at 13 months (about 4%) (Fig. 3).

Age-related changes in Bowman's capsule space

The increase in Bowman's capsule space is another striking feature of age-related changes of the kidney. Figure 4 shows that the enlargement of Bowman's capsule was progressive during 1 to 9 months of age in male rats and during 1 to 13 months in females. At 1 month of age there was no sex difference. Bowman's capsule space of 3-month-old male rats was almost the same as that of 9-month-old female rats, indicating the rate of enlargement was greater in male than female rats. Bowman's capsule space in male rats was 1.6 times of that in female rats at 3, 6 and 9 months of age

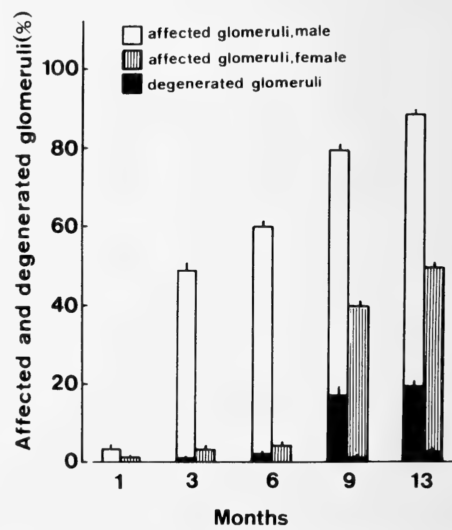

FIG. 3. Age-related increase in mean percentage of affected glomeruli and degenerated glomeruli in total number of glomeruli in 18 sections from medial part of the kidney in each rat (total counts of more than 2700 glomeruli). Open columns: percentage of affected glomeruli in male rats, hatched columns: percentage of affected glomeruli in female rats, solid columns: percentage of degenerated glomeruli in both sexes. Vertical bars indicate standard errors of means.

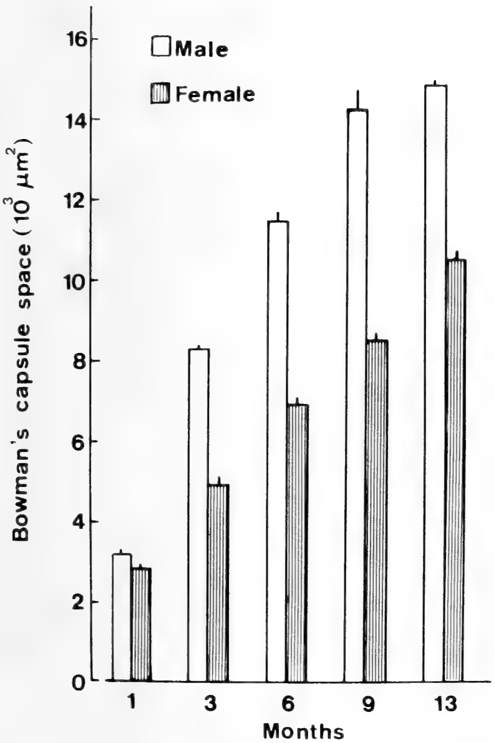

FIG. 4. Age-related changes in the mean maximum space of Bowman's capsules. Vertical bars indicate standard errors of means. Each column shows the mean of 5 rats.

(Fig. 4).

Figure 5 shows the coefficients of rank correlation between the weight of the kidney and Bowman's capsule space regardless of ages in both sexes. Rank correlation was highly significant at r=0.97 in males and r=0.93 in females for fitted regression lines. These results show that the increase in the weight of kidney is correlated with the space of Bowman's capsule.

DISCUSSION

The frequency of PGN was observed by light microscopy in Wistar/Tw rats until 13 months of age in both sexes. The onset of pathological lesions was characterized by histological and histoquantitative criteria. Male rats showed the development of lesions as early as at the age of 3 months and definite lesions developed at 6 months. In contrast, in female rats lesions developed 6–7 months later than in male rats. However, water intake and urinary output were conceivably within the range of normal functional variation until 13 months of age in both sexes, as has been reported previously [3, 4]. According to Hackbarth and Harrison [18] the kidney is endowed with a great compensatory ability, allowing

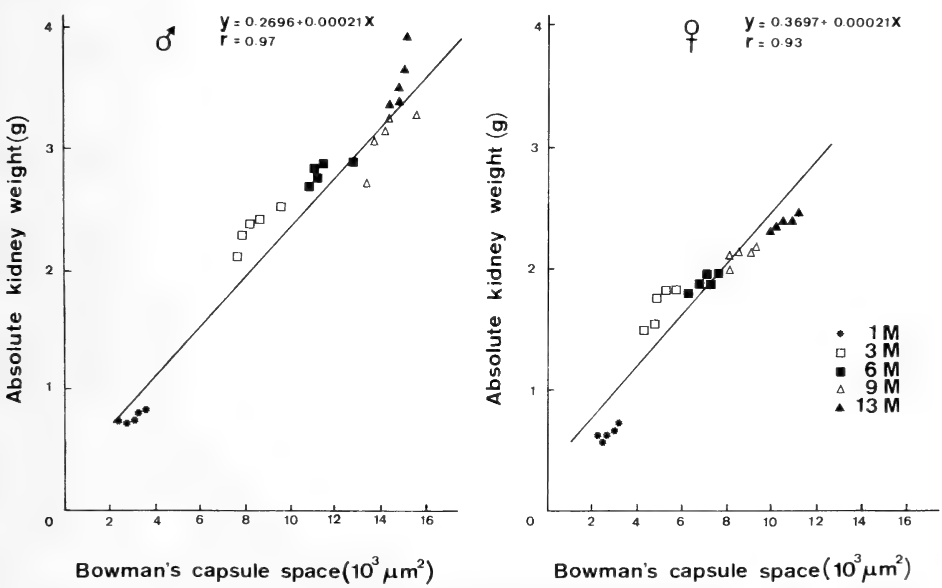

FIG. 5. Relationships between the weight of kidney and the space of Bowman's capsule regardless of ages (months; M) in male and female rats. Rank correlation (r) is statistically significant in both sexes of rats.

it to maintain near normal function even in chronic kidney disease or with extensive histological changes. Thus, the absence of any marked physiological abnormalities may be the characteristics of compensatory ability of the kidney of rats younger than 13 months of age in Wistar/Tw strain. Moreover, our Wistar/Tw strain male rats showing enlargement of Bowman's capsule space with marked degenerated glomeruli about 70% at 17–18 months were accompanied by polydipsia and polyuria. These changes in water metabolism may indicate the marked changes in renal function due to degeneration of glomeruli.

The present study showed the possible relationships among the incidence of PGN, affected and degenerated glomeruli, the weight of kidney, Bowman's capsule space and the age and sex of animals. Elema *et al.* [19], Guttman and Kohn [20], Striker *et al.* [21] and Berg [6] reported that the glomerular lesion precedes tubular lesion. The present results were consistent with the findings of these workers, because we found that the primary change began in the glomerulus. There were many divergent views upon the enlargement of renal corpuscles. Using the same substrain as ours, Kobayashi and Kawashima [12] suggested that the increase in diameter of renal corpuscles at 17–18 months of age was due to the enlargement of Bowman's capsule *per se* and not to the glomerular enlargement. Bauer and Rosenberg [22] interpreted that the glomerular enlargement was a reflection of the dilatation of glomerular capillaries. These results altogether may indicate that the enlargement of renal corpuscle is probably due firstly to the dilatation of capillaries, and secondly to the repletion with casts. In addition, in the present study the observed enlargement of Bowman's capsule space together with marked tubular dilatation filled with casts of various sizes probably induced the increase in kidney weight as age advanced.

Based on histological observations Gray *et al.* [17] reported that Sprague-Dawley female rats showed the onset of disease during their second year of life. In their study Brown Norway (BN/Bi) rats were in an initial disease state at about 30 months of age in both sexes, and Wistar (WAG/Rij) male rats attained a similar state at 13–15 months of age, approximately 8 months earlier than female rats. In our Wistar/Tw male rats the initial lesions occurred at least 10 months earlier in both sexes than the Wistar rats used by other investigators.

From the present results together with the previous findings we may conclude that the presence of sex difference is evident in the process of PGN in Wistar/Tw rats and that the early lesions are usually followed by eventual development of polydipsia and polyuria at the age of about 17 and 24 months in male and female Wistar/Tw rats, respectively. Therefore, the development of polydipsia and polyuria may be pathological changes of the kidney.

ACKNOWLEDGMENTS

The authors wish to thank Dr. T. Machida for his helpful discussion. This study was supported in part by a Grant-in-Aid for Scientific Research from the Ministry of Education, Science and Culture, Japan.

REFERENCES

1 Kobayashi, Y. and S. Kawashima (1980) Polydipsia and polyuria in aged male rats of the Wistar/Tw strain. Proc. Japan Acad., Ser. B., **56**: 643–648.

2 Kobayashi, Y. and S. Kawashima (1984) Age-related changes in the water and electrolyte metabolism in male rats of the Wistar/Tw strain. Exp. Gerontol., **19**: 107–113.

3 Kawashima, S. and Y. Kobayashi (1982) Morphometric study of the hypothalamo-neurohypophyseal system in aged rats. J. Sci. Hiroshima Univ., Ser. B., Div. 1, **30**: 229–242.

4 Kobayashi, Y. and S. Kawashima (1982) Sex difference in water metabolism during aging and life span in rats of the Wistar/Tw strain. J. Sci. Hiroshima Univ., Ser. B, Div. 1, **30**: 243–248.

5 Foley, W. A., D. C. L. Jones, G. K. Osborn and D. J. Kimeldorf (1964) A renal lesion associated with diuresis in the aging Sprague-Dawley rat. Lab. Invest., **13**: 439–450.

6 Berg, B. N. (1965) Spontaneous nephrosis with proteinuria, hyperglobulinemia and hypercholesterolemia in the rat. Proc. Soc. Exp. Biol. Med., **119**: 417–420.

7 Berg, B. N. (1976) Pathology and aging. In "Hypothalamus, Pituitary and Aging". Ed. by A. V. Everitt and J. A. Burgess, C. C. Thomas Publ., Illionis, pp. 43–67.

8 Sworn, M. J. and M. Fox (1972) Donor kidney selection for transplantation. Br. J. Urol., **44**: 377–383.

9 Christian, J. J. (1976) Anterior pituitary in relation to renal disease. In "Hypothalamus, Pituitary and Aging." Ed. by A. V. Everitt and J. A. Burgess, C. C. Thomas Publ, Illinois, pp. 297–332.

10 Goldman, R. (1977) Aging of the excretory system: Kidney and bladder. In "Handbook of the Biology of Aging." Ed. by C. E. Finch and L. Hayflick, Van Nostrand Reinhold, New York, pp. 409–431.

11 Goyal, V. K. and P. C. Chatterjee (1980) Changes with age in mouse kidney. Exp. Gerontol., **15**: 151–160.

12 Kobayashi, Y. and S. Kawashima (1983) Histological changes in the kidney of aged rats of the Wistar/Tw strain showing polydipsia and polyuria. J. Sci. Hiroshima Univ., Ser. B., Div. 1, **31**: 149–154.

13 Kawashima, S., K. Kawamoto and Y. Kobayashi (1986) Aging of the Hypothalamo-neurohypophysial system and water metabolism in rats. Zool. Sci., **3**: 227–244.

14 Elema, J. D. and A. Arends (1975) Focal and segmental glomerular hyalinosis and sclerosis in the rat. Lab. Invest., **33**: 554–561.

15 Bras, G. and M. H. Ross (1964) Kidney disease and nutrition in the rats. Toxicol. Appl. Pharmacol., **6**: 247–262.

16 Coleman, G. L., S. W. Barthold, G. W. Osbaldiston, S. J. Foster and A. M.Jonas (1977) Pathological changes during aging in barrier-reared Fischer 344 male rats. J. Gerontol., **32**: 258–278.

17 Gray, J. E., M. J. van Zwieten and C. F. Hollander (1982) Early light microscopic changes of chronic progressive nephrosis in several strains of aging laboratory rats. J. Gerontol., **37**: 142–150.

18 Hackbarth, H. and D. E. Harrison (1982) Changes with age in renal function and morphology in C57BL/6, CBA/HT6 and $B6CBAF_1$ mice. J. Gerontol., **37**: 540–547.

19 Elema, J. D., J. Koudstaal, H. B. Lamberts and A. Arends (1971) Spontaneous glomerulosclerosis in the rat. Arch. Pathol., **91**: 418–425.

20 Guttman, P. H. and H. I. Kohn (1960) Progressive intercapillary glomerulosclerosis in the mouse, rat and chinese hamster, associated with aging and X-ray exposure. Am. J. Pathol., **37**: 293–307.

21 Striker, G. E., R. B. Nagle, P. W. Kohnen and E. A. Smuckler (1969) Response to unilateral nephrectomy in old rats. Arch. Pathol., **87**: 439–442.

22 Bauer, W. C. and B. F. Rosenberg (1960) A quantitative study of glomerular enlargement in children with tetralogy of Fallot. Am. J. Pathol., **37**: 695–712.

ZOOLOGICAL SCIENCE 4: 875–880 (1987)

Ultrastructural Observations of the Developing Basophilic Granulocytes in the Loach Kidney

Kiyoto Ishizeki

Department of Oral Anatomy, School of Dentistry, Iwate Medical University, Morioka 020, Japan

ABSTRACT—The developing basophils in the intertubular space of the loach kidney were examined electron microscopically. These basophils could be classified into early, intermediate, and mature stages based on ultastructural appearance. The majority of the cells identified as in the early stage had a developing rough endoplasmic reticulum and Golgi apparatus, and several immature granules that consisted only of a fine granular matrix. Among these cells, typically large lymphoid cells that contained a nucleus with a prominent nucleolus, many ribosomes, a few large mitochondria, and occasionally vesicles containing flocculent material were considered to be the most immature cells of the basophil series. Intermediate cells contained well-developed Golgi apparatus, rough endoplasmic reticulum, and numerous immature and mature electron-dense homogeneous granules, and they were similar morphologically to the myelocytes of the mammalian basophils. In the intertubular tissues, cells with an eccentric oval nucleus and numerous electron-dense homogeneous granules ultrastructurally resembled the mature basophils found in the peripheral blood. In conclusion, the loach has basophils clearly distinguishable from other granulocytes and the ultrastructural features of its granules closely resemble those of higher vertebrates.

INTRODUCTION

In higher vertebrates, basophils are common blood cells. However, in lower vertebrates such as teleost fishes, basophils have been found in some, but not in other families. Some light microscopic [1, 2], histochemical [3] and electron microscopic [4, 5] studies failed to find basophils in several teleost fishes, but several studies [6–10] revealed the presence of basophils in the blood of some teleost fishes. Lester and Desser [11] demonstrated electron microscopically the blood basophils of the white sucker (*Catostomus commersoni*) which contained large, round, membrane-bound electron-dense granules consisting of fine granular material. Catton [12], Kamishiro [13] and Bielek [14] reported that these basophils are produced in the kidney of some teleost fishes. However, detailed ultrastructural studies of the developing basophils in teleost fishes have not been reported.

In the present study, developing basophils in the intertubular space of the loach kidney were examined by electron microscopy, to clarify their morphological characteristics.

MATERIALS AND METHODS

Commercially supplied adult loaches, *Misgurnus anguillicaudatus* (5–10 g in weight, 10–15 cm in length) were used.

For electron microscopy, specimens of the kidney and whole blood were centrifuged and the resulting pellets were fixed in cold 2.5% glutaraldehyde buffered in sodium cacodylate (pH 7.4) for 1 hr, and then postfixed in 1% OsO_4 for 1 hr at 4°C. The fixed materials were then dehydrated by an ethanol series and finally embedded in Epon 812. The specimens were sectioned on an LKB-ultratome using a diamond knife. Ultrathin sections were stained with uranyl acetate and lead citrate, and examined with a JEM-100B electron microscope at 80 kV. Blood smear preparations obtained from decapitated animals were stained with May-Grünwald Giemsa solution and were used for light microscopic observations.

Accepted May 6, 1987
Received March 4, 1987

RESULTS

Loach blood contained three kinds of granulocytes: basophils, heterophils and eosinophils. However, basophils were easily distinguished, because they differed clearly from the other granulocytes in staining features, hemopoietic sites, and fine structural features of specific granules as previously reported [15].

Light microscopically, the basophil was not found so frequently in smear preparation as other granulocytes. Almost all the basophils observed were oval or round, and contained a large nucleus and granules which were stained dark blue (Fig. 1a). The ultrastructure of such basophils (Fig. 1b) in the peripheral blood exhibited an eccentric oval nucleus with condensed heterochromatin and many electron-dense homogeneous granules (Fig. 1c). A few rough endoplasmic reticulum, mitochondria and immature granules with a fine granular matrix were also recognizable. In the present observations, the basophils showing these morphological features were identified as mature basophils of the loach.

In the intertubular space of the kidney, various kinds of developing basophils could be seen. Among these cells, the most immature cells were of large lymphoid-shaped and had an oval nucleus with a high percentage of euchromatin and a prominent nucleolus. A few large mitochondria

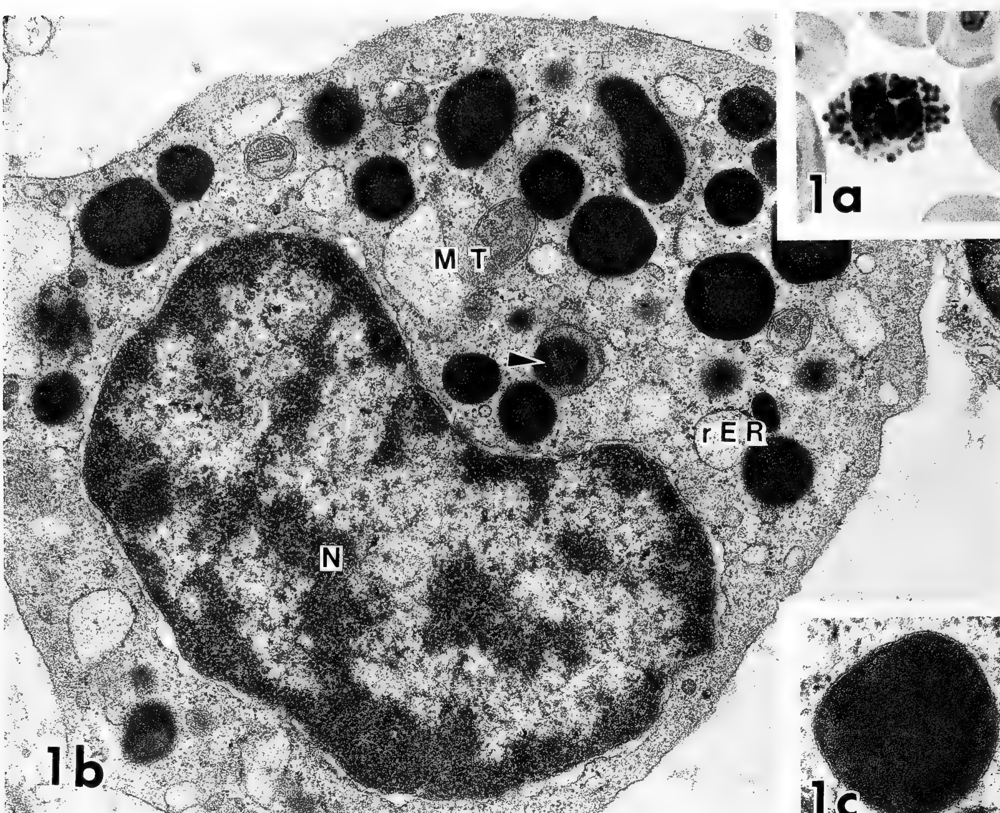

Fig. 1. a: Light micrograph of the mature basophil in the blood smear preparation. A large oval nucleus and granules stained dark blue can be seen. ×1,500. b: Oval nucleus (N) with condensed heterochromatin, many large round homogeneous granules, a few mitochondria (MT), rough endoplasmic reticulum (rER) and immature granules containing a fine granular matrix (arrowhead) can be seen in the cytoplasm. ×20,400. c: High magnification of mature granule that consists of an electron-dense homogeneous matrix. ×46,000.

and many ribosomes were distributed throughout the cytoplasm, but other organelles were undeveloped (Fig. 2a). Occasionally, the cytoplasm contained a few vesicles that were partially filled with flocculent material (Fig. 2a, inset). In addition, more developed basophils were distinguished by an increased amount of heterochromatin at the nucleus rim, developing Golgi apparatus and rough endoplasmic reticulum (Fig. 2b). The immature granules (0.3–0.6 μm in diameter) were spherical and consisted of an electron-intermediated fine granular matrix (Fig. 2b, inset).

Furthermore the cells which were identified as in the intermediate stage (Fig. 3a, b) were relatively large and were characterized by a well-developed Golgi apparatus and an increased number of electron-dense homogeneous granules (0.8–1.1 μm in diameter). Eccentric nuclei had more condensed heterochromatin than those of the early stage cells and were invaginated slightly near the Golgi apparatus, which consisted of several cisternae, enclosed the progranules arising from the ends of the outer cisternae (Fig. 3b, arrow). The other characteristics at this stage were mingling of immature and mature granules. Immature granules were similar to those seen in the early stage cell, and mature granules showed an electron-dense homogeneous matrix.

In the intertubular tissue, cells similar in ultrastructural appearance to those of mature basophils in the peripheral blood were observed (Fig. 4). This type of cell had an eccentric condensed nucleus and many mature dense granules, but other organelles tended to decrease. Mature granules had neither precise crystalline cores nor myelin figures, such as those observed in amphibian [16–18] or human basophils [19]. Thus, in the present observation, these cells were classified as

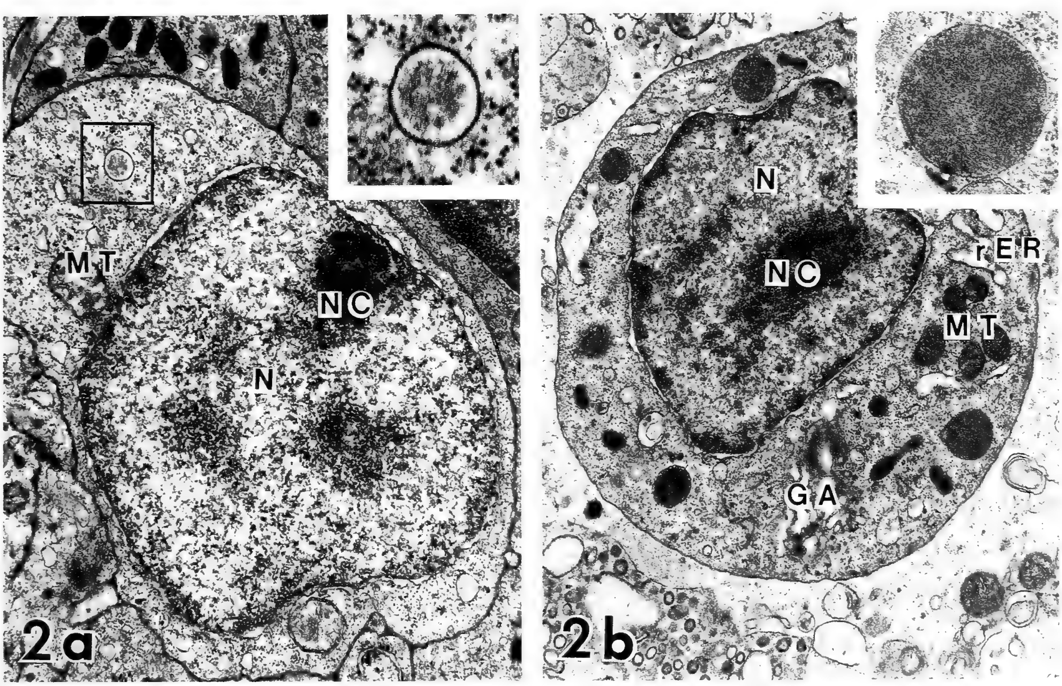

FIG. 2. a: A very early immature basophil that contains a large oval nucleus (N) with prominent nucleolus (NC). A few large mitochondria (MT) and many ribosomes of the polysome type are present. Note that the vesicle contains flocculent material (frame). ×13,800. Inset: High magnification of area shown in the frame. ×40,000. b: An early stage of a basophil having a large oval nucleus (N), prominent nucleolus (NC), rough endoplasmic reticulum (rER), mitochondria (MT) and developing Golgi apparatus (GA). Note the small number of immature granules that consist of fine moderately-dense granular matrices. ×11,000. Inset: Immature granule seen at an early stage at a high magnification. ×23,400.

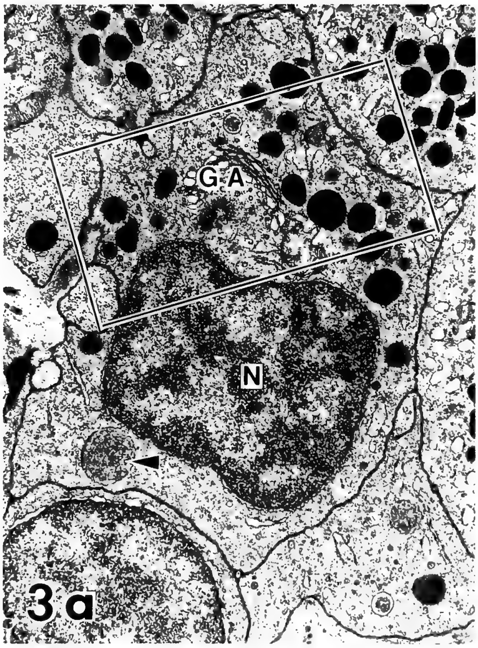

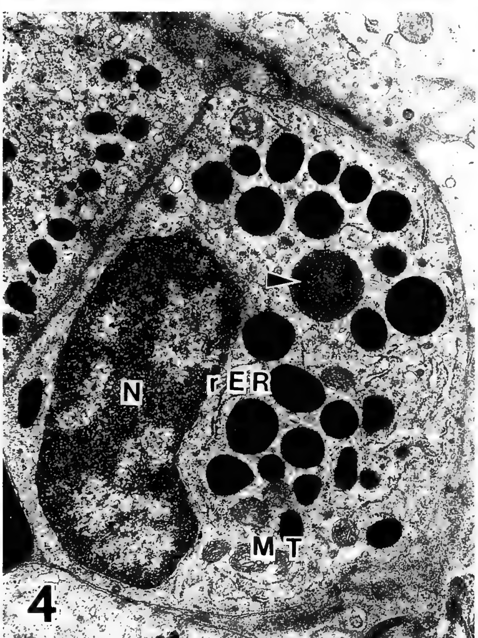

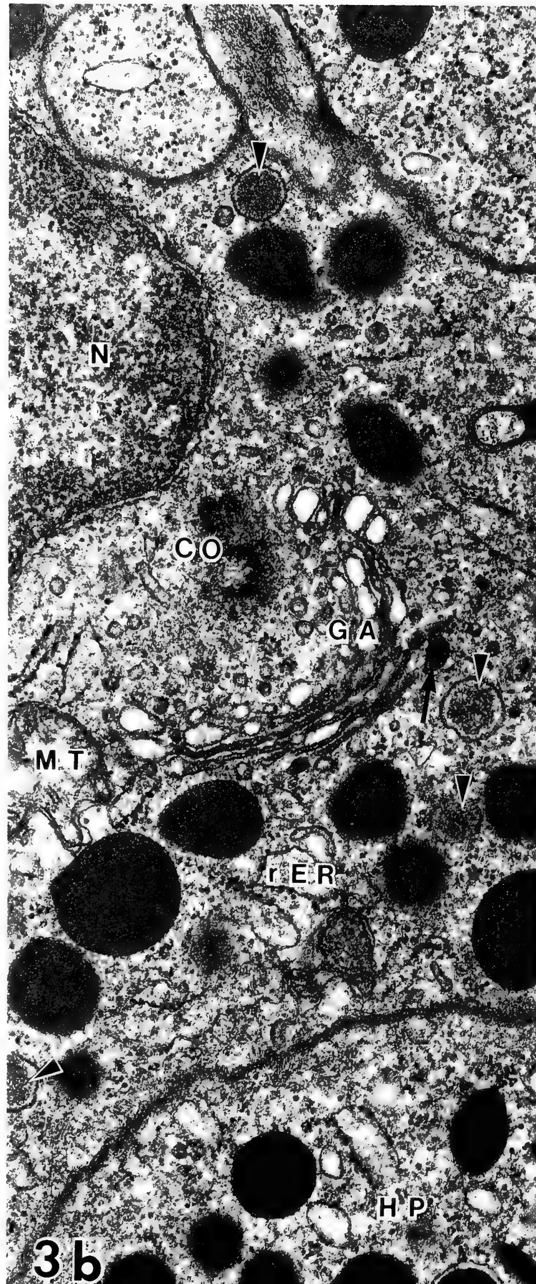

FIG. 3. a: A basophil at the intermediate stage. Many immature granules and mature granules, well-developed Golgi apparatus (GA) around the centriole and eccentric nucleus (N) with moderately clumped heterochromatin characterized the cell of this stage. Arrowhead shows immature granule with a fine granular matrix. ×11,000. b: High magnification of portion of the Golgi apparatus (GA) shown in (a). Immature granules can be seen at the end of the Golgi cisterna (arrow) and in the surrounding area (arrowhead). Note the

mature basophils.

DISCUSSION

In the teleost fishes, basophils have been reported in only a few species [6–11]. They derive from the intertubular space of the kidney [12–14]. In the loach kidney, there were many maturing basophils, which relates to the hemopoietic nature of this tissue.

Generally, the morphological change of mammalian developing basophils is similar to that of eosinophils or neutrophils [20–22], and mature basophils possess a lobulated nucleus [23–25]. However, in the loach, such segmented basophils, though matured cells, were not found light-microscopically: it was therefore difficult to directly apply mammalian criteria to the development of loach basophils. Therefore, in the present study, basophils were classified into three stages of maturation by ultrastructural appearance.

The cytoplasmic granule, as seen in large lymphoid-cells (Fig. 2a), was similar to the immature granules of the basophil series. Also, this type of granule resembled the progranulocyte (myeloblast) of the amphibian (*Plethodon glutinosus*; [17]) and rabbit basophilic myelocytes [23]. Heterophils as well as basophils also arose from the intertubular space of the kidney, the two cell types were morphologically distinct because heterophils contained granules with more electron-dense material than those of basophils even though progranules. Therefore, the cells of this type were identified as the most immature basophils of the loach. Also, among the basophils classified as in the early stage, cells containing a few granules with a fine granular matrix alone were also seen, but by the appearance of rough endoplasmic reticulum and heterochromatin, which is condensed in the nuclear periphery, they seemed to be more developed than the cell shown in Figure 2a. The mammalian basophilic myelocytes and metamyelocytes are characterized by a centrally located large nucleus, well-developed Golgi apparatus and rough endoplasmic reticulum, and two or three types of cytoplasmic granules [20–23]. Such cells seemed to be morphologically similar to the cell types that were classified as being at the intermediate stage in this study.

In mammalian basophils such as in humans [19, 22, 24], rabbits [23], minks [26] and in amphibian basophils [18, 27], two types of granules, particulate and homogeneous matrix, have been observed. Furthermore, Lester and Desser [11] reported that the basophils in the peripheral blood of the white sucker (*Catostomus commersoni*) possess two types of granules with large, round membrane-bound granules: some were uniformly electron-dense, while others were in a granular matrix. Both granules resembled ultrastructurally the immature or mature granules of the loach basophils, but generally granules with a fine granular matrix have been described in mature basophils [18, 24, 27]. Although the stage of appearance of these granules varies among animal species, the structure of such granules might reflect the phylogenetic characteristic of the basophils.

In the present investigation, basophil granules occurred as condensed vacuoles containing flocculent material at the end of the Golgi cisternae, and progressed to a fine granular matrix and were finally transformed into electron-dense homogeneous granules, which were numerous in near-mature or mature basophils. Thus, the large homogeneous granules were a mature form of fine granular matrices and consequently, the loach basophils consist of one population of granules.

Although it is unknown whether the granule contents of the basophils vary with the species, if teleost basophils have similar granules, the present findings would be important for classifying basophils. Further study is needed to examine whether this cell is functionally analogous to basophils of the higher vertebrates.

heterophilic granules with more electron-dense crystalloid structures. HP, heterophil, N, nucleus, MT, mitochondria, Co, centriole, rER, rough endoplasmic reticulum. ×29,500.

FIG. 4. Mature basophil in the kidney showing condensed nucleus (N), many electron-dense mature granules, a few rough endoplasmic reticulum (rER) and mitochondria (MT). One large immature granule is indicated by the arrowhead. This type of cell is similar to the mature basophils in the peripheral blood. ×12,300.

ACKNOWLEDGMENT

The author wish to thank Prof. T. Nawa for critical reading of the manuscript.

REFERENCES

1 Chlebeck, A. and Phillips, G. L. (1969) Hematological study of two buffalofishes, *Ictiobus cyprinellus* and *I. bubalus* (Catostomideae). J. Fish. Res. Bd. Canada, **26**: 2881–2886.

2 Conroy, D. A. (1972) Studies on the haematology of the atlantic salmon (*Salmo salar* L.). Symp. Zool. Soc. Lond., **30**: 101–127.

3 Barber, D. L. and Westermann, J. E. M. (1975) Morphological and histochemical studies on a PAS-positive granular leukocyte in blood and connective tissue of *Catostomus commersonnii* Lacépède (Teleostei: Pisces). Am. J. Anat., **142**: 205–220.

4 Cannon, M. S., Mollenhauer, H. H., Eurel, T. E., Lewis, D. H., Cannon, A. M. and Tompkins, C. (1980) An ultrastructural study of the leukocytes of the channel catfish, *Ictalurus punctatus*. J. Morphol., **164**: 1–23.

5 Savage, A. G. (1983) The ultrastructure of the blood cells of the pike *Esox lucius* L. J. Morphol., **178**: 187–208.

6 Duthie, E. S. (1938) The origin, development and function of the blood cells in certain marine teleosts. part 1. Morphology. J. Anat., **73**: 396–414.

7 Weinreb, E. L. (1963) Studies on the fine structure of teleost blood cells. 1. Peripheral blood. Anat. Rec., **147**: 219–238.

8 Watson, L. J., Shechmeister, I. L. and Jackson, L. L. (1963) The hematology of goldfish, *Carassius auratus*. Cytologia, **28**: 118–130.

9 Srivastava, A. K. (1968) Studies on the hematology of certain freshwater teleosts. IV. Leucocytes. Anat. Anz. Bd., **123**: 520–533.

10 Williams, R. W. and Warner, M. C. (1976) Some observations on the stained blood cellular elements of channel catfish, *Ictalurus punctatus*. J. Fish Biol., **9**: 491–497.

11 Lester, R. J. G. and Desser, S. S. (1975) Ultrastructural observations on the granulocytic leucocytes of the teleost *Catostomus commersoni*. Can. J. Zool., **53**: 1648–1657.

12 Catton, W. T. (1951) Blood cell formation in certain teleost fishes. Blood, **6**: 39–60.

13 Kamishiro, K. (1955) Untersuchungen über die Leukozyten der Fishe (Pisces). Kyoto daigaku igakubu daini kaibou ronbunshu, **3**: 1–43. (In Japanese, Abstract in Germany).

14 Bielek, K. (1981) Developmental stages and localization of peroxidatic activity in the leucocytes of three teleost species (*Cyprinus carpio* L.; *Tinca tinca* L.; *Salmo gairdneri* Richardson). Cell Tissue Res., **220**: 163–180.

15 Ishizeki, K., Nawa, T., Tachibana, T., Sakakura, Y. and Iida, S. (1984) Hemopietic sites and development of eosinophil granulocytes in the loach, *Misgurunus anguillicaudatus*. Cell Tissue Res., **235**: 419–426.

16 Tooze, J. and Davies, H. G. (1968) Light and electron microscopic observations on the spleen and the splenic leukocytes of the newt *Triturus cristatus*. Am. J. Anat., **123**: 521–555.

17 Curtis, S. K., Cowden, R. R. and Nagel, J. W. (1979) Ultrastructure of the bone marrow of the salamander *Plethodon glutinosus* (Caudata: Plethodontidae). J. Morphol., **159**: 151–184.

18 Ishizeki, K. (1982) The cytodifferentiation in the basophilic granulocytes of the newt (*Triturus pyrrhogaster*) in organ culture. J. Iwate Med. Assoc., **34**: 551–567. (In Japanese, Abstract in English).

19 Hastie, B. and Chir, B. (1974) A study of the ultrastructure of human basophil leukocytes. Lab. Invest., **31**: 223–231.

20 Bessis, M. (1973) The granulocytic series. In "Living Blood Cells and their Ultrastructure". Springer-Verlag, Berlin, Heidelberg, New York, pp. 285–355.

21 Cawley, J. C. and Hayhoe, F. G. J. (1973) The basophil. In "Ultrastructure of Haemic Cells: A Cytological Atlas of Normal and Leukaemic Blood and Bone Marrow". W. B. Saunders Company Ltd., London, Philadelphia, & Toronto, pp. 24–29.

22 Rhodin, J. A. G. (1974) Blood and lymph. In "Histology: A Text and Atlas". Oxford University Press, New York, London & Toronto, pp. 93–138.

23 Wetzel, B. K., Horn, R. G. and Spicer, S. S. (1967) Fine structural studies on the development of heterophil, eosinophil, and basophil granulocytes in rabbits. Lab. Invest., **16**: 349–382.

24 Zucker-Franklin, D. (1967) Electron microscopic study of human basophils. Blood, **29**: 878–890.

25 Dvorak, A. M., Galli, S. T., Morgan, E., Galli, A. S., Hammond, E. and Dvorak, H. F. (1981) Anaphylatic degranulation of guinea pig basophilic leukocytes. I. Fusion of granule membranes and cytoplasmic vesicles: formation and resolution of degranulation sacs. Lab. Invest., **44**: 174–190.

26 Davis, W. C., Spicer, S. S., Greene, W. B. and Padgett, G. A. (1971) Ultrastructure of cells in bone marrow and peripheral blood of normal mink and mink with the homologue of the Chediak-Higashi trait of humans. II. Cytoplasmic granules in eosinophils, basophils, mononuclear cells and platelets. Am. J. Pathol., **63**: 411–431.

27 Campbell, F. R. (1970) Ultrastructure of the bone marrow of the frog. Am. J. Anat., **129**: 329–356.

ZOOLOGICAL SCIENCE 4: 881–888 (1987)

Body Color and the Preference for Background Color of the Siamese Fighting Fish, *Betta splendens*

Tsuneo Moriya and Yoko Miyashita

Department of Biology, Sapporo Medical College, Sapporo, 060, Japan

ABSTRACT—The preference of the fish, *Betta splendens,* for black or white background color was observed using an experimental tank which was divided into white and black halves. This fish has originally a greater preference for black than for white.

When fish were kept for one week in the tank with a black background, this preference for black was enhanced, while keeping fish in a white tank increased the time the fish spent in the white area. These results show that the environmental color affects the background color preference. Next, we examined the relationship between preference for background color and fish body color. The difference of preference for background color in the female and male was examined because they exhibit a pronounced difference in their body colors, the male being darker than the female when they are exposed to the same background. Males exhibited a greater preference for black than females did. We also compared the preference for background color of reserpinized fish, which had darker bodies than that of control fish (reserpine-untreated). Reserpinized fish preferred a black background more than control fish did. Throughout the observation, there was no significant difference between the number of appearances of control and reserpinized fish in the white area of the experimental tank. However, the average time control fish spent in the white area at each appearance was always longer than that of the reserpinized fish.

INTRODUCTION

Some species of lower vertebrates change their body color according to the background color. This is regarded as camouflage against predators and such changes are called "protective color changes" [1]. In addition to being camouflage, the body color and color patterns have been considered to serve for communication [2–5]. The Siamese fighting fish, *Betta splendens,* demonstrates unique color changes on various occasions, such as antagonistic and reproductive displays [6]. When two males are housed together in a tank, they fight each other, opening their opercula and spreading the tail fin, and the body color becomes darker. The fish beaten in the fight becomes pale and two longitudinal black lines appear on its body sides [6]. Since the loser can avoid attack by its opponent after changing its body color, it is considered that the body color functions as a communicatory signal. Thus, it is plausible to assume that animals are aware of their own body color. If this is the case, animals might be able to move positively toward an appropriate environment suitable for their hue. Kohda and Watanabe [7] reported that the cross-striped fish, Oyanirami *Coreoperca kawamebari,* prefers a vertically, rather than a horizontally, striped background. They suggested that the cross-stripes, appearing vertically when the fish is swimming or resting, could function as a cryptic pattern among vertical plants in the aquatic habitat.

Brown and Thompson [8] demonstrated that fish adapted to black background choose black more frequently than fish adapted to white background in eight species of fish. The above mentioned papers [7, 8] reported that fish select some background area corresponding to their body color and/or color pattern; however, it has not yet been clarified whether they perceive their own body color or some hormonal factors act on the brain, causing them to choose a suitable background.

The formation and change of body color of

Accepted May 1, 1987
Received January 22, 1987

animals, including teleost fish, are controlled by neural or/and hormonal regulatory systems [9]. It is possible that certain nervous or hormonal conditions which regulate the skin color have some behavioral effects [10]. Karplus and Samuel [11] demonstrated that MSH injected into white-adapted *Xenopus* tadpoles induced a significant shift in their preference toward black background, and they speculated that the effect of MSH was mediated by its action on the brain rather than its skin darkening action.

In the present study, in order to expand our knowledge of the relationship between the preference for background color and body color, we have tried to learn the fundamental preference for background color in the Siamese fighting fish, *Betta splendens*. We also examined whether the exposure of fish to a black or white background affects their background color preference. In the third part of this study, we analyzed whether the body color of the fish affects its background color preference or not.

MATERIALS AND METHODS

Adult Siamese fighting fish, *Betta splendens*, hatched in our laboratory were maintained singly in vessels. For the adaptation to background color, the fish were kept in a white or black plastic tank 43×43×20 cm deep made of opaque plastic plates for one week under a 15 hr-light and 9 hr-dark cycle. The water in each tank was adjusted to 10 cm in depth and maintained at 25°C. The fish were individually identified and designated by the letters A–S and a–l. After the adaptation to white or black background color, single fish was transferred to an experimental tank 43×43×20 cm deep divided into white and black halves and their preference for background color was observed. The movement of the fish in each tank was monitored with a video camera (Olympus VX–304) for 5 hr from 10 AM to 3 PM under conditions of continuous illumination. For the purpose of analysis, the time fish stayed in the white area and the number of appearances in the white area from the black area for 30-min periods was checked from video tapes using a quick visual searching system.

In the treatment with reserpine, an inducer of body darkening in fish [12], half the number of fish which had been kept in a white tank for one week were immersed in water containing 3×10^{-6} M reserpine (Daiichi Seiyaku Co. Ltd., Tokyo) for 20 hr in a dark room. As the control, the other half were kept in water containing no reserpine. Reserpine treatment caused a darkening effect on the body color even with a white background. This effect continued for more than one week in the white tank (details shown in Miyashita [12]). In contrast, the control fish became pale in a white background.

The data were tested statistically using Student's t-test, the Cochran-Cox test, the paired t-test and the Kruskal-Wallis test [13]. For these statistical tests (except for the Kruskal-Wallis test), we employed the computer programs prepared by Ishii *et al.* [14].

RESULTS AND DISCUSSION

Betta splendens, especially females, rapidly changed their body colors according to the background color. When the fish were transferred into a black tank from a white one, their body colors became dark, and when they were returned to the white tank, the body color became pale. This change occurred within two minutes after transfer and the altered body color was maintained as long as the fish stayed in the same tank.

First, we examined the influence of previous exposure to a black or a white background on the background color preference. Female fish were kept in either a black or a white tank for one week (black or white adaptation). Then they were subjected to a choice between white and black environments. The time the fish spent in the white area and the number of appearances in the white area from the black one are shown in Table 1. In both groups, the number of appearances in the white area decreased with the observation time ($r(70)=-0.595$, $p<0.001$ and $r(70)=-0.562$, $p<0.001$ for the black-adapted and the white-adapted group, respectively). There was no significant difference between the two groups in total number of appearances (mean±S.E. were 47.0 ± 10.8 (n=7) and 52.9 ± 7.5 (n=7) for the

TABLE 1. The background color preference of the female *Betta splendens* after adaptation to white or black environments

Time (hr)/Fish	Group 1 Black-adapted fish						
	A	B	C	D	E	F	G
0.0–0.5	25 (3)	133 (5)	306 (19)	58 (4)	274 (8)	219 (12)	289 (15)
0.5–1.0	345 (6)	104 (3)	221 (11)	0 (0)	449 (10)	532 (12)	469 (10)
1.0–1.5	102 (3)	225 (3)	211 (13)	0 (0)	284 (13)	526 (10)	227 (9)
1.5–2.0	132 (3)	212 (7)	195 (6)	47 (2)	168 (10)	242 (7)	434 (14)
2.0–2.5	252 (3)	104 (1)	302 (4)	54 (2)	132 (9)	235 (3)	370 (8)
2.5–3.0	60 (3)	119 (3)	263 (2)	0 (0)	103 (5)	0 (0)	225 (8)
3.0–3.5	88 (2)	0 (0)	171 (5)	0 (0)	177 (4)	243 (3)	173 (5)
3.5–4.0	30 (1)	0 (0)	86 (3)	0 (0)	71 (5)	211 (3)	153 (6)
4.0–4.5	0 (0)	104 (1)	112 (2)	0 (0)	308 (2)	12 (1)	264 (6)
4.5–5.0	0 (0)	63 (1)	171 (2)	0 (0)	95 (3)	36 (1)	104 (4)
Total	1034 (24)	1064 (24)	2038 (67)	159 (8)	2061 (69)	2256 (52)	2709 (85)
Time (hr)/Fish	Group 2 White-adapted fish						
	H	I	J	K	L	M	N
0.0–0.5	328 (9)	770 (13)	4 (1)	160 (9)	347 (9)	488 (6)	650 (9)
0.5–1.0	535 (20)	707 (12)	0 (0)	239 (5)	511 (5)	200 (8)	648 (14)
1.0–1.5	516 (7)	825 (10)	8 (1)	392 (2)	462 (10)	339 (9)	183 (9)
1.5–2.0	1639 (10)	694 (8)	69 (1)	777 (5)	161 (11)	107 (9)	191 (6)
2.0–2.5	265 (5)	619 (7)	121 (3)	900 (5)	374 (5)	204 (4)	186 (6)
2.5–3.0	951 (4)	435 (6)	23 (3)	1220 (2)	64 (8)	150 (7)	806 (4)
3.0–3.5	747 (2)	215 (5)	7 (1)	860 (3)	251 (1)	133 (4)	765 (6)
3.5–4.0	232 (7)	368 (3)	4 (1)	273 (2)	220 (5)	271 (5)	200 (5)
4.0–4.5	46 (1)	254 (2)	75 (2)	603 (3)	118 (4)	0 (0)	521 (3)
4.5–5.0	340 (2)	74 (1)	103 (3)	603 (1)	427 (8)	12 (1)	284 (3)
Total	5599 (67)	4961 (67)	414 (16)	6027 (36)	2935 (66)	1904 (53)	4434 (65)

The time the fish stayed in the white area is expressed in seconds. The number of appearances in the white area is shown in parentheses. The total times and total numbers of appearances for 5 hr were analyzed statistically according to Student's t-test. All the individual values for time and number of appearances in 30-min periods were analyzed according to the Kruskal-Wallis test. See text for statistical evaluation.

black-adapted and the white-adapted group, respectively). In the black-adapted fish, the time spent in the white area for 30-min periods gradually decreased with the passage of time ($r(70) = -0.448$, $p < 0.001$). In contrast, in the white-adapted fish, no changes in the time spent in the white area were observed. The mean total time the fish spent in the white area during the entire observation period (5 hr) was 1617 ± 336 sec ($n=7$) for black-adapted fish and 3753 ± 783 sec ($n=7$) for white-adapted fish and there was a significant difference between them ($t=2.507$, $p<0.05$). Even in the white-adapted fish, the time was only 20% of the entire observation period. These results show that this fish strongly prefers a black background to a white background. Their preference for background color seems to be similar to that of the blunt-nosed minnow and doughbelly, which show a smaller degree of modification of background choice as a result of residence in an area with a black or a white background, as reported by Brown and Thompson [8].

Even within the same group, there were statistically significant differences among individuals for the time ($H_{cor}(7)=30.6$) and the number of

appearances ($H_{cor}(7)=31.3$) in black-adapted fish, as well as in white-adapted fish, for which the respective figures were $H_{cor}(7)=32.7$ and $H_{cor}(7)=22.8$, $p<0.001$. Each fish might have a unique character as far as its color preference is concerned.

In order to eliminate the individual variations and to confirm the above observation, we examined the preference for background color for each fish after alternately keeping it in a white or black tank for one week using 19 females. As shown in Figure 1, when the fish were kept in a black background for one week, they showed a strong preference for black, and when the same fish were kept in a white background for the same period, the time the fish stayed in the white area increased, except for four fish, L, O, R and S. The change in background preference according to the pre-adaptation was statistically significant ($t=3.972$, $p<0.001$, paired t-test). These results strongly suggest that the tone condition of the environment in which the fish had stayed affected later preference for background color.

However, it is possible that the long-term exposure to a white or black background brings about some difference in the hormonal and/or neural conditions as well as in the body color and that one or both of these differences could affect the background color preference.

In order to confirm whether the body color is related to background color preference or not, we examined the background preference of the female and male fish. This was done because their body hues are distinguishably different even while in the same background; the male is always darker than the female in a white background. After adaptation to a white background for one week, background preference was observed. As shown in Figure 2, males exhibited a greater preference for the black background than females. The above observations suggest that differences in the body color of fish might directly reflect the preference for background color; darker fish prefer to stay longer in the black background than pale fish. However, we can't disregard the possibility that this difference in the choice of background color is due to sexual differences.

Therefore, we tried to compare the differences in the preference of fish having different hues in the same environmental color using the same sex.

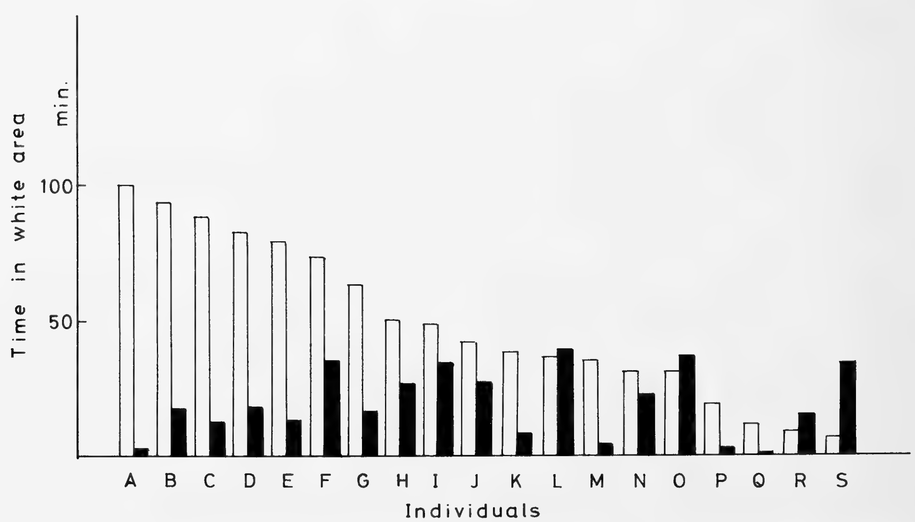

Fig. 1. The influence of previous exposure to a black or white background on the color preference of the fish, *B. splendens*.

Nineteen female fish (A–S) were used. White columns show the time that the fish stayed in the white area for 5 hr after white adaptation. Black columns show the time that the same fish stayed in the white area after black-adaptation. The difference in time for each fish was statistically significant ($p<0.001$, paired t-test).

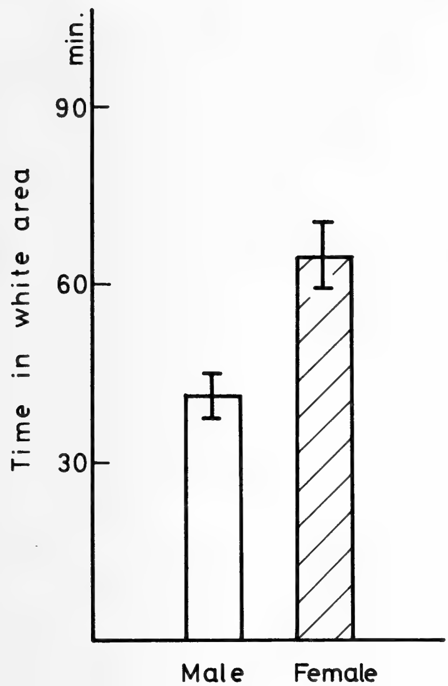

For this purpose, the fish were treated with reserpine.

Throughout the observation period, reserpine-treated fish (black fish) always showed a strong preference for black compared to the control fish and no change in staying time was observed in either group (Fig. 3). As shown in Table 2, in both the male or female groups, as well as in the mixed male-female group, there was a significant difference between the control and reserpinized groups. The difference in preference between females and males was also observed in the control group (Table 2). This result confirmed a previous experimental series which showed a difference in the

FIG. 2. The difference between preference for background color of the female and male of *B. splendens*.

Columns show the time that fish stayed in the white area throughout the observation time (5 hr). Bars show the standard errors. There is a significant difference in time between males (n=12) and females (n=16) ($p<0.01$, Cochran-Cox test).

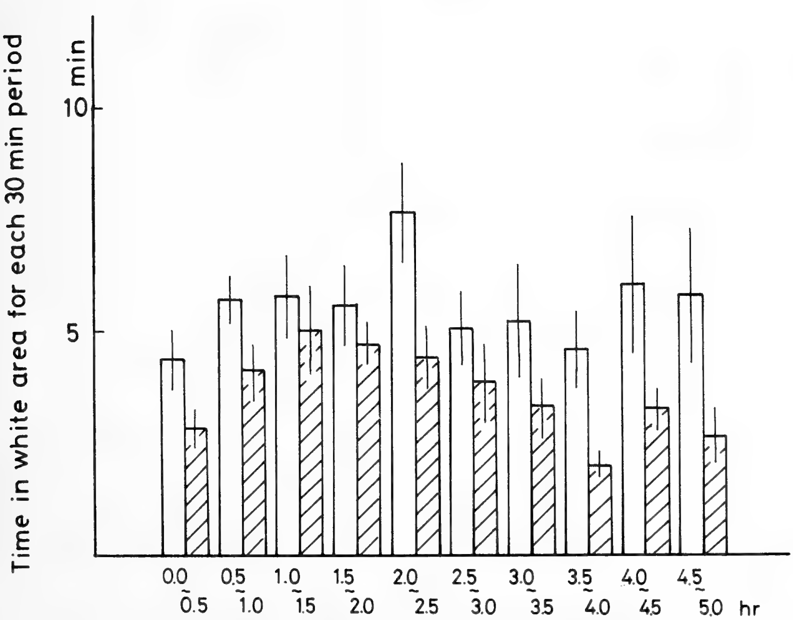

FIG. 3. The difference between preference for background color of reserpinized and control fish in *B. splendens*.

Columns show the time that the fish stayed in the white area for each 30-min period. White columns; control group (consisted of seven males and eight females). Hatched columns; reserpinized group (consisted of six males and ten females). Bars show the standard errors.

preference for background color between the female and the male (Fig. 2). However, this difference disappeared in the reserpinized groups (Table 2), indicating that the difference of preference for black or white is mainly due to the difference of body hue rather than the sexual difference.

The number of appearances of both the control and reserpinized fish in the white area decreased in correlation with the observation time ($r(150)=-0.516$, $p<0.001$ for the control group; $r(160)=-0.327$, $p<0.001$ for the reserpinized group) (Fig. 4). There was no significant difference between the two groups (mean number of appearances±S.E. was 40.4±3.6 (n=15) and 45.9±3.6 (n=16) for the control and reserpinized groups, respectively). This indicates that the movements of the fish to the white area from the black area were not affected by reserpine.

The changes in duration time for each appearance in the white area throughout the entire observation time (5 hr) are shown in Figure 5. In the control fish, the duration in the white area gradually increased from 40 sec to 160 sec with the passage of time. This result suggests that control fish become used to staying in the white area after transfer to the experimental tank. In contrast, the time the reserpinized fish spent in the white area was almost constant (between 30 and 40 sec) throughout the observation period. These results show that the reserpinized fish move into the white area from the black area as frequently as the control fish do, but that they return to the black area more quickly than the control fish. Interestingly, the time the reserpinized fish spent in the white area seems to correspond to the time it would have taken to change the body color from black to white had they not received reserpine. This suggests that they might be aware of their unchanged body color and try to move into black background color.

The information is lacking about how they recognize their own body color. We can only speculate that they see their body color or that they are affected by some physiological changes regulating the integumental color, such as the elevation of the MSH level in the plasma. It has been reported that, in the amphibian tadpole (*Xenopus laevis*), the content of MSH in the blood significantly increased after the adaptation to a black background, and decreased after the adaptation to a white one [15]. Karplus and Samuel [11] reported that the *Xenopus* tadpole kept in a white background showed a significant preference for white, and that injection of MSH induced an increase in their preference for black. They assumed that MSH acts on the brain and induces a preference for black. The increase of MSH content in the plasma is also known in black-adapted trout [16, 17] and eel [18]. In this study, we kept fish in a black or white background for one week before they were used in an experimental

TABLE 2. The difference in preference for background color between reserpinized and control group *B. splendens*

Group	Duration time in white area for 30 min* Control	Reserpinized
Male plus female	332±20 (n=150)[a]	216±13 (n=160)[a′]
Male	269±26 (n= 70)[b]	190±16 (n= 60)[b′]
Female	388±28 (n= 80)[c]	231±18 (n=100)[c′]

*: expressed in sec (mean±S.E.)
These data were obtained from the same experimental series shown in Figure 3. All the values for time the fish spent in the white area for 30-min periods were analyzed.
Difference between a and a′, $p<0.001$, $t=4.96$ (t-test).
Difference between b and b′, $p<0.05$ (Cochran-Cox test).
Difference between c and c′, $p<0.01$, $t=4.73$ (t-test).
Difference between b and c, $p<0.01$, $t=3.11$ (t-test).
No significant difference between b′ and c′, $t=1.71$ (t-test).

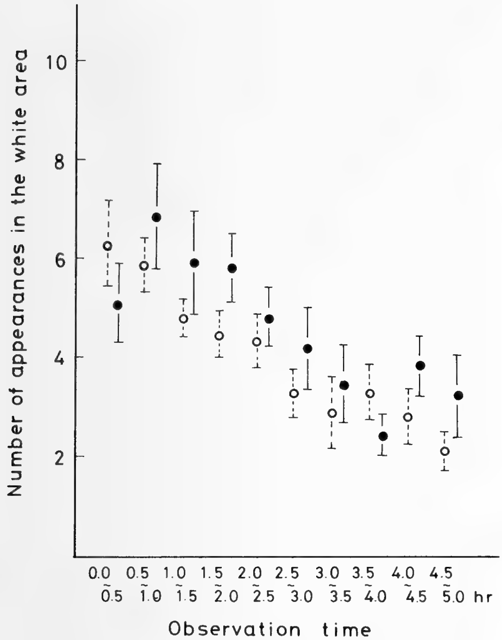

Fig. 4. The change in number of appearances of the fish, *B. splendens,* in the white area for 30-min periods throughout the observation time.

White circles show the mean number of appearances for control fish. Black circles show the mean number of appearances for reserpinized fish. Bars show the standard errors.

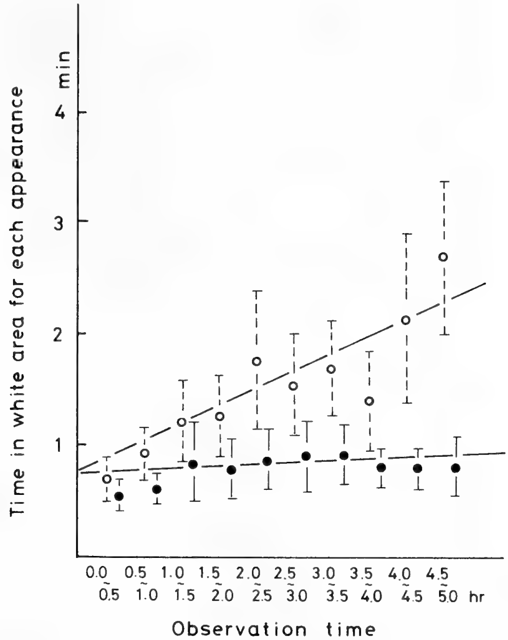

Fig. 5. The changes in time the fish, *B. splendens,* spent in the white area for each appearance in the white area.

White circles show the mean time for control fish. Black circles show the mean time for reserpinized fish. Bars show standard errors. The line ($y=16.4x+48.2$) for the control group was obtained by a least square calculation with a correlation coefficient of $r(150)=0.304$, ($p<0.001$).

series. During this period, the level of MSH in the plasma might have changed. We observed that black-adapted fish showed a slightly stronger preference for black compared with the reserpinized fish (data not shown). We can't exclude the possibility that, in the black-adapted fish, increased endogenous MSH caused their preference for black. However, in the reserpine-treatment expriments, two groups of fish (control and reserpinized fish) were both kept in a white background for the same period (one week). Thus, we can assume that the level of MSH in reserpinized fish might be almost the same as that in control fish. In spite of having the same level of MSH, reserpinized fish preferred to stay in a black background more than control fish did. This datum gave us the impression that the body color affected background color preference.

In the lower vertebrates, protective color change is very important for the protection against predators. However, it is not the only method. Animals can also move to a better background color to hide, as it appears to be the case in Siamese fighting fish, *Betta splendens.*

REFERENCES

1 Brown, F. A., Jr. (1961) Chromatophores and color change. In "Comparative Animal Physiology". Ed. by C. L. Prosser, Saunders Co., Philadelphia & London, pp. 915–950.

2 Kohda, Y. (1983) The effects of color patterns on aggressive behaviors of a freshwater serranid fish, *Coreoperca kawamebari.* Zool. Mag., **92**: 356–360.

3 Kohda, Y. and Watanabe, M. (1982) Agonistic behavior and color pattern in a Japanese freshwater serranid fish, *Coreoperca kawamebari.* Zool. Mag., **91**: 61–69.

4 Kohda, Y. and Watanabe, M. (1982) Relationship of color pattern to dominance order in a freshwater serranid fish, *Coreoperca kawamebari.* Zool. Mag., **91**: 149–145.

5 Kohda, Y. and Watanabe, M. (1983) Reproductive behavior and color pattern in a freshwater serranid fish, *Coreoperca kawamebari.* Zool. Mag., **92**: 207–215.

6 Robertson, G. M. and Sale, P. F. (1975) Sexual discrimination in the Siamese fighting fish (*Betta splendens* Regan). Behavior, **54**: 1–25.

7 Kohda, Y. and Watanabe, M. (1986) Preference for vertical-striped backgrounds by the Oyanirami *Coreoperca kawamebari,* a freshwater serranid. Ethology, **72**: 185–190.

8 Brown, F. A., Jr. and Tompson, D. H. (1937) Melanin dispersion and choice of background in fishes, with special reference to *Ericymba buccata.* Copeia, **3**: 172–181.

9 Fujii, R. and Oshima, N. (1986) Control of chromatophore movements in teleost fishes. Zool. Sci., **3**: 13–47.

10 Kastin, A. A., Sandman, C. A., Stratton, L. O., Schally, A. V. and Miller, L. H. (1975) Behavioral and electrographic changes in rat and man after MSH. Prog. Brain Res., **42**: 143–150.

11 Karplus, I. and Samuel, D. (1978) The effect of exposure to black background and to MSH on black-white background preference in the amphibian *Xenopus laevis* (Daudin). Horm. Behav., **11**: 151–159.

12 Miyashita, Y. (1985) Melanophore responses and color change in female Siamese fighting fish (*Betta splendens*)—A brief note. J. Lib. Arts Sci., Sapporo Med. Coll., **26**: 35–39.

13 Siegel, S. (1956) Nonparametric Statistics for Behavioral Sciences, McGraw-Hill, New York.

14 Ishii, S., Kohno, S., Wakabayashi, K., Wada, M. and Kubokawa, K. (1983) N88-BASIC Jitsuyou Puroguramu Shyu (N88-BASIC Programs for Biologist), Vol. 2, Baifukan, Tokyo.

15 Wilson, J. F. and Morgan, M. A. (1979) Alpha melanotrophin-like substances in the pituitary and plasma of *Xenopus laevis* in relation to color change responses. Gen. Comp. Endocrinol., **38**: 172–182.

16 Bowley, T. J., Rance, T. A. and Baker, B. I. (1983) Measurement of immunoreactive α-melanocyte-stimulating hormone in the blood of rainbow trout kept under various conditions. J. Endocrinol., **97**: 267–275.

17 Rodrigues, K. T. and Sumpter, J. P. (1984) Effects of background adaptation on the pituitary and plasma concentrations of some pro-opiomelanocortin-related peptides in the rainbow trout (*Salmo gairdneri*). J. Endocrinol., **101**: 277–284.

18 Baker, B. I., Wilson, J. F. and Bowley, T. J. (1984) Changes in pituitary and plasma levels of MSH in teleosts during physiological color change. Gen. Comp. Endocrinol., **55**: 142–149.

ZOOLOGICAL SCIENCE 4: 889–896 (1987)

Interspecific Differences in Some Courtship Behavioral Properties among the Four Species Belonging to the *Drosophila auraria* Complex[1]

YUZURU OGUMA, HARUO KUROKAWA, SUMIO M. AKAI[2], HISASHI TAMAKI and JIRO KAJITA

Institute of Biological Sciences, University of Tsukuba, Sakura-mura, Ibaraki 305, Japan

ABSTRACT—The four species comprising the *Drosophila auraria* complex were examined for their sexual activities, with regard to the forms of consecutive behavior exhibited during courtship. The mating frequencies and mating indices of the four species showed no diurnal changes, though under a dim red light, no insemination was observed during an initial 30-min observation period. The forms of courtship behavior observed on video tape recordings were analyzed for six parameters, i.e., time to initiation of courtship, total time of courtship, number of courtship bouts, length of courtship bout, number of tappings, and number of wing displays. Significant species differences were found in some courtship parameters.

INTRODUCTION

A large number of observations of courtship behavior have been performed using many *Drosophila* species including *D. auraria* [1]. One of the objectives of these investigations was to assign specific values to the behavioral elements in a courtship sequence which could be used as taxonomic characteristic for clarifying phylogenetic relationships.

The *D. auraria* complex consists of four sibling species, i.e., *D. auraria, D. biauraria* and *D. triauraria,* which are widely distributed in Japan and Korea, and *D. quadraria,* which has been recorded only in Taiwan. Although interspecific crosses are successful and can produce hybrid offspring in the laboratory, each species retains a completely or almost completely discrete gene pool even in a sympatric area in the natural population [2–4]. It is thus concluded that some form of ethological isolating mechanism has become well developed, being strong enough to separate the gene pool of one species from those of the others. The major aim of our consecutive works is to elucidate the role of male courtship behavior, which constitutes the behavioral basis of sexual isolation.

Grossfield [5, 6] reported that mating success in the *D. auraria* complex was highly dependent on light. This fact suggests that a visual stimulus may be indispensable for partner recognition in this group. The diurnal rhythmicity of courtship behavior in *D. auraria* has also been investigated by Hardeland [7].

The present paper describes interspecific differences in some properties of courtship behavior among the four species belonging to the *D. auraria* complex.

MATERIALS AND METHODS

Species used

Species used in this experiment were *D. auraria* (A541, Tsukuba), *D. biauraria* (B16, Tokyo), *D. triauraria* (T544, Tsukuba) and *D. quadraria* (Q, Taiwan, Texas stock No. 3075.1). These stocks had been maintained in mass laboratory cultures for several years at the time of initiation of the study.

Accepted May 12, 1987
Received April 4, 1987

[1] Special Research Project on Instinct, University of Tsukuba.

[2] Present address: Yamanashi Gakuin Junior College, Kofu, Yamanashi 400, Japan.

Rearing conditions

Flies were raised and aged in the standard *Drosophila* medium (sucrose–dried yeast–corn meal) seeded with live yeast at 25 ± 0.5°C and 60% R. H. under an artificial light (200–300 lux) and dark cycle (LD 14:10), the light period being between 5:00 and 19:00. Virgin flies emerging within 8 hr were sexed under CO_2 anesthesia, and aged in groups of 30 males or 20 females in food vials for a given period as described in Results. For observation of behavior using a video recording, a single male stored in a vial was employed.

Sexual maturity

For the record of mating success which was employed for measuring the degree of sexual maturity according to the time after eclosion and the diurnal change in sexual activity, two kinds of measurement were obtained from mass mating test. Ten females were placed with 15 males in each mating vial ($\phi\, 3 \times 10$ cm), and 20 replicates were run for each test. Both male and female flies were removed from the vial with an aspirator as soon as they had paired. The number of matings in every 5-min interval was scored during a 30-min observation period, and then a mating index was calculated using the formula proposed by Spiess *et al.* [8]. Mating frequency was measured according to the proportion of females mated within 30 min.

In order to estimate the time taken to attain sexual maturity after eclosion, mating frequencies were examined for flies which had been aged for 1, 3, 4, 6 and 12 days, respectively.

Diurnal changes

To study diurnal changes in mating activity, both mating frequencies (%) and mating indices were measured either every two hours during the light period or every three hours during the dark period. The dark condition was furnished by a dim red light.

Percentage of insemination under dark conditions

Ten 4-day-old females were placed with fifteen 4-day-old males in each mating vial under the illumination conditions shown in Table 2. The prepared vials were left for 2, 12, 24 and 48 hr, respectively. After each of the given time periods had passed, the females were dissected and their ventral receptacles were examined for sperm.

Observation of courtship behavior

In order to analyze the parameters of courtship behavior, each of 20 single pairs was recorded for a 30-min period using a video recorder set (camera, Sony SLD–325; video recorder, PVM–171; video-recorder monitor, ACV 1150D) at 10× magnification. Afterward, the forms of behavior were analyzed by replaying the tapes. The observation chamber measured 15 mm in diameter and 5 mm in depth. The observation and the recording were carried out from 9:00 to 12:00 a.m.

Parameters of courtship behavior

There are basically three male courtship behavior elements, i.e., orientation/following, wing display and attempted copulation. All of these forms of behavior were observed and noted via a video monitor. The parameters determined from the playbacks were as follows: time to initiation of courtship, number of courtship bouts in a 30-min observation period, length of courtship bout, total time of consecutive courtship behavior, number of tappings, number of wing displays per 10-min courtship period, latency to copulation and duration of copulation. The time to initiation of courtship meant a measure of the time taken for the initiation of the first form of male courtship behavior after introducing the fly into the observation chamber. The calculation of the number of tappings or wing displays per 10 min was done as follows: if the total courtship time is 2 min with 30 episodes of tapping and 5 episodes of wing display in a 30-min observation period, we multiply them by five. Therefore the figures for the two parameters become 150 and 25, respecitvely.

RESULTS

The time taken for flies to attain sexual maturity can be estimated by observing the daily changes in their mating frequency (Fig. 1). There was no significant difference among the four species in their mating frequencies at the 4 days. The values reached a maximum at 4 to 6 days after eclosion.

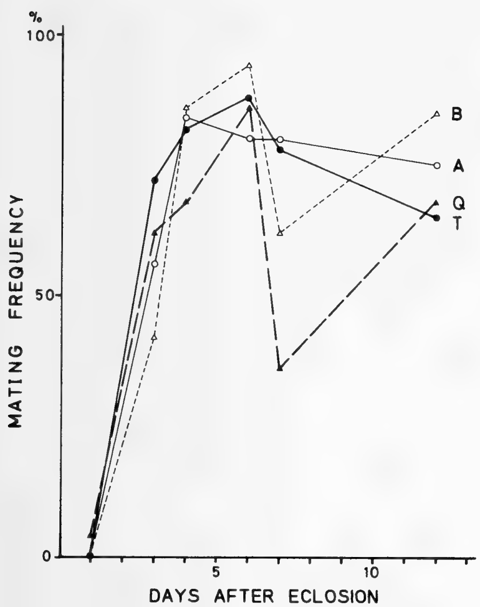

FIG. 1. Changes in sexual activity (percentage of insemination) with age. Ten females and 15 males in a vial were tested for a 30-min observation peiod.
A: *D. auraria,* B. *D. biauraria,* T: *D. triauraria,* Q: *D. quadraria*

Accordingly, observation of courtship behavior was carried out using 4- to 6-day-old flies in the subsequent experiment.

Diurnal changes in the mating frequency and the mating indices are summarized in Table 1. No mating was observed within the first 30-min observation period under the dim red light during the dark phase. Neither following nor tapping was observed under this condition. The male fly began to actively court the female under a low light intensity of 2–3 lux. No particular change in the diurnal activity of mating was revealed for any of the species. *D. auraria* showed 70% mating frequencies on average while *D. biauraria, D. triauraria* and *D. quadraria* showed higher levels. This tendency could also be seen in the mating index, that is, the mating indices of *D. auraria* ranged from 70.5 to 87.2, while those of the others ranged from 104.1 to 137.4. Thus the latter three species seemed to be sexually more active than *D. auraria* during the light period.

The results of the insemination test under dark conditions are shown in Table 2. There was a slight difference in light dependency among the four species. Under dark conditions the percentage of insemination in *D. auraria* increased gradually with time and reached 89.7% at 12 hr after the beginning of the test. However, *D. biauraria* showed a much lower value and *D. triauraria* and *D. quadraria* showed values intermediate between those of *D. auraria* and *D. biauraria*.

The sequence of male courtship behavior in the *D. auraria* complex fundamentally coincided with that described by Spieth [1]. The general features of this behavior are as follows: After the male fly has been introduced into the observation chamber, he moves around for a while, and then orients toward a female. He follows and taps her with his fore leg and extends one wing at 90 degrees and vibrates it. A receptive female becomes to move slowly after a short time and the male can make contact with her, after which he attempts copulation, extending one wing to 90 degrees following copulation.

During copulation, the male rubs the female's abdomen with his mid legs and vibrates one of his wings. Toward the end of the copulation period, the female spins and kicks the male. The male rubs her more frequently and vibrates his wing in concert with her movements, then he withdraws and dismounts.

The frequency of each courtship element was found to be clearly different among the four species (Table 3). The results of the analyses of courtship behavior are shown in Table 4. The mean latency time to copulation and the duration of copulation are shown in Table 5. The six parameters obtained could be used to build up pictures of courtship for each species by Mann-Whitney U-test [9] (Tables 6–1, 6–2 and 6–3).

The species characteristics of male courtship behavior in the *D. auraria* complex are summarized as follows:

1. *D. auraria* Males spent a very long time from being introduced into the observation chamber to initiation of courtship (=time to initiation of courtship) (Tables 4 and 6–1). On the contrary, the total time of courtship (56.9 sec) was much shorter, and the number of courtship bouts (2.8 sec) was lower than the other three species (Tables

TABLE 1. Diurnal changes in mating frequency, mating index with the standard error of the mean (S.E.M.) and its coefficient of variation (CV) of the 4 species of the *D. auraria* complex under a light period of the diurnal cycle using 4-day-old flies

Run	Mating frequency (%)	Mating index with S.E.M.	CV (%)	Observation time	Run	Mating frequency (%)	Mating index with S.E.M.	CV (%)
	D. auraria					*D. triauraria*		
19	70.0	70.5±5.3	33.1	6:00	20	90.5	129.9±3.0	10.3
19	73.2	78.4±6.4	35.7	8:00	19	88.9	125.6±4.8	16.6
19	70.0	74.5±6.2	36.4	10:00	20	88.5	134.3±5.6	18.5
20	76.0	75.9±4.5	26.7	12:00	19	83.1	116.4±5.8	21.7
20	76.0	77.9±6.3	35.9	14:00	17	84.7	129.3±4.5	14.3
20	74.5	76.7±6.3	36.9	16:00	20	76.5	105.1±5.3	22.7
18	77.2	87.2±6.2	30.0	18:00	17	90.0	137.4±5.8	17.4
135	73.8	77.2±2.3	34.2	Mean	132	86.0	125.2±2.1	19.3
	D. biauraria					*D. quadraria*		
19	76.8	114.8±5.4	20.7	6:00	19	82.6	132.5±6.2	20.3
19	83.2	104.6±3.8	16.0	8:00	20	76.5	118.4±4.4	16.7
20	82.5	122.5±5.0	18.4	10:00	20	77.5	132.5±5.4	18.1
20	76.5	104.1±5.7	24.4	12:00	19	73.2	117.2±6.4	23.6
20	77.0	113.8±5.2	23.2	14:00	20	76.0	120.4±7.7	28.4
20	80.5	115.7±4.8	18.6	16:00	20	76.0	127.4±5.7	22.2
20	82.0	111.9±8.2	32.9	18:00	20	84.0	134.0±5.7	18.9
138	79.8	112.5±2.2	23.2	Mean	138	78.0	126.1±2.4	22.0

The group comparisons showing a significant difference (P<0.001, by t-test) in mating indices are marked with a brace (}).

TABLE 2. Percentage of inseminated females under constant light (LL), constant dark (DD) and a normal diurnal cycle (LD)

	N	2 hr (%)		X^{2}_{y}*	12 hr (%)		X^{2}_{y}	24 hr (%)		X^{2}_{y}	48 hr (%)		X^{2}_{y}
		LL	DD		LL	DD		LD	DD		LD	DD	
D. auraria	100	95.0	58.0	36.0	98.0	89.7	n.s.	100	96.0	n.s.	100	100	n.s.
D. biauraria	100	75.0	0.0	116.8	95.0	4.0	162.0	92.0	60.0	26.3	100	92.0	n.s.
D. triauraria	100	84.0	44.0	33.0	95.0	42.0	62.7	93.0	52.0	40.1	99.0	76.0	22.1
D. quadraria	50	99.0	20.0	90.3	98.0	62.0	18.1	98.0	65.0	15.9	99.0	100	n.s.

All tests were performed in vials containing 10 femals and 15 males.
* All chi-squared values were calculated with the Yates' correction [9] and are significant (P=0.001). n.s. means not significant.

4 and 6–2). Attempted copulation was not observed in the first 30-min observation period (Table 3), but a few were found when the observation time was extended to 60 min.

2. *D. biauraria* Many of the males showed wing display (85.0%) and tapping (75.0%) (Table 3). The mean numbers of tappings and wing displays per 10 min were 41.0 and 15.6, respectively, each of which was significantly higher than the others (Table 6–3). The mean time of initiation to

TABLE 3. Frequency (%) of males showing courtship behavior and each courtship element in the 30-min observation period

	Run	Courtship	Tapping	Wing display	Attempted copulation	Copulation
D. auraria	40	60.0	30.0	5.0	0	0
D. biauraria	20	95.0	75.0	85.0	30.0	20.0
D. triauraria	20	100	75.0	30.0	75.0	70.0
D. quadraria	20	100	60.0	5.0	50.0	40.0

TABLE 4. Comparison of parameters of courtship behavior in the males

	Run	Time of initiation of courtship (sec±S.E.M)	Total time of courtship (sec±S.E.M)	Number of courtship bouts with S.E.M	Length of courtship bout (sec±S.E.M)	Mean number per 10 min courtship period	
						Tapping	Wing Display
D. auraria	40	546.4±83.6	56.9± 15.1	2.8±0.5	26.6±10.8	17.2±8.8	1.0±0.5
D. biauraria	20	71.2±22.5	464.5± 83.5	12.0±2.6	60.9±16.4	41.0±9.2	15.6±3.9
D. triauraria	20	118.8±47.9	903.1±137.9	4.2±0.7	233.4±71.5	10.9±5.6	4.6±1.0
D. quadraria	20	161.3±29.4	531.7± 71.7	6.4±3.5	59.3± 9.9	0.3±0.1	0.1±0.1

TABLE 5. Comparison of latency to copulation and duration of copulation among the three species in the 30-min observation period

	N	Latency (sec±S.E.M.)	Duration (sec±S.E.M.)
D. biauraria	4	1105.3±232.4 *	321.8±25.9
D. triauraria	14	719.9±146.0	357.5±13.6
D. quadraria	8	236.2± 49.5 *	289.1± 8.6

* Significant (P=0.01) by Mann-Whitney U-test.

courtship (71.2 sec) was significantly shorter than those of *D. auraria* and *D. quadraria* (Tables 4 and 6–1). The male courted the female with short gaps and short lengths of courship bouts in the 30-min observation period (Tables 4 and 6–2). Although the male courted the female frequently, the percentage of pairs copulated (20.0%) was low in the 30-min observation period (Table 3).

3. *D. triauraria* A very long length of the courtship bout (233.4 sec) revealed that the male of this species courted the female with a long period of orientation and following with only few episodes of tapping. This characteristic feature was comprehensible by the fact that the total time of courting (903.1 sec) was about half the time of the observation period (Tables 4 and 6–1). After the long time of courtship, most of the males were able to attain the copulation (70.0%) (Table 3) with a few episodes of tapping and wing display.

4. *D. quadraria* The males courted the females frequently almost without any episodes of wing display and tapping (Tables 3 and 4), and only half the number of males showed attempted copulation. The time to initiation of courtship of this species was 161.3 sec, a value intermediate between those of *D. auraria* and *D. biauraria.* The characteristic feature of courtship behavior in this species was that the males showed only a few episodes of tapping and wing display despite the long courtship bout.

TABLE 6–1. Results of Mann-Whitney U-test for courtship parameters, time to initiation of courtship and total time of courtship

	auraria	*biauraria*	*triauraria*	*quadraria*	
auraria		U=20 p<0.0001	U=41 p<0.0001	U=56 p<0.0001	time to initiation of courtship
biauraria	U=53 p<0.0001		U=185.5 not sig.	U=100 0.01<p<0.05	
triauraria	U=33 p<0.0001	U=107 0.01<p<0.05		U=110 0.01<p<0.05	
quadraria	U=37 p<0.0001	U=170 not sig.	U=121 0.01<p<0.05		
	total time of courtship				

TABLE 6–2. Results of Mann-Whitney U-test for courtship parameters, number of courtship bouts and length of courtship bout

	auraria	*biauraria*	*triauraria*	*quadraria*	
auraria		U=92 p<0.0001	U=252.5 0.01<p<0.05	U=221 0.001<p<0.01	number of courtship bouts
biauraria	U=116.5 0.001<p<0.01		U=74 0.0001<p<0.001	U=106.5 0.01<p<0.05	
triauraria	U=85 0.0001<p<0.001	U=130 not sig.		U=175.5 not sig.	
quadraria	U=78 0.0001<p<0.001	U=163 not sig.	U=136 not sig.		
	length of courtship bout				

TABLE 6–3. Results of Mann-Whitney U-test for courtship parameters, number of tappings and wing displays per 10-min priod of courtship behavior

	auraria	*biauraria*	*triauraria*	*quadraria*	
auraria		U=175.5 0.0001<p<0.001	U=279 not sig.	U=330 not sig.	number of tappings
biauraria	U=57 p<0.0001		U=110 0.01<p<0.05	U=92 0.001<p<0.01	
triauraria	U=199.5 not sig.	U=61.5 0.0001<p<0.001		U=162 not sig.	
quadraria	U=399 not sig.	U=21 p<0.0001	U=148 not sig.		
	number of wing displays				

DISCUSSION

There were some differences in the degree of sexual activity between the four species of the complex. *D. biauraria, D. triauraria* and *D. quadraria* were sexually more active, whereas *D. auraria* showed a lower level of activity (Table 1). *D. auraria* took the longest time of initiation to first courting (Tables 4 and 6–1). The percentage of females inseminated in the first 30-min observation period was drastically decreased under dim red illumination for all of the four species. The results presented in Table 2 coincide partly with those reported by Grossfield [6]. It is apparent that all of the four species are light-dependent species. As Grossfield reported, this fact suggests that a visual signal is a very important factor for initiating courtship by the male flies of the *D. auraria* complex. As shown in Table 2, the percentage of insemination in *D. auraria* was less decreased by constant dark condition than the other three species. This implies that *D. auraria* males may rely mainly on a visual signal for orientation, and the others, such as acoustic or olfactory signals, are employed for their success in copulation.

Male flies of *D. triauraria* from which both of the wings were removed frequently showed attempted copulation, but hardly any successful mounting was observed in a 30-min observation period (unpublished data). In this connection, the percentage of insemination at 12 hr with males from which the wings were removed was decreased to below half that occurring with untreated males in all of the four species. The vibration sound emitted by the wing display of males, especially upon attempted copulation, may act acoustically to decrease the threshold of female receptivity. This explanation was confirmed by observation using the infrared rays under dark conditions (Oguma and Kurokawa, unpublished data).

The sequence of male courtship behavior in the *D. auraria* complex observed here is basically similar to that described by Spieth [1], but the courtship parameters were quantitatively different with one another in the four species (Tables 4, 6–1, 6–2 and 6–3).

The present study was carried out using single pairs in small observation chambers without food. The length of courtship bout is to some extent determined by the female's behavior [10, 11] and the size of the observation cell [12, 13]. Ewing and Ewing [13] pointed out the importance of flying off which terminates courtship in the completely unrestrained conditions existing in the wild. The length of courtship bout was much longer (233.4 sec) in *D. triauraria* than those of the other three species (Table 4). Our results suggest that long length of courtship bouts for *D. triauraria* was not attributable to the size of the observation chamber or to the female's behavior but rather to the courtship behavior of the *D. triauraria* males themselves. Our reasons for interpreting the observation in this way are as follows: When a *D. triauraria* male encounters a female of an alien species in the small chamber, he follows and taps her but then terminates the courtship, resulting in a very short length of courtship bout (unpublished data). This fact means that a *D. triauraria* male's ability to continue courtship with a conspecific female is not restricted by the cell size but by a visual signal together with another signal of a contact chemical. The length of courtship bout is thus considered to be one of the most important parameters for analysis of the basis of species recognition. We further intend to carry out experiments in this way on analyzing male courtship using interspecific combination of flies.

ACKNOWLEDGMENTS

We thank the late Prof. H. Ikeda, Ehime University, for his invaluable advice. We also thank Messrs. K. Omori and Y. Ito for their assistance. We are indebted to Dr. H. Takamori for using his program of Mann-Whitney U-test. This study has been supported by a grant from the Special Research Project on Instinct, University of Tsukuba.

REFERENCES

1 Spieth, H. T. (1952) Mating behavior within the genus *Drosophila* (Diptera). Natur. Hist., **99**: 395–474.

2 Kurokawa, H. (1960) Sexual isolation among the three races A, B and C of *D. auraria*. Jpn. J. Genet., **35**: 161–166.

3 Kurokawa, H. (1967) Population genetics on three

races of *D. auraria* Peng. III. Geographical and ecological distribution of the races, A, B, and C, with special regard to its speciation. Jpn. J. Genet., **42**: 109–119.

4 Kurokawa, H., Oguma, Y. and Tachibana, N. (1982) Sexual isolation among four species of *D. auraria* complex. Drosophila Inf. Serv., **58**: 98–99.

5 Grossfield, J. (1968) The relative importance of wing utilization in light dependent courtship in *Drosophila*. Studies in Genetics, IV. Univ. Texas Publ., No. 6818: 147–156.

6 Grossfield, J. (1971) Behavioral differentiation of three races of *D. auraria*. J. Heredity, **62**: 72–73.

7 Hardeland, R. (1972) Species differences in the diurnal rhythmicity of courtship behaviour within the *melanogaster* group of the genus *Drosophila*. Anim. Behav., **20**: 170–174.

8 Spiess, E.B., Langer, B. and Spiess, L. D. (1966) Mating control by gene arrangements in *Drosophila pseudoobscura*. Genetics, **54**: 1139–1149.

9 Sokal, R.R. and Rohlf, F. J. (1981) Biometry, Freeman, San Francisco.

10 Connolly, K. and Cook, K. (1973) Rejection responses by female *Drosophila melanogaster*: their ontogeny, causality and effects upon the behaviour of the courting male. Behaviour, **44**: 142–165.

11 Crossley, S. and McDonald, J. (1979) The stability of *Drosophila melanogaster* courtship accross matings. Anim. Behav., **27**: 1041–1048.

12 Robertson, H. M. (1982) Female courtship summation in *Drosophila melanogaster*. Anim. Behav., **30**: 1105–1117.

13 Ewing, L. S. and Ewing, A. W. (1984) Courtship in *Drosophila melanogaster*: Behaviour of mixed-sex groups in large observation chambers. Behaviour, **90**: 184–202.

ZOOLOGICAL SCIENCE 4: 897–902 (1987)

A New Species of *Zetomimus* (Acari: Oribatei) from Japan

NORIHIDE OHKUBO

Tsu Nōgyō-Kairyō-Fukyūsho, 446–34, Sakurabashi 3-chome, Tsu 514, Japan

ABSTRACT—A new species *Zetomimus brevis* is described. It is semiaquatic and able to walk on the surface of water, that is exceptional for oribatid mites. Some concepts about the taxonomy of the genus are mentioned.

INTRODUCTION

Hull [1] created *Zetomimus* for two species, *Oribata furcata* Warburton et Pearse [2] and *Oribates boothianus* Hull [3]. Balogh [4] treated *Ceratozetes argentinensis* Hammer [5] as the member of *Zetomimus*. The three species were indicated to be monodactyle in their original descriptions. Later, Shaldybina [6] found *Z. furcatus* has two side claws on legs III and IV. She treated *Hammobates* Hammer [7] as a synonym of *Zetomimus* because the genus *Hammobates* is characterized by that legs I and II are monodactyle but legs III and IV are tridactyle just like *Z. furcatus*. Though *Z. argentinensis* is not proved to have more claws, it is natural to be classified to the genus considering its characteristic features such as body contours, arrangement of notogastral setae and areae porosae and so on. As for *Z. boothianus,* its assignment to the genus is doubtful. As the author unfortunately does not know its rediscovery, the species is not mentioned in this paper furthermore.

In this paper, a new species of *Zetomimus* is described from Japan. All the members of the genus hitherto known were collected from aquatic or semiaquatic environment. The Japanese one is usually found by pond or paddy field, having the ability to walk on the surface of water like the European species, *Z. furcatus* [8], and never sinking in the water. It may well be said that *Zetomimus* species live a semiaquatic life.

In the following description, a metallograph was used in order to study surface textures of integument. Some of surface structures such as wrinkles and scales are only detected by the metallograph and they are hardly observable in the use of a usual microscope under transparent illumination. In such cases the expressions "faint" or "faintly" are used in the present paper.

Accepted April 15, 1987
Received March 4, 1987

Zetomimus brevis sp. n.
(Figs. 1–3)

Dimensions For 7 specimens, body length 360(383)400 μm, width 275(289)300 μm.

Prodorsum Rostrum with a pair of short, parallel ridges that become dull dents anteriorly. Between the ridges, rostrum nearly truncated at the tip, and faintly wrinkled dorsally (Fig. 1C). In dorsal view, these structures are not visible and rostrum seems to be simply rounded (Fig. 1A). Lateral rostral margin forming a narrow but conspicuous ridge with a thin outside blade, continued from rostral dent, covering tip of genal process and becoming anterior carina *ca*.

Rostral seta fairly barbed dorsolaterally, arising from a short, weakly swollen ridge. Tutorium smoothly curved at the border, and pointed at its free tip. The tip nearly at the level of insertion pore for rostral seta. Antiaxial surface of tutorium with long, conspicuous wrinkles. A few light spots of internal structure found outside the base of tutorium.

Lamella overhanging laterally, bending down abruptly under bothridium and being continued to the root of bothridium. Its surface with faint wrinkles and dots dorsally and long wrinkles ventrally. Lamellar costa only faintly developed. Cuspis cylindrical, smooth, 0.55 times as long as

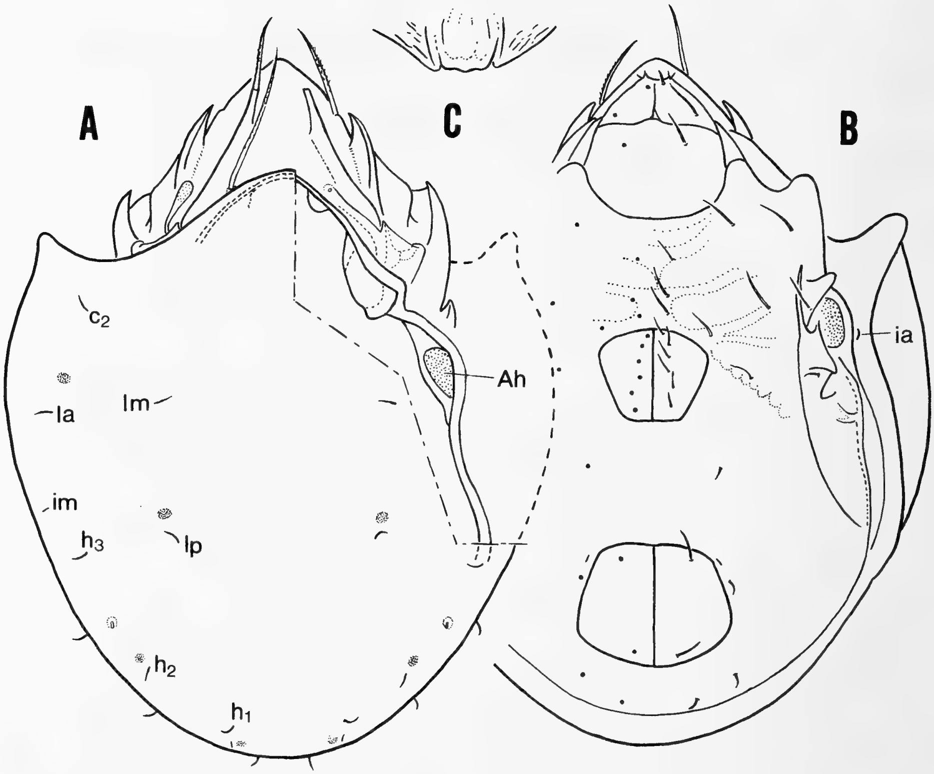

Fig. 1. *Zetomimus brevis* sp. n.

A. Dorsal aspect, also showing posterior border of prodorsum and an organ *Ah* by removing right shoulder of notogastral plate; B. Ventral aspect; C. Rostral tip in anterior view.

lamella and shorter than the mutual distance between the bases of both cuspidis. Its diameter almost the same throughout its length. Cuspidis converging anteriorly; the mutual distance of their tips 0.75 times as long as that of their bases. Lamellar seta as long as lamella, having a few scale-like, minute barbs dorsally.

Dorsal surface of prodorsum smooth. Translamella is absent. The lateral contour of prodorsum almost straight midway. Pore for interlamellar seta located in front of dorsosejugalis, but only partly concealed by notogastral plate. Under transparent illumination the anterior border of notogaster is easily overlooked, because the edge is a fairly thin, free blade protruding beyond a thick, conspicuous dorsosejugalis. The blade narrowest at the anteriormost part, becoming wider posteriorly to form pteromorph. Interlamellar seta arising on a long, weakly swollen ridge which continues from the side of bothridium. The seta inclines anteriorly with mimute barbs dorsally; the barbs denser than those of lamellar seta but sparser than those of rostral one.

Bothridium spindle-shaped in anterolateral view, protruding laterad posteriorly. Scale *sdm* pointed and scale *psdm* scarcely expanded at its free border; the border between the two scales consisting of two edges, upper and lower. Scale *svm* narrow, concealed under *sdm* in dorsal view, while scale *svl* is large but thin; border between these two scales strongly curved inward. Sensillus club-shaped, seemingly almost smooth but scattered with very faint, minute scales on distal half. Exobothridial seta slender.

Podosoma Genal process well developed. Its dorsal carina *dr* covered by carina *ca*; the two

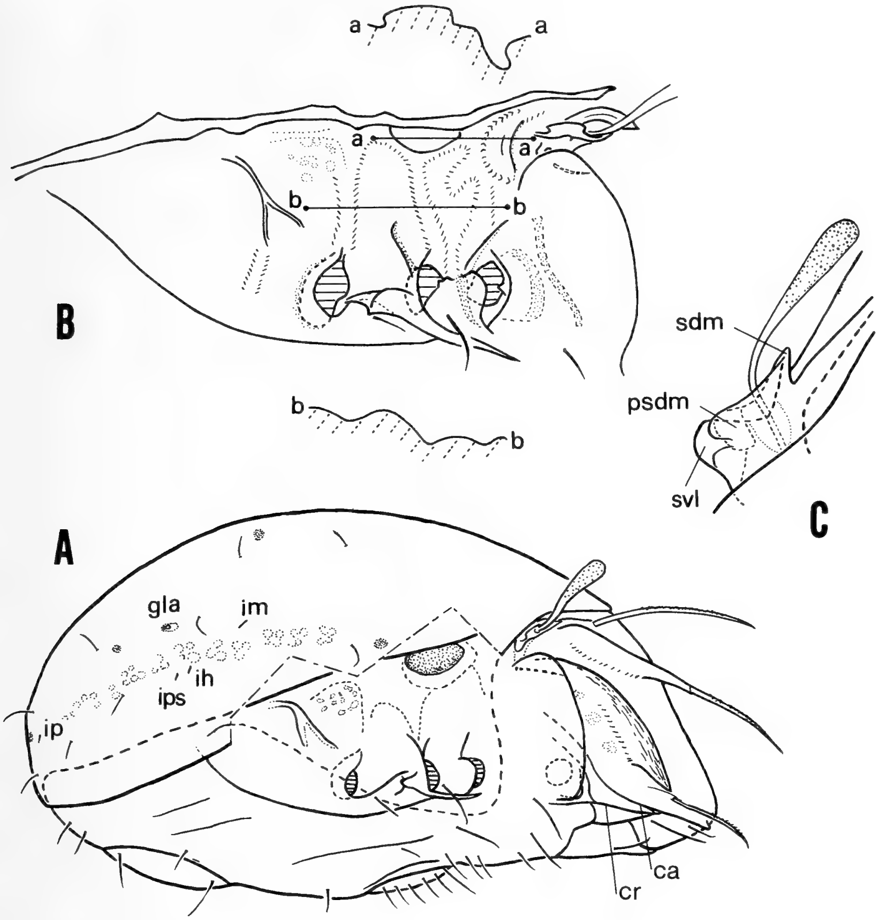

FIG. 2. *Zetomimus brevis* sp. n.

A. Lateral aspect, pteromorph removed; B. Podosoma in latero-ventral view (a–a and b–b show schematic section); C. Bothridium and sensillus in dorsal view.

carinae fusing posteriorly. Central carina *cr* strong, becoming posteriorly acetabular tectum I. Ventral fin thin, posteriorly covered by mentotectum.

Pedotectum II rather trapezoidal in lateral view. A short ridge extending upward from the upper end of pedotectum II. Custodium sharply pointed, separated from acetabular tectum III, discidium and circumpedal carina. Another short ridge extending upward from acetabular tectum III. Discidium resembling a triangular pyramid; the anterior plane continued to the posterior plane of pedotectum II, the upper plane convex, and the lower plane concave.

A very deep and large reniform cavity is present behind bothridium where so-called organ *Am* is absent. Area porosa *Ah* especially well developed, consisting of an externally excavated, membranous integument with dots and a strongly sclerotized circular ring; the organ extending horizontally and facing downward. Behind the organ *Ah* found an area where many clear spots are scattered. A bifurcate ridge running behind the area.

Epimeral region Epimeral plates smooth at the middle but faintly sculptured with short wrinkles at both sides. Epimeral setae relatively long; setae *1a, 2a, 3a* and *4c* the shortest among them, setae *3b, 4a* and *4b* longer, and setae *1b, 1c* and *3c* the

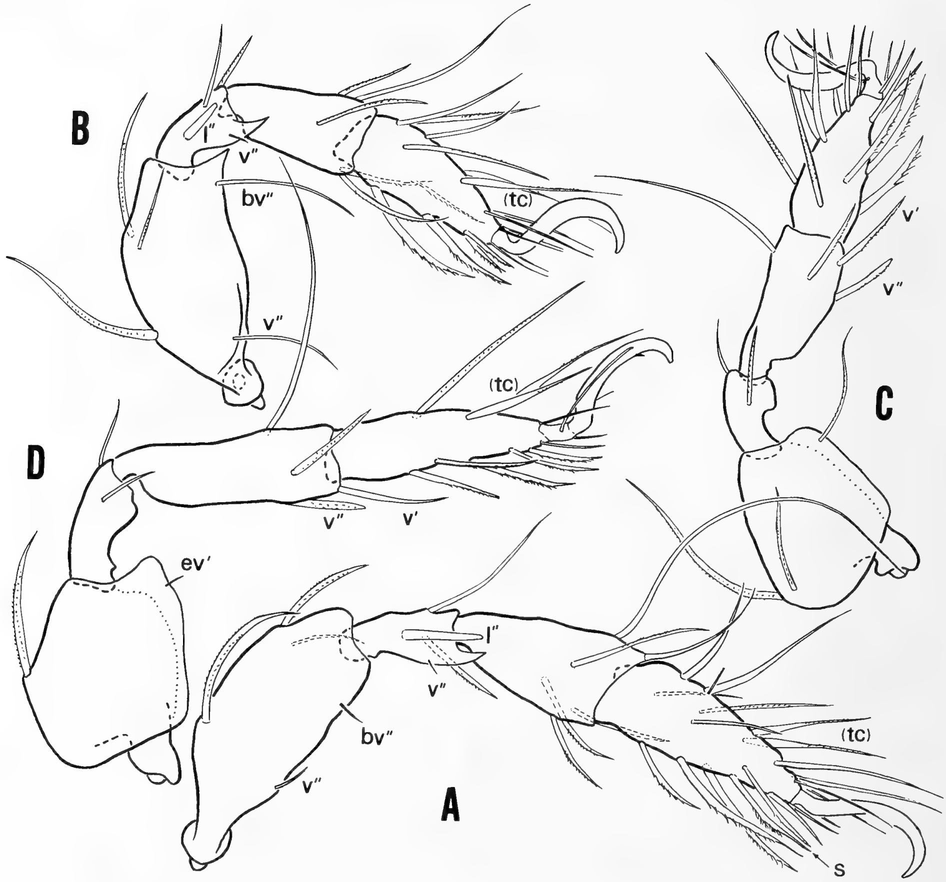

FIG. 3. *Zetomimus brevis* sp. n.
A, B, C and D show antiaxial side of legs I, II, III and IV, respectively.

longest, about 1.7 times longer than the shortest ones. Setae *1a, 2a, 3a* and *4c* smooth, setae *1b* and *1c* finely barbed, and the others only faintly barbed. All epimeral setae slightly inclined anteriorly.

Ano-genital region Genital aperture oblique to body axis, opening anterolaterally (Fig. 2A). The aperture especially wider anteriorly, 1.3 times wider than long, anterior border being smoothly rounded. Genital plate smooth, convex along genital setae and slightly concave outside them. Six genital setae slender, arranged in a row on the plate; the anteriormost seta as long as epimeral seta *3a* and 1.3 times as long as the other genital ones. Aggenital setae slender, shorter than anal ones.

Anal aperture slightly long sideways. Anal plates smooth and convex. Anal setae slender, shorter than genital ones. Adanal fissure short, located just near the aperture. Adanal setae slender, half as long as anal setae. Ventral plate smooth in ano-genital region.

Notogaster Notogastral plate clearly decolorized near anterior border and along pteromorphous margin. The surface looking smooth but very faintly sculptured irregularly. Anterior border narrowly hanging over prodorsum. Lateral border under pteromorph strongly undulating. Ten pairs of setae slender, only slightly curved; no seta on pteromorphs. Distance of seta c_2 from

anterior border of pteromorph about half as long as distance c_2–*la*. Seta *la* inserted at about mid-distance along length of pteromorph. Seta *lm* at the level of seta *la*. Mutual distance of setae *lm* wide, twice as long as distance *la*–*lm*. The mutual distance of setae *lp* 0.8 times as long as that of setae *lm* and almost equal to distance c_2–*la*. Seta h_3 just behind the level of seta *lp*. Distance between *lp*–h_3 almost equal to that between *la*–*lp*. Distance h_3–h_2 almost equal to distance h_2–h_1, and a little longer than mutual distance of setae h_1. Distance ps_3–ps_2 about equal to distance ps_2–ps_1, and about twice as long as mutual distance of setae ps_1.

Four pairs of areae porosae round, indistinct; *Aa*, A_1 and A_2 near setae *la*, *lp* and h_2, respectively, while A_3 at the middle level between setae ps_1 and h_1. Five pairs of lyrifissures short; lyrifissure *ia* just near *Ah*.

Legs Setation: trochanters 1–1–2–1, femora 5–5–3–2, genua 3(1)–3(1)–1(1)–2, tibiae 4(2)–4(1)–3(1)–3(1), tarsi 18(2)–15(2)–15–12. Tarsi I and II monodactylous. Tarsi III and IV hetero-tridactylous; side claws very thin, curving only slightly. An acute ventral spur on each of genua I, II and femur II. Lamelliform ventral ridge on femora III and IV as well as trochanters III and IV. Remarkable setae are as follows. Tarsi: all setae *tc* swollen at basal half. Tibiae: v'' III and IV dully pointed, thicker and shorter than v' III and IV, respectively. Genua: l'' I and II very thick and dully pointed, v'' I and II minute. Femora: bv'' I and v'' I thin, ev' IV minute. Trochanters: v' IV minute, while setae on other legs barbed, thin and very long.

Type-series Holotype (NSMT-Ac 9794 in spirit) and 7 paratopotypes: Ishinden-Kōzubeta, Tsu, Mie, May 4, 1986, collected and extracted by N. Ohkubo from dead leaves that are cast at the shore of a pond. All specimens will be deposited in the collection of the National Science Museum (Nat. Hist.), Tokyo.

Remarks The type species *Z. furcatus* has been collected from Europe frequently. Though the information on its morphology is not sufficient, the illustrations that were given by Warburton and Pearce [2], Willmann [8], Schweizer [9] and Shaldybina [6] indicate some specific characters: 1) long cuspis, 2) fairly thick base of cuspis, 3) barbation on sensillus (except in [8]), and 4) relatively pointed tip of sensillus (except in [8]). The body length (500 μm [2] and 440 μm [8]) is greater than that of the present new species. Argentine species *Z. argentinensis* is characterized by 1) very long cuspis, 2) presence of hairs on sensillus, 3) large areae porosae, 4) more posterior position of setae ps_3, 5) long notogastral setae, 6) more setae on tibia II and 7) longer and shorter setae on leg II. Its body length 500 μm. Two species were recorded from Chile: *Z. cristatus* (Hammer [7]) and *Z. spinosus* (Hammer [7]). The former species is different from the new species in 1) long cuspis, 2) short lamellar seta, 3) distinct areae porosae on notogaster, 4) anterior position of genital seta g_2, 5) lateral position of adanal seta ad_3 and 6) thick lateral claws of leg IV. The body length 580 μm. The latter species is characterized by 1) anteriorly tapering cuspis, 2) widely separated lamellae and 3) anterior position of genital sete g_2 and g_3. The body length 380 μm.

DISCUSSION

The genus *Zetomimus* Hull was not popular at first and its type species was rather known as a member of *Ceratozetes* until Balogh [10] accepted the genus as a well isolated taxon. Later, Shaldybina [11] constructed new system of Ceratozetoidea where she gave a family level taxon Zetomimidae to the genus. Her taxon was adopted in the identification keys of Balogh [4]. During the present study, however, the author notices that *Zetomimus* fairly resembles *Ceratozetes*. Behan-Pelletier [12] presented fine diagnosis of *Ceratozetes*. Examining his description, one can find that the present new species has almost all features of *Ceratozetes* as to adult. The genus *Zetomimus* is distinguishable only by some additional features as mentioned after. The family Ceratozetidae contains many genera which have little resemblance to *Ceratozetes*. The author, therefore, is doubtful about the family level separation of the two genera.

The genus *Zetomimus* is distinguished from *Ceratozetes* as follows: 1) legs I and II monodactyle and legs III and IV tridactyle, 2) notogaster

relatively wide, 3) lamella and cuspis relatively narrow, 4) sensillar head club-shaped, 5) area porosa A_1 situated just before seta *lp*, 6) median part of rostral tip not excavated. The next features have a possibility to become generic characters: 1) organ *Ah* extremely developed, 2) the border between *sdm* and *psdm* of bothridium only slightly curved, and 3) the presense of membranous secretion under pteromorphs and near dorsosejugalis.

ACKNOWLEDGMENT

The author wishes to thank Dr. J. Aoki, Yokohama National University, for reading the manuscript.

REFERENCES

1 Hull, J. E. (1916) Terrestrial Acari of the Tyne Province. Trans. Nat. Hist. Soc. Northumberland, **4**: 381–410.

2 Warburton, C. and Pearce, N. D. F. (1905) On new and rare British mites of the family Oribatidae. Proc. Zool. Soc. London, **2**: 564–569, 2 pls.

3 Hull, J. E. (1915) Acari from bird's nests, with description of a new species. Naturalist, **707**: 398–399.

4 Balogh, J. (1972) The Oribatid Genera of the World. Budapest, pp. 1–188, 71 pls.

5 Hammer, M. (1958) Investigations of the oribatid fauna of the Andes Mountains. I. The Argentine and Bolivia. Biol. Skr. Dan. Vid. Selsk., **10**: 1–129, 34 pls.

6 Shaldybina, E. S. (1975) Ceratozetoidea. In "A Key to Soil-Inhabiting Mites (Sarcoptiforms)". Ed. by M. S. Gilyalov, Moscow, p. 491. (in Russian)

7 Hammer, M. (1962) Investigations of the oribatid fauna of the Andes Mountains. III. Chile. Biol. Skr. Dan. Vid. Selsk., **13**: 1–95, 30 pls.

8 Willmann, C. (1931) Moosmilben oder Oribatiden (Cryptostigmata). Tierw. Deutschl., **22**: 79–200.

9 Schweizer, J. (1956) Die Landmilben des schweizerischen Nationalparkes. 3e partie: Sarcoptiformes. Ergeb. wiss. Unters. shweiz. Nationalparkes, **34**: 215–377.

10 Balogh, J. (1965) A synopsis of the world oribatid (Acari) genera. Acta Zool. Hung., **11**: 5–99.

11 Shaldybina, E. S. (1966) Postembrionic development of horned mites of superfamily Ceratozetoidea Balogh, 1961 and their system. In "1st Conference of Acarology. Abstracts". Nauka, pp. 225–226. (in Russian)

12 Behan-Pelletier, V. M. (1984) *Ceratozetes* (Acari: Ceratozetidae) of Canada and Alaska. Can. Entomol., **116**: 1449–1517.

ZOOLOGICAL SCIENCE 4: 903–911 (1987)

Redescription of *Villa myrmeleonostena* (Insecta, Diptera, Bombyliidae), A Parasitoid of Ant Lion in Japan

KINTARO BABA, AKIRA NAGATOMI[1], HISAKO NAGATOMI[2] and NEAL L. EVENHUIS[3]

Kurokawa-mura, Kitakambara-gun, Niigata Pref. 959–28, [1]Entomological Laboratory, Faculty of Agriculture, Kagoshima University, Kagoshima 890, [2]Biological Laboratory, Kagoshima Women's College, Hayato 899–51, Japan, and [3]Department of Entomology, B. P. Bishop Museum, Honolulu, Hawaii 96817, U.S.A.

ABSTRACT—*Villa myrmeleonostena* (Baba) comb. n. from Japan is redescribed and illustrated. The larva of this species is parasitic upon the ant lion.

INTRODUCTION

Baba [1] gave the biological notes upon a bee fly species from Japan, whose larva parasitizes the ant lion. Later, Baba [2] named this species *Argyromoeba* (?) *myrmeleonostena.* In this paper, *Villa myrmeleonostena* (Baba, 1953) comb. n. is redescribed and illustrated and its biology is introduced according to Baba [1, 2].

Genus ***Villa*** Lioy

Villa Lioy, 1864, Atti Ist. Veneto Sci. ser. 3, Vol. 9: 732. Type species: *Anthrax concinnus* Meigen, 1820 [=*abbadon* (Fabricius, 1794)]. By designation of Coquillett (1910).
Anthrax, authors, not Scopoli.

For diagnosis of *Villa,* see Engel [3], Hesse [4], Oldroyd [5], Hull [6], Hall [7] and Greathead [8].

This genus contains numerous species and is present in all of the continents (e.g., Bowden [9, 10]; Hull [6]; Painter and Painter [11]).

Oldroyd [5] wrote, "Clear-winged species of *Villa* are among the easiest Bombyliidae to recognize generically, but the most difficult to identify specifically."

Accepted May 23, 1987
Received April 18, 1987

[1] To whom reprints should be requested.

Villa myrmeleonostena (Baba) comb. n.
(Figs. 1–11)
[Japanese name: Arijigoku-tsuriabu]

Argyromoeba (?) *myrmeleonostena* Baba, 1953, Arijigoku no Seibutsushi [=Biology of the Ant Lion], p. 69. Type locality: Niigata Prefecture, Honshu.

According to Hall [7], "palpus usually about half length of proboscis or more. Thoracic bristles well-developed. Pulvilli present or absent" in the North American *Villa* and its related genera. In *V. myrmeleonostena* from Japan, the thoracic and scutellar bristles are lacking, the palpus is small and inconspicuous and difficult to recognize, and the pulvilli are absent.

According to the key to the Palaearctic species by Engel [3], *V. myrmeleonostena* falls into the couplet 7 and is similar to *V. albida* Becker, 1916 from Hungary (♂), but may easily be distinguished from the latter by having the following characters: bristles on mesonotum lacking and abdominal terga 4–6 with black erect hairs at sides.

Male Head (Figs. 1–5): Dark brown to black, and more or less pale gray pollinose; frons, face (except clypeus), and antennal segments 1–2 with black, trim, rather stout hairs; postocular rim (including cheek), ocellar triangle and proboscis with short, black haris which are recumbent on postocular rim; posterior border of postocular rim covered with white, trim hairs directed posteriorly, which become black on lower part; frons, face

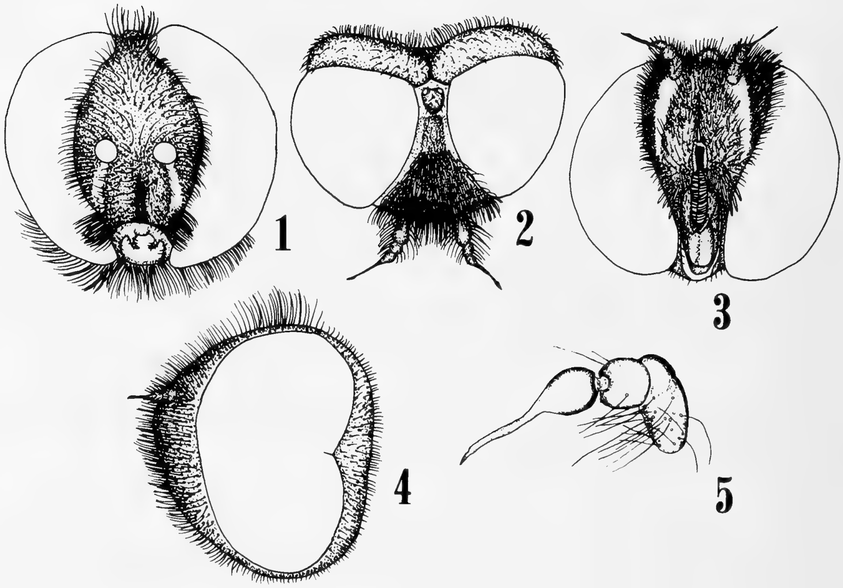

FIGS. 1–5. *Villa myrmeleonostena,* male. 1–4. Head, anterior, dorsal (ocellar triangle is kept horizontal), facial and lateral views. 5. Antenna, dorso-inner view (based on 2nd specimen).

(except clypeus), and postocular rim with small, pale (or pale brown) scales; half width of head from a direct frontal view 0.9 times distance from antenna to median ocellus and 1.0–1.1 times width of frons at antennae; ocellar triangle 0.8–1.0 times as wide as long; space between antennae 2.0–2.4 times width of ocellar triangle; width of frons at median ocellus 0.16–0.18 times distance from antenna to median ocellus, 0.18–0.20 times width of frons at antenna, 0.4–0.5 times narrowest part of face, and 1.3–1.5 times width of ocellar triangle; distance from lower margin of clypeus to antenna 1.2–1.3 times that from antenna to median ocellus; clypeus 0.3–0.4 times as wide as long and 5.5–12.0 times as wide as narrowest part of parafacials; antenna 0.5 times as long as distance from antenna to median ocellus and 2.8–3.3 times as long as width of frons at median ocellus; when measured along inner surface, antennal segment 3 (including short apical spine) 1.9–2.1 times as long as and 0.6 times as thick as segment 1, and 3.5–5.0 times as long as and 0.8 times as thick as segment 2; in segment 3, basal wide part 0.4–0.6 times as long as apical narrow part (including spine); proboscis (along ventral surface) 0.8–0.9 times as long as clypeus; data based on 5 specimens.

Thorax (Fig. 6): Dark brown to black, and more or less pale gray pollinose; mesonotum, scutellum,

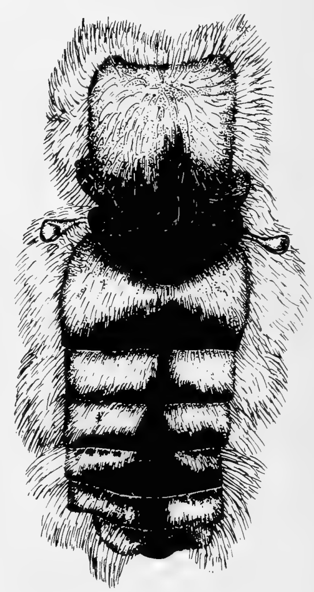

FIG. 6. Thorax and abdomen of *Villa myrmeleonostena,* male, dorsal view.

meta-, and upper part of meso-, and anteroupper part of pteropleura covered with long, white haris which are trim, vertically erect, and transversely running on anterior part of mesonotum; pro-, lower part of meso-, sterno- (except bare large anterolower part), and pteropleura (before metapleura) with black hairs which are long, dense, trim, and rather stout on propleura and running transversely above fore coxae; hypo- and lower part of pteropleura bare; halter creamy white or creamy pale brown, and partly tinged with dark brown.

Wing (Figs. 7–8): Hyaline; veins brown to dark brown; subcostal cell more or less brown fumose; supernumerary crossvein sometimes present connecting R_{2+3} and R_4 (see Fig. 8).

Legs (Figs. 9–11): Dark brown to black; coxa and femur more or less pale gray pollinose and with black hairs; femur also covered with small, pale (or pale brown) scales; fore tibia at dorsal surface and mid and hind tibiae throughout surfaces clothed with spicules; pulvilli absent; relative lengths of segments (excluding coxa and trochanter) of fore leg 66 (63–69): 67 (66–69): 20 (18–21): 9(8–10): 7 (6–7): 5 (5): 11 (11–12), of mid leg 75 (73–77): 80 (77–82): 24 (23–26): 9 (8–9): 7 (6–7): 5 (5–6): 11 (11), of hind leg 100: 108 (104–111): 37 (35–38): 15 (13–17): 11 (10–13): 7 (7–8): 13 (13–14) and in hind leg, relative thickness of femur, tibia, and tarsal segments 1–3, 10 (9–11): 7 (7): 4 (4–5): 3 (3–4): 3 (3–4); (N=4).

FIG. 7. Wing of *Villa myrmeleonostena*, male.

Abdomen (Fig. 6): Dark brown to black, and more or less pale gray pollinose; dorsum with white hairs which are dense on the sides and become chiefly or partly black on sides of terga 4–6; tergum 2 (except sides) with a large semicircular apical band which is covered with black scales; terga 3–7 (except sides) with white scales which become black along posterior borders (except that of tergum 7) and along mid lines; venter with black hairs which become white on sides of sternum 2; venter also with black scales which become pale (or pale brown) on sides.

Length: Body 6.4–8.8 mm (N=8); wing 7.0–8.8 mm (N=6); hind femur 2.1–2.4 mm (N=4).

Female Similar to male except as follows. Head: Space between antennae 1.8–2.0 times width of ocellar triangle; width of frons at median ocellus 0.25–0.29 times distance from antenna to

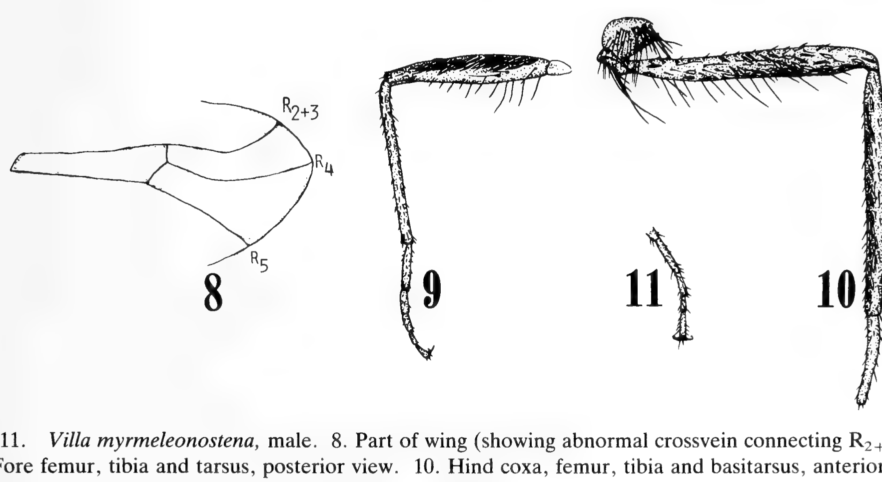

FIGS. 8–11. *Villa myrmeleonostena*, male. 8. Part of wing (showing abnormal crossvein connecting R_{2+3} and R_4). 9. Fore femur, tibia and tarsus, posterior view. 10. Hind coxa, femur, tibia and basitarsus, anterior view. 11. Hind tarsal segments 2–5, ventral view.

median ocellus, 0.30–0.33 times width of frons at antennae, 0.6–0.7 times narrowest part of face, and 1.8–2.0 times width of ocellar triangle; antenna 1.9–2.3 times as long as width of frons at median ocellus; when measured along inner surface, antennal segment 3 (including apical short spine) 1.7–1.8 times as long as and 0.7–0.8 times as thick as segment 1, and 4.0–5.5 times as long as and 0.8–0.9 times as thick as segment 2; data based on 5 specimens.

Thorax: Mesonotum (except sides and anterior border) and scutellum (except posterior border) covered with white scales and clothed with fine, erect black hairs which become partly white on scutellum and posterior border of mesonotum.

Wing: As in male.

Legs: Relative lengths of segments of fore leg 66 (65–67): 67 (65–69): 20 (19–20): 8 (8): 7 (6–7): 6 (5–6): 12 (12), of mid leg 76 (76): 78 (74–82): 27 (24–31): 9 (8–9): 7 (6–7): 6 (5–6): 11 (10–11), of hind leg 100: 107 (106–108): 38 (34–41): 13 (13–14): 10 (9–11): 8 (7–8): 13 (12–15) and in hind leg, relative thickness of femur, tibia, and tarsal segments 1–3, 12 (11–12): 7 (7–8): 5 (5): 4 (4): 4 (3–4); (N=3).

Abdomen: As in male.

Length: Body 7.4–8.6 mm (N=8); wing 7.2–8.6 mm (N=8); hind femur 2.1–2.3 mm (N=3).

Distribution Japan (Honshu).

Specimens examined (10♂♂, 9♀♀): Niigata Pref.: 2♂♂, 1♀, Kinoto, 18 & 29. vii. 1948, K. Baba; 1♂, Araihama, 19. vii. 1959, K. Baba; 4♂♂, 3♀♀, Senami, 4–14. vii. 1985, K. Baba; 2♂♂, 5♀♀, Senami, 4–24. vii. 1986, K. Baba; 1♂, Senami, 28. viii. 1986, K. Baba.

There is a single male specimen from Yakushima (Kagoshima Pref.) (Kurio, 27. vii. 1967, A. Nagatomi). Its size is as follows: body 10.2 mm; wing 9.8 mm; hind femur 2.75 mm. No significant difference is found between this specimen (from Yakushima) and *myrmeleonostena* (from Niigata Pref.). The male genitalia are not yet examined, however.

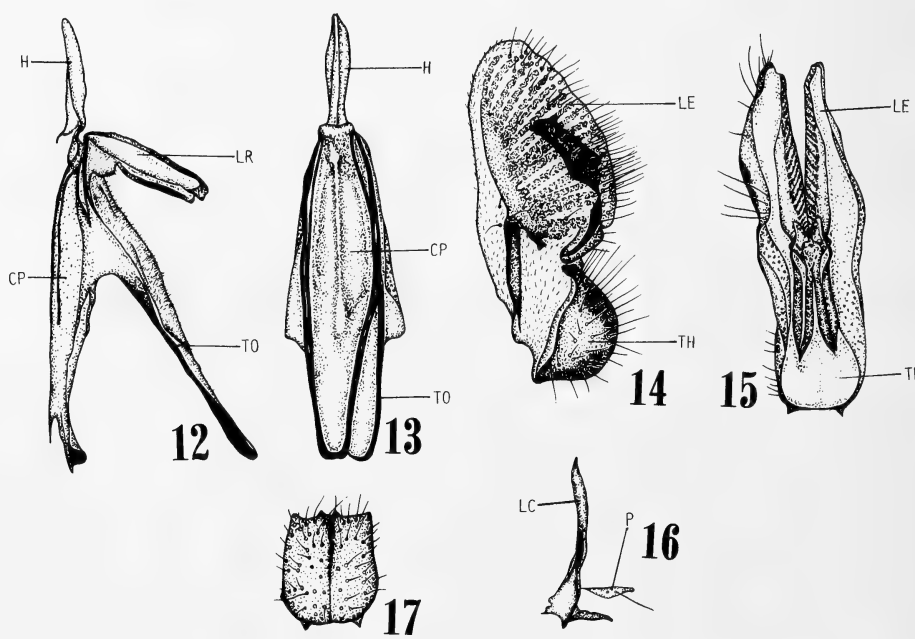

Figs. 12–17. Mouthparts of *Villa myrmeleonostena*, female. 12. Lateral view. 13. Ventral view. 14. Lateral view. 15. Dorsal view. 16. Lateral view. 17. Theca, ventral view. CP, cibarial pump; H, hypopharynx; LC, lacinia; LE, labellum; LR, labrum; P, palpus; TH, theca; TO, torma.

Mouthparts of *Villa myrmeleonostena* (Figs. 12–17)

Nagatomi and Soroida [12] described and illustrated the female mouthparts in 3 genera (*Anthrax, Bombylius* and *Ligyra*) and 3 species of Bombyliidae.

The structure of the mouthparts in *V. myrmeleonostena* is given below, based on 2♂♂, 1♀.

Differing from the 3 genera and 3 species (♀♀) above as follows: Hypopharynx not longer than labrum and mid-distal interlabellar process lacking.

Male Labrum longer than wide, and much shorter (0.4–0.5 times) than cibarial pump; dorsal part of labrum willow leaf-like, narrower apically, and with basal lesser half desclerotized; ventral part of labrum pipe-like, concave dorsally, parallel-sided, with apical margin nearly transverse, and with a V-shaped pale spot near apex. Hypopharynx thin dorsoventrally, shorter (0.9 times) than labrum, longer than wide, widest behind middle (or roughly parallel-sided), and desclerotized at basal part. Cibarial pump wider (1.7–2.0 times) than labrum, wider (2.8–3.3 times) than breadth between dorsal cornua, much longer (3.7–4.8 times) than wide, widest before middle, and gradually narrower posteriorly. Torma long and its base situated before (i. e. near anterior end) middle of cibarial pump; a pair of more sclerotized lateral lines not fused at posterior ends. Palpus elliptic, small and inconspicuous, 1-segmented, and longer than wide. Lacinia about as long as labrum. Labellum shorter (0.7 times) than cibarial pump, longer (1.7–1.9 times) than theca, and with 2 longitudinal darker spots. Length: Labrum 0.40–0.43 mm; cibarial pump 0.93–1.03 mm.

Female (Figs. 12–17) No significant difference is found between sexes. Length: Labrum 0.38 mm; cibarial pump 0.89 mm.

Specimens dissected: 2♂♂, Senami, Niigata

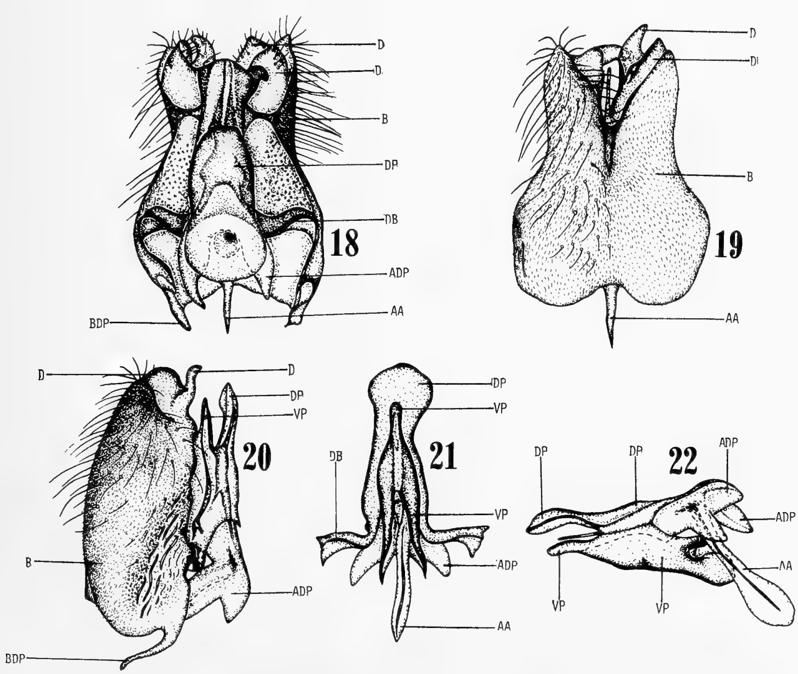

FIGS. 18–22. Male genitalia of *Villa myrmeleonostena*. 18. Dorsal view. 19. Ventral view. 20. Lateral view. 21. Ventral view. 22. Lateral view. AA, anterior bar of aedeagus; ADP, aedeagal dorso-anterior plate; B, basistyle; BDP, basistylar dorso-inner anterior process; D, dististyle; DB, dorsal bridge; DP, dorsal plate; VL, ventral lobe; VP, ventral plate.

Pref., 10 & 24. vii. 1986, K. Baba; 1♀, Senami, Niigata Pref., 14. vii. 1985, K. Baba.

Genitalia of *Villa myrmeleonostena*
(Figs. 18–32)

Hull [6] and Theodor [13] described and illustrated the male genitalia in many genera and species of the family Bombyliidae.

The following descriptions of the genitalia of *V. myrmeleonostena* contain the familial and generic characters. It is not possible to extract the specific characters, because only one species is examined. The term of each part of the male genitalia is the same as that in Nagatomi [14] on the lower Brachycera.

Male genitalia (Figs. 18–25) Basistyle neither thickened nor folded into dorsal piece, and composed only of ventral piece, but one narrow dorsal band present before dististyle; fused basistyles (from ventral view) widened at anterior part, longer than wide, gently concave at anterior margin and deeply so at posterior margin; basistyle (except anterior part) with ventral hairs; basistylar dorso-inner anterior process is strip-like, and a cove formed by this process and basistyle is narrow. Dististyle short in relation to basistyle and composed of outer wide and inner narrow processes, having hairs.

The so-called aedeagus composed of the dorsal and ventral plates, dorsal bridge, anterior bar of aedeagus, and aedeagal dorso-anterior plate (including a pair of diverging processes). Dorsal plate longer than wide; distal part of dorsal plate flattened dorsoventrally, wider anteriorly, and longer than distal part of ventral plate (which is probably composed of ventral plate and a part of dorsal plate). Ventral plate pointed and forming a tube at apex, and its basal part composed of a pair of long diverging processes. Anterior bar of aedeagus flattened laterally and wider and rounded anteriorly (=toward base of abdomen).

Tergum 9 widely concave at anterior margin, straight at posterior margin, with anterolateral angle pointed ventrally, and with dorsal long hairs which are absent on anterior part (whose middle area is large).

Cercus triangular in shape from dorsal view, rounded at posterior margin from lateral view, and widely bordered with membranous area covered with hairs.

There is no distinctly sclerotized sternum 10.

Specimens dissected (3♂♂): 1♂, Kinoto, Niigata Pref., 18. vii. 1948, K. Baba; 2♂♂, Senami, Niigata Pref., 10 & 24. vii. 1986, K. Baba.

Female genitalia (Figs. 26–32) Tergum 7 and sternum 7 much wider than long and the former slightly longer and slightly wider than the latter. Tergum 8 and tergum 9+10 much narrower than the preceding sgment. Each side of tergum 8 and tergum 9+10 developed into a ventral piece. Each of sternum 10 and cercus divided into a pair of sclerites which are flattened laterally. Sternum 8 flattened dorsoventrally, somewhat narrower than tergum 8, much wider than long, with anterior and lateral margins forming a semicircular line, and with anterior part desclerotized.

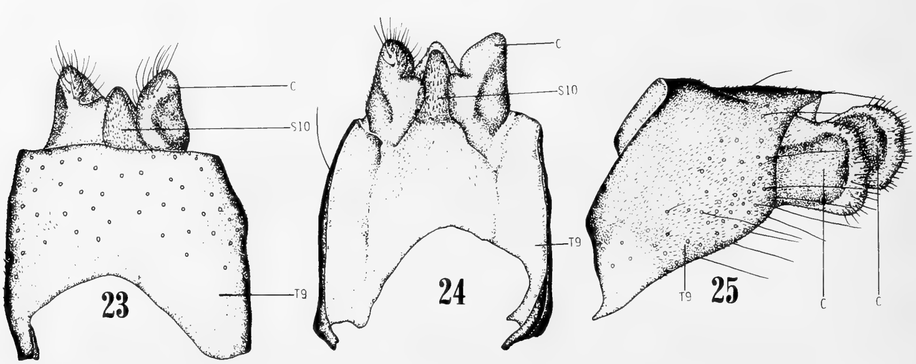

Figs. 23–25. Male genitalia of *Villa myrmeleonostena*. 23. Dorsal view. 24. Ventral view. 25. Lateral view. C, cercus; S10, sternum 10; T9, tergum 9.

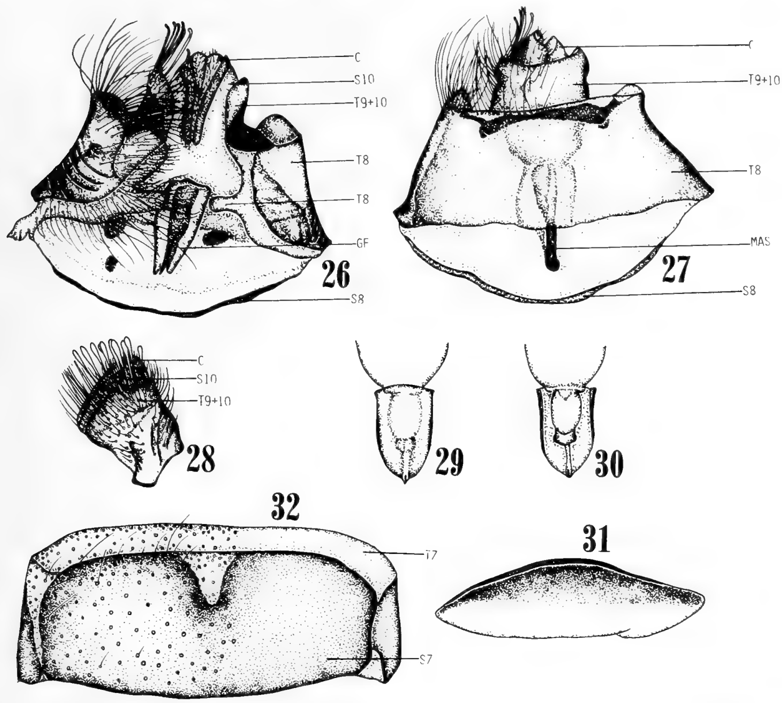

FIGS. 26–32. Female genitalia of *Villa myrmeleonostena*. 26. Ventral view. 27. Dorsal view. 28. Lateral view. 29–30. Genital fork, dorsal and ventral views. 31. Sternum 8, dorsal view. 32. Ventral view. C, cercus; GF, genital fork; MAS, midanterior stick in tergum 8; S7, sternum 7; S8, sternum 8; S10, sternum 10; T7, tergum 7; T8, tergum 8; T9+10, tergum 9+10.

Dorsal piece of tergum 8 trapezoidal, wider anteriorly, much wider than long, with a conspicuous midanterior stick, and with long soft hairs at posterior margin. Ventral fold of tergum 8 widely bordered with membrane which is covered with long soft hairs; this membrane developed into a process at middle and absent on posterior margin of ventral fold except outer angle; posterior part of ventral fold haired. Dorsal piece of tergum 9+10 wider than long, rectangular, and with an anterolateral sclerite+membrane (the membrane may be connected with postero-outer part of ventral piece); posterolateral part of tergum 9+10 with a vertical row of rod-like long spines, 10 or so in number; tergum 9+10 covered with long soft hairs. Inner border of sternum 10 darker and with soft hairs. Cercus membranous and haired.

Genital fork longer than wide, somewhat pentagonal, and with posterolateral long margins and midanterior short line sclerotized; as a part of genital fork, there is a U-shaped ventral sclerite.

Specimens dissected (3♀♀): 1♀, Senami, Niigata Pref., 14. vii. 1985, K. Baba; 1♀, Senami, Niigata Pref., 24. vii. 1986, K. Baba; 1♀, Senami, Niigata Pref., 19. vii. 1986, K. Baba.

Biology of *Villa myrmeleonostena*
(Figs. 33–36)

For biology and immature stages of the family Bombyliidae, see Clausen [15], Hull [6] and du Merle [16].

Ant-lion parasites in the family Bombyliidae have been recorded from the New World genus *Dipalta* Osten Sacken and the Old World genus *Micomitra* Bowden. *Anthrax confluensis* Roberts, and anomalous representative of this ubiquitous genus from Australia have also been recorded as parasitic on immatures of Myrmeleontidae. *A. confluensis* may belong in a new genus, but detailed phylogenetic study will have to be undertaken first to confirm this. For further details on the life history of *Micomitra stupida* (Rossi)

parasitic on Myrmeleontidae, see Steffan [17].

Baba [1, 2] gave an article on the biology of *V. myrmeleonostena.* An abstract of this article is given below.

The habitat The bee fly in question was collected on sand dune of the beaches in northern part of Niigata Prefecture and that at Akashi in Hyogo Prefecture. The investigation was made at the former.

The adult The parent fly appears in July and August. It visits the flower, e.g. *Fagara schinifolia* Engl. (=inuzansho). The copulation was seen on the flower. The fly hovers over sand dune under a burning sun, gradually descends and quietly alights on the sand, but takes flight at once and hovers again.

The hosts The parasite larva is found exclusively within the cocoon of the ant lion, that is, *Grocus bore* (Tjeder) (=kuro-ko-usuba-kagerō). There were 191 examined cocoons of *G. bore,* of which 97 were parasitized. Whereas in *Distoleon contubernalis* (MacLachlan) (=ko-kasuri-usuba-kagerô), out of 45 cocoons examined, only 1 was parasitized. The data above were obtained during 3 years from 1933 to 1935, at Kinoto, Niigata Prefecture. In 1985–86, at Senami, Niigata Prefecture, there were 88 examined cocoons of *G. bore,* of which 17 were parasitized.

The egg, 1st instar larva, and 2nd instar larva (within the host body) The stages above are not found. However, it is certain that the 1st instar larva (=planidium) enters into the host larval body. The molting time into the 2nd instar is unknown. The larva must spend a long time within the host body, waiting for the host pupation.

The larva upon the host pupal surface The youngest parasite larva found in the host cocoon is filiform and 4–5 mm long (Fig. 33). It crawls out from the host at the pupation time. When new host pupal thorax appears from the host larval cuticle, half or over half of the parasite body is usually seen already. It remains unknown whether the parasite larva at this time is the 2nd instar or the 3rd. It is always located at the venter of the host pupa between middle and hind legs and winds itself semicircularly round the host body. It becomes full-grown after 7–10 days (Fig. 34), passes a prepupal stage for 4–6 days upon the host body which is shrank completely, and then pupates.

The pupa The parasite pupa (Figs. 35 and 36) bores a hole through the host cocoon and reaches to the ground. The head and thorax appear out of the sand and emergence from the pupa takes place there. The pupal period is somewhat more than 10 days.

The habitat and life history of hosts Grocus bore (Tjeder) (=kuro-ko-usuba-kagerô): The larva of this species is common at sand dune of the beaches, but is also seen at that of the rivers and lakes. It makes a pitfall. The larva, devoted whole 1 to 3 years to mature, cocoons and pupates from late June to early August. In August, a number of new, ant lion pitfalls are seen.

Distoleon contubernalis (MacLachlan) (=ko-kasuri-usuba-kagerô): This species may not be regular as the host. The larva is seen both at seasides and at hilly places. At seasides, it lives in stationary sand dune under young pine trees. It does not make a pitfall.

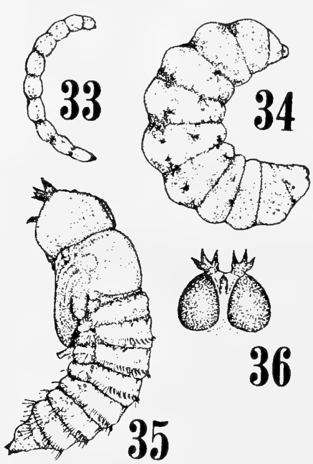

FIGS. 33–36. *Villa myrmeleonostena.*(after Baba [1]). 33. The youngest larva on host pupal surface. 34. Full-grown larva. 35. Pupa. 36. Pupal head.

ACKNOWLEDGMENTS

We wish to express our sincere thanks to Dr. Kanetosi Kusigemati (Kagoshima University) and Dr. Hiroshi Shima (Kyushu University) for their aid in various ways.

REFERENCES

1 Baba, K. (1936) Studies of the ant lion, IV. On the bee fly parasitic upon the pupa of the ant lion. Shizen Kenkyu (=Nature Study), **6**: 16–23. (In Japanese)

2 Baba, K. (1953) Arijigoku no Seibutsushi (=Biology of the Ant Lion). Essa Entomol. Soc., Niigata, 107 pp. (In Japanese)

3 Engel, E. O. (1932–37) Bombyliidae. 25. In "Die Fliegen der palaearktischen Region". Ed. by E. Lindner, Vol. 4, Pt. 3. E. Schweizerbart'sche Verlagsbuchhandlung, Stuttgart, pp. 1–619.

4 Hesse, A. J. (1956) A revision of the Bombyliidae (Diptera) of southern Africa. Part II; Part III. Ann. S. Afr. Mus., **35**: 1–464, 465–972.

5 Oldroyd, H. (1969) Diptera Brachycera. Section (a). Tabanoidea and Asiloidea. Handbooks for the identification of British Insects, Vol. 9, Part 4. Royal Entomol. Soc. of London, 132 pp.

6 Hull, F. M. (1973) Bee flies of the world: the genera of the family Bombyliidae. Smithsonian Institution Press, Washington, D. C. 687 pp.

7 Hall, J. C. (1981) Bombyliidae. In "Manual of Nearctic Diptera". Ed. by J. E. McAlpine, B. V. Peterson, G. E. Shewell, H. J. Teskey, J. R. Vockeroth and D. M. Wood, Res. Br., Agric. Can. Monogr., **27**(1): 589–602.

8 Greathead, D. J. (1981) The *Villa* group of genera in Africa and Eurasia with a review of the genera comprising *Thyridanthrax* sensu Bezzi 1924 (Diptera: Bombyliidae). J. Nat. Hist., **15**: 309–326.

9 Bowden, J. (1975) Family Bombyliidae. In "A Catalog of the Diptera of the Oriental Region". Ed. by M. D. Delfinado and D. E. Hardy, Vol. II. The University Press of Hawaii, Honolulu, pp. 165–184.

10 Bowden, J. (1980) Family Bombyliidae. In "Catalogue of the Diptera of the Afrotropical Region". Ed. by R. W. Crosskey, British Museum (Nat. Hist.), London, pp. 381–430.

11 Painter, R. H. and Painter, E. M. (1965) Family Bombyliidae. In "A Catalog of the Diptera of America North of Mexico". Ed. by A. Stome, C. W. Sabrosky, W. W. Wirth, R. H. Foote and J. R. Coulson, U. S. Dept. of Agriculture, Washington, D. C., pp. 407–446.

12 Nagatomi, A. and Soroida, K. (1985) The structure of the mouthparts of the orthorrhaphous Brachycera (Diptera) with special reference to blood-sucking. Beitr. Entomol., **35**: 263–368.

13 Theodor, O (1983) The Genitalia of Bombyliidae (Diptera). The Israel Academy of Sciences and Humanities, Jerusalem, 275 pp.

14 Nagatomi, A. (1984) Male genitalia of the lower Brachycera (Diptera). Beitr. Entomol., **34**: 99–157.

15 Clausen, C. P. (1940) Entomophagous insects. McGraw-Hill Book Co., New York, 688 pp.

16 du Merle, P. (1975) Les hôtes et les stades pré-imaginaux des Diptères Bombyliidae: revue bibliographique annotée. Bull. Sect. région. Quest Paláearctique (Organisation Internationale de Lutte Biologique). 1975 (4): 1–289.

17 Steffan, J. R. (1967) *Exoprosopa stupida* (Rossi) parasite de fourmilions dans l'ancien monde (Dipt., Bombyliidae). L'entomologiste (Paris), **23**: 78–79.

ZOOLOGICAL SCIENCE 4: 913–918 (1987)

Proposal of New Terminology for the Morphology of Nauplius Y (Crustacea: Maxillopoda: Facetotecta), with Provisional Designation of Four Naupliar Types from Japan

TATSUNORI ITÔ

Seto Marine Biological Laboratory, Kyoto University, Shirahama, Wakayama 649–22, Japan

ABSTRACT—New terminology for the morphology of first stage nauplius y larvae, mainly for the plates on their cephalic shield, is proposed. The proposed terminology aids in the identification of plates which vary in place and/or shape among naupliar types, and simplifies the description of nauplius y larvae. Four nauplius y larvae from Japan which are cited to explain the terminology are provisionally designated as separate types, symbolized as VIII–a, IX, X, and XI, the last being for the nauplius which was formerly described as a larva of *Hansenocaris pacifica* Itô.

INTRODUCTION

The nauplius y type IV larvae originally described by Hansen [1] and later reviewed by Schram [2] are characterized by the sculpture made of many clear "plates" on the cephalic shield. Many undescribed nauplii which are more or less similar to type IV in cephalic-shield sculpture are present in Tanabe Bay on the Pacific coast of Japan, where three types of nauplius y larvae have already been reported [3]. During the past three years I have raised many different nauplii into "cypris y" stages in the laboratory (for an abstract of the first successful case see [4]). The results of these rearing experiments should be taxonomically useful because the current taxonomy within the Facetotecta is based only upon the cypris y stage and remains tentative [5]. However, the lack of adequate terminology to describe cephalic-shield plates of different shapes and different arrangements poses an unexpected problem. Steuer [6] tried to identify plates of his material with their counterparts in Hansen's type IV larva by labeling them alphanumerically, and Schram [2] named plates in an advanced manner (see Fig. 1A). Although Schram's terminology, which was based upon the smallest form of his type IV larvae, seemed to be usable for my material, its application to various nauplius y larvae in Japan has often been very difficult even for larvae at the same stage (first naupliar stage) as his smallest form. Therefore, I have had to modify Schram's terminology to make it more universal. This improved terminology for first stage larvae, which is described in the present paper, will facilitate our forthcoming descriptive works on nauplius y larvae.

Provisional designation of naupliar types

Three of the four nauplii cited in the present paper (Fig. 2) are selected from undescribed forms found in Tanabe Bay on the Pacific coast of Japan. They are provisionally named as types VIII–a, IX, and X, though they will be fully described in forthcoming papers. The other one cited in this paper is called type XI; this nauplius was formerly described by Itô [3] as a nauplius of *Hansenocaris pacifica* Itô, 1985. Closer examination has revealed that this form is not the larva of *H. pacifica* but belongs to a separate species, the cypris y stage and the naupliar development of which are to be described elsewhere.

Comments on larval stages and general morphology

To judge from my successful rearing experi-

Accepted May 21, 1987
Received April 22, 1987

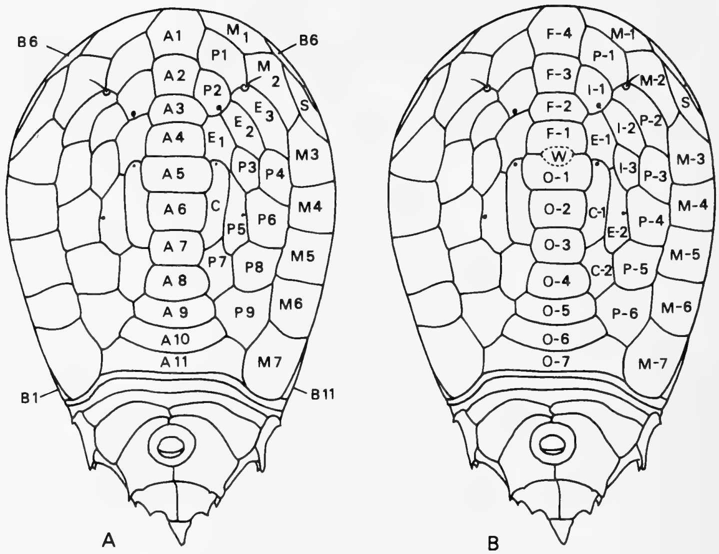

FIG. 1. Diagrams showing relationship between Schram's terminology (A) and new terminology (B) for cephalic-shield plates. The diagram A was redrawn from Schram [2] with permission. Abbreviations— A: axial; B: brim; C: crescentic; E: elongate; F: frontal; I: intercalary; M: marginal; O: occipital; P: polygonal; S: superlateral; W: window.

ments, the number of naupliar stages of facetotectans is typically five. The four naupliar types from Japan cited in the present paper represent the first naupliar stages of four separate species. It is apparent from certain characteristics in the structure of the cephalic shield that the original type IV larva described by Hansen [1] is also the first naupliar stage of a separate species. Characteristics available for identification of each stage will be dealt with elsewhere.

In the present paper the term "cephalic shield" is used to denote a particular dorso-anterior part of integument of the nauplius y larvae. The remainder of the integument is not yet named; I would like to call it "faciotruncal" integument. The border between these two parts is occasionally unclear, especially in a larva at an intermolt phase, so one might doubt the necessity for discriminating the cephalic shield from the faciotruncal integument. However, they are actually separate units of the naupliar integument. After a molting, a nauplius y larva often leaves two partial exuviae; the dome-shaped one with no appendages is the cephalic shield and the other one with appendages is the faciotruncal integument. When a nauplius starts to molt, the cephalic shield splits from the faciotruncal integument except along its rear edge and is pushed up by the emerging body which exits through this anteriorly facing gap. The connection between these two parts of the cast integument is weak and they easily detach from each other; the true contour of the cephalic shield can be clearly determined by examining such a cast one.

TERMINOLOGY

As can be seen in Figure 2 (especially A and E), the cephalic-shield plates principally form almost concentric circles interrupted by a midlongitudinal belt of plates. This latter belt is separated into two parts by a single special plate called "window" (abbreviated as "W"; in the following description, parenthesized symbols represent abbreviated forms of plate names); the plates which form the anterior belt are called "frontal" plates and numbered toward the front (F–1 to F–4), and the plates which form the posterior belt are called "occipital" plates and are numbered toward the

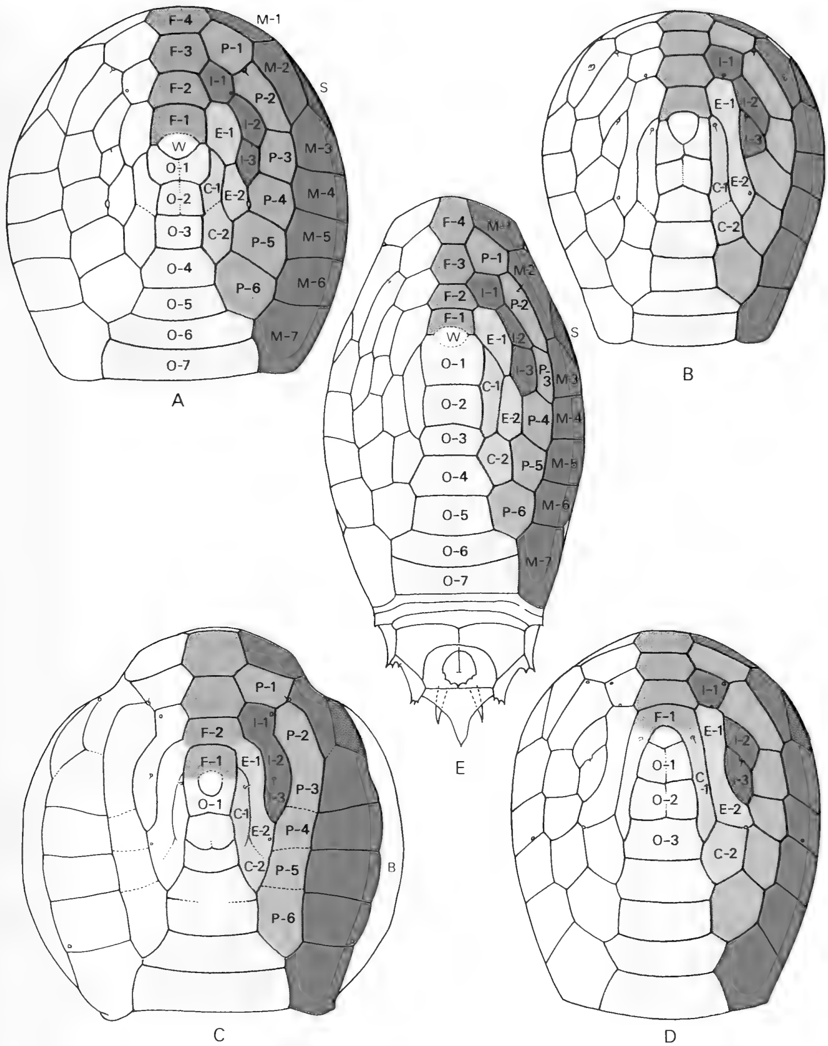

FIG. 2. Diagrams showing cephalic-shield plates of four naupliar types from Japan and Hansen's type IV larva. A: Type X; B: Type IX; C: Type VIII–a; D: Type XI; E: Hansen's type IV (window is not illustrated in the original figure by Hansen). For abbreviations see Fig. 1.

rear (O–1 to O–7). These frontal, window, and occipital plates may all be called "axial" plates (the reason is mentioned later).

The following explanation refers to the plates (or plate groups) of only one half of the cephalic shield, because the plate arrangement is symmetrical about the axials. The plates of all non-axial plate groups are numbered toward the rear.

Two plates which are placed alongside some of the anterior occipitals are called "crescentic" plates (C–1 and C–2). Two plates which are placed antero-lateral to the crescentics are called "elongate" plates (E–1 and E–2). Three plates which are placed antero-lateral to the elongates are called "intercalary" plates (I–1 to I–3). Six plates which border the outer sides of the intercalaries, E–2, C–2, and a few posterior occipitals are called "polygonal" plates (P–1 to P–6). Seven plates which border the outer sides of the polygonals are called "marginal" plates (M–1 to M–7).

There is a triangular plate which wedges itself between M–2 and M–3; it is called the "superlateral" plate (S). The externalmost part of the cephalic shield except for its rear edge (the rear edge of O–7) is called "brim" (B) as a whole (Fig. 2C).

FURTHER EXPLANATION AND DISCUSSION

Schram's "axial" plates (A1 to A11; in Schram's terminology, an abbreviated plate name is represented by a combination of a capital letter and a number with no hyphen between them) accord with the longitudinal belt of frontal, window, and occipital plates of my terminology (cf. Fig. 1A and B). The reason for dividing this simple belt of plates is given below.

With a light microscope we usually observe the cephalic shield which is mounted horizontally on a slide glass in dorsal view, not in frontal (anterior) view. To observe a cast cephalic shield in frontal view is actually impossible. This practical condition causes a difficulty in the observation of anterior plates. In certain nauplii the frontal region is rounded and in normal preparations is situated almost parallel to the line of sight. In such specimens, anterior axial plates appear to be closely appressed and accurate observations of their borders are difficult. This problem is more severe at later developmental stages because their axial plates are changed into numerous smaller plates by division. If Schram's terminology, in which the anteriormost plate is labeled the first axial (A1), were applied to nauplii whose first axial could not be surely ascertained, no axial plate could be confidently labeled, even an easily observable one on the top of the cephalic shield. My system avoids this difficulty because it starts from an easily identifiable plate, namely the window, which is placed almost on the top of the cephalic shield. As already reported by Itô [3], in two types of nauplius y from Tanabe Bay the window is a special plate above the nauplius eye; it is characterized by its smoothness (though partially filled with a mesh-like texture in certain nauplii), whereas other plates are usually not smooth, but of mesh-like texture.

Although the window is usually detectable in the first stage nauplius y larvae as shown in Figure 2, it is possible that we meet unusual nauplii in which the window is not detected. For describing such unusual nauplii the term "axial" in the sense of Schram would be still available and I think it should be reserved. It is also useful as a general term for a context in which there is no necessity to distinguish frontal, window, or occipital plates; in fact, I have already used it in this sense in former paragraphs.

Hansen [1] did not indicate the window in his type IV nauplius, but there is little doubt that it had a window because other similar nauplii have the window (Schram's larva 2 from Akeröya [2]; the nauplius illustrated by Steuer [6] based upon the material from Adriatic Sea). In Figure 2E, I indicate a possible situation of its window with reference to Schram's larva 2 from Akeröya. Schram clearly illustrates the window in his type IV larvae (especially in his Fig. 3E), and also mentions that "a circular platelete is present inside the original axial plate No. 5." The circular platelet (misspelled as "platelete") in his sense accords with the window. However, the window is not always a platelet embraced by A5 (0–1 in my terminology). The window of the type X nauplius is placed medially just between F–1 and O–1 (Fig. 2A), and it would be difficult to say that the window belongs to O–1. In the type IX nauplius (Fig. 2B), O–1 is subdivided with a faint ridge and the window is wedged deeply between the halves. In contrast, the window of the type XI nauplius does not appear to wedge itself deeply into the O–1, which is also subdivided as in type IX. The window of the type VIII–a nauplius is encircled with a single large plate, which seems to be a fusion of F–1 and O–1. Such a fused plate encircling the window can be called a "circum-window" plate.

Of the "crescentic" plates, C–1 is the same as Schram's single "crescentic" plate. However, I call a plate posterior to it the second crescentic (C–2), while Schram calls it "P7", namely the seventh polygonal. The main reason for considering Schram's P7 a "crescentic" plate is that the P7 has a tendency to fuse with the crescentic (cf. Fig. 2A, B, C). Another reason can be understood best in connection with the other polygonals *sensu*

Schram, which are dealt with later.

The first elongate plate (E–1) accords with the homonymic plate (E1) in the sense of Schram, but E–2 is called P5 in Schram's terminology. As can be seen in types IX and XI nauplii (Fig. 2B, D), E1 and P5 *sensu* Schram are fused with each other; hence, I treat P5 as an "elongate" plate. Similarly, P2, E2 and P3 have a tendency to fuse (cf. Figs. 1 and 2) and are regarded as members of the same plate-group. As there is no available name for them in Schram's terminology, the new term "intercalary" is introduced.

Among the intercalary plates of the type XI nauplius, I–2 and I–3 seem to form a unit isolated from I–1 (Fig. 2D). Similar arrangements are also seen in the other nauplii shown in Figure 2; for example, in the type IX nauplius (Fig. 2B), I–2 and I–3 are broadly connected with each other, while the connection between I–1 and I–2 is very narrow. In the intercalary plates, type X and Hansen's type IV nauplii are similar to type IX. In the type VIII–a nauplius, the three intercalary plates are fused with each other, but I–1 is still discernible from the others because the fused plate has a neck which indicates the border between I–1 and I–2.

My concept of the polygonal plates differs greatly from Schram's. Schram's polygonal plates occur as two groups separated by a radial row of three "elongate" plates (Fig. 1A). In types VIII–a and XI nauplii, there is no such radial row of plates; hence, elongate plates in the sense of Schram would be meaningless for these nauplii. Schram numbered the plates within the posterior group of polygonals outwards as he supposed transversal rows. However, such numbering is impossible for types IX, VIII–a and XI nauplii. I find it much more useful to recognize a row of plates which originates from P1 (the same as P–1) and extends posteriorly; thus, Schram's P2, P3, P5, and P7 are abandoned and, instead, a continuous row of six polygonal plates (P–1 to P–6) is formed. In the type VIII–a, five polygonal plates (P–2 to P–6) are almost fused with each other, which demonstrates the usefulness of this grouping.

The marginal (M–1 to M–7) and superlateral plates are the same as the homonymic ones in Schram's terminology. The brim is also the same as the homonymic part in Schram's terminology, though I do not yet recognize any first stage nauplius which has plates within the brim (Fig. 2 and [3]). The brim is usually not seen in dorsal view, but in the type VIII–a larva it is clearly seen even in dorsal view, except for an anterior portion (Fig. 2C).

The type XI nauplius has a peculiar single plate which has two "arms" extending posteriorly alongside the window, O–1, O–2, and O–3 plates (Fig. 2D). There is no doubt that this plate is made by fusion of F–1 and a pair of C–1 plates. A similar plate with two "arms" is present also in the type VIII–a nauplius (Fig. 2C), but it is made of F–2 fused with the E–1 and E–2 plates on each side.

Among the four nauplii from Tanabe Bay shown in Figure 2, the one closest to Hansen's type IV nauplius in the sculpture of the cephalic shield is the type X nauplius, although the proportions of its cephalic shield are greatly different. In contrast to these two similar nauplii, whose cephalic-shield plates may be regarded as the model of the proposed terminology, the other nauplii show various degrees of modification, mainly due to fusion and slight translocation of plates as already mentioned. However, it is important to acknowledge that their modified plates can readily be identified using the proposed terminology. These nauplii may be assumed to be closely related compared with other nauplii whose cephalic-shield sculpture can not be described using this terminology, like the type I nauplii described by Hansen [1] and Schram [7] or the Pacific type I described by Itô [5]. I expect that such similarity and dissimilarity in the fundamental structure of the cephalic-shield sculpture will be reflected in the taxonomy within the Facetotecta in the future.

The proposed terminology, which has been elaborated here specifically for application to the first naupliar stage, is also available for later naupliar stages to a certain extent, although it must be supplemented by other terms. An adaptation of this terminology to later stages will be demonstrated in a forthcoming paper which is in preparation.

ACKNOWLEDGMENT

I would like to express my sincere thanks to Dr. Mark J. Grygier for reviewing the manuscript. This study is supported in part by the Grant-in-Aid for Scientific Research, No. 62540567, from the Ministry of Education, Science and Culture, Japan.

REFERENCES

1 Hansen, H. J. (1899) Die Cladoceren und Cirripedien der Plankton-Expedition. Ergebnisse der Plankton-Expedition der Humboldt-Stifung, 2 (G.d): 1–58, pls. I–IV.

2 Schram, T. A. (1972) Further records of nauplius y type IV Hansen from Scandinavian waters. Sarsia, **50**: 1–24.

3 Itô, T. (1986) Three types of "nauplius y" (Maxillopoda: Facetotecta) from the North Pacific. Publ. Seto Mar. Biol. Lab., **31**: 63–73.

4 Itô, T. (1984) Nauplius y and cypris y (problematic crustacean larvae) from Japan. Zool. Sci., **1**: 1000.

5 Itô, T. (1986) A new species of "cypris y" (Crustacea: Maxillopoda) from the North Pacific. Publ. Seto Mar. Biol. Lab., **31**: 333–339.

6 Steuer, A. (1905) Über eine neue Cirripedien larve aus dem Golfe von Triest. Arb. Zool. Inst. Univ. Wien, **15**: 113–118.

7 Schram, T. A. (1970) On the enigmatical larva nauplius y type I Hansen. Sarsia, **45**: 53–68.

ZOOLOGICAL SCIENCE 4: 919–927 (1987)

Rediscovery of *Heptacarpus jordani* (Rathbun) with Notes on Morphological Variations (Decapoda, Caridea, Hippolytidae)

KEN-ICHI HAYASHI and TOSHIRO CHIBA[1]

Department of Aquaculture and Biology, Shimonoseki University of Fisheries, Shimonoseki, Yamaguchi 759–65, and [1]Kesennuma Municipal Office, Kesennuma, Miyagi 988, Japan

ABSTRACT—*Heptacarpus jordani* (Rathbun) is rediscovered from northern Japan. Based on samples collected during one year from *Zostera* belts, morphological variations and population growth are examined. A part of the key to the Asian species of the genus is revised.

INTRODUCTION

During the survey of the shore fauna in Kesennuma City, Miyagi Prefecture, northern Japan, a considerable number of specimens representing a single species of the hippolytid genus *Heptacarpus* were collected. They belonged to the species group with an epipod on the first three pereopods, and resembled *H. jordani* (Rathbun), reported originally from Hokkaido in 1902 [1], and subsequently from Sagami Bay in 1914 [2], but thereafter no material has been collected [3]. Variations in some important characters of these specimens, however, made the specific identification rather difficult. Thus, three specimens were sent to the Smithsonian Institution, where the holotype was deposited. Direct comparison revealed some discrepancies between them. In order to examine the morphological variability, we collected this species monthly for one year from Hajikami-akedo, near the mouth of Kesennuma Bay. The examination of many specimens proved that the present material represented the rediscovery of *H. jordani* after 70 or 80 years and demonstrated that this species showed considerable morphological variations. Hayashi [3] presented a key to the Asian species of the genus *Heptacarpus,* but it is necessary to revise that of the species group with an epipod on the first three pereopods.

Accepted May 22, 1987
Received September 26, 1986

MATERIALS AND METHODS

Material was collected from three localities at Kesennuma City, Miyagi Prefecture by one of the authors (TC). The monthly collection was made from littoral *Zostera* belts at Hajikami-akedo, just outside of the mouth of the Kesennuma Bay during October, 1983 to September, 1984. The scoop net used there had a 60 cm×60 cm mouth frame and covered with fine net of 6 mm mesh. The intertidal vegetation at a depth of about 0.5–1.0 m at low tide was swept over an area of about 200 m×50 m with this net by hand. Small collections were added from two other localities both facing the Kesennuma Bay: at Tajiri, Oshima Island, where specimens were collected from *Sargassum* belts by another small hand net, and at Nagaiso-hama, the shrimps were obtained from growing cages of the abalone juveniles hanging in the area.

After preservation in 10% neutral formalin, the samples collected prior to October, 1983 were examined morphologically in detail and the other samples were used for studies of morphological variation and of population growth including fecundity, breeding season and recruitment.

The specimen size was represented by the carapace length (cl), from the orbital margin to the posterior end of the carapace. Three specimens (1♂, 2♀) were deposited in the collection of the United States National Museum of Natural History (USNM), and 14 specimens (11♂, 1 ovig. ♀,

2♀) in the Shimonoseki University of Fisheries (SUF). The specimens with the abbreviations in parentheses are deposited in the respective institution. The remaining material without abbreviation is in the private collection of the author (TC).

Hajikami-akedo, Apr. 28, 1971 – 1♀ (SUF); Mar. 6, 1982 – 6♂ (SUF); June 27, 1983 – ♂ (USNM), 4♂ (SUF), 1 ovig. ♀ (SUF), 1♀ (USNM), 2♀ (SUF); Oct. 5, 1983 – 17♂, 41♀; Nov. 19, 1983 – 60♂, 23♀; Dec. 19, 1983 – 43♂, 4 ovig. ♀, 20♀; Jan. 20, 1984 – 21♂, 11 ovig. ♀, 4♀; Feb. 15, 1984 – 12♂, 5 ovig. ♀, 6♀; Mar. 15, 1984 – 13♂, 4 ovig. ♀, 2♀; May 4, 1984 – 2♂, 4 ovig. ♀, 1♀; May 19, 1984 – 6♂, 3 ovig. ♀; June 16, 1984 – 12♂, 2 ovig. ♀, 4♀; July 28, 1984 – 5♂, 2♀, 13 juv.; Aug. 25, 1984 – 2♂, 46♀, 15 juv.; Sept. 22, 1984 – 10♂, 55♀, 6 juv.

Tajiri, Sept. 5, 1982 – 21♀ (USNM); Dec. 12, 1983 – 21♂, 1♀.

Nagaiso-hama, Jan. 14, 1984 – 1♂, 1♀.

RESULTS

Heptacarpus jordani (Rathbun)
(Figs. 1–4)

Spirontocaris jordani Rathbun, 1902, p. 44, fig. 17 [1].
Spirontocaris jordani: Balss, 1914, p. 44 [2].
Heptacarpus jordani: Holthuis, 1947, p. 12 [4].
Heptacarpus jordani: Hayashi, 1979, p. 25 [3].

Diagnosis: Moderate size species (Fig. 1). Females larger than males. Rostrum shorter than carapace, with 5–9 teeth on dorsal margin and 1 or 2 teeth on ventral margin; posterior 1 or 2 dorsal teeth usually situated on carapace (Fig. 2*a*); ventral teeth situated near rostral apex. Carapace smooth, always with antennal spine. Pterygostomial spine usually present in females and present or absent in males (Fig. 2*b*).

Abdomen smooth. Pleuron of fourth somite usually not pointed, but that of fifth somite always pointed (Fig. 2*c*). Telson with 3–6, usually 4, pairs of spines. Posterior margin pointed at middle, flanked by 2, or rarely 3, pairs of spines and 1, or rarely 2, pairs of plumose setae (Fig. 2*d*). These spines and setae sometimes arranged asymmetrically.

First segment of antennular peduncle with 2–6, usually 4, spinules on distal margin. Large spine present on second and third segments (Fig. 2*a*). Mouthparts typical of the genus (Fig. 3). First pereopod rather elongated in mature males.

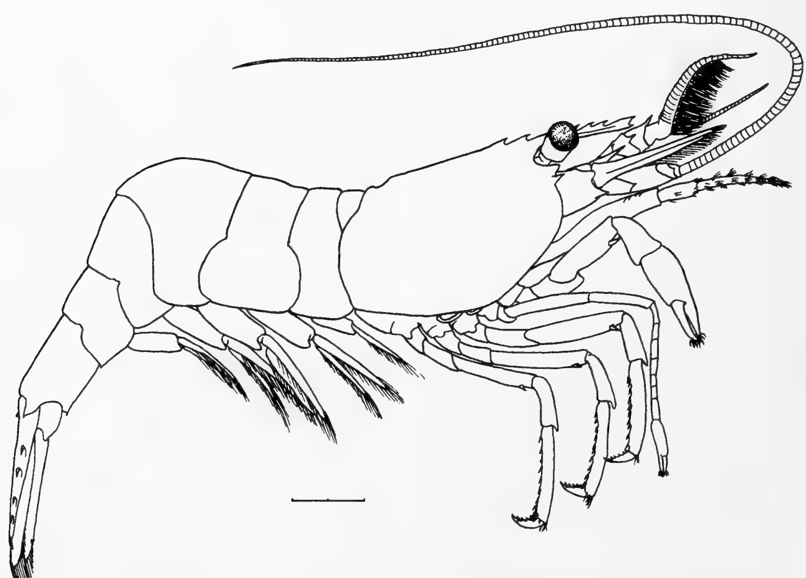

FIG. 1. *Heptacarpus jordani* (Rathbun). Male, 5.0 mm in carapace length. Scale represents 2.0 mm.

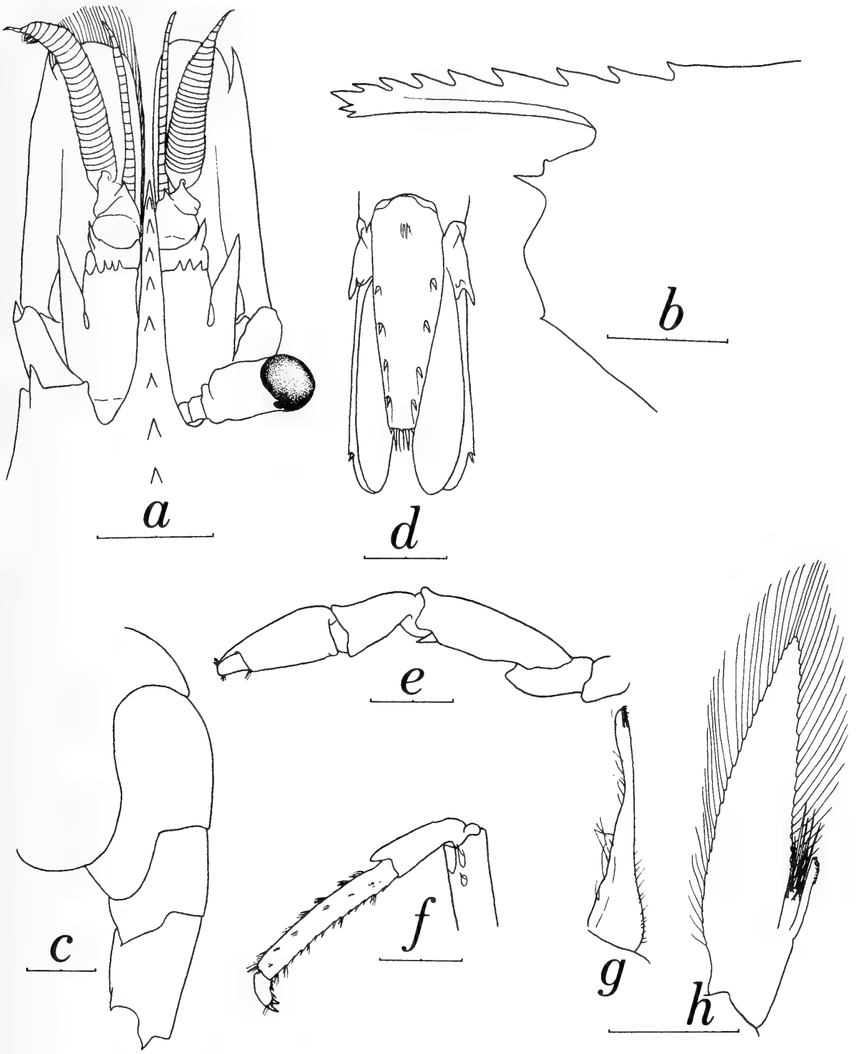

FIG. 2. Body parts of *Heptacarpus jordani* (Rathbun). *a–c,* female, 7.3 mm in carapace length (cl); *d,* female, 7.6 mm in cl; *e, f,* female, 8.9 mm in cl; *g, h,* male, 6.0 mm in cl. *a,* anterior part of body in dorsal view, left eye and setation of right antennal scale removed; *b,* anterior part of carapace in lateral view; *c,* third to sixth abdominal somites; *d,* tail fan, setation of uropods omitted; *e,* first pereopod; *f,* distal four segments of third pereopod; *g,* first pleopod; *h,* endopod of second pleopod. Scales for *a–f* represent 2.0 mm and scale for *g, h* represents 1.0 mm.

Merus usually with a subterminal spine in both sexes (Fig. 2*e*). Meri of last three pereopods with 1–3 spines, usually 2 or 3 spines on third (Fig. 2*f*), 1 or 2 spines on fourth and single spine on fifth pereopod.

Endopod of male first pleopod elongated, distal part slightly broadened with some retinacula (Fig. 2*g*). Appendix masculina on male second pleopod shorter than appendix interna, with many long stiff setae (Fig. 2*h*).

The live individuals are unicolored, without stripes or bands, but rather variable from light-brown to dark-brown or dark green. In general the color merges into the habitats, from which they were collected, and is lighter in males than in females. The antennal flagella are always light

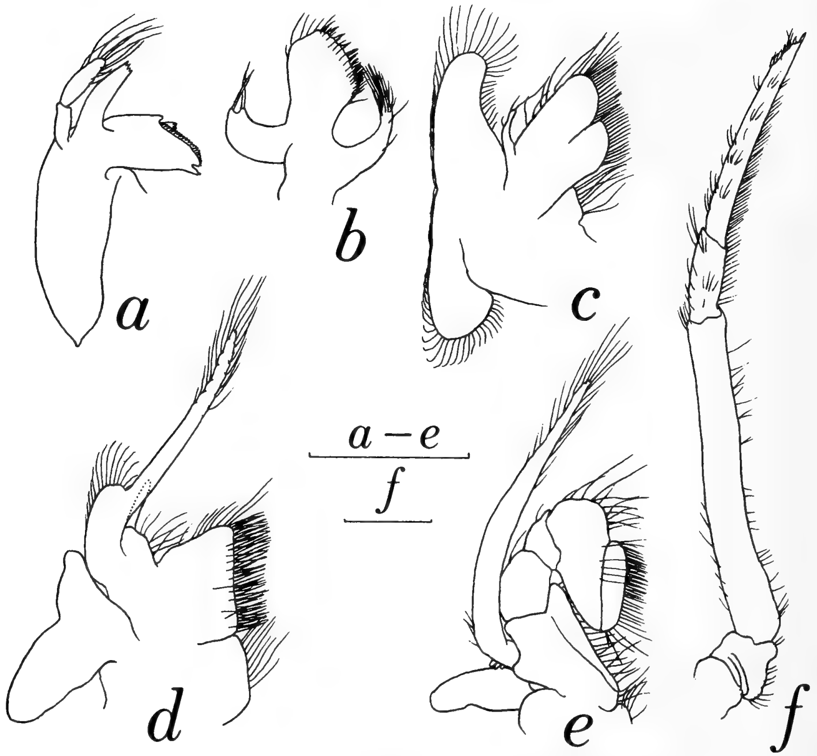

FIG. 3. Mouthparts of *Heptacarpus jordani* (Rathbun). Male, 4.3 mm in carapace length. *a,* mandible; *b,* first maxilla; *c,* second maxilla; *d,* first maxilliped; *e,* second maxilliped; *f,* third maxilliped. Scales represent 1.0 mm.

TABLE 1. Variations in rostral formulae of *Heptacarpus jordani* (Rathbun)

Rostral formula (dorsal/ventral)	No. of specimens		
	Male (%)	Female (%)	Juvenile (%)
6/0	0	1 (0.4)	0
10/1	1 (0.5)	0	0
9/1	5 (2.4)	15 (6.5)	0
8/1	96 (45.3)	100 (43.3)	2 (5.9)
7/1	99 (46.7)	85 (36.8)	14 (41.2)
6/1	9 (4.2)	18 (7.8)	15 (44.1)
5/1	0	0	3 (8.8)
9/2	0	1 (0.4)	0
8/2	2 (0.9)	7 (3.0)	0
7/2	0	3 (1.3)	0
6/2	0	1 (0.4)	0
Total	212	231	34

brown and the distal parts of the posterior pereopods are somewhat lighter than the other parts of body.

Variations: A total of 495 specimens, 217 males, 244 females including 34 ovigerous females and 34 juveniles, were examined for morphological variations of some important characters. They showed considerable variations and differed partly from the holotype.

The carapace length of the largest specimens was 6.2 mm in male and 10.2 mm in female. The ovigerous females were 6.1–8.6 mm in cl.

The variations in the rostral formulae are shown in Table 1. The combination of 7 or 8 dorsal with 1 ventral teeth was common in both sexes, more than 90% in males and 80% in females, but the juveniles had commonly 6 or 7 dorsal teeth.

Appearance of spines on the pterygostomial angle varied with sexes (Table 2). The juveniles were all provided with a spine on both sides. The females were also provided with the spine in most

TABLE 2. Presence or absence of a spine on pterygostomial angle, fourth abdominal pleuron and merus of first pereopod of *Heptacarpus jordani* (Rathbun)

	No. of specimens								
	Pterygostomial angle			Fourth abdominal pleuron			Merus of first pereopod		
	Male (%)	Female (%)	Juv. (%)	Male (%)	Female (%)	Juv. (%)	Male (%)	Female (%)	Juv. (%)
Present on both sides	76 (35.0)	208 (85.3)	34 (100)	2 (0.9)	18 (7.3)	1 (2.9)	202 (94.4)	234 (95.9)	30 (100)
Present on one side	21 (9.7)	32 (13.1)	0	10 (4.6)	21 (8.6)	6 (17.7)	9 (4.2)	9 (3.7)	0
Absent on either side	120 (55.3)	4 (1.6)	0	205 (94.5)	206 (84.1)	27 (79.4)	3 (1.4)	1 (0.4)	0
Total	217	244	34	217	245	34	214	244	30

TABLE 3. Variations of dorsal spines on telson and marginal spinules on first antennular segment of *Heptacarpus jordani* (Rathbun)

Spines or spinules	No. of specimens					
	Telson			Antennular peduncle		
	Male	Female	Total (%)	Male	Female	Total (%)
6–6	0	2	2 (0.5)	—	—	
6–5	—	—		1	2	3 (0.6)
6–4	—	—		3	4	7 (1.4)
5–5	3	4	7 (1.6)	23	19	42 (8.5)
5–4	25	24	49 (11.2)	60	61	121 (24.4)
5–3	1	0	1 (0.2)	4	6	10 (2.0)
4–4	150	185	335 (76.5)	93	87	180 (36.4)
4–3	9	27	36 (8.2)	26	46	72 (14.5)
4–2	1	1	2 (0.5)	1	0	1 (0.2)
3–3	2	3	5 (1.1)	5	37	42 (8.5)
3–2	1	0	1 (0.2)	1	12	13 (2.6)
3–1	—	—		0	1	1 (0.2)
2–2	—	—		0	3	3 (0.6)

In asymmetrical number of spines or spinules, the arrangement does not precisely represent the side of the actual specimen.

specimens, and it was restricted to one side only in 32 specimens (13.1%) or entirely absent on both sides in 4 specimens (1.6%). On the other hand, the males may have a tendency to lose this spine with growth. More than half of the males examined had no spine on either side. Nearly 16% of males less than 3.9 mm in cl had no spine, but this ratio increased to 42% at 4.0–4.4 mm, 62% at 4.5–4.9 mm and finally 76% in those larger than 5.0 mm in cl.

The pleural spine on the fourth abdominal somite was rather variable (Table 2), but usually absent in most specimens (88%) that showed no sexual dimorphism.

In most specimens of both sexes, the merus of the first pereopod was provided with a single subterminal spine on both sides in more than 95%. A few, only 3 males and 1 female, had no such spine on either side (Table 2).

The spines on the telson, usually 4 pairs, were rather variable from 2 to 6 spines, which were usually paired or sometimes asymmetrically arranged (Table 3).

The first antennular peduncle was provided with 1 to 6 marginal spinules on one side, and usually with 4 spinules but 3 or 5 spinules were also observed in considerable ratio (Table 3).

The outer spines on the meri of the last three pereopods were 1 to 4, usually 2 or 3, on third, 1 to 3, usually 1 or 2, on fourth and usually 1 spine on fifth pereopod.

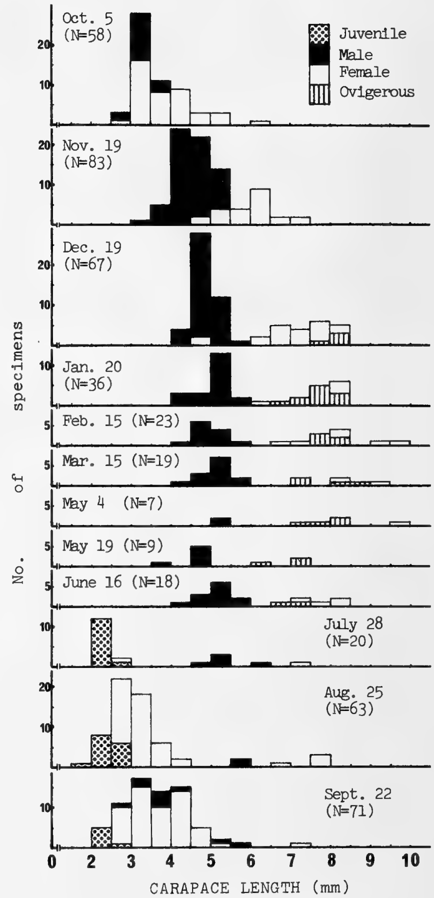

FIG. 4. Carapace length composition of *Heptacarpus jordani* (Rathbun) collected from *Zostera* belts at Hajikami-akedo, Kesennuma City during the period from October 1983 to September 1984.

Biology: The carapace length composition of *H. jordani* collected monthly from Hajikami-akedo during October, 1983 to September, 1984 is shown in Figure 4. The ovigerous females appeared first in December and the ratio of them to the adult females was 18%. This value rapidly increased to more than 70% in January and the high percentage continued to May, except February. The breeding season ended in June.

The new recruits, 1.9–2.6 mm in cl, appeared from July to September. The male is distinguished by the differentiation of the appendix masculina when they grew up to 2.7 mm in cl. Sexual size differences already appeared in September, though not large. After then animals gradually grew up and the differences became conspicuous. The mean carapace length attained 6.0 mm in females and 4.5 mm in males in November. The males attained about 5.0 mm in January, while the females continued to grow until February, in which they were as large as 8.0 mm. The largest male was 6.2 mm in cl and nearly the same size as the smallest ovigerous female. From December to early May the sexual size differences attained 2.6 to 3.0 mm. In late May the larger animals of both sexes disappeared and the mean size value decreased considerably. The males recovered the value in June or July, when the females, however, were nearly 1.0 mm smaller than those in early

May. The female-male ratio varied from month to month and the male dominated from November to June, except February and early May.

Based on 11 ovigerous females (6.1–8.2 mm in cl), 6 collected in January, 1 in May and 4 in December, number of eggs and egg size were examined. The total number of eggs of these females was counted, and 10 eggs selected at random from each ovigerous female were measured the long and short diameters with the micrometer.

Two specimens less than 7.0 mm in cl bore only 350 and 653 eggs, respectively. The remaining 9 specimens, more than 7.4 mm in cl, bore 866–1111 (mean 991) eggs. The log of egg numbers shows a significant linear correlation with the log of the carapace length of the female ($p<0.05$). The fitted regression equation is given by $E=5.4049L^{2.507}$ ($r=0.68$), where E is number of eggs and L is the carapace length of the mother shrimp in mm.

The short diameter was 0.58–0.72 (mean 0.64 ± 0.03) mm, and became slightly larger in eggs incubated in large number. The long diameter was 0.70–0.98 (mean 0.83 ± 0.06) mm, and became larger in the advanced developmental stages, though the short diameter did not change during developmental stages.

Other shrimps collected together with *H. jordani* were the following eight species; *Heptacarpus futilirostris, H. grebnitzkii, Eualus leptognathus, E. sinensis, Spirontocaris ochotensis, Pandalus prensor, Crangon affinis,* and *Metacrangon angusticauda. H. jordani* and *H. grebnitzkii* were the dominant shrimps in littoral vegetations at the present research fields.

DISCUSSION

Dr. Fenner A. Chace, Jr. of the Smithsonian Institution examined the holotype and compared it with a part of the present material. The holotype is a large female, 9.2 mm in cl, and shows differences in two important characters from most specimens of the present material. The meral spine on the first pereopod has been thought to be one of the key characters in the genus *Heptacarpus* and used to separate two related species from each other, such as absent in *H. futilirostris,* while present in *H. rectirostris* [5]. This character, however, varies slightly in the present species as stated previously. More than 95% of the specimens have a single such spine, but the holotype has no spine on either side as in 4 specimens of the present material.

The pleural spine on the fourth abdominal somite is present on both sides in the holotype, though nearly 90% of the samples have no spine. Similar differences were shown in the case of *H. commensalis* [3].

With regard to these two points, no specimens showing the combination of characters noted in the holotype were found among nearly 500 specimens examined. The holotype, therefore, seems to be a rather aberrant form. There are no other distinct discrepancies between the holotype and the present specimens.

The breeding season of this species was mainly in the winter and spring, like the most Japanese members of this genus [6–10] and the related genus *Eualus* [11], and *H. pictus* from the East Pacific Ocean [12]. Judging from the breeding season and the carapace length distribution, the life span of this species is thought to be 12 months at Kesennuma area. In comparison with other species the ovigerous females were rather scarce, which may indicate that spawning or releasing larvae takes place in deeper waters. Two peaks of the ovigerous season, which were observed in *H. pandaloides* at Ishinomaki Bay (Kurata [6] as *H. propugnatrix*) were not apparent in the present species.

H. jordani bears an epipod on all maxillipeds and the first three pereopods. This character is shared with five Asian species: *H. commensalis, H. futilirostris, H. grebnitzkii, H. minutus* and *H. rectirostris*. The most striking feature, by which *H. jordani* is separated from five other species, is the presence of 3–5, usually 4, marginal spinules on the first antennular segment. A single spinule is present in *H. commensalis, H. futilirostris* and *H. rectirostris* and 2 spinules in *H. grebnitzkii,* though the spination is uncertain in *H. minutus*.

Of these six species the rostral formulae differ markedly in *H. minutus* with many ventral teeth, and the arrangement differs in *H. grebnitzkii* by having dorsal and ventral teeth restricted in the central or proximal part. *H. jordani* is similar to

the three other species in number and arrangement of the teeth.

In *H. futilirostris* males are much larger than females but in *H. commensalis, H. grebnitzkii* and *H. rectirostris* females are larger than males like the present species. The sexual size difference of *H. minutus* is uncertain, because it has been known from the male holotype only. *H. commensalis* is much smaller than the other species, only 3.3 mm in cl of the ovigerous female.

In view of the morphological variations of *H. jordani,* it is necessary to partly revise the key to the Asian species of the genus. The following key to the Asian *Heptacarpus* species with an epipod on all maxillipeds and the first three pereopods is offered to modify the couples after couplet 5 of the key adopted by Hayashi [3].

5 Rostrum longer than carapace, with 6 teeth on dorsal margin and 7 teeth on ventral margin. First pereopod without meral spine. Pleuron of fourth abdominal somite without spine. .... *H. minutus* (Yokoya)

5 Rostrum with fewer than 4 teeth on ventral margin. 6

6 Rostrum longer than or as long as carapace. 2–4 teeth present on central part of ventral margin. First antennular peduncle with 2 spinules. First pereopod with meral spine. Pleuron of fourth abdominal somite without spine. Males smaller than females. .... *H. grebnitzkii* (Stimpson)

6 Ventral rostral teeth present distally. 7

7 First antennular peduncle with 3–5 marginal spinules. Rostrum shorter than carapace, with 7–8, rarely 6 or 9, teeth on dorsal margin and 1 or 2 teeth on ventral margin. First pereopod usually with meral spine, but rarely absent. Pleuron of fourth abdominal somite usually without spine. Males smaller than females. .... *H. jordani* (Rathbun)

7 First antennular peduncle with single marginal spinule. 8

8 First pereopod with meral spine. Pleuron of fourth abdominal somite with spine. Rostrum with 5–6 teeth on dorsal margin and 3–4 teeth on ventral margin. Males smaller than females. .... *H. rectirostris* (Stimpson)

8 First pereopod without meral spine. 9

9 Body large. Rostrum shorter than carapace. Mature males larger than females with elongated third maxilliped and strengthened first pereopod. Free living, usually in coastal weed belts.................... *H. futilirostris* (Bate)

9 Body small. Rostrum as long as or longer than carapace. Mature males smaller than females and any thoracic appendages neither elongated nor strengthened. Usually commensal with littoral coelenterates. .... *H. commensalis* Hayashi

ACKNOWLEDGMENTS

We wish to express our gratitude to Dr. Fenner A. Chace, Jr., of the Smithsonian Institution for examining the holotype of *Spirontocaris jordani* Rathbun and comparing it with a part of our material, as well as critical reading of the manuscript. We are indebted to Mr. H. Onodera of the Hashikami Fisheries Cooperative Association for collecting the shrimps at Nagaiso-hama.

REFERENCES

1 Rathbun, M. J. (1902) Japanese stalk-eyed crustaceans. Proc. U.S. Nat. Mus., **26**: 23–55.

2 Balss, H. (1914) Ostasiatische Decapoden. II. Die Natantia und Reptantia. Abh. Bayer Akad. Wiss., Suppl. **2** (10): 1–101, pl. 1.

3 Hayashi, K. (1979) Studies on hippolytid shrimps from Japan—VII. The genus *Heptacarpus* Holmes. J. Shimonoseki Univ. Fish., **28**: 11–32.

4 Holthuis, L. B. (1947) The Decapoda of the Siboga Expedition. Part IX. The Hippolytidae and Rhynchocinetidae collected by the Siboga and Snellius Expeditions with remarks on other species. Siboga Exped. Monogr., **39a**[8]: 1–100.

5 Miyake, S. and Hayashi, K. (1968) Studies on hippolytid shrimps from Japan—IV. Two allied species, *Heptacarpus rectirostris* (Stimpson) and *H. futilirostris* (Bate), from Japan. J. Fac. Agr. Kyushu Univ., **14**: 432–447.

6 Kurata, H. (1963) Ecology of shrimps on eel-grass bed. I. *Spirontocaris propugnatrix.* Bull. Hokkaido Reg. Fish. Res. Lab., **26**: 81–85.

7 Kurata, H. (1968) Larvae of Decapoda Natantia of Arasaki, Sagami Bay—II. *Heptacarpus futilirostris* (Bate) (Hippolytidae). Bull. Tokai Reg. Fish. Res. Lab., **55**: 253–258.

8 Kurata, H. (1968) Larvae of Decapoda Natantia of Arasaki, Sagami Bay—III. *Heptacarpus geniculatus* (Stimpson) (Hippolytidae). Bull. Tokai Reg. Fish.

Res. Lab., **56**: 137–142.

9 Yamashita, K. and Hayashi, K. (1979) Larvae of Decapoda Macrura in the vicinity of Miyazima, the Seto Inland Sea, I. *Heptacarpus rectirostris* (Caridea, Hippolytidae). Proc. Jap. Soc. Syst. Zool., **17**: 45–51.

10 Yamashita, K. and Hayashi, K. (1980) Larvae of Decapoda Macrura in the vicinity of Miyazima, the Seto Inland Sea, II. *Heptacarpus pandaloides* (Stimpson) and *H. geniculatus* (Stimpson) (Caridea, Hippolytidae). Proc. Jap. Soc. Syst. Zool., **19**: 16–23.

11 Oya, F. and Oka, K. (1985) Growth and breeding ecology of the hippolytid shrimp *Eualus sinensis* (Yu). Zool. Sci., **2**: 257–263.

12 Bauer, R. T. (1976) Mating behavior and spermatophore transfer in the shrimp *Heptacarpus pictus* (Stimpson) (Decapoda: Caridea: Hippolytidae). J. Nat. Hist., **10**: 415–440.

ZOOLOGICAL SCIENCE 4: 929–931 (1987)

[COMMUNICATION]

In Vitro Synthesis of Connectin in an Extract of Chicken Embryo Muscles

Atsushi Asakura[1,2], Yoichi Nabeshima[2] and Koscak Maruyama[2,3]

[1]*Department of Biochemistry, Cancer Institute, Japanese Foundation for Cancer Research, Toshima-ku, Tokyo 170, and* [2]*Department of Biology, Faculty of Science, Chiba University, Chiba 260, Japan*

ABSTRACT—Incorporation of ^{35}S-methionine into connectin during protein synthesis in an extract from chicken embryo muscles was detected by autoradiography after immunoprecipitation with anti-connectin antibodies followed by SDS gel electrophoresis. Any radioactivity of peptides smaller than connectin but larger than actin was not detected with anti-connectin antibodies reacted samples. On the other hand, incorporation of radioactive methionine into nebulin was not observed.

INTRODUCTION

Connectin (also called titin) is a very long, elastic filamentous protein of striated muscle and its MW is estimated as huge as 2.8 million from SDS gel electrophoresis mobility (cf. review [1]). Whether connectin is comprised of a single peptide or not has as yet remained uncertain. In the present study, it was attempted to observe *in vitro* synthesis of connectin by the incorporation of ^{35}S-methionine in a chick embryo muscle extract. Autoradiography of anti-connectin antibodies reacted sample revealed a faintly radioactive band corresponding to connectin.

MATERIALS AND METHODS

Breast muscles from five chick embryos incubated for 15 days were gently homogenized in an equal volume of cold salt solution containing 0.25 M KCl, 10 mM $MgCl_2$, 6 mM 2-mercaptoethanol and 10 mM Tris-HCl buffer, pH 7.4. The homogenate was centrifuged for 7 min at 7,000×*g*, and the supernatant was subjected to Sephadex G–25 column (1×15 cm), using the salt solution as elutant. Amino acid free protein-rich fractions including polysomes were collected for protein synthesis assay [2].

A reaction mixture, 0.2 ml, containing muscle extract, 0.15 M KCl, 10 mM $MgCl_2$, 6 mM 2-mercaptoethanol, 0.25 mM GTP, 2 mM ATP, 4 mM creatine phosphate, 10 μg creatine kinase, 40 μM amino acid mixture (minus Met), 200 μCi ^{35}S-Met (NEN Research Products) and 10 mM Tris-HCl, pH 7.4, was incubated for 1 hr at 37°C [2]. After incubation, 40 μl of the reaction mixture was treated with 20 μl of affinity chromatographed anti-β-connectin antibodies [3], anti-nebulin [3] and also non immune IgG for 1.5 hr at room temperature followed by the incubation with 20 μl of Affi-Gel Protein A (Bio Rad) for 1.5 hr at room temperature [4]. The precipitate was washed 5 times with a solution of 0.5 M NaCl and 20 mM Tris-HCl buffer, pH 7.5. The precipitate was added with an SDS solution (final concentrations, 5% SDS, 20 mM DTT, 5 mM EDTA, and 50 mM Tris-HCl, pH 6.7) and heated for 2 min at 100°C. A portion of the total reaction mixture and also a piece of adult chicken breast muscle, were also treated with SDS. SDS gel electrophoresis was carried out according to Laemmli [5] using 2.5%

Accepted June 16, 1987
Received June 3, 1987
[3] To whom reprint requests should be addressed.

polyacrylamide for stacking gel and 4.5% polyacrylamide for separation gel. The gel stained with Coomassie Brilliant Blue was incubated with a scintilating agent EN^{3}NANCE (NEW Research Products) for 30 min, washed with distilled water and dried. Fluorography was carried out for 7 days at −80°C.

RESULTS AND DISCUSSION

Figure 1 shows autoradiograms of a chicken embryo muscle extract incubated with radioactive methionine. In the whole mixture, strong radioactivity was recognized at the top of the gel, unknown band lower than nebulin, myosin, and other smaller proteins (Fig. 1c). In the Coomassie Brilliant Blue stained gel, bands corresponding to connectin and nebulin were very faint, if any (Fig. 1b). A strong radioactive band near nebulin (Fig. 1c) was significantly lower than the nebulin band (Fig. 1a). Furthermore, anti-nebulin antibodies precipitated sample did not show any radioactivity at the nebulin band (Fig. 1d). On the other hand, in the anti-connectin antibodies precipitated sample, faint but significant radioactivity was recognized in the connectin band (Fig. 1e). This radioactive band was not detected with anti-nebulin antibodies (Fig. 1d) and non immune IgG (Fig. 1f) precipitated samples. It is to be noted that strong radioactivities detected in the lower fronts of Figure 1d, e, f, might be due to contaminant proteins of low molecular weight, e.g. actin, that could not be washed out.

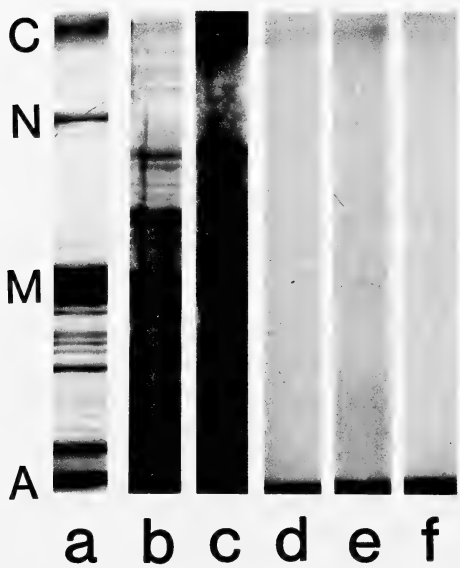

FIG. 1. Incorporation of ^{35}S-methionine into connectin synthesized *in vitro* in chicken embryo muscle extract. For conditions and method of detection, see text.

(a) Coomassie Brilliant Blue stained whole sample of adult chicken breast muscle. C, connectin; N, nebulin; M, myosin heavy chain; A, actin.
(b) Coomassie Brilliant Blue stained whole sample of embryo muscle extract after incubation.
(c) Autoradiogram of the whole sample.
(d) Autoradiogram of the anti-nebulin antibodies precipitated fraction.
(e) Autoradiogram of the anti-connectin antibodies precipitated fraction.
(f) Autoradiogram of the non-immune IgG precipitated fraction.

A trial to prepare mRNA for connectin from chick neonatal muscles was unsuccessful. This was very probably due to breakdown of very long mRNA during preparation procedures. Therefore, an embryo muscle extract containing polysomes for connectin was prepared and its *in vitro* translation was demonstrated in the present study. However, the extent of radioactive methionine incorporation was very low. This is not surprising because of breakdown of the mRNA even during a gentle homogenization of muscle tissues. It is to be mentioned that there were not any radioactive peptides smaller than connectin but larger than actin (Fig. 1e). This suggests that a large peptide of connectin is synthesized *in vivo* [cf. 6].

At present the largest mRNA encoding a muscle protein is that of Duchenne dystrophy gene and its size is 14 kb corresponding to a protein of MW of half a million [7]. Cloning of connectin gene will give a final answer to the nature of this gigantic protein.

REFERENCES

1 Maruyama, K. (1986) Int. Rev. Cytol., **104**: 81–114.
2 Heywood, S. M., Dowben, R. M. and Rich, A. (1967) Proc. Natl. Acad. Sci., **57**: 1002–1009.
3 Sugita, H., Nonaka, I., Itoh, Y., Asakura, A., Hu, D. H., Kimura, S. and Maruyama, K. (1987) Proc.

Jap. Acad., **63B**: 107–110.

4 Olliver, C. L. and Boyed, C. D. (1984) Methods Mol. Biol., **2**: 157–160.

5 Laemmli, U. K. (1970) J. Biol. Chem., **244**: 4406–4412.

6 Yoshidomi, H., Ohashi, K. and Maruyama, K. (1985) Biomed. Res., **6**: 207–212.

7 Monaco, A. P., Neve, R. L., Colletti-Feeper, C., Bertelson, C. J., Kurnit, D. M. and Kunkel, L. M. (1986) Nature, **223**: 646–650.

Development Growth & Differentiation

Published by

the Japanese Society of Developmental Biologists

Papers in Vol. 29, No. 5. (October 1987)

Development, Growth and Differentiation (ISSN 0012–1592) is published bimonthly by The Japanese Society of Developmental Biologists, Department of Biology, School of Education, Waseda University, Tokyo 160, Japan. 1987: Volume 29. Annual subscription U. S. $ 110.00 including air speed delivery except Japan. Application to mail at second class postage rate is pending at Jamaica, NY 11431, U. S. A.

Outside Japan: Send subscription orders and notices of change of address to Academic Press, Inc., Journal Subscription Fulfillment Department, 6277 Sea Harbor Drive, Orlando, FL 32887, U. S. A. Send notices of change of address at least 6–8 weeks in advance. Please include both old and new addresses. U. S. A. POSTMASTER: Send changes of address to *Development, Growth and Differentiation,* Academic Press. Inc., Journal Subscription Fulfillment Department, 6277 Sea Harbor Drive, Orlando, FL 32887, U. S. A.

In Japan: Send nonmember subscription orders and notices of change of address to Business Center for Academic Societies Japan, 16–3, Hongo 6-chome, Bunkyo-ku, Tokyo 113, Japan. Send inquiries about membership to Business Center for Academic Societies Japan,4–16, Yayoi 2-chome, Bunkyo-ku, Tokyo 113, Japan.

Air freight and mailing in the U. S. A. by Publications Expediting, Inc., 200 Meacham Avenue, Elmont, NY 11003, U. S. A.

(*Contents continued from back cover*)

ZOOLOGICAL SCIENCE

VOLUME 4 NUMBER 5 **OCTOBER 1987**

CONTENTS

(*Contents continued on inside back cover*)

INDEXED IN:
Current Contents/LS and AB & ES,
Science Citation Index,
ISI Online Database,
CABS Database

Issued on October 15
Printed by Daigaku Printing Co., Ltd.,
Hiroshima, Japan

ISSN 0289-0003

ZOOLOGICAL SCIENCE

An International Journal

Proceedings of the Fifty–Eighth Annual Meeting of the Zoological Society of Japan

October 7–9, 1987
Toyama

Vol. 4 No. 6 December 1987

published by Zoological Society of Japan

distributed by Business Center for Academic Societies Japan
VNU Science Press BV, Utrecht, The Netherlands

ZOOLOGICAL SCIENCE

The official Journal of the Zoological Society of Japan

ZOOLOGICAL SCIENCE is devoted to publication of original articles, reviews and communications in the broad field of Zoology. The journal was founded in 1984 as a result of unification of Zoological Magazine (1888–1983) and Annotationes Zoologicae Japonenses (1897–1983), the former official journals of the Zoological Society of Japan. ZOOLOGICAL SCIENCE appears bimonthly. An annual volume consists of six numbers of more than 1000 pages including an issue containing abstracts of papers presented at the annual meeting of the Zoological Society of Japan.

MANUSCRIPTS OFFERED FOR CONSIDERATION AND CORRESPONDENCE CONCERNING EDITORIAL MATTERS should be sent to:

Dr. Seiichiro Kawashima, Managing Editor, Zoological Science, Zoological Institute, Faculty of Science, Hiroshima University, 1–1–89 Higashisenda-machi, Naka-ku, Hiroshima 730, Japan, in accordance with the instructions to authors which appear in the first issue of each volume. Copies of Instructions to Authors will be sent upon request.

SUBSCRIPTIONS. ZOOLOGICAL SCIENCE is distributed free of charge to the members, both domestic and foreign, of the Zoological Society of Japan. To non-member subscribers within Japan, it is distributed by Business Center for Academic Societies Japan, 6–16–3 Hongo, Bunkyo-ku, Tokyo 113. Subscriptions outside Japan should be ordered from the sole agent, VNU Science Press BV, Europalaan 93, 3526 KP Utrecht, (postal address; P. O. Box 2093, 3500 GB Utrecht), The Netherlands. Subscription rates will be provided on request to these agents. New subscriptions and renewals begin with the first issue of the current volume.

[Publication of Zoological Science has been supported in part by a Grant-in-Aid for Scientific Publication from the Ministry of Education, Science and Culture, Japan.]

ZOOLOGICAL SCIENCE 4: 933–944 (1987)

REVIEW

Rectal Gland and Crypts of Lieberkühn: Is There a Phylogenetic Basis for Functional Similarity?

CHRISTOPHER A. LORETZ

Department of Biological Sciences, State University of New York at Buffalo, Buffalo, New York 14260, U.S.A.

INTRODUCTION

Clinicians are surely familiar with the debilitating and potentially fatal effects of intestinal malabsorption, especially secretory diarrhea. Secretory diarrhea can result from a variety of causes, all of which produce active fluid secretion to override the fluid absorption which normally occurs. The ultimate cause may be exogenous like enterotoxins (e.g., cholera toxin) of bacterial origin, or endogenous, such as hormone-secreting tumors (e.g., vasoactive intestinal peptide-(VIP-)oma in pancreatic cholera syndrome) or choleric enteropathy where, because of insufficient enterohepatic recycling, bile salts pass into the colon [1–6]. In many such cases, these agents act through the same intracellular mediators, for example, causing an elevation of cyclic AMP and the subsequent stimulation of active Cl^- secretion [1–6]. The secretory flux of Cl^- (and Na^+) draws water into the intestinal lumen, thereby producing the diarrhea. The loss of this fluid brings about the profound dehydration requiring clinical care. Physiologists appreciate the complexity of the simultaneous absorptive and secretory processes at the intestinal epithelium which contribute in their balance to the net overall Na^+ and Cl^- fluxes. In recent years, considerable attention and experimental ingenuity have been directed toward localizing and understanding these transport processes and their control. The list of hormonal and other mediators implicated in the regulation of gastrointestinal function is extensive [3, 7]. Many of these agents have multiple actions, including effects on the absorptive and secretory components of ion and water transport, intestinal vascular flow, and general intestinal smooth muscle tone (e.g., [3]).

For the physiologist studying ion transport, the simultaneous operation of absorptive and secretory mechanisms can confound even baseline transport studies on untreated tissues. Animal models with simpler transport schemes, perhaps involving only absorptive or secretory components, are useful in the study of particular aspects of intestinal ion transport and its control.

Although the intestinal epithelium is simple in the histological sense, its mixed cell composition and folding to produce villi and crypts seem more reflective of its multifunctional role in the organism [8, 9]. The intestinal epithelium of mammals (and most vertebrate classes) is arranged in a series of folds which involve the lamina propria (referred to as villi), or additionally the muscularis mucosae and submucosa (referred to as the plicae circulares or rings of Kerckring); the latter may, in fact, have a villous covering. There are also glandular pits penetrating into the underlying lamina propria of the mucosa, or even into the submucosa. There may occur submucosal glands (Brunner's glands), restricted in their distribution to the duodenum, as well as mucosal glands (crypts of Lieberkühn) which are found throughout the small intestine and colon. The villi and crypts are distinct in their

Received August 1, 1987

histology. In addition to the abundant absorptive cells and somewhat less abundant mucus cells common to most regions of intestinal epithelium, the crypts also contain Paneth cells and enterochromaffin/argentaffin cells. The Paneth cells, with their apical secretory granules, secrete lysozyme which serves a protective role through its ability to digest the cell coat of potentially harmful intestinal bacteria [8]. The enterochromaffin cells are endocrine cells of the gastroenteropancreatic series which can be individually identified by immunocytochemical staining [7]. In mammals, the crypts are also the site of active mitosis to regenerate the epithelial cells lost following their normal migration from the crypts to the villus tips. The segregation of the epithelium into villar and crypt regions with these subtleties of cell distribution invites speculation regarding the distribution of function.

REGIONAL SEGREGATION OF NaCl TRANSPORT FUNCTION

With respect to Na^+ and Cl^- transport, the villar and crypt regions have been characterized functionally based on several lines of experimental evidence. Osmotic shock to damage the villar portion of the jejunum did not diminish the secretory response to cholera toxin, suggesting a secretory function for crypt epithelium [10]. Cholera toxin exposure on the luminal side inhibits NaCl absorption very rapidly but net secretion is stimulated only after a longer delay, consistent with diffusion of toxin into the crypts [11]. Welsh *et al.* [12], using a visual technique, showed for the rabbit colon that the crypts are the site of active fluid secretion. When colonic tissue covered with paraffin oil was stimulated with PGE_2, the secreted fluid appeared as droplets only over the crypt duct openings. Weiser and Quill [13] reported greater increases in adenylate cyclase activity in isolated villus cells compared with crypt cells following exposure to cholera toxin; although these experimenters conclude correctly that the major adenylate cyclase response is at the villus, this finding does not address directly the issue of the location of ion transport systems. Field and coworkers [14] reported the intriguing finding that cyclic AMP reduced net Na^+ and Cl^- absorption by the winter flounder (*Pseudopleuronectes americanus*) intestine but did not stimulate the active Cl^- secretion characteristic of mammalian small intestine and colon. Similar data have been reported for two additional species, the flounder (*Platichthys flesus*; [15, 16]) and the goby (*Gillichthys mirabilis*; [17, 18]). Field *et al.* [14] related these data to the well documented absence in fish intestine of crypts of Lieberkühn ([19]; Figs. 1A, B and 2), consistent with the notion that active secretion originates in the crypts.

The absence of crypts, and also of active fluid secretion, in fish intestine is physiologically significant. Active Cl^- secretion along the length of the fish intestine would be maladaptive in both seawater and fresh water. Seawater-adapted teleosts make good their diffusive losses of water to the external environment by ingesting seawater. Absorption of Na^+ and Cl^- from the lumen reduces the osmolality of the luminal fluid, which drives water absorption. Low circulating levels of the fresh water-adapting hormone prolactin, which normally reduces intestinal water permeability, allow greater coupling between NaCl and water absorption [20, 21]. Following this absorption of seawater, the organism relies on another set of epithelial organs (gills, opercular membrane and skin), spatially separated from the intestine, to actively excrete Na^+ and Cl^-, leaving the fish with a net gain of free water. Active secretion of Cl^- by the intestine, to reduce the osmotic gradient, would be counterproductive to the overall goal of fluid absorption. Fluid secretion is probably not required to generate an aqueous milieu for chemical and enzymatic digestion (as might be argued for terrestrial vertebrates with a relatively dry diet) since drinking in seawater-adapted teleosts can be quite substantial [21–23]. Secretion of mucus, for the protection of the intestinal epithelium from digestive enzymes and to lubricate the flow of digesta, and of HCO_3^- [24] and K^+ [25, 26], for acid-base and ionic regulation, do occur.

In fresh water-adapted fishes, where the drinking rate is low and intestinal water permeability is low due to the action of prolactin, NaCl secretion would clearly be detrimental. Reduced coupling of water absorption to NaCl absorption limits intes-

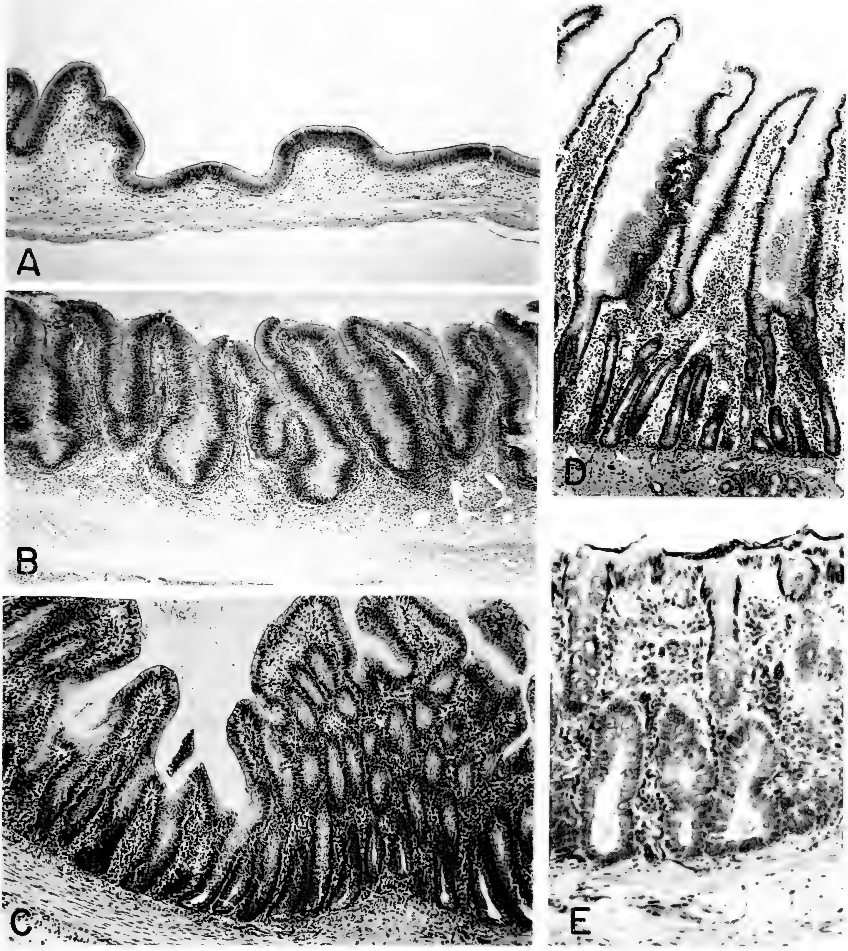

FIG. 1. Light photomicrographs of intestinal histology. (A): Goby (*Gillichthys mirabilis*) posterior intestine. There are no mucosal or other glands and the muscularis externa is very poorly developed. (×65) (B): Bowfin (*Amia calva*) posterior intestine. The epithelium is highly folded but no mucosal glands are apparent; the muscularis externa is highly developed and extends well below the field of view. (×60) (C): Cat ileum. Both villi extending into the lumen and crypts of Lieberkühn extending downward to the muscularis mucosae can be distinguished in this section. (×65) (D): Cat duodenum. In addition to villi and crypts, Brunner's glands are visible in the submucosa (lower right). (×60) (E): Cat colon. Crypts form the major portion of colonic mucosa with the villi reduced to the horizontal layer of surface cells. (×135)

tinal water gain while the kidney and urinary bladder produce a copious, hypotonic urine.

Although teleost fish lack crypts of Lieberkühn and the associated intestinal active fluid secretion, they do possess a number of other salt excretory organs: branchial "chloride cells", opercular membrane and skin, rectal salt gland and dendritic organ. The inability of teleost fish intestine to actively secrete NaCl and the simultaneous presence of other secretory structures stimulated my interest in the possible phylogenetic and functional relationships of one of the latter, secretory, organs. In particular, similarities between the rectal gland and the mammalian crypts of Lieberkühn will be addressed in this paper and one possible interpretation of the data will be presented. The discussion will be largely synthetic, making use of anatomical and physiological data.

RECTAL GLAND STRUCTURE AND HOMOLOGY

The argument for homology of the crypts of Lieberkühn and the rectal gland is based on morphological considerations. A morphological series, as an approximation to the intermediate stages of a phylogenetic or evolutionary series, can be constructed using the anatomies of extant species. Many of these data are old and careful reading of the original reports reveal that the general notion of homology, while not fully developed, is certainly not new. The morphologies of the various organs will be summarized herein and a morphological series constructed which includes the mammals. An abundant literature exists on the various morphologies of the fish rectal gland, which has gone by a variety of names since its earliest anatomical recognition by Severini in 1645 (in [27, 28]); rectal gland synonymies include:

- rectal gland
- caecum
- postanal gland
- bursa cloacae
- caecal gland or appendage
- appendix digitiformis
- appendix vermiformis
- superanal gland
- nodular gland

The first report of the glandular nature of the organ was in 1852 when Leydig described well vascularized clusters of ducts in macerated specimens; he compared the glandular structure of the rectal gland with that of Brunner's glands (in [27, 28]). As noted below for the coelacanth, there has also been some confusion in identity and nomenclature.

Probably the best known rectal gland is that of elasmobranchs such as the dogfish shark (*Squalus acanthias*; [27–32]; Fig. 2). The dogfish rectal gland is a digitiform dorsal diverticulum of the postvalvular intestine supported by dorsal mesorectum. Although a number of functions have been attributed to the rectal gland since its first description (including accessory reproductive structure, urinary bladder, renal accessory excretory structure, hormone secretion, and blood function; cf. [27, 28]), its function as a NaCl excretory organ, emptying its effluent into the terminal intestine via the rectal gland duct is now well established (e.g., [33–35]). In addition to active NaCl secretion by the gland measured directly, the secretory cells of the ducts bear all the hallmarks of ion-secreting epithelial cells, including abundant mitochondria and a well-developed tubulovesicular system and associated cisternae continuous with basolateral membrane invaginations. The Na^+–K^+–ATPase has been localized using histochemistry to this series of basolateral membranes [32, 36], and is responsible for generating the electrochemical gradient for Na^+ into the cell which drives the active secretion.

Arterial supply to the gland is from the rectal gland artery (synonymous with the posterior mesenteric artery and caecal artery, [27–29, 37, 38]), a branch from the dorsal aorta. Three courses of flow are possible for blood passing toward the rectal gland in the rectal gland artery. The rectal gland artery, upon reaching the gland, supplies a series of circumferential arteries and then continues along the dorsal surface of the rectal gland to beyond the junction of the gland with the intestine, where it joins the circulation of the postvalvular intestine. Blood delivered to the circumferential arteries can follow two routes. Blood can pass to a network of superficial venules and then via a pair of larger veins through the

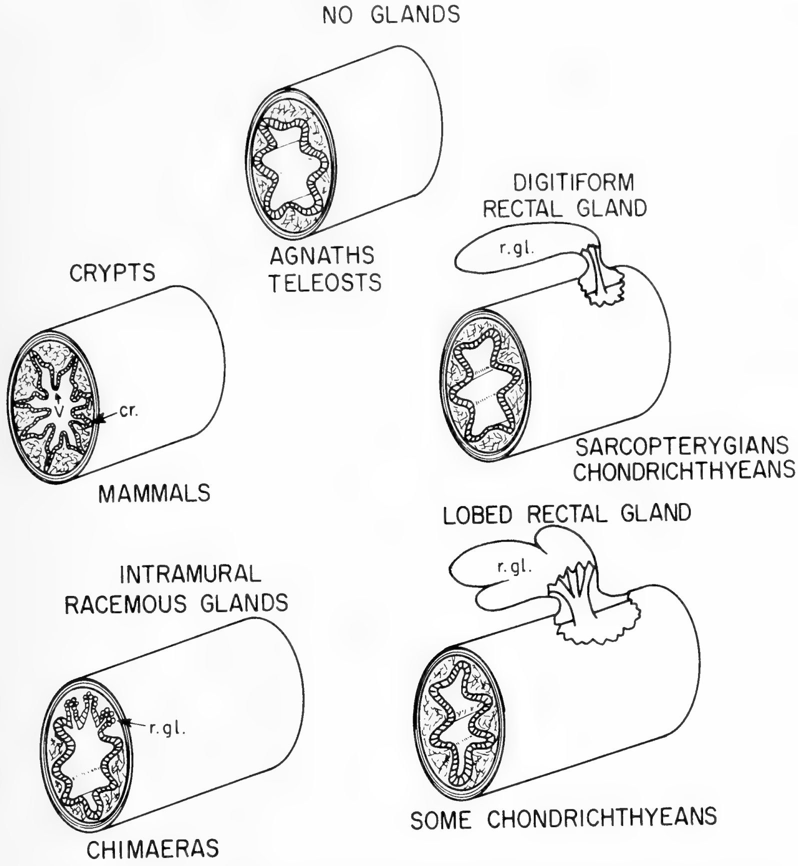

FIG. 2. Morphological series illustrating the variety of mucosal morphologies discussed in the text. The series of intestinal morphologies shows the gradual transition (counterclockwise in the figure) from mammalian crypts to the elasmobranch-type rectal gland. In these drawings, submucosal, muscularis externa and serosal layers are depicted for simplicity as single lines.

dorsal mesentery to the posterior cardinal vein system [37]. Alternatively, blood can be delivered to sinusoids in the deeper, secretory regions of the gland. This blood passes through capillaries surrounding the secretory ducts and is collected centrally in the rectal gland vein which passes into the intestine as the dorsal intestinal vein, a tributary of the hepatic portal vein. Clearly, there may be shunting of blood from the rectal gland artery to the vessels of the posterior intestine, bypassing the gland altogether. Satchell [38] has reported that subambient pressures in the dorsal intestinal vein produced by cyclic vasoconstriction of the rectal gland sinusoids may actually cause retrograde flow to the rectal gland of blood in the intestinal veins. He further proposed that the advantage of such flow would be the delivery of NaCl-rich blood (resulting from intestinal NaCl absorption) directly to the gland for secretion, before delivery of that blood to the general circulation.

The coelacanth (*Latimeria chalumnae*) postanal gland (=rectal gland or nodular gland) has a structure and vascular connections similar to those of the *Squalus* elasmobranch type [39, 40]. Although its salt secretory function has not been directly measured, the ultrastructural appearance of the parenchymal cells and high levels of Na^+–K^+–ATPase in the gland support such a role [39–41].

The lungfish (*Protopterus aethiopicus* and *P. dolloi*) cloacal gland (=rectal gland) is a descrete encapsulated gland which is located posterior to the urogenital sinus as opposed to the anterior position of other rectal glands [42]. There also occurs in lungfish another structure, the cloacal caecum (=urogenital sinus) whose placement is more typical of the elasmobranch rectal gland. In the earlier literature, the relationship of this cloacal caecum to the rectal gland of elasmobranchs was unknown. Its placement was noted to be similar to that of the elasmobranch rectal gland although a different (nonglandular) internal structure was acknowledged [43]. Description of the vascular connections has not been published. Ultrastructurally, the secretory cells of cloacal gland tubules exhibit the typical abundant mitochondria and basolateral cisternae seen in the secretory cells of other rectal glands. Interestingly, a cloacal gland is found only in the lungfish genus *Protopterus*. This is the only genus of lungfish which estivates for any length of time; Lagios and McCosker [42] hypothesize a role for the gland in osmoregulation during estivation based on this correlation.

In some elasmobranchs, such as *Hexanchus* and *Heptanchus*, the rectal gland is a postvalvular intestinal diverticulum of the *Squalus* type but consisting of 2–4 discrete lobes with separate lumina (Fig. 2); vascular supply and drainage are via the caecal artery and dorsal intestinal vein, respectively [27].

In the chimaeras, there is no extramural rectal gland but, instead, a series of 9–12 or more intramural racemous glands located either dorsolaterally (*Chimaera monstrosa*; Fig. 2) or circumferentially (*Hydrolagus colliei*). These glands are located in the gut wall immediately posterior to the last plicum of spiral valve and drain into the postvalvular intestine via separate ducts; these ducts enter at the bases of intestinal folds [27, 31, 42, 44]. Arterial supply is via the caecal artery and venous drainage presumably, although not described, via the intestinal veins. The organ is arranged as lobulated clusters of grape-like glands drained by tubular ducts. Both glands and ducts are formed of a simple cuboidal/columnar epithelium. The cells of the parenchyma are mitochondria rich, show the typical basolateral cisternae, and are rich in Na^+–K^+–ATPase activity as expected for an ion-secreting structure. As in some sharks, and reminiscent of crypts, particularly in the colon, the ducts contain numerous mucus cells [31].

Extramural rectal glands and intramural glands of the chimaeroid type are lacking in tetrapod vertbrates which, instead, possess numerous mucosal glands (crypts of Lieberkühn; Fig. 1C, D, E) or their apparent equivalents, the various cell nests and tubular glands of amphibians and reptiles, respectively [8, 19, 45, 46]. There are, in addition, submucosal secretory glands in the duodenum (Brunner's glands; Fig. 1D).

The intestines of teleosts and lamprey possess neither crypts of Lieberkühn nor rectal glands of the types described above [14, 17, 19, 47–50]. Instead, the middle and posterior intestinal segments are simple in organization. They are lined by a simple epithelium folded to various extents, producing villi (Fig. 1A, B and 2). The submucosal and muscularis externa layers are more or less developed according to species ([14, 17]; Fig. 1A, B). This cryptless epithelium is capable of performing many of the functions of mammalian intestine including the absorption of NaCl and water and the secretion of HCO_3^-, K^+ and mucus (e.g., [17, 22–26, 47]).

One function associated with the mammalian crypts of Lieberkühn is the proliferation from stem cells of epithelial cells to replace those lost at the villus [9]. In some teleost species, cell proliferation occurs at the bases of intestinal folds [48, 49] whereas in other species [50], and in the lamprey [51], proliferation occurs throughout the epithelium, with each generative cell supplying surrounding areas. Therefore, cell proliferation is not universally associated with crypts. As an aside, the localization of proliferative cells and the functional segregation of absorptive and secretory processes in mammalian intestine suggest the interesting notion that the functional role of an epithelial cell perhaps changes as the cell matures and migrates toward the villus tip.

Two major evolutionary questions arise with regard to the relationships between the crypts and the rectal gland in its various forms. First, are the

rectal gland and crypts of Lieberkühn homologous structures? And second, what are the phylogenetic relationships of the various intestinal morphologies? Both of these questions are difficult to answer, of course, because the fossil record does not yield anatomical details of the sort required. Given only the anatomy of extant species, then, there are several possible interpretations of the data. These are: (1) the presence of intestinal salt-secreting structures (crypts and rectal glands) is primitive with respect to the vertebrates, and some groups, notably the teleost fishes, have secondarily lost them, (2) the various intestinal excretory structures in several groups were derived independently from ancestors with the teleost-type intestinal morphology and have subsequently converged in appearance, or (3) crypts and rectal glands are advanced specializations shared by relatively closely related taxonomic groups.

With respect to the first question, a morphological series illustrates possible intermediate morphological stages in the evolution of these various organs (Fig. 2). No phylogenetic scheme is implied in Figure 2, only the logical arrangement of intermediate morphological stages from the digitiform *Squalus*-type to the crypt-like intramural type. The mammalian crypts of Lieberkühn (an example of tetrapod mucosal glands) are included as an extention of the fish series since it appears to represent an extreme case of multiple intramural glands of the chimaeroid type with circumferential distribution. The assignment of the aglandular teleost and agnathan intestines to an intermediate position in this continuous series (circular, as it is diagrammed) between the crypt-like glands and the digitiform-type gland reflects the earlier argument of the unsure evolutionary origin of this condition, i.e., being an aglandular primitive condition or an advanced condition where secretory glands were secondarily lost.

The taxonomic distribution of intestinal salt-secreting glands is presented in Figure 3. Various rectal gland phylogenies have been proposed but, according to Forey [39], no single phylogeny can be supported despite the accepted homology of the different rectal gland types. Considering the broad distribution of secretory glands in their various forms and the claims of Fange and Fugelli [31] and

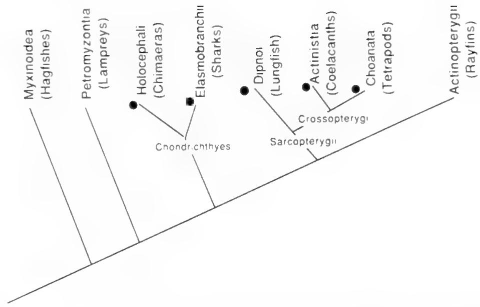

FIG. 3. Phylogeny of the major groups of vertebrates (adapted from [52, 53]). Filled circles indicate those groups with intestinal secretory gland (rectal glands) or tissues (crypts of Lieberkühn).

Lagios and Stasko-Concannon [44] that the intramural glands are primitive with respect to the extramural rectal gland, the most parsimonious scheme might include the appearance of crypts in early gnathostomes with their subsequent development into extramural glands in some groups (sharks, lungfish and coelacanth) and their secondary loss in rayfinned fishes. Remarkably, Pang *et al.* [52] earlier described the identical taxonomic distribution for ureotelism in vertebrates. This parallelism might suggest that ureotelism and intestinal secretory glands are both shared characters associated with the evolution of a particular osmoregulatory strategy (as opposed to each being derived independently in serveral groups). Strengthening this argument is the fact that both ureotelism and rectal gland secretion are adaptations to the marine environment. Urea retention is diminished in elasmobranches acclimated to brackish water (cf. [54]) and the rectal glands in sharks adapted to fresh water and in freshwater stingrays, although normal in anatomical position, are extremely small [55, 56].

In addition to the similarity of vascular connections, the ontogeny of the elasmobranch rectal gland supports the proposed homology. Early reports [27, 28] describe the developmental origin of the rectal gland as an outgrowth from the dorsal intestinal wall. The gland originates as a single outpocketing to give rise to the rectal gland stalk and duct; subsequent repeated evaginations from this anlage produce the secretory ducts of the parenchyma [28]. The dorsal placement of both adult elasmobranch glands and intramural glands

of the *Chimaera*-type reflect this ontogeny. Crofts [27] and Fange and Fugelli [31] claim the chimaeroid type to be primitive with respect to the elasmobranch digitiform gland based on its less defined structure; the intramural embryonic origin might substantiate their claim. Lagios and Stasko-Concannon [44] concur with regard to the "primitive" status of intramural glands and analogize the transformation into a compact extramural rectal gland with the evolutionary development of the endocrine pancreas from diffusely-arranged endocrine cells in the gut wall.

Ultrastructural similarity also lends support to the proposed homology. Mitochondria-rich cells characterize the glandular epithelium of the rectal glands of elasmobranchs, the coelacanth, the chimaeras, and the absorptive cells of the crypts of Lieberkühn [9, 29, 30, 32, 40, 42, 44]. Although a similar ultrastructural appearance is consistent with the proposed homology, this is merely supportive considering the widespread occurrence of mitochondria-rich cells in transporting epithelia of diverse ontogenetic origin (such as fish skin and opercular membrane from ectoderm; [57–60]).

Separate from the issue of rectal gland-crypt homology presented here, Crofts [27] considered vertebrate intestinal caeca (where present) to be homologs of the rectal gland; she based this argument on gross anatomical similarity and the alleged presence in the rectal gland of simple lymphoid tissue similar to that seen in caeca. Crofts [27], in her detailed description, states that the lymphoid tissue is commonly found in the associated mesentery and is sometimes pressed against the rectal gland. Some anatomists (e.g., Morgera in [27]) included the mammalian appendix in the homology as well. Hoskins [28], Bulger [29], Fange and Fugelli [31], and others (cf. [27]), however, do not find lymphoid tissue in the substance of the rectal gland, thus weakening the caecal homology argument.

PHYSIOLOGICAL AND ENDOCRINOLOGICAL SIMILARITIES BETWEEN RECTAL GLAND AND CRYPTS

Physiological and endocrinological studies on intestine and rectal gland demonstrating functional similarity are supported by the proposed homology. The intestine of mammals, the best studied of tetrapods, has several electrolyte transport functions. Two of these are relevant here: (1) NaCl absorption and (2) Cl^- secretion. Current concensus places the Na^+ and Cl^- absorptive function in the villus epithelium and the Cl^- secretory function in the crypt epithelium [1, 12]. The intestine of at least three species of teleost fish possesses only the absorptive transport component; in two flounder species and the goby, cyclic AMP did not stimulate active Cl^- secretion as it does in mammals [14–18]. Non-teleost fishes have received little attention; the presence of a valvular intestine (spiral valve) in a number of these forms presents morphological complexities to *in vitro* study, and a consequent paucity of data. Should the proposed homology be correct and if an intramural secretory organ (such as the chimaeroid type rectal gland or the crypts of Lieberkühn) represents the primitive condition as some argue, then it can be concluded that the salt secretory function in the intestine of some fishes has been removed to an extramural gland, and in other fishes has been lost altogether. In teleosts, the abundant branchial and epidermal salt-secreting chloride cells may functionally replace the crypts or rectal gland in the role of salt secretion. Since ion transport processes of the valvular intestine of elasmobranchs which lack crypts, or of other species with rectal glands, have not been reported, the expected absence of secretory capability of this tissue cannot be addressed at present.

The advantage for fishes of removing NaCl secretion to an extramural site is clear. In teleosts, by transferring the secretory role to chloride cells of the skin, opercular and branchial regions, the problem alluded to earlier of simultaneous absorption and secretion across the intestine is relieved. The intestine could maintain a relatively high permeability to water (in the seawater-adapted fish, for example) facilitating absorption, while the chloride cell-containing epithelia could maintain a relatively low permeability to water limiting osmotically-driven water efflux. Another effective strategy (in the sharks, for example) is the use of an extramural rectal gland to produce a concen-

trated NaCl solution which is delivered to the posterior-most segment of intestine where it might be rapidly voided, thereby limiting the time available for osmotic water loss from the organism across intestinal tissues. Judging from the concentration of secreted fluid (ca. 500 mM NaCl; [33–35]), the water permeability of the rectal gland ducts is reasonably low. The intramural glands of holocephalans, which drain into the intestine in a more crypt-like manner would be less efficient in NaCl removal although the placement of their ducts in the postvalvular segment of intestine is surely adaptive compared with the broad distribution of crypts in tetrapods.

In the context of ion transport, functional similarity of the homologous crypt and rectal gland epithelia is supported by the currently accepted models for transport [1, 2, 34, 35]. A simple diagram of the cellular model for active Cl^- secretion, including the major relevant features is shown in Figure 4. Secretion depends ultimately on the basolateral Na^+–K^+–ATPase to maintain a low intracellular activity of Na^+. The system operates as a two-step mechanism involving the apical (luminal) and basolateral (blood-side) cell membranes. Coupled transport driven by the electrochemical gradient for Na^+ brings Na^+ and Cl^- into the cell. Cl^-, accumulated above electrochemical equilibrium, exits in a conductive manner down its gradient into the lumen as secreted Cl^-. Accumulated Na^+ is recycled across the basolateral membrane by the Na^+–K^+–ATPase. Under open circuit conditions, as would be the case *in vivo,* macroscopic electroneutrality is maintained by the diffusion of Na^+ through the cation-selective paracellular pathway from blood side to the lumen in response to the lumen-negative electrical potential difference established by Cl^- exit. This general model for Cl^- secretion applies not only to rectal gland and crypt cells but also to secretory cells of the teleost skin and opercular membrane and mammalian tracheal epithelium [57, 61].

In contrast to Cl^- secretion, there is a greater diversity of transport mechanisms for the NaCl-absorptive component of intestinal ion transport. There are abundant reviews of these processes available for the interested reader [1, 2, 62, 63].

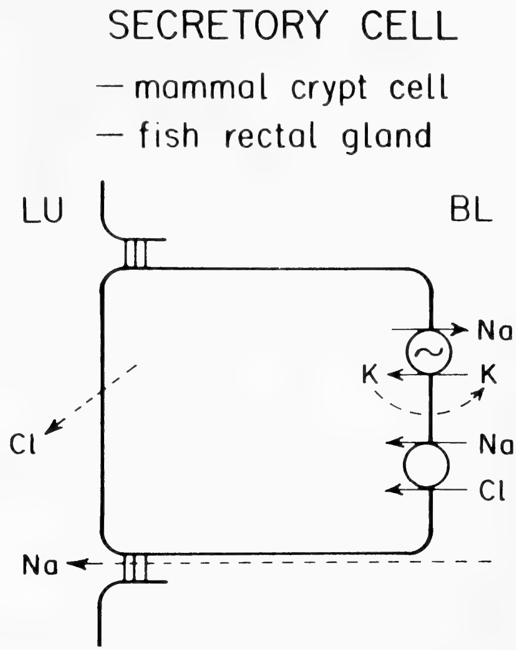

FIG. 4. Cellular model for active Cl^- secretion by mammalian crypt cells and fish rectal gland. LU indicates the luminal side of the epithelium and BL the blood side. The basolateral membrane Na^+–K^+–ATPase maintains a low intracellular Na^+ activity which drives the coupled entry of Na^+ and Cl^-. Cl^- exits by a conductive mechanism across the luminal membrane. Na^+ and K^+ recycle across the basolateral cell membrane. Under open-circuit conditions, Na^+ diffuses through the paracellular pathway to the luminal side. (Adapted from [1, 2, 34–36, 85]). An identical mechanism is proposed for Cl^- secretion by chloride cells in fish skin and opercular membrane [59, 60].

Functional similarity between the rectal gland and crypts of Lieberkühn extends also to endocrine mechanisms of control of ion transport. Active secretion of fluid by both rectal glands and intestinal crypts is stimulated by cyclic AMP. Moreover, in both systems, chemical messengers which act via cyclic AMP produce similar effects. For example, VIP stimulates both tissues to secrete; in both systems, VIP is thought to act via an increase in cyclic AMP [64–69]. Shuttleworth and Thorndyke [70] report that in sharks the natural agonist may not be VIP but, instead, the newly discovered peptide “rectin”. Similarly, somatostatin inhibits VIP-induced secretion in

some mammalian intestinal segments and in shark rectal gland [66, 67, 71–73]. Although details of the schemes have yet to be elucidated fully, intracellular Ca^{2+} acting as an intracellular messenger stimulates secretion by both mammalian intestine and shark rectal gland; this stimulatory effect of Ca^{2+} may be dependent on other intracellular messengers [74–77].

The cryptless teleost intestine bears some functional resemblance to the absorptive portion of mammalian intestine located at the villus [1], specifically with respect to control by hormonal and intracellular mediators like Ca^{2+}. Na^+ and Cl^- absorption by some mammalian intestinal segments is stimulated by somatostatin [71, 72, 78]; urotensin II, a naturally-occurring teleost analog of somatostatin [79] stimulates Na^+ and Cl^- absorption across teleost intestine [47, 80, 81]. Regulation by the calcium messenger system of coupled NaCl absorption in the goby is similar to the general scheme proposed for coupled NaCl-absorptive systems in mammalian intestine [74, 75, 82]; elevated intracellular Ca^{2+} activity inhibits absorption (acting through calmodulin) whereas depressed Ca^{2+} activity stimulates.

One contribution of studies on fish tissues can be stated at present with respect to the regulatory effect of somatostatin on NaCl transport. As noted above, somatostatin reduces VIP-induced ion and fluid secretion by the mammalian intestine [71–73]; this effect could result from either a direct effect to block the secretory process of the crypts or an offsetting stimulation of absorption at the villi. The ability of somatostatin to inhibit VIP-induced secretion in rectal gland [67] and of urotensin II to stimulate basal absorption in teleost intestine [81] suggest the dual actions of somatostatin, antisecretory and absorptive, in reducing net intestinal secretion in mammals; several years ago, this question of dual action was unresolved [1].

DO RAYFINNED FISHES REALLY LACK INTESTINAL SECRETORY GLANDS?

A special note must be made of a little known accessory secretory structure in teleost fishes. Marine species of the catfish family Plotosidae possess a dendritic organ located caudal to the urinary papilla [83, 84]. The dendritic organ is a highly folded, external epithelial organ; apparent secretory cells are located in short crypts or acini opening to the surface of the tissue leaflets. In the plotosid *Cnidoglanis macrocephalus,* ligation of the dendritic organ produces an increase in plasma sodium concentration, indicating a salt-excretory role for the organ [84]. A salt excretory function and the location of the organ near the anus invite speculation as to possible homology with the rectal gland. The salt-secreting cells of the dendritic organ are similar ultrastructurally to branchial chloride cells, elasmobranch rectal gland cells and avian nasal salt gland cells [83] reinforcing the suggestion of a role in salt secretion. The placement of the glands supports an ectodermal, rather than endodermal, origin, however. It appears, therefore, that teleosts (at least those examined to date) do not possess an intestinal NaCl secretory apparatus.

CONCLUSION

More study is needed to validate further the use of piscine models in intestinal transport research. Particularly, detailed studies on the biophysical mechanisms, as well as schemes for cellular and endocrine regulation involving larger numbers of putative messengers, are desirable. With further refinement, the teleost intestine may emerge as a model system for mammalian villar transport, with its coupled Na^+–Cl^- or Na^+–K^+–$2\,Cl^-$ absorption (where present) and K^+ secretion. The shark rectal gland has already been acknowledged as a model for Cl^- secretion not only by intestine, but also by sweat gland and salivary gland [85]. The teleost intestine and elasmobranch rectal gland can be models for the NaCl absorptive and Cl^- secretory components, respectively, of mammalian intestine. As presented here, the basis for such use can, in addition to functional similarity, also include their phylogenetic relationship. At the very least, though, results of studies on one system can provide useful insight into other systems and aid in the framing of interesting and informative hypotheses for future testing.

ACKNOWLEDGMENTS

Great thanks are due to Dr. J. W. Crim for collecting intestinal tissues from *Amia* and to Professor H. A. Bern for his encouragement and enthusiasm.

REFERENCES

1 Field, M. (1981) In "Physiology of the Gastrointestinal Tract". Ed. by L. R. Johnson, Raven Press, New York, pp. 963–982.

2 Binder, H. J. (1981) In "Physiology of the Gastrointestinal Tract". Ed. by L. R. Johnson, Raven Press, New York, pp. 1003–1019.

3 Walsh, J. H. (1981) In "Physiology of the Gastrointestinal Tract". Ed. by L. R. Johnson, Raven Press, New York, pp. 59–144.

4 Ruskone, A., Rene, E., Chayvialle, J. A., Bonin, N., Pignal, F., Kremer, M., Bonfils, S. and Rambaud, J. C. (1982) Digestive Dis. Sci., **5**: 459–466.

5 Freel, R. W., Hatch, M., Earnest, D. L. and Goldner, A. M. (1983) Am. J. Physiol., **245**: G808–G815.

6 Westergaard, H. and Dietschy, J. M. (1986) In "Physiology of Membrane Disorders", 2nd edition. Ed. by T. E. Andreoli, J. F. Hoffman, D. D. Fanestil and S. G. Schultz, Plenum Publ. Co., New York, pp. 873–885.

7 Vigna, S. R. (1986) In "Vertebrate Endocrinology: Fundamentals and Biomedical Implicaions". Ed. by P. K. T. Pang and M. P. Schreibman, Academic Press, New York, pp. 261–278.

8 Bloom, W. and Fawcett, D. W. (1986) A Textbook of Histology, 11th edition, W. B. Saunders Co., Philadelphia.

9 Trier, J. S. and Madara, J. L. (1981) In "Physiology of the Gastrointestinal Tract". Ed. by L. R. Johnson, Raven Press, New York, pp. 925–961.

10 Roggin, G. M., Banwell, J. G., Yardley, J. H. and Hendrix, T. R. (1972) Gastroenterology, **63**: 981–989.

11 deJonge, H. R. (1975) Biochim. Biophys. Acta, **381**: 128–143.

12 Welsh, M. J., Smith, P. L., Fromm, M. and Frizzell, R. A. (1982) Science, **218**: 1219–1221.

13 Weiser, M. M. and Quill, H. (1975) Gastroenterology, **69**: 479–482.

14 Field, M., Smith, P. L. and Bolton, J. E. (1980) J. Membr. Biol., **55**: 157–163.

15 MacKay, W. C. and Lahlou, B. (1980) In "Epithelial Transport in the Lower Vertebrates". Ed. by B. Lahlou, Cambridge Univ. Press, Cambridge, pp. 151–162.

16 MacKay, W. C., Lahlou, B. and Porthe-Nibelle, J. (1978) C. R. Acad. Sci. Paris, **287**: 1239–1242.

17 Loretz, C. A. (1983) Comp. Biochem. Physiol., **75A**: 205–210.

18 Mooney, S. M. and Loretz, C. A. (1987) Comp. Biochem. Physiol., **86A**: 367–372.

19 Andrew, W. and Hickman, C. P. (1974) Histology of the Vertebrates, C. V. Mosby Co., St. Louis.

20 Loretz, C. A. and Bern, H. A. (1982) Neuroendocrinology, **35**: 292–304.

21 Potts, W. T. W., Foster, M. A., Rudy, P. P. and Howells, G. P. (1967) J. Exp. Biol., **47**: 461–470.

22 Smith, H. W. (1930) Am. J. Physiol., **93**: 480–505.

23 Smith, H. W. (1932) Q. Rev. Biol., **7**: 1–26.

24 Dixon, J. M. and Loretz, C. A. (1986) J. Comp. Physiol. B, **156**: 803–811.

25 Frizzell, R. A., Halm, D. R., Musch, M. W., Stewart, C. P. and Field, M. (1984) Am. J. Physiol., **246**: F946–F951.

26 Ando, M. and Utida, S. (1986) Zool. Sci., **3**: 605–612.

27 Crofts, D. R. (1925) Proc. Zool. Soc. Lond., **1925**: 101–188.

28 Hoskins, E. R. (1917) J. Morphol., **28**: 329–367.

29 Bulger, R. E. (1963) Anat. Rec., **147**: 95–107.

30 Bulger, R. E. (1965) Anat. Rec., **151**: 589–608.

31 Fange, R. and Fugelli, K. (1963) Sarsia, **10**: 27–34.

32 Van Lennep, E. W. (1968) J. Ultrastr. Res., **25**: 94–108.

33 Burger, J. W. and Hess, W. N. (1960) Science, **131**: 670–671.

34 Epstein, F. H., Stoff, J. S. and Silva, P. (1983) J. Exp. Biol., **106**: 25–41.

35 Epstein, F. H., Stoff, J. S. and Silva, P. (1984) In "Chloride Transport Coupling in Biological Membranes and Epithelia". Ed. by G. A. Gerencser, Elsevier Sci. Publ, B. V., pp. 347–357.

36 Eveloff, J., Karnaky, K. J., Jr., Silva, P., Epstein, F. H. and Kinter, W. B. (1979) J. Cell Biol., **83**: 16–32.

37 Kent, B. and Olson, K. R. (1982) Am. J. Physiol., **243**: R296–R303.

38 Satchell, G. H. (1986) New Zealand J. Zool., **13**: 101–105.

39 Forey, P. L. (1980) Proc. R. Soc. Lond. B, **208**: 369–384.

40 Lemire, M. and Lagios, M. (1979) Acta Anat., **104**: 1–15.

41 Griffith, R. W. and Burdick, C. J. (1976) Comp. Biochem. Physiol., **54B**: 557–559.

42 Lagios, M. D. and McCosker, J. E. (1977) Copeia, **1977**: 176–178.

43 Parker, W. N. (1892) Trans. R. Irish Acad. Dublin, **30**: 109–230.

44 Lagios, M. D. and Stasko-Concannon, S. (1979)

Cell Tissue Res., **198**: 287–294.

45 Patten, S. F., Jr. (1960) Exp. Cell Res., **20**: 638–641.

46 Andrew, W. (1963) Ann. N. Y. Acad. Sci., **106**: 502–517.

47 Loretz, C. A., Howard, M. E. and Siegel, A. J. (1985) Am. J. Physiol., **249**: G284–G293.

48 Gas, N. and Noaillac-Depeyre, J. (1974) C. R. Acad. Sci. Paris, **279**: 1085–1088.

49 Stroband, H. W. J. and Debets, F. M. H. (1978) Cell Tissue Res., **187**: 181–200.

50 Trier, J. S. and Moxey, P. C. (1980) Cell Tissue Res., **206**: 379–385.

51 Youson, J. H. and Langille, R. M. (1981) Can. J. Zool., **59**: 2341–2349.

52 Pang, P. K. T., Griffiths, R. W. and Atz, J. W. (1977) Am. Zool., **17**: 365–377.

53 Schaeffer, B. and Williams, M. (1977) Am. Zool., **17**: 293–302.

54 Prosser, C. L. (1973) In "Comparative Animal Physiology", 3rd edition. Ed. by C. L. Prosser, W. B. Saunders Co., Philadelphia, pp. 1–78.

55 Oguri, M. (1964) Science, **144**: 1151–1152.

56 Gerst, J. W. and Thorson, T.B. (1977) Comp. Biochem. Physiol., **56A**: 87–93.

57 Marshall, W. S. and Nishioka, R. S. (1980) J. Exp. Zool., **214**: 147–188.

58 Foskett, J. K., Logsden, C. D., Turner, T., Machen, T. E. and Bern, H. A. (1981) J. Exp. Biol., **93**: 209–224.

59 Foskett, J. K., Bern, H. A., Machen, T. E. and Conner, M. (1983) J. Exp. Biol., **106**: 255–281.

60 Degnan, K. J. (1984) In "Chloride Transport Coupling in Biological Membranes and Epithelia". Ed. by G. A. Gerencser, Elsevier Sci. Publ. B. V., pp. 359–391.

61 Welsh, M. J. (1986) In "Physiology of Membrane Disorders", 2nd edition. Ed. by T. E. Andreoli, J. F. Hoffman, D. D. Fanestil and S. G. Schultz, Plenum Publ. Co., New York, pp. 751–766.

62 Schultz, S. G. (1981) In "Physiology of the Gastrointestinal Tract". Ed. by L. R. Johnson, Raven Press, New York, pp. 983–989.

63 Powell, D. W. (1986) In "Physiology of Membrane Disorders", 2nd edition. Ed. by T. E. Andreoli, J. F. Hoffman, D. D. Fanestil and S. G. Schultz, Plenum Publ. Co., New York, pp. 751–766.

64 Schwartz, C. H., Kimberg, D. V., Sheerin, H. E., Field, M. and Said, S. I. (1974) J. Clin. Invest., **54**: 536–544.

65 Waldman, D. B., Gardner, J. D., Zfass, A. M. and Makhlouf, G. M. (1977) Gastroenterology, **73**: 518–523.

66 Carter, R. F., Bitar, K. N., Zfass, A. M. and Makhlouf, G. M. (1978) Gastroenterology, **74**: 726–730.

67 Stoff, J. S., Rosa, R., Hallac, R., Silva, P. and Epstein, F. H. (1979) Am. J. Physiol., **237**: F138–F144.

68 Krejs, G. J., Browne, R. and Raskin, P. (1980) Gastroenterology, **78**: 26–31.

69 Davis, G. R., Santa Ana, C. A., Morawski, S. G. and Fordtran, J. S. (1981) J. Clin. Invest., **67**: 1687–1694.

70 Shuttleworth, T. J. and Thorndyke, M. C. (1984) Science, **225**: 319–321.

71 Dharmsathaphorn, K., Binder, H. J. and Dobbins, J. W. (1980) Gastroenterology, **78**: 1559–1565.

72 Dharmsathaphorn, K., Racusen, L. and Dobbins, J. W. (1980) J. Clin. Invest., **66**: 813–820.

73 Dharmsathaphorn, K., Sherwin, R. S. and Dobbins, J. W. (1980) Gastroenterology, **78**: 1554–1558.

74 Donowitz, M. (1983) Am. J. Physiol., **245**: G165–G177.

75 Donowitz, M. and Welsh, M. J. (1986) Ann. Rev. Physiol., **48**: 135–150.

76 Forrest, J. N., Jr., Dornbusch, J. N., Ross, B. and Murdaugh, A. (1987) Bull. Mt. Desert Is. Biol. Lab., **18**: 10–13.

77 Shuttleworth, T. J. (1983) Am. J. Physiol., **245**: R894–R900.

78 Guandalini, S., Kachur, J. F., Smith, P. L., Miller, R. J. and Field, M. (1980) Am. J. Physiol., **238**: G67–G74.

79 Pearson, D., Shively, J. E., Clark, B. R., Geschwind, I. I., Barkley, M., Nishioka, R. S. and Bern, H. A. (1980) Proc. Natl. Acad. Sci. USA, **77**: 5021–5024.

80 Mainoya, J. R. and Bern, H. A. (1982) Gen. Comp. Endocrinol., **47**: 54–58.

81 Loretz, C. A., Freel, R. W. and Bern, H. A. (1983) Gen. Comp. Endocrinol., **52**: 198–206.

82 Loretz, C. A. (1987) J. Exp. Zool., in press.

83 van Lennep, E. W. and Lanzing, W. J. R. (1967) J. Ultrastr. Res., **18**: 333–344.

84 Kowarsky, J. (1973) Comp. Biochem. Physiol., **46A**: 477–486.

85 Epstein, F. H. (1979) Yale J. Biol. Med., **52**: 517–523.

ZOOLOGICAL SCIENCE 4: 945–954 (1987)

REVIEW

Insect Circadian Activity with Special Reference to the Localization of the Pacemaker

Yoshihiko Chiba and Kenji Tomioka

Environmental Biology Laboratory, Biological Institute, Yamaguchi University, Yamaguchi, 753 Japan

Circadian rhythm, an endogenous biological rhythm with a period approximating the length of a day is ubiquitous among the physiological organization of eukaryotes, forming the basis of daily rhythm in animal life. Characteristic features of this rhythm are, on one hand, persistence in a constant environment, where at least light intensity and temperature are kept as constant as possible and, on the other hand, entrainability to environmental (particularly light) cycles of an appropriate length (in general, not much deviated from 24 hr). The internal mechanism has been hypothesized as including, at the very least, a pacemaker (primary generator of temporal information) and photoreceptors which disperse photic information toward the pecemaker for entrainment.

If a tissue includes the pacemaker, then the following criteria should be met. 1) Removal or disconnection of the tissue from the rest of the body should cause the overt rhythm under study to disappear or to become quite atypical. 2) The tissue itself should show circadian rhythm in complete isolation from the rest of the body. 3) Either the phase or the period of the overt rhythm should be transplanted by transplanting the tissue to an individual deprived of rhythmicity. It would, of course, be ideal if all these criteria are satisfied, but difficulties arising mainly from technical problems do not always allow us to investigate the latter two criteria completely.

Pacemaker tissues which have so far been demonstrated to meet all or at least two of the criteria —1) plus one other— are the suprachiasmatic nuclei of mammals [1, 2], pineal body of birds [3, 4], and eyes or parieto-visceral ganglion of molluscs [5–7]. Studies on the function of the pacemaker at the cellular level have also begun in some animals [8].

In insects where the candidate pacemaker tissue was reported earlier than in any other animals [9], essential progress has occurred only recently. The purpose of this paper is to review the studies on the localization of pacemakers controlling the circadian timing of insect behavior or locomotion, in order to augment previous pertinent reviews [10–12].

THE OPTIC LOBE

Disconnection of the optic lobes from the midbrain

Nishiitsutsuji-Uwo and Pittendrigh [9] first reported that the bilaterally paired optic lobes possibly house some crucial structure (driving oscillator) underlying the circadian locomotor rhythm of the cockroach, *Leucophaea maderae.* This was based on experimental results meeting the criterion that the overt circadian rhythm free-ran under a 24 hr cycle of light and darkness (LD) after bilateral optic nerve severance, but disappeared when the optic tracts were cut to isolate the optic lobe neurally from the midbrain (cerebral lobes).

Each optic lobe has three neuropiles (synaptic regions), the lamina, medulla, and lobula (Fig. 1). Electrical cauterization experiments yielded re-

Received May 30, 1987

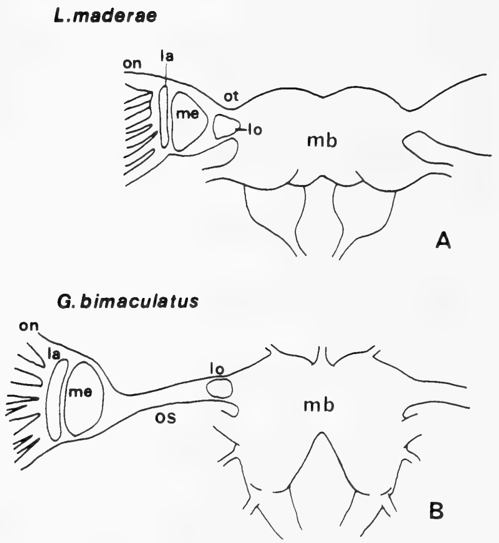

Fig. 1. Schematic drawings of cricket (A) and cockroach (B) brains illustrating the optic nerves (on), optic tract (ot), optic stalk (os) and the region of neuropiles, lamina (la), medulla (me), and lobula (lo). The optic lobes, each including these neuropiles, lies bilaterally between the midbrain (mb) and the compound eyes.

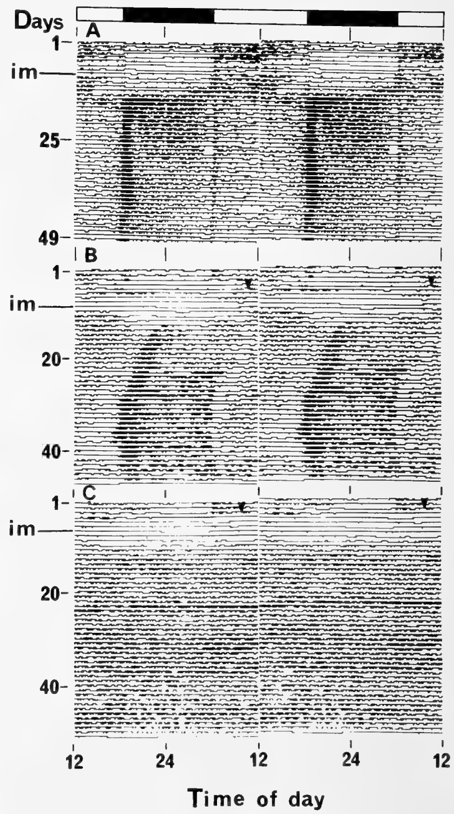

Fig. 2. Activity records of three crickets. A: Intact cricket showing entrained rhythm reversing itself from diurnal to nocturnal 4 to 5 days after imaginal molt. B: Cricket with optic nerves severed bilaterally, showing free-running rhythm. Note the occurrence of rhythm reversal. C: When optic lobes were bilaterally ablated, circadian rhythmicity disappeared. Crickets were 8th instar nymphs at time of operation (arrow)—one instar before adult.

sults suggesting that the cell bodies area adjacent to the second optic chiasma and to the lobula play a particularly important role [13]. Similarly, it has been expressed that the medulla plus the lobula system may be crucial but that the most distal synaptic region, the lamina, is not necessary for the manifestation of rhythm. Rather, it functions as a pathway conveying photic information from the compound eyes to the postulated pacemaker located somewhere in the deeper part [14].

The indispensability of the optic lobe was also demonstrated in crickets (*Teleogryllus commodus* [15], and *Gryllus bimaculatus* [16]). The latter has a medulla and lobula which are connected by a long optic stalk in contrast to the cockroach which has the two neuropiles located close together (Fig. 1). In the optic lobe ablation experiment, the optic stalk was cut at its distal end near the medulla, leaving the greater part of the stalk plus the whole lobula attached to the midbrain. However, the bilateral ablation caused the rhythm to disappear or sometimes to become quite atypical (Fig. 2). Thus, whether the view of Sokolove [13] or Roberts [14] applies to the cricket deserves careful investigation.

The third insect which, to be rhythmic, may require the optic lobe is the beetle, *Carabus problemsticus*; bilateral optic lobe ablation resulted in the disappearance of the rhythm [17].

Transplantation of the optic lobe

If the optic lobes, disconnected from the midbrain by cutting the optic tracts, are left *in situ*, the locomotor rhythm reappears in a few weeks. In addition, the rhythm returned in a cockroach

which had lost rhythmicity through optic lobe ablation, when the optic lobe was transplanted from another individual [18]. The transplanted lobe had reestablished structural connections with the midbrain of the host. The free-running period of the restored rhythm was similar to the period of the donor animal's rhythm before surgery. Page [19] also succeeded in replacing one of the bilaterally paired lobes with a lobe transplanted from another individual having a different free-running period. The recipient's activity showed the two rhythmic components (Fig. 3); one may be controlled by the recipient's original lobe and the other by the donor's. There is no other explanation for these data except that the oscillation regulating locomotor activity must originate in the optic lobes.

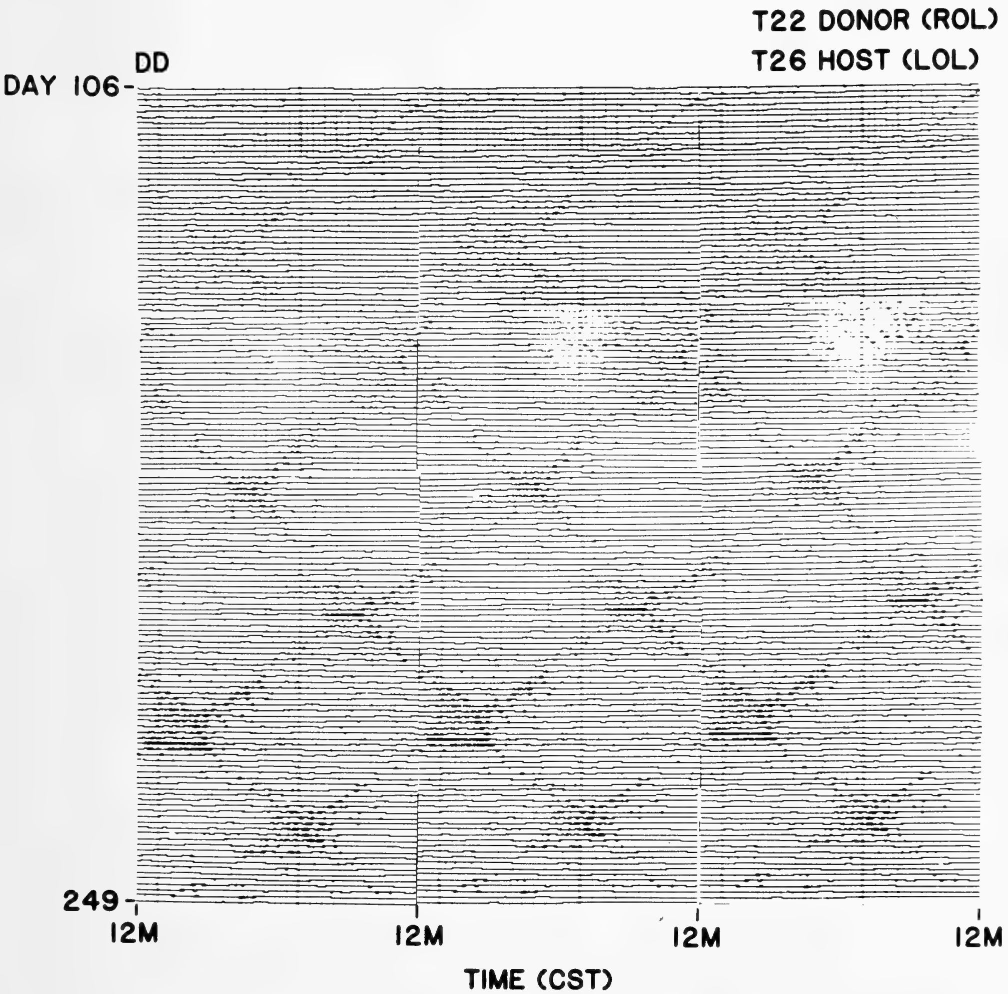

FIG. 3. Activity record of an animal with a unilateral optic lobe transplant [19]. The host animal had been raised from birth in LD 13:13 (T26) and the donor had been raised in LD 11:11 (T22). The right optic lobe (ROL) of the donor was transplanted. The host retained its left optic lobe (LOL). The record begins 106 days after transplantation and 33 days after section of the host optic tract; the record is 'triple-plotted', and shows 72 hr across. Two clear components to the activity rhythm appear to be free-running independently. An increase in the activity level is evident when the two components come into phase, and activity is nearly eliminated when the components are in anti-phase [19]. (Courtesy of Dr. Terry Page)

Circadian nervous activity of optic lobe efferents

In the cricket, *G. bimaculatus,* lamina-medulla tissue ablation causes the circadian locomotor rhythm to disappear [16]. The "lamina-medulla-compound eye" system (LMCS) exhibited clear circadian rhythms in the multiple unit activities recorded extracellularly from the cut end of the optic stalk with a suction electrode under constant conditions. In LL, all specimens exhibited a rhythm with a peak discharge frequency in the subjective night and with a free-running period longer than 24 hr. However, in specimens kept under DD or in those with the optic nerve severed, two types of circadian patterns were observed: one type showed a "diurnal" increase and the other a "nocturnal". Removal of the cerebral lobe and/or subesophageal ganglion, which minimizes the possibility of hormonal control over the system being measured, did not affect these rhythms (Fig. 4). Even though humoral controls were not excluded completely, the results may be regarded as fairly conclusive evidence that the "lamina-medulla"-complex contains a neural mechanism, i.e. a circadian pacemaker [20]. Isolation of the pacemaker tissue from both neural and humoral factors is necessary to make the evidence more conclusive, as is already being tried in the cockroach [21].

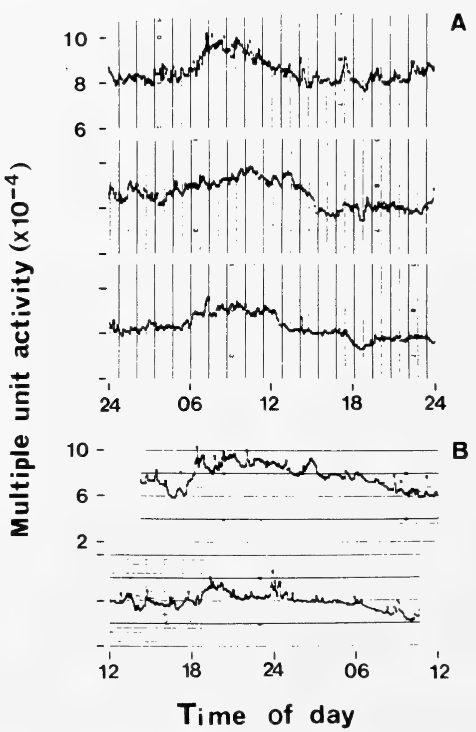

FIG. 4. Circadian rhythms of the lamina-medulla efferents after both optic stalk and optic nerve transection under constant light. The multiple unit activity showed either diurnal (A) or nocturnal (B) increases. In both cases, both the cerebral lobe and subesophageal ganglion were excised. The operation was performed at 10:00 on day 1. The record should be read from top to bottom [16].

Circadian rhythm of the amplitude of the electroretinogram (ERG)

Studies on ERG amplitude rhythm also suggest that the optic lobe contains a circadian pacemaker. In the beetle, *Blaps gigas,* ERG rhythms of the bilateral compound eyes free-ran under DD with specific circadian periods and thereby desynchronized with each other, indicating that bilateral pacemakers function independently [22]. The ERG rhythm disappeared after lobula ablation in the beetle, *Anthia sexguttata* [23].

The cricket, *G. bimaculatus,* also showed circadian ERG rhythm under DD peaking in the subjective night. The rhythm persisted in the LMCS isolated from the lobula and the midbrain (Fig. 5). A 24 hr LD cycle given unilaterally entrained the rhythm of the ipsilateral LMCS isolated from the lobula and the midbrain, but did not entrain the contralateral normal LMCS kept in DD. Consequently, the two eyes were desynchronized, implying that the LMCS constitutes a complete circadian system composed of a receptor (photoreceptor), pacemaker and effector (photoreceptor), and that the bilaterally paired systems can function independently of each other [24, 25].

The question of whether the locomotion and ERG share a common pacemaker was answered to some extent by studies with the cockroach. Bisection of the optic lobe distal to the lobula abolished the ERG rhythm of the cockroach, *L. maderae,* suggesting that the pacemaker is probably located near the lobula, as in the case of the locomotor rhythm [26].

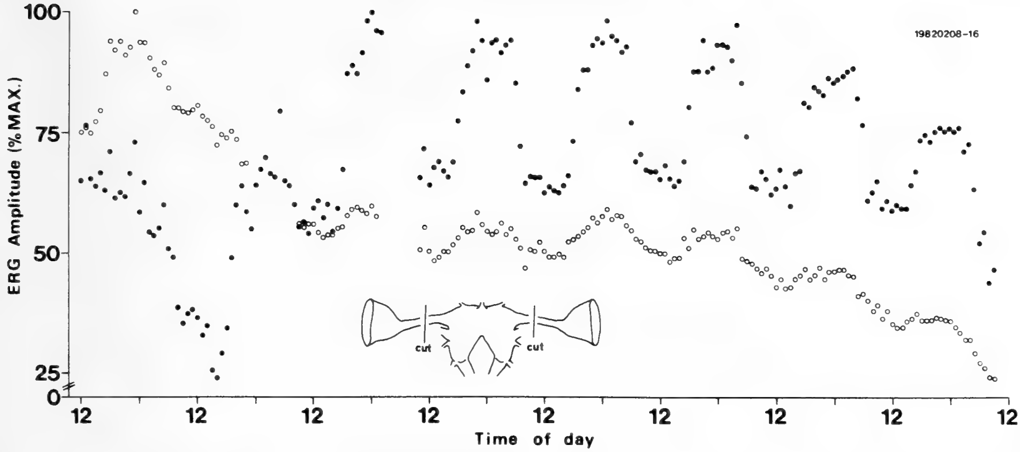

FIG. 5. ERG amplitude rhythms in a cricket after bilateral severance of the optic stalk. ○: right eye, ●: left eye. Record was taken in DD. Taus of right and left eyes were 23.2 and 23.4 hr, respectively. Data partly missing on days 2 and 3 due to technical failure [24].

Bilaterally paired pacemaker

If the bilateral pacemakers with their intrinsic periods work independently from each other, then locomotion under the control of the pacemakers shows a perturbed rhythm soon after the animal is held under constant conditions. But, the perturbation seldom occurs. That this is attributable to the existence of a bilateral connection between the postulated pacemakers was demonstrated both functionally and morphologically.

The functional demonstration was based on two lines of evidence [27]. First, the free-running period in locomotion shown by the cockroach with a unilateral lobe ablated did not change significantly under DD, no matter which of the bilateral lobes was left intact, but was significantly longer than that shown by the intact cockroach. Second, the postulated pacemaker entrained to the LD cycle received by the contralateral photoreceptor.

From a morphological aspect [28], abundant axons and axon terminals were observed degenerated in one optic lobe following extirpation of the other. Roth and Sokolove [28] also utilized a postaxotomy change in RNA distribution and retrograde axonal transport of the enzyme horseradish peroxidase to visualize the perikarya of neurons which directly interconnect the optic lobes of the cockroach, *Leucophaea maderae*.

The cricket, *Teleogryllus commodus,* which had the optic nerves cut on one side during the last larval instar, showed two activity (stridulation) components with different periods in LL; one period was longer, the other shorter than 24 hr. It is likely here that the two underlying pacemakers are only weakly coupled [29].

EXTRA- "OPTIC LOBE" PACEMAKER

The locomotor rhythm persisted in the silkmoths, *Antheraea pernyi* and *Hyalophora cecropia,* after ablation of the bilateral optic lobes and, in addition, the unilateral cerebral lobe. Because the rhythm vanished by total brain ablation or severance of the circumesophageal connectives, the pacemaker may be situated not in the optic lobes, but in the cerebral lobes [30].

The postulated pacemaker receives photic information through the extraocular photoreceptor for entrainment and emits temporal information toward the thoracic nervous system through the neuronal pathway to control the flight rhythm. The housefly, *Musca domestica*, [31] and the mosquito, *Culex pipiens pallens*, [32] may also have the pacemaker in the cerebral lobes.

The mosquito, deprived of the greater part of the optic lobes (Fig. 6), still maintained a circadian activity rhythm free-running both in DD (Fig. 7) and in LL (Fig. 8) but synchronizing with a 24 hr LD cycle. Surgical operations such as brain

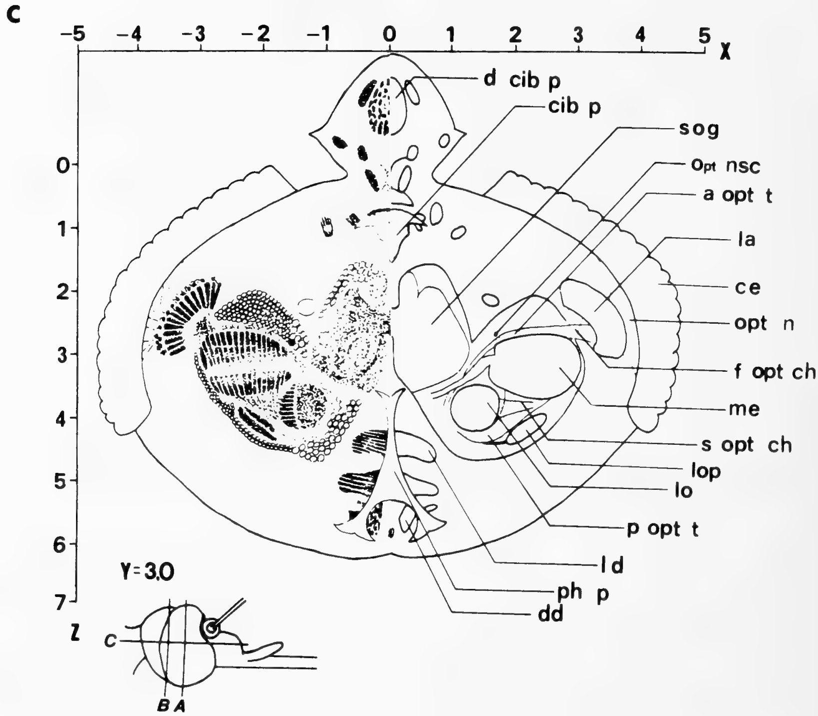

FIG. 6. The structure of the mosquito brain; a horizontal section at level C of the head indicated at bottom left. At this level, all neuropiles in the optic lobe are seen in one section, but the cerebral lobes do not appear. a opt t: anterior optic tract, ce: compound eye, cib p: cibarial pump, d cib p: dilators of cibarial pump, dd: dorsal dilators, f opt ch: first optic chiasma, la: lamina, ld: lateral dilators, lo: lobula, lop: lobula plate, me: medulla, opt nsc: optic lobe neurosecretory cell, opt n: optic nerve, ph p: pharyngeal pump, p opt t: posterior optic tract, sog: suboesophageal ganglion, s opt ch: second optic chiasma (Kasai and Chiba, unpublished).

ablation to eliminate rhythm were not successful because of high mortality. Therefore, the parts of central nervous system crucial for controlling the overt rhythm are unknown, although they might well be in the cerebral lobes, as in the silkmoth and housefly. The adult mosquito has no ocelli [33]; there might be an extraocular photoreceptor enabling the LD cycle to entrain the rhythm.

The moquito's circadian activity is characterized by a diphasic pattern with two peaks per cycle [34–36]. The peaks are assumed to be of a physiologically different nature [37] or to be controlled by separate oscillators [35, 36]. Whatever the mechanism is, they occurred in the altered mosquitoes, suggesting that the optic lobe is not involved in producing the diphase.

However, persistence of the rhythm in the optic-lobe-ablated insects does not in fact mean that the optic lobes contain *no* oscillator, in view of the idea that multiple oscillators form hierarchy underlying an overt rhythm [10, 38]. If the hierarchy exists, it is not unusual for the overt rhythm to linger at least for a few days, even though in atypical form, in the absence of the master oscillator (pacemaker). The possibility that the rhythm observed in the optic-lobe-ablated mosquito is residual is highly unlikely, because the rhythm persisted in all altered individuals in a typical form, and for as long as measurement continued (i.e., at least 10 days).

Cymborowski [40, 41] has insisted that the cricket, *Acheta domesticus,* has an intra-"cerebral lobe" pacemaker. This is based on the disappearance of rhythm and the occurrence of hyperactivity

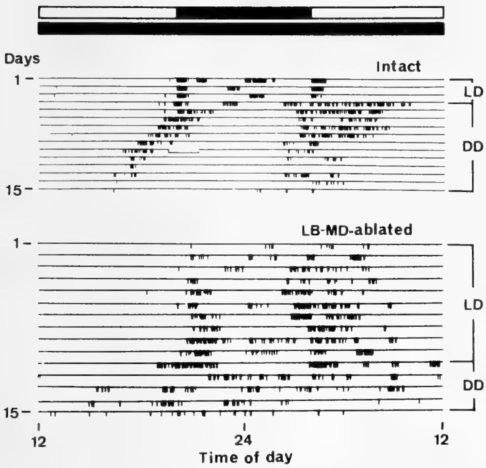

FIG. 7. Activity records of two typical female mosquitoes *Culex pipiens pallens,* held under LD 16:8 followed by constant darkness (DD). Lighting conditions indicated by white and black at top of figure. The post-operative mosquitoes (lower panels) showed significant rhythms under DD with taus of 23.7. 'LB-MD-ablated' mosquitoes lost the greater part of both optic lobes (including the lobula, lobula plate, and medulla) but retained, bilaterally, the distal portion with lamina [32].

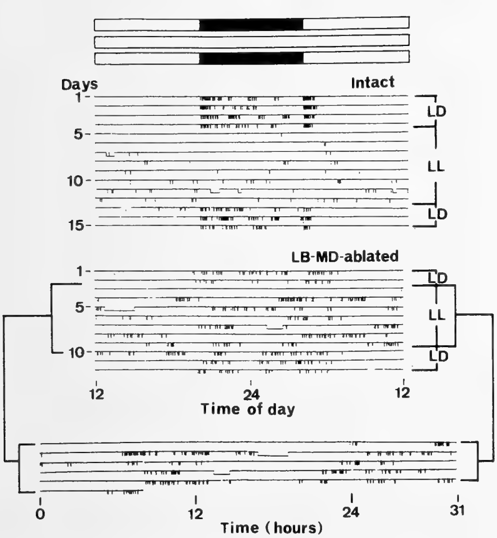

FIG. 8. Activity records of two typical female mosquitoes *Culex pipiens pallens,* under LD 16:8 followed by constant light (LL). The LL records for the post-operative mosquito (lower two panels) are replotted on a *c.* 30 hr time axis in the lower panel to clarify the presence of a rhythm with a tau of *c.* 15 hr. For further explanation, see Fig. 7.

caused by the ablation of neurosecretory cells in the pars intercerebralis. The rhythm resumed, however, with a brain transplanted from a normal animal. In the grasshopper, *Ephippiger ephippiger,* the bilateral removal of the optic lobes did not essentially affect the sound production but caused a change in its waveform [42]—another example alluding to the existence of a cerebral lobe pacemaker.

CIRCADIAN TIMING OF BEHAVIORS DURING POST-EMBRYONIC DEVELOPMENT

Once-in-a-lifetime developmental behaviors such as molting and eclosion in many insects are under circadian control. Remarkable evidence has been accumulated for endocrinological mechanisms of the circadian timing of adult eclosion [43], larval-larval molting [44], larval-prepupal development [45, 46], and pupation-associated gut-purge [47, 48].

The adult ecdysis (eclosion) clock of the silkmoth is located in the cerebral lobe [43]. This was demontrated by the exchange of brains between two different species with different daily timings of emergence. An extraocular photoreceptor in the cerebral lobes functions for synchronization with the LD cycle. The eclosion involving a stereotyped sequence of behaviors is triggered by a peptide hormone—the eclosion hormone released from the brain under control of the circadian clock. This peptide acts directly on the CNS to release the ecdysial motor programs [49–51]. The eclosion is preceded by movements to detach the old cuticle from the new one. In the moth, *Manduca sexta,* this preparatory behavior, triggered by the declining titer of ecdysteroids, is timed by the action of a temperature-sensitive clock residing outside the brain, whereas the timing of eclosion is influenced by both the phase of the ecdysteroid decline and by the brain clock. The two distinct clocks thus act in this moth late in development.

In the moth, *Samia cynthia,* a brain clock times the prothoracicotropic hormone release which is necessary for gut purge. However, the final timing of this preparatory behavior for pupation is controlled by a clock in the prothoracic gland that

gates the release of ecdysone. The prothoracic gland itself includes the photoreceptor for entrainment. These conclusions came from experiments which localized illuminations and transplanted glands from one larva to another [48, 49].

SUMMARY AND PERSPECTIVE

Optic lobe and midbrain

Insects may be divided into two groups depending on whether or not circadian locomotor rhythm persists after optic lobe ablation. One group includes the cockroach and cricket which undoubtedly have a pacemaker in the optic lobes [19, 20]. In the other group, however, which includes the silkmoth [43], housefly [31] and mosquito [32], proof of the existence of a pacemaker in the midbrain still eludes us. Therefore, in comparing the two groups, one cannot say more than that the crucial part in controlling the locomotor rhythm is different. An interesting view is that the difference is related to the method of metamorphosis [43]; the locus of the pacemaker is the optic lobes in insects undergoing incomplete metamorphosis and the midbrain in those undergoing complete metamorphosis. A study with the beetle [23] casts doubts on this view, which still deserves further study.

Neural and hormonal controls

As to the pathway conveying a time cue (temporal information) from the optic lobe pacemaker to the outside of the brain, there have been conflicting views. Nishiitsutsuji-Uwo and Pittendrigh [9] postulated that the lateral neurosecretory cells (LNSC) in the pars intercerebralis function as a junction station where the pathway is changed from nervous to hormonal. This postulation was soon superseded by the view that the pathway is all neural and is never changed to hormonal in the brain [53, 54].

However, things are not quite settled; recent reports say that surgical operations on the pars intercerebralis frequently lead to abolishment of the rhythm [15, 40, 41, 55]. Connection of the optic lobe pacemaker to the pars intercerebralis still leaves much room for investigation, especially from the standpoint, appearing in the following section, that multiple oscillators form a circadian system.

In *Drosophila melanogaster,* an arrhythmic mutant gained rhythmicity with the donor's period when receiving a brain from a short period mutant by transplantation [39]. Although it was not mentioned whether the transplanted brain included the optic lobe or not, in any event, this result suggests that a humoral control is involved in the manifestation of locomotor rhythm.

Multiple oscillators

Kinetic studies using a *Drosophila* pupae population have resulted in the two-oscillator model to explain the mechanism of daily timing of eclosion [56]. It says that a temperature sensitive oscillation controls the timing of eclosion directly but is entrained to a light sensitive one which is defined as the master oscillation. The definite phases of oscillation, recurring at the interval of about a day, are called "gates" which allow insects to emerge if developmental maturation is attained. The concrete feature corresponding to the assumed oscillators is still unknown, but the concept of "multiple oscillators underlying an overt rhythm shown by a single physiological process" has been accepted as a most attractive paradigm for experimentation. It has contributed toward the analysis of circadian systems related not only to post-embryonic behaviors [44, 47, 48] but also to adult locomotion [19, 29, 55]. In the cricket, *T. commodus,* the neurosecretory cells in the pars intercerebralis may be related in some way to the manifestation of rhythm, since their ablation sometimes abolished stridulation and locomotor rhythm [15, 56]. Singing activity of the cricket lost circadian rhythmicity, which reappeared in synchrony with a 24 hr temperature cycle. The reappearance was accompanied by some characteristics exemplified by the presence of transients, suggesting the existence of an extra-"optic lobe" temperature sensitive oscillation [58]. On the other hand, the existence of "separate oscillators for multiple physiological processes" has been assumed in *Drosophila* (adult locomotion and eclosion) [59], the moth *Pectinophora* (oviposition, eclosion and hatching [60]), the flesh fly

Sarcophaga (the initiation of larval wandering, pupal eclosion and the induction of pupal diapause [61]) and the cockroach (locomotion and growth layer formation in the endocuticle [62]).

How these oscillators, if they really exist, are organized to form a circadian system is a problem arising after the localization of oscillators.

Cellular mechanisms

The localization of the oscillator (pacemaker) is a step further into the study of the cellular mechanisms of oscillation. This analytical step, already taken in rodent suprachiasmatic nuclei [1, 2] and the bird pineal body [3, 4], has not been reported in insects.

However, a *Drosophila* study yielded an interesting view concerning the cellular mechanism of behavior rhythm, although it is not directly related to localization of the pacemaker. Fluorescence intensity of isolated salivary gland cells of wild-type *D. melanogaster* larvae showed significant rhythmicity in the cytoplasmic and nuclear areas. But in arrhythmic mutant (*per*^{0}) cells, arrhythmic and rhythmic changes were registered, the latter showing lower amplitudes. The decreased amplitude and the lower number of significant cellular rhythms in *per*^{0} mutants might be viewed as leading to an apparent arrythmicity at the behavioral level [63].

Gene control

To use biotechnological means for revealing the essential mechanism of oscillation would have great impact. In *D. melanogaster,* three mutants are known with respect to a free-running period in emergence and locomotion; one is arrhythmic (*per*^{0}), the other two having free-running periods of 19 hr (*per*^{s}) and 28 hr (*per*^{l}) [64]. These mutants are all related to a gene *per* located between zeste and white on the distal in the X chromosome, one of the most extensively investigated region of *Drosophila* genome [65]. The *per* gene DNA region was almost identified after much controversy [66, 67]. Transfer of this gene from the wild type to an arrhythmic mutant restored circadian behavioral rhythm [68, 69]. It is highly possible that this DNA codes for a proteoglycan [70].

ACKNOWLEDGMENTS

We thank Dr. Terry Page of Vanderbilt University who kindly permitted us to reproduce Figure 3 and provided us with a glossy print. Thanks are also due to Mr. Yutaka Yamamoto for his help in preparing the manuscript. This work was supported by grants from the Japanese Ministry of Education, Science and Culture (Nos. 60304010, 60304011, 61840024).

REFERENCES

1 Inouye, S. T. and Kawamura, H. (1979) Proc. Natl. Acad. Sci. USA, **76**: 5962–5966.
2 Sawaki, Y., Nihonmatsu, I. and Kawamura, H. (1984) Neurosci. Res., **1**: 67–72.
3 Deguchi, T. (1979) Nature, **282**: 94–96.
4 Takahashi, J. S., Hamm, H. and Menaker, M. (1980) Proc. Natl. Acad. Sci. USA, **77**: 2319–2322.
5 Block, G. D. and McMahon, D. G. (1984) J. Comp. Physiol., **A**, **155**: 387–395.
6 Jacklet, J. W. (1969) Science, **164**: 562–563.
7 Strumwasser, F. (1974) In "The Neurosciences: Third Study Program". Ed. by F.O. Schmitt and F.G. Worden, MIT Press, Cambridge, Mass., pp. 459–478.
8 Jacklet, J. W. (1984) Int. Rev. Cytol., **89**: 251–294.
9 Nishiitsutsuji-Uwo, J. and Pittendrigh, C. S. (1968) Z. vergl. Physiol., **58**: 14–46.
10 Brady, J. (1974) Adv. Insect Physiol., **10**: 1–115.
11 Saunders, D. S. (1976) Insect Clocks. Pergamon Press, Oxford.
12 Page, T. L. (1981) In "Handbook of Behavioral Neurobiology, Vol. 4 (Biological Rhythms)". Ed. by J. Aschoff, Plenum Press, New York, pp. 145–172.
13 Sokolove, P. G. (1975) Brain Res., **87**: 13–21.
14 Roberts, S. K. (1974) J. Comp. Physiol., **88**: 21–30.
15 Loher, W. (1972) J. Comp. Physiol., **79**: 173–190.
16 Tomioka, K. and Chiba, Y. (1984) Zool. Sci., **1**: 375–382.
17 Balkenol, M. and Weber, F. (1981) Mitt. Dtsch. Ges. allg. angew. Entomol., **3**: 223–227.
18 Page, T. L. (1982) Science, **216**: 73–75.
19 Page, T. L. (1983) J. Comp. Physiol., **153**: 353–363.
20 Tomioka, K. and Chiba, Y. (1986) J. Insect Physiol.,**32**: 747–755.
21 Page, T. L. (1986) Japan-US Seminar on Biological Rhythm (July 30–Aug. 2, 1986, Hawaii), organized by Y. Chiba and J. Feldman.
22 Koehler, W. K. and Fleissner, G. (1978) Nature, **274**: 708–710.
23 Fleissner, G. (1982) J. Comp. Physiol., **149**: 311–316.
24 Tomioka, K. and Chiba, Y. (1982) Naturwissen-

schaften, **69**: 395–396.

25 Tomioka, K. and Chiba, Y. (1985) J. Interdiscipl. Cycle Res., **16**: 73–76.

26 Wills, S. A., Page, T. L. and Colwell, C. S. (1985) J. Biol. Rhythm, **1**: 25–37.

27 Page, T. L., Caldarola, P. C. and Pittendrigh, C. S. (1977) Proc. Natl. Acad. Sci. USA, **74**: 1277–1281.

28 Roth, R. L. and Sokolove, P. G. (1975) Brain Res., **87**: 23–39.

29 Wiedenmann, G. (1983) J. Comp. Physiol., **150**: 51–60.

30 Truman, J. W. (1974) J. Comp. Physiol., **A, 95**: 281–296.

31 Helfrich, C., Cymborowski, B. and Engelmann, W. (1985) Chronobiol. Int., **2**: 19–32.

32 Kasai, M. and Chiba, Y. (1987) Physiol. Entomol., **12**: 59–65.

33 Clements, A. N. (1963) The Physiology of Mosquitoes. Pergamon Press, Oxford.

34 Chiba, Y., Yamakado, C. and Kubota, M. (1981) Int. J. Chronobiol., **7**: 153–164.

35 Clopton, J. R. (1985) J. Comp. Physiol., **A, 155**: 1–12.

36 Jones, M. D. R. (1982) Physiol. Entomol., **7**: 281–289.

37 Chiba, Y., Kubota, M. and Nakamura, Y. (1982) J. Interdiscipl. Cycle Res., **13**: 55–60.

38 Moore-Ede, M. C., Scemelzer, W. S., Kass, D. A. and Herd, J. A. (1976) Fed. Proc., **35**: 2333–2338.

39 Handler, A. M. and Konopka, R. J. (1979) Nature, **179**: 236–238.

40 Cymborowski, B. (1973) J. Insect Physiol., **19**: 1423–1440.

41 Cymborowski, B. (1981) J. Interdiscipl. Cycle Res., **12**: 133–140.

42 Dumortier, B. (1972) J. Comp. Physiol., **77**: 80–112.

43 Truman, J. W. (1972) In "Circadian Rhythmicity". Ed. by J. F. Bierhuizen, Centre for Agricultural Publishing and Documentation, Washington, pp. 111–135.

44 Truman, J. W. (1972) J. Exp. Biol., **57**: 805–820.

45 Truman, J. W. and Riddiford, L. M. (1974) J. Exp. Biol., **60**: 371–382.

46 Fujishita, M. and Ishizaki, H. (1982) J. Insect Physiol., **28**: 77–84.

47 Mizoguchi, A. and Ishizaki, H. (1982) Proc. Natl. Acad. Sci. USA, **79**: 2726–2730.

48 Mizoguchi, A. and Ishizaki, H. (1984) J. Comp. Physiol., **A, 155**: 639–647.

49 Truman, J. W. (1978) J. Exp. Biol., **74**: 151–174.

50 Truman, J. W. (1971) Am. Zool., **21**: 655–661.

51 Truman, J. W. and Weeks, J. C. (1983) Soc. Exp. Biol. Symp., **37**: 223–241.

52 Truman, J. W. (1984) J. Comp. Physiol., **A, 155**: 521–528.

53 Bardy, J. (1971) In "Biochronometry". Ed. by M. Menaker, National Academy of Sciences, Washington, D.C., pp. 517–524.

54 Robert, S. K., Skopik, S. D. and Driskill, R. J. (1971) In "Biochronometry". Ed. by M. Menaker, National Academy of Sciences, Washington, D.C., pp. 505–515.

55 Tomioka, K. (1985) J. Insect Physiol., **31**: 653–657.

56 Sokolove, P. G. and Loher, W. (1975) J. Insect Physiol., **21**: 781–799.

57 Pittendrigh, C. S. (1960) Cold Spring Harbor Symp. Quant. Biol., **25**: 159–184.

58 Rence, B. and Loher, W. (1975) Science, **190**: 385–387.

59 Engelmann, W. and Mack, J. (1978) J. Comp. Physiol., **127**: 229–237.

60 Pittendrigh, C. S. and Minis, D. H. (1978) In "Biochronometry". Ed. by M. Menaker, National Academy of Sciences, Washington, D.C., pp. 212–250.

61 Saunders, D. S. (1986) Chronobiol. Int., **3**: 71–83.

62 Lukat, R. (1978) Experientia, **34**: 477.

63 Weizel, G. and Rensing, L. (1981) J. Comp. Physiol.,**143**: 229–235.

64 Konopka, R. J. and Benzer, S. (1971) Proc. Natl. Acad. Sci. USA, **68**: 2112–2116.

65 Konopka, R. J. (1979) Fed. Proc., **38**: 2602–2605.

66 Bargiello, T. A. and Young, N. W. (1984) Proc. Natl. Acad. Sci. USA, **81**: 2142–2146.

67 Reddy, P., Zehring, W. A., Wheeler, D. A., Pirrotta, V., Hadfield, C., Hall, J. C. and Rosbash, M. (1984) Cell, **38**: 701–710.

68 Bargiello, T. A., Jackson, F. R. and Young, M. W. (1984) Nature, **312**: 752–754.

69 Zehring, W. A., Wheeler, D. A., Reddy, P., Konopka, R. J., Kiriacou, C. P., Rosbash, M. and Hall, J. C. (1984) Cell, **39**: 369–376.

70 Reddy, P., Jacquier, A. C., Abovich, N., Peterson, G. and Rosbash, M. (1986) Cell, **46**: 53–61.

Proceedings of the Fifty-Eighth Annual Meeting of the Zoological Society of Japan

October 7–9, 1987

Toyama

Suffixal letters of abstract number refer to the abbreviated subfields of zoology

PH : physiology
CB : cell biology
GE : genetics
IM : immunology
BI : biochemistry
DB : developmental biology
EN : endocrinology
MO : morphology
BB : behavior biology
EC : ecology
TS : taxonomy and systematics

ZOOLOGICAL SCIENCE 4: 957 (1987)

PRESIDENT'S MESSAGE

I would like to take the opportunity to make a few comments on the occasion of the Fifty-eighth Annual Meeting of the Zoological Society of Japan, held in Toyama.

First of all, I would like to express my sincere gratitude to the chairman of the Organizing Committee, Professor Manabu K. Kojima of Toyama University, as well as to the members of the local committee who have endeavored to produce such a fruitful meeting. In addition, I would like to thank the nearly 1,000 members in attendance for their contribution to the success of this meeting.

As you know, our Society is now enjoying its 108th year since being founded through the efforts of our predecessors, and serves as the focal point of zoolgical research in Japan. It goes without saying, however, that our Society's importance arises not from its venerable age, but from its many members who are active at the forefront of research, and I want to emphasize that we should remain a youthful, fresh society which promotes the exchange of information and understanding among members.

The progress being made recently in Life Sciences is quite rapid, and researchers now have great expectations of the information emanating from our Society. I believe we all should make aggressive efforts toward the progress of the Zoological Society of Japan.

In 1984, on the occasion of the 100th anniversary of the founding of the Society and after many years of preparation, we began publishing our new official journal, *Zoological Science*. At the 1984 annual meeting, our former president Dr. Hideshi Kobayashi discussed six goals of our Society in the president's message (see *Zoological Science*, **1** (6): 852–853). Upon my being elected president last year, I vowed to continue to pursue those goals which were established in the pivotal year 1984. I am pleased to note that Dr. Kobayashi will henceforth work towards the progress of *Zoological Science* as Editor-in-Chief. For the enhanced, international development of our journal, I hope our members will support the publication and continue to submit thier high quality manuscripts for the journal.

Our Society is characterized by its dedication to the very wide field of Zoology, and by a membership comprising both elder and young members. It is my desire that our members do not restrict themselves to one narrow field, but instead have an interest in all of biology. With a view towards broadening our scope from the minutely detailed experiments in our laboratories, to the observation of biological phenomena on a global scale, we should strive to improve communication among biologists of different fields.

Recently, the Science Council of Japan inquired about the progress being made by our Society. We must not let ourselves become satisfied only with the existence of our Society; instead, it is necessary for us to assert to the world in this day of strong expectations for Life Sciences, our important role and compelling reason for existence.

We must preserve the free atmosphere and flavor of our Society in which every member can devote himself to his basic and independent research. At the same time, we would like our Society to be a humane, professional group which can contribute to the many problems human beings confront, from bioethical issues which arise in the genetic engineering pursued in biotechnology, to the problems of population, food, and environment.

My sincere wishes for the great success of each and every one of our members.

October 8, 1987

NOBUO EGAMI
The President of the Zoological Society of Japan

ZOOLOGICAL SCIENCE 4: 958 (1987)

[THE ZOOLOGICAL SOCIETY PRIZE]

Biochemical Studies on Fertilization

Motonori Hoshi

Biological Laboratory, Faculty of Science, Tokyo Institute of Technology, Tokyo 152

Fertilization is one of a few exceptional events in which allogeneic cell interactions are allowed to take place. The process is achieved through successive changes of two highly differentiated cells, eggs and spermatozoa. These changes are both spatially and temporally well regulated and can be synchronously induced in large populations of homogeneous cells at least in some marine invertebrates like sea urchins and starfish. This provides us good experimental systems to understand the molecular mechanisms underlying cell-to-cell interactions and other important cellular events. While spermatozoa are naked cells, eggs are generally encased within one or a few egg coats mostly made of glycoconjugates. Egg coats are the place where major events ending up in the gamete fusion are performed. By using suitable marine invertebrates, we have studied the three principal events; sperm binding, acrosome reaction and sperm penetration.

Sperm Binding to the Vitelline Coat Sperm bind species-specifically to the vitelline coat as a transitory but obligatory step for fertilization in various animals. In the ascidian *Ciona intestinalis,* a hermaphrodite, the binding is a step of self/not-self recognition and is possible to be analyzed separately from other events like the acrosome reaction. *Ciona* sperm are known to recognize the molecular architecture, especially the terminal L-fucose, of a glycoprotein (the sperm receptor) in the vitelline coat. It was attempted to identify a sperm surface protein that binds complementarily to the sperm receptor. On the basis of experimental evidence, we have proposed a theory that a glycosidase on the surface of ascidian sperm, α-L- fucosidase in the specific case of *Ciona,* serves as the binding protein by forming a quasi-stable complex in sea water with a potential substrate, the sperm receptor.

Egg-Jelly Components Responsible for the Induction of Acrosome Reaction Where fertilizing sperm undergo the acrosome reaction is yet an open question in almost all animals. In the starfish, however, it is well established that fertilizing sperm undergo the acrosome reaction when they meet the egg-jelly coat. Thus jelly components responsible for inducing the acrosome reaction were searched in *Asterias amurensis.* Three components are proved responsible for the induction; acrosome reaction-inducing substance (ARIS), its co-factor (Co-ARIS) and an oligopeptide(s). ARIS and Co-ARIS are indispensable for the induction in normal sea water and presumably activate Ca-channels in the sperm plasma membrane. The peptide is not obligatory but it facilitates the reaction by increasing the intracellular pH of sperm. ARIS is a sulfated glycoprotein of a extremely high molecular weight, and sulfate residues and saccharide portions are essential for its activity. Three sulfated steroid saponins are chemically identified as Co-ARIS. The activity of Co-ARIS depends mainly on the side chain of steroid and sulfate residue.

Enzymatic Lysins Enzymatic lysins were screened by comparing effects of various enzyme inhibitors on the fertilization of intact and naked eggs. Lysins for the vitelline coat were searched in an ascidian *Halocynthia roretzi* where the coat is rather easily removed by using needles without injuring eggs. Either or both of two trypsin-like proteases, spermosin and acrosin, and a chymotrypsin-like protease are shown to be vitelline coat lysins. It is also shown by a similar method that sea urchin sperm use an arylsulfatase and a sialidase as jelly coat lysins, and an arylsulfatase and a chymotrypsin-like protease as vitelline coat lysins.

ZOOLOGICAL SCIENCE 4: 959 (1987)

[THE ZOOLOGICAL SOCIETY PRIZE]

Chronobiology of Behavior

Yoshihiko Chiba

Environmental Biology Laboratory, Yamaguchi University, Yamaguchi 753

Behaviors are timed with reference to 24-h day as the result of synchronization of *circadian rhythm* with its *environmental counterpart.* The timing is affected also by the physiological state related to *the purpose of behavior.* We have been investigating how these three factors are involved in timing host-seeking or biting behavior of the female mosquito, *Culex pipiens pallens.*

Virgin females show a diphasic activity under LD 16:8 h, peaking at lights-off ('dusk') and lights-on ('dawn'). After insemination, however, she becomes active from 'dusk' to midnight and lowers the 'dawn' peak. This modification is caused by the male accessory gland (MAG) substance in the seminal fluid. The effect of MAG homogenate, assayed by injection into virgin female, shows a dose-dependency; 0.5 MAG equivalent is critical, eliciting a half-maximal response. More than 95% of the females captured on baits in the field are inseminated prior to host-seeking and biting. Modification of the circadian pattern by insemination may have some adaptive significance in achieving the purpose of the ensuing behaviors. The virgin female activity is under circadian control, free-running under constant conditions, synchronizing with environmental cycles or showing a temperature compensation (Q_{10}=0.91–0.96). The internal mechanism of circadian rhythm has been postulated to include, at the very least, a pacemaker (primary generator of temporal information) and photoreceptor which disperses photic information toward the pacemaker for entrainment. Mosquitoes deprived of the greater part of their optic lobes still maintained the circadian rhythm in DD and LL, and showed the diphasic activity entrained roughly to a 24-h LD cycle. Thus, the pacemaker or a crucial part for controlling the rhythm is presumably within the cerebral lobes, but not within the optic lobes we demonstated almost conclusively to house the pacemaker in the cricket. The entrainment may be attained primarily by the photic information conveyed through an extraocular receptor. The other photoreceptive pathway, 'compound eye plus optic lobe' (CE–OL), may function either to strengthen the synchronization or to mask the overt rhythm. The surgical experiment provided a clue to a question of subspecific difference in sensitivity to light between *pallens* distributed over the ground and its subspecies *molestus* inhabiting underground constructions. The spatially scotophilous *molestus* is temporarily photophilous, being very active in the light fraction of a 24-h LD cycle or under LL, where *pallens* is hardly active. But the optic lobe ablation makes *pallens* photophilous, indicating that the subspecific difference is related to 'CE–OL' function.

Our interest covers the connections between the physiology of individual females and the field observations on population or community. In individual females, mating and biting are not daily events; the former occurs once in a lifetime and the latter recurs at the interval of a few days while eggs are matured and laid. The daily activity peaks observed in the laboratory correspond to the so-called 'gate' which allows mosquito to assume one of these behaviors. How does, for example, each inseminated female, select her own biting time in such a wide gate that lasts for several hours from dusk to midnight? On the other hand, biting populations of multiple species and their host form a community revealing a 24-h rhythm in, for example, diversity. Is the community rhythm explained simply as the addition of the rhythms of component species? These ecological questions also deserve future study.

PH 1

COMPARISON OF OSMOREGULATORY CAPACITY BETWEEN THE AMPHIDROMOUS AND LANDLOCKED RINOGOBIUS (GOBIIDAE) AFTER TRANSFER TO 50% SEA WATER.

K. IWATA and T. SAIJYO. Biol. Labo., Fac. of Edu., Wakyama Univ., Wakayama.

Among the genus of Rinogobius living in Japan, R. guirinus and R. brunneus are the amphidromous species, and R. brunneus living in Lake Biwa and R. flumineus are the landlocked species. When the fishes were directly transferred to 50% SW, a high mortality was observed in the landlocked species, but no fish was died in the amphidromous species. In the landlocked species the blood osmolarity increased to 400 mOsm within 24 hrs after transfer. However, the lacustrine species surviving for 7 days in SW slightly surpassed R. flumineus in the hypoosmoregulatory capacity. In the amphidromous species, the blood osmolarity decreased within 48 hrs, although the levels were somewhat higher than the FW levels. Na-K-ATPase activities in the gill of the amphidromous species increased much above the FW levels for 7days in SW, but any change was not observed in the landlocked species. On the other hand, those levels increased greatly when all the species examined were adapted to deionized water.

It is suggested that the amphidromous species preserve an ability to survive well in SW during their FW lives, but the landlocked ones lose some function to remove an excess ion from their bodies during SW entry.

PH 2

WATER INFLUX THROUGH THE INTEGUMENT OF TREEFROG, Hyla arborea japonica.

H. Nakashima and Y. Kamishima. Dept. of Biol., Facult. of Sci., Okayama Univ. okayama 700

Anurans take the water they need through the integument. The water intake in japanese treefrogs was mainly confined to the ventral pelvic skin. Water influx through this portoin was 0.3µl/cm²/min. The water influx was markedly increased in animals kept under dehydrated condition, showing 1.12µl/cm²/min. Isoproterenol, an adrenergic β-agonist, enhanced the influx 7 times as much as the controls, showing 2.13µl/cm²/min. However, the influx rate of animals in breeding season was 0.08µl/cm²/min which was much lower than the animals in off-breeding season. Enhancement by the β-agonist was also reduced in these animals. Prolactin administration to the animal in off-breeding season caused the same depriviation of the water influx with that of animals in breeding season. Morphological modifications of the tissue was observed in accordance with the physiological activities. When water influx was high,the skin appeared thinner and flatter, and the outermost layer of the epidermis was strongly stained with several dyes, while the skin with less water influx appeared granular in texture, and the epidermal cells were larger and showed no special chromophilic nature.

PH 3

AMINO ACIDS METABOLISM STIMULATES WATER ABSORPTION ACROSS THE SEAWATER EEL INTESTINE.

M. Ando. Lab. of Physiol. Fac. of Integrated Arts & Sci., Hiroshima Univ., Hiroshima.

To elucidate how intracellular L-alanine enhances water absorption across the eel intestine, effects of metabolic inhibitors were examined. The enhancement by 5 mM L-alanine was inhibited by aminooxyacetate, an aminotransferase inhibitor. After blocking pyruvate synthesis by the drug, the water absorption was accelerated by pyruvate, whose effects were inhibited by oxythiamine, a dehydrogenase inhibitor. Furthermore, the effects of L-alanine was inhibited by 2,4-dinitrophenol, and O_2 consumption of the tissue increased after treatment with alanine. These results indicate that L-alanine is metabolized via the TCA cycle to produce ATP. L-glutamine also enhanced the water absorption through a common metabolic pathway with L-alanine. However, the responses to 1-2 mM L-glutamine was faster and greater than those to 5 mM L-alanine. Therefore, it seems likely that L-glutamine is a major fuel for the water absorption across the seawater eel intestine.

PH 4

NEURAL CONTROL OF FERTILIZATION IN THE GENITAL CHAMBER OF THE FEMALE CRICKET, *TELEOGRYLLUS COMMODUS*.

T.Sugawara. Dept. Biol., Saitama Med. Sch., Saitama.

Stimulation of mechanosensory cells in the postero-lateral wall of the genital chamber elicited reflex contraction in the spermathecal duct via the genital chamber nerve. The contraction of circular muscles of the duct occurred in the basal part connecting with the chamber, and was propagated in the peristaltic manner upward to the spermathecal bulb. It was observed that this contraction produced sperm flow downward to the chamber. The spermatozoa were transported with tails first. Sensory cells were found in the copulatory papilla. They are clustered in both sides of the spermathecal duct, and send dendrites along the duct toward its opening to the chamber. They may respond to the sperm descent.

The process of fertilization during the rest phase of oviposition in the female cricket was thus revealed as follows: (1) the egg introduced into the genital chamber stimulates the mechanosensory cells in the chamber wall, (2) the reflex contractions occur both in the muscles covering the chamber and in the spermathecal duct, (3) the sperm is squeezed out and the egg is fertilized, (4) the sperm stimulates the sensory cells in the copulatory papilla, (5) the gate-opener muscles (M9s) reflexly contract, and finally (6) the egg is ejected into the ovipositor.

PH 5

RESPONSES OF NONSPIKING GIANT INTERNEURONS TO MAGNETIC FIELD AND VISUAL STIMULATION IN THE CRAYFISH.

Y.Okada and T.Yamaguchi. Dep. of Biol., Fac. of Sci., Okayama Univ., Okayama.

In the protocerebrum of the crayfish, there are five pairs of nonspiking giant interneurons (NGIs) which are presynaptic to the oculomotor neurons. Three of them form a cluster and respond with graded hyper- or depolarizing potentials to ipsi- or contralateral eye illumination, respectively (Okada and Yamaguchi,1986). The present study of the responsiveness of these neurons to the magnetic field stimulation (MFS) and visual stimulation (VS) revealed the following features. (1) The NGIs respond with hyper- or depolarizing potentials without action potentials to MFS of each statocyst. (2) Hyperpolarizing current injection through a recording electrode into a NGI increases the amplitude of depolarizing response elicited by MFS or VS and decreases that of hyperpolarizing response. Depolarizing current injection shows the reversed effect on the responses. (3) When MFS and VS are applied in succession, the polarity of response to preceding stimulation affects on the amplitude of the response of following stimulation. (4) These results suggest that the responses of NGIs to MFS are modulated by those to VS or vice versa.

PH 6

MORPHOLOGICAL AND FUNCTIONAL FEATURES OF NEURONS INNERVATING THE REPRODUCTIVE ORGANS IN THE FEMALE CRICKET.

T.Kimura, Y. Kotoh and T.Yamaguchi. Dept. of Biol., Fac. of Sci., Okayama Univ., Okayama.

In the female cricket, rhythmic movements of the spermathecal duct are induced by 10^{-8}M 5-HT and they are inhibited by 10^{-8}M octopamine. Ni^{++} back-filling reveals that the female reproductive organs (genital chamber, spermathecal duct, spermatheca) are innervated by several dorsal unpaired median neurons (DUMR4 neurons) emerging through the fourth nerve roots from the terminal abdominal ganglion and two paired neurons extending the axons through one of the nerve roots. One of the paired neurons is a 5HT-like immunoreactive neuron, and the immunoreactivity is seen in its soma and terminals which are distributed among the muscle layers of genital chamber, copulatory papilla and the spermathecal duct near the junction with the genital chamber. The most probable conclusion from another immunohistochemical evidence is that the DUMR4 neurons are octopamine-like immunoreactive.

PH 7

FUNCTIONAL ROLE OF NONSPIKING NEURONS IN THE CERCUS-TO-GIANT INTERNEURON SYSTEM OF CRICKETS.

Y.Baba and T.Yamaguchi. Dept. of Biol., Fac. of Sci., Okayama Univ., Okayama

The nonspiking interneurons (NIs) responding only with slow potentials to wind stimulation of the filiform hairs (T- and L-hairs) on the cerci are present in the terminal abdominal ganglion of crickets, and 15 NIs (NI-1 - NI-15) are distinguishable by the features of their morphology and responsiveness to the stimulation. The directional sensitivity of NIs is rather complex: for instance, NI-2 responds well with depolarizing potential to anterior wind, and NI-7 responds with depolarizing potential to lateral wind in the ipsilateral side to its soma as well as with hyperpolarizing potential to lateral wind in the contralateral side. The results of selective wind stimulation of T- and L-hairs on the cerci shows that each NI integrates the sensory inputs from these hairs in a characteristic way. Double staining of a medial giant interneuron and a NI reveals that the dendrite of medial giant interneuron is wound with branchlets of NI-1, NI-2 and NI-5. These results imply that the NIs may play an important role in the spatial information processing in the cercus-to -giant interneuron system.

PH 8

SEXUAL DIMORPHISM AND PROGRAMMING CELL DEGENERATION IN THE FLIGHT MUSCLES OF ADULT CRICKETS.

T.Yamaguchi, S.Kogawauchi, S. Shiga, K. Yamada and T.Kimura. Dept.of Biol., Fac. of Sci., Okayama Univ., Okayama.

The depressor muscle, M90 of male adult is larger than that of female adult, and the elevator muscles, M112a and M119, and depressor muscle, M129a, of female adult is larger than those of male adult. In both sexes, an increase in weight of the muscles, M112a, M119 and M129a, is first seen during four days following the imaginal ecdysis. After the weight reaches the maximum value, a rapid decrease in the weight and the marked change in the color of muscles take place: the young muscles assume pale-red color, and old muscles do white color. In the case of M112a, the muscle histolysis with accompanying the disappearance of birefringence occurs about 20 days after the ecdysis. However, in the motoneurons innervating the muscle, M112a , there is no significant atrophy and the morphological profiles are well preserved, and they fire normally during flight performance.

PH 9

DESCENDING STATOCYST INPUT TO THE UROPOD MOTOR SYSTEM OF CRAYFISH

M.Takahata and M. Hisada. Zool. Inst., Fac. Sci., Hokkaido Univ., Sapporo 060.

The responses of uropod motoneurons and related interneurons to magnetic field stimulation were analysed intracellularly in an animal with its statolith replaced with fine ferrite granules. The motoneuron activity was recorded from the dendritic branches in the terminal abdominal ganglion while the activity of descending statocyst interneurons was monitored at the circumesophageal commissure. All the motoneurons examined showed subthreshold, depolarizing PSPs in response to descending interneuron activity. No hyperpolarizing response was observed. The PSPs seemed to be mediated polysynaptically since there was no 1:1 correspondence between the descending spikes and the PSPs. The only candidate at present for the neuron interposed between the descending statocyst interneuron and the uropod motoneuron is the local nonspiking interneuron: no other class of neurons in the terminal abdominal ganglion such as local spiking interneurons and interganglionic interneurons responded to the magnetic field stimulation except the descending statocyst interneurons. The response of nonspiking interneurons was either depolarizing or hyperpolarizing, but in neither case the 1:1 correspondence was observed between the descending spikes and the PSPs of a nonspiking interneuron. The connection between the descending statocyst interneurons and the uropod motoneurons thus seems to be mediated by a network of interneurons probably involving both the nonspiking and spiking interneurons.

PH 10

CRAYFISH STATOCYST INTERNEURONS HAVE OVERLAPPING DENDRITIC FIELDS IN SEVERAL SENSORY NEUROPILES IN THE BRAIN.

H. Nakagawa and M. Hisada, Zool. Inst., Fac. Sci., Hokkaido Univ., Sapporo

Seven descending interneurons (S1 to S2) which respond tonically to statocyst stimulation were identified in the crayfish brain. Statocyst was stimulated by artificially bending the statocyst hairs in situ while recording intracellularly from candidate neurons at the circumesophageal connective. After physiological identification, the neurons were stained with intracellular injection of $NiCl_2$ and subsequent silver intensification. Morphological characteristics of these seven interneurons are (1) the cell bodies in the anterior cluster, (2) dendrites projecting to the optic, parolfactory and antennal lobes and to the dorsal parts of both the deuto- and tritocerebrum, (3) lack of dendrites projecting to the olfactory and accessory lobes except S3. The projections of these interneurons in the optic lobe and the deutocerebral area agree well with the fact that the equilibrium responses are controlled by both statocyst and visual inputs. The function of the additional tritocerebral projections remain to be analyzed. The morphology of these neurons clearly indicates that they are multimodal, highly complex interneurons rather than simple relay interneurons. By comparing the input statocyst and the axonal location in the circumesophageal connective, S1, S2 and S7 are thought to be respectively identical with C_1, C_2 and I_2 among four statocyst interneurons described by Takahata and Hisada (1982).

PH 11

A WHOLE-MOUNT SILVER INTENSIFICATION METHOD FOR ELECTRON MICROSCOPY

M.Sato and M.Hisada. Zool. Inst., Fac. of Sci., Hokkaido Univ. Sapporo.

Nickel chloride filled neurons of the crayfish can be examined using both light (LM) and electron microscopy (EM). The method of whole mount silver intensification for LM was improved by changing the schedule and the ratio of the contents, pH and osmotic mol, of the developer base solution. The injected nickel cations were precipitated with rubeanic acid. The tissue, which included the neuron, was pre-fixed and treated with that solution. After treatment, it was post-fixed and embedded in epoxy resin, and then sectioned (50μm thick). The sections were analyzed under LM, and resectioned for EM. LM observation showed that the neurites were clearly blackened by fine silver grains, and under EM, they contained electron dense deposits of 10-100nm in diameter. This method makes it possible to observe both the gross morphology and the ultra structure of one neuron, which until now has required the observation of 2 or more neurons. Moreover, to investigate connections between two distinct neurons by using together this method and the HRP-method, it is possible to distinguish neurites of the different cells on the basis of differences in staining characteristics.

PH 12

LASER DESTRUCTION OF DENDRITE TO FACILITATE THE ANALYSIS OF NEURAL CIRCUIT.

M. Hisada, M. Takahata and T. Toga. Zool. Inst., Hokkaido Univ., Sapporo.

We have devised a laser irradiation apparatus in combination with a dissection microscope. By manipulating a single lens in the optical pathway the device works either as a epi-illumination fluorescence microscope or a microbeam irradiation source of about 30 μm in diameter. By staining a single neuron in situ intracellularly with Lucifer Yellow dye, we are able to observe the morphology of the whole neuron for identification during the intracellular recording of the neural activity when the device is used as a fluorescence microscope. With the microbeam, a desired portion of the stained neuron can be destructed and eliminated out from the functional entity in a few seconds by the photochemical reaction. The severance does not affect the function of the rest of the cell appreciably except a temporal slight depolarization. We have tested this method in the crayfish ganglion to assess the role of some neurites in the local nonspiking, ascending and motor neurons. In the nonspiking and the ascending neurons, the differential distribution of sensory input terminals among the neurites was revealed by the selective elimination of the neurites. In the flexor inhibitor motoneuron, excitatory interaction between the sibling neurons remained intact after the severance of axon indicating the interaction is in a local, nonspiking mode. The device has hence proved to be quite useful to assess the functional differentiation of individual dendrites in a single neuron. Potential use of this device includes the elimination of an entire cell in a nerve ganglion or in a developing embryo to assess the role of the cell as a whole.

PH 13

THE EFFECTS OF CALCIUM AND CALMODULIN OF THE INITIATION OF SPERM MOTILITY IN RAINBOW TROUT.

W. Yamao and M. Morisawa. Ocean Research Institute, University of Tokyo, Tokyo.

K^+ efflux and subsequent Ca^{++} influx trigger the first step of initiation of trout sperm motility. In order to know the second step which may be regulated by the intruded Ca^{++}, we studied the effects of calmodulin antagonists on the motility of rainbow trout sperm. There was no effect of W-5, but W-7 and trifluoperazine (TFP) at the concentration around 10^{-5}M inhibited the motility of live sperm. On the other hand, W-7 didn't inhibited the motlity of demembranated sperm, suggesting that calmodulin regulates the sperm motility at the plasma membrane. In contrast, TFP inhibited the motility of demembranated sperm, implicating the presence of other regulatory mechanism in the axoneme which is sensitive to TFP. With regard to the effects of Ca^{++} concentrations on the live and demembranated sperm, the former were motile in the medium containing Ca^{++} at the concentration more than 10^{-6}M and immotile in less than 10^{-7}M, but the latter were immotile in the medium containing Ca^{++} at the concentration more than 10^{-6}M and motile in less than 10^{-7}M Ca^{++}. These results suggest that Ca^{++} at the concentration between 10^{-6}M-10^{-8}M affects the plasma membrane or axoneme, and regulated sperm motility of trout sperm. The regulatory mechanism may be controled by Ca^{++} regulatory protein, calmodulin.

PH 14

EFFECTS OF PROTEIN KINASE INHIBITORS ON THE PHOSPHORYLATION OF PROTEINS AND MOTILITY IN RAINBOW TROUT SPERMATOZOA.

M.Morisawa[1], T.Hirabayashi[1] and H.Hayashi[2]
[1]Ocean Res. Institute, Univ. Tokyo, Tokyo and [2]Institute of Mol. Biol.,Fac. Sci. Nagoya Univ., Nagoya.

We showed that cyclic AMP-dependent phosphorylation of tyrosine residues in 15K protein triggers the final step of the initiation of trout sperm motility. We investigated here the effects of protein kinase inhibitors on the cAMP dependent phosphorylation of sperm proteins with molecular weights of 15K, 25K, 32K, 68K and motility of demembranated sperm. H-7, a known inhibitor of protein kinase C did not inhibit both phosphorylation of 15K protein and sperm motility. Inhibitors of cAMP dependent protein kinase such as H-8, H-9, protein kinase corepeptide inhibited phosphorylation of all proteins including 15K protein and sperm motility. Poly (Glu,Tyr)4:1, specific inhibitor of tyrosine kinase inhibited only the phosphorylation of 15K protein and sperm motility. However, it did not inhibit the phosphorylation of other proteins. Antiserum of phosphotyrosin inhibited sperm motility but not phosphorylation of proteins. These results suggest that tyrosine kinase is phosphorylated and activated by A-kinase, and phosphorylation of 15K protein through this process causes the initiation of sperm motility in rainbow trout.

PH 15

THE PROCESS OF ACQUISITION OF SPERM MOTILITY IN SALMONID FISH.

S. Morisawa[1], K. Ishida[2], & M. Morisawa[3].
[1]Biol. lab., St. Marianna Univ., Kawasaki, [2]Teikyo Univ., [3]Ocean Res. Inst., Tokyo Univ., Tokyo.

Testis spermatozoa of salmonid fish are morphologically mature in the breeding season, however, they do not have the potential for motility. Spermatozoa acquire the potential during passage through the sperm duct after leaving the testis. During the course the HCO_3^- concentration and pH in the seminal plasma increased. When testis sperm of rainbow trout lacking motility were incubated in artificial seminal plasma containing HCO_3^- at pH 8.2, motility potential developed. The maturation of motility potential was less at lower or higher pHs. During the incubation period, the intracellular cAMP level increased to a level similar to that of sperm duct spermatozoa.

The motility of demembranated testis sperm of chum salmon caught in the bay was much less than for river fish, and demembranated sperm of river fish were similarly motile in testis and sperm duct spermatozoa.

These suggest that in the process of acquisition of motility potential 1) axonemal maturation 2) membrane maturation and 3) accumulation of cAMP, are each indispensable, as the HCO_3^- concentration and pH value of seminal plasma increase from the testis to sperm duct.

PH 16

SPERM-ACTIVATING SUBSTANCE FROM HERRING EGG

H. Ohtake[1], S. Tanimoto[2] and M. Morisawa[3].
[1]Dept. of Physiol., Dokkyo Univ. Sch. Med., Tochigi, [2]Dept. of Biol., Fac. of Sci., Toho Univ., Chiba, [3]Lab. of Physiol., Ocean Res. Inst., Univ. of Tokyo, Tokyo.

It is well established that spermatozoa of marine teleosts initiate motility when they are discharged to the fluid of high osmolarity such as sea water. The motility of herring spermatozoa was also initiated in hypertonic sea water. However motility was low. When herring egg or supernatant from egg and sea water suspension (egg water) was added to spermatozoa which exhibited low motility in sea water, spermatozoa become active. Thus it is likely that the motility of spermatozoa was initiated by osmolarity and was then activated with the substance released from the egg. The most effective egg water was obtained when herring eggs were immersed in sea water, while no or less sperm - activating factor was found in distilled water or diluted sea water isotonic to the seminal plasma. This suggest that the substance is released from the eggs when they exposed to sea water at spawning. The activating effect vanished when egg water was incubated with pronase. The factor is heat stable. From the procedure that 6 ml of egg water (10 g eggs / 100 ml sea water) was loaded on Sephadex G-75(1.8ø * 40 cm) and eluted with artificial sea water (2 ml / tube), single peak with activity was obtained in the fractions between 40 - 50.

PH 17

INTRACELLULAR CA^{++} INDUCES INITIATION OF AXONEMAL MOVEMENT IN XENOPUS SPERM FLAGELLUM.

T.Inoda and M.Morisawa. Ocean Research Institute, University of Tokyo, Tokyo.

We recently reported that a decrease in osmolality surrounding spermatozoa at spawning causes the initiation of sperm motility in *Xenopus*. (Inoda and Morisawa, Comp. Biochem. Physiol. in press). We reported here that EGTA, chelating agent for divalent cations, had no effect on the motility when EGTA was present in external medium, whereas spermatozoa were quiescent in the medium containing calcium ionophore, A23187. Subsequent addition of Ca^{++} induced the initiation of sperm motility, suggesting that intracellular Ca^{++} plays an important role in the initiation of sperm motility in frogs. (Dev.Growth.Differ., 1987, 29(4),abstract). We further showed that when spermatozoa of *Xenopus* were treated with 0.4 % Triton X-100 and suspended in the reactivating medium containing $MgATP^{--}$, axonemal movement did not occur if Ca^{++} was depleted from the medium. However, when Triton-extracted spermatozoa were suspended in the reactivating medium containing $MgATP^{--}$ and Ca^{++}, axonemal movement occurred. The motility became active concomitant with increase in Ca^{++} concentrations and maximum motility was obtained at the concentration between 0.1-1 mM Ca^{++}. These results suggest that intracellular Ca^{++} regulates on-off switch of the initiation mechanism of *Xenopus* sperm motility.

PH 18

ACTIVITY OF THE ACCESSORY OLFACTORY BULB TO CHEMICAL STIMULI DELIVERED TO THE VOMERONASAL MUCOSA IN TURTLES

T. Hatanaka[1] and T. Hanada[2], [1]Dept. Biol. Fac. of Educ., Univ. of Chiba, Chiba, [2]Inst. of Biol. Sci., Univ. of Tsukuba, Ibaraki.

To investigate the receptivity of the vomeronasal receptors, induced wave responses and unitary discharge of the accessory olfactory bulb neurons were recorded in three species of aquatic turtles, Geoclemys reevesii, Pseudemys scripta, and Clemmys japonica. Response amplitude and pattern to various stimuli were compared in the three species. And relation of the induced wave pattern and the unitary discharge was discussed.

Induced wave responses were yielded by not only vapor stimuli like as iso-amyl acetate and some fatty acids but also liquid stimuli like as some salts solution and acids solution. But amino acids were not so effective with few exceptions. Rank orders of effectiveness of chemicals were almost coincident in the same species, but differed among species. Unitary responses of the bulb neurons were composed with facilitation and suppression of firing. Some discharge patterns resembled to the rise and fall patterns of the induced wave. But unit had a tendency to respond with same pattern to various stimuli. So, particular relation of stimulant and response pattern was not detected.

PH 19

CYCLIC NUCLEOTIDE-INDUCED CONDUCTANCE INCREASE IN SOLITARY OLFACTORY CELLS.

N. Suzuki, Zool. Inst., Fac. of Sci., Hokkaido Univ., Sapporo.

To test the possible involvement of cyclic nucleotides as intracellular messengers in the olfactory transduction process, I have studied the effects of various nucleotides, their analogs and phosphodiesterase inhibitors on the membrane conductance in enzymatically isolated bullfrog olfactory receptor cells by means of a whole-cell clamp perfusion technique. Of six different cyclic nucleotides, cGMP and cAMP were most effective and induced a phasic increase in membrane conductance. However, structurally different cyclic nucleotides, 2',3'-forms, were ineffective. The conductance increases induced by cGMP and cAMP were not influenced by the presence of di- or triphosphate nucleotides, indicating a direct action of these cyclic nucleotides on the membrane. The conductance increase by cGMP was identified as being due to an increase in cationic permeability of the receptor membrane, and its adaptation process was found to be controlled by divalent cations such as Ca^{2+} and Mg^{2+}. Dibutyryl cAMP and 8-bromo cAMP induced delayed and prolonged conductance increases. Furthermore,IBMX and theophylline prolonged the decay of cAMP-induced conductance increase. Results suggest that a phosphodiesterase may be distributed in the olfactory receptor membrane.

PH 20

ADAPTATION OF ODOR RESPONSES IN THE OLFACTORY RECEPTOR CELLS MAY BE CONTROLLED BY INFLUX OF EXTRACELLULAR DIVALENT CATIONS.

T. Kurahashi and T. Shibuya. Inst. of Biol. Sci., Univ. of Tsukuba, Ibaraki.

In this study, the adaptation phenomena of odor responses were investigated from several point of view, by using solitary cell preparation and patch clamp method.

In the standard Ringer's solution, many of the depolarizing responses in the solitary olfactory receptor cells evoked by 10 mM n-amyl acetate showed phasic time course. And the odorant-induced current (OIC), which observed under the voltage-clamp condition, showed similar time course. When the double pulse stimulus was applied to the cell, amplitude of OIC which was induced by second stimulus was always smaller than first. The second current amplitude became larger as the interval of each stimulus became longer. The amplitude was almost recovered with a rest of more than 10 seconds.

When the extracellular divalent cations (Ca, Mg) were removed and double pulse stimulus was applied, in contrast with above observation, the amplitude of second OIC was almost same with first. Moreover, in such an environment, there was little reduction in amplitude of OIC even for the continuous stimulus.

These results may indicate that the extracellular divalent cations correlate with the adaptation of the odor response.

PH 21

THE STRUTURE AND ODOR RESPONSE OF OLFATORY BULB IN THE PIGEON Columba livia

T.Hanada and T.Shibuya, Inst. of Biol. Sci., Univ. of Tukuba, Ibaraki.

Historogical structure of the pigeon olfactory bulb(OB) was observed by staining with Bodian's silver method. The structure was fundementary similar to that in other vertebrates. However, the mitral and granule cells were smaller than those of rat. From this structure, the pigeon OB seemed to have sufficient functions as the primary olfactory center. OB induced waves(16-17Hz) were remarkably obserbed to two kinds of odors (n-Amyl acetate and d-Limonene) known as the common chemical substances for olfactory experiment. Unitary spike activities to the odors were mainly recorded at the external plexiform layer and mitral cell layer. Several units had different response patterns, excitation , inhibition and complex types to odors. The same odor evoked with different response patterns among units. Moreover, many units showed variable response patterns with increase of concentration. These response patterns were similar to that of a reptilian OB (Gecko).
IN OB units of the pigeon, a response range with excitation pattern in concentration (10^{-7} - 10^{0}) of n-Amyl acetate narrower than in other animal OB units.

PH 22

RESPONSE OF TARSAL CONTACT CHEMORECEPTOR OF THE Citrus-FEEDING SWALLOWTAIL BUTTERFLY Papilionidae RELEASING OVIPOSITION BEHAVIOR

K.Kusumi and T.Shibuya. Inst. of Biol. Sci., Univ. of Tsukuba, Ibaraki.

Citrus unshiu is one of the most favorite host plants of the Citrus-feeding swallowtail butterflies, Papilionidae. The stimulation of the extract of C. unshiu leaves to the tarsi of the female Papilio xunthus evoked oviposition behavior clearly. Many chemosensory sensilla (designated as "type-A") were observed with many other cuticular structures ("type-B and -C") by SEM. The "type-A" sensilla were more abundant in the female than in the male, especially on the tarsi of forelegs which were necessary for "drumming", pre-oviposition behavior. The tip recording method was applied to these sensilla of a female P. protenor, it become obvious that the electrical resistance of them was much smaller than that of others ("type-C"). This fact suggested the presense of pores on the sensilla, which was one of the most remarkable features of a contact chemoreceptor. The sensilla initiated larger spikes to the leaf extract.The number of the spikes increased with increase of the extract concentration.

It seems that the "type-A" sensilla have a function as contact chemoreceptor to the ovipositional substance.

PH 23

RESPONSES OF CONTACT-CHEMORECEPTOR CELLS TO THE WING-RAISING FACTOR ON ANTENNAE IN THE MALE LOBSTER COCKROACH, Nauphoeta cinerea.

A.Watanabe and T.Shibuya. Inst. of Biol. Sci., Univ. of Tsukuba, Ibaraki.

It is well known that the contact-sexual pheromone (wing-raising factor) contained in cuticular wax of the lobster cockroach releases a wing-raising display as an initial action pattern in mating behavior of the male cockroach.

This investigation was undertaken to study receptive mechanisms in the antennal contact-chemoreceptor cells related to initiation of wing-raising display. The tip recording method was applied to lead out activities of receptor cells in a single sensillum on the male antenna. A glass capillary was filled with stimulating suspension, which was composed of 0.1 M NaCl and extracted wing-raising factor and treated with ultrasonic waves. Spike-responses (6-20Hz, 10-20mV) to the wing-raising factor were recorded in many sensilla. One type of sensilla contained receptor cells which responded to wing-raising factor. Another type of sensilla contained, at least, two kinds of receptor cell responsible to 0.1M NaCl or wing-raising factor with defferrent spikes in amplitude. Morphological type of sensilla responsible to wing-raising factor may be the sensillum chaeticum.

PH 24

α-GLUCOSIDASE ON THE TASTE RECEPTOR MEMBRANE OF THE FLY, Phormia regina.

M.Ozaki and T.Amakawa. Dept. of Biol., College of Gen. Edu., Kobe Univ., Kobe.

In the labellar chemosensillum of the blowfly, Phormia regina, α-glucosidase was thought to distribute at the tip of the sensory process with the active site exposing outside of the cell. We investigated the activity of the α-glucosidase in the intact sensilla by floating method. The binding abilities of the α-glucosidase to polysaccharides, sugars and inhibitor were compared with those of sugar receptor (investigated electrophysiologically) or those of a candidate protein for the P site (a sugar receptor site to sucrose, L-fucose etc.)(investigated by affinity electrophoresis). The results on starch, L-fucose, fructose and nojirimycin suggested that α-glucosidase is different from sugar receptor molecule.

After the sensillum tip was dipped in the DOC solution and the tip of the sensory process was torn to small vesicles, the sensory process was reconstructed and the responsiveness recovered. When the sensillum tip was dipped in 10 mM nojirimycin bisulfate (α- glucosidase inhibitor) after the DOC treatment, however, the recovery of the responsiveness was 2 fold later. Thus, α-glucosidase may have a role concerning with membrane fusion by recognizing sugar chain on the surface of the reseptor membrane.

PH 25

EFFECTS OF PROTEIN KINASE INHIBITORS AND PHORBOL ESTERS ON THE SUGAR-RECEPTOR CELL OF THE FLY.

T.Amakawa and M.Ozaki. Div. of Biol., Col. of Gen. Educ., Kobe Univ., Kobe.

We gave protein kinase inhibitors and protein kinase C activators (phorbol esters) inside the chemo-sensory process of the taste receptor cell of the fly, Phormia regina. Their effects on the electrophysiological response from sugar receptor cell were as follows. Protein kinase C inhibitor (H-7) reduced but phorbol esters (TPA and DPBA) enhanced the decrease of the impulse frequency, during stimulation (adaptation).

Cyclic nucleotide dependent protein kinase inhibitors (H-8 and HA1004) decreased the impulse frequency immediately after the beginning of stimulation and depressed overall magnitude of response (excitability). These results suggested that at least two different types of protein kinase, kinase A or G and kinase C, are deeply concerned with the sugar taste response by regulating excitation and adaptation, respectively.

Thus, we believe protein phosphorylation plays important roles in taste receptor cell as widely recognized in visual and secretory cells.

PH 26

ISOLATION OF MUTANTS IN HYGRORECEPTION OF DROSOPHILA MELANOGASTER.

F. Yokohari, T. Ito and T. Tanimura
Biol. Lab., Fac. Sci., Fukuoka Univ., Fukuoka.

We attempted to isolate mutants in hygroreception of Drosophila melanogaster, in order to introduce genetic approaches in study of insect hygroreceptor. For the isolation of X-linked mutants, wild-type males were mutagenized with ethelmethane sulphonate. The treated males were crossed with virgin females of the attached-X chromosome. F_1 males were individually crossed with attached-X females and the isogenic lines were established. Prior to the experiment, ca. 50 male flies were transferred to a empty vial and kept in a desiccator with dry silica gel for 4 - 5 hrs. They were transferred to transparent acrylic box (200mm long x 15mm wide x 5 or 10 mm high), in which humidity gradient was set up, and kept for 20 min in the dark. Then the distribution of the flies were photographed. The number of flies in each side was counted on the photograph. Among 868 lines tested, flies of 18 strains could not detect the humidity difference. Electroantenograms (EAGs) to humidity stimulus were recorded and compared between the wild-type and the mutant flies. EAGs of 8 strains showed remarkably smaller value than the wild-type flies. Survey of antennal sensilla by SEM found possible hygroreceptive sensilla in the sacculus of antennal flagellum, but no difference was found in the external structure of the sensilla among EAG-small strains tested and wild-type.

PH 27

THE STRUCTURE OF THE MUSHROOM BODY AND RESPONSES OF THE PROTOCEREBRAL NEURONS IN THE HONEYBEE BRAIN

H.Yamamoto and T.Shibuya. Inst. of Biol. Sci., Univ. of Tsukuba, Ibaraki.

The mushroom body in the honeybee brain was morphologically studied. The mushroom body was reconstructed 3-dimensionally from serial sections of the brain stained with Bodian's method. The mushroom bodies were observed as paired structures. Each of them consisted of two cup-like calyces and a stalk with α- and β-lobes.

To know the physiological aspect of the mushroom bodies, responses of the protocerebral neurons to odor (geraniol and n-propanol) and light were recorded. Some of them were stained by fluorescent dye injection of lucifer yellow CH.

4 classes of neurons were recorded as follows; 1)bimodal neurons responded to both odor and light (OL neurons), 2)unimodal neurons responded to odor (O neurons), 3)unimodal neurons responded to light (L neurons), and 4)neurons responded neither to odor nor light. Among neurons identified morphologically, there were one L neuron and one OL neuron. The L neuron run from right to left bilaterally in the protocerebrum and branched in the lobula and the medulla. The cell body of the OL neuron was observed at the ventral side of calyces and many branches between α-lobes. The OL neuron, compared with O neurons, exhibited weaker responses to odor and showed gentle dose-response curve.

PH 28

THE STIMULATING EFFECT OF 1,6-ANHYDRO-β-D-HEXOPYRANOSES ON THE LABELLAR TASTE RECEPTORS OF THE FLESHFLY.

I.Shimada[1], H. Hori[2], H. Ohrui[2] and H. Meguro[2]. [1]Dept. of Biol. Sci., Tohoku Univ. and [2]Dept. of Food Chem., Fac. of Agric., Tohoku Univ., Sendai.

Most sugars posess reducing properties due to their free anomeric centers and are generally unstable model substances for the study of structure-activity relationship in taste. Eight 1,6-anhydro-β-D-hexopyranoses which have stable conformations without free anomeric centers were examined their effectiveness on the labellar taste receptors of the fleshfly. 1,6-Anhydro-β-D-idopyranose with three successive equatorial hydroxyl groups was found the most effective on the sugar receptor, which again supports the validity of the proposed model of pyranose(P) site (Shimada et al., 1974 and Shimada, 1987). 1,6-Anhydro-β-D-galactopyranose, on the other hand, was revealed to stimulate the salt receptor. Mixtures of both anhydrohexoses clearly stimulated the sugar and salt receptors at the same time. Furthermore, 1,6-anhydro-β-D-altropyranose alone could stimulate both the sugar and salt receptors, too. This may suggest the different sites for sweetness and bitterness in human taste.

PH 29

DAILY RHYTHM OF SUCROSE INTAKE IN THE BLOWFLY, Phormia regina M.

A.Shiraishi, T.Frusho, S.Okamura and H.Tsutsumi[1]. Dep.Biol.,Fac.Sci.,Kyushu Univ,Fukuoka. [1]Amakusa.Marine Laboratory.Kyushu Univ,Kumamoto.

Daily sucrose intake in the blowfly, Phormia regina M was measured with the apparatus prepared in our laboratory. Three kinds of electrical signals, muscle potential from alimentary canal during sucrose intake, artifact accompanying movement of labellar lobes during intake or during licking of the surface of solution and touch artifact of legs to solution, respectively were measured. These three electrical signales were counted at an interval of every 1 h during 3 or 4 days. Sucrose was dissolved into 0.001 M NaCl to keep electric conductivity of solution.

Daily sucrose intake in the blowfly showed the circadian rhythm. Usually, blowflies took sucrose under light condition but did not take the solution under dark condition, even though blowflies were starved more than 24 h. Blowflies were kept previously under 12 h light cycle (6:00 - 18:00, light) or under constant light for 4 days. These individual blowflies were put into the apparatus and were measured the activity under constant dark. These flowflies were started to take sucrose after 12 h and continuously took sucrose during 12 h and stopped. The rhythm of sucrose intake was observed more than 48 h.

PH 30

EFFECT OF PHOTOPERIODIC CYCLES ON THE PHOTOTAXIS OF A WATER STRIDER, GERRIS PALUDUM.

T. Harada and K. Taneda. Dept. of Biol. Fac. of Sci.,Kochi Univ.,Kochi.

We have investigated the effect of the breeding photoperiodic cycle on the positive phototaxis of a water strider, Gerris paludum. First instar nymphs just after hatching were bred under long-day (LD=10:14) or short-day (LD=14:10) photoperiodic cycles until they became adults. Then the adult specimens were bred under long-day or short-day photoperiodic cycles. All the breedings and determinations were made at constant temperature(20-22°C). The direction of movement of each adult specimen with reference to that of the light source was periodically determined during all the breeding periods. The degree of positive phototaxis was expressed as the percent number of specimens whose motile tracks were confined within 30 degrees toward the light source. When the adult specimens were bred under the short-day (or long-day)cycles, they showed a low (or high) degree of positive phototaxis regardless of the nymphal breeding photoperiodic cycles. Thus, the phototactic behavior of the adult specimen was considerably affected by the photoperiodic cycle. However, the photoperiodic cycle experienced during the nymph stage seemed to have little influence on the phototactic behavior of the adult specimen.

PH 31

SEASONAL CHANGE IN THE PHOTOTAXIS OF A WATER STRIDER,GERRIS LACUSTORIS.

T. Harada and K. Taneda. Dept. of Biol. Fac. of Sci.,Kochi Univ.,Kochi.

Seasonal change in the degree of positive phototaxis of the water strider, Gerris lacustoris which had been bred in an outdoor aquarium, was investigated using artificial beam light as a stimulus during the full period of occurrence (from April through September). The degree of positive phototaxis was expressed as the percent number of specimens whose motile tracks were confined within 30 degrees toward the light source. In April, the degree was considerably high. The high value persisted until June. Then the degree gradually decreased until the onset of diapause (September). The decreasing curve in the degree of phototaxis was similar to decreases in the day length. There was a silght difference in the seasonal change between male and female specimens. Diurnal variation in the degree of phototaxis was not observed on any day. When the specimens were bred for more than 15 days under a long-day photoperiodic cycle, they showed a higher degree of phototaxis than the controls. The ecological significance of the change in positive phototaxis of this species was also discussed on the basis of the present findings.

PH 32

THE ROLE OF THE PINEAL AND THE EYES IN THE CIRCADIAN ORGANIZATION IN THE NEWT.

A.Chiba, M.Kikuchi and K.Aoki. Life Sci. Inst., Sophia Univ., Tokyo

The roles of the pineal and the eyes in the circadian organization in the newt were studied by examining the effects of pineal lesions and bilateral optic enucleations on locomotor activity rhythms both under light-dark cycles and in constant darkness. Under light-dark cycles, both pineal lesioned newts and blinded newts showed the locomotor activity rhythms which were entrained to the light-dark cycles. After transfer to constant darkness, pineal-lesioned newts failed to maintain circadian rhythmicity. The blinded newts showed free-running rhythms in constant darkness. The free-running periods of the blinded newts, however, were different from the periods observed before blindings.

The effects of pineal lesions on locomotor activity rhythms were also examined in the blinded newts. Pineal lesions after blindings often cause arrhythmicity not only in constant darkness but also under light-dark cycles.

These data suggest that both the pineal and the eyes are involved in circadian organization in the newts.

PH 33

KEY STIMULI RELEASING COURTSHIP AND SPAWNING BEHAVIOR IN HIMÉ SALMON (LANDLOCKED RED SALMON, ONCORHYNCHUS NERKA)

M.Satou[1], H.Takeuchi[1], K.Takei[1], T.Hasegawa[1], T.Matsushima[1], N.Okumoto[2] and K.Ueda[1]. [1]Zool. Inst., Fac. of Sci., Univ. of Tokyo, Tokyo, [2]Nat. Inst. Aquaculture, Tochigi.

Signals releasing courtship behavior in male himé salmon were examined in model presentation experiments. To test the courtship behavior, two-dimensional square or rectangular models of various sizes and patterns were presented to the male and the frequency of "quivering" elicited by model was measured. It was found that key stimuli for eliciting courtship behavior consisted of three aspects of visual cues, i.e., shape (horizontally elongated rectangle with a size, 6 cm high x 24 cm long), pattern (black above, white below), and movement which simulated some features of the female sexual behavior. To test the spawning behavior, three-dimensional models (size: 6 cm high x 24 cm long x 4 cm wide) were vibrated vertically (frequency: 21 Hz) by a motor-controlled vibrator and the frequency of "spawning act" elicited by the model was measured. Two types of three-dimensional model were used: a simplified "female" model with a pattern of black above and white below and a transparent model with exactly the same dimensions. The results showed that both the vibrational and visual cues were important in eliciting spawning. The importance of the position of visual cues relative to that of the vibrational cues was also shown. The results suggest that in addition to the presence of both vibrational and visual targets, the matching of both targets' positions is important for eliciting spawning behavior.

PH 34

THANATOSIS OF THE CRICKET

T. Katayama and M. Sakai
Dept. of Biol., Fac. of Sci., Okayama Univ., Tsushima-Naka-3-1-1, Okayama

Thanatosis is a death feigning posture that can be found widely in the animal kingdom. It can be induced artificially when animals are forcibly brought into an abnormal posture. So far, however, physiological study on thanatosis has been only made in stick insects (Godden 1972). We found that thanatosis could be induced in crickets (Gryllus bimaculatus) that continued for several minutes. Animals could respond to a weak auditory stimulus by ventilatory movements during thanatosis and woke up quickly any time when a strong stimulus was given. This was not the case in animals under anesthesia with CO_2, ethyl ether or low temperature (5°C). The duration of thanatosis was shortened when animals were in a noisy condition or tested after they were disturbed. The thanatosis could be induced as far as the suboesophageal ganglion was not inactivated. Spontaneous discharges of the hindleg motoneurons and descending neurons tended to decrease during thanatosis while those of the cercal giant interneurons were not. These results suggest that inhibitory interneurons impinging upon the motor system underlie the generation of thanatosis.

PH 35

SOCIAL BEHAVIOUR OF *AMOEBA PROTEUS* (V).

H. Horikami and K. Ishii.
Lab. Biol., Hosei Univ., Tokyo

We found that *Amoeba proteus* (AP), strain G, could form compact groups in higher cell density in fresh saline. Then, the processes of the group formation and the dispersion were investigated to get a clue to the grouping mechanism by photomacrography with interval timer.

(1) In higher cell density (more than ca. 2 cells/mm^2), a frequency of simultaneous collision of more than 3 cells became high to be a small group in a short time. Such groups grew up to a large compact group by collisions each other within 1 Hr.

(2) An isolated group dispersed gradually. In a case of the group of 10 cells it took ca. 30 min before the dispersion, and it was more than 1 Hr in the group of 50 cells.

(3) The dispersion time of the all groups was about 3 Hrs in a control experiment. And periodic formation of the group was not observed during 12 Hrs.

(4) However, APs after the dispersion of the group could form groups again in the fresh saline.

From these results, the group formation in APs is probably due to trapping effect based on reciprocal chemical information.

PH 36

CHICKS BLINDED BY FORMOGUANAMINE DO NOT DEVELOPE LID SUTURE MYOPIA.

T. Oishi[1], J. K. Lauber[2] and Y. Obara[3].
[1]Dept. of Biol., Fac. of Sci., Nara Women's Univ., Nara, [2]Dept. of Zool., Univ. of Alberta, Edmonton, Canada, [3]Dept. of Agr. Chem., Fac. of Agr., Meijo Univ., Nagoya.

The involvement of the retina in avian lid suture myopia was investigated by use of formoguanamine (FG), which induces blindness in chicks. In control chicks reared under a diurnal lighting schedule of LD 12:12, unilateral eyelid suture at 3 days of age induced a typical lid suture myopia response on the operated side by 4 weeks of age, e.g., enlarged eye: 1.542±0.056g (suture eye) vs. 1.244 ±0.017g (control eye); increased anterior chamber depth: 3.48±0.21mm (sutured eye) vs. 2.14±0.03mm (control). On the other hand, in FG-treated blind chicks also reared under LD 12:12, there was no difference in eye parameters between sutured and non-sutured eyes. All globe parameters measured were very similar in FG-treated and control non-sutured chicks. Corneal diameter and anterior chamber depth in the eyes of FG-treated chicks (6.11±0.06mm and 1.46±0.08mm, respectively) were significantly smaller than in control non-sutured eye (6.76±0.03mm and 2.14±0.03mm, respectively). Thus, the retina is necessary for the induction of lid suture myopia, and also for normal corneal growth.

PH 37

CHANGE IN DENDRITIC MORPHOLOGY OF FLIGHT MOTOR NEURONS DURING METAMORPHOSIS IN THE SILK MOTH, BOMBYX MORI.

H.TSUJIMURA. Lab. of Boil., Tokyo Univ. of Agr. and Tech., Fuchu, Tokyo.

During metamorphosis, some larval motor neurons (DLM motor neurons) which innervate mesothoracic dorsal longitudinal muscles degenerate but others survive and become adult flight motor neurons. In this study we show changes in dendritic morphology of these DLM motor neurons by axonal cobalt back-fill and silver intensification methods.

In early stages of metamorphosis some larval dendritic branches degenerated and dendritic field of DLM motor neurons decreased. Moreover, relative position of the dendrite in the ganglion shifted somewhat. In middle pupal stage new branches started to grow from remaining dendrite and many filopodial extensions occurred on the surface of the dendritic branches. In late pupal stage large field of complex dendritic branches were completed and this became adult one.

This result shows that neural circuits for controlling the motor neuron activity are reorganized during metamorphosis. This reorganization may plays a role in alteration of behavior from larval pattern to adult one and development of flight behavior during metamorphosis.

PH 38

STIMULUS SELECTION IN A FOOD REINFORCED COLOR-PATTERN DISCRIMINATION IN THE GOLDFISH, CARASSIUS AURATUS.

K. Ohnishi. Dept. of Physiol., Nara Medi. Uni., Kashihara

To examine whether the goldfish select an attribute independently from visual stimuli in the learning process, the fish were trained to discriminate between a pair of the stimuli having two different attributes (color and pattern). Normal and telencephalonless goldfish were given the food only when the fish selected a runway of two runways training apparatus. The inner walls of the runways were covered with the stimulating color papers which were positioned according to Gellerman alternation sequence. Brightness of the color papers whose spectral reflectance was measured was physically equal. When the fish were trained with green-vertical (green paper with vertical black patterns) and blue-horizontal, the animals showed remarkable learned behaviors (over 75% correct responses from about the 10th day after the start of training trials): acquisition by the telencephalonless fish was slightly slower than by the normal fish. Two days later from the training trials on the 20th or 40th day, memory tests were performed in these animals. They could discriminate between white-vertical and white-horizontal, but not blue and green, while the fish trained with blue and green or green-vertical and blue-vertical could discrimnate between blue and green (over 75% correct responses from about the 20th day). These results suggest that the fish select more impressible attribute (pattern) from the visual stimuli with multi-attributes (color and pattern) and memorize it alone in the extratelencephalic nervous systems.

PH 39

LIGHT REQUIREMENT FOR GREEN PIGMENTATION OF THE WILD SILKWORM ANTHERAEA YAMAMAI COCOONS: LOCAL IRRADIATION AND PARABIOSIS EXPERIMENTS.

Y. Kato. Dept. of Biol., International Christian Univ., Mitaka, Tokyo.

Green pigmentation of silk glands in A. yamamai, which is followed by green cocoon formation, requires high intensity of light. I tried to determine where photoreceptive site will be localized. When neck-ligated animals or isolated abdomens were partially irradiated after gut purge stage, silk glands exhibited green pigmentation in any cases. Next, two decapitated animals were connected with a vinyl tube, one of the partner exposed to light and the other covered with a card-board box. The results showed that silk glands of covered animals became green as well as those of exposed ones. Surprisingly, light irradiation to the part of connecting tube in which haemolymph were flowing was effective. Thus, these suggest that haemolymph may function as a possible photoreceptive site.

PH 40

DEVELOPMENT OF THE OPTOKINETIC RESPONSE AND THE ACTIVITY OF THE DIRECTIONALLY SELECTIVE UNITS IN THE MIDBRAIN OF THE MEDAKA (ORYZIAS LATIPES)

Y.Kasuya and K.Aoki. Life Sci.Inst., Sophia Univ., Tokyo.

The development of the behavioral acuity in optokinetic response in the larva and adult Medaka (0-180 days after hatching) was investigated. The behavioral acuity of optokinetic response improved drastically during 15 days from 55 to 70 days after hatching. In spite of 1-1.5 hr after hatching, 70-80 % of larval fish could swim as the same direction of the rotating stimulus, 1-3 days after hatching there was significant decrease in the direction detecting ability and also significant difference was observed in the appearance of the opposite following fish. Directionally selective visual units of 21 in motion detecting 48 units were recorded in the midbrain in Medaka during stimulation by a rotating striped drum. Directionally selective units were also obtained in the Medaka in the optic tectum and in and around the anterior dorsal tegmentum which was already found in the gold fish and in the Japanese dace, respectively. Further, these units were obtained in and around the optic tract and posterior part of the midbrain tegmentum, and nucleus rotundus.

PH 41

THE MECHANISMS OF NYSTAGMOGENIC AREA IN THE MESO-DIENCEPHALON OF JAPANESE DACE, TRIBOLODON HAKONENSIS.

K. Aoki and M. Takahashi, Life Sci. Inst., Sophia Univ., Tokyo.

Optokinetic nystagmus (OKN) of Japanese dace (Tribolodon hakonensis) was induced by the electrical stimulation of the thalamic-pretectal region in the brain. Nystagmus always occured in both eyes and lasted during the stimulation of 10 sec. The amplitude of nystagmus ranged from 3° to 14° (7.6° on the average). The stimulation of the right region induced nystagmus with the slow phase to the right, and vice versa. The strengths of the stimulus to induce nystagmus were 5-10 µA, and variation of the pulse repetition rate (10-200/sec) for nystagmus affected on the velocity of the slow phase. Optimal pulse repetition rates which could induce maximum slow phase velocity were 50-100/sec, and induced slow phase velocities were 4-22°/sec. Although OKN could be induced by electrical stimulation under the light condition, in some cases, OKN was inhibited by ambient room light. In those cases, the nystagmus with spontaneous eye movement was observed within the evoked eye movements. Under the dark condition and with high stimulus pulse repetition rate (200/sec), the long lasting after-nystagmus was observed from nystagmus continued after the stimulation quite longer than that induced by visual stimulaion.

PH 42

EFFECTS OF MOVING STRUCTURED BACKGROUND ON THE NEURONAL ACTIVITIES OF OPTIC TECTUM IN THE JAPANESE TOAD

H.-j.Tsai[1], M.Satou[2], A.Shiraishi[3] and K.Ueda[4]. [1]Dept. of Biol. Sci. & Biotechn., Tsinghua Univ., Beijing, China,[2-4]Zool. Inst., Fac. of Sci., Univ. of Tokyo, Japan

Toad's visual system can extract informations about the object's motion from the background. It can also discriminate the 'real' object's motion from the 'self-induced' visual motion. Firstly, to study the underlying neural mechanism of this characteristic, the effects of moving structured background (visual noise) on the responses of single neuron in the optic tectum to a moving object (black square) were examined. The background was moved either 'in-phase' (at the same velocity and in the same direction) or 'anti-phase' (at the same velocity, but in opposite direction) with the object. Class T5 neurons responded to an object moving against the stationary background. When the object and the background were moved 'in-phase,' the responses were strongly inhibited in most cases. On the other hand, in the case of 'anti-phase' movements, the responses were inhibited only mildly, not inhibited at all or facilitated. These in-phase and anti-phase effects were considerably modulated when the neuron's excitatory receptive field (ERF) or its surrounding area was masked.
Secondly, the neuron's responsiveness was tested under a condition that the object was maintained stationary state in the center of ERF, while the background was moved and then stopped. Many neurons started to respond with a burst of spikes within a few sec after the moving background was stopped. This 'motion after effect' became stronger, when the object large enough to mask the whole ERF was used.

PH 43

DIAGNOSIS OF THE LEVEL OF VIGILANCE ±N IN A FREE MOVING MOUSE.

A.Higashi, Natl.Inst.for Physiol. Sci., Okazaki,444,Japan.

Sleep-wake phenomina might be expressed as the momentarily changing reverse vectors, and each vector corresponding to the activity to reach at the absolute sleep and wake equilibrium potentials spontaneously by way of the body surface. Based on such an assumption, it will be presumed that the momentarily changing vigilance level might also be generated from the momentarily changing sleep-wake vectors. In order to analyze the relation between the conscious activity and sleep-wake phenomina, the method of dynamic behavioral stage analysis (DBSAM) and the method of micro-sleep and micro-wakefulness processing (MMP) in a free moving mouse have been developed. In this report, the relation between the practical measurements and logics of data processing for DBSAM and MMP, and a working hypothesis of conscious activity is outlined. The first step to consider this relation could be shown as is in Fig.1.

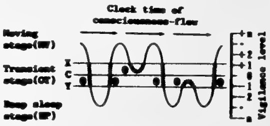

Fig.1; Relation between sleep-wake phenomina and conscious activity. C;Vigilance 0. X and Y; boundaries. 1,2,3 and 4; entering sleep, awaking, quiet and light sleep stage, respectively.

PH 44

PROSTAGLANDINS FOR MOVEMENT ON SPERMATOZOA AND OVIPOSITION BEHAVIOR IN CRICKET, GRYLLUS BIMACULATUS.

M.Ishii, N.Yamaguchi and N.Ai. Dept. of Biol.,Tokyo Gakugei Univ., Koganei, Tokyo.

We clearly observed that full-matured sperm taken out from spermatophore just after copulation in G.bimaculatus adult female had not any mobility of spermatozoa at all. But after transportation of sperm from spermatophore to female spermatheca,spermatozoa stored up inside of spermatheca rose gradually flagellar movement with high frequent stroke. In this experiment, we had attention to show effective concentration to rise spermatozoa movements. In this case, flagellum movement and relative velocity of spermatozoon were measured as the indicator of mobility. Otherwise,PGE2, PGD2 and PGF2-alfa were prepared as activators for spermatozoal movement. When fresh spermatozoa were soaked in several kind of PG solution with different concentration, reletive velocity of spermatozoon was measured by using of blood count set. As the experimental result, PGD2 and PGF2-alfa were not effective to the movement with low concentration. But PGE2,on the contrary, was more effective to it with lower concentration as 10^{-5} or less. In this experiment, we could get graph of dose-response. So, in circadian rhythm of oviposition, inthe period of egg deposition had not any PGE2 at all(10^{-7} or less),but oviposition period had higher conc.PGE2 (10^{-5} or more).

PH 45

EVIDENCE FOR A ROLE OF THE CENTRAL PAIR COMPLEX IN FORMING PLANAR WAVEFORMS IN FLAGELLA.

S. Ishijima[1], K. Sekiguchi[2] and Y. Hiramoto[3]. [1]Biological Laboratory, Tokyo Institute of Technology, O-okayama, Meguro-ku, Tokyo, [2]Jobu University, Shinmachi and [3]The University of the Air, Wakaba, Chiba-shi.

Electron micrography has revealed that American horseshoe crab sperm flagella have the typical 9+2 structure, whereas Asian horseshoe crab sperm flagella have a 9+0 axoneme which lacks central pair and central sheaths but possesses other structures; inner and outer arms, radial spokes and nexin links. Beat patterns of the American and the Asian horseshoe crab sperm were recorded by means of a Nac microscopic high speed video at the rate of 200 fields per second and were analyzed in order to study the role of the central pair of the axoneme in flagellar movement. The American horseshoe crab sperm beat with planar waves, similar to those of sea urchin and starfish sperm flagella, at the rate of 29.9 Hz. On the other hand, the Asian horseshoe crab sperm beat with right-handed helical waves at the rate of 17.6 Hz. These results suggest that the central complex (central pair and central sheaths) plays an important role in forming planar waves, whereas it is not essential for the conversion of microtubule sliding into axonemal bends.

PH 46

EFFECTS OF SEMINAL PLASMA FACTOR ON THE DEMEMBRANATED SEA URCHIN SPERM FLAGELLA.

M.Okuno Dept. Biol., Coll. Arts & Sci., Univ. Tokyo, Tokyo, Japan.

The mammalian seminal plasma contains a factor (SPF) which inhibits the movement of the reactivated mammalian (Lamirande et al, Biol. Reproduct., 28, 788, 1983), salmonid fish and sea urchin (Okuno et al, Zool. Sci., 3, 976, 1986) sperm flagella. The factor inhibited the reactivated flagellar movement at approximately 30 µg/ml. However, the preexisting bends on the flagellar axoneme propagated very slowly (less than 1 µm/sec) near the critical concentration. The bend angle and the curvature of both the principal and the reverse bend maintained constant during the propagation. The length of the bent region maintained also constant while the straight inter-bend region elongated. These results seems to suggest the active area of the axoneme propagates the axoneme maintaining its length and the distortion regardless of the propagation velocity.

When the axoneme was digested with trypsin followed by the incubation with SPF the sliding disintegration of the outer doublet was inhibited. However, considerable number of the axoneme peeled off at the distal region. In addition the preliminary experiment revealed that the stiffness of the axoneme was increased by the incubation with SPF. These results suggested that the SPF increased the viscoelastic resistance of the axoneme.

PH 47

ROLES OF CALCIUM AND CYCLIC AMP ON MOTILITY INITIATION OF HAMSTER SPERMATOZOA.

K. Ishida[1], M. Waku[1] and M. Morisawa[2]. [1]Dept. of Urol. Teikyo Univ. Sch. of Med. and [2]Lab. of Physiol. Ocean Res. Inst. Univ. of Tokyo, Tokyo.

When calcium was removed from sperm cells of hamster by diluting them into the medium containing both EGTA and calcium ionophore A23187, they are completely quescent. Spermatozoa initiated motility by an addition of excess amount of calcium, suggesting that calcium plays an important role in the initiation of sperm motility. The level of cyclic AMP content and activity of adenylate cyclase and phosphodiesterase were reduced by removing calcium from the cell by the above method. Addition of calcium enhanced both activity of the adenylate cyclase and phosphodiesterase, and the intra-spermatozoal cyclic AMP level. These results suggest that activation of the adenylate cyclase resulting an increase in cyclic AMP by the presence of calcium in the cell is a prerequisite to the initiation of sperm motility. Since both cyclic AMP generating system and sperm motility were stimulated by the presence of external calcium, it is likely that accumulation of intraspermatozoal calcium by transport from the outside into the cell causes the synthesis of cyclic AMP through the activation of the adenylate cyclase and then, cyclic AMP induces the initiation of sperm motility in hamster.

PH 48

EFFECTS OF ORGANIC SOLVENTS ON THE SLIDIN DISINTEGRATION OF CHLAMYDOMONAS FLAGELLA.

M. Noguchi, M. Takahashi and H. Segawa. Dept. of Biol., Fac. of Sci., Toyama Univ., Toyama.

Effects of organic solvents on the sliding disintegration of *Chlamydomonas* flagella and on hydrolysis of ATP during the disintegration were examined. The sliding disintegration was monitored by changes in turbidity. Isolated flagella were demembranated and used after a brief treatment with trypsin. The maximal turbidity change was observed at 30 µM ATP in the standard solution. In the presence of methanol or glycerol, turbidity change decreased with increasing concentration of the solvents. On the other hand, the amount of hydrolyzed ATP increased with increasing methanol concentration, whereas it decreased with increasing glycerol concentration. Thus the inhibitory effect of glycerol on sliding disintegration was accompanied with the inhibition of the ATPase activity. In contrast the inhibitory effect of methanol on sliding disintegration was accompanied with the activation of the ATPase. These results suggest that methanol inhibit the sliding by uncoupling the mechanochemical coupling on the interaction between dynein and adjacent microtubule, and that glycerol inhibit the sliding by reducing the rate of ATP hydrolysis.

PH 49

FLAGELLAR BENDING PATTERNS DURING RESPONSES TO ELECTRICAL STIMULATION OF THE OUTER DYNEIN ARM LESS *CHLAMYDOMONAS* MUTANT, *ODA*38.

Kenjiro Yoshimura and Keiichi Takahashi. Zool. Inst., Fac. of Sci., Univ. of Tokyo, Tokyo.

Flagellar responses to electrical stimulation were analysed in the *oda*38 mutant of *Chlamydomonas reinhardtii* which lacks the outer dynein arms. The flagella of the mutant normally beat with the ciliary pattern. When the cell was held on a suction electrode and stimulated by an electric pulse (1ms, 0.04-0.07μA), the flagella beat with the flagellar pattern for about 0.6sec, after which the ciliary type beating was resumed. The changes in bending pattern at the onset of the response were analysed quantitatively. We identified the following two kinds of changes. First, the sliding velocity of the microtubules in the propagating reverse bend decreased uniformly along the length of the bend. This change was different from that in the wild type cell, in which the sliding velocity decreased more in the more distal region of the reverse bend. This suggests that the inner and outer dynein arms play different roles at the onset of the response. Second, there were the interruptions of the effective stroke and prolongation of the recovery stroke similar to those observed in the wild type cells.

PH 50

RELATIONSHIP BETWEEN INTRACELLULAR cAMP LEVEL AND SWIMMING DIRECTION IN PARAMECIUM CELL MODEL.

A.Izumi[1] and Y.Nakaoka[2]. [1]Lab. of Cell Biol., Univ. of the Air, Chiba and [2]Dept. of Biophys. Engineer., Fac. of Engineer. Sci., Oosaka Univ., Toyonaka.

We have reported that cAMP regulates the swimming direction in Paramecium cell models as well as Ca^{2+} . In one type of triton-extracted model(model II) calmodulin antagonists inhibit Ca^{2+}-induced backward swimming and cAMP enhances the inhibitory effect. The other type of triton-extracted model(model I) is insensitive to calmodulin antagonists and the sensitivity is obtained by addition of cAMP. Sucrose-treated model cannot swim forward without cAMP, even in the absence of Ca^{2+}. These cAMP effects are inhibited by an inhibitor of cAMP-dependent protein phosphorylation. An intracellular protein(forward swimming-inducing substance : FSIS)had equivalent effects to cAMP. These results suggest that FSIS increases intracellular cAMP level. To clear this suggestion, intracellular cAMP levels of three types of cell model in various condition, were measured by a radioimmunoassay. cAMP levels were higher, when the models swam forward. It was suggested that cAMP formed by intracellular FSIS (and perhaps cAMP-dependent protein phosphorylation) is required for Paramecium cells to swim forward.

PH 51

EFFECTS OF THE LENGTH OF A FLAGELLUM ON ITS MOVEMENT.

S.A.Baba[1], Y.Mogami[1], A.Yogo[2] and Y.Imamura[3], [1]Dep. of Biol., Fac. of Sci., Ochanomizu Univ., Tokyo, [2]Dep. of Regul. Biol., Fac. of Sci., Saitama Univ., Urawa and [3]Terumo Co., Tokyo.

The length of a flagellum is a crucial physical quantity that may restrict mechanical performance of the contractile machinery of the flagellum. To study the length effect on flagellar movement, we analyzed bending waves in echinoderm sperm flagella of various lengths obtained by severing their distal part. The bending waves in flagella of all lengths analyzed, from some 2 μm through the full length of intact flagella, could be fairly accurately described by equations of the same form as used to describe those in intact flagella, in which the angular direction ϕ is a sine function of the distance s measured along the flagellum and time t as follows,

$$\phi(s, t) = \phi_a(s) \cos\{2\pi ft + S_\phi(s)\} + \phi_b(s),$$

where f is the beat frequency, and ϕ_a, S_ϕ, ϕ_b are the amplitude, phase and bias of ϕ. The beat frequency of severed flagella longer than half the full length remained essentially at the normal level of intact flagella, whereas that of shorter flagella increased linearly with their decreasing length. The curves of maximum rate of anglular change, $2\pi f\phi_a(s)$, and of phase, $S_\phi(s)$, were shifted upward and downward, respectively, in the range of length shorter than half the full length. However, the curve of bias $\phi_b(s)$ remained unchanged within the whole range of length.

PH 52

COMPUTER SIMULATION OF TACTIC BEHAVIOR IN PARAMECIUM.

T. Tominaga and Y. Naitoh, Inst. Biol. Sci., Univ. Tsukuba, Ibaraki 305

To understand mechanisms governing tactic behaviors of free-swimming unicellular organisms, a computer model was constructed to simulate distribution of the cells in two different environmental conditions adjoining with each other. Basic assumptions for constructing the model were, (1) the cells first distribute at random on a finite line, (2) then environmental condition in one half side of the line is suddenly changed, (3) each cell passes over a border point between two halves of the line with a certain probability depending on its pass direction, (4) moving rate of the cell changes with time after it passes over the border and (5) the cells on the line do not disturbe their movements with each other. Thus simulated distribution was compared with the actual distribution of the specimens of Paramecium caudatum in a thin square chamber. Temperature of half of the chamber was suddenly lowered to a certain degree. Time change in the distribution of the specimens was examined. We found some discrepancies between simulated and actual distributions. The discrepancies were mostly dependent on the presence of the cells swimming along the border between two differnt temperature-regions.

PH 53

CORRELATION BETWEEN TENTACLE MOVEMENT AND MEMBRANE POTENTIAL RESPONSES IN NOCTILUCA MILIARIS.

K. Oami and Y. Naitoh, Inst. of Biol. Sci., Univ. of Tsukuba, Ibaraki 305.

To understand mechanisms controlling tentacle movement of the marine dinoflagellate Noctiluca miliaris, membrane potential responses and tentacle movement were recorded simultaneously, and examined their time relationship. A slow flexion took place during a slow depolarization of the tentacle regulating potentials (TRPs). Rate of the flexion markedly increased after the specimen showed a negative spike. The flexion reached its maximum several hundreds milliseconds after the negative spike. The tentacle extended during a hyperpolarization after the negative spike. The flexion was markedly enhanced by raising external Ca concentration, while the TRPs were little affected. On the contrary, the tentacle stopped its movement at its most extended state when the external Ca ions were eliminated, while the TRPs could be seen. A quick flexion was associated with the flash triggering potential (FTP). In contrast to the TRPs-associated flexion, the FTP-associated flexion did not need external Ca ions.

PH 54

CILIARY RESPONSES IN THE GILL OF THE ABALONE.

Akira Murakami and Keiichi Takahashi. Zool. Inst., Fac. of Sci., Univ. of Tokyo, Tokyo.

Responses of cilia on the gill of the abalone, Nordotis gigantea, to electrical stimulation and to 5-hydroxytryptamine (5HT) were investigated. A single gill plate was isolated and folded around one of a pair of platinum electrodes in the perfusion chamber. The lateral cilia on the isolated gill plate were motionless or beat slowly with a beat frequency <10 Hz. When stimulated with an electric pulse (duration 0.5 ms), the cilia were arrested. The duration of the arrest changed from $<$ a second to $>$ 2 minutes as the stimulus intensity increased from 10 to 20 V. The response was Ca-dependent. 5HT (10^{-6} M) stimulated the lateral cilia to beat faster; the frequency of the stimulated beat was usually $>$ 15 Hz. The duration of the arrest response was reduced in the medium containing 5HT. The ciliary beat activation by 5HT also ocurred in Ca-free sea water. The results indicate that the respiratory current of the abalone is regulated by mechanisms similar to those reported for the feeding current in Mytilus (Takahashi and Murakami, 1968 etc.).

PH 55

CILIARY RESPONSES IN SEA URCHIN LARVAE OF LATE DEVELOPMENTAL STAGES.

Yoshihiro Mogami[1], Kikuyo Fujima[2] and Shoji A. Baba[1]. [1]Dept. Biol. Ochanomizu Univ. Tokyo, [2]NEC Micom. Tech. Tokyo.

Spontaneous ciliary responses of cilia of major ciliary bands (epaulets) in free swimming eight-armed pluteus of sea urchin (*Hemicentrotus pulcherrimus*) were analized with the aid of high speed video-microscopy. Larvae swimming forwards frequently showed backward swimming with reversal beating of epaulet cilia. Revarsal beating usually returned to normal beating *via* intermediate beating with less polarized bend formation. It was, in some cases, followed by the cessation of beating in a position near the end of recovery stroke of reversal beating. After a period of cessation arrested cilia slowly inclined posteriorly to the position of the end of effective stroke of normal beating, where they beat with small amplitude (inactive beating) and then quickly moved to the arrest position. After several times of flip-flop between arrest and inactive beating the cilia resumed normal beating, never associated with reversal beating. The difference between the changeover to normal beating from reversal beat and from ciliary arrest suggests the functionally irreversible changes of the ciliary motile machinery during the transition from reversal beating to arrest response.

Unusual metachronal coordination of coexsitense of dexioplectic and laeoplectic waves in individual larvae was confirmed. The direction of bidirectional wave propagation was maintained also in reversal beating.

PH 56

MULTIMODAL INHIBITORY INNERVATION OF THE GILL OF APLYSIA JULIANA.

M. Kurokawa* and K. Kuwasawa. Dept. Biol., Tokyo Metropolitan Univ., Tokyo. *Present address: Meiji Inst.Health Science., Odawara.

We have reported that the gill musculature of Aplysia receives excitatory innervation by motor neurons located in three neural classes, the abdominal ganglion, the branchial ganglion and the gill neural plexus. In this study, four types of inhibitory innervation were found in the gill.

(1) IJPs were induced in gill muscle cells by the branchial nerve stimulation.
(2) Motor neurons of the neural plexus in the gill received inhibitory innervation from the abdominal ganglion. The inhibition persisted for a long period after cessation of the branchial nerve stimulation. (3) A certain neuron in the branchial ganglion received IPSP input from the branchial nerve. (4) The motor neuron in the abdominal ganglion (AGN) received presynaptic inhibition at its periphery to gill muscle cells.

As AGN also received periodic bursts of IPSPs in the abdominal ganglion, this central inhibition of AGN may result in depression of both longitudinal gill shortening, which is directly evoked by AGN, and pinnule contraction evoked by the motor neurons in the branchial ganglion, which are activated by EPSPs from AGN. The presynaptic inhibition may allow AGN to cause the pinnule contraction without the longitudinal shortening.

PH 57

SYNAPTIC TRANSMISSION BETWEEN SECOND- AND THIRD-ORDER NEURONS OF COCKROACH OCELLI.

M. Mizunami and H. Tateda. Dept. of Biol. Fac. of Sci. Kyushu Univ. Fukuoka.

We examined how the steady (tonic) and dynamic (transient) potential changes in the second-order ocellar neurons are transmitted to the third-order neurons of the cockroach, Periplaneta americana.

The transfer function to steady inputs, measured by simultaneous recordings from second- and third-order neurons, was sigmoidal. The threshold of transmission was a little negative than the membrane potential of dark- or light-adapted state.

Dynamics of transmission has been studied by comparing the responses of second and third-order neurons using sinusoidally-modulated light. We found that 1) the waveforms of responses of third-order neurons were more transient than those of second-order neurons, 2) the amplitudes of responses of third-order neurons increased exponentially with the increase in the amplitudes of potential changes in second-order neurons and 3) potential changes of higher frequencies in second-order neurons produced larger responses in third-order neurons. The former two retained after an application of TTX, and were due to sigmoidal nature of input-output characteristics of the synapse. The enhancement of responses to high-frequency inputs, the latter one, was mainly due to active membrane properties of third-order neurons, because it was reduced by an application of TTX.

PH 58

DESCENDING OCELLAR INTERNEURONS OF THE AMERICAN COCKROACH.

T. OHYAMA and Y. TOH. Dept. of Biol., Fac. of Sci., Kyushu Univ., Fukuoka.

In the cockroach, ocellar interneurons descending directly from the ocellar nerve to the thorax have been reported (Toh & Sagara, 1984; Mizunami & Tateda, 1986). However, their morphology in the thorax and detailed physiology were not known. In the present study, two descending ocellar interneurons were morphologically and physiologically identified. They are identical with D-I and D-II neurons of Mizunami and Tateda (1986). The D-I and II neurons have a cell body in the brain and extend distally into the ocellar nerve. The D-I neuron sends an axon ipsilaterally through the suboesophageal ganglion. The D-I axon was confirmed to reach the prothoracic ganglion. The D-II neuron sends an axon contralaterally through the suboesophageal ganglion. The D-II axon was confirmed to reach the second abdominal ganglion. Both axons extend side-branches and fine processes in the hemisphere of each ganglion ipsilateral to the axon. These neurons responded with only a few off spikes to ocellar illumination, but responded with a train of spikes to cercal stimulation. The train of spikes was inhibited by ocellar illumination. It has been proposed in many insects that the ocellus controls activities of the CNS. The present data appears to comprise physiological evidence of such ocellar function.

PH 59

RESPONSE OF THE TEMPORAL ORGAN TO THE AIR-BORNE CHEMICALS IN JAPANESE HOUSE CENTIPEDE.

N.Doi and Y.Toh, Dept. of Biol., Fac. of Sci., Kyushu Univ., Fukuoka.

The temporal organ of the Japanese house centipede, Thereuonema hilgendorfi, has been identified to be CO_2 receptors: the receptor cell decreases impulse frequencies by CO_2 stimulation. The temporal organ also responds to many air-borne chemicals. Acidic chemicals(eg., fatty acid) decrease impulse frequencies whereas basic chemicals (eg., amine) increase them. Yamana et al. (1986) supposed that the effect of air-borne chemicals may be secondary effects: air-borne chemicals change pH at receptor site, which results in changes of molar fraction of CO_2. It is shown in the present study, however, that presence or absence of CO_2 do not affect responses of the receptor cells to air-borne chemicals. This result suggests changes of molar fraction of CO_2 may not be always involved in chemical responses of the temporal organ. Yamana et al.(1986) also supposed that the possibility of pH effect is intrinsic to the receptor cell. However, in the present study, increasing of pH of air-born chemicals did not always result in increasing impulse frequencies. These results suggest that the possibility of the air-borne chemicals may be directly accepted by the receptor cell.

PH 60

VISUAL SYSTEM OF THE TIGER BEETLE (CICINDELA CHINENSIS) LARVA I.STRUCTURE

Y.Toh and A.Mizutani, Dept. of Biol., Fac. of Sci., Kyushu Univ., Fukuoka.

Larvae of the tiger beetles live in the burrows. They ambush and catch preys. The neural mechanism underlying such unique visual behavior appears an interesting subject to examine. In the present study structure of the ocellar system of the Cicindela larva has been examined. The larva possesses six ocelli on either side of the head. The six ocelli are classed into two large ocelli (ca. 450 um), two medium ones (ca. 150 um) and two small ones (ca. 75 um). Each ocellus possesses a corneal lens, beneath which a rhabdom layer occurs. The number of retinular cells included in the six ocelli is estimated about 20,000. Retinular axons enter the optic neuropil located beneath the ocelli. The optic neuropil is stratified into two layers (lamina and medulla). Retinular axons synapse with monopolar neurons in the lamina. Lateral connections among lamina monopolar neurons also occur. Lamina monopolar neurons extend into medulla, and synapse with branches of medulla intrinsic neurons. The medulla intrinsic neurons swell up to 10 um in the posterior region of the neuropil, and extend to the brain as an optic nerve. The optic nerve contains about 150 axons. These results suggest occurrence of the neural circuit for movement detection in the optic neuropil.

PH 61

VISUAL SYSTEM OF THE TIGER BEETLE (CICINDELA CHINENSIS) LARVA II.ELECTROPHYSIOLOGY,
A.Mizutani and Y.Toh, Dept. of Biol., Fac. of Sci., Kyushu Univ., Fukuoka.

The ocellar system of the *Cicindela* larva was studied electrophysiologically. Of the six ocelli two large ocelli and one medium ocellus have been examined. The two large ocelli are directed dorso-anteriorly and dorso-posteriorly, respectively, and the medium ocellus is directed anteriorly. Visual fields (measured by ERG amplitudes) of adjacent ocelli partially overlap each other. The flicker fusion frequency of large ocelli measured by ERG is about 50 Hz. Spike responses of the higher order neurons to illumination were intracellularly recorded in the optic neuropil. Response patterns are as follows: 1)sustained inhibition of spontaneous discharges during illumination 2)phasic-tonic discharges during illumination 3)phasic-tonic inhibition during illumination 4)off-discharges 5)on- and off- discharges. Receptive fields of some higher order neurons were coincident to or included in that of some ocellus, whereas receptive fields of other neurons were wide enough to cover those of more than two ocelli. It is inferred from observed variation in response pattern and receptive field of the higher order neurons that extensive visual information processing would take place in the optic neuropil.

PH 62

MICROVILLI-BEARING GANGLION CELLS IN ONCHIDIUM STALK EYE.
Y.KATAGIRI[1], N.KATAGIRI[2] and Y.SHIMATANI[1]
Dept. of Physiol[1]. and Anatomy[2], Tokyo Women's Medical College, Tokyo.

The ganglion cells (GCs) in the *Onchidium* stalk eye are found separately or in a cluster in the neuropil along the periphery of the retina which consists of visual cell type 1, type 2 and supporting cells. GC is approximatly oval in shape and has a large oval nucleus and an axon. It is distinguished from other retinal cells by large size (15-40 µm in diameter), a position in the eye, electron lucent cytoplasm, and absence of photic vesicles and pigment granules. In serial sections, a mass of microvilli (MV) surrounded by its own cytoplasm are found in the GC. MV are short and less compare to those of visual cells. MV in GC has not been known in other molluscan eyes. GC contains many dense lamellar bodies in the cytoplasm which are also rich in other organelles; Golgi apparatus, mitochondria, rough endoplasmic reticulum, ribosomes, glycogen granules, dense vesicles, filaments and microtubules. Fine structure of GCs is similar to those of GCs in eyes of *Bulla* and *Aplysia* except for MV. Although it is unknown whether MV of GC in the *Onchidium* stalk eye are a photosensitive organelle or not, large action potentials respond to light are recorded from the GC.

PH 63

NEUROANATOMY OF THE TERMINAL NERVE SYSTEM IN THE DWARF GOURAMI.
Y.Oka[1], M.Ichikawa[2],M.Satou[1] and K. Ueda[1].
[1]Zool. Inst., Fac. of Sci., Univ. of Tokyo,[2]Dept. of Anat. & Embryol., Tokyo Metro. Inst. of Neurosci., Tokyo.

It has recently been suggested that the terminal nerve (NT) system is involved in the control of sexual behavior in teleosts. We have examined neuroanatomically the NT system in a tropical fish, dwarf gourami, as a basis to study its involvement in the sexual behavior. The ganglion cells of the NT (NT cells)in the transitional area between the olfactory bulb (OB) and the telencephalon strongly reacted to a monoclonal anti-LHRH (LRH13, a gift from Dr. Wakabayashi of Gunma Univ.) as well as to a polyclonal anti-LHRH. The LHRH-ir fibers were abundant in the OB, ventral telencephalon (V) and several other areas. A distinct bundle of axons emanating from the NT cells ran through the V and the preoptic area (POA), and some of them entered the optic nerve (ON). The NT cells could also be labelled by the cobaltic lysine applied to the cut end of the ON. The dendrites ramified in the OB, while the axons ran through the V and the lateral POA, and entered the ON. Thus, the LHRH-ir NT system might affect the olfactory and visual functions as a neuromodulator and/or neurotransmitter. It might also affect the V and POA, which have been suggested to be involved in the control of sexual behavior in teleosts.

PH 64

EFFECT OF DENERVATION ON THE EXCITATORY AND INHIBITORY INNERVATION IN THE INSECT MUSCLE FIBERS.
H. Washio, Lab. Neurophysiol.
Mitsubishi-Kasei Inst. of Life Sci.
Machida, Tokyo

Insect skeletal muscle fibers are known to be innervated multiterminally and sometimes polynerrally. The coxal depressor muscle (177d and e) of the cockroach, *Periplaneta americana* receives innervation from a slow excitatory (Ds) and three common inhibitory motoneurons, possiblly from one of the dorsal unpaired median neurons. In the previous work on denervated coxal muscles of the cockroach it was shown that the excitatory neuromuscular transmission disappeared in about 2 days and resumed in about 3 weeks after nerve section at 26°C. In this study I have demonstrated that there is the different time course of these failure and resumption of excitatory and inhibitory inputs in the cockroach leg muscle fibers. Although almost simultaneous failure of those innervations took place at 26°C, the disappearance of the excitatory input has been found to preceede the inhibitory's a few days at 15°C. Also the resumption of the excitatory transmission took place more than two weeks before the one of the inhibitory after motor nerve crush at 26°C. The result suggests that the neurotrophic influence of nerve on the muscle may be specific for the type of innervation in insect muscles.

PH 65

STRUCTURAL DIVERSITY OF THE HEMOGLOBINS FROM THE TWO CLOSELY RELATED BIVALVES BARBATIA VIRESCENS AND BARBATIA LIMA

T.Suzuki*, M.Shiba*, T.Furukohri* and M. Kobayashi**
*Dep.Biol., Fac.Sci., Kochi Univ., Kochi,
**Dep.Biol.,Fac.Sci.,Niigata Univ., Niigata

The subunit structures of intracellular hemoglobins from *Barbatia lima* and *B.virescens* were investigated. *B.virescens* hemoglobin consisted of only 30,000 daltons component, whose structure was determined to be heterodimer. The two constituent chains were isolated by HPLC. The Mr of the chains was estimated to be 17,000 by SDS-PAGE. On the other hand, *B.lima* hemoglobin consisted of two components. One was a subunit with Mr of 60,000, whose structure was determined to be tetramer (usual $\alpha_2\beta_2$ structure). The two chains were isolated by HPLC. The other was a polymeric subunit. SDS-PAGE showed that the Mr of this subunit is 32,000, therefore the didomain structure was suggested. No N-terminal residue was found by Edman method. We made CNBr cleavage and enzymatic digestion of the didomain subunit, and isolated the peptides containing N-terminal region. The sequence was determined as follows; N-terminal 36 residues of the first domain are Ac-(BVSZ)KIEEVTQPANKNLIRSTWNVMAGDRGNGVELM, and the first 37 residues of the second domain are MGVTERIEEVTQPANKGLIRETWNIVAGDRKNGVELM. The homology between domains was very high.

PH 66

HATCHABILITY AND HEMOGLOBIN OF DAPHNIA MAGNA EMBRYO

M. Ninomiya and M. Kobayashi. Dept. of Biol., Fac. of Sci., Niigata Univ. Niigata

The developmental rate of embryos in the brood pouch of *Daphnia magna* was markedly affected by temperature. The hatchability of embryos stayed constantly high at temperature below 27 C but decreased acutely with a temperature increase above this point. Fifty percent hatchability point was obtained at 29 C for embryos in the brood pouch of pale animals and at 30 C for embryos in the brood pouch of red animals. The hatchability of embryos in the brood pouch increased with an increase in oxygen tension and reached a steady high level. Fifty percent hatchability was obtained at oxygen tension of 12.6 torr for embryos in the brood pouch of pale animals and 8.6 torr for embryos in the brood pouch of red animals. The oxygen tension for 50 % hatchability of embryos isolated from the brood pouch was 32.7 torr, and no significant difference was found between embryos isolated from pale and red animals

D. magna hemoglobin was separated electrophoretically into at least 6 distinct components. There was a difference between the relative amount of hemoglobin components in pale animals and that in red ones. Parthenogenetic eggs also had different amount of hemoglobin components, compared to that in adult animals.

PH 67

APLYSIA MYOGLOBIN WITH AN UNUSUAL HEME ENVIRONMENT

A. Matsuoka and K. Shikama. Biol. Inst., Tohoku Univ., Sendai.

The radular muscle of *Aplysia*, the gastropod sea mollusc, is one of the most remarkable red muscles found in invertebrates. We have succeeded in isolating native oxymyoglobin directly from the radular muscle of *Aplysia kurodai*, a common species around the Japanese coast, and have examined its structural, spectral and stability properties.

Unlike mammalian myoglobins, *Aplysia kurodai* myoglobin contains only a single histidine residue at the proximal position, lacking the usual distal one. Moreover, the hydropathy profile along the amino acid sequence of *Aplysia* Mb is completely different from that of sperm whale Mb, especially on the distal side of the heme.

Aplysia MbO_2 is very similar in its spectrum to those of mammalian oxymyoglobins; the α-peak being higher than the β-peak and the absorbance ratio (α/β) being 1.03. Its stability, however, is quite different from those of mammalian oxymyoglobins, and *Aplysia* MbO_2 is found to be extremely susceptible to autoxidation. Its rate is one-hundred times higher at pH 9.0, and its pH dependence is unusual and much less steep, when compared with sperm whale MbO_2 as a reference.

PH 68

SEASONAL VARIATION OF SPECTRAL SENSITIVITY IN CRAYFISH RETINULA CELLS AND ITS MONOCOLNAL ANTIBODIES.

T.Hariyama, Y.Tsukahara[1], H.Yamamoto, T.Takeuchi[2] and F.Tokunaga[3]
[1]Research Center for Applied Information Sciences, [2]Dept of Biol.,Fac.of Sci., [3]Dept of Phys.,Fac.of Sci., Tohoku Univ., Sendai

Spectral sensitivity curves (SSC) were obtained from crayfish retinula cells by intracellular recordings with on axis stimulation throughout the year. During summer, only one type of SSC(λ max 600 nm) was obtained and the eye has retinal. In other seasons, four types of SSC were obtained. These eyes contain both retinal and 3-dehydroretinal. The SSC of the two of the four and of the summer's were well fit to the absorption spectra computed from Ebrey's (1977) nomogram for retinal (λ max 560, 600 nm). The rest of the four were also fit for 3-dehydroretinal (λmax 600, 640 nm). The selective light adaptation for the isolated rhabdom showed that the visual pigment based on retinal absorbed shorter wavelenth than the visual pigments of the rhabdom with 3-dehydroretinal and retinal. These results suggest that the synthesis of the winter type opsin was induced by 3-dehydroretinal, sumer type opsin was induced by retinal. In order to confirm these hypothesis, we prepared monoclonal antibody against rhodopsins. There is no significant diffrence of molecular weight of rhodopsins in summer and in winter.

PH 69

RETINYL AND 3-DEHYDRORETINYL ESTERS IN THE CRAYFISH RETINA

T.Suzuki[1], Y.Maeda[2], Y.Toh[3] and E.Eguchi[4]
[1]Dept. of Pharmacol.,Hyogo Coll. of Med., Nishinomiya,[2]Dept. of Chem.,Yokohama Natl. Univ.,Yokohama,[3]Dept. of Biol.,Kyushu Univ. Fukuoka,[4]Dept. of Biol.,Yokohama City Univ. Yokohama.

The crayfish Procambarus clarkii has rhodopsin and porphyropsin in the retina, and the ratio of the two pigments varies with seasons. In order to clarify the origin of visual pigment chromophore we studied retinyl esters in the crayfish retina. 3-Dehydroretinyl and retinyl esters were found in the retina and more than 95% of them were in 11-cis configuration in dark-adapted animals. When light-adapted animals were kept in dark, visual pigments gradually regenerated and all-trans retinoids accumulated in the stored ester. A major fatty acid of the stored ester was docosahexaenoic acid (C22:6). The results of fractionation experiment and microscopic observation indicated that the retinyl esters were stored in photoreceptor cells as oil droplet. The ratio of dehydroretinal /retinal in the visual pigment was always higher than that of dehydroretinol/retinol in the stored ester. The present results show that the retinyl and dehydroretinyl esters are the precursor of visual pigment chromophore and suggest a mechanism of selective utilization of 3-dehydroretinyl ester for pigment synthesis.

PH 70

CLONING OF C-DNA'S FOR OCTOPUS RHODOPSIN AND RETINOCHROME

J. Uematsu[1] , T. Hara[1] and F. Tokunaga[2]
[1] Dept. of Biol., Fac. of Sci., Osaka Univ.,Toyonaka, [2] Dept. of Phys., Fac. of Sci., Tohoku Univ., Sendai.

In order to elucidate the amino acid sequences of octopus rhodopsin and retinochrome, we have tried to prepare their c-DNAs. The c-DNA library was constructed by Okayama-Berg method. About 300 positive transformants for bovine rhodopsin c-DNA were isolated. By further screening 15 transformants were expected to encode rhodopsin. Restriction enzyme digestions showed their lengths were 300 - 600 bp.

We synthesised the oligonucleotides induced from partial amino acid sequences of the squid retinochrome. These oligonucleotides were used as probes for screening colonies containing retinochrome c-DNA. The oligonucleotide encoding the amino-terminal region of retinochrome did not give positive signals for any colonies. The oligonucleotide encoding one of BrCN fragments of retinochrome provided 14 positive colonies expected to contain retinochrome c-DNA. Restriction enzyme digestions showed the lengths of their c-DNA were 500 - 750 bp.

We are now trying subcloning of their c-DNA fragments to the plasmid vector, pTZ, to determine their base sequences.

PH 71

THE ROLE OF RETINAL-BINDING PROTEIN IN THE CHROMOPHORE EXCAHNGE BETWEEN RHODOPSIN AND RTETINOCHROME SYSTEMS OF THE SQUID RETINA.

A. Terakita, R. Hara and T. Hara
Dept. of Biol., Fac. of Sci., Osaka Univ., Toyonaka, Osaka 560, Japan

Our previous works on retinal-binding protein (RALBP) with aporetinochrome and opsin suggested that RALBP plays important roles on retinoid turnover in the squid retina. The role of RALBP on the exchange of retinal between metaretinochrome (MRet) and metarhodopsin (MRh) was then examined by the use of 3-dehydroretinal (retinal$_2$) as a tracer of retinal chromophore.

In the fresh dark-adapted retina, RALBP dominantly combines with 11-cis-retinal. When mixed with excess all-trans-retinal and retinol, RALBP takes up each of them, releasing endogenous retinoid ligands.

When an all-trans-retinal-rich RALBP was incubated in the dark with MRet$_2$-carrying membranes (retinal$_2$ as chromophore), the RALBP took up 11-cis-retinal$_2$ from MRet$_2$ and gave the all-trans-retinal to produce retinochrome in the membranes.

On further incubation of this 11-cis-retinal$_2$-rich RALBP with MRh-carrying membranes, the RALBP took up all-trans-retinal from MRh and gave the 11-cis-retinal$_2$ to form Rh$_2$ in the membranes.

These findings showed that RALBP may act as a shuttle of retinal between MRh and MRet to regenerate each of the photopigments, Rh and Ret, in the visual cells.

PH 72

RHODOPSIN AND RETINOCHROME IN THE NAUTILUS RETINA

A. Kishigami, R. Hara and T. Hara
Dept. of Biol., Fac. of Sci., Osaka Univ., Toyonaka, Osaka 560, Japan

Just like the dibranchiate cephalopods, the nautilus (*Nautilus pompilius*) has two kinds of photopigments, rhodopsin and retinochrome, in the retina. Retinochrome roughly amounts to about 4% of rhodopsin. These pigments were examined in digitonin extracts as follows.

The λ_{max} of rhodopsin lies at very short wavelengths (465nm). On irradiation with blue light, rhodopsin yields a photosteady state mixture with metarhodopsin ($\sim$510nm), which is photoregenerated to rhodopsin by orange light. Rhodopsin is stable in the presence of 100mM NH_2OH, whereas metarhodopsin is slowly decomposed into retinaloxime, showing a time-course consisting of two phases, fast and slow.

On irradiation with orange light, retinochrome (λ_{max}:$\sim$510nm) readily bleaches to metaretinochrome, which again yields retinochrome on addition of all-trans-retinal. As the result, nautilus retinochrome can catalyse the conversion of free all-trans-retinal to 11-cis in the light. Retinochrome is fairly stable in 20mM NH_2OH, but metaretinochrome is destroyed quickly.

According to the analysis by SDS-PAGE, the molecular weight of retinochrome was 26K, while that of rhodopsin was 84K, far larger than 45K in the squid, *Todarodes*.

PH 73

DEPENDENCY OF RHODOPSIN PHOTOLYSIS ON PHOTON DENSITY OF PICOSECOND LASER PULSE

T.Yoshizawa, Y.Shichida, S.Matuoka and H.Kandori.
Dept. of Biophysics., Fac. of Science, Kyoto University, Kyoto.

A photon density of picosecond laser pulse is essentially so high that it often causes unphysiolosical events due to multi-photon effect in investigating the primary processes of rhodopsin. Three typical examples of the multi-photon effect were shown in the following.

Excitation of cattle rhodopsin with a weak pulse induced the generation of photorhodopsin which decayed to bathorhodopsin with time constant of 45 psec, while excitation with an intense pulse induced the generation of another bathochromic product due to multi-photon effect. This product was stable in the picosecond time scale.

Relative quantum yield of isorhodopsin to rhodopsin was 0.39 which was obtained by irradiation with a weak laser pulse. The value was close to that obtained by steady illumination. Irradiation with intense pulse gave bigger ratios due to multi-photon effect. This result was close to a previous result by other groups.

11-cis-locked 7-membered rhodopsin was excited with a weak pulse, and one intermediate was observed in the early picosecond time scale. Excitation with an intense pulse induced the generation of another product due to multi-photon effect.

PH 74

CHICKEN RHODOPSIN GENE.

M. Takao[1], A. Yasui[2] and F. Tokunaga[1].
[1]Dept. of Phys., Fac. of Sci. and [2]Res. Ins. for Tuberculosis and Cancer, Tohoku Univ., Sendai.

Chicken genomic library was screened with a bovine opsin cDNA probe. A clone isolated under high stringency hybridization conditions contained DNA sequence highly homologous to all the five exons of bovine and human opsin genes. Sequence comparison of the putative open reading frame in the chicken DNA fragment of 4.3 kb with bovine opsin cDNA revealed 82 % identity for the nucleotide and 84 % for the deduced amino acid sequence, indicating that this DNA fragment contains the whole chicken opsin gene. In the 5'-noncoding region upstream of TATA box, several separated segments of 8 to 13 nucleotides long are commom in chicken and mammalian opsin genes, suggesting that these sequences might be related to the cell type specific expression of the opsin genes in these organisms.

PH 75

OPSIN LOCALIZATION DURING RETINAL DEVELOPMENT IN THE *BALB/C* AND *RDS* MUTANT MOUSE.

J. Usukura [1] and D. Bok [2]. [1] Dept. of Anatomy, Univ. of Tokyo, Tokyo. [2] JSEI UCLA, USA.

Electron microscope immunocytochemistry and Western blot were used to detect the presence and localization of opsin in the developing photoreceptor of *rds* mutant and their *BALB/c* normal control. Western blot analysis of isolated retinal membranes detected first at 10 postnatal days in both strains. Opsin levels rose progressively with development in normal retinas. In contrast, levels in the *rds* retina became undetectable by 30 days after peaking at 15 days. Specific binding of anti-opsin antibodies was first observed by immunocytochemistry at postnatal 5 days in the distal plasma membrane of the connecting cilium in both *BALB/c* and *rds* retinas. Thereafter, labeling intensity increased progressively with development in the *BALB/c* retina. Anti-opsin binding to photoreceptors in the *rds* mouse retina predominated in the plasma membrane of the connecting cilium at 5 postnatal days, but opsin was present at higher density in the inner segment plasma membrane at 5 - 20 postnatal days when compared to *BALB/c* photo- receptors. Opsin rich vesicles were observed in the subretinal space of the *rds* retina during this period. By 30 days, labeling of the ciliary and inner segment plasma membrane decreased to near background levels.

PH 76

EFFECT OF VITAMIN-A DEFICIENCY ON ERG RESPONSE AND 3-OH-RETINAL CONTENT IN THE SILKWORM COMPOUND EYES.

S.Hori[1], I.Shimizu[1], S.Yoshida[2], T.Yoshizawa[2]. [1]Lab. for Plant Ecological Study ,Fac. of Sci., Kyoto Univ., [2]Dept. of Biophys., Fac. of Sci., Kyoto Univ.

Identification and analysis of 3-OH-retinal with HPLC was carried out on various stages of Bombyx mori pupa and adults reared on mulberry leaf.

3-OH-retinal first appeared on 7 day after pupation in the eye region of pupa, and its amount rapidlly increased during 2 days before ecolosion. ERG response of developing compound eye was also detected from 7 day pupa.

When reared on vitamin-A-deprived artificial diet, the silkworm adults lost the ERG response of their compound eye. 3-OH-retinal was not detected in the vitamin-A-deficientcompound eyes. They recovered ERG response by infection of lutein at middle pupal stage. However, 3-OH-retinal and retinal was not detected from the adult compound eye of injected animals. Animals injected with beta-caroten, retinoic acid and bicyclic retinal did not show the recovery of ERG response.

PH 77

Effects of Ca^{2+} and Zn^{2+} on the ERP of octopus retina.

K. Ohtsu. Ushimado Marine Laboratory, Fac. of Sci., Okayama Univ., Okayama.

In a Ca^{2+}-free condition, the early receptor potential (ERP) of the retina of Octopus ocellatus reacts normally to the first test flash but is depressed upon following test flashes (flash-induced depression, FID). Recovery from FID usually takes an hour but strikingly accelerates to within several minutes upon addition of 1 mM $CaCl_2$. If the retina is transferred to not only Ca^{2+}- but Na^+-free artificial sea water (ASW) following test flashes in Na^+-free ASW, however, FID is greatly reduced. This suggests in view of the Na-Ca exchanger that Ca^{2+} which flowed into the photoreceptor cell through membrane channels opened by the test flashes in Na^+-free ASW could not be pumped out in the following Na^+/Ca^{2+}-free ASW because of the lack of the counter ion, Na^+. On the other hand, immediate immersion of the retina into Na^+/Ca^{2+}-free ASW without the two test flashes in Na^+-free ASW resulted in remarkable FID but recovered in a few minutes. This suggest a Ca^{2+} release from the internal calcium store, which causes quick recovery from FID, as well as the inability for Na-Ca exchange. FID was also abolished by the addition of 1 mM $ZnCl_2$. Zn^{2+} might substitute partially for Ca^{2+}. Alternately, Zn^{2+} might inhibit the pumping out of Ca^{2+} by affecting the Na-Ca exchanger because it has been known that the ion inhibits the function of Ca-ATPase.

PH 78

BIPOLAR-BIPOLAR COUPLING AND RECEPTIVE FIELD SIZES OF CARP BIPOLAR CELLS

T.Saito[1] and T.Kujiraoka[2]. [1]Inst. of Biol. Sci., The Univ. of Tsukuba, Niihari-Gun, Ibaraki, [2]Dept. of Physiol. St. Marianna Univ. Sch. of Med.,Miyamae-ku, Kawasaki

ON and OFF bipolar cells were identified in the carp retina by means of intracellular recording and dye injection. The receptive field centers, determined by measuring the response amplitudes obtained by centered spots of different diameters were 0.3-1.0 mm in diameter for ON bipolars and 0.3-0.4 mm for OFF bipolars These central receptive field values were much larger than dendritic field diameters measured from histological methods.

Simultaneous intracellular recordings were made from pairs of neighboring bipolar cells. Current of either polarity injected into one member of bipolar cell pair elicited a sign-conserving, sustained potential change in the other bipolar cell. The coupling efficiency was nearly identical for both depolarizing and hyperpolarizing currents. This electrical coupling was reciprocal, summative, and it was observed between cell types of similar function and morphology. Dye coupling was observed in 4 cases out of 34 stained cells. These results suggest that there is a spatial summation of signals at the level of bipolar cells, which makes central receptive fields much larger than their dendritic fields.

PH 79

TRANSMITTER RELEASED FROM PHOTORECEPTORS IN THE CARP RETINA.

K.-I. Takahashi and M. Murakami, Dept. Physiol., Keio Univ. Sch. Med., Tokyo.

We have developed a new technique which enabled us to measure a reversal potential in cone horizontal cells despite of the presence of electrical coupling between cells (J. Physiol., 386: 165-180, 1987). This technique was applied to rod horizontal cells. The carp retina was superfused with a solution containing high-calcium, barium, and potassium channel blockers. A calcium action potential was triggered in the cells in situ when they were depolarized electrically or by application of the excitatory amino acid (EAA). At its overshoot, light responses and electrically evoked synaptic potentials appeared with polarities reversed to those elicited at the resting state. In addition, their reversal potentials coincided with the maximal depolarization of the EAA-induced response. Since our previous report revealed that the maximal depolarization was also the reversal potential of the EAA response, the ionic mechanisms of three kinds of responses in the rod horizontal cells were identical. From these results, it is suggested that the EAA is a leading candidate for the transmitter released not only from cones but also from rods, and that the synaptic mechanism from rods to horizontal cells is the same as that of the cone system.

PH 80

POSSIBLE in situ INACTIVATION MECHANISM OF cGMP PHOSPHODIESTERASE IN FROG ROD OUTER SEGMENTS.

S. Kawamura and M. Murakami
Dept. Physiol., Keio Univ. Sch. Med., Tokyo.

Activation of cGMP phosphodiesterase (PDE) in rod disk membrane is an intermediary process of phototransduction. Though the turn-on (activation) mechanism of this enzyme is now well understood, the turn-off process has not been well elucidated: previous results so far done under in vitro condition showed that the inactivation of this enzyme is a much slower process than the recovery of the photoreceptor potential. We suggest a possible rapid turn-off mechanism of this enzyme that is attained under in situ condition.

The Michaelis constant (Km) of PDE is about 0.1 mM in the dark. When PDE is activated and the maximum PDE activity (Vmax) increases in the light, the Km also increases to about 1 mM. This Km increase is observed only in a crude preparation that probably preserves cell intactness. Using the crude preparation, we found that the Km increase does not seem to require components other than the proteins that are known to be involved in PDE activation. The Km increases within 200 msec after a light flash. When one takes the in situ cGMP concentration (<10 μM) into account, the rapid Km increase may function as a rapid turn-off mechanism of PDE in situ.

PH 81

THE EFFECT OF LIGHT DEPRIVATION ON THE FLY VISUAL SYSTEM DEMONSTRABLE WITH CYTOCHROME OXIDASE HISTOCHEMISTRY

K. Mimura, Fac. of Liberal Arts, Nagasaki University, Nagasaki.

Cytochrome oxidase histochemistry was used to examine the effect of the visual deprivation on the development of the neuron network in the optic lobe (Mimura, 1986). Flies, in which unilateral compound eye were covered immediately after emergence, were raised under normal light and dark conditions (LD). The results indicated that asymmetry in staining between the covered and uncovered sides was produced and, then, deprivation produced a decrease in the cytochrome oxidase staining of the retina and optic lobe. This difference in staining between both sides was not seen in 1-5 days post-emergence, but became evident after the sixth day post-emergence. No difference was seen in the central part of the brain. When flies were raised in LD after being raised in DD until the 5th day post-emergence, cytochrome oxidase staining was delayed. These results confirm the previous behavioral experiments of visual deprivation (Mimura, 1987), and suggest that visual deprivation during the early period of post-emergence leads to a long-lasting decrease in neuronal activity.

PH 82

SPECTRAL SENSITIVITIES OF THE COMPOUND EYE OF SOME BEETLES.

J. T. Lin, M. MIZUNAMI, Y. TOH and H. TATEDA. Dept. of Biol., Fac. of Sci., Kyushu Univ., Fukuoka.

Some coleoptera show bright colorful appearance, whereas some show somber monochromatic appearance. It appears to be an interesting subject to see relation between body colors and spectral types of the compound eye in such coleoptera. However, there have been few electrophysiological accounts about spectral sensitivities of coleopteran photoreceptors. In the present study, spectral sensitivities of the compound eye in three species of beetles, *Cicindela chinensis* D., *Liocola brevitarsis* L. and *Coccinella septempunctata bruckii* M., have been studied by intracellular recordings.

Three types of color receptors, λmax at ca. 360 nm (4 cells), 420 nm (6 cells) and 520 nm (9 cells), were recorded in *C. septempunctata*. Two types of color receptors were found in the other two; λmax at ca. 370 nm (4 cells) and 530 nm (21 cells) in *C. chinensis* and λmax at ca. 375 nm (5 cells) and 515 nm (12 cells) in *L. brevitarsis*. Blue cells were not recorded in the latter two insects, but they would be included. The failure of recordings in blue cells may be due to their small sine. It is conjectured from present data that color receptor types may be rather independent of color appearance of beetles.

PH 83

SPECTRAL SENSITIVITIES OF THE ANTERIOR LATERAL EYES OF ORB WEAVING SPIDERS.

S. Yamashita. Biol. Lab., Kyushu Inst. of Design, Fukuoka.

Spectral sensitivities of the anterior lateral eyes of the orb weaving spiders, *Argiope bruennichii* and *A. amoena* were examined by recording extracellular ERGs and intracellular receptor potentials. Both ERGs and intracellular receptor potentials consisted of two rapid initial peaks followed by a slow phase. In the red-adapted eye, the amplitude of the first peak decreased markedly and the maximum amplitude for the second peak was observed at about 480-520 nm. In contrast, the second peak was markedly depressed in the blue-adapted eye and the maximum amplitude for the first peak was observed at about 540-580 nm. These observations suggest that the anterior lateral eye contains two types of receptors and that they are coupled to each other. Receptor cells were simultaneously impaled in a pair and electrical coupling was demonstrated between the receptors by passing a current into one cell and recording a resulting potential in the other cell.

PH 84

ELECTRON MICROSCOPIC IMMUNOCYTOCHEMISTRY OF THE *DROSOPHILA* VISUAL PIGMENT.

Y. TOMINAGA and T. TANIMURA. Dept. Biol., Fac. Sci., Fukuoka Univ. Fukuoka.

The peripheral retinula cells (R1-6) of *Drosophila* compound eyes contain different types of rhodopsin from those of the central retinula cells (R7 & 8). Using a monoclonal antibody specific for R1-6 rhodopsin, we have studied the subcellular localization of R1-6 rhodopsin and the turnover mechanism of photoreceptor membranes by electron microscopic immunocytochemistry.

Heavy labelling was seen on the rhabdomeric microvilli of R1-6. Multivesicular bodies in R1-6 were also heavily labelled by the anti-opsin antibody, and coated vesicles near the bases of microvilli were sometimes labelled. Secondary lysosomes presumably originated from multivesicular bodies were also labelled. These cytoplasmic organelles must be involved in the breakdown processes of rhabdomeric microvilli membranes.

Flies grown on the carotenoid-deficient medium lacks rhodopsin. R1-6 cells of these flies were scarcely stained by the antibody. By feeding retinoids, opsin synthesis can be triggerd in these flies. We examined the time course of opsin synthesis. The number of gold particles on the rhabdomeric microvilli membranes gradually increased. The labelling was found on the same cytoplasmic membrane components, such as rough ER, Golgi bodies, smooth ER, suggesting that these organelles may be related to the renewal of photoreceptor membranes.

PH 85

THE EFFECTS OF VITAMIN A DEFICIENCY ON THE COMPOUND EYES OF SILKWORM MOTH.

E.Eguchi, S.Hori* and I.Shimizu*.
Dept. of Biol., Yokohama City Univ., Yokohama.
*Lab. for Plant Ecological Studies, Fac. of Science, Kyoto Univ., Kyoto.

The structure and function of the compound eyes of silkworm moths (Bombyx mori) raised with vitamin A free diet (A free moth) were investigated and compared with those raised with normal diet (normal moth).

From the observations of thin-sections by electron microscope, it was found that the structure of rhabdoms of A free moth were maintained almost the same as that of normal moth, but the disorganization and vacuolation were occationally seen in the rhabdom. The observations of freeze-fractured specimens revealed the significant difference on the densities of intramembrane particles on P-face of rhabdom microvilli membrane between them, namely the density of A free moth is ca.300/μ^2 which is less than 10% of normal moth.

Electrophysiological measurements of the response amplitudes to graded stimulus light intensities by ERG method showed that the eyes of A free moth had significantly higher threshold (approximately 2-3 in log unit of light intensity) than the normal moths, and some showed no response even to the brightest light stimulus used in the experiment.

PH 87

A COMPARATIVE STUDY OF THE EFFECTS OF ALPHA ADRENERGIC REAGENTS ON MELANOPHORES OF TELEOSTS.

F. Morishita and K. Yamada. Zool. Inst., Fac. of Sci., Hiroshima Univ., Hiroshima.

Using specific agonists and antagonists, the subtypes of α-adrenoceptors mediating melanosome aggregation in melanophores were examined on the goby (Odontobutis obscus), catfish (Corydoras paleatus), rainbow trout (Salmo gairdnerii), goldfish (Carassius auratus) and dark chub (Zacco temminckii).

Among the agonists used, the melanosome-aggregating effect of clonidine (Clo, an α_2 agonist) on melanophores of the rainbow trout, goby and goldfish was far greater (EC50s, 33.5, 81.8 and 460 nM) than that of methoxamine (Mex, an α_1 agonist; EC50s, 3.0, 5.7 and 3.8 μM). However, the effect of Clo on melanophores of the catfish was far less (EC50, 22.4 μM) as well as that of Mex (EC50, 66.8 μM). For the cells of the dark chub, Clo acted as a partial agonist, and besides, at concentrations of more than 1 μM, the effect of Clo was weaker than that of Mex. Oxymetazoline, another α_2 agonist, had practically no effect on melanophores of the present teleosts. Although the melanophore responses to the agonists differed among fish species, the inhibitory effect of yohimbine, an α_2 antagonist, on the cell responses to the agonists was always greater than that of prazosine, an α_1 antagonist, suggesting that α_2 adrenoceptor is dominant in the dermal melanophores of the present teleosts.

PH 86

SUBCLASSIFICATION OF α- AND β-ADRENOCEPTORS IN MELANOPHORES OF GOBY, *TRIDENTIGER OBSCURUS*.

H. Katayama[1], Y. Isogai[2], F. Morishita[3] and K. Yamada[3]. [1]Mukaishima Mar. Biol. Stat., Hiroshima Univ., Mitsugi-gun,Hiroshima-ken, [2]Toyo-Jozo Co. LTD., Tagata-gun, Shizuoka-ken, and [3]Zool. Inst., Fac. Sci., Hiroshima Univ., Hiroshima.

Melanophores of the goby have both α- and β-adrenoceptors. Adrenergic α-agonosts induce pigment aggregation of melanophores, while both α-antagonists and β-agonists tend to inhibit pigment aggregation. To study effects of drugs on melanophores, responses of denervated melanophores in an isolated, split caudal fin were recorded photoelectrically with a microscope. The order of pigment aggregating potency of the α-agonists used was norepinephrine(NE)>clonidine(CL)>naphazoline(NP)>tetrahydrozoline (TH)>methoxamine(MX)>phenylephrine(PH). CL and NP are selective α_2-agonists. TH, MX and PH are α_1-agonists. Yohimbine, a specific α_2-antagonist more potently inhibited pigment aggregation caused by NE than prazosin, an α_1-antagonist. These results indicate that α-receptor of the melanophores is α_2 type. Specific β_2-agonists, salbutamol(SAL) and terbutaline(TER), and a specific β_1-agonist dobtamine(DOB) inhibited pigment aggregation induced by NE. The order of the lower limit of effective concentration that inhibit pigment aggregation was SAL<DOB<TER. These results suggest that β-receptor of the melanophores is β_2 type.

PH 88

MOTILITY OF CULTURED IRIDOPHORES OF THE FRESHWATER GOBY ODONTOBUTIS OBSCURA.

T. Iga, J. Kinutani and N. Maeno. Dept. of Biol., Fac. of Sci., Shimane Univ., Matsue.

The movements of iridophores in the dermis of the freshwater goby Odontobutis obscura were regulated by sympathetic adrenergic nerves and hormones. Electron microscopic observations suggested that the movements of the iridophores were of a translocation of the platelets within the cells. Nerve stimulation induced a dispersion of the platelets and αMSH caused an aggregation of the organelles at the cell center. In the present experiments, the motility of cultured iridophores was examined in relation to the migration of the platelets and changes in cell boundaries. Iridophores isolated from the scales were cultured in L-15 medium containing 5% fatal calf serum for about 1 week before use. αMSH induced an aggregation of the platelets, which moved almost linearly toward the centosphere. The migration velocity was measured as 0.1-0.5 μm/min. Melatonin produced a platelet dispersion. It took 3 to 4 hrs to recover the original state. During the movements the cell boundaries remained fixed.

PH 89

ADENOSINE RECEPTORS MEDIATING MELANOSOME DISPERSION IN MELANOPHORES OF THE MEDAKA.

S. Namoto and K. Yamada. Zool. Inst., Fac. of Sci., Hiroshima Univ., Hiroshima.

Adenosine causes a rapid and reversible dispersion of melanosomes in norepinephrine-treated aggregated melanophores of the medaka, Oryzias latipes, indicating the presence of adenosine receptors in the cells. To ascertain the precise nature of the receptors, cell response to various agonists were examined. The melanosome-dispersing potency of agonists used was in the following order: 5'-N-ethylcarboxamide-adenosine (NECA) > 2-chloroadenosine = adenosine = ATP > N^6-L-phenylisopropyladenosine (PIA) > cyclohexyladenosine (CHA). The potency of NECA (an A_2 agonists) was about 100-fold greater than that of A_1 agonists (PIA and CHA). Dipyridamole, a purine transport inhibitor, had no effect on the purine actions, suggesting that P-site, a intracellular purine-sensitive site, is not involved in the cell responses. Theophylline competitively inhibited the melanosome-dispersing action of adenosine, while forskolin, an activator of adeneylate cyclase, augmented the adenosine action. These findings suggest that adenosine receptors in the medaka melanophores are A_2 in nature and further that the stimulation of the receptor mediates activation of adenylate cyclase, which induces the dispersion of melanosomes through increase in the intracellular level of cAMP.

PH 90

ADENOSINE INHIBITS THE RELEASE OF NEUROTRANSMITTER FROM ADRENERGIC MELANOSOME-AGGREGATING NERVES IN TILAPIA.

N. Oshima, H. Kasukawa and R. Fujii. Dept. of Biol., Fac. of Sci., Toho Univ., Chiba.

In order to study the mechanism of presynaptic inhibition in adrenergic chromatic nervous system, the action of adenosine on the release of neurotransmitter from nervous elements was examined.

Split fin preparations of the tilapia, Sarotherodon niloticus, were loaded with ^{3}H-norepinephrine (NE), and rinsed with fresh saline. After they were transferred into a small plastic chamber, sampling of the bathing medium was carried out every 2 min. The number of disintegrations of ^{3}H in the sampling medium was counted in a liquid scintillation counter.

When electrical stimulation was applied, the release of ^{3}H-NE was significantly increased. The increase was suppressed by adenosine dose-dependently, and the minimal effective concentration was about 10^{-6} M. Such inhibitory effect of adenosine was blocked by theophylline, implying that adenosine interacts with presynaptic adenosine receptors. ATP also showed the same effect. Since ATP (adenosine) has been shown to be liberated as a co-transmitter from nerve terminals along with NE (cf. Fujii and Oshima, 1986), the mechanism of auto-regulation is suggested in chromatic nervous system in fish. On the other hand, NE itself did not repress the ^{3}H-NE release from adrenergic nerves of the tilapia.

PH 91

CHANGES IN BODY COLOR AND MECHANISMS CONTROLLING MELANOPHORE MOVEMENT IN UPSIDE-DOWN CATFISH.

H.Nagaishi, H.Nishi, R.Fujii and N.Oshima. Dept. of Biol., Fac. of Sci., Toho Univ., Chiba.

Upside-down catfish (Synodontis nigriventris) are noted for their unique habit of swimming and resting bottom up. Their ventral side is dark alike the dorsal part.

When the fish were adapted to the white or black background, the brightness of both dorsal and ventral parts changed. Melanophores present in the dorsal and ventral skins were shown to be controlled adrenergically, since they responded to norepinephrine by a remarkable pigment aggregation, which was readily antagonized by the specific blocker, phentolamine.

In the night, the dorsal part of the body surface seemed to be paler than the ventral part. This is probably due to the difference in the size and number of melanophores existing in each side: In ventral part, smaller melanophores are present in larger numbers.

When melatonin was added into the aquarium water, the fish were blanched in spite that they were on the black background, and swam actively. In addition, upside-down catfish was found to prefer the black background to the white one. Thus, the intimate relationship between the behavior and the change in the body brightness was suggested.

PH 92

SKIN COLORATION AND ITS CONTROLLING MECHANISMS IN THE BLUE-GREEN DAMSELFISH.

H.Kasukawa, K.Miyaji, N.Oshima and R.Fujii. Dept. of Biol., Fac. of Sci., Toho Univ., Chiba.

In the blue-green damselfish (Chromis caerules) skin, which normally displays yellowish green hue, three sorts of chromatophores, i.e. xanthophores, iridophores and a melanophore are present, and constitute a dermal chromatophore unit resembling that of anurans or reptiles. The iridophores showed analoguos fine structures as those in the blue damselfish, Chrysiptera cyanea. Those cells are categorized into the motile and non-motile ones, and each cell reflected rays of varying, but a single spectral peak by a non-ideal multilayer thin-film interference. The motile cell possessed only alpha- and beta-adrenoceptors, mediating changes of spectral shifts towards longer or shorter wavelength, respectively. The changes may be due to the simultaneous increase or decrease in the distance between adjoining reflecting platelets. On the other hand, the non-motile iridophore reflecting rays of single spectral peak may possess neither intracellular motile machinery nor receptors involved. Although the integument of this fish reflects several colors microscopically, it looks greenish as a whole, being due to an integrative effect of different purer colors reflected from iridophore sorts. The darkening is induced by a reverse process.

PH 93

THE ROLE OF Ca IONS IN PIGMENT-AGGREGATION RESPONSES OF MEDAKA XANTHOPHORES.

M. Iwakiri, Dept. of Biol., Fukuoka Univ. of Educ., Munakata.

Using denervated xanthophores in isolated scales of the medaka, Oryzias latipes, effects of Ca^{2+} antagonists and EGTA were examined on the cell responses to various pigment aggregating reagents. KCl (more than 30 mM) and noradrenaline (more than 1 μM) induced a full aggregation of pigment within the cells. Caffeine at concentrations less than 1 μM induced a weak pigment aggregation, while at higher doses it caused a marked pigment dispersion. Pigment-aggregation response of xanthophores to KCl was inhibited by verapamil, La^{3+} and EGTA, respectively, but not by procaine. The cell response to noradrenaline was also inhibited by verapamil, La^{3+} and EGTA, respectively. However in this case, the inhibitory effect of EGTA was considerably low and besides verapamil was observed to inhibit the cell response through its competitive action to noradrenaline at the receptor site. Caffeine-induced aggregation response of the cell was inhibited by procaine, La^{3+} and EGTA, respectively, but not by verapamil. These findings suggest that each cell response to the respective reagent requires Ca^{2+} from different sourses, i.e. the cell response to KCl requires the extracellular Ca^{2+}, while the intracellular Ca^{2+} is involved in both noradrenaline- and caffeine-induced cell responses.

PH 94

TRANSMISSION OF LIGHT-SENSITIVE RESPONSE OF XANTHOPHORES IN SCALES OF THE MEDAKA.

I. Kawai. Aichi Pref. Col. of Nursing, Nagoya.

Usually, xanthophores in isolated scales of the medaka, Oryzias latipes, maintained a fully pigment-dispersed state in physiological saline under darkness. The cells responded to light with a rapid and full aggregation of pigment granules and then with a gradual redispersion, finally attaining the half pigment-aggregated state. When a part of the scale was illuminated locally, in some xanthophores located in the outside of the illuminated area, aggregation of pigment also occurred to a certain extent. The subsequent illumination of the whole scale induced not only the aggregation response of non-stimulated xanthophores but also aggregation of the prestimulated cells. These light-sensitive responses of xanthophores were inhibited by the presence of Ca^{2+} antagonists, such as papaverine and verapamil. The findings suggest that the light-sensitive response is transmitted from the stimulated xanthophores to the other cells. The data also suggest that the chromatic nerves are not involved in the transmission of cell response, because such phenomena were consistently observed in both innervated and denervated cells. Ca^{2+} might take part in the transmission of the light-sensitive response as well as in the aggregation response itself.

PH 95

THE METABOLIC PATH TO FOR CHROMOPHORES OF INSECT VISUAL PIGMENTS.

T.Seki, S.Fujishita. Dept. of Health Sci., Osaka Kyoiku Univ., Hirano Campus, Osaka.

Retinoids and carotenoids in a compound eye of insects in several orders were analysed by using HPLC-system detecting absorbances at two wavelengths, UV and visible.

Xanthophyll was found in all the insects whether they use retinal or 3-OH retinal as the chromophore of visual pigments. This result indicate that the xanthophyll present in the compound eye does not necessaryly become the precursor of the chromophore of visual pigments.

In Mantodea, Orthoptera and Phasmida, far more retinyl ester than retinal was found in the compound eye, and in the case of Odonata which uses both retinal and 3-OH retinal as the visual pigment chromophore, far more retinyl ester and 3-OH retinyl ester than chromophore retinals were found in the compound eye. The predominant geometric isomer of the esters was 11-*cis*. These esters must be the precursor and the stock form of the chromophore retinals.

In Diptera and Lepidoptera which are the higher orders in Insecta and use 3-OH retinal as the chromophore retinal, little 3-OH retinyl ester was found in some species. In these species xanthophyll must be the precursor of the chromophore retinal. They may have obtained the ability to isomerize all-*trans* 3-OH retinal, which is the product by the imaginal xanthophyll dioxygenase activity, into 11-*cis* 3-OH retinal.

PH 96

IONIC MECHANISMS OF THE SLOW POST-SYNAPTIC POTENTIAL IN THE HEART EXCITATORY NEURONE OF THE AFRICAN GIANT SNAIL, *Achatina fulica* Férussac.

Y.Furukawa and M.Kobayashi. Physiol. lab., Fac. of Integrated Arts & Sci., Hiroshima University, Hiroshima.

Ionic mechanisms of the slow excitatory post-synaptic potential (SEPSP) of the heart excitatory neurone (PON) induced by the activity of two cerebral neurones were investigated under the voltage-clamped condition. By experiments of the ionic substitution and of the Cs^+-injection, SEPSP was found to be due mainly to the decrease of 'background' K^+-conductance. In some preparations, the transient increase of conductance was also seen. The increased conductance was assumed to be Ca^{2+}-conductance as synaptic response was increased by the injection of EGTA. Serotonin (5-HT) produced similar slow depolarization in PON, and both slow depolarizations induced by 5-HT and the cerebral cells were depressed by the 5-HT antagonist, methysergide. The slow depolarizaion by 5-HT was also mainly due to the decrease of 'background' K^+-conductance and two different 5-HT-sensitive K^+-channels were identified by the patch-clamp experiments. Serotonin also increased the voltage-dependent Ca^{2+}-conductance in PON. These results suggest that the neurotransmitter of the two cerebral cells may be 5-HT.

PH 97

REGULATION OF HEART ACTIVITY IN THE GIANT AFRICAN SNAIL, ACHATINA FULICA.

K. Fujii. Dept. of Biol., Fac. of Sci., Toho Univ., Chiba.

Molluscan heart is known to be myogenic, being regulated by the central nervous system. Working on the African giant snail, Achatina fulica, the controlling mechanism for the heart activities was studied. First, the presence of serotonin and FMRFamide in both the central nervous system and the heart was immunohistochemically examined and confirmed. The FMRFamide-positive nerve fibers in the heart were larger in number than the serotonin-positive nerve fibers, especially in the auricle. Using isolated heart preparations, the effects of the above-mentioned and the related substances were then studied. Serotonin, FMRFamide, dopamine and norepinephrine were found to augment the activities, while ACh acted inhibitorily. Serotonin acted excitatorily on the heart beat and amplitude. FMRFamide also acted excitatorily on the heart beat, but showed no effect on the amplitude. Effect of serotonin was more potent than FMRFamide. Dopamine showed a similar effect to that of serotonin. Norepinephrine caused a decrease of amplitude at 10^{-5}M. ATP at higher concentrations lowered the amplitude. Adenosine had the same effect but to a lesser degree. The receptor analysis of these drugs is under investigation.

PH 98

EXCITATORY AND INHIBITORY PATHWAYS OF CARDIO-REGULATORY NERVES IN THE CENTRAL NERVOUS SYSTEM IN AN ISOPOD, BATHYNOMUS DOEDERLEINI.

K.Tanaka and K.Kuwasawa. Dept. of Biol., Fac. of Sci., Tokyo Metropolitan Univ., Tokyo.

Each of two anterior cardiac nerves contains three cardio-regulatory axons, a cardio-inhibitor (CI) and two cardio-accelerators(CA1 and CA2). We found that CI, CA1 and CA2 arise from, respectively, the 3rd root of the 1st, 2nd and 3rd thoracic ganglia (T1G, T2G and T3G). In fact, we identified a candidate cell for CA2 neurone in T3G.

In isolated single-ganglion(T2G or T3G) preparation, impulse discharge of CA1 or CA2 was activated by stimuli applied to anterior and posterior connectives of T2G or T3G, and by stimuli of the 1st, 2nd and 3rd roots of T2G or T3G. CA1 and CA2 activities were inhibited by stimuli to connectives. T1G was necessary for the inhibition of CA1 and CA2 produced by stimuli of peripheral nerves.

CI was activated by stimuli of connectives anterior and posterior to T1G. In preparations containing T1G to T3G, CA1 and CA2 were inhibited by stimuli of peripheral nerves, while CI was activated by the stimulation.

These results show that there are excitatory inputs were transmitted to CA1 and CA2 in their own ganglia. Reciprocal relation between CI and CAs activities in response to stimuli applied to the periphery was eliminated in the preparation whose cerebral ganglion was removed. The reciprocal coupling mechanism between excitation of CI and inhibition of CAs may exsist in T1G.

PH 99

NEUROPHYSIOLOGICAL AND PHARMACOLOGICAL STUDIES ON THE CARDIO-ARTERIAL VALVE OF *BATHYNOMUS DOEDERLEINI*

Y.Fujiwara and K.Kuwasawa. Dept. of Biol., Fac. of Sci., Tokyo Metropolitan Univ., Tokyo.

The haemolymph flow to the arteries is modulated with dilation and constriction of their own valves.

The lateral cardiac nerves(LCNs) running along lateral arteries(LAs) were found to consist of one or two axons innervating the valve. The repetitive stimulation applied to LCNs always increased the haemolymph flow. All LCNs may be valve inhibitory (dilator) nerves.

When the heart was perfused with ACh, pressure pulses of the outflow into LAs were increased. This shows that ACh dilated the valve. Such inhibitory effects were also somewhat observed with muscarine, arecoline and atropine.

5-HT and octopamine decreased amplitude of pressure pulses. This shows that these drugs caused costriction of the valves. Noradrenalin, adrenalin, dopamine and glutamate produced no effect on pressure pulses.

We supposed that ACh may be a candidate for, at least, a transmitter of the inhibitory (dilatory) valve nerve. Since constriction of the valves should not be produced by neuronal mechanisms, it was suggested that 5-HT and octopamine may act the part of the excitatory humoral modulator on the cardio-arterial valves of the lateral arteries.

PH 100

NEURAL CONTROL OF THE HEART AND THE PERICARDIUM IN AN AMPHINEURAN MOLLUSC (LIOLOPHURA JAPONICA).

S.Matsumura, K.Kuwasawa. Dept. Biol., Fac. of Sci., Tokyo Metropolitan Univ., Tokyo.

Simultaneous extracellular recording from the heart and the pericardium showed that the heart and the pericardium beat at different rates. It is likely that the heart and the pericardium possess myogenic nature. ACh(10^{-10}M) produced inhibitory effects on the heart, 5-HT(10^{-8}M) produced excitatory effects on the heart. Inhibitory and excitatory nervous control of the heart may involve cholinergic and serotonergic mechanisms, respectively.

Cardioexcitatory responses were elicited by repetitive electrical stimuli applied to the ventral and the lateral nerve cords (VNC and LNC). The responses elicited by stimuli to VNC were observed even after the denervation of LNC. Cardioinhibitory responses were elicited only by stimuli to the LNC. In Cryptochiton, it has been determined whether the cardioexcitation caused by nerve stimulation is a direct effect of innervation to the heart or not. We confirmed that the excitatory effects were caused by cardioregurato-ry nerves, running from LNC and VNC. The inhibitory nerve possibly arises from LNC alone.

The pericardium was activated by stimuli to LNC and VNC and inhibited by stimuli to the LNC. The effects of nerve stimulation on the heart and the pericardium did not always coincide. Excitatory and inhibitory nerves to the heart are not common with those to the pericardium.

PH 101

INNERVATION OF IDENTIFIED NEURONS IN THE VISCERAL-GANGLIONIC NERVOUS SYSTEM OF *PLEUROBRANCHAEA NOVAEZEALANDIAE*

K. Kuwasawa and M. Kurokawa. Dept. of Biol., Fac. of Sci., Tokyo Metropolitan Univ., Tokyo.

The visceral ganglion has a pair of the connectives connected with the cerebro-pleural ganglion and the branchial nerve running to the gill and the visceral nerve to visceral organs including the circulatory system. Microscopic sections cut from the ganglion showed that the ganglion consists of about twelve ganglionic neurons. It was observed anatomically and electrophysiologically that the visceral nerve sends branches to the penis ganglion, arteries, the hermaphroditic duct, the pericardium, the renal pore, the ventricle and auricle of the heart. There is a single-cell ganglion on the visceral nerve usually at the site from where the nerve to the hermaphroditic duct arises.

The cells in this nervous system were filled with Co^{++} and/or Ni^{++} by simultaneous pressure and iontophoretic injection. Some processes of the cells were stained through a distance of 20mm which reach their effectors. Two of the largest neurons sends axons to the aorta and the hermaphroditic duct. There is an electrical coupling between them. One medium sized cell sends an axon to a region of the renal pore. The cell in the single-cell ganglion sends axons to the visceral ganglion, the pericardium and the glandular sac located at the branchial end of the auricle.

PH 102

DISTRIBUTION OF BIOACTIVE AMINES IN THE CENTRAL NERVOUS SYSTEM OF A MOLLUSC, *PLEUROBRANCHAEA NOVAEZEALANDIAE*

M. Otokawa[1] and K. Kuwasawa [2] [1]Fac. of Social Sci., Hosei Univ., Tokyo. [2]Dept. of Biol., Fac. of Sci., Tokyo Metropolitan Univ., Tokyo.

Tissue extracts from the central nervous system were analysed for bioactive amines by HPLC on a column (Chemcosorb 5-ODS-H) with an electrochemical detector (BAS, LC-4B). Electrochemically active substances were identified by the retention time.

In the cerebro-pleural ganglion average amounts of norepinephrine (NE), dopamine (DA) and 5-hydroxytryptamine (5-HT) were, respectively, 33.0, 265.9 and 170.1 pmoles.

In the buccal ganglion averages of NE, DA and 5-HT were 3.5, 39.6 and 30.0 pmoles, respectively.

In the left pedal ganglion averages of NE, DA and 5-HT were 4.8, 15.6 and 228.5, respectively.

In the right pedal ganglion they were 15.7, 166.2 and 144.5 pmoles, respectively.

In the visceral ganglion trace amounts of NE and DA were detected, but 5-HT was not observed. Immunocytochemichal study also suggested the absence of 5-HT containing neuron in the ganglion.

The glandular sac and pinnules of the gill innervated by nerves of the visceral ganglion were shown to have considerable amounts of DA and 5-HT.

PH 103

ANALYSIS OF RHYTHM COORDINATION BETWEEN THE AURICLE AND VENTRICLE IN THE OYSTER CRASSOSTREA GIGAS

H. Uesaka[1], H. Yamagishi[2] and A. Ebara[3]. [1]Facom·Hitac.Ltd., Ibaraki, [2]Inst. of Biol. Sci., Univ. of Tsukuba, Ibaraki, [3]Inst. of Physics, Sci. Univ. of Tokyo, Tokyo.

The mechanism of coordination of the auricular and ventricular rhythms mediated by mutual stretching was analyzed in the oyster heart from phase-response curves (PRC) for brief stretches. The PRCs were biphasic showing phase delay and advance as a function of the phase where the stretch was applied. The auricle and ventricle were considered as cardiac oscillators with similar dynamic properties for brief stretches, due to their PRCs being remarkably alike.

Entrainment of the beat rhythm by repeated stretches was predicted from the PRC and confirmed. When the interval of the stretches was close to the beat interval, the oscillator established a fixed phase relationship with the stretches at a phase predicted from the PRC and the beat rhythm was stably entrained. Alterations of the auricular and ventricular intervals recorded *in situ* in the uncoordinated state could be interpreted as repeated phase responses.

The regular heart rhythm of the oyster must be achieved by mutual stable entrainment of the auricular and ventricular rhythms mediated by mutual stretching.

PH 104

HIBERNATION-LIKE STATE IN CARDIAC FUNCTION OF NONHIBERNATING CHIPMUNKS.

N.Kondo. Dept. of Muscle Physiol. Mitsubishi-kasei Inst. of Life Sci., Machida, Tokyo

In an attempt to elucidate whether changes in cardiac properties observed during hibernation occur before entering into hibernation, seasonal variations in electromechanical responses were studied on myocardium of nonhibernating chipmunks. Characteristic properties of hibernating preparations were as follows: 1)frequency-dependent decrease in tension, 2)reduced amplitude of action potential plateau(APp) which is augmented by 4-aminopyridine(4-AP), 3)inhibition of APp and tension by substitution of Ca by Sr. In nonhibernating preparations, a frequency-dependent increase in tension was observed between June and September, while between October and next May, tension showed a frequency-dependent decrease. APp showed a high amplitude between May and September, but a reduced amplitude between October and next April which was increased by 4-AP. Sr markedly increased tension with a prolongation of APp in preparations obtained during summer season. In those obtained during winter season, Sr caused a marked inhibition of tension and APp. These indicate that changes in cardiac function are already triggered before hibernation begins, suggesting possible involvement of as yet unknown substance(s).

PH 105

EFFECT OF HYPOXIC CONDITION ON THE ISOLATED HEART BEAT OF THERMALLY ACCLIMATED GOLDFISH

H. Tsukuda. Dept. of Biol., Fac. of Sci., Osaka City Univ. Osaka.

The heart excised from 10°C- or 25°C-acclimated goldfish was immersed in physiological saline at 10°C with or without glucose and the frequency and the amplitude of ventricular contraction was recorded under hypoxic condition (about 25% oxygen) for three hours. The ventricular activity was evaluated by the "power" which is the product of frequency and amplitude.

The relative power (percentage to the initial value) was significantly higher and the decreasing rate was smaller in 25°C-acclimated fish than in 10°C-acclimated fish. After 30, 60, 120 and 180 min, the power decreased irrespective of exogenous glucose supply to 36, 19, 8 and 3% in average in 10°C-acclimated fish and 63, 55, 47 and 39% in 25°C-acclimated fish.

These results indicate that the ventricular activity of cold-acclimated fish is more sensitive to hypoxic condition than that of warm-acclimated fish and that exogenous glucose is scarcely available to ventricular contraction under hypoxic condition, especially in warm-acclimated fish, in contrast with the case under normoxic condition.

PH 106

ACTIVATION OF CONTRACTURES IN INSECT SKELETAL MUSCLES.

T.Yamaguchi[1],H.Washio[2]. [1]Dept.Biol. Intern. Christ. Univ., Mitaka, Tokyo, [2]Lab. Neurophysiology, Mitsubishi-Kasei Inst. Life Science, Machida, Tokyo.

To clarify the activating mechanism of contractures of insect skeletal muscle, 4X 10^{-4}M L-glutamate- and 100mM potassium-induced contractures were examined in the retractor unguis muscle of cockroach (Periplaneta americana). Both contractures were completely eliminated when the muscles were immersed in calcium free saline containing 2 mM EGTA. If then, calcium ions were added to these muscles, a delayed glutamate and a tonic potassium contractures were initiated, respectively. If the muscles were previously immersed for 10 min in a saline containing 10mM Mn^{++}, glutamate contracture was reduced by ca. 70%, while the phasic contracture of potassium was reduced by about half of the control. 1μM Nifedipine reduced both L-glutamate and potassium contractures at different rates, whereas procaine at the same rate. The latter drug suppressed the phasic component of potassium contracture. These results support the hypothesis that in insect muscle, contractures are initiated by external calcium ions which enter the membrane and then, act by two ways, one to SR and the other directly to contractile apparatus. This was also supported by the fact that a phasic contracture was induced by caffeine.

PH 107

ADRENERGIC PATHWAY IN NEURO-MUSCULAR TRANSMISSION IN THE RED MUSCLE OF PUFFER FISH.

S.Yukiyama and T.Hidaka* Dept. of Biol.Fac. of Sci., and *Fac. of Gen. Edu., Kumamoto Univ., Kumamoto.

In the pectoral fin red muscle of puffer fish, Takifugu poecilonotus and T. rubripes, excitatory junction potential(ejp), inhibitory junction potential(ijp) and the diphasic junction potential composed of ejp and ijp were elicited by the single nerve stimulation. Miniature ejp (mejp) and miniature ijp (mijp) were observed in the resting muscle. The previous study showed that this transmission was mediated by the cholinergic pathway.

Besides this pathway, the presence of another pathway was suggested from effects of adrenergic agonists and antagonists. While α-agonist, noradrenaline and phenylephrine, increased the amplitude of ejp and ijp, α-antagonist, phentolamine and prazosin increased both ejp and ijp. While β-agonist, isoproterenol and terbutaline, enhanced ijp, β-antagonist, propranolol, reduced it. These results suggested that α_1-receptor related to the generation of ejp and α_1- and β_2-receptors related to that of ijp.

On the other hands , α-agonist, noradrenaline, decreased the frequency of mejp and β-agonist , terbutaline , accelerated the generation of mijp. These results suggest the possibility that α- and β-receptors are present not only on the postjunctional membrane but also on the presynaptic membrane.

PH 108

EFFECTS OF PICROTOXIN ON CA CURRENT AND TENSION IN ISOLATED FROG MUSCLE FIBRES.

V. Jacquemond, K. Takeda[1] and O. Rougier. Lab. Physiol. Elements Excitables, Univ. Claude Bernard, Villeurbanne, France. [1]Visitor from Lab. Physiol., Fac. Educ., Tottori Univ., Tottori.

Single twitch fibres were isolated from semitendinosus muscle of Rana esculenta and prepared for double-mannitol-gap voltage-clamp method (Ildefonse et al., 1985, Biochem. Biophys. Res. Commun. 129, 904). Test solution used contained 1.8 mM $CaCl_2$, 122 mM $TEA\text{-}CH_3SO_3H$, 3 mM 4-aminopyridine, 10 mM HEPES-KOH and 5 mM glucose. It had normal Ca but most Cl was substituted, and most K channels were blocked in it. Holding potential (estimated to be ca. -90 mV) adjusted so as to have a contractile threshold at -50 mV was applied to maintain normal resting potential. 5 mM picrotoxin inhibited slow inward Ca current greatly (to below ca. 30% of control values in a fibre), but simultaneously recorded peak tension was increased (ca. 2.5 times in the fibre), provided the interval between applied depolarizing voltage steps (50 and 70 mV in amplitude) was kept long enough (2 minutes). These effects of picrotoxin on Ca current and tension were reversible and could be repeated in the same fibre. The results have shown that, in the experimental conditions used, picrotoxin potentiates contraction when it is inhibiting Ca current.

PH 109

MODULATORY ACTIONS OF THE CATCH-RELAXING PEPTIDE ON MOLLUSCAN MUSCLES.

T.Hirata and Y.Muneoka. Physiol. Lab., Fac. Integrated Arts and Sci., Hiroshima Univ., Hiroshima.

The catch-relaxing peptide (CARP: H-Ala-Met-Pro-Met-Leu-Arg-Leu-NH_2) is a novel neuropeptide isolated from the pedal ganglia of the mussel Mytilus edulis (Hirata et al., 1987). This peptide showed not only relaxing action on catch tension in the anterior byssus retractor muscle (ABRM) of the mussel at low concentrations (threshold, 0.3-1.0 nM) but also some other actions on various molluscan muscles. In the ABRM, CARP potentiated or inhibited phasic contraction in response to repetitive electrical pulses of stimulation. In general, the peptide showed potentiating action at lower concentrations (threshold, 0.3-0.5 nM), and inhibitory action at higher concentrations (threshold, 1-50 nM). CARP also inhibited contractions of the ABRM in response to ACh and FMRFamide. In the radula protractor and retractor muscles of the prosobranch mollusc Rapana, contractions in response to electrical pulses, ACh and glutamate were inhibited by CARP. Cardiac activities of Meretrix, Tapes and Mytilus were also inhibited by CARP. Thus, CARP seems to have modulatory actions on many molluscan muscles, and the actions seem to be brought about by direct effect of the peptide on muscle fibres.

PH 110

PHARMACOLOGICAL PROPERTIES OF RELAXING RESPONSE OF MYTILUS SMOOTH MUSCLE TO THE CATCH-RELAXING PEPTIDE.

T.Hirata,N.Fujimoto and Y.Muneoka. Physiol. Lab., Fac. Integrated Arts and Sci., Hiroshima Univ., Hiroshima.

Pharmacological properties of relaxation of catch in the ABRM of Mytilus in response to the catch-relaxing peptide (CARP) were examined and compared with those of relaxation in response to 5-HT, dopamine and repetitive electrical pulses of stimulation. Butaclamol (10^{-5} M), a dopamine blocker,did not affect relaxing responses to CARP, 5-HT and repetitive electrical pulses. Mersalyl ($5x10^{-4}$ M), a 5-HT blocker, slightly depressed but did not blocked relaxing response to CARP. Propranolol (10^{-3} M) depressed or blocked relaxing responses to 5-HT,dopamine and repetitive electrical pulses, whereas it enhanced that to CARP. Phenoxybenzamine (10^{-4} M) enhanced relaxation by CARP, 5-HT and repetitive electrical stimulation, but it did not affect relaxation by dopamine. Simple exposure of the ABRM to La^{3+} (5 mM) did not affect relaxing response to CARP, but, after the muscle had been exposed to La^{3+} in the presence of a depolarizing agent, relaxing response to CARP was abolished, as in the cases of 5-HT and dopamine. Cyclic AMP levels in the ABRM were increased by 5-HT, but were not significantly affected by CARP. CARP seems to relax catch tension by acting directly on muscle fibres, though its presynaptic action could not be ruled out.

PH 111

EFFECTS OF NEUROPEPTIDES ON THE HEART BEAT OF MOLLUSCS

M.Kobayashi, K.Hori, T.Hirata and Y.Muneoka Physiol. Lab., Fac. of Integrated Arts and Sciences, Hiroshima Univ., Hiroshima

Effects of several neuropeptides on the heart beat of a prosobranch Rapana thomasiana and a pulmonate Achatina fulica were studied. From the structure-activity relations of Phe-Met-Arg-Phe-NH_2 (FMRFamide) related peptides on the heart it was found that Arg^3, Phe^4 and the C-terminal amide were essential to FMRFamide-like effects both in Rapana and Achatina. In Rapana, FMRFamide enhanced the amplitude of beat in atrium and ventricle, while in Achatina it enhanced the beat of ventricle but reduced that of atrium. A novel neuropeptide (Catch-relaxing peptide, CARP) extracted from Mytilus had potent inhibitory effects on the Rapana heart, with the threshold of 3 X 10^{-10}-10^{-9} M. It appeared to be acting postsynaptically. Benzoquinonium blocked the inhibition of heart beat by acetylcholine and nerve stimulation but not blocked the inhibitory effects of CARP. CARP may be acting as a neurohormone to the Rapana heart. This peptide had no significant effects on the Achatina heart.

PH 112

CHANGE OF CARDIAC PUMPING ACTION IN VIVO IN THE LOBSTER, PANULIRUS JAPONICUS; EFFECTS OF PERICARDIAL NEUROHORMONES.

T. Kuramoto. Inst. Biol. Sci., Univ. of Tsukuba, Ibaraki 305.

Electrical activity of the heart and blood pressure in the lateral pericardial cavity were recorded during various behavioral states of the lobster. Each beat of the heart was followed by a fall in the pericardial pressure. The fall was regarded as one pumping action of the heart in vivo. Magnitude of the fall altered significantly from state to state and ranged from 0.2 to 1 g/cm^2 (5 hold change in maximum). The amount of fall gradually increased after an increase in heart rate, and decreased with decrease of the heart rate. The fall was decreased by a transient inhibition of the heart beat following a food application, while feeding behavior caused it to increase up to 1 g/cm^2. Similarly, it was often enhanced after vigorous body movements. Injection of pericardial hormones, octopamine or proctolin (10 μM), into the pericardial cavity caused the fall to increase to over 1 g/cm^2. The increase had a slow time course similar to that observed in the feeding behavior. Injection of serotonin (10 μM) or physiological solution had no significant effect on the fall. Thus, proctolin and octopamine might increase the pumping efficiency of the lobster heart in vivo.

PH 113

CA-BINDING PROTEINS IN GUINEA PIG SMOOTH MUSCLES.

N.Oishi[1] and H.Sugi[2]. [1]RI Center and [2]Dept. Physiol., Sch. Med., Teikyo Univ., Tokyo.

In order to understand the regulation of Ca^{2+} ion in excitation-contraction coupling, investigations of the activator Ca^{2+} that triggers cotraction are essential. By histochemical studies, the sub-sarcolemmal store of the activator Ca^{2+} that translocates to contractile machinery during contraction is demonstrated in vertebrate and invertebrate smooth muscles (Atsumi and Sugi, 1976; Sugi and Daimon, 1977). To search for the candidates for the Ca^{2+}-accumulator, we surveyed Ca^{2+}-binding proteins (CaBPs) from plasma membranes of guinea pig smooth muscles, taenia coli and aorta. An plasma membrane-enriched fraction was processed for sodium dodecylsulfate-polyacrylamide gel electrophoresis, and CaBPs were detected on the electroblot by $^{45}Ca^{2+}$-autoradiography. CaBPs with Mr of about 58,000 and 100,000 were routinely detected. And that with about 37,000, 55,000 and 140,000 were occasionally observed. The 37,000 protein was the most abundant CaBP in homogenate, while the large part of it was recovered in the soluble fraction. Further identification is in progress.

PH 114

PHYSIOLOGICAL AND MORPHOLOGICAL STUDY OF FISH SWIMBLADDER MUSCLE.

Y. Taniguchi, S. Suzuki and H. Sugi Dept. Physiol., Sch. Med., Teikyo Univ., Tokyo.

The swimbladder muscle of a crying fish, *Sebastiscus marmoratus*, was studied physiologically and morphologically. A single electric stimulus gave rise to an isometric twitch lasting 15 msec at 20° C. With repetitive stimuli, the tension showed a rapid spontaneous decrease to zero. High external potassium caused only a small contracture tension at 4° C but not at 20° C. These facts suggest that the rate of Ca^{2+} reuptake by the sarcoplasmic reticulum (SR) is very large. On the other hand, the muscle did not respond to a single electric stimulus at low temperature, suggesting that part of excitation-contraction coupling processes is inhibited at low temperature because the action potential and the Ca^{2+}-activated tension in the skinned fibers are not affected by temperature. Electron microscope observations revealed that, while the muscle was producing the maximal tension by caffeine, the SR was dilated and formed many small vesicles, and the electron-opaque pyroantimonate-Ca^{2+} complex was scattered on myofibrils, suggesting possible structural changes of the SR during the Ca^{2+} release.

PH 115

TWO MECHANICALLY DISTINCT TYPES OF MUSCLE FIBERS IN THE TIBIALIS ANTERIOR OF THE FROG.

H. Iwamoto and H. Sugi. Dept. Physiol., Sch. Med., Teikyo Univ., Tokyo

In the tibialis anterior muscle of *Rana japonica* were found two types of muscle fibers which had distinct mechanical properties. The fibers of one type produced net work within a certain range of frequencies when they were oscillated sinusoidally and showed a large loop in the Nyquist plot, while the fibers of the other type did not produce work at any frequency and showed only a small loop in the plot. The effect of external pH on their mechanical performance was studied because it has been reported to affect the intracellular concentration of inorganic phosphate, which is known to promote work production. Their mechanical properties were invariable in the pH range between 6.6 and 7.8, suggesting that they are not readily altered by external conditions. The two types of fibers were not found in a muscle at the same time. Since the work-producing type has hitherto been obtained in spring and summer while the other in the rest of a year, those differences may reflect seasonal modifications of the kinetics of the crossbridge action.

PH 116

COMPARISON OF THE EFFECT OF OUABAGENIN AND BAY K 8644 ON SCATTERED LIGHT INTENSITY FLUCTUATION IN VENTRICULAR MUSCLE.

T.Kobayashi[1] and D.Bose[2]. [1]Dept. of Physiol., Sch. of Med., Teikyo Univ., Tokyo and [1]Dept. of Pharmacol. and Ther., Fac. of Med., Univ. of Manitoba, Winnipeg.

Light intensity fluctuation of coherent light scattered by a strip of ventricular muscle during diastole (SLIF) is believed to be due to asynchronous cellular motion within the myocyte as result of sponteneous release of calcium from sarcoplasmic reticulum (SR). Ouabagenin produces inotropy by increasing intracellular free Ca, and in toxic concentration it produces abnormal aftercontractions (AC) by sponteneous Ca release from the SR. On the other hand the Ca channel agonist BAY k 8644 also produces inotropy but this is associated with a decrease in Ca release from SR, indicated by inhibition of 'post-rest potentiation'. This study was performed to see if the effect of these agents on the power spectra of SLIF were different. Both frequency and amplitude of SLIF were increased after 1 uM ouabagenin but these changes were most marked after onset of toxicity rather than during the positive inotropic response and were reversed by 2mM EGTA. In contrast, 1uM Bay k 8644 decreased SLIF at all level of inotropic response. These results suggest that SLIF is a better indicator of intracellular Ca overload and toxic oscillatory contraction rather than an increase in contractile state.

PH 117

EFFECTS OF THIOCYANATE ION ON THE CONTRACTILE AND MEMBRANE PROPERTIES OF RAT CARDIAC MUSCLE

R. Sugaya, H. Iwamoto and H. Sugi. Dept. Physiol., Sch. Med., Teikyo Univ., Tokyo

The effects of SCN^- on the contractile and membrane properties of the rat papillary muscle were studied. Equimolar substitution of SCN^- for Cl^- in Tyrode solution caused a monotonic decrease in the resting potential. Meanwhile the amplitude of the action potentials decreased with the resting potential but the force showed a transient enhancement followed by a gradual decrease. The deporalization caused by varying external K^+ concentration could basically reproduce these changes in the action potential and the force. However, the amplitude of the action potential and the force were smaller in SCN^--Tyrode. During the recovery period after the removal of SCN^-, further suppression of the force was observed. These results suggest at least three actions of SCN^- on the cardiac muscle: 1) reduction of resting potential, by which force is enhanced, 2) suppression of the generation of action potentials, and 3) suppression of the contractile force, presumably due to the incorporation of SCN^- into the muscle cell.

PH 118

LOCAL MOVEMENT OF INTACT SINGLE MUSCLE FIBERS OF THE FROG DURING INCREASE IN LOAD.

T. Takei, T. Tsuchiya and H. Sugi, Dept. of Physiol., Sch. of Med., Teikyo Univ., Tokyo.

Local movement of a muscle fiber is known to take place during the creep in isometric contraction and during ramp release and its role in muscle contraction has long been discussed. To know it further, local movement during step or ramp inrease in load in intact single muscle fibers of the frog was measured at low temperature (3-4 C).
Carbon powders were attached at the several points on the surface of a fiber so that the total muscle length might be divided equally and the local movement was recorded using high speed video system (200 frames/sec). Following step increase in load from isometric tension (Po) to 1.2-1.4Po, length of all segments increased equally. When the step increase in load, however, was large (1.6-1.8Po), a fiber tended to show "give" and only one of several segments was remarkably extended. In ramp increase in load to 1.3-1.4Po, the velocity of lenthening continued to increse and all segments were lengthened nearly equally. These results provide the evidence that large load induces localized elongation of a fiber.

PH 119

COOPERATIVE INTERACTIONS OF MYOSIN HEADS WITH ACTIN FILAMENT STUDIED USING SLIDING MOVEMENT OF MYOSIN-COATED BEADS ALONG ACTIN CABLES.

H. Sugi[1], S. Chaen[1] and T. Shimmen[2]. [1]Dept. Physiol., Sch. Med., Teikyo Univ., Tokyo and [2]Dept. Bot., Fac. Sci., Univ. Tokyo, Tokyo.

To study the role of double-headed myosin molecule structure in muscle contraction, the motion of latex beads coated with partially p-phenylenedimaleimide (p-PDM)-inactivated rabbit skeletal muscle myosin along the actin cables of giant Chara cell was examined. One kind of myosin samples consisted of myosin molecules with two native or two inactivated heads, while the other kind of samples consisted of myosin molecules with zero, one or two inactivated heads. For a given level of ATPase activity, the motion of beads was faster when they were coated with the former sample than when they were coated with the latter sample. If the velocity of bead motion was plotted against the fraction of myosin molecules with two native heads, all the data points fell around the same curve, suggesting that the bead motion is caused only by myosin molecules with two native heads. This implies that the two heads of each myosin molecule in muscle interact with actin filament in a cooperative manner to produce force and motion.

PH 120

PROPERTIES OF A HIGH-MOLECULAR WEIGHT CALCIUM BINDING PROTEIN ISOLATED FROM PLASMA MEMBRANE-ENRICHED FRACTION OF A MOLLUSCAN SMOOTH MUSCLE

T.Yamanobe[1], T.Mimura[1] and H.Sugi[2].

[1]Central Lab. Analyt. Biochem. and [2]Dept. Physiol., Sch. Med., Teikyo Univ., Tokyo.

In the anterior byssal retractor muscle (ABRM) of Mytilus edulis, Ca ions are accumulated at the inner surface of the plasma membrane, and are released into the myoplasm to cause contraction (Atsumi and Sugi, 1976) To study the mechanism of Ca accumulation and release at the plasma membrane, we have isolated a 450K Ca-binding protein characteristic of the plasma membrane-enriched fraction of ABRM (Yamanobe, Mimura and Sugi, 1985). SDS polyacrylamide gel electrophoresis indicates a decrease in the mobility of the 450K protein when Ca is removed, as with other Ca-binding proteins reported. The protein exhibits distinct changes in fluorescence and UV absorption by the change in pCa from 7 to 5. Ca binding assay shows that the protein has 7~9 Ca-binding sites with half-maximal binding at pCa 5.5.
These results are consistent with the view that the 450K protein may be involved in the regulation of mechanical activity of the ABRM in physiological range of pCa. Experiments are progress to elucidate the physiological role of the 450K protein in the contraction-relaxation cycle of the ABRM.

PH 121

GENETIC ANALYSIS OF SYNAPTIC TRANSMISSION

R. HOSONO Dept. Biochem. Sch. Med. Kanazawa Univ. Kanazawa.

The cha-1·unc-17 complex gene of C. elegans consists of at least two complementation groups, cha-1 and unc-17. The cha-1 region encodes ChAT, but the function of the unc-17 region is unclear. We measured ChAT activity, and choline and ACh levels of the gene mutant alleles. We found that in the unc-17 mutants the ChAT activity and choline levels are normal but ACh levels are abnormally high. Experimental results suggested that the unc-17 region encode functions necessary for storage and/or release of ACh.

To find related genes with unc-17, we further isolated resistants to trichlorfon. Six strains were allocated to unc-13(cn490), unc-17(cn355), tcf-1(cn252), unc-18(cn347), unc-10(cn257), and unc-3(cn4146). In addition to the unc-17 region, mutations in unc-13, tcf-1, and unc-18 caused abnormal accumulation of ACh. These genes seem to be functionally related because they share common phenotypes, that is, uncoordinated movement, resistance to inhibitors to acetylcholine esterase, growth retardation and small body size in adulthood. These mutations were induced by insertion of transposable element Tc1, making it possible to clone the gene with the element as probe. We found an unique Tc1-containing 6.8 kb BglII fragment in TN347 strain (unc-18(cn347)) and are now trying to clone the DNA fragment.

CB 1

INTRA- AND INTERSPECIES COMPARISON OF HEAT-EXTRACTED PROTEINS IN *Paramecium*.

Y. Tsukii, Lab. Biol., Hosei Univ., Chiyoda-ku, Tokyo 102

Morphological species of Ciliates consists of number of sibling species called syngens. Though syngens show little morphological diversity, advances in comparative studies, especially of isozyme patterns, gave a taxonomical basis for the identification of syngens of *P. aurelia* and *Tetrahymena pyriformis*.

On the other hand, isozyme studies have so far failed to discriminate syngens of *P. caudatum*. So, I attempted to compare heat-extracted proteins among syngens of *P. caudatum* as well as those among other ciliate species.

Moderately-starved cells were boiled for a few minutes and then centrifuged. The supernatants were compared by SDS-PAGE. Twenty to 30 protein bands were identified in each sample of 16 strains from four different syngens of *P. caudatum*. A few syngen specific bands were observed. Nearly all bands were, however, common among them, and, thus, it was unsuccessful to identify each syngen.

Morphological species (*P. caudatum*, *P. aurelia*, *P. jenningsi*, *P. multimicronucleatum*, *P. trichium*, *Tetrahynema thermophila*, *Bleharisma japonicum*) were discriminated well by this method, and their evolutionary relationships based on the percentages of common bands between different species coincide with those already known.

CB 2

DEGENERATION OF EPIDERMAL MELANOPHORES DURING METAMORPHOSIS IN THE FROG, *HYLA ARBOREA*

M. Yasutomi. Lab. of Biol., Aichi Medical College, Nagakute, Aichi.

Epidermal melanophores of the skin decrease in number or disappear during metamorphosis in many species of frog. This phenomenon is thought to be an adaptation for rapid color change (physiological color change), a property which the animals acquire after metamorphosis. We have reported that the decrease was due to the migration of them to the dermis in *Rana japonica*. In this frog, at metamorphic stage epidermal melanophores rather loosely associated with epidermal cells. The basement membrane became thinner and sometimes small breaks were seen in it. In *Hyla arborea*, epidermal melanophores disappear after metamorphosis. Through metamorphic climax the basement membrane was compact and epidermal melanophores were surrounded tightly by epidermal cells. Some of the epidermal melanophores included dense and round bodies which were probably lysosomes. Occasionally, the lysosome-like bodies contained melanosomes. Such cells were electron dense and the cytoplasm showed features of autolysis. From these facts, we concluded that the disappearance of epidermal melanophores during metamorphosis in *H. arborea* was not due to the migration of them to the dermis but to the degeneration in the epidermis.

CB 3

Myosin in normal and neoplastic fish pigment cells: Its occurrence and a mode of intracellular localization.

T. Akiyama[1], S. Hirai[2] and J. Matsumoto[1]. [1]Dept. Biol, Keio Univ., [2]Inst. Parsteur, France.

The occurrence of myosin in swordtail erythrophores, goldfish melanophores and erythrophoroma (GEM 81) cells was demonstrated by means of polyacrylamide gel electrophoresis (PAGE) using sodium dodecylsulfate (SDS) and sodium pyrophosphate (Nappi) and immunoblot using the antibody against chick gizzard myosin (heavy chain). The band appearing at the position of approximately 200 kd in SDS-PAGE was equivocally decorated with the antibody and Nappi electrophoresis had separated out native myosin free from any degradation. Myosin was also detectable in the two melanogenic variants induced from GEM 81, which were capable or not of pigment motile response. Immunofluorescence disclosed that myosin occurs at least in two forms in fish pigment cells; 1) a loose meshwork connecting dot-shaped aggregates, 2) stress fiber type-filaments. The former was prominent in normal pigment cells and heavily melanized GEM cells with motile response whereas the latter was so in non- or less melanized, poorly responsive GEM cells. This would suggest involvement of myosin in pigment translocation.

CB 4

IMMUNOCYTOCHEMICAL LOCALIZATION OF LAMININ IN THE ANTERIOR PITUITARY OF MALE RATS AT PUBERTY.

S.Kusaka, S.Yamashita, S.Yamaguchi, S.Kusunoki
Life Science, Lab., Advance CO., LTD., Tokyo

Laminin, one of the major components of basement membrane(BM), was detected immunocytochemically in various tissues or organs. Recently, Tougard et al reported that laminin was localized in the BMs and inside grandular cells, especially gonadotrophs, of the rat anterior pituitary. We have immunochemically demonstrated the localization of laminin in the BMs and LH cells of 10,20,30,40,50,60 and 90 day old rat pituitaries. After decapitation, pituitary glands were removed and fixed in a formol-sublimate(3:7) solution at 4℃ and embedded in Paraplast. 3μm thick sections were then prepared and immersed in 0.4% pepsin in 0.01N HCl at 37℃ for 60 minutes. Sections were processed by the immunoperoxidase method. Laminin was localized in the BM of the capillaries in all days' pituitary. In the 30 day old pituitary, there was a slight detection of laminin in some LH cells, the number of which increased with the age of the pituitaries, but decreased in the 90 day old. In addetion, in the over 50 day old pituitary, laminin was detected in the BM of the lobule-like structure.

These results suggested : 1) LH cells produced the laminin, possibly reflecting sexual maturation in rat, and 2) the BM may have formed at a particular stage in the growth of functional development of the pituitary gland.

CB 5

USE OF NUCLEOTIDES IN ENZYME-IMMUNO-HISTO IN SITU HYBRIDIZATION.

T.Koji, M.Tanno, T.Moriuchi and P.K.Nakane
Dept. of Cell Biol., Tokai Univ. Sch. Med. Isehara, Kanagawa.

To understand better the physiology of cells and tissues, one requires studies on the states of nucleic acids and protein metabolism at the cell level. To localize specific mRNA, we developed a new method using T-T dimerized haptenic cDNA probe. Subsequent to hybridization with cell mRNAs, the T-T cDNA was localized immunohistochemically. In this study while usin the T-T cDNA, our efforts were focused on to eliminate the deteriorative effects of formamide (e.g. instability, nonspecific reaction, morphological damage), the reagent usually used to decrease the melting points of double stranded nucleic acids. As an alternative to the formamide we examined the use of a mixture (Nm) of nucleotides (AMP, GMP, UMP, CMP) to reduce the melting point. The effects of Nm on re-annealing of single-stranded pBR 322 were investigated by agarose gel-electrophoresis. It was found that Nm (20-200 mg/ml) reduced the rate of the reannealing On dot blot hybridization using Nm, we obtained similar sensitive and specific results to that with formamide. On frozen sections of rat pituitary glands fixed by perfusion of 4% paraformaldehyde/PBS, prolactin mRNA may be localized using Nm instead of formamide and the tissues were better preserved when Nm was used than whe formamide was used.

CB 6

TRANSFORMATION OF MOUSE C3H 10T1/2 CELLS BY LOW-DOSE-RATE γ- AND β-IRRADIATION.

T. Yamaguchi. Biol.Inst., Fac.Gen.Educ., Ehime Univ., Matsuyama.

Cultured C3H 10T1/2 cells in confluency were irradiated with either β-rays from tritiated water (HTO) or ^{60}Co γ-rays. The duration of exposure was 20 h at either 4°C or 37°C, and the total dose was varied by changing the dose-rate. The absorbed dose from HTO was calculated using a water content value of 0.84. The value of 0.84 water was determined in a mass culture of the cells by a method in which [carboxyl-^{14}C]-inulin was used to measure the amount of extracellular water. The dose-survival and dose-transformation curves for γ-irradiaion at 4°C were nearly the same as those after a single acute X-ray dose. When γ-irradiation was administered at 37°C, both the lethality and transformation-induction were lower than those after the corresponding doses at 4°C, indicating the existence of repair from damage during irradiation at 37°C. The same effect of temperature was observed in the case of HTO-exposure. The effect per Gy, however, was higher for β-rays than for γ-rays in both the responses. Resulting relative biological effectctiveness (RBE) values of tritium β-rays were 1.4 at D_0 for cell killing and 1.6 - 1.7 for cell transformation within the dose range examined (1 to 6 Gy of β-rays), irrespective of the temperature during irradiation.

CB 7

A CYTOPLASMIC FACTOR WHICH CONTROLS THE SEROTYPE EXPRESSION IN SEROTYPE MUTANT STRAIN OF PARAMECIUM TETRAURELIA.

S.Koizumi and S.Kobayashi. Dept. of Biol., Miyagi Coll. of Educ., Sendai.

Mutant strain d48 in Paramecium tetraurelia cannot produce immobilization antigen A. Gene A encoding i-antigen A is present in micronucleus, but not in macronucleus because of lacking during macronuclear reorganization. To clarify the cell cycle stage at which gives rise to the lack of gene A, wild 51 macronucleoplasm from cells at about 10th cell cycle was transplanted into various stages of d48 cells: Recipient cells of d48 received 51 nucleoplasm by 2-3hr after the sensitive period were possible to express A in high frequencies(50-70%). Exconjugant clones of d48 derived from crosses with 51 frequently expressed serotype A when pair separation was delayed. The results exhibit that some protective substance for lacking gene A is also present in cytoplasm of wild type cells. To obtain the direct evidence for such a substance in cytoplasm, transfer of cytoplasm at various stages of 51 cells into d48 cells 1-2hr after the sensitive period were carried out: Transfer of cytoplasm during macronuclear reorganization caused the frequent expression of serotype A in recipient cell lines, but other stages of cytoplasm did not. Transplantation of nucleoplasm throughout the vegetative stage was effective to express serotype A in the recipient cells of d48.

CB 8

PREVENTION OF RADIATION-INDUCED INTERPHASE DEATH BY RNA- AND PROTEIN-SYNTHESIS INHIBITORS

T.Yamada[1], H.Ohyama[2] and K.Inui[1]. Divs. [1]Biol. & [2]Radiat.Health, National Institute of Radiological Sciences, Chiba.

Mammalian thymocytes are highly radiosensitive and show "interphase death" within a few hours after low doses of irradiation. However, the mechanisms of this type of death remain ill-defined. We have demonstrated that rat thymocyte interphase death involves a discrete, abrupt transition from the normal state, such as cell volume reduction to a definite small size, and is not merely the consequence of progressive and degenerative changes, and is an example of "apoptosis", the mode of death frequently observed when cell deletion is programmed.

In the present study, the effect of inhibitors of RNA- and protein-biosynthesis on interphase death as an expression of the death program was examined using thymocytes prepared from Wistar strain rats. Thymocyte suspension was incubated for 4 hours immediately after X irradiation, and dead cells were counted at the end of the incubation. Inhibitors such as cycloheximide, puromycin, chromomycin and actinomycin D given to the suspension suppressed completely appearance of the stained (dead) cells, and transition to small-sized cells. These results provide further support for the view that interphase death is apoptosis.

CB 9

A STUDY ON TRIPLOID HYBRID CELLS IN RHODEINE CYPRINID FISHES.

K.Yamamoto and Y.Ojima. Dept. of Biol., Fac. of Sci., Kwansei Gakuin Univ., Nishinomiya.

Two kinds of triploid hybrids by reciprocal cross between *Rhodeus ocellatus ocellatus* and *Acheilognathus limbata* (RA3n:R♀ × A♂ ; AR3n:R♂ × A♀) were obtained by cold shock treatment of feritlized eggs. A whole of the triploid hybrid fingerling was treated by trypsin solution and cells obtained were cultured. The cells after 5 times of subcultivation were used.

Both of the triploid hybrid cells had 72 chromosomes consisting of diploid sets of the female and a haploid set of the male. Ag-NORs were located on the 3 acrocentric chromosomes.

The multiplication rate of RA3n was relatively high in comparison with that of cultured cells of R.o.o. carrying two NORs. The directly prepared or the primary cultured cells had two active NORs, despite of triploidy. However, the cultured cells in this study had three active NORs. There might be a certain correlation between the high multiplication rate of RA3n and reactivation of a NORs.

Furthermore decrease of the chromosome number and increase of Ag-NORs were observed in RA3n after further subculture.

CB 10

THE ORIGIN OF THE NATIONAL MONUMENT, "SCARLET CRUCIAN CARP" (HIBUNA) IN THE HARUTORI LAKE, KUSHIRO, HOKKAIDO, JAPAN.

Y.Ojma. Dept. of Biology, Faculty of Sci. Kwansei Gakuin Univ. Nishinomiya.

" Scarlet Crucian Carp " (Hibuna) in the Harutori Lake of Kushiro, Hokkaido was designated a Natural Monument of Japan in 1937. Since then, however, no one had the opportunity to closely examine the origin of this special Hibuna because of its protected status.

The present study was undertaken in an aim to deal cytogenetically with the origin of the Hibuna, in comparison with the Japanese genus *Carassius* and the Gold-fish.

The results clearly showed that there are two kinds of Hibuna, diploidy and triploidy, in the Harutori Lake. The diploid Hibuna, 2n=100, showed the same chromosome constitution and C-band pattern as the Gold-fish. The individuals with triploid chromosomes, 2n=154, were the same as that of the *C. a. langsdorfii* in chromosome constitutions and C-band patterns.

CB 11

MICROINJECTION METHOD AND ITS APPLICATION IN *TETRAHYMENA*.

H. Ohba and Y. Watanabe, Inst. of Biol. Sci., Univ. of Tsukuba, Ibaraki

Microinjection of cytoplasm, antibody, protein or DNA into cells has been proved to be very useful method for assaying the *in vivo* activity of introduced substances. But, this method was not easily practiced in *Tetrahymena* mainly because of stiff layers of the cell membranes. Here we have succeeded in injection using a glass micropipette of keen tip (less than 0.5 um in diameter) at the angle of 65 degree and using the individual cells immobilized in proteose-peptone medium containing 2.5% methyl cellulose. Maximal injection volume was about 20 % of cell volume (3 nl).

We used this method to inject a guinea pig antiserum against p85 which was the gene product of *cdaA1* (cell division arrest mutant) into wild-type cells. p85 has been proved to be localized in basal bodies at cell equator just before cell division and in oral apparatus (J. Biochem. 100, 797, '86), suggesting the involvement of p85 in determination of cell division plane and in food uptake. By the antiserum injection, inhibition of cell division occurred probably due to ceasing of food vacuole formation, whereas no *cdaA1* phenocopy was exhibited. We are now testing the effects of other antisera against p85 to demonstrate the involvement of p85 in division plane determination.

CB 12

EFFECTS OF MACRONUCLEAR ELIMINATION ON GERMINAL MICRONUCLEUS DURING CONJUGATION OF PARAMECIUM.

K. Mikami, Res. Inst.for Sci. Educ., Miyagi Univ. of Educ., Sendai.

During conjugation, the micronucleus (MIC) produces gametic nuclei after meiosis. Then the nuclei exchange reciprocally and fertilize. To probe function of the macronucleus (MAC) on the micronuclear behavior, MAC was pipetted out by glass needle at various stages of conjugation in Paramecium caudatum. MIC shows crescent shape at meiotic prophase. When MAC was removed at 2-2.5 hours of conjugation, however, MIC skipped over typical crescent stage and then divided once or twice. Results showed that MAC gave information for"crescent"just prior to the crescent stage and information for nuclear division just prior to dividing stage of meiosis. It is likely that macronuclear gene products required for micronuclear division transfer easily through boundary of mating cells.

After meiosis, one nucleus remains and other 3 degenerate at about 12 hours of conjugation. The results suggest that the information for it is given 4 to 6 hours (crescent stage) of conjugation.

When MAC was removed before 2nd meiotic division, MIC did not enter into the partner. When both of MIC and MAC were removed from a cell at 6 hours, gametic MIC of the partner migrated to the enucleated cells. The results suggests that MAC about at the 2nd meiotic stage is indispensable for micronuclear migration.

CB 13

MORPHOGENESIS OF MIRROR-IMAGE SYMMETRY DOUBLET CELLS IN THE CILIATE STYLONYCHIA PUSTULATA.

J. Yano. Zool. Inst., Fac. of Sci., Hiroshima Univ., Hiroshima.

Mirror-image symmetry doublets were obtained when dividing cells were exposed to heat shocks. Two ventral surfaces of doublets were located on the same side. The adoral zone of membranelles (AZM) and the cirri in the left component were arranged in the same pattern as the normal singlets, except for the lack of the right marginal cirri. In the right component, the ciliary organelles were mirror-symmetrically disposed as compared to those in the left component. However, the right component had no cytostome, and the membranelles of its AZM were antero-posteriorly rotated 180°. In cell division of doublets, the oral primordium appeared just posterior to the AZM in each components. The sites of primordia of the other ciliary organelles were arranged in mirror-image symmetry. In almost all the right components, the membranelles of the new AZM were inverted. The normal and inverted membranelles rarely developed from the oral primordium of the right component. Therefore, the pattern formation of ciliary organelles in the right component seems to be undergone by the reversal of the right-left axis.

CB 14

SOME CHARACTERS OF ENCYSTMENT-INDUCING SUBSTANCES OF THE CILIATE EUPLOTES ENCYSTICUS.

F. Yonezawa. Zool. Inst., Fac. of Sci., Hiroshima Univ., Hiroshima.

It has been reported that cell-free fluid (CFF) contains some substances which are responsible for encystment of E. encysticus (Yonezawa, 1986). The purpose of this work is to partially characterize the substances. 20 liters of CFF was concentrated at a reduced pressure to about 50 ml by a rotary evaporator at 40 ℃. After centrifuging concentrated CFF (conc-CFF) at 3000rpm for 20 minutes, the supernatant was dialyzed against redistilled water. Encystment-inducing activity was detected in dialyzed conc-CFF but not in external fluid. Heating to 100 ℃ did not appreciably affect inducing activity within the first one hour of exposition, whereas after three hours the activity dropped to about a half of the original. Incubation of dialyzed conc-CFF with lipase (200 μg/ml) or α-glucosidase (25 μg/ml) for 24 hours at 30 ℃ did not lead to a complete inactivation of the substances. On the contrary, activity was completely destroyed after 24-hour-treatment with trypsin (200 μg/ml) at 30 ℃. After centrifuging dialyzed conc-CFF at 10000g for 30 minutes, the supernatant was chromatographed with Sephadex G-75 column. The peak of elution pattern (OD at 280 nm) appeared in the fraction 62, whereas the peak of activity was detected in the fraction 72.

CB 15

CYTOSKELETON OF HELIOZOAN AXOPODIA IN ECHINOSPHAERIUM AKAMAE.

S.Ikegawa[1], H.Ishida[1], Y.Shigenaka[1] and E.Masuyama[2]. [1]Lab. Cell Biol., Fac. Integr. Arts & Sci., Hiroshima Univ. and [2]Dept. Life Sci., Hiroshima Women's Univ., Hiroshima.

Heliozoan axopodia of Echinosphaerium akamae radiate from the spherical cell body. The core of each axopodia is formed of the regular arrangement of many microtubules as main cytoskeletal elements. By treatment with 65% D_2O, we found that the axopodia could be isolated completely from cell body. Electron microscopy revealed that the isolated axopodium maintained the regular arrangement of microtubules. We subjected the isolated axopodia and the cell body extracts to SDS-PAGE. The result showed that two remarkable bands appeared in isolated axopodia extract, corresponding to tubulin on account of the electron microscopical results. To identify the proteins of these two bands further, we subjected the heliozoan extract to Western blot, and analyzed by using antibody against tubulin of rat brain (ADVANCE Co., Ltd.). This antibody reacted with only one band (Mr=46000). Althogh another band (Mr=50000) was not recognized, it behaved together with the low band during the process of isolation axopodia. These results strongly suggest that the proteins of two bands must be tubulin of axopodia of Echinosphaerium akamae.

CB 16

MECHANISM OF AXOPODIAL RETRACTION AND CONTRACTION IN HELIOZOA.

Y. Shigenaka, S. Ikegawa, H. Ishida and H. Terada. Lab. Cell Biol., Fac. Integr. Arts & Sci., Hiroshima Univ., Hiroshima

Against various types of stimuli, heliozoan axopodia react by demonstrating slow retraction and/or instantaneous contraction. In general, the former retraction occurs when certain chemical drugs or big prey organisms are given to the cell. On the other hand, the latter contraction might be induced as small-sized protozoans are attached to the distal portions of axopodia. In this case, the contractile tubules are considered to induce the contraction by self-twisting and supercoiling of them. At this time, the axonemal microtubules, which are contained as cytoskeletal elements in the axopodium, depolymerize simultaneously at the final step. We also examined the localization of calcium during axopodial contraction using a potassium pyroantimonate assay. Ca-Sb deposits were detected on the contractile tubules only during twisting and coiling of this organelle, and on the axonemal microtubules during their disassembly. Our results indicate that axopodial contraction is enforced by twisting and coiling of contractile tubules and by folding of axonemal microtubules, which might be mediated by influx of Ca^{2+} through axopodial membrane and efflux of Ca^{2+} stored in vesicles.

CB 17

ULTRASTRUCTURAL CHANGES IN THE PARORAL REGION DURING CONJUGATION BETWEEN DOUBLET CELLS AND SINGLET CELLS IN PARAMECIUM TETRAURELIA

Y. Yashima. Dept. of Biol., Sch. of Lib. Arts and Sci., Iwate Med. Univ., Morioka.

During nuclear migration, one of the meiotic nuclei lies in the paroral region and survives, but the remaining seven nuclei lie outside the paroral region and degenerate. To better understand the morphological changes associated with conjugation, conjugation was induced between singlet cell and doublet cell, and was observed by TEM. According to TEM observation, 2-3 hours after the beginning of conjugation, the paroral region was unchanged with the exception of the contact region. In particular, there were no microtubules in the paroral region at this time. When a micronucleus moved into the paroral region, microtubules were observed around the nucleus, and as the micronuclei in the paroral regions moved in the direction of the contact membrane, the microtubules tended to increase around these nuclei. Just before the beginning of the nuclear exchange, a microtubule meshwork had formed around the micronuclei in the paroral regions, but there were almost no microtubules around the micronuclei outside these regions. There were some electron dense granules (0.08-0.12μm in diameter) around these extraparoral nuclei, but no electron dense granules were present around the intraparoral micronuclei. These results suggest that 1) the microtubules are related to the nuclear movement in the paroral region and 2) electron dense granules may be related to nuclear degeneration.

CB 18

ISOLATION AND CHARACTERIZATION OF REPRODUCTIVE FORM OF HOLOSPOLA OBTUSA, A MACRONUCLEUS-SPECIFIC BACTERIUM OF PARAMECIUM CAUDATUM.

Y.KOJIMA and M.FUJISHIMA. Dept. of Biology, Fac. of Sci., Univ. of Yamaguchi, Yamaguchi

The gram-negative bacterium Holospola obtusa is a macronucleus-specific symbiont of Paramecium caudatum. This bacterium shows molphologically distinct five types in its life cycle: an infectious long form of buoyant density 1.16 g/ml, three intermediate forms of buoyant densities 1.13 g/ml, 1.11 g/ml and 1.09 g/ml, and a reproductive short form. The former four types have been isolated by Percoll density gradient centrifugations. But the reproductive form is not yet isolated by the same method, because the bacterium is easily digested by host lysosomal enzymes in the homogenate. We intend to extract and characterize holospolas DNA, but the long forms were hardly lysed by ordinary methods for DNA extraction. Therefore, an isolation method of the reproductive form is needed to establish. In this study, we succeeded to isolate the reproductive short forms. Cells borne the reproductive forms were mildly lysed in NP-40 containing medium and their macronuclei were isolated. Then, the nuclei were homogenized, centrifuged in Percoll, and reproductive forms in a band of the tube were harvested. The isolated bacterium was found to be easily lysed in a lysozyme, SDS-containing medium.

CB 19

CHANGES OF PROTEIN COMPOSITION IN THE LIFE CYCLE OF HOLOSPORA OBTUSA, A MACRONUCLEAR SPECIFIC SYMBIONT OF PARAMECIUM CAUDATUM.

M. Fujishima and Y. Kojima. Biol. Inst. Fac. of Sci., Yamaguchi Univ., Yamaguchi.

The gram-negative bacterium H. obtusa invades into the host cytoplasm via the food vacuole, infects its macronucleus exclusively and grows in the nucleus. The bacterium can be isolated from host homogenates by Percoll density gradient centrifugations. We have ever clarified that the bacterium changes its length, morphology of nucleoid and buoyant density in the life cycle: four long forms of which longitudinal lengths are 15 μm and buoyant densities are 1.16, 1.13, 1.11 and 1.09 g/ml and a short form of which length and buoyant density are 1.5 μm and 1.09 g/ml. During early stage of the infection process, the long form of 1.16 g/ml decreases its buoyant density to 1.09 g/ml. Then, each long form divides to become about 10 short forms at the third day after the infection. When the host grows, this short form also grows by binary fissions. But, when the host starves the short form stops to grow and becomes long forms. In the present study, we compared protein compositions among the bacteria of buoyant densities of 1.16, 1.11 and 1.09 g/ml by 2D-PAGE. It has been found that the composition is similar between those of 1.16 and 1.11 g/ml, but that of 1.09 g/ml is very different from others.

CB 20

EFFECT OF GLUCOSE ON FOOD VACUOLE FORMATION IN PARAMECIUM MULTIMICRONUCLEATUM.

S.Mishima[1], Y.Harada[2]. [1]Biol. Lab., Coll. Gen. Educ., Ibaraki Univ., Mito and [2]Dept. of Biophys. Engn., Fac. of Engn. Sci., Osaka Unv.,Toyonaka.

Paramecium multimicronucleatum usually ingests bacteria, which are tightly packed into food vacuoles. However, we found that when glucose was added to the culture medium in concentrations of 20 mM or more, paramecia did not form tightly packed vacuoles but formed loosely packed ones. In the glucose solution, paramecia made food vacuoles. The volume of each vacuole in the acid stage was measured in three media: (1) bacteria (2) glucose (3) bacteria and glucose. When compared, the volume in medium (3) was the sum of (1) and (2). Furthermore, though it is known that starved paramecia first make a huge vacuole after the addition of large amounts of bacteria, in medium (3) starved paramecia still formed large initial vacuoles even at lower bacteria concentrations. These results suggest that glucose as well as bacteria may be recognized as food or nutrient by paramecia. Other sugars, such as ribose and sucrose, had similar effects, but the other important soluble nutrients, such as amino acids, had no effect on food vacuole formation.

CB 21

EXPRESSION OF JUMYO GENE OF PARAMECIUM TETRAURELIA IN DIFFERENT CULTURE CONDITIONS.

Y. TAKAGI. Dept. of Biol., Nara Women's Univ., Nara.

Jumyo (*jum*) gene of *Paramecium tetraurelia* is thought to be a pleiotropic gene controlling short clonal lifespan (Sh) and slow division (S) (Y.Takagi & K.Izumi, 1987, Biomed. Gerontol.11:115-116.). Under condition of the daily isolation culture, the *jum/jum* clones usually show lifespans shorter than 20 fissions and have fission rates slower than 1.5 fissions a day. Although an intraclonal variation of lifespans was commonly observed as shown by some lines with lifespans longer than 50 fissions while some other lines with very short lifespans, the longer lifespans were not due to the phenotypic reversion of Sh but instead due to the two or more life cycles linked by missing autogamy. Thus, the *jum* gene shows a complete penetrance with a stable expressivity well distinguishable from long lifespan (L) and fast division (F) of the wild type. Under condition of the mass culture, however, the phenotypic reversion from S to F was really the case. Mutants (d4-SL4), wild types and their F_2 segregants of S, all showed the F phenotype of 3-4 fissions a day during the logarithmic phase of growth in 200 ml flask cultures. The reversing factor(s) appears to be associated with cell density yet remains completely unknown.

CB 22

PHAGOCYTIC RESPONSE TOWARD FATTY ACIDS IN AMOEBA PROTEUS

A.Kihara,K.Ishii Lab.Biol.,Hosei Univ.,Tokyo

Amoeba could be extended its pseudopodium around a oil drop of some water-soluble fatty acid (e.g. nonanoic acid), and food-cup did not contact directly with it. This response was elicited from any surface of advancing amoeba.

Amoeba which immersed in nonanoic acid solution altered prominently its shape depending on the concentration. When the concentration was lower than 100nM, amoeba moved normally. At the concentration of 100nM or 150nM, amoeba first extended many pseudopodia vigorously all around then became the flatly spread shape, however the pseudopodia were getting scanty and were devoid of amoeboid movement in the solution beyond 150nM. According to these results, it seems that the pseudopodium formation is accelerated by the fatty acid at the moderate concentration, though it is inhibited at the higher concentration.

It was established that the larger food-cup was produced toward the bigger oil drop. Some stable concentration gradation caused by diffusion may be produced in the medium around the fatty acid drop, and these gradation, the food-cup formation seems to depend on, should be expanded as the increase of diameter of the oil drops. This feeding mechanism may make it possible that amoeba adjust the food-cup width to the various size of edible materials lacking of direct contact.

CB 23

REGULATION OF THE INTRACELLULAR CALCIUM STORAGE IN AN AMOEBA, COCHLIOPODIUM SP.

I. Yamaoka, S. Yamashita and R. Murakami. Biol. Inst., Fac. Sci., Yamaguchi Univ., Yamaguchi.

Amoeba *Cochliopodium* sp. has an ability to store of calcium in the body. Calcium are stored in spherical granules (about 0.3 μm in diameter) which are enveloped by a limiting membrane and situated at the peri-nuclear region. Phosphorus also are detected in the granules by the X-ray microanalysis. A factor to regulate the calcium storage in the granule was examined.

Alkaline phosphatase activities were detected histochemically in the inside of the membrane of the granules. When the amoeba was cultured on the agar containing 2.0 mM EGTA the granules disappeared within 6 hours of culture. When the amoeba treated with EGTA was transferred to normal medium, these granules reappeared, restoration of the granules was inhibited by 2.5mM levamisol, a specific inhibitor of alkaline phosphatase.

These results suggest that alkaline phosphatase is involved in calcium storage in the granules and that by using of inhibitor of the enzyme activity the calcium storage can be inhibited.

CB 24

COMPARISON OF ULTRASTRUCTURES AMONG RESTING CYSTS OF SEVERAL HYPOTRICH CILIATES.

T. Matsusaka. Dept. of Biol., Fac. of Sci., Kumamoto Univ., Kumamoto.

Among hypotrich ciliates, the resting cysts of the family Oxytrichidae, so far reported, have common ultrastructures; e.g. 3-layered cyst wall, electron dense cytoplasm, and total absence of ciliary organelles. These features seem to be a useful marker to consider hypotrich phylogeny.

The cysts of 4 Oxytrichid ciliates examined demonstrated typical ultrastructures described above and their endocysts reacted positively to anti-CW190 (an endocyst protein isolated from Histriculus cavicola) as detected by immunoelectron microscopy, although the intensity of reaction was variable among species. In Holosticha sp., its cyst showed similar ultrastructures and reaction to anti-CW190 to those of Oxytrichidae. The cysts of Holosticha adami and Pseudourostyla levis had 2-layered cyst wall, cytoplasm of moderate electron density, and basal bodies but not ciliary shafts, and was negative to anti-CW190. In Euplotes encysticus, the cyst had 4-layered cyst wall, cytoplasm of moderate electron density, and intact ciliary organelles, and was negative to anti-CW190. These findings may suggest that Oxytrichidae may be a fairly homogeneous group, that Urostylidae may be a relative to Oxytrichidae, and that Euplotidae may be a quite different group from the other 2 families.

CB 25

CORTICAL MORPHOGENESIS DURING BINARY FISSION IN SEVERAL HYPOTRICH CILIATES: A COMPALATIVE STUDY.

T. Matsusaka, O. Noguchi, N. Shimizu. Dept. Biol., Fac. Sci., Kumamoto Univ., Kumamoto.

In many hypotrich ciliates, cortical morphogenesis during binary fission have been reported, but only a few papers have compared it among different families. In the present study, cortical morphogenesis were compared on protargol impregnated specimens of 5 different hypotrich families including 11 species (Oxytrichidae, 4 species; Urostylidae, 4 species; Pseudourostylidae, 1 species; Strongylidiidae, 1 species; Euplotidae, 1 species).

The present observations and earlier papers clearly distinguished Euplotidae from the other 4 families by its subsurface stomatogenesis and different cirral migratory pattern. The other 4 families might have common ancestor, since their stomatogenesis occur at cell surface and cirral migratory pattern is fundamentally the same. Among these 4 families, Oxytrichidae may be quite homogeneous group, because they showed essentially the same patterns of stomatogenesis, cirral migration and dorsal bristle formation. On the contrary, Urostylidae may be divided into several groups, since they showed variations in stomatogenetic and dorsal bristle formation.

CB 26

AGE-RELATED CHANGES IN THE RELEASE OF SEROTONIN FROM RAT PLATELETS

Y. Yonezawa, H. Kondo and T. A. Nomaguchi
Dept. of Biol., Tokyo Metropolitan Inst. of Gerontol., Itabashiku, Tokyo.

Platelets contain various coagulation factors, cell growth regulators, serotonin (a vasoconstriction factor), and others. In order to determine whether platelet functions change with aging, we studied serotonin release from Wistar rat platelets with thrombin. Serotonin contents in young male(7M) and female(6-7M) rat platelets were 740 ng and 660 ng/3x10^8 platelets, respectively. In males, those increased at middle age(12-14M) and significantly decreased at old age(24-25M). The same changes were obtained when those in serum were measured. In females, serotonin contents in both platelets and serum did not change during aging. No serotonin was detected in plasma of all rats measured. Serotonin release was induced from rat platelets with 1.0-2.0 U/ml thrombin and reached a maximum with 4.0 U/ml. In males, the amount of this release was lower at middle age than at young age, but increased at old age to much higher level than at younger ages. In females, the release from platelts of young and middle rats was greater about 1.5-2 times than that from male rats, but decreased markedly at old age(25-26M). These results conclude that serotonin contents in platelets and its release from platelets of Wistar rats with thrombin greatly changed during aging.

CB 27

ANALYSIS OF CELL SURFACE ANTIGENS IN INTERDIGITATING CELLS OF MICE USING MONOCLONAL ANTIBODY.

S.Tanaka[1], H.Uda[1], T.Maruyama[2]. [1]Dep. of Pathology, Kagawa Med. School, Kagawa, [2]Shionogi Lab., Toyonaka, Osaka.

Recently it has become known that the skin is an immunological organ. Langerhans' cells (Lc) play a major role of immunological response in the skin. After sensitization by antigens, Lc are assumed to migrate to draining lymph nodes and interpret the antigen to T lymphocytes. But there is no obvious evidence. We prepared an antibody for interdigitating cells (IDC) of mice. The obtained antibody recognized a cell surface antigen which is a glycoprotein of about 15K daltons. According to study by light and electron microscopic immunohistochemistry, this antibody reacts to Lc, IDC, marginal zone histiocytes (MZH) and some undetermined histiocytes. However it reacts with almost no follicular dendritic cells (FDC), lymphocytes and fibroblasts. Because our antibody attached to IDC as readily as to Lc and MZH, then we can assume that there is the same antigen on IDC, Lc and MZH, and that this antigen is different from those on FDC, lymphocytes and fibroblasts to which the antibody would not attach. The fact that this antibody reacted some undetermined histiocytes will require further study and clarification.

CB 28

FUNCTIONAL MORPHOLOGY OF THE AGRANULAR CELL OF THE SALIVARY GLAND IN THE CATTLE TICK HAEMAPHYSALIS LONGICORNIS, WITH SPECIAL EMPHASIS ON THE DIFFERENCE BETWEEN BOTH SEXES.

H. Yanagawa, S. Shiraishi and T. A. Uchida. Zool. Lab., Fac. of Agr., Kyushu Univ., Fukuoka.

Elimination of the excess water and chloride during condensation of blood components is a major physiological problem for blood-sucking ticks. In the cattle tick H. longicornis, the excess water and electrolytes are returned to the host by means of salivary secretion. In female ticks, the agranular cells of Type III acini change conspicuously their volume and structure during feeding; especially, the e-cell and the abluminal interstitial cell develop greatly at the late stage of feeding, ending up with an elaborate system of membraneous infoldings containing numerous free ribosomes and elongated mitochondria, which is a common feature of fluid-transporting epithelia. Thus, these cells may contribute to maintaining osmotic and ionic balance. On the other hand, in male ticks which need not to suck a large quantity of blood, the e-cell and the abluminal interstitial cell are poorly developed in volume, although the fundamental structure of both cells is similar to those in females. This corresponds well with the much lower abilities in fluid secretion of male salivary glands.

CB 29

ULTRASTRUCTURES OF ADDUCTOR MUSCLES OF BIVALVE, Lima vulgaris.

A.Matsuno and H.Kuga. Dept. of Biol., Fac. of Sci., Shimane Univ., Matsue.

The adductor of Lima vulgaris (bivalve) shows long-distanced contraction and relaxations to open the valves wide. It seems that the adductor works well in this way compared with ones of other bivalves. The adductor is composed of translucent and opaque portions. The translucent portion is composed of cross-striated muscle cells that are similar to those of vertebrates: They have regular array of sarcomeres, and have thick (about 14 nm in diameter) and thin (about 7 nm) myofilaments. The opaque portion is composed of smooth muscle cells that show hexagonal profiles in cross section and elongated shapes. These cells contain also thick and thin myofilaments homogeneously distributed. Thin ones measure about 7 nm in diameter. Thick ones show various sizes (10-80 nm) as they distribute disordered way in longitudinal direction of the cell. We tried to estimate the size of thick myofilaments by the statistical analysis: Diameters measured from micrographs were classified into groups at 10 nm intervals, and the frequency in each class was shown along the vertical axis. The distribution of diameters semmed to fit the normal distribution curve that has a peak at 45-55 nm in diameter. Thick myofilaments of these sizes are commonly observed in molluskan retractor, but they are rare in adductors of bivalves.

CB 30

RUNNING PATTERN OF 10-NM FILAMENTS IN ASCIDIAN SMOOTH MUSCLE.

K. Terakado. Dept. of Regul. Biol., Fac. of Sci., Saitama Univ., Urawa.

The organization of intermediate (10-nm) filaments in smooth muscle cells was examined under an electron microscope. The material used was a body-wall muscle of the ascidian Halocynthia roretzi. The intermediate filaments ran in groups through spaces in a continuous network of myofibrils, connecting them at the regions of dense bodies longitudinally, obliquely and transversely to form an intimately associated, dual network. In their transverse passage, the intermediate filaments ran across myofibrils along I-zones (analogous regions to the I-bands of striated muscle) exclusively, interconnecting successive dense bodies. The pattern of attachment of intermediate filaments to dense bodies was predominantly "one-sided". The filament themselves were not incorporated into the contractile apparatus, and they remained folded or unfolded between myofibrils in synchrony with the contraction-relaxation cycles. The filaments terminated, usually in small groups, in the cell surface.

These results suggest that the intermediate filaments mechanically maintain the organization and arrangement of myofibrils via an intimate association with the myofibrils in the regions of the dense bodies, in such a way that the filaments do not impede muscle function.

CB 31

CHANGES OF VOLUME AND BIREFRINGENCE OF SPERM NUCLEI DURING SPERMIOGENESIS IN TESTES OF CEPHALOPODS.

H. Sato[1], K. Kato[2] and Y. Sato[3]. [1]Sugashima M. B. L., Nagoya Univ., Toba, [2]Biol. Lab., Nagoya City Univ., Nagoya and [3]Biol. Lab., Shoin Womens Univ., Kobe.

Process of sperm maturation was followed during spermiogenesis of Octopus vulgaris by Nomarski and polarization optics and transmitting EM. During the spermiogenesis, sperm nuclei elongated from 9.0 μm to 21 μm, width reduced from 8.9 μm to 1.2 μm. Thus, nuclear volume decreased from 364 μm^3 to 21.5 μm^3, indicating 1/16 condensation. Sperm heads gradually gained birefringence (BR). Same sequencial trends were confirmed in Octopus ochellatus and Ommatostrephes sloani pacificus. Sign of BR of these sperm are negative. From the series of imbibition experiments with various refractive indices, nature of the sperm BR was determined as intrinsic with slight contribution of positive BR due to the oriented manchette microtubules. Based on results obtained from pronase and DNase treatments, we confirmed that the BR of sperm nuclei was yielded by highly oriented DNA molecules and the co-efficient of BR, $(n_e - n_o)$, was measured as 0.8 to 2 x 10^{-2}, almost identical with the pure DNA gel. However, we presume the molecular alignment of DNA in mature sperm head could not be a simple straight bundles but should be a form of tightly packed coiled-coil chromonema with DNA molecules as their backbone.

CB 32

USE OF LASER RAYS FOR PRESERVING *DROSOPHILA* EMBRYOS BY FREEZING.

Y. Kuroda[1], Y. Takada[1] and T. Kasuya[2]. [1] Lab. of Phenogenet., Dept. of Ontogenet., Nat. Inst. Genet., Mishima. [2] Inst. of Phys. and Chem. Res., Wako, Saitama.

An attempt was mede to use the laser rays for preserving early embryos of *Drosophila melanogaster* at -196°C. The point to be solved for freezing *Drosophila* embryos was how to introduce protective agents into the inside of eggs through the vitelline membrane. In the present study, UV laser microbeam was applyed to cut the micropile to allow glycerol to enter into the inside of eggs. Dechorionated eggs were exposed to laser microbeam at the micropile under a microscope, incubated in culture medium involving 15% glycerol at 25°C for 16 hours, and frozen in liquid nitrogen at -196°C. After several days, eggs were thawed and incubated at 25°C. Larvae hatched at a low frequency and grew to adult flies. The entrance of glycerol into the inside of eggs after exposure to laser rays was confirmed by the stainability of eggs with neutral red. The survival of eggs after freezing was better when irradiated eggs were incubated with glycerol for more than 16 hours. The appropriate stage of embryos, the incubation medium and the speed of freezing and thawing are now under stady to obtain higher viability of eggs after freezing.

CB 33

ANALYSIS OF CELL PROLIFERATION DURING THE HATCHING PROCESS OF THE FRESHWATER SPONGE *Ephydatia fluviatilis*.

T.Matsuzaki and A.Shima. Zool.Inst., Fac. of Sci., Univ. of Tokyo, Tokyo.

The gemmules of the freshwater sponge were exposed to gamma-rays of ^{137}Cs at various time points during hatching incubation at 27°C and delay in hatching was examined. There were two radiation sensitive periods, one around the beginning of incubation and the other at about 27 hrs prior to hatching. The former period corresponds to the beginning of the transition of cells from resting stage to proliferating phase, the latter to the onset of DNA replication in S phase as revealed by DNA content measurement using DAPI-DNA microfluorometry. With regard to hatchability, irradiation at the latter period only was effective for reduction. Further, changes in number of nuclei per cell were counted on photomicrographs of gemmular cells at different time points throughout hatching incubation. The fraction of binucleated diploid cells decreased and that of mononucleated diploid cells increased with the advancement of incubation time. From these results, we presumed that upon the incubation of gemmules diploid twin nuclei in one thesocyte replicated synchronously their DNA, and then formed 4 diploid nuclei *via* nuclear division. Thereafter a tetranucleated cell divided into 4 mononucleated diploid cells just before hatching.

CB 34

CHARACTARIZATION OF THE PERMANENT PORCINE DIPLOID ENDOTHELIAL CELL LINE IN CULTURE.

K.Yamamoto[1], M.Yamamoto[1] and N.Hasegawa[2]. [1] Dept.Biol.,Tokyo Metropol.Inst.Gerontol., Tokyo, [2] Div.Cell Biol.,Yakult Inst.Microbiol.Res., Kunitachi.

The characterization of a porcine aortic endothelial cell line PAE-20 is described. This cell line underwent spontaneous transformation at about 80 PDL. The transformed cells are presently growing indefinitely (510 PDL) and exhibit normal mode of chromosome number. An abnormal chromosome, 3p+, were observed in all metaphase chromosomes in the transformed cells (120-492 PDL). The plating efficiency in the transformed cells was higher than that in the normal cells. The transformed cells at 474 PDL exhibited low efficiency of colony formation in soft agar. The transformed cells, however, possessed antibodies to Factor VIII-related antigen and high potential to produce prostacyclin up to 495 PDL. The angiotensin converting enzyme activity of the cells decreased linealy up to 81 PDL, and maintained barely detectable levels in the transformed cells. Fibronectin of the cell surface decreased significantly after the cells spontaneously transformed, but the transformed cells possessed the same antibody to the fibronectin antigen as the normal cells when cells were cultured in dishes coated with human fibronectin.

CB 35

ALTERATIONS IN ISOZYMES OF A SPONTANEOUSLY TRANSFORMED PORCINE ENDOTHELIAL CELL LINE DURING LONG-TERM SERIAL CULTURE.

M.Yamamoto and K.Yamamoto. Dept.Biol., Tokyo Metropol.Inst.Gerontol., Tokyo.

Tweleve isozymes were determined in the porcine diploid endothelial cell line PAE-20 that spontaneously transformed at about 80 PDL and continuously subcultivated over a 3-year period. Lactate dehydrogenase B(LDHB) gradually decreased up to 69 PDL and lost at 84 PDL. Lactate dehydrogenase A (LDHA) increased in the transformed cells (84-474 PDL). The transformed cells demonstrated a distinctly decreased ratio of LDHB to LDHA compared to the normal cells. A lower migrating isozyme of malic enzyme gradually decreased in the transformed cells. Isozyme expressions of malate dehydrogenase, isocitrate dehydrogenase and mannose phosphate isomerase varied in the transformed cells. Expressions of seven isozymes (phosphoglucose isomerase, glucose 6-phosphate dehydrogenase, phosphoglucomutase, purine nucleoside phosphorylase, glutamate oxaloacetate transaminase and peptidase A and B) were stable in all PDL examined here. Total choresterol contents lineally increased at 21-69 PDL but gradually decreased up to 510 PDL. Changes in the choresterol contents may be related to isozyme phenotypes of malic enzyme and malate dehydrogenase (lipid synthetic enzymes).

CB 36

EFFECTS OF CHEMICAL CARCINOGENS ON THE CULTURED CELLS DERIVED FROM THE FINS OF THE CENTRAL MUDMINNOW (UMBRA LIMI; PISCES).

I. Suyama and H. Etoh. Natl. Inst. Radiol. Sci., Chiba.

The ULF-23, a cell line from the fins of U. limi, was established and cultivated at 25°C. From the growth curve the doubling time was estimated to be 72 h. Fluorescense profiles of the cells stained with PI were obtained by a cytofluorometer. From these data the cell cycle times were estimated as follows; G_0+G_1 = 59 h, S = 9 h, and G_2+M = 4h. The ULF-23 and ULO, another cell line from the ovary of Umbra, were treated with chemical carcinogens for sister chromatid exchange (SCE) analyses. Chemicals used were MNNG (10^{-7} to $2x10^{-5}$M), MAM acetate ($2x10^{-7}$ to 10^{-4}M) and ENU ($2x10^{-8}$ to $2x10^{-5}$M). After treatments with the chemicals SCE in second mitosis was observed. SCE values of control cells were 9-12/cell. SCEs in ULF cells treated with MNNG were increased with increasing concentrations and reached to 27 at 10^{-5}M. No increases in SCE were observed in ULF cells treated with MAM acetate below 10^{-5}M and in ENU-treated ULO cells within the range tested. The yield of SCE with chemicals was lower than in cultured mammalian cells, but the usefulness in cytogenetic studies of cultured Umbra cells was confirmed.

CB 37

Effects of human serum from various ages on proliferation and migration of human lung and skin fibroblasts.

H. Kondo, Y. Yonezawa and T. A. Nomaguchi. Dept. Biol., Tokyo Metropol. Inst. Gerontol., Itabashiku, Tokyo.

It has been reported that both serum and blood plasma from old animals inhibit cell growth in plasma clot culture. However, we have demonstrated that sera from rabbits and most rats in old age did not inhibit cell proliferation. In order to determine whether human serum from the old stimulates or inhibits cell proliferation, we measured cell proliferation activity of human serum from various ages (16-89 years) on the 3rd and 7th days. The results showed that sera from the old of either sex stimulated proliferation of human fetal lung fibroblasts (TIG-1) as well as FBS. This is also the case when using human old skin fibroblasts. Next, we tried to determine cell migration activity of human serum (16-64 years) since cell growth with plasma clot culture method includes cell proliferation, cell migration and others. Human sera from their 60s caused lower migration of TIG-1 cells, human adult and old skin fibroblasts. There was statistical significance between both age groups in female only when TIG-1 cells were tested. These results implied that serum from the old did not greatly inhibit proliferation and migration of human fetal lung fibroblasts, adult and old skin fibroblasts.

CB 38

CHROMOSOME REPLICATION OF SYNCHRONIZED INDIAN MUNTJAC CELLS

M.Ikeda[1] & T.Ueda[2]. [1]Dept. of Biol.,Keio Univ., Yokohama.Dept.ofDevelop. Biol., Mitsubishi Kasei Inst. of Life Sciences, Tokyo.

Fusion between mitotic and S-phase cells induces the formation of prematurely condenced chromosomes (PCC) in the interphase partner. Mitotic HeLa cells were fused with S-phase muntjac cells which were syncronised with excess thymidine and N_2O high-pressure. Viewed through a light microscope, S-phase PCC appears to be fragmented and heterogenous; early S-phase is characterized by extremely attenuated filaments. Mid-S-phase is heterogenous, with attenuated regions of little staining containing some large and small blocks of stained material and a late S-phase PCC has elongated duplicated chromosomes with gaps. Autoradiographs of S-phase PCC by pulse and pulse-chase experiments showed $_3$H thymidine incorporated first into unstained region, then into lightly stained fragments, and finally into dark stained chromosomes. Stained with Chromomycin A_3(a G-C specific dye), the fiberous material can be clearly observed in Giemsa unstained regions. On the other hand, no staining can be observed when the same PCC is treated with Hoechst 33258 (a A-T specific dye).

CB 39

CHNGES IN CHARACTER OCCURRING DURING SUCCESSIVE SUBCULTURES IN SMF CELL LINE.

T.KUBO[1], N.EBITANI[2] and S.NADAMITSU[3]. [1]Biol. Lab., Sophia Univ., Tokyo, [2]Biol. Lab., Shohoku Coll., Atsugi and [3]Biol. Lab. Hiroshima Women's Univ., Hiroshima.

The SMF cell line has been established in the fins of the marine teleost fish, *Sebastiscus marmoratus*. Two clonal cell lines were obtained from the above cells at different PDNs viz (a) TN-1 from the cells at small PDN and (b) TN-2 from the cells at large PDN. Some characteristics were compared among primary cells (P) and the SMF cells at small and large PDNs (S-SMF and L-SMF) and also the TN-1 and TN-2 cells. MORPHOLOGY - P and TN-1 cells were fibroblast-like and showed regular arrangement. S-SMF cells were fibroblast-like but didn't show regular arrangement. L-SMF cells were fibroblast-like but were short and wide to some extent, and their arrangement was irregular. TN-2 cells were not fibroblast-like, but rather epithelial-like. MODAL NUMBER OF CHROMOSOMES - P: 2n=48, S-SMF: 2n =96, L-SMF: 2n=50, TN-1: 2n=98, TN-2: 2n=50 NUMBER OF METACENTRIC CHROMOSOMES AND AgNORs - P: 2 and 4, S-SMF: 4 and 8, L-SMF: 2 and 4, TN-1: 4 and 8, TN-2: 2 and 4. Chromosome loss was observed in SMF cells subcultured successively for a long term. In view of the number of metacentric chromosomes and AgNORs, the chromosome loss was not random, but meiotic chromosomal segregation might have taken place.

CB 40

CONDITIONED MEDIUM OF BOVINE AORTIC ENDOTHELIAL CELLS CONTAINS A GROWTH FACTOR(S) THAT STIMULATES THE PROLIFERATION OF HUMAN ENDOTHELIAL CELLS.

K. Kaji and M. Matsuo. Isotopes Lab., Tokyo Metro. Inst. Gerontol., Tokyo.

Bovine aortic endothelial cells (ECs) grew in MEM supplemented with 10 % fetal bovine serum (FBS), but human ECs derived from the umbilical cord could not grow in the same culture medium. We tested the possibility that bovine ECs produce a endothelial cell growth factor(s) (ECGF), and the factor acts in an autocrine fashion to stimulate ECs proliferation. Quiescent bovine aortic ECs were exposed to MEM for 4 days and the conditioned medium was harvested. The conditioned medium added 10-40 % to MEM plus 10 % FBS stronly stimulated the proliferation of human ECs, and the cell number increased by 2-4 times in 3 days. The ECGF activity was nondialyzable, trypsin sensitive, acid unstable and heat stable. The ECGF activity eluted from heparin-Sepharose at 0.6 M and 1.5 M NaCl, and the activity of the latter fraction was inhibited by 10-100 μg/ml of heparin. The cell homogenate of bovine ECs also contained ECGF activity which eluted from heparin-Sepharose at 1.5 M NaCl. On the other hand, human ECs homogenate contained very little ECGF activity, if any.

These data showed existing evidence for autocrine growth control by bovine ECs, but not by human ECs.

CB 41

WOUND HEALING OF RAT FETUS SKIN.

S.Ihara, E.Nagao, Y.Motobayashi, A.Kistler and N.Shioya. Dept. of Plast. Surg. Kitasato Univ. Sch. of Med., Sagamihara.

As the first step to make clear the feature of fetus wound healing process, we have made a model in which wounded rat fetus skin was cultured in vitro. When a small open wound (2mm ϕ) was made in the 18d fetus skin and the skin piece was cultured, kept floating, in DMEM plus 1% Ultroser G, a thin network (NW) was formed horizontally across the wound edge within 24h after the beginning of culture. Two to 4 days after, fibroblast-like cells appeared and increased in NW. NW formation did not depend on the presence of Ultroser G, but the cell growth depended. SEM study showed that NW consisted of thin filaments (40-60nm ϕ) which were branched in places. Its appearance resembled collagen fibrils or fibrin fibers. However, no fibrous collagen-specific striation could be observed by TEM. SDS-PAGE analysis showed that the major component of NW was a 55kd polypeptide (P55) which was insensitive to bacterial collagenase, and no α-chain of collagen was detected in NW. Meanwhile, the amino acid sequence (9 amino acids) of a tryptic digest from P55 was not identical to the whole sequences of human fibrinogens α, β and γ. Therefore, P55 may be a new kind of ECM component which is produced by the healing fetus skin.

CB 42

ESTABLISHING A D-GALACTOSAMINE INDUCED HEPATIC INJURY MODEL USING PRIMARY CULTURED RAT HEPATOCYTES

J.Kijima[1], J.Arai[1], S.Kusunoki[1], T.Furuya[2], [1]Life Science Lab., Advance CO.,LTD., Tokyo, [2]Dept. of Pharmaco., Kitasato Univ., Tokyo.

The In vitro hepatic injury model using primary cultured rat hepatocytes was shown to be quite suitable for the first screening of some natural extracts because many samples of these extracts could be screened in a short time and the amounts of samples required were very small.

After 24 h preincubation, the hepatocytes were exposed to a medium containing either D-galactosamine (GalN) or GalN and a natural extract. After a lapse of 72 h the GPT and LDH activity and the albumin concentration in the medium were measured. We had thus established a GalN induced hepatic injury model using primary cultured rat hepatocytes. We compared the effect of Ganoderma lucidum mycelium extract (GLM1), Ganoderma lucidum fruits body extract (GLF1, GLF2) and Alismatis rhizoma extract (AR1) with Glycyrrhetinic acid using this model.

This model showed a significant increase in GPT and LDH activity and a decrease in albumin synthesis in the GalN challenge medium. Four samples where 300 μg/ml were added to hepatocytes inhibited the increase of GPT activity. Only GLF2 significantly prevented the increase of LDH activity by GalN. It seems that this assay was therefore effective.

CB 43

PROTECTIVE EFFECT OF NATURAL EXTRACTS ON TWO TYPES OF HEPATIC INJURY MODELS

T.Nakamura[1], H.Miyazaki[1], S.Kusunoki[1], T. Furuya[2], [1]Life Science Lab.,Advance Co.LTD., Tokyo, [2]Dept. of Pharmaco. Kitasato Univ., Tokyo

We observed that some natural extracts have a protective effect on primary cultured rat hepatocytes against hepatic injury induced by D-galactosamine (GalN). The effects of GLM1, GLF1,GLF2 and AR1 were studied through an in vivo hepatic injury model in rats induced by carbon tetrachloride (CCl_4) and GalN.

Eight week old, 180-220g male Wistar rats were used and permitted free access to food and water. Samples of the natural extracts (dosage 1, 10, 100 mg/kg bw ip) were administered 30 minutes before treatment with CCl_4 (dosage 1.0 ml/kg bw po) and GalN (dosage 500 mg/kg bw ip).

An increase in serum transaminase (GOT, GPT) and LDH activities was observed after CCl_4 and GalN treatment. All samples, dosage of 100 mg/kg, inhibited the increase of GOT, GPT and LDH activities in the CCl_4 induction hepatic injury model.

On the other hand, an increase of GOT,GPT and LDH activities induced by GalN was inhibited by the administration of GLM1 and GLF2 (dosage 100 mg/kg). Histopathological findings resembled biochemical findings.

These results demonstrated a correspondence between in vivo and in vitro findings.

GE 1

RESTRICTION FRAGMENT LENGTH POLYMORPHISM OF RIBOSOMAL DNA IN GENUS APODEMUS

H.Suzuki[1], K.Tsuchiya[2], M.Sakaizumi[3], S.Sakurai[1], Y.Harada[4], K.Moriwaki[4]. [1]Central Res. Lab., The Jikei Univ. School of Med., Tokyo, [2]Miyazaki Med. College, [3]The Tokyo Metropol. Inst. Med. Sci., [4]Natl. Inst. Genet., Mishima.

Southern blot analysis for ribosomal DNA (rDNA) in six Apodemus species (A. slvaticus, A. flavicollis, A. semotus, A. agrarius, A. argenteus, A. speciosus) using 14 restriction enzymes revealed that a major rDNA repeating unit type (repetype) of each species was specified by characteristic topological arrangement of restriction sites.

In the non-transcribed spacer region near the 28S gene, most of A. speciosus collected from 20 different locations in Japan gave two EcoRI bands (1.3 kb and about 5kb) attributed to EcoRI site variation within individual. No correlation was noticed between two karyotype groups (2n=46 and 48) and the EcoRI site variation. Small island populations, however, had either one of two EcoRI bands in their genome predominantly: Tokara, Yaku and Miyake had 5 kb and Tsushima 1.3 kb. These results suggest that fixation of variant repetypes occurs rapidly in a small population, irrespective of repetypes.

GE 2

EXPRESSION OF A^y GENE IN THE SKIN OF THE MOUSE.

C.Sato, T.Takeuchi. Biol. Inst., Tohoku Univ., Sendai.

Mammalian melanocytes are capable of producing two types of melanins, black pigment (eumelanin) and yellow pigment (pheomelanin). In the house mouse, the type of melanin is known to be determined by the agouti (a) locus, which is thought to be expressed in the hair follicle. Mouse with genotype (a/a) exibits eu-melanin, whereas genotype (A^y/a) exibits pheomelanin.

Our previous experiments showed that L-DOPA enhanced pheomelanogenesis in TM10 cells in vitro. The contents of this pre-cursor in melanogenesis were estimated in the skin of yellow mouse and black mouse. The amount of L-DOPA in A^y/a skin was greater than that in a/a skin.

Homogenate from the skin of 3.5 day (A^y/a) mouse was used for immunizing the mouse of (a/a) genotype. Then the spleen cells from (A^y/a) mouse were fused with P6 myeloma cells. ELISA assay showed that one hybridoma cell line secreted antibody which react solely to (A^y/a) mouse skin. By immunofluorescence technique, this antibody was found to react to epidermis, hair follicles, dermal cells in the skin of 2.5 day newborn mouse.

GE 3

ENZYMATIC ANALYSIS OF THE INSEMINATION REACTION IN DROSOPHILA I.

N. Asada[1], and T. K. Watanabe[2]. [1]Dept. of Biology, Faculty of Science, Okayama Univ. of Science, Okayama, [2]Genet. Stock Center, Nat. Inst. of Genetics, Mishima.

Phenoloxidase and protease are concerned in the insemination reaction which is the phenomenon occurs in copulated female accompanied by reaction mass formation and plays important roles on isolation in Drosophila. The production of reaction mass takes place within a few minutes after copulation both in intra- and interspecific crosses. In the latter crosses, reaction mass was maintained in uterus, then melanized in vivo and in vitro following the detection of phenoloxidase activity resulted in restraining the fecundity. In the former crosses, however, reaction mass remained the original color, then reduced in size gradually and disappeared by proteolysis prior to oviposition.

Because formation and disappearance of reaction mass show temperature dependency, specific enzyme-blockers injected in vivo significantly inhibited above phenomena, and enzyme activities were detected, each enzyme(s) are thought to be key one(s) for formation and transition of reaction mass in intraspecific crosses. Above phenomena seem to be the consequence of the female's discrimination system of male's secretion by humoral immune involved in phenoloxidase-protease system in Drosophila.

GE 4

HETEROMORPHIC CHROMOSOMES IN SEA URCHIN, TYPE B OF ECHINOMETRA MATHAEI, FROM OKINAWA

T.Uehara[1] and K. Taira[2]. [1]Dept. of Biol., Univ. of Ryukyus, Okinawa. [2]Shuri Junior High Sch., Okinawa

Since sea urchins have many chromosomes of small size, it is difficult to distinguish the homologus ones. Therefore, existence of the heteromorphic chromosomes in sea urchins has been left unsolved until now. Type B urchin is one of the four types of E. mathaei. Diploid chromosome number in all of the four types is 42 in which one strikingly large chromosome pair exists. The largest chromosomes consist of two metacentric ones in three urchins of A,C and D type. In Type B, karyotypes of one largrst chromosome pair of 52 fertilized eggs from three pairs were analysed. Twenty five cells with homomorphic chromosome pair and 27 cells with heteromorphic chromosome one were counted. Furtheremore, in Type D♀ x B♂, two kinds of the heteromorphic chromosome pairs were observed. One consists of a metacentric chromosome from Type D and a telocentric one from Type B, and the other composed of a metacentric chromosome from Type D and a submetacentric one from Type B. These results show that there are dimorphic chromosomes in the sperm from Type B.

GE 5

ESTABLISHMENT OF THE MULTIPLE RECESSIVE TESTER MEDAKA HOMOZYGOUS FOR THE 3 LOCI.

A.Shimada and A.Shima. Zool.Inst., Fac. of Sci., Univ. of Tokyo, Tokyo.

The establishment of a multiple recessive tester stock is the prerequisite for using specific-locus method in the Medaka *Oryzias latipes*. We have previously produced a multiple recessive tester stock homozygous for 5 loci, *i.e.*, *b*, *Da*, *gu*, *pl* and *r*. For practical use, however, we found some problems like low viability and low fecundity in this stock. Then attempts were made to change some loci in order to obtain more suitable tester stock. We deleted the *Da*, *pl* and *r* loci and introduced the *lf* locus as a new marker. The homozygotes for the locus *lf* are known to have no leucophores throughout the life, while the leucophores in the wild type can be recognized around brain of embryo about 3 days after fertilization. The new tester stock Medaka thus obtained are homozygous for the *b*, *gu* and *lf* loci, have high viability and fecundity and are judged to be suitable for use in the specific-locus test. The data on numbers of F_2 offspring obtained during the production of this tester were used for segregation analyses of the 3 locus-pairs, *b*-*gu*, *b*-*lf* and *gu*-*lf*, respectively. Since P values were clearly greater than 0.05, the observed results were in good agreement with those to be expected for the independent assortment of each two pairs of alleles.

GE 6

RADIATION INDUCTION OF SPECIFIC-LOCUS MUTATIONS IN THE MULTIPLE RECESSIVE TESTER MEDAKA.

A.Shima and A.Shimada. Zool.Inst., Fac. of Sci., Univ. of Tokyo, Tokyo.

We succeeded in establishing the multiple recessive tester Medaka *Oryzias latipes* homozygous for 3 or 5 loci. In order to determine if our tester Medaka are valid for detection of induced recessive mutations by the specific-locus method, we set out to examine gamma-ray-induced mutation frequencies at the *b*, *lf*, *gu*, and *pl* loci. The total numbers of loci examined were 187,073 and 147,713 for the postspermatogonial and spermatogonial cells, respectively. No spontaneous mutant that survived more than 4 days after hatching has yet been obtained. Because we chose as markers genes whose phenotypes are expressed rather early during development, we very often observed deaths of mutant embryos prior to hatching. The approximate ratio of numbers of such mutants as died before hatching to those of viable (survived more than 4 days after hatching) mutants was 10:1, indicating that the vast majority of the mutation are not viable probably due to deletions rather than point mutations. We presented data which showed that gamma-irradiation induced specific locus mutations in the Medaka were fairly well in accordance with the comparable results on mice obtained above all by W.L. Russell.

GE 7

NEW MUTANT IN THE MEDAKA.

H.Tomita. Lab. of Freshwater Fish Stocks, Fac.of Sci., Nagoya Univ., Nagoya.

The mutant(*ha*), deformity of inner ears was already established. The new mutant which is similar pheotype to the mutant(*ha*)was found. The offspring of crosses between the new mutant and the *ha* mutant were all normal. These mutants belong to different alleles each others. The new mutant is recessive autosomal and polymeric(*ha*-2,*ha*-3). At the embryonic and larval stages, the auditory vesicle swelled and protruded. This protrusion turned to normal at about 10 mm body length. At about 20mm body length, the fishes swimmed round. In the inner ears, the ultriculus fused with the scculuse and became swelled vesicle and the semicircular cannals developed incompletely and sometimes were absent.

The *rs*-2 -and *rs*-3 mutants were established at last year. The former had small scales and the latter was partial lack of scales(partial naked). They are autosomal and recessive. The *rs*-2 is independent of the *b* and *dm* alleles. The *rs*-3 is independent of the *b*, *ci*, *dm*,*rs*-2 and *vc* alleles.

GE 8

KARYOTYPE EVOLUTION AND GEOGRAPHICAL DISTRIBUTION OF BIARMED CHROMOSOME GROUP OF RICEFISH, GENUS *ORYZIAS*, IN YUNNAN, CHINA AND EASTERN ASIA.

H. Uwa, R.-F. Wang[2] and Y.-R. Chen[2]. Dept. of Biol., Shinshu Univ., Matsumoto and [2]Kunming Inst. of Zool., Acad. Sinica, Kunming, China.

Karyotypic studies were made in two species of ricefishes collected from Yunnan, south-western China. *Oryzias latipes* collected from the eastern Yunnan Plateau had 2n, 46 chromosomes consisting of 3 metacentric, 8 submetacentric, 2 subtelocentric, and 10 acrocentric pairs , the arm number (NF) being 68 (2n=46, NF=68, 3M+8SM+2ST+10A). The karyotype was characteristic by having a "large" metacentric pair and nucleolus organizer regions (NORs) on the short arms of a submetacentric pair. A diminutive species *O. minutillus* collected from Xishiangbanna, the southern low mountain areas of Yunnan, showed 2n, 42 chromosomes consisting of 21 acrocentric pairs, NF being 42 (2n=42, NF=42, 21A). NORs were located at the telomeric regions of an acrocentric pair. Geographical distribution of these ricefishes were seemed to be correlated with river systems and climatic zones.

Karyotype of *O. latipes* from Yunnan was closely related to that from eastern China and western Korea (2n=46, NF=68-70), but distinct from that from eastern Korea and Japan (2n=48, NF=68-70).

Relationship between karyotype evolution and geographical distribution of ricefishes was discussed among four species of the biarmed chromosome group collected from eastern Asia; *O. mekongensis* (2n=48, NF=58), *O. latipes* (2n=46-48, NF=68-70), *O. curvinotus* (2n=48, NF=82), and *O. luzonensis* (2n=48, NF=96).

GE 9

GENETIC DIVERSITY OF THE EAST ASIAN POPULATIONS OF THE FRESHWATER FISH, ORYZIAS

M. Sakaizumi[1], H. Uwa[2], and S. R. Jeon[3]
[1]The Tokyo Metropol. Inst. Med. Sci., Tokyo, [2]Fac. Sci., Shinshu Univ., Matsumoto, and [3]College of Nat. Sci., Sangmyung Women's Univ., Seoul.

Allozyme studies have revealed that the wild populations of medaka are composed of four major groups, the Northern Population and the Southern Population from Japan, the East Korean Population, and the China-West Korean Population. In Korean Peninsula two groups were separated by the backbone mountain, which is a major boundary of Korean freshwater fish fauna. Introgression of 'western' alleles into the East Korean Population was observed in the southern area of the peninsula. But little traits of Japanese two major populations were found in Korea, suggesting strong isolation between the populations of the Japan Islands and Korean Peninsula. The populations of Yunnan District in China showed a similar genetic profile to that of the China-West Korean Population. On the other hand, the medaka collected in Hong Kong was different from any of the four major groups. These results suggest that the China-West Korean Population has a great distribution range and that the population of Hong Kong belongs either to the fifth group of O. latipes or to a different species closely related to it.

GE 10

KARYOTYPE POLYMORPHISM OF A SMALL RICEFISH, ORYZIAS MINUTILLUS.

T. Ashida and H. Uwa[2]. Nagano-ken Fujimi High School, Suwa-gun and [2]Dept. of Biol., Fac. of Sci., Shinshu Univ., Matsumoto.

Members of the genus Oryzias so far studied could be karyotypically divided into three groups; monoarmed chromosome type, biarmed chromosome type, and fused chromosome type. Karyotypes of O. minutillus from Bangkok (2n=34, NF=44; 4M+1SM+12A) and Chiang Mai (2n=30, NF=44; 6M+1SM+8A), Thailand, had 4 and 6 pairs of "large" metacentric chromosomes, respectively, and it had been considered to be a member of the fused chromosome group (Magtoon and Uwa, 1985). Nucleolus organizer regions (NORs) were located on the short arms of a submetacentric pair.

Recently, we found specimens of O. minutillus collected from Phuket in southern Thailand had 2n, 42 chromosomes consisting of 21 acrocentric pairs (2n=42, NF=42; 21A). NORs were located at the telomeric regions of an acrocentric pair. The hybridization test among specimens from three localities revealed that they could breed and F1 offspring were fertile. O. minutillus collected from Xishiangbanna in Yunnan, China, also had a karyotype (2n=42, NF=42; 21A) similar to that from Phuket. From these results, karyotype of specimens from Phuket (and Xishiangbanna) might be basic for O. minutillus, and those from Bangkok and Chiang Mai might be caused by Robertsonian centric fusion and pericenrtic inversion.

GE 11

CHROMOSOME ANALYSIS OF THE MOUSE SPERMATOZOA BY THE INTERSPECIFIC IN-VITRO FERTILIZATION METHOD

M. Shimada, Y. Kamiguchi, H. Tateno and K. Mikamo, Dept. of Biol. Sci., Asahikawa Med. Col., Asahikawa.

We modified our interspecific in-vitro fertilization method with zona-free hamster ova for analyzing human sperm chromosomes in order to study mouse sperm chromosomes.

The main points of the modification are as follows: (1) Use of TYH medium for sperm capacitation instead of mBWW medium used previously. (2) Use of MEM alpha medium containing 30 % fetal bovine serum for postinsemination culture instead of TC medium 199 containing 10 % fetal bovine serum. (3) Determination of the optimum moment of insemination by observing the changing aspects of movement patterns of spermatozoa. (4) Insemination of ova with sperm suspension of a low concentration, 1 X 10^4 sperms/ml, for a short time, 5-6 minutes.

Most of mono-, di- and trispermic eggs were successfully activated by this method, showing expulsion of the 2nd polar body and active growth of male and female pronuclei. Among them, 71 % of both mono- and dispermic eggs developed up to the stage of the 1st cleavage metaphase.

We described the procedures of this method and some results thereby obtained.

GE 12

ACUTE AND LATE EFFECTS ON OOCYTES IN CHINESE HAMSTERS X-IRRADIATED DURING NEONATAL STAGES

H. Tateno[1,2], K. Mikamo[1], Y. Kamiguchi[1] and K. Tanaka[2]. [1]Dept. of Biol. Sci., and [2]Central Lab. for Res. & Ed., Asahikawa Med. Col., Asahikawa.

In our previous studies, it was shown that diplotene and early dictyate oocytes of neonatal Chinese hamsters were highly radiosensitive and they were completely destroyed by 100 rad X-rays. In the present study, we exposed females at 6 days of age to three doses of X-rays (10, 25 and 50 rad) in order to examine acute and late effects of these lower dosages on their oocytes.

Nearly 95% of oocytes survived 10 and 25 rad X-rays, but only 30% of oocytes could survive 50 rad. Fertility span of females exposed to 10 and 25 rad X-rays was not significantly different from that of non-irradiated females. On the other hand, the fertility span was significantly shortened in the females exposed to 50 rad. They clearly showed delay in sexual maturation and precocious cessation of estrous cycles owing to the shortage of oocytes. There was no significant increase in incidences of chromosome aberrations and dominant lethal mutations in the oocytes ovulated from all irradiated females. These results showed that the X-rays irradiated on diplotene and early dictyate oocytes induced only acute oocyte-killing, but did not induce late effects due to genic damages.

GE 13

ASSESSMENT OF GENETIC EFFECTS OF ENVIRONMENTAL MUTAGENS USING HUMAN SPERM CHROMOSOME ANALYSIS

Y. Kamiguchi, H. Tateno, M. Shimada and K. Mikamo, Dept. of Biol. Sci., Asahikawa Med. Col., Asahikawa.

Using our interspecific in-vitro fertilization system between human spermatozoa and zona-free hamster ova, we studied cytogenetic effects of X-rays and an alkylating agent, methylmethansulfonate (MMS), on human sperm chromosomes. Total number of 4959 spermatozoa were karyotyped in the former experiment,and 3095 in the latter.

(1) Incidences of spermatozoa with structural chromosome aberrations were 14.1 % (0 rad), 18.9 % (25 rad), 28.5 % (50 rad), 42.6 % (100 rad) and 68.0 % (200 rad) in the X-ray experiment, and were 14.6 % (controls), 22.8 % (5 µg/ml), 29.5 % (10 µg/ml), 53.5 % (25 µg/ml) and 81.7 % (50 µg/ml) in the MMS experiment. Dose-dependent increase of affected spermatozoa was linear in both experiments. (2) In the X-ray experiment, the incidence of breakage-type aberrations was far higher than that of exchange-type aberrations, both of them showing linear increase with increase of dosage. (3) In the MMS experiment, breakage-type aberrations increased linearly with increasing dosage, whereas exchange-type aberrations increased quadratically, reaching 32 % of total aberrations in the highest dose group. Importance of this method in assessing genetic effects of mutagens on human was stressed.

GE 14

COMPARATIVE CHROMOSOMAL STUDIES OF ANEMONEFISHES (PERCIFORMES)

A.Takai, S.Kosuga, and Y.Ojima, Dept. of Biol., Fac. of Sci., Kwansei Gakuin Univ., Nishinomiya.

Karyotypes and distribution of nucleolus organizer regions (NORs) and C-banded heterochromatin of seven anemonefishes were comparatively studied. Chromosome number was 2n=48 in all species and karyotypes were similar as follows : Amphyprion clarkii, A.ocellaris, and A. polymunus (12M+24SM+12ST,A, NF=84); A. frenatus and A.perideraion (12M+22SM+14ST,A, NF= 82); A. ephippium (10M+28SM+10ST,A, NF=86); Premnas biaculeatus (12M+30SM+6ST,A, NF= 90). NORs were located at terminal regions of the short arms of 2nd or 3rd largest subtelocentric pair in all species except A.ocellaris in which NORs were located at pericentric regions of the long arms of the 2nd largest submetacentrics. C-bands were located in centromeric regions of several chromosomes, but the distributional patterns were different among the species. Only A.polymnus had many telomeric C-bands. The present results suggest that the karyotypes of A. ephippium and P. biaculeatus are somewhat differentiated from the other four species and a close relation between changes of C-banded heterochromatin distribution and species differentiation. NORs seem to be located in the identical chromosomes among the species.

IM 1

LATE LARVAL HEMOPOIESIS OF BULLFROG RANA CATESBEIANA,USING MONOCLONAL ANTIBODIES.

K.Hatakeyama and K.Sugiyama. Dept.Biol., Fac.Sci.,Hiro-aki Univ.,Hirosaki.

Four mouse monoclonal antibodies,named mAb Rc-T-1(reported as T1-3A5 previously), mAb Rc-G1(as 2A-4),mAb Rc-G2(as 2B-9) and mAb Rc-P(as 1B-10),were prepared against lymphocytes of bullfrog Rana catesbeiana previously and have been characterized of their reactivities among various lymphoid tissues of frog by indirect immunofluorescence antibody staining. An application of these mAbs to the late larval hemopoietic cells during the metamorphosis(Cooper Stages 25-34)demonstrated that both neutrophils(recognizable by mAb Rc-G1 and mAb Rc-G2) and small monocyte-like cells(recog.by mAb Rc-G2)were mainly originated from the larval mesonephros and from the liver in part. Whereas,the platelet antigen Rc-P positive cells were originated from the larval liver and showed a considerable higher cell population in PBL during larval stages,but a noticeable decreasing of these cells was shown at the postmetamorphic froglet,in contrast to the Rc-G1 and Rc-G2 positive cells. Much of thymocyte antigen (Pc-T-1) was detected at the begining stage(st.25/26)of hind limb formation already . Rc-T-1 positive cells were also detected significantly on the lymphoid cells from mesonephros(st.25/26)and PBL with a faint reactivity.

IM 2

C-REACTIVE PROTEIN (CRP) IN RAT. -THE SITE FOR ITS SYNTHESIS AND INTERACTION WITH MACROPHAGE (MØ)-

W. NUNOMURA[1,2], H. WATANABE[1] and H. HIRAI[1]. 1) Tumour Laboratory and 2) Nippon Bio-Test Laboratories Inc., Tokyo.

Although CRP is one of typical acute phase proteins, its physiological role(s) and mechanism for the synthesis have not been fully elucidated. In this study, we investigated the site(s) for the synthesis and interaction with MØ in rat CRP.

By immunohistochemical method, CRP was strongly stained in liver by chemical inflammation provoked injection of turpentine. CRP was localized in cytoplasm of hepatocytes and also detected on the surface of polynuclear leucocytes infiltrated in the injured tissues.

In primary culture of rat hepatocytes, CRP was synthesized and released into the medium. Cytokines from rat MØ faciliated the production of CRP, while those from thymocytes and splenocytes had no effect. On the other hand, the incubation of rat CRP with MØ resulted in the generation of O_2^-.

These results suggest that the restoration of injured tissues are facilitated by cooperation of CRP and MØ.

IM 3

ENHANCED RNA SYNTHESIS IN ACTIVATED RAT PERITONEAL MAST CELLS (PMC)

H.Fujimaki [1] and A.D.Befus [2]
[1]Div. of Basic Med. Sci., Natl. Inst. for Environ. Studies, Ibaraki [2]Dept. of Micro.& Infect Dis., Univ. of Calgary, Canada.

The well recognized heterogeneity in rat mast cell populations may be due to differences in the phases of differentiation in a single cell lineage, or to microenvironmental influences. Therefore, to determine the molecular basis of mast cell heterogeneity we have initiated investigation of mast cell RNA. Preliminary experiments showed that RNA levels are low in normal adult PMC.Thus we have attempted to increase RNA synthesis of PMC activated with 48/80 or worm antigen. Firstly, Sprague-Dawley rats were injected IP with 48/80. One,5,10 and 25 days later rats were killed and PMC were isolated and purified using a discontinuous Percoll gradient. One day before the rats were killed ^{3}H-uridine was also given IP. In vivo labeling with uridine showed no enhanced RNA synthesis in purified PMC. Secondly, purified PMC from normal rats were treated with 48/80 or sensitizing antigen in vitro and were cultured for 1, 3 and 24 hours in the presence of ^{3}H-uridine. The uptake of uridine in activated PMC increased compared to non-activated PMC. These observations provide important tool to study underlying mechanisms of mast cell heterogeneity.

IM 4

ANTI-MOPC-315(H-2^d) PLASMACYTOMA RESPONSES IN MAJOR HISTOCOMPATIBILITY COMPLEX-IDENTICAL STRAINS OF MICE : Natural Tolerance to the Tumor-Specific Antigenic Determinants in a Susceptible Strain of Mice

M.Hosono, K.Yano, Y.Katsura and K.Takahashi*
Dept. Bacteriol.& Serol.,Chest Dis. Res. Inst., Kyoto University, Kyoto and *Aburabi Lab., Shionogi-Seiyaku Co., Ltd., Koga-gun, Shiga.

BALB/c-originated MOPC-315 plasmacytoma bears tumor specific transplantation antigens(TSTA) recognizable by and rejected in the syngeneic BALB/c mice as well as in the other H-2-identical allogeneic strains except for DBA/2 mice. The trait of unresponsiveness to the TSTA in the latter mice is genetically inherited codominantly. Among BALB/c-DBA/2 hybrids, white mice, homozygous at the BALB/c-albino locus, were entirely resistant to the tumor. Preimmunization of adult BALB/c mice with nucleated and anucleated cells of DBA/2 but not of any other mice used, promoted tumor regression, indicating an induction of positive immunological memory. In contrast, administration of those antigens, into neonatal BALB/c mice rendered them unresponsiveness to the TSTA at adulthood, indicating that immunological tolerance or negative immunological memory was induced. These results provide evidence that in susceptible mice, natural tolerance has already occurred with regard to their own bodies' antigenic determinants which cross-react with the TSTA, supporting the "clonal deletion model" for an unresponsiveness to "foreign" antigens.

IM 5

STUDIES ON THE PLATELET-LIKE STRUCTURES(PLS) IN HEMOLYMPH FROM LAND SLUG, INCILARIA SPP. USING BIOTINYL LECTINS AND AVIDIN-HORSERADISH PEROXIDASES(I)

E.Furuta[1], K.Yamaguchi[2] and A.Shimozawa[1]
[1]Dept. of Anat. and [2]Lab. of Med. Sci. Dokkyo Univ. Sch. of Med.,Tochigi

Three morphologically and functionally distinct hemolymph cells, Type I,II and III, were present in collected hemolymph from land slug, Incilaria spp.,In additon, vast numbers of PLS can be seen in most of the light and electron micrographs. In order to know the origin of PLS, four different biotinyl lectins and avidin-horseradish peroxidases were used. Type I cell (phagocyte) and PLS were preferentially stained with wheat germ agglutinin, Ricimus communis agglutinin and Ulex europeus agglutinin in vitro. However, they were negative for Concanavalin A staining and Type II cells were not positively stained with each lectin. Moreover, when hemolymph cells were cultured with SH7 medium, Type I cells gradually split into several PLS during 3rd or 4th day incubation. And in vivo, PLS are not normally present in hemolymph but they may be formed rapidly in response to trauma. Because, after injection of a high concentration of carbon or latex beads into the hemocoel of land slug, great numbers of PLS are present. These results suggest that PLS are derived from Type I cell and retained same recognizing ability of Type I cell, so they can clamp foreign materials.

IM 6

STUDIES ON THE PLATELET-LIKE STRUCTURES IN HEMOLYMPH FROM LAND SLUG, INCILARIA SP. USING BIOTINYL LECTINS AND AVIDIN-HRPO(II).

K. Yamaguchi[1], E. Furuta[2] and A. Shimozawa[2].
[1]Lab. of Med. Sci. and [2]Dept. of Anat., Dokkyo Univ. Sch. of Med., Tochigi.

We reported previously that the cells of 3 morphologically distinct types were present commonly in the hemolymph of land slug, Incilaria fruhstorferi and bilineata; Type I cell was macrophage-like, Type II cell was lymphocyte-like and Type III was fibroblast-like. Besides these 3 type-cells, numerous platelet-like structures(PLS) were usually observed in collected hemolymph.

In order to define the origin of PLS, biotinyl lectin-avidin horseradish peroxidase method was used. In light microscopical examination, Type I cell and also PLS were stained positively with WGA, UEA and RCA. However, in electron microscopic observation, only PLS was weakly stained with WGA, but Type I cell was not stained with any lectin. These results suggest that the condition of fixation may not be suitable for the hemolymph cells in the present experiment. Since the hemolymph was prefixed with very low concentration of glutaraldehyde(0.08%) for long time(20hrs) at room temperature as the same method in our previous experiments, the hemolymph cells might not be fixed enough before DAB treatment was done. Another reason may be considerable that the concentration of biotinyl lectins(20µg/ml) is lower than the sufficient one.

IM 7

MELANO-MACROPHAGE CENTER LIKE STRUCTURES IN THE HEART OF THE MEDAKA, ORYZIAS LATIPES.

H.Nakamura[1], A.Shimozawa[1] and S.Kikuchi[2]. [1]Dept. of Anat., Dokkyo Univ. Sch. of Med., Shimotsuga-gun and [2]Kominato Marine Biol. Lab., Fac. of Sci., Chiba Univ., Chiba.

It is known that the endocardial lining cells (ECCs) in the heart of some teleosts take up foreign particles such as carbon and yeasts. In the medaka, Oryzias latipes, not only ECCs but also the cells in the subendocardial spaces showed phagocytosis and the ingested carbon particles persisted in these cells for over 2 years. Most of the subendocardial cells (SECs) contained yellowish-brown pigments and often accumulated to form nodules resembling in appearance that of melano-macrophage centers(MMC) observed within the spleen and kidney. By light microscopy, SECs stained positive by PAS and Schmorl reactions suggesting that they contained lipofuscin and ceroid series. Perl's reaction was slightly positive (but not constantly). By electron microscopy, macrophages containing large heterogeneous inclusions together with some lymphocytes were observed. No sheath-like structures were found around them.

Such MMC-like structures were also found in the atrium of the black molly, Poecilia sphenops, but not in the flounder, Paralichthys olivaceus.

The possible homology between these structures and the MMCs in the hemopoietic organs has still to be resolved.

IM 8

INTERNAL DEFENSE FACTORS IN THE APPLE SNAIL, POMACEA CANALICULATA.

A.Shozawa, C.Suto & N.Kumada. Dep. of Med. Zool.,Nagoya Univ. Sch. of Med., Nagoya.

Several workers have recently reported the production of active oxygen species by molluscan hemocytes. They suggested possibilities of cell-mediated cytotoxicity by the hemocytes as observed in vertebrate leucocytes. Hemocytes of the fresh water snail, P. canaliculata, show active phagocytosis, a major role of the host defense. We tried to detect active oxygen species produced by the snail hemocytes. Hemagglutination activity of the hemolymph was also examined.

Active oxygen species were detected by cytochemical methods using nitroblue tetrazolium (NBT) or diaminobenzidine (DAB). The hemocytes showed NBT-reduction and DAB-reaction. Those responses were inhibited by superoxide dismutase or sodium azide, respectively. The cells stimulated with phorbol myristate acetate or zymosan showed significantly higher responses than resting cells. This suggests that the snail hemocytes produce active oxygen species during phagocytosis or upon stimulation by membrane-activators.

Hemolymph samples were tested for hemagglutination against rabbit, chicken and sheep erythrocytes. Only rabbit cells were agglutinated and the titers were 8-32. This reaction was inhibited by EDTA.

BI 1

AMINO ACID SEQUENCE OF STARFISH OOCYTE DEPACTIN.

T. Takagi[1], K. Konishi[1], I. Mabuchi[2,3] and H. Hosoya[3]. [1]Biol. Inst., Fac. Sci., Tohoku Univ., Sendai, [2]Dept. Biol. College of Arts and Sci., Univ. Tokyo, Tokyo, [3]Natl. Inst. for Basic Biol., Okazaki.

Amino acid sequence of starfish (Asterias amurensis) oocyte depactin was determined. It is composed of 150 amino acid residues and the N-terminus is free proline. The molecular weight is calculated to be 17,590, in good agreement with the value estimated by SDS-PAGE. Prediction of the secondary structure shows that depactin contains 64 % alpha helix. Comparison of depactin sequence with those of other proteins shows no significant homology. The amino acid sequence of starfish oocyte depactin is shown in Fig. 1.

```
1         10        20        30        40
PQSGTALDENVKEEIRAFKMDQSKVKVPWMLLEIVQNDDR
          50        60        70        80
IDVVKVTKKAGPSDNLETLREELKQREVVYFVLDYEPSEE
          90        100       110       120
KRAKHNIPKGKTYPLTCFWSMETANIKLKMKYSSTVGTLK
          130       140       150
SATSTLKTYLEAHDFDDLSEEAIGDKIKNF
```

Fig. 1. Amino acid sequence of starfish oocyte depactin.

BI 2

EFFECTS OF PHOSPHATIDYL INOSITOL 4,5-DIPHOSPHATE (PIP_2) ON F-ACTIN-SEVERING ACTIVITY OF 45K PROTEIN FROM SEA URCHIN EGGS

M.Ohnuma and I.Mabuchi. Dept. of Biol., Coll. of Arts & Sci., Univ. of Tokyo, Tokyo.

It has been reported that PIP_2 affects actin-modulating activities of two actin-modulating proteins, profilin and gelsolin. 45K protein is a Ca^{2+}-dependent F-actin-severing protein obtained from sea urchin eggs. We investigated effects of PIP_2 on the actin-severing activity of 45K protein by measuring high-shear viscosity and the rate of actin depolymerization induced by dilution. F-actin solution was diluted with a solution that contained 45K protein in the presence of Ca^{2+}. F-actin depolymerized rapidly. This was considered to be due to the severing activity of 45K protein. However when 45K protein was preincubated with PIP_2 before dilution, it did not seem to sever F-actin even in the presence of Ca^{2+}. Thus, it was considered that PIP_2 blocked the severing activity of 45K protein. On the other hand, other related materials, PIP, PI, IP_3 and PS, did not affect the severing activity of 45K protein. 45K protein forms 1 to 1 complex with actin in the presence of Ca^{2+} and this complex (45K-A) caps the barbed end of F-actin. 45K-A reduced the depolymerization rate induced by dilution. Preincubation of 45K-A with PIP_2 before dilution did not affect the depolymerization rate. Therefore, PIP_2 may not influence the capping activity of 45K-A.

BI 3

2D-PAGE ANALYSES OF C-PROTEIN ISOFORMS EXPRESSED IN DEVELOPING, DENERVATED AND DYSTROPHIC CHICKEN PECTORALIS MUSCLES

T. Kojima, K. Sano, and T. Obinata. Dept. of Biol., Fac. of Sci., Chiba Univ., Chiba

C-Proteins in chicken slow, fast, and cardiac muscles have been distinguished by immunochemical methods, and developmental changes in the expression of C-protein isoforms have been pointed out (Reinach et al., 1982; Obinata et al., 1984). In this investigation, we established a method to characterize C-protein variants on 2D-gel by a combination of the electrophoretic system which were deviced by Hirabayshi (1981) and immunoblotting. We were able to distinguish four C-protein isoforms in chicken striated muscles, based on the difference in size and pI, namely, a fast-type (FC), a cardiac-type (CC), and two slow-type (SC-1 & SC-2) C-proteins. At neonatal ages, both pectoralis (PM) and posterior latissimus dorsi (PLD) muscles expressed FC and SC-1. During postnatal development, expression of SC-1 was down-regulated in PM, while in PLD, SC-1 was replaced by SC-2. Therefore, adult PM contained solely FC, and adult PLD did FC as well as SC-2. Interestingly, however, when the muscles were suffered with muscular dystrophy or denervated, expression of both SC-1 and SC-2 was induced in PM, whereas SC-1 was re-expressed in PLD. As a result, PM and PLD became almost the same with regard to the expression of C-protein isoform.

BI 4

DIFFERENCE BETWEEN MAMMALIAN AND CHICKEN MUSCULAR DYSTROPHY AS REVEALED BY TROPONIN T ISOFORM EXPRESSION.

K. Takeuchi*, S. Ohshima*, T. Totsuka+, T. Shimizu# and T. Obinata*. *Dept. of Biol., Fac. of Sci., Chiba Univ., Chiba, +Inst. of Develop. Res., Aichi Pref. Colony, Aichi, and #Dept. of Neurol., Fac. of Med., Univ. of Tokyo, Tokyo.

We have shown that progression of chicken muscular dystrophy is accompanied with change in troponin T (TNT) isoform expression (Zool Sci, 3, 1066, 1986). The present work was carried out to clarify whether the TNT isoform-change occurs also in mammalian muscular dystrophy. Variations of TNT was detected by 2D-PAGE in combination with immunoblotting. We observed that TNT changes during postnatal development of normal mouse skeletal muscle; at neonatal ages, several spots of TNT were detected, which focused in a acidic pH region, while mature muscle gave more spots which differed in both MW and pI. Progression of muscular dystrophy in two strains of mice, namely dy and mdx, did not cause change in TNT isoform, even 3 months after birth when the symptom of dystrophy was obvious. Several types of human muscular dystrophy were also examined, but the difference in TNT isoform was scarcely detected between normal and dystrophic muscles. These results indicate that the change in TNT isoform can be a marker of the muscular dystrophy of chicken but not of mammals.

BI 5

ANALYSIS OF PHOSPHORYLATED GIZZARD MYOSIN WITH PTOTEIN KINASE C BY NATIVE PPi PAGE.

H.Takano-Ohmuro, T.Kaminuma and K.Kohama* Tokyo Met. Inst. Med. Sci., Bunkyo-ku, Tokyo and *Dept. of Pharmacol., Fac. of Med., Univ. of Tokyo, Tokyo

We previously reported that of the gizzard smooth muscle myosin (GM, un-phosphorylated form) phosphorylated at its regulatory myosin light chian (20,000 Mr, L_{20}) with myosin light chain kinase (MLCK) produces faster moving bands (GMP 1:heterodimer myosin with 1 unphosphorylated L_{20} and 1 mono-phosphorylated L_{20}, GMP2: homodimer myosin with 2 mono-phosphorylated L_{20}s) on navive pyrophosphate polyacrylamide gel electrophoresis (PPi PAGE) [J.Biochem. 100, 259-268 & 1681-1684]. However, when the GM was phosphorylated with protein kinase C (PKC) at its L_{20}, only one band which comigrated with GM was observed on PPi PAGE. In addition, GM sequentially phosphorylated with PKC and MLCK or with MLCK and PKC gave only one band which comigrated with GM on PPi PAGE.

We conclude that the mobility increase shown by GM phosphorylated with MLCK on PPi PAGE is not attributable to an increase in the negative charge of L_{20} due to phosphorylation. This conclusion is also supported by the result that phosphorylated skeletal or cardiac myosin with MLCK did not show mobility increase on PPi PAGE (J.Biochem. 100, 259-268).

BI 6

CHANGES OF TROPOMYOSIN ISOFORMS DURING EMBRYONIC DEVELOPMENT OF THE SEA URCHIN, *HEMICENTROTUS PULCHERRIMUS*.

T.Ishimoda-Takagi, S.Koui, T.Maruyama and Y.Fukushima. Dept. of Biol., Tokyo Gakugei Univ., Tokyo.

Multiple isoforms of tropomyosin (TM) are present in sea urchin eggs. We examined changes of TM isoforms during embryonic development of the sea urchin, *Hemicentrotus pulcherrimus*. TM included in the crude egg and embryo extracts were co-precipitated with exogenous F-actin by ultracentrifugation. Egg and embryonic TM isoforms were analyzed by two-dimensional urea-shift gel electrophoresis. Three isoforms of TM were detected in the egg extract. These three TM isoforms were also detected until mesenchyme blastula stage. However, in gastrula extract TM isoforms decreased drastically, and two other components bound to actin instead. Although a third of specimens from prism to early pluteus larvae revealed the gastrula-type pattern, three TM isoforms were restored in the rest of specimens from these stage larvae. The extracts from late pluteus larvae retained three TM isoforms. The two components observed in the gastrula extract were not likely to be degraded products of TM isoforms or stage-specific TM isoforms. We could obtain three TM isoforms from gastrula embryos as well as unfertilized eggs. These results might suggest that the stage-specific actin-binding proteins which competed with the binding of TM isoforms with actin appeared in gastrula stage embryos.

BI 7

LOCALIZATION OF 400 kDa FRAGMENT OF CONNECTIN FILAMENT IN MYOFIBRILS OF CHICKEN BREAST MUSCLE.

Y. Itoh, T. Suzuki, K. Ohashi and K. Maruyama. Dept. Biol., Fac. Sci., Chiba Univ., Chiba.

Connectin is an elastic filamentous protein of MW of three million. It links myosin filaments to Z lines in myofibrils. By proteolytic action, 400 kDa fragments are easily formed and can be isolated by gel filtration. We have prepared polyclonal antibodies against the 400 kDa peptides. There are two kinds of monoclonal antibodies reactive with this fragment (SM1 and 3B9).

With an indirect immunofluorescence technique, fluorescent bands in A-I junction region moved toward Z lines, when myofibrils were stretched from 2.5 to 3.5 μm sarcomere length. SM1 label also moved, but 3B9 one did not. Immunoelectron microscopic investigations are under way.

The present work clearly shows that the 400 kDa fragment exists in the connectin filament between the end of myosin filament and A-I junction region. The latter portion is elastic.

BI 8

PURIFICATION AND CHARACTERIZATION OF 45kDa ACTIN BINDING PROTEIN FROM BOVINE AORTA SMOOTH MUSCLE.

M. Oosawa, S. Shimaoka and K. Maruyama. Dept. Biol., Fac. Sci., Chiba Univ., Chiba.

During the purification of 84kDa gelsolin from bovine aorta smooth muscle by the procedure of Ebisawa et al. (Biomed. Res., 6:161-173,1985), a 45 kDa protein was isolated by hydroxyapatite, DEAE cellulose, and gelfiltration chromatography.

The 45 kDa protein markedly slowed down the polymerization process of actin and elongation step of actin nuclei only in the presence of Ca ions.

Peptide mapping clearly showed that it is different from actin. However, the amino acid composition was very similar to that of gelsolin. Gelsolin was easily split into 45 and 47kDa fragments (CT 45; CT 47) by the action of chymotrypsin. The present 45kDa protein had two isoforms one of which was very similar to CT 47, though the chain weights were slightly different. The IP of the 45 kDa protein differed from that of CT 45 fragment of gelsolin.

A further work is in progress to clarify the relationship of the 45kDa protein with the gelsolin fragments.

BI 9

EFFECTS OF CHICKEN I-PROTEIN ON THE RECONSTITUTION OF MYOSIN FILAMENTS.

K.Ohashi, K.Ishikawa and K.Maruyama. Dept. of Biol., Fac. of Sci., Chiba Univ., Chiba.

I-protein is an myofibrillar protein that is localizing at the A-I junctional region of myofibrils and has inhibitory action on the actomyosin ATPase activity under low ionic conditions. Chicken myosin was assembled into filaments under various pH and concentration of KCl. When myosin assembly was carried out by dilution in the I-protein containing solutions, myosin filaments were constituted under higher pH and higher KCl concentration than when assembled without I-protein. For example, myosin filaments were constituted in the solution of 70 mM KCl and 10 mM potassium phosphate buffer, pH 6.5 when equimolar I-protein was added, while not without I-protein. In the solution of 20 mM KCl and 10 mM potassium phosphate buffer, pH 6.5, almost all I-protein could bind to myosin filaments when the molar ratio of added I-protein to myosin was lower than 5% and unbound I-protein coexisted when I-protein was added more than 5%. Approximately equimolar I-protein could bind to myosin filaments when excess of I-protein was added. In this case, myosin filaments were aggregated into higher density clusters than the control experiment without I-protein. Electron microscopic observation revealed that I-protein assembled myosin filaments side by side and end to end into large bundles and sheets.

BI 10

PHOSPHORYLATION OF DROSOPHILA MYOSIN LIGHT CHAINS AND ITS EFFECTS ON ATPase ACTIVITY.

S. Takahashi[1], H. Takano-Ohmuro[2] and K. Maruyama[1]. [1]Dept. Biol., Fac. Sci., Chiba Univ., Chiba, and [2]Tokyo Metropol. Inst. Med. Sci.,Bunkyo, Tokyo.

Takano-Ohmuro et al. (J. Biochem.,94: 967-974,1983) reported that Drosophila myosins have different light chain isoforms in fibrillar(f) and tubular(t) muscles: Lf1(34kDa), Lf2, Lf2'(30), Lf3(20) and Lt1(31), Lt2, Lt2', Lt3(20).

The present P32-ATP incorporation experiments showed that Lf1, Lt1, Lf2'and Lt2' were phosphorylated. Dephosphorylations of these light chains by the treatment of myosin with two kinds of phophatases resulted in the shifts of Lf1, Lt1, Lf2' and Lt2' spots to Lf2,L2t spots.

We have been able to isolate myosins light chains of which were either completely phosphorylated or dephosphorylated from adult Drosophila flies by modifying preparation procedures. The Ca-activated and Mg-activated ATPase activities of phosphorylated myosin was markedly higher than those of dephosphorylated ones. The present results suggest that Drosophila myosin ATPase activity is regulated by phosphorylation of light chains.

BI 11

CONNECTIN LOCALIZATION AND PASSIVE TENSION GENERATION IN MYOSIN-EXTRACTED MYOFIBRILS OF SKINNED FIBERS OF FROG SKELETAL MUSCLE.

T. Suzuki[1], H. Higuchi[2], S. Kimura[1] and K. Maruyama[1]. [1]Dept. Biol., Fac. Sci., Chiba Univ. and [2]Dept. Physiol., Jikei Univ. Med. Sch.,Tokyo 105.

When myosin was partially extracted with 0.35 M KCl leaving the center region of A band in frog skinned fibers, connectin filaments remained between unextracted myosin filaments and Z lines. Immuno electron microscopic studies revealed that three stripes in the regions from 0.65 to 0.8 um from the center of A band remained as in intact myofibrils. Resting tension development decreased only a little.

On the other hand, when skinned fibers were treated with 0.6 M KCl, all the myosin molecules were dissolved away leaving the I band intact. Connectin stripes disappeared completely. Instead, there were deposits of antibodies around the region 0.3 um apart from the Z lines. It appears that connectin filaments freed from the M band region were pulled back toward Z lines. The resting tension generation dropped completely by this 0.6 M KCl treatment.

Thus the present observations strongly support the view that connectin filaments linking myosin filaments to Z lines are responsible for passive tension generation.

BI 12

MAGNESIUM POLYMERS OF ACTIN FORMED UNDER THE INFLUENCE OF β-ACTININ AND GELSOLIN.

S. Shimaoka, M. Oosawa and K. Maruyama, Dept. Biol., Fac. Sci., Chiba Univ., Chiba.

It is known that Mg polymer is formed when actin is polymerized by Mg ions in the presence of β-actinin or fragmin. The Mg polymer shows low viscosity and amorphous aggregates under an electron microscope. This is due to formation of fragile actin filaments of short length.

In the present study, the effect of gelsolin was tested if Mg polymer is formed. Viscosity and flow birefringence measurements suggested its formation, but these were due to short actin filament formation under electron microscope. β-actinin was effective to produce Mg polymers under the same conditions.

It was observed that, when phalloidin had been added to actin monomers, Mg polymer was not formed in the presence of β-actinin. Short actin filaments were formed. When phalloidin was added to preformed Mg polymer, partial changes into short actin filaments took place.

In the presence of β-actinin short and fragile actin filaments are formed and they were deteriorated by uranyl acetate used for negative staining. Phalloidin may stabilize the fragile actin filaments. It is of interest that gelsolin did not result in such weak structure of actin filaments.

BI 13

THE ISOMERASE ACTIVITY OF SEPIAPTERIN REDUCTASE

S. Katoh and T. Sueoka. Department of Biochemistry, Josai Dental University, Sakado, Saitama 350-02

Sepiapterin reductase is known as an NADPH-oxidoreductase required for catalyzing the last two step of the biosynthetic pathway of tetrahydrobiopterin (BH_4), an essential cofactor for the formation of biological monoamines, from GTP. In the presence of NADPH, sepiapterin reductase can reduce two monoketo tetrahydropterin (PH_4) intermediates of BH_4 such as C1'-keto PH_4 (6-lactoyl PH_4) and C2'-keto PH_4 (6-1'-hydroxy-2'-oxopropyl PH_4) to form BH_4. On the other hand, we have found now that the large amount of this enzyme convert C1'-keto PH_4 into a novel PH_4 other than BH_4 in the absence of NADPH by HPLC-analysis of PH_4 using amperometric detector. The retention time of the novel PH_4 on HPLC column was similar to that of C2'-keto PH_4. The novel PH_4 converted into 6(R)-L-erythro-BH_4 by the enzyme with NADPH and the oxide of this product by I_2 in acid was L-erythro biopterin in HPLC analysis using authentic isomers of four 6(R)-BH_4 and four biopterins as control. The novel PH_4 has the keto group since it formed hydrazone. By these results and the recent analysis on ^{1}H-NMR, the structure of the novel PH_4 was identified as 6(R)-L-erythro-1'-hydroxy-2'-oxopropyl tetrahydropterin (C2'-keto PH_4). Thus sepiapterin reductase has 6-lactoyl tetrahydropterin isomerase activity besides the activity of an NADPH-oxidoreductase.

BI 14

REACTION PROCEDURE IN THE FORMATION OF TETRAHYDROBIOPTERIN FROM DIKETO TETRAHYDROPTERIN INTERMEDIATE

T.Sueoka[1], S.Katoh[1], M.Masada[2] and M.Akino[3]. [1]Dept.of Biochem.,Josai Dental Univ.,Sakado, [2]Dept.of Biol., Tokyo Metropolitan Univ., Tokyo, [3]Dept.of Industrial Chem., Kokugakuin Univ.,Tokyo.

In the biosynthetic pathway of tetrahydrobiopterin(BH_4) from GTP, two monoketo tetrahydropterin(PH_4), C1'-keto PH_4 and C2'-keto PH_4 were found as the intermediate between pyruvoyl PH_4 (dyspropterin) and BH_4. We have analyzed the reaction procedure in the reduction of pyruvoyl PH_4 to BH_4 by the function of sepiapterin reductase in vitro. Pyruvoyl PH_4 was synthesized from dihydroneopterin P_3 by the incubation with $MgCl_2$, and pyruvoyl PH_4 synthase purified from fat bodies of the silkworm. Pyruvoyl PH_4 sample, which was prepared from its synthesizing reaction mixture after deproteinization through Millipore filter, was added with homogeneous sepiapterin reductase prepared from rat erythrocytes in the presence of NADPH at 37 ℃ in Tris-HCl buffer(pH 7.4 and 8.6). Time-dependent variation of the PH_4 components in the reaction system was measured by HPLC-electrochemical analysis. And C2'-keto PH_4 was certainely recognized as the intermediate between pyruvoyl PH_4 and BH_4 from the observation of the pattern of a typical successive reaction. However, C2'-keto PH_4 also appeared in addition of the final product BH_4 when C1'-keto PH_4 was incubated with this enzyme and NADPH . It might be undeniable that, besides C2'-keto PH_4, C1'-keto PH_4 is also the intermediate of this reaction.

BI 15

THE RELATIONSHIP BETWEEN PAPILIOCHROME AND THE TYPE A RED PIGMENT.

T. Okabe, K. Morimoto and Y, Umebachi. Dept. of Biol., Fac. of Sci., Kanazawa Univ., Kanazawa.

Papiliochromes are the wing-pigments of Papilio butterflies. There are three kinds of Papiliochrome, II (pale yellow), M (deep yellow), and R (reddish brown). These pigments are all related to kynurenine, dopamine, and β-alanine. The II and M are formed from kynurenine and N-β-alanyldopamine. On the other hand, the type A red pigment of Pachliopta aristolochiae contains β-alanine but is not related to kynurenine. The pigment shows a remarkable color change with pH, that is, red in alkaline and yellow in acid. The color change occurs at about pH 3. This suggests that the pigment is a kind of quinone. On acid hydrolysis (1 N HCl, 100°C, 1 - 5 hr) the pigment releases β-alanine and indole compounds. But the possibility also exists that the indole compounds may be secondary products during acid hydrolysis. But there is almost no doubt that the pigment is a β-alanine-containing quinone pigment. The possibility has been suggested that the type A red pigment is formed from N-β-alanyldopamine or N-β-alanylnorepinephrine. When N-β-alanyldopamine is incubated with tyrosinase, an orange pigment is formed. The pigment also shows the color change with pH and releases β-alanine on acid hydrolysis.

BI 16

SYNTHESIS OF PAPILIOCHROME II BY PHENOLOXIDASE FROM A PRAYING MANTID.

M.Yago, H.Sato and H.Kawasaki. Dept. of Biochem., School of Dentistry, Iwate Medical Coll., Morioka.

Papiliochrome II(P-II), a yellow pigment of the wings of Papilio butterflies, was found and has been studied in detail by Y.Umebachi and his coworkers. According to their results, the pigment is composed of kynurenine(Kyn) and N-ß-alanyldopamine (NBAD), and decomposes into Kyn and N-ß-alanylarterenol(NBANA). It seems that in Papilio xuthus, free Kyn and free NBAD enter the wings from haemolymph and combine there. It is unclear which enzymes are involved in the combining process. The results of the present experiment indicated that phenoloxidase from a praying mantid catalyzed the synthesis of P-II from L-Kyn and NBAD. The enzyme from the left colleterial gland of Tenodera aridifolia sinensis Saussure is involved in oothecal sclerotization and hydroxylates the sidechain of N-acyldopamines. When L-Kyn and NBAD were incubated with the enzyme in 0.2M phosphate buffer(pH 5.0) for 24hrs at 28°C, yellow pigment was formed. After being purified, it was subjected to various analyses. Its uv absorption spectra and its chromotographical results were the same as that of P-II. On heating in 1mM HCl at 100°C for 30min, Kyn and NBANA were identified as hydrolysis products. Thus the yellow pigment was found to be P-II.

BI 17

ACTIVATION OF LACCASE-TYPE PROPHENOLOXIDASE IN THE CUTICLE OF INSECT. IV. PROPERTIES OF THE ACTIVATOR

H.I.Yamazaki. Biol.,Lab., Atomi Gakuen Women's Univ., Saitama

The phenoloxidase activating system in insect cuticle is supposed to play a central role of the hardening and darkening process in the course of larval-pupal ecdysis. In this system, the laccase-type of phenoloxidase seems to be a key enzyme. The previous observations suggested that laccase in the cuticle might be formed from the pro-form by an activator with proteolytic activity.

The changes of the laccase in the cuticle were analysed by SDS-PAGE during larval-pupal ecdysis. After electrophoresis, laccase including the pro-form was located by immunoblotting method using anti-laccase antiserum. Three immuno-reactive bands were released from the cuticle by SDS treatment at 2 hours after ecdysis, but no bands were detectable after 24 hours.

As a preliminary attempt to elucidate the activation mechanism, the activator for pro-laccase was partially purified by ammonium sulfate precipitation and gel filtration from early pupal cuticles. The suitable temperature for activation was 0°C and the pH was 6-7. Under the conditions, the partial purified activator, which contained proteinase activity, could activate pro-laccase to the active form.

BI 18

A FEW ADDITIONAL PIECES OF INFORMATION ON THE β-ALANINE IN INSECT CUTICLE.

Y. Umebachi, Y. Tagi and M. Sakai. Dept. of Biol., Fac. of Sci., Kanazawa Univ., Kanazawa.

Umebachi (1979, 1984) reported in lepidopteran scales and dipteran exuviae that the β-alanine content and the amount of the ketocatechol released on acid hydrolysis are inversely related to each other. After that, an attempt to investigate the subject using the protein fraction solubilyzed from exuviae has been made. As the material, the mutant strains yellow, black and ebony of Drosophila melanogaster were used. The 4 % HCl-methanol extract of the exuviae were hydrolyzed in acid, and the β-alanine and ketocatechol were determined, The above-mentioned relationship between β-alanine and ketocatechol has proved to hold true here also. This shows that the HCl-methanol extract can be useful for the investigation of the cross-linking in cuticle. After the extraction with HCl-methanol, the residue was further extracted with 1 N NaOH at 25°C. The extract was suitable for the investigation of β-alanine but not for the study of ketocatechol. After the extraction with NaOH, the final residue also contained β-alanine, which was small in quantity but high in molar ratio. The final residue may be useful in studying the nature of the bonding between protein and chitin.

BI 19

STRUCTURES AND ORGANIZATION OF GENES FOR THE MAJOR PLASMA PROTEINS OF Bombyx mori

S.Mori, S.Izumi and S.Tomino
Dept. Biol. Tokyo Metropol. Univ., Tokyo

Genomic sequences for the major plasma proteins (30K proteins) of B. mori were cloned and their structures were analyzed. An EMBL 3 library was constructed from the Mbo I partial digests of larval fat body DNA and was screened for the 30K protein-mRNA sequence with 30K-C6 cDNA probe. Among seven clones isolated, three clones carried tandem array of 30K protein genes 7 Kb apart on a genomic DNA segment, implying that these genes constitute a family. Sequence analysis provided evidence that one of these clones, termed 30K-E1 bears two 30K protein genes, 6G1 and 21G1 corresponding to 30K-C6 and 30K-C21 cDNAS, respectively, in an opposite orientation. mRNA sequencing demonstrated occurence in 6G1 gene of an intron with approximately 800 bases in length in the upstream region adjacent to the protein-coding sequence. Initiation site of the 6G1 gene transcription was determined at nucleotide level. The 5' flanking segment of the transcription initiation site contained sequences highly homologous to the regulattory elements predicted for the eukaryotic class II genes, including TATA-box, CAT-box, enhancer elements and ecdysteroid-receptor binding site.

BI 20

HYDROCARBONS OF PHILOSAMIA SILKWORM LIPOPHORIN

C. Katagiri and H. Kihara.
Biochem. Lab., Inst. of Low Temp. Sci., Hokkaido Univ., Sapporo.

Hydrocarbons are important constituents of insect cuticle and are known to provide a water-proofing layer to protect the insect from desication. Considerable amounts of hydrocarbons have been reported to be present in a circulating lipoprotein, lipophorin, of cockroach and locust in addition to diacylglycerol and cholesterol. Lipophorin is known to transport hydrocarbons from the site of synthesis to the site of deposition, e.g., cuticle. Lipophorin of Philosamia silkworm diapausing pupae, on the other hand, contains only a trace of hydrocarbons. The present study demonstrates that silkworm lipophorin also transport hydrocarbons and that, after pupal ecdysis, it contains appreciable amounts of hydrocarbons (15% of total lipid). The pupal lipophorin which contains hydrocarbons was subjected to physicochemical measurements. The data suggest that the silkworm lipohorin after pupal ecdysis is composed of centrosymmetrical three layers which has been proposed as the possible structure of the cockroach and locust lipophorins; an outer shell with apolipophorin I and phospholipid, a middle layer with diacylglycerol and apolipophorin II, and a core with hydrocarbons.

BI 21

SOLUBLE TYPE OF VITELLIN BINDING PROTEIN IN OOCYTE FROM LOCUSTA MIGRATORIA.

K.Yamasaki. Dept.Biol.Tokyo Metropol.Univ. Tokyo.

Vitellin binding protein(VBP) is involved in the uptake mechanism of vitellogenin into oocyte. VBP locallizes mainly on the surface area of oocyte during vitellogenesis and is found in membrane fraction. The VBP is insoluble in aqueous solution. On the other hand,soluble type of VBP exists in the soluble fraction from oocyte homogenate. One of the functions of the soluble VBP is supposed as a responsible element in condensation apparatus of vitellin.

Soluble VBP was precipitated by $(NH_4)_2SO_4$ from soluble fraction of oocyte homogenate. The VBP was soluble in aqueous solution and the binding activity was immobilized by cellulose acetate. The VB activity was estimated by electro-washing method on cellulose acetate membrane. The VBP fraction was treated with 1% sodium dodecyl sulfate(SDS) and VBP was precipitated by the addition of cold acetone. After removal of residual SDS, VBP was found in the precipitate. The precipitate was reextracted with octyl-β-glucoside. VB activity was found in the precipitate and was specific for vitellin. In the extract,microvitellin binding activity was detected and could not find binding activity for vitellin.

BI 22

DEVELOPMENTAL CHANGES IN PROPERTIES OF LIPOPHORIN OF THE SILKWORM, BOMBYX MORI.

K. Miura and I. Shimizu. Research Section of Environmental Biology, Laboratory for Plant Ecological Studies, Faculty of Science, Kyoto University, Kyoto.

Lipophorins were isolated from the hemolymph of the males of the silkworm by KBr density gradient ultracentrifugation. The larve and pupae of an early stage had a single lipophorin of a density 1.12g/ml, which contained two apoproteins. On the other hand adult moths had a low density lipophorin (d=1.06) in addition to the high density type (d=1.12). Total fatty acid content of adult low density lipophorin was more than twice those of larval, pupal and adult high density lipophorin. Adult low density lipophorin contained a large amount of the third apoprotein, apolipophorin-III (apo-III) in addition to the two apoproteins. Apo-III was also detected in larval and pupal hemolymph and lipophorin-free subnatant fraction obtained by the centrifugation using immunoblotting. It was demonstrated that apo-III content in hemolymph increased suddenly on the day before eclosion and that an apo-III-rich low density lipophorin was already constructed in the pharate moths.

BI 23

LIPID TRANSFER PROTEIN FROM LOCUST, LOCUSTA MIGRATORIA

Y.Hirayama, H.Chino. Biochem.Lab.,Inst. of Low Temper.Science, Hokkaido Uiv.,Sapporo.

A new protein was found in the hemolymph of the locust, *Locusta migratoria*, which serves to transfer lipid between resting lipophorin and adipokinetic hormone (AKH) activated lipophorin; therefore named lipid transfer protein (LTP).

To isolate this LTP, a low ionic precipitation , DEAE-sepharose CL-6B column chromatography and density gradient ultracentrifugation were employed. After these steps, an electrophoretically pure protein was obtained. The purified LTP displayed a density of about 1.21 g/ml; thus, LTP may be a lipoprotein. Sodium dodecyl sulfate polyacrylamide gel electrophoresis revealed that this protein is comprised of three apoproteins, apo-LTP-I (MW 310,000), apo-LTP-II (MW 89,000), and apo-LTP-III (MW 78,000).

Lipid transfer protein may play a role in equilibrating the density of lipophorin by transferring lipids, mostly diacylglycerol, between lipophorin molecules. The ability of LTP to transfer diacylglycerol between AKH-activated lipophorin and resting lipophorin suggests that LTP may also facilitate diacylglycerol mobilization from fat body to flight muscle during flight.

BI 24

IN VITRO STUDY OF THE ADIPOKINETIC HORMONE ACTION ON LIPOPHORIN IN LOCUSTS.

H. Chino, Y. Kiyomoto and T. Hiraoka. Inst. of Low Temperature Sci., Hokkaido Uni., Sapporo.

Experiments were performed to demonstrate *in vitro* the action of adipokinetic hormone (AKH) on lipophorin in locusts. The hemolymph was first collected from male adult locusts by injecting EDTA-Ringer(flush method) and dialysed against insect Ringer to remove EDTA. The dialysed hemolymph was then incubated with fat body in the presence of AKH. After incubation, the medium was subjected to density gradient centrifugation for futher analyses. We made the following observations after incubation: 1) The density of lipophorin was shifted from 1.12g/ml to 1.06g/ml. 2) the content of diacylglycerol in lipophorin was elevated by several times. 3) Apolipophorin-III (apoIII) became bound with lipophorin. 4) The size of lipophorin became larger and heterogeneous. All these changes are very similar to those observed *in vivo* for lipophorin after injection of AKH. It was also demonstrated that the above changes require Ca^{2+} essentially. We further tested a reconstruction system in which purified lipophorin and apoIII were incubated with fat body in the presence of AKH. Similar but incomplete changes were observed; we failed to demonstrate clearly the dramatical shift of the density of lipophorin after incubation.

BI 25

PHOSPHORYLATION OF VITELLOGENIN (Vg) AND VITELLIN (Vn) FROM THE SILKWORM, BOMBYX MORI.

S.Y.Takahashi, Dept.of Biol.,Fac.of Liberal Arts, Yamaguchi Univ.,753 Yamaguchi.

In our previous paper, two types of cyclic nucleotide-dependent protein kinases, namely G- and A-Kinases, in silkworm eggs have been reported. The relative activities of them varied significantly during the course of development. In developing egg G-kinase activity was relatively high in the middle of embryonic development, and diminished just before hatching, indicating that the kinase played an important role during embryonic development. In order to know the biological significance of this kinase we have studied about endogenous substrate proteins of the kinase. The silkworm Vn and Egg specific protein (ESP) were effectively phosphorylated both by the highly purified G-kinase.

Two moles of phosphate were incorporated into vitellin. When the ovarian extract was incubated in the acetate buffer,pH5.2,one of the major ovarian protein,ESP, was rapidly degraded, whereas Vn was not, indicating that Vn was resistant to proteolysis by theprotease in the ovary, which had been also characterized in our previous paper as a thiol proteinase. By contrast, if ovarian extract was incubated in the phosphorylation reaction mixture with either A-or G-kinase before incubation in the digestion mixture, Vn becameto be degraded. The degradation of vitellin appeared to be closely related to the phosphorylation.

From the results we suggested that the phosphorylation of Vn probably lead to the structural changes of the protein molecule and enhanced its susceptibility to digestion by endogenous protease.

BI 26

HEMOLYMPH AND EGG PROTEINS OF BEAN BUG. II. PROPERTIES OF INSECTICYANIN FROM EGG AND HEMOLYMPH.

Y. Chinzei[1] , T. Haruna[1] , H. Numata[2] and S. Nakayama[3] , [1] Dept. of Med. Zool., Mie Univ., [2] Dept. of Biol., Osaka City Univ., [3] Tezukayama Coll., Nara.

We purified a blue-protein, insecticyanin (INS egg) from eggs of the bean bug, *Riptortus clavatus*. Eggs were from 1 to 24 hours old and INS egg was purified by gel filtration and ion exchange chromatography. Molecular weight (MW) of INS egg was estimated 320,000 daltons by polyacrylamide gel electrophoresis (PAGE) and 335,000 by gel filtration chromatography. By SDS-PAGE analysis, INS egg showed only one band, MW of which was 76,000. This indicates INS egg is composed of four subunits. INS has absorbance peaks at 280, 370 and 620 nm of wave length which suggestes that INS egg is associated with biliverdin. INS egg does not contain lipid but does sugars; Gas-liquid chromatography analysis shows 13 % neutral sugar, mainly mannose. INS egg has high mole % (17 %) of aromatic amino acids, which suggests close similarity to arylphorin type storage proteins. Isoelectric point (pI) of INS egg is 7.85. One of the four INS in hemolymph (INS hem) has the same pI as INS egg, but the others are 7.60, 7.40 and 7.25. Almost all properties of INS hem are the same as INS egg except pI.

BI 27

HEMOLYMPH AND EGG PROTEINS OF BEAN BUG. III. IMMUNOLOGICAL PROPERTIES AND QUANTITATIVE CHANGES OF INSECTICYANIN.

H. Numata[1], Y. Chinzei[2] and T. Haruna[2]
[1]Dept. of Biol., Osaka City Univ., Osaka, [2]Dept. of Med. Zool., Mie Univ., Tsu.

We found four insecticyanins (INS 1-4) in the hemolymph of the bean bug, Riptortus clavatus by Western immunoblotting analysis with the antiserum against purified egg insecticyanin (INS egg). Hemolymph INS 1-4 were grouped into two types of rocket (A and B) by rocket immunoelectrophoresis using the same anti-INS egg serum. INS 1 -3 and INS egg was shown to be an A type rocket, but INS 4 was a B type. Quantitative changes of hemolymph INS were analysed by rocket immunoelectrophoresis during the diapause (D) and nondiapause (ND) development of females. In the nymphal stage, both INS A and B were observed at high levels but decreased toward adult emergence to undetected levels. In ND female adults, INS A increased again but INS B did not; in D female adults, INS B did and INS A did not. We also analysed quantitative changes of INS A and B of ND and D female and male whole body. INS A and B at high levels in nymphal stage decreased at adult emergence in all kind of insects (ND and D, or female and male). In ND female adults, INS A increased again, but not in males. In D females and males both INS A and B increased significantly and accumulated gradually during diapause development.

BI 28

CHARACTERIZATION OF DYSPROPTERIN SYNTHETASE FROM FAT BODIES OF SILKWORM LARVAE

M.Masada and M.Akino*
Dept.Biol., Tokyo Metrop.Univ., Tokyo *Dept. Ind.Chem., Kougakuin Univ., Tokyo

The properties of the purified dyspropterin synthetase that catalyzes the conversion of dihydroneopterin triphosphate to dyspropterin in the presence of Mg^{2+} were further studied. Effect of Mg^{2+} concentration on the activity showed a biphasic pattern. The K_m values of Mg^{2+} for the enzyme were calculated to be 2.0×10^{-3} and 2.1×10^{-4}M, respectively. The K_m values of dihydroneopterin triphosphate at 1 and 5 mM of Mg^{2+} were almost the same. Some divalent cations such as Ca^{2+}, Mn^{2+} and Ba^{2+} also stimulated the enzyme activity. However, when Ca^{2+} or Ba^{2+} was added to the reaction mixture containing a low concentration of Mg^{2+}(1 mM), the activity was greatly accelerated.

A rabbit was immunized with the homogeneous preparation of dyspropterin synthetase.When examined by Ouchterlony double immunodiffusion method the anti-serum preparation formed a single precipitation line with both the purified dyspropterin synthetase and crude preparation from fat bodies of silkworm larvae. The specificity of anti-serum for dyspropterin synthetase was confirmed by its ability to precipitate the dyspropterin synthetase activity.

BI 29

MIP, MICROTUBULE-ASSEMBLY INHIBITOR PROTEIN. IMMUNOLOGICAL AND PHYSICOCHEMICAL STUDIES.

S.Kotani, A.Ikai, S.Maekawa and H.Sakai.
Dept. of Biophys. and Biochem., Fac. of Sci., Univ. of Tokyo, Tokyo.

Microtubule-assembly inhibitor protein (MIP) is an acidic protein with an apparent molecular weight of 33,000 which inhibits microtubule assembly in vitro (Kotani, S., Murofushi, H., Nishida, E., and Sakai, H., J. Biochem. 96, 959-969). Anti-MIP antibody was affinity purified from rabbit anti-MIP antisera raized against chemically modified MIP. MIP localizes in cell nuclei in interphase cultured cells as revealed by immunofluorescent light microscopy. Immunoblotting shows that MIP exists in a variety of mammalian cells and tissues. Kidney appears to be a better source of TIP than brain, an original source of MIP. Kidney MIP, which is indistinguishable from brain MIP in several respects, is isolated by the same procedure as for brain TIP and physicochemically characterized. MIP contains 20% aspartic acid and 25% glutamic acid in consistent with its acidic nature. Hydrodynamically, MIP is a monomer with $S_{20,w}$ = 1.9 and M_r = 30,000. The frictional ratio, f/f_o =1.7, indicates that TIP is not a globular molecule but has either an elongated or an expanded structure. Spectrochemical analysis reveals that MIP has a largely unordered structure.

BI 30

ANALYSIS OF TUBULIN ISOTYPES IN CILIA AND FLAGELLA.

K.Nakamura, Y.Kubo, E.Masuyama and T.Kusano. Dept. of Living Sciences, Hiroshima Women's Univ. Uzina, Hiroshima.

Tubulin from diverse sources including cilia and flagella exists in its native form as a heterodimer of one α-tubulin and one β-tubulin. Moreover there has been much evidence from isoelectric focusing (IEF), immunological methods, and genetic analysis that each tubulin has several isotypes. Recent reports have suggested that the heterogeneity is correlated to the assembly and the various functions of microtubules. Thus, it is important to analyze the isotypes of tubulins of axonemes for understanding the roles of tubulins in cellular motility. In the present experiments, we have developed an method to analyze the isotypes of tubulin using IEF and SDS-PAGE. This technique has been applied to compare the isotypes of axonemal tubulin between gill cilia and sperm flagella of oyster, and the following results have been obtained.

(1) Both axonemes consist of identical seven isotypes, but the densitometric profiles of isotypes revealed slight difference between them.

(2) Immunoblotting after IEF have revealed the presence of at least three isotypes which react with an antibody against chicken brain tubulin.

BI 31

NUCLEOSIDE TRIPHOSPHATE SPECIFICITY OF CILIARY MOTILITY OF TETRAHYMENA

T. SHIMIZU[1], K. FURUSAWA[1], M. HATO[1], Y. TANAKA[1] AND M. OKUNO[2]. [1]Res. Inst. Polym. Text., Tsukuba, Ibaraki and [2]Dept. Biol., Coll. Arts & Sci., Univ. Tokyo, Tokyo.

The nucleoside triphosphate specificity of ciliary motility was investigated by using *Tetrahymena* models prepared by NP-40 (detergent) treatment after U. Goodenough (J. Cell Biol. **96** (1983) 1610). The enzymatic specificity of 22S dynein was also studied with respect to its apparent Km and Vmax for each nucleotide. Some of the nucleotides were synthesized chemically and/or enzymatically and their purity was checked by HPLC. Among 11 ATP analogues tested at 1 mM, only 2'-dATP, 3'-dATP and N-methyl-ATP induced ciliary reactivation but others, 8-Br-ATP, 8-azido-ATP, N,N-dimethyl-ATP, εATP, formycin-triphosphate (FTP), purine riboside triphosphate (PRTP), periodate-treated ATP (oATP), periodate- and $NaBH_4$-treated ATP (orATP), were ineffective. Those which induced the reactivation were good substrates for dynein with apparent Km's of 10 uM or less and with Vmax comparable to that of ATP itself. The apparent Km's for those unable to induce the reactivation were higher except FTP. The Vmax value for each nucleotide was lower that that for ATP except for FTP, oATP or 8-Br-ATP. The study indicates high specificity of dynein and ciliary motility toward intact adenine ring.

BI 32

ANT-ATP AS A SUBSTRATE OF DYNEIN ATPase AND FLAGELLAR MOTILITY

K.Inaba, M.Okuno, and H.Mohri. Department of Biology,College of Arts and Sciences, University of Tokyo,Komaba,Meguro-ku, Tokyo.

We synthesized Ant-ATP,which has fluorescent anthraniloyl moiety at OH group of ribose,to elucidate the mechanism of flagellar bend formation and its propagation in relation to mechanochemical cycle of dynein ATPase.This fluorescent analogue of ATP was efficiently hydrolized by 21S dynein from sea urchin sperm flagella,with Km=50μM which was half of that when ATP was used as a substrate.Vmax was the same with both ATP and Ant-ATP. Inhibition of the hydrolysis of Ant-ATP was a little weaker than that in the case of ATP,using vanadate.UV cleavage of 21S dynein heavy chains in the presence of Ant-ATP and vanadate was less efficient and the rate of the decrease of dynein heavy chains was 60% of that in the presence of ATP and vanadate.Ant-ATP also induced the motility of demembranated sperm.When ATP was used the apparent Michaelis constant for beat frequency(Kmf) was 0.22mM and the maximum frequency(fmax) was 36Hz,whereas Kmf was 0.14mM and fmax was 20Hz for Ant-ATP.ATP-induced sperm motility was inhibited in the presence of Ant-ATP uncompetitively.These results suggest that the life time of dynein-ADP-Pi complex is essential for flagellar motility.

BI 33

THE PROPERTIES OF INNER ARM ATPASE FROM SEA URCHIN SPERM FLAGELLA

S.WADA, M.OKUNO and H.MOHRI
Dept., Biol., Coll. Arts & Sci., Univ. Tokyo, Tokyo.

In order to clarify the role of inner arms on flagellar movement of sea urchin spermatozoa, an ATPase fraction probably originating from the inner arms was partially purified. We named it 12S, since the sedimentation coefficient of this fraction was 12S. The properties and functions of 12S were compared with those of 21S dynein (the outer arms).

The Michaelis Constants (Km) of 12S was about 4 times of that of 21S ATPase. This indicated that the kinetic characteristic of 12S on ATPase activity was different from that of 21S. And the A-band polypeptide of 12S was different from that of 21S based on the peptide mappings by V-8 protease.

As reported last year, 12S fraction has the ability of rebinding to the outer doublet microtubules of the axonemes, when it was observed the electron microscopy. That was confirmed not only by electron micrographs but also by SDS-PAGE and the measurement of ATPase activity. The low-salt-extracted axoneme which was incubated with 12S fraction and digested with trypsin, the axoneme regain the ability to slide out the microtubules. This indicate that 12S may be one of the element in the sliding systems of flagellar movement.

BI 34

IMMUNOLOGICAL ANALYSIS OF DYNEIN HEAVY CHAINS BETWEEN CILIARY AND FLAGELLAR OUTER-ROW ARMS.

E.Masuyama[1], H.Ishida[2], K.Nakamura[1], and Y.Shigenaka[2]. [1]Dep. of Living Sic., Hiroshima Women's Univ., [2]Fac. Integr. Arts & Sic., Hiroshima Univ., Hiroshima.

When *Tetrahymena* ciliary 22S dynein was digested with thermolysin, two protease-resistant fragments which were designated TH-1 and TH-2 were obtained. The fragments were characterized by high ATPase activities and consisted of two principal polypeptides (TH-1: 173K and 80K and TH-2: 173K and 120K). Polyclonal antibodies against these dynein fragments were prepared and used to investigate the origin of these fragments and the structure relationships between the polypeptides of the fragments. By immunoblotting analysis, anti-TH-1 and anti-TH-2 cross-reacted strongly with γ- and β-heavy chain of 22S dynein, respectively. The two antibodies recognized only the 173K polypeptide of each fragment. We also used these antibodies to further investigate the immunological similarities of dynein polypeptides between cilia and flagella. Anti-TH-2(β) cross-reacted with heavy chain of flagellar dynein from oyster sperm, but anti-TH-1(γ) showed no cross-reactivity. Thermolytic active fragment originating from β-heavy chain of flagellar dynein was prepared and compared with TH-2 about these polypeptide components.

BI 35

EFFECTS OF AN ACYLPEPTIDE(K26-5) ON THE TRITON-EXTRACTED SPERM MODEL.

E. YOKOTA[1,2], I. MABUCHI[1], A. KOBAYASHI[3], and H. SATO[2].
[1]Dept. Biol., Coll. Arts and Sci., Univ. Tokyo, [2]Sugashima MBL., Nagoya Univ., Toba, and [3]Dept. Agric. Chem., Okayama Univ., Okayama.

An acylpeptide called K26-5, which was isolated from the culture medium of a soil bacterium Bacillus sp. 503, has been shown to inhibit motility of the Triton-extracted sea urchin sperm models at concentrations below 10 µM, although it does not affect the sliding between outer doublet microtubules in the trypsin-treated axoneme. We investigated the mechanism of K26-5 inhibition of the Triton models of sperm Anthocidaris crassispina. The inhibition of motility was canceled by the addition of both cAMP at concentrations above 1 µM and Triton-soluble fraction of the flagellum. We tried to purify active factors in the fraction with hydroxylapatite and DEAE-cellulose (DE 52) column chromatographies. Consequently, fractions that canceled the K26-5 inhibition coincided with peaks of activity of cAMP-dependent protein kinase. Both incorporation of Pi into the Triton model and the activity of the partially purified cAMP-dependent protein kinase were inhibited by K26-5. From these results,it is speculated that K26-5 affects the cAMP-dependent phosphorylation in the Triton model, and thereby inhibits the mechanism that converts sliding into bending.

BI 36

CONDITIONS FOR MINIMIZING THE DEGRADATION OF PROTEINS IN TETRAHYMENA CELL HOMOGENATE

M. Nakamura, M. Hirono and Y. Watanabe
Inst. Biol. Sci., Univ. of Tsukuba, Ibaraki.

As a first step for isolating various actin-binding proteins from Tetrahymena cells, we investigated the conditions for minimizing the degradation of proteins in the cell homogenate because of a potent endogenous protease activity in Tetrahymena cells. We first adopted the homogenizing solution in which Dictyostelium actin was successfully purified (Uyemura et al. (1978) J. Biol. Chem.253, 9088-9096), and degradation of Tetrahymena proteins in various conditions, such as presence of triethanolamine, concentrations of sucrose and tetra-sodium pyrophosphate, pHs, and temperatures were examined by densitometric analysis of SDS-PAGE. As a result, we finally found that most Tetrahymena proteins detectable on SDS-PAGE remained unchanged at 4 °C for 5 hr in a solution containing 0.5 % Nonidet P-40, 0.4 mM dithiothreitol, 10 µg/ml leupeptin, and 80 mM tetra-sodium pyrophosphate, pH 8.0 .

BI 37

ISOLATION AND PARTIAL CHARACTERIZATION OF TETRAHYMENA ACTIN.

M. Hirono, Y. Kumagai and Y. Watanabe.
Institute of Biological Sciences, Univ. of Tsukuba, Ibaraki.

We have previously reported the cloning and sequencing of the Tetrahymena actin gene and the localization of the gene product. In this report, we succeeded in isolating Tetrahymena actin using an antiserum against the synthetic N-terminal peptide deduced from the DNA sequence as an indicator. The method is as follows. The acetone powder of Tetrahymena cells was extracted with a buffer of low ionic strength. Then, the extract was fractionated by the Q-Sepharose chromatography. By further gel filtration (Superose12 prep grade or Sephacryl S-200 HR) and ion exchange (Q-Sepharose) chromatographies and ammonium sulfate precipitation, the actin was purified nearly homogeneity. The isolated actin could be polymerized into filaments in the presence of 100 mM KCl, which showed typical features of ubiquitous actin filaments. We also found that Tetrahymena actin was less effective than muscle actin as an activator of the Mg^{2+}-ATPase of muscle myosin subfragment 1. The results consolidate our notion that Tetrahymena actin we found from gene analysis is a unique actin having considerable divergency in its amino acid sequence.

BI 38

CALMODULIN-BINDING PROTEINS IN TETRAHYMENA CILIA WHICH CAN INTERACT WITH MICROTUBULES

J. Ohnishi and Y. Watanabe, Inst. of Biol. Sci., Univ. of Tsukuba, Ibaraki.

Previously we detected at least 36 kinds of calmodulin-binding proteins (CaMBPs) in Tetrahymena cilia by ^{125}I-CaM overlay method. Therefore, we tried to purify native CaMBPs by CaM affinity column chromatography. However, the yield of CaMBPs was unexpectedly low. When a sample for CaM column was applied on ethyl N-phenylcarbamate column which was known to be used for purification of tubulin, most CaMBPs behaved along with tubulin. So we speculated that the association of CaMBPs with microtubules or tubulin occurred and this was the cause of low yield. To validate the speculation, interaction between CaMBPs and Tetrahymena axonemal microtubules polymerized in vitro was examined by cosedimentation experiment. As a result, at least 6 CaMBPs were cosedimented with microtubules and the ways of interactions were classified into two groups: i) CaMBPs which interact with microtubules only during polymerization (30kD, 26kD, 22kD), ii) CaMBPs which interact with microtubules during polymerization and with polymerized microtubules (69kD, 45kD, 37kD). Such CaMBPs were integrated in and exposed on outerdoublet microtubules. Thus, it is highly likely that they are involved in a Ca^{2+}-dependent regulation of axonemal motility of Tetrahymena cilia.

BI 39

DYNEIN-MICROTUBULE COMPLEX.

S.OHBA,K.OHHATA AND T.MIKI-NOUMURA. Dept of Biology,Ochanomizu University,Tokyo.

We studied dynein-microtubule interaction,using binding of dynein ATPase isolated from Tetrahymena cilia to singlet MTs reassembled from porcin brain tubulin. The interaction was analysed by measuring turbidity with spectrophotometer and density of gel bands in erectrophoresis with densitometer. Sometimes dynein-microtubule complex was confirmed and visualized by electron and dark-field microscopes.

At first,we examined whether dynein ATPase promots or increases polymerization of tubulin into MTs. Various conc.of dynein were incubated with 0.8mg/ml tubulin. The pellet of formed complex was applied to gel electorophoresis to analyse the amounts of polymerized MTs after centrifugation. We could not find any difference among the amounts of polymerized MTs.

When prewarmed solution containing 0.25 mg/ml dynein was added to polymerized MTs of 0.3mg/ml,turbidity incresed,indicatimg binding of dynein to MTs to form complex. We found that MTs in the complex did not depolymerize after dilution of specimen with buffer solution to below critical concentration of tubulin,while MTs in control experiment depolymerized into tubulin completly. ATP addition to the diluted specimen dissociated dynein from the complex,and brought about complete depolymerization of the MTs. On the other hand, addition of Ca ions or incubation at 0°C decomposed complex into each molecule, dynein and tubulin. These behabior indicated that bound dynein molecules kept MTs from depolymerization by dilution,but did not protect them from depolymerizing effect by Ca ion or 0°C. We are now studying on mechanism of these different response of dynein-microtubule complex to the depolymerizing effects.

BI 40

CLONING AND SEQUENCING OF THE GENE FOR TETRAHYMENA CALCIUM BINDING PROTEIN (TCBP).

T.Takemasa[1], K.Ohnishi[2], T.Kobayashi[3], T.Takagi[3], K.Konishi[3], Y.Watanabe[1]. [1]Inst. Biol. Sci. Univ. of Tsukuba, Ibaraki. [2]Natl. Inst. of Health, Japan. [3]Biol. Inst., Fac. of Sci., Univ. of Tohoku, Sendai.

We previously reported the purification and characterization of calcium-binding protein (TCBP) from Tetrahymena (J.B.C.,258,13978-13985,1983). Here, we attempted cloning and sequencing of the gene for TCBP. To design several oligonucleotide probes for the screening of a Tetrahymena genomic library, regions of minimal codon degeneracy were selected from the amino acid sequence of TCBP. Using four different probes, we detected only one common hybridizing band by Southern blot analysis of Tetrahymena genomic DNA fragments digested with restriction enzymes. Under these conditions, the genomic library constructed with pBR322 was screened and several hybridizing clones were isolated. Partial DNA sequence of a clone has revealed that, i) Molecular weight of TCBP is larger than 10 KD, ii) TCBP has at least 3 calcium binding sites, iii) TCBP gene is interrupted by at least one intron (87 nucleotide long) having consensus sequence at both ends (GT-AG), iv) TAA codes for glutamine.

BI 41

A RELATION BETWEEN CHANGES IN THE LOCALIZATION OF HEAT SHOCK PROTEINS (HSPS) AND AQUISITION OF THERMOTOLERANCE

O.Numata[1], T.Yoshida[2], H. Ohba[1] and Y.Watanabe[1]. [1]Inst. of Biol. Sci., Univ. of Tsukuba, Ibaraki, and [2]Dept. of Biol., Joetsu Univ. of Education.

Using immunofluorescence microscopy, we have characterized changes in the localization of hsp71 of T. pyriformis after sublethal heat treatment (HT)(34°C). After 1h, hsp71 was localized around the nucleoli. About 2h after the HT, hsp71 migrated from nuclei to cytoplasms, and 3h after the HT, it existed only in a cytoplasmic aggregate. To examine the relationship between these changes and aquisition of thermotolerance, we investigated the effect of a prior sublethal HT(34°C) on the viability of cells at 37°C. When Tetrahymena cells in log phase at 26°C were shifted directly to 37°C, they did not substantially survive (<1% viability). However, when treated at 34°C for 1h and then shifted to 37°C they survived normally for at least 3h. The length of the 34°C treatment of the cells (1h to 3h) had no differential effect on their subsequent survival properties at 37°C. This indicates no relationship between changes in the localization of hsp71 and aquisition of thermotolerance. On the other hand, in thermotolerant cells, we observed that all of hsp26, 33 and 71 were localized in the large cytoplasmic aggregates and that intensity of the immunofluorescence for each hsp pronouncedly increased.

BI 42

THE PROPERTIES OF PROTEASE Tl

Y.Motobayashi[1], S.Ihara[2], and K.Yoshizato[3] [1]Dept. of Biochem., [2]Develop. Biol. Lab., Dept. of Plastic Surg.,Kitasato Univ. Sch. of Med., Kanagawa and [3]Dept. of Biol., Tokyo Metro. Univ., Tokyo

The tail of a metamorphosing tadpole of Bullfrog, Rana catesbeiana, contains Protease Tl which is a cystein endoproteinase and preferentially degrades actin. This enzyme hydrolyzes Boc-Val-Leu-Lys-MCA and Bz-Phe-Arg-MCA but neither Arg-MCA (hydrolyzed by cathepsin B) nor Z-Arg-Arg-MCA (hydrolyzed by cathepsin H). Therefore it differs from these cathepsins.

The amino acid composition of this enzyme was compared with those of cathepsinB, H, L and papain according to the composition divergence test. Protease Tl was not similar to those cystein proteinase. The purified Protease Tl from the regressing tail muscle was digested by trypsin and three fragments (F3, F12, F23) were obtained. Automatic amino acid sequence determination with these peptides were carried out using an Applied Biosystems sequencer model 470. The sequences of F3, F12 and F23 were Asp-Gly-Val-Tyr-Gly-Ala-Glu-Leu-Arg, Asn-Leu-Val-Ile-x-Phe-Asn-Pro and Phe-Pro-Ile-Glu-Glu-Ile-x-Tyr-Leu-Asn-Ile-Val-Asn-Leu-Gln-Pro-Ile, respectively. Homology was searched between these sequences and all entries of National Biomedical Resarch Foundation data base library. No significant homology was detected, and thereby Protease Tl was confirmed to be a new protein.

BI 43

THE THIOL PROTEINASE FROM METAMORPHOSING TADPOLE TAIL OF RANA CATESBEIANA.

S.Fujita, K.Kobayashi and S.Horiuchi.
Life Sci.Inst., Sophia Univ., Tokyo.

The proteinase from the tadpole tail of Rana catesbeiana appears to act on the proteolysis in metamorphic tail resorption, and its activity is inhibited by leupeptin, as reported in the 57th annual meeting of the Zoological Society.
This enzyme is more purified (650-fold) by S-Sepharose rechromatography and the yield is 35%. The molecular weight of this enzyme is determined by FPLC on Superose as 20,000. This enzyme is separated to double protein bands by 7.5% acrylamide gel electrophoresis. The enzyme activity is inhibited by leupeptin, monoiodoacetic acid, E-64 and p-chloromercuribenzoic acid, which are known as inhibitors for thiol proteinases. Pepstatin, an inhibitor for cathepsin D, and diisopropyl phosphofluoridate (DFP), an inhibitor for serine proteinases have almost no effect. L-cysteine activates the enzyme activity on degradation of hemoglobin, and other proteins especially myoglobin degradation.

BI 44

MOLECULAR PROPERTIES OF THE EXTRACELLULAR HEMOGLOBIN FROM THE PLANORBID SNAIL, INDOPLANORBIS EXUSTUS.

T. Ochiai[1], I. Usuki[2] and Y. Enoki[3]. [1]Dept. of Biol., Fac. of Sci., [2]Dept. of Biol., Coll. of Gen. Educ., Niigata Univ.,Niigata 950-21. [3]2nd Dept. of Physiol., Nara Med. Univ., Kashihara, Nara 634

Sedimentation pattern of the native hemoglobin of the planorbid snail, Indoplanorbis exustus, gave a symmetric single boundary of 35.5S($s^0_{20,w}$). The molecular weight was determined to be 2.04×10^6 by sedimentation equilibrium. Iron and heme contents were 0.300 and 2.89%, corresponding to minimum molecular weights of 18,600 and 21,300, respectively. The millimolar coefficient of cyanomet derivative at 537nm was 10.3, and the absorbancy at 280nm of 1% solution of oxyhemoglobin was 21.1. SDS-PAGE in the absence of 2-mercaptoethanol gave one major band, corresponding to a molecular weight of 2.8×10^5, and many minor bands. On the other hand, in the presence of 2-mercaptoethanol, one major band, corresponding to a molecular weight of 1.7 x 10^5, and several minor bands appeared. The former value is too small for the consideration that the former is the dimer of the latter. From these results, we propose a tentative model that the native molecule is composed of 12 polypeptide chains and each chain contains 8 hemes.

BI 45

CHARACTERIZATION OF SARCOPLASMIC RETICULUM FROM SCALLOP STRIATED ADDUCTOR MUSCLE

M. Abe[1], J. Nakamura[1], K. Konishi[1] and T. Watanabe[2]. [1]Biol. Inst. Sci., [2]Dept. of Biol., Tohoku Univ., Sendai.

A highly active preparation of sarcoplasmic reticulum (SR) from scallop cross-striated adductor muscle was obtained according to the method reported at the 57th Annual Meeting and characterized.
Although, fragmented mitochondria were seen in the electron micrograph of the preperation and succinate-cyt.c reductase activity was detected, both Ca uptake and Ca-ATPase activities were not affected by NaN_3. Na,K-ATPase and 5'-Nucleotidase activities were undetectable.
The optipmum pH for Ca uptake was 7.0 and the uptake was rapidly decreased by increasing pH. At pH 7.5 which was optimum pH for Ca-ATPase, only very low activity of Ca uptake was obtained. Half maximum activation of Ca-ATPase was obtained at 1.5×10^{-7}M free Ca. This value was almost simillar to that for Ca uptake activity. The activation energy of Ca-ATPase was 20 kcal/mol estimated by Arrhenius analysis over the range of 0 to 20 °C. Lineweaver-Burk plot of Ca-ATPase activity against ATP concentration showed biphasic dependency, two values of Km were obtained 10 µM and 0.1-0.3 mM. The obtained SR accumulated 20 nmol Ca / mg protein in the absence of Ca precipitating reagents.

BI 46

COMPARATIVE BIOCHEMISTRY OF THE EJACULATED SUBSTANCES BETWEEN SILKWORM AND FLUIT FLY.

M.OSANAI and P.S.CHEN, Dept. Biol., Tokyo Metropol.Inst. Gerontol., 173-Tokyo, Japan; Zool.Inst., Univ.Zürich, 8057Zürich, Swiss.

Unlike Bombyx mori, Drosophila melanogaster do not form spermatophore for the sperm maturation. The sperm acquire motility in the vesicula seminalis. However, in Bombyx, like Drosophila, high GPT activity was found in the male reproductive system and spermatophore, especially in the v. seminalis (44 % of total activity). In the male reproductive system of Drosophila, concentration of Arg was low, but those of urea and ammonia were high. Secretion of accessary gland contained much phospho-serine. These substances were transferred to female uterus with sperm during mating. Most amino acids increased distinctly at 30 min after the end of mating and declined, suggesting protein degradation in uterus. Like in Bombyx, urea increased at the post-mating period, while Orn showed a rather low concentration. Orn must be metabolized in part to Glu. In this connection, it is notable that Ala rose markedly at 30 min following mating. As in the silkmoth, the energy metabolism of fruit fly sperm involves also Arg, Orn, urea, Ala and OXO. This is obvious due to the facts that Drosophila sperm are motile at the time of transfer, whereas Bombyx sperm become functionally mature in the spermatophore after their transfer to the female genital tract, bursa copulatrix.

BI 47

BIOSYNTHESIS OF PUPAL CUTICULAR PROTEINS OF Bombyx mori: cDNA CLONING AND ASSAY OF mRNA LEVEL DURING LARVAL-PUPAL TRANSFORMATION.

H.Nakato, M.Toriyama, S.Izumi and S.Tomino
Dept. Biol. Tokyo Metropol. Univ., Tokyo

We have cloned mRNA sequence coding for the pupal cuticular proteins (PCP) of B. mori and studied the change in the PCP-mRNAs during larval-pupal transformation. Three components of chitin-binding PCPs, termed PCP1, PCP2 and PCP3, were resolved by gel electrophoresis of the extract from the pupal integument. Immunoblot analysis of the cuticular extracts indicated that PCPs accumulate in a stage-specific manner in the integument. A λgt11 cDNA library was constructed from poly(A)$^+$ RNA of the epidermal cells immediately after the larval-pupal ecdysis, and two clones were isolated by screening the recombinant plaques with antibody probe. Restriction mapping analysis indicated that cDNA inserts in these clones are structurally different. RNA blot analysis demonstrated that mRNAs for PCP accumulate in the epidermal cells immediately before larval-pupal ecdysis then disappear within two days. The PCP-mRNAs complementary to two cDNA clones were different not only in their molecular size but also in the developmental profiles. These results suggest the possibility that genes for PCPs constitute multi-gene family and each gene in the family responds independently, yet in a concerted manner to the change in endocrine environment.

BI 48

CHARACTERIZATION OF THE CONSTITUENT FATTY ACIDS IN PHOSPHATIDYLINOSITOL DURING EARLY DEVELOPMENT IN RANA NIGROMACULATA.

M. Ryuzaki. Dept. of Biol., Kitasato Univ. School of Medicine, Sagamihara.

Qualitative and quantitative changes in phosphatidylinositol (PI) were analyzed in the eggs, embryos and tadpoles of R. nigromaculata, at various stages of development. Total lipids were extracted by the method of Folch ('54). Individual phospholipids were separated by thin-layer chromatography on layer of silica gel HR impregnated with sodium carbonate. The weight percentage of PI to total phospholipid and to total lipid was about 8-15% and 1-3%, respectively, during embryonic life. At the early stages of unfertilized egg and two-cell embryo, the predominant fatty acids were palmitic, stearic, oleic and linoleic acid. From the early gastrula stage and beyond, the percentage of linoleic acid declines and there is an increase in palmitic acid at the 1-position of PI. A large amount of arachidonic acid was observed at the 2-position of PI in the unfertilized egg, hatching embryo and post-hatching tadpole stages, relative to palmitic and stearic acid. Palmitic and stearic acid were increased at the 2-position of PI in the other embryo and feeding tadpole stages, relative to arachidonic acid, indicating a shift in these molecular species. Thus, there were marked changes in the positional distribution of the constituent fatty acids in PI during early development of R.nigromaculata.

BI 49

EFFECTS OF CYTOSINE ARABINOSIDE ON 2',3'-CYCLIC NUCLEOTIDE 3'-PHOSPHODIESTERASE (CNP) AND GLUTAMATE DECARBOXYLASE (GAD) IN THE ORGANOTYPIC CULTURE OF NEWBORN MOUSE CEREBELLUM.

D.SATOMI. Dept. of Biol., Coll. of Arts and Sci., Univ. of Tokyo, Tokyo.

The quantitative changes of CNP, a marker enzyme of myelin, and GAD, the rate limiting enzyme for the biosynthesis of γ-aminobutyric acid (GABA), during early developmental stages in the organotypic culture of newborn mouse cerebellum were examined by HPLC. Explants were incubated in the presence and absence of cytosine arabinoside, an inhibitor of DNA synthesis. Under standard conditions, the activity of CNP increased rapidly from 8 day in vitro (8 DIV) to 22 DIV. Myelin was observed after 15 DIV under light microscope. GAD activity increased linearly from 2 DIV to 22 DIV. In the same period, the amount of GABA also increased and synapse formation occurred. In the presence of cytosine arabinoside(10 μg/ml), the level of CNP activity was low during incubation. Whereas GAD activity increased nearly same manner as control. Morphologically, myelination did not occur and ependymal cells could not observed.

From these results, it was supposed that the low CNP activity and the lack of myelin were due to the failure of oligodendroglial differentiation, and that the GABAergic neurons in explants could differentiate and synthesize GABA without axonal myelination.

BI 50

LIPIDS IN TWO FRACTIONS OF HAMSTER CAUDA EPIDIDYMAL SPERMATOZOA

M. Awano[1], S. Oshio[2], A. Kawaguchi[1] and H. Mohri[1]. [1]Dept. Biol., Coll. Arts and Sci., Univ. Tokyo and [2]Dept. Urol., Teikyo Univ. Sch. Med., Tokyo.

Hamster cauda epididymal spermatozoa were separated into two fractions in a continuous Percoll-gradient centrifugation. The density of the upper and the lower fractions were 1.04 and 1.10 g/ml, respectively. We analyzed the lipids in the two fractions. In both fractions, palmitic (16:0), stearic (18:0), docosapentaenoic (22:5), docosahexaenoic(22:6) were found as the major fatty acids. The percentages of these major fatty acids were similar in both fractions. However, the ratio of 18:2 / 18:0 in the lower fraction was higher than that in the upper fraction. Phospholipids were the major lipid class in both fractions (80% of the total lipids). Phosphatidylcholine (PC) and phosphatidylethanolamine (PE) were the major phospholipids (80% of the total phospholipids). The principal poly-saturated fatty acids of the hamster spermatozoa were found in only PC and PE. The ratio of each class phospholipid was similar in both fraction but the total amount of phospholipids in the upper fraction was 1.4-fold of that of the lower fraction. The ratio sterol/ phospholipids was 0.17 in both fractions. The change of phospholipids content may reflect on the difference of their density and relate to the process of sperm maturation.

BI 51

UPTAKE OF ^{48}V-LABELED VANADIUM COMPOUNDS BY THE ASCIDIAN BLOOD CELLS.

J.Hirata[1], H.Michibata[1], M.Kawamura[2] and T.Ido[3]
[1]Biol. Inst., Fac. of Sci., Toyama Univ., Toyama, [2]Fac. Agr., and [3]Cyclotron RI CTR, Tohoku Univ., Sendai, Japan.

We have recently reported that among several types of ascidian blood cells, the signet ring cell is the very vanadocyte, that involves in the accumulation of vanadium ion, by means of Ficoll density gradient and neutron activation analysis (Michibata et al., J. Exp. Zool., 1987).

In the present experiment, influx of ^{48}V-labeled compounds into the blood cells was examined. The blood cells of Ascidia ahodori were incubated with ^{48}V-vanadate (V) or -vanadyl (IV) ions in the buffer solution. At time intervals, the cell suspension was loaded onto silicone oil in 1.5 ml microtube and then the cell pellet was recovered by centrifugation. The radioactivity of the pellet was measured by γ-counter. Consequently, it became clear that the vanadyl ion (IV) was incorporated faster into the blood cells than the vanadate ion (V) and the influx was saturated 2 hours after the incubation. This result indicates that the ascidian blood cells have higher affinity for vanadium ion in IV oxidation state than that in V oxidation state.

Moreover, to clarify which blood cells incorporate selectively ^{48}V-vanadyl ion, the blood cells incubated with ^{48}V for 2 hours were fractioned by the Ficoll gradient technique. The result shows that only the signet ring cells incorporate selectively ^{48}V-labeled vanadyl ion.

BI 52

CORRELATION BETWEEN VANADIUM IONS AND TUNICHROME IN THE ASCIDIAN BLOOD CELLS.

H.Michibata
Biol. Inst., Fac. of Sci., Toyama Univ.,Toyama, Japan.

Recently, Nakanishi's group isolated a tunichrome from the ascidian blood cells and determined the chemical structure (Bruening et al., J. Am. Chem. Soc., 1985). Based on the results that the crude tunichromes had an ability to reduce V(V) to V(IV) and existed in the morula cells which had been thought to be the vanadocytes, they have believed that the isolated tunichrome acted as a reductant of vanadium ions when the ascidian blood cells accumulated vanadium from seawater.

However, we verified that the morula cells contained no vanadium, while the signet ring cells, which contained no tunichromes, accumulated a large amount of vanadium ions. Moreover, upon species survey of the tunichrome, it became clear that some vanadium-rich ascidians had no tunichromes, conversely, some iron-rich ascidians contained the tunichromes (Oltz, Ph.D. thesis, Columbia Univ., 1987). The role of the tunichromes in the accumulation of vanadium in the ascidian blood cells is, therefore, skeptical.

Independently, we isolated a vanadium binding substance from the ascidian blood cells, which substance was colorless and could maintain vanadium ions in vanadyl form (IV). We suppose that the VBS acts as a carrier of vanadium ions in the ascidian blood cells. Further study to verify this function is in progress.

BI 53

EXTRACTION OF VANADIUM BINDING SUBSTANCE AND CHEMICAL NATURE OF ITS MODEL COMPLEX.

T.Miyamoto[1], H.Michibata[1], T.Numakunai[2] and H.Sakurai[3]
[1]Biol. Inst., Fac. of Sci., Toyama Univ., Toyama, [2]Asamushi Mar. Biol. St., Tohoku Univ., Aomori and [3]Fac. of Pharmaceut., Univ. of Tokushima, Tokushima, Japan

We reported previously that a vanadium binding substance (VBS) was purified from the blood cells of Ascidia sydneiensis samea. The VBS has an ability to maintain vanadium ion in a reducing form (VO(IV)), contains a reducing sugar and has an apparent affinity for exogenous vanadium ions in IV and V oxidation states (Michibata et al., Biochem. Biophys. Res. Com., 1986).

In further study, the similar substance has been extracted from the blood cells of A. ahodori, suggesting a possibility that the VBS exists in the blood cells of every ascidians that contain a large amount of vanadium.

In order to know the chemical nature of the VBS, using a glucose 1-phosphate as a representative of reducing sugars, glucose 1-phosphate-vanadyl sulfate (IV) and -sodium orthovanadate (V) complexes were prepared. When those complexes were loaded onto SE-Cellulose, the former was eluted in the same fractions with the VBS and the maximal UV absorbance and ESR parameters observed in this complex were very similar with those in the VBS. The latter also exhibited smaller ESR signals, indicating that the vanadate (V) was partially reduced to IV oxidation state by the complexing with the glucose 1-phosphate.

BI 54

COMPARISON OF VERTEBRATE CARDIAC MUSCLE PROTEINS BETWEEN ATRIA AND VENTRICLES

M.Oh-Ishi and T.Hirabayashi. Inst. of Biol. Sci., Univ. of Tsukuba, Ibaraki

Protein of atrial and ventricular muscles of 23 species vertebrates which covered all extant classes were examined by two-dimensional gel electrophoresis in order to find the difference in components between atria and ventricles. Their protein constituents were very similar and the similarity was more than 0.935 as calculated according to Aquadro and Avis, but clear differences were found in myosin heavy chain or light chain regions with lamprey, amphibia, reptiles, birds and mammals. Lamprey atrial myosin light chain 1 was electrophoretically distinct from that of the ventricles on 12-20 % SDS-PAGE. Frog atrial myosin light chain 1 was also distinct from ventricular one. Molecular weights of snake and lizard atrial myosin heavy chains were slightly smaller than those of ventricular ones.

Number of different protein spots between atria and ventricles of birds was smaller (similarity was 0.982-0.990) than that of mammals (similarity was 0.935-0.957). This fact suggested that the ventricular tissue was more specialized for its function in mammals than in birds, as compared with their atrial tissues.

BI 55

EXTRACTION, PURIFICATION AND BIOCHEMICAL CHARACTERIZATIONS OF COLLAGENS FROM SEA URCHIN ASTHENOSOMA IJIMAI

K.SHIMIZU and K.YOSHIZATO
Dept. of Biology, Fac. of Sci.,Tokyo Metropolitan Univ., Tokyo

There has been no attempt to obtain collagen molecules from spieces of sea urchin in an amount which allows chemical and biological characterizations. Sea urchin collagens were extracted and chemically purified from this extract by a salting-out with 10% NaCl, followed by a precipitation with 0.02M Na_2 HPO_4 in a neutral pH. The purified collagen was completely digestible with a non-specific protease-free bacterial collagenase. The collagens thus obtained were similar to those of manmals in respects to a SDS-PAGE pattern and amino acid compositions. The collagens of sea urchin have a smaller value for a specific optical rotation (-310°) and a lower denaturing temperature (23.1° C) than those of manmals (-400° and 39.8° C, respectively). Immunobloting analyses showed that collagens of sea urchin did not cross-react with anti serums against collagens of type I,II,III, IV and V of manmals.

BI 56

PROPERTIES OF Ca^{2+}-BINDING 15K PROTEIN LOCALIZED IN THE MITOTIC APPARATUS OF SEA URCHIN EGG

H. Hosoya[1], I. Mabuchi[2], S. Takagi[3], O. Iwaasa[3] and K. Konishi[3]. [1]Dept. Ultrastruc. Res., Tokyo Metro. Inst. Med. Sci., Tokyo, Dept. Cell Biol., Natl. Inst. Basic Biol., Okazaki, [2]Dept. Biol., Col. Arts and Sci., Univ. Tokyo, Tokyo, and [3]Dept. Biol., Fac. Sci., Tohoku Univ., Sendai.

We have already reported about Ca^{2+}-binding 15K molecular weight protein, which is found to localize in the mitotic apparatus of sea urchin egg, Hemicentrotus pulcherrimus, during mitosis and to play an important role in cell division through the experiment using antibody raised against the 15K protein.

In order to clarify the properties of this protein, we studied the effect of the 15K protein on the polymerization of cytoskeletal proteins such as actin and tubulin. The 15K protein inhibited actin polymerization in the presence of Ca^{2+}. The polymerization of microtubule proteins was inhibited in the absence of Ca^{2+}, but was not inhibited in the presence of Ca^{2+}. With tubulin further purified and free from MAPs, the 15K protein had no effect on tubulin polymerizarion both in the presence and absence of Ca^{2+}.

BI 57

IMMUNOCYTOCHEMICAL LOCALIZATION OF 260K PROTEIN IN TRITON-TREATED CORTEX OF SEA URCHIN EGG.

T.Yoshigaki, S.Maekawa and H.Sakai. Dept. of Biophys. and Biochem., Fac. of Sci., Univ. of Tokyo, Tokyo 113.

An actin binding protein having an apparent molecular weight of 260,000 (260K protein) is purified from the cortex fraction of sea urchin eggs. It causes actin filaments to bundle in vitro.

Immunoblotting analysis showed that the 260K protein is different from porcine brain fordrin and bovine smooth muscle filamin. Several lines of evidences including those from rotary shadowed images indicated clear differences between the 260K protein and sea urchin spectrin.

Immunofluorescence microscopy of isolated cortices was performed using monospecific antibodies to the 260K protein. The staining showed the localization of the 260-K protein in fertilization cone, microvilli and cleavage furrow. In unfertilized and fertilized eggs, the staining pattern was well correlated with that of actin filaments visualized by rhodaminyl-phalloidin. The localization of the 260K protein in the isolated cortices was investigated more precisely by immunogold staining method. The high density of gold particles was observed just beneath the plasma membrane and along the fibrous structure inside protrusions which seemed to be microvilli.

BI 58

PROLIFERATION OF C6 GLIOMA CELLS TO FORM CONDENSED OR LINEAR COLONIES, AND THEIR DIFFERENTIATION BY cAMP ANALOGUE.

T. Kobayashi. Department of Biochemistry, Jikei University School of Medicine, Tokyo

It is well known that confluent C6 glioma cells alter their morphology from epitherial type to that of astroglia. They usually made round and condensed colonies, though they sometimes happened to make linear colonies presumably because their cell division occurred in one direction and cells were chained in line. To make the above story simple and reproducible, C6 cells were passed many generations and mutants were then screened with respect to morphologies of colonies. Isolated subclones were classified into four groups: type C (Condensed), type S (Slashed), type L (Linear) and type D (Dispersed). All of them expressed differentiated morphologies like astroglial cells especially when they were confluent and trerated with cAMP analogue. Each morphology, however, differed in detail. Type C cells resembled protoplasmic astrocytes bearing spiny processes, while type S cells resembled fibrous astrocytes. Type L cells were bipolar and type D cells were mixture of bipolar, unipolar and fibrous astrocytes. I expect that these subclonal cell types reflect several aspects of glial cell differentiation.

BI 59

AMIDASE ACTIVITIES OF ASCIDIAN (HALOCYNTHIA RORETZI) HEMOLYMPH TOWARD PEPTIDYL-MCAS.

K. Tanaka and F. Shishikura, Dept. Biology, Nihon Univ. Sch. Med., Tokyo.

Amidase activities of hemolymph plasma of the ascidian, H. roretzi, were tested by various peptidyl-4- methyl-coumaryl-amides (PEPTIDE INSTITUTE, INC., Osaka) used as substrates for proteolytic enzyme assays of human blood plasma and other sources. Hemolymph was collcted into aseptic plastic tubes and centrifuged at 3000rpm for 5min. The plasma was stored at -80°C. The reaction mixture (1ml) containing plasma (50-100ul), substrate (5×10^{-4}M, 50-100ul) and 50mM Tris-HCl buffered Pantin's ASW(pH8) was incubated at 25°C for 0 - 120min. The reaction was terminated by addition of 17% AcOH (2ml). The AMC released was measured fluorometrically at Ex.380nm and Em.460nm. The plasma showed amidase activities toward ten substrates out of 26; strongly toward Boc-L-G-R-MCA (substrate for horseshoe crab clotting enzyme, HCC), moderately toward Boc-F-S-R-MCA , Boc-V-P-R-MCA and Boc-V-L-K-MCA, but scarcely toward substrates for KK, Urok, chymotrypsin and cathepsin. The optimum pH was 8. The activity for HCC was increased by the pretreatment of plasma with pieces of tunic which can induce aggregation of hemolymph cells. The pretreatment over 30min, however, decreased the effect. These results suggested that ascidian hemolymph plasma involved a contact-induced enzymatic cascade as well as mammalian blood plasma.

BI 60

PURIFICATION OF AMIDOLYTIC ENZYMES FROM THE ASCIDIAN, HALOCYNTHIA RORETZI, HEMOLYMPH PLASMA.

F. Shishikura and K. Tanaka. Dept. of Biol. Nihon Univ. Sch. of Med., Tokyo.

In a previous work we have shown that H. roretzi hemolymph plasma was highly susceptible toward Boc-Leu-Gly-Arg-MCA which was recently introduced as a substrate for the horseshoe crab clotting enzyme.

In this report we developed a purification procedure of amidolytic enzymes toward Boc-Leu-Gly-Arg-MCA from H. roretzi plasma, including 80% saturated ammonium sulfate fractionation, gel filtration on Toyopearl HW-65F, chromatofocusing on a Mono P column (Pharmacia), affinity chromatography on a p-aminobenzamidine coupled column (ABA-5PW, Toyo-Soda) and a repeated gel filtration on Superose 12 (Pharmacia).

Three active enzyme fractions, designated A, B, and C, were obtained from the first gel filtration and only A was used for the further purification.

The isolated enzyme was demonstrated to be homogeneous judged from gel filtration and SDS-polyacrylamide gel electrophoresis. An apparent molecular weight of active enzyme was about 40,000 dalton and its isoelectric point was 5.5-5.6 based on Mono P chromatography.

BI 61

OCCURRENCE OF POLYAMINE OXIDASE AND N^8-ACETYLSPERMIDINE-DEACETYLATING ACTIVITY IN CATFISH TISSUES.

T. Kumazawa and O. Suzuki. Department of Legal Medicine, Hamamatsu University School of Medicine, Hamamatsu.

Polyamine oxidase (PAO) and acetylspermidine deacetylase are considered to play a role for polyamine re-utilization after their acetylation in mammalian tissues.

In the present study, we have found the presence of PAO and N^8-acetylspermidine-deacetylating activity in tissues of the catfish, Parasilurus asotus.

PAO activity was highest in the intestine, followed by the liver, kidney and brain with N^1-acetylspermine as substrate. Substrate specificity was tested for the intestinal enzyme, and the highest activity was found with N^1-acetylspermine, followed by N^1-acetylspermidine and N^1,N^{12}-diacetylspermine. The optimal pH and apparent Km value for N^1-acetylspermine were 8.3 and 19.6 μM for the intestinal enzyme, respectively.

N^8-actylspermidine-deacetylating activity was highest in the kidney, followed by the intestine, liver, skin and brain with ^{14}C-N^8-acetylspermidine as substrate. The optimal pH and apparent Km value were 7.9 and 89.6 μM for the kidney enzyme, respectively.

These results suggest the presence of a system of polyamine re-utilization after their acetylation also in catfish tissues.

BI 62

STRUCTURE OF THE PROCESSING SITE OF RAT LIVER CATHEPSIN D.

S. Yonezawa. Dept. of Zool., Fac. of Sci., Hokkaido Univ., Sapporo.

The mature form of cathepsin D is generally thought to be a "two-chain" structure of the light and heavy chains, which are produced by proteolytic cleavage of a single chain. We examined the structure around the processing site of the single chain form of rat liver cathepsin D and compared it with the known structures of cathepsins D from other mammals. When carboxymethylated rat liver cathepsin D was digested with trypsin, followed by Con A-Sepharose 4B chromatography and gel filtration on Sephadex G50, two tryptic glycopeptides were obtained, one of which was homologous to a C-terminal segment of porcine cathepsin D. Two chymotryptic peptides which included the connecting region between the light and heavy chains were obtained from BrCN-treated enzyme by a procedure which involves digestion with chymotrypsin, gel filtration on Sephadex G50 and HPLC separation of peptides. A part of the identified rat sequence around the processing site is shown below, in comparison with the known sequences of porcine (P), human(H) and bovine(B) cathepsins D.

(shown in single letters)

```
Rat: GSGSLSGYLSQDTVSVPCK  S   T  LGGIKVE
     ...................         ..  .
P  : 77GSGSLSGYLSQDTVSVPSN97 ? ? ?  VGGIKVE
H  : GSGSLSGYLSQDTVSVPCQSASSASALGGVKVE
B  : GSGSLSGYLSQDTVSVPCNPS S  S SPGGVTVQ
        <----- L-chain          H-chain->
```

BI 63

WHY DOES THE APHID rRNA LACK THE HIDDEN BREAK ?

K.Ogino, H.Eda and H.Ishikawa. Dept.of Biol. Coll. Arts & Sci., Univ. of Tokyo, Tokyo.

Due to the hidden break the 28S rRNAs of insects and most protostomes are separated into the two parts. We had found that the break is created by excising RNA fragments with length of several tens of nucleotide from a certain part of the initial transcript to leave the gap in the sequence.
Among insects aphid species are distinct from the other insects in that their rRNAs invariably lack the hidden break.
To know what makes this difference, we constructed an aphid genomic library and studied the structure of aphid rDNA with respect to the region corresponding to the gap which the other insect rRNAs have in common. Sequence comparison revealed that while the other rRNAs are supposed to form an AU-rich loop in that region, the corresponding loop of the aphid rRNA is not AU-rich. Nor does the loop of the aphid rRNA contain the UAAU tract that can be a signal for the introduction of the hidden break, suggesting that in this particular region the aphid rRNA resembles those of deuterostomes which do not contain the hidden break.

BI 64

AN INTRACELLULAR SYMBIONT OF THE PEA APHID HAS HOST GENE-LIKE REPETITIVE SEQUENCES IN THE GENOMIC DNA.

S.Sato and H.Ishikawa. Dept.of Biol., Coll. Arts & Sci., Univ.of Tokyo, Tokyo.

While intracellular symbionts of the pea aphid had been well studied from the structural and nutritional viewpoints, they were seldom characterized as genetic elements. In particular, nothing has been known about the host-symbiont interaction at the genomic level. As the first step to study the gene expression of the intracellular symbiont, we characterized its genomic organization. Since we noticed that the isolated DNA of the symbiont contains aphid rDNA-like sequence, we constructed a genomic library of the symbiont using EMBL4 as a vector. By screening the library with cloned aphid rDNA fragments as probes, we picked up several clones containing sequence homologous to the host sequences. One of the clones was mapped and analyzed extensively. Dot-blot hybridization revealed that the cloned sequence occurs about 20 to 30 times in the symbiont genome. Southern blot hybridization suggested that most of the sequences are tandemly arranged in the genome.
Since the sequence is highly homologous to those of the host and other eukaryotic rDNA it cannot be the symbiont's own rDNA but likely the sequence which had been transferred from the host insect.

BI 65

TESTIS-SPECIFIC α-HYDROXY ACID OXIDIZING ENZYME OF DROSOPHILA VIRILIS

Y.Taka and T.Aotsuka. Dept. of Biology, Fac. of Science, Tokyo Metropolitan Univ., Tokyo.

We investigated α-hydroxy acid oxidizing enzymes of Drosophila virilis with electrophoresis. When homogenates of Drosophila virilis were run on polyacrylamide gels and stained with the reaction mixture of lactate, PMS and NBT, two major isozymes were detected. The one (isozyme A) was found in both sexes, but the other (isozyme B) was found only in males. We performed dissections in order to determine the localization of the isozymes. Then, isozyme B existed only in testis.
Isozyme B could also be visualized with the reaction mixture of lactate, peroxidase and dianisidine. In anaerobic condition, however, no band appeared with this system. These results suggested that, in the oxidation of lactate by isozyme B, O_2 is the electron acceptor and H_2O_2 is prodused. Examination of substrate specificity on the polyacrylamide gels showed that isozyme B oxidizes a variety of α-hydroxy acids.
Genetic analysises indicated that isozyme A and isozyme B are encoded by different loci on differnt chromosomes.

BI 66

ROLE OF CYCLIC GMP IN HORMONAL CONTROL MECHANISM OF CRAYFISH, PROCAMBARUS CLARKII

M.Shibata, K.Tozawa, T.Ozaki[1] And T. Ohoka Dep of Biol., Fac. of Sci., Tokyo Metropol. Univ., Tokyo and [1]Natl.Inst. for Physiol. Sci., Okazaki.

A prominent increase of cGMP level was found in crayfish heart and intestine, after administration of CHH(crustacean hyperglycemic hormone) fraction of sinus gland in an in vitro experiment. The increased cGMP level was 15 fold in intestine and 40 fold in heart, but cAMP level almost unchanged. Membrane bound and hormone sensitive guanylate cyclase was prepared from heart and intestine of destalked animal, but the sensitivity was rapidly lost after 5 min incubation at 30° as well as the cyclase activity decreased to 1/6 of initial level.
CHH fraction showed a stimulatory effect on spontaneous, periodical movement of intestine and an inhibitory effect on that of heart. These effects were mimicked by cGMP derivatives, dibutyryl cGMP and 8-bromo cGMP, not by dibutyryl cAMP. To investigate the molecular mechanism of hormone action, phosphorylated proteins were analysed by SDS-PAGE and autoradiography. After incubation of tissue homogenate or membrane fraction in presence of $[\gamma\text{-}^{32}P]$ATP, several radioactive protein bands were detected. More than 3 bands were hormone dependent and required calcium ion for phosphorylation. Two protein bands from membrane were found to be phosphorylated in presence of cGMP.

BI 67

RELATIONSHIP BETWEEN NEURAL PROCESS FORMATION AND GANGLIOSIDES IN RAT PRIMARY CULTURE NEURONS.

M.Ogiso[1], M.Ohta[1], S.Hirano[1], T.Noguchi[1], K. Kajiwara[2], and E.Sugaya[2]. [1]Dept. of Physiol., Toho Univ. Sch. of Med., Tokyo. [2]Dept. of Physiol., Kanagawa Dental Coll., Yokosuka.

In cerebral cortex from fetal rat, the physiological roles of gangliosides, which are enriched in neural tissues, were examined in primary culture using serum-free medium. Colchicine and cytochalasin B were added to the culture to inhibit process formation. Ganglioside composition during the formation of neural processes was analyzed by extraction in chroloform-methanol, DEAE-Sephadex column chromatography, and HPTLC separation. In colchicine-treated cells, GD_{1a} ganglioside significantly decreased and process formation was inhibited at 10^{-7} M. Cytochalasin B caused looping of neural processes and disappearance of GM_1 ganglioside. In comparison with data obtained using medium containing 15% fetal calf serum, some differences in ganglioside composition were observed. The differences may suggest cell-to-cell interaction between neurons and glial cells at the ganglioside level on the cell surface.

BI 68

EFFECTS OF METHYLMERCURY ON CELLULAR ACTIVITIES IN TISSUES OF RAT AND HAMSTER.

S.Omata, T.Hiranuma, K.Hirasawa and H.Sugano. Dept. of Biochem., Fac. of Sci., Niigata Univ., Niigata.

The uptake by and elimination of Hg from tissues of the hamster after administration of MeHg were very rapid compared with the rat, and the brain/blood Hg ratio of the hamster was much higher than that of the rat. These results prompted us to study differences in effects of MeHg on cellular activities of these animals. Among several neurotransmitter enzymes examined, only the activity of glutamic acid decarboxylase in the hamster brain showed a significant decrease at the symptomatic period(14-day). Lipid peroxidation in the hamster brain was increased significantly over the period of 5-14 days, and in the rat brain it showed a significant increase only at the symptomatic period. In the sciatic nerves of the symptomatic animals, activities of choline acetyltransferase and acetylchokinesterase were reduced in the rat to the extent larger than in the hamster. Decrease in the activity of GSH peroxidase in the hamster brain was greater than that in the rat at 14-day, while GSH S-transferase activity were increased in both brains of two species. In vivo protein synthesis was significantly reduced in the brain regions of the rat at latent and symptomatic periods, while that of the hamster showed a minor change. Similar difference in MeHg effects between rat and hamster was observed in in vitro amino acid incorporation experiments with the brain post-mitochondrial supernatant fractions obtained from these animal species.

BI 69

PURIFICATION AND IMMUNOLOGICAL CHARACTERIZATION OF MEMBRANE-BOUND AND SOLUBLE ALKALINE PHOSPHATASES IN THE MIDGUT OF SILKWORM, BOMBYX MORI.

M.Azuma, N.Okada, H.Yamamoto and M.Eguchi. Lab.of Appl.Genet. Dept.of Appl.Biol. Kyoto Inst.of Techn., Kyoto.

We have purified the membrane-bound(m-ALP) and soluble ALP(s-ALP) from the alimentary canal(midgut) of silkworms and some properties were investigated. Purification was successfully achieved by introducing the affinity chromatography (Con A-Sepharose 4B for m-ALP; 4-aminobenzyl phosphonic as ligands for s-ALP). Both ALPs were homogenous as judged by polyacrylamide gel electrophoresis(PAGE). They were found to be similar Mr=68,000 in gel filtration and a single subunit in denaturing SDS-PAGE with Mr=60,000. They also have similar amino acid compositions and pI(4.8). The pH optima of both ALPs were shown to lie at 10.8(m-ALP) and 9.7(s-ALP), and the m-ALP was extremely stable in pH 10-12 accords with the physiological milieu in Bombyx midgut lumen.

The antibody against m-ALP recognized m-ALP but not s-ALP. Rocket-immunoassay showed that m-ALP distributed similar levels along the length of midgut except for the most anterior portion. Although we have not determined the distribution of s-ALP immunologically, 70% of its activity existed in the posterior midgut. These results suggest m-ALP and s-ALP are distinct isozymes and undertook different roles.

BI 70

ATP-DEPENDENT PROTEASE IN BOVINE ADRENAL CORTEX.

S.Watabe, H.Kouyama, K.Hara, S.Tatunami, K.Shino and N.Yago. Radioisotope Res. Inst., St. Marianna Univ. Sch. Med., Kawasaki.

Mitochondria contain a protease which requires ATP for its catalytic activity. ATP-Dependent protease is most abundant in adrenal cortex and we purified the enzyme to homogeneity from bovine adrenocortical mitochondria (S.Watabe & T.Kimura (1985) J.Biol.Chem. 260 14498). The purified enzyme catalyzes protein-dependent ATP hydrolysis as well as ATP-dependent proteolysis. ATP Hydrolysis, however, is not a requisite of peptide bond hydrolysis, since nonhydrolyzable ATP analogs support peptide degradation. Large proteins, on the other hand, were not degraded in the presence of ATP analogs. Degradation of low concentration of labeled proteins /peptides was enhanced by unlabeled proteins/peptides, suggesting that substrate proteins/peptides were allosteric effectors. Activation of proteolysis by peptides was observed only in the presence of ATP but not in the presence of ATP analogs.

Mitochondria contain both activators and substrates for ATP-dependent protease. The protease efficiently degraded a mitochondrial protein of 27,000 M.W. and some other proteins, while most of mitochondrial proteins were remarkably resistant against digestion with mitochondrial ATP-dependnet protease in the presence of ATP. Fractionation of mitochondrial extract with a Sephadex G-100 column revealed that the 27K protein was eluted at two different positions, one at void volume and the other at M.W. 30 - 40K. The protein may be one of natural substrates for the protease and might be involved in some regulatory mechanisms.

BI 71

Purification of metalloendoprotease from sea urchin sperm.

C.Ohtaka, K.Akasaka and H.Shimada (Zool. Inst., Fac. Sci.,Univ. Tokyo, Tokyo)

Previously we reported the presence of Zn^{2+}-dependent and histone H1-specific metalloendoprotease in sea urchin sperm. In this paper, we describe the preliminary result on purification of this protease.
Mature male gonads (frozen, 2.6kg) of sea urchin (Hemicentrotus pulcherrimus) were homogenized in Tris buffer containing 1% Triton X-100. The extract was subjected to three cycles of DEAE cellulose column chromatography. The enzyme activity was eluted from the last DEAE cellulose column by 10-130 mM NaCl. The active fractions were concentrated by 80%-saturated ammonium sulfate, dialysed against 20 mM Tris buffer, and applied to the gel filtration through Sepharose CL-6B. Perhaps because of the low ionic strength, the enzyme became aggregated during dialysis with the significant loss of the activity, and eluted from the column as two distict peaks at the high molecular weight regions. SDS-PAGE analysis of this peak fraction revealed the presence of three distinct bands at 40-45 KDa which seemed to correspond to this protease. The protease thus purified preferentially hydrolyzed histone H1, and its activity was clearly stimulated by Zn^{2+}.

BI 72

GROWTH ASSOCIATED HISTONE KINASE OF REGENERATING RAT LIVER NUCLEI.

K. Asami. Div. of Biol., Natl. Inst. of Radiological Sci., Chiba-shi.

Liver histone H1 is phosphorylated at about 24 h after partial hepatectomy, when the DNA synthesis starts. X irradiation prior to partial hepatectomy inhibits the phosphorylation. Thus, phosphorylation of histone H1 will be related with DNA synthesis. To know the enzymes responsible for the phosphorylation, changes in the nuclear protein kinase activities were examined. The cAMP-dependent protein kinase activity changed from 15 to 24 h after hepatectomy. But the deviations of the data were so large that the change was not significant statistically. The effect of X irradiation was also non-significant. On the other hand, cAMP-independent kinase (non-A kinase) activity increased from 18 to 24 h after hepatectomy. The increase was not observed in the irradiated nuclei. The non-A kinase activity was not inhibited by isoquinolinesulfonamide compounds, H-7 and HA1004, but inhibited by quercetin. These results indicated that this enzyme would the growth-associated histone kinase. However, this enzyme preferred casein as a substrate to histone H1. The casein kinase activity was inhibited by heparin only partially and it was rather high in the irradiated nuclei. The nuclei may contain a casein kinase (NII) as well.

BI 73

PURIFICATION OF LDH-A and B ISOZYMES FROM THE MEDAKA, ORYZIAS LATIPES.

T. Sasaki , Y. Hyodo-Taguchi , I. Iuchi, and K. Yamagami . Life Sci. Inst., Sophia Univ., Tokyo and Div. Biol. Nat. Inst. Radiol. Sci., Chiba.

Lactate dehydrogenase (LDH; EC1.1.1.27) of medaka is known to consist of A, A', B and C subunits, the genetic and developmental expression of which was studied in inbred and outbred fish. Recently, LDH-B_4 was preliminarily purified from outbred medaka and some of its properties were studied (Ohyama et al., 1986). We further purified and characterized LDH-A_4 and B_4 of medaka muscle.

Crude muscle extracts were fractionated by an affinity chromatography using Blue-Separose CL-4B. B_4 was obtained by eluting with 1 mM NAD-3 mM lactate as a major component. By the following elution using 1 mM NADH, A_4 was obtained with other proteins. Each of them was further purified on an HPLC system using DEAE-silica column.

The molecular weight (mw) of native A_4 and B_4 was 117 kd. Mws of the subunits A and B were 27.0 kd and 27.5 kd, respectively. The optimal pHs of A_4 and B_4 in reductive reaction were 6.3-6.5 and 6.4-6.6, respectively. Substrate-inhibition was observed like LDHs of other animals. The Km values of A_4 and B_4 were 0.62 mM and 0.18 mM, respectively.

BI 74

Purification and Properties of Arginine Kinase Y.Yazawa, Dept. of Nutritional Physiol., Hokkaido Univ. of Education at Asahikawa, Asahikawa, Hokkaido.

Arginine kinase(AK) was purified from smooth muscle of sea-cucumber with ammonium sulfate fractionation, DEAE-Toyopearl column chromatography, gel filtration, and hydroxylapatite column chromatography. The preparation appeared to be homogeneous on SDS-PAGE. The M.W. of 43K was estimated from SDS-PAGE and 86K was estimated from gel filtration under physiological conditions. According to results of amino acid analysis, sea-cucumber AK contained 378 amino acids. The pH-activity curve for the forward reaction showed optimum at pH 5.0 and the specific activity was 93 umol Arg/mg. min. In the reverse reaction, a plateau was shown between pH8.5 and 9.6. and the specific activities were 1 umol Pi mg. min. The highest activation of AK by bivalent cation was observed in tne presence of Mg^{2+}.

BI 75

DECREASE OF SERUM ARGININE CONC. IN TUMOR -BEARING ANIMALS

T.Nishikawa[1], S.Kusunoki[1] and H.Namiki[2]. [1]Life Science Inst., Advance Co., Ltd., Tokyo and [2]Dept. of Biol., Sch. of Educ., Waseda Univ., Tokyo.

We have reported that serum arginine almost undetectably disappeared after partial hepatectomy of rats. Further study demonstrated that the phenominon was due to the elevation of arginase activity in the serum brought out from the regenarating liver.

Carcinoma is resemble to regenerating liver in terms of being proliferating. We, therefore, made an attempt to measure the enzyme activity in tumor-bearing animals. Significant elevation of the enzyme activity or decrease of arginine conc. was observed as well in sera of animals (mice and rats) bearing cancer of lung, liver or breast. In case of human, significant increase of enzyme activity was also noticed in that of patiants bearing same kinds of cancer. Postoperative observation showed that the elevated activity returned to the normal level within a month.

Whether the arginase originates in the tumor itself or in its peripheral tissues which has been dameged by its proliferation is not yet clarified. Increase of the enzyme activity may, however, be useful as a marker for cancer or hepatopath.

BI 76

HEPARIN-BINDING PROPERTY AND A NEW METHOD FOR PURIFICATION OF A CELL-ADHESIVE GLYCOPROTEIN VITRONECTIN.

M. Hayashi[1], T. Yatohgo[2], H. Kashiwagi[2], and M. Izumi[1]. [1]Dept. of Biol., Ochanomizu Univ., Tokyo, and [2]Inst. Clin. Med., Tsukuba Univ., Ibaraki.

Vitronectin (serum spreading factor, S-protein) is a cell-adhesive glycoprotein in human plasma and connective tissues. Heparin-binding activity of purified vitronectin can be activated by 8 M urea, 6 M guanidine-HCl, or heating at 100 C for 5 min [Hayashi et al., J. Biochem. 98, 1135 (1985); Barnes et al., J. Biol. Chem. 260, 9117 (1985)]. We found that fresh human plasma contained a few % of endogeneous heparin-binding form of vitronectin. Therefore, the heparin-binding vitronectin seems to be a functionally and structurally distinct form of vitronectin.

Furthermore, we developed a strikingly simple method by which vitronectin was purified from human plasma/serum. Heparin-binding activity of vitronectin in serum was also activated by 8 M urea. The activated vitronectin was purified approximately 250-fold by heparin affinity chromatography. This procedure produced 3 - 6 mg pure vitronectin from 100 ml of human serum within 2 days.

BI 77

ISOLATION AND COMPARATIVE ANALYSIS OF LECTINS FROM ALBUMEN GLANDS (A. G.) OF LAND SNAILS, THREE STRAINS OF *EUHADRA*.

O. Ikeda and T. Inoue. Dept. Biol., Tokyo Gakugei Univ., Tokyo.

Lectins from A. G. of land snails, *Euhadra peliomphala*, *E. subnimbosa* and *E. quaesita* in feeding, were isolated and studied biochemically. These lectins agglutinated only human A type erythrocyte. The agglutination was inhibited by D-GalNAc and D-GlcNAc. Each isolation of three lectins was carried out using affinity choromatography with D-GlcNAc-sepharose 4B. On O'Farrell's two-dimensional polyacrylamide gel electrophoresis (2D-PAGE), the lectins were composed of two groups of polypeptide spots. They showed charge isomers, which electric points were around 5, and major groups had about 21.5K of morecular weight. These spots were not shown in the 2D-PAGE patterns of A. G. in hibernation, so that the amount of lectin in A. G. was suggested to varied with season. Otherwise they were shown in that of egg, so that the lectin in A. G. was suggested to migrate to egg. In immunological studies, antibody which raised against isolated lectins from three strains showed reaction toward all of their parent antigens each other.

BI 78

HEMAGGLUTINATING ACTIVITY IN THE HEMOLYMPH OF *Bombyx mori*

K. Amanai, S. Sakurai and T. Ohtaki
Department of Biology, Faculty of Science, Kanazawa University, Kanazawa 920

Sheep red blood cells treated with trypsin and glutaraldehyde were agglutinated significantly by the larval hemolymph of *Bombyx mori*. Developmental change in hemagglutinating activity in hemolymph measured from the 4th instar to adult stage. The activity was relatively high at the end of the 4th instar and the time of gut purge. This activity seemed to be under the control of ecdysteroid during the 5th instar. This indicated an important role of hemagglutinin in the course of metamorphosis. Protein with hemagglutinating activity was precipitated by 30% saturated ammonium sulfate. The precipitation was applied to a column of Sephacryl S-300 and eluted in the excluded fraction. It was then applied to DEAE-Sephacel column equiliblated with 20 mM ammonium acetate buffer, pH 6.0 and eluted with 1M buffer. Active fractions were subjected to high performance ion-exchange chromatography of Tsk-gel 5 PW. The overall yield after HPIEC was only 0.1%, which was too low for further purification. Improvement of the yield and further purification by affinity chromatography using glucuronic acid as a ligand is under the progress.

BI 79

EFFECTS OF A JUVENILE HORMONE ANALOGUE ON MANNOSE CONTENT IN GLYCOPROTEINS AND MANNOSIDASE ACTIVITY IN THE HAEMOLYMPH OF THE SILKWORM, Bombyx mori.

S. Nakayama. Tezukayama Coll., Nara

Fifth instar larvae of the silkworm, Bombyx mori were treated with a juvenile hormone analogue (JHA) and changes in the content of mannose in glycoproteins and the activity of mannosidases in the haemolymph were examined.

Administration of JHA to the 3-day-old fifth instar larva had little effect on the growth rate, but caused the delay of spinning, resulting in the increased weight of the larva as well known. The JHA administration decreased the content of mannose in the glycoproteins in the haemolymph. The activity of mannosidases in the haemolymph was conspicuously increased in response to JHA administration. The mannosidase activity in the haemolymph increased, then mannose content in haemolymph glycoproteins decreased. These results suggest that the content of mannose in the glycoproteins in the haemolymph is controlled by the mannosidase activity in the haemolymph.

BI 80

LOCALIZATION OF β-1,3-GLUCAN RECEPTOR IN HEMOLYMPH OF SILKWORM, BOMBYX MORI.

M. Ochiai and M, Ashida. Biochem. Lab., The Institute of Low Temp. Sci., Hokkaido Univ., Sapporo

The prophenoloxidase(proPO) activating system of insect hemolymph is a cascade, which is triggered by β-1,3-glucan of fungal cell wall or peptidoglycan of bacterial cell wall. The system is considered to play important roles in the defence reaction. β-1,3-glucan receptor, a protein with affinity to β-1,3-glucan, triggers the system and is involved at the first step within the cascade when it is triggered by β-1,3-glucan. Previously, we reported a method to purify β-1,3-glucan receptor from silkworm hemolymph, but the localization and the action mechanism of the protein remained to be studied although such studies are fundamental to advance our understanding the function of the proPO activating system and recognition mechanism of fungi in insect.

Polyclonal antibodies against β-1,3-glucan receptor were prepared. As immunoblotting of proteins extracted from fat body, integument, hemocytes or in plasma indicated that β-1,3-glucan receptor is present both in hemocytes and in plasma, the localization of β-1,3-glucan receptor was examined on ultra thin sections of hemocytes with immunocytochemical techniques. β-1,3-glucan receptor was demonstrated to be present in particular cell types among hemocytes in silkworm hemolymph.

BI 81

PURIFICATION OF PEPTIDOGLYCAN-RECEPTOR FROM HEMOLYMPH OF SILKWORM LARVAE.

H.Yoshida and M.Ashida. Biochem. Lab.,Inst. of Low Temperature Science, Hokkaido Univ., Sapporo.

Peptidoglycan(PG), a component of cell wall in bacteria, has various activities including potentiation of immune system and promotion of slow-wave sleep in mammal, etc.

Prophenoloxidase(proPO) activating system in the hemolymph of silkworm larvae is triggered by PG or β-1,3-glucan, a cell wall component of fungi. PG and β-1,3-glucan are recognized with separate receptors in the activating system in the hemolymph.

We purified PG-receptor(PG-Rec), protein with affinity to PG, which is necessary for the activation of the system with PG. Homogeneous PG-Rec was prepared from hemolymph of silkworm larvae with column chromatography using PG-coupled Sepharose 4B, hydroxylapatite and MONO-Q(Pharmacia).

From the following observations, we concluded that PG-Rec is a component recognizing PG in the proPO activating system. 1) Pro-PO activating system of silkworm plasma passed through PG-Sepharose column is triggered by β-1,3-glucan but not by PG, indicating that PG-Rec is removed from the preparation. The system of the preparation mixed with purified PG-Rec was activated by PG. 2) Purified PG-Rec bound with PG.

BI 82

Purification and caracterization of BAEEase in hemolymph of the Silkworm, Bombyx mori.

Y.Nakamura and M.Asida. The Institute of Low Temp.Sci., Hokkaido Univ.,Sapporo

When the prophenoloxidase(proPO) activating system in insect plasma is triggered by elicitors sudh as β-1,3-glucan and peptidoglycan, at least two zymogens of serine enzymes are activated. They are BAEEase, an enzyme hydrolyzing Benzoylarginine ethylester, and proPO activating enzyme. In silkworm plasma BAEEase is short-lived and previously we demonstrated that the instability is due to the presence of its inhibitor. In the present study we first tried to seperate proPO activating system from the inhibitor to get stable BAEEase. 0-50 fraction (free of the inhibitor and at the same time containing proPO activating system) was prepared from silkworm plasma by a method involving ultracentrifugation and ammonium sulfate fractionation. The proPO activating system in 0-50 fraction was triggered with β-1,3-glucan and the resultant BAEEase was purified by column chromatography on hydroxylapatite, Sephadex G-150, MONO Q and Superose 12 in FPLC system. On SDS-PAGE, the purified protein migrated under non reduced conditions as a band with an apparent M.W. of 39K, showing that purified BAEEase was homogeneous. From the result of column chromatography of BAEEase and merker proteins on Superose 12 the native form was shown to have an approximate M.W. 39K. Other properties of BAEEase including substrate specificity was also reported.

BI 83

AN ATTEMPT TO GET INSIGHT INTO THE COMPLEXITY OF PROPHENOLOXIDASE ACTIVATING SYSTEM OF THE SILKWORM, *Bombyx mori*.

M. Ashida. Biochem. Lab., Institute of Low Temp. Sci., Hokkaido Univ., Sapporo.

The prophenoloxidase activating system of insect plasma is triggered with elicitors such as β-1,3-glucan and peptidoglycan. Separate proteins with affinity to each of the elicitors(β-1,3-glucan receptor and peptidoglycan receptor) are present in plasma and the interaction of the elicitor with the respective receptor initiates the activation of the system, leading to the activation of at least two serine enzyme precursors, proBAEEase(a precursor of an esterase hydrolyzing benzoylarginine ethylester) and proPPAE(a precursor of prophenoloxidase activating enzyme).

It has not been clear, however, how many components constitute the system. In the present study, the system of silkworm plasma was fractionated with ammonium sulfate into a few fractions and the system was attempted to be reconstituted using possible combinations of the fractions. The results indicate that there exist at least two more components in silkworm prophenoloxidase activating system in addition to β-1,3-glucan receptor, peptidoglycan receptor, proBAEEase, proPPAE and prophenoloxidase.

BI 84

INTACT GRAM-NEGATIVE BACTERIA DO NOT TRIGGER PROPHENOLOXIDASE ACTIVATING SYSTEM(PRO-PO CASCADE) OF INSECT.

K. Kinoshita, H. Yoshida and M. Ashida. Biochem. Lab., The Institute of Low Temp. Science, Hokkaido Univ., Sapporo.

The pro-PO cascade of insect is triggered by purified peptidoglycan(PG) but not by lipopolysaccharide(LPS). It remained, however, to be studied if intact Gram-negative bacteria trigger proPO cascade.

We cultured *B. subtilis*, *E. coli* and *P. ovalis* in synthetic media to logarithmic phase. These bacteria were incubated with silkworm plasma obtained by a method of Yoshida and Ashida[Insect Biochem. 16, 539 (1986)] or injected into hemocoel of silkworm larvae to examine the abilities of them to trigger pro-PO cascade. Both *E. coli* and *P. ovalis* did not trigger the cascades present in plasma(*in vitro*) and in hemocoel(*in vivo*) at the concentration of 8×10^7 bacteria/ml, whereas *B. subtilis* triggers the cascade both *in vitro* and *in vivo*. Gram-negative bacteria are phagocytosed in insect hemocoel by hemocytes and the enhanced phagocytic activity is displayed by hemocytes treated with -1,3-glucan or LPS. The enhancement by LPS has been explained as the result of the activation of proPO cascade [Ratcliffe *et al*. Science 226, 557 (1984)]. The results of the present study, however, indicate that activated components of proPO cascade is not likely to be a cause for the observed enhancement of phagocytosis of bacteria by endotoxin.

DB 1

YOLK FORMATION OF THE OOCYTE IN THE SEA URCHIN, *ASTENOSOMA IJIMAI*

J.Tsukahara. Dept. of Biol., Fac. of Sci., Kagoshima Univ., Kagoshima.

Ultrastructural changes of the oocyte of *A. ijimai* during vitellogenesis are studied. At the previtellogenesis stage of the oocyte (diameter; less than 350µm),the surface of the oocyte is almost smooth. The oocyte is surrounded by one layer of flattened follicle cells during oogenesis. Many mitochondria and a number of Golgi apparatus, annulated lamellae, bundles of microfilaments and streated structures are scattered in the oocyte cytoplasm.

At the beginning of the stage of vitellogenesis, cytoplasmic process appeare all over the surface of the oocyte. Near the base of the process a pinocytotic vesicle is formed. Primary yolk granules, which are less than 1µm in diameter, are observed near the cisternae of the Golgi apparatus. It is suggested that these yolk granules may be formed primary in the cisternae of the Golgi apparatus. A number of pinosomes become attached to the surface of the immature yolk granules. From cytochemical studies two types of yolk granules are formed during vitellogenesis. One of them includes a lot of fatty substances, and the other includes of acid mucopolysaccharides and proteins.

DB 2

PURIFICATION AND CHARACTERIZATION OF CREATINE PHOSPHOKINASE(CPK) FROM SEA URCHIN SPERMATOZOA

M. Kurita, H. Tsuchida, M. Yamaguchi and N. Suzuki. Noto Marine Lab. Kanazawa Univ., Uchiura

It is known that sperm activating peptides cause an electrophoretic mobility shift of a major sperm plasma membrane protein. The protein is supposed to be guanylate cyclase, although the molecular weight of the protein is very close to that of creatine phosphokinase(CPK) localized in sperm tail. This study was performed to make sure whether speract caused the molecular weight change of sperm tail CPK.

Sperm tail CPK was purified as follows: sperm tails were suspended into 0.5% NP-40, 5% glycerol, 5mM $MgCl_2$, 125mM KCl, 1mM DTT, 1mM EGTA, 0.2mM ADP, 0.2mM PMSF, 10µg/ml soybean trypsin inhibitor, 20mM HEPES, 10mM Tris (pH 7.0), homogenized and centrifuged at 100,000xg. The supernatant was applied onto a Reactive Red 120-Agarose column. The CPK activity was eluted by 0.5M KCl from red agarose column. CPK was further purified by DEAE Bio-Gel chromatography. The purified CPK migrated as a single band (MW 137,000) on SDS-polyacrylamide gel electrophoresis. The protein was stained by Shiff's reagent, suggesting that the enzyme is a glycoprotein.

DB 3

PURIFICATION AND STRUCTURE OF SPERM ACTIVATING PEPTIDES FROM THE EGG JELLY OF THE SEA URCHIN DIADEMA SETOSUM

K. Yoshino[1], M. Yamaguchi[1], N. Suzuki[1], K. Nomura[2] and H. Kajiura[3]

1 Noto Marine Lab. Kanazawa Univ., Uchiura 2 Dept. of Biochem. Tokyo Metropolitan Inst. of Gerontol., Tokyo and 3 Natl. Inst. for Basic Biol., Okazaki

The egg jelly of the sea urchin *Diadema setosum* stimulated the respiration rate of its own spermatozoa in slightly acidic sea water (pH 6.6). However, speract (Gly-Phe-Asp-Leu-Asn-Gly-Gly-Gly-Val-Gly), resact (Cys-Val-Thr-Gly-Ala-Pro-Gly-Cys-Val-Gly-Gly-Gly-Arg-Leu-NH_2), alloresact (Lys-Leu-Cys-Pro-Gly-Gly-Asn-Cys-Val) and mosact (Asp-Ser-Asp-Ser-Ala-Gln-Asn-Leu-Ile-Gly) did not show any respiratory stimulation toward *D. setosum* spermatozoa. These results suggest that the egg jelly of *D. setosum* contains peptides specific for *D. setosum* spermatozoa. The present study is concerned in purification and sequencing of the peptides from *D. setosum* egg jelly. Two new peptides were isolated and their amino acid sequences were as follows: Gly-Cys-Pro-Cys-Gly-Gly-Ala-Val and Gly-Cys-Pro-Trp-Gly-Gly-Ala-Val. These peptides half-maximaly stimulated the respiration rates of *D. setosum* spermatozoa at about 0.1 nM.

DB 4

SPECIFICITY OF SPERM ACTIVATING PEPTIDES

N.Suzuki[1],M.Yamaguchi[1],K.Yoshino[1],M.Kurita[1] H.Tanaka[1],K.Nomura[2] and H.Kajiura[3].
1; Noto Marine Lab. Kanazawa Univ. Uchiura, 2; Dept. Biochem. Tokyo Metropolitan Inst. of Gerontol., Tokyo and 3; Natl. Inst. for Basic Biol., Okazaki.

Twenty one different sperm activating peptides have been isolated and sequenced from egg jelly of eight species of sea urchins distributed into three taxonomic orders. Speract and its ten derivatives were obtained from five species (*H.purcherrimus*, *P.depressus*, *S.purpuratus*, *A.crassispina* and *L.pictus*) in the order Echinoida. They stimulated respiration of spermatozoa of sea urchins in the order Echinoida. Resact, alloresact and its five derivatives isolated from the egg jelly of sea urchins(*A.punctulata* and *G.crenularis*) in the order Arbacioida were effective for *G.crenularis* spermatozoa. Mosact and its two derivatives purified from the egg jelly of *C.japonicus* in the order Clypeasteroida were specific only for own spermatozoa. These results support a theory that sperm activating peptides isolated from sea urchin eggs of one taxonomic order interact with sperm cells of other species within the same order, but not within another order.

DB 5

PARTICIPATION OF SPERACT IN THE ACROSOME REACTION OF HEMICENTROTUS PULCHERRIMUS

M. Yamaguchi, T. Niwa, M. Kurita and N. Suzuki, Noto Marine Labo., Kanazawa univ. Uchiura.

Speract-free macromolecular fraction was prepared from the egg jelly of the sea urchin *H. pulcherrimus* by gel filtration and tested for the acrosome reaction inducing ability with or without exogenous synthetic speract. The macromolecular fraction without speract showed only about half of the activity of the original whole jelly for the induction of the acrosome reaction, while the activity of the fraction with speract was comparable to that of the original jelly. Speract itself, however, did not induce the acrosome reaction in the absence of the macromolecular fraction of jelly. The acrosome reaction was accompanied by the elevation of cyclic AMP concentrations in sperm cells, which depended on the concentration of the macromolecular fraction. The addition of speract to the fraction promoted both the induction of the acrosome reaction and the elevation of cyclic AMP concentrations cooperatively with the fraction. These results suggests that a major factor responsible for the acrosome reaction is a macromolecular component of the jelly and that speract promotes the reaction as a co-factor through ionic changes or the elevation of cyclic AMP concentrations.

DB 6

INDUCTION OF SEA URCHIN SPERM ACROSOME REACTION BY ANTIBODY AGAINST WGA BINDING PROTEIN ON THE SPERM PLASMA MEMBRANE.

Y.Sendai[1], T.Ohta[2] and K.Aketa[1]. [1]Akkeshi Mar. Biol. Stat., Hokkaido Univ., Akkeshi Hokkaido. [2]Dept. of Biol., Aichi Univ. of Educ., Kariya.

In the sea urchin *Strongylocentrotus intermedius*, wheat germ agglutinin (WGA) binds to the acrosomal region of sperm, and inhibits the egg jelly-induced acrosome reaction (AR) by interfering with both Ca^{2+} influx and Na^+/H^+ exchange (Sendai and Aketa, Zool. Sci., 3, 1033, 1986). In the present study, we partially purified a WGA binding protein (WGAbp) on the sperm plasma membrane, obtained polyclonal antibody to WGAbp (anti-WGAbp pcAb), and investigated the effect of pcAb on AR.

WGAbp purified from sperm plasma membrane was a glycoprotein of 260kD on the SDS-PAGE in the absence of 2-mercaptoethanol. Anti-WGAbp pcAb caused increases in both intracellular $Ca^{2+}$and pH, resulting in AR. Increases in intracellular Ca^{2+} and pH caused by pcAb were suppressed by WGA. PcAb-induced AR and egg jelly-induced AR were inhibited under the same conditions (low-pH ASW, 50 mM K^+ASW, Na^+ free ASW, 100 μM verapamil ASW).

These results suggest that the WGAbp is involved in the regulation of ion fluxes associated with AR in *S. intermedius* sperm. It is a strong candidate for the receptor of signal of AR inducing substance.

DB 7

POSSIBLE PARTICIPATION OF ENDOGENEOUS CHYMOTRYPSIN-LIKE PROTEASE IN THE ACTIVATION OF Ca^{2+} CHANNELS AT THE ACROSOME REACTION OF SEA URCHIN SPERM.

K.Matsumura and K.Aketa. Akkeshi Mar. Biol. Stat., Hokkaido Univ., Akkeshi Hokkaido.

We previously reported that synthetic chymotrypsin inhibitors and substrates inhibited acrosome reaction(AR) of Strongylocentrotus intermedius by egg jelly but not by ionophores (Matsumura and Aketa, 1986).

Inhibitory effect of BTEE on AR, like that on chymotrypsin activity, was reversible. Egg jelly-induced AR was inhibited by succinyl-Leu-Leu-Val-Tyr-MCA, not by succinyl-Ala-Ala-Pro-Phe-MCA. The substrate with high specificity for chymotrypsin-like protease in sperm extract inhibited AR more strongly than that with low specificity.

Measurements of changes of intracellular $[Ca^{2+}]$($[Ca^{2+}]_i$) and pH(pH_i) following the addition of egg jelly revealed that BTEE depressed transient increase of $[Ca^{2+}]_i$, but did not affect initial increase of pH_i. It only delayed the succeeding decrease of pH_i. Verapamil inhibited the egg jelly-induced AR, but it did not inhibit the ionophore-induced AR. The effect of verapamil on the egg jelly-caused changes of $[Ca^{2+}]_i$ and pH_i was similar to that of BTEE.

These results suggest that sperm chymotrypsin-like protease activates, directly or indirectry, Ca^{2+} channels which take part in AR of sea urchin sperm.

DB 8

PROBABLE PARTICIPATION OF GTP-BINDING PROTEIN IN THE ACROSOME REACTION OF SEA URCHIN SPERM.

K.Mikami-Takei and I.Yasumasu. Dept. of Biol., Sch. of Educ., Waseda Univ., Tokyo.

We found some evidences that suggest the participation of GTP-binding protein (G protein) in the acrosome reaction of sea urchin sperm. Incubation of dry sperm in an ice bath for 1-5 hrs cause a considerable decrease in the percentages of jelly water-induced acrosome reaction (the rate of acrosome reaction). GTPγS, a nonhydrolyzable guanine nucleotide activating G protein function, prevented, to some extent, the acrosome reaction from the decrease in its rate. Incubation with GDPβS, another nonhydrolyzable guanine nucleotide blocking G protein function, decreased the rates of acrosome reactions. Cholera toxin (CT) and pertussis toxin (PT), known specific ADP-ribosyltransferase that transfer ADP-ribose from NAD to G protein, increased the rate of acrosome reactions induced by jelly water. Treatment of sperm homogenate with (U-^{14}C)NAD and PT or CT showed (^{14}C)-incorporation to acid-insoluble fraction depending on the concentrations of CT and PT.

DB 9

ACTIVATION OF SEA URCHIN EGGS BY HALOTHANE AND ITS INHIBITION BY DANTROLENE

A. Fujiwara, K. Sudoh and I. Yasumasu
Dept. of Biol., School of Education
Waseda University, Tokyo.

Halothane, known to induce Ca^{2+} release from sarcosome, stimulated eggs of the sea urchin, *Hemicentrotus pulcherrimus*, to cause fertilization membrane formation in normal and Ca^{2+} free artificial sea water. In the absence of external Ca^{2+}, halothane-induced formation of fertilization membrane was inhibited by dantrolene, an inhibitor of Ca^{2+} release from sarcosome, but was not blocked by nifedipine, a Ca^{2+} antagonist specific to Ca^{2+} channels in plasma membrane. Ca^{2+} release from sedimentable fraction isolated from eggs was induced by halothane and was inhibited by dantrolene, but was not blocked by nifedipine. In normal artificial sea water, halothane-caused egg activation was not inhibited either by dantrolene or by nifedipine, but was blocked in the presence of both compounds. $^{45}Ca^{2+}$ influx was substantially stimulated by halothane in eggs exposed to $^{45}CaCl_2$. Halothane-induced $^{45}Ca^{2+}$ influx into eggs was inhibited by nifedipine but wss not blocked by dantrolene. When Ca^{2+} release from intracellular organellae is blocked, Ca^{2+} transport through Ca^{2+} channels in plasma membrane probably acts as a "fail-safe" system to induce an increase in cytosolic Ca^{2+} level, resulting in egg activation.

DB 10

VOLTAGE CLAMP STUDY OF IONIC CURRENT DURING FERTILIZATION IN SEA URCHIN EGG.

S.Obata and H.Kuroda, Sugashima Marine Biol. Lab., Sch. Sci., Nagoya University.

We measured ionic current underlying the fertilization potential (fertilization current) of the sea urchin, Anthocidaris crassispina, egg using two-microelectrode voltage clamp method. At a holding potential of -80mV (resting potential of an unfertilized egg), the fertilization current was inward and transient. Fertilization membrane began to elevate about the time when the current reached peak. Therefore, this transient inward current corresponds to the 2nd component of the fertilization potential. As a holding potential was more positive, the amplitude of the inward current decreased and changed to outward. Reversal potential of the current in standard artificial sea water (ASW) was +21mV. To study the effects of Na^+ and K^+ on this current, we measured the fertilizationcurrents at various holding potentials in low Na^+ ASW (43mM Na^+) or high K^+ ASW (35mM K^+ + 240mM Na^+). The reversal potentials were -26mV in low Na^+ ASW, +7mV in high K^+ ASW. These values differ from the equilibrium potential of Na^+ or that of K^+ in each ASW.

These data indicate that the 2nd component of the fertilization potential does not depend on voltage-sensitive channels. It was confirmed that conductances of both Na^+ and K^+ were responsible for the component using voltage clamp method.

DB 11

THE INITIAL ELECTRICAL SIGNAL OF SPERM-EGG INTERACTION.

K.Takemoto and H.Kuroda. Sugashima Marine Biol. Lab., Sch. Sci., Nagoya Univ., Toba.

The fertilization potential of sea urchin eggs consists of three components (A,B and C). Component A seems to be generated by a step-like depolarization. The depolarization is the initial electrical change caused by the sperm-egg interaction, and is referred to the initial depolarization(ID). The effect of external Na^+ concentration $[Na^+]_o$ and the membrane potential on ID was examined. The amplitude of ID depended on $[Na^+]_o$. The reversal potential was, however, nearly 0mV and was far negative than E_{Na}. These results suggest that sperm causes ID of the egg membrane by increasing the permeability of not only Na^+ but other ions. The egg hyperpolarized more negative than -100mV often elicited transient depolarization (TD) without fertilization potential on insemination. The time constant of its rising phase and the amplitude were similar to that of ID. Such depolarizations were also observed in low $[Na^+]_o$ sea water less than 21.5mM. TD had a relatively long duration of about 10 sec in conparison with its steep rising and falling phases. Thr summation of ID also occured in hyperpolarized eggs. In these eggs, multiple sperm asters were observed. These results suggest that a single initial or transient depolarization is elicited by a sperm-egg interaction.

DB 12

PARTIAL PURIFICATION AND CHARACTERIZATION OF THE ACID SEA WATER EXTRACT FROM UNFERTILIZED SEA URCHIN EGGS. III.

A.Nishikawa[1], S.Nakamura[1], M.K.Kojima[1] and N.Suzuki[2]. [1]Dept. of Biol., Fac. of Sci., Toyama Univ., Toyama 930, [2]Noto Marine Lab., Kanazawa Univ., Ishikawa 927-05.

The acid sea water extract from unfertilized sea urchin eggs (EE) can induce acceleration of cleavage in fertilized sea urchin eggs. Our previous work show that EE contains at least two kinds of acceleration factors of cleavage (AFC: MW≧12,000 and MW<12,000). In this study, we progressed the purification of AFC with lower mol wt. Filtered EE with collodion bags (Sartorius) was concentrated to about 100-fold by evaporation in the boiling water. The concentrate was applied to Bio Gel P-6, and two major peaks were detected by absorption at 260 nm. We confirmed that only the first peak contains AFC. Then fractions of the first peak were concentrated and applied to Bio Gel P-2. Three major peaks were detected by absorption at 260 nm, and only the first peak was identified as a fraction containing AFC. The mol wt of this AFC was estimated about 500 by gel filtration with Bio Gel P-2. As a next step, this fraction was applied HPLC (ODS C-18), and 3-4 sharp peaks were obtained. Now we are undertaking to identify peak(s) containing AFC.

DB 13

POSSIBLE INVOLVEMENT OF C-KINASE IN FERTILIZATION AND DEVELOPMENT OF SEA URCHIN EGGS.

K.Aketa and K.Matsumura,Akkeshi Mar.Biol.Stat., Fac.Sci.,Hokkaido Univ.,Akkeshi,Hokkaido.

Activation of phospholipase C at fertilization should produce diacylglycerol(DG) together with inositol trisphosphate(IP_3). DG is known to activate C-kinase with participation of calcium which is released by IP_3 from storage organella. Thus, activation of C-kinase at fertilization can be expected. We have examined this possibility using H7,inhibitor of C-,G- and A-kinase, and HA1004, inhibitor of G- and A-kinase.

H7(50μM) prevents onset and completion of visible cortical change of eggs of the sea urchin,*Strongylocentrotus intermedius*. The first sign of H7 effects is delay of onset of cortical change(fertilization membrane formation). Either interruption of membrane formation,formation of low membrane or complete lack of membrane formation are observed depending on eggs and treatments.

H7 does not block entry of spermatozoa,causing polyspermy.

H7 prevents also artifical activation by A23187.

H7 retards and stops development of normally fertilized eggs. At 25 μM,eggs can not develop beyond early blastula. Eggs in 12.5μM can not form mesenchymal cells

HA1004 does not exert any effect on eggs even at 200uM.

The above results suggest that phosphorylation of some specific proteins by C-kinase is required for cortical change and specific steps of development of *St.intermedius* eggs.

DB 14

AMMONIA CAUSES INVISIBLE CORTICAL CHANGE OF SEA URCHIN EGGS LEADING TO CHANGE OF SUSCEPTIBILITY TO CONCANAVALIN A AND RELEASE OF TRYPSIN-LIKE PROTEASE.

Y. Yamada and K. Aketa (Akkeshi Marine Biological Station, Faculty of Science, Hokkaido University, Akkeshi, Hokkaido)

Ammonia is known to initiate events such as nucleus swelling, which normally begins after fertilization, but bypasses the earyl events such as cortical granule (CG) exocytosis. Certainly, nucleus swelling occurs in unfertilized eggs(unf-eggs) of *Strongylocentrotus intermedius* by NH_4Cl without visible surface change. However, concanavalin A(Con A) specifically causes agglutination of the unf-eggs treated with NH_4Cl(10 mM). Ricinus communis agglutinin (RCA I and II) and wheat germ agglutinin have no effect. Fluorescein-conjugated Con A (FITC-Con A) binds weakly to unf-egg surface, but it does strongly to unf-egg surface treated with NH_4Cl. Binding is cancelled with α-methyl mannose. FITC-Con A nonspecifically binds to fertilization membrane. Release of trypsin-like protease is observed from unf-eggs treated with NH_4Cl. The change in susceptibility to Con A is completely inhibited by trypsin inhibitors. These results suggest that NH_4Cl causes partial CG exocytosis and some changes of the egg surface by releasing trypsin-like protease.

DB 15

ANALYSIS OF THE BREAKDOWN OF CORTICAL GRANULES IN SEA URCHIN EGGS BY MICROINJECTION USING VIDEO-MICROSCOPY

T. Mohri(1), Y. Hamaguchi(1) and Y. Hiramoto(2). (1) Biological Laboratory, Tokyo Institute of Technology, Tokyo, (2) University of The Air, Chiba.

We observed the breakdown of cortical granules in sea urchin (mainly Clypeaster japonicus) eggs using video-microscopy when Ca-EGTA buffer as Ca^{2+}, IP_3 (inositol 1, 4, 5-trisphosphate), GTP and GTPγS were microinjected into the sea urchin eggs. The duration to the first breakdown of a cortical granule after microinjection of Ca-EGTA buffer, IP_3 and GTPγS were determined to be about 0.5 sec, 1.0 sec and 2.4 sec, respectively. Durations after injection of Ca-EGTA buffer were not different from those in case of untreated eggs when Ca-EGTA buffer was injected into the eggs treated with cytochalasin B (5.2×10^{-7} -5.2×10^{-4} M), hypo-and hypertonic sea water (0.5-2.0 Osm). When the eggs were treated with sea water containing 40mM NH_4Cl at pH 7.0-8.5, the durations were prolonged (pH 7.0-8.0) or the breakdown of cortical granules did not occur (pH 8.5) until about 30 min after treatment. However, over 30 min after NH Cl treatment, the durations decreased gradually to the values of the untreated eggs.

DB 16

EFFECT OF ZINC ON FORMATION OF THE FERTILIZATION MEMBRANE IN SEA URCHIN EGGS.

S. Nakamura, C. Ohmi, A. Nishikawa and M.K. Kojima. Dept. of Biol., Fac. of Sci., Toyama Univ., Toyama 930.

The effect of Zn on formation of the fertilization membrane was observed in eggs of sea urchin, Anthocidaris crassispina. When the eggs were transferred into Zn-sea water by 10 sec after insemination, more than 5 µM Zn inhibited to form the fertilization membrane. This inhibition was irreversible. Although time of the first cleavage was delayed in the dose dependent manner, the cleavage occurred normally up to 1 mM Zn. Light and electron microscope examinations reveal that the exocytosis of cortical granules progress normally. However, the detachment of vitelline layer from the plasma membrane and the hardening of the vitelline layer were blocked in sea water containing more than 5 µM Zn. SDS gel electrophoresis of the membrane-associated cortical granules shows the presence of one Zn-binding protein, apparent mol wt of 68,000. Now we are trying to purify this protein.

DB 17

STRUCTURE AND LOCALIZATION OF TYROSINE-DERIVED CROSSLINKS IN THE FERTILIZATION MEMBRANE PROTEINS OF SEA URCHIN EGGS

K. Nomura[1] and N. Suzuki[2]. [1]Dept. of Biochem., Tokyo Metro. Inst. of Gerontol., Itabashi and [2]Noto Marine Lab., Kanazawa Univ., Uchiura.

The fertilization membrane(FM) of a sea urchin egg hardens within several min after it is lifted. In this process ovoperoxidase (OPO) released from cortical granule catalyzes the H_2O_2 oxidation of Tyr-residues in the FM proteins, forming dityrosine (DT), trityrosine (TT) and some other derivatives. The crosslinks, DT and TT in the HCl hydrolysates of various FM samples from H. pulcherrimus were quantitated by fluorometry (Ex283/Em410) after separation by HPLC (ODS column, 0.1% TFA, CH_3CN 0–30%).

The contents of DT and TT (res/10,000 total AA res) were as follw: Normal FM (5.5;1.5), Soft FM ((+)-Aminotriazole-fertilized) (0.2;trace), Hatching enzyme digest, whole (4.7;1.7), salt-out (2.6;1.1), sol (12.1;3.6), Sephadex G-75 Fr.B (Mw 10–30k) (12.2;3.6), NFM SDS sol (0.6;trace), residue (5.6;2.2), NFM Urea sol (1.6;0.4), residue (6.9;1.1), DEAE-Sephacel Fr.A, presumably, OPO (1.2;0.1).

The proteins of Mw >100k seem to be cross-linked much more than the smaller ones, but the reaction is not strictly specific for some limited proteins. A DT-containing peptide was isolated from the Pronase digest of NFM and its amino acid composition was determined as ($DT/Asx_3/Ser_2/Glu/Pro_2/Gly/Tyr$). Another fluorescent substance, unidentified yet, may be the third crosslinking amino acid.

DB 18

FERTILIZATION-INDUCED CHANGE OF THE RESPIRATORY RATE IN RED AND WHITE HALVES OF SEA URECHIS EGGS.

E. Tazawa[1], A. Fujiwara[2] and I. Yasumasu[2]. [1]Biol. Inst., Yokohama City Univ., Yokohama and [2]Dept. of Biol., Waseda Univ., Tokyo.

Red and white halves of sea urchin eggs obtained by centrifugation exhibited dramatic change in the respiratory rate following fertilization in the same manner as in normal eggs. CN^--insensitive respiration, observed for several minutes after fertilization was higher in its rate in red halves than in white halves. CN^--insensitive respiratory systems probably localized in some organellae. The rate of CN^--sensitive respiration in unfertilized white halves was higher than in fertilized red ones, whereas fertilized red halves exhibited markedly higher respiratory rate than in fertilized white halves. Amount of mitochondria was assumed to be lower in white halves than in red ones, on the basis of the rate of respiration stimulated by TMPD and DNP. Mitochondrial Ca^{2+} pool size in red halves was markedly higher than in white halves. Mito chondrial Ca^{2+} pool size in red and white halves, as well as normal eggs decreased following fertilization. Mitochondria isolated from fertilized and unfertilized eggs, which exhibited the same rate of respiration to each other. have been reported to exhibite low respiratory rate when they were charged with Ca. Ca release from mitochondria probably contribute to fertilization-induced activation of mitochondrial respiration.

DB 19

INTERNAL MOTION OF DNA IN MALE PRONUCLEI OF SEA URCHIN EGGS BY FLUORESCENCE ANISOTROPY UNDER THE MICROSCOPE

K.Hirano, Hamamatsu Photonics, Tsukuba.

Change in the internal motion of DNA in the male pronuclei was investigated by measuring stationary fluorescence isotropy under the microscope equipped with many filters. Sea urchin eggs and sperm were stained with 10 μM Hoechst 33342 in tha sea water. Fluorescence intensities polarized parallel and perpendicular to the direction of polarized excitation light were measured by the ultra-high sensitive TV camera and the image processor with rotating the polarizing filter.

Fluorescence anisotropy of sperm nulcei on the slide glass was 0.351±0.029 and that of male pronuclei in the fertilized eggs was reduced to 0.340±0.030 at 5 min after insemination. About that time the pronuclei grew spherical. Thereafter pronuclei continued swelling gradually, but the value of anisotropy was maintained up to 10 min (0.339±0.013). The value was increased and reached to 0.358±0.009 at 15 min, then returned to the value of 10 min-pronuclei. The pronuclear fusion occurred within this period of time. These results show that the degree of the internal motion of DNA molecules in the male pronuclei is settled in spite of the increasing volume, and that DNA temporarily grow ridid during the pronuclear fusion.

DB 20

MONOCLONAL ANTIBODIES AGAINST PROTEIN COMPONENTS IN PARTIALLY PURIFIED MICROTUBULE-ORGANIZING GRANULE (MTOG) FRACTION.

K.Ohta, M.Toriyama, S.Maekawa, S.Endo and H.Sakai. Dept. of Biophys. and Biochem., Fac. of Sci., Univ. of Tokyo, Tokyo

We previously showed that protein components competent to form asters in vitro could be fractionated from isolated mitotic apparatus (MA) and whole eggs. We prepared monoclonal antibodies against the protein components in partially purified MTOG fraction from whole eggs which was obtained by phosphocellulose column chromatography. Eight positive clones were screened by immunoblottings. Four clones (HP1,2,5,6) reacted with the major 51-kD protein specifically. Localizations in MA of the antigens for these 4 clones corresponed to that of the 51-kD protein which was previously reported. HP1 and 2 reacted with the homologous protein species in MAs isolated from several kinds of sea urchin eggs. Molecular weights of these immunoreactive species were close to 51,000. Other 4 clones generated antibodies against the minor components in the partially purified MTOG fraction. Molecular weights of the antigens were 63,000 (HP3,8), 140,000 (HP4), 100,000~110,000 (HP7). The 140-kD protein was shown to localize in MA. Microinjection experiments using HP series are in progress to study functions of the antigens.

DB 21

ASTER FORMATION INDUCED BY ENDOTHERMICAL POLYMERIZATION

M. Yamanaka[1], F. Tamaki[2] and S. Ishizaka[2].
[1]Dept. of Physics, Nihon Univ., Tokyo, [2]Inst. of Biol. Sci., Univ. of Tsukuba, Ibaraki.

A pair of asters is formed in the time course between mitosis and cytokinesis. The position where the cleavage furrow appears is determined by the boundary of these asters. Thus, unequality of cell division depends on the relative sizes of the two asters.

The principal component of the astral rays is tubulin which polymerizes endothermically (in a homogeneous system). We attempted to induce aster formation endothermically in a designed temperature gradient.

Tubulin was extracted from porcine brain by Shelanski's method. Joule's heat was generated at the fine tip of a glass microelectrode in a cold solution of tubulin. The electric current and the temperature of the tubulin solution were regulated to control the region that exceeds the critical temperature. The polymerizing process was observed by a polarizing microscope.

As a result, astral rays extended radially from the microelectrode tip. When the supply of Joule's heat was stopped, the astral rays depolymerized. Two sets of astral rays were formed from the tips of two microelectrodes.

DB 22

SPIRAL ARRAYS OF MICROTUBULES IN SEA URCHIN EGGS.

A. HANAYAMA, and T. MIKI-NOUMURA.
Dept. of biology, Ochanomizu Univ. Tokyo.

Spiral arrays of mictorubules were obsereved in fertilized eggs of sea urchin; Strongyrocentrotus purpuratus by P.Harris in 1979 and T.E.Schroeder in 1985.

We induced the spiral MTs in eggs of sea urchins(H. pulcherrimus, A. manni) with hexylene glycole S.W. (HG-SW). HG has been known as a MT inducing and stabilizing agent. To identify MTs, we stained the eggs with antitubulin-antibody using indirect immunofluorescence technique.

When eggs were exposed to 4% HG-SW after fertilization, radially oriented MTs appeared in the subcortical region of eggs and persisted for more than 1h. In 0.75% to 1.0% HG-SW, the spiral MTs appeared at pronuclear fusion and disappeared at streak stage. The eggs divided into two cells normally. The spiral MTs were not obsereved in blastmeres after two cell stage. Immunofluorescent micrographs revealed the three dimendional structure, in which MTs arranged spirally around an axis. Although we tried to find some relations between the spiral axis and the animal-vegetal axis, we were unable to find any relation. The spiral MTs were also observed in Ca-ionophore-activated eggs, but not in ammonia-activated eggs.

From these results, we concluded that HG increased tubulin polymerization to form a similar structure to the spiral arrays of MTs in eggs, induced by temperature in S. purpuratus. The appearance and dissappearance of spiral MTs seem to be programed in the subcortical region of eggs and triggerd by fertilization or activation by calcium.

DB 23

THE CYTOSKELETON AT THE 4TH CLEAVAGE OF SEA URCHIN EMBRYOS.

M. Abe and I. Uemura. Dep. of Biology, Tokyo Metropolitan Univ., Tokyo.

At the 4th cleavage of sea urchin embryos, the vegetal cells undertake unequal cleavage resulting a macromere and a micromere. Dan found that the interphase nucleus with a tiny aster at its front side of the vegetal blastomere moves toward the vegetal pole and forms mitotic apparatus there. The mechanism of this nuclearmovement has not beencleared. So far we identified only one centriole around the moving nucleus by the transmission electron microscopy. The mitotic apparatus at the 4th cleavage was hardly observed unless isolated in the microtuble preserving solution. By improving microtuble-preserving and fixing method, we succeeded to observe the mitotic apparatus of the 4th cleavage by immunofluorescent microscopy, using anti-tubulin monoclonal antibody. We found two centrosomes at the both sides of the interphase nucleus in each blastomeres of the 8 cells embryo, when the nuclei of the vegetal cells had not moved yet.

Tanaka reported the inhibition of nucleus movement and unequal cleavage caused by cytochalasin B treatment (Tanaka 1978), suggesting the vital role of actin filament in nuclear movement. We had been attempting to retain , and succeeded to observe the actin filaments near the cleavage furrow at the 1st cleavage by immuno-electron microscopy.

DB 24

STRUCTURAL ANALYSIS OF THE CONTRACTILE RING OF THE SEA URCHIN EGG.

S.Yonemura[1], S.Tsukita[2], S.Tsukita[2] and I.Mabuchi[1]. [1]Dept. of Biology, College of Arts and Sci., Univ. of Tokyo, Tokyo, [2]Dept. of Ultrastructural Research, The Tokyo Metropolitan Institute of Medical Science, Tokyo.

The contractile ring of the sea urchin egg, Hemicentrotus pulcherrimus was examined by electron microscopy. Cortices of the eggs were isolated on a substratum at telophase maintaining the ultrastructural integrity of the contractile ring.

When the section was cut tangentially through the contractile ring, highly oriented microfilaments were clearly identified. Some microfilaments were observed to be randomly oriented. The HMM-S1 decoration experiment revealed that these microfilaments are composed of actin and that antiparallel actin filaments were involved in the ring. Each actin filament was seen to originate from granular structures closely associated with the plasma membrane. Between adjacent actin filaments, thin cross-linkers were occasionally observed. The contractile ring in this preparation was characterized by thick filaments about 12-18nm in diameter, suggesting that myosin molecules were organized into long filamentous structures. These results are disscussed with special reference to the molecular organization of the contractile ring.

DB 25

CONTRACTION WAVE ON THE CELL CORTEX OF THE GRASSHOPPER NEUROBLASTS DURING MITOSIS.

K.Kawamura. Biology, Rakuno Gakuen Univ., Ebetsu, Hokkaido.

Grasshopper neuroblasts divide unequally with a definite polarity to produce a large daughter neuroblast and a small ganglion cell. During prometaphase and metaphase, the spindle located in the cap cell side, thereafter shifting to the ganglion cell side during anaphase. Therefore, unequal division of the neuroblast along with the cap cell-ganglion cell axis is accomplished by two factors; the direction of the spindle-axis and the shifting of the spindle body.

The present study deals with cortical movements of neuroblasts treated with Cytochalasin B to analyse the relation between mitosis and cytokinesis.

Cortical movements along nuclear axis or spindle axis were recorded by projecting the 16mm cine-film of dividing neuroblasts through a narrow slit onto a sheet of photographic paper moving at a constant speed. In Cytochalasin B-treated neuroblasts, the periodical contraction wave commenced on the cortex of one pole, and then spread toward opposite pole.

The periodicity of cortical movements of the neuroblast seems to be well coincided with mitotic events. Polarity of unequal division may be maintained principally by the action of cell cortex throughout mitoticcycle.

DB 26

ELECTRON MICROSCOPIC STUDIES ON UNEQUAL DIVISION OF GRASSHOPPER NEUROBLASTS

N.Yamashiki. Biology, Rakuno Gakuen Univ., Ebetsu, Hokkaido.

Grasshopper neuroblasts, which repeat unequal division with a definite polarity, have a contact with cap cells (cc) on one side of the surface, and with ganglion cells (gc) on the opposite side. The previous study on the ultrastructure of dividing neuroblasts showed the electron dense layer beneath the cell membrane on cc-side from late prophase till middle anaphase. The layer, however, was rather indistinct with the routine method of TEM. In the present study, neuroblasts were immersed in glutaraldehyde solution containing 0.02% saponin and then treated with tannic acid. The cell membrane on cc-side was well preserved, although that on gc-side was perforated. In the dense layer observed clearly on cc-side during metaphase and early anaphase, some actin-like filaments ran parallel to the cell surface. At middle anaphase, the cell membrane in all regions was perforated. As the dense layer on cc-side became also discontinuous, another dense layer with perforations appeared on the equator. At early telophase the dense layer in the furrow region became distinct. The cc-side cortex seems to be more resistant to saponin than the gc-side, and the resistability changes as mitosis proceeds. The dense layer which appeared in the equator shortly before cytokinesis may be derived from cc-side cortex.

DB 27

LOCALIZATION OF ACTIN NETWORKS DURING EARLY DEVELOPMENT OF TUBIFEX EMBRYOS

T. Shimizu. Zool. Inst., Fac.of Science, Hokkaido University, Sapporo 060, Japan.

In precleavage zygotes of Tubifex, actin filaments segregate to the animal and vegetal poles forming the polar actin filament networks (AFNs). In this study the fate of the polar AFNs during early development of Tubifex embryos has been followed using rhodamine-phalloidin. During the first two cleavages, which are unequal and meridional, the polar AFNs are retained at the regions of cells corresponding to the poles of the precleavage zygote; thereby, they are segregated to the CD-cell at the 2-cell stage then to the D-cell at the 4-cell stage. As the mitotic apparatus forms in the D-cell, however, the vegetal polar AFN translocates toward the animal pole of the cell where the mitotic apparatus is located and unites with the animal polar AFN there. This redistribution of the AFNs is impaired by colchicine-treatment, suggesting the involvement of microtubules. Thereafter, the unified AFN is found to be associated with nuclear regions of the macromeres of the D-cell line, and finally partitioned to the teloblst-precursors 2d and 4d and an endodermal cell 4D. Cytochalasin B-experiments indicate that the AFNs play a cytoskeletal role in generating and maintaining the spatial organization of the cytoplasm which gives rise to the intracellular localization of the cytoplasm and the mitotic apparatus orientations.

DB 28

THE POPULATION OF GERM CELLS IN THE DEVELOPING QUAIL

Y. Araki, N. Yamamoto. Dept. of Physiol., Gifu Univ., Sch. of Med., Gifu.

The numbers of germ cells were estimated in the testes and ovaries of embryos from fourth to fifteenth days of incubation. Serial sections on the gonad were examined under a magnification of x400, and germ cells situated in the cortex and medulla counted in every tenth section. In order to estimate the total number of germ cells, the counts were simply multiplied by 10. Moreover the proportion of germ cell numbers to volumes of developing gonad($10^{-3}mm^3$) was estimated and compared with that of male and female. That of the left medulla or right entire gonad in the female was about 52 or 18 cells on the fourth day, about 18 or 8 cells on the ninth day and about 4 or 3 cells on the fifteenth day and showed a decrease against that in the male (about 33 or 18 cells on the fourth day, about 45 or 28 cells ninth day and about 37 or 39 cells on the fifteenth day). On the other hand, that of the left cortex in the female gonad was about 18 cells on the fourth day, about 50 cells on the ninth and fiteenth days, and was similar to that of the male (11 cells on the fourth day, 39 cells on the ninth day and about 54 cells on the fifteenth day).

These results indicate that the medulla in the female was morphologically regressed but the medulla in the male developed into a testis and the left cortexes developed into an ovary in the female and temporarilly developed into an ovary-like structure in the male.

DB 29

INCREASED CELL PROLIFERATION IN THE PLACODE OF UROPYGIAL RUDIMENT OF THE QUAIL EMBRYO

Y. Fukui. Dep. Biol., Tokyo Women's Medical College, Tokyo.

In early morphogenesis of feathers and scales of avian embryos epidermal placodes are formed and DNA synthesis ceases for a certain period in the placodes. The uropygial gland is also one of the epidermal derivatives in birds. In Japanese quail (*Coturnix coturnix japonica*) embryos epidermal basal cells of the uropygial region remain cuboidal until day 7 of incubation. At day 8 they begin to elongate, become columnar, and develop placode-like structure at day 9.

To examine the proliferative activity of the basal cells, we recorded positions of ^{3}H-thymidine-labeled epidermal basal nuclei in ARG serial sections using a digitizer connected to a personal computer. The distribution pattern of labeled nuclei was reconstituted and displayed on CRT as two-dimensional computer graphics. Columnarization of cuboidal basal cells was confirmed in three-dimensional reconstitution of the same serial sections. Unlike the feather and scale placodes, the uropygial placode possesses no resting period of DNA synthesis. Labeling index of the uropygial placode increased considerably compared with that of nonplacode epidermis. No dermal condensation was observed under the uropygial placode.

DB 30

THE EFFECT OF HALOTHANE AND ENFLUREN GAS ON THE HATCHED CHICKEN. — ON THE RECOVERY OF LIVER DAMAGE BY SHOSAIKOTO —

H. HASEGAWA, H. TANAKA and K. NONOYAMA. Dept. of Biol. Aichi Univ. of Education, Kariya.

The authors previously investigated on the influence of halothane gas to the hatched chicken on the relationship between the concentration of the gas and the degree of growth inhibition, the variation of serum LDH and the ultramicrostructure of the chicken liver. In this experiment, the authors studied on the clinical condition of the anesthetic gas (halothane, 1 % and enfluren, 2 %) to the hatched chicken. The variation of serum GOT and GPT (by NADH-UV absorption method), α-GTP (by p-Nitroanilid substrate colorimetric method), LDH pattern and scanning electron microscopic observation of liver tissue were investigated on the chicken.

The chickens treated with halothane and enfluren gas for 100 hours and after that fed normally without anesthetic gas were all died between 8-10 days and their body weight recoveries were not recognized.

The serum GOT value of the anesthetized hatched chicken with halothane and enfluren for 100 hours was 67.0-68.4 IU/L unit respectively (control, 340). GOT values of the chicken of anesthetized and Shosaikoto-administered were 653-610, 5th day; 625-413, 12th day; 401-376, 22th day respectively. Serum LDH patterns were varied from control to anesthetic gas treatment as follows: control LDH 1, 76.8; 2, 13.0; 3, 5.8; 4, 7.1; 5, 3.4: halothane and enfluren treatment for 100 hours LDH 1, 37.3-36.2; 2, 17.7-16.8; 3, 16.5-10.5; 4, 8.3-9.6; 5, 24.2-26.9: Shosaikoto administration after 22th day LDH 1, 64.9-67.6; 2, 16.3-14.2; 3, 7.2-6.1; 4, 6.9-7.0; 5, 4.9-5.1 respectively.

DB 31

STRUCTURE AND EXPRESSION OF EMBRYONIC CHICKEN PEPSINOGEN.

K. Hayashi, S. Yasugi and T. Mizuno. Zool. Inst., Fac. of Sci., Univ. of Tokyo, Tokyo.

Chicken proventricular mesenchyme is known to be able to induce production of an embryonic pepsinogen (ECPg) in proventricular and gizzard endoderms and hypoblast, but not in small intestinal and allantoic endoderms, though they form complex proventriculus-type glands. In the present study, we examined the transcription of ECPg-mRNA in these endoderms by Northern hybridization with ECPg-cDNA as a prove. ECPg-mRNA was transcribed specificaly in embryonic proventriculi in certain period of normal development (maximum at day 15). When the esophagus, proventriculus and gizzard endoderms were recombined and cultured with the proventricular mesenchyme, they equally exhited ECPg-mRNA. In contrast, the small intestinal and allantoic endoderms did not express ECPg-mRNA in the same experimental conditions, though the proventricular morphogenesis occurred. ECPg-gene was isolated from chicken genomic library and its structure was determined. This will be a useful tool for study what occurs in the process of ECPg induction and why the competence for ECPg expression is different among various kinds of endoderm.

DB 32

PROGRAMMED CELL DEATH AND CELL CYCLE DURING CHICK LIMB MORPHOGENESIS.

S. Toné, S. Tanaka and Y. Kato. Dept. of Dev. Biol., Mitsubishi-Kasei Inst. of Life Sci., Machida

It is well known that interdigital mesenchymal cells are programmed to die during normal limb development of amniote. We have previously shown that (1) Presumptive dead cells were withdrawn from cell cycle and dead ca. 20 hrs. after last DNA synthesis. (2) Administration of BrdU, a thymidine analog at this critical last S phase suppressed the programmed cell death. These results suggest the presence of death-related gene(s).

What triggers programmed cell death? In order to delineate the program for cell death, especially early phase, at first we investigated cell kinetics of presumptive dead cells.

Interdigital cells at various developmental stages were pulse labelled in ovo with BrdU, immunohistochemically stained with anti-BrdU antibody (for detection of S cell) and simultaneously stained with DAPI (for DNA amount), and analysed by cytofluorometry. Individual cells can be assigned into several cell populations in terms of amount of DNA synthesis and DNA amount. These analyses revealed that presumptive dead cells were withdrawn at G_2 phase from cell cycle and gradually loose their genomic DNA, suggesting that cell death may be caused by a failure of transition from G_2 to M phase.

DB 33

THE GRADIENT OF REACTIVITY TO THE GROWTH PROMOTING ACTIVITY OF ZPA EXISTS IN THE CHICK LIMB BUD

H. Aono and H. Ide. Biol. Inst., Tohoku Univ., Sendai.

The growth promoting activity of ZPA (the zone of polarizing activity) was examined using in vitro coculture system. The limb bud posterior tissue fragments (containing ZPA) showed stronger growth effect on limb bud mesodermal cells of anterior region than on those of posterior region, and there existed a gradient of reactivity along the anteroposterior axis. Other fragments (anterior, distal or proximal) promoted cell growth in position-non-specific manner. To compare with the mitogen(s) which could be thought to be secreted by posterior fragment, growth promoting activities of FGF, EGF and insulin were tested in the same culture conditions. FGF showed position-dependent growth promotion which is similar to that of ZPA, while EGF and insulin promoted growth in the cells of any regions to the same extent. Serum-rich medium (10%FCS) also promoted cell growth but the promotion was observed only in the cell culture of central axial region. These results suggest that the cells of posterior region secrete FGF-like growth factor(s), which controls normal limb development and experimental duplicate formation.

DB 34

LIMB BUD SPECIFIC PROTEIN IS SYNTHESIZED IN EARLY CHICK EMBRYO

S.Nishimiya and H.Ide. Biol. Inst., Tohoku Univ., Sendai.

From the comparison of protein composition between limb bud and trunk (as a control) of chick embryo, a limb bud specific protein was found.

Both limb bud and trunk tissues from stages 21-27 embryos were respectively homogenized and fractioned by centrifugation. Nuclear and mitochondrial fraction and microsomal fraction obtained were dissolved in lysis solution and resolved by two-dimensional gel electrophoresis. proteins in gels were visualized by silver staining.

Among protein spots from microsomal fraction, there was a spot specific to limb bud. It appeared at stages 22-23 and disappeared at stages 26-27. It was moderately basic protein and its relative molecular mass was about 130kD. There was no limb bud specific spot from the nuclear and mitochondrial fraction.

Comparisons were also made between proximal and distal regions and between anterior and posterior regions within a limb bud. But no significant differences were found in any of these comparisons.

DB 35

CHARACTERIZATION OF THE AV-1 ANTIGEN WHICH SHOWS POSITION SPECIFIC EXPRESSION IN CHICK LIMB BUDS.

K.Ohsugi[1,2], T.Momoi[2] and H.Ide[1]. [1]Biol. Inst.,Tohoku Univ., Sendai, [2]Natl. Inst. for NeuroScience., Tokyo.

The AV-1 antigen shows position specific expression in the mesoderm of stage 19-28 chick limb buds. In stage 28 wing buds, the AV-1 antigen expresses in the restricted regions between the radius and ulna, and between the anterior two metacarpals. Here, we characterized the AV-1 antigen molecule. The results of cell fractionation, immuno-blot analysis, indirect immuno-staining and WGA-agarose column chromatography revealed that the AV-1 antigen was a glycoprotein of molecular weight 130 k dalton and was localized on the plasma membrane. The antigenicity of the AV-1 antigen was stable against collagenase or some endo-glycosidase treatments but was not stable against heat (80°C) or some protease treatments. This indicated that the AV-1 antigenicity was due to the protein portion and not the glycoconjugate portion.

DB 36

DISTRIBUTION OF MELANOBLASTS IN EPIDERMIS OF CHICK EMBRYO : AN ANALYSIS WITH MONOCLONAL ANTIBODY SPECIFIC FOR CHICKEN MELANOBLASTS.

K. Kitamura and M. Sezaki. Dept. of Dev. Biol., Mitsubishi-Kasei Institute of Life Sciences, Machida.

A monoclonal antibody (III2A6) raised in mouse in response to homogenates of dorsal skin of chick embryo was found to exhibit a unique reactivity towards the retinal pigment epithelium of the eye and the cultured neural crest-derived cells. III2A6 strongly reacted with the melano-blasts with premature melanosome rather than melanocytes with mature melanosome. Melanoblasts from other avian, such as quail, showed no staining with III2A6. Immunoblot analysis showed that III2A6 culture supernatant strongly reacted with a polypeptide of 28KDa in addition to those of 23 and 78KDa.

Temporo-spatial appearance of III2A6-positive cells in dorsal region was studied using immunofluorescence assays. These cells were firstly detected in the overlayer region of neural tube of stage 22, migrated into superficial dermis and homed into epidermis of shoulder part of trunk of stage 23. In the subsequent stages, the regional homing to epidermis of these cells was noted (1) in pteryla and apterium and (2) in feather rudiment. III2A6 is thought to be useful tool for investigation of differentiation and migration of melanoblast.

DB 37

INDUCTION OF FUNCTIONAL DIFFERENTIATION IN CHICK STOMACH EPITHELIUM BY REAGGREGATED PROVENTRICULAR MESENCHYMAL CELLS IN VITRO

K. Takiguchi. Zool. Inst., Fac. of Sci., Univ. of Tokyo, Tokyo.

We developed in vitro organ culture system for embryonic chick proventriculus to express pepsinogen. Explants were cultured on Millipore filters in Medium 199 with Earle's salts supplemented with 50% 12-day embryo extract at 38°C in 95% air and 5% CO_2.

In these culture conditions, pepsinogen, a functional marker protein of proventriculus, was expressed in 6-day proventricular rudiment after 3 days of cultivation. Epithelial-mesenchymal recombination experiments showed that 6-day oesophageal, proventricular and gizzard epithelia express pepsinogen when recombined and cultured with the proventricular mesenchyme, while 6-day small intestinal epithelium does not. These results were consistent with the results obtained by grafting on the chorioallantoic membrane and showed that the culture conditions are permissive for pepsinogen expression.

Both 6-day proventricular and gizzard epithelia expressed pepsinogen when recombined and cultured with reaggregated proventricular mesenchymal cells. These results indicate that the reaggregated proventricular mesenchymal cells retains inductive potency for pepsinogen expression of stomach epithelia.

DB 38

RE-ORGANIZATION OF F-ACTIN AND CELL POLARITIES IN ESOPHAGEAL EPITHELIUM OF THE CHICK EMBRYO.

T.Fujimoto, R.Murakami and I.Yamaoka. Biol. Inst., Fac. Sci., Yamaguchi Univ., Yamaguchi.

The lumen of esophagus of the chick embryo closes at 5-6 days of incubation and re-opens at 6-8 days. The morphology of the epithelium changes from pseudo-stratified epithelium to compact mass of cells, then to simple columnar epithelium. Changes in the distribution of F-actin and ultrastructures associated with the mor-phogenesis of the epithelium were studied by use of rhodamine-phalloidin and TEM.

In the open area, F-actin was intensely detected just under the cell membrane near the apical junctional areas of the epithelial cells. When the lumen became closed, F-actin was scarecely found in the epithelial cell mass, and the polarities of epithelial cells except the basal cells became disorganized. Re-opening of the lumen was initiated as the appearance of several intercellular spaces in the cell mass. F-actin reappeared around the spaces. Apical junctions also formed. The basal-apical polarities of the epithe-lial cells were restored around the spaces. The spaces fused or enlarged to form the lumen.

These results suggest that the re-organization of the F-actin and apical junctional complex is essential for the establishment of the lumen.

DB 39

DIFFERENTIATION OF THE EPITHELIUM LINING GIZZARD-DUODENAL JUNCTION OF THE CHICK EMBRYO.

S.Matsushita. Dept. of Biol., Tokyo Women's Medical College, Tokyo.

The differentiation of the epithelium lining the junctional region of gizzard(G) and duodenum(D) of the chick embryo was studied.

SEM observation showed that from 10 days of incubation villus formation proceeds in D and G-D boundary can be noticed at the point where D leaves G. Mucus secretory activity of G epithelium, as revealed by alcian blue-staining in paraffin sections and phosphotungstic acid(PTA)-stained granules in ultrathin sections, was prominent at 6 days and later. PTA-stained granules were found also in the anterior and middle region of D at 6 and 8 days. At 10 days, epithelial cells with the granules in D were reduced in number, and at later days they were only occasionally found. The immunofluorescence study with the affinity-purified anti-sucrase antibodies showed that the sucrase appeared only in D from 10 days. Thus, at early stages the anterior and middle part of D contains epithelial cells with G-like differentiation, which are almost lost when intestinal(D-like) differentiation manifests in D. Immunoelectron microscopy of chorioallantoic grafts of 6-day G-D fragment revealed that there exist some cells with both G- and D-like differentiation characters(PTA-stained granules and sucrase) in G-D boundary.

DB 40

TROPOMYOSIN ISOFORMS IN CHICKEN GIZZARD SMOOTH MUSCLE.

M.Hosoya[1], T.Ishimoda-Takagi[2] and T.Hirabayashi[1]
[1]Inst. of Biol. Sci. Univ. of Tsukuba, Ibaraki, [2]Dept. of Biol., Tokyo Gakugei Univ., Tokyo.

In the chicken gizzard smooth muscles of 7,10,14 day embryos we found four high- and six low-molecular-type tropomyosin(TM) isoforms in addition to the α- and β- ones. These proteins were identified as TM by (1) isoelectric point, (2) anomalous electrophoretic mobility in the presence of urea, (3) stability against heat treatment, (4) inclusion in Bailey's tropomyosnin fraction, (5) binding ability to muscle actin, and (6) cross-reactivity with antisera against TMs from chicken gizzard, skeletal muscle and brain. In the differentiation of gizzard smooth muscle, the ratio of accumulated TM to γ-actin was found to be reasonably constant after hatching, while it appeared to be lower than expected during the embryonic deveropment (7-14 days). The relative amounts of the isoforms found in this experiments at the earlier stages were predominant enough to bring up the ratio to γ-actin to those observed at the stages after hatching. The coordinate accumulation of actin and TM was expected even at the embryonic stages, just as observed after hatching.

DB 41

COORDINATE ACCUMULATION OF TROPONIN SUB-UNITS IN CHICKEN BREAST MUSCLE.

M. Kawabata and T. Hirabayashi. Inst. of Biol. Sci., Univ. of Tsukuba, Ibaraki.

The accumulation of troponin subunits in developing chicken breast muscle was determined by two-dimensional gel electrophoresis and an image analyzing system. All troponin T isoforms, including those hidden behind creatin kinase, were detected on the two-dimensional pattern by the addition of 6M urea in the second dimension SDS-polyacrylamide gel electrophoresis. These troponin T isoforms were classified into four types in developmental order by the isoelectric point and molecular weight: leg-muscle type (L), neonatal breast-muscle type (BN), young chicken breast-muscle type (BC) and adult breast-muscle type (BA). L-, BN-, and BC-type troponin Ts were transiently expressed at specific ranges of developmental stages. BA-type troponin T, first detected at around 7th day after hatching, was retained in adult. Three kinds of individual variations were detected in the way of BA-type expression, while troponin C and troponin I gave no change during development or among individuals. Quantitative analysis of two-dimensional patterns of troponin subunits showed a moderate coordination among the three components all through postnatal development, when total amount of all the types of troponin T was considered.

DB 42

LOCALIZATION OF AN EMBRYO-SPECIFIC MYOSIN LIGHT CHAIN (L-23) IN SMOOTH, CARDIAC, AND SKELETAL MUSCLE CELLS IN VITRO.

Y. Ogasawara, K. Takaoka and T. Obinata. Dept of Biol. Chiba Univ., Chiba.

A novel myosin light chain (MLC), L-23, exists in various muscles in chick embryo and also in nervous tissues. As a first step to clarify the role of L-23, we examined its location in cultured muscle cells by an immunofluorescence method. We prepared two monoclonal antibodies (McAb), EL-64 & EL-49, with L-23 as an immunogen; the former was specific for L-23, while the latter crossreacted with alkaline MLCs of smooth, cardiac, and skeletal muscles, and of nonmuscle cells. The McAbs were applied to cultured gizzard, ventricular, and pectoralis muscle cells. In the case of gizzard, both EL-64 and EL-49 stained stress fiber-like structures. Both McAbs stained brightly young cardiac myocytes to give striations. When the McAbs were applied to skeletal muscle cells, EL-64 stained myoblasts and young myotubes without giving any particular structures, although EL-49 gave a typical striated pattern. Cardiac myocytes and skeletal myotubes cultured for about a week were hardly stained with EL-64. Thus, the assembly of L-23 into the structures differed among the various muscles. We assume that the difference in affinity between L-23 and various myosin heavy chains is responsible for such phenomena.

DB 43

DISASSEMBLY AND REASSEMBLY OF MYOFIBRILS DURING DISSOCIATION AND REASSOCIATION OF CARDIAC MUSCLE CELLS

T. Yagi, H. Abe, S. Tsukita and T. Obinata

Previous investigation has shown that when muscle tissue was dissociated with trypsin, myofibrils are disassembled, but they were recovered without protein synthesis as muscle cells reaggregated (Fischman 1970). In the present study, we re-examined myofibrillar disassembly and reassembly during dissociation and reassociation of chicken embryonic heart cells as to 1) how cell adheion affects the initiation of myofibrillar assembly and 2) whether depolymerization of actin filaments into G-actin is caused during disassembly of myofibrils. By means of electron microscopy, we observed that when cell aggregates were formed in rotating cultures, assembly of myofibrils was initiated mostly at the site of cellular adhesion, suggesting that cell adhesion site can be a trigger for the assembly. Amount of G-actin as well as total actin in the cells were measured before and after dissociation of the tissues and during cell aggregation by DNase I inhibition assay. Either total actin or G-actin scarcely differed in amount during disassembly of myofibrils. However, free actin filaments in the cytoplasm increased significantly. Therefore, we suggest that actin filaments were not depolymerized but become free from Z-line during disassembly of myofibrils.

DB 44

CYTODIFFERENTIATION OF THE PROSTATE-LIKE GLANDULAR EPITHELIUM INDUCED FROM URINARY BLADDER EPITHELIUM OF THE ADULT RAT.

N. Suematsu, Zool. Inst. Fac. of Sci. Univ. of Tokyo, Tokyo.

Urinary bladder epithelium of the adult rat formed prostate-like glands, when combined with fetal urogenital sinus mesenchyme and cultured beneath the renal capsule of male rat hosts. With the progression of the gland formation, the bladder epithelium lost its alkaline phosphatase activity and antigenicity against anti-functional bladder epithelium-antiserum. Like the normal prostate, the induced epithelium expressed acid phosphatase, non-specific esterase and antigenicity against anti-human prostatic acid phosphatase-antiserum, but did not show androgen receptors nor an antigen against anti-4week-ventral prostate epithelium-antiserum. The SDS-PAGE patterns of proteins in the glandular epithelium induced from the urinary bladder epithelium and in the normal urinary bladder and prostatic epithelia revealed that the induced gland loses some bands identified in the bladder epithelium and became to express other bands similar to but not identical with those of the normal prostatic epithelium, suggesting that the induced gland does not differentiate as completely as the normal prostate. It is possible that this is linked with the absence of androgen receptors in the induced glandular epithelium.

DB 45

LOCALIZATION AND CHARACTERISTICS OF MICROTUBULES IN MATURE MYOTUBES IN CULTURE.

O. Saitoh*,**, T. Obinata** . *Zool. Inst., Fac. of Sci., Univ. of Tokyo, Tokyo and **Dept. of Biol., Chiba Univ., Chiba.

In the previous report, we have shown that microtubules are the cytoskeletal element which is most reponsible for elongation of developing myotubes. In this study, the distribution of microtubules in well-developed myotubes were examined by an indirect immunofluorescent microscopy. When mature myotubes were reacted with anti-tubulin antibody, fluorescence was observed with striations along myofibrils as well as with filamentous structures parallel to the longitudinal axis of the cells. Similar striation patterns were also observed when myotubes were treated with the antibody to MAP2. Microtubulular fraction was isolated from chicken embryonic muscles in the presence of taxol and the constituents of muscle microtubules were examined by SDS-PAGE and immunobotting. We detected a MAP2-like peptide which was 300 kDa in size and reacted with anti-MAP2 antibody in addition to tubulin. Treatment of myotubes with either colcemid or taxol caused local accumulation of actin which led to modulation of myofibrillar structures. From these observations, we suggest that microtubules exist in association with myofibrils and play some role in supporting the myofibrillar structures.

DB 46

THE CYTOSKELETAL SYSTEMS AND LOCOMOTION OF EPITHELIAL CELLS-A POSSIBLE ROLE OF MICRO-TUBULES.

S.Takeuchi. Zool.Inst.,Fac.Sci.,Univ. Tokyo, Tokyo.

In order to know the role of microtubule during locomotion, the epithelial cells in culture were treated with colcemid, and the effects of it were examined with the methods as follows: phase contrast microscopy, interference reflexion microscopy(IRM), secondary immunofluorescence method, and cytochemistry.

The epithelial sheets were completely inhibited to spread along the surface of Millipore filter(pore size, 0.3μm), when cultured for 96hr on Wolff-Haffen's medium containing colcemid(>0.05μg/ml). The marginal cells of epithelium explanted on the glass surface, started to retract, when cultured more than 40 min after transferred into a medium(L- 15, 20% horse serum) containing colcemid(0.05μg/ml). The loss of focal and close contacts under the leading lamella was confirmed with IRM. In the cells, no fibrous structures were recognized either with anti-tubulin anti-body or with rhodamine phalloidin, suggesting not only microtubules but F-actin were disintegrated with colcemid.

From these, microtubules were supposed to be responsible not only for mechanical maintenance of the leading lamella but for the organization of focal contacts from which the microfilament bundles were reported to elongate(Füchtbauer et al.1983).

DB 47

RECONSTITUTION OF HYDRA DISSOCIATED CELL--REEXAMINATION OF EXPERIMENTAL METHODS AND ABOUT INITIATION OF HEAD FORMATION DURING RECONSTITUTION.

K.Noda and C.Kanai. Lab of Electron microscopy,Tokyo Metropolitan Inst. of Gerontol.

The effect on reconstitution of aggregates of dilution ratio of dissociation medium was examined in P. robusta. M-29 solution (Its components were reported in 1986) is able to be diluted to 20% with 1mM TES buffer for reconstitution to perfect form in aggregates larger than 300μ. Components and their ratio of M-29 are the same as those of the culture solution for individuals. Difference in ratio of Ca ion in reconstitution medium is influential for survival ratio in aggregate smaller than 250μ during reconstitution.

Hours required for tentacle bud formation in reconstitution were compared with those of regeneration of tissue fragments with two cell layers and mesoglea. As a result, it is suggested that aggregates larger than 400μ can be initiated for head formation within 6-8hrs after the beginning of reconstitution. The mesoglea is not found even under electron microscope in 6-8 h-aggregates, which have partially arranged endodermal epithelial cells along the ectodermal epithelial cells covered on the entire surface of aggregates.

These phenomena are discussed briefly in contrast to those of embryogenesis.

DB 48

NERVE NET FORMATION IN REGENERATING TISSUES OF HYDRA I. PATTERN FORMATION OF RFamide-LIKE IMMUNOREACTIVE NERVE NET.

O.Koizumi & Y. Nakashima, Physiol. Lab., Fukuoka Women's Univ., Fukuoka.

The pattern formation of hypostomal nerve net was examined in regenerating head of hydra. Using a whole mount technique with indirect immunofluorescence, the spatial pattern of neurons showing RFamide-like immunoreactivity (RLI) was visualized. An antiserum to RFamide binds to two subsets of neurons in head: sensory cells of the apex of the hypostome and the ganglion cells of the lower hypostome and the tentacle. During initial stages of head-regeneration, only the ganglion cells arose at the regenerating tip. At later stages, the sensory cells began to appeare at the apex of the dome and at the same time the ganglion cells disappeared from the apex and relocated at the side of the dome close to the location of the tentacle ring. Head-regeneration deficient mutant, reg-16, shows very poor and delayed appearance of RLI+ sensory cells during head regeneration, while the appearance of RLI+ ganglion cells are normal. These results and the behavior of tentacle specific antigen visualized by a monoclonal antibody, TS19, support "the two part pattern during head regeneration" (Bode et al., 1986, 1987).

DB 49

THE DEFORMATION AND POLYMORPHISM OF POLYPS FORMED BY CONTACT BETWEEN TWO SPECIES OF HYDROZOAN'S COLONIES.

H.Namikawa and Y.Kakinuma. Dept. of Biol., Fac. of Sci., Kagoshima Univ., Kagoshima.

Two species of hydrozoans, Stylactis sp. and Leuckartiara sp., were transplanted to one petri dish and observed the influence of mutual interference on the formation of colonies of both species. After the contact of two colonies. Regardless of deformation, both species still coexised on the same petri dish. At the contacted part of stolons of two species the ectoderm tissues became thick, and the number of nematocysts of two species was increased.
The nematocysts formed a line in the stolon; each nematocyst facing to each one of the other species. The regression and regeneration of tissues were observed between 24 and 48 hours after the discharge of nematocysts. Fertheremore the elongating stolons of two species contained each other. In the case of Stylactis sp., polyp budding form polyps and abnormal development of tentacles were also founed.
When the amount of food for colonies were reduced to a half, the diffrentiation of finger like polyps gave rise and polymorphism of polyps was also observed at the contacted part of stolons of both species.

DB 50

ELECTRON MICROSCOPIC STUDIES OF THE REDIFFERENTIATION OF COPULATORY APPARATUS FROM THE DEDIFFERENTIATED CELLS ORIGINATED IN THE OLD COPULATORY APPARATUS IN A FRESHWATER PLANARIAN, BDELLOCEPHALA BRUNNEA.

M. Kudoh and W. Teshirogi. Dept. of Biol., Fac. of Sci., Hirosaki Univ., Hirosaki.

The regression of the copulatory apparatus of planarians is caused by the excision of the regenerating head-blastema at an interval of three days after decapitation. In this case, the copulatory apparatus disintegrated to cell clusters, then dissociated to neoblast-like cells and finally transformed into ordinary mesenchymal cells in 60 days after decapitation.

When a head of the worm which has regressed the copulatory apparatus was regenerated by discontinuance of excision of the head-blastema, a new copulatory apparatus was redifferentiated from the dedifferentiated cells, that is, the neoblast-like cells reaggregated to clusters and then differentiated to penis and other parts of the copulatory apparatus.

In this redifferentiation of the penis, new secretary epithelial cells were made from dedifferentiated cells originating in the old penis and the same holds good for nerves and muscles. However, it was not clear whether the neoblast-like cells are multipotent cells or totipotent cells. This problem is yet to be solved in the future.

DB 51

WOUND CLOSURE IN PLANARIAN EPIDERMIS. II. SCANNING ELECTRON MICROSCOPIC EXAMINATION OF THE PROCESS OF EPITHELIZATION.

S. Ishii. Div. Cell Sci., Cent. Res. Lab., Fukushima Med. Col., Fukushima.

The process of epidermal wound healing in planarians has not yet been fully understood, several different hypothetical views being prevalent. This study consists of SEM examination applied to D. japonica regenerants in various stages of the healing (0 min. to 40 hrs. postamputation). In order to avoid agonal distortion of specimens during fixation, they were quickly fixed with sulphuric acid (1.2 sec.). Owing to the initial wound contraction (for 10 min. after amputation) many epidermal rugae develop around the wound, giving rise to a special rim of confused array of epidermal cells. Cell crowding in the rim seems to stimulate migratory activities of epidermal cells toward the wound. Two steps of epidermal migration could be distinguished: 1) Initially formed marginal aggregates of cells, freed from the basement membrane, extend locally across the wound to form a very thin incomplete provisional covering called "epithelioid" (30 to 60 min. postamputation). 2) The ensuing steady advance of migration, probably due to a total sliding mechanism of the epidermis, results in a swallow of the wound, entirely replacing the degenerating epithelioid (24 to 40 hrs. postamputation).

DB 52

THE INSINKING PROCESSES OF NUCLEI OF PHARYNGEAL EPITHELIAL CELLS IN PHARYNX REGENERATION OF PLANARIAN, DUGESIA JAPONICA.

E. Asai, Dep. of Biol., Kanazawa Med. Univ., Ishikawa.

The insinking processes of nuclei of pharyngeal epithelial cells were observed in the pharynx regeneration in the head piece cut transversely in prepharyngeal region of planarian, Dugesia japonica, and the following results were obtained. (1) About 6 days after the cut, the nuclei of the outermost epithelial cells of pharyngeal rudiment begin to sink into underlying muscle cell layers. (2)Several basal nucleic as well as cytoplasmic projections seem as if they were trying to find suitable spaces between the muscle cells. After finding the most suitable space for sinking, the cells retract the other projections and concentrate on one projection with which to penetrate the muscle cell layers. (3)In the cytoplasm of insinking cells, numerous free ribosomes, several chromatoid bodies, many mitochondria(Mt.), rod-shaped bodies, rER, Golgi complexes, a few microtubules, small vesicles and glycogen particles were observed. (4)Around the insinking nucleus several Mt. were present. This suggests that much of the energy needed for insinking is supplied by Mt.. (5)One of the advantages of insinking of the cell nucleus seems to be that apical cytoplasm can extend much longer without the nucleus than with the nucleus when the pharynx is protruded to take the food.

DB 53

HISTOCOMPATIBILITY IN TWO SPECIES OF FRESHWATER SPONGES, EPHYDATIA MÜLLERI AND EPHYDATIA JAPONICA.

Y. Watanabe and Y. Yanagihara. Dept. of Biol., Ochanomizu Univ., Tokyo.

The taxonomic position of two freshwater sponges, E.mülleri and E.japonica has been identified by the roughness of their skeletal spicules, i.e., the former has rough, spiny megascleres and the latter has smooth ones. Because of skeletal variations between two species, there have been discussed that E.japonica should be a variety of E.mülleri and synonymize with the latter.

By the use of histocompatibility between these two species, we aimed to approach this problem outside spicular morphology. We examined the fusibility in the sponges derived from gemmules of 18 specimen from 6 localities. In two specimens with similar spicule composition in the same population, they were each other compatible fusible; that in ones with different spicules, they did not fuse. Cytotoxic rejection reactions occured even between the sponges in the same population. On the other hand, the sponges with similar spicular composition from different locality, were found to be incompatible.

These results showed that the morphological variations of megascleres may be influenced to some extent by environmental factors, though it is rather considered to be dominated genetically. Another approaches should be required to make sure that the incompatibility is interspecific rejection or intraspecific one.

DB 54

DEVELOPMENT OF COELOMIC CELLS, GAMETOGENESIS AND GONADOGENESIS IN ASCIDIA AHODORI.

Y.M.Sugino & M.Ishikawa. Dept. of Biol., Fac. of Sci., Ehime Univ., Matsuyama.

The differentiation of coelomic cells, gametogenesis, and the organogenesis of the ovary in the ascidian Ascidia ahodori were studied by light microscopy.

Paraffin sections stained by the azan method showed that the adults have at least 6 types of coelomic cells: the lymphocyte-like, blue, purple, brown-vacuolated, single-vacuolated, and red morula cells. The lymphocyte-like cells are already observed in the swimming larva. All other kinds of the cells appear 20-43 days after metamorphosis. The single-vacuolated cells, which seem to be the so-called signet ring cells, develop later than the other vacuolated cells.

Early oocytes appear in the 43-day individual whereas spermatogenic cells are detected initially in the 80-day individual. Both mature eggs and spermatozoa, however, become observed simultaneously in the 100-day individual. Formation process of female reproductive organs is divided into the following 3 steps. When the ovarian primordium becomes observed first, it shows a hollow epithelial structure composed of an oogenetic and a non-oogenetic part. The ciliated epithelium of the ovarian epithelium differentiates in the 60-day individual. Finally, formation of the oviduct is completed in the 100-day individual.

DB 55

REINITIATION OF MIOSIS IN ASCIDIAN EGG BY THE INJECTION OF CALCIUM ION.

N. Sensui. Zoological Inst., Faculty of Sci., Univ. of Tokyo, Tokyo.

In *Ciona savignyi*, an injection of $CaCl_2$ (more than 20mM, 65pl) into unfertilized egg induced the deformation of the egg and the 1st polar body formation like a fertilized egg. These changes were also induced by the injection of Ca^{2+}-EGTA. However, the injection of KCl, NaCl or $MgCl_2$ did not induce these changes. In the egg injected with $CaCl_2$, microvilli elongation and aggregation were observed as seen in the normal fertilized egg. In the eggs injected with EGTA (200mM, 65pl), these changes were suppressed for 60 min after insemination, then the deformation occurred slowly and abnormally, but the 1st polar body was not formed. Most of the eggs injected with $CaCl_2$ did not form the 2nd polar body after the 1st polar body formation. In these eggs, the 2nd polar body formation was often induced by insemination or the treatment with Ca^{2+}-ionophore. These results suggest that the deformation and the 1st polar body formation need Ca^{2+} and that the Ca^{2+} plays an important role in the changes after the fertilization and also that there are at least two steps in the miotic process of the ascidian egg.

DB 56

SELF-FERTILITY OF THE ASCIDIAN, CIONA SAVIGNYI.

T. Numakunai[1], Z. Hoshino[2] and M. Hoshi[3]. 1Mar. Biol. Stat. Fac. of Sci. Tohoku Univ., 2Dept. of Biol. Fac. of Educ. Iwate Univ., 3Lab. of Biol. Fac. of Sci. Tokyo Inst. of Technol.

In the species *C. savignyi*, which spawns at dawn, self-fertility of gonad eggs, oviduct eggs and eggs released under natural light cycle was surveyed. To observe self-fertilization of the released eggs two methods were used: (1) spawning in running sea water and catching the eggs in a trap, (2) spawning in a glass container. In the glass container a high percentage of self-fertilization was observed, whereas in the trap almost all the eggs were not self-fertilized. Each animal showed a different rate of self-fertilization from day to day. In the glass container, embryos at different developmental stages were observed. When the animals with great self-fertility were transferred to a trap in running sea water, almost all the eggs were found unfertilized. To get gonad eggs, *C. savignyi* gonads were dissected, and fully matured eggs were selected. Fertilization was confirmed by observing cleavage 1 hour, 2 hours and 3 hours after insemination. Newly collected animals showed a small percentage of self-fertilization in both gonad eggs and oviduct eggs. When animals were kept in the laboratory, especially under continuous light, almost all the gonad eggs and oviduct eggs were self-fertilized. The first cleavage was observed 1 hour later than in cross-fertilization. The self-fertility of *C. savignyi* is affecte more easily by conditions under which the animal is kept.

DB 57

FORMATION OF PIGMENT BODIES IN THE BRAIN VESICLE OF AN ASCIDIAN EMBRYO, STYELA PLICATEA (LESUERUR).

H. Ohtsuki and M. Yoshida. Biol. Inst., Fac. of Education, Oita University, Oita.

Formation of pigment boidies in otolith and ocellus of the developing ascidian embryos was investigated by whole mount method (Whittaker, 1973) and with serial paraffin sections (2 μm thick).

Two pigment bodies, which were nearly shperical and about the identical size (3.5 μm, diameter), appeared simultaneously in the presumptive otolith cell and in the ocellus pigment cell at 5.5 to 6 hr after fertilization (23-24 °C).

The pigment body in the otolith continued to increase its size during development, until the hatching stage (10 hr after fertilization) and became ovoid form (13 μm and 11.5 μm, axis length). It was composed of two blocks (ventral and dorsal) at the time of its appearance. At the swimming larval stage, one of the two blocks of the otolith pigment body looked like concave lens and the other, convex one.

The ocellus pigment body grew up by 6 hr after fertilization (5.5 μm, diameter) and it retained its shperical form, from the stage of first visible indication of it to the swimming larval stage. It was encircled with a small vesicle at postero-dorsal wall of the brain vesicle in the swimming larvae.

DB 58

INSULIN-LIKE SUBSTANCES MAY BE A GROWTH FACTOR OF STEM CELLS IN ASCIDIANS.

K. Kawamura and M. Nakauchi. Dept. of Biol., Fac. of Sci., Kochi Univ., Kochi.

In the polystyelid ascidian, *Polyandrocarpa misakiensis*, hemoblasts are the multipotent stem cell, 4-5 μm in diameter, that participates in the formation of several organ rudiments during palleal budding. In this work, we examined how the dynamics of stem cell population were regulated in the process of ascidian blastogenesis. Insulin prepared from the bovine pancreas (1 μg, 0.1 μg, 0.01 μg/ml) could enhance the mitotic activity of 1.5-day- or 2-day-old buds two or three folds as much as that of controls. The promotive effect of insulin on DNA synthesis first appeared on the mesenchymal blood cells, exclusively the hemoblasts and large lymphocytes, at 30 hours of bud development. Double staining of sectioned buds with insulin-FITC and DAPI (DNA-specific fluorescent dye) showed that insulin bound only to the periphery of the nucleus of hemoblasts. Anti-human insulin antibody prepared from guinea pig cross-reacted with the large vacuoles of morula cells in the blood and the inner-most layer of the tunic. Histological studies showed that the morula cells underwent autolysis at the earliest stage of bud development. These results strongly suggest that insulin-like growth factor(s) derived from the morula cells operate on the hemoblasts, and then the activated hemoblasts are assigned to several organ rudiments, contributing to the asexual development of ascidians.

DB 59

CLONING OF cDNA AS A PROBE FOR ANALYSING MOLECULAR MECHANISMS INVOLVED IN EPIDERMAL CELL DIFFERENTIATION IN THE ASCIDIAN EMBRYO.

K.Takamura, K.Makabe, T.Nishikata and N. Satoh. Dept. of Zool., Kyoto Univ., Kyoto.

In order to study molecular mechanisms involved in epidermal cell differentiation in ascidian embryos, we produced several monoclonal antibodies which specifically recognized epidermal cells of Halocynthia roretzi embryos (Nishikata et al., Dev.Biol. 121, 408-416, 1987). Among them, the Epi-2 antigen, about 100kd in MW, first appears at the tailbud stage and is present until at least the swimming larval stage. Studies with inhibitors of protein and RNA synthesis suggested that an activation of the gene encoding the antigenic polypeptide occurs at the late gastrula stage.

In this study, we first produced cDNA library against poly(A)$^+$RNA isolated from the tailbud embryos. The cDNAs were inserted into LacZ promotor region of an expression vector λgt11. Induction of the expression by IPTG resulted in synthesis of proteins encoded by cDNAs. Proteins produced were blotted onto nitrocellulose membranes, on which the proteins were cross-reacted with the Epi-2 antibody. Reacted clones were visualized with S^{35}-labeled second antibody. Thus, we screened a cDNA of about 1kb in length encoding the epidermis specific antigen. The cDNA was recloned by inserting into plasmid with T7 promotor, and the antisense RNA was selected as the molecular probe.

DB 60

RECONSTRUCTION OF THE ROWS OF STIGMATA DURING REGENERATION IN THE COMPOUND ASCIDIAN, POLYANDROCARPA MISAKIENSIS.

Y. Taneda and C. Ono. Fac. Educ., Yokohama Natl. Univ., Yokohama.

In ascidians, the rows of stigmata is approximately constant in number among the species. The compound ascidian, Polyandrocarpa misakiensis has a capacity to regenerate whole animal from a fragment. We revealed that the number of the rows of stigmata in the regenerated returned to the original number in intact zooid. Thus, we studied how to return the rows. Two modes of increasing pattern were observed. In one case, the rows of stigmata were once disappeared. New rows were produced afterwords. In another case, the increasing of the rows was caused by addition of the rows without disappearance of them.

When a zooid was cut into two parts leaving them on a slide, they usually fused together into single zooid. In some cases, an excess sperture was produced at the fused area. We revealed that the fused zooid had more rows than control and new rows were produced on the branchial wall near the fused area. Not only the reconstruction of the rows in the regenerated but also the increasing of them and the formation of excess aperture in the fused supports the existence of positional information along antero-posterior axis of the zooid.

DB 61

STRUCTURES OF COLONIAL MARGIN IN ASCIDIANS INVOLVED IN SELF-NONSELF RECOGNITION.

E.Hirose, K.Hashimoto*, and H.Watanabe. Shimoda Mar. Res. Ctr., Univ. of Tukuba, Shimoda and *Meiji Inst. of Health Science, Odawara.

Six species of botryllid ascidians, Botryllus scalaris, B. primigenus, Botrylloides simodensis, B. lentus, B. fuscus, and B. violaceus, were used. For SEM observations, interior surface of colonial margin was exposed by following methods: materials embedded in paraffin were cut into pieces, deparaffinized, and dried at critical point. Styrene resin was also used for embedding medium.

There were more than two types of test cells in the tunic. "Amoeboid test cell" was common to all species. "Granular test cell" was seen only in the species, in which the allogeneic recognition took place in the sub-cuticular region, but not in the other species. Thus, the "granular test cell" might have an important role for allo-recognition.

The external surface of the tunic was composed of cuticule. There were minute protrusions on the cuticule. Since the density of the protrusions decreased toward the edge of the colonial margin, the cuticle might grow at the edge of the colonial margin. Each species has the different shape of the protrusion and the difference might be related to xenogeneic recognition.

DB 62

THE MUTANT GENE ter CAUSES GERM CELL DEFICIENCY, NOT ACCOMPANIED BY TESTICULAR TERATOCARCINOGENESIS, IN A C57BL/6J GENETIC BACKGROUND IN MICE.

M.Noguchi[1], H.Kato[2], K.Moriwaki[3], and T. Noguchi[3,4], [1]Biol. Inst., Fac. of Sci., Shizuoka Univ., Shizuoka, [2]Central Inst.for Exp.Animals, Kawasaki, [3]Natl. Inst. of Genetics, Mishima, [4]Deceased Nov. 24, 1983.

A recessive mutant gene ter causes germ cell deficiency, accompanied by a high incidence of testicular teratomas in 129/Sv-ter strain mice (T.Noguchi & M.Noguchi, 1985). In order to examine the influence of a genetic background on the ter action, we have backcrossed animals carrying the mutation to C57BL/6J for N1-N8 generations. We found that germ cell deficiency occurred in 20-29% of offspring from N1-N8(+/ter) x 129/Sv-ter(+/ter), which would be the ter/ter genotype, but that testicular teratocarcinogenesis did not occur in ter/ter males after the 5th backcross. Also, we analysed biochemical markers produced by the alleles at 9 loci on 7 chromosomes, which differ between 129/Sv-ter and C57BL/6J strains, in N3-N8 generations. All of these alleles in N5-N8 animals were found to be those of C57BL/6J. Thus, it is concluded that this introduction of the ter gene onto the C57BL/6J background causes germ cell deficiency in homozygoutes and that gene(s) other than ter in 129/Sv are involved in determining susceptibility to testicular teratocarcinogenesis.

DB 63

FUNCTIONAL MORPHOLOGY OF EPITHELIAL CELLS RELATING TO SPERM STORAGE IN THE JAPANESE HOUSE-DWELLING BAT, PIPISTRELLUS ABRAMUS.

T.Mōri and T.A.Uchida. Zool. Lab. Fac. of Agr. Kyushu Univ., Fukuoka.

Spermatozoa were stored in both the uterus and the uterotubal junction (UTJ), and there was no infiltration of polymorphonuclear leucocytes into both parts.

The heads of spermatozoa were in close contact with epithelial microvilli covered by developed fuzz filaments in the uterus, while they were lodged in indentations of the non-ciliated epithelial cells in the UTJ. Although the endometrial epithelial cells did not endocytose cationized ferritins as well as dead spermatozoa, in the UTJ the ferritins were concentrated within endocytotic vesicles and vacuoles of the epithelial cells. The phenomenon seems to explain the mechanism of epithelial engulfment of spermatozoa in the UTJ.

The epithelial cells of the uterus and UTJ showed both alkaline phosphatase and glucose-6-phosphatase activities; they contained secretory granules which seem to play a role in antisepsis of dead spermatozoa and seminal plasma remaining in the uterus.

Thus, spermatozoa appear to be provided with nutritive substances from the epithelial cells and to be alive under suitable conditions, kept safely by the action of the secretory material from the epithelial cells in the uterus and kept clearly by the epithelial engulfment in the UTJ.

DB 64

DISTRIBUTION AND DIRECTION OF THE SITE IN MITOSIS IN THE SEMINIFEROUS TUBULE OF THE IMMATURE MOUSE.

M. Chiba. Dept. of Biol., Fukushima Med. Coll. Fukushima.

Early indications of the spermatogenic waves in the mouse seminiferous tubules were sought. Whole testes from 9-day-old mice were fixed in Bouin's, embedded in paraffin and cut serially at 10 µm. The Mallory's stain was used. Two-dimensional reconstruction maps were made through photomicrographs. The sites in spermatogonial mitoses were recorded along the length of the tubules. The types of sprematogonia were not identified. Other reconstruction maps were made to show the zigzag tubules as if they had been extended. Examination of the reconstructed tubules showed that the extent of the site in spermatogonial mataphase varied considerably.When a mark was allotted to the center of each site and the distance between the adjacent marks was measured, the average length was calculated to be 0.6 mm. Prophase spermatogonia were often seen near the site. On examination, such spermatogonia were situated mostly in the distal position. Location of the centers in prophase revealed that they were distributed more regularly along the tubule with the average interval of 1.2 mm. These findings may indicate that in the mouse the spermatogenic waves are taking place 9 days after birth.

DB 65

SURFACE PROTEIN ON ROUND SPERMATIDS FROM RAT TESTES.

M.NAKAMURA,R.MATSUDA*,S.OKINAGA & K.ARAI. Dept. of OB/GYN, Sch. of Med., Teikyo Univ. Tokyo 173 and *Dept. of Biol., Tokyo Metropolitan Univ. Tokyo 158.

Spermatids undergo drastic morphological changes and mature to be sperm. In this process, mRNA synthesis is active. However, there are few reports concerning the analysis of mRNA dependent protein synthesis in spermatids. This study was performed to analyze membrane bound proteins sensitive to actinomycin D.

Purified population of rat spermatids was obtained using unit gravity sedimentation on 2-4% linear gradient of BSA in PBS. Cells were incubated at 32°C with [^{35}S]methionine and actinomycin D. Plasma membranes were isolated by centrifugation on discontinuous gradients and SDS-PAGE in one and two dimentions was performed. For autography, gels were dried under vacuum and films were exposed to gels.

A labelled major protein of spermatids in the membrane bound proteins had a molecular weight of 24K. Actinomycin D (30 ug/ml) had no effect on newly synthesized proteins of the cytosol, while it inhibited the labelling of the membrane proteins significantly. Membrane bound 24K protein was extracted with 2% cholic acid. Elution profile of 24K protein from Sephadex G-200 column showed that this protein came off with larger proteins. This protein might play an important role in differentiation of round spermatids to sperm.

DB 66

Analysis of the mechanism of zona reaction in the mammalian egg IV.

T. Oikawa*, Joe Fukui* and Osamu Ikeda**, *; DRB Center, Yamagata 990, Japan, **; Tokyo Univ. of Arts and Sci., Tokyo 184, Japan

Very recently,during examination of the biochemical changes of zona pellucida before and after fertilization, we found a phenomenon that two kinds of lectins (BS-1 and BS-2) can discriminate the zona pellucida of unfertilized egg from that of fertilized one. So, for the purpose to know whether this phenomenon can be induced by cortical granule material (CGM) or not, we did an experiment to examine whether it is possible to induce the zona reaction-like changes on the zona pellucida of unfertilized egg by pretreatment with A23187 or not. As the result, it became clear that, if we artifitially activate unfertilized egg with A23187, we can induce the zona reaction-like biochemical changes on the zona pellucida of unfertilized egg. These data suggest that the biochemical differences detected with BS-1 and BS-2 lectins on the zonae pellucidae of unfertilized and fertilized eggs refrect the zona reaction itself which was induced by CGM at the time of fertilization. On the basis of the data obtained here, the mechanism of the zona reaction in the mammalian egg was discussed.

DB 67

INITIATION OF ANAPHASE CHROMOSOME MOVEMENT IN MOUSE UNFERTILIZED OOCYTES BY MEANS OF MICROINJECTION

Y. Hamaguchi. Biol. Lab., Tokyo Inst. of Technol., Tokyo.

When two kinds of calcium buffers that contained EGTA and EDTAOH (N-hydroxyethyl-ethylenediamine-N,N',N'-triacetic acid) were injected into the oocytes obtained from hormonally superovulated ICR mice, cortical granules disappeared at Ca concentration of >1 μM. Anaphase chromosome movement was observed at >4 μM in 96% at 37°C within 60 min after injection as reported at fifty sixth annual meeting of this society. Moreover, when inositol 1,4,5-trisphosphate (IP_3) (0.2-20 μM) were injected into the oocytes, anaphase took place in a manner dependent on IP_3 concentration, but 20 μM IP_3 solution containing 50 mM EGTA did not initiate anaphase when injected. However, when EDTAOH solutions (10-200 mM) were injected with or without 50 mM EGTA, anaphase also took place in a manner dependent on EDTAOH concentration. In this case, however, cortical granules of EDTAOH-injected oocytes appeared as before, when observed by differential interference microscopy, and the zona pellucida was dissolved as that of uninjected oocytes when treated with 0.1% chymotrypsin, which indicates that exocytosis did not take place. Therefore, it seems likely that EDTAOH initiates anaphase chromosome movement in Ca-independent manner.

DB 68

PERIOD OF ACTION OF MOUSE BLASTOCYST HATCHING ENZYME AND ITS HISTOCHEMICAL LOCALIZATION IN EMBRYOS

H. Sawada[1], K. Yamazaki[2], E. Hojo[2], Y. Kato[2], T. Someno[3], and M. Hoshi[1] ([1]Biol. Lab., Fac. of Sci., Tokyo Inst. of Technol., Tokyo, [2]Mitsubishi-Kasei Inst. of Life Sci., Tokyo, [3]Res. Labs., Pharmaceut. Grp., Nippon Kayaku Co., Tokyo)

We previously reported that a trypsin-like protease participates in hatching of mouse blastocyst by examining the effects of various protease inhibitors on hatching. In the present study, we attempted to demonstrate the period of action of hatching enzyme (HE: trypsin-like enzyme) and the localization of HE.

Embryos were obtained from pregnant ICR mice at 88 h after hCG administration, and was cultured at 37 °C in α-MEM containing 3 mg/ml BSA in the presence or absence of 0.1 mM TLCK at an appropriate time. The HE in embryos were stained at 37 °C for 3 h by using Z-Gly-Gly-Arg-MNA and Fast Blue B.

The period of action of HE was estimated by examining the effects of timing of TLCK treatment on hatching. The results suggest that the HE plays a role at 80-95 h after hCG treatment. 4 h or 10 h pulse treatments of TLCK were not sufficient to block hatching. Histochemical study demonstrated that the HE was localized in trophectoderm but not restricted to mural trophectoderm as reported by Perona and Wassarman (1986). In our procedure, the embryos were not stained in the absence of substrate or in the presence of TLCK and leupeptin, potent inhibitors against hatching, suggesting the specific staining of HE. Contrary, in their procedure, the embryos were stained similarly even in the absence of substrate or in the presence of the inhibitors.

DB 69

BISMUTH STAINING OF PREIMPLANTATION MOUSE EMBRYOS.

I.Takeuchi and Y.Takeuchi. Aichi Prefec. Colony, Inst. Dev. Res., Kasugai, and Gifu Col. Med. Technol., Seki.

The changes in the distribution of the structures contrasted with bismuth staining following glutaraldehyde fixation (Locke and Huie, 1977) were examined in the preimplantation mouse embryos. In the 1-cell embryos, the fibrillar centers (FC) located at the periphery of condensed nucleoli, and the perichromatin granules (PG) somewhat distributed in the nucleoplasm, were stained. In the nuclei of 2-cell embryos, PG increased in number, and numerous interchromatin granules (IG), well stained with bismuth, appeared in the nucleoplasm. In the cytoplasm of 2-cell embryos, the onset of appearance of bismuth-stained crystalloid inclusions was noted. In the 4-cell embryos, the dense fibrillar components (DFC) and granular components (GC) emerged around the condensed nucleoli, and both nucleolar components greatly increased in amount in the subsequent 8-cell and blastocyst-stage embryos, while the condensed nucleoli tended to be fragmented and disappear. In the nucleoli from the 4-cell embryos onward, bismuth deposited in the FC and the adjoining DFC. Cytoplasmic crystalloid inclusions increased in number along with the process of embryonic development.

DB 70

REGULATORY FUNCTIONS OF ADENOSINE 3',5'-CYCLIC MONOPHOSPHATE IN 1-METHYLADENINE PRODUCTION BY STARFISH FOLLICLE CELLS.

*M. Mita, *N. Ueta and **Y. Nagahama. *Dept. of Biochem., Teikyo Univ. Sch. of Med., Tokyo, **Lab. of Reprod. Biol., Nat. Inst. for Basic Biol., Okazaki.

Resumption of meiosis in starfish oocytes is induced by 1-methyladenine (1-MeAde) produced by ovarian follicle cells under the influence of gonad-stimulating substance (GSS). The present study was conduced to examine the importance of cyclic AMP in the GSS-induced increase in 1-MeAde production by starfish, *Asterina pectinifera*, follicle cell suspensions.

GSS treatment significantly stimulated 1-MeAde production during 1-2 hr incubation. The treatment also caused a 4 to 5-fold increase in intracellular levels of cyclic AMP, but not cyclic GMP. GSS is required at all times to maintain elevated levels cyclic AMP. 3-Isobutyl-1-methylxanthine, a phosphodiesterase inhibitor, stimulated both 1-MeAde and cyclic AMP production in a dose-dependent manner. Other substances, such as concanavalin A and proteases, which are known to induce 1-MeAde production in starfish follicle cells, also stimulated cyclic AMP production. Thus, in all cases examined, the induction in 1-MeAde production parallels the elevation in cyclic AMP levels. It is concluded that cyclic AMP mediates the action of GSS upon 1-MeAde production in starfish follicle cells.

DB 71

AN INCREASE IN OOCYTE CYCLIC AMP LEVEL INITIATES OOCYTE MATURATION IN THE BRITTLE-STAR AMPHIPHOLIS KOCHII.

M. Yamashita. Zool. Inst., Fac. of Sci., Hokkaido Univ., Sapporo.

Maturation of the brittle-star oocytes was induced by an external application of cAMP (10 mM), an inhibitor of cyclic nucleotide phosphodiesterase (25 mM theophylline, 25 mM caffeine) or an activator of adenylate cyclase (100 μM forskolin, 0.6 μM cholera toxin). Experiments in which the oocytes were treated with forskolin or theophylline for various periods of time, demonstrated that there was a positive correlation between the oocyte cAMP level measured by radioimmunoassay and the extent of germinal vesicle breakdown (GVBD) induced in each treatment: Both increased as the treatment period became longer and about three-fold increase in cAMP level induced 50% GVBD.

Oocyte maturation was also induced by microinjection of cAMP (5.7 μM/oocyte) or the catalytic subunit (0.7 μM/oocyte) of cAMP-dependent protein kinase (A kinase) into the immature oocytes. Microinjection of heat-stable inhibitor protein (0.5 μM/oocyte) of A kinase inhibited cAMP-induced oocyte maturation.

These results indicate that an increase in oocyte cAMP level initiates maturation of the brittle-star oocytes, probably via activation of A kinase.

DB 72

POSSIBLE INACTIVATION OF MATURATION-SPECIFIC PROTEIN KINASE IN STARFISH OOCYTES BY Ca-ACTIVATED PHOSPHOPROTEIN PHOSPHATASE.

K.Sano, Marine Biological Station, Hokkaido University, Akkeshi, Hokkaido

In Asterina pectinifera, maturation-specific protein kinase (M-sp PK), which is specifically observed in maturing oocytes (K.Sano,1985,Develop. Growth & Differ.,27, 263-275), is shown to be inactivated by adding Ca to the supernatant of maturing oocytes (K.Sano,1987,ibid.,29,399). To clarify the mechanism of inactivation by Ca, effects of various enzyme inhibitors were examined. Inactivation by Ca was suppressed by the inhibitors of phosphoprotein phosphatase such as glycerol-2-phosphate and pyrophosphate, suggesting that M-sp PK is inactivated by a Ca-activated phosphoprotein phosphatase which is present in maturing oocytes in addition to -SH oxidation. Next, we have characterized protein kinase activity which is activated by adding dithiothreitol to the supernatant of immature oocytes (1987,ibid.). The newly activated kinase was found to be Ca-, cAMP-independent and sensitive to iodoacetamide, using histone Hl as substrate. This indicates that the newly activated kinase is the M-sp PK. The inactivation of M-sp PK by two types of mechanisms suggests that inactive form of M-sp PK may be activated by some unknown mechanism such as phosphorylation in addition to the activation by -S-S- to -SH transition. Supported by Grant-in-Aid for Sci. Res. (61480024).

DB 73

A MONOCLONAL ANTIBODY TO 56- AND 58-KILODALTON-POLYPEPTIDES PRESENT IN THE EGG OF THE STARFISH, ASTERINA PECTINIFERA.

M. Kataoka, S. Yajima and S. Ikegami, Dept. Applied. Biochem., Fac. Applied Biological Science, Hiroshima Univ., Fukuyama.

In order to prepare a monoclonal antibody that reacts specifically with components of eggs and embryos of the starfish Asterina pectinifera, Balb/c mice were immunized with a 150-200 mM NaCl eluate of a DEAE-cellulose column that had been loaded with an egg extract. Spleen cells were removed from the mice and fused with myeloma SP-2 cells. Hybridoma cells that secreted immunoglobulin G reacting specifically with the polypeptides with molec ular weights of 56,000 and 58,000 were selected. The immunoglobulin G reacted to extracts of eggs, morulae, gastrulae and ovaries, but not with those of testes, pyrolic cacea, body walls and tube-feet. The immunoglobulin G did not reacted with extracts of eggs of the starfish Asterias amurensis or sea urchin Hemicentrotus pulcherrimus, suggesting that it is rather specific.

This work was supported in part by a grant from the Nissan Science Foundation.

DB 74

DISULFIDE-REDUCING AGENTS INCREASE 1-METHYL ADENINE-BINDING TO CORTICES ISOLATED FROM STARFISH OOCYTES.

M. Yoshikuni[1], K. Ishikawa[2], & Y. Nagahama[1]
[1]Lab. of Reprod. Biol., Natl. Inst. for Basic Biol., Okazaki, [2]Dept. of Biol., Fac. of Sci., Shizuoka Univ., Shizuoka.

Several disulfide-reducing agents, such as dithiothreitol, 2,3-dimercapto-1-propanol, cysteine ethyl ester and cysteine methyl ester, have previously been reported to induce oocyte maturation in starfish, Asterina pectinifera. In the present study we found that these agents enhanced the effectiveness of 1-methyladenine (1-MeAde) to induce oocyte maturation. This enhancement occurred at relatively low concentrations where these agents by themselves were ineffective in inducing oocyte maturation. Pretreatment of oocytes with these agents shortened the hormone-dependent period for 1-MeAde-induced oocyte maturation. Treatment of oocyte cortices with the agents caused a marked (about 2-fold) increase in specific [^{3}H]1-MeAde binding. The binding increased directly in relation to the potency of the agents in enhancing 1-MeAde action. Further analysis of this binding by the Scatchard plots indicated that dithiothreitol increased the Bmax without affecting the affinity of 1-MeAde binding. These results strongly suggest that disulfide-reducing agents enhance the maturational action of 1-MeAde by increasing the number of 1-MeAde binding sites in oocyte cortices.

DB 75

ARACHIDONIC ACID-INDUCED INHIBITION ON THE 1-METHYLADENINE-INDUCED OOCYTE MATURATION IN *ASTERINA PECTINIFERA*.

H. Tosuji and T. Nakazawa. Dept. of Biol., Fac. of Sci., Toho Univ., Funabashi.

In *Asterina pectinifera*, we reported that the arachidonic acid-induced oxygen consumption was exhibited (Zool. Sci. 3, 1037). This oxygen consumption existed in particlar fraction of the oocyte homogenate, and was inhibited by lipoxygenase inhibitors.

The arachidonic acid-induced oxygen consumption was also found in *Asterias amurensis*. In this species the arachidonic acid-induced oocyte maturation was found and this arachidonic acid-induced oocyte maturation was inhibited by arachidonic acid cascade inhibitors. In *Asterina*, the oocyte maturation is not induced by arachidonic acid (Meijer *et al*, 1984), on the contrary, arachidonic acid inhibited 1-methyladenine-induced oocyte maturation. This inhibition depended the pre-treatment time of arachidonic acid, and showed competitive inhibition to 1-methyladenine. But on the 1-methyladenine recepter of oocyte, the binding of 1-methyladenine was not affected by the concentration of arachidonic acid. It suggests that exogenous arachidonic acid is oxydized and its product which might induce oocyte maturation in *Asterias*, inhibit the 1-methyladenine-induced oocyte maturation competitively in *Asterina pectinifera*.

DB 76

CHANGES IN ISOELECTRIC POINT OF TUBULIN DURING STARFISH OOCYTE MATURATION

N. Hosoya[1], H. Shirai[2], H. Hosoya[3], Y. Nagahama[2] and H. Mohri[1]. [1]Dept. Biol., Coll. Arts and Sci., Univ. Tokyo, Tokyo, [2]Dept. Reprod. Biol., Natl. Inst. Basic Biol., Okazaki, and [3]Tokyo Metro. Inst. Med. Sci., Tokyo.

Microtubule structures in starfish oocytes (Asterina pectinifera) exhibited remarkable changes during maturation process induced by 1-methyl adenine (Shirai et al, in preparation). In order to analyze these changes biochemically we checked the changes in isoelelctric point (pI) of tubulin molecules.

The changes in pI of tubulin were detected using isoelectric focusing, immunostaining and two-dimensional gel electrophoresis. α-tubulin in maturing oocytes shifted to more acidic two isoforms at around germinal vesicle breakdown, returned again to the original (immature) ones after first polar body emission, subsequently shifted to acidic ones during the process of second polar body emission, and finally returned to the original ones. On the other hand, pI of β-tubulin did not change remarkably. When maturation was inhibited by 6-dimethyl amino purine, one of the inhibitors of phosphorylation, the changes in pI of α-tubulin were inhibited. From these results, the changes in pI seem to couple tightly to maturation process.

DB 77

INHIBITION OF MOUSE OOCYTE MATURATION BY A SYNTHETIC PROTEASE INHIBITOR, TLCK.

Naohiro Hashimoto*, Takeo Kishimoto**, and Yoshitaka Nagahama**. *Mitsubishi-Kasei Inst.Life Sci., Machida and Dev.Reprod. Biol.Centr., Yamagata, **Dep.Dev.Biol., Natl.Inst.Basic Biol., Okazaki.

Involvement of proteases in mouse oocyte maturation was studied using a synthetic protease inhibitor, Nα-tosyl-L-lysine chloromethyl ketone (TLCK). When isolated follicles were cultured with both 1 μg/ml ovine LH and TLCK (0.02-0.5 mM) for up to 6 h, LH-induced germinal vesicle breakdown (GVBD) was blocked to 2% by 0.5 mM TLCK. However, TLCK did not affect LH-induced elevation of follicle cell cAMP. Thus, follicle cells seem to respond to LH normally, suggesting that TLCK affects oocytes. Then denuded (cumulus-free) oocytes were liberated from follicles after preincubation with 0.5 mM TLCK for 3 h and further incubated with TLCK. Spontaneous GVBD in these oocytes was completely blocked throughout 5 h of incubation. When follicles were preincubated with TLCK for 1 h, GVBD at 5 h after liberation was decreased to 66% in denuded oocytes whereas 20% in cumulus-enclosed oocytes. It is likely that this enhancement of inhibition in cumulus-enclosed oocytes is due to facilitated transport of TLCK from cumulus cells into oocytes through gap junctions. The results suggest that a trypsin-type protease in oocytes plays a regulatory role in mouse meiotic maturation.

DB 78

WRINKLED BLASTULA OF THE SEA-STAR, ASTERINA MINOR: BEHAVIOR OF BLASTOMERES

M. Murase, M. Komatsu and C. Oguro

Department of Biology, Faculty of Science, Toyama University, Toyama 930, Japan

The wrinkled blastula stage has been reported in a number of asteroid species during normal development. However, nothing has been known on the details of the behavior of blastomeres during the wrinkled blastula stage.

In the present study, behavior of blastomeres was observed with a SEM and vital staining of the embryo. Before the commencement of wrinkling, blastomeres on the surface of the blastula were stained by immersing the embryo into 0.05% neutral red solution. By this treatment, blastomeres situated in the blastocoel were not stained.

When fine furrows appeared, 10 hours after fertilization, unstained blastomeres were located at the bottom of the furrows. At the most wrinkled stage, cell masses composed of stained blastomeres were separated by cell masses of unstained blastomeres which were mostly composing egression tracts. After the recovery from the wrinkling, the embryo became a coeloblastula. The blastoderm of this blastula showed a mosaic pattern which was composed of stained and unstained cell masses. When the embryo became a brachiolaria, the surface of the embryo still retained a mosaic pattern.

These results may indicate that the wrinkled blastula stage in this species is a process of cell rearrangement for the appropriate distribution of the blastomeres which were situated on the surface and in the blastocoel of the blastula before the wrinkling.

DB 79

SCANNING ELECTRON MICROSCOPIC OBSERVATIONS ON THE VITELLARIA OF THE BRITTLE STAR, OPHIOPLOCUS JAPONICUS

M. Komatsu, M. Murase, T. Wada and C. Oguro
Department of Biology, Faculty of Science, Toyama University, Toyama 930, Japan

It was observed with a light microscope that the larva of Ophioplocus japonicus is a vitellaria (Shōsaku et al., 1981). Four ciliary bands appear in the vitellaria, 3.5 days after fertilization, when tube feet emerged on each hydrocoel lobe.

In the present study, the embryos from the gastrula to the juvenile through the metamorphosis were observed with a SEM. Surface of the early gastrula was uniformly covered with cilia, 20 hours after fertilization. Four hours later, ciliary bands were not observed in the late gastrula. One and half days after fertilization, the presence of ciliary bands was first recognized in the early vitellariae. They were furnished with 5 hydrocoel lobes with rudiments of the tube feet. Three and half days after fertilization, vitellariae had 4 definite ciliary bands. Just before the commencement of the absorption of the larval part, cilia on the ciliary bands rapidly decreased in number and length. Five days after fertilization, no trace of ciliary bands was observed in the metamorphosing larva with the reduced larval part.

The present study shows that ciliary bands are formed in the early vitellaria, not like reported previously.

DB 80

EFFECTS OF INHIBITORS OF RNA SYNTHESIS ON EMBRYONIC DEVELOPMENT OF THE STARFISH ASTERINA PECTINIFERA.

H. Isomura, N. Tsuchimori, N. Itoh and S. Ikegami , Applied. Biochem., Fac. Applied Biological Science, Hiroshima Univ., Fukuyama, Hiroshima.

The rate of RNA synthesis is low during the morula stage and increases sharply at the beginning of blastulation. When fertilized eggs of the starfish, Asterina pectinifera, were cultured in artificial sea water containing formycin at a concentration of 25 µg/ml, RNA synthesis of the embryos was inhibited by approximately 40 % at 6 hr after fertilization and the development of the embryos stopped at the early blastula stage with the cell number of 1,024. The contents of UTP and CTP in the formycin-treated embryo were low as compared with those of control embryo whereas the contents of ATP and GTP was the same for both types of embryo. When cytidine (100 µg/ml) and uridine (100 µg/ml) were introduced into a culture of fertilized eggs which were placed in artificial sea water containing 25 µg/ml of formycin, they were able to develop to the late blastula stage, suggesting that the inhibition of RNA synthesis by formycin is due to the inhibition of biosynthesis of CTP and UTP.

This work was supported in part by a a grant from Nissan Science Foundation.

DB 81

EPITHELIAL CELLS OF THE STARFISH EMBRYO OPEN AND CLOSE THE SEPTATE JUNCTION IN RESPONSE TO SOLUTES PRESENT OUTSIDE THE BODY

M. DAN-SOHKAWA[1], C. KANAI[2] and K. NODA[2]
Dept. of Biol., Osaka City University, [2]Tokyo Metropolitan Inst. of Gerontol.

Septate junction and tight junction are classified as impermeable junctions, whose primary function is considered to prevent water and solutes to permeate freely into the body cavity by way of intercellular spaces. It is known, however, that in some vertebrate epithelia water and soluble materials are allowed to permeate through paracellular pathways when certain concentrations of low molecular weight substances, such as NaCl, urea and glycine, are present outside the body.

We show, in this study, that this paracellular transepithelial permeation also takes place in the body wall epithelium of the starfish embryo. What is more, three additional conditions to the apical hypertonicity, mentioned above, were found to evoke the paracellular permeation in this simple epithelium, namely Ca^{++}-free environment, 0°C and pH statuses over 9.

Macromolecules, such as FITC-labeled IgG and dextrans, were introduced into the blastocoel by taking advantage of the inflowing water to visualize the paracellular permeation.

DB 82

BLASTOCOEL FORMATION IN THE MONOLAYERED CELL SHEET OF SEA URCHIN EMBRYOS.

Y.D. Noda, *Y. Nakajima, and *M. Ikeda. Dept. of Biol., Ehime Univ., Matsuyama. and *Dept. of Biol., Keio Univ., Yokohama.

In the 8- or 16-cell stage embryo of the sea urchin, Mespilia globulus, the blastomeres begin to transform into flattened cell shape when the eggs removed fertilization membrane were cultured in Ca-deficient sea water (Nakajima & Noda '85). These flattened cells divide vertically to the substratum and form the monolayered cell sheet. Microvilli occur only on the free surface of the flattened cell. The surface facing the substratum is smooth. The cilium of the blastula stage cell is formed on the free surface.

When normal embryos develope into a blastula, monolayered cell sheet embryos begin to make a sphere (i.e.,blastocoel) between the cell sheet and the glass substratum. Starfish eggs of denuded fertilization membrane develope into a monolayered cell sheet. Microvilli are made on the cell surface facing the substratum and the free edges of the sheets begin to curl upward after 9th cleavage, then their sheets become a blastula-like structure (Dan-Sohkawa, '76, Kadokawa et al., '86). The cell sheets of sea urchin in Ca-deficient sea water do not occur 'closing movement' of starfish sheet. But, some sheets form a hollow sphere surrounding a center of blastocoel, and become a blastula-like structure.

DB 83

CELL CYCLE STUDY OF MICROMERES IN THE EMBRYOS OF THE SEA URCHIN, HEMICENTROTUS PULCHERRIMUS.

S.Tanaka[1], K.Nakajima and K.Dan[2].
[1]Lab. of Develop. Biol. Mitsubishi-Kasei Inst. of Life Sci., Machida-shi, [2]Misaki Marine Biological Station, Miura-shi

To investigate cell cycle kinetics of micromeres of a sea urchin embryo, a method was developed so as to dissociate and prepare every cell onto a glass slide obtained from one embryo, from which the fertilization membrane was removed. At early 8 cells stage, embryos were pulse labeled(30min)with 5-bromodeoxyuridine (BrdU) which was detected immunocytochemically using anti-BrdU antibody. Cell cycle related parameters such as DNA content, total protein content and BrdU amounts were successsively measured with specified cells utilizing a system composing of a microfluorometer, TV cameras, video recorders and microcomputers. Small micromeres were clearly identified by scattered plots of two parameters of BrdU /protein and protein of each cell from one embryo. A parameter of DNA /protein was also found to correlate well with that of BrdU/protein and be useful in identifying small micromeres. According to these methods, it was suggested that small micromeres progressed only one cell cycle of about 4h during a period ranging from 32 cells stage through about 250 cells stage.

DB 84

INTRACELLULAR CA^{2+} POOLS RELATING TO GROWTH OF SPICULES AND PSEUDOPODIA IN MICROMERE-DERIVED CELLS OF SEA URCHIN.

K.Mitsunaga[1], S.Shinohara[1], Y.Fijono[2] and I.Yasumasu[1]. [1]Dept. of Biol., Sch. of Educ., Waseda Univ., Tokyo and [2]Dept. of Pharmacol., Teikyo Univ. Sch. of Med., Tokyo.

Relation of intracellular Ca^{2+} pools to growth of spicules and pseudopodia was studied using Ca^{2+} transport inhibitors.

Spicule formation in the cultured micromere-derived cells was inhibited by ruthenium red and verapamil. Mitochondrial Ca^{2+} pool was reduced by these compounds at concentrations effective to block spicule formation, though extra-mitochondrial Ca^{2+} pool was enlarged by ruthenium red and was diminished by verapamil. Ruthenium red also induced excess growth of pseudopodia and stimulated ^{32}P incorporation into protein, though verapamil inhibited both of them. Their rates correlated with extra-mitochondrial Ca^{2+} pool size. The growth of pseudopodia and activity of C-kinase in micromere-derived cells were inhibited by H-7 but were not by HA1004.

These results suggest that mitochondrial Ca^{2+} pool is indispensable for spicule formation. Growth of pseudopodia in spicule forming cells requires protein phosphorylation catalyzed by C-kinase which is regulated by Ca^{2+} in extra-mitochondrial pool or cytosolic free Ca^{2+}.

DB 85

IN VITRO FORMATION OF SEA URCHIN SPICULES IN SEA WATER CONTAINING BLASTOCOELIC FLUID

M.Kiyomoto and J.Tsukahara. Dept. of Biol., Fac. of Sci., Kagoshima Univ., Kagoshima.

Okazaki('75) reported that descendants of isolated micromeres of sea urchin embryo formed larval spicules when they were cultured in sea water containing horse serum. If they were cultured in sea water without horse serum they couldn't form spicules. Under the normal development descendants of micromeres become primary mesenchyme cells and form a larval spicule in the blastocoel of sea urchin embryo. So some facters necessary for spicule formation may exist in blastcoel.

In the present study isolated micromeres were cultured in sea water containing blastcoelic fluid (BCF) obteined from centrifuged embryos. The descendants of micromeres could form spicules in this medium. The activity of spicule formation was higher in the BCF obteined from mesenchyme blastula, lower from gastula and not detected from early blastula. Such active substances were non-dialyzable and lost their activity after tripsin treatment. The cross experiments between H. pulcherrimus and P. depressus have shown that such substantces are not species specific.

DB 86

ELECTROPHORETIC ANALYSIS OF COLLAGEN-LIKE PROTEIN IN WATER-SOLUBLE EXTRACELLULAR MATRIX OF SEA URCHIN EMBRYO.

HAZIME MIZOGUCHI. Div. of Biol., Jun. Col. of Rissho Univ. Saitama.

To investigate whether extracellular matrix of sea urchin embryo contains collagen, electrophoretic analysis of water-soluble extracellular matrix of the embryo was performed with sodium dodecyl sulfate polyacryamide gel electrophresis.

Water soluble extracellular matrix(WSE) was obtained as follows. Embryos were dissociated with the medium (sea water containing glycine-EDTA), which was then centrifuged at 3,000 rpm for 5 min. The supernatant was dialyzed against distlled water. WSE was digested with pepsin over night at 4°C followed by collagenase over night at 25°C, and boiled for 1 min. Samples thus obtained were electrophoresed on 7.5% or 15% sodium dodecyl sulfate polyacrylamide gels at constant current. Gels were observed after silver staining.

Collagen-like protein was observed in WSE obtained from gastrulae and plutei. It was however not detected in that of 16 cell embryos and blastulae.

These results suggest that collagen-like protein is contained in the extracellular matrix of sea urchin embryos after gastrula stage.

DB 87

EXPRESSION OF A PRIMARY MESENCHYME CELL SURFACE SPECIFIC GLYCOPROTEIN, msp 130, AND ITS POTENTIAL ROLE ON THE CELL MIGRATION.

H. Katow, Biology Laboratory, Rikkyo Univ., Tokyo.

A monoclonal antibody, B2C2, raised against sugar moieties of sea urchin primary mesenchyme cell (PMC) surface specific glycoprotein, msp 130 (Anstrom, et al, '87, Development, in press) has been utilized for immunohistological studies. The antibody was also applied for examinations on the role of the glycoprotein during PMC migration in blastulae of the sea urchin, *Clypeaster japonicus*.

Indirect immunohistologies indicated that 1) the antibody binds only to the PMCs ingressed, but not to those in the embryos raised 2) in sulfate-deficient sea water, 3) with tunicamycin, or 4) with monensin. In those embryos the PMCs were formed but their migration did not occur. Transmission electron microscopies indicated that in monensin treated embryos the transitional vesicles of Golgi complex were abnormally inflated, which suggested that the cytoplasmic organ is associated with intracellular transportation of msp 130 to the cell surface. *In vitro* PMC migration studies conducted in mixtures of fibronectin which promotes PMC migration (Katow & Hayashi, '85, J.C.B) and the antibody indicated moderate to rather weak inhibitory effect of B2C2.

B2C2 has been kindly provided by Dr.R. Raff, Indiana University, USA.

DB 88

EXPRESSION OF PRIMARY MESENCHYME CELL (PMC) LINEAGE SPECIFIC ANTIGEN DURING DEVELOPMENT OF SEA URCHIN EMBRYO (II).

K. Shimizu°, H. Katow* and R. Matsuda°.
°Dept. of Biol. Tokyo Metropolitan Univ. and *Lab. of Biol. Rikkyo Univ., Tokyo.

PMC specific antigens have been studied by using monoclonal antibodies, P4 (Shimizu , et al. Develop. Growth and Differ. 29:389 , 1987) and B2C2 (kindly provided by Dr. R. A. Raff; Leaf et al. Develop. Biol. 121:29-40, 1987). P4 and B2C2 reacted with the same cell surface glycoproteins. From peptide mapping analysis, it was suggested that both antibodies recognized the same N-linked carbohydrate (CHO) chain. During developmnt, the P4 epitope appeared earlier than the B2C2 epitope. At the vegital plate stage of *Clypeaster japonicus*, presumptive PMCs already reacted with P4, however, PMCs did not react with B2C2 until they completed ingression. Besides, embryos of *Anthocidaris crassipina* grown in sulfate-free sea water reacted only with P4, but not B2C2. These results suggest that P4 and B2C2 epitopes localize at different regions of the same CHO chain. Biological function of P4 antigen was also examined. PMCs of *C. japonicus* embryos were obtained by Cytochalasin B treatment and were cultured in the presence or absence of P4. P4 inhibited PMC migration. This result indicates that the P4 antigen may play an important role for migratory activity of PMC. (Supported by grant-in-aid from the Ministry of Education, Science and Culture of Japan.)

DB 89

RELATIONSHIP BETWEEN PRIMARY MESENCHYME CELL BEHAVIOR AND THE SUBSTRATUM OF THE SEA URCHIN EMBRYOS TREATED WITH LITHIUM IONS.

S. Amemiya. Misaki Marine Biological Station, University of Tokyo, Kanagawa.

In the normal development of sea urchin embryos, primary mesenchyme cells accumulate in a ring-like pattern between the equator and vegetal pole after migrating along the basal lamina in the blastocoel. The author previously reported the basal lamina to consist of a network of fibrils and amorphous materials situated in the spaces among the fibrils. Some of the fibrils projecting from the basal lamina and lying alongside the ectodermal wall in the blastocoel may possibly constitute the substratum for primary mesenchyme cell migration. In this report, the extracellular matrix involved in the formation of the primary mesenchyme cell pattern was examined. Scanning electron microscopical observation revealed extracellular matrix fibrils to be well developed around this pattern. In embryos treated with lithium ions, the pattern formed in the animal hemisphere where extracellular matrix fibrils developed well. Spicules formed in mesenchymal aggregates that had accumulated in the animal hemisphere, thus indicating that the functions of primary mesenchyme cells are maintained essentially in embryos treated with lithium ions.

DB 90

SEA URCHIN DNA POLYMERASE γ:INTRACELLULAR LOCALIZATION AND CHANGES IN ACTIVITY DURING EMBRYOGENESIS.

M.Shioda. Dept. of Physiol.Chem. & Nutri., Fac. of Med., Univ. of Tokyo, Tokyo.

DNA polymerase γ is known to participate in mitochondrial DNA replication. In the present study, intracellular localization and changes in activity of the enzyme were examined in sea urchin (*Hemicentrotus pulcherrimus*) eggs and embryos. On differential and isopycnic centrifugation of egg or embryo homogenate, bulk of DNA polymerase γ activity recovered in the 10,000g precipitate and equlibrated at buoyant density of 1.216 g/cm^3, respectively. These results indicate that DNA polymerase γ is localized predominantly in mitochondria. The enzyme activity per embryo remained constant throughout the egg, cleavage and early blastula stages, thereafter, it began to increase. The amount of mitochondrial DNA per embryo also began to increase from cleavage or early blastula stage, suggesting that mitochondrial DNA replication begins to occur from this stage. The enzyme activity per mitochondrial DNA remained almost constant during embryogenesis. These results indicate that mitochondria contain a constant amount of DNA polymerase γ regardless of whether mitochondrial DNA replication occurs or not. This suggest that different regulation mechanisms operate in mitochondrial and nuclear DNA replication as to the amount of replicative enzyme.

DB 91

OCCURRENCE OF CASEIN KINASE TYPE PROTEIN KINASE IN THE CHROMATIN FROM SEA URCHIN EMBRYOS.

Y.Masuyama, M.Motojima, and I.Yasumasu. Dept. of Biol., Sch. of Educ., Waseda Univ., Tokyo.

Cyclic nucleotides-independent and polyamines-enhanced protein kinase was estimated in isolated chromatin from sea urchin embryos. Spermine (5mM) enhanced by about 2 holds the rate of phosphorylation of endogenous proteins by protein kinase reaction. this enzyme activity was relatively high in embryos at the morula stage and the gastrula stage, and was quite low at the swimming blastula stage. In extract of nuclei with 0.4M NaCl, protein kinase activity , which phosphorylated casein and phosvitin but not histone 2b, was found and was activated by spermine. Heparin did not influence this enzyme activity in the isolated chromatin, but inhibited it in the extract. Isolated nuclei having been extracted with 0.4M NaCl hardly exhibited Spermine-stimulated ^{32}P incorporation into endogenous proteins. A sharp peak of this enzyme activity was obtained by a casein-phosvitin-Sepharose column chromatography of this 0.4 M NaCl extract. Ion exchange chromatography by Mono Q (Pharmacia FPLC system) exhibited two peaks of casein kinase activities. These probably correspond to casein kinase 1 and 2, respectively.

DB 92

METHYLATION OF NUCLEIC ACID IN SEA URCHIN EMBRYOS DURING EARLY DEVELOPMENT.

M.FUJII, K.FUSHIMI and I.YASUMASU. Dept. of Biol. Sch. of Educ. Waseda Univ., Tokyo.

The rate of the incorporation of [^{3}H-methyl] group from [^{3}H-methyl]methionine into the nucleic acid of the sea urchin embryos changed during early development. The rate of the incorporation into DNA up to 6hr after fertilization, the cleavage stage, was remarkably and at 24hr, the gastrula stage, was slightly high. The rate was low at 12hr, the blastura stage, also low after 36hr, the prism and pluteus stage. The rate of [^{3}H-methyl]incorpolation into RNA was undetectable up to 18hr, and thereafter it was substantially increased, the highest rate was found at 36hr. These rates of [^{3}H-methyl]incorporation were decreased by addition of 5'-isobuthyl-5'-deoxyadenosin, an analogue of S-adenosyl-methionine. This compound resulted in abnormal development of sea urchin embryos. The profile of the change in incorporation of [^{3}H-methyl]group from S-adenosyl-[^{3}H-methyl]methionine into DNA was essentially similar to that of [^{3}H-methyl]incorporation into DNA from [^{3}H-methyl]methionine in embryos. But the incorporation in isolated nuclei at 6hr was almost the same as at 18hr. Labelled DNA in nuclei was isolated, digested with EcoRI and analysed by 1%agarose gel electrophoresis. Pattern of ^{3}H-radioactivity at 6hr evidently differ from that at 18hr.

DB 93

Onset of arylsulfatase gene expression and DNA methylation of sea urchin (*H. pulcherrimus*) embryos

K. AKASAKA, H. SASAKI and H. SHIMADA Zool. Inst. , Fac. Sci., Univ. of Tokyo, Tokyo.

In the sea urchin (*H. pulcherrimus*) embryo, the abundance of arylsulfatase mRNA decreased until early blastula stage (9h after fert. 15 C) and began to increase reaching about 1000-fold of that in prism stage, and then decreased again. The extent of DNA methylation of the embryos was estimated by HapII and MspI digestion method. The second cytosine residues within the CCGG recognition sites of the bulk DNA were significantly methylated (CG methylation) through the development up to prism stage. Degree of DNA methylation was especially high at prism stage.

The extent of methylation of arylsulfatase gene was estimated by Southern hybridization using arylsulfatase ^{32}P-cDNA as a probe. Arylsulfatase DNA became highly methylated (CG methylation) after fertilization, demethylated at the onsetof thegene expression (early blastula), and highly methylated again with the cessation of the gene expression of this gene (prism embryo).

DB 94

FORMATION AND DIFFERENTIATION OF GONADAL MEDULLA IN *RANA NIGROMACULATA* AND *RHACOPHORUS ARBOREUS*.

Akihiko Tanimura and Hisaaki Iwasawa. Biol. Inst., Niigata Univ., Niigata.

Gonadal development was observed in *R. nigromaculata* and *Rh. arboreus* in light and electron microscopy. Concerning the mode of gonadal sex differentiation, the former is a direct differentiated type and the latter is a semidifferentiated type. In both species, the gonadal medulla derived from the epithelial cells of the rudimentary gonad, and the medulla was in contact with the cortex. In *R. nigromaculata*, the medullary cells had a cytoplasm rich in organella, and were in close contact with each other. The mass of medullary cells was covered with a continuous basal lamina. On the other hand, in *Rh. arboreus*, the basal lamina covering the mass of medullary cells was fragmentary, and the contact among the medullary cells was rather loose. In both species, the dorsal portion of the medulla was elongated, extending to the mesonephric region, and differentiated into an efferent duct in male specimens. The medulla developed to the testicular rete in male specimens, and to the inner epithelium of the ovarian cavity in female ones.

DB 95

THE POSITIONAL EFFECT OF PRESUMPTIVE PRIMORDIAL GERM CELLS (PPGCS) ON THEIR DIFFERENTIATION INTO PGCS IN XENOPUS LAEVIS.

K. Ikenishi and Y. Tsuzaki Dept. of Biol., Fac. of Sci., Osaka City Univ., Osaka.

In order to know whether the location of "germ plasm"-bearing cells [presumptive primordial germ cells (pPGCs)] is crucial for their differentiation into PGCs in Xenopus, ^{3}H-thymidine labeled pPGCs were implanted into the anterior or posterior halves of the endoderm in unlabeled host neurulae. Labeled PGCs in the genital ridges of experimental tadpoles were investigated by autoradiography.

The proportion of tadpoles with labeled PGCs was significantly higher when labeled pPGCs were implanted into the posterior endoderm (p-tadpoles) than when labeled pPGCs were implanted into anterior endoderm (a-tadpoles). The average number of labeled PGCs in the p-tadpoles was much higher than that in the a-tadpoles. Besides, labeled PGCs in the p-tadpoles were found to be distributed throughout the genital ridges while those in the a-tadpoles were localized in the anterior part of the ridges. These facts indicate that the location of pPGCs in the endoderm affects their successful migration into the genital ridges. Therefore, it is reasonable to think that not only the presence of the "germ plasm" but also the proper location in endoderm are prerequisite to PGC differentiation of the germ line cells.

DB 96

MORPHOGENESIS OF THE GONADAL ANLAGE IN THE LIZARD EMBRYOS (TAKYDROMUS TACHYDROMOIDES)

T. Oka. Dep. of Biol., Fac. of Educ., Tokyo Gakugei Univ., Tokyo

The differentiation of the gonadal anlage was examined by light and electron microscopy in Takydromus embryos incubated at 25°C. In three day old embryos a proliferation of the coelomic epithelium which consisted of "dark" and "light" cells, was observed on the ventromedial surfaces of the mesonephros. This proliferation occurred especially rapid in the laterally placed nephrostomal area of the developing genital ridge. At the same time a cellular mass was segregated from the mesonephric blastema. In slightly older embryos the medullary cords approached the neighbouring mesonephric corpuscle and joined at the external border of Bowman's capsule and at the developing interrenal blastema. The medullary cords were composed of flattened "dark" and "light" cells with elliptical large nuclei and moderately developed rough endoplasmic reticulum. These flattened cells were very similar to the cells of germinal epithelium in the ultrastructural appearance. These results suggest that the cells of the medullary cords mostly derived from the germinal epithelium and the epithelium of the juxta-gonadic coelom in the undifferentiated gonad, although some cells may be derived from the mesonephric blastema.

DB 97

GONADAL SEX DIFFERENTIATION AND CHANGES IN THE NUMBER OF GERM CELLS IN ONYCHODACTYLUS JAPONICUS.

Takashi Nomura and Hisaaki Iwasawa. Biol. Inst., Niigata Univ., Niigata.

Changes in the number of germ cells (nGC) in the course of gonadal sex differentiation were examined in O. japonicus. In both male and female specimens, there was a high positive correlation between gonadal size and snout-vent length (SVL). The mode of sex differentiation of this species belongs to a differentiated type. Gonadal sex differentiation was recognized in some specimens in stage 67 (SVL 19-22mm). At this time, nGC in sexually indifferent gonads was 400-600. In the female specimens in this stage, secondary gonia appeared, and then increased in number. Therefore, nGC became more numerous in the ovaries than in the testes. Simultaneously with the appearance of auxocytes, the individual variation in nGC became greater. In female specimens having 39mm or larger SVL, nGC ranged 2000-10000. Nevertheless, there was found a correlation between nGC and SVL in the female specimens. And there was a positive correlation between the diameter of auxocytes and SVL. In male specimens, on the other hand, there was a positive correlation between nGC and SVL, and nGC reached about 6000 in the metamorphosing larvae having a 40mm SVL (st.71).

DB 98

ROLE OF PHOSPHORYLATION IN THE ACTIVITY OF YEAST MATURATION-PROMOTING FACTOR (MPF).

K.Tachibana[1,2], N.Yanagishima[2] and T.Kishimoto[1]. [1]Dept. of Devl. Biol., Natl. Inst. Basic Biol., Okazaki and [2]Dept. of Biol., Fac. of Sci., Nagoya Univ., Nagoya.

We examined the effect of the presence of phosphorylated groups on the meiosis-reinitiating activity of yeast MPF which was extracted from cdc20 mutant cells of Saccharomyces cerevisiae synchronized at M-phase. In contrast to the current assumption that MPF is a phosphoprotein stabilized by phosphorylated small molecules such as β-glycerophosphate and ATP, yeast MPF was still active after the treatment with alkaline phosphatase when injected into immature Xenopus oocytes. Further, even when treated with ATP-γ-S, yeast MPF lost its activity after the removal of ATP-γ-S. Thus, MPF need not necessarily be in a phosphorylated form in order to be active. On the other hand, the meiosis-reinitiating activity was detected when both yeast MPF and the phosphorylated small molecules were present simultaneously and almost undetectable when either of them was present alone. Such complementary effect was also observed when injection of yeast MPF was followed by that of the phosphorylated small molecules. Thus, the phosphorylated small molecules seem to have another effect, such as preventing the activity of phosphatases that might be present in recipient Xenopus oocytes rather than stabilizing the MPF molecule itself.

DB 99

HOW IS THE FLAGELLAR LENGTH OF MATURE SPERM DETERMINED ? I. COMPARISON BETWEEN NEWT AND XENOPUS IN VITRO.

S. Uno and S.-I. Abé, Dept. of Biol., Fac. of Science, Kumamoto Univ., Kumamoto.

We have developed cell culture systems which support meiotic divisions and early, mid-spermiogenesis in Cynops pyrrhogaster and Xenopus laevis(Int. Rev. Cyt.109,1987). In order to study how the flagellar length of mature sperm is determined, we compared the flagellar growth in spermatids between newt and Xenopus; the flagellar length of newt is more than 10 times as that of Xenopus.

The dissociated newt primary spermatocytes were embedded in collagen matrix and those from Xenopus were inoculated in pLL-coated dishes at cell density of 2-7 x 10^4/ dish. The cells were cultured at 22°C in L-15 medium containing no serum. Some primary spermatocytes were marked. At regular intervals after second meiotic divisions, 2 dishes were fixed and the flagellar length in spermatids were measured.

In Xenopus, the flagella increased in length up to 27μm in average by the 6th day and stopped the growth. In contrast, in newt, flagella elongated to about 110μm and did not increase the length after the 10th day. 10μg/ml actinomycin D had no effect on flagellar elongation in either animal. But, 10μM cycloheximide inhibited the flagellar growth by 80-90% in both animals. These results indicate that the flagellar elongation is under the translational control.

DB 100

ACROSOME FORMATION IN NORMAL AND FUSED SPERMATIDS FROM XENOPUS LAEVIS AND THE EFFECT OF CYCLOHEXIMIDE(CH) IN VITRO.

S. Asakura and S.-I. Abé, Dept. of Biol., Fac. of Science, Kumamoto Univ., Kumamoto.

In order to study the mechanism of acrosome formation, we observed the process of acrosome formation in vitro in normal and artificially fused spermatids and examined the effect of CH.

Dissociated primary spermatocytes were inoculated in pLL-coated dishes and cultured in L-15 medium without serum at 22°C. Cell fusion was induced between spermatids derived from single primary or secondary spermatocytes by treatment with hypotonic media for 5-10 min.

Both in normal and fused spermatids, a number of small vacuoles exist just after the second division. These vacuoles increased in size while decreased in number and finally formed a single large acrosome within 30 hr. 10μM CH inhibited the formation of acrosomes completely both in normal and fused spermatids. When CH was washed off, acrosomes reformed. The sensitive period to CH was initial 15 hr after the second division. Neither cytochalasin B nor colchicine inhibited acrosome formation in normal or fused spermatids. When spermatids were fused after an acrosome was formed in each spermatid, two acrosomes fused to form a single larger acrosome. These results indicate that acrosomes are formed by fusion of small vacuoles and that some proteins synthesized within spermatids are responsible for the fusion of vacuoles.

DB 101

ISOLATION OF ACROSOME REACTION INDUCING SUBSTANCE FROM AMPHIBIAN OVIDUCT.

N. Yoshizaki. Dept. of Biol., Fac. of Gen. Educ., Gifu Univ., Gifu.

An acrosome reaction inducing substance (ARIS) was isolated from the pars recta portion of the oviduct of the frog, Rana japonica. The ARIS was first obtained as secretory granules and then fractionated on a Sepharose 6B column after removal of the granules' limiting membranes. The ARIS has a molecular weight of 195 kD in a reduced condition. The activity of the ARIS was assayed as follows. Coelomic eggs treated with both the ARIS and spermatozoa together showed a dilation of vitelline coats, whereas eggs treated with either one of them alone did not. Electron microscopic observation disclosed vesicles in the most affected part of the vitelline coats which might be the remains of acrosome-reacted spermatozoa. When spermatozoa were treated directly with the ARIS, membrane vesicles, presumably composed of plasma and acrosomal membranes, appeared on the surface of the spermatozoa. Immunofluorescent staining using an antiserum raised against the ARIS in the rat showed the localization of the ARIS in the cells of pars recta and in the vitelline coat of uterine eggs. This implies that during the ovulation the ARIS is deposited in the vitelline coat where the acrosome reaction occurs in normal fertilization.

DB 102

BINDING PROPERTIES OF ACROSOME-REACTED TOAD SPERM

K.Takamune and Ch.Katagiri
Zool. Inst., Fac. of Science, Hokkaido Univ., Sapporo.

Treatment of fresh sperm of Bufo japonicus with FITC-conjugated peanut agglutinin (PNA) was found to provide a reliable measure of acrosome-reacted sperm. This was based on the specific binding of PNA to the inner acrosomal membrane (IAM) as defined both by the electron microscopical localization of ferritin-PNA on the IAM and its competitive inhibition by galactose. The sperm treated with the oviducal pars recta secretory granules (PRGs) were not stained with FITC-PNA, although they had evidently been acrosome-reacted. However, a high proportion of sperm treated with PRG showed a binding of FITC-labeled PRG also to IAM, and the surface of mid-piece and tail. Analyses of the similar binding pattern of sperm with various FITC-labeled substances revealed that PRG, vitelline coats (VCs) of uterine and fertilized eggs, and VCs of coelomic eggs pretreated with PRG showed a significantly higher binding than the background exhibited by PNA and coelomic egg VCs. These special binding properties of IAM provide a good means of elucidating the molecular mechanism of acrosome reaction and its induction by oviducal pars recta substances.

DB 103

CHARACTERIZATION OF VITELLINE COAT LYSIN FROM TOAD SPERM.

H. Yamasaki and Ch. Katagiri. Zool. Inst., Fac. of Sci., Hokkaido Univ., Sapporo.

A mild sonication supernatant of sperm of the toad, Bufo japonicus, can easily digest the vitelline coat (VC) of uterine eggs, hardly the VC of coelomic eggs, but not the VC of activated eggs. Both this VC lysis and fertilization were inhibited in the presence of Boc-Gln-Arg-Arg-MCA, suggesting the involvement of proteases in fertilization process. Starting from sonication supernatant, a strong VC lysin possessing the hydrolytic activity on Boc-Gln-Arg-Arg-MCA was purified by anion exchange chromatography (Mono Q HR5/5) and gel-filtration (Superose 12 HR 10/30). The activity of purified lysin was inhibited by such serine protease inhibitors, as DFP, SBTI and p-APMSF, but not by chymostatin, E-64 and EGTA. The molecular weight of VC lysin was estimated to be 32K on the basis of the fluorographic image of ^{3}H-DFP-binding. The VC lysin was most active at pH 7.0-7.6 and under the lower ionic strength equivalent to fresh water. These results suggest that the hydrolytic activity studied here represents the VC lysin of Bufo sperm that is involved in fertilization by digesting VC of uterine eggs.

DB 104

EXPRESSION OF THE MURINE DIHYDROFOLATE REDUCTASE GENE IN XENOPUS LAEVIS OOCYTES IN CULTURE.

K. Toga, N. Itoh, K. Mori and S. Ikegami, Dept. Applied. Biochem., Fac. Applied Biological Science, Hiroshima Univ., Fukuyama, Hiroshima.

When 4 ng of plasmid pSV2-dhfr which contains the simian virus 40 early promoter upstream to murine dihydrofolate reductase cDNA was microinjected into the germinal vesicle of a Xenopus laevis oocyte, ^{35}S-labeled murine dihydrofolate reductase was produced during a 48-hr culture in the OR-2 medium containing [^{35}S]methionine. On the other hand, the production of the reductase was low and not consistent in oocytes the germinal vesicle of which was microinjected with 4 ng of plasmids containing the adenovirus major late promoter upstream to murine dihydrofolate reductase cDNA. These results suggest that the simian virus 40 early promoter is more efficient than the adenovirus major late promoter in the transcriptional machinery in the germinal vesicle of the toad.

DB 105

DIFFERENTIATION OF VITELLINE ENVELOPE (VE) IN GROWING OOCYTES OF XENOPUS LAEVIS, STUDIED BY ANTI-VE SERUM.

S.Yamaguchi[1], J.L.Hedrick[2], Ch.Katagiri[1]. [1]Zool. Inst., Fac. Sci., Hokkaido Univ., Sapporo, [2]Dept. Biochem. and Biophys., Univ. Calif., Davis, U.S.A.

Differentiation of vitelline envelope in growing oocytes of Xenopus was studied using the rabbit antiserum specific to VE components. Light- and electrone microscopic observations, employing FITC-labeled antiserum and IgG-conjugated colloidal gold respectively, revealed that the VE antigens were first detectable throughout the cytoplasm of the previtellogenic oocytes at Dumont's st. I, localized preferentially in the periphery of oocytes at st. II, followed by decrease in the oocyte cytoplasm at later stages. The same antigens localized outside the oocytes first at late st. I as patches, increased its thickness sharply during st. II-III and gradually toward st. IV-VI. The antigens were frequently observed in and around the highly extended oocyte microvilli during late st. I-III, but were never found in follicle cells at all stages observed. Western blot analyses employing each 10 oocytes revealed that the extracellular VE components appeared first at st. II, whereas the intracellular antigens detected from st. I on contained unique components which are distinct from those in the VE after secretion.

DB 106

SCANNING ELECTRON MICROSCOPIC STUDIES OF THE PRIMITIVE STREAK AND MIGRATING MESODERMAL CELLS OF THE MOUSE EMBRYO.

K.Hashimoto and N.Nakatsuji. Div. of Dev. Biol., Meiji Inst. of Health Sci., Odawara.

We observed the ingression and migration of mesodermal cells(MCs) from the primitive streak of the embryonic ectoderm in early primitive-streak-stage(6.5-7.0 d)ICR mouse embryos. The first sign of the ingression of the MCs in 6.5-6.75 d embryos was disruption of the epithelial ectoderm and underlying basal lamina(BL). Cells at the periphery of this region spread on the BL and extended many long filopodia to the BL, while those in the central and anterior parts of the primitive streak had many blebs. Later, a few long slender filopodia grew out from each bleb toward the basal surface of the visceral endoderm layer.

We saw several MCs on the BL migrated away from the periphery of the mesodermal cell layer where cells kept contact with each other. These cells were spread on the BL, and having a large cell process with long filopodia extending from the tip. These individually migrating cells and MCs at the periphery protruded many long filopodia toward the direction of migration. The filopodia attached to the BL or a meshwork of the extracellular fibrils present on the BL. Thus, extracellular matrix seems to play an important role in the migration of MCs.

DB 107

CLONAL ANALYSIS OF KIDNEY AND LIVER TISSUES USING BEIGE MOUSE AGGREGATION CHIMAERAS.

N.Nakatsuji. Div. of Developmental Biology , Meiji Institute of Health Science, Odawara.

Anomalous giant granules of beige (bg) mice have been used as a cell marker in the study of cell lineages of mast cells. Such giant granules are known to exist in other tissues including kidney proximal tubules and liver parenchymal cells. We found that these granules give yellow or orange auto-fluorescence when fixed with formaldehyde. Thus, they can be used as a convenient cell marker recognizable in serial paraffin sections without need of any histochemical processing.

Chimaeric mice were produced by aggregation of 8-cell stage embryos of beige (C57BL - bg/bg, Jackson Laboratories) and A/J strain mice. Kidney and liver tissues were fixed in 10% Formalin, dehydrated through ethanol - buthanol series, embedded in paraffin, and serially sectioned at 10μm of thickness. After removal of paraffin with xylene, sections were mounted in glycerin and examined with a fluorescence microscope.

In the liver tissue, there were patches of beige parenchimal cells with very complicated irregular shapes. In the kidney cortex, the boundary of a patch usually coincided with the tubule structure. Beige cells occupied either whole cross sections of the proximal tubules or only part of them, thus showing polyclonal origin of a tubule.

DB 108

LONG-TERM RETENTION OF LABELED DNA STRAND IN MOUSE SKIN FOLLICULAR MELANOBLASTS

T.Morita, S.Horiuchi, K.Ito, Y.Koshida, Dept. of Biol., Coll. of Gen. Educ., Osaka Univ., Osaka.

A hypothetical mechanism for selective segregation of DNA strand at cell division in stem cell populations has been proposed by Cairns. It has been assumed that UV inactivation of melanoblasts having 5-bromodeoxyuridine-labelled DNA (BrdU-DNA) may result in the depigmentation of hair during the regeneration of hair follicles. The long-term retention of BrdU-DNA in follicular melanoblasts was examined to test the hypothesis. BrdU injected was incorporated into DNA during stimulated proliferation of melanoblasts after plucking. UV light from an FL 20 S.E. lamp was directed on the back of mice at 6 or 12 weeks after BrdU injection. The proportion of white to fully pigmented hair was estimated during 7 to 16 weeks after UV irradiation. In UV-irradiated mice, the white hair ratio was 20%, and finally reached 50%, but in non-irradiated or no-BrdU mice, the ratio was less than 1%. In mice which were plucked 3 times at intervals of 3 weeks after BrdU injection and irradiated with UV, the white hair ratio was 20%. BrdU-DNA in the cell nucleus was examined by the immunoperoxidase staining using a mouse monoclonal antibody against BrdU. Cells containing BrdU-DNA could be detected in follicular cells up to 9 weeks after BrdU injection.

DB 109

VIDEO-IMAGE ANALYSIS OF COAT-COLOR PATTERNS IN ARTIFICIALLY-PRODUCED CHIMERIC MICE BY MEANS OF A PERSONAL COMPUTER-BASED SYTEM.

C. Tachi. Zool. Inst., Faculty of Science, Univ. of Tokyo, Tokyo.

A personal computer-based program package, VIAS.CM (Video Image Analysis System for Chimeras and Mosaics), developed by the author is particularly suited for the quantitative analysis of the sampled video-images of the coat color patterns on the pelts of the artificially-produced chimeric mice. No similar system has been described in the literature. It was shown that the use of VIAS.CM, or an equivalent system, is indispensable for the analysis of coat color patterns due to complex phenotypic expression of hair pigmentation, such as those created on the coat of BALB/c -- C3H/HeJ mice. In VIAS.CM, it is possible to estimate the relative content of eumelanin and pheomelanin differentially, and calculate the mixing ratios between BALB/c and C3H/HeJ components. From the results of grey value profiles taken along mid-dorsal axis, it wa susggested that number of melanoblast clones in mice is probably much larger than so far proposed and 22 in terms of mimimum recognizable stripes (28 after correction for the random clumping) unilaterally in the trunk region.

DB 110

Morphological studies on Purkinje cells in the neo- and archicerebellum of rats.

H.Keino, E.Aoki and S.Kashiwamata. Dept. Perinatol. Inst. Dev. Res., Aichi.

It is generally known that the neocerebellum is severely damaged by various agents such as bilirubin and virus, but the archicerebellum is scarcely affected. We previously showed histochemically that Purkinje cells in lobule VII contain more acidic materials than those in lobule X. In this study, ultrastructural observations were done on Purkinje cells of adult and neonatal (7-day-old) Sprague-Dawley strain Gunn rats. Purkinje cells of newborns showed less organelles than those of adult rats. Packed cisternae of the smooth ER, some of which were tightly associated with mitochondria, were conspicuous in Purkinje cells in lobles VII and X of adult rats, while the cisternae of rough ER, which were arranged in parallel with the nuclear membrane, were markedly less in the former loble than in the latter. Well-developed Golgi apparatus were recognized in Purkinje cells in both lobules of adult and neonatal rats: No striking morphological differences of Golgi apparatus were observed between the neo- and archicerebellum, but the number was found more in lobule VII than in lobule X. The well-developed Golgi apparatus of Purkinje cells in lobule VII may also indicate higher activity of the membrane synthesis (neonatal rats) and turnover (adult rats) compared with those in lobule X.

DB 111

INTERACTION BETWEEN MELANOCYTE AND KERATINOCYTE FROM GENETICALLY DIFFERENT EPIDERMIS OF NEONATAL HUMAN FORESKINS.

T. Hirobe[1], E. Flynn[2] and G. Szabo[2].
Div. of Biol., Natl. Inst. Radiol. Sci., Chiba and Lab. Elect. Microsc., Harvard Sch. Dent. Med., Boston, USA

Pure black (Negroid) and white (Caucasoid) melanocyte cultures in melanocyte-growth-factor-supplemented medium were co-cultured with pure black and white keratinocyte cultures in Minimum Essential Medium containing 10 % fetal bovine serum, and pigment donation was observed with light and electron microscopes.

Melanosome donation from black melanocytes to white keratinocytes was observed to have a similar tendency to that of black melanocyte donation to black keratinocytes. Similarly, pigment donation from white melanocytes to black keratinocytes was observed to have the same manner as donation from white melanocytes to white keratinocytes. This suggests that pigment donation occurs between melanocytes and keratinocytes derived from genetically different human foreskins.

White melanocytes co-cultured with black keratinocytes became more dendritic and more pigmented than the control group. The result suggests that some substance produced by black keratinocytes is involved in regulating melanogenesis of white melanocytes.

DB 112

TISSUE MOVEMENT SPECIFIC TO THE MESENCHYME WHICH CAN INDUCE BRANCHING MORPHOGENESIS OF MOUSE SALIVARY EPITHELIUM.

H. Nogawa[1] and Y. Nakanishi[2].
[1]Biol. Lab., Coll. of Arts and Sci., Chiba Univ., Chiba and [2]Dept. of Chem., Fac. of Sci., Nagoya Univ., Nagoya.

We studied two behavioral activities of mesenchymes from mouse embryonic submandibular gland, lung, stomach, mandible and skin, comparing with their ability to induce submandibular epithelium to branch. Submandibular epithelium branched well in recombination with submandibular or lung mesenchyme, less well with stomach mesenchyme and never with mandibular or dermal mesenchyme. Studies of the first behavioral activity of contraction of collagen gels revealed that all the five kinds of mesenchymal cells were able to contract collagen gels in various degrees and that dermal cells with no branch-inducing ability had the highest gel-contracting activity among them. In studies of the second activity of separation of plastic beads placed in a mesenchymal mass, submandibular or lung mesenchyme separated the beads well and the other mesenchymes separated the beads in a degree corresponding to their branch-inducing activities. Time-lapse cinematography showed that the separation of beads was caused by the flowing movement of the mesenchymal tissue, suggesting that this movement may have an important role in bundling of collagen fibres and widening of clefts.

DB 113

DIFFERENTIATION OF EPITHELIAL CELLS IN THE GOLDEN HAMSTER OVIDUCT

H.Abe and T.Oikawa , Developmental and Reproductive Biology Center, Yamagata

The oviduct epithelium of the golden hamster consists of two kinds of cells, ciliated cells and secretory cells. The ultrastructural changes in the process of the differentiation of the two cells in postnatal hamster oviduct were investigated by means of electron microscopy. In the epithelium of the ampulla of newborn hamster, differentiated ciliated cells or secretory cells were not identified. In these undifferentiated cells, free ribosomes were well developed, but rough endoplasmic reticulum (RER) and Golgi complex were undeveloped. Ciliated cells were first identified on 4.5 days. They gradually increased in number until 12.5 days, then increased at an increasing rate until 20.5 days. In contrast, nonciliated cells of 12.5-day-old hamster contained well-developed RER and Golgi complex. These cells began together the production of secrtory granules from 15.5 days. The number of these cells was constant from 15.5 to 25.5 days. Most of the epithelial cells differentiated into either ciliated cells or secretpry cells by 20.5 days. These results indicate that ciliated cells begin to differentiate on 4.5 days after birth, and 11 days later nonciliated cells begin the production of secretory granules.

DB 114

DEVELOPMENT OF COLLAGENOUS MATRIX IN THE FIBROCARTILAGE OF THE OS PENIS OF THE RAT.

R.Murakami, K.Miyake and I.Yamaoka.
Biol. Inst., Fac. Sci., Yamaguchi Univ., Yamaguchi.

Distal segment of the os penis of the rat is a fibrocartilage whose development is dependent on androgens. Collagenous components in the fibrocartilage of the rat were analyzed by SDS-PAGE, immunoblot and immunofluorescence using anti-types I and II collagen sera.

Major collagens in the fibrocartilage were types I and II. Type I collagen appeared in the extracellular matrix of immature cartilage at about 1 week. Type II collagen appeared at about 4 weeks surrounding mature chondrocytes which developed as small clusters in the distal segment of the os penis. Both types of collagens co-existed in the cartilage matrix in adult males. When the rudiments of the distal segment in rat fetuses were cultured *in vitro* in the presence of testosterone, fibrocartilage containing both types I and II collagens developed. In the absence of testosterone, only a loose connective tissue positive for anti-type I collagen serum developed.

These results suggest that androgen is necessary at least for the synthesis of type II collagen in the fibrocartilage of the os penis of the rat.

DB 115

THE EFFECT OF 12-*O*-TETRADECANOYL-PHORBOL-13-ACETATE (TPA) ON THE DIFFERENTIATION OF THE MOUSE NEURAL CREST CELLS *IN VITRO*.

S.Tanaka[1], K.Ito[2] and T.Takeuchi[1]. [1]Biol. Inst., Tohoku Univ., Sendai. [2]Dept. of Biol., Col. of Gen. Educ., Osaka Univ., Toyonaka.

In the mouse neural crest cell culture, only crest cells associated with epithelial sheet from the explanted neural tube differentiate into melanocytes. When the explanted neural tubes were removed in the early phase of the culture period, however, the differentiation into melanocytes never occurred in spite of the appearance of adrenergic neurons (Ito and Takeuchi, 1984).

When the tumor promoter TPA, which has been shown to influence cell differentiation in several *in vitro* systems (Sieber-Blum and Sieber,1981; Weston et. al.,1986), was added to the culture medium, the differentiation of the mouse neural crest cells into fully developed melanocytes was observed. On the other hand, α-MSH, which induces the differentiation of melanoblasts into mature melanocytes, did not induced the differentiation of neural crest cells into melanocytes. This result seems to indicate that TPA promotes the differentiation of the mouse neural crest cells into melanocytes.

DB 116

EFFECT OF 5-AZACYTIDINE ON RAT EMBRYONIC DEVELOPMENT IN VITRO.

M. Matsuda, R. Kimura and R. Shoji. Dept. Embryol., Inst. Dev. Res., Aichi Prefec. Colony, Kasugai, Japan.

Rat embryos (day 9.5 of gestation) were cultured in vitro for 48 h in rotating bottles containing rat serum with or without 5-azacytidine (0.2 ug/ml) and assessed for embryonic growth and development at regular intervals. After 48 h in culture in rat serum, development of the embryos was at a rate almost identical to that seen in vivo 11.5-day embryos. When the embryos were cultured for 48 h in rat serum with 5-azacytidine, their heads were smaller compared with control embryos and cephalic neural folds remained open, although they closed after 33 h in control culture. However, somite number, crown-rump length and morphological features except head were almost the same as control embryos. Histological observations of the abnormal embryos showed that unfused neural folds at the hindbrain, an abnormal elevation of neural folds at the midbrain and the lack of the apices of the forebrain. These embryos also showed the abnormal migration of neuroepithelial cells. The abnormal cell migration may cause the irregular elevation of neural folds, which prevent the fusion of neural folds.

DB 117

FOFMATION OF ELASTIC FIBERS BENEATH MOUSE ORAL EPITHELIUM IN VITRO AND IN VIVO.

T.Yamaai, Dept. of Oral Anat., Okayama Univ. Dent. Sch., Okayama.

The formation of the elastic fibers in the mouse oral proper layer was examined on in vitro and in vivo by the method of the light microscopy. The upper jaws from 17-day fetuses of C3H mice which placed in milli-cell culture cups were cultured in DM-160 medium with 10% fetal calf serum for 7 to 14 days. The elastic fibers were stained by resorcin-fuchsin.

The evidence for the elastic fibers was found in the upper jaws from 17 days of pregnancy and indicated quite clear by a week after birth. However, the elastic fibers were appeared in the only buccal side of the dental lamina beneath the oral epithelium. On the other hand, an amount of the elastic fibers in the cultured upper jaw on the 7th day was already more abundant than it in vivo. In addition they were existed on the buccal and palatal sides of the dental lamina. There were many types of cells on the surface of the oral epithelium of the cultured upper jaws. Since they were arranged in as a mosaic, it seemed no specific arrangement from place to place of the surface of the oral epithelium as compared with that of in vivo. The cultured upper jaws adhered to the surface of the milli pore filter and were maintained under normal condition.

DB 118

SPICULE FORMATION IN SEA URCHIN EMBRYOS KEPT IN Cl^--DEFICIENT ARTIFICIAL SEA WATERS

Y. Fujino[1], K. Mitsunaga[2], A. Fujiwara[2] and I. Yasumasu[2]
[1]Dept. of Pharmacol., Teikyo Univ. Sch. of Med., Tokyo and [2]Dept. of Biol., Sch. of Educ., Waseda Univ., Tokyo

In artificial sea waters (ASW's) in which Cl^- concentrations were reduced to 30 % of normal concentration in ASW by its replacement with Br^-, ClO_4^-, NO_3^- and $HCOO^-$, and to 70 % by its substitution with acetate, propionate and BrO_4^-, early development of sea urchin embryos was apparently normal and developed to quasi-normal plutei with spicules. The replacements of more than 80 % of Cl^- amount with the former gruop of anions, made spicule rods somewhat poor and the substitutions of more than 40 % Cl^- amount with the latter anions strongly blocked spicule rod formation. In embryos kept in the former Cl^- deficient ASW's, anions replaced with Cl^- were transported into embryos in relation to the rate of spicule formation and the transports of these anions were inhibited by nifedipine or DIDS, which blocked formation of spicules. In embryos kept in the latter ASW's, the rates of uptake of these anions, with which Cl^- in ASW's was substituted, were quite poor and did not relate with the rate of Ca^{2+} uptake. Uptake of these anions was not affected by nifedipine and DIDS. These suggest that Ca^{2+} uptake through Ca^{2+} channels is coupled with co-transport of anions through anion channels.

DB 119

SPECIFIC BINDING OF LECTINS WITH THE CHROMATIN OF SEA URCHIN EMBRYOS DURING THE COURSE OF DEVELOPMENT.

S.Kinoshita[1], K.Yoshii[2] and Y.Tonegawa[3]. [1]Dept. of Biol., Saitama Medical School, Saitama, [2]Biol. Lab., St. Marianna Univ., Sch. of Med., Kawasaki and [3]Dept. of Regulation Biol., Saitama Univ., Urawa.

Embryonic cells of sea urchin were made permeable by treating with glycerol for the purpose of allowing penetration of lectins into the cell, and it was found that some lectins showed notable affinity with the nucleus.

Isolated chromatin was incubated with several kinds of fluorescent dye-labeled lectins, and the amount of lectins bound with the chromatin was measured by fluorometry. It was found that lectins could be classified into three groups according to the mode of binding with the chromatin: (a) Extent of binding increased notably at the gastrula stage (Con A and RCA-120); (b) Extent of binding showed a temporary decrease at the gastrula stage (TTA); and (c) Very low level of binding was maintained throughout all stages, and no particular change was observed at any stage of development (WGA, SBA and UEA-I).

DB 120

AP4A-HYDROLYZING ENZYMES IN SEA URCHIN EMBRYOS

M.Morioka & H.Shimada (Zool.Inst., Fac.Sci. Univ.Tokyo, Tokyo)

Based on our findings that the level of soluble AP4A drastically decreased at the onset of S phase with the concomitant increase its binding to the nuclear matrix, we suggested that AP4A is involved in the initiation of S phase in sea urchin embryos. However, the amount of AP4A being bound to the nuclear matrix was not large enough to explain the fate of AP4A disappeared from the soluble fraction at the onset of S phase. In this paper, we report some features of the AP4A-hydrolyzing enzymes in sea urchin embryos.

The embryo contains several enzymes which hydrolyze AP4A to ATP and AMP but not to ADP. One of these enzymes was partially purified by DEAE-cellulose column chromatography, Sephadex G-75 gel filtaration and AMP-Sepharose affinity chromatography. The molecular weight of the enzyme was 20,000 and the Km value for AP4A was 3μM. The enzyme required Mg^{++} for the maximal activity, while it showed little activity in the presence of EDTA. The activity was completely inhibited by $ZnCl_2$ and markedly inhibited by $CaCl_2$. AP4A-hydrolyzing activity was very low in the unfertilized egg. Tough the enzyme became activated immediately after fertilization, the activity did not change corresponding to a cell cycle.

DB 121

DIFFERENTIATION OF SEROTONERGIC GANGLION CELLS IN SEA URCHIN LARVAE, MESPILIA GLOBULUS.

Y. NAKAJIMA. Dept. of Biology, Keio Univ., Yokohama.

This work was undertaken in order to ascertain the relationship between the preoral serotonergic nerve of pluteus and the cells composing the apical plate with long cilia, which is supposed to function as a sensory organ in blastula and gastrula. Localization of serotonergic cells in animalized blastulae induced by the treatment with Evans Blue, vegetalized embryos produced by LiCl, and open and flattened embryos made by the treatment with Ca-deficient sea water were examined by indirect immunofluorescence microscopy.

In the animalized 24 h-old embryo, serotonergic cells appeared not in apical zone but in the second quarter of animal-vegetal axis. In later stages, numerous serotonergic cells and cell processes became visible mainly in this zone. Serotonergic cells were not detected in vegetalized exogastrulae. In "open" embryos, cellular differentiation proceeded normally after the transfer into sea water, and serotonergic cells and cell processes appeared as a ringlet in the epithelium around the tip of archenteron.

These findings indicate that serotonergic preoral ganglion cells of echinopluteus derive from the ectodermal epithelium surrounding the apical plate cells.

DB 122

Crt ANALYSIS OF POLY(A)$^+$RNA POPULATION IN VEGETALIZED SEA URCHIN EMBRYOS.

M. Komukai and I. Yasumasu
Dept. of Biol., Sch. of Educ., Waseda Univ., Tokyo.

The change in the poly(A)$^+$RNA population between Li^+-treated and normal sea urchin embryos was analyzed by cDNA-RNA hybridization. Poly(A)$^+$RNA was isolated from gastrulae or 24 hr vegetalized embryos which were treated by 60 mM LiCl for 3 hr (from 16 cell to 64 cell stage). ^{3}H-labeled cDNA was synthesized *in vitro* using AMV reverse transcriptase with poly(A)$^+$RNA from vegetalized embryos as a template. This ^{3}H-cDNA had a specific radioactivity of 1.8 x 10^5 dpm/ug. The cDNA was hybridized with a large excess of poly(A)$^+$RNA from either vegetalized or normal embryos (RNA/cDNA>1.1x10^3), and the extent of the hybrids was detemined by a S1 nuclease assay. The reaction occurred over 3 orders of Crt. Plateau value of the fraction of S1 nuclease-resisitant cDNA hybridized with gastrula poly(A)$^+$RNA was substantially lower than that with its own vegetalized poly(A)$^+$RNA. This subtracted value indicates the qualitative difference between normal and vegetalized poly(A)$^+$RNA population.

DB 123

EFFECT OF APHIDICOLIN ON THE GASTRULATION OF SEA URCHIN EMBRYOS

H. Fujisawa and S. Amemiya. Fac. of Educ., Saitama Univ., Urawa, and Misaki Marine Biological Station, Fac. of Sci., Univ. of Tokyo, Miura.

In sea urchin embryos, we noticed that the rate of increase in cell number at the time of archenteron invagination was generally higher than that during the preceding swimming blastula stage. We also found that the cell number of embryos animalized with Zn ion was larger than that of the embryos vegetalized with Li ion. From these facts we postulated that in normal embryos, partial cell proliferation in the animal hemisphere contributes the invagination of the archenteron. In order to test this, we observed the effect of aphidicolin, an inhibitor of DNA alpha-polymerase, on gastrulation. The sea urchins used in this experiment were Hemicentrotus pulcherrimus and Clypeaster japonicus. Aphidicolin (0.2 µg/ml sea water) was added to the embryos at the mid-blastula stage. The drug effectively suppressed cell proliferation from that stage, although the embryos were able to form the archenteron. This result shows that the increase in cell number occurring at the onset of gastrulation does not play any role in the invagination of the archenteron.

DB 124

IONIC EFFECT ON THE REVERSAL FORMATION OF CILIA IN THE ISOLATED GUT OF SEA URCHIN EMBRYOS.

H.Suzukawa & M.Ishikawa , Dept.of Biol., Fac.of Sci.,Ehime University, Matsuyama.

It has been reported by Amemiya('79) that when isolated guts of sea urchin embryos were incubated in a normal sea water for several hours, cilia were recognized on the opposite cell surface to their original growing positions after closure of the blastopore. In the present study, effects of several ions and ion-transport blockers on reversal formation of cilia in the isolated gut were investigated.

It was found that free from Ca^{2+} and Mg^{2+} in the culture medium does not influence on cilium formation. Verapamil(Ca^{2+} blocker) and ouabain(Na^{+}-K^{+}ATPase blocker) not inhibit cilium formation. Defect of Na^{+} and ethacrinic acid(Cl^{-},HCO_3^{-} blocker) inhibit elongation of the cilium after initial appearance of it. Reversal formation of the cilium does not occur in the K^{+}-free medium or allyl isochiocyanate(H^{+}-K^{+} blocker), but when the isolated gut is removed into the above conditional medium soon before initial appearance of the cilium, elongation of the cilium is not inhibited.

From above mentioned results, it may be suggested that existence of K^{+} in the culture medium is necessary for reversal formation of cilia in the isolated gut.

DB 125

PURIFICATION OF EXOGASTRULA-INDUCING PEPTIDES IN EMBRYOS OF THE SEA URCHIN, ANTHOCIDARIS CRASSISPINA.

K.Ishihara, Y.Tonegawa, T.Yoshizumi and T. Suyemitsu. Dept. of Regulation Biology, Fac. of Sci., Saitama Univ., Urawa.

We tried to purify the exogastrula-inducing factors from supernatant of the embryo homogenate of the sea urchin, Anthocidaris crassispina. Successive colume chromatography with DEAE-cellulose, Sephadex G-100 and G-50 revealed only one fraction which was active for inducing exogastrula. The fraction was separated by CM-sepharose CL-6B column into 8 fractions among which 3 fractions of Fr.D, Fr.E-2 and Fr.VI were biologically active. SDS-polyacrylamide gel electrophoresis of these fractions showed the presence of a single band in Fr.D and Fr.VI, and two bands in Fr.E-2 with M.W. of 4,800, 7,200, 5,500 and 8,300, respectively. Reverse phase HPLC of these fractions gave also a single peak from Fr.D and Fr.VI, and two peaks which were eluted separately from Fr.E-2.

These fractions were named as peptide A, D, B and C, and analyzed the amino acid composition. N-terminal amino acid sequences were found to be Asp-Ser- for peptides A and B, and to be Asp-Thr- for peptides C and D by direct Edman degradation. C-terminal sequences were found to be -Thr-Glx for peptide A, -Glx-Thr for peptides B and C, and -Ser-Ala for peptide D by the amino acid analyses of hydrolyzed peptides with carboxypeptidase Y.

DB 126

THE PRIMARY STRUCTURES OF THE EXOGASTRULA-INDUCING PEPTIDES IN EMBRYOS OF THE SEA URCHIN, ANTHOCIDARIS CRASSISPINA.

T.Suyemitsu, Y.Tonegawa, S.Noguchi and K. Ishihara. Dept. of Regulation Biology, Fac. of Sci., Saitama Univ., Urawa.

The complete amino acid sequences of the exogastrula-inducing peptides A, C and D in embryos of the sea urchin, Anthocidaris crassispina were determined. The homogenous peptides were cleaved with lysine endopeptidase or arginine endopeptidase. The resulting peptides were purified by reverse phase HPLC. Sequencing of the fragments was achieved with automated Edman degradation.

The exogastrula-inducing peptides A, C and D were composed of 52, 58 and 53 amino acid residues and their molecular weights were calculated to be 5,754, 6,463 and 5,735, respectively. The sequence of the peptide A was AspSerValTyrGlnCysAsnArgAsp ThrAsnSerCysAspGlyPheGlyLysCysGluLysSerThr PheGlyArgThrThrGlyGlnTyrIleCysAsnCysAspAsp GlyTyrArgAsnAsnAlaTyrGlyGlyCysSerProArgThr GluOH. The sequence of the peptide C was AspThrLysGlyGlyCysGluArgAlaThrAsnAsnCysAsn GlyHisGlyAspCysValGLuGlyArgTrpGlyGlnTyrTyr CysLysCysThrLeuProTyrArgValGlyGlySerGluSer SerCysTyrMetProLysAspLysGluGluAspValGluIle GluThrOH. The sequence of the peptide D was AspThrValAlaArgCysGluArgAspThrLysAsnCysAsp GlyHisGlyThrCysGlnLeuSerThrPheGlyArgArgThr GlyGlnTyrIleCysPheCysAspAlaGlyTyrArgLysPro AsnSerTyrGlyGlyCysSerProSerSerAlaOH.

DB 127

STIMULATION OF PROTEIN SYNTHESIS IN THE MITOCHONDRIA OF SEA URCHIN AND STARFISH BEFORE GASTRULATION.

T.Kawashima and T.Nakazawa. Dept. of Biol.,Fac. of Sci.,Toho Univ.,Funabashi.

A transient increase in protein synthesis in vitro was observed at the mesenchyme blastula stage of sea urchin and starfish embryos. This stimulated activity was inhibited by chloramphenicol but not by cycloheximide, and was localized in the mitochondrial fraction. Reconstituting experiments in which poly U-dependent protein synthesis was carried out showed the mitochondrial peptide elongation factor to be essential for increasing the protein synthetic activity in mesenchyme blastula, but aminoacyl tRNA synthetase and ribosome fraction containing initiation factor not to be involved in this increase.To clarify the nature of protein synthesized in the mitochondrial fraction of starfish embryos, [^{3}H]-amino acid-incorporated protein was purified with column chromatograhy. Properties of the synthetic protein will be examined in future.

DB 128

CORRELATION BETWEEN PROTEIN PHOSPHORYLATION AND DIFFERENTIATION IN SEA URCHIN EMBRYOS.

S.Shinohara[1], M.Motojima[1], K.Mitsunaga[1], Y.Fujino[2] and I.Yasumasu[1]. [1]Dept. of Biol., Sch. of Educ., Waseda Univ. and [2]Dept. of Pharmacol., Teikyo Univ. Sch. of Med., Tokyo.

H-7, an inhibitor of C-kinase, inhibited morphogenesis, especially spicule formation, in sea urchin embryos and pseudopodial cable growth, in which spicule rods were to be produced, in cultured micromere-derived cells. HA1004, an inhibitor of A-kinase, did not block them. ^{32}Pi incorporation into proteins was markedly inhibited by H-7 but was not by HA1004 both in embryos and in cultured cells. These results suggest that spicule formation, especially outgrowth of the cables, is probably supported by protein phosphorylation mediated by C-kinase. In embryos, which were introduced to H-7 and HA1004 at 16 hr after fertilization, proteins were analyzed by SDS-PAGE at the gastrula and the pluteus corresponding stages. The abnormal embryos kept with H-7 in a period between the mesenchyme blastula and the pluteus equivalent stage contained 41 K protein, which was found in blastulae and was absent in plutei. ^{32}P incorporation into 43, 41, 28 and 25 K proteins was somewhat inhibited by H-7 but was not by HA1004.

DB 129

CATHEPSIN B ACTIVITY IN SEA URCHIN EGGS AND EMBRYOS.

Y. Okada and Y. Yokota. Biol. Lab., Aichi Pref. Univ., Nagoya.

Cathepsin B activity was studied in sea urchin eggs and embryos. Cathepsin B was purified approximately 70-fold from unfertilized eggs of *Hemicentrotus pulcherrimus* by ammonium sulfate fractionation, column chromatography on CM-cellulose and gel filtration through Sephadex G-100 with a recovery of 4%. Gel filtration gave a molecular weight more than 200,000. It is assumed that cathepsin B may be in the form of complex with other proteins. The enzyme showed the highest activity arround pH 5.5 to carbobenzoxy-Arg-Arg-methylcoumarylamide, and Km to the same substrate was estimated to be 0.01 mM at pH 5.5.

Localization of cathepsin B in unfertilized eggs and the activity of cathepsin B in the embryo during development was investigated in *Anthocidaris crassispina*. Ninety-eight percents of the activity in the egg were detected in the nuclear and mitochondrial fractions. This result suggests that cathepsin B may be distributed mainly in the yolk granules. During the embryogenesis, remarkable changes in the activity of cathepsin B, which is assumed to participate in the disintegration of a major yolk protein, were not observed.

DB 130

PROPERTIES OF THE CONTRACTION-INDUCING FACTOR IN THE ABORAL INTESTINE OF THE SEA URCHIN AND ITS MONOCLONAL ANTIBODY.

N. Takahashi[1], N. Sato[2], M, Takahashi[1] and K. Kikuchi[2]. [1]Marine Biomed. Inst. and [2]Dept. of Pathology, Sapporo Med. Coll., Sapporo.

The characteristics of gonadal contraction-inducing factor(s) (CF) in the aboral intestine of the sea urchin Strongylocentrotus intermedius were determined on the basis of measurements of gonad responses to CF under various conditions. CF was found to show heat stability and resistance toward several kinds of proteases. Its molecular weight was within the range of 2000 to 4ooo.

The monoclonal antibody (MoAb) of this factor was obtained from hybridomas secreting it, by the mechanical response of gonad to mixture of CF with the MoAb, the enzyme-linked immnosoluvent assay (ELISA) and the avidin-biotin method (ABC). The spleen cells of BALB/c mice immunized two times with 0.5 ml supernatant (40,000 rpm) from aboral intestine were hybridized with NS-1, a hypoxanthine phosphoribosyltransferase-deficient myeloma line of BALB/c mice. The hybridomas responsing to CF by the ELISA and the ABC method and inhibiting gonadal contraction were selected for the MoAb of CF. The MoAb was designated as "#11-B-2". We are presently working to establishing the MoAb of the receptor of CF.

DB 131

OOGENESIS AND TIMING OF COPULATION DURING FEEDING IN THE ADULT TICK, HAEMAPHYSALIS LONGICORNIS.

Y.Yano, T.Mōri, S.Shiraishi and T.A.Uchida. Zool. Lab., Fac. of Agr., Kyushu Univ., Fukuoka.

In the unfed stage, the ovarian oocytes in the late stage of prophase of the meiosis I were connected with each other through intercellular bridges; some oval mitochondria were present in groups in the scanty cytoplasm. At 4-day phase in the feeding stage, the oocyte protruded into the haemocoel increasing its cytoplasmic volume and was attached to the ovarian wall by the funicle cells originated from the ovarian epithelium. The microvilli of both the oocyte and the funicle cell developed well on the boundary zone between them, and many mitochondria became scattered in the egg cytoplasm. Myoepithelial cells with contractile filaments were recognized and appeared to be derived from the ovarian epithelium. Copulation seemed to occur after the above differentiation of the epithelial cells. At the engorged and detached stage, vitellogenesis and egg-shell synthesis have almost completed in the oocyte with polarity. Because of the invagination between the adjacent funicle cell membranes, it may be easy for the oocyte to fall into the ovarian lumen. Spermatozoa found in the lumen were in close contact with the microvilli of the ovarian epithelial cells containing a large quantity of rER, or lodged in indentations of the funicle cell membranes.

DB 132

REPEATED REGENERATION OF THE GERMAN COCKROACH LEGS.

A. Tanaka, M. Ohtake-Hashiguchi and E. Ogawa. Dept. of Biol., Fac. of Sci., Nara Women's Univ., Nara.

Two series of repeated-regeneration experiments were carried out on each fore-, mid- and hindleg of both sexes during the entire postembryonic development. One was autotomy at trochantero-femoral articulation; the other was amputation from basal coxa. In both experiments, one of the six legs was operated before the regeneration critical period in the 1st instar. If a regenerate appeared in the following instar, it was repeatedly operated; if not, operation was postponed until a regenerate appeared. In autotomy regenerates repeatedly appeared almost every instar until the adult stage, while in amputation no regenerates were present just after postoperative molts. Regenerated femur and tibia developed well after autotomy, whereas those after amputation were considerably smaller. All the regenerated legs had tetramerous tarsi. Regenerated legs from autotomized stumps showed incomplete homoeotic regeneration as to the kind of legs. Regenerates from foreleg stumps showed intermediate tibia/femur ratios between normal foreleg and midleg, and those from the hindlegs, intermediate between normal hindleg and midleg. Possible modifiers were suggested for the homoeotic and tetramerous regeneration.

DB 133

REGENERATION OF ANTENNAE IN *Riptortus clavatus* (HETEROPTERA) IN RELATION TO AMPUTATION LEVELS AT THE FIRST INSTAR

K.IKEDA and H.NUMATA. Dept. of Biol., Fac. of Sci., Osaka City Univ. Osaka.

The structure of regenerated antennae of adults was observed with a scanning electron microscope after the amputation at various sites at the first instar.

The excessive growth of each segment depended on the length of the distal segment of the remaining antenna (RDS). If RDS was longer than a certain length, the more distal the segment was, the more the excessive growth was. Moreover, the structures peculiar to the normal distal segment, e.g. sensory hairs, grooved pegs, appeared on RDS which grew most excessively. If RDS was shorter than the critical length, however, the second distal segment grew most excessively, and the structures peculiar to the normal distal segment appeared on both RDS and the distal part of the second distal segment. When a whole antenna was removed, the antenna was never regenerated.

After the amputation at the first (proximal) or the second segment, a new segment often arose from RDS. When the amputation was at the proximal part of the third segment, a new segment sometimes arose from the second distal segment.

DB 134

EXPERIMENTAL EGG ACTIVATION IN THE SAWFLY, ATHALIA ROSAE (TENTHREDINIDAE, HYMENOPTERA)

M. Sawa and K. Oishi. Div. of Sci. of Biological Resourses, Grad. School of Sci. and Technol., Kobe Univ., Kobe.

Mature unfertilized eggs (ripe oocytes) dissected from ovaries of the turnip sawfly (*Athalia rosae*), if soaked in distilled water, are activated and initiate parthenogenetic development (Naito 1982). In the present study, we examined the effects of various treatments on egg activation. Effect of osmorality was examined by dissecting and maintaining the ripe oocytes in in NaCl, KCl, $CaCl_2$, $MgCl_2$, and sucrose at various concentrations. Frequency of activated eggs, determined at blastoderm stage, decreased with increasing concentrations of the solutions. Egg activation was prevented at about 300 mOsm in $CaCl_2$, $MgCl_2$, and sucrose. NaCl, however, inhibited egg activation completely at 200 mOsm, while KCl did so only at 600 mOsm. Effect of pH was examined using 0.15M phosphate buffer. Most eggs were activated at pH 5.0, but none at 7.0 and 9.0. Finally effects of various other treatments were examined. Ripe oocytes were dissected out, kept in NaCl (300 mOsm), and variously treated: Brief (3 min) desiccation (up to 70% activated), passage through a narrow capillary tubing (up to 34 %), puncture with a sharp glass needle (up to 50%). Altogether the present results appear to indicate the involvement of the egg surface membrane potential in the egg activation in this system.

DB 135

THREE STORAGE PROTEINS IN THE COMMON CUTWORM, SPODOPTERA LITURA.

S. Tojo. Lab. Nematol. & Entomol., Fac. Agricul., Saga University, Saga.

In the common cutworm, Spodoptera litura, whole of two proteins named SL-1 and SL-2, and part of one protein named SL-3 were found to be sequestered into the fat body from the haemolymph during the pharate pupal stage.SL-1 and SL-2 appeared in the haemolymph for the first time in the early last larval instar and their appearance was blocked by juvenile hormone application at this stage. While SL-3 increased during larval-larval ecdysis in the penultimate larval instar and the juvenile hormone treatment could not inhibit its rapid increase in the haemolymph in the last larval instar. All of these proteins decreased in the body during the pharate adult development and disappeared shortly after the adult emergence.

The properties of these proteins were similar , all of which had molecular weight of around 500,000 and were composed of subunit of around 80,000. SL-1 and SL-2 were similar in the amino acid composition, but differed from SL-3, which contained exceptionally high level of phenylalanine and tyrosine and resembled calliphorin in the amino acid composition.

From these resurts, it was concluded that SL-1 and SL-2 were pupal storage proteins and SL-3 was arylphorin.

DB 136

HISTOLOGICAL STUDIES ON THE G. PROSTATICA OF THE SILKMOTH, BOMBYX MORI.

H.KASUGA, M.OSANAI and T.AIGAKI. Dept. of Biol., Tokyo Metrop. Inst. Geront., Tokyo.

The secretion of glandula (g.) prostatica contains an endopeptidase, initiatorin, which causes in the spermatophore the motility acquisition of apyrene sperm, the dissociation of eupyrene sperm, the activation of a carboxypeptidase producing free Arg, and the Arg degradation cascade for yielding energy. G. prostatica is distinguished to four parts from the external genitalia to g. alba due to histological differences of the exocrine cells and their secretions. 1. A thin duct consisting of flat epithelial cells which is surrounded by a spincter. 2. A layer of exocrine cells projected to the tube, making many folds in it. At the lower part, there is a valve shuting in the newly emerged adult to avoid an outflow of secretions. 3. An exocrine gland consisting of a cubical epithelium of three cell-layers. Secretion contains heterogeneously neutral fat, droplet of acidy fat and PAS-positive material. 4. An exocrine gland of a cylindrical epithelium. Cells contain much large and small secretion glanules stained brown and dark green with toluidine blue, respectively. Neutral fat and a material unstained with any dyes are found in this secretion. At the ejaculation, cytoplasm in the glandular epithelium cells is also excreted in part and the intracellular granules diappear.

DB 137

A histological study of capsules during pupal-adult metamorphosis in Samia cynthia ricini.

S.TAKAHASHI, G.ENOMOTO and Y.NAKAJIMA. Dept. of Biol. Nara Women's Univ. Nara.

Changes of capsules taking place during pupal-adult metamorphosis were studied in Samia cynthia ricini. Pieces of cellulose acetate membrane were implanted into pupae within 10 hr after ecdysis. Hemocytes reacted rapidly against CEA and formed thick capsule around it. Capsules, 24 hr after implantation, consisted of an inner layer of necrotic cells nearest the melanized surface of implant and an outer layer of numerous flattened cells. When the insect entered the period of apolysis (70-hr old), large, basophilic cells appeared between the two layers. These cells also surrounded the implant and finally formed an epitheliumlike mono-layer. There was a secretion which covered the whole inside of the layer. In the outside of the layer, flattened cells disappeared for a time , but accumulated again in later stages of pharate adult. Origin and nature of cells of the newly formed layer are unknown. In conclusion, during pupal-adult metamorphosis, hemocytic capsules having formed in an early pupal stage were decomposed like other larval tissues, and a turnover of capsule cells occurred.

DB 138

EVEN DISTRIBUTION OF SCALE MOTHER CELLS IN THE PUPAL WING DISC OF SMALL WHITE CABBAGE BUTTERFLY, PIERIS RAPAE.

A.Yoshida and K.Aoki. Life Sci. Inst., Sophia Univ., Tokyo.

We studied the even distribution pattern of one of the two kinds of scale mother cells, termed S1, in the pupal wing disc of Pieris. During the phase S1's were differentiated, right wing discs were examined with scanning electron microscope, while whole mounts of left wing discs were stained by Feulgen reaction and examined with optical microscope.

The results are as follows. First, S1's are differentiated from the homogeneous epidermal cells of the wing disc without cell divisions. Second, the number of S1's increases and finally S1's are separated by one or two undifferentiated cell(s). Third, S1 does not divide during that phase, while some undifferentiated epidermal cells divide in the definite area of the wing disc. Forth, the distribution pattern of S1 is the same between in the areas with cell divisions and without cell divisions.

All the results can be accounted for by assuming that all undifferentiated cells are going to give rise to S1's and the earlier differentiated S1's inhibit the adjacent undifferentiated cells to give rise to S1's.

DB 139

MUTATIONS AFFECTING NUCLEAR MIGRATION AND F-ACTIN ORGANIZATION IN DROSOPHILA EARLY EMBRYOS.

K.Hatanaka and M.Okada. Inst. Biol. Sci., Univ. of Tsukuba, Ibaraki.

Maternal effect mutations, N26, N441 and par share a similar phenotype showing defective nuclear migration with little effect on synchrony in cleavage mitosis. A phenocopy of these mutants can be induced by treatment of wild-type embryos with cytochalasins immediately after egg laying. In addition to abnormal nuclear migration, these mutants showed cleavage-stage specific defects in F-actin organization: formation of aggregates in the cortical F-actin meshwork, and retarded transition in F-actin distribution inside the yolk mass(Zool.Sci.,2,952,1985). Distribution of F-actin was normal after the syncytial blastoderm. N26 and N441 were located at 10A6-B3 and 11A7-B9, respectively. Both are far from all known actin loci. Phenotypes of hemizygous mutants showed that N441 and par were amorphic and N26 was hypomorphic. A double mutant of N441 and N26 showed an extreme phenotype with completely spherical nuclear distribution at a late cleavage stage, suggesting that $N441^+$ and $N26^+$ contribute independently and cooperatively to normal F-actin organization, which is required for normal nuclear migration.

DB 140

EFFECTS OF GENE DOSAGE ALTERATION ON RIBOSOMAL PROTEIN EXPRESSION IN DROSOPHILA MELANOGASTER.

H.B.Tamate[1 2], M.Rosbash[3], and M.Jacobs-Lorena[2]. [1]Yamagata Univ.Sch.Med. [2]Case Western Reserve Univ. [3]Brandeis Univ. USA

To study the regulatory mechanism for the coordinate synthesis of ribosomal proteins (r-proteins), the effect of altered gene dosage on the r-protein expression was analyzed in transgenic flies carrying extra copies of r-protein 49 gene. The abundance of the rp49 mRNA in ovaries was quantitated by RNA blot analysis. The same blots were also hybridized with other r-protein DNA probes. The rp49 mRNA was overrepresented in most of the transgenic lines, while the abundance ot other r-protein mRNAs remained unaltered. Despite the larqer difference in rp49 mRNA content, the proportion of the rp49 mRNA that is associated with polysomes did not differ in control and transgenic flies. There was no apparent difference in 2D-gel pattern of newly synthesized r-proteins in transgenic and control flies. These results suggest that the rp49 expression is controlled mainly at post-translational level, probably at protein turnover.

DB 141

HOMOLOGY TO A MITOCHONDRIAL LARGE rRNA OF THE poly(A) RNA RESPONSIBLE FOR POLE CELL FORMATION IN DROSOPHILA

S.Kobayashi and M.Okada. Inst. Biol. Sci., Univ. of Tsukuba., Ibaraki.

Pole cells, determined for germ line, are prevented from forming by uv irradiation at the posterior pole of cleavage embryos. Injection of poly(A)$^+$RNA extracted from cleavage embryos restores the pole cell forming ability to uv-irradiated embryos. Screening a cDNA library, prepared from poly(A)$^+$RNA of cleavage embryos, we isolated a single cDNA clone (pDE20.6) of the RNA with pole cell inducing ability. A computer analysis of the nucleotide sequence revealed that the cDNA is highly homologous to the mitochondrial large rRNA (lrRNA) gene of Drosophila. No nuclear gene homologous to the cDNA was detected by the Southern blot analysis. In cleavage embryos, the poly(A)+RNA complementary to the pDE20.6 cDNA was found dominantly in post-mitochondrial fraction (P3 fraction) but less in mitochondrial fraction (P2fraction). P3 fraction included almost no mitochondria. After the pole cell formation stage, pDE20.6 poly(A)$^+$RNA in P3 fraction decreased to 0.1%-0.3% level of the cleavage embryos. These results indicates that poly(A)$^+$RNA transcribed from the lrRNA gene is transferred to the cytosol to play a role in pole cell formation, and degraded after pole cell formation.

DB 142

SOMATIC CELL SPECIFIC ANTIGEN IN DROSOPHILA EMBRYOS.

F. Maruo*, M. Kurabayashi and M. Okada. Inst. Biol. Sci., Univ. of Tsukuba.

We have generated monoclonal antibodies (MAbs) against Drosophila ovaries to find developmentally regulated molecules during embryogenesis. One of the MAbs, E7-10, detected the antigen that is produced in nurse cells, shifted to the oocyte, and differentially distributed in early embryo cells. The distribution of the antigen was surveyed immunocytochemically with the MAb on polyester wax sections of embryos and first instar larvae. The antigen was found throughout cytoplasm of freshly laid eggs, later gathered in cytoplasm of every energid. At the blastoderm stage this antigen accumulated in the cytoplasm of the basal region of the somatic cells, and some antigen was also seen in the surface region of the central yolk mass. In the blastoderm and organogenesis stages, the antigen was found in all somatic cells, and then it gradually decreased from cytoplasm of all somatic cells to disappear by the end of embryogenesis . The antigen was neither found in pole cells nor in primordial germ cells in the embryonic and larval gonads. The MAb bound to a single band of MW 46 Kd in the immunoblot analysis. These observations indicate that during embryogenesis a common molecule is present in all somatic cells but not in germ line cells.

DB 143

EFFECT OF COLCHICINE ON CLEAVAGE OF AMPHIBIAN EGGS.

A. Yomota[1] and T. Sawai[2] Dept. of Biol. [1]Fac. of Sci. [2]Fac. of Gen. Ed. Univ. of Yamagata., Yamagata

It is known that the cleavage plane is determined by some stimulus transmitted to the cortex through astral rays of mitotic apparatus.

In this experiment, we examined the timing of determination of the cleavage plane in Cynops and Xenopus eggs by injecting colchicine at various times before the onset of cleavage.

When colchicine was injected into eggs more than 10 min before the start of cleavage in Cynops and more than 3 min before that in Xenopus, no furrow was formed. Ten min in Cynops eggs and 3 min in Xenopus ones corresponded to 0.10 in Dettlaff unit and the telophase of nuclear division. In both species, when the colchicine injection was made within 0.10D, the cleavage furrow was formed on the animal hemisphere but not on the vegital one. Colchicine injection at various times after the furrow appearance caused a cleavage arrest in various degrees.

These results indicate that, in the animal half, the cleavage plane of amphibian eggs would be determined by colchicine sensitive factor about 0.10D before the cleavage, and that the similar factor would be also take part in the furrow formation in the vegital half.

DB 144

ANALYSIS OF STAGE-SPECIFIC EFFECTS OF Li ON AMPHIBIAN MORPHOGENESIS.

Y. Yamaguchi & A. Shinagawa, Dept. Biol., Fac. Sci., Yamagata Univ. Yamagata 990.

Li+ is known to have teratogenic effects on amphibian morphogenesis. However, there is no information about precise relations between the timing of Li+ treatment and the consequent malformation excepting some studies suggesting the stage-specificity of the teratogenic response by the embryo to Li+ treatment. This study attempts to analyze precisely these relations by applying a relatively high concentration (0.4M) of Li+ on Xenopus embryos for a short period (5 min) at various stages up to the neurula stage.

Embryos treated at a stage from 16=cell to mid-blastula showed a syndrome of malformation as if dorsalized while those treated at a stage from mid-blastula to late gastrula showed another syndrome of malformation as if ventralized. These two syndromes of malformation was most efficiently induced by treatment at morula to early blastula stages and that at a mid-blastula stage, respectively. Neither treatment before the 16-cell stage nor that after the late gastrula stage induced significant malformation.

Thus, there are two distinct periods at which a Xenopus embryo is sensitive to Li ions and the way of its response to Li+ is quite different.

DB 145

MECHANISMS IN A XENOPUS EGG WHICH DETERMINE THE ORIGINATING SITE OF SURFACE CONTRACTION WAVES.

A. Shinagawa[1], S. Konno[1,2], Y. Yoshimoto[3,4], Y. Hiramoto[3,4]. [1]Dep. Biol., Fac. Sci., Yamagata Univ., [2]Devl. & Rep. Biol Cent., Yamagata, [3]Div. Cell Prolif., Natl. Int. Basic Biol., Okazaki, [4]Dep. Biol., Broadcast Univ., Chiba.

The originating site of SCWs is examined in Xenopus eggs after various treatments such as colchicine-injection, egg-inclination and enucleation. SCWs originate (1) at the sperm entrance point in fertilized eggs, regardless of the egg orientation, when injected with colchicine at 0.2-0.3, (2) at the uppermost site in fertilized eggs, regardless of the egg orientation, when injected at 0.8-0.9, (3) at the animal pole in activated eggs, regardless of the egg orientation, when injected at 0.2-0.3, (4) at the animal pole in the normally oriented activated eggs but often at the uppermost site as well as at the animal pole in the 90°-rotated activated eggs when injected at 0.8-0.9, and (5) at the uppermost site in enucleated eggs, regardless of above treatments. It is concluded from these results that the originating site of SCWs is determined by such cytoplasmic factors as have tendency to concentrate primarily around the male nucleus and secondarily around the female nucleus but around the uppermost region of the egg when no nucleus is present.

DB 146

VITELLINE ENVELOPE FORMATION IN URODELE OOCYTE.

K. Onitake, K. Mori and E. Ohzu. Dept. of Biol., Fac. of Sci., Yamagata Univ., Yamagata 990, Japan.

The vitelline envelope (VE) of anuran eggs has an important roles of polyspermy block after fertilization, but little is known about the function of urodele VE. In this study, we examined the VE formation of the newt, Cynops pyrrhogaster, during oogenesis with the immunohistochemical (indirect method) and histochemical (PAS-staining) methods. Developmental stages of oocytes were identified according to Dumont (1972). The anti-VE sera were obtained from an injecting rabbits of isolated VEs from matured eggs. Antisera were absorbed with homogenates of the VE-free matured eggs.

In stage II, immunofluorescence was first observed in some large vesicles of cytoplasm. In late stage II-stage III, the vitelline envelope began to form, and immunofluorescence was first observed on the surface of the oocyte as isolated patches. In stage IV, the VE formed a continuous layer over the surface of the oocyte. The oocyte of stage I and the follicle cells were not stained with FITC-labelled antibody. The same results were obtained from PAS-staining.

It is suggested that the vitelline envelope of the newt were formed mainly with the products from oocyte.

DB 147

PORLAR BODY FORMATION IN XENOPUS EGGS.

T. Kubota. Dept. of Biol., Fuc. of Sci., Kagoshima Univ., Kagoshima.

Xenopus laevis eggs dejellyed with thioglycollate and electrically activated were used at 20 C. In eggs fixed with Zenker fluid and stained with Feulgen, the second meiosis was at metaphase, anaphse, and telophase, respectively, at 0-6, 8-15, and 20 min after activation, and the first sign of polar body formation was found as a minute protrusion of the surface close to a spindle pole at 4 min. Eggs without their membrane were suspended between Steinberg solution and undiluted Percoll, and observed from side with a phase microscope.(1) an extruded and constricted cytoplasmic mass was not spherical. The mass became spherical after separation from the egg surface. (2)the separated second polar body and often the first remained there by some holding structure. This peculiar device may be related for amphibian eggs to rotate following activation. Colchicine injection after activation resulted in suppression of the polar extrusion. Dipping of activated eggs into a 10$\mu g/ml$ cytochalasin-containing medium had no effect on the polar body formation, presumably because of little permeation of cytochalasin into the egg. Polar bodies were formed in eggs part of whose cytoplasm was removed by its outflow produced by rupture of the the vegetal egg surface, or by its suction with a micropipette, suggesting that polar extrusion does not always necessitate the inner pressure originating from egg-surface tension.

DB 148

A POSITIVE FERTILIZATION POTENTIAL IN THE SALAMANDER, HYNOBIUS NEBULOSUS EGG.

Y. Iwao. Biol. Inst., Fac. Sci., Yamaguchi Univ., Yamaguchi.

In order to determine what kind of mechanisms of polyspermy block is operating in the salamander, Hynobius nebulosus egg, the electrical responses at fertilization and the behavior of accessory sperm nuclei in the egg cytoplasm were investigated.

The unfertilized eggs had a membrane potential of about -10 mV. The eggs elicited a rapidly-rising positive fertilization potential of about +40 mV. The positive potential lasted more than 30 min. All the eggs exhibited monospermy and developed normally. The same positive activation potential was produced by pricking, electric shock, or ionophore A23187. The positive potential was reduced to about -20 mV by 100 mM choline-Cl in the external medium. When the partially-jellied eggs were inseminated, 3-4 sperm entered each egg. The eggs underwent a multipolar cleavage and abnormal development. The accessory sperm nuclei never degenerated at all in the egg cytoplasm and formed extra bipolar spindles.

These indicate the primitive Hynobius eggs lack an intracellular polyspermy block, but the positive fertilization potential may contribute to a fast block to polyspermy. Thus, the Hynobius eggs exhibit an evolutionally intermediate state between anurans and higher urodeles.

DB 149

AN INHIBITION OF CYTOKINESIS IN NEWT'S EGGS WITH WGA TREATMENT.

T. ESAKA. Dept. of Biol., Science Education Inst. of Osaka Pref., Osaka.

Eggs of Cynops pyrrhogaster deprived of jelly and vitellin membrane were treated with WGA(100 μg in 1 ml of modified Steinberg's solution : 0.34 % NaCl, 0.005% KCl, 0.008 % $Ca(NO_3)_2 \cdot 4H_2O$, 0.0025 % $MgSO_4 \cdot 7H_2O$, and 0.0001 % phenol red, buffered to pH 7.2 with 0.05 % HEPES and NaOH) before first cleavage. In the eggs, furrow formation was initiated normally at each cycle of cleavage, but cytokinesis was inhibited. Rhodamine conjugated WGA seemed to bind uniformly to the egg surface, which is confirmed with a fluorescence microscope, while injected WGA was not effective to provoke the inhibition of cytokinesis.

Time-lapse VTR and 16 mm cinematograph showed that the appearance of surface contraction waves were not inhibited. The study with serial paraffine sections and with TEM proved that the division of nucleus and appearance of diastema were normal, and the egg surface was uniformly coated with WGA about 0.1 μm in thickness. To identify for the WGA layer, ferritin conjugated WGA was used.

DB 150

REGIONAL CHARACTERISTICS IN PROTEIN PATTERN OF 8-CELL STAGE OF X. LAEVIS.

A. Osada and A. S. Suzuki. Dept. of Biol. Fac. of Gen. Edu. Kumamoto Univ. Kumamoto.

Regional pattern of proteins in 8-cell stage of X. laevis was analyzed by two-dimensional SDS-polyacrylamide gel electrophoresis. The blastomeres of 8-cell stage were separated into four groupsö animal-dorsal(AD), animal-ventral(AV), vegetal-dorsal(VD), and vegetal-ventral(VV). Each group was separately sonicated in 70% ethanol-detergent buffer solution and centrifuged at 12,000g for 15 min. The supernatants were applied tó 2D SDS-PAGE. Each gel was stained by highly sensitive silver stain method.

we could found regional differences in several spots on each gel. Six spots were significantly different between AV and VV, five spots were also different between AD and VD. However, only two spots were different between AD and AV, VD and VV, respectively. These differences were qualitative or quantitative. The present experiment suggested the possibility that there are animal-specific and vegetal-specific proteins, because two spots were observed only in animal half and one spot was only in vegetal half. These results suggest that there is already regional specificity of protein pattern in 8-cell stage.

DB 151

IMMUNOBLOTTING DETECTION OF MYOSIN TO MUSCLE DIFFERENTIATION CAUSED BY MESODERMAL INDUCING SUBSTANCES.

M.Asashima, K.Shimada and H.Nakano. Dept. of Biol.,Yokohama City Univ., Kanazawa-ku, Yokohama 236.

Mesodermal inducing substances(F1) purified from carp swim bladder were used as the inductor in this experiment. F1 induces mesodermal tissues such as muscle and notochord in the ectoderm of early gastrula. To detect and analyse myosin molecule to muscle differentiation, immunoblotting method (western blotting) was employed. Following culture days (0,5,10 and 15 days) of the explants with or without the inducer, the samples were extracted with lysis buffer, and run on 7.5% polyacrylamide gel. At this time silver staining was also carried out to compare with the immumoblotting bands. The ectoderm only explants without inducer could not detect any myosin specific bands in both immunoblotting and silver staining in 15 days culture. But the explants with inducer after 10 days culture had recognized clear specific band at the high molecular(M.W. about 220K) which is corresponded to standard myosin band. This myosin specific band could observed in the explants from 10 days culture, but not 0 and 5 days culture explants. These immunoblotting data are discussed with the histological H-E staining observation and immunohistochemical study.

DB 152

MONOCLONAL ANTIBODY PRODUCTION AGAINST THE 38-KD PROTEIN LACKING IN XENOPUS MUTANT EMBRYOS.

Y.Tsuzaki and K.Ikenishi, Dept. of Biol., Fac. of Sci., Osaka City Univ., Osaka.

A maternal-effect mutant female in *Xenopus* (designated as no. 65) whose offspring always arrested the development at gastrulation was incidentally found (submitted). 2D-gel analysis revealed that an acidic, 38-kD protein which was always present in the wild-type unfertilized eggs was absent in the counterparts of female no. 65. It is known in *Ambystoma mexicanum* that the mutant embryos from o/o female which also showed the developmental arrest at gastrulation could develop beyond gastrulation when a protein fraction from the wild-type eggs of embryos was microinjected (Briggs & Justus, 1968).

In order to know whether this is the case in the female no. 65, it is necessary to obtain sufficient amount of the 38-kD protein, which is not denatured, for microinjection. So, we tried to make monoclonal antibody against the protein extracted from polyacrylamide gels. Culture supernatants of the hybridoma cell lines were primarily screened by ELISA with the extracted protein, and further examined with western blotting of 2D-gel electrophoresis of protein samples from the homogenate of wild-type, 2-cell eggs. The cloning of some cell lines which were positive in the blotting is now in progress.

DB 153

THE NEURAL TRANSMISSION OF NEURAL INDUCING SIGNAL EVOKED BY NEURALIZED CELL.

N.Sasaki, K.Yamazaki-Yamamoto, T.Kameda & K.Shimizu, Lab.of Biol.,Div.of Child.Educ., Seinan-Gakuin Univ.,Fukuoka

During the morphogenesis of amphibian embryo,the neural plate is formed in the ectoderm by the underlaying chordamesoderm. In this study, we showed the neuralized cells induced by the chordamesoderm obtained the potency to produce a neuro-inducing signal (homoiogenetic one), and this signal transmitted within ectodermal cell layer played an important role in the spatial extension of the neural plate of embryo. Followings were the experiments;

(1) In chimera experiment with *Hynobius* and *Cynops*,young ectoderm was implanted into an area of neural plate of early neurula. The ectoderm cells were transformed into neural cells.

(2) An isolated neural plate could induce neural tissues in young ectoderm. On the other hand, the myotome of neurula, by which the implanted ectoderm in (1) was underlaid had no ability for provoking neural differentiation in the ectoderm.

(3) The pieces of presumptive ectoderm of *Cynops* gastrula were transplanted into a front and adjoining lateral side of the neural plate of *Cynops* neurula. These ectoderm cells were transformed into neural ones. In the contrast,those of ectoderm transplanted into abdorminal area could not differentiate into neural cells.

DB 154

ISOLATION OF NEURAL RECEPTOR PROTEIN ON THE INNER SURFACE OF THE COMPETENT ECTODERM OF CYNOPS GASTRULA.

M.R.M. DIAZ[1],K. TAKESHIMA[2], K. TAKATA[2] and N. TAKAHASHI[3]. [1]Dept. of Biol., Fac. of Sci., Nagoya Univ. [2]Radioisotope Ctr., Nagoya Univ. and Nagoya City Univ. Sch. of Med., Nagoya.

Results of previous studies have pointed to the specificity by which neural inducers like Con A and the living organizer react with glycoproteins on the inner surface of the competent ectoderm to bring about neural formation. This finding has led us to suspect the presence of receptor proteins which can be isolated and identified. As a preliminary, therefore, affinity between Con A-Sepharose beads and the inner surface of the ectodermal explants reacted together for 30 min and 24 hrs was observed by SEM. Intense affinity was manifested by skirts, filopodia, lobopodia, blebs, stalks and half-sunken beads. Con A-Sepharose bead-bound ectodermal explants were treated with deoxycholate and DNAse, and centrifuged in Percoll solution. The isolated bead fraction was then washed with 0.5M α-methylmannoside and the eluate radioiodinated and ran in SDS PAGE. Two major bands, 80kd and 50kd, and a few minor bands were observed. To determine whether any of these bands turly corresponds to neural receptor proteins, monoclonal antibodies have been raised against the surface antigens of the competent ectoderm.

DB 155

ANALYSIS OF PROTEIN INVOLVED IN NEURAL INDUCTION BY CON A IN THE NEWT ECTODERMAL EXPLANT.
T. TAKABATAKE[1], A. MUTO[1], S. OSAWA[1], K. TAKESHIMA[2] and K. TAKATA[2]. [1]Dept. of Biol., Fac. of Sci., Nagoya Univ. and [2]Radioisotope Ctr., Nagoya Univ., Nagoya.

Treatment of the presumptive ectoderm of newt early gastrula with Con A brings about neural differentiation. In the absence of Con A, it differentiates into epidermis. Using this as a model for neural induction, O'Farrell 2-D-electrophoresis was done to detect proteins appearing in neural or epidermal differentiation. Also, in order to compare these with proteins in normal development, proteins of the neural plate and epidermis were analyzed.

The ectodermal explants were treated with ^{35}S-Met, cultured for 3 hrs and the labeled protein samples were used for electrophoresis. Following O'Farrell's method (1977), the acidic and basic sides were ran separately. In the acidic side, spots which specifically accompany neural induction were not observed, but one spot, which disappeared in the presence of neural induction, and some spots specifically accompanying epidermal development were observed. In the basic side, induced ectoderm showed one strongly stained spot. To determine the time of appearance of the spots, the culturing time after ectoderm excision was prolonged. Some differneces were observed in the Con A-treated and untreated explants with respect to time.

DB 156

EFFECTS OF PROTEIN-SYNTHESIS INHIBITORS AND TUNICAMYCIN ON NEURAL-INDUCING ACTIVITY OF NEWLY-MESODERMALIZED ECTODERM.
J.Matsuda and A.S.Suzuki. Dept.of Biol., Fac.of Gen. Edu., Kumamoto Univ., Kumamoto.

Presumptive ectoderm of *Cynops* gastrula was mesodermalized by swimbladder of *Carassius sp*. The newly-mesodermalized ectoderm(nME) acquired very strong neural-inducing capacity. In the present study, nMEs were treated with cychloheximide(0.5μg/ml), puromycin(20μg/ml), and tunicamycin(1-5μg/ml) for 3 hrs.

Neural-inducing capacity of cycloheximide-treated nME decreased one-seventh of the control, puromycin-treated nME was one-tenth of the control. Tunicamycin-treated nME also showed lower neural-inducing capacity: one-tenth of the control in the case of 5ug/ml. It seems to be concluded that neural-inducing capacity of the newly-mesodermalized ectoderm is coupled with protein synthesis. It is also suggested that cell surface(sugar-containing complexes) of the nME cells plays a important role in neural-inducing activity as same as in reacting activity of the competent ectoderm cells.

Changes in protein pattern of the newly-mesodermalized ectoderm was also analyzed by two-dimensional polyacrylamide gel electrophoresis. We could observed the qualitative and quantitative differences in several spots between nME and control ectoderm within 24 hrs.

DB 157

DISTRIBUTION OF TRANSPLANTED *X. BOREALIS* ANIMAL-CAP CELLS ONTO PROSPECTIVE NEURAL REGIONS OF *X. LAEVIS* GASTRULA.
A. S. Suzuki and K. Harada. Dept. of Biol. Fac. of Gen. Edu. Kumamoto Univ. Kumamoto.

Small pieces(0.2x0.3mm) of the animal cap of *X. borealis* gastrula(stage 10) were transplanted onto various regions of the noninvoluting marginal zone of albino *X. laevis* gastrula(stage 10). Distribution of the donor cells were analyzed by quinacrine fluorescence staining.

Transplanted pieces on the dorsal median plane extended remarkably in the animal-vegetal direction during gastrulation and finally formed a ventral side of the central nervous system(CNS), particularly of the anterior part. Both dorsal-lateral and lateral regions converged toward the dorsal midline, extending in the animal-vegetal direction. The former constituted a lateral side of the anterior CNS and the latter formed a lateral side of the posterior CNS. Lateral-ventral and ventral regions remarkably converged toward the constricting blastopore and the epidermis surrounding the anus consisted of their descendant cells. The present data suggest that the prospective CNS lies as a belt-shaped area in the noninvoluting marginal zone of early gastrula and the limiting line of the prospective CNS is between 0.6mm and 0.7mm above the blastopore on the dorsal side.

DB 158

EFFECT OF ANTIBIOTICS ON PH OF NEWT BLASTOCOEL FLUID AND ANALYSIS OF THE CONTENTS OF THE FLUID
T. Asao. Biol. Lab. Sch. Med. St. Marianna Univ. Kawasaki

As we have already reported blastocoel fluid of newt gastrula is fairly alkaline. In order to know the main cause that induced such a phenomenum and to analyze the role of the alkalinity of blastocoel fluid in an embryonic development, inhibition experiments using several antibiotics were performed. Antimycin A stopped the development and also lowered the pH of the fluid to 7.6. Calcium ionophore inhibited invagination but gave hardly effects in the change of pH. Cycloheximide inhibited the neural plate formation. Abnormal effects were not observed with the treatment of ouabain, monensin and malonic acids. Quantitative analysis of inorganic ions of the fluid showed that only the Ca ion contents of antimycin A-treated gastrula was twice larger than that of control. The alkalinity of blastocoel fluid may be related to the energy consuming Ca pumping action. On the other hand, the organic substances of the fluid were qualitatively estimated by thin layer chromatography and SDS polyacrylamide gel electrophoresis. Small ninhydrin reactive substances were detected in thin layer chromatography and a low molecular protein (about 26 k dalton) was clearly found in polyacrylamide gel electrophoresis. The electrophoretic band pattern showed that several silver stained proteins were contained in the fluid.

DB 159

ALKALINE PHOSPHATASE ACTIVITY DURING DEVELOPMENT IN THE BULLFROG

A. Kashiwagi. Lab. for Amphibian Biol., Fac. of Sci., Hiroshima Univ., Hiroshima.

The change of alkaline phosphatase (Alp) activity during development in various organs of *Rana catesbeiana* was examined by acrylamide gel electrophoresis and spectrophotometer. Alp was extracted from the pancreases, livers, kidneys and intestines of embryos at five Shumway's stages, tadpoles at 13 Tayler and Kollros' stages and juvenile frogs. The results showed that Alp activities greatly differed with organs and developmental stages. In the pancreas, a light band appeared at stage III and existed in all subsequent stages. In the liver, a wide band which had the same mobility as that of the pancreas appeared at stage III, disappeared by one week after completion of metamorphosis, and was three weeks later changed for another more cathodic band. In the kidney, a single band appeared at stage III and remained in subsequent stages. In the intestine, the first band appeared at stage 25, became a major band at stage III, and then disappeared at stage XX. A minor band with faster mobility appeared during stages VII to XIV. A new band which was often accompanied by one minor band with slow mobility appeared at stage XXV and remained thereafter. Alp activity in all organs except the liver increased rapidly at late tadpole stages, decreased temporarily during metamorphosis and increased again after completion of metamorphosis.

DB 160

PIGMENT CELL DIFFERENTIATION IN CYTOCHALASIN-TREATED EXPLANTS OF *XENOPUS* EMBRYO.

H. Ide. Biol. Inst., Tohoku Univ., Sendai

To make clear the distribution pattern of presumptive pigment cells in *Xenopus* embryos, neural tubes of tail bud embryos and whole dorsal region of gastrula-neurula embryos were isolated and cultured in a medium containing cytochalasin B, in which morphogenetic movement such as neural tube formation or neural crest cell migration was blocked and the cells differentiated in their original positions. Two types of pigment cells, melanophores and xanthophores differentiated in the explants. In the neural tube explants, melanophores and xanthophores differentiated only on the dorsal surface, the neural crest region. In the explants of whole dorsal region, the melanophores differentiated in the trunk neural fold region, and first aligned in four rows running parallel with anteroposterior axis. The xanthophores also differentiated in the neural fold region. Both pigment cells differentiated also in the isolated dorsal ectoderm sheets of late gastrula embryos. These results suggest that the commitment of the differentiation pathwat to the pigment cells begins at late gastrula stages and the committed cells differentiate to the melanophores and xanthophores *in situ* in the explants without morphogenetic movements.

DB 161

ONTOGENY OF LEUKOCYTES IN LARVAL *XENOPUS* AS STUDIED BY MONOCLONAL ANTIBODY.

H. Ohinata, S.Tochinai, and Ch. Katagiri, Zool. Inst., Fac. of Sci., Hokkaido Univ.

The monoclonal antibody (mAb) reactive to all types of leukocytes was developed for studying the chronological appearance of leukocytes in *Xenopus laevis*. The mAb-positive cells were first detectable around st.35/36 mostly in the mesenchymal tissues throughout the body and blood vessels, but few in the ventral blood island where the red blood cells (RBCs) had been differentiating since st.28. In the liver, the positive cells appeared in the liver at st.37/38, and accumulated significantly in the subcapsular region from st.47 on. In the prospective mesonephric region, the aggregations of non-lymphoid leukocytes were first detectable in the mesenchyme surrounded by the Wolffian duct, dorsal aorta, and vena cava, before the first appearance of lymphocytes in the thymus at st.47. In later stages, the positive cells were apparently localized along the medial wall of the mesonephros. Thymocytes became positively stained after st.46-47, following the appearance of strongly-positive dendritic cells at st.44/45 thymus rudiments. At st.49, many leukocytes were detected in both red and white pulps in the spleen.

DB 162

EFFECTS OF TRIIODOTHYRONINE ON THE EPIDERMAL CELL DEATH OF THE ANURAN TADPOLES.

A. Nishikawa and K. Yoshizato. Department of Biology, Faculty of Science, Tokyo Metropolitan University, Tokyo.

In order to know the mechanism of cell death induced by thyroid hormone at metamorphosis, we cultured the tail epidermal cells (T) and the back skin epidermal cells (B) of *Rana catesbeiana* tadpoles and compared the effects of triiodothyronine (T_3) between T and B on (1) DNA synthesis, (2)keratinization and (3)protein synthesis.

(1) Imunofluorescent micrographs using anti-BrdU showed that T_3 (10^{-8}M) decrease the number of cells in the S-phase in T but not in B, indicating that T_3 surpress the progression of T into the S-phase.

(2) The increase of transglutaminase activity and the number of SDS-insoluble cells (keratinized cells) were promoted by T_3 (10^{-8}M) more markedly in T than B.

(3) Two-dimensional electrophorogrammes of the extracts of T and B labelled with ^{35}S-methionine revealed more than 100 protein spots. The extent of staining in the 30 spots was changed by the treatment with T_3 (10^{-8}M). The fourteen spots of them were found only in T, the eight spots were found more intensely in T than in B, and the rest were found equally in T and B.

From these results, thyroid hormone induced changes in protein synthesis, which might be involved in the regulation of cell cycle in T and the promotion of keratinization of T and B.

DB 163

LOCALIZATION OF LECTIN-BINDING SITES IN ANURAN LARVAL SKIN.

T. Kinoshita, H. Takahama and F. Sasaki. Dept. of Biol., School of Dent. Med., Tsurumi Univ., Yokohama.

Localization of lectin-binding sites in tail skin of Rana japonica tadpole was examined at pre- (st. X) and climactic metamorphosis (st. XXIII). Binding sites of lectins were explored using MPA and GS-1 directly labeled with FITC for light microscopy and with colloidal gold for electron microscopy. In tail skin at st. X, MPA bound only to apical cells of epidermis. In tail skin at st. XXIII, however, MPA bound not only to apical epidermal cells but also to basal cells, especially to degenerating epidermal cells. Furthermore, MPA bound to dermal collagen layers. GS-1 also bound to apical epidermal cells at st. X. The number of binding sites of GS-1 to apical cells of epidermis decreased at st. XXIII. At the same time, GS-1 bound to macrophages which had increased in number from st. X through XXIII within epidermis and dermis. Apparently it was not to fibroblast-like cells which phagocytosed degrading dermal collagen fibers. These results suggest that MPA and GS-1 are useful to detect qualitative differences among cells and extracellular matrixes in anuran larval skin during metamorphosis.

DB 164

ULTRASTRUCTURAL CHANGES IN INTESTINAL CONNECTIVE TISSUE OF XENOPUS LAEVIS DURING METAMORPHOSIS.

A. Ishizuya-Oka and A. Shimozawa. Dept. of Anat., Dokkyo Univ., Sch. of Med., Tochigi.

We studied by transmission electron microscopy the development of intestinal connective tissue of Xenopus laevis tadpoles from stage 50 to 66 (Nieuwkoop & Faber), to clarify ultrastructural relations between the intestinal epithelium and the connective tissue during metamorphosis.

Throughout the larval period to stage 60, the connective tissue consists of immature fibroblasts surrounded by a sparse extracellular matrix. At the beginning of the transition from larval to adult epithelial form around stage 60, extensive changes are observed in the connective tissue. The cells become more numerous and different types appear as the collagen fibrils increase in density. Through gaps in the thickened basal lamina, frequent cell contacts between the epithelium and the connective tissue are established. Thereafter, with the progression of fold formation, the fibroblasts around the trough of the fold become aligned parallel to the curvature of the epithelium.

These observations indicate that the developmental changes in the connective tissue are closely related spatio-temporarily to the epithelial transition during the metamorphic climax.

DB 165

CHANGES OF HEART BEATS DURING NORMAL EMBRYONIC DEVELOPMENT AND ORGAN CULTURE

M.Taguchi[1], M.Uemura[2] and M.Asashima.[1]
[1]Dept.of Biology,Yokohama City Univ.Yokohama 236.[2]Med.Sci.,Dept.of Ped.Teikyo Univ.,Itabash-ku,Tokyo 173

Heart beat rates in normal development and organ culture were investigated using the material of newt. Heart rate at 20°C was assayed before and after metamorphosis. In normal development,heart beats began from st.33 (32beats/min) and its rate went up to st.52 (80beats/min). Then its rate went down to st.60 (55beats/min). Heart beats rate was temperature sensitive showing the linear equation between 4°C to 30°C. These rates were depend on their developmental stages. On the other hand the beat rate of organ cultured hearts was depend on starting stage and there culture days. In organ culture started from st.33 its beating rate showed 22beats/min in one day,and then its rate showed the maximum peak after 54-58 days showing 65beats/min. After this culture period the rate went down following culture days. In culture started from st.47,the peak of their heart rate showed after 14-21 days,but in cultured heart from st.58 it had no peak after 70 days. The heart beat rate in organ culture was also showed tempereture sensitive between 4°C and 30°C. These organ culture data of heart beats seem to reflect the resemble states of the heart in normal embryonic development.

DB 166

DEVELOPMENT OF THE WATER TRANSPORTING SKIN OF TREEFROGS DURING THE METAMORPHOSIS.

Y. Kamishima, and H. Nakashima. Dept. of Biol., Facult. of Sci., Okayama Univ. Okayama 700

Water intake in japanese treefrogs was mainly carried out through the ventral pelvic skin and was positively controlled by a neural agent through an adrenergic β-receptor. However, this integumental water transport was observed only in adult frogs and neural agents failed to facilitate the function in premetamorphic larvae. In aquatic larvae, no morphological differences were observed between dorsal and ventral epidermal cells. At the metamorphic climax when disorganization and reformation of the integument took place, the pelvic skin differenciated into a charateristic one in which epidermal cells showed microvillus-like processes, and wider interspaces. The outermost layer of pelvic epidermal cells also showed characteristic features with dense granules and perforated cytoplasm during this period. The dorsal skin lacked all these features even after the metamorphosis.

When the skin is activated to permeate the water, outermost cells of the epidermis took strongly metachromasic dyes. These cells showed strong cytoplasmic density and appeared as masses of intermingled long processes which were formed during the metamorphosis and a characteristic feature of the ventral pelvic skin.

DB 167

FREQUENT OCCURRENCE OF RENAL TUMORS IN THE HYBRIDS BETWEEN *BUFO JAPONICUS* AND *B.RADDEI*

M.Nishioka and Y.Kondo. Lab. for Amphibian Biol.,Fac.of Sci.,Hiroshima Univ.,Hiroshima

It was remarkable that most of the hybrids between a female *Bufo j. japonicus* and a male *B. raddei* died of renal tumors. While 73(11.6%) of the normally cleaved eggs obtained in 1982 became young toads,many of them died by 1987. When the cause of death was examine in 27 toads, it was found that 22 suffered from renal tumors. These toads consisted of 10 females, nine males and three young ones of unkown sex. Eight, one, twelve and one died in 1982, 1983, 1984 and 1986, respectively. Of the other five dead toads, one was a five-year-old male which suffered from a pancreatic tumor, and four were yearlings in which the cause of death was undetermined. Eleven other toads are now living. One of them appeared to have a tumor in the body cavity from examination by touch, while the other ten seemed to be still healthy. In the control series, none of *B. j. japonicus* and *B. raddei* died of tumors during the five years 1982 - 1987. When the renal tumors of the dead toads were histologically examined, it was found that some mesonephric tubules became first abnormal and were filled with pathologic cells. Hydronephrosis and necrosis occurred in the morbid portion, whereas the Malpighian bodies remained almost normal for a time. In the hybrids between *Bufo raddei* and *B. j. gargarizans* or *B. viridis*, tumors occurred very rarely in the pancreas or Bidder's organ.

DB 168

ABUNDANT TUMORS WHICH RECENTLY OCCURRED IN THE LABORATORY FOR AMPHIBIAN.

M. Nishioka and H. Ueda Lab. for Amphibian Biol.,Fac.of Sci.,Hiroshima Univ.,Hiroshima

It was a wonder that several kinds of tumors were suddenly detected in 1982 and widespread in the following years in the anurans kept in our laboratory. When dead or dying anurans were examined at ages of one to 11 years, a specific tumor was found in a definite kind of anurans. Of the toads which were produced in 1980 and died by 1987, 46(17.6%) of the 262 female hybrids between *Bufo japonicus* from Japan or China and *B. bufo* or *B. viridis* from Europe suffered from ovarian tumors, while 9(2.0%) of the 440 male hybrids suffered mostly from tumors in the Bidder's organ. At present, 45 (28.0%) of the 161 living hybrids suffer from abdominal tumors.

On the other side, many pancreatic tumors and a few others occurred in *Rana plancyi*, *R. nigromaculata*, their inter- and intraspecific hybrids produced in 1980. Of the 487 dead frogs examined during 7 years from 1982 to 1987, 101(20.7%) suffered from various tumors. Tumors were also detected in 80 dead frogs of the hybrids, backcrosses and allopolyploids produced in 1975-1984 except 1980 among five species and two subspecies of pond frogs. Fifty-seven of them died of pancreatic tumors, while the remaining 23 suffered from ovarian, renal, hepatic and some other tumors. It was remarkable that a highly contagious disease occurred in 1985 and spread thereafter in our laboratory.

DB 169

SPERMATOGENESIS OF HALICHONDRIA OKADAI

K.Tanaka-Ichihara[1] and Y.Watanabe[2]. [1]Inst. of Comprehen. Med. Sci., Sch. of Med., Fujita-Gakuen Health Univ., Aichi. [2]Dep. of Biol., Fac. of Sci., Ochanomizu Univ. Tokyo.

Spermatogenesis of H.okadai was examined by light and electron microscopy. At the outset of spermatogenesis, number of choanocyte chambers suddenly decreased. Simultaneously, many amoeboid cells became sighted in the mesohyl. These cells, uniflagellated and with nucleolated nuclei, were observed only in the early stage of spermatogenesis. They differentiated to primary spermatocytes, and entered into the meiosis retaining flagella. Primary spermatocytes were enclosed by a single layer of flattened cells. Thus, Spermatic cysts were formed. Two meiotic divisions to secondary spermatocytes and spermatids almost synchronously ocurred in a spermatic cysts. Four spermatids derived from a single spermatocyte were connected each other through their cytoplasmic bridges. Each mature spermatozoon contained a condensed nucleus of 1.5 µm in diameter, a ring-shaped mitochondrion, a pair of centrioles, a flagellum of 20 µm in length, and an acrosome-like structure comprising several tens of rods of 44 nm in diameter and 300 nm in length.

In summary, spermatozoa were generated from flagellated amoeboid cells that were thought to be originated from choanocytes.

DB 170

ROLES OF MAJOR ACROSOMAL PROTEINS OF ABALONE SPERM IN THE VITELLINE COAT LYSIS.

N. Usui[1] and K. Haino-Fukushima[2]. [1]Dept. of Anat., Teikyo Univ. Sch. of Med. and [2]Dept. of Biol., Fac. of Sci., Tokyo Metropólitan Univ., Tokyo.

Major soluble components released from the acrosomal vesicles during the acrosome reaction of the abalone *Haliotis discus* sperm are two proteins of molecular weights 15,500 and 20,000. Crude acrosomal contents and a sample which contained predominantly 15.5K protein possessed lytic activity on the vitelline coat (VC) ('84).

To elucidate role(s) of each protein in the lysis of the VC, *H. discus* oocytes were treated with various mixtures of the acrosomal proteins; (a) 20K and a trace amount of 15.5K, (b) 15.5K alone, (c) 20K alone and (d) a 1:1 mixture of both proteins. The mixtures of both proteins (a, d) induced swelling of the VC but each protein alone (b, c) was incapable of dissolving the VC. Thin-sectioning revealed that 15.5K protein could not induce any morphological change in the VC, whereas the surface electron-dense layer of the VC was dissolved by 20K protein, and that the 1:1 mixture (d) led to the lysis of the surface layer and extreme loosening of the VC main part,i.e., a feltwork of fine filaments.

These observations indicate that the 20K protein contained in the anterior half of the acrosomal vesicle first dissolves the outer layer so that the posteriorly-located 15.5K protein acts on the inner main part.

DB 171

A PROTEIN COMPONENT OF THE "TRUNCATED CONE" IN JAPANESE ABALONE SPERM

Y.Shiroya, S.Maekawa* and Y.T.Sakai. Biol. Lab., Wayo Women's Univ., Chiba. *Dept. of Biophys. & Biochem., Fac. of Sci., Univ. of Tokyo, Tokyo.

We have previously reported that the unique structure lying at the acrosomal apex in abalone (*Haliotis discus*) sperm named the "truncated cone" transforms into the cylindrical structure during the acrosome reaction (D.G.D. 26, 25, 1984). The present study deals with characterization of the protein components of this structure by immunological technique.

The truncated cones were isolated from abalone sperm by treating sperm heads with a Nonidet P-40 solution followed by discontinuous sucrose gradient centrifugation. After treating with Ca^{2+}-free sea water, the insoluble fraction of the truncated cone was enriched in proteins of 60, 86 and 200kD, as determined by SDS-PAGE. Indirect immunofluorescence staining using affinity-purified monospecific antibodies against 60, 86 and 200kD proteins showed that only the anti-60kD protein antibody stained the apex of the acrosomal vesicle. The exclusive localization of the 60kD protein to the truncated cone of both the isolated apical half of the acrosome and acrosome-reacted sperm was clearly confirmed by immunoelectron microscopy. These results indicate that the 60kD protein is a component of the truncated cone.

DB 172

Determination of the Structure of Lysin Binding Sites on Vitelline Coat: Fractionation of Solubilized Vitelline Coat

M.Shitara & K.Haino-Fukushima. Dep.of Biol. Fac.of Sci.,Tokyo Metropolitan Univ.,Tokyo

Vitelline coat lysin of marine Mollusca, Tegula pfeifferi irreversibly binds to the vitelline coat (VC),bringing about the lysis of VC.VC of this species is composed of sulfated-glycoprotein and is solubilized by alkaline degradation. We reported previously that the solubilized VC (sol.VC) also bears LBS nearly equivalent to those found in intact VC.

In the present study,we found that Pronase digestion of sol.VC totally destroys LBS. Amino acid analysis indicated that residues including Val,Phe,Leu,Ile,and Lys are absent from the Pronase digested VC. We also found that total loss of LBS on sol.VC is caused by cleavage of N-glycosidic bond. Deglycosylation of sol.VC by TFMS, which leaves N-glycosidic bond unaffected, failed to show any remarkable effect on LBS. On the other hand, the 90K fragment was recovered when sol.VC was degraded in succession by V8 protease digestion, serial periodate oxidation,and TFMS deglycosylation. This fragment contains only 2 LBS despite the presence of 75 N-glycosidic bonds. From these results,it is evident that LBS requires not only N-glycosidic bond but certain amino acid sequence to be recogonized by Lysin.

DB 173

ROLE OF DIFFERENT KINDS OF ZONA PELLUCIDA ON THE ACROSOME REACTION OF GOLDEN HAMSTER SPERMATOZOA.

N.Uto[1], R.Yanagimachi[2]. [1]Dept. of Biol. Hamamatsu Univ. School of Med., Hamamatsu, [2]Univ. of Hawaii School of Med., Honolulu, Hawaii, U.S.A.

The occurence of hamster acrosome reaction on zona in cumulus free eggs was studied. Different types of egg were inseminated with preincubated hamster spermatozoa and then the sperm acrosome reaction on zona of them was investigated.

The zona of homologous hamster eggs were most effective on hamster spermatozoa. In younger oocytes, the inducing ability of their zona were relatively accomplished state. In pronuclear stage, the zona of them did not loss the ability so much in spite of post zona reaction. When hamster living eggs were treated with salt-solution or fixatives, the ratio of acrosome reaction on zona in these eggs decreased a little but retained in spite of some denaturalization with reagents. Furthermore, heterogenous kinds of egg i.e. mouse, rat, guinea pig, hen and human eggs were compared. The zona of human egg induced the acrosome reaction well. On the other hand, in zona of other kind eggs, we hardly could observe the spermatozoa that underwent not only acrosome reaction but penetration into zona.

In these studies it was suggested that the characteristics of hamster zona is different relatively from other kinds of animals. The proper itself was discussed everywhere.

DB 174

EGG JELLY COMPONENTS RESPONSIBLE FOR THE INDUCTION OF ACROSOME REACTION IN THE STARFISH, ASTERINA PECTINIFERA.

Y. Okita[1], T. Amano[1], T. Matsui[2] and M. Hoshi[1]. [1]Biol. Lab., Fac. of Sci., Tokyo Inst. of Technol., Tokyo and [2]Div. of Biomed. Polymer Sci., Inst. for Compre. Med. Sci., Fujita-Gakuen Health Univ., Toyoake.

ARIS, a high-molecular weight sulfated glycoprotein in the egg jelly, requires diffusible jelly components for inducing the acrosome reaction (AR) in a starfish, Asterias amurensis that belongs to the Forcipulata.

Similarly, both ARIS and a diffusible fraction (M_8) of the jelly were proved essential for the induction of AR in another species of starfish belonging to the Spinulosa, Asterina pectinifera. The AR was induced also by combinations of the calcium ionophore A23187 and either monensin or M_8, or of ARIS and NH_4Cl. M_8 increased the internal pH of sperm monitored by using a fluorescent probe, 9-aminoacridine. Both NH_4Cl and monensin are known to increase the internal pH. Thus ARIS presumably has a function in stimulating Ca^{2+}-uptake into sperm in Asterina as known in Asterias.

The basic mechanisms underlying AR induction by the egg jelly appear common at least to the two species of starfish so far studied and may be very similar throughout the Class, Asteroidea.

DB 175

EFFECTS ON THE SPERM OF EGG JELLY COMPONENTS RESPONSIBLE FOR INDUCING THE ACROSOME REACTION IN THE STARFISH, ASTERINA PECTINIFERA

T. Matsui[1], T. Amano[2], Y. Okita[2] and M. Hoshi[2]. [1]Div. of Biomed. Polymer Sci., Inst. for Compre. Med. Sci., Fujita-Gakuen Health Univ., Toyoake and [2]Biol. Lab., Fac. of Sci., Tokyo Inst. of Technol., Tokyo.

A high-molecular weight sulfated glycoprotein and diffusible substance(s) in the egg jelly were essential for the induction of acrosome reaction (AR) in the starfish *Asterina pectinifera* as known in *Asterias amurensis*. Either component did not induce the acrosome reaction by itself, but within a few minutes it made sperm species-specifically unable to undergo the AR in response to the egg jelly. The AR was not induced in such sperm by increasing the external Ca^{2+} concentration or pH. Similarly, if the sperm was incubated as short as a minute with egg jelly in Ca^{2+}-deficient seawater, they never underwent the AR even after calcium was sufficiently supplemented. A combination of calcium ionophore A23187 and monensin, however, did induce the AR even in thus pretreated sperm.

These results suggest that the jelly components modulate the transmembrane control systems simultaneously, transiently and irreversibly ending up in the acrosome reaction.

DB 176

INITIATION OF SPERM HISTONE DEGRADATION BY EGG JELLY COMPONENTS IN THE STARFISH, ASTERINA PECTINIFERA.

T. Amano, Y. Okita, and M. Hoshi. Biol. Lab., Fac. of Sci., Tokyo Inst. of Technol., Tokyo.

Egg jelly induces two distinct sperm reactions, the acrosome reaction and histone degradation in the starfish, *Asterina pectinifera*. We have studied whether the jelly components required for these reactions are the same or not.

A glycoprotein (ARIS) and a diffusible fraction of the jelly were required for inducing histone degradation as well as acrosome reaction. Both reactions were susceptible to calcium channel antagonists, verapamil and diltiazem. Once sperm were treated with the egg jelly in Ca^{2+}-free sea water, they became unable to undergo these reactions even after Ca^{2+} was fortified. Calcium ionophore A23187 did not induce either reaction. However, histone degradation without acrosome reaction was induced by treating sperm with a low concentration of egg jelly, or monensin, or simply lowering the concentration of Na^{+} in sea water to 50 mM or less.

Thus jelly components required for the two reactions are the same or very similar, but the mechanisms underlying these reactions seem different at least partly.

DB 177

FURTHER STUDIES ON ARTIFICIAL PARTHENOGENESIS OF STARFISH EGGS PRODUCED BY SUPPRESSION OF POLAR BODY FORMATION.

C. Saitoh[1], S. Washitani-Nemoto[2], and S. Nemoto[1]. [1]Tateyama Marine Lab., Ochanomizu Univ., Tateyama, and [2]Lab., of Biol., Hitotsubashi Univ., Tokyo, Japan.

As we previously reported (Biol. Bull., '84), caffeine produced parthenogenetic development of starfish eggs by two-step actions, i.e. the activation of the eggs and the inhibition of polar body (PB) formation. To know the role of these two steps in production of parthenogenesis, we separated the steps by using two drugs; calcium ionophore for egg activation, and cytochalasin B (Cyt. B) for the inhibition of PB formation. The drugs were applied to *Asterina pectinifera* eggs at some stages during meiosis. Cleavages did not occur in eggs treated with the ionophore alone, which formed 2 PBs and showed monoaster cycling only. Additional treatments with Cyt. B caused cleavages in more than 80% of the eggs that failed to form either both 1st and 2nd PB or 2nd PB. The embryos derived from both types of eggs developed as tetraploids like caffeine-induced embryos. SDS, inhibiting PB formation, induced cleavages in eggs without fertilization membrane formation. These results indicate that the inhibition of polar body formation is prerequisite for production of parthenogenetic development in starfish eggs.

DB 178

RELATION BETWEEN CLEAVAGE INDUCED BY INHIBITION OF POLAR BODY FORMATION AND NUMBER OF CENTRIOLES, IN PARTHENOGENETICALLY ACTIVATED STARFISH EGGS.

K. H. Kato[1], A. Hino[2], S. W. Nemoto[3] and S. Nemoto[4] [1]Coll. Gen. Educ., Nagoya City Univ., Nagoya, [2]Fac. Sci., Nagoya Univ., [3]Lab. Biol., Hitotubashi Univ., [4]Fac. Sci. Ochanomizu Univ.

Starfish oocytes can be artificially activated by caffeine, during the course of maturation division induced by 1-MeAde. When caffeine treatment was carried on so as to inhibit the formation of polar body(s), a high percentage of cleavage and parthenogenetic development was attained (Obata and Nemoto, 1984). There is a possibility that the number of centrioles remaining in the egg has relation to the capacity of eggs to cleave. In this study, we examined with TEM the number of centrioles, in the aster at maturation divisions and at parthenogenetically induced mitotic divisions. In parthenogenetically developed embryos, it was confirmed by consecutive serial sections, that there was a pair of centrioles in an aster of the third division. The centriole number in the aster of the first maturation division was two (a pair) and that of the second was one. In normally fertilized eggs, there was a pair of centrioles in the aster of the second division. A schematic diagram on the number of centrioles and their duplication timing during meiosis and mitosis in normal fertilization and parthenogenesis was presented.

DB 179

MASS ISOLATION OF GERMINAL VESICLES FROM STARFISH OOCYTES.

N. Hashimoto[1], K. Yamamoto[2] and S. Nemoto[1]
[1]Tateyama Marine Lab., Ochanomizu Univ., Tateyama, and [2]Dept. of Biol., Fac. of Gen. Educ., Gifu Univ., Gifu, Japan.

Germinal vesicles (GV) of primary oocytes contain some factors necessary for the completion of meiosis and development.

To know the character of the factors, we developed a simple isolation procedure for GVs by using fully grown oocytes of the starfish, Asterina pectinifera. Oocytes were treated with pronase to remove the vitelline coat, and then with cytochalasin B to decrease the rigidity of cell surface. The oocytes were then centrifuged on a discontinuous sucrose-density gradient. GVs and enucleated fragments came to rest in separate layers according to their density. The isolated GVs were fairly uniform in size and morphorogy, and surrounded with a very thin layer of cytoplasm, in which microtubules were observed. The GVs isolated by this procedure appeared morphologically very similar to those in the oocytes. When the content of the isolated GVs was introduced into enucleated fragments by microinjection, cyclic appearance of male pronuclei was observed.

DB 180

SPECIES SPECIFICITY OF FACTORS IN THE GERMINAL VESICLE REQUIRED FOR SPERM PRONUCLEUS FORMATION IN STARFISH OOCYTES

K. Yamamoto[1], N. Hashimoto[2] and S. Nemoto[2]
[1]Dept. of Biol., Fac. of General Edu., Gifu Univ., Gifu and [2]Tateyama Marine Lab., Ochanomizu Univ., Chiba.

The transformation of the sperm nuclei into the male pronuclei is known to be dependent on the germinal vesicle (GV) material in most animal eggs including starfish. In the present study we examined whether GV material exhibits any species specificity on the activity of inducing sperm-pronucleus formation using three different starfish.

Inseminated nonnucleate fragments obtained from immature Asterina pectinifera oocytes were injected with GV contents of either Astropecten scoparius or Astropecten polyacanthus oocytes. Following application of 1-methyladenine (1-MA) the fragments were examined with Nomarski optics. Sperm pronuclei developed in these fragments about 3 hrs after 1-MA treatment, suggesting that the factors in GV have similar nature in Asteroidea.

Furthermore, our preliminary experiments in which nonnucleate fragments of starfish (A. pectinifera) oocytes were injected with GV contents of sea cucumber (Holothuria hilla) oocytes suggest the factors in GV have no specificity among echinoderms.

DB 181

SUCCESSION OF THREE DISTINCT LEVELS IN THE CAPACITY OF FORMING FERTILIZATION ENVELOPE DURING MATURATION OF STARFISH EGGS.

K. Chiba, and M. Hoshi. Biol. Lab., Fac. of Sci., Tokyo Inst. of Technol., Tokyo.

When oocytes of Asterina pectinifera were treated with calcium ionophore A23187 before 1-methyladenine (1-MA) addition (A phase), fertilization envelope (FE) was formed near the surface of oocytes. But between 1-MA addition and germinal vesicle break down (GVBD)(B phase), A23187-induced FE formation was inhibited. After GVBD (C phase), this inhibition was canceled and a fully elevated FE was formed by A23187. Thus we raised a question whether the phase-dependent difference is due to differences in intracellular calcium concentration (Ca_i) after A23187 treatment. To answer this question, Ca_i was fixed by the microinjection of calcium buffers. Fixation of Ca_i at 2.8uM resulted similarly as A23187 treatments. Electron microscopic observation showed that exocytosis of cortical granules was blocked only in A23187-treated oocytes of B phase. These results indicate that an increase in Ca_i is not necessarily sufficient for inducing the exocytosis as believed generally. There seems to be a post-calcium-increase step(s) that is modulated on the course of maturation.

DB 182

ELECTROPHYSIOLOGICAL PROPERTIES AND EFFECTS OF SH-BLOCKING REAGENT ON THE CAPACITY FOR FERTILIZATION MEMBRANE FORMATION IN STARFISH OOCYTES.

H. Nakamura. Akkeshi Mar. Biol. Stat. Hokkaido Univ., Akkeshi, Hokkaido

Immature starfish oocytes have been reported not to form fertilization membrane(F.M.) upon insemination under natural conditions. However, since we have observed that immature starfish oocytes occasionally formed F.M. upon insemination, differences of the electrophysiological properties(Elec. Prop.) between F.M.-forming oocytes and none-forming oocytes were investigated using Asterina pectinifera. Effects of SH-blocking reagent on the capacity of the oocytes for F.M. formation was also examined. F.M.-none-forming oocytes showed a constant Elec. Prop. On the other hand, F.M.-forming oocytes showed four different types of Elec. Prop. When F.M.-forming oocytes were treated with iodoacetamide, the capacity for F.M. formation was abolished. Although the Elec. Prop. of the treated oocytes changed to those of another type, there seemed to be no direct correlation between the type of Elec. Prop. and capacity for F.M. formation.

These results suggest that the acquisition of the capacity for F.M. formation in oocytes may be correlated with the increase in SH-groups in their surface area, and that the Elec. Prop. of immature oocyte can be shifted from one type to another by oxidizing surface SH-groups.

DB 183

ARTIFICIAL INDUCTION OF MEIOSIS-RESUMPTION IN OYSTER OOCYTES.

K. Osanai, K. Kyozuka and R. Kuraishi.
Mar. Biol. Stn., Tohoku Univ., Aomori.

Crassostrea gigas oocytes obtained by dissecting the ovary were at the germinal vesicle stages. The oocytes undergo germinal vesicle breakdown in sea water containing serotonin (5-hydroxytrypt-amine), but are arrested at the first metaphase of meiosis. The present examination showed that alkaline sea water (pH 9.3) induced the resumption of meiosis from the first metaphase. Alkaline sea water containing calcium ionophore A23187 (CaI, 0.5-10 μM) was more effective than alkaline sea water or CaI in pH 8.3 sea water, and induced meiotic changes from the first metaphase to the pronuclear stage within 1 hr. When metaphase I oocytes were incubated in alkaline sea water containing 5 or 10 μM CaI (Alkaline CaI), the oocytes began to extrude the first polar body and the second polar body about 15 min and 35 min after incubation, respectively. After the incubation for 60 min, some oocytes formed the polar lobe. Alkaline CaI seems to induce also mitotic change following the meiosis.

The present result suggests that the successive changes of meiosis require the rise of pH and the increase of calcium ions in oocytes.

DB 184

EFFECTS OF LIGHT ON OOCYTE MATURATION AND SPAWNING IN AMPHIOXUS, Branchiostoma belcheri tsintauense.

T. Watanabe[1], M. Yoshida[1], and H. Shirai[2].
[1]Mar. Biol. Stn. Okayama Univ. Ushimadocho, Okugun, Okayama and [2]Lab. Reprod. Biol. Natl. Inst. for Basic Biol. Myodaijicho, Okazaki, Aichi.

According to Wu, Institute of Oceanology, Academia Sinica, China, adult amphioxus spawns mature gametes in laboratory after sunset when a large number (about 2,000) of animals are kept in a tank with airation. Such activities usually last for about 1 hr and are observed intermittently through the breeding season (June to August).

The time-dependent activity infers involvement of a light-dependent mechanism in the reproductive behavior, particularly the timing of oocyte maturation and egg discharge. The present experiments showed that mature oocytes were detected only in afternoon and spawning occurred 1-1.5 hr after sunset. Day length-prolongation by artificial illumination shifted the spawning time accordingly, but its shortening by early darkening did not.

We conclude that the spawning time is controlled at least by two factors; one is darkening, an external factor which directly triggers mature egg-discharge and the other is susceptibility to darkness, an intrinsic factor which gradually develops during the course of day in mature animals.

DB 185

PURIFICATION OF TWO KINDS OF SIALOGLYCOPROTEINS FROM MATURE CARP EGGS AND THEIR IMMUNOHISTOCHEMICAL LOCALIZATION.

S.Kudo[1], S.Inoue[2], and Y.Inoue[3]. [1]Dept. of Anatomy, Gunma Univ. School of Medicine, [2]School of Pharmac. Sci., Showa Univ. and [3] Dept. of Biophs. Biochem., Univ. of Tokyo

Mature carp eggs crushed were extracted with a solution of 0.8% NaCl. The mixture was filtered through gauze and the filtrate was centrifuged at 5,000 rpm for 30 min.The supernatant was mixed with 1 vol. of 90% phenol, and this mixture was stirred at room temperature for several hours. The aqueous phase was separated by centrifugation for 15 min and dialyzed against distilled water, followed by lyophilization. The partially purified material containing sialoglycoproteins (SGPs) and phosvitin was applied to a DEAE-Sephadex A-25 column pre-equilibrated with 0.01 M Tris-HCl buffer(pH 8.0) and eluted with a linear gradient of NaCl (0.1-0.5 M). The SGP peak was then subjected to Sephacryl S-200 chromatography following pre-equilibration with the same buffer, in order to separate SGPs from phosvitin, and eluted with 0.1 M NaCl in the same buffer, to obtain two kinds of SGPs (4-1 and 4-3). SGP 4-1 contained much more sialic acid than SGP 4-3 and agglutinated fish sperm, whereas SGP 4-3 did not. Application of antibodies against SGP 4-1 and SGP 4-3 revealed that they were immunohistochemically localized in the cortical alveoli of carp eggs.

DB 186

ELECTRON MICROSCOPIC OBSERVATION OF MICROPYLAR CELLS IN THE OVARIAN FOLLICLES OF MEDAKA, Orizias latipes.

S.Nakashima and T.Iwamatsu. Dept. of Biol., Aichi Univ. of Educ., Kariya.

The formation and morphological changes of micropylar cells during the course of vitellogenesis and maturation of oocytes of Medaka, Orizias latipes were examined with electron microscope. The micropylar cell was distinguished from neighboring cells as a large mushroom-shaped cell and was stained with methylene blue slightly deep blue compared with other follicle cells. In previtellogenic stage, this large cell stained with methylene blue was not observed and all cells in the follicle layer showed the same stainability. The special large cell was observed in the stage which yolk vesicles appear. In this stage a bundle of tonofilaments extending from desmosomes was observed in the cytoplasm of both micropylar cell and neighboring cells. Bundles of the tonofilaments were gradually developed in the micropylar cell with the progress of vitellogenesis and maturation of the oocyte. On the contrary, these filaments gradually diminished in the other follicle cells. The apical part of the cytoplasmic process with meandering tonofilaments extended in the cortical region of the oocyte. The main cell body contains well developed Golgi bodies, tonofilaments and rough endoplasmic reticulum.

DB 187

FERTILIZATION POTENTIAL OF THE MEDAKA (ORYZIAS LATIPES) EGG.
S.Ito and K.Shimamoto. Dept of Biol., Fac. of Sci., Kumamoto Univ., Kumamoto.

Fertilization of the medaka egg in 10% Ringer, generates a depolarization of a few mV just before the appearance of a characteristically longer hyperpolarization. The depolarization appears to result from a nonspecific leak triggered by sperm-egg fusion; and the amplitude of the depolarization is reported to be independent of $[Ca^{2+}]$ (Nuccitelli, 1980). We have investigated the ionic dependence of this depolarization. An initial small depolarization(3-4mV; duration, 5-8 sec) is followed by a rising phase of a spike-like depolarization ranging from 10-60 mV when recordings are made in appropriate Ca^{2+} concentrations(1-18 mM) dissolved in isotonic sucrose(210 mM) solution. The amplitude of this spike-like depolarization is proportional to log $[Ca^{2+}]$ ranging from 0.33-18 mM. Calcium antagonist, i.e. 10mM cobalt or 10μg/ml verapamil dissolved in 10% Ringers do not block the depolarization. We conclude that the spike-like depolarization of the medaka egg is dependent on $[Ca^{2+}]$, however the mechanism underlying the genesis of the depolarization may be different from the generation of Ca-action potentials in excitable tissues.

DB 188

PROPERTIES OF FERTILIZATION POTENTIAL IN THE MEDAKA, ORIZIAS LATIPES EGGS.
M. Nakaya and Y. Iwao. Biol. Inst., Fac. Sci., Yamaguchi Univ., Yamaguchi.

Upon fertilization of Oryzias latipes eggs, cortical alveoli breakdown (CABD) is preceded by a fertilization potential (FP) that has a small depolarization (DP) followed by a large hyperpolarization (HP). To investigate the relationship between the CABD and the FP, the centrifuged eggs (450 g, 10 min) were inseminated in 10% Ringer. The magunitude of DP in the eggs whose cortical alveoli (CA) had been accumulated at vegetal pole (VP eggs) were smaller than accumulated at animal pole (AP eggs). The time lapsed from the onset of DP to the peak of HP in the VP eggs was longer than in the AP eggs. These indicate a close correlation between the CABD and the HP of the FP in the fertilized eggs.
Upon activation by pricking or Ca-ionophore A23187, the eggs elicited an activation potential similar to the FP in 1.8 mM CaCl (resting potential; about -60 mV), but the DP was not detected in 10% Ringer (resting potential; about -10 mV). The DP as well as the HP is caused by the ionic channels on the egg-membrane, but the appearance of DP is voltage-dependent.
When the naked eggs were inseminated in Ringer, short-lived recurring DPs (1-2 mV) were observed, besides the DP followed by the HP of the FP. These step-like DPs may correlated with sperm-egg collisions.

DB 189

ON THE INITIATION TIME OF Ca^{2+} RELEASE AND EXOCYTOSIS BY MICROINJECTION OF VARIOUS AGENTS IN THE MEDAKA EGG.
T. Iwamatsu[1], Y. Yoshimoto[2], K. Onitake[3] and H. Hiramoto. [1]Dept. Biol., Aichi Univ., Kariya,[2]Biol. Lab. Univ. Air, Chiba, and [3]Dept. Biol., Fac. Sci., Yamagata Univ., Yamagata.

The real initiation time of Ca^{2+} release from cytoplasmic stores and exocytosis of cortical alveoli in Oryzias latipes eggs were examined by microinjection of inositol 1,4,5-triphosphate (IP$_3$), ionophore A23187, Ca^{2+}, cGMP and GTP under Ca^{2+}-free conditions. Intracellular release of Ca^{2+} by microinjection was analysed by measuring luminescence of aequorin loaded in unfertilized eggs. Microinjection of IP$_3$ or A23187 could rapidly induce a propagative Ca^{2+}release without delay, while microinjection of Ca^{2+} or cGMP could induce it with a time lag. In these microinjections, the Ca^{2+} release commenced at the cytoplasmic region close to the egg surface. Furthermore, a propagative exocytosis was rapidly triggered by Ca^{2+}- or IP$_3$-microinjection, but slowly by cGMP- or GTP-microinjection. However, cAMP- and ATP-microinjections that triggered no Ca^{2+}release, failed to induce exocytosis. Cyclic GMP or GTP failed to induce exocytosis, when was simultaneously microinjected with Co^{2+}. Unlike cGMP and GTP, IP$_3$ and Ca^{2+} could induce exocytosis even in the presence of Co^{2+}. The inhibitory effect of Co^{2+} was also observed on exocytosis by sperm stimulation.
These results in the medaka egg suggest that the cytoplasmic Ca^{2+} and GTP induce indirectly Ca^{2+} release from cytoplasmic stores,probably via a membrane factor such as IP$_3$, and that both IP$_3$ and Ca^{2+} act to the same process of exocytosis, different from that as cGMP and GTP act.

DB 190

IMMUNOCYTOCHEMICAL ANALYSIS OF THE EGG ENVELOPE FORMATION OF MEDAKA.
T. S. Hamazaki, I. Iuchi and K. Yamagami. Life Sci Inst., Sophia Univ., Tokyo.

The egg envelope (chorion) of Oryzias latipes has a liver-derived constituent. This substance is produced in the liver under the influence of estrogen, and incorporated finally into the oocyte chorion from the inside.
In the present study, an indirect immunocytochemical observation of the ovary using anti-chorion glycoprotein antibody and protein A-colloidal gold particle revealed that a high immunoreactivity was present in the inner layer (IL) of the oocyte chorion, but not in the outer layer (OL) of chorion, the chorionic fibrils, the follicle cells, nor the theca cells. Moreover, the dense cored vesicles (DCV) showed no reactivity, which were considered to contain the precursor substance of the IL, and appeared in the cytoplasm of the oocyte only the initial phase of the IL formation. However, the vesicles with an intermediate electron density, occurring throughout the period of the IL formation, showed a little immunoreactivity. Thus, the possibilities arise that the OL of medaka egg envelope has two sublayers, inner one of which is made up of the DCV, and the IL is made up of the liver-derived constituent together with a few other constituents which might be synthesized in the oocyte itself.

DB 191

SOME PROPERTIES OF HATCHING ENZYME AS EXAMINED BY MONOCLONAL ANTIBODIES.

S. Yasumasu[1], S. Katow[2], I. Iuchi[1] and K. Yamagami[1]., [1]Life Sci. Inst., Sophia Univ., [2]Natl. Inst. Health Jpn., Tokyo.

Two enzymes, high choriolytic enzyme (HCE) and low choriolytic enzyme (LCE), have been considered to participate in digesting the chorion cooperatively at the hatching time of medaka embryos (Yasumasu et al., 1987).

We obtained various clones producing the monoclonal antibodies (MAbs) against either LCE or HCE. Tested by the immunoblotting method, anti-LCE-MAbs were found to be specific for LCE, while anti-HCE-MAbs were not completely specific for HCE but a little cross-reactive to LCE. Competition experiments showed that anti-HCE-MAbs could be classified into two groups in respect to their recognition sites.

One of anti-HCE-MAbs (7-E-2) inhibited the choriolytic activity of HCE but not its caseinolytic (proteolytic) activity. In addition, 7-E-2 inhibited also the association of HCE with chorion.

These results suggest that the binding action and the proteolytic (catalytic) activity were segregated and that a step of its binding to chorion prior to hydrolyzing it may be involved in chorion digesting process.

DB 192

MORPHOLOGICAL OBSERVATION ON THE REGENERATING SCALES IN THE SKIN OF FLOUNDER.

N.Makino[1] and S.Kikuchi[2], [1]Dept.of Biol., Fac. of Sci., Chiba Univ., Chiba and [2]Kominato Lab., Fac. of Sci., Chiba Univ., Awa-gun.

In the flounder, the skin of both body sides differs not only pigmentation but also the scale shape. Color anomalies occur frequently in hatchery-reared flounder. Including color anomalies, ctenoid scales are observed in the melanized skin and cycloid scales in the non-melanized skin. Present work deals with regenerating scales in the melanized and non-melanized skin of flounder, Paralichthys olivaceus. Operation was performed surgecal removement of the skin. Scales were formed in parallel with regeneration of the skin in both sides. Reformation of melanophores in ocular side was observed 10-20 days after operation. On the tip of regenerating scale, formation of ctenium began, and they grew gradually into ctenoid scales. In blind side cteium formation did not occur in regenerating scales and they grew into the cycloid scales. Also in the regeneration, formation of ctenoid scale was observed only in theskin in which melanophores well develop.

DB 193

MORPHOLOGICAL OBSERVATION ON AUTO-TRANSPLANTED SCALES IN THE FLOUNDER.

S.Kikuchi[1], N.Makino[2] and H.Nakamura[3], [1]Kominato Lab., Fac. of Sci., Chiba Univ., Awa-gun, [2]Dept. of Biol., Fac. of Sci., Chiba Univ., Chiba and [3]Dept. of Anat., Dokkyô Univ. Sch. of Med., Shimotsuga-gun.

In the flounder, Paralichthys olivaceus, there are two types of scales, ctenoid in melanized black region and cycloid in non-melanized white region of the skin. In the present work auto-transplantation of scale was performed in order to examine effect of melanophore on the formation of ctenoid scale. Transplantation was performed as follows: Scales were pulled out and used as transplants. An isolated scale with a fragment of the skin was inserted into empty scale pocket which was made by removement of pre-existed scale before transplantation. In surrowndings of the blind side, melanophores proliferated and formed in crowds small black spot. After 3 months grafted ctenoid scale barely stayed under suppression of regenerating scale. Formation of ctenium did not found in the natural and regenerating cycloid scales in the melanized region. In transplantation of cycloid scales in ocular side, transplants were gradually restroyed in parallel with formation of regenerating ctenoid scales. In the present work formation of ctenium on the natural and the transplanted scales did not occur.

EN 1

THE ROLE OF CALCITONIN IN THE GOLDFISH

Y. Sasayama, F. Mizutani and C. Oguro.
Fac. of Sci., Toyama Univ., Toyama

In teleosts, the role of calcitonin (CT) in Ca metabolism has not been clarified. In the present study, at first, the effect of CT on the serum Ca level was examined in the goldfish. Synthetic salmon CT was administered (100mU or 3U/100g bw) directly to the arterial bulb. However, the serum Ca level did not show any changes during 24 hr. Secondly, effects of CT on other aspects in Ca metabolism than the serum Ca level was studied. Young goldfish was kept in water containing 45Ca (120 μCi/l) for 17 days. They were injected intraperitoneally with the extract of the ultimobranchial gland (UBE) of the adult goldfish (1/2 gland/individual) for 5 times during this experiment.

In the result, in UBE-injected group, 45Ca activity of scales, otoliths and other hard tissues was higher than that in the control. It was noted that the radioactivity of gall bladder in the experimental group is extremely higher than that in the control. In feces, the value of the former was higher than that of the latter, too. These facts suggest that CT functions to accelerate the accumulation of Ca into hard tissues and the excretion of Ca into alimentary tract via gall bladder, although CT does not seem to participate in the serum Ca control.

EN 2

MINERAL CONCENTRATIONS OF BODY FLUIDS IN CYCLOSTOMES AND CARTILAGINOUS FISHES

Y. Sasayama, N. Suzuki and C. Oguro.
Fac. of Sci., Toyama Univ., Toyama

Mechanisms of the excretion of salts via alimentary tract has not been clarified so far in cyclostomes and cartilaginous fishes. In the present study, mineral concentrations of the serum, the bile and the fluid stagnated in alimentary tract were determined in 2 species of cyclostomes and in 4 species of cartilaginous fishes. Those are all sea-water fishes. The values obtained were compared with those determined in bony fishes which we examined previously.

In bony fishes, minerals in the fluid stagnated in alimentary tract show a constant tendency of descent or ascent with going down to the end of the tract. In cyclostomes, however, it became clear that mineral levels do not change throughout the tract, except for Pi. In addition, it was noted that in the lamprey Na is already diluted at stomach to 1/22 of the sea-water level. Ca and Mg were concentrated to 2 times. It is well known that cartilaginous fishes do not drink sea-water. Therefore, the importance of alimentary tract on the mineral excretion has been neglected so far. However, present study revealed that handlings of minerals in the tract are different from species to species. Furthermore, it was known that in the bile Cl level is fairly higher than that in bony fishes.

EN 3

EFFECTS OF ADRENALECTOMY ON SERUM Na, K AND GLUCOSE CONCENTRATIONS IN THE SNAKE, RHABDOPHIS TIGRINUS.

C. Oguro, E. Ohba and Y. Sasayama
Department of Biology, Faculty of Science, Toyama University, Toyama 930, Japan

Function of the adrenal gland in the reptile has not been completely clarified. One of the main reasons is that the surgical removal of the adrenal gland is very difficult because of the intimate relation of the adrenal tissue to the kidney and large blood vessels. However, a technique for complete adrenalectomy without defect in kidney function was developed in snakes in this laboratory. Using this technique, effects of adrenalectomy on serum Na, K and glucose concentrations were studied in the snake, *Rhabdophis tigrinus* tigrinus.

Ten days after adrenalectomy, serum K concentration was increased by 35% (16.7→22.3 mg/100 ml) and serum glucose concentration was decreased by 68% (125→39 mg/100 ml). But, serum Na concentration (400 mg/100 ml) was not changed.

Therefore, it was concluded that the adrenal gland of *R. t. tigrinus* functions to maintain serum glucose concentration at a normal level and to suppress the increase of serum K concentration. However, the adrenal gland does not seem to have an important role in the control of serum Na concentration.

The similar results have been reported in two species of lizards, *Trachysaurus rugosus* and *Varanus gouldii*. Taking these facts into account, it is highly probable that in squamate reptiles the adrenal gland has a major role in the control of serum K and glucose concentrations but has very minor role in the control of serum Na concentration.

EN 4

RELEASE OF CALCITONIN FROM THE ULTIMOBRANCHIAL GLAND OF THE BULLFROG IN VITRO

C. Oguro, T. Ishijima and Y. Sasayama
Department of Biology, Faculty of Science, Toyama University, Toyama 930, Japan

It has been known that calcitonin (CT) from the ultimobranchial gland (UB) has a role in the regulation of serum Ca concentration in anuran amphibians. However, nothing is known on the regulatory mechanism of CT secretion from the UB in amphibians. It was reported that secretion of CT in vitro from the rat thyroid C cells is enhanced by a high Ca concentration in the culture medium.

In the present study, isolated UB of the bullfrog were cultured for 72 hours in various Ca concentrations. CT released into culture media and contained in the UB after the culture were determined in rat bioassay.

Four kinds of culture media were used; [1] frog saline (Ca, 1.1 mM), [2] 2X Ca frog saline (Ca, 2.2 mM), [3] 3X Ca frog saline (Ca, 3.3 mM), [4] phosphate added frog saline (Ca, 1.1 mM; Pi, 1.45 mM). Every culture media contained o.1% glucose. Every culture media and the UB after the culture showed hypocalcemic potency when given to rats. The highest activity was obtained in medium [3]. Medium [2] showed the next highest followed by medium [1]. Presence of phosphorus seems to inhibit the release of CT from the UB in this culture condition, since the hypocalcemic potency of medium [4] was lower than that of other media.

From the results obtained, it was concluded that isolated UB of *Rana catesbeiana* releases CT into culture media and the release is promoted by a high Ca concentration in the medium.

EN 5

EFFECTS OF PARATHYROIDECTOMY AND ULTIMOBRANCHIALECTOMY ON THE SERUM Pi CONCENTRATION IN BULLFROG TADPOLES

Y. Sasayama, M. Kiyozuka and C. Oguro.
Fac. of Sci., Toyama Univ., Toyama

It has been known that in mammals parathyroid hormone and calcitonin affect not only Ca but also Pi metabolism. Therefore, it has been suggested that these calcemic hormones may have emerged for the regulation of Pi rather than for Ca. In lower vertebrates, however, the relationship between these hormones and the serum Pi level has not been clarified so far. In the present study, effects of parathyroidectomy and ultimobranchialectomy on the serum Pi level were studied in the bullfrog tadpole.

Parathyroidectomy and the sham-operation brought about significant rises in the serum Pi level 7 days after. When comparison was made in those values between the both groups, the level of the former tended to be higher than that of the latter. This result shows that parathyroid gland may be concerned with the serum Pi regulation, although the degree of the participation is small.

Also in ultimobranchialectomy and the sham-operation, serum Pi level increased significantly 7 days after. Between the both groups, however, there was no significant difference. This result suggests that ultimobranchial gland does not participate in the control of the serum Pi concentration.

EN 6

EFFECT OF PARATHYROID EXTRACT ON CULTURED BONE OF CYNOPS PYRRHOGASTER.

C. Oguro, Y. Minamimura and Y. Sasayama.
Department of Biology, Faculty of Science, Toyama University, Toyama 930, Japan.

In urodelan amphibians, parathyroid gland (PT) plays a role in the maintenance of normal serum Ca concentration in species belonging to phyletically higher groups. Thus, it was reported that in Cynops pyrrhogaster PT is one of the major organs for the maintenance of serum Ca concentration.

On the bases of the results in preliminary experiments, it was suggested that the target organ of PT is the bone. In the present study, the effect of bullfrog parathyroid extract (PTE) on the cultured bone of C. pyrrhogaster was observed by the ^{45}Ca release from the bone which had been labelled with ^{45}Ca. The incubation was done at 20°C. The rate of ^{45}Ca release to the media was 17.3% at the end of incubation. This value was lower than the values reported in fetal bones of mammal and bird.

Femur and humerus obtained from the ^{45}Ca labelled individuals were incubated in media with or without PTE. The ^{45}Ca release in the PTE containing media was higher than that from the control media in every sampling time(4,8,12,24 and 48 hrs). The difference between experimental and control groups was statistically significant($P<0.05$). ^{45}Ca release from the dead bone was unstable and thus the results noted above were noticed to be physiological. From these results, it is concluded that in C. pyrrhogaster parathyroid hormone exerts its effect directry to the bone and promotes the release of Ca to the blood for the maintenance of serum Ca concentration normal.

EN 7

SEASONAL CHANGES OF PLASMA CA, MG AND INORGANIC PHOSPHORUS LEVELS IN MALE SNAKES.

M.Yoshihara[1], M.Uchiyama[1], T.Murakami[1], H.Yoshizawa[2] and C.Oguro[3]. [1]Dept. of Oral Physiol., Sch. of Dentistry at Niigata, The Nippon Dental Univ., Niigata, [2]Dept. of Oral Histol., Matsumoto Dental Coll., Shiojiri, [3]Dept. of Biol., Fac. of Sci., Toyama Univ., Toyama.

There is no information currently in the literature concerning possible seasonal fluctuations of plasma Ca levels in male reptiles. In the present study, seasonal changes of plasma Ca, Mg and inorganic phosphorus (Pi) levels of the rat snake, Elaphe quadrivirgata, were investigated.

Snakes used were sexually mature males and they were bled 5-14 days after capture. Blood samples obtained in December and February were obtained from artificially hibernating snakes maintained in an incubator at 5°C from early November. Plasma Ca levels in pre- and post-hibernating (October, November and April) and hibernating (December and February) seasons were significantly lower (8%) than those in the active season (June-September, 3.57 ± 0.02 mM/l, n=167). On the contrary, plasma Mg levels in pre- and post-hibernating and hibernating seasons were significantly higher (12 and 55%) than those in the active season (1.57 ± 0.03 mM/l, n=105). Plasma Pi level in pre- and post hibernating seasons was significantly lower (17%) and that during hibernation was significantly higher (17%) than that in the active season (1.23 ± 0.03 mM/l, n=98). These results indicate that in E. quadrivirgata seasonal changes occur in plasma Ca, Mg and Pi levels.

EN 8

DEVELOPMENT AND SALINITY TOLERANCE IN TADPOLES OF THE CRAB-EATING FROG.

M.Uchiyama[1], T.Murakami[1], C.Wakasugi[2] and S.Sudara[3]. [1]Dept. of Oral Physiol., The Nippon Dental Univ., Niigata., [2]Dept. of Histol., The Nippon Dental Univ., Niigata and [3]Dept. of Marine Science, Chulalongkorn Univ., Bangkok, Thailand.

It has been reported that the tadpoles of the crab-eating frog, Rana cancrivora, inhabit brackish environment. The present study was performed to clarify physiological mechanism of their great tolerance for salinity. For this purpose, ontogeny, salinity tolerance and histology were investigated. The rate of embryonic development was fairly rapid (96 hrs) in 10% sea water at about 25° C. Tadpoles before the limb bud stages were able to survive in media up to 40% sea water but died within 8 hrs after being placed acutely in 50% sea water or more high salinity. On the other hand, tadpoles (stages I-XVIII) adapted in higher salinities when acclimatization was carried out in steps by changing the salinity 10-20% every 2-7 days. In the histological examinations, hypertrophy of the epidermis was demonstrated in the tadpoles adapted to the higher salinities although no salt gland was observed. Eosinophilic cells were observed in the internal gills of tadpoles adapted to 10-100% sea water. These structures might be useful for the adaptation to the environment of various salinities.

EN 9

SUPPRESSION OF LH RELEASE BY SHORT DAYS.

M. Wada
Dept. Gen. Educat., Tokyo Med. Dent. Univ., Ichikawa, Chiba

In my previous paper, I reported that a pattern of LH release changed during early photostimulation from "episodic" to "constant" release in Japanese quail and that short days were not enough to suppress LH release after the release pattern is once changed to "constant" release. To test an effect of short days on LH secretion, one to 7 photopulse were given to quail kept under 8L16D. One hour photopulses at the photosensitive phase induced sustained LH secretion; plasma concentration of LH maintained increased levels even after the pulses being no more delivered. Plasma LH concentrations were tended to decrease, however, by 20 days after the initial treatment in the quail given 1, 2, or 3 pulses each day. On the other hand, LH concentrations in the quail delivered 5 or 7 pulses were not decreased to the initial basal LH level by 20 days after the treatment. The increased LH levels were around 1 ng/ml, which were lower than those in long day control birds. The cloacal protrusion of these birds maintained a developed state even in the short days. Another experiment indicated that low temperature is also required for short days to express full suppression on LH secretion.

EN 10

EFFECTS OF LONG-DAY PHOTOPERIODS ON CHANGES OF PLASMA GONADOTROPINS AND SEX STEROIDS IN JAPANESE COMMON PHEASANTS DURING BREEDING SEASON

H. Sakai, M. Sato, S. Wakabayashi, K. Hirano[1], Y. Oono[1], and M. Kasuga[1], Dept. of Biol., Nihon Univ. School of Dentistry, Tokyo, and [1]Saitama Prefectural Poultry Experiment Station, Saitama.

Eight-month old pheasants were reared under long-day photoperiods (16L:8D) from February to study the relationship of changes in plasma gonadotropins and sex steroid hormones in wild birds. Male LH and female progesterone were already high in February both in long-day and natural photoperiod groups, and no significant difference was observed between them. On the other hand, egg laying and increase in plasma levels of male FSH, female LH, FSH and estrogen by long-day photo stimulation preceded natural photoperiod group by 4 to 8 weeks with different features of change. Testosterone levels of male groups increased for the same period, but their levels during breeding period were different. This study showed that long-day photo stimulation preceding the breeding period hasten hormone secretion but not necessarily the hormonal changes observed in natural condition. These results suggest that further study of the gonadal responsibilities will be needed to account for these results.

EN 11

EFFECT OF PROLACTIN ON WATER DRIVE SYNDROME OF THE SALAMANDER HYNOBIUS NIGRESCENS.

Masato Hasumi and Hisaaki Iwasawa.
Biol. Inst., Niigata Univ., Niigata.

Hibernating adult males of *Hynobius nigrescens*, which were bred outdoors throughout the year, were divided into 8 groups (initial control, intact cont., saline, 5 IU PRL injection for 12 days, 50 IU 12 days, 5 IU 20 days, 50 IU 20 days, 5 IU 20 days in a poolless container) just before the breeding season. These animals were injected intraperitoneally with ovine prolactin (PRL) every other day, and the position of the salamanders, on land or in water, was examined every 2-6 hours. The salamanders were observed to wander back and forth between water and land up to whole submergence. The specific gravity of the whole body was greater than unity in all the individuals irrespective of the treatments, and no significant difference was found among the groups. The connective tissue inside the skin was tight in PRL-injected animals kept in a poolless container. Cornified epidermis and mucous glands filled with mucus were seen in intact animals (initial control), whereas these structures were not seen in any in the PRL-injected groups. In the field, the mucous glands of some males shortly after migration into a breeding pond were filled with mucus yet, but little mucus was seen in the glands of typical aquatic-phase males.

EN 12

SEASONAL VARIATION OF THE PROLACTIN (PRL) EFFECT ON ACTIVE Na TRANSPORT ACROSS AMPHIBIAN SKIN.

M. TAKADA, Dept. of Physiol., Saitama Med. Sch., Moroyama, Saitama

1. The long-term effect of PRL. Long-term application of PRL, i.e., 20 μg/g body weight injected into autumn newts (*Cynops pyrrhogaster*) every other day for 2 weeks, induced an increase in resistance to active Na current (R_{Na}), and a resulting decrease in the potential difference (PD) and the short circuit current (SCC), but barely changed the electromotive force of the active Na current (E_{Na}). Such long-term application of PRL to spring newts induced a decrease in PD and SCC but exerted no effect on the E_{Na} and R_{Na}.
2. The short-term effect of PRL. Ten μg/ml of PRL was applied to the dermal side of isolated skin of the tadpole (*Rana catesbeiana*) during metamorphosis. PRL induced a transient increase in SCC across the skin of both spring and autumn tadpoles. Percent increase in SCC of the skin of spring tadpoles was larger than that of autumn ones in Cl-Ringer's condition. By contrast, the PRL effect was only slightly or not at all present in the skin of both spring and autumn tadpoles in SO_4-Ringer's solution.

EN 13

FACILITATION OF MASCULINE SEXUAL BEHAVIOR BY SYNTHETIC INHIBITOR OF SEROTONIN IN SEPTAL LESIONED MALE RATS.

Y. Kondo, A. Shinoda, K, Yamanouchi[1], and Y. Arai[2]. Dept. Psychol., Fac. Letters, Gakushuin univ., 1) Dept. Human Sci., Fac. Human Sci., Waseda univ., and 2) Dept. of Anat., Juntendo univ. Sch. Med., Tokyo.

Previously, we reported the suppression of masculine sexual behavior following lesioning in the medial preoptic or lateral septal area (MPOL and LSL) in male rats. In this study, we examined the effect of a synthetic inhibitor of serotonin, p-chlorophenylalanine (PCPA), on masculine sexual behavior in these rats.

Orchidectomized rats received either bilateral LSL or bilateral MPOL. Three weeks later, all animals were treated with testosterone(T) by implantation of Silastic tubings. Observations of masculine behavior were carried out 10 and 20 days after T implantation. Each observation was followed by 4 daily injections of PCPA (100mg/Kg) or saline. Saline-treated males with LSL or MPOL showed significantly less masculine behavior than sham controls. Administration of PCPA markedly facilitated masculine behavior in control and LSL males. However, PCPA failed to increase masculine behavior in MPOL males. The results suggest that the lateral septum has facilitatory influences upon a regulating system of masculine behavior which may be inhibited by serotonergic neurons, while the medial preoptic area may be more important for masculine behavior.

EN 14

EFFECT OF ANDROGEN ON EARLY POSTNATAL DEVELOPMENT OF THE MEDIAL PREOPTIC NUCLEUS(MPN) IN THE RAT.

S. Murakami[1], S. Ito[2] and Y. Arai[1]. Depts of Anat[1] and Ob-Gyn[2], Juntendo Univ. Sch. of Med. Tokyo.

The medial preoptic nucleus(MPN) is an intensely stained neuron group in the rostroventral periventricular gray of the preoptic area. Its volume is significantly greater in females than in males. This sex difference is dependent on neonatal androgen. Treatment of female rats with 50 µg of testosterone propionate(TP) for 5 days from the day of birth effectively reduced the nuclear volume to the level just comparable to that of normal males. In order to elucidate the possible mechanisms involved in the volume reduction of the MPN following neonatal androgen treatment, the number of degenerating cells in the MPN during early postnatal period was examined in females and TP-treated females. At postnatal days 7 and 10, TP-treated females had significantly more pycnotic cells in the MPN than females. Furthermore, most of the pycnotic cells were distributed in the peripheral zone of the MPN. These results suggest that neonatal androgen may promote the loss of MPN neurons during developmental stages, and this may account for the reduction of the volume of the MPN by neonatal treatment with TP.

EN 15

STRUCTURAL RELATIONSHIPS OF HYPOPHYSIAL VASCULARIZATION AND ADENOHYPOPHYSIAL CYTOLOGY IN THE SNAKE, ELAPHE QUADRIVIRGATA

I.Koshimizu and Y.Oota. Biol. Inst., Fac. of Sci., Shizuoka Univ., Shizuoka.

The vascular supply of hypophysis and distribution of the adenohypophysial cells were studied in the snake. The median eminence is supplied by a very dense primary capillary plexus deriving from branches of the infundibular arteries. The primary capillary plexus converge into several large portal vessels. The pars distalis (PD) receives its blood supply via the portal vessels. In the PD, the portal vessels give off the sinusoid system which has intimate contact with the PD cells. Histologically, the PD can be divisible into cephalic and caudal lobes, which are marked by differential distribution of glandular cells. Immunohistochemically, the prolactin-immunoreactive cells are found exclusively in the cephalic lobe, whereas the growth hormone-immunoreactive cells are distributed in the caudal lobe. Structurally, the anterior group of portal vessels is mainly supplied in the cephalic lobe, whereas the posterior group of portal vessels enters the caudal lobe.

EN 16

AN ELECTRON MICROSCOPE STUDY OF THE PARS TUBERALIS OF THE TURTLE, GEOCLEMYS REEVESII

Y.Oota and K.Miyata. Biol. Inst., Fac. of Sci., Shizuoka Univ., Shizuoka.

The morphology and cytophysiology of the pars tuberalis (PT) were studied in the turtle. The PT is well developed and can be divisible into three parts : juxta neural PT (juxPT), the portal zone and the PT interna (PTint). The cells of the juxPT spread over the ventral surface of the median eminence. In the portal zone, the PT cells envelope the portal vessels connecting the median eminence and the pars distalis. The PTint forms a continuous tissue to the pars distalis. Most of the PT cells are chromophobic nature, however, a small number of cells showing positive immunoreaction to thyrotropin-antisera are demonstrated in the juxPT. Similarly, cells showing positive immunoreaction to follicle stimulating hormone-antisera are identified in the PTint. With the electron microscopy, the PT cells can be readily classified into two types : secretory cells and follicular cells. Although there is some morphological variability, characteristic secretory cells containing electron-dense granules are demonstrated in the juxPT and PTint.

EN 17

EFFECTS OF LHRH ON EEG ACTIVITY AND PLASMA ANDROGEN LEVELS IN JAPANESE TOADS.

Y. Fujita and A. Urano. Dept. of Regul. Biol., Fac. of Sci., Saitama Univ., Urawa.

A series of our studies has suggested that initiation of reproductive behavior in hibernating toads is controlled by various neurohormones, such as LHRH and TRH. We showed that systemically applied LHRH enhanced amplitudes of EEGs in the toads. In this study, we measured changes in the plasma androgen levels after LHRH administration to examine whether EEG enhancement is induced by direct central action of LHRH or indirect action through the hypothalamo-hypophysial-gonadal axis. Animals were immobilized by pith, and were cannulated through the femoral artery and vein for a intravenous application of LHRH and collection of plasma samples 2-36 hr after the LHRH administration, respectively. Intravenous LHRH at dose levels of 10 and 100 g that could arouse toad EEG activity did not elevate the plasma androgen levels. Moreover, the increases in androgen levels by 4-hr continuous LHRH infusion did not temporally coincide with the EEG enhancement in the same individuals. Intraventricularly applied LHRH yielded a similar result. These results indicate that LHRH may act directly on the brain and enhance its electrical activity.

EN 18

HYPOTHALAMIC LHRH CONTENT FOLLOWING NOREPINEPHRINE INFUSION INTO CEREBRAL VENTRICLE IN NEONATALLY HIGHLY ESTROGENIZED RATS.

M. Aihara[1], S. Hayashi[2] and K.Wakabayashi[3]. [1]Dept.Biol., Toho Univ., Funabashi, [2]Dept. Anat/Embryol., Tokyo Met.Inst.Neurosci., Fuchu & [3]Inst.Endocr.,Gunma Univ.,Maebashi.

Administration of 10 µg estradiol benzoate (EB) for 10 consecutive days to newborn female rats of the Sprague-Dawley strain induced extreme reduction in gonadotropic activity in adulthood. However, the hypothalamic LHRH content of these rats was higher than that in intact cycling rats. In this study, we examined the effects of intracerebroventricular (ICV) infusion of norepinephrine (NE) on hypothalamic LHRH content. Animals were ovariectomized and received ICV cannulation at 70 days of age. They received subcutaneous injection of 30 µg EB 2 weeks later. Two days later, they were killed 6 min after ICV infusion of 100 µg NE. The hypothalamus was frozen immediately. The LHRH content in the frontal slices of 400 µm thickness was measured by RIA. Two clear peaks in the rostro-caudal LHRH distribution were detected which were divided at the suprachiasmatic nucleus region. In neonatally non-treated rats, the caudal peak was significantly reduced by ICV infusion of NE. In contrast, in neonatally estrogenized rats, no significant decrease in the peak value of LHRH was observed. These results indicate that neonatal administration of EB affected the hypothalamic noradrenergic system which is intimately related to LHRH secretion.

EN 19

CHARACTERIZATION OF LUTEINIZING HORMONE BINDING INHIBITOR(S) SECRETED FROM CULTURED MOUSE SERTOLI CELLS.

M. Takase, K. Tsutsui and S. Kawashima. Zoological Institute, Faculty of Science, Hiroshima University, Hiroshima.

We have found and previously reported the secretion of some LH binding inhibitor(s) (LH-BI) from mouse Sertoli cells in culture. In order to assess basic features of LH-BI, Sertoli cell-cultured media (SM) were subjected to heating at 100°C for 20 min, and incubation with trypsin (2.5 mg/ml) or charcoal (20 mg/ml). After heating and trypsinization of SM 1.8-fold and 1.3-fold increases in LH binding, respectively, were observed in Leydig cells cultured in intact non-treated SM, but the increases were not statistically significant. Charcoal treatment of SM induced 4.4-fold increase of LH binding as compared to intact SM ($p < 0.05$). In order to know whether mouse Sertoli cells in culture secrete LHRH or E_2, RIA for LHRH and E_2 in SM was performed. LHRH was undetectable (<4.46 pg/ml original medium) in acetic acid-ethanol extracts from lyophilized SM. Ether extract from SM contained 66.8 pg E_2 per ml original medium. These results may suggest that the possible candidate for LH-BI may be steroidal substance, e.g. E_2, rather than proteinic substance.

EN 20

EFFECTS OF COMPLETE SUPRACHIASMATIC DEAFFERENTATION ON THE POSITIVE FEEDBACK RESPONSE TO ESTROGEN AND PROGESTERONE ON LH RELEASE.

K. Nomura, S. Takahashi and S. Kawashima. Zool. Inst., Fac. of Sci., Hiroshima Univ., Hiroshima.

Estrous cycle and ovulation were prevented by complete deafferentation (CSD) of the suprachiasmatic nucleus (SCN) in female rats. In this study, positive feedback effects of estradiol benzoate (EB) or progesterone (P) on LH release were examined in ovariectomized CSD rats. In control rats, LH surge was induced by EB or P following EB treatments. In CSD rats, EB failed to rise LH levels. Significant elevation in LH level occurred in CSD rats by P following EB, but the amplitude was less than that observed in the controls. However,P-induced LH release was abolished when the lesions by CSD extended further anteriorly to the medial preoptic nucleus. In control rats, LHRH content was significantly greater before EB-induced LH surge than that during the surge in both preoptic-anterior hypothalamic (POA-AH) and medial basal hypothalamic (MBH) regions. In CSD rats this difference was not observed, and their LHRH content of POA-AH was greater, but that of MBH was less than those of the controls. These results suggest that the SCN is involved in the regulation of EB-induced LH release rather than P-induced LH release, and in the stimulation of LHRH neurons to release LHRH.

EN 21

AGE-RELATED CHANGES IN GROWTH HORMONE BINDING TO THE LIVER OF FEMALE RATS

S. Takahashi[1], S. Kawashima[1], J. Meites[2]. [1]Zool. Inst., Fac. of Sci., Hiroshima Univ., [2] Dep. of Physiol., Michigan State Univ., East Lansing, USA.

Growth hormone (GH) secretion decreases with aging in male and female rats. Liver is one of the target organs of GH and secretes somatomedin-C (SM-C) in response to GH. Age-related changes in binding of ^{125}I-bovine GH to liver membrane fractions were measured in female Long-Evans rats at 2, 6, 12, and 20 months of age. Specific GH binding was not different between 2 and 6 months of age but it increased significantly at 12 and 20 months of age. Scatchard analyses showed that the plots were curvilinear and consisted of high- and low-affinity binding sites. The age-related increase in binding sites was mainly due to an increase in the number of low-affinity binding sites. Serum levels of SM-C in 20-month-old rats were about half of those in 6-month-old rats. Twice daily injections of ovine GH (2 mg/kg body weight) for 7 days depressed liver GH binding and increased serum SM-C levels in 19-month-old female rats, but had no effect on GH binding in 2-month-old female rats. These results suggest that the increase in liver GH binding sites and the decrease in SM-C secretion were associated with the decrease in GH secretion in old female rats.

EN 22

THE ROLE OF INTERNALIZATION ON DOWN-REGULATION OF FSH RECEPTORS.

A. Shimizu, K. Tsutsui and S. Kawashima. Zool. Inst., Fac. of Sci., Hiroshima Univ., Hiroshima.

The role of internalization of FSH-receptor complexes on down-regulation of FSH receptors was investigated in cultured Sertoli cells of C57BL/6NCrj mice. NaN_3 was used as an inhibitor of internalization. Sertoli cells were cultured for 8 days or 4 day-plus-4 day combinations in either the following media : 1) F12/DME (control group), 2) F12/DME, then F12/DME containing 5µg/ml FSH (down-regulated group), 3) F12/DME, then F12/DME containing 5µg/ml FSH and 10^{-5}, 10^{-4} or 10^{-3}M NaN_3, 4) F12/DME containing FSH and NaN_3, then F12/DME containing FSH. In all cultures, surface, internalized and degraded radioactivities were measured. The rate constant of internalization (k_i) in control and down-regulated groups was estimated. It was shown that surface and internalized radioactivities were decreased by FSH and the decrease was suppressed by coexistence of NaN_3. In contrast, degraded radioactivity was increased by FSH and this increase was also suppressed by NaN_3. In addition, k_i of down-regulated group was significantly larger than that of control group (6.94×10^{-2} vs. $4.11\times10^{-2}min^{-1}$, respectively). These results indicate that down-regulation of FSH receptors may be due to the translocation of surface receptors into the cells and as a result the number of available surface receptors is decreased.

EN 23

PROPERTIES OF TESTICULAR FSH RECEPTORS OF SHORT-TAILED BANDICOOT RAT, NESOKIA INDICA.

K. Tsutsui[1], S. Kawashima[1], R. Kapania[2], V. Kumar[2] and R. N. Saxena[2]. [1]Zool. Inst., Fac. of Sci., Hiroshima Univ., Hiroshima and [2]Dept. of Zool., Univ. of Delhi, India.

Basic properties of testicular FSH receptors of short-tailed bandicoot rat, *Nesokia indica* were characterized in the present study. Specific FSH binding was detectable only in the testis among various organs, and it reached an equilibrium after 2 hr of incubation at 35 ℃. The FSH binding was inhibited by mammalian FSH preparations as a function of the concentration, but not by highly purified rat LH and PRL. Scatchard plot analyses of FSH binding to the testicular preparations of *Nesokia indica* showed straight lines, suggesting the presence of a single class of binding sites. The dissociation constants (Kds) for FSH of adults of *Nesokia indica* were 1.416 (0.964 - 2.667, 95% confidence interval) nM in December, 1986 and 1.348 (0.885-2.849) nM in April, 1987. In contrast, Kds of the albino rat were 0.459 (0.357 - 0.641) nM at 19 days of age and 0.444 (0.308-0.806) nM at 3 months. These results showed that the specific FSH binding sites were present in the testis of *Nesokia indica* but the affinity of FSH binding in *Nesokia indica* was lower than that in the albino rat.

EN 24

STIMULATION OF GROWTH OF THE NUCLEAR VOLUME AND NEURONAL PROCESS LENGTH BY ESTRADIOL-17β IN RAT HYPOTHALAMIC AND LIMBIC NUCLEI.

M. Uchibori and S. Kawashima*. Suzugamine Women's College and *Zool. Inst., Fac. of Sci., Hiroshima Univ., Hiroshima.

We have studied the morphometric effects of estradiol-17β (E_2) on some E_2 concentrating neural substrates in rats castrated on the day of birth. They were given 10 µg E_2 daily for 10 postnatal days and killed on Days 11 and 31. The results were as follows. (1) The ventromedial nucleus (VMN): In males E_2 significantly stimulated the growth of nuclear volume on Day 11 but not on Day 31. In females, it significantly increased the volume both on Days 11 and 31. The total neuronal process length of E_2-treated rats was significantly greater than that of controls on Days 11 and 31 in males, and on Day 31 in females. (2) The stria terminalis (ST): Stimulation of the growth of nuclear volume by E_2 was observed only on Day 31 in males. E_2 significantly increased the total neuronal process length on Days 11 and 31 in males, but not in females. (3) The suprachiasmatic nucleus (SCN): The nuclear volume was not significantly different between E_2-treated and control rats on Days 11 and 31 in both sexes. The total neuronal process length in the SCN was significantly greater in E_2-treated rats of both sexes than controls on Day 31, but not on Day 11.

Thus, the effects of E_2 on these morphological parameters were evident in the VMN but not so marked in the ST and SCN.

EN 25

EFFECTS OF ESTRADIOL-17β ON THE SURVIVAL OF NEURONS FROM NEONATAL RAT HYPOTHALAMUS-PREOPTIC AREA IN PRIMARY CULTURE.

K. Takagi[1], H. Shimizu[1], M. Uchibori[2], and S. Kawashima[1]. [1]Zool. Inst., Fac. of Sci., Hiroshima Univ. and [2]Suzugamine Women's Coll., Hiroshima.

Dissociated cells of neonatal rat hypothalamus-preoptic area were grown in primary culture, and effects of estradiol-17β(E_2) on the survival of neurons were studied. Cells were cultured in culture media with or without E_2(100 ng/ml), and the number of viable neurons were counted at 3, 6, and 9 days of culture. The survival of neurons tended to be greater in E_2-added cultures than control cultures at all culture ages and in all triplicate observations. In Second series of expriments, cytosine-β-D-arabinofuranoside(AraC, 10^{-5} M/ml) was added to the culture media from 3 days to 6 days in culture with or without E_2, in order to inhibit the non-neuronal cell proliferation. AraC is known to inhibit mitosis. The survival of neurons was considerably increased by AraC treatment, and effects of E_2 cultured with AraC were likewise observed as in cultures without AraC.

These results suggest that E_2 has some stimulatory influence on the neuronal survival, and that the influence is maintained when the non-neuronal cell proliferation is inhibited with apparent elevation of the basal level of the survival.

EN 26

BEHAVIOR OF ARGININE VASOTOCIN-PRODUCING NEURONS OF THE MEDAKA *Oryzias latipes* IN DIFFERENT ENVIRONMENTAL SALINITY.

K.Haruta, T.Yamashita and S.Kawashima. Zoological Institute, Faculty of Science, Hiroshima University, Hiroshima.

A wild population of the medaka collected in a pond in Hiroshima City was used. Immunoreactive arginine vasotocin(AVT) neurons and axons were identified by their reactivity to anti-arginine vasopressin serum which was proved to crossreact with AVT. Immunoreactive AVT neurons were present in the nucleus preopticus of the hypothalamus. The nucleus can roughly be divided into pars magnocellularis and pars parvocellularis. The number of magnocellular AVT neurons showed an instantaneous changes after transfer from fresh water(FW) to sea water(SW) or from SW to FW. when FW-adapted fish were transferred to SW, The number of these neurons increased 30 minutes after the transfer. Then, the number decreased with the lapse of time. Radioimmunoassay of AVT showed that AVT content in the pituitary decreased two hours after the transfer to SW but increased after that approaching the initial control level. On the contrary, when SW-adapted fish were transferred to FW. The number of AVT neurons increased one day after the transfer, but it then decreased reaching the level of FW-adapted fish after one week. The present results suggest that AVT is one of the important hormonal factors involved in the osmoregulation of the medaka.

EN 27

SYNAPTIC PATTERN OF THE MEDIAL PREOPTIC NUCLEUS OF RATS.

M.Miyakawa and Y.Arai. Dept. Anat. Juntendo Univ. Sch. Med., Tokyo.

Medial preoptic nucleus(MPN) is located along the ventricular wall of the anteroventral part of the preoptic area. The important role in cyclic ovulation and the presence of abundant estrogen receptors have been reported on the MPN. This nucleus is sexually dimorphic being larger in the female than in the male. In the present study, synaptic pattern of the MPN was examined in male, female and neonatally androgen-treated female rats at 70 days of age. The numbers of axo-somatic synapses, axodendritic shaft synapses and axodendritic spine synapses were counted differentially in 9,000 sq.um area of the identical part in each animal. The number of axosomatic synapses was small and almost the same in all groups. The numbers of both axodendritic shaft and spine synapses were significantly larger in male rats than in females. The synaptic pattern of females treated with 50µg testosterone propionate for the first 5 days of life was not different from that of intact females. Synapses containing large granular vesicles showed similar pattern of sexual dimorphism. Further analysis is necessary to clarify the effect of sex steroid on the differentiation of synaptic pattern of the MPN.

EN 28

NEUROGENESIS IN THE MEDIAL PREOPTIC NUCLEUS OF THE RAT: BROMODEOXYURIDINE (BRDU)-ANTIBRDU MONOCLONAL ANTIBODY METHOD.

M. Nishizuka and Y. Arai, Dept. Anat., Juntendo Univ. Sch. Med., Tokyo.

To determine the time of origin of neurons in the medial preoptic nucleus (MPN), 20 mg bromodeoxyuridine(BrdU), a thymidine analogue, was intraperitoneally injected in pregnant rats on gestational day 10, 11, 12, 13, 14, 15, 16, 17, 18, or 19. Rat pups were also subcutaneously injected with 20 mg BrdU on postnatal day (PD)1. The offspring and PD1-treated rats were killed on PD12 or thereafter. The brains were fixed and tissue sections were immunocytochemically stained using with antiBrdU monoclonal antibody. When BrdU was given on embryonic day (ED)13-18, a number of immunopositive cell nuclei were detected in the MPN of male and female rats. Particularly, the treatment on ED14-16 caused immunolabelling in a substantial number of MPN cell nuclei. In contrast, BrdU exposure on ED10-12, 19, or PD1 failed to label any MPN cell. Based on these, we conclude that the majority of MPN neurons of male and female rats were formed in ED14-16, and a population of neurons was added on ED 13,17, and 18. The present study ascertained availability of BrdU-anti BrdU method in study of neurogenesis.

EN 29

A MECHANISM OF EXPERIMENTAL ANTERIOR PITUITARY HEMORRHAGE IN MICE.

C.Iga and Y.Kobayashi. Dept.of Biol.,Fac. Sci.,Okayama Univ.,Okayama.

Intense hemorrhage has been reported in the anterior pituitary of mice immediately after i.p. injection of hypertonic solutions including electrolytes and non-electolytes(Kobayashi et al.,1982). Futher detail was studied on a mechanism of this experimental anterior pituitary hemorrhage. All adult male mice received i.p. injection of 35% glucose at a doseof 0.03ml/g B.W. showed intense anterior pituitary hemorrhage within 20min. A new finding is that this incidence of bleeding was redused by combined treatment with an anesthetic and a dopamine D_2 antagonist. Under pentobarbitar anesthesia(50µg/g B.W.) the pituitary hemorrhage occurred in mice 4 out of 20(100%→20%). Metoclopramide(a dopamine D_2 antagonist, 30µg/g B.W.for 3days) also resulted in the low level of bleeding only 6 out of 16(100%→37.5%). Combined pretreatment with pentobarbitar and metoclopramide showed no anterior pituitary hemorrhage in all mice. While bromocriptine(a dopamine D_2 agonist, 5µg/g B.W.) stimulated the incidence of pituitary bleeding 16 out of 20(80%) at a low dose(0.02ml/g B.W.) that occurred pituitary bleeding only 1 out of 20(5%).

EN 30

AGE-ASSOCIATED CHANGES IN THE DISTRIBUTION OF CYTOCHROME P-450PB IN THE RAT LIVER.

T. Machida[1], S. Kawashima[1], and C. F. A. van Bezooijen[2]. [1]Zool. Inst., Fac. of Sci., Hiroshima Univ., Japan and [2]TNO Inst. of Gerontol., The Netherlands.

Cytochrome P-450 (P-450) is a family of heme proteins that serve as the terminal oxidase in a mixed-function-oxidase system. Several forms of P-450 isozymes are known to specifically induced in the liver by the treatment of animals with specific drugs. In the present experiments, distribution of a P-450 isozyme induced by phenobarbital (PB) was immunohistochemically investigated in the liver of the male rats of different ages. In the liver of 3-month-old rats, an intense staining against anti-P-450PB antiserum was invariably observed in the hepatocytes of the perivenous (PV) zone, while cells in the periportal (PP) zone reacted only slightly to the antiserum. At this age, difference in the distribution of P-450PB between PV and PP cells was statistically significant in all the four lobes of the liver, although the predominant localization of P-450PB in the PV cells was most conspicuous in the caudal lobe. Prominent localization of P-450PB in the PV hepatocytes became less obvious at 18 months of age and came to be almost undetectable at 30 months. The result demonstrated the age-related decline of the heterogeneously distributed P-450PB in the liver lobules of male rats.

EN 31

EFFECTS OF ABDOMINAL VAGOTOMY ON THE HYPOTHALAMIC AND PITUITARY FUNCTION IN MALE MICE.

T.S. Nakazawa, T. Machida and S. Kawashima. Zoological Institute, Faculty of Science, Hiroshima University, Hiroshima.

Possible involvement of vagus nerve in the control of hypothalamic and pituitary function in male mice was examined.

Male mice of the CD-1 strain were castrated and/or abdominal vagotomized at 2 or 8 months of age, and changes in the size of neuronal nuclei in the hypothalamus-preoptic area and plasma levels of gonadotropins were investigated one week after operation. Bilateral castration or removal of left testis caused a significant reduction in the size of neuronal nuclei of the POA, while removal of right testis failed to affect the size of neuronal nuclei. On the other hand, vagotomy induced a significant enlargement of neuronal nuclear size of the POA, the VMN and the ARC. Neuronal nuclei of these regions in vagotomized mice exhibited a consistent decrement in their sizes following castration, although vagotomy-induced enlargement of nuclear size still persisted after castration. Significant changes were not induced by vagotomy in plasma levels of LH and FSH. The results indicate that the vagus nerve is not modulating the effect of castration <u>per se</u> but may have some other intrinsic effects on the hypothalamic control of pituitary function in male mice.

EN 32

THE EFFECT OF AN AROMATASE- AND A 5α-REDUCTASE-INHIBITOR UPON THE OCCURRENCE OF POLYOVULAR FOLLICLES, PERSISTENT ANOVULATION, AND PERMANENT VAGINAL STRATIFICATION IN MICE TREATED NEONATALLY WITH TESTOSTERONE.

T. Iguchi, R. Todoroki, N. Takasugi and V. Petrow*. Dept. Biol. Yokohama City Univ. Yokohama and *Dept. Physiol. Duke Univ. Med. Ctr. North Carolina, U.S.A.

Female C57BL/Tw mice were given 5 daily injections of 20μg testosterone (T), 100μg 4-hydroxy-4-androstene-3,17-dione (4-HA), 100μg 6-methylene-4-pregnene-3,20-dione (6-MP), 4-HA+6-MP, T+4-HA, T+6-MP and T+4-HA+6-MP starting on the day of birth. The incidence of polyovular follicles (PF) at 30 days was significantly increased by neonatal treatment with T. By contrast, the PF incidence was significantly reduced by injections of 4-HA with T. Neonatally T- or T+6-MP-treated 90-day-old mice had ovaries without corpora lutea. By contrast, T+4-HA (64%)- and T+4-HA+6-MP (82%)-treated mice had ovaries with corpora lutea. There were no significant differences in the vaginal epithelium of T-treated mice as compared with those of T+4-HA-, T+6-MP- or T+4-HA+6-MP-treated mice. They showed vaginal stratification. The present results indicate that 1) development of PF and persistent anovulation are due to the direct action of estrogen (E) derived from T; 2) T itself can induce ovary-independent vaginal changes, although 5α-reduced androgen and E derived from T seem to be more effective in this regard.

EN 33

OCCURRENCE OF HERNIA AND PERMANENT CARTILAGINIFICATION OF PELVIS IN MICE TREATED NEONATALLY WITH TAMOXIFEN

S. Irisawa, T. Iguchi and N. Takasugi. Dept.Biol. Yokohama City Univ. Yokohama.

Male and female C57BL/Tw mice were given 5 daily injections of 100 μg tamoxifen (Tx) starting on the day of birth, 3, 5, 7, or 10 days of age. Bladder hernia with or without caecum hernia occured in mice given Tx starting within 5 days. The incidence of hernia in female (100%) and male (50%) mice reached plateau at 90 days. Pubic symphysis in Tx mice was significantly longer than that of the controls. Permanent inhibition of pelvic ossification was found in all Tx mice. Development of pelvis was studied in mice of 18-day-fetus to 540 days, using X-rays and differential staining of cartilage and bone. In control mice, ilium was ossified even in 18-day-fetus. But pubis and ischium showed cartilaginous state until at 30 days. After 30 days, they joined together to form a ossified pelvis. In contrast, ossification of the junctional area of pubis and ischium was permanently inhibited in Tx mice. Permanent cartilaginification of pelvis was found in all mice given Tx starting within 10 days of age, but not in mice given Tx after 30 days. Neonatal treatments of mice with clomiphene and nafoxidine induced neither cartilaginification of pelvis nor hernia. These results suggest that inhibition of pelvic ossification is Tx specific effect.

EN 34

CORRELATION BETWEEN PLASMA LEVELS OF TWO GONADOTROPINS AND SEX STEROIDS IN TOADS.
M.Itoh, M.Inoue, and S.Ishii. Dept. of Biol., Sch. of Edu., Waseda Univ. Tokyo.

We previously reported that plasma gonadotropin (GTH) levels of Bufo japonicus showed distinct annual changes. Regression analysis revealed that LH had positive and significant correlation with total androgen in males (r=0.95) and with estradiol (E2) in females (r=0.79). We performed more detailed survey of plasma GTH and sex steroid levels around the breeding period. Blood samples were collected from toads resting under the ground, migrating to a pond, moving around the pond, swimming in the pond and moving on the ground after breeding. In males, GTHs increased suddenly when they came near the pond. Testosterone (T) and 5α-dihidrotestosterone (DHT) started to increase in advance to the rise of GTHs. Low (r=0.27-0.36) but significant correlations were obtained between FSH and T, and two GTHs and DHT. In females, changes of GTHs were similar to those in males. Progesterone (P) showed a rapid increase in paralled with GTHs when toad approached the pond . A rise of E2 preceeded surges of GTHs and P. Correlation analyses revealed that GTHs were positively correlalated with P (r=0.70 and 0.76) but negatively with E2 (r=-0.45 and -0.44). Thus, we could confirm in the field observation that egg maturation and ovulation are induced by P under the influence of GTH in amphibians.

EN 35

PURIFICATION OF GONADOTROPINS OF THE CYNOMOLGOUS MONKEY, MACACA FASICULARIS
[1]H. Ando, [1]S. Ishii and [2]T. Yoshida [1] Dept. of Biol. Waseda Univ., Tokyo 160. and [2]Tsukuba Primate Center for Medical Science N.I.H., Ibaraki 305.

FSH and LH were purified from acetone dried powder of cynomolgous monkey pituitary glands by the ammonium sulfate precipitation method and the successive column chromatographies of the Pharmacia FPLC system with Phenyl-Superose, Superose 12 and Mono Q (for FSH) or Mono S (for LH). Gonadotropic activities were monitored by the following two radioreceptor assay systems : one, for FSH activity, using rat testis receptors and radioiodinated rat FSH, and the other, for LH activity, using rat Leydig cell receptors and radioiodinated human LH. FSH and LH activities were completely separated into different fractions by the Phenyl-Superose chromatography. Final preparations after Mono Q or Mono S were highly active, as increases in the specific activity from the starting material were 720-fold and 410-fold for FSH and LH, respectively. The specific activities of FSH and LH were 1.9-fold and 4.6-fold higher, respectively, than those respective hormones of rhesus monkey (Yamji et al., 1973; Monroe et al., 1970). By the SDS-PAGE, the final FSH and LH preparations migrated as a diffused band at the position of M.W. 22000. The subunits of FSH and LH seem to have a similar molecular weight.

EN 36

BINDING ACTIVITIES OF LUTEINIZING HORMONE-ISOHORMONES IN CYNOMOLGUS MONKEY PITUITARIES.
T.Yoshida[1], K.Ohtoh[2] and F.Cho[1]. [1]Tsukuba Primate Center for Medical Science, N.I.H. and [2]The Corporation for Production and Research of Laboratory Primates, Ibaragi.

Competitive binding activities of luteinizing hormone(LH)-isohormones were studied by the radioreceptor assay using rat Leydig cell fractions as the receptor preparation. Male cynomolgus monkey(Macaca fascicularis) pituitaries were fractionated by isoelectrofocusing technique. Seven LH-isohormones(pI=7.0, 7.5, 8.0, 8.8, 9.1, 9.8~10.3 and 11.5) were obtained. The competitive binding activity of each isohormone was compared with that of hCG by the radioreceptor assay using labeled hCG as the radioligand in the presence or absence of 150mM NaCl. In the absence of NaCl, the binding-inhibition curves of hCG and neutral isohormones yielded similar slopes, while alkaline and highly alkaline isohormones yielded steeper slopes than those of hCG and neutral isohormones. In the presence of NaCl, the binding rates of isohormones except one species were considerably diminished, but binding rates of hCG and highly alkaline isohormone(pI=11.5) were not affected. From these results, we suggest the difference of functional states of the hormone-receptor complex between highly alkaline LH-isohormone as well as hCG and other LH-isohormones.

EN 37

INDUCTION OF GONADOTROPIN SURGE BY STEROID HORMONE IMPLANTATION IN OVARIECTOMIZED GOLDFISH
M. Kobayashi, K. Aida, and I. Hanyu. Dept. of Fisheries, Univ. of Tokyo, Tokyo.

Female goldfish show a GtH surge at the time of ovulation. The occurrence of this ovulatory GtH surge is considered to be mainly controlled by environmental and physiological cues. The present study examined the involvement of some steroid hormones in relation to the occurrence of this GtH surge.

Female goldfish were ovariectomized and testosterone, estradiol, or both steroids were implanted by silastic tubing. As a control, empty tubing was implanted. These fish were kept below 12°C for three months after the implantation, and then the water temperature was raised to 20°C, which is the same method for induction of spontaneous ovulation in goldfish. After the water temperature was raised, some of the steroid implanted fish, especially in the testosterone implanted group, showed a GtH surge which was quite similar to that of the normal ovulatory GtH surge. Control fish showed no marked change in the plasma GtH levels.

These results indicate that the ovarian steroids are one of the important physilogical cues for the GtH surge in goldfish.

EN 38

TWO-CELL TYPE MODEL OF FOLLICULAR ESTRADIOL-17β PRODUCTION IN THE SALMONIDS

Y. Nagahama and S. Adachi
Lab. of Reprod. Biol., Natl. Inst. for Basic Biol., Okazaki.

Our earlier studies based mainly on the use of in vitro incubation experiments using isolated thecal and granulosa cells of vitellogenic amago salmon, Oncorhynchus rhodurus, led to the proposal of a two-cell type model for the follicular production of estradiol-17β. In this model, the thecal cell, under the influence of gonadotropin, secretes aromatizable androgens, mainly testosterone, which are converted to estradiol-17β by granulosa cells. In the present study we have found evidence which indicates that this two-cell type model is applicable to the production of follicular estradiol-17β in four other species of salmonids, the chum salmon (O. masou), the masu salmon (O. masou), the rainbow trout (Salmo gairdneri) and the white-spotted char (Salvelinus leucomaenis). We have also found that the thecal cell from amago salmon and the granulosa cell from rainbow trout could produce the same effect as has been observed using combinations of thecal and granulosa cells from the same species. The reciprocal use of amago salmon granulosa cells and rainbow trout thecal cells is also effective. These findings imply that there may be little species specificity of each of these cells among salmonids.

EN 39

ISOLATION OF ALDOSTERONE-RELEASING SUBSTANCE FROM THE BULLFROG ADENOHYPOPHYSES.

S.Iwamuro and S.Kikuyama. Dept. Biol., Sch. of Educ., Waseda Univ., Tokyo.

We have previously observed that the bullfrog anterior hypophysis contain principle(s) which enhances plasma aldosterone levels in hypophysectomized Xenopus.

Attempt was made to isolate the active substance(s) from the bullfrog adenohypophyses by extraction with acid-aceton and separation by C18 SEP-PAK cartridge, Sephadex G-50 column and RP-HPLC. The 4-5 KD fraction obtained by gel filtration chromatography showed a prominent bioactivity. When this fraction was subjected to RP-HPLC as the final step of purification, an active principle emerged as a main peak at a concentration of approximately 50% AcCN. It has a molecular weight of 4,400 as determined by SDS-PAGE. The isoelectric point is 7.9 as determined by analytical electrofocusing. This substance is as potent as porcine ACTH in promoting aldosterone release from the adrenal glands of hypophysectmized Xenopus juveniles. However, the amino acid composition does not resemble that of ACTHs ever known, since it lacks Arg and Tyr which are invariably contained in the amino acid residues of 1-24 ACTH.

EN 40

ISOLATION OF NEWT PROLACTIN

K. Matsuda, K. Yamamoto and S. Kikuyama. Dept. of Biol., Sch. of Educ., Waseda Univ., Tokyo.

Attempt was made to isolate prolactin(PRL) from the pituitary gland of the newt, Cynops pyrrhogaster pyrrhogaster. PRL-containing fraction was obtained from the acetone-dried pituitary powder by extraction with acid acetone. Then, the extract was subjected to polyacrylamide gel electrophoresis. PRL band was identified immunologically by Western blotting method using antiserum against bullfrog PRL. PRL was eluted from the fast-moving protein band which was identified as PRL, using an electroeluter. The eluate had a marked bioactivity to stimulate collagen synthesis in the tail fin of bullfrog tadpoles. The PRL fraction thus obtained was subjected to reversed phase HPLC. PRL emerged as the main peak at a concentration of approximately 70% acetonitrile. It gave a single band on SDS-polyacrylamide gel electrophoresis and had a molecular weight of 23,700. The isoelectric point was 4.3 when determined by electrofocusing.

EN 41

CHANGES IN HORMONE LEVELS IN TOAD TADPOLES DURING METAMORPHOSIS

K. Niinuma[1], K. Yamamoto[1], N. Mamiya[1], S. Kikuyama[1], M. Tagawa[2], T. Hirano[2].
[1]Dept. of Biol., Sch. of Educ., Waseda Univ., Tokyo. [2]Ocean Res. Inst., Tokyo Univ., Tokyo.

It has been known that thyroid hormone, aldosterone(ALDO) and prolactin(PRL) are involved in metamorphosis. These hormone levels were measured in Bufo japonicus formosus larvae by radioimmunoassay. Since they are of relatively small size, PRL and ALDO were assayed with pooled plasma samples. Thyroxine(T_4) and triiodothyronine (T_3) were extracted from the individual body with methanol, recovery being about 60%. PRL levels elevate as metamorphosis progresses. However, the maximum concentration in toad tadpoles is about one twentieth of that of bullfrog tadpoles. ALDO levels elevate during prometamorphosis, reach maximum at mid-climax and decline at the end of metamorphosis. Both T_4 and T_3 concentrations elevate during prometamorphosis and reach maximum at climax. Relatively lower levels of PRL may account for the rapid metamorphosis in this species.

EN 42

PLASMA PROLACTIN AND OSMOLALITY IN CRAB-EATING FROGS

S. Kikuyama, K. Yamamoto, K. Matsuda, T. Ogasawara*, S. Hasegawa* and T. Hirano*
Dept. of Biol., Sch. of Educ., Waseda Univ., Tokyo. *Ocean Res. Inst., Tokyo Univ., Tokyo

Prolactin (PRL) levels in the plasma of marine frogs, Rana cancrivora kept in various concentrations of sea water (SW) were measured by radioimmunoassay using antiserum against bullfrog PRL. Osmolality of the plasma of frogs kept in fresh water (FW) was 339±10 mOsm/kg. When the animals were transferred into 50 and 75% SW, it elevated upto 556±2 and 735±8 mOsm/kg, respectively, which are slightly above the values of environmental SW. It was confirmed that the elevation of plasma osmolality in the SW-adapted frogs is largely due to the increase in the plasma urea concentration. Average PRL concentration in the plasma of the FW-adapted frogs was 158±39 ng/ml. It declined to 56±10 and 29±8 ng/ml when put into 50 and 75% SW, respectively. Involvement of PRL in osmoregulation in this species is suggested.

EN 43

PRIMARY STRUCTURE OF BULLFROG GROWTH HORMONE

T.Kobayashi[1,2] S.Kikuyama[2] A.Yasuda[3] H.Kawauchi[3] K.Yamaguchi[4] H.Sano[4]
1)Dept. of Basic Human Sciences, Sch. of Human Sciences, Waseda Univ., Saitama. 2)Dept. of Biol., Sch. of Educ., Waseda Univ., Tokyo. 3)Sch. of Fisheries, Kitasato Univ., Iwate. 4)Tokyo Res. Lab., Kyowa Hakko Co. Ltd., Tokyo

Growth hormone(GH) was isolated from adenohypophyses of bullfrog, Rana catesbeiana, by acid-acetone extraction, anion-exchange chromatography and reverse-phase high performance liquid chromatography(rp-HPLC). Amino acid composition of bullfrog GH thus obtained resembles other vertebrate GHs, possessing 4 half-cystines. To determine the amino acid sequence of bullfrog GH, purified GH was reduced, carboxymethylated and subsequently cleaved with cyanogen bromide. GH was also digested with enzymes such as lysyl endopeptidase and trypsin. The resulting fragments were separated by rp-HPLC and subjected to sequence analysis by Edman method. Thus, about 140 amino acids sequence of bullfrog GH has been determined. The amino-terminal 40 amino acid residues show 53%, 70%, 50% and 30% sequence identity with human, chicken, eel and salmon, respectively. The carboxy-terminal 40 residues show 53%, 83%, 83%, and 63% sequence identity with human, chicken, eel and salmon, respectively.

EN 44

ROLE OF INFUNDIBULAR PRIMORDIUM ON THE DIFFERENTIATION OF PITUITARY CELLS IN TOAD TADPOLES (BUFO JAPONICUS).

K. Kawamura and S. Kikuyama, Dept. Biol., Schl. Educ., Waseda Univ., Tokyo 160.

Aim of the present study is to see whether the differentiation of pituitary cells is dependent on infundibular primordium. Anterior part of the neural plate ectoderm was surgically removed from open neurulae. In the operated animals, the melanin granules of dermal melanophore were permanently concentrated, showing no background response. These animals completed metamorphosis slightly later than sham-operated control. The brain regions were fixed and stained with specific antisera against adenohypophyseal hormones. In the experimental group, infundibulum was absent, and the epithelial hypophysis was located away from the normal site without morphological contact with the brain tissue. Neither MSH nor ACTH cells were detectable whereas PRL, GH and TSH cells were invariably present in the epithelial hypophysis. These results implicate an important role of the infundibular primordium on the differentiation of pituitary POMC cells. If these cells originate from the stomodeal ectoderm as is described in classical embryology, induction from the brain seems to be necessary for the differentiation of the cells. It is also conceivable that the pituitary POMC cells are derived from the neuroectoderm itself.

EN 45

Immunocytochemical study of TSH cells in toad tadpoles during metamorphosis.

S. Kurabuchi[1], S.Tanaka[2] and S. Kikuyama[3].
[1]Dept.of Histol., the Nippon Dental Univ., Tokyo. [2]Dept. of Morphol., Inst. of Endocrynol., Gunma Univ., Maebashi. [3]Dept. of Biol., Sch. of Educ., Waseda Univ., Tokyo.

TSH producing cells in the pars distalis of Bufo japonicus formosus tadpoles at different metamorphic stages were identified by peroxidase-anti-peroxidase method using anti-human TSHβ serum. The first sign of immunoreaction appeared in a very cells at stage 35, the reaction being very weak. At stage 40, immunoreactivity and number of TSH-positive cells suddenly increased and they were maintained throughout metamorphosis. In tadpoles deprived of thyroid primordium at external gill stage, immunoreactive TSH cells never appeared even after their hatch-mate completed metamorphosis. When thyroidectomized tadpoles were artificially metamorphosed by thyroxine (T_4), considerable number of TSH-positive cells with an intense immunoreactivity appeared in the pituitary gland. In the pituitary gland which had been autotransplanted to the tail region of the hypophysectomized tadpoles at tail-bud stage, TSH cells were abundant when examined at climax. These results suggest that thyroid hormone is necessary for the development of TSH cells.

EN 46

STIMULATION OF DRINKING BY CAPTOPRIL, AN ANGIOTENSIN I -CONVERTING ENZYME INHIBITOR, IN THE GOLDFISH, CARASSIUS AURATUS.

H. Kobayashi[1] and Y. Okawara[2], [1]Res. Lab., Zenyaku Kogyo Co. Ltd., Nerima, Tokyo and [2]Dept. Pharmacol., School of Med., Univ. of Calgary, Calgary, Canada.

Single intraperitoneal (ip) injections of angiotensin II (ANG II) stimulated water intake for 60 min in a dose related manner in the goldfish, *Carassius auratus*. Single ip injections of captopril (SQ14225), an angiotensin I -converting enzyme (ACE) inhibitor, at lower doses (0.4 and 4.0 µg/fish) stimulated water intake for 60 min. This stimulation cannot be ascribed to an increase in levels of plasma ANG I, since ANG I (2.2 µg/fish) did not stimulate drinking in the presence of SQ14225 (two injections of 9.9 µg /fish). It is suggested that the elevated plasma ANG I concentrations achieved after blockade of ACE was converted into ANG II approximately 50 min after SQ14225 injections (4.0 µg/fish), when the injected SQ14225 was effectively metabolized. Thus, the newly elevated level of ANG II may have been responsible for the vigorous drinking. Higher doses of SQ14225 (40 and 200 µg/fish) did not affect the water intake for 60 min, indicating that the rate of basal water intake is independent of the renin-angiotensin system in the goldfish.

EN 47

ATRIAL NATRIURETIC PEPTIDE(ANP)-LIKE IMMUNOREACTIVITY OF FISH HEARTS.

H.Uemura[1], M.Naruse[2], T.Hirohama[1], S.Nakamura[1] and T.Aoto[1]. [1]Biol. Lab., Kanagawa Dent. Coll., Yokosuka, [2]Dept. of Med., Tokyo Women's Coll., Tokyo.

Hearts of the banded dogfish (*Triakis scyllia*), four species of freshwater (FW) teleosts (*Cyprinus carpio*, *Anguilla japonica*, *Lepomis macrochirus*, *Channa maculata*) and three species of seawater(SW) teleosts (*Hexagrammos otakii*, *Pagrus major*, *Trachurus japonicus*) were studied ultrastructurally and immunohistochemically using antiserum against α-human ANP. Immunoreactive ANP(IR-ANP) in heart tissue and plasma was estimated by RIA.

ANP-immunostained cardiocytes were found in both the atria and ventricles of all species except *Hexagrammos*, being present in far greater number in the former than latter. In *Triakis*, *Pagrus* and *Trachurus*, very little stained material could be detected in only a few cardiocytes. These three species and *Hexagrammos* had fewer electron-dense granules in cardiocytes and a much lesser amount of IR-ANP in the heart tissue compared to the other species. The plasma content of IR-ANP was about 31-91 and 3-16 pg/ml in the FW and SW species, respectively. From these findings, it thus appears that the overall extent of synthesis and release of ANP-like material is greater in the FW species than SW species.

EN 48

EFFECTS OF SALINITY ON ANP-LIKE SUBSTANCE AND ULTRASTRUCTURES IN EEL CARDIOCYTES.

S. Nakamura, T. Hirohama, H. Uemura and T. Aoto. Biol., Lab., Kanagawa Dent. Coll., Yokosuka.

Atrial cardiocytes were investigated immunohistochemically, using antiserum against α-human ANP, and ultrastructurally for (*Anguilla japonica*) adapted to either fresh water or 100% artificial sea water. Dense ANP immunoreactive material (ir-ANP) and numerous secretory granules (about 200 nm) were found situated about the nucleus of cardiocytes in fish adapted to fresh water (control). In fish transferred from fresh water and adapted to sea water for 24 hr, the amount of ir-ANP and number of granules decreased somewhat whereas in fish kept in sea water for one week, they resumed initial values to some extent. Furthermore, in fish transferred to fresh water for 24 hr after having adapted to sea water for one week, these values were recovered to essentially those of the control. From these results, it is evident that the amounts of ir-ANP and number of granules in cardiocytes are closely related, that eel ir-ANP is immunologically related to human ANP, and that ir-ANP in eels plays physiologically important role in adaptation to change of environmental salinity.

EN 49

ATRIAL NATRIURETIC PEPTIDE (ANP)-LIKE PEPTIDE IN THE CARDIOCYTES OF DEVELOPING AND ADULT TOADS.

T. Hirohama, S. Nakamura, H. Uemura and T. Aoto. Biol. Lab., Kanagawa Dent. Coll. Yokosuka.

The ontogeny of ANP-like immunoreactivity and ultrastructures of the cardiocytes in developing and adult toads (*Bufo japanicus formosus*) were studied, using antiserum against α-human ANP. The number of the electron-dense granules (about 115 nm) that could be observed in periphery of the cardiocytes was quite few and all atrial cardiocytes showed weak ANP-immunoreactivity in larvae as early as the limb-bud stage. The number of granules increases rapidly during metamorphosis, and could be seen frequently in the atrial cardiocytes of young toads with tail remnants. In adults, ranules of two different sizes (about 115 nm and 200 nm) could be seen in atrial cardiocytes. Stronger ANP-immunoreactivity and a greater number of secretory granules were found in the right atrium compared to the left atrium of an adult heart. The numbers of granules in breeding (April) and non-breeding (August) animals did not differ significantly. Throughout the life, only a trace of immunoreactivity was detected in ventricular cardiocytes. These results indicate that atrial cardiocytes of toads synthesize a peptide immunologically related to human ANP and which may be essential to land life.

EN 50

IN VIVO CHARACTERIZATION OF ANGIOTENSIN II RECEPTORS AND CONVERTING ENZYMES IN THE QUAIL AND EEL.

Y. Takei. Dept. Physiol., Kitasato Univ. Sch. Med., Sagamihara, Kanagawa 228

As an initial step for comparison of angiotensin II (ANG II) receptors and converting enzymes among vertebrates, pressor potency of ANG I's and II's from the rat, fowl and eel, and effects of ANG II competitive inhibitors and converting enzyme inhibitors on pressor effects of angiotensins, were examined in the quail and eel. Among all angiotensin II's examined, ANG II from the native class of vertebrate (fowl ANG II for quail and eel ANG II for eel) exhibited the greatest pressor potency in the respective species. Among ANG II competitive inhibitors examined, only [Sar^1, Ile^8] ANG II blocked pressor effects of ANG II in both species. Since all ANG II's and competitive inhibitors have similar in the rat, ANG II receptors appear to be different in the rat, quail and eel. Among all ANG I's examined, ANG I from the native class again had greatest pressor potency in the quail and eel. Among converting enzyme inhibitors examined, bradykinin potentiator B and SQ14225 blocked the pressor effect of ANG I in the eel, and only SQ14225 was an effective inhibitor in the quail. Since all inhibitors examined are effective in the rat, converting enzymes also may be different in the rat, quail and eel.

EN 51

INHIBITION OF HCG-INDUCED OOCYTE MATURATION BY PMSF IN INTACT FOLLICLES OF XENOPUS LAEVIS.

K. Ikeo and K. Ishikawa, Biological institute, Faculty of Science, Shizuoka University, Shizuoka.

Human chorionic gonadotropin (HCG) (50 IU per 2 ml medium) induces oocyte maturation [designated as germinal vesicle breakdown (GVBD)] in intact follicles of Xenopus laevis. The objective of the present study was to investigate protease involvement in regulating oocyte maturation induced by HCG.

Experiments were carried out using intact follicles containing follicle cells and oocytes to assess the effect of phenyl methanesulfonylfluoride (PMSF) as an irreversible inhibitor of serine protease. When intact follicles were previously exposed for 60 min at 21°C to PMSF, PMSF (0.7-1.4 mM) was effective in inhibiting HCG-induced GVBD. Intact follicles developed an insensitivity to PMSF some 4 hours after HCG addition which preceded onset of GVBD by one hour. In addition, PMSF inhibited to some degree progesterone production induced by HCG.

In this study, it was suggested that serine proteases in intact follicles may play roles in mediating progesterone production and induction of GVBD by HCG.

EN 52

DIFFERENTIAL ONTOGENIC APPEARANCE OF THE SUBUNITS OF GLYCOPROTEIN HORMONES (LH, FSH AND TSH) IN BULLFROG PITUITARY IN RELATION WITH HYPOTHALAMIC RELEASING HORMONES.

S.TANAKA, Y.TANIGUCHI, M.K.PARK[1] AND K.KUROSUMI. Dept. of Morphol. and [1]Hormone Assay Center, Inst. of Endocrinol., Gunma Univ., Maebashi.

The ontogeny of gonadotrophs and thyrotrophs in bullfrog pituitary was demonstrated by the immunocytochemical technique using anti-human TSHβ serum in addition to monoclonal antibodies (MCAs) against bullfrog LHβ, FSHβ and their α-subunit. Immunoreactive (IR) α-subunit and TSHβ were observed before premetamorphosis (St.24), but IR-FSHβ and LHβ were not. IR-FSHβ appeared earlier than IR-LHβ. At TK St.XV a few gonadotrophs containing FSH and LH were found in ventrocaudal region. However, most gonadotrophs contained only FSH throughout metamorphosis. The number of IR-α-subunit cells was always higher than the total number of IR-β-subunits cells. The ontogenic study suggested that hypothalamic TRH and LHRH may be related with the appearance of each subunit of glycoprotein hormones. At St.24, IR-TRH was first found in the pars nervosa, the primitive median eminence (ME) and some other parts of the brain. During prometamorphosis, a few TRH fibers terminated near some of the pars distalis cells, suggesting direct action of TRH upon these cells. IR-LHRH fibers in the ME were found from TK St.XIII onwards. IR-β-subunits of FSH and LH increased, as the number of IR-LHRH fibers increased (St.XV- XIX).

EN 53

EFFECTS OF SERIALLY ADMINISTERED MDP AND URIDINE ON NOCTURNAL SLEEP IN RATS.

M.Kimura, K.Honda, Y.Komoda and S.Inoué. Inst. Med. Dent. Eng., Tokyo Med. Dent. Univ., Tokyo.

The differential compound-dependent sleep-promoting activity is demonstrated by our 10-h intracerebroventricular (i.c.v.) nocturnal infusion of muramyl dipeptide (MDP, 2.0 nmol) and uridine (10 pmol) in freely behaving rats. The combination-dependent sleep enhancement is also observed by the 10-h i.c.v. simultaneous infusion of MDP and uridine. A serial i.c.v. infusion of uridine (5 pmol/5h) and MDP (1.0 nmol/5h) resulted in a increase in both slow wave sleep (SWS) and paradoxical sleep (PS) which gradually appeared during the uridine-infusion period, and lasted for a few hours even after the termination of the MDP-infusion. The total amount of SWS and PS was significantly larger than that of the baseline level. The time-course pattern of the sleep modulation was quite different from that in the similar experiment in which uridine was replaced by saline. Thus, the pre-existing uridine modified the effect of MDP. In conclusion, the single, the simultaneous, and the sequencial administrations resulted in the different temporal changes in sleep-waking activity. Sleep seems to be regulated by an interaction of multiple sleep factors.

EN 54

MECHANISMS OF DEVELOPMENT OF UTERINE ADENOMYOSIS IN MICE

T. Mori
Zoological Institute, Faculty of Science, University of Tokyo, Bunkyo-ku, Tokyo 113

Adenomyosis is an abnormal growth of glands and stroma into and beyond the smooth muscle layers of uterus. I have reported that ectopic pituitary isografting induces an early and high incidence of adenomyosis in mice associated with hyperprolactinemia. The goal of the present study is to clarify the mechanisms of the development of this uterine lesion.

The results showed that spontaneous development of adenomyosis was significantly suppressed by removal of ovaries between 4 and 10 weeks but not between 10 and 16 weeks of age. It was further found that temporary administration of bromocriptine, a potent suppressor of pituitary prolactin release, between 4 and 11 weeks of age only inhibited spontaneous development of adenomyosis with age. These results suggest that there is a critical period during youth for the spontaneous development of adenomyosis at advanced age. Furthermore, the results showed some morphological disorders of uterus such as glandular hyperplasia, disintegration of muscle cells, dilation of blood vessels, accumulation of collagen in the musculature on the development of experimentally induced-adenomyosis.

The relevance of these histological findings to the hormonal milieu induced by ectopic pituitary grafting is discussed.

EN 55

DIFFERENCES IN FOOD- AND WATER-INTAKES AND GLUCOSE TOLERANCE BETWEEN HIGH AND LOW MAMMARY TUMOR STRAINS OF MICE.

S.Ozawa, T.Iguchi, N.Takasugi and H.Nagasawa*. Dept. Biol. Yokohama City Univ. Yokohama and *Dept. Agri. meiji Univ. Kawasaki.

We have measured the differences in food- and water-intakes, urination, blood glucose level and glucose tolerance between high(SHN) and low(SLN) mammary tumor virus (MTV)-expressed strains and MTV-unexpressed strains (C57BL, BALB/c and ICR) of mice. Three-month-old male and female mice of the five strains were used for this present study. Food- and water-intakes in male and female SHN mice were significantly higher than those in the corresponding sexes of any strains of mice. Nevertheless, SHN mice were not larger in body weight than SLN mice. Urinary volume was significantly higher in SHN than in SLN strain in both sexes. Blood glucose levels were significantly higher only in female SHN mice than in other strains. Glucose tolerance in male SHN mice was significantly lower than in the other strains. These results suggest that SHN mice possess abnormal glucose metabolism. Previous studies demonstrated that there is a close relationship between diabetes and tumor growth. Therefore, it is strongly suggested that the higher incidences of mammary tumors in SHN mice are ascribed partially, at least, to glucose metabolic abnormality, leading to a diabetic state.

EN 56

MAMMARY TUMOR CAUSES HYPERGLYCEMIA IN MICE

N.Nishimura, T.Iguchi, and N.Takasugi.
Dept.Biol., Yokohama City Univ., Yokohama.

Blood glucose levels (BGL) were examined in 7-month-old female SHN mice with spontaneous mammary tumor (MT). BGL in mice with MT were significantly higher than in mice without MT. BGL increased in proportion to the size of MT from 0 to 30 mm in diameter, but decreased when MT reached a diameter bigger than 30 mm. Serum insulin levels in mice with MT were significantly higher than in mice without MT. There were no differences in weights of pancreas and adrenals in mice between the presence and absence of MT. Langerhans' islets having cells with pycnotic nuclei were found in 5 of 10 mice with MT. No difference was found in occupancy of A (10%) and B cell areas (80%) of normal islets between groups of mice with and without MT. Transplantation of MT into male SHN mice raised BGL; mice with MT grafts showed an increase in BGL in proportion to the size of MT grafts. The BGL increase was also found in 10-month-old C57BL female mice with MT grafts. No differences in weights of pancreas and adrenals were found between groups of male SHN and female C57BL mice with and without MT. These findings indicate that 1) there is a correlation between occurrence of MT and hyperglycemia. 2) blood glucose levels increase in proportion to the size of MT. 3) serum insulin levels are markedly high despite the hyperglycemia in female SHN mice with MT.

EN 57

MULLERIAN-INHIBITING ACTIVITY IN CIRCULATION OF QUAIL EMBRYO

A. Ohuchi and T. Noumura.
Dept. Regul.Biol., Fac. Sci., Saitama Univ., Urawa.

We have demonstrated that the Müllerian-inhibiting substance (MIS) in circulation can cause regression of the Müllerian ducts (Md) at a site distant from the testes in the chick embryo (Proc. Japan Acad., 62B, 257, 1986). Then, comparable experiments have been performed in the quail embryo.

Two experimental approaches were designed in the quail embryos which were cultivated in the chicken egg shells: briefly, 2-day quail embryo and egg contents were transferred into a half of the chicken egg shell, sealed the opening with plastic wrap, and continued to incubate at 37.6°C. In the first series, two testes from 8-day embryo were grafted onto the chorioallantoic membrane (CAM) of 6-day female embryo. After four days, female host embryos showed signs of regression in their Mds. In the second series, Md from 7-day female embryo was grafted onto CAM of 8-day male embryo. After three days, only the Mds grafted onto male embryos showed clear signs of regression.

These results suggest that the circulating levels of MIS in the quail embryo, as well as in the chick embryo, may be effective to cause regression of Mds.

EN 58

IMMUNOCYTOCHEMICAL STUDIES ON THE PANCREATIC ENDOCRINE TISSUE IN SOME LOWER VERTEBRATES

K.Miyata[1], Y.Oota[1] and M.Nozaki[2].
[1]Biol. Inst., Fac. of Sci., Shizuoka Univ., Shizuoka and [2]Primate Res. Inst., Kyoto Univ., Inuyama.

Immunocytochemically, the pancreatic endocrine tissue was studied to consider the phylogenetic aspects of cell types and topographical distribution of cells. In the present study, 7 species of lower vertebrates including cyclostome (Eptatretus burgeri), elasmobranchs (Triakis scyllia), teleosts (Carassius auratus), amphibians (Cynops pyrrhogaster pyrrhogaster and Rana tagoi) and reptiles (Geoclemys reevesii and Elaphe quadrivirgata) were examined. For immunocytochemical study, avidin-biotin peroxidase complex method was used. The following antisera obtained from rabbits were used : anti human glucagon, anti human insulin, anti mammalian somatostatin and anti porcin pancreatic polypeptide (PP). Cells containing PP-immunoreactivities are not revealed in all the animals tested. In Eptatretus burgeri, insulin- and somatostatin-immunoreactive cells are found. Although there are species differences in cell distribution, at least three cell types are identified in the rest animals.

EN 59

AN IMMUNOCYTOCHEMICAL STUDY ON THE HATSCHEK'S PIT OF THE AMPHIOXUS

M. Nozaki[1], A. Gorbman[2], and K. Miyata[3].
[1]Primate Res. Inst., Kyoto Univ., Inuyama, [2]Dept. of Zool., Univ. of Washington, Seattle, WA, USA, and [3]Dept. of Biol., Shizuoka Univ., Shizuoka.

Hatschek's pit of the amphioxus has long been postulated to be the ancestor of the vertebrate pituitary gland, with no convincing evidence. In this study, the Hatschek's pit of Branchiostoma belcheri was examined immunocytochemically with regards to a possible hormonal content. Antibodies to various hormonal peptides were used as immunocytochemical probes.

Substance P- and Met-enkephalin-positive immunoreactions were observed in distinct cells of the margin parts of the pit, which correspond to the distribution of electron microscopically granulated cells. Faint immunoreactions to anti-human (h)-LHβ and anti-h-CG were observed in the deepest part of the pit, but other antibodies to pituitary glycoprotein hormones or subunits gave no immunoreaction there (i.e., h-FSHβ, h-TSHβ, salmon (s)-GTH, s-TSH, carp-GTH). No immunoreactivity was obtained with antibodies to hypothalamic hormones (mammalian-LHRH, SRIH-14, AVP), pituitary single hormones (h-PRL, h-GH, porcine (p)-ACTH, α-MSH, s-PRL, s-GH), pancreatic hormones (h-insulin, h-glucagon, p-PP, s-insulin, s-glucagon, s-SRIH-25), or brain-gut peptides (p-CCK, p-VIP, neurotensin).

EN 60

THE EFFECT OF SALMON MELANOTROPIC HORMONES ON ISOLATED MEDAKA MELANOPHORES.

S. Negishi[1], I. Kawazoe[2] and H. Kawauchi[2].
[1]Dept. of Biol., Keio Univ., Yokohama, and [2]Lab. of Mol. Endocr., Sch. of Fish. Sci., Kitasato Univ., Sanriku, Iwate.

The isolated medaka melanophores, which are light sensitive, are utilized to determine MSH activity. Though the scale bioassay of Oryzias are rather insensitive to MSH, the isolated melanophores bioassay, which respond to light with pigment dispersion and dark with aggregation, are remarkably sensitive to MSH. The dark-asgregated melanophores disperse by α-MSH I, N-des-Ac-α-MSH I and β-MSH I isolated from chum salmon, despite of complete lack of illumination. The minimum concentration which is required for melanosome dispersion was 10^{-15} M α-MSH I, 10^{-13} M N-des-Ac-α-MSH I and 10^{-11} M β-MSH I. Melanophores of most cold-blooded vertebrate, which are sensitive to MSH, respond to the hormone at 10^{-6}-10^{-10} M. Therefore, the isolated medaka melanophores are surprisingly sensitive to α-MSH. Light sensitive medaka xanthophores also disperse by similar concentration of α-MSH, though the rate of pigment dispersion is 3 times slower than melanophores. Chum salmon endorphin I (EP) enhances Oryzias melanophore dispersing activity of β-MSH I about 40%, but does not cause pigment dispersion by itself. The mechanism of the enhancement by EP has been unclear. EP may possibly change the affinity of β-MSH to receptors on melanophores.

EN 61

EFFECTS OF AGING ON URINARY AND SERUM PARAMETERS FOR RENAL FUNCTION IN THE WISTAR/TW MALE RATS:I. 3- TO 13-MONTHS-OLD.

Y. Kobayashi, M. Senoo* and K. Hattori.
Dept. of Pharmacol. and *Cent. Res. Lab., Shimane Med. Univ., Izumo.

The Wistar/Tw strain male rats show polydipsia and polyuria after 16 months of age. Morphological changes in renal glomeruli have reported from 3-months-old males. In the present study, urinary and serum parameters for renal function such as urinary volume, urinary protein concentration, urinary and serum creatinine concentration were measured from 3 to 13 months of age. For comparison, the Wistar strain males were used. Urinary volume was smaller in the Wistar/Tw strain through the period and it was significant at 6 months of age. Urinary protein concentration was almost 2-fold in the Wistar/Tw strain through the period and daily excretion of urinary protein was significantly higher at 6 months of age, suggesting the early occurrence of renal failure in the Wistar/Tw strain. Urinary creatinine concentration was not different. Serum creatinine concentration was significantly lower in the Wistar/Tw strain at 4-months-old. Then, relative glomerular filtration rate was significantly lower in the Wistar/Tw strain at 4 months of age, suggesting the dysfunction of glomeruli of the Wistar/Tw males in this period. Serum total protein concentration, blood urea nitrogen value, serum albumin concentration were not different between the strains.

EN 62

CHANGES OF ANDROGEN SECRETION AND HYPERTROPHY OF LEYDIG CELLS AFTER HEMICASTRATION IN MALE RATS.

T.Furuya, K.Miyoshi and M.Hokano. Dept. of Anatomy, Tokyo Medical College, Tokyo.

The hormonal and testicular histological effects of hemicastration were examined using rodent models. Wistar strain rats were hemicastrated at 5, 10, 15, 20, 30 and 40 days of age, and autopsied 30 days after surgery. Hypertrophy decreased as the age at hemicastration approached 15 days and did not occur in rats operated on 20 days of age or older. Serum gonadotropins, plasma testosterone and DHT were measured by RIA. A significant increase in FSH level was noted in the rats hemicastrated at 5, 10, 20 and 40 days when compared to the normal rats, but no difference in LH level was detected. A higher concentration of plasma testosterone was detected in 50 day-old control rats than in hemicastrated rats. In contrast, 70 day-old hemicastrated rats showed plasma testosterone levels higher than in control rats. Plasma DHT in 60 and 70 day-old hemicastrated rats was higher than in control rats. Leydig cells in 70 day-old hemicastrated rats showed more active morphological features than in control rats. The size of Leydig cells, nuclei and mitochondria were larger and sER were more prominent than those in intact rats. Hemicastration at post-pubertal age increases Leydig cell size and androgen production.

EN 63

MORPHOMETRIC ANALYSIS OF SEXUAL DIMORPHISM IN MOUSE PELVIS

Y. Takahashi. Zool. Inst., Fac. of Sci., Univ. of Tokyo, Tokyo.

Sexual dimorphism of the pelvis of the mouse was analysed morphometrically in normal male and female. In adult mice, relative length of pubis was larger in the female, while relative length of ischium and pubic symphysis was larger in the male. Caudal border of ischium was convex in the male, while it was straight or slightly concave in the female. Study of ontogeny of the dimorphism showed that relative length of pubis and shape of caudal border of ischium were different as early as 1 week after birth between male and female. Difference in relative length of pubic symphysis was already apparent at 3 weeks. Relative length of ischium was different at 8 weeks. These observations revealed that the sexual dimorphism appears earlier than ever described. Comparison of adult male, female, and androgen-insensitive mutant male (Tfm/Y) indicated that relatively long pubis and short pubic symphysis were characteristic of female, and that relatively long ischium and convex shape of caudal border of ischium were characteristic of male. This suggests that the former features are estrogen-dependent and the latter ones are androgen-dependent.

EN 64

CHANGE IN BOMBYXIN CONTENT IN THE BRAIN OF *Bombyx mori*.

A.Mizoguchi[1], H.Ishizaki[1], H.Nagasawa[2] and A.Suzuki[2]. [1]Biol.Inst., Fac. of Sci., Nagoya Univ., Nagoya, [2]Dept. of Agr. chem., The Univ. of Tokyo, Tokyo.

Bombyxin from *Bombyx mori*, previously called 4K-PTTH, exhibits the prothoracicotropic hormone(PTTH) activity on the pupal prothoracic glands(PG) of *Samia cynthia ricini*, but does not on the *Bombyx* PG. For the purpose of elucidating the physiological role of this peptide in *Bombyx*, we examined the change in bombyxin content in the brain during *Bombyx* development. The 'PTTH' activity in *Bombyx* brain extracts on *Samia* PG was high(4 units/brain) in the animals immediately after final larval ecdysis(on day-0 of fifth instar, V_0), gradually decreased in the course of larval development(V_3,V_6), and was undetectable in the newly ecdysed pupae(P_0) and pharate adults(PA)(< 0.5 units/brain). Immunoblotting study of the brain extracts using bombyxin antibodies also revealed the quantitative change of bombyxin compatible with the change in the biologic activity. Immunohistochemistry of the *Bombyx* brain demonstrated that bombyxin which accumulated in the 4 pairs of large medial neurosecretory cells was most abundant in the V_0 brain among the developmental stages tested (V_0,V_3,V_6,P_0,PA). The dramatic change of bombyxin content in the brain suggests that this peptide is involved inthe regulation of the development of *Bombyx*.

EN 65

DEVELOPMENTAL CHANGE OF THE CEPHALIC NEUROSECRETORY CELL ACTIVITY OF *BOMBYX MORI* AS REVEALED BY IMMUNOHISTOCHEMISTRY USING MONOCLONAL ANTIBODIES RAISED AGAINST PTTH.

C.Suzuki[1], H.Ishizaki[1], H.Kataoka[2] and A. Suzuki[2]. [1]Biol. Inst., Fac. of Sci., Nagoya Univ., Nagoya, [2]Dept. of Agr. Chem., Fac. of Agr., Univ. of Tokyo, Tokyo.

Mouse spleen cells were cultured for 4 days with an extensively purified *Bombyx* PTTH(22K-PTTH) and fused with NS-1 to produce monoclonal antibodies. Two clones (L101 & L104) produced IgMs which immunostained the brain neurosecretory cells in the medial and lateral regions and the peripheral nerve fibers of corpora allata, the neurohaemal organ for PTTH release. The immunohistochemical results showed that the amount of immunoreactive material disappeared at around the head critical periods for PTTH necessary to larval moulting and larval-pupal commitment. Attempts so far made to demonstrate the immunobinding of these antibodies with PTTH activity turned out unsuccessful. Furthermore, immunoblot analyses with L101 after SDS-PAGE of *Bombyx* brain extracts revealed a single band of 23 kD which disappeared when a heated extract was tested; PTTH is heat-stable. These facts suggset that these antibodies were not directed to PTTH but to other brain peptides which resemble it closely in their purification behavior and are synthesized and released in close association with PTTH.

EN 66

CHANGE IN HEMOLYMPH JUVENILE HORMONE TITER IN THE SILKWORM, Bombyx mori.

S.Niimi, S.Sakurai and T.Ohtaki
Department of Biology, Faculty of Science, Kanazawa University. Kanazawa 920.

Juvenile hormone (JH), released from corpora allata, participates with ecdysteroids in hormonal control of larval molting and metamorophosis in insects. A simple, micro assey system of JH may be indispensable for the study of the role of JH in insect post-embryonic development. We prepared antiserum against JH-I, a major JH of Bombyx mori. Relative reactivity JH-I, II, III and JH-I acid was]00, 20.4, 3.4 and]00%, respectively.

By RIA using this antiserum, change in JH titer in hemolymph was determined from early 4th throug the 5th instar. The titer in the 4th instar was relatively high in early half of the instar and then declined to one-fouth. The titer increased again simultaneously with the molting to the 5th instar but the maximum level was half of that in early 4th instar. It then decreased to low level and increased again after the onset of spinning. During those two large peaks, amall but significant peak was found in late feeding stage. This peak in female occurred one day earlier than that in male.

Change in JH titer was expressed in a summation of JH-I and JH-I acid since the antiserum we used showed the same cross-reactivity to JH-I and acid. We are making an effort to measure the each amount.

EN 67

CHRACTERIZATION OF ECDYSTEROID BINDING PROTEIN (Ecd-BP) IN WING IMAGINAL DISCS OF BOMBYX MORI.

Y.Ishikawa, S.Sakurai and T.Ohtaki
Department of Biology, Faculty of Science, Kanazawa University, Kanazawa 920

Ecdysteroid binding protein(Ecd-BP) in the wing imaginal discs of Bombyx mori was studied using ^{3}H-ponasterone A (PNA) with high specific activity.

Equilibrium Kd of the BP in cytoplasmic and nuclear fractions were 4.1 and 4.3 nM, respectively. Numbers of binding site (NBS) were 49.2 fmole/mg cytosol protein and 341.5 fmole/mg nuclear protein. According to Scatchard analysis, 87.3 $\pm$ 3.2% of the total binding capacities was found in nuclear fraction. Addition of Mg^{++}increased the binding capacity in cytoplasmic fraction, but addition of Ca^{++}decrased it.

Effects of three reagents on the binding capacity were examined. SH blocking reagents, iodoacetic acid and N-ethylmaleimide, inhibited the binding between PNA and Ecd-BP. Arachidonic acid, that exhibited dose-response inhibition on androgen receptor binding capacity in rat glandula prostatica, increased Ecd-BP binding capacity.

Purification of the binding protein is under the progress using ligand affinity chromatography.

EN 68

ECDYSTEROID CONJUGATES IN MATURE LARVAE OF THE FLESH FLY, Sarcophaga peregrina.

K.Sakurai, S.Sakurai and T.Ohtaki
Department of Biology, Faculty of Science, Kanazawa University. Kanazawa 920.

In mature larvae of the flesh fly, Sarcophsga peregrina, ecdysone is rapidly metabolized into polar metabolites (free ecdysteroids and OA and OB), which could be separated on TLC. Very polar metabolity, OA, liberated free ecdysteroid by treatment with snail enzyme. IS-RP-HPLC analysis indicated that the very polar metabolites, OA, are consisted with two major compounds, whose side chain may be modified according to RIA date using two types of antiserum. Hydrolysis of these conjugated ecdysteroids by treatment with phosphatase revealed that one of them was phoaphate ester and the other was not.

When the less polar metabolite was analysed on RP-HPLC, these was no UV absorption in the fraction with high radioactivity. UV spectrum of this fraction showed the maximum absorption at 2]2 nm whereas no absorption at 243 nm which is characteristic to conjugated enone of ecdysteroids. Thus OB appeared to be a fragment of side chain, becouse OB fraction exhibited a high radioactivity which was originally located in the side chain.

EN 69

3-DEHYDROECDYSONE: A MAJOR ECDYSTEROID PRODUCED BY PROTHORACIC GLAND OF THE TOBACCO HORNWORM, MANDUCA SEXTA.

S. Sakurai[1], S. Kiriishi[1], J.T. Warren[2], D.B. Rountree[2] and L.I. Gilbert[2]
[1]Dept. of Biol., Fac. of Sci., Kanazawa Univ. Kanazawa 920 and [2]Dept. of Biol., Univ. of North Carolina, N.C. 27514, U.S.A

It is generally accepted that prothoracic glands produce ecdysone. When protein fraction of hemolymph was added to the in vitro incubation of larval or pupal prothoracic glands of Manduca sexta, ecdysteroid content of the medium was increased by 8-fold. Comparative increase was observed when only the medium preconditioned with prothoracic glands was added with the protein fraction. A combination of analytical techniques (NMR, CD, MS) demonstrated that the major ecdysteroid released from the glands is a mixture of 2-dehydroecdysone and 3-dehydroecdysone (1:2), which is promptly converted into ecdysone if incubated with the hemolymph protein fraction.

Comparative study showed that the major ecdysteroid secreted by ring gland of Sarcophaga peregrina and prothoracic gland of Bombyx mori is ecdysone whereas the glands of Papilio xuthus, P. protenor, P. machaon and Mamestra brassicae released dehydroecdysones as a major ecdysteroid.

EN 70

IN VITRO BIOSYNTHESIS OF JUVENILE HORMONE III BY THE CORPORA ALLATA OF THE COCKROACH, DIPLOPTERA PUNCTATA, DURING LARVAL LIFE.

S.Kikukawa[1] and S.S.Tobe[2], [1]College of Liberal Arts, Toyama Univ., Toyama and [2]Dept. of Zool., Univ. of Toronto, Toronto.

The rates of Juvenile Hormone (JH III) release by the corpora allata (CA) were determined in female larvae (I to IV instars) of the viviparous cockroach, Diploptera punctata, using an in vitro radiochemical assay. Higher rates were observed in the latter half of larval stadia I-III, whereas JH release was undetectable in the latter half of the final (IV) stadium. These findings suggest that the 'critical period' for JH sensitivity may not be correlated with the period of increased JH synthesis. Thus, a reexamination of the 'critical period' was necessitated, using allatectomy and denervation of the CA. These data provide insights into the endocrinological programming of larval-larval molts and metamorphosis.

EN 71

ISOLATION AND CHARACTERIZATION OF ECDYSTEROID CONJUGATES FROM OVARIES OF BOMBYX MORI

E.Ohnishi[1], Y.Fujimoto[2], M.Hiramoto[2], and N.Ikekawa[2]. [1]Dept. of Biology, Fac. of Sci., Nagoya Univ., Nagoya and [2]Dept. of Chem., Fac. of Sci., Tokyo Inst. of Technol., Tokyo.

In ovaries of Bombyx mori, ecdysteroids accumulate in free as well as conjugated forms. Major components of the free forms have been identified as follows: ecdysone, 20-hydroxyecdysone, 2-deoxyecdysone, 2-deoxy-20-hydroxyecdysone, 2,22-dideoxy-20-hydroxyecdysone and bombycosterol. Isolation of the conjugates was achieved by the combination of liquid chromatography on Sephadex G15, silicic acid, and Sephadex LH-20 with high performance liquid chromato graphy. Six ecdysteroid conjugates have sofar been isolated. Upon incubation with snail juice or alkaline phosphatase from calf intestine, they yielded free ecdysteroids of the structures above mentioned, indicating that they are phosphate esters. This supposition was supported by the results of fast atom bombardment mass spectrometry. Analysis by use of proton magnetic resonance revealed that 4 of them are 22-phosphate and 2 are 3-phosphate. Further analysis is now in progress.

EN 72

EXTRACTION AND PARTIAL PURIFICATION OF SUMMER-MORPH-PRODUCING HORMONE IN THE ASIAN COMMA BUTTERFLY, POLYGONIA C-AUREUM L.

K. Endo, T. Masaki and K. Kumagai*. Environ. Biol. Lab., Biol. Inst., Fac. of Sci., Yamaguchi Univ, Yamaguchi. * Biol. Inst., Fac. of Liberal-Arts, Yamaguchi Univ., Yamaguchi.

In the Asian comma butterfly, Polygonia c-aureum, a physiological system underlying the photoperiodic control of seasonal morphs was shown to involve a factor producing summer morphs (SMPH). The Polygonia SMPH as well as a Bombyx factor showing SMPH-activity could be extracted with 2% NaCl, but unsuccessful with acetone or 80% ethanol. Doses of the SMPH and 4K-PTTH (bombixin) were evaluated by Polygonia and Papilio pupal assays, respectively. Bioassay for SMPH was made on the basis of the color of the wings.

The SMPHs were thought to be peptide hormones since it could be precipitated by ammonium sulfate and were inactivated by hydrolizing the extracts with trypsin. Molecular sizes of Polygonia and Bombyx SMPHs were estimated to be about 4,500, which were judged as being almost the same size as bombixin (4K-PTTH: M.W. 4,400) on the basis of the gel-filtration pattern through Sephadex G-50. But, based on the chromatographs of reversed-phased HPLC, the factors showing SMPH- and 4K-PTTH-activities were judged as being different.

EN 73

IN VITRO SYNTHESIS OF VITELLOGENIN BY FAT BODY AND OVARY OF ARMADILLIDIUM VULGARE.

S. Suzuki*, K. Yamasaki** & Y. Katakura***. *Biol. Lab. Kanagawa Pref. Col., Yokohama. **Dept. Biol. Tokyo Metropol. Univ., Tokyo. ***Dept. Biol. Keio Univ., Yokohama.

Vitellogenin (Vg) synthesis was investigated in vitro tissue culture at each molting stage during vitellogenesis. Synthesized Vg was analyzed by polyacrylamide gel electrophoresis.

The fat body synthesized four forms of Vg, mainly Vg·1-2, and the rate of Vg synthesis was correlated with the molting cycle: low levels at stages A-C, E and a maximal level at stage D. Each form of Vg appears to be synthesized respectively in the fat body. The ovary also synthesized a slight amount of Vgs at stages D and E of the molting cycle. The lower forms (Vg·3-4) were synthesized, not the higher (Vg·1-2) in the ovary. The fat body from Y-organ ectomized females maintained very low synthetic level of Vgs. By the injection of 20-hydroxyecdyson, a slight induction of Vg synthesis was observed in vitro fat body culture.

These results indicate that in A. vulgare most of the Vg may be synthesized by the fat body at stage D of the molting cycle, although vitellogenin synthesis could not be induced by the molting hormone.

EN 74

ON THE MORPHOLOGICAL COLOR CHANGE AND NEUROSECRETORY SYSTEM IN THE MANTIS, TENODEA ARIDIFOLIA

K.Iwatani and Y.Oota. Biol. Inst., Fac. of Sci., Shizuoka Univ., Shizuoka.

Like other insects, mantises display two types of morphological color change : green and dark body coloration (BC). The BC changes in relation to environmental factors such as temperature, photoperiod and humidity. Usually, the pigment modifications are associated with developmental stages. The present experiment was undertaken to investigate the fine structural changes of the brain-corpora cardiaca (CC)-corpora allata (CA) system during different phases of the developmental stages at various experimental conditions. During first instar, the larvae display the dark BC. In the proceeding instar, the BC of larvae exhibit a responsible reactions. Environmental factors such as constant lightness, green background and wet humidity cause green BC. On the other hand, constant darkness, brown background and dry humidity cause dark BC. On the basis of electron microscopic studies of the brain-CC-CA system, considerable difference is demonstrated in the CC. One of the remarkable feature of the CC in the dark BC animal is the presence of numerous electron-opaque granules.

EN 75

ANNUAL CHANGES IN BIDDER'S ORGAN IN BUFO JAPONICUS FORMOSUS: HISTOLOGICAL OBSERVATION.

Yoshiyuki Moriguchi and Hisaaki Iwasawa. Biol. Inst., Niigata Univ., Niigata.

Annual changes in germ cells and follicle cells in Bidder's organ were studied histologically. Secondary oogonia and leptotene•zygotene•pachytene-stage oocytes markedly increased in number in June. In July, however, the development of oocytes was remarkably retarded, and remained in this condition through the autumn months, and no yolk accumulation was observed in hibernating toads, though yolk deposition began in the summer months in ovarian oocytes. Numerous degenerated oocytes were seen in March. It seems, therefore, that most oocytes in Bidder's organ degenerate during the hibernating period. The fine structure of oocyte-follicle complex in Bidder's organ was quite similar to that in the oocytes in the previtellogenic stage in the ovary. In Bidder's organ, however, a considerable amount of interstitium was seen, and the nuclei of the follicle cells were more ellipsoidal in shape, especially in August-September specimens, than those in the ovary. Well-developed oocyte-follicular cell interdigitations were seen through the year, and no remarkable change was recognized in this structure.

EN 76

ULTRASTRUCTURAL STUDY ON RESPONSIVENESS OF SPERM TRANSPORT ROUTE AT HCG-INDUCED SPERMIATION IN RANA NIGROMACULATA.

Tohru Kobayashi and Hisaaki Iwasawa. Biol. Inst., Niigata Univ., Niigata.

The responsiveness of the sperm transport route was examined electron-microscopically 0 and 20 min. and 2 and 4 days after hCG injection (low dose; 3.3, high dose; 15 IU/g B.W.) in adult summer frogs. In the control frogs, the cells of efferent duct-linked seminiferous tubules with the nephron were characterized by filament-rich cytoplasm in all regions of the intratestis, ductuli efferense, and intrakidney. After the treatment, a remarkable development of ER and Golgi complex was seen in these cells, and the swelling of cytoplasm was also observed irrespective of the passage of spermatozoa. In the cells of the renal tubules, no noticeable changes were seen, even though spermatozoa passed through the tubules. The epithelial cells of the ampullar portion of the Wolffian duct released PAS-positive granules after the treatment, and the release of numerous granules was recognized 4 days after the high dose-treatment. The passage of spermatozoa in each route was recognized at the all fixative times in the high dose-treated group, but was not recognized in the route beyond the intratesticular efferent duct in the low dose-ones.

EN 77

CIRCANNUAL CHANGES IN PLASMA CONCENTRATION OF GLUCOSE IN TOADS, BUFO JAPONICUS.

K.Kubokawa and S.Ishii. Dept.Biol., Waseda Univ., Tokyo.

Studying circannual changes of plasma corticosterone and aldosterone levels, Jolivet-Jaudet et al.(Ref.1,2) suggested a possibility that aldosterone is the main glucocorticoid and corticosterone is the main mineralocorticoid in the toad, *Bufo japonicus*. In order to examine this possibility, we studied the monthly change of the plasma glucose level with the same materials which were used in the previous corticoid studies. Among plasma levels of corticoid and weights of the liver and fat body, only aldosterone showed a high and significant positive correlation with glucose. The peaks of glucose and aldosterone were preceded by a sharp peak of the fat body and followed by a rapid increase of the ovarian weight which is due to the yolk accumulation. This sequence of events supports the idea that aldosterone stimulates supply of glucose to the plasma from the fat body. In breeding period, we measured the plasma concentration of glucose. The glucose level increased tremendously when toads came into water. It have shown that PRL, T4, LH and FSH also increased. These results indicate that when toads breed in the pond, a number of regulatory mechanisms becomes active simultaneously. Ref. 1. Jolivet-Jaudet,G. et al.(1984)Zool.Sci.1,317: 2.Jolivet-Jaudet, G.et al.(1984)Gen.Comp.Endcrinol.53,163.

EN 78

EVOLUTION OF GONADOTROPIN MOLECULES IN VERTEBRATES

Susumu Ishii, Department of Biology, Waseda University, Nishi-Waseda 1-6-1, Tokyo 160

We have limited information to discuss the molecular evolution of gonadotropins, as the complete or even partial amino acid sequence of gonadotropin has been reported only in mammals and fishes. The author calculated the sum of the difference of the content of each amino acid residue for all amino acids except Cys and Trp between two hormones, and used the sum as a quantitative index to show the difference of the two hormones. The index between homologous FSH and LH was least in amphibians and largest in mammals. This indicates that the difference of FSH and LH molecules is larger in phylogenically higher vertebrates. When LHs of various vertebrates were compared with Bufo LH, the index was also larger when higher vertebrates were compared. When FSH was similarly compared, the indice or differences did not show any tendency. Detailed comparisons of various LHs with Bufo LH revealed that the content of Pro was larger in higher vertebrates, while the contents of Lys and Asp (or Asn) were less in higher vertebrates. These results show that the evolution of the LH molecule has a certain direction, while that of the FSH molecule is relatively random. The observed change of the LH molecule may be the first example of the molecular orthogenesis in peptide hormones.

EN 79

EFFECT OF PROLACTIN AND TESTOSTERONE ON THE NEWT MAUTHNER NEURON.

Y. Suzuki and S. Kikuyama*
Lab. Biol., Dept. Lib. Arts, Asia Unib., Musashino-shi, Tokyo and *Dept. Biol., Sch. Edu., Waseda Univ., Shinjiku-ku, Tokyo.

There is evidence that Mauthner neurons in the medulla oblongata play a roll in tail movement in some amphibians as well as in fishes. During the breeding season the male newt (Cynops pyrrhogaster) vibrates his tail vigorously to perform the courtship behavior in front of the female. Morphological study revealed that the nuclear volume of the Mauthner neuron both in male and female newts captured in the breeding season was larger than that in the newts in the non-breeding season and that in the breeding season the nuclear volume is much greater in the male than in the female. Implantation of testosterone (T) pellet to hypophysectomized newts increased the nuclear volume of the Mauthner neuron to some extent. Administration of prolactin (PRL) makedly increased the nuclear volume of the Mauthner neuron in the newts bearing T pellet. The present result, together with the previously obtained results that treatment of the male newt with PRL and T elicits the courtship behavior and cloacal gland development, indicates that PRL is playing important rolls in reproduction in the male newt.

EN 80

CHANGES IN PRL CELL BY THE ADDITION OF TRH OR DA IN VITRO.

T. Shinkai[1], M. Takahashi[2] and H. Ooka[1].
[1]Dept. of Biol., and [2]Cell Cult. Lab., Tokyo Metropol. Inst. of Gerontol., Tokyo.

Rat pituitary PRL cells are subdivided into three types : small secretory granule type (PI), mean granule type (PII) and large granules type (PIII). We observed morphological changes in female rat PRL cells in primary culture for 4 days by the addition of TRH or DA using immunocytochemical technique. PRL cells which were cultured in the absence of TRH or DA had large granules, parallel-arrayed rough endoplasmic reticulum (RER) and developed Golgi apparatus (GA). Ultrastructurally, they were similar to PIII. TRH (10^{-7}M) increased PRL levels in vitro. The secretory granules changed into those of PII by the addition of TRH but other features of the cells were not similar to PII. Many PRL cells showed highly active synthesis and secretion, and a few of them had RER which changed into vacuoles. These results suggest that the PRL cells stimulated by TRH contain immature granules which resemble those of PII in shape and size. DA (10^{-4}M) decreased PRL levels in vitro. Decay of RER and GA, and increase of lysosome were observed in the cytoplasm. These ultrastructural features of PRL cells indicate inactive synthesis and release of PRL.

EN 81

AGE-RELATED CHANGES IN PROLACTIN RELEASE BY LACTOTROPIC CELLS OF FEMALE RATS IN VITRO.

M.Takahashi[1], T.Shinkai[2] and H.Ooka[2], [1]Cell Cult.Lab.,[2]Dept.of Biol., Tokyo Metropol. Inst. of Gerontol.,Tokyo.

To study the possible mechanisms involved in hyperprolactinemia in aged rats, anterior pituitary cells from young(6 mo.) and old(22 mo.) female rats were cultured in vitro to examine the basal prolactin(PRL) release and responsibility to dopamine and TRH. The basal PRL release of 10^3 PRL cells from young and old rats were 23.5 and 21.8 ng,respectively, however, no significant difference was found between the two values($p>0.05$). Dopamine at concentration in the range from 10^{-7} to 10^{-3} M inhibited the PRL release of the cells from young rats in a dose-dependent manner. Similar inhibitory effect of dopamine was also observed for the cells from old rats . Contrary this, the PRL cells from old rats were more responsible to TRH than those from young rats with respect to the PRL release, that is, the PRL release of the cells from old rats was significantly stimulated by 10^{-10} M TRH, whereas the cells from young rats was responsible to 10^{-9} M TRH. The present results suggest that the increased susceptibility of the PRL cells to TRH in aged rats may be involved in age-related hyperprolactinemia in vivo.

EN 82

INDUCTION OF METAMORPHOSIS IN THE LARVAL LAMPREY. III. THE EFFECT OF PINEALECTOMY.

Shintaro Suzuki. Dept. of Comp. Endocrinol., Inst. of Endocrinol., Gunma Univ., Maebashi.

The Larval lampreys, Lampetra reissneri were pinealectomized by making a longitudinal incision. After one week these larvae were treated with potassium perchlorate. At 50 days after treatment metamorphosis was induced in the larger larvae. Completely metamorphosed larvae were obtained at 100 days after treatment. In these larvae thyroid follicles were formed from endostyle, as seen in spontaneous metamorphosis. However,in the smaller larvae partial metamorphosis was induced.Oral apertures, branchiopores, and eyes were at different metamorphic stages, and the cell type 1 of the endostylar cells degenerated and no thyroid follicles were formed, even after prolonged treatment. On the other hand, the larvae which were not treated with potassium perchlorate after pinealectomy did not metamorphose, and the plasma thyroxine levels were high, as in intact larvae. In the larvae treated with potassium perchlorate after pinealectomy, the plasma thyroxine levels were very low. These results suggest that pineal complex is not involved directly in the metamorphosis of the larval lamprey.

EN 83

A COMPARATIVE STUDY FOR IN VITRO RESPONSE OF THYROID GLANDS BY THYROID STIMULATING HORMONES IN MAMMALS AND AVES

M. Sato, H. Sakai, S. Wakabayashi and T. Yoshida* Dept of Biol., Nihon Univ. School of Dentistry, Tokyo, and *Tsukuba Primate Center for Medical Science, N.I.H., Tsukuba-gun.

To establish thyroid stimulating hormone (TSH) bioassay, in vitro responses of thyroid glands by TSH were determined with Japanese quails, newly hatched cockerels, mice and monkeys. When quail thyroid glands were tissue-cultured in medium containing TSH preparation, the release of thyroxine (T4) from the glands showed significant increase after 2 hours. With mice and monkeys, it took more than 6 hours to reveal the same significant T4 increase, and the ratios of increase in both animals were similar. On the other hand, thyroid glands of any of the animals showed the same response using TSH from any of the animals. Seasonal changes in the response of avian thyroid glands were observed. Different response from mice could be ascribed to diurnal effects. These observations indicate that the responses of thyroid glands between mammals and aves differ, and that the thyroid glands used did not show high specificity to TSH from the animals.

EN 84

CHANGES IN THYROID HORMONE CONCENTRATIONS IN DEVELOPING CHUM SALMON.

Masatomo Tagawa and Tetsuya Hirano. Ocean Research Institute, Univ. Tokyo, Tokyo.

In order to examine the role of thyroid hormones during early developmental stages of chum salmon, techniques were developed and validated for quantitative extraction of thyroid hormones from eggs, embryos and juveniles, and changes in the hormone concentrations in tissue and plasma were examined.

Significant amounts of both thyroxine (T4) and triiodothyronine (T3) were found in unfertilized eggs, and the same levels were maintained until hatching. The embryonic thyroid follicles were still small in number and in size at hatching. During the course of yolk absorption, whole body concentrations of T4 and T3 decreased steadily, and then tended to increase temporarily toward the end of yolk absorption. Both T4 and T3 were detected in plasma during later stage of yolk absorption, and their concentrations increased gradually. T3 levels in both whole body and plasma were always lower than the T4 levels. Embryonic thyroid gradually developed during the yolk absorption, and looked mildly activated thereafter. These findings suggest an important role of maternal thyroid hormones during early development, followed by activation of the larval thyroid after the yolk absorption.

EN 85

cDNA CLONING OF THE PORCINE THYROTROPIN β-SUBUNIT

T.Hirai[2], H.Takikawa[2], Y.Kato[1]. Dept. of [1]Protein Chemistry and of [2]Pharmaceutical Chemistry, Inst. of Endocrinol., Gunma Univ., Maebashi.

A porcine anterior pituitary cDNA library was constructed in expression vector λgt11. Three clones for the precursor of the β-subunit of thyrotropin (pre-TSHβ) were identified by hybridization with a synthetic nucleotide probe (85mer) and with a DNA fragment encoding human TSHβ (Hayashizaki et al. 1985)[a].
The nucleotide sequence of these clones were determined. These clones cover a part of the signal sequence, the entire sequence of mature protein, and 3'-untranslated sequence. The nucleotide sequence showed that the mature protein of porcine TSHβ consist of 118 amino acid residues. In comparison with the amino acid sequence of secretory form of porcine TSHβ (Pierce et al. 1971)[b], there are four differences, and the extended carboxyl terminus of six amino acid residues. The nucleotide sequence of cording region have a homology of 90% for human, 93% for bovine, 84% for mouse, and 83% for rat. Northern analysis showed that the length of porcine pre-TSHβ mRNA is about 500 bases with no heterogeneity.

a) FEBS LETTERS 188, 394-400
b) Recent Prog. Horm. Res. 27, 165-212

EN 86

PURIFICATION AND CHARACTERIZATION OF BULLFROG THYROTROPIN

M.Sakai, H.Takasu, S.Kikuyama, S.Tanaka[1], Y.Hanaoka[1] and H.Hayashi[1]
Dept. of Biol., Sch. of Educ., Waseda Univ., Tokyo. [1]Inst. of Endocrinol., Gunma Univ., Maebashi

Thyroid-stimulating hormone(TSH) was purified from the pituitary glands of bullfrogs, Rana catesbeiana, using ethanol precipitation, hydrophobic interaction and anion exchange chromatography, and affinity chromatography employing monoclonal antibodies against bullfrog LH and FSH β. This preparation was eluted from TSK G3000SW column as a single peak and its molecular weight was estimated to be about 32,000. Its bioactivity, as measured by the *in vitro* release of T_4 from the thyroid glands taken from hypophysectomized prometamorphic bullfrog tadpoles was about 2 times higher than that of bovine TSH. Thus, we concluded that this preparation is exactly TSH. Isoelectric focusing electrophoresis revealed that this TSH is of multiple isoelectric points, ranging from 4.5-5.0. Bullfrog TSH was separated into two subunits by reverse-phase HPLC after dissociation. One of these was bound to a monoclonal antibody against bullfrog FSH α, and the other to a polyclonal antibody against human TSH β, but not to monoclonal antibodies against bullfrog FSH and LH β. Bullfrog TSH β thus identified, consisting of about 100 amino acid residues,seems to be of more acidic and hydrophilic nature than human one.

EN 87

THE PRESENCE OF THYROID HORMONE BINDING PROTEINS IN PLASMA OF BULLFROG.

K. Yamauchi, S. Koya, R. Horiuchi and H. Takikawa.
Institute of Endocrinology, Gunma University, Maebashi.

Using affinity labeling with N-bromoacetyl [^{125}I]-L-triiodothyronine (T_3), the presence of a distinct T_3 binding protein (T3BP) was demonstrated in the plasma of metamorphosing tadpoles and adult bullfrogs, respectively. The both proteins showed higher affinity for T_3 than for L-thyroxine. Tadpole type T3BP was found anodal to albumin on polyacrylamide gel electrophoresis, and was 54 K dalton protein composing of four subunits. The molecular features resembled those of human thyroxine binding prealbumin. On the other hand, adult type T3BP was found cathodal to albumin, and was 56 K dalton protein composing a single peptide. The replacement of tadpole type T3BP by adult type T3BP took place at stage XXIV. Since thyroid hormone levels in bullfrog blood increase during prometamorphosis and decrease at metamorphic climax, tadpole type T3BP might be important as thyroid hormone carrier.

EN 88

EFFECTS OF PHOTOPERIOD AND TEMPERATURE ON PLASMA T_3 AND T_4 LEVELS IN THE DJUNGARIAN HAMSTER.

A. Masuda[1], K. Tsutsui[2] and T. Oishi[1].
[1]Dept. of Biol., Nara Women's Univ., Nara, [2]Dept. of Zool., Hiroshima Univ., Hiroshima.

We investigated the effects of photoperiod and temperature on plasma thyroid hormones and testosterone levels in the Djungarian hamster. In Experiment I, adult male hamsters were maintained in conditions of four combinations of photoperiods and temperatures (LD16:8-25°C; LD8:16-25°C; LD16:8-7°C; LD8:16-7°C). After 8 weeks, plasma T_3, T_4 and testosterone were measured by radioimmunoassay. Plasma T_3 level was significantly higher at low temperature than at high temperature, regardless photoperiods. At high temperature, plasma T_4 level was significantly higher in long day than in short day. Plasma testosterone level was also higher in long day than in short day. In Experiment II, male hamsters were maintained in three conditions (long day, short day and short day with testosterone implantation) for 19 weeks. Plasma T_4 level of testosterone implanted hamsters in short day was higher than that of short day control and similar to the value of long day control. In conclusion, 1) Plasma T_3 level was increased by low temperature. 2) Plasma T_4 level was increased by long photoperiod, probably due to the high plasma testosterone level.

MO 1

OVARIAN STRUCTURE AND OOGENESIS OF PYCNOGONIDS

K.Miyazaki and T.Makioka. Inst. of Biol. Sci., Univ. of Tsukuba, Ibaraki.

The subphylum or class Pycnogonida is a small group of marine arthropods. Some problems remain concerning the phylogenetic relationships of pycnogonids among the arthropod groups. In the present study, we examined the ovarian structure and oogenesis in 10 species, including 4 families, of adult pycnogonids in order to compare them with those in the chelicerates and mandibulates. In most species, the tubular ovary was localized in the trunk and legs on the dorsal side of the gut. A cord-shaped germarium including the oogonia was present in the dorsal ovarian epithelium through almost the entire length of the ovary as in chelicerates. The growing oocytes occurred in the ovarian cavity as in mandibulates, and in most species, they were found only in the pedal ovarian branches. However, they were not arranged in a line in order of size as seen in mandibulate ovarioles. In Propallene longiceps, the tubular ovary was localized only in each leg, and the germarium was not found. No follicle cells occurred in any species as in horseshoe crabs. Thus, pycnogonids have both chelicerate-like and mandibulate-like characteristics in ovarian structure and oogenesis.

MO 2

Ultrastructure of the tooth of sea urchin, Hemicentrotus pulcherrimus.

O.Ochi and M.Watanabe. Dept.of Biol.,Fac. of Sci.,Ehime Univ.,Matsuyama.

Morphological investigations on teeth of Hemicentrotus pulcherrimus isolated by maceration in antiformin or decalcified by ascorbic acid solution and energy dispersive X-ray microanalyses on the teeth were performed. No great difference between the tooth and the other Echinoid one described by Märkel, Chen, et al. is recognized.
The teeth are divided into the plumula (growth region), the shaft and the chewing part. They are used up during chewing and continually renewed. The tooth skeleton is composed of two rows of tooth elements sticking alternately one within the other. Each element consists of the primary and secondary plates and the lamellae-needle-complex, and its carcareous deposits are formed intercellularly by syncytial odontoblasts. Secondary calcareous deposits unite the tooth elements to form the complete tooth skeleton. The secodary deposit and the greater part of the tooth element are composed of almost $CaCO_3$, but hardest part of the tooth, the stone part, has a high amount of $MgCO_3$ (about 2 per cent).

MO 3

ABSENCE OF THE PINEAL IN THE ELECTRIC TELEOST, GYMNARCHUS NILOTICUS.

K. Tsuneki. Dept. of Biol., Shimane Univ., Matsue.

Although there are several vertebrate genera that lack the pineal (e. g. Myxine, Torpedo, Crocodilus, etc.), no teleosts have been known to lack the pineal. However, in the course of histological study of the brain of various teleosts, I found that the electric teleost, Gymnarchus niloticus, lacks the pineal. In the epithalamic roof, the saccus dorsalis is highly folded, but there is no pineal stalk here. In front of the saccus dorsalis, the paraphysis extends rostrodorsally. The tip of the paraphysis is sacculated, but it does not contain the pineal end-vesicle.

For comparison, I studied the epithalamic region of several electric teleosts (e. g. Malapterurus, Electrophorus, Eigenmannia, Sternarchella, etc.). All these possessed a well-developed pineal. According to the literature, blind or semi-blind teleosts living in the cave or in the deep sea possess a well-developed pineal.

The reason why only Gymnarchus niloticus lacks the pineal is unknown, but this is the first demonstration that there is a teleost without the pineal.

MO 4

STUDIES ON THE KIDNEYS AND URINARY BLADDERS OF THREE ANTARCTIC TELEOSTS.

Mizuho Ogawa, Dept. of Biology, Fac. of Liberal Arts and Science, Saitama Univ., Urawa, Saitama, 338, Japan.

The structures of the kidneys and urinary bladders of the three Antarctic teleosts, Pagothenia borchgrevinki, Trematomus bernacchii and T. hansoni were compared.

It was reconfirmed that their kidneys are aglomerular. It was found that their bladders are well developed in size. In the first two species, the bladder epithelium is composed of tall columnar cells continuous with the collecting tubule and which gradually transform to low columnar cell near the cloaca. The epithelium of T. hansoni, however, is composed of simple cuboidal cells that cover the whole surface of the bladder. Although T. hansoni is a mid-water fish, P. borchgrevinki is adapted to life in and under the platelet ice and T. bernacchii dwells on or near the sea floor. These two fishes are exposed to different osmolalities during the freezing and the thawing seasons. It is therefore necessary for them to produce dilute urine under hypotonic condition during the thawing season. This situation appears to be similar to that occurring the bladder of euryhaline marine fishes during their migrations into brackish environments.

A functional difference in the urinary bladder between these two Antarctic teleosts and T. hansoni is suggested.

MO 5

LIGHT AND ELECTRON MICROSCOPIC STUDIES ON THE LUNG OF HYNOBIUS NEBULOSUS TOKYOENSIS.

T.Gomi, Y.Kikuchi, A.Kimura, Y.Ishikawa, T.Hashimoto and K.Kishi. Dept. of Anat., Sch. of Med., Toho Univ., Tokyo.

The lungs of the Hynobius nebulosus tokyoensis were observed by light and electron microscopy (SEM, TEM). In this species, the lungs were mainly divided into two groups, airway portion and respiratory portion. Smooth muscles were well developed in the airway portion. Elastic fibers and collagen fibers were more developed in the respiratory portion than in the airway portion. In the airway portion, ciliated cells and goblet cells were seen to exist. In the respiratory portion, epithelial cells were cuboidal or columnar in shape. In the cytoplasm of these cells, osmiophilic lamellated bodies were found to exist, and their secreting figures were observed. Moreover, these cells possessed the features of both Type I and Type II alveolar cells, demonstrating membranous cytoplasmic projections which extended from the lateral surface of the cell and covered the capillaries. The most characteristic feature was the presence of the secretory granules containing material of moderate electron density, which were found under the cell surface. These granules proved to be PAS and colloidal iron reaction positive. Sudan black B positive granules existed in the cytoplasm of the alveolar epithelial cell.

MO 6

FIN RESORPTION IN TAIL OF THE AXOLOTL DURING METAMORPHOSIS.

H.Takahama, T. Kinoshita, F. Sasaki and K. Watanabe. Dept. of Biol., School of Dent. Med., Tsurumi Univ., Yokohama.

Morphological changes of the dermis in the tail fin of an axolotl(Ambystoma mexicanum) which induced metamorphosis by T3 administration were observed by light and electron microscopy. The endocytotic capacity for FITC-dextran injected into the animals was compared between fibroblasts and macrophages. At the non-metamorphic stage the fibroblasts which undercoated basement lamella are spindle-shape and contain many smooth-surfaced vesicles near the cell membrane. Intermediate junctions are seen between the fibroblasts. The macrophages have higher endocytotic capacity for FITC-dextran than the fibroblasts. At the metamorphic stage prominent degenerative changes occur only in the apical regions of the tail fin. In these region orthogonal arrangement of collagen fibers disappears in the basement lamella and the disordered collagen fibers accumulate. Many of the fibroblasts and macrophages are seen among the collagen fibers. Collagen-containing structures (phagosomes) are observed in the cytoplasm of the fibroblasts in those degenerative regions, where some fibroblasts and nerve tissue degenerate and the macrophages phagocytose them. However, there is no evidence that the macrophages directly phagocytose the degraded collagen fibers.

MO 7

THE DIFFERENT LIFE CYCLES IN BIPALIUM SP. (PERH. B.PENNSYLVANICUM BY R.OGREN)OF NON-FISSION TYPE SPECIES.

N.Makino and Y.Shirasawa. Dept.of Biol., Tokyo Med., Coll., Tokyo.

Materials were first collected at Hino Shi in 1982. Authors made a paper open to the public about their characteristic structure of copulatory organ in 1984. They were unknown species in our own and other lands. They have three longitudinal lines keep dark color in median line of the dorsal side, showing dark green on the whole and have no line and lighty in the ventral side.In the breeding season,they have copulated at 100 to 200 mg within one year old, from the latter part of March to July in Tokyo.Their egg laying are very active,for they can lay egg 1 by 1 over 10 cocoons at last.After the copulation,they lay egg for some months, and after last egg laying,they die natural death within several months.But authors observed that materials were born in 1985, did the copulation only in April of the next year,and laid one cocoon only in July in 1987. Then,the weight of adults became over 1000 mg. Recently,author received a paper of new Bipalium from Dr.R.Ogren, The new Bipalium;B.pennsylvanicum by R. Ogren seems to the same worm with our new material,and the body weight of B.penn.are less than 300 mg. Thus,the same species in adult have different body weight and different aging,and about egg laying, there is nothing to choose between the two in different adults. Interestingly,their cells are composed of 2n=15 by the air-drying method.

MO 8

THE KARYOTYPES OF GENUS; BIPALIUM IN BOTH THE FISSION AND NON-FISSION TYPES.

N.Seo, N.Makino and Y.Shirasawa. Dept. of Biol., Tokyo Med., Coll., Tokyo.

Genus; Bipalium have active regenerative ability, and have two characteristics; fission and non-fission type. The non-fission type worms are usual species in Japan and propagate only bisexual reproduction and they have thick and short of external forms, for example, B. fuscatum, B. fusco-lineatum, B. hilgendorfi and B. pennsylvanicum(new species) etc. The fission type worms have been reared in our laboratory about three species; B. nobile, B. kewense and B. multilineatum and they have very long slender of external forms. These two types of Bipalium are different from the structure of the copulatory organs also. Authors have been studied the relation of regeneration and cell division in Bipalium. From this angle of vision, authores studied the analysis of karyotypes in Bipalium, both fission and non-fission types. Fission type species ; cosmopolitan worm, B. kewense in our material is 2n=18, though L.Winsor reported 2n=16. B. multilineatum which do not bisexual reproduction in Tokyo is 2n=10. Giant Bipalium, B. nobile which does sexual and asexual reproduction is investigated both regular and translocated types in chromosomes, namely 2n=10. Non-fission type species; B. pennsylvanicum is composed of 2n=15 and B. fuscatum is 2n=10.
For the analysis of karyotypes, the air-drying method was used.

MO 9

OBSERVATIONS ON THE REGENERATION OF THE SAGITTAL SMALL PIECES IN THE LAND PLANARIAN, BIPALIUM NOBILE.

Y. Shirasawa and N. Makino. Dept. of Biol. Tokyo Med. Coll., Tokyo.

Morphological and histochemical studies on the head-regeneration of the sagittal small pieces have been made in B. nobile. The head-frequency of the sagittal pieces showes a decrease of 50% under the transverse one. And the former took much more times for the head-regeneration than the latter. There was no difference in the head frequency between the pre- and the post pharyngeal region. In several hours after the cutting, most sagittal pieces curved toward the lateral cut surface and the rest formed a ring by the adhesion of the anterior and the posterior surface. Unlike the transverse pieces, almost all the sagittal pieces did not move actively. The lateral cut surface was covered by the stretched dorsal epidermis in about 24hrs. The histological preparations stained by AF(Gomori's aldehyde fuchsin) demonstrated that also in the sagittal pieces, the AF-positive granules released from the intestine appeared in the parenchyma at the stage of 3-5 days. And that in this stage, the anterior end of the ventral nerve cord approached to the anterior cut surface, and the nerve cells observed in this portion were slightly AF-positive. Electron microscopically, these cells had developed nucleoli, small dense bodies in the proximal of the nuclei, many free lobosomes and secondary lysosomes.

MO 10

FINE STRUCTURAL LOCALIZATION OF ACID PHOSPHATASE ACTIVITY IN THE REGENERATING FRESH-WATER EARTHWORM, BRANCHIURA SOWERBYI.

M. Shirasawa and N. Makino. Dept. of Biol., Tokyo Med. Coll., Tokyo.

The morphology and AcPase activity were investigated electron microscopically in the fresh-water earthworm, Branchiura sowerbyi and were compared among the early stages of the head-regeneration. On the cut-surface of regenerating worms, the enzyme was localized in the lysosomes of the propagating epidermal cells. In their Golgi zones, the vacuoles and the reticular parts were strongly and the cisternae were slightly positive. But in intact worms, these activities were not conspicuous. In the intestinal epithelial cells, the dense bodies came from the Golgi vacuoles were strongly and the cisternae were slightly positive. Some of these, in regenerating worms, showed the diffusion of the lead phosphate and resulted in autolysis. The intestinal granular cells had the most remarkable activity in intact worms, but the activity, in the large granules, rapidly declined in the regeneration. The nerve cells of the ventral ganglia had strong AcPase activity, unlike other cells mentioned above, in the well-developed Golgi citernae. The Golgi vacuoles and the irregularly shaped dense bodies were also positive. In regenerating worms, the activity of the cisternae was the most remarkable in the stage of 1-2 days.

MO 11

ULTRASTRUCTURAL INVESTIGATIONS OF MELANOCYTE AND MACROPHAGE IN THE MOUSE HARDERIAN GLAND.

K. Shirama and M.Hokano. Dept. of Anatomy, Tokyo Medical College, Tokyo.

The presence of dendritic cells containing melanin granules have been demonstrated employing silver impregnation and with electron microscopy in the interstitial tissue of the mouse Harderian gland. Two types of melanocytes, either with or without the various developmental stages of melanin granules, were found in the gland. The cell with developing granules was more dendritic and contained a large number of cytoplasmic organelles. The other cell was ellipsoidal or slender in shape and contained few cytoplasmic organelles and a large number of fully melanized granules, but no developing granules. In general, the granules of the Harderian gland melanocyte resembled granules from other organs(particularly the skin of the eyelids). The general size range of the granules was 0.2-0.9 μm. Each granule was enclosed by a membrane.

The Harderian gland macrophages contained fully pigmented melanin granules of various sizes. The granules were enclosed by a membrane either singly or in groups. Some of the melanin granules within the phagosomes showed signs of degranulation,revealing the underlying matrix.

MO 12

UNUSUAL VESICULAR STRUCTURE IN PHOTOSENSITIVE CHROMATOPHORES.

M. Obika. Dept. of Biol., Keio Univ., Yokohama.

Dermal chromatophores of some vertebrates are photosensitive, responding to photic stimuli with rapid intracellular pigment translocation. Ultrastructural studies on melanophores, xanthophores and leucophores of Oryzias latipes and tail fin melanophores of Xenopus laevis tadpoles have revealed that these photosensitive chromatophores possess characteristic vesicles that bulge out from cell surface. The size and number of vesicles are variable but they always contain membranous components such as small vesicles, either spherical or tubular, or lamellated membranes. No other cytoplasmic organelles are observed in this area. Studies on serial sections indicate that each vesicle is connected to the cell body by a stalk that contains fuzzy, filamentous inclusions. Microtubules are only rarely encounterd in the stalks of Oryzias melanophores. No significant difference in the internal structure of the vesicles has been found between the dark- and light-adapted chromatophores. From their distribution and structural characteristics, these unusual vesicular compartments found in photosensitive chromatophores of the fish and the toad appear to be the likely candidates of photoreceptors.

MO 13

IMMUNOCYTOCHEMICAL AND ELECTRON MICROSCOPIC STUDIES ON THE GLIAL CELLS IN THE BRAINS OF ELASMOBRANCHS.

A.Chiba[1] and Y.Honma[2]. [1]Dept. of Biol., Nippon Dental Univ., Niigata and [2]Sado Mar. Biol. Stat., Fac. of Sci., Niigata Univ., Niigata.

Immunocytochemical and electron microscopic studies were conducted to elucidate the cytological features of glial cells in the brains of elasmobranchs. For this purpose, three species of elasmobranchiate fishes, *Scyliorhinus torazame*, *Mustelus manazo* and *Dasyatis akajei*, collected from the coastal waters of Sado Island were used.

By means of the peroxidase anti-peroxidase method, S-100 protein-like immunoreactivity was demonstrated in the tanycytes and astrocytes including Bergmann's glia in the cerebellar cortex. These cells with their endfeet formed a distinct boundary membrane on the brain surface (*membrana limitans gliae superficialis*) and the periphery of the blood vessels (*m.l.g. perivascularis*). By the electron microscopic immunoperoxidase method, S-100 protein-like antigen appeared to be localized in the cytoplasmic matrix. Glial fibrillary acidic protein-like immunoreactivity was also detected in the tanycytes and astrocytes. Conventional electron microscopy demonstrated three types of glial cells, astrocytes, oligodendrocytes and microglia in these fishes.

MO 14

ULTRASTRUCTURAL CHANGES IN THE RENAL GLOMERULUS OF MALE AND FEMALE WISTAR/TW RATS.

Win Win Yee, S. Takahashi and S. Kawashima. Zoological Institute, Faculty of Science, Hiroshima University, Hiroshima.

Changes in the renal glomerulus between male and female Wistar/Tw rats were electron microscopically examined at 1, 3, 6, 12 and 18 months of age. Common changes were observed after 3 months in male rats and 6 months old female rats in the glomerular capillaries basement membrane (GBM), epithelial cell foot processes (EpF), and epithelial cell cytoplasm. Initial lesions detected in a few scattered area in 3-month-old male rats were the slight thickening of the GBM with some fusion of the EpF and the appearance of vesicles and vacuoles in the epithelial cells. Lesions became more extensive as age advanced, and at 18 months profound lesions were detected . In female rats the initial lesions were not apparent until 6 months of age . Every 12-month-old female rat showed focal changes of the GBM thickening with some fusion of the EpF and at 18 months focal changes became segmental ones . From 12 months there were striking sex differences in the development of renal lesions . Only aged male rats showed extensive thickening of the GBM with nodular folds which intermingled with mesangial matrix , extensive fusion and then denudation of the EpF and degeneration of the epithelial cell cytoplasm.

MO 15

METAMORPHOSIS OF LARVAL TRACHEAE AND FORMATION OF PUPAL ABDOMINAL TRACHEAE IN DROSOPHILA MELANOGASTER

T.Matsuno.Kyoto Prefec.Univ.of Med.,Kyoto.

Adult tracheal discs are present on the spiracular tracheae in the third instar larvae. After pupation the tracheae posterior to the fifth spiracles exclude air and do not function for gas exchange. Cells of discs proliferate, migrate along the tracheae and replace larval tracheal cells to form adult tracheae.

Pupal abdominal tracheae (PAT) which function during the pupal stage arise from the fourth and fifth spiracular tracheae in the third instar larvae. Growing through cell division,PAT rudiments become elliptic lobes lying on the larval tracheae (transverse connectives). The lobes swell and bulbous buds are formed on the side being in contact with the larval tracheae. After pupation PAT rudiments stand up and tracheoles are discernible in some cells of buds. Tracheole cells elongate and PAT formation is completed.
The branching pattern of PAT consists of 'leaves' (tracheole cells) and 'branches'. 'Leaves' crowd at the tips of 'branches'. 'Branches' appear to correspond to buds. Bud formation seems to reqire contact between PAT rudiments and the larval tracheae.

MO 16

REPAIR AND REGROWTH OF THE DETACHMENT SITE OF THE CORAL FUNGIA FUNGITES

H.Yamashiro[1], and K.Yamazato[2]. [1]Radioisotope Lab. and [2]Dep. of Biol. Fac. of Sci., Univ. of the Ryukyus, Okinawa.

Structural changes of the detachment sites in both disc and stalk after detachment were studied in the hermatypic solitary coral F. fungites. Truncated end of the remained stalk was covered rapidly with intracalicular soft tissues within a day or two. Then the stalk regenerated the complete polyp with mouth and tentacles (about 10 days later). Regenerated skeletal elements on the stalk were formed by direct growth of corresponding structures in the former stalk. In a disc, the detachment plane was covered with the intracalicular soft tissues and then thin calcareous plates (about 10 µm thick) expanded horizontally from the lower ends of the septa or columellae. Before detachment, more or less in most specimens, interseptal spaces already had been narrowed, filled up or plugged up, partly or fully, with calcareous matter caused by the thickening of the septa, columellae and synapticulae. When the interseptal spaces become to be small and also the skeletal pulverization is insufficient to detach, the soft tissues below the detachment plane are suffocated, degenerate and sometimes result in the death of the stalk.

MO 17

THE DIFFERENTIATION OF THE NAUPLIUS EYE IN CYPRIS LARVAE OF A BARNACLE, BALANUS AMPHITRITE HAWAIIENSIS BROCH.

M.Takenaka, T.Yamamoto and M.Yoshida. Ushimado Marine Lab., Okayama Univ., Okayama.

The nauplius eye in cypris larvae is symmetrical in form and composed of two pigment cells and fourteen visual cells. The pigment cells form three concave depressions. Visual cells are correspondingly divided into three groups, two lateral and one ventral components.

At the metamorphosis into the adult stage, the three components of the nauplius eye are separated and differentiate into the adult ocelli independently. Each lateral component develops into the adult lateral ocelli, forming newly pigment cells and tapetum cells, while the ventral component develops into the adult median ocellus.

It is concluded that the adult photoreceptors are originated from the ocellar components of the planktonic nauplii.

MO 18

MONOAMINE CONTAINING CELLS IN THE TASTE BUDS OF THE MOUSE VALLATE PAPILLA.

M.Kudoh. Dept. of Biol., Fukushima Med. College, Fukushima.

The taste buds in the vallate papillae of the mice were observed by means of fluorescence histochemistry (aqueous glyoxylic acid method) and electron microscopy (glyoxylic acid-Mg^{2+}-$KMnO_4$ method). The specific fluorescence appeared faintly in the taste bud of both untreated and nialamide-treated mouse, and was intensively enhanced by the administration of the monoamine precursors such as 5-HTP and L-DOPA. Electron microscopic observations of OsO_4-fixed materials revealed that by the injection of the amine precursors a large number of small clear vesicles approximately 40-60 nm in diameter appeared throughout the cytoplasm of the type III cells which are supposed to be the gustatory cells ,and these vesicles aggregated especially around Golgi body and in the presynaptic regions of the nerve terminals. Electron microscopic histochemistry demonstrated that after injection of the amine precursors,numerous small dense vesicles, of which the size and the density of the content are variable, are found among the small clear vesicles in the cytoplasm of the type III cells. It is suggested from the present observations that the type III cells may be capable of taking up amines and storing them in the small clear vesicles. The stored amines might play a role in neurotransmission in taste transduction.

MO 19

MORPHOLOGICAL OBSERVATIONS ON NEUROSECRETORY CELLS OF A FRESHWATER OLIGOCHAETE, TUBIFEX HATTAI.

H. Jaana. Biol. Lab., Asahikawa College, Hokkaido Univ. of Education, Asahikawa.

The distribution of neurosecretory cells and the morphological characteristics of them were studied by light and electron microscopes. Their cytological activity was also examined during an egg-laying period. Cells stained intensely with paraldehyde-fuchsin were observed in a subpharyngeal ganglion (Sub.G) and ventral segmental ganglia (Seg.G), while weakly-positive cells were detected in the cerebral ganglion (Cer.G), Sub.G and Seg.G. Electron microscopy revealed three types of granular cells in the Cer.G (type I, II and III cells). Two other types of granular cells (type IV and V cells) were intermingled with type II cells in the Sub.G and Seg.G. Among them only type II cells showed morphological changes during an egg-laying period. The number of granules of type II cells decreased after oviposition, while well-developed rough ER and Golgi apparatus emerged in their cytoplasm. Several hours later, swollen parts of axons accumulating granules came to be observed frequently. It was suggested that the release of granules of type II cells may trigger the oviposition, or the release after oviposition may activate epithelial cells of the clitellum which have taken part in a cocoon formation.

MO 20

STRUCTURE OF SEMINIFEROUS TUBULES AND TESTICULAR VASCULAR PATTERNS IN AGING CHINESE HAMSTERS (*CRICETULUS GRISEUS*).

H. Ninomiya[1], K. Yamazaki[2], S. Kondo[2] and E. Hohjoh[2].
[1]Dept. of Labo. Animal Sci., Azabu Univ., Sagamihara, [2]Technical Sect., Mitsubishi-Kasei Inst. of Life Sci., Machida, Tokyo.

The age-related changes of the histological structures and vascular systems in the testes of the Chinese hamster(17-43 months) were examined both at the light and electron microscopic (TEM and SEM) levels. Scanning electron microscopy was used for the examination of testicular vasculatures as their acrylic resin casts. The senile changes noted were: depletion of spermiogenesis, edema of interstitial tissues, tubular sclerosis, degeneration and/or hyperplasia of Leydig cells, dilation of seminiferous tubules, arterial stasis, and embolism. Degenerative changes were also observed in the endothelial cells of intertubular and peritubular capillaries surrounding seminiferous tubules. The observation on the resin casts showed that those capillaries were torn-off and strangulated. The aetiology and pathogenesis of these changes in seminiferous tubules are briefly discussed in relation to blood supply.

MO 21

REMOVAL OF COLLAGEN BUNDLES IN MURINE UTERUS DURING POSTPARTUM INVOLUTON.

K.Shimizu,T.Harada,M.Hokano. Dept.of Anat. Tokyo Med.Coll., Tokyo.

The localization of collagenolytic activity within the mouse uterus (IVCS strain) was investigated during postpartum involution.The rate of collagenase activity was measured by analyzing of tissue levels of hydroxyproline from the day of parturition to the 20th postpartum day (Woessner's method). Collagenase activity was high during the first two postpartum days. Collagen distribution in tissues was analyzed by viewing birefringence induced by the picrosirius technique (Sweat's method). An attempt was made to interrelate the quantitative analysis with the histologic distribution of collagen during the first two postpartum days. Histologic and quantitative evidence indicated that (1) the collagenous compartments of the endometrium and myometrium differ in their response to the postpartum rise in collagenase activity. Collagen degradation occurs primarily in the endometrium, i.e. the myometrial collagen remains but much of the endometrial collagen is removed. (2) Endometrial collagen is degraded particulary in the immediate subluminal compartment.

MO 22

MORPHOLOGICAL VARIATIONS IN THE KILLIFISH BRAIN PRODUCED BY DOMESTICATION

Y. Sato, Dept. of Anat., Yokohama City Univ. Sch. of Med., Yokohama

The external and internal features of the brains of the medaka, Oryzias latipes and its albino form, the "hi-medaka", were examined. On the dorsal aspect the proportion of the size of the telencephalon to the whole brain in greater in the hi-medaka than in the medaka. But the proportion of the size of the optic tectum is greater in the medaka than in the hi-medaka. The optic tectum of these killifish shows the same strata as in other bony fishes: stratum marginale (SM), st. opticum (SO), st. fibrosum et griseum sup. (SFGS), st. griseum centrale (SGC), st. album centrale (SAC), and st. periventriculare (SPV). The SO and SFGS received retinotectal afferent fibers. The SO and SFGS together occupy about 32% of the total tectal thickness in the medaka, but only about 26% in the hi-medaka. Since the hi-medaka is an artificially produced strain, these morphological variations imply that the structure of the optic tectum has been affected by domestication.

MO 23

ON THE MORPHOGENESIS OF FREE NEUROMAST OF FRESHWATER TELEOST, ORYZIAS LATIPES.

S.Nagai, M.Otsuka and K.Ishii. Dept. of Biol., Dokkyo Univ. School of Med. Mibu.

The developmental process of the free neuromast in embryo and larva of Oryzias latipes alb. was studied using an electronmicroscope and a scanning one. Distinction of hair cells and supporting cells, and interlocking formation by desmosomes and invagination were observed at 120 hours after fertilization. In addition, initial formation of cupula pore with stereociliae and kinocilium was observed at 125 hours. The number of hair cells increased according to the development of embryo: one cell at 120 hours and 2 cells at 125 hours after fertilization; 5 cells just after hatching; 11 cells for 2-day old and 15 cells for 7-day old larvae, respectively. The formation of afferent neurons was found at 132 hours after fertilization while that of efferent neurons was observed just after hatching. Secretory granules in supporting cells were observed from 120 hours after fertilization.

MO 24

A GOLGI STUDY ON THE CUTANEOUS NERVES AND THEIR TERMINALS IN THE SALAMANDER, *HYNOBIUS NEBULOSUS*.

N. Iwahori, Dept. of Anat., Fac. of Med., Nagasaki Univ., Nagasaki.

The morphology of the cutaneous nerves and their terminals was studied in the salamander using the rapid Golgi method. The cutaneous nerves are derived from the spinal and some cranial nerves and travelled superficially among muscles as a number of discrete bundles which contained numerous axons of diverse diameters. Upon arriving at the dermal-epidermal transitional region, the cutaneous nerves swung in a tangential direction and branched out into numerous collaterals to form a dense fiber network. Many fibers emerged from the fiber network and proceeded toward the surface, branching profusely to terminate mainly in the epidermis. The majority of the fibers terminated as free nerve endings; only a few ended with some terminal expansion. The free nerve endings were seen in the middle and deep epidermal areas forming a dense terminal plexus, while the expanded tip terminals were impregnated mainly in the middle epidermal region. The distribution area of the terminals derived from one cutaneous nerve fiber overlapped to a considerable extent with that from other nerve fibers. In addition to the above fibers, in the upper dermal regions, a few fine fibers were seen to travel toward the mucous glands to terminate in conjunction with glandular tissue.

MO 25

MORPHOLOGICAL CHANGES OF ACHR-AGGREGATES DURING MUSCLE REGENERATION OF URODELE.

T.Tabuchi and S.Inoue. Dep. of Comp. Endocrinol., Inst. of Endocrinol., Gunma Univ. Maebashi.

Acetylcholine receptor(AChR)-aggregates of urodele limb muscles were observed during development and regeneration. The binding of tetramethyl rhodamine-labelled α-bungarotoxine(TMR-αBT) to AChR, and the histochemical reaction for acetylcholine esterase were observed in the same sample. The materials used were the upper arms of the larval Hynobius nigrescens and the musculus flexer digitorum communis of adult Cynops pyrrhogaster.

During the larval period of Hynobius, AChR-aggregates appeared in spot and/or plate forms. They became linearly arranged dring metamorphosis and then acquired the mature shape of the neuromuscular junction (n-m-j).

During the regeneration of lower arms of Cynops, the labelling intensity of the n-m-j of stump muscles decreased to some extent throughout almost all the phases of regeneration. In the early period of regeneration, spot and plate form AChR-aggregates became lost. After 3 post-amputation weeks, they reappeared not only in the original n-m-j location in the stump muscles but also near the cut ends of muscles. These spot and plate aggregates were considered to form the new n-m-j through a similar way as in development.

MO 26

A HISTOLOGICAL STUDY ON THE NERVE INNERVATION IN THE HEART OF CLEMMYS JAPONICA.

H. Ishihara. Biolog.Lab., Fac. of Sci.& Engineer., Aoyama Gakuin Univ., Tokyo.

The morphology of nerve innervation and nerve endings in the heart of Clemmys japonica was investigated according to the silver impregnation method devised by the present author. In the adventitia, the nerve plexus was relatively well developed. The nerve bundles which separated from fundus plexus were distributed over the adventitia. The nerve bundles were covered with neuroplasmamass containing numerous nuclei. They were observed to run a wavy course. After repeating ramification, the nerve bundles became thinner and thinner in structure and then radiation was seen running to all direction. The nerve bundles which had entered myocardium, together with capillaries or by themselves diverged from adventitial plexus. The nerve bundles penetrated the muscle fiber, after repeated branching was seen to form rich plexuses. In this plexus, nerve cells and triangular cells attaching to the nerve fiber were frequently observed. A fine nerve fiber which ran paralel or obliquely in the muscle layer was detected. Various nerve endings were very often found in the myocardium and adventitia. Further, the fine nerve fibers were observed to run parallel to the capillaries or surrounding them. In addition, the nerve fibers bearing nuclei here and there were found to run in serpentine course.

MO 27

INNERVATION OF THE SHORT THUMB MUSCLES OF THE FRUITBAT *Pteropus medius*

Khin Maung Saing. Inst. of Biological Sciences, Univ. of Tsukuba , Ibaraki 305, Japan.

The thumb of the fruitbat found in Burma is well developed in structure and function compared to insectivorous bats. As the forelimb morphology in bats plays an important role in locomotion, functional specializations concerning gross anatomy, innervation and lipid content of the short thumb muscles of the fruitbat were examined. Three muscles i.e. flexor pollicis brevis, adductor pollicis and abductor pollicis brevis were present. All muscles were innervated by metacarpal nerve I derived from a single nerve trunk composed of combined median and ulnar nerves. All muscles had diffuse type of motor endplates. Single motor endplates on single muscle fibres were found predominantly. But occasionally a single axon supplied two motor endplates on different muscle fibres or two diferent axons ended in two motor endplates on a single muscle fibre. Complex and intermediates types of neuromuscular spindles, Pacinian corpuscles and encapsulated Golgi tendon organs were found.All spindles had nuclear bag and nuclear chain types of intrafusal muscle fibres. Three extrafusal muscle fibre types i.e. red, white and intermediate based on lipid content were noted. Correlaship of function to structures in the thumb of the fruitbat is discussed with comparison to other mammals including insectivorous bats and monkey.

MO 28

THE ULTRASTRUCTURE OF SIF (SMALL INTENSELY FLUORESCENT) OR SGC (SMALL GRANULE-CONTAINING) CELLS AND NERVE TERMINALS IN THE CARDIAC GANGLIA OF THE SHREW MOLE, Urotrichus talpoides.

S.Kikuchi
Dept.of Biol., Sch.of Lib.Arts and Sci., Iwate Med.Univ., Morioka.

The cardiac ganglia in the atria and interatrial septum of the shrew mole contain clusters of small cells which show a strong glyoxylic acid-induced fluorescence of dopamin. Ultrastructurally these cells are characterized by large nerve terminals and an abundance of dense-cored vesicles in the cytoplasm. These SGC(SIF) cells are in glomus-like structures within the ganglia in close proximity to capillaries, of which endothelial cells are fenestrated in the area of contact with the SGC cells and their processes. Each SGC cell with a thick process is innervated by at least one large nerve terminal, together with several small ones. A large nerve terminal frequently makes synaptic connections with two or three SGC cells surrounding it. Three types of synaptic connections, afferent, efferent and reciprocal, are found on the SGC cells. These characteristics resemble those of the SGC cells in the carotid body and aortic body rather than the other autonomic ganglia or paraganglia, suggesting a chemoreceptive function of SGC cells in the cardiac ganglia. The chemoreceptors may be not confined to the arotic regions but more widely distributed in the heat.

MO 29

WHERE DO NEURONS RELEASE THEIR CHEMICAL MESSENGERS? — TRANSMISSION AND SCANNING ELECTRON MICROSCOPIC STUDY.

Y. ENDO*, Dept. of Anatomy, Yamanashi Med. Coll., Yamanashi.

Generally, it is believed that neurons release their chemical messengers toward the effector cells through a synapse. I investigated exocytotic release of secretory granules from the neurons of the posterior pituitary, adrenal medulla and enteric nervous system of the rats stimulated with perfusion of high K^+ Ringer solution. Tannic acid-glutaraldehyde-osmium tetroxide fixation was applied. Unexpectedly, as far as observed, exocytosis of large-cored vesicles occurred at non-synaptic sites where no structural specialization of membrane was found. Scanning electron microscopy of the enteric nervous system using a HCl-digestion method indicated that varicose neuronal processes were exposed elswhere to the surface of unmyelinated nerve fascicles. Exocytosis of large-cored vesicles occurred not only at these exposed area but also at the interspace between neuronal processes and Schwann cells.

*Present adress: Dept. of Applied Biology, Kyoto Institute of Technology, Matsugasaki, Sakyo-ku, Kyoto 606.

MO 30

OBSERVATIONS OF LIMB WOUNDS IN MICE OF WHICH LIMB WERE SURGICALLY AMPUTATED

T.Nobunaga[1] and S.Inoue[2]. [1]Inst. for Exper. Animals, Tohoku Univ., Sendai and [2]Inst. of Endocrinol., Gunma Univ., Maebashi.

As previously reported, the wound healing of the amputated limbs in the fetus seemed to proceed faster than the amputated limb of the newborn mouse. The surfaces of the amputated limbs in utero at 6 post-operative days showed slight moundings.

We further studied the amputated limbs which were harvested at 6 and 49 days after birth, the limbs having been amputated in utero at 13 or 14 days after mating in proestrus (in utero operated + 6 day-or 49 day-limb series). The external appearance of the in utero operated + 6 day limb series was not so different from the amputated limbs in utero at 6 post operative days. However, the limbs at 49 days after birth (in utero operated + 49 day limb series) were cone shaped, showing large amount of fibrocartilage-like callus formation at the ends of the amputated bones.

BB 1

LEARNING ABILITIES AND OTHER BEHAVIORAL CHARACTERISTICS OF EXCELLENT AND DULL LINES OF ddY MICE.

N.Mishima, Y.Maeda, T.Mizuta, R.Iguchi. Dep. of Biology, Fac. of Pharm.,Tokushima-Bunri Univ., Tokushima.

The present experiment was aimed to study behavioral characteristics of 8th generations of "Excellent line" (Ex-8) and "Dull line"(Dull-8) which were obtained by selective brother-sister breedings of ddY mice exhibiting "good"and"poor" retentions in 1-trial passive avoidance task,respectively. In the retention test of the task, Dull-8 displayed significantly lower avoidance than non-selective ddY mice (control), but there was no difference between Ex-8 and the control. On the other hand, Ex-8 established much more quickly active avoidance task in T-maze and two appetitive tasks; Skinner box and radial maze than Dull-8. Although the two lines were selected by results of retention test but not acquisition session, Ex-8 had superior learning abilities and Dull-8 had inferior abilities than the control in the all tasks as far as we tested. On the contrary, there are no significant difference in general activities such as wheel running activity or open field activity. These results suggest that there exsists significant differences in some characters specific to learning ability, but not general activity between the two lines.

BB 2

ONTOGENETIC CHANGES IN LEARNING AND MEMORY ABILITIES OF ddY MICE IN AVOIDANCE TASKS.

H.Nakano., R.Iguchi and N.Mishima, Dep. of Biol.,Fac.of Pharm., Tokushima Bunri-Univ.

Development of learning and memory abilities of ddY mice were studied in various tasks as a function of age. Passive avoidance task was acquired with similar numbers of trials to adult mice, on the day of eye opening. However, the mice (15 days old) could not learn active avoidance tasks such as 1-way and 2-way T-maze tasks. Learnings of the two tasks became possible between 16-19 days and 18-22 days, respectively. On the other hand, long term memory was scarecely established by 15 days old mice, but rapid improvement of the memory retention appeared between 17-19 days. These results demonstrate that avoidance learning and its memory are suddenly developed between eye opening and weaning. On the contrary, open field activity or wheeling activity, at weaning was about 50% of adult levels. Catecholamine levels of brain were measured at various ages since our previous data suggested possible involvement of dopaminergic system in learning and memory mechanism of adult mice. At 20 days, DA was only 52 % and NE was 50% of each adult levels.These results show that emergence of learning and memory abilities are not dependent upon maturation of CA system or general activity.

BB 3

FEMALE MICE PREFER ODORS OF AGGRESSIVE MALES.

S.Hayashi. Dept.Biol.,Fac.Educ.,Kagoshima Univ. Kagoshima.

A dominant male develops preputial glands and attacks subordinate ones customarily even in a population where a dominance relationship has been established. In this experiment, advantages of these aggressions and functions of preputial glands were investigated .

Preputial glands of a male mouse increased when the animal could smell of strange male odors and increased markedly when it could display aggressions. The development of the glands did not continue without males to fight with or attack. When 11 aggressive males were isolated for 24 days, the weight of their preputial glands decreased from 46.5 mg to 32.2 mg, on the average.

On the other hand, female mice preferred a box which had contained an aggressive male over that contained a submissive one in 5-min test. These female preferences for a dominant male disappeared after resection of the preputial glands. Effects of preputialectomy were more noticeable in aggressive males than in submissive males.

Aggressiveness of a male mouse and some adequate rivals seem to be essential to maintain developed preputial glands and sexual attractivity.

BB 4

HORMONAL FACTORS INVOLVED IN COUNTER-MARKING BEHAVIOR IN MICE.

M.Daumae and T.Kimura. Dept. of Biol., Coll. of Arts and Sci., Univ. of Tokyo, Tokyo.

Counter-marking in mice was investigated by analyzing urine deposition pattern on filter paper previously marked with other male and female mice urine. Intact males deposited larger numbers of urine spots and more amount of urine on the area with female urine than on the area with male urine, but castrated males marked both area equally. Ovariectomized and androgenized females deposited larger number of urine spots than intact female, but they, as well as intact females, showed no marking preference towards previously marked area with male or female urine. Neonatally androgenized females deposited larger numbers of urine spots in total than intact females, and marked more amount of urine on male urine area than on female urine area. Ovariectomy erase the marking preference for male urine in these neonatally androgenized females. Although further experiments are needed, these results suggest that (1)male-type urination pattern (large numbers of small spots) is established by neonatal androgen, (2)preference for counter-marking on female urine area is induced by later androgen only in mice showing male-type pattern, and (3)estrogen possibly enhances counter-marking on male urine area.

BB 5

ANALYSIS OF FEMALE-ATTRACTING ACTIVITY OF MALE MOUSE URINARY FACTORS AND PREPUTIAL GLAND SECRETION.

K. Ninomiya[1], T. Kimura[1] and K. Mori[2]. [1]Dept. of Biol., Coll. of Arts and Sci. and [2]Dept. of Agr. Chem., Fac. Agr., Univ. of Tokyo, Tokyo.

Two androgen-dependent compounds(dehydro-exo-brevicomin[I] and 2-sec-butyl dihydrothiazole[II]) in male mouse urine are known to attract females when mixed with castrated male urine, but stereospecificity of these compounds has not been studied. As both enantiomers of [I] were synthesized by one of us(Mori), We compared the effects of each when mixed with castrated male urine plus [II](racemate). Although the study is still in preliminary stage, results so far obtained strongly suggest that the coexistence of both enantiomers is necessary for female-attraction. This is rather exceptional and interesting case, since most of other pheromones show one-sided stereospecificity.

We reported in the last Meeting that preputial gland secretion mixed in male urine is another essential factor for female-attraction. To confirm this, we mixed [I] and [II](both racemate) with castrated or castrated-preputialectomized male urine. When tested with both mixtures, female mice significantly preferred the former. This indicates that factor(s) in preputial gland secretion which is probably androgen-independent is indispensable for attracting females.

BB 6

IMPAIRMENT AND RECOVERY OF OLFACTORY BEHAVIOR FOLLOWING LESION OF THE ACCESSORY OLFACTORY BULB IN RAT.

M.Ichikawa. Dept. Anat. & Embryol., Tokyo Metropol. Inst. for Neurosci., Tokyo.

We have reported that synaptic reorganization occurs in rat medial amygdaloid nucleus(MAN) following denervation of fibers from accessory olfactory bulb (AOB)[1,2,3]. However, functional significance of synaptic reorganization following the denervation of afferent fibers has been unknown. To clarify the relationship between synaptic reorganization and functional recovery, as a first step, we studied the change of olfactory behavior following denervation of the AOB fibers. It is known that male rat shows the preference in odor of female rat. In the present study, thus, the preference of male rat in female odor was examined before and after a lesion of the AOB. The preference decreased to 10 % of intact after the AOB lesion (6 - 10 days after the lesion). Thereafter, the preference of AOB lesioned rat increased gradually and showed about 80 % of intact at 2 month survival time. The present study indicates that time course of recovery of odor preference after lesion of the AOB is similar to the time course of recovery of the synaptic density in MAN following a lesion of the AOB[2].

1. Ichikawa, M. Zool. Sci., 3 (1986) 982.
2. Ichikawa, M. Brain Res., 420 (1987) 243
3. Ichikawa, M. Brain Res., 420 (1987) 253

BB 7

COLOUR LEARNING IN THE BLOWFLY, *LUCILIA CUPRINA*.

T.Fukushi Dept. of Biol., Miyagi Coll. of Educ., Sendai.

The compound eyes of flies provide a variety of spectral types of receptor that could be used in colour vision. By means of learning experiment, colour vision has been proven in *Musca* (Fukushi, 1976), *Drosophila* (Menne and Spatz, 1977) and *Lucilia* (Fukushi, 1985). What use does a fly make of its colour learning capacity under natural circumstances where objects with many hues of colour exist?

The Australian sheep blowflies *Lucilia cuprina* were trained to a colour by presenting a droplet of the sugar solution on a patch with various colours. Then, the flies were tested on visits to colours in the arena where four kinds of colour patches were arranged so that the fly encountered each colour in the same probability in random walks.

The flies visited preferably the colour to which they had trained. The effect of training was most remarkable in blue and yellow. Green was discrimanated from blue but confused with yellow. The red-trained fly behaved in the test situation as black-trained one, suggesting that the fly is hardly discernible red.

BB 8

PHOTIC ENVIRONMENT, BIOLUMINESCENCE AND VISION OF A SQUID, *Watasenia scintillans*.

Y.Kito[1], M.Seidou[1], M.Michinomae[2] and A. Tokuyama[2], [1]Dept of Biol., Osaka Univ. and [2]Dept. of Biol., Kounan Univ., Kobe.

Mechanism of bioluminescence of this squid has been clarified (1,2) and the light is thought as emitted from some fluorescent substance, excited by the luciferase system. This paper suggests that bioluminescence of the squid is not corresponded with blue monochromatic light of the deep sea environment but with a particular trichromatic vision recently found (3). Half bandwidth of light from large photophores of the fourth arm was broad and 4600 cm^{-1} (Em max:475 nm) as detected by spectrograph. Fluorescence from the small photophore of mantle were determined with microspectrofluorometry. Bandwidth and Em max were varied according to characteristic shape and color of the photophore. Then, fluorescent substance was extracted and partially purified by HPLC. Two substances (Em max:460 and 490 nm) with MW<20K were found. Thus, various fluorescences from photophores are explained as emitted from mixtures of a certain proportion of the two fluorescent substances. The light may facilitate mutual communication among species.

1. T.Goto in Marine natural products, Acad. Press,1980.
2. F.I.Tsuji, Proc. NAS.,82,(1985) 4629
3. S.Matsu et al., J.Gen.Physiol. in press

BB 9

LARVAL RELEASE RHYTHM IN THE GRAPSID CRAB SESARMA PICTUM.

M. Saigusa. College of Liberal Arts and Sciences, Okayama Univ., Okayama.

Sesarma pictum is a terrestrial crab which inhabits banks at the seashore. Females incubate eggs in early summer, and after a few weeks they release zoea-larvae at the water's edge. This study examined the daily timing of larval release in the laboratory.

For this purpose ovigerous females were collected from the field at Kasaoka, Okayama Pref., and maintained under artificial 24-h light-dark cycles.

When they were exposed to a light regime whose phase was much the same as in nature, i.e. light-off at 20:00 and light-on at 5:00, the daily timing of larval release roughly coincided with the times of high water in the field. The correlation between the release timing and tidal cycles was recognized over 2-3 weeks. The phase of this free-running rhythm was clearly bimodal, not unimodal.

Both phases of this circa-tidal rhythm gradually delayed under a 24-h LD in which light-off was set at 1:00. However, it could not be confirmed whether the release timing was actually related to the onset of darkness, because of poor number of experiments.

BB 10

THE LOCOMOTOR ACTIVITY IN THE HAGFISH, EPTATRETUS BURGERI, UNDER THE VARIOUS LENGTH OF LIGHT-DARK CYCLES.

S.Ooka[1] and H.Kabasawa[2]. [1]Atomi College, Tokyo, [2]Keikyu Aburatsubo Marine Park Aquarium, Miura.

The locomotor activity in the hagfish, Eptatretus burgeri, was recorded by means of an infra-red light photocell system. The animal showed nocturnal activity in 12L:12D and had clear circadian rhythm in constant darkness.

The animals were exposed to various light-dark cycles greater and less than 24 hours which were gradually changed with 20 minutes interval successively for 7 months. The animals showed stable entrainment in 24±1 hours. Entrainment to greater and less than 24±1 hours produced a gradual decrease in activity time, and an entrance of activity to light time. The activity crossed over the light time, then settled in the adjacent dark time. The animals showed similar "beats" through the experiments. The maximum range of locomotor activity cycles was about 24±3 hours.

These results are explained in correlation with the effect of light pulse on the length of circadian rhythm in a previous work.

BB 11

LOCOMOTOR RHYTHM OF THE MUTANT CRICKET, GRYLLUS BIMACULATUS.

K. Hamada, H. Ito and I. Nakatani. Dept. of Biol., Fac. of Sci., Yamagata Univ., Yamagata.

The mutant cricket with white compound eyes was segregated from normal black eyed one in our laboratory. Melanin granules do not exist in the iris and the retinular pigment cells of the white eyed cricket. The records of locomotor activities of the crickets were done under the condition of two illuminating intensities (about 60 lx. and 600 lx.) in light period and with or without of dark shelter in a plastic box in which a cricket is confined, respectively. These records were continued from the stage of last instar nymph to two weeks after of the imaginal molt under 12-h light and 12-h dark photoperiodical condition at 24°C. Nocturnal rhythms in the wild cricket and diurnal rhythms in the mutant cricket were can not observed through the stage of larva to imago, while several mutant crickets showed nocturnal rhythms through larval to imaginal stage when they reared with shelter. The difference of locomotor rhythm due to illumination intensity was not remarkable. These results may be show that the compound eye of mutant cricket to illumination slightly sensitive than the wild cricket.

EC 1

PLEVALENCE OF INTESTINAL HELMINTHS OF THE FROG(RANA BREVIPODA PORESA AND RANA JAPONICA)

Y. Sasaki and N. Makino. Dept. of Biology, Tokyo Med. Coll.,Tokyo.

Prevalence of enteric helminths were parasitic on the frog(Rana brevipoda porosa and Rana japonica) were studied during a 3 month period (Sep. from Jul.) This investigation is a part of studies that are going on one year. Fifty frogs (Rana b.p.) per month were captured at Inzai cho, Inba gun, Chiba Prefecture. Sex ratios of 150 frogs were approximately equal (48%♂:52%♀). Frogs (Rana j.) were collected small in number at the same place, and they were also examined in order to compare with Rana b.p.. The cestodes; Ophiotaenia sp. were observed at a low rate in the small intestine of Rana b.p..The nematodes;Oswaldocruzia sp. showed a high prevalence in the stomach and the duodenum of Rana j.. This nematodes were observed that they were laying eggs in September.The mature and immature trematodes; Diplodiscus amphichrus j. were observed in the small intestine of Rana b.p.and Rana j.. The nematodes ; Cosmoserca japonica displayed a very high prevalence in the rectum of both frogs. There were many females. And we always observed eggs and larvae for 3 months. Females laid eggs in the physiological salt solution and larvae hatched out in no time. Interestingly, some frogs were parasitic on larvae only in the rectum. Above-mentioned effects were no significant difference between males and females of host.

EC 2

THE ECOLOGICAL STUDY OF INLAND ANT-LION

T.Ohhashi,Biological Institute.Hyogo Univercity of Teacher Education,Hyogo.

Larvae of Hagenomyia micans MacLachian mainly constructed the pit under an overhanging precipice along a path and in case of Myrmeleon formicarius Limme under the floor of a temple and a shrine.Both species inhabited frequently in the same place.It seemed that there was no difference in habitat between the two species.

It was observed that both species passed the first winter in either the first or the second instar and second winter in the third(last)instar.It seemed to take three years from the egg to the adult in some cases.The reproductive activity of H.micans was a little later than that of M.formicarius.

These ant-lion larvaes mainly captured ants.Third instar larvae of M. formicarius living in larger-sized pits captured lager-sized and various prey.

EC 3

SEXUAL REPRODUCTION IN FOUR SYMPATRIC SPECIES OF THE CORAL GENUS MONTIPORA FROM OKINAWA.

T. Yeemin and K. Yamazato. Dept. of Biology, Univ. of the Ryukyus, Okinawa.

The mode and timing of sexual reproduction, mating pattern and embryogenesis were studied in four species of coral genus Montipora, namely, M. aequituberculata, M. peltiformis, M. digitata and M. sp.1, on the reefs of Sesoko Island, Okinawa. All species had an annual gametogenic cycle and were simultaneous hermaphrodites, bearing male and female gonads in the same polyps. Three species released gametes on a few nights following the full moon in June and the other, M. peltiformis in July, August and September. Eggs (bearing zooxanthellae) and sperm were packaged in a single cluster in each polyp before spawning. Egg diameters ranged from 312 µm (M. digitata) to 416 µm (M. sp.1). Fertilization and development were external. Cross-fertilization was the major mating pattern. Only M. sp.1 was capable of self-fertilization. Embryogenesis and larval development were observed. Developmental patterns and rates were similar in all the four species. First cleavage occurred at approximately 2 hours after spawning. The majority of larvae had settled within 4-7 days in aggregates on small tiles and limestone substrate under laboratory conditions.

EC 4

REPLODUCTIVE ECOLOGY OF A SCLERACTINIAN CORAL GALAXEA FASCICULARIS LINNAEUS (GAMATEGENESIS AND FERTILIZATION).

M. Minei and K. Yamazato. Dept. of Biology, Univ. of the Ryukyus, Okinawa.

Galaxea fascicularis has two types : Soft and Hard. In 1987, the spawning of Soft type was observed on June 17-19 in the freshly collected colonies and on June 18 and July 17 in the field, and that of Hard type on July 16-18 and August 15-17 in the freshly collected colonies. Main spawning season of Soft type was June while that Hard type was August. All spawning occured about 7 days after full moon.

G. fascicularis have been reported as hermaphroditic coral. However, our studies showed that G. fascicularis had female colony that contain eggs only in the mesentery and hermaphroditic colony that contain both eggs and testes in the mesentery. The ratio of female and hermaphroditic colonies are about 3 : 2. Male colony was not found.

On both types almost all eggs from female colony ćould be fertilized and develop. However, eggs from hermaphroditic colony did not develop by self or cross fertilization. Thus, eggs from hermaphoroditic colony had no function.

EC 5

DISTRIBUTION OF THE DEEP SEA SHRIMP, EUALUS BIUNGUIS IN THE JAPAN SEA.

H.Ito. Nansei Reg.Fish.Res.Lab.,Hiroshima.

Eualus biunguis is genarally known as a deep sea shrimp in the Northern Pacific Ocean. An ecological survey was carried out on the shrimp from 1969 to 1971 in the central areas of the Japan Sea.

The results obtained are as follows:
1) The animal inhabits the coastal waters of Hokkaido,Honshu,and Peter the Great Bay. It is also distributed in offshore reefs and bank areas such as Yamato-tai,Kita-Yamato-tai,Shin-Oki-tai,and Hakusan-se. The southern extremity is located around 36°06' N and this may be considered the southern most distribution of the species in the northern hemisphere.
2) The shrimp is distributed in the strata from a depth 208m down to 1250m,but most frequentlly dwells within the depth range of 600m and 1000m.
3) Judging from the carapace length composition of males and females,there is no evidence of sexual habitat segregation in the strata of the water depths

EC 7

MECHANISM OF DIEL ACTIVITY OF CONTRACTION AND EXPANSION OF A FAVIID CORAL, GONIASTREA ASPERA.

Y.Nakano and K.Yamazato. Dept. of Biol., Univ. of Ryukyus, Okinawa.

We studied the adaptive strategy and the mechanisms of diel activity of contraction and expansion of the polyps of a faviid coral, Goniastrea aspera. This coral occupies the upper limit of coral distribution, that is, the infralittoral subzone, and is found abundant on the reef near Sesoko Marine Science Center. The polyps of this coral contract during the day and expand during the night in the field. Our study revealed the following in the laboratry:
1) They remained expanded under continuous light and contracted under continuous darkness.
2) When the light-dark periods shortened (L:D= 6:6, 3:3), the contraction-expansion periods became shorter accordingly.
3) Under the red or green light, they expanded.

These results suggest that the contraction and expansion behavior of the polyps were directly controlled by light condition. However, the behavior was indirectly by the energy supply of zooxanthellae The behavior is closely connected with photosynthesis.

EC 6

HISTOCOMPATIBILITY GRAFTING BIOASSAY IN A CORAL PORITES (SYNARAEA) RUS

K. Miyara and K. Yamazato. Dept. of Biol. , Univ. of the Ryukyus, Okinawa.

The screlactinian coral Porites (Synaraea) rus is living over approximately 1 km on the reef of south-eastern coast of Sesoko Is. , Okinawa. They were dioecious and made of six color-morphs. Twenty seven colonies containing either one or both sexes of five color-morph from this reef were used for histocompatibility grafting bioassay during six months. All iso-graft pairs (N = 27, for control) fused ($p<0.001$), while allo-graft pairs (N = 224) showed fusion reaction only in the case of the same color-molph with the same sex (N = 65, $p < 0.005$) with few exception. Moreover the colony size (in a diameter) that could be expected to have been derived from fragments (N = 87, mean diameter = 8.8 cm, measured within two weeks after the typhoon No. 12) tended to increase in number of colonies within each population. However, the number of small size colony that were expected to have been recruited from planulae did not increase.

In conclusion, P. (S.) rus in Sesoko Is. occur in clonal populations characterized by each color-morph, which were derived from fragmentation.

EC 8

REGRESSION OF THE VALVULA CEREBE OF PERCIDA.

K. UCHIHASI SEKIHAN LABORATOTY, AKASHI.

As for the habitats of the species of Percida, I classified them into five, i.e., the surface layer, the ridge area, the middle layer, the bottom layer and the deep sea bottom, from each of which I got the sample. Next I made median longitudinal sections (15-20 μ) of valvula cerebelli, stained them with Nissl's method and examined them. As the result of the survey, I found out that the shapes of valvula cerebelli of every one of the forms that have differentiated from primitive Thunnus alalunga to Allolepis , pollandi, are going on with regression. This fact shows the adaptive radiation of Percida, and I also presume that this is because there may have been the diversification of the oceans including the enlargement of the floors of the oceans during the Cretaceous period. Now, while Clupeida, which came into being during the Jurassic period, shows the progresive differentiation of its valvula cerebelli, Percida which appeared during the Cretaceous period shows excessive regression.

TS 1

KARYOLOGICAL AND TAXONOMIC STUDIES OF THE DUGESIA SPECIES IN SOUTHEAST ASIA. XI. CHROMOSOMES OF DUGESIA JAPONICA JAPONICA AND DUGESIA SP. FROM TAIWAN.

S.Tamura[1], I.Oki[1], M.Kawakatsu[2], M.Takai[3], K.-Y.Lue[4], H.Hori[5], A.Muto[6], and S.Osawa[6]. [1]Ôsaka Pref.Inst.Publ.Health, Ôsaka, [2]Biol. Lab., Fuji Women's Coll., Sapporo, [3]Biol. Lab., Saga Med.Coll., Saga, [4]Natn.Taiwan Normal Univ., Taipei, Taiwan, [5]Gen-Iken, Hiroshima Univ., Hiroshima, and [6]Lab.Molec. Gen., Dept.Biol., Fac.Sci., Nagoya Univ., Nagoya.

The animals of Dugesia species from additional 5 localities of Taiwan were examined cytologically.

The 8 karyotypes of animals of Dugesia japonica japonica were found from 4 localities (Uulai, Hsiaoi, Liukuei, and Chihpên Hot Spring). They are as follows: 2x=16, 3x=24, (3x-1)+1LB=24, (3x-1)+1LB+SB=24+SB, (3x-1)+2LB=25, 3x & (3x-1)+1LB=24 & 24, 3x +1LB & (3x-1)+2LB=25 & 25, and (3x-1)+2LB & (3x-1-1)+3LB=25 & 25. The mixokaryotypes were found in animals from Uulai, Hsiaoi and Chihpên localities.

The chromosome numbers (including no. of SB chromosomes) of Dugesia sp. from Lanhsü Island are as follows: 19, 19 & 21 & 25, 19 & 24 & 25 & 26, and 19 & 21 & 24 & 25 & 26. The karyotypes are unidentified yet. Judging from the shape of each chromosome of Dugesia sp. of Lanhsü Island, the species is different from D. japonica and Dugesia sp. (species of Taiwan) reported in 1979 (Kawakatsu et al.).

TS 2

KARYOLOGICAL AND TAXONOMIC STUDIES OF THE DUGESIA SPECIES IN SOUTHEAST ASIA. XII. A SYNTHETIC REPORT ON THE TAXONOMY OF FRESHWATER PLANARIANS FROM TAIWAN.

M.Kawakatsu[1], I.Oki[2], S.Tamura[2], M.Takai[3], K.-Y.Lue[4], H.Hori[5], A.Muto[6], and S.Osawa[6]. [1]Biol.Lab., Fuji Women's Coll., Sapporo, [2]Ôsaka Pref.Inst.Publ.Health, Ôsaka, [3]Biol. Lab., Saga Med.Coll., Saga, [4]Natn. Taiwan Normal Univ., Taipei, Taiwan, [5]Gen-Iken, Hiroshima Univ., Hiroshima, and [6]Lab.Molec. Gen., Dept.Biol., Fac.Sci., Nagoya Univ., Nagoya.

For the past 20 years, the freshwater planarian fauna of Taiwan and the karyology of this animal group have become very clear.

Dugesia japonica japonica Ichikawa et Kawakatsu, 1964. This species is commonly found both in the lowland and alpine regions of Taiwan. Its chromosome number is essentially n=8 and 2x=16. Some other homo- and mixokaryotypes were also found. D. j. ryukyuensis Kawakatsu, 1976, is not distributed in Taiwan.

Dugesia sp. (species of Taiwan). This species is only recorded from the swampy places in the vicinity of Taipei. Its karyotype includes a pair of subtelocentric chromosomes (2x=16). There is a high possibility that the species is identical with D. austroasiatica Kawakatsu, 1985.

Dugesia sp. (species of Lanhsü Island). Although its karyotypes are unidentified yet, this species is only found in Lanhsü Island now.

TS 3

HYBRIDIZATION EXPERIMENTS IN CYPRINIDA (II). CROSS BETWEEN CARASSIUS CARASSIUS AND CTENOPHARYNGODON IDELLUS.

M.Kasama and H.Kobayasi. Dept. of Biol., Jap. Women's Univ., Tokyo.

Intergeneric cross was performed with Carassius carassius and Ctenopharyngodon idellus . About 41 % of eggs produced from this cross was developed into embryos. Almost all of embryos hatched, but many of hatched larvae suffered from edamatous syndrome, bend body and circulatory failture. Finally 56 hybrids could be reared until the adult form. Forty-one of them were analyzed morphologically and karyologically at the age of about one and a half years, and the others were subsequently reared in the laboratory.

Based upon 17 characters selected on the basis of marked and consistent differences between parental species, the hybrid index was within the range considered intermediate. But only 4 of 17 characters were intermediate, and 10 were closer to C. carassius. The phenotype of hybrid was more similar to C.carassius than intermediate.

The chromosome number of all hybrids was 124. These chromosomes were distinguished into 28 metacentrics, 50 submetacentrics and 46 acrocentrics, which was karyotype incorporating two genomes of C. carassius and one of C.idellus.

These data confirm that the hybrids are rather similar to C.carassius than intermediate. And it seems that the trend of resembalance to C.carassius in almost all characters results from the unbalanced reception of inheritance from parental species.

TS 4

MARINE HYDROIDS FROM OKINAWA ISLANDS.

M. Yamada. Biol. Lab., Oshamambe Branch, Science University of Tokyo, Oshamambe, Hokkaido.

The marine hydroid fauna of Okinawa Islands was studied chiefly in the vicinity of Sesoko Marine Science Center of the Univ. of the Ryukyus in 1985-86. Four athecate and nine thecate species were able to be identified. In addition to them over ten species were found, but these were not identifiable owing to their lacking of gonophores. Most of the species identied are the species already known from the Japanese waters but two ones are newly added to the Japanese fauna. Among the species identified the biogeographically interesting ones are as follows: Asyncoryne ryniensis Warren which is ever known from South Africa and the Seychelles is first recorded from the Pacific; Myrionema amboinense Pictet known from the Philippines and the Indo-Pacific is also first recorded from Japan. The finding of Eugymnanthea inquilina is the southernmost record from Japan. It is indicated that the marine hydroid species in Okinawa Islands are mostly temperate or subtropical ones and no boreal species were found.

TS 5

URBAN TARDIGRADES IN HOKURIKU AREA.

K.Utsugi. Dept. of Biol.,Tokyo Women's Medical College, Tokyo.

For studying the urban tardigrades, mosses or lichens were collected at 105 stations from 11 cities in the Hokuriku area(Tsuruga,Fukui,Kanazawa,Nanao,Takaoka, Toyama,Uotsu,Itoigawa,Joetsu,Kashiwazaki and Niigata) during a period from 1984 to 1987.

The presence of tardigrades were microscopically examined in the precipitates after macerating the mosses or lichens for a few hours. Then most of the specimens were treated with heat and mounted in Gum-chloral for phase microscope observation. Some of them were fixed in 5 % formalin after heat treatment and prepared for SEM observation.

19 species were found at 53 stations in 11 cities. 6 species including Macrobiotus harmsworthi, M.hufelandi, M.intermedius, M.occidentalis, Milnesium tardigradum and Echiniscus japonicus were commonly found in many stations,however,the other 13 species including M.richtersi, Hypsibius sp. H.dujardini, Isohypsibius schaudinni, Diphascon scoticus, Echiniscus baius*, E. lapponicus, E.rugospinosus*, E.testudo quadrifilis*, Pseudehiniscus suillus, P. facettalis, P.ramazzotti f.facettalis and Cornechiniscus lobatus were rarely found in urban areas.

Among these tardigrades, three species indicated by "*" were reported for the first time in Japan.

TS 6

BIOCHEMICAL EVIDENCE FOR THE GENETIC DISTINCTION BETWEEN Ciona intestinalis AND Ciona savignyi.

A. Hino, T. Kobayashi[2] and K. Numachi[2].
[1]Dept. of Biology, Nagoya Univ., Aichi and [2]Otsuchi Marine Research Center, Ocean Res. Institute, Univ. of Tokyo, Iwate.

Ciona intestinaris and C. savignyi are distinguished from each other by several minor but distinct feature (Hoshino and Nishikawa, '85). An electrophoretic investigation was designed to obtain further information on the taxonomic and genetic relationship between these two morphologically similar species. Mature specimens of both species were collected at Onagawa bay. Ovary and intestine were mixed and homogenized, then these supernatant were subjected to horizontal electrophoresis in 12.5% starch gel (6mm thick). Gels were holizontally sliced into 1mm thick pieces and stained in the required fashion. MDH, AK and EST-2 showed a single (monomorphic) bands and all of their mobility were different between species. In ICDH, single- and double-banded phenotypes which corresponded homo and heterozygous state were detected. These bands showed same mobility between species. Polymorphic patterns were also obtained in PHI, EST-2 and catalase and the mobility of their bands was different between two species. The allele frequencies of seven loci were calculated from each 32 individual samples. Based on these data, the genetic distance (Nei,'72) between Ciona intestinaris and C. savignyi was computed at 0.869.

TS 7

GENETIC POLYMORPHISM DEDUCED FROM RESTRICTION PATTERNS OF DNA IN THE GENUS, CIONA

K. Owada and M. Hoshi. Biol. Lab., Fac. of Sci., Tokyo Inst. of Technol., Tokyo.

Genetic polymorphism was studied in the genus Ciona; C. intestinalis from Otsuchi, Yamada, Misaki, Nagoya, Toyama and Maizuru and C. savignyi from Asamushi, Yamada and Misaki. Nuclear DNA extracted from individuals was digested with Bam HI. The degradation products were electrophoretically analyzed by ethidium bromide (EtBr) staining and by Southern hybridization. A 6.6kb mouse rDNA fragment including 18S and 28S DNAs and the non-transcribed spacer region (NTS) were used as a probe.

Polymorphic patterns were observed in EtBr-stained gel. The visible bands suggesting highly repetitious sequence were detected at 2.8, 6.5, 8.5, 9.0, 14.0 and 17.0kb. The bands of 2.8, 6.5 and 9.0kb comprised rRNA gene. The repetitious bands were observed in most of C. savignyi but in less than 50% of C. intestinalis.

The rDNA 18S-28S probe detected five bands of 2.8, 6.5, 7.4, 8.5 and 9.0kb. These patterns showed variability of the NTS within rDNA repeating units. The 7.4kb band was found at Misaki and 8.5kb band at Asamushi in C. savignyi. This diversity suggests a heterogeneity in the sequence and/or length of NTS.

Restriction patterns are remarkably different among the populations from different localities, which suggests a regional isolation of Ciona reproduction.

TS 8

BIOCHEMICAL STUDY ON THE TAXONOMIC RELATIONSHIP OF THE TWO MORPHOLOGICALLY VERY SIMILAR SEA-URCHINS, ECHINOSTREPHUS ACICULATUS AND E. MOLARIS.

N. Matsuoka and H. Suzuki. Dept. of Biol., Fac. of Sci., Hirosaki Univ., Hirosaki.

The genus Echinostrephus of the family Echinometridae (Echinoida: Echinoidea) comprises only two living sea-urchin species. They are E.aciculatus A.Agassiz and E.molaris(Blainville). These two species are very similar morphologically and therefore have often been confused with each other. The taxonomic relationship of these two morphologically very similar sea-urchin species was examined by means of gel electrophoresis of 18 different enzyme systems. The results demonstrated that the two species shared common allozymes at 25 of the 26 genetic loci studied here and that the Nei's genetic identity value(I=0.963) obtained between the two species was comparable to those already reported between conspecific local populations of many other animals. Their genetic similarity verified by the present electrophoretic study and their morphological and ecological similarity strongly suggest that E. aciculatus and E. molaris may belong to one and the same species.

TS 9

APPLICATION OF A TWO-DIMENSIONAL POLYACRYLAMIDE GEL ELECTROPHORESIS METHOD TO SYSTEMATIC STUDY OF LAND SNAILS IN SUBGENUS LUCHUPHAEDUSA.

J.Miyazaki, R.Ueshima, and T.Hirabayashi. Inst. Biol. Sci., Univ. of Tsukuba, Ibaraki.

The radiation process and the phylogeny of land snails in subgenus *Luchuphaedusa* are intriguing subjects, since its distribution in the southwestern Japan is peculiar and is not interrupted by biogeographical boundaries suggested by other examples, and the phylogenetic relationships of members in this group are not clear. We compared by 2D PAGE the large form of *Tyrannophaedusa* (*Luchuphaedusa*) *ophidoon* with 8 members of this subgenus and 2 species of different subgenera of the same genus, and obtained the similarity ranging from 0.989 to 0.667. The similarity between the large form and *T.* (*Decolliphaedusa*) *bilabrata* was lowest, while two species of the other subgenus, *Nesiophaedusa*, were very similar to the large form. The difference was very small between two specimens of the large form. The small form of *T.* (*L.*) *ophidoon* was significantly different from the large form. We estimated the relationship of the large and small forms to be closely related species or distantly differentiated intraspecific populations by comparing our result with available data obtained previously.

TS 10

A NEW SPECIES OF GENUS JULIA FROM OKINAWA ISLAND

S.Mizofuchi[1] and T.Yamasu[2] [1]Dept.Biol., Coll. Sci., Univ. Ryukyus, [2]Div.Gen.Educ., Univ. Ryukyus, Okinawa.

Several hundred living specimens of genus *Julia* were collected at Sunabe, Okinawa in 1986 and 1987. We found about 20 specimens showing some different characteristics from other known species of the same genus.

General morphology of these specimens is similar to that of *J. mishimaensis* except for some remarks. The specimens are light greenish yellow both on the body and the shell. Several red spots are scattered near the top of each valve. Each rhinophore provide with double brown bands at the mid portion.

We found they fed on *Caulerpa fastigiata* exclusively and not on *C. ambigua* as the other four species of the same genus did. Spawning habits of the adults are closely similar to those of *J. mishimaensis*. Shape of radular teeth are different from those of other species. The tooth is wider in width and thinner in thickness. Comb-like sculpture on the lateral sides of the teeth is faint than those of the other species.

Considering morphological features and habits of the specimens, it seems to be reasonable that the specimen is a new species in genus *Julia*.

TS 11

A NEW SPECIES OF MARINE INTERSTITIAL OSTRACODA OF THE GENUS PSAMMOCYTHERE FROM KUSHIRO, HOKKAIDO.

S. Hiruta. Biol. Lab., Kushiro College Hokkaido Univ. of Educ., Kushiro.

A new species of the genus *Psammocythere* (Ostracoda) was collected from a sandy shore at Kushiro, Hokkaido. This is the fourth record of the genus from the world. The new species resembles *Ps. santacruzensis* Gottwald, 1983 from Galapagos in appendage morphology, but the structure of carapace is clearly different from each other.

The family psammocytheridae which contains only the genus *psammocythere* is considered as a sister group of all the other cytheracean groups, because the former has four-segmented endopodite of the legs (except leg 1 in male), while the latter has three-segmented endopodite (Gottwald, 1983). The primitive character (four-segmented endopodite) has been preserved in interstitial environment.

Judging from the worldwide distribution of the genus *Psammocythere* and the fossil record of the superfamily Cytheracea to which the genus belongs, it is considered that the genus would colonize in marine interstitial habitat during the lower Mesozoic at the latest.

TS 12

ON THE ANAL OPERCULUM OF HARPACTICOID COPEPODS.

Y. Kikuchi. Itako Hydrobiol. Stat., Fac. of Sci., Ibaraki Univ., Itako-machi.

For several years, I have examined on morphology of anal operculum of freshwater and terrestrial harpacticoid copepods using SEM and phase contrast microscope. The anal opercula are various in shapes: semi-circular, triangular, transverse narrow plate and comb. Some of the anal opercula being semi-circular attached to one to five spines on its hind margin, for instance, as *Epactophanes richardi*. *Elaphoidella grandidieri*, semi-terrestrial species, have comb-shaped anal operculum of muscular membrane.

The anal opercula of several species of genus *Canthocamptus* were transverse narrow plate, triangular and semi-circular. Consequently they were able to be distinguished in each species by the morphological differences of anal operculum.

Functions of anal operculum are a little known. It seems that anal operculum shields harpacticoid anus from harm or danger. Anal opercula of terrestrial harpacticoid copepods trended to elongate by comparison with freshwater ones. It has been suggested, or implied that anal operculum is advantageous for preventing evapolation from anus in low humid conditions as leaf litters of forest.

TS 13

THE PREZOEA STAGE IN DECAPOD CRUSTACEANS

R. Quintana and K. Konishi. Zool. Inst., Fac. of Sci., Hokkaido Univ., Sapporo 060.

Some basic problems on prezoea larva are reviewed. A discussion on misunderstandings due to its nature and very short duration (normally few minutes) is made. Recent evidences have proved that the prezoea occurs as a normal stage in the ontogenic development of a wide variety of decapod crustaceans.

Transverse sections of the prezoea stage of Pagurus brachiomastus (Thallwitz) were made to determine the fine structure of the prezoeal cuticle and the exoskeleton of the first zoea, by using transmission electron microscopy. The thin cuticle covering the newly hatched prezoea is 15-17 nm thick, which is approximately 24 times thinner than the zoeal cuticle. High resolution revealed a trilaminar structure of the prezoeal cuticle, which is composed of an outer layer, approximately 4.4 nm thick, a mid lighter layer, 3.5 nm thick, and an inner layer, 7.7 nm thick.

During the prezoeal stage, the inner zoeal exoskeleton consists of an epicuticle and exocuticle, measuring approximately 0.36 μm thick. At this stage, there were no indications of the formation of endocuticle.

TS 14

IDENTIFICATION OF BIFURCATE PARAOCULAR PROCESS AND POSTOCULAR FILAMENTARY TUFT OF "CYPRIS Y" (CRUSTACEA)

T. Itô[1], M. Takenaka[2]. [1]Seto Mar. Biol. Lab., Kyoto Univ., Shirahama, Wakayama, [2]Ushimado Mar. Lab., Okayama Univ., Ushimado, Okayama.

Ultrastructures of the bifurcate paraocular process and the postocular filamentary tuft in "cypris y" were examined using TEM. The bifurcate paraocular process is accompanied proximally with a mass of complex lamellar structures that are apical branches of cilia arising from what appear to be nerve cells, and each cilium contains 9+0 microtubules. It is concluded that the bifurcate paraocular process is an external portion of the organ of Bellonci, which is well known in cirripedes and some other crustaceans. There is little doubt that the bifurcate, frontal filaments known in nectiopodans are also an external portion of the same organ. The postocular filamentary tuft is continuous with two kinds of compactly aggregated, prominent cells, in which one is characterized by the possession of dense mitochondria, the other is characterized by granular inclusions. The filaments rise from the latter kind of cell. This organ, although it is not connected with any duct, is similar in ultrastructure to the cement glands known in cirripede and rhizocephalan cyprids.

TS 15

DISCOVERY OF A NEW SPECIES OF THE PHYLUM LORICIFERA FROM THE IZU-OGASAWARA TRENCH

Y. Shirayama[1] and R.M. Kristensen[2]. [1]Ocean Res. Inst., Univ. of Tokyo, Tokyo, [2]Inst. Cell Biol. Anatomy, Zool. Inst., Univ. Copenhagen, Copenhagen Ø, Denmark

A new species of the most recently described phylum, Loricifera Kristensen, 1983, was discovered from the red clay collected at ST. 9 of a cruise of RV Hakuhō Maru, ORI, UT. The station was situated close to the axis of the Izu-Ogasawara Trench at a depth of 8260 m. The present species was found to belong to the genus *Pliciloricus* (Pliciloricidae) and is the most closely related to *P. profundus* Higgins and Kristensen, 1986 in the presence of single pair of P-flosculi, the type of mouth cone and clavoscalids, and the claw-shaped spinoscalids. Unique to the present species is its bulb-like shape of the lorica, the mucous coat of the larval lorica and the 30 sculptured plates in the adult thorax. This is the first record of loriciferans from the Indo-Western Pacific area. In addition, the habitat of the present species is completely different from the other congeneric species. Though the former was discovered from very fine sediment of the hadal depth, all described species so far have been collected exclusively from sublittoral coarse sands off the southeastern coast of the USA. Moreover, in contrast to the interstitial nature of the other species, the present species probably burrows within the sediment. These findings suggest that loriciferans have great ability to adapt to various kinds of habitat and the phylum is distributed ubiquitously throughout marine environments.

TS 16

THE STRUCTURE OF THE DIGITS IN ORZELISCUS TARDIGRADA AND ITS TAXONOMIC SIGNIFICANCE

H.NODA (SETO MAR.BIOL.LAB.,KYOTO UNIVERSITY SHIRAHAMA, WAKAYAMA.)

The detailed structure of the digit of the genus Orzeliscus is described.

Digit is composed of four parts; a stump-shaped proximal portion of the stalk rising directly from the tibia, a round distal portion of the stalk, a ventral club-shaped swelling, and a dorsal rod forming itself a middorsal ridge of the swelling. The swelling is somewhat depressed dorsoventrally and is fringed with a narrow membrane.

Some previously unknown similarities in legs are recognized between Orzeliscus, which was formerly belonged to Batillipedidae but which currently belongs to Halechiniscidae, and Batillipes (Batillipedidae). "E,toe disc", "D,brace", "C,distal stalk enlargement" and "A,distal portion of stalk" in Batillipes in the sense of McKirdy(1975) correspond to the ventral swelling, the dorsal rod, the distal portion of the stalk and the proximal portion of the stalk in Orzeliscus, respectively.

Based upon this observation, the taxonomic problems between the two families are discussed.

TS 17

SYSTEMATIC POSITION OF THE FAMILY MARINONISCIDAE (CRUSTACEA: ISOPODA)

N.Nunomura. Toyama Science Museum, Toyama

A new family Marinoniscidae was created for the specimens collected in the tidal zone, Amakusa, Kyushu and later the second species was collected in the supertidal zone of Okinoerabu Island, Ryukyu Islands.

Judging from absence of pseudotracheae and having a single genital papilla, Marinoniscidae should be included in the group, Crinocheta-Oniscoidea. Among this group, Marinoniscidae resembles the families Scyphacidae, Halophilosciidae and Olibrinidae both in many morphological features and halophil habitat. Marinoniscidae has some primitive features such as long 6-7 segmented flagellum of antennae, presence of 12 teeth on the outer lobe of maxillule and presence of distinct incisions on palp of maxilliped, otherwise, Marinoniscidae has also some advanced features such as a single tuft of molar process of mandibles and presence of noduli lateralis. From the results compared above, Marinoniscidae and other above-mentioned families considered to have been derived independently from some stock of Diplocheta in not so recent years.

TS 18

ON SOME ISOPOD CRUSTACEANS FROM THE JAPAN TRENCH.

S. Gamô. Dept. of Biol., Fac. of Educ., Yokohama Natl. Univ., Yokohama.

Four new deep-sea asellote isopods were taken from far off Kinkazan by the marine biological research of the Japan Trench and its vicinities, which was carried out by R/V Hakuho-Maru of the Ocean Res. Inst., Univ. of Tokyo, during the cruise KH-81-4 (6 Jul.- 4 Aug., 1981). The specimens were collected by beam-trawl and box-corer.

1) Macrostylis sp. (A)., a female, 5.8 mm long, collected from 6386-6450 m deep. Body compact, elliptical in dorsal view, more than 3 times as long as its width. Eye absent. 2) M. sp. (B)., a female, 5.2 mm, from 6380 m. Body compact, elliptical, nearly 2 1/2 times as long as its width. Eye absent. These species differ from the other members of the genus by their elliptical shape of body. 3) Janirella sp., a female, 2.6 mm, from 6380 m. Body elliptical, with sparse spines. Each body segment has 1-3 lateral projections with 2-3 apical spines. Eye absent. This species is allied to J. tuberculata Birstein, 1963, from 5350-7817 m. 4) Janirallata sp., a female, 10.9 mm, from 1890-1900 m. Body flattened, oblong. Each body segment has 2 lateral projections with serrated borders and 1-2 long apical setae. Eye present. This species resembles J. serrata Birstein, 1963, from 1641 m.

TS 19

ALPHEID SHRIMPS (CRUSTACEA, DECAPODA) FROM THE PACIFIC COAST OF N.- AND S.-AMERICAS IN THE COLLECTION OF THE ZOOLOGISCHES MUSEUM, UNIVERSITAT HAMBURG, W. GERMANY.

Y. Miya. Fac. of Liberal Arts, Nagasaki Univ., Nagasaki.

In the collection of the Zoologisches Museum, Universität Hamburg there are found 12 species of Alpheidae collected from the Pacific coast of N.- and S.-Americas. They were taken from various localities from San Pedro, California southward to Tocopila, N. Chile in date from the 1890s to the 1910s by captains of merchant ships for the Museum Godeffroy. Then they were placed under the control of the ZMUH. During the World War II the museum was destroyed, but the specimens were stored away in a safe place.

The species are listed as follows: Alpheus clamator, A. cf. chilensis, A. cristulifrons, A. cylindricus, A. formosus, A. lottini, Synalpheus charon, S. fritzmuelleri, S. spinifrons, S. townsendi brevispinis, Betaeus emarginatus, B. truncatus. Among them A. cristulifrons and A. formosus are newly recorded from the Pacific coast and should be enumerated as the amphi-American species. Morphological characteristics of S. t. brevispinis, which is represented by a young male specimen (6.8 mm in body length) from Iquique, Chile, are closely compared with 3 other subspecies.

TS 20

GENETIC AND ENVIRONMENTAL EFFECTS ON THE VARIATIONS IN REPRODUCTIVE CHARACTERISTICS IN HYNOBIUS NIGRESCENS

Hisashi Takahashi and Hisaaki Iwasawa. Biol. Inst., Niigata Univ., Niigata.

In 6 populations of H. nigrescens living at various altitudes, and with various spawning dates, the relationships of clutch size, egg size and total egg volume to female body size were studied. Body size significantly differed among populations, being larger in earlier breeding populations. There was a negative correlation between body size and total egg volume in all the populations examined. On the other hand, as for the relationship of clutch size and egg size to body size, the populations were divided into 2 groups; the body size correlated with clutch size in one group, and correlated with egg size in the other one. Adjusted means of clutch size, egg size and total egg volume, which mean the averages except for the effect of difference in body size, significantly differed among populations. It is conceivable that the interpopulational variations in the adjusted means of clutch size and egg size are caused by the difference in the allocation of ooplasm among populations. These phenomena may be due to genetic factors. It seems that the difference in the' adjusted means of total egg volume among populations is affected by environmental factors, such as breeding periods.

TS 21

MORPHOLOGICAL FEATURES OF HYNOBIUS SP. (URODELA) OF CENTRAL JAPAN.

H. Nambu. Toyama Science Museum, Toyama.

Morphological features of Hynobius sp. collected from the mountain areas of Japan Sea side of Central Japan were studied comparing with species belonging to "nebulosus group", H.lichenatus, H. tokyoensis, H.nebulosus and H.takedai.

The present species is characterized by unique skull feature, unique shape of vomer teeth series, less number of teeth and lack in the 5th toe of hind limb.

Nasal, prefrontal, frontal and vomer of this species are not developed, but parietal is well developed. Skull length of this species is apparently smaller than that of H.lichenatus. In vomer teeth series of this species, outer branch is short and principal branch is narrow in comparison with that of the other species compared. Number of vomer, upper jaw and mandible teeth are smaller than that of the other species compared. The 5th toe of hind limb is almost lacking, although in other species, the 5th toe is developed. Number of trunk vertebrae of this species, H.lichenatus, H.takedai and H.nebulosus from Tottori are 17. However, that of H. tokyoensis and H.nebulosus from Okayama and Nagasaki are 18.

From the results obtained, it is concluded that the present species is apparently discernible from the Hynobius species hitherto described and is new to science.

TS 22

CHARACTERISTICS OF ADAPTATION TO TORRETIAL ENVIRONMENT FOUND IN BUFO TORRENTICOLA LARVAE.

Hisaaki Iwasawa and Kenichi Saito.
Biol. Inst., Niigata Univ., Niigata.

Eggs of B. torrenticola (B.t.) and of B. japonicus formosus (B.j.f.) were reared at 8, 18 °C and room temperature, and the larval morphology of the two species was compared. In young B. t. larvae, the external gills were remarkably underdeveloped. In the swimming larvae, the body was rather depressed, and well-developed musculature and poor fin were seen in the tail. The tail was relatively shorter in B. t. The oral part was strikingly well-developed in B. t.; the area of this part was ca. 8 mm^2 in full-grown larvae (St. 41), and this value was 3.2 times larger than in B. j. f. The labial processes were well-developed and the average number was 139 in the larvae of St. 41, and was 8.4 in B. j. f. in the same stage. The neuromasts were well developed in B. t. Metamorphic changes in the oral part occurred more suddenly in B. t. At 18 °C, B. t. larvae metamorphosed on the 52nd day after fertilization on average, and B. j. f. ones on the 45th day. The adaptation to torrential environment in B.t. larvae was seen most clearly in the sucker-like development of the oral part.

TS 23

PHYLOGENY OF *RANA LIMNOCHARIS* AND TWO ALLIED SPECIES.

M.Nishioka and M.Sumida. Lab. for Amphibian Biol.,Fac.of Sci.,Hiroshima Univ.,Hiroshima

Phylogenetic relations were biochemically examined among five populations, the Okayama, Hiroshima, Okinawa, Iriomote and Taiwan, of *Rana limnocharis*, two populations, the Philippine and Tai, of *Rana cancrivora* and the New Guinea population of *Platymantis papuensis*. Nineteen kinds of enzymes extracted from skeletal muscles and livers and two kinds of blood proteins of 64 frogs in total were analyzed by the method of starch-gel electrophoresis. It was found that there were 31 loci controlling these enzymes and blood proteins. At each locus, there were 2∿6 alleles, 3.8 on the average, which revealed 2∿8 phenotypes, 4.4 on the average. The mean proportion of heterozygous loci per individual, the mean proportion of polymorphic loci per population and the mean number of alleles per locus in the eight populations of the three species were 5.8%, 18.4% and 1.18, respectively.

A dendrogram generated from Nei's genetic distances (D) by the UPGMA method showed that the Okayama, Hiroshima and Okinawa populations resemble one another very closely (D=0.018 ∿ 0.053) and considerably distinct from the Taiwan and Iriomote populations (D=0.170 ∿ 0.321) in *R. limnocharis*. There is a high degree of dissimilarity between *R. limnocharia* and *R. cancrivora* (D=1.430∿1.747) and remarkably greater genetic dissimilarity between these two species and *P. papuensis* (D=3.217 ∿ 3.269).

TS 24

ISOZYMIC DIFFERENTIATION AND SPECIATION IN RANA NARINA FROM THE RYUKYU ARCHIPELAGO AND TAIWAN

M. Matsui, Biol. Lab.Yoshida Coll., Kyoto Univ., Kyoto.

Isozyme variation was studied in 96 individuals of Rana narina from throughout the species range (Amami-Oshima, Toku-no-shima, Okinawajima, Ishigakijima, Iriomotejima, and Taiwan). Starch gel electrophoresis was done to resolve 11 enzyme systems encoded by 15 presumptive loci. The calculated Nei's and Rogers' genetic distances indicated the presence of extreme genetic divergences among island populations. Although two allopatric populations from Iriomotejima were genetically almost identical (Nei's D= 0.03), two syntopic populations from Ishigakijima showed a clear genetic division from each other (D= 0.44). The result well agreed to the morphological evidence. The large-sized type was genetically very similar to two populations from Iriomotejima (D= 0.08), but the small-sized stood in the isolated position from other populations. The distribution pattern of several electromorphs (e.g., Ldh-B-a,b,d) indicated the occurrence in the past of multiple invasions by this frog complex into the Ryukyu Archipelago. Constructed UPGMA phenogram indicated the presence of five distinct lineages (Amami+ Toku, Okinawa, Ishigaki-small, Ishigaki-large+ Iriomote, Taiwan), and suggested the possibility of further taxonomic divisions in this species.

TS 25

BIOCHEMICAL VARIATION IN CYNOPS PYRRHOGASTER FROM WESTERN JAPAN.

T. Hayashi[1] and M. Matsui[2].
[1]Dept. of Zool., Fac. of Sci., Kyoto Univ., Kyoto and [2]Biol. Lab., Yoshida Coll., Kyoto Univ., Kyoto.

Using starch gel electrophoresis, we analysed 15 loci of 12 enzymes in 40 populations of C. pyrrhogaster collected from Kinki, Chugoku, Shikoku and Kyushu Districts. The UPGMA phenogram based on Nei's genetic distance (D) showed the following: (1)Three poplations from southern Kyushu are genetically differentiated from the other populations (mean D value = 0.145). (2)The latter group is divided into two subgroups with the mean D value being 0.050. One subgroup consists of populations from western Chugoku, Shikoku and middle and northern Kyushu, and the other from eastern Chugoku and Kinki. C. pyrrhogaster has been morphologically divided into six local races, of wich three (Hiroshima, Sasayama and Intermediate races) occur in western Japan. The analysis of allozymic variation revealed the following: (1)The division between Sasayama and Hiroshioma races are supported. (2)The division between Sasayama and Intermediate races is not supported. (3)Hiroshima race is not homogeneous but contains two distinct groups.

TS 26

MICROHABITAT OF TWO SYMPATRIC EUBRANCHIID NUDIBRANCHS, *E. RUSTYUS* AND *E. OLIVACEUS* (AEOLIDACEA) FROM CAPE ARAGO NEAR COOS BAY, OREGON.

Y.J.Hirano[1], J.H.R.Goddard[2] and Y.M.Hirano[3]
[1,3]Mukaishima Mar. Biol. Lab., Fac. of Sci., Hiroshima Univ. [2]Oregon Inst. Mar. Biol., Univ. of Oregon, U.S.A.

Eubranchus rustyus (Marcus, 1961) and *E. olivaceus* (O'Donoghue, 1922) were found together from a hydroid, *Plumularia* sp. growing on the seaweed, *Cystoceira* sp. in Cape Arago. *E. rustyus* always occurred on the part of *Plumularia* stalk and *E. olivaceus* always around the base of *Plumularia*. Although other species of hydroids, such as *Calycella* sp. and *Halecium* sp. were found around *Plumularia* stolon, observation of nematocysts in the cerata apparently showed that *E. rustyus* eats *Plumularia* hydranth and *E. olivaceus* eats *Plumularia* hydrorhiza. *Obelia* spp., which had been reported as major food resources of *E. olivaceus*, was not found nearby.

Difference of microhabitat between *E. rustyus* and *E. olivaceus* is considered to be caused by partition of feeding parts on the same hydroid. It is interesting as contrasted with the relationship between two *Eubranchus* species (*E. misakiensis* and *E. horii*) in Japan which occur together and eat completely different species of hydroids (Hirano & Hirano, 1985).

TS 27

TWO SYNGENS OF EUPLOTES HARPA (CILIOPHORA).

H.Kanemoto. Zool., Inst., Fac. of Sci., Hiroshima Univ., Hiroshima.

Using the encysting euryhaline ciliate Euplotes harpa, the way of sexual reproduction, number of mating types, and kinds of breeding systems have been investigated. In this species, two sibling species, syngen 1 and 2, were found, which have separate breeding systems from one another. Stocks of syngen 1 were collected from the Seto Inland Sea and the Sea of Japan, and undergo both inter- and intraclonal conjugations as the way of sexual reproduction. Viability of exconjugants from interclonal conjugations varied from cross to cross. When crossing two different stocks from areas being relatively far apart, viability of exconjugants was extremely low. But when crossing two stocks from the same area, viability was always high. On the other hand, viability of exconjugants from intraclonal conjugations was always more than 75%. This syngen has a multiple mating type system with seven mating types. Stocks of syngen 2 were collected from Ariake Bay and Beppu Bay, and undergo two kinds of conjugation the same as syngen 1 do. Viability of exconjugants from interclonal conjugation as well as those from intraclonal conjugation was constantly high. This syngen has a multiple mating type system with six mating types. There is no morphological difference between syngen 1 and 2, but no conjugations occur between them.

TS 28

AUTOGAMOUS STOCK IN SYNGEN 1 OF EUPLOTES WOODRUFFI (CILIOPHORA).

T. Kosaka. Zool., Inst., Fac. of sci., Hiroshima Univ., Hiroshima

All of the stocks studied belong to syngen 1 that is a brackish-water dweller, which are capable of undergoing conjugation, but not autogamy. One of 29 stocks that were recently collected and isolated from brackish water (5.5 - 10.5 ‰ in salinity) in Ariake Bay, Kyusyu, however, could undergo autogamy as well as conjugation. The others carried out only conjugation when another mating type stock was mixed together. All of the exautogamous F_1 clones from the autogamy stock were also capable of carrying out autogamy, but non-autogamy clones were not found among them. The length of autogamy immaturity measured on 12 of the exautogamous clones was between 33 and 51 cell divisions. The viability of exautogamonts was 75 to 100 % in 8 clones, 50 to 60 % in 3 clones, and 20 % in 1 clone. All exautogamous clones derived from the autogamy stock were capable also of making conjugating pairs with different mating type stocks of syngen 1, and produced viable exconjugant clones. However, autogamy seemed to occur more often than conjugation even when a mixture of the autogamy clone with non-autogamy clone was done.

TS 29

Studies on the classification of gregarines by crossinfection.

K. Hoshide and T. Inoue. Biol.Lab.,Fac. of Educ.,Yamaguchi Univ.,Yamaguchi.

We tried to identify the species of gregarines which parasitized different species of hosts by crossinfection. Gregarina blattarum was reported from various species of cockroaches, Blatta orientalis ,Blattella germanica,Ischroptera pennsylvanica and Periplaneta americana. All gregarines from the above hosts are thought to be the same species because they have the same morphology. A gametocyst of Gregarina blattarum was collected from the feces of Blattella germanica. The gametocyst was kept in a moistchamber. After two days it dehiscenced innumerable oocysts. We mixed these oocysts with bait and fed it to B.germanica,B.japonica, Periplaneta americana and P. japonica. B. germanica and B. japonica were infected with the gregarine but P. americana and P. japonica were not infected by this method. The crossinfection occurred only between different species of hosts in the same genus but did not occur in different genera. Judging from our results, the species of gregarine in Blattella germanica must be different from that in Periplaneta americana. The classification of gregarines which parasitized different genera of hosts must be reconsidered.

TS 30

LARVAL MORPHOLOGY AND METAMORPHOSIS OF THE MARINE BRYOZOAN PSEUDOCELLEPORINA TRIPLEX.

S. F. Mawatari[1] and Y. Nodasaka[2]. [1]Zool. Inst., Fac. Sci., Hokkaido Univ. and [2]Lab. Elec. Microsc., Sch. Dent., Hokkaido Univ.

The larval morphology and the metamorphosis of the marine bryozoan Pseudocelleporina triplex was examined by light and electron microscopy. The primary morphological characteristics of the larva are: (1) The pear-shaped body, (2) a large corona that forms most of the larval surface, (3) no eyespots, (4) a large apical disk without distinct blastemas, (5) a moderate pallial sinus and (6) a large internal sac. The larva is not referable to any previously reported larval types in having (1) a deep oral groove lined by a heavily ciliated epithelium, (2) a mass of large gland cells that secrete mucous into the oral groove and (3) no long vibratile plum.

Through the rapid morphogenesis after settlement, the most part of the cystid epidermis of the ancestrula was formed by the internal sac, but the remaining small portion by the pallial epithelium. This type of cystid formation is intermediate between the two well-known types, that is, the Bugula type in which the internal sac forms the entire epidermis and Watersipora type in which both the internal sac and pallial epithelium contribute half-and-half to the body wall epidermis of the ancestrula.

TS 31

PECULIAR MORPHOLOGICAL CHARACTERS OF THE HOPLONEMERTEAN SAGAMINEMERTES NAGAIENSIS WITH CONSIDERATION OF ITS SYSTEMATICS.

F. Iwata. Zool. Inst., Fac. of Sci., Hokkaido Univ., Sapporo.

In 1957 Iwata reported a new monostiliferous hoplonemertean Amphiporus nagaiensis. Subsequently Friedrich (1968) commented that this species should be placed in a new genus Sagaminemertes. The present revision on the material of S. nagaiensis has confirmed Kirsteuer's (1973) conclusion that this species belongs with the reptantic polystiliferous hoplonemerteans. Iwata originally missed two fundamental features, that the mouth and rhynchodaeum have separate apertures and that the proboscis armature consists of a sickle-shaped basis bearing about 20 minute stylets. However, morphological characters peculiar for the present species lies on that a distinct precerebral region is wanting and the mouth opens below the ventral commissure of the brain which is situated at the anterior end of the head. Furthermore the circulatory system involves the cephalic lacunae which do not anastomose anteriorly and a cerebral lacuna derived from the cephalic lacunae and dorsal vessel.

Sagaminemertes nagaiensis resembles in its internal characters Siboganemertes weberi Stiasny-Wijnhoff, 1923, to which the family Siboganemertidae and the subtribes Archireptantia were established in 1936.

TS 32

EVOLUTION OF SPERM POLYMORPHISM IN THE DROSOPHILA OBSCURA SPECIES SUBGROUP.

H. Takamori[1] and H. Kurokawa[2]. [1]Dept. of Biol., Tokyo Gakugei Univ., Tokyo and [2]Inst. of Biol. Sci., Univ. of Tsukuba, Ibaraki.

A polymorphic condition in spermatozoa (short/middle/long) characteristically exists in the Drosophila obscura species subgroup (Beatty and Sidhu, 1970; Policansky, 1970). In this study, the sperm length was newly measured in 1 species of the subgenus Scaptodrosophila and 3 species of the D. obscura species subgroup and remeasured in 4 species of this subgroup.

The males of D. alpina which is thought to be the most primitive form in the D. obscura subgroup showed an incompletely dimorphic pattern in sperm size. D. coracina, a member of the subgenus Scaptodrosophila which phylogenetically occupies the most primitive position in the genus Drosophila and is closest to the D. obscura species group (Throckmorton, 1975), produced monomorphic sperm. It is conceivable that males of an ancestral form of the D. obscura subgroup may have consistently produced monomorphic sperm, and evolved to produce dimorphic (short/long) sperm. The distribution of the sperm length in D. bifasciata appeared to be incompletely trimorphic, and complete trimorphism appears in D. obscura. Thus it is presumed that the long sperm gradually evolved into 2 types (middle/long) and eventually produced the complete trimorphic type.

TS 33

KARYOTYPES IN THREE JAPANESE SPECIES OF IRREGULAR SEA URCHINS.

K.Saotome, Yokohama City Institute of Health, Yokohama.

The unsolved problems still remain as to taxonomy of irregular sea urchins based on morphological viewpoints. One of them is classification of family in the suborder Laganina, which is divided into different numbers of family like 1,5,6 or 14 by several investigators (Shigei,1974). As cytogenetical techniques were considered to provide valuable information for echinoid taxonomy, chromosome numbers and karyotypes were examined in the order Clypeasteroida.

Chromosome numbers of three species; Clypeaster japonicus, Scaphechinus mirabilis and Astriclypeus manni were all 2n=46 (Saotome,1986). However, each species had its own karyotypes;1)in C.japonicus, the number of submetacentric pairs was larger than that of meta- or subtelocentric ones,2)karyotype of S.mirabilis was composed of many submeta- and subtelocentric pairs, and 3)A.Manni had many metacentric pairs.

As karyotype differed considerably between S.mirabilis and A.manni, it is reasonable that they belong to different families each other.

If chromosomes of many species are examined, karyological data may provie useful information for classification of family in the suborder Laganina.

TS 34

DISTRIBUTION OF PUSILLUS GROUP BATS OF THE GENUS RHINOLOPHUS WITH SPECIAL REFERENCE TO THEIR CESTODE FAUNA.

I. Sawada. Biol. Lab., Nara Sangyo Uni., Nara

The Rhinolophus bats are divided into the following five groups: arcuatus, pusillus, ferrumequinum, hipposideros and luctus. The bats of the pusillus group (small type bats) in Asia contain R. cornutus cornutus, R. c. orii, R. perditus, R. pumilus and R. imaizumii of Japan, R. monoceros of Taiwan, and R. pusillus and R. acuminatus of Thailand. Vampirolepis isensis is commonly parasitic on R. c. cornutus of various places in Japan with Tanaga-shima at their southernmost limit, on R. c. orii of Amami-oshima and Tanegashima, on R. perditus of Ishigaki-shima and on R. imaizumii of Iriomote-shima. At present, R. pusillus and R. acuminatus of Thailand were found not infected with any cestodes. R. monoceros of Taiwan was found infected with V. isensis.

According to the cestode fauna of these bats, R. monoceros of Taiwan may have a distributional connection with the bats of the pusillus group of Japan.

TS 35

SOME ADDITIONS TO SYSTEMATICALLY INTERESTING MICROSCOPICAL ANIMALCULES IN JAPAN.

M.Sudzuki[1] and S.Ohki[2] [1]Biol.Lab.,Nihon Daigaku Univ.,Omiya, [2]Saitama Institute of Environmental Pollution,Urawa.

Psammonobiotus communis Golemansky,1967, Proichtydioides sp.1 and Xenotrichula sp.1 were detected from the sample collected on 30,Aug.,86 at the sand beach by a lake Saiko around Mt.Fuji.The 1st one is a species regarded as "a psammobiont marine Testacea" (Golemansky,74;Chardez,77,80 & Sudzuki,79ab) but one exception by Golemansky(1967,70)who discovered it in a hygropsammon of a lake Ohridsko.So,our case means a second example. Body 40μm long,22μm wide and 18μm high.The 2nd is a gastrotrich species yet undescribed but belonging to a genus Proichtydioides (consisting of 1 species,remanei Sudzuki,1971),whose systemaric position is left untouched.This time 4 specimens were observed. Head: 30x14-15μm,trunk:40x12-15μm,foot:10-15 x 5μm,toes:20-24 μm.No pharyngeal pores,no eyes.Different from remanei in having 2-3 pairs of"Haftrörchen"(exclusively provided by marine order,Macrodasyoidea)on hind part of the trunk and relatively long head,foot toes.The 3rd is of also undescribed Gastrotricha but under Xenotrichula,all of which are reported to live in maritime beach.Filinia cornuta(Weisse,1874) is dealt with a rare brackish rotifer(Koste,1978).6 specimens collected on 8 May,87 from a site near a Yamato bridge on a creek,Kasumigawa,Saitama.Body 115-167μm;blades lateral 20-25μm, caudal 35-40μm;D-egg 45x35μm;Water=22.5 °C; pH=7.7;BOD=17.5mg/l,DO=6.9mg/l;Cl^-=54.3mg/l

TS 36

EXAMINATIONS OF THE ASTEROID SPECIMENS COLLECTED BY VON SIEBOLD AND A REVIEW OF THE EARLY TAXONOMICAL STUDIES ON JAPANESE ASTEROIDS.

M. Shigei[1], L.B. Holthuis[2] and T. Yamaguchi[3]
[1]Misaki Mar. Biol. Stat., Univ. of Tokyo, Kanagawa, [2] Rijksmuseum v. Natuur. Hist., Leiden, Netherlands, [3] Aitsu Mar. Biol. Stat., Univ. of Kumamoto, Kumamoto.

The asteroid specimens collected by Siebold were first examined by Müller and Troschel, who described in 1842, 5 species new to science. Next to them, Herklots who had been a curator of the Rijksmuseum van Natuurlijke Historie at Leiden in 1846-1872, made a apart of descriptions on 2 new species and prepared some plates for "Fauna Japonica VI (Echinoderms)" which was not published finally.

Recently, we could examine the specimens described by these authors and at the same time surveyed the plates and the manuscripts by Herklots at the Rijksmus. v. Natuur. Hist.. The results are as follows: (1) Müller and Troschel's Asteriscus (= Asterina) pectinifera, Luidia maculata and Archaster (= Craspidiaster) hesperus are valid species. (2) Müller and Troschel's Astropecten japonicus and Astropecten armatus are synonyms of A. scoparius Valenciennes and A. polyacanthus Müller and Troschel. (3) Herklots' species, Astropecten Mülleri is Ctenopleura fisheri Hayashi and Asteriscus spinifer is Coscinasterias acutispina (Stimpson).

TS 37

MATSUMORI TANEYASU AND "RYÔU HAKUBUTSU ZUFU"

N. Isono. Dept. of Biology, Keio Univ., Yokohama.

Matsumori Taneyasu (1825-1892), an amateur naturalist, left several manuscripts on natural history. Among them, the most interesting one is "Ryôu Hakubutsu Zufu" (Fauna and Flora of Yamagata and Akita Districts). It is composed of 7 parts (59 volumes): "Jûrui Zufu" (mammals), "Kinrui Zufu"(birds), "Hachû Zufu"(reptiles and amphibians), "Gyorui Zufu" (fishes), "Kaira Zufu" (molluscs, crustaceans etc.), "Tobimushi Zufu" (insects) and "Shokubutsu Zufu" (plants). In total, about 1,900 individuals of animals are illustrated.

It has the following characteristics: (1) It was the only illustrated manuscript written at the period of transition from Honzô-gaku (natural history of Chinese origin) to modern biology. (2) It was one of the earliest attempts to describe local fauna and flora in Japan. (3) He tried to make his own system of classification, though it was based mainly on the old idea of Honzô-gaku. (4) Many excellent illustrations are found, especially in the parts of birds, fishes and insects. (5) It gives many important and useful informations for studying the past fauna and flora as well as the domesticated plants of those days.

Oji International Seminar
on
Perspectives in Marine Biology Contribution to Cell and Developmental Biology
in Commemoration of 100th Anniversary of the Misaki Marine Biological Station

Chairman of the Organizing Committee of the Seminar:
TAKEO MIZUNO, *Misaki Marine Biological Station, Faculty of Science, University of Tokyo*

INTRODUCTORY REMARKS

Takeo Mizuno: Misaki Marine Biological Station, Faculty of Science, University of Tokyo, 1024 Koajiro, Misaki, Miura-shi, Kanagawa 238-02, Japan

---

The international seminar was held at the Sanjo-kaikan Hall of University of Tokyo (Hongo, Tokyo, Japan) on 2 - 4, April, 1987, in commemoration of the centennial of the Misaki Marine Biological Station, which was established as the first research and educational institute for marine biology in Japan. Total number of participants was 193 (168 domestic, and 25 from Belgium, Canada, China, France, Sweden and U.S.A.).

The Papers presented at the seminar were all substantial and the topics were grouped into five: Initiation of development (P. Guerrier, T. Kishimoto, V.D. Vacquier, M. Hoshi, D. Epel and C. Sardet), Cytoskeleton and Cell Motility (M. Morisawa, Keiichi Takahashi, S. Inoué, Y. Hiramoto, H. Sato, D. Mazia, G. Schatten and H. Sakai), Gene expression and morphogenesis (H. Shimada, T. Humphreys, A. Kuroiwa, R.A. Ruff, P.D. Burke and H. Katow), Comparative physiology (A. Gorbman, B. Fernholm, R. Gilles, T. Hirano, M.G. Haygood, I. Tasaki, G. Matsumoto, Kunitaro Takahashi and N. Le Douarin), and Perspectives in marine biology (K. Dan, J.Y. Liu and J.D. Ebert). These papers appealed and gave many information to the participants. It was deeply significant that such an exciting international seminar was held at the moment when many marine biological stations in the world entered their second century.

THE MISAKI MARINE BIOLOGICAL STATION AND ZOOLOGY IN JAPAN.

K. Dan Misaki Marine Biological Station, Miura-shi, Kanagawa-ken

Pre-station period (1877-1886)

Establishment of the Tokyo University. Opening of the Zoology Dept. Contributions by Prof. Edward Sylvester Morse and Prof. Charles Otis Whitman as the 1st and 2nd professors in zoology.

1st period (1887-1910) - taxonomy

The Misaki Marine Biological Station was initiated in the Town of Misaki in 1887, Prof. Kakichi Mitsukuri as an acting director. Moving of the Station to the present site, Koajiro (1897). For selection of these sites, a previous report on Misaki fauna by Prof. Ludwig H.P. Döderlain (Medical Faculty) has a grave influence (Arch. f. Naturgesch., 49:102-123, 1883). Cooperations of Prof. C.D. West (Engineering Faculty) and Mr. Alan Owston (Head of the Owston & Snow Co.) by offering their boats for the Station's use. Discoveries of many rare animals by a genius collector, Kumakichi Aoki; e.g. Branchiocerianthus imperator (hydrozoan), Hyalonema sieboldi (glass sponge), Ikeda taenioides (echiuran), Metacrinus rotundus (crinoid), Chlamydoselachus anguineus and Mitsukurina owstoni (selachians) etc. Beginning of artificial pearlculture by Tohkichi Nishikawa.

2nd period (1910-1930) - embryology

Development of Lingula anatina by Prof. Naohide Yatsu and development of Balanoglossus misakiensis by Yoshinobu Miyashita.

3rd period (1930-1950) - cell physiology

Echinoderm development and cell division mechanism by Isao Motomura and by Katsuma Dan. Sea urchin fertilization by Masao Sugiyama. Acrosome reaction of spermatozoa by Jean Clark Dan. Starfish maturation substance by Haruo Kanatani. Egg physiology in general by Yukio Hiramoto.

4th period (1951-1987) - biochemistry

Identification of the starfish maturation substance as 1-methyl adenine by Haruo Kanatani. Sperm motility and naming of "tubulin" by Hideo Mohri. Study of microtubule by Hikoichi Sakai. Biochemistry of fertilization by Motonori Hoshi.

Concluding remark

It was warned that blind spot of contemporary marine biology is utter lack of genetical information among marine animals which is a serious retarding factor in the days of molecular genetics.

FACTORS REGULATING OOCYTE MATURATION

P. Guerrier[1], I. Néant[1] and H. Shirai[2]. [1]Station Biologique, 29211 Roscoff, France, [2]Natl. Inst. for Basic Biol., Okazaki, Japan.

In the prosobranch mollusk Patella vulgata as well as in the starfish oocyte maturation involves a neurohormonal signal which stimulates the follicle cells. In the starfish, where intracellular pH is already high, experimental evidences suggest that mimetics as well as the hormone must trigger an intracellular calcium translocation in order to activate female asters and MPF precursor molecules. In Patella, calcium is only required to release oocytes from the metaphase 1 block, whereas GVBD depends upon a change in intracellular pH. Interspecific cytoplasmic transfers from Patella to starfish demonstrate that both MPF precursor activation and amplification directly depend on this change in pH. MPF activity is associated with protein phosphorylation. In the starfish, there are two phosphorylation bursts, the first one being protein synthesis independent. In Patella, there is only one burst up to first metaphase. In presence of emetine, this burst occurs and a normal spindle constitutes. However, like in the starfish, dephosphorylation soon occurs, spindle desintegrates and resting nuclei are produced. In both cases, it thus appears that MPF formation does not require the synthesis of an initiator. However, it appears that the second burst observed in the starfish as well as maintenance of metaphase 1 conditions and chromosone condensation activity in Patella directly depend on a continuous supply of new short lived proteins. These must be modified through phosphorylation since we observed that all the cytological effects of emetine could be reproduced in the presence of 150-600 μM 6-dimethylaminopurine, a drug that directly inhibited protein kinase activity without affecting protein synthesis.

MATURATION-PROMOTING FACTOR: PRELIMINARY CHARACTERIZATION, PRODUCTION AND ACTION.
Takeo Kishimoto. Dept. of Devl. Biol., Natl. Inst. for Basic Biol., Okazaki, Japan.

Fully grown ovarian oocytes with germinal vesicles are arrested at prophase of the first meiosis. In starfish, the resumption of meiosis is triggered by 1-methyladenine produced in the follicle cells around each oocyte. This hormone acts on the oocyte surface to produce a cytoplasmic maturation-promoting factor (MPF), which in turn brings about germinal vesicle breakdown and subsequent meiotic maturation. While 1-methyladenine activity is specific to starfish in inducing maturation, MPF activity appears in a wide variety of eukaryotic cells at M-phase including mitotically dividing cells as well as maturing oocytes, and it acts in a non-specific manner across different phyla. MPF is produced in starfish oocytes even after the injection of the oncogenic product of H-*ras*$^{val\ 12}$, whereas the proto-oncogenic protein is inactive. During oocyte maturation, MPF activity fluctuates in exact correspondence with meiotic cycles having a peak at each metaphase. Further, the disappearance of MPF activity initiates the metaphase-anaphase transition. Thus, MPF seems to be a metaphase-promoting factor during M-phase of eukaryotic cell cycle rather than just a maturation-promoting factor. Preliminary characterization shows that starfish oocyte MPF is a protein having a molecular weight of 300 kd with a sedimentation coefficient value of 5S and yeast MPF, extracted from *cdc20* mutant cells of *Saccharomyces cerevisiae*, is a protein with 6S. Approximate 5S appears to be a common molecular size of MPF from various origins.

When injected into immature starfish oocytes with follicles, MPF induces disruption of desmosome-like junctions connecting the processes of the follicle cells with the oocyte surface, resulting in follicular envelope breakdown. Further, such breakdown is caused by MPF even in enucleated oocytes with follicles. Thus, MPF affects the cell surface to dissociate oocyte-follicle cell junctions independently of the presence of nucleus. Considering that MPF affects also the nucleus to cause nuclear membrane breakdown and chromosome condensation, the site of the direct action of MPF appears to be in the cytoplasm. The elucidation of the mechanism of such bi-directional function of MPF will be a most important endeavor for an understanding of the initiation of metaphase.

PROTEINS OF THE PLASMA MEMBRANE OF SEA URCHIN SPERMATOZOA INVOLVED IN SPERM-EGG INTERACTION.
James S. Trimmer and Victor D. Vacquier. A-002, University of California, San Diego, La Jolla, California 92093 USA.

Monoclonal antibodies (Mab) have been isolated which bind to external domains of glycoproteins of the plasma membrane of *S. purpuratus* spermatozoa. Of 95 Mabs isolated, 85 bind to a 210K protein, 1 to a 80K protein, 1 to a 60K protein, and 8 to a group of 6 proteins ranging in relative molecular mass from about 340 to 25K. This latter group is termed the anti-HMW (high molecular weight) Mabs. The 210K sperm membrane protein is the most immunogenic component of the sea urchin sperm membrane in mice. Anti-210K Mabs can be divided into two classes: those which do, and those which do not, inhibit the egg jelly-induced acrosome reaction (AR). Fab fragments of Mab J10/14 are potent inhibitors of the AR. Immunofluorescence localizes the 210K on a collar of plasma membrane 1μm wide over the anterior nuclear fossa of the sperm head, and also on the entire flagellum (Cell, 40, 697, 1985). J10/14 Fab induces transitory increases in sperm intracellular calcium 23-fold above the basal level. Such Mab induced increases in calcium are not accompanied by an increase in intracellular pH or the AR. Egg jelly treatment of sperm results in a 6-fold increase in intracellular calcium, an increase in intracellular pH of about 0.2 units and induction of the AR. If J10/14 Fab treatment to increase intracellular calcium, is combined with ammonium chloride to increase intracellular pH, the AR is induced. This shows that calcium entry alone does not drive the increase in intracellular pH, and also that increases in both calcium and pH are needed to induce the AR (PNAS 83, 9055, 1986). The 210K protein may function as a calcium channel. The 8 anti-HMW Mabs immunoprecipitate, and also react on Western blots, with a group of sperm membrane proteins of 340, 320, 210, 170, 60 and 25K. The externally disposed common antigenic site on these proteins is periodate insensitive, but protease sensitive. These Mabs induce increases in both intracellular calcium and pH, and they also induce the AR. The HMW Mabs appear to mimic the effects of egg jelly on sperm. They identify a small subset of sperm membrane proteins which may be receptors for the fucose sulfate glycoconjugate of egg jelly, which is the natural inducer of the AR. Detailed studies of these proteins may lead to a greater understanding of the transduction of transmembrane signals which underlie induction of the AR at fertilization.

INDUCTION OF THE ACROSOME REACTION IN STARFISH.

Motonori Hoshi. Biol. Lab., Fac. of Sci., Tokyo Inst. of Technol., Tokyo

The acrosome reaction was discovered in marine invertebrates, first in sea urchins and then in starfish, by J. C. Dan at Misaki Marine Biological Station in the early '50s. Since then the jelly coat of eggs has been claimed to contain a physiological inducer of the acrosome reaction. Yet molecular features of the active principle in the jelly coat are barely understood.

It has been shown in the starfish, *Asterias amurensis*, that a cooperation of two jelly components, namely ARIS and Co-ARIS, is required for inducing the acrosome reaction in normal sea water. ARIS, acrosome reaction-inducing substance, is a sulfated, fucose-rich glycoprotein. It is capable to induce the acrosome reaction in high Ca^{2+} or high pH sea water even in the absence of Co-ARIS. Its activity seems dependent mainly upon the saccharide portion and the sulfate moiety. Co-ARIS does not induce the acrosome reaction in the absence of ARIS or its derivatives. Three closely related steroidal saponins have been identified as the major Co-ARISs. The sulfate moiety and the side chain of steroid are important for the biological activity of Co-ARIS, while the saccharide chain seems not necessarily to be strictly specified for its activity.

ARIS and Co-ARIS cooperatively increase the concentration of intracellular Ca^{2+} probably through activation of Ca^{2+}-channels. The jelly coat also contains a third factor, presumably an oligopeptide(s), that is not obligatory for the induction of the acrosome reaction but facilitates it by increasing the intracellular pH of sperm. Upon encountering the jelly coat, the spermatozoa respond to a co-operation of these three components of the jelly coat and eventually undergo the acrosome reaction in a few seconds.

THE SECOND CENTURY: NEW CHALLENGES AND NEW STRATEGIES FOR STUDYING EGG ACTIVATION.

D. Epel and R. Swezey. Hopkins Marine Station, Department of Biological Sciences, Stanford University, Pacific Grove, CA 93950 USA.

The visualization of fertilization with the microscope preceded by just a few years the founding of the Misaki Marine Laboratory. This lecture focusses on a new technique for studying egg activation, examining enzyme activities in electrically-permeabilized eggs and embryos of sea urchins. Glucose-6-phosphate dehydrogenase (which was first studied here at Misaki) exhibits high and equal activity in *homogenates* prepared from either eggs or embryos and there is no change in activity at fertilization. However, unfertilized, *permeabilized* eggs show highly repressed activity, equivalent to only 1-2% of the available enzyme. When permeabilized after fertilization, however, the activity of this enzyme increases 8-15 fold. Thus, a post-fertilization change in activity is only seen in permeabilized cells. This same behaviour is also seen for five other enzymes we have assayed, suggesting that a general step-up in activity takes place which is only apparent in the permeabilized cell. Our experimental analysis indicates that this activation occurs *in vivo* and is controlled by both Ca^{+2} and pH. Clearly, understanding the nature of this change will provide new insights into the fertilization process.

This study is one example of new types of approaches which will become increasingly important for this 2nd century of study of egg activation - staying as close as possible to the *in vivo* situation. Another approach will come from the development of optical "reporter" molecules which can assess directly the status of intracellular enzymes etc. A third approach, is microinjection of enzymes and antibodies to assess function *in vivo*. Fertilization is one of the best understood developmental programs - a major challenge for the next century will be understanding how the responding elements are set up during oogenesis to be unfolded at fertilization.

FERTILIZATION IN MARINE INVERTEBRATES

Christian Sardet. Biologie Cellulaire Marine CNRS, Station Marine, F-06230 Villefranche sur mer

Our recent research deals with 3 questions: -Is sperm attracted to the egg? -Does it enter in a particular region of the egg? -What events does it trigger in the egg?

In some chosen species, these questions can be answered with great clarity, and it has been a major contribution of Marine Stations to provide a place to explore the diversity of species, discover and develop appropriate biological systems.

In Siphonophores (planktonic cnidarians), the egg secretes an extracellular material (the cupule) that attracts the spermatozoids in a specie specific manner. The attractant (a small acidic protein) modifies the trajectories of spermatozoids in such a way that they remain trapped near the source of attractant (collaboration with D. Carré, M.P. Cosson and J. Cosson).

If in most species sperm enter anywhere, in many species, the spermatozoid enters in the animal hemisphere, near the maturation pole (insects, cnidarians, fish, amphibians,...). The ascidian egg where sperm is said to enter at the vegetal pole appeared one of the rare exception. Our recent studies on denuded ascidian eggs (Phallusia mammillata) indicate however that sperm enter preferentially in the animal hemisphere. Using time lapse video recording and an Imaging Photon Detector to detect light emission from aequorin loaded eggs (collaboration with L.F. Jaffe and J.E. Speksnijder), we have analyzed the reaction of the ascidian egg to the entering sperm. A large localized increase in intracellular calcium (≅3 μM) propagates (≅7 μm/sec) across the egg. As it reaches the animal pole, it is followed by a wave of cortical contraction that propagates from the animal to the vegetal pole in 2 minutes (≅2 μm/sec), moving simultaneously subcortical organelles and extracellular markers to the vegetal pole. Periodic oscillations in the level of intracellular calcium and cytoplasmic contraction-relaxation of the egg precede second polar body formation. Subcortical organelles that have accumulated at the vegetal pole finally move toward the sperm aster and the futur posterior pole of the embryo.

THE INDUCTION OF MOTILITY IN SPERMATOZOA BY IONS AND CYCLIC AMP.

M. Morisawa. Ocean Research Institute, University of Tokyo, 1-15-1, Minamidai Nakano-ku, Tokyo, 164 Japan.

After leaving from the testis, the spermatozoa pass into sperm duct or epididymis. From there they are released into the place in which fertilization occurs. Throughout this travel, the spermatozoa are suspended into fluid environments differing properties: The chemical and physical nature of fluids in vas deferens and spawning ground progressively or drastically changes. In the course of trip, function of spermatozoa are also changing: They acquire the potential for motility during passage through the sperm duct or epididymis and then they initiate motility at spawning or at ejaculation, and it has been implicated that composition of the surrounding fluid may result the induction of sperm function.

A number of factors which seem to be responsible for the acquisition or initiation of sperm motility have been proposed since these phenomena were treated by Tournade or Gray in early twenty century, and they are still poorly understood.

These problems are recently reinvestigating by the author and colleagues using salmonid fish spermatozoa and it was suggested that change of HCO_3^- and H^+ concentrations in the sperm duct is the external factors for the acquisition of sperm motility and gradual increase in intracellular cAMP which occurs during transit of sperm in the sperm duct is involved in the expression of the acquired potential for motility.

We further demonstrated a cascade process of the initiation of sperm motility in salmonid fishes: Seminal K^+ at the concentration of approximately 35-85 mM suppresses the motility of sperm even though they have already acquired the potential for motility at the posterior end of the sperm duct and decrease in environmental K^+ at spawning in river fresh water causes instantaneous and drastic increase in intracellular cAMP and then phosphorylation of axonemal protein with a molecular weight of 1,5000(15K protein) by newly synthesized cAMP triggers the final step of the initiation cascade of sperm motility. Studies based on these evidence further suggested that similar process occurs and regulates sperm motility in marine invertebrates such as sea urchins, tunicates and mammals.

THE MOTILE MECHANISM OF THE SEA URCHIN SPERM: ANALYSES WITH REACTIVATED "MODEL" SYSTEMS.

Keiichi TAKAHASHI. Zoological Institute, Faculty of Science, University of Tokyo, Hongo, Tokyo.

Echinoderm spermatozoa have been shown to be very useful in the study of flagellar motility and its control. We have used demembranated sea urchin sperm flagella to determine the mechanical properties of ATP-driven microtubule sliding that powers the flagellar motion and to elucidate the mechanism by which the sliding is controlled to generate patterns of flagellar beat. Some of our recent results are reviewed.

To study the dynamic properties of microtubule sliding, particularly the force-velocity relation, glass microneedles that have previously been calibrated for their compliances are attached to the demembranated flagellum. The positions of the microneedles are monitored by projecting their microscopic images onto a photodiode-array position sensor. Microtubule sliding is initiated by perfusing a reactivating solution containing ATP and elastase and the force and velocity of the sliding between the microtubules attached to the needles are determined by analyzing the deflection of the needles caused by the sliding force. A piezoelectric device is used to change the distance between the microneedles so that abrupt length steps can be applied to the flagellum during the force generation. This made it possible to carry out a "slack test" for more reliable determination of the mechanical parameters of sliding than has previously been possible. The results indicate that the shape of the force-velocity curve differs substantially from that of the familiar hyperbolic force-velocity curve of skeletal muscle and is independent of the ATP concentration over a wide range.

VIDEO MICROSCOPY OF MITOSIS.

Shinya Inoué, Marine Biological Laboratory, Woods Hole, MA 02543, U.S.A.

The application of video technology has provided enhanced image contrast, resolution, and recording speed in microscopy, as well as making possible noise reduction, thin optical sectioning, 3-D reconstruction, and discrimination and quantitation of image features (for summary, see Inoué, 1986, Video Microscopy, Plenum Press, NY). With video microscopy, time-lapse analyses of cell division and mitosis can be carried out at high optical resolution using well-corrected optics and aided by the excellent image quality and versatile playback capabilities of the optical memory disk recorder (OMDR; laser disk recorder/player).

I will demonstrate, in *Haemanthus* endosperm cells that Drs. A.S. and J. Molè-Bajer and I recorded in rectified Plan Apo polarization optics: (1) the behavior of chromosome arms in anaphase; (2) very thin serial optical sections showing the dichroism of microtubules decorated via anti-tubulin to 5 nm colloidal gold spheres. Finally, I will present stereo-paired images reconstructed, using a novel computer program, from sequential optical sections stored in the OMDR (Inoué, S. and T.D. Inoué, 1986, Ann. N.Y. Acad. Sci. 483: 392-404). These images show surprising distributions of microtubules including: splaying and extensive mixing of kinetochoric and polar microtubules towards the spindle poles; some very long, curved microtubules criss-crossing the others which run more or less parallel to the spindle axis; and distal ends of polar microtubules wrapping tightly around the metaphase and anaphase chromosome arms, forming a loosely woven basket of microtubule helixes. These arrangements of microtubules were confirmed in the living cell, but their functional roles are yet to be understood (Inoué, S., A.S. Bajer, and J. Molè-Bajer, 1985, in M. DeBrabander and J. DeMey, eds., Microtubules and Microtubule Inhibitors, Elsevier, Amsterdam, pp. 269-276).

MICROMANIPULATION OF DIVIDING ECHINODERM EGGS.

Yukio Hiramoto. University of the Air, 2-11 Wakaba, Chiba 260, Japan.

The location and nature of the motive force for chromosome movement and spindle elongation during anaphase were analyzed in sea urchin eggs by micromanipulation and Colcemid-UV method in which Colcemid could be applied to a restricted region of the cell. Chromosome behavior and spindle elongation during mitosis were observed by differential interference microscopy and birefringence indicating the state of microtubules at various regions of the cell were measured by polarization microscopy, while various micro-operations were made to the mitotic apparatus by micromanipulation and the Colcemid-UV method.

By micromanipulation experiments, it was found that poleward chromosome movement occurred in the spindle after removing the aster(s), the region of the spindle near its polar end, or protoplasm at the interzonal region of the spindle by sucking it out with a micropipette, or severing the spindle in two parts at the equatorial plane or at the region between the equatorial plane and the polar end. The Colcemid-UV method revealed that chromosome movement occurs only in birefringent region of the spindle, irrespective of the presence or absence of birefringence in other regions of the same spindle. It was concluded that chromosome movement during anaphase is driven by microtubule-dependent engine(s) located near chromosomes.

The spindle elongation during anaphas was inhibited by removing asters attached to the ends of the spindle by micromanipulation or destructing them by Colcemid-UV method. A hypothesis was presented that the spindle elongation is caused by forces generated at the surface of astral microtubules acting in the direction away from each centrosome attached to the end of the spindle.

MODULATION OF SPINDLE ASSEMBLY IN DIVIDING SEA URCHIN EGGS.

H. Sato, T. J. Itoh, T. Ohara[1] and Y. Sato[2]. [1]Sugashima Marine Biol. Lab., Nagoya Univ., Toba, Mie 517 and [2]Shoin Women's Univ., Biol. Lab., Nada-ku, Kobe 657.

Well preserved isolated spindles from the first cleavage of dividng sea urchin eggs revealed that3,000 to 5,000 orderly arranged microtubules as the major cytoskeletal components. Considering the sensitive nature of the spindle birefringence, it is highly probable that the spindle assembly is regulated by the labile association of pooled tubulin and the kinetic centers such as the kinetochores and MTOC's in centrosomes. In order to examine molecular basis of spindle assembly, mitotic arresters and Chlortetracycline were used as the molecular probes.

When fertilized sea urchin eggs of Hemicentrotus pulcherrimus, Pseudocentrotus depressus or Clypeaster japonicus were exposed to dilute solutions of alkylresorcinols, i. e., T-1, its derivatives, Ansamycin, Culvularin or Macbecin I, spindles were tend to arrested in metaphase and also turned into barrel-shape. Anaphase chromosome movement can be initiated but with very slow pace. Efficacy of these drugs is comparable with detergent and can be interpreted as freezing the dynamic state of equilibrated molecular association of tubulin along the microtubules. Bundles of straight microtubules with an even length composed barrel-shaped spindles, and we thought it might reflects the stabilized state of tubulin polymers caused by the local increase of molecular hydrophobicity. We confirmed this unusual spindle shape also due to the discoidal redistribution of MTOC's in centrosomes.

Chlortetracycline was employed as a fluorescent chelate probe to determine the distribution of membrane-associated calcium in dividng sea urchin eggs. Following the change of the fluorescent pattern durint mitosis, we found that the CTC-fluorescence coincided with that of ER-like membrane which were revealed in electron micrographs. Tetracaine, which was known to displace membrane-bound calcium, reduced fluorescence and spindle birefringence. Results obtained suggested that intracellular free calcium ions were sequestered in the membrane system associated with the mitotic apparatus during mitosis. (Supported by Grants-in-Aids for Scientific Research;59380026, 60480020 and 61304008.)

THE CENTROSOME: ORGAN OF CELL ARCHITECTURE

D. Mazia Hopkins Marine Station of Stanford University
Pacific Grove, CA 93950, U.S.A.

A century ago, the centrosome was recognized by Boveri as a major permanent organ of the cell. At the present time, the centrosome commands renewed attention and it is prominent in the present symposium. (Contributions of Schatten, Sakai, Sato and Mazia).

The cell cycle includes a centrosome cycle: a consistent cycle of changes of the shapes of centrosomes. Compact centrosomes flatten, spread and divide, thus forming the poles for the next mitotic cycle. Since the centrosomes generate microtubules, the shape of the mitotic apparatus (e.g. pointed poles or flat poles) will depend on the stage of the centrosome cycle relative to the stage of the chromosome cycle.

The general facts of the centrosome cycle have now been confirmed in many kinds of cells including types of cells (e.g. in higher plants) in which the very existence of centrosomes has been denied previously. Currently, immunofluorescence studies with anticentrosome antibodies are especially revealing.

It is proposed that the centrosome is the architectural organ of the cell; <u>the conformations of centrosomes generate cell morphologies that are based on microtubules</u>. A model of the structure of the centrosome present it as a very long flexible linear element, carrying large numbers of sites that determine the origins and directions of individual microtubules. There is new evidence for the model, but specific molecular characteristic of centrosomes are still unknown.

Reference: Mazia, D. 1987. Int. Rev. Cytol., 100:49-92.

CENTROSOMAL INHERITANCE AND MOTILITY DURING FERTILIZATION.

G. Schatten and H. Schatten Integrated Microscopy Resource for Biomedical Research, University of Wisconsin, 1117 West Johnson Street, Madison, WI 53706 U.S.A.

The organization of the cytoskeleton and the regulation of motility have been investigated during fertilization in sea urchins and in mice. Microfilaments interacting with non-erythrocyte spectrin or fodrin are found at the regions of sperm-egg fusion in sea urchins, but not in mice. Latrunculin, a new microfilament inhibitor, interferes with sperm incorporation in sea urchins but not in mice, reinforcing the suggesting that these two system accomplish fertilization in different manners. In sea urchins, an actin-spectrin gel interacts with the plasma membrane at the site of sperm incorporation whereas spermhead incorporation in the mouse occurs without any apparent microfilament involvement; the formation of the second polar body requires microfilament activity.

Centrosomes are traced in sea urchins with a human autoimmune antibody and a mouse monoclonal antibody generated against <u>Drosophila</u> intermediate filament protein, which reacts with a 68 Kd antigen in sea urchins. The sperm contributes this structure which spreads and duplicates as shown by Boveri at the turn of the century.

Surprisingly the mouse sperm does not bind centrosomal antibodies, and instead it appears that this structure is maternally inherited in this mammal. Parthenogenesis experiments support this unexpected conclusion.

Centrioles are not found in the unfertilized mouse oocyte, as studied with serial thick sections and high voltage electron microscopy. Though the sperm contributes a centriole-like structure at fertilization, it does not seem to be involved in the formation of the first mitotic spindles. Instead mitoses occur in the absence of centrioles. Remarkably centrioles are not observed until the second trimester of fetal development.

These studies demonstrate that, contrary to expectations, fertilization in this mammal raises several significant questions involving the fundamentals of cell organization and motility.

ASTER FORMATION IN VITRO INDUCED BY 51K PROTEIN, A COMPONENT OF THE CENTROSOME.

K. Ohta, M. Toriyama, S. Endo and H. Sakai. Dept. of Biophys. and Biochem., Fac. of Sci., Univ. of Tokyo, Tokyo.

The pericentriolar material of sea urchin egg consists of the clusters of granules with a diameter of ~90 nm originally found by Endo in 1979. After isolation and homogenization of the mitotic apparatus (MAs) at low temperature, granules in the suspension formed many small asters when mixed with tubulin. The protein fraction responsible for this aster-forming activity was solubilized and partially purified by phosphocellulose column chromatography. This fraction which contained more than several components with a major protein having a molecular weight of 51,000 and an isoelectric point of 9.8 (51K protein fraction) was reconstituted into granules by dialysis and initiated astral microtubules in the presence of tubulin with the plus end distal to the center of the asters.

The antibody was raised in mouse against the 51K protein and affinity-purified. The antibody stained only the center of asters reconstructed from both the granules in the homogenized MAs (centrosomal fragments) and those reconstituted from the 51K protein fraction. The antibody also stained the centrosome as well as the peripheral region of the centrospheres and the half spindles. Therefore, the 51K protein is a component of the centrosome and it is involved in the formation of the clusters of granular material (Endo, 1979) in the centrosome and plays a role in the initiation of astral and spindle microtubules at mitosis.

SEA URCHIN ARYLSULFATASE AND ITS EXPRESSION DURING DEVELOPMENT.

H.Shimada. Inst. of Zool., Fac. of Sci., Univ. of Tokyo, Tokyo.

Arylsulfatase (ARSase) of sea urchin embryos which begins to increase at the hatched blastula stage is an extracellular protein which becomes localized in the cell surface of the embryo during gastrulation (Rapraeger and Epel, 1981). However, little is known about its role in embryogenesis and the mechanism controlling its expression during sea urchin development.

We have recently purified the ARSase from the sea urchin embryo. The Enzyme consists of ten identical 63KD-subunits, and it occupies as much as 0.5% of the total proteins of pluteus larvae. The activity of purified ARSase was markedly inhibited by 20 mM sulfate ions. It showed the maximal activity between pH 5 and 6, and showed little activity around pH 8 (the pH value of sea water). Thus, the enzyme seems to be inactive in an extracellular environment. Moreover, the purified ARSase did not hydrolyze any sulfated polysaccharides extracted from the sea urchin embryo. These results, together with its extracellular localization, suggest the ARSase of the sea urchin embryo functions as one of the cell-surface structural proteins rather than functions as an enzyme.

By use of the inhibitors of transcription and translation, we found that the low level of ARSase observed in the blastula is dependent on the translation of maternal mRNA, and the increase in the ARSase activity after this stage is due to transcription of the genomic ARSase gene. In order to further confirm this conclusion, the Northern analysis of the embryonic mRNAs were performed using the ARSase cDNA as the probe. The ARsase cDNA was cloned in our laboratory by use of the chemically synthesized DNA fragment corresponding to the amino acid sequence of a part of the purified ARSase polypeptide. The result of the Northern analysis agreed well with the results obtained by use of the inhibitors of transcription and translation. It was found that transcription of the ARSase gene starts at the pre-hatched blastula stage, and continues thereafter, while a detectable amount of the ARSase mRNA is stored in the unfertilized eggs. The size of the ARSase mRNA was estimated to be about 2.9 kb.

MOLECULAR CLONING AND DEVELOPMENTAL EXPRESSION OF HOMEO BOX CONTAINTING GENES IN SEA URCHIN EMBRYOS.

Tom Humphreys, University of Hawaii, Pacific Biomedical Research Center, 41 Ahui Street, Honolulu, Hawaii 96813, USA.

Hybridization of Drosophila Homeo Box DNA seqeunces to Southern transfers of sea urchin genomic DNA indicated the presence of 5-10 homeo boxes. Screening of a sea urchin genomic recombinant DNA library, with Drosophila probes from both Antennapedia-like and engrailed homeo boxes has so far yielded six unique homeo boxes confirmed by nucleotide sequencing.

Four of these homeo box sequences are Antennapedia-like with 66-72% nucleotide sequence homology to the Antennapedia gene homeo box. They encode amino acid homeo domains that show 70-88% homology with the Drosophila Antennapedia gene homeo box domain. One of the sequences isolated, though definitely a homeo box sequence, shows no special homology to any other homeo box which has been sequenced. The amino acid sequence encoded by this homeo box shows 42-47% homology to all of the approximately 30 known homeo domain sequences. The one engrailed-like homeo box in the sea urchin genome was isolated and sequenced. Its encoded amino acid sequence was 70% homologous to the Drosophila engrailed homeo domain and 77% homologous to the mouse engrailed homeo domain.

The expression of these homeo box sequences in sea urchin embryo was examined by isolating RNA from various stages of the embryo and preparing Northern transfers of this RNA to react to the various sea urchin gene probes. These experiments detected one homeo box gene which was expressed very actively during the embryonic stages. This sea urchin homeo box was most homologous to the Antennapedia homeo box with 88% homology in the encoded amino acid sequences. Transcripts of 6.9 kb and 7.5 kb could first be detected in blastula stage. They increase several fold by gastrula stage and then decreased significantly as development preceded to pluteus stage. Insitu-hybridization showed that these transcripts appeared in the dorsal (aboral) ectoderm of the embryo.

MOLECULAR ANALYSIS OF THE CHICKEN GENE CONTAINING THE HOMEO BOX

A. Kuroiwa and E. Yokoyama. Division of Molecular Neurobiology, Tokyo Metropolitan Institute for Neurosciences, 2-6 Musasidai, Fuchu-city, Tokyo, Japan

In the course of Drosophila embryonic development, segmentation genes and homeotic genes control a formation of metameric structure of body segment and a determination of the identity of each segment, respectively. All homeotic genes and some segmentation genes, so far cloned, contain "homeo box" sequence in the 3' exon. The homeo box is translated into a certain part of a protein and such a region act as a DNA binding domain of the protein, that regulate a expression of other genes. The homeo box is found not only in invertebrate but also in vertebrate gemon. Genes carrying homeo box in vertebrates are expected to have a similar function as in Drosophila.

In order to analyze a function of the homeo box genes in chicken embryonic development, I have isolated 15 different genomic clones containing a Antp-type homeo box. As in the case of Drosophila, (i.e. ANT-C and BX-C), chicken homeo box genes make several clusters in the genom and homeo domain locate near the end of open reading frame. At leaset 3 homeo box gene cluters are found in the chicken genom. Choxl cluser has 5 homeo box genes in 52Kb DNA in same transcriptional orientation (CHoxl. 0-1.4). ClusterII has 3 homeo box genes in 57Kb DNA (a, 26-2,26-1) and claster III has 3 homeo box genes in 35Kb DNA (x,226,Y). Since the homeo box sequence and gene arrangement of the CHoxI cluster are almost identical as the gene in HoxI cluster of mouse, CHoxI is a chicken homologue of HoxI. All these genes encode a characteristic mRNA(s), experessing in embryonic development and adult central nervous system.

By in situ hybridization analysis, CHoxl.4 is found to express in entire spinalcord and certain region of somites of 4 days embryo.

A MOLECULAR ANALYSIS OF HETEROCHRONY IN THE EVOLUTION OF DIRECT DEVELOPMENT IN SEA URCHINS.

Rudolf A. Raff Department of Biology, Indiana University
Bloomington, Indiana 47405, U.S.A.

If we are to understand the evolution of animal morphology we must define the mechanisms by which evolutionary changes occur in embryonic development. An excellent experimental system to study such processes is provided by direct developing sea urchins closely related to those with a typical mode of development. A significant number of sea urchin species have eliminated the typical pluteus larva, and instead produce large yolkly eggs that rapidly and directly develop into juvenile sea urchins. Development in such forms is radically modified in several ways. The most evident changes result from heterochronies in which larval features are lost and development of adult features is accelerated.

We are investigating the development of an Australian direct developing sea urchin, Heliocidaris erythrogramma. This species is sufficiently closely related to Strongylocentrotus purpuratus that cDNA and monoclonal antibody probes to primary mesenchyme cells of S. purpuratus cross react readily. We have been able to establish the homology of mesenchyme and other cell lineages between the two species, and have begun to investigate the heterochronies in two aspects of cell behavior. The first is in changes in cell cleavage dynamics. The second is in timing changes in cell lineage-restricted gene expression. The use of molecular probes to mesenchyme cells demonstrates that the predicted heterochronies are demonstrable at the cellular and molecular levels. A large number of primary mesenchyme cells are present by the completion of gastrulation, and they initiate an adult pattern of gene expression.

STUDIES OF MESENCHYME IN SEA URCHIN EMBRYOS

Robert D. Burke, Allan W. Gibson, and Colin R. Tamboline.
University of Victoria, Victoria, B.C. V8W 2Y2 Canada

A distinctive aspect of sea urchin development is the mesenchyme. These cells, which migrate into the blastocoel from the vegetal plate and the tip of the archenteron, are associated with the principal morphogenetic events in the formation of the pluteus larva. Classically two subsets are recognized; primary and secondary mesenchyme. Studies we have undertaken using monoclonal antibodies have enabled us to document the ontogeny of morphologically indistinguishable subsets of mesenchyme, such as pigment cells. The antibody, Sp-1 recognizes a 110 kd glycoprotein characteristic of presumptive pigment cells. Using this antibody the release of these cells from the vegetal plate, their migration through the blastocoel and insertion in the epidermis has been documented.

Mesenchyme is known to give rise to skeletogenic cells, pigment cells and a population of cells that span the blastocoel. Our studies indicate that a number of components of the extracellular matrix are associated with the skeletogenic and blastocoelar cells. The antibody Sp-12 is specific to several peripheral membrane components of all the classes of mesenchyme. A glycoprotein recognized by this antibody is a major component of the extracellular matrix of adult body wall and is present in the embryo from the mesenchyme blastula stage. Sp-14 is an antibody that binds to a fibrillar component of the ECM of early embryos. This material is present in the blastocoel and associated with the primary mesenchyme. Primary mesenchyme cells and mesenchyme from dissociated embryos appear to produce both Sp-12 and Sp-14 positive material in vitro. We hypothesize that an important role of the mesenchyme in the sea urchin embryo is to produce or modify the extracellular matrix of the blastocoel.

ROLE OF A SITE IN FIBRONECTIN MOLECULE IN MIGRATION OF PRIMARY MESENCHYME CELL IN SEA URCHIN EMBRYOS.

H. Katow, Biology Laboratory, Rikkyo University, Toshima-ku, Tokyo 171.

The cell migration is an elemental process along with the cell division in the morphogenesis in multicellular animals including sea urchin embryos.

In the most sea urchin embryos the primary mesenchyme is a group of cells to be formed primarily in the blastulae as a mass of free cells, and they possess a property of migration. The migration is held until the formation of cell aggregates prior to the spicule differentiation. During the migration the cells have an extracellular glycoprotein, fibronectin, on their surface. Anti-fibronectin antibodies inhibit the cell migration in vivo.

In vitro the cells are able to bind with exogenous fibronectin, and their migration responds to the amount of the molecule in culture medium. In proper amount, 40μg/ml in Pseudocentrotus depressus, fibronectin increases not only the number of cells which were promoted the migration but also the distance of the migration performed by each of these cells.

The synthetic peptides that contain a particular amino acid sequence, Gly-Arg-Gly-Asp-Ser, which is known to represent the cell binding domain of fibronectin also inhibit the binding of the molecule to the cell surface as well as the fibronectin-promoted migration of the cells in vitro. The synthetic peptides can be injected into a large number of blastulae simultaneously using a micro-mass injection technique, and they inhibit the cell migration in the blastocoel. The inhibition of cell migration by these synthetic peptides is erased by addition of extra amount of fibronectin to the culture medium. The inhibition, therefore, is regarded as of a competitive.

All these results indicate that the amino acid sequence in cell binding domain of fibronectin molecule is the very site at which the molecule binds to the primary mesenchyme cells, and that the site is utilized in the cell migration in the blastocoel.

THE HAGFISH AS A RESOURCE IN THE STUDY OF EVOLUTIONARY ENDOCRINOLOGY

Aubrey Gorbman, University of Washington, Seattle, Washington 98195, U.S.A.

The hagfish Eptatretus burgeri has figured prominently in the history of the Misaki Marine Biological Laboratory, particularly since Prof. Bashford Dean of Columbia University came in 1900 to study development of Eptatretus. It was one of the principal research materials of Prof. Hideshi Kobayashi during his directorship of the laboratory, and later. The hagfish at Misaki has two broadly significant attributes that have attracted researchers from all over the world. First, it is the most primitive vertebrate available for study today. Hence, it is the best source of information to the zoologist from which to extrapolate and judge the evolution of any vertebrate system. The second cyclostome group, the lampreys, are much more like other lower vertebrate taxa, especially primitive cartilaginous fishes. A second feature of the Japanese Eptatretus that attracts study is the seasonality of its breeding cycle; it is probably the only seasonally breeding hagfish species, an indication that it may be less degenerate than other hagfish species, and therefore more representative of its proto-vertebrate primitive ancestor.

Several examples of hagfish study, one of them completed at the Misaki laboratory, will be presented briefly. One deals with the brain-pituitary regulatory relationship. A second deals with development of the head and pituitary gland. Profound differences in these and other features between cyclostomes and higher vertebrates, and between hagfishes and lampreys are contributing to phyletic reasoning in two ways: 1) they provide criteria against which the full extent of evolution of vertebrate systems may be judged, and 2) they indicate a diphyletic origin of the two cyclostome groups, now included in a single class.

REPRODUCTIVE BIOLOGY IN HAGFISH —— A MARINE BIOLOGICAL ENIGMA.

B. Fernholm Research Department, Swedish Museum of Natural History
S-104 05 Stockholm, Sweden

During the last one hundred years no other marine chordate has been the subject of so much research into its reproductive biology with so little result as hagfish. I will try to analyze the reasons for this and point out potentially fruitful approaches.

1. Hagfish are exclusively marine animals living fairly deep, at least during spawning time. Therefore direct observation in the sea is difficult.
2. Hagfish dig into soft bottoms thereby making direct observation difficult.
3. Most of the studied species of hagfish do not seem to have a well difined spawning time.
4. The investigated species seem to have particular spawning places which are difficult to find.
5. In several species of hagfish it is particularly difficult to find males, especially males with mature sperm cells.

Hagfish of different species occur in all oceans and many attempt to find their eggs and embryos have been made, mainly in Scandinavia, England, California, and Japan. One hundred years ago the first efforts to obtain ripe eggs from females were made in Scandinavia, keeping females with large eggs in wooden cases in the sea for 6 months. No eggs were laid. I have used plastic and metal cases in Japan and Scandinavia in a similar way. Many seemingly normal eggs, all unfertilized, were deposited.

The most successful attempts to secure embryos have been those in California using long lines and hooks. Since that method is less efficient than baited traps for catching large numbers of hagfich it has not been in much use recently. The method depends on the hooked hagfish sliming and wriggling and thereby catching nearby deposited eggs in its slime and was recommended already around the turn of the century as the best method to obtain eggs and embryos.

I plan to use the long line method in Sweden, in addition to improved cases having muddy bottoms.

VOLUME CONTROL PROCESSES IN ANIMAL CELLS

R.GILLES

Laboratory of animal physiology, University of Liège, 22, quai Van Beneden, B-4020 Liège, Belgique

This brief overview will compare the physiological responses of cells from homeosmotic and euryhaline poecilosmotic species to osmotic challenges.Both cell types are perfectly able to regulate their volume following an osmotically induced swelling. However, mammalian cells cannot survive in diluted media while cells of euryhaline poecilosmotic species do. This shows that adaptation and survival of cells to changes in the osmolality of their environmental medium cannot be related solely to their possibility of volume regulation. In fact, their possibility to cope with the disrupting effects changes in intracellular concentrations of inorganic ions can have on the structure and activity of different macromolecules must also be taken into consideration. In this respect, the amino-compounds usually found in rather large amounts in cells of marine euryhaline poecilosmotic species could have an important part to play. They indeed seem to have a "stabilizing" effect on protein structure that can oppose the "disrupting" effects of inorganic ions. Further, their use as major osmolytes in the cells of euryhaline species allows a control of the intracellular level of inorganic monovalent ions otherwise used as major osmotic effectors. The cells can thus avoid the important disrupting effects of changes in these ions concentration.

The mechanisms discussed can be considered as clues to survival and settlement of species in coastal ecotones with fluctuating salinities.

OSMOREGULATORY ROLES OF PROLACTIN AND GROWTH HORMONE IN TELEOSTS.

Tetsuya Hirano. Ocean Research Institute, University of Tokyo, Tokyo.

It has been well established that prolactin (PRL) plays an important role in maintaining hydromineral balance of euryhaline teleosts in fresh water, whereas cortisol has been known as a seawater-adapting hormone. An improvement in seawater adaptability has also been shown when some salmonids are treated with mammalian growth hormone (GH). The opposite effects of PRL and GH are intriguing considering the close similarity between their primary structures. Recently, PRL and GH have been isolated and characterized from chum salmon pituitaries. Chum PRL was about 100 times more potent than ovine PRL in causing plasma Na retention in hypophysectomized killifish. When injected into seawater-adapted juvenile rainbow trout, PRL produced a dose dependent increase in plasma Na, and chum PRL was 2-10 times more active than ovine PRL. On the other hand, when juvenile rainbow trout were transferred from fresh water to seawater after 3 injections of chum salmon GH, plasma Na levels were significantly lower then the saline-injected control. In addition, only a single injection of chum GH was sufficient to reduce plasma Na levels of chum fry transferred from fresh water to seawater. Changes in plasma levels of PRL and GH during transfer of chum salmon and rainbow trout to different salinities were followed using recently established homologous radioimmunoassays. When immature chum salmon were transferred from seawater to fresh water, PRL levels increased, whereas GH levels fell. Furthermore, when transferred from fresh water to seawater, they exhibited a significant increase in plasma GH without any change in PRL levels.

The importance of GH and cortisol in seawater adaptation was also assessed in mature chum salmon. Mature fish, especially females after completion of ovulation, are difficult to maintain in seawater, mainly due to a gradual increase in plasma ion concentrations. When plasma levels of various hormones were examined, an increase in plasma GH and cortisol was observed in parallel with the increase in plasma ions. Whether GH acts directly on osmoregulatory surfaces or indirectly through cortisol remains to be studied.

SYMBIOSIS BETWEEN ANOMALOPID (FLASHLIGHT) FISHES AND LUMINOUS BACTERIA.

Margo G. Haygood[1] and Daniel H. Cohn[2]. [1]Scripps Institution of Oceanography, La Jolla, CA 92093, USA and [2]University of Washington, Seattle, WA 98195, USA.

Fishes from a number of families have light organs that contain extracellular symbiotic luminous bacteria. In most cases the bacteria have been cultured and identified, but in the anomalopids (flashlight fish) the symbionts have proved impossible to culture thus far. In the flashlight fishes, the bacteroids are contained in two conspicuous suborbital light organs.

DNA extracted from the light organs of the Caribbean flashlight fish, *Kryptophanaron alfredi*, was hybridized with a probe derived from the luciferase genes of *Vibrio harveyi*, a free-living luminous bacterium. The probe showed stronger homology to the luciferase genes of the symbiont than to those of *Vibrio fischeri*, a readily cultured luminous symbiont. This result suggested a relatively close evolutionary relationship between the luciferase genes of the symbiont and *V. harveyi*, and was consistent with previously published kinetic analyses of the luciferases from these organisms.

A clone bank was constructed with DNA from the *K. alfredi* light organ and the luciferase genes were cloned. The nucleotide sequence of *lux*A was determined. Comparison with the published *V. harveyi luxA* sequence showed that the two sequences were 75% homologous at the nucleotide sequence level and 83% homologous at the amino acid sequence level. Codon usage in the symbiont gene differed from the *V. harveyi* gene and exhibited a marked bias. This result raises the possibility that the symbiont may have acquired the luciferase gene by lateral gene transfer.

Comparison of luciferase genes from other anomalopid species may provide an independent test of the proposed phylogeny of the fish species. In addition, examination of nucleotide sequence divergence of the bacterial genes within the context of evolution of the fish hosts may provide a rare opportunity to estimate nucleotide substitution rates in a relatively recently evolved bacterial gene family.

MECHANICAL AND THERMAL SIGNS OF EXCITATION PROCESSES IN THE NERVOUS SYSTEM.

I. Tasaki National Institute of Mental Health, Bethesda, MD 20892, U.S.A.

By using synthetic piezoelectric and pyroelectric materials, sensitive divices were constructed for detection of mechanical and thermal changes in the nervous system. To record rapid mechanical changes in excitable cells and tissues, piezoelectric banders (purchased from Gulton Industries) were employed in conjunction with an operational amplifier (AD515, OPA111 or 128). It was found possible to demonstrate rapid swelling during excitation in squid giant axons, crab nerves, lobster and frog retinae, frog spinal cord preparations etc. These findings strongly suggest that movement of water is involved in excitation processes. In the squid giant axon, the peak of swelling was found to coincide with the peak of the action potential recorded intracellularly from the site of mechanical recording. It is suggested that the excitation process is associated with an increase in the water content of the excitable membrane sites.

To detect heat production associated with excitation processes, thermal detectors were constructed by using multi-layers of polyvinylidene fluoride (manufactured by Kureha Chemical Industry). Using these detectors, it was found possible to measure a rapid rise in temperature of about 1/100,000 degree. Rapid heat production was detected during excitation of crab nerves, vagal nerves of the guinea pig, frog retinae and spinal cords, etc. It is probable that the observed heat production during excitation of nerve fibers is associated with exchange of bound calcium for univalent cations. In stimulation of the dark-adapted frog photoreceptor cells by a brief light pulse, the energy released by the cells in the form of heat was found to be more than one million times as large as the energy of the light pulse absorbed by the photopigment. In isolated spinal cord preparations of the bullfrog, it was shown that the observed heat production is associated with synaptic transmission of nerve impulses.

SQUID : ANIMALS INDISPENSABLE FOR EXPERIMENTATION

Gen Matsumoto. Electrotechnical Laboratory, Tsukuba Science City, Ibaraki 305.

The important problems in neuro-physiology have been successfully approached through the study of animals with particularly large neurons that are amenable to experimentation. The squid *Loligo, Doryteuthis* and *Sepioteuthis* have large nerve cells suitable for studying molecular events of synaptic communication between the cells and neural transmission along the axon.

Molecular organizations of the axonal cytoskeletons underlying the plasma membranes of squid giant neurons have been well analyzed, biochemically and morphologically. It has been found that the axolemma is specialized into two domains (microtubule- and microfilament-associated domains) by its underlying cytoskeletons. Intensive studies on the subaxolemmal cytoskeletons will lead to better understanding of their physiological roles in membrane excitation.

Axoplasm from the giant axon can be dissociated, allowing bidirectional organelle movements to be visualized along individual cytoplasmic filaments with video-enhanced differential interference contrast microscopy. The axoplasm deserves as a typical system for elucidating molecular basis of motile force generation.

Difficulties in squid experiments result from regional and seasonal limitations on the availability of natural squid stocks. These limitations are now partially eliminated by successfully maintaining the squid in an aquarium in the laboratory.

NEURAL TYPE DIFFERENTIATION AND Na CHANNELS IN THE CLEAVAGE-ARRESTED AND ISOLATED BLASTOMERES OF THE ASCIDIAN EMBRYO.

K. Takahashi, Y. Okamura and H. Okado. Dept. of Neurobiology, Inst. of Brain Research, Faculty of Medicine, University of Tokyo, Tokyo.

As previously reported, when the cell-cleavage of the Halocynthia embryo of the protochordate is arrested at the early developmental stages, such as 1- to 8-cell, and the arrested embryo is cultured further until the normal hatching time, the membrane of a large and multinuclear blastomere expresses one of four types of excitability, such as neural, epidermal, muscular and non-excitable types. The differentiation of excitability will be different depending upon the cytoplasmic factors in the blastomere and the cell-cell interaction with neighboring blastomeres. In the present study, the cell autonomous differentiation was analysed using blastomeres from the cleavage-arrested 4-cell embryo of Halocynthia roretzi. All four blastomeres in the 4-cell embryo evoked a long-lasting Ca action potential, suggesting epidermal type differentiation in terms of the excitability, but the other cell type may appear when each blastomere was cultured separately.

The 4-cell embryo was dechorionated by pronase, and the cleavage-arrested blastomeres were isolated and identified by the vital staining patterns of mitochondria. The isolated blastomere was continuously cultured at 10 °C in Jamarine artificial sea water containing extra 20 mM $CaCl_2$. Voltage-clamp measurements were performed more than twice for each blastomere. Changes in Na, Ca delayed K and anomalous K channels were examined during development and compared between anterior A3 and posterior B3 blastomeres. At the final stage of the development all blastomeres were penetrated again in order to determine differentiation types in terms of the existence of various ionic channels. Both anterior A3 and posterior B3 showed an increase in egg type Na channels with a shift of the critical level to hyperpolarized direction after 20 hours development. After 50 hours the increased Na channels in A3 which includes presumptive neural region were altered into the differentiated type with the depolarized critical level, while B3 blastomere showed an increase in differentiated Ca or differentiated Ca plus delayed K channels.

INTERSPECIFIC CHIMAERAS : A TOOL TO STUDY THE DEVELOPMENT OF THE NERVOUS SYSTEM

Nicole M. Le Douarin, Institut d'Embryologie du CNRS et du Collège de France, 49bis, Avenue de la Belle-Gabrielle 94736 NOGENT-sur-MARNE CEDEX (FRANCE)

In the Vertebrate embryo, the peripheral nervous system (PNS) arises mainly from a pluripotent structure, the neural crest. A fate map of the neural crest, constructed by using the quail-chick marker system, showed that it is regionalized into areas from which only a definite set of phenotypes originate. However, if the position of the neural crest cells is changed by heterotopic transplantations before the onset of their emmigration, it appears that virtually all the cell types forming the PNS ganglia can arise from any region of the neural crest, provided it is transplanted in the appropriate position in the embryo. This reveals the critical role played by the microenvironment experienced by the neural crest cells during their differentiation (1) and raises two questions : 1- what are the tissue factors selecting among the neural crest cell potentialities ; 2 - what is the state of committment of the neural crest cells during migration, and when they reach the site of gangliogenesis. Experiments carried out both in vivo and in vitro revealed that the precursors of sensory and autonomic neurons have different requirements for survival and differentiation. The role of the primordium of the central nervous system in the development of sensory neurons has been demonstrated along with the effect of BDNF on the survival of the early sensory precursors (2, 3). A clonal analysis of neural crest cell developmental potentialities is in progress and has already shown that during the process of migration the crest cells are highly heterogenous with respect to their state of committment (4).

ADVANCES IN MARINE BIOLOGY OF CHINA.

Ruiyu Liu (J.Y. Liu) Institute of Oceanology, Academia Sinica, Qingdao, China

Great progress has been made in marine biology of China since the founding of the People's Republic.

Based on the materials obtained through a series of comprehensive oceanographic and fishery resources surveys over entire China seas, hundreds of papers and tens of monographs have been published on the fauna and flora of Chinese seas, and hundreds of new taxa described. Based on these data, the "Fauna Sinica" and "Flora Phycologica Marina Sinica" are now in compilation. In the ecological studies, the characteristics of community structure and seasonal changes of quantitative distribution of plankton and benthos (as well as nekton and micro-organisms) were analysed and described; the biology and ecology of some of the important species have been studied in detail; delineation of marine faunal and floral regions in China seas have also been made; and the prediction of natural resources of important fishes and shrimps, necessary for marine fishery production and management, has been successively practiced. Sea ranching experiments by releasing juvenile shrimps and fishes into the sea for the enhancement of living resources (shrimp and fish stocks) have been successfully carried out in Jiaozhou Bay and many other bays and coastal areas in Huanghai and Bohai Sea, and the East and South China Sea, the production of shrimps in these areas is therefore increased in recent several years.

Experimental ecology, physiology and biochemistry studies on marine organisms have been conducted and great strides made. New findings in the studies on the nucleus-cytoplasm interrelationship during the early developmental stages of amphioxus, ascidians and fishes by nucleo-transplantation technique revealed that the segregation of the cytoplasm was gradually established during organogenesis and embryogenesis, but not during the fertilization after the entrance of the spermatozoid. Scientists led by the late Prof. T.C. Tung and his student Prof. S.C. Wu believed and have experimentally proved with their cytochemical studies that the cytoplasm played an important role in cell differentiation and in the transfer of genetic information. In their comparative photosynthetic study of the marine algae, Prof. C.K. Tseng and his student have put forth new proposal concerning three independent lines of evolution leading to the Rhodocyanophytae, the Chromophytae and the Chlorophytae. In the study of neurophysiology, marine biologists found the giant nerve fiber of the ventral nerve cord (with a diameter of 150-250 um) of the shrimp, *Penaeus orientalis*, is characterized by a very high conductivity of 80-200 m/sec, much higher than that of higher vertebrates. Phototaxis measurements of the pelagic fishes, *Decapterus maruadsi*, *Pneumatophorus japonicus*, etc. have been made and the results are useful and helpful for the improvement of the perse seine fishing technique.

Based on the findings obtained in the experimental ecology studies of induced maturation, spawning, larval breeding, nutrition and growth of juvenile and young fishes, shrimps, molluscs and seaweeds, effective methods for the mass production of fries of fishes and shrimps, spats of mussels, scallops, clams abalone and pearl oysters, juveniles of jelly fish and sea cucumber, and sporelings of kelp, purple laver and other species of sea weeds have been popularized in mariculture production. Production of shrimp, mollusc and seaweed culture increased drastically in recent years; annual production of cultivated shrimps in China reached 80,000 tons in 1986.

The international academic exchanges and cooperations in the fields of marine biology developed fast and are strengthened recently.

In the past 37 years, marine biologists of China have contributed much in the development of marine fisheries production, as well as the progress of marine biological sciences, and shall certainly contribute much more in the future to the socialist contruction and mordenization of our country.

PERSPECTIVES IN MARINE BIOLOGY.
J.D. Ebert, Carnegie Institution of Washington and Chesapeake Bay Institute, The Johns Hopkins University, Baltimore, Maryland.

It is a signal honor to celebrate with you the one-hundredth anniversary of the founding of the Misaki Marine Biological Station. Your invitation to speak about the future of marine biology was welcome, for the revolutionary thrust of science and technology today has the potential of eclipsing, even within the next decade, all of the advances wrought in the preceding century. I take as my theme our opportunity--indeed our imperative-- as marine biologists to work in the true service of mankind, to respond to real human needs, to battle man's ancient enemies of hunger, disease and ignorance--in short to truly enhance the quality of human lives through basic research. "We cannot escape from the past", wrote Rene Dubos in his paean to the symbiosis of humankind and the Earth, "but neither can we avoid inventing the future". But what future will we invent? How will we shape the world's marine biological laboratories as they enter their second centuries? Often the question is put: "How effectively can we harness the special power of biotechnology, that is derived from genetic engineering and immunology, to better understand the development and function of marine organisms?" The answer is found in the program of our international seminar. However, our challenge goes beyond the thrust of today's technology and its applications to the often unspoken question, "Is there a continuing justification for marine laboratories?" Today's biotechnology permits us to focus, ever more rapidly, on ourselves, even to contemplate sequencing the human genome. Is there still a pivotal role for fundamental research in such fields as biodiversity and marine biomedicine, or must we focus our efforts on the preservation of the marine environment and marine resources through coastal mariculture and other economically attractive technologies? I will address these questions, which are critical to the future of marine biology.

CLOSING REMARKS.
S. Kinoshita. Dept. of Biol. Saitama Medical School, Saitama.

On behalf of the organizing comittee of this symposium I would like to thank all of you, speakers, chairpersons, and all participants, for the success of this very active meeting.

These three days were very repleted days filled with stimulative and exciting presentations and discussions. The memory of this symposium will be the best monument for the centenial aniversary of the Misaki Marine Biological Station. Our Misaki Marine Biological Station is now making her first step to the second century. On the day of her new start, we are very happy to know that so many friends are together with us in solidarity.

And at last, but never at least, we are grateful for the Japan Society for the Promotion ofScience and the Fujihara Foundation of Science, by whose support this symposium was able to be held in such a splendid success.

Thank you and meet you again soon.

ZOOLOGICAL SCIENCE 4: 1138 (1987)

[Book Review]

New Horizons in Sperm Cell Research

HIDEO MOHRI, editor.
Japan Scientific Societies Press, Tokyo, and Gordon and Breach Science Publishers, New York.
1987, 546 pp.

This clearly organized book is based on papers presented at the Fifth International Symposium on Spermatology, held at Fujiyoshida, Japan, in 1986. Forty one invited and selected contributed papers are arranged according to the seven main topics considered at the meeting: 1. Spermatogenesis, Maturation, and Capacitation; 2. Evaluation and Control of Fertility; 3. Sperm Metabolism and Motility; 4. Sperm-egg Interactions; 5. Evolutionary Aspects of Sperm; 6. Male Contraception; 7. X- and Y-bearing Sperm.

Papers gathered under the last two headings represent the most accessible account of current trends devoted to analyzing the control of fertility in mammals including human. Four papers particularly give us a comperehensive bird-view of the extent to which methods to develop repeatable means of separating male- from female-determining spermatozoa have been accomplished. One of the more intriguing parts of the volume is the demonstration that certain products of post-meiotic gene expression are elaborated by developing germ cells in mice. Questions concerning the function of the products expressed by the haplotype gene remain open, but hopefully the elucidation of the significance of this gene expression should be done coupled with the *in vitro* culture of testis germinal explants that has now been successfully performed in amphibian system.

Mammalian spermatozoa enjoy greater focus among the investigations gathered under the first four headings. However, the papers addressed to these topics confirm that the comparative approach to the functional aspects of spermatozoa is highly rewarding. Such investigations include the elucidation of the molecular cascade which leads to the events such as motility and the membrane fusion of the acrosome reaction, first discovered in the spermatozoa of lower vertebrates and echinoderms and now known to be shared among many mammals as well. In this respect, what is diverse may be the environmental conditions provided by the male and female reproductive tracts, so that the efforts to elucidate the molecular basis for postgonadal maturation of sperm in diverse animal groups are warranted. A study on the biochemical characterization of isolated plasma membrane of sea urchin sperm also illustrates that invertebrates can still offer a paradigm for studies of gamete interactions.

Papers collected under the fifth heading represent the comparative and phylogenetic approaches that were particularly emphasized during the Symposium. These include the comparative examination of sperm ultrastructure for elucidating the taxonomical problems at specific levels, in several invertebrates including molluscs and annelids. Another example of the comparative approach may be seen in the analysis of the production of polymorphic spermatozoa, notably found in oligochaete annelids. The occurrence of such dimorphism might be relevant to the more conceptual questions as to why grossly excessive numbers of sperm are produced by males, if indeed spermatozoa exist only to fertilize, as discussed in one paper in this section. These issues, together with the most fundamental questions raised by C. R. Austin under the title "Are Sperms Really Necessary?", certainly inspire the readers of Zoological Science who have a deep concern for the broad aspects of sexual reproduction, including its genetic basis.

CHIAKI KATAGIRI
Hokkaido University
Sapporo, Japan.

ZOOLOGICAL SCIENCE 4: 1139 (1987)

[Book Review]

Emotions—Neuronal and Chemical Control

YUTAKA OOMURA, editor.
Japan Scientific Societies Press, Tokyo and S. Kager AG, Basel.
1986, 446 pp.

This book is a collection of 38 rather independent papers introducing mainly recent studies on the neural and chemical control of behaviors and physiological activities which compose the basis of our understanding of EMOTION. The papers are grouped into four chapters with the following titles: 1) Chemosensory Control of Feeding and Drinking, 2) Sensation-Energy Balance, 3) Neuroendocrine Affected Behavior and 4) Psycophysiological Correlates of Emotion. Many of the authors, as well as the editor, of this book are authorities of various fields of neurophysiology or psycophysiology, and studies presented in most of the papers are of the high level.

The editor seems to attempt to elucidate mechanisms existing behind "EMOTION" by integrating recent accomplishments in the field of studies on neural and neurochemical control mechanisms of feeding and drinking, since 20 papers of the first two chapters dealt with this problem. I do not know whether the editor thought his attempt successful or not, since he did not give his own conclusion in this book. Accordingly, each reader should conclude by him- or herself. However, this book still keeps its scientifically high quality and is useful to obtain current information on the control mechanism of food intake and related physiological functions. Neuroendocrine mechanisms are discussed in three papers of the third chapter and one paper of the last chapter. Some of them are too remote to emotion, although they can be highly evaluated. Two papers on the aggressive behavior also comprises an interesting part of this book.

The article most faithful to the title of the book is the paper by E. T. Rolls, entitled "A theory of emotion, and its application to understanding the neural basis of emotion". In this article, the author aims to clarify the neural bases of emotion and to provide a theoretical basis to understand the complex neural system which is involved in emotion. He first discussed the function of emotion, and presented the function of the amygdala and orbitofrontal cortex which are indispensable to understand the neural bases of emotion. This important and interesting article occupies only 20 pages out of 446 pages. The editor could have provided more space to this article. In the last chapter, in addition to the paper by Rolls, there are a few papers which are more directly related to emotion.

In conclusion, I felt that emotion is still far behind our scientific understanding, although neurophysiologists and psycophysiologists have achieved a great advance in these years. Many readers of this book might be inspired to challenge this hard target to attack.

SUSUMU ISHII
Waseda University
Tokyo, Japan.

ZOOLOGICAL SCIENCE 4: 1140 (1987)

[Book Review]

Indo-Pacific Fish Biology

Teruya Uyeno, Ryoichi Arai, Toru Taniuchi and Keiichi Matsuura, Editors.
The Ichthyological Society of Japan, Tokyo.
distributed by Business Center for Academic Societies Japan, Tokyo.
1986, 985 pp.

This is a comprehensive volume published as the Proceedings of the Second International Conference on Indo-Pacific Fishes held at the Tokyo National Museum, Ueno Park, Tokyo from July 29 to August 3, 1985 under the sponsorship of the National Science Museum.

It is honored by a foreward by His Imperial Highness Crown Prince Akihito as the Honorary President of the Conference. Almost all the representative Japanese ichthyologists of today and many authorities concerned from abroad comprising 24 countries assembled at the Conference. Since most of the appropriate reviewers of this book are contributors, I took the liberty of substituting for them. This book is compiled in three major parts in phylogenetic order, Agnatha, Chondrichthyes and Osteichthyes. At the beginning is placed a brief statement on the history of Japanese ichthyology. Recent advances in ichthyology, as in many other branches of zoology, were due to the application of modern biological methodology. These include transmission and scanning electron microscopies, biochemical techniques, and electrophysiological approaches, all of which have served as powerful exploratory tools as described in this book.

Part I Agnatha consists of eight papers selected from the symposium, the largest ever to be organized on the biology of cyclostomes. Part II Chondrichthyes composed of thirty papers deals with paleontology, systematics and zoophysiology, reproduction, growth, and behavior on elasmobranchs and chimaeroids. Part III Osteichthyes constitutes naturally the largest part, being the most frequent in any water, most important natural resourses for food and most frequently used research materials among the fish classes. Fifty-five papers are devoted to zoophysiology, systematics, biology of larvae, reproduction, ecology and evolutionary genetics.

Since the Devonian period, the age of fishes, stretching back less than half-a-billion years, most major branches of living fish classes were found as records preserved in rocks. The change from water to terrestrial life was first initiated in the Devonian by the early amphibians and completed by the reptiles in the late Paleozoic era. Later, from their reptilian ancestors, the warm-blooded birds and mammals were developed. Since goodbye fins and gills and welcome limbs and lung, these land dwellers have adapted themselves to almost every conceivable mode of life on land. In contrast, fishes have enjoyed inhabiting waters ever since those days. The modification and diversification of the basic design and function are so great in fishes as can be seen in this book that the fish world is comparable in taxonomic size to the rest of the vertebrates. However, it may be said that fishes have, nevertheless, maintained fundamentally the same basic design. Therefore, for a firm understanding of any vertebrate, knowledge on fish is considered essential.

Undoubtedly, this volume will become to be one of the dog-eared reference books for not only fish biologists but also those studying terrestrial vertebrates. The editors and the Ichthyological Society of Japan are to be commended for their contribution to its publication.

Seiichiro Kawashima
Editor, Zool. Sci.
Hiroshima University
Hiroshima, Japan.

ANNOUNCEMENT

The editors express their gratitude to the following reviewers, who evaluated papers for ZOOLOGICAL SCIENCE from September 1, 1986 to August 31, 1987. Without their assistance the journal could not function.

Aketa, K.
Akino, M.
Amemiya, S.
Ando, K.
Aoki, J.
Arai, R.
Arai, Y.
Asahina, S.
Asami, K.
Ashida, M.

Baba, K.
Bern, H. A.

Chiba, Y.

Egami, N.
Eguchi, E.
Eguchi, G.
Endo, K.

Fujii, R.
Fujimoto, M.
Funakoshi, K.

Gorbman, A.
Gotoh, T.

Hamaguchi, Y.
Hara, T.
Hashimoto, H.
Hayashi, K.-I.
Hayashi, S.
Hidaka, T.
Hihara, F.
Hiramoto, Y.
Hirano, H.
Hirano, T.
Hisada, M.
Hiwatashi, K.
Hoshino, K.

Ichikawa, M.
Ichikawa, T.
Ide, H.
Iga, T.
Ijiri, K.
Imai, H.
Imamura, T.
Inoue, S.
Inoué, S.
Ishihara, K.
Ishii, S.
Ishizaki, H.
Itô, T.
Iuchi, I.
Iwamatsu, T.
Iwasawa, H.

Kamishima, Y.
Katagiri, Ch.
Katakura, Y.
Kato, K.-I.
Kawahara, A.
Kawamoto, K.
Kawanabe, H.
Kikuchi, T.
Kikuyama, S.
Kinoshita, S.
Kobayashi, M.
Kobayashi, Y.
Kohno, S.-I.
Koji, T.
Kondo, H.
Kondo, N.
Konishi, K.
Koshida, Y.
Kimura, T.
Kuramoto, M.
Kuroda, Y.
Kurokawa, H.
Kuwasawa, K.

Mabuchi, I.
Machida, M.
Maruyama, K.
Matsui, M.
Matsumoto, A.
Matsumura, S.
Matsuoka, N.
Matsushima, O.
Miki-Noumura, T.
Mohri, H.
Mori, T.
Morino, H.
Morita, H.
Moriya, T.
Muneoka, Y.
Murakami, A.

Nagahama, Y.
Nagata, S.
Naito, N.
Naitoh, Y.
Naka, K.-I.
Nakamura, K.
Nakane, T.
Nakasone, Y.
Nakauchi, M.
Nishizuka, M.
Nomaguchi, T.
Noumura, T.

Ochi, O.
Ogawa, M.
Oguro, C.
Ohnishi, E.
Ohoka, T.
Ohta, Y.
Ohtaki, T.

ANNOUNCEMENTS

THE 59TH ANNUAL MEETING OF THE ZOOLOGICAL SOCIETY OF JAPAN

The 59th Annual Meeting of the Zoological Society of Japan will be held at the Sapporo Medical College from October 8 to 10, 1988. Further information and application forms will be sent to the domestic members in the April issue of 'Biological Science News' (No. 197). The deadline for application is July 15, 1988.

For application from foreign countries, please contact:

Professor Mituhiko Hisada
Organizing Committee of the 59th Annual Meeting
of the Zoological Society of Japan
c/o Zoological Institute, Faculty of Science,
Hokkaido University,
Kita 10-jyo Nishi 8-chome, Kita-ku,
Sapporo 060, Japan.
Phone: 011–716–2111, Ext. 2749.

ZOOLOGICAL SCIENCE AWARD

Annual awards for the best original papers have been established through the donation of Narishige Scientific Instrument Laboratory, Tokyo. The sum of about 500,000 yen will be awarded annually at the Annual Meeting of the Zoological Society of Japan to a few papers published in ZOOLOGICAL SCIENCE during the preceding calendar year. Every original papers published in this journal will automatically be candiates for the award. The aim of the award is to encourage contributions to this journal. Selection Committee for the award will be organized every year.

ZOOLOGICAL SCIENCE AWARD 1987 was given to the following three papers.

Hiroshi Nojiri, Moriyuki Sato and Akihisa Urano: Increase in the vasopressin mRNA levels in the magnocellular neurosecretory neurons of water-deprived rats: *in situ* hybridization study with the use of synthetic oligonucleotide probe. Vol. 3, No. 2, pp. 345–350, 1986.

Ryohei Kanzaki and Tatsuaki Shibuya: Identification of the deuterocerebral neurons responding to the sexual pheromone in the male silkworm moth brain. Vol. 3, No. 3, pp. 409–418, 1986.

Masakane Yamashita: *In vitro* maturation of the brittle-star *Amphipholis kochii* oocytes induced by cyclic AMP. Vol. 3, No. 3, pp. 467–477, 1986.

AUTHOR INDEX

A

B

C

D

I

J

K

O

P

Q

R

S

T

U

V

W

Y

Development Growth & Differentiation

Published by

the Japanese Society of Developmental Biologists

Papers in Vol. 29, No. 6. (December 1987)

Development, Growth and Differentiation (ISSN 0012–1592) is published bimonthly by The Japanese Society of Developmental Biologists, Department of Biology, School of Education, Waseda University, Tokyo 160, Japan. 1987: Volume 29. Annual subscription U. S. $ 110.00 including air speed delivery except Japan. Application to mail at second class postage rate is pending at Jamaica, NY 11431, U. S. A.

Outside Japan: Send subscription orders and notices of change of address to Academic Press, Inc., Journal Subscription Fulfillment Department, 6277 Sea Harbor Drive, Orlando, FL 32887, U. S. A. Send notices of change of address at least 6–8 weeks in advance. Please include both old and new addresses. U. S. A. POSTMASTER: Send changes of address to *Development, Growth and Differentiation,* Academic Press. Inc., Journal Subscription Fulfillment Department, 6277 Sea Harbor Drive, Orlando, FL 32887, U. S. A.

In Japan: Send nonmember subscription orders and notices of change of address to Business Center for Academic Societies Japan, 16–3, Hongo 6-chome, Bunkyo-ku, Tokyo 113, Japan. Send inquiries about membership to Business Center for Academic Societies Japan,4–16, Yayoi 2-chome, Bunkyo-ku, Tokyo 113, Japan.

Air freight and mailing in the U. S. A. by Publications Expediting, Inc., 200 Meacham Avenue, Elmont, NY 11003, U. S. A.

ZOOLOGICAL SCIENCE

VOLUME 4 NUMBER 6 **DECEMBER 1987**

CONTENTS

Indexed in:
Current Contents/LS and AB & ES,
Science Citation Index,
ISI Online Database,
CABS Database

Issued on December 15
Printed by Daigaku Printing Co., Ltd.,
Hiroshima, Japan

λ